

The chemistry of **peroxides**

The chemistry of peroxides, volume 2

Edited by Z. Rappoport © 2006 John Wiley & Sons, Ltd ISBN: 0-470-86274-2

Patai Series: The Chemistry of Functional Groups

A series of advanced treatises founded by Professor Saul Patai and under the general editorship of Professor Zvi Rappoport

The **Patai Series** publishes comprehensive reviews on all aspects of specific functional groups. Each volume contains outstanding surveys on theoretical and computational aspects, NMR, MS, other spectroscopic methods and analytical chemistry, structural aspects, thermochemistry, photochemistry, synthetic approaches and strategies, synthetic uses and applications in chemical and pharmaceutical industries, biological, biochemical and environmental aspects.

To date, over 110 volumes have been published in the series.

Recently Published Titles

- The chemistry of the Cyclopropyl Group (Volume 2)
- The chemistry of the Hydrazo, Azo and Azoxy Groups (Volume 2, 2 parts)
- The chemistry of Double-Bonded Functional Groups (Volume 3, 2 parts)
- The chemistry of Organophosphorus Compounds (Volume 4)
- The chemistry of Halides, Pseudo-Halides and Azides (Volume 2, 2 parts)
- The chemistry of the Amino, Nitro and Nitroso Groups (2 volumes, 2 parts)
- The chemistry of Dienes and Polyenes (2 volumes)
- The chemistry of Organic Derivatives of Gold and Silver
- The chemistry of Organic Silicon Compounds (2 volumes, 4 parts)
- The chemistry of Organic Germanium, Tin and Lead Compounds (Volume 2, 2 parts)
- The chemistry of Phenols (2 parts)
- The chemistry of Organolithium Compounds (2 volumes, 3 parts)
- The chemistry of Cyclobutanes (2 parts)
- The chemistry of Peroxides (Volume 2, 2 parts)

Forthcoming Titles

- The chemistry of Organozinc Compounds
- The chemistry of Anilines

The Patai Series Online

Starting in 2003 the **Patai Series** is available in electronic format on Wiley InterScience. All new titles will be published as online books and a growing list of older titles will be added every year. It is the ultimate goal that all titles published in the **Patai**

Series will be available in electronic format.

For more information see under **Online Books** on:

www.interscience.wiley.com

The chemistry of **peroxides**

Volume 2

Part 1

Edited by

ZVI RAPPOPORT

The Hebrew University, Jerusalem

2006



John Wiley & Sons, Ltd

An Interscience® Publication

The chemistry of **peroxides**

Volume 2

Part 2

Edited by

ZVI RAPPOPORT

The Hebrew University, Jerusalem

2006



John Wiley & Sons, Ltd

An Interscience® Publication

Copyright © 2006

John Wiley & Sons Ltd, The Atrium, Southern Gate, Chichester,
West Sussex PO19 8SQ, England

Telephone (+44) 1243 779777

Email (for orders and customer service enquiries): cs-books@wiley.co.uk

Visit our Home Page on www.wiley.com

All Rights Reserved. No part of this publication may be reproduced, stored in a retrieval system or transmitted in any form or by any means, electronic, mechanical, photocopying, recording, scanning or otherwise, except under the terms of the Copyright, Designs and Patents Act 1988 or under the terms of a licence issued by the Copyright Licensing Agency Ltd, 90 Tottenham Court Road, London W1T 4LP, UK, without the permission in writing of the Publisher. Requests to the Publisher should be addressed to the Permissions Department, John Wiley & Sons Ltd, The Atrium, Southern Gate, Chichester, West Sussex PO19 8SQ, England, or emailed to permreq@wiley.co.uk, or faxed to (+44) 1243 770620.

Designations used by companies to distinguish their products are often claimed as trademarks. All brand names and product names used in this book are trade names, service marks, trademarks or registered trademarks of their respective owners. The Publisher is not associated with any product or vendor mentioned in this book.

This publication is designed to provide accurate and authoritative information in regard to the subject matter covered. It is sold on the understanding that the Publisher is not engaged in rendering professional services. If professional advice or other expert assistance is required, the services of a competent professional should be sought.

Other Wiley Editorial Offices

John Wiley & Sons Inc., 111 River Street, Hoboken, NJ 07030, USA

Jossey-Bass, 989 Market Street, San Francisco, CA 94103-1741, USA

Wiley-VCH Verlag GmbH, Boschstr. 12, D-69469 Weinheim, Germany

John Wiley & Sons Australia Ltd, 42 McDougall Street, Milton, Queensland 4064, Australia

John Wiley & Sons (Asia) Pte Ltd, 2 Clementi Loop #02-01, Jin Xing Distripark, Singapore 129809

John Wiley & Sons Canada Ltd, 22 Worcester Road, Etobicoke, Ontario, Canada M9W 1L1

Wiley also publishes its books in a variety of electronic formats. Some content that appears in print may not be available in electronic books.

Library of Congress Cataloging-in-Publication Data:

LCCN: 83014844

British Library Cataloguing in Publication Data

A catalogue record for this book is available from the British Library

ISBN-13: 978-0-470-86274-2

ISBN-10: 0-470-86274-2

Typeset in 9/10pt Times by Laserwords Private Limited, Chennai, India

Printed and bound in India by Thomson Press, New Delhi

This book is printed on acid-free paper responsibly manufactured from sustainable forestry in which at least two trees are planted for each one used for paper production.

Dedicated to

Masaaki Mishima

and

Hiroshi Yamataka

Contributing authors

- Waldemar Adam Institute of Organic Chemistry, University of Würzburg, am Hubland, D-97094 Würzburg, Germany and Department of Chemistry, University of Puerto Rico, Rio Piedras, Puerto Rico 00931, USA. Fax: +1 787 807 0389; e-mails: wadam@chemie.uni-wuerzburg.de and wadam@adam.uprr.pr
- Wataru Ando Department of Chemistry, University of Tsukuba, Tennodai, Tsukuba, Ibaraki 305-8577, Japan. Fax: +81 29 851 4796; e-mail: wataru.ando@aist.go.jp
- Wilhelm J. Baader Instituto de Química, Universidade de São Paulo-Av. Prof. Lineu Prestes, 748 Bl., 12S CEP 05508-900, São Paulo—SP, Brazil. Fax: +55 113 815 5579; e-mail: wjbaader@iq.usp.br
- Robert D. Bach Department of Chemistry and Biochemistry, University of Delaware, Newark, Delaware 19716, USA. Fax: +1 302 831 6335; e-mail: rbach@udel.edu
- Mario D. Bachi Department of Organic Chemistry, The Weizmann Institute of Science, Rehovot 76100, Israel. Fax: +972 8934 4142; e-mail: mario.bachi@weizmann.ac.il
- Erick L. Bastos Instituto de Química, Universidade de São Paulo-Av. Prof. Lineu Prestes, 748 Bl., 12S CEP 05508-900, São Paulo—SP Brazil. Fax: +55 113 815 5579; e-mail: elbastos@iq.usp.br
- Albrecht Berkessel Department of Organic Chemistry, University of Cologne, Greinstr. 4, D-50939 Köln, Germany. Fax: +49 221 470 5102; e-mail: berkessel@uni-koeln.de
- Olga Bortolini Dipartimento di Chimica, Università della Calabria, Via Bucci, cubo 12C, I-87036 Rende (CS), Italy, Fax: +39 098 449 3307; e-mail: o.bortolini@unical.it
- Jean Cadet Laboratoire 'Lésions des Acides Nucléiques', LCIB-UMR-E n°3 CEA-UJF, Département de Recherche Fondamentale sur la Matière Condensée, CEA/Grenoble, F-38054 Grenoble Cedex 9, France. Fax: +33 43 878 5090; e-mail: jcadet@cea.fr
- Giovanni Cerioni Dipartimento Farmaco Chimico Tecnologico, Università di Cagliari, Via Ospedale 72, I-09124, Cagliari, Italy. Fax: +39 070 675 8553; e-mail: cerioni@unica.it

- James Chadwick Department of Chemistry, The Robert Robinson Laboratories, University of Liverpool, Liverpool, L69 7ZD, UK. Fax: +44 151 794 3553
- Valeria Conte Dipartimento di Scienze e Tecnologie Chimiche, Università di Roma "Tor Vergata", via della Ricerca Scientifica, I-00133 Roma, Italy. Fax: +39 067 259 4328; e-mail: valeria.conte@uniroma2.it
- Paolo Di Mascio Departamento de Bioquímica, Instituto de Química, Universidade de São Paulo, Ar. Prof. Lineu Prestes, 748 CP 26077, CEP 05513-970, São Paulo, SP, Brazil. Fax: +55 113 815 5579; e-mail: pdmascio@iq.usp.br
- Jens Hartung Fachbereich Chemie, Organische Chemie, Technische Universität Kaiserslautern, Erwin-Schrödinger-Straße, D-67663 Kaiserslautern, Germany. e-mail: hartung@chemie.uni-kl.de
- Vidyadhar Jadhav Center for Molecular Design and Synthesis, Department of Chemistry, Korea Advanced Institute of Science and Technology, Taejon 305-701, Korea. Fax: +82 42 869 5818
- Sung Soo Kim Department of Chemistry, Inha University, Incheon 402-751, South Korea. Fax: +82 32 867 5604; e-mail: sungsoo@inha.ac.kr
- Yong Hae Kim Center for Molecular Design and Synthesis, Department of Chemistry, Korea Advanced Institute of Science and Technology, Taejon 305-701, Korea. Fax: +82 42 869 5818; e-mail: kimyh@kaist.ac.kr
- Edward E. Korshin Department of Organic Chemistry, The Weizmann Institute of Science, Rehovot 76100, Israel. Fax: +972 8934 4142; e-mail: edward.korshin@weizmann.ac.il
- Joel F. Liebman Department of Chemistry and Biochemistry, University of Maryland, Baltimore County, 1000 Hilltop Circle, Baltimore, MD 21250, USA. Fax: +1 410 455 2608; e-mail: jliebman@umbc.edu
- Francesca Mocci Dipartimento di Scienze Chimiche, Università di Cagliari, Cittadella Universitaria di Monserrato, SS 554 Bivio per Sestu, I-09024, Monserrato (CA), Italy
- Paul M. O'Neill Department of Chemistry, The Robert Robinson Laboratories, University of Liverpool, Liverpool, L69 7ZD, UK. Fax: +44 151 794 3553; e-mail: P.M.oneill01@liv.ac.uk
- Michael Orfanopoulos Department of Chemistry, University of Crete, G-71409 Iraklion, Greece. Fax: +30 281 039 3601; e-mail: orfanop@chemistry.uoc.gr
- Min Young Park Center for Molecular Design and Synthesis, Department of Chemistry, Korea Advanced Institute of Science and Technology, Taejon 305-701, Korea. Fax: +82 42 869 5818
- Sarah L. Rawe Department of Chemistry, The Robert Robinson Laboratories, University of Liverpool, Liverpool L69 7ZD, UK. Fax: Fax: +44 151 794 3553

- Suzanne W. Slayden Department of Chemistry, George Mason University, 4400 University Drive, Fairfax, VA 22030-4444, USA. Fax: +1 703 993 1055; e-mail: sslayden@gmu.edu
- Cassius V. Stevani Instituto de Química, Universidade de São Paulo-Av. Prof. Lineu Prestes, 748 Bl., 10S CEP 05508-900, São Paulo—SP, Brazil. Fax: +55 113 815 5579; e-mail: stevani@iq.usp.br
- Manolis Stratakis Department of Chemistry, University of Crete, G-71409 Iraklion, Greece. Fax: +30 281 039 3601
- Ingrid Svoboda Fachgebiet Strukturforchung, FB 11, Material-und Geowissenschaften, Technische Universität Darmstadt, Petersenstr. 23, D-64287 Darmstadt, Germany. e-mail: svoboda@tu-darmstadt.de
- Alexei V. Trofimov Institute of Biochemical Physics, Russian Academy of Sciences, ul. Kosygina 4, Moscow 119991, Russian Federation and Institute of Organic Chemistry, University of Würzburg, am Hubland, D-97094 Würzburg, Germany. Fax: +7 495 137 4101; e-mail: avt_2003@mail.ru
- Nadine Vogl Department of Organic Chemistry, University of Cologne, Greinstr. 4, D-50939 Koln, Germany. Fax: +49 221 470 5102; e-mail: Nadine.Vogl@uni-koeln.de
- Georgios C. Vougioukalakis Department of Chemistry, University of Crete, G-71409 Iraklion, Greece. Fax: +30 281 039 3601
- Jacob Zabicky Institutes for Applied Research and Department of Chemical Engineering, Ben-Gurion University of the Negev, Beer-Sheva 84105, Israel. Fax: +972 8647 2969; e-mail: zabicky@bgu.ac.il
- Cong-Gui Zhao Department of Chemistry, University of Texas at San Antonio, San Antonio, TX 78249, USA. Fax: +1 210 458 7428; e-mail: cong.zhao@utsa.edu

Foreword

The earlier volume in *The Chemistry of Functional Groups* dealing with organic compounds including the O–O functional group in peroxides, hydroperoxides and related groups was edited by S. Patai and published in 1983. In the intervening 23 years there have been significant advances in the field, some of which are covered in books such as W. Ando's *Organic Peroxides*, Wiley (1992), and some were covered in chapters in Patai's Supplement E2 (1993).

The present volume comprises 17 chapters, written by 27 authors from 11 countries, and deals with theoretical aspects and structural chemistry of peroxy compounds, with their thermochemistry, ^{17}O NMR spectra and analysis, extensively with synthesis of cyclic peroxides and with the uses of peroxides in synthesis, and with peroxides in biological systems. Heterocyclic peroxides, containing silicon, germanium, sulfur and phosphorus, as well as transition metal peroxides are treated in several chapters. Special chapters deal with allylic peroxides, advances in the chemistry of dioxiranes and dioxetanes, and chemiluminescence of peroxide and with polar effects of their decomposition. A chapter on anti-malarial and anti-tumor peroxides, a hot topic in recent research of peroxides, closes the book.

Unfortunately, two planned chapters did not materialize, on polyoxides and on structural chemistry of organometallic and heteroatomic peroxides. The literature coverage is mostly up to the end of 2004.

I would be grateful to readers who draw my attention to mistakes in the present volume, or to the omission of chapters which deserve to be included in such a treatise.

ZVI RAPPOPORT

Jerusalem,
October 2005

The Chemistry of Functional Groups

Preface to the series

The series 'The Chemistry of Functional Groups' was originally planned to cover in each volume all aspects of the chemistry of one of the important functional groups in organic chemistry. The emphasis is laid on the preparation, properties and reactions of the functional group treated and on the effects which it exerts both in the immediate vicinity of the group in question and in the whole molecule.

A voluntary restriction on the treatment of the various functional groups in these volumes is that material included in easily and generally available secondary or tertiary sources, such as Chemical Reviews, Quarterly Reviews, Organic Reactions, various 'Advances' and 'Progress' series and in textbooks (i.e. in books which are usually found in the chemical libraries of most universities and research institutes), should not, as a rule, be repeated in detail, unless it is necessary for the balanced treatment of the topic. Therefore each of the authors is asked not to give an encyclopaedic coverage of his subject, but to concentrate on the most important recent developments and mainly on material that has not been adequately covered by reviews or other secondary sources by the time of writing of the chapter, and to address himself to a reader who is assumed to be at a fairly advanced postgraduate level.

It is realized that no plan can be devised for a volume that would give a complete coverage of the field with no overlap between chapters, while at the same time preserving the readability of the text. The Editors set themselves the goal of attaining reasonable coverage with moderate overlap, with a minimum of cross-references between the chapters. In this manner, sufficient freedom is given to the authors to produce readable quasi-monographic chapters.

The general plan of each volume includes the following main sections:

- (a) An introductory chapter deals with the general and theoretical aspects of the group.
- (b) Chapters discuss the characterization and characteristics of the functional groups, i.e. qualitative and quantitative methods of determination including chemical and physical methods, MS, UV, IR, NMR, ESR and PES—as well as activating and directive effects exerted by the group, and its basicity, acidity and complex-forming ability.
- (c) One or more chapters deal with the formation of the functional group in question, either from other groups already present in the molecule or by introducing the new group directly or indirectly. This is usually followed by a description of the synthetic uses of the group, including its reactions, transformations and rearrangements.
- (d) Additional chapters deal with special topics such as electrochemistry, photochemistry, radiation chemistry, thermochemistry, syntheses and uses of isotopically labeled compounds, as well as with biochemistry, pharmacology and toxicology. Whenever applicable, unique chapters relevant only to single functional groups are also included (e.g. 'Polyethers', 'Tetraaminoethylenes' or 'Siloxanes').

This plan entails that the breadth, depth and thought-provoking nature of each chapter will differ with the views and inclinations of the authors and the presentation will necessarily be somewhat uneven. Moreover, a serious problem is caused by authors who deliver their manuscript late or not at all. In order to overcome this problem at least to some extent, some volumes may be published without giving consideration to the originally planned logical order of the chapters.

Since the beginning of the Series in 1964, two main developments have occurred. The first of these is the publication of supplementary volumes which contain material relating to several kindred functional groups (Supplements A, B, C, D, E, F and S). The second ramification is the publication of a series of 'Updates', which contain in each volume selected and related chapters, reprinted in the original form in which they were published, together with an extensive updating of the subjects, if possible, by the authors of the original chapters. Unfortunately, the publication of the 'Updates' has been discontinued for economic reasons.

Advice or criticism regarding the plan and execution of this series will be welcomed by the Editors.

The publication of this series would never have been started, let alone continued, without the support of many persons in Israel and overseas, including colleagues, friends and family. The efficient and patient co-operation of staff-members of the publisher also rendered us invaluable aid. Our sincere thanks are due to all of them.

The Hebrew University
Jerusalem, Israel

SAUL PATAI
ZVI RAPPOPORT

Sadly, Saul Patai who founded 'The Chemistry of Functional Groups' series died in 1998, just after we started to work on the 100th volume of the series. As a long-term collaborator and co-editor of many volumes of the series, I undertook the editorship and I plan to continue editing the series along the same lines that served for the preceding volumes. I hope that the continuing series will be a living memorial to its founder.

The Hebrew University
Jerusalem, Israel
May 2000

ZVI RAPPOPORT

Contents

1	General and theoretical aspects of the peroxide group Robert D. Bach	1
2	The structural chemistry of acyclic organic peroxides Jens Hartung and Ingrid Svoboda	93
3	Thermochemistry of peroxides Suzanne W. Slayden and Joel F. Liebman	145
4	^{17}O NMR spectroscopy of organic compounds containing the O—O group Giovanni Cerioni and Francesca Mocci	171
5	Synthesis of cyclic peroxides Edward E. Korshin and Mario D. Bachi	189
6	Synthetic uses of peroxides Albrecht Berkessel and Nadine Vogl	307
7	Analytical and safety aspects of organic peroxides and related functional groups Jacob Zabicky	597
8	Silicon and germanium peroxides Wataru Ando	775
9	Selective formation of allylic hydroperoxides via singlet oxygen ene reaction Michael Orfanopoulos, Georgios C. Vougioukalakis and Manolis Stratakis	831
10	Polar effects in decomposition of peroxidic compounds and related reactions Sung Soo Kim	899

11	Peroxides in biological systems Jean Cadet and Paolo Di Mascio	915
12	Sulfur and phosphorus peroxides Vidyadhar Jadhav, Min Young Park and Yong Hae Kim	1001
13	Transition metal peroxides. Synthesis and role in oxidation reactions Valeria Conte and Olga Bortolini	1053
14	Contemporary dioxirane chemistry: Epoxidations, heteroatom oxidations and CH insertions Waldemar Adam and Cong-Gui Zhao	1129
15	Contemporary trends in dioxetane chemistry Waldemar Adam and Alexei V. Trofimov	1171
16	Chemiluminescence of organic peroxides Wilhelm J. Baader, C. V. Stevani and Erick L. Bastos	1211
17	Biomimetic Fe(II) chemistry and synthetic studies on antimalarial and antitumour endoperoxides Paul M. O'Neill, James Chadwick and Sarah L. Rawe	1279
	Author index	1347
	Subject index	1439

List of abbreviations used

Ac	acetyl (MeCO)
acac	acetylacetone
Ad	adamantyl
AIBN	azoisobutyronitrile
Alk	alkyl
All	allyl
An	anisyl
Ar	aryl
Bn	benzyl
Bu	butyl (C ₄ H ₉)
Bz	benzoyl (C ₆ H ₅ CO)
CD	circular dichroism
CI	chemical ionization
CIDNP	chemically induced dynamic nuclear polarization
CNDO	complete neglect of differential overlap
Cp	η^5 -cyclopentadienyl
Cp*	η^5 -pentamethylcyclopentadienyl
DABCO	1,4-diazabicyclo[2.2.2]octane
DBN	1,5-diazabicyclo[4.3.0]non-5-ene
DBU	1,8-diazabicyclo[5.4.0]undec-7-ene
DIBAH	diisobutylaluminium hydride
DME	1,2-dimethoxyethane
DMF	<i>N,N</i> -dimethylformamide
DMSO	dimethyl sulphoxide
ee	enantiomeric excess
EI	electron impact
ESCA	electron spectroscopy for chemical analysis
ESR	electron spin resonance
Et	ethyl
eV	electron volt

Fc	ferrocenyl
FD	field desorption
FI	field ionization
FT	Fourier transform
Fu	furyl(OC_4H_3)
GLC	gas liquid chromatography
Hex	hexyl(C_6H_{13})
<i>c</i> -Hex	cyclohexyl(<i>c</i> - C_6H_{11})
HMPA	hexamethylphosphortriamide
HOMO	highest occupied molecular orbital
HPLC	high performance liquid chromatography
<i>i</i> -	iso
ICR	ion cyclotron resonance
Ip	ionization potential
IR	infrared
LAH	lithium aluminium hydride
LCAO	linear combination of atomic orbitals
LDA	lithium diisopropylamide
LUMO	lowest unoccupied molecular orbital
M	metal
<i>M</i>	parent molecule
MCPBA	<i>m</i> -chloroperbenzoic acid
Me	methyl
MNDO	modified neglect of diatomic overlap
MS	mass spectrum
<i>n</i>	normal
Naph	naphthyl
NBS	<i>N</i> -bromosuccinimide
NCS	<i>N</i> -chlorosuccinimide
NMR	nuclear magnetic resonance
Pen	pentyl(C_5H_{11})
Ph	phenyl
Pip	piperidyl($\text{C}_5\text{H}_{10}\text{N}$)
ppm	parts per million
Pr	propyl (C_3H_7)
PTC	phase transfer catalysis or phase transfer conditions
Py, Pyr	pyridyl ($\text{C}_5\text{H}_4\text{N}$)

R	any radical
RT	room temperature
<i>s</i> -	secondary
SET	single electron transfer
SOMO	singly occupied molecular orbital
<i>t</i> -	tertiary
TCNE	tetracyanoethylene
TFA	trifluoroacetic acid
THF	tetrahydrofuran
Thi	thienyl(SC ₄ H ₃)
TLC	thin layer chromatography
TMEDA	tetramethylethylene diamine
TMS	trimethylsilyl or tetramethylsilane
Tol	tolyl(MeC ₆ H ₄)
Tos or Ts	tosyl(<i>p</i> -toluenesulphonyl)
Trityl	triphenylmethyl(Ph ₃ C)
Xyl	xylyl(Me ₂ C ₆ H ₃)

In addition, entries in the 'List of Radical Names' in *IUPAC Nomenclature of Organic Chemistry*, 1979 Edition, Pergamon Press, Oxford, 1979, p. 305–322, will also be used in their unabbreviated forms, both in the text and in formulae instead of explicitly drawn structures.

CHAPTER 1

General and theoretical aspects of the peroxide group

ROBERT D. BACH

*Department of Chemistry and Biochemistry, University of Delaware, Newark, Delaware
19716, USA*

Fax: +1 302 831 6335; e-mail: rbach@udel.edu

I. INTRODUCTION	2
II. BACKGROUND AND HISTORICAL PERSPECTIVE	3
III. BOND DISSOCIATION ENERGIES OF SELECTED PEROXO COMPOUNDS	5
IV. THE CHEMISTRY OF PEROXYNITROUS ACID	7
A. Historical Overview	7
B. Peroxynitrite Anion and Peroxynitrous Acid. Ground State Properties	8
C. Higher-lying Metastable States of Peroxynitrous Acid	10
D. Dissociative Pathways for Peroxynitrous Acid	13
E. HO–ONO Reactivity	14
1. Two-electron oxygen atom transfer to N, S, P and Se nucleophiles	14
2. Epoxidation of ethylene and propylene	17
3. Peroxynitrite anion oxidations	21
4. A comparison of peroxynitric acid and peroxynitrous acid	21
5. One-electron oxidation. The oxidation of methane with metastable peroxynitrous acid	22
6. The 1,2-rearrangement of peroxynitrous acid to nitric acid	25
V. THE CHEMISTRY OF DIOXIRANES	26
A. Background	26
B. Molecular Orbital Treatments of Dioxirane	27
C. The Electronic Structure of Dioxirane and Carbonyl Oxide	29
D. Oxygen Atom Transfer from Dioxiranes and Carbonyl Oxides	32
1. A comparison of DFT theory with higher-level methods	34
2. Epoxidation of alkenes with carbonyl oxides and dioxiranes	35
3. Relative rates of dioxirane epoxidation in solution	40
4. Oxidation of saturated hydrocarbons	44

The chemistry of peroxides, volume 2

Edited by Z. Rappoport © 2006 John Wiley & Sons, Ltd ISBN: 0-470-86274-2

VI. THE EPOXIDATION OF ALKENES WITH PERACIDS	48
A. Early Mechanistic Studies	48
B. Hartree–Fock Level Theoretical Calculations	48
C. Synchronous versus Asynchronous Transition States	50
D. Gas-phase Epoxidation of Selected Alkenes	58
E. Factors Influencing the Rate of Epoxidation	58
F. Epoxidation of Allylic Alcohols	65
VII. OXYGEN ATOM TRANSFER FROM SELECTED HYDROPEROXIDES	67
A. The Oxidation of Amines	67
B. The Oxidation of N, S, P and Se Containing Nucleophiles	70
C. Electronic Factors Influencing Oxygen Atom versus Hydroxyl Transfer	72
D. Model Studies on Enzymatic Oxidation of Heterocycles and Aromatic Rings	77
VIII. MISCELLANEOUS OXYGEN TRANSFER REACTIONS	82
IX. ACKNOWLEDGMENTS	84
X. REFERENCES AND NOTES	85

I. INTRODUCTION

Since dioxygen (O_2) is the second most abundant molecule in the atmosphere, it should not be too surprising that O–O bonds play such a major role in our lives. In a great many instances dioxygen is the source of the oxygen atoms used in the formation of peroxy compounds. The peroxy linkage is vital to both the incorporation of oxygen in the human body by biochemical syntheses and biochemical decomposition of molecules in our metabolism. It also is a major player in oxidative degradation, combustion, atmospheric and stratospheric chemistry, as well as in smog reactions. Thus, both the formation and decomposition of compounds containing the O–O bond pervade our lives in many ways and a thorough understanding of the mechanistic nuances of such chemical processes are of vital importance to us all.

More than two decades have passed since the last critical review in this Patai series was presented by Cremer¹. This comprehensive review considered mainly the conformational aspects, physical properties, molecular orbitals of relatively small peroxy compounds such as XO_2 , X_2O_2 , peroxides, peroxyacids and ozonides ($X = H, C, N, O$ and F). At that time, the peroxy systems were considered to be among the most difficult functional groups for computational treatment² owing to the very nature of the oxygen–oxygen bond. In fact, early theoretical studies on the conformational properties of hydrogen peroxide presented difficulties in just computing the O–O rotational barrier³ in HO–OH; processes involving O–O bond cleavage were treated with great caution. Many of these difficulties were simply a manifestation of the level of theory available at that time and the speed and sophistication of the computers available. The most commonly available method of calculation was Hartree–Fock theory (HF) and it soon became obvious that such single reference methods were not adequate for calculations involving the numbers of electron lone-pairs inherent to the O–O bond.

In the past decade more efficient code and faster computers have allowed the use of electron-correlated methods of calculation and this has opened this area of theoretical chemistry to a wide range of research groups. The present sequel will be focused mainly on recent theoretical studies on a variety of oxidative processes involving oxygen atom transfer. We will include an extensive description of the very recent chemistry of peroxy-nitrous acid (HO–ONO), dioxiranes, peracids and alkyl hydroperoxides. Since chemically realistic molecular systems can now be treated at an adequate level of electron-correlated

theory, new and exciting mechanistic details of oxidation chemistry can be gleaned from such computations that simply were not available to earlier investigators.

II. BACKGROUND AND HISTORICAL PERSPECTIVE

During the formative years of the development of theoretical procedures for the treatment of oxidative processes involving the peroxy moiety, the Hartree–Fock level of theory was most often applied. There were essentially no serious efforts to treat the O–O bond at the extended Huckel⁴ level or by the semiempirical CNDO/2⁵ or INDO⁶ methods. In fact, most such semiempirical methods are not specifically parameterized even today for the O–O bond. When the earlier versions of the Gaussian suite of programs (G-70) were widely distributed among academic institutions, the use of *ab initio* calculations for mechanistic studies became widespread although most researchers were still restricted to the use of a minimal basis set (STO-3G). This 1970 version had basis sets with s and p functions only and no gradient optimization methods or electron-correlation corrections were available. As Gaussian 80 and G82 became even more widely distributed, second-order Møller–Plesset perturbation theory (MP2) with the ability to handle d functions came into limited use with SCF gradients and MP2 first derivatives. Although the Gaussian^{7a} suite of programs was widely used, other codes such as Gamess, ACES, MOLPRO, CADPAC, Jaguar etc.^{7a–f} were added to the arsenal of the theoretical chemist. In fact, many such programs became sufficiently ‘user friendly’ that a number of experimentalists became adept at doing theoretical calculations to augment their laboratory experiments.

As Gaussian 92 became more widely available to the general research population, standard protocol was to use MP2 or higher-order Møller–Plesset theory up to MP4 to calculate the electron-correlation correction. However, the computational expense involved still typically mandated that the geometry be optimized at the HF level. While the use of HF theory proved satisfactory in some smaller systems, it also often led to major errors in the overall energetics of reactions, especially where lone-pair electrons were involved. The size of the practical basis set had expanded to 3-21G and many applications employed the 6-31G basis set and some even with d-functions on all heavy atoms [6-31G* or 6-31G(d)]. Minimal basis sets such as STO-3G were no longer publishable by the late 1970s while 4-31G basis sets were still acceptable for publication in major journals up to the late 1980s. By the mid 1980s the 6-31G(d) basis set had become the standard for most applications unless the size of the system was prohibitive.

The G92 program marked the introduction of density functional theory (DFT) although general skepticism prevented its more general use until the G94 code became available. During the early 1990s it was possible to optimize the geometry of some systems using the electron-correlated MP2 method and this recipe coupled with an MP4 energy correction became the most generally accepted method to study systems up to eight heavy atoms (nonhydrogen atoms). This general protocol was accepted by all but the most rigorous theoreticians to be at least adequate. However, this was not a panacea since calculations of transition structures involving the problematic O–O bond and related molecules sometimes led to structural problems even with the MP2 method. This problem was exacerbated by the fact that analytical second derivative calculations were not yet available, so the optimized structure could not be characterized by a frequency calculation as a minimum (all real frequencies) or a first-order saddle point (a transition state with one imaginary frequency).

In the mid-nineties more highly correlated methods such as CCSD⁸ and QCISD⁹ became available through distribution of the ACES and Gaussian 94 programs. Geometry optimization with these more cpu intensive programs was restricted for the most part to six heavy atoms. About this time multiconfigurational self-consistent-field (MCSCF) or

complete active space (CASSCF) methods became the rage. Such calculations were highly touted as being very accurate and especially good for fairly small biradicaloid systems where more than one reference state was anticipated. However, while this may be true for highly symmetrical alkenes and dienes, the choice of the active space actually used in more complex systems is highly subjective and can lead to serious problems. A cautionary note typically accompanies the suggested use of these multireference methods; these are not the 'black box' calculations so typically available today. During these earlier years most practitioners preferred to use the Gamess^{7b} code for MCSCF calculations since it was faster than Gaussian. However, a major drawback of these CAS methods existed in that a second-level electron-correlation correction to the total energies was essential in order to be able to compute relative energies of saddle points on a reaction surface.

The implementation of Gaussian 98 and the introduction of much faster computers coincided with the rise of the G1, G2 and CBS-Q methods, another milestone in computational chemistry, since chemical accuracy was now available for compounds up to six heavy atoms. Currently, the G3 and CBS-Q methods can treat systems up to ten heavy atoms without too much difficulty, affording bond energies in most cases within 1–2 kcal mol⁻¹ accuracy.

It was not until the introduction and widespread use of density functional theory (DFT) that reliable calculations on larger molecules became possible. This method is much faster than MP2, implicitly corrects for at least part of the electron correlation and also provides geometries and overall energetics in many cases comparable to those of higher-level methods. The B3LYP variant of the DFT code has proven to be especially tractable for systems as large as fifty heavy atoms even with a respectable size basis set. In many applications now being reported a 6-311+G(d,p) or 6-311+G** basis set is applied to the more difficult problems. The plus basis (+) is especially useful for the peroxy moiety since its function is to better describe anions or electron lone-pairs through the introduction of a large p-orbital on each heavy atom. In addition to the d-orbitals on each heavy atom (d), polarization functions (p) are included on each hydrogen atom to provide a better description of secondary- and hydrogen-bonding interactions. Today the B3LYP variant of DFT calculations is the method of choice for most investigators working on practical theoretical problems of oxidative chemistry. Direct comparison of B3LYP data with that of other methods by a number of investigators has proven its general applicability.

The scientific community has also been particularly fortunate that the software required to locate such complex minima and transition structures has kept pace with the accompanying explosion in hardware. It is now common place for individual investigators to have in their own laboratory a multiprocessor computer of equal computing power to the regional supercomputer laboratories of just a decade ago. However, without the more advanced code for locating such complex molecules we could not take advantage of such hardware developments. A decade ago most geometry optimization methods used the algorithm developed by Schlegel¹⁰ and introduced in the early Gaussian versions as the 'Berny algorithm'. Today, with such added options as modredundant optimization (redundant coordinate optimization¹¹) the number of gradient cycles required to locate the minimum-energy geometry of a saddle point is more than cut in one-half. The author of this review, an experimentalist, published his first theoretical paper on electrophilic addition to alkenes using extended Huckel theory in 1970^{12a}. He has had the good fortune to watch the evolution of theoretical chemistry to the point where one can now do a systematic theoretical study of alkene epoxidation with peracids and dioxiranes on chemically relevant molecules. At present, state-of-the-art calculations modeling enzymatic reactions are feasible. It is from this backdrop that we now present the more successful theoretical studies on several new and emerging areas of oxidative chemistry involving the O–O bond.

III. BOND DISSOCIATION ENERGIES OF SELECTED PEROXO COMPOUNDS

The chemistry of peroxides is to a first approximation simply dictated by the fact that the bond energy of the generic O–O bond is quite low. Consequently, many reactions of the peroxo moiety are thermally induced since it is assumed that O–O bond cleavage can be accomplished at relatively low temperatures. This is something of an enigma since homolysis produces alkoxy radicals (RO[•]) that are not especially stable. However, the lack of thermodynamic stability of most peroxides is also at the root of a major problem; difficulty in isolation and characterization of a great many peroxo compounds means that the accuracy of O–O bond dissociation energies (BDE) is sometimes questionable. Molecules possessing an O–O bond, which is electronically challenged with four pairs of lone-pair electrons, pose an interesting theoretical puzzle. Just what is responsible for the relatively weak O–O bond? Since by nature the oxygen radicals that result from O–O bond cleavage are less stable than many typical radicals, including carbon radicals, one could anticipate a much stronger O–O bond¹³.

Average bond energies (kcal mol⁻¹) of oxygen atoms bound to carbon (C–O ≈ 84), nitrogen (N–O ≈ 53) and fluorine (F–O ≈ 44) are all presumed to be substantially greater than that of oxygen bound to itself. Consequently, a relatively low bond energy (O–O ≈ 34 kcal mol⁻¹) has typically been ascribed to a generic peroxide¹. The unusual reactivity of peroxides is generally attributed to weakness of the O–O bond linkage and hence the ease with which it is homolytically cleaved. The kinetics of the thermal decomposition of a number of peroxides has been studied, and these bond dissociation enthalpies (BDE) have been used to derive O–O bond strengths. It was concluded that the strength of the O–O bond in dialkyl peroxides is about 37 (±1) kcal mol⁻¹ and is independent of the alkyl group. The BDE of the O–O bond in diacyl peroxides was estimated by this method to be only 30 (±1) kcal mol⁻¹. Established estimates of the amount of energy required to cleave homolytically a generic peroxide ZO–OY ranges from 47 for hydrogen peroxide down to about 29 kcal mol⁻¹ for dialkyl peroxodicarbonates (Table 1)^{1,14}. A more accurate value has recently been determined for H₂O₂, which corresponds to 50.5 kcal mol⁻¹ for the BDE at 298¹⁵.

It has been assumed that the enthalpy for homolysis of related peroxides such as ZO–OY can be derived from the mean BDE for ZO–OZ and YO–OY. For example, the enthalpy for O–O dissociation in peroxyacetic acid (ΔH_{298} 38.5 kcal mol⁻¹) has been derived^{14a} from the enthalpies of HO–OH (47 kcal mol⁻¹) and CH₃COO–OCOCH₃ (30 kcal mol⁻¹). It was the use of this relatively low BDE for diacyl peroxides to predict O–O bond energies that led to the low estimate for peracids. One major source of discrepancy between the accepted experimental O–O bond energies and theoretical values lies in the fact that the experimental O–O bond energies for diacyl peroxides are in error. The bond dissociation enthalpies used to derive the O–O bond energies were predicted on the basis of the assumption that a unimolecular one-step O–O bond dissociation was involved. The mechanism of O–O bond cleavage in diacyl peroxides is more complex than had been assumed initially and ¹⁸O oxygen scrambling was shown by Bach and coworkers to be quite facile by a unique ‘peroxo Oxy-Cope’ rearrangement^{16a}.

A variety of bond dissociation enthalpies at 298 K have been calculated at the G2MP2, CBS-Q and G2 levels of theory and a summary of typical O–O BDEs are presented in Table 1. It becomes immediately obvious that the estimate of the O–O BDE of a generic peroxide should be increased by 10 kcal mol⁻¹ to *ca* 44 kcal mol⁻¹.

The bond dissociation energy of hydrogen peroxide has been accurately predicted by high-level *ab initio* theory¹⁶. It was disclosed very early that Hartree–Fock theory, in the absence of electron-correlation correction, simply cannot be applied to problems involving O–O bond dissociation. For example, the predicted O–O bond energy in peroxyformic acid is only 1.0 kcal mol⁻¹ by Hartree–Fock theory, whereas at the

TABLE 1. Calculated O–O bond dissociation energies (ΔH_{298} , kcal mol⁻¹) at different levels of theory^a. Bond dissociation energies in the last column (BDE_{exp.}, kcal mol⁻¹) are experimental^{15, 18}

	B3LYP/6-31+G(d,p)	G2MP2	G2	CBS-Q	BDE _{exp.}
HO–OH		51.40	50.45	50.72	50.5
CH ₃ O–OH	37.5	46.04	44.96	44.68	44.6
CH ₃ O–OCH ₃	28.7	40.68	39.43	38.52	37.8
(CH ₃) ₃ CO–OH	36.7	48.30	45.00 ^b		
tricyclic Flavin hydroperoxide (FIHOOH) ^c	32.7				
(CH ₃) ₃ CO–OC(CH ₃) ₃			45.20		
H(C=O)O–OH		49.16	48.41	47.95	
(N=O)O–OH		22.83	21.96	20.44	
CH ₃ (C=O)O–OH		48.32	47.55	47.12	
CF ₃ (C=O)O–OH		48.90			
CH ₃ (C=O)O–O(C=O)CH ₃		37.89			
CH ₂ =C(CH ₃)O–OH		22.73			
H ₃ SiO–OH		52.46			
H ₃ SiO–OSiH ₃		55.45			
(CH ₃) ₃ SiO–OH		53.10			
(CH ₃) ₃ SiO–OSi(CH ₃) ₃			54.81	56.83	

^a For a more complete discussion including additional citations, see References 16–20.

^b Calculated by the G3 method.

^c The BDE value for tricyclic flavin hydroperoxide is taken from Reference 20c.

MP4//MP2/6-31G* level ΔE values for HO–OH and HCO₂–OH are predicted to be 49.2 and 50.7 kcal mol⁻¹, respectively¹⁷. The fact that these two BDEs are significantly higher than the accepted average bond energy of 34 kcal mol⁻¹ prompted a systematic theoretical study of O–O bond energies by Bach and his group¹⁶.

It is also noteworthy that both peroxyntrous acid and isopropenyl hydroperoxide have exceptionally low O–O BDE while silyl peroxides have systematically higher BDEs^{16b}. The pronounced decrease in the O–O bond energy of CH₃O–OCH₃ relative to HO–OH obviously reflects the greater stability of the CH₃O radical as compared to the HO radical. The substituent effects on the O–O bond enthalpy appear to be nearly additive since the G2 mean O–O bond enthalpy for dimethyl peroxide and hydrogen peroxide yields a BDE of 45.0 kcal mol⁻¹, equal to the G2 value for O–O bond energy in methyl hydroperoxide. These data should prove to be a worthwhile addition to the literature on this topic since it is the O–O bond energies that control much of the chemistry of peroxides.

Early theoretical studies on the epoxidation reaction were carried out at the MP2 level of theory and were mainly concerned with just identification of transition structures¹⁷. However, as the field matured it became necessary to also reproduce accurate activation barriers for these oxygen atom transfer reactions. It soon became evident that the B3LYP method typically underestimates the O–O BDE as noted for selected examples in Table 2. At a relatively high level of theory¹⁶, with an adequate basis set, it is possible to get bond strengths in quite good agreement with experiment^{15, 18}. It is especially relevant to point this out because this DFT variant is the most commonly applied method for calculations involving oxidation mechanisms. The B3LYP method has been used successfully in a variety of the procedures involving O–O cleavage and affords activation barriers in good agreement with experiment^{12b, 19, 20}. For example, the calculated activation barrier for the *m*-chloroperoxybenzoic acid epoxidation of cyclohexene agrees within 1 kcal mol⁻¹ with the experimental value^{19d}. DFT theory has also been used to calculate the O–O BDE in a series of fluoro-substituted peroxides²¹ and it has been applied to the optimization of

TABLE 2. Comparison of the calculated barriers (kcal mol^{-1}) for the oxidation of alkenes, dimethyl sulfide, trimethylamine and trimethylphosphine with peroxyxynitrous acid, peroxyformic acid and dimethyldioxirane (DMDO)

Reactants	Peroxyxynitrous acid (20.3) ^a	Peroxyformic acid (46.9) ^a	DMDO
Ethylene	18.3 ^b	18.8 ^b	19.4 ^c
Propylene	15.5 ^b	16.0 ^b	
Dimethyl sulfide	9.6 (6.9) ^d	6.6 ^e	9.4 ^e
Trimethylamine	5.3 (1.6) ^d	0.9 ^e	6.3 ^e
Trimethylphosphine	1.5 (-0.1) ^d	0.5 ^e	1.0 ^e

^a The O–O bond energies (D_{O}) calculated with G2 theory are given in parentheses.

^b At the QCISD(T)/6-31G*//QCISD/6-31G* level.

^c The barrier for ethylene epoxidation with DMDO was calculated at the QCISD(T)//QCISD(full)/6-31G* level. The barrier for ethylene oxidation with the parent dioxirane is lower ($16.6 \text{ kcal mol}^{-1}$ at the same level).

^d At the QCISD(T)/6-31G*//MP2/6-31G* level, the barriers calculated at the MP4/6-31G*//MP2/6-31G* level are shown in parentheses.

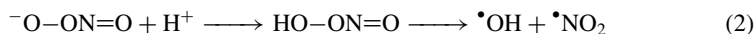
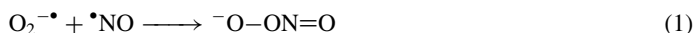
^e At the MP4/6-31G*//MP2/6-31G* level.

transition structures, modeling oxygen transfer from a tricyclic 4a-flavin hydroperoxide to trimethylamine, dimethyl sulfide, dimethyl selenide and trimethylphosphine^{21b}.

IV. THE CHEMISTRY OF PEROXYNITROUS ACID

A. Historical Overview

It has now been more than a decade since Beckman and his collaborators²² first disclosed their observations that the combination of two relatively unreactive, yet biologically relevant free radicals, superoxide anion and nitric oxide, would produce a new highly reactive physiologically important reagent. The interaction of these two presumably innocuous species appears to be diffusion controlled and produces a thermally stable peroxy anion, peroxyxynitrite (equation 1)²³.



At physiological pH the anion will be partially protonated (pK_a 6.8)²³ to produce a new and potent biological oxidizing agent, peroxyxynitrous acid, the first such peroxy acid known to be produced *in vivo*. This highly reactive oxidizing agent has a half-life of less than a second at 37°C . Although $\text{HO}-\text{ONO}$ decomposes at physiological pH, its nitrite anion is stable in base solution for months. Peroxyxynitrite anion ($\text{}^-\text{O}-\text{ON}=\text{O}$) is 36 kcal mol^{-1} higher in energy than its nitrate isomer ($\text{}^-\text{O}-\text{NO}_2$).

There were initially two proposals put forth to account for the powerful oxidizing capacity of peroxyxynitrous acid. Beckman and coworkers²² suggested that peroxyxynitrite dissociation produced a strong oxidant able to initiate many reactions currently used that imitated the action of hydroxyl radical. It was also proposed that this new oxidant could actually be the hydroxyl radical according to equation 2. The first and perhaps simplest explanation advanced for the atypical reactivity of this peroxy acid was O–O bond homolysis to produce the nitrogen dioxide radical ($\bullet\text{NO}_2$) and hydroxyl radical ($\bullet\text{OH}$) as the proximate oxidant²⁴. Hydroxyl radical is generally recognized as the most reactive of all biologically relevant ‘oxy radicals’. However, initial reports by Koppenol and coworkers²⁵

precluded the formation of $\bullet\text{OH}$ from the decomposition of $\text{HO}-\text{ONO}$ based upon thermodynamic calculations and kinetic measurements. The measured activation parameters for peroxyxynitrite decomposition ($\Delta H^\ddagger = 18 \pm 1 \text{ kcal mol}^{-1}$ and $\Delta S^\ddagger = 3 \pm 2 \text{ eu}$) suggested that the entropy of activation was too small to be consistent with the *ca* $12 \text{ cal mol}^{-1} \text{ K}^{-1}$ typically observed for $\text{O}-\text{O}$ bond homolysis in peroxides²⁵.

The second proposal is a bit more imaginative and arises from the above arguments that $\text{O}-\text{O}$ bond homolysis is much too slow to be involved in oxidations by peroxyxynitrate. Pryor and coworkers^{23,26} invoked the intermediacy of a metastable form of peroxyxynitrous acid ($\text{HO}-\text{ONO}^*$) in equilibrium with its ground state. This so-called ‘excited state’ of peroxyxynitrous acid has, to date, eluded detection or characterization by the experimental community. However, recent high-level theoretical calculations by Bach and his collaborators²⁷ have presented plausible evidence for the intermediacy of such a short-lived species with a highly elongated $\text{O}-\text{O}$ bond and have confirmed its involvement in the oxidation of hydrocarbons (see below). The discovery²³⁻²⁶ of this novel series of biologically important oxidants has fostered a new area of research in both the experimental and theoretical communities. In this chapter we will describe many of the more pertinent theoretical studies on both the physical properties and chemical reactivity of peroxyxynitrous acid.

B. Peroxyxynitrite Anion and Peroxyxynitrous Acid. Ground State Properties

Initially, McGrath and Powland²⁸ calculated various $\text{HO}-\text{ONO}$ conformers at the HF/6-31G(d) and MP2/6-31G(d) levels. They concluded that there are a total of eight conformers of $\text{HO}-\text{ONO}$, but realistically only the three most stable conformers were important. Subsequent calculations by Jin and collaborators²⁹ at the B3LYP/6-311+G(d,p) level concurred with these findings and studied the overall potential energy surface (PES) for $\text{HO}-\text{ONO}$ isomerization. The nomenclature presented in Figure 1 is the same as that developed earlier by McGrath and Powland^{28b}.

The different rotational isomers of peroxyxynitrous acid $\text{ONO}'-\text{OH}$ are labeled by their respective dihedral angles ($\langle \text{ONO}'-\text{O} \rangle$) and ($\langle \text{NO}'-\text{OH} \rangle$) designated 0, 30, 60, 90 and

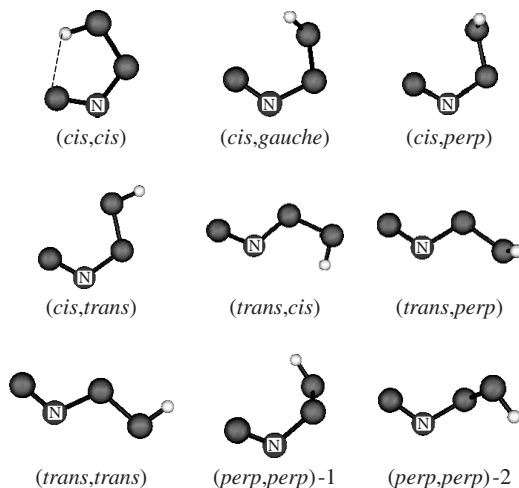


FIGURE 1. Equilibrium structures of $\text{HO}-\text{ONO}$ conformers

180° as *cis*, *gauche*, *perp* and *trans*, respectively. For example, the conformer with *cis* ONO'–O and *trans* NO'–OH is denoted by (*cis,trans*). Jin and coworkers²⁹ confirmed the earlier eight conformers of HO–ONO (Figure 1) to be stationary points. The three stable conformers are (*cis,cis*), (*cis,perp*) and (*trans,perp*), respectively, all have real vibrational frequencies²⁹, while the other five different conformers, (*cis,gauche*), (*cis,trans*), (*trans,cis*), (*trans,trans*) and (*perp,perp*), are treated as transition states because these structures all have an imaginary frequency.

Of the three stable conformers of HO–ONO, the (*cis,cis*) conformer with a five-membered hydrogen-bonded ring lies lower in energy than the others. Three different channels in the isomerization process of HO–ONO were found. The (*cis,perp*) is a bridge transferring from (*trans,perp*) to the (*cis,cis*) conformer²⁹.

The calculated barrier heights of these channels indicate that the (*trans,perp*) conformer can be more easily observed than the (*cis,cis*) and (*cis,perp*) conformers by experiment. However, as is noted below, at higher levels of theory the *cis,perp* appears to be the global minimum.

In earlier theoretical studies Shen and coworkers used Hartree–Fock self-consistent-field (HF) calculations with different basis sets to study water complexes of anionic ONO–O[−].³⁰ Two stable ONO–O[−] isomers, *cis* and *trans*, formed hydrogen bonds with H₂O molecules at different positions. Second-order Møller–Plesset perturbation theory (MP2) with a 6-311+G(d,p) basis set has also been applied to the study of ONO–O[−], (H₂O)_n (*n* = 1 or 2) complexes³¹. Koppenol and Klasinc studied the *cis* and *trans* conformers as well as the transition state for torsional motion of ONO–O[−] at the HF/6-31(d) level³². In their calculations, the *trans* conformer is slightly more stable than the *cis* form, and the rotational barrier was thought to be quite high. However, correlated methods (MP2) were also used to study this molecule, and they predict that the *cis* conformer is more stable than the *trans* conformer^{33,34}.

The metal salts of peroxyinitrite have also been studied using *ab initio* methods. We use the same nomenclature as McGrath and Powland's early paper on ONO–OH^{28b}, which distinguishes different conformers by their dihedral angles. For example, the structure with a *cis* ONO–O arrangement and the alkali atom bonded to the terminal oxygen with a perpendicular orientation is called '*cis,perp*'. Figure 1 describes the conformational aspects of the conformers studied.

Comparisons of ONO–OLi, ONO–ONa and ONO–OK establish several conformational trends³⁵. When the alkali atom size increases from Li to K, the relative stability between *cis,cis* and *trans,cis* decreases for the five-membered ring. The rotation of the OM bond away from the planar *cis,cis* conformation (i.e. NO–OM torsion) also becomes easier as the alkali atom changes from Li to Na to K. For the latter, the *cis,perp* minimum disappears, and *cis,trans* ONO–OK is a transition state that gives an activation barrier of 9–10 kcal mol^{−1} for NO–OK torsion. The B3LYP method predicts that *trans,perp* (or *trans,trans* in the case of ONO–ONa) will be 2–4 kcal mol^{−1} higher in energy than *trans,cis* ONO–OM. The transition state energies for converting *cis,cis* ONO–OM to *trans,cis* or *trans,perp* ONO–OM do not show a systematic trend with respect to the alkali atom, although the barriers (relative to the *cis,cis* structure) are in the 20–30 kcal mol^{−1} range.

A comparison of HF, MP2 and density functional methods in a system with Hartree–Fock wave function instabilities, ONO–OM (for M = Li, Na and K), shows that DFT methods are able to avoid the problems that *ab initio* methods have for this difficult class of molecules. The computed MP2 frequencies and IR intensities were more affected by instabilities than HF. The hybrid B3LYP functional reproduced the experimental frequencies most reliably. The *cis,cis* conformation of ONO–OM was highly preferred because of electrostatic attraction and was strongest in the case where M = Li. The small Li cation can fit in best in the planar five-membered ring. This is completely different from the nonionic

ONO–OH, which has only a slight preference for the *cis,cis* conformation and low barriers for NO–OH torsion^{28b}. The rotational barrier for ONO–O torsion was significant [20, 27 and 22 kcal mol⁻¹ for M = Li, Na and K, respectively, at the B3LYP/6-311+G(d) level of theory], as is the case for anionic ONO–O⁻ (27 kcal mol⁻¹)^{33,36}.

C. Higher-lying Metastable States of Peroxynitrous Acid

As noted above, the peroxynitrite anion (NOO–O⁻), formed by the direct combination of nitric oxide (NO) and superoxide anion (O₂⁻), is stable in alkaline solution. At physiological pH the anion is partially protonated, and its fate in aqueous media has been a primary point of contention. It was suggested that this strong oxidant might be a source of very potent biologically relevant hydroxyl radicals^{22b, 23, 25, 26}. One of the more intriguing aspects of HO–ONO chemistry is the earlier suggestion that O–O bond homolysis was slow, and the reactive species is a vibrationally excited form of HO–ONO^{22b}. However, its very short lifetime of *ca* 10⁻¹¹ s would preclude its involvement in bimolecular reactions, and Pryor and coworkers^{26a} advocated the existence of a higher-energy metastable form of peroxynitrous acid (HO–ONO*) that is in steady-state equilibrium with ground-state HO–ONO. Conventional wisdom has proposed homolysis to produce either •OH and •NO₂ or a caged radical (*OH··•NO₂). Careful experimentation has suggested that the yield of hydroxyl radicals at room temperature in deoxygenated and bicarbonate free water at pH 6.8 is about 10%²⁴.

However, reports of the yields of hydroxyl radicals from the decomposition of HO–ONO have ranged from 0 to 40%^{24a}. To date, no experimental evidence has been presented for the presence of such a metastable species. There have been numerous theoretical studies that have described the geometry^{37a}, decomposition pathways^{37b} and reactivity^{37c–e,38} of peroxynitrous acid. There is no low-energy channel in the dissociation of peroxynitrous acid that leads to the often anticipated products HNO and singlet oxygen (¹O₂)^{37b}. The lowest-energy pathway remains the formation of a radical pair (*OH + •NO₂) that may recombine to form nitric acid among other products. High-level *ab initio* calculations of the ground state (GS) and the low-lying excited states of peroxynitrous acid predict that the O–O bond dissociation is 18.8 ± 1 kcal mol⁻¹. Vertical excitation energies suggest two low-lying excited state bands at 296 and 240 nm with the 1¹A'' state being bound³⁹. A thermally excited form (HO–ONO*) of peroxynitrous acid has until recently eluded description.

Bach and his coworkers have only recently reported²⁷ *cis* and *trans* higher-lying singlet minima of peroxynitrous acid (HO···ONO) at several levels of theory, including CASSCF. The ground state (GS) structures of HO–ONO have been studied theoretically by a number of groups^{16a, 27, 37, 38}. While the *cis* form is the ground state at B3LYP, the perpendicular conformer is slightly more stable at the QCISD and CASSCF levels (Figure 2).

A search for the so-called 'excited state', that would presumably have a highly elongated O–O bond, required a relatively high level of theory. A potential problem associated with the location of such a biradicaloid species on the unrestricted potential energy surface (PES) is that despite attempting to optimize the geometry with an unrestricted (UB3LYP) description, the wave function can converge to the restricted PES ($\langle S^2 \rangle = 0$). However, you can be assured of at least starting the geometry search with an unrestricted initial guess by mixing HOMO and LUMO (guess = mix^{7a}, $\langle S^2 \rangle = 1.0$). Following this protocol, using a fairly flexible basis set [6-311+G(d,p) or larger] with a relatively small step size, a singlet species (A' symmetry) was located having an elongated O–O distance

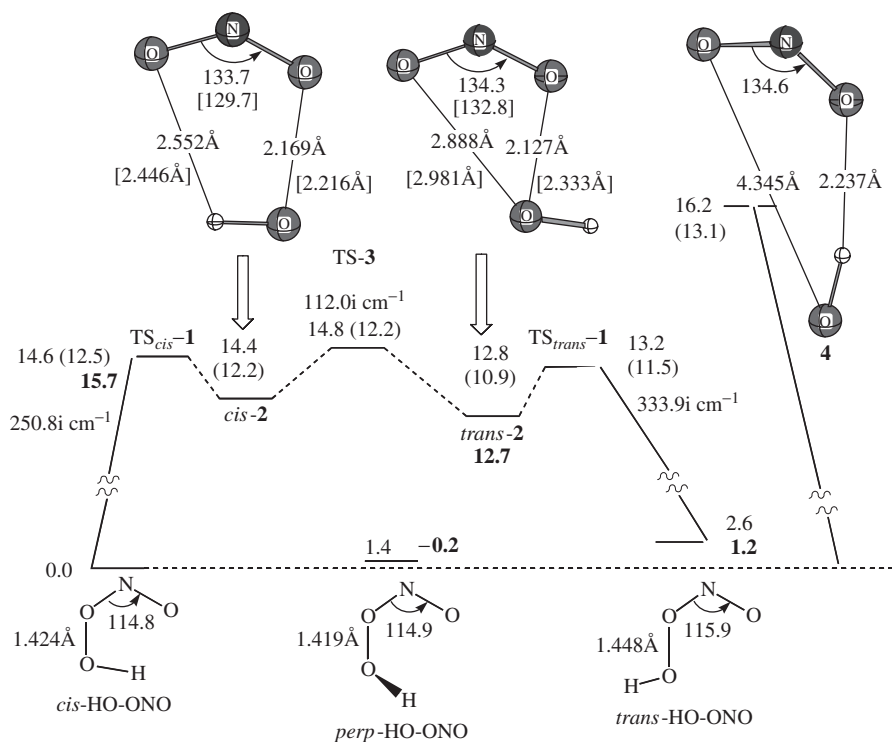


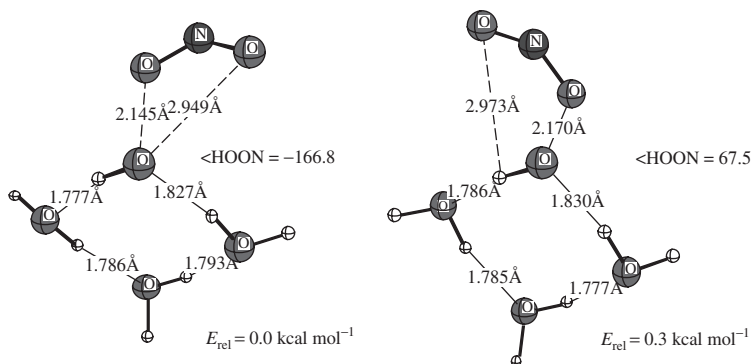
FIGURE 2. Energy diagram (kcal mol⁻¹) for the O–O bond elongation of *cis*- and *trans*-HO–ONO to form their respective higher-lying singlet biradicaloid minima. Plain numbers are at the UB3LYP/6-311+G(3df,2p) level. Bold numbers correspond to UQCISD(T)/6-311+G(d,p)//UQCISD/6-311+G(d,p). Geometrical data in brackets are at the CAS(12,10)/6-311+G(d,p) level

of 2.17 Å that was only 14.4 kcal mol⁻¹ [UB3LYP/6-311+G(3df,2p)] higher in energy than its *cis*-peroxynitrous acid GS precursor (Figure 2, *cis*-2). A second higher-lying minimum (*trans*-2) derived from the *trans* conformer of HO–ONO was observed and was 12.8 kcal mol⁻¹ higher in energy than ground-state HO–ONO. At the UQCISD(T) level, *trans*-2 was 12.7 kcal mol⁻¹ higher in energy than GS *cis*-HO–ONO, in excellent agreement with the DFT calculations. The ONO fragment of the metastable states appeared to correlate with the ²A₁ state of the NO₂ radical with an ONO bond angle of 134°. The transition state for O–O bond stretching (TS_{*cis*-1}, R_{O–O} = 1.947 Å, ν = 314.5i cm⁻¹) was found to be only 0.2 kcal mol⁻¹ higher in energy than *cis*-2. The TS associated with formation of a slightly more stable singlet, *trans*-2, was 13.2 kcal mol⁻¹ above the GS *cis* minimum for HO–ONO (TS_{*trans*-1}, R_{O–O} = 1.889 Å, ν = 333.9i cm⁻¹). The TS for interchanging *cis*-2 and *trans*-2 (TS-3) involves a simple in-plane migration of the OH group between the two terminal oxygens of the ONO radical fragment (ν = 112.0i cm⁻¹). The expectation values of the S² operator (⟨S²⟩ = 0.76 and 0.73) for *cis*-2 and *trans*-2 suggested a significant contamination of the singlet wave function with triplet character.

A complete active space (CASSCF) calculation^{7b}, to assess the multireference character of the wave function, used an active space comprising 12 electrons and 10 active orbitals [CAS(12,10)]. With a 6-311+G(d,p) basis set, the optimized geometries of *cis*-2 and *trans*-2 were quite close to those obtained with the DFT method (Figure 2). Another indication of the closeness of the DFT and CASSCF geometries was gleaned from single-point Brueckner Doubles calculations^{7a} on the energy differences between the GSs and *cis*-2 and *trans*-2. At the BD(TQ)/6-311+G(d,p) level, the energy difference between GS *cis*-HO-ONO and *cis*-2 was 15.5 kcal mol⁻¹ with the DFT geometry and 15.2 kcal mol⁻¹ with the CASSCF geometries. These energy differences were also in good accord with the DFT energies provided in Figure 2. Similarly, the energy differences between minimum GS *perp*-HO-ONO and *trans*-2 were 14.0 and 13.0 kcal mol⁻¹ at the DFT and CASSCF geometries, respectively. A CIPT2^{7d} correlation correction to the CASSCF wave function suggested an energy difference between the GS *perp*- and *trans*-2 of 4.9 kcal mol⁻¹. A multireference configuration interaction (MRCI)^{7d} calculation with the above active space (6.8 million contracted configurations) gave energy differences between GS and metastable conformers of 11.7 and 9.0 kcal mol⁻¹ for *cis*-2 and *trans*-2, respectively. The O-O bond dissociation enthalpy for GS *cis*-HO-ONO was calculated to be 22.0 kcal mol⁻¹ at the G2 level of theory^{16a}. The calculated dissociation limits for the GS *cis*-, GS *perp*- and GS *trans*-HO-ONO were 17.3, 15.9 and 14.6 kcal mol⁻¹. With zero-point energy corrections [ZPE at B3LYP/6-311+G(3df,2p)] these dissociation limits were 15.3, 14.3 and 13.4 kcal mol⁻¹, values well above the energies of the higher-lying minima located.

The O-O dissociation energy of 15.3 kcal mol⁻¹ for GS *cis*-HO-ONO was in good accord with the Gibbs experimental enthalpy and free energy of activation (18 ± 1 kcal mol⁻¹, $\Delta S^\ddagger = 3$ eu and 17 ± 1 kcal mol⁻¹, $\Delta S^\ddagger = 12$ eu, respectively) for the isomerization of peroxyxynitrite to its nitrate form (presumably by a dissociative mechanism). However, the calculated Gibbs free energy (5.9 kcal mol⁻¹) for dissociation of *cis*-HO-ONO ($\Delta S = 36$ eu) was significantly less than the experimental value for O-O dissociation in solution. While gas-phase and solution entropies are not directly comparable, the existence of *cis*-2 and *trans*-2 in the gas phase remains an open question. Similar questions concerning the weakly bound HO• and •NO₂ radicals reported by Houk and coworkers^{37c} (structure 4, Figure 2) were also raised by Musaev and Hirao^{40a}. The relationship of the above gas-phase calculations to HO-ONO under physiological conditions now becomes the more relevant question. This question cannot be addressed directly, but can be estimated with full geometry optimizations of *cis*- and *trans*-2 using the COSMO solvent model⁴¹. In THF solvent, the energy difference between GS *cis*-HO-ONO and *cis*-2 and *trans*-2 was 12.3 and 10.2 kcal mol⁻¹ [B3LYP/6-311+G(d,p)]. In methanol solvent, these energy differences increased to 13.9 and 12.4 kcal mol⁻¹, and in water media, the energy increases were 14.3 and 12.7 kcal mol⁻¹ [15.4 and 14.2 kcal mol⁻¹ with the larger 6-311+G(3df,2p) basis set]. Significantly, *cis*-2 and *trans*-2 both existed as energy minima in polar media with elongated O-O distances (2.140 Å and 2.089 Å) for *cis*-2 and *trans*-2 in water.

Since hydrogen bonding is not explicitly treated in the COSMO solvent model, the stability of *trans*-2 H-bonded to water molecules can be examined. Minima were located for *trans*-2 H-bonded to one, two, three and four H₂O molecules with O-O distances of 2.13, 2.12, 2.15 and 2.11 Å, respectively [BLYP/6-311+G(d,p)]. As anticipated, the overall complexation energy increased almost linearly with increasing numbers of H₂O molecules (-5.6, -15.9, -28.2 and -34.7 kcal mol⁻¹, respectively). Attempts to optimize *cis*-2 H-bonded to three waters resulted in a *perp*-2•3H₂O complex (<HOON = 68°). The energy difference between this complex and *trans*-2 H-bonded to 3H₂O was only 0.3 kcal mol⁻¹ (see below). By contrast, the interaction between the radical pairs in 4^{37c} (Figure 2) was sufficiently weak that the complex completely dissociated upon inclusion of just two H₂O molecules^{40a}.



Both *cis*- and *trans*-**2** when H-bonded to $3\text{H}_2\text{O}$ resulted in perpendicular complexes ($\langle \text{HO}-\text{ON} = 91.4^\circ$ and 116.2° , $\Delta E = 0.3 \text{ kcal mol}^{-1}$). The energy differences between *trans*-**2**• $3\text{H}_2\text{O}$ and the corresponding GS *perp*-HO-ONO• $3\text{H}_2\text{O}$ were 12.1 and 12.2 kcal mol⁻¹ for the *perp*-**2**• $3\text{H}_2\text{O}$ complex, thereby supporting the existence of these higher-lying singlets in aqueous media. It was suggested that solvated forms of *cis*-**2**• $3\text{H}_2\text{O}$ and *trans*-**2**• $3\text{H}_2\text{O}$ are representative of the elusive higher-lying biradicaloid minima that have been advocated by Pryor²⁶ as the metastable forms of peroxynitrous acid (HO-ONO*) largely responsible for the rich chemistry associated with this highly reactive oxidant.

D. Dissociative Pathways for Peroxynitrous Acid

Density functional theory has also been recently applied to several dissociative pathways of HO-ONO and its anion (ONO-O⁻) in aqueous solution. For example, the Gibbs free energy for the homolysis of peroxynitrous acid (HO-ONO → HO• + •ONO) is calculated to be $\Delta G(\text{aq.}) = 11.1 \text{ kcal mol}^{-1}$, a value in good agreement with experiment ($13.6 \text{ kcal mol}^{-1}$). For peroxynitrite homolysis (ONO-O⁻ → NO₂ + O•⁻) the calculated $\Delta G(\text{aq.}) = 13.0 \text{ kcal mol}^{-1}$ was obtained for ion-molecule complexes with water⁴².

The mechanism of the forward and reverse reaction of HOO• radical with NO has also been examined at the B3LYP/6-311+G(3df,2p) level⁴³. The dominant pathway for the formation of HO + NO₂ from the reaction of these two radicals involves the direct fragmentation of intermediate HO-ONO. The alternate pathway, isomerization of HO-ONO to nitric acid, is $5.2 \text{ kcal mol}^{-1}$ higher in energy.

The reaction between hydroxyl radical and NO₂ has also been characterized by Dolco and Röthlisberger⁴⁴ using the B3LYP method. These two radicals combine spontaneously to form HNO₃ and *cis*, *cis* peroxynitrous acid. Formation of the *trans*, *perp* rotamer had a small activation barrier of $4.5 \text{ kcal mol}^{-1}$. When this work was extended to the aqueous solution phase, HO-ONO was found to have a hydrophilic end (OH) and a hydrophobic portion (the ONO fragment) that induces a solvent cage. This group was the first to show that an explicit solvation model was required in order to get an adequate description of the conformational aspects of HO-ONO. The relative energy difference between the *cis* and *trans* conformers was enhanced in aqueous solution and the rotational barrier is increased to 21 kcal mol^{-1} due to solvent reorganization, a value much higher than that predicted in the gas phase^{44b}.

A high-level *ab initio* study of related reactions of alkyl nitrates (RO-NO₂) at the G3 and B3LYP/6-311++G(d,p) levels has revisited the reactions of alkyl peroxy radicals (ROO•) with nitric oxide. Activation barriers for the isomerization of RO-ONO to RO-NO₂ were found to be too high to account for the formation of alkyl nitrates

in tropospheric reactions. Since such isomerization reactions result in the loss of the high-energy O–O bond, they are typically highly exothermic based upon the analogous HO–ONO \rightarrow HO–NO₂ isomerization that has a calculated energy difference of 29.1 kcal mol⁻¹ at the G3 level⁴⁵.

E. HO–ONO Reactivity

1. Two-electron oxygen atom transfer to N, S, P and Se nucleophiles

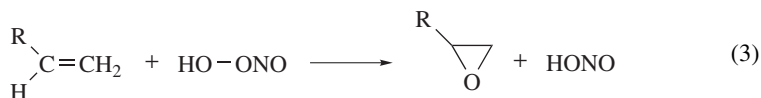
The similarity of the structure of peroxyxynitrous acid to the simplest peroxy acid, peroxyformic acid, immediately raised the question as to its relative reactivity as an oxygen atom donor. This became particularly relevant when it was recognized that the O–O bond dissociation energy ($\Delta G^\circ = 21$ kcal mol⁻¹)^{16,25} of HO–ONO was much lower than that of more typical peroxides. Consequently, peroxyxynitrous acid (HO–ONO) can be both a one- and two-electron oxidant. Since the O–O bond in HO–ONO is so labile, its chemistry is also consistent in many cases with that of the free hydroxyl radical.

Although one-electron oxidations may occur with the intermediacy of the hydroxyl radical, viscosity tests that serve to inhibit the diffusion of HO• have provided evidence against the formation of free hydroxyl radicals^{26a}. This prompted the suggestion by Houk and coworkers^{37e} that the hydroxyl radical is formed in a tight cage in aqueous solution, still capable of performing one-electron oxidations.

Two-electron oxidations (oxygen atom transfer) of amines, sulfides^{26b} and selenides⁴⁶ by HO–ONO have been observed experimentally. Earlier theoretical studies by Houk and coworkers^{37e} suggest that HO–ONO should provide oxidative reactivity comparable to that of organic peroxyacids. Transition structures were located for the concerted peroxyxynitrous acid oxidations of H₂S, NH₃ and ethylene. The activation energies of these reactions were calculated to be 13–18 kcal mol⁻¹ [B3LYP/6-31G(d)], confirming that these two-electron oxidations by HO–ONO are energetically feasible. For comparison, transition structures were also calculated for the peroxyformic acid oxidation of H₂S, NH₃ and ethylene at the B3LYP/6-31G* level; these are very similar in both energetics and geometries to those calculated earlier by Bach and coworkers at the MP2/6-31G* level¹⁷. Each transition structure involves substantial stretching of the O–O bond and only slight hydrogen transfer to the departing ONO⁻ anion fragment in much the same manner as peracid oxidation. This should not be too surprising since these two peroxides are formally isoelectronic.

The relatively short half-life of peroxyxynitrous acid hampers experimental studies of its reactions as an oxidizing agent. Therefore, theoretical methods can play a particularly useful role in describing the chemistry of peroxyxynitrous acid. For comparison of the HO–ONO fragment geometries found in transition structures, the geometric parameters of HO–ONO at various levels of theory are presented in Figure 3.

For practical reasons the two-electron oxidations of such prototypical substrates as alkenes, sulfides, amines and phosphines with peroxyxynitrous acid have been studied since this type of oxygen atom transfer reaction is similar to the corresponding oxidations with peroxyformic acid, where both experimental⁴⁷ and computational data are available^{12b, 17, 19a, 38, 48}. The oxidative reactions (equations 3–6) of these key substrates can serve as models for the oxidizing activity of HO–ONO in biochemical transformations involving substrates with the same functional groups or fragments^{49,50}. In this manner it can be ascertained whether biochemical reactions can share their basic mechanistic features with oxidations of the prototype molecules.



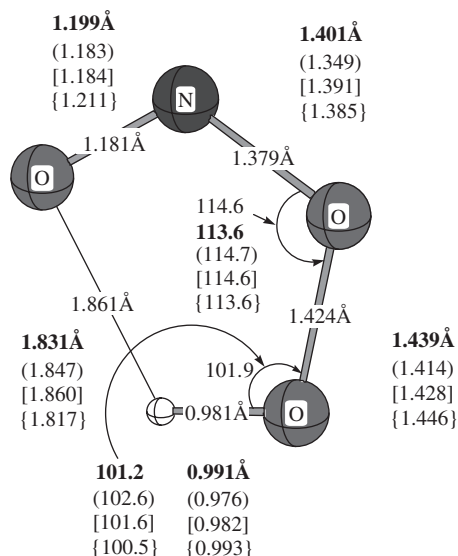
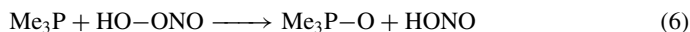
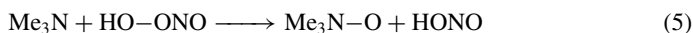
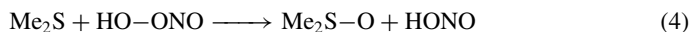


FIGURE 3. The geometry of the lowest-energy (*cis,cis*) conformation of peroxyacetic acid calculated at B3LYP/6-311+G(3df,2p), QCISD/6-31G* (bold numbers), CISD/6-31G* (in parentheses), B3LYP/6-311G** (in square brackets) and MP2(full)/6-31G* (in curly brackets) computational levels



Bach and coworkers³⁸ reported two-electron oxidations by HO–ONO of methyl substituted nucleophiles Me₃N, Me₂S and Me₃P. It is generally believed that methyl substitution provides more realistic substrates for such model studies^{17a}. The TSs are given in Figure 4. Relatively low activation barriers of 7.4, 7.5 and 0.6 kcal mol⁻¹ respectively at the B3LYP/6-311G(d,p) level attest to the reactivity of HO–ONO as an oxygen atom donor. A comparison of the activation barriers of peroxyacetic acid, peroxyformic acid and dimethyldioxirane at higher levels of theory are given in Table 2.

A comparison of the mechanisms of reaction of dimethyl sulfide and dimethyl selenide with peroxyacetic acid (ONO–OH) and peroxyacetic acid (ONO–OH) has also been reported by Musaev and Hirao^{40a} at the B3LYP/6-311+G(d,p) level of theory. The gas phase reactions with peroxyacetic acid were found to proceed by an oxygen atom transfer (two-electron oxidation) to produce the corresponding oxides, DMSO and DMS₂SeO, and the NO₂⁻ anion. As anticipated, the activation barrier was found to be 6–7 kcal mol⁻¹ lower for the third row Se nucleophile. The reaction of the neutral peroxide, HO–ONO, was suggested to be far more complex with the potential for both a concerted and stepwise mechanism for the oxidation of DMS in the gas phase. The stepwise process first involves homolysis to the radical pair, HO• + •NO₂, which can then coordinate with DMS to afford the intermediate adduct, (CH₃)₂S(OH)(NO₂), as exemplified below for a model compound of ebselen (Figure 5). There is a small barrier for the transfer of a hydrogen atom to form the thermodynamic products DMSO and HNO₂. In solution, it was suggested that the two pathways would be in competition.

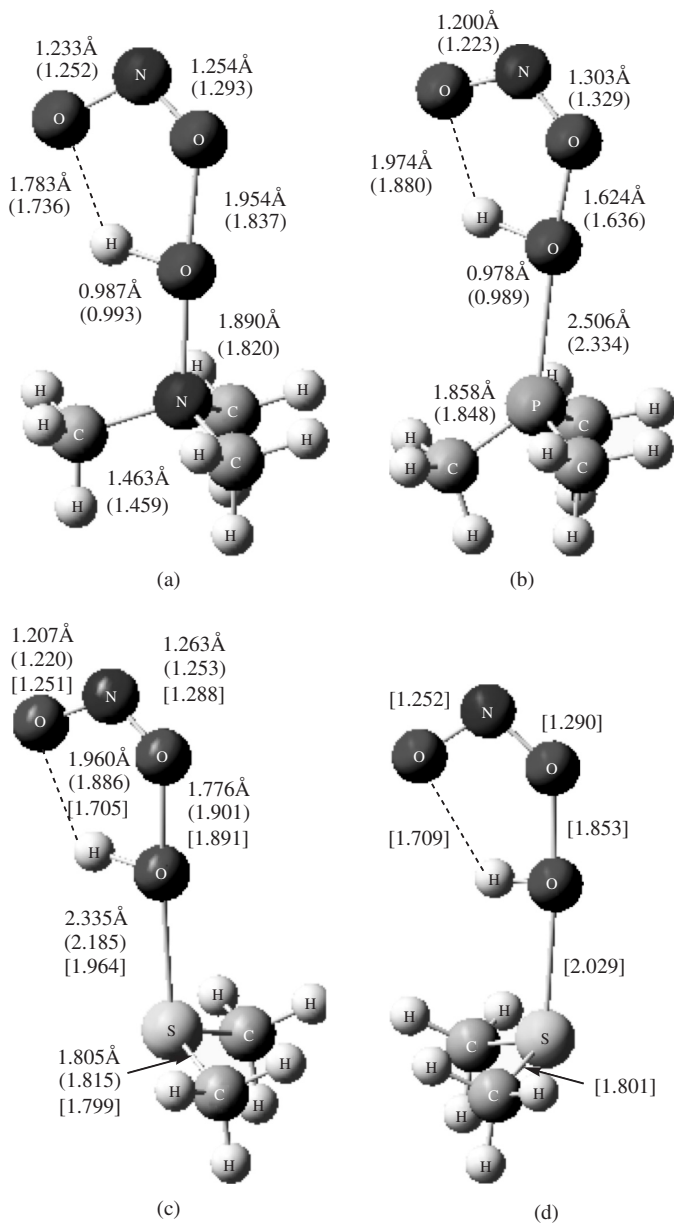


FIGURE 4. Transition structures for the oxidation of trimethylamine (a), trimethylphosphine (b) and dimethyl sulfide (c,d) with peroxy-nitrous acid optimized at the B3LYP/6-311G**, MP2(full)/6-31G* (in parentheses) and QCISD/6-31G* (in brackets) levels

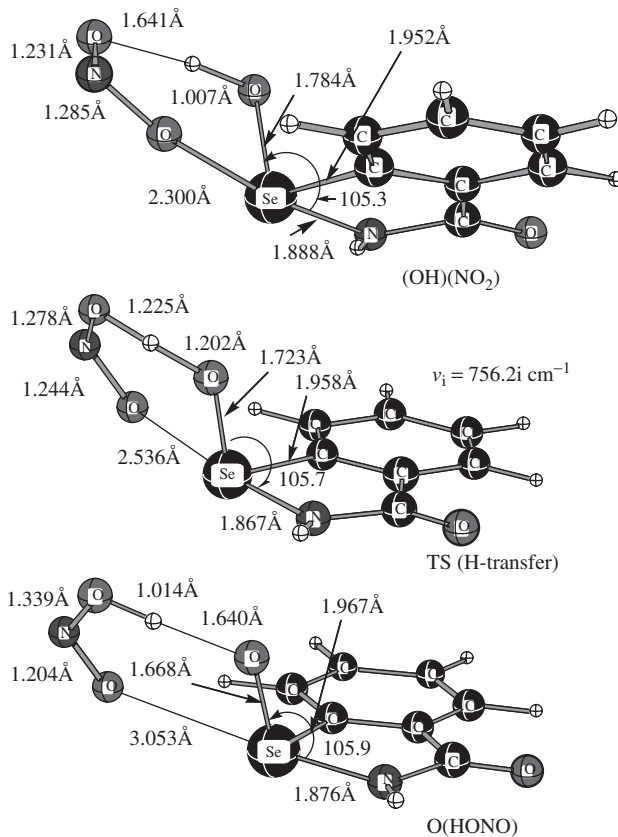


FIGURE 5. B3LYP/6-311G(d,p) optimized intermediates and the transition structure for the reaction of ebselen with peroxyxynitrous acid. For details see Reference 40a

A similar mechanistic dichotomy was suggested for the reactions of these two oxidants with a model compound of ebselen (1,2 benzoselenazol-3(2H)-one)^{40b}. The concerted two-electron pathway was found to be more favorable at the enthalpy level. However, inclusion of entropy effects favors a stepwise mechanism (Figure 5). Musaev and coworkers also reexamined the possible involvement of the weakly bound hydrogen bonded structure, $^{\bullet}\text{OH} \cdots \text{ONO}^{\bullet}$, (Figure 6), arising from homolysis of $\text{HO}-\text{ONO}$ that was first described by Houk and coworkers^{37c}. However, it was soon discovered that at the Gibbs free-energy level, with entropy corrections, this weakly bound structure is not stable relative to the $^{\bullet}\text{OH} + \text{ONO}^{\bullet}$ dissociation limit in the gas phase. It was also shown that the weak interaction between these radicals vanishes when increasing numbers of water molecules are explicitly included in the optimization. This point was also addressed above in the section on metastable $\text{HO}-\text{ONO}$.

2. Epoxidation of ethylene and propylene

High-level calculations of alkene epoxidation reactions with peroxyformic acid, $\text{HO}-\text{O}(\text{C}=\text{O})\text{H}$, which is isoelectronic with peroxyxynitrous acid [$\text{HO}-\text{O}(\text{N}=\text{O})$], have indicated

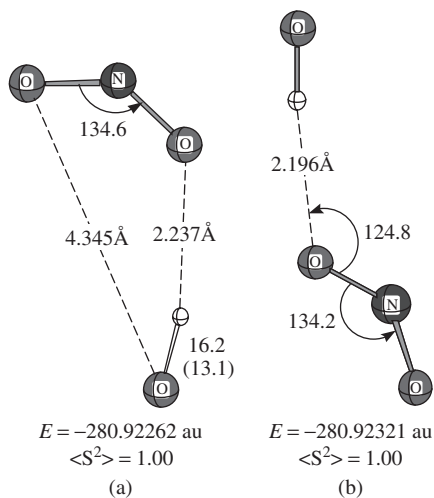


FIGURE 6. Two isomers (a and b) of the weakly bound hydrogen-bonded $\bullet\text{OH}\cdots\text{ONO}\bullet$ optimized at the UB3LYP/6-311+G(d,p) level of theory

a symmetrical transition structure with C–O bond lengths that are either equal (ethylene) or close to each other (propylene)³⁸. B3LYP computational results for alkene epoxidation reactions with peroxyformic acid are in good agreement with the data of higher-level calculations (QCISD(T)//QCISD, CASSCF, BD)^{12b}. It has been suggested that B3LYP calculations perform quite well for the transition structure geometries of epoxidation reactions. Both experimental and B3LYP data have recently appeared that also suggest that peracid epoxidations of alkenes proceed by a symmetrical transition structure⁵¹. Recent extended high-level CASSCF studies aimed specifically at this question have confirmed the original suggestion that if the wave function of the alkene is electronically symmetrical then one should anticipate a highly symmetrical TS⁵². These studies have also confirmed the spiro nature of most such symmetrical TSs and have basically disproved the existence of planar TSs⁵³ under typical conditions.

The oxidation of the simplest symmetrically substituted alkene, ethylene, is noteworthy in that an asymmetric ‘spiro’ transition state is observed. When constrained to C_s symmetry with equal forming carbon–oxygen bond lengths, the energy increases by only 0.1 kcal mol⁻¹. The spiro TS has the plane of the HO–ONO (or peracid) at right angles to the axis of the C=C bond. In an idealized spiro TS this angle is exactly 90°. While the formation of sulfoxides from sulfides by peroxyxynitrous acid is well-established^{26b}, epoxidations have not yet been observed in solution.

Both MP2 and B3LYP calculations resulted in unsymmetrical transition structures for ethylene and propylene epoxidations with peroxyxynitrous acid (Figure 7). The difference in the C–O bond distances between the ethylene carbons and the spiro-oxygen in b of Figure 7 is 0.393 Å at the B3LYP/6-311G** level and even larger (0.575 Å) at the MP2 level. Geometry optimization at the B3LYP/6-311+G(3df,2p) level also gave unsymmetrical transition structures with geometrical parameters close to those calculated with the smaller 6-311G** basis. The geometry optimizations carried out at the CISD and QCISD levels, however, led to an almost symmetrical transition structure for ethylene [a, the differences in the C–O bond distances are 0.001 Å at both the QCISD/6-31G* and CISD/6-31G* levels, Figure 7] and propylene [(a), Figure 8]. The harmonic frequencies

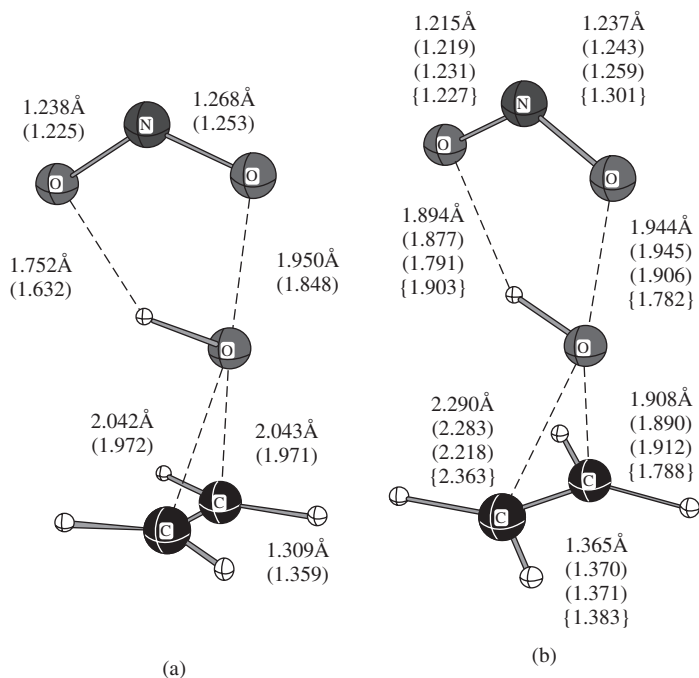


FIGURE 7. Geometrical parameters of symmetrical transition structure **a** for ethylene epoxidation with peroxyxynitrous acid optimized at the QCISD/6-31G* and CISD/6-31G* (values are in parentheses) levels and unsymmetrical transition structure **b** resulting from the geometry optimizations at the B3LYP/6-311+G(3df,2p), B3LYP/6-311G**, (values in parentheses), B3LYP/6-31G* (values in square brackets) and MP2(full)/6-31G* (in curly brackets) levels. The full set of QCISD/6-31G* geometrical parameters for **A** is given as the most reliable data

calculated for **A** at the CISD/6-31G* level confirm that it is a transition structure (one negative eigenvalue of the Hessian). Thus, the nature of the transition structures differs significantly at the MP2 and B3LYP levels relative to those calculated at the CISD/6-31G* and QCISD/6-31G* levels. Contrariwise, the B3LYP calculations of ethylene and propylene epoxidation reactions with peroxyformic acid give symmetrical-type transition structures in agreement with the QCISD and CISD results³⁸.

The triplet instability of both RB3LYP and RHF solutions is responsible for the difference in the symmetry of the ethylene–peroxyxynitrous acid transition structure. In general, an unsymmetrical transition structure with alkene epoxidation when an alternative symmetrical structure is possible, appears to be associated with an unstable wave function.

For the epoxidation of propylene with HO–ONO, both the QCISD and CISD calculations result in a Markovnikov-type transition structure, where the electrophile is slightly skewed toward the least substituted carbon, with a small difference in the bond lengths between the spiro-oxygen and the double-bond carbons (0.106 and 0.043 Å, respectively; Figure 8). The B3LYP calculations also lead to an unsymmetrical Markovnikov-type transition structure (**b**). However, the MP2/6-31G* geometry optimization results in an anti-Markovnikov-type structure (**c**) (Figure 8). The CCSD(T)/6-31G* and BD(T)/6-31G* barriers for ethylene epoxidation with HO–ONO calculated with the QCISD/6-31G*

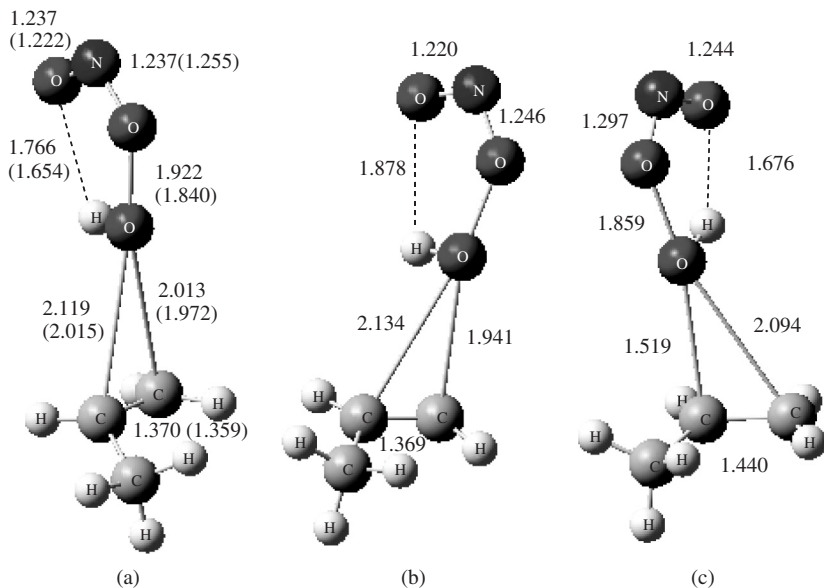


FIGURE 8. Geometrical parameters of the nearly symmetrical transition structure (a) for propylene epoxidation with peroxyinitric acid optimized at the QCISD/6-31G* and CISD/6-31G* (values are in parentheses) levels and unsymmetrical transition structures (b) and (c) resulting from the geometry optimizations at the B3LYP/6-311G** and MP2(full)/6-31G* levels, respectively

optimized geometries are 18.4 and 19.9 kcal mol⁻¹, respectively^{12b}. The BD(T) barrier coincidentally is the same as the BD(T)/6-31G**/QCISD/6-31G* barrier for the epoxidation of ethylene with peroxyformic acid. The CCSD(T)/6-31G**/CCSD/6-31G* (19.4 kcal mol⁻¹)¹ and CCSD(T)/6-31G**/QCISD/6-31G* barriers for both reactions are also close to each other. A basis set extension to the 6-311G** basis set does not result in a significant change of the CCSD(T) barrier for the C₂H₄ + HO-ONO reaction (19.1 kcal mol⁻¹). The B3LYP calculations with the 6-311G** and 6-31G* basis sets lead to transition structure geometries and activation barrier values (12.8 and 13.4 kcal mol⁻¹, respectively) for the epoxidation of ethylene (Figure 7) that are quite similar. The basis set extension to the 6-311+G(3df,2p) basis set results in a modest increase in the barrier to 14.8 kcal mol⁻¹. These B3LYP barrier heights are, however, underestimated when compared with the QCISD(T)//QCISD and QCISD(T)//CISD barriers (18.4 and 19.3 kcal mol⁻¹, respectively). The B3LYP barrier is also underestimated for the epoxidation of propylene with HO-ONO (a barrier of 10.2 kcal mol⁻¹) when compared to the QCISD(T)/6-31G**/QCISD/6-31G* barrier (15.5 kcal mol⁻¹)^{12b}. A similar trend of the B3LYP functional in underestimating the activation barrier has been found for the alkene epoxidation reactions with peroxyformic acid³⁸. As noted for the epoxidation of alkenes with HO-O(C=O)H, the activation barriers calculated at the QCISD(T)/6-31G* level with the B3LYP optimized geometries are close to those computed at the more computer-time-demanding QCISD(T)/6-31G**/QCISD/6-31G* and QCISD(T)/6-31G**/CISD/6-31G* levels of theory. It was gratifying to observe the same trend with HO-ONO, notwithstanding the fact that the B3LYP and QCISD (or CISD) transition state geometries differ from each other to a much greater extent than those for epoxidations with peroxyformic acid³⁸.

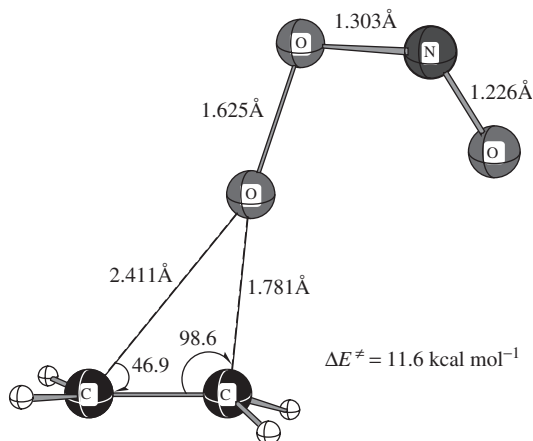


FIGURE 9. B3LYP/6-31G* transition structure for oxidation of ethylene with anion $\text{ONO}-\text{O}^-$

3. Peroxynitrite anion oxidations

The peroxynitrite anion appears to be a relatively poor one-electron oxidant, although DFT calculations indicate that it is capable of alkene epoxidation^{37c}. The fact that it has a substantially longer lifetime than peroxynitrous acid in solution makes this a much more viable oxidant. The transition structure for the oxidation of ethylene by peroxynitrite is shown in Figure 9. This reaction is exothermic ($\Delta E = -21.0 \text{ kcal mol}^{-1}$) with an activation barrier of $11.6 \text{ kcal mol}^{-1}$ based upon isolated reactants. However, the lower barrier is most likely just a consequence of the fact that the system is negatively charged. As expected, for the gas phase, there is an ion-molecule complex that is $4.8 \text{ kcal mol}^{-1}$ more stable than the reactants. This transition structure differs markedly from that found for neutral $\text{HO}-\text{ONO}$; the transition structure is highly asymmetrical. This is a nucleophilic addition transition state, and the second phase of the reaction would involve cyclization of the oxirane ring and expulsion of NO_2^- . This reaction would be especially facile for electron-deficient alkenes, analogous to the Michael-type epoxidation of enones by basic hydrogen peroxide. The oxidation of the more nucleophilic amines and sulfides, on the other hand, will be highly disfavored. Reactions of peroxynitrite are further complicated by its rapid reaction with spurious carbon dioxide. In fact, some earlier studies that did not take this into account gave questionable results. There is effectively no barrier to the exothermic ($\Delta E = -25.7 \text{ kcal mol}^{-1}$)^{37c} formation of the peroxynitrite adduct with CO_2 ($\text{ONO}_2\text{CO}_2^-$, Figure 10). Homolysis of the O-O bond to form $^*\text{NO}_2$ and the carbonate radical ($^*\text{CO}_3^-$) requires only $8.7 \text{ kcal mol}^{-1}$. The optimized structure exhibits a nearly 90° dihedral angle about the O-O bond^{37c}.

Musaev and Hirao have also reported theoretical studies on the reaction mechanisms of dimethyl sulfide and dimethyl selenide with peroxynitrite ($\text{ONO}-\text{O}^-$)^{40a}.

4. A comparison of peroxynitric acid and peroxynitrous acid

Peroxynitric acid ($\text{O}_2\text{NO}-\text{OH}$) is another important reactive two-electron oxidative species in this series of nitrogen-containing peroxides. The activation barriers reported by Houk and coworkers^{37d} for two-electron oxidation of NH_3 , H_2S and $\text{H}_2\text{C}=\text{CH}_2$ are similar to those found for $\text{HO}-\text{ONO}$ ^{37d}. It differs from peroxynitrous acid mainly in its

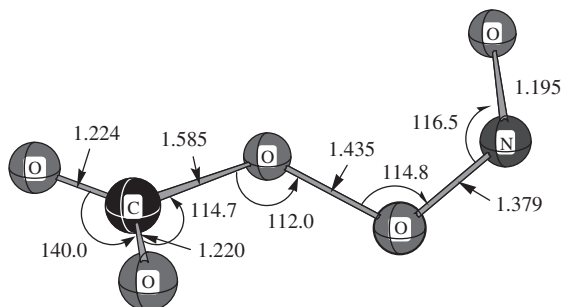


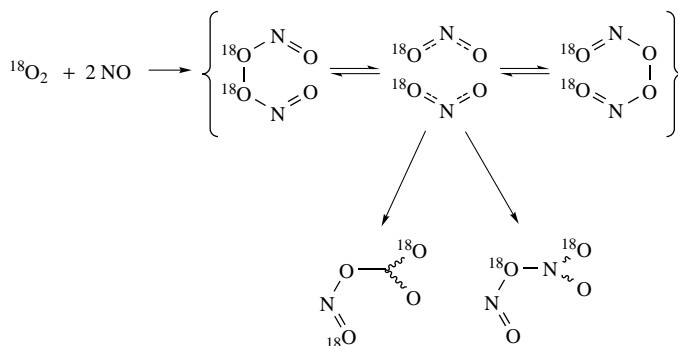
FIGURE 10. B3LYP/6-31G*-optimized structure for anion ONO-OCO_2^-

stability as a function of pH. The O–O bond strength in $\text{O}_2\text{NO-OH}$ is calculated^{37d} to be *ca* 20 kcal mol⁻¹ greater than that of HO–ONO. The central N–O bond of $\text{O}_2\text{NO-OH}$ is weaker than its O–O bond in agreement with experimental observation that dissociation produces NO_2 and OOH. The O–O BDE of $\text{O}_2\text{NO-OCO}_2^-$ is 26 kcal mol⁻¹ greater than that of ONO-OCO_2^- which accounts for its insensitivity to the presence of CO_2 .

A theoretical study reported earlier by McKee⁵⁴ of the N_2O_4 potential energy surface produced a new and interesting N_2O_4 isomer that ostensibly couples two NO_2 radicals through oxygen–oxygen bonds (ONO–ONO). This intermediate arises by the oxidation of nitric oxide (NO) by dioxygen. This interesting intermediate actually has a calculated negative O–O BDE due to the electronic reorganization energy acquired through the formation of GS NO_2 radicals. Subsequently, Houk and his coworkers⁵⁵ extended this study to include the rearrangement of this unusual peroxide. The well-known [3,3]-sigmatropic shift of 1,5-hexadiene (the Cope rearrangement)⁵⁶ provides an excellent template for the corresponding O–O bond cleavage and ‘inorganic Cope rearrangement’ of ONO–ONO as shown in Scheme 1. These data are consistent with the ¹⁸O₂ labeling distribution derived from trapping of intermediate ONO–NO₂.

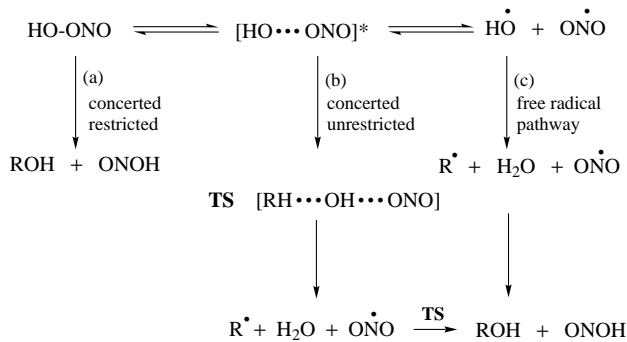
5. One-electron oxidation. The oxidation of methane with metastable peroxyxynitrous acid

Two fundamental questions of pertinence to the relevance of higher-lying metastable states of peroxyxynitrous acid are their relative stability in aqueous media and possible



SCHEME 1

involvement in biological reactions. In principle, hydrocarbon oxidation can take place by at least three pathways (Scheme 2). The concerted or two-electron pathway has been described by Rauk and coworkers^{37c}. The free radical pathway, advocated by many, has also been part of the controversy. The recent description of a metastable form of peroxyntrous acid (HO–ONO*) further complicates this mechanistic picture²⁷.



SCHEME 2

While it is well established that HO–ONO can be involved in such two-electron processes as alkene epoxidation and the oxidation of amines, sulfides and phosphines³⁸, the controversy remains concerning the mechanism of HO–ONO oxidation of saturated hydrocarbons. Rauk and coworkers advanced the hypothesis that the reactive species in hydrocarbon oxidations by peroxyntrous acid, and in lipid peroxidation in the presence of air, is the discrete hydroxyl radical formed in the homolysis of HO–ONO^{37c}. The HO–ONO oxidation of methane (equation 7) on the restricted surface with the B3LYP and QCISD methods gave about the same activation energy ($31 \pm 3 \text{ kcal mol}^{-1}$) irrespective of basis set size^{37c}.



Recent studies by Bach and coworkers^{27b} at the B3LYP/6-311+G(d,p) level also suggest a classical activation barrier for methane oxidation on the restricted ($\langle S^2 \rangle = 0.0$), two-electron surface, of $\Delta E^\ddagger = 31.1 \text{ kcal mol}^{-1}$ (TS-6_R, Figure 11). However, the more important question is whether hydrocarbon oxidation proceeds by a one-electron process involving the metastable form of peroxyntrous acid.

The initial prereaction complex (MIN-5) between GS HO–ONO (*cis*-conformer) and CH₄ is stabilized by only $0.4 \text{ kcal mol}^{-1}$ (Figure 11).

As in the case of the HO–ONO molecule itself, a transition state (TS-6) for the O–O bond elongation process was observed, where HO–ONO is complexed with a molecule of methane (C⋯O distance 3.54 \AA). This metastable O–O bond elongation TS-6 is only $10.2 \text{ kcal mol}^{-1}$ higher in energy than isolated reactants and had $\langle S^2 \rangle = 0.34$. The structure of the HO–ONO fragment is almost identical with the TS for formation of *cis*-metastable HO–ONO from GS HO–ONO with an O–O bond distance of 1.871 \AA and a $\langle S^2 \rangle = 0.4$. The difference in energy between this minimum and TS-6 is only $0.6 \text{ kcal mol}^{-1}$ and an $\langle S^2 \rangle = 0.76$ is consistent with its biradicaloid nature. The TS for hydrogen abstraction from methane occurs on the one-electron surface and confirms the involvement of the ‘excited’ form of peroxyntrous acid. MIN-10 is a structure that can be described as NO₂ and CH₃ radicals interacting with a water molecule. As a consequence of

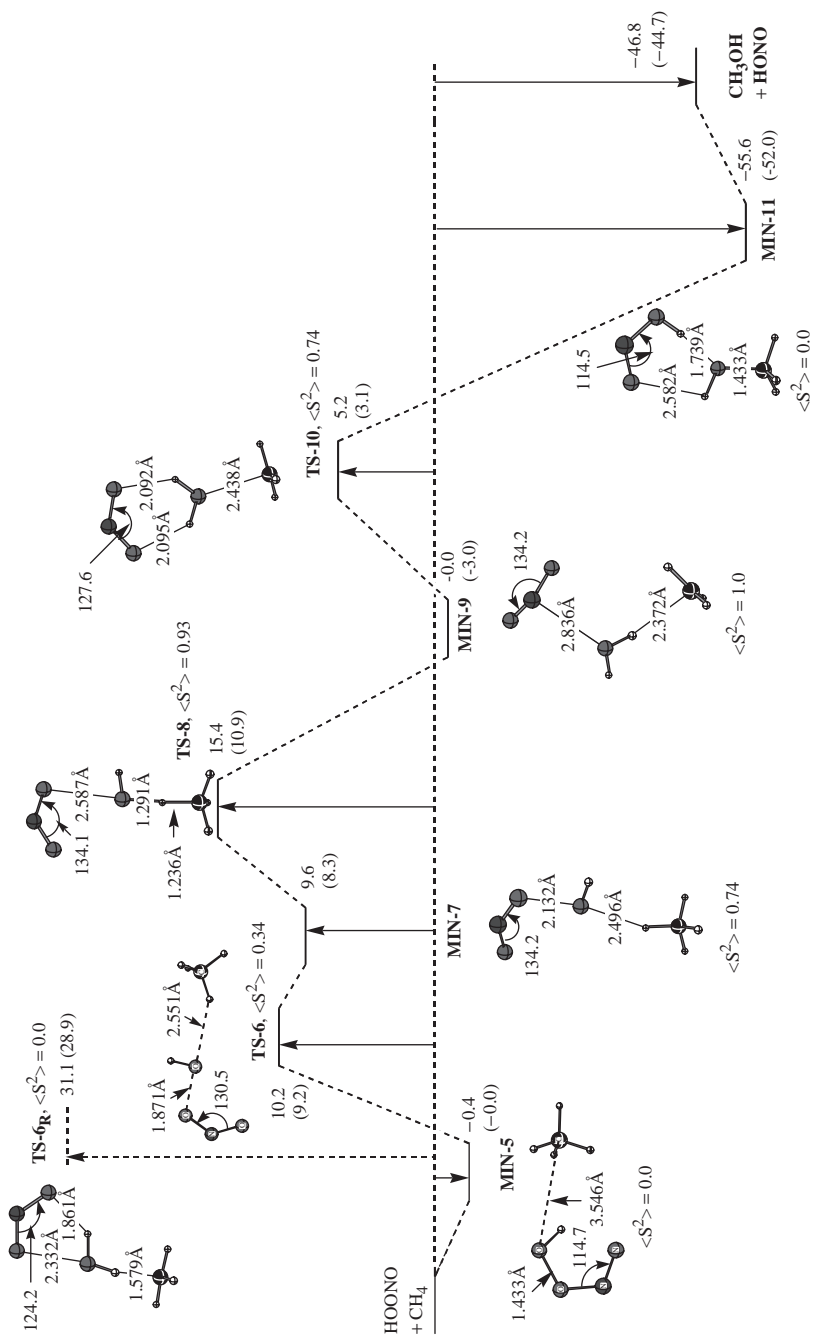


FIGURE 11. B3LYP/6-311+G(d,p) energy diagram for the reaction of HO-ONO and CH₄. Relative energies in kcal mol⁻¹ are with respect to isolated reactants (values in parentheses are with ZPE correction)

its biradical nature the calculated $\langle S^2 \rangle = 1.0$. The transition structure for concerted transfer of a hydroxyl radical to produce methanol, with hydrogen transfer to the NO_2 radical fragment forming H-ONO (TS-10), is just $5.2 \text{ kcal mol}^{-1}$ higher in energy than MIN-9. This transition structure ($\langle S^2 \rangle = 0.74$) is almost symmetrical with the $\text{O} \cdots \text{H}$ distances between the NO_2 and the H_2O fragment of 2.092 and 2.095 \AA and an $\text{O} \cdots \text{C}$ distance of 2.44 \AA . An IRC calculation reveals that this TS connects the $\text{H}_3\text{C}^\bullet \cdots \text{H}_2\text{O} \cdots \bullet\text{NO}_2$ complex to the $\text{CH}_3\text{OH} \cdots \text{HONO}$ complex (MIN-11), and that during that reaction pathway the first process is the C-O bond formation and after the barrier is crossed a H transfer from the developing $\text{CH}_3 - \text{OH}_2^+$ takes places leading to products, MIN-11. This final H-bonded product complex is $55.6 \text{ kcal mol}^{-1}$ more stable than isolated HO-ONO and methane. The very large difference in activation energies between closed-shell TS-6_R and TS-8 ($\Delta\Delta E^\ddagger = 15.7 \text{ kcal mol}^{-1}$) strongly supports the direct involvement of the metastable form of peroxyxynitrous acid (HO-ONO^*) advocated with tremendous insight by Pryor and coworkers²⁶ at the very outset of this rich new area of chemistry.

6. The 1,2-rearrangement of peroxyxynitrous acid to nitric acid

Another relevant pathway for peroxyxynitrous acid decomposition in aqueous solution is O-O bond dissociation and rearrangement of HO-ONO to nitric acid, HO-NO_2 , since it could potentially involve the 'excited' form of peroxyxynitrous acid (HO-ONO^*). Location of the TS for this formal 1,2-OH shift has proven to be difficult but both Sumathi and Peyerimhoff^{37a} and Dixon and collaborators^{37b} have reported activation barriers for this reaction ($39.0 \text{ kcal mol}^{-1}$, B3LYP and $21.4 \text{ kcal mol}^{-1}$, MP2). Presumably the latter second-order perturbation method does not treat the diradical nature of the TS adequately^{37a}. More recently Bach and coworkers^{27b} reported an activation barrier of $40.8 \text{ kcal mol}^{-1}$ with an O-O distance of 2.53 \AA and an O-N distance of 2.382 \AA in the transition state for OH to migrate from O in the ONO fragment to N in the NO_2 fragment of HO-NO_2 (Figure 12). In the TS the OH is essentially stationary between the two ONO oxygen atoms and animation of the single imaginary frequency ($\nu_i = 690.0i \text{ cm}^{-1}$) showed largely a rocking motion of the ONO nitrogen toward the OH group. This concerted rearrangement takes place on the restricted PES ($\langle S^2 \rangle = 0.0$). While the magnitude of the barrier may seem surprisingly high for such a loosely bound TS, it should be remembered that all 1,2-rearrangements to a lone pair of electrons are 4-electron processes that are formally forbidden and hence have a very high barrier. Thus, all three studies^{37a,b} conclude that the facile rearrangement of HO-ONO to HO-NO_2 involves dissociation to its free radical components and simple recombination.

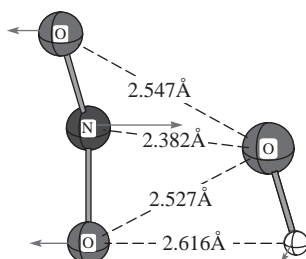


FIGURE 12. Transition structure for the isomerization of peroxyxynitrous acid to nitric acid optimized at the B3LYP/6-311+G(d,p) level of theory. Classical reaction barrier, TS total energy and imaginary frequency (vectors represented by the arrows) are $40.8 \text{ kcal mol}^{-1}$ (with respect to *cis*-GS HO-ONO), -280.86143 au and $690i \text{ cm}^{-1}$, respectively

V. THE CHEMISTRY OF DIOXIRANES

A. Background

For most of the past century rather simple oxidizing agents such as hydrogen peroxide, alkyl and aryl hydroperoxides and peracids have been used as the preferred oxidizing agents in a variety of synthetic applications. However, over the past two decades a second major area of peroxo chemistry has evolved that has found specific uses for dioxiranes in complex organic syntheses. In the earlier stages of development rather primitive dioxiranes were prepared or generated *in situ* by oxygen transfer from water-soluble peroxo compounds such as OXONE to simple ketones. The characterization of dioxiranes has been seriously hampered by the fact that the parent dioxirane has only been observed as a labile species in the gas phase and its geometry determined by microwave spectroscopy⁵⁷. The most commonly used dioxirane, dimethyldioxirane (DMDO), was isolated from an acetone solution by Jeyaraman and Murray⁵⁸ and can be kept at room temperature for several days. Methyl(trifluoromethyl)dioxirane (TFDO) was first isolated by Curci and coworkers⁵⁹ and has served well as a highly reactive oxygen atom donor. Since these are very labile oxidants, we must rely heavily upon calculations at a high level of theory for structural information (Figure 13).

Dimesityldioxirane, a crystalline derivative, has been isolated by Sander and colleagues⁶⁰ and subjected to X-ray analysis. The microwave and X-ray data both suggest that dioxiranes have an atypically long O–O bond in excess of 1.5 Å. Those factors that determine the stability of dioxiranes are not yet completely understood but what is known today will be addressed in this review. A series of achiral, and more recently chiral oxygen atom transfer reagents, have been adapted to very selective applications in the preparation of complex epoxides and related products of oxidation. A detailed history and survey of the rather remarkable evolution of dioxirane chemistry and their numerous synthetic applications is presented in Chapter 14 of this volume by Adam and Cong-Gui Zhao. Our objective in this part of the review is to first provide a detailed theoretical description of the electronic nature of dioxiranes and then to describe the nuances of the mechanism of oxygen atom transfer to a variety of nucleophilic substrates.

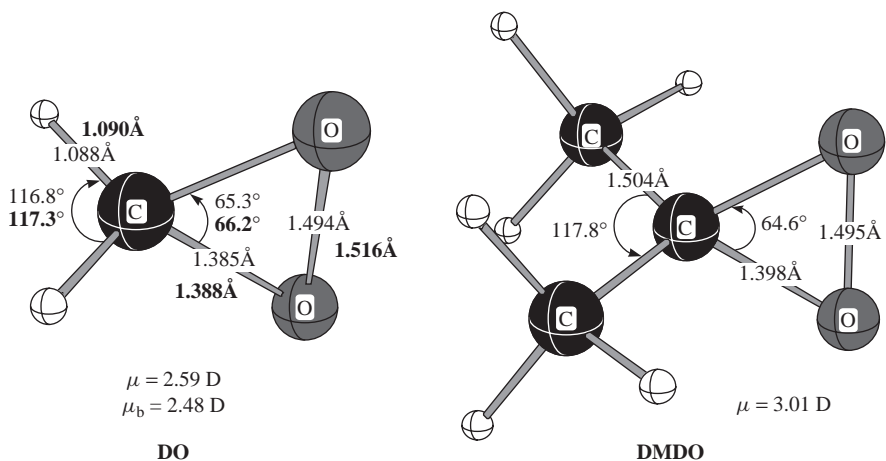


FIGURE 13. B3LYP/6-311+G(3df,2p)-optimized structures of dioxirane (DO), dimethyldioxirane (DMDO) and methyl(trifluoromethyl)dioxirane (TFDO). Bold numbers for DO are experimental microwave-structural data.⁵⁷

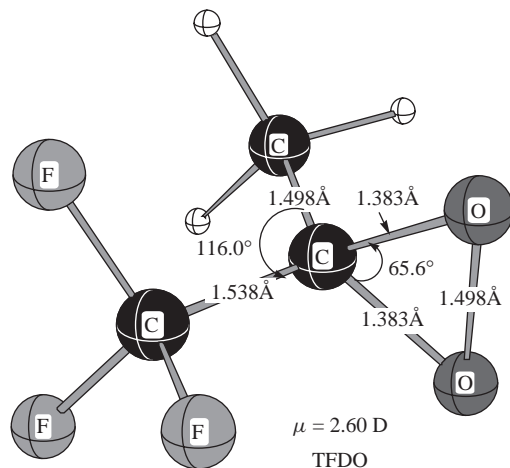
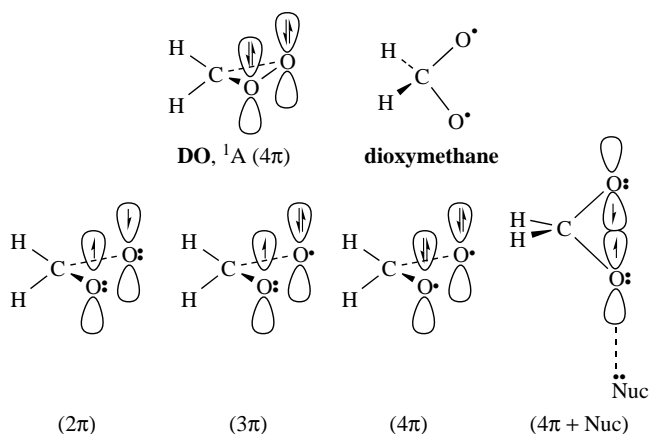


FIGURE 13. (continued)

B. Molecular Orbital Treatments of Dioxirane

The dioxirane ring presents a unique type of O–O bond in that this three-member ring peroxide is marginally stable at best and its atypical reactivity as an oxidizing agent was initially attributed to its ring strain energy. This turns out not to be the case, since as explained below dioxiranes are not that highly strained. However, it was also discovered very early on that these cyclic peroxides have several higher-lying singlet excited states that may also contribute to their reactivity. In a seminal theoretical study Wadt and Goddard^{61a} reported generalized valence bond (GVB) calculations that described the ground state of the parent dioxirane (DO) as a singlet that has its oxygen lone-pair electrons (π -type 2p orbitals) doubly occupied on both oxygen atoms. This ground state (GS) in the Goddard nomenclature⁶¹ is thus referred to the $^1A(4\pi)$ state of DO (Scheme 3).



SCHEME 3

Since the O–O bond in DO is presumably quite weak, it has been suggested that the methylenebisoxo form of DO, dioxymethane, could potentially make a contribution to the overall chemistry of DO. The ground state of dioxymethane, a singlet diradical of 1A symmetry, is derived simply by elongating the O–O bond until a singlet minimum is found where the π -type atomic 2p orbitals on both oxygens are singly occupied and the two oxygen lone-pairs reside in the O–C–O plane.

Goddard⁶¹ predicted this diradical singlet $^1A(2\pi)$ state of dioxymethane to be 11.1 kcal mol⁻¹ higher in energy than GS DO. The corresponding 3π state of dioxymethane, with one of the π -type atomic 2p orbitals singly occupied and the other doubly occupied, was only slightly higher in energy (2.8 kcal mol⁻¹) than the $^1A(2\pi)$ ground-state of dioxymethane. The $^1A(4\pi)$ state, a singlet minimum with an electron distribution similar to GS DO except for the elongated O–O bond, was 11.3 kcal mol⁻¹ higher in energy than GS dioxymethane and 22.4 kcal mol⁻¹ above ground-state dioxirane. In this earlier study the O–O bond distances were assumed to be the same as the equilibrium bond in GS-dioxymethane. The relative energies of DO and dioxymethane were later estimated to be almost identical by Karlström and coworkers⁶² at the multiconfiguration self-consistent-field (MCSCF) level with DO being only 1.6 kcal mol⁻¹ lower in energy than diradical dioxymethane. The adiabatic energy barrier for the ring opening of DO to form dioxymethane was calculated to be 15.2 kcal mol⁻¹.

Subsequently, Bach and coworkers^{48c,63} studied the structure and relative energy of dioxirane and dioxymethane at a variety of theoretical levels including complete active space self-consistent field (CASSCF). Their most reliable estimate of the energy at the QCISD(T)/6-31G(d) level with the geometry computed at the QCISD/6-31G(d) level (QCISD(T)/6-31G(d)//QCISD/6-31G(d)) suggested that DO was 12.4 kcal mol⁻¹ more stable than ground-state diradical dioxymethane. For the 2π state (1A_1) of dioxymethane an O–O distance of 2.37 Å (MRDCI+Q/6-31G*) was found for this diradical GS of DO and its HOMO (b_2) is comprised of an antibonding combination of two oxygen lone-pairs oriented along the original O–O σ bond axis. The higher-lying 3π and 4π excited states of dioxymethane (Scheme 3) were estimated to be 11.5 and 26.5 kcal mol⁻¹ higher in energy than the lowest-energy $^1A(2\pi)$ state of this diradical ground state^{48c,63}. At the MP2/6-31G(d) level the O–O bond lengths of GS DO and the singlet diradical 2π , 3π and 4π states of dioxymethane were found to be 1.53, 2.35, 2.14 and 2.20 Å, respectively. It is a very unique type of singlet minima containing an O–O bond that can exhibit four such different bond lengths. This type of excited state is reminiscent of the metastable form of peroxytrifluoroacetic acid described above.

It is also worthy of note that by symmetry considerations it is the higher energy 4π state of dioxymethane that must be involved in oxygen transfer from dioxirane to a nucleophile. For example, oxygen transfer from DMDO to a typical nucleophilic two-electron σ - or π -donor (e.g. :Nuc = alkene, amine, phosphine, sulfide) proceeds via an S_N2 -like displacement along the O–O bond axis with concomitant breaking of the O–O bond and formation of an O ← :Nuc bond. The ground state of dioxirane correlates with the 4π configuration of methylenebisoxo affording the oxidized product and ground-state formaldehyde^{20a}. The primary electronic event for this σ,σ approach (π,π for Nuc = alkene) of a :Nuc involves transfer of electron density from the O–O bond and the :Nuc to the dioxirane O–O σ^* orbital as the 4π state intervenes. The orientation of the single electrons in both the 2π and 3π states would afford the excited state of the carbonyl group in acetone. The 4π state is the only one of the three excited states that can produce acetone in its ground state. The above symmetry arguments presented for dioxirane also hold for DMDO. Consistent with this idea the 2π diradical of dimethyldioxirane, with geometry optimization at the QCISD/6-31G* level, was calculated to be 19.1 kcal mol⁻¹

[QCISD(T)] and $18.1 \text{ kcal mol}^{-1}$ at the MRCI+Q/6-31G* level (numerically optimized) higher in energy than ground-state DMDO^{48c,63}.

A CASSCF study by Cantos and coworkers⁶⁴ also suggested that the ground-state of dioxymethane was located $11.1 \text{ kcal mol}^{-1}$ above DO and predicted a barrier for ground-state conversion of DO to dioxymethane of $25.8 \text{ kcal mol}^{-1}$. More recently, Anglada⁶⁵ has reported a high-level *ab initio* MRD-CI (multireference single- and double-excitation configuration interaction) estimate suggesting that dioxymethane is only $5.8 \text{ kcal mol}^{-1}$ higher in energy than dioxirane. An activation barrier of $21.4 \text{ kcal mol}^{-1}$ was predicted for the ring opening of DO into dioxymethane. At this higher level the equilibrium geometries for DO, the TS for O–O bond elongation and dioxymethane were found to be 1.512, 2.108 and 2.359 Å. The calculated geometry for DO is in excellent agreement with the microwave data given in Figure 13.

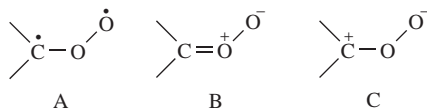
Hoffmann and coworkers⁶⁶ have presented structural data on a series of dioxiranes substituted with electronegative substituents including difluorodioxirane. Difluorodioxirane is of particular interest because it has been described as potentially the most stable of the series of dioxiranes we have described. Cremer and coworkers⁶⁷ have predicted on the basis of *ab initio* calculations that in contrast to the parent dioxirane (CO_2H_2), difluorodioxirane (CO_2F_2) should possess considerable thermodynamic stability. Difluorodioxirane is the only known dioxirane that is stable in the gas phase at room temperature.

C. The Electronic Structure of Dioxirane and Carbonyl Oxide

One of the most important features of the ozonolysis reaction of alkenes is one in which ozone adds to the C=C bond to form a primary ozonide (1,2,3-trioxolane). The Criegee mechanism⁶⁸ suggests that this unstable intermediate decomposes into a carbonyl compound and a carbonyl oxide that recombine to form a final isomeric ozonide (1,2,4-trioxolane). Direct spectroscopic evidence for a substituted carbonyl oxide has only recently been reported by Sander and coworkers⁶⁹ for the NMR characterization of dimethyl carbonyl oxide. Kraka and coworkers⁷⁰ have theoretically modeled dimethyl carbonyl oxide and confirmed the structural aspects reported by Sander and coworkers⁶⁹ on the basis of NMR data.

These highly reactive 1,3-dipolar species readily isomerize and undergo 1,3-cycloaddition reactions in addition to their cyclization to the corresponding dioxirane⁷¹. It is within this latter context that we describe the more recent theoretical studies on carbonyl oxides and their relationship to dioxiranes. As a result of the lability of carbonyl oxides much of the research on this class of compound has been of a theoretical nature^{62,67,72,73}.

There is a significant energy difference between a carbonyl oxide and its dioxirane that presents a driving force for cyclization. The activation barrier for the reverse reaction, ring opening to the higher-energy carbonyl oxide, has a prohibitive barrier. One of the earlier studies reported by Karlström and Roos⁷³ at the MCSCF level suggested a transition state for the rearrangement of the parent carbonyl oxide to dioxirane that was $23.9 \text{ kcal mol}^{-1}$ above ground-state carbonyl oxide. This barrier is reduced to $19.1 \text{ kcal mol}^{-1}$ at the QCISD(T) level^{48c}. At the MP4SDTQ/6-31G(d)//MP2/6-31G(d) level dioxirane is $29.2 \text{ kcal mol}^{-1}$ more stable than its isomeric carbonyl oxide. Calculations on carbonyl oxides have to be done with some caution because, as pointed out by Bach and his coworkers^{48c}, the calculated C–O and O–O bond lengths for these intermediates are highly sensitive to the level of theory used. The electronic character of carbonyl oxide changes from diradical (A) to zwitterionic (B and C) as the level of theory and basis set is augmented (Scheme 4). Increasing the number of methyl groups on the carbonyl oxide also increases its dipolar character⁷⁴.



SCHEME 4

Bernhardsson and coworkers^{75a} have recently used CASPT2 calculations (electron-correlation correction to the CAS wave function) to model carbonyl oxides in solution. Solvation effects in acetonitrile solvent also suggest that the zwitterionic form would be favored with an elongation of the O—O bond length and a decrease in the C—O bond^{75b}. *Ab initio* calculations have been recently reported for monofluorocarbonyl oxide⁶⁷, difluorocarbonyl oxide⁷⁶, methylcarbonyl oxide and cyclopropenone carbonyl oxide⁷⁷. In the recent literature the idea that carbonyl oxide can be an important source of OH radicals has also been presented⁷⁸.

The electronic structure and vibrational frequencies for dimethyl-substituted carbonyl oxide and its cyclic isomer dimethyldioxirane have also been reported by Kim and Schaefer⁷⁹ (Figure 14) at the coupled cluster level with single and double excitation (CCSD), and the CCSD with connected triple excitations [CCSD(T)]. The relative energetics and isomerization barriers for dimethyldioxirane were also computed in that study with relatively large basis sets. At the highest level of theory employed, TZP [triple- ζ (TZ) quality basis set with one set of polarization functions] CCSD(T), dimethyldioxirane is predicted to be lower in energy than its carbonyl oxide by 23.2 kcal mol⁻¹ with the inclusion of zero-point vibrational energy (ZPVE) corrections. The energy barrier for the cyclization of dimethylcarbonyl oxide to DMDO (Figure 15)⁷⁹ was reported to be 19.5 kcal mol⁻¹ at the same level of theory. The molecular structure of dimethyl-substituted carbonyl oxide has C_s symmetry with a staggered conformation. The predicted C—O bond distance of 1.28 Å at the TZP CCSD(T) level of theory shows some double-bond character, which implies that the electronic structure of dimethylcarbonyl oxide prefers the zwitterionic form. The transition state for the cyclization of dimethyl carbonyl oxide to dimethyldioxirane has C_1 symmetry (Figure 15)⁷⁹.

Another route to the formation of carbonyl oxides is the reaction of methylene (CH₂) with dioxygen. This oxidative process involving methylene with O₂ is one of the most important reactions in the combustion of unsaturated hydrocarbons. The reaction between CH₂ (X^3B_1) + O₂ has been studied by Anglada and Bofill^{77a} in the gas phase by carrying out CASSCF and CASPT2 calculations with the 6-31G(d,p) and 6-311+G(3df,2p) basis

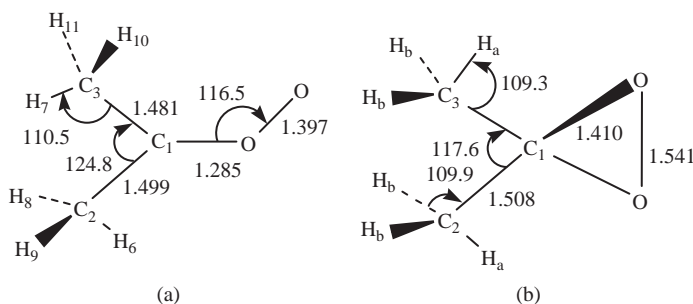


FIGURE 14. Predicted geometries for (a) the dimethyl-substituted carbonyl oxide and (b) dimethyldioxirane at the TZP CCSD(T) level of theory. Bond lengths are given in Å

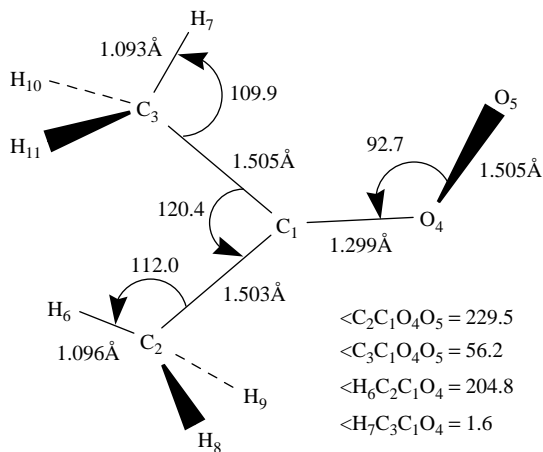
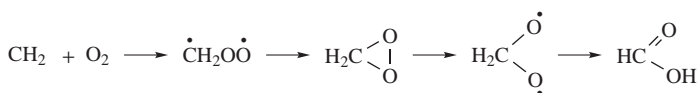


FIGURE 15. Predicted geometries of the transition state for rearrangement of the carbonyl oxide to the dioxirane at the DZP CCSD(T) level of theory



SCHEME 5

sets. The reaction proceeds by the addition of O_2 to methylene and may proceed on either a singlet or a triplet potential energy surface. In both cases, the initial product is the carbonyl oxide (H_2COO) that may isomerize to dioxirane and beyond as shown in Scheme 5⁸⁰.

The reaction in its singlet multiplicity is computed to be exothermic by $50.9 \text{ kcal mol}^{-1}$ with an activation enthalpy of $1.9 \text{ kcal mol}^{-1}$ at 298 K. The triplet reaction is computed to be exothermic by $26.9 \text{ kcal mol}^{-1}$ with an activation enthalpy of $5.4 \text{ kcal mol}^{-1}$ at 298 K. According to classical transition state theory, the branching ratio for the reaction in its triplet state multiplicity changes from negligible at 298 K to about 26% at 1800 K, and this ratio equals the formation of atomic oxygen, $\text{O}(^3\text{P})$. The carbonyl oxide can isomerize to dioxirane with an activation enthalpy of $18.7 \text{ kcal mol}^{-1}$ or to formic acid which dissociates into HCO and OH with an activation enthalpy of $32.5 \text{ kcal mol}^{-1}$ ^{77b}. The triplet H_2COO ($\text{A}^3\text{A}''$) decomposes into H_2CO (X^1A_1) + O ($^3\text{P}_g$). The process is computed to be exoergic by about 27 kcal mol^{-1} and has an activation enthalpy of $2.9 \text{ kcal mol}^{-1}$.

At the same time Fang and Fu reported on the identical reaction also using CASSCF methods with a relatively large active space⁸¹. CAS(14,12)/cc-pVDZ calculations are reported for the reaction of $^3\text{CH}_2 + ^3\text{O}_2 \rightarrow \text{products}$. On the singlet potential energy surface, a transition state has been located with an energy barrier of $1.65 \text{ kcal mol}^{-1}$, which is in good agreement with the experimental estimation of $1.0\text{--}1.5 \text{ kcal mol}^{-1}$. For the triplet case, the formation of CH_2OO has an energy barrier of $5.79 \text{ kcal mol}^{-1}$, and the triplet CH_2OO produced could be further decomposed into $\text{CH}_2\text{O} + \text{O}(^3\text{P})$ with an energy barrier of $2.92 \text{ kcal mol}^{-1}$. The geometries of some key points were also located at the CAS(8,6)+1+2/cc-pVDZ level of theory for comparison.

It has been argued by Cremer and coworkers^{82a} that the parent carbonyl oxide, CH_2COO , does not readily decompose into $\text{HCO}+\text{OH}$ radical because of a relatively high activation enthalpy of 31 kcal mol^{-1} . However, a relatively low activation pathway ($\Delta\Delta H_f^0 = 14.4 \text{ kcal mol}^{-1}$) was found for methyl-substituted carbonyl oxides that were capable of undergoing a 1,5-hydrogen migration to produce a vinyl hydroperoxide. This methyl-substituted vinyl hydroperoxide readily undergoes O–O bond cleavage to produce the OH radical. This led to the important conclusion that gas-phase ozonolysis of substituted alkenes leads to the formation of hydroxyl radicals—a reaction of serious consequences for the chemistry of the atmosphere. The origin of the weakness of the O–O bond in vinyl hydroperoxides has been noted previously^{16a}. The two competing potential pathways for the decomposition of dimethyl carbonyl oxide are shown in Scheme 6. A theoretical investigation of a series of reactions that project mechanisms for the formation of formic acid in the atmosphere from the simplest Criegee intermediate, CH_2COO , has also been reported^{82b}.

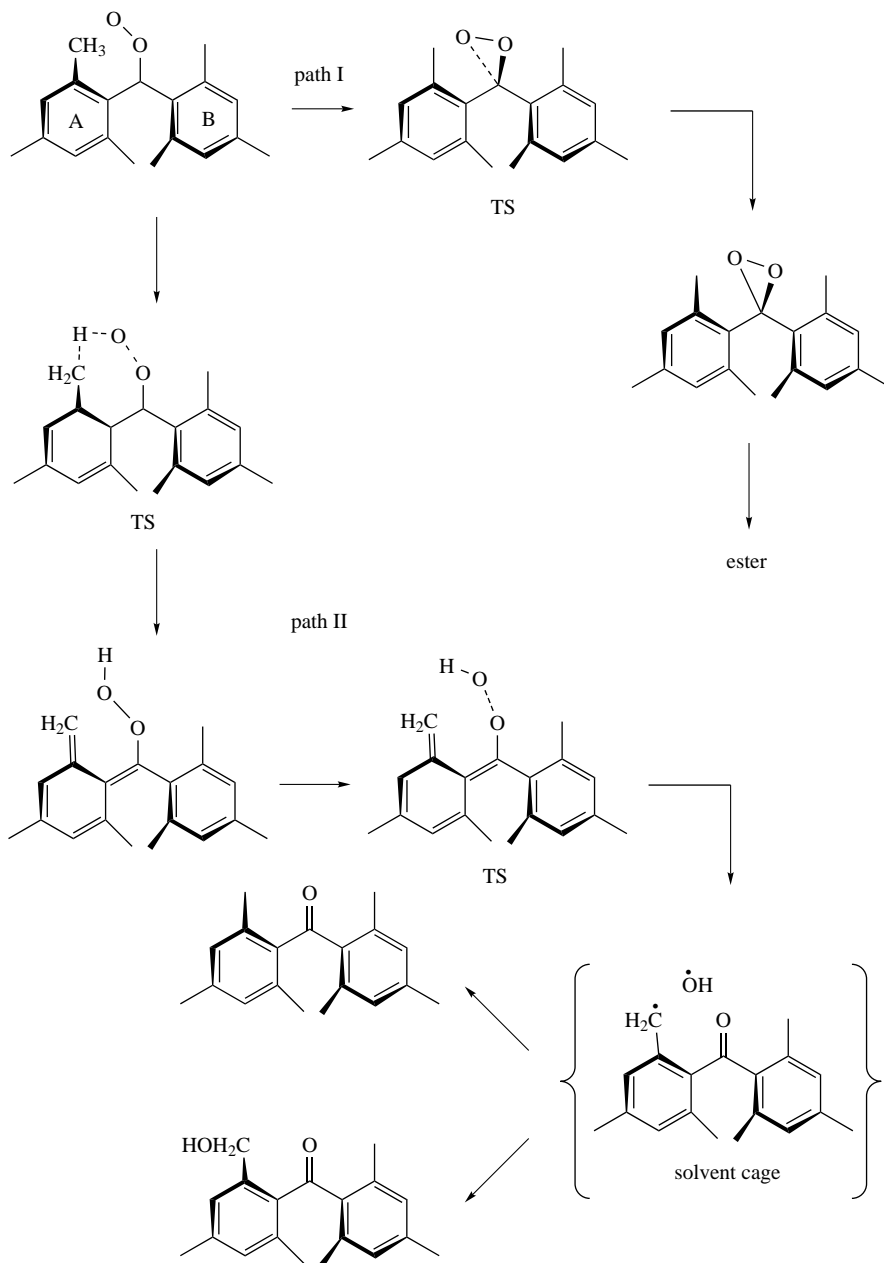
Schindler and coworkers verified the formation of hydroxyl radicals kinetically⁸³ and further RRKM calculations by Cremer and coworkers placed the overall concept on a more quantitative basis by verifying the measured amount of OH radical⁸⁴. An extensive series of calculations on substituted alkenes placed this overall decomposition mechanism and the involvement of carbonyl oxides in the ozonolysis of alkenes on a firm theoretical basis⁷⁸. The production of OH radicals in solution phase was also suggested on the basis of a series of DFT calculations^{85a}. Interestingly, both experiment and theory support a concerted [4 + 2] cycloaddition for the ozone–acetylene reaction rather than a nonconcerted reaction involving biradical intermediates^{85b}.

Using statistical-dynamical methods and transition state theory, Zhang and coworkers demonstrated that excited carbonyls dissociate promptly to produce OH radicals (11%) or isomerize to form dioxirane (32%) or are collisionally stabilized (57%)⁸⁶.

In a recent paper Anglada, Cremer and coworkers have discovered several new facets of the alkene ozonolysis mechanism that impacts the area of alkene epoxidation as well⁸⁷. A comparison of the reactivity of the three isomeric oxidizing carbonyl oxides, dioxirane and methylenebisoxo with ethylene was achieved using CASPT2, CCSD(T) and B3LYP with a relatively large 6-311+G(2d,2p) basis set. Contrary to expectation, carbonyl oxide prefers to react with ethylene via a [4 + 2] cycloaddition reaction (activation enthalpy, $\Delta H^\ddagger = 1.0 \text{ kcal mol}^{-1}$) to produce 1,2-dioxolane with a reaction enthalpy of $-65 \text{ kcal mol}^{-1}$ rather than the epoxidation reaction ($\Delta H^\ddagger = 11.3 \text{ kcal mol}^{-1}$) forming oxirane and formaldehyde. Epoxidation of ethylene by dioxirane is also slower, having a calculated activation enthalpy of $13.7 \text{ kcal mol}^{-1}$. The biradical methylenebisoxo was observed to undergo a pseudo-[4+2] cycloaddition ($\Delta H^\ddagger = 1.8 \text{ kcal mol}^{-1}$) leading to 1,3-dioxolane in a highly exothermic reaction ($\Delta H = -84.5 \text{ kcal mol}^{-1}$). These combined data will require a reevaluation of many aspects of the ozonolysis reaction.

D. Oxygen Atom Transfer from Dioxiranes and Carbonyl Oxides

Dioxiranes are three-membered ring peroxides that serve as paradigm examples of electrophilic species. Dimethyldioxirane (DMDO), in particular, is a powerful oxidant with unusual synthetic utility that can be produced *in situ* by the reaction of acetone with Caroate ($2\text{KHSO}_5\cdot\text{KHSO}_4\cdot\text{K}_2\text{SO}_4$). Consequently, a great many such synthetic procedures are carried out in acetone solvent. Methyl(trifluoromethyl)dioxirane (TFDO) was synthesized a few years later by Curci and coworkers⁵⁹, demonstrating that electron-withdrawing groups can markedly increase the reactivity of dioxiranes. Most of the theoretical calculations on the mechanism of dioxirane epoxidation have been accomplished at the DFT level since this topic came under general scrutiny when this method came into vogue.



SCHEME 6

1. A comparison of DFT theory with higher-level methods

In the past several years the B3LYP variant of density functional theory (DFT) has been used extensively for calculations involving oxygen atom transfer. A comparison of the performance of DFT calculations with other high-level *ab initio* methods has presented credible evidence that this relatively efficient DFT functional is quite adequate for answering mechanistic questions about the epoxidation of alkenes. A systematic study by Bach and coworkers^{12b} on the epoxidation reactions of ethylene, propylene, and *cis*- and *trans*-2-butene with peroxyformic acid and of ethylene with dioxirane and dimethyldioxirane has provided an internally consistent series of activation energies and geometries for comparison. The transition structures for the epoxidation of ethylene and propylene with peroxyformic acid and of ethylene with dioxirane and dimethyldioxirane were calculated at the B3LYP level, as well as at the QCISD and CCSD levels. The B3LYP method provided symmetrical transition structures with nearly identical C–O bond distances, whereas the MP2 calculations favor unsymmetrical transition structures as noted for TS-a (Figure 16).

An interesting comparison of the electronic character of peroxyformic acid and dioxirane has been provided by Deubel⁸⁸ through an analysis of the donor–acceptor interactions in a series of transition states (TS) for the epoxidation of alkenes. It was suggested that alkenes are attacked by peroxyformic acid (PFA) in an electrophilic way. A relationship between the electronic character of the reagent and its reactivity has been suggested: the more electrophilic the attack on the C=C bond, the faster the reaction. In contrast, dioxirane (DO) has been identified as both an electrophilic and nucleophilic oxidant, depending upon the substituents on the C=C double bond. The substrates with electron-withdrawing groups are attacked by DO in a nucleophilic way. These reactions have comparably low activation barriers. For instance, acrylonitrile epoxidation with dioxirane is significantly faster than the corresponding reaction with PFA and proceeds via a transition state earlier on the reaction coordinate and with a larger extent of asymmetry.

The geometrical parameters of the transition structures calculated using the B3LYP functional are close to those found at the QCISD and CCSD levels. While the activation

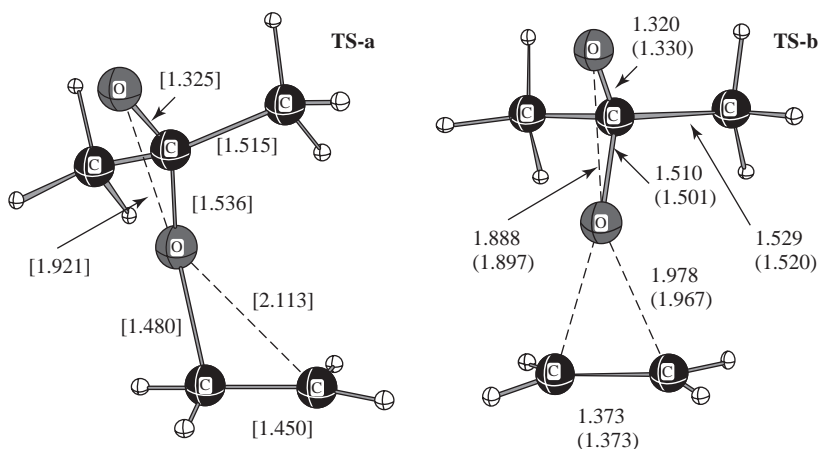


FIGURE 16. Transition structures for the epoxidation of ethylene with DMDO optimized at the MP2/6-31G* level (TS-a) and at the B3LYP/6-31G* level (TS-b, numbers in parentheses are at the QCISD/6-31G* level)

barriers for the epoxidation reactions calculated at the B3LYP/6-31G* and B3LYP/6-31+G* levels are very close to the MP4SDTQ/6-31G**/MP2/6-31G* and MP2/6-31G**/MP2/6-31G* values, these activation energies are systematically lower for peracid epoxidation (up to 5–6 kcal mol⁻¹) than the barrier heights calculated at such higher correlated levels as the QCISD(T)/6-31G**/QCISD/6-31G*, CCSD(T)/6-31G**/CCSD/6-31G* and BD(T)/6-31G**/QCISD/6-31G* levels. *The opposite trend is true for dioxirane epoxidation, where the activation barriers are slightly overestimated.* DFT calculations on the epoxidation reactions of ethylene and propylene with peroxyformic acid using the BH&HLYP functional also lead to symmetrical transition structures, but the calculated barriers are overestimated when compared with the QCISD(T) results. The activation barriers calculated for these epoxidation reactions at the QCISD(T)/6-31G**/B3LYP/6-31G* level are very close to those computed at the QCISD(T)/6-31G**/QCISD/6-31G* level.

One of the objectives of the present review is to provide some guidance that suggests the most reasonable or affordable method of calculation balanced against the accuracy of the method. Some generalized conclusions derived from the above systematic comparison include:

(1) In contrast to the results of the MP2 calculations, the nature of the transition structures in the alkene epoxidation reactions calculated at the B3LYP level agree well with those computed using higher correlated methods such as QCI and CC. Therefore, while the MP2 calculations are biased in favor of unsymmetrical transition structures, the B3LYP method is capable of providing the correct transition structure geometry for simple unconjugated alkenes if the B3LYP solution for the wave function is stable.

(2) The transition structures for the epoxidation of ethylene and propylene with peroxyformic acid and of ethylene with dioxirane and dimethyldioxirane calculated at the B3LYP, QCISD and CCSD levels are symmetrical with a spiro orientation of the electrophilic oxygen, whereas the MP2 calculations favor unsymmetrical transition structures. The geometries of the transition structures calculated using the B3LYP functional are close to those found at QCISD, CCSD, CCSD(T) levels as well as those found at the CASSCF(10,9) and CASSCF(10,10) levels for the transition structure of the epoxidation of ethylene.

(3) The activation barriers for the epoxidation reactions calculated at the B3LYP/6-31G* and B3LYP/6-31+G* levels are systematically lower (up to 5–6 kcal mol⁻¹) than the barrier heights calculated at such higher correlated levels as the QCISD(T)/6-31G**/QCISD/6-31G*, CCSD(T)/6-31G**/CCSD/6-31G* and BD(T)/6-31G**/QCISD/6-31G*, although the transition structure geometries calculated at these levels of theory are in good agreement. In contrast, the BH&HLYP/6-31G* barrier for the epoxidation of ethylene and propylene with peroxyformic acid is overestimated by up to 8 kcal mol⁻¹ when compared with the barriers calculated at the QCISD(T), BD(T) and CCSD(T) levels of theory. The activation barriers calculated at the QCISD(T)/6-31G**/B3LYP/6-31G* level appear to be close enough to those computed at the QCISD(T)/6-31G**/QCISD/6-31G* level to adopt this protocol for relatively large systems.

2. Epoxidation of alkenes with carbonyl oxides and dioxiranes

Since Kim and Schaefer have shown that dimethylcarbonyl oxide is 23 kcal mol⁻¹ higher in energy than its corresponding cyclic dioxirane (DMDO)⁷⁹, one might assume that the barrier for oxygen atom transfer from the higher-energy carbonyl oxide should be lower. However, alkene epoxidation by carbonyl oxide is 20–30 kcal mol⁻¹ more exothermic than oxidation by dioxirane^{48d}. As a result of the greater exothermicity of the reactions with carbonyl oxide, the barriers are as much as 10 kcal mol⁻¹ lower than for oxidation by dioxirane^{48d}. This concept was examined more closely for the oxidation of

ethylene since the carbon–carbon double bond is weakly nucleophilic and considerable experimental data on the formation of epoxides from alkenes are available. However, since carbonyl oxides are not sufficiently stable to be employed as a laboratory reagent, their inclusion here is more of a theoretical nature. It should also be recalled as noted above that carbonyl oxides, at least in the gas phase, prefer a [4+2] cycloaddition pathway in reactions with alkenes instead of the anticipated epoxidation TS⁸⁷.

The transition states for the epoxidation of ethylene by carbonyl oxide and dimethylcarbonyl oxide are shown in Figure 17. The orientation of approach of the electrophilic oxygen is approximately symmetrical in nature but the TS is essentially planar with the O–O–C fragment lying along the C=C bond axis^{48d}. This is distinctly different from the transition structures for dioxirane and peracid epoxidation where a spiro, but typically symmetrical, TS is observed. Additionally, the developing C–O bonds are considerably longer, indicating a more reactant-like structure in agreement with Hammond’s postulate.

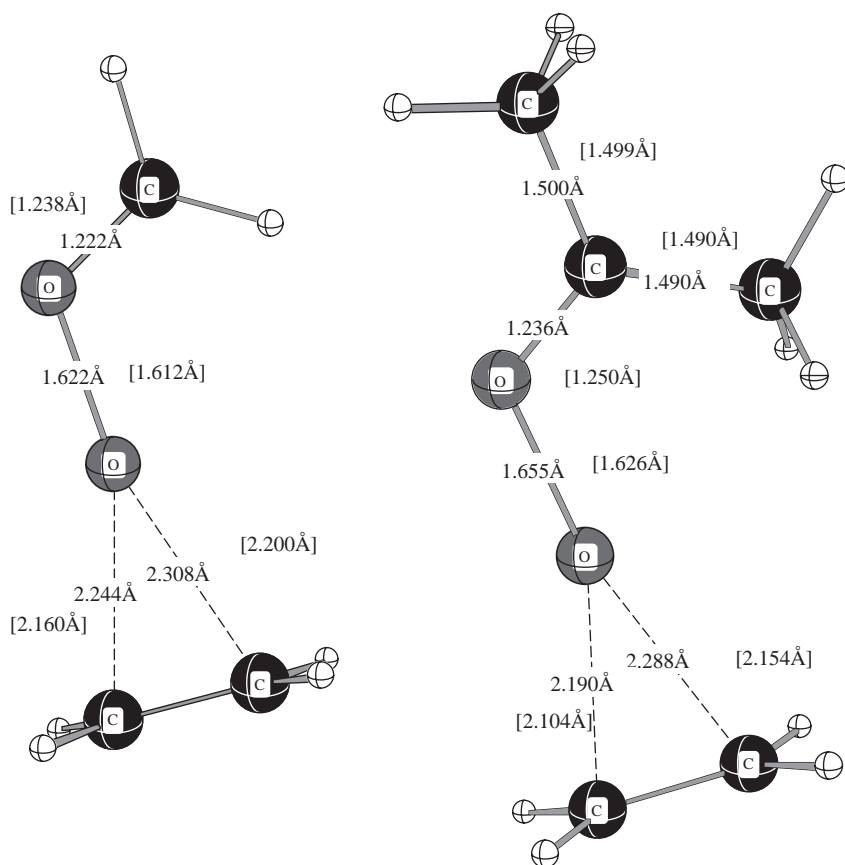


FIGURE 17. Transition structures for the epoxidation of ethylene by carbonyl oxide [$\Delta(E+ZPVE)^\ddagger = 10.2 \text{ kcal mol}^{-1}$] and dimethylcarbonyl oxide [$\Delta(E+ZPVE)^\ddagger = 10.3 \text{ kcal mol}^{-1}$] optimized at the B3LYP/6-311+G(d,p) level of theory. Bond lengths given in brackets are at the MP2/6-31G(d) level, and the corresponding barriers are 14.8 and 12.9 kcal mol⁻¹^{48d}

Ethylene epoxidation with unsubstituted carbonyl oxide is *ca* 5 kcal mol⁻¹ more exothermic than with dimethylcarbonyl oxide, yielding an even earlier transition state.

In contrast to dioxirane oxidation, the transition states for carbonyl oxide oxidation are not affected as much by RHF-UHF wave function instability problems, and there is good agreement between the MP2, MP4 and QCISD(T) barrier heights. Methyl substitution on the carbonyl oxide has very little effect on the barrier heights, but it can be anticipated that methyl substitution of the alkene would lower the barriers significantly^{19d}. The calculated changes in the barriers due to solvation are much smaller than for dioxirane oxidation, primarily because the differences between the reactant and transition state dipoles are smaller.

In summary, transition structures with dioxirane and dimethyldioxirane are unsymmetrical at the MP2/6-31G* level, but are symmetrical at the QCISD/6-31G* and B3LYP/6-31G* levels. The transition states for oxidation of ethylene by carbonyl oxides do not suffer from the same difficulties as those for dioxirane and peroxyformic acid. Even at the MP2/6-31G* level, they are symmetrical (Figure 17). The barriers at the MP2 and MP4 levels are similar and solvent has relatively little effect. The calculated barriers agree well with experiment⁷¹. In a similar fashion, the oxidation of ethylene by peroxyformic acid has been studied at the MP2/6-31G*, MP4/6-31G*, QCISD/6-31G* and CCSD(T)/6-31G* and B3LYP levels of theory^{48d}. The MP2/6-31G* level of theory calculations lead to an unsymmetrical transition structure for peracid epoxidation that, as noted above, is an artifact of the method. However, QCISD/6-31G* and B3LYP/6-31G* calculations both result in symmetrical transition structures with essentially equal C—O bonds.

In the past several years dioxiranes have rapidly grown into one of the more useful oxidative reagents in the arsenal of the synthetic chemist. Its unique ability ranges from the transfer of an oxygen atom to the C—H bond of a saturated hydrocarbon to that of oxidation of atoms containing a lone pair of electrons such as amines and sulfides. Their use now rivals that of peracids in the epoxidation reaction due in part to their application under neutral conditions and to comparable or even enhanced rates of reaction⁸⁹. However, by far the most common application for dioxiranes remains the oxidation of a carbon-carbon double bond. A concerted oxygen atom transfer for the dioxirane epoxidation reaction has been advocated by both Bach^{12b} and Houk⁹⁰ and their coworkers. It is generally accepted that an S_N2-like attack of the alkene π -bond on the dioxirane peroxide σ O—O bond is responsible for the epoxidation step. The *spiro* orientation is a manifestation of a weak back-bonding interaction of the HOMO of the alkene with the σ^* O—O orbital of the dioxirane. Sarzi-Amade and coworkers reported a comparison of the transition structures for the epoxidation of ethylene and *Z*-2-butene with the parent dioxirane (DO) and DMDO that also suggested a symmetrical spiro approach to the C=C⁹¹.

In marked contrast to the generally accepted mechanism, the involvement of a radical pair produced by an alkene-induced O—O bond homolysis was suggested by Minisci and coworkers⁹². In a combined experimental and theoretical study Curci, Houk and coworkers⁹³ sought to differentiate between a radical pathway and the commonly accepted concerted mechanism. Both product and kinetic studies tended to exclude a radical pathway. Computational studies at the B3LYP/6-31G* level on the epoxidation of isobutylene with DMDO predicted an activation energy ($\Delta E^\ddagger = 15.3$ kcal mol⁻¹) significantly lower than the O—O bond dissociation energy of DMDO of 23.1 kcal mol⁻¹ estimated by Cremer and coworkers^{94a}. Thus, both theory and experiment support a concerted epoxidation mechanism. However, several authentic transition structures (first-order saddle points) have recently been located for the addition of the excited state of both DO and DMDO to ethylene and *Z*-2-butene involving a radicaloid pathway. These open-shell TSs are

connected to the corresponding epoxide products in a two-step mechanism and are lower in energy than the aforementioned closed-shell pathway.

This mechanistic dichotomy has many things in common with the recent developments in peroxyformic acid chemistry²⁷ and deserves further study.

A typical closed-shell transition structure for DMDO epoxidation is exemplified by the epoxidation of *E*- and *Z*-2-butene. Baumstark and Vasquez have reported experimental studies that demonstrate the greater reactivity of *Z*-alkenes in the DMDO epoxidation of *E/Z*-pairs of alkenes^{94b}. As anticipated, approach of the dioxirane ring to the *Z*-double bond in the less hindered manner, away from the methyl groups of DMDO,

TABLE 3. B3LYP/6-31G(d) activation barriers (ΔE^\ddagger , kcal mol⁻¹) for the epoxidation of a series of alkenes with peroxyformic acid (PFA) and dimethyldioxirane (DMDO). The barriers in parentheses are at the B3LYP/6-31+G(d,p) level of theory. Other computational approaches are indicated by footnotes. The barriers have been computed with respect to isolated reactants

Alkene	PFA	DMDO
Ethylene	14.1 (14.9) 17.0 ^a [16.4] ^b	18.2 (17.7) [15.2] ^b
Propene	12.0 (12.6) 14.8 ^a [16.0] ^c	16.6 (16.0)
<i>t</i> -Butylethylene	11.2 (12.3) 14.0 ^a	
1-Octene	11.2 (12.2) 14.1 ^a	15.8 (15.2)
Isobutene	10.8 (11.2) 13.0 ^a [13.7] ^c	15.3 (14.0) 16.0 ^a
<i>E</i> -2-Butene	10.5 (11.0) 12.8 ^a [13.4] ^c	15.5 (14.8) [14.6] ^c
<i>Z</i> -2-Butene	10.0 12.1 ^a	14.1 (13.4)
<i>Z</i> -2-Pentene	9.3 (10.0) 11.6 ^a	
Cyclopropene	12.0 (12.5) 14.5 ^a	
Cyclobutene	11.0 (11.5) 13.7 ^a	
Cyclopentene	9.3 (9.7) 12.1 ^a	
Cyclohexene	9.7 (10.1) 12.1 ^a	13.5 (12.6) 14.7 ^a
Cycloheptene	9.8 (10.2) 12.2 ^a	
<i>Z</i> -Cyclooctene	9.1 (9.6) 11.5 ^a	
<i>E</i> -Cyclooctene	5.6 (6.1) 8.2 ^a	
1-Methyl- <i>E</i> -cyclooctene	4.0 (4.3) 5.9 ^a	
Norbornene (<i>exo</i>)	9.7 (10.3) 12.9 ^a	13.3 (13.0)
Norbornene (<i>endo</i>)	12.5 (13.2) 15.4 ^a	15.9 (15.8)
Benzonorbornadiene (<i>exo</i>)	9.6 (10.2) 12.2 ^a	
Benzonorbornadiene (<i>endo</i>)	14.6 (15.1) 17.0 ^a	
Bicyclo[3.3.1]non-1-ene	5.2 (5.7) 7.7 ^a	
Trimethylethylene	8.9 (9.1) 11.0 ^a	13.7 (12.8)
Tetramethylethylene	7.8 (7.9) 9.8 ^a	14.0 (12.8)
1,3-Butadiene	11.7 (12.4) 14.3 ^a [15.9] ^c	14.9 (14.6)
<i>trans</i> -2- <i>cis</i> -4-Hexadiene	9.4 (9.6) 11.5 ^a	
<i>E</i> -Stilbene	13.2 (13.3) 15.1 ^a	
<i>Z</i> -Stilbene	11.8 (12.6) 14.6 ^a	
Styrene	11.2 (11.7) 14.2 ^a	14.3(13.8)
<i>Z</i> -3-Methyl-3-penten-2-ol	9.2 ^d	
Allyl alcohol	7.5 ^e 11.4 ^f	

^a Classical activation barriers computed at the B3LYP/6-311+G(3df,2p)//B3LYP/6-31+G(d,p) level of theory.

^b The numbers in brackets for ethylene are at the QCISD(T)//QCISD/6-31+G(d,p) level of theory.

^c The numbers in brackets for propylene, isobutylene, *E*-2-butene and 1,3-butadiene entries are at the QCISD(T)//QCISD/6-31G(d) level of theory; QCISD(T)/6-31G(d)//B3LYP/6-311+G(3df,2p) gas-phase intrinsic barriers (ΔE^\ddagger) for the epoxidation of *E*-2-butene with dimethyldioxirane (DMDO) and peroxyformic acid are 14.3 and 13.2 kcal mol⁻¹, respectively.

^d Classical activation barrier computed at the B3LYP/cc-pVTZ level.

^e Classical activation barrier computed at the B3LYP/6-311G(d,p) level.

^f Classical activation barrier computed at the QCISD(T)//QCISD/6-31G(d) level.

is 3.4 kcal mol⁻¹ lower in energy. DMDO epoxidation of *E*-2-butene has a calculated barrier ($\Delta E^\ddagger = 15.5$ kcal mol⁻¹, B3LYP/6-31G*)^{90b} that is 2.3 kcal mol⁻¹ higher than that of the less encumbered *Z*-alkene. At the B3LYP/6-31+G(d,p) level the activation barriers for *E*- and *Z*-2-butene differ by only 1.4 kcal mol⁻¹^{19d}. The calculated barrier at the QCISD(T)/QCISD/6-31G(d) level is 14.6 kcal mol⁻¹. These data are summarized in Table 3.

The approach of DMDO to *E*-2-butene is *spiro* in nature with nearly equally developing C–O bond distances (Figure 18). The O–O bond in the TS is elongated to 1.879 Å. The calculated gas-phase enthalpy of activation ($\Delta H^\ddagger = 13.5$ kcal mol⁻¹) is higher than the experimental $\Delta H^\ddagger = 7.4$ kcal mol⁻¹ for the DMDO epoxidation of cyclohexene⁹⁵ in acetone solvent while the calculated entropy of activation ($-\Delta S^\ddagger = 39.7$ cal mol⁻¹ K⁻¹) is in better agreement with experiment ($-\Delta S^\ddagger = 35.5$ cal mol⁻¹ K⁻¹).

Electron-withdrawing fluorine substitution on both peracids and dioxiranes has a rather large impact upon the reaction rate of oxygen atom transfer. Although the reactivity of dioxiranes has traditionally been ascribed to a driving force due to relief of ring strain and the favorable enthalpy attending the formation of a strong C=O π -bond, the recent reassessment of the strain energy of DMDO (SE = 11 kcal mol⁻¹)^{20b} suggests that the enhanced reactivity just may be due to the relatively low-lying O–O σ^* orbital of the dioxirane. However, the involvement of the low-lying excited states of dioxiranes cannot be discounted at this time. The increased reactivity (≥ 1000 -fold) of methyl (trifluoromethyl) dioxirane (TFDO) compared to DMDO has been accredited largely to the inductive effect of the CF₃ group on the dioxirane ring. Since experimental rate data that

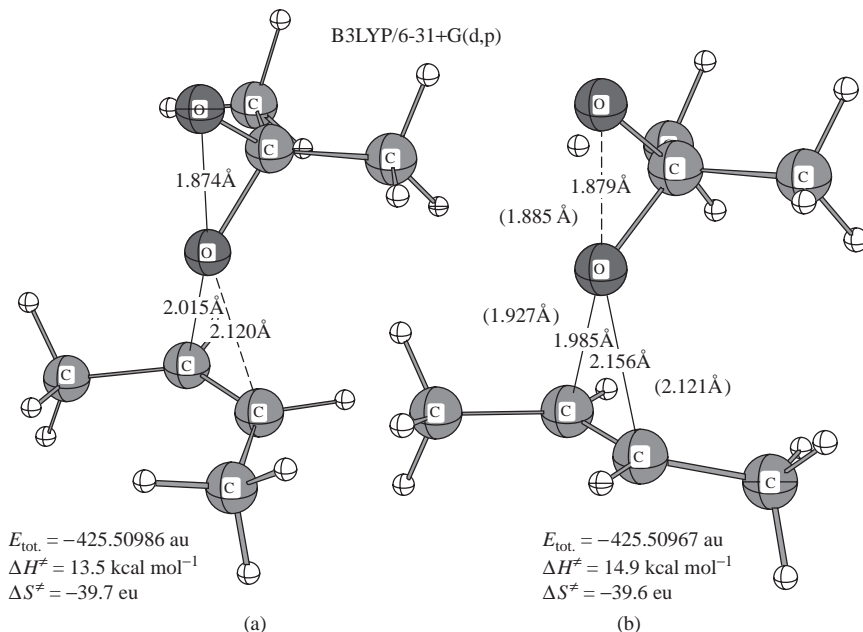


FIGURE 18. Transition structures for the epoxidation of *Z*-2-butene (a) and *E*-2-butene (b) with DMDO, optimized at the B3LYP/6-31+G(d,p) level of theory. Bond distances in parentheses for *E*-2-butene are at the QCISD/6-31G(d) level of theory. Thermal corrections to enthalpy (H) and entropy values have been calculated at the B3LYP/6-31G(d) level of theory

TABLE 4. B3LYP/6-31G(d) activation barriers (ΔE^\ddagger , kcal mol⁻¹) for the epoxidation of a series of alkenes with dimethyldioxirane (DMDO) and methyl(trifluoromethyl)dioxirane (TFDO). The barriers in parentheses are at the B3LYP/6-31+G(d,p) level of theory. Other computational approaches are indicated by footnotes. The barriers have been computed with respect to isolated reactants

Alkene	DMDO	TFDO
Ethylene	18.2 (17.7) [15.2] ^a	11.3 (11.1)
Propylene	16.6 (16.0)	9.6 (9.1)
1-Octene	15.8 (15.2)	8.2 (8.0)
Isobutylene	15.3 (14.0) 16.0 ^b	7.3 (6.8)
<i>E</i> -2-Butene	15.5 (14.8) [14.6] ^c	6.9 (6.9)
<i>Z</i> -2-Butene	14.1 (13.4)	5.6 (5.6)
Cyclohexene	13.5 (12.6) 14.7 ^b	5.3 (5.2)
Norbornene (<i>exo</i>)	13.3 (13.0)	5.5 (5.5)
Norbornene (<i>endo</i>)	15.9 (15.8)	
Trimethylethylene	13.7 (12.8)	4.8 (4.9)
Tetramethylethylene	14.0 (12.8)	4.8 (4.7)
1,3-Butadiene	14.9 (14.6)	7.6 (7.3)
Styrene	14.3 (13.8)	6.7 (6.3)

^a The barrier in brackets for ethylene is at the QCISD(T)//QCISD/6-31+G(d,p) level.

^b Classical activation barriers computed at the B3LYP/6-311+G(3df,2p)//B3LYP/6-31+G(d,p) level.

^c The barrier in brackets for *E*-2-butene is at the QCISD(T)//QCISD/6-31G(d) level of theory; QCISD(T)/6-31G(d)//B3LYP/6-311+G(3df,2p) gas-phase intrinsic barrier (ΔE^\ddagger) for the epoxidation of *E*-2-butene with dimethyldioxirane (DMDO) is 14.3 kcal mol⁻¹.

make this comparison in reactivity are relatively sparse, a theoretical gas-phase study on a series of alkenes has provided the best source of comparison to date. These data^{19d} are summarized in Table 4.

From this series of calculations it is noted that the gas-phase reactivity of TFDO is substantially greater than that of DMDO. This rate difference has been ascribed largely to the inductive effect of the CF₃ group. Fluoro-substituted dioxiranes have also played a unique role in the chiral epoxidation of alkenes. Houk and coworkers⁹⁶ have identified a novel stereoelectronic effect that increases the rate of epoxidation when the fluorine substituent is *anti* to the oxygen of the developing C=O group in the TS for epoxidation.

3. Relative rates of dioxirane epoxidation in solution

Theoretical data reported by Bach and coworkers^{19d} strongly support the surprising contention that the inherent gas-phase reactivity of DMDO is comparable to that of a typical peracid like peroxyformic acid. How can this assertion be resolved based upon the observed greater reactivity of DMDO in relatively polar or protic solvents? It is well-established experimentally that protic solvents disrupt the internal H-bond in a peracid and markedly slow the rate of epoxidation. Moreover, the rate of oxygen transfer from a peracid responds only modestly to acid catalysis⁹⁷. In contrast, Baumstark and Vasquez^{94b} showed that the protic solvents *enhance* the rate of DMDO epoxidation of *p*-methoxystyrene. Murray and Gu⁹⁵ showed that the protic solvents methanol and acetic acid increase the rate of epoxidation of cyclohexene by DMDO at 25 °C by factors of 5 and 7.5 compared with acetone. In moist acetone, the rate is enhanced both by the polarity of the medium and the effects of hydrogen bonding on the distal oxygen of DMDO in the TS for epoxidation. Indeed, Curci and coworkers⁹⁸ have reported a rate ratio of 74 for the epoxidation of cyclohexene with DMDO in acetone versus perbenzoic acid (PBA) in CH₂Cl₂. The classical activation barrier (ΔE^\ddagger) of 12.6 kcal mol⁻¹ for the gas-phase

TABLE 5. Calculated [B3LYP/6-311+G(d,p)] activation parameters (kcal mol⁻¹ and eu) for the epoxidation of cyclohexene and isobutene with dimethyldioxirane (DMDO), peroxybenzoic acid (PBA), *m*-chloroperoxybenzoic acid (*m*-CPBA) and peroxyformic acid (PFA). Solvent corrections were performed with the COSMO model. The numbers in bold are experimental values^{95,136}. Numbers in parentheses are at the B3LYP/6-311+G(3df,2p)//B3LYP/6-311+G(d,p) level of theory

	DMDO/ cyclohexene	PBA/ cyclohexene	<i>m</i> -CPBA/ cyclohexene	PFA/ isobutene	DMDO/ isobutene
ΔE^\ddagger (gas phase)	12.6 (14.7)	12.0 (14.3)	10.9 (13.4)	11.2 (13.0)	14.0 (16.0)
ΔH_{298}^\ddagger (gas phase)	12.6	11.9	10.9		14.2
ΔG_{298}^\ddagger (gas phase)	24.0	23.1	22.2		25.0
ΔS_{298}^\ddagger (gas phase)	-38.1	-37.6, -32.9	-38.1, -27.8		-36.3
ΔE^\ddagger (CHCl ₃)	11.3				
ΔH_{298}^\ddagger (CHCl ₃)	11.4, 5.0				
ΔG_{298}^\ddagger (CDCl ₃)	16.9				
ΔE^\ddagger (CH ₂ Cl ₂)		12.2	11.4		
ΔH_{298}^\ddagger (CH ₂ Cl ₂)		12.1	11.3, 10.9		
ΔE^\ddagger (acetone)	10.7		10.6		10.9
ΔH_{298}^\ddagger (acetone)	10.7, 7.4		10.6		11.1, 9.3
ΔG_{298}^\ddagger (acetic acid)	16.6				
ΔE^\ddagger (benzene)		12.2			
ΔH_{298}^\ddagger (benzene)		12.1, 10.4			

DMDO epoxidation of cyclohexene (Table 5) is reduced by 4.1 kcal mol⁻¹ when a single water molecule is hydrogen-bonded to the distal oxygen of DMDO (a *bimolecular* process relative to a prereaction cluster of DMDO, H₂O) and by 6.3 kcal mol⁻¹ with two complexed water molecules [B3LYP/6-311+G(d,p)]. The H-bonded DMDO-CH₃OH prereaction cluster has a stabilization energy of -6.9 kcal mol⁻¹. The calculated barriers for the DMDO epoxidation of *E*-2-butene with and without water catalysis are 11.0 and 14.4 kcal mol⁻¹ at the same level of theory (Figure 19)^{19d}.

These composite data strongly suggest that the presence of adventitious water or other hydrogen donors can markedly affect the observed rate of epoxidation. For example, Murray and Gu have reported $\Delta H^\ddagger = 5.0$ kcal mol⁻¹ for the DMDO epoxidation of cyclohexene in CDCl₃ and 7.4 kcal mol⁻¹ in acetone as solvent⁹⁵. Curci and coworkers also reported an E_a value of 9.3 kcal mol⁻¹ for the DMDO epoxidation of isobutylene in acetone⁹³. These barriers are significantly lower than the 13–18 kcal mol⁻¹ gas-phase barriers reported^{19d} at the B3LYP level of theory (Tables 3 and 4). Activation barriers of 12.6, 11.4 and 10.7 kcal mol⁻¹ for the DMDO epoxidation of cyclohexene in the gas phase, CHCl₃ and acetone, respectively, were estimated by using the COSMO solvent model [B3LYP/6-311+G(d,p), Table 5]. However, the current solvent correction models do not explicitly treat hydrogen-bonding interactions. Importantly, the calculated activation barriers for peracid cyclohexene epoxidation, 12.0 (PBA, gas phase) and 10.9 kcal mol⁻¹ (MCPBA, gas phase), are not as sensitive to the solvent as is DMDO. For example, estimated barriers for the PBA/cyclohexene in CH₂Cl₂ and in benzene both had the same calculated ΔE^\ddagger values of 12.2 kcal mol⁻¹. These results and the comparison with experimental data are given in Table 5. As is evident, the activation enthalpies for the peracid epoxidation of cyclohexene in CH₂Cl₂ and benzene are in very good agreement with experiment. A summary of the relative calculated activation barriers for the epoxidation of ethylene with PFA and DMDO at various levels of theory is given in Table 6. The effect of the flexibility of the basis set upon the activation barrier for epoxidation of a series of selected alkenes at the QCISD level is presented in Table 7.

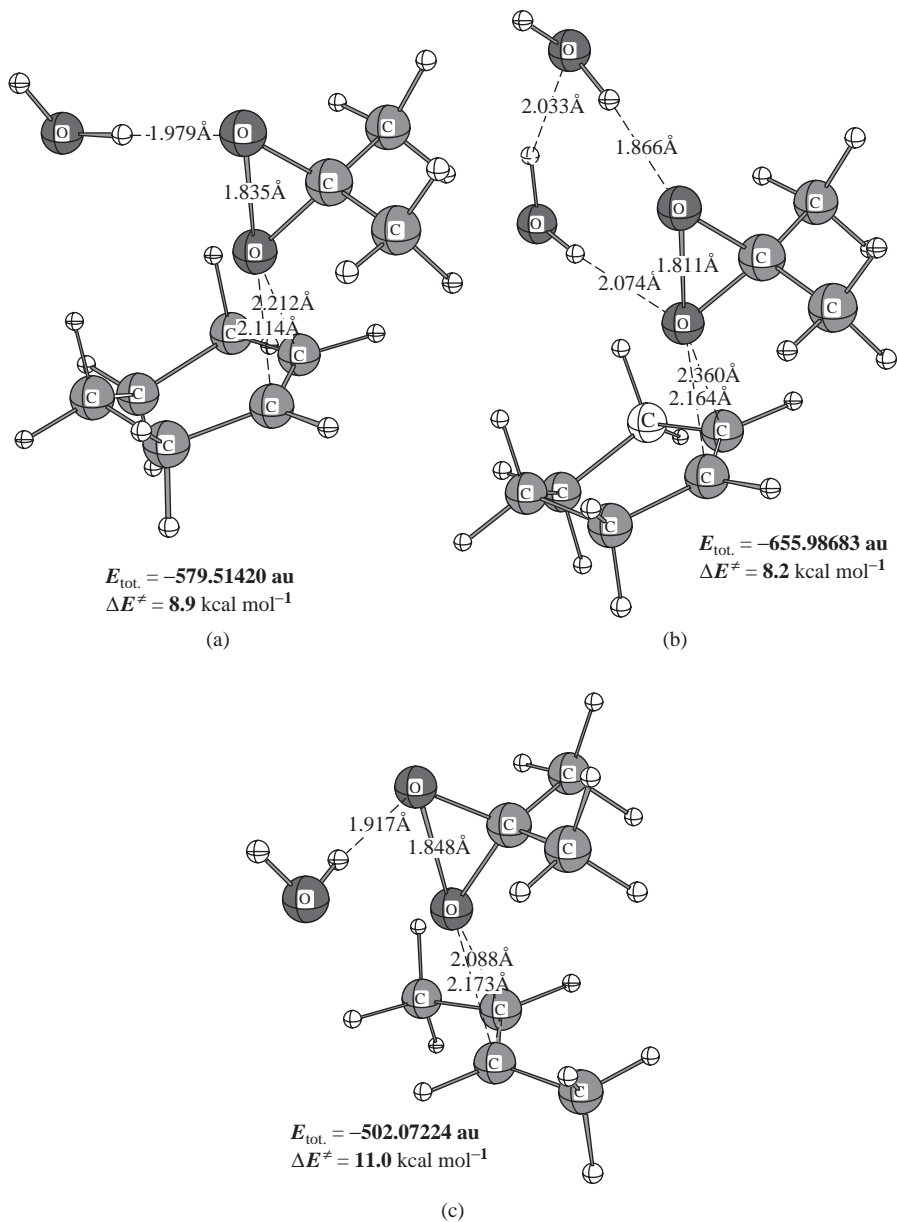


FIGURE 19. B3LYP/6-311+G(d,p)-optimized transition structures for the epoxidation of cyclohexene with DMDO in the presence of one (a) and two (b) water molecules. The transition structure for the epoxidation of *E*-2-butene (c) is optimized at the same level of theory in the presence of one water molecule. The classical barriers are estimated using total electronic energies of the transition structures, cyclohexene (-234.71316 au), *E*-2-butene (-157.27453 au), DMDO with one water molecule (-344.81523 au) and DMDO with two water molecules (-421.28672 au)

TABLE 6. Classical reaction barriers (ΔE^\ddagger , kcal mol⁻¹) for ethylene epoxidation with peroxyformic acid (PFA) and dimethyldioxirane (DMDO) at various levels of theory

Method	Ethylene + PFA	Ethylene + DMDO
B3LYP/6-31G(d)	14.1	18.2
B3LYP/6-31+G(d,p)	14.9	17.7
B3LYP/6-311+G(3df,2p)//B3LYP/6-31+G(d,p) ^a	17.0	19.6
B3LYP/6-311+G(3df,2p)	16.9	19.1
QCISD(T)//QCISD/6-31G(d)	18.8	19.4
QCISD/6-31+G(d,p)	23.4	22.3
QCISD(T)//QCISD/6-31+G(d,p)	16.4	15.2
B3LYP/6-311+G(3df,2p)//QCISD/6-31G+(d,p)	17.0	18.9
QCISD(T)/6-31G+(d,p)//B3LYP/6-311+G(3df,2p)	16.2	14.9
CCSD(T)//CCSD(T)/6-31G*	19.4	18.4
CCSD(T)/6-31+G(d,p)//CCSD(T)/6-31G* ^b	17.1	15.5

^a The TS geometry was optimized at B3LYP/6-31+G(d,p) with a single-point energy correction at B3LYP/6-311+G(3df,2p).

^b Geometry optimization with the triples contribution gave a symmetrical TS for PFA epoxidation but an asymmetric approach to the double bond with DMDO (C–O bonds of 1.830 and 2.301 Å).

TABLE 7. Summary of the reaction barriers (kcal mol⁻¹) for the epoxidation of simple alkenes with peroxyformic acid (PFA) and dimethyldioxirane (DMDO)

Reaction	ΔE^\ddagger	Method
Ethylene + PFA	16.4	QCISD(T)//QCISD/6-31+G(d,p)
	18.7	QCISD(T)//B3LYP/6-31G(d) ^a
	18.8	QCISD(T)//QCISD/6-31G(d) ^b
	17.4	QCISD(T)//B3LYP/6-311G(d,p) ^b
	18.6	QCISD(T)/6-311+G(3df,2p)//QCISD/6-31+G(d,p)
Propylene + PFA	15.9	QCISD(T)//B3LYP/6-31G(d) ^b
	16.0	QCISD(T)//QCISD/6-31G(d) ^b
Isobutylene + PFA	13.7	QCISD(T)//B3LYP/6-31G(d) ^a
	13.8	QCISD(T)//QCISD/6-31G(d) ^a
<i>E</i> -2-Butene + PFA	13.3	QCISD(T)//B3LYP/6-31G(d) ^a
	13.4	QCISD(T)//QCISD/6-31G(d)
	10.8	QCISD(T)/6-31+G(d,p)//QCISD/6-31G(d)
	11.2	CBS-Q//QCISD/6-31G(d) ^c
	13.2	QCISD(T)/6-31G(d)//B3LYP/6-311+G(3df,2p)
1,3-Butadiene + PFA	15.9	QCISD(T)//QCISD/6-31G(d)
<i>E</i> -2-Butene + DMDO	14.6	QCISD(T)//B3LYP/6-31G(d)
	14.6	QCISD(T)//QCISD/6-31G(d)
	14.3	QCISD(T)/6-31G(D)//B3LYP/6-311+G(3df,2p)
	9.7	CBS-Q//QCISD/6-31G(d) ^c
Ethylene + DMDO	15.2	QCISD(T)//QCISD/6-31+G(d,p)
	19.3	QCISD(T)//B3LYP/6-31G(d) ^b
	19.4	QCISD(T)//QCISD/6-31G(d) ^b

^a Reference 122.

^b References 38 and 124.

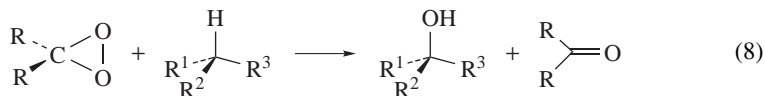
^c Based upon CBS-Q energy calculations on the QCISD/6-31G(d) optimized geometries of TS and corresponding isolated reactants.

Experimental rate data reported by Murray and Gu⁹⁵ for the DMDO epoxidation of cyclohexene also suggest that an increase in solvent polarity results in an increase in the rate of epoxidation. The increased reactivity in polar solvents can be assigned to enhanced polarization of the TS relative to the reactants. Theoretical solvation studies by Houk, Jorgensen and coworkers are consistent with these observations^{90b} and suggest that in methanol solvent a strong H-bond forms between the two oxygens of DMDO with CH₃OH and another H-bond to the distal oxygen in the TS. Miaskiewicz and Smith⁹⁹ provided a comparison of activation barriers on intra- and intermolecular H-bonding interactions. Solvent polarity effects using the SCI-PCM solvent model¹⁰⁰ show a decrease in the activation energy for DMDO epoxidation of 2-methyl-2-butene from 13.6 kcal mol⁻¹ in the gas phase to 9.5 kcal mol⁻¹ (B3LYP/6-31G*) when a dielectric constant of 20 is used (acetone solvent). The calculated activation enthalpy of 9.9 kcal mol⁻¹ was in very good agreement with the aforementioned experimental $\Delta H^\ddagger = 7.4$ kcal mol⁻¹ for epoxidation of the disubstituted alkene, cyclohexene, in acetone solvent.

A systematic study of the effects of hydrogen bonding and solvation has also been reported by Sarzi-Amade and coworkers¹⁰¹. Using 2-propen-1-ol as a substrate at the B3LYP/6-31G* level, it was shown that the electron-withdrawing effect of the hydroxy substituent in allyl alcohol has a mild rate-retarding effect upon the rate of oxidation. However, theory predicts a slightly greater reactivity for allyl alcohol with respect to the epoxidation of propylene in the gas phase but inclusion of solvation effects (Tomasi solvent model¹⁰², acetone) leads to a reversal in reactivity in agreement with experiment.

4. Oxidation of saturated hydrocarbons

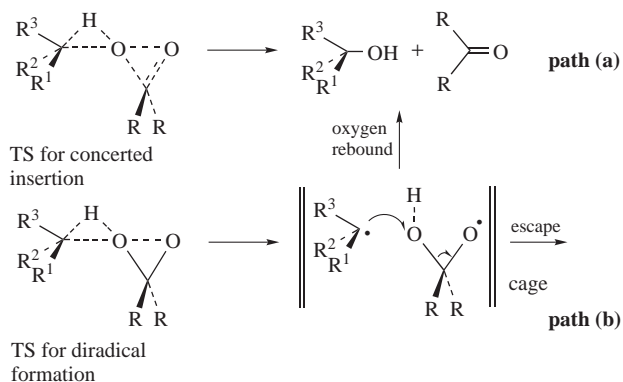
Part of the mystique surrounding the often assumed high reactivity of dioxiranes stems from the observation that dioxiranes such as methyl(trifluoromethyl)dioxirane (TFDO) are capable of oxidizing saturated hydrocarbons to their alcohols at relatively low temperatures¹⁰³ in high yields and with impressive stereoselectivities (equation 8).



The enhanced propensity of dioxiranes to insert oxygen into unactivated alkane C–H bonds was ascribed initially to the high ring strain energy (SE) of dioxiranes that has sometimes exceeded 30 kcal mol⁻¹. Since the SE of these three-membered peroxides has recently been substantially reduced (SE = *ca* 11–18 kcal mol⁻¹), a different explanation is required^{20b}.

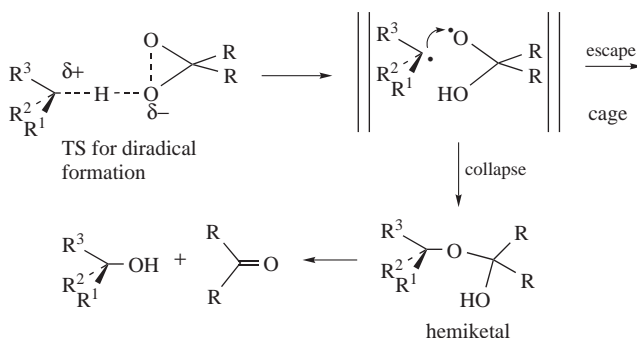
The mechanism of this unique oxidation has been the subject of controversial debate focused on a concerted versus a stepwise dichotomy. Curci, Adam and coworkers¹⁰³ advanced a one-step (concerted) electrophilic oxygen insertion (Scheme 7, path a) that is experimentally very difficult to distinguish from a stepwise process (path b) in which the TS proceeds to a caged radical pair that undergoes a very rapid ‘oxygen rebound mechanism’ by an S_H2 reaction forming the observed products (ketone plus alcohol) with retention of configuration. What is considered by many to be compelling evidence for a concerted oxidation comes from complete retention of configuration for oxygen insertion into a chiral center¹⁰³, and from the absence of radical rearrangements in radical clock studies¹⁰⁴. Radical clocks gave unrearranged products and are more consistent with concerted oxenoid insertion.

Despite the fact that a concerted oxygen insertion reaction appeared to be in complete agreement with existing experimental studies, Minisci and his group strongly advocated a



SCHEME 7

stepwise mechanism supported by the formation of radical intermediates. The ‘molecule induced mechanism’ shown in Scheme 8¹⁰⁵ describes a radical pair that can either collapse to products or produce out-of-cage free radicals that lead to a variety of products^{92,106}.

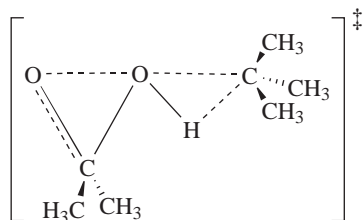


SCHEME 8

It was subsequently discovered that spurious dioxygen, present for most synthetic applications, could scavenge a small amount of the free radicals that escaped from the solvent cage, disrupting the free radical chain process, and give the typically observed alcohol insertion product. A much different product distribution was observed when dioxygen was rigorously excluded. This mechanistic anomaly was responsible for a lot of the confusion!

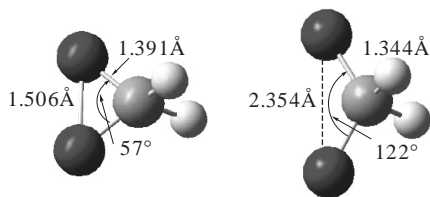
Theoretical studies with the DFT method provided strong support for the concerted pathway. The hydroxylation of hydrocarbons on the restricted energy surface (RB3LP) provided TSs with the requisite O–O bond elongation and substantial transfer of the C–H hydrogen to the attacking oxygen atom as shown below. Calculations at the G2 level by Bach and coworkers¹⁰⁷ suggested that C–H bond homolysis is not thermodynamically favorable in hydrogen abstraction reactions of methane, propane and isobutane with either DMDO, the parent dioxirane DO, or DFDO.

Intrinsic reaction coordinate following (IRC) analysis by both Bach and coworkers¹⁰⁷ and Du and Houk¹⁰⁸ showed that these TSs were connected to both reactant and product without the formation of a radical intermediate consistent with an oxygen insertion into the C–H bond (see inset). Shustov and Rauk¹⁰⁹ advocated a bifurcation on the descent



pathway on the product side at a point just below the TS that led to radical products. All three studies evidenced a UHF-RHF wave function stability. At that time such a problem was typically resolved by showing that the UHF solution is only marginally lower in energy and the restricted TS is assumed to be valid. However, in those cases where significant diradical character is involved such a transition structure may be flawed and a lower-energy TS on the unrestricted or open-shell potential energy surface may well be possible as noted below. This mechanistic controversy has been hampered due to experimental difficulties such as the aforementioned lack of stability of dioxiranes and by the fact that it is very difficult to obtain pure solutions of the more synthetically useful dioxiranes although solutions of TFDO are relatively stable, compared to the parent dioxirane (DO), and can be stored at -20°C for 48 h with only minor losses. This presents an ideal case where theory can perhaps provide an answer more readily than experiment.

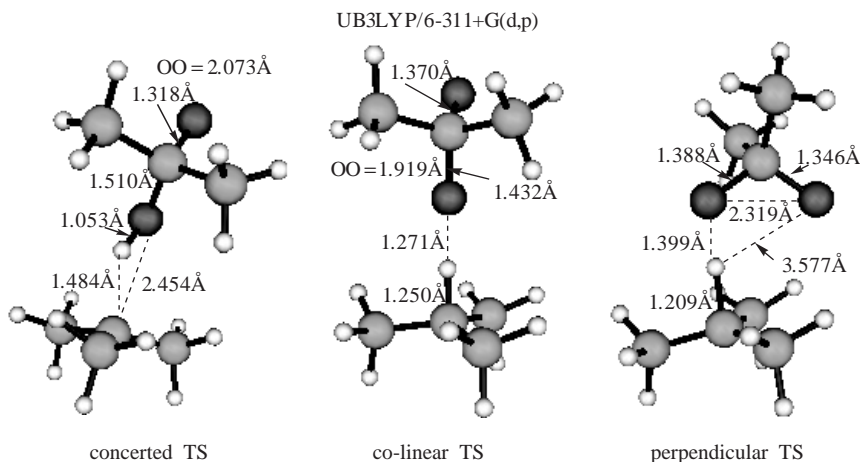
This mechanistic dichotomy is in one sense largely semantic in nature. The pertinent questions to answer are what is the lifetime of free radical species on the reaction coordinate and what is the rate of the subsequent S_H2 hydroxylation of the intermediate carbon radical (or radicaloid)? Although in many cases when an RHF-UHF wave function instability is noted, the resulting restricted TS may be adequately described and its geometry does not differ significantly from a TS located on the unrestricted surface. However, as noted above for the peroxyxynitrous acid oxidation of saturated hydrocarbons²⁷, where a unique type of singlet free radical intermediate is possible, the open-shell potential energy surface should also be examined. Dioxiranes are capable of experiencing O—O bond elongation to produce several singlet diradical intermediates that are energetically accessible on the PES for alkane oxidation. As noted above, Anglada⁶⁵ reported a high-level *ab initio* MRD-CI estimate suggesting that the diradical singlet form of DO is only 5.8 kcal mol⁻¹ higher in energy than its ground state. An activation barrier of 21.4 kcal mol⁻¹ was predicted for the ring opening of DO to this excited singlet.



Recent DFT calculations by Sarzi-Amade and his collaborators¹¹⁰ may well have resolved this mechanistic difference between a biradicaloid TS (Scheme 7, path b) and a mechanism involving discrete long-lived free radicals (Scheme 8). Oxygen insertion into the C—H bond of isobutane by DMDO was studied computationally at the unrestricted B3LYP level. Transition structures that were diradicaloid in nature were found to lead to

insertion products via radical pair intermediates. These UB3LYP TSs were lower in energy than TSs located previously on the restricted PES (RB3LYP) supporting the possibility of radical pair formation in reactions of dioxiranes with saturated hydrocarbons.

In a subsequent exemplary theoretical study¹⁰⁵ they were able to locate two transition structures on the UB3LYP/6-311+G(d,p) surface that not only differed geometrically from the previously reported^{107–109} concerted TSs (RB3LYP) but were lower in energy.



The classical activation barrier (ΔE^\ddagger) for lower-energy diradical TS for isobutane oxidation was 12.2 kcal mol⁻¹ lower in energy than the closed-shell concerted TS ($\Delta E^\ddagger = 32.0$ kcal mol⁻¹) and involved approach of the alkane C–H *perpendicular* to the plane of the three-membered ring peroxide. A second TS ($\Delta E^\ddagger = 24.5$ kcal mol⁻¹) was somewhat higher in energy but the initial product of hydrogen abstraction had a much better orientation for the S_H2 hydroxylation step. Collapse of the intermediate 2-hydroxy isopropoxy radical–*t*-butyl radical pair to product acetone and *t*-butyl alcohol proceeded with a barrier of only 0.4 kcal mol⁻¹. They concluded that the PES on the open-shell pathway was indeed consistent with the ‘molecule induced homolysis’ and that genuine diradical TSs were involved. The question remains as to whether this is actually a ‘one-step nonconcerted’ process or a very rapid two-step process. Clearly, this theoretical analysis supports the contention that biradical TSs are involved in this oxidative process and conforms to the suggestions made by Curci and Adam¹⁰³ based upon experimental studies with chiral substrates. This approximate reaction pathway was intuitively predicted by these experimentalists, suggesting that after a slow step the ‘*alternative to direct collapse into products—some radical character develops*’ or ‘*cage radical pairs are formed after the slow step*’¹⁰³.

Thus, it would appear that serious consideration must be given to at least partial involvement of open-shell species in the reactions of dioxiranes with both saturated and unsaturated hydrocarbons. Perhaps it should not be too surprising that those peroxides that have readily accessible low-lying singlet excited states like dioxiranes or metastable states like peroxyxynitrous acid can exhibit open-shell chemistry. For example, UB3LYP/6-31G(d) calculations on oxygen insertion by trifluoroperoxyacetic acid into the C–H bonds of methane and isobutane strongly support the viability of a one-step nonconcerted mechanism invoking a transition state with high diradical character and strong polarization¹¹¹. Such a process is ostensibly a two-step oxidation where the O–H bond forms first and

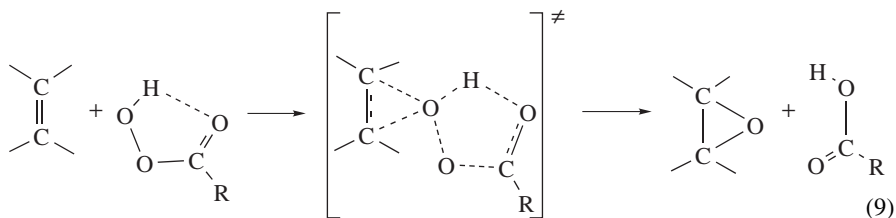
the C–O bond effecting oxygen insertion occurs subsequently but only a single transition state is observed and no minima corresponding to intermediates were located. Such diradicaloid transition states are difficult to treat theoretically and much additional work is needed before one can accurately assign such a mechanism.

VI. THE EPOXIDATION OF ALKENES WITH PERACIDS

A. Early Mechanistic Studies

Since the discovery of the peracid epoxidation reaction by Prilezajew in 1909¹¹², epoxides, as a class of compounds, have played a major role in organic chemistry both synthetically and in industry. Epoxides continue to provide synthetic intermediates as building blocks for the synthesis of more complex molecules. For most of the last century epoxides were prepared from alkenes primarily by their interaction with peracids. Certainly, the peracid functionality is among the more cleverly designed synthetic reagents since it can transfer an oxygen atom to a C=C bond by a 1,5-intramolecular hydrogen transfer to the carbonyl oxygen and still retain its highly stabilized carboxylic acid group. The use of chiral epoxides in synthetic chemistry gained particular favor in the 1970s with the discovery of the metal-catalyzed epoxidation that utilized the Sharpless epoxidation¹¹³. During the last several decades a wide variety of oxygen atom transfer reagents have been disclosed and several of the most useful oxidizing agents are described elsewhere in this treatise. We will not include metal-catalyzed epoxidation reactions since they have recently been extensively reviewed¹¹⁴.

The mechanism of the peracid epoxidation of alkenes, a subset of this general class of reactions, has been the subject of experimental study for many years^{115,116}. More than fifty years ago Bartlett proposed^{117a} a mechanism where the terminal oxygen atom of the peroxy acid was transferred to the carbon–carbon double bond with simultaneous transfer of the proton of the peracid to the carbonyl oxygen. This was the accepted mechanism for many years and became known as the ‘butterfly mechanism’ because of the approximate shape of the proposed transition state (equation 9). The actual origin of this term is not known to us, but it was not in the original lecture delivered by Bartlett in a Frontiers in Chemistry lecture at Wayne State University in 1950^{117b}. In subsequent publications Bartlett and coworkers^{117c} reinforced the idea that the proposed transition state (TS) for oxygen atom transfer was planar in nature with the peracid group along the C=C bond axis.



B. Hartree–Fock Level Theoretical Calculations

For more than forty years the Bartlett ‘butterfly’ TS was the generally accepted mechanism for peracid epoxidation and numerous experimental studies supported this transition structure^{115,116}. During these formative years theoretical calculations did not play a major role due to limitations of available methods that could adequately treat the peroxy functional group. Theoretical contributions in 1978 were at the Hartree–Fock (HF) level since

that was all that was available at that time. HF calculations by Plesnicar and coworkers¹¹⁸ with a very small basis set (STO-4G) suggested an unsymmetrical TS. However, early theoretical studies by Bach and coworkers^{48a} suggested a symmetrical approach of the peracid to the C=C and, more importantly, that the plane of the peroxyacid moiety preferred to be perpendicular to the C=C bond axis; the term '*spiro* transition state'⁴⁸ was coined to describe the local tetrahedral environment about the attacking electrophilic oxygen atom. The *spiro* nature of the TS was based largely upon the supposition that the TS could be stabilized if the attacking oxygen lone pair could back bond to the π^* orbital of the carbon-carbon double bond. In an idealized *spiro* orientation the H-O-C-C dihedral angle is 90.0°. It was recognized early on that in the absence of electron-correlation corrections, HF calculations were not capable of adequately describing reactions that involved O-O bond cleavage¹¹⁹. Thus, the possibility for serious contributions from theoretical studies did not present itself until 1991 when *ab initio* calculations with electron correlation was feasible. The first report^{17b} of a transition structure for the peroxyformic acid epoxidation of ethylene at a correlated level of theory, second-order Moller-Plesset theory (MP2), was constrained to be symmetric and suggested an approximate *spiro* orientation (TS-b, Figure 20). IRC calculations by Bach and coworkers^{17b} corroborated the basic tenets of the accepted mechanism where the 1,5-intramolecular hydrogen shift to the carbonyl oxygen took place *after the barrier was crossed*. These data were consistent with

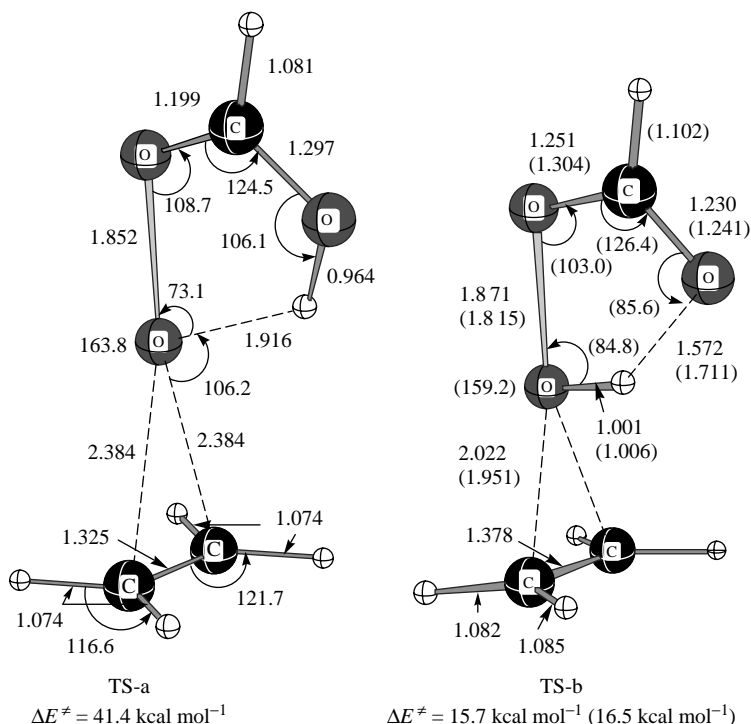


FIGURE 20. The transition states for peroxyformic acid zwitterion + ethylene (TS-a) and peroxyformic acid + ethylene (TS-b) at the HF/6-31G* and the MP2/6-31G* level (in parentheses). The energy is at the MP4SDTQ//HF/6-31G* level and MP4SDTQ//MP2/6-31G* (in parentheses)

a relatively small kinetic isotope effect (KIE), $k_{\text{H}}/k_{\text{D}} = 1.17$, for the O–H group on the peracid¹²⁰. The peroxyformic acid O–H distance in the TS for ethylene epoxidation was only slightly elongated at 1.006 Å in support of the IRC data. It is particularly noteworthy that Hartree–Fock calculations gave a completely erroneous TS where the 1,5-hydrogen shift occurred *prior* to the oxygen atom transfer (TS-a, Figure 20). Since the O–O bond dissociation energy (BDE) for a peracid is essentially zero at the HF level^{16a}, stretching the O–O bond in the TS is without energetic consequences. Despite this obvious deficiency, a number of theoreticians continue to employ HF calculations for such reactions including QM/MM methods^{20c}.

At that period of time, this rather primitive transition structure for the peracid epoxidation of ethylene was sufficiently novel to warrant publication as a communication^{17b}! Today, calculating transition structures for epoxidation of a variety of complex alkenes with the actual peracid used experimentally, such as *meta*-chloroperoxybenzoic acid (*m*-CPBA), is commonplace^{19d}.

C. Synchronous versus Asynchronous Transition States

Calculations at the second-order Moller–Plesset (MP2) theory level were not without problems because the TSs for even simple alkenes, although *spiro* in nature, were highly unsymmetrical¹²¹. Although the concerted nature of the mechanism has been generally accepted, the MP2 results initiated controversy over the synchronous versus asynchronous (equal or unequal developing C–O bonds) approach of the peracid to the C=C double bond. MP2 theory was used initially for most *ab initio* calculations involving O–O bond cleavage and seemed to provide adequate energetics for such epoxidation reactions but very poor geometries^{17, 122}. For example, the MP2 method gave an unsymmetrical transition structure¹²¹ for the peroxyformic acid epoxidation of ethylene, where the two developing C–O bonds were of unequal length (C–O = 1.805 and 2.263 Å) that was 0.2 kcal mol⁻¹ lower in energy than a symmetrical *spiro* structure (a second-order saddle point)¹²³. However, the asymmetric nature of this TS was shown by Bach and coworkers^{17a} to be an artifact of the MP2 method since more highly correlated methods [QCISD, CCSD, CCSD(T)] gave very symmetrical *spiro* transition structures with synchronous formation of the developing C–O oxirane bonds for symmetrically substituted alkenes¹²⁴.

For example, a variety of computational methods suggested a *spiro* TS, with nearly identical developing C–O bonds, for the peroxyformic acid epoxidation of ethylene with the exception of the MP2 method (Figure 21). Similarly, a slightly asymmetric TS was noted for the epoxidation of isobutylene, with the exception of the MP2 method where the developing C–O bonds differed widely (1.899 and 2.192 Å, Figure 22). The calculated differences in the two developing C–O bonds for the epoxidation of a series of alkenes with the MP2, B3LYP and QCISD methods are given in Table 8.

The most convincing evidence for an essentially synchronous peracid epoxidation of simple alkenes came from a combined experimental and theoretical study by Singleton, Houk and coworkers¹²⁵. Experimental KIEs for the reaction of *m*-CPBA with 1-pentene, determined by the clever methodology developed by Singleton and Thomas¹²⁶ utilizing the combinatorial high-precision determination of ¹³C and ²H KIEs at natural abundance, confirmed the symmetrical or nearly symmetrical nature of this epoxidation TS. These data were corroborated by B3LYP/6-31G* calculations on propylene that supported a synchronous transition state for peroxyformic acid epoxidation.

Conjugated and α,β -unsaturated C=C double bonds exhibit decidedly different behavior toward peracids. Bach and coworkers^{19b} have reported that both 1,3-butadiene and acrylonitrile afford asymmetric TSs consistent with their polarizable conjugated double bonds. The unsymmetrical character of the transition structures for both the epoxidation of

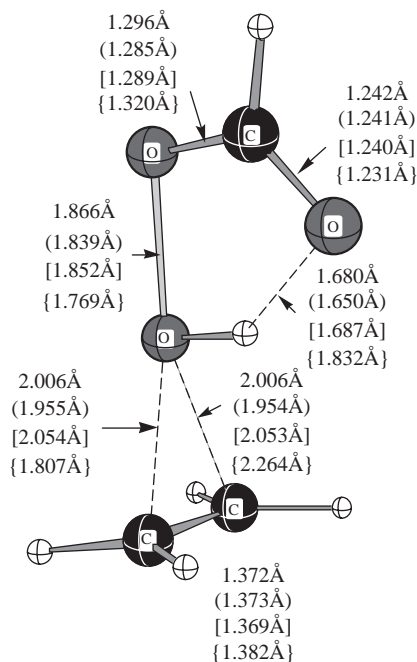


FIGURE 21. Selected geometrical parameters of the transition structures for the epoxidation of ethylene with peroxyformic acid calculated at the QCISD/6-31G*, CCD/6-31G* (in parentheses), B3LYP/6-31G* (in square brackets) and MP2(FC)/6-31G* (in curly brackets) levels

TABLE 8. Differences (Å) in the O–C1 and O–C2 calculated distances of transition structures for the epoxidations of alkenes with peroxyformic acid using different methods

Substrate	ΔR (MP2/6-31G*)	ΔR (B3LYP/6-31G*)	ΔR (QCISD/6-31G*)
Ethylene	0.458	0.000	0.000
Propylene	0.537 ^a	0.117	0.021
Isobutylene	-0.293 ^b	0.190 ^c	0.044 ^d
Z-2-Butene		0.001	
E-2-Butene		0.034	
1,3-Butadiene	0.519	0.417 ^e	0.305 ^f
Acrylonitrile	0.465	0.460 ^g	0.358

^a Two transition structures were found at the MP2/6-31G* level. The difference in the CO distances is given for a Markovnikov-type structure. While Markovnikov-type transition structures (albeit much more symmetrical) were found at the B3LYP and QCISD levels, this MP2 TS is 0.2 kcal mol⁻¹ higher than an anti-Markovnikov TS (for which the distance difference is -0.363 Å).

^b The MP2 transition structure exhibits a regiochemical preference for C1, in contrast to the B3LYP and QCISD results.

^c 0.237 Å at the B3LYP/6-311+G(3df,2p) level.

^d 0.069 Å at the CISD/6-31G* level.

^e 0.424 Å at the B3LYP/6-311+G(3df,2p) level.

^f 0.209 Å at the CISD/6-31G* level.

^g 0.439 Å at the B3LYP/6-311+G(3df,2p) level.

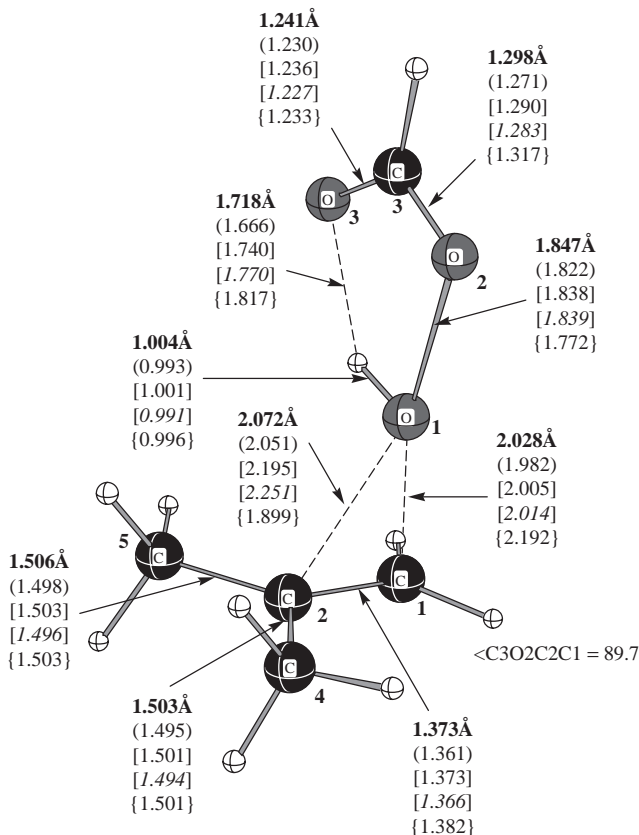


FIGURE 22. Selected geometrical parameters of the transition structure for the epoxidation of isobutylene with peroxyformic acid calculated at the QCISD/6-31G*, CISD/6-31G* (in parentheses), B3LYP/6-31G* (in square brackets), B3LYP/6-311+G(3df,2p) (in italic in square brackets) and MP2/6-31G* (in curly brackets) levels

1,3-butadiene and acrylonitrile (Figure 23) corresponds to a concerted reaction pathway although the C–O bond formation is asynchronous. Animation of the B3LYP/6-31G* vibrational mode corresponding to the negative eigenvalue of the Hessian for the transition structure of 1,3-butadiene and peroxyformic acid shows the transfer of the oxygen to C1 accompanied by O1–O2 bond elongation with $sp^2 \rightarrow sp^3$ rehybridization at the terminal carbon as it moves out of the plane toward the electrophilic oxygen. There is comparatively little motion of C2 in the TS [(a), Figure 23], and essentially no O–H bond motion is observed. By contrast, in the transition structure for the epoxidation of isobutylene with peroxyformic acid (Figure 22), the oxygen atom approaches the center of the C=C bond and both C1 and C2 carbons experience $sp^2 \rightarrow sp^3$ rehybridization with the lighter hydrogen atoms at C1, showing more motion than the two methyl groups. This type of S_N2 attack by the π -bond along the O–O bond axis is consistent with the endocyclic restriction test developed by Woods and Beak¹²⁷ to probe the geometry for alkene epoxidation. The dihedral angles between the peracid moiety and the C–C bond

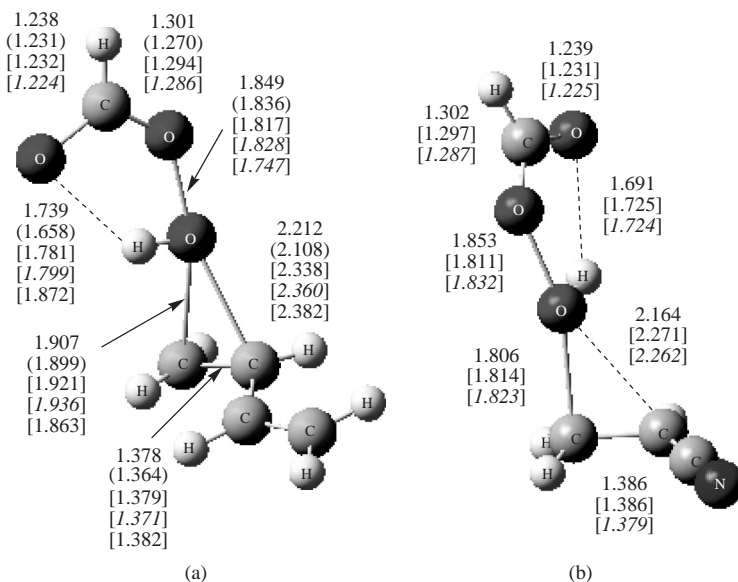


FIGURE 23. Selected geometrical parameters for the transition structures for the epoxidation of 1,3-butadiene (a) and acrylonitrile (b) with peroxyformic acid calculated at the QCISD/6-31G*, CISD/6-31G* (in parentheses), B3LYP/6-31G* (in square brackets) and MP2/6-31G* (in curly brackets) levels. The B3LYP/6-311+G(3df,2p) values are given in italic in square brackets. Bond lengths are given in Å

axis ($\angle O3C3C2C1$) in TS (a) and TS (b) are skewed by 101.0° and 109.7° , to the CC axis of the double bond, indicating a deviation from an ideal (90°) *spiro* orientation as a consequence of the polarizability of the multiply bonded substituents on the π bond. The activation barrier for the epoxidation of acrylonitrile with peroxyformic acid is about $5\text{--}6\text{ kcal mol}^{-1}$ higher than that for the epoxidation of 1,3-butadiene (Table 9, Figure 23).

The unsymmetrical nature of peracid epoxidation TSs derived from MP2 calculations were at first considered to be corroborative evidence for the correct approach of the peracid since inverse KIE reported by Hanzlik and Shearer¹²⁰ was suggestive of an unsymmetrical TS. Experimentally determined kinetic isotope effects (KIEs) are one of the few available experimental tools that can probe the geometry of a transition state. Significant secondary isotope effects should be anticipated in an electrophilic addition to an alkene when there is a discernible change in hybridization from sp^2 to sp^3 in the transition state at the isotopically substituted position. In a classic experiment, Hanzlik and Shearer¹²⁰ used this concept to define the geometry of the transition state and the timing of the bonding changes in the epoxidation of a specifically deuteriated *p*-phenylstyrene (4-vinylbiphenyl) with *m*-chloroperoxybenzoic acid (Figure 24).

Since the sp^2 carbon atoms become more sp^3 -like in the resulting epoxide, the energy of activation for an $sp^2 \rightarrow sp^3$ change in hybridization is *lower* for a deuterium-substituted double bond and the KIE is inverse with $k_H/k_D < 1.0$. The failure to observe an isotope effect for the arylethylene- α - d_2 ($k_H/k_D = 0.99$) and the observation of a significant KIE for the β , β - d_2 -substituted styrene ($k_H/k_D = 0.82$) suggested that only the arylethylene- β - d_2 -carbon had undergone a discernible change in its hybridization from sp^2 to sp^3 . These data led Hanzlik and Shearer¹²⁰ to the generalization that all transition structures

TABLE 9. Activation barriers and reaction enthalpy changes (kcal mol⁻¹) for the epoxidation of alkenes with peroxyformic acid calculated at various computational levels

Substrate	ΔE^\ddagger				
	B3LYP ^a	B3LYP/ 6-311+G (3df,2p)	QCISD(T)// B3LYP ^a	MP4SDTQ// MP2 ^a	QCISD(T)// QCISD ^a
Ethylene	14.1		18.7	16.3	18.8
Propylene	12.0		15.9	—	16.0
Allyl alcohol	7.5 ^c		11.4 ^c	7.7	(11.4) ^b
1-Butene (<i>syn</i>)	12.3				
(<i>Z</i>)-2-Butene	10.0				
(<i>E</i>)-2-Butene	10.4			10.4	
Isobutene	10.8		13.8	10.6	13.7
1,3-Butadiene (<i>syn</i>)	11.7	14.3	15.7	12.4	15.7
1,3-Butadiene (<i>anti</i>)	11.8		15.9	12.5	15.9
Styrene	11.2	13.9 ^e			
1-Octene (<i>syn</i>)	11.2	14.2			
Trimethylethylene	8.9				
Tetramethylethylene	7.8				
Allyl alcohol	4.0				
Z-3-Methyl-3-penten-2-ol	(4.2) ^d				
Acrylonitrile (<i>syn</i>)	17.4			17.1	
Acrylonitrile (<i>anti</i>)	17.3		20.8	16.8	21.0

^a The 6-31G(d) basis set was used for geometry optimizations.

^b QCISD(T)/6-31G(d)//MP2/6-31G(d) calculation; the same value was obtained for the QCISD(T)/6-311G(d,p)//B3LYP/6-311G(d,p) barrier.

^c The 6-311G(d,p) basis set was used for both single-point energy calculations and geometry optimizations.

^d Classical activation barrier with the 6-31G(d,p) basis set.

^e The basis set 6-311G(d,p) was used for geometry optimization of the *anti*-TS.

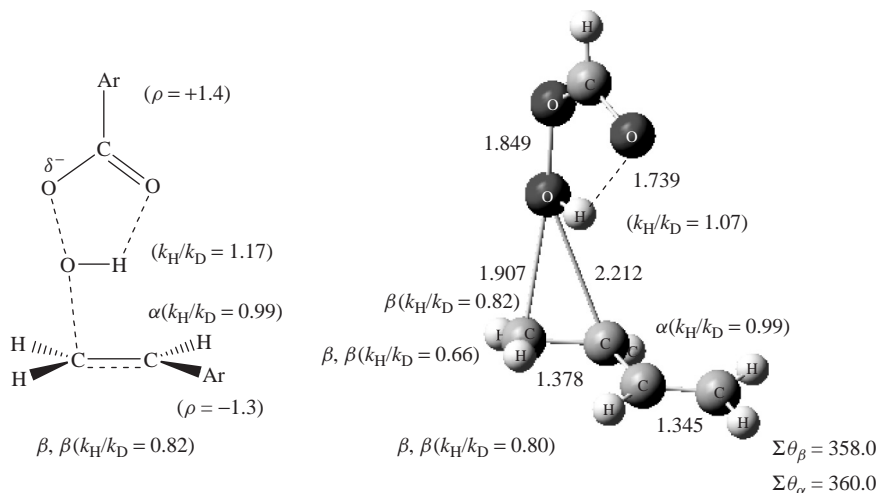


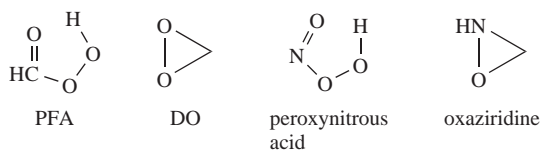
FIGURE 24. Proposed transition structure for epoxidation of an aryl-substituted styrene (4-vinylbiphenyl, left) and the transition structure for epoxidation of 1,3-butadiene (right, calculated at the QCISD/6-31G* level). The theoretical isotope effects were calculated at the MP2/6-31G* level using the Bell tunneling correction. For a discussion see Reference 19b. Bond lengths are given in Å

for epoxidation resemble the geometry of the transition structure for epoxidation of 1,3-butadiene given in Figure 24, where only one C–O bond of the oxirane product is formed, and that the unsymmetrical nature of the TS was not simply a consequence of a mono-substituted alkene.

As a theoretical model, diastereotopically distinct isotopic substitution in 1,3-butadiene was utilized by Bach and coworkers^{19b} to provide an independent test of the ability of high-level *ab initio* calculations to accurately predict a transition structure for epoxidation. The calculated KIE for deuterium substitution at the α -carbon in the TS for epoxidation of 1,3-butadiene (Figure 24) (H_a) is 0.99, in excellent agreement with the experimental value for an aryl-substituted styrene. The KIE for diastereotopically distinct hydrogen (H_b) on the β -carbon *cis* to the vinyl substituent is 0.80, while that for H_c is predicted to be 0.82. The calculated β,β - d_2 KIE is 0.66 for this transition structure with H_c , reflecting the extensive rehybridization at C_β . The calculated primary KIE for the position of the transferring hydrogen of KIE = 1.07 is lower than experiment (KIE = 1.17)¹²⁰ but consistent with an O_1-H_1 bond distance of 0.995 Å (MP2/6-31G* geometry) and a TS where the hydrogen is transferred after the barrier is crossed. Thus, both the MP2 and QCISD geometries suggest an unsymmetrical approach. For the sake of comparison, several computational methods were compared for the peroxyformic acid epoxidation of 1,3-butadiene (Figure 23) and all showed an unsymmetrical approach.

A systematic examination of the transition structures for the peroxyformic acid epoxidation at various levels of theory confirms the above suggestion that the MP2 method does provide adequate geometries for a conjugated carbon–carbon double bond in 1,3-butadiene (Figure 23). However, the inverse KIEs measured by Hanzlik and Shearer¹²⁰ for 4-vinylbiphenyl are specific to conjugated alkenes and should not be used as evidence of an asynchronous epoxidation TS for simple nonconjugated alkenes⁵³.

In general, alkene epoxidations can be classified formally, as to the nature of the substrate and type of oxidant, into four main groups: (i) symmetrical alkene (e.g. ethylene) and symmetrical oxidizing agents [peroxyformic acid (PFA), dioxirane (DO) and peroxynitrous acid, see Scheme 9], which can form a *spiro*-type transition structure where the plane of the oxidant is at *ca* 90° to the double bond; (ii) symmetrical alkene and unsymmetrical oxidant [e.g. oxaziridine]; (iii) unsymmetrical alkenes (propylene, isobutylene and 1,3-butadiene) and symmetrical oxidant; (iv) unsymmetrical alkene and unsymmetrical oxidant. With case (i), where the TS has an approximate C_s plane of symmetry geometrically, in the absence of significant diradicaloid character in the wave function, a highly symmetrical TS should be anticipated on the basis of electronic considerations. In the other cases, an asymmetrical approach to the alkene double bond should occur since the electronic distribution of the wave function is asymmetric. However, for most closed-shell systems the electronic perturbation should be minimal and an approximate symmetrical *spiro* TS typically results. Since the O–O bond in a peracid is a fairly typical O–O bond with a relatively high bond energy for a peroxo bond (*ca* 45–50 kcal mol⁻¹), the extent of diradicaloid participation should be minimal. Obviously, with dioxiranes where the O–O bond can have several higher-lying biradicaloid singlet states, the opposite situation may well be observed. These generalizations do not preclude a variety of



SCHEME 9

other possible transition structures if a planar approach of the oxidizing reagent to the C–C bond axis is preferred on steric grounds. In this section we will discuss the transition structures for the first three of these oxidizing agents with symmetrical, unsymmetrical and conjugated alkenes that have been reported in the more recent literature.

Just such an example of a planar TS has been reported recently by Sarzi-Amade and his coworkers^{51b}, who managed to locate only a planar-like TS and a planar TS (the peroxy acid plane contains the C=C bond axis), for *anti*- and *syn*-sesquiorbornenes. They are substrates that, because of steric constraints, cannot easily accommodate *spiro*-like TSs. These planar TSs are ‘nonconcerted’ since they are strongly unsymmetrical and only one of the C–O bonds of the oxirane ring is significantly formed. IRC analysis, while confirming that formation of one C–O bond fully precedes that of the other, also suggests that all this can take place without formation of intermediates, that is, within a ‘nonconcerted one-step process’.

As noted elsewhere, one should only anticipate an asynchronous TS for alkene epoxidation when the possibility for significant diradical character is evident. In a systematic study of alkene epoxidation by the four classes of oxidant noted above (Scheme 9), Houk and coworkers described the varying asynchronous nature of the epoxidation TSs at the B3LYP/6-31G* level of theory^{90a}. These results were compared to the corresponding TSs derived from MP2 calculations. In general, it was noted that all of the epoxidations exhibit *spiro* transition states; those with peroxyformic acid and dioxirane are early TSs and involve synchronous oxygen transfer. Ethylene epoxidation with peroxyxynitrous acid and oxaziridine are later TSs with an asynchronous oxygen atom transfer. However, as described above in Section IV.E (Figures 7 and 8) the HO–ONO epoxidation of ethylene at the more highly correlated QCISD level has an essentially symmetrical TS. When the C=C is substituted by methoxy, methyl, vinyl and cyano groups, the TS becomes more asynchronous as noted above. The activation barriers are lowered for all substituents but cyano with both peracid and dioxirane epoxidation.

This controversy^{12b, 17a, 90a, 121, 125} concerning the use of MP2 calculations for epoxidation reactions was rather short-lived since more efficient density functional calculations (DFT) came into general use and generally produced symmetrical *spiro* transition structures. Consequently, the use of MP2 theory for O–O bond cleavage reactions has been largely discontinued. Most have assumed that the question of symmetrical versus asymmetrical approach of the peracid had been resolved. Recall that this same problem with MP2 calculations existed for the early calculations for dioxirane epoxidation (see Section V.D).

During the past decade DFT calculations have been utilized to show various aspects of the epoxidation reaction and the activation energies for numerous epoxidation reactions have been reported^{17b, 19}; the *spiro* orientation, with symmetrically substituted alkenes, has always been of lower energy than a planar approach where the peroxyacid is parallel to the C=C bond axis ($\angle \text{H–O–C–C} = 0.0^\circ$). The symmetrical nature of the transition structure for peracid epoxidation was also verified by Bach and coworkers¹²⁴ at the complete active space [CASSCF (10,9)] level where it was demonstrated that the choice of active space is critical to determining the nature of the TS. A comparison of these CASSCF results with those of such highly correlated methods as MP2, QCI, CC and BD presented very strong evidence that a symmetrical *spiro* TS is involved in peracid epoxidation of symmetrically substituted *nonconjugated alkenes*. The preferred *spiro* approach is thought to be due to a small back bonding interaction of the distal oxygen lone-pair of electrons with the C=C π^* orbital^{148a, 128}. This favorable electronic interaction is maximized with a tetrahedral array around the developing oxirane oxygen and ‘turned off’ in the planar transition structure. These energy differences have been reported by several groups^{88, 90a, 129, 130} to be relatively small and it has been almost universally assumed that the *spiro* TS is operating. Recent

experimental^{51a} and theoretical^{51b} studies involving sterically encumbered alkenes also suggest that the *spiro* TS is favored over a planar one.

However, a recent report by Leszczynski and coworkers⁵³ has called both the preferred transition structure for peracid epoxidation and the use of DFT calculations for such reactions into question. Based upon a series of CASSCF calculations, including the CASSCF(12,12)/6-311++G(d,p) level, they suggested a nearly planar orientation of the peroxyformic acid relative to the ethylene double bond (first-order saddle point). It was concluded that the electronic structure of this TS could only be described correctly by quantum-mechanical methods that are based upon multideterminantal approaches. This question was reexamined by Bach and Dmitrenko⁵² at several levels of theory including CASSCF, and convincing evidence was again presented that the *spiro* orientation is in fact the preferred approach for alkene epoxidation with peracids and that the B3LYP variant of DFT calculations remain a useful and reasonably accurate method of choice for such studies. The problem with the planar TS suggested by the recent CASSCF results⁵³ was most likely a consequence of choosing an unbalanced active space as noted much earlier¹²⁴. A similar exercise for dioxirane epoxidation by Dmitrenko and Bach¹³¹ also confirmed a *spiro*, essentially symmetrical, approach of the dioxirane ring for the transition state. It should be emphasized that the PES for the approach of the electrophilic oxygen to the C=C π -bond is very shallow and minor changes in geometry may occur without a significant energy penalty.

Several general conclusions may be drawn concerning the mechanism of peracid epoxidation of alkenes:

(1) The epoxidations of propylene and isobutylene with peroxyformic acid proceed in a concerted way via slightly unsymmetrical Markovnikov-type transition structures where the differences in the bond distances between the double-bond carbons and the *spiro* oxygen are only 0.021 and 0.044 Å at the QCISD/6-31G* level. In contrast, the more polarizable nature of the carbon-carbon double bond of α,β -unsaturated systems results in a highly unsymmetrical transition structure for the epoxidation of 1,3-butadiene with an order-of-magnitude difference in the carbon-oxygen bond distances of 0.305 Å at the QCISD/6-31G* level. A highly unsymmetrical transition structure has been also found for the epoxidation of acrylonitrile.

(2) Epoxidations of methyl-substituted alkenes and α,β -unsaturated systems as 1,3-butadiene and acrylonitrile with peroxyformic acid follow a concerted asynchronous pathway.

(3) Methyl substitution leads to a decrease in the epoxidation barriers from 18.8 kcal mol⁻¹ for ethylene to 13.7 kcal mol⁻¹ for isobutylene at the QCISD(T)/6-31G**/QCISD/6-31G* level.

(4) While the activation barrier for the epoxidation of 1,3-butadiene with peroxyformic acid (15.9 and 11.7 kcal mol⁻¹ at the QCISD(T)/QCISD and B3LYP levels, respectively) is close to that for propylene epoxidation (16.0 and 12.0 kcal mol⁻¹ at the QCISD(T)/QCISD/6-31G* and B3LYP/6-31G* levels, respectively), the barrier for acrylonitrile epoxidation is higher (21.0 and 17.3 kcal mol⁻¹ at the QCISD(T)/QCISD/6-31G* and B3LYP/6-31G* levels, respectively). This increase in the barrier height reflects the decreased nucleophilicity of double bonds bearing electron-withdrawing substituents. The closeness of the barriers for propylene and 1,3-butadiene epoxidations supports the conclusion that both reactions have similar mechanisms albeit they differ in the asynchronous character of their transition structures.

(5) A comparison of the barriers for alkene epoxidations calculated at the QCISD(T)/6-31G**/B3LYP/6-31G* level with the QCISD(T)/6-31G**/QCISD/6-31G* and CCSD(T)/6-31G**/QCISD barriers leads to the conclusion that using the B3LYP geometries in the

QCISD(T) and CCSD(T) calculations can be cost effective and, at the same time, a reliable computational approach to study epoxidations of alkenes with peroxy acids.

D. Gas-phase Epoxidation of Selected Alkenes

Although experimental mechanistic studies of electrophilic addition to alkenes has been a major area of research for many years¹³², more recent questions have been probed mainly by computational means. We are now in a position to visualize the transition structures for a great many such reactions with unique alkenes or those that are difficult to prepare with high strain energy (SE)¹³³. For example, Bach, Adam and coworkers^{19d} have reported that epoxidation barriers are only slightly greater for highly strained alkenes such as cyclopropene (SE = 55.2 kcal mol⁻¹)¹³⁴ and cyclobutene (SE = 28.4 kcal mol⁻¹) than for cyclopentene (SE = 4.1 kcal mol⁻¹), which possibly reflects the fact that the resulting epoxide products are also strained. The SE for the simplest epoxide, oxirane or ethylene oxide is 26.3 kcal mol⁻¹^{20b} with an accompanying reduction in SE with each alkyl substituent¹³³. The lack of correlation of rate with strain energy is quite evident in the relatively small $\Delta\Delta E^\ddagger = 0.8$ kcal mol⁻¹ for cyclopropene versus cyclobutene (Table 10, Figure 25). All three TSs exhibit a highly symmetrical approach to the carbon-carbon double bond with a *spiro*^{128b, 124} orientation (90°) of the plane of the peracid with respect to the C=C bond axis.

Alkenes strained by twist or π -bond torsion, such as *E*-cyclooctene, exhibit much lower barriers due to relief of strain in the TS for the oxygen transfer step. While the epoxidation of symmetrically substituted alkenes normally involve a symmetrical approach to the π -bond, the TSs for epoxidation of *E*-cyclooctene and *E*-1-methylcyclooctene exhibit highly asymmetric transition structures. The $\Delta\Delta E^\ddagger = 3.3$ kcal mol⁻¹ for *E*- versus *Z*-cyclooctene is clearly a reflection of the relative SE of these two medium ring alkenes (16.4 vs 4.2 kcal mol⁻¹)¹³⁴. The classical activation barrier (ΔE^\ddagger) for the highly strained bicyclo[3.3.1]non-1-ene is also quite low (Table 10, Figure 26). In these twist-strain alkenes, the approach of the peracid deviates markedly from the idealized *spiro* approach suggesting that this part of the potential energy surface is quite soft.

Although it is generally accepted that the *exo* approach to norbornene is favored over the *endo*, the magnitude of the $\Delta\Delta E^\ddagger$ is rarely measurable experimentally unless some fraction of the *endo* product can be detected. The *exo* approach to norbornene is favored over the *endo* orientation by nearly 3 kcal mol⁻¹ for both PFA and DMDO, while the *exo* TS for benzonorbornadiene is favored by nearly 5 kcal mol⁻¹ (Figure 27). The preferred *exo* approach does not appear to result from steric interactions. It is of particular interest that the ΔE^\ddagger for norbornene is only 0.9 kcal mol⁻¹ *greater* than that for cyclohexene despite the SE = 19.2 kcal mol⁻¹ for the strained bicyclic alkene. Thus, in the absence of twist-strain we observe little rate enhancement due to strain energy.

E. Factors Influencing the Rate of Epoxidation

We have discussed how the different methods of calculation can influence the nature of the transition states for peracid epoxidation. The method of calculation also has an impact on the calculated activation barriers (Table 9). A comparison of the barriers for alkene epoxidations calculated at the QCISD(T)/6-31G(d)//B3LYP/6-31G(d) level with the QCISD(T)/6-31G(d)//QCISD/6-31G(d) and CCSD(T)/6-31G(d)//QCISD barriers lead to the conclusion that using the B3LYP geometries in the QCISD(T) and CCSD(T) calculations can be both a cost-effective and reliable computational approach to study epoxidations of alkenes with peracids^{19b}. A comparison of the calculated barrier heights for a series of typical alkenes at different levels of theory is given in Table 9. In general,

TABLE 10. B3LYP activation barriers (ΔE^\ddagger , kcal mol⁻¹) for the epoxidation of a series of alkenes with peroxyformic acid (PFA) showing the effect of the basis set (the first barriers are at the B3LYP/6-31G(d) level of theory, the barriers in parentheses are at the B3LYP/6-31+G(d,p) level)

Alkene	PFA	
Ethylene	14.1 (14.9)	17.0 ^a [16.4] ^b
Propylene	12.0 (12.6)	14.8 ^a [16.0] ^c
<i>t</i> -Butylethylene	11.2 (12.3)	14.0 ^a
1-Octene	11.2 (12.2)	14.1 ^a
Isobutene	10.8 (11.2)	13.0 ^a [13.7] ^c
<i>E</i> -2-Butene	10.5 (11.0)	12.8 ^a [13.4] ^c
<i>Z</i> -2-Butene	10.0	12.1 ^a
<i>Z</i> -2-Pentene	9.3 (10.0)	11.6 ^a
Cyclopropene	12.0 (12.5)	14.5 ^a
Cyclobutene	11.0 (11.5)	13.7 ^a
Cyclopentene	9.3 (9.7)	12.1 ^a
Cyclohexene	9.7 (10.1)	12.1 ^a
Cycloheptene	9.8 (10.2)	12.2 ^a
<i>Z</i> -Cyclooctene	9.1 (9.6)	11.5 ^a
<i>E</i> -Cyclooctene	5.6 (6.1)	8.2 ^a
1-Methyl- <i>E</i> -cyclooctene	4.0 (4.3)	5.9 ^a
Norbornene (<i>exo</i>)	9.7 (10.3)	12.9 ^a
Norbornene (<i>endo</i>)	12.5 (13.2)	15.4 ^a
Benzonorbornadiene (<i>exo</i>)	9.6 (10.2)	12.2 ^a
Benzonorbornadiene (<i>endo</i>)	14.6 (15.1)	17.0 ^a
Bicyclo[3.3.1]non-1-ene	5.2 (5.7)	7.7 ^a
Trimethylethylene	8.9 (9.1)	11.0 ^a
Tetramethylethylene	7.8 (7.9)	9.8 ^a
1,3-Butadiene	11.7 (12.4)	14.3 ^a [15.9] ^c
<i>trans</i> -2- <i>cis</i> -4-Hexadiene	9.4 (9.6)	11.5 ^a
<i>E</i> -Stilbene	13.2 (13.3)	15.1 ^a
<i>Z</i> -Stilbene	11.8 (12.6)	14.6 ^a
Styrene	11.2 (11.7)	14.2 ^a
<i>Z</i> -3-Methyl-3-penten-2-ol	9.2 ^d	
Allyl alcohol	7.5 ^e	11.4 ^f

^a Classical activation barriers computed at the B3LYP/6-311+G(3df,2p)//B3LYP/6-31+G(d,p) level.

^b The numbers in brackets for ethylene are at the QCISD(T)//QCISD/6-31+G(d,p) level.

^c The numbers in brackets for propylene, isobutylene, *E*-2-butene and 1,3-butadiene entries are at the QCISD(T)//QCISD/6-31G(d) level of theory; CBS-Q//QCISD/6-31G(d) gas-phase intrinsic barriers (ΔE^\ddagger) for the epoxidation of *E*-2-butene with dimethyldioxirane (DMDO) and peroxyformic acid are 9.7 and 11.2 kcal mol⁻¹, respectively.

^d Classical activation barrier computed at the B3LYP/cc-pVTZ level.

^e Classical activation barrier (ΔE^\ddagger) computed at the B3LYP/6-311G(d,p) level.

^f Classical activation barrier computed at the QCISD(T)//QCISD/6-31G(d) level.

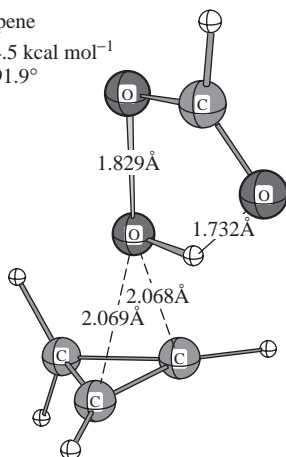
methyl substitution on the C=C leads to a decrease in the epoxidation barriers from 18.8 kcal mol⁻¹ for ethylene to 13.7 kcal mol⁻¹ for isobutylene at the QCISD(T)/6-31G(d)//QCISD/6-31G(d) level (Table 9).

One of the more intriguing features of peracid epoxidation is that the strength of the O–O bond has little impact on the rate of oxygen atom transfer. For example, peroxyacetic acid and peroxytrifluoroacetic acid have nearly identical O–O BDE (G2MP2, $\Delta H^0 =$

cyclopropene

$\Delta E^\ddagger = 14.5 \text{ kcal mol}^{-1}$

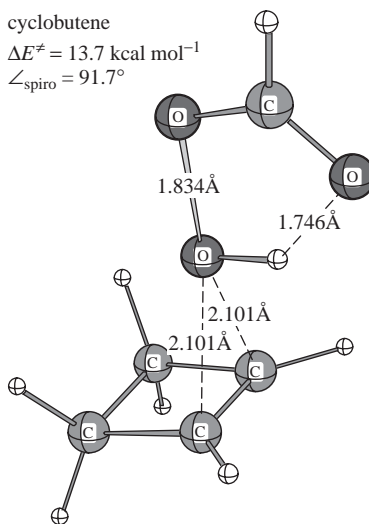
$\angle_{\text{spiro}} = 91.9^\circ$



cyclobutene

$\Delta E^\ddagger = 13.7 \text{ kcal mol}^{-1}$

$\angle_{\text{spiro}} = 91.7^\circ$



cyclopentene

$\Delta E^\ddagger = 12.1 \text{ kcal mol}^{-1}$

$\angle_{\text{spiro}} = 91.2^\circ$

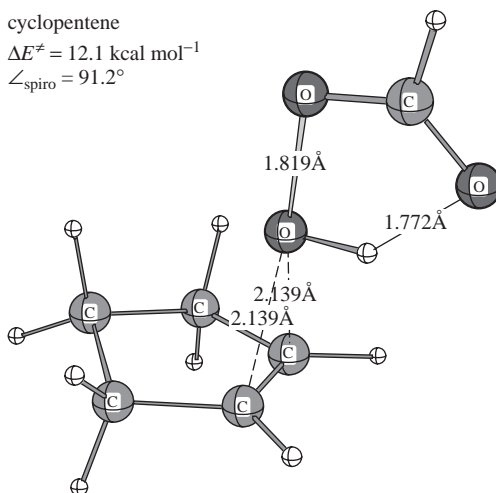


FIGURE 25. Transition structures for the epoxidation of cyclopropene, cyclobutene and cyclopentene with peroxyformic acid (PFA), optimized at the B3LYP/6-31+G(d,p) level of theory. The classical activation barriers are given at B3LYP/6-311+G(3df,2p)//B3LYP/6-31+G(d,p). Dihedral angles (\angle_{spiro} represents $\angle\text{HOCC}$) indicate the deviation from an ideal *spiro* approach (\angle_{spiro} is 90°) of the HO group in PFA onto the C=C bond of the alkene

46.4 and $47.0 \text{ kcal mol}^{-1}$)^{16a} but the latter peracid exhibits a $\geq 10^5$ greater reactivity toward alkenes. The enhanced reactivity of $\text{CF}_3\text{CO}_2\text{H}$ has been attributed to the effect of electron-withdrawing groups on the peroxy acid moiety on the charge distribution in the transition state for epoxidation. Conventional wisdom would suggest that the inductive effect of the electron-withdrawing CF_3 group would increase the electron density at the

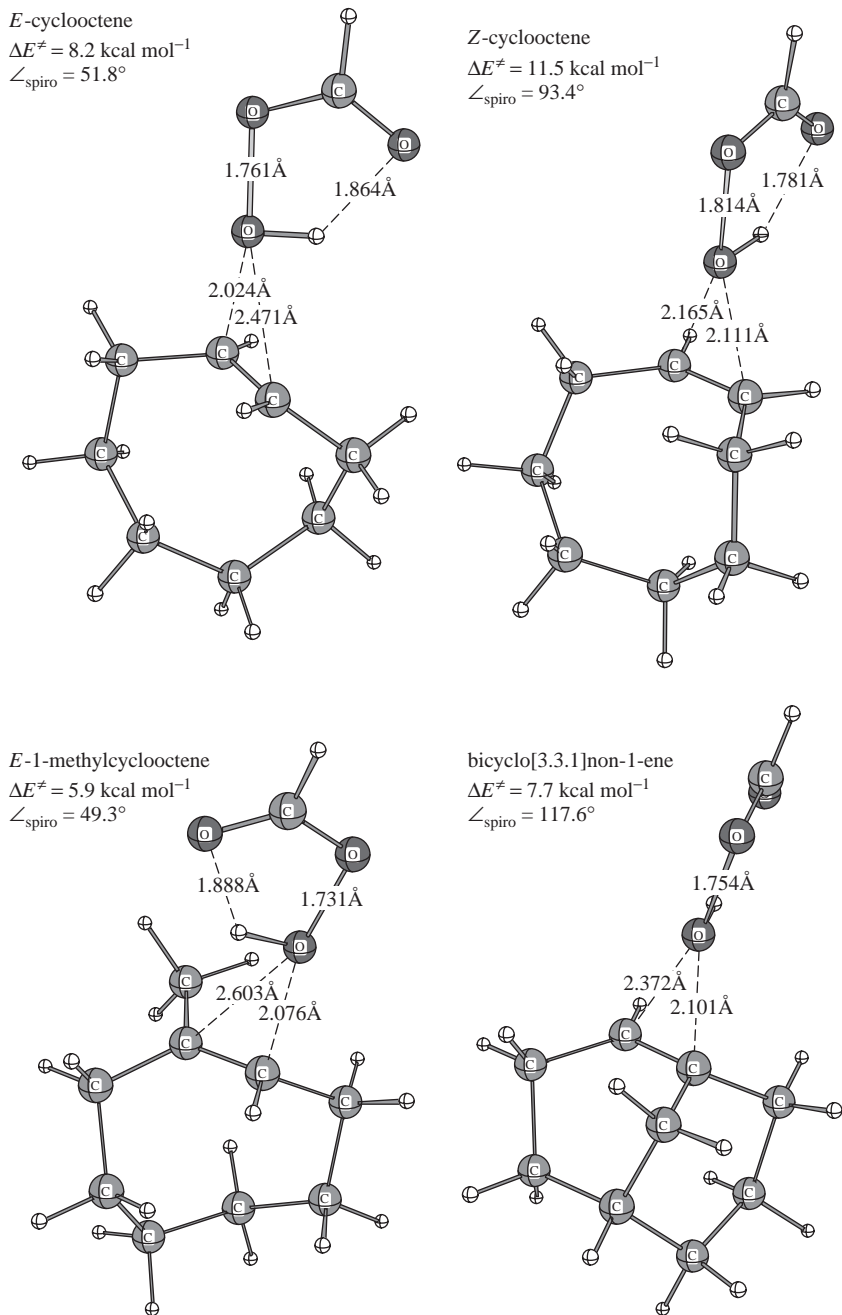


FIGURE 26. Transition structures for the epoxidation of selected cyclic alkenes with peroxyformic acid (PFA), optimized at the B3LYP/6-31+G(d,p) level of theory. The classical activation barriers are given at B3LYP/6-311+G(3df,2p)//B3LYP/6-31+G(d,p)

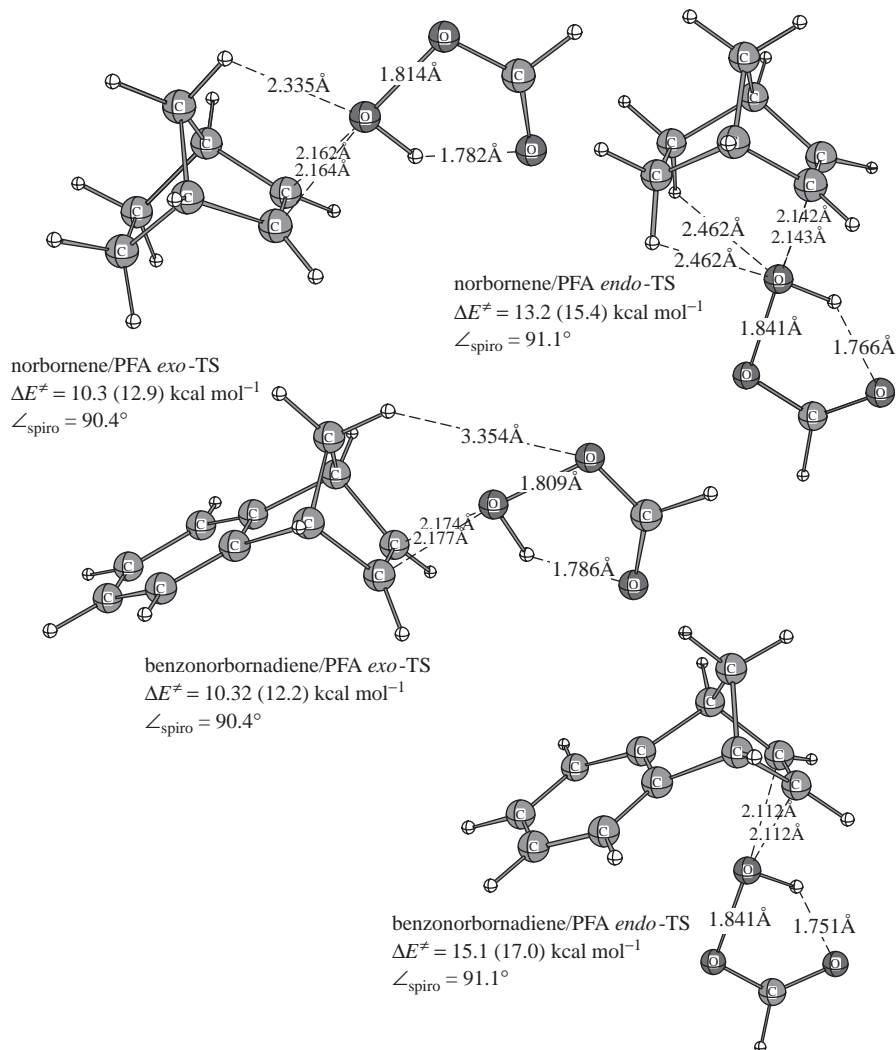


FIGURE 27. Transition structures for the epoxidation of norbornene and benzonorbornadiene, optimized at the B3LYP/6-31+G(d,p) level of theory. The classical activation barriers are given at B3LYP/6-31+G(d,p). The barriers in parentheses are at B3LYP/6-311+G(3df,2p)/B3LYP/6-31+G(d,p). Dihedral angles (\angle_{spiro} represents $\angle\text{HOCC}$) indicate the deviation from an ideal *spiro* approach (\angle_{spiro} is 90°)

developing carboxylate oxygen anion in the TS and by its stabilizing influence assist in *heterolytic* O—O bond scission. Using *E*-2-butene as a common substrate, Bach^{20a} varied the substituent on the peroxy acid, R—CO₃H, where R = H, CH₃, CF₃, F and OCH₃. A summary of the calculated activation barriers is given in Table 11 (for more details see Reference 20a).

TABLE 11. Calculated activation barriers (ΔE^\ddagger , kcal mol⁻¹), H-bonding energies ($E_{\text{H-bonding}}$, kcal mol⁻¹) in the peroxy acid^a and exothermicities ($\Delta E_{\text{reaction}}$, kcal mol⁻¹) of the epoxidation reactions of *E*-2-butene with substituted peroxy acids at the B3LYP//B3LYP/6-31+G(d,p) level of theory

Peroxy acid	ΔE^\ddagger	$\Delta E_{\text{reaction}}$	$E_{\text{H-bonding}}^a$
H(C=O)O—OH	11.01	-50.77	2.94 (8.27)
F(C=O)O—OH	6.41	-54.51	1.07 (5.31)
CH ₃ (C=O)O—OH	13.48	-49.18	4.59 (10.47)
CF ₃ (C=O)O—OH	6.39	-53.05	1.94 (5.85)
CH ₃ O(C=O)O—OH	12.81	-49.51	3.22 (10.04)

^a Intramolecular hydrogen-bonding energy in the peroxy acid; the numbers in parentheses are calculated from the difference in total energy of the TS and the structure with the H-bonding disrupted by a 180° rotation of the OH group [B3LYP/6-31+G(d,p), SP]

The activation barrier for epoxidation of *E*-2-butene with peroxyformic acid ($\Delta E^\ddagger = 11.0$ kcal mol⁻¹) is 2.5 kcal mol⁻¹ lower in energy than the activation energy for epoxidation with peroxyacetic acid. No inductive effect is observed for the methoxy group where the barrier for epoxidation with the percarbonate, CH₃O-CO₃H, is slightly increased ($\Delta E^\ddagger = 12.8$ kcal mol⁻¹). However, the predicted effect of electron-withdrawing fluorine substituents is observed with the classical activation barriers for epoxidation with CH₃CO₃H versus CF₃CO₃H ($\Delta \Delta E^\ddagger = 7.1$ kcal mol⁻¹). The activation barrier for the directly substituted fluoroperoxyformic acid, FCO₃H, is identical ($\Delta E^\ddagger = 6.4$ kcal mol⁻¹) to that of CF₃CO₃H and ironically both have the same O—O distance (Figure 28) in the TS (1.769 Å).

Although no experimental rate comparisons are available with trifluoroperacetic acid since the reactions 'are too fast to measure'¹³⁵, the enhanced reactivity of CF₃CO₃H is usually ascribed to the fact that the developing trifluoroacetate anion leaving group is much more stable than the acetate anion. Intuitively, this should mean that additional negative charge should build up on the CF₃COO⁻ fragment in the TS. However, examination of the charges on the alkene fragment and the substituted carboxylate fragment are essentially identical and are quite comparable for all five TSs examined! In each case the charge on the OH fragment is essentially zero (Figure 28). Clearly, this suggests that conventional wisdom does not provide an explanation for this increased reactivity that has traditionally been ascribed to inductive stabilization of the developing anionic leaving group. The transition structures for both of the fluoro-substituted TSs come earlier along the reaction coordinate as evidenced by the shorter O—O bond (1.769 Å) relative to that of the peroxyformic and peroxyacetic acid TSs (1.83 Å). An earlier TS is also consistent with the longer C—O bonds in the developing epoxide ring.

From this theoretical analysis it may be concluded that the arguments pertaining to classical inductive effects cannot explain the increased rates of epoxidation due to either increased alkyl substitution on the double bond or the effect of electronegative substituents on the peracid. Our best rationale at this time is that the electron-withdrawing substituents lower the energy of the O—O σ^* orbital of the peracid, which has the effect of moving the TS closer to the reactants side of the reaction coordinate with a complementary lowering of the activation barrier. Consistent with this suggestion, and in consonance with the Hammond postulate, there is a linear relationship between the number of alkyl groups on the double bond and the overall heat of the reaction forming the epoxide product and the neutral carboxylic acid. The G2 energies of reaction (ΔE) for epoxidation of ethylene, propylene, isobutylene and trimethylethylene are -47.7, -50.2, -52.0 and -55.1 kcal mol⁻¹, respectively.

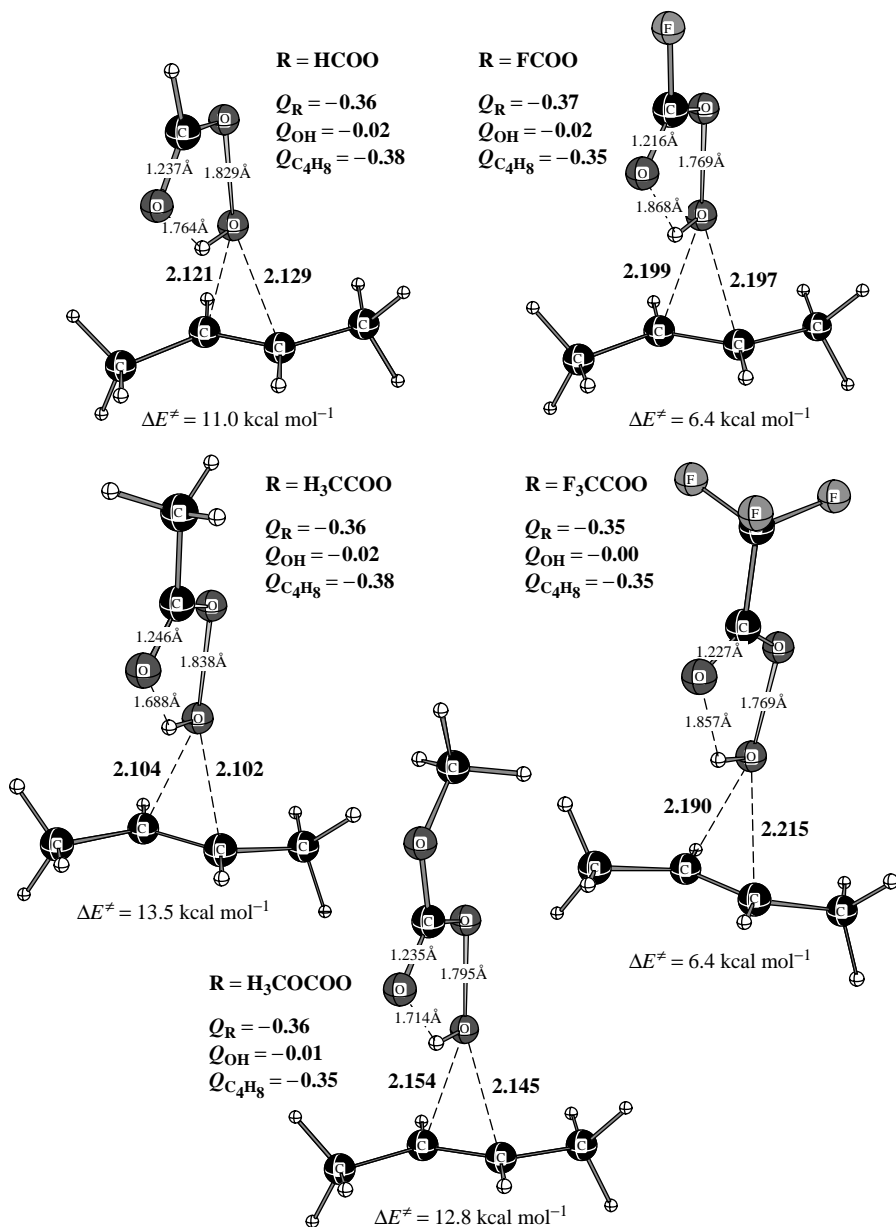


FIGURE 28. Effect of substitution in peracids on the activation barriers (kcal mol^{-1}) and charge distribution (electrons) for the epoxidation of *E*-2-butene. Charge distributions in B3LYP/6-31+G(d,p) optimized transition structures are calculated using NBO, B3LYP/6-31+G(d,p)

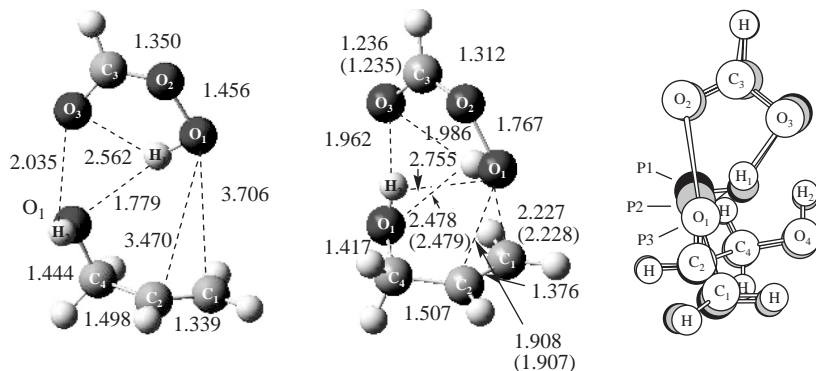
Another intriguing aspect of peracid epoxidation is the effect of pH upon the rate of epoxidation. Bach and coworkers⁹⁷ have reported experimental studies showing that the rate of *m*-CPBA epoxidation of *Z*-cyclooctene was only increased 6.8-fold upon the addition of the catalyst trifluoroacetic acid. The predicted activation barrier for epoxidation of ethylene with fully protonated peroxyformic acid is indeed quite low ($\Delta E^\ddagger = 6.4 \text{ kcal mol}^{-1}$). This relatively low activation barrier is largely a consequence of the fact that the system is positively charged. It was argued that under typical reaction conditions in nonpolar solvents, an effective concentration of protonated peroxy acid is not attainable, and the stability of the product epoxide is in question. At the same level of theory [QCISD(T)/6-31G(d)//QCISD/6-31G(d)] the gas-phase barrier of the uncatalyzed epoxidation reaction is $18.8 \text{ kcal mol}^{-1}$. The increase in rate of alkene epoxidations observed upon addition of carboxylic acids of moderate acidity was rationalized in terms of a pre-equilibrium forming a reactant cluster between the peroxy acid and the undissociated acid catalyst (HA). The hydrogen bond between HA and the peroxy acid, activating the latter, is capable of lowering the gas-phase barrier for epoxidation of ethylene by peroxyformic acid by about 3 kcal mol^{-1} with respect to the uncatalyzed process.

F. Epoxidation of Allylic Alcohols

The pioneering studies by Henbest^{136a,b} mark the first demonstration that the stereochemical course of the peracid epoxidation reaction may be steered through synergistic interplay between conformational and hydrogen-bonding effects^{136c} in chiral allylic alcohols. This mechanistic concept has been designated by Adam and Wirth^{137a} as *hydroxy-group directivity*. For 3-hydroxycyclohexene it was shown¹³⁶ that the *cis* epoxide was favored, which signifies that the perbenzoic acid attacks the π -bond from the same side that bears the allylic alcohol functionality. Acyclic allylic alcohols lack the inherent advantages of cyclic ones in regard to conformational preferences, unless imposed through appropriate substitution. The concept of allylic strain serves this purpose^{137b}, which allows differentiation of the two π -faces of the olefinic *syn* double bond by adequate alignment of the hydroxy group through steric effects. Bach and his coworkers¹³⁸ provided the first computational verification of these concepts by demonstrating that the hydrogen-bonding interaction of peroxyformic acid with allyl alcohol (Figure 29) directed the electrophilic oxygen to the *syn* π -face of the C=C. This preliminary study was followed by a much more extensive study by Sarzi-Amade and coworkers^{130a}.

Calculations at the B3LYP/6-31G* and B3LYP/6-311+G**//B3LYP/6-31G* theory levels about the mechanism of epoxidation of chiral acyclic allylic alcohols (3-methyl-3-buten-2-ol and (*Z*)-3-penten-2-ol) lead to the following observations based upon the location of more than twenty TSs. Hydrogen bonding is operative in *syn* TSs with the OH group acting as hydrogen-bond donor while the carbonyl oxygen and the peroxy oxygens of the peracid compete with each other as hydrogen-bond acceptor. The geometry of all TSs should be classified as *spiro* butterfly, i.e. with the peroxy acid plane close to a perpendicular orientation to the C=C bond axis. No TSs were located that could be classified as planar or butterfly (i.e. with the peroxy acid plane oriented along the C=C bond axis). Hydrogen bonding stabilizes *syn* TSs and influences their geometry; however, it never succeeds in imposing a planar butterfly structure.

A complementary paper was reported soon after by Adam, Bach and coworkers¹³⁹ where eight transition structures for the epoxidation of the chiral allylic alcohol (*Z*)-3-methyl-3-penten-2-ol with peroxyformic acid were computed by the B3LYP density functional method with 6-31G(d) and 6-31G(d,p) basis sets. The four lowest-energy transition structures and their respective prereaction clusters were fully re-optimized by employing 6-311+G(d,p) and correlation-consistent polarized valence triple- ζ cc-pZTV basis sets.



Reactant cluster	TS		IRC		
			P1	P2	P3
<O ₂ C ₃ O ₃ = 128.1	<O ₂ C ₃ O ₃ = 128.0 (128.1)	Reaction coord	0.00	-1.49	-4.48
<C ₃ O ₂ O ₁ = 112.0	<C ₃ O ₂ O ₁ = 105.3 (105.3)	Relative energy	0.00	-5.19	-40.9
<O ₂ O ₁ H ₁ = 101.8	<O ₂ O ₁ H ₁ = 91.7 (91.8)	Distances:			
<O ₄ C ₄ C ₂ = 111.9	<O ₄ C ₄ C ₂ = 112.5 (112.5)	O ₁ -O ₂	1.77	1.95	2.34
<C ₄ C ₂ C ₁ = 123.0	<C ₄ C ₂ C ₁ = 122.3 (122.3)	O ₁ -C ₁	2.76	2.02	1.56
<C ₁ C ₂ C ₄ O ₄ = 107.1	<C ₁ C ₂ C ₄ O ₄ = 25.5 (25.6)	O ₁ -C ₂	1.91	1.67	1.48
<O ₁ C ₂ C ₄ O ₄ = 23.1	<O ₁ C ₂ C ₄ O ₄ = 65.0 (-65.0)	O ₁ -H ₁	0.99	1.02	1.20
<C ₂ C ₁ O ₁ H ₁ = 43.7	<C ₂ C ₁ O ₁ H ₁ = 110.8 (110.0)	H ₁ -O ₃	1.99	1.84	1.52
<C ₂ C ₁ O ₂ C ₃ = 24.2	<C ₂ C ₁ O ₂ C ₃ = 89.0 (88.9)	H ₁ -O ₄	2.48	2.41	2.42
<O ₃ C ₃ O ₂ O ₁ = 8.4	<O ₃ C ₃ O ₂ O ₁ = 4.7 (4.7)	H ₂ -O ₃	1.96	1.94	1.88
MP2/6-31G(d):	MP2/6-31G(d):	O ₃ -C ₃	1.24	1.26	1.31
$\Delta E_{\text{stab.}} = -9.8 \text{ kcal mol}^{-1}$	$\Delta E^\ddagger = 8.6 \text{ kcal mol}^{-1}$	C ₃ -O ₂	1.31	1.28	1.24
MP4//MP2/6-31G(d):	MP4//MP2/6-31G(d):				
$\Delta E_{\text{stab.}} = -10.7 \text{ kcal mol}^{-1}$	$\Delta E^\ddagger = 7.7 \text{ kcal mol}^{-1}$				

FIGURE 29. Reactant cluster, transition state, TS, and the IRC path study (right drawing) of the epoxidation of allyl alcohol with peroxyformic acid showing the movement of atoms from the transition state (dark, P1) toward the products (light, P3) with an intermediate structure, P2. The calculation was done at the MP2/6-31G(d) level. The reaction coordinate is in units of amu bohr, the relative energies are in kcal mol⁻¹ and the distances are in Å. Geometric parameters in parentheses are at the MP2/6-31G(d,p) (see text) level of theory

The relative energies of the transition structures were found to be highly sensitive to the basis set applied. The transition state for *threo* product formation, *anti*-(2*S*,3*R*,4*S*)-TS, with the lowest total energy (at B3LYP/611+G(d,p) and B3LYP/AUG-cc-pZTV) of all the TSs examined, has a planar peracid moiety and is a precursor for the 1,4-migration of the peracid hydrogen atom to the peroxy carbonyl oxygen atom. The proton affinity, according to G2 calculations¹³⁸, is much larger for the carbonyl oxygen atom than for the distal peroxy oxygen. This suggests that gas-phase H-bonding to the carbonyl oxygen should be stronger.

The transition state for *erythro* epoxidation, *syn*-(2*R*,3*R*,4*S*)-TS, is only 0.9 kcal mol⁻¹ higher in energy and possesses a nonplanar peracid approaching the C=C bond in a manner intermediate between *spiro* and planar. The relative energy and nonplanarity of this *syn* transition structure is highly sensitive to the basis set applied. It was shown that

this approach agrees well with the experimental *threo/erythro* product ratio, in particular when the corrections for a solvent effect are made within the self-consistent isodensity polarized continuum model (SCI-PCM).

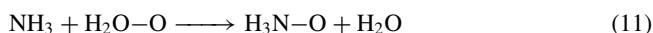
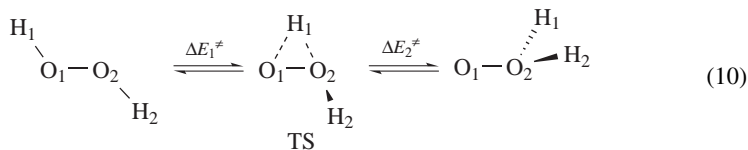
Cyclic allylic alcohols have different steric requirements than the acyclic substrates discussed above. Sarzi-Amade and coworkers^{130b} addressed the mechanism of epoxidation of 2-cyclohexen-1-ol by locating all the transition structures (TSs) for the reaction of peroxyformic acid (PFA) with both pseudoequatorial and pseudoaxial cyclohexenol conformers. Geometry optimizations were performed at the B3LYP/6-31G* level, and the total energies were refined with single-point B3LYP/6-311+G**//B3LYP/6-31G* calculations.

Solvent effects were approximated with the CPCM method. It was reported that all TSs exhibit a *spiro*-like structure, that is, the dihedral angle between the peroxy acid plane and the forming oxirane plane is closer to 90° than to 0°. A stabilizing hydrogen-bonding interaction was found in the *syn* TSs. The *syn,exo* TSs with hydrogen bonding at the PFA peroxy oxygens were found to be more stable than *syn,endo* TSs hydrogen bonded at the PFA carbonyl oxygen. The calculations correctly predict the experimental dominance of attack leading to *syn* epoxide for both cyclohexenol conformers.

VII. OXYGEN ATOM TRANSFER FROM SELECTED HYDROPEROXIDES

A. The Oxidation of Amines

Hydrogen peroxide is the simplest hydroperoxide and for obvious reasons this is where the early theoretical attempts at computational descriptions of the OOH group were concentrated. A molecular orbital treatment of HO–OH was thoroughly reviewed in the last volume of this continuing series by Cremer¹. In this section we will examine principally the computational attempts to examine the mechanism of oxygen atom transfer from HO–OH and related hydroperoxides. As described above, the computational problems associated with reactions involving O–O bond cleavage have only recently been resolved to a satisfactory treatment. Early attempts to transfer an oxygen atom from HO–OH to the simplest nucleophile, ammonia, proved to be challenging because the TS for oxidation of ammonia first involved a 1,2-transfer of hydrogen to the distal oxygen of HO–OH. Therefore, the preliminary calculations by Bach and coworkers pertaining to reactions involving O–O bond cleavage in HO–OH were centered around the 1,2-hydrogen shift in HO–OH to form the zwitterionic structure, water oxide [H₂O[−]–O⁺] (equation 10)^{119,140}. First, it should be recalled that, in general, a 1,2-hydrogen shift to an adjacent lone pair of electrons is formally a four-electron forbidden reaction and consequently will have a high activation barrier¹⁴¹. The activation barrier for the 1,2-hydrogen shift in HO–OH to form water oxide (or oxywater) has a calculated $\Delta E_1^\ddagger = 55.4 \text{ kcal mol}^{-1}$ (MP4SDTQ/6-31G*). The barrier for the reverse reaction reforming hydrogen peroxide is only 6.1 kcal mol^{−1} (ΔE_2^\ddagger). The transition structure for the HO–OH oxidation of ammonia involved water oxide (equation 11) and the barrier was consequently quite high at 53.4 kcal mol^{−1}.



By contrast, the oxidation of ammonia with CH₃O–OH proceeded more normally with the 1,2-hydrogen shift to the departing methoxide ion occurring after the barrier was crossed but a relatively high barrier was reported ($\Delta E^\ddagger = 46.5 \text{ kcal mol}^{-1}$)^{19a}.

Since water oxide was a potentially new and unusually high-energy intermediate, its existence as an observable intermediate was questioned almost immediately. An *ab initio* molecular electronic structure investigation of the oxywater–hydrogen peroxide isomerization by Schaefer and coworkers¹⁴² was initiated using self-consistent-field (SCF), configuration interaction including all single and double excitations (CISD), and coupled cluster with single and double excitations (CCSD) methods with a triple-zeta plus double-polarization (including f functions on the oxygen atoms) quality (TZ2P+f) basis set. The CCSD method with connected ‘triple excitations’ [CCSD(T)] was also used to obtain oxywater’s equilibrium geometry. A classical barrier to isomerization of water oxide of $5.7 \text{ kcal mol}^{-1}$ (equation 10, ΔE_2^\ddagger) was predicted at the highest level of theory. After correction for zero-point vibrational energies, the comparable ground-state activation energy is $3.2 \text{ kcal mol}^{-1}$. Although these *ab initio* predictions could be decreased by 1 or 2 kcal mol^{-1} at yet higher levels of theory, there can be little doubt that oxywater is a genuine minimum on the H_2O_2 potential energy hypersurface. It was concluded¹⁴² that oxywater is a high-energy minimum that awaits synthesis.

These high-level calculations encouraged Schwarz and his collaborators¹⁴³ to initiate an experimental study to seek out this very elusive but interesting potential oxygen donor. Collisional activation, charge reversal and six different neutralization–reionization mass spectrometric experiments with $\text{H}_2\text{O}_2^{\bullet+}$ radical cations and $\text{H}_2\text{O}_2^{\bullet-}$ radical anions were performed in order to probe the predicted existence of neutral water oxide, $\text{H}_2\text{O}-\text{O}$, the long sought after tautomer of hydrogen peroxide, $\text{HO}-\text{OH}$. The experiments together with *ab initio* calculations indicate that $\text{H}_2\text{O}-\text{O}$ is a local minimum on the $[\text{H}_2\text{O}_2]$ potential energy surface, and the elusive molecule seems to be formed as a transient upon neutralization of the corresponding radical cation $\text{H}_2\text{O}-\text{O}^{\bullet+}$ in the gas phase.

There have also been attempts to examine the relative stability of water oxide in a highly hydrogen-bonded aqueous environment¹⁴¹. The reduction in the barrier to produce an effective water oxide reagent from $\text{HO}-\text{OH}$ in protic media must reflect both the amelioration of the 1,2-hydrogen shift barrier and a decrease in electron density at the ‘electrophilic’ oxygen; however, the greatest effect comes from stabilization of water oxide itself by hydrogen bonding since this zwitterionic water oxide structure is more basic than $\text{HO}-\text{OH}$ itself. This surface was examined initially (MP2/6-31G*) by including several water molecules in the TS for rearrangement¹⁴¹. Although H_2O_2 hydrogen bonded to two water molecules affording a cyclic structure is stabilized by $21.9 \text{ kcal mol}^{-1}$, the hydrogen-bonded cyclic array, involving water oxide, is $42.7 \text{ kcal mol}^{-1}$ lower in energy than its separated entities, and only $7.0 \text{ kcal mol}^{-1}$ above the energy of isolated H_2O_2 plus two water molecules¹⁴¹. A more recent DFT study [B3LYP/6-311++G(d,p)] of the solvent effect on the equilibrium between these two isomeric forms of hydrogen peroxide has arrived at basically the same conclusion¹⁴⁴. A proton relay can lower the barrier for the formation of hydrogen-bonded water oxide when the proton is passed successively between water molecules relative to a direct 1,2-hydrogen shift. However, even with three water molecules the barrier is $29.5 \text{ kcal mol}^{-1}$, which places this type of oxidant out of the practical range of most chemical reactions.

Although water oxide, once formed, proved to be a remarkably efficient oxygen atom donor, it is quite likely that it is simply too high in energy to be a viable oxidant. A second problem with the preliminary calculations by Bach and coworkers¹¹⁹ is that NH_3 is not a realistic nucleophile for such studies; it is what was feasible at that time¹⁴⁵. This inadequacy has only recently been ameliorated by Ottolina and Carrea¹⁴⁶, who used the more nucleophilic trimethylamine (TMA) as the attacking nucleophile and got an entirely different and much more chemically realistic hypersurface for the $\text{HO}-\text{OH}$ oxidation of amines. The prior results at the MP2 level compared favorably with the results of the B3LYP/6-31+G* method, so the basic problem was in the nucleophile and not with the

type of calculation. With both methods the transition structure for the HO–OH oxidation of TMA came much earlier on the reaction coordinate and resembled the anticipated S_N2 -like displacement of the nitrogen nucleophile along the O–O σ^* orbital with transfer of the hydrogen to the distal OH to form a neutral water leaving group *after the barrier is crossed*, as exemplified in Figure 30. These authors also reported the effect of one water molecule on the reduction of the activation barrier ($\Delta\Delta E_1^\ddagger = 8.4 \text{ kcal mol}^{-1}$). An IRC analysis [B3LYP/6-31+G(d)] suggested that the single water molecule did not act

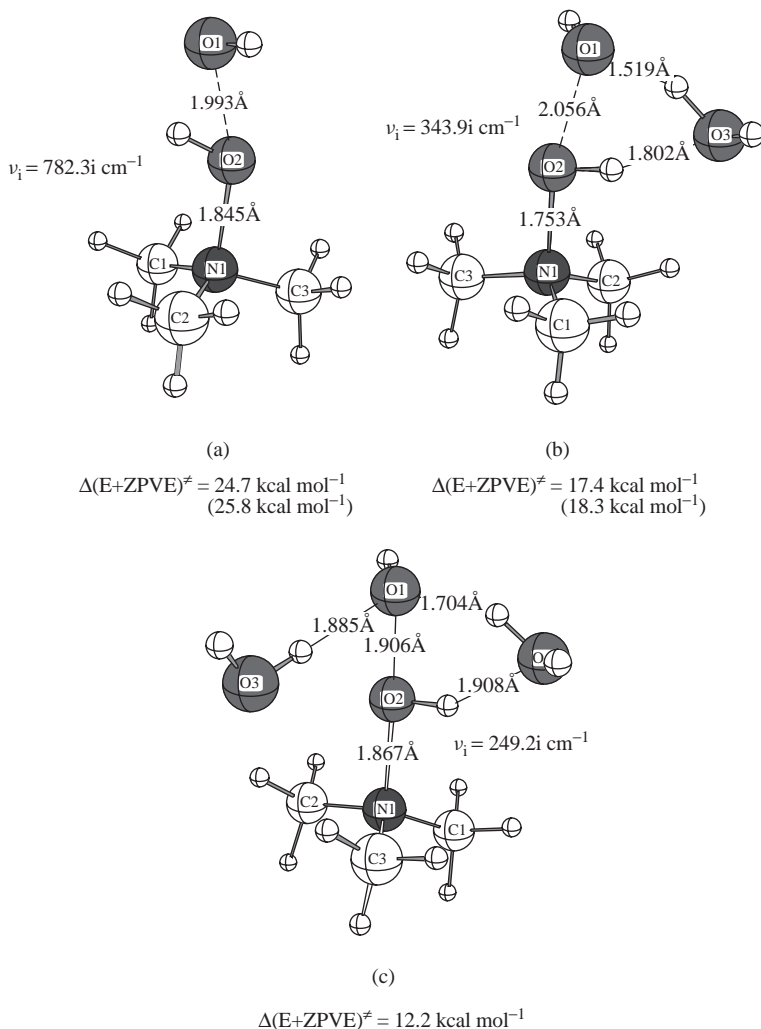


FIGURE 30. B3LYP/6-31+G(d,p)-optimized transition structures for the oxidation of trimethylamine by hydrogen peroxide (a), with one water molecule (b), and two water molecules (c). The values of the imaginary frequency and the barriers [$\Delta(E+ZPVE)^\ddagger$] are at the B3LYP/6-31+G(d,p) level. The barriers given in parentheses are at the B3LYP/6-31+G(d) level¹⁴⁶

as a proton relay but produced a rather strong hydrogen bond to the departing OH group ($r_{\text{O}\cdots\text{H}} = 1.57 \text{ \AA}$).

The overall surface for the HO–OH oxidation of TMA was recently reexamined¹⁴⁷ at the B3LYP/6-31+G(d,p) level using a slightly larger basis set that contained polarization functions on the hydrogens to treat more effectively hydrogen-bonding interactions. Although the TS with TMA¹⁴⁶ came somewhat earlier than that with ammonia as the nucleophile, the major component of the reaction vector still corresponds to the 1,2-hydrogen shift to the distal oxygen as noted by the magnitude of the activation barrier ($\Delta E^\ddagger = 24.7 \text{ kcal mol}^{-1}$) and the relatively large imaginary frequency ($782i \text{ cm}^{-1}$) for the rate-limiting step²¹. In this relatively simple case the hydrogen is transferred to the distal oxygen to produce a neutral water molecule *in concert with the formal transfer of the proximal OH group to the nitrogen* nucleophile of the tertiary amine (TS-a, Figure 30).

When one water molecule is included in the oxidation step (TS-b, Figure 30), a major contribution to the eigenvector in the TS is an interaction of a developing proton on the water molecule with the departing OH group. An IRC analysis [B3LYP/6-31+G(d,p)] clearly exhibits a proton relay from the water molecule (O_3) to the departing OH group (O_1) to form a neutral water leaving group after the barrier is crossed. This observation differs from the IRC reported earlier¹⁴⁶ and may possibly be due to the fact that polarization functions were not included in the basis set (see above). The imaginary frequency associated with the TS for the oxidation step diminishes as the effect of water catalysis increases with one and two water molecules. The catalytic role of the hydrogen-bonded water molecules diminishes the necessity for the high-energy 1,2-hydrogen shift to stabilize the departing hydroxide ion as discussed in more detail below.

The activation barrier decreases with each additional water molecule but the overall catalytic role of the second water molecule (TS-c, Figure 30) on the position of the hydrogen shift is much in the same way as noted for a single water molecule. A proton relay from the closest H-bonded water molecule to the developing OH anion (O_1) in the TS is in evidence late along the reaction coordinate as shown by an IRC calculation. The O–O distance is reduced to 1.91 \AA in TS-c, reflecting the stabilizing influence of the two H-bonded waters to the developing hydroxide anion. The final product, trimethylamine oxide, is produced after a second sequential proton relay from the N–OH (from O_2) to form the three neutral water molecules and the $(\text{CH}_3)_3\text{N–O}$ product. The overall reduction in the gas-phase activation energy [from isolated reactants TMA and $\text{HO–OH}\cdot (\text{H}_2\text{O})_n$] for one and two water molecules is 7.3 and $12.5 \text{ kcal mol}^{-1}$. Obviously, in bulk water solvent this reaction would proceed rapidly even with solvation of the nucleophile, that tends to lower the nucleophilicity of the amine (see below).

B. The Oxidation of N, S, P and Se Containing Nucleophiles

The early attempts to study sulfide oxidations computationally were plagued by many of the problems described above for amine oxidation. The use of HO–OH as the model oxidant was problematic because it was again difficult to pin down the position of the migrating proton in the transition state for the oxygen transfer step. Calculations at the MP2 level reported by Bach and coworkers^{19a} suggested that the 1,2-hydrogen shift could either precede the oxygen transfer step or occur after the barrier was crossed. Although the activation barriers for the HO–OH oxidation of dimethyl sulfide (DMS) were in general too high to be compatible with experimental data, it was shown that hydrogen bonding of the hydroperoxide itself or associated water molecules could effectively reduce the activation energy in agreement with experiment. Most of these problems have been recently resolved by a definitive DFT study by Chu and Trout¹⁴⁸ that has served to exclude the involvement of water oxide in the oxidation of sulfides. Solvent effects were examined in this study by both including explicitly water molecules and with the polarizable

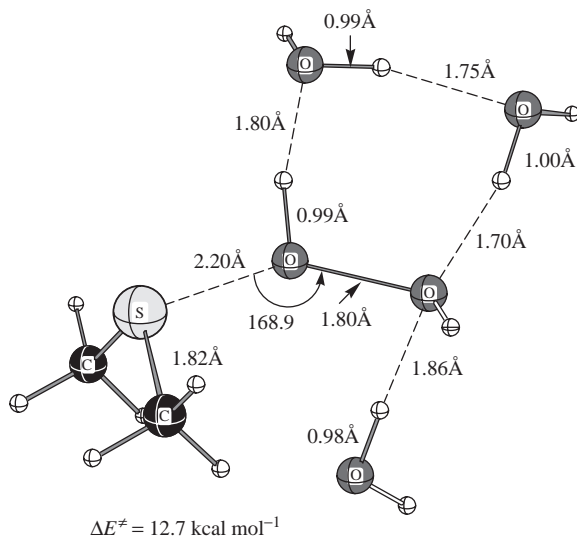


FIGURE 31. Transition structure for the HO–OH oxidation of dimethyl sulfide with three water molecules fully optimized at the B3LYP/6-31++G(d,p) level. The reaction barrier (ΔE^\ddagger) was calculated at the MP4//B3LYP/6-31++G(d,p) level with respect to the reactant cluster

continuum model. When explicit water molecules were included, specific interactions including hydrogen bonding with 2–3 water molecules was shown to provide enough stabilization for the charge separation of the O–O bond cleavage in HO–OH. The energy barrier of the oxidation of DMS by hydrogen peroxide was estimated to be $12.7 \text{ kcal mol}^{-1}$ [MP4//B3LYP/6-31++G(d,p)] within the experimental range of the oxidation of analogous compounds ($10\text{--}20 \text{ kcal mol}^{-1}$). This is a very satisfactory result when compared to the activation energy ($13.5 \text{ kcal mol}^{-1}$) for thioxane oxidation by hydrogen peroxide in aqueous solution^{149,150}. The basic mechanism with the effective catalysis by three water molecules is represented by the transition structure shown in Figure 31¹⁴⁸. Two of the water molecules serve to solvate the departing OH^- as the O–O bond elongated to 1.8 \AA in the TS for this nucleophilic $\text{S}_\text{N}2$ -like displacement. A proton relay is very likely involved as seen above with the water-catalyzed tertiary amine oxidation since the final product, dimethyl sulfoxide $[(\text{CH}_3)_2\text{S-O}]$, is produced after it transfers a proton.

The major reaction coordinates of the reaction are the breaking of the O–O bond of H_2O_2 and the formation of the S–O bond. The transfer of hydrogen to the distal oxygen of hydrogen peroxide occurs after the system has passed the transition state. Therefore, a two-step oxidation mechanism in which, first, the transfer of a hydrogen atom occurs to form water oxide and, second, the transfer of oxygen to the substrate occurs was deemed unlikely. Several important conclusions to be drawn from this study include:

- (1) For moderate pH values, perhaps between 2 and 12, the reaction coordinate leading to oxidation of dimethyl sulfide by H_2O_2 involves O–O bond cleavage with the formation of the S–O bond. Under these conditions, water molecules can stabilize the transition complex via specific interactions including formation of hydrogen bonds with H_2O_2 .
- (2) Hydrogen transfer does occur during oxidation of DMS, but it is not the determining factor of the activation barrier. Hydrogen transfer can occur via multiple different pathways depending on the local solvent configuration.

(3) Water molecules can stabilize the charge separation in the TS by local polarization and via formation of hydrogen bonds with H_2O_2 .

(4) For hydrogen transfer reactions involving H_2O_2 and DMS oxidation with a single water molecule, including solvent via a polarizable continuum model, has only a minor effect on the activation energies ($<1 \text{ kcal mol}^{-1}$ in most cases). This is consistent with the experimental observation that the rates of oxidation of organic sulfides are not a strong function of the solvent dielectric constant.

C. Electronic Factors Influencing Oxygen Atom versus Hydroxyl Transfer

The rate of heterolytic O–O bond cleavage in oxygen atom transfer reactions is largely a function of the stability of the oxyanion leaving group accompanying heterolytic O–O bond cleavage. For example, the O–O bond cleavage in a peracid [$\text{R}(\text{C}=\text{O})\text{O}-\text{OH}$] gives a fairly stable carboxylate anion ($\text{p}K \text{ a ca } 5$), while an alkyl hydroperoxide affords a relatively unstable alkoxide ion ($\text{p}K \text{ a ca } 16-19$). Oxygen atom transfer from the $-\text{OOH}$ moiety can proceed by two basic pathways: (a) the formal transfer of the hydroxyl group closely followed by an intramolecular hydrogen transfer along the reaction coordinate or (b) a hydroxylation process where the intact OH group is transferred and the leaving alkoxide anion exists as a minimum connected to the TS. The former is best exemplified by the peracid epoxidation of an amine (Figure 32, a) that proceeds by the formal transfer of an essentially neutral $\text{OH}^{20\text{a}}$ group to the nitrogen atom of the amine followed by an intramolecular 1,4-proton transfer to the carbonyl oxygen of the departing carboxylate leaving group. In a similar fashion, the epoxidation of a simple alkene is attended by the

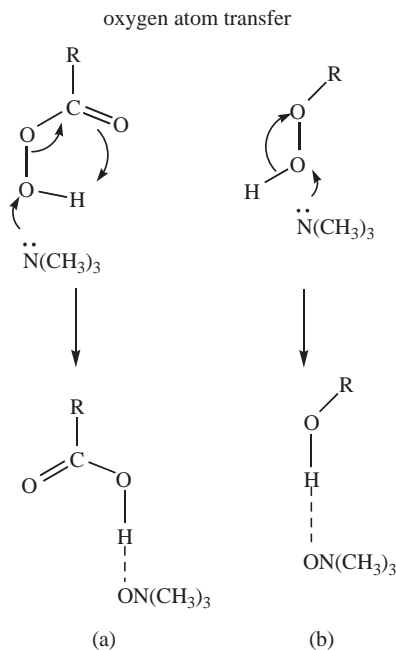
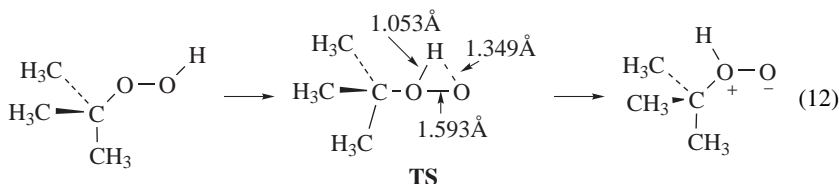


FIGURE 32. Mechanistic pathway for oxygen atom transfer from peroxyformic acid (a) and alkyl hydroperoxides (b) to trimethylamine

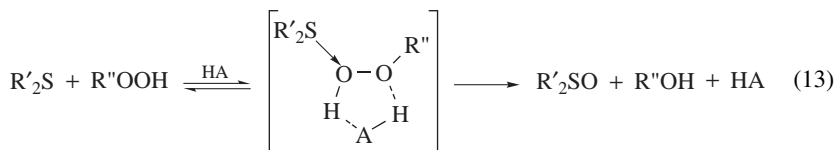
cleavage of a relatively weak peracid O—O bond (*ca* 48 kcal mol⁻¹) and the formation of an epoxide and a neutral carboxylic acid. The energetics of the reaction are quite favorable with a typical ΔH_{298} of epoxidation on the order of 48–59 kcal mol⁻¹^{19d}.

Oxygen atom transfer from an alkyl hydroperoxide, however, has additional energy requirements. Since this is typically a heterolytic O—O bond cleavage, the instability of the developing anionic alkoxide can influence the reaction pathway. For example, the heterolytic cleavage of the O—O bond in *t*-BuO—OH affords the relatively poor *t*-butoxide leaving group (*pK*_a 19). Consequently, the S_N2-like attack on the distal oxygen by a nucleophile such as an amine is attended by a 1,2-proton transfer (Figure 32, b) to the departing alcoholate in order to produce neutral *tert*-butyl alcohol and the N-oxide product. The activation barrier for oxygen atom transfer from a hydroperoxide, like HO—OH, is also controlled, to a very large extent, by the energetics of this 1,2-hydrogen transfer step. As noted above, concerted 1,2-hydrogen transfer reactions to an adjacent lone pair are four-electron processes and as such are formally forbidden^{17c}. For example, the 1,2-hydrogen shift in *t*-BuO—OH to form the high-energy *tert*-butyl alcohol oxide intermediate (equation 12) has an activation barrier of 49.5 kcal mol⁻¹.



This highly endothermic rearrangement ($\Delta E = 40.1$ kcal mol⁻¹) has a very late TS as evidenced by the short O—H bond to the proximal oxygen. When the reaction vector is composed mostly of light-atom hydrogen migration, as in equation 12, the imaginary frequency is quite high at $\nu_i = 1233i$ cm⁻¹. Contrariwise, when the reaction vector consists mainly of heavy-atom OH motion as in peracid alkene epoxidation^{20a}, the single imaginary frequency of the first-order saddle point is only about 300i to 450i cm⁻¹ (see Table 12 for a summary)²¹.

Much of what is understood today about the influence of solvent on rates of oxidation reactions with hydrogen peroxide, alkyl hydroperoxides and peroxyacids can be attributed to the seminal studies by Edwards and his collaborators over thirty years ago¹⁴⁹. They provided convincing experimental data that showed that a hydroxylic solvent (e.g. ROH) can participate in a cyclic transition state where a proton relay can in principle afford a neutral leaving group attending heterolytic O—O bond cleavage (equation 13).



On the basis of kinetic data, it was suggested that appreciable charge separation in the activated complex (equation 13) could be avoided by means of such proton transfers, where HA is a general acid (H₂O, ROH, RO—OH). Upon change from a polar protic solvent to the nonpolar solvent dioxane, the reaction was observed to be second-order in hydrogen peroxide and the second molecule of H₂O₂ obviously played the role of HA in the 1,4-proton shift. The rate of oxidation was shown to increase linearly with the *pK*_a of solvent HA. In general, it was concluded that solvent interactions provide a

TABLE 12. Reaction barriers (kcal mol⁻¹) calculated with respect to the isolated oxidizing agent and substrate. Numbers in parentheses are barriers calculated with respect to the prereaction complex. Classical activation energies (ΔE^\ddagger) at the B3LYP/6-31G(d) level are given in plain numbers, Bold numbers correspond to B3LYP/6-31+G(d,p) calculations. The single imaginary frequencies (Imag. freq.) are at the B3LYP/6-31G(d) level. Fl = Flavin

Substrate	Oxidizing agent	ΔE^\ddagger (kcal mol ⁻¹)	Imag. freq. (cm ⁻¹)
Ethylene	H(C=O)O—OH	14.1; 14.9	448.0i
<i>E</i> -2-Butene	H(C=O)O—OH	10.5; 11.0	411.1i
	<i>t</i> -BuOOH	32.2; 32.2	438.0i
(CH ₃) ₃ N	H(C=O)O—OH	3.3; 3.0	283.2i
	<i>t</i> -BuO—OH	30.5; 29.0 (40.9)	800.4i
	tricyclic FIHO—OH 14	12.2; 12.3	312.8i
(CH ₃) ₂ S	H(C=O)O—OH	5.6; 3.7	303.0i
	MeO—OH	27.1 (32.4)	697.9i ^a
	MeO—OH ··· MeO—OH (dimer)	10.8; 10.5 (22.5; 19.4)	283.8i ^a
	<i>t</i> -BuO—OH	30.0; 27.2 (36.5; 32.2)	672.5i
	tricyclic FIHO—OH 14	14.1; 12.7	286.4i
(CH ₃) ₂ Se	H(C=O)O—OH	-3.7; -6.5	248.1i
	<i>t</i> -BuO—OH	12.1	535.9i
	tricyclic FIHO—OH 14	2.6; -3.2	206.4i
(CH ₃) ₃ P	H(C=O)O—OH	-0.2; -0.3	280.5i
	<i>t</i> -BuO—OH	15.3; 14.0 (20.7)	358.4i
	tricyclic FIHO—OH 14	3.9; 4.4	327.0i

^a The single imaginary frequency was calculated at the B3LYP/6-31+G(d,p) level.

mechanistic path which avoids significant charge separation in the activated complexes for displacements on peroxide molecules by neutral nucleophiles and that the effectiveness of the protic solvent is correlated with their relative acidities. An excellent example of the importance of the role of solvent participation is the oxidation of dimethyl sulfide by *t*-BuO—OH. Curci and coworkers¹⁵⁰ showed that in aprotic solvents sulfide oxidation is second-order in hydroperoxide and that the second molecule of RO—OH plays the role of a protic solvent catalyst HA as exemplified in equation 13. The calculated activation barrier for the oxidation of DMS by monomeric CH₃O—OH is 32.4 kcal mol⁻¹ relative to its prereaction complex (Table 12) as a consequence of the relatively poor methoxide leaving group²¹. A marked reduction in activation barrier for the oxidation of DMS was observed when the dimer of CH₃O—OH is employed ($\Delta\Delta E^\ddagger = 13$ kcal mol⁻¹). More importantly, there is a change in mechanism that becomes immediately obvious upon examination of the imaginary frequencies of the two TSs (Figure 33). The TS for oxygen atom transfer from monomeric CH₃O—OH to DMS has a large degree of hydrogen atom motion involving a 1,2-hydrogen shift ($\nu_i = 698i$).

As discussed above for amine oxidation, the activation barrier for sulfide oxidation can be reduced markedly by hydrogen-bonding interactions that stabilize the alkoxide anion leaving group resulting from O—O bond cleavage. This catalytic effect serves to reduce the energetic requirements for the obligatory 1,2-hydrogen shift in the TS for the oxygen transfer step. The marked reduction in the imaginary frequency from $\nu_i = 698i$ to 284i cm⁻¹ for the dimeric CH₃O—OH oxidation (Figure 33) is consistent with very little displacement of the hydrogen atom during vibration of the imaginary frequency as visualized graphically in Figure 34. In frame A, both hydrogens of the OOH groups are involved in hydrogen bonding to produce the prereaction dimer that is weakly H-bonded to the sulfur atom. In the dimeric TS (Figure 33) the second CH₃O—OH is strongly H-bonded to the separating peroxo bond. After the barrier is crossed in frame C (Figure 34)

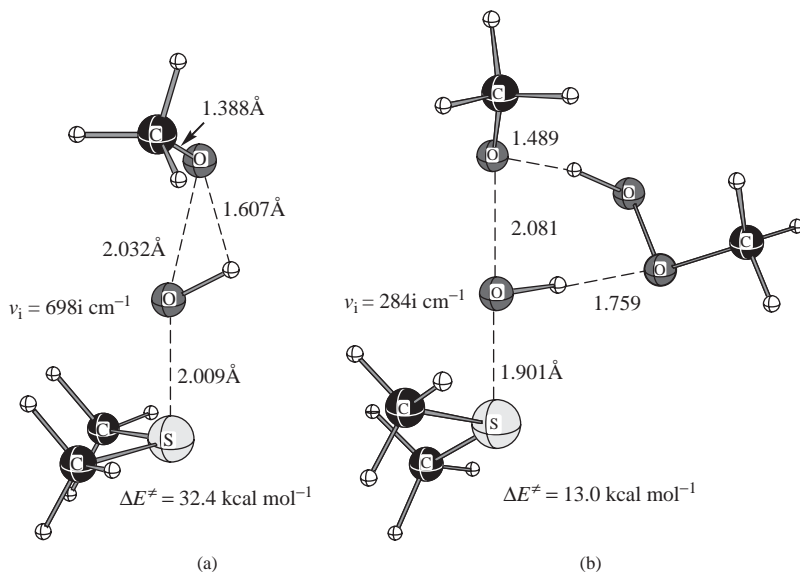


FIGURE 33. Transition structures [B3LYP/6-31+G(d,p)] for the oxidation of dimethyl sulfide with (a) monomeric $\text{CH}_3\text{O}-\text{OH}$ and (b) dimeric methyl hydroperoxide

the proton from the catalytic $\text{CH}_3\text{O}-\text{OH}$ is transferred to the departing methoxide ion and the proton now residing on the ‘protonated sulfoxide’ is poised to neutralize the incipient $\text{CH}_3\text{O}-\text{O}^-$ anion. This type of proton relay obviates the need for the 1,2-proton direct shift thereby reducing activation barrier.

It is not surprising that the proton relay for sulfide oxidation (Figure 34) can be extended to the involvement of both $\text{HO}-\text{OH}$ and $\text{RO}-\text{OH}$ dimers in the oxidation of amines¹⁴⁷. The dimeric forms of the hydroperoxides can reduce the activation barriers as evidenced by the $\text{HO}-\text{OH}$ and $\text{CH}_3\text{O}-\text{OH}$ dimeric oxidation of TMA (Figure 35). The activation barrier for TMA oxidation with dimeric $\text{HO}-\text{OH}$ is effectively reduced by $12.1 \text{ kcal mol}^{-1}$ relative to the same oxidation of TMA with monomeric $\text{HO}-\text{OH}$ ($25.8 \text{ kcal mol}^{-1}$, Figure 30).

For the $\text{HO}-\text{OH}$ dimeric TS with TMA, an IRC calculation clearly shows a proton relay in operation that serves to reduce the activation barrier by ameliorating the energetic requirements for a direct 1,2-hydrogen shift. The H-bonded hydrogen of the participating $\text{HO}-\text{OH}$ group is transferred to the developing anionic OH group [H10 to O7, TS(a)] being displaced to produce a neutral water molecule leaving group *after the barrier is crossed*. This behavior is comparable to the above $\text{HO}-\text{OH}$ oxidation of TMA catalyzed by a single water molecule (Figure 30)¹⁴⁶ where a proton relay from water was advocated in the TS. The involvement of a proton relay with dimeric $\text{HO}-\text{OH}$ is potentially a reflection of the much greater acidity of $\text{HO}-\text{OH}$ than H_2O as is also reflected in the lower classical barrier ($\Delta\Delta E^\ddagger = 3.7 \text{ kcal mol}^{-1}$). The very short H-bond of the OOH group ($r_{\text{OH}} = 1.45 \text{ \AA}$) in the $\text{CH}_3\text{O}-\text{OH}$ dimer TS is also suggestive of a proton relay (Figure 35). The relatively low activation energy ($19.5 \text{ kcal mol}^{-1}$) for the dimeric TMA oxidation is reduced by $8.2 \text{ kcal mol}^{-1}$ when compared to the monomeric $\text{CH}_3\text{O}-\text{OH}$ oxidation of TMA¹⁴⁷. The barrier for the oxidation of TMA by dimeric $\text{CH}_3\text{O}-\text{OH}$ is also $9.5 \text{ kcal mol}^{-1}$ lower than oxidation by monomeric *t*-butyl hydroperoxide (Table 12).

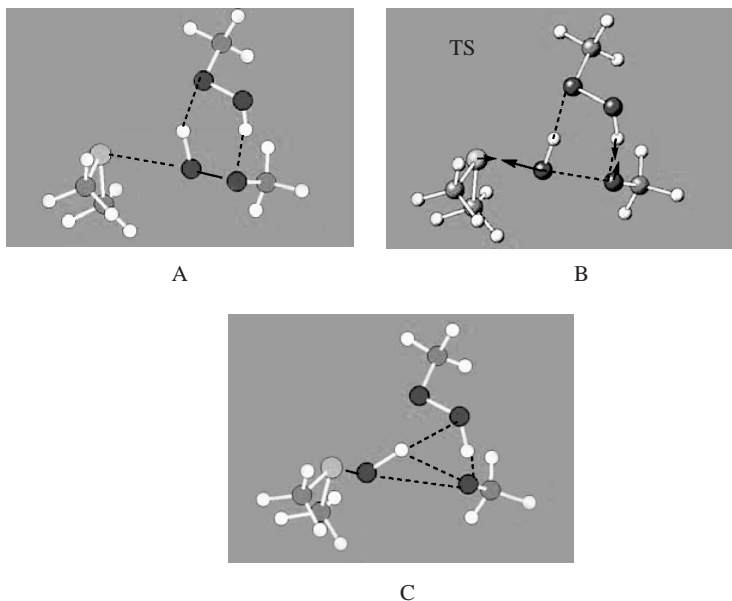


FIGURE 34. Graphical visualization of the imaginary vibration ($\nu_i = 2841 \text{ cm}^{-1}$) characterizing the transition structure (**B**) for the oxidation of DMS with MeO-OH dimer. Structures **A** and **C** correspond to the extreme points of the vibration. The TS optimization and frequency calculation are at the B3LYP/6-31+G(d,p) level

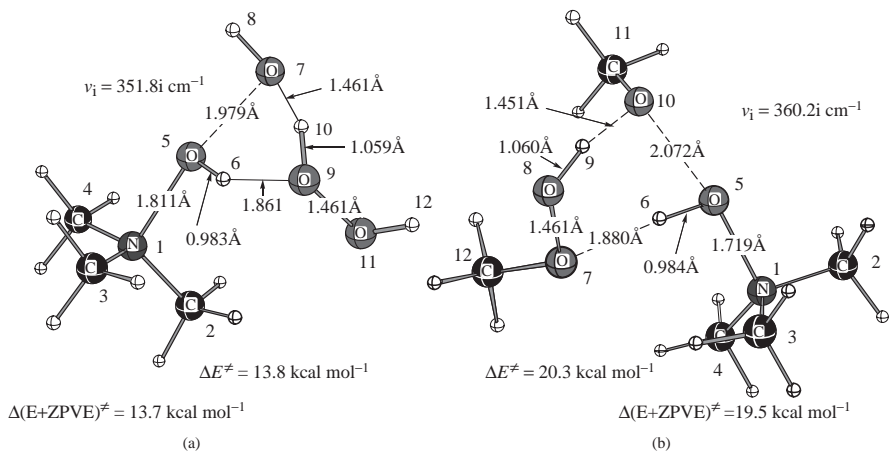
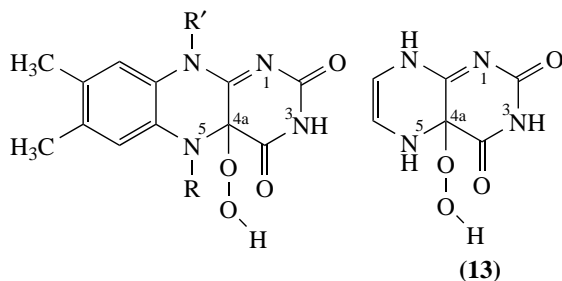


FIGURE 35. Transition structures for the oxidation of trimethylamine (TMA) with the dimer of hydrogen peroxide (a) and the oxidation of TMA with dimeric $\text{CH}_3\text{O-OH}$ (b) optimized at the B3LYP/6-31+G(d,p) level of theory

D. Model Studies on Enzymatic Oxidation of Heterocycles and Aromatic Rings

One of the most important oxygen atom transfer reactions in biochemistry involves catalysis by flavoenzymes¹⁵¹. These tricyclic isoalloxazine moieties are among the more versatile of the redox cofactors in biochemistry. C4a-hydroperoxyflavin (4a-FIHO-OH) has been implicated as the key hydroperoxide intermediate that serves as the oxygen atom donor. These enzymes are able to oxidize a number of substrates including the aromatic ring in hydroxy-substituted phenols^{152a}. *p*-Hydroxybenzoate hydroxylase (PHBH) has become the paradigm aromatic hydroxylase because of extensive kinetic and X-ray structural studies^{152b}. When the N5 nitrogen in C4a-hydroperoxyflavin is alkylated with an ethyl group, the *N*5-ethyl group prevents the elimination of H₂O₂, and this model C4a-hydroperoxyflavin (4a-FIeTO-OH) can be prepared and isolated in the laboratory¹⁵³. The intrinsic reactivity of the *N*5-ethyl derivative **12b** has been extensively studied by Bruice in a series of papers where it has been reacted with amines, sulfides, alkenes and I⁻, and its reactivity has been compared to common oxidants such as hydroperoxides and peracids¹⁵³.



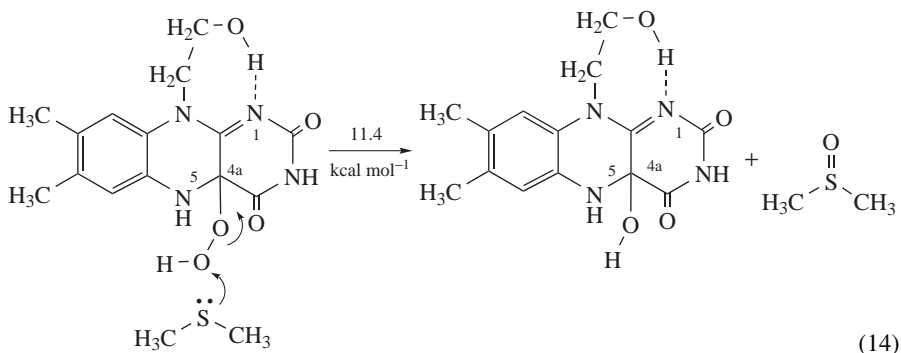
(12) R' = 2'-OH ribityl side chain; R = H (FIHOOH)

(12a) R' = CH₃, R = H (Lumiflavin)

(12b) R' = CH₃, R = C₂H₅ (FIeTOOH)

(14) R' = C₂H₄OH, R = H (FIHOOH 3)

It is particularly noteworthy that the state-of-the-art in theoretical chemistry has now reached the point where reasonably reliable *ab initio* calculations can be carried out on model enzymatic reactions, albeit most of the important residues at the active site must be ignored at this level. Theoretical calculations at the B3LYP/6-31+G(*d,p*) level reported by Canepa, Bach and Dmitrenko^{20c} have been used to study the oxidation of dimethyl sulfide by a tricyclic model C4a-flavin hydroperoxide (R = H, R' = CH₂CH₂OH). The C-(4a)-flavin hydroperoxide (FIHO-OH **14**) contains the tricyclic isoalloxazine moiety, the C-4a-hydroperoxide functionality, and a hydroxyethyl group to model the effect of the 2'-OH group of the ribityl side chain of native FADHO-OH. The intrinsic gas-phase reactivity of this tricyclic hydroperoxyflavin is *ca* 10⁹ greater than of *t*-BuO-OH (Table 12). The S_N2-like attack of the nucleophile on the distal oxygen of the hydroperoxide and the relative reactivity of the peracid are in excellent agreement with the earlier experimental data of Bruice¹⁵³. The oxidation of DMS by model 4a-FIHO-OH **14** had an activation barrier of only 11.4 kcal mol⁻¹ (equation 14)^{20c}.



It was shown that isolated N1- and N5-protonated cations of model 4a-FIHO-OH exhibit artificially low barriers as a consequence of their location in a high-energy region of the potential energy surface domain. In fact, charged structures, either cations or anions, will typically give an artificially low activation barrier^{20c}.

A mechanistic study of the oxidation of a series of related heteroatoms containing nucleophiles by a model 4 α -flavin hydroperoxide **14** has also been recently reported by Bach and Dmitrenko²¹ (Table 12). Using the paradigm model theoretical oxygen atom donor peroxyformic acid as a measure, the barriers for the epoxidation of ethylene, *E*-2-butene and DMS with bicyclic model **13** are an average of 9 kcal mol⁻¹ greater than that for peroxyformic acid. Peroxyformic acid is also much more reactive toward DMS than methyl hydroperoxide ($\Delta\Delta E^\ddagger = 23$ kcal mol⁻¹). It is also evident that DMS is a much better gas-phase nucleophile than ethylene, as evidenced by their difference in activation barriers ($\Delta\Delta E^\ddagger = 11$ kcal mol⁻¹) for reaction with peroxyformic acid. While CH₃O-OH and *t*-BuO-OH have comparable barriers for the oxidation of DMS (27.2 and 27.1 kcal mol⁻¹), tricyclic model flavin FIHO-OH **14** exhibits a much lower activation barrier of only 14.3 kcal mol⁻¹. Thus, one may consider this tricyclic model flavin hydroperoxide to be a 'tertiary alkyl hydroperoxide' with electronegative substituents that is a much better oxygen donor than *t*-BuO-OH. This increased reactivity is due at least in part to the p*K*_a of the departing 'alcohol' due to the inductive stabilization of the alcoholate leaving group by the electronegative elements surrounding C4. The experimentally estimated p*K*_a of 4a-FIEtO-OH is 9.4, while the p*K*_a of *t*-BuOH is approximately twice that. The role of Coulombic stabilization on the stability of the leaving group alcoholate in the oxygen transfer step has been presented earlier by Bach and Su^{17c}.

Bach and Dmitrenko²¹ have reported density functional calculations at the B3LYP/6-31+G(d,p) level that were used to study the mechanism of the oxidation of xenobiotics catalyzed by flavin-containing monooxygenases (FMOs)¹⁵⁴. The xenobiotics were modeled by the oxidation of methyl-substituted N-, S-, P- and Se-containing nucleophiles. A mechanism for distinguishing oxygen atom versus hydroxyl transfer from RO-OH to (CH₃)₃N, (CH₃)₂S, (CH₃)₃P and (CH₃)₂Se was presented based upon the concept that the type or mechanism of oxidative process is related to the magnitude of the single imaginary frequency for the transition state for oxygen atom transfer (Table 12). Classical activation barriers for oxygen atom transfer from model tricyclic isoalloxazine C-4a-hydroperoxide (FIHO-OH) to dimethyl sulfide, trimethylamine, trimethylphosphine and dimethyl selenide suggest that the reactivity of this biologically important oxidizing agent is intermediate between that of *tert*-butyl hydroperoxide and a peracid. The gas-phase reactivity of FIHO-OH **14** toward these four nucleophiles is estimated to be 10⁷-10¹² greater than that of *t*-BuO-OH but 10²-10⁶ less than that of peroxyformic

TABLE 13. Reaction barriers (ΔE^\ddagger) and reaction energetics (ΔE_{react}) calculated with respect to the isolated oxidizing agent, FIHO–OH **14**, and substrate. Plain numbers correspond to B3LYP/6-31+G(d,p) calculations. Energy refinement at the B3LYP/6-31+G(3df,2p)//B3LYP/6-31+G(d,p) level of theory is given in bold

Substrate	ΔE^\ddagger (kcal mol ⁻¹)	ΔE_{react} (kcal mol ⁻¹)
(CH ₃) ₃ N	12.3, 13.5	-5.3
(CH ₃) ₃ P	5.0, 5.0	-90.7
(CH ₃) ₂ S	12.7, 11.8	-43.7
(CH ₃) ₂ Se	-3.2	-38.2

acid. The intrinsic gas-phase barriers for the oxidation of (CH₃)₃N and (CH₃)₂S with model FIHO–OH **14** differ by only 1 kcal mol⁻¹. The experimentally observed 10⁶ rate difference for amine oxidation with protein-bound FIHO–OH¹⁵⁴ versus synthetic flavinhydroperoxide (FIeO–OH)¹⁵³ in solution was attributed simply to solvent effects; no special activation of the amine by the local enzymatic environment is required for this xenobiotic oxidation^{21, 156}.

The oxidation of a heteroatom bearing a lone pair of electrons (e.g. amine, sulfide or phosphine) with increased nucleophilicity of the heteroatom typically results in an early TS, especially with phosphines. Since the N–O bond in an N-oxide is particularly weak, this can sometimes be an endothermic reaction, in contrast to the highly exothermic oxidation of a phosphine with its associated very strong P–O bond (Table 13).

The subject of the relative nucleophilicity and the role of solvent polarity in the hydroperoxide oxidation of heteroatoms has been a subject of controversy for a number of years. The predilection to assign phosphorus a much greater nucleophilic capacity than nitrogen or sulfur is based upon nucleophilic constants that were determined in methanol solvent¹⁵⁵. Second-row elements have always been considered to be more nucleophilic than those of the first row. Indeed, trimethylphosphine is far more reactive than Me₃N toward both *t*-BuO–OH ($\Delta\Delta E^\ddagger = 15.0$ kcal mol⁻¹) and C4a-hydroperoxyflavin **14** ($\Delta\Delta E^\ddagger = 7.9$ kcal mol⁻¹). The oxygen atom transfer step for this highly exothermic reaction (-90.7 kcal mol⁻¹) comes much earlier along the reaction coordinate (Figure 36) with an O–P distance in the TS of 2.29 Å, a fairly short O–O distance (1.70 Å) and a correspondingly very low activation energy ($\Delta E^\ddagger = 5.0$ kcal mol⁻¹). In contrast, the overall reaction energy for the oxidation of Me₃N with tricyclic hydroperoxide is only -5.3 kcal mol⁻¹ and this later TS is reflected in a higher energy of activation ($\Delta E^\ddagger = 13.5$ kcal mol⁻¹). The relative reactivity of the N and P nucleophiles toward tricyclic FIHO–OH stands in marked contrast to the relative reactivities of these two nucleophiles toward the more reactive oxygen atom donor peroxyformic acid. The rate ratios for oxidation with tricyclic FIHO–OH **14** relative to *t*-BuO–OH for N, S, Se and P nucleophiles can be estimated from the calculated activation barriers to be 2×10^{12} , 4×10^{11} , 2×10^{11} and 10^7 .

In an earlier report Bach and coworkers^{17a} suggested that Me₃N and Me₃P had nearly the same gas-phase barriers with peroxyformic acid ($\Delta\Delta E^\ddagger = 0.5$ kcal mol⁻¹, MP4//MP2/6-31G*) and that their relative reactivity in protic solvent is better attributed to a much greater ground-state solvation of the more basic tertiary amine than the polarizability of the phosphorus. In a more recent study²¹, a 3.3 kcal mol⁻¹ barrier difference was observed with HCO₃H in favor of the P nucleophile at B3LYP/6-31+G(d,p) (3.0 versus -0.3 kcal mol⁻¹, Table 12). Thus, the less reactive *t*-BuO–OH is a more discriminating oxidant with a later TS and the difference in barrier heights for N versus P oxidation widens. These data also point out that rate differences should be compared for a common set of nucleophiles and that when you use oxidants of different reactivity you should

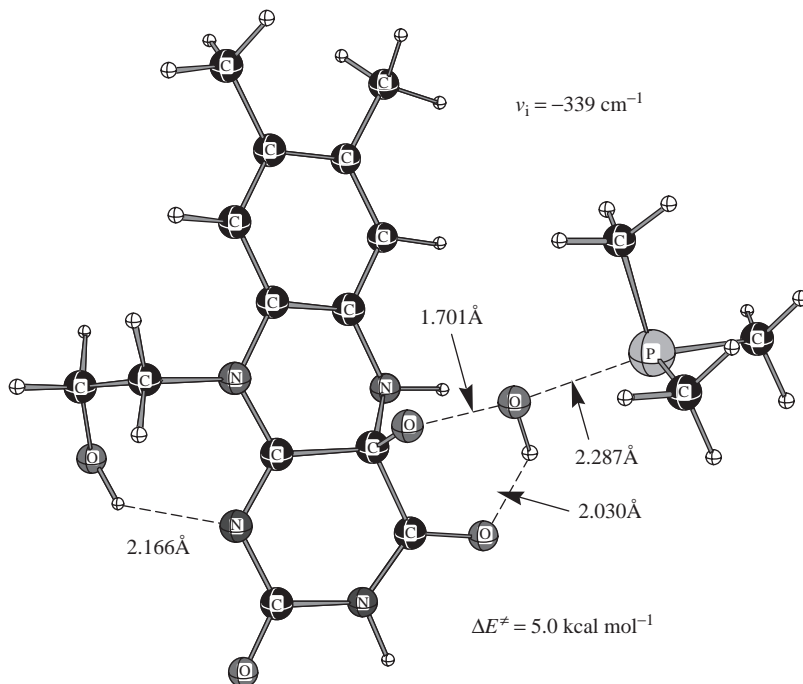


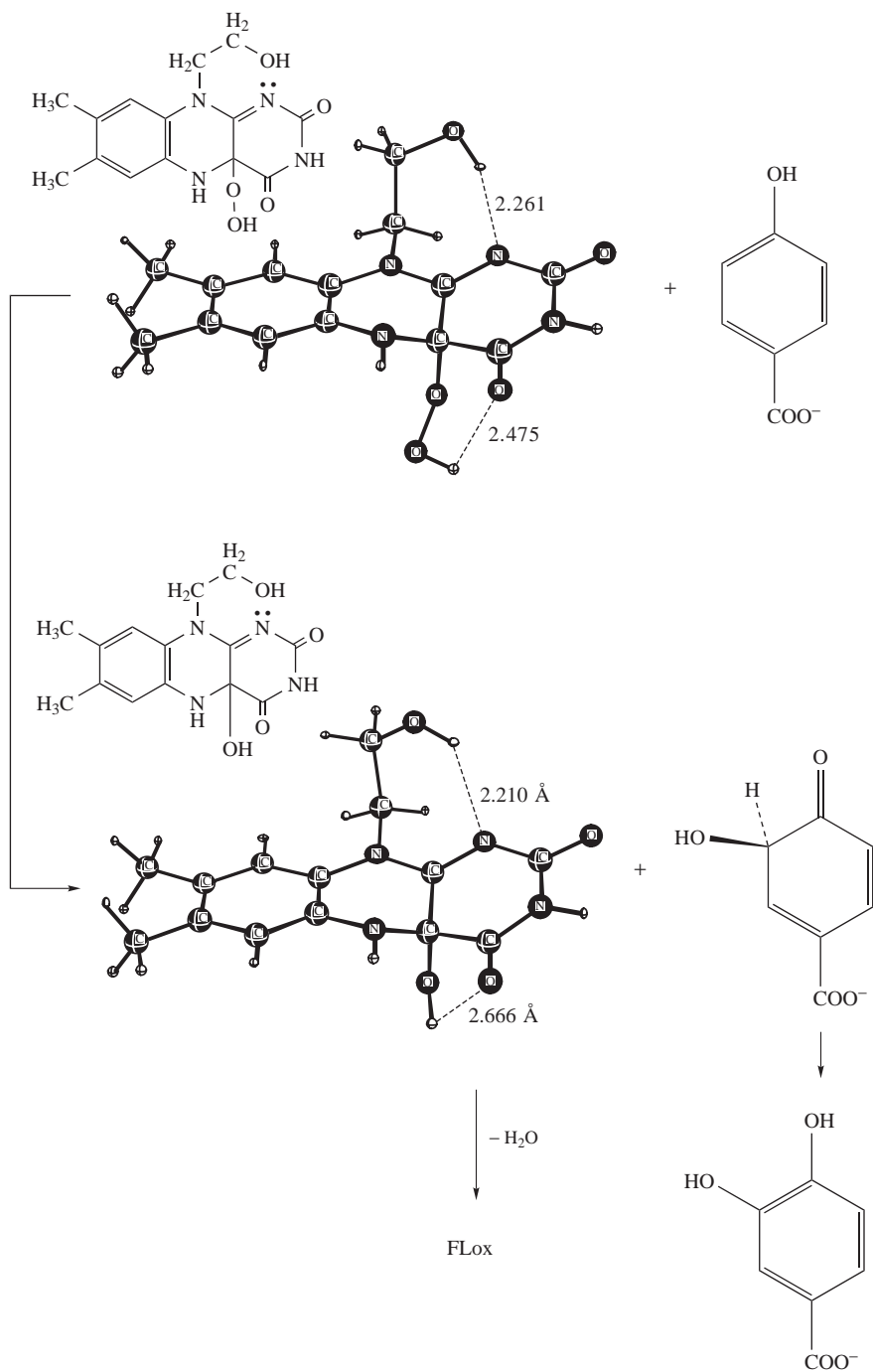
FIGURE 36. Transition structure for the oxidation of $(\text{CH}_3)_3\text{P}$ with tricyclic FIHO-OH **14** optimized at the B3LYP/6-31+G(d,p) level of theory. Imaginary frequencies are at the B3LYP/6-31G(d) level

anticipate different rate ratios. The differences in activation barriers for N versus P as well as S versus Se oxidation decrease markedly as the oxygen donor propensity of the oxidizing agent increases ($t\text{-BuO-OH} < \text{flavinhydroperoxide} < \text{peracid}$).

As demonstrated above on relatively simple nucleophiles, native FADHO-OH¹⁵¹, as modeled in this work by tricyclic FIHO-OH **14**, is intermediate in reactivity between a peracid and RO-OH. Despite this it is still, surprisingly, capable of enzymatically oxidizing the aromatic ring in *p*-hydroxybenzoic acid (*p*-OHB). The two primary active site residues involved in the hydroxylation step in PHBH have been assigned to Tyr-201 and Arg-214. It is generally assumed that oxidation of the aromatic ring in *p*-OHB produces the hydroxylated cyclohexadienone tautomeric intermediate shown in Scheme 10. A recent model study by Bach and Dmitrenko¹⁵⁶ on the enzymatic oxidation of *p*-hydroxybenzoic acid (PHBH) included two of the primary residues present at the active site at a level of theory where the reaction energy differences were reasonably accurate. This study provided a mechanistic rationale for the oxidation of this aromatic ring and also addresses the related question whether the H-bonding interactions of ionized *p*-OHB with Tyr-201 actually increase the rate of hydroxylation.

There have been relatively few theoretical studies aimed at the mechanism of PHBH processes. Vervoort and coworkers¹⁵⁷ have suggested on the basis of AM1 calculations that a correlation exists between $\ln k_{\text{cat}}$ for the conversion of a series of 4-hydroxylated substrates and the energy of their highest occupied molecular orbital (HOMO).

Peräkylä and Pakkanen¹⁵⁸ studied the proton-transfer step in the *ortho*-hydroxylation of *p*-OHB. On the basis of HF/3-21G calculations, they arrived at the conclusion that the



SCHEME 10

intermediate in the hydroxylation step is the radical OH adduct of *p*-hydroxybenzoate. There have also been several attempts to define the hydroxylation step in PHBH using quantum mechanical/molecular mechanical (QM/MM) methods. Ridder and coworkers¹⁵⁹ demonstrated a correlation of calculated activation energies with experimental rate constants for an enzyme-catalyzed aromatic hydroxylation. Billeter and coworkers¹⁶⁰ studied the hydroxylation of *p*-hydroxybenzoate in its various anionic states and concluded that the dianion was the most probable form of *p*-OHB at the hydroxylation step. Both of these QM/MM studies used the closed-shell semiempirical AM1 method to study the hydroxylation step that involves O–O bond dissociation. As noted above, this level of theory is not capable of treating the O–O bond cleavage step in this enzymatic reaction^{21a}. In this series of calculations, guanidine was included to model the role of Arg-214 and to maintain a net charge of ‘-1’ on the overall complex. Phenol was used to model Tyr-201, and it is H-bonded to *p*-OHB to examine its effect on the activation barrier for hydroxylation of *p*-OHB with FIHO–OH **14**. One of the problems associated with this type of enzyme-modeling approach is that the model amino acid residues are not geometrically constrained by the interacting environment of the active site. A second difficulty is accurately measuring the influence of hydrogen bonding and Coulombic interactions in the ground state versus the transition state. Free energy relationships in a classical physical organic sense suggest that the mechanism of the hydroxylation step is best described as an electrophilic aromatic substitution¹⁶¹. On the basis of the spectra of substituted cyclohexadienones, Anderson and coworkers also suggest that a simple nucleophilic model may be correct¹⁶². Consistent with these fundamental concepts Bach and Dmitrenko¹⁵⁶ suggested that electrophilic aromatic substitution proceeds by an S_N2-like attack of the aromatic sextet of *p*-OHB phenolate anion on the distal oxygen of FIHO–OH **14**. The transition structure for oxygen atom transfer was fully optimized [B3LYP/6-31+G(d,p)] and had a classical activation barrier of 24.9 kcal mol⁻¹ when measured from prereaction complex R-A (Figure 37). The O–O distance in TS-B was 1.84 Å and the distance to nucleophilic carbon of *p*-OHB, *ortho* to the phenolate oxygen, was 2.08 Å (Figure 37).

From these data the following conclusions were drawn:

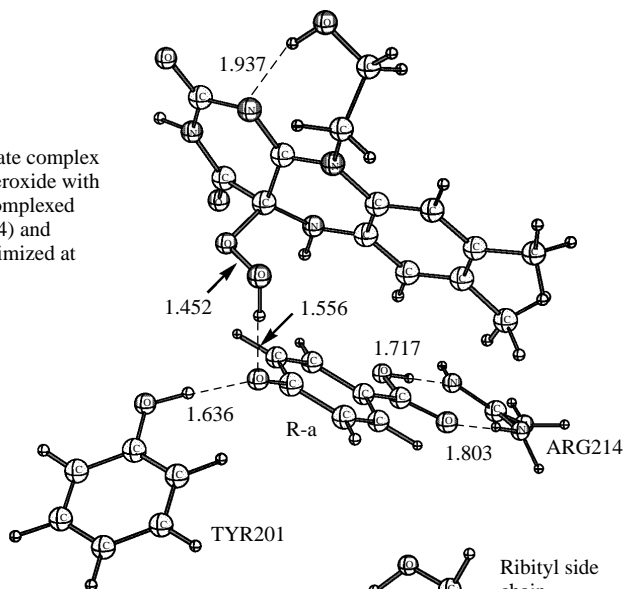
(a) The B3LYP data suggest that C-(4a)-flavinhydroperoxide (FIHO–OH **14**) is quite puckered with a N4-C4a-C10a-N10 dihedral angle of 41.8°. The ultimate alcohol product of the oxygen transfer reaction (FIHOH) and its precursor alcoholate leaving group (FIHO⁻) are also both seriously puckered, and the latter has a strong H-bond between the 2'-OH group and N1 (1.89 Å).

(b) Prereaction complex R-a (Figure 37) has an overall stabilization energy of 53.4 kcal mol⁻¹ relative to isolated reactants. The activation barrier for oxidation of R-A (TS-b) is 24.9 kcal mol⁻¹. The single imaginary frequency of 401.5i cm⁻¹ is consistent with oxygen atom transfer early on the reaction coordinate to a relatively stable alcoholate leaving group (FIO⁻). The magnitude of the barrier for anionic TS-b suggests that the role of the Tyr-201 is to orient the *p*-OHB substrate and to properly align it for the oxygen-transfer step. Although the negatively charged phenolate oxygen does activate the C-3 carbon of *p*-OHB phenolate anion toward oxidation relative to *ortho* oxidation of the carboxylate anion, it appears that H-bonding the Tyr-201 residue to this phenolic oxygen stabilizes both the GS and the TS and therefore plays only a minor role, if any, in lowering the activation barrier.

VIII. MISCELLANEOUS OXYGEN TRANSFER REACTIONS

Since this is not an exhaustive search of the literature for all theoretical contributions from the past twenty years, we have elected to include selected interesting articles pertaining to unique calculations on the peroxo bond.

Prereaction ground-state complex for 4α -flavinhydroperoxide with *p*-hydroxybenzoate complexed to guanidine (ARG214) and phenol (TYR201) optimized at B3LYP/6-31+G(d,p)



TS for oxidation of *p*-hydroxybenzoate (as its phenoxide anion). $\Delta E^\ddagger = 24.9 \text{ kcal mol}^{-1}$ (B3LYP/6-31+G(d,p))

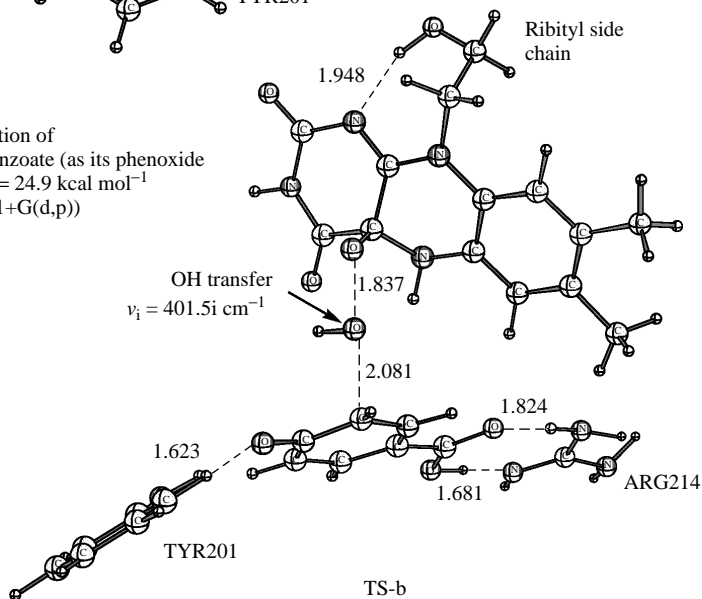


FIGURE 37. Prereaction complex (R-a) and transition structure (TS-b) with the 'natural' (enzymatic) orientation of the *p*-OHB substrate with respect to the FIHO–OH 14

Although hydrogen peroxide and alkyl hydroperoxides in general are not sufficiently reactive to epoxidize alkenes, there are some exceptions. Experimental observations show that direct olefin epoxidation by H_2O_2 , which is extremely sluggish otherwise, occurs in fluorinated alcohol (R_fOH) solutions under mild conditions requiring no additional

catalysts. Theoretical calculations¹⁶³ of ethylene and propylene epoxidation by H_2O_2 in the gas phase and in the presence of methanol and of two fluorinated alcohols, presented in this paper, show that the fluoro alcohol itself acts as a catalyst for the reaction by providing a template that stabilizes specifically the transition state (TS) of the reaction. Thus, much like an enzyme, the fluoro alcohol provides a complementary charge template that leads to the reduction of the barrier by 5–8 kcal mol⁻¹. Additionally, the fluoro alcohol template keeps the departing OH and hydroxyalkenyl moieties in close proximity and, by polarizing them, facilitates the hydrogen migration from the latter to form water and the epoxide product. The reduced activation energy and structural confinement of the TS over the fluoro alcohol template render the epoxidation reaction observable under mild synthetic conditions¹⁶³.

Examination of the hydroperoxy radical and its closed-shell ‘analogues’ including the analysis of the potential energy surfaces of the protonated forms of the HOO, HOF and the HO–OH was also recently reported by Bil and Latajka¹⁶⁴. The geometrical parameters of the protonated forms of the analyzed molecules were optimized at the level of B3LYP, MP2, MP3, MP4SDQ, CISD, CCD and the QCISD methods using 6-311++G(2d,2p) basis set. The unimolecular chemistry of the system $[\text{HO–OH}]\text{H}^+$ has also been investigated by Uggerud and coworkers^{165a} using *ab initio* quantum-chemical methods. In analogy with the isoelectronic systems $[\text{H}_2\text{NNH}_2]\text{H}^+$ and $[\text{HONH}_2]\text{H}^+$, the lowest-energy pathway for decomposition of protonated hydrogen peroxide is loss of an oxygen atom in its triplet electronic state, giving H_3O^+ as the ionic product. This process requires a crossover from the singlet to the triplet potential energy surface, and the minimum-energy crossing point was located. The proton affinity was also calculated and found to be in good accordance with experimental data. Uggerud and coworkers have also reported on the oxidative power of protonated hydrogen peroxide^{165b}. It was suggested that the oxidation of alkanes by protonated hydrogen peroxide does not occur by insertion of O into C–H, but by a multistep sequence in which a simple hydride transfer is the essential step. Earlier calculations by Bach and Su¹⁶⁶ have provided a model for the approach of protonated hydrogen peroxide in the oxidation of saturated hydrocarbons.

Ab initio molecular orbital theory at the correlated level of MP4SDTQ/6-31G**//MP2/6-31G** has been applied to investigate the reactions of NO^+ and NOH_2^+ with methane. Reinvestigation of the theoretical reaction of CH_4 with NO^+ by Olah and coworkers¹⁶⁷ showed that the reaction path involves attack on carbon instead of C–H bond insertion. In contrast to NO^+ , with superelectrophilic NOH_2^+ methane preferentially reacts via proton transfer to give CH_5^+ or by hydride abstraction. The results of the reaction of methane with NO^+ were compared with such strong electrophiles as D^+ , CH_3^+ , C_2H_5^+ , OH^+ and F^+ , and the consequences on the reaction mechanism were discussed. The studies reaffirm the general pattern of electrophilic substitution of methane with strong electrophiles to proceed via five-coordinate carbocations involving 3c-2e C–H bond insertion.

Panin and Tulub¹⁶⁸ have reported RHF(UHF)CMP2 and CASSCF calculations of potential energy surfaces’ sections of neutral particles and their corresponding protonated cations X–OH^+ ($\text{X} = \text{C}, \text{N}, \text{O}$). It was shown that all cations should be relatively stable both with respect to X–O bond breaking and intramolecular rearrangements. Reactions of electron capture by these cations were also studied, providing evidence that under electric discharge in an atmosphere saturated with water vapor both neutral and charged molecules may serve as building units for more complicated systems.

IX. ACKNOWLEDGMENTS

The author is indebted to the efforts of his very talented senior associate, Dr. Olga Dmitrenko, for her assistance in the preparation of this review. He is especially thankful

for her many intellectual contributions over the last six years to the papers of his cited in this summary of theoretical contributions to the chemistry of peroxides. The association with his former colleague, Professor Berny Schlegel, at Wayne State University in Detroit, is largely responsible for the transformation of this once hard-core experimentalist into the realm of theoretical chemistry. The author is also appreciative of the many collaborative efforts with his experimental colleagues during these many years. The financial support from the National Science Foundation and the National Computational Science Alliance under CHE990021N and use of the NCSA SGI Origin2000 and University of Kentucky HP Superdome have made it possible for the author to continue doing research since his retirement in 1996.

X. REFERENCES AND NOTES

1. D. Cremer, in *The Chemistry of Peroxides* (Ed. S. Patai), Wiley, Chichester, 1983, pp. 1–84.
2. B. M. Gimeric, *J. Am. Chem. Soc.*, **100**, 1996 (1978).
3. (a) M. P. Melrose and R. G. Parr, *Theoret. Chim. Acta*, **8**, 150 (1967).
(b) P. A. Christiansen and W. E. Palke, *J. Chem. Phys.*, **67**, 57 (1977).
4. R. Hoffmann and W. N. Lipscomb, *J. Chem. Phys.*, **36**, 2179 (1962).
5. J. A. Pople, D. P. Santry and G. A. Segal, *J. Chem. Phys.*, **43**, S129 (1965).
6. J. A. Pople, D. Beveridge and P. Dobosh, *J. Chem. Phys.*, **47**, 2026 (1967).
7. (a) M. J. Frisch, G. W. Trucks, H. B. Schlegel, G. E. Scuseria, M. A. Robb, J. R. Cheeseman, V. G. Zakrzewski, J. A. Montgomery, R. E. Stratmann, J. C. Burant, S. Dapprich, J. M. Millam, A. D. Daniels, K. N. Kudin, M. C. Strain, O. Farkas, J. Tomasi, V. Barone, M. Cossi, R. Cammi, B. Mennucci, C. Pomelli, C. Adamo, S. Clifford, J. Ochterski, G. A. Petersson, P. Y. Ayala, Q. Cui, K. Morokuma, D. K. Malick, A. D. Rabuck, K. Raghavachari, J. B. Foresman, J. Cioslowski, J. V. Ortiz, B. B. Stefanov, G. Liu, A. Liashenko, P. Piskorz, I. Komaromi, R. Gomperts, R. L. Martin, D. J. Fox, T. Keith, M. A. Al-Laham, C. Y. Peng, A. Nanayakkara, C. Gonzalez, M. Challacombe, P. M. W. Gill, B. G. Johnson, W. Chen, M. W. Wong, J. L. Andrés, M. Head-Gordon, E. S. Replogle and J. A. Pople, *Gaussian 98 (Revision A.7)*, Gaussian, Inc., Pittsburgh, PA, 1998.
(b) The GAMESS (General atomic and molecular electronic structure system) program: M. W. Schmidt, K. K. Baldridge, J. A. Boatz, S. T. Elbert, M. S. Gordon, J. H. Jensen, S. Koseki, N. Matsunaga, K. A. Nguyen, S. Su, T. L. Windus, M. Dupuis and J. A. Montgomery, *J. Comput. Chem.*, **14**, 1347 (1993).
(c) ACES II is a program product of the Quantum Theory Project, University of Florida. J. F. Stanton, J. Gauss, J. D. Watts, M. Nooijen, N. Oliphant, S. A. Perera, P. G. Szalay, W. J. Lauderdale, S. A. Kucharski, S. R. Gwaltney, S. Beck, A. Balková, D. E. Bernholdt, K. K. Baeck, P. Rozyczko, H. Sekino, C. Hober, and R. J. Bartlett.
(d) MOLPRO is a package of *ab initio* programs designed by H.-J. Werner and P. J. Knowles. The authors are R. D. Amos, A. Bernhardsson, A. Berning, P. Celani, D. L. Cooper, M. J. O. Deegan, A. J. Dobbyn, F. Eckert, C. Hampel, G. Hetzer, P. J. Knowles, T. Korona, R. Lindh, A. W. Lloyd, S. J. McNicholas, F. R. Manby, W. Meyer, M. E. Mura, A. Nicklaß, P. Palmieri, R. Pitzer, G. Rauhut, M. Schütz, U. Schumann, H. Stoll, A. J. Stone, R. Tarroni, T. Thorsteinsson and H.-J. Werner.
(e) CADPAC: The Cambridge Analytic Derivatives Package Issue 6, Cambridge, 1995. A suite of quantum chemistry programs developed by R. D. Amos with contributions from I. L. Alberts, J. S. Andrews, S. M. Colwell, N. C. Handy, D. Jayatilaka, P. J. Knowles, R. Kobayashi, K. E. Laidig, G. Laming, A. M. Lee, P. E. Maslen, C. W. Murray, J. E. Rice, E. D. Simandiras, A. J. Stone, M.-D. Su and D. J. Tozer.
(f) *Jaguar 4.1*, Schrödinger, Inc., Portland, OR, 1991–2000.
8. (a) J. Cizek, *Adv. Chem. Phys.*, **14**, 35 (1969).
(b) G. D. Purvis and R. J. Bartlett, *J. Chem. Phys.*, **76**, 1910 (1982).
(c) G. E. Scuseria, C. L. Janssen and H. F. Schaefer III, *J. Chem. Phys.*, **89**, 7382 (1988).
(d) G. E. Scuseria and H. F. Schaefer III, *J. Chem. Phys.*, **90**, 3700 (1989).
9. J. A. Pople, M. Head-Gordon and K. Raghavachari, *J. Chem. Phys.*, **87**, 5968 (1987).

10. (a) H. B. Schlegel, *J. Comput. Chem.*, **3**, 214 (1982).
(b) H. B. Schlegel, *Adv. Chem. Phys.*, **67**, 249 (1987).
(c) H. B. Schlegel, in *Modern Electronic Structure Theory* (Ed. D. R. Yarkony), World Scientific, Singapore, 1995, p. 459.
11. (a) C. Peng, P. Y. Ayala, H. B. Schlegel and M. J. Frisch, *J. Comp. Chem.*, **17**, 49 (1996).
(b) A. E. Reed and F. Weinhold, *J. Chem. Phys.*, **78**, 4066 (1983).
12. (a) R. D. Bach and H. F. Henneike, *J. Am. Chem. Soc.*, **92**, 5589 (1970).
(b) R. D. Bach, M. N. Glukhovtsev, C. Gonzalez, M. Marquez, C. M. Estevez, A. G. Baboul and H. B. Schlegel, *J. Phys. Chem. A*, **101**, 6092 (1997).
13. (a) A. C. Baldwin, in *The Chemistry of Peroxides* (Ed. S. Patai), Wiley, Chichester, 1983, p. 97.
(b) G. Bouillon, C. Lick and K. Shank, in *The Chemistry of Peroxides* (Ed. S. Patai), Wiley, Chichester, 1983, p. 279.
(c) S. Oae and K. Fujimori, in *The Chemistry of Peroxides* (Ed. S. Patai), Wiley, Chichester, 1983, p. 585.
(d) K. Fujimori, in *Organic Peroxides* (Ed. W. Ando), Wiley, Chichester, 1992, p. 319.
(e) J. A. Kerr, *Chem. Rev.*, **66**, 465 (1966).
14. (a) R. Curci and J. O. Edwards, in *Catalytic Oxidations with H₂O₂ as oxidant* (Ed. G. Strukul), Chap. 3, Reidel-Kluwer, Dordrecht, 1992.
(b) R. Curci, in *Advances in Oxygenated Processes* (Ed. A. L. Baumstark), Vol. 2, Chap. 1, JAI Press, Greenwich, 1990, pp. 1–59.
15. M. W. Chase, C. A. Davies, J. R. Downey, D. J. Frurip, R. A. McDonald and A. N. Syverud, JANAF Thermodynamical Tables, *J. Phys. Chem. Ref. Data, Suppl.*, **1**, 14 (1985).
16. (a) R. D. Bach, P. Y. Ayala and H. B. Schlegel, *J. Am. Chem. Soc.*, **118**, 12758 (1996).
(b) C. M. Estevez, O. Dmitrenko, J. E. Winter and R. D. Bach, *J. Org. Chem.*, **65**, 8629 (2000).
17. (a) R. D. Bach, J. E. Winter and J. W. McDouall, *J. Am. Chem. Soc.*, **117**, 8586 (1995).
(b) R. D. Bach, A. L. Owensby, C. Gonzalez and H. B. Schlegel, *J. Am. Chem. Soc.*, **113**, 2338 (1991).
(c) R. D. Bach and M.-D. Su, *J. Am. Chem. Soc.*, **116**, 5392 (1994).
18. (a) X. Luo, P. R. Fleming and T. R. Rizzo, *J. Chem. Phys.*, **96**, 5659 (1992).
(b) J. R. Barker, S. W. Benson and D. M. Golden, *Int. J. Chem. Kinet.*, **9**, 31 (1977).
19. (a) R. D. Bach, M.-D. Su and H. B. Schlegel, *J. Am. Chem. Soc.*, **116**, 5379 (1994).
(b) R. D. Bach, M. N. Glukhovtsev and C. Gonzalez, *J. Am. Chem. Soc.*, **120**, 9902 (1998).
(c) R. D. Bach, C. Canepa and M. N. Glukhovtsev, *J. Am. Chem. Soc.*, **121**, 6542 (1999).
(d) R. D. Bach, O. Dmitrenko, W. Adam and S. Schambony, *J. Am. Chem. Soc.*, **125**, 924 (2003).
20. (a) R. D. Bach, Peroxide Chemistry, in *DFG Research Report on Peroxide Chemistry: Mechanistic and Preparative Aspects of Oxygen Transfer* (Eds. W. Adam and C. R. Saha-Möller), Wiley-VCH, Weinheim, 2000, pp. 569–600.
(b) R. D. Bach and O. Dmitrenko, *J. Org. Chem.*, **67**, 3884 (2002).
(c) C. Canepa, R. D. Bach and O. Dmitrenko, *J. Org. Chem.*, **67**, 8653 (2002).
21. (a) For a critique of problems related to the use of HF theory for the peroxy bond see Reference 21b.
(b) R. D. Bach and O. Dmitrenko, *J. Phys. Chem. B*, **107**, 12851 (2003).
22. (a) J. S. Beckman, T. W. Beckman, J. Chen, P. M. Marshall and B. A. Freeman, *Proc. Natl. Acad. Sci. U.S.A.*, **87**, 1620 (1990).
(b) J. P. Crow, C. Spruell, J. Chen, C. Gunn, H. Ischiropoulos, M. Tsai, C. D. Smith, R. Radi, W. H. Koppenol and J. S. Beckman, *Free Radical Biol. Med.*, **16**, 331 (1994).
23. For a comprehensive review of the overall impact of peroxyacid see: R. W. Pryor and G. L. Squadrito, *Am. J. Physiol.*, **268**, L699 (1995).
24. (a) C. E. Richeson, P. Mulder, V. W. Bowry and K. U. Ingold, *J. Am. Chem. Soc.*, **120**, 7211 (1998).
(b) G. R. Hodges and K. U. Ingold, *J. Am. Chem. Soc.*, **121**, 10695 (1999).
25. W. H. Koppenol, J. J. Moreno, W. A. Pryor, H. Ischiropoulos and J. S. Beckman, *Chem. Res. Toxicol.*, **5**, 834 (1992).
26. (a) W. A. Pryor, X. Jin and G. L. Squadrito, *J. Am. Chem. Soc.*, **118**, 3125 (1996).
(b) W. A. Pryor, X. Jin and G. L. Squadrito, *Proc. Natl. Acad. Sci. U.S.A.*, **91**, 11173 (1994).

27. (a) R. D. Bach, O. Dmitrenko and C. M. Estevez, *J. Am. Chem. Soc.*, **125**, 16204 (2003).
(b) R. D. Bach, O. Dmitrenko and C. M. Estevez, *J. Am. Chem. Soc.*, **127**, 3140 (2005).
28. (a) M. P. McGrath and M. M. Francl, *J. Phys. Chem.*, **92**, 5352 (1988).
(b) M. P. McGrath and F. S. Powland, *J. Phys. Chem.*, **98**, 1061 (1994).
29. H. W. Jin, Z. Z. Wang, Q. S. Li and X. R. Huang, *J. Mol. Struct. (Theochem)*, **624**, 115 (2003).
30. M. Shen, Y. Xie, H. F. Schaefer III and C. A. Deakyne, *J. Chem. Phys.*, **93**, 3379 (1990).
31. H.-H. Tsai, T. P. Hamilton, J.-H. Tsai and J. S. Beckman, *Struct. Chem.*, **6**, 323 (1995).
32. W. H. Koppenol and L. Klasinc, *Int. J. Quant. Chem.*, **20**, 1 (1993).
33. M. Krauss, *Chem. Phys. Lett.*, **222**, 513 (1994).
34. J.-H. M. Tsai, J. G. Harrison, J. C. Martin, T. P. Hamilton, M. van der Woerd, M. J. Jablonski and J. S. Beckman, *J. Am. Chem. Soc.*, **116**, 4115 (1994).
35. H.-H. Tsai, T. P. Hamilton, J. H. M. Tsai, J. G. Harrison and J. S. Beckman, *J. Phys. Chem.*, **100**, 6942 (1996).
36. J.-H. M. Tsai, *Ph.D. Dissertation*, Department of Physics, University of Alabama at Birmingham, 1994.
37. (a) R. Sumathi and S. D. Peyerimhoff, *J. Chem. Phys.*, **107**, 1872 (1997).
(b) D. A. Dixon, D. Feller, C. G. Zhan and J. S. Francisco, *J. Phys. Chem. A*, **106**, 3191 (2002).
(c) G. V. Shustov, R. Spinney and A. Rauk, *J. Am. Chem. Soc.*, **122**, 1191 (2000).
(d) L. P. Olson, M. D. Bartberger and K. N. Houk, *J. Am. Chem. Soc.*, **125**, 3999 (2003).
(e) K. N. Houk, K. R. Condroski and W. A. Pryor, *J. Am. Chem. Soc.*, **118**, 13002 (1996).
38. R. D. Bach, M. N. Glukhovtsev and C. Canepa, *J. Am. Chem. Soc.*, **120**, 775 (1998).
39. Y. Li and J. S. Francisco, *J. Chem. Phys.*, **113**, 7976 (2000).
40. (a) D. G. Musaev and K. Hirao, *J. Phys. Chem. A*, **107**, 1563 (2003).
(b) D. G. Musaev, Y. V. Geletii and C. L. Hill, *J. Phys. Chem. A*, **107**, 5862 (2003).
41. V. Barone, M. Cossi and J. Tomasi, *J. Comput. Chem.*, **19**, 404 (1998).
42. S. Pfeiffer, B. Mayer and R. Janoschek, *J. Mol. Struct. (Theochem)*, **623**, 95 (2003).
43. R. S. Zhu and M. C. Lin, *J. Chem. Phys.*, **119**, 10667 (2003).
44. (a) K. Dolco and U. Röthlisberger, *Chem. Phys. Lett.*, **297**, 205 (1998).
(b) K. Dolco and U. Röthlisberger, *J. Phys. Chem.*, **104**, 6464 (2000).
45. L. L. Lohr, J. R. Barker and R. M. Shroll, *J. Phys. Chem. A*, **107**, 7429 (2003).
46. S. Padmaja, G. L. Squadrito, J. N. Lemercier, R. Cueto and W. A. Pryor, *Free Radical Biol. Med.*, **21**, 317 (1996).
47. (a) H. O. House and R. S. Ro, *J. Am. Chem. Soc.*, **80**, 2428 (1958).
(b) Y. Ogata and I. Tabushi, *J. Am. Chem. Soc.*, **83**, 3440 (1961).
48. (a) R. D. Bach, C. L. Willis and J. M. Domagals, in *Applications of MO Theory in Organic Chemistry* (Ed. I. C. Szizmadia), Vol. 2, Elsevier, Amsterdam, 1977, p. 221.
(b) R. D. Bach, J. L. Andrés and F. Davis, *J. Org. Chem.*, **57**, 613 (1992).
(c) R. D. Bach, J. L. Andrés, A. L. Owensby, H. B. Schlegel and J. J. W. McDouall, *J. Am. Chem. Soc.*, **114**, 7207 (1992).
(d) A. G. Baboul, H. B. Schlegel, M. N. Glukhovtsev and R. D. Bach, *J. Comput. Chem.*, **19**, 1353 (1998).
49. M. N. Hughes and H. G. Nicklin, *J. Chem. Soc. A*, 450 (1968).
50. (a) H. Masumoto and H. Sies, *Chem. Res. Toxicol.*, **9**, 262 (1996).
(b) Y. Kono, H. Shibata, K. Adachi and K. Tanaka, *Arch. Biochem. Biophys.*, **311**, 153 (1994).
51. Recent experimental (a) and theoretical (b) studies involving sterically encumbered alkenes also suggest that the spiro TS is favored over a planar one:
(a) T. Koerner, H. Slebocka-Tilk and R. S. Brown, *J. Org. Chem.*, **64**, 196 (1999).
(b) M. Freccero, R. Gandolfi, M. Sarzi-Amadé and A. Rastelli, *J. Org. Chem.*, **67**, 8519 (2002).
52. R. D. Bach and O. Dmitrenko, *J. Phys. Chem. A*, **107**, 4300 (2003).
53. S. Okovytyy, L. Gorb and J. Leszczynski, *Tetrahedron Lett.*, **43**, 4215 (2002).
54. M. L. McKee, *J. Am. Chem. Soc.*, **117**, 1629 (1995).
55. L. P. Olson, K. T. Kuwata, M. D. Bartberger and K. N. Houk, *J. Am. Chem. Soc.*, **124**, 9469 (2002).
56. (a) A. C. Cope and E. M. Hardy, *J. Am. Chem. Soc.*, **62**, 441 (1940).
(b) J. J. Gajewski, *Hydrocarbon Thermal Isomerizations*, Academic Press, New York, 1981.

57. R. D. Suenram and F. J. Lovas, *J. Am. Chem. Soc.*, **100**, 5117 (1978).
58. R. Jeyaraman and R. W. Murray, *J. Am. Chem. Soc.*, **106**, 2462 (1984).
59. R. Mello, M. Fiorentino, O. Sciacovelli and R. Curci, *J. Org. Chem.*, **53**, 389 (1988).
60. A. Kirschfeld, S. Muthusamy and W. Sander, *Angew. Chem.*, **106**, 2261 (1994); *Angew. Chem., Int. Ed. Engl.*, **33**, 2212 (1994).
61. (a) W. R. Wadt and W. A. Goddard III, *J. Am. Chem. Soc.*, **97**, 3004 (1975).
(b) L. B. Harding and W. A. Goodard III, *J. Am. Chem. Soc.*, **100**, 7180 (1978).
62. G. Karlström, S. Engström and B. Jönsson, *Chem. Phys. Lett.*, **67**, 343 (1979).
63. R. D. Bach, A. L. Owensby, J. L. Andrés and H. B. Schlegel, *J. Am. Chem. Soc.*, **113**, 7031 (1991).
64. M. Cantos, M. Merchan, F. Tomas-Vert and B. O. Roos, *Chem. Phys. Lett.*, **229**, 181 (1994).
65. J. M. Anglada, *J. Phys. Chem. A*, **102**, 3398 (1998).
66. J. Song, Y. G. Khait and M. R. Hoffmann, *J. Phys. Chem. A*, **103**, 521 (1999).
67. D. Cremer, T. Schmidt, J. Gauss and T. P. Radhakrishnan, *Angew. Chem., Int. Ed. Engl.*, **27**, 427 (1988).
68. R. Criegee, *Angew. Chem., Int. Ed. Engl.*, **14**, 745 (1975).
69. W. Sander, A. Kirschfeld, W. Kappert, S. Muthusamy and M. Kiselewsky, *J. Am. Chem. Soc.*, **118**, 6508 (1996) and references cited therein
70. E. Kraka, C. P. Sosa and D. Cremer, *Chem. Phys. Lett.*, **260**, 43 (1996).
71. W. H. Bunnelle, *Chem. Rev.*, **91**, 335 (1991).
72. (a) D. Cremer, T. Schmidt, W. Sander and P. Bischof, *J. Org. Chem.*, **54**, 2515 (1989).
(b) J. Gauss and D. Cremer, *Chem. Phys. Lett.*, **163**, 549 (1989).
(c) D. Cremer, *J. Am. Chem. Soc.*, **103**, 3619 (1981).
(d) D. Cremer, *J. Am. Chem. Soc.*, **101**, 7199 (1979).
(e) W. Sander, K. Schröder, S. Muthusamy, A. Kirschfeld, W. Kappert, R. Böse, E. Kraka, C. Sosa and D. Cremer, *J. Am. Chem. Soc.*, **119**, 7265 (1997).
(f) A. Patyk, W. Sander, J. Gauss and D. Cremer, *Angew. Chem., Int. Ed. Engl.*, **28**, 898 (1989).
73. G. Karlström and B. O. Roos, *Chem. Phys. Lett.*, **79**, 416 (1981).
74. C. Selçüki and V. Aviyente, *Chem. Phys. Lett.*, **288**, 669 (1998).
75. (a) A. Bernhardsson, R. Lindh, G. Karlström and B. O. Ross, *Chem. Phys. Lett.*, **251**, 141 (1996).
(b) A. Bouchy, M. T. C. Martins-Costa, C. Millot and M. F. Ruiz-Lopez, *J. Mol. Struct. (Theochem)*, **536**, 1 (2001).
76. M. Rahman, M. L. McKee, P. B. Shevlin and R. Szyrbicka, *J. Am. Chem. Soc.*, **110**, 4402 (1988).
77. (a) J. Anglada and J. M. Bofill, *J. Org. Chem.*, **62**, 2720 (1997).
(b) B.-Z. Chen, J. M. Anglada, M.-B. Huang and F. Kong, *J. Phys. Chem. A*, **106**, 1877 (2002).
78. R. Gutbrod, E. Kraka, R. N. Schindler and D. Cremer, *J. Am. Chem. Soc.*, **119**, 7330 (1997).
79. S.-J. Kim and H. F. Schaefer III, *J. Phys. Chem. A*, **104**, 7892 (2000).
80. R. A. Alvarez and C. B. Moore, *J. Phys. Chem.*, **98**, 174 (1994).
81. D.-C. Fang and X.-Y. Fu, *J. Phys. Chem. A*, **106**, 2988 (2002).
82. (a) R. Gutbrod, R. N. Schindler, E. Kraka and D. Cremer, *Chem. Phys. Lett.*, **252**, 221 (1996).
(b) P. Aplincourt and M. F. Ruiz-Lopez, *J. Am. Chem. Soc.*, **122**, 8990 (2000).
83. R. Gutbrod, E. Kraka, R. N. Schindler and D. Cremer, *J. Am. Chem. Soc.*, **119**, 7330 (1997).
84. M. Olzmann, E. Kraka, D. Cremer, R. Gutbrod and S. Andersson, *J. Phys. Chem. A*, **101**, 9421 (1997).
85. (a) D. Cremer, E. Kraka and C. Sosa, *Chem. Phys. Lett.*, **337**, 199 (2001).
(b) D. Cremer, E. Kraka, R. Crehuet, J. Anglada and J. Gräfenstein, *Chem. Phys. Lett.*, **347**, 268 (2001).
86. D. Zhang, W. Lei and R. Zhang, *Chem. Phys. Lett.*, **358**, 171 (2002).
87. R. Crehuet, J. M. Anglada, D. Cremer and J. M. Bofill, *J. Phys. Chem. A*, **106**, 3917 (2002).
88. D. V. Deubel, *J. Org. Chem.*, **66**, 3790 (2001).
89. R. W. Murray, R. Jeyaraman and L. Mohan, *J. Am. Chem. Soc.*, **108**, 2470 (1986).
90. (a) K. N. Houk, J. Liu, N. C. DeMello and K. R. Condroski, *J. Am. Chem. Soc.*, **119**, 10147 (1997).
(b) C. Jensen, J. Liu, K. N. Houk and W. L. Jorgensen, *J. Am. Chem. Soc.*, **119**, 12982 (1997).

91. M. Freccero, R. Gandolfi, A. Sarzi-Amade and A. Rastelli, *Tetrahedron*, **54**, 6123 (1998).
92. A. Bravo, F. Fontana, G. Fronza, F. Minisci and L. Zhao, *J. Org. Chem.*, **63**, 254 (1998).
93. J. Liu, K. N. Houk, A. Dinoi, C. Fusco and R. Curci, *J. Org. Chem.*, **63**, 8565 (1998).
94. (a) D. Cremer, E. Kraka and P. G. Szalay, *Chem. Phys. Lett.*, **292**, 97 (1998).
(b) A. L. Baumstark and P. C. Vasquez, *J. Org. Chem.*, **53**, 3437 (1988).
95. R. W. Murray and D. Gu, *J. Chem. Soc., Perkin Trans. 2*, 2203 (1993).
96. A. Armstrong, I. Washington and K. N. Houk, *J. Am. Chem. Soc.*, **122**, 6297 (2000).
97. R. D. Bach, C. Canepa, J. E. Winter and P. E. Blanchette, *J. Org. Chem.*, **62**, 5191 (1997).
98. R. Curci, A. Dinoi and M. F. Rubino, *Pure Appl. Chem.*, **67**, 811 (1995).
99. K. Miaskiewicz and D. A. Smith, *J. Am. Chem. Soc.*, **120**, 1872 (1998).
100. J. B. Foresman, T. A. Keith, K. B. Wiberg, J. Snoonian and M. J. Frisch, *J. Phys. Chem.*, **100**, 16098 (1996).
101. M. Freccero, R. Gandolfi, A. Sarzi-Amade and A. Rastelli, *Tetrahedron*, **54**, 12323 (1998).
102. V. Barone, M. Cossi and J. Tomasi, *J. Comput. Chem.*, **19**, 404 (1998).
103. W. Adam, R. Curci, L. D'Accolti, A. Dinoi, C. Fusco, F. Gasparrini, R. Kluge, R. Paredes, M. Schulz, A. K. Smerz, L. A. Veloza, S. Weinkötz and R. Winde, *Chem. Eur. J.*, **3**, 105 (1997).
104. P. A. Simakov, S. Y. Choi and M. Newcomb, *Tetrahedron Lett.*, **39**, 8187 (1998).
105. Schemes from: M. Freccero, R. Gandolfi, M. Sarzi-Amade and A. Rastelli, *J. Org. Chem.*, **68**, 811 (2003).
106. (a) F. Minisci, L. Zhao, F. Fontana and A. Bravo, *Tetrahedron Lett.*, **36**, 1895 (1995).
(b) F. Minisci, L. Zhao, F. Fontana and A. Bravo, *Tetrahedron Lett.*, **36**, 1697 (1995).
(c) A. Bravo, F. Fontana, G. Fronza, F. Minisci and A. Serri, *Tetrahedron Lett.*, **36**, 6945 (1995).
(d) A. Bravo, F. Fontana, G. Fronza, A. Mele and F. Minisci, *J. Chem. Soc., Chem. Commun.*, 1573 (1995).
107. M. N. Glukhovtsev, C. Canepa and R. D. Bach, *J. Am. Chem. Soc.*, **120**, 10528 (1998).
108. X. Du and K. N. Houk, *J. Org. Chem.*, **63**, 6480 (1998).
109. G. V. Shustov and A. Rauk, *J. Org. Chem.*, **63**, 5413 (1998).
110. M. Freccero, R. Gandolfi, M. Sarzi-Amade and A. Rastelli, *Tetrahedron Lett.*, **42**, 2739 (2001).
111. M. Freccero, R. Gandolfi, M. Sarzi-Amade and A. Rastelli, *Tetrahedron*, **57**, 9843 (2001).
112. N. Prilezajew, *Chem. Ber.*, **42**, 4811 (1909).
113. (a) M. G. Finn and K. B. Sharpless, *Asymmetric Synthesis*, **5**, 247 (1986).
(b) K. B. Sharpless and T. R. Verhoeven, *Aldrichimica Acta*, **12**, 63 (1979).
114. For reviews on metal-catalyzed epoxidation see: (a) D. V. Deubel, G. Frenking, P. Gisdakis, W. A. Herrmann, N. Rosch and J. Sundermeyer, *Acc. Chem. Res.*, **37**, 645 (2004).
(b) T. Katsuki, in *Catalytic Asymmetric Synthesis*, 2nd edn. (Ed. I. Ojima), Wiley-VCH, New York, 2000.
(c) E. N. Jacobsen and M. H. Wu, in *Comprehensive Asymmetric Catalysis* (Eds. E. N. Jacobsen, A. Pfaltz and H. Yamamoto), Springer, New York, 1999, pp. 1309–1326.
(d) J. N. Jacobsen, in *Catalytic Asymmetric Synthesis* (Ed. I. Ojima), Chap. 4.2, VCH, New York, 1993.
115. For summaries and incisive reviews, see: (a) B. Plesničar, in *The Chemistry of Peroxides* (Ed. S. Patai), Wiley, Chichester, 1983, p. 521.
(b) H. Mimoun, *Angew. Chem., Int. Ed. Engl.*, **21**, 743 (1982).
(c) J. Rebeck, Jr., *Heterocycles*, **15**, 517 (1981).
(d) V. G. Dryuk, *Tetrahedron*, **32**, 2855 (1976).
(e) *Organic Peroxides* Vol. II (Ed. D. Swern), Chap. 5, Wiley-Interscience, 1971.
116. For an excellent review on substrate-directable chemical reactions, see A. H. Hoveyda, D. A. Evans and G. C. Fu, *Chem. Rev.*, **93**, 1307 (1993).
117. (a) P. D. Bartlett, *Rec. Chem. Progr.*, **11**, 47 (1950).
(b) The Frontiers in Chemistry lectures at Wayne State University, Detroit, were published as a series of lectures in the Record of Chemical Progress up until 1971 when this journal was discontinued.
(c) A. A. M. Roof, W. J. Winter and P. D. Bartlett, *J. Org. Chem.*, **50**, 4093 (1985).
118. B. Plesničar, M. Tasevski and A. Azman, *J. Am. Chem. Soc.*, **100**, 743 (1978).
119. R. D. Bach, J. J. W. McDouall, A. L. Owensby and H. B. Schlegel, *J. Am. Chem. Soc.*, **112**, 7065 (1990).

120. R. P. Hanzlik and G. O. Shearer, *J. Am. Chem. Soc.*, **97**, 5231 (1975).
121. S. Yamabe, C. Kondou and T. Minato, *J. Org. Chem.*, **61**, 616 (1996).
122. R. D. Bach, M. N. Glukhovtsev and C. Gonzalez, *J. Am. Chem. Soc.*, **120**, 9902 (1998).
123. The peroxyformic acid-ethylene TS calculated at the MP2 level and reported in Reference 17b (prior to the availability of MP2 frequencies in 1991) was constrained to be symmetrical with identical C–O bonds. This structure, however, was a first-order saddle point with an HF/6-31G* frequency calculation pointing to the dangers of using frequency calculations at a level lower than the geometry optimization.
124. R. D. Bach, M. N. Glukhovtsev, C. Gonzalez, M. Marquez, C. M. Estevez, A. G. Baboul and H. B. Schlegel, *J. Phys. Chem. A*, **101**, 6092 (1997).
125. D. A. Singleton, S. R. Merrigan, J. Liu and K. N. Houk, *J. Am. Chem. Soc.*, **119**, 3385 (1997).
126. D. A. Singleton and A. A. Thomas, *J. Am. Chem. Soc.*, **117**, 9357 (1995).
127. K. W. Woods and P. Beak, *J. Am. Chem. Soc.*, **113**, 6281 (1991).
128. (a) T. J. Lang, G. J. Wolber and R. D. Bach, *J. Am. Chem. Soc.*, **103**, 3275 (1981).
(b) R. D. Bach and G. J. Wolber, *J. Am. Chem. Soc.*, **106**, 1410 (1984).
129. K. N. Houk and I. Washington, *Angew. Chem., Int. Ed.*, **40**, 2001 (2001).
130. (a) M. Freccero, R. Gandolfi, M. Sarzi-Amadè and A. Rastelli, *J. Org. Chem.*, **64**, 2030 (1999).
(b) M. Freccero, R. Gandolfi, M. Sarzi-Amadè and A. Rastelli, *J. Org. Chem.*, **65**, 8948 (2000).
131. O. Dmitrenko and R. D. Bach, *J. Phys. Chem. A*, **108**, 6886 (2004).
132. R. C. Fahey, *Top. Stereochem.*, **3**, 237 (1968).
133. R. D. Bach and O. Dmitrenko, *J. Org. Chem.*, **67**, 2588 (2002).
134. R. D. Bach and O. Dmitrenko, *J. Am. Chem. Soc.*, **126**, 4444 (2004).
135. H. Hart, *Acc. Chem. Res.*, **4**, 337 (1971).
136. (a) H. B. Henbest and R. A. L. Wilson, *J. Chem. Soc.*, 1957, (1958).
(b) H. B. Henbest, *Proc. Chem. Soc.*, 159 (1963).
(c) K. J. Shea and J.-S. Kim, *J. Am. Chem. Soc.*, **114**, 3044 (1992).
137. (a) W. Adam and T. Wirth, *Acc. Chem. Res.*, **32**, 703 (1999).
(b) R. W. Hoffmann, *Chem. Rev.*, **89**, 1841 (1989).
138. R. D. Bach, C. M. Estevez, J. E. Winter and M. N. Glukhovtsev, *J. Am. Chem. Soc.*, **120**, 680 (1998).
139. W. Adam, R. D. Bach, O. Dmitrenko and C. R. Saha-Möller, *J. Org. Chem.*, **65**, 6715 (2000).
140. R. D. Bach, J. J. W. McDouall, A. L. Owensby and H. B. Schlegel, *J. Am. Chem. Soc.*, **112**, 7064 (1990).
141. R. D. Bach, A. L. Owensby, C. Gonzalez, H. B. Schlegel and J. J. W. McDouall, *J. Am. Chem. Soc.*, **113**, 6001 (1991).
142. H. H. Huang, Y. Xie and H. F. Schaefer III, *J. Phys. Chem.*, **100**, 6076 (1996).
143. D. Schroder, C. A. Schalley, N. Goldberg, J. Hrusak and H. Schwarz, *Chem. Eur. J.*, **2**, 1235 (1996).
144. T. Okajima *J. Mol. Struct. (Theochem)*, **572**, 45 (2001).
145. On a personal note, it took a number of weeks for a very good postdoctoral to locate the above TS for HO–OH and NH₃ at the MP2 level. This TS was recently repeated at the B3LYP level by the author in less than an hour! The problem initially was not the MP2 method but rather that for the weakly nucleophilic ammonia the 1,2-hydrogen shift precedes the oxygen transfer step. With TMA the hydrogen shift follows the O–O bond cleavage. This could not be closely examined at that time because MP2 second derivatives were not yet available to perform a frequency calculation. Additionally, the algorithms currently available with the luxury of being able to first calculate the force constants before doing the gradient calculations make the location of even more complex TSs almost trivial. These marked improvements in geometry optimization techniques are due in a large part to the important contributions to this art made by my former colleague at Wayne State University, Professor Bernard Schlegel.
146. G. Ottolina and G. Carrea, *Chem. Commun.*, 1748 (2001).
147. R. D. Bach and O. Dmitrenko (unpublished results).
148. J.-W. Chu and B. L. Trout, *J. Am. Chem. Soc.*, **126**, 900 (2004).
149. For a discussion of solvent-assisted proton transfer in alkyl hydrogen peroxides see: M. A. P. Dankleff, R. Curci, J. O. Edwards and H. Y. Pyun, *J. Am. Chem. Soc.*, **90**, 3209 (1968).
150. R. Curci, R. DiPrete, J. O. Edwards and G. Modena, *J. Org. Chem.*, **35**, 740 (1970).

151. (a) T. C. Bruice, in *Flavins and Flavoproteins* (Eds. R. C. Bray, P. C. Engel and S. G. Mayhew), de Gruyter, Berlin, 1984, pp. 57–60.
(b) C. Walsh, in *Enzymatic Reaction Mechanisms*, W. H. Freeman and Co., San Francisco, 1979, pp. 406–463.
152. (a) F. Müller, *Biochem. Soc. Trans.*, **13**, 443 (1985).
(b) M. Ortiz-Maldonado, S. M. Aeschliman, D. P. Ballou and V. Massey, *Biochemistry*, **40**, 8705 (2001).
153. (a) S. Ball and T. C. Bruice, *J. Am. Chem. Soc.*, **101**, 4017 (1979).
(b) S. Ball and T. C. Bruice, *J. Am. Chem. Soc.*, **102**, 6498 (1980).
(c) T. C. Bruice, J. B. Noar, S. Ball and U. V. Venkataram, *J. Am. Chem. Soc.*, **105**, 2452 (1983).
(d) T. C. Bruice, *J. Chem. Soc., Chem. Commun.* 14 (1983).
154. (a) D. M. Ziegler, *Annu. Rev. Pharmacol. Toxicol.*, **33**, 179 (1993).
(b) L. L. Poulsen and D. M. Ziegler, *Chem. Biol. Interact.*, **96**, 57 (1995).
(c) D. M. Ziegler, *Drug Metab. Rev.*, **34**, 503 (2002).
155. (a) F. A. Carey and R. J. Sundberg, *Advanced Organic Chemistry*, 3rd edn., Part A, Plenum Press, New York, 1990, p. 284.
(b) T. H. Lowry and K. S. Richardson, *Mechanism and Theory in Organic Chemistry*, 3rd edn., Harper & Row, New York, 1987, p. 367.
156. R. D. Bach and O. Dmitrenko, *J. Am. Chem. Soc.*, **126**, 127 (2004).
157. J. Vervoort, I. M. C. M. Rietjens, W. J. H. van Berkel and C. Veeger, *Eur. J. Biochem.*, **206**, 479 (1992).
158. M. Peräkylä and T. A. Pakkanen, *J. Am. Chem. Soc.*, **115**, 10958 (1993).
159. (a) L. Ridder, A. J. Mulholland, I. M. C. M. Rietjens and J. Vervoort, *J. Am. Chem. Soc.*, **122**, 8728 (2000).
(b) L. Ridder, A. J. Mulholland, J. Vervoort and I. M. C. M. Rietjens, *J. Am. Chem. Soc.*, **120**, 7641 (1998).
(c) L. Ridder, B. A. Palfey, J. Vervoort and I. M. C. M. Rietjens, *FEBS Lett.*, **478**, 197 (2000).
160. S. R. Billeter, C. F. W. Hanser, T. Z. Mordasini, M. Scholten, W. Thiel and W. F. van Gunsteren, *Phys. Chem. Chem. Phys.*, **3**, 688 (2001).
161. M. Ortiz-Maldonado, D. P. Ballou and V. Massey, *Biochemistry*, **38**, 8124 (1999).
162. G. Merenyi, J. Lind and R. F. Anderson, *J. Am. Chem. Soc.*, **113**, 9371 (1991).
163. S. P. de Visser, J. Kaneti, R. Neumann and S. Shaik, *J. Org. Chem.*, **68**, 2903 (2003).
164. A. Bil and Z. Latajka, *Chem. Phys.*, **305**, 243 (2004).
165. (a) E. L. Oiestad, J. N. Harvey and E. Uggerud, *J. Phys. Chem. A.*, **104**, 8382 (2000).
(b) A. M. Leere Oiestad, A. C. Petersen, V. Bakken, J. Vedde and E. Uggerud, *Angew. Chem., Int. Ed.*, **40**, 1433 (2001).
166. R. D. Bach and M.-D. Su, *J. Am. Chem. Soc.*, **116**, 10103 (1994).
167. G. A. Olah, N. Hartz, G. Rasul and G. K. S. Prakash, *J. Am. Chem. Soc.*, **117**, 1336 (1995).
168. A. I. Panin and A. V. Tulub, *Int. J. Quant. Chem.*, **77**, 580 (2000).

CHAPTER 2

The structural chemistry of acyclic organic peroxides

JENS HARTUNG

*Fachbereich Chemie, Organische Chemie, Technische Universität Kaiserslautern, Erwin-Schrödinger-Straße, D-67663 Kaiserslautern, Germany
e-mail: hartung@chemie.uni-kl.de*

and

INGRID SVOBODA

*Fachgebiet Strukturforschung, FB 11, Material-und Geowissenschaften, Technische Universität Darmstadt, Petersenstr. 23, D-64287 Darmstadt, Germany
e-mail: svoboda@tu-darmstadt.de*

I. INTRODUCTION	94
II. BASIC PRINCIPLES	95
A. H ₂ O ₂ and H ₂ OO	96
B. Structure and Bonding in Acyclic Organic Peroxides	100
1. Lone pair repulsion	100
2. Steric effects	101
3. Orbital effects	101
4. Hydrogen bonding	103
5. Conclusion	105
III. ORGANIC PEROXY COMPOUNDS	105
A. Alkyl Hydroperoxides	105
1. Structural aspects	110
2. The anomeric effect	110
3. Hydrogen bonding	111
B. The Alkyl Hydroperoxide Anion as Ligand	114
1. Covalent radii versus experimental M–O bond lengths	114
2. Dihedral angles associated with the peroxy ligand	119
3. Tetrahedral distortion	119
C. Dialkyl Peroxides	119

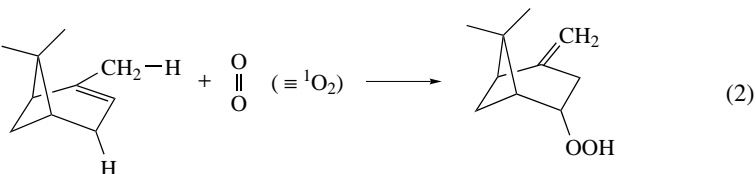
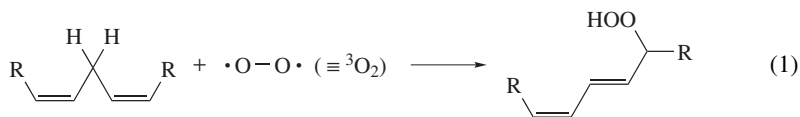
The chemistry of peroxides, volume 2

Edited by Z. Rappoport © 2006 John Wiley & Sons, Ltd ISBN: 0-470-86274-2

D. Peroxids	125
1. Alkanoyl peroxids	125
2. Aroyl peroxids	127
3. The percarboxylate anion as ligand	127
E. Peresters	127
F. Diacyl Peroxides	128
IV. POLYOXO COMPOUNDS	131
A. Trioxides	131
B. Tetroxides and Higher Polyoxides	133
V. NATURAL PRODUCTS	133
A. Sesquiterpenes	133
1. Alkyl hydroperoxides related to artemisinin and its derivatives	133
2. Miscellaneous sesquiterpene hydroperoxides	134
B. Triterpenes	136
C. Acetogenins	136
VI. CONCLUDING REMARKS	138
VII. REFERENCES	138

I. INTRODUCTION

Autoxidations of hydrocarbons with molecular oxygen in its electronic ground state ($^3\text{O}_2$) and pericyclic transformations of olefins with singlet oxygen ($^1\text{O}_2$) furnish acyclic organic peroxides (equations 1 and 2)^{1,2}. Since nature provides O_2 in seemingly unlimited quantities, compounds with O—O single bonds occur almost ubiquitously in our environment³. Depending on where, in which quantities and from what substrates they are produced, peroxides act as atmospheric pollutants⁴, primary oxidants⁵, secondary metabolites⁶ or therapeutics⁷.



The common aspect of peroxide chemistry is the inherent weakness of the O—O single bond⁸. This fact and some fundamental conformational properties have been related to Coulomb repulsion between the lone pairs at the O—O bond. More recent MO calculations, however, have shown that this picture is far from complete⁹. A timely treatise on structural aspects of acyclic organic peroxides therefore has to consider information from diffraction experiments and spectroscopy on one side and data from computational investigations on the other¹⁰. The controversy on how to adequately describe the peroxide functionality by theoretical procedures has been settled¹¹. An application of methods that include electron correlation provides O—O distances that agree within accepted error limits with data from solid state geometries or gas phase studies¹². The Pople 6-31G* basis set, or an equivalent, generally poses a lower limit in order to address conformational aspects of

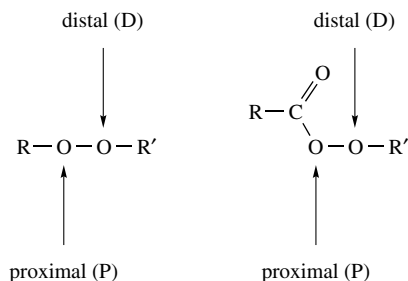


FIGURE 1. Nomenclature for O atoms in constitutionally asymmetric peroxides ($R = \text{alkyl, aryl; } R' = \text{H, metal, transition metal, group 13-17 elements}$)

the peroxide bond adequately. An application of diffuse and/or polarization functions has been recommended in order to improve the results¹³. In view of this background, it is the major aim of this chapter to organize the structural fundamentals of acyclic organic peroxides—compounds with notable industrial, synthetic and environmental significance. The literature has been covered back to 1983 since an earlier book chapter on this topic is available¹⁴. In order to facilitate the discussion, the O atoms in constitutionally asymmetric peroxides have been labeled according to the notation outlined in Figure 1.

II. BASIC PRINCIPLES

Neutral organic peroxides are characterized by the four atom unit $\text{C}-\text{O}-\text{O}-\text{X}$, where C denotes an organic substituent and X either H, alkyl, aryl, acyl, a metal ion, a transition metal fragment or a main group element. O—O distances r from crystal structures of H_2O_2 (1.453 Å)¹⁵, KO_2 (1.28 Å)¹⁶ and O_2 (1.208 Å)¹⁷ have been correlated with the associated MO bond order n to provide the empirical relationship $r(n) = -0.245n + 1.681$ Å (Figure 2). The accepted value for a O—O single bond measures 1.45 ± 0.02 Å. Reports on longer O—O bonds (1.5–1.7 Å) have been attributed to systematic errors introduced by crystal instability during continuous exposure to X-rays¹⁸. Comparatively short bonds (1.2–1.3 Å), in particular in metal compounds, have been interpreted in terms of a superoxo mode of binding¹⁹.

The major groups of acyclic organic peroxides may be obtained by successively substituting H atoms in H_2O_2 with alkyl, aryl, acyl, alkoxy-carbonyl or heteroatom substituents (Figure 3). A formal O insertion into the O—O bond provides polyoxides, i.e. compounds with at least three O atoms in a row. Substituents R have the potential to modify the

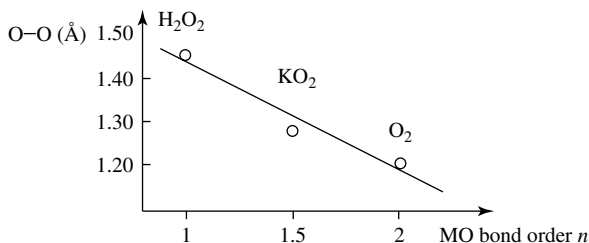


FIGURE 2. Correlation between experimentally observed O—O bond lengths and MO bond order n : $r(n) = -0.245n + 1.681$ Å ($R^2 = 0.97$)

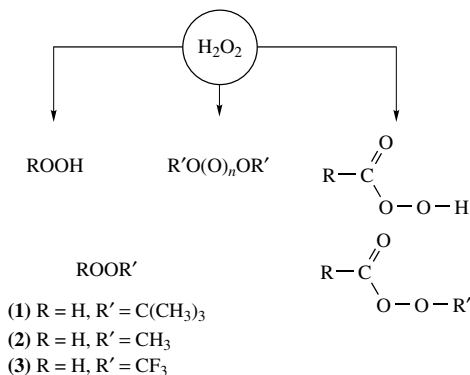


FIGURE 3. A synopsis of the most important groups and selected examples of acyclic peroxides ($\text{R} = \text{alkyl, aryl, alkoxy carbonyl}$; $\text{R}' = \text{H, NO}_2, \text{R}$)

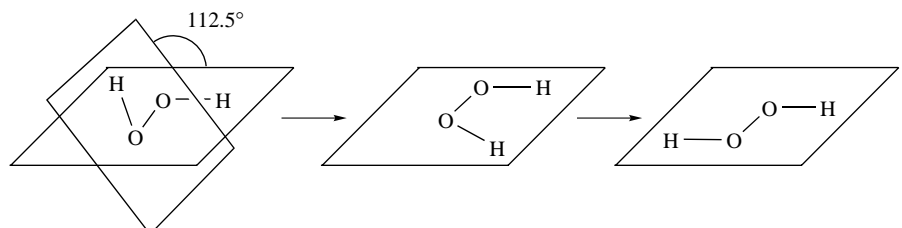
properties of the peroxide functionality by means of electronic and/or steric effects, hyperconjugation and hydrogen bonding, which is reflected in different bond dissociation energies (BDE)⁸, redox potentials²⁰, $\text{p}K_{\text{a}}$ ²¹ or $\text{p}K_{\text{HB}}$ ²² values. The $\text{p}K_{\text{a}}$ values of compounds of the type ROOH, for example, gradually decrease with the electron-withdrawing property of R along the series $(\text{H}_3\text{C})_3\text{COOH}$ (1) ($\text{p}K_{\text{a}} = 12.8$), H_2O_2 (11.6), CH_3OOH (2) (11.5), CF_3OOH (3) (8.9) to $\text{CH}_3\text{C}(\text{O})\text{OOH}$ (8.2)²³.

A. H_2O_2 and H_2OO

Hydrogen peroxide (dihydrogen dioxide, H_2O_2) and water oxide (H_2OO) are the smallest acyclic peroxides. H_2O_2 crystallizes at ambient pressure in the tetragonal space group $\text{D}_4^4\text{-}P4_12_12$ with four molecules in the unit cell ($\text{H}_2\text{O}_2\text{-I}$)^{15,24}. The two O atoms in H_2O_2 are separated by 1.453 Å. The H–O bond measures 1.008 Å, the bond angle O–O–H = 102.7° and the dihedral angle H–O–O–H = 90.2° (neutron diffraction analysis)¹⁵. A phase transition from $\text{H}_2\text{O}_2\text{-I}$ into a stronger hydrogen-bonded high-pressure modification $\text{H}_2\text{O}_2\text{-II}$ at 7.5 GPa has been reported on the basis of results from Raman and X-ray measurements²⁵. H_2O_2 is persistent in both modifications. Decomposition into O_2 and H_2O occurs at the onset of melting at elevated pressure.

The data from microwave spectroscopy have been interpreted with a dihedral angle H–O–O–H = 120.0° for the gas-phase equilibrium structure of H_2O_2 ²⁶. The non-planarity of the peroxide gives rise to a stereogenic O–O axis¹⁰. The computed total parity violating energy shift of $-1.9 \times 10^{-19} \text{ kJ mol}^{-1}$ between the two enantiomers, however, is too small in order to be measured with contemporary devices²⁷.

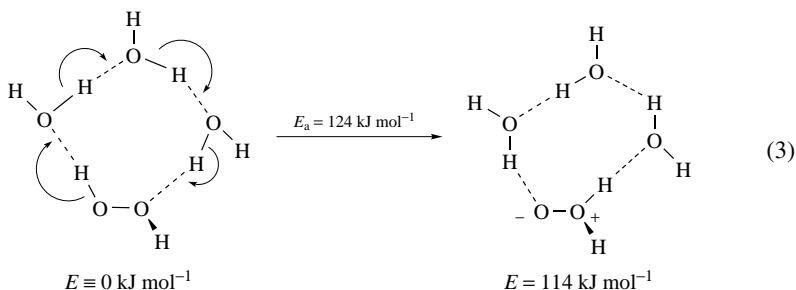
Theory (CCSD) predicts that the rotation about the O–O bond in H_2O_2 is associated with changes of the O–O length and the O–O–H angle in going from the equilibrium structure (*gauche*: O–O = 1.453 Å, H–O–O–H = 112.5°, $E_{\text{rel}} \equiv 0.0 \text{ kJ mol}^{-1}$), to the energetic maximum (*synperiplanar*: O–O = 1.463 Å, H–O–O–H = 0°, $E_{\text{rel}} = 30.4 \text{ kJ mol}^{-1}$), and further to the *antiperiplanar* arranged rotamer (O–O = 1.464 Å, H–O–O–H = 180°, $E_{\text{rel}} = 4.5 \text{ kJ mol}^{-1}$, Table 1)²⁸. The computed H–O–O angle increases along the series *antiperiplanar* conformer (98.4°) via the *gauche* configured conformer (99.9°) to the *synperiplanar* arranged structure (104.1°). The energies of these H_2O_2 conformers have been correlated with the experimentally observed two barriers in the potential energy curve for the torsional movement about the O–O bond in

TABLE 1. Calculated parameters (\AA , $^\circ$) of selected H_2O_2 conformers (CCSD)²⁹


Entry	Conformation	E_{rel} (kJ mol^{-1})				
			O—O (\AA)	O—H (\AA)	O—O—H ($^\circ$)	H—O—O—H ($^\circ$)
1	<i>gauche</i>	0.0	1.453	0.963	99.9	112.5
2	<i>synperiplanar</i>	30.4	1.463	0.963	104.1	0.0
3	<i>antiperiplanar</i>	4.5	1.464	0.962	98.3	180.0

H_2O_2 ($\Delta E = 4.6 \text{ kJ mol}^{-1}$ and 29.4 kJ mol^{-1})²⁷. Upon lengthening of the O—O bond in the equilibrium structure of H_2O_2 (O—O = 1.446 \AA , H—O—O = 100.9° , H—O—O—H = 111.9°), the calculated (B3LYP) ΔG value gradually increases, until a shallow maximum near 3 \AA with a planar arrangement of the four atoms is reached (O—O = 3.0 \AA , H—O—O = 78.9° , H—O—O—H = 180.0°)²⁹. Beyond this point, two hydroxyl radicals are released.

A formal 1,2-hydrogen atom shift in H_2O_2 furnishes water oxide (H_2OO), the high energy tautomer of hydrogen peroxide (equation 3)³⁰. The existence of water oxide has recently been probed using collisional activation, charge reversal and six different neutralization–reionization mass spectrometric experiments with $[\text{H}_2, \text{O}_2]^{*+}$ radical cations and $[\text{H}_2, \text{O}_2]^{*-}$ anions³¹. The results of these studies suggest that H_2OO exists as transient in the gas phase and may play a role in oxidation reactions involving H_2O_2 . Theory predicts that water oxide is a non-planar molecule with an O—O bond of 1.563 \AA , a bond angle H—O—O of 99.5° and a torsion angle H—O—O—H of 108.5° (MP4SDTQ)³². The calculated energetic barrier ($\Delta E^\ddagger = 222 \text{ kJ mol}^{-1}$, B3LYP) and the reaction enthalpy ($\Delta_{\text{R}}H = 192 \text{ kJ mol}^{-1}$) of the unimolecular tautomerization $\text{H}_2\text{O}_2 \rightarrow \text{H}_2\text{OO}$ in the gas phase is lowered, if water molecules are included into the reaction sequence (for the reaction in the presence of $3 \text{ H}_2\text{O}$: $\Delta E^\ddagger = 124 \text{ kJ mol}^{-1}$, $\Delta_{\text{R}}H = 114 \text{ kJ mol}^{-1}$)^{30,32}. The origin of this effect has been attributed to the formation of a hydrogen-bonded cluster of H_2O_2 and H_2O , which is a prerequisite for the change of the reaction mechanism from an intra- to an intermolecular process (equation 3).



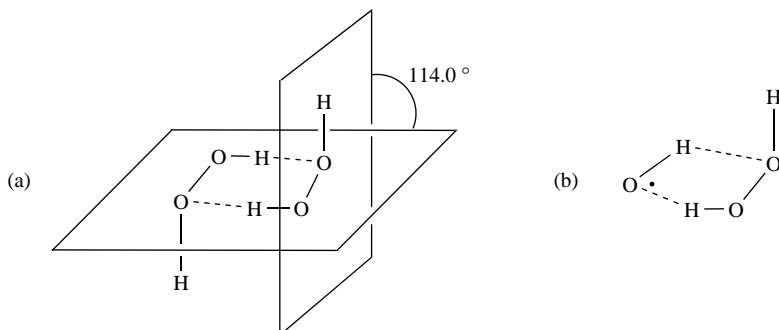


FIGURE 4. Visualization of (a) the hydrogen-bonded H₂O₂ dimer (IR, MP2) and (b) the predicted hydrogen-bonded adduct between the HO• and H₂O₂ (UB3LYP)^{34,36}

The carbonyl oxides, i.e. the carbon analogs of water oxide, are well-established intermediates in the ozonolysis of olefins and may be independently prepared by treatment of diazo compounds with singlet oxygen³³.

In (H₂O₂)₂, which has been trapped and characterized in an argon matrix (IR spectroscopy), either unit serves as proton donor and acceptor. The computed binding energy for the equilibrium structure, which shows a plane of four O atoms with the H atoms from the bridge transposed either 0.14 Å above or below this plane, is 27 kJ mol⁻¹ in the gas phase (MP2, Figure 4)³⁴. The observed geometric changes in the H₂O₂ subunit are small in going from the monomer to (H₂O₂)₂.

Hydrogen bonding between H₂O₂ and the hydroxyl radical has been explored in a computational study (UB3LYP) in order to find evidence that might explain the unusual kinetic behavior of the HO• + H₂O₂ reaction at elevated temperatures^{35,36}. Theory predicts that the two components form a hydrogen-bridged, conformational flexible five-membered adduct with a 17 kJ mol⁻¹ binding energy (UB3LYP, UMP2). Hydrogen bonds of a similar strength have been calculated for adducts between H₂O₂ and CO (20 kJ mol⁻¹, binding via the C atom; MP2)³⁷ or N₂ (24 kJ mol⁻¹, MP2)³⁸.

H₂O₂ cocrystallizes with organic compounds to form perhydrates³⁹. The most prominent example of this kind is the adduct between urea and H₂O₂ (UHP, space group *Pnca*, Figure 5)⁴⁰. A view of the unit cell along *b* indicates that molecules of urea and H₂O₂ [neutron diffraction: H—O = 1.005 Å, O—O = 1.457 Å, H—O—O = 102.5°, H—O—O—H = 99.0°] are stacked above one another. Adjacent columns exhibit H₂O₂ molecules of opposite configuration along the O—O axis. Three types of hydrogen bonds are present in the crystal of UHP: (i) double hydrogen bonds between two N—H groups of one urea molecule toward the two peroxide O of *one* H₂O₂ molecule, (ii) O—H...O=C bonds and (iii) three-centered bonds between an N—H proton and a peroxide O atom (Figure 5).

In the crystal structure of potassium hydrogen phthalate hemiperhydrate (**4**), the H₂O₂ molecule adopts an *antiperiplanar* arrangement, presumably for the reason of maximum ion-dipole interaction between the lone pairs at O and the potassium cation⁴¹. The observed O—O distance of 1.418 Å in **4** (Figure 6) is shorter than the value of 1.481 Å that was found in hydrogen peroxide dihydrate. The origin of short O—O bonds in crystal structures of perhydrates in general has been associated with a random substitution of H₂O₂ by water molecules. If the two structures are isotypic, the peaks from powder data

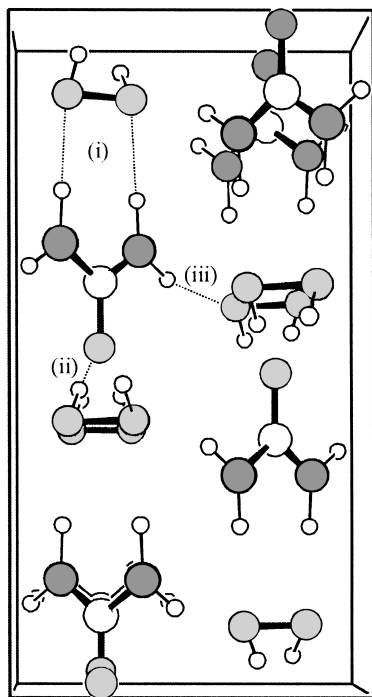


FIGURE 5. The solid state geometry of urea hydrogen peroxide [UHP, view along b ; the O atoms are depicted in gray and the N atoms in black; for description of H bonds (i)–(iii), see text]⁴⁰

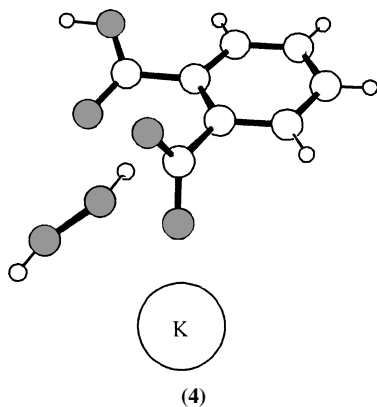


FIGURE 6. The geometry of potassium hydrogen phthalate hemiperhydrate (**4**) in the solid state (ball and stick presentation with the oxygen atoms depicted in gray)⁴¹

originating from water substitution are difficult to separate from those belonging to H_2O_2 , thus giving rise to misleading geometric information. This issue has been thoroughly addressed in a neutron diffraction study on potassium oxalate perhydrate at 123 K⁴². The O–O distance of 1.458 Å obtained from this study is longer than a value of 1.355 Å, which has been documented in an earlier report dealing with neutron diffraction powder data of the deuteriated derivative.

B. Structure and Bonding in Acyclic Organic Peroxides

1. Lone pair repulsion

Peroxides of the type $\text{R}-\text{O}-\text{O}-\text{R}'$ preferentially adopt a *gauche* conformation (Figure 7a). This geometry lowers Coulomb repulsion between the lone pairs at O, which are more significant in the *synperiplanar* and *antiperiplanar* arranged rotamers than in the *gauche* conformer (Figure 7b,c)²⁸. The interaction between the non-bonding orbitals at oxygen has been correlated with the inherent weakness of the O–O bond [212.5 kJ mol⁻¹ for $\text{HO}-\text{OH}$ ⁴³, 187.3 kJ mol⁻¹ for $\text{H}_3\text{CO}-\text{OH}$ (**2**)⁴⁴, 158.8 kJ mol⁻¹ for $\text{H}_3\text{CO}-\text{OCH}_3$ (**5**) (Figure 7d)⁴⁵ and 126 kJ mol⁻¹ for $\text{H}_3\text{CC}(\text{O})\text{O}-\text{O}(\text{O})\text{CCH}_3$ ⁴⁵ (all values experimental data)].

Diverging values for the hydrogen bond basicity ($\text{p}K_{\text{HB}}$) have been correlated with differences in the degree of lone pair repulsion in cyclic and acyclic peroxides²². Di(*tert*-butyl)peroxide (**6**), for example, has a $\text{p}K_{\text{HB}}$ of 0.13 in its hydrogen-bond-forming reaction with *p*-fluorophenol. This value is close to the number obtained for sterically hindered ethers. Ascaridole (**7**), on the other hand, exhibits a significantly higher $\text{p}K_{\text{HB}}$ of 0.92. These data have been interpreted by the release of lone pair interactions in conformational flexible acyclic peroxides, such as di(*tert*-butyl)peroxide (**6**) (Figure 7e). In small to medium sized rings, the endoperoxide functionality may not adopt a similar energetically favorable conformation. The larger $\text{p}K_{\text{HB}}$ of ascaridole (**7**) (Figure 7f) points to a considerable degree of lone pair repulsion that may be reduced upon H-bond formation.

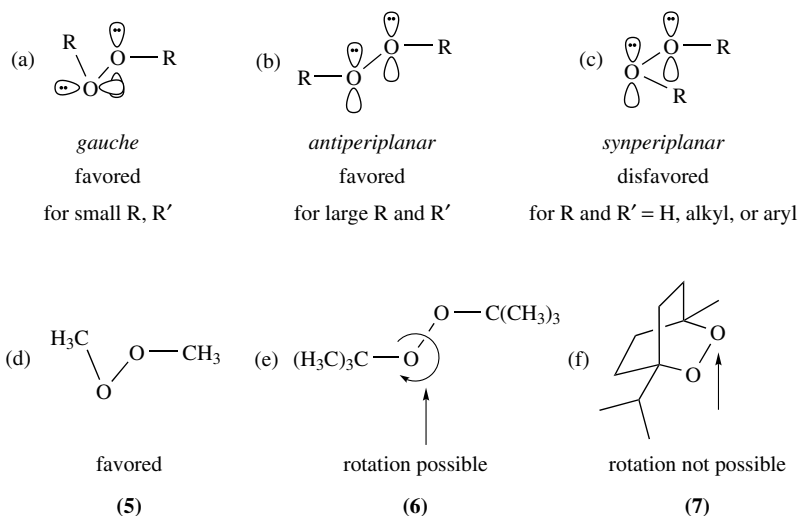


FIGURE 7. Conformational aspects of peroxide chemistry

2. Steric effects

The torsion angle R–O–O–H in alkyl hydroperoxides lies in the range of $100 \pm 20^\circ$, which is comparable to the value for H₂O₂, either in the gas phase or in the solid state (Tables 1 and 2)^{15,26}. In peroxides of the type R¹–O–O–R² (for R¹, R² = alkyl, aryl, vinyl, alkynyl) a progressive increase of the peroxide dihedral angle with the steric demand of R¹ and R² is observed (Table 2).

3. Orbital effects

In peroxides of the type X–O–O–Y, the O–O bond length is inversely correlated with the X–O and the O–Y distance. For example, in F₂O₂, the F–O bond measures 1.575 Å, which is longer than the F–O distance of 1.41 Å in F₂O. The O–O bond (1.217 Å), on the other hand, is considerably shorter than the standard value of 1.453 Å in H₂O₂⁵². A further peculiarity of F₂O₂ is associated with an experimental barrier of 126 kJ mol⁻¹ for rotation about the O–O bond. This number exceeds the bond dissociation energy of 84 kJ mol⁻¹ for cleavage of the F–O bond according to the sequence FOOF → FOO• + F•^{52,53}. These effects may be explained by taking hyperconjugation between a lone pair at oxygen (n) and the σ* orbital of the F–O bond into account. This interaction raises the O–O bond order, while the strength of the F–O connectivity is reduced. The net effect of the n → σ*_{X–O} and/or n → σ*_{Y–O} interaction is associated with a lowering of the electron population in the non-bonding orbitals at O thus reducing electrostatic repulsion between these entities (Figure 8 and Table 3). The computed stabilization energy originating from this type of hyperconjugation increases along the sequence CH₃OOCH₃ (**5**) (4.2 kJ mol⁻¹), CH₃OOH (**2**) (8.9 kJ mol⁻¹) to CF₃OOCF₃ (**12**) (9.0 kJ mol⁻¹, all values B3LYP)⁹. The

TABLE 2. Geometric parameters of selected peroxides R¹–O–O–R²

Entry	Compound	(H ₅ C ₆) ₃ COOH		(H ₅ C ₆) ₃ COOC(C ₆ H ₅) ₃		Reference
		(8)	(9)	O–O (Å)	R ¹ –O–O–R ² (°)	
1	–	H	H	1.453	90.2 ^a , 120 ^b	15, 26
2	2	CH ₃	H	1.443	114 ^b	46
3	1	C(CH ₃) ₃	H	1.472	95 and 114 ^{a, c}	47
4	8	C(C ₆ H ₅) ₃	H	1.455	100.8 ^a	48
5	5	CH ₃	CH ₃	1.457	119 ^d	49
6	6	C(CH ₃) ₃	C(CH ₃) ₃	1.478	164.0 ^a	50
7	9	C(C ₆ H ₅) ₃	C(C ₆ H ₅) ₃	1.480	180 ^a	51

^a X-ray analysis.

^b Microwave spectroscopy.

^c Two independent molecules.

^d Electron diffraction.

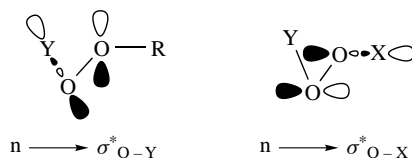
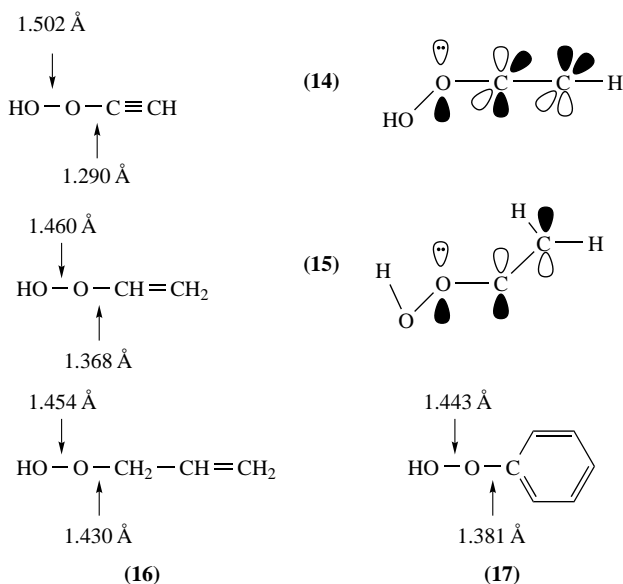


FIGURE 8. Hyperconjugation between the lone pairs at O and the σ*_{X–O} and σ*_{Y–O} orbitals^{9,52}

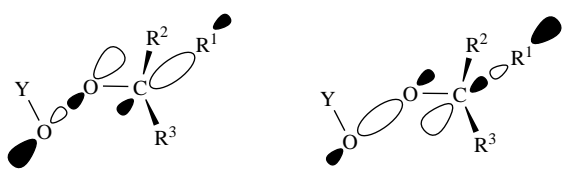
TABLE 3. Geometric parameters of substituted peroxides X–O–O–Y (electron diffraction)

Entry	F ₃ COOF		F ₃ COOCl	F ₃ COOCF ₃	F ₃ C–O–O–NO ₂		Reference	
	(10)	(11)	(12)	(13)	(13)	(13)		
	X	Y	Compd.	O–O (Å)	X–O (Å)	Y–O (Å)	X–O–O–Y (°)	
1	CH ₃	CH ₃	5	1.457	1.420	1.420	119	49
2	CF ₃	H	3	1.447	1.376	0.974	95	54
3	CF ₃	F	10	1.366	1.419	1.449	97	54
4	CF ₃	Cl	11	1.447	1.372	1.699	93	54
5	CF ₃	CF ₃	12	1.419	1.399	1.399	123	55
6	CF ₃	NO ₂	13	1.414	1.378	1.523	105	56

FIGURE 9. The effect of π -type interactions on C–O and O–O distances in alkynyl, vinyl and phenyl hydroperoxide **14–17**.⁵⁷

most efficient $n \rightarrow \sigma^*_{X-O}$ and $n \rightarrow \sigma^*_{Y-O}$ overlap is attainable in the *gauche* conformer. This arrangement is therefore consistently associated with the shortest O–O bond of all rotamers [for CF₃OOCF₃: O–O = 1.47 Å at C–O–O–C = 0°, 1.44 Å at 80° and 1.46 Å at 180°; C–O: 1.39 Å for C–O–O–C = 0°, 1.40 Å for 80° and 1.39 Å for 180°; B3LYP].

A π -type interaction between the lone pair at O and a π^* -orbital of a peroxide bound aryl, alkenyl or alkynyl substituent may lead to a shortening of the associated C–O bond (Figure 9). This model has been applied in order to explain the unusually short C–O distance of 1.290 Å, which has been calculated for ethynyl hydroperoxide (**14**)

TABLE 4. Tetrahedral distortion in the peroxide bound alkyl substituent⁹


Entry	Compd.	R ¹ R ² R ³ C	Y	R ¹ -C-O (°)	R ² -C-O (°)	R ³ -C-O (°)	Reference
1	1	(H ₃ C) ₃ C	H	101.7	109.3	111.6	47
2	6	(H ₃ C) ₃ C	C(CH ₃) ₃	100.6	109.1	112.5	50
3	8	(H ₅ C ₆) ₃ C	H	103.9	107.4	110.1	48
4	9	(H ₅ C ₆) ₃ C	C(C ₆ H ₅) ₃	99.5	109.9	110.6	51

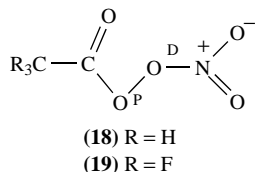
(B3LYP)⁵⁷. Theory predicts an O–O bond dissociation energy of 30 kJ mol⁻¹ for the latter compound. This value suggests that homolysis of the peroxide bond occurs upon rotation thus leading to the generation of a ketyl and a hydroxyl radical. In a similar way, vinyl hydroperoxide (**15**) and phenyl hydroperoxide (**17**) exhibit smaller calculated C–O distances than allyl hydroperoxide (**16**) because the $n \rightarrow \pi^*$ overlap is no longer possible in the latter case (Figure 9, B3LYP).

A common structural motif in peroxides of the type R₃C–O^P–O^D–Y (R = alkyl, aryl, fluorine, Y = R₃C or H) is a marked distortion of the R₃C fragment from tetrahedral geometry. The R–C bond, which is located in the C–O^P–O^D plane, exhibits the smallest of the three R–C–O angles (Table 4)^{9,50}. This tetrahedral distortion has been interpreted, on the basis of an electron population analysis, with a $\sigma_{R-C} \rightarrow \sigma^*_{O-O}$ and/or $\sigma_{O-O} \rightarrow \sigma^*_{R-C}$ hyperconjugation.

Acetyl peroxyhydrate (**18**) and perfluoroacetyl peroxyhydrate (**19**), two important atmospheric oxidation products of hydrocarbons (formation of **18**) or chlorofluorocarbon replacements, such as CF₃CH₃ (formation of **19**), preferentially adopt a *gauche* conformation (C–O–O–N = 84.7° for **18** and 85.8° for **19**; electron diffraction)⁵⁸. The two peroxides are characterized by comparatively short O–O bonds on one side and long O^D–N connectivities (Table 5) on the other. The observed O^D–N distances may be explained on the basis of an $n_{O^P} \rightarrow \sigma^*_{O^D-N}$ orbital overlap. This type of interaction lowers the O^D–N bond order and could explain the low bond dissociation energies of this connectivity in peroxides **18** and **19** (118 ± 4 kJ mol⁻¹ for both compounds). It should be noted that this interpretation does not reflect a possible π -type interaction between a lone pair at O^D and virtual orbitals of the nitro group and therefore requires future investigation.

4. Hydrogen bonding

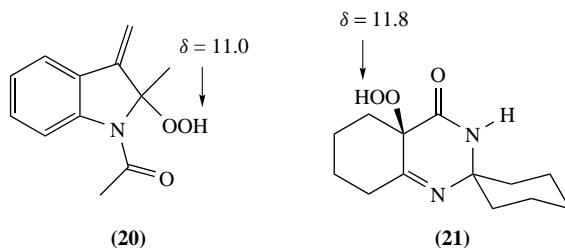
Alkyl hydroperoxides, which lack additional functional groups, prefer intermolecular to intramolecular hydrogen bonding⁵⁹. Neat cumene hydroperoxide, for example, forms a cyclic six-membered hydrogen-bridged dimer, in which the O^P atom serves as acceptor for the hydroperoxide proton. In CCl₄ solution, the π -electrons of the aromatic subunit act as an acceptor for the OH proton. The strength of a hydrogen bond between solvent molecules and cumene hydroperoxide gradually increases along the series CHCl₃ <

TABLE 5. Geometric parameters for acetyl peroxyhydrate (**18**) and perfluoroacetyl peroxyhydrate (**19**) (electron diffraction)⁵⁸

Entry	Compound	O–O (Å)	C–O (Å)	O ^D –N (Å)	O–O–C (°)	C–O–O–N (°)
1	18	1.418	1.395	1.492	107.3	84.7
2	19	1.408	1.360	1.526	107.6	85.8

$C_6H_6 < CH_3NO_2 < \text{anisole} < \text{benzophenone} < CH_3CN < \text{di}(tert\text{-butyl})\text{peroxide}$ (**6**) < acetone < dioxane < diethyl ether (IR spectroscopy). ¹H NMR chemical shifts provide a more qualitative approach for analyzing the effect of hydrogen bonding between the hydroperoxide proton and solvent molecules. 1-Acetyl-2-hydroperoxy-2-methyl-3-methyleneindoline (**20**) (Figure 10), for example, exhibits in acetone solution a sharp resonance for the OOH proton at 11.0, which is indicative of hydrogen bonding with the carbonyl O of solvent molecules. In CDCl₃ or CD₂Cl₂ the OOH signal is broad and ranges from 8.2 to 10.0 ppm, depending on the concentration, which is indicative of intermolecular hydrogen bonding between molecules of hydroperoxide **20**⁶⁰. Dimethyl sulfoxide is another solvent that interacts strongly with the hydroperoxy group, thus leading to a marked downfield shift of the OOH signal in ¹H NMR spectra of alkyl hydroperoxides, for instance to 11.8 ppm in 5', 6', 7', 8'-tetrahydro-4a'-hydroperoxyspiro[cyclohexane-1, 2'(2'H)-quinazoline]-4'(3'H)-one (**21**)⁶¹.

Peracids prefer a *synperiplanar* to a *gauche* or even an *antiperiplanar* arranged equilibrium structure in the liquid and the gas phase⁶². A *synperiplanar* geometry is the prerequisite for formation of a comparatively strong intramolecular hydrogen bond of 25–30 kJ mol⁻¹ with the C=O group. This obviously compensates the effects of lone pair repulsion and hyperconjugation that otherwise would favor the *gauche* rotamer. The relevance of the cyclic hydrogen-bonded structure is noted in a lower acid strength of, e.g. peracetic acid (pK_a = 8.2) in comparison to acetic acid (pK_a = 4.75)^{21,23}. Unlike their carboxylic acid derivatives, peracids exist in solution *and* in the gas phase preferentially as monomers (Figure 11a,b). If aggregation occurs, the Swern dimer (Figure 11c) is disfavored with respect to a macrocyclic alternative, because in the former case the peroxidic oxygen and in the latter the carbonyl group serves as H-bond acceptor^{63,64}.

FIGURE 10. ¹H NMR chemical shifts of hydroperoxides **20** in (CD₃)₂CO and **21** in (CD₃)₂SO^{60,61}

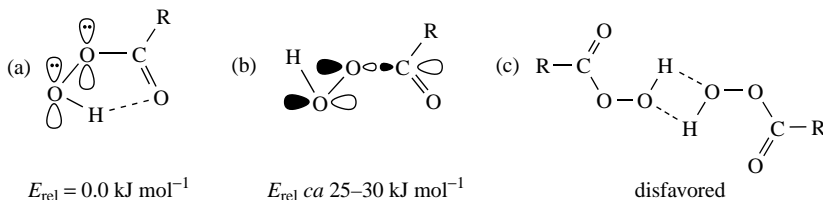


FIGURE 11. Hydrogen bonding (a) versus hyperconjugation (b) in peracids and a disfavored mode of hydrogen bonding (c)^{62–64}

In X-ray diffraction studies, hydrogen atoms are frequently difficult to locate. In case of solid state structures of peracids, the majority of information about hydrogen bonding therefore originates from an analysis of non-bonded O...O distances. A separation between O^D of the peracid functionality and a heavy atom from an accepting unit that falls below the sum of the corresponding van der Waals radii is indicative of a hydrogen bond between these entities⁶⁵. The majority of likewise investigated structures points to either *gauche* or *antiperiplanar* arranged C(O)OOH groups.

5. Conclusion

Acyclic organic peroxides are characterized by an O–O single bond with a mean distance of $1.45 \pm 0.02 \text{ \AA}$. Conformational preferences of the peroxide functionality are guided by the necessity to lower repulsive interactions between the four lone pairs at the O atoms thus leading to a preference for the *gauche* arrangement on the basis of electrostatic and hyperconjugative interactions. In bulky dialkyl peroxides, the release of strain may favor the *antiperiplanar* conformation, while peracids that form strong intramolecular H bonds tend to favor the *synperiplanar* geometry in the liquid and the gas phase.

III. ORGANIC PEROXY COMPOUNDS

More than 200 structures from X-ray diffraction studies of acyclic organic peroxides have been disclosed in the literature since 1983. Structural information prior to 1983 was reviewed in an earlier book chapter¹⁴ and therefore has been omitted from this synopsis. Emphasis has been laid on a documentation of the most important structural information. The survey, however, remained incomplete since a considerable number of structures had been disclosed in the literature and/or the CSD database⁶⁶ without providing the associated atomic coordinates. Further, structures with unusually short or long O–O connectivities have been omitted from the statistics for the reasons outlined in Section II.

A. Alkyl Hydroperoxides

A survey of crystal structures of 66 alkyl hydroperoxides (Table 6, Sections II and V) provided a mean O–O bond length of $1.46 \pm 0.01 \text{ \AA}$ (mean value \pm standard deviation) and an O–O–C angle of $108 \pm 1.5^\circ$ (mean value \pm standard deviation). The torsion angle H–O–O–C was reported for 54 structures and varied between 169.9° and 11.8° (Table 6, entries 9 and 37). The geometric parameters at the O–O bond in alkyl hydroperoxides follow the guidelines for structure and bonding that have been disclosed in Section II. The aspects of tetrahedral distortion, the anomeric effect and hydrogen bonding, however, deserve a comment.

TABLE 6. Geometric parameters of alkyl hydroperoxides at the peroxide bond

Entry	Compound name (CSD code)	O-O [Å]	C-O [Å]	C-O-O-H [°]	Reference
<i>Aliphatic hydroperoxides</i>					
1	{(4 <i>R</i> ,5 <i>R</i>)-[(Hydroperoxydiphenylmethyl)-2,2-dimethyl-1,3-dioxolan-4-yl]diphenylmethanol (QEDTEY)}	1.466	1.431	128.6	67
2	19-(Hydroperoxymethyl)-4 β ,5-epoxy-2-oxa-5 β ,10 α -androstan-3,17-dione (GAKFIH)	1.465	1.439	111.8	68
3	2-Azido-6,6-dimethylbicyclo[3.1.1]heptane-2-hydroperoxide (22) (VIQGOR)	1.459	1.452	103.3	69
4	2,5-Dimethyl-2,5-dihydroperoxyhexane (23) (XINFAB)	1.470	1.454	110.6	70
<i>Allylic hydroperoxides</i>					
5	1-Hydroperoxy-3-isopropyl-2-methylenecyclohex-4-ene-3-carboxylic acid (TECWON)	1.460	1.440	73.7	71
6	Aristolane (DAWCAF10)	1.453	1.447	96.6	72
7	8-Desacetoxy-11 β H,13-dihydroperoxyferolide (NUBDIX)	1.463	1.458	158.5	73
8	Dihydrochysanolide hydroperoxide (BUSYAP)	1.477	1.457	- ^a	74
9	<i>cis</i> -3,4 <i>a</i> ,5,7 <i>a</i> -Tetrahydro-6,7 <i>a</i> -diphenylcyclopental [1,2- <i>e</i>]-1,2,4-trioxin-5 β -yl hydroperoxide (24) (FEXYOW10)	1.466	1.409	169.9	75
10	5,6,7,8-Tetrahydro-6-hydroxy-8-hydroperoxy-2,2,6,8-tetramethyl-7-methylenecyclohexan-5-one (25) (YAWXOJ)	1.472	1.450	134.6	76
11	1-Hydroperoxy-8-[<i>tert</i> -butyl(dimethyl)siloxy]bicyclo[4.4.1]undeca-2,5-diene-4,11-dione (CADGAP)	1.453	1.430	- ^a	77
12	(3 <i>aR</i> ,4 <i>aS</i> ,8 <i>aR</i> ,9 <i>aR</i>)-Decahydro-4 <i>a</i> -hydroperoxy-8 <i>a</i> -methyl-3,5-dimethylenenaphtho[2,3- <i>b</i>]furan-2(3 <i>H</i>)-one (CHIZEY)	1.464	1.447	- ^a	78
13	1-Hydroperoxy-5-hydroxy-1,3,6,8-tetra- <i>tert</i> -butylphenanthren-4(1 <i>H</i>)-one (GEMDIL)	1.418	1.467	- ^a	79
14	10 β -Hydroperoxyestr-4-ene-3,17-dione (CUHZAG)	1.460	1.444	- ^a	80
<i>Benzyl hydroperoxides</i>					
15	10-Hydroperoxy-9-anthrone (<i>Z</i>)-1,2-di-9-anthrylethene-1,2-diyl acetal (PEPDOD)	1.445	1.357	- ^a	81
16	α -(9-Anthryloxy)-9-hydroperoxy-10-methylene-9,10-dihydroanthracene diethyl ether solvate (PEPDUJ)	1.453	1.451	103.4	82
<i>Propargyl hydroperoxides</i>					
17	1-Ethynyl-4-hydroperoxy-1,2,3,4-tetrahydro-1-naphthol (VUYXES)	1.476	1.455	126.4	83
18	2,5-Dimethyl-2,3-dimethylhydroperoxyhex-3-yne (XINFEE)	1.454	1.449	115.9	70

19	<i>N-Heterocyclic hydroperoxides</i>						
20	3-(1-Hydroperoxy-2-phenylallyl)-4-isopropylloxazolidin-2-one (WUKFAJ)	1.465	1.412	104.6	84		
21	1-Acetyl-2-hydroperoxy-2-methyl-3-methyleneindoline (20) (EABNIE)	1.465	1.413	107.2	60		
22	2,4,5-Triphenyl-4 <i>H</i> -imidazol-4-yl hydroperoxide (FUJYOY)	1.464	1.418	90.7	85		
23	5,6-Dihydro-6-hydroperoxy-5-hydroxy-2,4(1 <i>H</i> ,3 <i>H</i>)-pyrimidinedione (FUFDIH)	1.451	1.394	105.8	86		
24	<i>rac</i> -4-Hydroperoxy- <i>trans</i> -5-hydroxy-4-methylimidazolidin-2-one (BOBHOV)	1.470	1.439	113.0	87		
25	<i>cis</i> -3-(2-Chloroethyl)-2-[(2-chloroethylamino)4-(hydroperoxy)tetrahydro-2 <i>H</i> -1,3,2-oxazaphosphorin-2-one (BUWTES)	1.462	1.442	- ^a	88		
26	3,4,4 <i>a</i> ,5,6,7,8,8 <i>a</i> -Octahydro-8 <i>a</i> -hydroperoxy-2-quinolone (NUNJEL)	1.460	1.442	95.6	89		
27	5-Hydroperoxy-2,4,4,6-tetraphenyl-4,5-dihydropyrimidine (ZEDLOY)	1.458	1.435	- ^a	90		
28	2-(Trimethylsilyl)-3-methyl-3 <i>H</i> -benzof[imidol-3-yl]hydroperoxide (26) (TABLUD)	1.453	1.429	78.8	91		
29	5,5-Bis(2-hydroperoxy-2,2-diphenylethyl)barbituric acid ethanol solvate (EACJIB)	1.450	1.446	102.1	92		
30	5',6',7',8'-Tetrahydro-4 <i>a</i> -hydroperoxy Spiro(cyclohexane-1,2'(2' <i>H</i>)-quinazoline)-4'(3' <i>H</i>)-one (21) (DORHUN)	1.463	1.430	- ^a	61		
31	<i>S,N-Heterocyclic hydroperoxides</i>						
32	<i>rac</i> - <i>cis</i> -2-(2,6-Dichlorophenyl)-2,3,4,5,6,7-hexahydro-3-hydroperoxy-1,2-benzisothiazole 1-oxide (27) (BANGEC)	1.458	1.421	102.7	93		
33	2-(4'-Bromophenyl)-3-hydroperoxy-2,3,4,5,6,7-hexahydro-1,2-benzisothiazole-1,1-dioxide (ZUKPOK)	1.479	1.404	60.0	94		
34	2-(2,5-Dichloro-4-isopropylloxyphenyl)-3-hydroperoxy-2,3,4,5,6,7-hexahydro-1,2-benzisothiazole 1,1-dioxide (XUXHUT)	1.474	1.405	122.1	95		
35	1-Benzoylamino-8 <i>a</i> -hydroperoxy-1,5,6,7,8,8 <i>a</i> -hexahydro-(4 <i>H</i>)-cyclohepta[<i>c</i>]isothiazole 2,2-dioxide (NEMWIL)	1.461	1.430	84.9	96		
36	2,3-Dihydro-4,5-dimethyl-3-(hydroperoxy)-2-[4-(methoxycarbonyl)phenyl]isothiazole 1,1-dioxide (AFUPOG)	1.461	1.417	106.6	97		
37	<i>rac</i> -Methyl 4-(<i>cis</i> -2,3-dihydro-3-hydroperoxy-4,5-dimethyl-1-oxoisothiazol-2-yl)benzoate (IDUKAT)	1.458	1.426	100.6	98		

(continued overleaf)

TABLE 6 (continued)

Entry	Compound name (CSD code)	O—O [Å]	C—O [Å]	C—O—O—H [°]	Reference
<i>Hydroperoxyacetals</i>					
36	1-Hydroxy-2-bromocyclohexyl hydroperoxide (28) (XAHPOL)	1.473	1.423	104.4	99
37	Methyl 2-(2-hydroperoxy-2,4,4-triphenyl-3-oxetanylidene)acetate (MIWPEN)	1.471	1.400	11.8	100
38	12-Hydroperoxy-8 α ,12-epoxy-11-homodrimane (ROQQOD)	1.454	1.429	111.9	101
39	4-Methoxy-4-methyl-2,3-dioxabicyclo[3.3.1]nonyl hydroperoxide (RALZOT)	1.464	1.416	89.6	102
40	<i>cis</i> -4-Nitrobenzaldehyde oxime <i>O</i> -(2,5-dihydro-5-hydroperoxy-2-methoxy-3-(methoxycarbonyl)-5-(3-methoxyphenyl)-2-furyl) ether (BEYQUR)	1.461	1.413	55.7	103
41	1-Hydroxy-1'-hydroperoxydicyclohexyl peroxide (SEGDIR)	1.465	1.427	96.2	104
42	9-Methylamino-1 <i>H</i> -phenalen-1-one (1,4-dioxan-2-yl hydroperoxide) solvate (29) (SOYFIV)	1.461	1.410	107.7	105
43	3-Hydroperoxy-3-phenyl-3,4-dihydro-1 <i>H</i> -2-benzopyranone (LINWEK)	1.463	1.417	101.2	106
44	(1 α ,3 α ,4 α)-3,4-Dihydro-1-methoxy-3,4-diphenyl-1 <i>H</i> -2-benzopyran-3-yl hydroperoxide (EABPAY)	1.465	1.428	123.7	107
45	8 α -Hydroperoxy-2,2,5,7,8-pentamethylchroman-6(8 <i>aH</i>)-one (30) (FENWUQ)	1.458	1.483	114.7	108
46	3,4-Dihydro-3-trifluoroethoxy-4- <i>tert</i> -butyl-1 <i>H</i> -2-benzopyran-yl hydroperoxide (31) (ZELMAE)	1.461	1.440	93.9	109
47	1-Methoxy-1,3,4-triphenyl-3-hydroperoxyisochroman (VAMPOO)	1.458	1.415	118.4	110
48	4-Chloro-3-hydroperoxy-1-methoxy-1,3-diphenylisochroman (GIGKOW)	1.461	1.427	110.2	111
49	1-Methoxy-4-methyl-3-peroxy-1,3-diphenylisochroman (CAWYII)	1.466	1.424	— ^a	112
50	1,3-Diphenyl-1-methoxy-3-hydroperoxyisochroman (JIMHES)	1.463	1.418	121.8	113
51	3 β -Acetoxy-5 α -hydroperoxy-7 α -isopropoxy-5 α -B-homo-6-oxacholestane (NOQBAAW)	1.450	1.412	74.7	114
52	3 β -Acetoxy-5 α -hydroperoxy-7 α -methoxy-5 α -B-homo-6-oxaandrostane (NOQBBA)	1.464	1.428	85.4	114
53	<i>Bis</i> (<i>hydroperoxy</i>)acetals [1,2-Bis(diphenylphosphonyl)ethane] bis(2,2-dihydroperoxypropane) (32) (XAHMIC)	1.464	1.429	96.8	115
		1.458		86.6	

54	5 β -Cholestane-3 α ,3 β -dihydroperoxide (RIHTEH)	1.444 1.443 1.454 1.463	1.440 1.428 1.420 1.427	- ^a - ^a 76.0 104.9	116 117
55	2-[4,4-Bis(hydroperoxy)hexyl]phenol (33) (MALSUN)				
	<i>Miscellaneous alkyl hydroperoxides</i>				
56	(Z)-1-Hydroperoxy-N-[(Z)-3-(methoxycarbonyl)-2-propenylidene] cyclohexylamine N-oxide (RAYMOT)	1.462	1.399	125.1	118
57	Sodium [pyridoxylidene- α -(hydroxyphenyl)alaninato](pyridoxylidene- α - hydroperoxyphenyl)alaninato)cobaltate(III) (PONPEN)	1.438	1.398	- ^a	119

^aNot reported.

1. Structural aspects

Three examples serve to document the effect of tetrahedral distortion in peroxides, in which the O–O unit is connected to an acyclic or to a cyclic framework^{9,50}. 2,5-Dimethyl-2,5-dihydroperoxyhexane (**23**) ($C2/c$, O–O = 1.47 Å, C–O–O–H = 110.6°, Figure 12) exhibits in the solid state two larger and one smaller O–C–C angle (O–C1–C2 = 101.3°, O–C1–C3 = 110.5° and O–C1–C4 = 110.7°), similar to the situation outlined for *tert*-butyl hydroperoxide (**1**) and triphenylmethyl hydroperoxide (**8**) (Table 4)⁷⁰. Comparable distortions are observed for the peroxide bound C atoms in 1-hydroxy-2-bromocyclohexyl hydroperoxide (**28**) ($P\bar{1}$, O–O = 1.47 Å, C–O–O–H = 104°, Figure 12) and the bis(hydroperoxy) acetal **33** in the solid state ($P2_12_12_1$, O–O = 1.454 Å, C–O–O–H = 104.9 and 76.0°; O–C1–C2 = 102.7°, O–C1–C3 = 113.1°, O–C1–O = 109.8°, Figure 12)¹¹⁷. In the former case, the endocyclic angle O2–C1–C6 = 103.6° is markedly smaller than the angles O2–C1–C2 = 112.5° and O1–C1–O2 = 110.4°⁹⁹.

2. The anomeric effect

The hydroperoxy functionality in α -position to an endocyclic O atom, such as in the 2-hydroperoxy 1,4-dioxane subunit of the aggregate **29** ($P\bar{1}$, O–O = 1.461 Å, C–O–O–H = 104°, Figure 13)¹⁰⁵, prefers the axial to the equatorial position. In the former case, one of the lone pairs of the endocyclic O atom and the σ^* -orbital of the

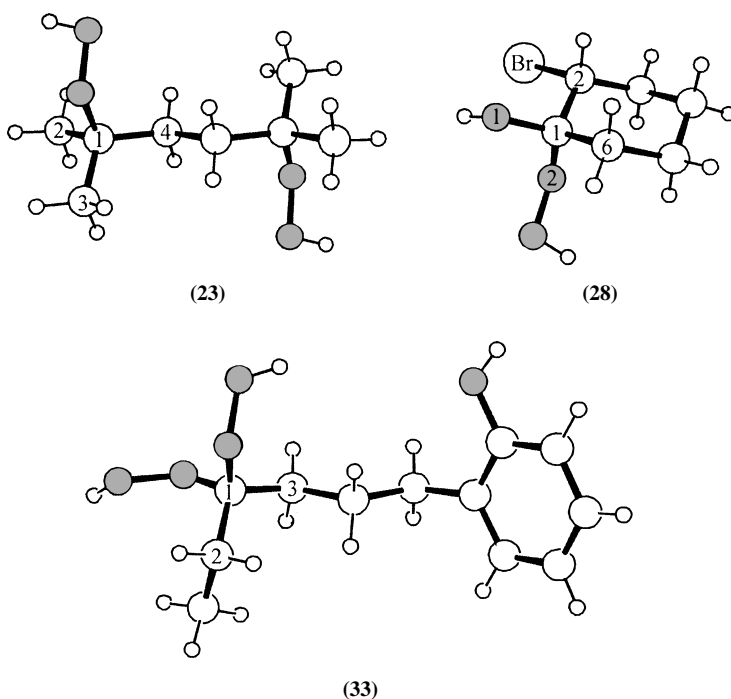


FIGURE 12. Geometries of alkyl hydroperoxides **23**, **28** and **33** in the solid state (ball and stick presentation with the O atoms depicted in gray)^{70,99,117}

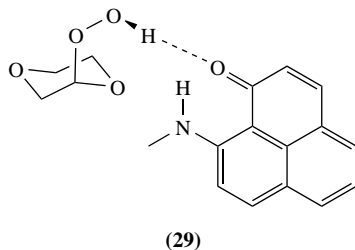


FIGURE 13. The geometry of 9-methylamino-1*H*-phenalen-1-one (1,4-dioxan-2-yl hydroperoxide) solvate (29) in the solid state¹⁰⁵

exocyclic C–O bond are in coplanar arrangement, thus stabilizing the conformer with the axial positioning of the hydroperoxide functionality due to favorable stereoelectronic effects.¹²⁰

3. Hydrogen bonding

The packing of alkyl hydroperoxide molecules is determined by their shape and a variety of intermolecular forces such as hydrogen bonding. The OOH entity either serves as proton donor (O–H) or as acceptor (A). Localization of the hydroperoxide H atom in crystal structures is feasible, either directly from the difference Fourier map, or indirectly, if, e.g., O–O⋯O or O–O⋯N distances fall below the sum of the van der Waals radii of two O atoms (3.04 Å) or one O and one N atom (3.07 Å, Table 7)^{65,121}. The majority of likewise determined hydrogen bonds refer to intermolecular connectivities, which are characterized by O–H⋯A angles between 145–178° and O–O⋯O or O–O⋯N distances that range between 2.66–2.97 Å in the former and 2.74–2.94 Å in the latter case. According to a general guideline, intermolecular O⋯O and O⋯N distances of this magnitude point to predominantly electrostatic interactions with strengths between 17–63 kJ mol⁻¹¹²¹.

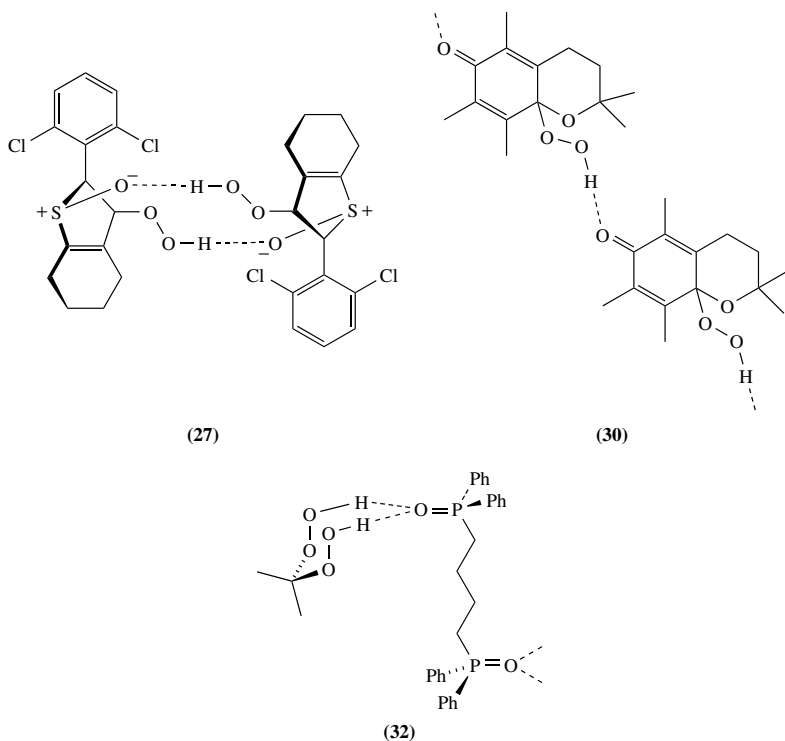
The largest number of hydrogen bonds in crystal structures of alkyl hydroperoxides refer to intermolecular bonds between the hydroperoxide proton and functionalities of the type O=X, where X denotes a sulfur (e.g. 27), carbon (e.g. 30) or a phosphorous atom (e.g. 32, Figure 14, Table 7)^{93,108,115}. The geometry of [1,2-bis(diphenylphosphinoyl)ethane] bis(2,2-dihydroperoxypropane) (32) in the solid state is a rare example of a bifurcated hydrogen bond between an OOH donor and an O=X proton acceptor.

The second largest number of hydrogen bonds in crystal structures of alkyl hydroperoxides refers to interactions of the type OO–H⋯OR¹R², where R¹ is an alkyl group and R² denotes H, alkyl or R¹O. The OO⋯OR¹R² distances vary between 2.67–2.91 Å and the associated O–H⋯O angles range from 152 to 177°. In some compounds, formation of intramolecular hydrogen bonds of the type OO–H⋯O=X would in principle have been feasible. The number of examples documented in the literature so far is clearly in favor of the intermolecular type of H bonding.

In *cis*-3,4*a*,5,7*a*-tetrahydro-6,7*a*-diphenylcyclopenta[1,2-*e*]-1,2,4-trioxin-5β-yl hydroperoxide (24) (*P*2₁/*c*, O⋯O = 2.87 Å, O⋯H = 1.99 Å, O⋯H–O = 172°), hydrogen bonding occurs between the OOH proton and the ether O (Figure 15). On the basis of p*K*_{HB} data alone, an association via the endoperoxide entity of the molecule would have been expected^{22,75}. The affinity for H-bond formation toward ether O atoms is documented in the number of cocrystallization adducts between ether molecules and alkyl

TABLE 7. Parameters associated with hydrogen bonds of the type $O^P O^D - H \cdots A$ in the solid state

Entry	A	$O^D \cdots A$ (Å)	$O^D - H \cdots A$ (°)	Reference
	O=C			
1	ketone	2.66–3.01	162–177	72, 77, 79
2	carboxylic acid	2.68	162	71
3	lactone	2.71–2.97	150–171	68, 73, 74
4	amide	2.67–2.75	164–166	84
5	urea	2.81	157	92
6	urethane	2.72	175	60
	O=S			
7	sulfoxide	2.68–2.83	147–175	93, 98
8	sulfone	2.78	145–155	94, 97
	O=P			
9	phosphinoxide	2.76–2.82	172–173	115
10	phosphamide	2.75	175	88
	–O–			
11	peroxide	2.68–2.96	152–177	76, 102, 117
12	alcohol	2.67–2.81	152–174	83
13	ether	2.68–2.87	156–172	75, 81
	–N=			
14	heterocycle	2.77–2.81	168–177	85
15	oxime	2.94	155	103
16	azide	2.84	170	69

FIGURE 14. Intramolecular hydrogen bonds: the carbonyl, sulfoxide and phosphine oxide group as acceptor for the hydroperoxide proton^{93, 108, 115}

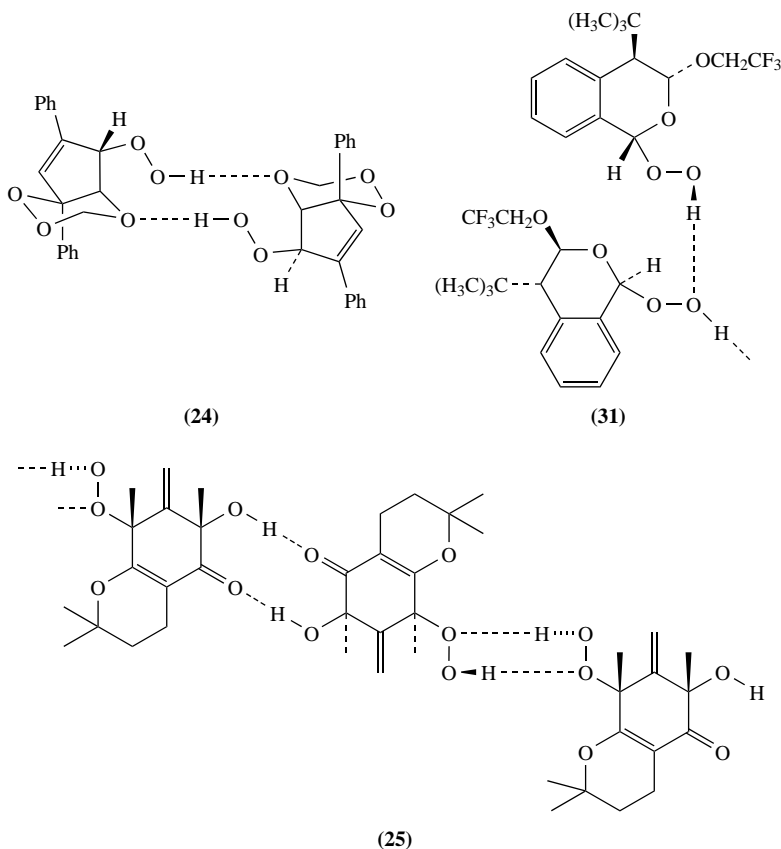


FIGURE 15. Intramolecular hydrogen bonds of the type $\text{OO-H}\cdots\text{OR}^1\text{R}^2$ ($\text{R}^1 = \text{alkyl}$, $\text{R}^2 = \text{H}$, alkyl, RO)^{75, 76, 109}.

hydroperoxides, such as in α -(9-anthroyl)- α -(9-anthryloxy)-9-hydroperoxy-10-methylene-9,10-dihydroanthracene diethyl ether solvate ($P\bar{1}$, $\text{O}\cdots\text{O} = 2.69 \text{ \AA}$, $\text{O}\cdots\text{H} = 1.77 \text{ \AA}$, $\text{O}\cdots\text{H}-\text{O} = 156^\circ$, Table 6, entry 16)⁸².

A rare example of H-bond formation between the OOH proton and the proximal O atom of a hydroperoxide group as acceptor is observed in 5,6,7,8-tetrahydro-6-hydroxy-8-hydroperoxy-2,2,6,8-tetramethyl-7-methylenechroman-5-one (**25**) ($P\bar{1}$, $\text{O}\cdots\text{O} = 2.96 \text{ \AA}$, $\text{O}\cdots\text{H} = 2.12 \text{ \AA}$, $\text{O}\cdots\text{H}-\text{O} = 160^\circ$)⁷⁶. This mode of binding is reminiscent of the self-aggregation of cumene hydroperoxide molecules in the liquid phase⁵⁹. The distal O atom of the OOH group is the accepting unit in the crystal structure of 3,4-dihydro-3-trifluoroethoxy-4-(*tert*-butyl)-2(1*H*)-benzopyranlyl hydroperoxide (**31**) ($P2_1/a$, $\text{O}\cdots\text{O} = 2.76 \text{ \AA}$, $\text{O}\cdots\text{H} = 2.13 \text{ \AA}$, $\text{O}\cdots\text{H}-\text{O} = 152^\circ$)¹⁰⁹. In a similar way hydrogen bonds between the OOH functionality and an endoperoxide O atom have been observed, such as in the crystal structure of the antimalaria active compound 4-methoxy-4-methyl-2,3-dioxabicyclo[3.3.1]nonyl hydroperoxide ($P2_1/c$, $\text{O}\cdots\text{O} = 2.86 \text{ \AA}$, $\text{O}\cdots\text{H} = 2.02 \text{ \AA}$, $\text{O}\cdots\text{H}-\text{O} = 176^\circ$, Table 6, entry 39)¹⁰².

Functionalities of the type $R^1-N=R^2$ that are present in unsaturated *N*-heterocycles, oximes or azides constitute the third important class of hydrogen-bond acceptors for the hydroperoxy group. This type of aggregation has been reported so far in 4 crystal structures. The observed $OO\cdots NR^1R^2$ distances range from 2.77 to 2.94 Å, while the associated $O-H\cdots N$ angles vary between $155-177^\circ$. In 2-azido- β -pinene-2-hydroperoxide (**22**, Figure 16), the carbon bound N atom of the azide group serves as acceptor for the OOH proton (P_{21} , $O\cdots N = 2.84$ Å, $H\cdots N = 2.05$ Å, $O-H\cdots N = 170^\circ$)⁶⁹. Association of 2-(trimethylsilyl)-3-methyl-3*H*-benz[*f*]indol-3-yl hydroperoxide (**26**) in the solid state occurs via the heterocyclic N atom as accepting unit for the hydroperoxide proton (P_{21} , $O\cdots N = 2.76$ Å, $H\cdots N = 1.90$ Å, $O-H\cdots N = 168^\circ$)⁹¹.

B. The Alkyl Hydroperoxide Anion as Ligand

A survey of crystal structures of 29 compounds (Table 8), in which the alkyl hydroperoxide anions serves as ligand to metal ions, transition metal ions or group 13–17 elements, provides a mean $O-O$ bond length of 1.46 ± 0.03 Å, an $O-O-C$ angle of $109 \pm 2.1^\circ$ and a $M-O-O$ angle of $112 \pm 6.9^\circ$. More specialized aspects that deserve to be addressed separately refer to the nature of the $M-O$ bond, the magnitude of the dihedral angle $M-O-O-C$ and the tetrahedral distortion of the peroxide bound C atom.

1. Covalent radii versus experimental $M-O$ bond lengths

The experimentally observed $(M-O)_{\text{exp}}$ distances fall into three categories, if compared to the sum of covalent radii $(M-O)_{\text{cov}}$ based on values from a CSD recommendation (Table 9)⁶⁵: (i) $(M-O)_{\text{exp}}$ values that fall short of $(M-O)_{\text{cov}}$, (ii) $(M-O)_{\text{exp}}$ distances that are longer than $(M-O)_{\text{cov}}$ and (iii) $(M-O)_{\text{exp}}$ data that fit $(M-O)_{\text{cov}}$.

(i) Bonds between the distal O atom of the *tert*-butylperoxy ligand and the transition metal ions Cu(II), Hf(IV), and to some extent Co(III) and Ti(IV), are shorter than

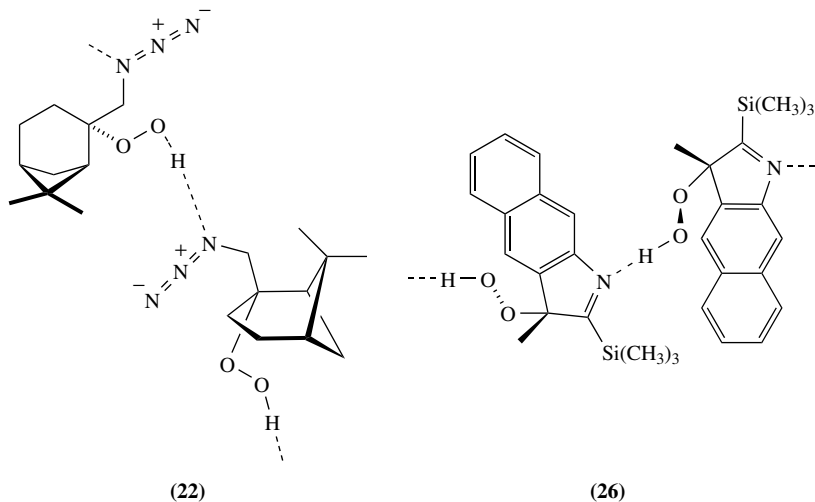


FIGURE 16. The formation of intramolecular hydrogen bonds: nitrogen functionalities as acceptor for the hydroperoxide proton^{69,91}

TABLE 8. Geometric parameters for the M–O–O–C entity

Entry	Compound name (CSD code)	O–O (Å)	C–O (Å)	M–O–O–C (°) ^a	Reference
<i>Group 1</i>					
1	Dodecakis(μ^3 - <i>tert</i> -butylperoxy)lithium (34) (NADCUQ)	1.457 1.477	1.440 1.471	– ^b	122
<i>Group 4</i>					
2	(<i>tert</i> -Butylperoxy)chloro[bis(η^5 -cyclopentadienyl)titanium(IV)] (35) (MUPFAE)	1.467	1.458	156.6	123
3	Bis[μ^2 - <i>N,N,N</i> -tris(2-oxoethyl)amine]bis(<i>tert</i> -butylperoxy- <i>O,O'</i>)-ditanium(IV) (36) (ZUKJIY)	1.469	1.471	138.1 ^c	124
4	(<i>tert</i> -Butylperoxy- <i>O</i>)ethylbis(η^5 -pentamethylcyclopentadienyl)hafnium(IV) (37) (FAWDIQ)	1.487	1.436	126.2	125
<i>Group 7</i>					
5	[Dimethyl(phenyl)methylperoxy][hydrogen[tris(3- <i>tert</i> -butyl-5-isopropylpyrazol-1-yl)borato]manganese(II)] (HIZDID)	1.410	1.463	176.9	126
<i>Group 8</i>					
6	<i>cis</i> -Bis(acetylacetonato)(<i>tert</i> -butylperoxy)(1-methylimidazole)cobalt(III) (38) (LACSEN)	1.466	1.443	143.8	127
7	<i>cis</i> -Bis(acetylacetonato)(<i>tert</i> -butylperoxy)(pyridine)cobalt(III) (LACSAJ)	1.452	1.453	119.3	127
8	<i>cis</i> -Bis(dibenzoylmethane)(<i>tert</i> -butylperoxy)(pyridine)cobalt(III) (LACVEQ)	1.454	1.486	135.5	127
9	(Allylperoxy)(pyridyl)(<i>meso</i> -tetraphenylporphyrinato)cobalt(III) (KEBM(IN))	1.401	1.408	107.5	128
10	[<i>N,N'</i> -(Dipropyl)enetriamine]bis(salicylideneiminato)][2,4,6-tri- <i>tert</i> -butyl-1-peroxy]quinolato]cobalt(III) (SCQUCO)	1.496	1.423	127.8	129
11	2-Benzylpropylperoxy- <i>(N,N</i> -bis[2-(2-pyridyl)ethyl]pyridine-2,6-dicarboxamide)cobalt(III) (FEFBOH)	1.488	1.432	161.6	130
12	Isopropylperoxy- <i>(N,N</i> -bis[2-(2-pyridyl)ethyl]pyridine-2,6-dicarboxamide)cobalt(III) (FEFDUP)	1.445	1.423	109.2	130
13	Cumeneperoxy- <i>(N,N</i> -bis[2-(2-pyridyl)ethyl]pyridine-2,6-dicarboxamide)cobalt(III) (FEDYUI)	1.485	1.443	175.9	130

(continued overleaf)

TABLE 8 (continued)

Entry	Compound name (CSD code)	O—O (Å)	C—O (Å)	M—O—O—C (°) ^a	Reference
14	Cyclohexylperoxy-(<i>N,N</i> -bis[2-(1-pyrazolyl)ethyl]pyridine-2,6-dicarboxamide)cobalt(III) (FEFFIF)	1.456	1.437	92.9	130
15	Cyclohexylperoxy-(<i>N,N</i> -bis[2-(2-pyridyl)ethyl]pyridine-2,6-dicarboxamide)cobalt(III) (FEFBUN)	1.460	1.426	112.2	130
16	<i>n</i> -Propylperoxy-(<i>N,N</i> -bis[2-(2-pyridyl)ethyl]pyridine-2,6-dicarboxamide)cobalt(III) (FEFFAX)	1.451	1.398	100.7	130
17	(Benzoato- <i>O,O'</i>)(<i>tert</i> -butylperoxy)[1,3-bis(pyridyl-2-imino)isoindoline- <i>N,N,N''</i>]cobalt(III) (DASBOO)	1.445	1.421	119.1	131
18	Bis(dimethylglyoximate)(4-ethoxycarbonyl- <i>but</i> -3-en-2-ylperoxy)(pyridine)cobalt(III) (DAZLIZ)	1.415	1.428	100.1	132
	<i>Group 9</i>				
19	(<i>ter</i> -Butylperoxy)(pyridyl)(hydrogen[tris(3,5-diisopropylpyrazolyl)borato]- <i>N,N'</i>)palladium(II) (39) (PIHQIG)	1.437	1.433	112.3	133
20	<i>trans</i> -(<i>μ</i> -(<i>iso</i> propylperoxy)(dimethyl)(1,10-phenanthroline)platinum(IV) (BOVLED)	1.465	1.456	108.2	134
	<i>Group 11</i>				
21	(Dimethylphenylmethylperoxy)(hydrogen[tris(3,5-diisopropylpyrazolyl)borato]copper(II) (PESVOY)	1.453	1.457	179.3	135
	<i>Group 13</i>				
22	Bis[(<i>μ</i> ²- <i>tert</i> -butylperox- <i>O,O</i>)(<i>di-tert</i> -butyl)gallium(III)] (40) (PAJKIU)	1.486	1.450	121.2	136
23	Bis[(<i>μ</i> ²- <i>tert</i> -butylperox- <i>O,O</i>)(<i>di-tert</i> -butyl)indium(III)] (41) (KECYOG)	1.484	1.433	110.9	137

24	<i>Group 14</i> [Bis(ethylperoxy)](tetraphenylporphyrinato(-2)-N,N',N'',N''') germanium(IV) (KEVHUO)	1,477	1,436	121.7	138
25	<i>Group 15</i> (<i>tert</i> -Butylperoxy)(methyl)[tetraphenylporphyrinato(-2)]antimony(V) hexafluorophosphate (XITCAE)	1,469	1,436	143.4	139
26	(<i>tert</i> -Butylperoxy)(tetraphenyl)antimony(V) (42) (JOFPEP)	1,476	1,453	147.5	140
27	[Bis(<i>tert</i> -butylperoxy)(triphenyl)antimony(V) (BUPOSB)]	1,480 1,473	1,472 1,450	145.5 144.4	141
28	<i>Group 17</i> 1-(<i>tert</i> -Butylperoxy)-1,2-benziodoxol-3-(1 <i>H</i>)-one (43) (SUFKOT)	1,459	1,452	109.9	142
29	1-[1,1-Dimethyl-3-(trimethylsilyl)prop-2-ynyl]peroxy-1 λ ,3'-2-benziodoxol-3(1 <i>H</i>)- one (PALJAN)	1,482	1,432	110.1	143

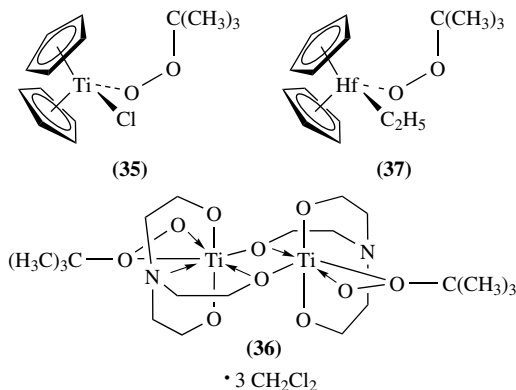
^a η^1 mode of binding.

^b η^1 and η^2 mode of Li binding.

^c η^2 mode of binding.

TABLE 9. Experimental M–O distances versus calculated covalent M–O bond lengths ($r_{\text{cov}} = 0.68 \text{ \AA}$ for O)⁶⁵

Entry	M (r_{cov} (Å))	(M–O) _{cov} (Å)	(M–O) _{exp} (Å)	Reference
1	Li (0.68)	1.36	1.85–1.91 for η^1 1.87–2.11 for η^2	122
2	Ge (1.17)	1.85	1.85–1.87	138
3	Ga (1.22)	1.90	2.01	136
4	Co (1.33)	2.01	1.84–1.92	127–132
5	Mn (1.35)	2.03	1.96	126
6	I (1.40)	2.08	2.03–2.04	142, 143
7	Sb (1.46)	2.14	1.98–2.11	139–141
8	Ti (1.47)	2.15	1.91 for η^1 1.91–2.26 for η^2	123 124
9	Pd (1.50)	2.18	2.03	137
10	Pt (1.50)	2.18	1.82	134
11	Cu (1.52)	2.20	1.82	135
12	Hf (1.57)	2.25	1.97	125
13	In (1.63)	2.31	2.19	137

FIGURE 17. Modes of *tert*-butylperoxy ligand binding to selected transition metal fragments in the solid state^{123–125}

the calculated $(\text{M}-\text{O})_{\text{cov}}$ value. This observation has been explained on the basis of hyperconjugation between one of the lone pairs of O^{D} and vacant virtual orbitals at the transition metal center. The short Hf–O bond in the 16-electron hafnium(IV) complex **37** ($P2_1/c$, Hf–O = 1.970 Å, Hf–O–O–C = 126.2°), for instance, has been interpreted as Hf–O multiple bonding (Figure 17)¹²⁵. A formal 4-electron donation from O^{D} of the peroxy ligand lowers the electron density within the peroxide lone pairs and reduces the electron deficiency at the Hf metal center. The alternative mode of η^2 ligation seems to be disfavored, for reasons of steric repulsion between a *tert*-butyl group and two pentamethylcyclopentadienyl auxiliaries. The short Ti–O bond between the η^1 -coordinated *tert*-butylperoxy ligand and the transition metal center in (*tert*-butylperoxy)chloro[bis(η^5 -cyclopentadienyl)titanium(IV)] (**35**) has been interpreted similarly ($P2_1/c$, Ti–O = 1.909 Å, Ti–O–O–C = 156.6°, Figure 16)¹²³. In bis[μ^2 -*N,N,N*-tris(2-oxoethyl)amine]bis(*tert*-butylperoxy-*O,O'*)-dititanium(IV) (**36**),

on the other hand, the *tert*-butylperoxy ligand exhibits an asymmetric η^2 ligation ($P\bar{1}$, Ti–O = 1.913 and 2.269 Å, Ti–O–O–C = 138.1°, Figure 17)¹²⁴, which has been correlated with the electrophilicity of this reagent. Such an arrangement allows heterolysis of the O–O functionality in the reaction with a nucleophile, without changing significantly the core geometry of the ensemble.

(ii) M–O distances that exceed the calculated $(M-O)_{\text{cov}}$ value have been encountered in (lithium *tert*-butyl peroxide)₁₂ (**34**) (Table 10). The origin of this effect has been related to the ionic character of the Li–O bond. The phenomenon of peroxide bridging by Li⁺ in addition to the η^1 mode of binding has been associated with an additional stabilization of the negative charge located at O^D.

(iii) Alkyl hydroperoxide derivatives of the elements Mn, Ga, In, Sb, Ge and I are characterized by $(M-O)_{\text{exp}}$ distances that follow the values obtained by adding the tabulated covalent radii of M and O. Such connectivities may therefore be described as predominantly σ -donor bonds with a significant covalent character.

2. Dihedral angles associated with the peroxy ligand

The torsion angle in compounds of the type [M]–O–O–C(CH₃)₃, where [M] denotes a monovalent otherwise coordinatively saturated fragment, varies for the η^1 mode of coordination between 92.9–179.3°. Most values are larger than the dihedral angle H–O–O–C(CH₃)₃ (**1**) of 95° and 114° (two independent molecules in the unit cell). The steric demand imposed by the fragments associated with [M] must therefore be larger than that of H, although the steric effect is to a certain degree counterbalanced by M–O distances, which are longer than the O–H bond.

3. Tetrahedral distortion

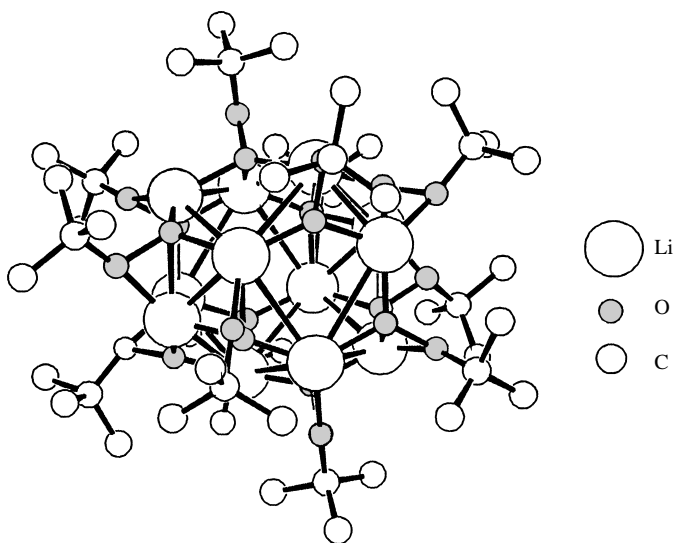
In, e.g., *tert*-butylperoxy ligands, the methyl substituent that is located in an *antiperiplanar* arrangement with respect to the atoms O^D–O^P–C1 is characterized by a bond angle of O–C1–C2 = 102 ± 1°, while the two remaining CH₃ groups exhibit angles of 110 ± 1° (Table 10). This geometry may be explained on the basis of a maximum of $\sigma_{\text{C1-C2}} \rightarrow \sigma^*_{\text{O-O}}$ hyperconjugation⁵⁰. The observed narrow range for the O–C1–C2 angles obviously poses an appropriate balance between the stabilization gained by the orbital interaction and the angle strain caused by the bend⁹.

C. Dialkyl Peroxides

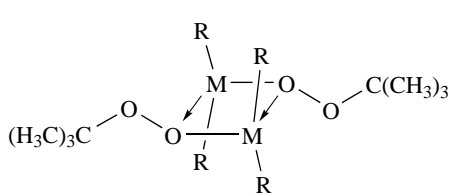
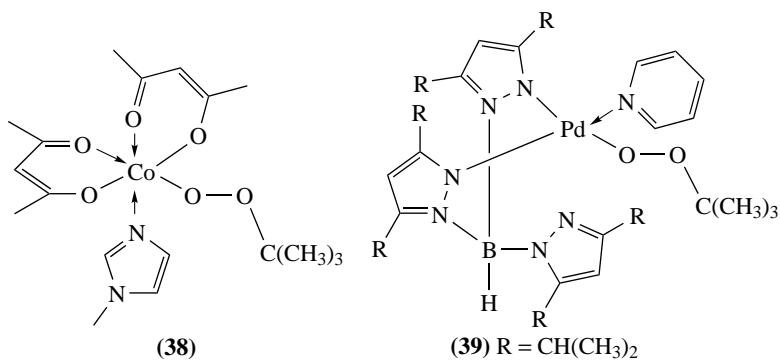
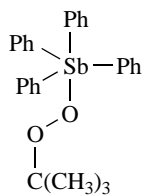
A survey of crystal structures of 29 dialkyl peroxides (Table 11 and Sections II and V) provided a mean O–O bond length of 1.48 ± 0.01 Å and a O–O–C angle of 107 ± 1.3° (with respect to the larger alkyl substituent) and 106 ± 2.4° (for the smaller alkyl group). The torsion angle C–O–O–C shows a scatter between 180° and 125.8°.

As the steric demand of substituents at the peroxide bond increases, the C–O–O–C torsion angle gradually changes from 119° in dimethyl peroxide (**5**) to 180° in bis(triphenylmethyl)peroxide (**9**) (Table 2). Although this general statement is based on structural information that originates for some compounds from gas phase experiments, while solid state geometries were used in other instances, it poses a useful guideline for a conformational classification of dialkyl peroxides. Polar groups, e.g. Cl, OH, CN, that are bound at the peroxide C atom preferentially exhibit an *antiperiplanar* arrangement, probably in order to minimize electrostatic repulsion.

The largest number of reports on solid state geometries of dialkyl peroxides refers to compounds with either two tertiary substituents, molecules with one tertiary and

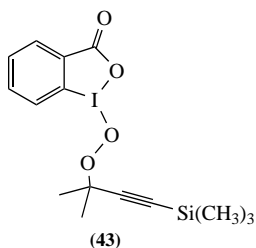
TABLE 10. Bond angles $O^P-C1-C2$ in compounds of the type $M-O^D-O^P-C(CH_3)_3$ 

(34)

(40) $M = Ga, R = C(CH_3)_3$ (41) $M = In, R = C(CH_3)_3$ 

(42)

TABLE 10. (continued)



Entry	Compound	M	O ^P -C1-C2 (°)	O ^P -C1-C2 (°)	O ^P -C1-C2 (°)
1	34	Li	102.8	109.2	110.4
2	35	Ti	101.5	110.3	110.4
3	37	Hf	101.4	111.0	112.3
4	38	Co	102.1	109.4	111.1
5	39	Pd	102.7	109.0	110.8
6	40	Ga	100.7	110.5	110.5
7	41	In	102.7	110.3	110.3
8	42	Sb	101.7	110.0	110.2
9	43	I	101.0	110.7	111.3

one secondary alkyl group, and primary or secondary alkyl substituents that exhibit a polar functionality at the peroxide C. These peroxides show C-O-O-C angles of 150–180°. In bis(heptachlorocyclopent-2-enyl) peroxide (**44**, Figure 18) ($P\bar{1}$, O-O = 1.474 Å), the C-O-O-C entity exhibits *antiperiplanar* geometry to form a plane from which the two Cl atoms that are bound to the peroxide C atoms are translated into opposite direction¹⁴⁷. A similar geometry is found in the antiplanar arranged conformer of bis(cyanodiphenylmethyl) peroxide (**47**) ($C2/c$, O-O = 1.490 Å, C-O-O-C = 180°, Table 11)¹⁵³. One of the *ipso* carbons, i.e. the atoms that link the phenyl group to the peroxide bound C, is located within the O-O-C plane. The associated $\sigma_{C-C_{ipso}}$ orbital therefore may interact with the peroxide σ_{O-O}^* orbital. This causes the bond angle C1_{*ipso*}-C-O = 102.2° to be smaller than the angles C2_{*ipso*}-C-O = 112.2° and C_{*nitrile*}-C-O = 108.1°¹⁵³.

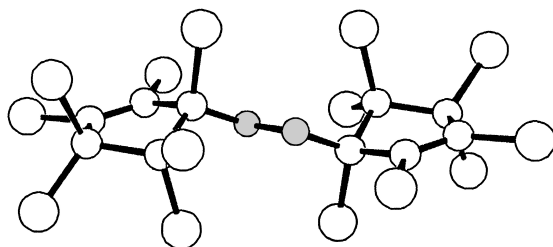
The peroxide dihedral angles in the two diastereomeric dichromanyl peroxides **48** ($P2_1/c$, O-O = 1.469 Å, C-O-O-C = 149.4°) and **49** ($P\bar{1}$, O-O = 1.485 Å, C-O-O-C = 180°, Figure 19) deviate considerably, which may be caused by packing effects¹⁰⁸.

Conformational restraints may lead to unexpectedly small torsion angles. Thus, the staggering of two cyclopentadienyl ligands in cationic Rh(III) complex **45** ($R3$, O-O = 1.468 Å) induces a conformation at the peroxide functionality that is characterized by a C-O-O-C angle of 144.9°, although both peroxide substituents constitute tertiary alkyl groups¹⁴⁹. The unsymmetric substituted methyl peroxide **46** ($P2_12_12_1$, O-O = 1.478 Å) seemingly does not follow the general guideline for peroxide torsion angles since it exhibits a comparatively large C-O-O-C dihedral angle of 151.7° in the solid state (Figure 20)¹⁵⁰. This observation is probably related to the fact that the second peroxide substituent in **46** is a tertiary C atom and part of a sterically demanding tricyclic skeleton.

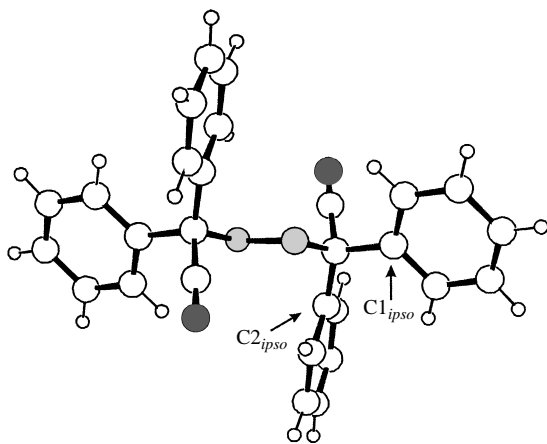
TABLE 11. Summary of O—O distances and C—O—O—C torsion angles in dialkyl peroxides

Entry	Compound name (CSD code)	O—O (Å)	C—O—O—C (°)	Reference
<i>Dialkyl peroxides</i>				
1	Bis(1,1'-hydroxy-2,2'-phenylethyl) peroxide (YEDHOE)	1.479	153.8	144
2	5- <i>tert</i> -Butylperoxy-5-(oxiran-2-yl)-1-(prop-2-ynyl)pyrrolidin-2-one (QAMTED)	1.479	154.2	145
3	1-Methyl-9-(<i>p</i> -methoxyphenyl)bicyclo[4.3.0]nona-6,8-dien-5-yl <i>tert</i> -butylperoxy ether (CIXFOF)	1.485	177.7	146
4	Bis(heptachlorocyclopent-2-enyl) peroxide (44) (BEMSUH)	1.474	180.0	147
5	Bis[2,2,6,6-tetramethylpiperidinyloxy-carbonyl(diphenyl)methyl] peroxide (FEBFIB)	1.491	180.0	148
6	(μ^2 -Peroxo)-bis(η^5 -cyclopentadienyl-diphenylmethyl)rhodium(III) perchlorate (45) (BOBZIB)	1.486	144.9	149
<i>Alkyl alkyl peroxides, alkyl benzyl peroxides, and allyl propargyl peroxides</i>				
7	1-Methyl-6,10-dimethylene-9-methylperoxy-4-oxatricyclo[7.4.0.0 ^{0:7}]tridecan-5-one (46) (CEJRI5)	1.478	151.7	150
8	Bis(1,3,5-tri- <i>tert</i> -butyl-4-oxo-2,5-cyclohexadien-1-yl) peroxide (SIP1OQ)	1.508	180	151
9	1,1'-Bis[1-hydroxy-1,4,4-trimethyl-4-(<i>tert</i> -butylperoxy)but-2-yn-1-yl]ferrocene (LORMIO)	1.451	160.0	152
10	<i>trans</i> -Bis(cyanodiphenylmethyl) peroxide (47) (OCUCIY)	1.490	180.0	153
11	1-[Bis(2,6-dimethoxyphenyl)phenylmethyl]-2-[4-[bis(2,6-dimethoxyphenyl)cyclohexa-2,5-dien-1-yl]peroxide (PIRSIS)	1.472	127.6	154
12	Bis[9-(<i>o</i> -isopropylphenyl)-9-fluorenyl] peroxide (BOMBEX)	1.496	180.0	155
13	Bis[9-(<i>o</i> -phenyl)fluorenyl] peroxide (BIRXAB)	1.491	180.0	156
14	1,4-Bis[(1-methyl-1-phenylethyl)peroxymethyl]benzene (MUGKUU)	1.476	163.1	157
<i>Peroxyacetals</i>				
15	(1,1'-Dihydroxy)dicyclohexyl peroxide (DUCXEE)	1.482	156.1	158
16	1,1'-Bis(1,3,5-trimethyl-4-oxo-2,5-cyclohexadienyl)peroxydiethyl ether (DEZTIL)	1.477	142.3	159
17	Bis[3,5,5-trimethyl-1-(1,2-dioxolan-3-yl)] peroxide (NAHPER)	1.479	180.0	160
18	12 α ,12 α' -Peroxy-bis(8 α ,12-epoxy-11-homodrimane) (ROOQUJ)	1.482	174.0	101

19	(8a <i>R</i> ,8a' <i>R</i>)-Bis(2,2,5,7,8-pentamethyl-6-oxo-6,8a-dihydrochroman-8a-yl) peroxide (48) (FENXEB)	1.469	149.4	108
20	(8a <i>R</i> ,8a' <i>S</i>)-Bis(2,2,5,7,8-pentamethyl-6-oxo-6,8a-dihydrochroman-8a-yl) peroxide (49) (FENXAX)	1.485	180.0	108
21	<i>meso</i> -Bis(1-hydroxyheptyl) peroxide (RABGAD)	1.479	180.0	161
22	<i>meso</i> -Bis(1-hydroxyonyl) peroxide (RABFUW)	1.469	180.0	161
23	1-Hydroxy-1'-hydroperoxydicyclohexyl peroxide (SEGDIR)	1.478	120.5	104
<i>Peroxyaminals</i>				
24	<i>N</i> -[2-(Methoxycarbonyl)benzoyl]-(α -aminoisobutyryl)- α -aminoisobutyric acid <i>N</i> '-[2-(<i>tert</i> -butylperoxy)-2-propyl]amide (AHANUS)	1.436	140.2	162
25	<i>N</i> -[2-(1,3-Dioxo-1,3-dihydro-2 <i>H</i> -isindol-2-yl)-2-methylpropanoyl]- α -aminoisobutyric acid <i>N</i> '-[2-(<i>tert</i> -butylperoxy)-2-propyl]amide (AHAPAA)	1.447	176.0	162
26	Bis(1,3,5-trimethyl-5,6-dihydrobenzo[k]phenanthridin-6-yl) peroxide (WQQKAO)	1.491	125.8	163
27	α -(Pentafluoroamido)-2,3,4,5,6-pentafluorobenzyl peroxide (DOWMEH)	1.462	164.1	164

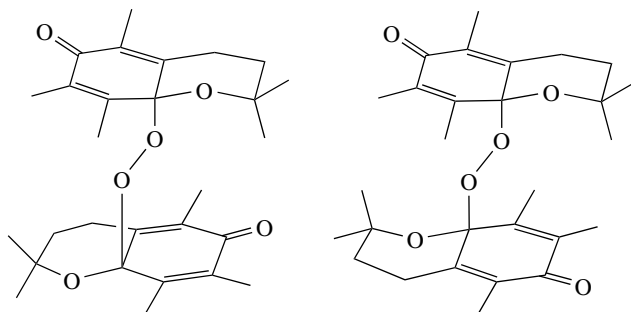


(44)



(47)

FIGURE 18. The geometry of dialkyl peroxides **44** and **47** in the solid state (ball and stick presentation with the O atoms depicted in gray and the N atoms in black; the larger white circles in peroxide **44** denote chlorine atoms; for **47**: $C1_{ipso}-C-O = 102.2^\circ$, $C2_{ipso}-C-O = 112.2^\circ$, $C_{nitrile}-C-O = 108.1^\circ$)^{147, 153}



(48)

(49)

FIGURE 19. Diastereomeric peroxides with different C-O-O-C angles in the solid state: 149.4° for **48** and 180° for **49**¹⁰⁸

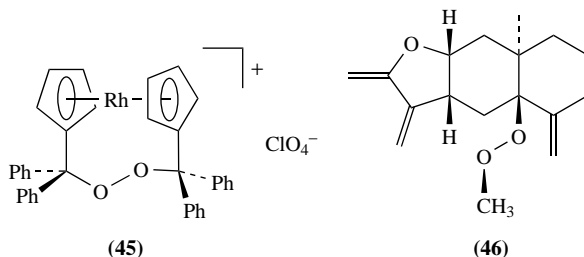


FIGURE 20. Constitution formulae of dialkyl peroxides with noteworthy C—O—O—C angles: 144.9° for **45** and 151.7° for **46**^{149,150}

D. Peracids

A survey of results from 10 crystal structures of peracids (Table 12 and Section II) provided a mean O—O bond length of 1.458 ± 0.009 Å and an O—O—C angle of $109 \pm 0.8^\circ$. The torsion angle H—O—O—C was reported in 3 structures. It varies between 180° and 165.9° .

1. Alkanoyl peracids

The packing of peracid molecules in the solid state, e.g. phthalimidoperoxyalkanoic acids, was extensively studied with the aim to find compounds of high solid state stability to serve as potential low-temperature laundry bleaches. In 1,3-dihydro-1,3-dioxo-2*H*-isoindole-2-peroxyhexanoic acid (**50**) ($P2_1/c$, O—O = 1.462 Å, O···O = 2.72 Å) and a number of its derivatives, the position of the peracid proton was located indirectly by analyzing relevant O···O distances that fall below the sum of the van der Waals radii of two O atoms. The CO₂H functionality acts in peracid **50** as proton donor and as accepting unit, thus linking two molecules into chains (Figure 21)¹⁶⁵. In the solid state structure of 1,3-dihydro-1,3-dioxo-2*H*-isoindole-2-peroxybutanoic acid ($P\bar{1}$,

TABLE 12. Geometric parameters of peracid peroxide bonds

Entry	Compound name (CSD code)	O—O(Å)	C—O—O—H(°)	Reference
1	1,3-Dihydro-1,3-dioxo-2 <i>H</i> -isoindole-2-peroxybutanoic acid (HIHPAP)	1.461	— ^a	165
2	1,3-Dihydro-1,3-dioxo-2 <i>H</i> -isoindole-2-peroxypentanoic acid (HIHPET)	1.446	— ^a	165
3	1,3-Dihydro-1,3-dioxo-2 <i>H</i> -isoindole-2-peroxyhexanoic acid (50) (HIHPPIX)	1.462	— ^a	165
4	3-Oxo-1,2-benzisothiazole-2(3 <i>H</i>)-perethanoic acid 1,1-dioxide (TEJMEA)	1.474	— ^a	166
5	3-Oxo-1,2-benzisothiazole-2(3 <i>H</i>)-peroxypropanoic acid 1,1-dioxide (51) (HEKZIG)	1.469	180.0	167
6	<i>p</i> -(Acetamido)perbenzoic acid (52) (ZUHBIT)	1.452	179.0	168
7	<i>p</i> -(Propanoylamido)perbenzoic acid (ZUHBOZ)	1.456	170.1	168
8	<i>p</i> -(Butanoylamido)perbenzoic acid (ZUHBUF)	1.454	180.0	168
9	<i>p</i> -(Pentanoylamido)perbenzoic acid (ZUHJAN)	1.448	165.9	168

^a Not reported.

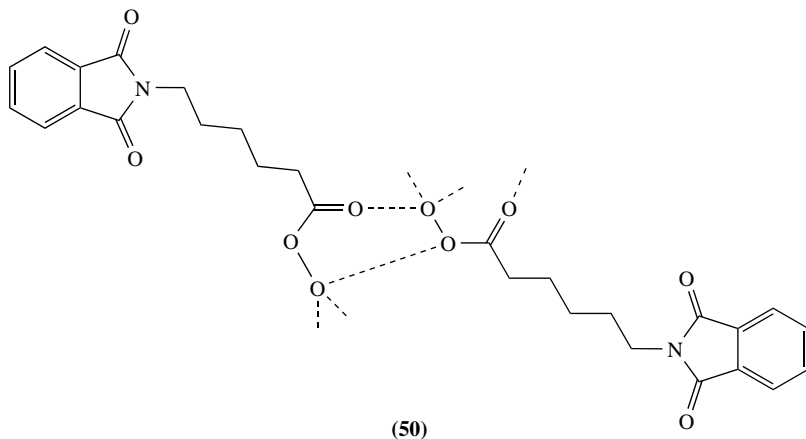


FIGURE 21. Association of percarboxylic acid **50** in the solid state (the peroxide protons were not localized directly and were therefore omitted from the graphics)¹⁶⁵

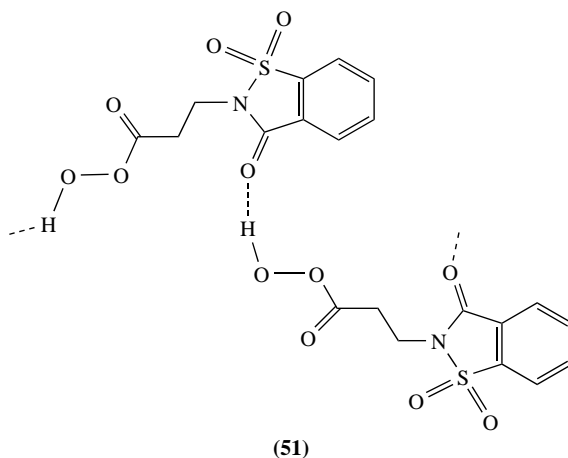


FIGURE 22. Intramolecular hydrogen bonding observed for *N*-saccharinperpropanoic acid **51** in the solid state¹⁶⁷

O—O = 1.461 Å, O···O = 2.75 Å; Table 12, entry 1), i.e. the twofold lower homologue of **50**, hydrogen bonding occurs between the peracid proton and one of the phthalimido O atoms¹⁶⁵.

The percarboxylic acid proton of 3-oxo-1,2-benzisothiazole-2(3*H*)-peroxypropanoic acid 1,1-dioxide (**51**) (*Pnma*, O—O = 1.469, C—O—O—H = 180.0°) was located on the difference Fourier map¹⁶⁷. Hydrogen bonding in the peracid **51** (Figure 22) occurs from the peracid proton to the carbonyl O of the saccharin entity (O···O = 2.618 Å) to provide chains of peracid molecules that are stacked via additional C—H···O contacts (not shown in Figure 22) in sheets along the *b* axis.

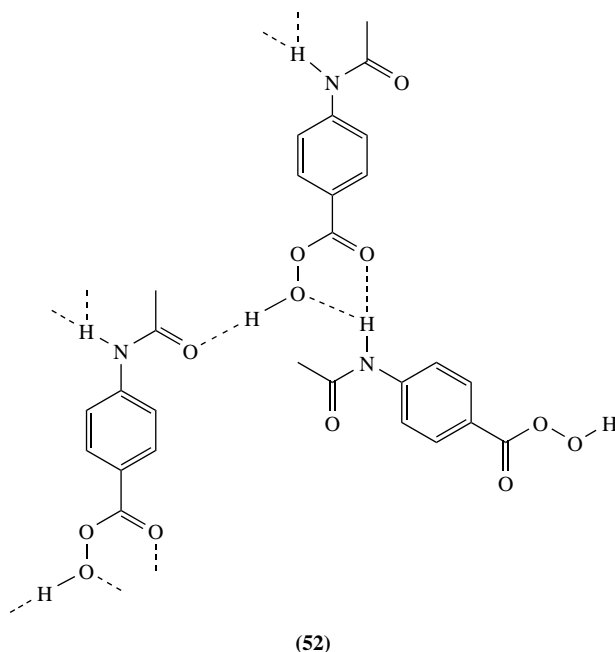


FIGURE 23. Intramolecular hydrogen bonding in the crystal structure of *p*-(acetamido)perbenzoic acid (52)¹⁶⁸

2. Aroyl peracids

The structures of four *p*-(alkanoylamido)perbenzoic acids have been investigated (Table 12, entries 6–9). The compounds are characterized by a planar arrangement of the peracid functionalities and an extensive network of hydrogen bonding.¹⁶⁸ In *p*-(acetamido)perbenzoic acid (52) (*Cc*, O–O = 1.452 Å, C–O–O–H = 180°, O···O = 2.573 Å, H···O = 1.759 Å, O–H···O = 169.3°) hydrogen bonds are formed between the OOH and the acetamido carbonyl O, and from the amido proton toward the peracid carbonyl O¹⁶⁸ (Figure 23).

3. The percarboxylate anion as ligand

Acylperoxy-bridged dicopper(II) complex 53 (*C2/c*, O–O = 1.463, C(O)–O–O = 110.3°, O–O–Cu = 123.3° and 122.4°, C–O–O–Cu = 94.3° and 116.2°, Figure 24) constitutes a rare example for which a percarboxylate serves as ligand for a transition metal complex¹⁶⁹.

E. Peresters

A survey of crystal structures from 12 peresters (Table 13 provided a mean O–O bond length of 1.46 ± 0.01 Å and C(O)–O^P–O^D angle of $111 \pm 1.6^\circ$ and $108 \pm 1.5^\circ$ for O^P–O^D–C.

The majority of crystal structures of peresters, which have been disclosed in the CSD data base in the last two decades, relate to formal condensation products between

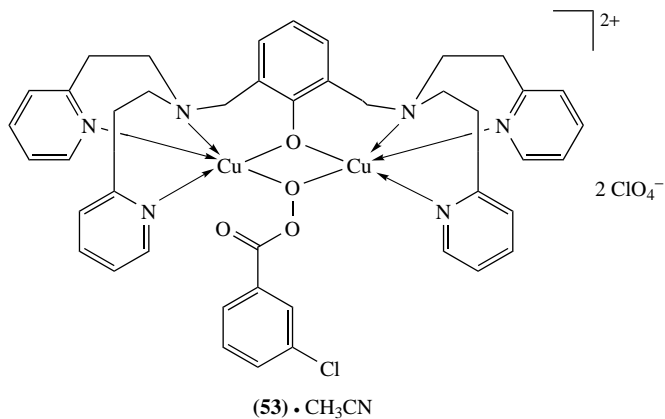


FIGURE 24. The *meta*-chloroperbenzoate anion as bridging ligand in binuclear copper(II) complex **53**¹⁶⁹

carboxylic acids and *tert*-butyl hydroperoxide (**1**). The dihedral angle $C(O)-O^P-O^D-C = 119.3^\circ$ in *tert*-butylperoxy 2,3,4,5,6-penta-*O*-acetyl-D-gluconate (**54**) ($P2_12_12_1$, $O-O = 1.463 \text{ \AA}$) is close to the value for *tert*-butyl hydroperoxide (**1**) (95° and 104° , two crystallographically independent molecules), which points to a comparatively small steric demand of the acyl group in peresters. Due to its structural similarity to dialkyl peroxides, it is reasonable that the *ortho* ester **56** ($P2_1$, $O-O = 1.481 \text{ \AA}$, $C-O-O-C = 145.1^\circ$) exhibits a significantly larger peroxide dihedral angle than **54**¹⁷⁰.

The structures of *tert*-butyl peresters are characterized by the familiar sequence of one small $O-C-CH_3$ angle and two that are close to the tetrahedral angle. The smallest value is consistently associated with the methyl group that is located in the O^P-O^D-C plane, thus pointing to hyperconjugative distortion of the peroxide bound alkyl substituent (for **54**: $O^D-C1-C2 = 101.1^\circ$, $O^D-C1-C3 = 109.7^\circ$, to $O^D-C1-C2 = 110.3^\circ$, Figure 25)^{50,170}. In a similar way, the back side angle $C-C(O)-O^P = 107.3^\circ$ of the perester carbonyl group [$O^D-O^P-C(O)-C = 169.6^\circ$] is smaller than that of the acetyl substituents ($110.3-112.3^\circ$).

A survey of the back side angles $C-C(O)-O^P$ of perester acyl groups in general provides values between $106.8-109.0^\circ$ in case of aliphatic carboxylic acids (entries 2-7, 11, 12, Table 13), while the corresponding angles for the benzoic acids derivatives (entries 8-10, Table 13) are grouped in the region of $109.2-110.6^\circ$ ¹⁷¹⁻¹⁷⁶.

In spite of the structural diversity of the peresters listed in Table 13, the dihedral angles $C(O)-O^P-O^D-C$ fall into a comparatively narrow range of $120 \pm 20^\circ$, thus favoring the *gauche* arrangement. Structures that exhibit considerably larger peroxide torsion angles are characterized by sterically demanding substituents at either side of the $O-O$ bond, such as the *tert*-butyl substituent and the 2,4,6-tri(*tert*-butyl)benzoyl group in peroxide (**55**) ($P2_1$, $O-O = 1.479 \text{ \AA}$, $C(O)-O^P-O^D-C = 173.4^\circ$, Figure 26)¹⁷⁴.

F. Diacyl Peroxides

The set of diacyl peroxides that have been investigated by X-ray diffraction and disclosed in the literature in the last two decades is restricted to symmetric compounds with a mean $O-O$ bond length $1.45 \pm 0.01 \text{ \AA}$ (Table 14) and $O-O-C$

TABLE 13. Geometric parameters at the O—O bond in peresters

Entry	Compound name (CSD code)	O—O (Å)	C(O)—O ^P —O ^D —C (°)	Reference
<i>tert</i> -Butyl peresters				
1	2,3,4,5,6-Penta- <i>O</i> -acetyl-D-gluconic acid <i>tert</i> -butylperoxy ester (54) (GEQQOI)	1.463	119.3	170
2	<i>tert</i> -Butyl 3-methyl-3-(9-triptycy)peroxybutanoate (NUJLOT)	1.450	127.8	171
3	<i>tert</i> -Butyl 3-methyl-3-(1,4-dimethyl-9-triptycy)peroxybutanoate (NUJMAG)	1.467	142.8	171
4	<i>tert</i> -Butyl 3-methyl-3-(1,4-dimethoxy-9-triptycy)peroxybutanoate (NUJLUZ)	1.469	130.2	171
5	<i>N</i> -Phthaloyl- <i>cis</i> -1-aminocyclohexane-4-carboxylic acid <i>tert</i> -butyl perester (LUGCUL)	1.459	132.0	172
6	<i>N</i> -(3-Fluorophthaloyl)- <i>cis</i> -1-aminocyclohexane-4-carboxylic acid <i>tert</i> -butyl perester (LUGDEW)	1.461	128.4	172
7	<i>N</i> -(3,6-Difluorophthaloyl)- <i>cis</i> -1-aminocyclohexane-4-carboxylic acid <i>tert</i> -butyl perester (LUGDAS)	1.456	162.7	172
8	<i>tert</i> -Butyl 3-nitroperbenzoate (CEKKEI)	1.457	107.4	173
9	<i>tert</i> -Butyl 4-nitroperbenzoate (CEKKIM)	1.490	120.5	173
10	<i>tert</i> -Butyl 2,4,6-(tri- <i>tert</i> -butyl)perbenzoate (55) (VUPZEL)	1.479	173.4	174
<i>Miscellaneous Peresters</i>				
11	(1 <i>R</i> ,4 <i>R</i> ,5 <i>S</i> ,6 <i>S</i> ,7 <i>S</i>)-(<i>E</i>)-1-Hydroperoxy-5-hydroxy-4,14-cyclogermacra-9,11(13)-dien-12,6-olactone diacetate (DINLIV10)	1.456	95.4	175
12	3-Methyl-3-(1,7-dicarba- <i>closo</i> -dodecaboran[12]-1-carbonylperoxy)but-1-yne (XINPAL)	1.457	122.8	176

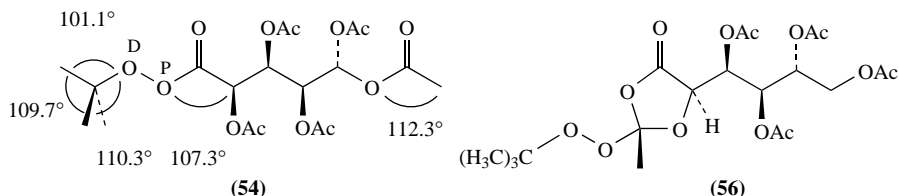


FIGURE 25. Carbohydrate derivatives of *tert*-butyl hydroperoxide (**1**): perester **54** and the *ortho* analogue **56**¹⁷⁰

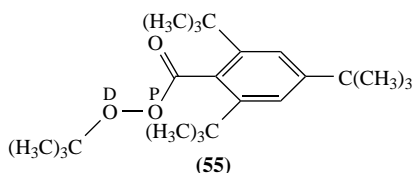


FIGURE 26. Conformation of perester **55** in the solid state¹⁷⁴

TABLE 14. Geometric parameters of diacyl peroxides at the peroxide bond

Entry	Compound name (CSD code)	O–O (Å)	C–O–O–C (°)	Reference
1	Disuccinyl peroxide (CEYLUN)	1.452	88.9	181
2	Diglutaryl peroxide (DIHYEY)	1.448	82.3	182
3	(<i>R,R,S,S</i>)-Bis{[(<i>E</i>)-2-phenyl-1-cyclopropyl]carbonyl}peroxide (COMKIY)	1.454	122.6	177
4	Bis[(1-phenyl-1-cyclopropyl)carbonyl]peroxide (BEPTIZ)	1.462	86.7	179
5	Dibenzoyl peroxide (DBEZPO01)	1.434	90.6	183
6	Bis(3,3'-dichlorobenzoyl) peroxide (CIMHIP)	1.454	92.0	184
7	Bis[4,4'-(dimethoxy)benzoyl] peroxide (DISJEU)	1.463	86.8	185
8	Bis[(<i>E</i>)-cinnamoyl] peroxide (57) (CIRZIM)	1.421	87.2	178
9	Bis[α -fluoro-(<i>E</i>)-cinnamoyl] peroxide (CUGBOV)	1.449	91.0	186

angles of $110 \pm 1.6^\circ$. The angle C–O–O–C of these structures is grouped in the narrow range of 82.3 – 92.0° (Table 14). The peroxide torsion angle of 122.6° in (*R,R,S,S*)-bis{[(*E*)-2-phenyl-1-cyclopropyl]carbonyl} peroxide ($P2_1/c$, O–O = 1.454 Å, Table 14, entry 3) deviates from the common value¹⁷⁷. The back side angle of the carbonyl group C–C(O)–O varies between 104.6° in bis[(*E*)-cinnamoyl] peroxide (**57**) ($P2_1$, O–O = 1.421 Å, C–O–O–C = 87.2, Figure 27)¹⁷⁸ to 110.7° in bis[(1-phenyl-1-cyclopropyl)carbonyl]peroxide ($C2/c$, O–O = 1.462 Å, C–O–O–C = 86.7, Table 14, entry 4)¹⁷⁹. The smallest back side angle for the carbonyl group O–C(O)–O = 102.4° was found in the solid structure of carbonate **58** ($P2_1/n$, O–O = 1.432 Å, C–O–O–C = 90.0° , Figure 27)^{178, 180}.

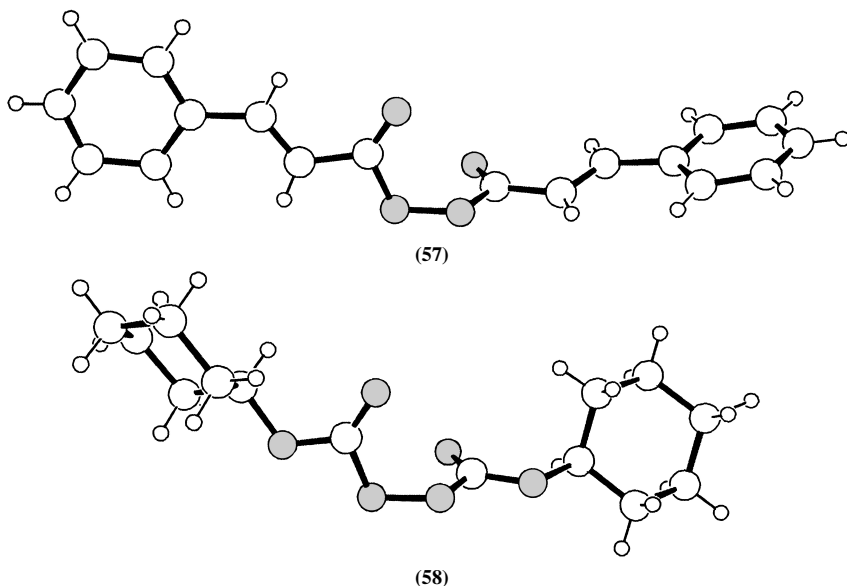


FIGURE 27. The geometry of diacyl peroxide **57** and bis(peroxy carbonate) **58** in the solid state (ball and stick presentation with the O atoms depicted in gray)¹⁸⁰

IV. POLYOXO COMPOUNDS

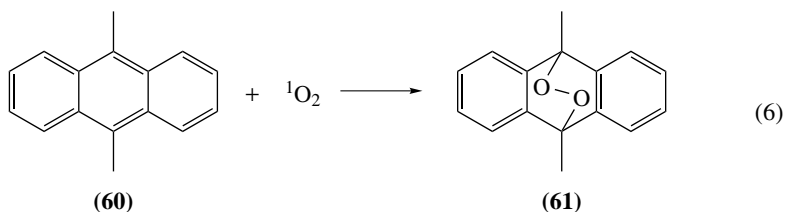
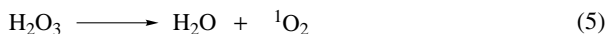
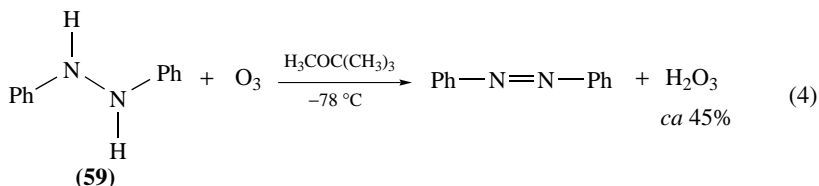
One of the significant differences between sulfur and oxygen chemistry is the reluctance of oxygen to form long chains of the type $\text{RO}-\text{O}_n-\text{OR}'$ ($n > 0$, $\text{R}, \text{R}' = \text{H}$, alkyl, aryl). The earliest reports on the preparation and characterization of the smallest polyoxo compound H_2O_3 dates back to 1963^{187, 188}. The synthesis, structural characterization and exploration of this chemistry has made tremendous progress within the last decades and has opened a new area in peroxide chemistry, which is associated with the question on the maximum possible chain length of a polyoxide chain before the system escapes spectroscopic characterization based on its lability^{189–191}.

A. Trioxides

Dihydrogen trioxide, H_2O_3 (hydrogen sesquioxide), has been prepared by ozonization of 1,2-diphenylhydrazine (**59**) at -78°C in *tert*-butyl methyl ether in approximately 45% yield (equation 4)¹⁹². Characterization of H_2O_3 and isotopic labeled derivatives thereof has been achieved by IR spectroscopy in combination with a computational analysis. The computed (B3LYP) equilibrium geometry of H_2O_3 ($\text{O}-\text{O} = 1.446 \text{ \AA}$, $\text{O}-\text{O}-\text{O}-\text{H} = 79.6^\circ$) is reminiscent of geometric parameters obtained for the energetically lowest conformer of H_2O_2 . H_2O_3 exhibits two stereogenic axes and therefore may exist as a set of three stereoisomers, i.e. the pair of (*P,P*)- and (*M,M*)-enantiomers and the (*P,M*)-configured *meso*-compound¹⁰.

Hydrogen sesquioxide is characterized by a ^1H NMR resonance at $\delta = 13.1$ in $(\text{CD}_3)_2\text{CO}$ (10.0 for H_2O_2). In the ^{17}O NMR spectrum [referenced versus $\text{H}_2\text{O} \equiv 0$ ppm, all values in $(\text{CD}_3)_2\text{CO}$], the resonances of H_2O_3 (421 ppm for the internal oxygens and 305 ppm for the central oxygen) are clearly separated from the signal of H_2O_2 (187 ppm). H_2O_3 exhibits a

half-life of 16 ± 1 min at 20°C , which is independent of the solvent. It decomposes among other products into singlet oxygen, which was characterized by (i) the $^1\text{O}_2$ chemiluminescence at $\lambda = 1272$ nm and (ii) trapping with 9,10-dimethylanthracene (**60**) to furnish $20 \pm 10\%$ of endoperoxide **61** (equations 5 and 6). The experimental activation energy for H_2O_3 decomposition of 70 ± 9 kJ mol $^{-1}$ is lower than the calculated BDE for homolysis of the HO–OOH bond (125 kJ mol $^{-1}$, B3LYP). It has been suggested that this deviation between theory and experiment originates from an involvement of H_2O_2 and/or H_2O as bifunctional catalyst(s) in a polar, i.e. non-radical, pathway for H_2O_3 decomposition.



A limited set of alkyl hydrotrioxides has been obtained as side product from syntheses of H_2O_3 via low-temperature ozonization of organic substrates. The compounds were characterized by ^1H and ^{17}O NMR in combination with computational studies¹⁹³. Preliminary investigations show that alkyl hydrotrioxides are labile compounds that share several chemical properties with the alkyl hydroperoxides. Bis(trifluoromethyl) trioxide (**62**), on the other hand, has been prepared from hexafluoroacetone, F_2 and O_2 on a 1.2 g scale¹⁹⁴. Trioxide **62** has a boiling point of -16°C and decomposes at 20°C . It has been investigated by X-ray diffraction at -170°C and shows marginal distortion from C_2 symmetry in the solid state (Figure 28). The unit cell ($P\bar{1}$, $Z = 2$) contains a 1:1 ratio of (*P,P*)- and (*M,M*)-configured trioxide **62**. The distances (O–O = 1.437 Å, C–O = 1.398 Å) and the dihedral angle C–O–O–O = 95.9° are similar to the values reported for bis(trifluoromethyl) peroxide. These observations imply that peroxides and trioxides probably share common structural characteristics.

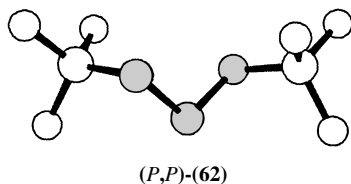


FIGURE 28. The geometry of bis(trifluoromethyl) trioxide (**62**) in the solid state [ball and stick presentation with the O atoms depicted in gray; the (*P,P*)-enantiomer of **62** was arbitrarily selected from the racemate that is present in the unit cell]¹⁹⁴

B. Tetroxides and Higher Polyoxides

H_2O_4 has been identified by a combination of IR and Raman spectroscopy as a product of electrical discharge reactions of water vapor and subsequent trapping of likewise prepared compounds at 80 K¹⁸⁹. A weak Raman band at 98 cm^{-1} has been assigned to the torsional mode of the O_4 skeleton. Dihydrogen tetroxide has been reported to decompose at temperatures above 173 K. The calculated [G2(MP2)] stability of polyoxo compounds gradually decreases along the sequence $\text{H}_2\text{O}_3 > \text{H}_2\text{O}_4 > \text{H}_2\text{O}_5 > \text{H}_2\text{O}_6$. According to the proposed mechanism and the associated activation barriers, it is expected that the BDE of 27 kJ mol^{-1} [G2(MP2)] for the central bond of H_2O_6 poses a lower limit for the stability of polyoxo compounds. In turn, peroxides of the type H_2O_n should become more persistent, in going from dihydrogen hexoxide to the heptoxide and to higher polyoxides¹⁹¹.

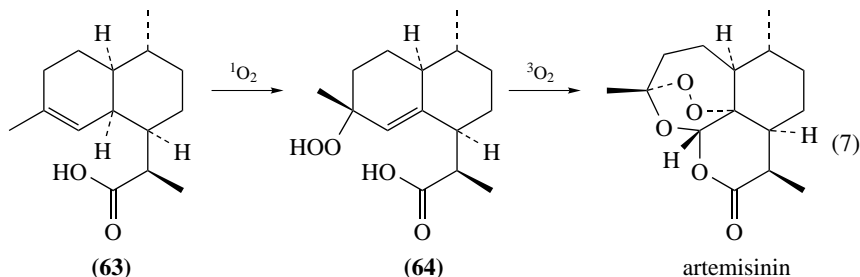
V. NATURAL PRODUCTS

The discovery that the peroxide functionality serves as pharmacophore in the antimalarial qinghaosu (artemisinin)—an amorphane sesquiterpene endoperoxide that cures patients who have been infected by multidrug resistant strains of *Plasmodium falciparum*—has initiated efforts to uncover the biological properties of naturally occurring peroxides⁷. An increasing number of predominantly sesquiterpene-derived hydroperoxides have been isolated in the last decades from marine and terrestrial sources, although frequently in low yields. One of the most important issues to be addressed in forthcoming studies therefore relates to the verification that these compounds constitute authentic secondary metabolites and are not artefacts produced during the work-up process.

A. Sesquiterpenes

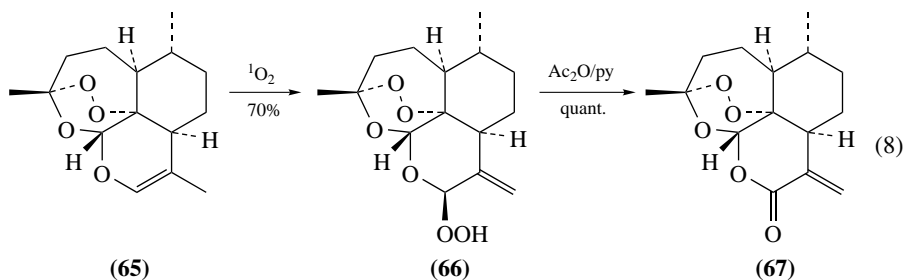
1. Alkyl hydroperoxides related to artemisinin and its derivatives

The biosynthesis of the unique 1,2,4-trioxane ring in artemisinin in *Artemisia annua* L. is under current investigation. Dihydroartemisinic acid (**63**) (equation 7) is likely to be one of the biosynthetic progenitors of this compound. Photooxygenation of sesquiterpene **63** with singlet oxygen in vitro, for example, provides allylic hydroperoxide **64**, which has recently been isolated from extracts of *Artemisia annua*. Singlet oxygen is formed in nature in photosensitized reactions between $^3\text{O}_2$ and, e.g., chlorophyll. Exposure of hydroperoxide **64** to air furnishes artemisinin and dihydro-*epi*-deoxyarteannuin B (not shown in equation 7)^{195, 196}.



Isotopically labeled artemisinin or hydroxylated derivatives thereof, which are required in order to investigate the metabolism of qinghaosu, have been prepared starting from

anhydrodihydroartemisinin (**65**) (equation 8)¹⁹⁷. Photooxygenation of substrate **65** with $^1\text{O}_2$ provides allylic hydroperoxide **66**, which has been investigated by X-ray diffraction. Compound **66** crystallizes in $P2_12_12_1$. The asymmetric unit comprises a pair of hydrogen-bonded molecules of **66**, which exhibit similar but not identical geometries (molecule 1: $\text{O}-\text{O} = 1.456 \text{ \AA}$, $\text{H}-\text{O}-\text{O}-\text{C} = -75.6^\circ$; molecule 2: $\text{O}-\text{O} = 1.449 \text{ \AA}$, $\text{H}-\text{O}-\text{O}-\text{C} = -67.0^\circ$)¹⁹⁷. Treatment of hydroperoxide **66** with Ac_2O and pyridine furnishes artemisitene (**67**), which serves as starting material for syntheses of, e.g., artemisinin metabolites.



2. Miscellaneous sesquiterpene hydroperoxides

3-(Angeloyloxy)-11-(hydroperoxy)-1-hydroxyeremophila-6,9-dien-8-one (**68**) (Figure 29) is an eremophilane hydroperoxide ($P2_12_12_1$, $\text{O}-\text{O} = 1.470 \text{ \AA}$, $\text{H}-\text{O}-\text{O}-\text{C} = 120.0^\circ$), which has been isolated from dried and ground leaves of the South American plant *Robinsonecio gerberifolius* that grows in high mountains of Mexico and Guatemala¹⁹⁸. The compound exhibits a moderate activity against a human prostate cancer cell line.

The octahydrohydroperoxy-(5*H*)-cyclopropa[*a*]-naphthalen-5-one **69** ($P2_12_12_1$, $\text{O}-\text{O} = 1.453$) has been extracted from the underground part of the plant *Aristolochia debilis*¹⁹⁹. The plant is used in traditional Chinese medicine to cure airway disorders. Hydroperoxide **69** has been prepared independently upon exposure of a suitable deperoxy derivative to air.

Furodysin hydroperoxide (**70**) ($P2_12_12_1$, $\text{O}-\text{O} = 1.471 \text{ \AA}$) has been isolated from a methanol extract of the nudibranch *Chromodoris funerea* (equation 9)²⁰⁰. This animal feeds on sponges of the genus *Dysidea*, which contain among others furodysin, a compound that exhibits fish-repellent properties. An analysis of secondary metabolites from the nudibranch showed that the animal not only tolerates furanosesquiterpenes but also sequesters, and modifies these chemicals for its own defense. There is cumulative evidence that endoperoxides, probably formed by singlet oxygen addition to furodysin

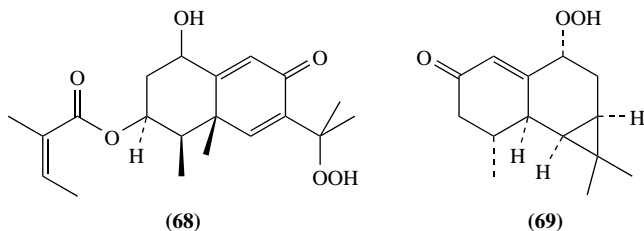
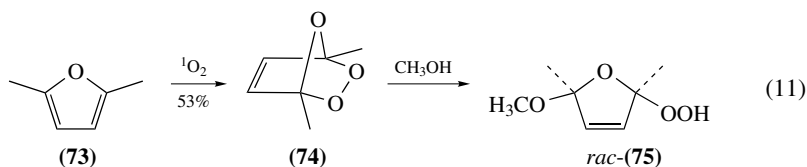
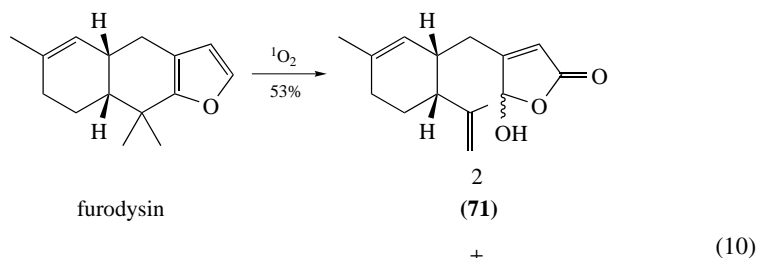
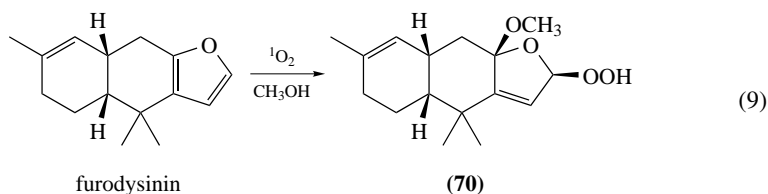


FIGURE 29. Sesquiterpene hydroperoxides, which have been obtained from natural sources and investigated by X-ray diffraction^{198, 199}

and/or furodysin, constitute at least some of the biologically active compounds in question. According to this interpretation the 2-hydroperoxy-5-methoxy-2,5-dihydrofuran **70** is not considered to be a genuine natural product. It is likely to originate from the reaction between CH_3OH and a furodysin-in-derived endoperoxide in the course of a methanol extraction of the animal. This assumption is supported by three independent studies. First, the extraction of *C. funerea* with dichloromethane furnished other furodysin-in-derived oxidation products than the hydroperoxide **71**. Second, the in vitro reaction of furodysin with $^1\text{O}_2$ gave a 2:1 mixture of γ -hydroxybutenolide **71** and the lactone **72**—compounds that have been identified in the dichloromethane-soluble part of the acetone extract of *C. funerea* (equation 10). Third, endoperoxide **74**, which is formed upon treatment of 2,5-dimethyl furan (**73**) with $^1\text{O}_2$, adds methanol, thus leading to 2,5-dimethyl-2-hydroperoxy-5-methoxy-2,5-dihydrofuran (**75**) (P_{21}/n , $\text{O}-\text{O} = 1.463 \text{ \AA}$, equation 11)²⁰¹.



More recently, the sesquiterpene $\Delta^{7,14}$ -isonakafuran-9-hydroperoxide (**76**) (P_{21} , $\text{O}-\text{O} = 1.458 \text{ \AA}$, $\text{H}-\text{O}-\text{O}-\text{C} = 63.3^\circ$, Figure 30) has been isolated from the dichloromethane/methanol extract of the marine sponge *Dysidea* sp. nov.²⁰². The peroxide is inhibitory to the marine fungus *Trichophyton mentagrophytes* and to murine leukemia cells. In view

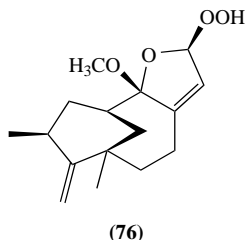


FIGURE 30. Constitution formula of $\Delta^{7,14}$ -isonakafuran-9-hydroperoxide (**76**)²⁰²

of the mechanistic scheme outlined above, it is necessary to verify in further studies whether or not the 2-hydroperoxy-5-methoxy-2,5-dihydrofuran subunit in **76** is a genuine structural motif of a secondary metabolite of *Dysidea* sp. nov, or if it originates from CH_3OH addition to a suitable precursor in the course of the extraction process.

B. Triterpenes

The methylene chloride soluble portion of a methanol extract from the wood of *Eurycoma longifolia* shows strong cytotoxic properties. One of the active constituents, longilene peroxide (**77**) (P_{21} , $\text{O}-\text{O} = 1.472 \text{ \AA}$, Figure 31), was isolated in a 0.0003% yield. The characteristic horse-shoe-like arrangement, which is observed in the crystal structure of squalene derivative **77**, has been associated with its biological activity^{203,204}.

Maytensifolin A (**78**) (P_{21} , $\text{O}-\text{O} = 1.472 \text{ \AA}$, Figure 32) is a friedelin-type hydroperoxy triterpene that was obtained in a 0.00013% yield from a chloroform extract of *Maytenus diversifolia*. No biological data have been reported for this compound so far²⁰⁵.

C. Acetogenins

Oxanthromicin (**79**) (Figure 33) is an optically active antibiotic that has been isolated from the fermentation broth produced by *Actinomadura* sp. SCC 1646²⁰⁶. The results

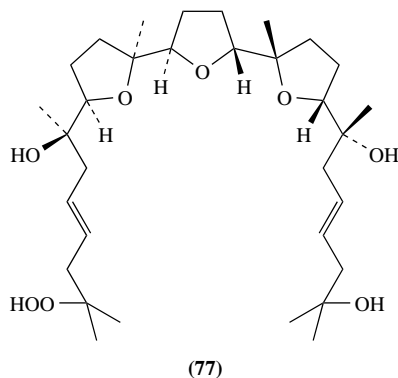


FIGURE 31. Structure formula of longilene peroxide (**77**) and its crystal structure (ball and stick presentation with the O atoms depicted in gray)²⁰³

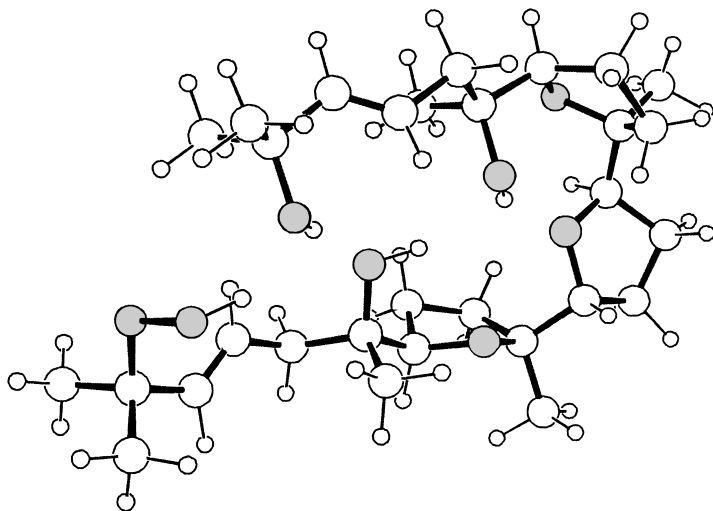
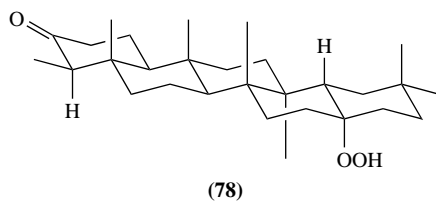
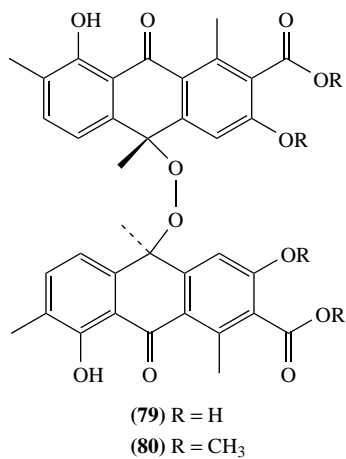


FIGURE 31. (continued)

FIGURE 32. Constitution formula of triterpene-derived hydroperoxide **78**²⁰⁵FIGURE 33. Constitution formula of the acetogenin oxanthromicin (**79**) and its tetramethyl derivative **80**²⁰⁶

from an X-ray diffraction analysis of tetramethyl oxanthromicin (**80**) clarified that the compound is a dimeric anthrone peroxide ($P2_1$, $O-O = 1.482 \text{ \AA}$, $C-O-O-C = 172.2^\circ$). The answer to the question whether or not enzymes participate in the peroxide-forming step remains to be pursued in future studies on the biosynthesis of optically active natural product **79**.

VI. CONCLUDING REMARKS

Structure determines reactivity. Reactivity in turn is the basis for the diverse chemistry of acyclic organic peroxides^{207,208}. Today, structure and bonding of peroxides are well understood. The most significant progress in this field of research within the last two decades originated in particular from the synergy between the disciplines of synthesis, analytical chemistry, spectroscopy, diffraction analysis and computational chemistry, thus leading to a set of five effects that control the most important structural aspects of acyclic organic peroxides: (i) the effect of lone pair repulsion that directs a peroxide entity preferentially into a *gauche* conformation, thus minimizing Coulomb interactions, (ii) the $n_O \rightarrow \sigma^*_{O-R}$ hyperconjugation that lowers the electron population within the lone pairs at oxygen, (iii) the $\sigma_{R-O} \rightarrow \sigma^*_{O-O}$ hyperconjugation that is associated with the tetrahedral distortion of a peroxide-bound alkyl substituent, (iv) strain effects between the two substituents at the peroxide group and (v) hydrogen bonding.

The unique reactivity of peroxides has led to numerous useful industrial and laboratory scale applications via heterolytic or homolytic cleavage of the $O-O$ bond. Many of these aspects have been investigated in considerable depth, while new topics emerge^{207,208}. The advent of CF_3OONO_2 (**13**) in significant quantities in our atmosphere in the years that followed the discovery and the large-scale application of chlorofluorohydrocarbon (CFC) substitutes is just one example. Trifluoromethyl peroxyxynitrate (**13**) is formed in the troposphere via OH^\bullet -initiated degradation of CFC replacements. It is nowadays considered a reservoir for CF_3O^\bullet , CF_3OO^\bullet or NO_2^\bullet and may therefore contribute to a depletion of stratospheric ozone²⁰⁹. In other atmospheric regions, CF_3OONO_2 (**13**) has been associated with NO_2^\bullet transport from industrial zones to almost unpolluted environments^{56,210}. Other aspects of peroxide chemistry that might require our future attention are associated with the chemistry of H_2O_3 , the biological role of peroxygenated secondary metabolites and the search for new peroxide-based drugs^{7,211}. Many of the future challenges are thus reflected in a vision that somehow has guided H_2O_2 chemistry from its very beginning, and hopefully will continue to do so: '*C'est en traitant le peroxide de barium par les acides que je suis parvenu à faire ces nouvelles combinaisons, qui, pour la plupart, sont très-remarquables et dignes de fixer l'attention des chimistes*'²¹².

VII. REFERENCES

1. N. A. Porter, *Acc. Chem. Res.*, **19**, 262 (1986).
2. M. Prein and W. Adam, *Angew. Chem., Int. Ed. Engl.*, **35**, 477 (1996).
3. (a) J. Emsley, *The Elements*, 3rd edn., Oxford University Press, Oxford, 1998, p. 148.
(b) D. A. Casteel, *Nat. Prod. Rep.*, **16**, 55 (1999).
4. (a) R. P. Wayne, *Chemistry of Atmospheres*, 2nd edn., Oxford University Press, New York, 1991.
(b) B. H. Singh, L. J. Salast and W. Viezee, *Nature*, **321**, 588 (1986).
(c) S. Seefeld, D. J. Kinnison and J. A. Kerr, *J. Phys. Chem. A*, **101**, 55 (1997).
5. K. B. Sharpless and T. R. Verhoeven, *Aldrichim. Acta*, **12**, 63 (1979).
6. V. Ullrich and R. Brugger, *Angew. Chem., Int. Ed. Engl.*, **33**, 1911 (1994).
7. C. W. Jefford, *Curr. Med. Chem.*, **8**, 1803 (2001).
8. (a) R. D. Bach, P. Y. Ayala and H. B. Schlegel, *J. Am. Chem. Soc.*, **118**, 12758 (1996).

- (b) M. Szwarc and J. S. Roberts, *J. Chem. Phys.*, **18**, 561 (1950).
(c) P. Molyneux, *Tetrahedron*, **22**, 2929 (1966).
9. S. L. Khursan and V. L. Antonovsky, *Russ. Chem. Bull.*, **52**, 1312 (2003).
10. E. L. Eliel, S. H. Wilen and L. N. Mander, *Stereochemistry of Organic Compounds*, Wiley, New York, 1994.
11. (a) D. Christen, H.-G. Mack and H. Oberhammer, *Tetrahedron*, **44**, 7363 (1988).
(b) C. M. Eestévez, O. Dmitrenko, J. E. Winter and R. D. Bach, *J. Org. Chem.*, **65**, 8629 (2000).
12. (a) D. Cremer, *J. Chem. Phys.*, **69**, 4440 (1978).
(b) E. Kraka, Y. He and D. Cremer, *J. Phys. Chem. A*, **105**, 3269 (2001).
13. (a) R. A. Blair and W. A. Goddard III, *J. Am. Chem. Soc.*, **104**, 2719 (1982).
(b) J. E. Carpenter and F. Weinhold, *J. Chem. Phys.*, **90**, 6405 (1986).
14. J. Z. Gougoutas, in *The Chemistry of Peroxides* (Ed. S. Patai), Chap. 12, Wiley, Chichester, 1983, pp. 375–415.
15. W. R. Busing and H. A. Levy, *J. Chem. Phys.*, **42**, 3054 (1965).
16. S. C. Abrahams and J. Kalnajs, *Acta Crystallogr.*, **8**, 503 (1955).
17. (a) C. S. Barrett, L. Meyer and J. Wasserman, *J. Chem. Phys.*, **47**, 592 (1967).
(b) H. Krebs, *Grundzüge der Anorganischen Kristallchemie*, Enke Verlag, Stuttgart, 1968, p. 133.
(c) I. L. Karle, *J. Chem. Phys.*, **23**, 1739 (1955).
18. M. J. Nolte, E. Singleton and M. Laing, *J. Am. Chem. Soc.*, **97**, 6396 (1975).
19. L. Vaska, *Acc. Chem. Res.*, **9**, 175 (1976).
20. S. Antonello, M. Musumeci, D. M. Wayner and F. Maran, *J. Am. Chem. Soc.* **119**, 9541 (1997).
21. M. Jonsson, *J. Phys. Chem.*, **100**, 6814 (1996).
22. M. Berthelot, F. Besseau and C. Laurence, *Eur. J. Org. Chem.*, 925 (1998).
23. A. J. Everett and G. J. Minkoff, *Trans. Faraday Soc.*, **49**, 410 (1953).
24. S. C. Abrahams, R. L. Collin and W. N. Lipscomb, *Acta Crystallogr.*, **4**, 15 (1951).
25. H. Cynn, C.-S. Yoo and S. A. Sheffield, *J. Chem. Phys.*, **110**, 6836 (1999).
26. J. Koput, *J. Mol. Spectrosc.*, **115**, 438 (1986).
27. (a) J. K. Laerdahl and P. Schwerdtfeger, *Phys. Rev. A*, **60**, 4439 (1999).
(b) A. Bakasov, T.-K. Ha and M. Quack, *J. Chem. Phys.*, **109**, 7263 (1998).
28. (a) J. Koput, *Chem. Phys. Lett.*, **236**, 516 (1995).
(b) L. Margulès, J. Demaison and J. E. Boggs, *J. Mol. Struct. (Theochem)*, **500**, 245 (2000).
29. N. Akiya and P. E. Savage, *J. Phys. Chem. A*, **104**, 4441 (2000).
30. T. Okajima, *J. Mol. Struct. (Theochem)*, **572**, 45 (2001).
31. D. Schröder, C. A. Schalley, N. Goldberg, J. Hřusák and H. Schwarz, *Chem. Eur. J.*, **2**, 1235 (1996).
32. (a) R. D. Bach, A. L. Owensby, C. Gonzalez, H. B. Schlegel and J. J. W. McDouall, *J. Am. Chem. Soc.*, **113**, 6001 (1991).
(b) R. D. Bach, J. L. Andrés, A. L. Owensby, H. B. Schlegel and J. J. W. McDouall, *J. Am. Chem. Soc.*, **114**, 7207 (1992).
33. R. L. Kuczkowski, in *Ozone and Carbonyl Oxides in 1,3-Dipolar Cycloaddition Chemistry*, Vol. 2 (Ed. A. Padwa), Chap. 11, Wiley, New York, 1984.
34. A. Engdahl, B. Nelander and G. Karlström, *J. Phys. Chem. A*, **105**, 8393 (2001).
35. (a) H. Hippler and J. Troe, *Chem. Phys. Lett.*, **192**, 333 (1992).
(b) H. Hippler, H. Neunaber and J. Troe, *J. Chem. Phys.*, **103**, 3510 (1995).
36. B. Wang, H. Hou and Y. Gu, *Chem. Phys. Lett.*, **309**, 274 (1999).
37. J. Lundell, S. Jolkkonen, L. Khriachtchev, M. Pettersson and M. Räsänen, *Chem. Eur. J.*, **7**, 1670 (2001).
38. J. Lundell, S. Pehkonen, M. Pettersson and M. Räsänen, *Chem. Phys. Lett.*, **286**, 382 (1998).
39. (a) D. Thierbach, F. Huber and H. Preut, *Acta Crystallogr.*, **B36**, 974 (1980).
(b) B. F. Pedersen, *Acta Chem. Scand.*, **23**, 1871 (1969).
(c) B. F. Pedersen, *Acta Chem. Scand.*, **21**, 779 (1967).
40. (a) C.-S. Lu, E. W. Hughes and P. A. Giguère, *J. Am. Chem. Soc.*, **63**, 1507 (1941).
(b) C. J. Fritchie Jr. and R. K. McMullan, *Acta Crystallogr.*, **B37**, 1086 (1981).
41. B. M. Kariuki and W. Jones, *Acta Crystallogr.*, **C51**, 1128 (1995).
42. B. F. Pedersen and Å. Kvik, *Acta Crystallogr.*, **A46**, 21 (1990).

43. X. Luo, P. R. Fleming and T. R. Rizzo, *J. Chem. Phys.*, **96**, 5969 (1992).
44. J. R. Barker, S. W. Benson and D. M. Golden, *Int. J. Chem. Kinet.*, **9**, 31 (1977).
45. (a) L. Jaffe, E. J. Prosen and M. Szwarc, *J. Chem. Phys.*, **27**, 416 (1957).
(b) A. Rembaum and M. Szwarc, *J. Am. Chem. Soc.*, **76**, 5975 (1954).
46. M. Tyblewski, T.-K. Ha, R. Meyer, A. Bauder and C. E. Blom, *J. Chem. Phys.*, **97**, 6168 (1992).
47. A. Y. Kosnikov, V. L. Antonovskii, S. V. Lindeman, M. Y. Antipin, Y. T. Struchkov, N. A. Turovskii and I. P. Zyat'kov, *Theor. Exp. Chem. (Eng. Transl.)*, **25**, 73 (1989).
48. V. L. Antonovskii, A. Y. Kosnikov, N. A. Turovskii, T. V. Timofeeva, S. V. Lindeman, Y. T. Struchkov and A. V. Ganyushkin, *Izv. Akad. Nauk SSSR, Ser. Khim.*, 68 (1990); *Chem. Abstr.*, **113**, 5393 (1990).
49. B. Haas and H. Oberhammer, *J. Am. Chem. Soc.*, **106**, 6146 (1984).
50. Y. L. Slovokhotov, T. V. Timofeeva, M. Y. Antipin and Y. T. Struchkov, *J. Mol. Struct.*, **112**, 127 (1984).
51. C. Glidewell, D. C. Liles, D. J. Walton and G. M. Sheldrick, *Acta Crystallogr.*, **B35**, 500 (1979).
52. (a) R. H. Jackson, *J. Chem. Soc.*, 4585 (1962).
(b) D. A. Dixon, J. Andzelm, G. Fitzgerald and E. Wimmer, *J. Phys. Chem.*, **95**, 9197 (1991).
53. J. K. Burdett, D. J. Gardiner, J. J. Turner, R. D. Spratley and P. Tchir, *J. Chem. Soc., Dalton Trans.*, 1928 (1973).
54. C. J. Marsden, D. D. DesMarteau and L. S. Bartell, *Inorg. Chem.*, **16**, 2359 (1977).
55. C. J. Marsden, L. S. Bartell and F. P. Diodati, *J. Mol. Struct.*, **39**, 253 (1977).
56. (a) F. A. Hohorst and D. D. DesMarteau, *Inorg. Chem.*, **13**, 715 (1974).
(b) R. Kopitzky, H. Willner, H.-G. Mack, A. Pfeiffer and H. Oberhammer, *Inorg. Chem.*, **37**, 6208 (1998).
57. N. Sebbar, H. Bockhorn and J. W. Bozzelli, *Phys. Chem. Chem. Phys.*, **4**, 3691 (2002).
58. A. Hermann, J. Niemeyer, H.-G. Mack, R. Kopitzky, M. Beuleke, H. Willner, D. Christen, M. Schäfer, A. Bauder and H. Oberhammer, *Inorg. Chem.*, **40**, 1672 (2001).
59. I. I. Shabalin and E. A. Kiva, *Opt. Spectrosc.-USSR*, **24**, 377 (1968).
60. S. Foote and S. I. Khan, *J. Org. Chem.*, **58**, 47 (1993).
61. K. J. McCullough, *Acta Crystallogr.*, **C42**, 688 (1986).
62. (a) S. L. Khursan and V. L. Antonovsky, *Russ. Chem. Bull.*, **52**, 1908 (2003).
(b) R. Benassi and F. Taddei, *J. Mol. Struct. (Theochem)*, **303**, 101 (1994).
63. D. Swern, L. P. Witnauer, C. R. Eddy and W. E. Parker, *J. Am. Chem. Soc.*, **77**, 5537 (1955).
64. D. Belitskus and G. A. Jeffrey, *Acta Crystallogr.*, **18**, 458 (1965).
65. A. Bondi, *J. Phys. Chem.*, **68**, 441 (1964).
66. F. H. Allen, O. Kennard and R. Taylor, *Acc. Chem. Res.*, **16**, 146 (1983).
67. M. Aoki and D. Seebach, *Helv. Chim. Acta*, **84**, 187 (2001).
68. S. Hrycko, P. Morand, F. L. Lee and E. J. Gabe, *J. Org. Chem.*, **53**, 1515 (1988).
69. A. G. Griesbeck, J. Lex, K. M. Saygin and J. Steinwascher, *Chem. Commun.*, 2205 (2000).
70. K. A. Lyssenko, M. Y. Antipin and V. N. Khrustalev, *Russ. Chem. Bull. (Engl. Transl.)*, **50**, 1539 (2001).
71. K. Peters, E.-M. Peters, T. Linker and L. Fröhlich, *Z. Kristallogr.*, **211**, 359 (1996).
72. I. S. A. Farag, M. A. El Kordy, A. Kirfel and G. Will, *Cryst. Res. Technol.*, **23**, 729 (1988).
73. R. K. Thalji, H. G. Pentes, N. H. Fischer and F. R. Fronczek, *Acta Crystallogr.*, **C54**, 861 (1998).
74. F. S. El-Ferally, D. A. Benigni and A. T. McPhail, *J. Chem. Soc., Perkin Trans. 1*, 355 (1983).
75. G. Bernardinelli, C. W. Jefford, J. Boukouvalas, D. Jaggi and S. Kohmoto, *Acta Crystallogr.*, **C43**, 701 (1987).
76. S. Matsumoto, Y. Itaka, S. Nakano and M. Matsuo, *J. Chem. Soc., Perkin Trans. 1*, 2727 (1993).
77. R. M. Corbett, Chee-Seng Lee, M. M. Sulikowski, J. Reibenspies and G. A. Sulikowski, *Tetrahedron*, **53**, 11099 (1997).
78. G. Appendino, M. Calleri, G. Chiari and D. Viterbo, *J. Chem. Soc., Perkin Trans. 2*, 903 (1984).
79. L. M. Engelhardt, F. R. Hewgill, J. M. Stewart and A. H. White, *J. Chem. Soc., Perkin Trans. 1*, 1845 (1988).
80. D. F. Covey, W. F. Hood, D. D. Beusen and H. L. Carrell, *Biochemistry*, **23**, 5398 (1984).

81. V. Langer and H.-D. Becker, *Z. Kristallogr.*, **206**, 117 (1993).
82. V. Langer and H.-D. Becker, *Z. Kristallogr.*, **206**, 121 (1993).
83. J. A. Moore, F. R. Fronczek and R. D. Gandour, *Acta Crystallogr.*, **C44**, 2027 (1988).
84. W. Adam, S. G. Bosio and N. J. Turro, *J. Am. Chem. Soc.*, **124**, 14004 (2002).
85. Z. Z. Hu, S. Takami, M. Kimura, Y. Tachi and Y. Naruta, *Acta Crystallogr.*, **C56**, e465 (2000).
86. J. L. Flippen-Anderson, *Acta Crystallogr.*, **C43**, 2228 (1987).
87. G. Rapi, M. Chelli, M. Ginanneschi, D. Donati and A. Selva, *J. Chem. Soc., Chem. Commun.*, 1339 (1982).
88. A. Camerman, H. W. Smith and N. Camerman, *J. Med. Chem.*, **26**, 679 (1983).
89. S. Alini, A. Citterio, A. Farina, M. C. Fochi and L. Malpezzi, *Acta Crystallogr.*, **C54**, 1000 (1998).
90. Y. Mori and K. Maeda, *Bull. Chem. Soc. Jpn.*, **67**, 1204 (1994).
91. G. A. Morales and F. R. Fronczek, *Acta Crystallogr.*, **C52**, 1266 (1996).
92. C.-Y. Qian, H. Nishino, K. Kurosawa and J. D. Korp, *J. Org. Chem.*, **58**, 4448 (1993).
93. C. Hartung, K. Illgen, J. Sieler, B. Schneider and B. Schulze, *Helv. Chim. Acta*, **82**, 685 (1999).
94. B. Schulze, S. Kirrbach, K. Illgen and P. Fuhrmann, *Tetrahedron*, **52**, 783 (1996).
95. F. G. Gelalcha and B. Schulze, *J. Org. Chem.*, **67**, 8400 (2002).
96. A. Kolberg, B. Schulze and J. Sieler, *Z. Kristallogr.*, **216**, 309 (2001).
97. B. Schulze, K. Taubert, F. G. Gelalcha, C. Hartung and J. Sieler, *Z. Naturforsch.*, **B57**, 383 (2002).
98. K. Taubert, J. Sieler, L. Hennig, M. Findeisen and B. Schulze, *Helv. Chim. Acta*, **85**, 183 (2002).
99. A. J. Carnell, W. Clegg, R. A. W. Johnstone, C. C. Parsy and W. R. Sanderson, *Tetrahedron*, **56**, 6571 (2000).
100. M. R. Iesce, F. Cermola, F. De Lorenzo, I. Orabona and M. L. Graziano, *J. Org. Chem.*, **66**, 4732 (2001).
101. K. I. Kuchkova, Y. M. Chumakov, Y. A. Simonov, G. Bocelli, A. A. Panasenko and P. F. Vlad, *Synthesis*, 1045 (1997).
102. T. Tokuyasu, A. Masuyama, M. Nojima, K. J. McCullough, H.-S. Kim and Y. Wataya, *Tetrahedron*, **57**, 5979 (2001).
103. M. R. Iesce, F. Cermola, A. Guitto and F. Giordano, *J. Chem. Soc., Perkin Trans. 1*, 475 (1999).
104. A. Y. Kosnikov, V. L. Antonovskii, S. V. Lindeman, Y. T. Struchkov, I. P. Zyat'kov and N. A. Turovskii, *Zh. Strukt. Khim.*, **29**, 125 (1988); *Chem. Abstr.*, **110**, 85979 (1989).
105. A. V. Yatsenko, V. A. Tafeenko, K. A. Paseshnichenko, T. V. Stalnaya and S. L. Solodar, *Z. Kristallogr.*, **213**, 466 (1998).
106. K. J. McCullough, R. Takeuchi, A. Masuyama and M. Nojima, *J. Org. Chem.*, **64**, 2137 (1999).
107. T. Sugimoto, K. Teshima, N. Nakamura, M. Nojima, S. Kusabayashi and K. J. McCullough, *J. Org. Chem.*, **58**, 135 (1993).
108. S. Matsumoto, M. Matsuo and Y. Iitaka, *J. Chem. Res.*, **58**, 601 (1987).
109. K. Teshima, S. Kawamura, Y. Ushigoe, M. Nojima and K. J. McCullough, *J. Org. Chem.*, **60**, 4755 (1995).
110. N. Nakamura, T. Fujisaka, M. Nojima, S. Kusabayashi and K. J. McCullough, *J. Am. Chem. Soc.*, **111**, 1799 (1989).
111. K. J. McCullough, T. Fujisaka, M. Nojima and S. Kusabayashi, *Tetrahedron Lett.*, **29**, 3375 (1988).
112. K. J. McCullough, M. Nojima, M. Miura, T. Fujisaka and S. Kusabayashi, *J. Chem. Soc., Chem. Commun.*, 35 (1984).
113. K. J. McCullough, N. Nakamura, T. Fujisaka, M. Nojima and S. Kusabayashi, *J. Am. Chem. Soc.*, **113**, 1786 (1991).
114. Z. Paryzek and U. Rychlewska, *J. Chem. Soc., Perkin Trans. 2*, 2313 (1997).
115. C. Pettinari, F. Marchetti, A. Cingolani, A. Drozdov and S. Troyanov, *Chem. Commun.*, 1901 (2000).
116. N. M. Todorovic, M. Stefanovic, B. Tinant, J.-P. Declercq, M. T. Markler and B. A. Solaja, *Steroids*, **61**, 688 (1996).

117. H.-J. Hamann and J. Liebscher, *J. Org. Chem.*, **65**, 1873 (2000).
118. M. R. Iesce, F. Cermola, A. Guitto, F. Giordano and R. Scarpati, *J. Org. Chem.*, **61**, 8677 (1996).
119. K. Jitsukawa, T. Yamamoto, T. Atsumi, H. Masuda and H. Einaga, *J. Chem. Soc., Chem. Commun.*, 2335 (1994).
120. A. J. Kirby, *Stereoelectronic Effects*, Oxford University Press, Oxford, 1996.
121. G. A. Jeffrey, *An Introduction to Hydrogen Bonding*, Oxford University Press, Oxford, 1997.
122. G. Boche, K. Mobus, K. Harms, J. C. W. Lohrenz and M. Marsch, *Chem. Eur. J.*, **2**, 604 (1996).
123. A. G. DiPasquale, W. Kaminsky and J. M. Mayer, *J. Am. Chem. Soc.*, **124**, 14534 (2002).
124. G. Boche, K. Mobus, K. Harms and M. Marsch, *J. Am. Chem. Soc.*, **118**, 2770 (1996).
125. A. van Asselt, B. D. Santarsiero and J. E. Bercaw, *J. Am. Chem. Soc.*, **108**, 8291 (1986).
126. H. Komatsuzaki, N. Sakamoto, M. Satoh, S. Hikichi, M. Akita and Y. Moro-oka, *Inorg. Chem.*, **37**, 6554 (1998).
127. F. A. Chavez, J. A. Briones, M. M. Olmstead and P. K. Mascharak, *Inorg. Chem.*, **38**, 1603 (1999).
128. W. Mikolajski, G. Baum, W. Massa and R. W. Hoffmann, *J. Organomet. Chem.*, **376**, 397 (1989).
129. A. Nishinaga, H. Tomita, K. Nishizawa, T. Matsuura, S. Ooi and K. Hirotsu, *J. Chem. Soc., Dalton Trans.*, 1504 (1981).
130. F. A. Chavez, J. M. Rowland, M. M. Olmstead and P. K. Mascharak, *J. Am. Chem. Soc.*, **120**, 9015 (1998).
131. L. Saussine, E. Brazi, A. Robine, H. Mimoun, J. Fischer and R. Weiss, *J. Am. Chem. Soc.*, **107**, 3534 (1985).
132. N. W. Alcock, B. T. Golding and S. Mwesigye-Kibende, *J. Chem. Soc., Dalton Trans.*, 1997 (1985).
133. M. Akita, T. Miyaji, S. Hikichi and Y. Moro-oka, *J. Chem. Soc., Chem. Commun.*, 1005 (1998).
134. G. Ferguson, M. Parvez, P. K. Monaghan and R. J. Puddephatt, *J. Chem. Soc., Chem. Commun.*, 267 (1983).
135. N. Kitajima, T. Katayama, K. Fujisawa, Y. Iwata and Y. Moro-oka, *J. Am. Chem. Soc.*, **115**, 7872 (1993).
136. M. B. Power, W. M. Cleaver, A. W. Apblett, A. R. Barron and J. W. Ziller, *Polyhedron*, **11**, 477 (1992).
137. W. M. Cleaver and A. R. Barron, *J. Am. Chem. Soc.*, **111**, 8966 (1989).
138. A. L. Balch, C. R. Cornman and M. M. Olmstead, *J. Am. Chem. Soc.*, **112**, 2963 (1990).
139. W. Satoh, S. Matsumoto, Y. Yamamoto and K. Akiba, *Heteroat. Chem.*, **12**, 431 (2001).
140. V. E. Shklover, Y. T. Struchkov, V. A. Dodonov, T. I. Zinov'eva and V. L. Antonovskii, *Metalloorg. Khim.*, **1**, 1140 (1988); *Chem. Abstr.*, **112**, 21063 (1990).
141. Z. A. Starikova, T. M. Shchegoleva, V. K. Trunov, I. E. Pokrovskaya and E. N. Kanunnikova, *Kristallografiya*, **24**, 1211 (1979); *Chem. Abstr.*, **92**, 86253 (1980).
142. M. Ochiai, T. Ito, Y. Masaki and M. Shiro, *J. Am. Chem. Soc.*, **114**, 6269 (1992).
143. M. Ochiai, T. Ito and M. Shiro, *J. Chem. Soc., Chem. Commun.*, 218 (1993).
144. A. Kobayashi, Y. Ikeda, K. Kubota and Y. Ohashi, *J. Agric. Food Chem.*, **41**, 1297 (1993).
145. S. J. Coles, D. E. Hibbs and M. Hursthouse, *Acta Crystallogr.*, **E57**, o66 (2001).
146. J. Fischer, P. G. Jones, U. Nippert and E. Winterfeldt, *Eur. J. Org. Chem.*, 3455 (1999).
147. S. Gab, W. V. Turner, F. Korte and L. Born, *J. Org. Chem.*, **47**, 173 (1982).
148. W.-w. Huang, H. Henry-Riyad and T. T. Tidwell, *J. Am. Chem. Soc.*, **121**, 3939 (1999).
149. J. Jeffery, R. J. Mawby, M. B. Hursthouse and N. P. C. Walker, *J. Chem. Soc., Chem. Commun.*, 1411 (1982).
150. G. Appendino, M. Calleri, G. Chiari and D. Viterbo, *Acta Crystallogr.*, **C40**, 97 (1984).
151. R. Stomberg and K. Lundquist, *Z. Kristallogr.*, **212**, 263 (1997).
152. E. A. Dikisar, V. L. Shirokii, A. P. Yuvchenko, A. V. Bazhanov, K. L. Moiseichuk, V. N. Khrustalev and M. Y. Antipin, *Zh. Obshch. Khim.*, **69**, 1315 (1999); *Chem. Abstr.*, **132**, 334588 (2000).
153. Y. Lam, G.-H. Lee and E. Liang, *Bull. Chem. Soc. Jpn.*, **74**, 1033 (2001).
154. S.-H. Jang, P. Gopalan, J. E. Jackson and B. Kahr, *Angew. Chem., Int. Ed. Engl.*, **33**, 775 (1994).

155. P. D. Robinson, Y. Hou and C. Y. Meyers, *Acta Crystallogr.*, **C55**, IUC9900147 (1999).
156. T. Pilati, M. Simonetta and S. Quici, *Cryst. Struct. Commun.*, **11**, 1027 (1982).
157. N. Kuznik, J. Zawadiak, D. Gilner, A. Wieckol, P. Wagner and M. Kubicki, *Acta Crystallogr.*, **C58**, 549 (2002).
158. A. Y. Kosnikov, V. L. Antonovskii, S. V. Lindeman, Y. T. Struchkov and I. P. Zyat'kov, *Kristallografiya*, **31**, 97 (1986); *Chem. Abstr.*, **104**, 139703 (1986).
159. C. W. Jefford, G. Bernardinelli and E. C. McGoran, *Helv. Chim. Acta*, **67**, 1952 (1986).
160. M. Ramm, *Z. Kristallogr.* **211**, 660 (1996).
161. G. L. Squadrito, M. G. Salgo, F. R. Fronczek and W. A. Pryor, *Methods in Enzymology*, **319**, 570 (2000).
162. A. Moretto, M. De Zotti, L. Scipionato, F. Formaggio, M. Crisma, C. Toniolo, S. Antonello, F. Maran and Q. B. Broxterman, *Helv. Chim. Acta*, **85**, 3099 (2002).
163. K. Peters, E.-M. Peters, J. Hinrichs and G. Bringmann, *Z. Kristallogr.*, **215**, 57 (2000).
164. G. G. Furin, A. O. Miller, Y. V. Gatilov, I. Y. Bagryanskaya and G. G. Yakobson, *J. Fluorine Chem.*, **28**, 23 (1985).
165. N. Feeder and W. Jones, *Acta Crystallogr.*, **C52**, 1516 (1996).
166. N. Feeder and W. Jones, *Acta Crystallogr.*, **C52**, 2323 (1996).
167. N. Feeder and W. Jones, *Acta Crystallogr.*, **C50**, 1347 (1994).
168. N. Feeder and W. Jones, *Acta Crystallogr.*, **C52**, 919 (1996).
169. P. Ghosh, Z. Tyeklar, K. D. Karlin, R. R. Jacobson and J. Zubieta, *J. Am. Chem. Soc.*, **109**, 6889 (1987).
170. P. Koll, R. Bruns and J. Kopf, *Carbohydr. Res.*, **305**, 147 (1998).
171. M. Oki, I. Fujino, D. Kawaguchi, K. Chuda, Y. Moritaka, Y. Yamamoto, S. Tsuda, T. Akinaga, M. Aki, H. Kojima, M. Norita, M. Sakurai, S. Toyota, Y. Tanaka, T. Tanuma and G. Yamamoto, *Bull. Chem. Soc. Jpn.*, **70**, 457 (1997).
172. S. Antonello, M. Crisma, F. Formaggio, A. Moretto, F. Taddei, C. Toniolo and F. Maran, *J. Am. Chem. Soc.*, **124**, 11503 (2002).
173. L. Golic and I. Leban, *Acta Crystallogr.*, **C40**, 447 (1984).
174. L. Antolini, R. Benassi, S. Ghelli, U. Folli, S. Sbardellati and F. Taddei, *J. Chem. Soc., Perkin Trans. 2*, 1907 (1992).
175. G. Chiari, G. Appendino and G. M. Nano, *J. Chem. Soc., Perkin Trans. 2*, 263 (1986).
176. A. S. Lyakhov, L. S. Ivashkevich, A. P. Yuvchenko, T. D. Zvereva, A. A. Govorova and Y. I. Petrushevich, *Kristallografiya*, **46**, 1054 (2001); *Chem. Abstr.*, **136**, 247624 (2002).
177. D. Bethell, D. J. Chadwick, M. M. Harding and G. Q. Maling, *Acta Crystallogr.*, **C40**, 1909 (1984).
178. D. Bethell, D. J. Chadwick, G. Q. Maling and M. M. Harding, *Acta Crystallogr.*, **C40**, 1628 (1984).
179. D. Bethell, D. J. Chadwick, M. M. Harding and G. Q. Maling, *Acta Crystallogr.*, **B38**, 1677 (1982).
180. A. Y. Kosnikov, V. L. Antonovskii, S. V. Lindeman, Y. T. Struchkov and I. P. Zyat'kov, *Kristallografiya*, **33**, 875 (1988); *Chem. Abstr.*, **109**, 180935 (1988).
181. S. V. Lindeman, V. E. Shklover, Y. T. Struchkov, E. K. Starostin and G. I. Nikishin, *Izv. Akad. Nauk SSSR, Ser. Khim.*, 2744 (1983); *Chem. Abstr.*, **100**, 94889 (1984).
182. S. V. Lindeman, Y. T. Struchkov, E. K. Starostin and G. I. Nikishin, *Izv. Akad. Nauk SSSR, Ser. Khim.*, 819 (1985); *Chem. Abstr.*, **102**, 229793 (1985).
183. J. M. McBride and M. W. Vary, *Tetrahedron*, **38**, 765 (1982).
184. A. Syed, P. Umrigar, E. D. Stevens, G. W. Griffin and R. J. Majeste, *Acta Crystallogr.*, **C40**, 1458 (1984).
185. A. Y. Kosnikov, V. L. Antonovskii, S. V. Lindeman, Y. T. Struchkov, I. P. Zyat'kov, G. A. Pitsevich and V. I. Gogolinskii, *Izv. Akad. Nauk SSSR, Ser. Khim.*, 937 (1985); *Chem. Abstr.*, **103**, 104638 (1985).
186. D. Bethell, D. J. Chadwick, M. M. Harding, G. Q. Maling and M. D. Wiley, *Acta Crystallogr.*, **C41**, 470 (1985).
187. G. Czapski and B. H. J. Bielski, *J. Phys. Chem.*, **67**, 2180 (1963).
188. J. A. Gormley, *J. Chem. Phys.*, **39**, 3539 (1963).
189. J. L. Arnau and P. A. Giguère, *J. Chem. Phys.*, **60**, 270 (1974).
190. A. Engdahl and B. Nelander, *Science*, **295**, 482 (2002).
191. D. J. Mckay and J. S. Wright, *J. Am. Chem. Soc.*, **120**, 1003 (1998).

192. (a) B. Plesničar, T. Tuttle, J. Cerkovnik, J. Koller and D. Cremer, *J. Am. Chem. Soc.*, **125**, 11553 (2003).
(b) D. Cremer, *J. Phys. Chem.*, **69**, 4456 (1978).
193. B. Plesničar, J. Cerkovnik, T. Tekavec and J. Koller, *Chem. Eur. J.*, **6**, 809 (2000).
194. K. I. Gobatto, M. F. Klapdor, D. Mootz, W. Poll, S. E. Ulic, H. Willner and H. Oberhammer, *Angew. Chem., Int. Ed. Engl.*, **34**, 2244 (1995).
195. T. E. Wallaart, N. Pras and W. J. Quax, *J. Nat. Prod.*, **62**, 1160 (1999).
196. (a) G. D. Brown and L.-K. Sy, *Tetrahedron*, **60**, 1139 (2004).
(b) G. D. Brown, G. Y. Liang and L.-K. Sy, *Phytochemistry*, **64**, 303 (2003).
197. F. S. El-Feraly, A. Ayalp, M. A. Al-Yahya, D. R. McPhail and A. T. McPhail, *J. Nat. Prod.*, **53**, 66 (1990).
198. A. Arciniegas, A. L. Perez-Castorena, S. Reyes, J. L. Contreras and A. R. de Vivar, *J. Nat. Prod.*, **66**, 225 (2003).
199. G. Rucker, R. Mayer, E. Breitmaier, G. Will, A. Kirfel and M. El Kordy, *Phytochemistry*, **23**, 1647 (1984).
200. B. Carté, M. R. Kernan, E. B. Barrabee and D. J. Faulkner, *J. Org. Chem.*, **51**, 3528 (1986).
201. K. Peters, E.-M. Peters, H. G. von Schnering, A. Griesbeck and K. Gollnick, *Z. Kristallogr.*, **168**, 153 (1984).
202. A. E. Flowers, M. J. Garson, K. A. Byriell and C. H. L. Kennard, *Aust. J. Chem.*, **51**, 195 (1998).
203. H. Itokawa, E. Kishi, H. Morita, K. Takeya and Y. Iitaka, *Chem. Lett.*, 2221 (1991).
204. H. Morita, E. Kishi, K. Takeya, H. Itokawa and Y. Iitaka, *Phytochemistry*, **34**, 765 (1993).
205. K.-H. Lee, H. Nozaki and A. T. McPhail, *Tetrahedron Lett.*, **25**, 707 (1984).
206. J. J. K. Wright, Y. Merrill, M. S. Puar and A. T. McPhail, *J. Chem. Soc., Chem. Commun.*, 473 (1984).
207. J. Hartung and M. Greb, *J. Organometal. Chem.*, **661**, 67 (2002).
208. J. Hartung, T. Gottwald and K. Špehar, *Synthesis*, 1469 (2002).
209. (a) M. J. Molina, A. J. Colussi, L. T. Molina, R. N. Schindler and T. L. Tso, *Chem. Phys. Lett.*, **173**, 310 (1990).
(b) R. A. Cox and G. D. Hayman, *Nature*, **332**, 796 (1988).
210. (a) V. R. Kotamarthi, J. M. Rodriguez, M. K. W. Ko, T. K. Tromp, N. D. Sze and M. J. Prather, *J. Geophys. Res. Atmos.*, **103**, 5747 (1998).
(b) M. K. W. Ko, N. D. Sze, J. M. Rodriguez, D. K. Weistenstein, C. W. Heisey, R. P. Wayne, P. Biggs, C. E. Canosamas, H. W. Sidebottom and J. Tracey, *Geophys. Res. Lett.*, **21**, 101 (1994).
211. X. Xu and W. A. Goddard III, *Proc. Natl. Acad. Sci. USA*, **99**, 15308 (2002).
212. L.-J. Thenard, *Ann. Chim. Phys.*, **8**, 306 (1818).

CHAPTER 3

Thermochemistry of peroxides

SUZANNE W. SLAYDEN

Department of Chemistry, George Mason University, 4400 University Drive, Fairfax, VA 22030-4444, USA

Fax: +1 703 993 1055; e-mail: sslayden@gmu.edu

and

JOEL F. LIEBMAN

Department of Chemistry and Biochemistry, University of Maryland, Baltimore County, 1000 Hilltop Circle, Baltimore, MD 21250, USA

Fax: +1 410 455 2608; e-mail: jliebman@umbc.edu

I. INTRODUCTION, SCOPE AND DEFINITIONS	146
A. Thermochemistry	146
B. Sources of Data	146
II. HYDROCARBON-SUBSTITUTED PEROXIDES	147
A. Quality of the Data	147
B. Enthalpies of Vaporization	147
C. Enthalpies of Isomerization	150
D. Formal Reactions and Relationships	151
1. Hydroperoxides	151
2. Peroxides	153
3. Mixed hydroperoxides and peroxides	154
E. Other Reactions	155
F. Polymeric Peroxides	155
III. PEROXIDES WITH SINGLE-BONDED OXYGEN FUNCTIONAL GROUPS	155
A. Hydroxyl Substituents	155
B. Hydroxyl and Alkoxy Substituents	157
IV. PEROXYCARBOXYLIC ACIDS AND THEIR DERIVATIVES	158
A. Peroxycarboxylic Acids	158
B. Percarboxylate Esters	160
C. Acyl Peroxides	162

The chemistry of peroxides, volume 2

Edited by Z. Rappoport © 2006 John Wiley & Sons, Ltd ISBN: 0-470-86274-2

V. CYCLIC PEROXIDES AND MULTIPLY-LINKED PEROXIDES	163
A. Dioxetanes	163
B. 1,2,4,5-Tetroxanes	164
C. Ozonides (1,2,4-Trioxolanes)	165
D. An Explosive Triperoxide	166
E. Arene Endoperoxides	166
VI. REFERENCES AND NOTES	167

I. INTRODUCTION, SCOPE AND DEFINITIONS

After a hiatus of more than 10 years since our earlier chapter on the thermochemistry of oxygen-containing compounds¹, it might be expected that a review of the literature of the thermochemistry of peroxides and hydroperoxides would produce new data and fresh insights. Unfortunately, we have been disappointed. In the intervening years we have found virtually no new thermochemical experimental studies on either the most structurally simple or even complex peroxides. Likewise, we have found few new data for those compounds with which it might be advantageous to compare the peroxides, such as ethers, acetals and alcohols, and the lack of which thwarted us in the previous volume. However, since this current study concerns peroxides only (ROOR' and ROOH both generically called 'peroxides') and is not part of a larger consideration of other oxygen-containing species, it is more complete in terms of the number of compounds cited with their accompanying thermochemical data and associated interpretation. Some of the current text refers to the findings from contemporary (1990 and later) investigations while others refer to studies earlier neglected by diverse thermochemical archivists and also by us.

A. Thermochemistry

The current chapter is devoted primarily to discussion of the 'standard enthalpy of formation', more colloquially called the 'heat of formation'. Enthalpies of formation are written as $\Delta_f H_m^0$ with an affixed s, lq or g to convey that the species of interest is found as a solid, liquid or gas, respectively. The temperature and pressure are tacitly 25 °C ('298 K') and 1 atmosphere (taken as either 101,325 or 100,000 Pa), respectively, and the energy units are kJ mol⁻¹ where, by definition, 4.184 kJ = 1 kcal. Enthalpies of reaction involving peroxides are discussed within the context of deriving or otherwise discussing an enthalpy of formation. Phase change enthalpies (vaporization, liquid → gas; sublimation, solid → gas; fusion, solid → liquid and their reverse) are discussed, especially vaporization since that quantity requires the fewest supplemental data for its prediction. By intent, we forego discussion of other thermochemical properties such as Gibbs energy, entropy, heat capacity and excess enthalpy. Ionization processes (gain or loss of an electron or of a proton) are likewise ignored.

B. Sources of Data

Unless otherwise noted, following our practice in other chapters in this series, enthalpies of formation and of vaporization were taken from the evaluated archival source by Pedley, Naylor and Kirby². Where primary sources were difficult to access, data were obtained from the electronic database at the National Institute of Standards and Technology³ and the original source is cited. Except for the more recently determined values, the peroxide enthalpies of formation that appear in Tables 1–4 here also appeared in our earlier

review¹: we acknowledge the error in recording some OH-containing species as solids rather than liquids.

II. HYDROCARBON-SUBSTITUTED PEROXIDES

A. Quality of the Data

The enthalpy of formation data appear in Table 1. Where there are numerous data for structurally related compounds, plotting the enthalpy of formation versus the number of carbons can reveal at a glance the quality of the data. For the alkyl hydroperoxides especially, the data are seen to be of mixed quality as evidenced by the lack of linearity in the plot (Figure 1). The error bars for the ethyl and *n*-propyl hydroperoxides are so large as to render the data meaningless. Also, the enthalpy of formation of *n*-propyl hydroperoxide is more negative than that of 1-hexyl hydroperoxide, another indication of its gross inaccuracy. The C₂ and C₃ hydroperoxide data will not be considered any further.

There is reported enthalpy of formation data for methyl hydroperoxide⁴. The enthalpy of formation of the methyl derivative for any functional group, MeZ, is expected to deviate somewhat from the linear relationship established by the *n*-alkyl members of the homologous series with the same Z¹⁴. It is unclear where the best straight line lies for the *n*-alkyl hydroperoxides and so the extent of deviation for methyl hydroperoxide is likewise unclear. However, methyl hydroperoxide, like other methyl derivatives with electron-withdrawing functional groups, should exhibit an enthalpy of formation that is more positive than other members of the series.

The liquid enthalpy of formation difference between 1-hexyl and 1-heptyl hydroperoxides is almost twice that of a normal enthalpy of formation methylene increment of about 25 kJ mol⁻¹. But which of these two, if either, is correct? For hydrocarbon substituents bonded to electronegative functional groups, the secondary isomers are more stable than the *n*-isomer. Accordingly, either the 1- or 4-heptyl hydroperoxide, or both, have an inaccurate enthalpy of formation because the primary isomer is reported to have the more negative enthalpy of formation. All of the enthalpies of formation for the C₆ and C₇ hydroperoxides cited in Reference 2 come from a single source¹⁵. There is a reported value⁴ for the gas phase enthalpy of formation of *tert*-butyl hydroperoxide that is 11 kJ mol⁻¹ less negative than the value in Reference 2.

There are much fewer data for the dialkyl peroxides. The gas phase enthalpy of formation difference between the diethyl and dibutyl peroxides of about 40 kJ mol⁻¹ per methylene group is about twice that of the normal methylene increment of *ca* 21.6 kJ mol⁻¹. The 219 kJ mol⁻¹ enthalpy of formation difference between the di-*tert*-butyl and di-*tert*-amyl peroxide is so large as to be incredible.

At this stage it may be worth conjecturing as to why some calorimetric studies of peroxides and hydroperoxides are seemingly unreliable. Recall that an ether that has been left standing too long autooxidizes to a peroxide, which then has a tendency to explode on heating or when shocked. In an experimental combustion process, this same tendency to explode may result in incomplete combustion with attendant carbon build-up. If so, there are thermodynamically ill-defined and irreproducible products that increase the variability and uncertainty in the measurements and essentially invalidate the results derived¹⁶.

B. Enthalpies of Vaporization

Where enthalpies of vaporization are not otherwise available, the 'CHLP protocol'¹⁷ is used to estimate these quantities according to equation 1. The quantities \tilde{n}_c and n_Q refer respectively to the number of quaternary (non-hydrogen-bearing sp³-hybrid) carbon

TABLE 1. Enthalpies of formation of hydrocarbon-substituted hydroperoxides and peroxides (kJ mol⁻¹)

Compound	$\Delta_f H_m^0$ (s)	$\Delta_f H_m^0$ (lq)	$\Delta_f H_m^0$ (g)	Reference
Hydroperoxides				
Methyl hydroperoxide		-196.	-131.	4, 5
Ethyl hydroperoxide		-242 ± 58.6	-198.9 ± 58.7	2
<i>n</i> -Propyl hydroperoxide		-318 ± 62.8		2
Isopropyl hydroperoxide			-197.1	4
<i>tert</i> -Butyl hydroperoxide		-293.6 ± 5	-245.9 ± 5	2
			-234.9	4
Cyclohexyl hydroperoxide		-273.2 ± 2.9	-214.9	2, 6
1-Hexyl hydroperoxide		-299.6 ± 5		2
2-Hexyl hydroperoxide		-310.1 ± 2.9		2
3-Hexyl hydroperoxide		-305.1 ± 7.5		2
1-Methylcyclohexane hydroperoxide		-330.4 ± 6.3		2
1-Heptyl hydroperoxide		-343 ± 5		2
2-Heptyl hydroperoxide		-346.4 ± 2.1		2
3-Heptyl hydroperoxide		-346.8 ± 4.2		2
4-Heptyl hydroperoxide		-333.8 ± 2.1		2
1,1-Dimethyl-4-penten-2-yn-1-yl hydroperoxide		63.3 ± 1.9	127.1 ± 1.9	6
Cumyl hydroperoxide [(2-hydroperoxy-2-propyl)benzene]		-148.3 ± 6.7	-78.4 ± 6.7	2
Tetralin-1-hydroperoxide ^a [1,2,3,4-tetrahydro-1-hydroperoxynaphthalene]	-185.7 ± 6.5			2
1-Methyltetralin-1-hydroperoxide [1-Methyl-1,2,3,4-tetrahydronaphthalene-1-hydroperoxide]	-157.2 ± 18.4			2
Decalin-9-hydroperoxide [<i>trans</i> -decahydro-9-hydroperoxynaphthalene]	-349.2 ± 6.3			2
Bishydroperoxides				
2,5-Dimethyl-3-hexyne-2,5-bis(hydroperoxide)	-257.6 ± 2.8		-130.2 ± 3.3	7 ^b
2,5-Dimethylhexane-2,5-bis(hydroperoxide)	-567.2 ± 3.5		-428.7 ± 3.7	7 ^b
Peroxides				
Dimethyl peroxide			-125.7 ± 1.3	2
Diethyl peroxide		-223.3 ± 1.3	-192.8 ± 2.5	2
Di- <i>n</i> -butyl peroxide		-394.3 ± 5	-354.3	8
Di- <i>tert</i> -butyl peroxide		-380.8 ± 2	-341.5 ± 2	9
Di- <i>tert</i> -amyl peroxide		-599.6		10
5-Methyl-5- <i>tert</i> -butylperoxyhex-3-yn-1-ene [<i>tert</i> -butyl 1,1-dimethyl-4-penten-2-yn-1-yl peroxide]		-28.9 ± 3.5	22.7 ± 3.5	6

TABLE 1 (continued)

Compound	$\Delta_f H_m^0$ (s)	$\Delta_f H_m^0$ (lq)	$\Delta_f H_m^0$ (g)	Reference
<i>tert</i> -Butyl cumyl peroxide [1,1-dimethylethyl 1-methyl-1-phenylethyl peroxide]		-263 ± 5.8	-193.9 ± 5.8	11
<i>tert</i> -Butyl <i>p</i> -isopropylcumyl peroxide [1-methylethyl-1-[(4- methylethyl)phenyl]ethyl 1,1-dimethylethyl peroxide]		-352.1 ± 5.0	-278.8 ± 7.1	11
Bisperoxides				
2,2-Bis(<i>tert</i> - butylperoxy)butane [bis(<i>tert</i> -butyl)- <i>sec</i> - butylidene]		-616.7		12
1,4-Phenylenebis(1- methylethylidene)]bis[(1,1- dimethylethyl) peroxide]	-568.6 ± 6.4		-457.0 ± 14.6	11
Polystyrene peroxide -CH ₂ -CH(C ₆ H ₅)-O-O-	27 ± 21			13
Mixed hydroperoxide and peroxide				
2,5-Dimethyl-2- hydroperoxide-5- <i>tert</i> - butylperoxyhexane		-636.0 ± 3.3	-561.8 ± 3.3	7

^a This compound is misnamed as the 5-hydroperoxy compound in Reference 2.

^b This reference reports the enthalpy of sublimation as the enthalpy of vaporization.

atoms and non-quaternary (hydrogen-bearing carbons or sp²-hybrid) carbon atoms, and *b* is a value that is characteristic of the functional group bonded to the hydrocarbon parent.

$$\Delta H_{\text{vap}}(\text{kJ mol}^{-1}) = 4.69\tilde{n}_c + 1.3 n_Q + 2.97 + b \quad (1)$$

The *b* value for peroxides was not evaluated in the original publication¹⁷, but we can do so here from the experimental enthalpies of vaporization that are available. There are three such for the alkyl hydroperoxides: 35 kJ mol⁻¹ for methyl hydroperoxide, 43.1 kJ mol⁻¹ for ethyl hydroperoxide and 47.7 kJ mol⁻¹ for *tert*-butyl hydroperoxide. The corresponding *b* values are 27.3, 30.8 and 29.8 kJ mol⁻¹, respectively. The mean value, 29.0 ± 1.5 kJ mol⁻¹, is the same as the *b* value for alcohols (29.4 kJ mol⁻¹). There are independent determinations of the enthalpies of formation of cyclohexyl hydroperoxide in the liquid and gaseous phases. The enthalpy of vaporization from the arithmetic difference between these two quantities differs by only 2 kJ mol⁻¹ from that calculated using equation 1 and the newly derived *b* constant.

There are three dialkyl peroxides with experimental enthalpies of vaporization: 30.5 kJ mol⁻¹ for diethyl peroxide, 40 kJ mol⁻¹ for di-*n*-butyl peroxide⁸ and 39.3 kJ mol⁻¹ for di-*tert*-butyl peroxide⁹. The calculated *b* values are 8.8, -0.46 and 5.6 kJ mol⁻¹, respectively. The mean is 4.6 ± 4.7 kJ mol⁻¹. Although the negative *b* value is non-

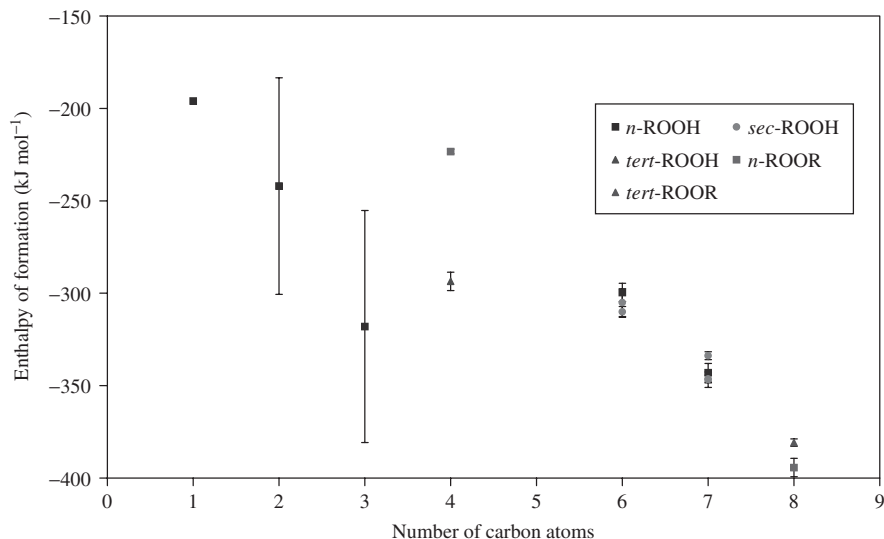


FIGURE 1. Enthalpies of formation of alkyl hydroperoxides and dialkyl peroxides vs. number of carbon atoms (lq, kJ mol⁻¹)

physical, the CHLP equation generally reproduces experimental enthalpies of vaporization only to within $\pm 5\%$. This average b value does not reproduce the experimental enthalpies of vaporization quite so accurately. However, the b value for ethers is 5.0 kJ mol^{-1} and so we accept the mean calculated value for the structurally related peroxides. From the estimated enthalpies of vaporization, the calculated liquid phase enthalpies of formation of isopropyl hydroperoxide, dimethyl peroxide and di-*tert*-amyl peroxide are -243 , -142.7 and $-551.9 \text{ kJ mol}^{-1}$, respectively.

Three peroxides with aromatic substituents have reported enthalpy of vaporization data, all from the same source¹¹. The enthalpies of vaporization of cumyl hydroperoxide and *tert*-butyl cumyl peroxide are the same, which makes us skeptical of at least one of these values. The calculated b value for cumyl hydroperoxide is 31.5 , consistent with the alkyl hydroperoxides. The calculated b value for *tert*-butyl cumyl peroxide is 15.4 and more than twice that for the mean of the dialkyl peroxides. The structurally related *tert*-butyl *p*-isopropylcumyl peroxide has a b value of 8.8 and so is consistent with the other disubstituted peroxides.

C. Enthalpies of Isomerization

Since we absolutely do not believe the enthalpy of formation of *n*-PrOOH, let us derive a plausible value for it from the isomerization of *i*-PrOOH, assuming that whatever its provenance it is the more accurate of the two. From the difference between the enthalpies of formation of *n*-propyl and isopropyl alcohol, the derived enthalpies of isomerization are $-17.7 \text{ kJ mol}^{-1}$ (g) and $-15.5 \text{ kJ mol}^{-1}$ (lq). Using these as the approximate enthalpies of isomerization of the related hydroperoxides, the derived enthalpies of formation of *n*-PrOOH are thus -179 kJ mol^{-1} (g) and -227 kJ mol^{-1} (lq) from the liquid enthalpy of formation of *i*-PrOOH that was estimated above.

The derived enthalpies for isomerization of *n*-BuOH to *t*-BuOH are $-31.9 \text{ kJ mol}^{-1}$ (lq) and $-36.7 \text{ kJ mol}^{-1}$ (g). From the enthalpies of formation² of *t*-BuOOH, the calculated enthalpies of formation of *n*-BuOOH are $-261.7 \text{ kJ mol}^{-1}$ (lq) and $-209.3 \text{ kJ mol}^{-1}$ (g). Using the more recently reported enthalpy of formation of *tert*-BuOOH in the gas phase⁴, the derived enthalpy of formation of *n*-BuOOH is $-198.2 \text{ kJ mol}^{-1}$. The linear least-squares analysis of the derived liquid enthalpies of formation of *n*-PrOOH and *n*-BuOOH and the experimental enthalpy of formation of *n*-HexOOH gives an intercept of $-161.3 \text{ kJ mol}^{-1}$ and a slope of $-23.4 \text{ kJ mol}^{-1}$, the latter value very close to that for the C₃–C₆ *n*-alkanols of -25 kJ mol^{-1} . From the regression constants, the liquid enthalpy of formation of *n*-HeptOOH is -325 kJ mol^{-1} , a value that is less negative, and thus more plausible when compared to its secondary isomers.

The enthalpy of isomerization of liquid 1-hexanol to either 2- or 3-hexanol is *ca* 15 kJ mol^{-1} , and the enthalpy of isomerization of liquid 1-heptanol to 2-, 3- or 4-heptanol¹⁸ is *ca* 13 kJ mol^{-1} . From the experimental enthalpy of formation of 1-hexyl hydroperoxide, the calculated enthalpy of formation of 2- and 3-hexyl hydroperoxide is *ca* -315 kJ mol^{-1} , which is about $5\text{--}10 \text{ kJ mol}^{-1}$ more negative than their experimental values. As noted earlier, the measured enthalpies of formation of 2- and 3-heptyl hydroperoxide are about the same as that of 1-heptyl hydroperoxide, while that of 4-heptyl hydroperoxide is actually less negative than for its primary isomer. Using instead the above-derived enthalpy of formation of 1-heptyl hydroperoxide of -325 kJ mol^{-1} , the enthalpy of formation of the secondary isomers would be *ca* -338 kJ mol^{-1} . This value is very close to the experimental enthalpy of formation of 4-heptyl hydroperoxide, but 8 kJ mol^{-1} less negative than the experimental values for 2- and 3-heptyl hydroperoxide. These latter enthalpies of formation are too negative compared to the experimental values for 2- and 3-hexyl hydroperoxide, with a methylene increment of *ca* 36 kJ mol^{-1} . The derived values are more plausible.

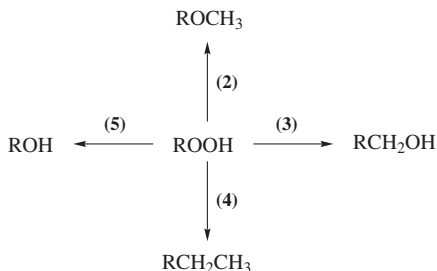
The formal isomerization enthalpies of methyl *n*-butyl ether to methyl *tert*-butyl ether and of di-*n*-butyl ether to *n*-butyl *tert*-butyl ether are about -24 kJ mol^{-1} (lq) and $-26.5 \text{ kJ mol}^{-1}$ (g), respectively. From these, and the experimental enthalpy of formation of di-*tert*-butyl peroxide, the enthalpies of formation of di-*n*-butyl peroxide are *ca* -333 kJ mol^{-1} (lq) and -288 kJ mol^{-1} (g), wildly divergent from the reported values.

D. Formal Reactions and Relationships

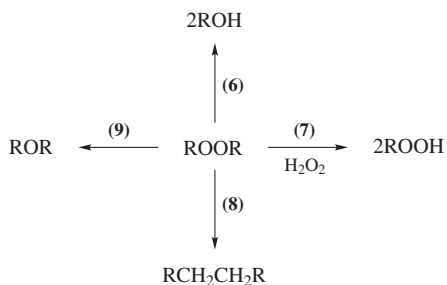
In our previous review¹, we attempted to establish some simple relationships among peroxides, ethers, alcohols and alkanes using a limited peroxide data set and a sometimes less than adequate data set for the comparison classes of compounds. The analysis is extended in this volume. The formal reactions, equations 2–5 and 6–9, that illustrate some typical comparisons are shown in Schemes 1 and 2.

1. Hydroperoxides

For the comparison of hydroperoxides with methyl ethers (equation 2), we find there is enthalpy of formation data only for dimethyl ether, isopropyl methyl ether and *t*-butyl methyl ether (again ignoring the ethyl and propyl hydroperoxides). The enthalpies of formal reaction 2 for R = Me, *i*-Pr and *t*-Bu (two gas phase enthalpies of formation for *t*-BuOOH) are -53.1 , -54.9 and -37.6 or $-48.6 \text{ kJ mol}^{-1}$, respectively, in the gas phase. In the liquid phase, the enthalpies of reaction are -7.4 , -35 (from the estimated enthalpy of formation of isopropyl hydroperoxide) and $-20.0 \text{ kJ mol}^{-1}$, respectively. Because the enthalpy of formation deviations from linearity for dimethyl ether and methyl hydroperoxide might not be identical, the reaction enthalpy might not be consistent with those



SCHEME 1



SCHEME 2

obtained from the other alkyl pairs. There is no obvious reason why the values should vary widely depending on the secondary/tertiary carbon classification of the hydrocarbon and on this basis we conclude that the gas phase enthalpy of formation of *t*-butyl hydroperoxide from Reference 4 appears to be more accurate.

For reaction 3 to replace an oxygen with a methylene group to form a primary alcohol, there are enthalpies of formation for only seven alcohols to compare with the nineteen hydroperoxides, almost all of them only for the liquid phase. The enthalpies of the formal reaction are nearly identical, $-104.8 \pm 1.1 \text{ kJ mol}^{-1}$, for R = 1-hexyl, cyclohexyl and *tert*-butyl, while we acknowledge the experimental uncertainties of ± 8.4 and $\pm 16.7 \text{ kJ mol}^{-1}$, respectively, for the enthalpies of formation of the secondary and tertiary alcohols. We accept this mean value as representative of the reaction. For R = 1- and 2-heptyl, the enthalpies of reaction are the disparate -83.5 and $-86.0 \text{ kJ mol}^{-1}$, respectively. From the consensus enthalpy of reaction and the enthalpy of formation of 1-octanol, the enthalpy of formation of 1-heptyl hydroperoxide is calculated to be *ca* -322 kJ mol^{-1} , nearly identical to that derived earlier from the linear regression equation. The similarly derived enthalpy of formation of 3-heptyl hydroperoxide is *ca* -328 kJ mol^{-1} . The enthalpy of reaction for R = *i*-Pr is only *ca* -91 kJ mol^{-1} , and also suggests that there might be some inaccuracy in its previously derived enthalpy of formation. Using the consensus enthalpy of reaction, a new estimate of the liquid enthalpy of formation of *i*-PrOOH is *ca* -230 kJ mol^{-1} .

For the formal reaction of replacing both oxygens in the hydroperoxide by methylene groups (equation 4), there are more comparison data available. Although there was seemingly no difference in the enthalpies of reaction 3 for a typical primary, secondary and tertiary hydroperoxide whose experimental enthalpies of formation we accepted, the situation changes with reaction 4. The enthalpies of reaction are quite different depending

on whether R is primary, secondary or tertiary. This has less to do with the peroxide in the formal reaction than with the formal conversion of the primary alcohol to the hydrocarbon, $RCH_2OH \rightarrow RCH_2CH_3$. The enthalpies of this reaction are: R = 1-hexyl, $153.2 \text{ kJ mol}^{-1}$; R = cyclohexyl, 166.2 and R = *tert*-butyl, $185.6 \text{ kJ mol}^{-1}$. We again note the error bars for cyclohexyl methanol and neopentyl alcohol. The enthalpies of reaction 4 for these same R groups are 49.5 kJ mol^{-1} , 61.3 kJ mol^{-1} and 79.8 kJ mol^{-1} , respectively. The other secondary groups (R = isopropyl, 2-hexyl, 3-hexyl) have somewhat lower enthalpies of reaction (49.5 , 57.8 , 54.7 kJ mol^{-1}) and again the isopropyl hydroperoxide enthalpy of formation seems to be inaccurate. The enthalpy of reaction for R = 1-heptyl of 68.3 kJ mol^{-1} is seemingly too large for a primary group and again calls into question the accuracy of its peroxide's enthalpy of formation. The enthalpy of reaction for R = 1-methylcyclohexyl is 90.2 , quite a bit larger than for the other tertiary group, *tert*-butyl. From the gas phase enthalpies of formation of 2,5-dimethylhexane-2,5-dihydroperoxide⁷ and 3,3,6,6-tetramethyloctane¹⁹, the enthalpy of reaction 4 is 54 kJ mol^{-1} per hydroperoxy group. This is comparable to the gas phase value for the same reaction of *tert*-butyl hydroperoxide² of 60 kJ mol^{-1} .

For the formal deoxygenation (decomposition) reaction 5, there is an enthalpy of formation value for every alcohol that matches a hydroperoxide²⁰. Using our 'exemplary' groups, R = 1-hexyl, cyclohexyl and *tert*-butyl, the liquid enthalpies of reaction are -77.9 , -75.0 and $-65.6 \text{ kJ mol}^{-1}$, respectively (there is no liquid phase enthalpy of formation reported for *t*-butyl peroxide from Reference 4). The secondary hydroperoxides' enthalpies of reaction average $-77 \pm 7 \text{ kJ mol}^{-1}$. For the three instances where there are also gas phase enthalpies of formation, the enthalpies of reaction are almost identical in the gas and liquid phases. The 1-heptyl ($-60.3 \text{ kJ mol}^{-1}$) and 1-methylcyclohexyl ($-50.6 \text{ kJ mol}^{-1}$) enthalpies of reaction are again disparate from the 1-hexyl and *tert*-butyl. If the enthalpy of reaction 5 for 1-hexyl hydroperoxide is used to calculate an enthalpy of formation of 1-heptyl hydroperoxide, it is -325 kJ mol^{-1} , almost identical to values derived for it above. The enthalpies of reaction for the liquid and gaseous phases for the tertiary 2-hydroperoxy-2-methylhex-5-en-3-yne are -78.2 and $-80.9 \text{ kJ mol}^{-1}$, respectively. For gaseous cumyl hydroperoxide, the enthalpy of reaction is $-84.5 \text{ kJ mol}^{-1}$.

The three solid phase tetralin and decalin hydroperoxides have enthalpies of reaction that are surprisingly comparable, $-93.9 \pm 6.4 \text{ kJ mol}^{-1}$, despite the sometimes large error bars associated with either the peroxide or corresponding alcohol and their differences in structure. Notably, the gas phase reaction enthalpy for the cumyl hydroperoxide is nearly identical to the solid phase reaction enthalpy for the 1-methyl-1-tetralin hydroperoxide, $-87.0 \text{ kJ mol}^{-1}$, for these structurally similar compounds and supports the hypothesis that the gas and condensed phase formal reaction enthalpies are nearly the same for all compounds. However, for 2,5-dimethylhexane-2,5-dihydroperoxide, the enthalpies of reaction 5 per hydroperoxy group for the solid and gaseous phase are not close: -57 and -76 kJ mol^{-1} , respectively. Compare them with the enthalpies of reaction for *tert*-butyl hydroperoxide of -66 (lq) and -67 or -78 (g) kJ mol^{-1} . For the unsaturated counterpart, 2,5-dimethylhex-3-yne-2,5-dihydroperoxide, the solid and gas phase enthalpies of reaction per hydroperoxy group are $-64.2 \text{ kJ mol}^{-1}$ and $-74.6 \text{ kJ mol}^{-1}$, respectively.

2. Peroxides

Of the five dialkyl peroxides with enthalpy of formation data, only those of unquestioned accuracy, dimethyl, diethyl and *tert*-butyl peroxide, are included in the analysis. The enthalpies of the formal hydrogenolysis reaction 6 are remarkably consistent for the methyl, primary and tertiary compounds: $-335.0 \pm 2.9 \text{ kJ mol}^{-1}$ for the liquid (using the estimated enthalpy of vaporization for dimethyl peroxide) and $-279.5 \pm 3.5 \text{ kJ mol}^{-1}$ for

the gas. From these quantities, the enthalpies of formation of *n*-butyl peroxide are calculated as $-319.6 \text{ kJ mol}^{-1}$ (lq) and $-272.1 \text{ kJ mol}^{-1}$ (g) and those for *tert*-amyl peroxide are $-424.0 \text{ kJ mol}^{-1}$ (lq) and $-379.1 \text{ kJ mol}^{-1}$ (g), all of them very different from their reported values.

The gas phase enthalpies of reaction 6 for the variously unsaturated peroxides are also consistent, with one exception. The values are: *tert*-butyl cumyl peroxide, $-288.5 \text{ kJ mol}^{-1}$; [1,4-phenylenebis(1-methylethylidene)]bis[(1,1-dimethylethyl)peroxide]¹¹ (normalized for two peroxy groups), $-287.1 \text{ kJ mol}^{-1}$; 1,1-dimethylethyl-1-methyl-1-[4-(1-methylethyl)phenyl]ethyl peroxide, $-276.6 \text{ kJ mol}^{-1}$; and 2-*tert*-butylperoxy-2-methylhex-5-en-3-yne, $-305.8 \text{ kJ mol}^{-1}$. The last species named also has a disparate liquid phase enthalpy of reaction, $-344.9 \text{ kJ mol}^{-1}$. The only solid phase reaction enthalpy, for [1,4-phenylenebis(1-methylethylidene)]bis[(1,1-dimethylethyl)peroxide] (normalized for two peroxy groups), is $-357.2 \text{ kJ mol}^{-1}$.

Disproportionation reaction 7 might be expected to be thermoneutral in the gas phase and perhaps less so in the liquid phase where there is the possibility of hydrogen-bonding²¹. Only for gas phase dimethyl peroxide is the prediction true, where the reaction enthalpy is -0.2 kJ mol^{-1} . The liquid phase enthalpy of reaction is the incredible $-61.5 \text{ kJ mol}^{-1}$. Of course, we have expressed some doubt about the accuracy of the enthalpy of formation of methyl hydroperoxide. For *tert*-butyl cumyl peroxide, the prediction for thermoneutrality is in error by about 6 kJ mol^{-1} in the gas phase and by *ca* 9 kJ mol^{-1} for the liquid. The enthalpy of reaction deviation from prediction increases slightly for *tert*-butyl peroxide: -14 kJ mol^{-1} for the gas phase, which is virtually the same result as in the liquid phase, -19 kJ mol^{-1} . The reaction enthalpy is calculated to be far from neutrality for 2-*tert*-butylperoxy-2-methylhex-5-en-3-yne. The enthalpies of reaction are $-86.1 \text{ kJ mol}^{-1}$ (g) and $-91.5 \text{ kJ mol}^{-1}$ (lq). This same species showed discrepant behavior for reaction 6. Nevertheless, still assuming thermoneutrality for conversion of diethyl peroxide to ethyl hydroperoxide in reaction 7, the derived enthalpies of formation for ethyl hydroperoxide are -206 kJ mol^{-1} (lq) and -164 kJ mol^{-1} (g). The liquid phase estimated value for ethyl hydroperoxide is much more reasonable than the experimentally determined value and is consistent with the other *n*-alkyl hydroperoxide values, either derived or accurately determined experimentally.

As was the case for the alkyl hydroperoxides in reaction 4, the enthalpies of the oxygen/hydrocarbon double exchange reaction 8 for dialkyl peroxides are different depending on the classification of the carbon bonded to oxygen. For R = Me, Et and *t*-Bu, the liquid phase values are -4 , 24.6 and 52.7 kJ mol^{-1} , respectively, and the gas phase values are 0.1 , 25.7 and 56.5 kJ mol^{-1} , respectively. For the formal deoxygenation reaction 9, the enthalpies of reaction are virtually the same for dimethyl and diethyl peroxide in the gas phase, $-58.5 \pm 0.6 \text{ kJ mol}^{-1}$. This value is the same as the enthalpy of reaction of diethyl peroxide in the liquid phase, $-56.0 \text{ kJ mol}^{-1}$ (there is no directly determined liquid phase enthalpy of formation of dimethyl ether). Because of steric strain in the di-*tert*-butyl ether, the enthalpy of reaction is much less negative, but still exothermic, $-17.7 \text{ kJ mol}^{-1}$ (lq) and $-19.6 \text{ kJ mol}^{-1}$ (g).

3. Mixed hydroperoxides and peroxides

2,5-Dimethyl-2-hydroperoxide-5-*tert*-butylperoxyhexane⁷ contains both a peroxy and a hydroperoxy group. The enthalpy of reaction 5, to give 2,5-dimethyl-2-hydroxy-5-*t*-butylperoxyhexane⁷, is $-59.9 \text{ kJ mol}^{-1}$ (lq) and $-58.8 \text{ kJ mol}^{-1}$ (g), comparable to those obtained from 1-methylcyclohexane hydroperoxide and *t*-butyl hydroperoxide. If the mixed peroxide were to undergo the formal reactions 5 and 6 simultaneously, the alcohol product would be 2,5-dimethylhexane-2,5-diol, for which there is only an enthalpy

of formation for the solid. From an estimated enthalpy of fusion²² of 18 kJ mol^{-1} , the liquid enthalpy of formation is -664 kJ mol^{-1} . The combined enthalpy of reaction is thus -384 kJ mol^{-1} , which is 19 kJ mol^{-1} less negative than for the same two reactions for di-*tert*-butyl peroxide and *tert*-butyl hydroperoxide combined. The deviation from thermoneutrality is large for the disproportionation reaction 7 of 2,5-dimethyl-2-hydroperoxy-5-*tert*-butylperoxyhexane. The enthalpy of reaction in the gas phase is $+23.4 \text{ kJ mol}^{-1}$.

E. Other Reactions

From the difference between the enthalpies of formation of 2,5-dimethyl-2,5-dihydroperoxyhexane and 2,5-dimethyl-2,5-dihydroperoxyhex-3-yne⁷, the enthalpies of hydrogenation of the alkyne are derived as $-298.5 \text{ kJ mol}^{-1}$ (g) and $-309.6 \text{ kJ mol}^{-1}$ (s). The gas phase value is quite a bit larger than that for its deoxygenated counterpart, 3-hexyne, of $-272.4 \text{ kJ mol}^{-1}$ (g)²³. However, the calculated solid phase enthalpy of hydrogenation of 2,5-dimethylhex-3-yn-2,5-diol⁷ to 2,5-dimethylhexane-2,5-diol is $-295.7 \text{ kJ mol}^{-1}$.

F. Polymeric Peroxides

Numerous polymers autooxidize to form peroxides. These compositionally, and thus calorimetrically, ill-defined products may be considered polymeric peroxides. However, one well-defined polymeric peroxide is that of polystyrene with the repeat unit $-\text{CH}_2-\text{CH}(\text{C}_6\text{H}_5)-\text{O}-\text{O}-$. Through a combination of combustion and reaction calorimetry (chain degradation to benzaldehyde and formaldehyde), a solid phase enthalpy of formation of this species was found¹³ to be $27 \pm 21 \text{ kJ mol}^{-1}$. Much the same procedure was used to determine the enthalpy of degradation²⁴ for the polyperoxide polymers of 2-vinylnaphthalene and the isomeric 1- and 2-propenylnaphthalene to form the related acylnaphthalene and formaldehyde. Numerically, the reaction enthalpy values for these last three polyperoxides were -206 ± 4 , -222 ± 8 and $-222 \pm 10 \text{ kJ mol}^{-1}$, to be compared with the aforementioned polystyrene with a value of $-209 \pm 8 \text{ kJ mol}^{-1}$. However, in the absence of enthalpy of formation data for the decomposition products in the naphthalene case, we hesitate to derive enthalpies of formation for these three species²⁵.

III. PEROXIDES WITH SINGLE-BONDED OXYGEN FUNCTIONAL GROUPS

The enthalpy of formation data for peroxides containing hydroxyl and alkoxy functional groups are in Table 2.

A. Hydroxyl Substituents

Of the seven hydroxyl-containing peroxides listed in Table 2, six are *tert*-butylperoxy derivatives. Although the *tert*-butyl group kinetically stabilizes the peroxide so that its combustion enthalpy can be measured, its presence makes finding suitable reference compounds such as hydrocarbons and ethers to compare in reactions 2–9 more difficult. Reaction 6 is the only reaction for which there are enthalpy of formation data for the requisite comparison compounds. Three hydroxy peroxides, all from the same source²⁶, have remarkably consistent enthalpies of reaction 6 in both the liquid and gas phases. The mean values derived from the *vicinal*-dioxygen substituted alcohols, 2-*tert*-butylperoxyethanol, 2-*tert*-pentylperoxyethanol and 3-*tert*-butylperoxy-1,2-propanediol, are $-304.0 \pm 4.1 \text{ kJ mol}^{-1}$ (lq) and $-257.1 \pm 6.0 \text{ kJ mol}^{-1}$ (g). However, these values

TABLE 2. Enthalpies of formation of hydroperoxides and peroxides containing single-bonded oxygen functional groups (kJ mol⁻¹)

Compound	$\Delta_f H_m^0$ (s)	$\Delta_f H_m^0$ (lq)	$\Delta_f H_m^0$ (g)	Reference
<i>Containing hydroxy groups</i>				
<i>tert</i> -Butylperoxymethanol		-480.6 ± 2.8	-421.0 ± 4.0	26
2- <i>tert</i> -Butylperoxyethanol ^a		-511.7 ± 2.3	-445.3 ± 3.0	26
2- <i>tert</i> -Pentylperoxyethanol ^b		-534.2 ± 1.6	-464.1 ± 3.0	26
1- <i>tert</i> -Butylperoxycyclohexanol		-589.1 ± 5.7		27
2,5-Dimethyl-5- <i>tert</i> -butylperoxy-2-hexanol		-696.9 ± 2.2	-621.6 ± 2.2	7
Bis(hydroxymethyl) peroxide	-665. ± 5.1		-571.7 ± 6.7	2
3- <i>tert</i> -Butylperoxy-1,2-propanediol		-719.2 ± 1.6	-631.2 ± 3.1	26
<i>Containing hydroxy and alkoxy groups</i>				
1- <i>tert</i> -Butylperoxy-3-methoxy-2-propanol		-666.3 ± 2.6		2
1- <i>tert</i> -Butylperoxy-3-ethoxy-2-propanol		-706.7 ± 3.0		2
1- <i>tert</i> -Butylperoxy-3-propoxy-2-propanol		-725.0 ± 3.0		2
1-Butoxy-3- <i>tert</i> -butylperoxy-2-propanol		-747.0 ± 3.0		2
1- <i>tert</i> -Butylperoxy-3-pentoxy-2-propanol		-771.2 ± 4.6		2

^a This compound was incorrectly named as 1-*t*-butylperoxyethanol in Reference 26.

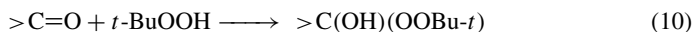
^b This compound was incorrectly named as 1-*t*-pentylperoxyethanol in Reference 26.

are about 20–30 kJ mol⁻¹ less negative than the corresponding reactions for di-*tert*-butyl peroxide or diethyl peroxide. It is likely that both the hydroxyperoxide species and the product diols are stabilized by intramolecular hydrogen-bonding, but to different extents, thus accounting for the net enthalpy difference. Not consistent with the aforementioned peroxides, 2,5-dimethyl-5-*tert*-butylperoxy-2-hexanol⁷ has an enthalpy of reaction 6, -272.6 kJ mol⁻¹ (g), which is only *ca* 10 kJ mol⁻¹ less negative than the corresponding reaction for di-*tert*-butyl peroxide. The liquid phase reaction enthalpy, -326 kJ mol⁻¹, using the estimated liquid enthalpy of formation of 2,5-dimethylhexane-2,5-diol²⁰ is also about 10 kJ mol⁻¹ less negative than for di-*tert*-butyl peroxide. In this case, the hydroxyperoxide and diol product would be expected to be less stabilized by intramolecular hydrogen-bonding.

tert-Butylperoxymethanol, 1-*tert*-butylperoxycyclohexanol and bis(hydroxymethyl) peroxide all yield a *gem*-diol (carbonyl hydrate) upon formal hydrogenolysis (reaction 6). The first and third peroxides produce methanediol and the second one produces 1,1-cyclohexanediol. Although it doesn't contain a hydroxyl group, the *gem*-diperoxide, 2,2-bis(*tert*-butylperoxy)butane¹² yields a *gem*-diol, 2,2-butanediol, upon formal hydrogenolysis. The gas phase enthalpies of formation for these hydrate species can be calculated from the hydration enthalpies of the corresponding carbonyl compounds²⁸. The gas phase enthalpy of reaction 6 for *tert*-butylperoxymethanol is -274 kJ mol⁻¹, very similar to the enthalpies of the corresponding reactions for di-*tert*-butyl peroxide and diethyl peroxide. From estimated enthalpies of vaporization for 1-*tert*-butylperoxycyclohexanol and

2,2-bis(*tert*-butylperoxy)butane using equation 1, the gas phase enthalpies of reaction 6 for these peroxides are -290 and -278 kJ mol^{-1} , respectively. The reaction enthalpy for the latter is normalized for the two peroxy groups undergoing cleavage. It is perhaps not surprising that the enthalpies of reaction for the *gem*-dioxxygen substituted species are not too different from the hydrocarbyl-substituted species since any anomeric effect in the peroxide is plausibly cancelled by a similar effect in the hydrate product.

The gas phase enthalpy of reaction 6 for bis(hydroxymethyl) peroxide is -192 kJ mol^{-1} , which deviates from the other hydrate-producing peroxides by nearly 89 kJ mol^{-1} . The enthalpy of reaction 8, 145 kJ mol^{-1} , is likewise discrepant by some 120 kJ mol^{-1} from that for diethyl peroxide, *ca* 26 kJ mol^{-1} . From the high-level calculations reported in Reference 28, the reaction enthalpy for the addition of H_2O_2 to formaldehyde is -59 kJ mol^{-1} . A similar reaction is equation 10 for the gas phase addition of *tert*-butyl hydroperoxide to a carbonyl group.



For formaldehyde reacting to give *tert*-butylperoxymethanol, the reaction enthalpy is -66.5 kJ mol^{-1} and for cyclohexanone reacting to give 1-*tert*-butylperoxycyclohexanol, the enthalpy of reaction is *ca* -45 kJ mol^{-1} . The average of these is compatible with the value reported from Reference 28. By contrast, the gas phase formal reaction 11 to produce bis(hydroxymethyl) peroxide is calculated to be exothermic by some -218 kJ mol^{-1} for the case of formaldehyde.



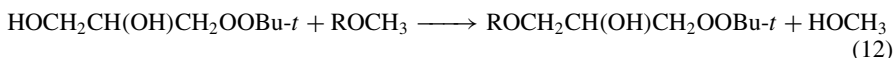
This is so much more than twice the enthalpy for monoaddition to formaldehyde that we are suspicious of the formation enthalpy reported for bis(hydroxymethyl) peroxide²⁹.

B. Hydroxyl and Alkoxy Substituents

There is a collection of liquid phase enthalpy of formation data for compounds with multiple oxygen-containing functional groups: alkoxy, hydroxy and alkylperoxy ($\text{ROCH}_2\text{CH}(\text{OH})\text{CH}_2\text{OOBu-}t$) and a collection of the corresponding species with the *tert*-butoxy group replacing the *tert*-butylperoxy group ($\text{ROCH}_2\text{CH}(\text{OH})\text{CH}_2\text{OBu-}t$) where $\text{R} = \text{Et}$, *n*-Pr, *n*-Bu and *n*-Pen. There are data for $\text{R} = \text{Me}$ for the peroxide only. Each of these collections constitutes a homologous series and so a plot of the enthalpies of formation vs. number of carbons should be linear. The value for $\text{R} = \text{Me}$ deviates, as many methyl derivatives do, from the otherwise straight line. A weighted, least-squares regression analysis of each series shows excellent linearity with $r^2 > 0.999$. The slope for the peroxide series is -21.1 ± 0.9 kJ mol^{-1} and the slope for the corresponding ether series is -22.3 ± 0.5 kJ mol^{-1} . These slopes are more typical of gas phase species (*ca* -21 kJ mol^{-1}) than of liquid phase species (*ca* -25 kJ mol^{-1}). We know of no other such homologous series with comparable slopes.

The similarity of the slopes guarantees that the enthalpies of reaction 9, which involve members of these two series, will be similar. The mean value of -46.8 ± 2.1 kJ mol^{-1} is about 12 kJ mol^{-1} less negative than the enthalpy of reaction 9 for diethyl peroxide, mentioned in the preceding section.

An alcohol/ether exchange reaction can be written for the peroxide collection as in equation 12.



There are liquid enthalpy of formation values for the methyl ethers for R = Me, *n*-Pr, *n*-Bu and *n*-decyl. Additional enthalpies can be extrapolated for the R = Et and *n*-Pen species from the linear regression analysis of the enthalpies of formation vs. number of carbons³⁰. However, the regression constants from this same analysis immediately reveal that any assumption of thermoneutrality for equation 12 is incorrect. The slope of $-25.3 \pm 0.1 \text{ kJ mol}^{-1}$ for the methyl ethers is much too different from the slope for the peroxide series for there to be a constant difference between enthalpies of formation for two compounds with the same R substitution (the two alcohol enthalpies of formation in equation 12 are constant). As expected, the derived enthalpies of reaction for equation 12 increase with increasing number of carbons: 13.9, 21.4, 24.0 and 25.6 kJ mol^{-1} .

A formal reaction corresponding to equation 6 for the 'de-etherated' parent species, 3-*tert*-butylperoxy-1,2-propandiol, is equation 13 for which the enthalpy of reaction is $-308.2 \text{ kJ mol}^{-1}$. This value is about 29 kJ mol^{-1} less negative than the corresponding reaction for di-*tert*-butyl peroxide.



IV. PEROXYCARBOXYLIC ACIDS AND THEIR DERIVATIVES

In this section we discuss the thermochemistry of some species with the general formulas, $\text{RC}(=\text{O})\text{OOH}$, $\text{RC}(=\text{O})\text{OOR}'$ and $\text{RC}(=\text{O})\text{OOC}(=\text{O})\text{R}$. These species have the generic names peracids (peroxycarboxylic acids), peresters (percarboxylate esters) and acyl peroxides. The enthalpy of formation values are in Table 3. Three formal reactions that are discussed here are conceptually the same as in the earlier sections. Because now there is a carbonyl group present, we rewrite equations 5, 6 and 9 as equations 14, 15 and 16.



A. Peroxycarboxylic Acids

The C_{12} , C_{14} , C_{16} and C_{18} peracids belong to a homologous series for which the measured solid phase enthalpies of combustion are self-consistent, as was discussed in detail by the original investigators³¹. From our weighted least-squares regression of the enthalpies of formation vs. number of carbon atoms in the peracid, the methylene increment for the series is $-29.5 \text{ kJ mol}^{-1}$. If these peracids were to undergo the formal deoxygenation reaction 14, the products would be the homologous carboxylic acids. For these acids, the methylene increment derived from a weighted least-squares regression is $-29.0 \text{ kJ mol}^{-1}$. (This value is virtually the same as that derived for all the solid C_{10} – C_{20} carboxylic acids, $-30.1 \text{ kJ mol}^{-1}$.) Since the methylene increments for the two acid series are the same, the enthalpy of reaction 14 is essentially constant: $-89.5 \pm 4.4 \text{ kJ mol}^{-1}$.

Because of the compound's thermal instability, the enthalpy of fusion of peroxydodecanoic acid (perlauric acid) was indirectly determined from freezing point measurements in various solutions³¹. The resulting value, $46.3 \pm 0.8 \text{ kJ mol}^{-1}$, is 10 kJ mol^{-1} larger than

TABLE 3. Enthalpies of formation of hydroperoxides and peroxides containing double-bonded oxygen functional groups (kJ mol^{-1})

Compound	$\Delta_f H_m^0$ (s)	$\Delta_f H_m^0$ (lq)	$\Delta_f H_m^0$ (g)	Reference
<i>Peracids</i>				
Peroxybenzoic acid	-367.0 ± 12.8			2
Peroxydodecanoic acid	-680.3 ± 8.4^a	-634 ± 10	-563.2 ± 8.4	2, 31
Peroxytetradecanoic acid	-749.9 ± 9.6			2
Peroxyhexadecanoic acid	-801.9 ± 9.2			2
Peroxyoctadecanoic acid	-857.3 ± 11.3			2
<i>Peresters</i>				
<i>tert</i> -Butyl				
(<i>E</i>)-peroxy-2-butenate		$-417. \pm 5.4$		32, 33
<i>tert</i> -Butyl peroxydecanoate		-688.4 ± 8.8		2
<i>tert</i> -Butyl peroxydodecanoate		-738.3 ± 10.0		2
<i>tert</i> -Butyl peroxytetradecanoate		-795.8 ± 10.5		2
Cumyl perbenzoate	-231.5 ± 12.1		-188.4 ± 12.8	2
[benzenecarboperoxoic acid, 1-methyl-1-phenylethyl ester]				
4- <i>tert</i> -Butoxy-4-oxo-(<i>E</i>)-2- buteneperoxoic acid methyl ester [OO- <i>t</i> -butyl O-methyl peroxyfumarate]		-746.8 ± 2.0		32, 33
(<i>E</i>)- <i>t</i> -BuOOC(O)CH= CHCOOMe				
4- <i>tert</i> -Butoxy-4- oxobutaneperoxoic acid methyl ester [OO- <i>t</i> -butyl O-methyl peroxysuccinate]				
<i>t</i> -BuOOC(O)CH ₂ CH ₂ COOMe		-878.2 ± 3.0		32, 33
Di- <i>tert</i> -butyl 2,4-hexadienoate [di- <i>t</i> -butyl peroxyfumarate]		-777.7 ± 4.8		34
4- <i>tert</i> -Butoxy-4-oxo-(<i>E</i>)-2- buteneperoxoic acid allyl ester [OO- <i>t</i> -butyl O-allyl peroxyfumarate]		-673.2 ± 4.2		32, 33
4- <i>tert</i> -Butoxy-4- oxobutaneperoxoic acid allyl ester [OO- <i>t</i> -butyl O-allyl peroxysuccinate]		-817 ± 4		33
Benzoylcarboxyperoxide phenyl ester [phenyl benzoylperoxycarbonate]				
PhC(=O)OOC(=O)OPh	-484.9 ± 8.4		-387.0 ± 8.7	2
Benzoyl(cyclohexyloxy)carbonyl peroxide [cyclohexyl benzoylperoxycarbonate]	-741.5 ± 8.4		-645.3 ± 9.4	2
Tetra- <i>tert</i> -butylperoxy- pyromellitate [tetra- <i>tert</i> -butyl 1,2,4,5-benzene tetracarboxylate]	-1536.1 ± 7.6			35
Tetra- <i>tert</i> -amylperoxy- pyromellitate	-1761.9 ± 6.7			35
1,4-Di- <i>tert</i> -butylperoxy pyromellitate ^b	-1661.8 ± 6.0			35
1,4-Di- <i>tert</i> -amylperoxy pyromellitate ^b	-1640.6 ± 6.1			35
<i>Acyl peroxides</i>				
Diacetyl peroxide		-535.2 ± 9.2		2
Dipropionyl peroxide		-620.0 ± 6.3		2

(continued overleaf)

TABLE 3 (continued)

Compound	$\Delta_f H_m^0$ (s)	$\Delta_f H_m^0$ (lq)	$\Delta_f H_m^0$ (g)	Reference
Dibutyl peroxide		-673.2 ± 4.2		2
Dibenzoyl peroxide	-369.6 ± 4.6		-271.7 ± 5.3	2
Bis(2-methylbenzoyl) peroxide	-500.5 ± 7.9			2
Bis(4-methylbenzoyl) peroxide	-451.5 ± 7.9			2
Dicinnamoyl peroxide	-356.1 ± 8.4			2

^a In Reference, 3, the enthalpy of combustion that is shown for the liquid is actually for the solid.

^b The substance is probably a mixture with the 1,5-isomer³⁶.

that for lauric acid, a difference that seems quite large for compounds that both exhibit intermolecular hydrogen-bonding in the solid state³⁷ and differ in molecular weight by only one oxygen atom. In contrast, the enthalpy of vaporization of lauric acid is some 25 kJ mol^{-1} larger than that for perlauric acid, 70.7 kJ mol^{-1} . While this latter value might be plausible in that intramolecular H-bonding stabilizes the gas phase of the peracid relative to the corresponding carboxylic acid, we note that the value for perlauric acid is an estimate³¹. Furthermore, the enthalpy of vaporization of peroxyacetic acid is only 2.6 kJ mol^{-1} larger than for acetic acid³⁸. From equation 1, the enthalpy of vaporization of perlauric acid is calculated from that of peroxyacetic acid, with an additional 10 non-quaternary carbon atoms, as 91.1 kJ mol^{-1} . This is much more reasonable, especially when compared to the enthalpy of vaporization of lauric acid, 95.7 kJ mol^{-1} .

The enthalpy of formation of solid peroxybenzoic acid was determined by a combination of combustion and reaction calorimetry. The enthalpy of reaction 14 is calculated to be $-18.2 \text{ kJ mol}^{-1}$. This result does not seem credible. There is no reason to doubt the enthalpy of formation of benzoic acid, and there is no apparent reason why the enthalpy of reaction should be so different from the aliphatic peracids.

B. Percarboxylate Esters

The three saturated long-chain *tert*-butyl peresters are members of a homologous series, and as such, the weighted least-squares regression analysis of the enthalpies of formation vs. number of carbons yields a methylene increment of $-26.7 \text{ kJ mol}^{-1}$, a typical value for liquids. The methylene increment for the *tert*-butyl esters of the C_8 , C_{10} , C_{12} and C_{14} acids is $-28.0 \text{ kJ mol}^{-1}$. The closeness of these two values ensures that the enthalpies of formal reaction 16 will be nearly constant. For the three pairs from Table 3, the value is $-70.3 \pm 8.1 \text{ kJ mol}^{-1}$. The standard deviation from the mean is quite large because the arithmetic difference for the C_{12} ester and perester, $-79.5 \text{ kJ mol}^{-1}$, is quite a bit more negative than the differences for the C_{10} and C_{14} pairs, -64.4 and $-66.9 \text{ kJ mol}^{-1}$, respectively. Unfortunately, the acids and esters are in different phases and so we are reluctant to attempt any comparison between them, such as a formal hydrolysis reaction or disproportionation with hydrogen peroxide.

The enthalpy of formation of the unsaturated *tert*-butyl peroxy-2-butenate may be reconciled as follows. Its hydrogenation product is *tert*-butyl peroxybutanoate, whose enthalpy of formation can be estimated from the regression constants generated from the long-chain *tert*-butyl peroxyalkanoates, above. So doing, the derived enthalpy of formation is $-526.9 \text{ kJ mol}^{-1}$. The formal enthalpy of hydrogenation, calculated as the difference between the two enthalpies of formation, is thus $-109.9 \text{ kJ mol}^{-1}$. From a collection of esters of α,β -unsaturated C_3 – C_5 acids² and their saturated counterparts¹⁴, the average enthalpy of hydrogenation is *ca* -114 kJ mol^{-1} , in good agreement.

There are enthalpies of formation for two phases of cumyl perbenzoate. However, the associated sublimation enthalpy that interconnects these phases, 43 kJ mol^{-1} , is much too small. In that the enthalpy of sublimation must exceed the enthalpy of vaporization, and the latter is at least 75 kJ mol^{-1} using the CHLP protocol¹⁷ (from the number of carbons alone), the enthalpy of formation data loses credibility. Furthermore, lacking the enthalpy of formation of the corresponding cumyl benzoate (in any phase) disallows comparison. This would seem to be an altogether normal species until it is recognized that the archetype arylcarboxylate ester, methyl benzoate, has provided complications for the calorimetrist³⁹.

In References 32 and 33 we find the liquid phase enthalpies of formation of the methyl and allyl esters of the *OO-tert*-butyl peroxyfumaric and peroxy succinic acids. The difference between the enthalpies of formation of each fumarate and succinate pair of preesters is the enthalpy of hydrogenation. The enthalpy of hydrogenation to the succinate of the methyl fumarate is $-131.4 \pm 3.6 \text{ kJ mol}^{-1}$, and of the allyl fumarate is $-143.8 \pm 5.8 \text{ kJ mol}^{-1}$. By comparison, the enthalpy of hydrogenation of a different, non-peroxy, fumarate ester—the diethyl species—was earlier directly measured to be -121.1 ± 0.2 and $-122.6 \pm 0.6 \text{ kJ mol}^{-1}$ (cf. References 40 and 41, respectively). In that these hydrogenation measurements were conducted in acetic acid solution rather than the neat liquid, we find the results to be in reasonably satisfactory accord. We can also derive a hydrogenation enthalpy value for the dimethyl fumarate as solid by combining the enthalpy of formation of this species⁴², $-741.0 \pm 2.0 \text{ kJ mol}^{-1}$, and that of its succinate counterpart⁴³, -832 kJ mol^{-1} . The hydrogenation enthalpy derived from these data is *ca* 91 kJ mol^{-1} , highly discrepant. (We do note that the enthalpy of formation of the related, solid phase, dimethyl malonate from Reference 43 is -793 kJ mol^{-1} while that of this species as liquid, necessarily more positive than that of the solid, was more recently reported⁴⁴ to be $-799.7 \pm 0.7 \text{ kJ mol}^{-1}$.) We are suspicious of the dimethyl succinate result and so likewise of the derived enthalpy of hydrogenation value.

Because the liquid phase enthalpy of formation of the corresponding *t*-butyl methyl succinate ester³² is available, $-950.9 \pm 3.0 \text{ kJ mol}^{-1}$, the enthalpy of reaction 16 can be calculated. The result, $-72.8 \pm 3.9 \text{ kJ mol}^{-1}$, is nearly the same as that for the esters and preesters above, $-70.3 \pm 8.1 \text{ kJ mol}^{-1}$.

The final comparison is between the enthalpies of formation³⁴ of di-*t*-butyl *E,E*-muconate (2,4-hexadienoate), $-917.1 \pm 3.9 \text{ kJ mol}^{-1}$, and its diperoxy ester counterpart, $-777.7 \pm 4.8 \text{ kJ mol}^{-1}$. The enthalpy of reaction 16 is $139.4 \pm 6.2 \text{ kJ mol}^{-1}$ or $69.7 \pm 3.1 \text{ kJ mol}^{-1}$ per carboxylate ester group, nearly the same as the differences for the other preesters.

An admittedly enigmatic result⁴⁵ involves the thermolysis of solution phase di-*t*-butyl diperoxyoxalate and a cyclic counterpart, 7,7,10,10-tetramethyl-1,2,5,6-tetraoxacyclodecane-3,4-dione. While the former reaction was shown to be exothermic by $238.5 \pm 8.4 \text{ kJ mol}^{-1}$ and the latter by $414.2 \pm 8.4 \text{ kJ mol}^{-1}$, the latter is slower by a factor of some 3000. The latter decomposition results in acetone, ethylene, CO_2 and 3,3,6,6-tetramethyl-1,2-dioxacyclohexane. The enthalpy of formation measurements of the cyclic peroxyoxalate and the 1,2-dioxane are coupled: if we knew the enthalpy of formation of 1,2-dioxane it would allow us to derive the enthalpy of formation of 7,7,10,10-tetramethyl-1,2,5,6-tetraoxacyclodecane-3,4-dione and the other way around.

Although there are measured enthalpies of formation of phenyl and cyclohexyl benzoylperoxycarbonate², there are none for the corresponding deoxygenated benzoylcarbonates that replace the $-\text{OO}-$ moiety by $-\text{O}-$. The difference between the gas phase enthalpies of formation of the peroxy compounds, *ca* $258 \pm 13 \text{ kJ mol}^{-1}$, is the hydrogenation enthalpy of the phenyl compound. This value is far in excess of the hydrogenation enthalpy of any other phenylated species; from the enthalpies of formation of gaseous phenol and cyclohexanol, the difference is but $189.98 \pm 2.3 \text{ kJ mol}^{-1}$.

However, this analysis does not tell us whether it is the phenyl and/or cyclohexyl peroxy species that is in error.

We now note a set of solid phase enthalpies of formation of peroxyperomellitates (1,2,4,5-benzenetetracarboxylates)³⁵. The difference between the enthalpies of formation of the tetra-*tert*-butyl and the tetra-*tert*-amyl species is $-225 \pm 12 \text{ kJ mol}^{-1}$, inexplicably large for a difference of four methylene groups, even found as solids. Which, or both, of these numbers is wrong? For the di-*t*-butyl and di-*t*-amyl diperoxy derivatives (the locations of the peroxy and carboxylic acid substituents are unstated but the isomers are expected to have comparable stabilities), the difference is $+21 \pm 9 \text{ kJ mol}^{-1}$. Although the absolute value difference is reasonable, the greater stability of the *tert*-butyl derivative is clearly wrong. Again, the data are problematic: while there are thermochemical data for other alkyl peromellitates, they are all for liquid phase species and we lack confidence in predicting the necessary enthalpies of fusion to interrelate all of these arenecarboxylate and peroxy-carboxylate data.

C. Acyl Peroxides

There are liquid enthalpies of formation for three homologous acyl peroxides: diacetyl, dipropionyl and dibutyryl². If the three enthalpy values are plotted versus the number of carbons in the compound, we immediately notice that the data do not lie on a straight line. It would seem either that at least one of the values is incorrect or that the diacetyl peroxide exhibits the expected less-negative methyl deviation from linearity. With respect to the latter supposition, we note that the enthalpies of formation of neither dimethyl ketone, nor acetic acid, nor methyl acetate deviate from their homologs (in fact, it is formic acid and methyl formate that deviate). If a weighted least-squares regression of the peroxide data is performed, the resulting slope (methylene increment) is $-32.5 \text{ kJ mol}^{-1}$, typically rather larger than for the liquid phase. If the enthalpy of formation of diacetyl peroxide is omitted, the difference between the remaining two species is the more normal $-26.6 \text{ kJ mol}^{-1}$. The error bars are the largest for the diacetyl peroxide.

Formal hydrogenolysis of diacyl peroxides (reaction 15) yields the carboxylic acids. Not surprisingly, the enthalpies of reaction for the dipropionyl and dibutyryl peroxides are the comparable -401.4 and $-394.4 \text{ kJ mol}^{-1}$, a result that is more than 60 kJ mol^{-1} more negative than for the liquid dialkyl peroxides. For the diacetyl peroxide, the reaction enthalpy is the disparate $-436.0 \text{ kJ mol}^{-1}$. The other reaction for which there are data for the product species is the deoxygenation reaction 16. There are liquid enthalpy of formation values only for acetic and propionic anhydride. The resulting enthalpies of reaction are -89.2 and $-59.1 \text{ kJ mol}^{-1}$, very different from each other, as we would expect. Although the latter value is close to the corresponding reaction with the dialkyl peroxides, the presence of the two carbonyl groups might affect the enthalpy of reaction. The enthalpy of reaction 16 for the peresters, above, was somewhat more negative than for the dialkyl peroxides, and so the enthalpy of reaction for the diacyl peroxides might be expected to be yet more negative. On the basis of this reaction, we cannot deduce which data, if any, are inaccurate.

There are solid phase enthalpy of formation data for four aromatic acyl peroxides: dibenzoyl peroxide and the bis-*o*- and bis-*p*-toluyl derivatives and dicinnamoyl peroxide. The last three were reported in the same publication⁴⁶. The first disconcerting observation is that the *p*-methyl substituted benzoyl peroxide is less stable than the *ortho* isomer by nearly 50 kJ mol^{-1} . We cannot reconcile the large difference between the enthalpies of formation of these two isomers, especially since the corresponding anhydrides have comparable enthalpies of formation, -521.0 ± 7.9 (*p*⁻) and -533.5 ± 7.9 (*o*⁻) kJ mol^{-1} . However, they too exhibit an unexpected stability order and were measured by the same

authors⁴⁶. The corresponding carboxylic acids, as originally measured⁴⁶ with the same inverted stability order, have since been redetermined⁵ and show the *para* isomer to be *ca* 3 kJ mol⁻¹ more stable. We note the dicinnamoyl peroxide and anhydride have enthalpies of formation⁴⁶ of -356.1 ± 8.4 and -347.8 ± 8.4 kJ mol⁻¹ and wonder how these species have essentially the same enthalpy of formation and why the peroxide is seemingly more stable than the anhydride? For solid dibenzoyl peroxide there are three measured values: -392.0 ± 6.3 , -368 ± 8.4 and $-369. \pm 4.6$ kJ mol⁻¹ from References 46, 47 and 48, respectively. While these disparities make it easy to disparage the thermochemical values for acyl peroxides, we find there are two archived values for benzoic anhydride that are relatively disparate, -430.9 ± 6.7 and $-415. \pm 2.$ kJ mol⁻¹ from References 46 and 49, respectively.

Because the accuracy of the data for three of the diacyl peroxides is in question, we will attempt to derive enthalpies of formation for them from the reverse of equations 15 and 16. The enthalpy of reaction 15 for dibenzoyl peroxide, using enthalpy of formation values of unquestioned accuracy⁴⁸, is -400.8 kJ mol⁻¹. This is the same as the *ca* -398 kJ mol⁻¹ for the liquid non-aromatic diacyl peroxides discussed above. Using the solid phase enthalpy of reaction for dibenzoyl peroxide and the appropriate carboxylic acid enthalpies of formation, the calculated enthalpies of formation of bis(*o*-toluyl) peroxide and bis(*p*-toluyl) peroxide are -432.2 and -457.6 kJ mol⁻¹, respectively. From the foregoing analysis, it would seem that the measured enthalpy of formation is accurate for the bis(*p*-toluyl) peroxide but is not for its isomer. The analysis for dicinnamoyl peroxide is complicated by there being two enthalpies of formation for *trans*-cinnamic acid that differ by *ca* 12 kJ mol⁻¹. One is from our archival source^{2,50} (-336.9 ± 12 kJ mol⁻¹) and the other is a newer measurement⁵¹ (-325.3 kJ mol⁻¹). The calculated enthalpies of formation of dicinnamoyl peroxide are thus -273.0 and -249.8 kJ mol⁻¹. Both of these results are *ca* 80–100 kJ mol⁻¹ less negative than the reported enthalpy of formation.

The enthalpies of reaction 16 for solid and gaseous dibenzoyl peroxide are -45.8 and -47.3 kJ mol⁻¹, respectively. These values are much smaller than those calculated for the liquid dialkyl peroxides (*ca* -56 kJ mol⁻¹), the acyl peresters (*ca* -70 kJ mol⁻¹) or the non-aromatic diacyl peroxides (-89 or -59 kJ mol⁻¹). However, we have no reason not to accept the result. It would be futile to use this result for further calculations concerning the solid phase enthalpies of formation of bis(*o*-toluyl) peroxide, bis(*p*-toluyl) peroxide and dicinnamoyl peroxide because all the peroxide and the anhydride product enthalpy of formation data are from the same suspect source⁴⁶.

V. CYCLIC PEROXIDES AND MULTIPLY-LINKED PEROXIDES

The peroxides discussed here are those that incorporate the peroxide linkage(s) within a cycle or that have multiple peroxide linkages. The enthalpies of formation of these species appear in Table 4.

A. Dioxetanes

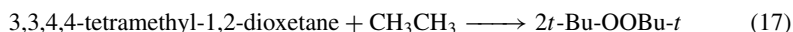
About 30 years ago, an enthalpy of formation was reported for 3,3,4,4-tetramethyl-1,2-dioxetane⁵². Both by direct microcalorimetric combustion measurements of the neat solid and by reaction calorimetry (of the solid itself, and in acetone solution to form acetone), a consensus value was derived. Now, is the enthalpy of formation 'plausible', notwithstanding the very large error bars? Consider reaction 6 for the dioxetane that produces 2,3-dimethyl-2,3-butanediol⁶⁰. The liquid phase enthalpy of reaction is -329 kJ mol⁻¹. It is remarkable that this value is compatible with that for the dialkyl peroxides, *ca* -335 kJ mol⁻¹, despite the ring strain that might be expected.

TABLE 4. Enthalpies of formation of cyclic peroxides and multiply-linked peroxides (kJ mol⁻¹)

Compound	$\Delta_f H_m^0$ (s)	$\Delta_f H_m^0$ (lq)	$\Delta_f H_m^0$ (g)	Reference
3,3,4,4-Tetramethyl-1,2-dioxetane	-284 ± 42	-277 ± 42		52
1,2,4,5-Tetroxane [formaldehyde diperoxide]	-165.9 ± 3.1		-153.7 ± 3.1	53
3,6-Diphenyl-1,2,4,5-tetroxane	134.0 ± 1.3		99.7 ± 1.3	54
Ozonide of $\Delta^{9,10}$ octalin ^a	-593.7			55 ^a
<i>trans</i> -3,5-Diphenyl-1,2,4-trioxolane (ozonide of <i>trans</i> -stilbene)	-123.8 ± 12.6			55 ^b
1,4-Dimethyl-2,3,7-trioxo-[2.2.1]bicyclohept-2-ene			-173 ± 20	56, 57
1,4-Diphenylbenzo-2,3,7-trioxanorbornene			111 ± 27	56, 58
Hexamethylenetriperoxide diamine (HMTD) [1,6-diaza-3,4,8,9,12,13-hexaoxabicyclo[4.4.4]tetradecane]	-360.3			59
Anthracene-9,10-endoperoxide	82.9 ± 3.4			2
5,6,11,12-Tetraphenyl-naphthacene-5,12-endoperoxide [rubrene peroxide]	516.5 ± 20.9			2

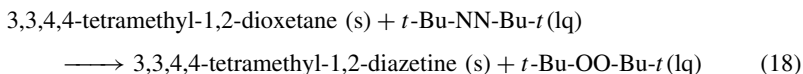
^a The structure of this compound is not characterized. See discussion in text.

Consider next the hypothetical process in equation 17.



Using all species in their liquid phase⁶¹ this reaction is found to be exothermic by -7 kJ mol⁻¹ while the related ring-opening reaction of cyclobutane is exothermic by *ca* -106 kJ mol⁻¹.

Another interesting comparison may be offered by reaction 18.



This reaction is 66 kJ mol⁻¹ endothermic. While the ring-opening reactions are nearly thermoneutral, contrary to expectation, this reaction would have been expected to be thermoneutral given it is homodesmotic and, additionally, maintains a four-membered ring on both sides of the reaction.

B. 1,2,4,5-Tetroxanes

Recently, the enthalpies of combustion and sublimation were measured for formaldehyde diperoxide, i.e. 1,2,4,5-tetroxane⁵³, from which the enthalpies of formation could be derived. These results were shown to be in good agreement with quantum chemical

calculations performed at a variety of levels, the highest being 6-311+G(d,p) within both the Hartree–Fock and B3LYP framework. Nonetheless, we are very much surprised by these values—in particular, the sublimation enthalpy of 11.2 kJ mol^{-1} seems too low. Recall, the sublimation enthalpy of any species equals the sum of the enthalpies of fusion and vaporization. Using the CHLP protocol¹⁷ we would estimate an enthalpy of vaporization of *ca* 22 kJ mol^{-1} and see no reason to doubt this value as a lower bound for the desired sublimation enthalpy. As such, we wonder if some of the sample decomposed exothermically during the phase change measurement, thereby decreasing the measured value for this quantity.

The gas phase enthalpy of formal reaction 8 that replaces the oxygens in the ring to produce cyclohexane is $+15.4 \text{ kJ mol}^{-1}$ for each peroxide unit replaced. From the results in an earlier section, we might have expected an enthalpy value of about 40 kJ mol^{-1} . The *gem*-diol, methanediol, is produced in formal reaction 6, the gas phase reaction enthalpy for which is -301 kJ mol^{-1} per peroxide unit. This is *ca* 22 kJ mol^{-1} more negative than the results in an earlier section that also produced *gem*-diols, *ca* -281 . Both of these reactions deviate from previous examples by nearly the same amount.

A related study⁵⁴ of 3,6-diphenyl-1,2,4,5-tetroxane resulted in enthalpies of formation of the solid and gaseous species of 134.0 ± 1.3 and $99.7 \pm 1.3 \text{ kJ mol}^{-1}$. Again, while computational theory and experiment are in good agreement, the sublimation enthalpy of 34.3 kJ mol^{-1} seems too low. We would have suggested a lower bound of *ca* 71 kJ mol^{-1} based on our enthalpy of vaporization estimation approach given above.

An additional problem with the enthalpies of formation of the two tetroxane species is irreconcilable. The -288 kJ mol^{-1} difference between the enthalpies of formation of the parent and diphenylated species is much too large. After all, the difference between the enthalpies of formation of 1,3-dioxolane and its 2-phenyl derivative⁶² is -93 kJ mol^{-1} and doubling this value for two substituents is but -186 kJ mol^{-1} . No explanation for this discrepancy is apparent.

C. Ozonides (1,2,4-Trioxolanes)

Direct calorimetric measurements of two ozonides have been reported. Both the enthalpy of combustion of the ozonides and the direct enthalpies of ozonation of the precursor olefin were measured. The first species to be studied was the purported ozonide of $\Delta^{9,10}$ octalin (1,2,3,4,5,6,7,8-octahydronaphthalene)^{55a}. It is doubtful that the product of the octalin ozonation reaction would be the ‘molozone’ formed by direct addition with no subsequent rearrangement (i.e. 11,12,13-trioxabicyclo[4.4.3]tridecane); but perhaps even less likely is the rearranged and hence ‘normal’ ozonide, the 11,12,13-trioxa[4.4.2.1]paddlane. From the published enthalpy of combustion of $-5628 \text{ kJ mol}^{-1}$, we derive an enthalpy of formation of this species, whatever it is, of $-593.7 \text{ kJ mol}^{-1}$.

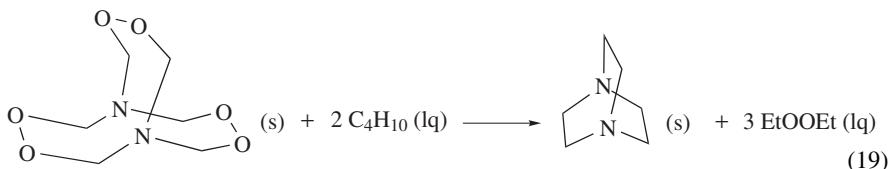
The second ozonide^{55b} is that from *trans*-stilbene, i.e. the 3,5-diphenyl trioxolane derivative. The ozonation experiment was done on both the *cis* and *trans* olefins resulting in reaction enthalpies of -471.5 and $-428.9 \text{ kJ mol}^{-1}$, respectively. The difference between these two values is *ca* 43 kJ mol^{-1} , which is close to the difference between the two olefins’ enthalpies of formation (one as liquid and the other as solid), $46 \pm 2 \text{ kJ mol}^{-1}$. This result vindicates the original authors’ suggestion of using the ozonation enthalpies as a method of determining the difference between enthalpies of formation of a *Z/E* pair of olefins.

There are photocalorimetric enthalpy data for two other ozonides, both coming from sensitized photochemical dioxygenation reactions in non-polar solvents⁵⁶. This study reports the enthalpies of the reactions of 2,5-dimethylfuran and 1,3-diphenylisobenzofuran to their corresponding endoperoxides to be exothermic by -45 ± 20 and $-92 \pm 25 \text{ kJ mol}^{-1}$ (the latter value is an average of the values given for different solvents). From

the gas phase enthalpy of formation of $-128.1 \pm 1.0 \text{ kJ mol}^{-1}$ of 2,5-dimethylfuran⁵⁷, we derive the enthalpy of formation of 1,4-dimethyl-2,3,7-trioxa-[2.2.1]bicyclohept-2-ene of $-173 \pm 20 \text{ kJ mol}^{-1}$. Likewise, from the gas phase enthalpy of formation of $203 \pm 10 \text{ kJ mol}^{-1}$ for 1,3-diphenylisobenzofuran⁵⁸, we thus deduce the enthalpy of formation of gaseous 1,4-diphenylbenzo-2,3,7-trioxanorbornene to be $111 \pm 27 \text{ kJ mol}^{-1}$. That these trioxa species are the ozonides of 1,2-dimethylcyclobutadiene and 7,8-diphenylbenzocyclobutadiene adds interest, but regrettably, no further information.

D. An Explosive Triperoxide

Finally, we note the enthalpy of formation of the explosive hexamethylenetriperoxide diamine (HMTD), more properly named 1,6-diaza-3,4,8,9,12,13-hexaoxabicyclo[4.4.4]tetradecane. Giving bomb calorimetry a potentially literal meaning, we find from a secondary source⁵⁹ an enthalpy of formation of -1731 kJ kg^{-1} or $-360.3 \text{ kJ mol}^{-1}$ in our more ‘appropriate’ thermochemist’s set of units. Again we ask if this result is plausible. Thermochemical data are sparse for medium and large ring species of any type. Let us neglect the strain in the bicyclic framework and distortion of the peroxide link⁶³, but also neglect any anomeric stabilization from the multiple N-CH₂-O units. Therefore, we would assume rough thermoneutrality for reaction 19. The calculated enthalpy of reaction is actually $+158 \text{ kJ mol}^{-1}$. The source of the large discrepancy is not obvious.



E. Arene Endoperoxides

Endoperoxides are the cyclic peroxides formed by adding diatomic oxygen in a 1,4-manner across a ring of an aromatic hydrocarbon, thereby replacing one benzenoid ring by a dioxabicyclo[2.2.2]octadiene, generally in the midst of the other rings. Direct combustion calorimetric measurements, as archivally chronicled, give a solid phase enthalpy of formation of anthracene-9,10-endoperoxide of $82.9 \pm 3.4 \text{ kJ mol}^{-1}$ and that of 5,6,11,12-tetraphenylnaphthacene-5,6-endoperoxide (rubrene peroxide) of $516.5 \pm 20.9 \text{ kJ mol}^{-1}$. By contrast, the archival values for the enthalpy of formation of the corresponding hydrocarbons are 129.2 ± 1.8 and $620.3 \pm 21.3 \text{ kJ mol}^{-1}$. The enthalpy of the formal oxygen addition reaction, the difference between the enthalpies of the endoperoxide and hydrocarbon, is exothermic by -46 ± 4 and $-103 \pm 30 \text{ kJ mol}^{-1}$ for anthracene and 5,6,11,12-tetraphenylnaphthacene, respectively. We are not surprised that the latter reaction is more exothermic than the former—naphthacene is less aromatic than anthracene and tetraphenylation of the latter plausibly induces increased strain. While in principle the reaction as written can be calorimetrically monitored, it clearly is too slow or else the arenes would autooxidize in air at a rapid rate.

Then we remember that as normally found, molecular oxygen has two unpaired electrons and so the reaction as written is both entropically discouraged and spin-forbidden. What about the reaction involving the excited state of oxygen, the $^1\Delta$ lying some 94 kJ mol^{-1} above the ground state? Even though the reaction is facile by comparison, that, too, seems to be a calorimetrically rarely performed measurement. One photocalorimetric study is that of Reference 56 wherein we find the exothermicity of this reaction for 9,10-diphenylanthracene and the non-benzenoid six-membered ring species

1,3-cyclohexadiene are -25 ± 20 and -80 ± 20 kJ mol⁻¹, respectively. The energetics of the reverse reaction—the decomposition of already formed endoperoxides—is relatively easily studied as it can be induced both thermally and photolytically. Of the anthracenes studied, the only one that can be directly compared⁶⁴ is the aforementioned 9,10-diphenyl derivative for which the deoxygenation reaction is endothermic by 25 ± 4 kJ mol⁻¹ in the solid state and 42 ± 8 kJ mol⁻¹ for the solution. The solid state result is identical, except for change of sign, to the reverse reaction.

VI. REFERENCES AND NOTES

1. S. W. Slayden and J. F. Liebman, 'Thermochemistry of ethers, alcohols, arenols, enols and peroxides', in *The Chemistry of Functional Groups, Supplement E: The Chemistry of Hydroxyl, Ether and Peroxide Groups, Vol. 2* (Ed. S. Patai), Wiley, Chichester, 1993.
2. J. B. Pedley, R. D. Naylor and S. P. Kirby, *Thermochemical Data of Organic Compounds* (2nd Edn.), Chapman & Hall, New York, 1986.
3. H. Y. Afeefy, J. F. Liebman and S. E. Stein, 'Neutral Thermochemical Data', in *NIST Chemistry WebBook, NIST Standard Reference Database Number 69* (Eds. P. J. Linstrom and W. G. Mallard), March 2003, National Institute of Standards and Technology, Gaithersburg MD, 20899 (<http://webbook.nist.gov>).
4. S. L. Khursan and V. S. Martem'yanov, *Russ. J. Phys. Chem. (Engl. Transl.)*, **65**, 321 (1991). The enthalpy of formation data cited from this source are from an unobtainable preprint.
5. The enthalpy of vaporization is from E. J. Blat, M. J. Gerber and M. B. Neumann, *Acta Physicochim. U.R.S.S.*, **10**, 273 (1939) as cited in Reference 3.
6. Yu. Ya. Van-Chin-Syan, T. N. Dolbneva, V. P. Vasil'ev, S. K. Chuchmarev and V. A. Puchin, *Russ. J. Phys. Chem. (Engl. Transl.)*, **56**, 1736 (1982).
7. Yu. Ya. Van-Chin-Syan, V. F. Korotyuk, Yu. V. Panchenko and S. K. Chuchmarev, *Russ. J. Phys. Chem. (Engl. Transl.)*, **57**, 1727 (1983) as taken from Reference 3.
8. A. V. Tobolsky and R. B. Mesrobian, *Organic Peroxides*, Interscience, New York, 1954, as cited in Reference 3.
9. H. P. Diogo, M. E. Minas da Piedade, J. A. M. Simões and Y. Nagano, *J. Chem. Thermodyn.*, **27**, 597 (1995).
10. T. S. A. Islam, *Dacca Univ. Stud., Part B*, **28**, 1 (1980) as cited in Reference 3.
11. In addition to the enthalpies of formation of peroxides cited, the enthalpies of formation of the following compounds were taken from Yu. Ya. Van-Chin-Syan, T. N. Dolbneva, M. A. Dikii and S. K. Chuchmarev, *Russ. J. Phys. Chem. (Engl. Transl.)*, **58**, 1783 (1984) as cited in Reference 3: 2-phenyl-2-propanol (solid, -250.4 ± 2.3 kJ mol⁻¹; gas, -162.9 ± 2.3 kJ mol⁻¹); $\alpha,\alpha,\alpha',\alpha'$ -tetramethyl-1,4-benzenedimethanol (solid, -543.0 ± 1.5 kJ mol⁻¹; gas, -406.2 ± 3.4 kJ mol⁻¹); 2-(4-isopropylphenyl)-2-propanol (solid, -343.7 ± 2.8 kJ mol⁻¹; gas, -242.9 ± 3.3 kJ mol⁻¹); 1,4-bis(2-hydroxy-2-propyl)benzene (solid, -543.0 ± 1.5 kJ mol⁻¹; gas, -406.2 ± 3.2 kJ mol⁻¹).
12. F. H. Dickey, J. H. Raley, F. F. Rust, R. S. Treseder and W. E. Vaughan, *Ind. Eng. Chem.*, **41**, 1673 (1949) as found in Reference 3.
13. K. Kishore and K. Ravindran, *Macromolecules*, **15**, 1638 (1982).
14. J. D. Cox and G. Pilcher, *Thermochemistry of Organic and Organometallic Compounds*, Academic Press, London, 1970; J. F. Liebman, J. A. Martinho Simões and S. W. Slayden, *Struct. Chem.*, **6**, 65 (1995).
15. W. Pritzkow and K. A. Muller, *Chem. Ber.*, **89**, 2318 (1956).
16. J. F. Liebman and M. V. Roux, unpublished analysis.
17. J. S. Chickos, D. G. Hesse and J. F. Liebman, *J. Org. Chem.*, **54**, 5250 (1989); J. S. Chickos, D. G. Hesse, J. F. Liebman and S. Y. Panshin, *J. Org. Chem.*, **53**, 3424 (1988).
18. The enthalpies of formation of the heptanols were taken from: K. B. Wiberg, D. J. Wasserman and E. Martin, *J. Phys. Chem.*, **88**, 3684 (1984).
19. The liquid enthalpy of formation of 3,3,6,6-tetramethyloctane of -373 kJ mol⁻¹ is from S. M. Shtekher, S. M. Skuratov, V. K. Daukshas and R. Ya. Levina, *Dokl. Akad. Nauk SSSR*, **127**, 812 (1959) as taken from Reference 3. An enthalpy of vaporization was calculated as 52.4 kJ mol⁻¹.

20. The enthalpies of formation of the saturated alcohols were taken from Reference 14 (2-, 3- and 4-heptanol) and K. B. Wiberg, D. J. Wasserman, E. J. Martin and M. A. Murcko, *J. Am. Chem. Soc.*, **107**, 6019 (1985) (1-methylcyclohexanol). The enthalpy of formation of 2-methylhex-1-ene-3-yn-2-ol is from Reference 32. The enthalpy of formation of solid 2,5-dimethylhexane-2,5-diol is from Reference 2 and the enthalpy of vaporization ($100.7 \pm 0.5 \text{ kJ mol}^{-1}$) is from Reference 18; the liquid phase enthalpy of formation is derived as -664 kJ mol^{-1} from an estimated enthalpy of fusion of 18 kJ mol^{-1} .
21. The enthalpies of formation of hydrogen peroxide [$-187.8 \text{ kJ mol}^{-1}$ (lq); $-136.3 \text{ kJ mol}^{-1}$ (g)] are from D. D. Wagman, W. H. Evans, V. B. Parker, R. H. Schumm, I. Halow, S. M. Bailey, K. L. Churney and R. L. Nuttall, *The NBS Tables of Chemical Thermodynamic Properties: Selected Values for Inorganic and C₁ and C₂ Organic Substances in SI Units*, *J. Phys. Chem. Ref. Data*, **11**, (1982), Supplement 2.
22. J. S. Chickos, W. E. Acree, Jr. and J. F. Liebman, *J. Phys. Chem. Ref. Data*, **28**, 1535 (1999) for estimating solid-liquid phase change enthalpies and entropies.
23. The enthalpy of hydrogenation of 3-hexyne is from D. W. Rogers, O. A. Dagdagan and N. L. Allinger, *J. Am. Chem. Soc.*, **101**, 671 (1979).
24. T. Mukundan and K. Kishore, *Macromolecules*, **22**, 4430 (1989).
25. Admittedly, we are not surprised that the decomposition enthalpies of styrene and 2-vinylnaphthalene peroxides are close to each other, as are those of the isomeric isopropenyl species. There is a rather reliable constant enthalpy of formation difference between phenyl and naphthyl derivatives, and as a corollary, a near-equality of the enthalpies of formation of 1- and 2-naphthyl derivatives, cf. the combined calculational and calorimetric studies of M. V. Roux, M. Temprado, R. Notario, S. P. Verevkin, V. N. Emel'yanenko, D. E. DeMasters and J. F. Liebman, *Mol. Phys.*, **102**, 1909 (2004) and references cited therein. It is perhaps more surprising that the α -methyl group on the unsaturated moiety (vinyl \rightarrow isopropenyl) causes such a small change.
26. Yu. Ya. Van-Chin-Syan, N. S. Kachurina, G. A. Petrovskaya and S. K. Chuchmarev, *Russ. J. Phys. Chem. (Engl. Transl.)*, **57**, 1751 (1983).
27. The value is from the liquid phase enthalpy of reaction between cyclohexanone and *tert*-butyl hydroperoxide from V. L. Antonovskii, E. V. Federova, N. E. Shtivel and V. D. Emelin, *Kinet. Katal.*, **30**, 1235 (1989).
28. K. B. Wiberg, K. M. Morgan and H. Maltz, *J. Am. Chem. Soc.*, **116**, 11067 (1994). The hydration enthalpies are derived from high-level quantum calculations that are consistent with solution phase enthalpies reported elsewhere in the literature.
29. The experimental enthalpy of formation of bis(hydroxymethyl) peroxide is derived from the enthalpy of the reaction between the peroxide and sodium hydroxide to yield hydrogen, sodium formate and water. Using the enthalpies of formation for dihydroxymethane and bis(hydroxymethyl) ether from Reference 21, the corresponding mono- and diaddition reaction enthalpies of formaldehyde to water are calculated to be exothermic by -102 and -52 kJ mol^{-1} , very nearly the expected 2:1 ratio.
30. The liquid enthalpies of formation of ethyl methyl ether (methoxyethane) and methyl *n*-pentyl ether (1-methoxypentane) were extrapolated as $-240.2 \text{ kJ mol}^{-1}$ and $-316.4 \text{ kJ mol}^{-1}$, respectively, from the data for 1-methoxypropane, 1-methoxybutane and 1-methoxydecane.
31. H. A. Swain, Jr., L. S. Silbert and J. G. Miller, *J. Am. Chem. Soc.*, **86**, 2562 (1964).
32. I. D. Zaikin, V. V. Shibanov and V. A. Fedorova, *Russ. J. Phys. Chem. (Engl. Transl.)*, **47**, 1236 (1973). See also Reference 33. There is an apparent contradiction concerning the structures of these compounds, as found in the original publications (translated) and in Reference 3. The translated title of the paper, correctly reproduced and with corresponding structures in the database, is 'Standard Heats of Formation of *t*-Butyl *OO*-Methyl Peroxyfumarate, *t*-Butyl *OO*-Methyl Peroxysuccinate, and *t*-Butyl Methyl succinate', implying a methyl peroxy linkage. No structures or synthesis information are given by the original authors. However, the later publication, Reference 33, reports the enthalpies of formation of these same substances and other dicarboxylic acid monoesters. Again, no structures are given. However, the substance of the report, and other publications by this same author, suggest a *tert*-butyl peroxy linkage.
33. I. D. Zaikin, *Russ. J. Phys. Chem. (Engl. Transl.)*, **51**, 786 (1977). See Reference 32. The title of the work (translated) taken directly from the reference is 'The Dissociation Energy of the Peroxide Linkage in Peroxyesters'. In Reference 3, for this data source, the structures of the

- peroxy and oxy are transposed from those in Reference 32. These are probably the correct structures.
34. R. N. Dolbneva, M. I. Darmograi and C. H. Wang, *Vestn. L'vov. Politekhn. In-ta*, 30 (1982); *Chem. Abstr.*, **97**, 162142c (1982).
 35. C. H. Wang, V. N. Dibrivnyi, V. A. Donchak and S. K. Chuchmarev, *Izv. Vyssh. Uchembn. Zared. Khim. Khim. Tekhnol.*, **24**, 1573 (1981); *Chem. Abstr.*, **97**, 29380n (1982).
 36. For a discussion of the energetics of isomeric benzene dicarboxylate esters, see P. Jiménez, J. Z. Dávalos, C. Turrión, H. Y. Afeefy and J. F. Liebman, *J. Chem. Soc., Faraday Trans.*, **94**, 887 (1999).
 37. D. Swern, L. P. Witnauer, C. R. Eddy and W. E. Parker, *J. Am. Chem. Soc.*, **77**, 5537 (1955).
 38. J. S. Chickos and W. E. Acree, Jr., *J. Phys. Chem. Ref. Data*, **32**, 519 (2003).
 39. M. V. Roux, M. Temprado, J. Z. Dávalos, P. Jiménez, R. S. Hosmane and J. F. Liebman, *Phys. Chem. Chem. Phys.*, **4**, 3611 (2002).
 40. R. B. Turner, W. R. Meador and R. E. Winkler, *J. Am. Chem. Soc.*, **79**, 4116 (1957).
 41. R. B. Williams, *J. Am. Chem. Soc.*, **64**, 1395 (1942).
 42. M. A. R. Matos, M. S. Miranda, V. M. F. Morais and J. F. Liebman, *J. Org. Biomol. Chem.*, **1**, 2930 (2003).
 43. P. E. Verkade, J. Coops and H. Hartman, *Recl. Trav. Chim. Pays-Bas*, **45**, 585 (1926).
 44. S. Verevkin, B. Dogan, H.-D. Beckhaus and C. Rüchardt, *Angew. Chem.*, **102**, 693 (1990).
 45. W. Adam and J. Sanabia, *J. Am. Chem. Soc.*, **99**, 2735 (1977).
 46. J. W. Breitenbach and J. Derkosch, *Monatsch. Chem.*, **82**, 177 (1951) as cited in Reference 3.
 47. E. G. Kiparisova and I. B. Rabinovich, *Dokl. Phys. Chem. (Engl. Transl.)*, **199**, 675 (1971).
 48. A. S. Carson, P. G. Laye and H. Morris, *J. Chem. Thermodyn.*, **7**, 993 (1975).
 49. A. S. Carson, D. H. Fine, P. Gray and P. G. Laye, *J. Chem. Soc. B*, 1611 (1971).
 50. G. S. Parks and H. P. Mosher, *J. Chem. Phys.*, **37**, 919 (1962).
 51. D. Zavoianu, I. Ciocazan, S. Moga-Gheorghe and C. Bornaz, *Rev. Chim. (Bucharest)*, **41**, 234 (1990) as cited in Reference 3.
 52. P. Leckten and G. Höhne, *Angew. Chem., Int. Ed. Engl.*, **12**, 772 (1973).
 53. J. M. Romero, L. C. Leiva, N. L. Jorge, M. E. Gómez Vara and E. A. Castro, *Acta Chim. Slov.*, **50**, 579 (2003).
 54. N. L. Jorge, L. C. A. Leiva, M. G. Castellanos, M. E. Gómez Vara, L. F. R. Cafferata and E. A. Castro, *The Scientific World Journal*, **2**, 455 (2002).
 - 55a. E. Dallwigk and E. Briner, *Helv. Chim. Acta*, **36**, 1166 (1953).
 - 55b. E. Briner and E. Dallwigk, *Helv. Chim. Acta*, **40**, 1978 (1957).
 56. J. Olmsted, III, *J. Am. Chem. Soc.*, **102**, 62 and 2825 (errata) (1980).
 57. S. P. Verevkin and F. M. Welle, *Struct. Chem.*, **9**, 215 (1998).
 58. A. Hussein and T. S. Akeshah, *Dirasat, Univ. Jordan*, **12**, 65 (1985).
 59. R. Meyer, *Explosives* (2nd Edn.), Verlag Chemie, Weinheim, 1982.
 60. The enthalpy of formation of 2,3-dimethyl-2,3-butanediol (pinacol), $-606.3 \pm 8.4 \text{ kJ mol}^{-1}$ (lq), is from J. P. Guthrie, *Can. J. Chem.*, **55**, 3562 (1977).
 61. The value for ethane was estimated using a derived enthalpy of liquefaction (the negative of the generally calculated enthalpy of vaporization), and numerically is *ca* -13 kJ mol^{-1} .
 62. S. P. Verevkin, B. Dogan, J. Hdrich, H.-D. Beckhaus and C. Rüchardt, *J. Prakt. Chem.*, **93**, 337 (1995).
 63. It is to be acknowledged that this species and other cage (bicyclic) peroxides have planar bridgehead nitrogen atoms, J. T. Edward, F. L. Chubb, D. F. Gilson, R. C. Hynes, R. Sauriol and A. Wiesenthal, *Can. J. Chem.*, **77**, 1057 (1999). This structural feature was not incorporated into our thermochemical analysis.
 64. N. J. Turro, M.-F. Chow and J. Rigaudy, *J. Am. Chem. Soc.*, **103**, 7218 (1981).

CHAPTER 4

¹⁷O NMR spectroscopy of organic compounds containing the –O–O–group

GIOVANNI CERIONI

Dipartimento Farmaco Chimico Tecnologico, Università di Cagliari, Via Ospedale 72, I-09124, Cagliari, Italy
Fax: +39 070 675 8553; e-mail: cerioni@unica.it

and

FRANCESCA MOCCI

Dipartimento di Scienze Chimiche, Università di Cagliari, Cittadella Universitaria di Monserrato, SS 554 Bivio per Sestu, I-09024, Monserrato (CA), Italy

I. INTRODUCTION	171
II. ORGANIC PEROXIDES	173
A. Ozonides	173
B. Trioxides	178
C. Peroxides	183
III. A BRIEF LOOK AT METALLO-ORGANIC AND BIOLOGICAL SYSTEMS	185
IV. REFERENCES	186

I. INTRODUCTION

This chapter deals mainly with ¹⁷O NMR spectroscopy of organic derivatives containing oxygen bound to oxygen. Occasional references are given for multinuclear NMR and theoretical calculations, when necessary for the completeness of the subject. They relate mainly to data published in the past thirteen years (from 1991 through 2003), supplementing the information contained in the earlier volume of this series concerning the peroxide functional group¹ and in a section of Chapter 9 of Boykin's book dealing with ¹⁷O NMR

The chemistry of peroxides, volume 2

Edited by Z. Rappoport © 2006 John Wiley & Sons, Ltd ISBN: 0-470-86274-2

spectroscopy in organic chemistry². Some references, mostly till 1990, can be also found in the chapter on ¹⁷O NMR spectroscopy in the book by Berger, Braun and Kalinowski³.

From the point of view of ¹⁷O NMR spectroscopy, there are two widely different classes of compounds among those containing oxygen–oxygen bonds: one class whose O–O bonds can be related to hydrogen peroxide, and a second class whose derivatives contain oxygen–oxygen bonds to be better related to those of the ozone molecule. In fact, hydrogen peroxide⁴ has an ¹⁷O NMR chemical shift of $\delta = 174$ ppm, very different from values measured for ozone⁵, $\delta = 1032$ (central) and 1590 (terminal) ppm. Organic compounds mostly belong to the first class, while important examples of the second type can be found among, e.g., heme dioxygen complexes. Papers dealing with derivatives of the first type will be the main subject of this review, whereas studies on the other type will not be reviewed here except that some representative examples will be given, in a separate section, together with a few examples of metallo-organic systems.

It might be convenient for the reader to briefly premise the advantages and drawbacks of ¹⁷O NMR spectroscopy, as its utilization is still not widespread among organic chemists. The main NMR spectroscopic properties of the ¹⁷O nuclide are gathered in Table 1.

We see from Table 1 that the only observable nuclide for oxygen, ¹⁷O, has a very low natural abundance, even in comparison with those of *popular* nuclides like ¹³C (1.108%) and ¹⁵N (0.37%). Moreover, its quadrupole moment prevents any practical utilization of polarization transfer techniques like INEPT or DEPT, now widely used in ¹³C and ¹⁵N NMR spectroscopies. A range of chemical shifts much wider than those of ¹³C and ¹⁵N is an important point in favour of utilization of ¹⁷O. All these properties did not prevent important applications of ¹⁷O NMR spectroscopy in organic chemistry, even from the times of continuous wave NMR spectroscopy. Interesting examples of such pioneering works can be found both at natural abundance^{4,6} as well as with enriched samples^{7,8}. However, also in the case of ¹⁷O NMR spectroscopy, FT NMR proved to be decisive for its development.

¹⁷O relaxation times are very short and an overnight accumulation allows one to obtain *ca* 2×10^6 transients; therefore, the disadvantage of low natural abundance is much reduced and good spectra of organic compounds of molecular weights ≤ 800 Da can be easily obtained using non-enriched samples. Further improvement is obtained by using low viscosity solvents, such as MeCN, at relatively high temperatures, usually 65–75 °C. The use of as high as possible fields and 10-mm tubes is recommended.

Summing up, one can say that, in the experience of the authors, an organic sample of about 400 Da molecular weight and a solubility of 100–200 mg in 3 ml of solvent requires no more than 3 hours of instrument time, usually much less. Biological samples, unfortunately, often do not meet these requirements and, subsequently, studies on these subjects are more rare, as is shown also in Section III of this chapter.

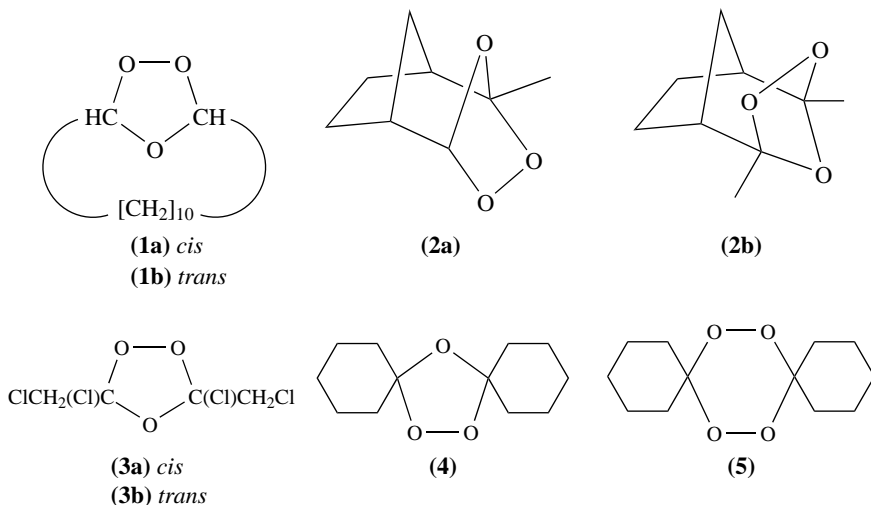
TABLE 1. ¹⁷O magnetic properties and NMR parameters

Property	Value
Nuclear spin I	5/2
Natural abundance	0.037%
Gyromagnetic ratio γ	-3.6266×10^7 (rad T ⁻¹ s ⁻¹)
Quadrupole moment Q	-2.578×10^{-2} (m ² $\times 10^{-26}$)
Resonance frequency (at 7.05 T)	40.662 (MHz)
Relaxation times	≤ 0.2 (s)
Chemical shift range	<i>ca</i> 2000 ppm

II. ORGANIC PEROXIDES

A. Ozonides

An important paper by Salomon, Clennan and coworkers on dialkyl peroxides⁹, where also one ozonide was reported, appeared in 1985. In this paper, a correlation among ^{13}C and ^{17}O chemical shifts was established, and the influence of several factors like concentration, temperature, solvent and, naturally, chemical structure was thoroughly studied but confined to dialkyl peroxides. There was a gap of several years before the appearance of a further note¹⁰ reporting data of seven 1,2,4-trioxolanes (ozonides), **1–4**, and of the 1,2,4,5-tetroxane **5**. Their ^{17}O NMR data are given in Table 2. Spectra were obtained at natural isotopic abundance, in toluene at 27°C .



A comparison of the chemical shifts of ozonides and cyclic peroxides⁹ shows that those of the former are at the upper end of the chemical-shift range (232–318 ppm) of the latter.

TABLE 2. ^{17}O NMR data of the peroxidic oxygens of **1–5**¹⁰

Compound	$\delta(\text{ppm})^a$	$\nu_{1/2}(\text{Hz})^b$
1a	306	510
1b	297	570
2a	310, 320	^c
2b	329, 333	^c
3a	327	750
3b	319	717
4	295	720
5	256	^d

^a Relative to 1,4-dioxane used as an external reference, +0.2 ppm relative to water.

^b Half-height line-widths.

^c Composite signals.

^d Not reported.

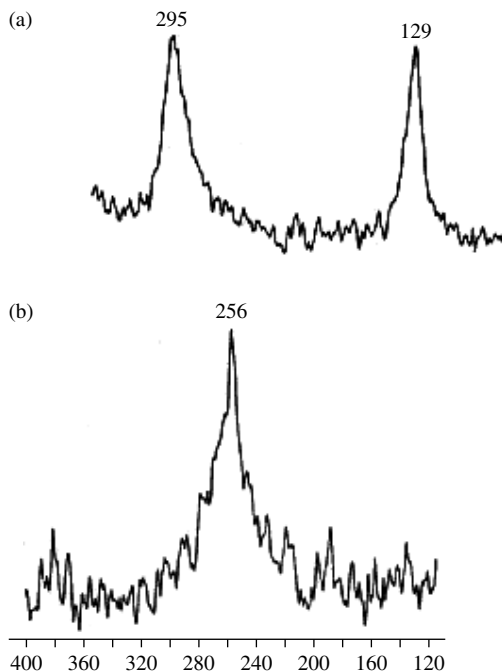


FIGURE 1. Partial ^{17}O NMR spectra of (a) **4** and (b) **5** relative to dioxane in toluene. Reproduced by permission of The Royal Society of Chemistry from Reference 10

Therefore, following the qualitative inverse relationship between ^{17}O NMR chemical shifts and the C–O–O–C dihedral angle observed for cyclic peroxides⁹, one can estimate this angle as being close to 0° . Consequently, the large shielding (*ca* 40 ppm) observed for **5** relative to **4** suggests a large deviation from planarity in both C–O–O–C dihedral angles of tetroxane **5**. Moreover, these results indicated that the use of ^{17}O NMR spectroscopy enables an easy and unequivocal differentiation between ozonides and 1,2,4,5-tetroxanes, which are often coproducts in the ozonolysis of olefins. This differentiation is, *inter alia*, obviously given by the lack of the ethereal signal of the peroxide at $\delta = 129$ ppm (Figure 1a) in the spectrum of tetroxane **5** (Figure 1b).

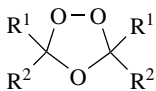
Following this work on ^{17}O NMR spectra of ozonides, there is an extensive paper by the Griesbaum group¹¹ where 35 ozonides (**6–14** with different stereochemistries) have been studied. The widely different structures examined allowed the influences of structural features on ^{17}O NMR spectra of ozonides to be shown. Five structurally different types of ozonides can be recognized: symmetrically tetrasubstituted (type **6**), unsymmetrically tetrasubstituted (type **7**), unsymmetrically tri- and tetrasubstituted (type **8**), unsymmetrically disubstituted (type **9–13**) and bicyclic ozonides (type **14**). ^{17}O NMR chemical shifts of peroxidic and ethereal oxygens are collected in Table 3. All spectra were obtained at natural isotopic abundance, in benzene- d_6 solution mainly at 25°C , although in some cases higher temperatures had to be used. These experimental conditions make for an easy comparison with the previously discussed data.

Examination of the data for derivatives **6** allows one to observe the influence of the electronegativity of substituents both on the ethereal oxygens and on the peroxidic atoms.

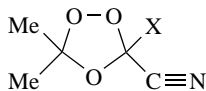
TABLE 3. ^{17}O NMR data of ozonides **6–14**¹¹

Compound	R ¹ or X	R ²	$\delta(\text{ppm})$ $-\text{O}-\text{O}-$	$\delta(\text{ppm})$ $-\text{O}-$
<i>cis</i> - 6a	Me	CH ₂ Cl	293.4	125.6
<i>trans</i> - 6a	Me	CH ₂ Cl	297.9	126.5
<i>trans</i> - 6b	Me	CN	327.7	143.8
6c ^a	Me	OC(=O)Me	310.4	162.4
<i>cis</i> - 6d ^b	Cl	CH ₂ Cl	327.0	172.0
<i>trans</i> - 6d ^b	Cl	CH ₂ Cl	319.0	162.0
<i>trans</i> - 6e	F	CH ₂ Br	303.1	155.6
7a	X=CN	—	288.6	336.4
7b ^c	X=Cl	—	291.4	329.2
8a ^{c,d}	H	Me	312.2	123.8
8b ^{c,d}	H	OMe	303.0	125.9
8c ^{c,d}	Me	CF ₃	282.0	325.3
8d ^{c,d}	Me	CH ₂ Cl	302.3	127.5
8e ^c	Me	Me	307.9	131.9
8f ^{c,d}	Me	CN	299.7	322.4
9	—	—	283.8	320.7
10(I) ^e	—	—	277.7	312.0
10(II) ^e	—	—	279.0	314.8
11(I) ^e	—	—	263.2	318.6
11(II) ^e	—	—	300.0	111.5
12(I) ^e	—	—	280.1	309.6
12(II) ^e	—	—	285.4	305.1
13(I) ^e	—	—	272.5	318.5
13(II) ^e	—	—	280.7	314.4
<i>cis</i> - 14a ^d	CN	CN	319.1	167.3
<i>cis</i> - 14b ^f	Me	H	303.4	129.8
<i>cis</i> - 14c ^f	C ₆ H ₅	H	304.5	129.1
<i>cis</i> - 14d ^{g,h}	Me	H	289.6	114.7
<i>cis</i> - 14e ^{g,i}	Me	H	298.6	111.0
<i>cis</i> - 14f ^{c,j}	H	H	294.8	103.4
<i>trans</i> - 14f ^{c,j}	H	H	305.0	106.7
<i>cis</i> - 14g ^k	H	H	293.4	102.9
<i>cis</i> - 14h ^l	H	H	298.1	99.6
<i>trans</i> - 14h ^l	H	H	299.0	102.4
<i>cis</i> - 14i ^m	H	H	296.2	101.9
<i>trans</i> - 14i ^m	H	H	294.8	102.9
<i>cis</i> - 14j ^{m,n}	Me	Me	292.6	132.0
<i>trans</i> - 14j ^{m,n}	Me	Me	300.5	130.8

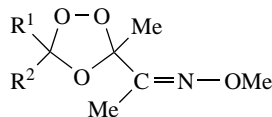
^a Unknown stereochemistry; spectrum recorded at 40 °C.^b Data from Reference 9.^c Spectra recorded at 30 °C.^d $n = 2$.^e Notation (I) and (II) indicates two different isomers of unknown stereochemistry.^f $n = 3$.^g $n = 4$.^h Substituted by CH₂=C(Me) in β position to the CH group.ⁱ Substituted by O=C(Me) in β position to the CH group.^j $n = 9$.^k $n = 10$.^l $n = 12$.^m $n = 14$.ⁿ Spectra recorded at 50 °C.



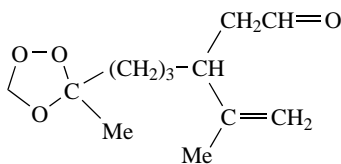
(6)



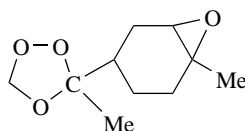
(7)



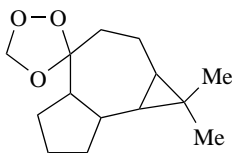
(8)



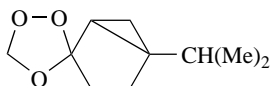
(9)



(10)



(11)



(12)

The ability of each substituent to exercise this influence is different for the two groups and thus two sequences are observed for the ether O atoms [$\text{CN} < \text{F} < \text{O}-(\text{C}=\text{O})-\text{Me} \approx \text{Cl}$] and the $-\text{O}-\text{O}-$ group [$\text{F} < \text{O}-(\text{C}=\text{O})-\text{Me} < \text{Cl} < \text{CN}$]. The effect of substitution is, in both cases, to cause a downfield shift, although it can be observed that the extent of these chemical shift changes is larger for the ether oxygen than for the $-\text{O}-\text{O}-$ group. A greater sensitivity of the ether oxygen compared to the peroxidic ones is observed also for methyl substitution (e.g. *trans*-**14i** vs. *trans*-**14j**) and seems to be a general rule.

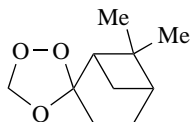
Both points discussed for derivatives **6** are very clearly seen again in derivatives **7a** and **7b**. The ethereal oxygen of **7b** is 20.4 ppm downfield compared to that of **7a**, while the opposite (7.2 ppm upfield) is observed for the peroxidic oxygen juxtapositioned near the substituent X. The influence of the electronegativity of the substituents is also clearly shown for **7** by the large $\Delta\delta$ (ca 30 ppm) observed between the two peroxidic oxygens.

An important result given by derivatives **8** is that unsymmetrical substitution alone is not sufficient to cause a difference in ^{17}O chemical shifts to be observed. Interestingly, it can be noted that the only two derivatives, **8c** and **8f**, yielding two different signals for the peroxidic oxygens are those substituted by strongly electron-withdrawing substituents. The authors observe that this is not the only prerequisite for doubling of the signals, as shown in the following.

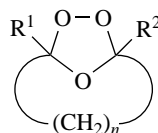
In fact, all derivatives **9–13** show doubling of the peroxidic signals except for **11(II)**. The authors pointed out that these data serve as a clear indication that hydrocarbon substituents, as well as substituents bearing electron-withdrawing heteroatoms, are sufficient to cause a chemical shift nonequivalence of the two peroxidic oxygens at ^{17}O NMR. Although the unknown stereochemistry of derivatives **10–13** does not allow us to discuss properly the origin of this nonequivalence, some reasonable hypotheses can be put forth.

For all the derivatives **10–13**, the most shielded signal is close to 280 ppm, with the exception of **11(I)** and to a lesser extent of **13(I)**. Such values allow, by comparison with previous data, to assign this signal to the oxygen bound to the annular unsubstituted

4. ^{17}O NMR spectroscopy of organic compounds containing the $-\text{O}-\text{O}-$ group 177



(13)

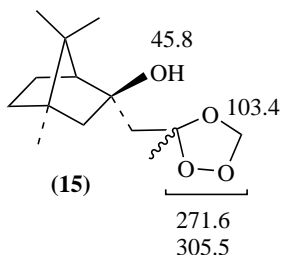


(14)

carbon. Moreover, application of the known criteria^{10,12} used to estimate the $\text{C}-\text{O}-\text{O}-\text{C}$ dihedral angle seems to indicate that there is not a significant variation from 0° except for **11(I)** and, possibly, for **13(I)**. The effect of substitution, observed on the nearby peroxidic oxygen, is thus deshielding, most probably due to steric crowding, as usually observed¹³ in ^{17}O NMR spectroscopy. Interestingly, we note that the largest $\Delta\delta$ values between the two peroxidic oxygens of the same derivative are measured for **11(I)** and **13(I)**. We mentioned above that for these two derivatives we may suspect a distortion from planarity of the $\text{C}-\text{O}-\text{O}-\text{C}$ dihedral angle, which is a very likely effect of steric compression.

Chemical shifts in type **14** derivatives are in agreement with the previously discussed results. It can be observed that unsymmetrical substitution, when applicable, was never sufficient to differentiate between the two peroxidic oxygens. Likewise, a little influence seems to be exercised by *cis/trans* annulation.

These observations were applied by Dimitrov, Hesse and coworkers¹⁴. On studying ozonization of a series of allylic and homoallylic alcohols prepared from (+) camphor and (-) fenchone, they were able to isolate a certain number of ozonides and to obtain the ^{17}O NMR spectrum of the diastereomeric mixture of one of them, i.e. derivative **15**, whose structure and ^{17}O NMR chemical shifts (δ , ppm) are shown below.

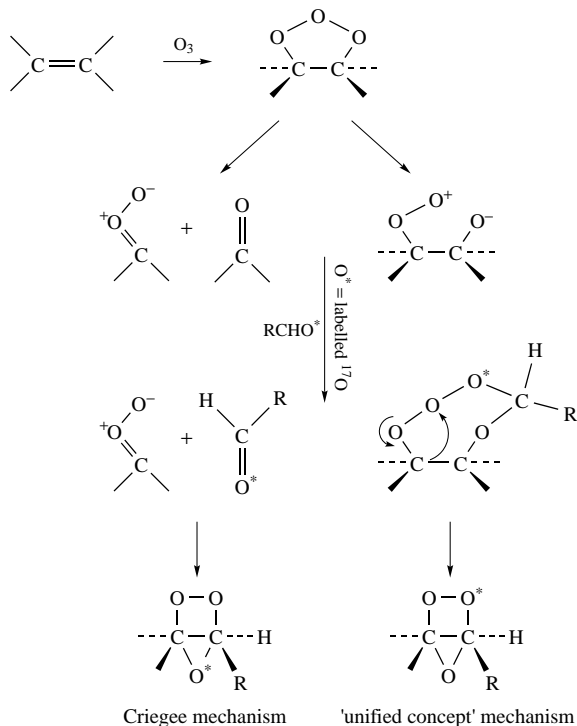


(15)

It was not possible to differentiate between the two diastereoisomers because of the quite large line-widths of the signals, *ca* 2000 Hz for the peroxidic oxygens and *ca* 1300 Hz for the ether oxygen. Such large line-width values could be due to the solvent (CDCl_3) used for this measurement as well as to the large line-broadening factor (400 Hz) applied to the FID. However, the overall influence of these experimental conditions does not put in doubt the authors' suggestion of a low $\text{C}-\text{O}-\text{O}-\text{C}$ dihedral angle for **15**.

In the work of Geletneky and Berger¹⁵, ^{17}O NMR proved to be decisive in clarifying the mechanism of ozonolysis, allowing one to choose between the Criegee mechanism¹⁶ and the 'unified concept'¹⁷. When using labelled compounds, the final position of the labelled oxygen atom will be different, depending on the reaction mechanism, and by the use of ^{18}O labelling and mass spectrometry evidence in favour of the 'unified concept' mechanism was reported^{18,19}. The two mechanisms are shown in Scheme 1.

The use of an ^{17}O -labelled aldehyde enables one to obtain a final ozonide labelled either at the ether oxygen or at the peroxide bridge, depending on which reaction mechanism is



SCHEME 1. Mechanism of ozonolysis. Reproduced by permission of Wiley-VCH Verlag GmbH from Reference 15

operating. This has been tested by ozonization of two olefins, styrene and ethylenecyclohexane. The spectra reported in Figure 2 clearly demonstrate that only the ether oxygen is labelled, thus giving substantial evidence in favour of the Criegee mechanism.

B. Trioxides

^{17}O NMR spectroscopy has found further application in a series of papers^{20–23} concerned with the ozonization of the C–H bond, a reaction leading, at low temperature, to the formation of alkyl hydrotrioxides ROOOH and hydrogen trioxide HOOOH. Through the use of ^{17}O -enriched ozone, the authors could characterize by ^{17}O NMR the trioxide group. In a preliminary communication²⁰, the Plesničar group studied the ozonization of isopropyl alcohol, observing the formation of both the isopropyl alcohol trioxide and the hydrogen trioxide, and this was confirmed by the ^{17}O NMR chemical shift assignments which gave excellent agreement with the computed shifts. These studies were extended in a subsequent paper²¹, where the Plesničar group studied the ozonization of isopropyl alcohol and isopropyl methyl ether in three different solvents: acetone- d_6 , methyl acetate and *tert*-butyl methyl ether, at -78°C . All the polyoxides formed were fully characterized by their ^1H , ^{13}C and ^{17}O NMR spectra. Their ^{17}O chemical shifts were compared to those of similar peroxides as well as calculated at various computational levels. ^1H and ^{13}C NMR data are collected in Table 4, ^{17}O NMR experimental data in Table 5 and calculated ^{17}O NMR chemical shifts in Table 6.

4. ^{17}O NMR spectroscopy of organic compounds containing the $-\text{O}-\text{O}-$ group 179

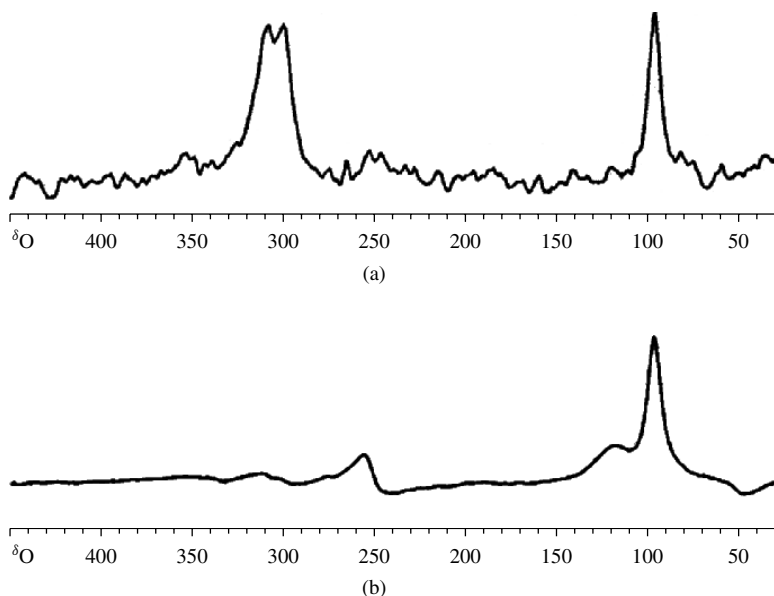


FIGURE 2. (a) Room-temperature ^{17}O NMR spectrum of the secondary ozonide of styrene obtained after ozonolysis in pentane at -78°C . (b) Room-temperature ^{17}O NMR spectrum of the secondary ozonide of styrene obtained after ozonolysis in pentane at -78°C in the presence of 1.0 equiv. of ^{17}O -labelled benzaldehyde. Reproduced by permission of Wiley-VCH Verlag GmbH from Reference 15

TABLE 4. ^1H and ^{13}C NMR chemical shifts of some trioxides²¹

Compound	^1H chemical shifts, δ^a	^{13}C chemical shifts, δ^a
HOOOH	13.02 ^b and 13.035 ^b	
$\text{Me}_2\text{C}(\text{OH})(\text{OOOH})^c$	1.44 (CH_3), 12.85 (OOOH)	25.7 (CH_3) 104.3 (C)
$\text{Me}_2\text{C}(\text{OMe})(\text{OOOH})$	1.38 (CH_3), 3.23 (OCH_3), 13.026 (OOOH)	23.1 (CH_3), 49.4 (OCH_3), 106.8 (C)

^a ppm downfield from TMS (-10°C), in acetone- d_6 .

^b Values obtained respectively for the reaction of isopropyl alcohol and isopropyl methyl ether.

^c OH value was not reported; see text.

TABLE 5. Experimental ^{a,b} ^{17}O NMR chemical shifts $\delta(\text{O})$ of some trioxides²¹

Compound	$\delta(\text{O}^1)$	$\delta(\text{O}^2)$	$\delta(\text{O}^3)$
$\text{HO}^1\text{O}^2\text{O}^3\text{H}$	305 (350)	421 (1450)	305 (350)
$\text{HO}^1\text{O}^2\text{H}$	187 (320)	187 (320)	
$\text{Me}_2\text{C}(\text{OH})(\text{O}^1\text{O}^2\text{O}^3\text{H})$	368 (950)	445 (2100)	305 (350)
$\text{Me}_2\text{C}(\text{OH})(\text{O}^1\text{O}^2\text{H})$	262 (1600)	220 (1600)	
$\text{Me}_2\text{C}(\text{OMe})(\text{O}^1\text{O}^2\text{O}^3\text{H})$	347 (580)	450 (1350)	306 (330)
$\text{Me}_2\text{C}(\text{OMe})(\text{O}^1\text{O}^2\text{H})$	237 (800)	224 (800)	
$\text{Ph}(\text{Me})\text{C}(\text{OH})(\text{O}^1\text{O}^2\text{O}^3\text{H})$	367 (2000)	451 (2300)	304 (490)

^a ppm downfield from the internal standard H_2^{17}O , in acetone- d_6 at -10°C .

^b Half-height line-widths in Hz (values in parentheses).

TABLE 6. Calculated ^{17}O NMR chemical shifts²¹

Compound	GIAO/MP2/6-31++G*	GIAO/MP2/6-311++G**
$\text{HO}^1\text{O}^2\text{O}^3\text{H}$	300 (O^1 , O^3) 435 (O^2)	306 (O^1 , O^3) 433 (O^2)
$\text{HO}^1\text{O}^2\text{H}$		192
$\text{Me}_2\text{C}(\text{OH})(\text{O}^1\text{O}^2\text{O}^3\text{H})^a$	374 (O^1), 461 (O^2), 295 (O^3) 362 (<i>O^1</i>), 470 (<i>O^2</i>), 311 (<i>O^3</i>)	
$\text{Me}_2\text{C}(\text{OH})(\text{O}^1\text{O}^2\text{H})$	271 (O^1), 216 (O^2)	
$\text{MeO}^1\text{O}^2\text{O}^3\text{H}$	327 (O^1), 453 (O^2), 293 (O^3)	315 (O^1), 488 (O^2), 282 (O^3)
$\text{MeO}^1\text{O}^2\text{H}$	212 (O^1), 236 (O^2)	215 (O^1), 243 (O^2)

^a Calculated for the most stable of the ‘open’ forms and the intramolecularly hydrogen-bonded form (in italics); see also text.

Very similar results to those shown in Tables 4 and 5 have also been obtained when the reaction solvents were methyl acetate and *tert*-butyl methyl ether.

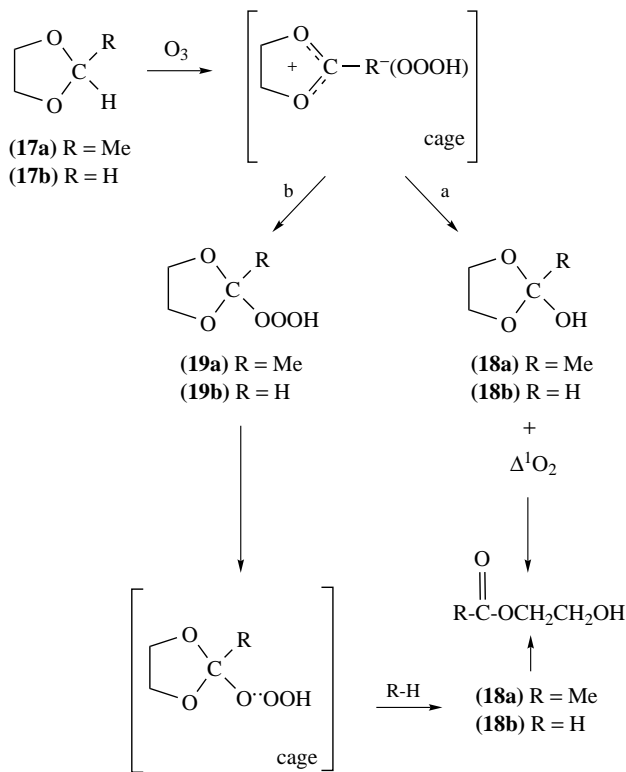
The slight difference observed for the ^1H NMR shifts of HOOOH (Table 4) is not significant. The authors have identified beyond doubt the HOOOH resonance by exchange, at -60°C , with CH_3OD or DOD and on the basis of the enriched ^{17}O NMR of polyoxides²¹. Moreover, hydrogen trioxide has been synthesized, in an independent experiment, by low-temperature ozonization of hydrazobenzene, a procedure yielding HOOOH in the absence of other hydrotrioxides. It was also pointed out that the different rate of decomposition of polyoxides and HOOOH furnishes a further unambiguous way to characterize all these species.

^1H NMR measurements of the concentration and temperature dependence of the OOOH signals of the hydrotrioxides $\text{Me}_2\text{C}(\text{OH})(\text{OOOH})$ (**16a**) and $\text{Me}_2\text{C}(\text{OMe})(\text{OOOH})$ (**16b**) gave very reliable indications concerning their various forms in oxygenated solvents. Most probably, **16a** and **16b** exist as intramolecularly hydrogen-bonded forms in equilibrium with monomeric, dimeric and oligomeric intermolecularly hydrogen-bonded forms, solvated by the basic solvents (acetone, methyl acetate and *tert*-butyl methyl ether). These findings are well supported by calculations. For **16a**, an energy difference of 1.9 kcal mol^{-1} has been computed (at MP2/6-31++G*) between the intramolecular hydrogen-bonded form and the most stable of the various ‘open’ conformations. This is to be compared with an energy difference of 8.2 kcal mol^{-1} found between cyclic dimeric and/or polymeric forms, and the solvated form for the system MeOOOH-OMe_2 . The quite good agreement between computed and experimental ^{17}O NMR chemical shifts is also noteworthy, particularly if we take into account the sensitivity of the shifts to conformational changes (Table 6). Similar results have been obtained also for HOOOH. Kinetic studies and additional calculations, which are outside the scope of this chapter, gave evidence in favour of a radical pair $[\text{R}\cdot\text{OOOH}]$ mechanism for the formation of the alkyl hydrotrioxides and HOOOH as well as for water-assisted decomposition of these species.

In a subsequent paper²² the Plesničar group extended these studies to two different substrates, cumene and triphenylmethane. However, while newly obtained HOOOH ^{17}O NMR spectra confirmed the previous results, it was impossible to obtain the ^{17}O NMR spectra of cumene and triphenylmethane hydrotrioxides. This was ascribed, by the authors, most probably to too large a line-width, due to the internal asymmetry of these derivatives, which prevented their observation. The derivatives were, in any case, characterized by ^1H and ^{13}C NMR spectroscopy.

In a further study²³, devoted also to seeking evidence of the elusive HO_3^- anion, ^{17}O NMR spectroscopy played a key role. Low-temperature ozonization of the 1,3-dioxolanes **17a** and **17b** in acetone- d_6 , methyl acetate and *tert*-butyl methyl ether yielded the hemioortho esters **18a** and **18b** and the dioxolane trioxides **19a** and **19b** (Scheme 2).

4. ^{17}O NMR spectroscopy of organic compounds containing the $-\text{O}-\text{O}-$ group 181



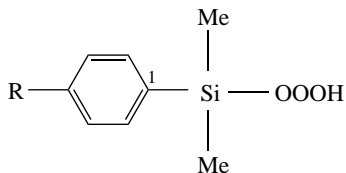
SCHEME 2

^{17}O NMR data were reported only for 2-methyl-1,3-dioxolane hydrotrioxide **19a** [$\delta_{\text{acetone-d}_6} = 305 (\text{O}^3), 455 (\text{O}^2), 355 (\text{O}^1)$ ppm; for clarity we use the same oxygen numbering of Table 4, although it differs from that used in the original paper] and the hemioortho ester **18a** [$\delta_{\text{acetone-d}_6} = 96.0$ ppm (OH)]. As in all these low-temperature and low-concentration experiments reported by Plesničar and colleagues^{20–23}, ^{17}O NMR signals could be detected only for the isotopically enriched groups. This point is diagnostic for the reaction pathways described in Scheme 2, since the enrichment (and subsequent detection) of the OH group of **18a** indicates that the reaction of the initially formed carbenium ion with HOOO^- takes place in the solvent cage. Further evidence in favour of the suggested mechanism is given by ^1H NMR kinetic experiments and calculations. As a last but significant point, it should be noted that HOOOH has not been observed in the dioxolane ozonization, contrary to the previously discussed ozonizations.

In a very recent paper²⁴ the same group investigated the mechanism of formation of HOOOH in the ozonization of 1,2-diphenylhydrazine and 1,2-dimethylhydrazine. Ozonization of the former is the most suitable reaction to obtain HOOOH solutions not contaminated by organic trioxides ROOOH , allowing one also to obtain relatively concentrated solutions of HOOOH , estimated to be $45 \pm 10\%$ at -60°C . The results fully agree with those previously discussed, for both ^1H and ^{17}O NMR.

Although ^{17}O NMR results (at natural abundance) could not be obtained, it is worth discussing briefly a related paper²⁵ of the same group, containing interesting data on

^{29}Si NMR of dimethylphenylsilyl hydrotrioxide **20a** and some analogous organosilicon peroxides and other derivatives. The relevant NMR data are collected in Table 7.



- (**20a**) R = H
 (**20b**) R = Me
 (**20c**) R = OMe
 (**20d**) R = Cl

The ^{29}Si chemical shifts show a clear deshielding effect on going from the OH to the OOOH derivative, the difference between $\text{PhSi}(\text{Me})_2\text{OH}$ and $\text{PhSi}(\text{Me})_2\text{OOH}$ being much larger than that between $\text{PhSi}(\text{Me})_2\text{OOH}$ and $\text{PhSi}(\text{Me})_2\text{OOOH}$. A similar trend, but in the opposite direction, is shown by the ^{13}C NMR chemical shifts of C_1 and Me. This trend could be suggestive of increasing electron demand by the silicon atom when the substitution changes from OH to OOOH.

The ^1H NMR chemical shifts of only the OOOH group were reported for all the derivatives studied. They are, in δ ppm from TMS, in acetone- d_6 solutions at -78°C : **20a** (13.96), **20b** (13.78), **20c** (13.78), **20d** (13.70).

For the sake of completeness of the ^{17}O NMR data on polyoxides, we mention briefly an older paper²⁶ on bis(trifluoromethyl) trioxide $\text{CF}_3\text{OOOCF}_3$ (**21**). The ^{17}O NMR data (δ , ppm) of **21**, 321 (terminal) and 479 (central), were already reported³ but a comparison with the new data on polyoxides obtained by Plesničar and colleagues^{20–24} can be of interest, particularly for the O^1 and O^2 oxygens, since the O^3H oxygens are rather different from the others (see Table 5 and **19a**), and their shifts are remarkably constant through all the measured derivatives ($\delta = 305 \pm 1$ ppm). The O^1 oxygens show a strong deshielding by substitution (shown by comparing O^1 and O^3), in a way somehow resembling that observed for aliphatic peroxides²⁷ but with large variations due to great structural differences of the groups bonded to O^1 . This effect is quite less pronounced for **21** (compare with HOOOH). The chemical shift variation of the central oxygen O^2 is, on the contrary, much bigger for **21** than for the other trioxides, again in comparison with HOOOH. It is also noteworthy that among the other trioxides $\Delta\delta(\text{O}^2)$ is relatively small, being equal to 10 ppm [$\delta(\text{O}^2) = 450 \pm 5$ ppm].

TABLE 7. Selected ^{13}C and ^{29}Si NMR chemical shifts^a for **20a** and analogues²⁵

Compound	C_1	Me	Si
$\text{PhSi}(\text{Me})_2\text{OOOH}$ (20a)	138.5	2.7	17.31
$\text{PhSi}(\text{Me})_2\text{OOH}$	139.6	2.8	14.31
$\text{PhSi}(\text{Me})_2\text{OH}$	143.5	3.1	3.30
$\text{PhSi}(\text{Me})_2\text{H}$	140.6	-1.1	-16.95
$\text{PhSi}(\text{Me})_2\text{OSi}(\text{Me})_2\text{Ph}$	143.1	3.9	-0.96
$\text{PhSi}(\text{Me})_2\text{OOSi}(\text{Me})_2\text{Ph}$	139.5	2.8	16.6

^a δ (ppm) downfield from internal TMS, in acetone- d_6 at -78°C .

C. Peroxides

Notwithstanding the promising results obtained, in the case of **21**, by the use of ^{17}O NMR in the early days of ^{17}O spectroscopy and an increasing importance of fluorinated peroxides²⁸, there is, to the best of our knowledge, only one other report by Barieux and Schirmann²⁹ of ^{17}O NMR experimental data on derivatives belonging to this class. They reported ^{17}O NMR data of thirteen peroxides, **22–34**, obtained using enriched samples. The data are collected in Table 8.

Hydrogen peroxide **22** has been measured in three different solvents, H_2O , dioxane and acetonitrile, showing a complete invariance of chemical shifts and an increase of half-height line-width only in dioxane solution (240 Hz). In all cases, the spectra had been measured at 65 °C. The chemical shift value(s) obtained are in good agreement with that (174 ppm) already reported⁴. *t*-Bu peroxide **23** has been measured in two different solvents, H_2O and hexane, and only the oxygen bound to the *t*-Bu group showed a small variation (249 ppm). The agreement with previous data³⁰ is good for the oxygen bound to the *t*-Bu group while the difference observed for the OH oxygen is noteworthy (221 ppm)³⁰. The invariance observed for the chemical shifts on changing solvent from H_2O to hexane is unusual, particularly for an oxygen bearing a hydrogen, but a proper comparison is made difficult by the different concentrations used, namely 1 M in hexane and 2 M in H_2O . Half-height line-widths were revealed to be more sensitive to the change of the solvent, ranging from 330 to 750 Hz. The measurement temperature was, in this case and in both solvents, room temperature. No indication of the solvent(s) used for the other derivatives was given and spectra have been obtained at various temperatures, mostly at room temperature. Peroxide **24** chemical shift fits well previous data, being in the upper part of the interval of similar derivatives (see Tables 2 and 3). By using the criteria^{10,12} to estimate the dihedral angle C–O–O–C established for cyclic peroxides, a value of this angle close to either 0° or 180° can be estimated for **24**, if we make the reasonable assumption that annulation has not too great an effect and that chemical shift values for dihedral angles of 0° or 180° are very similar, as observed for α -diketones^{31,32}. Assignment of the two oxygens of the peroxy bridge for compounds **25–28** and **31–34** is very tentative. Comparison among the data of Table 8 seems to favour attribution of the signals in the region 270–292 ppm to the peroxidic oxygens bonded to substituents

TABLE 8. ^{17}O NMR data of some peroxides RO–OR'²⁹

Compound	R	R'	δ (ppm) ^a	$\nu_{1/2}$ (Hz) ^b
22 ^c	H	H	180	130
23 ^c	<i>t</i> -Bu	H	246 206	750 650
24	2-pyranyl	2-pyranyl	287	800
25	H–(C=O)	H	273 255	350
26	Me–(C=O)	H	273 255	400
27	CF ₃ –(C=O)	H	280 260	400
28	Et–(C=O)	H	280 266	300
29	Me–(C=O)	Me–(C=O)	327	800
30	CF ₃ –(C=O)	CF ₃ –(C=O)	319	900
31	Cl–(C=O)	<i>t</i> -Bu	270 393	190 300
32	CF ₃ –(C=O)	<i>t</i> -Bu	273 372	300 600
33	Me–(C=O)	<i>t</i> -Bu	292 333	260 400
34	C ₄ H ₉ NH–(C=O)	<i>t</i> -Bu	273 313	800 1400

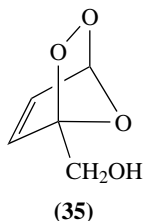
^a Relative to water.

^b Half-height line-widths.

^c Measured in various solvents; values in the Table refer to spectra obtained in H_2O ; see also text.

different from the *t*-Bu or H groups. High shielding can be noted for **30**, particularly in comparison with **32**. The reason for this is unclear.

Although ^{17}O NMR of the peroxide moiety has actually not been measured, an interesting application of this technique for studying the reactivity of furfuryl alcohol endoperoxide **35** was suggested by Braun and colleagues³³. (2 + 4)-Cycloaddition of ^{17}O -enriched singlet O_2 with furfuryl alcohol yields the thermally unstable **35**, labelled at both the peroxidic oxygens. Identification of the enriched oxygens in the stable degradation products allowed one to choose between several possible reaction pathways leading to them. Formation of hydroperoxide intermediates has also been deduced.



The ^{17}O NMR data of dimethyldioxirane **36** have already been reviewed², but the closely related spectrum of methyl(trifluoromethyl)dioxirane **37** was not reviewed and a comparison of its experimental data³⁴ with the computed values for the parent dioxirane **38** and of difluorodioxirane **39**³⁵ can be of interest. Experimental and computed data are gathered in Table 9.

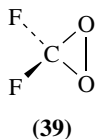
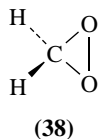
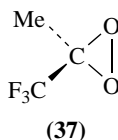
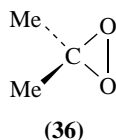


TABLE 9. Experimental^a and computed^b NMR data of dioxiranes **36**–**39**

Cmpd	^1H δ (ppm)	^{13}C δ (ppm)	^{19}F δ (ppm)	^{17}O δ (ppm)	T ($^\circ\text{C}$)
36	1.65	22.6 (Me) 102.2 (CO_2) [24.2 (Me) 108.2 (CO_2)]		302 [334]	0
37	1.97	14.51 (Me) 97.32 (CO_2) 122.2 (CF_3)	-81.5	297 [277]	-20
38		[91.4 (CO_2)]		[277]	
39		[133.4 (CO_2)]	[-82.8]	[403]	

^a δ (ppm) are relative to TMS for ^1H and ^{13}C NMR, to internal CFCl_3 for ^{19}F NMR and to external $\text{Me}_2\text{C}=\text{O}$ and then referred to H_2O for ^{17}O NMR.

^b SOS-DFPT/VQZ2P NMR chemical shifts, ^{13}C shifts are relative to TMS, ^{19}F shifts relative to CFCl_3 and ^{17}O shifts relative to gaseous water. Numbers in square brackets are computed shifts.

4. ^{17}O NMR spectroscopy of organic compounds containing the $-\text{O}-\text{O}-$ group 185

It can be observed from the experimental data that substitution of a Me by a CF_3 group does not cause an important change in ^{17}O NMR shift, the shift being $\Delta\delta = 5$ ppm. Agreement between experimental and computed ^{17}O NMR shifts is quite good, applying the relationship $\delta_{\text{gas}} = \delta_{\text{liq}} + 36.1$ ppm. Hence the large $\Delta\delta$ values computed for **36**, **38** and **39** are particularly noteworthy. Kraka and colleagues³⁵ discussed the case of **39** and suggested a substantial charge transfer from the fluorine to the oxygen atoms. More experimental measurements would be very valuable in order to extend knowledge of this fascinating and important class of molecules.

III. A BRIEF LOOK AT METALLO-ORGANIC AND BIOLOGICAL SYSTEMS

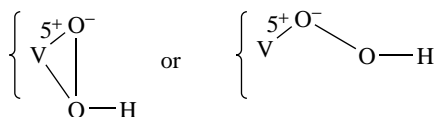
The experimental difficulties of ^{17}O NMR spectroscopy severely restrict the applicability of this technique to biological systems, notwithstanding the obvious importance that it could have in studying, e.g., dioxygen complexes. Some references can be found in an important review by Momenteau and Reed³⁶. Two papers discussed are of particular interest, one dealing with solution ^{17}O NMR spectroscopy of the $\text{Fe}-\text{O}_2$ moiety of hemo-protein models³⁷ and another on solid state ^{17}O NMR of [$^{17}\text{O}_2$] picket fence porphyrin, myoglobin and hemoglobin³⁸. Related to this last paper, although ^{17}O NMR work was confined to $\text{Fe}-\text{O}_2$ analogous of metalloporphyrins and metalloproteins, is another work on solid state ^{17}O NMR by the Oldfield group³⁹. It is noteworthy that both in solution and in the solid state the oxygens of the O_2 group show high deshielding, their shifts reaching values over 2500 ppm for the terminal oxygen in solution and around 2000 ppm in the solid state. Relevant in this last case are the very large observed values of the anisotropies of the shift tensors and the relatively small values of the ^{17}O nuclear quadrupole coupling constants of both oxygens (*ca* 5 MHz), to be compared with the values of 8.5 and 20 MHz found for ozone.

Coordination compounds containing either the peroxo group and/or peroxidic ligands are not rare and ^{17}O NMR spectroscopy has been applied to study and characterize several of them. However, the peroxo group seems rather difficult to be observed in the case of many such derivatives, probably because its signals are very broad. In most cases the structure of the peroxo derivatives is of the type shown below



with one (shown) or two three-membered cycles formed by the metal ion and the two peroxidic oxygens. The range of the ^{17}O NMR chemical shifts for these peroxo derivatives does not differ largely from that for the dioxirane cycle, being roughly centered at *ca* 400 ppm. Zamaraev and coworkers⁴⁰ reported observable ^{17}O NMR spectra of five Mo peroxo complexes, with a very narrow range of chemical shifts ($\delta = 450 \pm 5$ ppm) for the peroxo group and rather broad signals ($\nu_{1/2} = 2000-2500$ Hz). Comparable results⁴¹ have been obtained for nine Mo and W oxoperoxo and polyoxoperoxo complexes, although the range of chemical shifts was larger, being between 376 and 468 ppm. It was found that structural variations within complexes of the same metal did not cause important changes in ^{17}O NMR chemical shifts, while variations in the shifts were observed on changing the metal. Line-widths were, in all cases, very large, particularly for polyoxoperoxo complexes, being up to 6900 Hz. In two cases this broadness prevented the observation of the peroxo group. In contrast, the signals that originated from the oxo groups are very sharp (≤ 100 Hz!) except for the two unobserved polyoxoperoxo complexes. In the latter case, however, the oxo signals could be measured and their line-widths were *ca* 600 Hz.

In an interesting research⁴² on bromoperoxidase, the various peroxovanadates obtained using ¹⁷O-enriched H₂O₂ showed a broad range of chemical shifts. The main influences on changes in the shift were a different extent of protonation and the number of peroxy groups bonded to the vanadium centre. Two relatively shielded (263 and 233 ppm) signals were also observed. The authors tentatively assigned these signals to one of the two possible structures shown below.



The assignments were confirmed by studying model peroxovanadium compounds both at ¹⁷O NMR as well as at ⁵¹V NMR.

A recent paper by Babushkin and Talsi⁴³ characterized three vanadium alkylperoxy complexes of general formula VO(OObu-*t*)_{*k*}(Obu-*n*)_{3-*k*} where *k* = 1–3. Although the VO group could be observed by ¹⁷O NMR, the peroxy group could not be observed. This observation seems a further case of the apparent difficulty in observing the peroxy group. Indeed, on measuring the ¹⁷O NMR spectrum of a saturated CDCl₃ solution of 3-chloroperbenzoic acid at natural abundance at 25 °C, we found that the peroxidic oxygen signals are significantly broader than other signals of the same molecule, namely δ_{C=O} = 314.5 ppm *v*_{1/2} = 360 Hz, δ_{O-O} = 267 and 230 ppm *v*_{1/2} = 940 and 600 Hz, respectively⁴⁴. This experimental unfavourable feature could be the reason for the still scarce utilization of ¹⁷O NMR spectroscopy in this field, albeit actually modern instrumentation allows, in most cases, a ready and easy (total time of the experiment can be *ca* 30 min) measurement of ¹⁷O NMR spectra of organic peroxides.

IV. REFERENCES

1. S. Patai (Ed.), *The Chemistry of Hydroxyl, Ether and Peroxide Groups, Supplement E*, Wiley-Interscience, Chichester, 1993.
2. D. W. Boykin and A. L. Baumstark, in *¹⁷O NMR Spectroscopy in Organic Chemistry* (Ed. D. W. Boykin), Chap. 9, CRC, Boca Raton, 1991, pp. 252–258.
3. S. Berger, S. Braun and H.-O. Kalinowski, *NMR Spectroscopy of the Non-metallic Elements*, Wiley, Chichester, 1997.
4. H. A. Christ, P. Dihel, H. R. Schneider and H. Dahn, *Helv. Chim. Acta*, **44**, 865 (1961).
5. I. J. Salomon, J. N. Keith, A. J. Kacmarek and J. K. Raney, *J. Am. Chem. Soc.*, **90**, 5408 (1968).
6. P. Dihel, H. A. Christ and F. B. Mallory, *Helv. Chim. Acta*, **45**, 504 (1962).
7. D. J. Sardella and J. B. Stothers, *Can. J. Chem.*, **47**, 3089 (1969).
8. J. Reuben, *J. Am. Chem. Soc.*, **91**, 5725 (1969).
9. M. G. Zagorski, D. S. Allan, R. G. Salomon, E. L. Clennan, P. C. Heah and R. P. L'Esperance, *J. Org. Chem.*, **50**, 4484 (1985).
10. J. Lauterwein, K. Griesbaum, P. Krieger-Beck, V. Ball and K. Schlindwein, *J. Chem. Soc., Chem. Commun.*, 816 (1991).
11. F. Hock, V. Ball, Y. Dong, S.-H. Gutsche, M. Hills, K. Schlindwein and K. Griesbaum, *J. Magn. Reson., Ser. A*, **111**, 150 (1994).
12. D. W. Boykin and A. L. Baumstark, in *¹⁷O NMR Spectroscopy in Organic Chemistry* (Ed. D. W. Boykin), Chap. 3, CRC, Boca Raton, 1991, pp. 61–62.
13. D. W. Boykin and A. L. Baumstark, in *¹⁷O NMR Spectroscopy in Organic Chemistry* (Ed. D. W. Boykin), Chap. 3, CRC, Boca Raton, 1991, pp. 77–88.
14. K. Kostova, V. Dimitrov, S. Simova and M. Hesse, *Helv. Chim. Acta*, **82**, 1385 (1999).
15. C. Geletneky and S. Berger, *Eur. J. Org. Chem.*, 1625 (1998).

4. ^{17}O NMR spectroscopy of organic compounds containing the $-\text{O}-\text{O}-$ group 187

16. R. Criegee, *Angew. Chem., Int. Ed. Engl.*, **14**, 745 (1975).
17. P. R. Story, J. A. Alford, J. R. Burgess and W. C. Ray, *J. Am. Chem. Soc.*, **93**, 3044 (1971).
18. P. R. Story, C. E. Bishop and J. R. Burgess, *J. Am. Chem. Soc.*, **90**, 1907 (1968).
19. R. W. Murray and R. Hagen, *J. Org. Chem.*, **36**, 1103 (1971).
20. B. Plesničar, J. Cerkovnik, T. Tekavec and J. Koller, *J. Am. Chem. Soc.*, **120**, 8005 (1998).
21. B. Plesničar, J. Cerkovnik, T. Tekavec and J. Koller, *Chem. Eur. J.*, **6**, 809 (2000) and references therein.
22. J. Cerkovnik, E. Eržen, J. Koller and B. Plesničar, *J. Am. Chem. Soc.*, **124**, 404 (2002).
23. B. Plesničar, J. Cerkovnik, T. Tuttle, E. Kraka and D. Cremer, *J. Am. Chem. Soc.*, **124**, 11261 (2002).
24. B. Plesničar, T. Tuttle, J. Cerkovnik, J. Koller and D. Cremer, *J. Am. Chem. Soc.*, **125**, 11553 (2003).
25. B. Plesničar, J. Cerkovnik, J. Koller and F. Kovač, *J. Am. Chem. Soc.*, **113**, 4946 (1991).
26. I. J. Solomon, A. J. Kacmarek, W. K. Sumida and J. K. Raney, *Inorg. Chem.*, **11**, 195 (1972).
27. S. Berger, S. Braun and H-O. Kalinowski, *NMR Spectroscopy of the Non-metallic Elements*, Chap. 5, Wiley, Chichester, 1997, p. 333.
28. H. Sawada, *Chem. Rev.*, **96**, 1779 (1996).
29. J. J. Barieux and J. P. Schirmann, *Tetrahedron Lett.*, **28**, 6443 (1987).
30. R. Curci, G. Frisco, O. Sciacovelli and L. Troisi, *J. Mol. Catal.*, **32**, 251 (1985).
31. H. Cerfontain, C. Kruk, R. Rexwinkel and F. Stunnenberg, *Can. J. Chem.*, **65**, 2234 (1987).
32. G. Cerioni, A. Plumitallo, J. Frey and Z. Rappoport, *Magn. Reson. Chem.*, **33**, 874 (1995).
33. A. M. Braun, H. Dahn, E. Gassmann, I. Gerothanassis, L. Jakob, J. Kateva, C. G. Martinez and E. Oliveros, *Photochem. Photobiol.*, **70**, 868 (1999).
34. R. Mello, M. Fiorentino, O. Sciacovelli and R. Curci, *J. Org. Chem.*, **53**, 3890 (1988).
35. E. Kraka, Z. Konkoli, D. Cremer, J. Fowler and H. F. Schaefer III, *J. Am. Chem. Soc.*, **118**, 10595 (1996).
36. M. Momenteau and C. A. Reed, *Chem. Rev.*, **94**, 659 (1994).
37. I. P. Gerothanassis and M. Momenteau, *J. Am. Chem. Soc.*, **109**, 6944 (1987).
38. E. Oldfield, H. C. Lee, C. Coretsopoulos, F. Adebodun, K. D. Park, S. Yang, J. Chung and B. Phillips, *J. Am. Chem. Soc.*, **113**, 8680 (1991).
39. N. Godbout, L. K. Sanders, R. Salzmann, R. H. Havlin, M. Wojdelski and E. Oldfield, *J. Am. Chem. Soc.*, **121**, 3829 (1999).
40. E. P. Talsi, K. V. Shalyaev and K. I. Zamaraev, *J. Mol. Catal.*, **83**, 347 (1993).
41. F. P. Ballistreri, G. A. Tomaselli, R. M. Toscano, V. Conte and F. Di Furia, *J. Mol. Catal.*, **89**, 295 (1994).
42. M. Čásný, D. Rehder, H. Schmidt, H. Vilter and V. Conte, *J. Inorg. Biochem.*, **80**, 157 (2000).
43. D. E. Babushkin and E. P. Talsi, *React. Kinet. Catal. Lett.*, **71**, 115 (2000).
44. G. Cerioni and F. Mocchi, unpublished results.

CHAPTER 5

Synthesis of cyclic peroxides

EDWARD E. KORSHIN and MARIO D. BACHI

Department of Organic Chemistry, The Weizmann Institute of Science, Rehovot 76100, Israel

Fax: +972 8934 4142; e-mails: edward.korshin@weizmann.ac.il, mario.bachi@weizmann.ac.il

I. INTRODUCTION	190
II. SYNTHESIS OF 1,2-DIOXOLANES, 1,2-DIOXANES AND RELATED ENDOPEROXIDES	192
A. Peroxidation with Triplet Molecular Oxygen and Peroxy-radical Cyclization	192
1. Cycloaddition of triplet oxygen with diradicals and latent diradicals	192
2. Cycloaddition of triplet oxygen with cation radicals	204
3. Free radical cyclization of alkenyl hydroperoxides	212
4. Autoxidation through all-homolytic chain reactions	218
5. Thiyl and selenyl radical-mediated domino reactions of dienes and of vinylcyclopropanes with triplet oxygen	221
6. Peroxidation of vinylcyclopropanes and 1,5-dienes mediated by Co(II)/Et ₃ SiH	223
7. Halogen-mediated synthesis of cyclic peroxides through free radical chain reactions	225
B. Cyclization of Hydroperoxides through Intramolecular Nucleophilic Substitution and Addition	230
1. Nucleophilic substitution	233
2. Nucleophilic addition to carbon–carbon double bonds	238
3. Nucleophilic addition to the carbonyl group	245
C. Cycloaddition of Singlet Oxygen with 1,3-Dienes	252
III. SYNTHESIS OF 1,2,4-TRIOXANES	273
A. Peroxyacetalization of Carbonyl Functions with β -Hydroperoxyalcohols .	273
B. Peroxyacetalization of Carbonyl Functions with Strained Endoperoxide Systems	277
C. Coupling of Allylic Hydroperoxides and Alcohols with Carbonyl Compounds	285

The chemistry of peroxides, volume 2

Edited by Z. Rappoport © 2006 John Wiley & Sons, Ltd ISBN: 0-470-86274-2

D. Miscellaneous Syntheses of 1,2,4-Trioxanes	290
IV. REFERENCES	292

I. INTRODUCTION

The chemistry of cyclic peroxides has been associated with the isolation, identification and synthesis of naturally occurring endoperoxides as well as with the study of their physiological properties and their biosynthesis. Among the first studied endoperoxides are ascaridole that was isolated from a plant extract in 1911¹, and ergosterol endoperoxide (**1**) (Chart 1), which was first obtained by peroxidation of ergosterol in 1928² and subsequently isolated in 1947 from fungi³. A remarkable acceleration in the development of the chemistry of endoperoxides occurred in the 1970s as the result of the recognition of the central role of endoperoxides in various vital biological processes. Following the postulation of prostaglandin endoperoxides as biosynthetic products⁴⁻⁶, the highly unstable PGH₂ (**2a**)^{7,8} and PGG₂ (**2b**)^{8,9} were isolated, and identified as key intermediates in prostaglandins' biosynthesis from arachidonic acid. Shortly afterwards, the total syntheses of PGH₂ (**2a**) and PGG₂ (**2b**) by Johnson and coworkers¹⁰ and Porter and coworkers¹¹⁻¹³ were accomplished. The early studies on prostaglandin endoperoxides **2** as well as the studies on a variety of simplified analogues thereof were reviewed by Nicolaou and coworkers¹⁴, Johnson¹⁵ and Salomon¹⁶. The great interest in prostaglandin endoperoxides **2** stimulated the development of new sophisticated methods for the synthesis and for tuning the structures of this type of complex and reactive molecules.

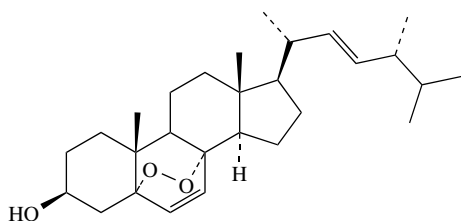
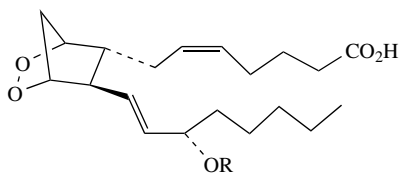
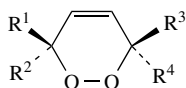
During the last decade progress associated with the chemistry, the isolation of naturally occurring endoperoxides and their biological properties has been regularly reviewed¹⁷⁻²². Monocyclic endoperoxides **3a-d** were isolated from different marine sponges^{17,18}. In fact, antitumor cyclic peroxy ketal (+)-chondrillin (**3a**) was the first discovered marine endoperoxide²³⁻²⁵. The marine cyclic peroxide plakortin acid (**4a**) is a potent antifungal and antibacterial agent, while its methyl ester plakortin (**4b**) is inactive²⁶.

In 1979, Liang and coworkers reported on the isolation and structure determination of the active component of a traditional antimalarial Chinese remedy, namely the bridged bicyclic endoperoxide yingzhaosu A (**5**)^{27,28}. At about the same time the powerful antimalarial agent, the tetracyclic 1,2,4-trioxane artemisinin (qinghaosu) (**6**), was isolated by Wu and coworkers from another Chinese folk medicament²⁹⁻³². These findings have motivated a worldwide intensive quest for additional antimalarial cyclic peroxides, from natural and synthetic origins³³⁻⁴⁴. A first generation antimalarial peroxide drug is being used on a low scale in endemic countries^{32,42,45-48}.

The structural and biological diversity of naturally occurring endoperoxides is further illustrated by the antimalarial cardamom peroxide (**7**) containing a 7-membered ring cyclic peroxide moiety⁴⁹, and by the tremorgenic verrucologen (**8**) containing an 8-membered endoperoxide system (Chart 1)⁵⁰.

The increasing need for new antimalarial drugs to overcome the continuing emergence of multi-drug resistant parasites and the challenge associated with the construction of some intricate peroxide systems have promoted the development of new synthetic methods. The synthesis and chemistry of cyclic peroxides have been reviewed earlier by Saito and Nittala⁵¹, by Clennan and Foote⁵², by McCullough⁵³, and by McCullough and Nojima⁵⁴. The synthesis of 1,2,4-trioxanes, 1,2,4,5-tetroxanes and related compounds was recently thoroughly reviewed^{33,40,44,53-56}.

Section II covers the synthesis of the cyclic peroxides with medium ring size from 5 to 7. Section III covers the synthesis of 1,2,4-trioxanes. Classification in sub-sections and sub-sub-sections is done according to the type of reaction by which the cyclic peroxide system is formed. Syntheses of dioxirans, 1,2-dioxetanes, trioxolanes (ozonides), tetroxanes, and macrocyclic peroxides are not discussed in this review.

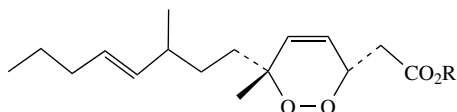
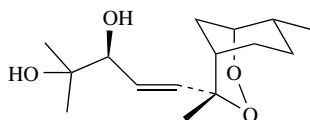
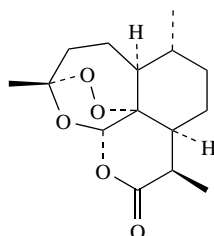
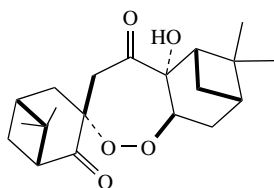
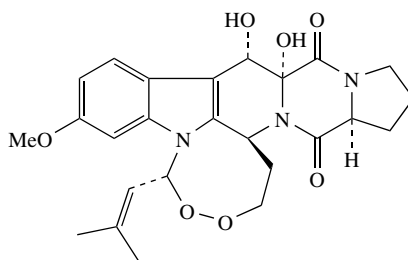
Ergosterol endoperoxide (**1**)PGH₂ (**2a**): R = H,PGG₂ (**2b**): R = OH

(+)-Chondrillin (**3a**): R¹ = C₁₆H₃₃,
R² = MeO, R³ = CH₂CO₂Me, R⁴ = H,

(-)-Chondrillin (**3b**): R¹ = MeO,
R² = C₁₆H₃₃, R³ = H, R⁴ = CH₂CO₂Me,

(-)-Plakorin (**3c**): R¹ = MeO,
R² = C₁₆H₃₃, R³ = CH₂CO₂Me, R⁴ = H,

(+)-Plakorin (**3d**): R¹ = C₁₆H₃₃,
R² = MeO, R³ = H, R⁴ = CH₂CO₂Me

Plakortin acid (**4a**): R = H,Plakortin (**4b**): R = MeYingzhaosu A (**5**)Artemisinin (qinghaosu) (**6**)Cardamom peroxide (**7**)Verruculogen (**8**)

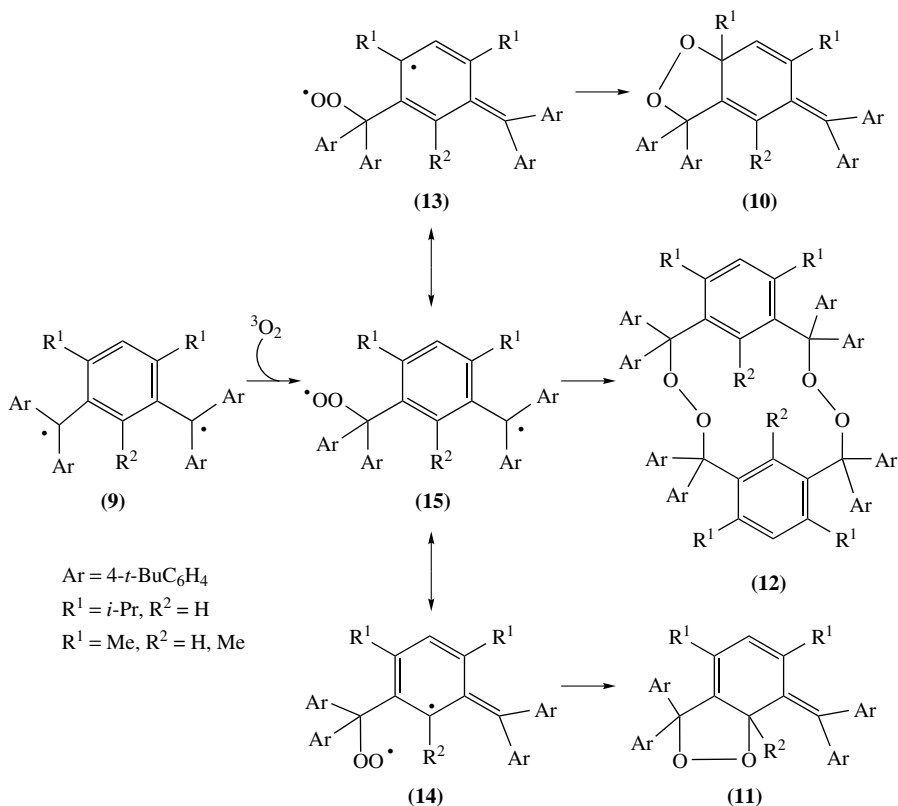
II. SYNTHESIS OF 1,2-DIOXOLANES, 1,2-DIOXANES AND RELATED ENDOPEROXIDES

A. Peroxidation with Triplet Molecular Oxygen and Peroxy-radical Cyclization

1. Cycloaddition of triplet oxygen with diradicals and latent diradicals

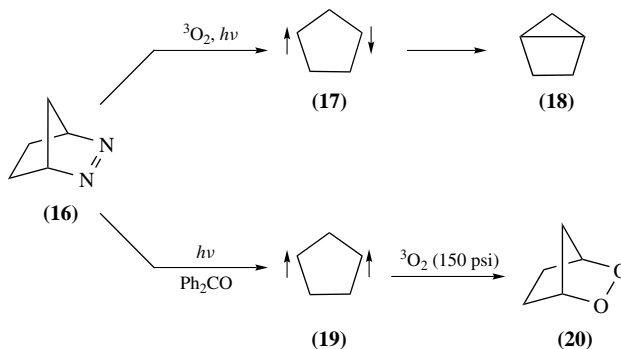
Reactive triplet diradicals have been conventionally detected through their trapping of triplet oxygen ($^3\text{O}_2$) in a reaction leading to cyclic peroxides or to the degradation product thereof^{57,58}. Although not many methods for the generation of carbon-centered diradicals are available and although most studies on their interaction with molecular oxygen focus on mechanistic aspects, they may have a viable synthetic potential. Persistent Schlenk hydrocarbon 1,5-diradicals of type **9**, which are stable under inert atmosphere, readily react with $^3\text{O}_2$ to give 1,2-dioxolanes **10** as the major reaction product (50–70% isolated yield), the minor products, 1,2-dioxolanes **11** and the dimeric endoperoxides **12** (Scheme 1)⁵⁹. While 1,2-dioxolanes **10** and **11** derive from the collapse of stabilized 1,5-peroxy-diradicals in their respective mesomeric forms **13** and **14**, peroxides **12** result from dimerization of the mesomeric 1,7-peroxy-diradicals **15**.

Save for a few exceptions, singlet diradicals are too short-lived to be trapped by molecular oxygen^{60–62}. Indeed, direct photolysis of azo-compound **16** under molecular



SCHEME 1

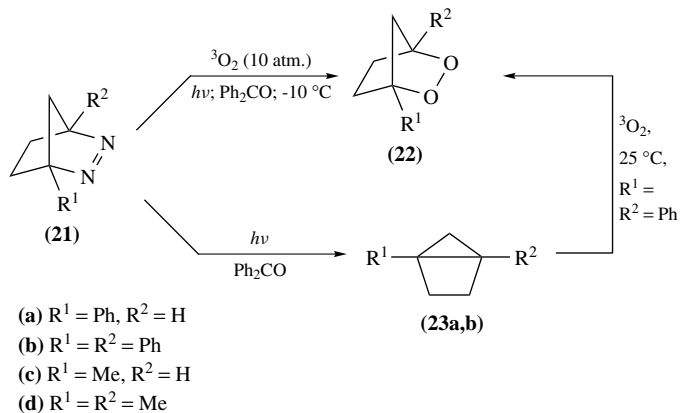
oxygen produces 1,3-cyclopentenediyl singlet diradical **17**, which instantaneously collapses into bicyclo[2.1.0]heptane **18** avoiding oxygen trapping (Scheme 2)⁶³. In contrast, benzophenone-sensitized laser photolysis ($\lambda \geq 350$ nm) of azoalkane **16** generates the more persistent triplet diradical **19**, which reacts with molecular oxygen (150 psi) to give the bridged bicyclic endoperoxide **20**⁶³. Due to the photolability of many endoperoxides^{51,52}, the yield of bicyclic peroxide **20** dramatically decreases as the reaction proceeds, resulting in 73% yield of **20** at 21% conversion and 54% yield at 43% conversion⁶³.



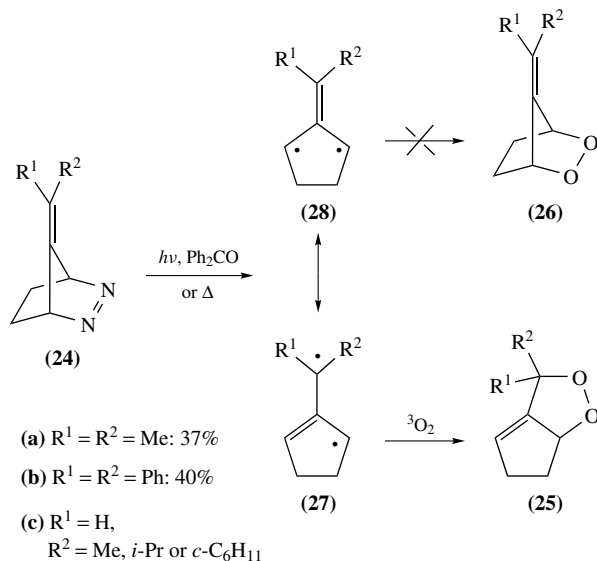
SCHEME 2

Increasing the stability of diradicals through aryl substitution at the radical centers augments the efficacy of intermolecular oxygen trapping^{58,61,64}. For example, benzophenone-sensitized laser photolyses of azoalkanes **21a** and **21b** at -10°C under 10 atmospheres pressure of oxygen afford 1-phenyl- **22a** and 1,4-diphenyl-2,3-dioxabicyclo[2.2.1]heptanes **22b** as the only reaction products (Scheme 3)⁶⁴. Peroxides **22a** and **22b** derive from the intermediacy of the corresponding triplet 1-phenylcyclopentane-1,3-diyl radical and 1,3-diphenylcyclopentane-1,3-diyl radical which efficiently trap molecular oxygen. Under similar conditions also alkyl-substituted azo-compounds **21c** and **21d** afford the corresponding bridged bicyclic endoperoxides **22c** and **22d**^{58,65,66}. The benzophenone-sensitized photolysis of phenyl-substituted azoalkanes **21a** and **21b** under argon results in the ring contraction products **23a** and **23b** respectively⁶⁴. Noteworthy is that 1,4-diphenylbicyclo[2.1.0]pentane **23b**, prepared from **21b** under oxygen-free conditions, is readily oxidized by triplet oxygen at room temperature to give endoperoxide **22b** (Scheme 3)⁶⁴.

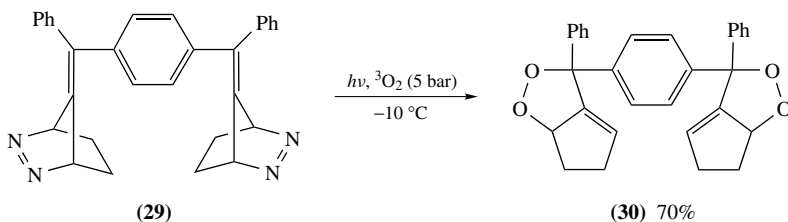
The benzophenone-sensitized photolyses of β,β -disubstituted alkylidene azoalkanes **24a** and **24b** lead to the formation of the fused bicyclic 1,2-dioxolanes **25a** and **25b** respectively, and not to bridged endoperoxides of type **26** (Scheme 4)⁶³. These results are rationalized by electron delocalization in the incipient diradical hybrids **28** to the diradical hybrids **27**, which are preferentially trapped by triplet oxygen. Similarly, fused bicyclic 1,2-dioxolanes **25c** are formed through thermolysis (80°C) of monoalkyl-substituted azoalkanes **24c** under oxygen atmosphere⁶⁷. Photolysis of the bis(azoalkane) **29** generated a couple of allylic diradicals similar to **27**, which are stabilized through hyperconjugation in a *para*-quinoid form, thus setting the grounds for an effective trapping of triplet oxygen to give the bis(endoperoxide) **30** in 70% isolated yield (Scheme 5)⁶⁸. Variations of this reaction are illustrated in Scheme 6. Benzophenone-sensitized photolysis of azoalkane **31** under 5 bar of oxygen gas at 20°C affords, through the intermediacy of diradicals **32** and **33**, exclusively a *ca* 1:1 diastereomeric mixture of fused bicyclic 1,2-dioxolanes **34**⁶⁹.



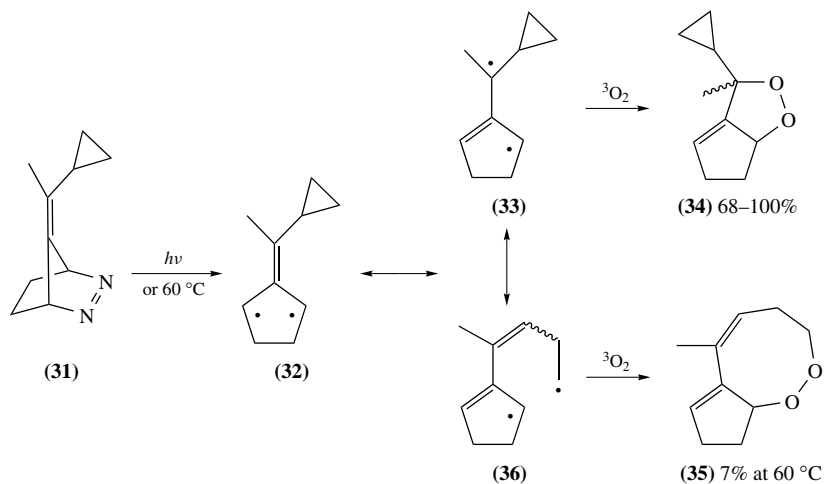
SCHEME 3



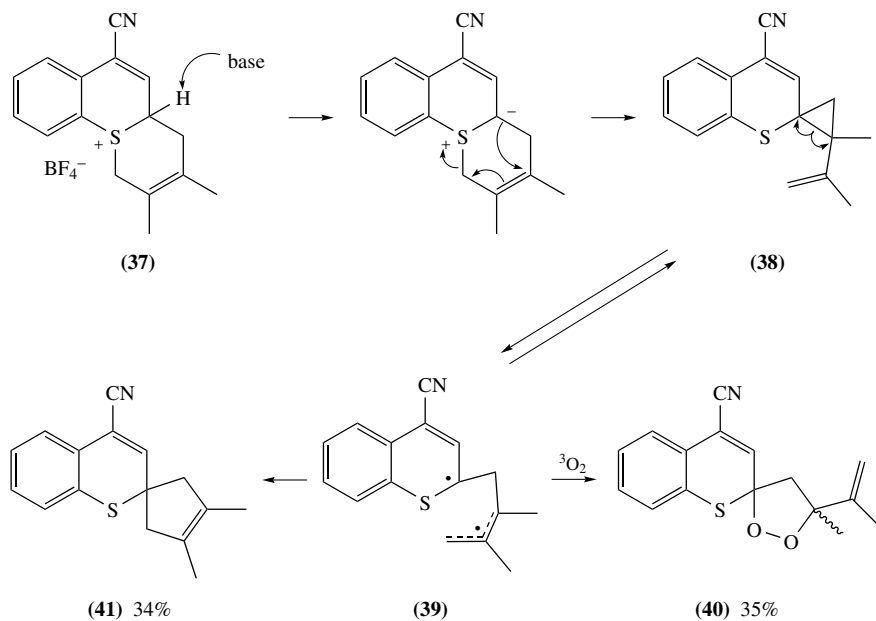
SCHEME 4



SCHEME 5



SCHEME 6



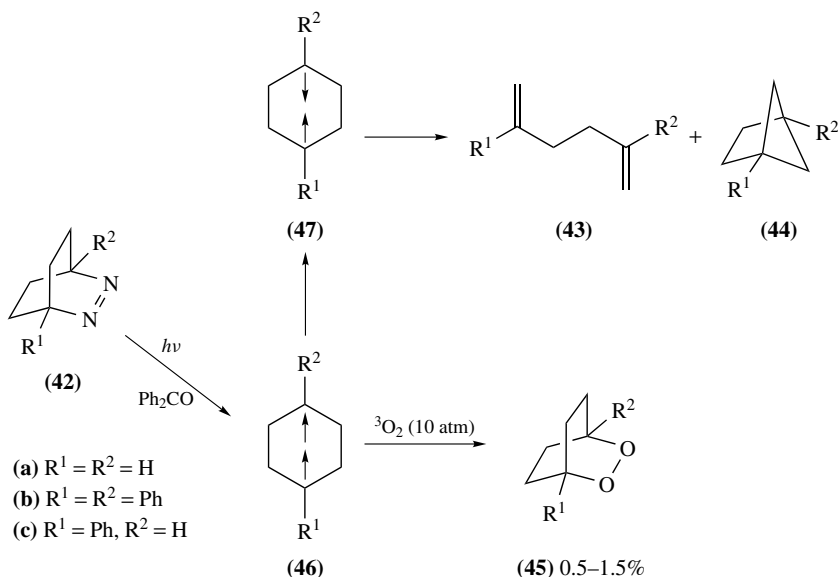
SCHEME 7

However, thermolysis of the same compound **31** at 60°C under oxygen gave, in addition to the major products **34** (68%), a small amount (7%) of the fused bicyclic 8-membered endoperoxide **35**, which derives from mesomeric diradical **36**⁶⁹.

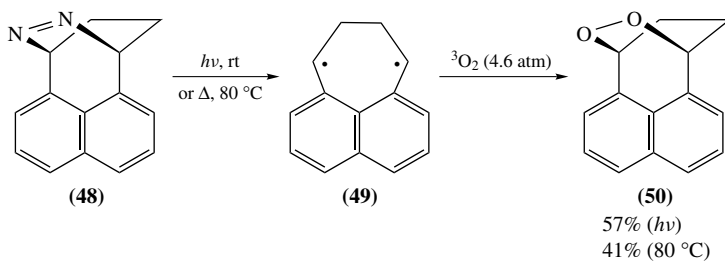
A specific way for the generation of 1,3-diradicals, based on a spontaneous ring cleavage of the highly substituted spirocyclopropanes of type **38**, is illustrated in Scheme 7⁷⁰.

Such a reaction may occur on treatment of the benzo-fused bicyclic sulfonium salt **37** with various bases under aerobic conditions. The incipient allylic diradical **39** is trapped as 1,3-diradical by molecular oxygen to give a mixture of up to 35% diastereomeric spiro-1,2-dioxolanes **40**. The spirocyclopentene **41** is obtained in a competing path in which allylic diradical **39** is cyclized as a 1,5-carbon-centered diradical⁷⁰.

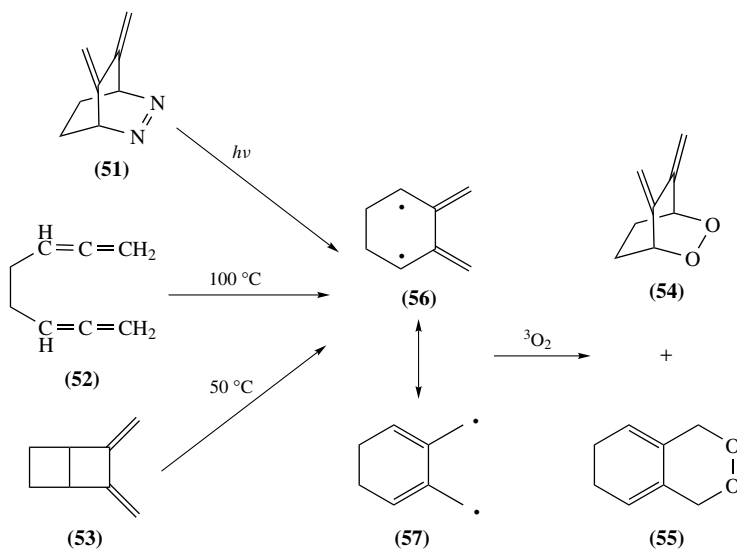
The reactions outlined in Schemes 8–11 indicate that 1,4-diradicals can trap triplet oxygen to give 6-membered cyclic peroxides in variable yields. For example, even under 10 atm oxygen pressure, Ph₂CO-sensitized photolyses of the azoalkanes **42** afford the dienes **43** and bicyclo[2.1.1]hexanes **44** as the major products while the bicyclic peroxides **45** are formed in very poor yields ($\leq 1.5\%$) (Scheme 8)^{64, 71, 72}. Failure in oxygen trapping was attributed to an extremely rapid spin intercrossing in the initial triplet 1,4-cyclohexadiyl diradicals **46** to generate the corresponding singlet diradicals **47**, which are transformed into oxygen-free products of types **43** and **44**⁷². In contrast, when azo-compound **48** is irradiated with a medium-pressure mercury lamp using a cutoff filter ($\lambda > 380$ nm), or when it is subjected to thermolysis at 80 °C under 4.6 atm of oxygen pressure, it generates 1,4-perinaphthadiyl diradical **49**, which readily reacts with triplet oxygen to give polycyclic peroxide **50** in 57% and 41% yield, respectively (Scheme 9)⁶⁰. Photolysis of azoalkane **51**⁷³, thermal Cope-rearrangement of 1,2,6,7-octatetraene **52**⁷⁴ and ring-cleavage of 2,3-dimethylenebicyclo[2.2.0]hexane **53**⁷⁵ under aerobic conditions provide a *ca* 1:1 mixture of bridged bicyclic peroxide **54** and fused bicyclic 1,2-dioxane **55**. The common denominator to these three reactions are mesomeric 2,3-dimethylene-1,4-cyclohexadienyl diradical **56** and diallyl diradical **57** intermediates, which undergo cycloaddition with ³O₂ (Scheme 10). 1,4-Diradicals **59** and **62** can be generated through an attractive photochemical Norrish type II reaction of the aromatic ketones **58** and **61** under oxygen. These diradicals are trapped with triplet oxygen to produce the monocyclic 3-hydroxy-1,2-dioxane-5-one **60**⁷⁶ and the bicyclic dioxane **63**⁷⁷ respectively, in moderate yields (Scheme 11).



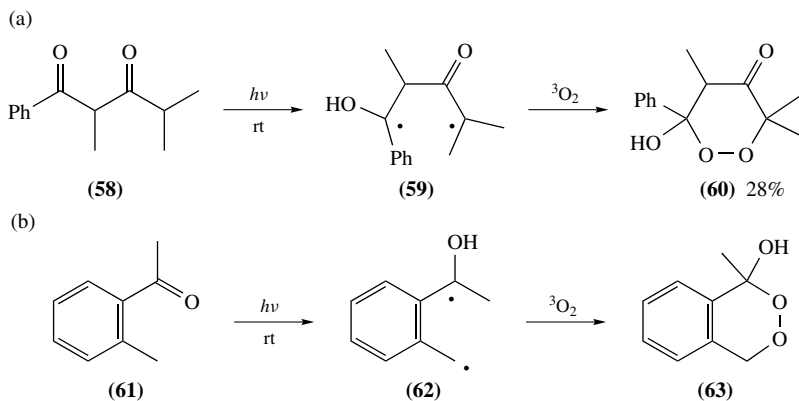
SCHEME 8



SCHEME 9

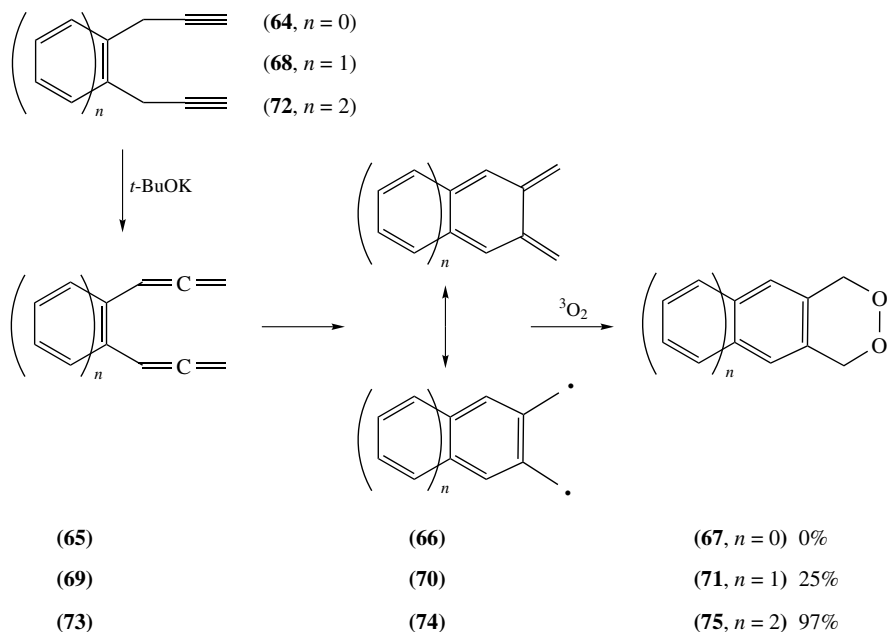


SCHEME 10



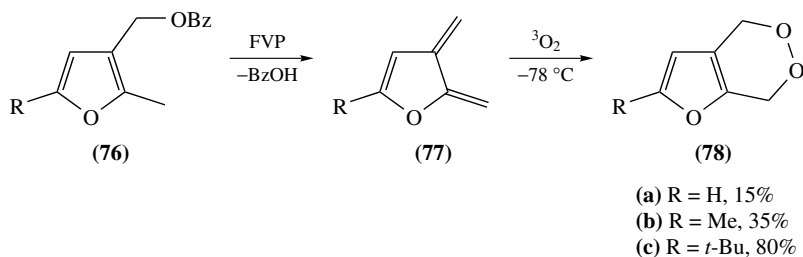
SCHEME 11

Some cisoid 1,3-dienes like *ortho*-quinodimethanes, which have a diradicaloid character ground state, can react with triplet oxygen to give cyclic peroxides. The effectivity of such a cycloaddition depends on the relative stability of the substrate and on reaction conditions. Thus, potassium *tert*-butoxide induced prototropic rearrangement of *cis*-4-octene-1,7-diyne (**64**) in aerobic conditions generates the *cis*-bis(allene) derivative **65** that cyclizes to a highly unstable *ortho*-quinodimethane **66**, which could not be trapped by triplet oxygen (Scheme 12)⁷⁸. However, under similar conditions the more stable *ortho*-naphthaquinodimethane (**70**), generated from **68**, affords the endoperoxide **71** in a moderate yield. The additionally stabilized *ortho*-anthraquinodimethane (**74**), formed from **72**, gives the corresponding peroxide **75** almost quantitatively (Scheme 12)⁷⁸. Similarly, naphthaquinodimethane **70** can be generated and subsequently trapped with oxygen through either photolytic or thermal nitrogen elimination from 1,4-dihydrobenzo[*g*]phthalazine⁷⁹. The furan-based *ortho*-quinodimethanes **77a–c**, generated by flash vacuum pyrolysis (FVP) of the corresponding benzoates **76a–c**, react with triplet oxygen to give the endoperoxides **78a–c** in variable yields (Scheme 13)⁸⁰. Triplet oxygen adds to *ortho*-quinodimethane **80**, generated by decarbonylation of 1,3-diphenylinden-2-one-norbornene adduct **79**, to give the polycyclic endoperoxide **81** (Scheme 14)⁸¹.

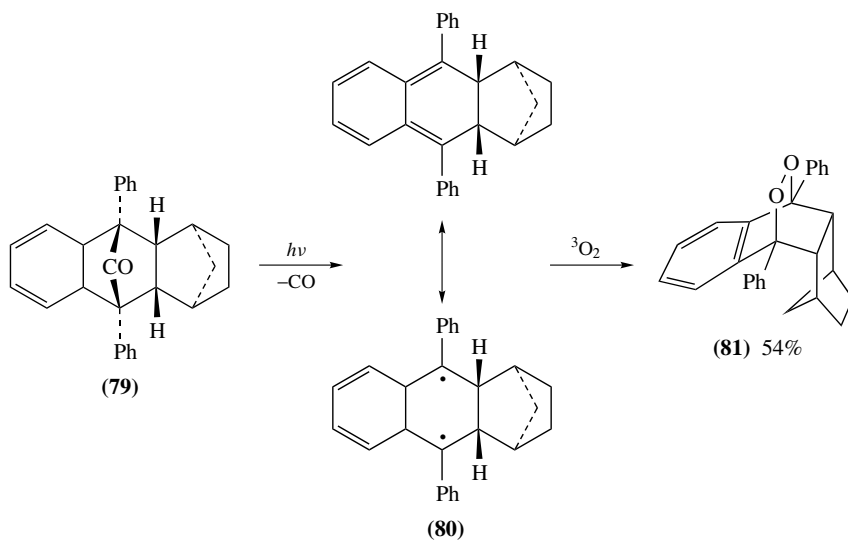


SCHEME 12

A number of semibullvalenes and some barbaralanes, which undergo a facile Cope rearrangement via bicyclooctadienyl diradicals, produce various cyclic peroxides on exposure to triplet oxygen^{82–84}. Thus, cyclopentano semibullvalene **82a** is peroxidized with air to give a mixture of 5-membered **83a** and 6-membered endoperoxide **84a** in a 1:2 ratio, whereas the cyclohexano derivative **82b** yields only the 6-membered cyclic peroxide **84b** (Scheme 15)⁸⁴. The energy in the highly strained mono(Dewar benzene) isomer of



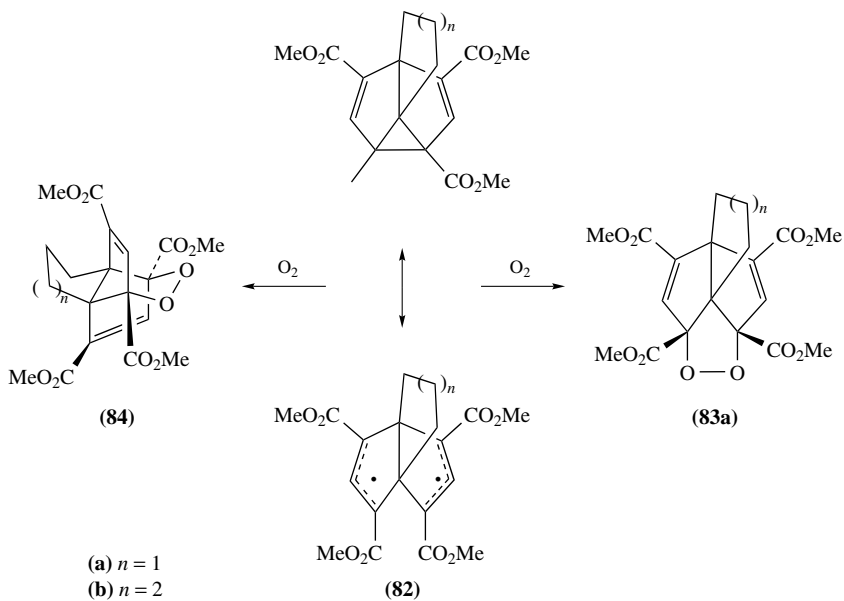
SCHEME 13



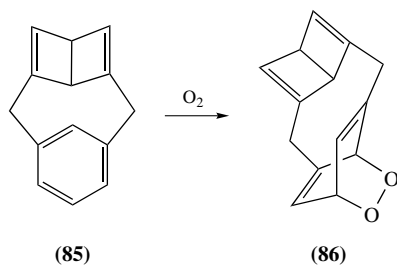
SCHEME 14

[1.1]metacyclophane (**85**) leads to dearomatization of the benzene ring, which is readily peroxidated by air to give cyclic peroxide **86** (Scheme 16)⁸⁵. A similar visible light induced peroxidation across the more substituted ring of the more stable [2.2]metacyclophane **87** gives stable endoperoxide **88** in good yield (Scheme 17)⁸⁶. Analogous peroxidations with triplet oxygen were described for some dihydropyrene derivatives⁸⁷. UV irradiation of arylidene- β -ionones **89** in the presence of oxygen leads to a high-yielding formation of the bridged endoperoxides **91** through a peroxidation of 2-oxabicyclo[4.4.0]deca-3,5-diene intermediates **90** (Scheme 18)⁸⁸.

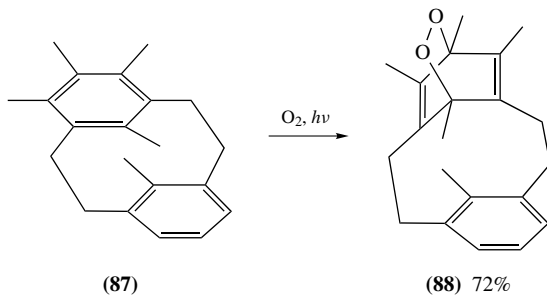
Some α,β -unsaturated ketones react on irradiation, as synthetic equivalents of 1,4-carbon-centered diradicals, which undergo cycloaddition with triplet oxygen to give the corresponding 3-hydroxy-1,2-dioxanes. In the case of the most reactive substrates, such a cycloaddition with $^3\text{O}_2$ can occur upon exposure to daylight, or even in the dark. For example, 2-alkylidencyclohexane-1,3-diones **92-keto** add oxygen across the diene system of **92-enol** without irradiation to give the fused bicyclic peroxides **93** in excellent yields (Scheme 19)^{89,90}. Pursuing a similar approach, syncarpic acid (**94**) was efficiently converted, via intermediates **95** and **96**, into the natural product, G3 factor



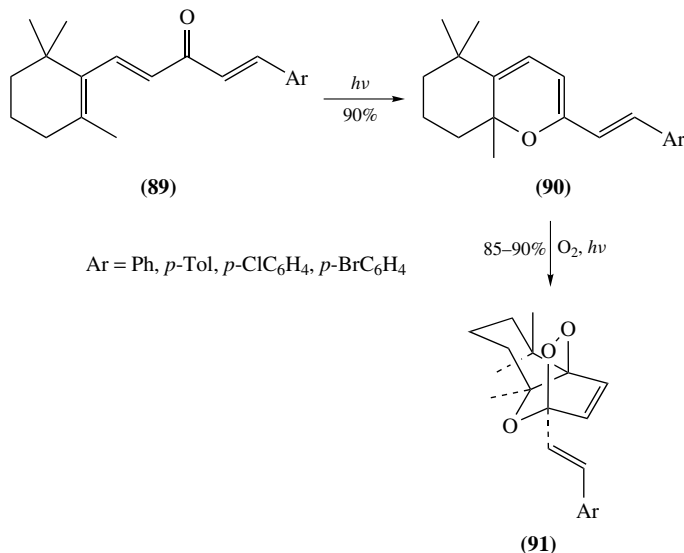
SCHEME 15



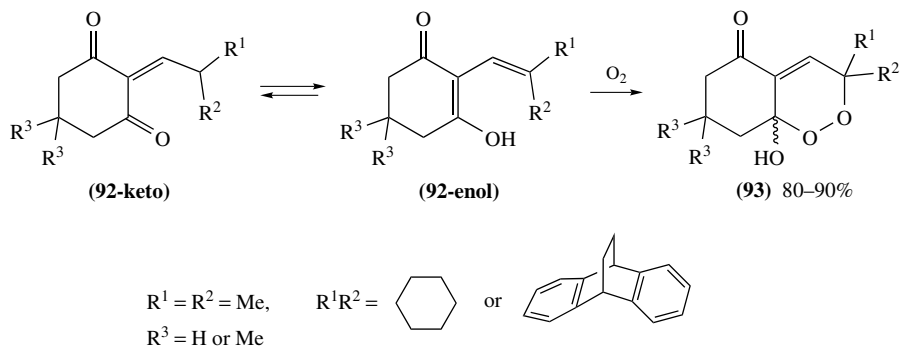
SCHEME 16



SCHEME 17



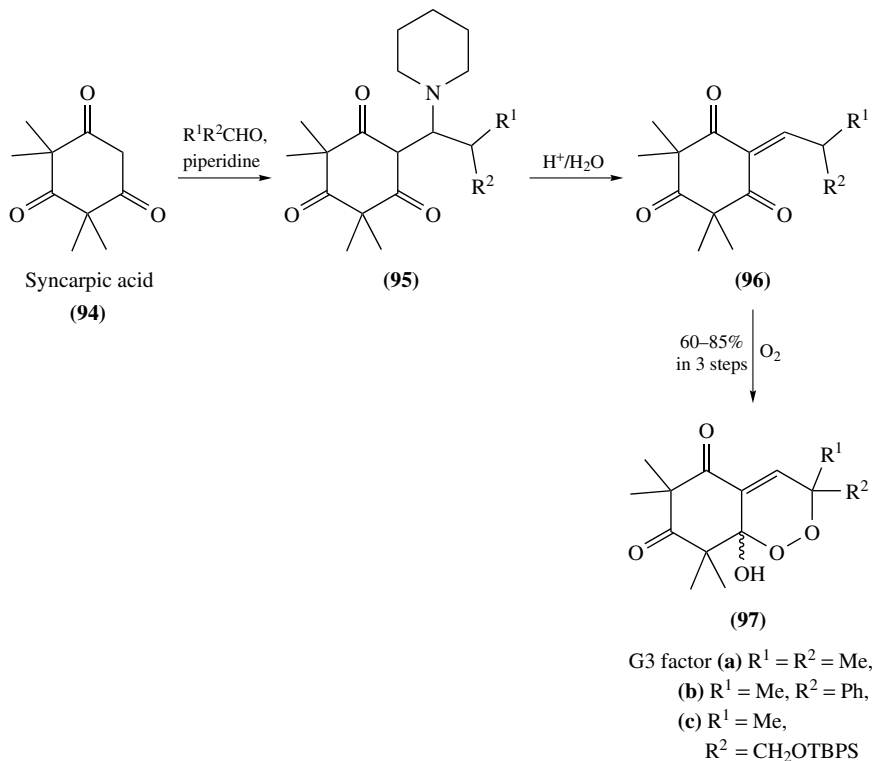
SCHEME 18



SCHEME 19

endoperoxide (**97a**), and into its analogues **97b** and **97c**, which exhibit antimalarial activity (Scheme 20)^{91,92}.

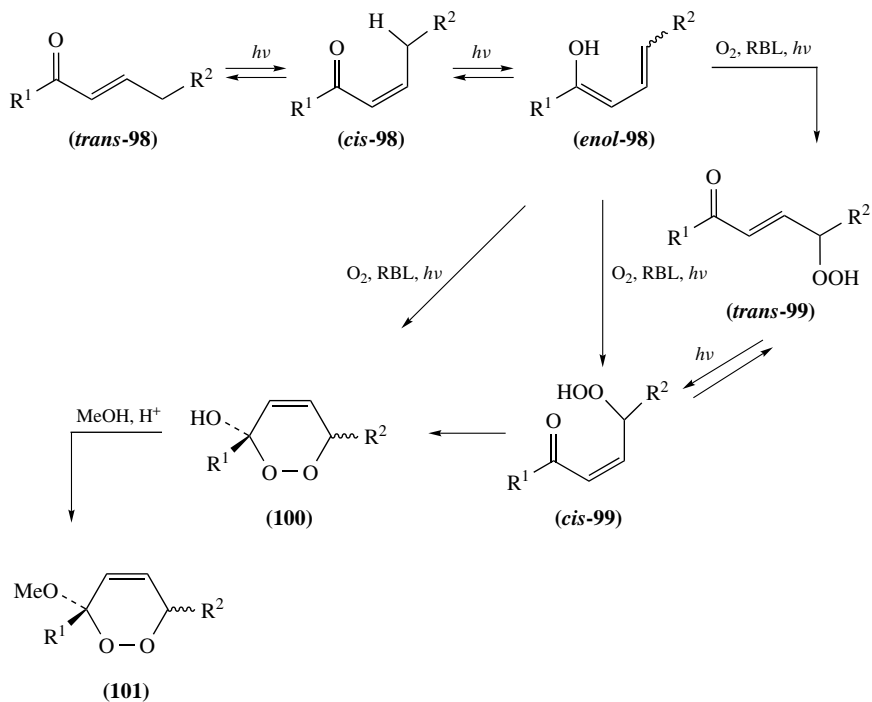
Unsaturated ketones of type *trans*-**98**, possessing just one carbonyl group, are less active toward molecular oxygen and their peroxidation requires sensitizers and sun-lamp irradiation. Snider and Shi reported that irradiation of unsaturated ketones **98a**, **98b** and of **98d** in $\text{CH}_2\text{Cl}_2/\text{MeOH}$ under oxygen in the presence of rose bengal (RB) for 8 h affords the corresponding cyclic peroxy hemiketals **100** in 70–90% yield as a mixture of C6-epimers (Scheme 21)^{93,94}. 3-Hydroxy-derivatives of type **100** are converted quantitatively to peroxyketals **101** on treatment with methanol catalyzed by TsOH. Of particular interest is the high-yielding conversion of **98d** to a mixture of racemic and epimeric natural endoperoxides **101d**, namely (\pm)-chondrillin (**3a** and **3b**) and (\pm)-plakorin (**3c** and **3d**)⁹⁴.



SCHEME 20

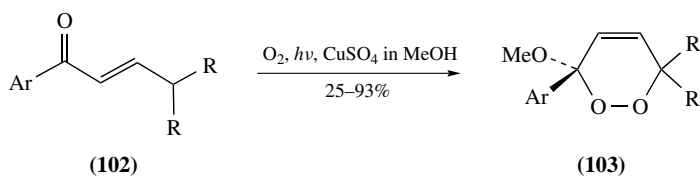
For a synthesis of non-racemic chondrillins **3a** and **3b**, as well as plakorins **3c** and **3d**, see Scheme 106 in Section II.B.3. Although the mechanism of the peroxidations with triplet oxygen is not clear yet, it was assumed to proceed via a series of intermediates **98** and **99** as shown in Scheme 21⁹⁴. It is noteworthy that RB, which plays a role of pre-sensitizer, is converted to rose bengal lactone (RBL) sensitizer. Such a direct peroxidation was found to be ineffective for free acids of type **98e** ($\text{R}^2 = \text{CH}_2\text{CO}_2\text{H}$). However, the silyl ester **98c** is successfully converted to cyclic hemiperoxyacetals **100c**, which through subsequent *in situ* desilylation by prolonged photolysis in the MeOH-containing reaction media afford the acid **101e** ($\text{R}^1 = \text{C}_{12}\text{H}_{25}$, $\text{R}^2 = \text{CH}_2\text{CO}_2\text{H}$) in total 52% yield⁹⁴.

Similar peroxidations with triplet oxygen can be induced by UV irradiation at 350 nm with CuSO_4 as a sensitizer in methanol⁹⁵. For example, under these conditions acyclic alkenyl aryl ketones of type **102** give the 6-membered cyclic peroxyketals **103** (Scheme 22), which exhibit significant antimalarial activity^{96,97}. Related CuSO_4 -sensitized photooxygenation of *cis*-4-acetoxypulegone (**104**) in $\text{CH}_2\text{Cl}_2/\text{MeOH}$ gives almost quantitatively a 2:3 mixture of the naturally occurring product, 6-membered bicyclic peroxy lactol (+)-isoacetylsaturejol (**105**) and its methylketal **106** (Scheme 23)⁹⁸. In contrast to the previous example, a singlet oxygen photooxygenation of the same substrate **104** using visible light irradiation and RB as a sensitizer affords another naturally occurring 5-membered bicyclic peroxide, namely (–)-acetylsaturejol (**107**), in 75% yield (Scheme 23)⁹⁸. The cyclic endoperoxide-lactols **109** were synthesized in moderate to good



- (a)** $R^1 = Me, R^2 = n-Bu$
(b) $R^1 = C_{12}H_{25}, R^2 = CH_2CO_2Me$
(c) $R^1 = C_{12}H_{25}, R^2 = CH_2CO_2TBS$
(d) $R^1 = C_{16}H_{33}, R^2 = CH_2CO_2Me$
(e) $R^1 = C_{12}H_{25}, R^2 = CH_2CO_2H$

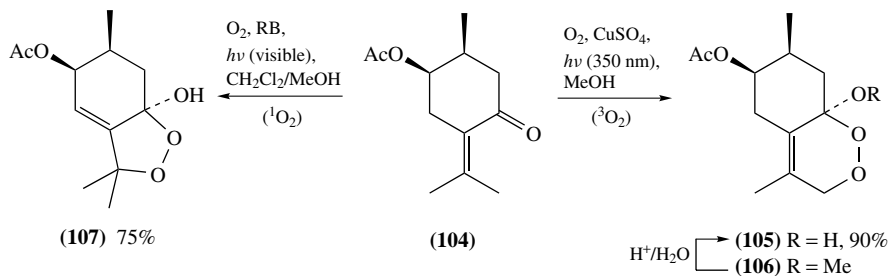
SCHEME 21



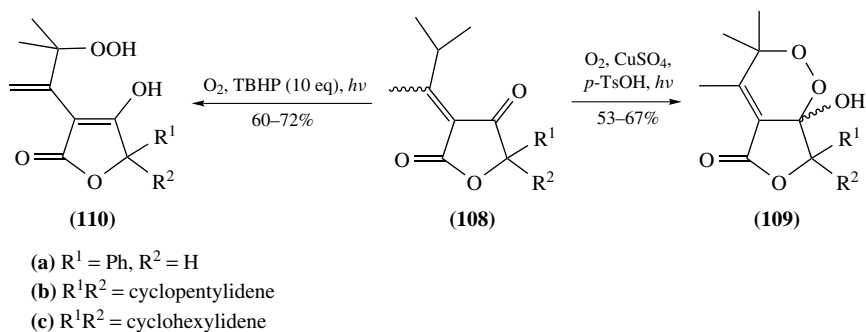
$Ar = p-An, p-Tol, Ph, p-FC_6H_4, p-ClC_6H_4, p-MeSC_6H_4, p-O_2NC_6H_4, p-CF_3C_6H_4, 3,4,5-(MeO)_3C_6H_2$

$R = Me, \text{ or } RR = \text{cyclobutylidene, cyclopentylidene, cyclohexylidene, cycloheptylidene}$

SCHEME 22



SCHEME 23



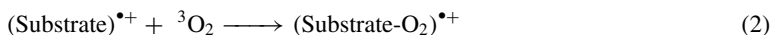
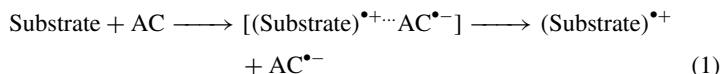
SCHEME 24

yield using a Snider-type triplet oxygen peroxidation of 3-alkylidenedihydrofuran-2,4-diones **108** (Scheme 24)⁹⁹. It is noted that while free radical autoxidation or oxygenation of **108b** in the presence of $(\text{PhCOO})_2$ affords **109b**, albeit in low yield, formally similar oxygenations in the presence of *tert*-butyl hydroperoxide (TBHP) give mainly hydroperoxides **110** (Scheme 24)^{99,100}.

2. Cycloaddition of triplet oxygen with cation radicals

Endoperoxides can be prepared through triplet oxygen peroxidation of cation radicals, derived from electron-rich cyclopropanes, arylalkenes and dienes under electron transfer conditions using appropriate one-electron oxidizing agents. The mechanism and some synthetic applications of these reactions were extensively discussed in several specialized reviews^{101-103a}. These processes are rationalized in terms of the cation radical chain mechanism, which was originally suggested by Bartlett¹⁰⁴, Tang and coworkers¹⁰⁵ and Haynes and coworkers¹⁰⁶⁻¹⁰⁸ for the explanation of Barton's spin-forbidden peroxidation of some 1,3-dienes with triplet oxygen^{109,110}. According to the definition of Foote, the process belongs to the type I photosensitized oxidation by which photosensitization activates the organic substrate and not the molecular oxygen¹¹¹. Such a process generally consists of 3 key, potentially reversible, steps: (i) One-electron transfer from the substrate to one-electron acceptor (AC) to give a cation radical of the substrate and one-electron reduced form of the acceptor (equation 1). (ii) Reaction of the cation radical with triplet oxygen to give the peroxy-radical cation as in equation 2. (iii) One-electron oxidation of the substrate by the peroxy-radical cation to produce the endoperoxide and a new cation radical of the substrate that acts as a chain carrier (equation 3). Reactions involving a

peroxidation of cation radicals are usually carried out in polar aprotic solvents such as acetonitrile that facilitates the ion-pair [(Substrate)^{•+} AC^{•-}] dissociation, thus shifting the electron transfer equilibrium to the right (equation 1).



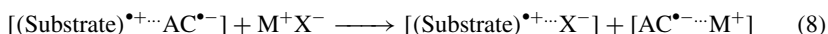
To secure the efficiency of the one electron transfer, electron acceptors like 9,10-dicyanoanthracene (DCA) or quinones in conjunction with UV or visible light irradiation are commonly employed. Although photosensitized reactions are usually associated with a singlet excited state (equations 4 and 5), some processes of this type can occur thermally in the dark.



The DCA-sensitized photooxygenation of electron-rich substrates is markedly accelerated (3–10 times) by the addition of biphenyl (BP), which acts as an effective one-electron carrier from the substrate to the excited state of the acceptor (equations 6 and 7).

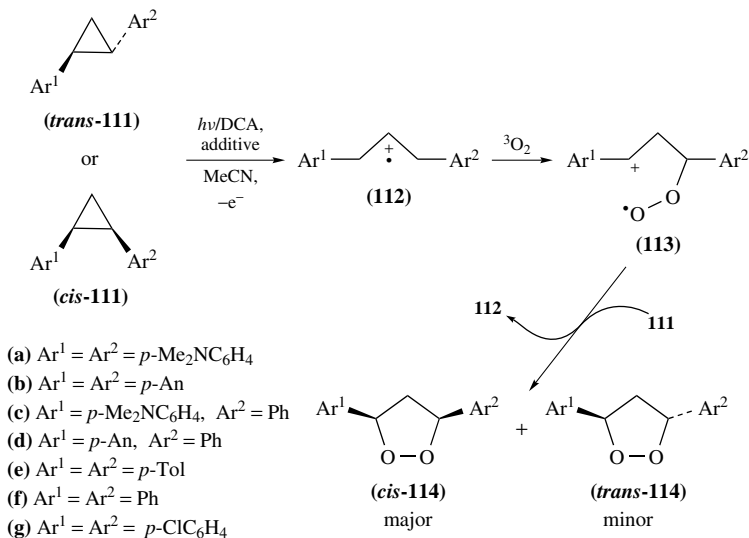


For the preparation of cyclic peroxides from less electron-rich substrates, addition of some metal salts (MX) with non-nucleophilic anions that can support solvolysis, is beneficial (equation 8).

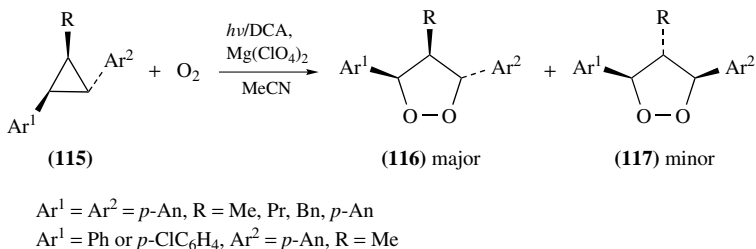


For example, DCA-sensitized photooxygenation of the electron-rich 1,2-diarylcyclopropanes *trans*-**111a-d** or *cis*-**111a-d** proceeds smoothly through the intermediacy of the cation radicals **112** and peroxy-radical cations **113** as discussed above, affording a mixture of 3,5-*cis*- and 3,5-*trans*-disubstituted 1,2-dioxolanes **114a-d** (*cis/trans*, *ca* 7:3) in quantitative yield (Scheme 25)^{112–114}. Photooxygenation of the less electron-rich 1,2-diarylcyclopropanes **111e-f** to 1,2-dioxolanes **114e-f** with BP requires addition of Mg(ClO₄)₂. Under these conditions 1,2-dioxolanes **114e-f** were obtained in 45–55% yield¹¹⁴. Analogously, irradiation of an oxygen-saturated acetonitrile solution of 1,2,3-trisubstituted cyclopropanes **115** in the presence of DCA as a sensitizer and Mg(ClO₄)₂ as an additive affords a *ca* 9:1 mixture of the 1,2-dioxolanes **116** and **117** in 70–95% yield (Scheme 26)¹¹⁵. In contrast to that, DCA-sensitized photooxygenation of 1,1-diphenyl-2-vinylcyclopropane (**118**) to give the corresponding 1,2-dioxolane **119** proceeds smoothly in the presence of BP without any salt additives (Scheme 27)^{116,117}.

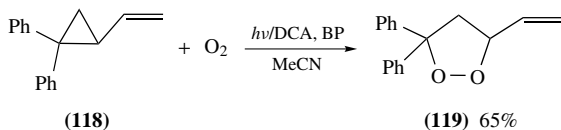
1,1,2,2-Tetraarylcyclopropanes, which are inert toward singlet oxygen (¹O₂), are readily photooxygenated in MeCN with triplet oxygen in the presence of DCA as a sensitizer and BP as a co-sensitizer to give 3,3,5,5-tetraaryl-1,2-dioxolanes (70–100%)^{118,119}. Similar high yields were obtained using 1,8-dihydroxyanthraquinone as a sensitizer instead of DCA, or LiClO₄ as a co-sensitizer instead of BP¹¹⁹. DCA-sensitized photooxygenations of *trans*-1,1-diaryl-2,3-diphenylcyclopropanes (Ar = *p*-An, *p*-Tol) in the presence



SCHEME 25



SCHEME 26

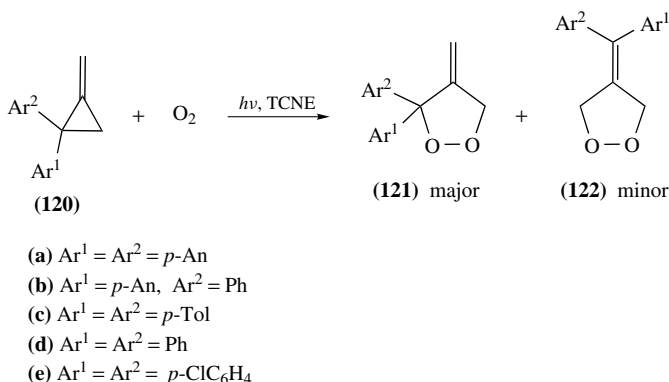


SCHEME 27

of BP afford a mixture of *cis*- (60–70%) and *trans*- (40–30%)-3,3-diaryl-4,5-diphenyl-1,2-dioxolanes in good yield¹²⁰. Employment of similar reaction conditions on the more electron-poor *trans*-1,1,2,3-tetraphenylcyclopropane results in just traces of the corresponding 1,2-dioxolane¹²⁰.

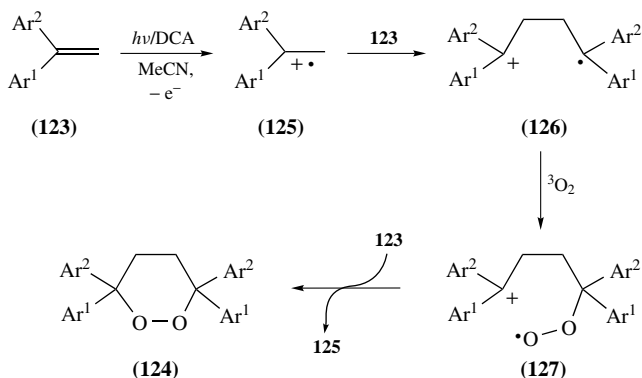
Dioxygenations of 2,2-diaryl-1-methylenecyclopropanes (**120**) proceed via detectable electron donor–acceptor charge transfer complexes^{121, 122} and can be accomplished using various strong π -electron acceptors, such as 1,2,4,5-tetracyanobenzene¹²¹, tetracyanoethylene (TCNE)^{118, 123}, chloranil, anthraquinone etc.¹²⁴. Thus, on irradiation of oxygen-saturated solutions of the substrates **120a** and **120b**, bearing highly electron-donating

aryl substituents, in MeCN or nitromethane, in the presence of TCNE, the corresponding, 3,3-diaryl-4-methylene-1,2-dioxolanes **121a** and **121b** are formed within 1 h in high yields (Scheme 28)^{118,123}. The less active substrates **120c–e** afford endoperoxides **121c–e** as major isomers (20–55%), as well as minor isomers **122c–e** (3–5%)¹¹⁸. It is noteworthy that dioxygenation of the more active substrates **120a** and **120b** may occur also in the dark, although it requires several days for getting comparable results^{118,123}.



SCHEME 28

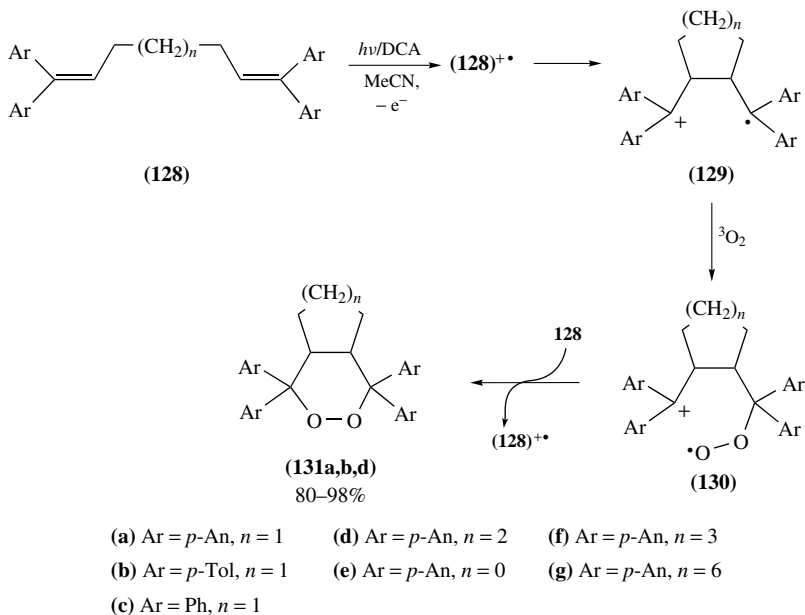
Electron-transfer induced photooxygenation of 1,1-diarylethylenes **123** with triplet oxygen to give 1,2-dioxanes **124** follows an attractive one-pot sequential chain process which includes the formation of a new C–C bond and the construction of a peroxide moiety (Scheme 29). Indeed, the incipient cation radical **125**, generated through a single electron abstraction from substrate **123**, dimerizes, forming a new carbon–carbon bond and a new 1,4-cation radical **126**. The latter reacts with triplet oxygen to give, through the peroxy-radical cation **127**, the 6-membered ring peroxide **124**, regenerating cation radical **125** that continues the chain (Scheme 29)¹⁰⁸. The DCA-photosensitized oxygenations give high yields of endoperoxides **124** if at least one of the aryl groups in **123** carries an electron-releasing substituent at the *para*- or *ortho*-position (e.g. $\text{Ar}^1 = p\text{-Me}_2\text{NC}_6\text{H}_4$,



SCHEME 29

p-An, *o*-An, *p*-Tol)^{125–131}. 10-Methylacridinium salts can be successfully used instead of DCA in such a photooxygenation^{131,132}. Similar oxygenations of more electron-poor substrates **123** (e.g., Ar¹ = Ar² = Ph) give the cyclic peroxides **124** in poor yields (15–30%), and the corresponding benzophenones as the major product^{130,132}. Alternatively, 3,3,6,6-tetraaryl-1,2-dioxane and related tetraaryl-analogues **124** can be effectively prepared in 80–90% yield by irradiation of pre-formed charge transfer complexes of **123** with SbCl₅ in methylene chloride at –78 °C in the presence of oxygen^{108,133}.

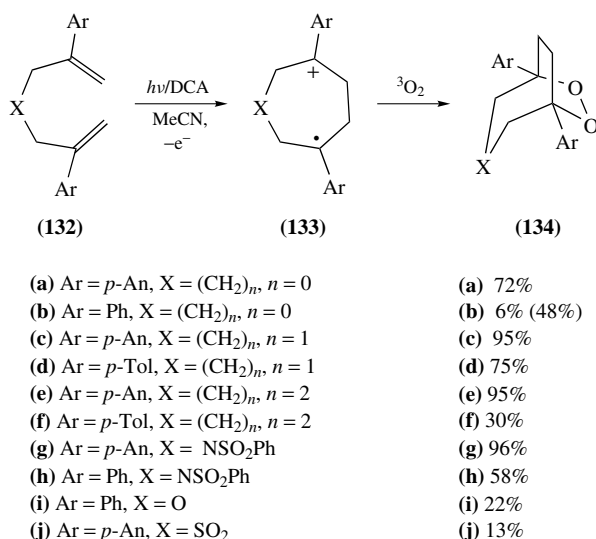
Analogous electron transfer photooxygenations of 1,3-bis(diarylethenyl)propanes **128a** and **128b**, and of 1,4-bis(di-*p*-anisylethenyl)butane **128d**, sequentially involving cation radicals (**128**)⁺⁺ of the corresponding substrate, 1,4-cation radicals of type **129** and peroxy-radical cations **130**, give the fused bicyclic peroxides **131a**, **131b** and **131d** respectively, in high yield (Scheme 30)¹⁰³. However, this reaction is arrested if the substrate, as in the case of **128c**, is less electron-rich, or when the cyclization, as in the cases of **128e–g**, would have lead to the construction of cation radicals of type **129** having 4-, 7- or 10-membered carbocyclic rings. In such instances degradation to the corresponding benzophenones prevails¹⁰³.



SCHEME 30

A number of the photoinduced electron transfer cyclization–peroxidation processes leading to bridged bicyclic endoperoxides were recently reported (Schemes 31–33). Scheme 31 describes the photooxygenation of bis(diarylethenyl)compounds of type **132**. In general, the effectivities of these photooxygenation processes strongly depend on the size of the monocyclic cation radical **133**, on the donating capacity of the aryl substituents, on the nature of linker X and on the nature of the photosensitization. Thus, all-carbon-tethered precursors **132** (X = (CH₂)_n, *n* = 0–2) that possess high electron-donating aryl substituents (Ar = *p*-An or *p*-Tol) do undergo a smooth DCA-photosensitized oxygenation via the corresponding 6- to 8-membered 1,4-cation radicals **133** to give

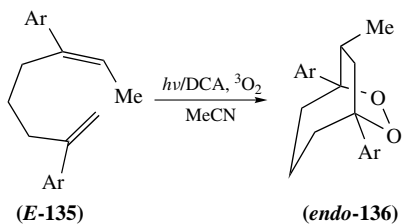
the corresponding endoperoxides **134a** and **134c–e** in high yields^{134–138}. Under these conditions, the yield of endoperoxide **134b** for diphenyl-substituted all-carbon-tethered substrate **132b** ($n = 0$) is very poor, but it can be improved to 48% by addition of $\text{Mg}(\text{ClO}_4)_2$ ¹³⁴. A similar positive effect of $\text{Mg}(\text{ClO}_4)_2$ on photooxygenation of electron-poor 2,6-diaryl-1,6-heptadienes of type **132** (Ar = Ph or *p*- FC_6H_4 , $n = 1$) was reported¹³⁸. Additional increase in the yields of bicyclic peroxides of type **134** has been achieved by replacing the sensitizer DCA with a stronger oxidizing agent like 2,4,6-triphenylpyrylium tetrafluoroborate¹³⁸. Elongation of the carbon tether between the two styryl units in substrates **132** ($n > 2$) significantly reduces the yield of endoperoxides **134**. For example, the *para*-methoxyphenyl-substituted derivatives **132** give the corresponding bridged bicyclic peroxides **134** in 9% (for X = $(\text{CH}_2)_n$, $n = 3$) and 3% (for X = $(\text{CH}_2)_n$, $n = 4$) yields¹³⁹. Heteroatom-containing dienes **132** (Ar = *p*-An or Ph, X = O, SO_2 , NSO_2Ph or NMs) were subjected to DCA-sensitized photooxygenation to give the corresponding bridged bicyclic endoperoxides, e.g. **134g–j**, in variable yields (Scheme 31)^{140,141}.



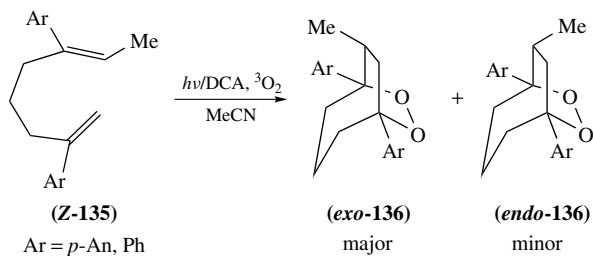
SCHEME 31

The effectivity of the photoinduced electron transfer cyclization–oxygenation of unsymmetrical 2,6-diaryl-1,6-heptadienes **135**, possessing one terminal and one internal C=C bond in the styryl units, as well as the resulting stereochemistry of the products, strongly depend on the stereochemistry of the substrates (Scheme 32)^{142,143}. Thus, DCA-sensitized photooxygenation of *E*-styryl derivative **E-135** (Ar = *p*-An) gives exclusively and stereoselectively the bridged bicyclic peroxide **endo-136** (65%) (Scheme 32a). In contrast, photooxygenation of the isomeric *Z*-styryl derivative **Z-135** is less selective and less efficient, leading to a mixture of *exo*-bridged bicyclic peroxide **exo-136** (33%) and *endo*-bridged bicyclic peroxide **endo-136** (9%) (Scheme 32b)¹⁴³. The photooxygenation of *E,E*- as well as *Z,Z*-3,6-diaryl-2,6-octadienes (**137**) was found to be highly stereoselective giving exclusively the *trans*-bridged bicyclic peroxides **trans-138** (Scheme 33a), whereas a similar treatment of *E,Z*-3,6-diaryl-2,6-octadienes (**E,Z-137**) led to a mixture of bicyclic peroxides **exo,cis-138** (major product) and **endo,cis-138** (minor product) (Scheme 33b)^{134,142,144}.

(a)

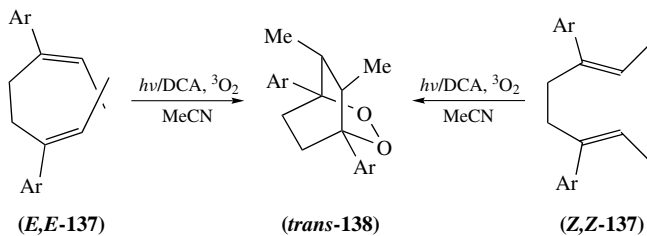


(b)

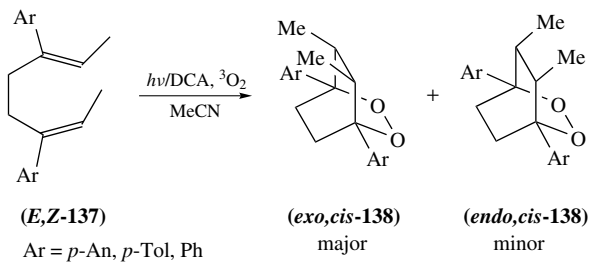


SCHEME 32

(a)

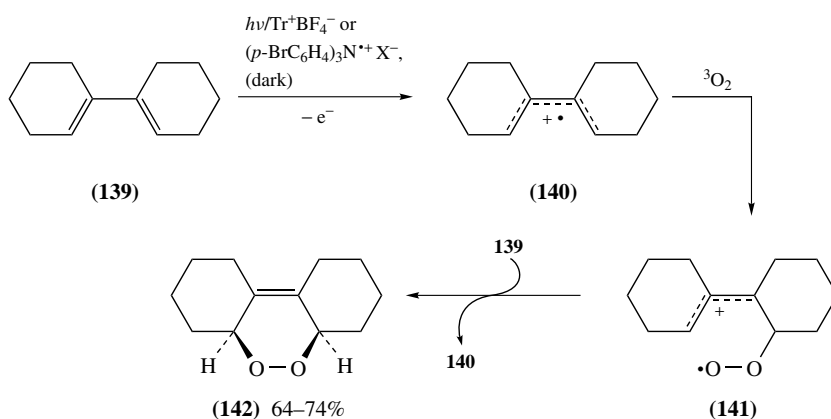


(b)

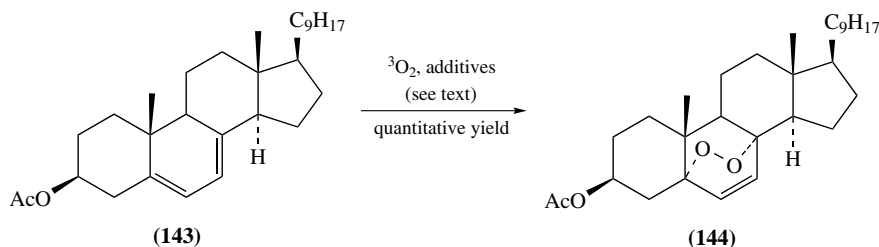


SCHEME 33

A direct [4 + 2]-cycloaddition of triplet oxygen to 1,3-dienes is spin-forbidden. Nevertheless, as originally discovered by Barton and coworkers^{109,110}, a number of *cis*-1,3-dienes do undergo peroxidation with triplet oxygen under electron-transfer conditions to give the corresponding 4,5-unsaturated-1,2-dioxanes. These processes are commonly chain reactions which proceed via cation radical of type **140** and peroxy-radical cation of type **141**, as discussed earlier in this section and illustrated in Scheme 34 for the case of electron transfer-mediated cycloaddition of triplet oxygen to 1,1'-bicyclohexenyl (**139**)^{104–106}. Indeed, the diene **139** readily reacts with triplet oxygen at -78°C in the presence of various Lewis acids (e.g., trityl tetrafluoroborate, Tr^+BF_4^-) under a daylight irradiation, or in the presence of amine cation radical salts such as tris(*p*-bromophenyl)aminium tetrafluoroborate in the dark, giving the single *cis*-fused tricyclic peroxide (**142**) in high yield (Scheme 34)^{107,110}. Similarly, a solution of ergosterol 3 β -acetate (**143**) in CH_2Cl_2 on exposure to air and laboratory light in the presence of a catalytic amount of trityl tetrafluoroborate, at -78°C , undergoes a fast peroxidation to give the corresponding endoperoxide **144** in quantitative yield and at a higher rate than a similar reaction with singlet oxygen (Scheme 35)¹¹⁰. A variety of Lewis acids such as BF_3 , SnCl_4 , AlCl_3 , SbCl_5 and even I_2 induce the photoperoxidation at -78°C of diene **143** to cyclic peroxide **144**^{106,109,110}. When Lewis acids like (*p*- BrC_6H_4) $_3\text{N}^+\text{SbCl}_6^-$, FeCl_3 , WCl_6 , MoCl_5 and VOCl_3 are added, this peroxidation is brought to completion, at -78°C in the dark within few minutes^{106,110}. Additional examples of this type of photooxygenation of 1,3-dienes are given in earlier original articles and reviews^{145–150}.

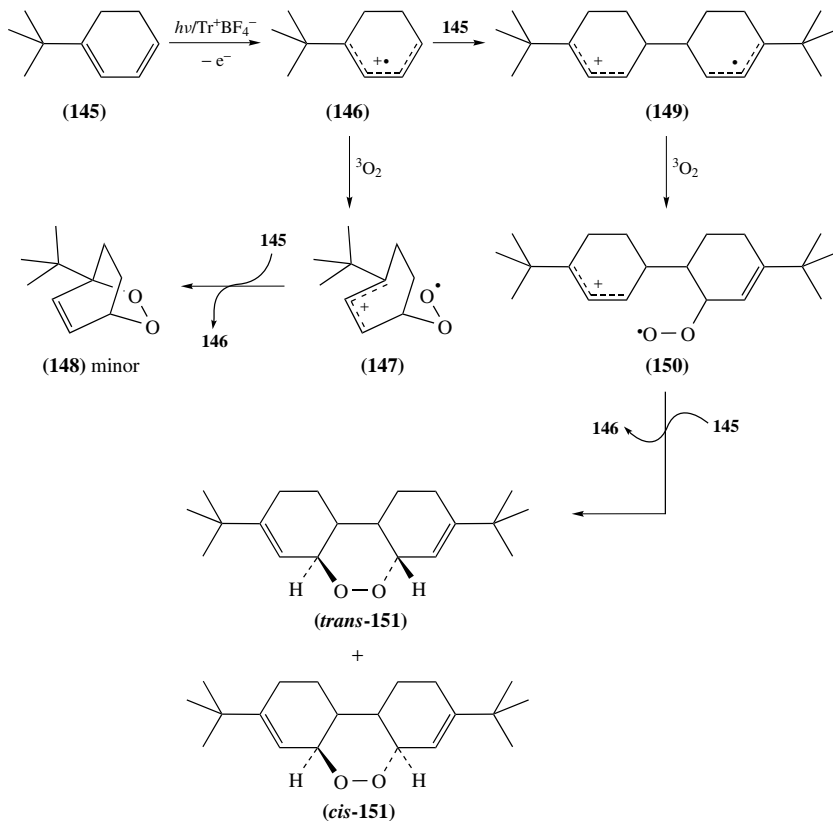


SCHEME 34



SCHEME 35

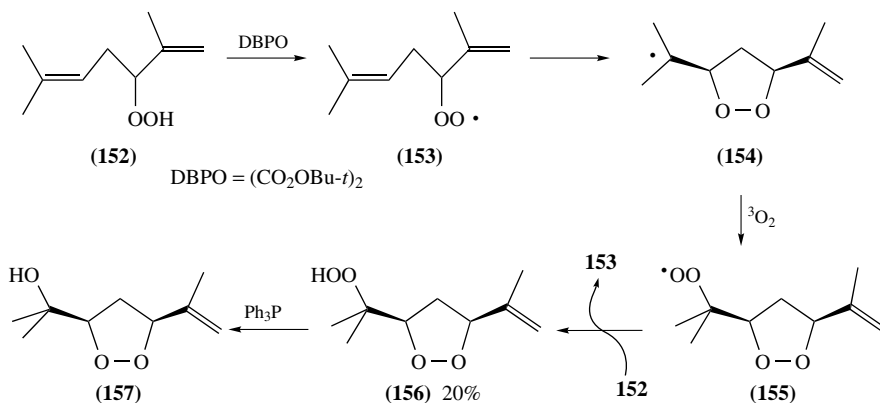
Following a mechanism similar to that described in Scheme 29, electron transfer photooxygenation of 1-*tert*-butylcyclohexa-1,3-diene (**145**) in the presence of Tr^+BF_4^- leads, through the intermediacy of cation radicals **146**, **149** and **150**, to the dimeric fused tricyclic peroxides **151** (total 40% yield, *cis/trans* ca 5:4) rather than to the monomeric bridged bicyclic peroxide **148** (5–10%) which derives from cation radical **147** (Scheme 36)^{148, 151}.



SCHEME 36

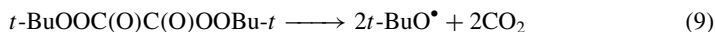
3. Free radical cyclization of alkenyl hydroperoxides

The original reports by Porter and coworkers^{152, 153} and Pryor and Stanley¹⁵⁴ in 1975 on the homolytic cyclization of alkenyl hydroperoxides provided one of the most useful and highly utilized methods for the synthesis of endoperoxides^{52, 155, 156}. This method is illustrated herein through the conversion of alkenyl hydroperoxide **152** into 3-hydroperoxyalkyl-1,2-dioxolane **156** (Scheme 37)¹⁵⁷. In this sequential reaction peroxy-radical **153**, obtained from alkenyl hydroperoxide **152** on the initiation step, undergoes 5-*exo*-addition to give the carbon-centered radical **154**. The latter is trapped by triplet oxygen yielding peroxy-radical **155**, that abstracts a hydrogen atom from the starting material **152**, thus giving hydroperoxy-1,2-dioxolane **156** and regenerating peroxy-radical **153** that continues the free radical chain reaction.

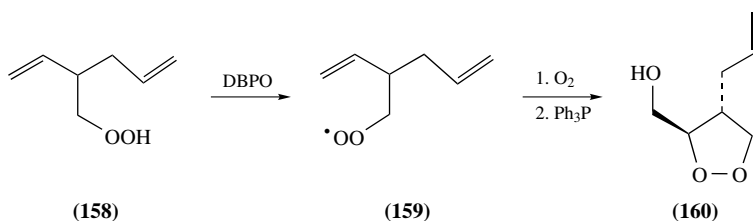


SCHEME 37

The strength of the O–H bond in ROO–H is comparable to that of allylic and benzylic C–H bonds and is *ca* 15–20 kcal mol⁻¹ weaker than the corresponding RO–H bond¹⁵⁸. Therefore, alkoxy radicals like *t*-BuO• are suitable initiators in reactions of the type described in Scheme 37. The hazardous di-*tert*-butyl peroxalate (DBPO)¹⁵⁹ (*t*_{1/2} *ca* 12 h at 20 °C in solution) (equation 9) and the safer di-*tert*-butyl hyponitrite (DTBN) (*t*_{1/2} *ca* 12 h at 40 °C) (equation 10)^{160,161} have been widely used for the generation of *tert*-BuO radicals under very mild conditions^{155,158}.



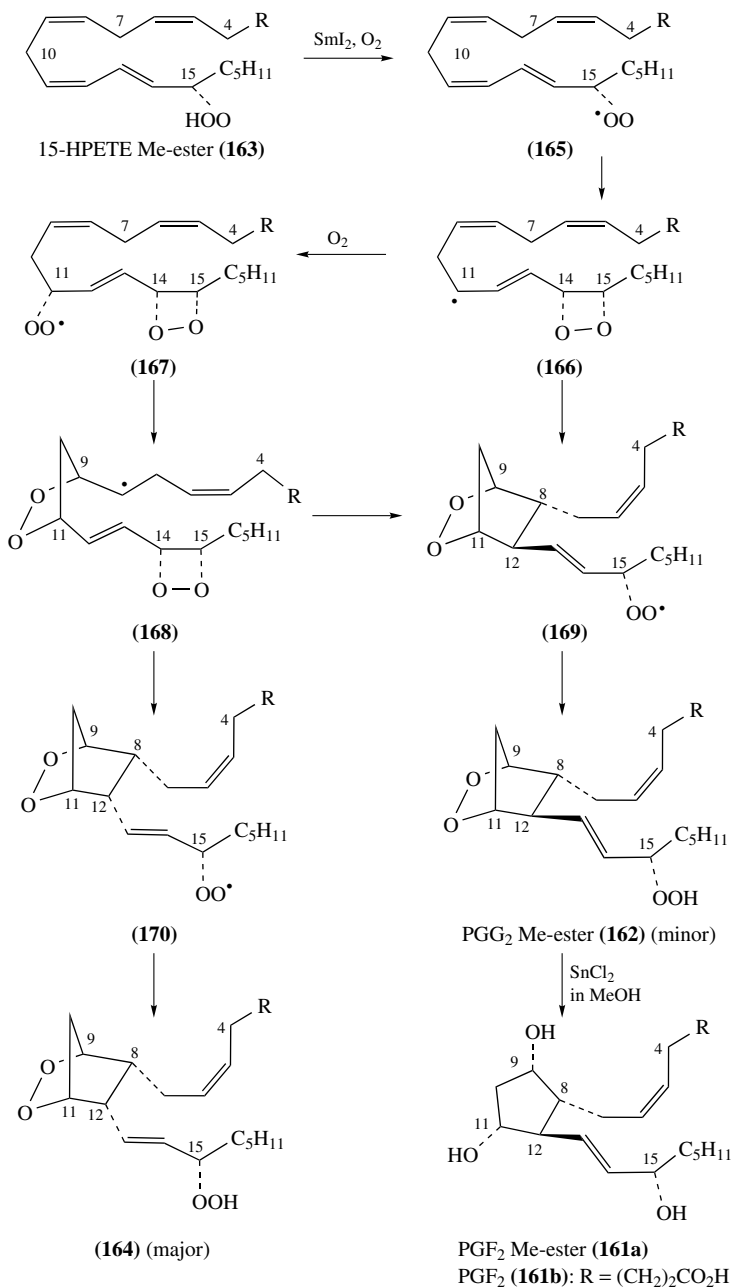
Most often, the rate of hydrogen abstraction by alkoxy radicals (RO•) from C–H and X–H bonds is higher than their addition rate to carbon–carbon double bonds. In contrast, slightly electrophilic peroxy-radicals like **153** have a strong tendency to add intramolecularly onto electron-rich C=C bonds through both the 5- and 6-*exo-trig* mode to give endoperoxide-containing carbon-centered radicals like **154** (Scheme 37). Usually, cyclizations of peroxy-radicals like **153** follow the well-established rules for cyclization of analogous carbon-centered radicals¹⁶². Since hydroperoxides cannot serve as good hydrogen atom donors to carbon-centered radicals, a mediating chain transfer agent is required. As found in many studies that were discussed in previous reviews, triplet oxygen is particularly useful for this purpose and was widely applied in synthesis^{155,156}. Application of this methodology to hydroperoxide **152**, that contains an allylic and a homoallylic tether, afforded the 3,5-*cis*-disubstituted 1,2-dioxolane hydroperoxide **156** in 20% isolated yield (Scheme 37)¹⁵⁷. Selective reduction of hydroperoxide function in **156** with Ph₃P at ambient temperature affords the corresponding hydroxy-endoperoxide **157** in good yield (Scheme 37). No product deriving from a 4-*exo* cyclization onto the double bond of the allylic tether was identified¹⁵⁷. Additional examples illustrating the predominant formation of 3,5-*cis*-disubstituted 1,2-dioxolanes through radical cyclizations of homoallylic hydroperoxides were reported¹⁶³. In the absence of particularly adverse factors, homoallylic peroxy-radicals undergo 5-*exo*- rather than 6-*endo*-cyclization¹⁶⁴. For example, cyclization of **158** via the dialkenyl peroxy-radicals **159** proceeds through an exclusive 5-*exo*-ring closure to give, after reduction with Ph₃P in the same vessel, 3,4-*trans*-disubstituted 1,2-dioxolane **160** (Scheme 38)¹⁶⁵.



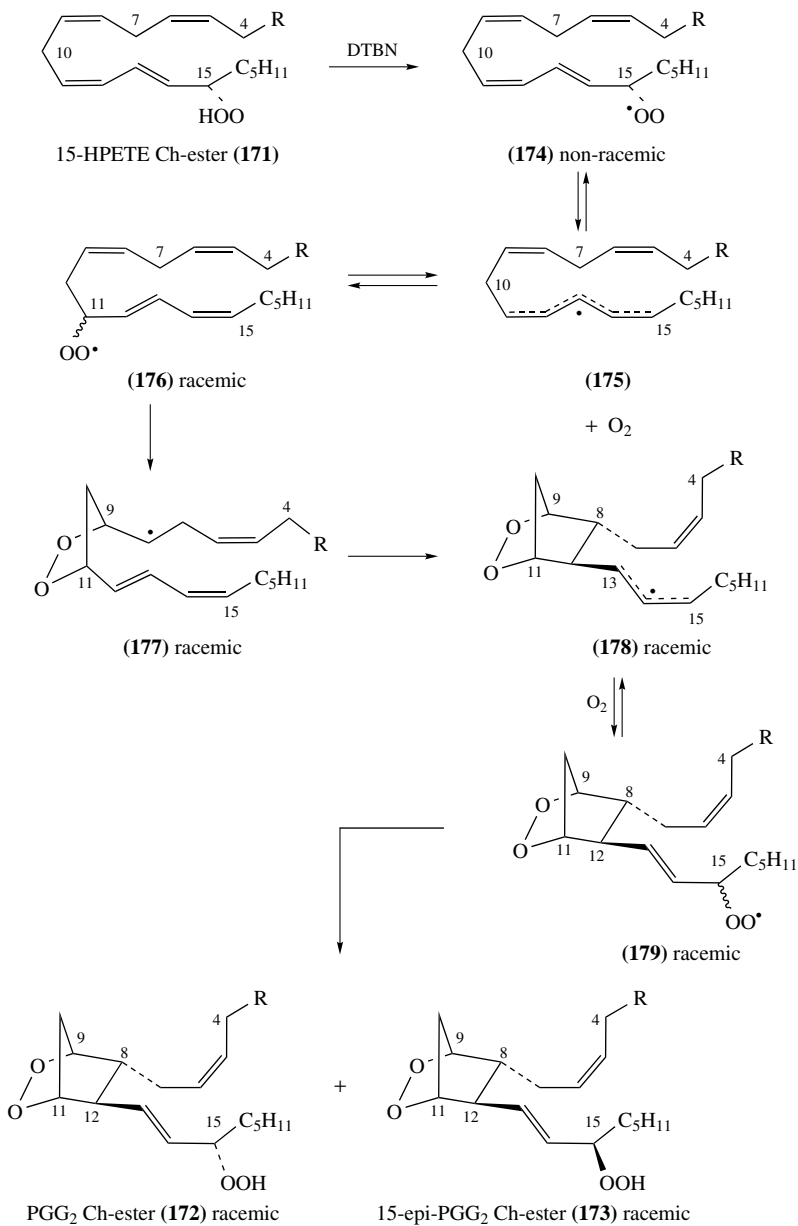
SCHEME 38

The free-radical oxidative 5-*exo* cyclization of homoallylic peroxy-radicals is closely associated with biologically important processes, such as those promoted by cyclooxygenases (COX) enzymes' oxidation of arachidonic acid to form optically pure prostaglandin endoperoxides PGH₂ (**2a**) and PGG₂ (**2b**)¹⁶⁶⁻¹⁷¹. The naturally occurring prostaglandin endoperoxides **2** are characterized by *trans*-arrangement of the side chains attached to the 2,3-dioxabicyclo[2.2.1]heptane at C8 and C12 of the prostaglandin system. While PGH₂ (**2a**) and PGG₂ (**2b**) have been prepared semisynthetically at the end of the 1970s starting from PGF_{2α} (**161b**) via a series of nucleophilic displacements¹⁰⁻¹³, early biomimetic free-radical approaches failed. Subsequent attempts to synthesize prostaglandin endoperoxides **2** by free-radical biomimetic routes led preponderantly to isomers having *endo*- and *exo-cis*-arrangements of the side chains of the bridged bicyclic system rather than to the natural products with their characteristic *trans* configuration¹⁷²⁻¹⁷⁵. An important advance of the biomimetic approach was made in 1994 by Corey and Wang with the synthesis of PGG₂ methyl ester (**162**) (Scheme 39)¹⁷⁶. In this synthesis the methyl ester of 15*S*-hydroperoxy-5,811*Z*,13*E*-eicosatetraenoic acid (15-HPETE) (**163**) was treated with triplet oxygen and a free radical initiator (presumably I₂SmOOSmI₂), prepared *in situ* from oxygen and SmI₂, to give a 1:3 mixture of the methyl esters of PGG₂ **162** and its *cis*-isomer **164** in 43% total yield (at 35% conversion)¹⁷⁶. IR, NMR and non-chiral chromatographic analyses of synthetic PGG₂ methyl ester (**162**) were found to be identical to those of a sample of PGG₂ methyl ester (**162**) deriving from a natural source. Additionally, the reduction product **161a** and a sample of PGF_{2α} methyl ester (**161a**) from natural origin were found to exhibit identical spectral data. According to the authors' suggestion, the overall free-radical sequential process proceeds according to the mechanism displayed in Scheme 39. Thus, the incipient chiral peroxy-radical **165** cyclizes by the 4-*exo-cis*-mode to form the 14,15-dioxetane carbon-centered allyl radical **166**, which is trapped by triplet oxygen to give allylperoxy-radical **167** that in turn ring-close through the 5-*exo*-addition mode at position 9. The resulting intermediate **168** was postulated to undergo an intramolecular addition-elimination step yielding a mixture of two isomeric peroxy-radicals **169** and **170**. The latter would then reversibly abstract hydrogen atom from the starting hydroperoxide **163** thus affording the PGG₂ methyl ester (**162**) and its *cis*-isomer **164**, regenerating a new peroxy-radical **165** that continues the sequential radical chain reaction.

The mechanism postulated by Corey and Wang for their biomimetic synthesis was contested by Porter and coworkers¹⁷⁷⁻¹⁷⁹. They studied the same autoxidation reaction using the cholesteryl ester of 15*S*-hydroperoxy-5,811*Z*,13*E*-eicosatetraenoic acid (15-HPETE) (**171**), instead of the methyl ester **163**, and DTBN as initiator instead of SmI₂/oxygen. Under similar reaction conditions to those reported by Corey and Wang, they obtained racemic PGG₂ cholesteryl ester (**172**) along with its racemic C15-epimer **173**, as well as racemic C8,C12-*cis*-isomers (Scheme 40)^{178, 179}. The formation of these racemic products is not in accord with the mechanism of Corey and Wang (Scheme 39) which would lead to enantiomerically pure products. Racemization and the subsequent transformations

R = (CH₂)₂CO₂Me

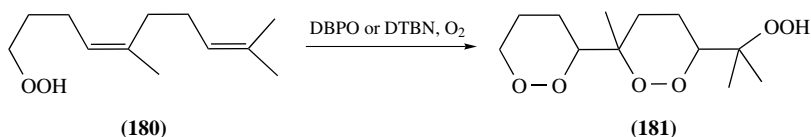
SCHEME 39



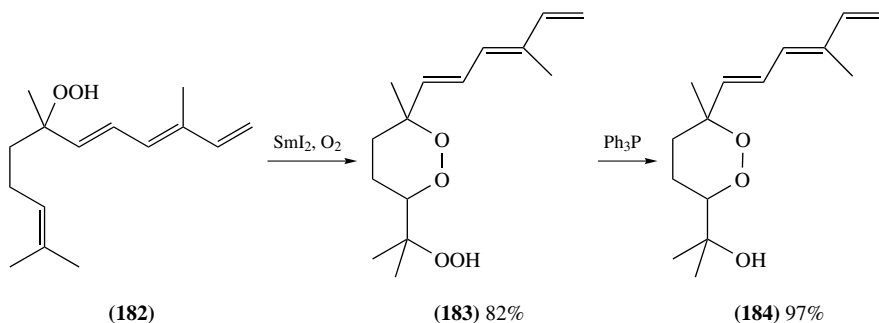
SCHEME 40

were rationalized by Porter and coworkers using the mechanism shown in Scheme 40. Accordingly, the incipient enantiomerically pure dienylperoxy-radical **174** undergoes a characteristic allylic peroxy-radicals β -fragmentation to molecular oxygen and highly delocalized dienyl carbon-centered radical **175**, which traps triplet oxygen at C11 to give the racemic peroxy-radical **176**^{169, 180–184}. Through a characteristic sequential homolytic process for oxidative cyclizations, peroxy-radicals **176** cyclize to carbon centered radicals **177** and then a second cyclization to delocalized enyl radical **178**. Addition of molecular oxygen to the latter gives a mixture of epimeric peroxy-radicals **179** and eventually, through hydrogen abstraction from hydroperoxide **171**, racemic PGG₂-cholesteryl ester (**172**) and 15-*epi* PGG₂-cholesteryl ester **173**. The racemic C8,C12-*cis*-isomers are formed from the common intermediate radical **177** in a parallel route of cyclization^{178, 179}.

Suitably substituted unsaturated hydroperoxides can undergo a serial oxidative 5-*exo*-¹⁸⁵ or 6-*exo*-cyclization as exemplified in Scheme 41 by the conversion of peroxide **180** to the corresponding bis(endoperoxide) **181**^{186, 187}. Reaction conditions of homolytic cyclizations of hydroperoxides are compatible with a variety of functional groups. For instance, the sensitive 4-methylhexa-1,3,5-trienyl system remained unchanged upon SmI₂/oxygen-induced cyclization of α -farnesyl hydroperoxide (**182**) to the highly unsaturated 1,2-dioxanehydroperoxide **183** (82%), which was then reduced (97%) to the alcohol **184** (Scheme 42)^{188, 189}. 6-*Exo*-cyclizations of peroxy-radicals are widely employed in the synthesis of naturally occurring cyclic peroxides and related compounds. Thus, oxidative cyclization of hydroperoxide **185** afforded a mixture of epimeric hydroperoxides **186** and **187** in 79% total yield when SmI₂/O₂ was used as initiator and 89% when DBPO/TBHP was used as initiator. Selective reduction of the hydroperoxy group to hydroxyl function afforded racemic yingzhaosu C (**188**) and its epimer **189** (Scheme 43)¹⁹⁰.

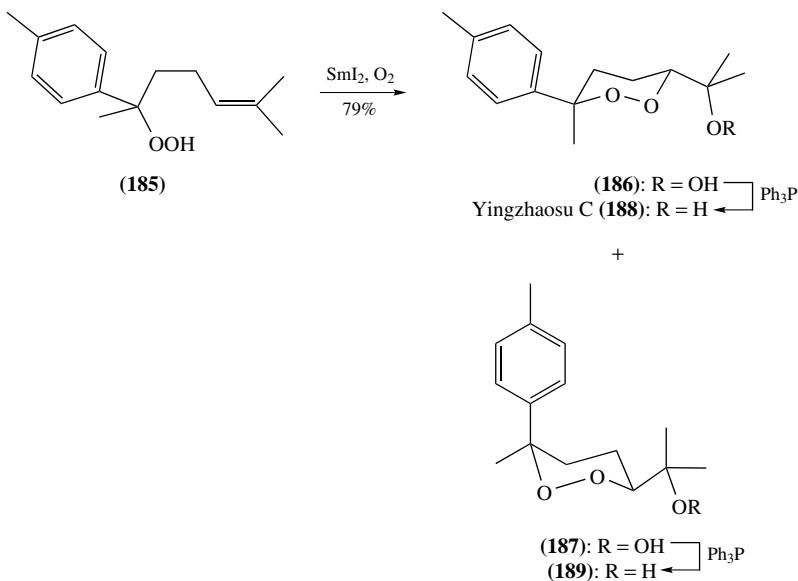


SCHEME 41



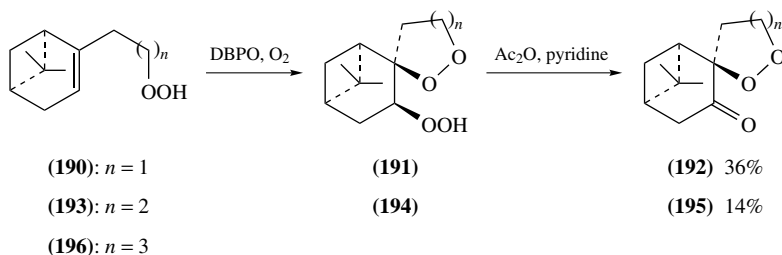
SCHEME 42

In the context of the synthesis of naturally occurring product cardamom peroxide (**7**), radical spirocyclizations of the hydroperoxides **190**, **193** and **196** were studied (Scheme 44)¹⁹¹. It was found that the DBPO-induced oxidative cyclization of **190** follows the 5-*exo*-mode to give the spiroendoperoxide **191**, which was subsequently converted



SCHEME 43

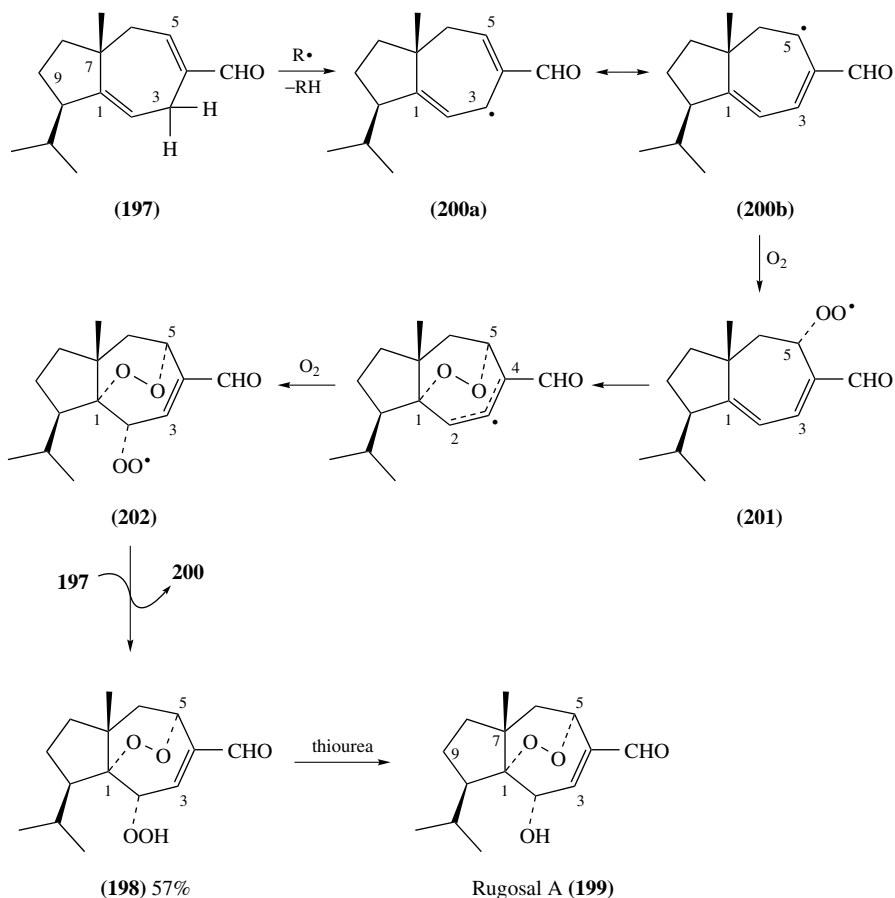
to the keto-derivative **192** (36%) by treatment in the same vessel with Ac_2O /pyridine. Application of the same reaction to **193** followed the 6-*exo*-mode to give, through the spirocyclic peroxide **194**, the keto-derivative **195** in 14% yield. An analogous cyclization of **196**, that would have required 7-*exo*-ring closure, failed.



SCHEME 44

4. Autoxidation through all-homolytic chain reactions

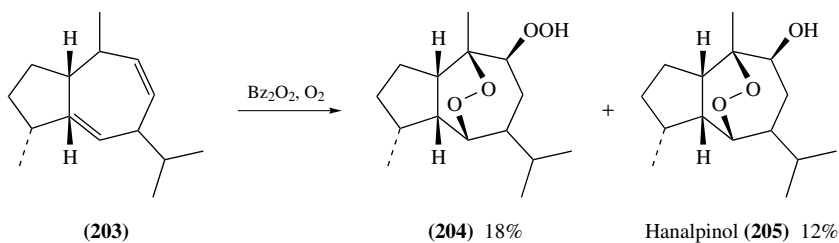
The syntheses of cyclic peroxides discussed in Section II.A.3 involve the generation of peroxy-radicals from hydroperoxides. An alternative approach that avoids handling and storing labile hydroperoxides is based on the generation of peroxy-radical through addition of triplet oxygen to carbon-centered radicals. In particular instances, the incipient carbon-centered radical is obtained in an all-homolytic autoxidation process. For example, autoxidation of carota-1,4-dien-14-al (**197**) afforded the bridged tricyclic peroxide-hydroperoxide **198** in 57% yield (Scheme 45)¹⁹²⁻¹⁹⁴. The radical chain mechanism is initiated by a spontaneous hydrogen atom abstraction from substrate **197** to



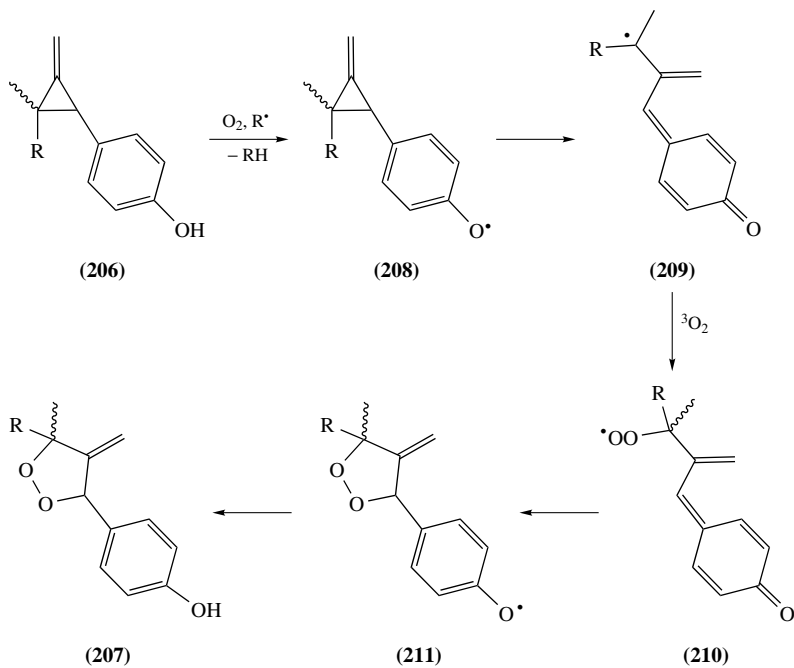
SCHEME 45

generate the incipient carbon radical **200a**. Subsequent entrapment of the mesomeric radical **200b** by triplet oxygen affords peroxy-radical **201**. Transannular 6-*exo*-cyclization followed by addition of a second equivalent of oxygen gives peroxy-radical **202**, and, after hydrogen atom abstraction, e.g. from starting material **197**, the product **198** along with free radical **200** that continues the chain. Chemoselective reduction of the hydroperoxy-function in **198** affords the naturally occurring rugosal A (**199**) (Scheme 45)^{193, 194}. In a similar process, dibenzoyl peroxide initiated autoxidation of guaia-6,9-diene (**203**) at 60 °C provides a mixture of structurally related hydroperoxide-endoperoxide **204** (18%) and natural cyclic peroxide hanalpinol (**205**) (12%) (Scheme 46)¹⁹⁵.

High-yielding autoxidative ring-enlargements of *para*-hydroxyphenylcyclopropanes **206** to the corresponding 1,2-dioxolanes **207** were considered to involve radical intermediates **208–211** (Scheme 47)¹⁹⁶. Autoxidation of a series of cyclopropylanilines **212** on exposure to atmospheric oxygen gives the corresponding 3-anilino-1,2-dioxolanes **213** as a mixture of diastereomers (*trans/cis* ca 55:45) (Scheme 48)¹⁹⁷. Presumably this reaction, which does not apply to *N*-substituted derivatives of **212**, follows an all-homolytic

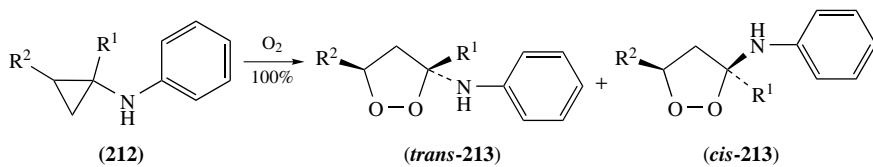


SCHEME 46

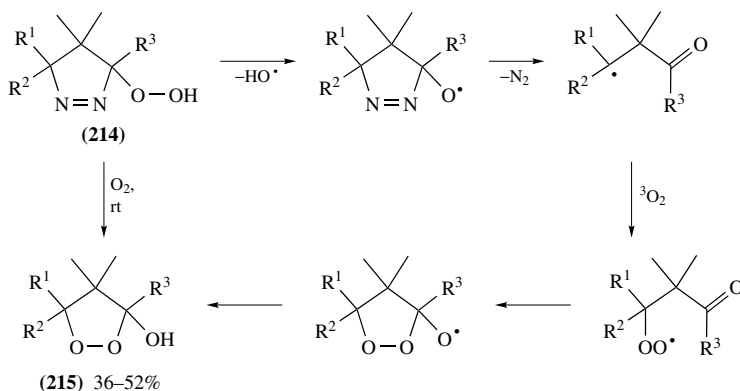


R = Me or Ph

SCHEME 47

(a) $\text{R}^1 = \text{R}^2 = \text{H}$ (b) $\text{R}^1 = \text{Me}, \text{R}^2 = \text{H}$ (c) $\text{R}^1 = \text{H}, \text{R}^2 = \text{Me}$ (*cis*- or *trans*-)

SCHEME 48



SCHEME 49

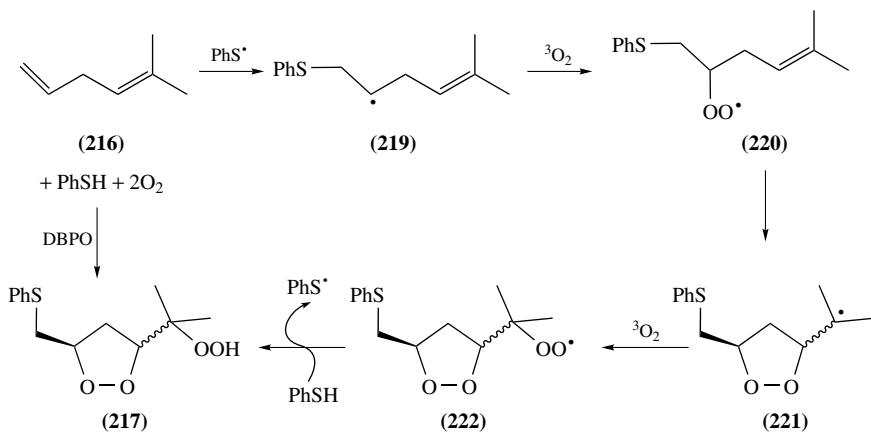
process including an oxidative ring opening of the cyclopropane ring¹⁹⁷. Pentasubstituted 3-hydroxy-1,2-dioxolanes **215** were obtained in moderate yields through homolysis of α -azohydroperoxides **214** under pure oxygen, probably by the mechanism described in Scheme 49^{198, 199}.

5. Thiol and selenyl radical-mediated domino reactions of dienes and of vinylcyclopropanes with triplet oxygen

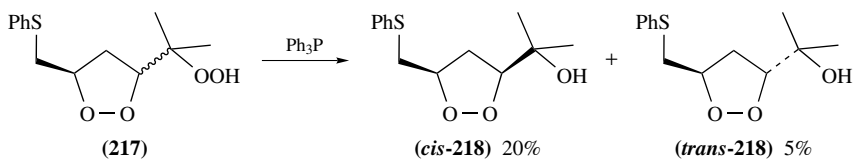
In the reactions described in Section II.A.4, the starting materials are characterized by particular structural and electronic features that favor a rapid generation of the incipient carbon-centered radicals. Regioselective addition of exogenous radicals to a terminal double bond of suitably engineered compounds provides a general method for the generation of carbon-centered radicals, designated to act as propagators of oxidative chain reactions leading to cyclic peroxides. Additional synthetic economy can be gained if the incipient carbon-centered radical is produced through the addition of an exogenous radical, for example PhS^\bullet (Scheme 53), that can be instrumental in a particular stage of a multi-step synthesis of functionalized cyclic peroxides as in Scheme 55.

Beckwith and coworkers were the first to apply the classical thiol-olefin co-oxygenation (TOCO) reaction^{200, 201} to the construction of cyclic peroxides, namely of 1,2-dioxolanes (Scheme 50)²⁰². In this reaction 5-methylhexa-1,4-diene (**216**), thiophenol and triplet oxygen are converted in a single domino radical reaction, initiated by DBPO, into hydroperoxide-endoperoxide **217** (Scheme 50a). *In situ* chemoselective reduction with Ph_3P resulted in a mixture of *cis*-3,5-disubstituted-1,2-dioxolane *cis*-**218** (major product) and its *trans*-isomer *trans*-**218** (minor product) (Scheme 50b). The incipient carbon-centered radical **219**, which is generated through the regioselective addition of phenylthiyl radical to the less substituted terminus of the $\text{C}=\text{C}$ bond, is trapped by triplet oxygen to give the acyclic peroxy-radical **220**. Subsequent 5-*exo*-cyclization affords the cyclic carbon-centered radical **221**, which is trapped by a second molecule of $^3\text{O}_2$ to give peroxy-radical **222**. The latter abstract hydrogen from thiophenol, producing a mixture of the epimeric hydroperoxide-endoperoxides **217** and phenylthiyl radical that continues the chain (Scheme 50a). While a similar TOCO reaction with 1,1-bis(vinyl)cyclohexane produces the corresponding 1,2-dioxolane (42%), the unsubstituted parent penta-1,4-diene failed to give the corresponding peroxide²⁰². Similar co-oxygenations of PhSH with trienes **223** and **225** afford the 3,5-*cis*-substituted 1,2-dioxolanes **224** and **226**, respectively (Scheme 51)^{203, 204}.

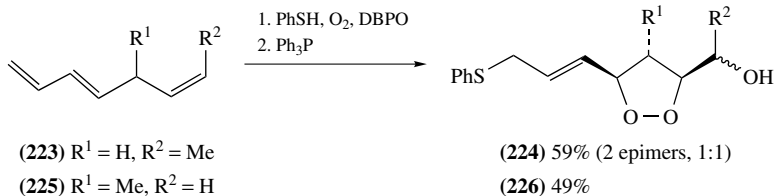
(a)



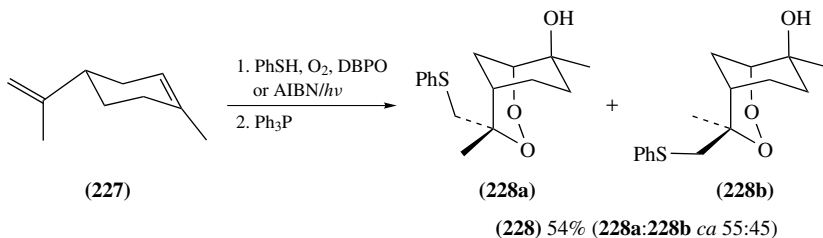
(b)



SCHEME 50



SCHEME 51



SCHEME 52

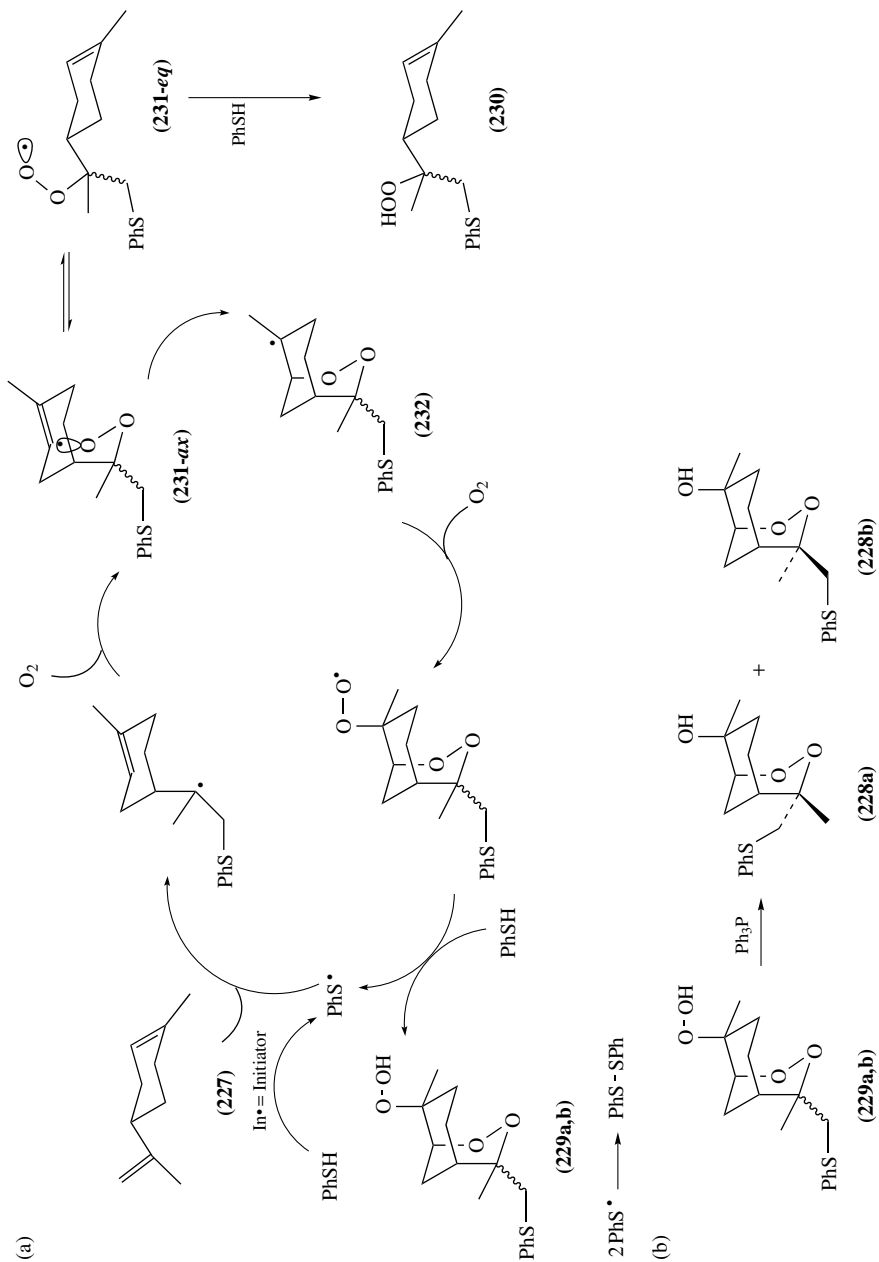
More recently, Bachi and coworkers extended and adapted the TOCO reaction to the synthesis of 2,3-dioxabicyclo[3.3.1]nonane derivatives like **228** (Scheme 52)^{205,206}. As detailed in Scheme 53a, the bridged bicyclic hydroperoxide-endoperoxides like **229** are obtained, from (*S*)-limonene (**227**), in a 4-component one-operation free-radical domino reaction in which 5 new bonds are sequentially formed. Particular experimental conditions are required in order to reduce the formation of by-products **230** and (PhS)₂, and to favor the critical 6-*exo*-ring closure of peroxy-radical **231** to carbon-centered radical **232**²⁰⁶. *In situ* chemoselective reduction of bridged bicyclic hydroperoxide-endoperoxides **229a** and **229b** gives the corresponding β -sulfanyl hydroxy-endoperoxides **228a** and **228b** which differ in the arrangement of substituents at C4 of the bicyclic system (Scheme 53b). The TOCO reaction of (*R*)-limonene (**233**) to give β -sulfanyl endoperoxides **234–239** is more effective when mediated by aromatic thiols than when mediated by aliphatic thiols (Scheme 54)²⁰⁶. Substitution of the methyl group of limonene **233** by the phenyl group as in **240** results in acceleration of the TOCO reaction and in a remarkable increase in yield of the corresponding bicyclic peroxide (72% for **241** as compared with 55% for **234**)²⁰⁷. Cyclic peroxides like **228a,b** and **234a,b** served as intermediate compounds for the synthesis of potent antimalarial endoperoxides like **242a**, **243a** and **243b** (Chart 2)^{208–210}.

The straightforward synthesis of β -sulfanyl-endoperoxides **228a** and **228b** from (*S*)-limonene (**227**) paved the way for an efficient total synthesis of the antimalarial natural product yingzhaosu A (**5**) as outlined in Scheme 55^{211,212}. Dehydration of **228a** and **228b** with SOCl₂/pyridine followed by low-temperature selective oxidation with *m*-CPBA affords a mixture of 8 isomeric β -sulfanyl endoperoxides **244**. Treatment of this mixture with TFAA and 2,6-lutidine gives, through a Pummerer rearrangement, unsaturated aldehydes **245** and **246**. Low-temperature hydrogenation of aldehydes **245** over PtO₂ in ethyl acetate at $-11\text{ }^{\circ}\text{C}$ to $-12\text{ }^{\circ}\text{C}$ proceeds chemo- and stereoselectively to give the single saturated aldehyde **247**. Subsequent TiCl₄-mediated Mukaiyama-type aldol reaction with bis(trimethylsilyl) enol ether **248** followed by *in situ* dehydration under mild basic conditions affords the unsaturated ketone **249**, which was diastereoselectively reduced to the yingzhaosu A (**5**). Thus, overall yield of **5** from *S*-limonene (**227**) (Schemes 52 and 55) is 7.3%²¹².

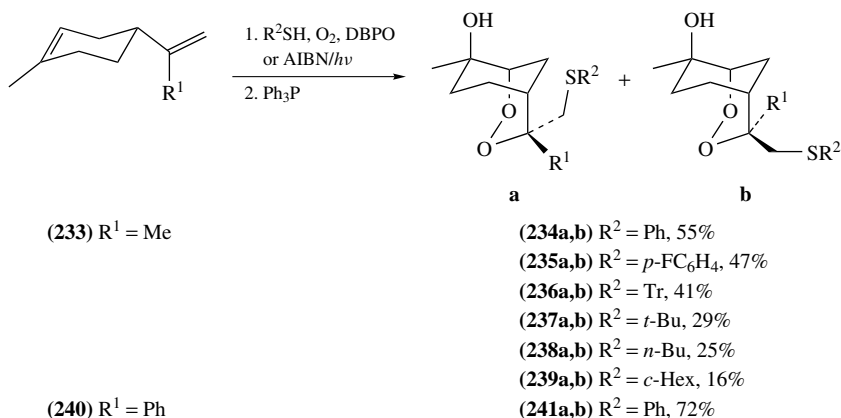
Feldman and Parvez widened the scope of the TOCO reaction for the synthesis of endoperoxides by the incorporation into the sequential free radical process of a cyclopropylcarbiny–homoallyl rearrangement. This process opens up an avenue to the synthesis of a variety of sulfur-free five-membered cyclic peroxides, starting from alkenylcyclopropane precursors^{213,214}. Thus, diphenyl diselenide- and diphenyl disulfide-catalyzed oxygenation of cyclopropane **250** afford stereoselectively *cis*-3-vinyl-5-phenyl-1,2-dioxolane (**251**) in good yield through the sequential free-radical process shown in Scheme 56^{213–215}. Ph₂Se₂-promoted TOCO reactions with 2-vinylcyclopropyl esters **252** give mixtures of *cis*- and *trans*-dioxolanes **253** (Scheme 57). When the ester group is directly linked to the cyclopropyl ring as in **252a–d**, a pronounced 3,5-*trans*-diastereoselectivity is observed^{214,216,217}, while *cis*-diastereoselectivity is observed in the same reaction with the vinylogous esters **252e** and **252f**^{214,216,217}. Ph₂Se₂-promoted oxygenation of tricyclopropane **254** results in the formation of mono-1,2-dioxolane **255**, while the tris(dioxolane) **256** is obtained upon Ph₂S₂-catalysis (Scheme 58)^{214,216}. Oxygenation of vinylspirocyclopropanes **257** under AIBN/UV-irradiation in the presence of Ph₂Se₂ or Ph₂S₂ leads to spiro-1,2-dioxolanes **258** in moderate to good yield (Scheme 59)²¹⁸.

6. Peroxidation of vinylcyclopropanes and 1,5-dienes mediated by Co(II)/Et₃SiH

The formal addition of hydrogen atom to the terminal double bond of vinylcyclopropanes and of 1,5-diene systems under triplet oxygen provides another sequential



SCHEME 53



SCHEME 54

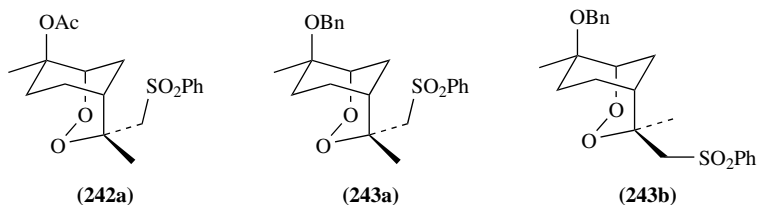


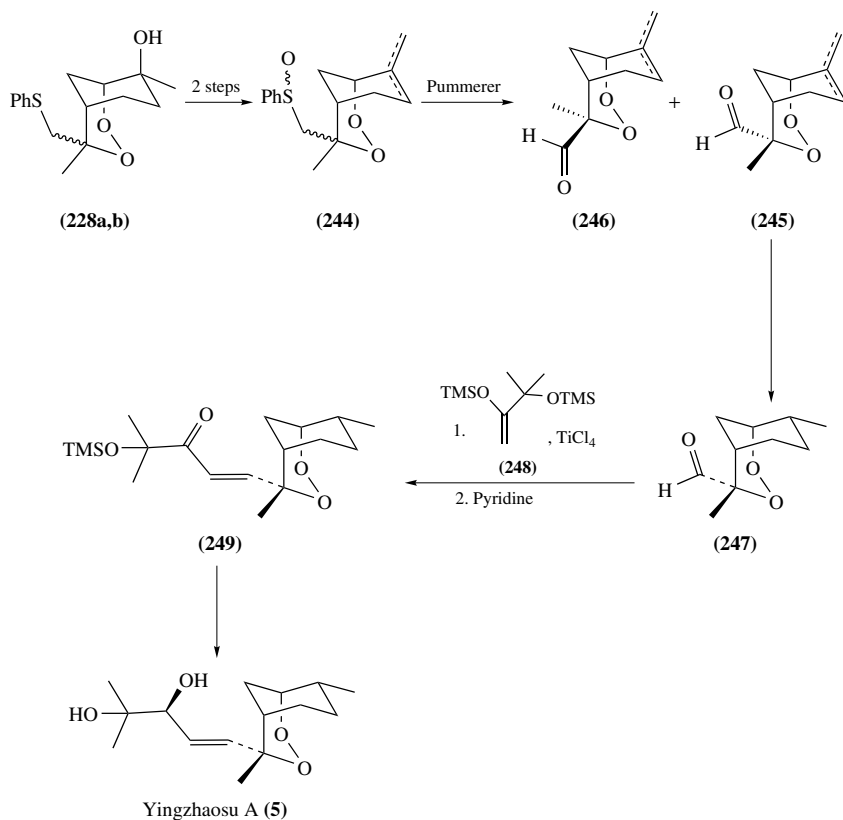
CHART 2

reaction useful for the synthesis of cyclic peroxides. Thus, treatment of vinylcyclopropane **250** with triethylsilane and 7% $\text{Co}(\text{modp})_2$ catalyst under oxygen atmosphere results in the formation of the triethylsiloxy-substituted 1,2-dioxolane **259** (Scheme 60)^{219, 220}. The analogous reaction with (*S*)-limonene **227** affords, after acidic deprotection, a mixture of the bridged bicyclic peroxide **260** (22%) and hydroperoxide **261** (36%) (Scheme 61a). Neat alkenyl hydroperoxide **261** undergoes spontaneous, albeit slow, autoxidation to the same endoperoxide **260**²²⁰.

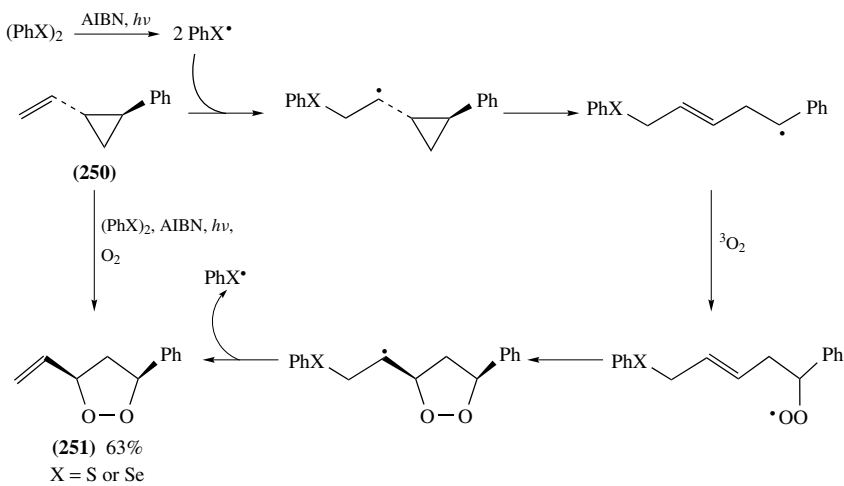
Regioselective hydrogen atom transfer from $\text{Co}(\text{III})$ -hydride complex gives carbon-centered radical **262**, which adds to triplet oxygen leading to peroxy-radical **263** and then, through intermediates **264**, **265** and **266**, to the silylated peroxide **267**, which after desilylation affords the yingzhaosu A analogue **260** (Scheme 61b)²²⁰. Peroxidation of 1,5-diene **268** with Et_3SiH and $\text{Co}(\text{modp})_2$ catalyst gives a mixture of the open-chain hydroperoxide **269** and the bridged bicyclic peroxide **270** (Scheme 62)²²⁰. It was postulated that this reaction follows the mechanism detailed in Scheme 61a for the peroxidation of limonene **227**²²⁰. Such a mechanism would involve ring closure of peroxy-radical **271** to give bridged bicyclic peroxide **270**, thus providing a rare example for peroxy-radical addition to an electron-deficient double bond.

7. Halogen-mediated synthesis of cyclic peroxides through free radical chain reactions

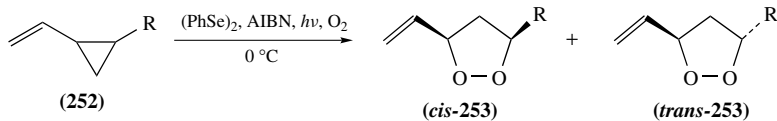
Haloperoxidation of unsaturated hydroperoxides based on heterolytic ring closure is extensively discussed in Section II.B.2. Herein, halogen-mediated peroxidations involving



SCHEME 55

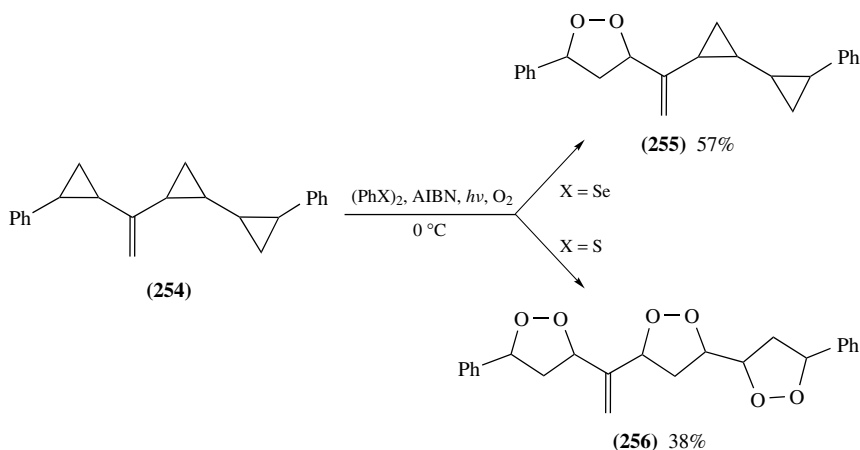


SCHEME 56

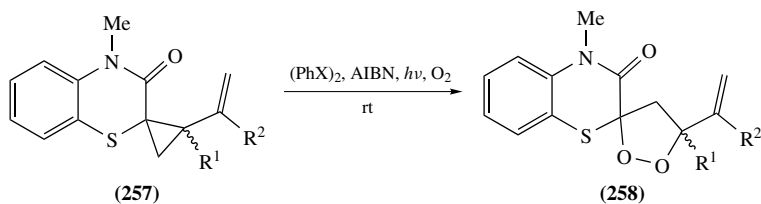


- | | |
|---|--------------------------------------|
| (a) R = CO ₂ Bu- <i>t</i> | (a) 66% (<i>cis/trans</i> , 1:1.8) |
| (b) R = COSPh | (b) 46% (<i>cis/trans</i> , 1:3.4) |
| (c) R = CO ₂ Ph | (c) 63% (<i>cis/trans</i> , 1:3.0) |
| (d) R = CO ₂ CH(CF ₃) ₂ | (d) 70% (<i>cis/trans</i> , 1:6.0) |
| (d) R = CO ₂ CH(CF ₃) ₂ , (-50 °C) | (d) 70% (<i>cis/trans</i> , 1:10.0) |
| (e) R = (<i>E</i>)-CH=CHCO ₂ Me | (e) 44% (<i>cis/trans</i> , 6.5:1) |
| (f) R = (<i>E</i>)-CH=CHCO ₂ CH(CF ₃) ₂ | (f) 58% (<i>cis/trans</i> , 2.2:1) |

SCHEME 57



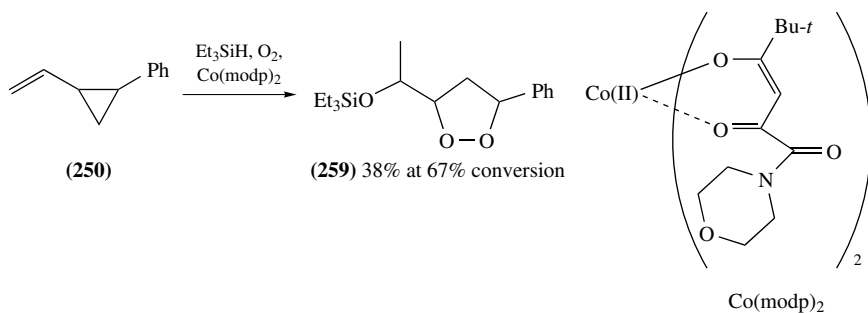
SCHEME 58



R¹, R² = Me or Ph, X = S or Se

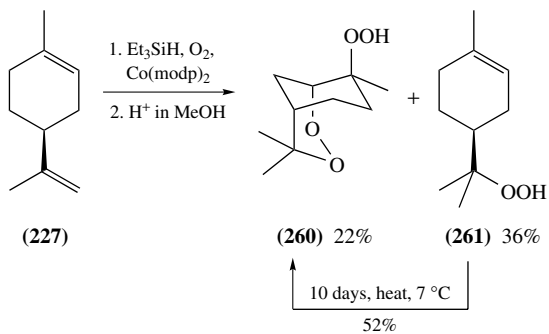
SCHEME 59

homolytic processes are described. Thus, treatment of hydroperoxide **158** with *N*-iodosuccinimide (NIS) affords the *trans*-isomer of iodomethyldioxolane **272** through a 5-*exo* homolytic cyclization (Scheme 63, compare with Scheme 38)^{165, 221}. Similarly, NIS-mediated cyclization of unsaturated hydroperoxide **273** affords the bridged bicyclic

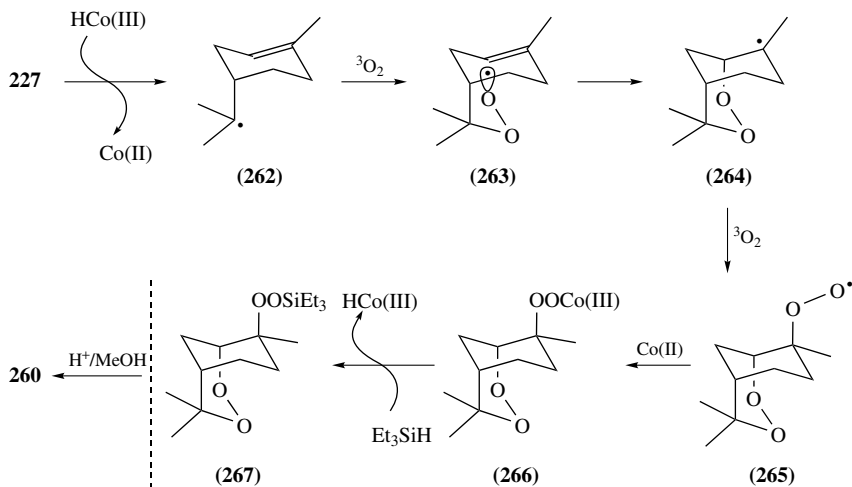


SCHEME 60

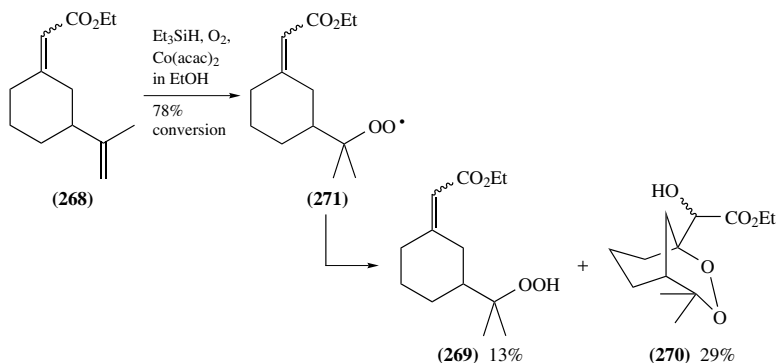
(a)



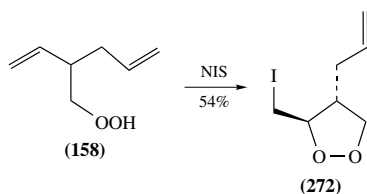
(b)



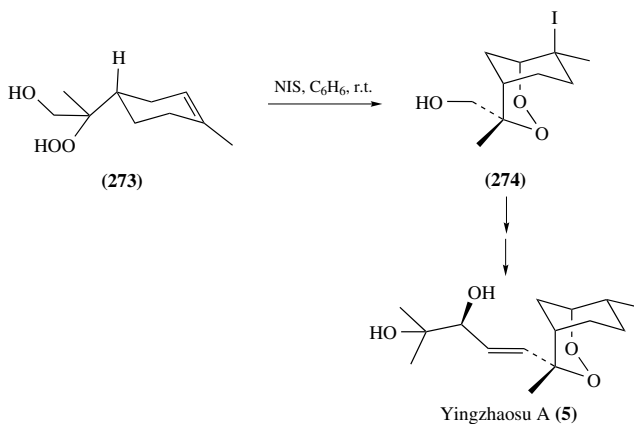
SCHEME 61



SCHEME 62



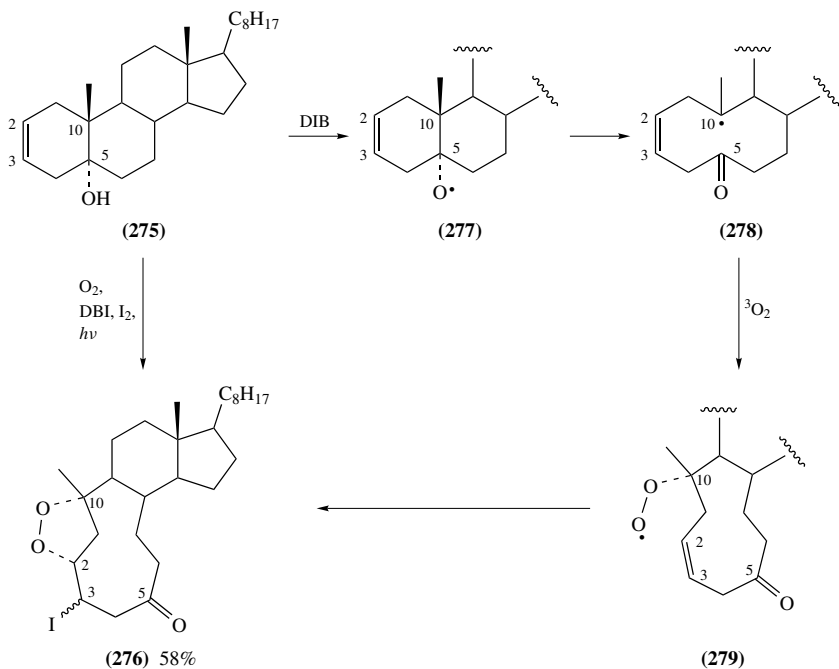
SCHEME 63



SCHEME 64

peroxide **274**, which was used as a key intermediate in a total synthesis of yingzhaosu A (**5**) (Scheme 64)²²².

Diacetoxyiodobenzene (DIB) in combination with iodine is an efficient reagent for iodoperoxidation of some tertiary hydroxy steroid derivatives^{223, 224}. For example, visible light irradiation of steroid alcohol **275** with DIB/I₂ under oxygen atmosphere induces a homolytic cascade reaction, leading to the fused 1,2-dioxolane **276** in good yield (Scheme 65). The incipient alkoxy radical **277** undergoes a homolytic β -cleavage to the



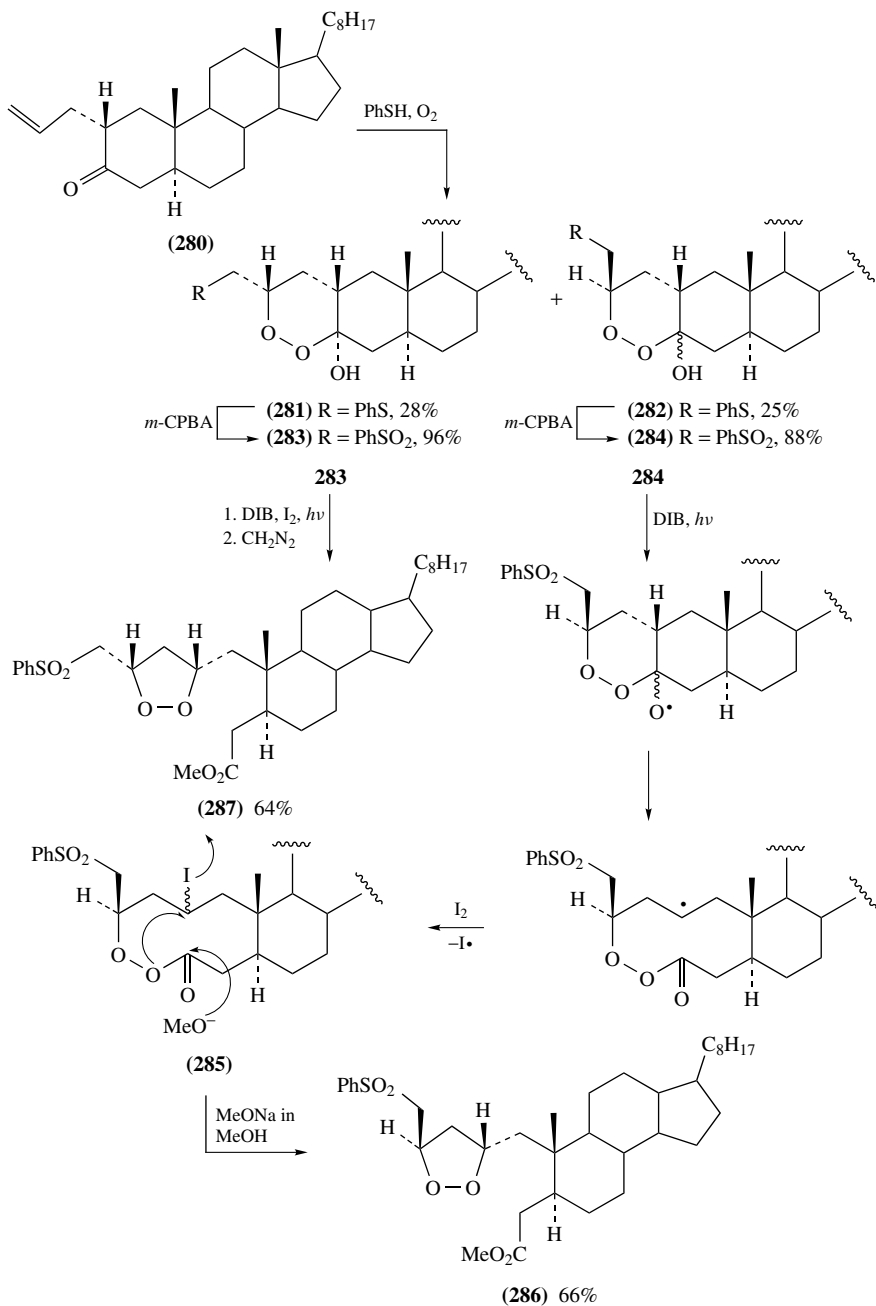
SCHEME 65

carbon-centered radical **278**, which is trapped by triplet oxygen to give peroxy-radical **279** that undergoes a iodinative ring closure to give the iododioxolane **276** (Scheme 65)^{223, 224}.

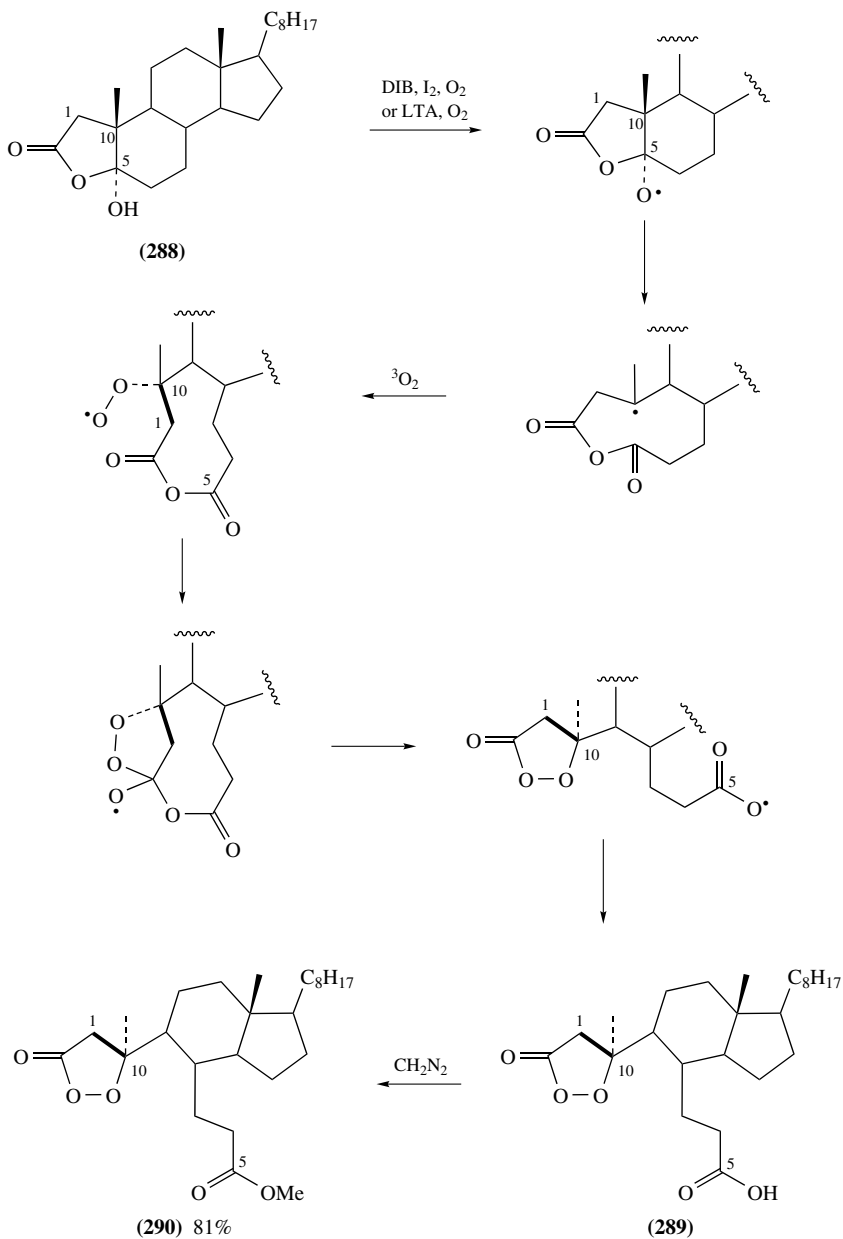
Scheme 66 describes a rather elaborate set of reactions. Hydroxyl-carrying epimeric cyclic peroxides like **281** and **282** were obtained by the thiol olefin co-oxygenation of steroid derivative **280**^{225, 226}. In principle, such a reaction can be either all homolytic (see Section II.A.5), or it can involve a homolytic TOCO reaction leading to a hydroperoxide intermediate which subsequently ring closes through a heterolytic addition to a carbonyl group (see Section II.B.3). Sulfone-endoperoxides **283** and **284**, obtained by oxidation of sulfides **281** and **282** respectively, carry a tertiary hydroxyl group that is instrumental in the aerobic photolytic DIB/I₂-mediated reactions. Indeed, irradiation of sulfone **284** under oxygen in the presence of DIB and iodine leads stereoselectively to the corresponding macrocyclic peroxides **285**, and eventually to the 1,2-dioxolane **286** in high yield^{225, 226}. Hydroxysulfone **283** under similar exposure to irradiation with DIB/I₂ and subsequent treatment with diazomethane was converted into 1,2-dioxolane **287**, the C3-epimer of **286** (Scheme 66)^{225, 226}. Structurally related steroidal β -peroxylactone ester **290** was obtained in excellent yield from the corresponding ketolactol **288** (Scheme 67)²²⁷⁻²²⁹. Precursor **289** is formed in a single homolytic sequential peroxidation reaction mediated either by DIB/I₂ or by lead tetraacetate (LTA) via the mechanism described in Scheme 67²²⁷⁻²²⁹.

B. Cyclization of Hydroperoxides through Intramolecular Nucleophilic Substitution and Addition

Cyclic peroxides can be prepared from hydroperoxides and their synthetic equivalents through processes involving intramolecular nucleophilic substitution at a carbon



SCHEME 66



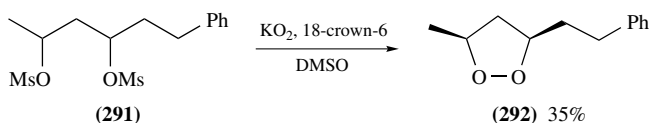
SCHEME 67

atom, as well as through intramolecular nucleophilic addition onto C=C and C=O bonds^{51, 52, 155, 230}.

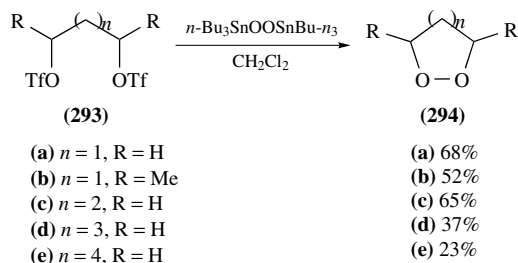
1. Nucleophilic substitution

In 1975 Corey and coworkers reported that bis(mesylate) **291**, upon treatment with potassium superoxide (KO₂) as a hydrogen peroxide precursor, is converted into 2,5-*cis*-disubstituted 1,2-dioxolane **292** in moderate yield (Scheme 68)²³¹. Salomon and Salomon synthesized a series of monocyclic 5–8 membered endoperoxides **294a–e** from the corresponding bis(triflates) **293a–e** and bis(tributyltin) peroxide (Scheme 69)²³². Application of this tin peroxide transfer reagent for the conversion of cyclopentane-1,3-bis(triflate) (**295**) into 2,3-dioxabicyclo[2.2.1]heptane (**20**) failed in solution, but proved to be possible in vacuum, albeit in poor yield (Scheme 70)²³³. Early semisynthetic approaches to naturally occurring prostaglandin endoperoxide PGH₂ methyl ester (**297**) involve the treatment of 1,3-dibromide **296** with KO₂ and 18-crown-6¹⁰, or with anhydrous hydrogen peroxide and silver trifluoroacetate (Scheme 71)^{11, 12}. Silver trifluoroacetate and H₂O₂ were used also for the synthesis of prostaglandin endoperoxide PGG₂ (**2b**)¹³ and of a series of cyclic peroxides, containing the 2,3-dioxabicyclo[2.2.1]heptane system²³⁴.

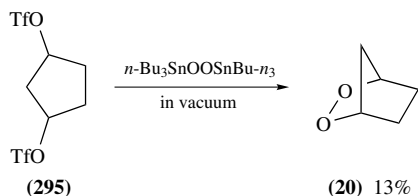
β -Bromohydroperoxides **299** that are readily available from the corresponding cyclopropanes **298** cyclize in good yield into 1,2-dioxolanes **300** on treatment with silver(I) oxide (Scheme 72)²³⁵. Ozonolysis of unsaturated iodide **301** in methanol gives



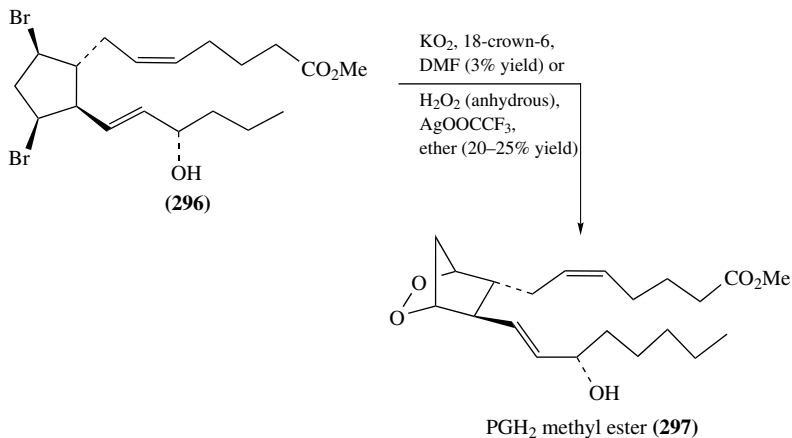
SCHEME 68



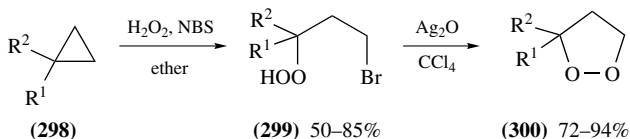
SCHEME 69



SCHEME 70

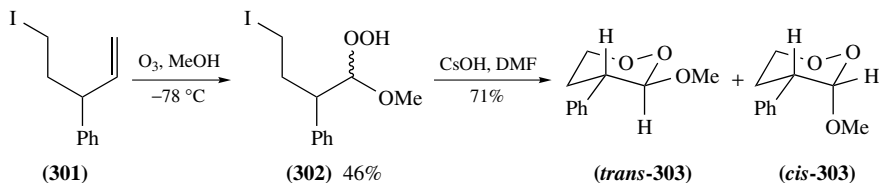


SCHEME 71



R¹ = Ph or *p*-BrC₆H₄, R² = H, Me or Ph

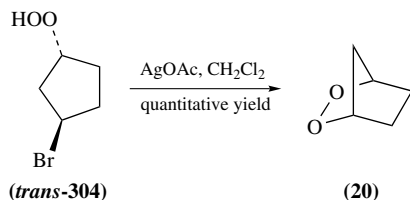
SCHEME 72



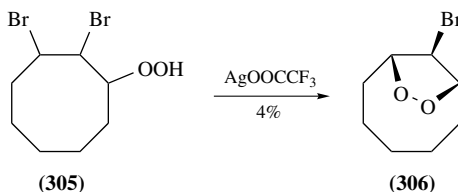
SCHEME 73

the hydroperoxy acetal **302** that yields a diastereomeric mixture of *trans*-**303** and *cis*-**303** (total 71%, *trans/cis* 63:37) on treatment with CsOH in DMF (Scheme 73)²³⁶. While silver acetate promotes a fast and quantitative formation of bicyclic endoperoxide **20** from *trans*- β -bromohydroperoxide *trans*-**304** (Scheme 74), the parallel reaction with its *cis*-isomer is sluggish²³⁷. The structurally more complex bridged bicyclic bromodioxolane **306** was obtained, albeit in very poor yield, by silver(I)-promoted ring closure of 2,3-dibromocyclooctyl hydroperoxide (**305**) (Scheme 75)²³⁸.

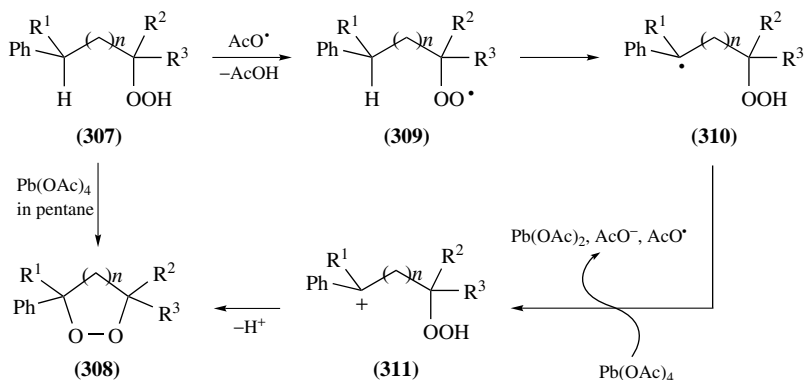
ω -Phenylhydroperoxides **307a–h** are converted into the corresponding 5–7-membered cyclic peroxides **308a–h**, in variable yields, upon treatment with lead tetraacetate (Scheme 76)^{239,240}. The best yields were observed for the endoperoxides **308d** (76%) and **308e** (66%)²³⁹. A plausible mechanism that may conform with the yield distribution of products **308** involves the transitory intermediates **309–311** (Scheme 76). Singlet



SCHEME 74



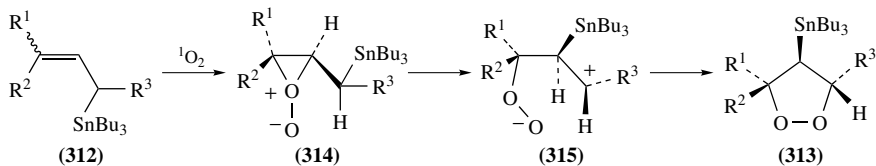
SCHEME 75



- (a) $n = 1$, $R^1 = \text{H}$, $R^2 = R^3 = \text{Me}$, 15%
 (b) $n = 1$, $R^1 = \text{H}$, $R^2 = R^3 = \text{Ph}$, 17%
 (c) $n = 1$, $R^1 = R^2 = R^3 = \text{Me}$, 27%
 (d) $n = 1$, $R^1 = \text{Ph}$, $R^2 = R^3 = \text{Me}$, 76%
 (e) $n = 1$, $R^1 = R^2 = R^3 = \text{Ph}$, 66%
 (f) $n = 2$, $R^1 = R^2 = R^3 = \text{Me}$, 22%
 (g) $n = 2$, $R^1 = \text{Ph}$, $R^2 = R^3 = \text{Me}$, 45%
 (h) $n = 3$, $R^1 = R^2 = R^3 = \text{Me}$, 10%

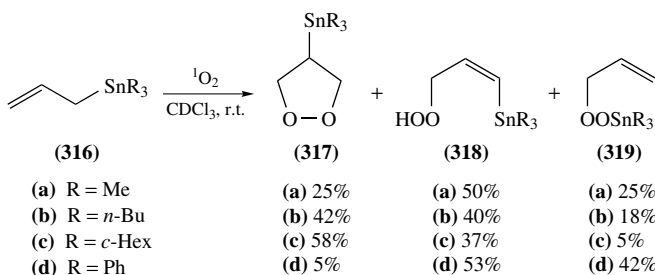
SCHEME 76

oxygen dioxygenation of chiral allylstannanes **312** affords stereoselectively 4-stannyl-3,5-disubstituted 1,2-dioxolanes **313** in variable yields (Scheme 77)^{241–243}. It was suggested that intermediate perepoxides **314** derived from the anti- S_E2' attack of $^1\text{O}_2$ on allylstannanes **312** rearrange through 1,2-migration of stannyl group to transient zwitterions **315**, which undergo cyclization to endoperoxides **313** (Scheme 77)^{242, 243}. No



- | | |
|---|---------|
| (a) $\text{R}^1 = E\text{-C}_5\text{H}_{11}$, $\text{R}^2 = \text{H}$, $\text{R}^3 = \text{CH}_2\text{CO}_2\text{Me}$ | (a) 15% |
| (b) $\text{R}^1 = E\text{-C}_5\text{H}_{11}$, $\text{R}^2 = \text{H}$, $\text{R}^3 = \text{OMOM}$ | (b) 0% |
| (c) $\text{R}^1 = \text{H}$, $\text{R}^2 = Z\text{-C}_5\text{H}_{11}$, $\text{R}^3 = \text{OMOM}$ | (c) 58% |
| (d) $\text{R}^1 = Z\text{-C}_5\text{H}_{11}$, $\text{R}^2 = \text{H}$, $\text{R}^3 = \text{OAc}$ | (d) 0% |
| (e) $\text{R}^1 = E\text{-C}_5\text{H}_{11}$, $\text{R}^2 = \text{Me}$, $\text{R}^3 = \text{OMOM}$ | (e) 46% |

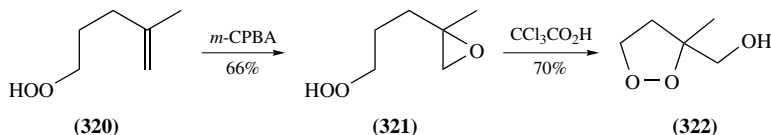
SCHEME 77



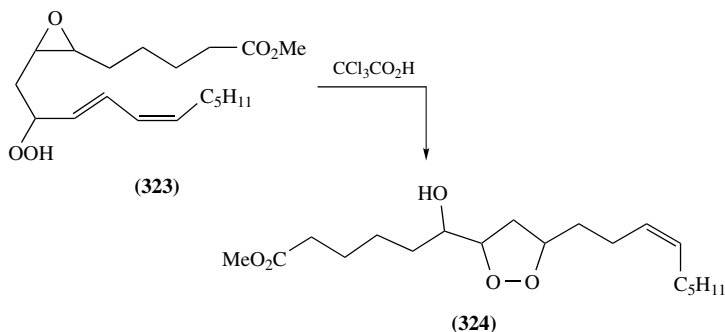
SCHEME 78

formation of endoperoxides was observed in reactions of structurally related allylsilanes with $^1\text{O}_2$ ²⁴³. In the photooxygenation of the simple allylstannanes **316** three types of products, namely **317–319**, are obtained. They derive respectively from a formal cycloaddition of $^1\text{O}_2$ to substrates **316**, a common H-ene-reaction of **316** with $^1\text{O}_2$ and H-ene-reaction followed by 1,5-translocation of the stannyl fragment (Scheme 78)^{244–246}. The yields of 1,2-dioxolanes **317** were found to be highly dependent on the tin ligands R, for example 5% (**317d**, R = Ph) and 58% (**317c**, R = *c*-Hex)²⁴⁶. Increase in the yield of **317c** (75%) was observed upon photooxygenation of **316c** at -78°C , whereas substituting the solvent CDCl_3 by a $\text{CDCl}_3/\text{MeCN}$ mixture decreases the yield of dioxolane **317c** to 33%²⁴⁶.

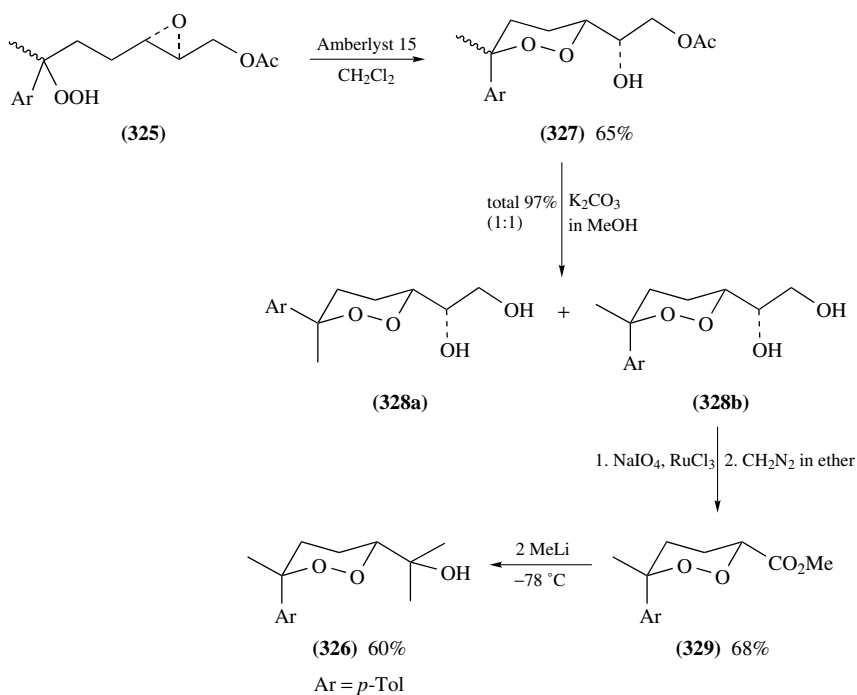
Acid-catalyzed intramolecular attack of nucleophilic hydroperoxide function on an oxirane ring results in formation of 3-(1-hydroxyalkyl)endoperoxides. For example, epoxidation of unsaturated hydroperoxide **320** affords oxirane-hydroperoxide **321** (66%), which through acid-catalyzed regioselective cyclization gives 1,2-dioxolane **322** (70%) (Scheme 79)¹⁶⁴. This type of reaction is applicable also to a more complex epoxide-hydroperoxide such as **323**, which cyclizes to polyfunctionalized 5-membered cyclic



SCHEME 79



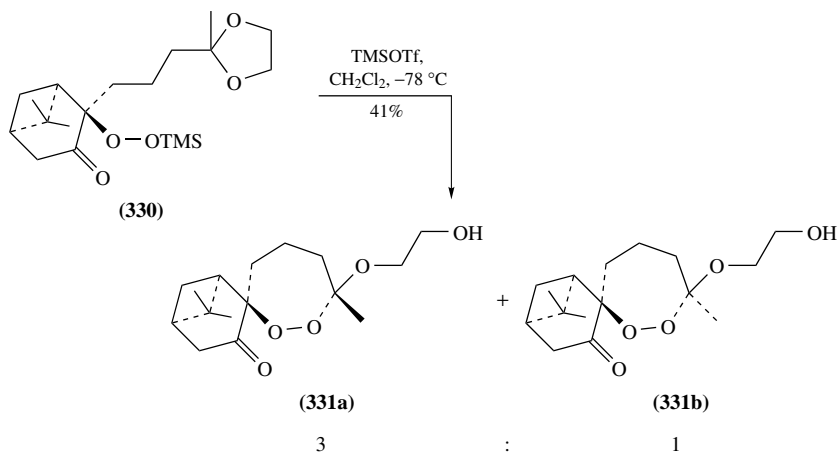
SCHEME 80



SCHEME 81

peroxide **324** (Scheme 80)¹⁶⁴. Chiral epoxide-hydroperoxide **325** was used as a key intermediate in the total synthesis of naturally occurring peroxide yingzhaosu C (**326**) (Scheme 81)^{247, 248}. Cyclization of **325** results in a diastereomeric mixture of 3,6,6-trisubstituted 1,2-dioxanes **327** (65%, *ca* 1:1), which is quantitatively deacetylated to the dihydroxy derivatives **328a** and **328b**. Oxidative cleavage followed by *in situ* esterification of diol **328b** gives the ester-endoperoxide **329** in good yield. Treatment of ester **329** with 2 equivalents of MeLi at -78°C affords the non-racemic yingzhaosu C (**326**). In addition to the natural product **326**, other stereoisomers were also synthesized^{247, 248}.

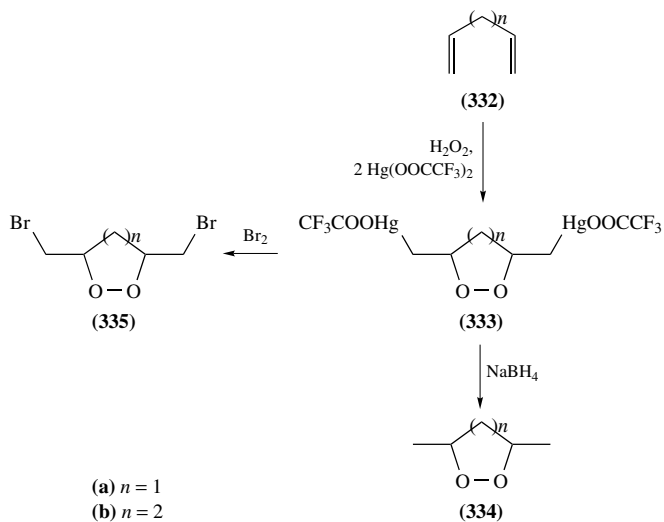
Synthesis of 7-membered spirobicyclic peroxides **331a** and **331b**, which belong to the cardamom peroxide (**7**) family, was recently accomplished through TMSOTf-catalyzed intramolecular peroxy-reacetalization of the 1,3-dioxolane moiety with the nucleophilic silylperoxide function in precursor **330** (Scheme 82)²⁴⁹.



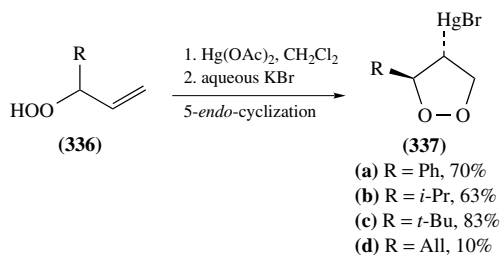
SCHEME 82

2. Nucleophilic addition to carbon-carbon double bonds

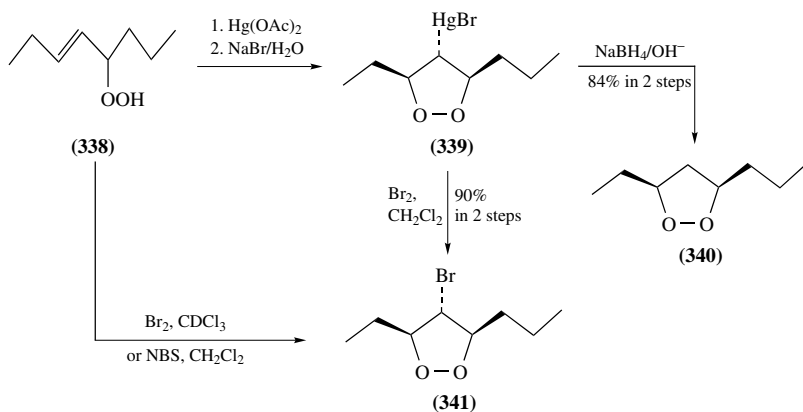
Intramolecular electrophile-assisted peroxidation of electron-rich C=C bonds with hydroperoxides proved to be a useful general method for preparation of a variety of 5- and 6-membered cyclic peroxides. Mercury salts and various sources of positively charged halogen are commonly used as electrophiles in processes of this type. For example, peroxymercuration of dienes **332a** and **332b** with anhydrous H₂O₂ and mercury trifluoroacetate lead to bis(mercurated) 1,2-dioxolane **333a** and 1,2-dioxane **333b**, respectively^{250–252}. Both 5- and 6-membered cyclic peroxides **333** can be reduced with NaBH₄ to parent endoperoxides **334** or brominated to the dibromo derivatives **335** (Scheme 83)^{250–252}. In contrast to peroxy-radical cyclizations which follow exclusively 5- and 6-*exo-trig* mode, electrophile-mediated intramolecular additions of hydroperoxides to the C=C bond frequently proceed through 5-*endo* mode^{253–256}. For example, mercuration followed by ligand exchange of allylic hydroperoxides **336** afford mercurated 1,2-dioxolanes **337** (Scheme 84)^{253, 256}. Similarly, peroxymercuration of disubstituted allylic hydroperoxide **338** leads to 3,5-*cis*-disubstituted 1,2-dioxolane **339**, which on reduction gives **340** and on bromination affords **341** in excellent yields (Scheme 85)²⁵⁵. The bromo derivatives **341** can be directly obtained from hydroperoxide **338** on treatment with molecular bromine or with NBS (Scheme 85)^{254, 255}. Additional examples of mercury salt mediated 5-*endo* cyclization of allylic hydroperoxides were reported^{255–257}. Intramolecular peroxymercuration of homoallylic hydroperoxides **342** follow the 5-*exo* mode, giving in high yield the corresponding mercurated 1,2-dioxolanes **343**, which can be subsequently hydridodemercurated to the corresponding cyclic peroxides **344** (Scheme 86)^{174, 175, 253, 256, 258}. Additional related 5-*exo*-cycloperoxyhalogenations of homoallylic hydroperoxides with NBS and NIS were reported^{165, 221, 259}. More rare examples of 5-*exo*-cycloperoxychlorination of homoallylic hydroperoxides **345** to the corresponding chlorinated 1,2-dioxolanes **346** are shown in Scheme 87²⁶⁰. High-yielding



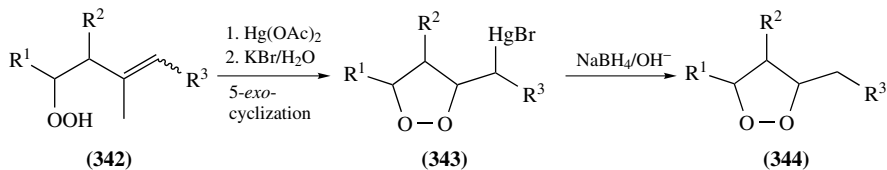
SCHEME 83



SCHEME 84

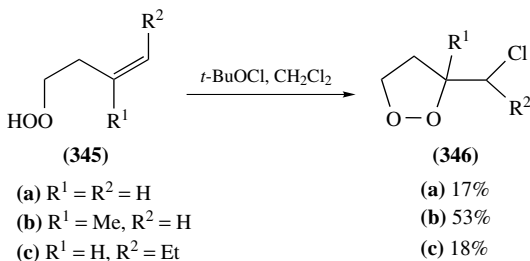


SCHEME 85

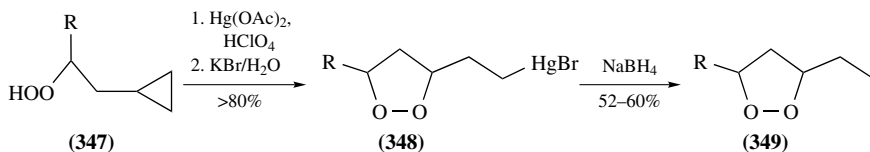


$R^1 = R^2$ and $R^3 = \text{H, Alk or Ar}$

SCHEME 86

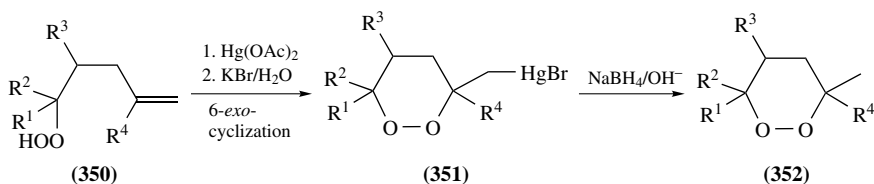


SCHEME 87



$R = \text{Me, Et, } i\text{-Pr, } c\text{-Hex}$

SCHEME 88



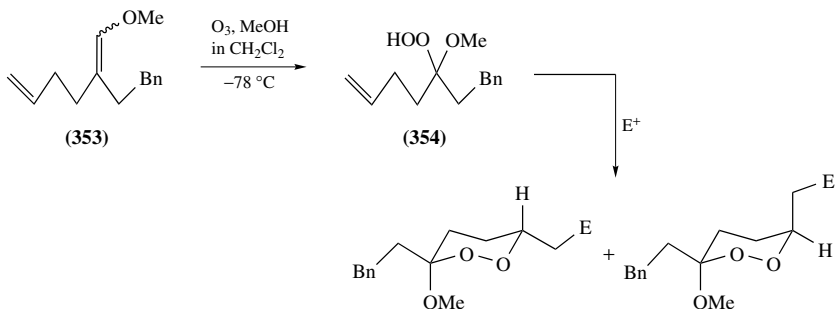
R^1, R^2, R^3 and $R^4 = \text{H, Alk or Ar}$

SCHEME 89

mercury(II)-mediated 5-*exo*-cyclizations of β -hydroperoxyalkylcyclopropanes **347** afford 3-(β -bromomercurioethyl)-1,2-dioxolanes **348**, which are conventionally reduced by NaBH_4 to mercury-free endoperoxides **349** (Scheme 88)²⁶¹.

A series of 1,2-dioxanes **352** were prepared, in moderate to high yield, by cycloperoxymercuration 6-*exo* ring closure of unsaturated hydroperoxides **350** to mercurated endoperoxides **351** followed by hydridodemercuration (Scheme 89)^{256, 262–264}. Cycloperoxymercuration of *trans*-hexen-4-yl hydroperoxide with $\text{Hg}(\text{NO}_3)_2$ follows concomitant

6-*exo* and 7-*endo* cyclization (*ca* 3:1)²⁵⁸. Unsaturated hydroperoxyketal **354**, readily available by a chemoselective ozonolysis of the enol ether **353** in methanol, undergoes an effective electrophile-assisted cyclization to give 6-iodomethyl-1,2-dioxanes **355** with I₂/pyridine and 6-mercuriomethyl derivatives **356** with mercuric acetate (Scheme 90)²⁶⁵. In contrast to the non-selective peroxyiodination of **354**, the corresponding peroxymercuration was found to be *cis*-stereoselective (*cis*-**356**/*trans*-**356** is *ca* 3:1)²⁶⁵.



E⁺ = I⁺ (I₂/pyridine in CH₂Cl₂, 0 °C)

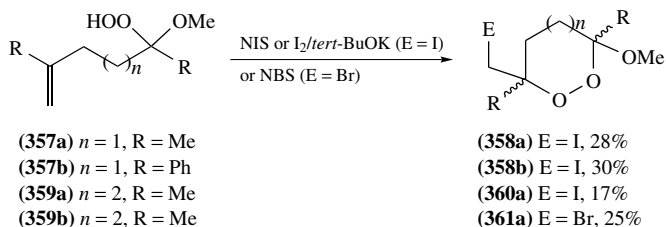
(*cis*-**355**) (total 50%, *cis/trans* 1:1) (*trans*-**355**)

E⁺ = HgBr⁺ [Hg(OAc)₂/KBr, CH₂Cl₂, r.t.]

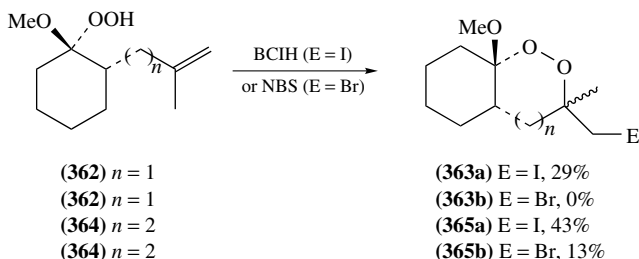
(*cis*-**356**) (total 55%, *cis/trans* 3:1) (*trans*-**356**)

SCHEME 90

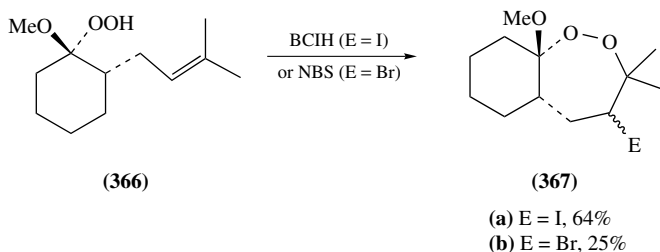
As recently shown by Nojima, McCullough and coworkers, halonium ion-mediated cyclizations of unsaturated hydroperoxyketals provide a general route for the synthesis of a variety of 6- and 7-membered monocyclic, fused and bridged bicyclic peroxides (Schemes 91–94)^{266, 267}. As sources for halonium ions, in addition to the common NIS and NBS, they widely used bis(*sym*-collidine)iodine(I) hexafluorophosphate (BCIH). Thus, on exposure to peroxyiodination, hydroperoxyketals **357a** and **357b** give the corresponding 3-iodomethyl-1,2-dioxanes **358a** and **358b**. The longer chain analogue **359a** affords the 7-membered ring iodoendoperoxide **360a** upon treatment with NIS and the corresponding bromo derivative **361a** when NBS is used (Scheme 91)²⁶⁶. Peroxyhalogenation of ω -unsubstituted unsaturated hydroperoxyketals **362** and **364** with BCIH or NBS lead to cyclization by the 6- and 7-*exo* mode to give the fused bicyclic endoperoxides **363** and **365** respectively (Scheme 92)²⁶⁶. A similar BCIH-mediated 6-*exo* peroxyiodination of *trans*-2-(2-methylprop-2-en-1-yl)cyclohexyl hydroperoxide was reported²⁶⁷. In contrast to the previous examples, BCIH and NBS-induced cyclizations of unsaturated hydroperoxyketal **366**, in which the C=C bond is not terminal, proceed in the 7-*endo* mode



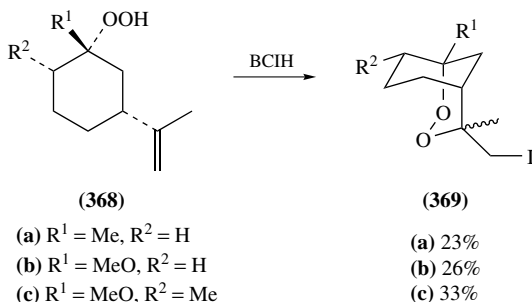
SCHEME 91



SCHEME 92



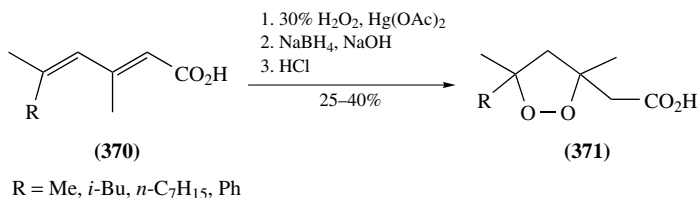
SCHEME 93



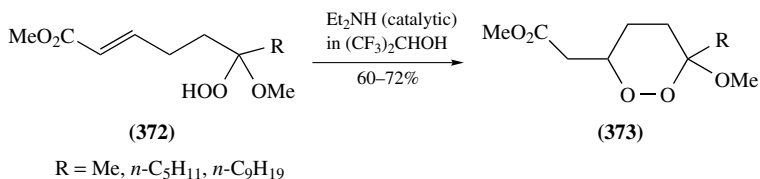
SCHEME 94

to give the 7-membered fused bicyclic peroxides **367a** (64%) and **367b** (25%) respectively (Scheme 93)²⁶⁶. *Cis*-3-isopropenylcyclohexyl hydroperoxide **368a** and hydroperoxyketals **368b** and **368c** undergo BCIH-mediated 6-*exo* cyclization to give the antimalarial active bridged bicyclic peroxides **369a–c** (Scheme 94)²⁶⁷. Some 8-membered endoperoxides, as well as 10- to 20-membered macrocyclic peroxides possessing 2 or 3 peroxide units in the ring were prepared through the BCIH-promoted *exo*-cyclizations of the corresponding unsaturated hydroperoxides^{268, 269}.

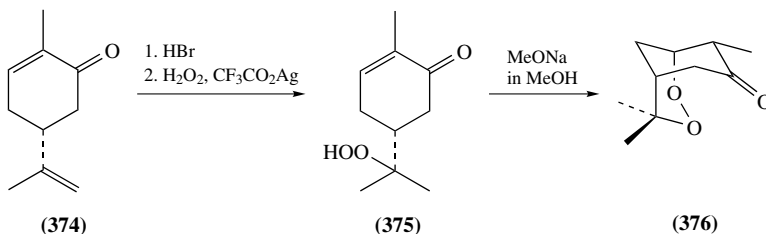
In addition to these extensive studies on electrophile-mediated intramolecular peroxydation of electron-rich C=C bonds, some examples of intramolecular hydroperoxide addition to electron-poor C=C bonds have been described. For example, several racemic analogues **371** of the naturally occurring plakinic acid were readily obtained by peroxymercuration followed by hydridodemercuration of the dienic acids **370** (Scheme 95)²⁷⁰. Intramolecular Michael addition of hydroperoxide function to the double



SCHEME 95



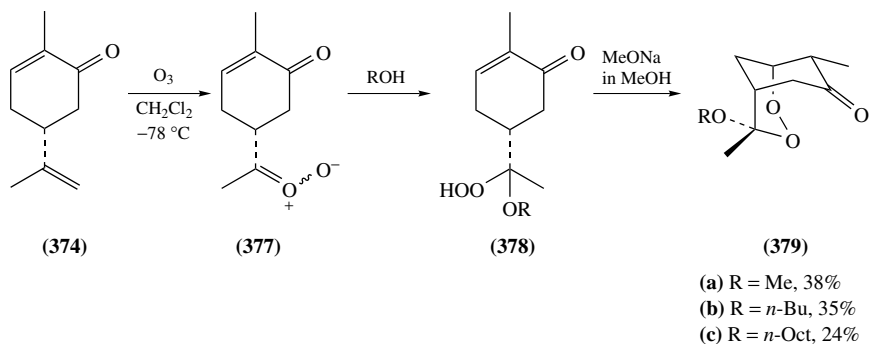
SCHEME 96



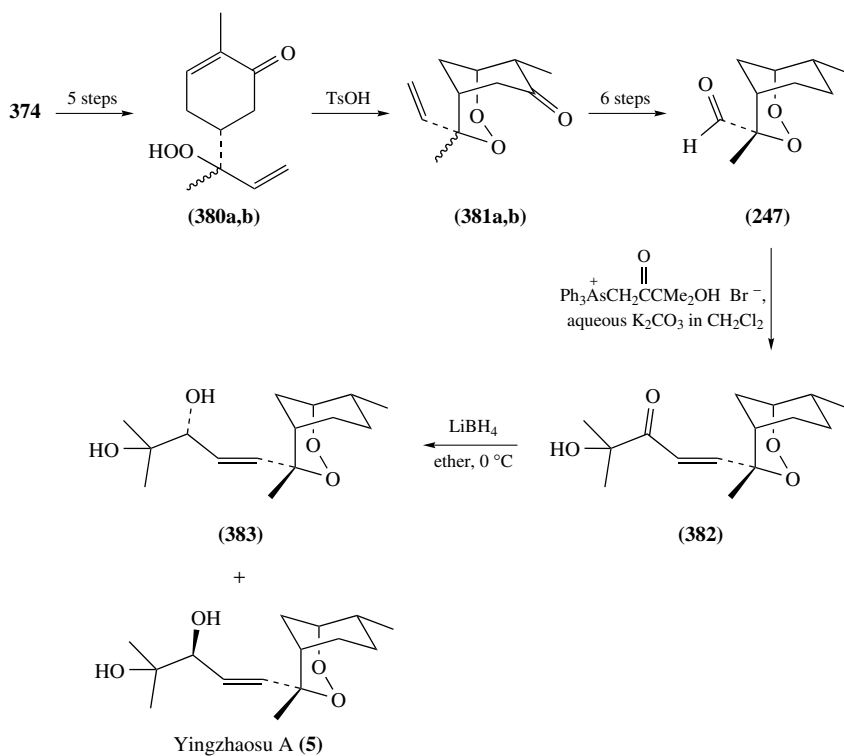
SCHEME 97

bond of the acrylic moiety of unsaturated hydroperoxyketals **372**, to afford the antimalarial 6-membered cyclic peroxides **373**, proceeds most effectively under Et₂NH catalysis in (CF₃)₂CHOH solution (Scheme 96)^{271,272}. Treatment of hydroperoxide **375**, derived from (*R*)-carvone (**374**), with MeONa/MeOH results in a 6-*exo* Michael cyclization to give 4,4,8-trimethyl-2,3-dioxabicyclo[3.3.1]nonan-7-one (**376**) (Scheme 97)²⁷³. Unsaturated hydroperoxyketals **378**, which are obtained through low-temperature ozonolysis of **374** with subsequent trapping of carbonyl oxide intermediate **377** by the appropriate primary alcohol, cyclize under basic conditions to bridged bicyclic endoperoxides **379** (24–38%) (Scheme 98)²⁷⁴.

Unsaturated hydroperoxides **380a** and **380b**, which were obtained from (*R*)-carvone (**374**) in 5 steps, were used for the construction of the 2,3-dioxabicyclo[3.3.1]nonane system in the first total synthesis of yingzhaosu A (**5**) (Scheme 99)^{275,276}. In this case the intramolecular addition of the hydroperoxide function to the electron-poor enone in **380a** and **380b**, to give the bridged bicyclic peroxides **381a** and **381b**, was induced by acid catalysis. Polyfunctionalized peroxides **381a** and **381b** were then converted through 5 additional steps and diastereomer separation into aldehyde-peroxide **247**. A Wittig-type olefination of the latter with an arsenium ylide afforded enone **382**, which was reduced with LiBH₄ to give a *ca* 2:3 mixture of yingzhaosu A (**5**) and its C14-epimer **383** (Scheme 99)^{275,276}. A similar acid-induced cyclization of **380a** and **380b** into **381a** and **381b** was also used for the preparation of a series of potent antimalarial endoperoxides, including a drug-candidate artefene^{273,277}.

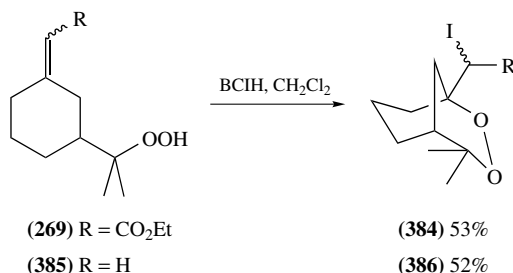


SCHEME 98



SCHEME 99

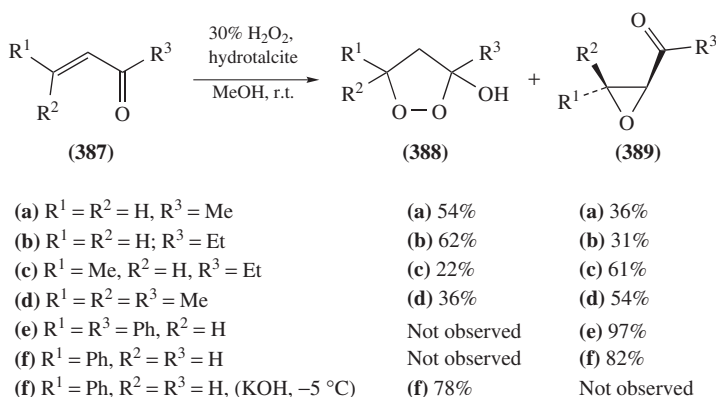
It is noteworthy that BCIH-mediated peroxyiodination of unsaturated hydroperoxide **269** follows an intramolecular addition of hydroperoxide onto an electron-poor $C=C$ bond to give the bridged bicyclic iodoperoxide **384** (Scheme 100)²⁶⁷. This reaction is as effective as the conversion of **385** to **386**, which involves iodonium-mediated intramolecular attack of a hydroperoxide group on an electron-rich double bond²⁶⁷.



SCHEME 100

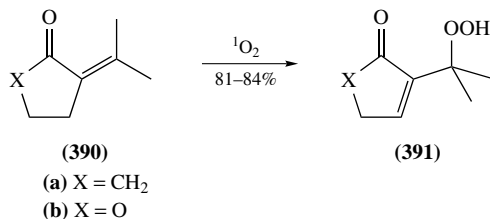
3. Nucleophilic addition to the carbonyl group

Intramolecular nucleophilic addition of hydroperoxide function to a carbonyl group is one of the earliest methods for formation of cyclic peroxides. Extension of studies from the 1950s and 1960s^{278–280} indicates that α,β -unsaturated ketones **387a–d** react with hydrogen peroxide at RT in the presence of hydrotalcite, a synthetic anionic clay mineral, to give 1,2-dioxolanes **388a–d** (Scheme 101)²⁸¹. Under these conditions, *trans*-chalcone (**387e**) and *trans*-cinnamaldehyde (**387f**) afford selectively the corresponding epoxides **389e** and **389f**^{281, 282}. The important role of reaction conditions and catalyst is illustrated by studies with cinnamaldehyde (**387f**), which within 1 h reacts with H₂O₂ at $-5\text{ }^{\circ}\text{C}$ and pH 10–11 (KOH catalyst) to afford the endoperoxide **388f** in high yield²⁸³; however, when longer reaction time and lower pH 8 are employed the primary product **388f** is converted into epoxide **389f**^{279, 283}.

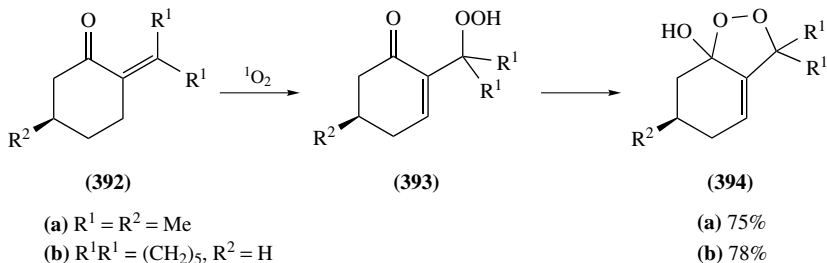


SCHEME 101

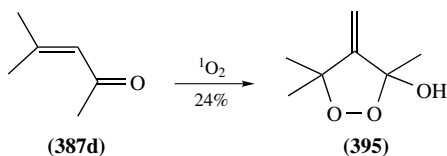
α,β -Unsaturated 5-membered cyclic ketone **390a** and lactone **390b** are known to undergo photooxygenation to hydroperoxy derivatives **391** in high yield (Scheme 102)²⁸⁴. In contrast, photooxygenation of the related 6-membered cyclic ketones **392** under analogous conditions directly affords the corresponding fused bicyclic peroxides **394** (Scheme 103)²⁸⁴. Probably this reaction involves a spontaneous cyclization of the keto-hydroperoxide intermediates **393**²⁸⁴. Photooxygenations of structurally related 7- and 8-membered α,β -unsaturated ketones also give the corresponding fused 1,2-dioxolanes, albeit in low yield²⁸⁵. Monocyclic 4-methylene-1,2-dioxolane **395** was similarly obtained



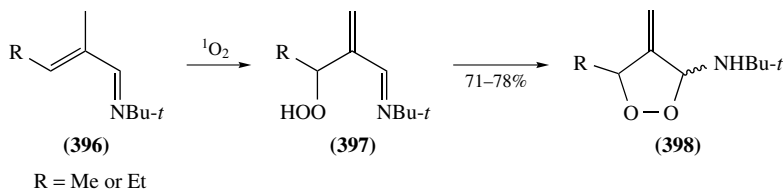
SCHEME 102



SCHEME 103



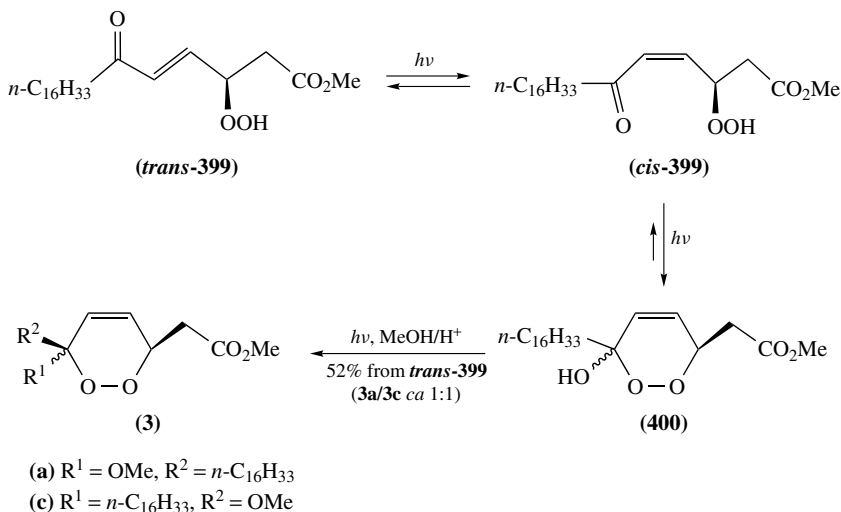
SCHEME 104



SCHEME 105

(24%) by photooxygenation of mesityl oxide (**387d**) (Scheme 104)²⁸⁴. Acyclic unsaturated *N-tert*-butyl aldimines **396** smoothly react with singlet oxygen to give, probably through the intermediary β -hydroperoxy aldimines **397**, the corresponding 3-amino-1,2-dioxolanes **398** in 71–78% yield (Scheme 105)²⁸⁶. In contrast to that, *N-tert*-butylimine of cyclopent-1-en-1-al gave only 19% yield of the corresponding fused bicyclic peroxide, whereas *N-tert*-butylimine of cyclohex-1-en-1-al was found to be unreactive under the common photooxygenation conditions²⁸⁶.

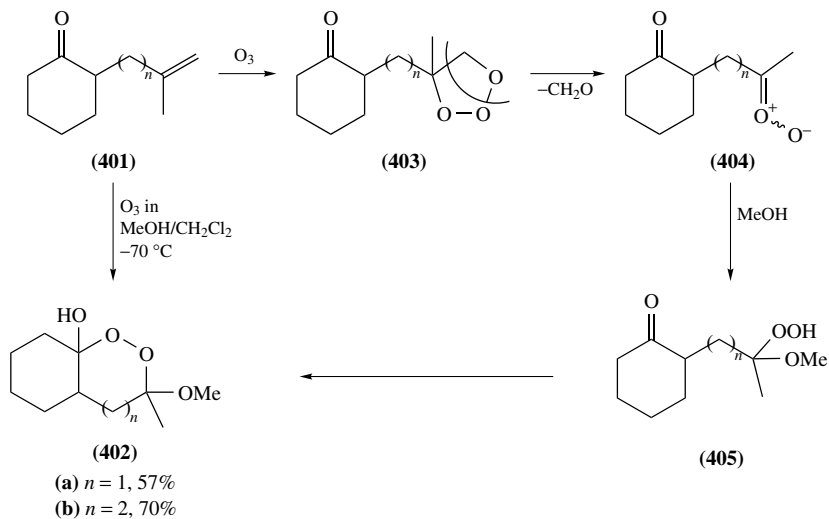
The final stage in Dussault's total syntheses of marine 3-methoxy-1,2-dioxines of type **3** is based on the cyclization of α,β -unsaturated γ -hydroperoxyketones **399** as exemplified in Scheme 106^{287,288}. Thus, photoisomerization of α,β -unsaturated γ -hydroperoxyketone



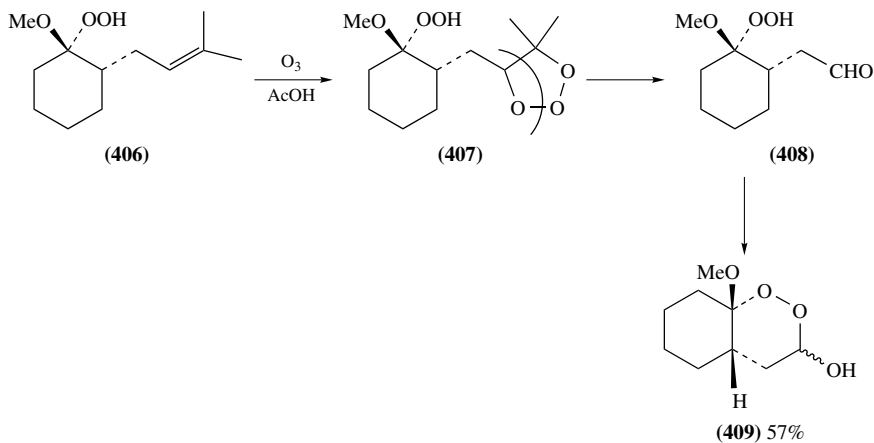
SCHEME 106

trans-**399** to *cis*-**399**, which cyclizes to a mixture of peroxy lactols **400a** and **400b**, is followed by ketalization with MeOH in acidic conditions to give a mixture of (+)-chondrillin (**3a**) and (–)-*ent*-plakorin (**3c**) in good yield (Scheme 106)^{287,288}. For the total synthesis of racemic compounds **3**, see Section II.A.1.

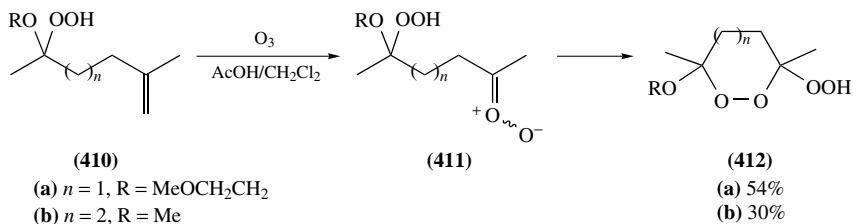
Some saturated 6- and 7-membered cyclic peroxy lactols are effectively obtained via intramolecular nucleophilic attack of hydroperoxide to electrophilic carbonyl or carbonyl oxide functionality. Both nucleophilic hydroperoxide and electrophilic carbonyl (carbonyl oxide) functionalities can be generated *in situ* by controlled ozonolysis of properly substituted alkenyl groups. Thus, low-temperature ozonolysis in MeOH/CH₂Cl₂ of unsaturated ketones **401a** and **401b** gives, in a one-pot process, the fused bicyclic peroxy lactols **402a** and **402b** respectively, both in high yield (Scheme 107)²⁸⁹. The reaction mechanism involves initial [3 + 2]-cycloadditions of ozone to the terminal C=C bond, thus generating highly unstable primary ozonides **403**, which are cleaved to carbonyl oxides **404** with extrusion of formaldehyde. The highly electrophilic species **404** are trapped with methanol to generate the carbonyl-containing hydroperoxyketals **405**, which are readily cyclized to the final peroxy lactols **402a** or **402b** (Scheme 107). The trisubstituted 1,2,3-trioxolane **407**, that is obtained by cycloaddition of ozone to the internal C=C bond of unsaturated hydroperoxyketal **406**, is cleaved with extrusion of acetone oxide and formation of the intermediate γ -hydroperoxy aldehyde **408** which readily cyclize to fused peroxy lactol **409** (57%) (Scheme 108)²⁸⁹. Ozonolyses of unsaturated acyclic hydroperoxyketals **410a** and **410b** in AcOH/CH₂Cl₂ give carbonyl oxide intermediates of type **411** that are intramolecularly trapped by hydroperoxide functionalities to furnish the corresponding monocyclic 6-membered **412a** and 7-membered **412b** hydroperoxy-endoperoxides (Scheme 109)²⁸⁹. A similar ozonolysis of the individual stereoisomer hydroperoxyketal **413** affords, through the substituted carbonyl oxide intermediate **414**, the fused bicyclic hydroperoxy-endoperoxide **415** in high yield (Scheme 110)²⁸⁹. Various cyclic 7- to 12-membered α -hydroxy- and α -hydroperoxy-substituted spiro tetraoxacycloalkanes were obtained by ozonolysis of the corresponding hydroperoxyketals in 2,2,2-trifluoroethanol (TFE)²⁹⁰.



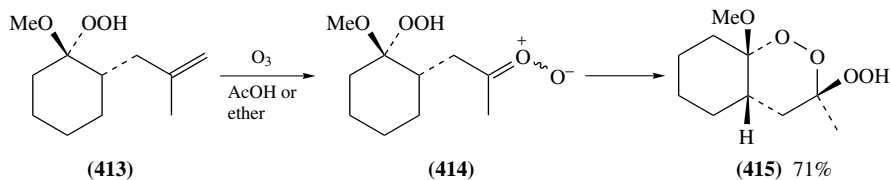
SCHEME 107



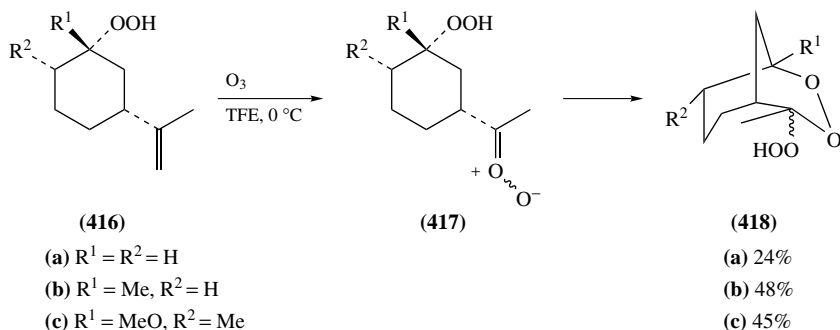
SCHEME 108



SCHEME 109

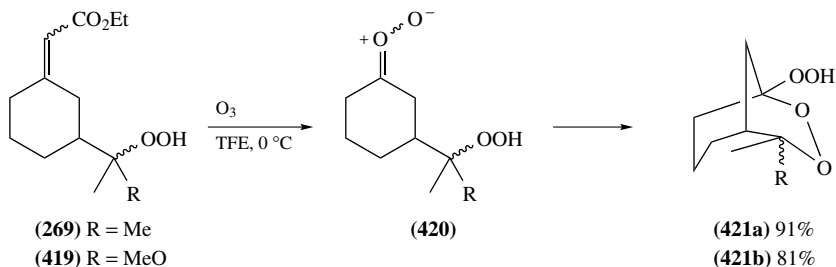


SCHEME 110



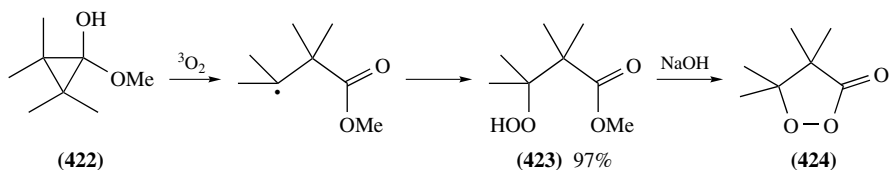
SCHEME 111

By the same pattern, unsaturated hydroperoxides of type **416** are ozonized to carbonyl oxide intermediates **417** that afford bridged bicyclic peroxides **418**, containing the 2,3-dioxabicyclo[3.3.1]nonane system of yingzhaosu A (**5**) (Scheme 111)^{291, 292}. Noteworthy is that ozonolyses of electron-poor C=C bonds in substrates **269** and **419** are highly effective for generation of the γ -hydroperoxy carbonyl oxide intermediates **420**, which are readily cyclized to give 2,3-dioxabicyclo[3.3.1]nonane derivatives **421a** and **421b** in very high yield (Scheme 112)²⁹².

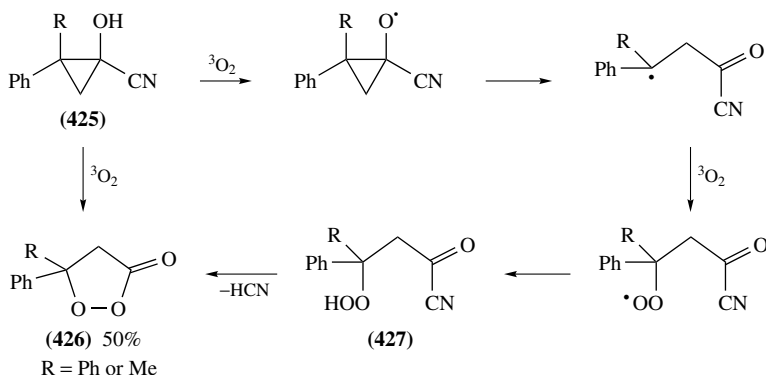


SCHEME 112

Some cyclopropanol derivatives undergo a facile autoxidation to give a hydroperoxide carrying a carbonyl group on a β -position. Such intermediates are prone to either catalyzed or spontaneous heterolytic ring closure to multisubstituted 1,2-dioxolanes. For example, tetramethylcyclopropanone methyl hemiketal (**422**) smoothly reacts with atmospheric oxygen to give, through the homolytic mechanism shown in Scheme 113, the hydroperoxide **423** in excellent yield. Base-catalyzed cyclization yields the peroxypropiolactone **424**²⁹³.



SCHEME 113

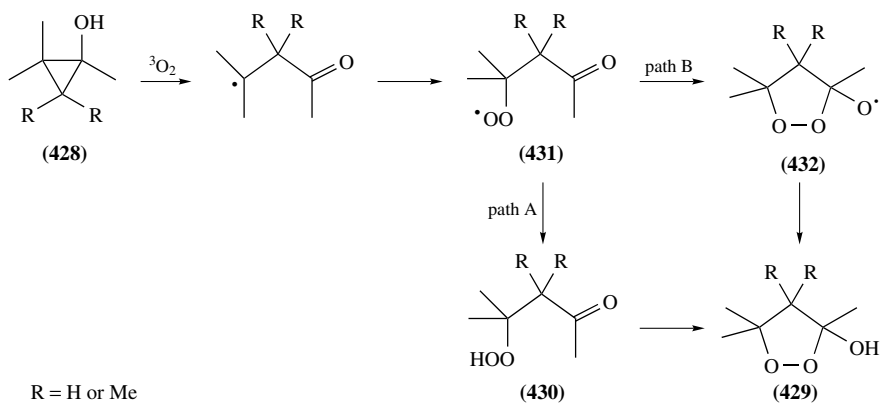


SCHEME 114

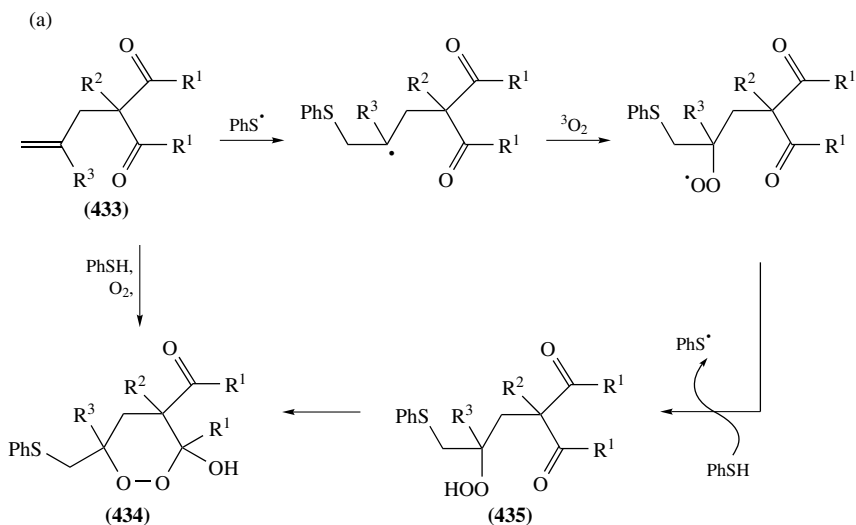
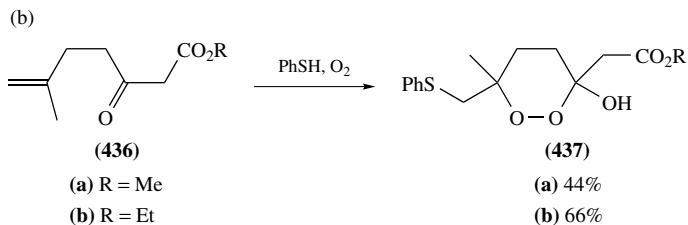
Replacement of the methoxy substituent by a better leaving group, such as the cyano group in cyanohydrin **425**, results in the spontaneous autoxidation to the corresponding peroxypropiolactone **426**, probably via the intermediate hydroperoxides **427**, as shown in Scheme 114²⁹⁴. 1,2,2-Trimethyl- and 1,2,2,3,3-pentamethylcyclopropanols of type **428** are slowly autoxidized by atmospheric oxygen (48 h at RT) to give the corresponding 3-hydroxy-1,2-dioxolanes **429** (Scheme 115)²⁹³. The formation of the cyclic peroxides **429** can be rationalized by two mechanisms: homolytic formation of hydroperoxide **430**, followed by its heterolytic cyclization (path A), and an all-homolytic process involving intermediate radicals **431** and **432** (path B) (Scheme 115); path A seems to us more probable. While the monocyclic 2,2-dimethyl-1-(2-pyridyl)cyclopropanol and some fused cyclopropanols produce the corresponding 5-membered endoperoxides in high yields upon exposure to atmospheric oxygen, the related O-protected cyclopropanols are resistant to oxidation^{295, 296}.

6-Membered fused bicyclic peroxy lactols **434a–c** were synthesized by application of the TOCO reaction to γ,δ -unsaturated β -diketones of type **433**. While the TOCO reactions described in Section II.A.5 involve all-homolytic processes, herein the radical chain reactions lead to the formation of γ -keto hydroperoxides **435**, which undergo spontaneous, probably heterolytic, cyclization to the final endoperoxides **434** (Scheme 116a)²⁹⁷. The best yields of cyclic peroxides **434** (up to 75%) were obtained for the derivatives of 2-methylcyclopentane-1,3-dione **433b** and **433c**, whereas 2-allylcyclohexane-1,3-dione (**433d**) failed to yield endoperoxide **434d**²⁹⁷. Allyl acetoacetic esters **436a** and **436b** undergo a similar TOCO reaction to form the corresponding monocyclic peroxy lactols **437a** and **437b** (Scheme 116b)²⁹⁷. For related examples in steroid series, see Scheme 66 in Section II.A.7.

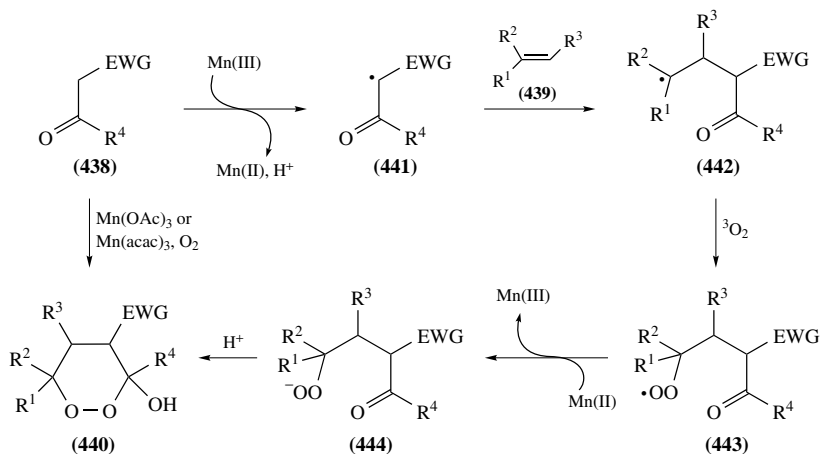
A highly versatile method for the synthesis of a variety of 6-membered monocyclic and fused bicyclic peroxy lactols **440** from activated ketones **438** (EWG = electron-withdrawing



SCHEME 115

(a) $R^1 = R^2 = \text{Me}$, $R^3 = \text{H}$, 36%(b) $R^1 R^1 = (\text{CH}_2)_2$, $R^2 = \text{Me}$, $R^3 = \text{H}$, 75%(c) $R^1 R^1 = (\text{CH}_2)_2$, $R^2 = R^3 = \text{Me}$, 71%(d) $R^1 R^1 = (\text{CH}_2)_2$, $R^2 = R^3 = \text{H}$, no endoperoxide formation

SCHEME 116



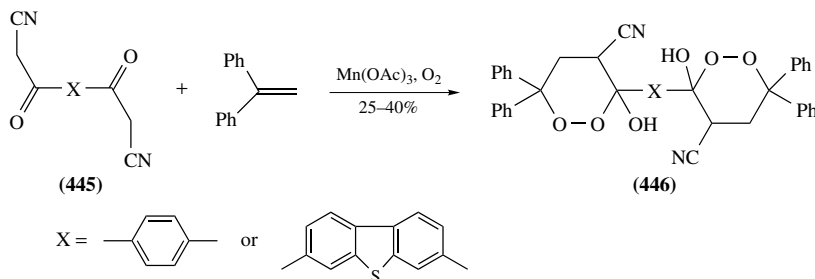
R^1 and $\text{R}^2 = \text{Ar}$, Alk , $\text{R}^3 = \text{H}$, $\text{R}^1 = \text{Ar}$ or Alk , $\text{R}^2 = \text{R}^3 = \text{H}$, $\text{R}^1\text{R}^3 = (\text{CH}_2)_3$ or $(\text{CH}_2)_4$, $\text{R}^2 = \text{H}$,
 $\text{EWG} = \text{CN}$, COR^5 , CO_2Alk , CONR_2^5 , SO_2R^5 , POR_2^5 , NO_2 , R^4 and $\text{R}^5 = \text{Alk}$, Ar or Het

SCHEME 117

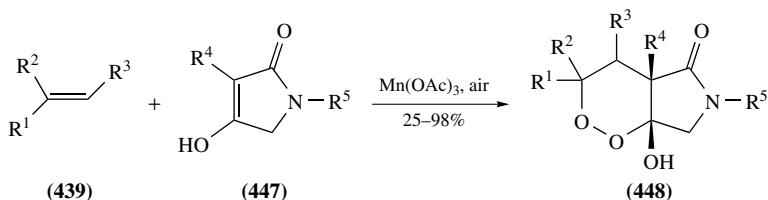
group) and electron-rich ethylenes **439** is detailed in Scheme 117^{298–307}. When activated ketones **438** and electron-rich 1-aryl (or alkyl-), 1,1-diaryl- or 1,1-dialkyl-substituted ethylenes **439** are used, the co-oxygenation process leads to endoperoxides **440** in 80–90% yield. Some 1,2-disubstituted alkenes of type **439**, such as cyclohexene, were found to be less effective. The reaction is commonly carried out in AcOH using 1–3 equivalents of one-electron oxidant like $\text{Mn}(\text{OAc})_3$ or $\text{Mn}(\text{acac})_3$. Other oxidants like CAN, LTA, potassium permanganate and chromium (VI) oxide were also employed^{304,308}. The role of the oxidant is to produce the incipient α -ketoalkyl radicals **441** from ketones **438**. These radicals being strongly electrophilic readily add to the less substituted terminus of electron-rich alkene **439** to generate the γ -ketoalkyl radicals **442**, which add to triplet oxygen thus forming the corresponding peroxy-radicals **443**. The latter are probably reduced by Mn(II) to give manganese salts of the peroxy-anions **444**, which cyclize in acidic media to form the 6-membered lactols **440** (Scheme 117). Protonated open-chain γ -keto hydroperoxides **444** may be in equilibrium with cyclic peroxy lactols **440**. Cases in which equilibrium is in favor of the former were reported^{309,310}. Ketone-olefin co-oxygenations of substrates like **445**, bearing 2 activated ketone fragments, lead to bis(endoperoxides) **446** in moderate yields (Scheme 118)^{307,311,312}. Similar co-oxygenations of cyclic activated carbonyl compounds of type **447** with alkenes **439** give fused bicyclic peroxides of type **448**; yields range from moderate when 1,2-disubstituted alkenes **439** are employed to excellent in reactions with 1,1-disubstituted alkenes **439** ($\text{R}^3 = \text{H}$) (Scheme 119)^{308,312–317}.

C. Cycloaddition of Singlet Oxygen with 1,3-Dienes

Singlet oxygen ($^1\text{O}_2$) can be generated on a synthetically useful scale either chemically or, preferably, photochemically through photosensitization mediated by a suitable dyestuff (e.g. methylene blue, rose bengal, porphines) in visible light^{51,52,318–322}. Singlet oxygen readily reacts with a variety of acyclic and cyclic 1,3-dienes (type II photooxidation)^{111,323} to give the corresponding unsaturated 6-membered cyclic peroxides. This is the earliest reported and one of the most general routes to endoperoxides. Indeed, as early as 1867



SCHEME 118

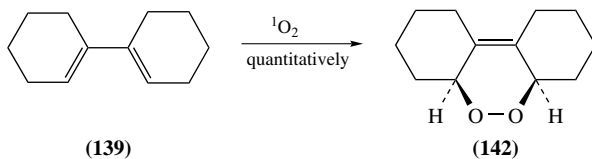


R^1 and $R^2 = \text{Ar, Alk}$, $R^3 = \text{H}$, $R^4 = \text{Ar or Alk}$, $R^2 = R^3 = \text{H}$, $R^1R^3 = (\text{CH}_2)_3$ or $(\text{CH}_2)_4$, $R^2 = \text{H}$,
 $R^4 = \text{H, CN, CO}_2\text{Alk}$, $R^5 = \text{H, Alk, Bn}$

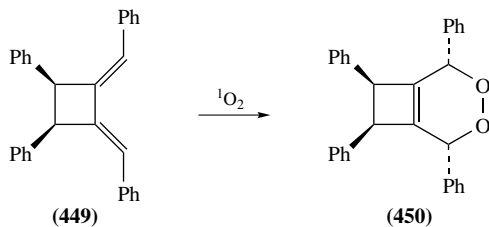
SCHEME 119

Fritzsche described a reversible addition of singlet oxygen to naphthacene³²⁴. Windaus and Brunken in 1928 reported the isolation of cyclic peroxide prepared by singlet oxygen cycloaddition to ergosteryl acetate². Literature on the preparation of endoperoxides using photooxidation of various acyclic and carbocyclic 1,3-dienes as well as of electron-rich aromatic and heteroaromatic compounds up to the end of the 1980s has been extensively reviewed^{51, 230, 323, 325–328}. Representative data on reversible binding of oxygen to aromatic compounds were recently reported by Aubry and coworkers³²⁹. Contemporary views on the mechanistic aspects of the reactions of 1,3-dienes with singlet oxygen leading to 6-membered cyclic peroxides and some synthetic applications of these processes have been discussed in several recent reviews by Clennan³²³, by Adam and coworkers^{330–333} and by Houk and coworkers^{334, 335}. A number of factors influencing the competition between the [4 + 2], [2 + 2] and ene-reaction on photooxidations of 1,3-dienes have been discussed in the review of Clennan³²³. Theoretical studies on the mechanism^{336–339} and quantitative experimental data about the formation of cyclic peroxides from 1,3-dienes and singlet oxygen useful for synthetic planning are available^{340–345}. Herein we focus on synthetic applications of the singlet oxygen photooxygenation of 1,3-dienes to form 6-membered cyclic peroxides; mechanistic aspects will be addressed only when required for synthetic considerations.

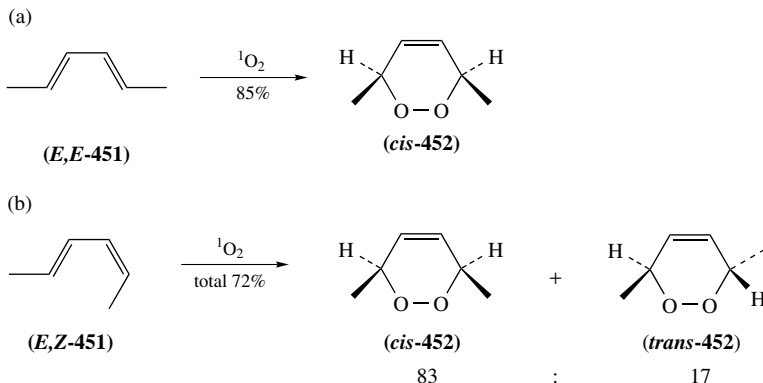
Due to the formal analogy to the classical Diels–Alder reaction, the mechanism of cyclic peroxide formation through cycloadditions of 1,3-dienes with $^1\text{O}_2$ was considered for a long time to involve a concerted suprafacial [4 + 2]-cycloaddition of a superdienophile, namely a singlet oxygen to 1,3-dienic system^{318, 326, 327, 346}. In such a case, the concerted or almost concerted cycloaddition must be *cis*-stereospecific and the stereochemical properties of the diene must be reflected in the three-dimensional structure of cyclic peroxide according to well-defined rules. Indeed, it was found in early stereochemical



SCHEME 120



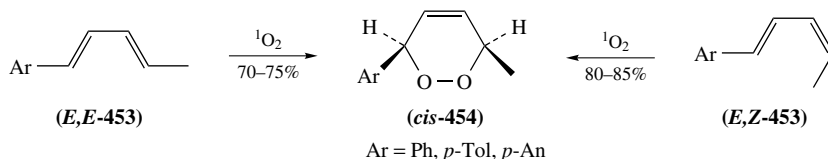
SCHEME 121



SCHEME 122

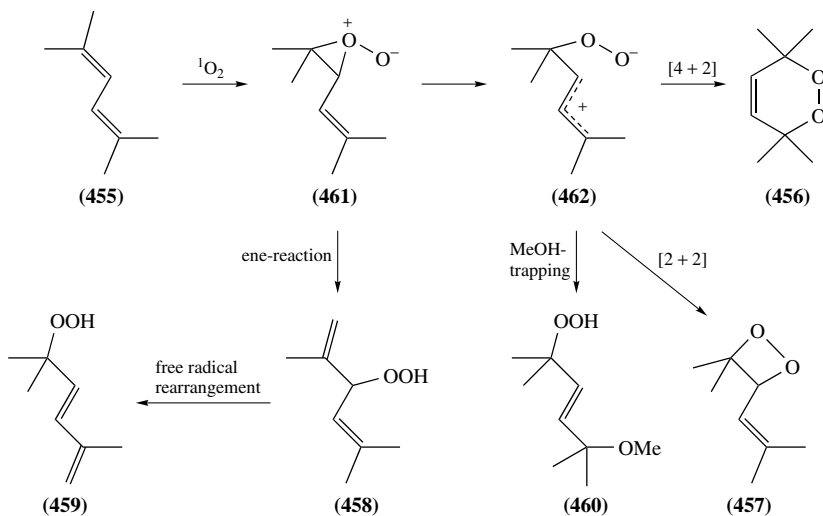
studies that singlet oxygen photooxidation of 1,1'-dicyclohexyl (**139**) leads quantitatively to the *cis*-cyclic peroxide **142** (Scheme 120)³²⁶, and the photooxidation of *s-cis*-fixed diene **449** produces *cis*-endoperoxide **450** (Scheme 121)³⁴⁷. Nevertheless, from the beginning of the 1980s a number of experimental data deriving from extensive stereochemical studies demonstrated that peroxidations of 1,3-dienes with singlet oxygen cannot be always rationalized on the grounds of a concerted [4 + 2]-cycloaddition mechanism. For instance, while photooxidation of *E, E*-hexa-2,4-diene (*E,E*-**451**) affords exclusively *cis*-endoperoxide *cis*-**452** in good yield (Scheme 122a), in accord with the expectation from a concerted [4 + 2]-cycloaddition, peroxidation of the corresponding *E,Z*-isomer *E,Z*-**451** gives the apparently concerted cycloaddition derivative *trans*-**452** only as the minor product (Scheme 122b)^{348, 349}. The major product in this reaction is the *cis*-**452**, which is not expected to derive from an electrocyclic process (Scheme 122b). Similar photooxidation of *Z,Z*-hexa-2,4-diene (*Z,Z*-**451**) also proceeds non-stereoselectively to give a mixture of endoperoxides *cis*-**452** (42%) and *trans*-**452** (10%)³⁴⁹. Analogous reactions

of singlet oxygen, either with *E,E*-1-aryl-1,3-pentadienes *E,E*-**453** or with the *E,Z*-isomers *E,Z*-**453**, give in both cases *cis*-endoperoxides *cis*-**454** (Scheme 123)³⁵⁰. When reactions of hexa-2,4-dienes (**451**) were carried out in methanol, up to 25% of a methanol adduct was observed³⁴⁹; its formation was rationalized by the involvement of zwitterionic intermediates^{349,351}.



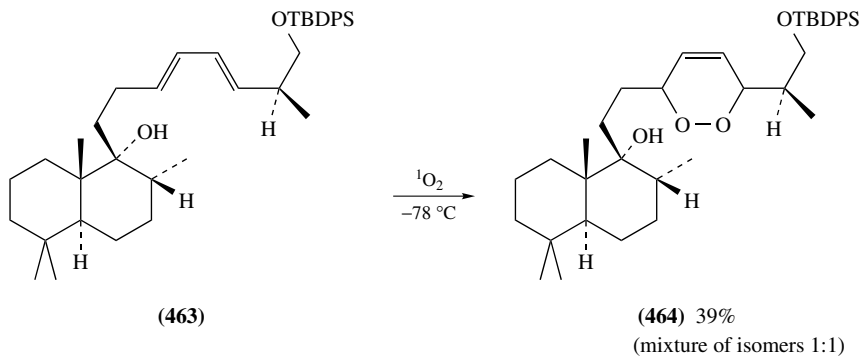
SCHEME 123

In a thorough study on photooxidation of 2,5-dimethyl-2,4-hexadiene (**455**) it was found that 1,2-dioxene **456**, 1,2-dioxetane **457**, hydroperoxy dienes **458** and **459** and, when methanol was used as solvent, also hydroperoxy(methoxy)octene **460** are formed (Scheme 124)³⁵²⁻³⁵⁶. Product distribution was found to be highly solvent dependent. These results led investigators to postulate a mechanism involving the intermediacy of perepoxide **461** and zwitterion **462** (Scheme 124). Accordingly, the product of [4 + 2]-cycloaddition **456**, the product of [2 + 2]-cycloaddition **457**, as well as the products **458** and **459** deriving from ene-addition would originate from polar intermediates **461** and **462**.³⁵²⁻³⁵⁶

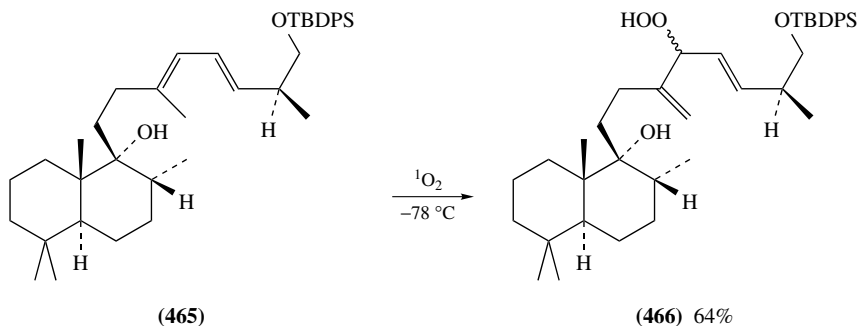


SCHEME 124

While the viability of singlet oxygen to undergo [4 + 2]-cycloaddition with dienes is highly dependent on the degree of substitution at both termini of the diene system and on the steric demands of the substituents, many types of functionalities can tolerate the mild conditions of photooxygenation. Thus, notwithstanding the two bulky substituents at both ends of the unsaturated system in *E,E*-diene **463**, it reacts with singlet oxygen at -78°C to give the corresponding 6-membered cyclic peroxide **464** (39%) as 1:1 mixture of isomers

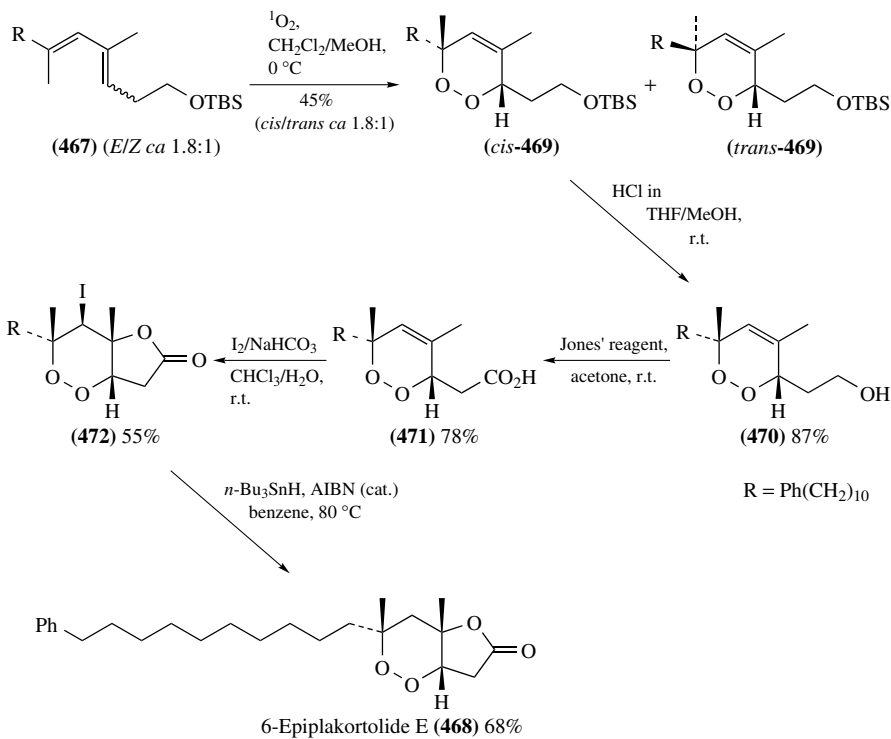


SCHEME 125

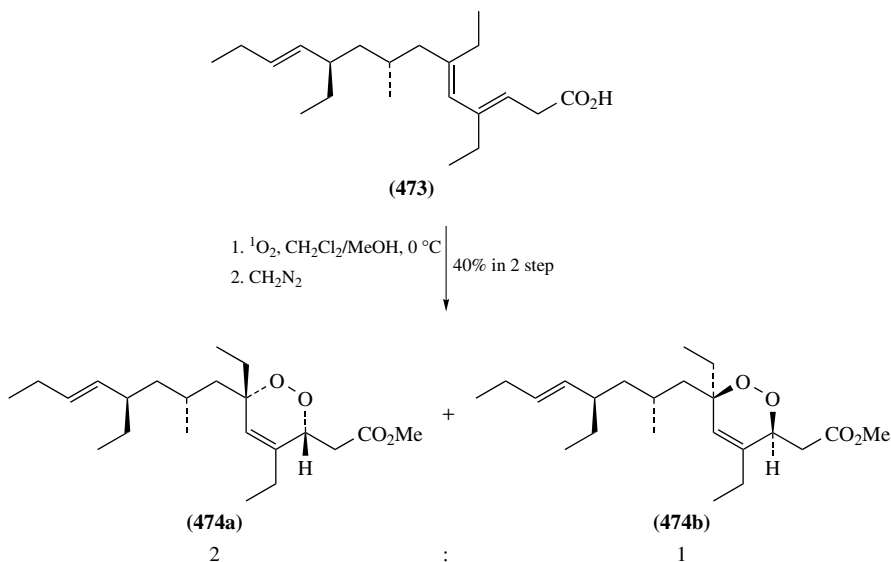


SCHEME 126

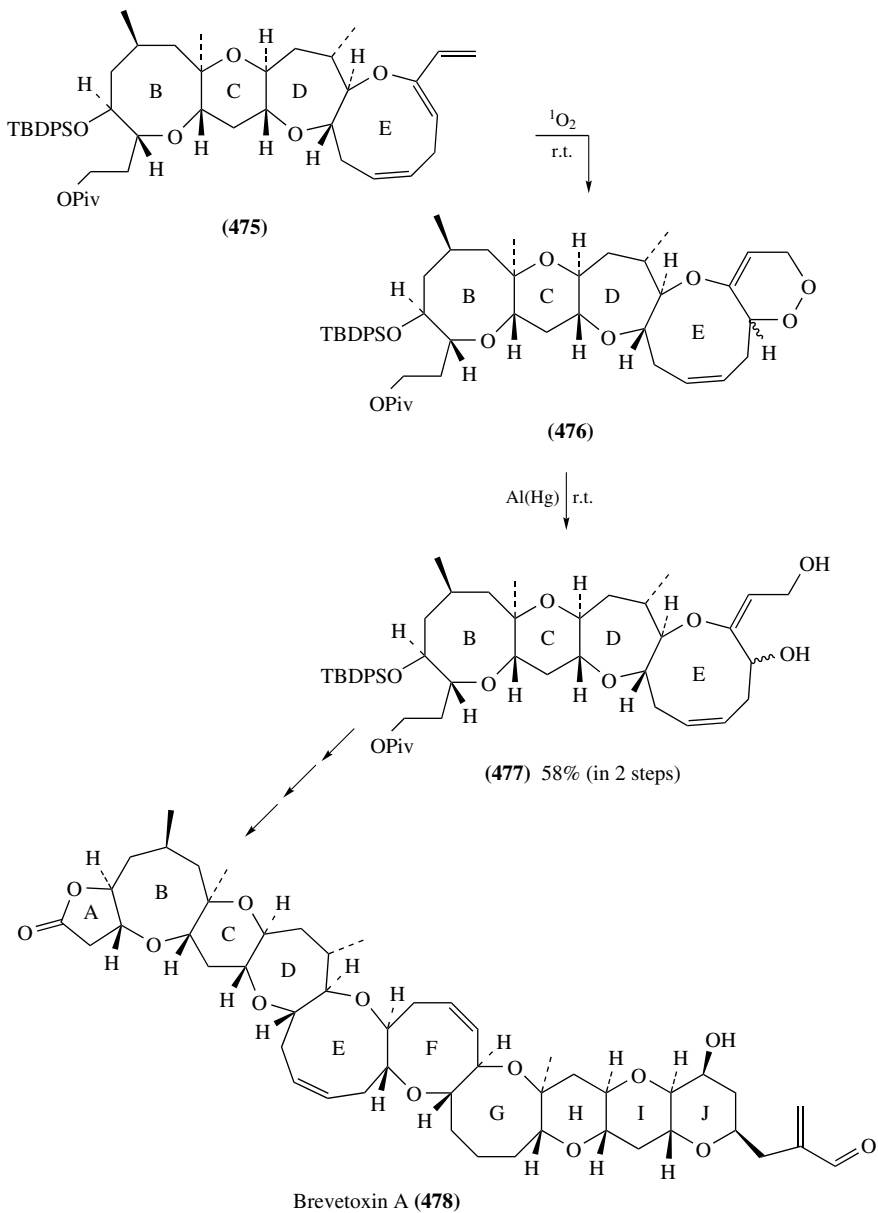
(Scheme 125)^{357, 358}. In contrast, no cyclic peroxide was obtained upon photooxygenation of the very similar 1,1,4-trisubstituted diene **465**; the major product in this reaction is hydroperoxide **466** (64% yield), which resulted from the ene-reaction (Scheme 126)^{357, 358}. Nevertheless, in some cases photooxygenations of 1,1,3,4-tetrasubstituted 1,3-dienes could be expedient for the synthesis of structurally complex 6-membered endoperoxides. Thus, using singlet oxygen [4 + 2]-cycloaddition with dienes **467** for constructing the endoperoxide framework, Jung and coworkers recently accomplished an efficient total synthesis of the racemic form of a naturally occurring cyclic peroxy lactone 6-epiplakortolide E (**468**) (Scheme 127)³⁵⁹. It seems that photooxygenation of a *ca* 1.8:1 *E/Z* mixture of dienes **467** proceeds stereoselectively to give endoperoxides *cis*-**469** and *trans*-**469**, retaining the 1.8:1 ratio (45% total yield). Acidic desilylation of the major component, *cis*-**469**, affords the alcohol **470**. Oxidation of the latter by Jones' reagent leads to acid **471**, which was subjected to iodolactonization to bicyclic endoperoxide-iodolactone **472**. Chemoselective free-radical reductive deiodination of **472** gives the target 6-epiplakortolide E (**468**) in good yield (Scheme 127)³⁵⁹. Yao and Steliou recently applied singlet oxygen [4 + 2]-cycloaddition to the chiral 1,1,3,4-tetrasubstituted 1,3-diene **473** in the final step of the total synthesis of bioactive naturally occurring cyclic peroxides **474** (Scheme 128)³⁶⁰. It is noteworthy that the non-conjugated C=C bond is not affected in this reaction, and in both diastereomeric endoperoxides **474a** and **474b** the biggest alkenyl substituent and the methoxycarbonyl moiety are *cis*-positioned.



SCHEME 127



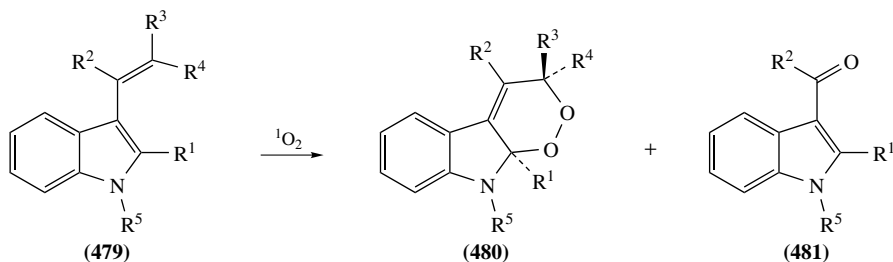
SCHEME 128



SCHEME 129

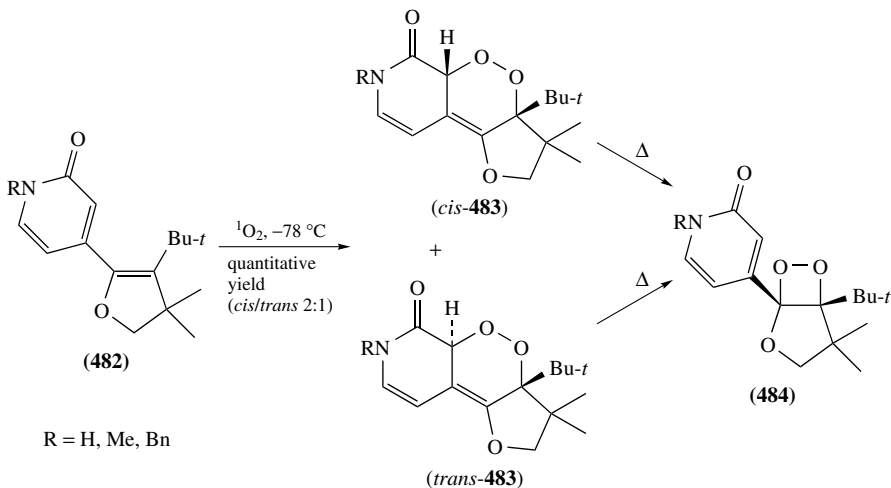
Singlet oxygen [4 + 2]-cycloadditions to 1,3-dienes are widely used in intermediary stages of the total syntheses of various non-peroxidic natural products and their analogues. For example, photosensitized oxygenations of 1-vinylcyclohexenes followed by LiAlH_4 or thiourea reduction of the resulting 6-membered fused cyclic peroxides was used for the stereoselective preparation of *Z*-2-(2-methylenecyclohexylidene)ethanols, advanced precursors in the synthesis of calcitriol (vitamin D_3)³⁶¹. Using singlet oxygen photooxygenation of the diene **475** to a 1:1 mixture of diastereomers of the endoperoxide **476**, followed by aluminum amalgam reduction to diol **477**, Nicolaou and coworkers recently accomplished a convergent total synthesis of the powerful neurotoxin brevetoxin A (**478**) (Scheme 129)³⁶². Singlet oxygen peroxidation of a model compound mimicking the monocyclic E-ring diene in **475** gives fused bicyclic endoperoxide related to **476** in 85% yield^{363, 364}.

A number of vinylarenes have been subjected to peroxidation with singlet oxygen to give the corresponding mono- and bis(endoperoxides)^{31, 323, 325}. A thorough study by Foote and coworkers on singlet oxygen photooxygenation of 3-vinylindole derivatives **479a–k** to cyclic peroxides **480a–k** and/or aldehydes **481a–k** demonstrated a high sensitivity of the process to steric and electronic features of the diene fragment (Scheme 130)³⁶⁵. In contrast to the highly stereoselective photooxygenations of 3-vinylindoles, singlet oxygen [4 + 2]-cycloaddition to (2,3-dihydrofuran-5-yl)-2-pyridones **482** at -78°C proceeds non-stereospecifically to give a mixture of *cis*- and *trans*-fused tricyclic peroxides **483**. Both of them rearrange upon heating into the more stable 1,2-dioxetanes **484** (Scheme 131)³⁶⁶. Additional related rearrangements of furan endoperoxides into the corresponding 1,2-dioxetanes were reported^{367, 368}.

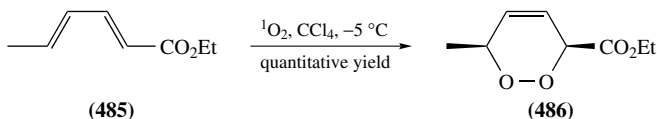


(a) $\text{R}^1 = \text{R}^2 = \text{R}^3 = \text{R}^4 = \text{H}, \text{R}^5 = \text{Me}$	(a) 96%	not detected
(b) $\text{R}^1 = \text{R}^2 = \text{R}^3 = \text{R}^4 = \text{H}, \text{R}^5 = \text{PhSO}_2$	(b) 96%	not detected
(c) $\text{R}^1 = \text{R}^5 = \text{Me}, \text{R}^2 = \text{R}^3 = \text{R}^4 = \text{H}$	(c) 91%	(c) 6%
(d) $\text{R}^1 = \text{R}^2 = \text{R}^4 = \text{H}, \text{R}^3 = \text{MeO}, \text{R}^5 = \text{Me}$	(d) 90%	(d) 8%
(e) $\text{R}^1 = \text{R}^2 = \text{R}^3 = \text{H}, \text{R}^4 = \text{MeO}, \text{R}^5 = \text{Me}$	(e) 98%	not detected
(f) $\text{R}^1 = \text{R}^2 = \text{R}^4 = \text{H}, \text{R}^3 = \text{MeO}, \text{R}^5 = \text{PhSO}_2$	(f) 91%	(f) 6%
(g) $\text{R}^1 = \text{R}^2 = \text{R}^3 = \text{H}, \text{R}^4 = \text{MeO}, \text{R}^5 = \text{PhSO}_2$	(g) 96%	not detected
(h) $\text{R}^1 = \text{R}^5 = \text{Me}, \text{R}^2 = \text{R}^4 = \text{H}, \text{R}^3 = \text{MeO}$	not detected	(h) 90%
(i) $\text{R}^1 = \text{R}^5 = \text{Me}, \text{R}^2 = \text{R}^3 = \text{H}, \text{R}^4 = \text{MeO}$	not detected	(i) 90%
(j) $\text{R}^1 = \text{R}^3 = \text{R}^4 = \text{H}, \text{R}^2 = \text{Me}, \text{R}^5 = \text{PhSO}_2$	(j) 83%	(j) 15%
(k) $\text{R}^1 = \text{R}^2 = \text{R}^4 = \text{H}, \text{R}^3 = \text{CO}_2\text{Et}, \text{R}^5 = \text{PhSO}_2$	(k) 80%	not detected

SCHEME 130



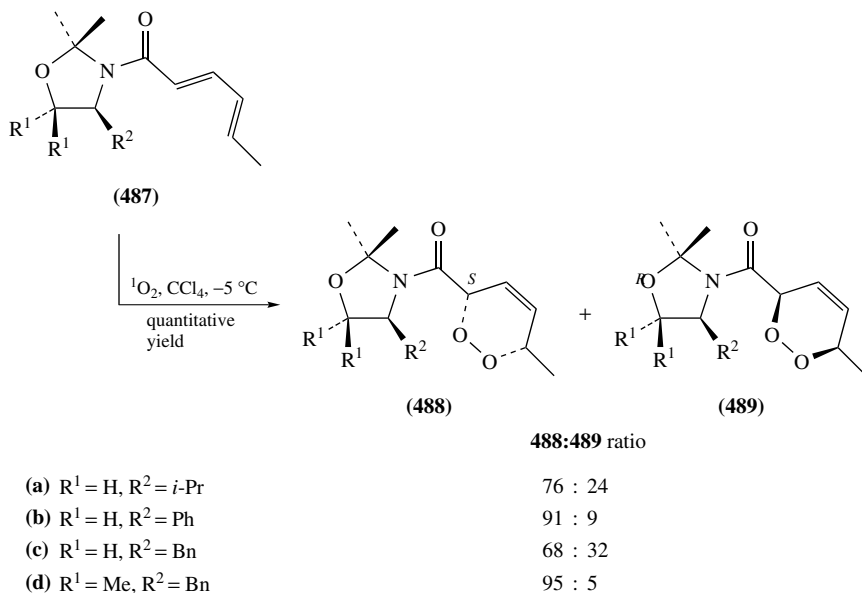
SCHEME 131



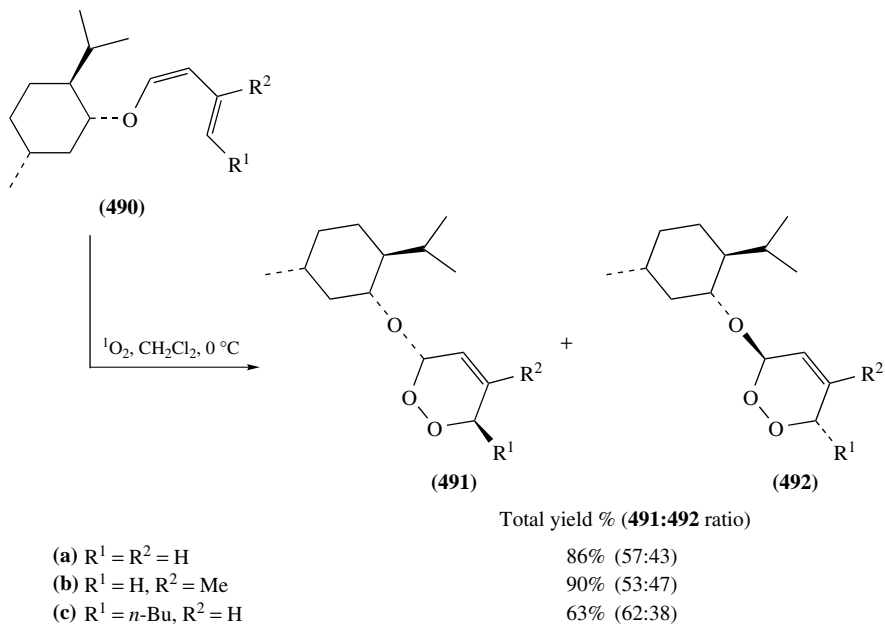
SCHEME 132

Contrary to earlier reports indicating that the electron-poor diene system in sorbates is inert toward singlet oxygen^{369,370}, an effective and stereoselective [4 + 2]-cycloaddition of $^1\text{O}_2$ to ethyl sorbate (485) giving the labile *cis*-endoperoxide 486 as the only detectable product was more recently described (Scheme 132)³⁷¹. Based on this finding, Adam and coworkers developed a method for the diastereoselective cycloaddition of singlet oxygen to optically active 2,2-dimethyloxazolidine derivatives of sorbic acid 487a–d, thus producing the chiral endoperoxides 488a–d and 489a–d (Scheme 133)^{332,371}. As expected, the major products, cyclic peroxides 488, result from $^1\text{O}_2$ approaching from the less hindered side of the dienic system in 487, whereas the minor products 489 are derived from singlet oxygen approaching from the opposite side. The diastereoselective ratio is correlated with the substitution pattern of the oxazolidinyl auxiliary, and depends on the degree of steric interaction between the substituent R^2 in the diene 487 and the incoming $^1\text{O}_2$ (Scheme 133)³⁷¹. Some other commonly used auxiliaries, as for example, chiral cyclohexanol esters and the Oppolzer's sultam, were found to provide inferior diastereofacial control in [4 + 2]-cycloaddition of singlet oxygen to the corresponding sorbates³⁷². Photooxygenation of chiral dienol ethers of type 490 proceeds in good yield but rather low diastereoselectivity to give the enantiomerically enriched 3-alkoxy-1,2-dioxines 491 and 492 (Scheme 134)³⁷³.

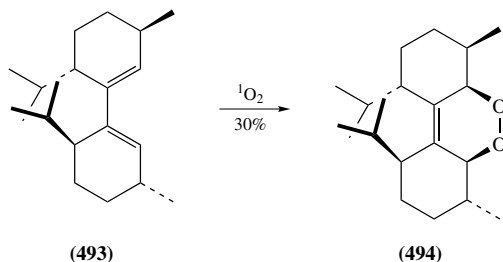
Singlet oxygen reacts through the [4 + 2]-cycloaddition mode with the sterically hindered and non-planar 1,3-diene system in 1,1'-dimenthene (493) to afford the *cis*-endoperoxide 494, albeit in moderate yield (Scheme 135)³⁷⁴. Cycloaddition of $^1\text{O}_2$ to more planar bis(dialine) (495) proceeds smoothly leading predominantly to the *trans*-endoperoxide *trans*-496 (70%), while *cis*-496, which would be expected to derive from a concerted process, constitutes the minor (15%) product (Scheme 136)^{375,376}.



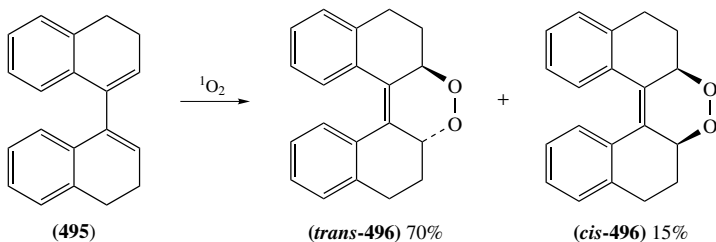
SCHEME 133



SCHEME 134



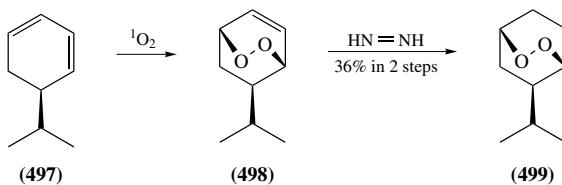
SCHEME 135



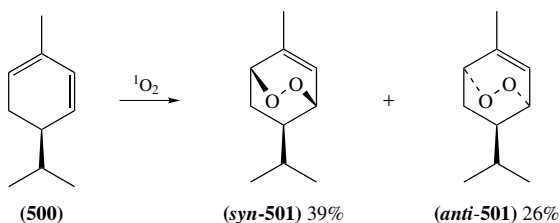
SCHEME 136

Singlet oxygen reacts with many carbocyclic 1,3-dienes to form the corresponding bridged endoperoxides, which can be further transformed into miscellaneous polyoxo functionalized carbocycles^{51, 52, 230, 323, 325}. The rate of photooxygenation of *n*-cyclic 1,3-dienes is gradually decreasing in the order: $n = 5 \gg 6 > 7 \gg 8$ ^{323, 345, 377}. While the rate of [4 + 2]-cycloaddition of singlet oxygen to 1,3-cycloheptadiene is comparable to that of *E,E*-2,4-hexadiene (*E,E*-451) (Scheme 122a), due to the optimal C1-C4 distance, cycloaddition of ¹O₂ to cyclopentadiene proceeds approximately 100 times faster. Due to adverse geometry of the diene system in 1,3-cyclooctadiene, its photooxygenation proceeds about 20 times slower than photooxygenation of acyclic diene *E,E*-451. Although unsaturated bridged endoperoxides are frequently unstable, their C=C bond can be hydrogenated with diimide to the more stable saturated derivatives^{51, 325}.

In general, the stereochemistry of singlet oxygen cycloaddition to cyclic 1,3-dienes is influenced by steric hindrance. In some cases significant remote electronic effects are observed. Overall, the synthetic and stereochemical outcome of such photooxygenations is so variable that it is hard to make reliable predictions even for simple substrates. For instance, upon treatment of 5-isopropyl-1,3-cyclohexadiene (497) with singlet oxygen, followed by *in situ* reduction with diimide, just one cyclic peroxide, *syn*-499, is obtained (36%) (Scheme 137), along with 3-hydroperoxy-1-isopropylcyclohexene (24%)³⁷⁸. These results were rationalized in terms of a preferential ene-reaction originating from ¹O₂ approaching from the freely accessible *anti*-face of the diene 497, whereas the *syn*-face [4 + 2]-cycloaddition leading to unsaturated endoperoxide *syn*-498 derives from singlet oxygen approaching from the more hindered side³⁷⁸. However, an additional methyl substituent in position 2 of the diene 500 diverts the reaction path to the formation of both diastereomeric bicyclic peroxides *syn*-501 (39%) and *anti*-501 (26%) (Scheme 138)³⁷⁹.

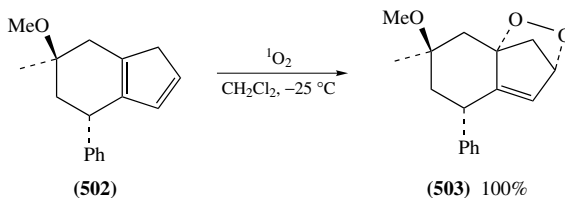


SCHEME 137

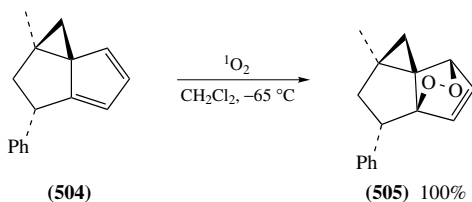


SCHEME 138

Contrary to a variety of common carbon dienophiles, singlet oxygen being the smallest 'dienophile' reveals only moderate bottom-face selectivity toward isodicyclopentadiene and its substituted derivatives^{380–382}. Nevertheless, [4 + 2]-cycloadditions of singlet oxygen to fused cyclopentadienes in some cases are highly stereoselective. Thus, photooxygenation of the fused cyclopentadiene **502** proceeds at -25°C with high face-selectivity ($>98\%$) to give the single cyclic peroxide **503** (Scheme 139)^{383,384}. A similar reaction of cyclopropanated derivative **504** with $^1\text{O}_2$ at -65°C occurs with very high, but opposite face-selectivity, leading to single endoperoxide **505** (Scheme 140)³⁸⁴. [4 + 2]-Cycloadditions of singlet oxygen to adamantylenecyclopentadiene³⁸⁵, as well as to the related 6,6-dialkylfulvenes^{386,387} and to 6-heteroatom-substituted fulvenes³⁸⁸ leading to formation of unstable bridged cyclic peroxides, were reported.

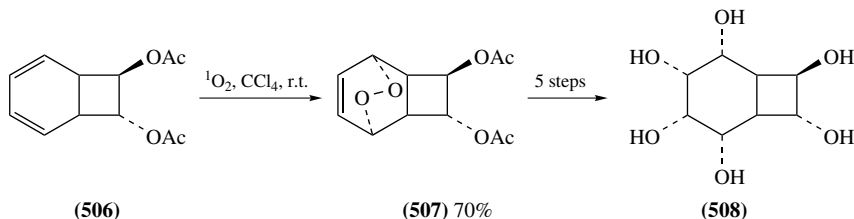


SCHEME 139

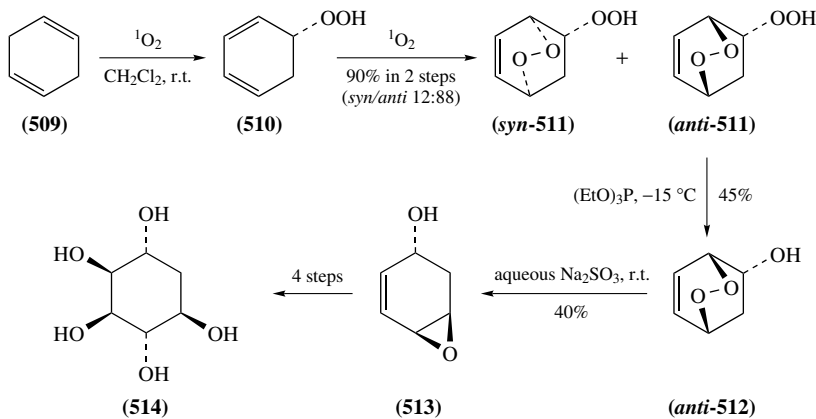


SCHEME 140

Singlet oxygen readily adds to parent 1,3-cyclohexadiene to give the corresponding endoperoxide, namely 2,3-dioxabicyclo[2.2.2]oct-5-ene, in good yield^{389, 390}. The latter as well as analogously generated bridged bicyclic endoperoxides, obtained from $^1\text{O}_2$ photooxygenation of 5,6-epoxy- or 5,6-diacetoxy-1,3-cyclohexadienes, serve as useful intermediates for the syntheses of various polyhydroxylated cyclohexanes^{391–396}. Similarly, singlet oxygen adds to *trans*-7,8-diacetoxycyclo[4.2.0]octa-2,4-diene (**506**) to give the tricyclic endoperoxide **507** (70%), which was converted into bis(homoinositol) (**508**) (Scheme 141)³⁹⁷. Photooxygenation of non-conjugated 1,4-cyclohexadiene (**509**) provides additional options for the synthesis of endoperoxides and of valuable polyhydroxylated compounds. For example, in a one-pot sequential process, **509** is converted to 5-hydroperoxy-1,3-cyclohexadiene (**510**), which reacts with a second equivalent of $^1\text{O}_2$ to afford a separable 12:88 mixture of *syn*- and *anti*-hydroperoxy-endoperoxides **511** in excellent overall yield (Scheme 142)^{393, 398, 399}. Selective deoxygenation of the hydroperoxide function in *anti*-**511** to hydroxy endoperoxide *anti*-**512** and subsequent stereoselective reductive rearrangement gives the unsaturated epoxy alcohol **513**^{399, 400}. Epoxy alcohol **513** served as a key intermediate in the synthesis of racemic⁴⁰⁰ and non-racemic *proto*-quercitol (**514**) (Scheme 142)⁴⁰¹.

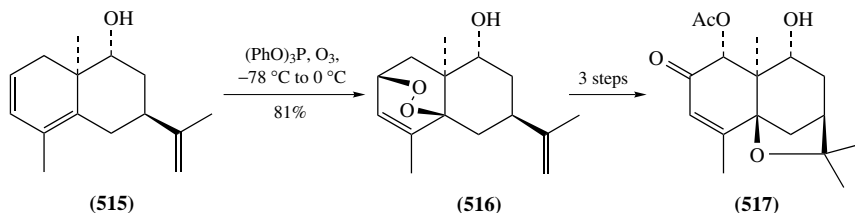


SCHEME 141

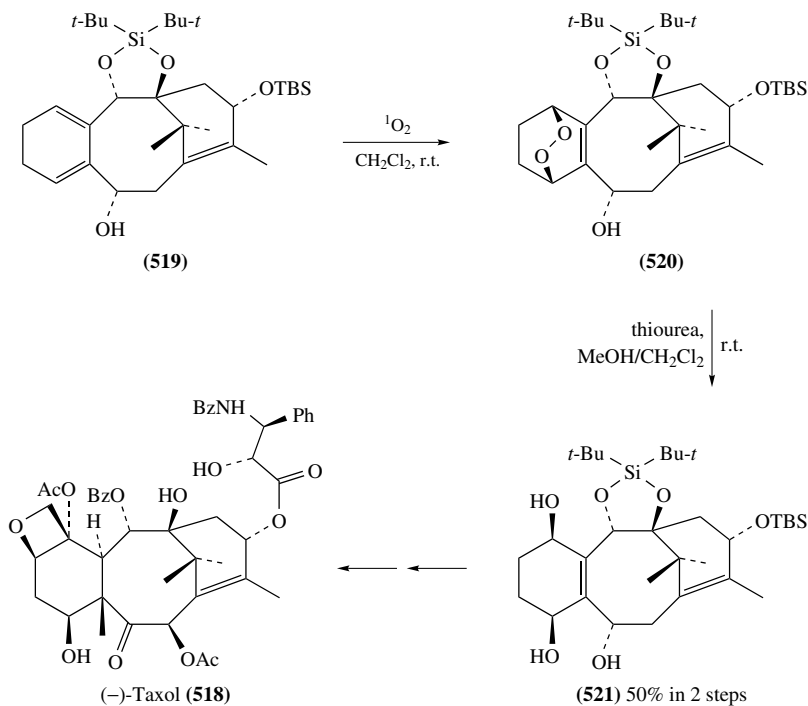


SCHEME 142

[4 + 2]-Cycloadditions of singlet oxygen to particular fused 1,3-cyclohexadienes can be highly diastereoselective, and therefore useful in the total syntheses of some complex natural products. For example, chemically generated $^1\text{O}_2$ effectively and stereoselectively adds to the termini of the 1,3-diene system in **515** to give a single endoperoxide **516** (81%),



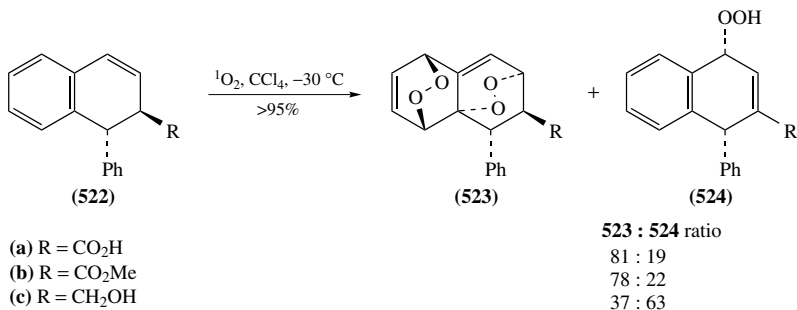
SCHEME 143



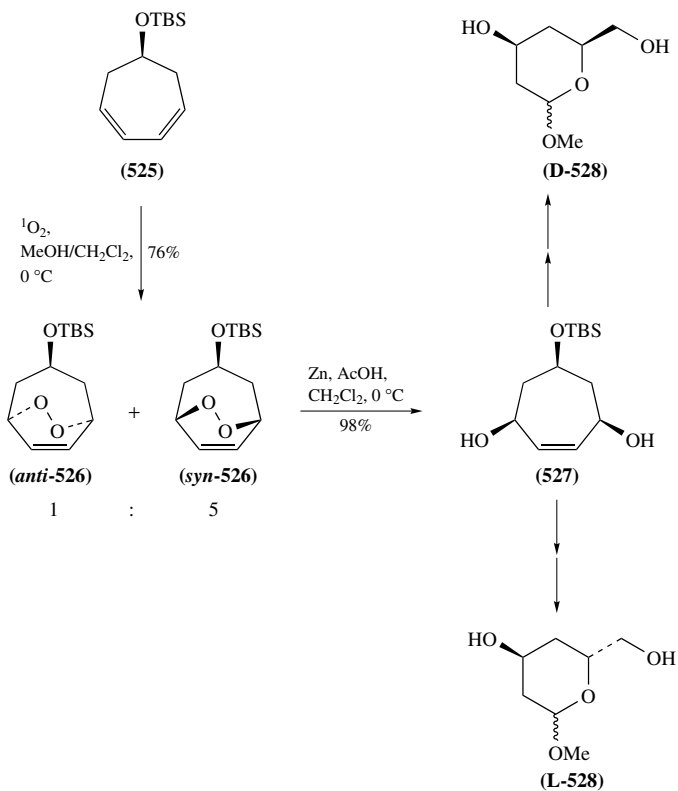
SCHEME 144

that was converted in 3 steps to the tricyclic compound **517** possessing the molecular framework of the naturally occurring sesquiterpenoid agarofuran (Scheme 143)⁴⁰². A crucial stage in a recent total synthesis of (–)-taxol (**518**) was based on the stereoselective [4 + 2]-cycloaddition of singlet oxygen with cyclohexadiene **519** to give the bridged bicyclic peroxide **520**, which was reduced to the *cis*-1,4-dihydroxycyclohex-2-ene **521** and eventually converted to taxol (**518**) (equation 144)⁴⁰³.

The photooxygenations of chiral 1,2-dihydronaphthalenes **522a–c** at -30°C are highly stereoselective due to a first attack of singlet oxygen from *anti*-face respective to substituent R. The ratios of bis(endoperoxides) **523** to hydroperoxides **524** are strongly influenced by the R-group (Scheme 145)⁴⁰⁴. While the reaction of $^1\text{O}_2$ with acid **522a** gives mostly bis(endoperoxide) **523a**, photooxygenation of the alcohol **522c** leads preferentially to hydroperoxide **524c**.

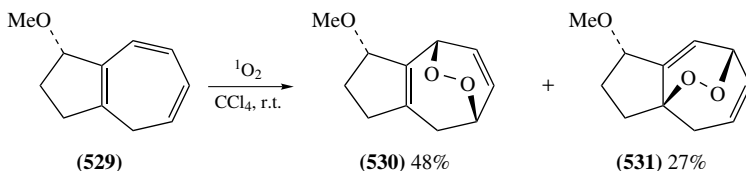


SCHEME 145

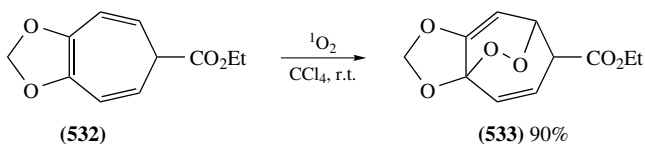


SCHEME 146

A sequence of transformations involving diastereoselective singlet oxygen photooxygenation of TBS-protected 3,5-cycloheptadienol **525** to predominantly *syn*-endoperoxide *syn-526* and some *anti-526*, followed by reduction into the all-*cis* triol **527** as described in Scheme 146, was used by Johnson for synthesis of enantiopure methyl 2,4-dideoxyhexapyranosides **D-528** and **L-528**^{405, 406}.



SCHEME 147

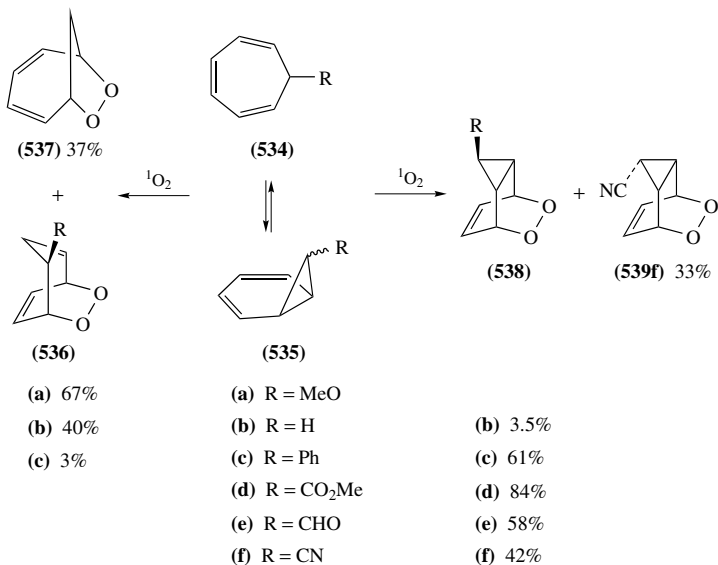


SCHEME 148

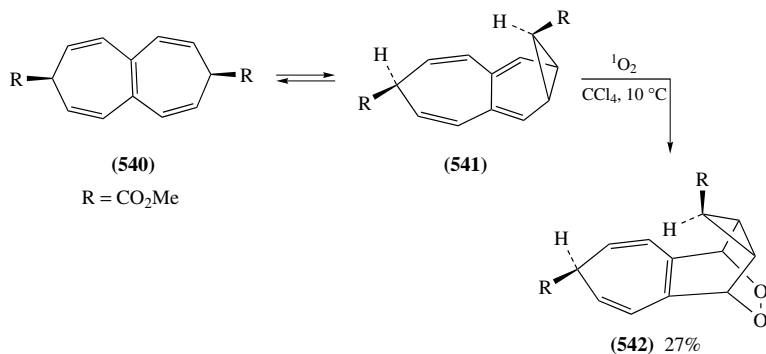
Highly *anti*-diastereoselective, but not regioselective, [4 + 2]-cycloaddition of singlet oxygen to 1-methoxy-1,2,3,4-tetrahydroazulene **529** leads to a mixture of tricyclic peroxides **530** and **531** (Scheme 147)⁴⁰⁷. A similar regiodiversity was earlier observed for a ¹O₂ peroxygenation of 3,4-dihydroazulen-1(2*H*)-one^{408,409}. Treatment of symmetric 1,3-dioxolane-fused cycloheptatriene **532** with singlet oxygen affords the single cyclic peroxide **533** in very high yield (Scheme 148)⁴¹⁰. Reaction of ¹O₂ with 7-methoxy-1,3,5-cycloheptatriene (**534a**) gives the bridged bicyclic peroxide **536a** in good yield through [4 + 2]-cycloaddition to the parent tropilidene form (Scheme 149)^{411,412}. In contrast to that, singlet oxygen peroxidation of monocyclic 7-substituted cycloheptatrienes **534c–f**, bearing electron-withdrawing substituents at C7, afford mostly the isomeric tricyclic peroxides **538c–f**, derived from norcaradiene valence isomer **535**, having a *syn*-relationship between peroxide fragment and the substituent R. Singlet oxygen photooxygenation of parent cycloheptatriene (**534b**) affords the [4 + 2]-cycloaddition adduct **536b** (40%), [6 + 2]-cycloaddition adduct **537b** (37%) and a small amount of the product **538b**, derived from the norcaradiene valence isomer **535b** peroxidation (Scheme 149)⁴¹³. The norcaradiene-derived endoperoxide **539f** with the *anti*-arrangement was isolated only in the reaction with **534f**, carrying the small cyano substituent⁴¹². Reactions of 2-, 3- or 4-carbomethoxy (or acetyl)-1,3,5-cycloheptatrienes with ¹O₂ give predominantly bicyclic peroxides structurally related to **537**⁴¹⁴. [4 + 2]-Cycloaddition of one molecule of singlet oxygen to the fused bis(cycloheptatriene) **540** proceeds through the norcaradiene valence isomer **541** leading to a single, thermally and chemically robust endoperoxide **542** (Scheme 150)⁴¹⁵.

A remarkable stereodirecting influence of remote oxygen-containing substituents on singlet oxygen cycloaddition to conformationally rigid 1,3-cyclohexadienes of type **543** was recently described (Scheme 151)^{416,417}. While photooxygenations of the diol **543a** and the diacetate **543b** involve mainly *syn*-addition to give, respectively, endoperoxides **544a** and **544b**, the dimethoxy derivative **543c** and ethylenedioxy derivative **543d** give preponderantly the corresponding *anti*-endoperoxides **545c** and **545d**. These, and additional results from experiments with carbonyl, cyclic ketal and thioketal derivatives were attributed to electrostatic interaction between approaching singlet oxygen and the heteroatom^{416,417}. Similar electronic effects were observed in studies on singlet oxygen [4 + 2]-cycloaddition to the naturally occurring alkaloid (–)-colchicine^{418,419}, but the opposite facial selectivity was reported for the isomeric (–)-isocolchicine⁴²⁰.

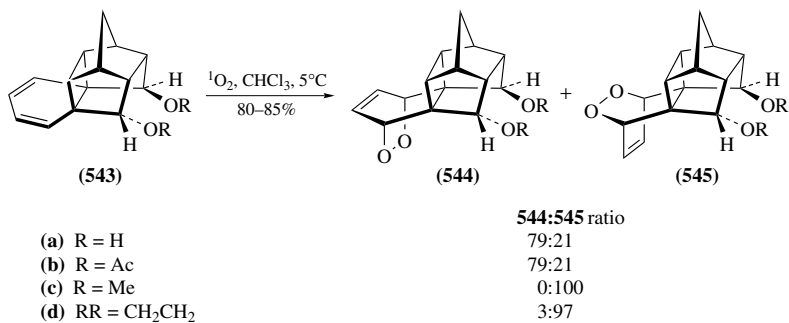
A large number of electron-rich polycyclic aromatic systems including anthracenes, azaanthracenes and larger homologues arenes undergo [4 + 2]-cycloaddition with singlet



SCHEME 149



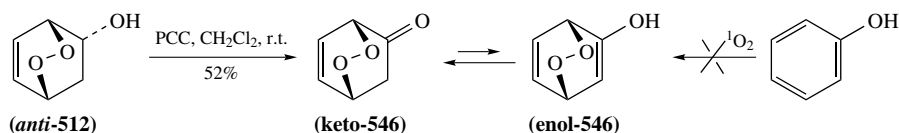
SCHEME 150



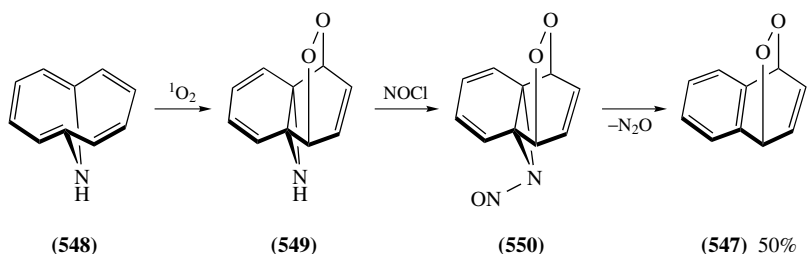
SCHEME 151

oxygen to give relatively stable endoperoxide adducts^{51,325}. The binding of singlet oxygen to aromatic compounds is frequently reversible, therefore many ‘aromatic endoperoxides’ can serve as a valuable source for the clean generation of $^1\text{O}_2$ free from other reactive oxygen species^{52,329}. Some water-soluble cyclic peroxides were used as singlet oxygen source in biological studies under physiological conditions^{329,421,422}. Some ^{18}O -labeled 1,4-substituted naphthalene endoperoxides were used in mechanistic studies⁴²³.

The photosensitized peroxidations of electron-rich aromatic compounds, including phenols, generally lead to the corresponding 4-hydroperoxy-2,5-cyclohexadienones rather than to endoperoxides⁵¹. Bicyclic peroxide **keto-546**, which is relatively stable at room temperature, is formally derived from the hypothetical [4 + 2]-cycloaddition of singlet oxygen to the 2 and 5 positions of phenol that would lead to **enol-546**. The peroxide **keto-546** was prepared by oxidation of the readily available hydroxy-peroxide **anti-512** with pyridinium chlorochromate (PCC) (CH_2Cl_2 , r.t.) (Scheme 152)³⁹⁹. Unsubstituted naphthalene doesn't produce endoperoxide **547** upon exposure to $^1\text{O}_2$ ⁵¹. Nevertheless, this endoperoxide has been synthesized from 1,6-imino[10]annulene **548** as shown in Scheme 153⁴²⁴. Singlet oxygen peroxidation of **548** occurs with concomitant C–C bond formation, leading to the tetracyclic peroxide **549**. Treatment of **549** with NOCl affords the unstable *N*-nitrosoaziridine **550**, which spontaneously extricates N_2O to give naphthalene endoperoxide **547** (Scheme 153)⁴²⁴.

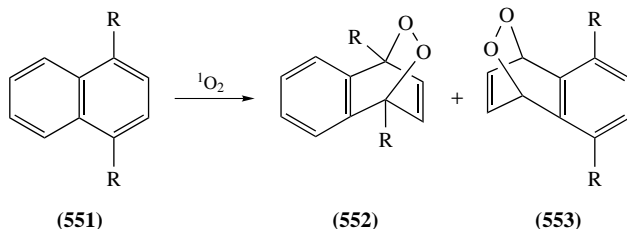


SCHEME 152



SCHEME 153

In contrast to parent naphthalene, naphthalene derivatives with electron-donating substituents at the 1,4-positions readily react with singlet oxygen to give the corresponding 1,4-endoperoxides^{51,325}. Photosensitized singlet oxygen peroxidation in water or in methanol of 1,4-disubstituted naphthalenes **551a–d** possessing highly hydrophilic substituents lead to a mixture of 1,4-endoperoxides **552a–d** and 5,8-endoperoxides **553a–d**; the former usually constitute the major products (Scheme 154)^{425,426}. Anthracene and 9,10-dialkyl-substituted anthracenes smoothly add $^1\text{O}_2$ onto the central ring to give the corresponding 9,10-endoperoxides^{51,325}. When electron-donating substituents are in the terminal ring, singlet oxygen can also add across the terminal ring^{427–429}. For example, brief $^1\text{O}_2$ photooxygenation of 1,2,3,4-tetramethylanthracene and its 9,10-diphenyl analogue afford the corresponding 1,4-endoperoxides in 85–90% yield⁴²⁹. Similarly,



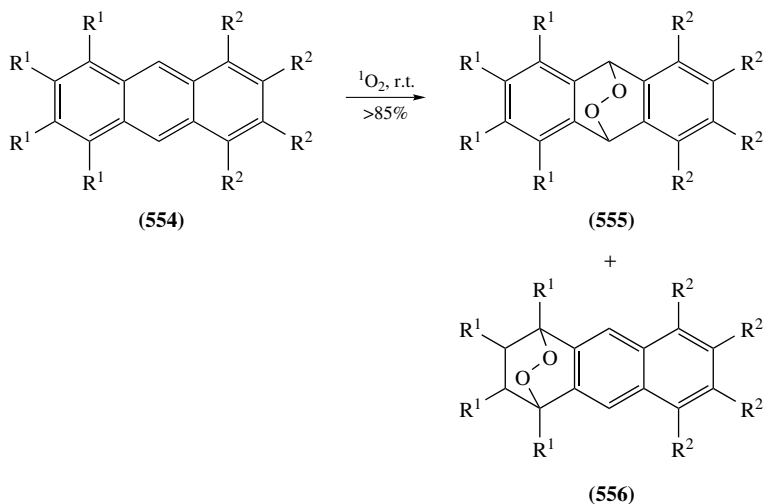
(a) R = CH₂CH[CONHCH₂CH(OH)CH₂OH]₂

(b) R = CH₂CH₂CO₂Na

(c) R = CH₂CH(CO₂Na)₂

(d) R = CH₂OCH₂CH(OH)CH₂OH

SCHEME 154



555:556 ratio

(a) R¹ = R² = Me

5:81

(b) R¹ = R² = Et

52:44

(c) R¹ = R² = *n*-Pr

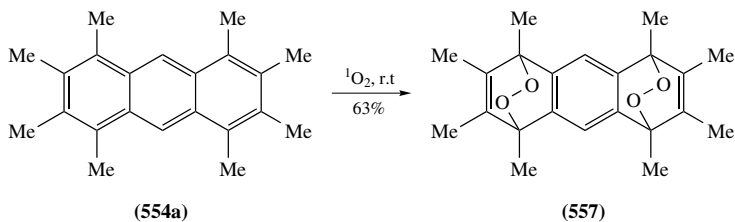
61:32

(d) R¹ = Et, R² = Ph

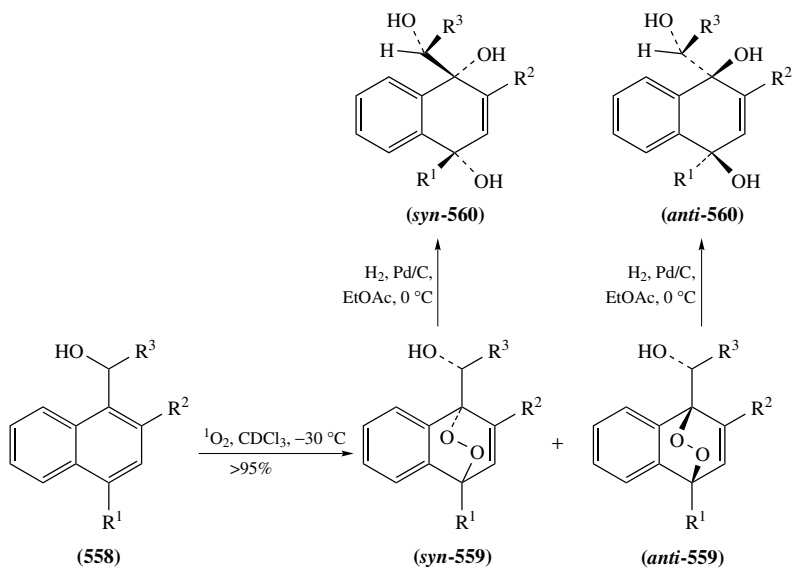
53:40

SCHEME 155

singlet oxygen cycloaddition to 1,2,3,4,5,6,7,8-octamethylantracene **554a** gives mainly the 1,4-endoperoxide **556a** accompanied by a small amount of the 9,10-isomer **555a** (Scheme 155)⁴³⁰. The higher alkyl-homologues **554b** and **554c** and the tetraphenyl-analogue **554d** give a mixture of 9,10-endoperoxides **555b–d** and 1,4-endoperoxides **556b–d**⁴³⁰. Upon prolonged photooxygenation, the octamethylantracene **554a** can add singlet oxygen onto both terminal rings with formation of the bis(endoperoxides) **557** (two isomers, *ca* 1:1) in good total yield (Scheme 156)^{430,431}.



SCHEME 156



syn-559 : anti-559 ratio
(at 95% conversion)

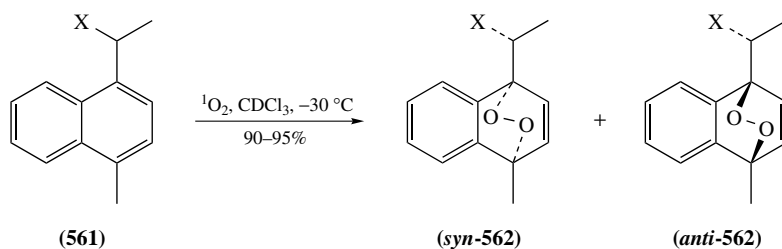
(a) R ¹ = R ³ = Me, R ² = H	85:15
(b) R ¹ = Me, R ² = H, R ³ = Et	88:12
(c) R ¹ = Me, R ² = H, R ³ = <i>t</i> -Bu	87:13 (at 30% conversion)
(c) R ¹ = Me, R ² = H, R ³ = <i>t</i> -Bu	5:95 (at 60% conversion)
(d) R ¹ = H, R ² = OMe, R ³ = Me	91:9
(e) R ¹ = H, R ² = OH, R ³ = Me	95:5 (69% total yield)
(f) R ¹ = H, R ² = R ³ = Me	6:94

SCHEME 157

Adam and coworkers recently discovered that singlet oxygen [4 + 2]-cycloaddition to chiral naphthalene derivatives, bearing a proximal stereogenic center attached to position 1 of the naphthalene core, frequently occurs with high π -facial diastereoselectivity.^{331, 332} Indeed, photooxygenations of naphthyl alcohols **558a,b,d,e** in CDCl₃ give predominantly the corresponding *syn*-endoperoxides **syn-559** accompanied by small amounts of *anti*-endoperoxides **anti-559** (Scheme 157)^{432, 433}. In contrast to the examples listed above,

reaction of $^1\text{O}_2$ with dimethyl derivative **558f** in CDCl_3 proceeds with high but opposite diastereoselectivity, and the *anti*-endoperoxide **anti-559f** is formed as the major product⁴³². Being much less reactive toward $^1\text{O}_2$ than its smaller alkyl homologues **558a** and **558b**, the *tert*-butyl substituted substrate **558c** demonstrates high *syn*-selectivity at 30% conversion, that reverses to very high *anti*-selectivity at 60% conversion. These observations indicate that *syn*-endoperoxides **syn-559** are the kinetically favored products, whereas the more stable peroxides **anti-559** result from thermodynamically controlled processes. In all the tested reactions, more polar solvents like perdeuterated acetone, acetonitrile or methanol significantly decrease the degree of diastereoselectivity. Acetylated, methylated or silylated derivatives of alcohol **558a** are photooxygenated efficiently, but without π -facial discrimination^{434,435}. For corroboration of the stereochemical assignments, both **syn-559** and **anti-559** type cyclic peroxides were stereoselectively reduced to the triols **syn-560** and **anti-560** respectively (Scheme 157)⁴³⁴. It is noteworthy that 2- and 4-(1-hydroxyethyl)phenols undergo essentially diastereoselective photooxygenation with singlet oxygen to give the corresponding chiral 4-hydroperoxy-3,5-cyclohexadienones⁴³⁶.

Not only a proximal hydroxy group, but also some other functionalities can effect the π -facial diastereoselectivity in the singlet oxygen cycloaddition^{432,435}. Indeed, while cycloadditions of $^1\text{O}_2$ to the cyanoalkyl naphthalene **561a** and aldehyde **561b** are not diastereoselective, the ester **561c** and the acid **561d** exhibit considerable *anti*-selectivity to give preferentially endoperoxides **anti-562c** and **anti-562d**, respectively (Scheme 158)⁴³². The presence of pyridine (2 equivalents) during photooxygenation of acid **561d** significantly increases *anti*-diastereoselectivity (*syn/anti* ca 10:90) without affecting the high yield of the endoperoxides **562d**. Reaction of the alcohol **561e** with singlet oxygen proceeds with equally high, but opposite diastereoselectivity to yield predominantly cyclic peroxide **syn-562e** (Scheme 158)⁴³². Photooxygenations of the naphthalene derivatives of type **561** bearing substituents $\text{X} = \text{Me}_3\text{Si}$ or Br were found to be highly diastereoselective (*dr* 95:5), but due to the inherent thermal lability of the resulting cyclic peroxides their relative stereochemistry has not been assigned⁴³⁵.



syn-562 : anti-562 ratio
(at > 90% conversion)

(a) X = CN	51:49 (at 40% conversion)
(b) X = CHO	60:40 (at 48% conversion)
(c) X = CO ₂ Me	22:78
(d) X = CO ₂ H	21:79
(d) X = CO ₂ H	10:90 (with 2 equiv. pyridine)
(e) X = CH ₂ OH	90:10

SCHEME 158

Photooxygenation of polysubstituted 9,10-dimethoxyanthracene followed by *in situ* Baeyer–Villiger-type rearrangement of the intermediate peroxide was used for constructing the aromatic part of (–)-balanol, a naturally occurring protein kinase C inhibitor⁴³⁷. Reactions of singlet oxygen with 5-membered aromatic heterocycles usually lead to complex mixtures of products. In some cases, the corresponding unstable bridged cyclic peroxides were isolated^{51, 325, 438}.

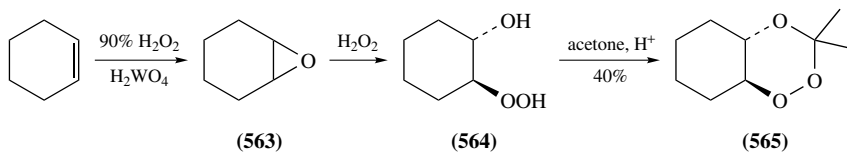
III. SYNTHESIS OF 1,2,4-TRIOXANES

The isolation and structural determination of the naturally occurring potent antimalarial sesquiterpene endoperoxides, artemisinin (qinghaosu) (**6**)^{28–31, 439} and the recognition of the 1,2,4-trioxane system as the pharmacophore responsible for its parasitocidal properties^{440–442} have motivated a worldwide quest for new trioxanes with effective therapeutic properties. The need for new compounds for structure to biological activity relationship (SAR) studies and for the investigation of the mode of action of 1,2,4-trioxanes have led to the development of a variety of new synthetic methodologies^{32, 33, 53–56, 443}. 1,2,4-Trioxane-based antimalarial drug design and the possible mechanisms of antimalarial action are thoroughly and regularly reviewed^{32–41, 46, 48, 55, 56, 443–455}. Several 1,2,4-trioxane derivatives of artemisinin (**6**)^{456–466}, and especially bis(trioxane) conjugates^{464–472}, were found to exhibit significant antiproliferative and antitumor activities which were recently reviewed^{32, 48}.

Considering the huge amount of available material, this section is more concise than the previous sections of this chapter. Synthetic modifications of naturally occurring artemisinin (**6**) are not discussed at all.

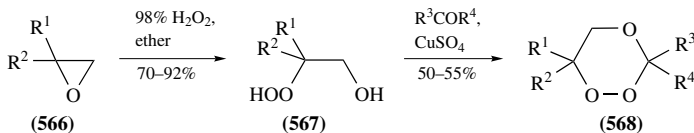
A. Peroxyacetalization of Carbonyl Functions with β -Hydroperoxyalcohols

The first example for the synthesis of 1,2,4-trioxane by acid-catalyzed peroxyacetalization of ketones and aldehydes with β -hydroperoxyalcohols was provided in 1957 in the context of a study on epoxidation of cyclohexene. Thus, trioxadecalin **565** was obtained from cyclohexene in a process involving epoxide **563** and β -hydroperoxycyclohexanol **564**, by treatment with concentrated H_2O_2 and tungstic acid in acetone (40% overall yield) (Scheme 159)⁴⁷³. Similarly, treatment of epoxides **566** with anhydrous H_2O_2 in ether gives the corresponding β -hydroperoxyalcohols **567**, which condense with carbonyls in the presence of copper(II) sulfate to form trioxanes **568** (Scheme 160)^{474, 475}. An analogous approach was more recently applied for preparation of dispiro-1,2,4-trioxanes from methylenecyclohexane epoxide⁴⁷⁶. An evident drawback of this method derives from the need of using highly hazardous concentrated hydrogen peroxide.



SCHEME 159

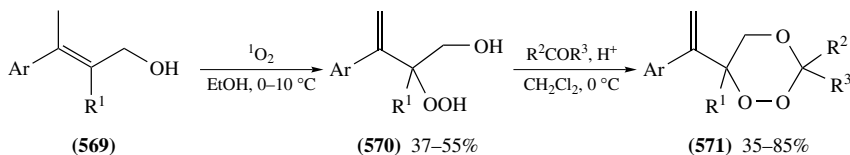
Allylic alcohols constitute an alternative valuable source for the preparation of β -hydroperoxyalcohols suitable for peroxyacetalization to 1,2,4-trioxanes. A number of 3-alkyl-substituted allyl alcohols undergo a highly regio- and stereoselective ene-reaction with singlet oxygen to generate the corresponding β -hydroperoxyalcohols⁴⁷⁷.



$\text{R}^1 = \text{R}^2 = \text{Me}$ or Ph , $\text{R}^3 = \text{R}^4 = \text{Me}$,

$\text{R}^1 = \text{R}^3 = \text{Ph}$, $\text{R}^2 = \text{R}^4 = \text{H}$

SCHEME 160



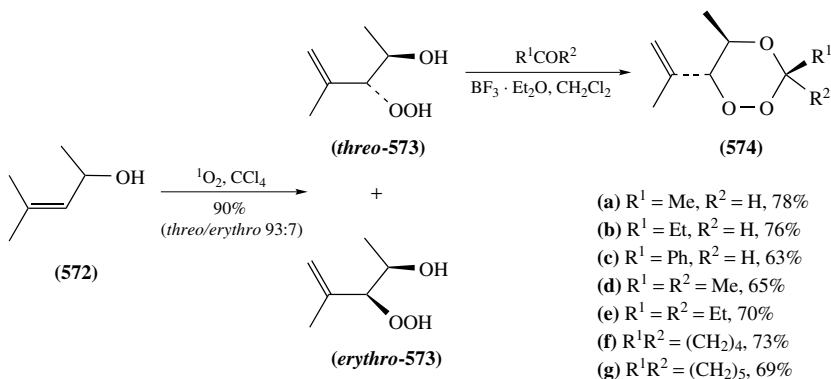
$\text{R}^1 = \text{H}$ or Me ,

$\text{R}^2 = p\text{-An}$, $\text{R}^3 = \text{H}$, $\text{R}^2 = \text{R}^3 = \text{Me}$, $\text{R}^2\text{R}^3 = (\text{CH}_2)_4$ or $(\text{CH}_2)_5$, $\text{R}^2\text{COR}^3 = 2\text{-adamantanone}$,

$\text{Ar} = 2,4\text{-Me}_2\text{C}_6\text{H}_3$ or $4\text{-XC}_6\text{H}_4$ ($\text{X} = \text{Cl}, \text{F}, \text{H}, \text{Me}, \text{OMe}$)

SCHEME 161

For example, such a photooxygenation of alcohols **569** lead to unsaturated alcohol-hydroperoxides **570**, which react with ketones and aldehydes to give 1,2,4-trioxanes **571** characterized by α -styryl-substituents at the 6-position (Scheme 161)⁴⁷⁸⁻⁴⁸¹. Geraniol and geraniol-derived allylic alcohols are similarly converted into the 3,3,6-trisubstituted 1,2,4-trioxanes^{482,483}. Ene-reaction of $^1\text{O}_2$ with secondary alcohol **572** proceeds with a high *threo*-diastereoselectivity to provide preferentially *threo*-**573**⁴⁸⁴. The latter is subjected to boron trifluoride-catalyzed peroxyacetalization with simple aldehydes and ketones, thus producing the corresponding trioxanes **574a-g** with a prerequisite *trans*-arrangement of substituent at C5 and C6 (Scheme 162)⁴⁸⁴. 1,2,4-Trioxanes-5-ones were obtained through a related peroxyacetalization using TMSOTf-mediated condensation of bis(trimethylsilylated) α -hydroperoxycarboxylic acids with aldehydes and ketones^{485,486}.



(a) $\text{R}^1 = \text{Me}$, $\text{R}^2 = \text{H}$, 78%

(b) $\text{R}^1 = \text{Et}$, $\text{R}^2 = \text{H}$, 76%

(c) $\text{R}^1 = \text{Ph}$, $\text{R}^2 = \text{H}$, 63%

(d) $\text{R}^1 = \text{R}^2 = \text{Me}$, 65%

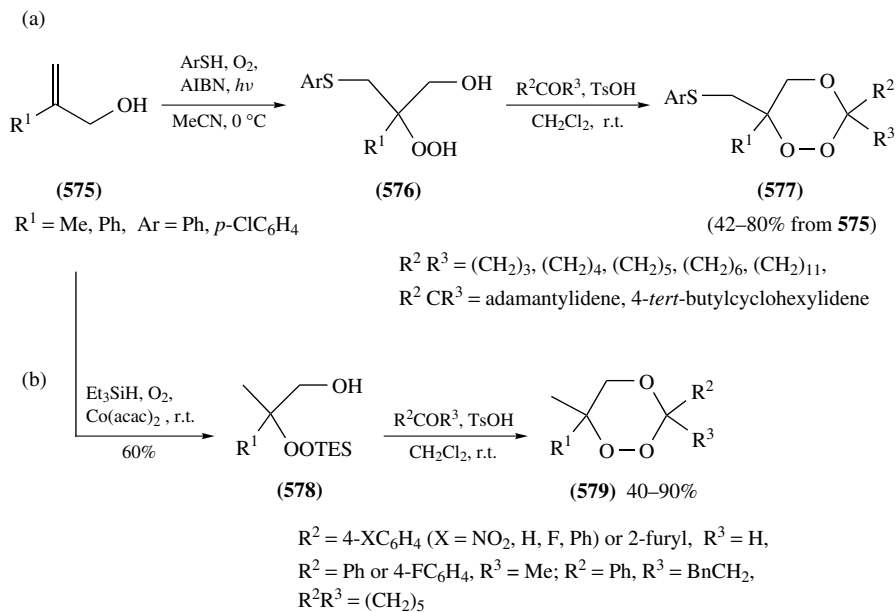
(e) $\text{R}^1 = \text{R}^2 = \text{Et}$, 70%

(f) $\text{R}^1\text{R}^2 = (\text{CH}_2)_4$, 73%

(g) $\text{R}^1\text{R}^2 = (\text{CH}_2)_5$, 69%

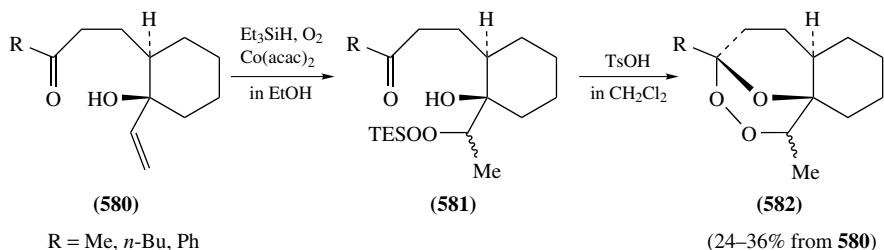
SCHEME 162

Two types of co-oxygenation processes leading to β -hydroperoxyalcohols that can be converted *in situ* to trioxanes are described in Scheme 163. Thiol olefin co-oxygenations of 3-unsubstituted allyl alcohols **575** (TOCO reaction, see also Schemes 51–54, Section II.A.5) afford the corresponding hydroperoxyalcohol intermediates **576**, which are condensed in the same vessel with ketones to give the corresponding trioxanes **577** in moderate to high yield (Scheme 163a)⁴⁸⁷. Likewise, Co(acac)-catalyzed Mukaiyama hydroperoxysilylation of allyl alcohols **575** efficiently produce triethylsilyl substituted β -hydroperoxyalcohols **578** (60%), which are condensed with aldehydes and ketones to give the corresponding trioxanes **579** (40–90%) (Scheme 163b)⁴⁸⁸. Spiro-1,2,4-trioxanes were obtained by the same method using bis(2,2,6,6-tetramethyl-3,5-heptanedionato)cobalt(II) as mediator⁴⁸⁹. A parallel Co(acac)-mediated co-oxygenation with cinnamyl alcohol affords 3-(triethylsilylperoxy)-3-phenylpropanol (64%) which, when subjected to peroxyacetalization with aldehydes and ketones, gives the corresponding 7-membered 1,2,4-trioxepanes (58–75%)⁴⁹⁰. Co(acac)-catalyzed triethylsilylperoxygenation of keto-substituted allylic alcohols **580** gives the corresponding β -triethylsilylperoxyalcohols **581**, which undergo an intramolecular condensation with a carbonyl function to give tricyclic 1,2,4-trioxanes **582** (24–36% from **580**) (Scheme 164)⁴⁹¹.

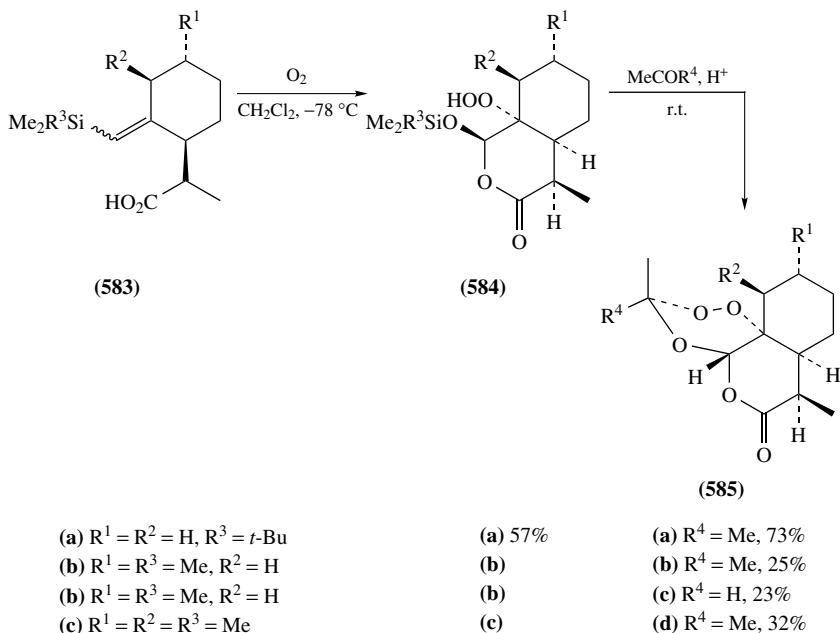


SCHEME 163

Avery and coworkers found that ozonolyses of vinylsilanes of type **583a–c** bearing properly positioned carboxylic function afford bicyclic lactones **584a–c** carrying the β -silyloxyhydroperoxide moiety (Scheme 165)^{492–494}. The particular array of substituents in lactones **584**, and their relative stereochemistry, are reflecting analogous features in the molecular core of artemisinin (**6**). Upon ozonolysis of **583a**, the TBS-protected intermediate **584a** was isolated in 57% yield and subsequently cyclized with acetone to give the *cis*-fused 1,2,4-trioxane **585a** (73%)⁴⁹². The more labile TMS-protected alcohols **584b** and **584c** deriving from **583b** and **583c** were converted to trioxanes **585b–d** in the same

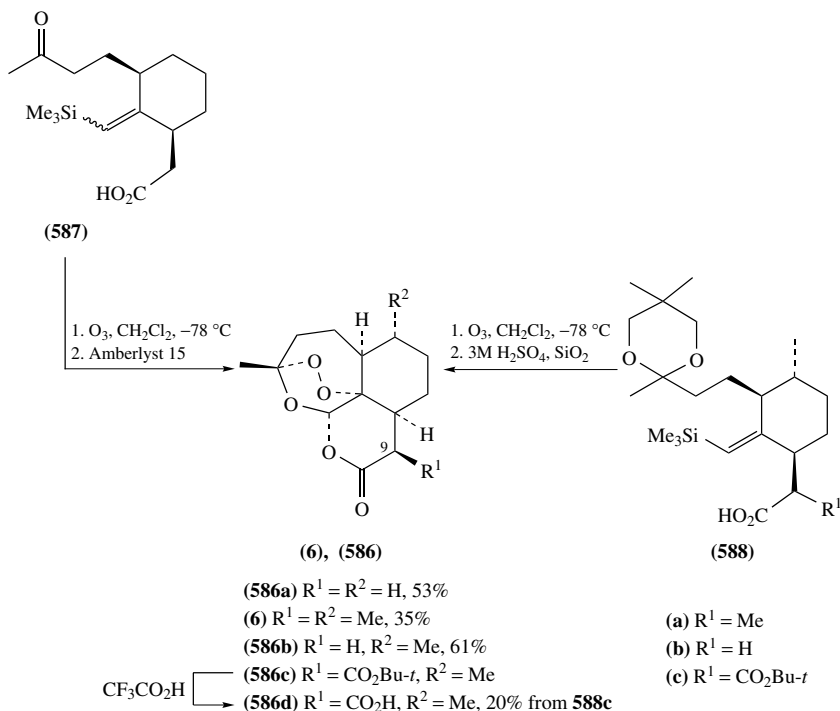


SCHEME 164



SCHEME 165

vessel (Scheme 165)^{493,494}. A direct route to artemisinin (**6**) and analogues thereof **586** was based on the employment of compounds of type **583** in which R² represents a suitable carbonyl-carrying side chain as described in Scheme 166. For example, the final stage in the synthesis of racemic 6,9-demethylated artemisinin analogue **586a** involves ozonolysis of the multifunctionalized precursor **587** and subsequent acid-catalyzed intramolecular peroxyketalization of the resulting β -silyloxyhydroperoxide system with the properly positioned carbonyl function (Scheme 166)⁴⁹⁵. Similarly, compound **588a** which was obtained from (*R*)-(+)-pulegone, and carries the carboxyl, TMS-vinyl and a ketal function was used as the key intermediate in the total synthesis of (+)-artemisinin (**6**) (Scheme 166)^{496,497}. A wide range of antimalarial artemisinin analogues, characterized by modifications at C9, including the 9-demethylated analogue **586b**, ester **586c**, and acid **586d**, were prepared from the corresponding ketals **588** or ketones of type **587**^{441,497–501}. The same methodology was applied also for the synthesis of simplified tricyclic analogues of artemisinin⁵⁰².

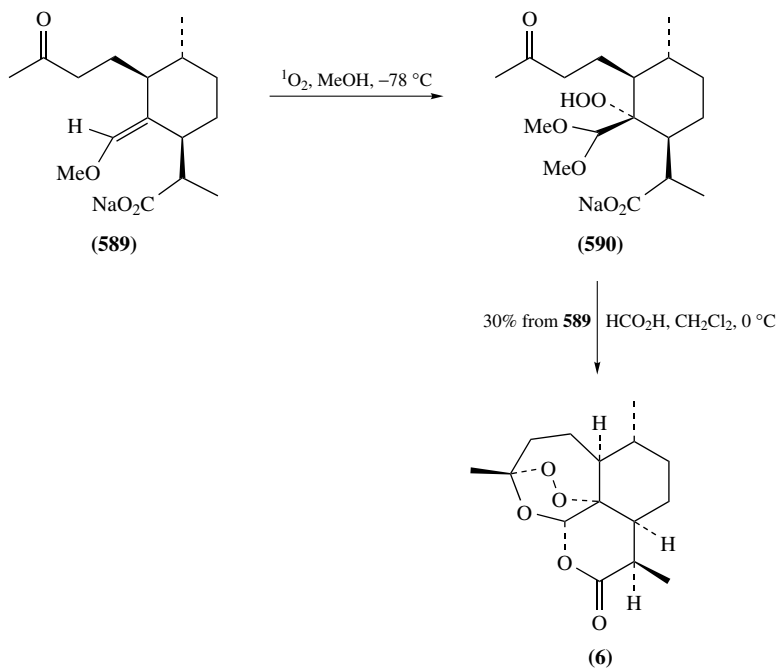


SCHEME 166

In 1983, Schmid and Hofheinz reported on the first total synthesis of artemisinin (**6**) (Scheme 167)⁵⁰³. It is based on a multi-step conversion of (–)-isopulegol to the key intermediate compound **589**, which has four of the five chiral centers of the target compounds in the correct absolute stereochemistry, as well as an array of substituents designed to complete the construction of the complex trioxane-lactone framework of artemisinin (**6**) in two additional steps. Low temperature peroxidation of the vinyl ether **589** with singlet oxygen in methanol affords an intermediate compound, presumably β -hydroperoxyacetal **590**, which undergoes an acid-catalyzed intramolecular sequential peroxyacetalization, transacetalization and lactonization reactions leading to artemisinin (**6**) in 30% yield (Scheme 167)⁵⁰³. Independently and simultaneously, Zhou and coworkers elaborated the total synthesis of **6** from (*R*)-(+)-citronellal based on a similar photooxygenation of the methyl ester of **589** in methanol and subsequent acid-catalyzed polycyclization of the product^{276, 504–506}. Very recently, the same 1O_2 oxygenation was applied by Yadav and coworkers for the simplified total synthesis of **6** from (+)-isolimonene⁵⁰⁷. Thus, albeit mechanistically not yet well elucidated, the low-temperature reaction of singlet oxygen with vinyl ethers in MeOH, followed by intramolecular peroxyacetalization and lactonization, provides a useful tool for constructing 1,2,4-trioxanes.

B. Peroxyacetalization of Carbonyl Functions with Strained Endoperoxide Systems

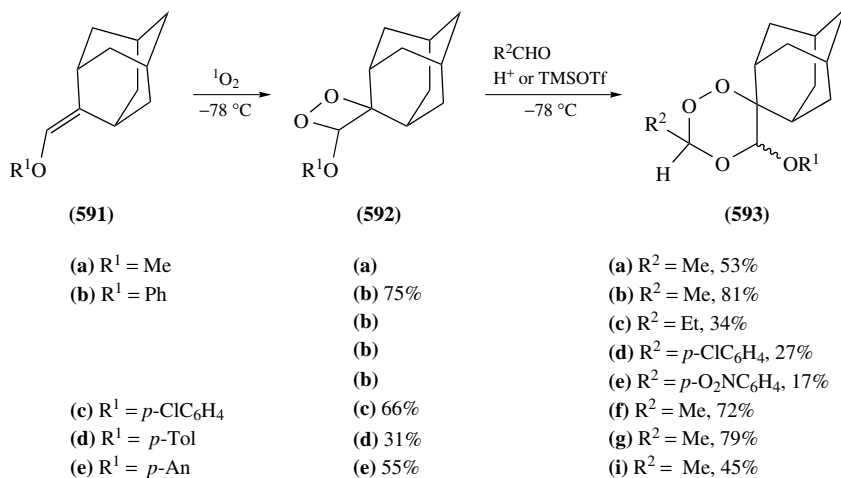
Lewis acid-catalyzed inter- or intramolecular condensation of carbonyl compounds with strained cyclic peroxides represents one of the most general and useful methods



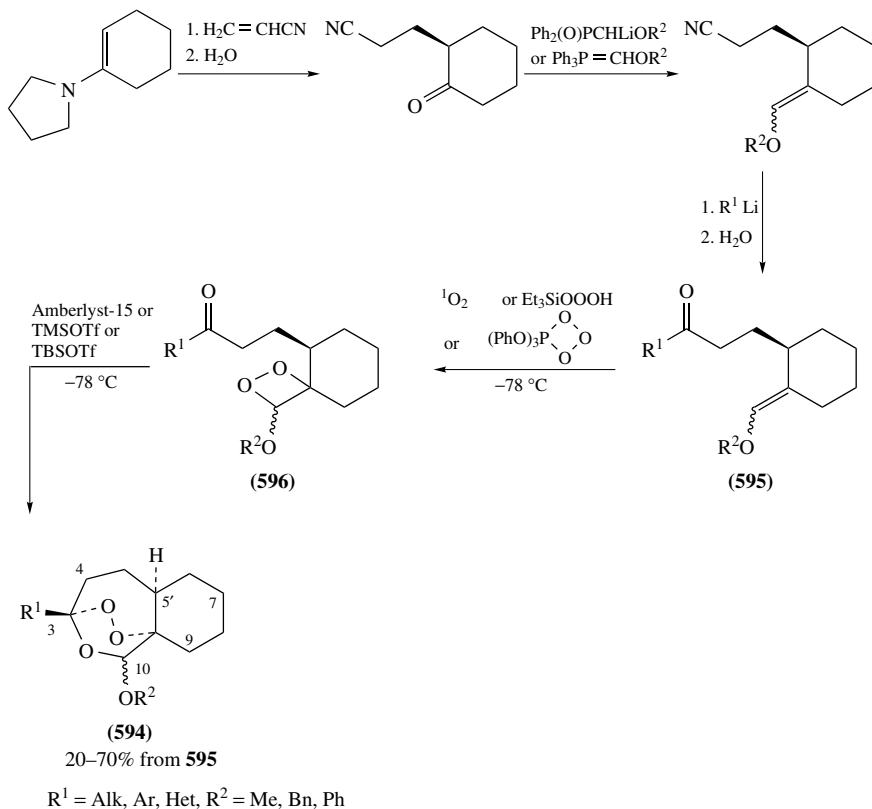
SCHEME 167

for synthesis of various 1,2,4-trioxanes. Alkyl(or aryl)oxy- spirocyclic and fused 1,2-dioxetanes as well as unsaturated bridged bicyclic 5- and 6-membered endoperoxides are commonly used in these reactions. For example, 2-(methoxymethylene)adamantane **591a** in solution of acetaldehyde at $-78\text{ }^\circ\text{C}$ easily undergoes [2 + 2]-cycloaddition with singlet oxygen to form the thermally unstable dioxetane **592a** that subsequently reacts with acetaldehyde to give 1,2,4-trioxane **593a** (total 53%) as a mixture of C5 epimers (Scheme 168)^{508,509}. While reactions of more robust 3-aryloxy-1,2-dioxetanes **592b–e**, deriving from the corresponding aryloxyethens **591b–e**, with excess acetaldehyde in the presence of TMSOTf afford the corresponding trioxanes **593b** and **593f–i** in good yields, the couplings of **592b** with other aliphatic and aromatic aldehydes were found to be less efficient (Scheme 168)^{509,510}. All the tested 1,2-dioxetanes **592b–e** failed to react with acetone under similar conditions^{509,510}. A number of fused 1,2,4-trioxanes were obtained (32–51%) on low-temperature photooxygenations of 2-(methoxymethylene)cyclohexanes in the presence of aldehydes^{508,511,512}.

Jefford and coworkers^{513,514} and Posner and coworkers^{515–519} elaborated an efficient and versatile methodology for the synthesis of tricyclic 1,2,4-trioxanes of type **594**, characterized by a molecular core which is structurally simpler than that of naturally occurring artemisinin (**6**). This general method, exemplified in Scheme 169 for the synthesis of 3,10-disubstituted derivatives **594**, allows also the introduction of a variety of structural changes at positions 3, 4, 5', 7, 9 and 10 of the tricyclic molecular core by employing analogues of **595** having a purposely designed array of substituents. 1,2-Dioxetanes of type **596** are generated by low-temperature [2 + 2]-cycloaddition of the electron-rich vinyl ether function in **595** with singlet oxygen^{513,514,517}, or of synthetic equivalents thereof, such as triethylsilyl hydrotrioxide^{515,517,519} and triphenylphosphite ozonide⁵²⁰. *In*



SCHEME 168

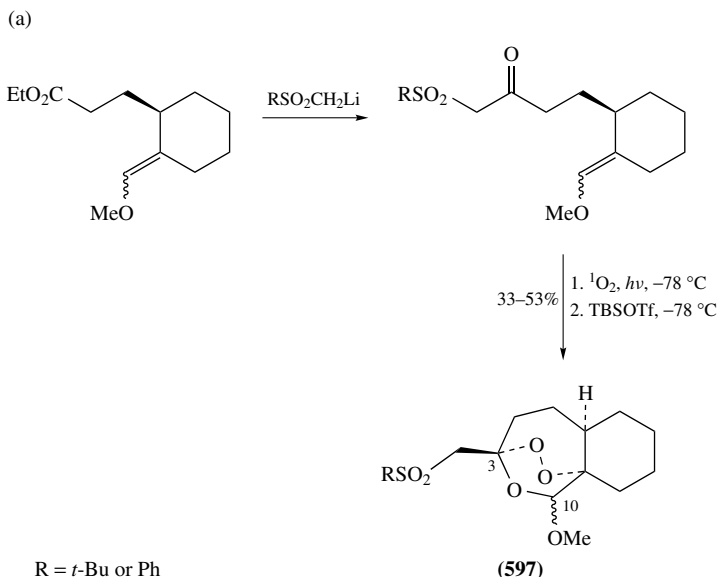


SCHEME 169

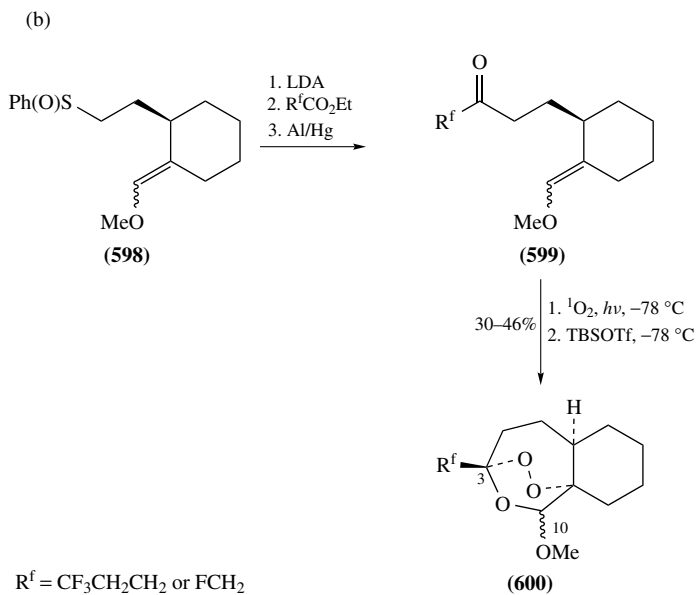
situ acid-induced intramolecular coupling of the carbonyl function with the alkoxy-1,2-dioxetane system in intermediates of type **596** gives the corresponding target compounds **594** (Scheme 169). The protocol outlined in Scheme 169 allows the introduction of a variety of substituents R¹ such as R¹ = H⁵¹⁴, R¹ = Me⁵¹³⁻⁵¹⁵, R¹ = (β -hydroxyethyl)⁵¹⁹, R¹ = Ph^{514,521}, R¹ = Ar and R¹ = Hetaryl⁵²¹⁻⁵²⁴. The scope of this method depends to a large extent on the feasibility of introducing structural modifications in the prototypic precursor **595** (R¹ = R² = Me). 3-Sulfonylmethyl-1,2,4-trioxanes **597** are obtained as shown in Scheme 170a⁵²⁰. The synthesis of fluoroalkylated ketones **599** (R^f = CF₃CH₂CH₂ and FCH₂) and subsequently the corresponding 3-(fluoroalkyl)-1,2,4-trioxanes **600** required an indirect route. Thus, acylation of δ -phenylsulfinyl vinyl ether **598**, with fluorinated carboxylic acid esters, followed by reductive desulfinylation was used for the preparation of trioxane precursors of type **599** (Scheme 170b)⁵²². 3-Trifluoromethyl-substituted trioxane of type **600** was also prepared from the corresponding precursor **599** (R^f = CF₃)⁵²⁵.

O'Neill, Posner and coworkers extended this methodology to an enantioselective synthesis of potent antimalarial agents 3-*p*-fluorophenyl-1,2,4-trioxanes **601a** and **601b** (Scheme 171)⁵²⁶. Thus, TMS-protected chiral enamine **602**, available from the condensation of cyclohexanone and (*R*)-(+)-prolinol followed by silylation of the free hydroxyl function, reacts with acrylonitrile in the presence of MgCl₂ to give the chiral 1,4-oxonitrile **603** (90% *ee*). Subsequent transformations of the chiral non-racemic intermediates **604** and **605** afforded, in good yield, a separable mixture of C10 methoxy-epimers (+)-**601a** and (+)-**601b**, both of 85% *ee*, having the same absolute stereochemistry as artemisinin (**6**) at the common stereogenic centers (Scheme 171)⁵²⁶.

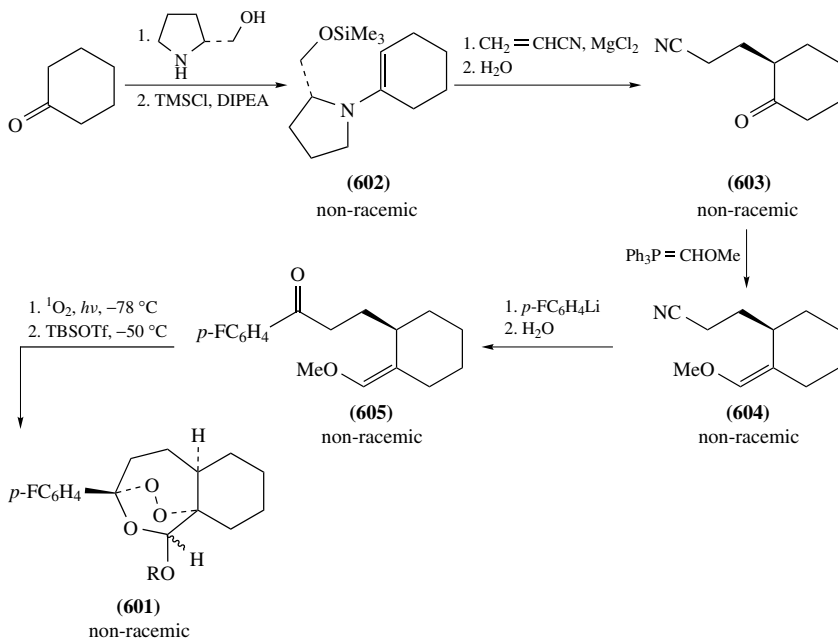
Additional examples for the syntheses of tricyclic trioxanes **606**, which are substituted at the position 7, are given in Scheme 172a^{515,519}, whereas compounds **607**, substituted at C4 and/or C9, are shown in Scheme 172b^{471,516-518,521,527}. Asymmetric syntheses of two non-racemic trioxanes **608**, bearing cyano- or ethoxycarbonyl substituents at the ring-junction (position 5'), are outlined in Scheme 172c^{528,529}. 10-Alkylthio- and arylthio-



SCHEME 170

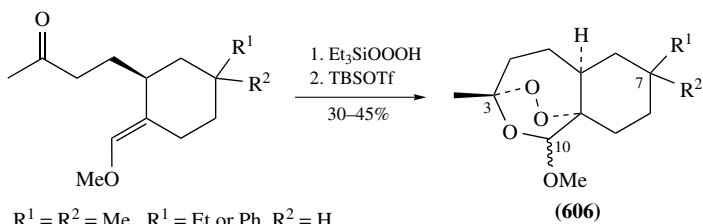


SCHEME 170. (continued)

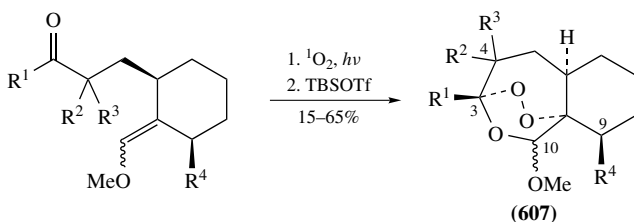
(a) $\text{RO} = \alpha\text{-MeO}$, 15%, 85% *ee*(b) $\text{RO} = \beta\text{-MeO}$, 25%, 85% *ee*

SCHEME 171

(a)

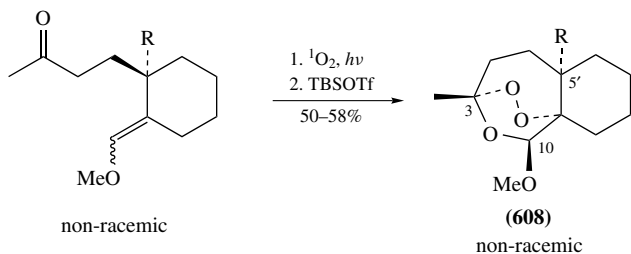


(b)

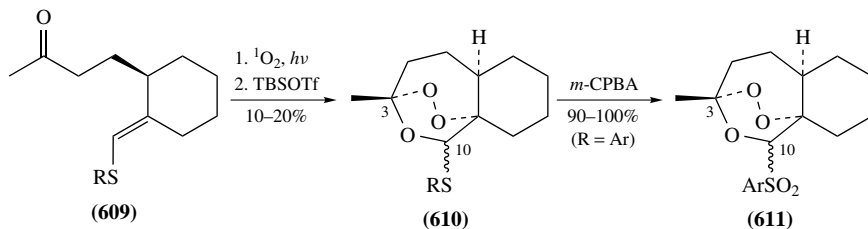


$\text{R}^1 = \text{Me or Ph}, \text{R}^2 = \text{Me, Bn, CH}_2\text{C}_6\text{H}_4\text{CH}_2\text{OH-}p, \text{CH}_2\text{OH, CH}_2\text{SiMe}_3, \text{CH}_2\text{SnMe}_3, \text{R}^3 = \text{R}^4 = \text{H},$
 $\text{R}^1 = \text{R}^2 = \text{Me}, \text{R}^3 = \text{H}, \text{R}^4 = \text{H or CH}_2\text{CH}_2\text{OH}$
 $\text{R}^1 = \text{Me or Ph}, \text{R}^2 = \text{R}^3 = \text{Me}, \text{R}^4 = \text{H}$

(c)

(a) $\text{R} = \text{CN}$ (b) $\text{R} = \text{CO}_2\text{Et}$ (opposite stereochemistry of the endoperoxide bridge)

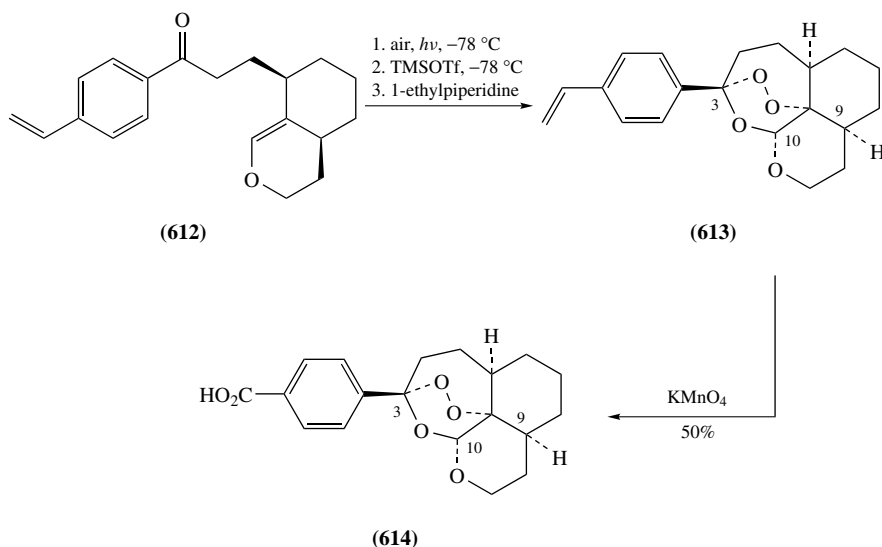
(d)

 $\text{R} = \text{Me, Ph, } p\text{-An, } p\text{-ClC}_6\text{H}_4$

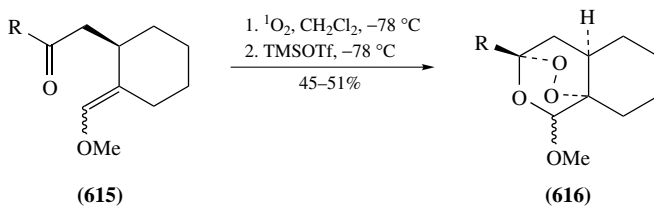
trioxanes of type **610** are obtained from the corresponding vinyl sulfide precursors **609** through photooxidation, followed by *in situ* intramolecular coupling of the resulting 1,2-oxetane and the carbonyl group as shown in Scheme 172^{d519,520,530}. *S*-Oxidation of the arylthio-trioxanes **610** affords the corresponding arylsulfonyl trioxanes **611**, which exhibit potent antimalarial activity^{520,530}. Hydroxyl functions in substituents at positions 4 and 9 of tricyclic trioxanes **607** were utilized for tethering with bis(electrophiles), yielding antimalarial, antiproliferative and antitumor active trioxane dimers⁴⁷¹.

The cyclic enol ether **612**, bearing highly sensitive styryl substituent at the ketone tether, was used for the synthesis of tetracyclic trioxane **613** (Scheme 173)⁵²⁴. The latter was oxidized with KMnO_4 to give antimalarial active, trioxane carboxylic acid **614** (Scheme 173)⁵²⁴. Several other cyclic enol ethers related to **612** were converted to bridged polycyclic trioxanes^{531–533}. Singlet oxygen photooxygenation of the vinyl ethers **615**, which carry a shortened carbonyl-containing chain, followed by treatment with TMSOTf affords bridged tricyclic trioxanes of type **616** (Scheme 174)⁵³⁴.

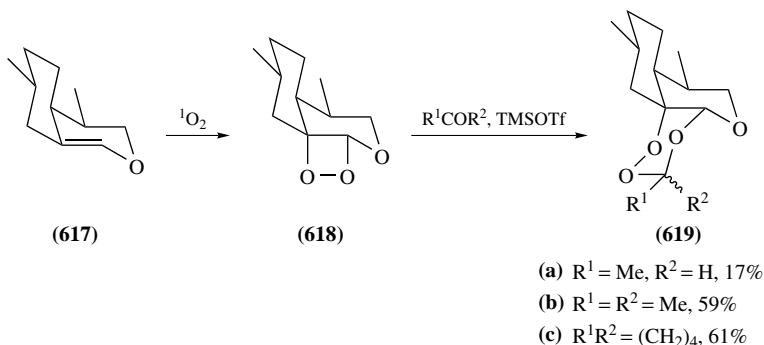
Photooxygenation of bicyclic enol ether **617** at -78°C affords intermediate 1,2-dioxetane **618**, which reacts with a premixed acetaldehyde without acidic additives or

**(614)**

SCHEME 173

**(615)****(616)**R = Me, MeOCH_2

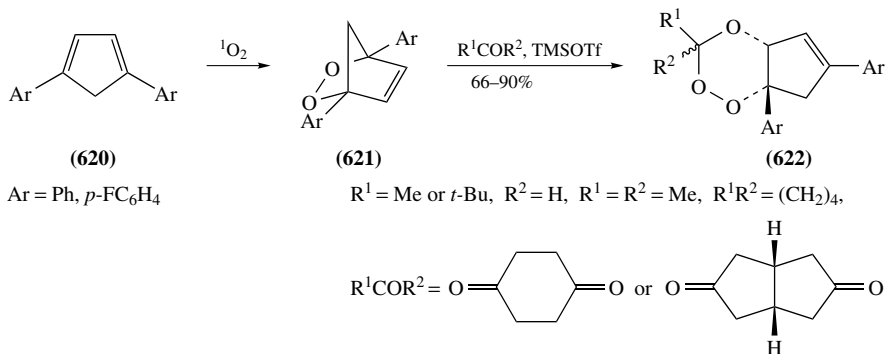
SCHEME 174



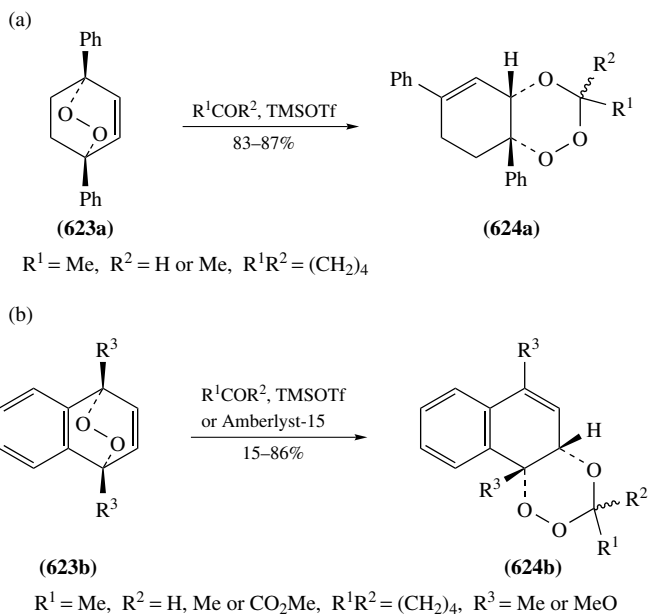
SCHEME 175

with ketones in the presence of TMSOTf to give trioxanes **619a–c** (Scheme 175)^{535, 536}. A number of related examples on synthesis of fused bicyclic and tricyclic 1,2,4-trioxanes from the corresponding cyclic enol ethers was reported^{508, 536–538}.

Relatively stable 5-membered bridged endoperoxides **621**, which are readily available in almost quantitative yield by photooxidation of the corresponding 1,4-diarylcyclopentadienes **620**, smoothly react with aliphatic aldehydes and ketones, in the presence of Amberlyst-15 or TMSOTf, giving the *cis*-fused cyclopenteno-1,2,4-trioxanes **622** (Scheme 176)^{510, 539–542}. Using reactions of endoperoxides **621** with chiral ketones^{543, 544}, or asymmetric resolution of racemic trioxanes **622**, some enantiomerically pure trioxanes of type **622** were prepared^{540, 545, 546}. 2,5-Diarylfurans analogues of **620** are converted into *cis*-fused dihydrofurano-1,2,4-trioxanes (14–26% yield)⁵⁴⁷. Bridged 6-membered cyclic peroxide **623a**, obtained from singlet oxygen cycloaddition to 1,4-diphenyl-1,3-cyclohexadiene, in the presence of TMSOTf reacts smoothly with acetaldehyde and with some ketones to give 5,6-*cis*-fused 1,2,4-trioxanes **624a** in high yield (Scheme 177a)⁵¹⁰. Similar reactions of cyclohexane-1,4-dione with bridged endoperoxides of type **623a**, deriving from the parent 1,3-cyclohexadiene and from α -terpinene instead of 1,4-diphenyl-1,3-cyclohexadiene, were recently applied in the syntheses of novel antimalarial trioxaquinone conjugates⁵⁴⁸. The condensations of aldehydes and ketones with 1,4-dimethyl- and 1,4-dimethoxynaphthalene endoperoxides **623b** afford the corresponding 1,2,4-trioxanes **624b** in variable yields (Scheme 177b)^{510, 539, 544, 549}.



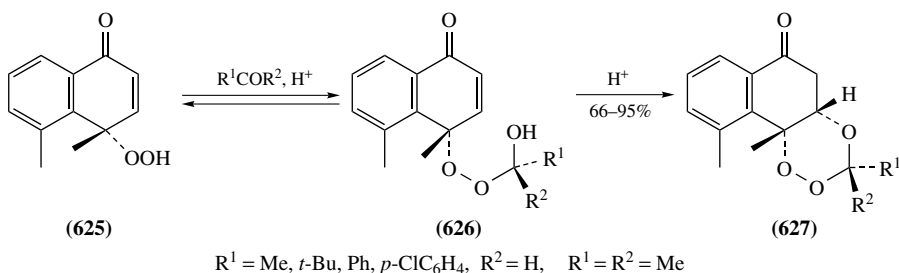
SCHEME 176



SCHEME 177

C. Coupling of Allylic Hydroperoxides and Alcohols with Carbonyl Compounds

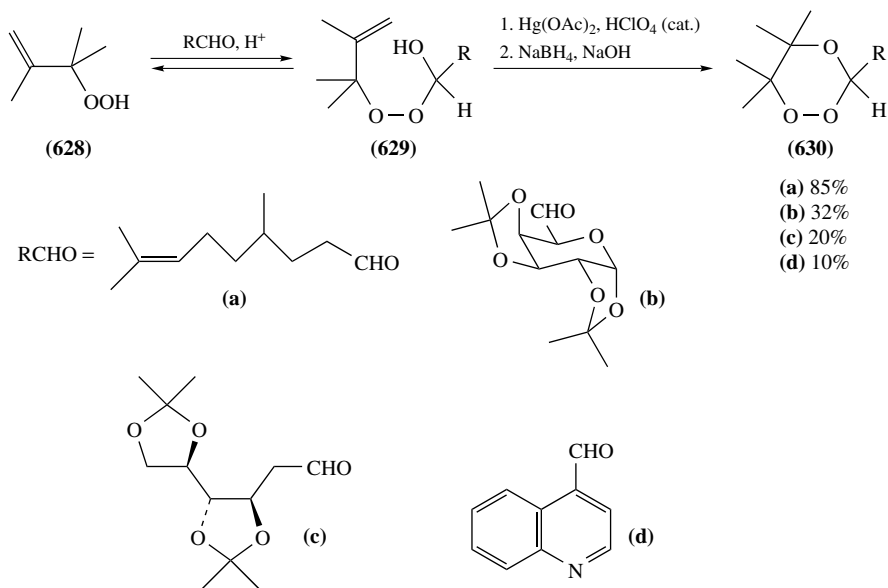
Under acidic conditions, allylic hydroperoxides reversibly add to the carbonyl group of aldehydes and ketones forming the corresponding allylic peroxyhemiketals, which can cyclize to an appropriately activated juxtaposed C=C group⁵⁵⁰. For example, the cyclic γ -hydroperoxy- α, β -unsaturated ketone **625** under catalysis with Amberlyst-15 reacts with aliphatic and aromatic aldehydes as well as with acetone to generate the hemiacetal- and hemiketal-intermediates **626**, which undergo a spontaneous Michael-type cyclization to form the cyclohexano-*cis*-fused 1,2,4-trioxanes **627** in high yields (Scheme 178)⁵⁵⁰. Related Michael-type cyclizations onto an aldimine C=N bond leading to 5-arylamino-1,2,4-trioxanes were also reported⁵⁵¹.



SCHEME 178

1,2,4-Trioxanes were prepared through the intramolecular oxymmercuration of various allylic peroxyhemiacetals and peroxyhemiketals⁵⁵²⁻⁵⁵⁵. For example, 1,2,4-trioxanes

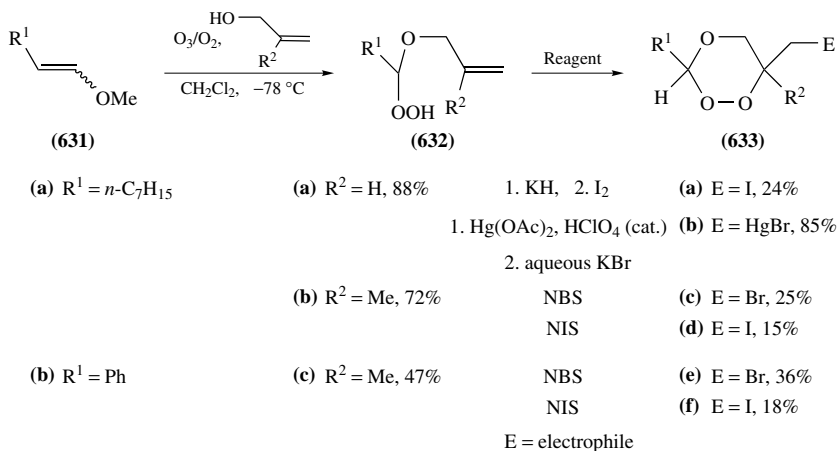
630a–d, functionalized at C3, are obtained through acid-catalyzed addition of 2,3-dimethylbut-1-en-3-yl hydroperoxide **628** to a variety of aldehydes generating the peroxyhemiacetals **629**, which are subjected to oxymercuration followed by hydride reduction (Scheme 179)⁵⁵⁵. Peroxyhemiacetals of type **629** (R = Alk) undergo NBS- and NIS-mediated cyclizations to give the 5-bromomethyl- and 5-iodomethyl-1,2,4-trioxanes respectively, in 25–60% yield⁵⁵⁶. A similar condensation of hydroperoxide **628** with 4-oxopentanal followed by NIS-mediated cyclization provides 5-iodomethyl-5,6,6-trimethyl-3-(3-oxo)butyl-1,2,4-trioxane, a useful building block for the preparation of trioxaquine-type antimalarial conjugates⁵⁵⁷. For related condensations involving tetra(allylperoxy)tin, see Reference 558.



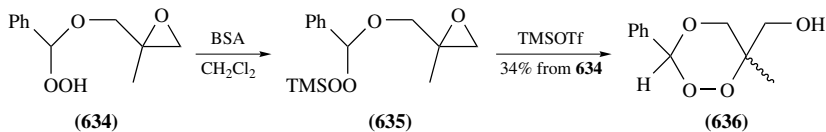
SCHEME 179

Related syntheses of trioxanes involve the generation of (*O*-allyl)hydroperoxyhemiacetals of type **632** by ozonolysis of enol ethers **631a** and **631b** in the presence of an allylic alcohol. Subsequent electrophile-mediated intramolecular addition of the hydroperoxy function to the C=C bond affords 6-iodomethyl- **633a,d,f**, and 6-bromomethyl-1,2,4-trioxanes **633c,e** in moderate yields, or 6-mercuriomethyl-1,2,4-trioxane **633b** in high yield (Scheme 180)²⁶⁵. A number of related electrophile-mediated 6-*exo*-cyclizations of unsaturated hydroperoxyacetals leading to monocyclic and spiro bicyclic 6-bromo(iodo)methyl-1,2,4-trioxanes as well as 7-*endo*-cyclizations forming 6-bromo(iodo)-1,2,4-trioxepanes were reported⁵⁵⁹. It was suggested that the NIS-induced cyclizations proceed through a free-radical pathway⁵⁵⁹.

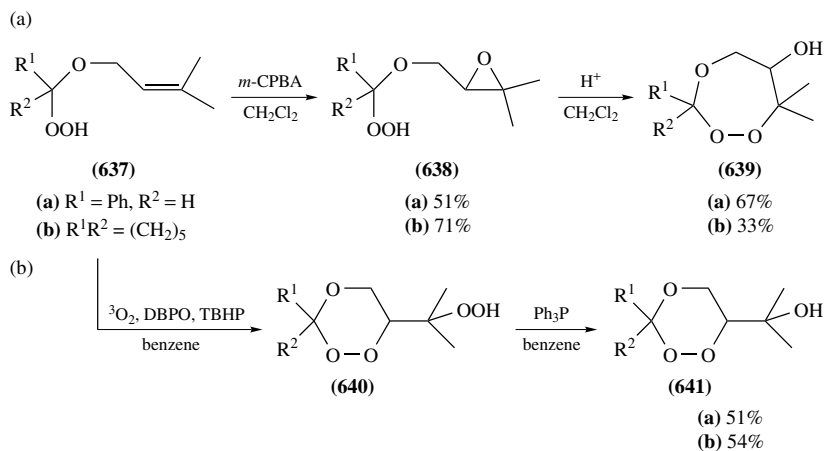
Epoxidation of **632c** with *m*-CPBA to **634**, followed by silylation with bis(trimethylsilyl)acetamide (BSA) to **635**, and TMSOTf-induced cyclization gives 6-hydroxymethyl-3-phenyl-1,2,4-trioxane **636** (Scheme 181)⁵⁶⁰. Epoxides **638**, which are characterized by geminal dimethyl substituents, are obtained by *m*-CPBA oxidation of the (*O*-3,3-dimethylallyl)hydroperoxy acetals **637**. While the structural change in **638**, as compared to epoxide **634**, direct the acid-catalyzed cyclizations to the *endo* mode yielding the 7-membered



SCHEME 180



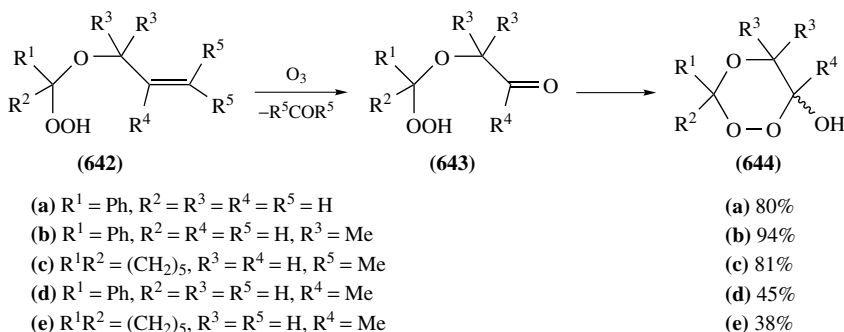
SCHEME 181



SCHEME 182

1,2,4-trioxepanes **639** (33–67%) (Scheme 182a), base-catalyzed cyclizations of **638** afford trioxanes **641**, albeit in low yields⁵⁶⁰. Direct *N*-halogenosuccinimide-mediated cyclizations of **637** commonly give mixtures of the corresponding trioxanes and trioxepanes in variable yields (up to 47% total yield) and ratios⁵⁵⁹. In contrast, DBPO-initiated free-radical cyclizations of **637** in the presence of triplet oxygen and TBHP proceed through the 6-*exo*

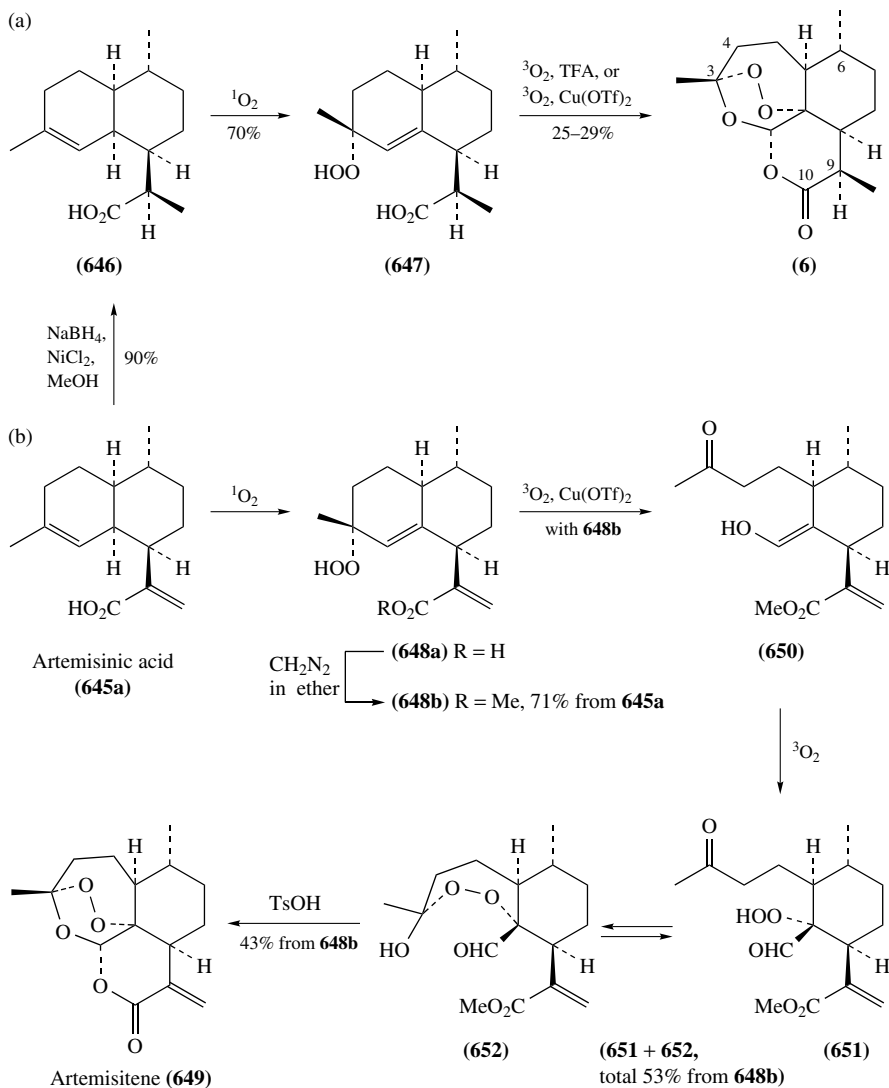
mode, leading to trioxane-hydroperoxides **640** and, after *in situ* deoxygenation with triphenylphosphine, to 6-hydroxymethyl-1,2,4-trioxanes **641** in good yield (Scheme 182b)⁵⁶⁰. Another useful method for ring closure of (*O*-allyl)hydroperoxyacetals **642a–e** involves ozonolysis of the allylic C=C bond to generate intermediates **643** bearing hydroperoxide and carbonyl functionalities (Scheme 183)⁵⁶¹. Thus generated oxo-hydroperoxides **643** undergo spontaneous cyclization to 6-hydroxy-1,2,4-trioxanes **644**. The method is versatile and yields depend on the array of substituents on substrates **642**⁵⁶¹.



SCHEME 183

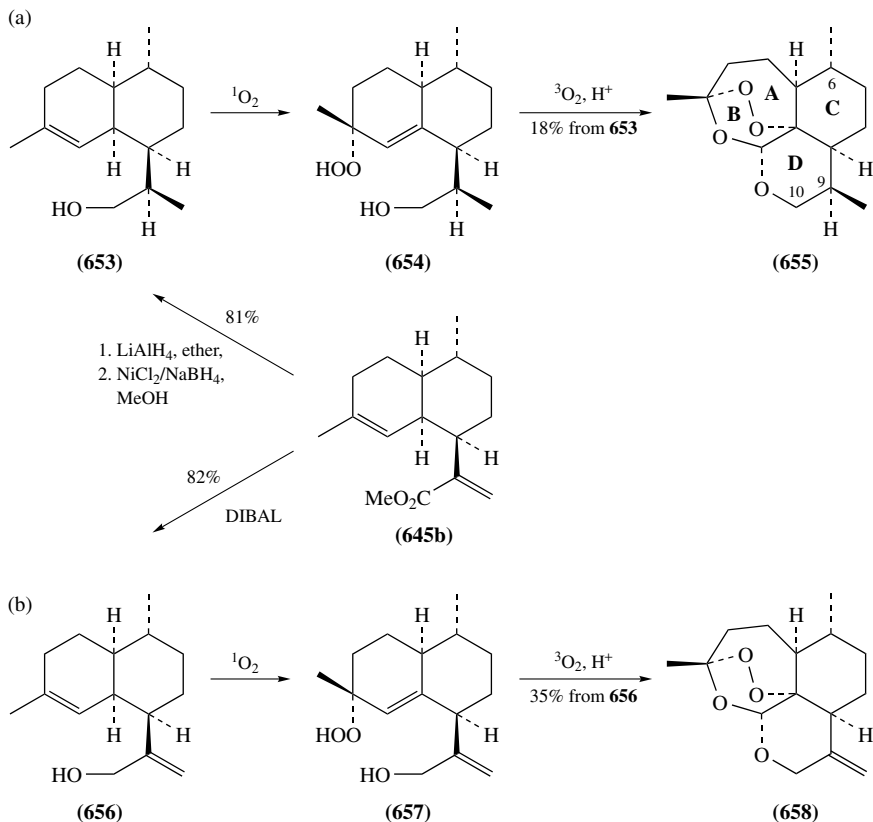
A number of research groups have followed a biomimetic approach to the synthesis of artemisinin (**6**). Such approaches are based on the use of artemisinic acid **645a**, a biogenetic precursor of artemisinin, as starting material. The synthesis of artemisinin (**6**) by Roth and Acton is based on stereoselective reduction of artemisinic acid **645a** to dihydroartemisinic acid **646**, followed by singlet oxygen photooxygenation to hydroperoxide **647** which, on treatment with $\text{CF}_3\text{CO}_2\text{H}$ in aerated hexane solution, undergoes a slow transformation into artemisinin (**6**) (Scheme 184a)^{562–564}. At about the same time, Haynes and Vonwiller described a similar efficient conversion of **646** into **6** using $\text{Cu}(\text{OTf})_2$ catalysis for the cyclization step⁵⁶⁵. In another synthetic path, they converted artemisinic acid **645a** to hydroperoxide **648b** and subsequently into artemisitene **649** (Scheme 184b)⁵⁶⁵. It was proved that a Hock-type ring cleavage of allylic hydroperoxide **648b** leads to keto-enol **650**, that can be isolated at low temperature⁵⁶⁶. This unusually stable simple enol undergoes slow autoxidation at RT, and facile oxygenation in aerobic conditions at -20°C in the presence of $\text{Cu}(\text{OTf})_2$, to give a tautomeric mixture of keto-hydroperoxide **651** and peroxy lactol **652**⁵⁶⁶. Finally, acid-catalyzed intramolecular acetalization–lactonization leads to artemisitene **649** (Scheme 184b). The same mechanism was attributed to the spontaneous autoxidation of natural dihydroartemisinic acid **646** into artemisinin (**6**)^{567–570}. An acid-catalyzed oxidative construction of the lactone–trioxane system, similar to that described above for the conversion of dihydroartemisinic acid **646** to artemisinin (**6**), was applied in the final stage of a total synthesis of **6** based on (–)- β -pinene as chiral non-racemic starting material⁵⁷¹.

Using various derivatives of artemisinic acid, the methodology outlined in Scheme 184 was extended to the synthesis of a number of modified artemisinin-type tetracyclic trioxanes. For example, the syntheses of 6,9-desdimethylartemisinin **586a**⁵⁷², 4- β -hydroxyartemisinin⁵⁷³, and C9-alkylated artemisinin analogues were reported^{574–576}. In some cases it is possible to avoid the lactonization step while preserving the ester functionality and interrupting the cyclization of aldehyde-peroxyhemiacetals of type **652**, at the step of formation of tricyclic 5-hydroxy-1,2,4-trioxane⁵⁷⁷.



SCHEME 184

Additional applications of the biomimetic approach are outlined in Scheme 185. Thus, reduction of unsaturated methyl ester **645b** to alcohol **653**, followed by an ene-reaction with singlet oxygen, gives the allylic hydroperoxide **654**. Application of the acid-catalyzed oxidative ring cleavage—recyclization process discussed above affords 10-deoxoarteminin **655** (Scheme 185a)⁵⁷⁸. The same strategy proved to be highly effective for the synthesis of 10-deoxoartemisene **658** starting from the ester **645b** (Scheme 185b)^{579,580}. It involves the oxidative transformation of **656** to allylic hydroperoxide **657** and its conversion to the tetracyclic 10-deoxoartemisene **658** by

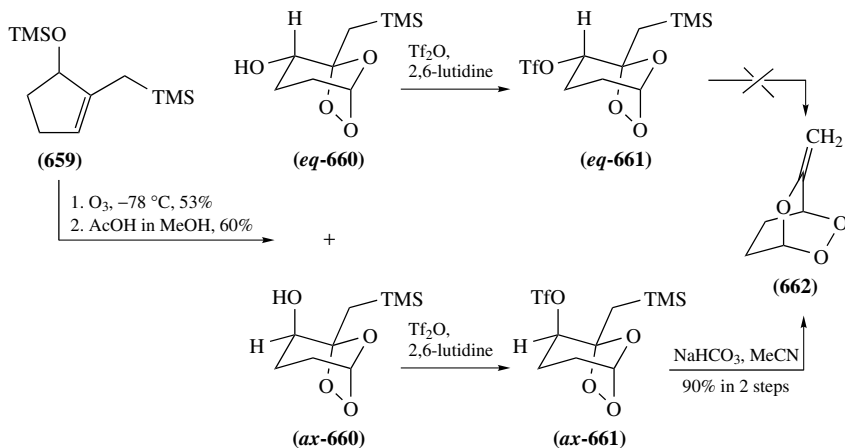


SCHEME 185

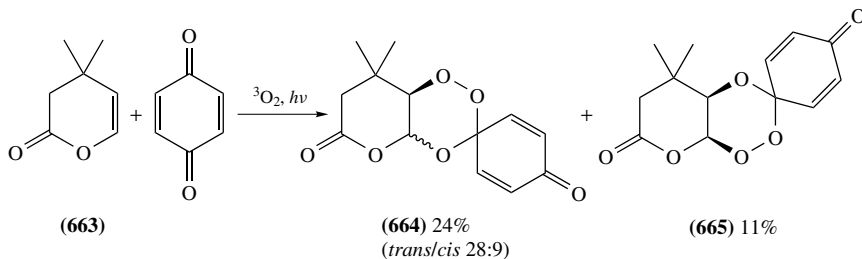
acid catalysis^{579, 580}. Additional applications of this method include syntheses of D-ring contracted⁵⁸¹ and D-ring enlarged analogues of 10-deoxoartemisinin **655**^{582, 583}, as well as a number of C10 alkylated or arylated derivatives of **655**^{463, 512, 583–591}.

D. Miscellaneous Syntheses of 1,2,4-Trioxanes

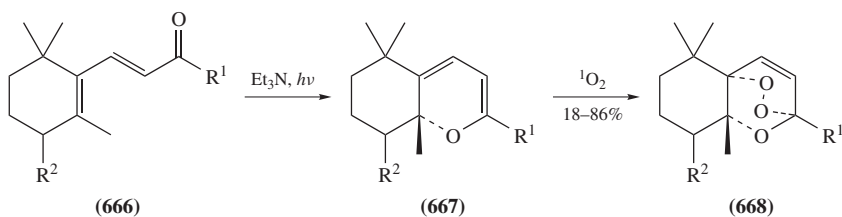
In this section are described three additional methods for the synthesis of 1,2,4-trioxanes that do not fit into any of the categories discussed in Sections III.A–C. Scheme 186 describes the ozonolysis of bis(silylated) cyclopent-2-enol **659** which, after hydrolysis, affords a mixture of ozonide-alcohols *eq*-**660** and *ax*-**660**, which are converted to the ozonide-triflates *eq*-**661** and *ax*-**661**⁵⁹². Treatment of ozonide *ax*-**661**, which is bearing an axially positioned strong nucleofuge with NaHCO_3 , that acts as an acid-scavenger, in acetonitrile leads to an efficient ring expansion of 1,2,4-trioxolane *ax*-**661** to the bridged bicyclic 1,2,4-trioxane **662**. Ozonide *eq*-**661**, which is carrying an equatorially attached nucleofuge, does not undergo such a transformation⁵⁹². Visible-laser photolysis of 3,4-dihydro-2*H*-pyran-2-one **663** and *para*-benzoquinone in aerobic conditions affords a mixture of regioisomeric 1,2,4-trioxanes **664** and **665** (35% total yield) (Scheme 187)⁵⁹³. In this reaction, triplet oxygen is incorporated into a relatively long-living Paterno–Büchi



SCHEME 186



SCHEME 187



$\text{R}^1 = \text{Me}, \text{CH}_2\text{CH}(\text{OH})\text{Me}, \text{CH}_2\text{CO}_2\text{Me}, \text{R}^2 = \text{H}$

$\text{R}^1 = \text{Me}, \text{R}^2 = \text{OH}, \text{OMe}, \text{OAll}, \text{OAc}$

SCHEME 188

triplet 1,4-diradical⁵⁹³. Tetrahydrobenzopyrans **667** are obtained through photocyclization of β -ionones **666** in the presence of Et_3N in anaerobic conditions⁵⁹⁴. Being electron-rich, cyclic dienes **667** readily undergo [4 + 2]-cycloaddition with singlet oxygen to give the tricyclic 1,2,4-trioxanes **668** (Scheme 188)⁵⁹⁵. More recently, it was found that UV irradiation at 350 nm of various β -ionones **666** under oxygen in the absence of base gives a direct access to 1,2,4-trioxanes **668** (Scheme 188)^{596,597}.

IV. REFERENCES

1. E. K. Nelson, *J. Am. Chem. Soc.*, **33**, 1404 (1911).
2. A. Windaus and J. Brunken, *Liebigs Ann. Chem.*, **460**, 225 (1928).
3. P. Wieland and V. Prelog, *Helv. Chim. Acta*, **30**, 1028 (1947).
4. B. Samuelsson, *J. Am. Chem. Soc.*, **87**, 3111 (1965).
5. D. H. Nugteren, R. K. Beerthuis and D. A. Van Dorp, *Recl. Trav. Chim. Pays-Bas*, **85**, 405 (1966).
6. M. Hamberg and B. Samuelsson, *J. Biol. Chem.*, **242**, 5336 (1967).
7. M. Hamberg and B. Samuelsson, *Proc. Nat. Acad. Sci. USA*, **70**, 899 (1973).
8. D. H. Nugteren and E. Hazelhof, *Biochim. Biophys. Acta*, **326**, 448 (1973).
9. M. Hamberg, J. Svensson, T. Wakabayashi and B. Samuelsson, *Proc. Nat. Acad. Sci. USA*, **71**, 345 (1974).
10. R. A. Johnson, E. G. Nidy, L. Baczynskij and R. R. Gorman, *J. Am. Chem. Soc.*, **99**, 7738 (1977).
11. N. A. Porter, J. D. Byers, R. C. Mebane, D. W. Gilmore and J. R. Nixon, *J. Org. Chem.*, **43**, 2088 (1978).
12. N. A. Porter, J. D. Byers, K. M. Holden and D. B. Menzel, *J. Am. Chem. Soc.*, **101**, 4319 (1979).
13. N. A. Porter, J. D. Byers, A. E. Ali and T. E. Eling, *J. Am. Chem. Soc.*, **102**, 1183 (1980).
14. K. C. Nicolaou, G. P. Gasic and W. E. Barnette, *Angew. Chem., Int. Ed. Engl.*, **17**, 293 (1978).
15. R. A. Johnson, *Adv. Prostagl. Thromb. Leukotr. Res.*, **14**, 131 (1985).
16. R. G. Salomon, *Acc. Chem. Res.*, **18**, 294 (1985).
17. D. A. Casteel, *Nat. Prod. Rep.*, **9**, 289 (1992).
18. D. A. Casteel, *Nat. Prod. Rep.*, **16**, 55 (1999).
19. G. A. Tolstikov, A. G. Tolstikov and O. V. Tolstikova, *Usp. Khim.*, **65**, 836 (1996); *Chem. Abstr.*, **126**, 143988 (1996).
20. D. J. Faulkner, *Nat. Prod. Rep.*, **17**, 7 (2000).
21. D. J. Faulkner, *Nat. Prod. Rep.*, **18**, 1 (2001).
22. D. J. Faulkner, *Nat. Prod. Rep.*, **19**, 1 (2002).
23. J. R. Wells, *Tetrahedron Lett.*, 2637 (1976).
24. E. Quinoa, E. Kho, L. V. Manes, P. Crews and G. J. Bakus, *J. Org. Chem.*, **51**, 4260 (1986).
25. S. Sakemi, T. Higa, U. Anthoni and C. Christophersen, *Tetrahedron*, **43**, 263 (1987).
26. D. W. Phillipson and K. L. Rinehart, Jr., *J. Am. Chem. Soc.*, **105**, 7735 (1983).
27. X. T. Liang, D. Q. Yu, W. L. Wu and H. C. Deng, *Acta Chim. Sin.*, **37**, 215 (1979).
28. X. Liang, in *Advances in Chinese Medicinal Materials* (Eds. H. M. Chang, H. W. Yeung, W. W. Tso and A. Koo), World Scientific Publ., Singapore, 1985, p. 427.
29. M.-Y. Liu, J.-M. Ni, J. F. Fan, Y.-Y. Tu, Z.-H. Wu, Y.-L. Wu and W.-S. Chou, *Acta Chim. Sin.*, **37**, 129 (1979).
30. D. L. Klayman, *Science*, **228**, 1049 (1985).
31. A. R. Butler and Y. L. Wu, *Chem. Soc. Rev.*, **21**, 85 (1992).
32. Y. Li and Y. L. Wu, *Curr. Med. Chem.*, **10**, 2197 (2003).
33. M. Jung, *Curr. Med. Chem.*, **1**, 46 (1994).
34. S. R. Meshnick, T. E. Taylor and S. Kamchonwongpaisan, *Microbiol. Rev.*, **60**, 301 (1996).
35. J. N. Cumming, P. Ploypradith and G. H. Posner, *Adv. Pharmacol.*, **37**, 253 (1997).
36. G. H. Posner, *Exp. Opin. Therap. Pat.*, **8**, 1487 (1998).
37. K. Borstnik, I. Paik and G. H. Posner, *Mini-Rev. Med. Chem.*, **2**, 573 (2002).
38. P. M. O'Neill and G. H. Posner, *J. Med. Chem.*, **47**, 2945 (2004).
39. R. K. Haynes and S. C. Vonwiller, *Acc. Chem. Res.*, **30**, 73 (1997).
40. J. A. Vroman, M. Alvim-Gaston and M. A. Avery, *Curr. Pharm. Des.*, **5**, 101 (1999).
41. C. W. Jefford, *Curr. Med. Chem.*, **8**, 1803 (2001).
42. M. Frederich, J. M. Dogne, L. Angenot and P. De Mol, *Curr. Med. Chem.*, **9**, 1435 (2002).
43. J. Wiesner, R. Ortmann, H. Jomaa and M. Schlitzer, *Angew. Chem., Int. Ed.*, **42**, 5274 (2003).
44. Y. Q. Tang, Y. X. Dong and J. L. Vennerstrom, *Med. Res. Rev.*, **24**, 425 (2004).
45. R. G. Ridley, *Exper. Parasitol.*, **87**, 293 (1997).
46. R. K. Haynes, *Curr. Opin. Infect. Dis.*, **14**, 719 (2001).
47. V. Dhingra, K. V. Rao and M. L. Narasu, *Life Sci.*, **66**, 279 (2000).
48. M. Jung, K. Lee, H. Kim and M. Park, *Curr. Med. Chem.*, **11**, 1265 (2004).

49. S. Kamchonwongpaisan, C. Nilanonta, B. Tamchompoo, C. Thebtaranonth, Y. Thebtaranonth, Y. Yuthavong, P. Kongsaree and J. Clardy, *Tetrahedron Lett.*, **36**, 1821 (1995).
50. J. Fayos, D. Lokensgard, J. Clardy, R. J. Cole and J. W. Kirksey, *J. Am. Chem. Soc.*, **96**, 6785 (1974).
51. I. Saito and S. S. Nittala, in *The Chemistry of Peroxides* (Ed. S. Patai), Wiley, Chichester, 1983, p. 311.
52. E. L. Clennan and C. S. Foote, in *Organic Peroxides* (Ed. W. Ando), Wiley, Chichester, 1992, p. 255.
53. K. J. McCullough, *Contemp. Org. Synth.*, **2**, 225 (1995).
54. K. J. McCullough and M. Nojima, *Curr. Org. Chem.*, **5**, 601 (2001).
55. A. K. Bhattacharya and R. P. Sharma, *Heterocycles*, **51**, 1681 (1999).
56. G. Bez, B. Kalita, P. Sarmah, N. C. Barua and D. K. Dutta, *Curr. Org. Chem.*, **7**, 1231 (2003).
57. R. M. Wilson, in *Organic Photochemistry, Vol. 7* (Ed. A. Padwa), Marcel Dekker, New York, 1985, p. 339.
58. W. Adam, S. Grabowski and R. M. Wilson, *Acc. Chem. Res.*, **23**, 165 (1990).
59. A. Rajca, S. Rajca, S. R. Desai and V. W. Day, *J. Org. Chem.*, **62**, 6524 (1997).
60. M. N. Burnett, R. Boothe, E. Clark, M. Gisin, H. M. Hassaneen, R. M. Pagni, G. Persy, R. J. Smith and J. Wirz, *J. Am. Chem. Soc.*, **110**, 2527 (1988).
61. W. Adam, H. Platsch and J. Wirz, *J. Am. Chem. Soc.*, **111**, 6896 (1989).
62. M. Abe, W. Adam, T. Heidenfelder, W. M. Nau and X. Y. Zhang, *J. Am. Chem. Soc.*, **122**, 2019 (2000).
63. R. M. Wilson and F. Geiser, *J. Am. Chem. Soc.*, **100**, 2225 (1978).
64. W. Adam, S. Grabowski, H. Platsch, K. Hannemann, J. Wirz and R. M. Wilson, *J. Am. Chem. Soc.*, **111**, 751 (1989).
65. W. Adam, P. Hossel, W. Hummer, H. Platsch and R. M. Wilson, *J. Am. Chem. Soc.*, **109**, 7570 (1987).
66. R. M. Wilson and J. W. Rekers, *J. Am. Chem. Soc.*, **103**, 206 (1981).
67. R. D. Little, L. Losinskidang, M. G. Venegas and C. Merlic, *Tetrahedron Lett.*, **24**, 4499 (1983).
68. W. Adam, S. E. Bottle, R. Finzel, T. Kammel, E.-M. Peters, K. Peters, H. G. von Schnering and T. Walz, *J. Org. Chem.*, **57**, 982 (1992).
69. W. Adam and R. Finzel, *J. Am. Chem. Soc.*, **114**, 4563 (1992).
70. H. Shimizu, S. Miyazaki and T. Kataoka, *J. Chem. Soc., Perkin Trans. 1*, 2227 (1996).
71. W. Adam, K. Hannemann and R. M. Wilson, *J. Am. Chem. Soc.*, **106**, 7646 (1984).
72. W. Adam, S. Grabowski, R. M. Wilson, K. Hannemann and J. Wirz, *J. Am. Chem. Soc.*, **109**, 7572 (1987).
73. W. R. Roth, M. Biermann, G. Erker and K. Jelich, *Chem. Ber.*, **113**, 586 (1980).
74. W. R. Roth, B. P. Scholz, R. Breuckmann, K. Jelich and H.-W. Lennartz, *Chem. Ber.*, **115**, 1934 (1982).
75. W. R. Roth and B. P. Scholz, *Chem. Ber.*, **115**, 1197 (1982).
76. M. Yoshioka, M. Oka, Y. Ishikawa, H. Tomita and T. Hasegawa, *J. Chem. Soc., Chem. Commun.*, 639 (1986).
77. P. Yates, A. C. Mackay and F. X. Garneau, *Tetrahedron Lett.*, 5389 (1968).
78. C. M. Bowes, D. F. Montecalvo and F. Sondheimer, *Tetrahedron Lett.*, 3181 (1973).
79. M. Gisin and J. Wirz, *Helv. Chim. Acta*, **59**, 2273 (1976).
80. C.-H. Chou and W. S. Trahanovsky, *J. Org. Chem.*, **60**, 5449 (1995).
81. D. W. Jones and A. Pomfret, *J. Chem. Soc., Perkin Trans. 1*, 263 (1991).
82. H. Quast, T. Herkert, A. Witzel, E.-M. Peters, K. Peters and H. G. von Schnering, *Chem. Ber.*, **127**, 921 (1994).
83. H. Quast, C. Becker, E.-M. Peters, K. Peters and H. G. von Schnering, *Liebigs Ann./Recl.*, 685 (1997).
84. R. Iyengar, R. Pina, K. Grohmann and L. Todaro, *J. Am. Chem. Soc.*, **110**, 2643 (1988).
85. G. W. Wijsman, D. S. van Es, W. H. de Wolf and F. Bickelhaupt, *Angew. Chem., Int. Ed. Engl.*, **32**, 726 (1993).
86. T. Sawada, K. Mimura, T. Thiemann, T. Yamato, M. Tashiro and S. Mataka, *J. Chem. Soc., Perkin Trans. 1*, 1369 (1998).
87. H. Cerfontain, A. Koeberg-Telder, B. H. Bakker, R. H. Mitchell and M. Tashiro, *Liebigs Ann./Recl.*, 873 (1997).

88. R. Singh and M. P. S. Ishar, *Tetrahedron Lett.*, **44**, 1943 (2003).
89. M. L. Bolte, W. D. Crow and S. Yoshida, *Austr. J. Chem.*, **35**, 1421 (1982).
90. K. Fuchs and L. A. Paquette, *J. Org. Chem.*, **59**, 528 (1994).
91. M. Gavrilan, C. Andre-Barres, M. Baltas, T. Tzedakis and L. Gorrichon, *Tetrahedron Lett.*, **42**, 2465 (2001).
92. F. Najjar, M. Baltas, L. Gorrichon, Y. Moreno, T. Tzedakis, H. Vial and C. Andre-Barres, *Eur. J. Org. Chem.*, 3335 (2003).
93. B. B. Snider and Z. P. Shi, *J. Org. Chem.*, **55**, 5669 (1990).
94. B. B. Snider and Z. P. Shi, *J. Am. Chem. Soc.*, **114**, 1790 (1992).
95. B. B. Snider, Z. P. Shi, S. V. O'Neil, K. D. Kreutter and T. L. Arakaki, *J. Org. Chem.*, **59**, 1726 (1994).
96. G. H. Posner, H. O'Dowd, P. Ploypradith, J. N. Cumming, S. Xie and T. A. Shapiro, *J. Med. Chem.*, **41**, 2164 (1998).
97. G. H. Posner and H. O'Dowd, *Heterocycles*, **47**, 643 (1998).
98. B. B. Snider and S. V. O'Neil, *Synth. Commun.*, **25**, 1085 (1995).
99. R. Schobert, R. Stehle and W. Milius, *J. Org. Chem.*, **68**, 9827 (2003).
100. R. Schobert, S. Siegfried, J. Weingartner and M. Nieuwenhuyzen, *J. Chem. Soc., Perkin Trans. 1*, 2009 (2001).
101. M. Chanon, M. Julliard, J. Santamaria and F. Chanon, *New J. Chem.*, **16**, 171 (1992).
102. L. Lopez, *Top. Curr. Chem.*, **156**, 117 (1990).
103. (a) K. Mizuno and Y. Otsuji, *Electr. Transf. I*, 301 (1994).
(b) K. Mizuno, T. Tamai, I. Hashida, I. Otsuji, Y. Kuriyama and K. Tokumaru, *J. Org. Chem.*, **59**, 7329 (1994).
104. P. D. Bartlett, *ACS Symp. Ser.*, **69**, 15 (1978).
105. R. Tang, H. J. Yue, J. F. Wolf and F. Mares, *J. Am. Chem. Soc.*, **100**, 5248 (1978).
106. R. K. Haynes, *Austr. J. Chem.*, **31**, 121 (1978).
107. R. K. Haynes, *Austr. J. Chem.*, **31**, 131 (1978).
108. R. K. Haynes, M. K. Probert and I. D. Wilmot, *Austr. J. Chem.*, **31**, 1737 (1978).
109. D. H. R. Barton, R. K. Haynes, P. D. Magnus and I. D. Menzies, *J. Chem. Soc., Chem. Commun.*, 511 (1974).
110. D. H. R. Barton, R. K. Haynes, G. Leclerc, P. D. Magnus and I. D. Menzies, *J. Chem. Soc., Perkin Trans. 1*, 2055 (1975).
111. C. S. Foote, *Photochem. Photobiol.*, **54**, 659 (1991).
112. K. Mizuno, N. Kamiyama and Y. Otsuji, *Chem. Lett.*, 477 (1983).
113. K. Mizuno, N. Kamiyama, N. Ichinose and Y. Otsuji, *Tetrahedron*, **41**, 2207 (1985).
114. T. Tamai, K. Mizuno, I. Hashida and Y. Otsuji, *J. Org. Chem.*, **57**, 5338 (1992).
115. N. Ichinose, K. Mizuno, T. Tamai and Y. Otsuji, *J. Org. Chem.*, **55**, 4079 (1990).
116. S. C. Shim and J. S. Song, *J. Org. Chem.*, **51**, 2817 (1986).
117. S. C. Shim and H. J. Lee, *Bull. Kor. Chem. Soc.*, **9**, 68 (1988).
118. T. Miyashi, M. Kamata and T. Mukai, *J. Am. Chem. Soc.*, **109**, 2780 (1987).
119. K. Gollnick, X. L. Xiao and U. Paulmann, *J. Org. Chem.*, **55**, 5945 (1990).
120. K. Gollnick and U. Paulmann, *J. Org. Chem.*, **55**, 5954 (1990).
121. H. Ikeda, T. Nakamura, T. Miyashi, J. L. Goodman, K. Akiyama, S. Tero-Kubota, A. Houmam and D. D. M. Wayner, *J. Am. Chem. Soc.*, **120**, 5832 (1998).
122. H. Ikeda, K. Akiyama, Y. Takahashi, T. Nakamura, S. Ishizaki, Y. Shiratori, H. Ohaku, J. L. Goodman, A. Houmam, D. D. M. Wayner, S. Tero-Kubota and T. Miyashi, *J. Am. Chem. Soc.*, **125**, 9147 (2003).
123. T. Miyashi, M. Kamata and T. Mukai, *J. Am. Chem. Soc.*, **108**, 2755 (1986).
124. Y. Takahashi, T. Miyashi and T. Mukai, *J. Am. Chem. Soc.*, **105**, 6511 (1983).
125. K. Gollnick and A. Schnatterer, *Tetrahedron Lett.*, **25**, 185 (1984).
126. K. Gollnick and A. Schnatterer, *Tetrahedron Lett.*, **25**, 2735 (1984).
127. S. L. Mattes and S. Farid, *J. Am. Chem. Soc.*, **108**, 7356 (1986).
128. K. Gollnick and S. Held, *J. Photochem. Photobiol., A: Chem.*, **59**, 55 (1991).
129. K. Gollnick and S. Held, *J. Photochem. Photobiol., A: Chem.*, **70**, 135 (1993).
130. K. Gollnick, A. Schnatterer and G. Utschick, *J. Org. Chem.*, **58**, 6049 (1993).
131. M. Kojima, A. Ishida and S. Takamuku, *Chem. Lett.*, 979 (1993).
132. M. Fujita, A. Shindo, A. Ishida, T. Majima, S. Takamuku and S. Fukuzumi, *Bull. Chem. Soc. Jpn.*, **69**, 743 (1996).

133. M. Kojima, A. Ishida and S. Takamuku, *Bull. Chem. Soc. Jpn.*, **71**, 2211 (1998).
134. T. Miyashi, A. Konno and Y. Takahashi, *J. Am. Chem. Soc.*, **110**, 3676 (1988).
135. T. Miyashi, H. Ikeda, A. Konno, O. Okitsu and Y. Takahashi, *Pure Appl. Chem.*, **62**, 1531 (1990).
136. Y. Takahashi, O. Okitsu, M. Ando and T. Miyashi, *Tetrahedron Lett.*, **35**, 3953 (1994).
137. A. G. Griesbeck, O. Sadlek and K. Polborn, *Liebigs Ann.*, 545 (1996).
138. M. Kamata, M. Ohta, K. Komatsu, H. S. Kim and Y. Wataya, *Tetrahedron Lett.*, **43**, 2063 (2002).
139. Y. Takahashi, M. Ando and T. Miyashi, *Tetrahedron Lett.*, **36**, 1889 (1995).
140. G. H. Posner, D. S. Wang, L. Gonzalez, X. L. Tao, J. N. Cumming, D. Klinedinst and T. A. Shapiro, *Tetrahedron Lett.*, **37**, 815 (1996).
141. G. H. Posner, L. Gonzalez, J. N. Cumming, D. Klinedinst and T. A. Shapiro, *Tetrahedron*, **53**, 37 (1997).
142. T. Miyashi, H. Ikeda and Y. Takahashi, *Acc. Chem. Res.*, **32**, 815 (1999).
143. Y. Takahashi, M. Ando and T. Miyashi, *J. Chem. Soc., Chem. Commun.*, 521 (1995).
144. H. Ikeda, T. Takasaki, Y. Takahashi, A. Konno, M. Matsumoto, Y. Hoshi, T. Aoki, T. Suzuki, J. L. Goodman and T. Miyashi, *J. Org. Chem.*, **64**, 1640 (1999).
145. J. Eriksen, C. S. Foote and T. L. Parker, *J. Am. Chem. Soc.*, **99**, 6455 (1977).
146. R. K. Haynes, J. M. Peters and I. D. Wilmot, *Austr. J. Chem.*, **33**, 2653 (1980).
147. R. K. Haynes and A. E. Hilliker, *Tetrahedron Lett.*, **27**, 509 (1986).
148. M. F. Arain, R. K. Haynes, S. C. Vonwiller and T. W. Hambley, *Austr. J. Chem.*, **41**, 505 (1988).
149. S. F. Nelsen, M. F. Teasley and D. L. Kapp, *J. Am. Chem. Soc.*, **108**, 5503 (1986).
150. S. F. Nelsen, *Acc. Chem. Res.*, **20**, 269 (1987).
151. M. F. Arain, R. K. Haynes, S. C. Vonwiller and T. W. Hambley, *J. Am. Chem. Soc.*, **107**, 4582 (1985).
152. M. O. Funk, R. Isaac and N. A. Porter, *J. Am. Chem. Soc.*, **97**, 1281 (1975).
153. N. A. Porter and M. O. Funk, *J. Org. Chem.*, **40**, 3614 (1975).
154. W. A. Pryor and J. P. Stanley, *J. Org. Chem.*, **40**, 3615 (1975).
155. N. A. Porter, in *Organic Peroxides* (Ed. W. Ando), Wiley, Chichester, 1992, p. 101.
156. J. Boukouvalas and R. K. Haynes, in *Radicals in Organic Synthesis* (Eds. P. Renaud and M. Sibi), Wiley-VCH, Weinheim, 2001, p. 455.
157. H. A. J. Carless and R. J. Batten, *Tetrahedron Lett.*, **23**, 4735 (1982).
158. J. Fossey, D. Lefort and J. Sorba, *Free Radicals in Organic Chemistry*, Mason, Paris, 1995.
159. P. D. Bartlett, E. P. Benzing and R. Pincock, *J. Am. Chem. Soc.*, **82**, 1762 (1960).
160. L. Dulog and P. Klein, *Chem. Ber.*, **104**, 895 (1971).
161. C. A. Ogle, S. W. Martin, M. P. Dziobak, M. W. Urban and G. D. Mendenhall, *J. Org. Chem.*, **48**, 3728 (1983).
162. D. P. Curran, N. A. Porter and B. Giese, *Stereochemistry of Radical Reactions: Concepts, Guidelines and Synthetic Applications*, VCH, Weinheim, 1996.
163. H. A. J. Carless and R. J. Batten, *J. Chem. Soc., Perkin Trans. 1*, 1999 (1987).
164. N. A. Porter, M. O. Funk, D. Gilmore, R. Isaac and J. Nixon, *J. Am. Chem. Soc.*, **98**, 6000 (1976).
165. A. J. Bloodworth, R. J. Curtis and N. Mistry, *J. Chem. Soc., Chem. Commun.*, 954 (1989).
166. P. Needleman, S. Moncada, S. Bunting, J. Vane, M. Hamberg and B. Samuelsson, *Nature*, **261**, 558 (1976).
167. C. D. Funk, *Science*, **294**, 1871 (2001).
168. N. A. Porter, *Acc. Chem. Res.*, **19**, 262 (1986).
169. N. A. Porter, S. E. Caldwell and K. A. Mills, *Lipids*, **30**, 277 (1995).
170. W. L. Smith and L. J. Marnett, *Biochem. Biophys. Acta*, **1083**, 1 (1991).
171. W. L. Smith, *Am. J. Physiol.*, **263**, 181 (1992).
172. D. E. O'Connor, E. D. Mihelich and M. C. Coleman, *J. Am. Chem. Soc.*, **103**, 223 (1981).
173. D. E. O'Connor, E. D. Mihelich and M. C. Coleman, *J. Am. Chem. Soc.*, **106**, 3577 (1984).
174. E. J. Corey, C. Shih, N. Y. Shih and K. Shimoji, *Tetrahedron Lett.*, **25**, 5013 (1984).
175. E. J. Corey, K. Shimoji and C. Shih, *J. Am. Chem. Soc.*, **106**, 6425 (1984).
176. E. J. Corey and Z. Wang, *Tetrahedron Lett.*, **35**, 539 (1994).
177. C. M. Havrilla, D. L. Hachey and N. A. Porter, *J. Am. Chem. Soc.*, **122**, 8042 (2000).

178. H. Y. Yin, C. M. Havrilla, J. D. Morrow and N. A. Porter, *J. Am. Chem. Soc.*, **124**, 7745 (2002).
179. H. Y. Yin, C. M. Havrilla, L. Gao, J. D. Morrow and N. A. Porter, *J. Biol. Chem.*, **278**, 16720 (2003).
180. N. A. Porter, J. K. Kaplan and P. H. Dussault, *J. Am. Chem. Soc.*, **112**, 1266 (1990).
181. K. A. Mills, S. E. Caldwell, G. R. Dubay and N. A. Porter, *J. Am. Chem. Soc.*, **114**, 9689 (1992).
182. N. A. Porter, K. A. Mills, S. E. Caldwell and G. B. Dubay, *J. Am. Chem. Soc.*, **116**, 6697 (1994).
183. N. A. Porter, K. A. Mills and R. L. Carter, *J. Am. Chem. Soc.*, **116**, 6690 (1994).
184. D. A. Pratt and N. A. Porter, *Org. Lett.*, **5**, 387 (2003).
185. J. A. Khan and N. A. Porter, *Angew. Chem., Int. Ed. Engl.*, **21**, 217 (1982).
186. N. A. Porter, A. N. Roe and A. T. McPhail, *J. Am. Chem. Soc.*, **102**, 7574 (1980).
187. A. N. Roe, A. T. McPhail and N. A. Porter, *J. Am. Chem. Soc.*, **105**, 1199 (1983).
188. S. Fielder, D. D. Rowan and M. S. Sherburn, *Synlett*, 349 (1996).
189. S. Fielder, D. D. Rowan and M. S. Sherburn, *Tetrahedron*, **54**, 12907 (1998).
190. J. Boukouvalas, R. Pouliot and Y. Frechette, *Tetrahedron Lett.*, **36**, 4167 (1995).
191. L. Cointeaux, J. F. Berrien and J. Mayrargue, *Tetrahedron Lett.*, **43**, 6275 (2002).
192. Y. Hashidoko, S. Tahara and J. Mizutani, *J. Chem. Soc., Chem. Commun.*, 1185 (1991).
193. Y. Hashidoko, S. Tahara and J. Mizutani, *J. Chem. Soc., Perkin Trans. 1*, 211 (1991).
194. Y. Hashidoko, S. Tahara and J. Mizutani, *J. Chem. Soc., Perkin Trans. 1*, 2351 (1993).
195. H. Morita, N. Tomioka, Y. Iitaka and H. Itokawa, *Chem. Pharm. Bull.*, **36**, 2984 (1988).
196. X. Creary, A. Wolf and K. Miller, *Org. Lett.*, **1**, 1615 (1999).
197. K. Wimalasena, H. B. Wickman and M. P. D. Mahindaratne, *Eur. J. Org. Chem.*, 3811 (2001).
198. A. L. Baumstark and P. C. Vasquez, *J. Heterocycl. Chem.*, **28**, 113 (1991).
199. A. L. Baumstark and P. C. Vasquez, *J. Org. Chem.*, **57**, 393 (1992).
200. M. S. Kharasch, W. Nudenberg and G. J. Mantell, *J. Org. Chem.*, **16**, 524 (1951).
201. A. A. Oswald and T. J. Wallace, in *The Chemistry of Organic Sulfur Compounds* (Eds. M. Kharasch and C. Y. Meyers), Pergamon Press, Oxford, 1966, pp. 217–232.
202. A. L. J. Beckwith and R. D. Wagner, *J. Am. Chem. Soc.*, **101**, 7099 (1979).
203. A. L. J. Beckwith and R. D. Wagner, *J. Chem. Soc., Chem. Commun.*, 485 (1980).
204. P. A. Barker, A. L. J. Beckwith and Y. Fung, *Tetrahedron Lett.*, **24**, 97 (1983).
205. M. D. Bachi and E. E. Korshin, *Synlett*, 122 (1998).
206. E. E. Korshin, R. Hoos, A. M. Szpilman, L. Konstantinovski, G. H. Posner and M. D. Bachi, *Tetrahedron*, **58**, 2449 (2002).
207. P. M. O'Neill, P. A. Stocks, M. D. Pugh, N. C. Araujo, E. E. Korshin, J. F. Bickley, S. A. Ward, P. G. Bray, E. Pasini, J. Davies, E. Verissimo and M. D. Bachi, *Angew. Chem., Int. Ed.*, **43**, 4193 (2004).
208. M. D. Bachi, G. H. Posner and E. E. Korshin, PCT Int. Appl. WO 99/12900 (1999); *Chem. Abstr.*, **130**, 237573 (1999).
209. M. D. Bachi, E. E. Korshin, P. Ploypradith, J. N. Cumming, S. J. Xie, T. A. Shapiro and G. H. Posner, *Bioorg. Med. Chem. Lett.*, **8**, 903 (1998).
210. M. D. Bachi, E. E. Korshin, R. Hoos, A. M. Szpilman, P. Ploypradith, S. Xie, T. A. Shapiro and G. H. Posner, *J. Med. Chem.*, **46**, 2516 (2003).
211. M. D. Bachi, E. E. Korshin, R. Hoos and A. M. Szpilman, *J. Heterocycl. Chem.*, **37**, 639 (2000).
212. A. M. Szpilman, E. E. Korshin, H. Rozenberg and M. D. Bachi, *J. Org. Chem.*, **70**, 3618 (2005).
213. K. S. Feldman and M. Parvez, *J. Am. Chem. Soc.*, **108**, 1328 (1986).
214. K. S. Feldman, *Synlett*, 217 (1995).
215. K. S. Feldman and R. E. Simpson, *Tetrahedron Lett.*, **30**, 6985 (1989).
216. K. S. Feldman and R. E. Simpson, *J. Am. Chem. Soc.*, **111**, 4878 (1989).
217. K. S. Feldman and C. M. Kraebel, *J. Org. Chem.*, **57**, 4574 (1992).
218. T. Iwama, H. Matsumoto, T. Ito, H. Shimizu and T. Kataoka, *Chem. Pharm. Bull.*, **46**, 913 (1998).
219. T. Tokuyasu, S. Kunikawa, A. Masuyama and M. Nojima, *Org. Lett.*, **4**, 3595 (2002).
220. T. Tokuyasu, S. Kunikawa, M. Abe, A. Masuyama, M. Nojima, H. S. Kim, K. Begum and Y. Wataya, *J. Org. Chem.*, **68**, 7361 (2003).

221. A. J. Bloodworth and R. J. Curtis, *J. Chem. Soc., Chem. Commun.*, 173 (1989).
222. See: J. Boukouvalas and R. K. Haynes, in *Radicals in Organic Synthesis* (Eds. P. Renaud and M. Sibi), Wiley-VCH, Weinheim, 2001, pp. 477–478.
223. A. Boto, C. Betancor, T. Prange and E. Suarez, *Tetrahedron Lett.*, **33**, 6687 (1992).
224. A. Boto, C. Betancor, T. Prange and E. Suarez, *J. Org. Chem.*, **59**, 4393 (1994).
225. R. Hernandez, S. M. Velazquez, E. Suarez and T. Prange, *Tetrahedron Lett.*, **37**, 6409 (1996).
226. A. Boto, R. Hernandez, S. M. Velazquez, E. Suarez and T. Prange, *J. Org. Chem.*, **63**, 4697 (1998).
227. A. Boto, R. Hernandez, E. Suarez, C. Betancor and M. S. Rodriguez, *J. Org. Chem.*, **60**, 8209 (1995).
228. A. Boto, C. Betancor, R. Hernandez, M. S. Rodriguez and E. Suarez, *Tetrahedron Lett.*, **34**, 4865 (1993).
229. R. Hernandez, J. J. Marrero, E. Suarez and A. Perales, *Tetrahedron Lett.*, **29**, 5979 (1988).
230. M. Balci, *Chem. Rev.*, **81**, 91 (1981).
231. E. J. Corey, K. C. Nicolaou, M. Shibasaki, Y. Machida and C. S. Shiner, *Tetrahedron Lett.*, 3183 (1975).
232. M. F. Salomon and R. G. Salomon, *J. Am. Chem. Soc.*, **99**, 3500 (1977).
233. R. G. Salomon and M. F. Salomon, *J. Am. Chem. Soc.*, **99**, 3501 (1977).
234. K. Takahashi and M. Kishi, *Tetrahedron*, **44**, 4737 (1988).
235. W. Adam, A. Birke, C. Cadiz, S. Diaz and A. Rodriguez, *J. Org. Chem.*, **43**, 1154 (1978).
236. P. H. Dussault and U. R. Zope, *J. Org. Chem.*, **60**, 8218 (1995).
237. N. A. Porter and D. W. Gilmore, *J. Am. Chem. Soc.*, **99**, 3503 (1977).
238. A. J. Bloodworth and B. P. Leddy, *Tetrahedron Lett.*, 729 (1979).
239. H. Kropf and H. Vonwallis, *Synthesis*, 237 (1981).
240. H. Kropf and H. Vonwallis, *Synthesis*, 633 (1981).
241. P. H. Dussault and R. J. Lee, *J. Am. Chem. Soc.*, **116**, 4485 (1994).
242. P. H. Dussault and U. R. Zope, *Tetrahedron Lett.*, **36**, 2187 (1995).
243. P. H. Dussault, C. T. Eary, R. J. Lee and U. R. Zope, *J. Chem. Soc., Perkin Trans. 1*, 2189 (1999).
244. H.-S. Dang and A. G. Davies, *Tetrahedron Lett.*, **32**, 1745 (1991).
245. H.-S. Dang and A. G. Davies, *J. Chem. Soc., Perkin Trans. 2*, 2011 (1991).
246. H.-S. Dang and A. G. Davies, *J. Organometal. Chem.*, **430**, 287 (1992).
247. X. X. Xu and H. Q. Dong, *Tetrahedron Lett.*, **35**, 9429 (1994).
248. X. X. Xu and H. Q. Dong, *J. Org. Chem.*, **60**, 3039 (1995).
249. L. Cointeaux, J.-F. Berrien, J. Mahuteau, M. E. Tran Huu-Dau, L. Ciceron, M. Danis and J. Mayrargue, *Bioorg. Med. Chem.*, **11**, 3791 (2003).
250. A. J. Bloodworth and M. E. Loveitt, *J. Chem. Soc., Chem. Commun.*, 94 (1976).
251. A. J. Bloodworth and M. E. Loveitt, *J. Chem. Soc., Perkin Trans. 1*, 522 (1978).
252. A. J. Bloodworth and J. A. Khan, *J. Chem. Soc., Perkin Trans. 1*, 2450 (1980).
253. N. A. Porter, P. J. Zuraw and J. A. Sullivan, *Tetrahedron Lett.*, **25**, 807 (1984).
254. E. Bascetta and F. D. Gunstone, *J. Chem. Soc., Perkin Trans. 1*, 2207 (1984).
255. J. L. Courtneidge, M. Bush and L. S. Loh, *Tetrahedron*, **48**, 3835 (1992).
256. A. J. Bloodworth, R. J. Curtis, M. D. Spencer and N. A. Tallant, *Tetrahedron*, **49**, 2729 (1993).
257. J. J. Helesbeux, D. Peyronnet, M. Labaied, P. Grellier, F. Frappier, D. Seraphin, P. Richomme and O. Duval, *J. Enz. Inhib. Med. Chem.*, **17**, 431 (2002).
258. J. R. Nixon, M. A. Cudd and N. A. Porter, *J. Org. Chem.*, **43**, 4048 (1978).
259. A. J. Bloodworth and M. D. Spencer, *Tetrahedron Lett.*, **31**, 5513 (1990).
260. A. J. Bloodworth and N. A. Tallant, *Tetrahedron Lett.*, **31**, 7077 (1990).
261. A. J. Bloodworth and D. Korkodilos, *Tetrahedron Lett.*, **32**, 6953 (1991).
262. A. J. Bloodworth, J. L. Courtneidge, R. J. Curtis and M. D. Spencer, *J. Chem. Soc., Perkin Trans. 1*, 2951 (1990).
263. N. A. Porter, M. A. Cudd, R. W. Miller and A. T. McPhail, *J. Am. Chem. Soc.*, **102**, 414 (1980).
264. N. A. Porter and P. J. Zuraw, *J. Org. Chem.*, **49**, 1345 (1984).
265. P. H. Dussault and D. R. Davies, *Tetrahedron Lett.*, **37**, 463 (1996).
266. T. Tokuyasu, A. Masuyama, M. Nojima and K. J. McCullough, *J. Org. Chem.*, **65**, 1069 (2000).

267. H. S. Kim, H. Begum, N. Ogura, Y. Wataya, T. Tokuyasu, A. Masuyama, M. Nojima and K. J. McCullough, *J. Med. Chem.*, **45**, 4732 (2002).
268. K. J. McCullough, T. Ito, T. Tokuyasu, A. Masuyama and M. Nojima, *Tetrahedron Lett.*, **42**, 5529 (2001).
269. T. Ito, T. Tokuyasu, A. Masuyama, M. Nojima and K. J. McCullough, *Tetrahedron*, **59**, 525 (2003).
270. A. J. Bloodworth, B. D. Bothwell, A. N. Collins and N. L. Maidwell, *Tetrahedron Lett.*, **37**, 1885 (1996).
271. N. Murakami, M. Kawanishi, S. Itagaki, T. Horii and M. Kobayashi, *Tetrahedron Lett.*, **42**, 7281 (2001).
272. N. Murakami, M. Kawanishi, S. Itagaki, T. Horii and M. Kobayashi, *Bioorg. Med. Chem. Lett.*, **12**, 69 (2002).
273. W. Hofheinz, H. Burgin, E. Gocke, C. Jaquet, R. Masciadri, G. Schmid, H. Stohler and H. Urwyler, *Trop. Med. Parasitol.*, **45**, 261 (1994).
274. P. M. O'Neill, N. L. Searle, K. J. Raynes, J. L. Maggs, S. A. Ward, R. C. Storr, B. K. Park and G. H. Posner, *Tetrahedron Lett.*, **39**, 6065 (1998).
275. X. X. Xu, J. Zhu, D.-Z. Huang and W.-S. Zhou, *Tetrahedron Lett.*, **32**, 5785 (1991).
276. W.-S. Zhou and X. X. Xu, *Acc. Chem. Res.*, **27**, 211 (1994).
277. C. Jaquet, H. R. Stohler, J. Chollet and W. Peters, *Trop. Med. Parasitol.*, **45**, 266 (1994).
278. I. N. Nazarov and A. A. Akhrem, *J. Gen. Chem. (USSR)*, **20**, 2183 (1950); *Chem. Abstr.* 1950 (1950).
279. G. B. Payne, *J. Org. Chem.*, **23**, 310 (1958).
280. A. Rieche, E. Schmitz and E. Grundemann, *Chem. Ber.*, **93**, 2443 (1960).
281. C. Cattivola, F. Figueras, J. M. Fraile, J. I. Garcia and J. A. Mayoral, *Tetrahedron Lett.*, **36**, 4125 (1995).
282. K. Yamaguchi, K. Mori, T. Mizugaki, K. Ebitani and K. Kaneda, *J. Org. Chem.*, **65**, 6897 (2000).
283. I. G. Tishchenko, V. N. Burd and I. F. Revinskii, *Russ. J. Org. Chem. (Eng. Transl.)*, **22**, 598 (1986).
284. H. E. Ensley, R. V. C. Carr, R. S. Martin and T. E. Pierce, *J. Am. Chem. Soc.*, **102**, 2836 (1980).
285. A. A. Frimer, M. Afri, S. D. Baumel, P. Gilinski-Sharon, Z. Rosenthal and H. E. Gottlieb, *J. Org. Chem.*, **65**, 1807 (2000).
286. T. Akasaka, K. Takeuchi, Y. Misawa and W. Ando, *Heterocycles*, **28**, 445 (1989).
287. P. H. Dussault and K. R. Woller, *J. Am. Chem. Soc.*, **119**, 3824 (1997).
288. P. H. Dussault, C. T. Eary and K. R. Woller, *J. Org. Chem.*, **64**, 1789 (1999).
289. T. Tokuyasu, T. Ito, A. Masuyama and M. Nojima, *Heterocycles*, **53**, 1293 (2000).
290. K. J. McCullough, H. Tokuhara, A. Masuyama and M. Nojima, *Org. Biomol. Chem.*, **1**, 1522 (2003).
291. T. Tokuyasu, A. Masuyama, M. Nojima, H. S. Kim and Y. Wataya, *Tetrahedron Lett.*, **41**, 3145 (2000).
292. T. Tokuyasu, A. Masuyama, M. Nojima, K. J. McCullough, H. S. Kim and Y. Wataya, *Tetrahedron*, **57**, 5979 (2001).
293. D. H. Gibson and C. H. DePuy, *Tetrahedron Lett.*, 2203 (1969).
294. A. Oku, T. Yokoyama and T. Harada, *Tetrahedron Lett.*, **24**, 4699 (1983).
295. S. Prathapan, K. E. Robinson and W. C. Agosta, *J. Am. Chem. Soc.*, **114**, 1838 (1992).
296. M. E. Scheller, P. Mathies, W. Petter and B. Frei, *Helv. Chim. Acta*, **67**, 1748 (1984).
297. J. Yoshida, S. Nakatani and S. Isoe, *Tetrahedron Lett.*, **31**, 2425 (1990).
298. J. Yoshida, S. Nakatani, K. Sakaguchi and S. Isoe, *J. Org. Chem.*, **54**, 3383 (1989).
299. S. Tategami, T. Yamada, H. Nishino, J. D. Korp and K. Kurosawa, *Tetrahedron Lett.*, **31**, 6371 (1990).
300. H. Nishino, S. Tategami, T. Yamada, J. D. Korp and K. Kurosawa, *Bull. Chem. Soc. Jpn.*, **64**, 1800 (1991).
301. C. Y. Qian, H. Nishino and K. Kurosawa, *Bull. Chem. Soc. Jpn.*, **64**, 3557 (1991).
302. C. Y. Qian, T. Yamada, H. Nishino and K. Kurosawa, *Bull. Chem. Soc. Jpn.*, **65**, 1371 (1992).
303. C. Y. Qian, H. Nishino and K. Kurosawa, *J. Heterocycl. Chem.*, **30**, 209 (1993).
304. T. Yamada, Y. Iwahara, H. Nishino and K. Kurosawa, *J. Chem. Soc., Perkin Trans. 1*, 609 (1993).

305. O. Y. Jie, H. Nishino and K. Kurosawa, *J. Heterocycl. Chem.*, **33**, 1291 (1996).
306. V. H. Nguyen, H. Nishino and K. Kurosawa, *Tetrahedron Lett.*, **37**, 4949 (1996).
307. V. H. Nguyen, H. Nishino and K. Kurosawa, *Synthesis*, 899 (1997).
308. S. Kajikawa, H. Nishino and K. Kurosawa, *Heterocycles*, **54**, 171 (2001).
309. C. Y. Qian, H. Nishino, K. Kurosawa and J. D. Korp, *J. Org. Chem.*, **58**, 4448 (1993).
310. M. T. Rahman and H. Nishino, *Tetrahedron*, **59**, 8383 (2003).
311. J. Ouyang, H. Nishino and K. Kurosawa, *J. Heterocycl. Chem.*, **32**, 1783 (1995).
312. F. A. Chowdhury, H. Nishino and K. Kurosawa, *Heterocycl. Commun.*, **7**, 17 (2001).
313. V. H. Nguyen, H. Nishino and K. Kurosawa, *Tetrahedron Lett.*, **38**, 1773 (1997).
314. F. A. Chowdhury, H. Nishino and K. Kurosawa, *Heterocycles*, **51**, 575 (1999).
315. F. A. Chowdhury, H. Nishino and K. Kurosawa, *Tetrahedron Lett.*, **39**, 7931 (1998).
316. V. H. Nguyen, H. Nishino and K. Kurosawa, *Heterocycles*, **48**, 465 (1998).
317. R. Kumabe, H. Nishino, M. Yasutake, V. H. Nguyen and K. Kurosawa, *Tetrahedron Lett.*, **42**, 69 (2001).
318. A. A. Frimer, in *The Chemistry of Peroxides* (Ed. S. Patai), Wiley, Chichester, 1983, p. 201.
319. R. W. Denny and A. Nickon, *Org. React.*, **20**, 133 (1973).
320. A. U. Khan, in *Singlet Oxygen, Vol. 1* (Ed. A. A. Frimer), CRC Press, Boca Raton, 1985, p. 39.
321. A. A. Trabanco, A. G. Montalban, G. Rumbles, A. G. M. Barrett and B. M. Hoffman, *Synlett*, 1010 (2000).
322. A. G. Griesbeck and A. Bartoschek, *Chem. Commun.*, 1594 (2002).
323. E. L. Clennan, *Tetrahedron*, **47**, 1343 (1991).
324. J. Fritzsche, *Compt. Rend.*, **64**, 1035 (1867).
325. A. J. Bloodworth and H. J. Eggelte, in *Singlet Oxygen, Vol. 1* (Ed. A. A. Frimer), CRC Press, Boca Raton, 1985, p. 92.
326. K. Gollnick and G. O. Schenck, in *1,4-Cycloaddition Reactions* (Ed. J. Hamer), Academic Press, Orlando, 1967, p. 255.
327. M. Matsumoto, in *Singlet Oxygen, Vol. 2* (Ed. A. A. Frimer), CRC Press, Boca Raton, 1985, p. 205.
328. M. Matsumoto, S. Dobashi, K. Kuroda and K. Kondo, *Tetrahedron*, **41**, 2147 (1985).
329. J. M. Aubry, C. Pierlot, J. Rigaudy and R. Schmidt, *Acc. Chem. Res.*, **36**, 668 (2003).
330. W. Adam and A. Griesbeck, in *CRC Handbook of Organic Photochemistry and Photobiology* (Eds. W. M. Horspool and P. Song), CRC Press, Boca Raton, 1995, p. 311.
331. W. Adam and M. Prein, *Acc. Chem. Res.*, **29**, 275 (1996).
332. W. Adam, C. R. Saha-Möller, S. B. Schambony, K. S. Schmid and T. Wirth, *Photochem. Photobiol.*, **70**, 476 (1999).
333. W. Adam, S. Bosio, A. Bartoschek and A. Griesbeck, in *CRC Handbook of Organic Photochemistry and Photobiology* (Eds. W. Horspool and F. Lenci), CRC Press, Boca Raton, 2004, pp. 25/1–25/19.
334. M. A. McCarrick, Y. D. Wu and K. N. Houk, *J. Org. Chem.*, **58**, 3330 (1993).
335. A. G. Leach and K. N. Houk, *Chem. Commun.*, 1243 (2002).
336. M. J. S. Dewar and W. Thiel, *J. Am. Chem. Soc.*, **99**, 2338 (1977).
337. M. Bobrowski, A. Liwo, S. Oldziej, D. Jeziorek and T. Ossowski, *J. Am. Chem. Soc.*, **122**, 8112 (2000).
338. A. Maranzana, G. Ghigo and G. Tonachini, *J. Am. Chem. Soc.*, **122**, 1414 (2000).
339. F. Sevin and M. L. McKee, *J. Am. Chem. Soc.*, **123**, 4591 (2001).
340. R. D. Ashford and E. A. Ogryzlo, *Can. J. Chem.*, **52**, 3544 (1974).
341. C. A. Long and D. R. Kearns, *J. Am. Chem. Soc.*, **97**, 2018 (1975).
342. A. A. Gorman, G. Lovering and M. A. J. Rodgers, *J. Am. Chem. Soc.*, **101**, 3050 (1979).
343. J. M. Aubry, B. Mandard-Cazin, M. Rougée and R. V. Bensasson, *J. Am. Chem. Soc.*, **117**, 9159 (1995).
344. A. G. Griesbeck, M. Fiege, M. S. Gudipati and R. Wagner, *Eur. J. Org. Chem.*, 2833 (1998).
345. F. Wilkinson, W. P. Helman and A. B. Ross, *J. Phys. Chem., Ref. Data*, **24**, 663 (1995).
346. A. A. Frimer, *Chem. Rev.*, **79**, 359 (1979).
347. J. Rigaudy, P. Capdevielle, S. Cambrisson and M. Maumy, *Tetrahedron Lett.*, 2757 (1974).
348. K. Gollnick and A. Griesbeck, *Tetrahedron Lett.*, **24**, 3303 (1983).
349. K. E. O'Shea and C. S. Foote, *J. Am. Chem. Soc.*, **110**, 7167 (1988).

350. J. Motoyoshiya, Y. Okuda, I. Matsuoka, S. Hayashi, Y. Takaguchi and H. Aoyama, *J. Org. Chem.*, **64**, 493 (1999).
351. C. W. Jefford, *Chem. Soc. Rev.*, **22**, 59 (1993).
352. K. Gollnick and A. Griesbeck, *Tetrahedron*, **40**, 3235 (1984).
353. L. E. Manring, R. C. Kanner and C. S. Foote, *J. Am. Chem. Soc.*, **105**, 4707 (1983).
354. L. E. Manring and C. S. Foote, *J. Am. Chem. Soc.*, **105**, 4710 (1983).
355. W. Adam and E. Staab, *Tetrahedron Lett.*, **29**, 531 (1988).
356. G. Vassilikogiannakis, M. Stratakis and M. Orfanopoulos, *J. Org. Chem.*, **63**, 6390 (1998).
357. L. M. Harwood, J. Robertson and S. Swallow, *Synlett*, 1359 (1999).
358. L. M. Harwood, A. C. Brickwood, V. Morrison, J. Robertson and S. Swallow, *J. Heterocycl. Chem.*, **36**, 1391 (1999).
359. M. Jung, J. Ham and J. Song, *Org. Lett.*, **4**, 2763 (2002).
360. G. Yao and K. Steliou, *Org. Lett.*, **4**, 485 (2002).
361. J. Ficini, C. Barbara and O. Ouerfelli, *Heterocycles*, **28**, 547 (1989).
362. K. C. Nicolaou, J. L. Gunzner, G. Q. Shi, K. A. Agrios, P. Gartner and Z. Yang, *Chem. Eur. J.*, **5**, 646 (1999).
363. K. C. Nicolaou, Z. Yang, M. Ouellette, G. Q. Shi, P. Gartner, J. L. Gunzner, K. A. Agrios, R. Huber, R. Chadha and D. H. Huang, *J. Am. Chem. Soc.*, **119**, 8105 (1997).
364. K. C. Nicolaou, P. A. Wallace, S. H. Shi, M. A. Ouellette, M. E. Bunnage, J. L. Gunzner, K. A. Agrios, G. Q. Shi, P. Gartner and Z. Yang, *Chem. Eur. J.*, **5**, 618 (1999).
365. X. J. Zhang, S. I. Khan and C. S. Foote, *J. Org. Chem.*, **58**, 7839 (1993).
366. M. Matsumoto, S. Nasu, M. Takeda, H. Murakami and N. Watanabe, *Chem. Commun.*, 821 (2000).
367. M. R. Iesce, M. L. Graziano, F. Cermola and R. Scarpati, *J. Chem. Soc., Chem. Commun.*, 1061 (1991).
368. W. Adam, M. Ahrweiler and M. Sauter, *Angew. Chem., Int. Ed. Engl.*, **32**, 80 (1993).
369. K. Gollnick, *Adv. Photochem.*, **6**, 89 (1968).
370. M. Matsumoto and K. Kuroda, *Tetrahedron Lett.*, **23**, 1285 (1982).
371. W. Adam, M. Guthlein, E.-M. Peters, K. Peters and T. Wirth, *J. Am. Chem. Soc.*, **120**, 4091 (1998).
372. W. Adam, S. G. Bosio, H.-G. Degen, O. Krebs, D. Stalke and D. Schumacher, *Eur. J. Org. Chem.*, 3944 (2002).
373. P. H. Dussault, Q. Han, D. G. Sloss and D. J. Symonsbergen, *Tetrahedron*, **55**, 11437 (1999).
374. F. Fabris, L. Leoni and O. De Lucchi, *Tetrahedron Lett.*, **40**, 1223 (1999).
375. G. Delogu, D. Fabbri, F. Fabris, F. Sbrogio, G. Valle and O. De Lucchi, *J. Chem. Soc., Chem. Commun.*, 1887 (1995).
376. F. Fabris, F. Sbrogio, O. De Lucchi, G. Delogu, D. Fabbri and G. Valle, *Gazz. Chim. Ital.*, **127**, 393 (1997).
377. F. Wilkinson and J. G. Brumer, *J. Phys. Chem., Ref. Data*, **10**, 809 (1981).
378. K. M. Davis and B. K. Carpenter, *J. Org. Chem.*, **61**, 4617 (1996).
379. R. Matusch and G. Schmidt, *Angew. Chem., Int. Ed. Engl.*, **27**, 717 (1988).
380. E. L. Clennan and K. Matusuno, *J. Org. Chem.*, **52**, 3483 (1987).
381. L. A. Paquette, R. V. C. Carr, E. Arnold and J. J. Clardy, *J. Org. Chem.*, **45**, 4907 (1980).
382. S. J. Hathaway and L. A. Paquette, *Tetrahedron*, **41**, 2037 (1985).
383. A. G. Griesbeck and T. Deufel, *Synlett*, 467 (1993).
384. A. G. Griesbeck, T. Deufel, K. Peters, E.-M. Peters and H. G. von Schnering, *J. Org. Chem.*, **60**, 1952 (1995).
385. X. Zhang, S. I. Khan and C. S. Foote, *J. Org. Chem.*, **60**, 4102 (1995).
386. W. Adam and I. Erden, *Angew. Chem.*, **90**, 223 (1978).
387. I. Erden, J. Drummond, R. Alstad and F. Xu, *Tetrahedron Lett.*, **34**, 2291 (1993).
388. X. Zhang, F. Lin and C. S. Foote, *J. Org. Chem.*, **60**, 1333 (1995).
389. R. W. Murray and M. L. Kaplan, *J. Am. Chem. Soc.*, **91**, 5358 (1969).
390. C. Kaneko, A. Sugimoto and S. Tanaka, *Synthesis*, 876 (1974).
391. N. Akbulut and M. Balci, *J. Org. Chem.*, **53**, 3338 (1988).
392. M. Balci, Y. Sutbeyaz and H. Secen, *Tetrahedron*, **46**, 3715 (1990).
393. H. Secen, E. Salamci, Y. Sutbeyaz and M. Balci, *Synlett*, 609 (1993).
394. H. Secen, S. Gultekin, Y. Sutbeyaz and M. Balci, *Synth. Commun.*, **24**, 2103 (1994).
395. Y. Kara, M. Balci, S. A. Bourne and W. H. Watson, *Tetrahedron Lett.*, **35**, 3349 (1994).

396. M. Balci, *Pure Appl. Chem.*, **69**, 97 (1997).
397. Y. Kara and M. Balci, *Tetrahedron*, **59**, 2063 (2003).
398. E. Salamci, H. Secen, Y. Sutbeyaz and M. Balci, *J. Org. Chem.*, **62**, 2453 (1997).
399. W. Adam, M. Balci and H. Kilic, *J. Org. Chem.*, **65**, 5926 (2000).
400. M. S. Gultekin, E. Salamci and M. Balci, *Carbohydr. Res.*, **338**, 1615 (2003).
401. M. S. Gultekin, M. Celik, E. Turkut, C. Tanyeli and M. Balci, *Tetrahedron: Asymmetry*, **15**, 453 (2004).
402. G. Zhou, X. Gao, W. Z. Li and Y. Li, *Tetrahedron Lett.*, **42**, 3101 (2001).
403. H. Kusama, R. Hara, S. Kawahara, T. Nishimori, H. Kashima, N. Nakamura, K. Morihira and I. Kuwajima, *J. Am. Chem. Soc.*, **122**, 3811 (2000).
404. T. Linker, F. Rebien and G. Tóth, *Chem. Commun.*, 2585 (1996).
405. C. R. Johnson, A. Golebiowski and D. H. Steensma, *J. Am. Chem. Soc.*, **114**, 9414 (1992).
406. C. R. Johnson, A. Golebiowski, D. H. Steensma and M. A. Scialdone, *J. Org. Chem.*, **58**, 7185 (1993).
407. M. Celik, N. Akbulut and M. Balci, *Helv. Chim. Acta*, **83**, 3131 (2000).
408. L. T. Scott and C. M. Adams, *J. Am. Chem. Soc.*, **106**, 4857 (1984).
409. N. Akbulut, A. Menzek and M. Balci, *Tetrahedron Lett.*, **28**, 1689 (1987).
410. A. Dastan, N. Saracoglu and M. Balci, *Eur. J. Org. Chem.*, 3519 (2001).
411. W. Adam and M. Balci, *J. Am. Chem. Soc.*, **101**, 6285 (1979).
412. W. Adam and M. Balci, *J. Org. Chem.*, **44**, 1189 (1979).
413. W. Adam and M. Balci, *J. Am. Chem. Soc.*, **101**, 7537 (1979).
414. M. E. Sengul and M. Balci, *J. Chem. Soc., Perkin Trans. 1*, 2071 (1997).
415. N. Saracoglu, A. Menzek, S. Sayan, U. Salzner and M. Balci, *J. Org. Chem.*, **64**, 6670 (1999).
416. G. Mehta, R. Uma, M. N. Jagadeesh and J. Chandrasekhar, *Chem. Commun.*, 1813 (1998).
417. G. Mehta and R. Uma, *J. Org. Chem.*, **65**, 1685 (2000).
418. R. Brecht, F. Haenel, G. Seitz, G. Frenzen, A. Pilz, W. Massa and S. Wocadlo, *Liebigs Ann./Recl.*, 851 (1997).
419. R. Brecht, F. Haenel and G. Seitz, *Liebigs Ann./Recl.*, 2275 (1997).
420. R. Brecht, F. Buttner, M. Bohm, G. Seitz, G. Frenzen, A. Pilz and W. Massa, *J. Org. Chem.*, **66**, 2911 (2001).
421. C. Pierlot, J.-M. Aubry, K. Briviba, H. Sies and P. di Mascio, *Meth. Enzymol.*, **319**, 3 (2000).
422. I. Saito, T. Matsuura and K. Inoue, *J. Am. Chem. Soc.*, **103**, 188 (1981).
423. G. R. Martinez, J.-L. Ravanat, M. H. G. Medeiros, J. Cadet and P. Di Mascio, *J. Am. Chem. Soc.*, **122**, 10212 (2000).
424. E. Vogel, M. Schafer-Ridder and U. Brocker, *Angew. Chem., Int. Ed. Engl.*, **15**, 228 (1976).
425. C. Pierlot and J. M. Aubry, *Chem. Commun.*, 2289 (1997).
426. C. Pierlot, J. Poprawski, J. Marko and J. M. Aubry, *Tetrahedron Lett.*, **41**, 5063 (2000).
427. N. J. Turro, M.-F. Chow and J. Rigaudy, *J. Am. Chem. Soc.*, **103**, 7218 (1981).
428. K. B. Eisenthal, N. J. Turro, C. G. Dupuy, D. A. Hrovat, J. Langau, T. A. Jenny and E. V. Sitzmann, *J. Phys. Chem.*, **90**, 5168 (1986).
429. J. Rigaudy, M. Lachgar and M. M. A. Saad, *Bull. Soc. Chim. Fr.*, **131**, 177 (1994).
430. X. Zhou, M. Kitamura, B. Shen, K. Nakajima and T. Takahashi, *Chem. Lett.*, **33**, 410 (2004).
431. J. Rigaudy, A. Caspar, M. Lachgar, D. Maurette and C. Chassagnard, *Bull. Soc. Chim. Fr.*, **129**, 16 (1992).
432. W. Adam and M. Prein, *Tetrahedron*, **51**, 12583 (1995).
433. W. Adam and M. Prein, *J. Am. Chem. Soc.*, **115**, 3766 (1993).
434. W. Adam, E.-M. Peters, K. Peters, M. Prein and H. G. von Schnering, *J. Am. Chem. Soc.*, **117**, 6686 (1995).
435. W. Adam and M. Prein, *Tetrahedron Lett.*, **35**, 4331 (1994).
436. M. Prein, M. Maurer, E.-M. Peters, K. Peters, H. G. von Schnering and W. Adam, *Chem. Eur. J.*, **1**, 89 (1995).
437. H. Miyabe, M. Torieda, K. Inoue, K. Tajiri, T. Kiguchi and T. Naito, *J. Org. Chem.*, **63**, 4397 (1998).
438. R. Scarpati, M. R. Iesce, F. Cermola and A. Guitto, *Synlett*, 17 (1998).
439. X.-D. Luo and C.-C. Shen, *Med. Res. Rev.*, **7**, 29 (1987).
440. A. Brossi, B. Venugopalan, L. D. Gerpe, H. J. C. Yeh, J. L. Flippen-Anderson, P. Buchs, X.-D. Luo, W. Milhaus and W. Peters, *J. Med. Chem.*, **31**, 645 (1988).

441. M. A. Avery, F. G. Gao, W. K. M. Chong, S. Mehrotra and W. K. Milhous, *J. Med. Chem.*, **36**, 4264 (1993).
442. Y. L. Wu and Y. Li, *Med. Chem. Res.*, **5**, 569 (1995).
443. C. W. Jefford, *Adv. Drug Res.*, **29**, 271 (1997).
444. M. A. Avery, *Adv. Med. Chem.*, **4**, 125 (1999).
445. G. H. Posner and P. M. O'Neill, *Acc. Chem. Res.*, **37**, 397 (2004).
446. G. H. Posner, J. N. Cumming and M. Krasavin, in *Biomedical Chemistry: Applying Chemical Principles to the Understanding and Treatment of Disease* (Ed. P. F. Torrence), Wiley, New York, 2000, p. 289.
447. K. Borstnik, I. H. Paik, T. A. Shapiro and G. H. Posner, *Int. J. Parasitol.*, **32**, 1661 (2002).
448. Y. K. Wu, *Acc. Chem. Res.*, **35**, 255 (2002).
449. P. L. Olliaro, R. K. Haynes, B. Meunier and Y. Yuthavong, *Trends Parasitol.*, **17**, 122 (2001).
450. R. K. Haynes, W. Y. Ho, H. W. Chan, B. Fugmann, J. Stetter, S. L. Croft, L. Vivas, W. Peters and B. L. Robinson, *Angew. Chem., Int. Ed. Engl.*, **43**, 1381 (2004).
451. A. Robert and B. Meunier, *Chem. Soc. Rev.*, **27**, 273 (1998).
452. A. Robert, O. Dechy-Cabaret, J. Cazelles and B. Meunier, *Acc. Chem. Res.*, **35**, 167 (2002).
453. U. Eckstein-Ludwig, R. J. Webb, I. D. A. van Goethem, J. M. East, A. G. Lee, M. Kimura, P. M. O'Neill, P. G. Bray, S. A. Ward and S. Krishna, *Nature*, **424**, 957 (2003).
454. G. A. Biagini, P. M. O'Neill, A. Nzila, S. A. Ward and P. G. Bray, *Trends Parasitol.*, **19**, 479 (2003).
455. S. R. Meshnick, *Int. J. Parasitol.*, **32**, 1655 (2002).
456. H. J. Woerdenbag, T. A. Moskal, N. Pras, T. M. Malingre, F. S. Elferaly, H. H. Kampinga and A. W. T. Konings, *J. Nat. Prod.*, **56**, 849 (1993).
457. H. Lai and N. P. Singh, *Cancer Lett.*, **91**, 41 (1995).
458. Y. Li, J. M. Wu, F. Shan, G. S. Wu, J. Ding, D. Xiao, J. X. Han, G. Atassi, S. Leonce, D. H. Caignard and P. Renard, *Bioorg. Med. Chem.*, **11**, 977 (2003).
459. T. Efferth, A. Sauerbrey, A. Olbrich, E. Gebhart, P. Rauch, H. O. Weber, J. G. Hengstler, M. E. Halatsch, M. Volm, K. D. Tew, D. D. Ross and J. O. Funk, *Molec. Pharmacol.*, **64**, 382 (2003).
460. T. Efferth, R. Bauer, J. O. Funk, M. Davey, M. Volm and R. Davey, *Eur. J. Cancer*, **38**, S99 (2002).
461. T. Efferth, H. Dunstan, A. Sauerbrey, H. Miyachi and C. R. Chitambar, *Int. J. Oncol.*, **18**, 767 (2001).
462. S. Oh, I. H. Jeong, W. S. Shin and S. Lee, *Bioorg. Med. Chem. Lett.*, **13**, 3665 (2003).
463. M. Jung, *Bioorg. Med. Chem. Lett.*, **7**, 1091 (1997).
464. M. Jung, S. Lee, J. Ham, K. Lee, H. Kim and S. K. Kim, *J. Med. Chem.*, **46**, 987 (2003).
465. A. C. Beekman, A. R. W. Barentsen, H. J. Woerdenbag, W. VanUden, N. Pras, A. W. T. Konings, F. S. Elferaly, A. M. Galal and H. V. Wikstrom, *J. Nat. Prod.*, **60**, 325 (1997).
466. A. C. Beekman, H. J. Woerdenbag, H. H. Kampinga and A. W. T. Konings, *Phytother. Res.*, **10**, 140 (1996).
467. J. P. Jeyadevan, P. G. Bray, J. Chadwick, A. E. Mercer, A. Byrne, S. A. Ward, B. K. Park, D. P. Williams, R. Cosstick, J. Davies, A. P. Higson, E. Irving, G. H. Posner and P. M. O'Neill, *J. Med. Chem.*, **47**, 1290 (2004).
468. G. H. Posner, I. H. Paik, S. Sur, A. J. McRiner, K. Borstnik, S. J. Xie and T. A. Shapiro, *J. Med. Chem.*, **46**, 1060 (2003).
469. G. H. Posner, J. Northrop, I. H. Paik, K. Borstnik, P. Dolan, T. W. Kensler, S. Xie and T. A. Shapiro, *Bioorg. Med. Chem.*, **10**, 227 (2002).
470. G. H. Posner, P. Ploypradith, M. H. Parker, H. O'Dowd, S. H. Woo, J. Northrop, M. Krasavin, P. Dolan, T. W. Kensler, S. J. Xie and T. A. Shapiro, *J. Med. Chem.*, **42**, 4275 (1999).
471. G. H. Posner, P. Ploypradith, W. Hapangama, D. S. Wang, J. N. Cumming, P. Dolan, T. W. Kensler, D. Klinedinst, T. A. Shapiro, Q. Y. Zheng, C. K. Murray, L. G. Pilkington, L. R. Jayasinghe, J. F. Bray and R. Daughenbaugh, *Bioorg. Med. Chem.*, **5**, 1257 (1997).
472. S. Ekthawatchai, S. Kamchonwongpaisan, P. Kongsaree, B. Tamchompoo, Y. Thebtaranonth and Y. Yuthavong, *J. Med. Chem.*, **44**, 4688 (2001).
473. G. B. Payne and C. W. Smith, *J. Org. Chem.*, **22**, 1682 (1957).
474. W. Adam and A. Rios, *J. Chem. Soc., Chem. Commun.*, 822 (1971).

475. V. Subramanyam, C. L. Brizuela and A. H. Soloway, *J. Chem. Soc., Chem. Commun.*, 508 (1976).
476. A. Haq, B. Kerr and K. J. McCullough, *J. Chem. Soc., Chem. Commun.*, 1076 (1993).
477. E. L. Clennan, *Tetrahedron*, **56**, 9151 (2000).
478. C. Singh, *Tetrahedron Lett.*, **31**, 6901 (1990).
479. C. Singh, D. Misra, G. Saxena and S. Chandra, *Bioorg. Med. Chem. Lett.*, **2**, 497 (1992).
480. C. Singh, D. Misra, G. Saxena and S. Chandra, *Bioorg. Med. Chem. Lett.*, **5**, 1913 (1995).
481. C. Singh, H. Malik and S. K. Puri, *Bioorg. Med. Chem.*, **12**, 1177 (2004).
482. C. Singh, N. Gupta and S. K. Puri, *Bioorg. Med. Chem. Lett.*, **12**, 1913 (2002).
483. C. Singh, N. Gupta and S. K. Puri, *Bioorg. Med. Chem. Lett.*, **13**, 3447 (2003).
484. A. G. Griesbeck, T. T. Eldreedy, M. Fiege and R. Brun, *Org. Lett.*, **4**, 4193 (2002).
485. C. W. Jefford, J.-C. Rossier and G. D. Richardson, *J. Chem. Soc., Chem. Commun.*, 1064 (1983).
486. C. W. Jefford, J. Currie, G. D. Richardson and J.-C. Rossier, *Helv. Chim. Acta.*, **74**, 1239 (1991).
487. P. M. O'Neill, A. Mukhtar, S. A. Ward, J. F. Bickley, J. Davies, M. D. Bachi and P. A. Stocks, *Org. Lett.*, **6**, 3035 (2004).
488. P. M. O'Neill, M. Pugh, J. Davies, S. A. Ward and B. K. Park, *Tetrahedron Lett.*, **42**, 4569 (2001).
489. P. M. O'Neill, S. Hindley, M. D. Pugh, J. Davies, P. G. Bray, B. K. Park, D. S. Kapu, S. A. Ward and P. A. Stocks, *Tetrahedron Lett.*, **44**, 8135 (2003).
490. C. H. Oh and J. H. Kang, *Tetrahedron Lett.*, **39**, 2771 (1998).
491. C. H. Oh, H. J. Kim, S. H. Wu and H. S. Won, *Tetrahedron Lett.*, **40**, 8391 (1999).
492. M. A. Avery, C. Jenningswhite and W. K. M. Chong, *J. Org. Chem.*, **54**, 1789 (1989).
493. M. A. Avery, W. K. M. Chong and J. E. Bupp, *J. Chem. Soc., Chem. Commun.*, 1487 (1990).
494. M. A. Avery, F. L. Gao, W. K. M. Chong, T. F. Hendrickson, W. D. Inman and P. Crews, *Tetrahedron*, **50**, 957 (1994).
495. M. A. Avery, C. Jenningswhite and W. K. M. Chong, *J. Org. Chem.*, **54**, 1792 (1989).
496. M. A. Avery, W. K. M. Chong and C. Jenningswhite, *J. Am. Chem. Soc.*, **114**, 974 (1992).
497. M. A. Avery, C. Jenningswhite and W. K. M. Chong, *Tetrahedron Lett.*, **28**, 4629 (1987).
498. M. A. Avery, J. D. Bonk, W. K. M. Chong, S. Mehrotra, R. Miller, W. Milhous, D. K. Goins, S. Venkatesan, C. Wyandt, I. Khan and B. A. Avery, *J. Med. Chem.*, **38**, 5038 (1995).
499. M. A. Avery, S. Mehrotra, J. D. Bonk, J. A. Vroman, D. K. Goins and R. Miller, *J. Med. Chem.*, **39**, 2900 (1996).
500. M. A. Avery, S. Mehrotra, T. L. Johnson, J. D. Bonk, J. A. Vroman and R. Miller, *J. Med. Chem.*, **39**, 4149 (1996).
501. M. A. Avery, M. Alvim-Gaston, J. A. Vroman, B. Wu, A. Ager, W. Peters, B. L. Robinson and W. Charman, *J. Med. Chem.*, **45**, 4321 (2002).
502. C. A. Haraldson, J. M. Karle, S. G. Freeman, R. K. Duvadie and M. A. Avery, *Bioorg. Med. Chem. Lett.*, **7**, 2357 (1997).
503. G. Schmid and W. Hofheinz, *J. Am. Chem. Soc.*, **105**, 624 (1983).
504. W.-S. Zhou, *Pure Appl. Chem.*, **58**, 817 (1986).
505. X. X. Xu, J. Zhu, D. Z. Huang and W.-S. Zhou, *Acta Chim. Sin.*, **41**, 574 (1983).
506. X. X. Xu, J. Zhu, D. Z. Huang and W.-S. Zhou, *Acta Chim. Sin.*, **42**, 940 (1984).
507. J. S. Yadav, R. S. Babu and G. Sabitha, *Tetrahedron Lett.*, **44**, 387 (2003).
508. C. W. Jefford, S. Kohmoto, J. Boukouvalas and U. Burger, *J. Am. Chem. Soc.*, **105**, 6498 (1983).
509. C. W. Jefford, J. Boukouvalas and S. Kohmoto, *Helv. Chim. Acta.*, **66**, 2615 (1983).
510. C. W. Jefford, J. Boukouvalas and S. Kohmoto, *J. Chem. Soc., Chem. Commun.*, 523 (1984).
511. Y. Imakura, T. Yokoi, T. Yamagishi, J. Koyama, H. Hu, D. R. McPhail, A. T. McPhail and K.-H. Lee, *J. Chem. Soc., Chem. Commun.*, 372 (1988).
512. M. K. Jung and R. F. Schinazi, *Bioorg. Med. Chem. Lett.*, **4**, 931 (1994).
513. C. W. Jefford, J. Velarde and G. Bernardinelli, *Tetrahedron Lett.*, **30**, 4485 (1989).
514. C. W. Jefford, J. A. Velarde, G. Bernardinelli, D. H. Bray, D. C. Warhurst and W. K. Milhous, *Helv. Chim. Acta*, **76**, 2775 (1993).
515. G. H. Posner, C. H. Oh and W. K. Milhous, *Tetrahedron Lett.*, **32**, 4235 (1991).
516. G. H. Posner and C. H. Oh, *J. Am. Chem. Soc.*, **114**, 8328 (1992).
517. G. H. Posner, C. H. Oh, L. Gerena and W. K. Milhous, *J. Med. Chem.*, **35**, 2459 (1992).

518. G. H. Posner, C. H. Oh, D. S. Wang, L. Gerena, W. K. Milhous, S. R. Meshnick and W. Asawamahasadka, *J. Med. Chem.*, **37**, 1256 (1994).
519. G. H. Posner, C. H. Oh, L. Gerena and W. K. Milhous, *Heteroatom Chem.*, **6**, 105 (1995).
520. G. H. Posner, J. P. Maxwell, H. O'Dowd, M. Krasavin, S. J. Xie and T. A. Shapiro, *Bioorg. Med. Chem.*, **8**, 1361 (2000).
521. J. N. Cumming, D. S. Wang, S. B. Park, T. A. Shapiro and G. H. Posner, *J. Med. Chem.*, **41**, 952 (1998).
522. G. H. Posner, J. N. Cumming, S. H. Woo, P. Ploypradith, S. J. Xie and T. A. Shapiro, *J. Med. Chem.*, **41**, 940 (1998).
523. G. H. Posner, H. B. Jeon, M. H. Parker, M. Krasavin, I. H. Paik and T. A. Shapiro, *J. Med. Chem.*, **44**, 3054 (2001).
524. G. H. Posner, H. B. Jeon, P. Ploypradith, I. H. Paik, K. Borstnik, S. J. Xie and T. A. Shapiro, *J. Med. Chem.*, **45**, 3824 (2002).
525. O. Provot, H. Moskowitiz and J. Mayrargue, *J. Fluor. Chem.*, **91**, 199 (1998).
526. P. M. O'Neill, A. Miller, J. F. Bickley, F. Scheinmann, H. O. Chang and G. H. Posner, *Tetrahedron Lett.*, **40**, 9133 (1999).
527. G. H. Posner, S. B. Park, L. Gonzalez, D. S. Wang, J. N. Cumming, D. Klinedinst, T. A. Shapiro and M. D. Bachi, *J. Am. Chem. Soc.*, **118**, 3537 (1996).
528. O. Provot, M. Hamzaoui, D. N. Huy, J. Mayrargue and H. Moskowitiz, *Heterocycl. Commun.*, **2**, 267 (1996).
529. M. Hamzaoui, O. Provot, F. Gregoire, C. Riche, A. Chiaroni, F. Gay, H. Moskowitiz and J. Mayrargue, *Tetrahedron: Asymmetry*, **8**, 2085 (1997).
530. G. H. Posner, H. O'Dowd, T. Caferro, J. N. Cumming, P. Ploypradith, S. J. Xie and T. A. Shapiro, *Tetrahedron Lett.*, **39**, 2273 (1998).
531. B. Ye and Y.-L. Wu, *J. Chem. Soc., Chem. Commun.*, 726 (1990).
532. Y.-J. Rong and Y.-L. Wu, *J. Chem. Soc., Perkin Trans. 1*, 2149 (1993).
533. C. H. Oh, J. H. Kang and G. H. Posner, *Bull. Kor. Chem. Soc.*, **17**, 581 (1996).
534. J. Cazelles, B. Camuzat-Dedenis, O. Provot, A. Robert, J. Mayrargue and B. Meunier, *J. Chem. Soc., Perkin Trans. 1*, 1265 (2000).
535. C. W. Jefford, Y. Wang and G. Bernardinelli, *Helv. Chim. Acta*, **71**, 2042 (1988).
536. C. W. Jefford, M. F. Deheza and J. B. Wang, *Heterocycles*, **46**, 451 (1997).
537. C. W. Jefford, D. Jaggi, J. Boukouvalas, S. Kohmoto and G. Bernardinelli, *Helv. Chim. Acta*, **67**, 1104 (1984).
538. C. W. Jefford, T. Hatsui, M. F. Deheza and G. Bernardinelli, *Chimia*, **46**, 114 (1992).
539. C. W. Jefford, D. Jaggi, J. Boukouvalas and S. Kohmoto, *J. Am. Chem. Soc.*, **105**, 6497 (1983).
540. C. W. Jefford, S. Kohmoto, D. Jaggi, G. Timari, J.-C. Rossier, M. Rudaz, O. Barbuzzi, D. Gerard, U. Burger, P. Kamalaprija, J. Mareda, G. Bernardinelli, I. Manzanares, C. J. Canfield, S. L. Fleck, B. L. Robinson and W. Peters, *Helv. Chim. Acta*, **78**, 647 (1995).
541. O. Dechy-Cabaret, F. Benoit-Vical, A. Robert and B. Meunier, *ChemBiochem.*, **1**, 281 (2000).
542. O. Dechy-Cabaret, A. Robert and B. Meunier, *Compt. Rend. Chim.*, **5**, 297 (2002).
543. C. W. Jefford, S. J. Jin and G. Bernardinelli, *Tetrahedron Lett.*, **32**, 7243 (1991).
544. C. W. Jefford, S. J. Jin and G. Bernardinelli, *Helv. Chim. Acta*, **80**, 2440 (1997).
545. C. W. Jefford, D. Misra, A. P. Dishington, G. Timari, J.-C. Rossier and G. Bernardinelli, *Tetrahedron Lett.*, **35**, 6275 (1994).
546. C. W. Jefford, D. Jaggi, S. Kohmoto, G. Timari, G. Bernardinelli, C. J. Canfield and W. K. Milhous, *Heterocycles*, **49**, 375 (1998).
547. C. W. Jefford, S. J. Jin, J.-C. Rossier, S. Kohmoto and G. Bernardinelli, *Heterocycles*, **44**, 367 (1997).
548. O. Dechy-Cabaret, F. Benoit-Vical, C. Loup, A. Robert, H. Gornitzka, A. Bonhoure, H. Vial, J. F. Magnaval, J. P. Seguela and B. Meunier, *Chem. Eur. J.*, **10**, 1625 (2004).
549. C. W. Jefford, E. C. McGoran, J. Boukouvalas, G. Richardson, B. L. Robinson and W. Peters, *Helv. Chim. Acta*, **71**, 1805 (1988).
550. C. W. Jefford, D. Jaggi, S. Kohmoto, J. Boukouvalas and G. Bernardinelli, *Helv. Chim. Acta*, **67**, 2254 (1984).
551. H. Yamamoto, M. Akutagawa, H. Aoyama and Y. Omote, *J. Chem. Soc., Perkin Trans. 1*, 2300 (1980).
552. A. J. Bloodworth and A. Shah, *J. Chem. Soc., Chem. Commun.*, 947 (1991).

553. A. J. Bloodworth and N. A. Tallant, *J. Chem. Soc., Chem. Commun.*, 428 (1992).
554. A. J. Bloodworth and K. A. Johnson, *Tetrahedron Lett.*, **35**, 8057 (1994).
555. A. J. Bloodworth, T. Hagen, K. A. Johnson, I. LeNoir and C. Moussy, *Tetrahedron Lett.*, **38**, 635 (1997).
556. A. J. Bloodworth and A. Shah, *Tetrahedron Lett.*, **34**, 6643 (1993).
557. O. Dechy-Cabaret, F. Benoit-Vical, A. Robert, J. F. Magnaval, J. P. Seguela and B. Meunier, *Comp. Rend. Chim.*, **6**, 153 (2003).
558. J. Cai and A. G. Davies, *J. Chem. Soc., Perkin Trans. 1*, 3383 (1992).
559. Y. Ushigoe, Y. Kano and M. Nojima, *J. Chem. Soc., Perkin Trans. 1*, 5 (1997).
560. Y. Ushigoe, A. Masuyama, M. Nojima and K. J. McCullough, *Tetrahedron Lett.*, **38**, 8753 (1997).
561. Y. Ushigoe, Y. Torao, A. Masuyama and M. Nojima, *J. Org. Chem.* **62**, 4949 (1997).
562. R. J. Roth and N. Acton, *J. Nat. Prod.*, **52**, 1183 (1989).
563. R. J. Roth and N. Acton, *J. Chem. Educ.*, **68**, 612 (1991).
564. N. Acton and R. J. Roth, *J. Org. Chem.*, **57**, 3610 (1992).
565. R. K. Haynes and S. C. Vonwiller, *J. Chem. Soc., Chem. Commun.*, 451 (1990).
566. S. C. Vonwiller, J. A. Warner, S. T. Mann and R. K. Haynes, *J. Am. Chem. Soc.*, **117**, 11098 (1995).
567. L.-K. Sy, G. D. Brown and R. K. Haynes, *Tetrahedron*, **54**, 4345 (1998).
568. L.-K. Sy and G. D. Brown, *Tetrahedron*, **58**, 909 (2002).
569. L.-K. Sy and G. D. Brown, *Tetrahedron*, **58**, 897 (2002).
570. S. C. Vonwiller, J. A. Warner, S. T. Mann and R. K. Haynes, *Tetrahedron Lett.*, **38**, 2363 (1997).
571. H.-J. Liu, W.-L. Yeh and S. Y. Chew, *Tetrahedron Lett.*, **34**, 4435 (1993).
572. R. K. Haynes, G. R. King and S. C. Vonwiller, *J. Org. Chem.*, **59**, 4743 (1994).
573. N. Acton, *J. Nat. Prod.*, **62**, 790 (1999).
574. J. A. Vroman, I. Khan and M. A. Avery, *Synlett*, 1438 (1997).
575. J. A. Vroman, I. A. Khan and M. A. Avery, *Tetrahedron Lett.*, **38**, 6173 (1997).
576. J. A. Vroman, H. N. ElSohly and M. A. Avery, *Synth. Commun.*, **28**, 1555 (1998).
577. K. Takasu, R. Katagiri, Y. Tanaka, M. Toyota, H. S. Kim, Y. Wataya and M. Ihara, *Heterocycles*, **54**, 607 (2001).
578. M. Jung, X. Li, D. A. Bustos, H. N. ElSohly and J. D. McChesney, *Tetrahedron Lett.*, **30**, 5973 (1989).
579. M. Jung, K. Lee and H. Jung, *Tetrahedron Lett.*, **42**, 3997 (2001).
580. M. Jung, K. Lee, H. Jung, H. Kendrick, V. Yardley and S. L. Croft, *Bioorg. Med. Chem. Lett.*, **14**, 2001 (2004).
581. R. K. Haynes, S. C. Vonwiller and H. J. Wang, *Tetrahedron Lett.*, **36**, 4641 (1995).
582. D. A. Bustos, M. Jung, H. N. ElSohly and J. D. McChesney, *Heterocycles*, **29**, 2273 (1989).
583. M. Jung, H. N. ElSohly and J. D. McChesney, *Synlett*, 43 (1993).
584. M. K. Jung, K. Lee, H. Kendrick, B. L. Robinson and S. L. Croft, *J. Med. Chem.*, **45**, 4940 (2002).
585. M. Jung and J. Bae, *Heterocycles*, **53**, 261 (2000).
586. M. Jung and S. Lee, *Heterocycles*, **45**, 1907 (1997).
587. M. Jung and S. Lee, *Heterocycles*, **45**, 1055 (1997).
588. M. Jung, A. C. C. Freitas, J. D. McChesney and H. N. ElSohly, *Heterocycles*, **39**, 23 (1994).
589. M. Jung, D. Yu, D. Bustos, H. N. ElSohly and J. D. McChesney, *Bioorg. Med. Chem. Lett.*, **1**, 741 (1991).
590. M. Jung, D. Bustos, H. N. ElSohly and J. D. McChesney, *Synlett*, 743 (1990).
591. R. K. Haynes and S. C. Vonwiller, *Synlett*, 481 (1992).
592. W. H. Bunnelle, T. A. Isbell, C. L. Barnes and S. Qualls, *J. Am. Chem. Soc.*, **113**, 8168 (1991).
593. W. Adam, U. Kliem, T. Mosandl, E.-M. Peters, K. Peters and H. G. von Schnering, *J. Org. Chem.*, **53**, 4986 (1988).
594. J. D. White and R. W. Skean, *J. Am. Chem. Soc.*, **100**, 6296 (1978).
595. J. A. Kepler, A. Philip, Y. W. Lee, M. C. Morey and F. I. Carroll, *J. Med. Chem.*, **31**, 713 (1988).
596. S. N. Huber and M. P. Mischne, *Nat. Prod. Lett.*, **7**, 43 (1995).
597. M. P. Mischne, S. N. Huber and J. Zinczuk, *Can. J. Chem.*, **77**, 237 (1999).

CHAPTER 6

Synthetic uses of peroxides

ALBRECHT BERKESSEL and NADINE VOGL

Department of Organic Chemistry, University of Cologne, Greinstr. 4, D-50939 Köln, Germany

Fax: +49 221 470 5102; e-mails: berkessel@uni-koeln.de;

Nadine.Vogl@uni-koeln.de

I. INTRODUCTION, SCOPE AND STRUCTURE OF THE REVIEW	308
II. SYNTHESIS OF PEROXIDES	309
A. Hydroperoxides	309
1. General methodology	309
a. Synthesis from hydrogen peroxide	310
b. Synthesis from superoxide anion	315
c. Synthesis by autoxidation	320
d. Synthesis by reactions with singlet molecular oxygen	324
e. Synthesis by ozonolysis	326
f. Synthesis from peroxide precursors	327
g. Synthesis from alkyl halides and 2-(alkoxy)prop-2-yl hydroperoxide	327
h. Synthesis by hydrolysis of peroxyesters	329
2. Chiral hydroperoxides	329
a. Separation of enantiomers/diastereomers via chromatography	329
b. Kinetic resolution	330
c. Stereoselective dioxygenation	339
d. Reaction with hydrogen peroxide	348
B. Synthesis of Dialkyl Peroxides	351
1. General methodology	351
a. Acid- or base-catalyzed synthesis of dialkyl peroxides	351
b. Metal-catalyzed synthesis of dialkyl peroxides	358
c. Synthesis of dialkyl peroxides by autoxidation	360
d. Synthesis from stannyl peroxides	362
C. Synthesis of Hydrogen Peroxide	362
III. SYNTHETIC USES OF PEROXIDES	362
A. Epoxidation of C=C Double Bonds	362
1. Uncatalyzed and base-catalyzed epoxidations	363
2. Organo-catalyzed epoxidations	370

The chemistry of peroxides, volume 2

Edited by Z. Rappoport © 2006 John Wiley & Sons, Ltd ISBN: 0-470-86274-2

a.	Phase-transfer catalysis	370
b.	Polyamino acid catalysis	373
c.	Bovine serum albumin catalyzed epoxidations	383
d.	Selenide-catalyzed epoxidation reaction	384
e.	Ketone-catalyzed epoxidation of allylic alcohols and unfunctionalized olefins	385
3.	Metal-catalyzed epoxidations	386
a.	Asymmetric epoxidation of electron-deficient olefins	386
b.	Epoxidation of allylic alcohols	391
i.	Asymmetric epoxidation of allylic alcohols catalyzed by chiral metal complexes	394
ii.	Asymmetric epoxidation of allylic alcohols employing chiral hydroperoxides	401
iii.	Epoxidation of allylic alcohols with special synthetic utility or academic interest	406
iv.	Diastereoselective epoxidation of ene diols	413
c.	Metal-catalyzed epoxidations of unfunctionalized olefins	416
i.	Ti, Zr, Hf	417
ii.	V, Nb, Ta	422
iii.	Cr, Mo, W	425
iv.	Mn, Tc, Re	442
d.	Compounds of arsenic in the epoxidation of unfunctionalized olefins	462
B.	Oxidation of Sulfides	472
1.	Uncatalyzed sulfoxidations	472
2.	Enzyme-catalyzed sulfoxidations	474
3.	Metal-catalyzed sulfoxidations	476
a.	Non-asymmetric metal-catalyzed sulfoxidations	477
b.	Asymmetric sulfoxidations with chiral catalysts	478
c.	Asymmetric sulfoxidations with chiral hydroperoxides	485
C.	Alcohol Oxidation	492
D.	Other C–H Oxidation Reactions	503
1.	Allylic and benzylic oxidations	503
2.	α -Hydroxylation of ketones	519
3.	Oxidation of alkenes to ketones	521
4.	Oxidative cleavage of double bonds	525
5.	Oxidation of aromatic compounds	527
6.	Oxidation of alkanes	531
E.	<i>N</i> -Oxidation of Organonitrogen Compounds	531
F.	Baeyer–Villiger Oxidation	538
G.	Vicinal Dihydroxylation of Alkenes and Alkynes	556
H.	Oxidative Halogenation of Hydrocarbons	572
IV.	REFERENCES	581

I. INTRODUCTION, SCOPE AND STRUCTURE OF THE REVIEW

Peroxides are compounds of great synthetic interest. Especially, alkyl hydroperoxides and hydrogen peroxide have gained more and more importance as cheap and readily available oxygen donors in catalytic oxygenations. Formerly unsafe oxidation procedures (due to the employment of highly concentrated and therefore explosive peroxide solutions) have been optimized or substituted by other and more effective and safe procedures. Over the last two decades, the need for oxidation technologies with enhanced efficiency

has increased. Waste minimization has become an imperative in the manufacture of fine and bulk chemicals, calling for the substitution of stoichiometric oxidation processes by catalytic ones. The desire for an easy recyclability of oxidation catalysts led to the development of immobilized variants which are used in combination with hydroperoxides or hydrogen peroxide as terminal oxidants. These and other recent aspects of oxidative transformations using alkyl hydroperoxides and hydrogen peroxide will be discussed in this chapter.

In this review, we focus mainly on the preparative utility of organic peroxides, and only few mechanistic investigations are discussed. This review covers synthetic methodologies for the preparation of alkyl hydroperoxides and dialkyl peroxides (Section II) and the synthetic use of these peroxides in organic chemistry (Section III). In Section II, general methods for the synthesis of organic hydroperoxides and dialkyl peroxides are discussed, as well as the preparation of enantiomerically pure chiral hydroperoxides. The latter have attracted considerable interest for asymmetric oxidation reactions during the last years.

In Section III, we have opted for a categorization based on the different types of oxidation reactions. In this chapter we concentrated mainly on alkyl hydroperoxides and hydrogen peroxide as oxidants, as these are more reactive, particularly in combination with metal catalysts, and have consequently found wider usage than dialkyl hydroperoxides. From the viewpoint of 'green chemistry', especially hydrogen peroxide has received much attention since, in the oxygen transfer step, only water is formed as by-product. Therefore, during the last two decades, much effort has been spent on the development of new efficient metal-catalyzed oxidation processes utilizing hydrogen peroxide as terminal oxidant. In the major part of Section III, metal-catalyzed oxidation reactions using either hydrogen peroxide or alkyl hydroperoxides are discussed, but we also review oxidation reactions which do not employ a catalyst or which use organic molecules or enzymes as catalysts. Due to the fact that selective asymmetric synthesis has become a major theme in organic chemistry, a large portion of this review deals with enantioselective and diastereoselective oxidation reactions, employing either achiral oxidants in combination with chiral catalysts or chiral hydroperoxides.

In this review we were unable to discuss every facet of this well investigated topic. Nevertheless, we think that the present review provides a good overview of the field of synthetic uses of alkyl hydroperoxides and hydrogen peroxide, especially in catalytic oxidation reactions. We apologize for omissions that the expert reader may discover here and there.

II. SYNTHESIS OF PEROXIDES

A. Hydroperoxides

The great versatility of alkyl hydroperoxides is mainly due to the fact that besides hydrogen peroxide and molecular oxygen, they serve as very useful organic oxygen sources in different kinds of oxidation reactions. Since asymmetric oxidations became more and more important during recent years, it was of interest to develop chiral hydroperoxides and to synthesize them in an enantiomerically pure form, in order to employ them as oxidants and as asymmetric inductors in various kinds of oxidation reactions. The different literature methods for hydroperoxide synthesis in general and for the synthesis of enantiomerically enriched/pure hydroperoxides are presented in the following.

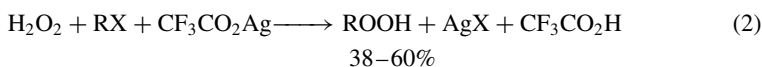
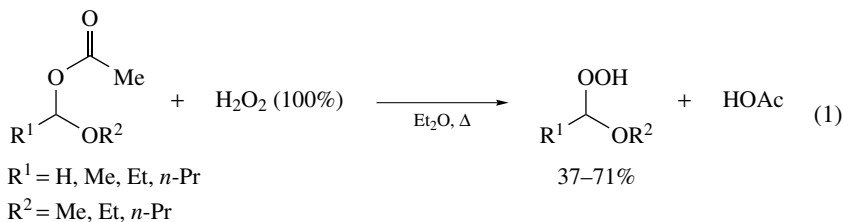
For reviews on the synthesis of alkyl peroxides see References 1 and 2.

1. General methodology

Literature procedures for the synthesis of hydroperoxides include the preparation from hydrogen peroxide (via reaction with alkyl halides, -phosphites, -sulfonates, alkenes,

alcohols, ethers), from superoxide anion, by autoxidation, by reaction with singlet molecular oxygen, by ozonolysis or from peroxide precursors. These methods are presented below.

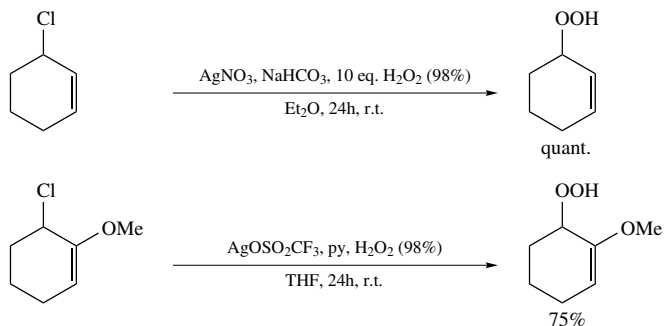
a. Synthesis from hydrogen peroxide. Due to the high nucleophilicity of hydrogen peroxide and particularly of its anion, which has been described in terms of the α -effect³, it is possible to prepare alkyl hydroperoxides via nucleophilic attack of hydrogen peroxide or its anion on alkyl sulfonates, alcohols, carboxylates or halides. Rieche and Bischoff developed a method for the preparation of α -hydroperoxydialkyl ethers by reaction of acetals with hydrogen peroxide (equation 1)⁴. By this procedure several α -hydroperoxydialkyl ethers have been obtained in yields between 37 and 71%. In 1976, Cookson and coworkers reported on the reaction of primary, secondary and tertiary alkyl bromides and iodides with hydrogen peroxide and silver trifluoroacetate or tetrafluoroborate yielding alkyl hydroperoxides in 38–60% (equation 2)⁵. While primary hydroperoxides are generally formed via the iodide, secondary and tertiary hydroperoxides are usually prepared via the bromide. Allylic hydroperoxides such as cyclohex-2-enyl hydroperoxide were prepared almost quantitatively by reaction of allylic chloride with silver nitrate, sodium bicarbonate and a tenfold excess of 98% hydrogen peroxide by the research group of Frimer (Scheme 1)⁶. The related 3-chloro-2-methoxycyclohexene was transformed to the allylic hydroperoxide by reaction with silver triflate, pyridine and 98% hydrogen peroxide in a yield of 75% (Scheme 1). Workup was very easy, consisting of filtration and evaporation of the solvent. The silver salt hydrogen peroxide sequence has been successfully used by Bascetta and Gunstone and by Porter and coworkers to prepare several hydroperoxides as shown in Scheme 2⁷.



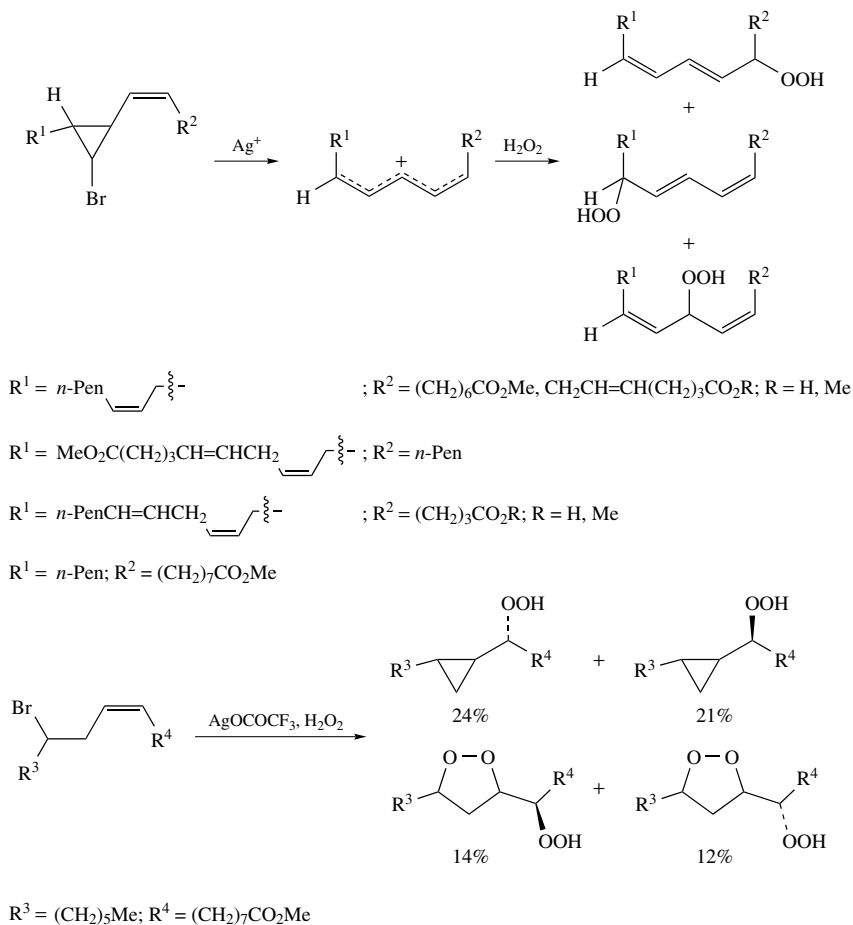
X = Br, I

R = *n*-Hex, 2-Bu, CMe₂Et, CMe₂Pr-*i*, CMe₂Bu-*t*, *n*-Pr₃C

Reaction of alkyl sulfonates with H₂O₂ also leads to the formation of alkyl hydroperoxides^{8–12}. Moderate yields were obtained for primary hydroperoxides using alkaline H₂O₂ while for secondary hydroperoxides, elimination competes with substitution and therefore yields are rather low. Tertiary alkyl hydroperoxides are obtained utilizing 30% H₂O₂ from tertiary alkyl sulfonates, which in turn are prepared from alkenes or alcohols with sulfuric acid. Using this method Porter and coworkers could prepare the unsaturated hydroperoxides depicted in Figure 1, which were obtained in yields of 40–60% from the corresponding mesylates⁸. Hydroperoxides **1a** and **1b** were also prepared from the corresponding mesylates by Corey and coworkers^{9,10}, Zamboni and Rokach prepared **1a**¹¹ and Just and coworkers prepared **1c**¹². With fatty acid hydroperoxide **1a** Zamboni and Rokach showed that the reaction proceeds with complete racemization¹¹. Therefore, Nagata and coworkers explored a different procedure for the synthesis of fatty acid hydroperoxide



SCHEME 1. Synthesis of allylic hydroperoxides

SCHEME 2. Hydroperoxide synthesis via silver ion promoted bromide substitution and oxidation with H_2O_2

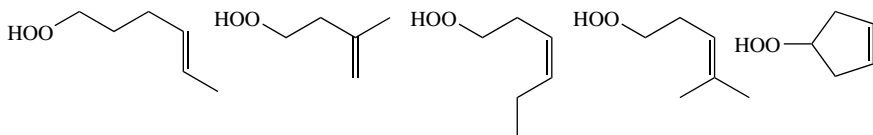
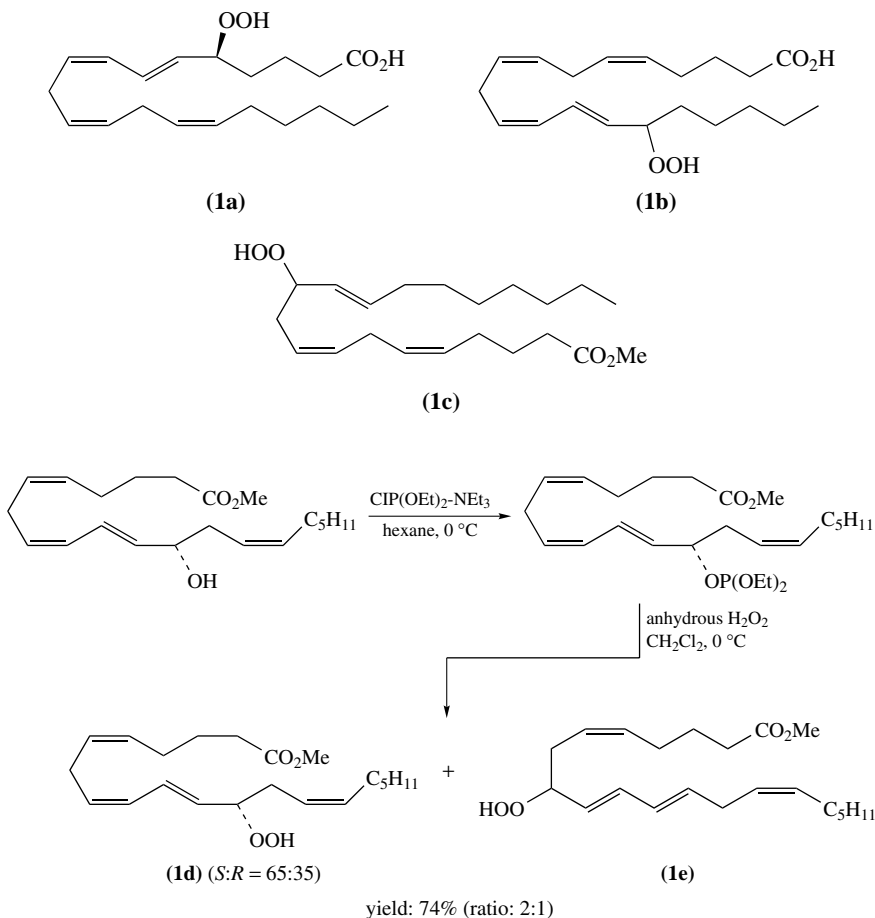
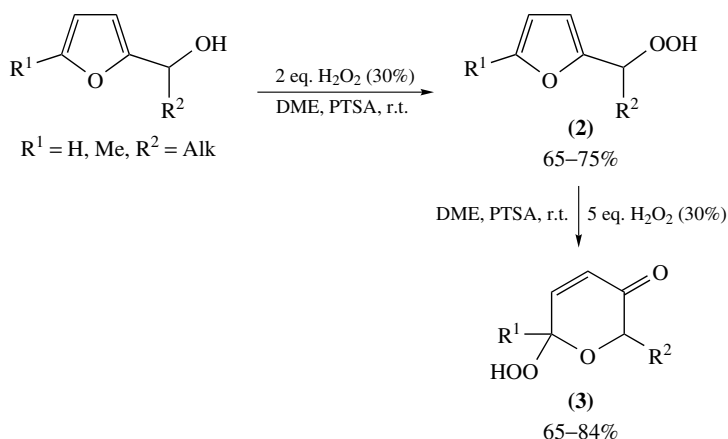


FIGURE 1

1d (Scheme 3)¹³. This was prepared via the corresponding phosphite, which can be synthesized by reaction of the alcohol with chlorodiethyl phosphite and triethylamine. The phosphite then undergoes nucleophilic substitution reaction with anhydrous H_2O_2 forming the hydroperoxide **1d** (enantiomeric ratio: *S/R* : 65/35) and isomeric hydroperoxide **1e** in a 2:1 mixture in 74% overall yield starting from the alcohol. Purification was possible by normal-phase HPLC. So in this case transformation of the phosphite to the hydroperoxide proceeds with partially retained configuration.

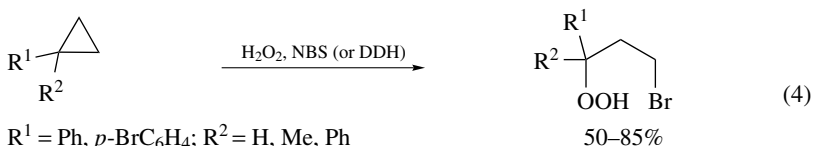
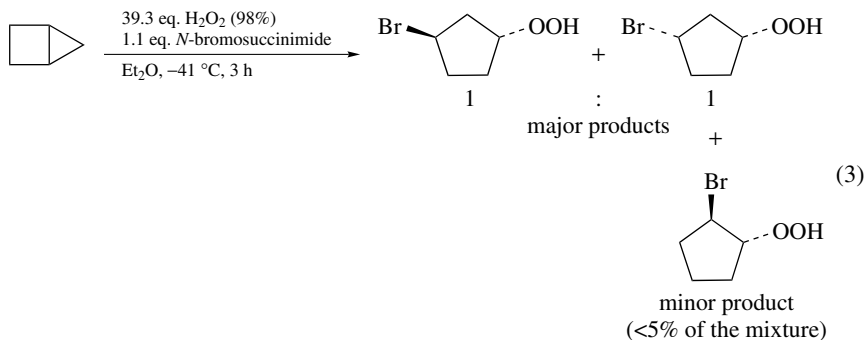
SCHEME 3. Synthesis of hydroperoxides **1d** and **1e** starting from the corresponding alcohol

An alternative method for the preparation of alkyl hydroperoxides is represented by the reaction of various electron-rich alkenes (like vinyl ethers), cyclopropanes or alcohols with hydrogen peroxide in the presence of acid or other electrophiles². The reaction is initiated by the addition of an electrophile, like H^+ , mercurinium ions or halogen electrophiles (generated from *tert*-butyl hypochlorite, 1,3-dibromo-5,5-dimethylhydantoin, *N*-bromosuccinimide and 1,3-diiodo-5,5-dimethylhydantoin) to the double bond or to the cyclopropane ring to form a carbenium ion. Alternatively, the same carbocation is formed via H^+ addition to the alcohol and elimination of water. The second step is the nucleophilic addition of hydrogen peroxide to the carbenium intermediate and H^+ elimination to form the hydroperoxide. In this way *tert*-pentyl hydroperoxide is readily formed from 2-methylbut-2-ene in the presence of catalytic amounts of sulfuric acid² and α -alkoxyhydroperoxides are synthesized from vinyl ethers. In 2001 Scettri and coworkers reported on the synthesis of 2-(1-hydroperoxyalkyl)furans (**2**) and 6-hydroperoxy-2*H*-pyran-3(6*H*)-ones (**3**) by acid catalyzed reaction of 2-furyl alcohols with hydrogen peroxide (Scheme 4)^{14,15}. The hydroperoxides **2** could be obtained in good yields of 65–75% in the presence of 2 equivalents of oxidant and after chromatographic purification. When the reaction is carried out with 5 equivalents of H_2O_2 , the hydroperoxides **2** undergo further oxidation to give hydroperoxides **3** in high yields (65–84%). Porter and Gilmore have shown that bicyclopentane reacts with *N*-bromosuccinimide and 98% hydrogen peroxide to provide the stereoisomeric cyclopentane bromohydroperoxides (equation 3)¹⁶ and an analogous reaction occurs with substituted cyclopropanes as published by Adam and coworkers (equation 4)¹⁷. By this method, γ -hydroperoxy bromides could be prepared in yields ranging from 50 to 85%. The stereochemistry of the addition of $Br^+ - H_2O_2$ to alkenes has been found to be *anti*. Electron-donating substituents on the alcohol or ether substrates help to improve the conversion due to their carbenium ion stabilizing effect. Therefore, (hemi)acetals are readily converted to α -alkoxyhydroperoxides as could be shown by Chmielewski and coworkers¹⁸. β -Hydroxyhydroperoxides are obtained from the acid catalyzed reaction of epoxides with 98% hydrogen peroxide as reported for example by Subramanyam and coworkers in 1976¹⁹. With a five-fold excess of H_2O_2 , the epoxides **4a–c** could be converted to the β -hydroxyhydroperoxides **5a–c** in yields of 55–95% (Scheme 5). Although in principle two ways of ring opening may occur, only one product is formed in each case, namely the one in which the hydroperoxy group is



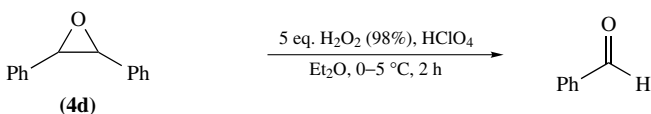
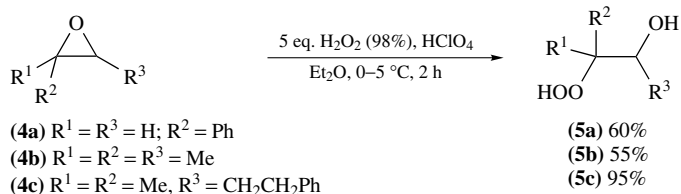
SCHEME 4. Hydroperoxide synthesis from an alcohol and H_2O_2

attached to the cationic carbon in the most stable intermediate carbenium ion. Stilbene oxide **4d** could not be transformed to the analogous β -hydroxyhydroperoxide; instead, two molecules of benzaldehyde were produced (Scheme 5).



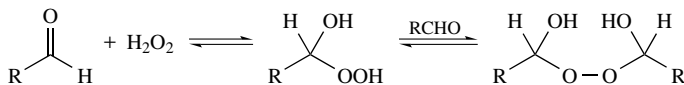
$\text{R}^1 = \text{Ph}$, *p*- BrC_6H_4 ; $\text{R}^2 = \text{H}$, Me, Ph

NBS = *N*-bromosuccinimide; DDH = 1,3-dibromo-5,5-dimethylhydantoin



SCHEME 5. β -Hydroxyhydroperoxide formation via acid-catalyzed epoxide ring opening with H_2O_2

One of the methods for α -hydroxyperoxide (perhydrate) synthesis consists in the addition of hydrogen peroxide to aldehydes or ketones (Scheme 6) as reported by Ganeshpure and Adam²⁰. In the presence of excess aldehyde, the perhydrate is further converted to



SCHEME 6. Synthesis of α -hydroxyhydroperoxides from aldehydes and H_2O_2

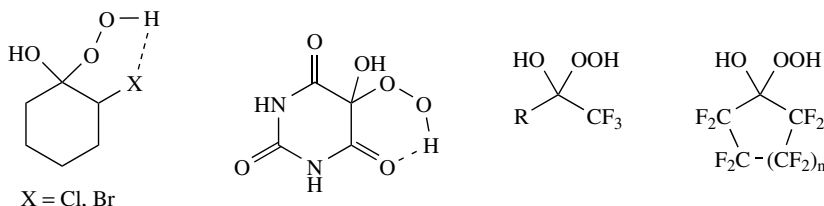
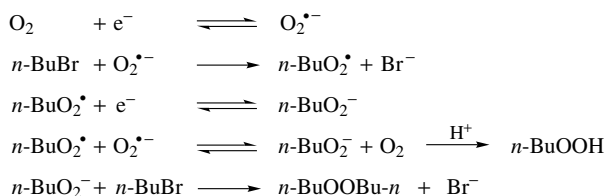


FIGURE 2

the bis(hydroxyalkyl) peroxide. Several perhydrates have been prepared in this way from aliphatic and aromatic aldehydes. Reaction of hydrogen peroxide with a ketone gives perhydrates that are significantly less stable and therefore isolation is difficult in most cases. Exceptions, which are reported, for example, by Witkop and coworkers²¹ or Kharasch and Sosnovsky²², are perhydrates that are either stabilized by intramolecular hydrogen bonding and/or electron-withdrawing groups like CF_3 or by the steric bulk of the substituents which prohibits dimerization (Figure 2).

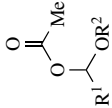
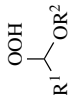
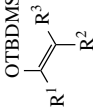
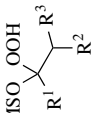
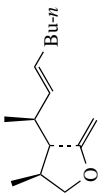
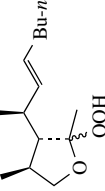

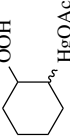
An overview of hydroperoxides that were prepared by reaction of various substrates with hydrogen peroxide is given in Table 1.

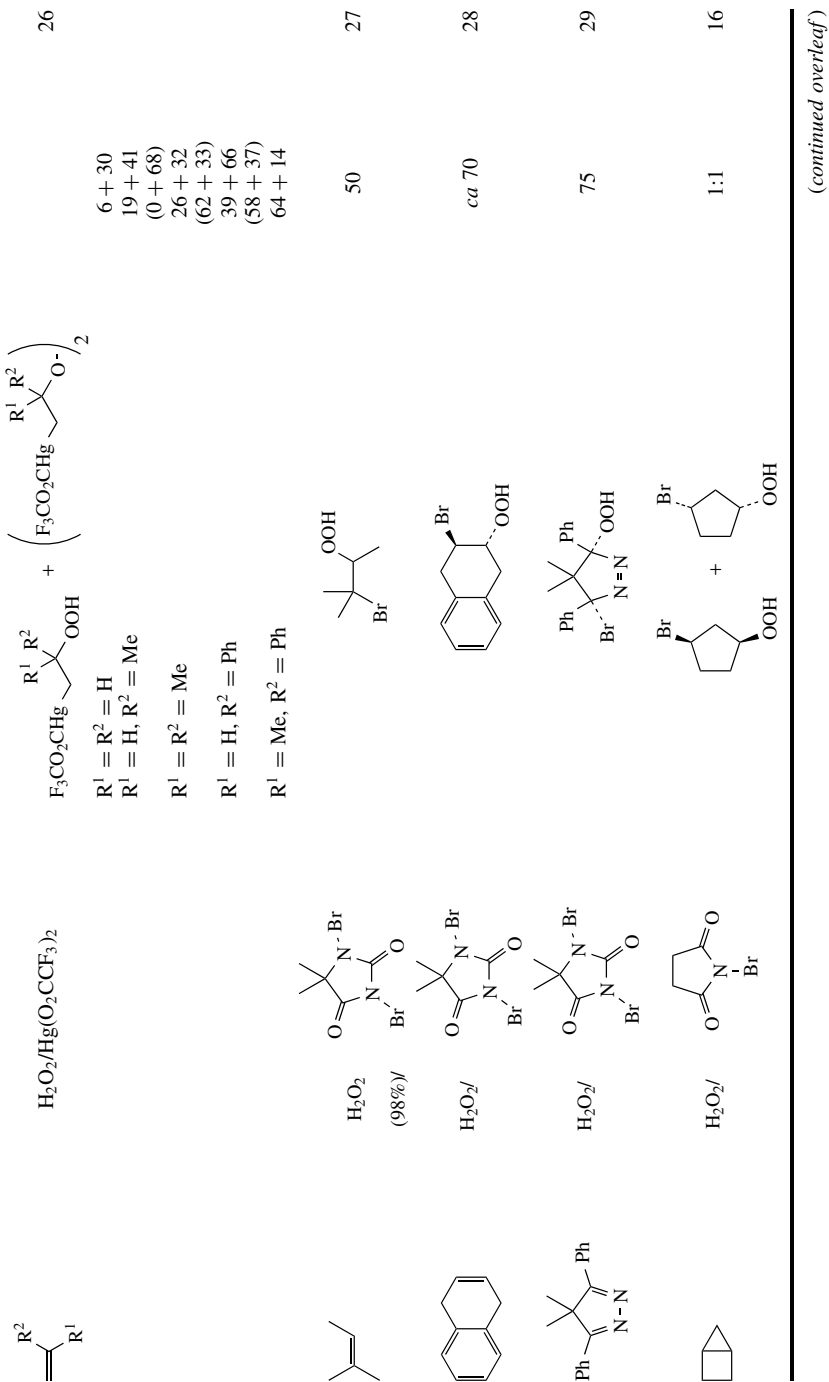
b. Synthesis from superoxide anion. Alkyl hydroperoxides can be synthesized via reaction of alkyl halides or sulfonates with the superoxide anion^{30,31}. Corey and coworkers^{32a} and Filippo and coworkers^{32b} reported that the carbon-oxygen bond-forming step proceeds with inversion of configuration. Solid superoxides react with substrates like triphenylmethyl chloride, but other alkyl halides are not reactive under these conditions. In contrast, tetraalkylammonium superoxide, which is prepared by electrochemical reduction of oxygen in dipolar aprotic solvents in the presence of tetraalkylammonium salts, has been shown to be an effective nucleophile in substitution with primary and secondary alkyl halides (Scheme 7). By this method, butyl hydroperoxides have been prepared by Dietz and coworkers³⁰ and Merritt and Sawyer³¹. Primary alkyl halides react faster than secondary ones and the latter faster than tertiary alkyl halides. Chlorides have been found to react slower than bromides or iodides³¹. Besides the alkyl hydroperoxide, also dialkyl peroxide and alcohol products were formed in this reaction^{32,33}. As a consequence, yields were sometimes low. The carbon-oxygen bond-forming reaction at secondary carbon occurs with nearly complete inversion of configuration. The utility of the method was demonstrated in 1988 by the synthesis of the hydroperoxide analogue of the AIDS drug



SCHEME 7. Synthesis of hydroperoxides from electrochemically generated superoxide and alkyl halides

TABLE 1. Preparation of alkyl hydroperoxides by reaction of different substrates with hydrogen peroxide

Substrate	Reagents	Products	Yield ^a (%)	Reference
	H ₂ O ₂	 R ¹ = H, R ² = Et R ¹ = Me, R ² = Et R ¹ = R ² = Et R ¹ = Et, R ² = <i>n</i> -Pr R ¹ = <i>n</i> -Pr, R ² = Me	41 71 50 37 42	4
 OTBDMS R ¹ R ² = -(CH ₂) ₄ -, R ³ = H R ¹ R ² = -(CH ₂) ₃ -, R ³ = H R ¹ = <i>c</i> -Pr, R ² = R ³ = H R ¹ = CH ₂ CH ₂ Ph, R ² = R ³ = H R ¹ R ² = -CH=CH(CH ₂) ₂ -, R ³ = H R ¹ = OMe, R ² = H, R ³ = <i>n</i> -Bu	H ₂ O ₂ /cat. TFA	 TBDMSO OOH	88 60 100 78 43 100	23
	H ₂ O ₂ /HOAc		>82	24
	H ₂ O ₂ /HgOAc		36	25



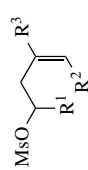
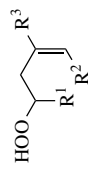
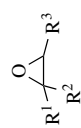
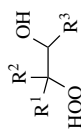
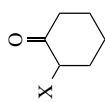
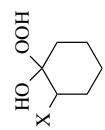
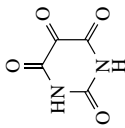
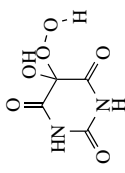


(continued overleaf)

TABLE 1. (continued)

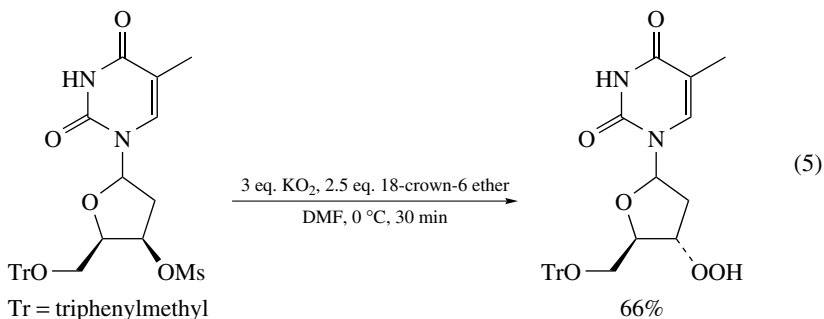
Substrate	Reagents	Products	Yield ^a (%)	Reference
	H ₂ O ₂ /NBS (or DDH)		60 50 65 50 85	17
	H ₂ O ₂ /H ⁺			15
	(2 eq.) (5 eq.)		65-75 (comp. 2) 65-84 (comp. 3)	
	50 eq. H ₂ O ₂ H ₂ O ₂		50 10-15	9 11
	90% H ₂ O ₂		10-30	12
	anhydrous H ₂ O ₂		ca 49	13

S : R = 65:35

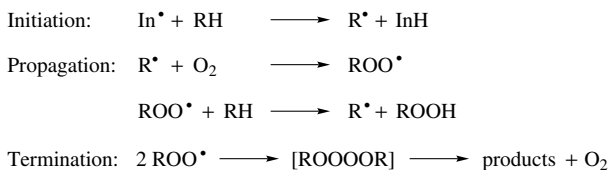
	$\text{H}_2\text{O}_2/\text{KOH}$		42	8
	$\text{H}_2\text{O}_2/\text{KOH}$		40-60	8
	H_2O_2 (98%)/ HClO_4		60 55 95	19
	H_2O_2 (30%)		92 70	22
	H_2O_2		72	21

^a Yields in brackets are obtained under different reaction conditions.

AZT from the corresponding mesylate by Schreiber and Ikemoto (equation 5)³⁴. Using 3 equivalents of KO_2 and 2.5 equivalents of crown ether in DMF at 0°C for 30 min, the hydroperoxide could be synthesized in 66% yield with inversion of configuration.



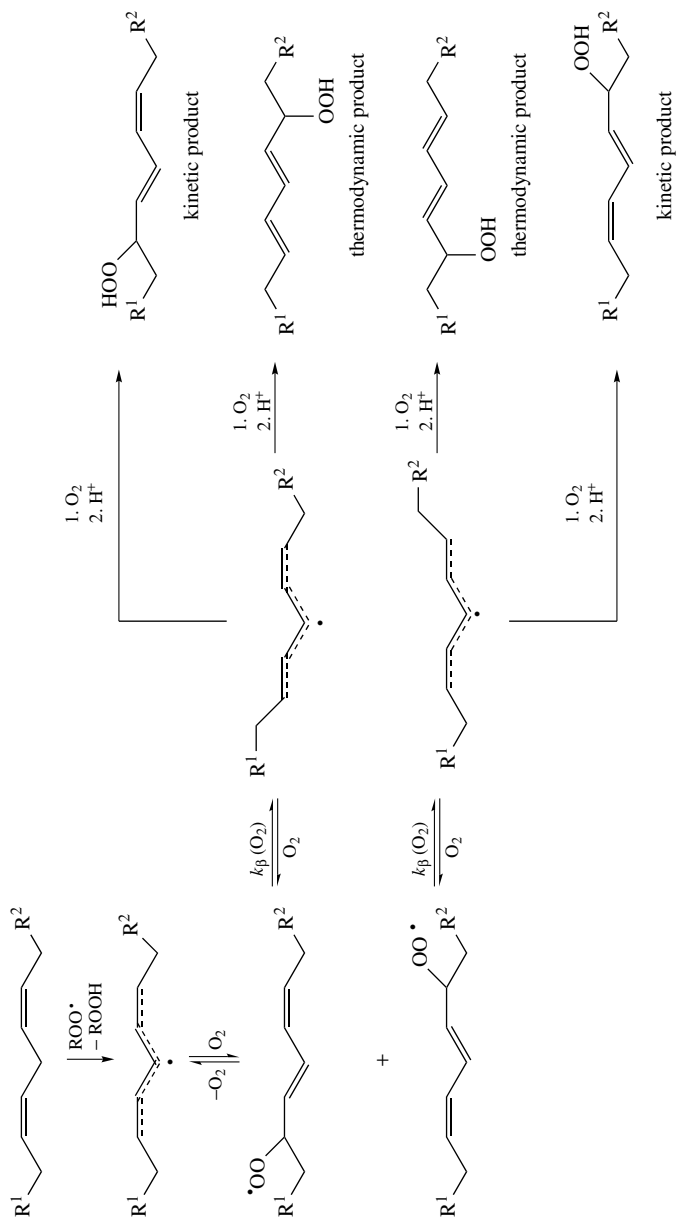
c. Synthesis by autoxidation. A further method for synthesizing alkyl hydroperoxides is the autoxidation of hydrocarbons, which is the spontaneous reaction of these molecules with molecular oxygen. This reaction includes the generation of the carbon radical by the initiator radical In^\bullet (initiation), reaction with molecular oxygen to form a peroxy radical (propagation) and hydrogen abstraction from a hydrocarbon molecule (Scheme 8).



SCHEME 8. Mechanism of hydrocarbon autoxidation

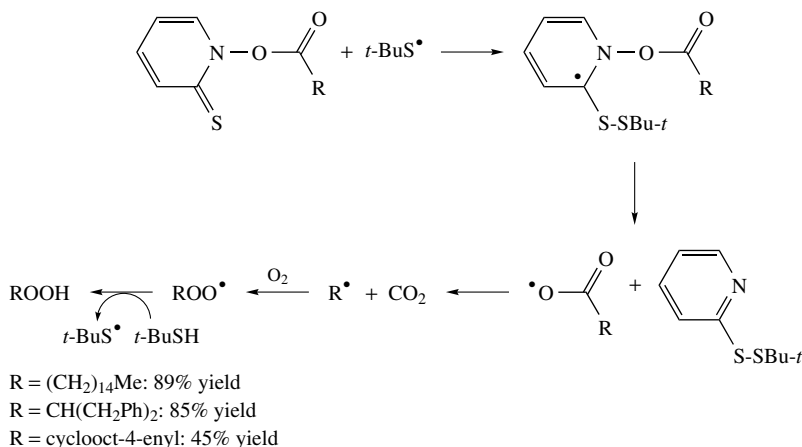
Autoxidation is concentration-dependent and the substrate should be present in high concentrations in order to promote autoxidation. A variety of molecules can serve as substrates for efficient autoxidation reactions, including enols, phenols, hydrazones, imines, alkenes, dienes and polyenes. In the case of alkenes and even more reactive dienes or polyenes, first an allylic hydrogen atom is abstracted, generating the resonance stabilized allylic radical which can exist as a mixture of *cis-trans* isomers. Homoconjugated dienes, such as linoleic acid, have been oxidized by the group of Porter at the terminal carbons of the diene unit forming the *trans-cis* and the *trans-trans* stereoisomers (Scheme 9)³⁵. In this reaction, a pentadienyl radical is formed first via H-atom abstraction from the central carbon atom, followed by O_2 addition mainly at one or the other end of the radical, giving a peroxy radical with *trans-cis* conjugated diene geometry. H-atom abstraction leads to the *trans-cis* product (kinetic product, preferentially formed at high substrate concentrations and in the presence of good H-donors). The thermodynamically favored product (*trans-trans*) is formed via β -fragmentation of the intermediate radical followed by oxygen coupling at the opposite end of the carbon radical.

A very efficient methodology for generating carbon radicals utilizes esters of *N*-hydroxypyridine-2-thione as radical precursors, and these have been used by Blood-



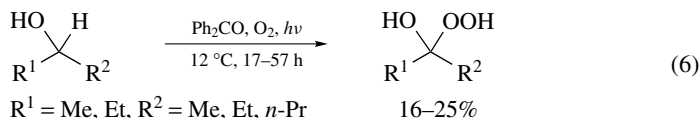
SCHEME 9. Autoxidation of homoconjugated dienes

worth and coworkers as well as Barton and coworkers for hydroperoxide preparation via autoxidation as shown in Scheme 10³⁶. The hydroperoxide products can be prepared in good yields (45–89%) via this route.

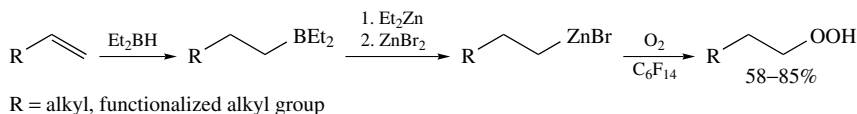


SCHEME 10. Preparation of hydroperoxides via oxygenation of carbon radicals generated from *N*-hydroxypyridine-2-thione esters as radical precursors

In 1958 and 1963 Schenck and coworkers reported on a method for the preparation of α -hydroxy hydroperoxides via photosensitized autoxidation of non-tertiary alcohols^{37,38}. These readily undergo photooxygenation using benzophenone as sensitizer producing α -hydroxy hydroperoxides in yields of 16–25% (equation 6). Ganeshpure and Adam reported on the use of the latter as oxygen transfer agents in organic synthesis²⁰.



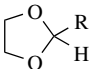
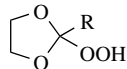
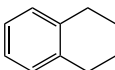
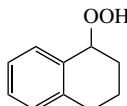
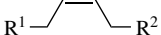
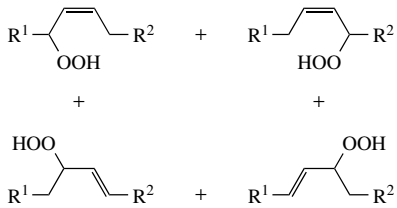
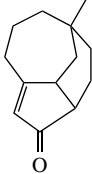
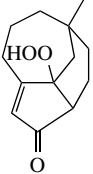
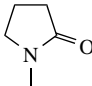
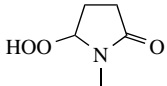
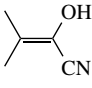
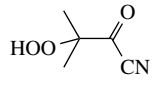
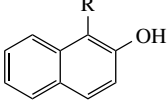
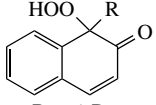
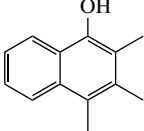
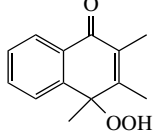
Zn-organometallics have been shown to act as alkyl hydroperoxide precursors. The transformation is carried out by oxidation of the Zn organometallics with molecular oxygen in perfluorinated solvents (Scheme 11)³⁹. The perfluorinated solvents have the advantage of dissolving large quantities of molecular oxygen and therefore less solvent is needed. Following this method organozinc bromides can be converted to the corresponding hydroperoxides in perfluorohexane in good yields (58–85%) and excellent chemoselectivity (hydroperoxide : alcohol ratio > 98:2).



SCHEME 11. Preparation of alkyl hydroperoxides by oxidation of zinc-organometallics

The results of alkyl hydroperoxide preparation by autoxidation of various substrates are shown in Table 2.

TABLE 2. Preparation of alkyl hydroperoxides by autoxidation

Substrate	Product	Yield (%)	Reference
 R = Me R = <i>i</i> -Pr		40 25 ^a 38 ^a	40
		n.g. ^b	41
		n.g. ^b	42
		n.g. ^b	43
		67	44
		>90	45
	 R = <i>i</i> -Pr R = <i>c</i> -Hex	75 77	46
		58	47

(continued overleaf)

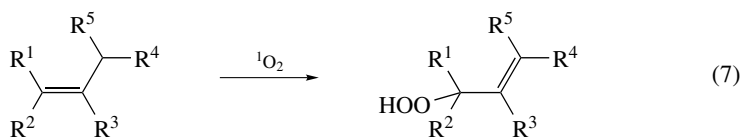
TABLE 2. (continued)

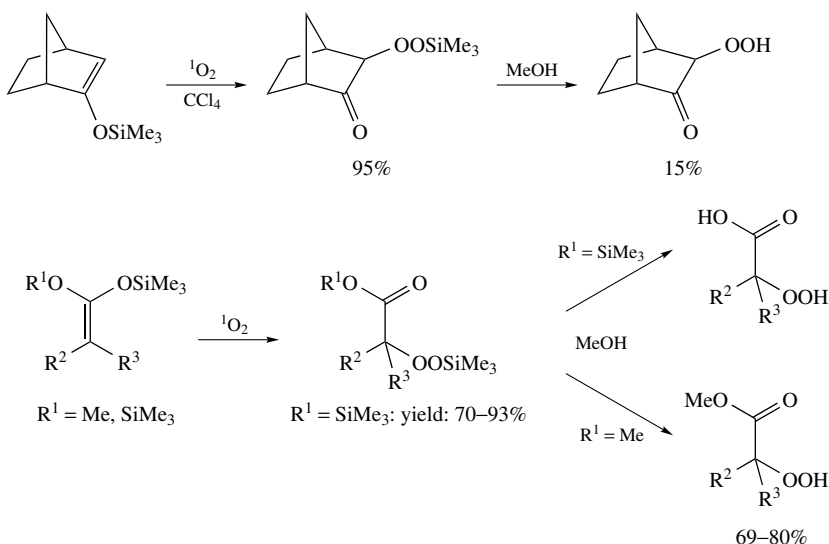
Substrate	Product	Yield (%)	Reference
		30 + 60	48
	ROOH		36
	R = (CH ₂) ₁₄ Me	89	
	R = CH(CH ₂ Ph) ₂	85	
	R = cyclooct-4-enyl	45	
		16–25	20
	R ¹ = Me, Et		
	R ² = Me, Et, <i>n</i> -Pr		
			39
	R = (CH ₂) ₄ Br	68	
	R = (CH ₂) ₄ OSi(<i>Pr</i> - <i>i</i>) ₃	61	
	R = OC(O)Bu- <i>t</i>	68	

^a α,α' -Azo-bis-isobutyronitrile was added as radical initiator.

^b Not given.

d. Synthesis by reactions with singlet molecular oxygen. Allylic hydroperoxides can be prepared by photosensitized reaction of alkyl substituted alkenes with singlet oxygen, which is generated under the reaction conditions (equation 7). Rose Bengal, methylene blue or porphyrins can serve as triplet sensitizers in order to generate oxygen in the singlet excited state. The reaction is an ene-type reaction and different mechanisms (concerted mechanism, via biradical, zwitterionic, peroxide intermediates) have been discussed in the literature⁴⁹. [4 + 2] and [2 + 2] cycloadditions are reactions that can compete with the ene reaction. Adam and del Fierro reported on the preparation of hydroperoxides from the corresponding silyl peroxides by desilylation with methanol⁵⁰. The silyl peroxides can be prepared by singlet oxygen oxygenation of silyl enol ethers or disilyl ketene acetals (Scheme 12) as reported by several authors^{50–52}. By this method α -hydroperoxyesters and α -hydroperoxy carboxylic acids could be prepared in moderate to good yields. Several examples of hydroperoxide synthesis via singlet oxygenation are summarized in Table 3.





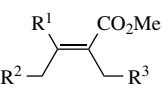
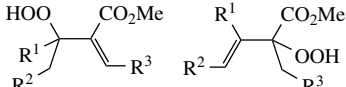
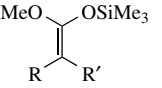
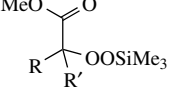
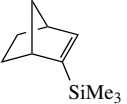
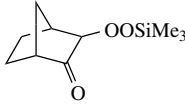
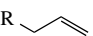
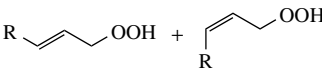
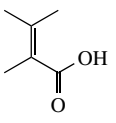
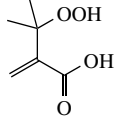
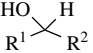
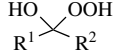
SCHEME 12. Synthesis of hydroperoxides from silyl enol ethers

TABLE 3. Preparation of alkyl hydroperoxides via singlet oxygen oxygenation

Substrate	Peroxide products	Conv. (%)	Yield (%)	Reference
			>99	53
			≥90	54
R = H, RR = -(CH ₂) ₂ -, -(CH ₂) ₃ -				
			75	55
		100		56

(continued overleaf)

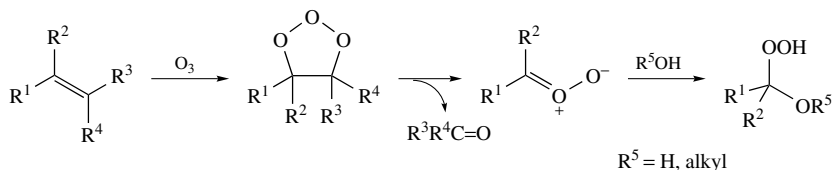
TABLE 3. (continued)

Substrate	Peroxide products	Conv. (%)	Yield (%)	Reference
 $R^1 = R^3 = H, R^2 = Me$ $R^1 = Me, R^2 = R^3 = H$ $R^1 = R^3 = Me, R^2 = H$ $R^1 = Ph, R^2 = R^3 = H$			>97:<3 88:12 51:49 56:44	57
 $R = t-Bu, R' = H$ $R = 1-Ad, R' = H$ $R = R' = Me$ $R = R' = Ph$			93 80 80 70	50
			95	52
 $R = t-Bu$ $R = SiMe_3$			>99:<1 22:78	58
			^a	59
 $R^1 = R^2 = Me$ $R^1 = Me, R^2 = Et$ $R^1 = Me, R^2 = n-Pr$ $R^1 = R^2 = Et$			25 23 16 18	38

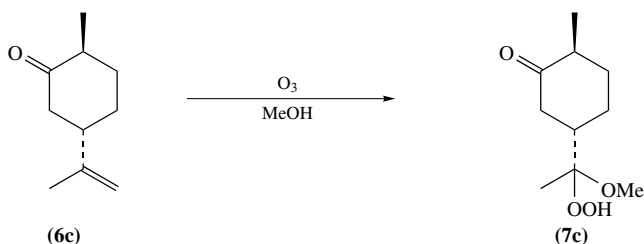
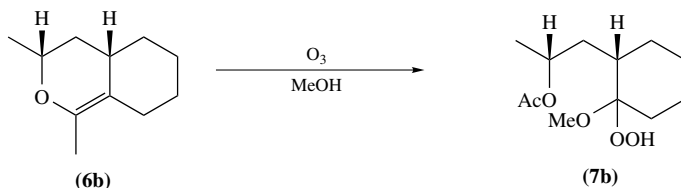
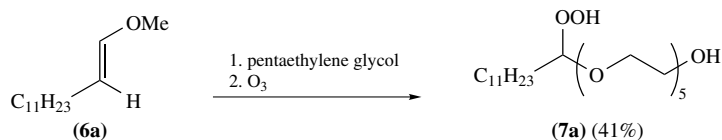
^a Product formed as an intermediate; yield $\geq 90\%$.

e. Synthesis by ozonolysis. Alkenes react with ozone to form—upon decay of the primary ozonide—carbonyl oxides. These zwitterions react with alcohols to give α -alkoxyhydroperoxides (Scheme 13). When water was used instead of an alcohol to react with the intermediate, α -hydroxyhydroperoxides were obtained²⁰. Following this procedure, Karlberg and coworkers synthesized the hydroperoxide **7a** from enol ether **6a** via ozonolysis in the presence of pentaethylene glycol⁶⁰ (Scheme 14) and Schreiber

presented the synthesis of α -alkoxyhydroperoxides **7b** and **7c** starting from dihydrofuran **6b** and alkene **6c**, respectively (Scheme 14)⁶¹.



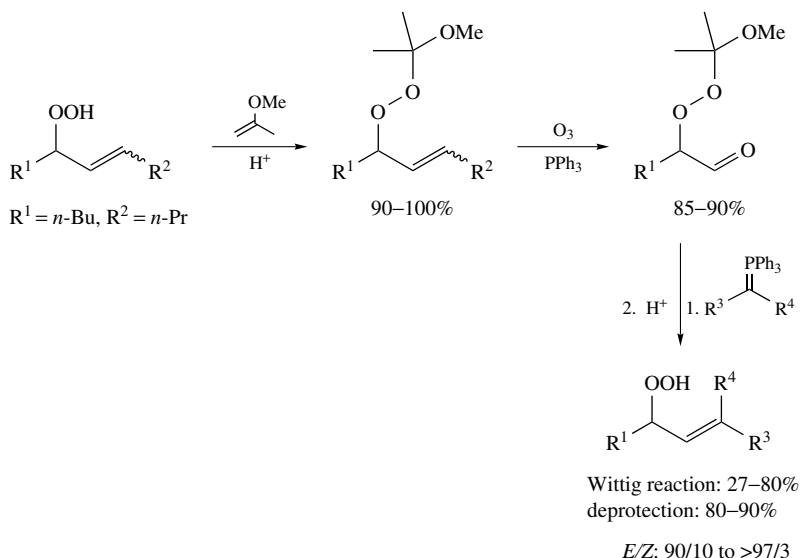
SCHEME 13. Synthesis of α -alkoxy hydroxy hydroperoxides by ozonolysis



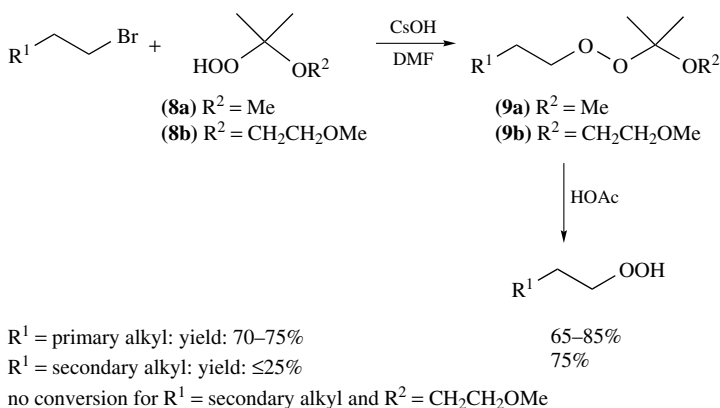
SCHEME 14. Preparation of α -alkoxyhydroperoxides via ozonolysis

f. Synthesis from peroxide precursors. In 1990, Dussault and Sahli presented a method for the structural modification of allylic hydroperoxides (Scheme 15)⁶². The reaction sequence includes protection of the hydroperoxide function as perketal, followed by ozonolysis of the alkene to give protected hydroperoxyaldehydes. This step proceeds in yields of 85 to 90% (for $R^1 = n\text{-Bu}$, $R^2 = n\text{-Pr}$). Horner–Emmons olefination or Wittig reaction with stabilized ylides provided allylic peroxides which were deprotected with aqueous acid to afford allylic hydroperoxides. The Wittig reaction step can be carried out with yields of 27–80% ($R^3 = \text{H, CO}_2\text{Et}$, $R^4 = \text{H, Me}$) and *E/Z*-selectivities of up to >97%. The deprotection proceeds with good yields of 80–90%.

g. Synthesis from alkyl halides and 2-(alkoxy)prop-2-yl hydroperoxide. An alternative method for the synthesis of primary and secondary hydroperoxides from the corresponding



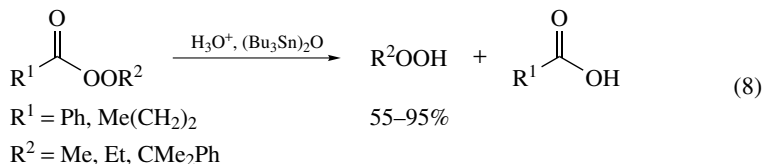
SCHEME 15. Preparation of hydroperoxides from peroxide precursors



SCHEME 16. Preparation of alkyl hydroperoxides from alkyl bromides

halides was presented by Dussault and coworkers (Scheme 16)⁶³. In this approach the hydroperoxides 2-methoxyprop-2-yl hydroperoxide (**8a**) and 2-(2-methoxyethoxy)prop-2-yl hydroperoxide (**8b**), both generated from 2,3-dimethylbutene by ozonolysis, reacted with alkyl halides and CsOH in DMF to afford the corresponding monoperoxyketals **9a** and **9b**. These protected alkyl hydroperoxides are hydrolyzed to give the alkyl hydroperoxides upon acidification. Reactions with primary bromides proceed cleanly to afford the perketals **9a** and **9b** in good yields (70–76%), while the reaction of secondary bromides or iodides was more problematic. 2-Bromooctane could not be transformed at all. The best results (perketal yields of 15–25%) with secondary halides were obtained by using **8a** in the presence of *t*-BuOK/18-crown-6 in benzene.

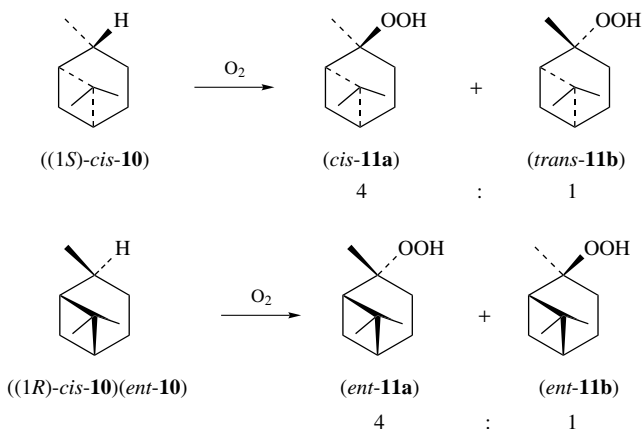
h. Synthesis by hydrolysis of peroxyesters. Primary hydroperoxides are generally difficult to synthesize. Their preparation is unsafe, and thus only few are available⁶³. As one example, ethyl hydroperoxide (and analogously also methyl and propyl hydroperoxide) is synthesized using the reaction of diethyl sulfate with dilute hydrogen peroxide in the presence of aqueous potassium hydroxide, but yields are low because of the base-catalyzed decomposition of hydroperoxides. In 2001, Baj and Chrobok reported on a new method for the efficient synthesis of primary hydroperoxides by hydrolysis of peroxyesters in the presence of bis(tributyltin)oxide (equation 8)⁶⁴. By this procedure, primary hydroperoxides with short alkyl chains, including some that have not been available before, can be synthesized in good yields (55–95%) due to the mild hydrolytic conditions.



2. Chiral hydroperoxides

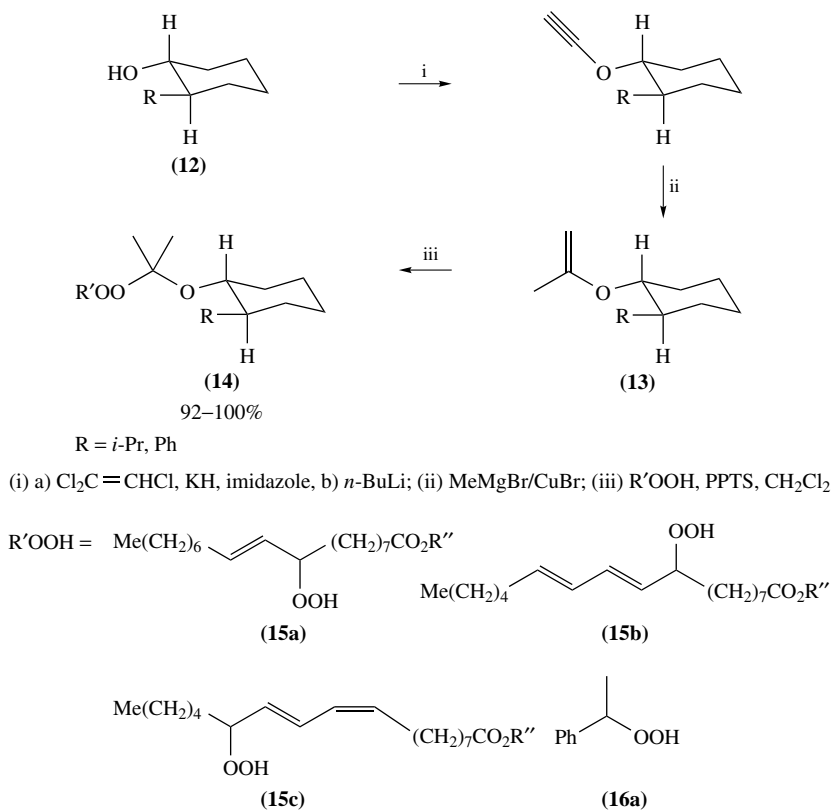
a. Separation of enantiomers/diastereomers via chromatography. Modified chiral cellulose stationary phases have been successfully applied by Kunath and coworkers to the enantioseparation of racemic hydroperoxides on analytical scale⁶⁵.

In the case of diastereomeric mixtures of chiral hydroperoxides, standard chromatography on achiral phase can be employed to separate the diastereomers. As one example for the preparation of optically pure hydroperoxides via this method, the ex-chiral pool synthesis of the pinane hydroperoxides **11** is presented by Hamann and coworkers⁶⁶. From (1*S*)-*cis*-pinane [(1*S*)-*cis*-**10**], two optically active pinane-2-hydroperoxides *cis*-**11a** and *trans*-**11b** were obtained by autoxidation according to Scheme 17. Autoxidation of (1*R*)-*cis*-pinane [(1*R*)-*cis*-**10**] led to the formation of the two enantiomers *ent*-**11a** and *ent*-**11b**. The ratio of *cis* to *trans* products was 4/1. The diastereomers could be separated by flash chromatography to give optically pure compounds.



SCHEME 17. Preparation of pinane hydroperoxides

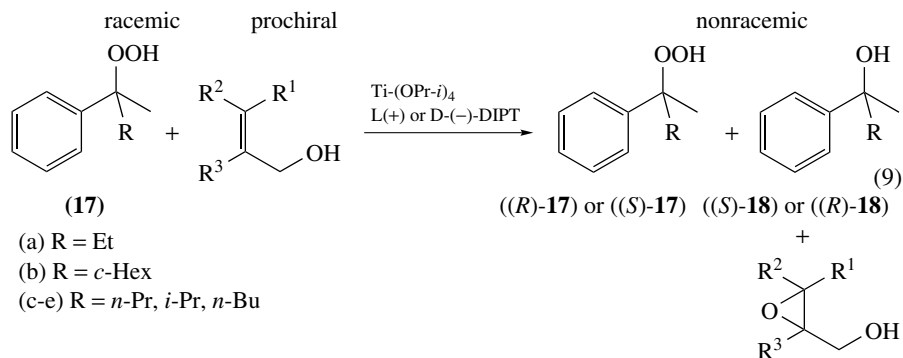
In 1988, Dussault and Porter reported on the resolution of racemic hydroperoxides via derivatization and subsequent separation of the resulting diastereomers by liquid-phase chromatography (Scheme 18)⁶⁷. The vinyl ethers **13**, readily prepared from the corresponding alcohols **12**, served as reagents for the derivatization. From **13** and the four racemic hydroperoxides **15a–c** and **16a** shown in Scheme 18, the perketals **14** were produced with pyridinium *p*-toluenesulfonate (PPTS) catalyst in yields between 92 and 100%. The mixture of the perketal-diastereomers **14** could then be separated by column chromatography. The perketal protecting group is easily removed with acetic acid/THF/water to liberate both enantiomers of the hydroperoxides **15a–c** and **16a** in enantiomerically pure form. With this method, optical purities of better than 96% *ee* were achieved and the enantiopure hydroperoxides were isolated in yields ranging from 64 to 95%.



SCHEME 18. Perketal formation of racemic hydroperoxides

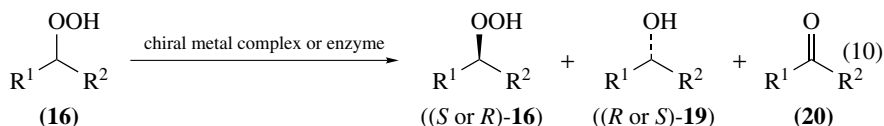
b. Kinetic resolution. Many methods have been published to synthesize enantiomerically pure or enriched hydroperoxides via kinetic resolution. One possibility is the Sharpless epoxidation. In this reaction, epoxy alcohols can be prepared with high enantioselectivity from allylic alcohols. At the same time, kinetic resolution of racemic chiral

hydroperoxides **17** occurs. Besides enantiomerically enriched hydroperoxides, also the opposite enantiomer of the corresponding alcohols **18** can be isolated in enantiomerically enriched form. Höft, Hamann and coworkers investigated the influence of the structure of components on the degree of resolution of tertiary hydroperoxides **17** (equation 9)^{66,68}.



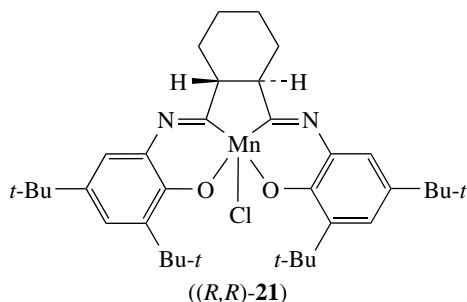
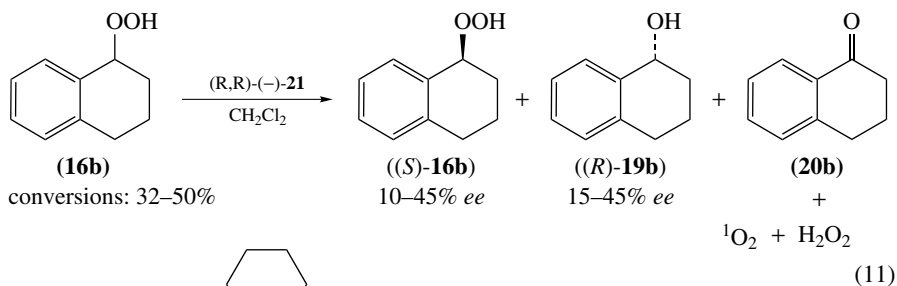
At 50% conversion of the hydroperoxide, *ee* values were determined and the best results were obtained using phenyl-substituted allylic alcohols [up to 29% *ee* of 1-cyclohexyl-1-phenylethyl hydroperoxide **17b** (R = *c*-Hex) employing either (*L*)- or (*D*)-DIPT and (*E*)- α -phenylcinnamyl alcohol as substrate]. In contrary, when allylic alcohols with hydrogen atoms or methyl groups at the double bond were used, the kinetic resolution of racemic hydroperoxides **17** occurred with enantiomeric excesses below 15% only. The authors also investigated the influence of the temperature on the obtained *ee* values in a range from 0 °C to 60 °C⁶⁸. The reaction rates increased with increasing temperature but at the same time the *ee* decreased. The *ee* values obtained were not influenced by increasing the amounts of Ti(OPr-*i*)₄, DIPT or allylic alcohol. An interesting result was that using (*Z*)-allylic alcohols in the presence of (*L*)-DIPT, an excess of the (*R*)-hydroperoxide was found, whereas (*E*)-allylic alcohols in the presence of the same enantiomer of DIPT afforded the (*S*)-hydroperoxide in enantiomerically enriched form. This shows that the configuration of the starting allylic alcohol dominates the stereochemical outcome of the reaction.

Kinetic resolution of racemic secondary hydroperoxides *rac*-**16** can be effected by selective reduction of one enantiomer with employing either chiral metal complexes or enzymes (equation 10). In this way hydroperoxides **16** and the opposite enantiomer of the corresponding alcohols **19** can be produced in enantiomerically enriched form. As side products sometimes the corresponding ketones **20** are produced.



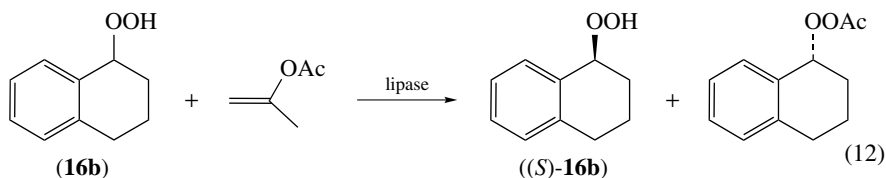
In 1996, Hamann and Höft were able to obtain 1,2,3,4-tetrahydronaphthyl hydroperoxide (THPO, **16b**) in enantiomerically enriched form starting from the racemic mixture by selective decomposition of one enantiomer in the presence of Jacobsen's catalyst **21**⁶⁹. Besides the enantiomerically enriched hydroperoxide (*S*)-**16b**, also the corresponding alcohol (*R*)-1-tetralol (**19b**) was isolated in enantiomerically enriched form (opposite

enantiomer, *ee* 15–45%) and the ketone 1-tetralone (**20b**), water and singlet oxygen were formed (equation 11). (*R,R*)-**21** selectively decomposed the (*R*)-(-)-THPO **16b** resulting in an enantiomeric excess of the (*S*)-enantiomer (*ee* 10–45%), while with (*S,S*)-**21** the (*S*)-enantiomer of **16b** was decomposed faster. The enantiomeric excess is dependent on the conversion and temperature. It could be increased by decreasing the temperature from room temperature to -20°C . The highest *ee* (45%) of (*S*)-**16b** was obtained with (*R,R*)-**21** at -20°C and a conversion of 50%.



An efficient method to prepare enantiomerically enriched hydroperoxides is the enzymatic kinetic resolution of racemic hydroperoxides using different kinds of enzymes (mainly lipases, chloroperoxidase, horseradish peroxidase). However, the scope of these reactions may be limited by the narrow substrate specificity of the enzyme.

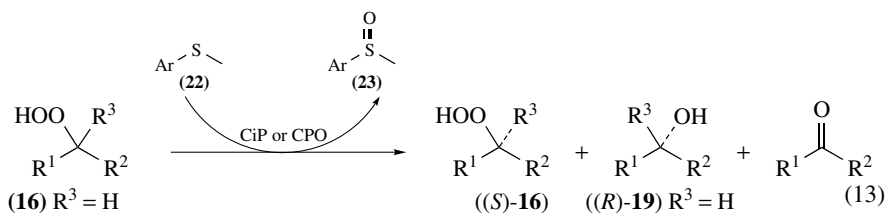
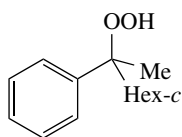
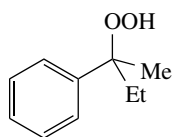
Höft reported about the kinetic resolution of THPO (**16b**) by acylation catalyzed by different lipases (equation 12)⁷⁰. Using lipases from *Pseudomonas fluorescens*, only low *ee* values were obtained even at high conversions of the hydroperoxide (best result after 96 hours with lipase PS: conversion of 83% and *ee* of 37%). Better results were achieved by the same authors using pancreatin as a catalyst. With this lipase an *ee* of 96% could be obtained but only at high conversions (85%), so that the enantiomerically enriched (*S*)-**16b** was isolated in poor yields (<20%). Unfortunately, this procedure was limited to secondary hydroperoxides. With tertiary 1-methyl-1-phenylpropyl hydroperoxide (**17a**) or 1-cyclohexyl-1-phenylethyl hydroperoxide (**17b**) no reaction was observed. The kinetic resolution of racemic hydroperoxides can also be achieved by chloroperoxidase (CPO) or *Coprinus* peroxidase (CiP) catalyzed enantioselective sulfoxidation of prochiral sulfides **22** with a racemic mixture of chiral hydroperoxides. In 1992, Wong and coworkers⁷¹ and later Höft and coworkers in 1995⁷⁰ investigated the CPO-catalyzed sulfoxidation with several chiral racemic hydroperoxides while the CiP-catalyzed kinetic resolution of phenylethyl hydroperoxide **16a** was reported by Adam and coworkers^{72,73} (equation 13). The results are summarized in Table 4.



conversions: 29–85%

5–96% *ee*

lipases: lipase PS, lipase AY, lipase M, pancreatin



(17a) $R^1 = Ph, R^2 = Et, R^3 = Me$

((R)-18a)

$R^1 = Ph, R^2 = Et, R^3 = Me$

Ar = Ph, *p*-Tol, *p*-MeOC₆H₄, *p*-O₂NC₆H₄, 2-naphthyl

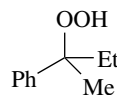
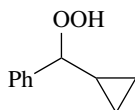
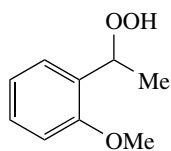
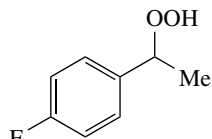
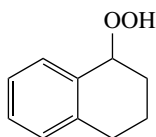
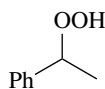


TABLE 4. Kinetic resolution of racemic hydroperoxides via CPO and CiP catalyzed enantioselective sulfoxidation

<i>rac</i> - 16/17	Sulfide 22	Enzyme	Conv. (16/17) [%]	Yield (%)			<i>ee</i> (%)			Ref- erence
				(<i>S</i>)- 16/17	(<i>R</i>)- 19/18	Ketone	(<i>S</i>)- 16/17	(<i>R</i>)- 19/18	23	
16a	Ar = Ph	CPO	46				62	71	86 ^a (<i>R</i>)	71
		CPO	64				89	50	70 (<i>R</i>)	71
		CPO	50				>99		92 (<i>R</i>)	70
		CiP	51	5	59	36	82	29	39 (<i>S</i>)	73
16a	Ar = <i>p</i> -Tol	CPO	50				>99		90 (<i>R</i>)	70
		CiP	68	28	57	15	>98	68	79 (<i>S</i>)	73
16a	Ar = <i>p</i> -MeOC ₆ H ₄	CPO	38				24	39	76 (<i>R</i>)	71
		CPO	71				91	38	61 (<i>R</i>)	71
		CiP	>95	38	52	10	95	65	79 (<i>S</i>)	73
16a	Ar = <i>p</i> -O ₂ NC ₆ H ₄	CiP	<2	47	33	20	55	65	—	73
16a	Ar = 1-Naph	CiP	53	35	46	19	81	76	89 (<i>S</i>)	73
16a	Ar = CH ₂ Ph	CiP	24	8	54	38	46	36	<10 (<i>S</i>)	73
17a	Ar = Ph	CPO	50				4		38 (<i>R</i>)	70
17a	Ar = <i>p</i> -Tol	CPO	50				0		18 (<i>R</i>)	70
16b	Ar = Ph	CPO	n.d. ^b				0	0	0	71
		CPO	50				4		64 (<i>R</i>)	70
16b	Ar = <i>p</i> -Tol	CPO	50				4		38 (<i>R</i>)	70
16c	Ar = Ph	CPO	45				56	68	58 (<i>R</i>)	71
16d	Ar = Ph	CPO	n.d.				n.d.	17	13 (<i>R</i>)	71
16e	Ar = Ph	CPO	n.d. ^b				n.d.	n.d.	0	71

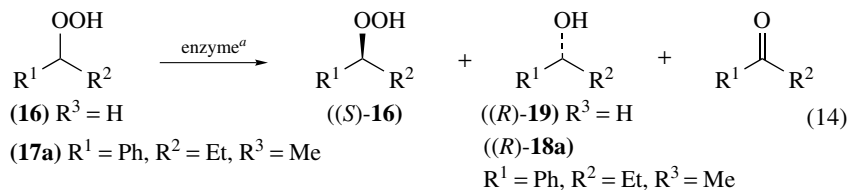
^a Could be raised up to 99% at very high sulfide conversions (94%), ratio sulfide : HP (1:1).

^b Not determined, conversion of the sulfide: 50%.

In this enzymatic transformation, three optically active compounds were prepared in one step. Besides the enantiomerically enriched hydroperoxide (*S*)-**16/17a**, also the opposite enantiomer of the corresponding alcohol (*R*)-**19/18a** and enantiomerically enriched (*S*)-sulfoxide **23** could be isolated (equation 13).

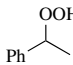
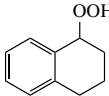
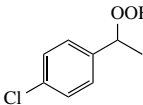
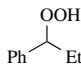
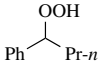
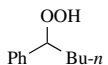
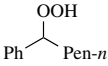
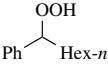
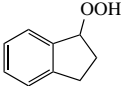
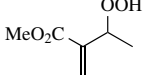
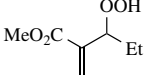
With substrates **16b** and **17a**, Höft and coworkers⁷⁰ observed only low *ee* values of up to 4% for the hydroperoxides. On the other hand, phenyl ethyl hydroperoxide (**16a**) could be isolated in high enantiomeric excess of >99% from the CPO-catalyzed reaction. The observed enantioselectivities of the sulfoxides varied, depending on the conversion of the sulfide and the hydroperoxide used, being highest with **16a** (92% *ee*). Unfortunately, the CPO-catalyzed resolution of chiral hydroperoxides is difficult on a preparative scale because of the high dilution necessary (0.5 μmol mL⁻¹). In the CiP-catalyzed kinetic resolution of **16a** better results were obtained compared to the CPO-catalyzed reaction (see Table 5).

A variety of further methods for the enzymatic kinetic resolution of racemic hydroperoxides (equation 14) has been published. For comparison they are summarized in Table 5.



^aIn the case of HRP, guaiacol was used as reducing agent.

TABLE 5. Kinetic resolution of several racemic hydroperoxides **16** by different enzymes or micro-organisms

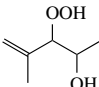
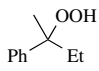
Entry	Hydroperoxide	Enzyme ^a	Time (h) ^b	Conv (%)	Yield (%)			<i>ee</i> (%)	<i>ee</i> (%)	Abs. Config.	Reference	
					16	19	20					
1		16a	HRP	5 min	50				>99	>99	(S)	66, 74, 75
			CiP	4		47	50	3	>98	90	(S)	72
			SeS	12 min	50				52	60	(R)	72, 76, 77
			A	4	64				88	30	(R)	78, 79
			A	0.5	94				>99	20	(R)	78, 79
			B	1.3	92				79	8	(R)	78
			C	4	19				6	0	(R)	78
			D	0.5	67				37	25	(S)	78
E	0.25	57				24	7	(S)	78			
F	1	23				9	23	(S)	78			
2		16b	HRP	3	50			95	97	(S)	66, 75	
3		16f	HRP	1.5	50			>95	>95	(S)	75	
			CiP	2		50	47	3	84	92	(S)	73
			SeS	18 min					48	56	(R)	77
			A	0.5	56				16	13	(R)	79
			D	0.5	65				40	37	(S)	79
4		16g	HRP	2.5	50			93	95	(S)	66, 75	
			CiP	72		36	31	33	31	54	(S)	73
			A	2	47				64	36	(R)	78
			B	2	36				3	3	(R)	78
D	0.75	55				7	9	(S)	78			
5		16h	HRP	1.5	50			<5	<5	(S)	66, 75	
			A	1.5	41				25	20	(R)	79
			D	0.5	83				29	11	(S)	79
6		16i	HRP	1.5	50			44	36	(S)	75	
			CiP ^c	408		37	20	43	<5	<5	(S)	73
			A	3	96				0	0	—	79
			D	1.3	53				14	7	(S)	79
7		16j	HRP	1.5	50			11	16	(S)	75	
8		16k	HRP	1.5	50			4	8	(S)	75	
9		16l	HRP	1	50			>99		(S)	75	
			CiP ^c	68		30	50	20	50	64	(R)	73
10		16m	HRP	5 min	50			97	>99	(S)	74	
11		16n	HRP	10 min	50			>99	>99	(S)	74	

(continued overleaf)

TABLE 5. (continued)

Entry	Hydroperoxide	Enzyme ^a	Time (h) ^b	Conv (%)	Yield (%)			<i>ee</i> (%)	<i>ee</i> (%)	abs. config.	Reference	
					16	19	20					
12		16o	HRP 24	7				<5	<5	(<i>S</i>)	66	
13		16p	HRP 3	50				15	14	(<i>R</i>)	66, 75	
			CiP 96		31	22	47	<5	<5	(<i>S</i>)	73	
			SeS 7 min						40	42	(<i>S</i>)	77
			A 0.5	74					55	26	(<i>R</i>)	79
	D 25 min	59					9	6	(<i>S</i>)	79		
14		16q	HRP 16	50				37	48	(<i>R</i>)	75	
15		16r	HRP 2	50				>95	>95	(<i>R</i>)	75	
			CiP ^c 20		52	33	15	50	65	(<i>R</i>)	72, 73	
			SeS 3 min	50					99	99	(<i>S</i>)	72, 76, 77
16		16s	CiP ^c 20		34	41	25	56	67	(<i>S</i>)	73	
17		16t	CiP ^c 336					>95			73	
18		16u	CiP ^c 144					>95			73	
19		16v	SeS 8 min	50				34	28	(<i>R</i>)	72, 76	
20		16w	SeS 13 min	50				80	96		72, 76	
21		16x	SeS 0.4 min	50				64	90	—	72, 76	
22		16y	SeS 9 min	50				14	30	(<i>S,S</i>)	72, 76	

TABLE 5. (continued)

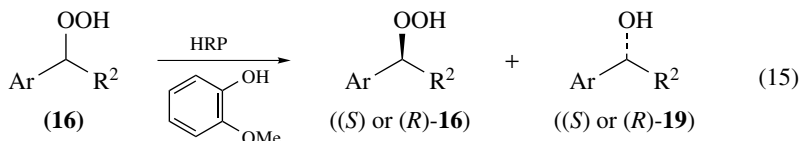
Entry	Hydroperoxide	Enzyme ^a	Time (h) ^b	Conv (%)	Yield (%)			<i>ee</i> (%)		abs. config. 16	Reference
					16	19	20	16	16		
23		16z	SeS	16	50			22	38	(<i>R,R</i>)	72, 76
	<i>threo</i>										
24		17a	A	0.5	19			5	30	(<i>R</i>)	79
			A	13 min	79			39	7	(<i>R</i>)	79

^a HRP = horseradish peroxidase (used together with guaiacol as reducing agent); CiP = Coprinus peroxidase; SeS = Selenosubtilisin; microorganisms: A = *Bacillus subtilis*; B = *Paecilomyces* sp.; C = *Bacillus* sp.; D = *Aspergillus niger*; E = *Botrytis cinerea*; F = *Penicillium v.*

^b For microorganisms A–F only the incubation times are given (no precultivation times).

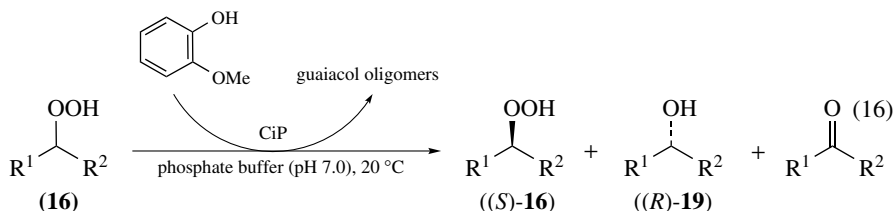
^c Product distribution instead of yield given, no conversion given.

Adam and coworkers reported on the horseradish peroxidase (HRP) catalyzed kinetic resolution of racemic hydroperoxides by enantioselective reduction in the presence of guaiacol^{72, 74, 75} (equation 15). The catalytic efficiency and stereoselectivity of HRP is highly dependent on the structure of the hydroperoxide substrate. While the enzyme selectively reduces sterically unencumbered (*R*)-alkyl aryl hydroperoxides, poor enzyme recognition is obtained with substrates bearing branched aliphatic chains (**16o–q**, see Table 5) and for sterically demanding hydroperoxy vinylsilanes. For these sterically more demanding hydroperoxides it was found that α -branching reduces the obtained *ee* more than β -branching, presumably due to size restrictions at the active site of the enzyme. With tertiary hydroperoxides such as **17a** and **17b** no conversion was observed. The structure of the hydroperoxide not only influences the enantioselectivity observed in these kinetic resolutions, but also the sense of specificity of the enzyme. For branched hydroperoxides as **16p** and **16q** (Table 5, entries 13, 14) the stereochemical course is opposite to that of *n*-alkyl aryl hydroperoxides **16a,b,f–l** (Table 5, entries 1–9) and hydroperoxide **16r** (Table 5, entry 15) (for the hydroxy-functionalized hydroperoxide **16r**, a change of the stereochemical description applies). HRP is very selective and only the (*R*)-enantiomer of alkyl aryl hydroperoxides is reduced even in the presence of excess guaiacol. Compared to other enzymes HRP is much less substrate specific. With this enzyme it was possible to conduct the kinetic resolution of racemic hydroperoxides in preparative amounts, as opposed to lipases and CPO-catalyzed methods. HRP is known to be composed of different isoenzymes⁸⁰. It was found that mostly isoenzyme C, the main component of the HRP, catalyzes the asymmetric reduction with turnover numbers that are 100-fold higher compared to isoenzyme A.

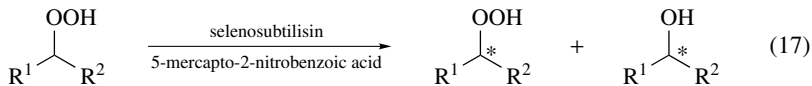


The same authors also investigated the kinetic resolution of racemic hydroperoxides with *Coprinus* peroxidase (CiP), isolated from the basidiomycete *Coprinus cinereus*

(equation 16)^{72,73}. The results observed were similar to the ones discussed before for horseradish peroxidase. With **16a** as substrate, the highest enantiomeric excesses of >98% of the (*S*)-enantiomer of **16a** were obtained (Table 5, entry 1). CiP shows—analogueous to HRP—good enantioselectivity for aryl alkyl hydroperoxides with short alkyl chains, but sterically more demanding hydroperoxides are poor substrates. The results obtained with CiP (Table 5, entries 1, 4, 6) showed that reactivity as well as selectivity are drastically reduced by increasing the chain length of the alkyl group in the substrate.

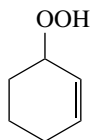


The application of CPO, HRP and CiP is limited to sterically unencumbered substrates and all these peroxidases produce the same absolute configuration of the chiral hydroperoxide. To overcome this limitation, the semisynthetic enzyme selenosubtilisin, a mimic for glutathione peroxidase, with the peptide framework of the serine protease subtilisin was developed by Bell and Hilvert⁸¹. This semisynthetic peroxidase catalyzes the reduction of hydrogen peroxide and hydroperoxides in the presence of 5-mercapto-2-nitrobenzoic acid. It was utilized by Adam and coworkers and Schreier and coworkers for the kinetic resolution of racemic hydroperoxides (equation 17)^{72,76,77}. The results obtained were very promising.



Although the selectivity of this semisynthetic enzyme is also strongly influenced by the structure of the substrate, its reactivity towards sterically encumbered substrates is significantly higher than that of the enzymes CiP and HRP. For example, sterically demanding hydroperoxides **16w** and **16x**, not accepted by HRP (Table 5, entries 20 and 21), could be resolved by selenosubtilisin with good to excellent turnover numbers (**16w**: $k_{\text{cat}} = 820 \text{ min}^{-1}$, **16x**: $k_{\text{cat}} = 3322 \text{ min}^{-1}$) and good catalytic efficiency (**16w**: $k_{\text{cat}}/K_m = 97 \text{ mM}^{-1} \text{ min}^{-1}$, **16x**: $k_{\text{cat}}/K_m = 47500 \text{ mM}^{-1} \text{ min}^{-1}$ [$K_m = \text{Michaelis affinity constant}$]). Tertiary hydroperoxides were accepted by selenosubtilisin, but for these substrates the semisynthetic enzyme showed reduced enantiomeric differentiation. Hydroperoxide substrates with both a hydrophobic and a polar residue (hydroperoxide **16r**, Table 5, entry 15) displayed increased affinity to selenosubtilisin. Substrate **16a** is reduced unselectively because the two substituents R^1 and R^2 are too similar to provide enantiomeric discrimination. A further advantage of selenosubtilisin compared to natural peroxidases is that it exhibits the opposite sense in enantioselectivity. Thus, it is possible to prepare also the (*R*)-enantiomer of alkyl aryl hydroperoxides in enantiomerically enriched form.

One of the major disadvantages of utilizing enzymes or semisynthetic enzymes for chemical transformations is the fact that large quantities of pure enzyme are needed for preparative scale. This disadvantage is contrasted with whole cell systems (bacteria, fungi, plant/animal cells) because they are easily available in large quantities through

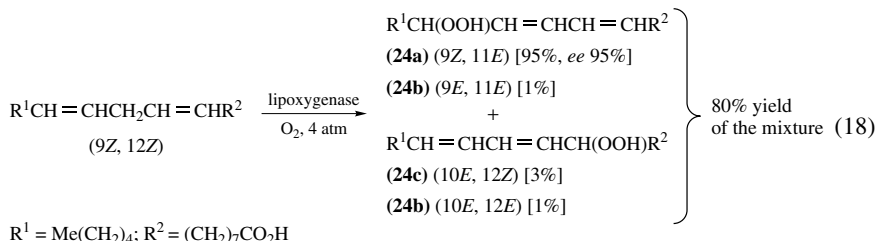
**(16 α)**

self-replication. In 1998 Adam and coworkers and Lukacs and coworkers^{78,79} reported for the first time about the kinetic resolution of organic hydroperoxides **16a** and **16g** by soil bacteria and fungi. The best results were obtained with *Bacillus subtilis*, which converted 64% of the racemic hydroperoxide **16a** within 240 min with an enantiomeric excess of 88% for the (*R*)-hydroperoxide and 30% for the (*S*)-alcohol. An even higher enantiomeric excess of the hydroperoxide (>99%) could be obtained with *B. subtilis* cultures that contained yeast extract in the growth medium. Under these conditions the enzyme activity was increased significantly and conversions were very high after short reaction times (94% after 0.5 h) (Table 5, entry 1). Therefore, yields of the enantiopure hydroperoxide were low. With these bacteria the sense of enantioselectivity is the same as observed before with the semisynthetic enzyme selenosubtilisin, but it is opposite to the sense of enantioselectivity observed with CPO, CiP or HRP. As observed before for enzymes, also with the soil bacteria the conversion rate and *ee* decreases with increasing steric demand of the hydroperoxide substrates but the structural tolerance seems to be higher than with isolated CPO, CiP or HRP. With *B. subtilis* a variety of secondary alkyl aryl hydroperoxides (see Table 5) and even the tertiary 2-phenylbutyl-2-hydroperoxide **17a** (Table 5, entry 24), which could not be resolved by isolated enzymes, have been resolved in moderate to good enantioselectivities⁷⁹. Even substrate **16h** (Table 5, entry 5), which did not display any enantioselectivity at 50% conversion utilizing HRP as catalyst, could be resolved, although with poor enantioselectivity (*ee* 25% at 41% conv.). The size limit for *B. subtilis* is marked by the *n*-butyl group in **16i**, which could not be resolved (no *ee*, Table 5, entry 6). The best fungal system was *Aspergillus niger*, which gave an *ee* value of 37% for hydroperoxide (*S*)-**16a** and 25% for the corresponding (*R*)-alcohol **19a** (Table 5, entry 1). This fungus displayed the opposite sense of enantioselectivity in the kinetic resolution of the hydroperoxides compared to the bacteria *B. subtilis*. The authors also reported on the immobilization of *B. subtilis* cells in alginate gel. It can be used for several cycles without loss of activity. Very interesting is the observation, that in immobilized form, the soil bacteria displayed even higher peroxidase activity than free cells.

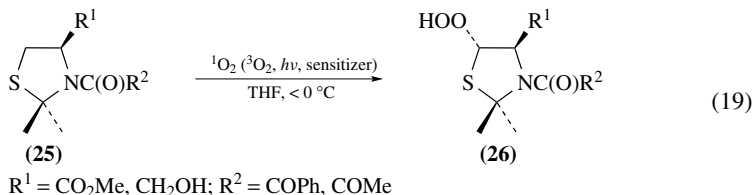
c. Stereoselective dioxygenation. Various kinds of substrates can be transformed into chiral hydroperoxides by stereoselective oxidation with dioxygen. In this kind of reaction, the asymmetric induction can either result from chiral catalysts like enzymes or can be substrate directed.

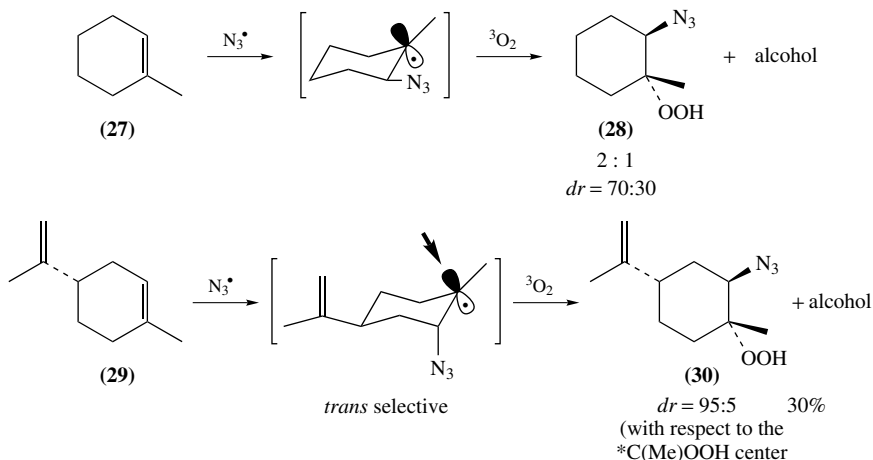
In 1990, Triantaphylidès and coworkers reported on the preparative enzymatic synthesis of linoleic acid (13*S*) hydroperoxide **24a** using soybean lipoxygenase-1⁸². In this dioxygenation asymmetry is induced by the catalyst, the enzyme. The reaction was later used by Dussault⁸³ and also by Baba and coworkers⁸⁴ as key step in the preparation of more complex peroxides. The enzyme is a non-heme iron dioxygenase which catalyzes the incorporation of dioxygen into polyunsaturated fatty acids to yield *E,Z* conjugated diene hydroperoxides **24a–d**. With this enzymatic method, the hydroperoxide **24a** could

be obtained with good selectivity (95% isomer purity, 95% *ee*) and in satisfactory yields (80%) on a preparative scale (equation 18).

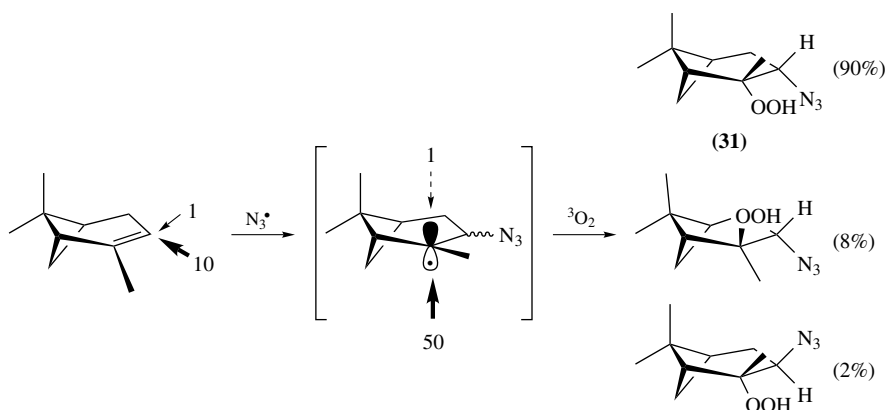


An example for substrate directed oxidation with singlet oxygen to prepare diastereomerically enriched hydroperoxides **26** was presented by Ando and coworkers in 1984 (equation 19)⁸⁵. These chiral hydroperoxides were generated by singlet oxygenation of the thiazoline derivatives **25**, and they were used for the asymmetric oxidation of sulfides (see Section III.B.3.c). The hydroperoxides were stable in dilute solution for a few hours and could be purified by chromatography, but decomposed upon concentration. The formation of product **26** was explained by assuming a Pummerer-type rearrangement of the intermediate persulfoxide via abstraction of an α -proton. A further example for substrate-directed oxidation with molecular oxygen is the azidohydroperoxidation reaction. This is a dioxygenation method for the preparation of 1,2-azidohydroperoxides. The reaction allows the chemo-, regio- and diastereoselective addition of azidyl radicals and molecular oxygen to acyclic and cyclic alkenes. It consists of a sequence of photoinduced electron transfer to generate the azidyl radical, which adds to alkenes or dienes, then trapping by oxygen, a second electron transfer and final protonation of the intermediate 1,2-azidohydroperoxo anion. Griesbeck and coworkers⁸⁶ investigated, for example, the simple diastereoselectivity of the azidohydroperoxidation of 1-methylcyclohexene (**27**) and limonene (**29**) (Scheme 19). With **27** a 2:1 mixture of azidohydroperoxide **28** and the corresponding alcohol was obtained both with a diastereomeric ratio of 70:30. In the case of limonene (**29**), one out of four possible diastereomeric azidohydroperoxides (**30**) was formed in large excess (*dr* 95:5, besides 30% of azidoalcohol). This result can be explained by a higher *cis*-asymmetric 1,4-induction in 4-substituted cyclohexyl radicals (N_3 is directed *trans* to the 2-propenyl group and then the oxygen attacks *trans* to N_3 and *cis* to 2-propenyl). For acyclic substrates, only moderate *erythro*/*threo* selectivity was obtained (65:35). The authors also investigated the induced diastereoselectivity of the azidohydroperoxidation of α -pinene (Scheme 20). The primary attack of the azidyl radical proceeds with a 10:1 selectivity *trans* to the sterically more demanding dimethyl-substituted methylene bridge, the subsequent oxygen attack with a 50:1 *endo*-selectivity (*trans* to the dimethylmethylene bridge). The major stereoisomer **31** was formed with 90% diastereoselectivity. In this substrate, the oxygen addition is directed by the shielding effect of the dimethylmethylene bridge.



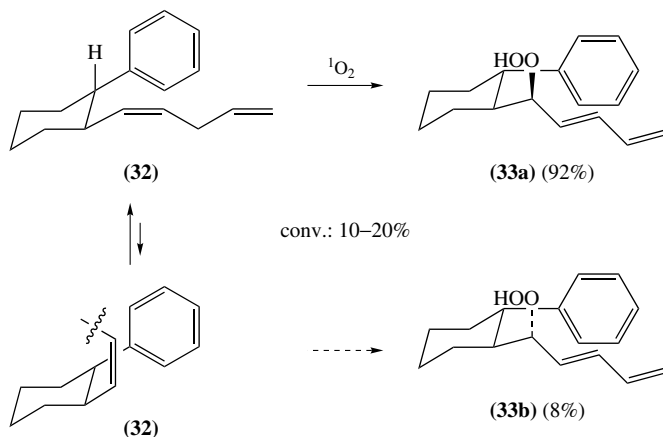


SCHEME 19. Azidohydroperoxidation of 1-methylcyclohexene and limonene

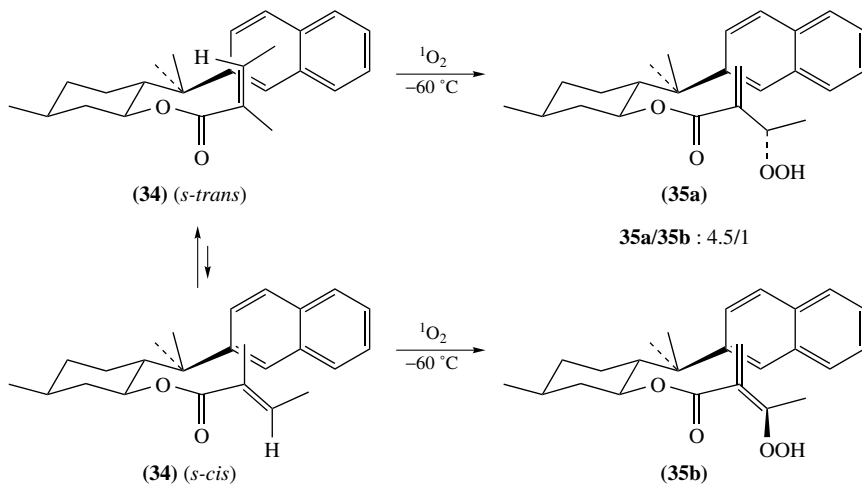
SCHEME 20. Azidohydroperoxidation of α -pinene

The most direct method for the synthesis of allyl hydroperoxides is the reaction between singlet oxygen and prochiral alkenes. Unfortunately, with this method, racemic products are produced, often as a mixture of regioisomers. Dussault reported several examples where dioxygenation could be carried out diastereoselectively due to a directing effect of adjacent groups in the employed substrates⁸³. The phenylcyclohexyl derivative **32** depicted in Scheme 21 is capable of controlling diene conformation as well as oxygen approach⁸⁷. Singlet oxygenation of **32** produced a 92:8 ratio of hydroperoxide diastereomers **33a** to **33b** (conversion of 10–20%). The (*E*)-alkene, which had a greatly reduced conformer bias, underwent oxygenation with distinctly reduced selectivity⁸⁷.

Dioxygenation of the chiral enoate **34** could also be conducted stereoselectively, although the selectivity was rather low (*dr* 4.5:1, Scheme 22). In compound **34** the naphthylmenthol auxiliary effectively blocked one face of the tethered enoate so that the oxygen can only be transferred from the non-blocked face. The observed



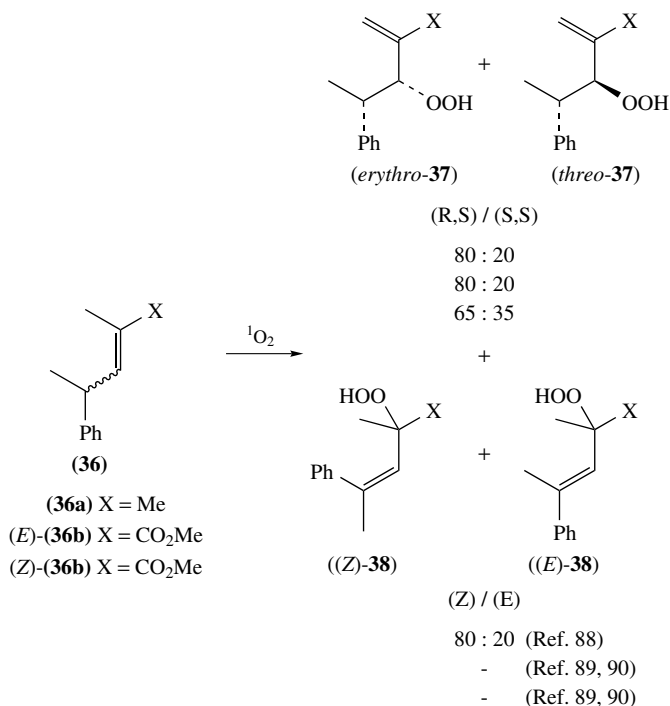
SCHEME 21. Auxiliary directed dioxygenation



SCHEME 22. Dioxygenation of enoates

diastereoselectivity of 4.5:1 (**35a:35b**) in the dioxygenation reaction and the improvement in stereoselection at lower temperatures mirrors the fact that the modest stereoselectivity is based upon an equilibrium favoring the *s-trans* conformer.

In a search for more effective approaches to the problem of stereoselective dioxygenation, alternative methods have been developed. While the inclusion of alkenes and $^1\text{O}_2$ within a chiral cyclodextrin cavity furnished hydroperoxides with modest *ee* values, neighboring stereocenters and chiral auxiliaries could induce highly stereoselective dioxygenation. In 1987 Kropf and Reichwaldt⁸⁸, and three years later Adam and coworkers^{89,90}, reported on the photooxygenation of phenyl-substituted alkenes **36** producing allylic hydroperoxides **37** and **38** with high diastereoselectivity (*dr* 80/20). In the best example



SCHEME 23. Regio- and stereoselective photooxygenation of phenyl-substituted alkenes

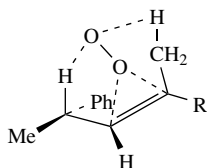
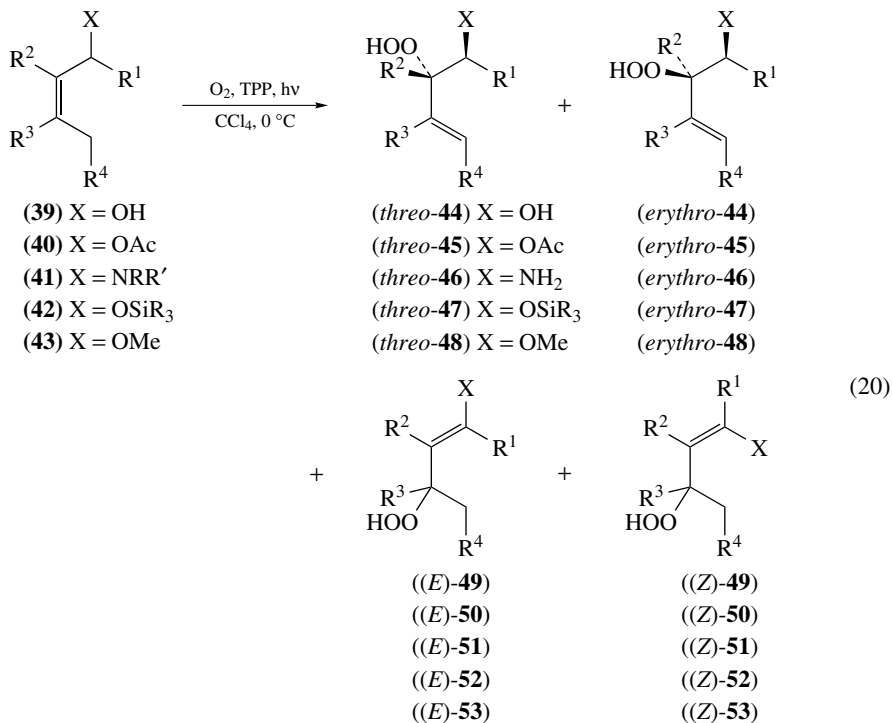


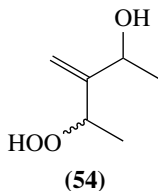
FIGURE 3

presented by Adam, the reaction was also completely regioselective (Scheme 23). Due to the same diastereoselectivity obtained, the authors proposed that the stereochemical control (*gem*-selectivity) results from a perepoxide like transition state in the product determining step as discussed by Stephenson and coworkers and Foote and coworkers (Figure 3, *cis*-effect)⁹¹ rather than the [4 + 2]-cycloaddition pathway, that was proposed by Ensley and coworkers in 1980⁹². This perepoxide-like transition state was further supported by stereochemical studies⁹⁰. For the (*Z*)-configured substrate **36b** a perepoxide-like geometry is not assisted by the *cis*-effect, because a suitable pair of allylic hydrogen atoms is not available and therefore lower reactivity as well as lower diastereoselectivity (*dr* 65:35) results. Later, Adam and coworkers investigated the regio- and diastereoselective ene reaction of singlet oxygen with chiral, secondary allylic alcohols **39**^{93,94}, acetates

40^{93,94}, amines **41** (and their acyl derivatives)⁹⁵, silyl enol ethers **42**⁹⁴ and enol ethers **43**⁹⁴ leading to products **44–53**, which is shown in equation 20 (Table 6).



R¹ = Me, Et, *i*-Pr, *t*-Bu; R² = H, Me; R³ = H, Me; R⁴ = H, *n*-Pr; NRR' = NH₂, NHAc, NPhth



While reaction of the acetate **40** as well as the acetyl- and phthalimide derivatives of chiral amine (**41b** and **41c**) proceeded with *erythro* diastereoselectivity (in accordance with the 'classical' *cis* effect, minimization of 1,3-allylic strain) (Table 6, entries 8, 10, 11), for the allylic alcohols **39**, primary allylic amine **41a**, silyl enol ethers **42** and enol ether **43** *threo* selectivity was observed (Table 6, entries 1–7, 9, 12–14) (see also Scheme 24). For allylic alcohols with an alkyl group R⁴ *cis* to the substituent carrying the hydroxyl group, diastereoselectivity was high (Table 6, entries 1–7); in contrast, stereoselection was low for allylic alcohols which lack such an R⁴ (*cis*) substituent (substrates **39h** and **39i**, see Figure 4).

TABLE 6. Results of the regio- and diastereoselective ene reaction of singlet oxygen with chiral allylic alcohols, acetates, amines (and acyl derivatives), silyl ethers and ethers

Entry	Substrate	X	R ¹	R ²	R ³	R ⁴	Diastereoselectivity		Regioselectivity		Ref- erence
							<i>threo</i> - 44–48	<i>erythro</i> - 44–48	44–48	49–53 [(<i>E</i>)/(<i>Z</i>)]	
1	39a	OH	Me	H	Me	H	93	7	96	4 ^a	93, 94
2	39b	OH	Me	H	H	H	93	7	>97	<3 ^b	93, 94
3	39c	OH	Et	H	H	H	94	6	>97	<3 ^b	94
4	39d	OH	<i>i</i> -Pr	H	H	H	94	6	>97	<3 ^b	94
5	39e	OH	<i>t</i> -Bu	H	H	H	95	5	>97	<3 ^b	93, 94
6	39f	OH	Me	Me	H	H	93	7	>97	<3 ^{b,c}	94
7	39g	OH	Me	H	H	<i>n</i> -Pr	94	6 ^d	>97	<3 ^b	94
8	40	OAc	Me	H	Me	Me	39	61	82	18	93
										[38/62]	
9	41a	NH ₂	Me	H	Me	H	>95	<5	>97	<3 ^b	95
10	41b	NHAc	Me	H	Me	H	28	72	>97	<3 ^b	95
11	41c	NPhth ^e	Me	H	Me	H	11	89	90	10	95
										[<3/>97 ^f]	
12	42a	SiMe ₃	Me	H	Me	H	80	20	74	26 ^g	94
13	42b	SiMe ₂ Bu- <i>t</i>	Me	H	Me	H	83	17	67	33 ^g	94
14	43	OMe	Me	H	Me	H	72	28	80	20 ^g	94

^a Regioisomer **49a** was obtained in the form of its ring tautomer 3-hydroxy-3,5,5-trimethyl-1,2-dioxolan, produced by ketonization of the initial enol and cyclization.

^b No products from **49a** and **49b** could be detected.

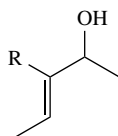
^c 8% of [(*S,S*), (*S,R*)-**54**] was formed as side products in a 23:77 ratio.

^d Only (*E*)-configured hydroperoxides **44g** were detected.

^e Phth = Phthaloyl.

^f No (*E*)-regioisomer was detected.

^g The intermediary enol ethers **52a** and **52b** and **53** were unstable under the reaction conditions.



(39h/39i)

39h: R = H: *threo/erythro*-**44h** : 54/46; ratio: **44h/49h**: 96/4^a

39i: R = Me: *threo/erythro*-**44i** : 66/34; ratio: **44i/49i**: >97/<3^{ab}

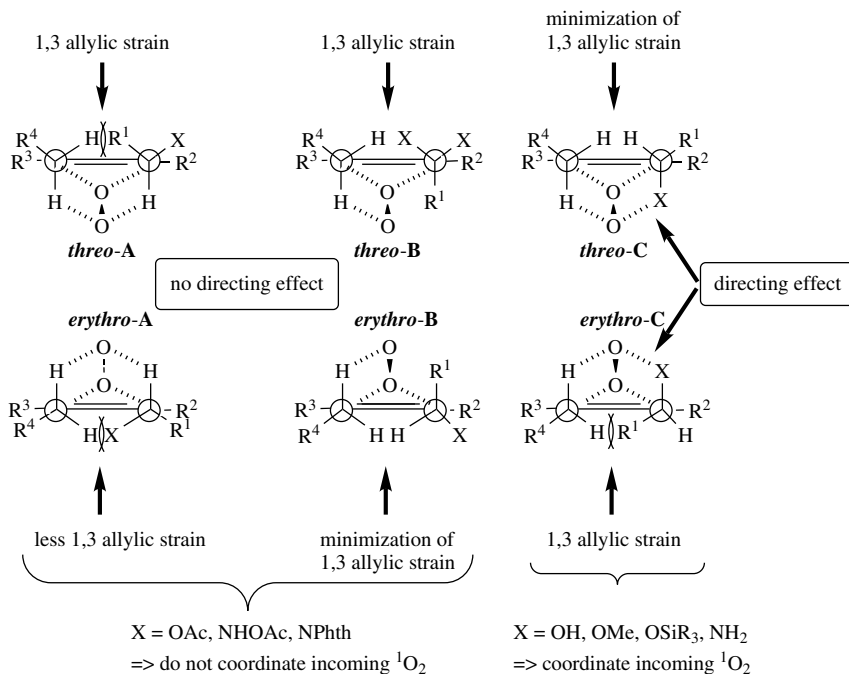
^aThe regioisomer was obtained in the form of its ring tautomer.

^b45% of [(*S,S*), (*S,R*)]-**54** was formed as side product in a

66:34 ration

FIGURE 4

These results are explained in terms of coordination of the nucleophilic hydroxy- (methoxy-, silyloxy-, amino-) functionality of the stereogenic center with the incoming electrophilic singlet oxygen (Scheme 24, right side, transition states **C**). Stereodifferentiation results from the preferred conformation of the allylic alcohol for oxygen transfer, which is mainly determined by 1,3-allylic strain (*threo*-**C** favored over *erythro*-**C**). The experiments also showed that the optimal dihedral angle of the allylic alcohol (C=C–C–O) in the transition state lies between 90° and 130° and the newly formed double bond in the

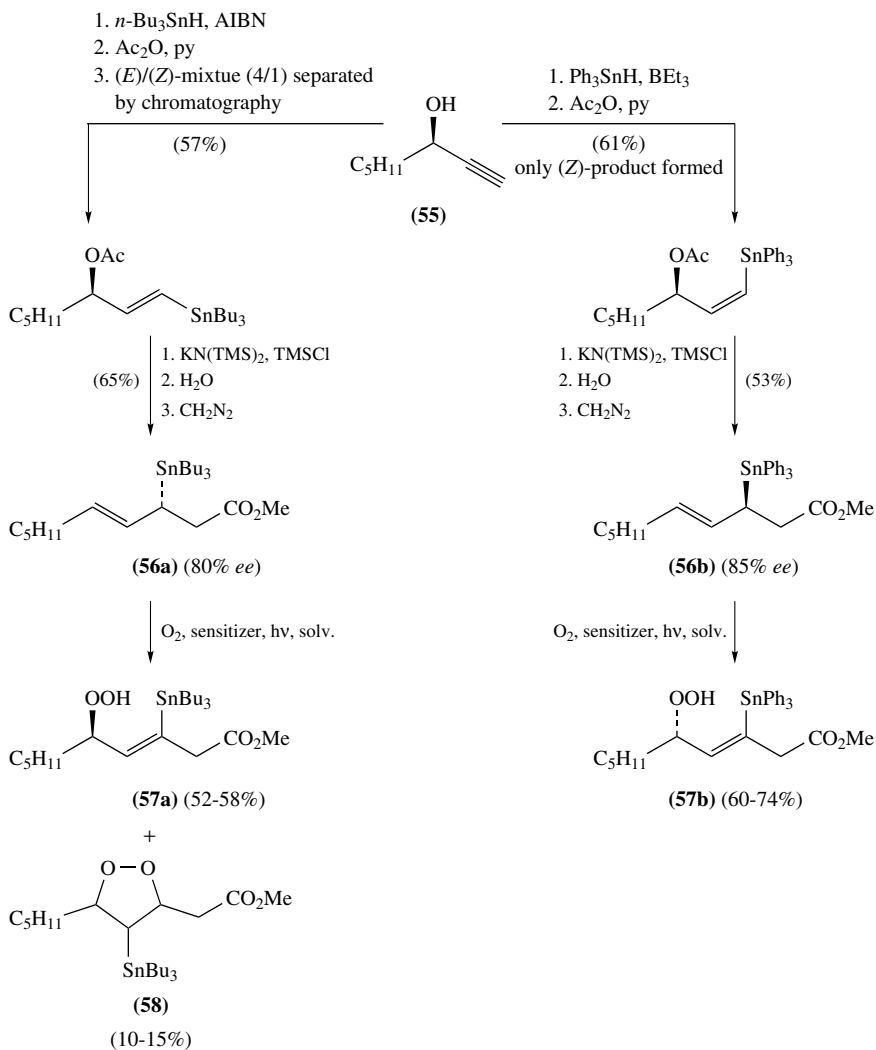


SCHEME 24. Possible transition state structures for ene reaction of $^1\text{O}_2$ with allylic substrates, with directing effect of the functional groups (right side, TS C) and without this directing effect (left side and middle, TS A and B)

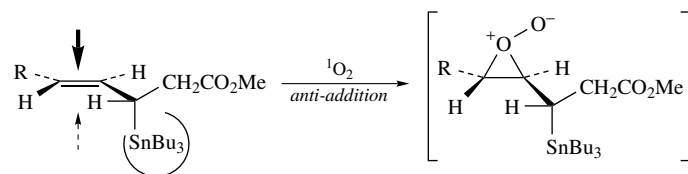
resulting hydroperoxides is exclusively formed in the (*E*)-configuration (substrate **39g**, Table 6, entry 7).

In 1991/1992, several reports of Dang and Davies dealing with the stannyl-directed regioselective dioxygenation of acyclic and cyclic allyl stannanes were published⁹⁶. In these reactions singlet oxygen shows a preference for *anti*/*s_E2'* electrophilic addition to chiral allylsilanes and -stannanes. Inspired by these observations Dussault developed a general strategy for the asymmetric synthesis of acyclic allylic hydroperoxides^{83,97}. Herein chiral propargylic alcohols **55** are stereoselectively converted to either enantiomer of an allylic hydroperoxide **57** through intermediate chiral allylstannanes **56** (Scheme 25). The reaction sequence includes the synthesis of the chiral allylstannanes from enantiomerically enriched propargyl alcohols **55** followed by dye-sensitized singlet oxygenation of intermediary chiral allylstannanes **56**. In the second step a single peroxide is selectively formed upon addition of $^1\text{O}_2$ to the chiral allylstannanes. This *anti*/*s_E2'* addition of oxygen to the substrate (Scheme 26) is typical for chiral allylsilanes and -stannanes⁹⁶. In the case of the allyltributylstannane **56a**, oxygenation also produced a small amount of the diastereomerically pure 4-stannyl-1,2-dioxolane **58**. This methodology complements the hydroxyl-directed singlet oxygenation developed by Adam and Nestler, which has already been discussed⁹⁴.

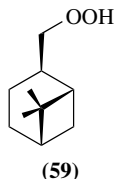
The oxidation of zinc organometallics to hydroperoxides with molecular oxygen in perfluorinated solvents has already been described in Section II.A.1. With this protocol



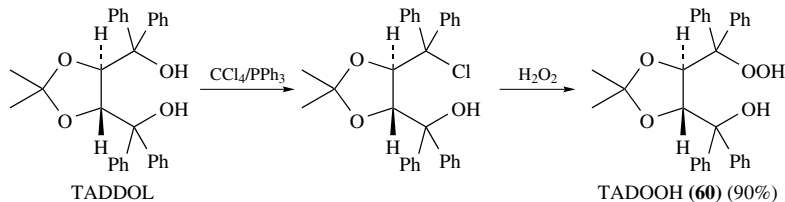
SCHEME 25. Stereoselective synthesis of allylhydroperoxides starting from propargyl alcohols

SCHEME 26. Favored *anti*/*s_E2'* addition of singlet oxygen to allylstannanes

also the synthesis of chiral hydroperoxides such as **59** has been achieved by Knochel and coworkers with 64% yield³⁹.



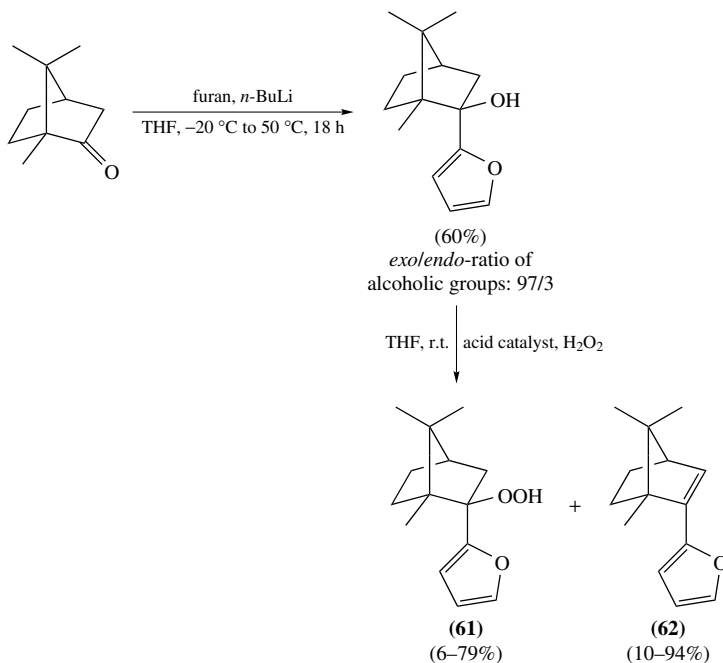
d. Reaction with hydrogen peroxide. A second method for the preparation of chiral hydroperoxides in enantiomerically enriched form consists in the substitution of suitable precursors by hydrogen peroxide. In this respect, the most widely used substrates are the corresponding chiral alcohols, which—upon treatment with hydrogen peroxide in acidic medium—can be transformed into chiral hydroperoxides. With this method, several enantiomerically enriched hydroperoxides were prepared by substitution reaction as, for example, the TADDOL-derived hydroperoxide **60**, developed by Aoki and Seebach⁹⁸ and the camphor-derived hydroperoxide **61** developed by Lattanzi and coworkers⁹⁹ (Schemes 27 and 28). TADOOH **60**, a chiral tertiary hydroperoxide, can be prepared from TADDOL by substitution of one hydroxyl group by chloride under Appel conditions (CCl_4 , PPh_3). Compound **60** can be isolated with 90% yield after substitution of the chloride by a hydroperoxy group using urea hydrogen peroxide.



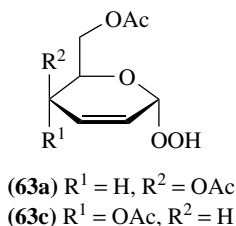
SCHEME 27. Preparation of the tertiary hydroperoxide **60** from TADDOL

Unlike TADOOH **60**, the reactive OOH group in the camphor-derived tertiary hydroperoxide **61** is directly bound to the stereogenic carbon center. **61** was prepared from (+)-(1*R*)-camphor by *endo*-selective addition of 2-furyl lithium to the ketone functionality. The obtained *exo/endo* ratio of the alcoholic group was 97/3. Stereoselective nucleophilic substitution with hydrogen peroxide (also urea-hydrogen peroxide was used) in acidic medium resulted in the formation of **61** in acceptable yields (Scheme 28). As a side product the bornene **62** was obtained. The product distribution and yields were largely dependent on the oxygen source [hydrogen peroxide or urea-hydrogen peroxide (UHP)] as well as the type and amount of the acid catalyst used (PTSA or amberlyst-15). The best results were achieved with 200%wt of amberlyst-15 and UHP after a reaction time of 19 hours. The hydroperoxide **61** could be prepared in 79% yield together with 15% of **62**.

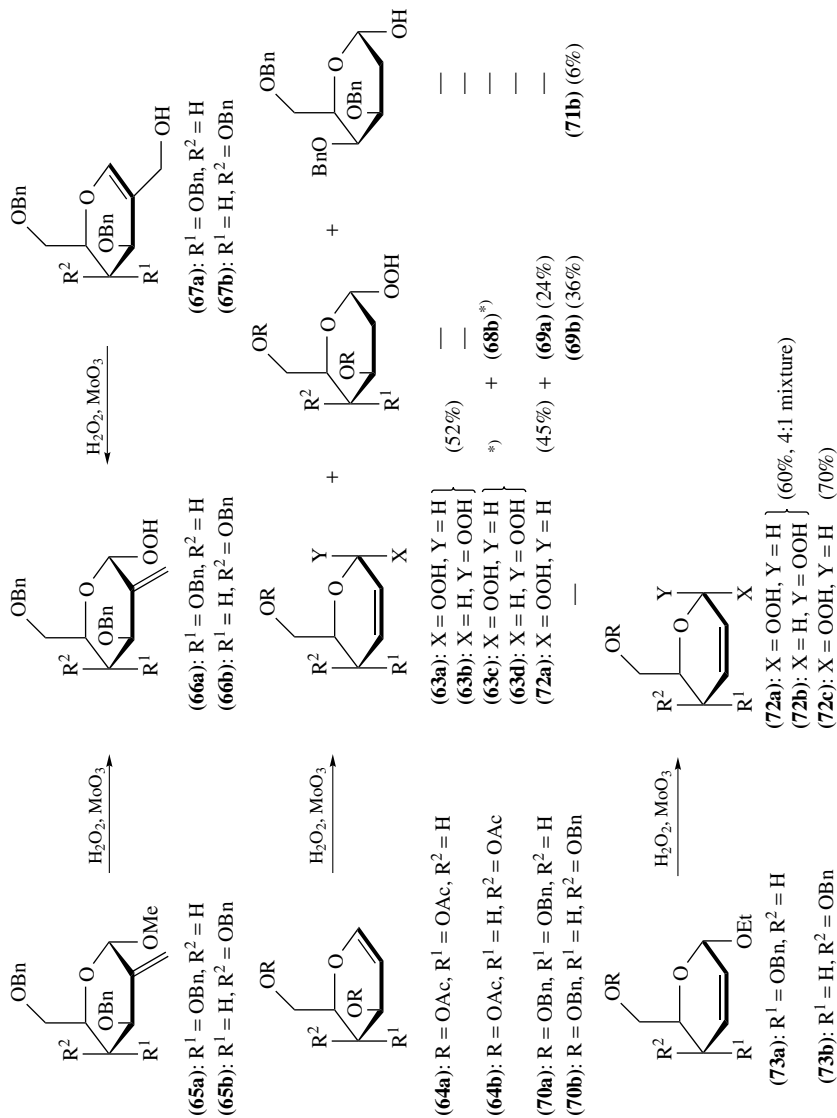
In 1987, Chmielewski and coworkers reported for the first time on the preparation of enantiomerically pure hydroperoxides **63a** and **63c** derived from carbohydrates¹⁸. The method employed consisted of the oxidation of 2,3-unsaturated glycosides (**64a** and **64b**, see Scheme 29) with hydrogen peroxide in the presence of a MoO_3 catalyst. The hydroperoxides **63a** and **63c** were isolated together with their β -anomers (**63b** and **63d**).



SCHEME 28. Stereoselective synthesis of camphor-derived tertiary hydroperoxides

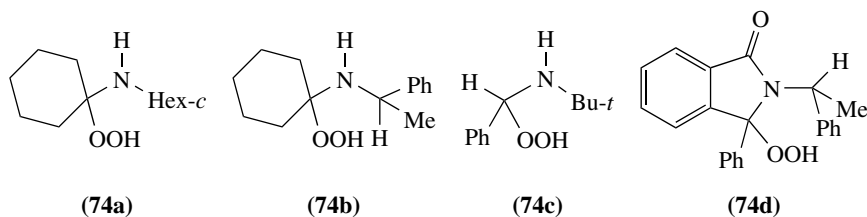
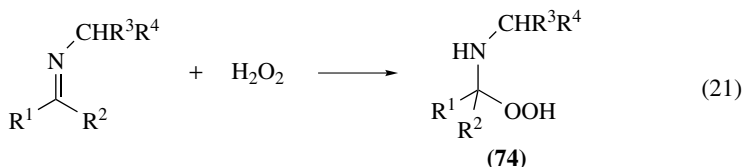


Hamann and coworkers⁶⁶ and Chmielewski and coworkers^{100, 101} could extend the range of carbohydrate-derived hydroperoxides (see Scheme 29)^{66, 100, 101}. The hydroperoxides **66a** and **66b** carrying an exocyclic double bond were prepared in 65–75% yield from the glycosides **65a** and **65b**, or alternatively from the hydroxymethylglycals **67a** and **67b** under the same conditions but with lower yields (30–40%). As by-products, two epoxides arising from intramolecular *O*-transfer in the presence of MoO₃ catalyst were obtained in yields of 6 and 2.5%. Oxidation of glucals **64a** and **64b** led to the formation of an anomeric mixture of hydroperoxides **63** as main products. Depending on the substitution pattern of the carbohydrate scaffold, saturated hydroperoxides **68/69** were formed besides the unsaturated hydroperoxides. In the case of the galactal **70b**, no unsaturated hydroperoxide **72b** was produced but saturated **69b** and the hemiacetal **71b**. The unsaturated carbohydrate hydroperoxides **72** can also be synthesized from the glycosides **73** by hydrogen peroxide oxidation. With **73a** as substrate, the two anomers **72a** and **72b** were formed in a ratio of 4:1 while with **73b** as substrate only the α -D-*threo* anomer **72c** was formed.



SCHEME 29. Preparation of chiral carbohydrate hydroperoxides

Chiral α -aminohydroperoxides **74a–d** can also be prepared via oxidation with hydrogen peroxide starting from the corresponding alcohols, or alternatively from Schiff's bases (equation 21)^{102,103}. For example, the α -aminohydroperoxides **74a–c** were prepared from the corresponding Schiff's bases and hydrogen peroxide. These hydroperoxides seem not to be stable under epoxidation conditions but cyclize to oxaziridines. A more stable α -aminohydroperoxide **74d** was prepared by Rebek and McCready from the corresponding alcohol by nucleophilic substitution with hydrogen peroxide¹⁰². The diastereomers that were formed in the H_2O_2 addition were separated by column chromatography.



B. Synthesis of Dialkyl Peroxides

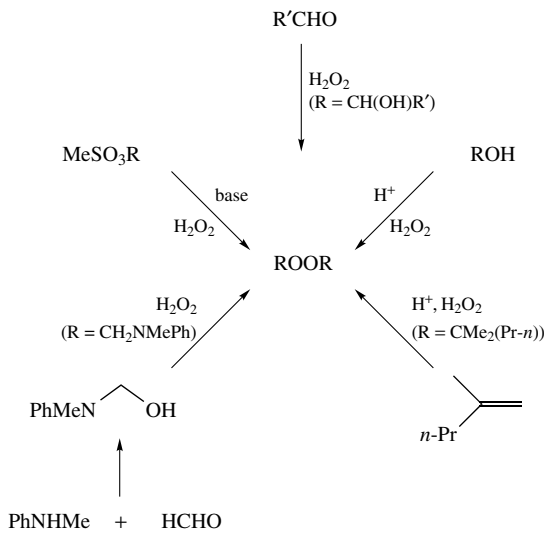
In this Section, we will focus on acyclic dialkyl hydroperoxides and we will not discuss cyclic peroxides. Dioxiranes are discussed in Chapter 14 and dioxetanes in Chapter 15 of this book.

1. General methodology

The methods for the preparation of dialkyl peroxides can in principle be divided into three categories: (i) acid- or base-catalyzed, (ii) metal-catalyzed and (iii) photochemical.

a. Acid- or base-catalyzed synthesis of dialkyl peroxides. The general methodology for this kind of reaction is the reaction of hydrogen peroxide or alkyl hydroperoxides with alkylating reagents in the presence of catalytic amounts of acid or base. Some examples for the preparation of symmetrical dialkyl peroxides are shown in Scheme 30. These compounds can be prepared from alkyl sulfonates^{104,105}, tertiary alcohols¹⁰⁶, alkenes¹⁰⁷, aldehydes¹⁰⁷ or α -dialkylaminomethanol (generated from secondary amines and formaldehyde)¹⁰⁸ by reaction with hydrogen peroxide leading to dialkyl peroxides, di-(tertiary alkyl) peroxides, di(α -hydroxyalkyl) peroxides and dialkyl aminomethyl peroxides.

Unsymmetrical dialkyl peroxides can be prepared by several methods. Some of them are summarized in Scheme 31. Primary¹⁰⁹, secondary or tertiary^{110,111} alkyl hydroperoxides can serve as substrates and are converted to the dialkyl peroxides by acid- or base-catalyzed nucleophilic substitution with alkylating agents like dialkyl sulfate¹⁰⁹, diazomethane¹⁰⁹, dialkyl sulfites, alcohols¹¹¹ or alkyl halides (e.g. in the presence of silver trifluoroacetate)^{5,110}. An overview of the results obtained utilizing the method mentioned above is given in Table 7.

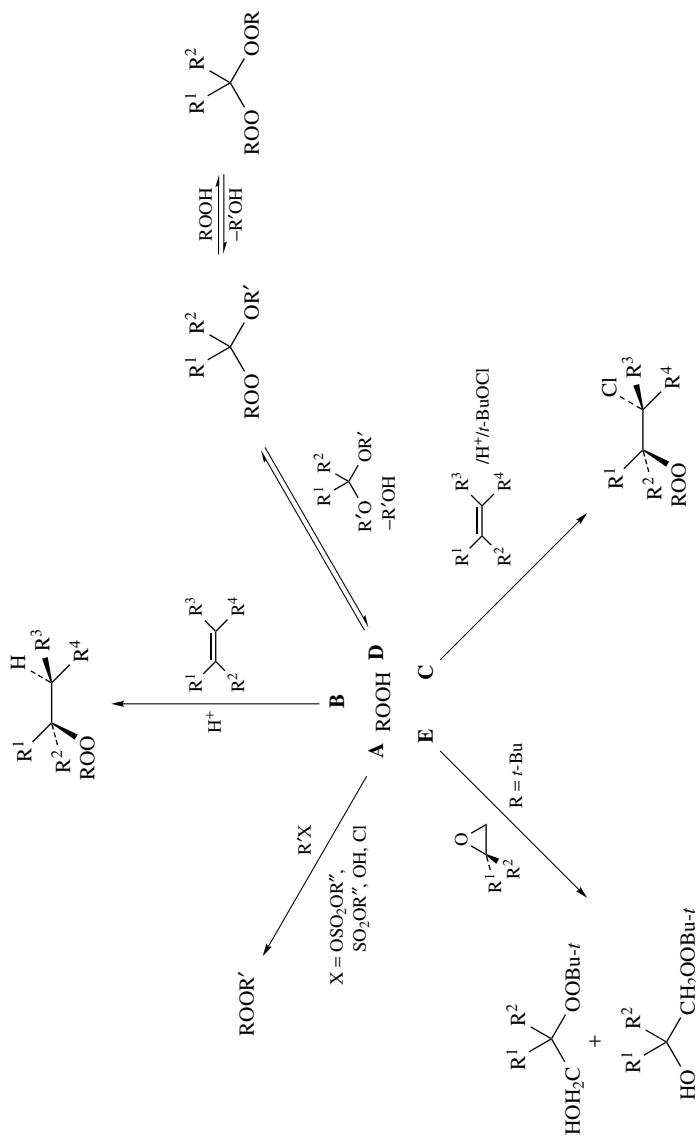


SCHEME 30. Preparation of symmetrical dialkyl peroxides

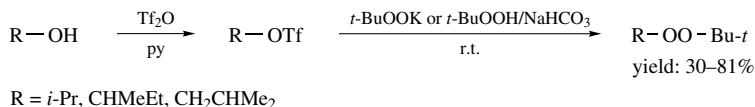
TABLE 7. Yields of dialkyl peroxides prepared by different methods

Dialkyl peroxide product	ROH (or alkene)/ H ₂ SO ₄ / H ₂ O ₂ (30%)	ROOH/ R'HSO ₄ (R'OH + H ₂ SO ₄)	MePhNH/ CH ₂ O/ H ₂ O ₂	<i>t</i> -BuOOK/ RBr	ROSO ₂ Me/ H ₂ O ₂ /KOH
Reference	106	106, 111	108	110	104
(<i>n</i> -BuO) ₂					48
(<i>s</i> -BuO) ₂					17
(<i>i</i> -BuO) ₂					10
(<i>n</i> -PenO) ₂					57
(<i>i</i> -PenO) ₂					50
(<i>n</i> -HexO) ₂					62
(2-HexO) ₂					28
(<i>n</i> -HepO) ₂					72
(<i>t</i> -BuO) ₂	up to 85 (HP ^a as side product)	92 ¹⁰⁶		100	
(Et ₃ CO) ₂		19 ¹¹¹			
<i>t</i> -BuOOCEt ₂ CEt ₃		41 ¹¹¹			
<i>t</i> -BuOOME				80	
<i>t</i> -BuOOEt				80–85	
<i>t</i> -BuOOPr- <i>i</i>				38	
<i>t</i> -BuOOBu- <i>n</i>				29	
<i>t</i> -BuOOBu- <i>i</i>				30	
<i>t</i> -BuOOCMe(Et)(Ph)	64 ¹¹³				
(<i>t</i> -PenOOBu- <i>t</i>)	68 ¹¹³				
[MePhNCH ₂ O] ₂			83		
[Me(<i>p</i> -Tol)NCH ₂ O] ₂			77		
(EtPhNCH ₂ O) ₂			85		
[Me(2,4,6-Me ₃ C ₆ H ₂) NCH ₂ O] ₂			70		
[BnPhNCH ₂ O] ₂			73		

^a HP = hydroperoxide.

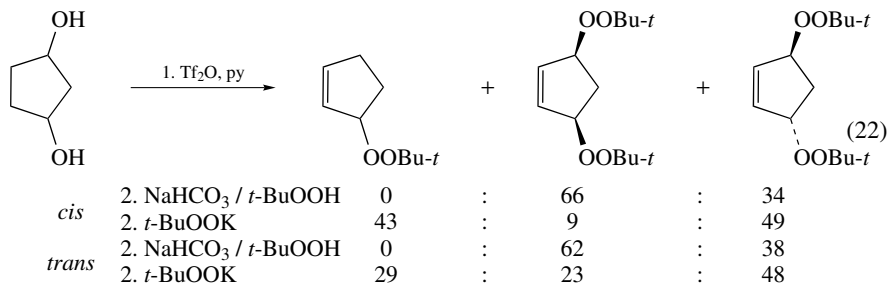


SCHEME 31. Preparation of unsymmetrical dialkyl peroxides

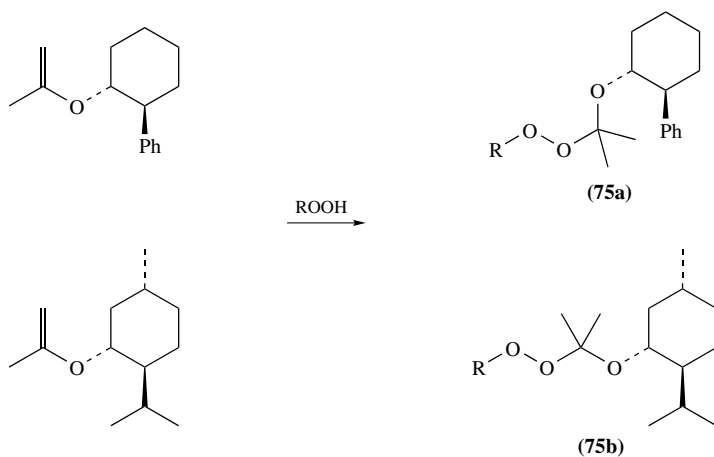


SCHEME 32. Synthesis of mixed dialkyl peroxides from triflates

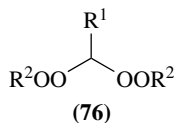
Salomon and coworkers reported on the synthesis of mixed peroxides from primary or secondary trifluoromethanesulfonates and either potassium *tert*-butyl peroxide or *tert*-butyl hydroperoxide in the presence of sodium bicarbonate under very mild conditions¹¹² (Scheme 32). With potassium *tert*-butyl peroxide high yields of primary–tertiary peroxides and moderate yields of secondary–tertiary peroxides could be obtained. Using this methodology 1,3-cyclopentane bis(*tert*-butyl) peroxides are readily prepared according to equation 22. Taking either *t*-BuOOK or NaHCO₃/*t*-BuOOH as peroxidic reagent, the stereochemistry of the starting cyclopentane-1,3-diol (*cis* or *trans*) is lost during the reaction. Independent of the relative configuration of the starting diols, *cis*-bisperoxide was favored under non-alkaline conditions and the *trans*-bisperoxide was predominantly formed when the alkaline potassium *tert*-butyl peroxide method was used. In the first case no elimination side product was obtained, while with KOObu-*t* as reagent *tert*-butyl 3-cyclopentenyl peroxide was observed as side product in significant amounts (29–43% of the product mixture). For monotriflates, products of higher purity are usually obtained by reaction with potassium *tert*-butyl peroxide rather than with hydroperoxide in the presence of sodium bicarbonate.



An alternative method for dialkyl peroxide synthesis is the nucleophilic addition of an alkyl hydroperoxide to an alkene under acid catalysis reported by Davies and coworkers (Scheme 31, path B)¹¹³. A similar reaction is the nucleophilic addition of alkylhydroperoxides to vinyl ethers under acid catalysis, producing perketals. Perketals can be deprotected under mild conditions (THF/water/acetic acid) and this hydroperoxide protection–deprotection sequence has been used by Dussault and Porter as a means for the resolution of racemic hydroperoxides (see also Section II.A.2)⁶⁷. In this respect more detailed studies were carried out with the perketals **75**, which were prepared via reaction of alkyl hydroperoxides with vinyl ethers (Scheme 33). Weissmermel and Lederer reported that in the presence of *tert*-butyl hypochlorite, α -chlorodialkyl peroxides can be formed in yields between 12% and 45% (Scheme 31, path C)¹¹⁴. α -Alkoxydialkyl peroxides and diperoxyacetals were prepared by Rieche and coworkers via acid catalyzed reaction of one or two equivalents of alkyl hydroperoxides with acetals, ketals or aldehydes (Scheme 31, path D)¹¹⁵ or by methylation of the corresponding α -alkoxy hydroperoxides with diazomethane (yields: 11%, 27%)¹¹⁶. The diperoxyacetals **76** were isolated in yields ranging from 39 to 77%.



SCHEME 33. Perketal formation by reaction of alkyl hydroperoxides with vinyl ethers



$\text{R}^1 = \text{Me, Et, } n\text{-Pr}$

$\text{R}^2 = n\text{-Pr, } i\text{-Pr, } t\text{-Bu}$

Between 1953 and 1983 several reports on the acid- and base-catalyzed reaction of hydroperoxides with epoxides, giving a mixture of β -hydroxydialkyl peroxides of different substitution, were published (Scheme 31, path E)^{117-120, 121}. A summary of the compounds and yields obtained is given in Table 8. Under base catalysis (10% NaOH) Kropf and coworkers reported that conversions were best in the heterogeneous solvent mixture tetrachloroethylene/water (yields up to 53%)¹²⁰. Reaction of hydroperoxides with epoxides bearing an electron-withdrawing substituent did not take place at all in the presence of NaOH as base (Table 8, entries 6, 16) and yields of dialkyl peroxides were generally lower with CHP compared to TBHP because of the lower nucleophilicity of the alkylperoxy anion. The authors also observed that the higher the steric demand of the epoxide, the lower the yields of the ring-opened product. A series of di(cycloalkyl) peroxides **77** could be synthesized by Druliner's group under phase transfer conditions by reaction of cycloalkylmethanesulfonates with potassium superoxide in the presence of a quaternary ammonium salt such as tetra-*n*-hexylammonium chloride as phase transfer catalyst¹²² (equation 23). By this method, the dicycloalkyl peroxides could be prepared in yields between 14 and 48%.

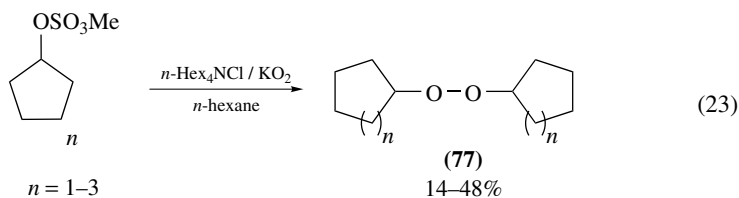


TABLE 8. Results of the synthesis of dialkyl peroxides through reaction of alkyl hydroperoxides with epoxides


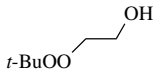
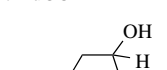
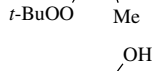
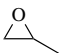
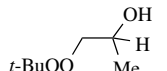
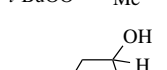
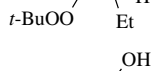
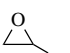
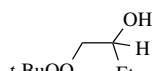
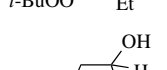
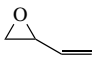
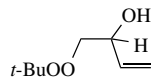
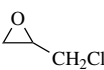
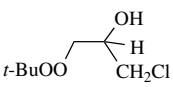
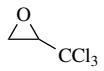
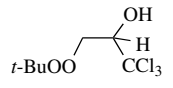
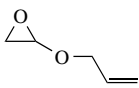
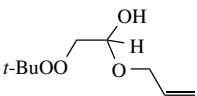
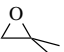
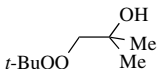
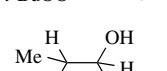
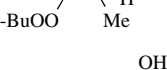

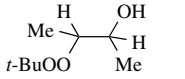

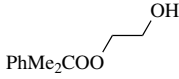
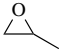
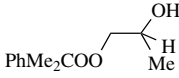
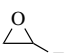
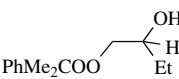

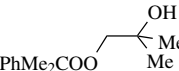
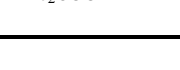
Entry	Substrate 1 ^a	Substrate 2	Product	Cat./method ^b	Yield ^c	Reference
1	TBHP			KOH	26 ^d	119
				NaOH (10%)	53 ^e	120
				A	61	117
2	TBHP			KOH	44 ^{d,f}	119
				NaOH (10%)	30 ^e	120
				A	42	117
3	TBHP			NaOH (10%)	28 ^e	120
				B	47	117
4	TBHP			B	33	117
5	TBHP			B	56	117
6	TBHP			NaOH (10%) B	0 ^e 15	120 117
7	TBHP			B	25	117
8	TBHP			H ₂ SO ₄ KOH	20 37 ^{d,f}	118 119
				NaOH (10%)	34 ^e	120
				A	45	117
9	TBHP			NaOH (10%) A	6 ^e 16	120 117
10	CHP			NaOH (10%) A	46 ^e 48	120 117
11	CHP			NaOH (10%) A	27 ^e 36	120 117
12	CHP			NaOH (10%) B	24 ^e 27	120 117
13	CHP			NaOH (10%)	30 ^e	120
				A	32	117

TABLE 8. (continued)

Entry	Substrate 1 ^a	Substrate 2	Product	Cat./method ^b	Yield ^c	Reference
14	CHP			NaOH (10%) A	2 ^e 7	120 117
15	PhCH ₂ CMe ₂ OOH			NaOH (10%)	44 ^e	120
16	TBHP or CHP or PhCH ₂ CMe ₂ OOH			NaOH (10%)	0 ^e	120
17	TBHP			B	41	117
18	TBHP			B	65	117

^a TBHP = *tert*-butyl hydroperoxide, CHP = cumyl hydroperoxide.

^b **A** = Al₂O₃ as catalyst, 4% hydroperoxide related to Al₂O₃; **B** = Al₂O₃ as catalyst, 10% hydroperoxide related to Al₂O₃; **C** = Al₂O₃ as catalyst, 20% hydroperoxide related to Al₂O₃.

^c Referred to oxirane.

^d In Et₂O/H₂O.

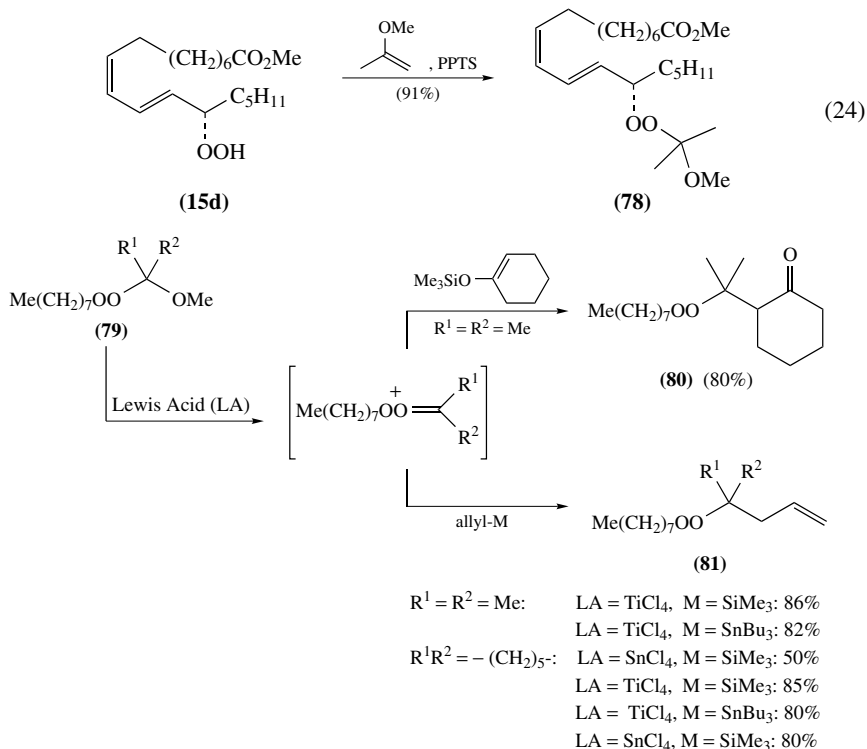
^e In tetrachloroethylene/H₂O.

^f Crude product.

^g R¹ = H, R² = Ph, C(O)Ph; R¹ = R² = CO₂Et; R¹R² = C(O)NHC(O)NHC(O).

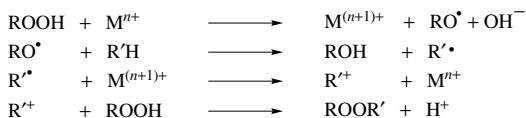
Dussault published a methodology for the synthesis of peroxide containing natural products. One step in the preparation of fatty acid derived hydroperoxides⁸³ was the protection of the hydroperoxy group of **15d** via acid-catalyzed reaction with 2-methoxypropene to give the diene monoperoxyketal **78** (equation 24), which is stable enough to survive reaction conditions such as Wittig olefination. The homologated hydroperoxides are liberated easily by acidic deprotection. This methodology can also be used for the preparation of enantiomerically enriched fatty acid hydroperoxides from racemic ones and has already been discussed in Section II.A.2 (Scheme 18)⁶⁷. The procedure includes the formation of diastereomeric dialkyl peroxides (monoperoxyketals) from racemic fatty acid hydroperoxides and 'Porter's enol ether', the 2-propenyl ether of *trans*-2-phenylcyclohexanol, followed by separation of the diastereomers by analytical or semi-preparative HPLC. The same author described a new methodology for the synthesis of dialkyl peroxides using a strategy in which peroxycarbenium ions are attacked by carbon nucleophiles (Scheme 34)¹²³. Dussault and Lee started from monoperoxyketals **79**, which are prepared as described above. Later it was observed that acetals also undergo displacements, but at significantly higher temperatures (-30°C compared to -78°C for peroxyketals). In the presence of Lewis acids such as TiCl₄ or SnCl₄, an alkoxy anion is split off, generating peroxycarbenium ions as intermediates which are able to undergo both inter- and intramolecular trapping with electron-rich alkene nucleophiles like allylsilanols or -stannanes. Intermolecular trapping leads to the new acyclic dialkyl peroxides **80** and **81** in good yields, whereas cyclic peroxides are formed by intramolecular trapping. For good

yields in this reaction, the order of adding the reagents is essential. Better yields were obtained by addition of the allylsilane (-stannane) to a solution of the monoperoxy ketal and the Lewis acid than vice versa.



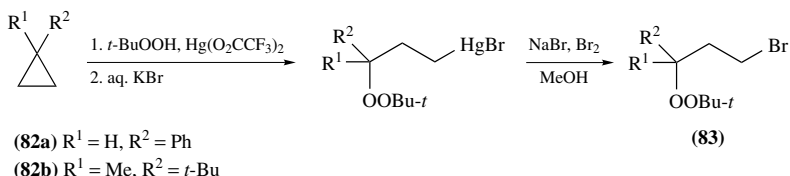
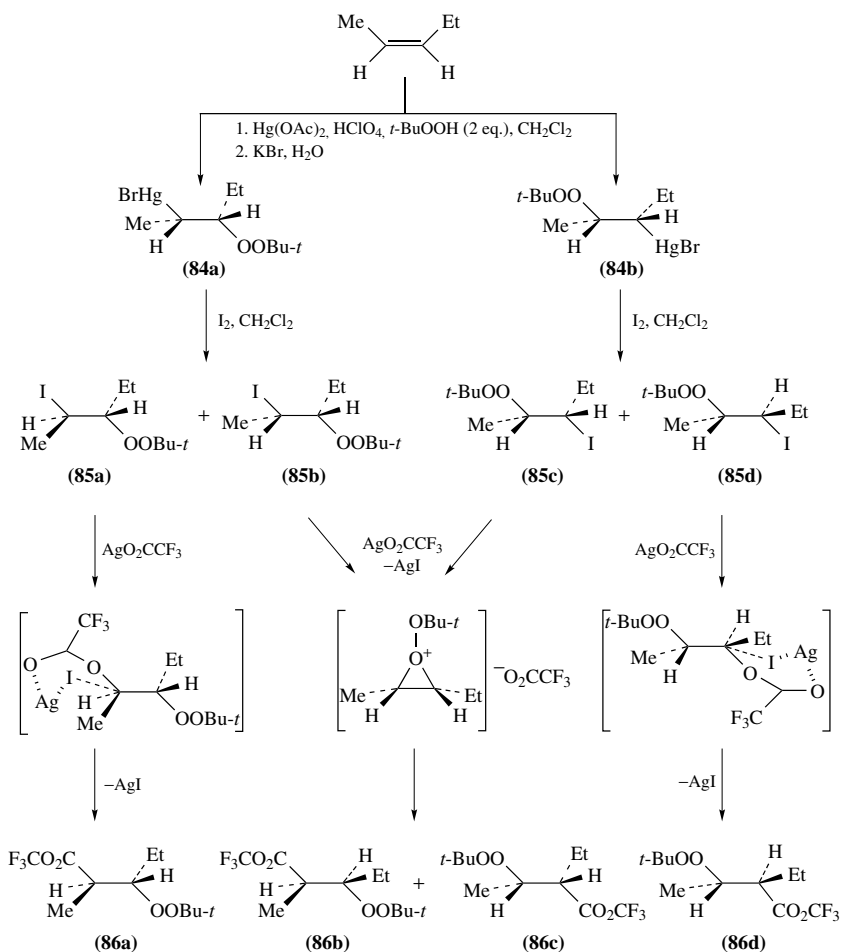
SCHEME 34. New dialkyl peroxides via addition of nucleophiles to peroxycarbenium ions

b. Metal-catalyzed synthesis of dialkyl peroxides. This methodology has been widely used to prepare dialkyl peroxides from alkyl hydroperoxides and various substituted alkanes or alkenes in the presence of metal ions like Cu⁺¹²⁴, Co²⁺¹²⁵ or Pb²⁺¹²⁶. Yields are generally better with copper catalysts. The general mechanism for this reaction is shown in Scheme 35.



SCHEME 35. Metal-catalyzed synthesis of dialkyl peroxides

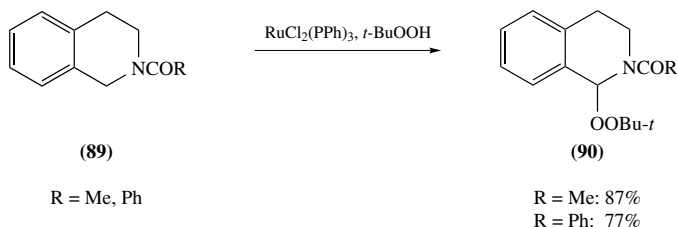
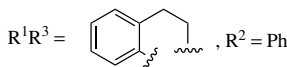
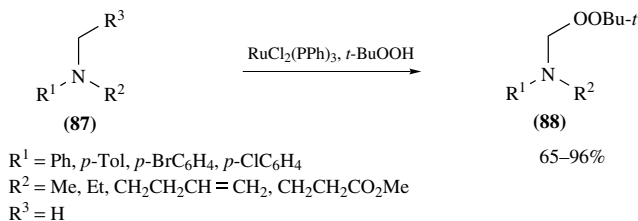
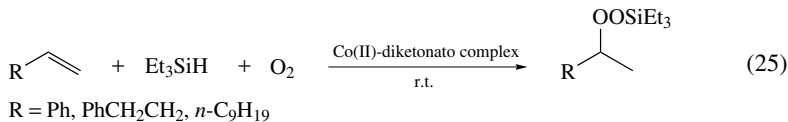
Cyclopropanes **82** can be converted to the corresponding γ -bromoalkyl *tert*-butyl peroxides **83** employing a method published in 1982 by Bloodworth and Courtneidge¹²⁷, which uses peroxymercuration and subsequent bromodemercuration (Scheme 36). Peroxymercuration is also useful to prepare α -iodo- β -*tert*-butylperoxyethanes **85** from olefins as shown by Bloodworth and coworkers in 1987¹²⁸ (Scheme 37). The *trans*-addition of

SCHEME 36. Synthesis of γ -bromoalkyl *tert*-butyl peroxide

SCHEME 37. Synthesis of dialkyl peroxides via peroxymercuration

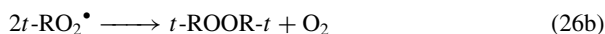
mercuric acetate and *tert*-butyl hydroperoxide to the olefin followed by acetate/bromine exchange leads to two regioisomers **84a** and **84b**, which react with iodine to give mixtures of stereoisomers **85a** and **85b** and **85c** and **85d**. These react with silver trifluoroacetate to give dialkyl peroxides **86a–d**.

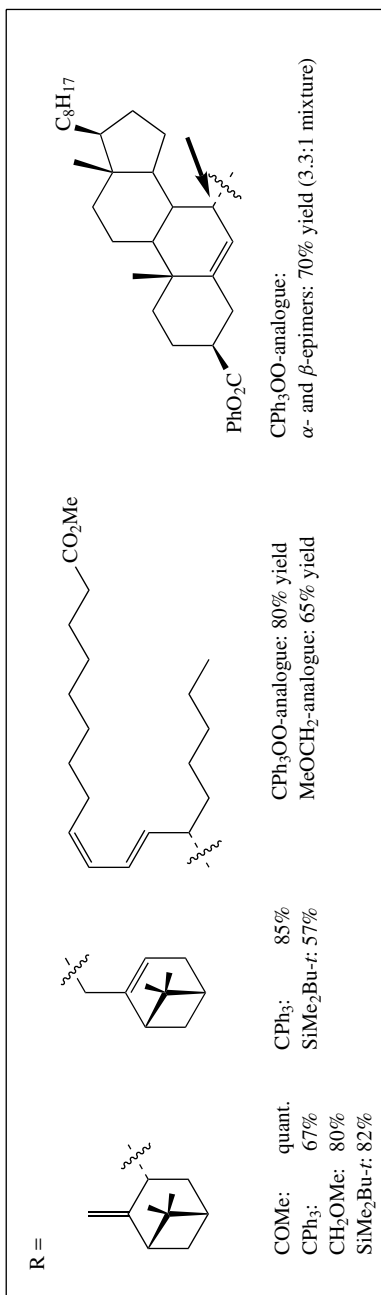
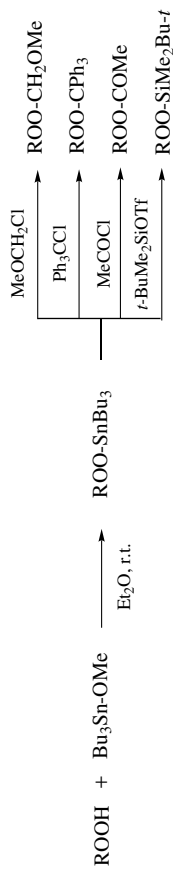
In 1989, a method for the peroxysilylation of alkenes using triethylsilane and oxygen was reported by Isayama and Mukaiyama¹²⁹ (equation 25). The reaction was catalyzed by several cobalt(II)-diketonato complexes. With the best catalyst Co(modp)₂ [bis(1-morpholinocarbamoyl-4,4-dimethyl-1,3-pentanedionato)cobalt(II)] product yields ranged between 75 and 99%. Dialkyl peroxides can also be obtained starting from tertiary amines **87**, amides **89** or lactams via selective oxidation in the α -position of the *N*-functional group with *tert*-butyl hydroperoxide in the presence of a ruthenium catalyst as presented by Murahashi and coworkers in 1988¹³⁰ (Scheme 38). With tertiary amines **87** as substrates the yields of the dialkyl peroxide products **88** ranged between 65 and 96%, while the amides **89** depicted in Scheme 38 are converted to the corresponding peroxides **90** in yields of 87% (R = Me) and 77% (R = Ph).



SCHEME 38. Ruthenium-catalyzed reaction of tertiary amines and amides with TBHP

c. Synthesis of dialkyl peroxides by autoxidation. Like alkyl hydroperoxides, also dialkyl peroxides can be synthesized by autoxidation of alkanes whereby low oxygen pressure is used. For the formation of dialkyl peroxides, alkylperoxy radicals have to couple with alkyl radicals or two alkylperoxy radicals combine to form dialkyl peroxides and molecular oxygen¹³¹ (equations 26a and 26b). A clean conversion can only take place when the intermediate alkyl radicals formed during the reaction are well resonance-stabilized. Therefore, the autoxidation of triphenylmethane resulting in the formation of bis(triphenylmethyl) peroxide upon acidification¹³² is a good example for this kind of reaction. Less stabilized radical intermediates show lower rate constants for the formation of dialkyl peroxides (see Table 9).





SCHEME 39. Synthesis of dialkyl peroxides from stanny peroxides

TABLE 9. Rate constants for the formation of di-tertiary alkyl peroxides from tertiary alkylperoxy radicals¹³¹

Peroxy radical	Me ₃ CO ₂ •	Me ₂ PhCO ₂ •	MePh ₂ CO ₂ •
$k[(M^{-1}s^{-1}) \times 10^{-3}]$	1.2	6.0	64

d. Synthesis from stannyl peroxides. In 1990, Haynes and Vonwiller could show that stannyl peroxides are useful precursors for the preparation of various peroxide derivatives, such as alkyl triphenylmethyl peroxides and alkyl methoxymethyl hydroperoxides (Scheme 39)¹³³. The stannyl hydroperoxides are prepared in quantitative yield from alkyl hydroperoxides and tributyltin methoxide. They are unstable and therefore are immediately converted to the dialkyl peroxides via reaction with reagents like acetyl chloride, triphenylmethyl chloride, chloromethyl methyl ether or *tert*-butyldimethylsilyl triflate. With primary and secondary hydroperoxides, the reaction sequence proceeds with good yield (57% to quant.), whereas with tertiary peroxides the intermediate peroxides sometimes undergo rearrangement reactions.

C. Synthesis of Hydrogen Peroxide

Hydrogen peroxide is one of the most essential chemicals for pulp bleaching, waste treatment and chemical production. It is the most promising major oxidant for green chemistry, because it is one of the oxidants with the highest atom economy (47% by weight of 'active' oxygen) and therefore is of great synthetic utility. Hydrogen peroxide is commercially available in different forms: aqueous solutions up to a concentration of more than 90%, urea hydrogen peroxide clathrate, percarbonate and perborate. The most commonly employed forms of hydrogen peroxide are the aqueous solutions, 30% and 50% being routinely applied for laboratory uses.

A variety of publications on the synthesis of hydrogen peroxide have appeared during the years¹³⁴, but will not be discussed further in this review.

III. SYNTHETIC USES OF PEROXIDES

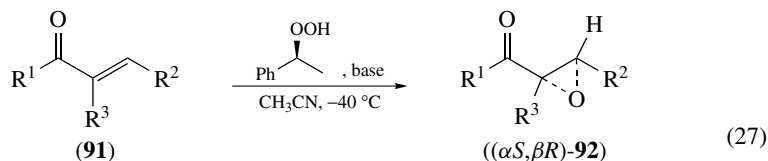
A. Epoxidation of C=C Double Bonds

The field of olefin epoxidation can be divided into three major categories: the epoxidation of (i) electron-poor olefins, (ii) allylic alcohols and (iii) unfunctionalized olefins. Each of these reactions has specific requirements. Because electron-poor olefins like α,β -unsaturated carbonyl compounds show reduced reactivity towards electrophilic oxidants, it is necessary to employ peracids with strong oxidizing ability like trifluoroperacetic acid¹³⁵ or better nucleophilic oxidants such as alkaline solutions of hydrogen peroxide or alkyl hydroperoxides (Weitz–Scheffer epoxidation via nucleophilic 1,4-addition¹³⁶). Many methods for these epoxidations have been published. Some require basic conditions and no catalyst is needed. These are discussed in Section III.A.1. Epoxidations of α,β -enones under bi- or triphasic conditions employing chiral phase transfer catalysts or polyamino acids as catalysts are reviewed in Section III.A.2. The few examples of metal catalyzed variants of this reaction are presented in Section III.A.3.a. Contrary to electron poor olefins, unsubstituted alkenes (electronically neutral) or allylic alcohols (electron-rich) show a higher reactivity in epoxidation reactions. Various epoxidation methods utilizing transition metal catalysis are established. These will be discussed in Section III.A.3 focusing on asymmetric variants and methods with remarkable synthetic

utility. The epoxidation of allylic alcohols and the epoxidation of unfunctionalized olefins will be discussed separately because of the difference in reaction mechanisms.

1. Uncatalyzed and base-catalyzed epoxidations

Compared to metal-catalyzed asymmetric epoxidation reactions, asymmetric versions of this reaction without the need of a catalyst (apart from a base) are rarely known. In 2000 Adam and coworkers reported a method for the asymmetric Weitz–Scheffer epoxidation of substituted enones **91** by the secondary, optically active hydroperoxide (*S*)-(1-phenyl)ethyl hydroperoxide (equation 27, Table 10)¹³⁷.



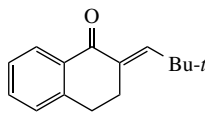
$\text{R}^1 = \text{Ph}, p\text{-Tol}, p\text{-MeOC}_6\text{H}_4, p\text{-BrC}_6\text{H}_4$

$\text{R}^2 = \text{Ph}, p\text{-Tol}, p\text{-MeOC}_6\text{H}_4, p\text{-O}_2\text{NC}_6\text{H}_4, \text{Me}, t\text{-Bu}$

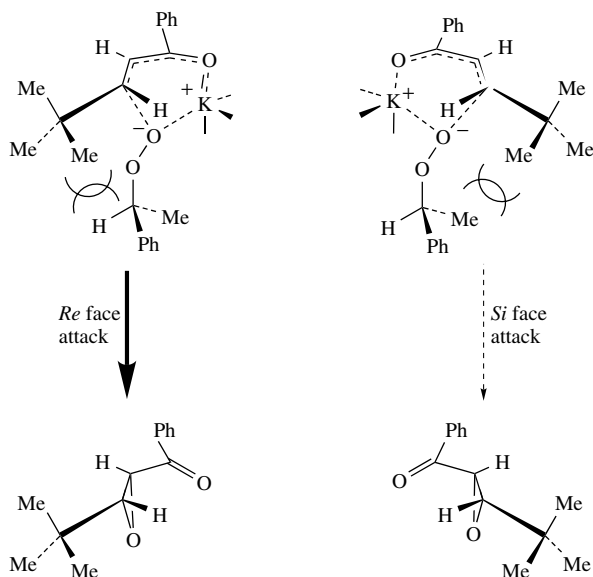
$\text{R}^3 = \text{H}$

With the help of this enantiomerically pure oxidant which was used in equimolar amount and an excess of potassium hydroxide as a base, it was possible to prepare epoxy ketones **92** with up to 99% yield and 90% *ee*. Substitution of the aromatic ring of the enone carbonyl function by *p*-Me, *p*-OMe or *p*-Br groups did not change the enantioselectivity. This is contrasted by the observation that *para*-substituents on the β -phenyl group influence the *ee* values considerably. Electron-withdrawing groups in this position lower the *ee* values while electron-donating groups like *p*-OMe increase the observed *ee* values. With DBU as base or KOH in the presence of 18-crown-6 cyclic ether the observed enantioselectivities dropped dramatically. Evidently, the potassium ion is important for the high enantiocontrol (Table 10). To explain the results, the authors proposed a transition state in which the favored attack of the optically active hydroperoxide on the *Re*-face of the *S*-*cis*-conformation of the enone is rationalized in terms of minimized steric repulsions between the substituents at the center of chirality of the hydroperoxide

TABLE 10. Enantioselective Weitz–Scheffer epoxidation of substituted enones $p\text{-XC}_6\text{H}_4\text{C}(\text{O})\text{CH}=\text{CR}$ with (*S*)-(1-phenyl)ethyl hydroperoxide

X	R	Base	Yield (%)	<i>ee</i> (%)
H	Ph	KOH	99	51
H	Ph	KOH/18-crown-6	94	6
H	Ph	DBU	84	9
Me, OMe, Br	Ph	KOH	95–98	48–54
H	<i>p</i> -Tol	KOH	97	57
H	<i>p</i> -MeOC ₆ H ₄	KOH	96	61
H	<i>p</i> -O ₂ NC ₆ H ₄	KOH	98	42
H	<i>t</i> -Bu	KOH	95	75
		KOH	90	90

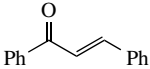
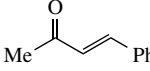
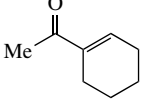
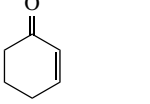
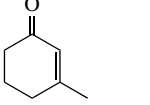
and the enone β -substituent. The simultaneous coordination of the metal ion to the α,β -enone and hydroperoxide (template effect) is responsible for the good enantioselectivity (Scheme 40).



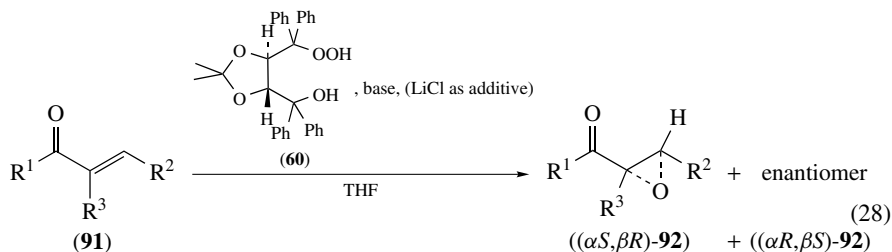
SCHEME 40. Metal template effect for the epoxidation of α,β -enones

Aoki and Seebach have developed the chiral, sterically demanding, tertiary hydroperoxide TADOOH **60** and investigated the capability of this optically pure oxidant to induce asymmetry in the Weitz–Scheffer epoxidation of enones **91a–e** (equation 28, Table 11)⁹⁸. In this reaction, good yields and high *ee* values of the corresponding epoxides **92** were obtained. The authors found out that the choice of base had a decisive influence on the yields and enantioselectivities obtained. In the series KOH, NaOH, LiOH, a reversal of the stereochemical course was observed (30:70, 45:55, 80:20 ratio of enantiomers) and high enantioselectivity was obtained only with LiOH or BuLi under totally aprotic conditions. This fact stresses the importance of the Li-counterion for good asymmetric induction. Two types of conditions were found to give the best results. The first one is the formation of the TADOOH–Li–salt by deprotonation with substoichiometric amounts of butyllithium, and reaction with the enone at low temperatures. By this method, the epoxyketone **92a** ($R^1 = R^2 = \text{Ph}$, $R^3 = \text{H}$) could be obtained after 120 hours in 80% yield and with an enantiomeric excess of the (2*S*,3*R*)-configured product of 97%. Better yields at shorter reaction times could be achieved by raising the temperature. In this case, lower enantioselectivities resulted (e.g. after 4 hours at 0 °C the epoxyketone **92a** was obtained in 94% yield and with an enantiomeric excess of 80%). By employing a catalytic amount of LiCl/DBU, a non-self-annihilating Lewis acid/base pair (temperature: $-78\text{ }^\circ\text{C} \rightarrow \text{r.t.}$), the yield of product **92a** after 7 hours was higher than with butyllithium (98%) but the enantiomeric excess of isolated epoxyketone was lower (68% *ee*). Other enones were also tested in the epoxidation reaction, employing butyllithium as base at $-30\text{ }^\circ\text{C}$. The products could be obtained in high yields and variable enantioselectivities (see Table 11). Aoki and Seebach proposed a model in which the enantioselectivity is

TABLE 11. Epoxidation of the α,β -enones **91** with chiral TADOOH **60** and BuLi (24 h at $-30\text{ }^\circ\text{C}$)

Substrate 91	Epoxide 92		
	yield (%)	enantiomeric ratio	
	91a	92	95:5 ($\alpha S,\beta R$)/($\alpha R,\beta S$)
	91b	74	89:11 ($\alpha S,\beta R$)/($\alpha R,\beta S$)
	91c	46	70:30
	91d	45	55:45 ($\alpha R,\beta R$)/($\alpha S,\beta S$)
	91e	74	91:9

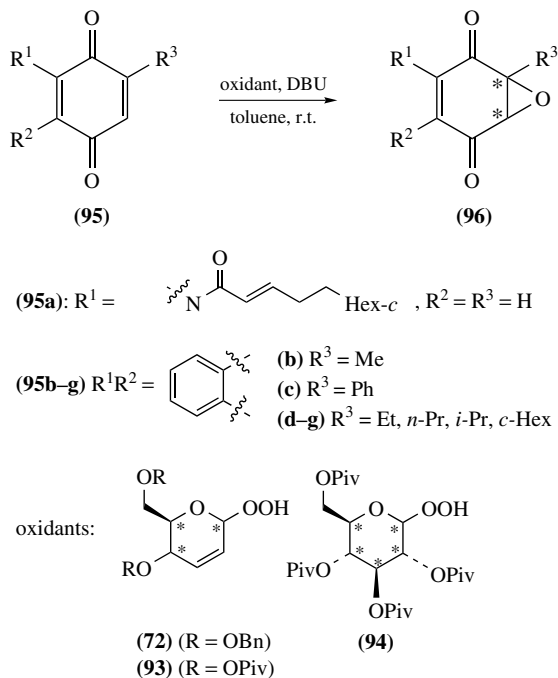
explained by a simultaneous coordination of the alkali ion to the carbonyl function of the substrate as well as the hydroperoxide.



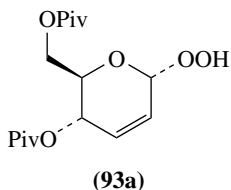
variation of base for substrate; $R^1 = R^2 = \text{Ph}$, $R^3 = \text{H}$:
 no conversion with NEt_3 , NEt_3/LiCl or DMAP
 65–98% yield with the other bases
er up to 98.5 : 1.5 (with BuLi as base)

base = NEt_3 , DMAP, KOH, NaOH, LiOH, BuLi, DBN, DBU

Besides the chiral, secondary hydroperoxides employed by Adam and coworkers and the tertiary hydroperoxide used by Seebach, the optically active carbohydrate hydroperoxides **72**, **93** and **94** have been tested by Taylor and coworkers in epoxidation reactions of the quinones **95** under basic conditions (Scheme 41)¹³⁸. The yields of the corresponding epoxides **96** that were obtained with this type of oxidant varied from 33 to 83% and the enantioselectivities were moderate and in some cases good (23 to 82%), depending

SCHEME 41. Epoxidation of quinones using chiral hydroperoxides **63**, **93** and **94**

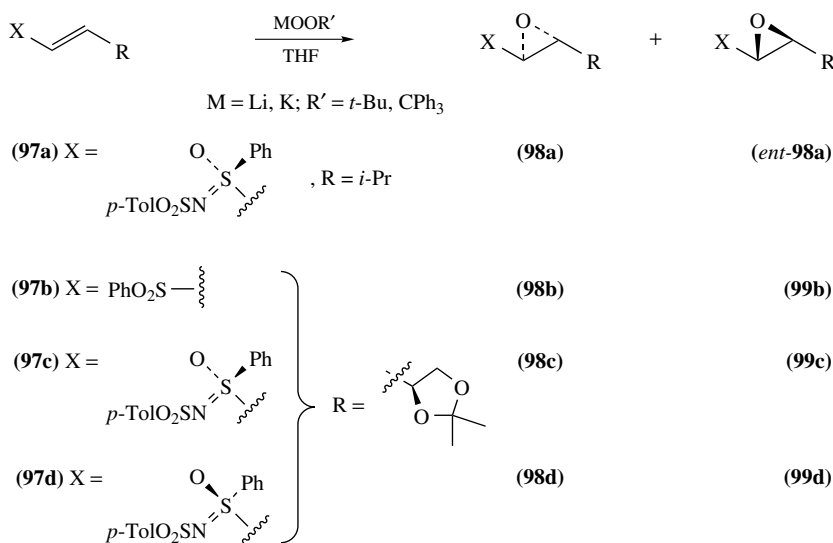
on the substitution pattern of the substrate as well as the carbohydrate hydroperoxide employed in the reaction. The best results were obtained with one diastereomer of **93**. With hydroperoxide **93a**, substrate **95c** could be epoxidized with a yield of 80% and an enantiomeric excess of 82%. With this chiral hydroperoxide vitamin K_3 and some of its analogues were epoxidized with yields of 30–80% and *ee* values ranging from 35 to 82%. The moderate enantioselectivity of 45% obtained for vitamin K_3 (**95b**) was the highest enantioselectivity reported for that substrate.



A further example for an uncatalyzed asymmetric epoxidation is the nucleophilic oxidation of vinyl sulfoximines with alkali alkyl peroxides. In 1993, it was reported by Jackson and coworkers that the epoxidation of vinyl *N*-tosylsulfoximines **97** ($X = \text{S(O)(Ph)NSO}_2\text{Tol-}p$, $R = \text{alkyl}$) using lithium *t*-butyl peroxide gives *N*-tosylsulfoximinooxiranes **98** in good yields (72–98%) and with extremely high diastereoselectivity (only one diastereomer was detected)¹³⁹. In these cases the asymmetric induction is substrate-induced. Epoxidation of **97**, bearing an alkyl group in α -position, turned out

to proceed much slower but nonetheless with the same high diastereoselectivity, leading to the same diastereomers. The combination of a bulky substituent at the β -position and any group larger than methyl at the α -position completely prevented any reaction. Recently this process was further investigated by the same group¹⁴⁰ (see Scheme 42, Table 12). Interestingly, with potassium *tert*-butyl peroxide they obtained almost no stereoselectivity. Epoxidation with lithium triphenylmethyl peroxide proceeded with very high diastereoselectivity (**98a/99a** : 25/1) whilst the same reaction with potassium triphenylmethyl peroxide resulted in formation of the epoxide with moderate selectivity of 4:1. The results clearly indicate an interaction between the lithium cation and the sulfoximine group during the reaction. Furthermore, the authors investigated the effect of an additional stereogenic center on the diastereoselectivity obtained (Table 12, entries 3 and 4). Potassium *tert*-butyl peroxide shows clear matched–mismatched effects while this is not the case for the other three peroxides (*t*-BuOOLi, Ph₃COOLi, Ph₃COOK). The diastereomeric ratios of epoxides **98** and **99** obtained with lithium triphenylmethyl peroxide as oxidant seem to be independent of the stereochemistry at the sulfoximine moiety (25:1).

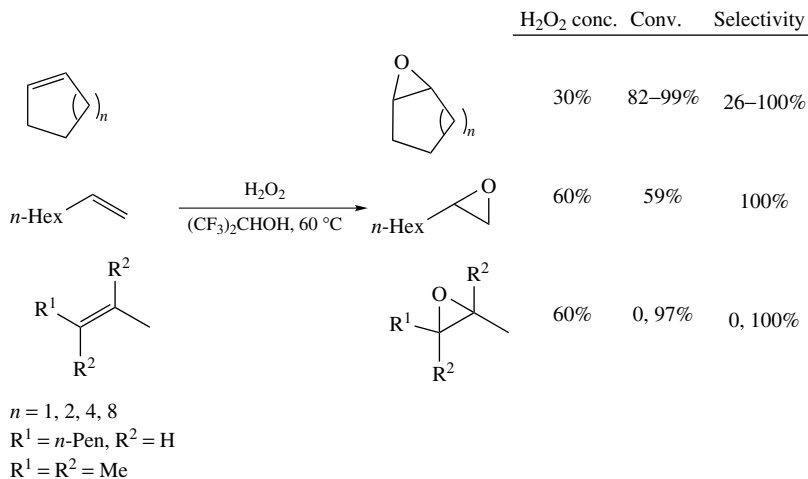
Next to the base-catalyzed asymmetric epoxidations of electron-deficient olefins with chiral hydroperoxides described above, a few examples of uncatalyzed epoxidations with



SCHEME 42. Diastereoselective epoxidation of vinylsulfoximines using different alkali peroxides

TABLE 12. Nucleophilic epoxidation of vinyl sulfoximines with alkali alkyl peroxides [diastereomeric ratios are given; in brackets the yields of the two diastereomers are shown]

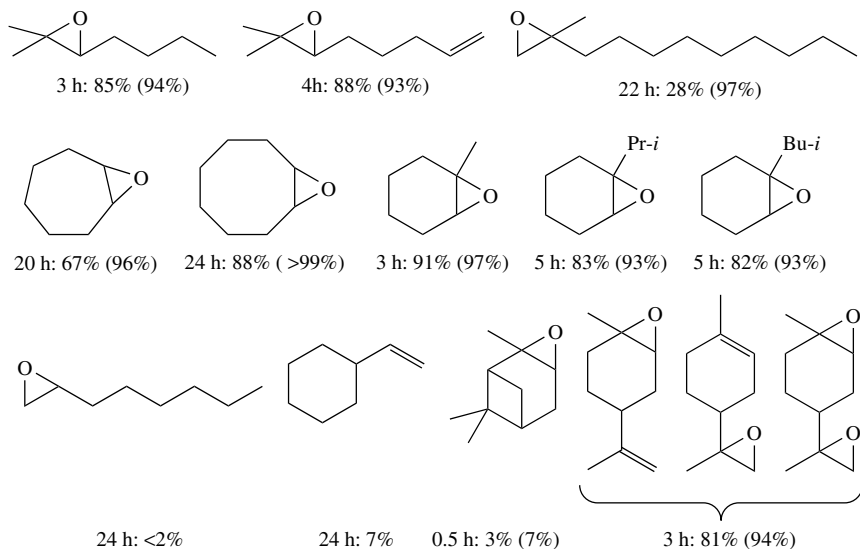
Alkene	Epoxides	<i>T</i> (°C)	<i>t</i> -BuOOLi [<i>dr</i> (yield)]	Ph ₃ COOLi [<i>dr</i> (yield)]	<i>t</i> -BuOOK [<i>dr</i> (yield)]	Ph ₃ COOK [<i>dr</i> (yield)]
97a	98a : 99a	−78	25:1 (97%)	25:1 (73%)	10:11 (76%)	4:1 (74%)
97b	98b : 99b	−20	4:3 (85%)	5:4 (78%)	4:1 (68%)	25:1 (76%)
97c	98c : 99c	−20	25:1 (68%)	25:1 (65%)	2:1 (80%)	25:1 (67%)
97d	98d : 99d	−20	2:1 (75%)	25:1 (76%)	6:1 (80%)	7:4 (74%)

SCHEME 43. Epoxidation of olefins with H₂O₂ in HFIP

hydrogen peroxide as oxidant are published in the literature. In 2000, Neimann and Neumann found that in 1,1,1,3,3,3-hexafluoro-2-propanol (HFIP) the epoxidation of olefins (as well as the Baeyer–Villiger oxidation, see Section III.F) can be carried out in the absence of a catalyst (Scheme 43)¹⁴¹. Hydrogen peroxide can be activated electrophilically due to the strong electron-withdrawing properties of fluorine in combination with the hydrogen-bonding properties of the OH hydrogen. Therefore, in HFIP as solvent various terminal, internal and cyclic aliphatic alkenes could be oxidized by 30% or 60% hydrogen peroxide at 60 °C with conversions ranging from 59–100% (3-nitrostyrene was epoxidized with only 39% conversion) and selectivities up to 100%. Styrene and 3-nitrostyrene yielded other oxidation products like phenylacetaldehyde and 3-nitrobenzaldehyde. One year later Sheldon and coworkers published an uncatalyzed epoxidation method in which they utilized fluorinated alcohols as solvents¹⁴². With trifluoroethanol at reflux or hexafluoro-2-propanol at room temperature it is possible to oxidize a variety of unfunctionalized alkenes to the corresponding epoxides with good conversions and selectivities. The epoxide products of this reaction together with necessary reaction time, conversions and selectivities (in parentheses) are shown in Scheme 44.

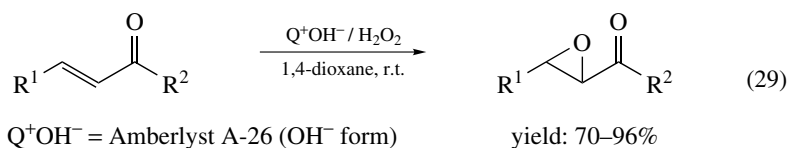
The best results were obtained by using relatively concentrated hydrogen peroxide (60%) in combination with a small amount of base like NaOAc, Na₂HPO₄ or Na₃EDTA in order to buffer the hydrogen peroxide solution. This method represents a useful strategy for the epoxidation of relatively reactive alkenes while less reactive substrates as α -pinene, 1-octene and vinylcyclohexane are poorly converted. In the same year Neumann and coworkers published their practical and theoretical studies on the alkene epoxidation by H₂O₂ in the presence of fluorinated alcohols¹⁴³. They could show that the fluoroalcohol itself acts as a catalyst by providing a charge template that stabilizes specifically the transition state of the reaction.

In 2001, Lakouraj and coworkers presented several reactions for which they employed amberlyst A-26 supported hydrogen peroxide as heterogeneous oxygen source¹⁴⁴. They found that this reagent has advantages over its homogeneous analog in terms of convenient reaction conditions, easier workup, high yield and selectivity. With this oxygen source it was possible to epoxidize α,β -unsaturated ketones in good yields (70–96%)



SCHEME 44. Products [yields and (selectivities)] of the uncatalyzed epoxidation in trifluoroethanol

(equation 29). The supported hydrogen peroxide is prepared *in situ* from 35% hydrogen peroxide and catalytic amounts of amberlyst A-26 (OH^-). Workup for this reaction is very easy and consists mainly of a simple filtration to separate the heterogeneous oxidant.



An alternative to the use of expensive fluorinated solvents is also represented by the method published in 2003 by Jacobs and coworkers¹⁴⁵. Hydrogen peroxide could be activated for electrophilic oxygen transfer in phenol as acidic solvent at temperatures between 20 and 60 °C (depending on the substrate) without the need of a metal catalyst (equation 30). With this method even acid-sensitive epoxides can be prepared very selectively accompanied by some diol and α -hydroxyphenyl ether. The best results are obtained by buffering the solution with a small amount of sodium acetate. In general, electron-rich double bonds are epoxidized with high reactivity while electron-poor double bonds are oxidized more slowly. Substituents on the aromatic ring of the solvent have a decisive influence on the reaction rate. Electron-withdrawing groups in *meta*- or *para*-position lead to an increase in rate, whereas alkyl groups in *meta*- or *para*-position lead to a decrease in reaction rate. The activation can be explained by formation of intermolecular hydrogen bonding between H_2O_2 and phenol (Figure 5, right side). Activation of hydrogen peroxide through hydrogen bonding to the solvent was also proposed by Neumann and coworkers¹⁴³, who reported on the H_2O_2 -activating effect of hexafluoroisopropanol (HFIP) (Figure 5, left side). A proof in favor of the proposed activation through hydrogen bonding is the fact that THF, which is an H-bonding acceptor, suppresses the

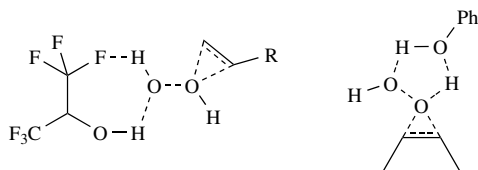
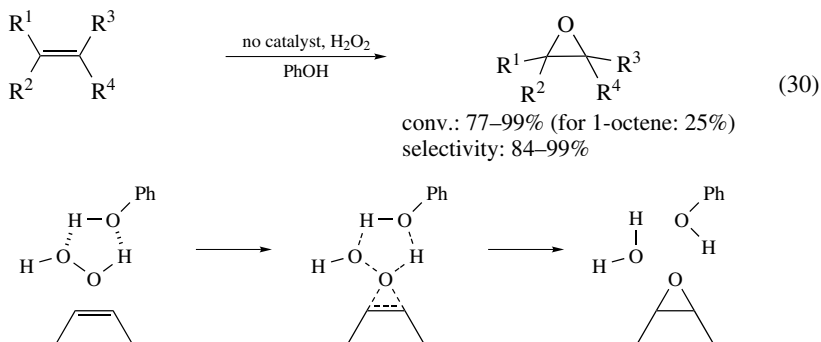


FIGURE 5

epoxidation reaction. The authors proposed the activation mechanism that is depicted in Scheme 45.

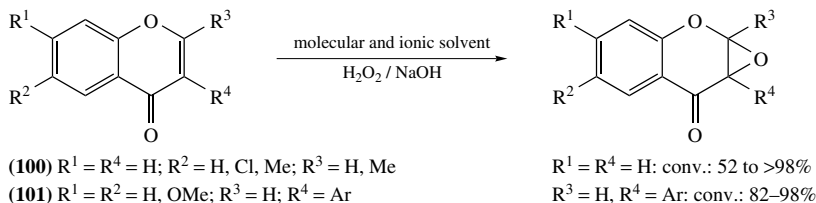
SCHEME 45. Hypothetical mechanism for epoxidation of alkenes by H_2O_2 in phenol

Very recently Bernini and coworkers reported on the epoxidation of chromones **100**, isoflavones **101** and chalcones **102** in ionic liquids using alkaline hydrogen peroxide as oxidant (Scheme 46)¹⁴⁶. The reactions in 1-butyl-3-methylimidazolium tetrafluoroborate proceed in good yields and faster than in conventional solvents. Depending on the substrate, at 0 °C or room temperature, reaction times for reaching high conversions were ≤ 2 hours. In the epoxidation reactions studied, no opening of the epoxide ring was observed.

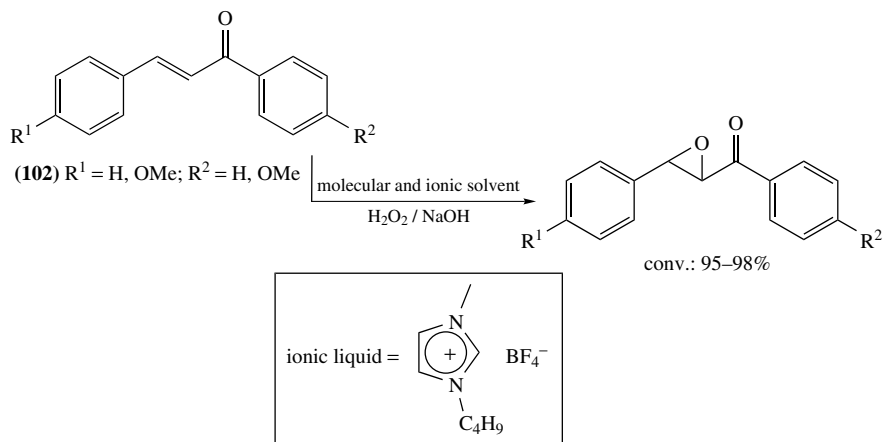
2. Organo-catalyzed epoxidations

One of the early examples for organocatalysis is the asymmetric Weitz–Scheffer epoxidation of electron-deficient olefins, which can be effected either by organic chiral phase transfer catalysts (PTC) under biphasic conditions or by polyamino acids. This reaction has gained considerable attention and is of great synthetic use.

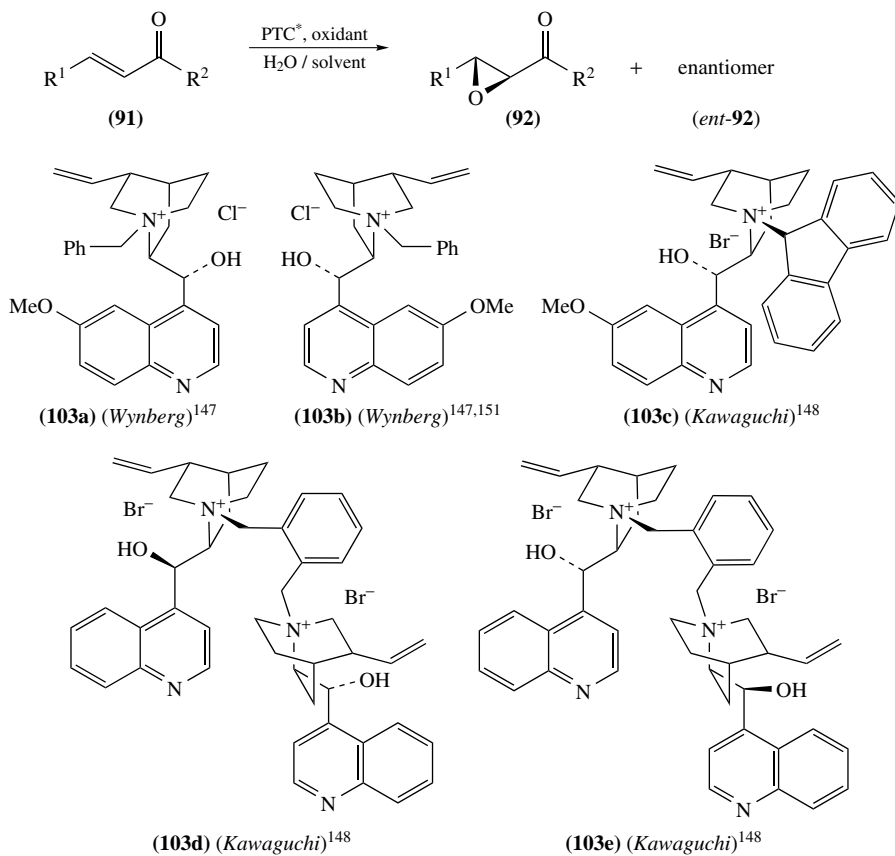
a. Phase-transfer catalysis. The biphasic approach utilizing phase-transfer catalysts was first investigated by Wynberg and coworkers in the mid-1970s (Scheme 47)¹⁴⁷. PTC **103a**



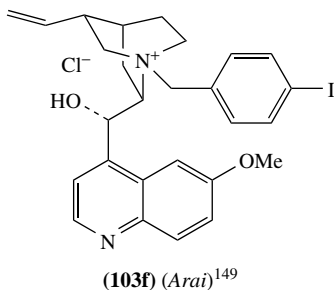
SCHEME 46. Epoxidation of chromones, isoflavones and chalcones



SCHEME 46. (continued)

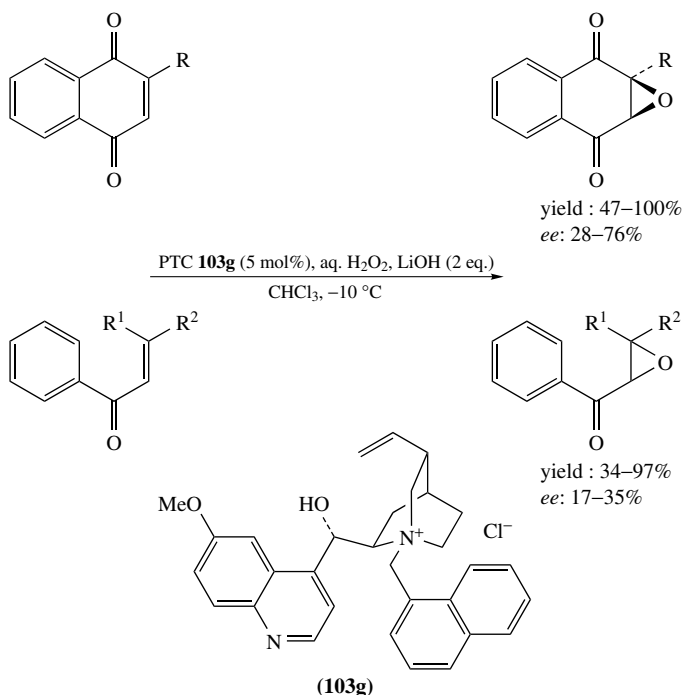


SCHEME 47. Phase-transfer catalyzed asymmetric epoxidation of enones



SCHEME 47. (continued)

and **103b** proved capable of catalyzing the asymmetric epoxidation of a wide range of acyclic enones and naphthoquinones, using aqueous hydrogen peroxide, *t*-butyl hydroperoxide or sodium hypochlorite as oxidant. Enantiomeric excesses up to 54% were observed. Utilizing the alkylated cinchona alkaloids **103c–e** Kawaguchi and coworkers were able to epoxidize cyclohexenone derivatives with enantiomeric excesses up to 63% (obtained with catalyst **103d** for the epoxidation of cyclohexenone)¹⁴⁸. Catalysts derived from cinchonine by alkylation with a range of *para*-substituted benzyl bromides (*p*-XC₆H₄CH₂Br, X = H, CF₃, Hal, NO₂) were presented by the group of Arai¹⁴⁹. The most effective and selective PTCs were the ones with an electron-withdrawing group at the *para* position



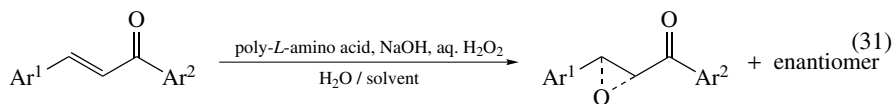
SCHEME 48. Catalytic asymmetric epoxidation of naphthoquinone derivatives under phase transfer catalyzed conditions

on the phenyl ring of the *N*-benzyl unit. The best results were obtained with compound **103f** ($X = I$), which allowed the epoxidation of a number of α,β -unsaturated ketones **91** ($R^1 = Ar, R^2 = Ar'$) to proceed with very high yields (88–100%) and moderate to very good enantioselectivities (65–92%) under mild reaction conditions. For alkyl-substituted enones ($R^1 = Alkyl$), considerably lower *ee* values were obtained than for aryl-substituted ones (*ee* 42–57%). In 1998, the same group reported about the epoxidation of substituted naphthoquinones and acyclic enones (*ee* values up to 76%) with a PTC derived from quinidine (Scheme 48)¹⁵⁰.

A summary of the epoxidation results obtained using different phase-transfer catalysts is given in Table 13.

Adam and coworkers reported on the asymmetric Weitz–Scheffer epoxidation of biologically relevant isoflavones **101** with various hydroperoxides [*t*-BuOOH, cumyl hydroperoxide, 1-phenyl ethyl hydroperoxide, *p*-chlorophenyl ethyl hydroperoxide] employing the chiral PTCs **103h–k** (Scheme 49)¹⁵². The authors were able to isolate the enantiomerically enriched isoflavone epoxides **104** with *ee* values of up to 98% (cumyl hydroperoxide as oxidant) and in very high yields. Taking a racemic mixture of 1-phenyl ethyl hydroperoxide (**16a**) as oxidant under Weitz–Scheffer conditions, a good enantiomeric excess of the epoxide **104c** (92% *ee*) but only moderate kinetic resolution of the hydroperoxide (33% *ee* of the (*S*)-enantiomer) were obtained. With enantiomerically pure hydroperoxide (*S*)-**16f** without any PTC, the epoxide **104c** could be isolated in 91% yield but only with 45% *ee*. Summarizing the results of further experiments of this group one can say that enantiofacial differentiation mostly results from the induction of the chiral catalyst while chiral hydroperoxides have only a minor effect. Changing the configuration at the hydroxyl-bearing site of the PTC (which seems to be the decisive region) leads to inversion in the sense of enantioselectivity of the epoxide obtained. The hydroxyl group itself is essential and cannot be exchanged by other groups. The authors postulate a transition state (TS) in which H-bonding between the substrate and the hydroxyl group of the PTC occurs. The enantioselectivity is explained on steric grounds.

b. Polyamino acid catalysis. The asymmetric epoxidation of chalcones utilizing basic hydrogen peroxide in the presence of a polyamino acid catalysts was discovered in 1980 by Julia, Colonna and coworkers (equation 31)^{153–156}. The reaction conditions were triphasic, consisting of the insoluble polyamino acid catalyst, an aqueous solution of sodium hydroxide and hydrogen peroxide and a solution of chalcone in an organic solvent. The catalysts are prepared from the *N*-carboxyanhydrides of the amino acids using different kinds of initiators, such as water, primary amine or polystyrene bonded amine¹⁵⁴. The yields of epoxyketones ranged from low to very high depending mainly on the polyamino acid employed (up to 96%).

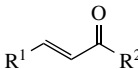


Similarly, good results were obtained with poly-(*L*)-alanine, poly-(*L*)-leucine and poly-(*L*)-isoleucine, whereas with poly-(*L*)-valine or random copolymers reduced chemical yields as well as asymmetric induction were obtained. Chemical and optical yields are closely related in all cases. The enantiomeric excesses obtained increased as the average chain length of the catalyst increased varying from 10 to 30 amino acids (*ee* values between 50 to 99%). For high *ee* values it seems to be essential that the polymer chain is at least 10 units¹⁵⁴. The degree of asymmetric induction decreases as the temperature is raised. The amount of catalyst only influences the chemical yield, not the optical yield of

TABLE 13. Comparison of the epoxidation results with different PTCs

Substrate:								
		R ¹	R ²	Cat.	Method ^a	Yield (%)	<i>ee</i> (%)	Reference
		various		103a–b	A1	50–100	0–54%	147
			C ₆ H ₄ CO ₂ Me- <i>o</i>	103a	A2	95	78	151
			R	103g	B	86	34	150
			R = Me			99	41	
			R = Et			95	40	
			R = <i>n</i> -Pr			93	70	
			R = <i>i</i> -Pr			100	28	
			R = <i>i</i> -Bu			60	64	
			R = <i>c</i> -Hex			47	76	
			R = Ph			84	40	
			R = C≡CPh					
				103c 103d	C	63 60	18 13	148
			R _x , R _y	103g	B	85	17	150
			R _x = H, R _y = Ph			97	35	
			R _y = <i>i</i> -Pr			34	26	
			R _y = <i>c</i> -Hex			88	21	
			R _y = Et			61	29	
			R _x = Et, R _y = H					
				103c 103d 103e	C	56 50–78 84	61 61–63 50	148
				103c 103d	C	60 100	45 44	148
				103c 103d	C	100 73	14 22	148

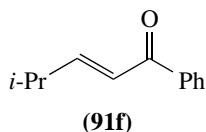
TABLE 13. (continued)

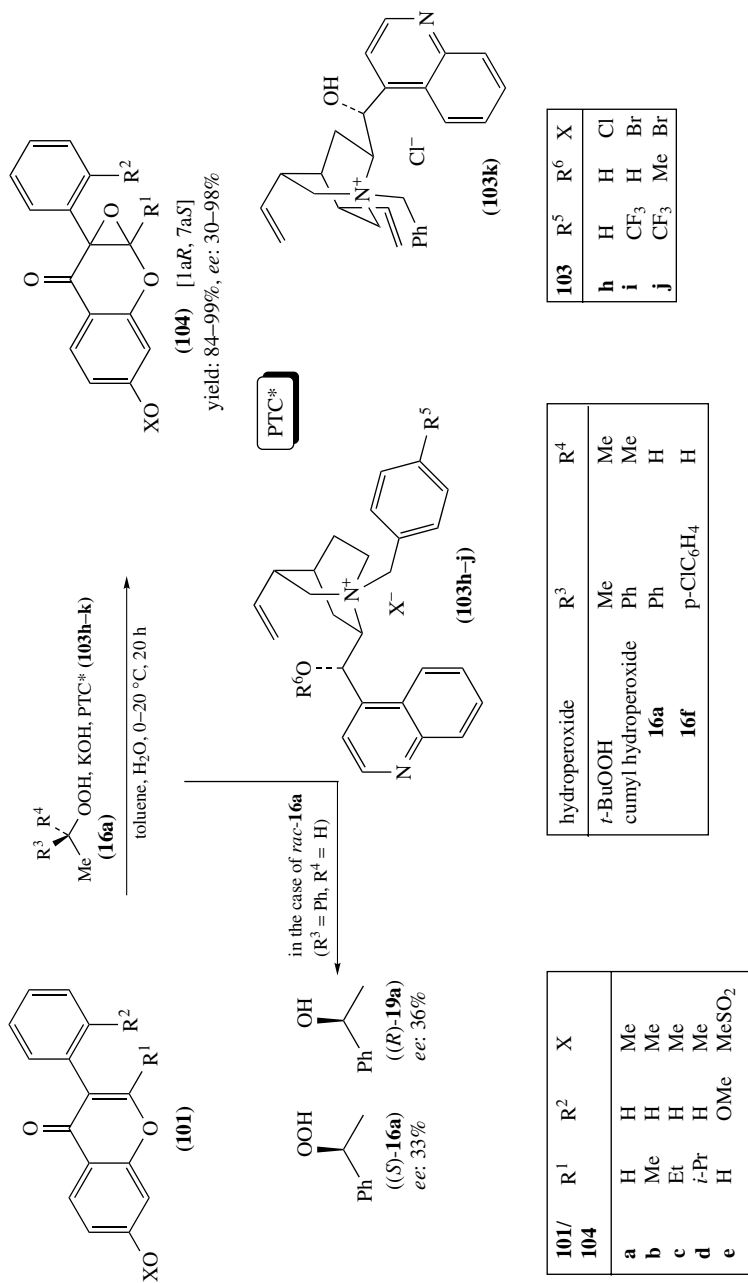
Substrate:							
							
R ¹	R ²	Cat.	Method ^a	Yield (%)	<i>ee</i> (%)	Reference	
Ph	Ph	103f	D	97	84	149	
<i>m</i> -MeC ₆ H ₄	Ph	103f	D	100	92	149	
<i>o</i> -ClC ₆ H ₄	Ph	103f	D	88	65	149	
Ph	<i>m</i> - or <i>p</i> -MeC ₆ H ₄	103f	D	95–99	87–89	149	
Alkyl	Ph	103f	D	41–90	42–57	149	

^a A1 = NaOH, aq. H₂O₂/toluene; A2 = NaOH, *t*-BuOOH/toluene; B = LiOH, aq. H₂O₂/CHCl₃, -10 °C; C = NaOH, TBHP or fluorenyl hydroperoxides, in toluene containing little amounts of water, between -10 °C and r.t.; D = LiOH, aq. H₂O₂/*n*-Bu₂O, 4 °C.

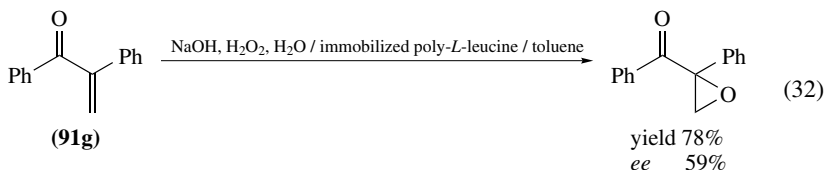
the epoxides. Other oxidizing agents, as for example *t*-BuOOH (basic), were also tested but with these low or no *ee* values could be obtained¹⁵⁵.

Colonna and coworkers proposed that H-bonding between the CO function of chalcone and the peptide group of the catalyst is responsible for the asymmetric induction¹⁵⁶. The results also indicated that the highest enantioselectivities were obtained with catalysts having a high content of α -helical conformation as poly-(*L*)-alanine, poly-(*L*)-leucine and the copolymer of (*L*)-leucine with (*L*)-alanine. With this method the catalyst can be readily separated from the reaction products, washed and reused. However, it showed reduced enantioselectivity due to degradation of the catalyst under the strong basic reaction conditions. Itsuno and coworkers prepared resin bound poly-(*L*)-leucine and poly-(*L*)-alanine¹⁵⁷, linking the polypeptide to aminomethylated polystyrene crosslinked with divinylbenzene, which is commercially available now. In this system the separation of the catalyst has been remarkably improved and it could be reused with only little loss of activity and asymmetric induction. Julia, Colonna and coworkers found that polymeric catalysts having a small degree of polymerization ($n < 10$) still have high catalytic activities (yields 36–67%, *ee* 80–88%), while non-supported poly(amino acids) ($n < 10$) gave only poor chemical and optical yield^{153–156}. The best result in the epoxidation of chalcone (92% yield, 99% *ee* of the epoxide) was obtained with the polymer-supported poly-(*L*)-leucine catalyst consisting of 32 (*L*)-leucine units (see Table 14, entry 21, method B1). The disadvantages of the Julia–Colonna epoxidation were the long reaction times, slow degradation of the catalyst by aqueous sodium hydroxide and the problem of converting less reactive substrates as, for example, compound **91f**, which could not be epoxidized under triphasic conditions with a poly-leucine catalyst (Table 14, entry 12)¹⁵⁸. Cyclopropyl groups or *tert*-butyl groups adjacent to the ketone moiety are well tolerated (Table 14, entries 6 and 22) and give good yields and *ee* values in the epoxidation reaction while isopropyl groups or methoxyisopropyl groups (Table 14, entries 24, 34) resulted in prolonged reaction times and decrease in enantioselectivity. In the same publication, Roberts



SCHEME 49. Weitz-Scheffer epoxidation of isoflavones **101** by various hydroperoxides and the chiral PTCs **103h–k**

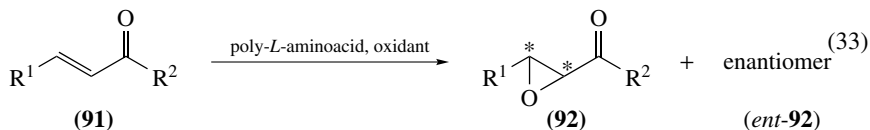
and coworkers presented the first example of an α -substituted β -unsubstituted enone **91g** undergoing asymmetric oxidation with 78% yield and 59% *ee* (equation 32)¹⁵⁸.



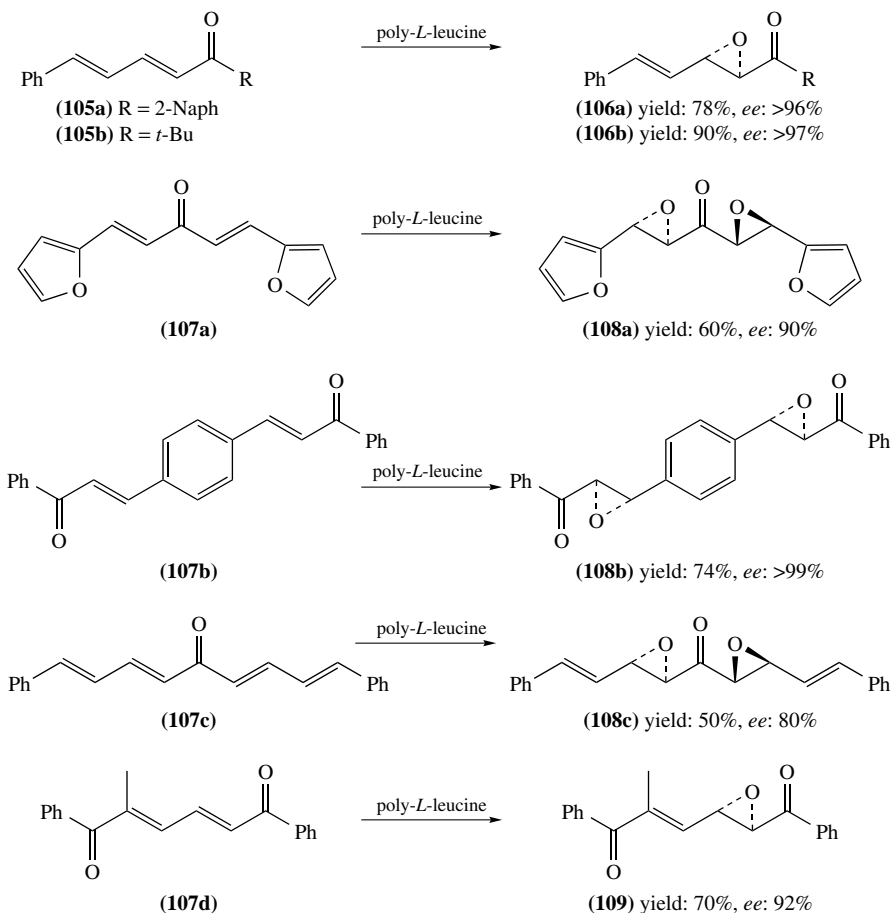
Improvements of this method were reported by Roberts and coworkers in 1997^{159, 160}. By exchanging aqueous hydrogen peroxide and inorganic base to urea hydrogen peroxide and a strong amidine base (DBU), the authors could switch from a triphasic system to a biphasic one and reduce reaction times for chalcone to under 30 minutes. Reactions were performed with poly-leucine or poly-(*L*)-neopentylglycine¹⁶¹ in an organic solvent such as THF and the oxidant was no longer required in excess. Different solvents (1,2-dimethoxyethane, *tert*-butyl methyl ether, ethyl acetate) gave similar results as THF, while dichloromethane, acetonitrile and toluene were less satisfactory. An alternative to DBU is represented by DBN but Hünig's base is much less effective, giving low conversion (37%) and enantiomeric excess (50%)¹⁶⁰. Enolisable substrates such as alkyl ketones showed good conversions under the modified reaction conditions. In order to obtain maximum rates and stereoselectivities it was necessary to activate the catalyst prior to use by stirring in a mixture of 4 M aqueous NaOH and toluene for 1–5 days, filtering and drying. Also, under biphasic conditions the catalyst can be recycled. It was found by Roberts' group that the activity dropped after reuse but could be recovered by submitting the catalyst to the activation procedure¹⁶². Because of the distinct uncatalyzed background reaction taking place under biphasic conditions (and therefore reduced *ee* values), Roberts and coworkers changed the reaction conditions to sodium percarbonate and poly-leucine in mixed 1,2-dimethoxyethane/water solvent system¹⁶³. This oxygen transfer agent has been reported earlier by the same group as an effective alternative to aqueous H₂O₂ for polyamino acid-catalyzed epoxidation under triphasic conditions¹⁶⁴. In this way the background reaction was diminished and the enantioselectivity remained unchanged and high throughout the course of the reaction (up to 96%). In this system, sodium percarbonate, which is a very cheap reagent, serves a dual role of oxidant and base. The ethereal–aqueous mixture was chosen due to easier dissolution of the sodium percarbonate and release of hydrogen peroxide and therefore shorter reaction times than with THF as solvent. With this method, lower catalyst-to-substrate ratios could be used without reducing the *ee* of the epoxidation product.

In 1999 and 2000, Roberts and coworkers reported the use of a silica-supported polyamino acid catalyst, which could be very effectively recovered by filtration^{161, 165}. For good substrates like *trans*-chalcone, the silica-adsorbed poly-(*L*)-leucine, poly-(*L*)-neopentylglycine and poly-(*L*)-alanine catalysts showed similar activity and selectivity compared to the corresponding non-immobilized polyamino acids (conv.: 60–95%, *ee*: 80–95%). Poly-(*L*)-valine and poly-(*L*)-phenylalanine showed a slight degree of catalytic activity on binding to silica but the optical activity of the products is negligible (yield and *ee* \leq 30%, similar to the results with non-immobilized catalysts). For less reactive substrates polyneopentylglycine and poly-leucine adsorbed onto flash silica were the best catalysts (conv.: 85–100%, *ee*: 92–97%) and they were significantly more effective and slightly more selective than the non-immobilized analogues (conv.: 45–97%, *ee*: 90–95%). This material showed higher activity than the resin-bound material which allowed the usage of only 2.5 mol% catalyst and the enantioselectivity was the same as observed for the free polyamino acid before. In 2003, Roberts and coworkers reported on

two improved procedures for the preparation of silica-supported poly-leucine producing a supported catalyst with excellent catalytic activity and selectivity (chalcone was epoxidized under biphasic conditions with conversions up to 98% (1h) and *ee* up to 97%)¹⁶⁶. Table 14 shows a comparison of the results obtained by employing different methods for the epoxidation of electron-deficient olefins with polyamino acids (equation 33).



It could also be shown that the epoxidation procedure is not limited to chalcones. Also, compounds **105a** and **105b** and **107a–d** could be epoxidized with good to excellent stereocontrol (Scheme 50)^{164, 171}. While substrates **105a** and **105b** and **107d** are selectively epoxidized on only one double bond to afford monoepoxides **106a** and **106b** and **109**,



SCHEME 50. Poly-(*L*)-leucine catalyzed epoxidation of chalcones

TABLE 14. Epoxidation results obtained under Julia-Colonna and Roberts' conditions

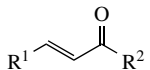
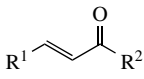
Entry	R ¹		R ²	Method ^a	Julia-Colonna conditions		Roberts' conditions		Reference
					yield (%)	ee (%)	yield (%)	ee (%)	
1	Ph		<i>o</i> -MeOC ₆ H ₄	A2	85	93			153
2	Ph		2-Furyl	A1	85	87			164
3	Ph		2-Pyridyl	A1	74	79			164
4	Ph		2-Thienyl	A2 ^b	96	80			155
5	Ph		3-Thienyl	A2 ^b	30	70			155
6	Ph		Cyclopropyl	A1	85	77			158, 167
7	2-furyl		2-Naphthyl	A1	75	>96			164
8	2-pyridyl		Ph	A1	84	72			164
9	4-pyridyl		<i>t</i> -Bu	A3	70	72			158
10	4-pyridyl		2-Naphthyl	A1	67	>96			164
11	<i>p</i> -MeOC ₆ H ₄		<i>o</i> -MeOCH ₂ OC ₆ H ₄	A2	64	66			168
12	<i>i</i> -Pr		Ph	A3	—	—			158
13	<i>t</i> -Bu		Ph	A3	85	90			158, 164
14	PhCH=CH		<i>t</i> -Bu	A1	90	>97			164
15	PhCO		Ph	A1	76	76			167
16	<i>t</i> -BuCO		<i>t</i> -Bu	B1	>95	>95			167
17	<i>t</i> -BuO ₂ C		Ph	B1	66	≥95			167
18	<i>n</i> -Bu ₃ Sn		Ph	A1	90	>99			169
19	<i>p</i> -O ₂ NC ₆ H ₄		Ph	A2 ^b	83	82			155
20	Ph		Ph	A2	85	93			153
				B1	92	99			157
				B2	66	93			157
				C1			85–90	>95	159–161
				C2			91 ^c	>95	161
				C3			60 ^c	80	161
				C4			19 ^c	81	161
				C5			36 ^c	21	161
				D			>99	96	163
				E1			95–100 ^c	93–95	161, 165
				E2			95 ^c	>95	161
				E3			60 ^c	80	161
				E4			20 ^c	30	161
				E5			34 ^c	30	161
21	Ph		2-Naphthyl	A1	90	93			164
				C1			91	91	162
22	Ph		<i>t</i> -Bu	A1	92	89			158
				A1	92	>98			167
				C1			71,76	94	159, 162
				C3			31 ^c	86	161
				E3			89 ^c	94	161
23	PhCH=CH		2-Naphthyl	A1	78	>96			164
				C1			85	96	171
24	Ph		CMe ₂ OMe	A1	70	63			158, 167
25	Ph		<i>o</i> -O ₂ NC ₆ H ₄	C1			91	91	170
26	Ph		<i>o</i> -MeC ₆ H ₄	C1			94	81	170
27	Ph		<i>o</i> -MeNHC ₆ H ₄	C1			62 ^c	96	170
28	Ph		<i>o</i> -H ₂ NC ₆ H ₄	C1			49 ^c , 81	94,98	161, 170
				C2			97 ^c	97	161
				C3			40 ^c	92	161
				C4			0 ^c	—	161
				C5			0 ^c	—	161
				E1			85 ^c	93–96	165
				E2			100 ^c	97	161
				E3			66 ^c	91	161
				E4			13 ^c	2	161
				E5			16 ^c	11	161

TABLE 14. (continued)

Entry	R ¹		R ²	Method ^a	Julia-Colonna conditions		Roberts' conditions		Reference
					yield (%)	ee (%)	yield (%)	ee (%)	
29	Ph		<i>p</i> -H ₂ NC ₆ H ₄	C1			0	—	170
30	Ph		PhC≡C	B1	57	90			158, 167
31	Ph		Me	C1			70	83	160
32	Ph		Et	C1			80	82	162
33	Ph		<i>n</i> -Pr	C1			85	94	162
34	Ph		<i>i</i> -Pr	A1	60	62			158, 167
				C1			47,56 ^c	89–92	161, 165
				C2			88 ^c	92	161
				C3			40 ^c	88	161
				C4/C5			0	—	161
				E1			78,95 ^c	92–93	161, 165
				E2			95 ^c	95	161
				E3			95 ^c	80	161
				E4/E5			0	—	161
35	Ph		<i>i</i> -Bu	C1			87	96	162
36	Ph		<i>n</i> -Pen	C1			45 ^c	95	161
				C2			97 ^c	90	161
				C3			34 ^c	86	161
				E1			90 ^c	95	161
				E2			100 ^c	97	161
				E3			49 ^c	80	161
37	<i>p</i> -ClC ₆ H ₄		Ph	A2 ^b	47	66			155
				A1	62	62			170
38	<i>p</i> -ClC ₆ H ₄		<i>o</i> -H ₂ NC ₆ H ₄	C1			91	>98	170
39	<i>p</i> -MeOC ₆ H ₄		<i>t</i> -Bu	C1			≥90	≥96	159
40	<i>c</i> -Hex		Ph	C1			91	89	159
41	PhCH=CH		Cyclopropyl	A1	73	74			158, 167
				F	52	98			167
42	(<i>E</i>)-ClCH=CH		Ph	C1			57	86	171
43	(<i>E</i>)- <i>t</i> -BuO ₂ CCH=CH		Ph	C1			95	90	171
44	(<i>E</i>)-MeO ₂ CCH=CH		Ph	C1			90	90	171
45	(<i>E</i> , <i>E</i>)-MeCO-CH=CHCH=CH		Ph	C1			43	90	171
46	(<i>E</i>)-Ph(O)CC(Me)=CH		Ph	C1			70	92	171
47	2-Naphthyl		Cyclopropyl	A1	56	90			158
				A1 ^d	61	90			158, 167
48	2-Quinoyl		Cyclopropyl	A1	94	79			158
49	Cyclopropyl		2-Naphthyl	A1	73	>98			158, 167
50	<i>p</i> -ClC ₆ H ₄ C(O)-		Ph	F	60	89			167
51	<i>t</i> -BuC(O)-		Ph	A1	79	82			167

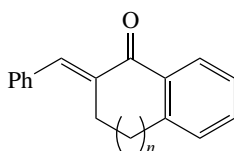
^a **A1** = triphasic (poly-(*L*)-leucine/aq. NaOH, aq. H₂O₂/substrate in organic solvent); **A2** = triphasic (poly-(*L*)-alanine/aq. NaOH, aq. H₂O₂/substrate in organic solvent); **A3** = triphasic (DAP-poly-(*L*)-leucine/aq. NaOH, aq. H₂O₂/substrate in organic solvent), [DAP = 1,3-diaminopropane as polymerisation initiator]; **B1** = triphasic (polymer supported poly-(*L*)-leucine/aq. NaOH, aq. H₂O₂/substrate in toluene); **B2** = triphasic (polymer supported poly-(*L*)-alanine (n = 20)/aq. NaOH, aq. H₂O₂/substrate in toluene); **C1** = biphasic (poly-(*L*)-leucine/urea•H₂O₂, DBU, THF); **C2** = biphasic (poly-(*L*)-neopentylglycine/urea•H₂O₂, DBU, THF); **C3** = biphasic (poly-(*L*)-alanine/urea•H₂O₂, DBU, THF); **C4** = biphasic (poly-(*L*)-valine/urea•H₂O₂, DBU, THF); **C5** = biphasic (poly-(*L*)-phenylalanine/urea•H₂O₂, DBU, THF); **D** = biphasic (Na₂CO₃•1.5 eq. H₂O₂, poly(leucine, DME/water); **E1** = biphasic (poly-(*L*)-leucine-SiO₂/urea•H₂O₂, DBU, THF); **E2** = biphasic (poly-(*L*)-neopentylglycine-SiO₂/urea•H₂O₂, DBU, THF); **E3** = biphasic (poly-(*L*)-alanine-SiO₂/urea•H₂O₂, DBU, THF); **E4** = biphasic (poly-(*L*)-valine-SiO₂/urea•H₂O₂, DBU, THF); **E5** = biphasic (poly-(*L*)-phenylalanine-SiO₂/urea•H₂O₂, DBU, THF); **F** = poly-(*L*)-leucine, NaBO₃, H₂O, NaOH, CH₂Cl₂, aliquat 336.

^b Cat.: poly-*S*-alanine.

^c Conversions given.

^d Poly-D-leucine instead of poly-(*L*)-leucine.

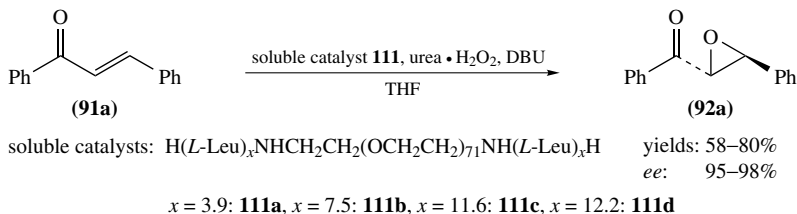
substrates **107a–c** are selectively epoxidized on the two double bonds in conjugation to the carbonyl group giving bisepoxides **108a–c**. In general, α -substituted enones, such as α -methylchalcone, are unreactive under polyleucine catalyzed conditions. An exception is represented by cyclic enones **110** derived from indanone ($n = 0$), tetralone ($n = 1$) or benzosuberone ($n = 2$), which have been reported by Porter and Skidmore to be epoxidized in yields of 72–76% and moderate to good *ee* values ranging from 59% ($n = 2$) to 88% ($n = 0$)¹⁷². This can be explained by the requirement of an *s-cis* conformation for epoxidation to occur, which was proposed by Enders and coworkers¹⁷³.



(110)

The potential of the Julia–Colonna epoxidation for the enantioselective synthesis of, for example, pharmaceuticals has been demonstrated by Roberts and coworkers^{159, 174}. But despite all efforts, the substrate spectrum of this peptide-catalyzed epoxidation of enones is still fairly narrow. For example, the synthetically most important endocyclic enones (such as cyclohexenones or quinones) or *Z*-enones in general are not suitable substrates. In order to rationally develop catalysts for these classes of substrates it is necessary to gain mechanistic knowledge about the Julia–Colonna epoxidation. For a long time almost nothing was known about the mechanistic details of activation. Julia, Colonna and coworkers and Roberts and coworkers could show that besides polyleucine, also polyalanine (α -helical structure), polyisoleucine (β -sheets) and poly(neopentylglycine) are effective catalysts for epoxidation, while polyvaline, polyphenylalanine and polyproline are less effective. The nature of the terminal group of homopolypeptide does not affect the degree of asymmetric induction but poly-(*L*)-amino acids lacking amidic hydrogens are chemically and stereoselectively inefficient catalysts. So hydrogen bonding between the carbonyl function of the substrate and the peptide group of the catalyst was proposed to be responsible for effective asymmetric induction¹⁵⁴. Roberts' investigations examining the importance of different regions of the catalyst chain led to the result that the dominant role in determining which enantiomer is created is played by the amino terminal region¹⁷⁵. In 1998, a series of oligopeptides of defined primary structure was prepared by Roberts and coworkers and their catalytic activity and selectivity under bi- as well as triphasic conditions was examined¹⁷⁶. The results of the mechanistic studies were that, under biphasic conditions, a 10mer of *L*-leucine is sufficient to affect good stereocontrol and five amino acid residues adjacent to the *N*-terminus dictate the stereochemistry of the product. Five *D*-leucine residues at the *N*-terminus of a 20mer of polyleucine were sufficient to overcome any catalytic effect of the 15 *L*-leucine residues of which the rest of the polymer chain consists. Catalyst H-(*D*-Leu)₅-(*L*-Leu)₁₅-PEG-PS yielded epoxide (also observed with poly-*D*-leucine) with an enantiomeric excess of 52%; with H-(*D*-Leu)₇-(*L*-Leu)₁₃-PEG-PS the same enantiomer was isolated with 83% *ee*. The NH₂ group itself is not crucial for good results. The influence of the *N*-terminal region depends on the presence of more than five and up to 15 residues adjacent to the C-terminus while the stereochemistry of the latter seems to be unimportant.

In 2001, soluble polymer catalysts **111**, poly-(*L*)-leucine bound to polyethylene glycol, were introduced by Roberts' group (Scheme 51)¹⁷⁷. In this catalyst a short peptide chain



SCHEME 51. Asymmetric epoxidation of chalcone with soluble poly(Leu) catalyst

of an average length of four amino acids is sufficient to yield products in high enantioselectivities and yields utilizing urea hydrogen peroxide as oxidant. FT-IR investigations have determined that the catalytically active poly(Leu) components of the copolymers have an α -helical structure. These and a number of further studies¹⁷⁸ on the effect of sequence on the catalytic efficiency can be found in the literature, both on ‘free’ peptides and on those bound to either soluble PEG polymers or to polystyrene supports by means of ester linkers. All these studies showed that (i) modifications at the *N*-terminal region of the peptide had the most pronounced effect on catalyst performance and (ii) there is a correlation between the degree of helicity and the catalytic activity of the oligopeptides.

In 2001, Berkessel and coworkers reported their studies on the elucidation of the mechanism of the Julia–Colonna asymmetric epoxidation¹⁷⁹. In order to find an answer to the most fundamental question of the minimum chain length of a catalytically competent peptide, a series of *L*-Leu 1–20mer peptides carrying 1–5 *N* terminal Gly residues on TentaGel SNH_2 was prepared. From their investigations the conclusion could be drawn that five *L*-Leu residues were sufficient to catalyze the Julia–Colonna epoxidation of chalcone with 96–98% *ee*, whereas the epoxide yields increase gradually and level off around the 14mer. From the fact that four amino acids are required to form one turn of an α -helix, it was concluded that one intact helical turn is the minimum structural element necessary for efficient asymmetric induction. In addition to the experiments, Berkessel and coworkers conducted molecular modelling studies which both suggested that the binding site for the partially negatively charged carbonyl oxygen atom of the substrate enone is the *N*-terminus, with its partial positive charge and three NH bonds not involved in intrahelical H-bonding (see Figure 6). This three-point attachment of the substrates to the *N*-terminus of the α -helix implies that it is the helical chirality of the peptide backbone and not the central chirality of the α -C which determines the epoxide configuration through face-selective delivery of a HOO^- anion. Furthermore, the proposed model explains why the *E*-configuration of the substrates is required. Docking of a *Z*-chalcone prohibits peroxide binding at the NH of the penultimate amino acid ($n - 1$), which is needed for effective and selective hydroperoxy anion transfer.

A short overview of the field of asymmetric epoxidation of α,β -unsaturated ketones catalyzed by poly(amino acids) was given by Lauret and Roberts in 2002¹⁸⁰. Recently, Kelly and coworkers reported on the preparation of soluble catalysts for the Julia–Colonna epoxidation using NH_2 -PEG-OMe as the support system¹⁸¹. The authors observed that the rate and *ee* of the epoxidation correlates with the helicity of the polypeptide and increases with increasing chain length. MeO-PEG-NH-poly(Leu) is largely the α -helical conformer and therefore an excellent epoxidation catalyst (>95% conversion and 97% *ee* for chalcone oxidation). In contrast MeO-Peg-NH-poly(Ala), which has the lowest α -helical content among the polymers tested, was also the poorest catalyst (only 10% conversion and 28% *ee* for chalcone oxidation). Also, quite recently Roberts and coworkers presented a modified version of the Julia–Colonna procedure with which several vinyl sulfones **112** could be epoxidized to the corresponding epoxides **113** in good yields (49–76%) and good to

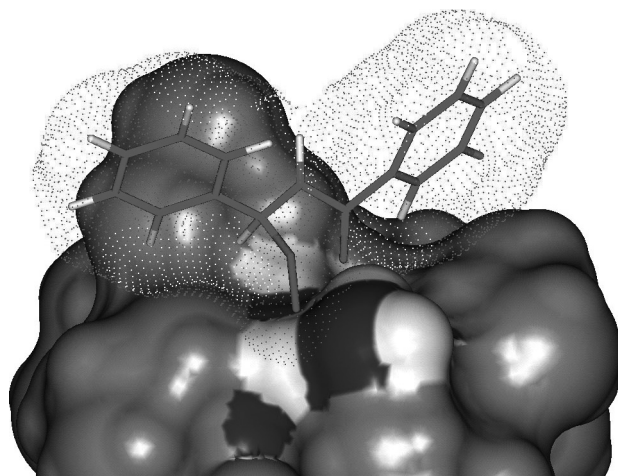
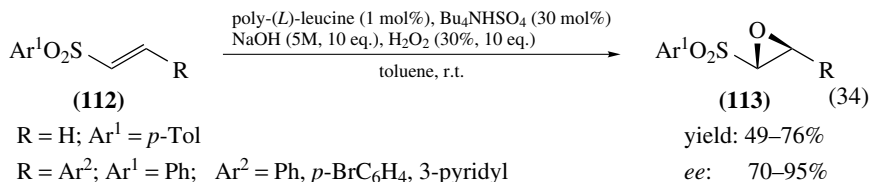


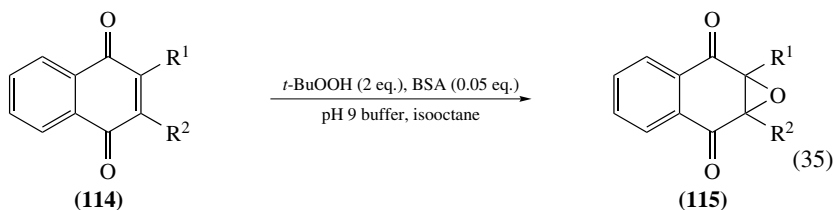
FIGURE 6

excellent optical purity (70–95%) (equation 34)¹⁸². In this procedure poly-(*L*)-leucine is prestirred with aqueous NaOH, 30% H₂O₂ and Bu₄NHSO₄ in toluene. After the catalyst has sequestered the peroxide from aqueous solution, the latter is removed to leave a biphasic system (toluene/gel-like polyamino acid), which efficiently oxidizes arylvinyl sulfones.



c. Bovine serum albumin catalyzed epoxidations. Colonna and coworkers have reported an epoxidation method for naphthoquinones **114** utilizing bovine serum albumin (BSA), a carrier protein in biological systems, as catalyst (equation 35)^{183–186}. The reaction was carried out in an aqueous buffer solution using H₂O₂ or *t*-BuOOH as oxygen sources. Yields of the corresponding epoxides **115** were moderate and ranged from 0 to 74% while the enantioselectivities obtained were up to 79% (obtained for 2-cyclohexyl-1,4-naphthoquinone). The studies showed that in most cases the enantioselectivity increases with decreasing pH of the buffer solution (pH 9 compared to pH 11)¹⁸⁴, which might be explained by the pH-depending isomerization of BSA. At pH 9, BSA is in a basic form, which is transformed into an isomerized aged form after long reaction time at 30 °C or by increasing the pH of the aqueous solution. Changes in the steric environment of the oxidant have a pronounced effect on the asymmetric induction without altering the chemical yield. Compared to H₂O₂ and cumene hydroperoxide, significantly higher enantiomeric excesses of the epoxides were obtained with TBHP (e.g. for substrate **114**: R¹ = H, R² = *i*-Bu: TBHP: 77% ee, H₂O₂: 8% ee, CHP: 36% ee)¹⁸⁴. The sense and magnitude of observed enantioselectivities were strongly dependent on the substituents on the substrate double bond. For example, 2-*t*-butyl-1,4-naphthoquinone was recovered unchanged while

2-isobutyl-1,4-naphthoquinone could be epoxidized with TBHP in pH 11 buffer in a yield of 62% and *ee* of 77%. In order to improve the obtained enantioselectivities, the effect of several organic cosolvents was investigated by Colonna and coworkers and turned out to be significant^{185, 186}. Much better asymmetric inductions were obtained with TBHP in a buffer solution containing 0.05 molar equivalents of isooctane. For example, the epoxide of 2-isobutyl-1,4-naphthoquinone could be isolated with an *ee* of 90% and therefore the enantiomeric excess could be improved by about 13% by the additional isooctane. Other cosolvents such as EtOH or DMSO slightly decreased the enantioselectivity (*ee* difference of 2–11%) and in CCl₄ racemic epoxide was obtained. The highest yield (66%) and enantioselectivity (>99%) was obtained with additional isooctane for the naphthoquinone substrate bearing a long alkyl chain (*n*-C₈H₁₇) at position R² (R¹ = H)¹⁸⁵.



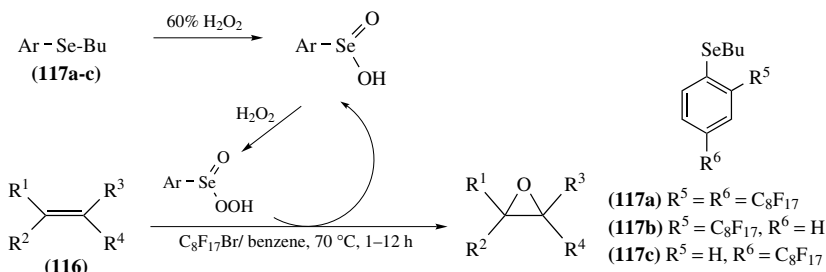
R¹ = H, Me, Et, *n*-Bu;

R² = Me, Et, *i*-Pr, *i*-Bu, *n*-Bu, *t*-Bu, *n*-C₆H₁₃, *n*-C₈H₁₇, *c*-Hex, Ph, Bn

yield: 22–66%

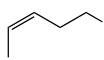
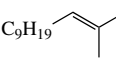
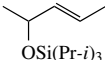
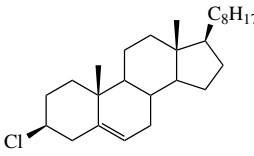
ee: 14 to >99%

d. Selenide-catalyzed epoxidation reaction. In 1999, Knochel and coworkers investigated the epoxidation of unfunctionalized and functionalized olefins **116** with perfluoroalkyl substituted selenides **117** (Scheme 52, Table 15)^{39, 187}. Two fluorinated alkyl chains on the catalyst are necessary to achieve good and selective solubility in fluorine media, which is essential for an effective recyclability of the catalyst. While with catalyst **117c** the reaction rates and yields decreased significantly after the third run (for cyclooctene from 80% to 40%), this is not the case with selenium compound **117a** (90% yield after several runs). With 5 mol% of the catalyst **117a**, various substrates could be epoxidized in good yields (63–97%) in a biphasic system of benzene and bromoperfluorooctane using 60% hydrogen peroxide as oxidant. Substrates which cannot be epoxidized under the conditions employed are terminal or aryl-substituted olefins. A stereogenic center adjacent to the double bond of the olefin does not induce diastereoselectivity, as can be seen from the results obtained by epoxidation of the secondary allylic silyl ether **116c**. The aryl butyl selenides **117a–c** are first oxidized *in situ* by hydrogen peroxide to the corresponding arylseleninic acid, then to the peracid, which catalyzes the epoxidation.



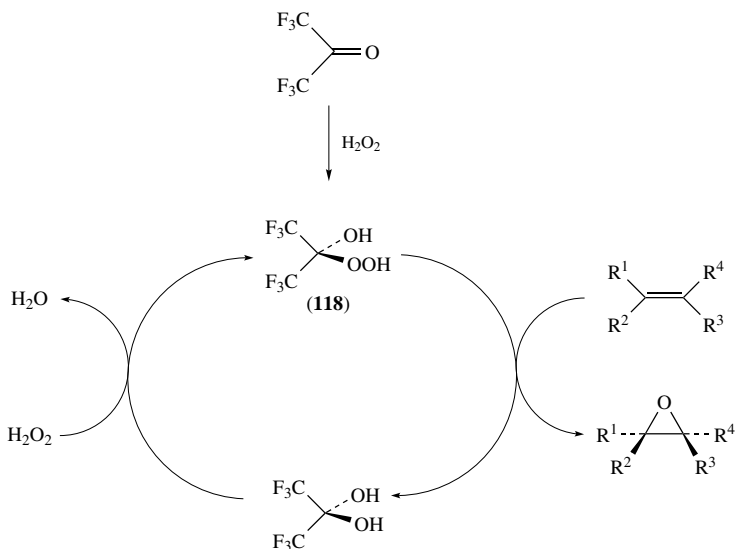
SCHEME 52. Selenium-catalyzed epoxidation of olefins

TABLE 15. Selenium-catalyzed epoxidation of several olefins employing catalyst **117a**

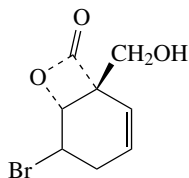
Substrate	Various alkenes				
		(116a)	(116b)	(116c)	(116d)
Epoxide yield (%)	63–93%	97%	93%	97%	80%
				<i>syn:anti</i> = 1:1	<i>syn:anti</i> = 4:1

e. Ketone-catalyzed epoxidation of allylic alcohols and unfunctionalized olefins.

α -Hydroxy hydroperoxides (perhydrates), generated from a ketone and hydrogen peroxide, possess an activated oxygen atom which is readily transferred electrophilically to a variety of organic compounds, among them also allylic alcohols and unfunctionalized olefins (see also Section III.B.1: use of perhydrates in uncatalyzed sulfoxidations)²⁰. The first report on the oxidation of alkenes to epoxides in high yield and selectivity with hydrogen peroxide and catalytic quantities of hexafluoroacetone or other fluoro(halo)acetone compounds was published in a patent in 1973 by Kim¹⁸⁸. With this method, 1-octene was quantitatively converted to the epoxide and other olefins such as propylene, allylic alcohol, *trans*-stilbene and 1,5-cyclooctadiene were epoxidized in 50–80% yield with high selectivity. Hexafluoroacetone is one of the most electrophilic ketones and therefore very reactive. It was employed by Heggs and Ganem as catalyst for the epoxidation of generally unreactive terminal olefins like 1-dodecene in the presence of hydrogen peroxide at room temperature, resulting in high yields of the corresponding epoxides¹⁸⁹ (Scheme 53). The corresponding

SCHEME 53. Epoxidation of olefins with hexafluoroacetone/H₂O₂

α -hydroxyhydroperoxide **118**, formed from hexafluoroacetone and hydrogen peroxide, was also used as stoichiometric oxidant for the epoxidation of various olefins yielding the epoxides generally in good yields (60–96%) at room temperature. Under the stoichiometric conditions, cyclohexene and cyclodecene were transformed to the epoxides in 96 and 90% yield at room temperature, respectively, while cyclohex-2-enyl acetate required reflux conditions. Electron-deficient cyclohex-2-enone and hindered olefin **119** did not undergo reaction at all.



(119)

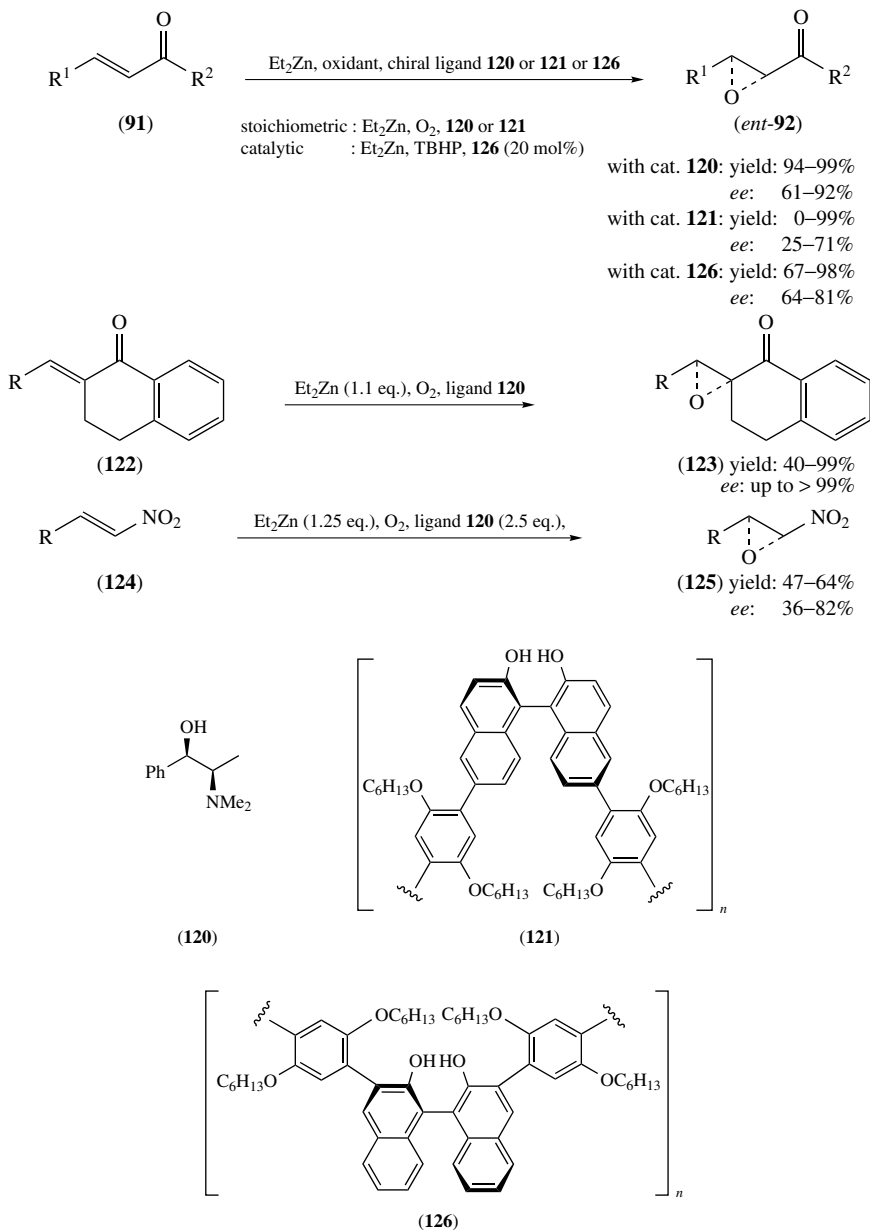
The catalytic version of this reaction with H_2O_2 as stoichiometric oxidant had to be carried out at reflux temperature, because at lower temperatures the catalytically active species, the perhydrate of hexafluoroacetone, was formed rather slowly. The epoxidation of allylic alcohols with **118** showed high π -facial stereoselectivity producing preferentially the *cis* isomers. The high diastereoselectivity observed with the perhydrate reagent, analogous to MCPBA, can be explained by hydrogen bonding between the allylic hydroxyl functionality and the oxidant. Acid-sensitive epoxides can be prepared by buffering the reaction solution with disodium hydrogen phosphate. This method represents one of the few examples of catalytic hydrogen peroxide activation without metal ions. An advantage of this oxidation procedure is that hexafluoroacetone, which is the precursor for one of the most reactive perhydrates **118**, is commercially available.

3. Metal-catalyzed epoxidations

For earlier reviews on this topic see, e.g., References 190 and 191.

a. Asymmetric epoxidation of electron-deficient olefins. Besides the methods for the organo-catalyzed epoxidation of α,β -unsaturated olefins, which have already been discussed in Section III.A.2, there are also some methods known in the literature which rely on the use of chiral ligands coordinated to the metal ion of a metal peroxide, which then undergoes a Weitz–Scheffer reaction. Several metals like zinc, lithium, magnesium and various lanthanides have been shown to catalyze this kind of reaction and will be discussed in the following.

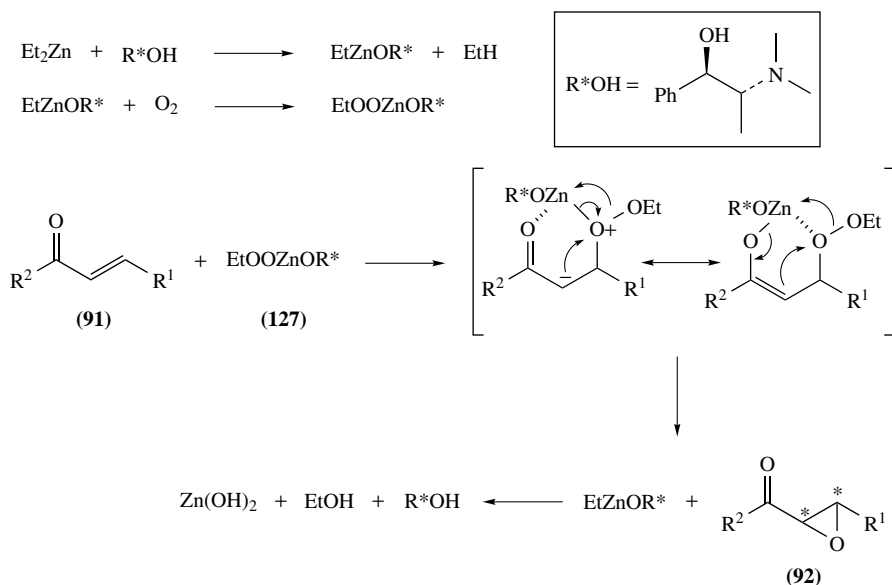
In 1996, Enders and coworkers reported the asymmetric epoxidation of (*E*)-enones **91** in the presence of stoichiometric amounts of diethylzinc and (1*R*,2*R*)-*N*-methylpseudoephedrine (**120**) under an oxygen atmosphere to give *trans*-epoxides **92** with excellent yields (94–99%), almost complete diastereoselectivity (>98% *de*) and with very good enantioselectivities (61–92%) (Scheme 54)^{173,192}. For the same reaction Pu and coworkers¹⁹³ utilized achiral polybinaphthyl **121** as ligand (in excess) instead of the chiral aminoalcohol. For each substrate, only one diastereomer was formed, but in most cases yields were lower than observed with the Enders' system. Enders' catalyst shows high asymmetric induction for alkyl-substituted enones (*ee* 82–92%), but for substrates bearing only aromatic substituents only modest enantioselectivity was obtained ($\text{R}^1 = \text{R}^2 = \text{Ph}$:



SCHEME 54. Zinc-mediated asymmetric epoxidation of electron-deficient olefins

$ee = 61\%$). For this special enone, i.e. chalcone, Pu's catalytic system proved to be slightly more enantioselective ($ee = 71\%$).

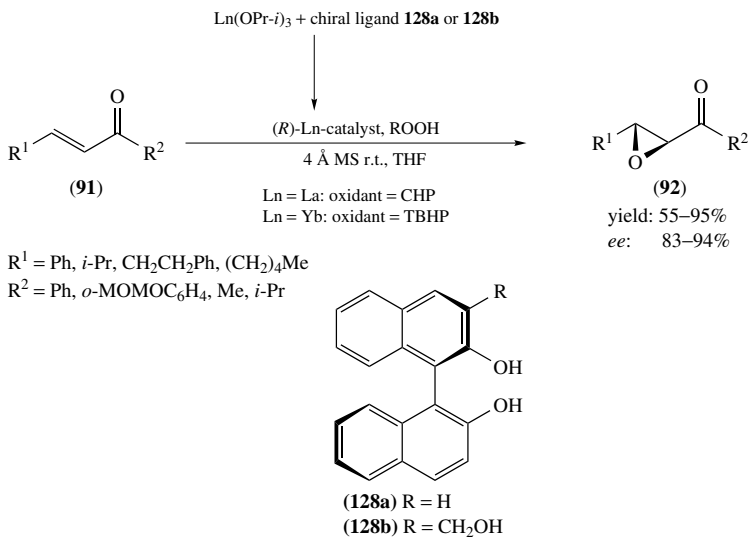
The Enders' catalyst has also been utilized successfully for the epoxidation of β -alkylidene- α -tetralones **122** giving epoxides **123**¹⁷³. In this reaction the authors found out that the enantioselectivity increases with the size of the substituent R, being highest for R = *i*-Pr (>99% ee). Besides α,β -unsaturated ketones, also some (*E*)-nitroalkenes **124** can be epoxidized by the catalytic system of Enders and coworkers¹⁹⁴, giving epoxides **125** with moderate yields (47–64%), complete diastereoselectivity and moderate to good ee values (36–82%). The highest enantioselectivity (82% ee) was obtained in the epoxidation of *trans*-1-nitro-3,3'-dimethyl-1-butene. It is worth mentioning that in all the examples the chiral ligand (1*R*,2*R*)-*N*-methylpseudoephedrine (**120**) can be recycled. The mechanism of this reaction was proposed as depicted in Scheme 55, proceeding via the intermediate ethylperoxyzinc alkoxide **127**. First, an ethylzinc alkoxide is generated from diethylzinc and (1*R*,2*R*)-*N*-methylpseudoephedrine. This intermediate is then converted to **127** by oxidation with molecular oxygen, which is the epoxidizing species in the process. The zinc alkoxide first complexes with the carbonyl oxygen of the enone and the ethylperoxy anion can then attack the β -position of the enone leading to the intermediate with two resonance structures as shown in Scheme 55. Cleavage of this intermediate (shown by the corresponding curved arrows) gives epoxyketones **92**. While the methods described above are all stoichiometric processes, Pu and coworkers developed a catalytic variant, using ligand **126** as asymmetric inductor¹⁹³. Oxygen was replaced by TBHP as stoichiometric oxygen source. With the catalytic method, chalcones as well as alkyl-substituted enones could be oxidized with good yields (67–98%) and enantioselectivity (ee 64–81%).



SCHEME 55. Proposed reaction mechanism for the zinc-mediated asymmetric epoxidation of α,β -enones

Shibasaki and coworkers have developed lanthanide–binol complexes $\text{LnM}_3(\text{binaphthoxide})$ [$\text{M} = \text{alkali metal}$], which have been shown to catalyze the epoxidation of

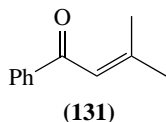
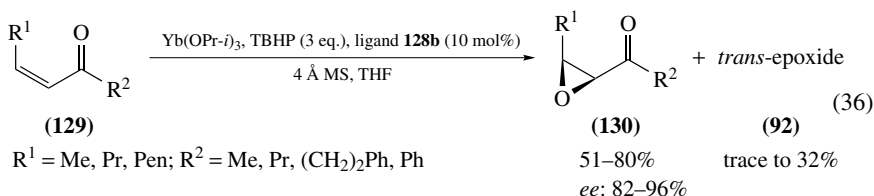
chalcone¹⁹⁵. The authors explained the activity of these bimetallic catalysts by the presence of a Brønsted basic and a Lewis acidic site which, through coordination, orientate substrate and reagent in the chiral environment such that reaction is rendered possible. With $\text{LaNa}_3[(R)\text{-BINOL}]_3$ as catalyst the epoxidation of chalcone with TBHP as oxidant affords the corresponding epoxide in 92% yield and 83% *ee*, but other enones could not be epoxidized. Later it was found that the asymmetric epoxidation of a wider range of (*E*)-enones was catalyzed by an alkali metal free lanthanum complex of the type depicted in Scheme 56¹⁹⁵. These complexes were formed by mixing (*R*)-BINOL and $\text{Ln}(\text{OPr-}i)_3$ [or $\text{Yb}(\text{OPr-}i)_3$] in an equimolar amount, in the presence of 4 Å molecular sieves and cumene hydroperoxide (or TBHP in the case of $\text{Ln} = \text{Yb}$). Yields of the epoxyketones **92** ranged from 85 to 93% and *ee* values were also quite high (83–86%). Chalcone was epoxidized with the same yield and enantioselectivity as observed before with the catalyst $\text{LaNa}_3[(R)\text{-BINOL}]_3$. Modification of the chiral ligand from (*R*)-BINOL **128a** to (*R*)-3-hydroxymethyl-BINOL **128b** led to a substantial increase in enantioselectivity (up to 94% *ee*). Shibasaki and coworkers observed that for each type of enone, there is an optimal lanthanide metal. While the La-128b-CHP system is the best one for aryl enones, alkyl enones are most effectively epoxidized by the ytterbium catalyst Yb-128b-TBHP ^{195,196}.



SCHEME 56. Lanthanide-BINOL-catalyzed epoxidations

The authors also investigated the mode of activation of these BINOL-derived catalysts. They proposed an oligomeric structure, in which one Ln-BINOL moiety acts as a Brønsted base, that deprotonates the hydroperoxide and the other moiety acts as Lewis acid, which activates the enone and controls its orientation towards the oxidant¹⁹⁵. This model explains the observed chiral amplification effect, that is the *ee* of the epoxide product exceeds the *ee* of the catalyst. The stereoselective synthesis of *cis*-epoxyketones from acyclic *cis*-enones is difficult due to the tendency of the *cis*-enones to isomerize to the more stable *trans*-derivatives during the oxidation. In 1998, Shibasaki and coworkers reported that the ytterbium-(*R*)-3-hydroxymethyl-BINOL system also showed catalytic activity for the oxidation of aliphatic (*Z*)-enones **129** to *cis*-epoxides **130** with good yields

(74–80%) and high stereoselectivity (93–96%), while in the epoxidation of aromatic (*Z*)-enones up to 32% of *trans*-epoxide **92** are obtained as side product and yields (51%, 60%) and enantioselectivities (82%, 88%) were slightly lower (equation 36)¹⁹⁷. Compared to (*E*)-enones, with the same enantiomer of the BINOL ligand, the opposite sense of stereochemistry is obtained at the β -carbon of *cis*-epoxides. The same catalyst was found to be active for catalyzing the epoxidation of the trisubstituted enone **131** with 78% yield and 87% *ee*¹⁹⁷. In 1998, Shibasaki and coworkers reported on a method for improving the asymmetric induction of the ytterbium-unsubstituted BINOL system, which is cheaper than the more active Yb-3-hydroxymethyl-BINOL catalyst, by addition of 4 to 5 equivalents of water [relative to Yb(OPr-*i*)₃] to the system generated *in situ* from Yb(OPr-*i*)₃ and BINOL (2:3)¹⁹⁶. For effective catalysis, it was still necessary to add molecular sieves. With this system, epoxides could be obtained with very good yields (82–99%) and enantioselectivities (*ee* 81–94%) (see Table 16). The authors explained the effect of water by the proposal that it binds to ytterbium and controls the orientation of the hydroperoxides as depicted in Figure 7.



The effect of additives on Shibasaki's lanthanide-BINOL catalysts has been investigated by Inanaga and coworkers. From a variety of additives, triphenylphosphine oxide turned out to be the best one improving, for example, the obtained *ee* for the chalcone epoxide from 73% to 96% (Table 16)¹⁹⁸. The explanation for the positive effect of the additive was the disruption of the oligomeric structure of the catalyst by coordination of the phosphine oxide. As a consequence, epoxidation takes place in the coordination sphere of the ytterbium where the reaction site might become closer to the chiral binaphthyl ring due to the phosphine oxide ligand with suitable steric bulkiness. In contrast to the Shibasaki

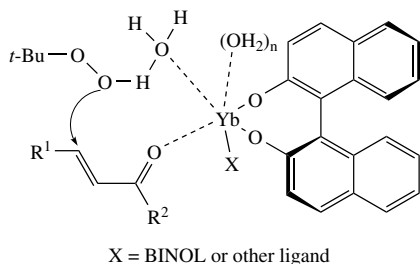
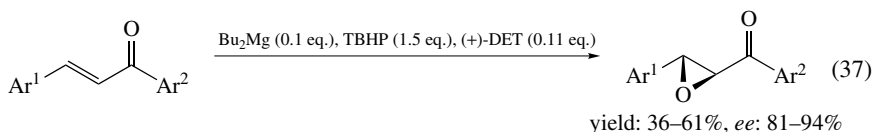


FIGURE 7

method, the modified procedure with triphenylphosphine additive is able to catalyze the epoxidation of alkyl ketones as well as aryl ketones.

An alternative method for the epoxidation of enones was developed by Jackson and coworkers in 1997¹⁹⁹, who utilized metal peroxides that are modified by chiral ligands such as diethyl tartrate (DET), (*S,S*)-diphenylethanediol, (–)-ephedrine, (–)-*N*-methylephedrine and various simple chiral alcohols. The best results were achieved with DET as chiral inductor in toluene. In the stoichiometric version, DET and lithium *tert*-butyl peroxide, which was generated *in situ* from TBHP and *n*-butyllithium, were used as catalyst for the epoxidation of enones. Use of 1.1 equivalent of (+)-DET in toluene as solvent afforded (2*R*,3*S*)-chalcone epoxide in 71–75% yield and 62% *ee*. In the substoichiometric method *n*-butyllithium was replaced by dibutylmagnesium. With this system (10 mol% Bu₂Mg and 11 mol% DET), a variety of chalcone-type enones could be oxidized in moderate to good yields (36–61%) and high asymmetric induction (81–94%), giving exactly the other enantiomeric epoxide than obtained with the stoichiometric system (equation 37).



An overview of the results obtained for the asymmetric epoxidation of (*E*)-enones **91** with the different catalytic systems is given in Table 16.

b. Epoxidation of allylic alcohols. The epoxidation of allylic alcohols can be conducted with several transition metal catalysts, for example Ti(IV)-, V(V), Mo(VI) and W(VI) complexes in the presence of alkyl hydroperoxides (above all, *tert*-butyl hydroperoxide). Whereas molybdenum complexes are more effective for the epoxidation of simple alkenes, the vanadium and titanium catalysts are most effective for the oxidation of allylic alcohols: The VO(acac)₂ catalyzed epoxidation of allylic alcohols with hydroperoxides takes place 200 times faster than for alkenes. Characteristic for the above-mentioned catalysts is their Lewis acidity, the high oxidation state (d⁰) and the low oxidation potential of the metal center. Ligands like alkoxides can easily be exchanged, which is necessary for the coordination of the substrate. The advantages of the metal-catalyzed epoxidation of allylic alcohols compared to unfunctionalized olefins are the milder reaction conditions and the faster oxygen transfer. This can be explained by formation of a metal template in which the allylic alcohol is covalently bound to the metal via the hydroxy group right next to the bidentately coordinated hydroperoxide (Figure 8). In this way the oxygen transfer can take place intramolecularly.

Aiming at easier workup conditions, immobilization of several transition metal catalysts, which show activity for the epoxidation of allylic alcohols, on polymer support has been investigated. For example, Suzuki and coworkers incorporated an oxo-vanadium ion into cross-linked polystyrene resins functionalized with iminodiacetic acid or diethylenetriamine derivatives (Scheme 57), which afforded a heterogeneous catalyst that can promote

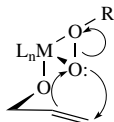


FIGURE 8

TABLE 16. Epoxidation of (*E*)-enones catalyzed by different metal/chiral ligand systems (yields are given; *ee* values are given in parentheses)

Enones 91		Ligand:		R = H		R = CH ₂ OH			
R ¹	R ²	Et ₂ Zn/O ₂ / 120 ^a	Et ₂ Zn/O ₂ / 121 ^b	Et ₂ Zn/TBHP/ 126 ^c	M = La/ CHP ^d	M = Yb/ TBHP + H ₂ O ^e	M = La/ CHP ^d	M = Yb/ TBHP ^g	[LiOOBu- <i>t</i> / (+)-DET]
Me	Ph	Ref. 173, 192	Ref. 193	Ref. 193	Ref. 195	Ref. 196	Ref. 198	Ref. 195	Ref. 199
Et	Ph	96 (85)							
<i>n</i> -Pr	Ph	99 (91)							
<i>i</i> -Pr	Ph	99 (87)		92 (76)			89 (93)	95 (94)	
<i>t</i> -Bu	Ph	97 (92)	18 (25)	93 (78)	93 (86)				
Ph	Ph		41 (71) ⁱ	67 (64)	93 (83)	99 (81)	99 (96)	93 (91)	61 (94) [71–75 (62)]
CH ₂ CH ₂ Ph	Me	94 (61)		92 (73)			92 (87)		
CH ₂ CH ₂ Ph	<i>t</i> -Bu	99 (90)							
Et	2,4,6-Me ₃ C ₆ H ₂	94 (82)							
<i>p</i> -Tol	Ph		34 (54)	93 (70)					
Ph	<i>p</i> -Tol								36 (84)
2-Naph	Ph		75 (54)						36 (87)
Ph	2-Naph		91 (47)						46 (92)
<i>p</i> -ClC ₆ H ₄	Ph			81 (79)					54 (81)

Ph	<i>o</i> -MeOCH ₂ OC ₆ H ₄	85 (85)			78 (83)	
Ph	Me		92 (94)			83 (94)
Ph	<i>i</i> -Pr		82 (93)		92 (93)	55 (88)
<i>n</i> -Pen	Me				67 (96)	71 (91)

^a Reaction in toluene at 0 °C, 2.4 eq. of ligand, 1.1 eq. of Et₂Zn.

^b Reaction in CH₂Cl₂ or toluene at 0 °C or -15 °C, 1.1 eq. of ligand, 1.05 eq. of Et₂Zn.

^c Reaction in Et₂O with 20 mol% ligand, 36 mol% Et₂Zn at r.t.

^d 5 mol% catalyst, 1.5 eq. CHP, THF, r.t., 4Å molecular sieves.

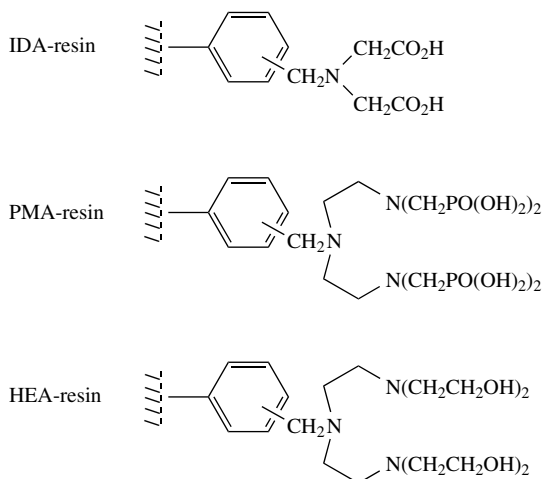
^e 5 mol% catalyst, Yb: ligand (2:3), H₂O as additive, 1.5 eq. TBHP, THF, r.t., 4Å molecular sieves.

^f 5 mol% catalyst, 15–30% Ph₃PO, THF, r.t., 4Å molecular sieves.

^g 5 or 8 mol% catalyst, 1.5 eq. TBHP, THF, r.t., 4Å molecular sieves.

^h Bu₂Mg (0.1 eq.), TBHP (1.5 eq.), (+)-DET (0.11 eq.), solvent: toluene/THF.

ⁱ Different reaction conditions were checked. Result with the highest *ee* is given here (in CH₂Cl₂, 0 °C, mole ratio: ligand: Et₂Zn: ketone 1: 0.95: 0.9).

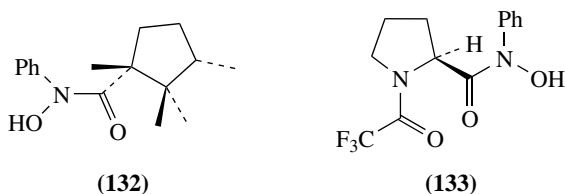


SCHEME 57. Polymer resins for complex formation with oxo-vanadium(V) ions

the epoxidation of allylic alcohols like geraniol with very high conversions (up to 100%) and in a high regioselective manner (up to 98% selectivity for allylic alcohol oxidation)²⁰⁰. The activity and selectivity of these catalysts is comparable to those of the homogeneous catalyst VO(acac)₂.

Because of the great synthetic utility, asymmetric versions of the epoxidation of allylic alcohols have been developed and will be discussed in the following. Two methods of asymmetric conduction of the reaction are known. The first one is the employment of chiral catalysts and the second possibility is the use of chiral oxidants, which will be presented separately.

i. Asymmetric epoxidation of allylic alcohols catalyzed by chiral metal complexes. The first methods for the enantioselective epoxidation of prochiral allylic alcohols were developed in 1977 by Sharpless and coworkers^{201,202}, who developed vanadium complexes with chiral hydroxamic acid ligands **132** and **133**, and by Yamada and coworkers²⁰³, who used chiral molybdenum complexes for this purpose. With the best vanadium complex, in which a proline-derived hydroxamic acid **133** coordinates to the metal, an *ee* of up to 80% was obtained for the epoxidation of α -phenylcinnamyl alcohol with TBHP. Yamada's molybdenum complex of *N*-ethylephedrine (Figure 9, left) in the presence of cumyl hydroperoxide afforded *ee* values up to 33%. An enantiomeric excess of 50% in the epoxidation of 3-methyl-2-buten-1-ol has been reported by Coleman-Kammula and Duim-Koolstra in 1983, who employed a MoO₂(acac)₂ catalyst in the presence of (*L*)-*N*-methylprolinol (Figure 9, right) and cumene hydroperoxide as oxidant²⁰⁴.



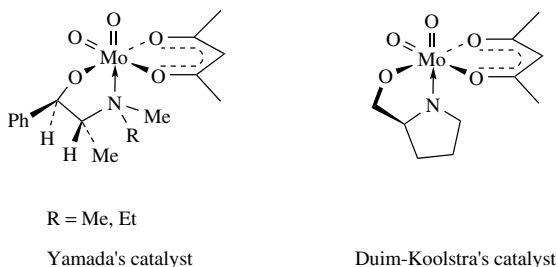
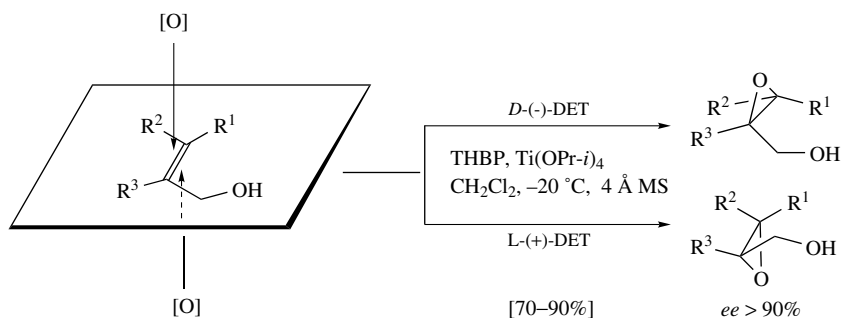


FIGURE 9

The real breakthrough in the field of enantioselective epoxidation was reached by Sharpless and Katsuki with the development of the catalytic system consisting of titanium tetrakisopropoxide and optically active diethyl- or diisopropyl tartrate (DET or DIPT) and water-free TBHP as oxygen donor (Scheme 58)^{205–207}. This milestone in synthetic organic chemistry, appropriately honored with the Nobel Prize in 2001, has kindled intensive research activity in catalytic oxidations. Both enantiomers of the epoxide can easily be obtained by this method utilizing either the (+)- or (–)-tartrate, which has to be used in excess (10–20% excess) in order to obtain optimal results²⁰⁸. The system is water-sensitive and the *ee* values drop drastically when water is present. Fairly water-soluble epoxy alcohols could only be isolated in poor yields (10–30%), but this problem was circumvented by employing dimethyl tartrate (DMT) as chiral inductor and by a modified workup²⁰⁵. The asymmetric induction of the optically active ligand in general is very high for a large variety of differently substituted primary allylic alcohols (*ee* >90%), except substrates with a sterically demanding *cis*-substituent. In addition, the catalytic system shows good regioselectivity. Isolated double bonds are not epoxidized. The use of 3 Å or 4 Å molecular sieves substantially increases the scope of the titanium(IV)-catalyzed asymmetric epoxidation²⁰⁸. Whereas without molecular sieves the catalytic version of the reaction generally lead to low conversion and enantioselectivity, in the presence of molecular sieves such reactions can be conducted with high conversions (>95%) and enantioselectivity (90–95% *ee*).



SCHEME 58. Sharpless–Katsuki epoxidation

For substrates (often low molecular weight allylic alcohols) that are difficult to obtain, due to problems of decomposition and/or water solubility, an *in situ* transformation was reported by Sharpless and coworkers in 1987²⁰⁸, making possible the effective synthesis

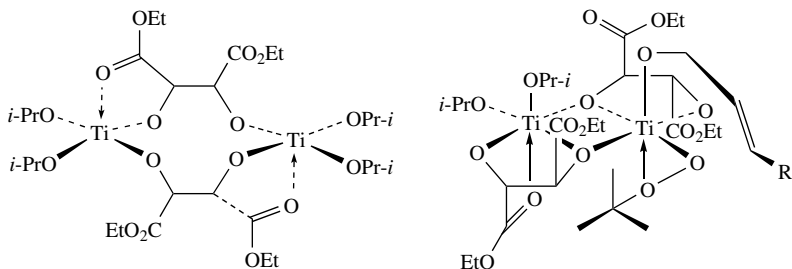


FIGURE 10

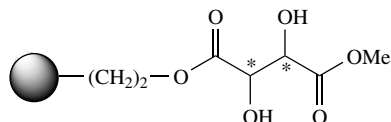
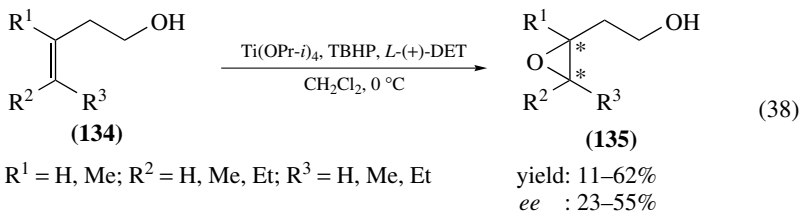
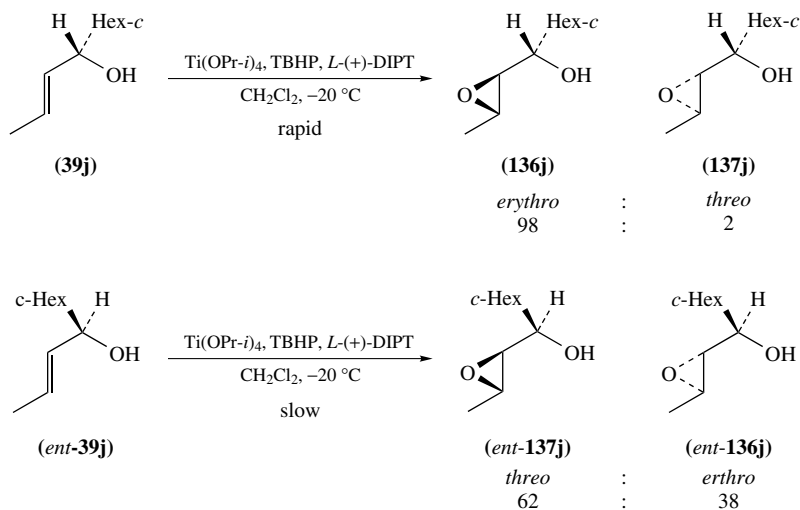


FIGURE 11

of many epoxy alcohol derivatives, which were previously difficult to obtain. The active chiral catalyst has been proposed to be a dimer in solution (Figure 10, left)^{205,207}. In the intermediately formed template structure, the tartrate ligand as well as the substrate and the oxidant are bound to the titanium metal whereby a chiral environment is generated and the oxygen atom can be transferred selectively from one side (Figure 10, right). The special synthetic utility of this reaction has been demonstrated throughout the years. For example, it is used as a key step reaction in the synthesis of carbohydrates, terpenes, leukotrienes, pheromones, macrocyclic natural products and many more compounds²⁰⁵. To avoid complex workup and to reuse the tartrate ester, the chiral ligand was attached to an insoluble polymer support by Farrall and coworkers (Figure 11)²⁰⁹. With this immobilized catalyst, an enantiomeric excess of 66% has been obtained for the epoxidation product of geraniol (95% with the normal procedure). The catalyst could be recycled, although a loss of activity of about one-third occurred after five cycles. Rossiter and Sharpless extended the Sharpless-epoxidation procedure to homoallylic alcohols **134** (equation 38)²¹⁰. The yields (11–62%) and enantiomeric purities (23–55%) of the corresponding epoxides **135** in this reaction were much lower than for 2,3-epoxy alcohols and the enantiofacial selection was opposite to that observed for allylic alcohols.



The epoxidation procedure can also be utilized for the kinetic resolution of secondary allylic alcohols **39** as shown by Sharpless and coworkers (Scheme 59)²¹¹. For example, secondary allylic alcohol **39j** can be epoxidized very rapidly by using the Sharpless

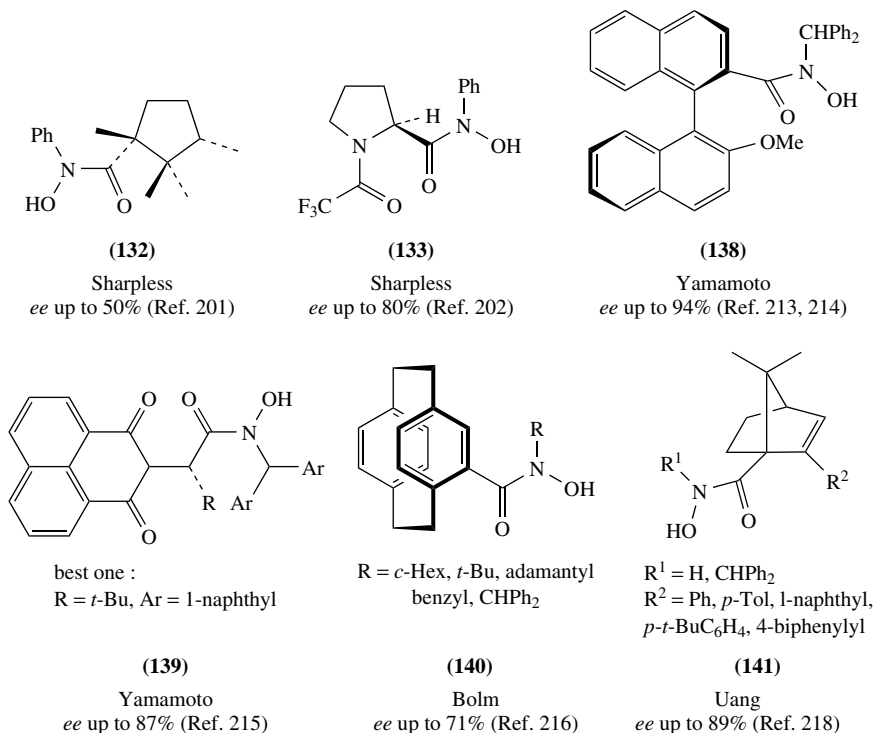
SCHEME 59. Titanium-catalyzed asymmetric epoxidation of both enantiomers of allylic alcohol **39j**

method giving preferentially the *erythro* epoxide (**136j/137j**: 98/2), because the oxygen is transferred from the less hindered side. The oxygen transfer in the epoxidation of *ent-39j* is sterically more hindered, which results in a very slow reaction giving a *threo/erythro* product mixture with low selectivity (*ent-137j/ent-136j*: 62/38).

For excellent reviews on the Sharpless asymmetric epoxidation, see References 191 and 212.

Besides the titanium system, also the structure of the vanadium systems was optimized in order to achieve high *ee* values. A compilation of published known hydroxamic acid ligands (**132**, **133**, **138–141**), which were used as chiral inductors in the vanadium-catalyzed epoxidation of allylic alcohols, together with the enantiomeric excesses achieved are summarized in Scheme 60. The catalytically active species is generated *in situ* by adding the ligand to $\text{VO(OPr-}i\text{)}_3$ prior to starting the reaction. With these systems a variety of differently substituted allylic alcohols could be oxidized with varying levels of selectivity. Table 17 compares the yields and enantioselectivities that were obtained with the different vanadium-hydroxamic acid catalysts and the results of the titanium-catalyzed Sharpless epoxidation.

While with the Sharpless ligand **132**²⁰¹ only moderate enantioselectivity was obtained (entries 7, 10), the results were improved by utilizing the proline-derived compound **133**²⁰² (entry 7). Significantly better asymmetric inductions were achieved by Yamamoto and coworkers employing the chiral vanadium catalyst **138**^{213, 214} with a hydroxamic acid ligand having an axially chiral binaphthyl group. Yields and *ee* of epoxide were moderate to good with this catalyst. In particular, the highest *ee* of 90% was obtained with 2,3-disubstituted allylic alcohols (entries 9, 13, 14), while mono- and trisubstituted substrates gave less satisfactory results ($\leq 78\%$). The observations were explained by a transition state in which the methoxy groups of the binaphthyl moiety are coordinated to the metal in order to make the complex conformationally more rigid. With the α -amino acid based ligand **139**²¹⁵, which was designed and optimized following a combinatorial strategy, Hoshino and Yamamoto obtained even better results. The selectivity of the product gradually increased with an increase in the steric hindrance of the side chain of the amino

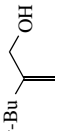
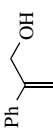
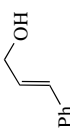
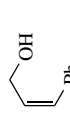
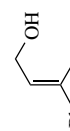
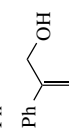
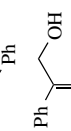
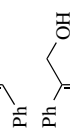


SCHEME 60. Optically active hydroxamic acid ligands for the vanadium-catalyzed asymmetric epoxidation of allylic alcohols,

acid. With this catalyst, yields and enantioselectivities were generally high. The epoxidation of monosubstituted allylic alcohols requires longer reaction time than that of di- or trisubstituted ones. Hydroxamic acid ligand **140** developed by Bolm and Kuhn with a paracyclophane chiral unit gave enantioselectivities up to 71% *ee*²¹⁶. As observed before by Yamamoto, monosubstituted allylic alcohols are less reactive, requiring higher temperatures for reasonable reaction times (substrate **142c**). Exchanging a methyl group in position C2 by a phenyl group decreases the enantioselectivity drastically (entries 7, 9) while the double bond geometry has no significant influence on enantioselectivity (entries 10, 11).

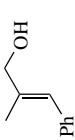
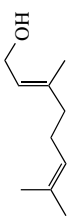
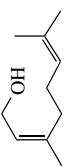

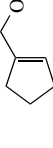
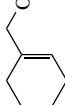
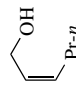
Later, in 2001, Bolm and coworkers reported a study on the influence of the steric demand of different hydroperoxides on this kind of reaction (Scheme 61)²¹⁷. As can be seen in Scheme 61, the use of a variety of achiral hydroperoxides revealed that the choice of hydroperoxide has a pronounced influence on the stereochemical outcome and that the presence of aryl groups in the oxygen source is detrimental for obtaining good *ee* values. Wu and Uang found out that decreasing the bulk of group R¹ and increasing the steric demand of R² enhances the enantioselectivity of the catalyst **141**²¹⁸. This observation is the opposite to what was found by Yamamoto and coworkers with their structurally different hydroxamic acid ligands. The best results were obtained with the ligand bearing a hydrogen at R¹ and a 4-biphenyl group at R². Wu and Uang reported that the presence of a phenyl group at position C2 compared to only a hydrogen atom at this position has a marked influence on selectivity, which is raised markedly in contrast to the findings with Bolm's paracyclophane-based ligand.

TABLE 17. Comparison of the epoxidation results obtained with different vanadium/hydroxamic acid catalysts and the Sharpless catalytic system (Ti/*L*-DET)^a (yields are given; *ee* and abs. configuration of the epoxides obtained are given in parentheses)

Entry	Substrates 142	Ti(OPr- <i>i</i>) ₄ ^b / (<i>L</i>)-DET/ TBHP	206	Ti(OPr- <i>i</i>) ₄ ^c / (<i>L</i>)-DET/ TBHP/MS	208	201	132/ TBHP	133/ TBHP	202	213, 214	138/ TiOOH	139/ TBHP	215	140/ TBHP	141/ TBHP	216	218
1								16 (40)									
2																	91 (81)
3				89 (>98%) ^e (<i>S,S</i>)								58 (87) (<i>S,S</i>)		74 (44) (<i>S,S</i>)		70 (<i>S,S</i>)	56
4								19 (38)									
5																	
6																	88 (73)
7			87(>95) (<i>S,S</i>)	n.d. (91) (<i>S,S</i>)		30 ^f (50) 84 ^{f,g} (40)	90 (80)					96 (95) (<i>S,S</i>)		87 (38) (<i>S,S</i>)		89 (89)	
8																	80 (46)

(continued overleaf)

TABLE 17. (continued)

Entry	Substrates 142	Ti(OPr- <i>i</i>) ₄ ^{b/} (<i>L</i>)-DET/ TBHP	Ti(OPr- <i>i</i>) ₄ ^{c/} (<i>L</i>)-DET/ TBHP/MS	132 / TBHP	133 / TBHP	138 / TiOOH	139 / TBHP	140 / TBHP	141 / TBHP
	Reference	206	208	201	202	213, 214	215	216	218
9			79 (>98 ^d) ^e (<i>S,S</i>)			96 (91) (<i>S,S</i>)	97 (95) (<i>S,S</i>)	85 (71) (<i>S,S</i>)	86 (55)
10			95 (91) (<i>S,S</i>)	86 ^f (30)		80 (66) (<i>S,S</i>)	95 (81) (<i>S,S</i>)	89 (45) (<i>S,S</i>)	83 (46)
11			79 (94) (<i>S,R</i>)			87 (41) (<i>S,R</i>)	97 (78) (<i>S,R</i>)	77 (41) (<i>S,R</i>)	85 (55)
12							94 (83) (<i>R,S</i>)		
13						59 (94) (<i>S,S</i>)			
14			77 (93) (<i>S,S</i>)			61 (87) (<i>S,S</i>)	82 (93) (<i>S,S</i>)	73 (55) (<i>S,S</i>)	
15							80 (82) (<i>S,R</i>)		

^a Cat. **141**: R¹ = H, R² = 4-biphenylyl, cat. **139**: Ar = 1-naphthyl, R = *t*-Bu; cat. **140**: R = adamantyl; TBHP = *tert*-butyl hydroperoxide, TiOOH = triphenylmethyl hydroperoxide.

^b Stoichiometric version.

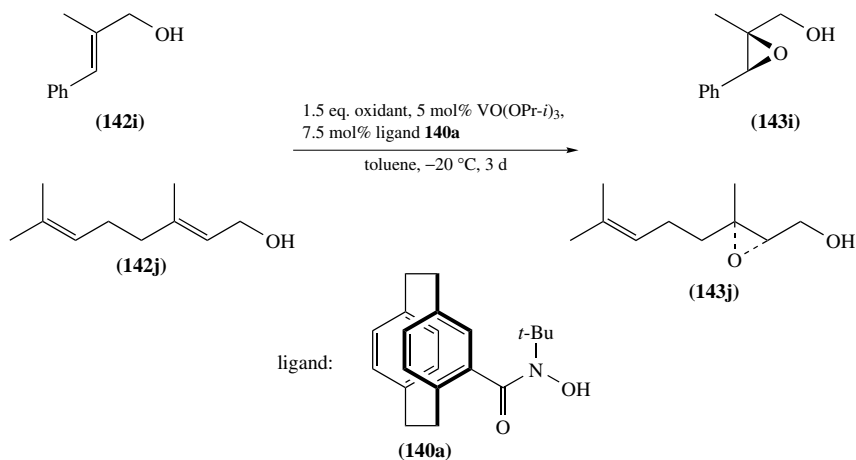
^c Catalytic version; 5% Ti(OPr-*i*)₄, 6–7.5% DET.

^d Recrystallized material.

^e DIPT instead of DET.

^f Conversion is given, not yield.

^g Higher temperature than above.

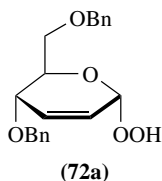


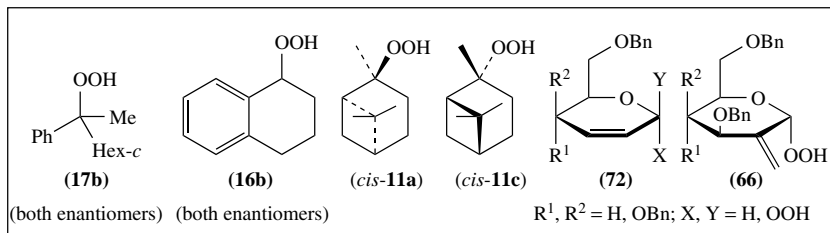
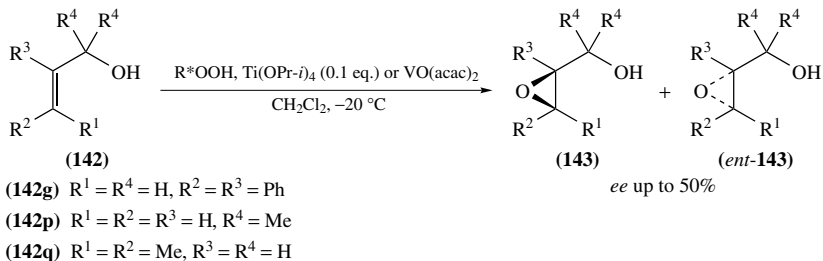
Oxidant	TBHP		CHP	TrOOH
yield (<i>ee</i>) 143i	81 (72)	80 (51)	86 (46)	70 (42)
yield (<i>ee</i>) 143j	88 (42)	86 (30)	93 (20)	42 (9 ^a)

^a Configuration is 2*R*, 3*R* in contrast to all the other cases.

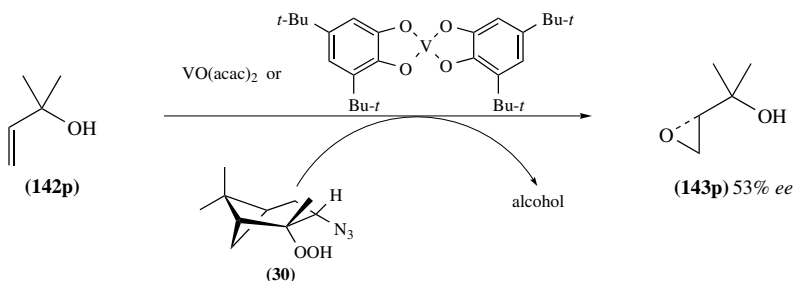
SCHEME 61. Vanadium-catalyzed epoxidation of allylic alcohols using different hydroperoxides

ii. Asymmetric epoxidation of allylic alcohols employing chiral hydroperoxides. Most of the catalytic systems for the asymmetric epoxidation of allylic alcohols are based on chiral metal complexes in combination with achiral hydroperoxides as oxygen donors. In this case the asymmetric induction is effected by the optically active ligands. Another possibility is to induce asymmetry with the help of chiral, enantiomerically pure oxidants in the presence of a catalyst which can be achiral. First results in this area were reported by Hamann and coworkers, who first tried to employ optically active hydroperoxides in the presence of Ti(OPr-*i*)₄ or VO(acac)₂ in order to conduct the epoxidation of prochiral allylic alcohols in an asymmetric way (Scheme 62)⁶⁶. The *ee* values obtained with the tertiary hydroperoxide **17b**, secondary hydroperoxide **16b**, as well as pinane hydroperoxides *cis*-**11a** and *cis*-**11c** were low ($\leq 15\%$). Slightly better results were obtained with the carbohydrate hydroperoxides **72** and **66**, which were also employed as oxidants in the vanadium-catalyzed epoxidation reaction^{66, 100, 101}. The best results were obtained with the titanium catalytic system (52% *ee*) as well as the vanadium catalyst (50% *ee*) for the allylic alcohol 3-methyl-2-buten-1-ol **142q**, using the carbohydrate hydroperoxide **72a**.



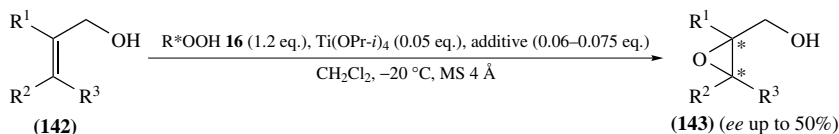


SCHEME 62. Titanium-catalyzed enantioselective epoxidation with different chiral hydroperoxides

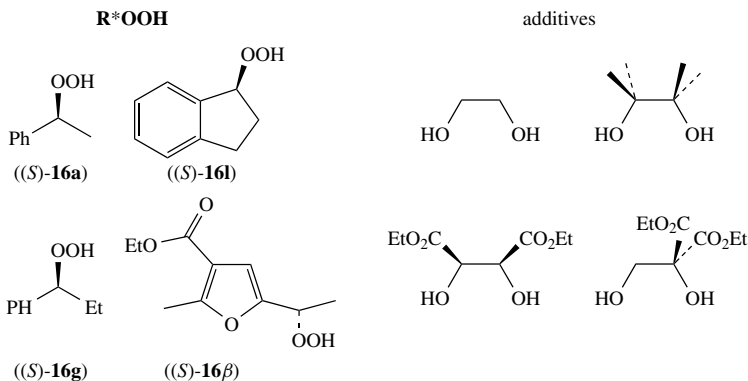
SCHEME 63. Asymmetric epoxidation with the azidohydroperoxy pinane **30**

The authors found that the configuration of the anomeric C-atom, to which the hydroperoxy group is bound, determines the absolute configuration of the epoxide formed. Remarkably, the allylic alcohol **142p**, which could not be epoxidized under Sharpless conditions, was oxidized by the carbohydrate hydroperoxides in combination with $Ti(OPr-i)_4$, albeit with low ee (11%).

In 2000, Griesbeck and coworkers⁸⁶ reported on the vanadium-catalyzed asymmetric epoxidation of 2-methyl-3-buten-2-ol (**142p**) using the chiral azidohydroperoxy pinane **30** as oxidant (Scheme 63). The enantiomeric excess of 53% in product **143p** was at that time the best result ever obtained in the epoxidation of a tertiary allylic alcohol. The use of optically active arylalkyl hydroperoxides in the titanium-catalyzed enantioselective epoxidation and sulfoxidation was reported by Adam and coworkers in 1995 (Scheme 64)^{219, 220}. In both reactions, enantiodifferentiation occurred but only low enantiomeric excess was obtained ($\leq 30\%$) with these sterically less demanding oxidants. The effect of several achiral diol ligands on the epoxidation reaction was investigated and it was found that with ethyl 2-hydroxy-2-(hydroxymethyl) malonate as achiral oligodentate ligand, the enantioselectivity in the epoxidation reaction could be raised up to 50% for the substrates 3-methyl-2-buten-1-ol and geraniol. This additive was ineffective in the oxidation of phenyl-substituted allylic alcohols. For allylic alcohols **142e, j–q** (see

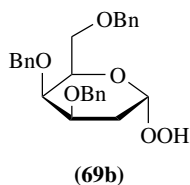


$\text{R}^1 = \text{H, Me, Ph}$; $\text{R}^2 = \text{H, Me, alkenyl, Ph}$; $\text{R}^3 = \text{H, Me, Ph}$



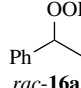
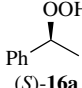
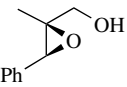
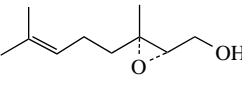
SCHEME 64. Titanium-catalyzed asymmetric epoxidation of allylic alcohols with secondary chiral hydroperoxides in the presence of diol additives

Table 17) with two substituents in position C3 the oxygen transfer by the chiral hydroperoxides occurred from the same enantioface of the double bond, while epoxidation of the (*E*)-phenyl-substituted substrates **142c,g,i** resulted in the formation of the opposite epoxide enantiomer in excess. In 2000 Hamann and coworkers reported a new saturated protected carbohydrate hydroperoxide **69b**⁶⁶, which showed high asymmetric induction in the vanadium-catalyzed epoxidation reaction of 3-methyl-2-buten-1-ol. The *ee* of 90% obtained was a milestone in the field of stereoselective oxygen transfer with optically active hydroperoxides. Unfortunately, the tertiary allylic alcohol 2-methyl-3-buten-2-ol was epoxidized with low enantioselectivity (*ee* 18%) with the same catalytic system⁶⁶.



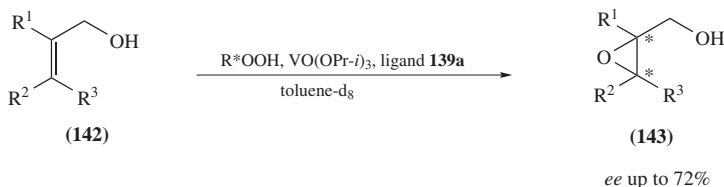
As already mentioned in Section III.A.3.b, Bolm and coworkers reported an interesting study of the effect of different hydroperoxides on the vanadium-catalyzed epoxidation of allylic alcohols (see Scheme 61)²¹⁷. Besides achiral hydroperoxides, also the chiral hydroperoxide **16a** in racemic and enantiomerically pure form was employed (see Table 18). The conclusion that could be drawn from these double asymmetric induction experiments, using chiral ligand and chiral hydroperoxide, is that the chiral ligand determined the absolute configuration of the epoxide. Both diastereomeric combinations of chiral ligand and chiral hydroperoxide react at about the same rates and therefore yields of the epoxide were similar (86–90% for **143i**, 91–93% for **143j**). However, a significant cooperative effect (one diastereomeric combination giving higher *ee*) was found.

TABLE 18. Enantiomeric excesses obtained in the vanadium-catalyzed asymmetric epoxidation of allylic alcohols using enantiomeric pure ligand **140a** and racemic as well as enantiomerically pure hydroperoxide **16a**

Epoxide	Ligand 140a configuration	Ph  <i>rac</i> - 16a	Ph  (<i>S</i>)- 16a
 (143i)	(<i>S</i>) (<i>R</i>)	49 (2 <i>S</i> ,3 <i>S</i>)	33 (2 <i>S</i> ,3 <i>S</i>) 63 (2 <i>R</i> ,3 <i>R</i>)
 (143j)	(<i>S</i>) (<i>R</i>)	23 (2 <i>S</i> ,3 <i>S</i>)	39 (2 <i>S</i> ,3 <i>S</i>) 27 (2 <i>R</i> ,3 <i>R</i>)

The racemic hydroperoxide *rac*-**16a** in combination with the (*S*)-enantiomer of the ligand **140a** produced the (2*S*,3*S*) enantiomers of the epoxides with 49% *ee* (**143i**) and 23% *ee* (**143j**). For substrate **142i**, the combination (*S*)-**16a**/*S*)-**140a** turned out to be the mismatched pair [33% *ee* of (2*S*,3*S*)-**143i**] and (*S*)-**16a**/*R*)-**140a** the matched pair [63% *ee* of (2*R*,3*R*)-**143i**], while for substrate **142j** the opposite was the case [(*S*)-**16a**/*S*)-**140a**: 39% *ee* of (2*S*,3*S*)-**143j**; (*S*)-**16a**/*R*)-**140a**: 27% *ee* of (2*R*,3*R*)-**143j**]. In employing the racemic hydroperoxide in this reaction, no kinetic resolution occurred.

In 2003, Adam, Vogl and coworkers reported on the vanadium-catalyzed epoxidation of prochiral allylic alcohols with enantiomerically pure hydroperoxides as asymmetric inductors (Scheme 65)²²¹. Unfortunately, as observed for the titanium-catalyzed system before, only modest enantioselectivities (up to 35%) were obtained with the secondary hydroperoxides for a variety of allylic alcohols. The authors investigated the ability of the sterically demanding tertiary hydroperoxide TADOOH (**60**), developed by Seebach's group, to induce asymmetry in the epoxidation reaction. This effort was much more successful. With good conversions (73 to >95% except for substrate **142d**) epoxides could be obtained with an enantiomeric excess up to 72% (obtained for substrate **142g**). The *ee* value of 52%, observed for substrate **142c**, is the highest enantioselectivity that has been



(**142b**) R¹ = Ph, R² = R³ = H

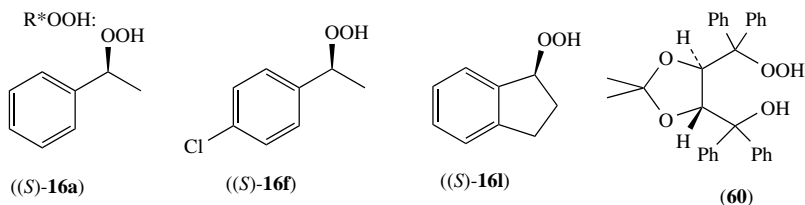
(**142c**) R¹ = R³ = H, R² = Ph

(**142d**) R¹ = R² = H, R³ = Ph

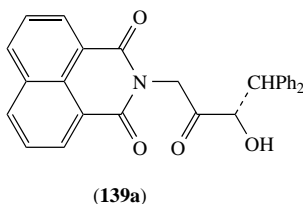
(**142g**) R¹ = R² = Ph, R³ = H

(**142i**) R¹ = Me, R² = Ph, R³ = H

SCHEME 65. Vanadium-catalyzed asymmetric epoxidation of allylic alcohols with chiral hydroperoxides



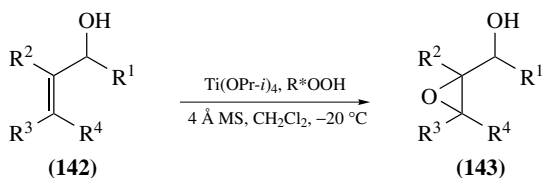
ligand:



SCHEME 65. (continued)

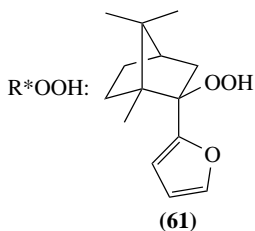
obtained for this substrate in the vanadium-catalyzed epoxidation with chiral hydroperoxides. After the reaction the optically active alcohol TADDOL can be completely recovered without loss of optical purity, which provides the opportunity to regenerate this chiral oxygen source. From the results obtained, a transition state was postulated in which the oxygen transfer takes place via a hydrogen-bonded template, held together by the vanadium metal. This assumption is supported by the observation that the enantioselectivity as well as the reactivity dropped drastically (18% conversion, 20% *ee* for substrate **142g**), when the hydroxyl-protected derivative TADOOme was used instead of TADOOH (**60**).

In 2003, Lattanzi and coworkers reported on the use of the tertiary camphor-derived hydroperoxide **61** in the titanium-catalyzed asymmetric epoxidation of allylic alcohols (equation 39)⁹⁹. Yields were moderate and ranged between 30 and 59%. Also, the enantioselectivities obtained were only moderate (24–46%). After the reaction, the enantiomerically pure camphor-derived alcohol can be recovered in good yields by chromatography without loss of optical purity and can be reconverted into the corresponding hydroperoxide.

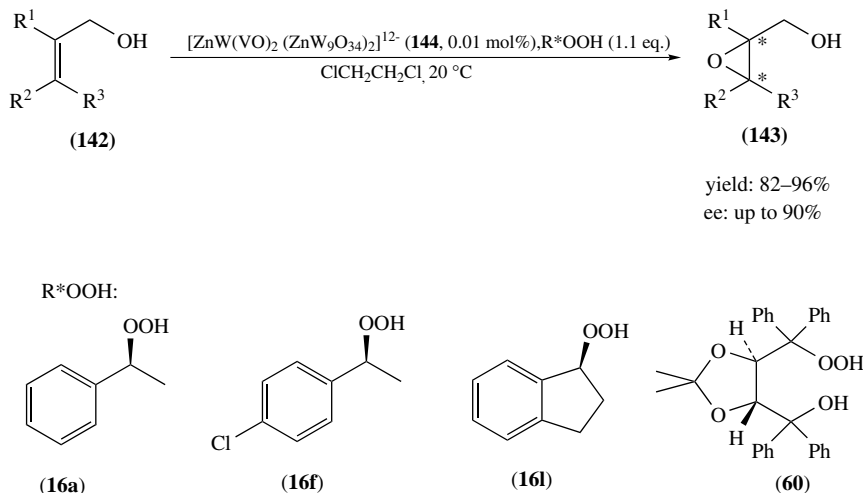


yield: 30–59%
ee : 24–46%

(39)



In 2003, Adam, Zhang and coworkers published a method for the asymmetric epoxidation of allylic alcohols catalyzed by an oxo-vanadium substituted sandwich-type polyoxometalate (POM) **144** with TADOOH **60** as chiral oxygen source²²². Upon screening of a group of differently substituted POMs, $[\text{ZnWM}_2(\text{ZnW}_9\text{O}_{34})_2]^{q-}$ ($M = \text{OV(IV), Mn(II), Ru(III), Fe(III), Pd(II), Pt(II), Zn(II)}$; $q = 10-12$) **144** turned out to be the most effective one (Scheme 66).



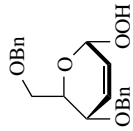
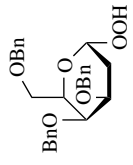
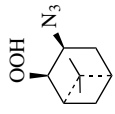
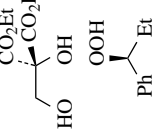
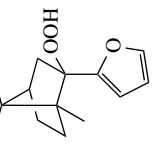
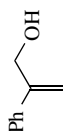
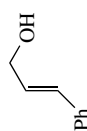
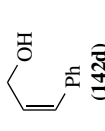
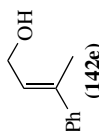
SCHEME 66. O = V(IV)-POM catalyzed asymmetric epoxidation of primary allylic alcohols with chiral hydroperoxides as chiral oxygen source

POM catalysts have the advantages of being stable homogeneous catalysts, which are resistant towards oxidation; they are easy to prepare and compatible with various oxygen sources. With **144**, conversions of >95%, diastereoselectivities of up to 91:9 and chemoselectivities (epoxidation/allylic alcohol oxidation) of up to >95:<5 could be obtained. In contrast to the POM-catalyzed epoxidation of allylic alcohols using H_2O_2 as oxidant, reactivity, chemoselectivity as well as stereoselectivity of the epoxidation reaction with hydroperoxides as oxygen source is significantly affected by the transition metal in the central ring. Therefore, this seems to be directly involved in the oxygen transfer. Other secondary optically active hydroperoxides were tested in the epoxidation reaction as well, but showed only low asymmetric induction (*er* 56:44). High enantiomeric ratios (85:15 to 95:5) could be obtained with *cis*-disubstituted allylic alcohols (see Table 19), monosubstituted substrates were oxidized with only moderate enantioselectivity (*er* 75:25) and geraniol is epoxidized with a low enantiomeric ratio of 59:41, but the regioselectivity was good. An interesting finding was that protection of the hydroperoxy functionality of TADOOH by a methoxy group led to the inactivation of the whole catalytic system and no reaction was observed.

An overview of the yields and enantioselectivities obtained in the asymmetric epoxidation of allylic alcohols with different published known optically pure hydroperoxides is given in Table 19. Here, only the results for the ‘best’ hydroperoxide of one type (highest asymmetric induction) are presented.

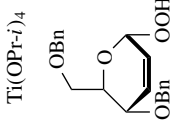
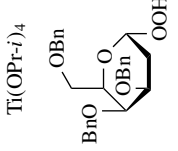
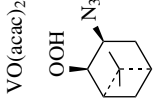
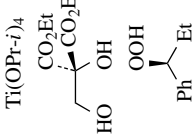
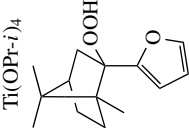
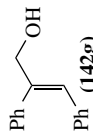
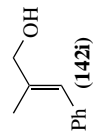
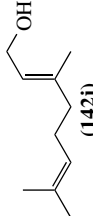
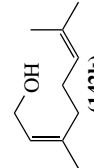
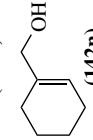
iii. *Epoxidation of allylic alcohols with special synthetic utility or academic interest.* In 1999, Adam and coworkers reported on the methyltrioxorhenium (MTO) catalyzed

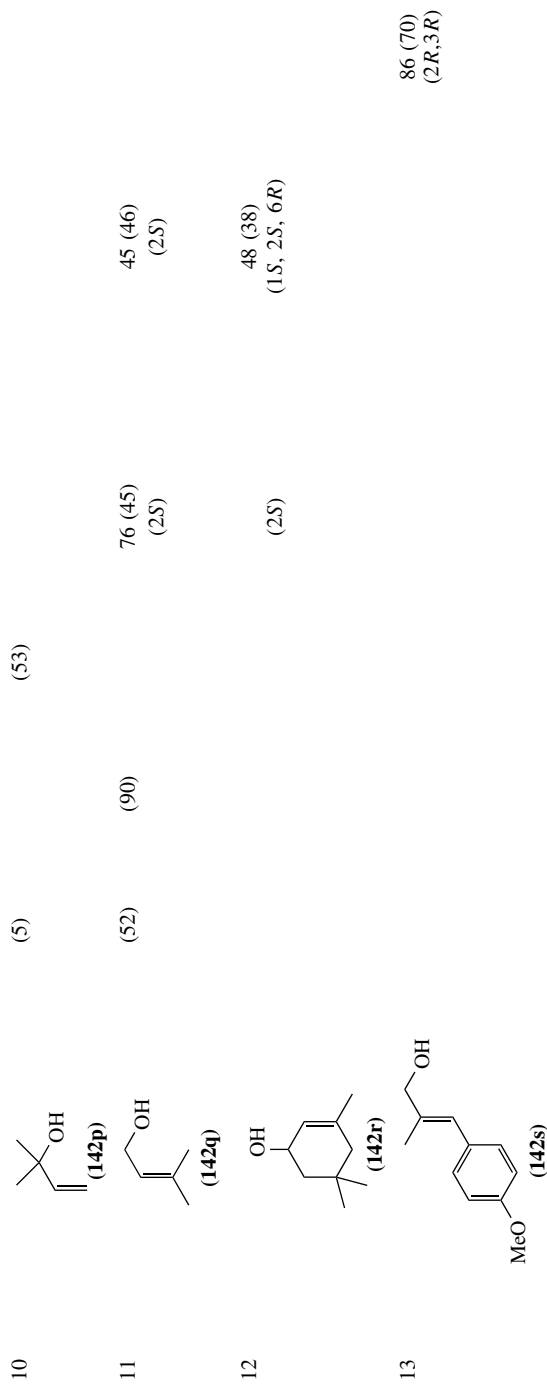
TABLE 19. Comparison of published results for the asymmetric epoxidation of allylic alcohols employing chiral hydroperoxides. (yields are given; *ee* and abs. configuration of the epoxides obtained are given in parentheses)

Entry	Ti(OPr- <i>i</i>) ₄ 	Ti(OPr- <i>i</i>) ₄ 	VO(acac) ₂ 	Ti(OPr- <i>i</i>) ₄ 	VO(OPr- <i>i</i>) ₃ ligand 139 ^a TADOOH 	POM ^b TADOOH	
1	 (142b)	66, 100	66	220	221	99	222
2	 (142c)			38 (9) (2 <i>R</i> ,3 <i>R</i>)	89 (52) (2 <i>S</i> ,3 <i>S</i>)		88 (50) (2 <i>R</i> ,3 <i>R</i>)
3	 (142d)			55 (13) (2 <i>S</i> ,3 <i>R</i>)	30 (41) (2 <i>R</i> ,3 <i>S</i>)		84 ^c (24) (2 <i>R</i> ,3 <i>S</i>)
4	 (142e)			77 (15) (2 <i>S</i> ,3 <i>S</i>)			88 (20) (2 <i>R</i> ,3 <i>R</i>)

(continued overleaf)

TABLE 19. (continued)

Entry	Ti(OPr- <i>i</i>) ₄ 	Ti(OPr- <i>i</i>) ₄ 	VO(acac) ₂ 	Ti(OPr- <i>i</i>) ₄ 	VO(OPr- <i>i</i>) ₃ ligand 139 ^a TADOOH	Ti(OPr- <i>i</i>) ₄ 	POM ^b TADOOH
5	 (142g)	66, 100 (9)	86	220 84 (6) (2 <i>R</i> ,3 <i>R</i>)	221 >95 (72) (2 <i>R</i> ,3 <i>R</i>)	99	222 94 (82) (2 <i>R</i> ,3 <i>R</i>)
6	 (142i)			89 (34) (2 <i>R</i> ,3 <i>R</i>)	73 (67) (2 <i>R</i> ,3 <i>R</i>)	30 (24) (2 <i>R</i> ,3 <i>R</i>)	92 (84) (2 <i>R</i> ,3 <i>R</i>)
7	 (142j)			83 (50) (2 <i>S</i> ,3 <i>S</i>)		54 (42) (2 <i>S</i> ,3 <i>S</i>)	96 (18) (2 <i>R</i> ,3 <i>R</i>)
8	 (142k)					59 (31) (2 <i>R</i> ,3 <i>R</i>)	
9	 (142n)					48 (36) (1 <i>R</i>)	

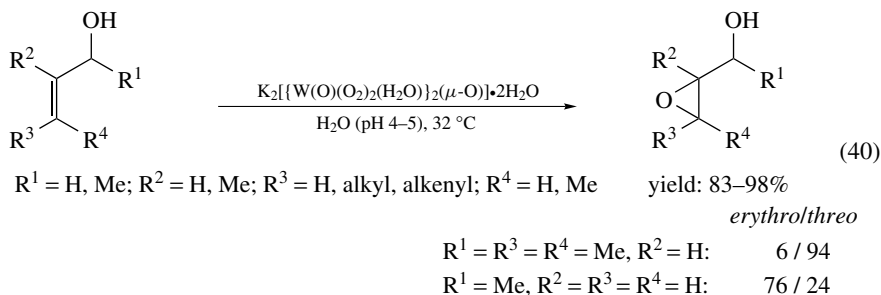


^a Ligand **139**: R = *t*-Bu, Ar = Ph.

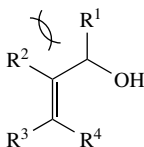
^b POM = [ZnW(VO)₂(ZnW₉O₃₄)₂]¹²⁻.

^c 9% *trans* epoxide was obtained (*ee* 16%)

epoxidation of cyclic allylic alcohols and cyclohexene derivatives with alkyl substituents in allylic position with urea hydrogen peroxide as oxygen source with high diastereoselectivity (see also Section III.A.3.c) (Scheme 67)²²³. The 3-alkyl-substituted cyclohexenes (R = Me, Et, *i*-Pr, *t*-Bu) are epoxidized with *trans* selectivity that increases with the size of the substituent (from *dr* 49:51 for R = Me to *dr* 9:91 for R = *t*-Bu) and which can be explained by steric effects. In the case of cyclic allylic alcohols, for which excellent chemoselectivities (epoxide/enone : >95/5) were observed, the diastereoselectivity changes to *cis*, because here a hydroxyl-directing effect through hydrogen bonding is present (*cis/trans*: 80/20). Compared to MCPBA (*cis/trans*: 84/16 up to 95/5) the *cis*-selectivity was slightly worse while it was much better than observed with dimethyldioxirane (DMD) as oxidant (almost no selectivity). For 2-cycloheptenol and 2-cyclooctenol hydrogen bonding is ineffective, and therefore diastereoselectivity is determined by steric interactions causing *trans*-selectivity (45/55 for 2-cycloheptenol epoxide and \leq 5/95 for 2-cyclooctenol epoxide). Recently, Mizuno and coworkers reported on an epoxidation method for allylic alcohols with high chemo-, regio- and diastereoselectivity catalyzed by a very efficient dinuclear peroxotungstate in the presence of only one equivalent of hydrogen peroxide as oxidant in water as solvent (equation 40)²²⁴. A variety of primary allylic alcohols could be oxidized with this catalyst with almost quantitative yields (85–98%) without formation of the corresponding aldehydes and carboxylic acids. In the case of *cis*- and *trans*-alcohols the configuration of the double bond was retained in the corresponding epoxide. For secondary allylic alcohols similar diastereoselectivities as obtained with the catalytic system VO(acac)₂/TBHP^{202, 225–228} were found (different from the results with DMD^{226, 228, 229} or titanium-silicalite TS-1/urea•H₂O₂^{226, 228, 230}). Epoxidation of alcohols with 1,3-allylic strain (see Figure 12) gives mainly *threo*-epoxy alcohols while alcohols without allylic strain lead to the formation of mainly *erythro*-oxidation product. A further advantage of this homogeneous system is the easy separation of products and catalyst by simple extraction and the reusability of the recovered catalyst without loss in catalytic activity.



1,2-allylic strain



1,3-allylic strain

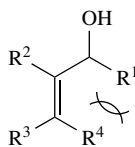
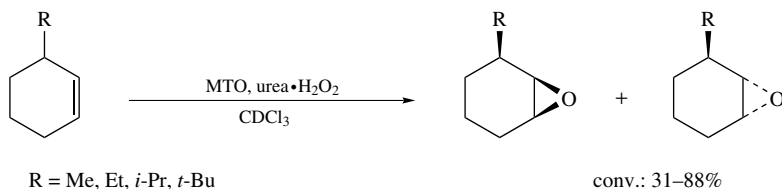
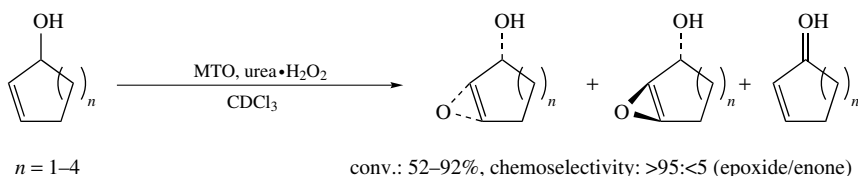


FIGURE 12



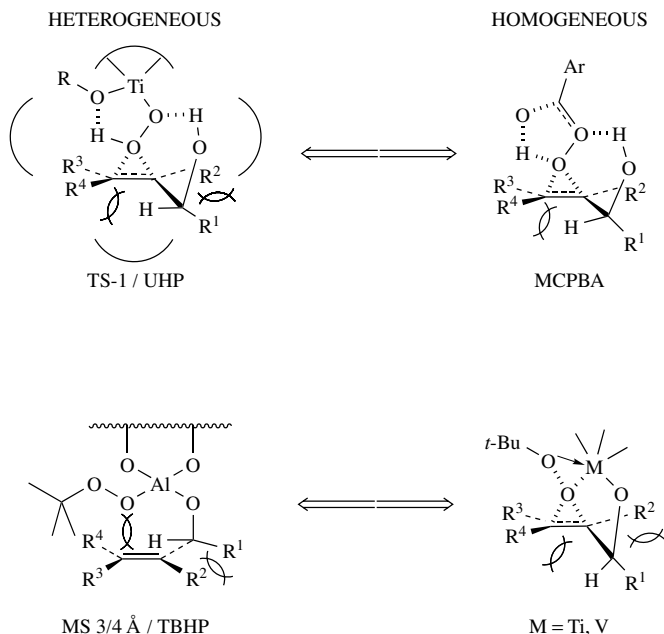
selectivity:	<i>cis</i>	:	<i>trans</i>
R = Me:	49	:	51
R = Et:	46	:	54
R = <i>i</i> -Pr:	27	:	73
R = <i>t</i> -Bu:	9	:	91



selectivity	<i>cis</i>	:	<i>trans</i>
$n = 1$	80	:	20
$n = 2$	81	:	19
$n = 3$	45	:	55
$n = 4$	≤5	:	≥95

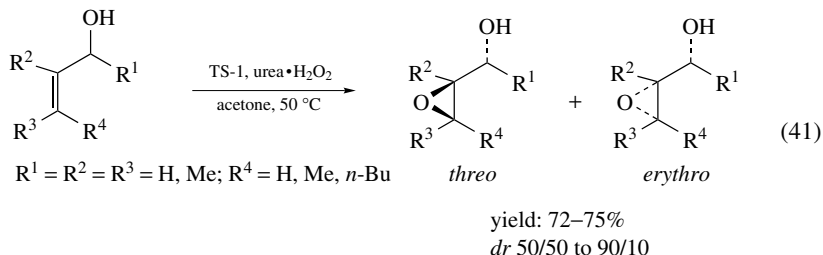
SCHEME 67. Steric and electronic effects in the diastereoselective catalytic epoxidation of cyclic olefins and allylic alcohols with MTO/UHP

Most of the published metal complexes for epoxidation reactions are homogeneous ones. During the last years, interest in developing heterogeneous catalysts has been increasing continuously because the key advantage of these supported catalysts is the ease of separation from the product mixture and their reusability. In 1996, Adam and coworkers reported on the first chemo- and diastereoselective epoxidation of acyclic chiral allylic alcohols with urea hydrogen peroxide catalyzed by TS-1 (equation 41)²²⁸, a titanium-silicalite, developed by the ENICHEM company²³¹. The catalytic system is environmentally benign, safe to handle and especially mild. With this heterogeneous catalyst, epoxide yields between 72 and 95% and diastereomeric ratios of up to 90:10 could be obtained. Depending on the extent of 1,3-allylic strain (between R¹ and R⁴) substrate specific selectivities were obtained leading preferentially to the *threo* product. Diastereoselectivity is high for substrates in which R² and R⁴ are not a hydrogen atom while the authors did not (or almost not) obtain diastereoselective epoxide formation when R² and/or R⁴ is a hydrogen atom. In contrast, 1,2-allylic strain does not have an influence on the diastereoselectivity of the epoxidation. Comparable selectivities were observed by the same group when utilizing Ti-β heterogeneous catalyst in combination with 85% H₂O₂ in acetonitrile and the highest *threo* selectivities (up to 95:5) were observed for substrates with 1,3-allylic strain²³⁰. An analogy between the heterogeneous system TS-1/UHP and the homogeneous MCPBA was found regarding diastereoselectivities which can be explained by a structurally similar active oxidizing species (Scheme 68). One year later,



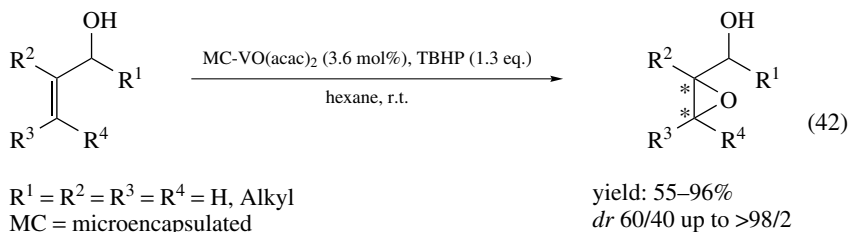
SCHEME 68. Comparison of the transition states of heterogeneous and homogeneous epoxidations of allylic alcohols

Scettri and coworkers presented an epoxidation procedure employing *tert*-butyl hydroperoxide/zeolite as oxidizing system²³². Primary alcohols could be epoxidized in the presence of MS 4 Å with yields ranging from 50 to >95%. For the epoxidation of secondary allylic alcohols high efficiency and selectivity was observed, the last one being similar to the diastereoselectivity observed with the homogeneous system VO(acac)₂/TBHP (similar type of oxygen transfer mechanism, see Scheme 68). When only 1,3-allylic strain is present in the molecule, the formation of the *threo*-epoxyalcohol is favored. When both 1,2- and 1,3-allylic strain are present in the molecule, 1,2-strain overcomes the 1,3-strain so that the *erythro*-product is generated in excess. In the absence of both strains moderate *erythro*-selectivity is obtained, which can be attributed to preferential steric interaction with the zeolite lattice. With the same oxidation system the authors also found that homoallylic alcohols can be epoxidized with moderate yields (29–53%) and long reaction times (96–120 hours).

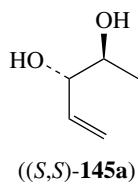


The results obtained with the heterogeneous systems are compared with the observed diastereoselectivities of the homogeneous systems $\text{Ti}(\text{OPr-}i)_4/\text{TBHP}/\text{CH}_2\text{Cl}_2$, $\text{MCPBA}/\text{CH}_2\text{Cl}_2$ and $\text{VO}(\text{acac})_2/\text{TBHP}/\text{C}_6\text{H}_6$ and are presented in Table 20.

A problem especially with oxidation catalysts is that the metals in their highest oxidation state tend to be less strongly associated with a support, so that the reaction conditions can lead to leaching of the metal complex from the support. To overcome this problem, microencapsulation, as an immobilization technique for metal complexes, has been introduced by Kobayashi and coworkers²³³. In the microencapsulation method, the metal complex is not attached by covalent bonding but is physically enveloped by a thin film of a polymer, usually polystyrene. With this technique leaching of the metal can be prevented. In 2002, Lattanzi and Leadbeater²³⁴ reported on the use of microencapsulated $\text{VO}(\text{acac})_2$ for the epoxidation of allylic alcohols. In the presence of TBHP as oxidant, it was possible to oxidize a variety of substrates with medium to good yields (55–96%) and diastereomeric ratios (60/40 to >98/2) (equation 42). The catalyst is easily prepared and can be reused several times without significant loss in activity.

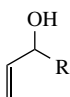
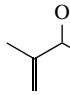
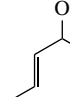
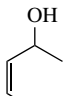
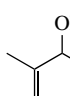
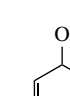
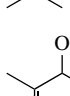
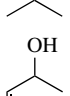


iv. Diastereoselective epoxidation of ene diols. The titanium/tartrate catalyzed enantioselective epoxidation of allylic alcohols (Sharpless reaction) is an effective method for the synthesis of epoxyalcohols in enantiomerically pure form. This reaction is limited by the fact that it works poorly for polyhydroxy substrates like, for example, compound **145a** because the bidentate oxidant TBHP cannot replace the formed tridentate epoxydiol via ligand exchange in order to regenerate the catalytically active titanium species. Therefore, optically active epoxydiols **147** (see Scheme 69) were hardly accessible in diastereomerically pure form.

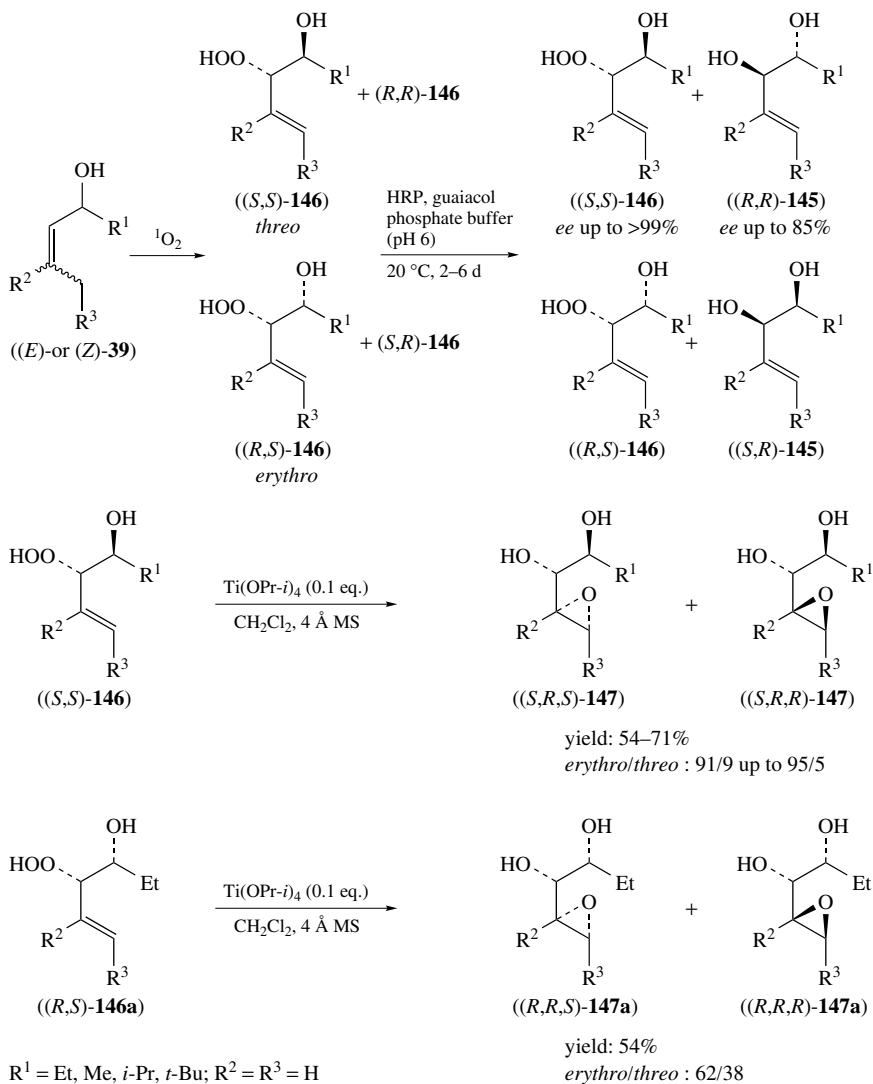


This problem was solved by Adam and coworkers in 1994–1998. They presented a high-yielding and diastereoselective method for the preparation of epoxydiols starting from enantiomerically pure allylic alcohols **39** (Scheme 69).²³⁵ Photooxygenation of the latter produces unsaturated α -hydroxyhydroperoxides **146** via Schenck ene reaction. In this reaction the (*Z*)-allylic alcohols afford the (*S,S*)-hydroperoxy alcohols **146** as the main diastereomer in a high *threo* selectivity ($dr \geq 92:8$) as racemic mixture. The (*E*)-allylic alcohols react totally unselectively (*threo/erythro* : 1/1). Subsequent enzymatic kinetic resolution of *rac*-**146** (*threo/erythro* mixture) with horseradish peroxidase (HRP) led to optically active hydroperoxy alcohols (*S,S*)- and (*R,S*)-**146** (*ee* >99%) and the

TABLE 20. Comparison of the diastereomeric ratios (*threo:erythro*) of epoxides obtained after oxidation of secondary allylic alcohols **39** utilizing different methods

Substrate	TS1/UHP/ acetone	Molecular sieves 3 or 4 Å/TBHP in CHCl ₃	Ti(OPr- <i>i</i>) ₄ / TBHP/ CH ₂ Cl ₂	MCPBA/ CH ₂ Cl ₂	VO(acac) ₂ / TBHP/ C ₆ H ₆	Mo(CO) ₆ / TBHP
	<i>dr</i>	<i>dr</i>	<i>dr</i>	<i>dr</i>	<i>dr</i>	<i>dr</i>
Reference	228	232	228	^a	^a	227
	R = Me	R = <i>n</i> -Pen	R = Me	R = Me	R = Me	R = Me
 (39k)	65:35	24:76	71:29	60:40	20:80	44:56
 (39l)	50:50		22:78	45:55	5:95	16:84
 (39h)	65:35	37:63	66:34	64:36	29:71	62:38
 (39b)	80:20		91:9	95:5	71:29	84:16
 (39f)	81:19	14:86 to 5:95 ^b	83:17	90:10	33:67	
 (39a)	95:5	82:18	95:5	95:5	86:14	95:5
 (39m)	90:10		95:5	90:10		
 (39g)	80:20		95:5	90:10 ^c	78:22	

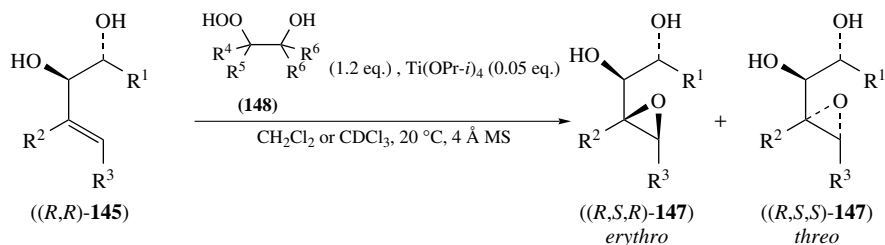
^a For substrates **39b,h,k,l** see Reference 202 and for substrates **39g,m** see Reference 228.^b Solvent: *n*-hexane instead of CHCl₃.^c In CDCl₃ as solvent.



SCHEME 69. Epoxy hydroxylation of chiral allylic alcohols to the corresponding epoxy diols

diols *(R,R)*- and *(S,R)*-**145** (*ee* up to 85%). Enantiomerically pure *(S,S)*-**146** (used in a ratio *(S,S)*-**146**:*(R,S)*-**146** $\geq 92:8$) served as substrate for the titanium-catalyzed so-called ‘epoxy-hydroxylation’ generating epoxy diols **147** with high diastereoselectivity [*(S,R,S)*-**147** (*erythro* product)/*(S,R,R)*-**147** (*threo* product): 91/9 up to 95/5]. The corresponding enantiomerically pure hydroperoxy alcohol *(R,S)*-**146a**, which is obtained by chemical separation of the 1:1 mixture of *erythro*:*threo* diastereomers by means of Ti-catalyzed separation, undergoes direct epoxidation to *(R,R,S)*-/*(R,R,R)*-**147a** but with lower reactivity as well as lower diastereoselectivity (*erythro*/*threo* : 62/38) than its *threo*-isomer.

In the direct epoxidation reaction the *in situ* generated allylic hydroperoxide acts as oxygen donor and oxygen acceptor and in the whole reaction sequence (photooxygenation, kinetic resolution, epoxidation) three additional chirality centers can be introduced regio- and diastereoselectively. The stereoselectivity in the case of (*Z*)-allylic alcohol as substrate results on one hand from the hydroxyl-directed photooxygenation of starting allylic alcohols with 1,3-allylic strain and, on the other hand, the additional coordination of the homoallylic hydroxyl group to the titanium metal in the epoxidation step. The second effect of the additional hydroxyl group is the rate enhancement compared to the conventional titanium-catalyzed epoxidation with TBHP (for the latter only traces of epoxide product are formed after several days). In contrast to the bidentate TBHP the tridentate hydroperoxy alcohols **146** can exchange with the epoxydiol products in the coordination sphere of the titanium metal, so that the catalytic cycle can continue. While the epoxy diols (*S,R,S*)-**147** are accessible diastereoselectively via the procedure described above, the corresponding enantiomers (*R,S,R*)-**147** cannot be prepared by this method. A short time later the same authors could present a novel synthetic concept for epoxy diols, in which the oxygen is not transferred intramolecularly but intermolecularly using β -hydroperoxy alcohols **148a–d** as novel oxygen donors (Scheme 70)^{235,236}. With this procedure also the (*R,S,R*)-configured diastereomers of **147** were accessible with high *erythro* selectivity (*dr* up to 96:4). Compounds **148a–d** are also tridentate and therefore can serve as effective oxidants for the diastereoselective epoxidation of γ,δ -unsaturated diols **145**, because they can efficiently replace the formed tridentate epoxy diol products **147** in the titanium template. With these oxygen sources very high yields (88 to >95%) and diastereoselectivities (*erythro*/*threo* : 76/24 up to >95/<5) of the products **147** were achieved. This high stereochemical control (*erythro* selectivity) is explained by the authors by the formation of a rigid transition state for the oxygen transfer. In this template the homoallylic hydroxyl group of the substrate additionally binds to the metal so that the substrate conformation is fixed in such a way that the oxygen can only be transferred from the side of the allylic oxygen functionality (see Reference 236). Also simple allylic alcohols display *erythro* selectivity, provided these monodentate substrates possess 1,2-allylic strain.



$\text{R}^1 = \text{H, Me, Et, } i\text{-Pr, } t\text{-Bu, Ph}$ **148a**: $\text{R}^4 = \text{R}^5 = \text{Me, R}^6 = \text{H}$

$\text{R}^2 = \text{H, Me}$ **148b**: $\text{R}^4 = \text{R}^5 = \text{R}^6 = \text{Me}$

$\text{R}^3 = \text{H, } n\text{-Pr}$ **148c**: $\text{R}^4 = \text{Ph, R}^5 = \text{R}^6 = \text{H}$

148d: $\text{R}^4 = \text{Ph, R}^5 = \text{Me, R}^6 = \text{H}$

yield: 88 to >95%

erythro/*threo* : 76/24 up to >95/5

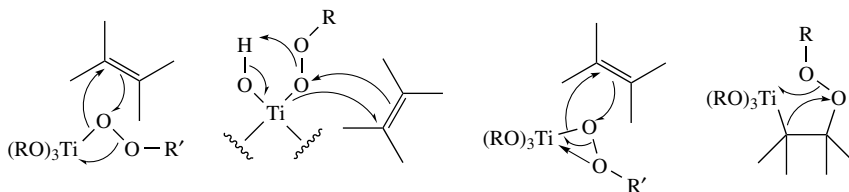
SCHEME 70. Titanium-catalyzed epoxidation of ene-diols **145** by β -hydroperoxy alcohols **148**

c. Metal-catalyzed epoxidations of unfunctionalized olefins. This kind of reaction plays a central role in synthetic organic chemistry and many complexes with a variety of different transition metals have been found to catalyze the epoxidation reaction

of unfunctionalized olefins. In this Section various published methods will be presented, classified by subgroups of the periodic table.

i. Ti, Zr, Hf. Characteristic for group IV transition metal catalysts for epoxidation reactions is the intermediate formation of a mono- or bidentate coordinated alkyl hydroperoxide, hydrogen peroxide or a bidentate coordinated peroxy group in the catalytically active species.

Coordination of a peroxide to Ti(IV) as depicted in Scheme 71 results in an activation of the oxidant for oxygen transfer. Different mechanisms have been proposed in the literature^{237–239}, including activation of intact hydroperoxide for epoxidation by coordination to the metal, titanium (IV) alkoxides, although not the most effective epoxidation catalysts, promote the reaction of alkenes with alkyl peroxides. Besides the asymmetric epoxidation of allylic alcohols (Sharpless epoxidation), in which they have gained the most popular role, they can also be employed as catalysts for the epoxidation of unfunctionalized olefins. A variety of alkenes have been epoxidized by Sheldon and coworkers using titanium(IV) alkoxides and alkyl hydroperoxides as the oxygen donor^{239–241}. The disadvantages of the reaction are that it is relatively slow and by-products are formed by addition of *tert*-butyl peroxide radicals to the substrate²⁴⁰. To overcome these limitations, heterogeneous silica-supported titanium(IV) catalysts have been developed. The first heterogeneous catalysts were silicon dioxide supported ones^{239,242}, patented in 1971 by the Shell Oil company. They were prepared by impregnating silica with TiCl_4 or an organotitanium compound, followed by calcinations. These catalysts are highly active and, for example, very good yields (93–94%) were obtained for the oxidation of propylene to the corresponding epoxide, which is a process of great industrial importance. The positive effect of the silicate ligands on the activity of the titanium catalyst was explained by the increase in Lewis acidity of the titanium center and the stabilization of the titanyl group by retarding polymerization, which is quite common for titanyl complexes. Titanium dioxide on silica gel, oxotitanium diacetylacetonate (reported by Sheldon and Vandoorn)²⁴⁰ and oxotitanium porphyrin (reported by Ledon and Varescon)²⁴³ have also been used as catalysts for epoxidations with TBHP, but their catalytic properties are worse than those of silicon dioxide supported titanyl derivatives.



SCHEME 71. Proposed mechanisms for titanium(IV)-catalyzed oxygen transfer to alkenes

Quite good results (epoxide yields up to 88%) were obtained by Grubbs and coworkers, who utilized polymer-supported TiCpCl_3 as epoxidation catalyst in the presence of TBHP, which proved to be a better catalyst than polymer-supported TiCp_2Cl_2 (epoxide yields up to 40%)²⁴⁴. Because of the great synthetic utility of the epoxidation reaction, intensive research has been pursued, aiming at further improvement of the titanosilicate structure with regard to better catalytic results, cheaper, safer and easier reaction conduction. Because of the hydrophilicity of the SiO_2 support layer, it was not possible to use simple and cheap aqueous hydrogen peroxide as oxygen donor, but highly concentrated H_2O_2 had to be used. During the last years, a variety of titanium-containing

compounds with zeolite structure have been developed²⁴⁵. First of all the TS-1, which is a titanium doped molecular sieve silicalite with ZSM-5 structure, was developed in 1981 by the ENICHEM company in Italy²³¹. This material is represented by the formula $x\text{TiO}_2 \cdot (1-x)\text{SiO}_2$ ($x = 0.01-0.025$) and it turned out to be a good catalyst for selective oxidations with aqueous hydrogen peroxide; it is not affected by the presence of water. The hydrophobic nature of the silicalite favors the diffusion of hydrophobic substrates to the active center, but admittance of water into the inner hollow spaces, and therefore deactivation of the catalyst, is prevented by the small micropores of the TS-1 (diameter of 6 Å). This advantage at the same time is a disadvantage because the small pore diameter limits the use of TS-1 to small molecules. TS-2 silicalite, with a molecular sieve ZSM-11 structure, was developed by Kumar and coworkers in 1990²⁴⁶. This compound showed similar catalytic activity and limitations in epoxidation reactions as TS-1 due to the same pore size as TS-1.

Further development of titanosilicates by Cambor and coworkers led to titanium doped zeolite β -(Ti- β)²⁴⁷, with a high silica content, a low alumina content and a 3-dimensional pore system having pore diameters of 7×7 Å. This Al-free Ti- β showed an enhanced activity and a much higher selectivity to the epoxide during alkene oxidation in the presence of H_2O_2 than the medium pore TS-1 catalyst. This hydrophilic catalyst shows high reactivity in protic solvents and also branched and cyclic olefins could be epoxidized with hydrogen peroxide with high selectivity and catalytic activity. The authors could show that with a decrease in Al content, and therefore acidic centers which might cause epoxide ring opening, the selectivity to the epoxide increases and the best results were obtained with Al-free catalyst. Side reactions could be diminished by deactivating the acidic functionalities of the β -(Ti- β) with the help of basic solvents.

The first report on mesoporous titanosilicates of the M41S-type was published by Beck and coworkers²⁴⁸ in 1992 and further developments on these M41S-type materials by others followed^{249, 250}. These heterogeneous catalysts in combination with either H_2O_2 or TBHP show moderate activity and chemoselectivity for the epoxidation of unfunctionalized olefins. A review on the use of mesoporous molecular sieve materials in catalysis has been published by Corma in 1997²⁵¹. These titanosilicates, which catalyze the epoxidation of olefins using organic hydroperoxides, can be divided into three classes based on the geometry of the arrangement of the pores: Ti-HMS (hexagonal, mesoporous SiO_2), MCM-41 (hexagonal) and MCM-48 (cubic). The size of pores varies from 16 to 100 Å and molecules have easy access to the catalytically active center, such that this class of titanosilicates is especially advantageous for the selective oxidation of sterically more demanding alkenes. In 1996, Thomas and coworkers together with a Chinese group developed the first synthetic zeolite-like material that contains five-fold coordinated titanium in a titanosilicate called JDF-L1, which has the formula $\text{Na}_4\text{Ti}_2\text{Si}_8\text{O}_{22} \cdot 4\text{H}_2\text{O}$ ²⁵². After pretreatment with dilute hydrochloric acid and aqueous hydrogen peroxide, this material is able to convert phenol and 1-naphthol to the corresponding quinones with hydrogen peroxide in acetone. With the aim to develop a new epoxidation catalyst that combines the benefits of the mesoporous and zeolitic materials and which is not limited to small olefins, Corma and coworkers reported on a material called ITQ-2, which is highly active and selective for the epoxidation of olefins with organic hydroperoxides such as TBHP and CHP²⁵³. This Ti-zeolite is prepared by grafting titanocene on ITQ-2 and consists of very thin silica layers of 2.5 nm height with an extremely high and well defined external surface. The catalyst shows good stability and can be reused.

In 2002, Wu and Tatsumi reported on the high *trans*-selectivity in epoxidation reactions with Ti-MWW (also known as MCM-22), a titanosilicate that contains both medium and

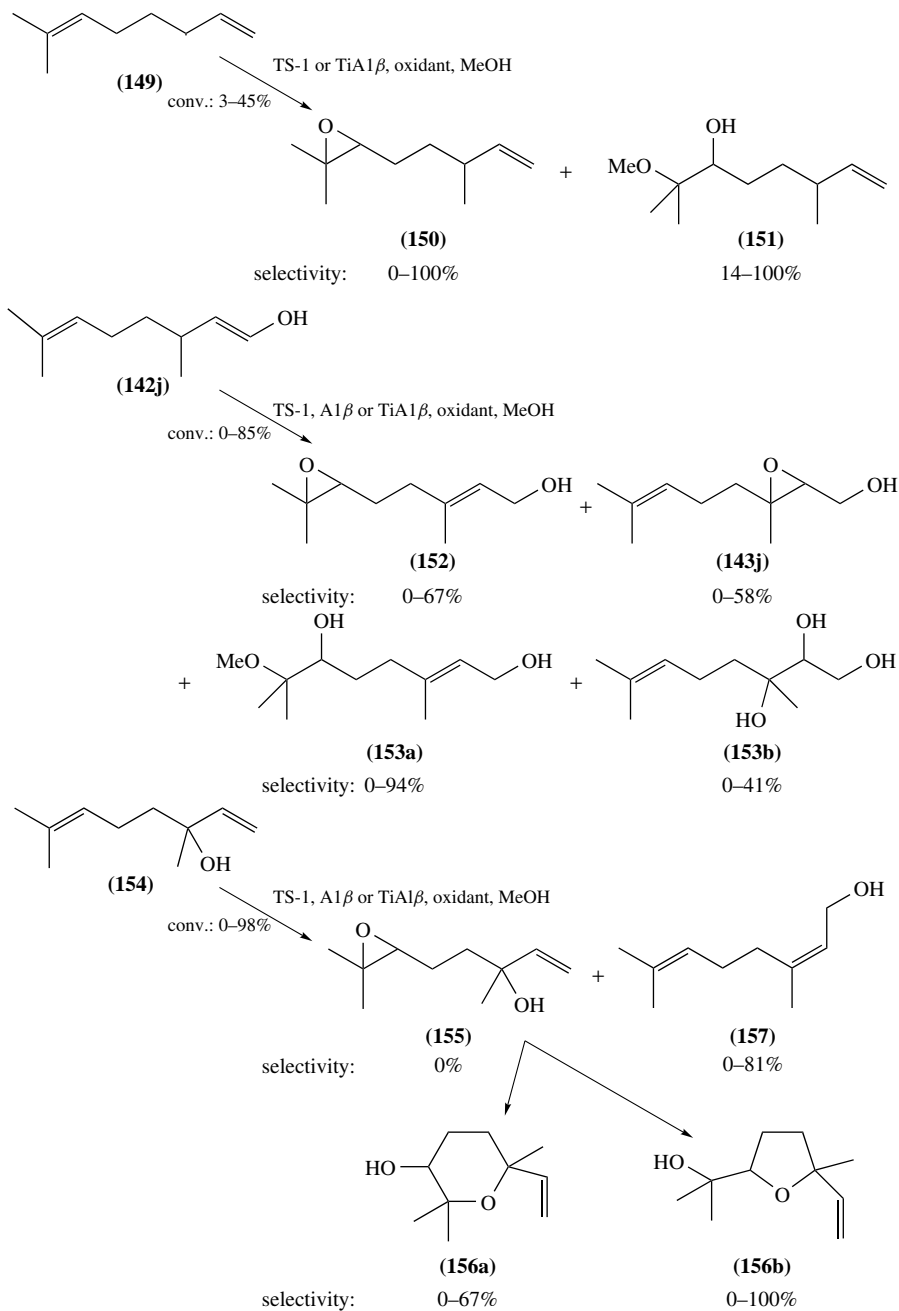
large pores, using 31% aqueous hydrogen peroxide solution²⁵⁴. An alkene mixture with a *cis/trans* ratio of 1:1 can be epoxidized with this catalyst with 80% selectivity for the *trans*-epoxide, being neither affected by reaction conditions nor by the types of alkenes. The authors could show that the *trans*-selectivity of Ti-MWW, which is in contrast to the *cis*-selective nature of conventional titanosilicates, results from its sinusoidal 10-membered ring channels.

In the same year Laha and Kumar reported on an epoxidation method using anhydrous urea hydrogen peroxide (UHP) (or aqueous H₂O₂ in the presence of separately added urea) over TS-1 and TS-2 redox molecular sieves²⁵⁵. This oxidizing agent minimizes acid-catalyzed isomerization and hydrolysis of the epoxides formed. Especially for allylic, open-chain and aromatic olefinic compounds, epoxide selectivity was higher when using UHP or *in situ* formed UHP instead of aqueous H₂O₂. The enhanced selectivity is explained by the controlled release of H₂O₂ from urea hydrogen peroxide. Furthermore, aldehyde formation by C=C double-bond cleavage is minimized by using UHP, *in situ* generated UHP (urea and aqueous H₂O₂) or by adding H₂O₂ slowly. Direct spectroscopic evidence for the formation of different titanium superoxo-complexes by interaction between TS-1/TS-2 and UHP was obtained from the characteristic continuous absorption band in the UV-vis region and the anisotropic EPR spectra for the superoxide radical attached to Ti(IV) centers on TS-1 and TS-2.

A study about the epoxidation of a variety of monoterpenes using TS-1 and TiAlβ catalysts and a range of different oxidants (H₂O₂, TBHP, UHP) was conducted by Hutchings and coworkers (Scheme 72)²⁵⁶. Dihydromyrcene **149** was selectively epoxidized at the more electron-rich double bond giving epoxide **150** and, depending on the catalytic system, also significant quantities of ring-opening products **151** were observed. Epoxidation of geraniol **142j** can occur at the allylic double bond (giving epoxide **143j**) and the unfunctionalized double bond (giving epoxide **152**) and also for this substrate both possible ring cleavage products **153a** and **153b** are observed. For both of these substrates replacement of aqueous H₂O₂ by non-aqueous oxidants (TBHP, UHP) led to an improvement of epoxide selectivity (for dihydromyrcene: up to 77%; for geraniol: up to 100%). Linalool **154** was epoxidized at the non-allylic double bond generating an epoxide **155** that underwent rapid intramolecular cyclization to five- and six-membered heterocycles **156a** and **156b**. Next to these products a side product **157** was also formed. The results obtained suggest that the ratio of the two products obtained is mainly dependent on the acid strength of the support rather than on the pore size of the catalyst.

The results obtained with several titanosilicate catalysts are summarized in Table 21.





Zirconium(IV) and hafnium(IV) complexes have also been employed as catalysts for the epoxidation of olefins. The general trend is that with TBHP as oxidant, lower yields of the epoxides are obtained compared to titanium(IV) catalyst and therefore these catalysts will not be discussed in detail. For example, zirconium(IV) alkoxide catalyzes the epoxidation of cyclohexene with TBHP yielding less than 10% of cyclohexene oxide but 60% of (*tert*-butylperoxy)cyclohexene²⁴⁰. The zirconium and hafnium alkoxides in combination with dicyclohexyltartramide and TBHP have been reported by Yamaguchi and coworkers to catalyze the asymmetric epoxidation of homoallylic alcohols²⁵⁷. The most active one was the zirconium catalyst (equation 43), giving the corresponding epoxides in yields of 4–38% and enantiomeric excesses of <5–77%. This catalyst showed the same sense of asymmetric induction as titanium. Also, polymer-attached zirconocene and hafnocene chlorides (polymer-Cp₂MCl₂, polymer-CpMCl₃; M = Zr, Hf) have been developed and investigated for their catalytic activity in the epoxidation of cyclohexene with TBHP as oxidant, which turned out to be lower than that of the immobilized titanocene chlorides²⁵⁸.



oxidant: H₂O₂, TBHP, UHP

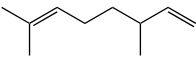
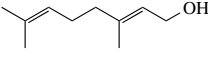
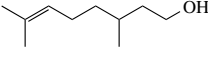
SCHEME 72. Oxidation of α -hydroxy-containing monoterpenes using titanium silicate catalysts


TABLE 21. Results of the epoxidation reactions of various alkenes using titanasilicate catalysts

Substrate	Catalyst ^a	Oxidant	Solvent	Time (h)	Temp. (°C)	Conv. (%)	Yield of epoxide (%) (<i>cis:trans</i>)	Yield of side-products (%)	Reference	
Cyclohexene	TiO ₂ -SiO ₂	TBHP	benzene	18	90	75 ^b	66	<1 ^c	240	
	O = Ti(TPP)	TBHP	benzene	27	70	45 ^b	36		243	
	 TiCpCl ₃	TBHP	—	18	80		88		244	
	 TiCp ₂ Cl ₂	TBHP	—	18	80		40		244	
	0.25%TiO ₂ /ITQ-2 1%TiO ₂ /ITQ-2/sil.	TS-1	TBHP	—	2	60	75	73		253
			TBHP	—	2	60	85	99		253
		TS-2	45% H ₂ O ₂	MeOH	12	40	38	8	30 ^e	255
			U + HP	MeOH	12	40	41	39	2 ^d	255
			UHP	MeOH	12	40	45	45	<1 ^d	255
			45% H ₂ O ₂	MeOH	12	40	40	10	30 ^f	255
U + HP	MeOH	12	40	42	39	3 ^d	255			
UHP	MeOH	12	40	44	43	1 ^d	255			
1-Octene	TiO ₂ -SiO ₂	TBHP	benzene	24	90	31 ^b	17	<1 ^c	240	
Cyclooctene	 TiCpCl ₃	TBHP	—	13	80		37		244	
	 TiCp ₂ Cl ₂	TBHP	—	20	80		25		244	
2-Hexene (<i>cis/trans</i> :41/59)	Ti-MWW	31% H ₂ O ₂	MeCN	2	60	51	50 (198:1)	<1 ^d	254	
		TBHP	MeCN	3	60	8	8 (70:30)	<1	254	
	TS-1	31% H ₂ O ₂	MeCN	2	60	29	28 (66:34)	1 ^d	254	
		TBHP	MeCN	2	60	3	3 (47:53)	<1	254	
	TS-2	31% H ₂ O ₂	MeCN	2	60	14	13 (67:33)	1 ^d	254	
		Ti-β	31% H ₂ O ₂	MeCN	2	60	16	14 (73:27)	2 ^d	254
		TBHP	MeCN	2	60	14	14 (93:7)	<1	254	
	Ti-MOR	31% H ₂ O ₂	MeCN	2	60	3	3 (52:48)	<1 ^d	254	
	Ti-Y	31% H ₂ O ₂	MeCN	2	60	4	2 (55:45)	2 ^d	254	
	Ti-MCM-41	31% H ₂ O ₂	MeCN	2	60	3	1 (62:38)	2 ^d	254	
TiO ₂ -SiO ₂	31% H ₂ O ₂	MeCN	2	60	0.8			254		
<i>trans</i> -2-Octene	Ti-MWW	31% H ₂ O ₂	MeCN	2	60	25	24		254	
	TS-1	31% H ₂ O ₂	MeCN	2		13	12		254	
<i>cis</i> -2-Octene	Ti-MWW	31% H ₂ O ₂	MeCN	2	60	10	10		254	
	TS-1	31% H ₂ O ₂	MeCN	2		21	20		254	
2-Heptene (<i>cis/trans</i> :1/1)	Ti-MWW	31% H ₂ O ₂	MeCN	2	60	28	28 (20:80)	<1 ^d	254	
3-Heptene (<i>cis/trans</i> :1/1)	Ti-MWW	31% H ₂ O ₂	MeCN	2	60	29	28 (28:72)	1 ^d	254	
2-Octene (<i>cis/trans</i> :1/1)	Ti-MWW	31% H ₂ O ₂	MeCN	2	60	17	17 (19:81)	<1 ^d	254	
Allyl alcohol	TS-1	45% H ₂ O ₂	MeOH	8	40	66	55	7 ^d	255	
		U + HP	MeOH	8	40	72	65	7 ^d	255	
		UHP	MeOH	8	40	74	73	1 ^d	255	
Allyl chloride	TS-1	45% H ₂ O ₂	MeOH	8	40	95	83	12 ^d	255	
		U + HP	MeOH	8	40	95	87	8 ^d	255	
		UHP	MeOH	8	40	96	93	3 ^d	255	

(continued overleaf)

TABLE 21. (continued)

Substrate	Catalyst ^a	Oxidant	Solvent	Time (h)	Temp. (°C)	Conv. (%)	Yield of epoxide (%) (<i>cis:trans</i>)	Yield of side-products (%)	Reference
Allyl bromide	TS-1	45% H ₂ O ₂	MeOH	8	40	94	82	12 ^d	255
		U + HP	MeOH	8	40	95	89	6 ^d	255
		UHP	MeOH	8	40	97	95	2 ^d	255
Methallyl chloride	TS-1	45% H ₂ O ₂	MeOH	8	40	64	49	15 ^d	255
		U + HP	MeOH	8	40	71	65	6 ^d	255
		UHP	MeOH	8	40	74	70	4 ^d	255
1-Hexene	TS-1	45% H ₂ O ₂	MeOH	12	40	35	10	25 ^d	255
		U + HP	MeOH	12	40	42	39	3 ^d	255
		UHP	MeOH	12	40	47	46	1 ^d	255
	Ti-MCM-41	H ₂ O ₂	MeOH	2	55	23	22	1 ^g	250
		H ₂ O ₂	MeOH	5	55	40	36	4 ^g	250
	TS-1	H ₂ O ₂	MeOH	2	60	16	14 ^h	2 ⁱ	256
	TiAlβ	TBHP	MeOH	24	60	45	32 ^h	13 ⁱ	256
	TS-1	H ₂ O ₂	acetone	24	60	39	8 + 19 ^j	12 ^g	256
	TiAlβ	TBHP	MeOH	24	60	33	8 + 22 ^j		256
	TiAlβ	UHP	MeOH	26	60	35	18 + 17 ^j		256
	TiAlβ	H ₂ O ₂	MeOH	20	60	64	55	9	256
	TiAlβ	H ₂ O ₂	MeOH	48	60	83	65	18	256

^a  = polystyrene, crosslinked with 20% divinylbenzene, ITQ-2 = very thin silica layers with a well defined external surface, sil. = silylated, U + HP = urea and hydrogen peroxide.

^b Conversion of hydroperoxide given.

^c 1-*t*-Butylperoxy-2-alkene.

^d Diols.

^e Cyclohexenol: <1%, cyclohexenone: 4%, *cis/trans*-1,2-cyclohexanediols: 24% [the structures of the cyclohexenol and cyclohexenone are not given].

^f Cyclohexenol: <1%, cyclohexenone: 4%, *cis/trans*-1,2-cyclohexanediols: 25% [the structures of the cyclohexenol and cyclohexenone are not given].

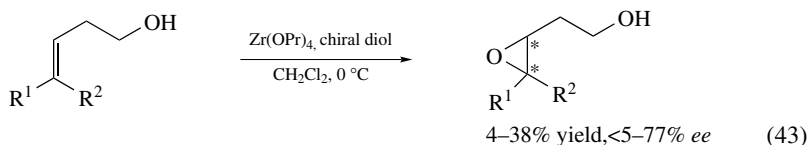
^g Side product: nerol.

^h Only one of two possible epoxides: 2,2-dimethyl-3-(3-methylpent-4-enyl)oxirane.

ⁱ Side product: 2-methoxy-2,6-dimethyloct-7-en-3-ol.

^j Allylic epoxide + non-allylic epoxide.

Epoxide yields were around 20% with the heterogeneous Zr catalysts and around 10% with the heterogeneous Hf catalysts.



R¹ = H, Me, Et;

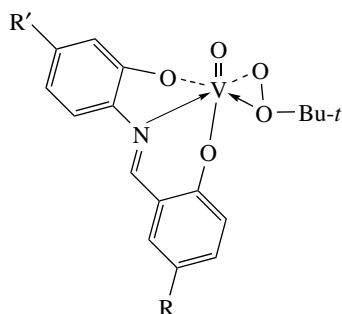
R² = H, Me, Et, Pr, *n*-Pen

chiral diol: dibutyltartramide, dibenzyltartramide, dicyclohexyltartramide, diisopropyl tartrate

ii. V, Nb, Ta. As for group IV metals described before, also in the case of group V transition metals the catalytically active species formed during the epoxidation reaction bears

a mono- or bidentate coordinated alkyl hydroperoxide, hydrogen peroxide or a bidentate coordinated peroxy group. Vanadium pentoxide was one of the first transition metal compounds used for catalytic epoxidation with TBHP as oxidant²⁵⁹. Like titanium(IV), vanadium(V) is a very effective catalyst for the epoxidation of allylic alcohols but is, compared to molybdenum catalysts, much less reactive (*ca* 10² times) for the epoxidation of unfunctionalized alkenes^{240, 241, 260}.

Several mechanisms of peroxide activation and oxygen transfer have been considered in the literature, and are similar to the mechanisms shown to operate in the Ti(IV)-alkylperoxide catalyzed epoxidations (see Scheme 71). The existence of oxovanadium(V)-alkylperoxy complexes (alkyl peroxide ligand coordinated in a mono- or in a bidentate fashion), which have been suggested by several authors to be the active species in the oxidation reactions^{202, 237, 238, 260, 261}, has been supported by ¹⁸O-labeling studies²³⁷. With stoichiometric quantities of the vanadium complex **158**²⁶² bearing a tridentate Schiff base ligand, Mimoun and coworkers observed a highly stereoselective epoxidation of several *cis*- and *trans*-olefins, yielding the corresponding *cis*- or *trans*-epoxides in moderate to good yields (40–98%). With complex **158**, allylic alcohols were not oxidized due to a displacement of *t*-BuOO⁻ by excess allylic alcohol. The epoxidation reaction was also inhibited by H₂O, alcohols and basic solvents and it was accelerated in non-coordinating, polar solvents like dichloroethane and nitrobenzene. The authors presented kinetic studies which showed that the olefins coordinate to the metal prior to the decomposition of the metal-olefin complex in the rate-determining step.

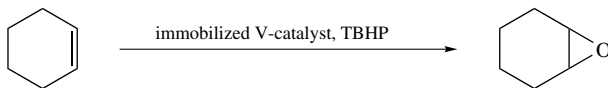


R = H, Cl; R' = H, Me, NO₂, Cl

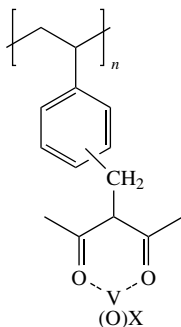
(158)

Immobilization of the oxovanadium ion on several polymer resins has been reported^{263–266} and the catalytic activity of these heterogeneous catalysts for alkene epoxidation with TBHP turned out to be better than that of the homogeneous analogs. The yields obtained with the different heterogeneous vanadium catalysts for the epoxidation of cyclohexene are shown in Scheme 73. Linden and Farona tested the catalytic activity of several oxovanadium(IV) catalysts immobilized on polymers containing ligands such as acetylacetonate, ethylenediamine or pyridine for the epoxidation of cyclohexene²⁶³. With TBHP as oxygen source and without any solvent, cyclohexene oxide could be obtained in yields between 15 and 26% after 6 hours at 80 °C with poly(vinylbenzylethylenediamine) oxovanadium(IV) sulfate [P-CH₂-en-VOSO₄] being the most efficient heterogeneous catalyst.

The same authors later on presented their results of the epoxidation of various cyclic and acyclic olefins employing a heterogeneous catalyst with an oxovanadium(IV) ion incorporated on a sulfonic acid ion-exchange resin and TBHP as oxidant²⁶⁵. Selectivities



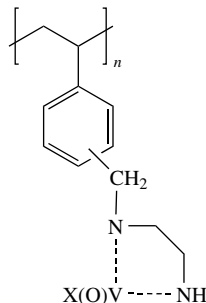
immobilized catalysts and the yields of cyclohexene oxide:



Farona et al.

X = SO₄: epoxide yield: 15%

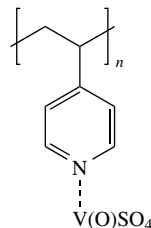
X = acac: epoxide yield: 21%



Farona et al.

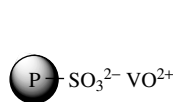
X = SO₄: epoxide yield: 26%

X = acac: epoxide yield: 21%



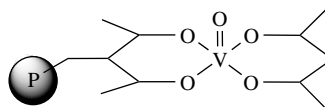
Farona et al.

epoxide yield: 15%



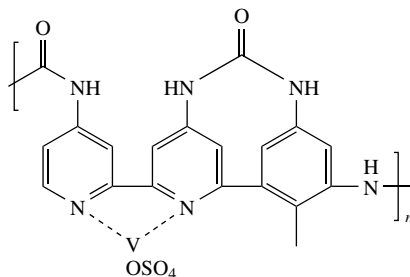
Farona et al.

epoxide yield: 74%



Bhaduri et al.

epoxide yield: <2%



Neckers et al.

epoxide yield: 46% (14% diol)

SCHEME 73. Epoxidation of cyclohexene utilizing immobilized vanadium catalysts

towards the epoxides were 100% and yields of the different epoxides ranged from trace up to 74% (for cyclohexene oxide), which is a very good result compared to 10–12% yield for cyclohexene oxide, obtained with VO(acac)₂ as homogeneous catalyst. Cyclic olefins have been found to be more susceptible to oxidation than acyclic alkenes, and yields decreased by substitution of one olefinic hydrogen atom by a methyl group. The sulfonated resin-anchored vanadyl could be recovered by filtration and reused many times before a significant decrease in activity is observed. In 1981, Bhaduri and coworkers reported the development of a polymer-supported oxobis(pentane-2,4-dionato)vanadium(IV) catalyst

and its use in the oxidation reaction of cyclohexene with TBHP as oxidant, but yields were rather low²⁶⁴. Vanadium complexes of bipyridine-based polyureas have been synthesized by Neckers and coworkers and used as catalysts for the epoxidation of several olefins and cyclic olefins bearing *endo*- and *exo*-double bonds²⁶⁶. With this catalyst, diols were obtained as side products (mainly in polar solvents). Without utilizing a solvent, olefins with only one double bond could be epoxidized with yields of 7–57% (yield of diols: 0–16%). The olefins with both *endo* and *exo* double bond were preferentially epoxidized at the *endo* site with selectivities between 86 and 98%. Yields of the epoxides ranged from 15 to 32% without a solvent (yields of diols: 12–31%), but could be improved in the non-polar benzene as solvent (40–50%, yields of diols: 3–8%). The catalyst could be recycled five times without significant loss of activity.

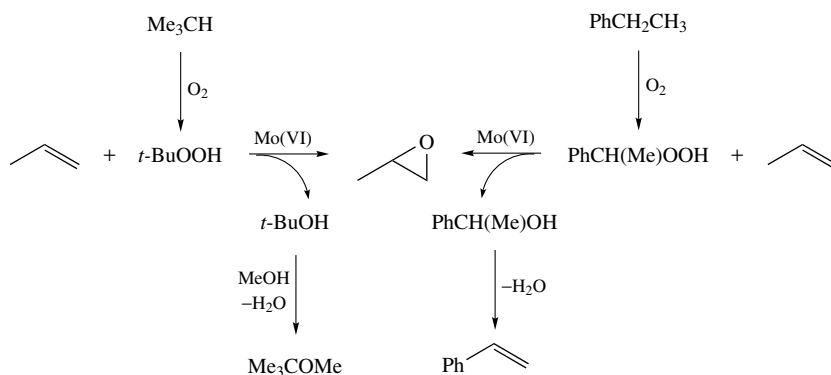
Like V(V), Nb(V) as well as Ta(V) alkoxides do catalyze the epoxidation of alkenes with TBHP as catalyst, but reaction times are long and yields are low due to side reactions (e.g. formation of (*tert*-butylperoxy)cyclohexene as major product from cyclohexene²⁴⁰). Grubbs and coworkers²⁴⁴ and Sala-Pala and coworkers²⁶⁷ could show that free and polymer-supported Cp_2NbCl_2 in the presence of hydrogen peroxide shows low or no catalytic activity for the epoxidation of alkenes (with cyclohexene only 36% epoxide selectivity).

iii. Cr, Mo, W. In contrast to group IV and V transition metals, the catalytic active oxidant is of another type for group VI transition metal-catalyzed epoxidations: The transition-metal-oxo complexes, in which the oxygen that is transferred is bonded to the metal via a double bond, are the active oxidizing species.

Chromium complexes in general are poor catalysts for the epoxidation of alkenes with TBHP due to the decomposition of the oxygen donor with formation of molecular oxygen²⁴⁰. Epoxidation reactions with this metal are known with other oxygen transfer agents than peroxides (e.g. iodosylbenzene) and will not be discussed here.

Molybdenum(VI) complexes are the most active catalysts for the epoxidation of unfunctionalized alkenes in the presence of hydroperoxides as oxygen donors, and many published examples exist for molybdenum-catalyzed epoxidations.

One molybdenum-catalyzed epoxidation, which is of industrial importance, needs special mention: the Halcon process²⁶⁸, which is the molybdenum-catalyzed epoxidation of propylene with TBHP or 1-phenylethyl hydroperoxide on a large scale (Scheme 74), and has been developed and patented by researchers from Halcon and Atlantic Richfield²⁶⁹.

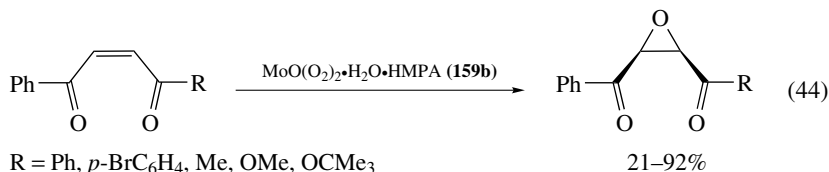


SCHEME 74. Halcon process

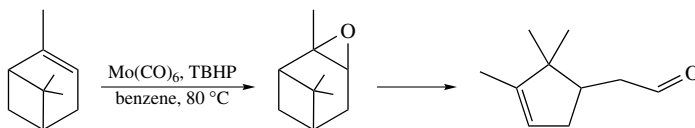
The first variant works with isobutane as the hydroperoxide precursor, which is oxidized to TBHP by molecular oxygen. During the epoxidation of propene, TBHP is transformed to *tert*-butanol, which is converted to methyl *tert*-butyl ether. The second procedure employs ethylbenzene, which is oxidized by molecular oxygen to phenyl ethyl hydroperoxide, which transfers an oxygen to propene and so is reduced to phenylethanol. This by-product of the process is converted to styrene, a versatile bulk chemical.

The ARCO-process²⁶⁹ is based on a homogeneous Mo catalyst, while the SHELL variant²⁷⁰ prepares propylene oxide using ethylbenzene or TBHP and a heterogeneous Ti(IV)/SiO₂ catalyst²⁷¹. A variety of molybdenum(VI) complexes have been found to catalyze the epoxidation of a variety of structurally different alkenes in the presence of different peroxides or hydrogen peroxide as oxidants: monomeric species^{191, 240}, clusters [Mo₃O(OAc)₆(H₂O)₃]²⁺(ClO₄⁻)₂ (by Szymanska-Buzar and Ziolkowski)²⁷² and [C₅H₅N⁺(CH₂)₁₅CH₃]₃[PMo₁₂O₄₀]³⁻ (by Ishii and coworkers)²⁷³. The catalytic results of reactions with these complexes are presented in Table 22. In contrast to the oxochromium-salen—and porphyrin complexes, oxomolybdenum-porphyrins are not able to oxidize olefins directly but they need TBHP for activation as reported by Ledon and coworkers²⁷⁴. As one example, in 1979 Sharpless and Verhoeven reported on the Mo(CO)₆-catalyzed epoxidation of various olefins using TBHP as oxidant with good yields (86–96%)²⁰². The disadvantages of this reaction were the long reaction times and the fact that the TBHP employed had to be dried.

In 1985, a patent by the Texaco company²⁷⁵ claimed the molybdenum-catalyzed epoxidation of α -olefins at high conversions and selectivities using 72% TBHP in *tert*-butanol with a slight excess of olefin at 95–135 °C. For these purposes they employed a Mo catalyst that was specially prepared from ammonium polymolybdates and glycol or aliphatic alcohols and overcame catalyst solubility problems. With this catalyst, for example, 1-octene could be epoxidized with 95% conversion and 95% selectivity within 1–2 hours. Monoperoxo-molybdenum complexes as MoO(O₂)L₂Cl₂ (L = DMF, HMPA) **159a**²⁷⁶ as well as diperoxo-molybdenum complexes as MoO(O₂)₂•H₂O•HMPA **159b** oxidize unsubstituted^{277, 278} alkenes, whereby the diperoxo-molybdenum complex turned out to be the more effective one, which also epoxidizes substituted substrates²⁷⁹. With stoichiometric amounts of the complex **159b**, good yields and very good *cis/trans* selectivities were obtained and the reactivity of olefins increased with increasing nucleophilicity as reported by Mimoun and coworkers^{278, 280}. For example, Sakamoto and coworkers reported that various *cis*-2-butene-1,4-diones could be epoxidized stereoselectively and with yields of 21–92% (equation 44)²⁷⁹.

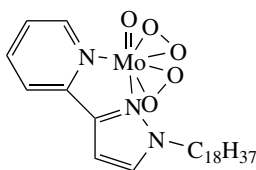


With complexes **159a**, various olefins were epoxidized in yields ranging from 0–43% and also cleavage products were obtained (ketones, aldehydes). The reactivity of substrates increased with the degree of substitution because the nucleophilic nature also increases in this order. In the catalytic process TBHP, CHP as well as H₂O₂ can serve as oxidants. While with TBHP the epoxides were formed with 98% selectivity and only traces of cleavage products were formed, with CHP lower epoxide selectivity was observed and more cleavage products were formed. With CHP and H₂O₂ stable and reactive peroxo complexes could be isolated by Mimoun's group²⁷⁶ and a mechanism for the reaction has been presented.

SCHEME 75. Epoxidation of α -pinene with $\text{Mo}(\text{CO})_6/\text{TBHP}$ leading to a rearrangement product

In 1981, Banthorpe and Barrow²⁸¹ investigated the $\text{Mo}(\text{CO})_6$ -catalyzed epoxidation of α -pinene with TBHP leading mainly to the undesired aldehyde due to rearrangement of the intermediary epoxide (Scheme 75). In addition, they had to use a radical scavenger in order to suppress allylic oxidations. An improved method with respect to an easy availability of the molybdenum catalyst employed 0.01 mol% of the readily available $\text{MoO}_2(\text{acac})_2$ in a 70% dry solution of TBHP in toluene. Conversions for α -olefins were 95–98% and in every case good epoxide selectivities were obtained (92–98%)²⁷¹. This catalytic system turned out to be especially effective also for terpene epoxidation. With 67% TBHP in toluene or Isopar E (residual water content <3%) reaction times were 1–2 hours at 100–125 °C. By running this type of reaction in a continuous reactor system at high temperatures between 160–200 °C, conversion of α -pinene was 97% and the epoxide was formed with 92% selectivity. The reaction time in this very effective process could be reduced to 0.5–5 minutes and all types of unsubstituted olefins could be oxidized²⁷¹.

In seven-coordinate molybdenum peroxo complexes of the type $\text{Mo}(\text{O})(\text{O}_2)_2\text{L}_2$, there is the problem of dissociation of the complex in the case of monodentate ligands like pyridine, HMPA, DMF or H_2O . Bidentate ligands like 2,2'-bipyridine, on the other hand, tend to give insoluble complexes. A solution to this problem was presented by Thiel in 1997 and 1998^{282, 283}. His group utilized the Mo-diperoxo complex **160** bearing a pyrazolylpyridine ligand.

**(160)**

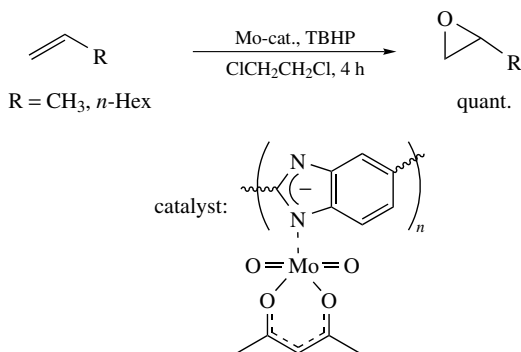
With this catalyst the epoxidation reactions can be carried out in the presence of TBHP (or H_2O_2 , although with lower activity) in non-polar organic solvents like chloroform, toluene or hydrocarbons with good to excellent yields (up to 100%). With this catalyst epoxides of non-functionalized olefins are obtained in good yields (>80%), whereas functionalized olefins with electron donor groups (styrene, conjugated dienes, enones) lead to a reduced activity of the catalytic system resulting in moderate to low yields of the corresponding epoxides. Allylic ethers give low yields and allylic alcohols do not react at all. Catalyst **160** converts chiral olefins like (*R*)-carvone or (*R*)-citronellal into 1:1 mixtures of diastereomeric epoxides.

Besides homogeneous systems, also heterogeneous molybdenum(VI) catalysts for olefin epoxidation have been reported in the literature. Among them are Mo complexes on anionites (Castel A-500p, Dowex 1X8 and Wofatit-AD-41)²⁸⁴, polymer immobilized Mo-peroxide (polymers bearing chelating or non-chelating nitrogen and oxygen donor fragments like benzimidazole, (aminomethyl)pyridine, imidazolylpyridine,

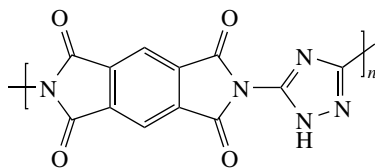
triazolyl containing polyimide)^{285–288}, Mo-oxide-Sn complexes on charcoal^{289,290}, Mo-zeolites^{291–293} and bimetallic B(III)-Mo(VI) complexes²⁹⁴. Of the three molybdenum complexes immobilized on different anionites developed by Sobczak and Ziolkowski, the one with $[\text{Mo}_2\text{O}_4(\text{oxalate})_2(\text{H}_2\text{O})_2]^{2-}$ deposited on Wofatit AD-41 containing $-\text{NMe}_2$ type coordination centers exhibited the highest catalytic activity in the epoxidation of cyclohexene with cumene hydroperoxide as oxidant²⁸⁴. With this heterogeneous catalyst cyclohexene was converted to its epoxide with 71% selectivity and a yield of up to 65%. Compared with the homogeneous system (79% selectivity, 74% yield), selectivity and yield with the heterogeneous system is somewhat lower.

Immobilized molybdenum peroxide complex, obtained by Kurusu and coworkers from the incorporation of Mo powder or MoO_3 with hydrogen peroxide into a chelating polymer (Diacon CR-20), showed good catalytic activity for the epoxidation of unfunctionalized olefins as well as allylic alcohols in the presence of *tert*-butyl hydroperoxide²⁸⁵. The rate of epoxidation increases with the number of alkyl groups as substituents on the double bond and, for unsubstituted olefins, the yields of epoxides ranged from 74 to 90%. The heterogeneous catalyst can be reused several times without loss of activity and it shows the possibility of regeneration after separation from the reaction medium by treatment with hydrogen peroxide.

A variety of polymer supported Mo(VI) catalysts with imidazole based ligands and two aminomethyl-2-pyridine (AMP) ligands were developed by Sherrington and coworkers and showed good catalytic activity as epoxidation catalysts in the oxidation of propene^{287,288}. Polybenzimidazole-supported molybdenum(VI) complex [PBI-MoO₂acac] turned out to be the best catalyst with respect to activity and recyclability (Scheme 76). In the high-pressure epoxidation of propene using TBHP (Halcon Process), propene oxide yields of up to 93% could be achieved after 4 hours and a yield of 89% was obtained even after a short time of one hour, which is much better than obtained with the homogeneous $\text{MoO}_2(\text{acac})_2$ (48% yield propene oxide after 1 hour). Also, 1-octene could be epoxidized in quantitative yields after 4 hours at 80–90 °C. This heterogeneous catalyst is especially long-lived and stable and can be reused several times. Remarkable is the increase in activity observed during recycling, with the aged catalyst (10 runs) giving quantitative conversion and selectivity in one hour (compared to 59% yield in the first run). An explanation for that might be the maximization of active Mo(VI) sites on the polymer upon longer exposure to TBHP. A polyimide-3,5-diamino-1,2,4-triazole (**161**) supported Mo catalyst in the presence of TBHP has been employed by Sherrington and coworkers for the epoxidation of cyclohexene giving yields up to 100% of the epoxide.

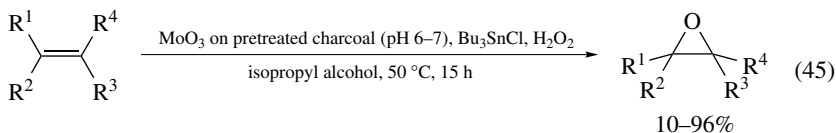


SCHEME 76. Epoxidation reaction using polybenzimidazole-supported Mo(VI) complex and TBHP



(161)

With the molybdenum oxide-tributyltin chloride on charcoal catalysts, which were introduced by Inoue and coworkers^{289,290}, a variety of unsubstituted olefins could be epoxidized selectively and with low to very good yields (10–96%) using 30% H₂O₂ (equation 45). The immobilized catalyst was prepared from Mo powder and aqueous H₂O₂ giving ‘molybdenum blue’, which is adsorbed on charcoal. This immobilized Mo complex itself is catalytically active, but upon addition of organotin compounds [best results with Bu₃SnCl and (Bu₃Sn)₂O] as cocatalysts the yields of epoxides could be raised significantly. The authors found that pretreatment of the charcoal support with inorganic acids or bases (0.1 N HCl or 0.1 N NaOH) to adjust the pH value to 6–7 increases the yields and epoxide selectivity and suppression of side reactions on charcoal was achieved by using butylating (*N,N*-dimethylformamide dibutyl acetal) or trimethylsilylating (1,1,1,3,3,3-hexamethyldisilazane) agents as modifiers. With this catalytic system cyclic as well as terminal and internal olefins have been epoxidized with yields depending on the structure of the substrate: Cyclic olefins (C₅ to C₈) could be oxidized with good yields (70–96%), and also internal olefins showed good reactivity (89% yield of 2-octene oxide), while terminal olefins were a bit less reactive (10–40%).

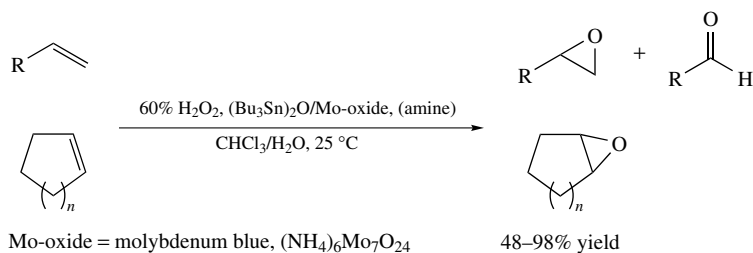


Lunsford and coworkers reported on the epoxidation of propene and cyclohexene using a molybdenum zeolite, prepared by introducing either Mo(CO)₆ or MoCl₅ into the zeolite, which showed initial good activity and selectivity for the epoxidation reaction in the presence of TBHP^{292,293}. The activity declined over a period of minutes, which was attributed to the formation of polyoxypropene, which fills the zeolite cavities and thus blocks the active sites. Also, leaching of Mo was observed. The selectivity for epoxidation was very high with TBHP and nearly the same for catalysts with various Mo loadings, but the activity of the catalyst increased with increasing Mo loading (highest for 6 wt%: 89% conversion after 8 hours at 75 °C)²⁹³.

The epoxidation with these Mo-zeolite materials occurs at Mo ions throughout the zeolite crystallites and not exclusively on the surface. This could be proven by poisoning experiments using tributylamine (deactivates the catalyst because it can enter the zeolite cavities) and triphenylamine (does not deactivate the catalyst because it is too big to enter the cavities). Especially in the last few years the development of new, defined oligomeric adducts, microporous materials consisting of both inorganic and organic components, the so-called polyoxometalates (POMs), and their use as catalysts in a variety of reactions has become a research field of great synthetic importance. The aim is to construct two- or three-dimensional coordination polymers that mimic conventional zeolites in that they exhibit reversible guest exchange and possibly selective catalytic activity. These compounds can either act as homogeneous catalysts or as heterogeneous ones depending on

the solvent used. In this respect also POMs bearing molybdenum as one of the metals have been developed and their catalytic activity for epoxidation of unfunctionalized olefins has been investigated.

In 1990 as one of the first groups Inoue and coworkers reported on the utilization of such a kind of Sn/Mo compound (generated *in situ*) for the epoxidation of terminal C5-C10 alkenes and cyclic alkenes with aqueous 60% H₂O₂ in a two-phase system (Scheme 77)²⁹⁵. At that time the authors did not know exactly about the composition of the catalytically active species but it has been suggested to be (Bu₃SnO)₂MoO₂, which showed similar activity to the *in situ* formed catalyst from molybdenum blue/(Bu₃Sn)₂O. From various molybdenum species [in the presence of bis(tributyltin) oxide] tested, ammonium heptamolybdate(VI)/(Bu₃Sn)₂O proved to be the best catalytic system and hydrophobic solvents like chloroform as the organic part of the two-phase system showed the best selectivities (83–97%). Amines as additives proved to have a strong effect on the reaction. While in the absence of amines poor epoxide yields were obtained with molybdenum blue, addition of ammonia greatly increased the yields for the epoxidation of cyclohexene and styrene (up to 96%) and aliphatic amines and pyridine gave similar results. The fact that the addition of trioctylmethylammonium chloride, a phase transfer catalyst, improved the selectivity for epoxidation as well (39% yield, 87% selectivity) led to the conclusion that the catalyst system also worked as a kind of PTC.



SCHEME 77. Mo-catalyzed epoxidation of cyclic and α -alkenes with H₂O₂ in two-phase solvents

Inoue's group proposed that the effect of the amine additive is either to stabilize the catalyst or to suppress the decomposition of the epoxide formed. For catalytic activity, the presence of an organotin compound is essential and the best results were obtained with Bu₂SnO, (Bu₃Sn)₂O and Oct₂SnO (yields between 61 and 78%). Several olefins could be epoxidized with the (Bu₃Sn)₂O-Mo species under biphasic conditions (with or without additional Me₃N) in low to good yields (48–98%). Twelve years later it was known that materials with the formula [(R₃Sn)₂MO₄] (M = Mo, W) possess a polymeric layered structure (see Figure 13) where small variations can be introduced by changing the nature and bulk of the organic residues R. With R = *n*-Bu, Romão and coworkers developed an active catalyst for the epoxidation of olefins with TBHP/decane or aqueous 30% H₂O₂ as oxygen transfer agent, the latter being the more active oxidant²⁹⁶. In the liquid phase epoxidation of cyclooctene (at 35–75 °C) with TBHP the Mo(VI) catalyst was much more active than the W(VI) species, yielding 88% of the epoxide as the sole product after 24 hours. The activity of [(*n*-Bu₃Sn)₂MoO₄] was higher in non-coordinating chlorinated solvents (ClCH₂CH₂Cl < CH₂Cl₂) than in coordinating solvents (MeOH < H₂O < EtOH < CH₃CN, only 14% conversion), because these compete with the peroxide for coordination to the molybdenum center. Under these conditions (6 h, r.t.) cyclic olefins, like cyclooctene, showed higher reactivity (quantitative yield of the epoxide, equation 46) than acyclic olefins with an internal double bond (52% conversion of 2-octene, 100%

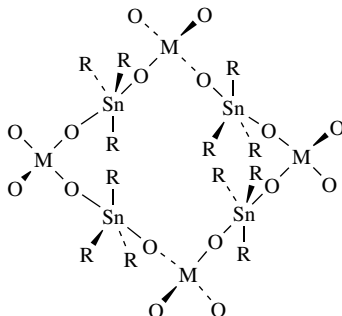
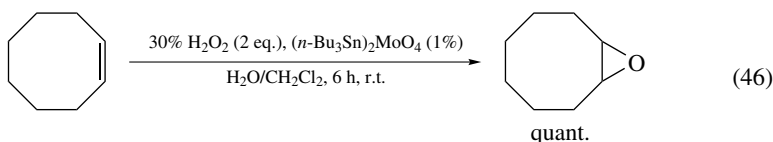
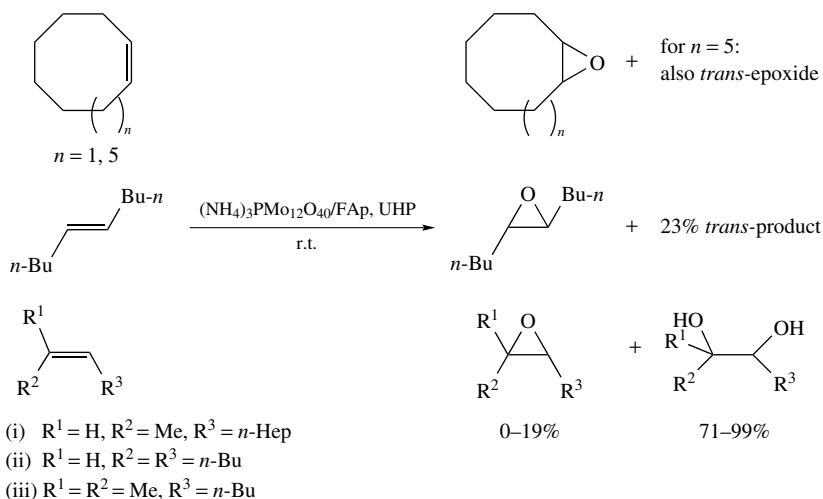


FIGURE 13

selectivity) and especially better reactivity than terminal double bonds (no conversion of 1-octene).



In 2002, Ichihara and coworkers reported on the employment of Keggin-type phosphometalates dispersed on fluorapatite (FAp) solid phase for the epoxidation of alkenes in the presence of urea hydrogen peroxide (Scheme 78)²⁹⁷. While the phosphotungstate $(\text{NH}_4)_3\text{PW}_{12}\text{O}_{40}$ was superior to phosphomolybdate $(\text{NH}_4)_3\text{PMo}_{12}\text{O}_{40}$ in the liquid phase, the opposite was the case in the solid-phase system. The solid-phase method is very

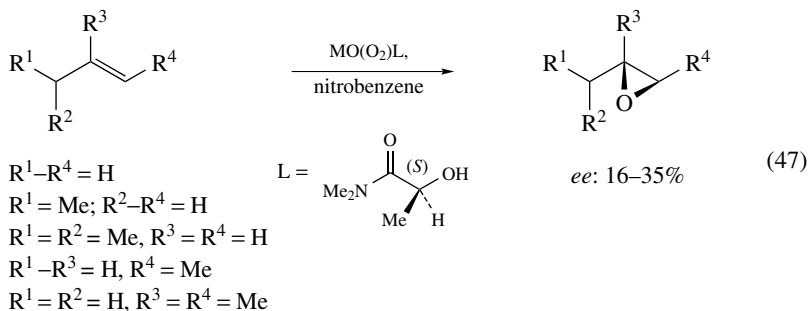


SCHEME 78. Solvent-free oxidation of cyclic and acyclic *cis*- and *trans*-alkenes using $(\text{NH}_4)_3\text{PMo}_{12}\text{O}_{40}$ on fluorapatite

convenient because the reactions are carried out by just mixing the solid catalyst (0.01 eq.), apatite and solid urea hydrogen peroxide (2 eq.) and then permeating by liquid substrate like cyclooctene. Oxidation of cyclic as well as acyclic *trans*-alkenes afforded the epoxides (low conversions for acyclic *trans*-alkenes), while *cis*-alkenes are converted to an epoxide–diol mixture.

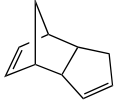
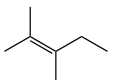
The results of the various published known methods for molybdenum-catalyzed epoxidation of different olefins are presented in Table 22.

Over the years asymmetric versions of the molybdenum-catalyzed epoxidation have been developed as well. First attempts by Otsuka and coworkers utilized $\text{MoO}_2(\text{acac})_2/\text{TBHP}$ in the presence of optically active carbohydrate derivatives and tartrate esters as chiral inductors for the epoxidation of 1-alkylcyclohexenes and squalene, but the enantioselectivities obtained were low (*ee* up to 14% for (3*S*)-2,3-oxidosqualene) (Scheme 79)²⁹⁹. The tartrate esters (1,2-diols) were more effective for asymmetric induction than the carbohydrate hydroperoxides (1,3- and 1,4-diols). Epoxide yields up to 70% and enantioselectivities of up to 35% have been reported by Schurig and coworkers for the epoxidation of low molecular weight alkenes employing stoichiometric amounts of a diperoxo-molybdenum complex with chiral bidentate ligands such as (*S*)-*N,N*-dimethylactamide (equation 47)³⁰⁰. Interestingly, the asymmetric induction decreased with higher sterical demand of the olefin and the rate of oxidation increased in this direction, presumably due to increasing strength of π -complexation. Later, Hamann and coworkers could improve this result significantly by employing the carbohydrate hydroperoxides **63c** and **69b** as oxidants and chiral inductors in the presence of a new Mo catalyst **162** (Scheme 80)⁶⁶. With these two systems 1-hexene was epoxidized with 38% *ee* and 50% *ee* respectively.



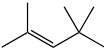
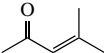
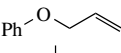
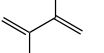
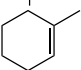
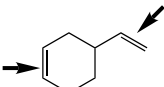
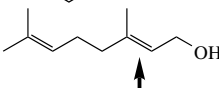
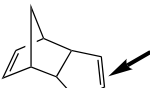
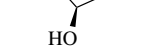
Compared to molybdenum(VI) complexes, which are probably the most active epoxidation catalysts in combination with alkyl hydroperoxides, the tungsten(VI) compounds show better reactivity with hydrogen peroxide as oxygen transfer agent. The fact that they do not have the same broad synthetic utility as the transition metal/alkyl hydroperoxide systems is due to retardation of the reaction in the presence of water or polar solvents or hydrolysis of the intermediary formed epoxides. One industrial important process which is catalyzed by $\text{WO}_4^{2-}/\text{H}_2\text{O}_2$ is the preparation of epichlorohydrin²⁴¹. The reaction is stereospecific and occurs with retention of configuration of both *cis* and *trans* alkenes. The reactive species is supposed to be a mono- or bidentate peroxide–tungsten complex but tungstates can also be polymeric in acidic, neutral and mildly basic solutions and therefore one has a complex mixture of tungstate species with different catalytic activities as reported by Kirshenbaum and Sharpless³⁰¹. $\text{WO}(\text{O}_2)_2 \cdot \text{HMPA} \cdot \text{H}_2\text{O}$, which was shown to be a more active stoichiometric oxidant than the analogous molybdenum species, epoxidizes olefins^{280, 302}. Some heterogeneous W(VI) catalysts, like the resin-attached tungstate³⁰³ or tungstic acid–tributyltin chloride on charcoal³⁰⁴, proved to be

TABLE 22. Comparison of the results of the molybdenum-catalyzed epoxidation of olefins

Substrate ^a	Catalyst ^b	Oxidant	Time (h)	Conv (%)	Yield (%)	Reference	
Propene	PBI-MoO ₂ acac ^c	TBHP	1		>99	287, 288	
1-Heptene	Mob/(Bu ₃ Sn) ₂ O	60% H ₂ O ₂	7	86	80	295	
1-Octene	Mob/(Bu ₃ Sn) ₂ O	60% H ₂ O ₂	3	95	88	295	
	(<i>n</i> -Bu ₃ Sn) ₂ MoO ₄	30% H ₂ O ₂	6	—	—	296	
	[C ₅ H ₅ N ⁺ (CH ₂) ₁₅ Me] ₃ [PMo ₁₂ O ₄₀] ³⁻	35% H ₂ O ₂	24	41	40	273	
	160	TBHP	1		58	283	
	MoO ^d -Bu ₃ SnCl-charcoal	H ₂ O ₂	15		40	290	
	PBI-MoO ₂ acac ^c	TBHP	4		>99	287	
2-Octene	(<i>n</i> -Bu ₃ Sn) ₂ MoO ₄	30% H ₂ O ₂	6	52	52	296	
	160	TBHP	1		96	283	
	MoO ^d -Bu ₃ SnCl-charcoal	H ₂ O ₂	15		89	290	
1-Decene	Mob/(Bu ₃ Sn) ₂ O	60% H ₂ O ₂	7	81	74	295	
	160	TBHP	1		55	283	
	MoO ^d -Bu ₃ SnCl-charcoal	H ₂ O ₂	15		41	290	
<i>cis</i> -2-Decene	(NH ₄) ₃ PMo ₁₂ O ₄₀ /Fap	UHP	24	83	6 ^e	297	
<i>cis</i> -5-Decene	(NH ₄) ₃ PMo ₁₂ O ₄₀ /Fap	UHP	72	90	19 ^f	297	
<i>trans</i> -5-Decene	(NH ₄) ₃ PMo ₁₂ O ₄₀ /Fap	UHP	72	8	8	297	
2-Methyl-2-heptene	(NH ₄) ₃ PMo ₁₂ O ₄₀ /Fap	UHP	48	100	0 ^g	297	
Cyclopentene	160	TBHP	1		100	283	
	MoO ^d -Bu ₃ SnCl-charcoal	H ₂ O ₂	15		87	290	
Cyclohexene	MoO ₂ (acac) ₂ /(Bu ₃ Sn) ₂	28% H ₂ O ₂	24		73	298	
	[Mo ₃ O(OAc) ₆ (H ₂ O) ₃] ²⁺ (ClO ₄) ₂ ⁵⁻	35% H ₂ O ₂		90	78	272	
	160	TBHP	1		93	283	
	polymer immobilized Mo ^h	TBHP	5		90	285	
	MoO ^d -Bu ₃ SnCl-charcoal	H ₂ O ₂	15		79	290	
	Mo-zeolite (6 wt% Mo)	TBHP	8	89		89	293
	[Mo ₂ O ₄ (OX) ₂ (H ₂ O) ₂] ²⁻ on Wofatit AD-41	PhCMe ₂ OOH				65	284
	PI-DAT-MoO ₂ acac ⁱ	TBHP	2		>99	287	
Cycloheptene	MoO ^d -Bu ₃ SnCl-charcoal	H ₂ O ₂	15		87	290	
Cyclooctene	Mob/(Bu ₃ Sn) ₂ O	60% H ₂ O ₂	1.25	100	98	295	
	(<i>n</i> -Bu ₃ Sn) ₂ MoO ₄	30% H ₂ O ₂	6		>99	296	
	(NH ₄) ₃ PMo ₁₂ O ₄₀ /Fap	UHP	24	91	85	297	
	160	TBHP	1		100	283	
	polymer immobilized Mo ^h	TBHP	22		89	285	
	MoO ^d -Bu ₃ SnCl-charcoal	H ₂ O ₂	15		96	290	
Cyclododecene ^j	(NH ₄) ₃ PMo ₁₂ O ₄₀ /Fap	UHP	24	34	23/11 (<i>trans/cis</i>)	297	
Styrene	160	TBHP	1		57 ^k	283	
	MoO ^d -Bu ₃ SnCl-charcoal	H ₂ O ₂	15		18	290	
α -Methylstyrene	Mob/(Bu ₃ Sn) ₂ O	60% H ₂ O ₂	7	84	70	295	
	MoO ^d -Bu ₃ SnCl-charcoal	H ₂ O ₂	15		10	290	
α -Pinene	0.01% MoO ₂ (acac) ₂	TBHP	1-2	97	87	271	
Cedrene	0.01% MoO ₂ (acac) ₂	TBHP	1-2	95	89	271	
	0.01% MoO ₂ (acac) ₂	TBHP	1-2	>99	93	271	
Allyl chloride	Mob/(Bu ₃ Sn) ₂ O ^l	60% H ₂ O ₂	10	52	48	295	
	160	TBHP	1		87 ^m	283	

(continued overleaf)

TABLE 22. (continued)

Substrate ^a	Catalyst ^b	Oxidant	Time (h)	Conv (%)	Yield (%)	Reference
	160	TBHP	1		98	283
	160	TBHP	1		40	283
	160	TBHP	1		5	283
	160	TBHP	1		69 ⁿ	283
	MoO ^d -Bu ₃ SnCl-charcoal	H ₂ O ₂	15		65	290
	[C ₅ H ₅ N ⁺ (CH ₂) ₁₅ Me] ₃ [PMo ₁₂ O ₄₀] ³⁻	35% H ₂ O ₂	24	65	57 + 4 ^o	273
	[C ₅ H ₅ N ⁺ (CH ₂) ₁₅ Me] ₃ [PMo ₁₂ O ₄₀] ³⁻	35% H ₂ O ₂	24	91	90	273
	[C ₅ H ₅ N ⁺ (CH ₂) ₁₅ Me] ₃ [PMo ₁₂ O ₄₀] ³⁻	35% H ₂ O ₂	8.5	94	87 ^p	273
	[C ₅ H ₅ N ⁺ (CH ₂) ₁₅ Me] ₃ [PMo ₁₂ O ₄₀] ³⁻	35% H ₂ O ₂	24	92	91	273
Limonene	polymer immobilized Mo ^h	TBHP	30		74	285
(<i>R</i>)-Limonene	160	TBHP	1		100 ^q	283
(<i>R</i>)-Carvone	160	TBHP	1		67 ^r	283
(<i>R</i>)-Citronellal	160	TBHP	1		76 ^r	283

^a When there are more than one double bond in the molecule, arrows mark the double bond where epoxidation takes place.

^b Mob = molybdenum blue; Fap = fluoroapatite.

^c PBI = polybenzimidazole support.

^d Molybdenum oxide.

^e Diol was obtained in 76% yield.

^f Diol was obtained in 71% yield.

^g Diol was obtained in 99% yield.

^h Molybdenum peroxide immobilized by coordination of a chelating polymer Diaion CR-20.

ⁱ PI-DAT = polyimide-3,5-diamino-1,2,4-triazole support.

^j Ratio *trans/cis*: 69/31.

^k Side product: 18% of *t*-butyl benzoate.

^l Prepared from MoO₂(acac)₂ and (Bu₃Sn)₂O.

^m Traces of 1,2-diol and pinacolone.

ⁿ 69% monoepoxide + <5% diepoxide.

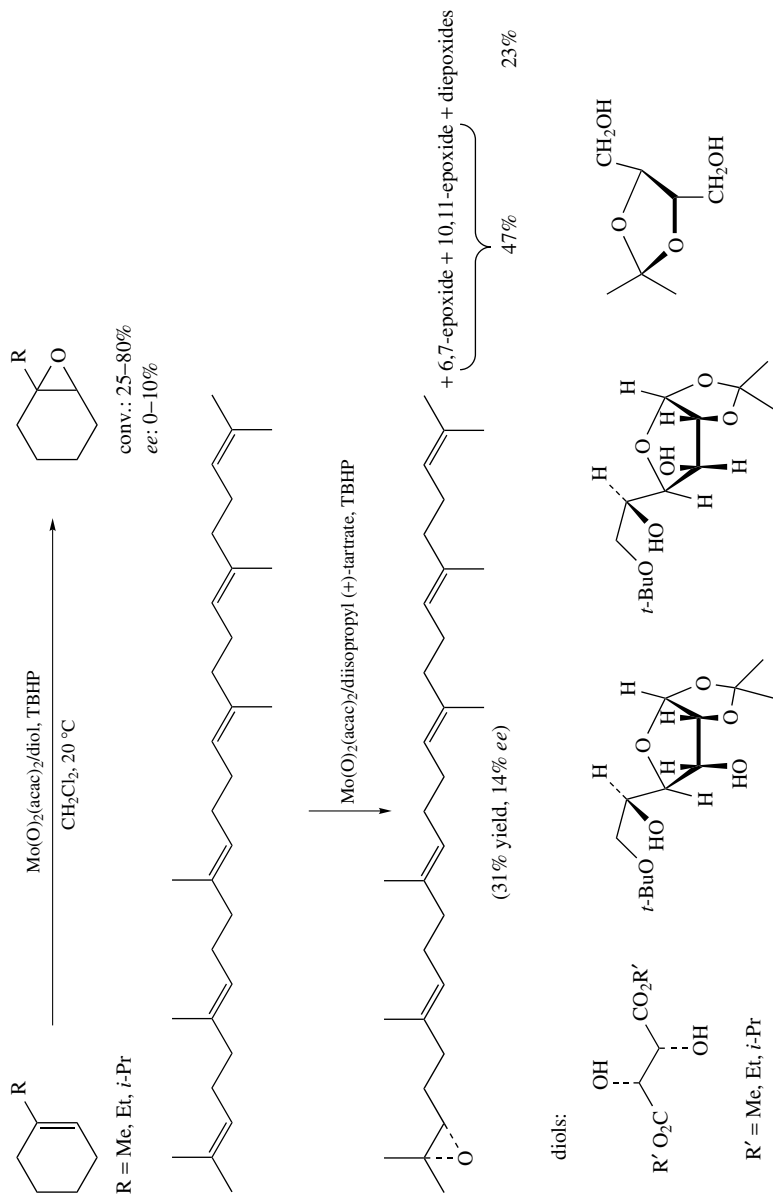
^o Product of epoxidation of the ring double bond: 57%, product of epoxidation of the terminal double bond: 4%, 3% diol formation.

^p 7% of enone.

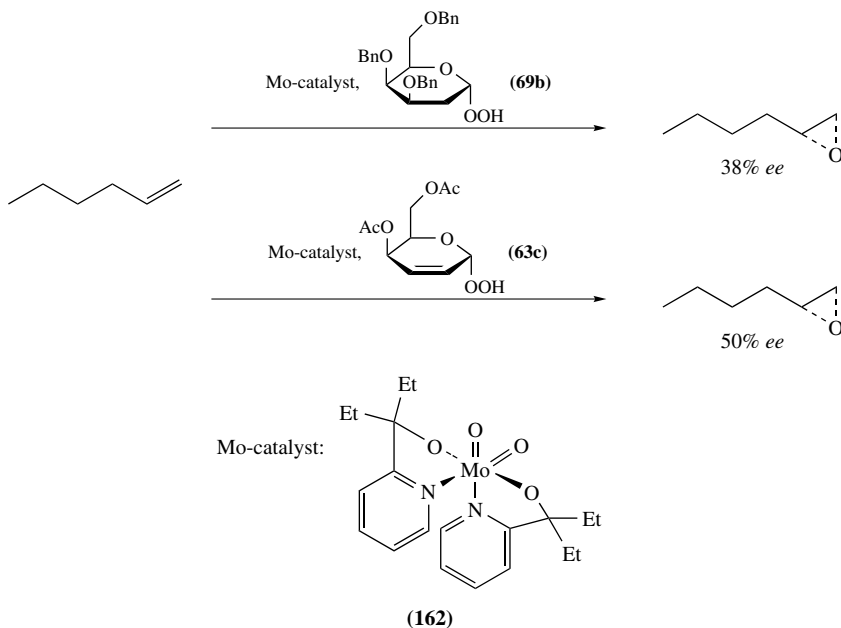
^q Divacant epoxides.

^r 2 diastereomers.

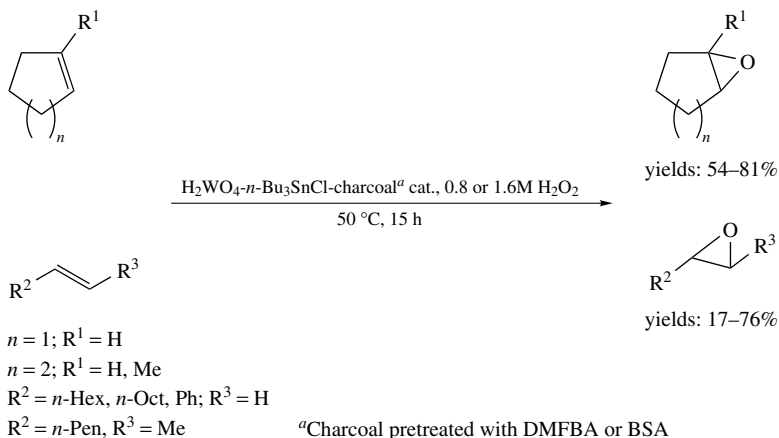
^s R is unknown.



SCHEME 79. Asymmetric epoxidation of olefins by TBHP catalyzed by a molybdenum catalyst in the presence of chiral diols



SCHEME 80. Mo-catalyzed asymmetric epoxidation of 1-hexene with chiral carbohydrate hydroperoxides



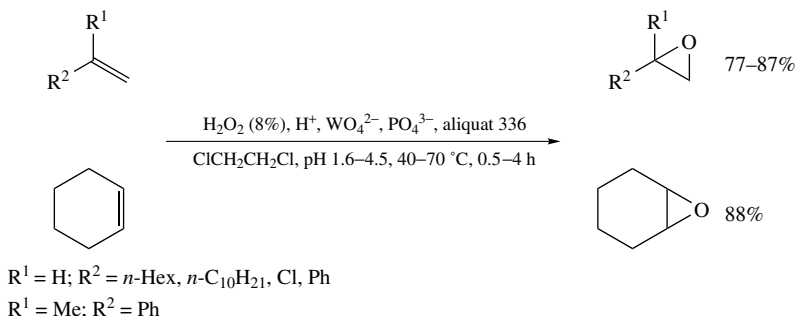
SCHEME 81. Tungstic acid–tributyltin chloride on a charcoal catalyst in the epoxidation of alkenes with hydrogen peroxide

more effective catalysts for the epoxidation of alkenes with hydrogen peroxide as oxidant than the tungstate salts. With the charcoal immobilized tungstic acid catalyst and 30% H_2O_2 , cyclic and acyclic olefins could be epoxidized to the corresponding epoxides (Scheme 81). Without an additive, significant amounts of diol and ether side products

were obtained, but in the presence of $n\text{-Bu}_3\text{SnCl}$, which turned out to be the best co-catalyst, hydrolysis was prevented and epoxides could be synthesized selectively (no side product). The authors proposed that a tightly-bonded complex between H_2WO_4 and the trialkyltin compound is formed $[(n\text{-Bu}_3\text{SnO})_2\text{WO}_2]$ in the reaction mixture with which the epoxidation can be performed with higher selectivity.

Yields were improved by utilizing chemically modified charcoal [treatment with N,N -dimethylformamide dibutyl acetal (DMFBA) or N,O -bis(trimethylsilyl)acetamide (BSA)] due to suppression of H_2O_2 decomposition and ranged between 18 and 81%. Conversion and selectivity seem to depend extremely on the pre-treatment of charcoal with solutions of various pH values being highest for solutions with pH 7.

A great step in the field of tungsten-catalyzed epoxidation reactions with hydrogen peroxide was taken when Venturello and coworkers published their results in 1983 on the direct epoxidation of various olefins using an *in situ* generated catalyst (from Na_2WO_4 and H_3PO_4 2:1) and hydrogen peroxide in acidic medium³⁰⁵. The reactions were carried out in a biphasic system (1,2-dichloroethane/ H_2O) with a very dilute aqueous H_2O_2 solution (<10%) and aliquat 336 (or also other PTCs) as a phase transfer cocatalyst, yielding epoxides in yields between 77 and 88% (Scheme 82). Epoxide selectivities were very high (80–90%) and the effectiveness of the method increases as the pH decreases. In spite of the acidic conditions, hydrolytic cleavage of the oxirane ring in general is prevented by the ‘protecting effect’ of the double phase and the short contact times of the products with the aqueous phase. The reaction is stereoselective and *trans* (cis) olefins are converted to *trans* (cis) epoxides. The limiting factors of this reaction were the excess of olefin necessary and the ring opening that occurred in the case of very acid-sensitive epoxides.

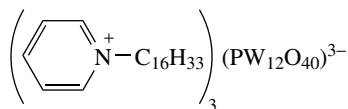


SCHEME 82. Epoxidation of olefins with the catalytic system $\text{Na}_2\text{WO}_4/\text{H}_3\text{PO}_4$ and H_2O_2 under phase transfer conditions

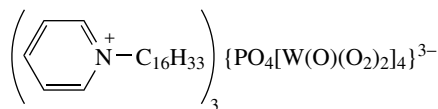
Two years later, the structure of the catalytically active species was elucidated by the same group to be a polytungstate-peroxy species $[\text{PO}_4[\text{W}(\text{O})(\text{O}_2)_2]_4]^{3-}$ that could be characterized with tetrahexylammonium as the counter ion³⁰⁶. The epoxidation with this catalyst is stereospecific and *cis*-2-hexene is transformed into *cis*-epoxide while *trans*-2-hexene is converted to the *trans*-epoxide. Venturello and D’Aloisio employed the preformed catalyst but with methyltrioctylammonium or dimethyl[diocetadecyl (76%) + dihexadecyl (24%)] ammonium as counteraction in the presence of dilute hydrogen peroxide, which led to improvement of the epoxide yields up to 94%³⁰⁷. In the case of acid-sensitive epoxide products, the method was slightly modified by adjusting the pH of the aqueous phase to a higher value (pH 3.3 instead of 2.3) in order to prevent ring opening.

Ishii and coworkers could develop a W-heteropoly acid catalyst **163**, prepared from 12-tungstaposphoric acid and cetylpyridinium chloride, which catalyzes the epoxidation of

a variety of olefins (performed or *in situ* generated) under biphasic conditions ($\text{CHCl}_3/\text{H}_2\text{O}$) in the presence of 35% H_2O_2 with good conversions (82–97%) and epoxide selectivities (up to >98%)³⁰⁸. The preformed catalyst was less effective than the *in situ* generated system. 4-Vinyl-1-cyclohexene was regioselectively oxidized at the ring double bond but no stereoselectivity was observed, while 5-vinylbicyclo[2.2.1]hept-2-ene could be epoxidized regio- and stereoselectively affording *exo*-2,3-epoxy-5-vinylbicyclo[2.2.1]heptane (90% conv., 90% selectivity).



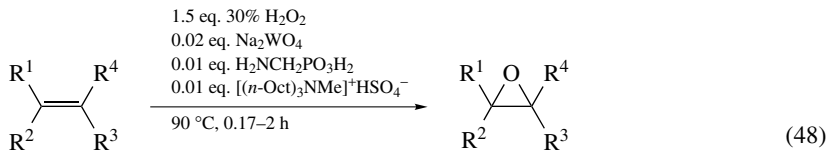
(163)



(164)

With catalyst **164** Ishii and coworkers could successfully epoxidize terpenes to the corresponding monoepoxides or diepoxides with good conversions (83–100%) and generally good selectivities (up to 99%) while employing very low amounts of catalyst (0.5%)³⁰⁹. Limonene was converted into limonene oxide in which the cyclohexene double bond was selectively epoxidized in almost quantitative yield. In terpenes bearing electron-withdrawing substituents (neryl acetate, geranyl acetate, citral, geranyl cyanide) the double bonds remote from the substituents were epoxidized in preference to the others.

In 1996/1997, Noyori and coworkers presented a very efficient solvent-free process (biphasic) for a variety of different oxidation reactions including epoxidation of olefins with a catalytic system consisting of 2 mol% Na_2WO_4 /1 mol% $(n\text{-Oct})_3\text{NMe}^+ \text{HSO}_4^-$ /1 mol% $\text{H}_2\text{NCH}_2\text{PO}_3\text{H}_2$ (see also Section III.B.3—metal-catalyzed sulfoxidation of thioethers and Section III.C—metal-catalyzed alcohol oxidation)^{310–312}. Reactions were performed at 40–90 °C with 30% aqueous H_2O_2 as oxygen source and additional aminomethylphosphonic acid, which is crucial for catalytic activity. This catalytic system is high yielding and affords clean conversions; it is safe to handle, simple to prepare and cost-effective. One of the oxidation reactions that are catalyzed is the epoxidation of cyclic, acyclic internal and terminal olefins (equation 48).



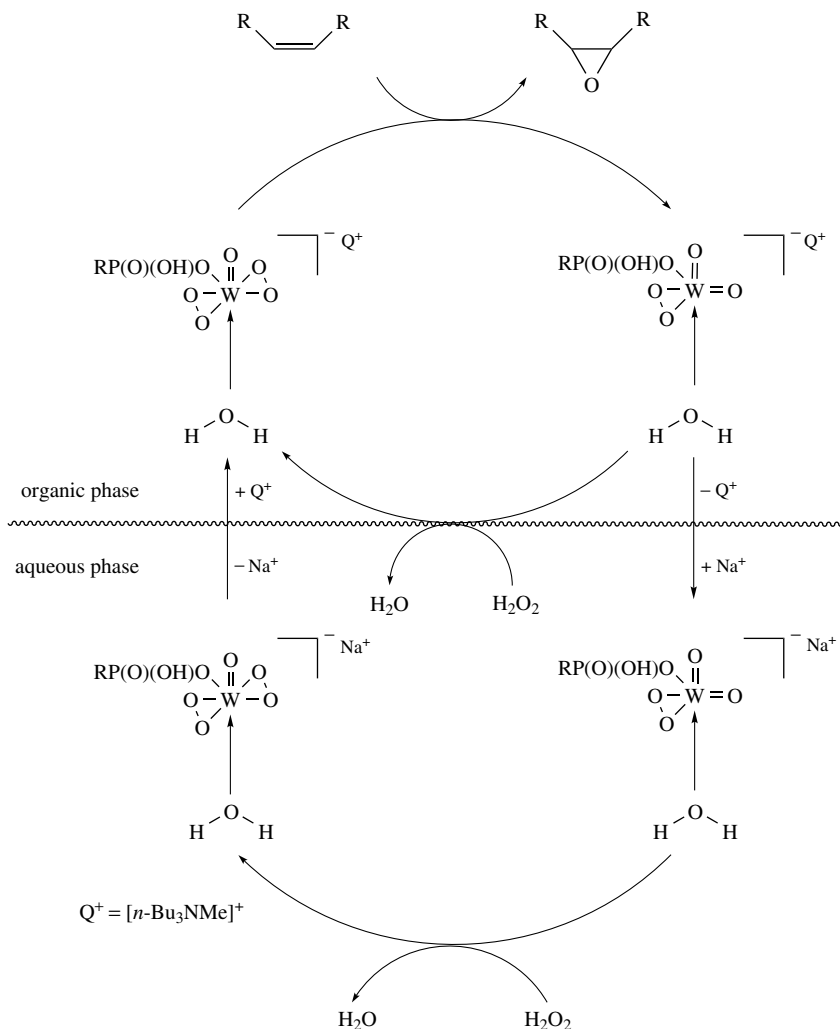
yields:

unfunctionalized alkenes: 76–99%

functionalized alkenes: 42–99%

Epoxide yields ranged from 76 to 99% for unfunctionalized olefins. One drawback of the method are the poor yields in the oxidations of styrene and its derivatives (<23% yield of epoxide) due to hydrolytic decomposition at the aqueous–organic interphase. The substrates of the biphasic H_2O_2 epoxidation are not limited to simple olefins, but functionalized substrates bearing an ester or ether functionality or α,β -enones could also be epoxidized by this procedure with good yields. Olefins bearing ether, alcohol, ketone and ester groups could be epoxidized with yields ranging from 42 to 99%³¹². Also, many otherwise unreactive terminal olefins showed good conversions to the corresponding

epoxides (e.g. epoxidation of generally unreactive 1-dodecene affords 1,2-epoxydodecane in 87% yield). Since the oxidizing species is electrophilic, the reaction rate is enhanced with increasing electron density of the olefinic bond³¹² and (*Z*)-olefins are more reactive than the (*E*)-analogues³¹². The epoxidations of 1,2-disubstituted olefins can be carried out stereospecifically with Noyori's catalytic system with retention of the configuration at the double bond. The authors proposed a catalytic cycle for this biphasic reaction which is illustrated in Scheme 83.



SCHEME 83. Catalytic cycle of the epoxidation reaction with Noyori's catalytic system

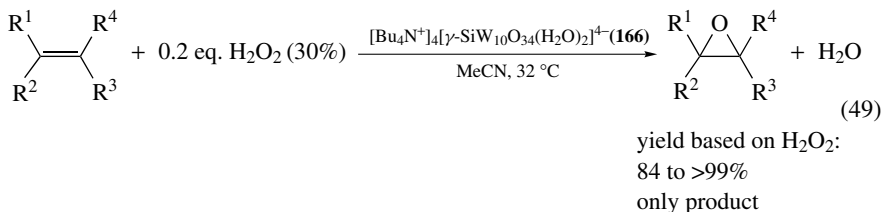
Alternatively, in 2000 researchers from Peroxid Chemie reported that with the catalytic system $[\text{Oct}_3\text{NMe}]_3[\text{PW}_{12}\text{O}_{40}]$ (0.06 mol%) using 70% H_2O_2 , olefins could be converted to the corresponding epoxides in high yields and selectivities (e.g. cyclooctene:

up to 98% conversion, 90–95% selectivity)²⁷¹. The oxidant is added in two steps and the catalyst can either be preformed or generated *in situ* from methyltriocylammonium chloride (0.15 mol%) and 12-tungstic phosphoric acid (0.05 mol%). Use of a solvent or a cocatalyst is not needed.

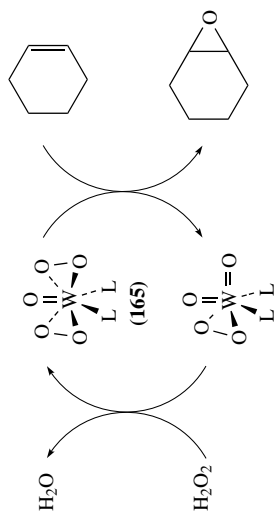
Over the years it has been shown that complexes prepared from organophosphorous ligands in combination with peroxotungstic acid or its quaternary ammonium salts exhibit efficient catalytic properties³¹³. In order to make an efficient recycling of the catalyst possible and get tungsten-free products and effluents, some of these catalysts were immobilized onto polystyrene, polybenzimidazole and polymethacrylate copolymers modified by the introduction of the phosphorous(V)-containing ligands.

In 2003, Gelbard reported on the epoxidation of alkenes with hydrogen peroxide using tungsten catalysts **165** that were immobilized by complexing to organophosphorous ligands, grafted onto porous polymers like the hydrophobic polystyrene and hydrophilic polymethacrylate resins of gel or macroporous type (Scheme 84)³¹⁴. The non-ionic complexing macroligands (polystyrene supported phosphoric amides and phosphonic amides) **165a–c** gave better results than the phosphine oxides **165d** and **165e** and afforded non-ionic catalysts with turnover frequencies higher than those of the analogous soluble catalysts. With the very stable complexes like the phosphoric amides, it was possible to effectively recycle the catalyst without significant loss in activity. Aminophosphorylated polymethacrylate supported ligands **165f** turned out to be a remarkable ligand for peroxotungstic species in the selective epoxidation of alkenes with hydrogen peroxide. With these ligands, no or almost no cleavage products like diols were obtained.

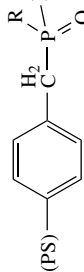
An extremely active and efficient catalyst for the epoxidation of unfunctionalized cyclic, internal and terminal olefins in the presence of aqueous 30% H₂O₂ could be presented by Mizuno and coworkers (equation 49)³¹⁵. The catalyst, a silicotungstate compound [Bu₄N⁺]₄[γ -SiW₁₀O₃₄(H₂O)₂]⁴⁻ (**166**), is synthesized by protonation of a divacant, lacunary, Keggin-type polyoxometalate (POM, [γ -SiW₁₀O₃₆]⁸⁻). Reactions are carried out with a five-fold excess of substrate relative to H₂O₂ (30% aqueous solution). The catalyst shows $\geq 99\%$ selectivity to epoxide formation, high efficiency of H₂O₂ utilization ($\geq 99\%$) and high stereospecificity. The configuration of the double bond was retained and *cis*-olefins were epoxidized much faster than the *trans*-isomers. In the competitive oxygenation of *cis*- and *trans*-2-octenes the ratio of the formation rate of *cis*-2,3-epoxyoctane to that of the *trans*-isomer was 11.5. It can easily be recovered from the homogeneous reaction mixture without loss of activity or selectivity and without decomposition. A fact that deserves special mention is that even olefins like cyclohexene, 1-methylcyclohexene, cyclooctene, cyclododecene and norbornene can be epoxidized with this catalytic system with high selectivity ($\geq 99\%$) and yields (84 to $>99\%$). Dienes such as 1,3-butadiene and 4-vinyl-1-cyclohexene were oxidized giving selectively the monoepoxides, whereby the double bond with the higher electron density was epoxidized regioselectively.



A very interesting type of POM catalyst with polyfluorinated quaternary ammonium salts as counterions for the oxidation of alkenes, alkenols and alcohols was developed by Neumann and coworkers in 2003³¹⁶. This catalyst with the general composition

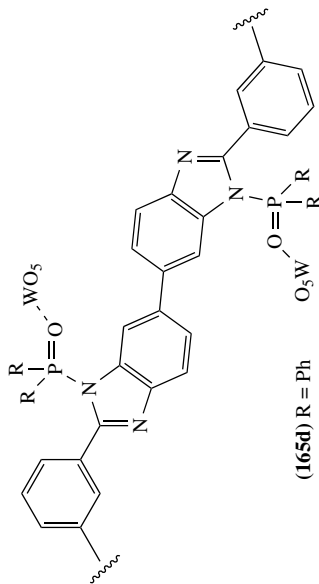


immobilized peroxotungstic catalysts : **165**



(165a)

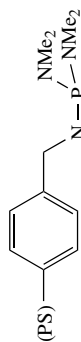
PS supported phosphine oxide



(165d) R = Ph

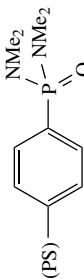
(165e) R = NMe₂

Polybenzimidazole supported phosphine oxide



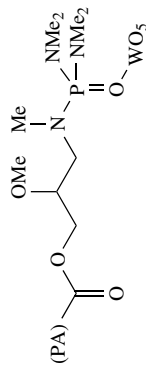
(165c)

PS supported phosphoramidate



(165b)

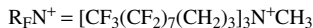
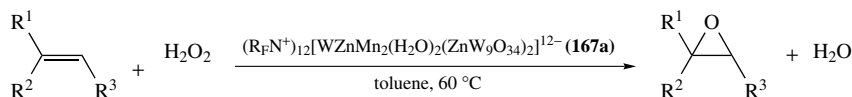
PS supported phosphonamide



(165f)

polymethacrylate supported phosphotriamides

SCHEME 84. Epoxidation of cyclohexene with tungsten catalysts immobilized on organophosphoryl macroligands



	Fluorous solvent	non-fluorous solvent
Conversion of alkenols	3–67%	8–82%
Conversion of alkenes		0–100%

SCHEME 85. Epoxidation of alkenes and alkenols with a perfluorinated quaternary ammonium salt of a polyoxometalate catalyst

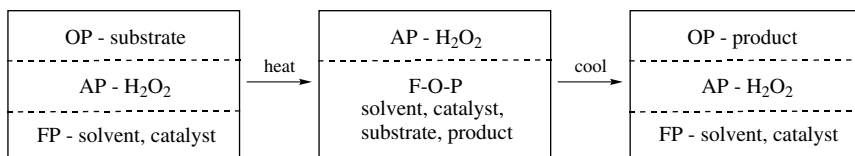
$[\{\text{CF}_3(\text{CF}_2)_7(\text{CH}_2)_3\}_3\text{N}^+\text{CH}_3]_{12}[\text{WZnM}_2(\text{H}_2\text{O})_2(\text{ZnW}_9\text{O}_{34})_2]^{12-}$ [$\text{M} = \text{Mn}(\text{II}), \text{Zn}(\text{II})$] (**167a** and **167b**) has been employed in fluorous biphasic oxidation catalysis with and without fluorous solvents in the cases of alcohol and alkenol oxidation and with toluene in the case of alkene epoxidation. The conversions of the alkenes using catalyst **167a** vary between 0 and 100%, depending on the substrate (Scheme 85). While acyclic unfunctionalized substrates like 1-octene were converted poorly or not at all, cyclic substrates showed much better reactivity for being oxidized (52–100% conv.). Conversions of alkenols in fluorous solvents were between 58 and 95% and in non-fluorous solvents they varied from 35 to 100%. Allylic alkenols showed greater reactivity towards epoxidation than non-allylic alkenols. The epoxidation was predominant for alkenols with primary alcohol moieties while for alkenols with secondary alcohol moieties alcohol oxidation is predominant. The catalyst is freely soluble in perfluorohydrocarbons and insoluble in common organic solvents at room temperature, but dissolves also in these solvents upon heating up to 60–80 °C. Therefore, in both cases—with or without fluorous solvent—one starts with a triphasic system, which is transformed to a biphasic reaction medium during the reaction upon heating: After the reaction, upon cooling, three phases are formed again, so that the product as well as the catalyst can be separated from the reaction medium very easily (Figure 14). The catalyst has been reused without significant loss in reactivity.

An overview of the published known results of tungsten-catalyzed epoxidation of unfunctionalized olefins with H_2O_2 as oxidant is given in Table 23.

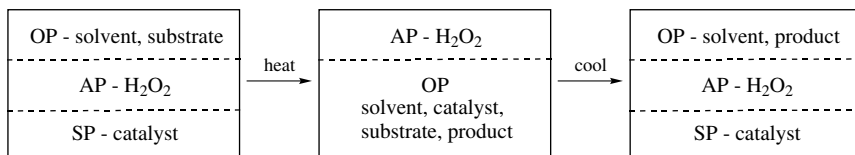
iv. Mn, Tc, Re. Compared to transition metals from groups IV–VI (except Cr), the catalytic properties of group VII and VIII (discussed later) transition metals with peroxides as oxidants are based on a different mechanism. While group IV–VI transition metal catalysts activate the peroxides through coordination towards nucleophilic attack by the alkene, the catalytic properties of group VII and VIII can be attributed to the fact that the transition metal serves as a relay for the oxygen atom transfer from the terminal oxidant to the alkene via an oxo-metal reactive intermediate. Characteristic for these transition metals is that they are easily capable of changing their oxidation state.

Different soluble Mn(II) salts like the manganese(II) triflate as well as salen and porphyrin complexes of manganese show the ability to catalyze the olefin epoxidation. In the case of manganese porphyrins, which have been studied in most detail because of their relation to the biological oxidation systems, different oxygen sources can be used³¹⁷: iodosylbenzene, sodium hypochlorite, molecular oxygen in the presence of an electron source, *N*-oxides, potassium hydrogen persulfate, oxaziridines and also hydrogen peroxide³¹⁸ or alkyl hydroperoxides³¹⁹. From these the manganese-catalyzed epoxidations with hydrogen peroxide or alkyl hydroperoxides will be discussed in the following. The

With fluorous solvent:



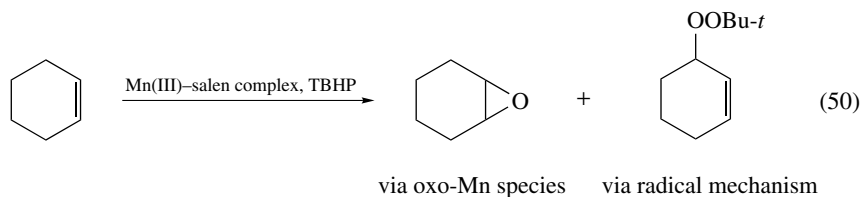
Without fluorous solvent:



OP = organic phase, AP = aqueous phase, FP = fluorous phase, SP = solid phase,
F-O-P = fluorous /organic phase

FIGURE 14. Phase behavior in the oxidation reaction with aqueous H_2O_2 catalyzed by $(\text{R}_F\text{N}^+)_{12}[\text{WZnM}_2(\text{H}_2\text{O})_2(\text{ZnW}_9\text{O}_{34})_2]^{12-}$ [$\text{M} = \text{Mn}(\text{II}), \text{Zn}(\text{II})$] with and without fluorous solvents

major problem in these catalytic systems is the homolytic cleavage of the peroxide bond, which leads to radical formation, the dismutation of peroxides and the oxidative destruction of catalysts by H_2O_2 . In the $\text{Mn}(\text{III})$ -salen catalyzed oxidation of alkenes using TBHP as oxygen source, two different oxidation pathways have been found to occur³²⁰: (i) formation of a *tert*-butylperoxyalkene via a radical chain mechanism (inhibited by a radical scavenger-like ionol) and (ii) epoxide formation via an oxo-manganese(V) complex (equation 50).



Without additives, radical formation is the main reaction in the manganese-catalyzed oxidation of alkenes and epoxide yields are poor. The heterolytic peroxide-bond-cleavage and therefore epoxide formation can be favored by using nitrogen heterocycles as cocatalysts (imidazoles³¹⁸⁻³²², pyridines^{320, 321}, tertiary amine *N*-oxides³²³) acting as bases or as axial ligands on the metal catalyst. With the Mn -salen complex $\text{Mn}-[N,N'$ -ethylenebis(5,5'-dinitrosalicylideneaminato)], and in the presence of imidazole as cocatalyst and TBHP as oxidant, various alkenes could be epoxidized with yields between 6% and 90% (in some cases ionol was employed as additive), whereby the yields based on the amount of TBHP consumed were low (10–15%). Sterically hindered additives like 2,6-di-*t*-butylpyridine did not promote the epoxidation.

TABLE 23. Comparison of the results of the tungsten-catalyzed epoxidation of unfunctionalized olefins

Substrate	Catalytic system ^a	Time [h]	Conversion [%]	Yield [%]	Reference
Propene	166	8	90	90	315
1-Butene	166	8	88	88	315
1,3-Butadiene	166	9	91	91 ^b	315
1-Octene	163	5	82	82	271, 308
	164			76	271, 309
	A	4	96	94	271, 311
	166	10	90	90	315
	167	13	0		316
	$[(n\text{-Hex})_4\text{N}^+]_3$ $[\text{PO}_4[\text{W}(\text{O})(\text{O}_2)_2]_4]^{3-}$	1.75		89	306
1-Nonene	A	2	90	86	271, 312
		4	95	94	312
1-Decene	A	4	99	99	311
1-Undecene	A	2–4	92–99	91–99	271, 310, 312
1-Dodecene	$\text{Na}_2\text{WO}_4/\text{H}_3\text{PO}_4/$ aliquat 336	1		87	271, 305
	A	4	98	97	271, 310, 311
(Z)-2-Octene	166	3	>99	>99	315
(E)-2-Octene	166	14	91	91	315
	167	13	3		316
(Z)-3-Octene	A	0.5	99	99	271, 310, 312
(E)-3-Octene	A	1–2	97–99	95–99	271, 310, 312
2-Methyl-2-heptene	167	13	64		316
2-Methyl-2-decene	A	1	99	99	271, 310, 312
2-Methyl-1-undecene	A	2	99	85	271, 312
3,4-Diethyl-3-hexene	A		93	76	271, 310, 312
Styrene	$\text{Na}_2\text{WO}_4/\text{H}_3\text{PO}_4/$ aliquat 336	3		77	271, 305
	A	1	34	23	312
<i>p-t</i> -BuC ₆ H ₄ CH=CH ₂	A	4	81	65	312
<i>p-n</i> -C ₉ H ₁₉ C ₆ H ₄ CH=CH ₂	A	2	72	69	312
α -Methylstyrene	$\text{Na}_2\text{WO}_4/\text{H}_3\text{PO}_4/$ aliquat 336	4		79	271, 305
Cyclohexene	$\text{Na}_2\text{WO}_4/\text{H}_3\text{PO}_4/$ aliquat 336	0.42–0.75		81–88	271, 305
	165		87–94	77–91 ^c	314
	166	6	84	84	315
	167	13	100		316
Cyclooctene	163	24	96	>94	271, 308
	A		98	98	271, 310, 312
	B		88–98	^d	271, 312
	166	2	99	99	315
	167	13	52		316
Cyclododecene	166	4	97	97	315
Vinylcyclohexene	163	2	96	>95 ^e	271, 308
5-Vinylbicyclo[2.2.1]- hept-2-ene	163	3	90	81 ^f	271, 308
1-Methylcyclohexene	166	4	95	95	315
	167	13	100		316
4-Methylcyclohexene	167	13	97		316
Norborene	166	4	>99	>99	315
Allyl chloride	$\text{Na}_2\text{WO}_4/\text{H}_3\text{PO}_4/$ aliquat 336	2.5		80	271, 305
γ -Terpinene	164		91	79 (11) ^g	271, 309
Neryl acetate	164		96	54 (32) ^g	271, 309
Geranyl acetate	164		100	86 (11) ^g	271, 309
Citral	164		84	71 ^h	271, 309

TABLE 23 (continued)

Substrate	Catalytic system ^a	Time [h]	Conversion [%]	Yield [%]	Reference
Nerol	164		85	55 ^h	271, 309
Geraniol	164		91	89 ^h	271, 309
Linalool	164		100	48 (22) ^g	271, 309
Limonene	164		94	91 ⁱ	271, 309
Functionalized substrates (ethers, alcohols, esters, ketones)	A		61–99	42–99	271, 312

^a **A** (Noyori's system) = Na₂WO₄/[n-Oct₃NMe]⁺HSO₄⁻/H₂NCH₂PO₃H₂. **B** = preformed cat.: [Oct₃NMe]⁺₃[PW₁₂O₄₀]³⁻ or *in situ* formation: (Oct₃NMe)Cl + H₃PW₁₂O₄₀.

^b Monoepoxide is exclusively formed.

^c Yield of diol: 0–13%.

^d Epoxide selectivity: 90–95%.

^e Selective epoxidation of the ring double bond but no stereoselectivity.

^f Product: *exo*-2,3-epoxy-5-vinylbicyclo[2.2.1]heptane obtained by regio- and stereoselective epoxidation.

^g Yield for monoepoxide; yield for diepoxide is given in parentheses.

^h 2,3-Epoxide selectively formed.

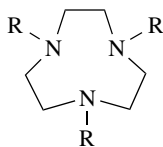
ⁱ Selective epoxidation of the ring double bond.

In the case of manganese porphyrin catalyzed epoxidations, the axial ligands have been used alone or together with other additives like carboxylic acids (Banfi and coworkers)³²¹ and soluble bases (Johnstone and coworkers)³²³. For example, Mansuy and coworkers showed that in the presence of imidazole, 2-methylimidazole or 4-imidazole chloromanganese(tetra-2,6-dichlorophenylporphyrin) catalyzes the epoxidation of various alkenes including 1-alkenes by H₂O₂^{318,322}. Under these conditions alkene conversion is complete within one hour at 20 °C and epoxide yields were very high (90–99%). Maximum yields were obtained using an imidazole/Mn ratio of 10 to 25. Epoxidations with this catalytic system are stereospecific corresponding to a *syn* addition of an oxygen atom to the double bond. The use of tertiary amine *N*-oxides is advantageous over imidazole ligands because of their better stability under the reaction conditions employed³²³.

In 1994, Mansuy and coworkers found that a simple ammonium salt, like ammonium acetate alone, is a very efficient cocatalyst for the metalloporphyrin-catalyzed epoxidation of simple alkenes by hydrogen peroxide³²⁴. Bases like sodium carbonate, sodium acetate or tetrabutylammonium hydroxide turned out to promote the porphyrin-catalyzed epoxidation without any other additive³²³. Adducts of hydrogen peroxide (with Na₂CO₃, urea, Me₃NO, Ph₃PO), which turned out to be particularly useful for reactions in which the concentration of H₂O₂ in solution needs to be controlled at a fixed level, have been employed by Johnstone and coworkers.

Besides porphyrin ligands also chiral 1,4,7-triazacyclononane and salen ligands have been investigated as asymmetric inductors in the manganese-catalyzed epoxidation of olefins. During their search for new catalysts for low temperature bleaching, Hage and coworkers from Unilever also investigated the capability of a manganese-containing system with 1,4,7-trimethyltriazacyclononane (tmtacn, **168a**) as ligand to epoxidize styrenes³²⁵. Using this ligand, the corresponding manganese complexes showed efficient epoxidation activity with hydrogen peroxide in a buffered solution (pH 9) giving the epoxides (epoxides of styrene and vinylbenzoic acid) with almost quantitative conversion of the olefins.

In 1996, an optimization of the oxidation protocol was described by De Vos and Bein who found a dependence of catalytic activity on temperature, solvent, and ligand structure³²⁶. Their investigations showed that different substituents on the nitrogen atoms of the triazacyclononane ligands **168** have a great effect on the activity



(168a) R = Me

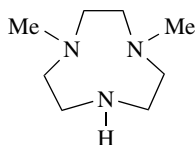
(168b) R = CH₂CH(OH)Et

(168c) R = CH₂CO₂⁻

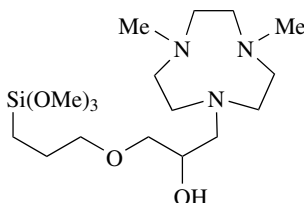
and selectivity of the catalyst. With ligand **168a** [trimethyltriazacyclononane (tmtacn), R = Me], cyclohexene and styrene could be epoxidized in acetone as solvent in yields of 79% and 98%, respectively. Especially with this catalyst acetone was essential as solvent in order to obtain good epoxide yields. This may be due to its function as a storage form of hydrogen peroxide. In other solvents like THF, acetonitrile or methanol, epoxide yields were significantly lower (<7%). With ligands **168b** and **168c**, epoxide yields were generally lower (1–60%) and a different solvent dependency was observed.

Two years later De Vos and coworkers reported on the enhancement of catalytic properties of Mn-tmtacn complexes for epoxidations with H₂O₂ by employing a catalytic amount of oxalate/oxalic acid buffer in order to favor epoxidation over peroxide disproportionation³²⁷. Using only a slight excess of hydrogen peroxide, reaction times were very short (≤ 2h) and a variety of structurally different olefins including unfunctionalized ones with internal or external double bond as well as olefins bearing functional groups could be oxidized. Deactivating functional groups in the substrate (CH₂OH, CH₂OCOR, COR, CO₂R, oxirane) are accepted and even double bonds in conjugation to a carbonyl group are epoxidized. The epoxide yields ranged from 35% to >99%. The positive effect of oxalic acid depends on its structure and is not only an acid effect, as was proven by employing other acids like acetic acid, which did not enhance the catalytic activity. Using the modified conditions the reaction was stereospecific (>98%), the epoxide selectivity was very high (66 to >99%) and no products of solvolysis were obtained.

In the case of olefins bearing more than one double bond, diepoxide formation was also achieved. Heterogenization of these kinds of ligands by either covalently attaching them to mesoporous siliceous support material (MCM-41)³²⁸ or by incorporation into zeolites³²⁹ was described and the corresponding Mn complexes were used as epoxidation catalysts by Bein and coworkers³²⁹ and by Jacobs and coworkers in 1999³³⁰. A very efficient heterogeneous catalyst was prepared from 1,4-dimethyl-1,4,7-triazacyclononane (dmtacn, **168d**) by reaction with (3-glycidyloxypropyl)trimethoxysilane. Compound **168e**, which is prepared in this way, is then immobilized on an amorphous SiO₂ surface by metal coordination via stirring with MnSO₄•H₂O.



(168d)



(168e)

Besides epoxides, also significant quantities of the corresponding *cis*-diols were formed with this catalyst, which did not result from solvolysis of the preformed epoxides. This

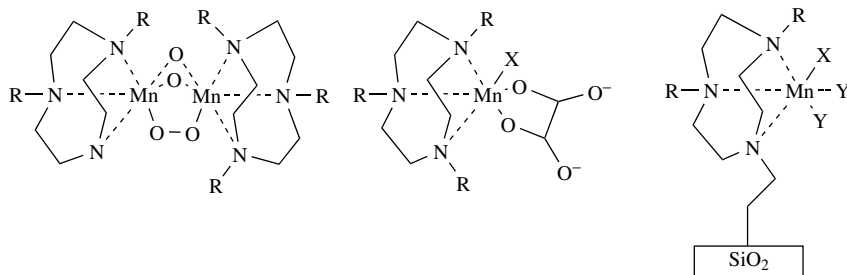


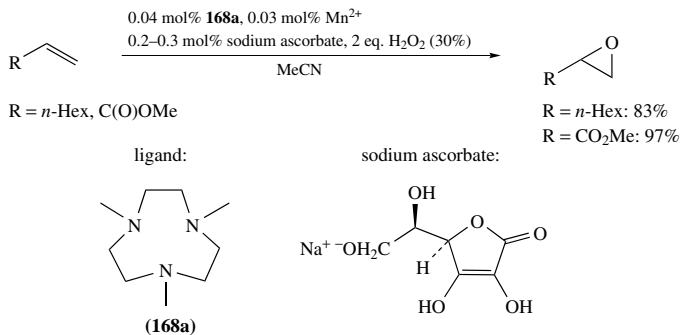
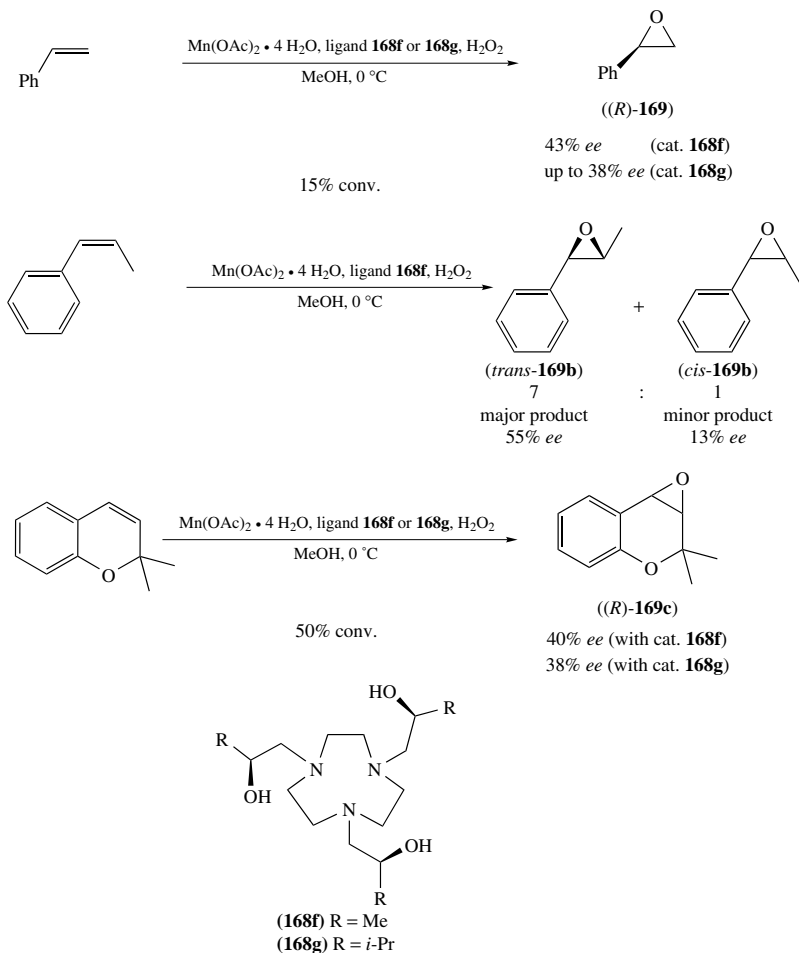
FIGURE 15. Structures proposed for homogeneous and heterogeneous Mn-tmtacn catalysts

fact is remarkable because the catalytic synthesis of *cis*-diols with H_2O_2 was only known for Os and Ru complexes bearing two *cis*-oxo ligands, which can form cyclic osmate- or ruthenate-esters. The authors proposed structures for the Mn-tmtacn oxidation catalysts in homogeneous solution with and without oxalic acid/oxalate buffer and for the heterogeneous Mn catalyst which are depicted in Figure 15. In solution, dinuclear species are easily formed (Figure 15, left) and are responsible for the catalase-like activity of the complex. Addition of oxalate leads to coordination of this compound to the Mn-tmtacn complex resulting in the formation of a mononuclear complex (Figure 15, middle), which does not catalyze the peroxide disproportionation and therefore a clean transfer of one oxygen atom occurs to form the epoxide. In the heterogeneous Mn complex (Figure 15, right) the formation of binuclear species is prevented due to the isolation of the ligand by the solid support and again peroxide disproportionation is diminished.

The zeolite-supported catalyst reported by Bein and coworkers (tmtacn/Mn incorporated into zeolite) was tested in the epoxidation of styrene and cyclohexene using H_2O_2 as oxidant³²⁹. The best results were obtained in acetone at 0°C and adding hydrogen peroxide in portions. Under these conditions conversions were 19% for styrene and 47% for cyclohexene with high epoxide selectivities of 98% and 95%, respectively. The catalyst was proposed to have a structure in which the active centers are shielded by the sterically demanding ligands being situated in the cavities of the zeolite.

Berkessel and Sklorz screened a variety of potential co-ligands for the Mn-tmtacn/ H_2O_2 catalyzed epoxidation reaction and found that ascorbic acid was the most efficient one³³¹. With this activator the authors could oxidize the terminal olefins 1-octene and methyl acrylate with full conversion and yields of 83% and 97%, respectively, employing less than 0.1% of the metal complex (Scheme 86). Furthermore, with *E*- and *Z*-1-deuterio-1-octene as substrates, it was shown that the oxygen transfer proceeded stereoselectively with almost complete retention of configuration ($94 \pm 2\%$). Besides the epoxidation, also the oxidation of alcohols to carbonyl compounds could be catalyzed by this catalytic system (see also Section III.C).

In 1996/97 the first applications of triazacyclononane manganese systems in combination with hydrogen peroxide for the enantioselective epoxidation were reported by Bolm and coworkers^{332,333}. In this procedure the epoxidation catalyst was formed *in situ* from Mn(II) acetate and enantiopure C_3 -symmetric **168f** or **168g** (Scheme 87). With H_2O_2 as oxygen source, styrene was epoxidized with poor conversion of 15% giving the corresponding (*R*)-configured epoxide **169a** with an enantiomeric excess of 43% (using catalyst **168f**) and 38% (using catalyst **168g**). (*Z*)- β -Methylstyrene was converted into a 7:1 mixture of the corresponding epoxides *trans*-**169b** (55% *ee*) and *cis*-**169b** (13% *ee*) using catalyst **168f**. Epoxidation of 2,2-dimethyl-2*H*-chromene using catalyst **168f** or **168g** led to the formation of epoxide **169c** with an enantiomeric excesses of 38–40%.

SCHEME 86. Mn-tmtacn/H₂O₂/Na ascorbate catalyzed epoxidation of terminal olefins

SCHEME 87. Enantioselective olefin epoxidation using chiral Mn/1,4,7-triazacyclononane complexes

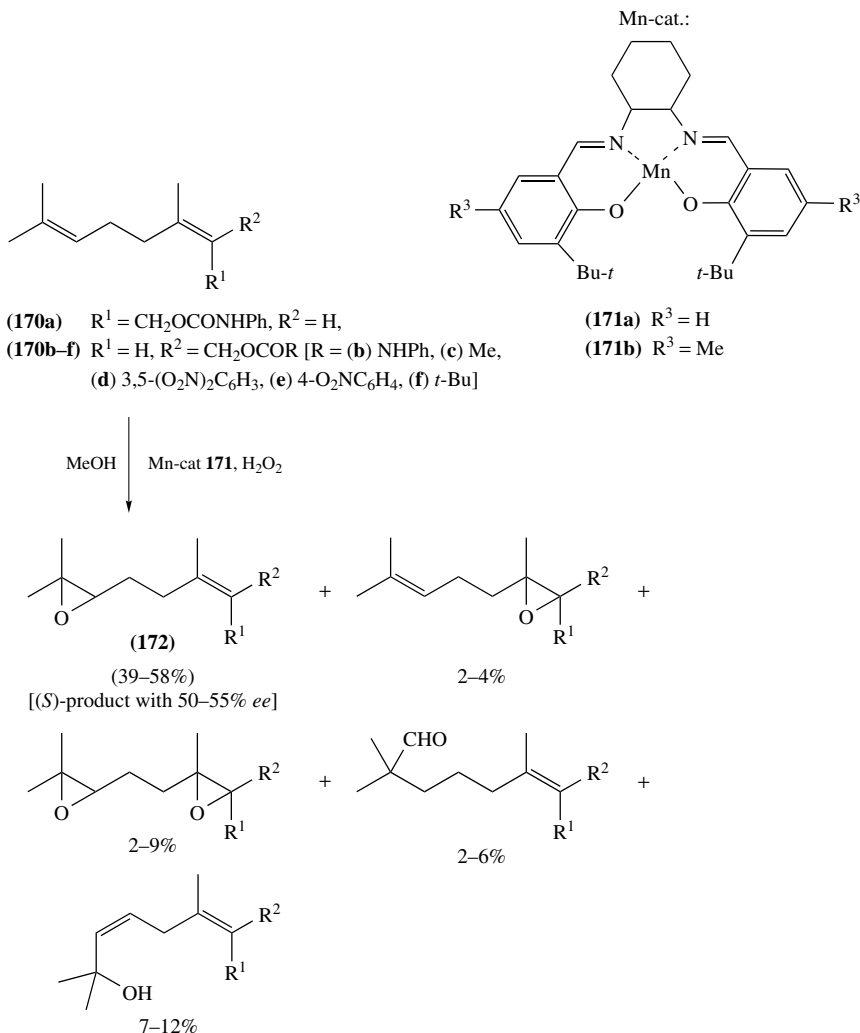
Bolm and coworkers observed that the enantiomeric excess decreases upon longer reaction times due to decomposition of the catalytically active species during the reaction, giving rise to other catalytically active species which yielded racemic product.

Recently, Lindsay Smith and coworkers reported on their mechanistic studies of the epoxidation of cinnamic acid in basic aqueous acetonitrile with hydrogen peroxide catalyzed by the Mn/tmtacn catalytic system³³⁴. The effect of several additives (potential co-ligands) on the reaction has been studied and the authors found that the oxidation rate decreased upon addition of biphenols, salicylic or anthranilic acid. Several diols, aliphatic amino acids, malonic acid and mandelic acid had a negligible effect on the reaction, while oxalic acid, ascorbic acid and naphthalene-2,3-diol-6-sulfonate gave a three- to five-fold increase in the rate of epoxidation. A Hammett correlation of rate data showed that the active oxidant is electrophilic and oxygen labelling experiments revealed that H₂O₂ and not H₂O is the source of the oxygen in the epoxide. The authors could show that MnSO₄/tmtacn/H₂O₂ in the presence of 5,5'-dimethoxy-2,2'-biphenol forms the complex O=Mn(V)(tmtacn)(biphenol), which is a stable complex and therefore a less effective oxidant for cinnamic acid. The experimental results also rule out peroxy acids or manganese peroxy acid complexes as key intermediates in the reactions with H₂O₂. In their publication Lindsay Smith and coworkers discuss possible mechanisms for this kind of reaction.

An important class of manganese complexes that is active for catalyzing the epoxidation of unfunctional alkenes is the one based on salen ligands and detailed reviews have been published by Katsuki³³⁵ as well as Muñiz-Fernández and Bolm³³⁶. In the epoxidation reactions with these kinds of manganese catalysts a variety of terminal oxidants can be employed like iodosylbenzene and its derivatives, sodium hypochlorite, molecular oxygen in combination with aldehyde and also hydrogen peroxide. From these, the reactions in which hydrogen peroxide was used will be discussed in the following. With this oxygen source, addition of a donor ligand is crucial in order to effect O–O bond cleavage of the intermediate hydroperoxide species [HO–O–Mn(III)] to form the catalytically active oxo-species. In general, *cis*-olefins conjugated with aryl, acetylenic and olefinic groups are the best substrates for salen-catalyzed epoxidation and also conjugated trisubstituted olefins bearing a methyl group *cis* to the hydrogen atom are good substrates. These classes of olefins exhibit high enantioselectivity (more than 90% *ee*). Significantly diminished enantioselectivity is observed for *cis*-olefins bearing only alkyl substituents and for *cis*-olefins conjugated with π -bonds at both terminal carbon atoms, while *trans*-olefins display moderate enantioselectivity. With manganese-oxo complexes the oxo-oxygen atom is transferred during the epoxidation step and the oxo-species is regenerated via oxidation with the terminal oxygen source like hydrogen peroxide. For the oxygen transfer step during epoxidation various mechanistic considerations have been proposed (olefin approach 'side-on', linear to the Mn=O bond or along the N-Mn bond axis³³⁵, reaction via concerted pathway, via radical intermediate or via metallaoxetane^{336,337}) in order to explain the obtained enantioselectivities of the reactions.

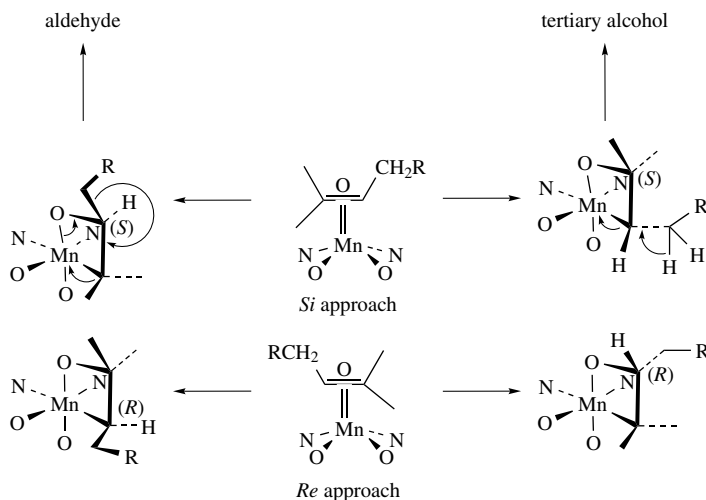
Brun and coworkers investigated the Mn-salen catalyzed epoxidation of nerol *N*-phenylcarbamate **170a** and geraniol derivatives **170b–f** with H₂O₂ as oxidant using complexes **171** (Scheme 88)³³⁷. Next to the epoxides (mono- and diepoxides) also tertiary alcohol and rearranged aldehyde were observed. With the analogous Mn–salen complex bearing the R³ = OMe substituent, no transformation was obtained. For the different substrates used results were similar, with epoxide **172** being the main product (39–58% yield) with an enantiomeric excess varying only slightly from 50 to 55% [(*S*)-enantiomer]. The authors proposed an epoxidation mechanism via oxometallacycle, with which the product and side product formation as well as stereoselectivity can be explained (Scheme 89).

Chiral Mn–salen complex **173a** in the presence of *N*-methylimidazole, which serves as axial ligand and H₂O₂ as oxygen source, has been employed by Pietikäinen for the

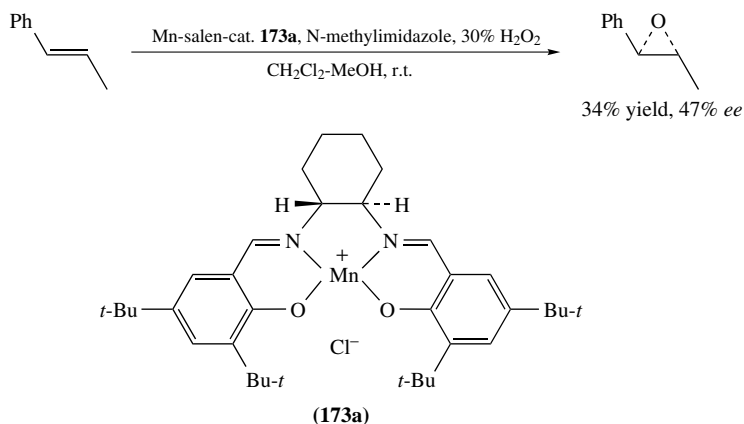
SCHEME 88. Mn-salen catalyzed epoxidation of geraniol and nerol using H_2O_2

epoxidation of 1-phenylpropene yielding the corresponding epoxide in 34% yield and with an enantiomeric excess of 47% of the $1R,2R$ -enantiomer (Scheme 90)³³⁸. Manganese–salen complexes **173b** and **173c** that have been used for epoxidation of olefin **174** in combination with hydrogen peroxide as terminal oxidant and the obtained yields and enantiomeric excesses of the corresponding epoxide **175** are shown in Scheme 91^{338, 339}. These include Mn–salen complex **173b** employed by Pietikäinen³⁴⁰ and chiral pentadentate dihydrosalen ligand **173c** developed by Schwenkreis and Berkessel³³⁹.

Various other chromene derivatives **176a–d** could be epoxidized with Katsuki's Mn-salen catalyst **173d** using either H_2O_2 or TMS_2O_2 as oxidant³⁴¹. With this catalytic system several axial ligands (none, *N*-methylimidazole, pyridine *N*-oxide) and additives (none,

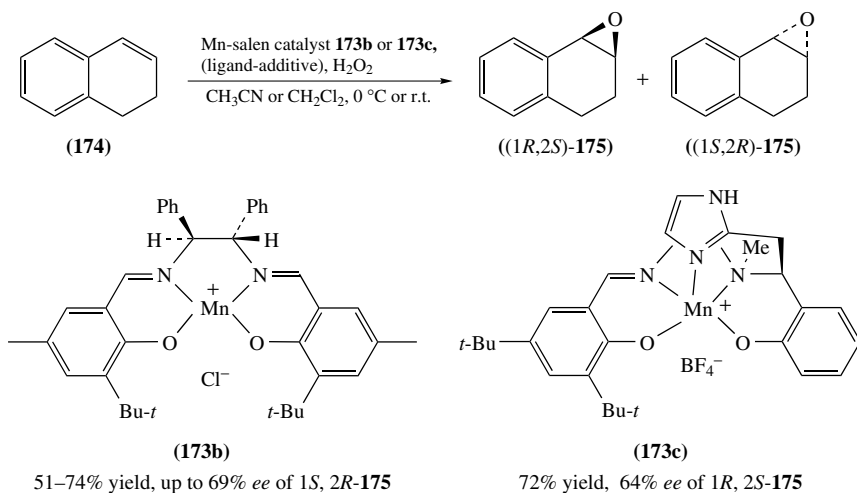


SCHEME 89. Mn-catalyzed epoxidation via oxametallacycles and pathways leading to side products

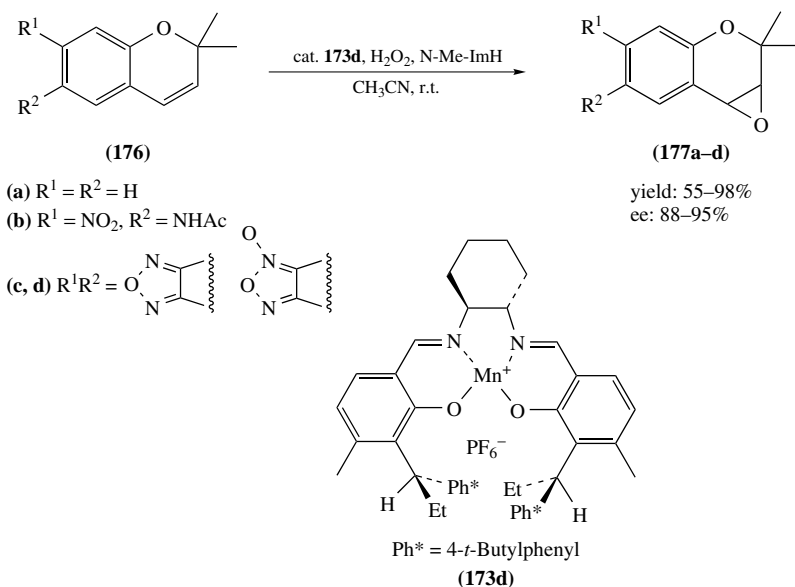
SCHEME 90. Epoxidation of *trans*-1-phenylpropene using chiral catalyst **173a**

NH_4ClO_4 , NH_4PF_6) have been tested and the best results were obtained in acetonitrile as solvent in the presence of *N*-methylimidazole using H_2O_2 as terminal oxidant (Scheme 92). Under these conditions chromene derivatives could be converted into the corresponding epoxides **177** in yields between 55 and 98% and *ee* values of 88–95%.

The effect of structural variation and the use of different carboxylate salts as cocatalysts was investigated by Pietikäinen³⁴⁰. The epoxidation reactions were performed with the chiral Mn(III)–salen complexes **173** depicted in Scheme 93 using H_2O_2 or urea hydrogen peroxide as oxidants and unfunctionalized alkenes as substrates. With several soluble carboxylate salts as additives, like ammonium acetate, ammonium formate, sodium acetate and sodium benzoate, good yields (62–73%) and moderate enantioselectivities (*ee* 61–69%) were obtained in the asymmetric epoxidation of 1,2-dihydronaphthalene. The results were better than with *N*-heterocycles like *N*-methylimidazole, *tert*-butylpyridine,

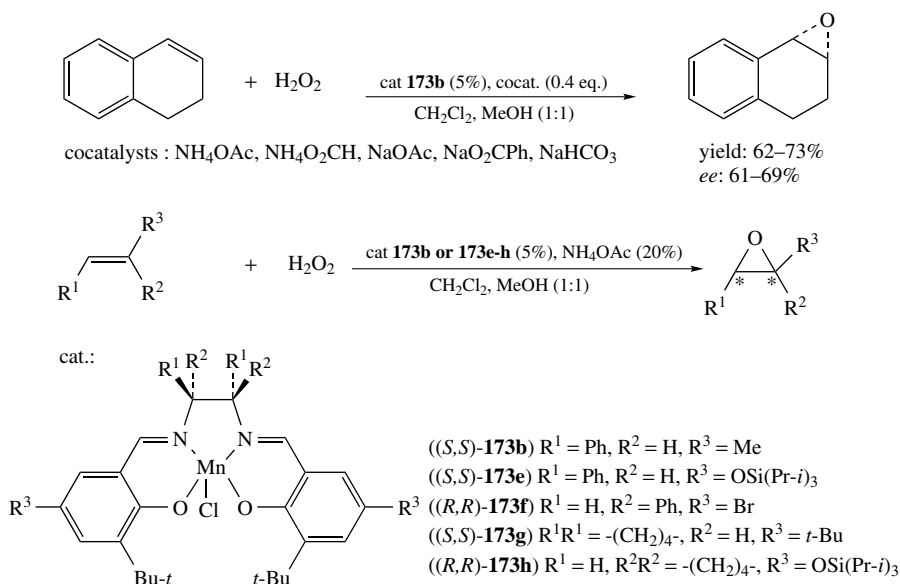


SCHEME 91. Asymmetric epoxidation of 1,2-dihydronaphthalene using chiral Mn–salen complexes **173b** and **173c**



SCHEME 92. Mn-catalyzed enantioselective epoxidation of chromene derivatives using H_2O_2

N-methylmorpholine *N*-oxide or 4-phenylpyridine *N*-oxide as cocatalysts. The yields and enantioselectivities obtained with H_2O_2 or urea hydrogen peroxide were comparable, with slightly better yields for the epoxidation with H_2O_2 (73% versus 68% for the epoxide of 1,2-dihydronaphthalene in the presence of NH_4OAc).




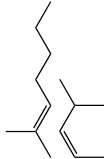
SCHEME 93. Asymmetric (Salen)Mn(III)-catalyzed epoxidation of unfunctionalized alkenes with H_2O_2 using carboxylate salts as cocatalysts



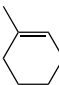
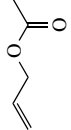
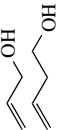
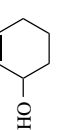
Steric and electronic effects of different substituents on the diamine moiety of the catalyst and on the aromatic ring of the salicylic moiety were investigated (catalysts **173b,e-h**). Similar results were observed in all cases with slightly better asymmetric inductions with catalyst (*S,S*)-**173g** and (*R,R*)-**173h** ($\Delta ee = 2\text{--}4\%$). Electron-donating substituents at 5 and 5' position of the salicylic aldehyde attenuated the reactivity and longer reaction times are needed for obtaining the same conversions. The role of the carboxylate cocatalyst might be that of a base that facilitates the deprotonation of hydrogen peroxide and therefore the formation of the hydroperoxy complex [(salen)Mn(III)–O–OH]. A second possibility is that the formation of the reactive species, the Mn(V)=O complex, proceeds via a peroxyacylmanganese species [(salen)Mn(III)–O–OC(O)R].

The results obtained in the manganese-catalyzed epoxidation reactions of various olefins are shown in Table 24.

Until 1991 manganese, in the form of its salts and complexes, has been the only transition metal of group VII that gained attraction as epoxidation catalyst. In 1991, Herrmann and coworkers reported that another simple organometallic compound of this group, the methyltrioxorhenium (MTO), serves as a highly effective catalyst for the oxidation of organic compounds by water-free hydrogen peroxide in *tert*-butanol solution³⁴². Re(VII) oxo and imido complexes, especially MTO, have gained importance throughout the years as very effective catalysts for a variety of reactions³⁴³ including oxidative transformations. With MTO as reactive oxidant it is possible to oxidize unfunctionalized olefins at room temperature or below in yields between 38 and 100%, but so far asymmetric epoxidation with MTO or chiral MTO derivatives has not been reported. Attempts by Herrmann and coworkers to carry out the MTO catalyzed epoxidation in an asymmetric way using Tröger's base as additive to form a chiral complex with MTO *in situ* were unsuccessful and only racemic epoxides were obtained³⁴⁴. With the Lewis-acidic MTO/ H_2O_2 catalytic system epoxide ring opening to form the diol was found, but Herrmann and coworkers

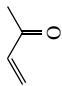
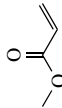
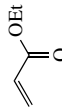
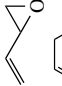
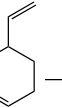
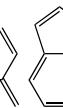
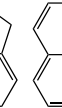
TABLE 24. Manganese-catalyzed epoxidation of olefins using hydrogen peroxide as oxygen source

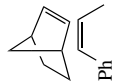
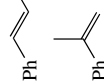
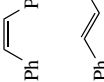

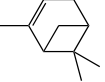
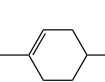
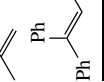


Substrate	Mn catalyst ^a	Solvent	Time (h)	Epoxide yield ^b (%)	Side products (%)	<i>ee</i> epoxide (%)	Abs. config.	Reference
	Mn(TPP)Cl/imidazole	MeCN/CH ₂ Cl ₂	1.5	26	5 ^c			318
	Mn(TMP)Cl/imidazole	MeCN/CH ₂ Cl ₂	1.5	66	2 ^c			318
	Mn(TDCPP)Cl/imidazole	MeCN/CH ₂ Cl ₂	1.5	93	2 ^c			318
	Mn-168a	acetone	3	98				326
	Mn-168b	MeOH	10	60				326
	Mn-168c	acetone	10	33				326
	Mn(III)-salen ^d /imidazole/TBHP ^e	MeCN	5 min	6	1 ^f			320
	Mn/tmtacn on zeolite support	acetone	12	18	<1 ^g			329
	Mn-168f	MeOH	5	15		43	(R)	332
	Mn-168a/oxalate buffer	MeCN	0.6	95				327
	Mn-168a/oxalate buffer	MeCN	0.3	>99				327
	Mn(TDCPP)Cl/imidazole	MeCN/CH ₂ Cl ₂	2	76 [^h >98:2]				322
	Mn-168a/oxalate buffer	MeCN	1	72 [98:2]				327, 330
	Mn-168e(immobilized on SiO ₂)	acetone	2	53 [86:14]	19 + 7 ^h			330
	Mn(III)-salen ^d /imidazole/TBHP	MeCN	5 min	26	2 ⁱ			320
	Mn(III)-salen ^d /imidazole/TBHP ^e	MeCN	5 min	79				320
	Mn(TDCPP)Cl/imidazole	MeCN/CH ₂ Cl ₂	2	40 [^h <2:98]				322
	Mn-168a/oxalate buffer	MeCN	1	35 [2:98]				327, 330
	Mn-168e(immobilized on SiO ₂)	MeCN	1	14 [11:89]	7 + 2 ^h			330
	Mn(TDCPP)Cl/Et ₃ NO/Bu ₄ NOH	MeOH/CH ₂ Cl ₂	24	72				323
	Mn(III)-salen ^d /imidazole/TBHP	MeCN	5 min	31	3 ⁱ			320
	Mn-168a/ascorbate	MeCN	2	83				331
	Mn(TDCPP)Cl/imidazole	MeCN/CH ₂ Cl ₂	1.5	99				318, 322
	Mn(TDCPP)Cl/NH ₄ O ₂ ·CMe	MeCN/CH ₂ Cl ₂		87				324
	Mn(TDCPP)Cl/hexylimidazole/benzoic acid	CH ₂ Cl ₂	0.25	92				321
	Mn(TDCPP)Cl/imidazole	MeCN/CH ₂ Cl ₂	1.5	99				318, 322
1-Dodecene 	Mn-168e(immobilized on SiO ₂)	MeCN	2	44 [86:14]	24 + 5			330

	Mn(TDCPP)/C/hexylimidazole/benzoic acid	CH ₂ Cl ₂	0.25	63 [0:100]	321
	Mn(TDCPP)/C/Et ₃ NO/Bu ₄ NOH	MeOH/CH ₂ Cl ₂	24	24	323
	Mn(TDCPP)/C/imidazole	MeCN/CH ₂ Cl ₂	1.5	91	318, 322
	Mn(TDCPP)/C/NH ₄ O ₂ CMe	MeCN/CH ₂ Cl ₂	0.17	95	324
	Mn(TDCPP)/C/hexylimidazole/benzoic acid	CH ₂ Cl ₂	5	100	321
	Mn(TDCPP)/C/Et ₃ NO/Bu ₄ NOH	MeOH/CH ₂ Cl ₂	2	98	323
	Mn(TDCPP)/C/Et ₃ NO/Bu ₄ NOH ^f	MeOH/CH ₂ Cl ₂	24	91	323
	Mn(TDCPP)/C/Et ₃ NO/Bu ₄ NOH ^k	MeOH/CH ₂ Cl ₂	2	89	323
	Mn(TDCPP)/C/Et ₃ NO/Bu ₄ NOH ^l	MeOH/CH ₂ Cl ₂	21	96	323
	Mn(III)-salen ^d /imidazole/TBHP ^e	MeCN	5 min	54	320
	Mn(TDCPP)/C/imidazole	MeCN/CH ₂ Cl ₂	1.5	91–97	318
	Mn(TDCPP)/C/NH ₄ O ₂ CMe	MeCN/CH ₂ Cl ₂	5 min	85	324
	Mn(III)-salen ^d /imidazole/TBHP	MeCN	5 min	29	320
	Mn(III)-salen ^d /py/TBHP	MeCN	3	28	320
	Mn-168a	acetone	79	71 ⁿ	326
	Mn-168b	MeOH	10	41	326
	Mn-168c	MeOH	10	32	326
	Mn-168a/oxalate buffer	MeCN	1	83	327
	Mn-168e(immobilized on SiO ₂)	MeCN	2	58	330
	Mn/tmtacn on zeolite	acetone	12	45	329
	Mn(TDCPP)/C/Et ₃ NO/Bu ₄ NOH	MeOH/CH ₂ Cl ₂	2.5	89	323
	Mn-168a/oxalate buffer	MeCN	0.3	>99	327
	Mn-168a/oxalate buffer	MeCN	1	92	327
	Mn-168a/oxalate buffer	MeCN	1	88	327
	Mn-168a/oxalate buffer	MeCN	0.3	63	327

(continued overleaf)

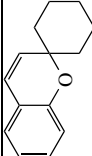
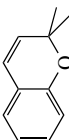
TABLE 24 (continued)

Substrate	Mn catalyst ^a	Solvent	Time (h)	Epoxide yield ^b (%)	Side products (%)	<i>ee</i> epoxide (%)	Abs. config.	Reference
	Mn-168a/oxalate buffer	MeCN	2	66				327
	Mn-168a/ascorbate	MeCN	2	97				331
	Mn-168a/oxalate buffer	MeCN	2	55				327
	Mn-168a/oxalate buffer	MeCN	1	80 ^r				327
	Mn-168a/oxalate buffer	MeCN	1	81 + 8 ^s				327
	Mn-168a/oxalate buffer	MeCN	1	84 + 7 ^s				327
	Mn-168e (immobilized on SiO ₂)	MeCN	3.5	25				330
	(<i>S,S</i>)-173b/NH ₄ OAc	MeOH/CH ₂ Cl ₂	2	63	15 + 2 ^h	75	1 <i>S</i> ,2 <i>R</i>	340
	173b/ <i>N</i> -methylimidazole	MeOH/CH ₂ Cl ₂	2–4	59–63		60	1 <i>S</i> ,2 <i>R</i>	338
	173c	CH ₂ Cl ₂	1	72		64	1 <i>R</i> ,2 <i>S</i>	339
	(<i>S,S</i>)-173b/NH ₄ OAc	MeOH/CH ₂ Cl ₂	4	73		68	1 <i>S</i> ,2 <i>R</i>	340
	(<i>S,S</i>)-173e/NH ₄ OAc	CH ₂ Cl ₂	5	54		64	1 <i>S</i> ,2 <i>R</i>	340
	(<i>S,S</i>)-173g/NH ₄ OAc	MeOH/CH ₂ Cl ₂	1	73		84	5 <i>S</i> ,6 <i>R</i>	340
	(<i>R,R</i>)-173h/NH ₄ OAc	MeOH/CH ₂ Cl ₂	6	54		89	5 <i>R</i> ,6 <i>S</i>	340

	Mn- 168e (immobilized on SiO ₂)	MeCN	5	54	28 + 3 ^h		330
	Mn- 168f	MeOH				7:1 55 (<i>trans</i>) 13 (<i>cis</i>)	332
	Mn(III)-salen ^d /imidazole/TBHP ^e	MeCN	5 min	86(Z): 4 (E)		47	320
	173a /N-methylimidazole	MeOH/CH ₂ Cl ₂		34–51			338
	Mn(TDCPP)Cl/hexylimidazole/benzoic acid	CH ₂ Cl ₂	0.12	100	16 ^f		321
	Mn(III)-salen ^d /imidazole/TBHP ^e	MeCN	5 min	56			320
	Mn(TDCPP)Cl/imidazole	MeCN/CH ₂ Cl ₂	2	94 [97:3]	2 ^u		322
	Mn(TDCPP)Cl/hexylimidazole/benzoic acid	CH ₂ Cl ₂	0.33	85 [100:0]			321
	Mn(TDCPP)Cl/NH ₄ O ₂ CMe	MeCN/CH ₂ Cl ₂		91 [97:3]			324
	Mn(TDCPP)Cl/imidazole	MeCN/CH ₂ Cl ₂	2	2 [0:100]			322
	Mn(TDCPP)Cl/hexylimidazole/benzoic acid	CH ₂ Cl ₂	5	0			321
	Mn(TDCPP)Cl/hexylimidazole/benzoic acid	CH ₂ Cl ₂	0.25	79 ^v			321
	Mn(TDCPP)Cl/hexylimidazole/benzoic acid	CH ₂ Cl ₂	0.17	73 ^w			321
	Mn(TDCPP)Cl/Et ₃ NO/Bu ₄ NOH	MeOH/CH ₂ Cl ₂	3.5	89 ^x			323
	(<i>S,S</i>)- 173g /NH ₄ OAc	MeOH/CH ₂ Cl ₂	4	84		96	340

(continued overleaf)

TABLE 24 (continued)

Substrate	Mn catalyst ^a	Solvent	Time (h)	Epoxide yield ^b (%)	Side products (%)	<i>ee</i> epoxide (%)	Abs. config.	Reference
	(<i>S,S</i>)- 173g /NH ₄ OAc	MeOH/CH ₂ Cl ₂	1.25	90		91	(+)	340
	Mn- 168f	MeOH	15	50 ^y		40	3 <i>R</i> ,4 <i>R</i>	332

^aTPP = tetraphenylporphyrin, TMP = tetramesitylporphyrin, TDCPP = tetra-2,6-dichlorophenylporphyrin.

^b*cis/trans* Ratio is given in brackets.

^cSide products detected: PhCHO and PhCH₂CHO.

^dMn(*N,N*-ethylenebis(5,5'-dinitrosalicylideneamino)).

^eIonol as additive.

^fPhCH₂CHO.

^gBenzaldehyde.

^hDiol + products of diol oxidation.

ⁱ*t*-BuOOBu-*t*.

^jNa₂CO₃•H₂O₂ as oxygen source instead of H₂O₂.

^kUrea•H₂O₂ as oxygen source instead of H₂O₂.

^lMe₃NO•H₂O₂ as oxygen source instead of H₂O₂.

^mAllylic products.

ⁿ1-*tert*-Butylperoxycyclohex-2-ene.

^o(*E*)-1,2-Cyclohexanediol.

^pCyclohex-2-ene.

^q2,3-Epoxycyclohexanone.

^r*Meso* diepoxide (40%) + (+/−)-diepoxide (60%).

^sDiepoxide + monoepoxide.

^tPhCHMeCHO.

^uPhCH₂COPh.

^v1:1:1 Ratio of *exo:endo* epoxides.

^w1:1 Ratio of diastereoisomeric epoxides.

^xRatio of epoxides: 0.69 [monoepoxide (oxidation of the double bond outside the ring)] : 0.18 [monoepoxide (oxidation of ring double bond)] : 0.12 [diepoxide].

^yConversion given.

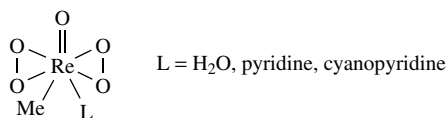
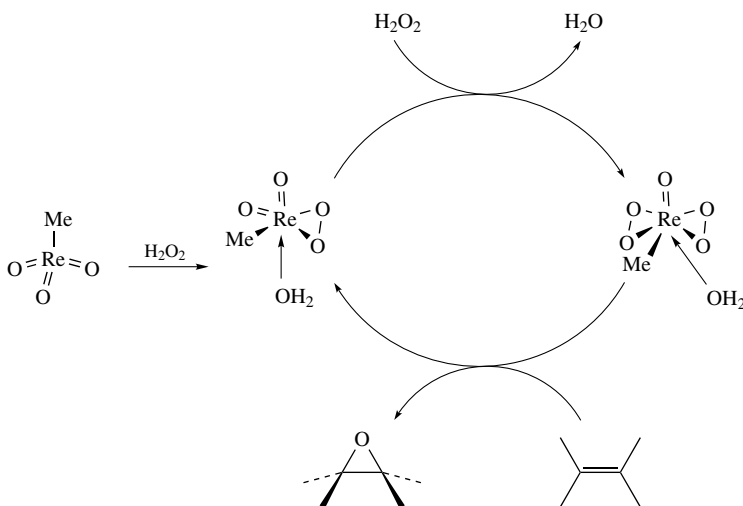
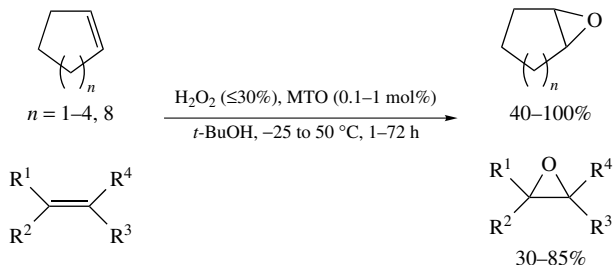


FIGURE 16

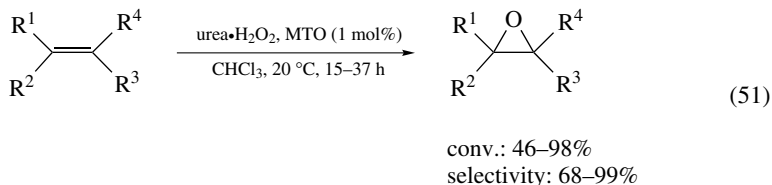
developed a method with which diol formation can be prevented. Simple addition of tertiary amines like pyridine, 4,4'-dimethyl-2,2'-bipyridine, quinine or cinchonine suppresses the ring opening, albeit the catalyst activity is also diminished^{342, 345}. Contrary to isoelectronic OsO₄, MTO does not react with olefins but is first transformed to the bis(peroxo) complex depicted in Figure 16. This catalytic active species, which can epoxidize olefins (according to Scheme 94)³⁴⁶, could be isolated by Herrmann and coworkers³⁴⁵⁻³⁴⁷ in the form of its diglyme adduct out of a MTO/H₂O₂ system and characterized by X-ray structural analysis.

SCHEME 94. Reaction mechanism for the MTO-catalyzed epoxidation by H₂O₂

With the MTO/H₂O₂/*t*-BuOH system alkynes can also be oxidized to form the enones. For example, 3-hexyne can be transformed to 4-hexen-3-one in 55% yield³⁴². Immobilization of MTO on polyvinylpyridines, which bear basic centers that can coordinate to Re, has been reported by the same authors. The immobilized MTO catalyst can simply be filtered off the solution after the reaction. Because of its great versatility as oxidation catalyst and its easy preparation and recyclability³⁴⁸, the epoxidation procedure with MTO is a suitable method for conversions on big scale and was improved over the years³⁴⁹. At the beginning relatively high catalyst concentrations (0.1–1 mol%) in the presence of a ≤ 30% solution of H₂O₂ were used in *tert*-butanol as solvent (Scheme 95)³⁴⁵. Related alkylrhenium(VI) complexes can be transformed to the same active species [MeReO(O₂)₂•H₂O] in the presence of hydrogen peroxide and therefore can also serve as catalysts. A comparison of the catalytic activity of various rhenium compounds is given in Reference 345. Because of its great oxidation activity, MTO can be used at room temperature and below. Although MTO is more active in the absence of bases like

SCHEME 95. MTO-catalyzed epoxidation with H_2O_2 in *tert*-butanol

pyridine, the epoxidation selectivity can be raised (due to suppression of epoxide ring opening) by pH adjustment, use of nitrogen ligands of the bipyridine or quinuclidine type or by employing a catalyst R-ReO_3 with an amino group in the R group. Under these conditions olefins could be epoxidized with yields ranging from 30 to 100%, but long reaction times (1–72 h) were needed especially for the more unreactive terminal olefins. If several double bonds are present in the substrate MTO shows selectivity towards the more electron-rich double bond. For example, in vinylcyclohexene the endocyclic double bond is oxidized first and in carvone the exocyclic double bond is attacked exclusively. The selectivity of the epoxidation reaction could be improved by Adam and Mitchell (up to 95%) in 1996 by employing urea hydrogen peroxide as oxygen source, because it contains no water and therefore epoxide opening which leads to diol formation is suppressed (equation 51)³⁵⁰. The employment of urea hydrogen peroxide has one major advantage over the addition of amines (which also suppress diol formation): while with amines, as already mentioned above, the activity of the catalyst drops significantly, this is not the case with addition of the urea hydrogen peroxide adduct. Urea acts as a kind of buffer in this system, so the acid-sensitive epoxides are more stable under the conditions employed, although extremely hydrolytic sensitive α -methylstyrene oxide still undergoes hydrolysis (next to 55% epoxide and 26% diol were formed).

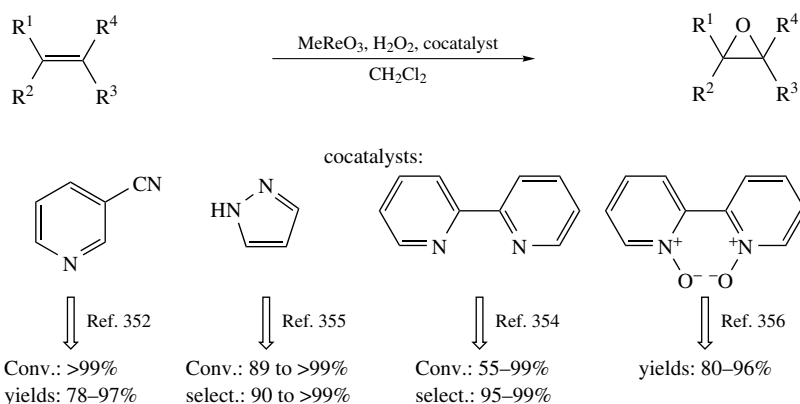


As observed earlier with the manganese catalytic systems, Sharpless and coworkers also found for rhenium that the selectivity towards epoxide formation could be enhanced by using pyridine or pyridine derivatives as ligands in a two-phase-system³⁵¹. The task of the pyridine is to raise the activity of the catalyst, to suppress epoxide decomposition and therefore diol formation and to raise the stability of the catalyst. The second effect of the nitrogen donor additives that has been observed by Herrmann and coworkers was that reaction times could be lowered (<24 h) and better yields were obtained³⁴⁴. An important feature of the Sharpless catalytic system was the possibility of using commercially available aqueous hydrogen peroxide as oxidant. An exception were terminal olefins for which the reaction took several days and selectivities were rather low (60%). This problem could be solved by Sharpless and coworkers who employed a pyridine/cyanopyridine mixture as MTO ligands (see Figure 16), which raised conversions up to 99% (yields between 78

and 97%) with very good epoxide selectivities at reaction times of 6–30 hours³⁵². Using this mixture of two ligands combines the advantage of pyridine as a basic nitrogen base to protect labile epoxides from ring opening and to diminish catalyst lifetime and the advantage of 3-cyanopyridine as a less basic pyridine to allow high conversions.

For the epoxidation of alkenes which form less acid-sensitive epoxides it is sufficient for obtaining good yields to only use 3-cyanopyridine as additive. Functional groups like alcohol, amides, chlorides, esters and ketones are compatible with this epoxidation method. Herrmann and coworkers reported that in the MTO-catalyzed epoxidation reaction in the presence of pyridines these have to be used in large excess (up to 40 mol% in the case of terpenes) because they are labile to oxidation to *N*-oxides, which is also catalyzed by MTO/H₂O₂³⁵³. A loss of activity due to adduct formation of the catalyst with pyridine *N*-oxide occurs, but the selectivity to epoxides remains high throughout the course of the catalysis, because the MTO-pyridine *N*-oxide complex is a highly selective epoxidation catalyst as well, although less active. The loss of activity can be compensated by extraction of pyridine *N*-oxide into the aqueous phase under biphasic conditions.

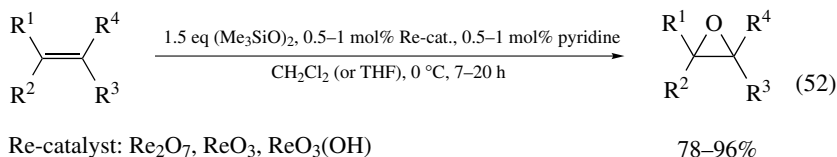
Rudler and coworkers reported that in the case of moderately acid-sensitive epoxides the use of biphasic reaction conditions (H₂O/CH₂Cl₂) proved to be sufficient in order to obtain the epoxides with good selectivity because under biphasic conditions the contact of epoxides with water is minimized³⁵⁴. Because of the lability of pyridines under the reaction conditions employed, alternative and more stable cocatalysts such as pyrazole (12 mol%, biphasic conditions)³⁵⁵, bipyridine (6 mol%, biphasic conditions H₂O/CH₂Cl₂)³⁵⁴ and bipyridine-*N,N'*-dioxide (1.2 mol%)³⁵⁶ were employed together with MTO (Scheme 96)³⁵⁷. Pyrazole is stable against oxidation and with this additive Herrmann and coworkers observed short reaction times (0.02–14 h, generally 1 h). Conversions (89 to >99%) as well as epoxide selectivities (90 to >99%) were very high. Bipyridine has been employed by Rudler and coworkers³⁵⁴ under biphasic conditions with good results. Later, in 1998, Nakajima and coworkers presented their results on this topic in which they proposed that it is not the bipyridine but the bipyridine-*N,N'*-dioxide, which is formed during the reaction, that is responsible for the suppression of the acidity of the MTO/H₂O₂ system³⁵⁶. With bipyridine-*N,N'*-dioxide as additive, a variety of olefins could be oxidized to the corresponding epoxides at room temperature with yields ranging from 80 to 96%.



SCHEME 96. MTO-catalyzed epoxidation of various olefins using H₂O₂ as oxidant in the presence of different cocatalysts

In 1999, Sheldon and coworkers could change the 2-phasic conditions to a 1-phasic system by using trifluoroethanol as solvent, and low catalyst loadings (0.1 mol% MTO, 5–10 mol% pyrazole as cocatalyst) were sufficient to obtain good epoxide yields³⁵⁸. By using this non-coordinating solvent the reaction rate could be increased markedly. For terminal alkenes, in most cases complete conversion was observed within 24 hours and yields were excellent (82 to >99%) due to the high selectivity observed with this catalytic system (except for styrene, which was also transformed to phenylethane-1,2-diol and benzaldehyde). Epoxidation of more reactive internal alkenes proceeded within minutes even upon cooling and with most epoxides >99% yield were obtained. The MTO-catalyzed process could be improved considerably by using a solution of H₂O₂ of higher concentration (70–85%)²⁷¹. Under these conditions, which render a very low catalyst loading possible (0.02–0.08 mol% MTO, <2 mol% base), very high epoxide yields were obtained (yields of 76–96%) and even very labile epoxides were obtained at reasonable times and with good yields.

Yudin and Sharpless reported on the utilization of much cheaper, readily available inorganic Re catalysts [Re₂O₇, ReO₃(OH), ReO₃ (0.5–1 mol%)] in combination with bis(trimethylsilyl) peroxide as oxidant and 0.5–1 mol% of pyridine (equation 52)³⁵⁹. In this oxidation process high epoxide yields (78–96%) were obtained using CH₂Cl₂ or THF as solvent. Traces of water or other protic species have been found to be essential for rapid turnover and accelerate the reaction.



Very recently, Bouh and Espenson presented an epoxidation method in which they employed MTO supported on niobia as heterogeneous catalyst in the presence of urea hydrogen peroxide³⁶⁰. With this catalytic system they could obtain very good epoxidation results for simple alkenes (70–100% yield at reaction times of 30–100 min) as well as for soybean oils (95–100% yield at reaction times of 30 min). No side products like the diols (through epoxide ring opening) were obtained in this reaction. The authors observed a dramatic decrease in epoxidation rate when water is present in the mixture. A further great advantage of the heterogeneous catalyst is its reusability.

Table 25 gives an overview of the conversions and yields obtained in the MTO-catalyzed epoxidation of various substrates employing different reaction conditions.

d. Compounds of arsenic in the epoxidation of unfunctionalized olefins. In 2000, Sheldon and coworkers reported that the combination of HReO₄ with tertiary arsines can act as catalytic system for the epoxidation of alkenes with aqueous hydrogen peroxide (Scheme 97)³⁶¹. Electron-donating groups in the arsine lower the rate, but increase the selectivity and therefore the yield of epoxide due to a depression of acid-catalyzed decomposition. The best cocatalyst for HReO₄ turned out to be Ph₂AsMe and the highest yields and highest reaction rates were obtained in 2,2,2-trifluoroethanol as solvent. Ph₂MeAsO gave identical results, which shows that arsine oxidation proceeds quickly and selectively. Employing an As:Re ratio of 2, several alkenes could be epoxidized at 75 °C with 60% H₂O₂ as oxidant providing the epoxides with yields generally between 61 and 99%, whereas the epoxide of allyl phenyl ether was obtained in only 26% yield.

TABLE 25. Results of the MTO-catalyzed epoxidation under different conditions

Substrate	Catalyst	Oxidant	Time (h)	Conv. (%)	Yield epoxide (%)	Yield diol (%)	Reference
Propene	0.8% MTO	anhydrous H ₂ O ₂	12		50 ^a	50 ^a	342
1-Hexene	0.33% MTO	anhydrous H ₂ O ₂	60		72		271, 345
	1–3% MTO/Nb ₂ O ₅	UHP	2	80			360
1-Heptene	0.5% MTO/12% pyrazole	35% H ₂ O ₂	8	95			355
	0.1% MTO/5% pyrazole ^b	60% H ₂ O ₂	21		>99		358
1-Octene	0.1% MTO/5% pyrazole ^b	60% H ₂ O ₂	21		>99		358
	1–3% MTO/Nb ₂ O ₅	UHP	2	80			360
1-Nonene	0.1% MTO/5% pyrazole ^b	60% H ₂ O ₂	21		>99		358
	1% MTO ^c	10% H ₂ O ₂	29	95			354
1-Decene	0.1% MTO/5% pyrazole ^b	60% H ₂ O ₂	21		>99		358
	0.33% MTO	anhydrous H ₂ O ₂	72		75		345, 271
1-Dodecane	0.5% MTO/12% py	30% H ₂ O ₂	48	82			271, 351
	0.5% MTO/10% cyanopy	30% H ₂ O ₂	17	>99			352
2-Butene	0.5% MTO/12% pyrazole ^b	35% H ₂ O ₂	14	>99			355
	0.1% MTO/5% pyrazole ^b	60% H ₂ O ₂	21		97		358
2-Butene	0.5% Re ₂ O ₇	(Me ₃ SiO) ₂	14		94		359
	0.8% MTO	anhydrous H ₂ O ₂	6		0	100 ^d	342
3-Hexene	0.8% MTO	anhydrous H ₂ O ₂	3		90		342
	1–3% MTO/Nb ₂ O ₅	UHP	2	70			360
trans-3-Decene	0.5% Re ₂ O ₇	(Me ₃ SiO) ₂	16		85		359
	0.5% Re ₂ O ₇	(Me ₃ SiO) ₂	11		79		359
3,3-Dimethylhexene	0.5% MTO/12% py	30% H ₂ O ₂	30		78		352
	0.5% MTO	anhydrous H ₂ O ₂	16		50–75		271, 342, 345
2,3-Dimethyl-2-butene	0.33% MTO	10% H ₂ O ₂	36		68		345
	0.1% MTO/10% pyrazole ^b	60% H ₂ O ₂	1.5		98		358
2-Methylhept-1-ene	1% MTO ^c	60% H ₂ O ₂	2	98			354
	0.1% MTO/10% pyrazole ^b	60% H ₂ O ₂	1		99		358
2-Methylhept-2-ene	0.8% MTO	anhydrous H ₂ O ₂	2		95		342
	0.5% MTO/12% py	30% H ₂ O ₂	24	97	91–96		271, 351
trans-4-Octene	0.5% MTO/12% py	30% H ₂ O ₂	6	99			271, 351
	0.5% Re ₂ O ₇ /1% py	(Me ₃ SiO) ₂	12		88		359
cis-4-Octene	0.5% MTO/12% py	30% H ₂ O ₂	2	99			351
	0.23–0.33% MTO	anhydrous H ₂ O ₂	3		48	40	271, 345

(continued overleaf)

TABLE 25 (continued)

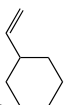
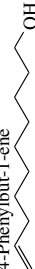
Substrate	Catalyst	Oxidant	Time (h)	Conv. (%)	Yield epoxide (%)	Yield diol (%)	Reference
Cyclohexene	0.5% MTO/12% pyrazole	35% H ₂ O ₂	1	>99	92		355
	0.8% MTO ^c	anhydrous H ₂ O ₂	0.1		0	97	342
	0.8% MTO ^f	anhydrous H ₂ O ₂	5		90	0	342
	0.16–0.33% MTO	anhydrous H ₂ O ₂	20		90		271, 345
	1% MTO	UHP	18	98	97	<1	350, 271
	0.5% MTO/12% py	30% H ₂ O ₂	6	96	95		271, 351
	0.02% MTO/2% N-base	70–85% H ₂ O ₂		97	96		271
	1–3% MTO/Nb ₂ O ₅	UHP	0.5	100			360
	0.5% MTO/12% pyrazole	35% H ₂ O ₂	1	>99			355
	0.1% MTO/10% pyrazole ^b	60% H ₂ O ₂	0.5		>99		358
Cycloheptene	1% MTO ^c	10% H ₂ O ₂	2	80	80		354
	1% MTO/6% bipyridine ^c	10% H ₂ O ₂	2	99	94		354
	0.33–0.47% MTO	anhydrous H ₂ O ₂	48		88		271, 345
	0.5% MTO/12% py	30% H ₂ O ₂	3	99	98		271, 351
	0.1% MTO/10% pyrazole ^b	60% H ₂ O ₂	1		>99		358
	0.1–0.33% MTO	anhydrous H ₂ O ₂	24		99		271, 345
	0.5% MTO/12% py	30% H ₂ O ₂	2	99	97		271, 351
	1–3% MTO/Nb ₂ O ₅	UHP	2	100			360
	MTO/(+)-Tröger's base	3.5M H ₂ O ₂	24	90	90		344
	0.5% MTO/12% pyrazole	35% H ₂ O ₂	0.02	89			355
Cyclododecene	0.1% MTO/10% pyrazole ^b	60% H ₂ O ₂	1		>99		358
	1% MTO ^c	10% H ₂ O ₂	2	100	>99		354
	0.33% MTO	anhydrous H ₂ O ₂	2		100		271, 342
	0.8% MTO	anhydrous H ₂ O ₂	2		0	70	342
	MTO/(+)-Tröger's base	3.5M H ₂ O ₂	2	70	70 ^g		344
	0.1% MTO/10% pyrazole ^b	60% H ₂ O ₂	0.5		>99		358
	1% MTO	UHP	19	88	84	4	350
	1–3% MTO/Nb ₂ O ₅	UHP	0.5	100			360
	0.33% MTO	anhydrous H ₂ O ₂			92		271, 342
	4-Methylcyclohexene						
Methyl oleate							

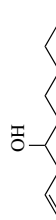
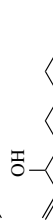
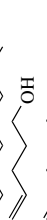


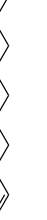




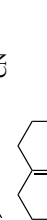
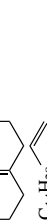

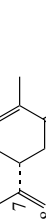
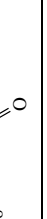

Camphene	1% MTO	UHP	30	92	87	0	350, 271
Styrene	1% MTO	UHP	19	46	44	0	350, 271
	0.5% MTO/12% py	30% H ₂ O ₂	16	83	84		271, 351
	0.5% MTO/10% cyanopy	30% H ₂ O ₂	6	>99	85		352
	0.5% MTO/12% pyrazole	35% H ₂ O ₂	3	>99	93		355
	1% MTO/1.2% BPD ^h	30% H ₂ O ₂	12		95		356
	0.1% MTO/5% pyrazole ^b	60% H ₂ O ₂	2		82 ⁱ		358
α -Methylstyrene	1% MTO	UHP	21	81	55	26	350, 271
	0.02% MTO/2% N-base	70–85% H ₂ O ₂		89	83		271
	0.5% MTO/12% py	30% H ₂ O ₂	6	92	82		351
	0.5% MTO/6% cyanopy/6% py	30% H ₂ O ₂	1.5	>99	74		357
	0.5% MTO/12% pyrazole	35% H ₂ O ₂	1	>99	87		355
<i>trans</i> -2-Methylstyrene	0.5% MTO/12% py	30% H ₂ O ₂	6	92–99	90–92		271, 351
	0.5% MTO/12% pyrazole	35% H ₂ O ₂	1	>99	94		355
<i>cis</i> -2-Methylstyrene	0.5% MTO/12% py	30% H ₂ O ₂	5	>99	99		271, 351
	0.5% MTO/12% pyrazole	35% H ₂ O ₂	1	>99	94		355
Indene	1% MTO	UHP	37	51	48	0	350, 271
	0.5% MTO/12% py	30% H ₂ O ₂	4	92	90		271, 351
	0.02% MTO/2% N-base	70–85% H ₂ O ₂		81	76		271
	0.1% MTO/10% pyrazole ^b	60% H ₂ O ₂	1		65 ^j		358
1,2-Dihydronaphthalene	0.5% MTO/12% py	30% H ₂ O ₂	5	99	96		351
	0.5% MTO/12% py	30% H ₂ O ₂	1	>99	99		355
1-Phenylcyclohexene	0.5% MTO/12% py	30% H ₂ O ₂	6	99	91		271, 351
	0.5% MTO/12% py	30% H ₂ O ₂	1	>99	95		357
	0.5% MTO/10% cyanopy	30% H ₂ O ₂	14	>99	99		357
	0.02% MTO/2% N-base	70–85% H ₂ O ₂		95	85		271
Dicyclopentadiene	0.02% MTO/2% N-base	70–85% H ₂ O ₂		100	82 ^k + 13 ^l		271
1,3-Hexadiene	1–3% MTO/Nb ₂ O ₅	UHP	2	45 ^m + 25 ⁿ			360
	0.8% MTO	30% H ₂ O ₂	3	[1.2:1] ^{o,p}			351
	0.67% MTO	anhydrous H ₂ O ₂	3			q	342
1,4-Cyclohexadiene	0.5% MTO/12% py	10% H ₂ O ₂	18		45 + 40 ^r		345
	0.5% MTO/12% py	30% H ₂ O ₂	6	[1:100] ^{o,p}			351
<i>cis,cis</i> -1,3-Cyclooctadiene	0.5% MTO/12% py	30% H ₂ O ₂	7	[1:1.3] ^{o,p}			351
	1% Re ₂ O ₇	(Me ₃ SiO) ₂	13		78		359

(continued overleaf)



TABLE 25 (continued)

Substrate	Catalyst	Oxidant	Time (h)	Conv. (%)	Yield epoxide (%)	Yield diol (%)	Reference
<i>cis</i> -1,5-Cyclooctadiene	0.8% MTO	anhydrous H ₂ O ₂	1.5		80		342
	0.5% MTO/12% py	30% H ₂ O ₂	5	[1:100] ^{a,p}			351
	0.5% HReO ₄	(Me ₃ SiO) ₂	12		68		359
	1% Re ₂ O ₇	(Me ₃ SiO) ₂	10		82		359
<i>trans</i> -Stilbene	1–3% MTO/Nb ₂ O ₅	UHP	2	100	83		360
	0.5% MTO/12% py	30% H ₂ O ₂	30	85	90		351
	0.5% MTO/12% pyrazole	35% H ₂ O ₂	4.5	>99	90		355
	1% MTO/1.2% BPD ^h	30% H ₂ O ₂	24		90 ^s		356
	0.5% Re ₂ O ₇	(Me ₃ SiO) ₂	10		96		359
	1% MTO	UHP	19	44	≥42	0	350
<i>cis</i> -Stilbene	0.5% MTO/12% py	30% H ₂ O ₂	30	99	97		351
	0.5% MTO/12% pyrazole	35% H ₂ O ₂	4	>99			355
	1% MTO/1.2% BPD ^h	30% H ₂ O ₂	24		95 ^t		356
	1–3% MTO/Nb ₂ O ₅	UHP	2	85			360
4-Penten-1-ol 	0.8% MTO	anhydrous H ₂ O ₂	0.1		40	50	342
	0.5% MTO/10% cyanopy	30% H ₂ O ₂	30	>99	86		352
	0.1% MTO/5% pyrazole ^b	30% H ₂ O ₂	21		>99		358
	0.5% Re ₂ O ₇	(Me ₃ SiO) ₂	7		95		359
	0.8% MTO	anhydrous H ₂ O ₂	2		50	40	342
	0.39% MTO	30% H ₂ O ₂	62		0	87	345
	0.8% MTO	anhydrous H ₂ O ₂	10		90		342
	0.8% MTO	anhydrous H ₂ O ₂	24		60		342
	0.8% MTO	anhydrous H ₂ O ₂	18		64		342
	0.8% MTO	anhydrous H ₂ O ₂	24		38		342
	0.5% MTO/12% py	30% H ₂ O ₂	7	97	86 ^u		351
4-Phenylbut-1-ene 	MTO/(+)-Tröger's base	3.5M H ₂ O ₂	1	<10	<10 ^s		344
	MTO/(+)-Tröger's base	3.5M H ₂ O ₂	3	50	35 ^s		344
	0.5% MTO/10% cyanopy	30% H ₂ O ₂	20	>99	89		352
	0.1% MTO/5% pyrazole ^b	60% H ₂ O ₂	21		97		358
	0.1% MTO/5% pyrazole ^b	60% H ₂ O ₂	21		>99		358
	0.5% MTO/10% cyanopy	30% H ₂ O ₂	19	>99	89		352

	0.5% MTO/10% cyanopy	30% H ₂ O ₂	27	>99	94	352
	0.5% MTO/10% cyanopy	30% H ₂ O ₂	17	>99	88	352
	0.5% MTO/10% cyanopy	30% H ₂ O ₂	18	>99	97 ^v	352
	0.5% MTO/10% cyanopy	30% H ₂ O ₂	20	>99	94	352
	0.5% MTO/10% cyanopy	30% H ₂ O ₂	30	>99	86	352
	0.5% MTO/10% cyanopy	30% H ₂ O ₂	20	>99	89	352
	0.5% MTO/10% cyanopy	30% H ₂ O ₂	19	>99	90	352
	0.5% MTO/10% cyanopy	30% H ₂ O ₂	24	>99	96	352
	1% MTO/1.2% BPD ^h	30% H ₂ O ₂	24		95 ^s	356
	1% MTO/1.2% BPD ^h	30% H ₂ O ₂	24		85 ^w	356
	0.5% Re ₂ O ₇	(Me ₃ SiO) ₂	18		92	359
	1% MTO/1.2% BPD ^h	30% H ₂ O ₂	2		80	356
	1% MTO/1.2% BPD ^h	30% H ₂ O ₂	24		91	356
	1% MTO/1.2% BPD ^h	30% H ₂ O ₂	24		85	356
	0.4% MTO	10% H ₂ O ₂	18		85	345
	1% MTO/1.2% BPD ^h	30% H ₂ O ₂	24		96 ^x	356

(continued overleaf)

TABLE 25 (continued)

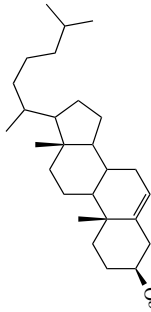



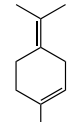
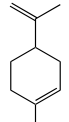
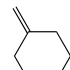
Substrate	Catalyst	Oxidant	Time (h)	Conv. (%)	Yield epoxide (%)	Yield diol (%)	Reference
	1% MTO/1.2% BPD ^b	30% H ₂ O ₂	12		94 ^v	356	
	1% MTO ^c	10% H ₂ O ₂	2	57	54	354	
	1% MTO/6% bipyridine ^c	10% H ₂ O ₂	2	94	89	354	
	0.5% MTO/12% py	30% H ₂ O ₂	14	61	60	357	
	0.5% MTO/12% pyrazole	30% H ₂ O ₂	14	>99	99	357	
	0.5% MTO/10% cyanopy	30% H ₂ O ₂	14	>99	99	357	
	0.5% MTO/12% py	30% H ₂ O ₂	1	>99	99	357	
	0.5% MTO/12% pyrazole	30% H ₂ O ₂	1	>99	99	357	
	0.5% MTO/12% cyanopy	30% H ₂ O ₂	2	63	60	357	
	0.5% MTO/12% py	30% H ₂ O ₂	4	98	98	357	
	0.5% MTO/12% pyrazole	30% H ₂ O ₂	2	>99	99	357	
	0.5% MTO/2% cyanopy	30% H ₂ O ₂	2	>99	99	357	
	0.5% MTO/12% py	30% H ₂ O ₂	2	>99	99 ^k	357	
	0.5% MTO/12% pyrazole	30% H ₂ O ₂	2	59	50 ^l	357	
	0.5% MTO/10% cyanopy	30% H ₂ O ₂	2	43	26 ^l	357	
	1% MTO ^c	10% H ₂ O ₂	1	92	86	354	
	0.02% MTO/2% N-base	70–85% H ₂ O ₂		100	85 ^{k,10} ^l	271	
	0.1% MTO/10% pyrazole ^b	60% H ₂ O ₂	1		99	358	
	0.5% MTO/12% py	30% H ₂ O ₂	4	99	96	351	

TABLE 25. (continued)

Substrate	Catalyst	Oxidant	Time (h)	Conv. (%)	Yield epoxide (%)	Yield diol (%)	Reference
	1% MTO ^c	10% H ₂ O ₂	48	27	27		354
	1% MTO ^c	10% H ₂ O ₂	24	0			354

^a Selectivity, not isolated yields is given. Data refers to converted olefin.

^b In trifluoroethanol.

^c Biphasic conditions: H₂O/CH₂Cl₂.

^d 40% yield of diol in the case where 50% epoxide was obtained.

^e At 82 °C.

^f At 10 °C.

^g 0% *ex.*

^h BPD = bipyridine *N,N'*-dioxide.

ⁱ Side products: phenylethane-1,2-diol and benzaldehyde.

^j Hydrolysis products as side products.

^k Bisepoxide.

^l Monoepoxide.

^m Yield of 3-hexene.

ⁿ Yield of 1-hexene.

^o Ratio: monoepoxide:diepoxide.

^p Diastereomeric ratio for diepoxide: i) diepoxides of 1,3-hexadiene and *cis,cis*-1,3-cyclooctadiene: 99% *anti*, ii) diepoxide of 1,4-cyclohexadiene: 96:4 (*anti:syn*), iii) diepoxide of *cis,cis*-1,5-cyclooctadiene: 99% *syn*.

^q 92% tetrahydrocyclohexane.

^r Diepoxide + monoepoxide.

^s *cis/trans* Ratio: <1:59.

^t *E/Z* Ratio of substrate: 3:97 leads to epoxide *cis/trans*-ratio: 97:3.

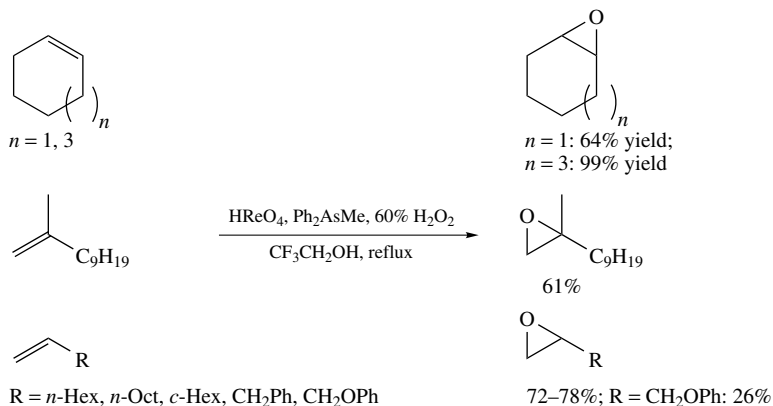
^u Only *exo*.

^v Initially formed epoxide cyclized completely to the tetrahydrofuryl alcohol, which was isolated in 97% yield.

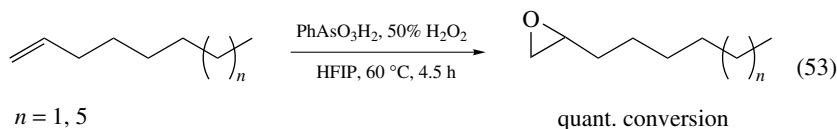
^w *cis/trans* Ratio: >99:1.

^x 7:8-Epoxide was formed as a 1:1 mixture of diastereomers.

^y α -Epoxide: β -epoxide = 4 : 1

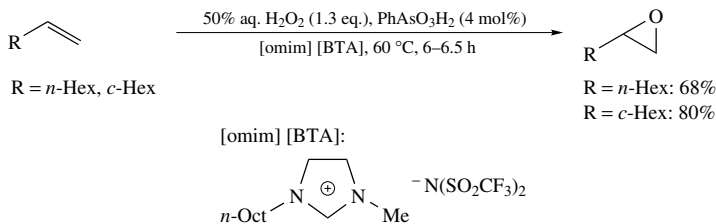
SCHEME 97. Epoxidation reaction catalyzed by the system $HReO_4/Ph_2AsMe$

Berkessel and Andreae reported that the catalytic activity of benzenearsonic acid in the epoxidation of olefins with hydrogen peroxide is potentiated in fluorinated alcohols such as HFIP³⁶². Since Brønsted acids do not effect epoxidation under these conditions, the formation of perarsonic acid appears to be the crucial feature of this catalyst. By using 1 mol% of benzenearsonic acid and 50% H_2O_2 in HFIP as solvent, 1-octene as well as 1-dodecene could be epoxidized quantitatively within 4.5 hours at 60 °C (equation 53). In order to get more insight into the mechanism of this reaction and the essential function of HFIP as activator, a more detailed kinetic study was carried out by Berkessel and Adrio³⁶³. It could be shown that with hydrogen peroxide as oxidant at low HFIP concentrations ($n_{HFIP}/n_{total} \leq 0.15$ [n = molar amount]) the epoxidation of cyclooctene (without employing a catalyst) as well as the epoxidation of 1-octene (using phenylarsonic acid as catalyst) show first-order dependence on the HFIP concentration. This was interpreted by a HFIP ‘charge template’ for the uncatalyzed epoxidation (as postulated by Neumann and coworkers¹⁴³) and by the formation of an arsenic acid mono-HFIP ester for the catalyzed reaction. At high HFIP concentration ($n_{HFIP}/n_{total} \geq 0.5$), the catalyzed and uncatalyzed oxidations were up to 5 orders of magnitude faster and show higher-order dependence on the HFIP concentration. This observation was interpreted in terms of the formation of HFIP clusters and the epoxidation taking place in a HFIP coordination sphere. The coordination sphere influences the enormous increases in epoxidation rates.



It could also be shown by Berkessel and coworkers that the ionic liquid 1-*n*-octyl-3-methylimidazolium bis(trifluoromethanesulfon)amide²⁹⁶ [omim] [BTA] can replace HFIP as solvent (Scheme 98)³⁶⁴. In this reaction medium, 1-octene and vinylcyclohexane, which are generally unreactive substrates under most of the known procedures in the literature, were epoxidized by phenylarsonic acid (4%) in 6 to 6.5 hours in the presence of 50% hydrogen peroxide with yields of 68 and 80%, respectively. The [BTA] anion seems to be essential for good epoxidation results, since other ionic liquids with different anions this anion did not affect the desired conversion. For the epoxidation in HFIP a charge

template consisting of olefin, hydrogen peroxide and fluorinated alcohol was postulated by Neumann and coworkers¹⁴³. In analogy to this ternary complex, a similar arrangement can be formulated for [omim] [BTA] as solvent and activator.



SCHEME 98. Arsonic acid-catalyzed epoxidation of olefins with hydrogen peroxide in ionic liquids

B. Oxidation of Sulfides

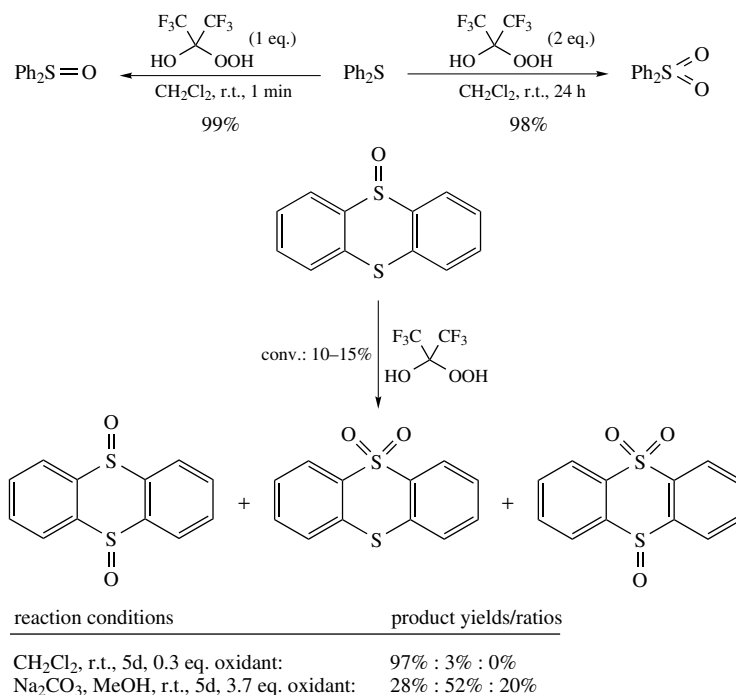
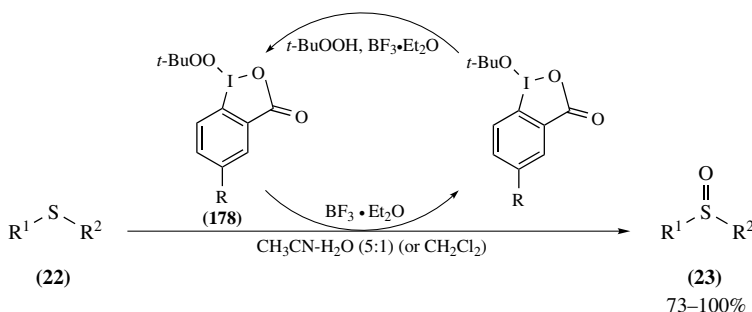
Sulfides are generally oxidized much faster than alkenes, and in the presence of excess oxidant further oxidation to the sulfone occurs. In the cases where the reaction is conducted in an asymmetric way, the chiral catalytic system may react faster with one enantiomeric sulfoxide to form the sulfone than with the other, so that kinetic resolution of the primarily formed sulfoxide may occur. In general, the reaction is carried out with alkyl hydroperoxides like TBHP in the presence of a metal catalyst like Mo, W, Ti or V complexes. In some cases the sulfoxidation with hydroperoxides can take place without the need of a metal catalyst. Both examples will be discussed in the following.

For an excellent review on asymmetric oxidation of sulfides see Reference 191.

1. Uncatalyzed sulfoxidations

The oxidation of sulfides to sulfoxides (1 eq. of oxidant) and sulfones (2 eq. of oxidant) is possible in the absence of a catalyst by employing the perhydrate prepared from hexafluoroacetone or 2-hydroperoxy-1,1,1-trifluoropropan-2-ol as reported by Ganeshpure and Adam (Scheme 99)²⁰. The reaction is highly chemoselective and sulfoxidation occurs in the presence of double bonds and amine functions, which were not oxidized. With one equivalent of the α -hydroxyhydroperoxide, diphenyl sulfide was selectively transformed to the sulfoxide in quantitative yield and with two equivalents of oxidant the corresponding sulfone was quantitatively obtained. 2-Hydroperoxy-1,1,1-fluoropropan-2-ol as an electrophilic oxidant oxidizes thianthrene-5-oxide almost exclusively to the corresponding *cis*-disulfoxide, although low conversions were observed (15%) (Scheme 99). Deprotonation of this oxidant with sodium carbonate in methanol leads to a peroxy anion, which is a nucleophilic oxidant and oxidizes thianthrene-5-oxide preferentially to the sulfone.

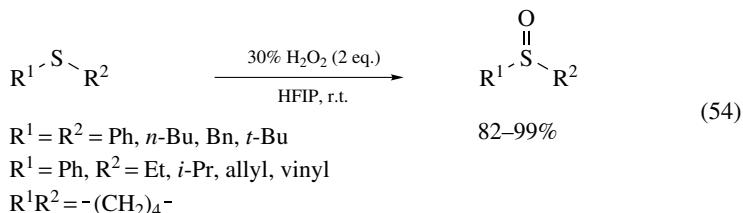
In 1997, Ochiai and coworkers³⁶⁵ reported on sulfoxidation reactions with the help of hypervalent (*tert*-butylperoxy)iodanes **178**, which were generated from 1-hydroxy-1,2-benziodoxol-3(1*H*)-ones and *tert*-butyl hydroperoxide in chloroform (Scheme 100). These compounds are stable in the solid state and can be stored at room temperature. With these reagents sulfides **22** can be oxidized to sulfoxides **23** in good yields ranging from 73 to 100%. The choice of solvent has marked influence on reaction rate and product distribution (sulfoxide/sulfone/side product). In toluene the sulfone was mainly formed, while in acetonitrile–water (5:1) at room temperature the sulfoxides were formed with high selectivity, although oxidation was slow. The rate of the reaction can be increased by addition of $\text{BF}_3 \cdot \text{Et}_2\text{O}$ as acid catalyst or alternatively by raising the temperature up to 50 °C. Also, the effect of different substituents on an aromatic group of the sulfides

SCHEME 99. Oxidation of sulfides with α -hydroxy hydroperoxidesSCHEME 100. Oxidation of sulfides with hypervalent (*tert*-butylperoxy)iodanes **178**

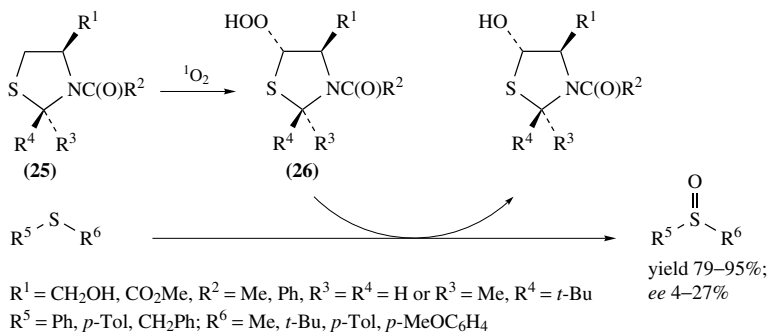
($\text{R}^1 = \text{Ar}$) has been investigated and the authors found out that electron-releasing groups increase the rate of oxidation (e.g. for OMe compared to H by up to 31 times in the presence of $\text{BF}_3 \cdot \text{Et}_2\text{O}$) and *vice versa*.

In 1998, Bégué and coworkers reported on a very selective conversion of sulfides to sulfoxides in hexafluoro-2-propanol (HFIP) as solvent using 30% H_2O_2 as oxidant without the need for a catalyst (equation 54)³⁶⁶. A variety of differently substituted ayclic sulfides and also a cyclic one could be cleanly oxidized to the sulfoxides in very good yields ranging from 82 to 99% and no sulfone formation was observed. C=C double bonds in the substrate are tolerated without being epoxidized. This excellent reactivity is explained

by the activation effect of HFIP. The latter—due to the electron-withdrawing character of the CF_3 group—forms a strong hydrogen bond with H_2O_2 and activates the hydroxyl leaving group.



The first results on the utilization of chiral hydroperoxides for the enantioselective oxidation of sulfides was published in 1986 by Takata and Ando³⁶⁷. The authors employed thiazoline derived hydroperoxides **26**, which were prepared *in situ* from singlet oxygen oxygenation, and investigated the uncatalyzed as well as the titanium-catalyzed sulfoxidation of various sulfides (Scheme 101). In the uncatalyzed case, yields were better than in the metal-catalyzed case and ranged between 79 and 95%. Optical purities were low and did not exceed 27%. In 2001, Seebach's group could successfully employ the TADOOH hydroperoxide (**60**) as chiral oxidant for the oxidation of methyl phenyl sulfide **22a** without the need of a catalyst⁹⁸ (Scheme 102). Depending on reaction time and temperature the sulfoxide (*S*)-**23a** is formed in yields between 61 and 91% and with an enantiomeric excess ranging from 64–86%. At -30°C sulfone formation is negligible ($< 1\%$), but at room temperature overoxidation of the sulfide takes place to form the sulfone **179a** in yields up to 27%. The authors present a mechanistic model which rationalizes the preferential formation of the (*S*)-methyl phenyl sulfoxide.

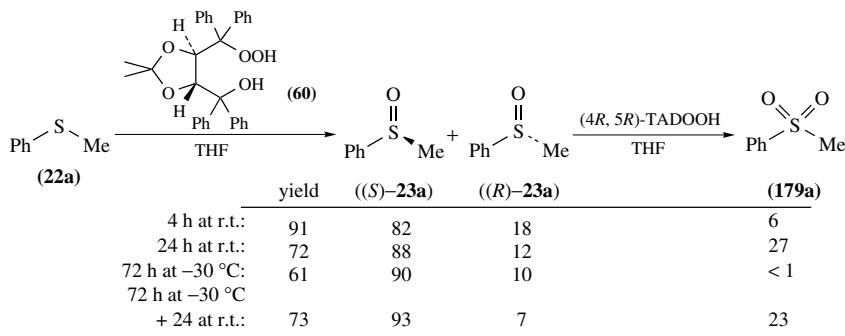


SCHEME 101. Uncatalyzed asymmetric sulfoxidation with chiral hydroperoxides as oxidants

2. Enzyme-catalyzed sulfoxidations

As already reported in Section II.A.2, the enzymes chloroperoxidase (CPO) and *Coprinus peroxidase* (CiP) catalyze the enantioselective oxidation of aryl alkyl sulfides. If a racemic mixture of a chiral secondary hydroperoxide is used as oxidant, kinetic resolution takes place and enantiomerically enriched hydroperoxides and the corresponding alcohols can be obtained together with the enantiomerically enriched sulfoxides. An overview of the results obtained in this reaction published by Wong and coworkers⁷¹, Höft and

coworkers⁷⁰ and Adam and coworkers⁷³ is given in Table 4, Section II.A.2. The enantioselectivity in the asymmetric oxidation was found to be dependent on the type of substrate and hydroperoxide, the concentration of the substrate and enzyme as well as the conversions of the substrates. In the CPO case, low substrate concentrations are used in order to minimize non-enzymatic reaction. By this method sulfoxides can be obtained with *ee* values up to >99%.



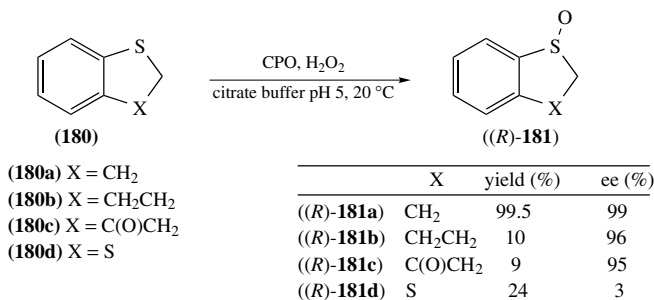
SCHEME 102. Oxidation of methyl phenyl sulfide **22a** by TADOOH **60**

In 1988, Colonna and coworkers reported the oxidation of aryl alkyl sulfides as well as dialkyl sulfides by CPO using TBHP as oxidant giving sulfoxides with enantiomeric excess ranging from 0 to 92%³⁶⁸. With H₂O₂ as oxidant significantly lower enantioselectivities of the sulfoxides were obtained (e.g. oxidation of *p*-tolyl methyl sulfide: 86% *ee* with TBHP, 35% *ee* with H₂O₂) and with cumene hydroperoxide as oxidant almost racemic product was observed. Electronic and especially steric effects influenced the outcome of the reaction and *para*-substitution led to higher asymmetric induction and chemical yield than *ortho*-substitution. Sulfides with alkyl groups larger than ethyl were not converted by CPO. The sulfoxide in this reaction was obtained from both enzyme-catalyzed and chemical oxidation and therefore *ee* values in some cases were rather low. Later, enantioselectivities could be improved by Colonna and coworkers by using modified reaction conditions in which the reactions were carried out with H₂O₂, added gradually to an aqueous buffer solution (pH 5) of the substrate at 25 °C³⁶⁹. Under these conditions hydrogen peroxide in most cases turned out to be more effective oxygen source than TBHP in terms of chemical conversion and enantiomeric excess, giving the corresponding sulfoxides in yields ranging from 10 to 100% and *ee* values of 5–99% depending on the structure and electronic properties of the substrate. The highest *ee* values were obtained with sulfoxides bearing electron-donating or poor electron-withdrawing groups on the aromatic ring, while strong electron-withdrawing substituents decreased the chemical conversion without affecting the enantioselectivity. Also, Wong and coworkers⁷¹ could obtain sulfoxides with high optical purity (97–100% *ee*, (*R*)-enantiomer) and good yields (66–92%) from the CPO-catalyzed oxidation of sulfides in dilute solution, using hydrogen peroxide as oxidant. Results obtained with both the Colonna and the Wong methods are summarized in Table 26.

Allenmark and Andersson investigated the CPO-catalyzed sulfoxidation of a series of rigid, aromatic cyclic sulfides **180a–d** (Scheme 103)³⁷⁰. The authors could show that the sulfoxidation of substrates **180** in principle works with good enantioselectivity (*ee* 95–99%) except of sulfide **180d** (only 3% *ee* of the sulfoxide **181d**). Unfortunately, yields were rather low (9–24%) and only **181a** was obtained with a high yield of 99.5%. The low yields could not be enhanced by addition of different cosolvents, longer reaction

TABLE 26. CPO-catalyzed oxidations of sulfides using H₂O₂ or TBHP as oxidants producing sulfoxides (*R*)-**23** (yields are given and *ee* values are given in parentheses)

Sulfide	CPO/TBHP/ pH 5 buffer (4 °C, 4–10 d)	CPO/TBHP/ pH 5 buffer (25 °C, 22 h)	CPO/H ₂ O ₂ / pH 5 buffer (25 °C, 1 h) (slow addition of H ₂ O ₂)	CPO/H ₂ O ₂ / pH 5 buffer (4 °C) (slow addition of H ₂ O ₂ and sulfide)
	Reference	368	369	369
PhSMe	100 (76)	90 (80)	100 (98)	90 (99)
<i>p</i> -TolSMe	60 (86)	80 (70)	98 (91)	92 (99)
<i>o</i> -TolSMe	27 (19)	56 (43)	27 (33)	
<i>p</i> -ClC ₆ H ₄ SMe	44 (85)	60 (70)	77 (90)	87 (97)
<i>o</i> -ClC ₆ H ₄ SMe		17 (45)	33 (85)	
<i>p</i> -FC ₆ H ₄ SMe		90 (70)	100 (97)	86 (97)
<i>p</i> -O ₂ NC ₆ H ₄ SMe	7 (39)	16 (80)	10 (80)	
<i>p</i> -MeOC ₆ H ₄ SMe	70 (92)	70 (61)	72 (90)	66 (100)
<i>o</i> -MeOC ₆ H ₄ SMe	33 (25)	30 (37)	24 (27)	
2-NaphthylSMe	0			
<i>p</i> -TolSEt	40 (30)	50 (68)	50 (68)	
<i>p</i> -TolSP <i>r-n</i>		30 (5)	53 (5)	
PhCH ₂ SMe	51 (91)	73 (55)	100 (90)	
<i>n</i> -BuSMe	54 (38)			
<i>p</i> -MeC(O)NHC ₆ H ₄ SMe		86 (70)	86 (67)	
<i>p</i> -TolSOct- <i>n</i>	13 (0)			
2-PyridylSMe	72 (65)	61 (89)	100 (99)	

SCHEME 103. CPO-catalyzed oxidation of cyclic sulfides **180** with H₂O₂

times or higher temperatures. Higher hydrogen peroxide concentrations led to a decrease in enantiomeric excess because then the background reaction became more pronounced. Employing TBHP as oxidant generally resulted in lower yields and *ee* values compared to hydrogen peroxide.

3. Metal-catalyzed sulfoxidations

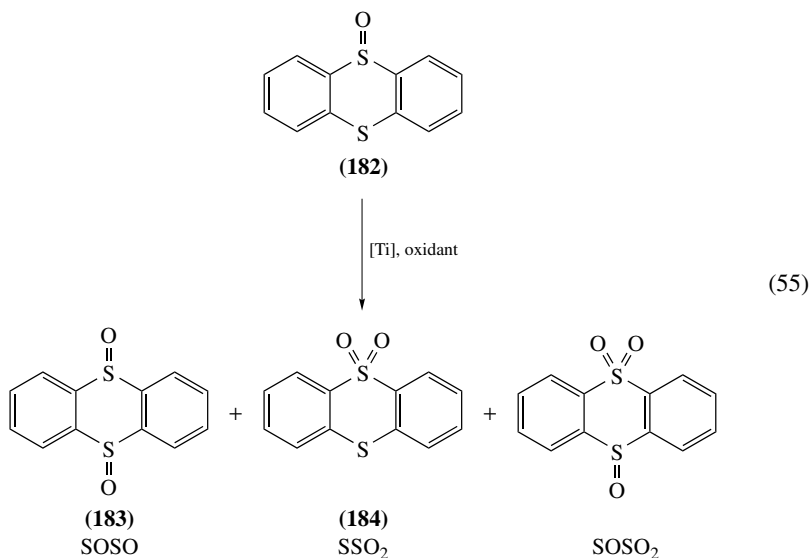
As already mentioned above, sulfides are oxidized to the corresponding sulfoxides with alkyl hydroperoxides in the presence of various metal catalysts like Mo, W, Ti and V. In the presence of excess hydroperoxide further oxidation to the sulfone occurs³⁷¹. Sulfides are generally oxidized much faster than alkenes, which is reflected in the selective oxidation of unsaturated sulfides exclusively at the sulfur atom. During the last years many asymmetric versions of this reaction have been developed and can be mainly divided

into two types: (i) sulfoxidations with chiral metal catalysts, and (ii) sulfoxidations in which the asymmetric induction results from a chiral hydroperoxide as oxidant, which will be discussed later in this Section. An early approach to an asymmetric reaction conduction was investigated by Modena and coworkers in 1976, who carried out the oxidation of unsymmetrical sulfides with TBHP/ $\text{VO}(\text{acac})_2$ in a mixture of benzene and a chiral alcohol, such as (-)-menthol, as solvent³⁷². Asymmetric induction was observed, although *ee* values were rather low (5–10%).

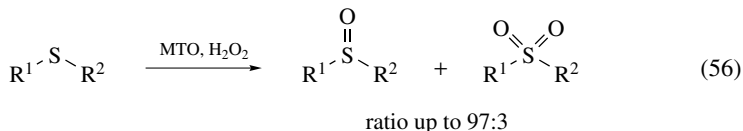
a. Non-asymmetric metal-catalyzed sulfoxidations. The extent of sulfide overoxidation to the sulfone, which in most cases accompanies the oxidation to the sulfoxide, depends on the electrophilicity of the oxidant. With the aim to determine electrophilicity of an oxygen transfer reagent, Adam and coworkers established a method with which they were able to classify oxidation systems in terms of electrophilicity³⁷³. Thianthrene-5-oxide **182** has been introduced as mechanistic probe, because in this compound a sulfide and sulfoxide functionality are oxidized competitively (equation 55). From the relative amounts of disulfoxide formation **183** (SOSO) and sulfone formation **184** (SSO_2) the so-called X_{SO} value can be calculated, and is <0.3 for electrophilic oxidants and >0.7 for nucleophilic oxidants. X_{SO} can be calculated from the equation:

$$X_{\text{SO}} = \frac{\text{SSO}_2 + \text{SOSO}_2}{\text{SSO}_2 + \text{SOSO} + 2x\text{SOSO}_2}$$

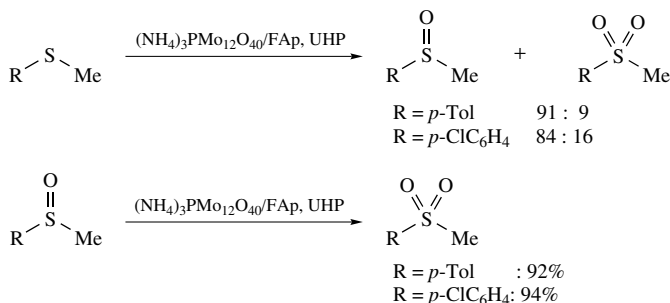
The X_{SO} value has been determined by this method for the homogeneous $\text{Ti}(\text{OPr-}i)_4/t\text{-BuOOH}$ system as well as some heterogeneous Ti-doped zeolites (Ti- β , Ti-MCM-41, Ti-IQC-2) and *t*-BuOOH or H_2O_2 as oxygen donors. All of the heterogeneous systems showed low X_{SO} values ranging from 0.06 to 0.19, indicating electrophilic character and selective formation of the sulfoxides. Compared to these catalysts the homogeneous system exhibits more nucleophilic character because of the higher X_{SO} value of 0.5, which is due to coordination of thianthrene-5-oxide to the titanium center at its sulfoxide functionality, such that oxidation occurs preferentially at the sulfide group to form the sulfone. In the case of heterogeneous Ti catalysts, this precoordination is hindered due to steric constraints and oxidation of the sulfide to the sulfoxide is favored.



In accordance with the highly electrophilic character of the MTO/H₂O₂ system ($X_{SO} = 0.07$) in the rhenium-catalyzed sulfoxidation, sulfoxides are generally generated with good chemoselectivities with only low sulfone formation (<29%), except in the presence of water, which enhances the sulfone formation (equation 56)³⁷⁴. The concentration of aqueous hydrogen peroxide seems to have a marked influence on the chemoselectivity, because water enhances the reactivity of the rhenium peroxo complex by hydrogen bonding such that sulfone formation is promoted³⁷⁴. Therefore, good chemoselectivities are only obtained with concentrated H₂O₂ (85%).

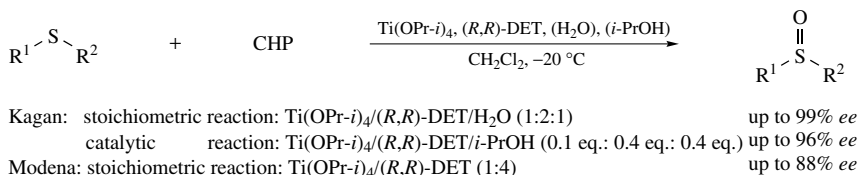


In 2002, Ichihara and coworkers reported on the utilization of a Keggin-type phosphomolybdate (NH₄)₃PMo₁₂O₄₀ on apatite as catalyst for the solvent-free epoxidation of olefins (see Section III.A.3.c) and the oxidation of sulfides and sulfoxides in the presence of urea hydrogen peroxide (Scheme 104)²⁹⁷. Chemoselectivities of the oxidation of the sulfides were good [product ratios (sulfide/sulfoxide): 84/16 up to 91/9] depending on the substrate, temperature and reaction time.



SCHEME 104. Solvent-free oxidation of sulfides and sulfoxides using (NH₄)₃PMo₁₂O₄₀ on apatite

b. Asymmetric sulfoxidations with chiral catalysts. Shortly after the discovery of the very effective Sharpless epoxidation procedure for allylic alcohols, this catalyst system was modified by Kagan and coworkers^{375–377}, and independently by Modena and coworkers³⁷⁸, for the enantioselective sulfoxidation of prochiral aryl alkyl sulfides (Scheme 105). In this procedure, unfortunately, the chiral titanium complex has to be



SCHEME 105. Asymmetric sulfoxidation using Kagan's or Modena's catalytic system

employed in stoichiometric amounts. The catalytic system developed by Kagan's group in 1984 (called the 'Orsay reagent') is based on the combination $\text{Ti}(\text{OPr-}i)_4/(R,R)\text{-DET}/\text{H}_2\text{O}$ 1:2:1 using TBHP at the beginning, but the oxidant being changed to cumyl hydroperoxide³⁷⁶ due to enhanced enantioselectivities. The catalytic system developed by Modena's group (called the 'Padova reagent') has the composition $\text{Ti}(\text{OPr-}i)_4/(R,R)\text{-DET}$ 1:4 using TBHP as oxidant. Both reagents gave similar trends in asymmetric sulfoxidations. The observed *ee* values with the 'Orsay reagent' using TBHP as oxidant ranged between 75 and 90% for alkyl aryl sulfides and 50–71% for dialkyl sulfides, while sulfone formation is avoided in the presence of water, even with excess TBHP³⁷⁷. Under Modena's conditions alkyl aryl sulfides are converted to the corresponding sulfoxides in yields of 41–99% and enantioselectivities of 14–88%. Kagan's group investigated the influence of several factors on the oxidation reaction. They found that an equimolar amount of water [compared to $\text{Ti}(\text{OPr-}i)_4$] is essential for obtaining good enantioselectivity (without water, racemic sulfoxides are observed). Many different functional groups on the phenyl group of the sulfide, like OH, CO_2Me , CH_2OH , NO_2 , pyridyl, are tolerated by the reagent system. Using cumyl hydroperoxide as oxygen source, the enantiomeric excess of the sulfoxide products ranged from 62 to 96% (yield between 71–97%). A careful control of temperature (between 16 and 35 °C) and reaction time in the premixing of $\text{Ti}(\text{OPr-}i)_4$, $(R,R)\text{-DET}$ and water (in a defined order: $\text{DET} + \text{Ti}(\text{OPr-}i)_4 \rightarrow$ wait for 2.5 min \rightarrow dropwise addition of H_2O during 1.5 min) is necessary in order to insure high *ee*³⁷⁵. By following this premixing protocol exactly, very high *ee* (95 to >99%) could be obtained for several substrates with Kagan's sulfoxidation reagent system. Aging of the freshly distilled $\text{Ti}(\text{OPr-}i)_4$ favored competitive formation of sulfones. The *ee* depends on the nature of the titanium alkoxide used, varying from $\text{Ti}(\text{OMe})_4$ (75% yield, 10% *ee* for (R) -*p*-tolyl methyl sulfoxide) to $\text{Ti}(\text{OPr-}i)_4$ (76% yield, 99% *ee* for (R) -*p*-tolyl methyl sulfoxide)³⁷⁹. In the absence of any alcohol (alcohols formed by preformation of the catalyst from $\text{Ti}(\text{OR})_4$ and $(R,R)\text{-DET}$ were removed in vacuum) and water, the catalytic system was almost inactive, giving the sulfoxide in poor chemical yield (19%) and low *ee* (3%). Reactivation occurred by addition of 4 equivalents of isopropanol and 1 equivalent of water [(R) -*p*-tolyl methyl sulfoxide: 70% yield, 85% *ee*]. Without additional water but isopropanol as additive, the best results for substrate *p*-tolyl methyl sulfide were obtained using $\text{Ti}(\text{OPr-}i)_4/(R,R)\text{-DET}/i\text{-PrOH}$ 1:2:4³⁷⁹. Larger as well as lower amounts of alcohol present in the mixture led to significantly lower *ee* values.

The results of the titanium-promoted asymmetric sulfoxidation of various sulfides using stoichiometric amounts of $\text{Ti}(\text{OPr-}i)_4/(R,R)\text{-DET}$ /hydroperoxide are shown in Table 27.

Later, also some catalytic or substoichiometric asymmetric processes were reported by several groups^{379–384}. The substoichiometric method developed by Kagan in 1987 at the beginning employed 0.2 eq. of $\text{Ti}(\text{OPr-}i)_4$, 0.4 eq. of DET and 0.2 eq. of water in the presence of molecular sieves 4 Å leading to enantioselectivities up to 90%. Lower catalyst amount led to a decrease in enantioselectivity (0.1 eq. $\text{Ti}(\text{OPr-}i)_4/0.2$ eq. $(R,R)\text{-DET}/0.1$ eq. H_2O : 85% yield, 70% *ee* for methyl *p*-tolyl sulfoxide)³⁷⁶. With catalytic amounts of the water-free system [0.1 eq. $\text{Ti}(\text{OPr-}i)_4/0.2$ eq. $(R,R)\text{-DET}/0.4$ eq. *i*-PrOH] Brunel and Kagan again observed beneficial effects of molecular sieves 4 Å³⁸⁰ (75% yield, 83% *ee* for (R) -*p*-tolyl methyl sulfoxide), as has already been reported by Hanson and Sharpless for the epoxidation of allylic alcohols³⁸⁵. The authors proposed that the molecular sieves efficiently regulate the formation of the chiral titanium complex and therefore have a positive effect on the enantioselectivity. Even better results could be obtained using 4 equivalents of chiral DET-ligand. Thus, the optimum catalytic reaction conditions were 0.1 eq. $\text{Ti}(\text{OPr-}i)_4/0.4$ eq. DET/0.4 eq. *i*-PrOH/1 eq. MS 4 Å, giving enantiomeric excesses up to 96%.

TABLE 27. Results of the titanium-catalyzed stoichiometric enantioselective sulfoxidation according to Kagan's and Modena's methods (yields are given and *ee* values are given in parentheses)

Substrate		Modena's method ^a	Kagan's method I ^b	Kagan's method II ^c	Kagan's method III ^d
R ¹	R ²				
ref.		378	377	376	375, 379
Ph	Me		80 (89) (<i>R</i>)	93 (93)	77 (99) (<i>R</i>)
<i>p</i> -MeC ₆ H ₄	Me	60 (88)	90 (90) (<i>R</i>)	93 (96)	77 (>99) (<i>R</i>)
<i>p</i> -BrC ₆ H ₄	Me		70 (80) (<i>R</i>)		
<i>p</i> -ClC ₆ H ₄	Me		95 (78) (<i>R</i>)	85 (91)	
<i>p</i> -MeO ₂ CC ₆ H ₄	Me		50 (91)		
<i>o</i> -MeO ₂ CC ₆ H ₄	Me		50 (60) (<i>R</i>)		
1-Naphthyl	Me				91 (91) (<i>R</i>)
2-Naphthyl	Me		88 (90)		81 (78) (<i>R</i>)
<i>p</i> -MeOC ₆ H ₄	Me		72 ^e (86)		78 (>99) (<i>R</i>)
<i>o</i> -MeOC ₆ H ₄	Me		70 (84)	97 (93)	75 (95) (<i>R</i>)
<i>p</i> -O ₂ NC ₆ H ₄	Me		63 (77)		51 (99) (<i>R</i>)
<i>p</i> -HOC ₆ H ₄	Me		90 (50)		
<i>p</i> -HOCH ₂ C ₆ H ₄	Me		71 (76)		
2-pyridyl	Me		63 (77)		
4-pyridyl	Me		51		
<i>p</i> -MeC ₆ H ₄	Et		71 (74) (<i>R</i>)		82 (87) (<i>R</i>)
<i>p</i> -MeC ₆ H ₄	<i>n</i> -Bu		75 (20) (<i>R</i>)		64 (38) (<i>R</i>)
<i>p</i> -MeC ₆ H ₄	<i>i</i> -Pr		56 (63) (<i>R</i>)		
<i>p</i> -MeC ₆ H ₄	CH ₂ Ph		41 (7) (<i>R</i>)		
2-Naphthyl	<i>n</i> -Pr		78 (24)		
<i>p</i> -ClC ₆ H ₄	CH ₂ CH ₂ OH	41 (14)			
Ph	<i>t</i> -Bu	99 (35)			
<i>o</i> -Anisyl	Ph				69 (14) (<i>R</i>)
CH ₂ Ph	Me	70 (46)	88 (58) (<i>S</i>)	84 (62)	87 (95) (<i>R</i>)
<i>n</i> -Oct	Me		77 (71)	71 (80)	63 (85) (<i>R</i>)
Ph(CH ₂) ₃	Me		84 (50)		
<i>c</i> -Hex	Me		67 (54)		
<i>t</i> -Bu	Me		72 (53) (<i>R</i>)		
<i>p</i> -MeOC ₆ H ₄ CH ₂	Me		40		
Et(Me)CH	Me		93 ^f (42, 38)		

^a Ti(OPr-*i*)₄/(*R,R*)-DET/TBHP (1 eq.: 4 eq.: 2 eq.).

^b Ti(OPr-*i*)₄/(*R,R*)-DET/H₂O/TBHP (1 eq.: 2 eq.: 1 eq.: 1.1 eq.) in CH₂Cl₂ at ca -20 °C.

^c Ti(OPr-*i*)₄/(*R,R*)-DET/H₂O/CHP (1 eq.: 2 eq.: 1 eq.: 1.1 eq.) in CH₂Cl₂ at -23 °C for 20 h.

^d Ti(OPr-*i*)₄/(*R,R*)-DET/H₂O/CHP (1 eq.: 2 eq.: 1 eq.: 2 eq.) in CH₂Cl₂ at -22 °C for 16 h; for exact conditions of the premixing procedure see References 375 and 379.

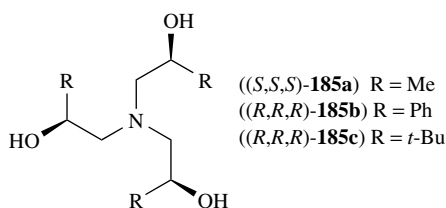
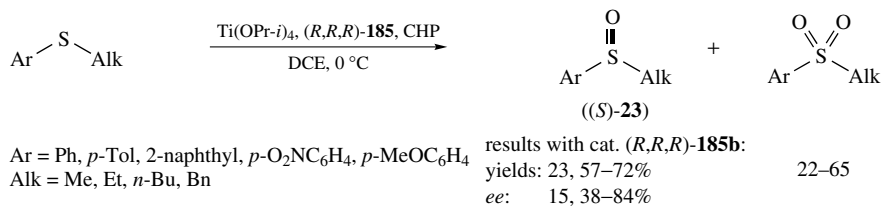
^e In addition there is 15% of sulfone.

^f Two diastereomers in the ratio 40:60.

The catalytic sulfoxidation system developed by Uemura and coworkers in 1993^{381,386} consisted of Ti(OPr-*i*)₄, (*R*)-BINOL, H₂O and TBHP in different compositions. The best results (highest *ee*) were obtained with low amounts of catalyst: 0.025 eq. Ti(OPr-*i*)₄, 0.05 eq. (*R*)-BINOL, 0.5 eq. H₂O and 2 eq. TBHP. With this method sulfoxides could be obtained with excellent enantioselectivities (*ee* 96%), although yields were low (28–44%) due to kinetic resolution of the formed sulfoxides to give the corresponding sulfones. More detailed investigations by Uemura and coworkers showed that an enantiomeric excess of 50% of the sulfoxides is obtained at the initial stage of the reaction and that an increase in *ee* results the longer the reaction takes place³⁸⁶. So the Ti-(*R*)-BINOL complex catalyzes

not only the asymmetric sulfoxidation but also the subsequent kinetic resolution^{381, 386}. Non-polar solvents turned out to be best for this reaction, and CCl_4 in particular was proven to be the best one. The system showed a great water tolerance, which allows the direct use of 70% aqueous TBHP, and water also increased the oxidation rate. The authors observed a positive non-linear effect in the asymmetric sulfoxidation of methyl *p*-tolyl sulfide, that is, the *ee* value of the product highly exceeds the *ee* value of the (*R*)-BINOL over a wide range. Furthermore, in most of these catalytic procedures the high *ee* values obtained are mainly due to a kinetic resolution process of the sulfoxide, the enantiomers of which undergo further oxidation with different rates and therefore yields are limited.

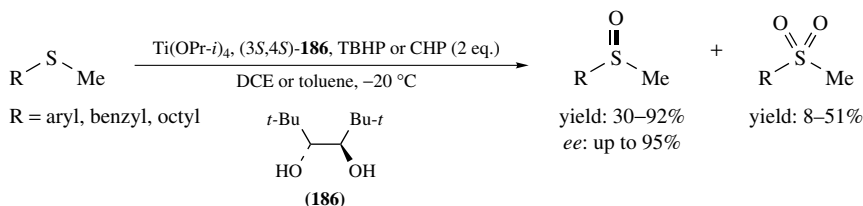
In 1996, Modena and coworkers reported on an enantioselective titanium-catalyzed sulfoxidation method employing enantiopure tetradentate trialkanolamines **185a–c** as ligands and hydroperoxides as oxidants (Scheme 106)³⁸². The best enantioselections were obtained with (*R,R,R*)-tris(2-hydroxy-2-phenylethyl)amine [(*R,R,R*)-**185b**] and either cumyl or trityl hydroperoxide as oxidant in chlorinated solvents at a temperature of 0 °C. Asymmetric sulfoxidation is accompanied by a second asymmetric process, the kinetic resolution via oxidation to sulfones, the latter being obtained in significant amount (around 15%). Both processes proceed with similar rates and work in the same direction: the (*S*)-sulfoxide is formed preferentially (*ee* of 29% for methyl *p*-tolyl sulfide) and the (*R*)-sulfoxide is oxidized faster to form the sulfone. Kinetic resolution of racemic methyl *p*-tolyl sulfoxide gives the (*S*)-sulfoxide with an *ee* of 33% after 50% conversion. The enantioselection is dependent on the nature of the alkyl moiety and the electronic effects of the aryl substituents. The best results are observed with aryl alkyl sulfides bearing branched alkyl chains (60–84% *ee*).



SCHEME 106. Titanium-catalyzed asymmetric oxidation of aryl alkyl sulfides using a chiral tetradentate trialkanolamine ligand

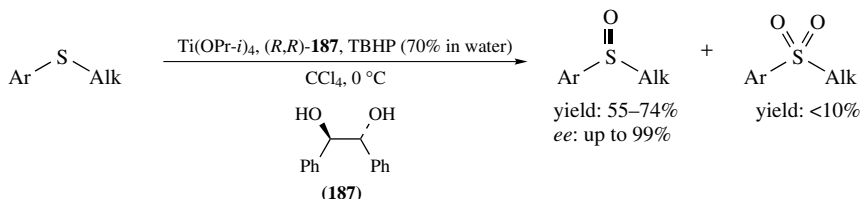
A new enantiopure, bidentate ligand (*3S,4S*)-2,2,5,5-tetramethyl-3,4-hexanediol [(*3S,4S*)-**186**] was developed by Yamanoi and Imamoto and investigated as asymmetric inducer in the titanium-catalyzed sulfoxidation reaction with various hydroperoxides as oxygen donors (Scheme 107)³⁸⁴. The catalytically active species was then prepared *in situ* from $\text{Ti(OPr-}i\text{)}_4$ and ligand (*3S,4S*)-**186**. The most efficient hydroperoxide in terms of enantioselectivity turned out to be cumyl hydroperoxide (95% *ee* compared to 30% *ee* in the case of methyl *p*-tolyl hydroperoxide), and molecular sieves 4 Å had a beneficial effect on the

reaction. Maximum enantiomeric excess was obtained in toluene as solvent at -20°C and at a $\text{Ti}(\text{OPr-}i\text{)}_4/\text{ligand}$ ratio of 1:2. Unfortunately, most of the dialkyl sulfides employed, were unreactive under these conditions.



SCHEME 107. Catalytic enantioselective sulfoxidation using chiral ligand **186**

Rosini and coworkers^{383,387} reported on a procedure that minimizes kinetic resolution ($<10\%$ sulfone formation), resulting in high yields and enantiomeric excess of the sulfoxides. The authors utilized a catalyst that was formed *in situ* by reacting $\text{Ti}(\text{OPr-}i\text{)}_4$, the enantiopure ligand (*R,R*)- or (*S,S*)-1,2-diphenylethane-1,2-diol [(*R,R*)-/(*S,S*)-**187**] and water (Scheme 108). The best results were obtained employing reagents and substrate in a ratio of sulfide/(*R,R*)-**187**/Ti/ $\text{H}_2\text{O} = 1/0.1/0.05/1$ with 2 equivalents of 70% aqueous TBHP at 0°C in CCl_4 under N_2 atmosphere and reaction times less than 2 hours, under which overoxidation to the sulfone is negligible. In the sulfoxidation reaction of aryl alkyl sulfides chemical yields of 60 to 73% and *ee* values ranging from 67 to 80% could be obtained for the sulfoxides, being almost independent of the nature of the aromatic group and of the size of the alkyl group. Exceptions are represented by substrates with aromatic groups bearing an electron-withdrawing substituent like NO_2 (44% *ee*) or such with branched and sterically demanding alkyl substituents (e.g. *i*-Pr: *ee*: 22%) present in the substrate, for which a marked decrease in enantioselectivity was found. Aryl benzyl sulfides, which are poor substrates in the Ti/DET catalyzed reaction, could be oxidized to the sulfoxide in good yields (55–74%) and high enantioselectivity (92–99%).



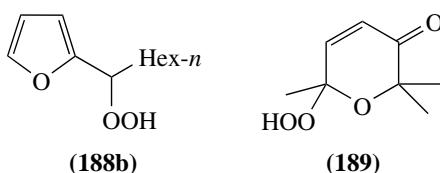
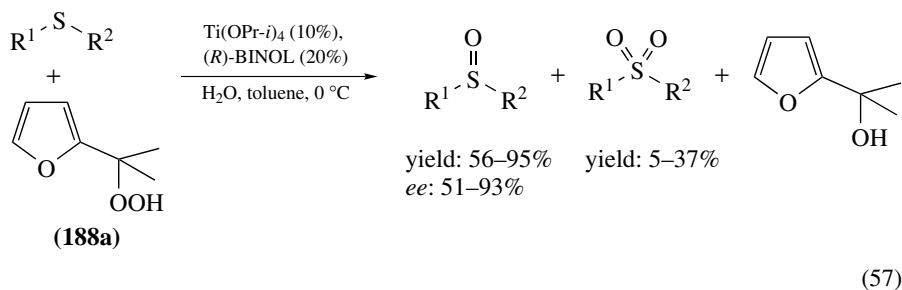
Ar = Ph, *p*-Tol, 2-naphthyl, *p*- $\text{O}_2\text{NC}_6\text{H}_4$, *p*- MeOC_6H_4 , *p*- BrC_6H_4

Alk = Me, Et, *n*-Bu, *i*-Pr, Bn

SCHEME 108. Ti-catalyzed enantioselective sulfoxidation employing enantiopure diol (*R,R*)-**187** as ligand

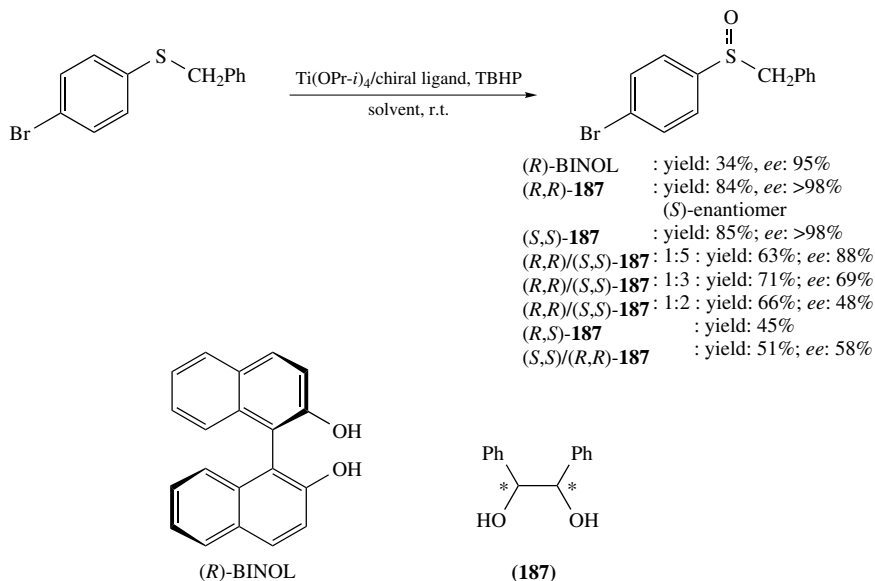
In 2001, Scettri and coworkers¹⁴ could show that titanium-catalyzed asymmetric sulfoxidation with a tertiary furyl hydroperoxide **188a** can be achieved under catalytic conditions by a modification of Uemura's approach³⁸⁶ employing (*R*)-BINOL as chiral ligand (equation 57). Under these conditions sulfoxides could be isolated in medium to good

yields (56–95%) and enantioselectivities (*ee* 51–93%). In accordance with the observations made earlier by Scettri and coworkers with the stoichiometric version of this reaction¹⁵ utilizing $\text{Ti}(\text{OPr-}i)_4/L\text{-DET}$ /hydroperoxides **188b** and **189**, the catalytic system depicted in equation 57 also showed rather low asymmetric induction in the first oxidation step producing the sulfoxide. The low *ee* values improved with time due to kinetic resolution of the sulfoxide by overoxidation to the sulfone. The hydroperoxides can be regenerated after chromatographic separation of the corresponding alcohols.

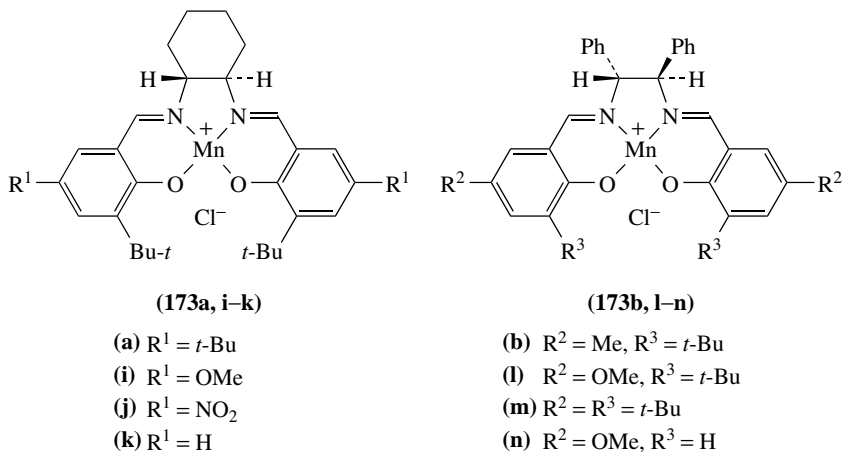


In 2002, Naso and coworkers reported on an enantioselective route to dialkyl sulfoxides which includes the asymmetric sulfoxidation of benzyl *p*-bromophenyl sulfide with TBHP catalyzed by chiral titanium complexes (Scheme 109)³⁸⁸. For this sulfoxidation reaction three structurally different optically pure ligands have been tested: (*R*)-BINOL, (+)-DET and (*R,R*)- or (*S,S*)-**187**. With (*R*)-BINOL as chiral ligand, CCl_4 turned out to be a better solvent than CH_2Cl_2 and interestingly, in the absence of water, no enantiomeric excess of the benzyl *p*-bromophenyl sulfoxide was observed. Increasing the reaction time up to 29 hours led to a higher *ee* (95%), but also to a significantly lower yield (34%) due to kinetic resolution of the sulfoxide by overoxidation to the sulfone. Sulfoxidation with the catalytic system $\text{Ti}(\text{OPr-}i)_4/(+)\text{-DET/CHP}$ under exclusion of water produced the corresponding (*R*)-configured sulfoxide in 46% yield and 58% *ee*. Utilizing (*S,S*)-**187** as chiral inductor, yield and *ee* varied with the solvent. The best result was obtained in hexane (81% yield, >98% *ee*) and water did not have great influence on the reaction. With this catalytic system a positive non-linear effect was observed: with a ligand of lower *ee*, sulfoxides with higher enantiomeric purity could be synthesized. With *meso*-**187**, large amounts of sulfone and racemic sulfoxide were formed.

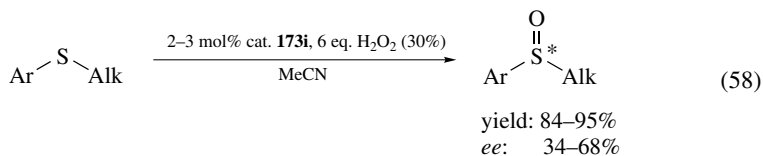
In combination with H_2O_2 (salen)Mn(III) complexes **173a, b, i–n** have also been employed by Jacobsen and coworkers as catalysts for the asymmetric oxidation of sulfides to sulfoxides, without a need for additives. From the structurally and electronically different Mn–salen catalysts screened, **173i** turned out to be the most active and selective one (equation 58)³⁸⁹. While dialkyl sulfides underwent uncatalyzed oxidation with H_2O_2 , aryl alkyl sulfides were oxidized only slowly compared with the catalyzed pathway. Using



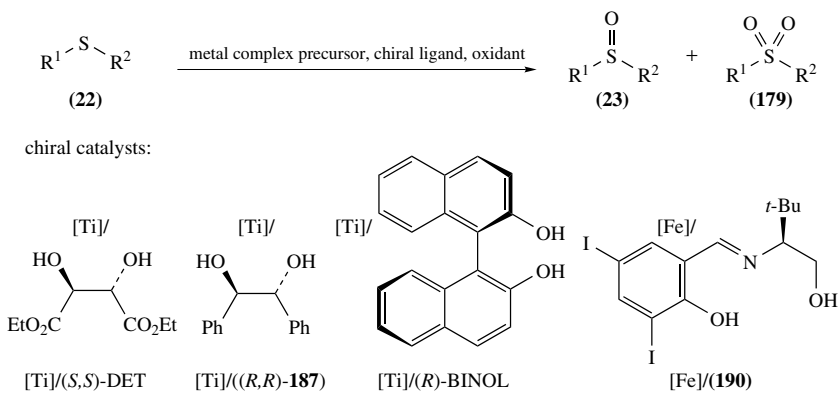
SCHEME 109. Enantioselective oxidation of benzyl *p*-bromophenyl sulfide by TBHP in the presence of chiral titanium catalysts



catalyst **173i** in the enantioselective sulfoxidation of various aryl alkyl sulfides, sulfoxide yields of 80–95% and enantiomeric excesses of 34–68% could be obtained.



Aiming at developing a practical sulfoxidation procedure with a cheap and non-toxic catalyst, Legros and Bolm very recently reported on an iron-catalyzed procedure which provides optically active sulfoxides with up to 90% *ee*³⁹⁰. The catalysis proceeds under biphasic (CH₂Cl₂/aqueous H₂O₂) and very simple reaction conditions (air and water do not affect the reaction) and utilizes a readily available chiral iron complex, which is formed *in situ* from iron acetate and ligand **190** (see Scheme 110), as well as inexpensive and safe 30% aqueous hydrogen peroxide. Several ligands with different substituents at the aromatic moiety were tested and the diiodo-substituted compound **190** turned out to be the most efficient one. In the sulfoxidation process no sulfones are formed, and therefore no kinetic resolution by overoxidation of the sulfoxide occurs. Enantiomeric excesses of the various sulfoxides ranged between 27 and 90%, being highest for *p*-nitrophenyl methyl sulfoxide, which showed especially low *ee* (44%, Table 28, entry 6) when being formed by the method developed by Rosini and coworkers³⁸⁷. Unfortunately, yields do not exceed 44% and could not be raised by higher catalyst loadings, higher amounts of oxidant or by performing the reaction under homogeneous conditions (substitution of CH₂Cl₂ by solvents miscible with water), without loss in enantioselectivity for the sulfoxides obtained.



SCHEME 110. Asymmetric sulfoxidation with various chiral metal catalysts

An overview of the results of the enantioselective sulfoxidation utilizing various chiral metal catalysts is given in Table 28.

c. Asymmetric sulfoxidations with chiral hydroperoxides. While the asymmetric sulfoxidation with chiral catalysts is a well investigated field of chemical research, much less effort has been spent on exploring the sulfoxidation reaction utilizing achiral metal complexes but optically active hydroperoxides as oxidant and asymmetric inductor. As already mentioned in Section III.B.1, Takata and Ando for the first time reported the asymmetric oxidation of prochiral sulfides with optically active hydroperoxides **26**, that were prepared *in situ* from thiazoline derivatives **25** by singlet oxygenation (Scheme 101)³⁶⁷. Next to the uncatalyzed reaction, the authors also tested Ti(OPr-*i*)₄ as an achiral catalyst in combination with the optically pure **26**. With this catalytic system, sulfoxide yields were lower than for the uncatalyzed sulfoxidation and ranged between 41 and 81%. Enantiomeric excesses were low but slightly better than observed for the uncatalyzed reaction (5–37%), which indicates that addition of Ti(OPr-*i*)₄ affects proximity of substrate and oxygen transfer agent through coordination in the transition state.

In 1997, Chmielewski and coworkers investigated the oxidation of methyl phenyl sulfide and methyl *p*-tolyl sulfide with chiral carbohydrate hydroperoxides, which have been

TABLE 28. Enantioselective sulfoxidation utilizing various chiral metal catalysts in catalytic quantities

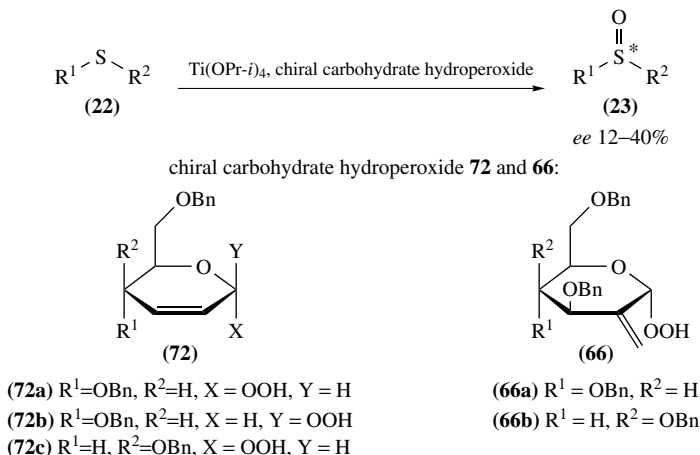
Entry	Substrate		Catalyst ^a	Water ^b	Oxidant	Yield sulfoxide (%)	<i>ee</i> sulfoxide (%)	Abs. config.	Reference
	R ¹	R ²							
1	Ph	Me	[Ti]/(<i>R,R</i>)-DET ^c	—	CHP	81	91	<i>R</i>	379, 380
			[Ti]/(<i>R,R</i>)-BINOL ^d	0.5	TBHP	28	96	<i>R</i>	386
			[Ti]/(<i>S,S</i>)- 187	1	TBHP	60[8] ^e	80	<i>R</i>	383
			[Ti]/(<i>R,R</i>)- 187	1	TBHP	63	80	<i>S</i>	387
			[Fe]/ 190	0.84	H ₂ O ₂	36	59	<i>S</i>	390
			[Ti]/(<i>S,S</i>)- 186	—	CHP	36 [45] ^e	87	<i>S</i>	384
			(<i>R,R</i>)- 173i	—	H ₂ O ₂	90	47	<i>S</i>	389
2	<i>p</i> -MeC ₆ H ₄	Me	[Ti]/(<i>R,R</i>)-DET ^f	0.52	CHP	90	96		376
			[Ti]/(<i>R,R</i>)-DET ^g	0.2	CHP	97	88		376
			[Ti]/(<i>R,R</i>)-DET ^c	—	CHP	77	96	<i>R</i>	379, 380
				0.5	TBHP	44	96	<i>R</i>	386
			[Ti]/(<i>R,R</i>)-DET ^h	0.2	TBHP	68	50		376
			[Ti]/(<i>R,R</i>)-DET ⁱ	0.25	CHP	94	84		376
			[Ti]/(<i>R,R</i>)-DET ^g	0.2	CHP	97	88		376
			[Ti]/(<i>R,R</i>)-DET ^j	0.1	CHP	85	70		376
			[Ti]/(<i>S,S</i>)- 187	1	TBHP	62 [8] ^e	80	<i>R</i>	383
			[Ti]/(<i>R,R</i>)- 187	1	TBHP	62	80	<i>S</i>	387
			[Ti]/(<i>S,S</i>)- 186	—	CHP	42 [40] ^e	95	<i>S</i>	384
			[Ti]/(<i>R,R,R</i>)- 185b	—	CHP	61 [37] ^e	45	<i>S</i>	382
			(<i>R,R</i>)- 173i	—	H ₂ O ₂	95	42	<i>S</i>	389
3	<i>p</i> -MeC ₆ H ₄	Et	[Ti]/(<i>R,R</i>)-DET ^c	—	CHP	68	78	<i>R</i>	379, 380
			[Ti]/(<i>R,R,R</i>)- 185b	—	CHP	63 [36] ^e	38	<i>S</i>	382
4	<i>p</i> -MeC ₆ H ₄	<i>n</i> -Bu	[Ti]/(<i>R,R</i>)-DET ^c	—	CHP	70	25	<i>R</i>	379, 380
			[Ti]/(<i>R,R,R</i>)- 185b	—	CHP	57 [42] ^e	44	<i>S</i>	382
5	<i>p</i> -MeOC ₆ H ₄	Me	[Ti]/(<i>R,R</i>)-DET ^c	—	CHP	73	92	<i>R</i>	379, 380
			[Ti]/(<i>S,S</i>)- 187	1	TBHP	56 [11] ^e	67	<i>R</i>	383
			[Ti]/(<i>R,R</i>)- 187	1	TBHP	55	69	<i>S</i>	387
			[Ti]/(<i>S,S</i>)- 186	—	CHP	30 [55] ^e	40		384
			[Ti]/(<i>R,R,R</i>)- 185b	—	CHP	64 [30] ^e	41	<i>S</i>	382
6	<i>o</i> -MeOC ₆ H ₄	Me	[Ti]/(<i>R,R</i>)-DET ^c	—	CHP	72	89	<i>R</i>	379, 380
			[Ti]/(<i>S,S</i>)- 186	—	CHP	45 [40] ^g	87	<i>S</i>	384
			(<i>S,S</i>)- 173i	—	H ₂ O ₂	94	34	<i>R</i>	389
7	<i>o</i> -MeOC ₆ H ₄	Ph	[Ti]/(<i>R,R</i>)-DET ^c	—	CHP	64	6	<i>R</i>	379, 380
8	<i>p</i> -ClC ₆ H ₄	Me	[Fe]/ 190	0.84	H ₂ O ₂	32	65	<i>S</i>	390
9	<i>p</i> -BrC ₆ H ₄	Me	[Ti]/(<i>R,R</i>)-BINOL ^d	0.5	TBHP	39	96	<i>R</i>	386
			[Ti]/(<i>S,S</i>)- 187	1	TBHP	50 [4] ^e	67	<i>R</i>	383
			[Ti]/(<i>R,R</i>)- 187	1	TBHP	58	67	<i>S</i>	387
			[Fe]/ 190	0.84	H ₂ O ₂	41	78	<i>S</i>	390
			[Ti]/(<i>S,S</i>)- 186	—	CHP	58 [40] ^e	65		384
(<i>S,S</i>)- 173i	—	H ₂ O ₂	93	56	<i>R</i>	389			
10	<i>o</i> -BrC ₆ H ₄	Me	[Ti]/(<i>S,S</i>)- 186	—	CHP	92	33		384
			(<i>R,R</i>)- 173i	—	H ₂ O ₂	80	68	<i>S</i>	389
11	<i>o</i> -IC ₆ H ₄	Me	(<i>S,S</i>)- 173i	—	H ₂ O ₂	95	65	<i>R</i>	389
12	<i>p</i> -O ₂ NC ₆ H ₄	Me	[Ti]/(<i>R,R</i>)- 187	1	TBHP	74	44	<i>S</i>	387
			[Fe]/ 190	0.84	H ₂ O ₂	21	90	<i>S</i>	390
			[Ti]/(<i>R,R,R</i>)- 185b	—	CHP	23 [65] ^e	15	<i>S</i>	382
			(<i>R,R</i>)- 173i	—	H ₂ O ₂	86	66	<i>S</i>	389
13	<i>m</i> -O ₂ NC ₆ H ₄	Me	(<i>S,S</i>)- 173i	—	H ₂ O ₂	84	63	<i>R</i>	389
14	<i>o</i> -O ₂ NC ₆ H ₄	Me	[Ti]/(<i>R,R</i>)-DET ^c	—	CHP	51	75	<i>R</i>	379, 380

TABLE 28 (continued)

Entry	Substrate		Catalyst ^a	Water ^b	Oxidant	Yield sulfoxide (%)	<i>ee</i> sulfoxide (%)	Abs. config.	Reference
	R ¹	R ²							
15	2-Naphthyl	Me	[Ti]/(<i>S,S</i>)- 187	1	TBHP	61 [9] ^e	71	<i>R</i>	383
			[Ti]/(<i>R,R</i>)- 187	1	TBHP	65	73	<i>S</i>	387
			[Fe]/ 190	0.84	H ₂ O ₂	44	70	(-)	390
			[Ti]/(<i>S,S</i>)- 186	—	CHP	46 [48] ^e	80	<i>S</i>	384
			[Ti]/(<i>R,R,R</i>)- 185b	—	CHP	52 [34] ^e	38	<i>S</i>	382
			(<i>R,R</i>)- 173i	—	H ₂ O ₂	84	46	<i>S</i>	389
16	Ph	Et	[Ti]/(<i>R,R</i>)- 187	1	TBHP	71	70	<i>S</i>	387
			[Fe]/ 190	0.84	H ₂ O ₂	30	44	<i>S</i>	390
			[Ti]/(<i>S,S</i>)- 186	—	CHP	40 [51] ^e	82	<i>S</i>	384
17	Ph	<i>n</i> -Bu	[Ti]/(<i>R,R</i>)- 187	1	TBHP	69	80	<i>S</i>	387
18	Ph	<i>t</i> -Bu	[Ti]/(<i>R,R,R</i>)- 185b	—	CHP	60 [36] ^e	66	<i>S</i>	382
19	Ph	<i>i</i> -Bu	(<i>R,R</i>)- 173i	—	H ₂ O ₂	94	43	<i>S</i>	389
20	Ph	<i>i</i> -Pr	[Ti]/(<i>R,R</i>)- 187	1	TBHP	60	22	<i>S</i>	387
21	Ph	CH ₂ Ph	[Ti]/(<i>R,R</i>)- 187	1	TBHP	73	>99	<i>S</i>	387
			[Fe]/ 190	0.84	H ₂ O ₂	40	27	<i>S</i>	390
			[Ti]/(<i>R,R,R</i>)- 185b	—	CHP	72 [22] ^e	84	<i>S</i>	382
22	Ph	CH=CH ₂	[Ti]/(<i>R,R</i>)-DET ^c	—	CHP	58	55	<i>R</i>	379, 380
23	<i>p</i> -MeC ₆ H ₄	CH ₂ Ph	[Ti]/(<i>R,R</i>)- 187	1	TBHP	65	98	<i>S</i>	387
24	<i>p</i> -MeOC ₆ H ₄	CH ₂ Ph	[Ti]/(<i>R,R</i>)- 187	1	TBHP	60	92	<i>S</i>	387
25	<i>p</i> -BrC ₆ H ₄	CH ₂ Ph	[Ti]/(<i>R,R</i>)-DET	0	CHP	46	58	<i>R</i>	388
			[Ti]/(<i>R,R</i>)-BINOL	0.5	TBHP	34	95	<i>R</i>	388
			[Ti]/(<i>R,R</i>)-BINOL	0	TBHP	69	0	<i>R</i>	388
			[Ti]/(<i>S,S</i>)- 187	0	TBHP	85 [5] ^e	>98	<i>R</i>	388
			[Ti]/(<i>R,R</i>)- 187	0	TBHP	84	>98	<i>S</i>	388
			[Ti]/(<i>S,S</i>)- 187 ^k	0	TBHP	63	88	<i>R</i>	388
			[Ti]/(<i>S,S</i>)- 187 ^l	0	TBHP	66	48	<i>R</i>	388
			[Ti]/(<i>R,S</i>)- 187	0	TBHP	45 [31] ^e	0		388
26	CH ₂ Ph	Me	[Ti]/(<i>R,R</i>)-DET ^c	—	CHP	72	90	<i>R</i>	379, 380
			[Ti]/(<i>S,S</i>)- 186	—	CHP	80[trace] ^e	3	<i>S</i>	384
27	<i>n</i> -Oct	Me	[Ti]/(<i>R,R</i>)-DET ^c	—	CHP	69	71	<i>R</i>	379, 380
			[Ti]/(<i>S,S</i>)- 186	—	CHP	83[trace] ^e	<1		384
28	Ph	<i>c</i> -Pr	(<i>R,R</i>)- 173i	—	H ₂ O ₂	84	40	<i>S</i>	389

^a [Ti]: Ti(OPr-*i*)₄.^b Molar ratio: water/sulfide.^c Ti(OPr-*i*)₄/(*R,R*)-DET/*i*-PrOH (0.1 eq.: 0.4 eq.: 0.4 eq.) in CH₂Cl₂ in the presence of MS 4 Å.^d Ti(OPr-*i*)₄/(*R*)-BINOL/H₂O/TBHP (0.025 eq.: 0.05 eq.: 0.5 eq. : 2 eq.) in CCl₄.^e In brackets: yield of isolated sulfone.^f Ti(OPr-*i*)₄/(*R,R*)-DET/H₂O (0.52 eq.: 1.04 eq.: 0.52 eq.) in CH₂Cl₂.^g Ti(OPr-*i*)₄/(*R,R*)-DET/H₂O (0.2 eq.: 0.8 eq.: 0.2 eq.) in CH₂Cl₂ in the presence of 1wt eq. MS 4 Å.^h Ti(OPr-*i*)₄/(*R,R*)-DET/H₂O (0.2 eq.: 0.4 eq.: 0.2 eq.) in CH₂Cl₂.ⁱ Ti(OPr-*i*)₄/(*R,R*)-DET/H₂O (0.25 eq.: 0.5 eq.: 0.25 eq.) in CH₂Cl₂.^j Ti(OPr-*i*)₄/(*R,R*)-DET/H₂O (0.1 eq.: 0.2 eq.: 0.1 eq.) in CH₂Cl₂ in the presence of 1wt eq. MS 4 Å.^k 67% *ee*.^l 33% *ee*.

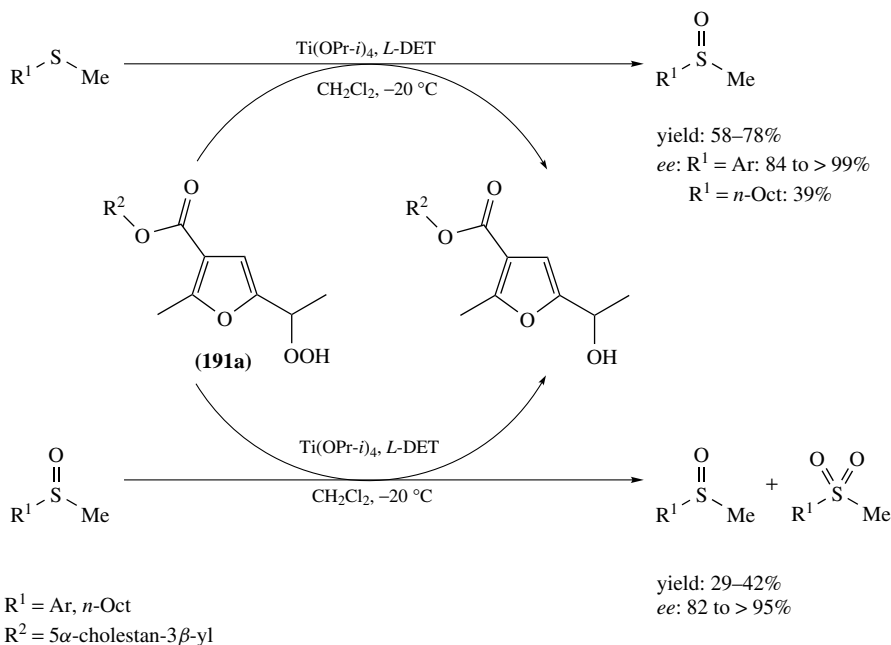
developed in their group (Scheme 111)^{66,100,101}. The yields for this reaction are not given; *ee* values range from 12 to 40%, with the highest asymmetric induction being obtained with hydroperoxide **72b** for methyl phenyl sulfide. As observed previously for the epoxidation of allylic alcohols (Section III.A.3.b), the sulfoxide formation by the carbohydrate



SCHEME 111. Titanium-catalyzed asymmetric oxidation of sulfides with carbohydrate hydroperoxides

hydroperoxide anomers **72a** and **72b** resulted in the opposite configuration of the sulfoxides.

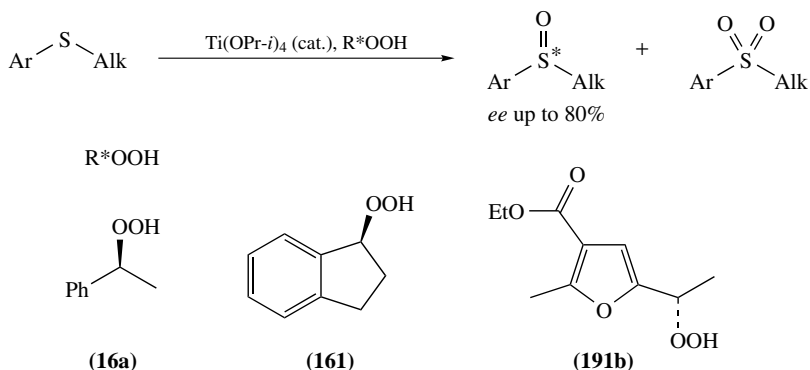
In 1996/1997, Scettri and coworkers reported on the employment of optically active, renewable furyl hydroperoxides **191** instead of cumyl hydroperoxides in the $\text{Ti(OPr-}i\text{)}_4/\text{DET}$ (or DIPT) catalyzed asymmetric sulfoxidation (Modena conditions, stoichiometric) and subsequent kinetic resolution (Scheme 112)^{391–393} The structure of the hydroperoxide seems to be important for the efficiency of the enantioselectivity and good yields and *ee* values were obtained by using functionalized furyl hydroperoxides. Various differently substituted sulfides were oxidized using $\text{Ti(OPr-}i\text{)}_4/(L)\text{-DET}$ or $(L)\text{-DIPT}$ as catalytic system in the presence of different secondary or tertiary furyl hydroperoxides **191** (shown in Scheme 112) as oxidants. The corresponding sulfoxides could be obtained in moderate to good yields (44–84%) and moderate to excellent enantiomeric excesses (50 up to >95%). The asymmetric sulfoxidation is accompanied by a kinetic resolution of the formed sulfoxide (yields of sulfone up to 15%). The two oxidation steps, asymmetric oxidation and kinetic resolution are enantioconvergent and therefore this results in high *ee*. Kinetic resolution of racemic sulfoxides as well as enantiomeric enriched ones was also conducted by the authors employing various furyl hydroperoxides. Starting from racemic sulfoxides, the enantiomerically enriched sulfoxides after kinetic resolution could be obtained in yields of 38 to 75% and enantiomeric excesses of 17 to >95%. This method could also be used for an enantiomeric enrichment of starting chiral sulfoxides (showing *ee* between 60 and 80%). In many cases the *ee* was improved to up to 95%. Next to the asymmetric sulfoxidation and kinetic resolution of sulfoxide, a third asymmetric process takes place: the kinetic resolution of racemic hydroperoxides **191** ($\text{R}^4 = \text{H, Et}$) producing enantiomerically enriched hydroperoxides and the corresponding alcohols. When the chiral hydroperoxides were employed as oxidants for the asymmetric sulfoxidation the corresponding alcohols could be isolated with *ee* values of 23 to 76%, while in the process of kinetic resolution of sulfoxides the racemic oxidant is kinetically resolved leading to *ee* values of 4–31%.



SCHEME 113. Ti/DET-catalyzed asymmetric sulfoxidation using a steroidal furyl hydroperoxide **191a** as oxidant

Scettri's group employed hydroperoxide **191a** (in the form of an inseparable 1:1 mixture of diastereomers) as oxidant for the titanium-catalyzed asymmetric sulfoxidation reaction (Scheme 113)³⁹⁴. Oxidation of differently substituted sulfides led to formation of the corresponding sulfoxides in yields between 58 and 78% and enantiomeric excesses of 39 to >95%, which results from the two enantioconvergent processes: asymmetric oxidation and kinetic resolution. While for aryl methyl sulfoxides *ee* values were high (84 to >95%), with dialkyl sulfides only moderate enantioselectivity was observed (*ee* 39%). The kinetic resolution of racemic sulfoxides employing the same catalytic system occurred with a highly preferential oxidation of the (*S*)-enantiomer, leading to the enantiomerically enriched (*R*)-sulfoxide (82 to >95% *ee*). With DIPT (diisopropyl tartrate) as chiral auxiliary significant lowering of *ee* was observed in the kinetic resolution of racemic sulfoxides (25–50%).

A further catalytic method for asymmetric sulfoxidation of aryl alkyl sulfides was reported by Adam's group, who utilized secondary hydroperoxides **16a**, **16l** and **191b** as oxidants and asymmetric inductors (Scheme 114)²¹⁹. This titanium-catalyzed oxidation reaction by (*S*)-1-phenylethyl hydroperoxide **16a** at -20°C in CCl_4 afforded good to high enantiomeric excesses for methyl phenyl and *p*-tolyl alkyl sulfides (*ee* up to 80%). Detailed mechanistic studies showed that the enantioselectivity of the sulfide oxidation results from a combination of a rather low asymmetric induction in the sulfoxidation (*ee* <20%) followed by a kinetic resolution of the sulfoxide by further oxidation to the sulfone



SCHEME 114. Titanium-catalyzed enantioselective sulfoxidation with secondary, optically pure hydroperoxides

(*ee* up to *ca* 80% at 85% sulfide conversion). The overoxidation is explained in terms of sulfoxide coordination to the titanium center to generate a template in which the oxygen is intramolecularly transferred from the bound hydroperoxide to the ligated sulfoxide in a stereocontrolled manner. In their publication the authors also presented a proposal for the intermediate template structure, which is shown in Figure 17. When racemic *p*-tolyl methyl sulfide was employed as substrate, kinetic resolution occurred, giving sulfone and enantiomerically enriched sulfoxide (up to 44% *ee* after 76% conversion).

Very recently, Lattanzi and coworkers reported on the use of enantiomerically pure camphor derived hydroperoxide **61** for the $\text{Ti(OPr-}i\text{)}_4$ catalyzed chemoselective asymmetric oxidation of aryl methyl sulfides (equation 59)³⁹⁵. The corresponding sulfoxides could be obtained in moderate yields (39–68%) and *ee* values up to 51%. The sulfoxidation to the sulfoxides is accompanied by further oxidation of the sulfone (kinetic resolution, yields of sulfone up to 9%). This process is stereodivergent with respect to the sulfoxidation step, which was found for the first time. Although the obtained enantioselectivities for the sulfoxides were only moderate, they proved to be among the best reported at that time with the use of enantiopure hydroperoxides as the only asymmetric inductor. The

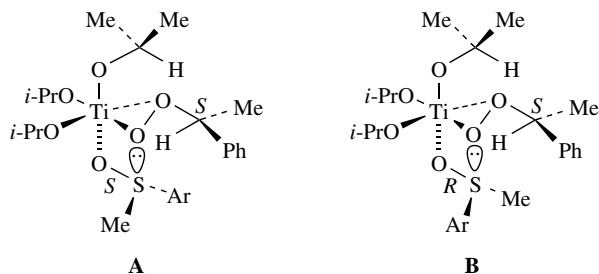
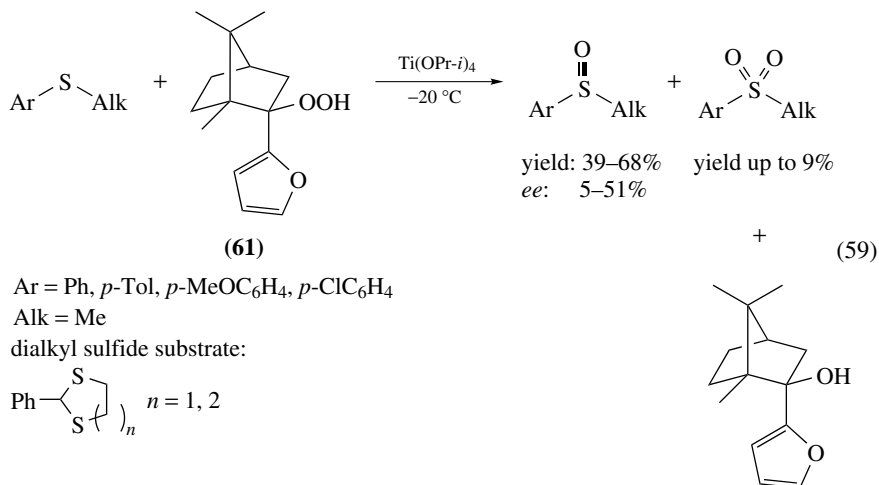


FIGURE 17

corresponding furyl alcohols, generated during the reaction, can be isolated by silica gel chromatography and recycled for the one-step synthesis of the hydroperoxides.



An overview of the obtained results of the titanium-catalyzed asymmetric sulfoxidation of various sulfides with different optically pure hydroperoxides as oxidant and asymmetric inductor is given in Table 29.

C. Alcohol Oxidation

Common alcohol oxidation methods employ stoichiometric amounts of toxic and reactive oxidants like CrO₃, hypervalent iodine reagents (Dess–Martin) and peracids that pose severe safety and environmental hazards in large-scale industrial reactions. Therefore, a variety of catalytic methods for the oxidation of alcohols to aldehydes, ketones or carboxylic acids have been developed employing hydrogen peroxide or alkyl hydroperoxides as stoichiometric oxygen sources in the presence of catalytic amounts of a metal catalyst. The commonly used catalysts for alcohol oxidation are different Mo/W(VI), Mn(II), Cr(VI), Re(VII), Fe(II) and Ru complexes³⁹⁶. A selection of published known alcohol oxidations with different catalysts will be presented here.

The first example of metal-catalyzed oxidation of alcohols using hydrogen peroxide appeared in 1979, when Jacobson and coworkers found that the hydrogen oxodiperoxo(pyridine-2-carboxylato)tungsten complex and its molybdenum analogue are catalytically active for oxidation of secondary alcohols with 90% H₂O₂ in methanol³⁹⁷. From these two complexes the tungsten species is much more efficient than the molybdenum one and, for different secondary alcohols, conversions between 19 and 70% were obtained. Later, Trost and Masuyama reported on the use of 30% H₂O₂ and (NH₄)₆Mo₇O₂₄·4 H₂O in the presence of potassium carbonate for alcohol oxidation under nearly stoichiometric conditions and the reaction needed several days (1–7 d)³⁹⁸. With this method secondary alcohols could be selectively oxidized to ketones in yields ranging from 42 to 90%, while primary alcohols are not oxidized. Interestingly, sterically more hindered alcohols like 2,6-dimethylcyclohexanol are oxidized more readily than sterically less hindered ones like cyclohexanol. Potassium carbonate accelerates the reaction and has the function of favoring alcohol oxidation over olefin epoxidation, so that unsaturated alcohols can be selectively oxidized to the unsaturated ketones.

TABLE 29. Results of the titanium-catalyzed asymmetric sulfoxidation with optically pure hydroperoxides (yields are given and *ee* values are given in brackets)

Sulfide	Ti(OPr- <i>i</i>) ₄	Ti(OPr- <i>i</i>) ₄	Ti(OPr- <i>i</i>) ₄	Ti(OPr- <i>i</i>) ₄	Ti(OPr- <i>i</i>) ₄	Reference
	 (26a)	 (72)	 (66)	 (16a)	 (191b)	
						$R^1 = \text{OEt}$ $R^1 = \text{OEt}$ $R^1 = b$ $R^2 = \text{Me}$ $R^2 = i\text{-Pr}$ $R^2 = \text{Me}$ $R^3 = \text{Me}$ $R^3 = \text{H}$ $R^3 = \text{Me}$
						367
Ph-S-Me (22a)			66, 101	219	393	394
			66a: [25] (S) 66b: [24] (S)	79 [79] (S) [19:81]	79 [91] (R)	59 [>95] (R)
<i>p</i> -Tol-S-Me (22b)	75 [37] (S)			88 [71] (S) [20:80]	53 [90] (R)	60 [>95] (R) 74 [84] (R)
<i>p</i> -Tol-S-Et (22c)				89 [72] (S) [17:83]		

(continued overleaf)

TABLE 29. (continued)

$p\text{-Tol-S-Pr-}i$ (22d)	82 [65] (S) [21:79]	
$p\text{-Tol-S-Bu-}n$ (22e)	82 [62] (S) [23:77]	
$\text{Ph-S-C}_6\text{H}_4\text{OMe-}p$ (22f)		41 [5](S)
$\text{PhCH}_2\text{-S-Me}$ (22g)		93 [8] (S) [68:32]
$\text{PhCH}_2\text{-S-Bu-}t$ (22h)		75 [74] (R)
$\text{PhCH}_2\text{-S-Tol-}p$ (22i)		51 [70] (R) ^c
$p\text{-MeOC}_6\text{H}_4\text{-S-Me}$ (22j)	97 [31] (S) [56:44]	

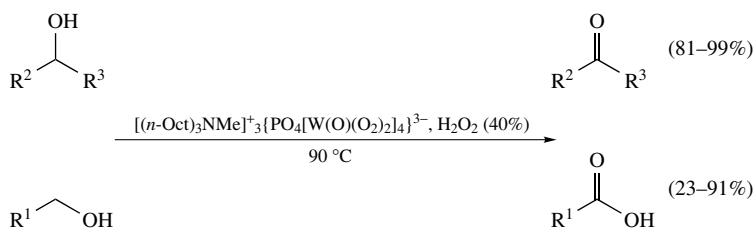
$p\text{-O}_2\text{NC}_6\text{H}_4\text{-S-Me}$ (22k)	93 [15] (S) [41:59]	58 [>95] (R)
2-naphthyl-S-Me (22l)	73 [24] (S) [32:68]	
$n\text{-Oct-S-Me}$ (22m)	92 [20] (S) [34:66]	77 [78] (R)
$p\text{-ClC}_6\text{H}_4\text{-S-Me}$ (22n)		51 [73] (R) ^c
$p\text{-BrC}_6\text{H}_4\text{-S-Me}$ (22o)		63 [92] (R)
$o\text{-BrC}_6\text{H}_4\text{-S-Me}$ (22p)		61 [92] (R)
		58 [94] (R)

^a Conversion of sulfides instead of sulfoxide yields are given; ratio in brackets show the chemoselectivity: **23** : **179**.

^b R = 5 α -cholestan-3 β -yl, chiral hydroperoxide was used as an inseparable 1:1 mixture of diastereomers.

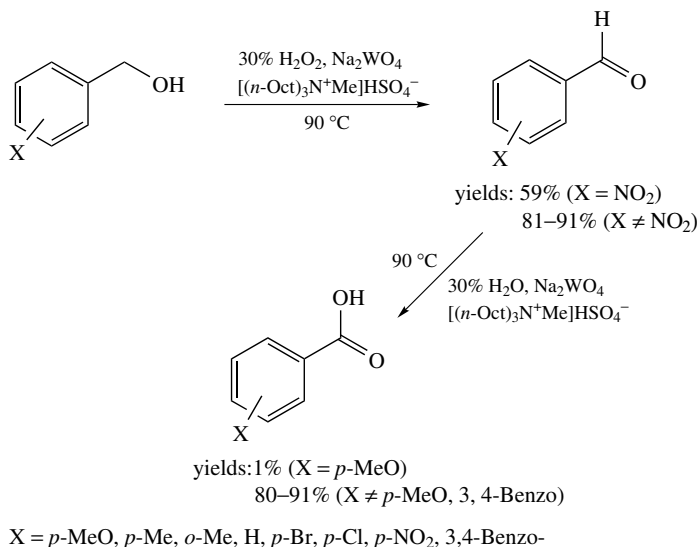
^c (L)-DIPT as chiral ligand.

Venturello and Gambaro investigated the employment of isolated $[(n\text{-Oct})_3\text{NMe}]^+{}_3\{\text{PO}_4[\text{W}(\text{O})(\text{O}_2)_2]_4\}^{3-}$ in combination with hydrogen peroxide in the alcohol oxidation without using a solvent and observed that this compound exhibits catalytic activity (Scheme 115)³⁹⁹. By this method several water-insoluble primary and secondary alcohols were oxidized to carboxylic acids and ketones in fair to good yields after short reaction times (10 min to 2 hours for secondary alcohols and 3–6 hours for primary alcohols). In substrates containing double bonds, epoxidation predominates the alcohol oxidation, but this trend can be reversed by using more dilute H_2O_2 (e.g. 16%) and less catalyst. Secondary alcohols containing no double bond were oxidized to the corresponding ketones in yields of 81 to 99%. For primary alcohols lower rates and selectivities were obtained. In most cases the main products are the carboxylic acids in yields of 23 to 90%. In contrast, benzyl- and 4-methylbenzyl alcohols were oxidized mainly to the aldehydes (77 and 84% yield) and carboxylic acids were only minor products (14 and 7%).



SCHEME 115. Alcohol oxidation with H_2O_2 under biphasic conditions catalyzed by $[(n\text{-Oct})_3\text{NMe}]^+{}_3\{\text{PO}_4[\text{W}(\text{O})(\text{O}_2)_2]_4\}^{3-}$

A tungstate-based heteropoly acid of the formula $[\pi\text{-C}_5\text{H}_5\text{N}^+(\text{CH}_2)_{15}\text{CH}_3]_3(\text{PW}_{12}\text{O}_{40})^{3-}$ (**163**) has been employed by Ishii and coworkers for the oxidation of secondary alcohols to ketones with aqueous 35% hydrogen peroxide as oxidant³⁰⁸. The products were obtained with excellent yields and selectivity (90 to >98% conversion, >98% selectivity). In the case of the primary alcohol 1-octanol the oxidation hardly took place under these conditions, providing octanal in poor yield (22% conv., 73% selectivity). An oxidation method for alcohols in general using aqueous hydrogen peroxide including primary or secondary alcohols and also benzylic alcohols catalyzed by Na_2WO_4 in the presence of a phase transfer catalyst $[(n\text{-Oct})_3\text{N}^+\text{Me}]\text{HSO}_4^-$ was reported by Noyori and coworkers (Scheme 116)^{400, 401}. The biphasic reaction can be carried out with or without organic solvent (toluene) at temperatures between 70 and 90 °C. Secondary alcohols are converted to ketones, whereas primary alcohols are oxidized to aldehydes or carboxylic acids, and benzylic alcohols are oxidized to benzaldehydes and benzoic acids depending on the reaction parameters. Many polar functional groups like ester, *t*-butyldimethylsilyl ether, epoxy, carbonyl, *N*-alkylcarboxamide and cyano are tolerated under the reaction conditions. This procedure is of low cost, safe and environmentally benign. Several benzyl alcohols, substituted with electron-withdrawing as well as electron-donating substituents, were oxidized by this method, giving the benzaldehydes in yields between 81 and 91%. One exception is *p*-nitrobenzyl alcohol, which was converted to the aldehyde with only 59% yield. A variety of benzyl alcohols can be converted directly to the corresponding benzoic acid derivatives using larger amounts of H_2O_2 (2.5–5 eq.) and 0.01 mol% of Na_2WO_4 and PTC. The yields obtained ranged from 80 to 91%. *p*-Methoxybenzyl alcohol could not be transferred directly into the carboxylic acid and only traces (1%) of acid were detected. In this second oxidation step side products (aryl formates) can be formed by a Baeyer–Villiger mechanism, which becomes significant with electron-donating substituents.

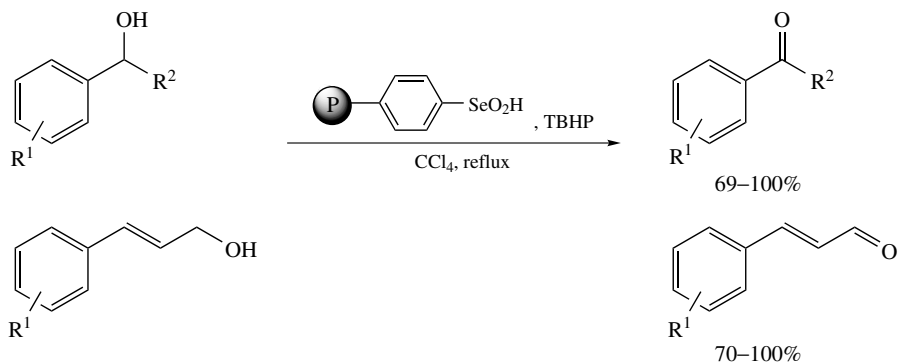


SCHEME 116. Oxidation of benzylic alcohols to benzaldehydes and benzoic acids with Na₂WO₄/PTC/H₂O₂

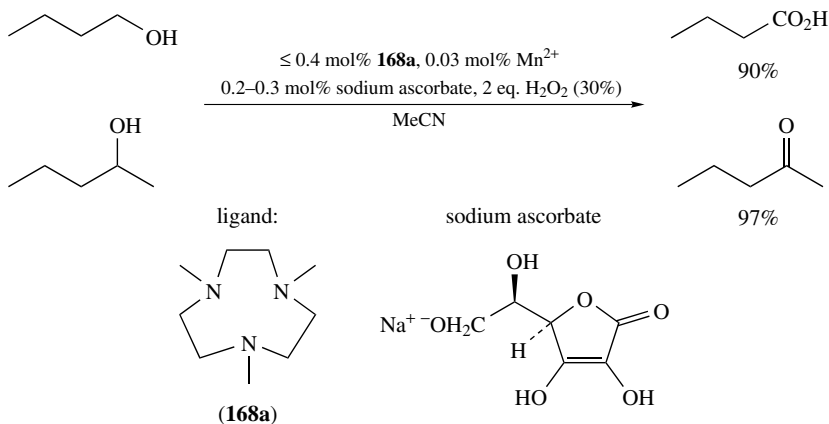
Taylor and Flood could show that polystyrene-bound phenylselenic acid in the presence of TBHP can catalyze the oxidation of benzylic alcohols to ketones or aldehydes in a biphasic system (polymer-TBHP/alcohol in CCl₄) in good yields (69–100%) (Scheme 117)⁴⁰². No overoxidation of aldehydes to carboxylic acids was observed and unactivated allylic alcohols or aliphatic alcohols were unreactive under these conditions. In 1999, Berkessel and Sklorz presented a manganese-catalyzed method for the oxidation of primary and secondary alcohols to the corresponding carboxylic acids and ketones (Scheme 118)³³¹. The authors employed the Mn–tmtacn complex (Mn/**168a**) in the presence of sodium ascorbate as very efficient cocatalyst and 30% H₂O₂ as oxidant to oxidize 1-butanol to butyric acid and 2-pentanol to 2-pentanone in yields of 90% and 97%, respectively. This catalytic system shows very good catalytic activity, as can be seen from the fact that for the oxidation of 2-pentanol as little as 0.03% of the catalyst is necessary to obtain the ketone in excellent yield.

During the years a variety of heterogeneous catalysts have turned out to be efficient and useful catalysts for a variety of oxidation reactions, including the oxidation of alcohols to ketones with H₂O₂. For a detailed review see Sheldon and Dakka (1994)⁴⁰³. The redox molecular sieve TS-1, a titanium(IV) silicalite catalyst, was one of the first heterogeneous catalysts developed for these purposes⁴⁰⁴. The chemoselectivity of TS-1-catalyzed oxidations is influenced by the solvent employed. For example, 2,3-butanediol can be oxidized to acetoin with high selectivity (91–96%) employing TS-1/35% H₂O₂ in water or methanol as solvent, but in acetone overoxidation to the diketone was observed⁴⁰³. Due to the pore dimensions of TS-1 (and also TS-2: 5.5 Å), the substrate spectrum is limited to small molecules.

Stoichiometric hexavalent chromium oxidants have been used for a variety of oxidation reactions⁴⁰⁵ but, due to environmental problems of chromium-containing waste, catalytic versions with soluble chromium catalysts have been developed, for example by Muzart⁴⁰⁶ using mainly TBHP as oxygen source. For instance, Muzart and coworkers



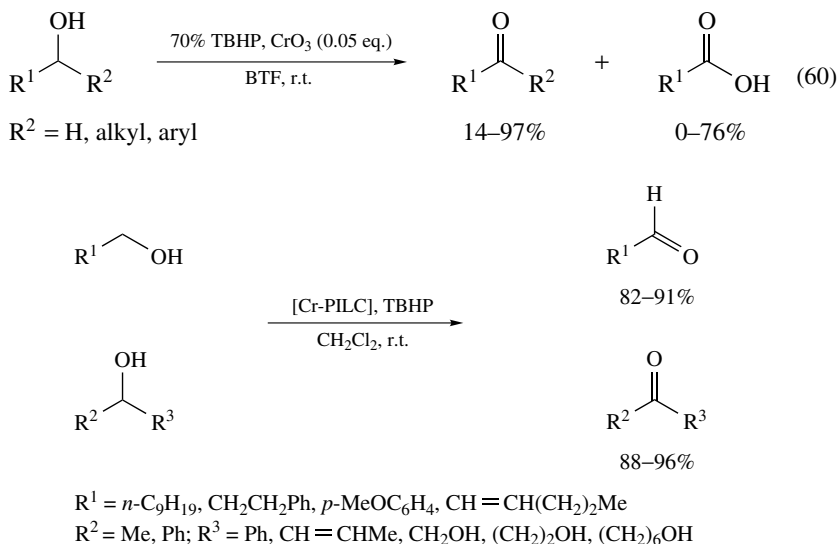
SCHEME 117. Alcohol oxidation under biphasic conditions using immobilized phenylseleninic acid/TBHP as catalyst



SCHEME 118. Mn/tmtacn/Na ascorbate catalyzed alcohol oxidation with H_2O_2

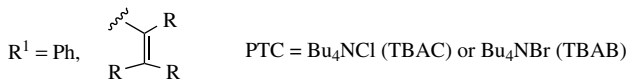
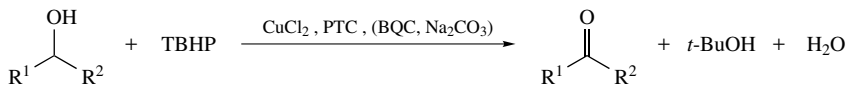
developed a CrO_3 -catalyzed method for the oxidation of alcohols to aldehydes or ketones using 70% TBHP in benzotrifluoride (BTF, an alternative to more toxic chlorinated solvents) (equation 60)⁴⁰⁷. The reactions were carried out with 0.05 equivalents of the catalyst and 4 equivalents of TBHP at room temperature in air, giving the corresponding aldehydes or ketones in yields ranging from 14 to 97%. For some alcohols the carboxylic acid was obtained besides the aldehydes or ketones. But even catalytic amounts of chromium present an environmental problem and therefore Sheldon investigated the use of chromium-substituted molecular sieves as recyclable solid catalyst for selective oxidations⁴⁰⁴. CrAPO-5 and CrAPO-11 turned out to be effective catalysts also for the oxidation of benzylic and other secondary alcohols to the corresponding ketones using TBHP or O_2 as the terminal oxidant^{408–410}. With these stable aluminophosphate molecular sieves the oxidation of secondary alcohols with TBHP can be carried out with moderate yields of the corresponding ketones (conversions: 54–79%) but ketone selectivity was very high (72–97%). For example, carveol could be selectively oxidized to carvone without any attack at its double bond. It is interesting to note that one of the two isomers of carveol (*cis/trans*) reacts faster than the other, which indicates that the catalyst exhibits shape

selectivity. 1-Phenyl-1,2-ethanediol was selectively oxidized at the secondary alcohol group to give α -hydroxyacetophenone (73% selectivity). Under an atmosphere of air yields based on TBHP greater than 100% were obtained, which can be explained by the fact that O_2 also acts as a terminal oxidant. The best results were obtained by a slow addition of 10% of TBHP. CrAPO-5 could be recycled by filtering, washing with chlorobenzene and recalcining at $500^\circ C$ for 5 hours. Recovered CrAPO-5 can be reused four times without any loss of activity. Next to the chromium–aluminophosphate sieves described above, also another type of heterogeneous chromium catalyst—the chromium(VI) pillared montmorillonites (Cr-PILC)—have been shown to catalyze the oxidation of primary and secondary alcohols to the corresponding aldehydes and ketones selectively using TBHP in CH_2Cl_2 as reported by Choudary and coworkers (Scheme 119)⁴¹¹. Allylic alcohols were selectively oxidized to the α,β -unsaturated aldehydes and ketones without oxidation of the double bond.



SCHEME 119. Selective oxidation of alcohols using a chromium-pillared montmorillonite catalyst and TBHP

In 1998 Sasson and coworkers⁴¹² and in 2003 Ferguson and Ajjou⁴¹³ presented a copper-catalyzed oxidation of benzylic and allylic alcohols using TBHP as oxidant (Scheme 120). Sasson and his coworkers employed $CuCl_2$ (or $CuCl$ or Cu powder) in the presence of tetrabutylammonium bromide (TBAB) as phase transfer catalyst in a biphasic (H_2O/CH_2Cl_2) system while Ajjou's biphasic method is solvent-free (substrate/ H_2O) and utilizes $CuCl_2$ in the presence of 2,2'-biquinoline-4,4'-dicarboxylic acid dipotassium salt (BQC), Na_2CO_3 and tetrabutylammonium chloride (TBAC) as phase transfer catalyst. The catalytically active species are formed *in situ* [$Cu(OH)Cl$ (Sasson)]. The yields that were obtained with Sasson's catalytic system ranged from 35 to 96% and with Ajjou's catalyst 100% conversion was obtained for a variety of benzylic, allylic and propargylic alcohols. For both systems it was found that alcohols bearing another group than phenyl or alkenyl at position R^1 showed only very little conversion [6–20% (Sasson), 20–39% (Ajjou)]. The chemoselectivity in almost all the cases was very high (100%). With H_2O_2 as oxidant



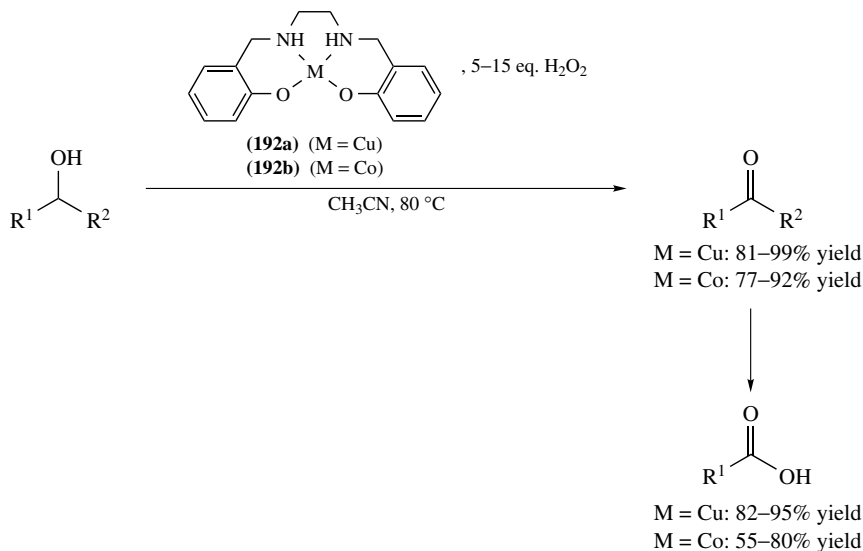
Sasson's method: CuCl_2 (1%), PTC (3%), aqueous TBHP, TBAB, CH_2Cl_2 , 25 °C, 24 h \Rightarrow 35–96% yield

Ajjou's method: CuCl_2 , BQC, Na_2CO_3 , TBAC, aqueous TBHP \Rightarrow 100% conversion

SCHEME 120. Cu-catalyzed effective oxidation of allylic or benzylic alcohols under biphasic conditions

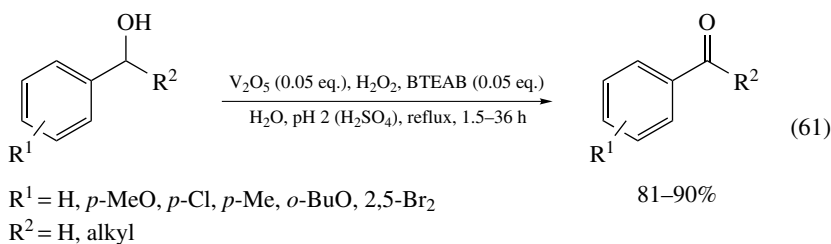
no products were formed. Sasson's group could show that the alcohol oxidation follows a heterolytic mechanism. In the solvent-free system the catalyst is stable and can be reused several times without loss of activity. The role of Na_2CO_3 is to keep the ligand BQC in basic form.

A copper(II)- and cobalt (II)-catalyzed oxidation of alcohols to the corresponding ketones and carboxylic acids with aqueous hydrogen peroxide in the presence of the metal catalysts **192a** ($M = \text{Cu}$) and **192b** ($M = \text{Co}$) depicted in Scheme 121 was reported by Punniyamurthy and coworkers^{414, 415}. A variety of differently substituted aromatic and aliphatic alcohols were oxidized with these catalysts. In most cases the carboxylic acids were obtained in good yields. For some substrates the oxidation stops at the stage of the ketone, which could also be isolated in good yields. Secondary alcohols showed greater reactivity towards oxidation than primary ones. In 2003, Li and coworkers reported on the first V_2O_5 -catalyzed oxidation of benzylic alcohols in the presence of dilute H_2O_2 producing aldehydes or ketones with yields between 81 and 90% (equation 61)⁴¹⁶. Addition



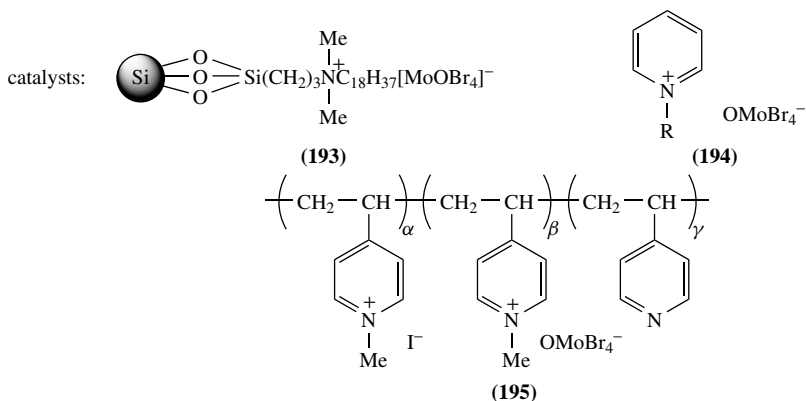
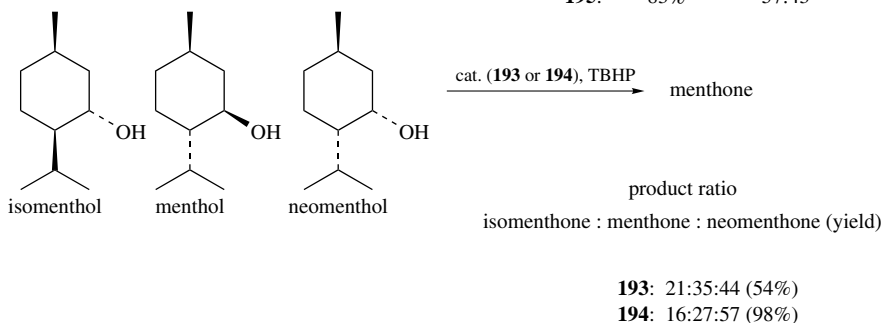
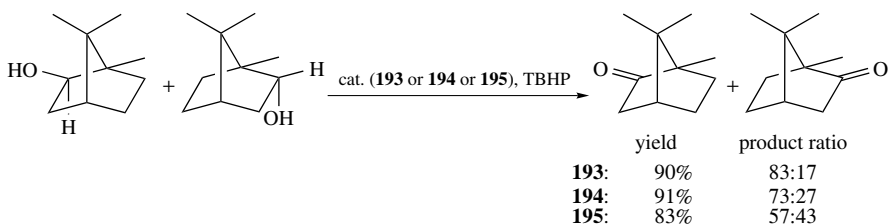
SCHEME 121. Copper- and cobalt-catalyzed alcohol oxidation using aqueous H_2O_2

of catalytic amounts of benzyltriethylammonium bromide (BTEAB) is essential for this reaction as well as a $\text{pH} < 5$, which is obtained upon acidification with acids like HBr, HCl, H_2SO_4 or H_3PO_3 . The authors found that the reaction rate increases with acidity and reactions were usually carried out at $\text{pH} 2$. Benzylic alcohols were oxidized much faster than aliphatic ones (1.5–10 h versus 30 h) and secondary alcohols faster than primary ones (1.5–2.5 h versus 6–10 h). Electron-withdrawing groups on the aromatic ring lead to a lower oxidation rate (34 h reaction time for *m*-nitrobenzyl alcohol). The authors propose a mechanism in which the reaction proceeds via a nucleophilic oxidation pathway (attack of intermediary formed benzyl cation on $\text{VO}(\text{O}_2)_2^-$).

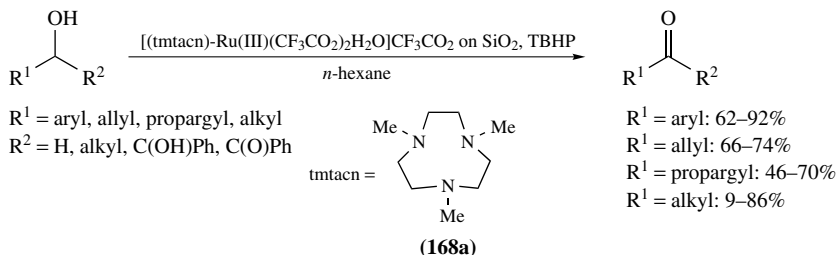


For an effective recyclability of the oxidation catalyst, immobilized metal catalysts have been developed over the years and tested in alcohol oxidation reactions. In 2000, Kurusu presented a silicagel or poly(*p*-vinylpyridinium) supported Mo-based oxidation catalyst for alcohol oxidation (Scheme 122)⁴¹⁷. Silica was chosen, because of its inertness to oxidation. With catalyst **193** it was possible to carry out the oxidation of alcohols with TBHP in benzene at 60 °C. Investigation of the oxidation of a 1:1 mixture of borneol and isoborneol leading to camphor (90% yield) showed that the *exo*-alcohol isoborneol is attacked more readily than the *endo*-alcohol borneol. The silica-supported catalyst **193** exhibited slightly higher selectivity (83/17) than pyridinium tetrabromooxomolybdate **194** (73/27) and significantly better selectivity than the poly(*p*-vinylpyridinium)- MoOBr_4^- catalyst **195** (57/43). The oxidation of a 1:1:1 mixture of isomenthol, menthol and neomenthol (providing menthone) showed a similar reactivity and selectivity of catalyst **193** and pyridinium tetraoxomolybdate. With these catalysts neomenthol is attacked most readily and isomenthol least readily. With **195** only low conversions were obtained (14%). Also, Che and coworkers investigated the immobilization of a Ru-complex of 1,4,7-trimethyl-1,4,7-triazacyclononane **168a** on silica beads, which could chemoselectively oxidize benzylic, allylic, propargylic and normal aliphatic alcohols to the corresponding aldehydes and ketones in *n*-hexane as solvent (Scheme 123)⁴¹⁸. Yields of this reaction ranged from 9 to 92%, while primary aliphatic alcohols could not be oxidized at all. The reaction is chemo- and stereoselective, as no overoxidation to the carboxylic acids nor epoxide formation (for unsaturated alcohols) is obtained in most of the cases and no isomerization of double bonds takes place. The silica-supported Ru catalyst can be recycled and reused without loss in activity.

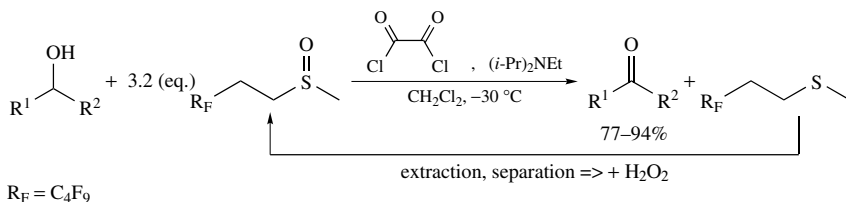
As a last example for alcohol oxidation utilizing hydrogen peroxide as oxygen source, a metal-free oxidation system will be presented in the following. In 2002, Crich and Neelamkavil presented an odor-free version of the Swern reaction, using a fluorinated sulfoxide as reagent (Scheme 124)⁴¹⁹. This sulfoxide, in conjunction with oxalyl chloride and Hünig's base, brings about the oxidation of diversely functionalized primary and secondary alcohols to aldehydes and ketones in excellent yields (77–94%). The fluorosulfoxide is efficiently recovered for reuse by a simple continuous fluoros extraction and subsequent oxidation with hydrogen peroxide.



SCHEME 122. Selective oxidation of borneols and menthols with immobilized Mo catalysts and TBHP



SCHEME 123. Heterogeneous Ru-catalyzed alcohol oxidation with the tmtacn ligand



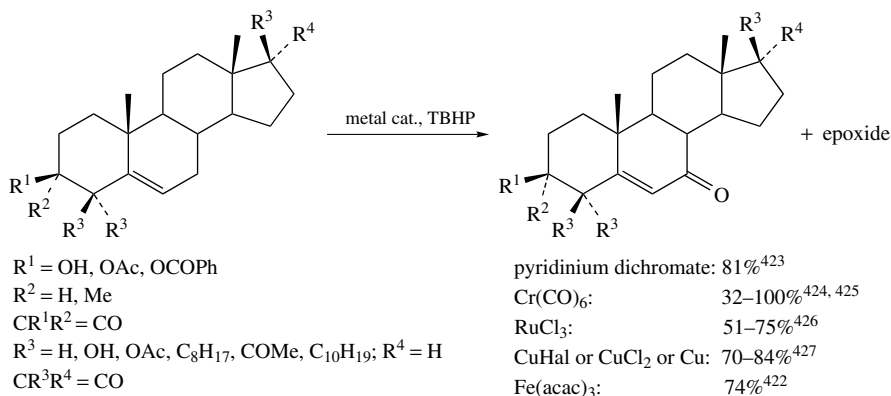
SCHEME 124. Odorless, fluoros Swern reaction

The summarized results for the oxidation of various alcohols by different methods are presented in Table 30.

D. Other C–H Oxidation Reactions

1. Allylic and benzylic oxidations

The allylic oxidation is a reaction of importance in organic chemistry with applications in areas ranging from agricultural products to pharmaceuticals⁴²⁰. A review on allylic oxidations until 1986 has been published by Muzart⁴²¹. The oxidation in allylic or benzylic position has free radical character and the intermediate radical formed is stabilized by the neighboring double bond. Traditionally, allylic oxidations were carried out using stoichiometric amounts of different chromium reagents. Of greater preparative interest has been the use of hydroperoxides combined with different types of catalyst. For example, a number of steroids could be oxidized in allylic position to produce the corresponding enones employing $Fe(acac)_3/ROOH$ ($R = Et, i\text{-}Pr, t\text{-}Bu, cumyl$)⁴²², pyridinium dichromate/TBHP⁴²³, $Cr(CO)_6/70\text{--}90\%$ TBHP^{424, 425}, $RuCl_3/TBHP$ ⁴²⁶, $CuX/TBHP$ ($X = Hal$) or $CuCl_2, Cu/TBHP$ (Scheme 125)⁴²⁷. With these catalysts also other alkenes have been shown to undergo allylic oxidation forming the corresponding enones.



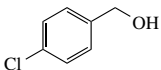
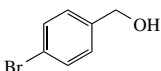
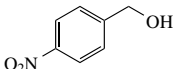
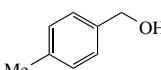
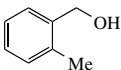
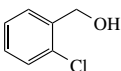
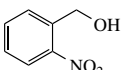
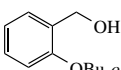
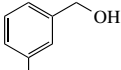
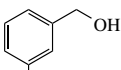
SCHEME 125. Metal-catalyzed allylic oxidation of steroids with TBHP

A catalytic method for the allylic oxidation of alkenes was first reported by Umbreit and Sharpless in 1977⁴²⁸, who utilized TBHP as oxidant and SeO_2 as catalyst for selective allylic oxidation. Yields were moderate providing allylic alcohols or ketones with 54–86% yield. The reaction did not proceed under strictly anhydrous conditions but with one equivalent of water present the oxidation proceeds smoothly at room temperature. In

TABLE 30. Comparison of the results of metal-catalyzed alcohol oxidation to ketones, carboxylic acids or aldehydes using H₂O₂ or TBHP

Substrate	Catalyst ^a	Oxidant	Solvent ^b	Time (h)	Yield (%) RCHO/ RC(O)R	Yield (%) RCO ₂ H	Reference	
	CuCl ₂ /TBAB	70% TBHP	CH ₂ Cl ₂	24	38	0	412	
	CrO ₃	70% H ₂ O ₂	CH ₂ Cl ₂	24	22	74	407	
			BTF	30	14	76	407	
	V ₂ O ₅ /BTEAB/ H ⁺	30% H ₂ O ₂	H ₂ O	6	84		416	
	A	TBHP	<i>n</i> -hexane	14	70		418	
	192a	30% H ₂ O ₂	CH ₃ CN	5		92	415	
	192b	30% H ₂ O ₂	CH ₃ CN	6		76	414	
	Na ₂ WO ₄ / D	30% H ₂ O ₂	—	3	87 ^c		401	
	Na ₂ WO ₄ / D	30% H ₂ O ₂	—	5		81 ^d	401	
	B	TBHP	CCl ₄	24	94		402	
	C	40% H ₂ O ₂	—	0.75	77	14	399	
	C	40% H ₂ O ₂ (3 eq.)	—	3		85	399	
		CuCl ₂ /TBAB	70% H ₂ O ₂	CH ₂ Cl ₂	24	75	0	412
CrO ₃		70% H ₂ O ₂	CH ₂ Cl ₂				407	
			BTF	48	84		407	
V ₂ O ₅ /BTEAB/ H ⁺		30% H ₂ O ₂	H ₂ O	2	81		416	
CrAPO-5		TBHP	C ₆ H ₅ Cl	16	74		408	
CrAPO-5		O ₂ /10% TBHP	C ₆ H ₅ Cl	5	30		408	
A		TBHP	<i>n</i> -hexane	16	93		418	
192a		30% H ₂ O ₂	CH ₃ CN	0.5	99		415	
192b		30% H ₂ O ₂	CH ₃ CN	3	92		414	
C		40% H ₂ O ₂	—	0.17	91		399	
Cr-PILC		TBHP	CH ₂ Cl ₂	10	96		411	
		CrO ₃	70% H ₂ O ₂	CH ₂ Cl ₂	3	83	0	407
				BTF	4.5	97	0	407
	CrAPO-5	TBHP	C ₆ H ₅ Cl	7	77		408	
	CrAPO-5	O ₂ /10% TBHP	C ₆ H ₅ Cl	19	34		408	
	A	TBHP	<i>n</i> -hexane	16	92		418	
	V ₂ O ₅ /BTEAB/ H ⁺	30% H ₂ O ₂	H ₂ O	1.5	81		416	
	C	40% H ₂ O ₂ (5 eq.)	ClCH ₂ CH ₂ Cl	4		<2	399	
	Na ₂ WO ₄ / D	30% H ₂ O ₂	toluene	5	90 ^c		401	
	Na ₂ WO ₄ / D	30% H ₂ O ₂	toluene	12		1 ^d	401	
	V ₂ O ₅ /BTEAB/ H ⁺	30% H ₂ O ₂	H ₂ O	8	83		416	
	192a	30% H ₂ O ₂	CH ₃ CN	3		93	415	
	192b	30% H ₂ O ₂	CH ₃ CN	5		78	414	
	Cr-PILC	TBHP	CH ₂ Cl ₂	15	91		411	

TABLE 30. (continued)

Substrate	Catalyst ^a	Oxidant	Solvent ^b	Time (h)	Yield (%)	Yield (%)	Reference
					RCHO/RC(O)R	RCO ₂ H	
	V ₂ O ₅ /BTEAB/ H ⁺	30% H ₂ O ₂	H ₂ O	7	84		416
	A	TBHP	<i>n</i> -hexane	16	71		418
	192a	30% H ₂ O ₂	CH ₃ CN	4.5		95	415
	192b	30% H ₂ O ₂	CH ₃ CN	7		74	414
	C	40% H ₂ O ₂ (3 eq.)	Cl ₂ HCCCHCl ₂	3		85	399
	Na ₂ WO ₄ / D	30% H ₂ O ₂	—	4.5	82 ^c		401
	Na ₂ WO ₄ / D	30% H ₂ O ₂	—	4		87 ^d	401
	192a	30% H ₂ O ₂	CH ₃ CN	4		94	415
	192b	30% H ₂ O ₂	CH ₃ CN	7		75	414
	Na ₂ WO ₄ / D	30% H ₂ O ₂	—	4.5	81 ^c		401
	Na ₂ WO ₄ / D	30% H ₂ O ₂	—	4		86 ^d	401
	192a	30% H ₂ O ₂	CH ₃ CN	8		82	415
	192b	30% H ₂ O ₂	CH ₃ CN	9		74	414
	Na ₂ WO ₄ / D	30% H ₂ O ₂	toluene/EtOAc	17	59 ^c		401
	Na ₂ WO ₄ / D	30% H ₂ O ₂	—	4		91	401
	B	TBHP	CCl ₄	5	100	—	402
	C	40% H ₂ O ₂ (3 eq.)	Cl ₂ HCCCHCl ₂	3		90	399
	V ₂ O ₅ /BTEAB/ H ⁺	30% H ₂ O ₂	H ₂ O	10	83		416
	Na ₂ WO ₄ / D	30% H ₂ O ₂	—	4.5	91 ^c		401
	Na ₂ WO ₄ / D	30% H ₂ O ₂	—	12		80 ^d	401
	C	30% H ₂ O ₂	—	0.5	84	7	399
	C	40% H ₂ O ₂ (3 eq.)	Cl ₂ HCCCHCl ₂	4	13	59	399
	Na ₂ WO ₄ / D	30% H ₂ O ₂	—	4.5	91 ^c		401
	V ₂ O ₅ /BTEAB/ H ⁺	30% H ₂ O ₂	H ₂ O	7.5	82		416
	A	TBHP	<i>n</i> -hexane	16	62		418
	C	40% H ₂ O ₂ (5 eq.)	—	5	19	60	399
	192a	30% H ₂ O ₂	CH ₃ CN	8		83	415
	192b	30% H ₂ O ₂	CH ₃ CN	9		72	414
	C	40% H ₂ O ₂ (3 eq.)	—	9		91	399
	V ₂ O ₅ /BTEAB/ H ⁺	30% H ₂ O ₂	H ₂ O	7	90		416
	C	40% H ₂ O ₂ (5 eq.)	—	4	7	55	399
	192a	30% H ₂ O ₂	CH ₃ CN	7		89	415
	192b	30% H ₂ O ₂	CH ₃ CN	7		76	414

(continued overleaf)

TABLE 30. (continued)

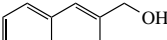
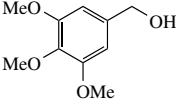
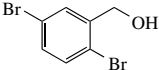
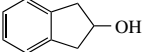
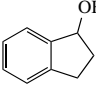
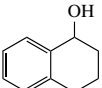
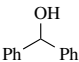
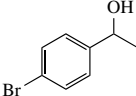
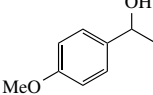
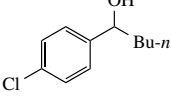
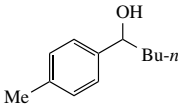
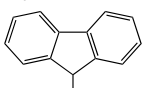
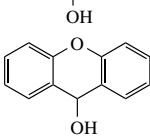
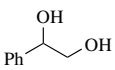
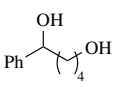
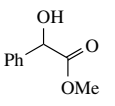
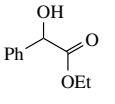
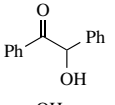
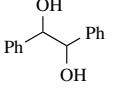
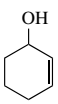
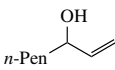
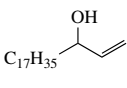
Substrate	Catalyst ^a	Oxidant	Solvent ^b	Time (h)	Yield (%) RCHO/ RC(O)R	Yield (%) RCO ₂ H	Reference
	Na ₂ WO ₄ / D	5% H ₂ O ₂	—	4.5	82 ^c		401
	192a	30% H ₂ O ₂	CH ₃ CN	2		93	415
	192b	30% H ₂ O ₂	CH ₃ CN	4		80	414
	V ₂ O ₅ /BTEAB/ H ⁺	30% H ₂ O ₂	H ₂ O	8.5	87		416
	E	TBHP	H ₂ O	24	27 ^e		413
	CuCl ₂ /TBAB	70% TBHP	CH ₂ Cl ₂	24	65		412
	CrO ₃	70% H ₂ O ₂	CH ₂ Cl ₂	3	77	0	407
	CrO ₃	70% H ₂ O ₂	BTF	4	81	0	407
	CrAPO-5	O ₂ /10% TBHP	C ₆ H ₅ Cl	19	56		408
	E	TBHP	H ₂ O	24	100 ^e		413
	CrAPO-5	O ₂ /10% TBHP	C ₆ H ₅ Cl	19	19		408
	CuCl ₂ /TBAB	70% TBHP	CH ₂ Cl ₂	24	71	0	412
	E	TBHP	H ₂ O	24	100 ^e		413
	F	30% H ₂ O ₂	THF	64	82		398
	V ₂ O ₅ /BTEAB/ H ⁺	30% H ₂ O ₂	H ₂ O	2.5	88		416
	192a	30% H ₂ O ₂	CH ₃ CN	0.5	89		415
	192b	30% H ₂ O ₂	CH ₃ CN	3	98		414
	B	TBHP	CCl ₄	24	100		402
	C	40% H ₂ O ₂	—	1	99		399
	E	TBHP	H ₂ O	24	100 ^e		413
	E	TBHP	H ₂ O	24	100 ^e		413
	E	TBHP	H ₂ O	24	100 ^d		413
	E	TBHP	H ₂ O	24	100 ^d		413
	V ₂ O ₅ /BTEAB/ H ⁺	30% H ₂ O ₂	H ₂ O	2.5	85		416

TABLE 30. (continued)

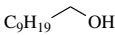
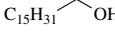
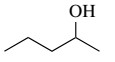
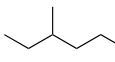
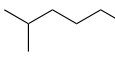
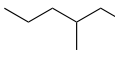
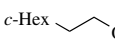
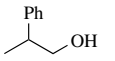
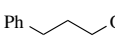
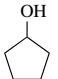
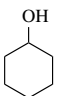
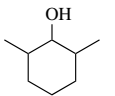
Substrate	Catalyst ^a	Oxidant	Solvent ^b	Time (h)	Yield (%) RCHO/ RC(O)R	Yield (%) RCO ₂ H	Ref- erence
	V ₂ O ₅ /BTEAB/ H ⁺	30% H ₂ O ₂	H ₂ O	2.2	87		416
	CrO ₃	70% H ₂ O ₂	CH ₂ Cl ₂	7	87	0	407
	CrO ₃	70% H ₂ O ₂	BTF	24	94	0	407
	E	TBHP	H ₂ O	24	100 ^e		413
	B	TBHP	CCl ₄	48		100	402
	CrO ₃	70% H ₂ O ₂	CH ₂ Cl ₂	24	29 ^f	0	407
	CrO ₃	70% H ₂ O ₂	BTF	65	35 ^f	0	407
	Cr-PILC	TBHP	CH ₂ Cl ₂	18	92 ^f		411
	B	TBHP	CCl ₄	48		69	402
	CrO ₃	70% H ₂ O ₂	CH ₂ Cl ₂	5	37	0	407
	CrO ₃	70% H ₂ O ₂	BTF	7.5	26	0	407
	CuCl ₂ /TBAB	70% TBHP	CH ₂ Cl ₂	24	96	0	412
	CrO ₃	70% H ₂ O ₂	CH ₂ Cl ₂	8	23	0	407
	CrO ₃	70% H ₂ O ₂	BTF	29	34	23	407
	A	TBHP	<i>n</i> -hexane	72	66		418
	B	TBHP	CCl ₄	24		98	402
	A	TBHP	<i>n</i> -hexane	16	85 ^g		418
	A	TBHP	<i>n</i> -hexane	12	57		418
	C	40% H ₂ O ₂	ClCH ₂ CH ₂ Cl	24	18 ^h		399
	E	TBHP	H ₂ O	2	87(100 ^e)		413
	CrO ₃	70% H ₂ O ₂	CH ₂ Cl ₂	5	48	5	407
	CrO ₃	70% H ₂ O ₂	BTF	23	85	0	407

(continued overleaf)

TABLE 30. (continued)

Substrate	Catalyst ^a	Oxidant	Solvent ^b	Time (h)	Yield (%) RCHO/ RC(O)R	Yield (%) RCO ₂ H	Reference
	CuCl ₂ /TBAB	70% TBHP	CH ₂ Cl ₂	24	35	0	412
	CuCl ₂ /TBAB	70% TBHP	CH ₂ Cl ₂	24	80	0	412
	163	35% H ₂ O ₂	<i>t</i> -BuOH	24	>98		308
	C	40% H ₂ O ₂	Cl ₂ HCCHCl ₂ 0.75		95		399
	F	30% H ₂ O ₂	THF	24	87		398
	F	30% H ₂ O ₂	THF	6d	59 ^f		398
	F	30% H ₂ O ₂	THF	7d	73 ⁱ		398
	CrO ₃	70% H ₂ O ₂	CH ₂ Cl ₂	8.5	71	0	407
	CrO ₃	70% H ₂ O ₂	BTF	24	91	0	407
	E	TBHP	H ₂ O	24	92(100 ^e)		413
	Cr-PILC	TBHP	CH ₂ Cl ₂	12	84		411
	CuCl ₂ /TBAB	70% TBHP	CH ₂ Cl ₂	24	31		412
	A	TBHP	<i>n</i> -hexane	16	66	84	418
	192b	30% H ₂ O ₂	CH ₃ CN	4		414	414
	B	TBHP	CCl ₄	63		100	402
	A	TBHP	<i>n</i> -hexane	16	74		418
	Mn- 168a / ascorbate	30% H ₂ O ₂ (2 eq.)	MeCN			90	331
	C	40% H ₂ O ₂ (3 eq.)	—	6		83	399
	C	40% H ₂ O ₂ (3 eq.)	—	6		83	399
	C	40% H ₂ O ₂ (4 eq.)	—	6	<1	70	399
	CuCl ₂ /TBAB	70% TBHP	CH ₂ Cl ₂	24	6	0	412
	163	35% H ₂ O ₂	<i>t</i> -BuOH	24	30		308
	C	40% H ₂ O ₂ (3 eq.)	—	6		85	399

TABLE 30. (continued)

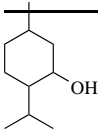
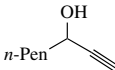
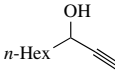
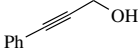
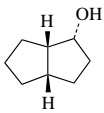
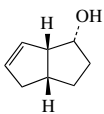
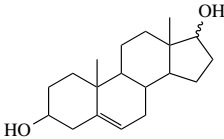
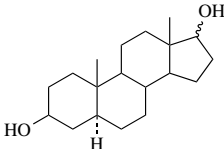
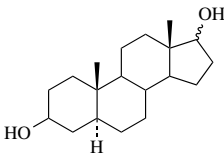
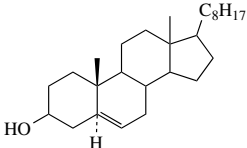
Substrate	Catalyst ^a	Oxidant	Solvent ^b	Time (h)	Yield (%)		Reference
					RCHO/RC(O)R	RCO ₂ H	
	192a	30% H ₂ O ₂	CH ₃ CN	8		93	415
	192b	30% H ₂ O ₂	CH ₃ CN	10		55	414
	C	40% H ₂ O ₂ (3 eq.)	—	6		83	399
	Cr-PILC	TBHP	CH ₂ Cl ₂	24	82		411
	192a	30% H ₂ O ₂	CH ₃ CN	9		90	415
	192b	30% H ₂ O ₂	CH ₃ CN	11		59	414
	Mn-168a/ascorbate	30% H ₂ O ₂ (2 eq.)	MeCN			97	331
	Cr-PILC	TBHP	CH ₂ Cl ₂	10	82		411
	C	40% H ₂ O ₂ (3 eq.)	—	6		40 ^j	399
	C	40% H ₂ O ₂ (3 eq.)	—	6		80	399
	C	40% H ₂ O ₂ (3 eq.)	—	6		80	399
	C	40% H ₂ O ₂ (3 eq.)	—	6		70	399
<i>c</i> -Hex 	C	40% H ₂ O ₂ (3 eq.)	—	6		83	399
	C	40% H ₂ O ₂ (3 eq.)	—	6		23 ^k	399
	C	40% H ₂ O ₂ (3 eq.)	—	6		76	399
	C	40% H ₂ O ₂	—	1.25	81		399
	CrAPO-5	TBHP	C ₆ H ₅ Cl	12	61		408
	CrAPO-5	O ₂ /10% TBHP	C ₆ H ₅ Cl	5	29		408
	V ₂ O ₅ /BTEAB/ H ⁺	30% H ₂ O ₂	H ₂ O	30	84		416
	A	TBHP	<i>n</i> -hexane	16	35		418
	192a	30% H ₂ O ₂	CH ₃ CN	4	99		415
	192b	30% H ₂ O ₂	CH ₃ CN	4	82		414
	163	35% H ₂ O ₂	<i>t</i> -BuOH	24	>98		308
C	40% H ₂ O ₂	—	0.75	86		399	
	C	40% H ₂ O ₂	—	0.5	97		399
	F	30% H ₂ O ₂	THF	4d	76		398

(continued overleaf)

TABLE 30. (continued)

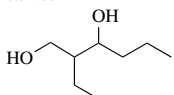
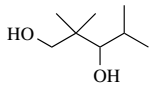
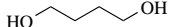

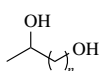
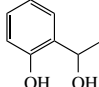
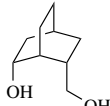
Substrate	Catalyst ^a	Oxidant	Solvent ^b	Time (h)	Yield (%) RCHO/ RC(O)R	Yield (%) Ref- RCO ₂ Herence
	192b	30% H ₂ O ₂	CH ₃ CN	4	77	414
	F	30% H ₂ O ₂	THF	4d	85	398
	E	TBHP	H ₂ O	24	39 ^c (<i>trans/cis</i> : 89/11)	413
<i>(trans/cis</i> : 83/17)						
	A	TBHP	<i>n</i> -hexane	12	95	418
	A	TBHP	<i>n</i> -hexane	16	89	418
	A	TBHP	<i>n</i> -hexane	12	9	418
	192a	30% H ₂ O ₂	CH ₃ CN	4	81	415
	CuCl ₂ /TBAB	70% TBHP	CH ₂ Cl ₂	24	20	0 412
163		35% H ₂ O ₂	<i>t</i> -BuOH	24	90	308
C		40% H ₂ O ₂	—	1.5	96	399
	CrO ₃	70% H ₂ O ₂	BTF	65	65	407
	A	TBHP	<i>n</i> -hexane	16	42	418
	F	30% H ₂ O ₂	THF	4d	88	398
	CuCl ₂ /TBAB	70% TBHP	CH ₂ Cl ₂	24	4	412
C		40% H ₂ O ₂ (3 eq.)	—	6	—	51 ^f 399
	Cr-PILC	TBHP	CH ₂ Cl ₂	24	86	411
	E	TBHP	H ₂ O	24	20 ^c	413
5 α -Cholestanol	CrO ₃	70% H ₂ O ₂	CH ₂ Cl ₂	5	47	407
	CrO ₃	70% H ₂ O ₂	BTF	24	95	407
Chromanol	E	TBHP	H ₂ O	24	100 ^c	413
	CuCl ₂ /TBAB	70% TBHP	CH ₂ Cl ₂	24	60	0 412

TABLE 30. (continued)

Substrate	Catalyst ^a	Oxidant	Solvent ^b	Time (h)	Yield (%) RCHO/ RC(O)R	Yield (%) RCO ₂ H	Ref- erence
	V ₂ O ₅ /BTEAB/ H ⁺	30% H ₂ O ₂	H ₂ O	36	88		416
	163	35% H ₂ O ₂	<i>t</i> -BuOH	24	>92		308
	C	40% H ₂ O ₂	—	2	88 ^m		399
	F	30% H ₂ O ₂	THF	5d	70		398
	E	TBHP	H ₂ O	24	83(100 ^e)		413
	A	TBHP	<i>n</i> -hexane	16	70		418
	A	TBHP	<i>n</i> -hexane	16	46		418
	F	30% H ₂ O ₂	THF	4d	73		398
	F	30% H ₂ O ₂	THF	5d	42		398
	F	30% H ₂ O ₂	THF	6d	90 ⁿ		398
	F	30% H ₂ O ₂	THF	2d	65 ⁿ		398
	F	30% H ₂ O ₂	THF	4d	80 ^o		398
	F	30% H ₂ O ₂	THF	6d	90 ⁿ		398

(continued overleaf)

TABLE 30. (continued)

Substrate	Catalyst ^a	Oxidant	Solvent ^b	Time (h)	Yield (%) RCHO/ RC(O)R	Yield (%) RCO ₂ H	Reference
carveol	CrAPO-5	TBHP	C ₆ H ₅ Cl	16	58		408
	163	35% H ₂ O ₂	<i>t</i> -BuOH	7	>98		308
	C	40% H ₂ O ₂	—	1	71 ^p		399
	163	35% H ₂ O ₂	<i>t</i> -BuOH	7	>98		308
	163	35% H ₂ O ₂	<i>t</i> -BuOH	24	>98		308
	163	35% H ₂ O ₂	<i>t</i> -BuOH	24	>98		308
	$n = 9$ F	30% H ₂ O ₂	THF	5d	79 ^f		398
	$n = 1$ Cr-PILC	TBHP	CH ₂ Cl ₂	24	89 ^f		411
	$n = 6$ Cr-PILC	TBHP	CH ₂ Cl ₂	24	94 ^f		411
	F	30% H ₂ O ₂	THF	5d	52 ^q		398
	F	30% H ₂ O ₂	THF	2d	88		398

^a TBAB = tetrabutylammonium bromide; BTEAB = benzyltriethylammonium bromide; **A** = [(168a)Ru(CF₃CO₂)₂(H₂O)]CF₃CO₂ on SiO₂; **B** = polystyrene bound phenylseleninic acid, BQC (2,2'-biquinoline-4,4'-dicarboxylic acid dipotassium salt, 1%), Na₂CO₃ (7%), TBAC (tetrabutylammonium chloride, 3%); **C** = [(*t*-Oct)₃NMe]⁺₃[PO₄[W(O)(O₂)₂]₄]³⁻, **D** = methyltriethylammonium hydrogen sulfate, **E** = CuCl₂ (1%), **F** = (NH₄)₆Mo₇O₂₄/K₂CO₃, Cr-PILC = chromium pillared montmorillonite.

^b BTF = benzotrifluoride.

^c 1.1–2 eq. H₂O₂.

^d 2.5–5 eq. H₂O₂.

^e Conversion given.

^f Oxidation of the secondary alcohol.

^g Monoketone.

^h +64% 1,2-epoxy-3-octanol +6% 1,2-epoxy-3-octanone.

ⁱ *endo:exo* ratio 3:1 (by NMR).

^j +20% 2-methyl-2-propanol.

^k +38% acetophenone.

^l +17% benzoic acid.

^m (–)-Menthone from (–)-menthol.

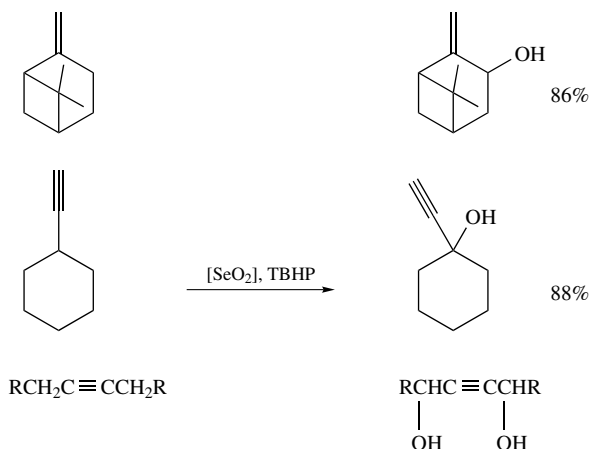
ⁿ Oxidation of the five-membered-ring alcoholic function.

^o Diketone formed; epiandrosterone was obtained in 17% yield.

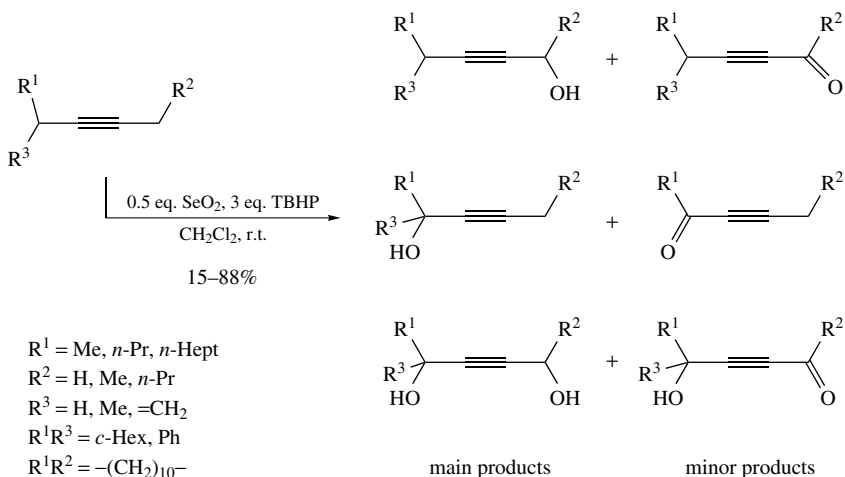
^p Secondary alcohol is oxidized to the ketone.

^q Product: 2-hydroxyphenyl methyl ketone.

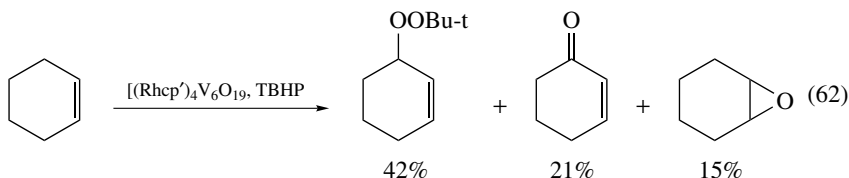
general, alkynes are more reactive towards allylic oxidation and internal alkynes show a preferred α,α' -dihydroxylation (Scheme 126). The great synthetic utility of this method has been demonstrated, for example, by using it as one reaction step in the synthesis of mokupalide (by Sum and Weiler)⁴²⁹ or several 3-acylindoles (by Campos and Cook)⁴³⁰.

SCHEME 126. Allylic oxidation of alkenes and alkynes with SeO_2/TBHP

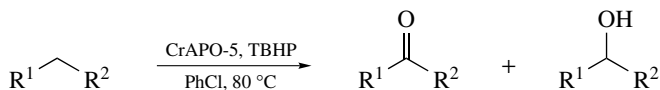
The same catalytic system (SeO_2/TBHP) has also been used by Chabaud and Sharpless in the allylic oxidation of alkynes⁴³¹. The oxidation products resulting from the SeO_2 -catalyzed allylic oxidation with TBHP are the allylic alcohol, the allylic diol, the allylic ketone, the ketol and the enynone (Scheme 127). The main product of the reaction is either the alcohol or the diol, depending on the substrate employed (together 76–100% of the whole yield). The yields of allylic oxidation products together range from 15 to 88%. From the observed results with unsymmetrical alkynes it could be concluded that the reactivity sequence for the carbon attached to the triple bond of alkynes is $\text{CH}_2 \sim \text{CH} > \text{CH}_3$.

SCHEME 127. SeO_2 -catalyzed allylic oxidation of alkynes using TBHP as terminal oxidant

In 1989, Isobe and coworkers reported on an organometallic polyoxometalate cluster $[(\text{Rhcp}')_4\text{V}_6\text{O}_{19}]$ ($\text{cp}' = \eta^2\text{-C}_5\text{Me}_5$) that catalyzes the oxidation of cyclohexene with TBHP as oxidant to give mainly allylic oxidation products (1-*tert*-butylperoxycyclohex-2-ene: 42% and cyclohex-2-en-1-one: 21%) and only little epoxide (15%) (equation 62)⁴³². The yield of 1-*tert*-butylperoxy cyclohex-2-ene increased with decreasing molar ratio of cyclohexene to TBHP, while the yield of cyclohex-2-en-1-one has a maximum at the ratio of 0.2.



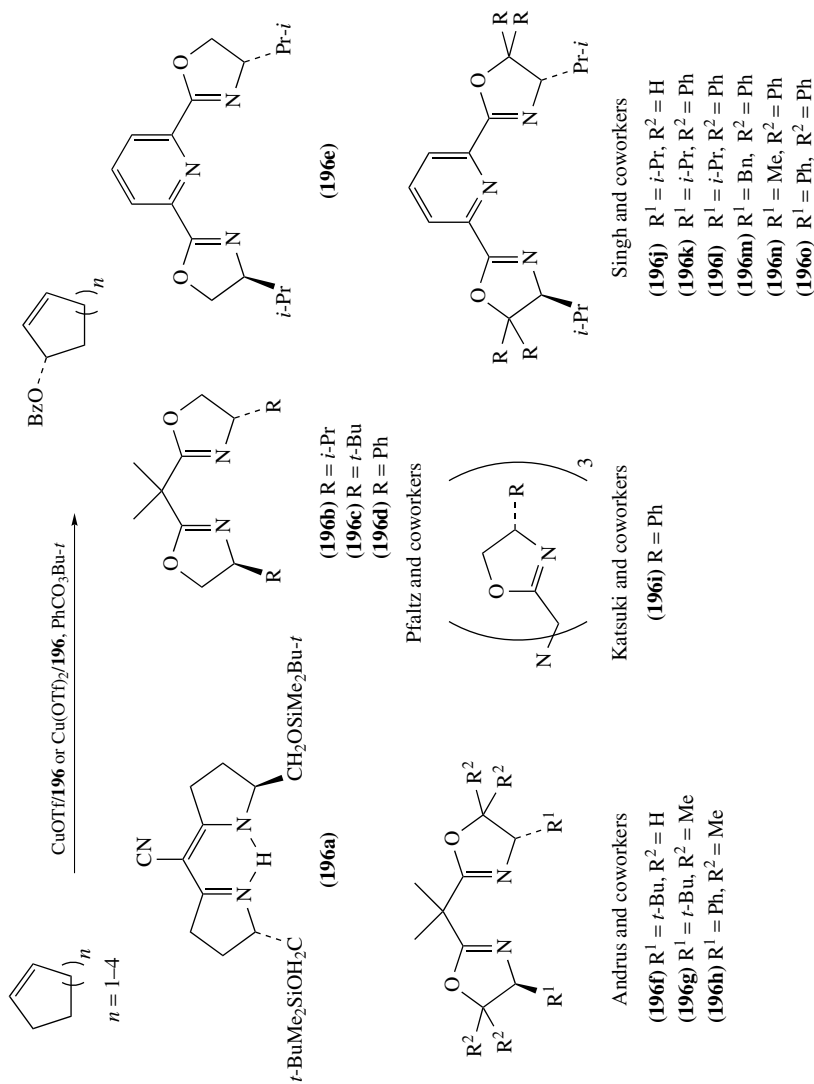
Sheldon and coworkers have developed chromium-substituted molecular sieves (CrAPO-5) as recyclable solid catalysts for several selective oxidations, among them also the allylic⁴³³ and benzylic^{404, 409, 410} oxidations using TBHP or O₂ as the terminal oxidants (equation 63), which yielded the corresponding benzylic ketones in moderate yield (conv.: 13–70%) and moderate to good selectivity (41%, 65–97%). The benzylic alcohols were formed as side products. Allylic oxidation also proceeded with good conversions, while selectivities were lower and both possible products, the allylic ketone (31–77% selectivity) and the allylic alcohol (0–47% selectivity), were formed. Chromium silicalite showed activity for selective benzylic oxidation in the presence of TBHP as well as giving mainly the allylic ketone (2-cyclohexen-1-one with 74% selectivity) and the allylic alcohol as minor product (2-cyclohexen-1-ol with 26% selectivity)^{404, 434}.



substrates for benzylic oxidation: \longrightarrow $\text{R}^1 = \text{Ar}$:
 $\text{R}^1 = \text{Ph, } p\text{-Tol, } p\text{-MeOC}_6\text{H}_4, 3\text{-pyridyl}$ conv. : 13–70%, select.: 41–97% (63)
 $\text{R}^2 = \text{Me, Et, } n\text{-Pr, } n\text{-Bu, Ph}$

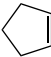
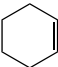
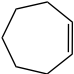

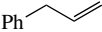
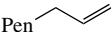
substrates for allylic oxidation: \longrightarrow $\text{R}^1 = \text{C}=\text{CR}^3\text{R}^4$:
 menthene, limonene, terpinolene, conv. : 85–96%, select.: 31–77% (ketone)
 α -pinene, β -pinene, 3-carene select.: 0–47% (alcohol)

Between 1995 and 1998 the groups of Pfaltz⁴³⁵, Andrus⁴³⁶, Katsuki⁴³⁷ and Singh⁴³⁸ reported on their results in the field of catalytic enantioselective allylic oxidations of olefins, mainly cycloalkenes, employing copper complexes with different chiral ligands of the bis- or trisoxazoline type **196** (Scheme 128, Table 31). In this reaction alkenes were transformed into optically active allylic benzoates using *tert*-butyl perbenzoate as the oxidant. The obtained results are summarized in Table 31. Besides the chiral bis- and trisoxazoline ligands, also ligands bearing only one oxazoline moiety **199a** and **199b** (Zondervan and Feringa 1996)⁴³⁹ and other chiral ligands like the bipyridine-type ligand **197** introduced by Kočovský and coworkers⁴⁴⁰, the bicyclic amino acids **198a** and **198b** used by Södergren and Andersson⁴⁴¹ and the proline **200** employed by Muzart and



SCHEME 128. Catalytic enantioselective Kharasch–Sosnovsky reaction catalyzed by different Cu-oxazoline chiral complexes

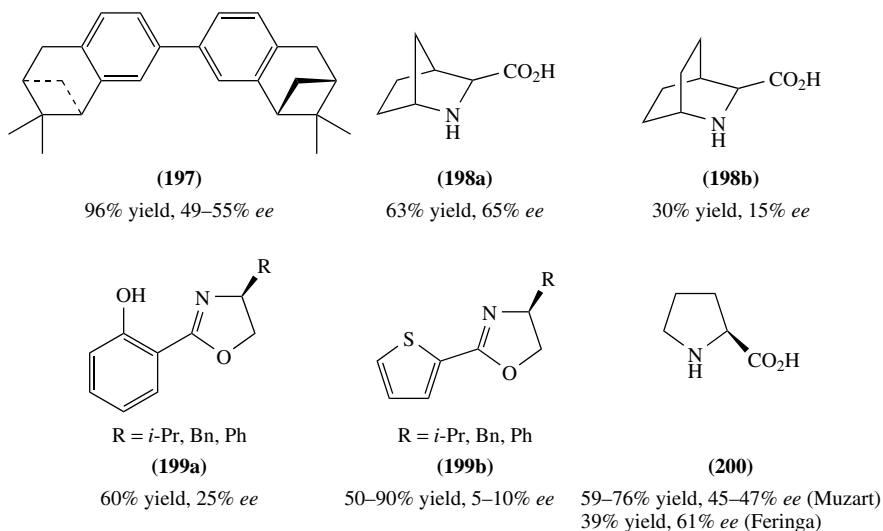
TABLE 31. Results of the Cu/oxazoline-catalyzed Kharasch–Sosnovsky reaction of various alkenes (yields are given and *ee* values are given in parentheses)

Alkene	CuOTf+	CuOTf complex of	Cu(OTf) ₂ +	Cu(OTf) ₂ + PhNHNH ₂
	196b , 196c or 196d	196f , 196g or 196h	196i	(or CuOTf) + molecular sieves + one of the ligands 196j–o
Reference	435	436	437	438
	66 (82) [cat. 196b] 61 (84) [cat. 196c] 84 (71) [cat. 196d]	44 (70) [cat. 196f] 41 (42) [cat. 196g] 49 (81) [cat. 196h]	2–68 (18–88) [cat. 196i]	59 (56) [cat. 196j] 70 (59) [cat. 196k] 80 (60) [cat. 196l]
	69 (64) [cat. 196b] 64 (77) [cat. 196c] 77 (67) [cat. 196d]	43 (80) [cat. 196f] 49 (67) [cat. 196g] 59 (46) [cat. 196h]	3–26 (28–72) [cat. 196i]	63 (45) [cat. 196j] 58 (81) [cat. 196k] 73 (75) [cat. 196l] 79 (62) [cat. 196m] 69 (23) [cat. 196n] 57 (11) [cat. 196o]
	44 (82) [cat. 196b]		5–34 (14–60) [cat. 196i]	39 (25) [cat. 196k] ^a 42 (82) [cat. 196l]
		44 (13) [cat. 196f] 43 (0) [cat. 196g]	11–18 (54–64) [cat. 196i]	28 (81) [cat. 196l]
Ph 		34 (36) [cat. 196f]		
Pen 		50 (30) [cat. 196f]	12 (23) [cat. 196i]	

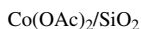
^a CuCN, chiral ligand in combination with TBHP/PhCO₂H was used.

coworkers^{442,443} and Feringa and coworkers⁴⁴⁴ have been used as chiral inductors in the Kharasch–Sosnovsky reaction. The reactivity and enantioselectivity of the corresponding copper complexes is compared on the basis of the allylic oxidation of cyclohexene. Yields and enantioselectivities for this reaction are given in Scheme 129. Ligand **197** leads to a better stereocontrol in the case of cycloalkenes with larger ring size (cycloheptene: 62–75% *ee*). Zondervan and Feringa found that the soft thiophene-oxazoline ligand **199b** leads to high conversion of alkene but only low enantioselectivity was observed, while the harder phenolic oxazoline ligand **199a** could introduce slightly higher asymmetry. Using proline **200** as ligand, Levina and Muzart could obtain the allylic benzoate of cyclohexene with an *ee* of 45%⁴⁴² and Feringa and coworkers reported an *ee* value of 61% for this reaction but with a low conversion of 39%⁴⁴⁴. With amino acid **198a**, bearing a more rigid cyclic backbone, higher asymmetric induction than with the proline ligand could be obtained in the Kharasch–Sosnovsky reaction, while ligand **198b**, bearing an additional methylene group, was less selective than **200** and **198a**.

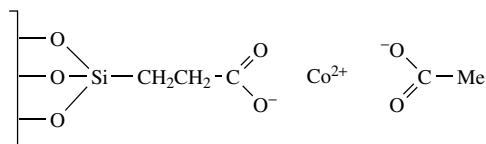
Salvador and coworkers reported on the use of cheap cuprous salts like CuBr, CuCl, CuI, a cupric salt CuCl₂ and copper metal as catalyst for the preparation of allylic oxidation products from Δ^5 -steroids using TBHP as oxygen source (see Scheme 125)⁴²⁷. Four years later Salvador and Clark presented two further catalysts, the homogeneous cobalt acetate **201a** and the heterogeneous cobalt catalysts **201b** and **201c** depicted in Figure 18,



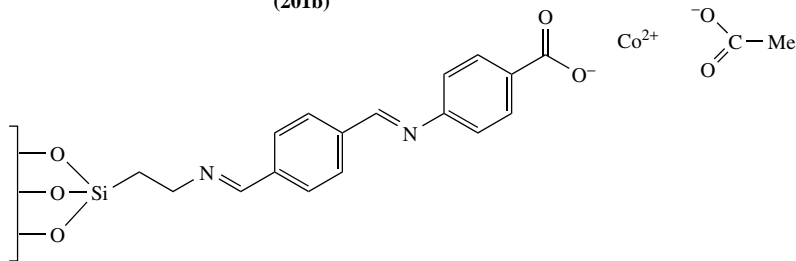
SCHEME 129. Yields and enantiomeric excesses of the enantioselective allylic oxidation (Kharasch–Sosnovsky reaction) of cyclohexene using different chiral ligands



(201a)



(201b)

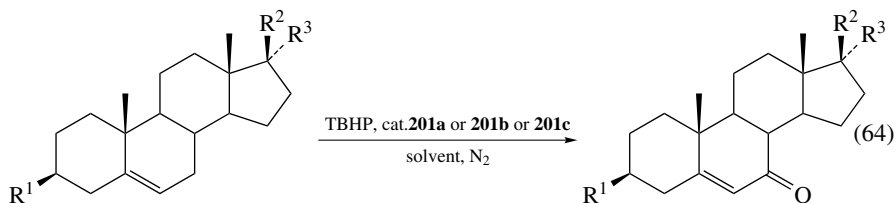


(201c)

FIGURE 18

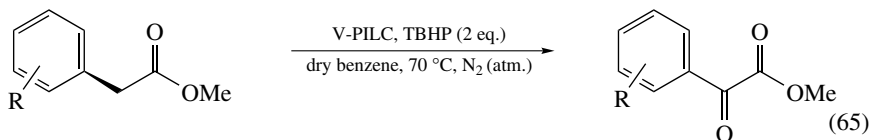
which they employed for the same type of allylic oxidation (equation 64)⁴⁴⁵. While product yields of the allylic oxidation are very similar under homogeneous conditions using Co(OAc)₂•4 H₂O catalyst (84 and 86%) and under heterogeneous conditions using catalysts **201a–c** (70–86%), the advantage of the heterogeneous process is the easy recovery

of the catalyst and the possibility of its reuse with only small reduction in product yields. The method is also effective in the presence of a secondary alcohol, which is not oxidized under the employed reaction conditions.



$R^1 = \text{H, OAc, Cl}; R^2 = \text{H, COMe, C}_8\text{H}_{17}, \text{OAc, OH}; R^3 = \text{H or } R^2R^3 = \text{O}$

An efficient synthesis of arylglyoxylic esters in good yields from arylacetic esters by oxidation in benzylic position using vanadium pillared clay (V-PILC) as catalyst and TBHP as oxidant was reported by Choudary and coworkers in 1993 (equation 65)⁴⁴⁶. The reaction is very selective towards the activated methylene sandwiched between aryl and ester groups. Other benzylic positions like in ethylbenzene or methylene groups next to ester groups like in methyl propionate are not oxidized by vanadium pillared clay. The authors found that electron-donating substituents at the aromatic moiety (especially in *para* position) facilitate the oxidation, while electron-withdrawing groups retard the reaction. While V_2O_5 immobilized on silica gel was as effective a catalyst as V-PILC, V_2O_5 alone turned out to be inactive. It was proposed that the enolate of the substrate (the ester), which is formed owing to acidic sites of the support, chelates the vanadium and is stabilized by extended conjugation with the aryl moiety. The chelated complex can then easily be oxidized to the α -keto esters.

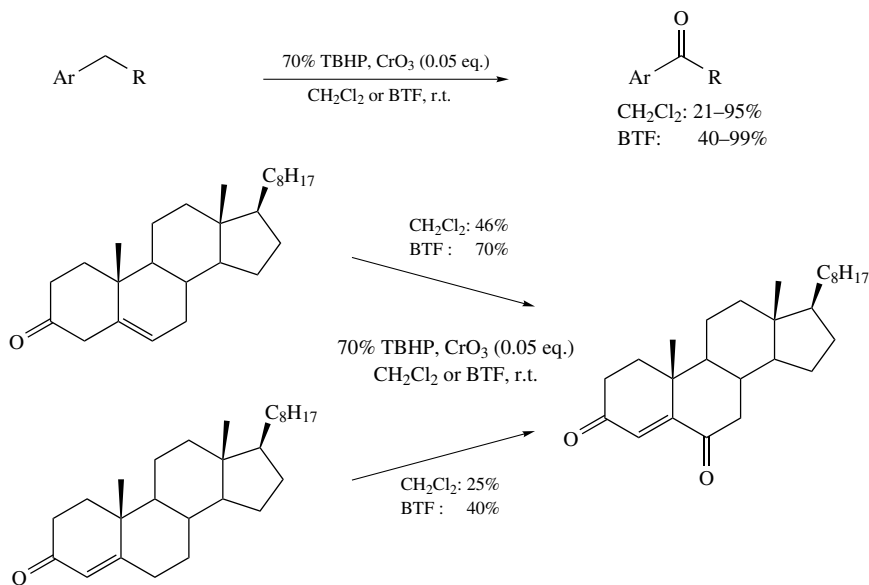
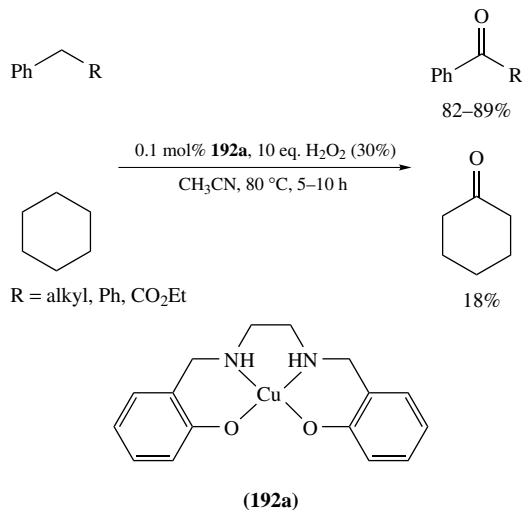


$R = \text{H, } p\text{-Me, } o\text{- and } p\text{-OMe, } o\text{- and } p\text{-NO}_2,$
 $o\text{- and } p\text{-Cl, } o\text{- and } p\text{-Bn, } p\text{-NH}_2$

V-PILC = vanadium pillard clay

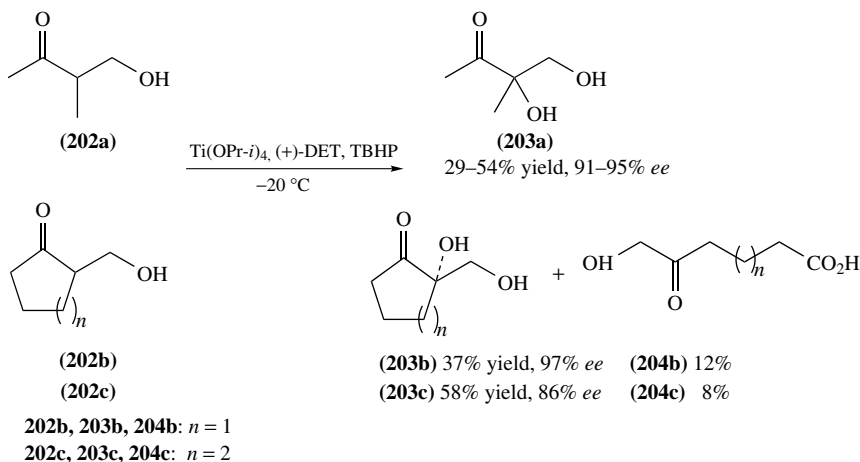
Muzart and coworkers investigated the CrO_3/TBHP catalyzed oxidation of various benzylic methylenes⁴⁴⁷ and the allylic oxidation of Δ^4 - and Δ^5 -cholesten-3-one to the corresponding ketones in CH_2Cl_2 ⁴²⁴ as well as benzotrifluoride (BTF) as solvent (Scheme 130)⁴⁰⁷. It could be shown that BTF in most cases improved the results even though the reactions were carried out with less TBHP than in CH_2Cl_2 (4 eq. compared to 7 eq.). Yields in CH_2Cl_2 varied from 21 to 94% and those in BTF from 40 to 99%.

In 2003, Velusamy and Punniyamurthy reported on a copper(II)-catalyzed C–H oxidation of alkylbenzenes and cyclohexane to the corresponding ketones with 30% hydrogen peroxide (Scheme 131)⁴⁴⁸. The reaction was catalyzed by the copper complex **192a** depicted in Scheme 131 and yields were high in the case of alkylbenzenes (82–89%) whereas cyclohexanone was obtained with a low yield of 18%. Chemospecificity was very high in every case; neither aromatic oxidation nor oxidation at another position of the alkyl chain was observed.

SCHEME 130. Benzylic and allylic oxidation with CrO_3 in CH_2Cl_2 or benzotrifluorideSCHEME 131. Copper(II)-catalyzed benzylic oxidation and oxidation of cyclohexane with 30% H_2O_2

2. α -Hydroxylation of ketones

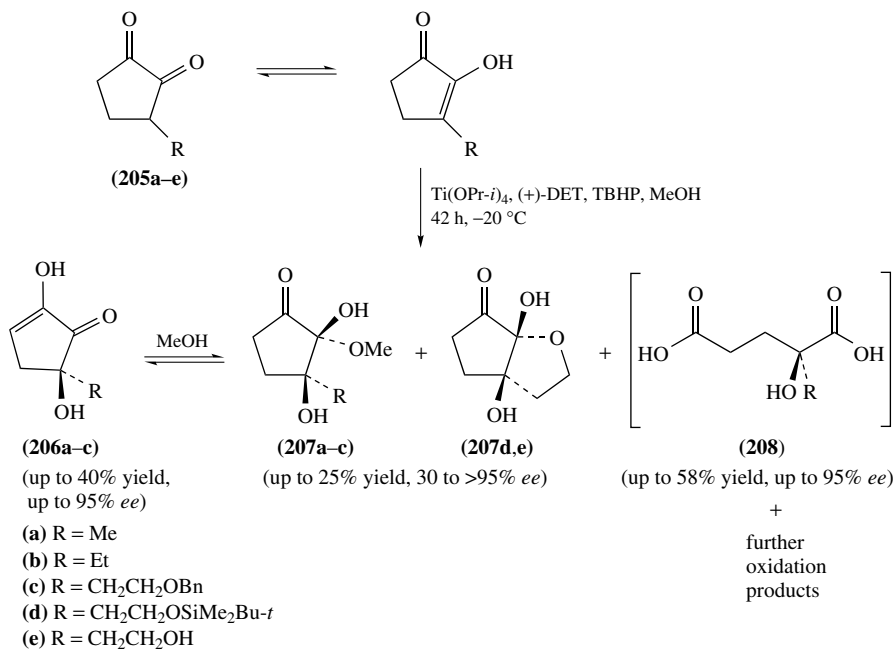
α -Hydroxy carbonyl compounds are useful building blocks in organic chemistry and especially the chiral ones are widely spread among natural products like carbohydrates, α -hydroxy acids etc. Some analogs have interesting biological properties and are used in

SCHEME 132. Direct asymmetric α -hydroxylation of 2-hydroxymethyl ketones

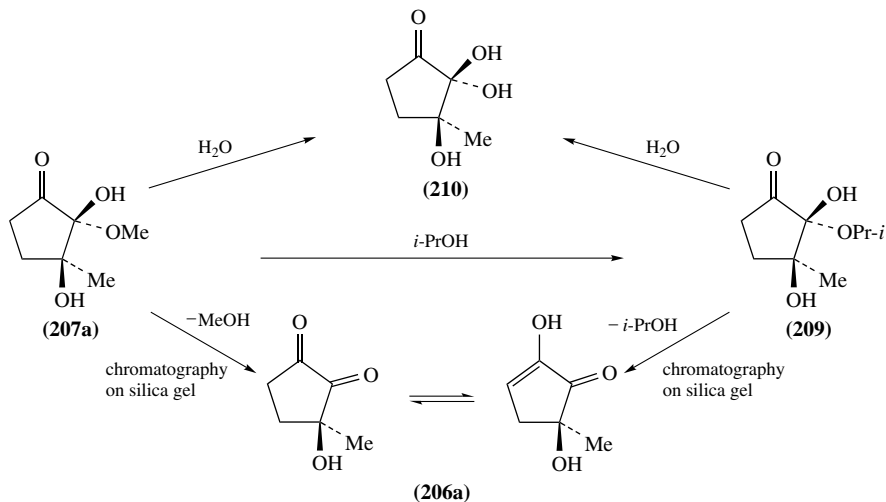
α,β -dihydroxy ketones **203a–c** with high enantiomeric purity (*ee* 86–97%) and moderate yields (37–58%) (Scheme 132)⁴⁵⁶. A variety of different substituted cyclic and acyclic 2-hydroxymethyl-substituted ketones underwent α -hydroxylation; however, the method is limited to this type of substrate. In the case of cyclic substrates, the hydroxylation was accompanied by the formation of a small amount of achiral keto acids **204b** and **204c** (8–12%). With the same catalytic system they could also hydroxylate 3-alkyl-1,2-cyclopentanediones **205a–e** with excellent enantioselectivity⁴⁵⁷. In this reaction two major types of oxidation products were obtained: the 3-hydroxylated products **206a–c** and **207a–e** and the ring-cleaved 3-hydroxylation products **208** (Scheme 133). In the case of **205a**, acetal **207a** is formed when the reaction is quenched with methanol. In isopropanol, **207a** undergoes an alkoxy exchange resulting in the formation of **209** (Scheme 134). In water, **209** forms the stable hydrate **210**. Acetal **207a** and **209** form the enol **206a** under anhydrous conditions, e.g. chromatography on silica gel. Oxidations under Sharpless conditions are sensitive to the reagent/substrate ratio and the authors found the best ratio for this special kind of reaction to be $\text{Ti(OPr-}i\text{)}_4\text{:205a}$ 0.8–1.5:1 and $\text{Ti(OPr-}i\text{)}_4\text{:DET}$ 1:1.2 to 1:2. The highest isolated yield of **206a** was 40%. Higher Ti/substrate ratios led to a reduction in enantioselectivity and yield of hydroxylation reaction. A variety of substrates have been hydroxylated under the conditions described above. The yield of α -hydroxylated products together varied between 3 and 40% with *ee* values of 30 to >98% and the yield of ring cleavage products ranged from 31 to 58%. Attempts to hydroxylate 3-methyl-1,2-cyclohexanediones **211** were unsuccessful resulting only in small yields (5–9%) of ring contraction products **212** (Scheme 135). No α -hydroxylation was obtained for 2-methyl-1,3-cyclopentanedione **213** as well; in this case only the product of the double-bond cleavage **214** was observed (8%). Therefore, the α -hydroxylation reaction using the Sharpless system $\text{Ti(OPr-}i\text{)}_4\text{/DET/TBHP}$ appears to be limited to 3-alkyl-1,2-cyclopentanediones.

3. Oxidation of alkenes to ketones

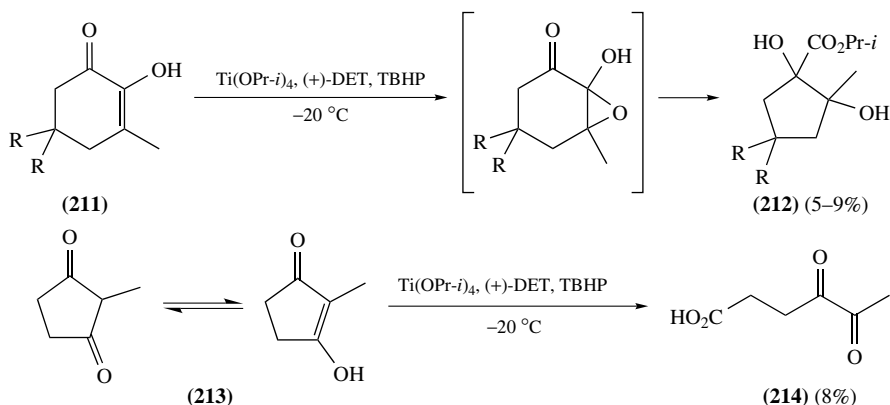
The selective oxidation of terminal alkenes to the corresponding methyl ketones was reported by Roussel and Mimoun in 1980 and can be carried out using *t*-butylperoxypalladium(II) trifluoroacetate (PPT) or alternatively catalytic amounts of



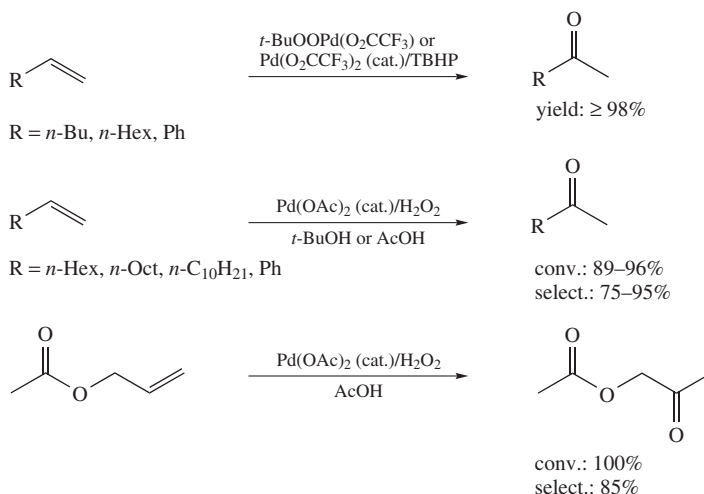
SCHEME 133. Asymmetric 3-hydroxylation of 3-alkyl-1,2-cyclopentanediones



SCHEME 134. Reacetalization, hydration and enolization of hydroxylated diketone

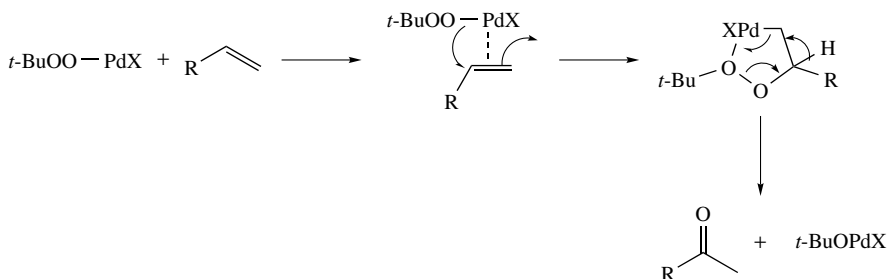


SCHEME 135. Oxidation of 3-methyl-1,2-cyclohexanedione and 2-methyl-1,3-cyclopentanedione using Sharpless system

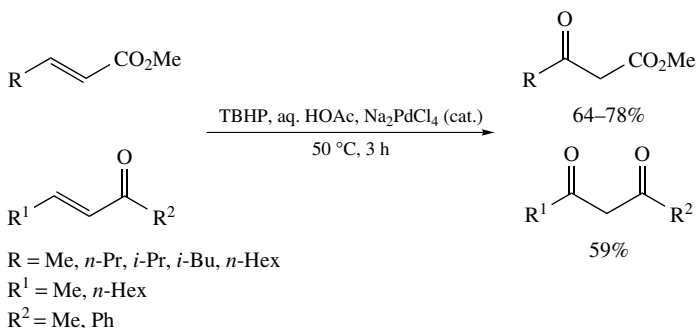


SCHEME 136. Palladium-catalyzed oxidation of terminal olefins to methyl ketones by TBHP or H_2O_2

$\text{Pd}(\text{OAc})_2$ in the presence of 30% H_2O_2 ⁴⁵⁸ or $\text{Pd}(\text{O}_2\text{CCF}_3)_2$ in the presence of TBHP (Scheme 136)^{238, 459}. With the latter catalytic system 1-hexene as well as 1-octene and styrene are converted to 2-hexanone, 2-octanone and acetophenone in benzene at 20°C in less than 10 minutes (50 min in the case of styrene) with a yield of $\geq 98\%$. The reaction is inhibited by water or other hydroxylic solvents. The proposed mechanism involves an alkylperoxyalkylpalladium(II) intermediate, formed via nucleophilic attack of the *t*-butylperoxy group on the coordinated alkene as shown in Scheme 137. With $\text{Pd}(\text{OAc})_2/\text{H}_2\text{O}_2$ internal olefins could not be oxidized and with PPT they were oxidized either very slowly or not at all; instead, a π -allylic complex is formed. A regioselective oxidation of α , β -unsaturated ketones and esters to the corresponding β -ketoesters and 1,3-diketones and β -ketoesters respectively, with TBHP or 30% hydrogen peroxide in 50%



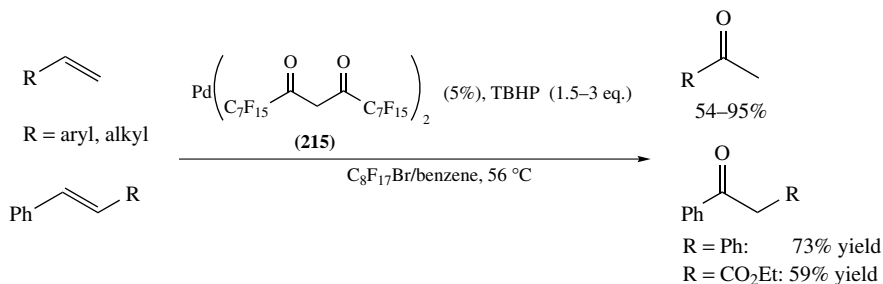
SCHEME 137. Proposed mechanism for the palladium-catalyzed oxidation of terminal alkenes to methyl ketones using TBHP oxidant



SCHEME 138. Regioselective oxidation of α,β -unsaturated carbonyl compounds catalyzed by Na_2PdCl_4 in the presence of TBHP

aqueous acetic acid using Na_2PdCl_4 as catalyst, was reported by Tsuji and coworkers (Scheme 138)⁴⁶⁰. In this reaction 1,3-dicarbonyl compounds, which are prepared only in low yields via Wacker reaction, can be synthesized in good yields (59–78%).

An organic/fluorous biphasic approach ($\text{C}_8\text{F}_{17}\text{Br}$ /benzene) to the synthesis of methyl ketones from terminal alkenes with TBHP in the presence of catalytic amounts of the palladium catalyst **215** was presented by Betzemeier and Knochel in 1998 (Scheme 139)³⁹.

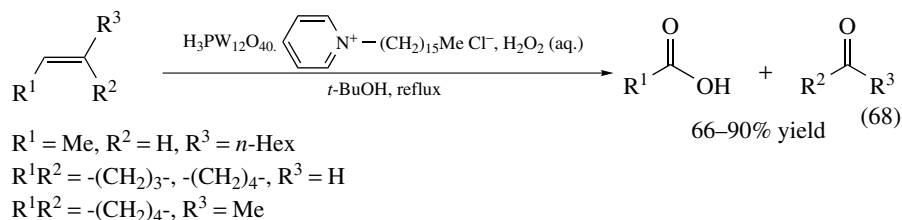


SCHEME 139. Oxidation of olefins to ketones with palladium catalyst **215** in a perfluorinated solvent

With this method styrene derivatives are oxidized in very good yields (complete conversion at 56 °C after 2–5 hours), whereas aliphatic alkenes require longer reaction time (8–20 h) and increased amounts of oxidant (3.5 eq.), and afford methyl ketones in moderate to good yields. Besides terminal olefins also stilbene and ethyl cinnamate have been converted to benzyl phenyl ketone and β -ketoester. The catalyst solution can be reused 8 times without decrease in yield.

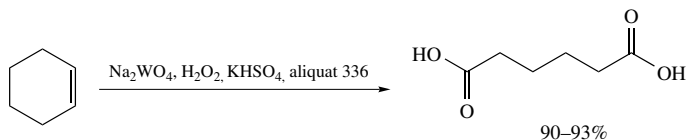
4. Oxidative cleavage of double bonds

The oxidative cleavage of the double bond in cyclohexene using hydrogen peroxide in the presence of catalytic amounts of a metal catalyst is a very useful synthetic method for the production of adipic acid and represents a real alternative to the widely used industrial method of producing adipic acid⁴⁶¹ (oxidation of cyclohexane to an alcohol/ketone mixture with air and Mn or Co salts as catalysts and further oxidation to adipic acid using either HNO₃ and NH₄-metavanadate/Cu-nitrate or air/Cu-Mn-acetate). The heteropoly acid [π -C₅H₅N⁺ (CH₂)₁₅Me]₃(PW₁₂O₄₀)₃⁻ (**163**) developed by Ishii and coworkers and mentioned above as effective *in situ* generated epoxidation catalyst has been shown to be also a good catalyst for the oxidative cleavage of double bonds (equation 68)³⁰⁸.

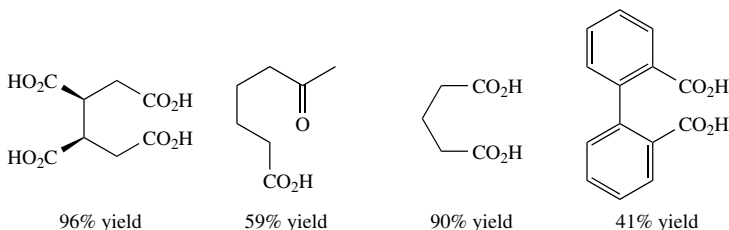


Especially internal alkenes like 2-octene, cyclopentene, cyclohexene or 1-methylcyclohexene could be oxidized with double bond cleavage (60–90% yield) while 1-octene was oxidized to heptanoic acid in a yield of 45%. In 1998, Noyori and coworkers used Na₂WO₄ in the presence of a phase transfer catalyst [Me(*n*-Oct)₃N⁺HSO₄⁻], which can be generated *in situ* from aliquat 336 and KHSO₄ by an ion exchange, to convert cyclohexene into adipic acid with H₂O₂ as oxygen source in an excellent yield of 90–93% (Scheme 140)⁴⁶². The one-pot transformation is achieved through multiple steps involving three kinds of oxidative reactions (olefin epoxidation, two alcohol oxidations and Baeyer–Villiger oxidation) and hydrolysis. With this procedure other substituted cyclohexenes and cyclopentene can be converted to the corresponding (di)carboxylic acid products as well in moderate to very high yields (41–96%, Scheme 140). Because of the fact that this reaction is easily carried out and that it is environmentally benign, the use of this experiment in an organic chemistry laboratory course at a university has been reported by Reed and Hutchison⁴⁶³. The catalyst can be recycled by separation of the aqueous phase and addition of fresh H₂O₂ and cyclohexene.

In 2002 the oxidative cleavage of nitrostyrenes double bonds to give carboxylic acids was described by Lakouraj and coworkers, who employed amberlyst A-26 supported hydrogen peroxide as heterogeneous oxygen source (equation 69)⁴⁶⁴. The supported hydrogen peroxide was prepared *in situ* from 35% hydrogen peroxide and catalytic amounts of amberlyst A-26 (OH⁻). One of the advantages of the heterogenized H₂O₂ was the easy workup, which is a simple filtration of the heterogeneous oxidant. The obtained yields for the conversion of nitrostyrenes to carboxylic acids are generally high (82–95%) with

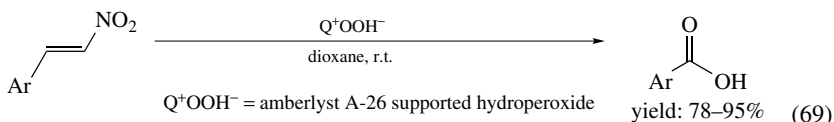


Products, that can be obtained by this method starting from cyclopentene and various cyclohexene derivatives:



Scheme 140. Direct oxidation of cyclohexenes and cyclopentene with 30% H_2O_2

the exception of substrates bearing strong electron-donating groups at the aromatic ring (NH_2 , NMe_2). With the latter, no conversion is observed.

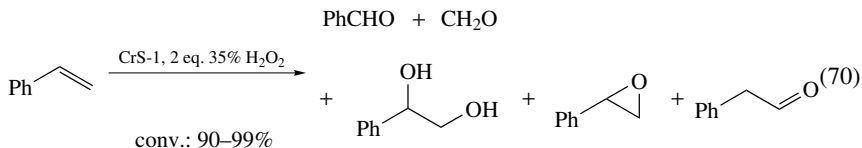


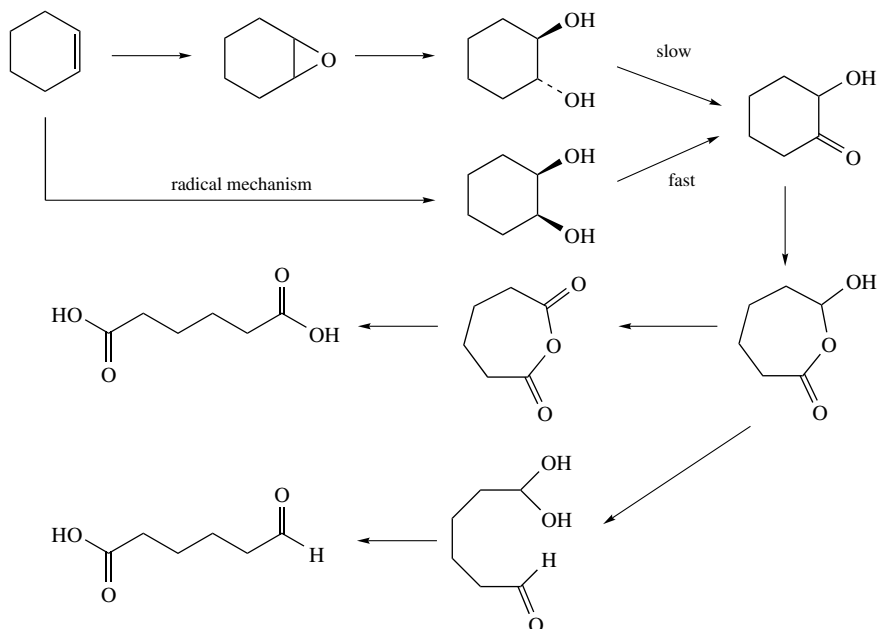
Ar = Ph, 4- XC_6H_4 , 3- YC_6H_4 , 2- $\text{O}_2\text{NC}_6\text{H}_4$, 3,4-(MeO) $_2\text{C}_6\text{H}_3$

X = Me, Cl, Br, Ph, NO_2 , MeO

Y = Br, NO_2 , MeO

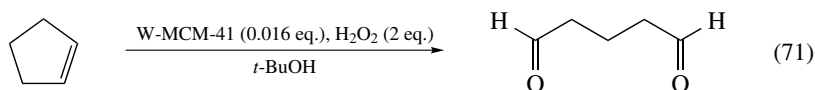
The redox molecular sieve CrS-1 has been shown by Sheldon and coworkers to be active for the oxidative cleavage of styrene to benzaldehyde at 70 °C using 35% H_2O_2 as oxidant (equation 70)⁴¹⁰. With almost complete conversions the major products were benzaldehyde (52–85% selectivity) and 1-phenyl-1,2-ethanediol (0–35% selectivity) together with small amounts of styrene oxide (16% selectivity) and phenylacetaldehyde (1–9% selectivity) as side products. The selectivity was dependent on the method employed for catalyst preparation. In 2003 Thomas and coworkers reported on the employment of a TAPO-5 molecular sieve catalyst for the same kind of reaction but without the need of an organic solvent⁴⁶⁵. TAPO-5 is a titanium framework substituted aluminophosphate, which is bifunctional and acts as Brønsted acid and as catalyst for oxygen transfer from H_2O_2 . Several oxidation products from cyclohexene have been detected in the product mixture, from which the authors gained insight into intermediates and the reaction mechanism (Scheme 141). Adipic acid could be obtained in yields of up to 30%. No significant leaching of the catalyst during catalysis was observed, but reused catalyst showed diminished activity.





SCHEME 141. Mechanistic pathway for the oxidation of cyclohexene to adipic acid using TAPO-5 catalyst

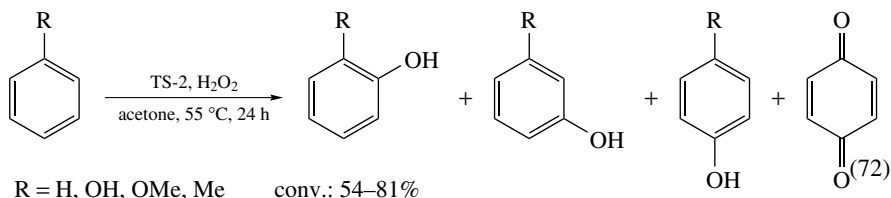
A catalyst for the oxidative cleavage of cyclopentene with hydrogen peroxide to form glutaraldehyde in good yield was reported by Dai and coworkers in 2003 (equation 71)⁴⁶⁶. The heterogeneous catalyst was a W-metal containing MCM-41, which was synthesized through a novel economic synthetic method using Na_2SiO_3 as Si source and ethyl acetate as hydrolyzer. Conversion of cyclopentene with this catalyst was complete after 24 hours and glutaraldehyde was generated with 71% selectivity. W-MCM-41 showed good anti-leaching properties and therefore could be recycled and reused without loss of activity, selectivity or collapse of its mesoporous structure after 7 runs.



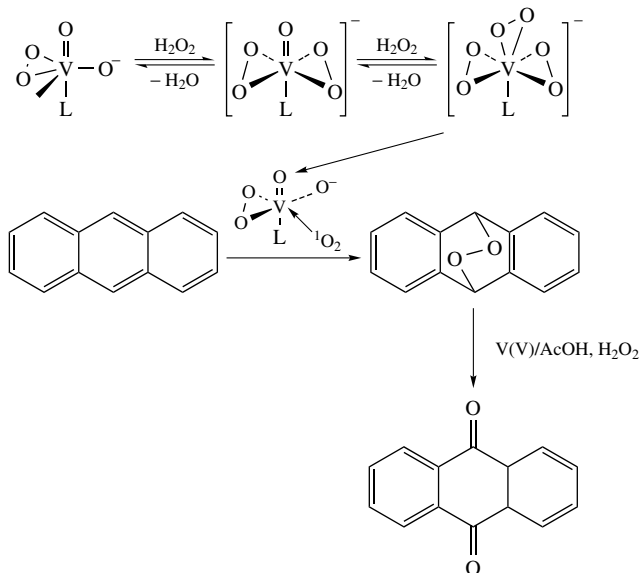
5. Oxidation of aromatic compounds

Besides a variety of other methods, phenols can be prepared by metal-catalyzed oxidation of aromatic compounds with hydrogen peroxide. Often, however, the selectivity of this reaction is rather poor since phenol is more reactive toward oxidation than benzene itself, and substantial overoxidation occurs. In 1990/91 Kumar and coworkers reported on the hydroxylation of some aromatic compounds using titanium silicate TS-2 as catalyst and hydrogen peroxide as oxygen donor (equation 72)²⁴⁶. Conversions ranged from 54% to 81% with substituted aromatic compounds being mainly transformed into the *ortho*- and *para*-products. With benzene as substrate, phenol as the monohydroxylated product

and *para*-benzoquinone are formed (57% conv., product distribution: 66:34).



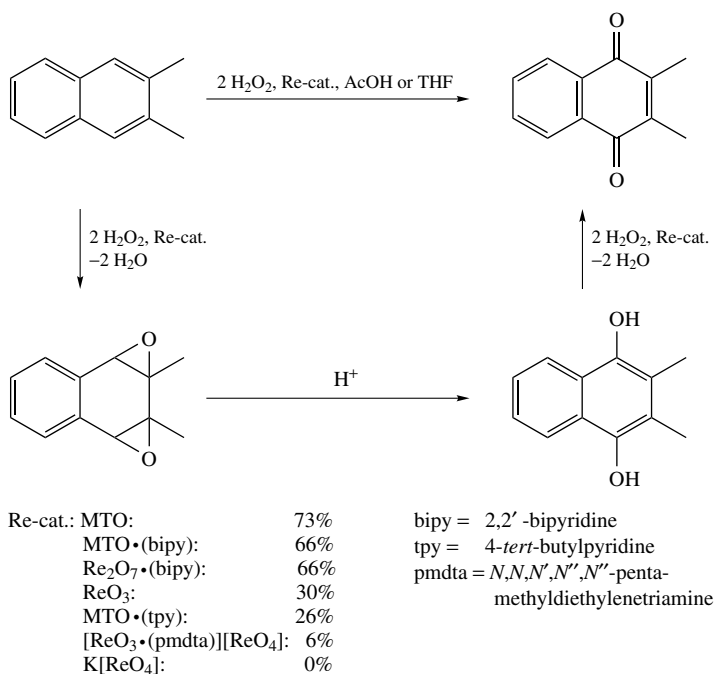
Moiseev and coworkers presented a vanadium(V)-catalyzed method for the synthesis of anthraquinones from anthracene and 2-ethylanthracene using hydrogen peroxide as terminal oxidant under acidic conditions (AcOH) (Scheme 142)⁴⁶⁷. The reaction was proposed to proceed via polar rather than via radical mechanism. Oxidation of anthracene was explained by Moiseev and coworkers by formation of a vanadium species with a singlet dioxygen molecule (as shown in Scheme 142) and capturing of the $^1\text{O}_2$ by an anthracene molecule⁴⁶⁸. The resulting short-living intermediate 9,10-dihydro-9,10-epidioxyanthracene is finally oxidized to anthraquinone by $\text{H}_2\text{O}_2/\text{V}^{\text{V}}/\text{AcOH}$.



Scheme 142. Vanadium-catalyzed oxidation of aromatic compounds using H_2O_2

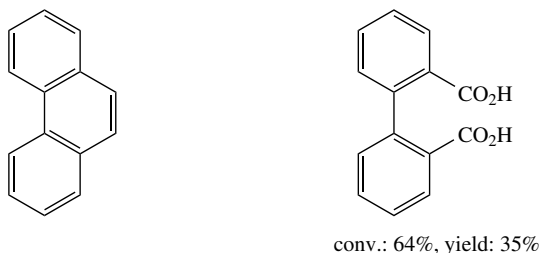
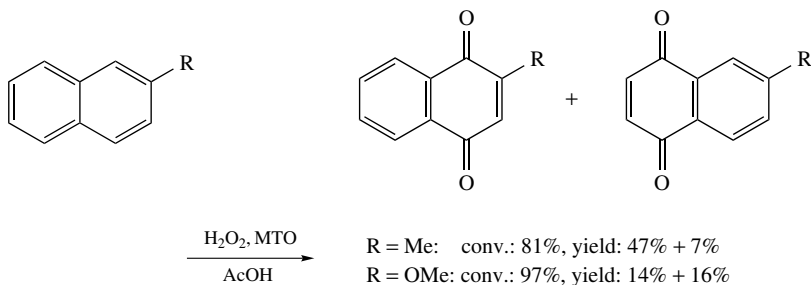
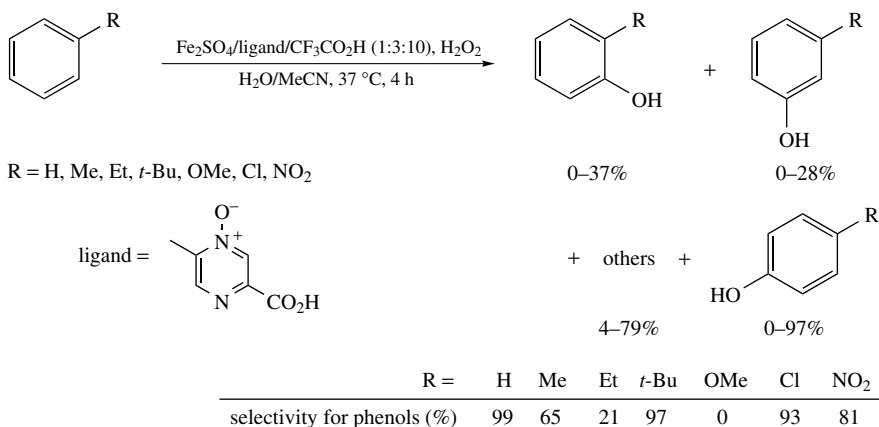
The incorporation of vanadium(V) into the framework positions of silicalite-2 has been reported by Hari Prasad Rao and Ramaswamy⁴⁶⁹. With this heterogeneous oxidation catalyst the aromatic hydroxylation of benzene to phenol and to a mixture of hydroquinone and catechol could be promoted. A heterogeneous ZrS-1 catalyst, which has been prepared by incorporation of zirconium into a silicalite framework and which catalyzes the aromatic oxidation of benzene to phenol with hydrogen peroxide, is known as well in the literature. However, activity and selectivity were lower than observed with the analogous TS-1 catalyst.

Herrmann and coworkers reported on the oxidation of aromatic compounds using a series of Re(VII) compounds, Re_2O_7 , MTO, EtReO_3 , $\eta^5\text{-C}_5\text{H}_5\text{ReO}_3$ and $\eta^5\text{-C}_5\text{H}_4\text{MeReO}_3$, as catalysts in the presence of hydrogen peroxide as oxidant (Scheme 143)^{346,470}. The oxidation of 2,3-dimethylnaphthalene in acetic acid with 85% aqueous H_2O_2 yielded 2,3-dimethyl-1,4-naphthoquinone. From the Re-catalysts tested, MTO revealed the highest activity for this reaction with a conversion of 73% after 4 hours at 20 °C. As catalytically active species, the peroxorhenium(VII) complex $[\text{R-ReO}(\text{O}_2)_2]\cdot\text{H}_2\text{O}$ was proposed. The reaction has been rationalized as involving the epoxidation of the naphthalene derivative, acid-induced ring opening yielding the corresponding hydroquinones, and oxidation to quinones (see Scheme 143). Using the catalytic system MTO/ H_2O_2 Adam and coworkers could oxidize naphthalene derivatives substituted in the 2-position and phenanthrene giving the corresponding naphthoquinones and biphenyl-2,2'-dicarboxylic acid, respectively (Scheme 144)⁴⁷¹. The oxidation occurs with moderate yields and good selectivity.



SCHEME 143. Oxidation of aromatic compounds using Re oxides as catalyst in the presence of H_2O_2

Recently, Bianchi and coworkers published an iron-catalyzed direct oxidation method of aromatic hydrocarbons to the corresponding phenols under biphasic conditions (Scheme 145)⁴⁷². As an efficient catalyst the authors employed an iron complex with 6-methylpyrazine-3-carboxylic acid *N*-oxide and trifluoroacetic acid as most efficient cocatalyst (increases the phenol selectivity). The aromatic compounds were employed in excess and high conversions relative to H_2O_2 were obtained (94% for benzene). Compared with the Fenton reagent this method allows higher selectivities to phenols, minimizing the overoxidation reactions to polyoxygenated derivatives. The great advantage of the biphasic conditions is first the quantitative distribution of the catalyst in the aqueous

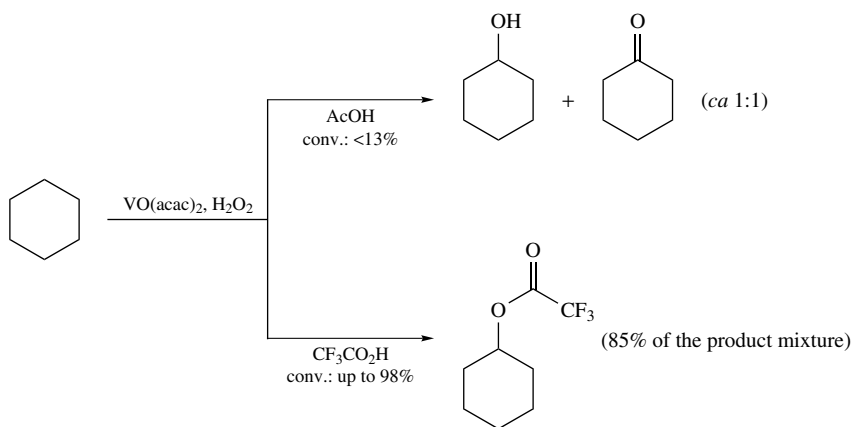
SCHEME 144. Oxidation of arenes with MTO/H₂O₂

SCHEME 145. Fe-catalyzed oxidation of aromatic hydrocarbons

phase, which can be separated and reused after the reaction without significant loss in activity, and second the reduced contact between the catalyst and the phenolic products, which minimizes overoxidation. The limitations of the procedure are the low selectivity in the case of very electron rich substrates such as anisole and the competition with the oxidation of aliphatic moieties (benzylic positions as in toluene and ethylbenzene).

6. Oxidation of alkanes

The selective oxidation of saturated hydrocarbons is a reaction of high industrial importance. Besides a variety of other oxidants, hydrogen peroxide as a very clean oxidant has also been used for these purposes^{321,322}. As an example, in 1989 Moiseev and coworkers reported on the vanadium(V)-catalyzed oxidation of cyclohexane with hydrogen peroxide (Scheme 146)⁴⁶⁸. When the reaction was carried out in acetic acid cyclohexanol and cyclohexanone were formed, but conversions were very poor and did not exceed 13%. Employing CF_3COOH as solvent, complete conversions could be obtained within 5 minutes. Here, cyclohexyl trifluoroacetate was the main product (85% of the products formed) resulting from the reaction of cyclohexanol (the primary product of the oxidation) with CF_3COOH .



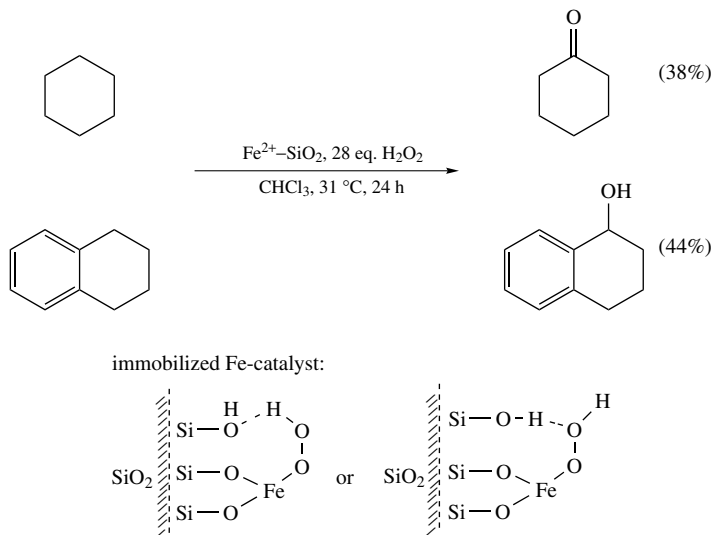
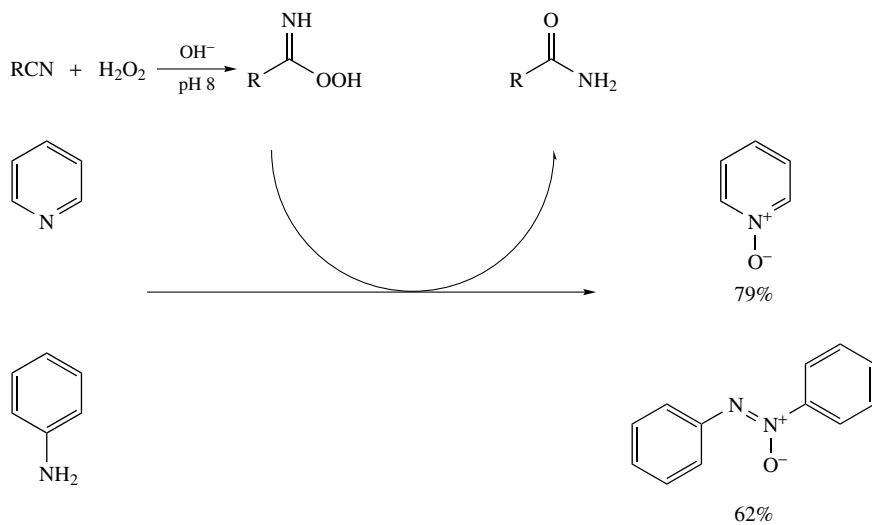
SCHEME 146. Vanadium-catalyzed oxidation of cyclohexane with H_2O_2

In 1992, Hari Prasad Rao and Ramaswamy reported on the oxyfunctionalization of alkanes with H_2O_2 using a vanadium silicate molecular sieve⁴⁶⁹. With this catalyst acyclic and cyclic alkanes were oxidized to a mixture of the corresponding alcohols (primary and secondary ones), aldehydes and ketones. Unfortunately, most of the early attempts were of rather limited success due to low turnover frequencies and radical producing side reactions as observed, for example, by Mansuy and coworkers in 1988³²².

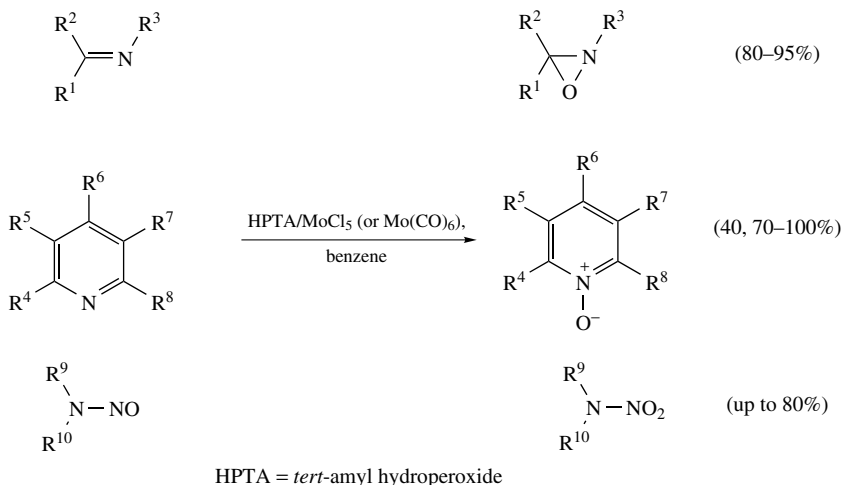
In 2001, Monfared and Ghorbani reported the use of a silica-supported iron(II) as a catalyst for the oxidation of hydrocarbons with hydrogen peroxide (Scheme 147)⁴⁷³. Besides epoxidation reactions, the catalyst also showed catalytic activity for the oxidation of alkenes to ketones. Tetrahydronaphthalene and cyclohexane could be oxidized with this system to α -tetralol (44% yield after 24 h at 31 °C) and cyclohexanone (38% yield after 24 h at 31 °C), respectively. The supported catalyst is inexpensive and easily prepared and it does not catalyze hydrogen peroxide decomposition. The authors postulated an iron(III)- η^1 -hydroperoxide adduct as intermediate, which is stabilized by hydrogen bonding between the hydroperoxide ion and the oxygen atom of the silica gel. However, a drawback of this method is the large excess of oxidant (ca 28 equivalents) that is required in order to obtain good conversions.

E. N-Oxidation of Organonitrogen Compounds

Several different organonitrogen compounds readily undergo metal-catalyzed oxidation using alkyl hydroperoxide or hydrogen peroxide as oxygen transfer agents. In 1961,

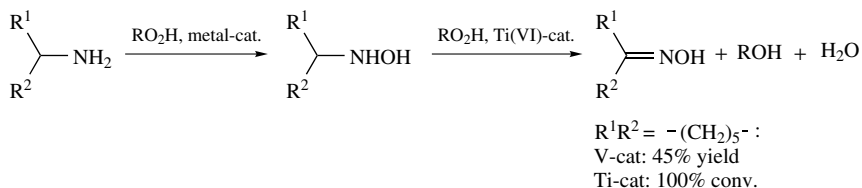
SCHEME 147. Oxidation of alkanes catalyzed by a silica-supported Fe catalyst and H_2O_2 SCHEME 148. Oxidation of amines with H_2O_2 in the presence of an organic nitrile

Payne and coworkers reported on an oxidation method for amines like aniline or pyridine using 30–50% hydrogen peroxide in the presence of an organic nitrile (Scheme 148)⁴⁷⁴. The active oxygen transferring species is proposed to be a peroxycarboximidic acid, which is formed by reaction of hydrogen peroxide with the nitrile. This species can then transfer an oxygen atom to the amine, being converted to the amide. By this method pyridine-*N*-oxide can be synthesized in 79% yield and azoxybenzene (from aniline) in



SCHEME 149. Molybdenum-catalyzed oxidation of nitrogen-containing compounds using *tert*-amyl hydroperoxide

62%, respectively. Imines can be oxidized to the oxaziridines in good yields (80–95%) using a molybdenum catalyst [MoCl_5 , $\text{Mo}(\text{CO})_6$] in the presence of *t*-amyl hydroperoxide (HPTA) (Scheme 149)⁴⁷⁵. Besides imines, also aromatic nitrogen heterocycles could be oxidized to the *N*-oxides with HPTA- MoCl_5 catalyst in yields of 70–100% (exception: 4-acetamidopyridine was *N*-oxidized yielding the *N*-oxide in only 40%) and nitrosamines were oxidized to nitramines in up to 80% yield with this Mo catalyst. As was reported by Russell and Kollar, primary aliphatic amines can be transformed to oximes with vanadium or molybdenum salts of naphthenic acids and by various titanium(IV) complexes/hydroperoxide systems in the presence of hydroperoxides like cumene hydroperoxide, $\text{PhCH}(\text{Et})\text{OOH}$ or *i*-BuOOH (Scheme 150)⁴⁷⁶.



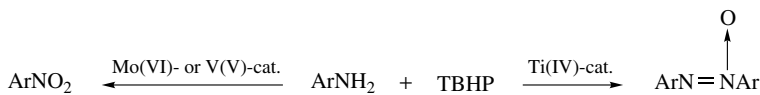
$\text{RO}_2\text{H} = \text{PhC}(\text{Me})_2\text{OOH}$, $\text{PhCH}(\text{Me})\text{OOH}$, *i*-BuOOH

metal cat.: V-, Mo-, Ti-salts of naphthenic acid, $\text{Ti}(\text{OBu})_4$, $\text{Ti}(\text{O}i\text{Bu})_2(2,6\text{-di-}i\text{-tert-butyl-}p\text{-cresyl})_2$, $\text{Ti}(\text{O}i\text{Cresyl})_4$

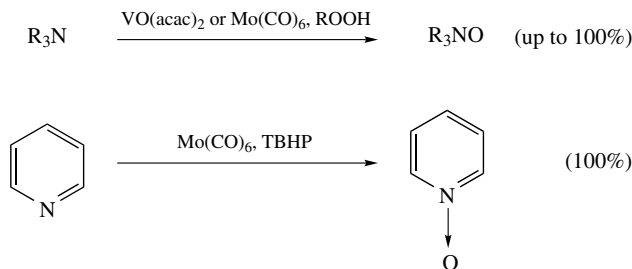
SCHEME 150. Ti-catalyzed oxidation of primary amines to hydroxylamines or oximes

Anilines could be oxidized to nitrobenzenes by Howe and Hiatt⁴⁷⁷ with molybdenum or vanadium catalysts in the presence of TBHP, while azoxybenzenes were produced by Koswig⁴⁷⁸ with titanium catalysts (Scheme 151).

Sheng and Zajacek reported that in the presence of $\text{VO}(\text{acac})_2$ or $\text{Mo}(\text{CO})_6$ catalysts tertiary amines are smoothly oxidized to the corresponding *N*-oxides with either TBHP



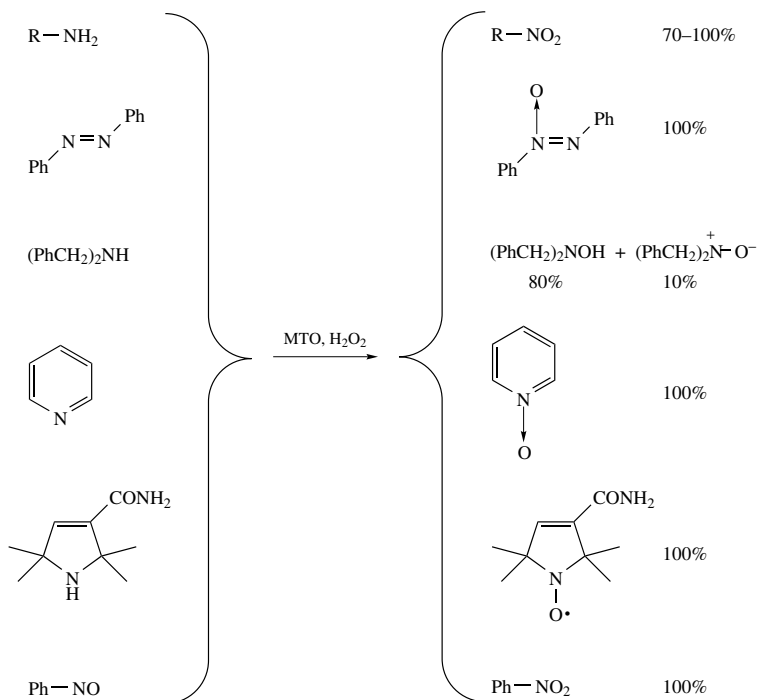
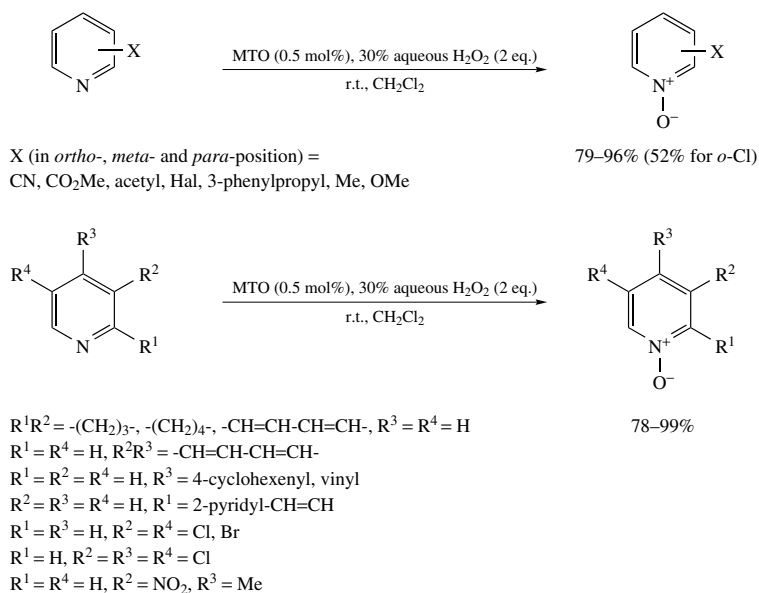
SCHEME 151. Metal-catalyzed oxidation of anilines by TBHP

ROOH = TBHP, *tert*-amyl hydroperoxideSCHEME 152. V- and Mo-catalyzed oxidation of tertiary amines to *N*-oxides with hydroperoxides

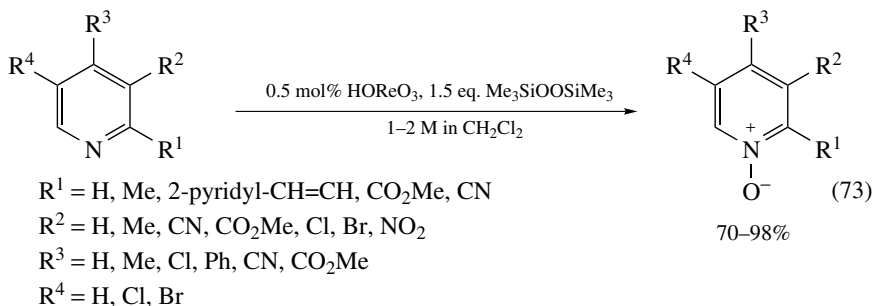
or *tert*-amyl hydroperoxide in quantitative yields (Scheme 152)⁴⁷⁹. Compared with the analogous peracid-catalyzed oxidations, the rates of the metal-catalyzed reactions with hydrogen peroxides are often significantly higher.

Methyltrioxorhenium (MTO) in the presence of hydrogen peroxide is a real allround talent with respect to oxidation reactions in general. Besides other oxidative transformations, it was reported by Murray and coworkers in 1996 that various *N*-oxidations of organonitrogen compounds can also be catalyzed by this system (Scheme 153)⁴⁸⁰. The conversions generally proceed at reaction times between 0.5 and 3 hours at room temperature (in some cases 0 °C or 60 °C) with good yields. Primary aromatic and aliphatic amines can be oxidized to the corresponding nitro compounds in good to excellent yields between 70 and 100%. In the case of aniline, azoxybenzene is obtained as side product (30% yield) and results from the reaction of the intermediate oxidation product nitrosobenzene with aniline to form azobenzene, which is then oxidized to azoxybenzene. With the MTO/H₂O₂ system the secondary amine dibenzylamine is oxidized to the corresponding hydroxylamine (80% yield) and to the nitron (10% yield). Pyridines are transferred to their *N*-oxides⁴⁸¹, nitrosobenzene to nitrobenzene and the 2,2,5,5-tetramethylpyrrolidine-3-carboxamide to the nitroxide, all three reactions with high yields. The latter reaction deserves special mention because the synthesis of nitroxides by standard methods is difficult with only the dioxirane method being comparable with the one described above.

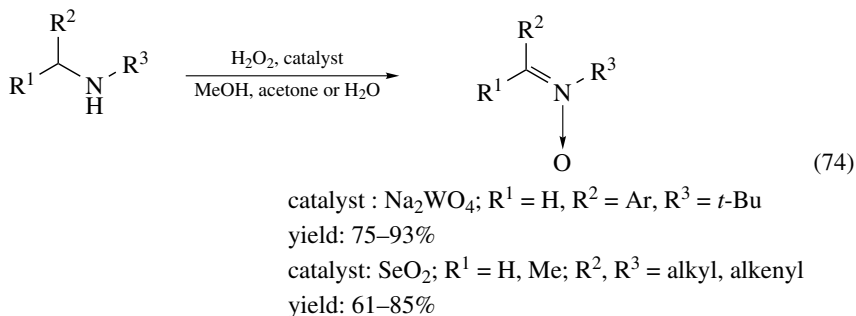
The oxidation of substituted pyridines to *N*-oxides was reported by Sharpless and coworkers to proceed with yields between 78 and 99% (Scheme 154)⁴⁸¹. A variety of substituents like electron donor as well as acceptor groups and alkenyl substituents are tolerated. In 1998, Sharpless and coworkers reported an alternative method for the preparation of pyridine-*N*-oxides in which the MTO/H₂O₂ catalyst could be replaced by cheaper inorganic rhenium derivatives (ReO₃, Re₂O₇, HReO₃) in the presence of bis(trimethylsilyl) peroxide (equation 73)⁴⁸². Yields of the prepared *N*-oxides after simple workup (filtration and bulb to bulb distillation) ranged from 70–98%. Molecular sieves slowed down the reaction while small amounts of water (0–15%) were essential for the reaction. Both electron-poor or electron-rich pyridines give high yields of their *N*-oxides and while *para*-

SCHEME 153. MTO-catalyzed *N*-oxidation reactions with H_2O_2 as oxidantSCHEME 154. Oxidation of pyridine derivatives using MTO/ H_2O_2

and *meta*-substitution does not affect the reaction course, *ortho*-substitution does (as can be seen from reaction times), depending on the nature of substituents.

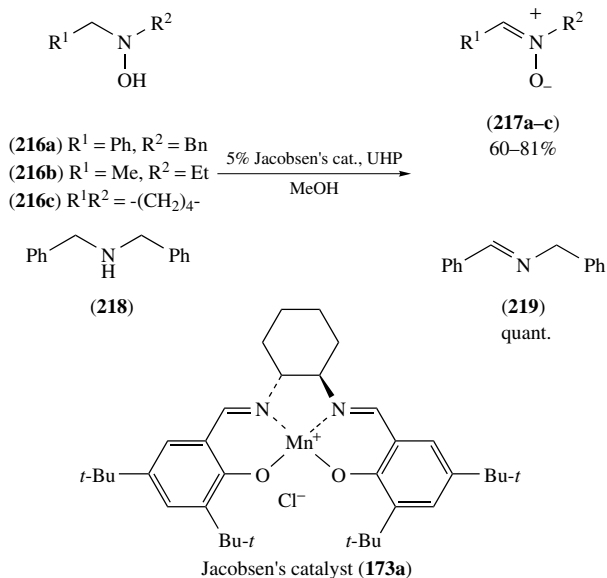


Secondary amines (dialkylamines, benzyl *tert*-butyl amines and cyclic amines) can be oxidized to the nitrones using hydrogen peroxide in the presence of catalysts like Na_2WO_4 or SeO_2 (equation 74)⁴⁸³.



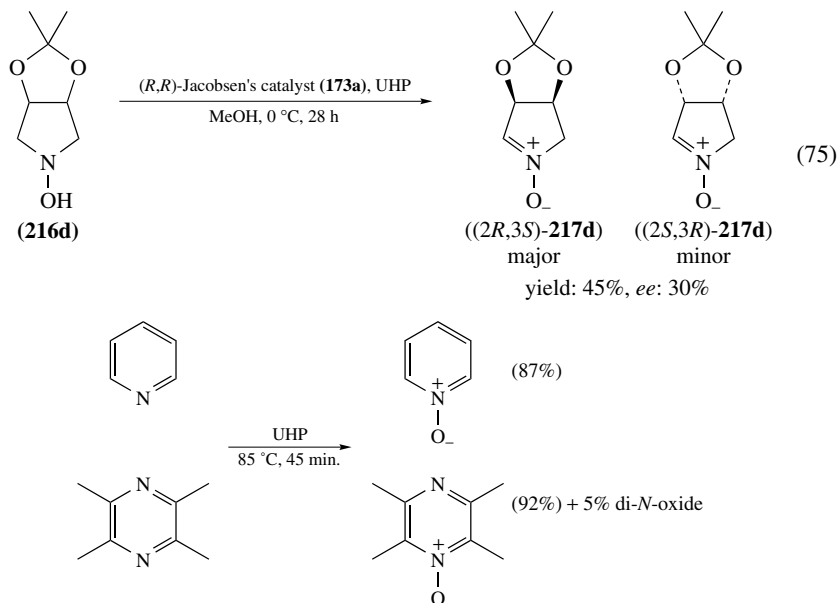
In 1999, Goti and coworkers reported on the conversion of hydroxylamines **216a–c** to the corresponding nitrones **217a–c** and of the secondary amine **218** to imine **219** by using Jacobsen's chiral manganese complex **173a** in combination with one of the following oxidants: H_2O_2 , $\text{urea}\cdot\text{H}_2\text{O}_2$, NaClO , PhIO (Scheme 155)⁴⁸⁴. The authors found the catalyst to be very efficient in catalyzing the conversion of hydroxylamines into nitrones giving the products in yields between 60 and 81%. With the same catalyst and UHP as oxidant, dibenzylamine could be oxidized to the corresponding imine in quantitative yield. The ability of the catalyst to induce asymmetry was tested using a protected *meso-cis*-dihydroxy-substituted cyclic hydroxylamine **216d** as substrate (equation 75). In methanol as solvent and a temperature of 0°C the nitronium **217d** could be obtained in 45% yield after 28 hours and with an enantiomeric excess of 30%, favoring the (2*R*,3*S*)-enantiomer. One reason for the low *ee* is the significant background reaction without a catalyst and therefore *ee* values are higher at lower temperatures. The use of 4-phenylpyridine *N*-oxide as additive increases the reaction rates but with UHP as oxidant the *ee* is decreased significantly.

Varma and Naicker published a solid-state oxidative protocol for the transformation of nitriles to amides and of *N*-heterocycles to *N*-oxides employing the urea hydrogen peroxide complex (Scheme 156)⁴⁸⁵. The *N*-oxides depicted in Scheme 156 were synthesized



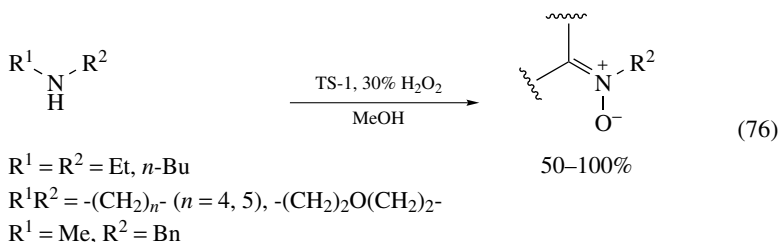
SCHEME 155. Oxidation of hydroxylamines to nitrones and a secondary amine to an imine employing Jacobsen's catalyst

with this oxygen source without the need for a catalyst at a temperature of 85 °C in 45 min and yields of 87 and 92%.



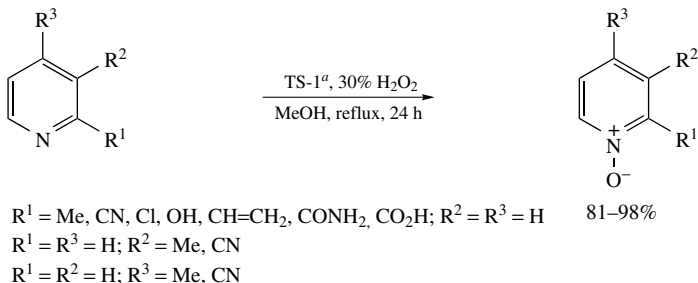
SCHEME 156. Oxidation of *N*-heterocycles using UHP as oxidant

In 1995, a heterogeneous catalytic method for the selective oxidation of secondary amines to nitrones was reported by Sudalai and coworkers, who employed the titanium silicate-1 (TS-1) as catalyst in the presence of 30% H_2O_2 (equation 76)⁴⁸⁶. Generally, acyclic and cyclic secondary amines are oxidized rapidly in a single step to yield the corresponding nitrones as the exclusive oxidation products in yields of 50–100%. A very efficient synthesis of heterocyclic *N*-oxides using redox-molecular sieves (TS-1, Ti-ZSM-5(30), Ti-MCM-41) and dilute hydrogen peroxide as oxidant in aqueous and non-aqueous (methanol and acetone as cosolvent) medium has been reported by Kulkarni and coworkers (Scheme 157)⁴⁸⁷. The yields of the *N*-oxidation reaction of substituted pyridines, quinolines and substituted isoquinolines using this catalytic system ranged from 35 to 98%. Pyridines having electron-donating substituent groups (Me, OH, vinyl) are oxidized rapidly to yield the *N*-oxides exclusively. Pyridines with electron-withdrawing substituents (CN, NO_2 , CONH_2) need longer time to reach full conversion. The activity of the heterogeneous catalysts employed TS-1 and TiZSM-5(30), and TiMCM-41 was compared using the oxidation of 3-cyanopyridine as test reaction. Ti-ZSM-5(30) and TS-1 catalysts gave better yields of the product (73% and 97%, respectively) than TiMCM-41 (53%), with TS-1 being the most efficient molecular sieve catalyst for this reaction.



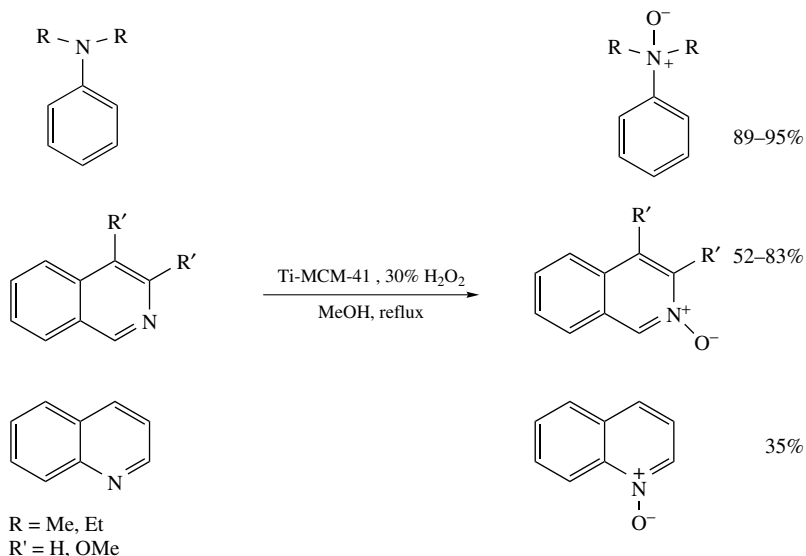
F. Baeyer–Villiger Oxidation

The Baeyer–Villiger oxidation of ketones is a reaction of considerable interest in organic chemistry since the lactone reaction products are important synthetic intermediates in agrochemical, chemical and pharmaceutical industries. Reviews dealing with the topic of Baeyer–Villiger oxidation have been published by Krow in 1993 and by Renz and Meunier in 1999, giving very detailed information on organic molecules that can be prepared by this method, reactivity of substrates, mechanism and kinetics⁴⁸⁸ and the metal-catalyzed Baeyer–Villiger oxidation of ketones was reviewed by Strukul in



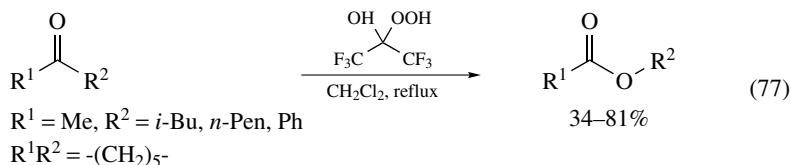
^a R^1, R^2 or $\text{R}^3 = \text{Me}$: TiZSM-5(30) as catalyst, 5–6 h

SCHEME 157. Synthesis of heterocyclic *N*-oxides over molecular sieve catalysts



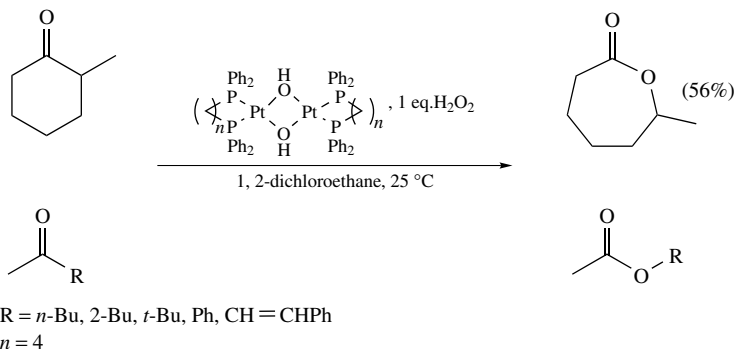
SCHEME 157. (continued)

1998⁴⁸⁹. Besides the peracid oxidants, which were mainly used originally, also the perhydrate 2-hydroperoxyhexafluoropropan-2-ol and hydrogen peroxide (in combination with a catalyst) can serve as oxygen sources. The employment of perhydrates as oxidants for the Baeyer–Villiger reaction of ketones like methyl isobutyl ketone, heptan-2-one, cyclohexanone and acetophenone was reported by Chambers and Clark (equation 77)^{20,490}. Refluxing the substrate together with the perhydrate in dichloromethane resulted in the formation of the corresponding esters in yields between 34–81%.



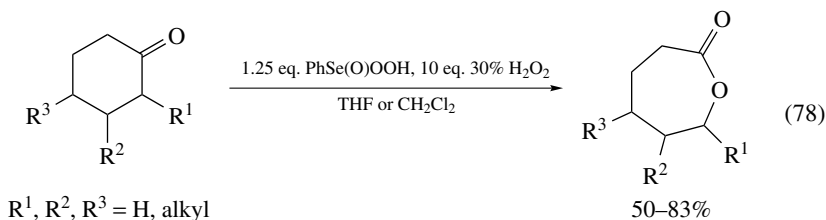
Following the approach of using hydrogen peroxide as oxidant, several new catalysts have been developed that can activate H_2O_2 as a clean oxidant by increasing its nucleophilicity and facilitating attack by the oxidizing species on the carbon of the carbonyl group⁴⁸⁹. Different catalyst systems reported for this include heterogeneous catalysts based on solid acids⁴⁹¹, zeolites^{492,493}, titanium silicate, Se⁴⁰², As⁴⁹⁴, sulfonated organic ion exchange resins^{493,495} and homogeneous catalysts based on Pt⁴⁹⁶, Zr⁴⁹⁷, Re^{498,499}, Se^{500,501}, As⁴⁹⁴ and Mo⁵⁰² and simple Brønsted acids³⁶².

In 1998, Strukul and coworkers presented a diphosphine–palladium complex, with which the Baeyer–Villiger oxidation of cyclic and for the first time also acyclic ketones could be catalyzed in the presence of various peroxidic oxidants (H_2O_2 , TBHP, KHSO_5 , carbamide peroxide) (Scheme 158)⁴⁹⁶. From these oxidants H_2O_2 turned out to be the most efficient one, whereas almost no conversion was obtained (<1% after several days) with TBHP. The authors could show that an increase in the bite angle of the diphosphine caused

SCHEME 158. Platinum-catalyzed Baeyer–Villiger oxidation using H₂O₂

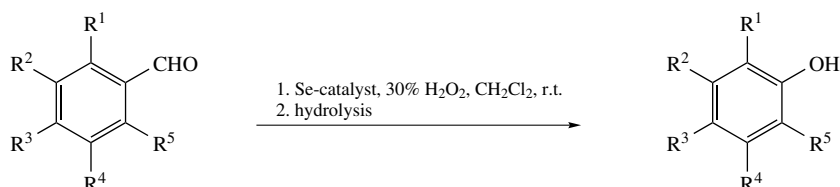
a decrease in the catalytic activity, and therefore the platinum complex with the dpbb ligand [1,4-bis(diphenylphosphino)butane] proved to be the most active catalyst, giving ϵ -caprolactone (starting from 2-methylcyclohexanone) with a yield of *ca* 56% after 4.5 hours at 25 °C. The selectivity of the reaction was extremely high (>99%) as the lactone was the only product observed. Besides cyclic ketones, also acyclic methyl ketones were tested as substrates and the tendency of migration increased in the following order: *prim*-alkyl < phenyl < *sec*-alkyl < vinyl < *tert*-alkyl. Two years later Strukul and coworkers reported on the immobilization of this platinum complex by ion exchange with sulfonated styrene–divinylbenzene copolymers and the use of this heterogeneous Pt complex as catalyst for the Baeyer–Villiger oxidation of 2-methylcyclohexanone⁵⁰³. Although the reaction could be effected with this immobilized catalyst, a significant decrease in activity was observed compared to the analogous homogeneous catalyst.

Selenium compounds, especially phenylselenenic acid, have been successfully employed as oxidation catalyst for a variety of reactions. In 1977, Grieco and coworkers carried out the Baeyer–Villiger oxidation of several mono- and bicyclic ketones using phenylselenenic acid as catalyst in the presence of 30% H₂O₂ as terminal oxidant yielding the corresponding lactones in 50–83% (equation 78)⁵⁰¹. With this catalytic system even substrates, which could not be oxidized to the lactone by other methods (peroxyacetic acid, MCPBA, anhydrous peroxyacetic acid, SeO₂/H₂O₂), were transformed to the lactone by phenylselenenic acid/H₂O₂ (63% yield after esterification).



Very good results were also obtained by Syper and Mlochowski, who tested a series of organoselenium compounds like organoselenenic acids and the corresponding diselenides as catalysts for the Baeyer–Villiger oxidation reaction of various aromatic ketones and aldehydes using hydrogen peroxide as oxidant^{504, 505}. All selenium compounds that can be oxidized by H₂O₂ to the corresponding seleninic acids can serve as efficient catalysts for the Baeyer–Villiger reaction. During their studies the authors also investigated the

effect of nitro substituents at the *ortho* and *para* position of benzeneseleninic acid on this oxidation reaction. The best results were obtained with the catalyst bearing a nitro group in *ortho* position and also the *ortho*, *para*-dinitro-substituted benzeneseleninic acid showed similarly good results (yields up to 98%). By this method a variety of phenols are accessible by Baeyer–Villiger oxidation of aromatic aldehydes and subsequent hydrolysis of the ester intermediate (Scheme 159).



$R^1 = \text{H, Me, OAlk, OBn, OCH}_2\text{OMe}$

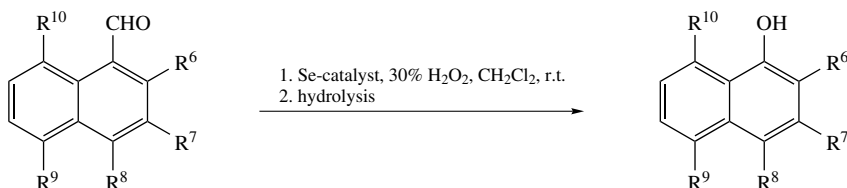
$R^2 = \text{H, Me, OMe}$

$R^3 = \text{H, Me, Ph, OMe, OBn, OCH}_2\text{OMe}$

$R^4 = \text{H, Me, OMe}$

$R^5 = \text{H, Me, OMe}$

14–98%



$R^6 = \text{H, OMe, OCH}_2\text{OMe}$

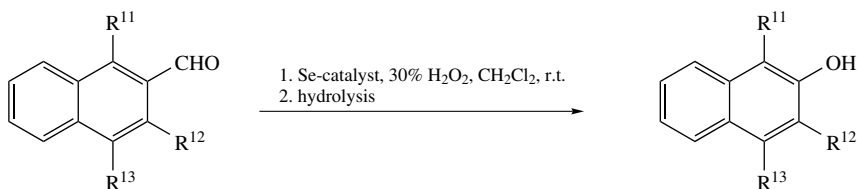
$R^7 = \text{H, OMe}$

$R^8 = \text{H, OMe}$

$R^9 = \text{H, Br}$

$R^{10} = \text{H, OMe}$

54–98%



$R^{11} = \text{H, OMe, OCH}_2\text{OMe}$

$R^{12} = \text{H, OMe}$

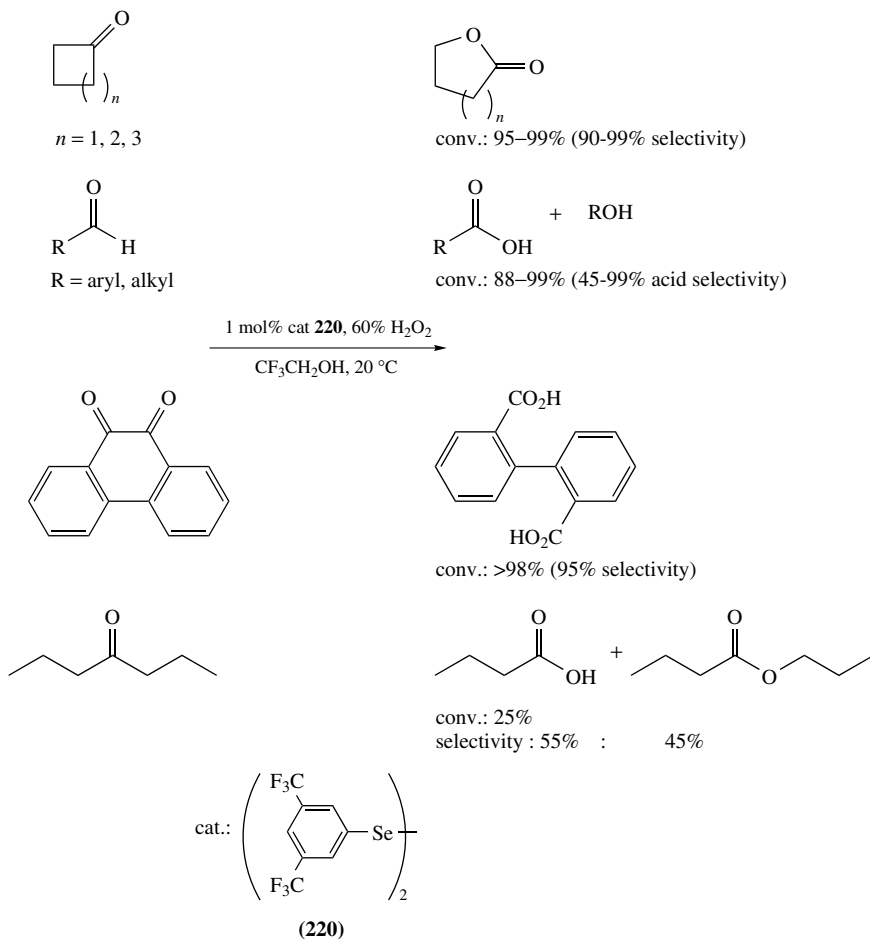
$R^{13} = \text{H, OMe}$

67–97%

Se-catalysts: 2-O₂NC₆H₄SeSeC₆H₄NO₂-2
 2,4-(O₂N)₂C₆H₃SeSeC₆H₃(NO₂)₂-2,4
 2-O₂NC₆H₄SeO₂H
 2,4-(O₂N)₂C₆H₃SeO₂H

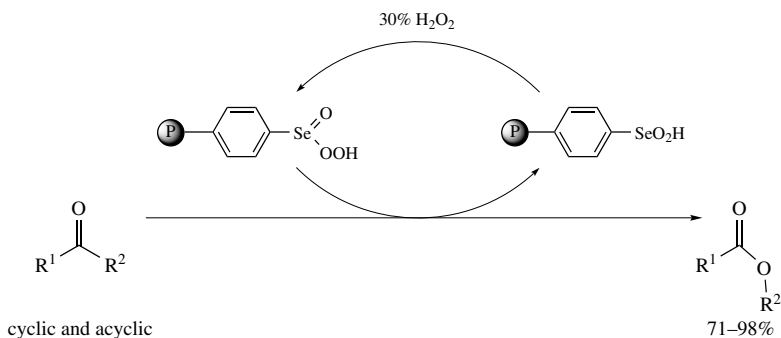
SCHEME 159. Selenium-catalyzed Baeyer–Villiger oxidation of aromatic aldehydes and phenol formation via hydrolysis of the intermediary esters

For the oxidation of aromatic aldehydes 30% H_2O_2 was sufficient to obtain good yields, but the ketone acetophenone and its derivatives reacted much more slowly and therefore 90% H_2O_2 had to be used in order to prepare the corresponding phenols in yields of 27 to 89% (for polymethoxyacetophenones bearing at least one OMe group on the aromatic ring). Sheldon and coworkers could show that diselenides with electron-withdrawing substituents (NO_2 , CF_3) in the *ortho*- and/or *para*-position of the aromatic ring serve as very efficient and selective catalysts for Baeyer–Villiger reaction in the presence of 60% aqueous hydrogen peroxide⁵⁰⁰. Bis[3,5-bis(trifluoromethyl)phenyl] diselenide **220** turned out to be most efficient in catalyzing the oxidation of a number of ketones in trifluoroethanol as solvent with good conversions (25–100%) (Scheme 160). Even better conversions were obtained in hexafluoroisopropanol, but this solvent is relatively expensive. The cycloalkanones give the corresponding lactones in good selectivities (90–99%) and show little tendency to give ring contraction to cycloalkanecarboxylic

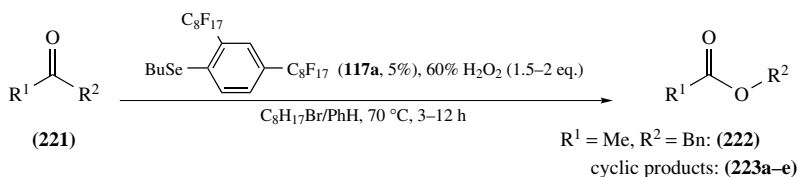


SCHEME 160. Diselenide-catalyzed Baeyer–Villiger oxidation of various carbonyl compounds with aqueous H_2O_2 as oxidant

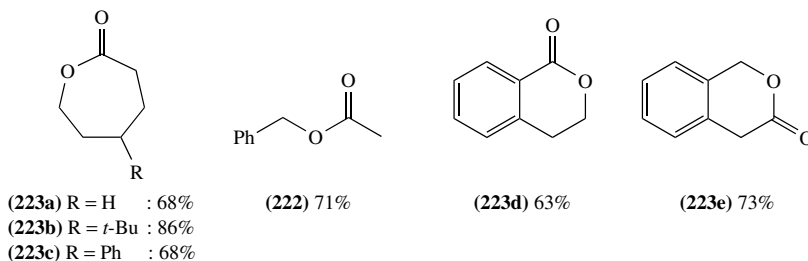
acids. Aldehydes or 1,2-diketones are transformed into the corresponding carboxylic acids (45–99% selectivity). In reactions where the lactone product is sensitive to hydrolysis, the fluorinated solvent is changed to CH_2Cl_2 in which the conversions are significantly lower but in which hydrolysis is suppressed. Since organoselenium compounds are toxic, product contamination can be avoided by using polystyrene-bound phenylseleninic acid. In 1983, for example, Taylor and Flood reported the use of polystyrene-bound seleninic acid in combination with hydrogen peroxide as catalytic system for the Baeyer–Villiger oxidation of ketones to lactones (Scheme 161)⁴⁰². The same system was also used for the dihydroxylation of alkenes and in combination with TBHP as catalyst for alcohol oxidation (see Section III.C). The products of the Baeyer–Villiger oxidation could generally be obtained in good yields of 71–98%. Fluorous biphasic catalysis is an alternative for this procedure, in which the catalyst is substituted with long perfluoroalkyl chains to achieve a selective solubility in perfluorinated solvents. Perfluoroalkyl-substituted aryl selenide **117a** (see Section III.A.2.d) has been found to catalyze the oxidation of ketones **221** to ester **222** and lactones **223a–e**³⁹. This reaction as well as the yields of several Baeyer–Villiger products are shown in Scheme 162.



SCHEME 161. Baeyer–Villiger oxidation using polymer-bound phenylseleninic acid and H_2O_2

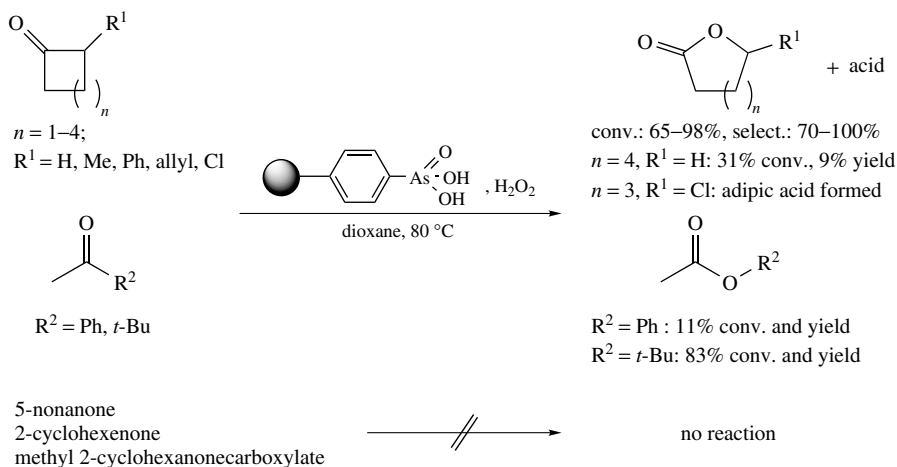


Products :



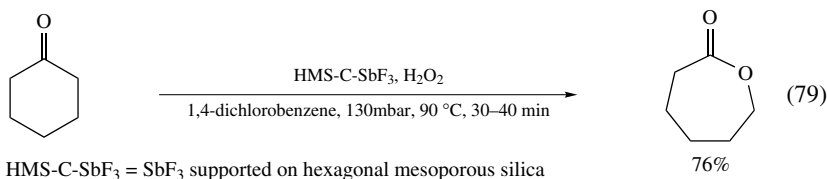
SCHEME 162. Selenium-catalyzed Baeyer–Villiger oxidation

Besides the selenium catalysts described above, also arsenic oxides like benzenearsonic acid showed catalytic activity for Baeyer–Villiger oxidation using hydrogen peroxide as oxidant⁴⁹⁴. A major drawback of arsenic oxides is their toxicity and the fact that in the presence of hydrogen peroxide they exhibit Brønsted and Lewis acidity causing extensive solvolysis of lactones. Therefore, Jacobson and coworkers developed a heterogeneous catalyst in which polystyrene is arsonated on the benzene ring⁴⁹⁴. This material proved to be a versatile catalyst for the Baeyer–Villiger oxidation of ketones by hydrogen peroxide under biphasic (water–dioxane/heterogeneous catalyst) as well as triphasic conditions (water/heterogeneous catalyst/chloroform) (Scheme 163). The rates of oxidation catalyzed by the arsonated polystyrene are about three times slower than that in the presence of equivalent quantities of benzeno- or toluenearsonic acids. The great advantage of the resin-supported arsenic acid is its recyclability by simple filtration without loss of activity. Besides this, also hydrolysis of the lactone and ester products, which is often a problem under homogeneous reaction conditions, can be prevented. Under biphasic conditions, oxidation of medium-size cycloalkanones (C4–C6), steroid ketones and branched chain aliphatic ketones are catalyzed with good yields, while larger cycloalkanones (cycloheptanone: 31% conversion, lactone : acid–by-product: 29:71), acetophenone (11% conversion) and straight-chain aliphatic ketones react slowly or not at all. The triphase system is useful for the preparation of lactones, which are insoluble in water. For example, estrone-3-methyl ether, which does not react with MCPBA in chloroform, can be oxidized in the triphasic system aqueous H₂O₂/arsonated polystyrene catalyst/chloroform with 60% yield.

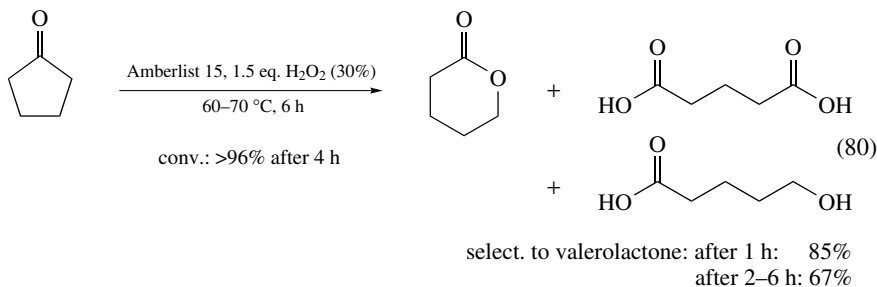


SCHEME 163. Baeyer–Villiger oxidation of ketones using arsonated polystyrene and H₂O₂

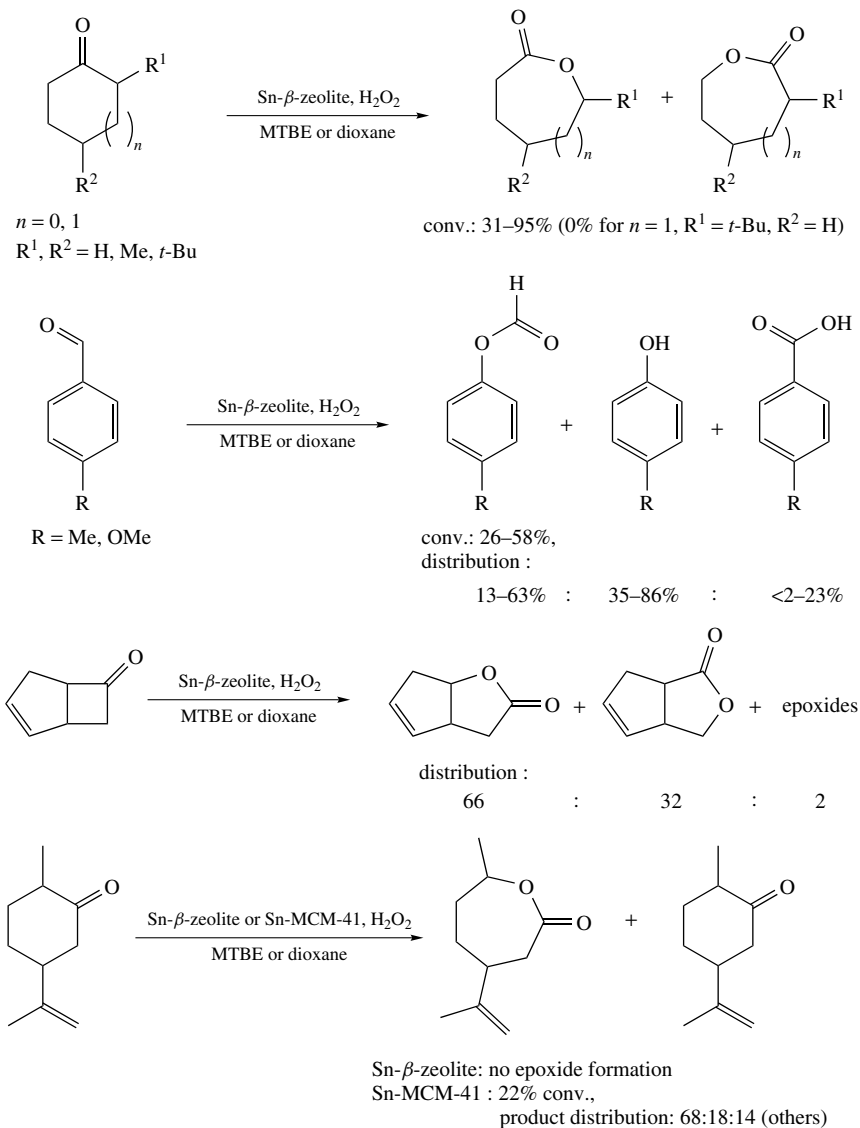
The oxidation of cyclohexanone to caprolactone using hydrogen peroxide as terminal oxidant can be selectively catalyzed by the heterogeneous acid catalyst SbF₃ supported on hexagonal mesoporous silica as reported by Lambert and coworkers in 2000 (equation 79)⁴⁹¹. The catalyst possesses Lewis- as well as Brønsted-acid sites and it shows higher efficiency for the Baeyer–Villiger oxidation than the silica gel analogues because of the high surface area. The best result that could be obtained with this catalyst was a 76% yield of caprolactone after 30–40 min reaction at 90 °C in vacuum (70–130 mbar). As a side reaction, some ring opening and polymerization of the lactone occurred.



In 1999, Fischer and Hölderich published a comparative study on the Baeyer–Villiger oxidation of cyclopentanone to δ -valerolactone using 30% aqueous H₂O₂ and several acidic heterogeneous catalysts (organic ion exchange resins, zeolites and Nafion® composite materials) without the need of a solvent (equation 80)⁴⁹³. Besides zeolite- β , which showed satisfactory results, the best catalyst in terms of activity and selectivity turned out to be the ion exchange resin Amberlist 15. With the Amberlist materials high conversions of cyclopentanone after 4 hours at 60–70 °C (almost 100%) and good lactone selectivities (maximum after 1 hour: 85%, after 2 hours: 67%) could be obtained, while zeolitic materials (HZSM-5, HMOR, HBEA, USY) (except zeolite- β : 80% conv.) were less active (conv. after 6 h: 30–60%). Glutaric acid, valeric acid and dicyclopentylidene diperoxide were formed as side products of the reaction. With Amberlist 15 as catalyst, selectivity and conversion increase with the excess of H₂O₂ whereby acceptable results are already obtained with 1.5 equivalents of oxidant.

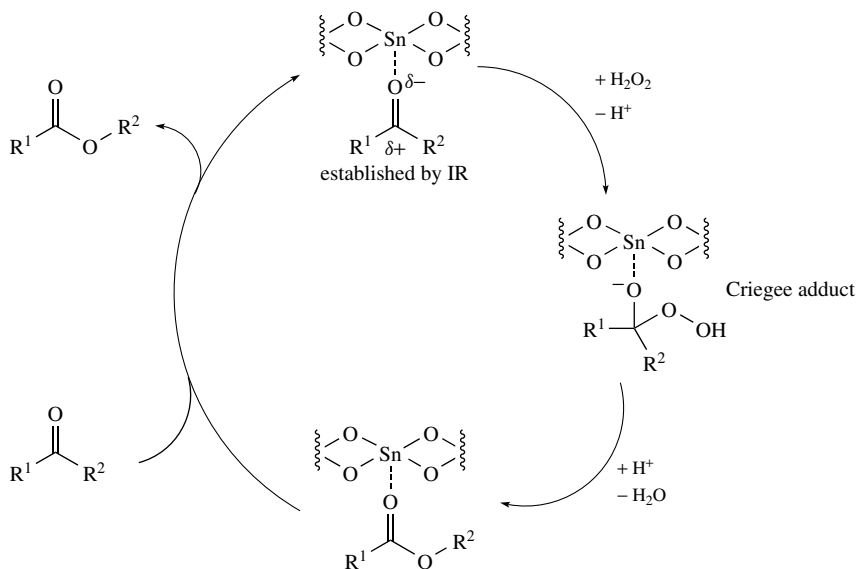
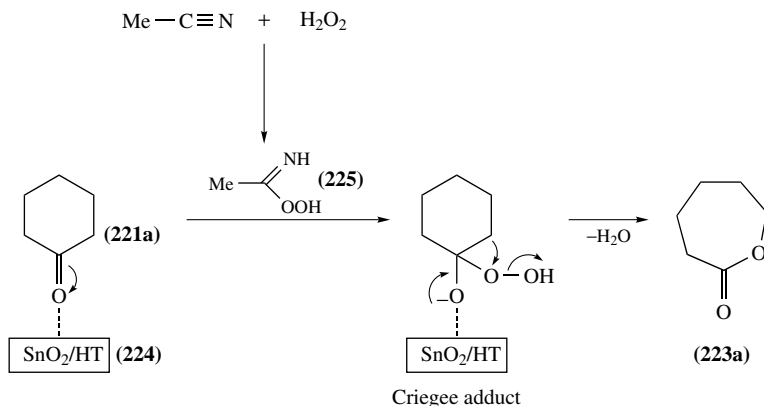


The disadvantage of some of the processes, which are based on the H₂O₂ activation by the catalyst, are low activity or selectivity. For example, homogeneous molybdenum peroxo picolinato and molybdenum peroxo pyridine-2,6-dicarboxylato complexes (by Jacobson and coworkers)⁵⁰² as well as supported Pt complexes (by Strukul and coworkers)⁵⁰³ showed low activity. A novel activation strategy has been reported by Corma and coworkers. Utilizing a novel heterogeneous Sn/zeolite- β catalyst (Scheme 164)^{506,507} and also a Sn-incorporated MCM-41 catalyst⁵⁰⁸, the authors could activate the carbonyl group of the ketone (instead of H₂O₂) for a Baeyer–Villiger reaction. Both catalysts show very good chemoselectivity for lactone formation in the presence of H₂O₂. With the Sn/zeolite- β catalyst the double bond of unsaturated ketones is not epoxidized under the reaction conditions and formation of dimeric peroxides (common by-products in Baeyer–Villiger reactions with H₂O₂) is not observed, while with the Sn-MCM-41 heterogeneous catalyst a small amount of epoxide product was also obtained (Scheme 164, bottom). Sn/zeolite- β provides shape selectivity, which can be seen from the fact that 2-*t*-butylcyclohexanone is not oxidized to the lactone, while other substituted cyclohexanones with similar size could be transferred (Scheme 164, top). Less reactive ketones such as acyclic or aromatic ones are not converted. Aromatic aldehydes can be oxidized by the Sn/zeolite- β catalyst either to the ester (phenol formation through hydrolysis) or to the carboxylic acid product,

SCHEME 164. Baeyer–Villiger oxidation using Sn- β -zeolite/ H_2O_2

whereby electron-donating groups direct towards ester/phenol formation while electron-withdrawing groups favor acid formation. The catalyst could be recycled (4 times) without loss of activity but the Sn-MCM-41 catalyst loses activity after recycling.

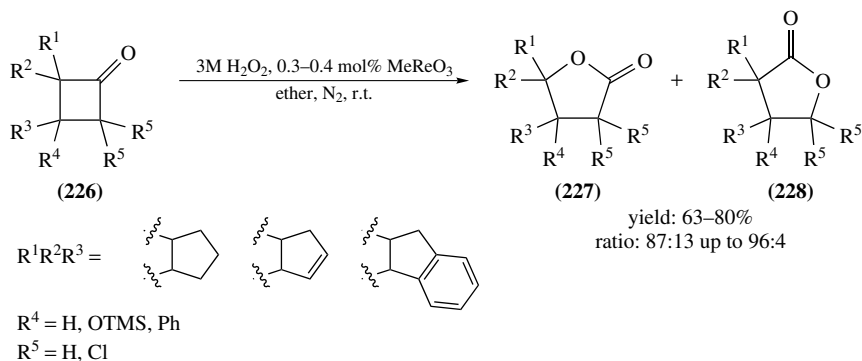
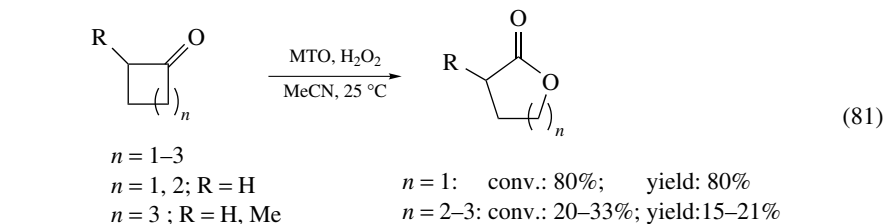
The results of infrared investigations and ^{18}O -labeling experiments support the mechanism depicted in Scheme 165, which includes carbonyl group activation by the catalyst and oxygen transfer via Criegee adduct. Two years later Pillai and Sahle-Demessie could

SCHEME 165. Catalytic cycle of the Baeyer–Villiger oxidation using Sn-zeolite- β /H₂O₂SCHEME 166. Baeyer–Villiger oxidation catalyzed by Sn-doped hydrotalcites in the presence of CH₃CN/H₂O₂

show that the Sn-doped hydrotalcite **224** depicted in Scheme 166 is an active and selective catalyst for the liquid-phase Baeyer–Villiger oxidation of cyclic ketones **221** in acetonitrile using H₂O₂ as oxidant⁵⁰⁹. Hydrotalcites are high surface area, homogeneous basic mixed hydroxides with a layered structure having the formula Mg₆Al₂(OH)₁₆CO₃·4 H₂O. The activity of the catalyst is attributed to the presence of active Sn sites in the interstitial position of hydrotalcite support, which activate the carbonyl group for a nucleophilic attack by the active peroxide species **225**. This active species is a peroxycarboximidic acid **225**, which is a good oxygen transfer agent and which is formed through nucleophilic

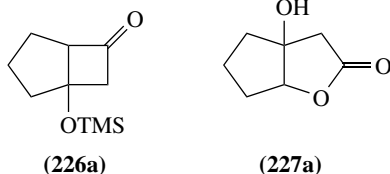
attack of the intermediary formed perhydroxyl anion on acetonitrile. Different ketones have been tested as substrates and yields between 16 and 42% have been obtained. The selectivity in every case was very high (100%) and turnover numbers (moles of reactant consumed/total number of metal sites) varied from 63 to 166.

Herrmann and coworkers were the first to report on the oxidation of cyclic ketones to the corresponding lactones employing MTO/H₂O₂(5–10%)/TBHP (equation 81)⁴⁹⁹. With this system conversions and yields were only good for ring-strained cyclobutanone (80% conversion and yield), while for the higher homologues yields were ≤ 21% after 3 days at 25 °C. The preformed bis(peroxo) complex [MeReO(O₂)₂·H₂O] has been shown to act as stoichiometric Baeyer–Villiger oxidant. Besides MTO, also ReO₃ is activated by 85% H₂O₂ to yield an efficient catalyst (valerolactone synthesis with 50% yield), which is more sensitive to water. γ -Butyrolactones **227** and **228** can be obtained in good yields and regioselectivity by Baeyer–Villiger oxidation with hydrogen peroxide catalyzed by MTO, as was shown by Faisca Phillips and Romão (Scheme 167)⁴⁹⁸. In general, conversions of substrates **226** were complete within 1–7.5 hours. Bicyclic and tricyclic compounds reacted faster due to increased ring strain. Electron-withdrawing groups retard the reaction and the oxygen is inserted between the carbon atom that is not substituted and the carbonyl group. Lactonization with MTO as catalyst proceeded chemoselectively in the presence of double bonds, aromatic rings and chlorine substituents and trimethylsiloxy substituted ketone **226a** was directly converted into a hydroxylated lactone **227a** in good yield (70%) and regioselectivity (96:4).



SCHEME 167. Synthesis of γ -butyrolactones by a MTO-catalyzed Baeyer–Villiger oxidation with H₂O₂

In 2003, Bernini and coworkers established a method for converting some flavonoid ketones into the corresponding lactones with hydrogen peroxide as oxidant catalyzed by MTO supported on poly(4-vinylpyridine) polymers (equation 82)⁵¹⁰. Conversions and

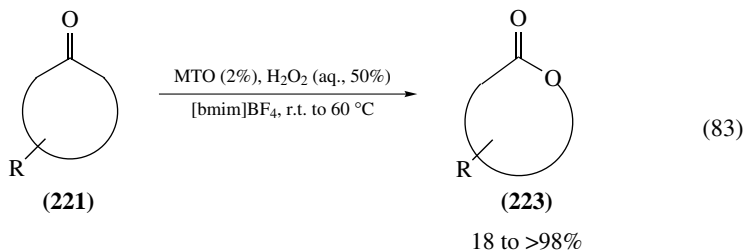
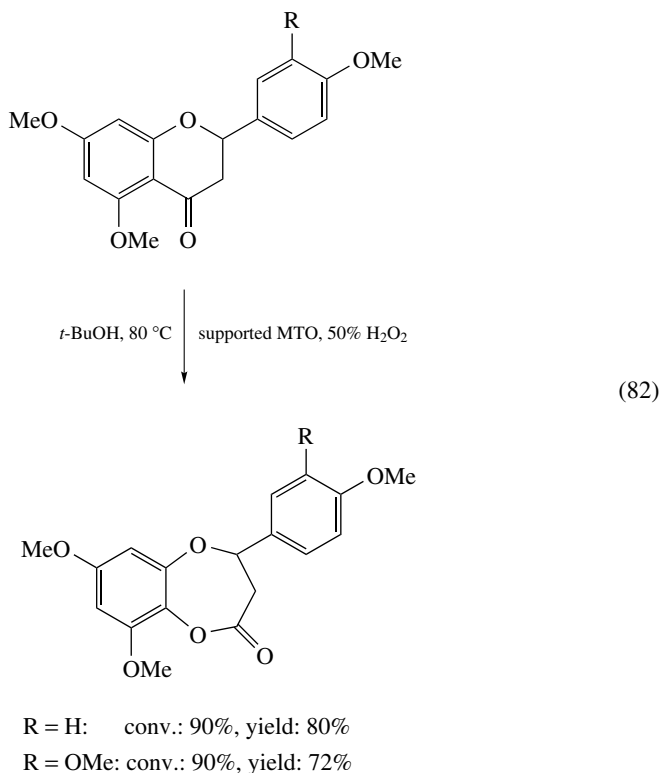


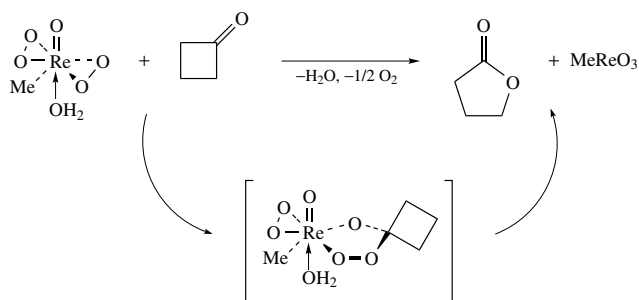
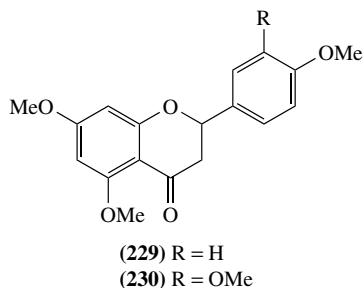
lactone selectivity were very good for these substrates (72% and 80% yield). Simple cyclic ketones such as cyclobutanone reacted slowly or were totally unreactive under these conditions (like cyclopentanone)⁵¹¹. Later, the same research group investigated an alternative to the heterogeneous catalyst: use and reuse of MTO as an efficient homogeneous catalyst in 1-butyl-3-methylimidazolium tetrafluoroborate ([bmim]BF₄) as ionic liquid⁵¹¹. The authors developed a recycling procedure in which the lactone was extracted with diethyl ether and the ionic liquid solution of the catalyst was recycled and reused, giving the same yields as in the first run. A variety of cyclic ketones **221** have been oxidized to the lactones **223** with low to high yields (18 to >98%, equation 83). MTO in ionic liquids was most effective for ring-strained cyclobutanone; γ -butyrolactone was quantitatively isolated after only one hour. The method was also tested for the methylated flavonones naringenin (**229**) and hesperitin (**230**), providing the corresponding lactones in very good yields (>98% and 95%) after two hours. Compared to the polymer-supported MTO/H₂O₂ system in butanol, the MTO/H₂O₂ catalytic system in [bmim]BF₄ was more efficient, affording milder reaction conditions, requiring smaller quantities of oxidant and producing the lactones with better yields. The mechanistic pathway for the MTO-catalyzed Baeyer–Villiger oxidation is shown in Scheme 168.

For a long time the asymmetric version of the metal-catalyzed Baeyer–Villiger reaction with hydroperoxides remained uninvestigated. The first promising developments in this area have been reported since 1994^{489,512}, using different metal/chiral ligand combinations and commercially available hydroperoxides like H₂O₂, TBHP or CHP. Strukul and coworkers for the first time investigated the asymmetric version of a Baeyer–Villiger transformation of racemic cyclic ketones substituted in position 2 by a kinetic resolution using hydrogen peroxide as oxidant in the presence of a variety of platinum(II) complexes **231** with various chiral diphosphine ligands (Scheme 169)⁵¹³. With these platinum complexes in the presence of hydrogen peroxide, the racemic chiral ketones depicted in Scheme 169 could be kinetically resolved with low to good enantiomeric excesses of 0–58%. The best asymmetric induction was obtained with complex **231d** bearing a chiral BINAP ligand, the dianion of 2-vanillin as second ligand and ClO₄[−] as counterion. With this system the highest enantiomeric excess of 58% was achieved with 2-(*n*-pentyl)cyclopentanone as substrate. Substrates with shorter side chains were converted to the corresponding lactones faster, but lower enantioselectivities were observed. Unfortunately, conversions did not exceed 12% and therefore low yields of lactones were obtained. ClO₄[−] as counterion seems to be essential for catalytic activity of the complex because it is a non-coordinating anion, which leaves a vacant coordination site on the central metal.

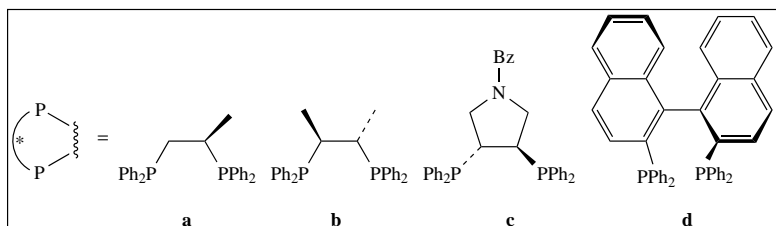
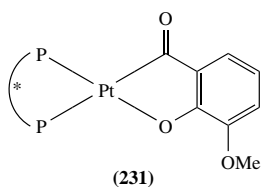
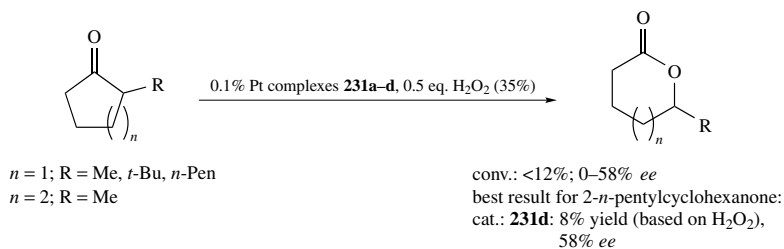
Later, the same group reported the use of new dinuclear chiral platinum(II) catalysts **232a–f** for the enantioselective Baeyer–Villiger oxidation of 2-methylcyclohexanone **221f**⁵¹⁴ and cyclic *meso*-ketones **221c, g, h**⁵¹⁵ again using hydrogen peroxide as oxidant (Scheme 170). The best catalysts are those in which the ligands, bearing the chiral information, possess C₂-symmetry and/or are capable of forming a seven-membered chelate ring with the Pt center. For all substrates tested, complex **232a** bearing two chiral BINAP ligands turned out to be the best catalyst in terms of yields and enantioselectivity of the cyclohexanones. **221c** and **221g** could be oxidized to give the corresponding lactones

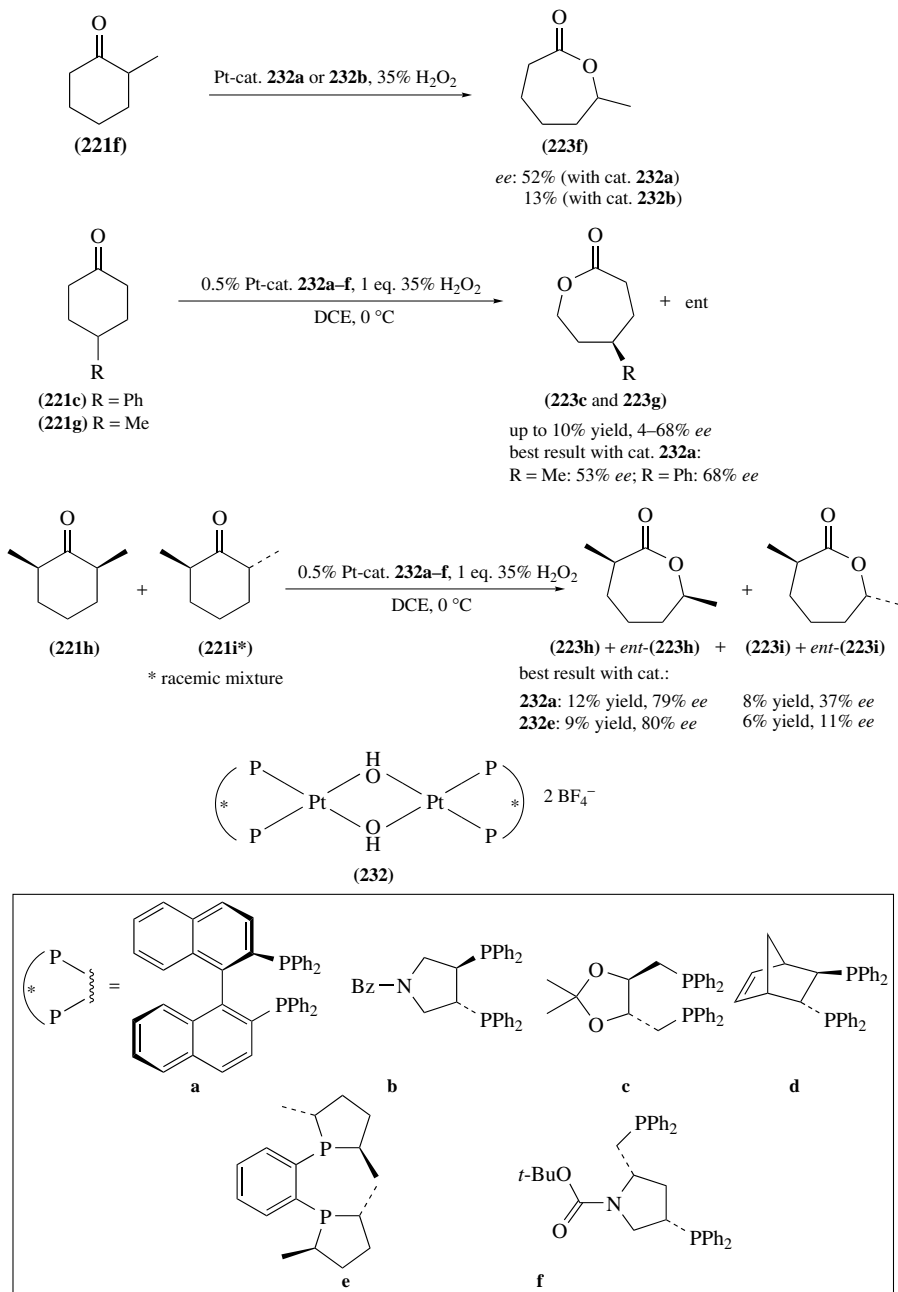
223c and **223g** in yields of 9% and 10% and enantiomeric excesses of 68% and 53%, respectively. In the case of the oxidation of the mixture of *meso*-cyclohexanone **221h** and racemic **221i**, two asymmetric transformations occurred at the same time: asymmetric induction on **221h**, producing the enantiomers **223h** and *ent*-**223h**, and the kinetic resolution of racemic **221i**, forming enantiomers **223i** and *ent*-**223i**. The asymmetric induction in the oxidation of **221h** is more selective (**223h** was obtained with *ee* up to 80%) than the kinetic resolution (**223i** was obtained with *ee* up to 37%). Yields in all cases were low ($\leq 10\%$) at 0 °C and could be raised up to 21% by conducting the reaction at a higher temperature of 25 °C, combined with a slight decrease in enantioselectivity. As a side reaction, peroxide formation was obtained from the acid-catalyzed reaction of hydrogen peroxide with the ketone (equation 84). This reaction can become quite significant and in some cases ketone amounts up to 50% were converted to the peroxide side product.



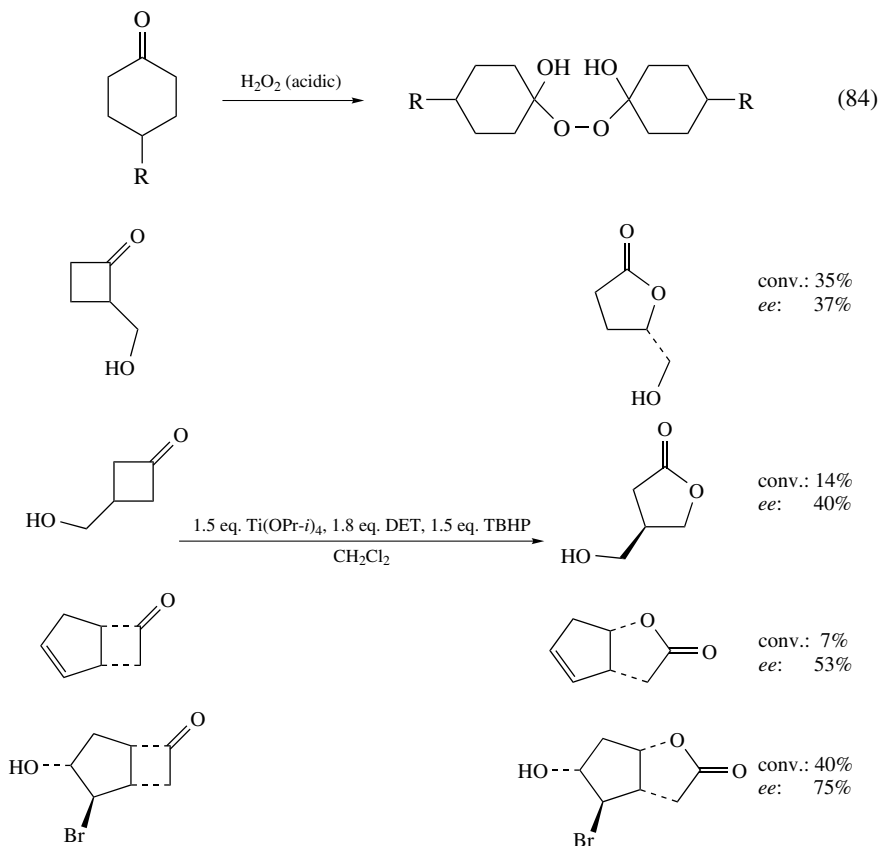


SCHEME 168. Mechanistic pathway for the oxidation of cyclobutanone catalyzed by MTO

SCHEME 169. Chiral Pt complexes **231** employed as asymmetric inducers in the kinetic resolution of racemic cyclic ketones formed by enantioselective Baeyer–Villiger oxidation



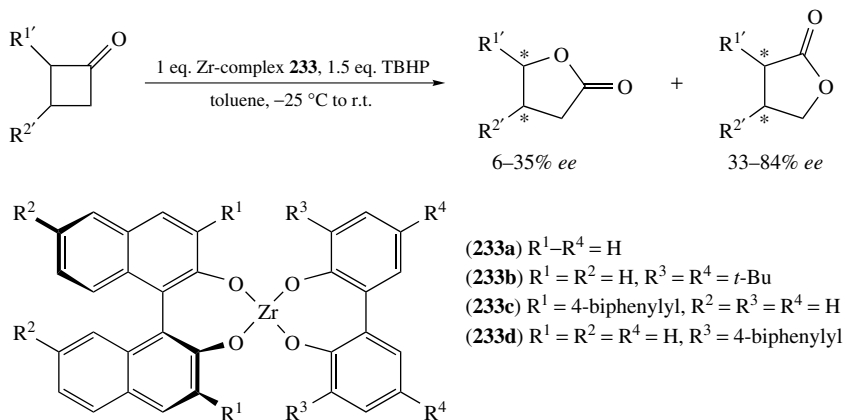
SCHEME 170. Pt-catalyzed enantioselective Baeyer–Villiger oxidation of cyclic *meso*-ketones with H_2O_2 using chiral diphosphine ligands



SCHEME 171. Titanium-catalyzed asymmetric Baeyer–Villiger oxidation of cyclobutanones

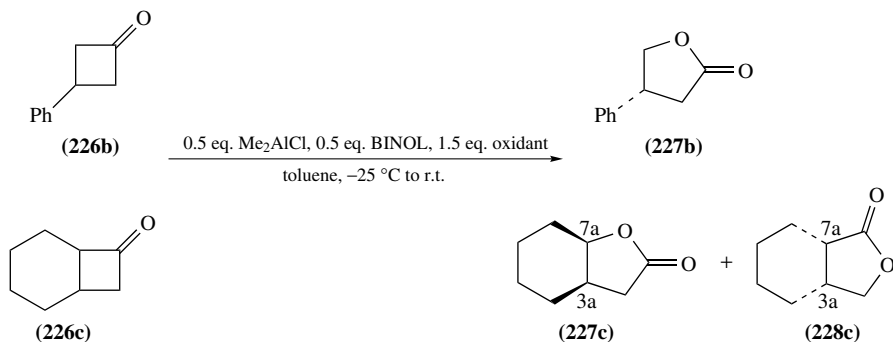
Another method for the asymmetric version of the Baeyer–Villiger reaction was presented by Lopp and coworkers in 1996⁵¹⁶. By employing overstoichiometric quantities of Ti(OP*i*-Pr)₄/DET/TBHP (1.5 eq./1.8 eq./1.5 eq.), racemic cyclobutanones were converted to enantiomerically enriched lactones with *ee* values up to 75% and moderate conversions up to 40% (Scheme 171). Bolm and Beckmann used a combination of axially chiral C₂-symmetric diols of the BINOL type as ligands in the zirconium-mediated Baeyer–Villiger reaction of cyclobutanone derivatives in the presence of TBHP (or CHP) as oxidant (Scheme 172)⁴⁹⁷. With the *in situ* formed catalysts **233a–d** the regioisomeric lactones were produced with moderate asymmetric inductions (6–84%). The main drawback of this method is the need of stoichiometric amounts of zirconium catalyst.

In 2001, Bolm and coworkers investigated the influence of structurally different achiral and chiral hydroperoxides on the enantioselectivity of the vanadium-catalyzed asymmetric epoxidation of primary allylic alcohols and the Baeyer–Villiger oxidation of racemic cyclobutanone derivatives using chiral ligands²¹⁷. The results of the former oxidation process are presented in Section III.A.3.b. Similar results were reported for the Baeyer–Villiger oxidation of two racemic cyclobutanone derivatives **226b** and **226c** using



SCHEME 172. Zirconium-mediated asymmetric Baeyer–Villiger oxidation

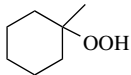
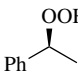
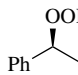
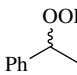
catalytic amounts (0.5 eq.) of $\text{Me}_2\text{AlCl}/\text{BINOL}$ (Scheme 173, Table 32). Here as well, it is dependent on the substrate which oxygen source is the best one. While trityl hydroperoxide was the best oxygen source for the oxidation of cyclobutanone **226b** (75% *ee* of the lactone **227b**), it was the worst one for the oxidation of **226c** [low *ee* of regioisomeric lactones: **227c** (22% *ee*) and **228c** (80% *ee*)]. The results with the enantiomerically pure hydroperoxide **16a** show that the absolute configurations are determined by the chirality of the ligand. A cooperative effect between the chiral ligand [(*R*)- or (*S*)-enantiomer] and the enantiomerically pure hydroperoxide (*S*)-**16a** was observed. The enantiomeric excess achieved with racemic hydroperoxide falls between the *ee* values of the experiments with the pure enantiomers.

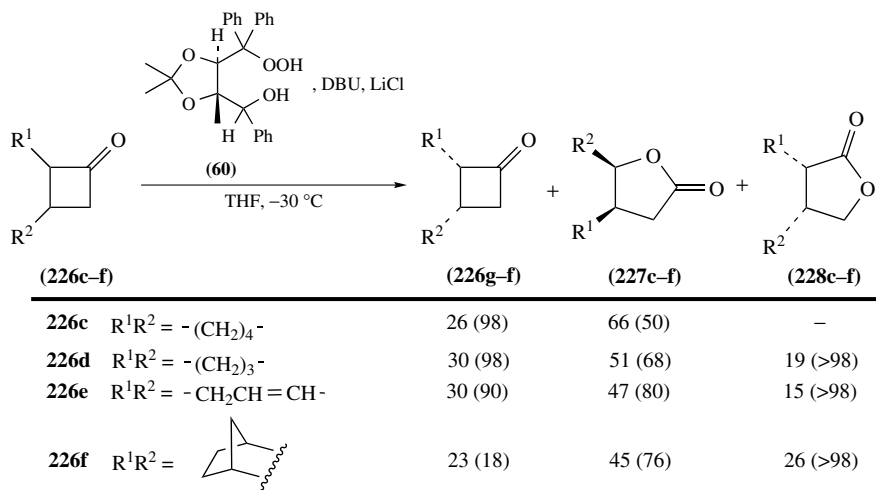


SCHEME 173. Aluminum-catalyzed Baeyer–Villiger oxidation using different oxidants

The use of a chiral hydroperoxide as oxidant in the asymmetric Baeyer–Villiger reaction was also described by Aoki and Seebach, who tested the asymmetric induction of their TADOOH hydroperoxide in this kind of reaction⁹⁸. Besides epoxidation and sulfoxidation, for which they found high enantioselectivities with TADOOH (**60**), this oxidant is also able to induce high asymmetry in Baeyer–Villiger oxidations of racemic cyclobutanone derivatives in the presence of DBU as a base and LiCl as additive (Scheme 174). The yields and *ee* values (in parentheses) of ketones and lactones are given in Scheme 174 as

TABLE 32. Results of the aluminum-catalyzed asymmetric Baeyer–Villiger oxidation using chiral BINOL ligand and achiral and chiral hydroperoxides

Oxidant	TBHP		CHP	TrOOH			
					(<i>S</i> - 16a)	(<i>R</i> - 16a)	(<i>rac</i> - 16a)
BINOL	(<i>S</i>)	(<i>S</i>)	(<i>S</i>)	(<i>S</i>)	(<i>S</i>)	(<i>R</i>)	(<i>S</i>)
<i>ee</i> 227b [(<i>S</i>)]	64	58	71	75	60	51 (<i>R</i>)	56
ratio 227c / 228c	3.3	2.1	2.7	4.5	11.2	4.5	8.3
<i>ee</i> 227c [(3 <i>aR</i> ,7 <i>aR</i>)]	27	36	34	22	5	18 ^a	11
<i>ee</i> 228c [(3 <i>aR</i> ,7 <i>aS</i>)]	95	94	96	80	89	92 ^b	89

^a Opposite enantiomer is formed: (3*aS*,7*aS*).^b Opposite enantiomer is formed: (3*aS*,7*aR*).

yield of different products are given and the corresponding *ee* values are given in parentheses.

SCHEME 174. Yields and *ee* values obtained for different products in the Baeyer–Villiger oxidation employing chiral TADOOH hydroperoxide (**60**)

well. Through this kinetic resolution enantiomerically enriched cyclobutanone derivatives **226c–f** (up to 98% *ee*) and enantiomerically enriched lactones **227c–f** and **228c–f** were obtained with *ee* values depending on reaction temperature, time and amount of base and additive. At high conversions of substrate **226c** (70%) the (*S,S*)-enantiomer of the substrate can be obtained with high enantiomeric purity (98% *ee*) but low yield (26%), while lactone **227c**, which is the only lactone formed, is obtained in a good yield (66%) but with an *ee* of only 50%. Lactone **227c** was obtained with higher enantiomeric purity (82% *ee*), when the conversion was lower (lower temperature and higher DBU and LiCl concentrations). In this case the optical purity of (*S,S*)-**226c** was reduced (76% *ee*). With cyclobutanones **226d–f**, regioisomeric lactones **228d–f** were also formed besides lactones **227d–f**. Under standard conditions (70% conv. with DBU/LiCl at -30°C in THF) substrates **226d** and **226e** showed similar yields and *ee* values as **226c**, producing

lactones **227d** and **227e** (47–51%, 68–80% *ee*) and **228d** and **228e** (15–19%, $\geq 98\%$ *ee*) in a ratio of *ca* 74:26. The tricyclic ketone **226f** reacts less selectively, giving **226f** in 23% yield with 18% *ee*, lactone **227f** in 45% yield and 76% *ee* and enantiomerically pure lactone **228f** in 26% yield (**227f**:**228f** ratio of 63:37).

In 2001, Albrecht Berkessel and Nadine Vogl reported on the Baeyer–Villiger oxidation with hydrogen peroxide in 1,1,1,3,3,3-hexafluoroisopropanol (HFIP) as solvent in the presence of Brønsted acid catalysts such as *para*-toluenesulfonic acid (equation 85)³⁶². Under these conditions cyclohexanone could be selectively transformed into the corresponding lactone within 40 min at 60 °C with a yield of 92%. Mechanistic investigations of Berkessel and coworkers revealed that this reaction in HFIP proceeds by a new mechanism, via spiro-bisperoxide **234** as intermediate, which then rearranges to form the lactone⁵¹⁷. The study illustrates the importance of HFIP as solvent for the reaction, which presumably allows the cationic rearrangement of the tetroxane intermediates.

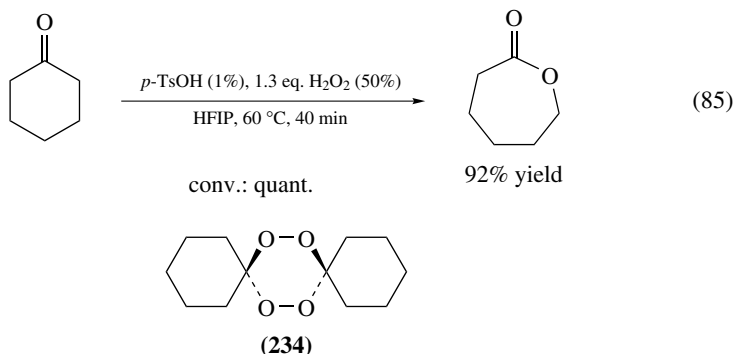


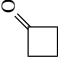
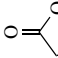
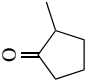
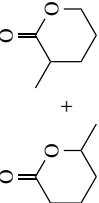
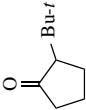
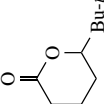
Table 33 summarizes the results of the Baeyer–Villiger oxidation of various ketones obtained with the different methods described above.

G. Vicinal Dihydroxylation of Alkenes and Alkynes

For a recent review on the catalytic asymmetric dihydroxylation, see Reference 518.

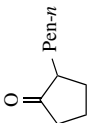
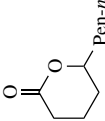
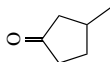
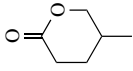
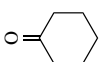
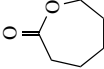
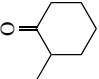
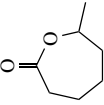
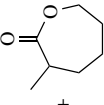
The dihydroxylation of alkenes and alkynes can be catalyzed by osmium, ruthenium and manganese oxo species, with osmium being the most versatile and selective catalyst for this process. Besides *N*-methylmorpholine *N*-oxide (NMO) or $K_3[Fe(CN)_6]$, also TBHP and hydrogen peroxide have been used as terminal oxidants. The ‘classical’ catalytic method for converting alkenes to the corresponding glycols employs hydrogen peroxide in the presence of catalytic amounts of osmium tetroxide (equation 86)⁵¹⁹. A survey of the yields obtained in the dihydroxylation reaction of various alkenes using catalytic amounts of OsO_4 and H_2O_2 as oxidant is given in the review of Schröder from 1980⁵¹⁹. Unfortunately, with this method overoxidation to ketols often occurs and therefore more effective methods have been developed over the years, some of them employing alkyl hydroperoxides, mainly TBHP^{520–523} or ethylbenzene hydroperoxide⁵²³ as oxidant. An early report on the use of the catalytic system OsO_4 /TBHP was published in 1948 by Byers and Hickinbottom⁵²⁴ and this method was modified by Sharpless and coworkers in 1976 and 1978 by employing additional Et_4NOH ⁵²⁰ or Et_4NOAc ⁵²¹ (Scheme 175). Addition of the ammonium salts increased the turnover rates by facilitating removal of glycol products from the coordination sphere of the osmium. Gaseous olefins could be dihydroxylated with OsO_4 /ethylbenzene hydroperoxide or TBHP in the presence of


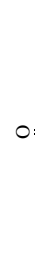

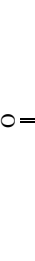
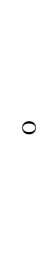
TABLE 33. Results of the Baeyer–Villiger oxidation of various ketones and aldehydes using different methods

Substrate	Catalyst/ method ^a	Amount of oxidant ^b (concentration)	Product(s)	Conv. (%)	Ketone yield (%), (<i>ee</i>)	Product(s) yield (%), (<i>ee</i>)	Reference
	A	2 eq. (50%)		>98		>98	511
	B	1.8 eq. (30%)		96		96	402
	220	2 eq. (60%)		89		89	500
	MTO (6%)	2.7 eq. (3M)		80		80	499
	C	0.2 eq. (90%)		98		98	494
	Sn/HT (1.5%)	4 eq. (30%)		16		16	509
	A	6 eq. (50%)		>98		>98	511
	B	1.8 eq. (30%)		95		95	500
	220	2 eq. (60%)		20		20	506
	MTO (6%)	2.7 eq. (3M)		32		32	493
Sn-β zeolite	1.5 eq. (35%)	50		50	493		
Amberlist 15	1.5 eq. (30%)	98		98	493		
Amberlist 15	1.5 eq. (30%)	60–70		60–70	27–33		
Nafion 13 (40)	1.05 eq. (30%)	0.2 eq. (90%)		93	79	494	
	A	6 eq. (50%)		>98		75 + 0	511
	B	1.8 eq. (30%)		43 + 43		43 + 43	402
	Sn-β zeolite	1.5 eq. (35%)		60 + 0		60 + 0	506
	231b or c	0.5 eq. (35%)		7–9 ^c		7–9 ^c	513
	C	0.2 eq. (90%)		84		(26) + 0 64 [20] ^d	494
	231d /HClO ₄	0.5 eq. (35%)		2 ^c (12)		2 ^c (12)	513

(continued overleaf)

TABLE 33. (continued)

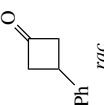
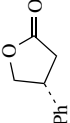
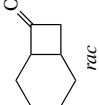
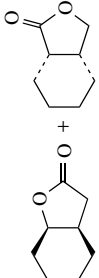
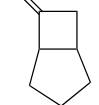
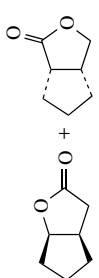
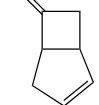
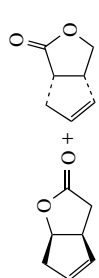


Substrate	Catalyst/ method ^a	Amount of oxidant ^b (concentration)	Product(s)	Conv. (%)	Ketone yield (%), (ee)	Product(s) yield (%), (ee)	Reference
	231d /HClO ₄	0.5 eq. (35%)				8 ^c (58)	513
	A	6 eq. (50%)		90		37 + 37	511
	117a (5%) ^e A B 220 MTO (6%) Sn-β zeolite Sn-MCM-41 HMS-C-SbF ₆ ⁸ <i>p</i> -TsOH (1%) C	1.5–2 eq. (60%) 6 eq. (50%) 1.8 eq. (30%) 2 eq. (60%) 2.7 eq. (3M) 1.5 eq. (35%) 1.5 eq. (35%) 1.3 eq. (50%) 0.2 eq. (90%)				68 20 0/ 94 21 52 35 76 92 63 [16] ^d	39 511 402 500 499 506, 507 508 491 362 494
	Sn/HT (1.5%) A PhSe(O)OOH Sn-β zeolite 231d /HClO ₄ C	4 eq. (30%) 6 eq. (50%) 10 eq. (30%) 1.5 eq. (35%) 0.5 eq. (90%) 0.2 eq. (90%)	 + 	42 38 80 78		0 + 42 38 + 0 83 + 0 65 + 12 18 ^c (45) 78	509 511 501 506 513 494

Sn/HT (1.5%) A	4 eq. (30%) 6 eq. (50%)		32 36	0 + 32 14 + 4	509 511
Sn/HT (1.5%) Sn- β zeolite 232a	4 eq. (30%) 1.5 eq. (35%) 1 eq. (35%)		26 70	26 68 10 (53)	509 506 515
B 232a	1.8 eq. (30%) 1 eq. (35%)		92	402 12 (79) +8 (37)	515
117a (5%) ^e PhSe(O)OOH Sn- β zeolite	1.5–2 eq. (60%) 10 eq. (30%) 1.5 eq. (35%)		91	86 67 89	39 501 506
117a (5%) ^e 232a	1.5–2 eq. (60%) 1 eq. (35%)		68 9 (68)	68 9 (68)	39 515

(continued overleaf)

TABLE 33. (continued)

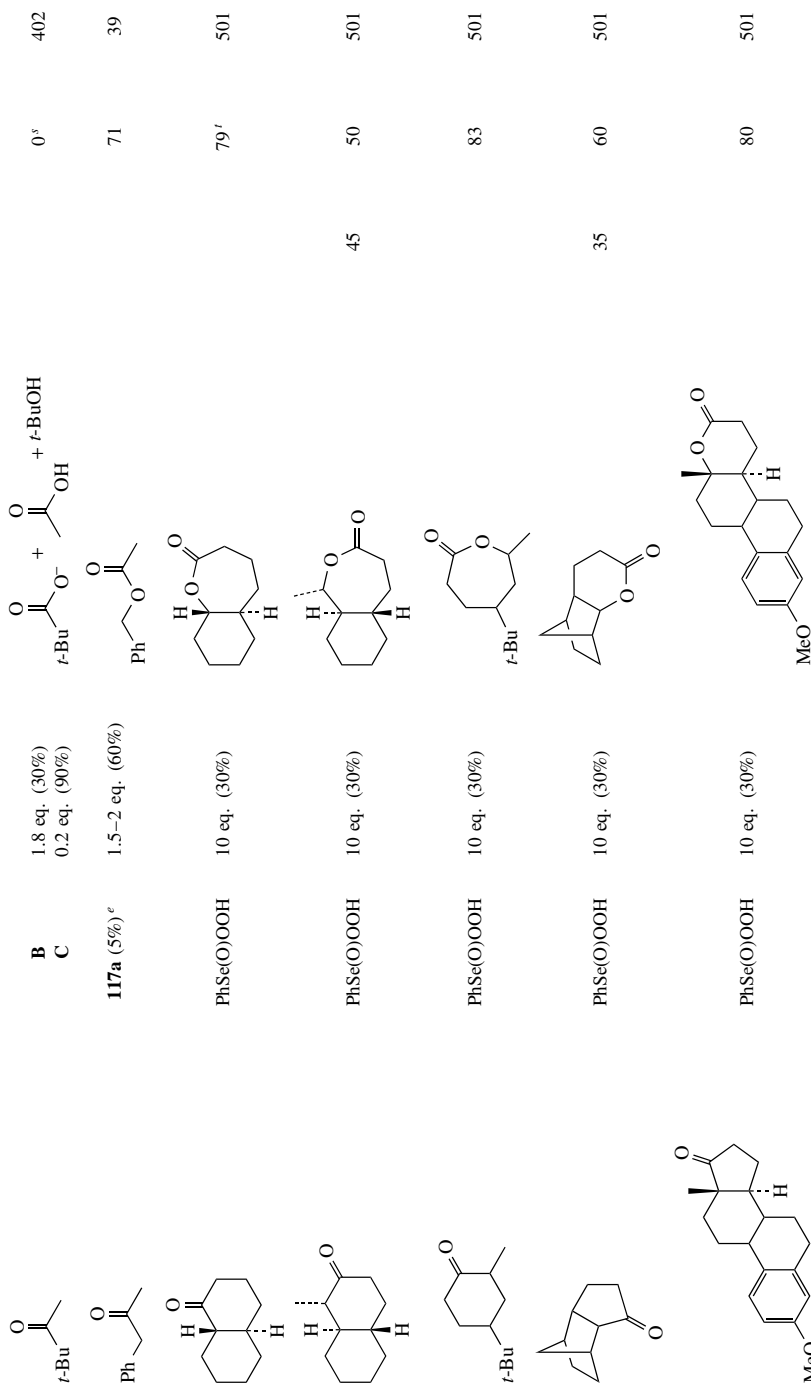
Substrate	Catalyst/ method ^a	Amount of oxidant ^b (concentration)	Product(s)	Conv. (%)	Ketone yield (%), (<i>ee</i>)	Product(s) yield (%), (<i>ee</i>)	Reference
	A 220	4 eq. (50%) 2 eq. (60%) 1.5 eq. (35%) 1.5 eq. (35%)		>98 100 95 >98	>98 99 94 >98	>98 99 94 >98	511 500 506, 507 508
	117a (5%) ^e	1.5–2 eq. (60%)		>98	63	63	39 500
	117a (5%) ^e	1.5–2 eq. (60%)		>98	73	73	39
	A supported MTO ^h	2 eq. (50%) 10 eq. (50%)		85 90	>98 80	>98 80	511 510
	A supported MTO ^h	2 eq. (50%) 8 eq. (50%)		82 90	95 72	95 72	511 510

	D 233a ⁱ <i>anti</i> - 233b ⁱ <i>anti</i> - 233c ⁱ 233d ⁱ MTO	1.5 eq. TiOOH 1.5 eq. TBHP 1.5 eq. TBHP 1.5 eq. TBHP 1.5 eq. TBHP 3M H ₂ O ₂		100 100 100 100 100 100	0 0 0 0 0 0	(75) ^j (31) (26) ^j (44) ^j (7) 68	217 497 497 497 498
	D	1.5 eq. CHP		100	0	2.7 : 1 ⁱ (34) (96)	217
	E 233a ⁱ 233b ⁱ	1.5 eq. (S)- 16a 0.7 eq. TADOOH 1.5 eq. TBHP 1.5 eq. TBHP		74 100	26(99) ^k 0	66 (50) ^m + 0 5.1 : 1 ^{i,n} (16) (84)	98 497
	E MTO	0.7 eq. TADOOH 3M H ₂ O ₂		100	0	12.5 : 1 ^{i,n} (6) (73)	497
	E 233a ⁱ 233b ⁱ MTO Sn-β zeolite	0.7 eq. TADOOH 1.5 eq. TBHP 1.5 eq. TBHP 3M H ₂ O ₂ 1.5 eq. (35%)		70 100 100 100	30(95) ⁿ 0 0 0	47(80) ^q +15(99) ^o 2 : 1 ^{i,n} (35) (65) 3 : 1 ^{i,n} (0) (33) 55 + 8 ^p 67 + 33	98 497 497 498

(continued overleaf)

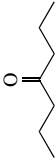
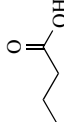
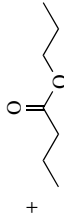
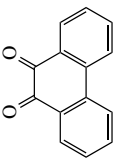
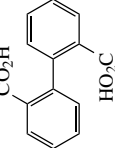
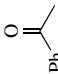
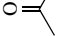
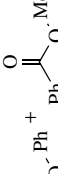
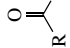
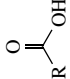
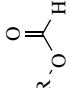
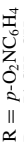


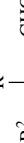

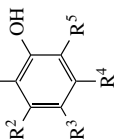
TABLE 33. (continued)

Substrate	Catalyst/ method ^a	Amount of oxidant ^b (concentration)	Product(s)	Conv. (%)	Ketone yield (%), (ee)	Product(s) yield (%), (ee)	Reference
	E	0.7 eq. TADOOH		77	23(59)	45(66) +26(99)	98
	233aⁱ MTO	1.5 eq. TBHP 3M		100	0	1.5 : 1' (37) (51) 66 + 10 ^p	497 498
	MTO	3M		94	6	69	498
	MTO	3M		100	0	67 + 3	498
	233aⁱ	1.5 eq. TBHP		100	0	(21)	497
	B	1.8 eq. (30%)				0 ^r	402

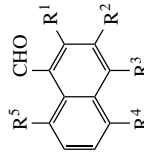
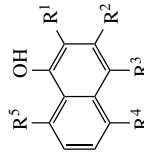
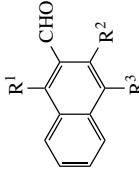
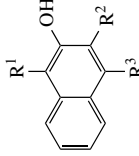
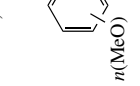
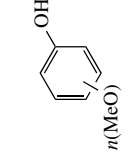
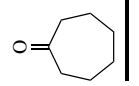
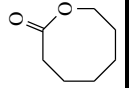


(continued overleaf)

TABLE 33. (continued)

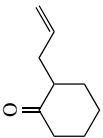
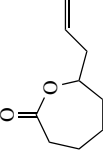
Substrate	Catalyst/ method ^a	Amount of oxidant ^b (concentration)	Product(s)	Conv. (%)	Ketone yield (%), (ee)	Product(s) yield (%), (ee)	Reference
	PhSe(O)OOH	10 eq. (30%)	 + 	25		14 + 11	501
	PhSe(O)OOH	10 eq. (30%)		>98		93	501
	C	0.2 eq. (90%)	 + 	11		11	494
	PhSe(O)OOH	10 eq. (30%)	 + ROH + 	88 99		84 + 0 + 0 45 + 54 + 0	501 501
				47		9 + 26 + 11	506
				98		96 + 0 + 0	501
				>90		89 + 0 + 0	501
				99		0 + 98 + 0	501
				58		50 + 1 + 8	506
	Se catalyst	2.5 eq. (30%)				14-98	504

R¹ = H, Me, OAlk, OBn, OCH₂OMeR² = H, Me, OMeR³ = H, Me, Ph, OMe, OBn, OCH₂OMeR⁴ = H, Me, OMeR⁵ = H, Me, OMe

 $R^1 = H, OMe, OCH_2OMe$ $R^2 = H, OMe$ $R^3 = H, OMe$ $R^4 = H, Br$ $R^5 = H, OMe$	Se catalyst	2.5 eq. (30%)		54–98	504
 $R^1 = H, OMe, OCH_2OMe$ $R^2 = H, OMe$ $R^3 = H, OMe$	Se catalyst	2.5 eq. (30%)		67–97	504
 $n = 1-4$	Se catalyst	3.5 eq. (90%)	 $n(MeO)$	27–89	504
	C	0.2 eq. (90%)		9 [12] ^d	494

(continued overleaf)

TABLE 33. (continued)

Substrate	Catalyst/ method ^a	Amount of oxidant ^b (concentration)	Product(s)	Conv. (%)	Ketone yield (%), (ee)	Product(s) yield (%), (ee)	Reference
	C	0.2 eq. (90%)		65		46 [19] ^d	494

^a A = MTO (2%)/[bmim]BF₄; B = polystyrene bound phenylseleninic acid; C = arsonated polystyrene; Se-catalyst: 2-O₂NC₆H₄SeSeC₆H₄NO₂-2; 2,4-(O₂N)₂C₆H₃SeSeC₆H₃(NO₂)₂-2,4; 2-O₂NC₆H₄SeO₂H; 2,4-(O₂N)₂C₆H₃SeO₂H; D = 0.5 eq. Me₂AlCl/(S)-BINOL; E = TADOOH (0.7 eq.)/DBU (0.7 eq.); Sn/HT = Sn doped hydrotalcite.

^b If not stated otherwise H₂O₂ was used as oxidant.

^c Yield based on H₂O₂ employed.

^d Yield of acid by-product is given in brackets.

^e In perfluorinated solvent: C₃F₇Br/PhH.

^f 71% 6-hydroxyhexanoic acid.

^g HMS-C-SbF₃ = SbF₃ supported on hexagonal mesoporous silica.

^h MTO supported on poly(4-vinylpyridine) 25% cross-linked with divinylbenzene.

ⁱ Stoichiometric amounts.

^j (S)-enantiomer formed in excess.

^k Configuration: (S,S).

^l No yields but ratio of regioisomers given.

^m Configuration: (R,R).

ⁿ *ent*-**223** and *ent*-**228** were formed.

^o Configuration (1*S*,5*R*).

^p Racemic products.

^q Configuration (1*R*, 5*S*).

^r Acetic acid and ethanol as products in 90% yield.

^s Ester/hydrolysis products: 69%/10%.

^t Reaction in the presence of phosphate buffer pH 7.

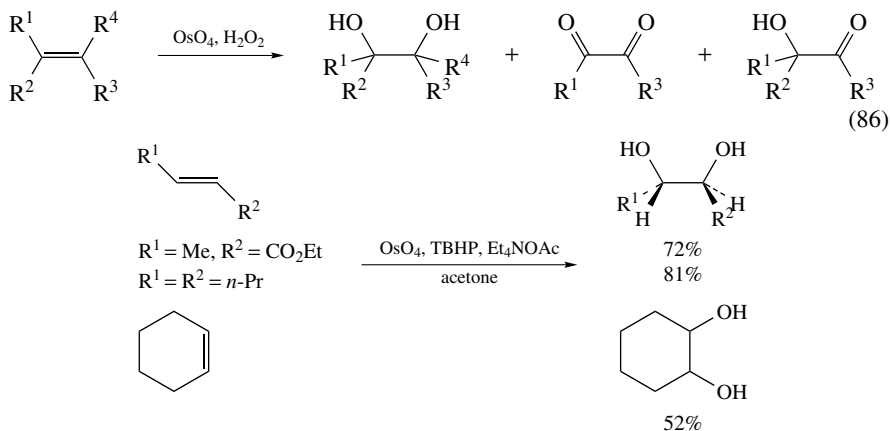
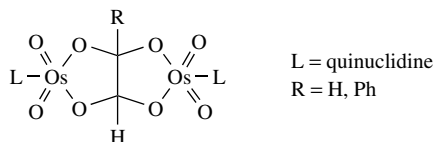
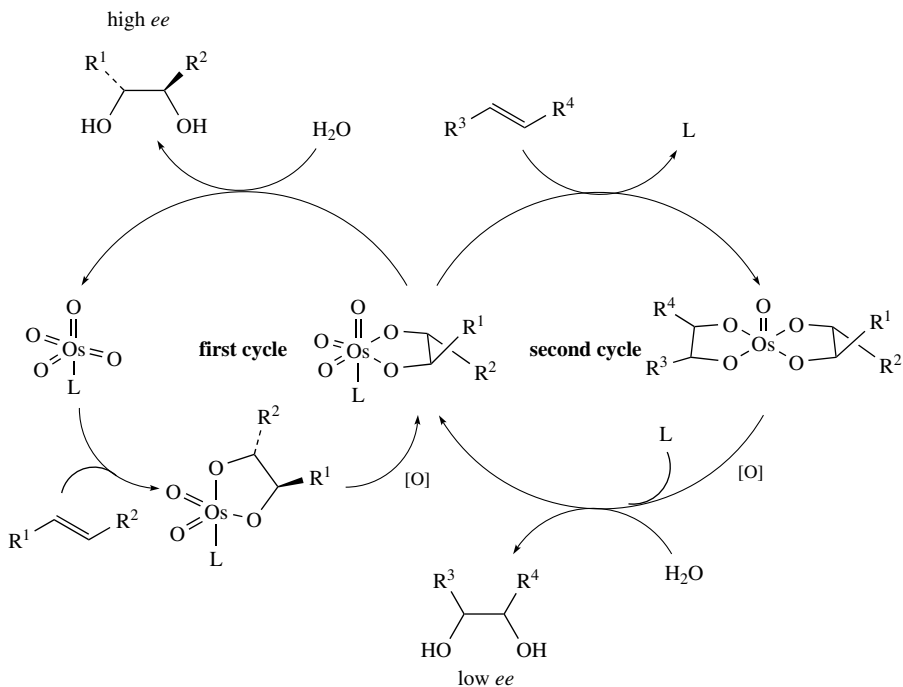
SCHEME 175. OsO₄-catalyzed dihydroxylation of olefins with TBHP in the presence of Et₄NOAc

FIGURE 19

hydroxide ion bases. For example, Wu and Kobylinski reported on the transformation of ethylene to ethylene glycol under these conditions in 84% yield⁵²³. The analogous OsO₄-catalyzed oxidation of alkenes with TBHP leads to α -diketones⁵¹⁹, and from this kind of reaction [OsO₄L + alkyne + TBHP (L = quinuclidine)] cyclic osmate esters (Figure 19) have been isolated as intermediates by Griffith and coworkers⁵²⁵.

The first efforts by Hentges and Sharpless to develop an asymmetric variant of the OsO₄-catalyzed dihydroxylation by employing chiral pyridine derivatives as *L*-2-(2-methyl)pyridine resulted in only low enantiomeric excess (3–18%)⁵²⁶. In 1980 and 1994, they presented a method for the asymmetric dihydroxylation of alkenes using stoichiometric amounts of OsO₄/chiral ligand producing the corresponding diols with moderate to good yields (62–90%) and enantiomeric excesses (5–83%) using acetate esters of cinchona alkaloids as chiral ligands^{526, 527}. The oxidation of the olefin can take place either in the first or the second catalytic cycle of the Os catalyst (Scheme 176). Sharpless and coworkers stated that dihydroxylations by the second cycle give no or low enantioselectivity in the case of alkaloid ligands⁵²⁸. More recent findings of the groups of Adolfsson and Sharpless revealed that even the second-cycle dihydroxylations may give substantial *ee* values^{529, 530}. In subsequent years many chiral ligands for osmium have been developed and their good asymmetric induction in dihydroxylation reactions has been shown. All of these methods either employ stoichiometric amounts of catalyst (OsO₄/chiral ligand) and therefore no peroxide as oxidant⁵³¹ or K₃Fe(CN)₆⁵³² as co-oxidant, and therefore will not be discussed further.

The main problem of OsO₄, even when employed in catalytic amounts, is its toxicity, and products may be contaminated with small amounts of non-hydrolyzed Os–diolate complexes. Therefore, heterogenization of the catalyst described by Jacobs and coworkers⁵²⁹



SCHEME 176. First and second cycle dihydroxylations with an osmium catalyst in the presence of a coordinating base

may be envisaged as a possible solution. Cainelli and coworkers⁵³³ and Herrmann and coworkers⁵³⁴ both followed the approach of using amine-functionalized polymers as supports for the immobilization of the osmium catalyst. Both authors used polyvinylpyridine (PVP) supported catalyst in combination with hydrogen peroxide, which proved to be the preferred oxidant under these conditions and, besides PVP, Cainelli and coworkers utilized several amine-type polymers **235** or **236** shown in Figure 20 in combination with different Os reoxidizing agents such as hydrogen peroxide, TBHP or trimethylamine oxide

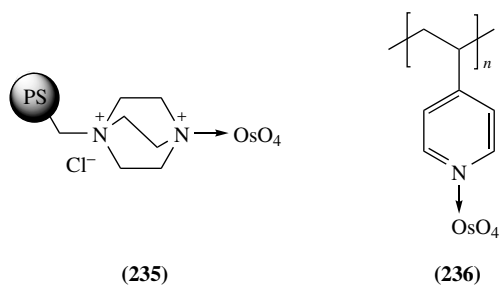
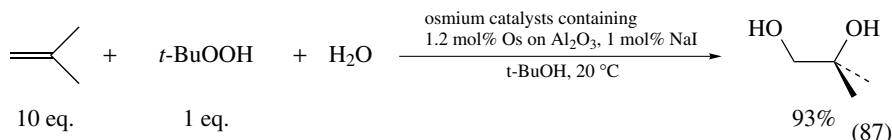


FIGURE 20

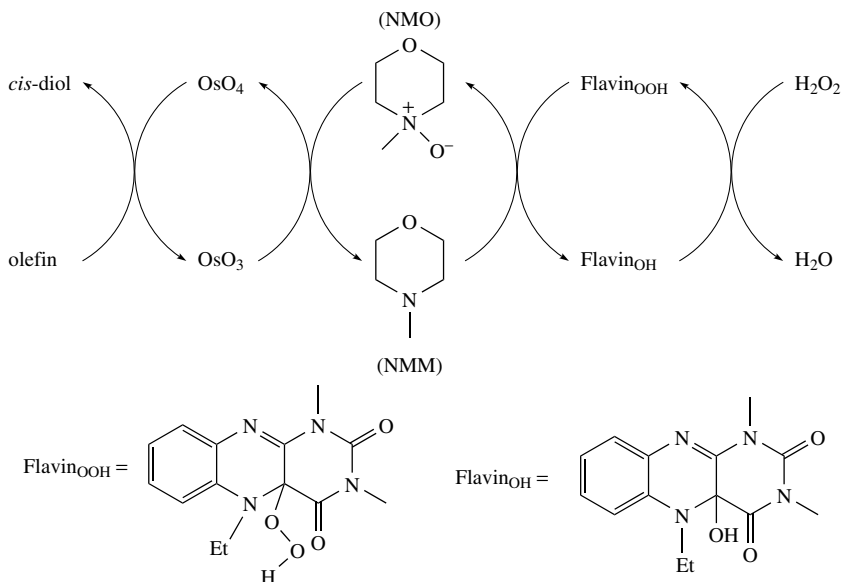
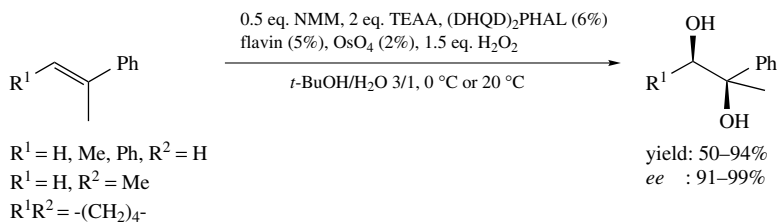
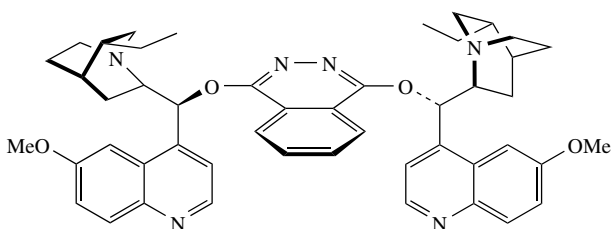
and obtained diol yields between 30 and 95%. While overoxidation to the ketol is often a problem with Os/H₂O₂, the PVP immobilized OsO₄ catalyst gives excellent diol yields (up to quantitative) as reported by Herrmann and coworkers⁵³⁴. The major drawback of this method is the need of a 40-fold excess of H₂O₂. With the osmium catalyst immobilized on amine-type polymers, overoxidation is obtained in some cases when H₂O₂ is employed as oxygen source.

Better results could be achieved using TBHP, which turned out to be also the oxidant of choice in the case of hindered olefins and of substrates with polar groups⁵³³. These methods rely on coordination of the polymer-supported bases to the Lewis acidic Os(VI) or Os(VIII) center and the concept of 'ligand accelerated catalysis', which means here that the addition of the metal to the olefinic double bond is accelerated by the polymer-supported amine ligand. Later, Jacobs and coworkers could show that the PVP supported OsO₄ material leaches active Os during the catalytic process and that the dihydroxylation takes place in the separated filtrate as fast as in the presence of the polymer-supported catalyst⁵²⁹. Also, enantiomerically pure chiral polymer-supported amines have been used for asymmetric versions of the OsO₄-catalyzed dihydroxylation; above all, cinchona alkaloids were employed. Inorganic and organic supports, soluble and insoluble polymers, or with different heteroaromatic groups at the stereo-determining C9-O position as well as heterogenized OsO₄²⁻ (by ion exchange) in combination with chiral ligand have been tested, but all using either K₃Fe(CN)₆/K₂CO₃ (1:1) or *N*-methylmorpholine-*N*-oxide as oxidant⁵³⁵. In the best cases the enantioselectivity observed was similar to the homogeneous reactions and ligand recycling was possible while OsO₄ remained in solution. During the last years also some asymmetric versions of this reaction catalyzed by immobilized Os catalysts were reported, in which TBHP or H₂O₂ could be used as terminal oxidant. Some of them will be presented in the following.

The research group of Michaelson developed some new heterogeneous Os catalysts for the dihydroxylation reaction, where Os complexes like Os₃(CO)₁₂ or OsCl₃ are adsorbed on inorganic oxides like, for example, MgO or Al₂O₃⁵³⁶. TBHP served as oxidant and cocatalysts (NaI, NaOH) were used in *t*-butanol as solvent (equation 87). In the presence of NaI the catalyst proved to be exclusively heterogenic and Os₃(CO)₁₂/Al₂O₃ can be reused several times without loss of activity. The same authors developed a heterogeneous catalyst, in which the iodide promoter was incorporated in the catalyst by use of an Amberlyst IRA-400 (ion exchange polymer)⁵³⁶.



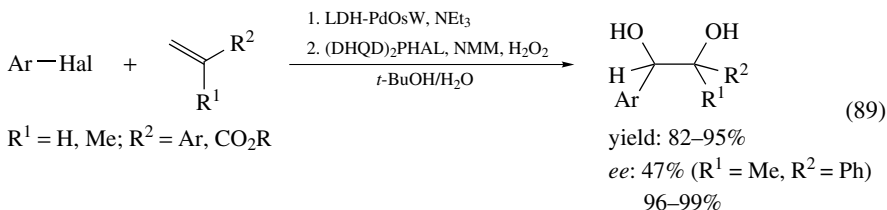
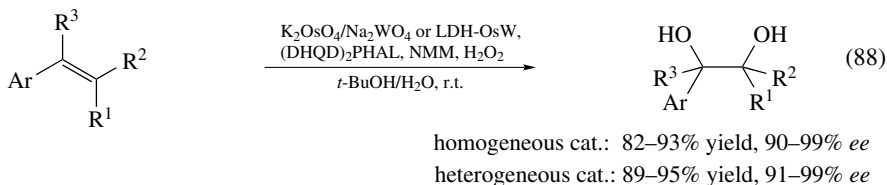
The use of H₂O₂ as terminal oxidant for the reoxidation of Os(VI) to Os(VIII) was often accompanied by overoxidation providing the diols in only low yields. A more effective coupled electron transfer–mediator system based on NMO and a flavin, using H₂O₂ as terminal oxidant, was developed by Bäckvall and coworkers in 1999 (Scheme 177)^{537–539}. This system combined the chemoselectivity of NMO with the ecologically favorable properties of H₂O₂. In this process Os(VI) is recycled to Os(VIII) through oxidation with NMO, generating NMM, which itself is recycled *in situ* by oxidation with the cheap and readily available terminal oxidant H₂O₂. Additional tetraethylammonium acetate (TEAA) improves the yields of the reaction. Yields of the dihydroxylation reaction employing the above catalytic system ranged from 72 to 95%^{537,538}. An asymmetric version of this reaction has also been developed utilizing hydroquinidine 1,4-phthalazinediyl diether

SCHEME 177. Coupled catalytic system for olefin dihydroxylation with H₂O₂ as terminal oxidant(DHQD)₂PHAL:SCHEME 178. Osmium-catalyzed catalytic asymmetric dihydroxylation of olefins by H₂O₂ as terminal oxidant

[(DHQD)₂PHAL] as chiral ligand (Scheme 178)^{538,539}. In order to obtain maximum enantioselectivity, the solvent was changed from acetone to *tert*-butanol (in some cases a mixture of acetone/H₂O proved to be the best solvent), the olefin was added slowly and an excess of ligand relative to osmium (Os:ligand 1:3) was used. Various phenyl-substituted internal and terminal olefins have been oxidized to the corresponding diols in

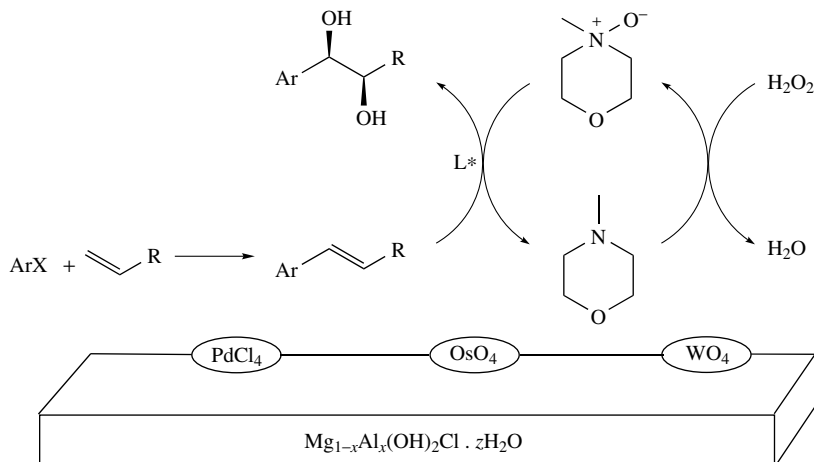
yields between 50% and 94% and enantiomeric excesses of 91–99%. Due to the fact that flavin is an efficient electron transfer mediator but rather unstable, Bäckvall and coworkers looked for an alternative and found that flavin can be replaced by stable vanadyl acetylacetonate⁵⁴⁰.

In 2001, Choudary and coworkers reported on the development of a bifunctional and a trifunctional catalyst for the one-pot synthesis of chiral diols^{541,542}. The authors found that the use of catalytic amounts of Na₂WO₄ in the presence of H₂O₂ in the osmium-catalyzed dihydroxylation of alkenes accelerated the generation of NMO *in situ* from NMM⁵⁴³, resulting in better diol yields, and both catalysts K₂OsO₄•2H₂O and Na₂WO₄•2H₂O could be recovered from the reaction. An analogous system was designed as heterogeneous bifunctional catalyst consisting of OsO₄²⁻ and WO₄²⁻ on a single matrix prepared by ion exchange from layered double hydroxides (LDH-OsW). This heterogeneous bifunctional catalyst showed high activity in the presence of NMM and H₂O₂ as terminal oxidant for the achiral as well as asymmetric dihydroxylation of several olefins (equation 88). A slow addition of hydrogen peroxide over several hours is essential for an effective reaction. The asymmetric dihydroxylation of *trans*-stilbene is carried out with additional 1,4-bis(9-*O*-dihydroquinidiny)phthalazine [(DHQD)₂PHAL] as ligand and chiral inductor, which provides the corresponding diol in 93% yield and 99% *ee*. For trisubstituted olefins, tetraethylammonium acetate (TEAA) turned out to be a better alternative to NMM. Homogeneous and heterogeneous systems were reused without loss in activity and selectivity. The trifunctional catalysts (homogeneous and heterogeneous), developed by the same research group, consisted of Na₂PdCl₄/K₂OsO₄/Na₂WO₄ in the homogeneous case or LDH-PdOsW in the heterogeneous case. With these catalytic systems it is possible to generate the prochiral olefins that serve as substrates for the asymmetric dihydroxylation, *in situ* via palladium-catalyzed Heck reaction of aryl halides and alkenes, followed by a very efficient and enantioselective dihydroxylation step (82–95% yield, up to 99% *ee*) in the presence of chiral ligand [(DHQD)₂PHAL], while the continuous supply of NMO is ensured through the oxidative cycle of NMM *in situ* by H₂O₂ as terminal oxidant (equation 89, Scheme 179). The preparation of chiral, vicinal diols starting from cheaper aryl halides and alkenes precursor is a low-cost process. The catalysts provide the diols with high yields and *ee* values and they are easily recyclable.



The results of the metal-catalyzed *syn*-dihydroxylation reaction of a variety of alkenes using hydrogen peroxide or TBHP as oxidants are shown in Table 34.

Whereas the *syn*-dihydroxylation reaction, which is described above, is performed in the presence of metal oxides KMnO₄ or OsO₄, the *anti*-dihydroxylation is carried out with



SCHEME 179. Catalytic cycle in the LDH-PdOsW-catalyzed synthesis of chiral diols using H_2O_2 as the terminal oxidant

peracids like peracetic acid or MCPBA. However, the atom efficiency of these oxidants are low because equimolar amounts of deoxygenated reagent are produced as waste. In 2003, Sato and coworkers could present a much more efficient route to the catalytic *anti*-dihydroxylation of olefins in an organic solvent and metal-free system, employing 30% hydrogen peroxide as oxidant (Scheme 180)⁵⁴⁴. The catalyst of this reaction was a resin-supported sulfonic acid, whereby similarly good results were obtained with nafion NR50 (0.04 eq., 0.8 mmol g^{-1} of SO_3H groups), nafion SAC-13 (powder supported on silica) and amberlyst 15 (ion exchange resin, polystyrene-supported sulfonic acid), while with resin-supported carboxylic acid (amberlite IRC76) the oxidation could not be catalyzed. The authors showed that the catalytic activity of the resin-supported sulfonic acid is much higher than that of homogeneous acid catalysts [yield of *anti*-2,3-hexanediol: 85% (with nafion SAC-13), 0–36% (with various homogeneous acids)]. The dihydroxylation with resin-supported sulfonic acid catalyst generally proceeds with good yields (40–100%) and selectivity for 1,2-diols and side products like epoxides, alcohols, ketones or ethers are not formed or only in traces. The reactivity of internal olefins is higher than that of terminal olefins. The dihydroxylation proceeds stereospecifically: (*E*)- and (*Z*)-2-hexene could be transferred to the *anti*- and *syn*-2,3-hexanediols selectively. What has to be pointed out is the easy recyclability of the catalyst by simple filtration and washing with H_2O . In this way the resin-supported sulfonic acid can be reused up to 10 times without decrease in catalytic activity.

H. Oxidative Halogenation of Hydrocarbons

Hydrogen peroxide has been shown to oxidize halide ions to halogens or positive halogen species in the presence of a metal catalyst. The generated halogens/hypohalites can then oxidize hydrocarbons to form alkyl or aryl halides.

In 1996, Detty and coworkers reported on the oxidation of sodium halides to positive halogens with hydrogen peroxide in two-phase systems of dichloromethane and pH 6 phosphate buffer, catalyzed by organotellurium catalysts **237** (Scheme 181)⁵⁴⁵. Mixtures of 1,2-dihalocyclohexane (**238**) and 2-halocyclohexanol (**239**) were formed upon reaction of the positive halogens formed with cyclohexene. From the three tellurium catalysts

TABLE 34. Dihydroxylation of olefins

Substrate	Catalyst ^a	Oxidant ^b	Yield diol (%)	ee diol (%) (config.)	Reference
	OsO ₄ /Et ₄ NOH	TBHP	73		520
	OsO ₄ /TEAA	TBHP	81		521
	OsO ₄	NMM/flavin/H ₂ O ₂	92		537
	OsO ₄	NMM/VO(acac) ₂ /H ₂ O ₂	83		540
	OsO ₄	NMM/flavin/H ₂ O ₂	95		537
	OsO ₄	NMM/VO(acac) ₂ /H ₂ O ₂	89		540
	OsO ₄ /(DHQD) ₂ PHAL/TEAA	NMM/flavin/H ₂ O ₂	80	95 (R)	538, 539
	OsO ₄	NMM/VO(acac) ₂ /H ₂ O ₂	83		540
	OsO ₄ /(DHQD) ₂ PHAL/TEAA	NMM/flavin/H ₂ O ₂	67	96 (R)	538, 539
	OsO ₄ /(DHQD) ₂ PHAL/TEAA	H ₂ O ₂	61	99	539
	LDH-OsW/(DHQD) ₂ PHAL	NMM/H ₂ O ₂	93	99 (R,R)	541
	LDH-PdOsW/(DHQD) ₂ PHAL ^c	NMM/H ₂ O ₂	85	99 (R,R)	541
	OsO ₄	NMM/flavin/H ₂ O ₂	74		537
	OsO ₄ /(DHQD) ₂ PHAL/TEAA	NMM/flavin/H ₂ O ₂	94	91 (R,R)	538, 539
	OsO ₄	NMM/flavin/H ₂ O ₂	72		537
		LDH-PdOsW/(DHQD) ₂ PHAL ^c	NMM/H ₂ O ₂	85–88	99 (R,R)
R ¹ = OMe, R ² = H			91	99 (R,R)	541
R ¹ = Me, R ² = H			89	97 (R,R)	541
R ¹ = Cl, R ² = H			86	99 (R,R)	541
R ¹ = R ² = Me			83	99 (R,R)	541
R ¹ = OMe, R ² = H					
	LDH-PdOsW/(DHQD) ₂ PHAL ^c	NMM/H ₂ O ₂	90	98 (2S,3R)	541
	R ¹ = H, R ² = Me		93	96 (2S,3R)	541
	R ¹ = OMe, R ² = Et				
	OsO ₄ /Et ₄ NOH	TBHP	61		520
	OsO ₄ /TEAA	TBHP	72		521
	235	TBHP	70		533
	235	TBHP	95		533
	235	TBHP			

(continued overleaf)

TABLE 34. (continued)


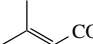

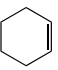
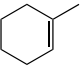
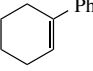
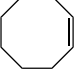
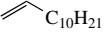
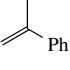
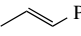
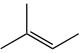
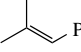
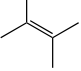
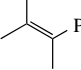
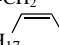
Substrate	Catalyst ^a	Oxidant ^b	Yield diol (%)	ee diol (%) (config.)	Reference
	235	TBHP	60		533
	235	TBHP	45		533
	235	TBHP	35		533
	OsO ₄ /Et ₄ NOH	TBHP	62		520
	OsO ₄ /TEAA	TBHP	52		521
	OsO ₄	NMM/flavin/H ₂ O ₂	91		537
	OsO ₄	NMM/VO(acac) ₂ /H ₂ O ₂	66		540
	OsO ₄	NMM/flavin/H ₂ O ₂	77		537
	OsO ₄ /(DHQD) ₂ PHAL/ TEAA	NMM/flavin/H ₂ O ₂	50	92 (<i>R,R</i>)	538, 539
	235	TBHP	68		533
Citronellol acetate 	OsO ₄ /TEAA	TBHP	83		521
	OsO ₄ /Et ₄ NOH	TBHP	73		520
	236	TBHP	45		533
	235	TBHP	75		533
	OsO ₄ /Et ₄ NOH	TBHP	71		520
	OsO ₄	NMM/flavin/H ₂ O ₂	93		537
	OsO ₄	NMM/VO(acac) ₂ /H ₂ O ₂	86		540
	OsO ₄ /(DHQD) ₂ PHAL/ TEAA	NMM/flavin/H ₂ O ₂	88	99	538, 539
	OsO ₄	NMM/flavin/H ₂ O ₂	95		537
	OsO ₄	NMM/VO(acac) ₂ /H ₂ O ₂	70		540
	OsO ₄ /Et ₄ NOH	TBHP	63		520
	OsO ₄ /Et ₄ NOH	TBHP	67		520
	OsO ₄ /Et ₄ NOH	TBHP	72		520
	235	TBHP	50		533
	OsO ₄ /Et ₄ NOH	TBHP	69		520

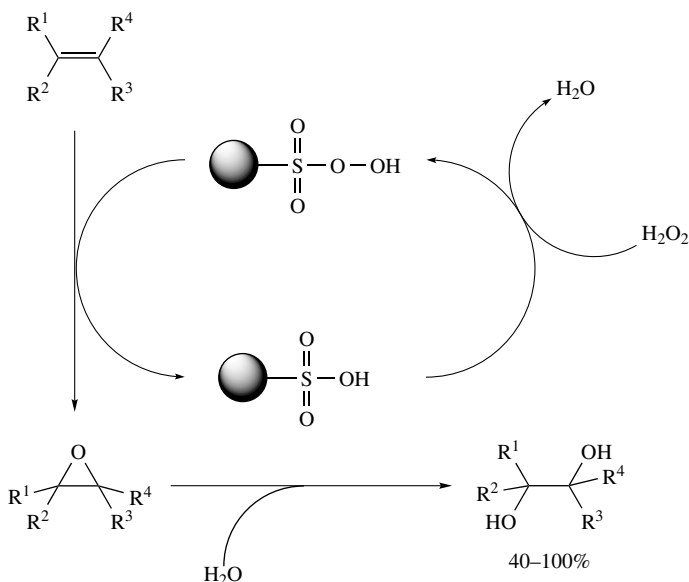
TABLE 34. (continued)

Substrate	Catalyst ^a	Oxidant ^b	Yield diol (%)	<i>ee</i> diol (%) (config.)	Reference
Oleic acid	OsO ₄ /Et ₄ NOH	TBHP	70		520
Oleic alcohol	OsO ₄ /Et ₄ NOH	TBHP	51		520
CH ₂ =CH ₂	OsO ₄ /CsOH	TBHP	84		523
<i>n</i> -C ₈ H ₁₇  C ₈ H ₁₆ CO ₂ Et	235	TBHP	60		533

^a TEAA = tetraethylammonium acetate; LDH-OsW = layered double hydroxides [Mg_{1-x}Al_x(OH)₂(Cl)_x · zH₂O] with OsO₄²⁻ and WO₄²⁻ ions; LDH-PdOsW = layered double hydroxides [Mg_{1-x}Al_x(OH)₂(Cl)_x · zH₂O] with PdCl₄²⁻, OsO₄²⁻ and WO₄²⁻ ions; (DHQD)₂PHAL = 1, 4-bis(9-*O*-dihydroquinidiny)phthalazine.

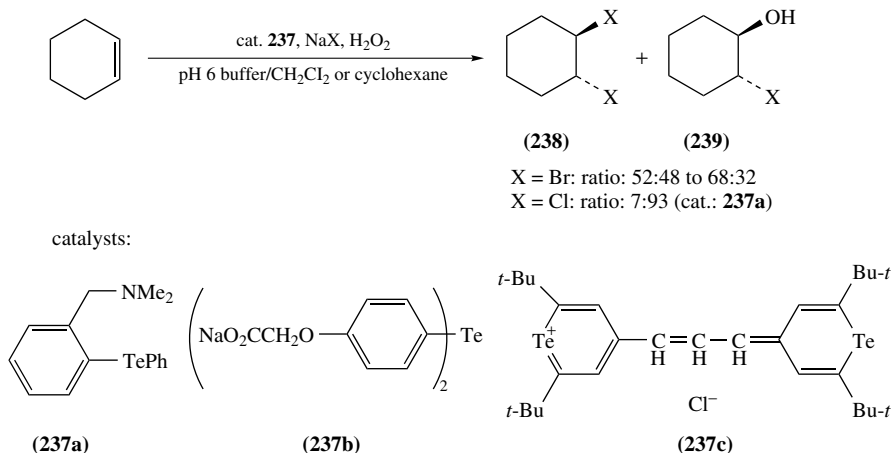
^b NMM = *N*-methylmorpholine.

^c Olefin that undergoes dihydroxylation is generated *in situ* from aryl halide and a terminal olefin via Pd-catalyzed Heck coupling.



SCHEME 180. Catalytic cycle for the *anti*-dihydroxylation of alkenes using resin-supported sulfonic acid catalyst

tested, **237a** turned out to be the most active with turnover numbers for cyclohexene and sodium bromide as substrates of >1000. The ratio of **238/239** with the different catalysts and NaBr ranged from 52:48 to 68:32. In the case of NaCl in the presence of catalyst **237a** a product ratio of 7:93 was observed, which shows the great effect of the choice of halide on the reaction. The authors proposed a mechanism for the reaction (Scheme 182) in which the first step is the oxidation of diorganotelluride to the hydroxy- (for **237a**) or dihydroxy-Te(IV) derivative (for **237b,c**). Nucleophilic attack by the halide at the ligated hydroxide gives diorganotelluride and hypohalous acid, which then brominates cyclohexene. The alternative route is the addition of halide to the tellurous oxide intermediate generating R₂Te(OH)X, which reductively eliminates hypohalous acid or eliminates halogen (also an active halogenating agent) after attack of halide at the halide ligand (see Scheme 182).

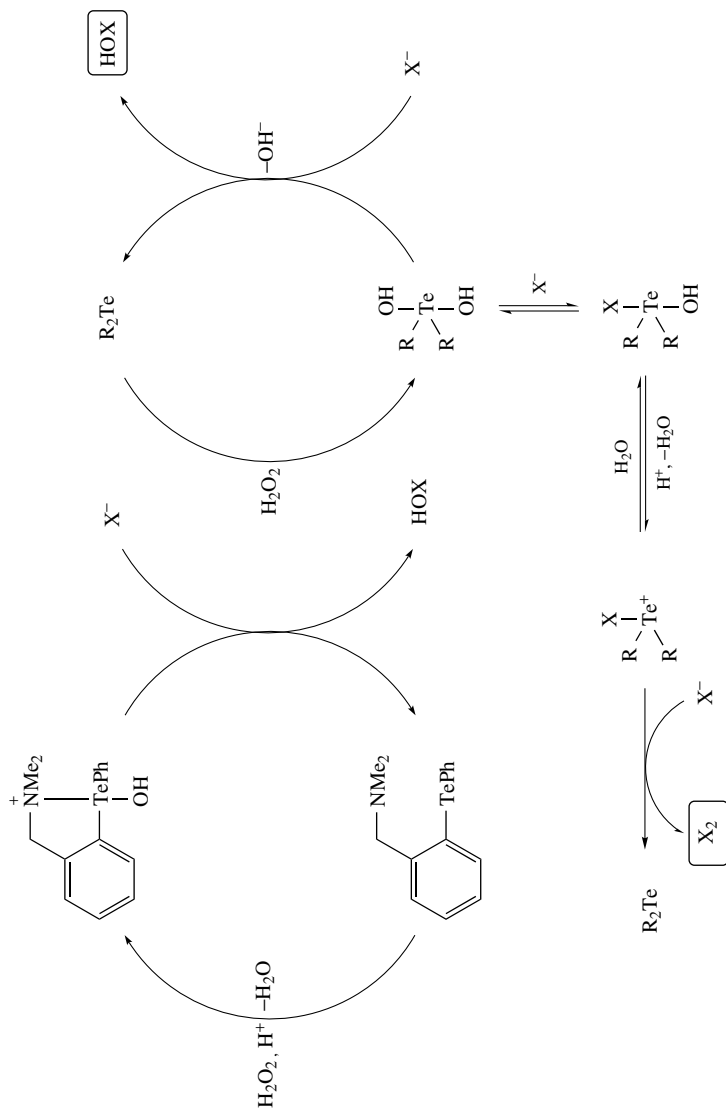


SCHEME 181. Tellurium-catalyzed dihalogenation and hydroxyhalogenation of cyclohexene with H_2O_2

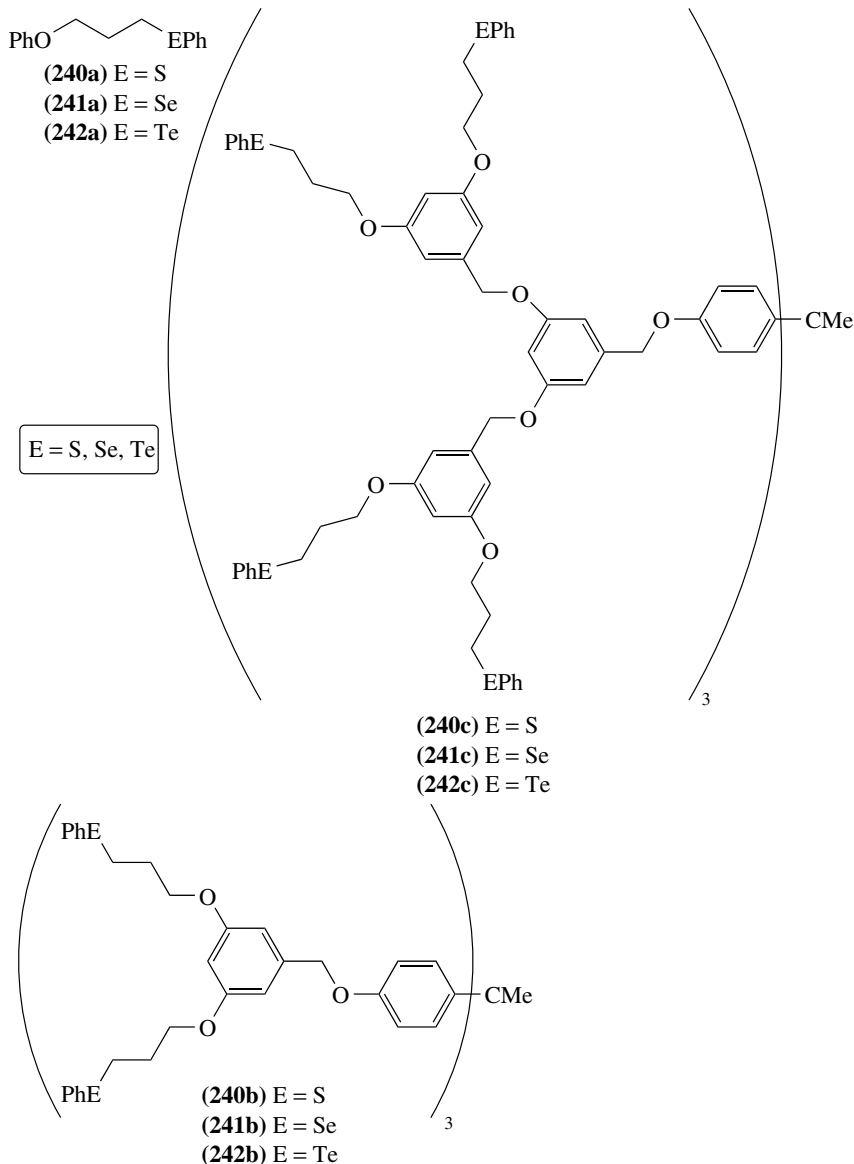
Five years later Detty and coworkers published their results on the catalysis of the halogenation reaction of cyclohexene under the same conditions but employing dendrimeric polyphenylselenides **241** and—tellurides **242** as catalysts⁵⁴⁶. These dendrimeric molecules terminating in phenylseleno- or phenyltelluro- groups are efficient catalysts in two-phase systems and, for example, the dendrimer bearing 12 PhSe groups has a turnover number of >60000 mol of H_2O_2 consumed per mole of catalyst. The analogous sulfides **240** showed no catalytic activity. The ratio of formed products **238/239** was in the range of 30:70 and 45:55.

In the same year, Detty and coworkers presented an organotelluride catalyst **243** for the oxidation of iodide with hydrogen peroxide (Scheme 183)⁵⁴⁷. With this catalytic system **243** (0.8 mol%)/NaI/ H_2O_2 various organic substrates were efficiently iodinated either in a two-phase system (aqueous buffer/organic solvent) or in the case of water-soluble substrates without organic solvent. 4-Pentenoic acids derivatives, the corresponding carboxylates or 4-pentenol were first iodinated at the double bond and then underwent lactonization to form five-membered rings with yields between 88 and 94% for the carboxylic acid and carboxylate substrates and 65% yield starting from the unsaturated alcohol. Activated aromatic compounds bearing one or more electron-donating substituents could also be iodinated with yields of 76–95% within 5 hours. The reactions could also be carried out with NaBr instead of NaI, but the bromination required longer reaction times and higher concentrations of Br^- , which can be attributed to the stronger Te–Br bond compared with the Te–I bond. Yields of bromination reactions ranged from <5 to 45%. The multistep mechanism of H_2O_2 activation with organotellurides has already been described in Scheme 182. The active halogenating species is either the free halogen or hypohalous acid generated during the reaction or a halotellurium salt intermediate ($\text{R}_2\text{Te}^+\text{X}$).

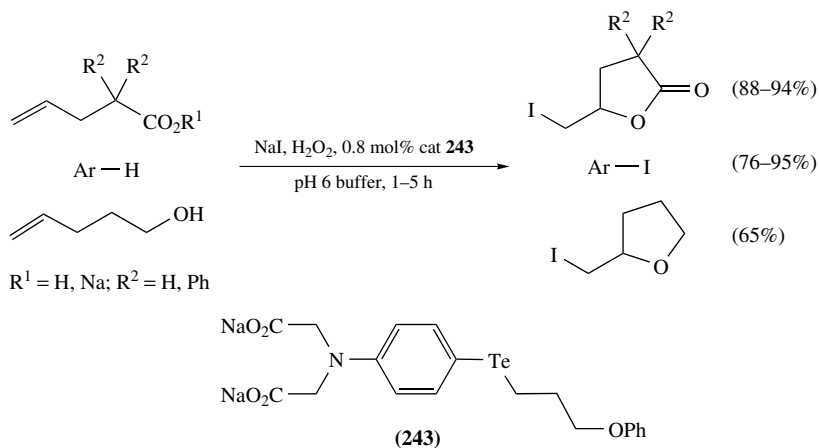
In 2003, Kulkarni and coworkers presented a method for the *para*-selective oxybromination of a variety of substituted phenols employing a novel heterogeneous catalytic system, the CrZSM-5 as catalyst, H_2O_2 as oxidant and KBr as bromine source⁵⁴⁸. Next to CrZSM-5 also other zeolites have been tested as catalysts, but although MoZSM-5 showed the highest conversion after 5 hours (89%), *para*-selectivity was lower (*para*: 36%; *ortho*: 31%; dibromination: 22%) than observed with the CrZSM-5 material (83%



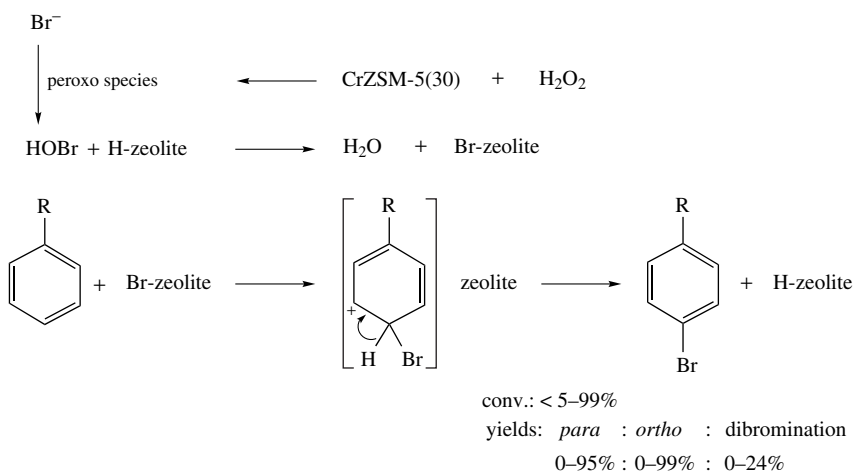
SCHEME 182. Proposed mechanisms for the tellurium-catalyzed generation of positive halogen or halogen



conversion; *para*: 58%; *ortho*: 25%; no dibromination). While electron-withdrawing substituents decrease the rate of ring bromination, electron-donating substituents increase it. The best results were obtained with acetic acid as solvent because hydrogen peroxide and acetic acid react to form peracetic acid, which is a stronger oxidant than hydrogen peroxide and oxidizes bromide to a positive bromine species more efficiently. The CrZSM-5(30) catalyst can be easily recovered and reused without loss of activity. The proposed mechanism of the reaction is shown in Scheme 184.



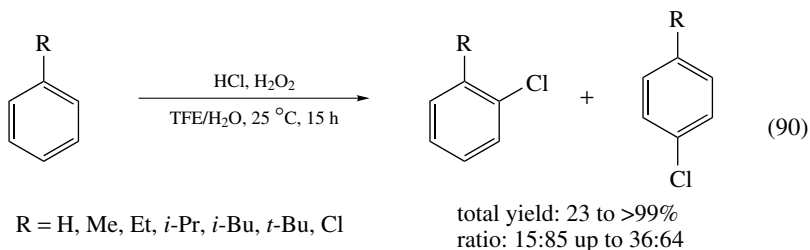
SCHEME 183. Iodination of organic substrates with sodium iodide and H₂O₂ using an organotelluride catalyst



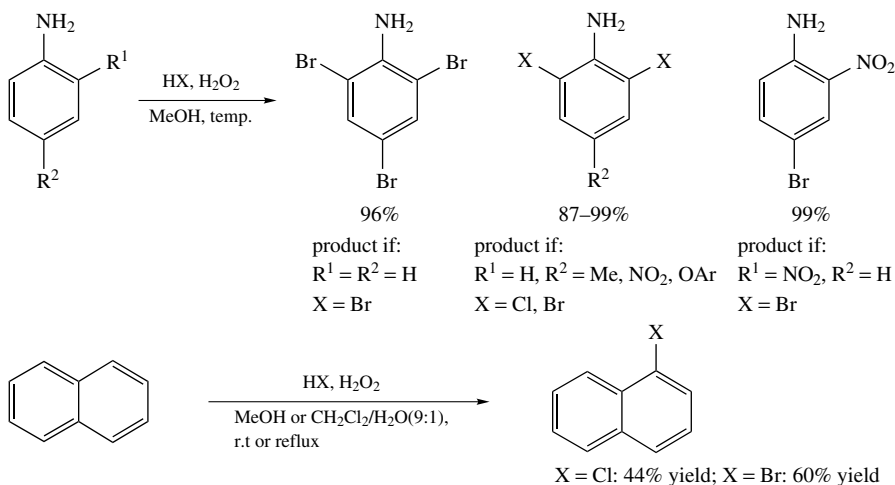
SCHEME 184. Mechanism for the CrZSM-5(30)-catalyzed *para*-bromination of various phenols with H₂O₂ as oxidant

Oxychlorination can in principle be carried out using HCl/H₂O₂, a 'green' chlorination method, which takes place by oxidation of chloride under acidic conditions in the absence of a catalyst to obtain HOCl and/or Cl₂, which can then chlorinate hydrocarbons. However, this method is limited by the facts that only very reactive substrates can be used and that a large excess of HCl is needed for good conversions. In 2003, Neumann and coworkers reported on a new method for aromatic chlorination using HCl/H₂O₂ in the presence of trifluoroethanol as solvent and activator (equation 90)⁵⁴⁹. This solvent catalyzes the chlorination by a charge template stabilization of the transition state, so that even arene substrates that do not undergo oxychlorination in other solvents can be chlorinated using the conditions of Neumann. Several aromatic compounds were oxychlorinated giving two

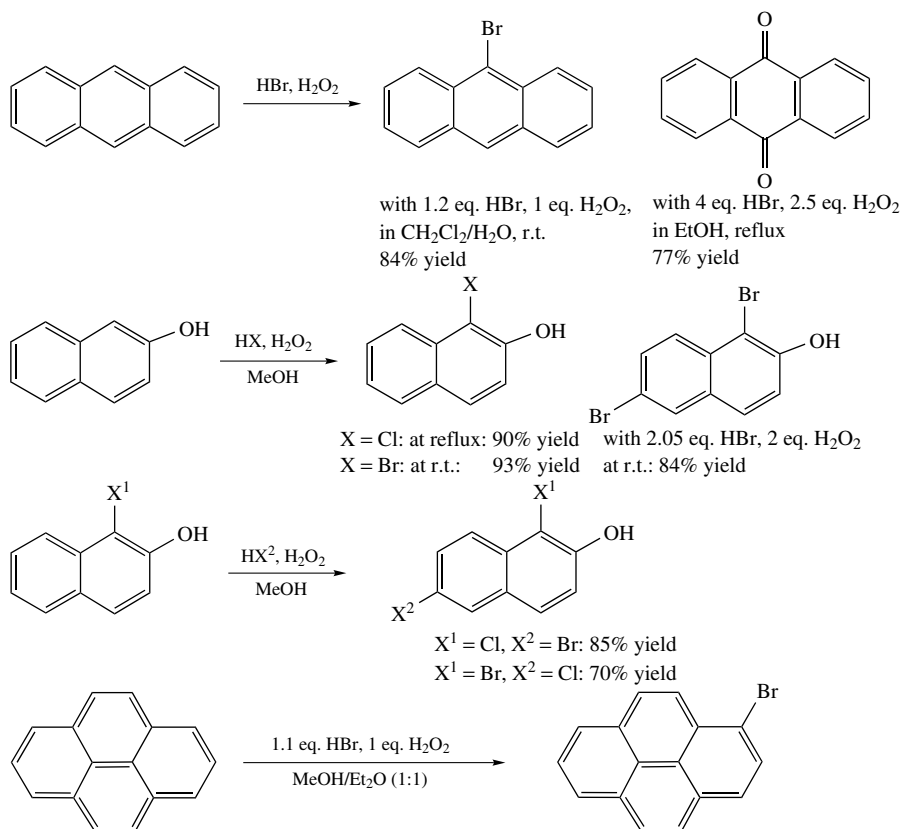
regioisomers (1,2- and 1,4-isomers) of the corresponding monochlorinated products (1,2- and 1,4-dichlorinated in the case of chlorobenzene as substrate) in yields between 23 and >99%. *p*-Xylene and mesitylene could also be converted to the chlorinated products in 98% and >99% yield, respectively.



A procedure for the environmentally benign chlorination and bromination of aromatic amines, hydrocarbons and naphthols without the need of a catalyst by *in situ* oxidation of hydrohalic acid with hydrogen peroxide was reported by Bedekar and coworkers (Scheme 185)⁵⁵⁰. The bromination of a variety of differently substituted aromatic amines (Me, NO₂, OAr in *para*-position) utilizing the *in situ* generation of hydrohalic acid led to dihalogenation in the *ortho* positions relative to the NH₂ group in very high yields (87–99%). In the case of *ortho*-NO₂-substituted aniline, monobromination in *para*-position (relative to NH₂) is obtained yielding the product in 99% and aniline itself underwent bromination in *para*- and both *ortho*-positions to give the tribrominated product in 96% yield. For the bromination of naphthalene and anthracene, the aqueous/methanolic solvent mixture was changed to CH₂Cl₂/water due to better yields of the formed 1-bromonaphthalene and 9-bromoanthracene (60% and 84%, respectively). Monochlorination of 2-naphthol had to be carried out using excess of hydrochloric acid and hydrogen peroxide in boiling methanol (90% yield) while in the analogous bromination good yield of monobrominated product (93%) was already observed at room



SCHEME 185. Chlorination and bromination of aromatic amines, hydrocarbons and naphthols with *in situ* generated active halogen



SCHEME 185. (continued)

temperature and with only 1.05 equivalents of HBr. 1,6-Dibromo-2-naphthol could be cleanly formed by using 2.05 equivalents of HBr and 2 equivalents of H₂O₂ (85% yield) starting from 1-Bromo-2-naphthol.

IV. REFERENCES

1. N. A. Porter, in *Organic Peroxides* (Ed. W. Ando), Chap. 2, Wiley, Chichester, 1992.
2. R. Hiatt, in *Organic Peroxides* (Ed. D. Swern), Vol. III, Chap. I, Wiley, New York, 1971.
3. (a) M. M. Heaton, *J. Am. Chem. Soc.*, **100**, 2004 (1978).
(b) S. Wolfe, D. J. Mitchell, H. B. Schlegel, C. Minot and O. Eisenstein, *Tetrahedron Lett.*, **23**, 615 (1982).
4. A. Rieche and C. Bischoff, *Chem. Ber.*, **94**, 2722 (1961).
5. P. G. Cookson, A. G. Davies and B. P. Roberts, *J. Chem. Soc., Chem. Commun.*, 1022 (1976).
6. A. A. Frimer, *J. Org. Chem.*, **42**, 3194 (1977).
7. (a) E. Bascetta and F. D. Gunstone, *J. Chem. Soc., Perkin Trans. 1*, 2217 (1984).
(b) N. A. Porter, D. H. Roberts and C. B. Ziegler Jr., *J. Am. Chem. Soc.*, **102**, 5912 (1980).
(c) N. A. Porter, C. B. Ziegler Jr., F. F. Khouri and D. H. Roberts, *J. Org. Chem.*, **50**, 2252 (1985).
8. N. A. Porter, M. O. Funk, D. Gilmore, R. Isaac and J. Nixon, *J. Am. Chem. Soc.*, **98**, 6000 (1976).

9. E. J. Corey, J. O. Albright, A. E. Barton and S. Hashimoto, *J. Am. Chem. Soc.*, **102**, 1435 (1980).
10. E. J. Corey, A. Marfat, J. R. Falck and J. O. Albright, *J. Am. Chem. Soc.*, **102**, 1433 (1980).
11. R. Zamboni and J. Rokach, *Tetrahedron Lett.*, **24**, 999 (1983).
12. G. Just, C. Luthe and M. T. P. Viet, *Can. J. Chem.*, **61**, 712 (1983).
13. R. Nagata, M. Kawakami, T. Matsuura and I. Saito, *Tetrahedron Lett.*, **30**, 2817 (1989).
14. A. Massa, A. Lattanzi, F. R. Siniscalchi and A. Scettri, *Tetrahedron: Asymmetry*, **12**, 2775 (2001).
15. A. Massa, L. Palombi and A. Scettri, *Tetrahedron Lett.*, **42**, 4577 (2001).
16. N. A. Porter and D. W. Gilmore, *J. Am. Chem. Soc.*, **99**, 3503 (1977).
17. W. Adam, A. Birke, C. Cádiz, S. Díaz and A. Rodríguez, *J. Org. Chem.*, **43**, 1154 (1978).
18. M. Chmielewski, J. Jurczak and S. Maciejewski, *Carbohydr. Res.*, **165**, 111 (1987).
19. V. Subramanyam, C. L. Brizuela and A. H. Soloway, *J. Chem. Soc., Chem. Commun.*, 508 (1976).
20. P. A. Ganeshpure and W. Adam, *Synthesis*, 179 (1996).
21. B. Witkop, S. Goodwin and T. W. Beiler, *J. Am. Chem. Soc.*, **76**, 5813 (1954).
22. M. S. Kharasch and G. Sosnovsky, *J. Org. Chem.*, **23**, 1322 (1958).
23. I. Saito, R. Nagata, K. Yuba and T. Matsuura, *Tetrahedron Lett.*, **24**, 1737 (1983).
24. F. E. Ziegler and R. T. Wester, *Tetrahedron Lett.*, **25**, 617 (1984).
25. E. Schmitz, A. Rieche and O. Brede, *J. Prakt. Chem.*, **312**, 30 (1970).
26. A. J. Bloodworth and M. E. Loveitt, *J. Chem. Soc., Perkin Trans. 1*, 1031 (1977).
27. K. R. Kopecky, J. E. Filby, C. Mumford, P. A. Lockwood and J.-Y. Ding, *Can. J. Chem.*, **53**, 1103 (1975).
28. A. Baumstark and P. C. Vasquez, *J. Org. Chem.*, **51**, 5213 (1986).
29. M. E. Landis, R. L. Lindsey, W. H. Watson and V. Zabel, *J. Org. Chem.*, **45**, 525 (1980).
30. R. Dietz, A. E. J. Forno, B. E. Larcombe and M. E. Peover, *J. Chem. Soc. B*, 816 (1970).
31. M. Merritt and D. T. Sawyer, *J. Org. Chem.*, **35**, 2157 (1970).
32. (a) E. J. Corey, K. C. Nicolaou and M. Shibasaki, *J. Chem. Soc., Chem. Commun.*, 658 (1975).
(b) J. San Filippo Jr., C.-I. Chern and J. S. Valentine, *J. Org. Chem.*, **40**, 1678 (1975).
33. R. A. Johnson, E. G. Nidy and M. V. Merritt, *J. Am. Chem. Soc.*, **100**, 7960 (1978).
34. S. L. Schreiber and N. Ikemoto, *Tetrahedron Lett.*, **29**, 3211 (1988).
35. (a) N. A. Porter, L. S. Lehman, B. A. Weber and K. J. Smith, *J. Am. Chem. Soc.*, **103**, 6447 (1981).
(b) H. Weenen and N. A. Porter, *J. Am. Chem. Soc.*, **104**, 5216 (1982).
36. (a) A. J. Bloodworth, D. Crich and T. Melvin, *J. Chem. Soc., Chem. Commun.*, 786 (1987).
(b) D. H. R. Barton, D. Crich and B. Motherwell, *J. Chem. Soc., Chem. Commun.*, 242 (1984).
37. G. O. Schenck and H.-D. Becker, *Angew. Chem.*, **70**, 504 (1958).
38. G. O. Schenck, H.-D. Becker, K.-H. Schulte-Elte and C. H. Krauch, *Chem. Ber.*, **96**, 509 (1963).
39. B. Betzemeier and P. Knochel, in *Peroxide Chemistry* (Ed. W. Adam), Chap. D8, Wiley, Weinheim, 2000.
40. J. Wolpers and W. Ziegenbein, *Tetrahedron Lett.*, **12**, 3889 (1971).
41. J. A. Howard and K. U. Ingold, *Can. J. Chem.*, **42**, 1250 (1964).
42. (a) E. N. Frankel, R. F. Garwood, J. R. Vinson and B. C. L. Weedon, *J. Chem. Soc., Perkin Trans. 1*, 2707 (1982).
(b) E. N. Frankel, R. F. Garwood, B. P. S. Khambay, G. P. Moss and B. C. L. Weedon, *J. Chem. Soc., Perkin Trans. 1*, 2233 (1984).
43. R. V. Venkateswaran and P. Goswami, *Tetrahedron Lett.*, **18**, 1943 (1977).
44. R. S. Drago and R. Riley, *J. Am. Chem. Soc.*, **112**, 215 (1990).
45. J. W. Jaroszewski and M. G. Ettlinger, *J. Org. Chem.*, **53**, 4635 (1988).
46. J. Carnduff and D. G. Leppard, *J. Chem. Soc., Perkin Trans. 1*, 2570 (1976).
47. H. Greenland, J. T. Pinhey and S. Sternhell, *Aust. J. Chem.*, **40**, 325 (1987).
48. A. Nishinaga, T. Shimizu, T. Fujii and T. Matsuura, *J. Org. Chem.*, **45**, 4997 (1980).
49. K. Gollnick and G. O. Schenck, *Pure Appl. Chem.*, **9**, 507 (1964).
50. W. Adam and J. del Fierro, *J. Org. Chem.*, **43**, 1159 (1978).
51. (a) W. Adam, O. Cueto and V. Ehrig, *J. Org. Chem.*, **41**, 370 (1976).
(b) G. M. Rubottom and M. I. Lopez Nieves, *Tetrahedron Lett.*, **13**, 2423 (1972).
52. C. W. Jefford and C. G. Rimbault, *Tetrahedron Lett.*, **18**, 2375 (1977).

53. N. Furutachi, Y. Nakadaira and K. Nakanishi, *J. Chem. Soc., Chem. Commun.*, 1625 (1968).
54. M. Matsumoto and K. Kondo, *Tetrahedron Lett.*, **16**, 3935 (1975).
55. (a) M. J. Kulig and L. L. Smith, *J. Org. Chem.*, **38**, 3639 (1973).
(b) M. J. Kulig and L. L. Smith, *J. Org. Chem.*, **39**, 3398 (1974).
56. B.-M. Kwon, R. C. Kanner and C. S. Foote, *Tetrahedron Lett.*, **30**, 903 (1989).
57. M. Orfanopoulos and C. S. Foote, *Tetrahedron Lett.*, **26**, 5991 (1985).
58. N. Shimizu, F. Shibata, S. Imazu and Y. Tsuno, *Chem. Lett.*, 1071 (1987).
59. W. Adam, A. Griesbeck and D. Kappes, *J. Org. Chem.*, **51**, 4479 (1986).
60. A. Bodin, M. Linnerborg, J. L. G. Nilsson and A. T. Karlberg, *Chem. Res. Toxicol.*, **16**, 575 (2003).
61. S. L. Schreiber, *J. Am. Chem. Soc.*, **102**, 6163 (1980).
62. P. Dussault and A. Sahli, *Tetrahedron Lett.*, **31**, 5117 (1990).
63. (a) P. Dussault and A. Sahli, *J. Org. Chem.*, **57**, 1009 (1992).
(b) P. H. Dussault, U. R. Zope and T. A. Westermeyer, *J. Org. Chem.*, **59**, 8267 (1994).
64. S. Baj and A. Chrobok, *Synlett*, 623 (2001).
65. A. Kunath, E. Höft, H.-J. Hamann and J. Wagner, *J. Chromatogr.*, **588**, 352 (1991).
66. H.-J. Hamann, E. Höft and J. Liebscher, in *Peroxide Chemistry* (Ed. W. Adam), Chap. D5, Wiley, Weinheim, 2000.
67. P. Dussault and N. A. Porter, *J. Am. Chem. Soc.*, **110**, 6276 (1988).
68. E. Höft, H.-J. Hamann and A. Kunath, *J. Prakt. Chem.*, **336**, 534 (1994).
69. H.-J. Hamann and E. Höft, *Tetrahedron: Asymmetry*, **7**, 2217 (1996).
70. E. Höft, H.-J. Hamann, A. Kunath, W. Adam, U. Hoch, C. R. Saha-Möller and P. Schreier, *Tetrahedron: Asymmetry*, **6**, 603 (1995).
71. H. Fu, H. Kondo, Y. Ichikawa, G. C. Look and C. H. Wong, *J. Org. Chem.*, **57**, 7265 (1992).
72. W. Adam, F. Heckel, C. R. Saha-Möller and P. Schreier, *J. Organomet. Chem.*, **661**, 17 (2002).
73. W. Adam, C. Mock-Knoblauch and C. R. Saha-Möller, *J. Org. Chem.*, **64**, 4834 (1999).
74. W. Adam, U. Hoch, C. R. Saha-Möller and P. Schreier, *Angew. Chem., Int. Ed. Engl.*, **32**, 1737 (1993).
75. W. Adam, U. Hoch, M. Lazarus, C. R. Saha-Möller and P. Schreier, *J. Am. Chem. Soc.*, **117**, 11898 (1995).
76. D. Häring, E. Schtüler, W. Adam, C. R. Saha-Möller and P. Schreier, *J. Org. Chem.*, **64**, 832 (1999).
77. D. Häring, M. Herderich, E. Schtüler, B. Withopf and P. Schreier, *Tetrahedron: Asymmetry*, **8**, 853 (1997).
78. W. Adam, B. Boss, D. Harmsen, Z. Lukacs, C. R. Saha-Möller and P. Schreier, *J. Org. Chem.*, **63**, 7598 (1998).
79. W. Adam, Z. Lukacs, C. R. Saha-Möller and P. Schreier, *J. Am. Chem. Soc.*, **122**, 4887 (2000).
80. O. Textorius, E. Welinder and S. E. G. Nilsson, *Doc. Ophthalmol.*, **60**, 393 (1985).
81. I. M. Bell and D. Hilvert, *Biochemistry*, **32**, 13969 (1993).
82. G. Iacazio, G. Langrand, J. Baratti, G. Buono and C. Triantaphylidès, *J. Org. Chem.*, **55**, 1690 (1990).
83. P. Dussault, *Synlett*, 997 (1995).
84. N. Baba, K. Yoneda, S. Tahara, J. Iwasa, T. Kaneko and M. Matsuo, *J. Chem. Soc., Chem. Commun.*, 1281 (1990).
85. (a) T. Takata, Y. Tamura and W. Ando, *Tetrahedron*, **41**, 2133 (1985).
(b) T. Takata, K. Hoshino, E. Takeuchi, Y. Tamura and W. Ando, *Tetrahedron Lett.*, **25**, 4767 (1984).
86. A. Griesbeck, J. Steinwascher and T. Hundertmark, in *Peroxide Chemistry* (Ed. W. Adam), Chap. B2, Wiley, Weinheim, 2000.
87. P. H. Dussault and M. R. Hayden, *Tetrahedron Lett.*, **33**, 443 (1992).
88. H. Kropf and R. Reichwaldt, *J. Chem. Res. (S)*, 412 (1987).
89. W. Adam and B. Nestler, *Liebigs Ann. Chem.*, 1051 (1990).
90. W. Adam, H. G. Brünker and B. Nestler, *Tetrahedron Lett.*, **32**, 1957 (1991).
91. (a) L. M. Stephenson, M. J. Grdina and M. Orfanopoulos, *Acc. Chem. Res.*, **13**, 419 (1980).
(b) M. Orfanopoulos, I. Smonou and C. S. Foote, *J. Am. Chem. Soc.*, **112**, 3607 (1990).

- (c) A. A. Frimer and L. M. Stephenson, in *Singlet Oxygen* (Ed. A. A. Frimer), Chap. 3, CRC Press, Boca Raton, 1985.
92. H. E. Ensley, R. V. C. Carr, R. S. Martin and T. E. Pierce, *J. Am. Chem. Soc.*, **102**, 2836 (1980).
93. W. Adam and B. Nestler, *J. Am. Chem. Soc.*, **114**, 6549 (1992).
94. W. Adam and B. Nestler, *J. Am. Chem. Soc.*, **115**, 5041 (1993).
95. W. Adam and H. G. Brünker, *J. Am. Chem. Soc.*, **115**, 3008 (1993).
96. (a) H. S. Dang and A. G. Davies, *J. Chem. Soc., Perkin Trans. 2*, 2011 (1991).
(b) H. S. Dang and A. G. Davies, *J. Chem. Soc., Perkin Trans. 2*, 1095 (1992).
(c) H. S. Dang and A. G. Davies, *J. Organomet. Chem.*, **430**, 287 (1992).
97. P. H. Dussault and R. J. Lee, *J. Am. Chem. Soc.*, **116**, 4485 (1994).
98. M. Aoki and D. Seebach, *Helv. Chim. Acta*, **84**, 187 (2001).
99. A. Lattanzi, P. Iannece, A. Vicinanza and A. Scettri, *J. Chem. Soc., Chem. Commun.*, 1440 (2003).
100. D. Mostowicz, M. Jurczak, H.-J. Hamann, E. Höft and M. Chmielewski, *Eur. J. Org. Chem.*, 2617 (1998).
101. H.-J. Hamann, E. Höft, D. Mostowicz, A. Mishnev, Z. Urbanczyk-Lipkowska and M. Chmielewski, *Tetrahedron*, **53**, 185 (1997).
102. J. Rebeck and R. McCreedy, *J. Am. Chem. Soc.*, **102**, 5602 (1980).
103. (a) E. Höft and A. Rieche, *Angew. Chem., Int. Ed. Engl.*, **4**, 524 (1965).
(b) E. G. E. Hawkins, *J. Chem. Soc. C*, 160 (1971).
104. F. Welch, H. R. Williams and H. S. Mosher, *J. Am. Chem. Soc.*, **77**, 551 (1955).
105. W. A. Pryor and D. M. Huston, *J. Org. Chem.*, **29**, 512 (1964).
106. N. A. Milas and D. M. Surgenor, *J. Am. Chem. Soc.*, **68**, 205 (1946).
107. S. Matsugo and I. Saito, in *Organic Peroxides* (Ed. W. Ando), Chap. 3, Wiley, Chichester, 1992.
108. L. Horner and K. H. Knapp, *Liebigs Ann. Chem.*, **622**, 79 (1959).
109. H. Hock and H. Kropf, *Chem. Ber.*, **88**, 1544 (1955).
110. F. F. Rust, F. H. Seubold and W. E. Vaughan, *J. Am. Chem. Soc.*, **72**, 338 (1950).
111. N. A. Milas and L. H. Perry, *J. Am. Chem. Soc.*, **68**, 1938 (1946).
112. M. F. Salomon, R. G. Salomon and R. D. Gleim, *J. Org. Chem.*, **41**, 3983 (1976).
113. A. G. Davies, R. V. Foster and A. M. White, *J. Chem. Soc.*, 2200 (1954).
114. K. Weissermel and M. Lederer, *Chem. Ber.*, **96**, 77 (1963).
115. A. Rieche, C. Bischoff and P. Dietrich, *Chem. Ber.*, **94**, 2932 (1961).
116. A. Rieche and C. Bischoff, *Chem. Ber.*, **94**, 2457 (1961).
117. H. Kropf, H. M. Amirabadi, M. Mosebach, A. Torkler and H. Vonwallis, *Synthesis*, 587 (1983).
118. W. H. Richardson and R. S. Smith, *J. Org. Chem.*, **33**, 3882 (1968).
119. M. R. Barusch and J. Q. Payne, *J. Am. Chem. Soc.*, **75**, 1987 (1953).
120. H. Kropf, M. Ball, H. Schröder and G. Witte, *Tetrahedron*, **30**, 2943 (1974).
121. H. Kropf, J. Thiem and H. Nimz, in *Houben-Weyl, Methoden der Organischen Chemie* (Eds. E. Müller, O. Bayer, H. Meerwein, K. Ziegler, H. Kropf and H.-G. Padeken), Vol. VI/1a, Chap. AIII, Georg Thieme Verlag, Stuttgart, 1979.
122. J. D. Druliner, *Synth. Commun.*, **13**, 115 (1983).
123. P. H. Dussault and I. Q. Lee, *J. Am. Chem. Soc.*, **115**, 6458 (1993).
124. M. S. Kharasch and G. Sosnovsky, *Tetrahedron*, **3**, 105 (1958).
125. W. Treibs and G. Pellmann, *Chem. Ber.*, **87**, 1201 (1954).
126. H. Kropf and D. Goschenhofer, *Tetrahedron Lett.*, 239 (1968).
127. A. J. Bloodworth and J. L. Courtneidge, *J. Chem. Soc., Perkin Trans. 1*, 1807 (1982).
128. A. J. Bloodworth, K. J. Bowyer and J. C. Mitchell, *J. Org. Chem.*, **52**, 1124 (1987).
129. S. Isayama and T. Mukaiyama, *Chem. Lett.*, 573 (1989).
130. S. Murahashi, T. Naota and K. Yonemura, *J. Am. Chem. Soc.*, **110**, 8256 (1988).
131. J. A. Howard, in *The Chemistry of Peroxides* (Ed. S. Patai), Chap. 8, Wiley, Chichester, 1983.
132. G. A. Russell and A. G. Bemis, *J. Am. Chem. Soc.*, **88**, 5491 (1966).
133. R. K. Haynes and S. C. Vonwiller, *J. Chem. Soc., Chem. Commun.*, 448 (1990).
134. (a) M. L. Kilpatrick, O. M. Reiff and F. O. Rice, *J. Am. Chem. Soc.*, **48**, 3019 (1926).
(b) J. H. Walton and G. W. Filson, *J. Am. Chem. Soc.*, **54**, 3228 (1932).

- (c) R. Bortolo, D. Bianchi, R. D'Aloisio, C. Querci and M. Ricci, *J. Mol. Catal. A: Chem.*, **153**, 25 (2000).
- (d) I. Yamanaka, T. Onizawa, S. Takenaka and K. Otsuka, *Angew. Chem., Int. Ed.*, **42**, 3653 (2003).
135. W. D. Emmons and A. S. Pagano, *J. Am. Chem. Soc.*, **77**, 89 (1955).
136. (a) C. A. Bunton and G. J. Minkoff, *J. Chem. Soc.*, 665 (1949).
(b) E. Weitz and A. Scheffer, *Chem. Ber.*, **54**, 2327 (1921).
137. W. Adam, P. B. Rao, H.-G. Degen and C. R. Saha-Möller, *J. Am. Chem. Soc.*, **122**, 5654 (2000).
138. C. L. Dwyer, C. D. Gill, O. Ichihara and R. J. K. Taylor, *Synlett*, 704 (2000).
139. P. L. Bailey, W. Clegg, R. F. W. Jackson and O. Meth-Cohn, *J. Chem. Soc., Perkin Trans. 1*, 343 (1993).
140. A. D. Briggs, R. F. W. Jackson, W. Clegg, M. R. J. Elsegood, J. Kelly and P. A. Brown, *Tetrahedron Lett.*, **35**, 6945 (1994).
141. K. Neimann and R. Neumann, *Org. Lett.*, **2**, 2861 (2000).
142. M. C. A. van Vliet, I. W. C. E. Arends and R. A. Sheldon, *Synlett*, 248 (2001).
143. S. P. de Visser, J. Kaneti, R. Neumann and S. Shaik, *J. Org. Chem.*, **68**, 2903 (2003).
144. M. M. Lakouraj, B. Movassagh and K. Bahrami, *Synth. Commun.*, **31**, 1237 (2001).
145. J. Wahlen, D. E. de Vos and P. A. Jacobs, *Org. Lett.*, **5**, 1777 (2003).
146. R. Bernini, E. Mincione, A. Coratti, G. Fabrizi and G. Battistuzzi, *Tetrahedron*, **60**, 967 (2004).
147. (a) R. Helder, J. C. Hummelen, R. W. P. M. Laane, J. S. Wiering and H. Wynberg, *Tetrahedron Lett.*, **17**, 1831 (1976).
(b) H. Wynberg and B. Greijdanus, *J. Chem. Soc., Chem. Commun.*, 427 (1978).
(c) H. Wynberg and B. Marsman, *J. Org. Chem.*, **45**, 158 (1980).
(d) H. Plum and H. Wynberg, *J. Org. Chem.*, **45**, 2498 (1980).
148. N. Baba, J. Oda and M. Kawaguchi, *Agric. Biol. Chem.*, **50**, 3113 (1986).
149. S. Arai, H. Tsuge and T. Shioiri, *Tetrahedron Lett.*, **39**, 7563 (1998).
150. S. Arai, M. Oku, M. Miura and T. Shiori, *Synlett*, 1201 (1998).
151. Y. Harigaya, H. Yamaguchi and M. Onda, *Heterocycles*, **15**, 183 (1981).
152. W. Adam, P. B. Rao, H.-G. Degen, A. Levai, T. Patonay and C. R. Saha-Möller, *J. Org. Chem.*, **67**, 259 (2002).
153. S. Julia, J. Masana and J. C. Vega, *Angew. Chem., Int. Ed. Engl.*, **19**, 929 (1980).
154. S. Banfi, S. Colonna, H. Molinari, S. Julia and J. Guixer, *Tetrahedron*, **40**, 5207 (1984).
155. S. Julia, J. Guixer, J. Masana, J. Rocas, S. Colonna, R. Annunziata and H. Molinari, *J. Chem. Soc., Perkin Trans. 1*, 1317 (1982).
156. S. Colonna, H. Molinari, S. Banfi, S. Julia, J. Masana and A. Alvarez, *Tetrahedron*, **39**, 1635 (1983).
157. S. Itsuno, M. Sakakura and K. Ito, *J. Org. Chem.*, **55**, 6047 (1990).
158. W. Kroutil, M. E. Lasterra-Sánchez, S. J. Maddrell, P. Mayon, P. Morgan, S. M. Roberts, S. R. Thornton, C. J. Todd and M. Tuter, *J. Chem. Soc., Perkin Trans. 1*, 2837 (1996).
159. B. M. Adger, J. V. Barkley, S. Bergeron, M. W. Cappi, B. E. Flowerdew, M. P. Jackson, R. McCague, T. C. Nugent and S. M. Roberts, *J. Chem. Soc., Perkin Trans. 1*, 3501 (1997).
160. P. A. Bentley, S. Bergeron, M. W. Cappi, D. E. Hibbs, M. B. Hursthouse, T. C. Nugent, R. Pulido, S. M. Roberts and L. E. Wu, *J. Chem. Soc., Chem. Commun.*, 739 (1997).
161. A. Dhanda, K. H. Drauz, T. Geller and S. M. Roberts, *Chirality*, **12**, 313 (2000).
162. J. V. Allen, S. Bergeron, M. J. Griffiths, S. Mukherjee, S. M. Roberts, N. M. Williamson and L. E. Wu, *J. Chem. Soc., Perkin Trans. 1*, 3171 (1998).
163. J. V. Allen, K. H. Drauz, R. W. Flood, S. M. Roberts and J. Skidmore, *Tetrahedron Lett.*, **40**, 5417 (1999).
164. M. E. Lasterra-Sánchez, U. Felfer, P. Mayon, S. M. Roberts, S. R. Thornton and C. J. Todd, *J. Chem. Soc., Perkin Trans. 1*, 343 (1996).
165. T. Geller and S. M. Roberts, *J. Chem. Soc., Perkin Trans. 1*, 1397 (1999).
166. S. Baars, K.-H. Drauz, H.-P. Krimmer, S. M. Roberts, J. Sander, J. Skidmore and G. Zanardi, *Org. Process Res. Dev.*, **7**, 509 (2003).
167. W. Kroutil, P. Mayon, M. E. Lasterra-Sánchez, S. J. Maddrell, S. M. Roberts, S. R. Thornton, C. J. Todd and M. Tuter, *J. Chem. Soc., Chem. Commun.*, 845 (1996).
168. J. A. N. Augustyn, B. C. B. Bezuidenhout and D. Ferreira, *Tetrahedron*, **46**, 2651 (1990).

169. J. R. Falck, R. K. Bhatt, K. M. Reddy and J. Ye, *Synlett*, 481 (1997).
170. W. P. Chen, A. L. Egar, M. B. Hursthouse, K. M. A. Malik, J. E. Mathews and S. M. Roberts, *Tetrahedron Lett.*, **39**, 8495 (1998).
171. J. V. Allen, M. W. Cappi, P. D. Kary, S. M. Roberts, N. M. Williamson and L. E. Wu, *J. Chem. Soc., Perkin Trans. 1*, 3297 (1997).
172. M. J. Porter and J. Skidmore, *J. Chem. Soc., Chem. Commun.*, 1215 (2000).
173. D. Enders, J. Q. Zhu and L. Kramps, *Liebigs Ann. Recl.*, 1101 (1997).
174. L. Carde, D. H. Davies and S. M. Roberts, *J. Chem. Soc., Perkin Trans. 1*, 2455 (2000).
175. P. A. Bentley, W. Kroutil, J. A. Littlechild and S. M. Roberts, *Chirality*, **9**, 198 (1997).
176. P. A. Bentley, M. W. Cappi, R. W. Flood, S. M. Roberts and J. A. Smith, *Tetrahedron Lett.*, **39**, 9297 (1998).
177. R. W. Flood, T. P. Geller, S. A. Petty, S. M. Roberts, J. Skidmore and M. Volk, *Org. Lett.*, **3**, 683 (2001).
178. (a) R. Takagi, A. Shiraki, T. Manabe, S. Kojima and K. Ohkata, *Chem. Lett.*, 366 (2000).
(b) P. A. Bentley, R. W. Flood, S. M. Roberts, J. Skidmore, C. B. Smith and J. A. Smith, *J. Chem. Soc., Chem. Commun.*, 1616 (2001).
179. A. Berkessel, N. Gasch, K. Glaubitz and C. Koch, *Org. Lett.*, **3**, 3839 (2001).
180. C. Lauret and S. M. Roberts, *Aldrichim. Acta*, **35**, 47 (2002).
181. D. R. Kelly, T. T. T. Bui, E. Caroff, A. F. Drake and S. M. Roberts, *Tetrahedron Lett.*, **45**, 3885 (2004).
182. J.-M. Lopez-Pedrosa, M. R. Pitts, S. M. Roberts, S. Saminathan and J. Whittall, *Tetrahedron Lett.*, **45**, 5073 (2004).
183. S. Colonna and A. Manfredi, *Tetrahedron Lett.*, **27**, 387 (1986).
184. S. Colonna, A. Manfredi, R. Annunziata and M. Spadoni, *Tetrahedron*, **43**, 2157 (1987).
185. S. Colonna, N. Gaggero, A. Manfredi, M. Spadoni, L. Casella, G. Carrea and P. Pasta, *Tetrahedron*, **44**, 5169 (1988).
186. S. Colonna, A. Manfredi and M. Spadoni, *Tetrahedron Lett.*, **28**, 1577 (1987).
187. B. Betzemeier, F. Lhermitte and P. Knochel, *Synlett*, 489 (1999).
188. L. Kim (Shell International Research Maatschappij N. V.), DE 2 239 681 (1973); L. Kim, *Chem. Abstr.*, **78**, 159400n (1973).
189. R. P. Heggs and B. Ganem, *J. Am. Chem. Soc.*, **101**, 2484 (1979).
190. (a) K. A. Jørgensen, *Chem. Rev.*, **89**, 431 (1989).
(b) V. K. Aggarwal, in *Comprehensive Asymmetric Catalysis* (Eds. E. N. Jacobsen, A. Pfaltz and H. Yamamoto), Chap. 18.3, Springer-Verlag, Berlin, 2000.
(c) E. N. Jacobsen and M. H. Wu, in *Comprehensive Asymmetric Catalysis* (Eds. E. N. Jacobsen, A. Pfaltz and H. Yamamoto), Chap. 18.2, Springer-Verlag, Berlin, 2000.
191. H. B. Kagan, in *Catalytic Asymmetric Synthesis* (Ed. I. Ojima), Chap. 6C, Wiley, New York, 2000.
192. D. Enders, J. Q. Zhu and G. Raabe, *Angew. Chem., Int. Ed. Engl.*, **35**, 1725 (1996).
193. H. B. Yu, X. F. Zheng, Z. M. Lin, Q. S. Hu, W. S. Huang and L. Pu, *J. Org. Chem.*, **64**, 8149 (1999).
194. D. Enders, L. Kramps and J. Q. Zhu, *Tetrahedron: Asymmetry*, **9**, 3959 (1998).
195. M. Bougauchi, S. Watanabe, T. Arai, H. Sasai and M. Shibasaki, *J. Am. Chem. Soc.*, **119**, 2329 (1997).
196. S. Watanabe, Y. Kobayashi, T. Arai, H. Sasai, M. Bougauchi and M. Shibasaki, *Tetrahedron Lett.*, **39**, 7353 (1998).
197. S. Watanabe, T. Arai, H. Sasai, M. Bougauchi and M. Shibasaki, *J. Org. Chem.*, **63**, 8090 (1998).
198. K. Daikai, M. Kamaura and J. Inanaga, *Tetrahedron Lett.*, **39**, 7321 (1998).
199. C. L. Elston, R. F. W. Jackson, S. J. F. MacDonald and P. J. Murray, *Angew. Chem., Int. Ed. Engl.*, **36**, 410 (1997).
200. (a) T. Yokoyama, M. Nishizawa, T. Kimura and T. M. Suzuki, *Chem. Lett.*, 1703 (1983).
(b) T. Yokoyama, M. Nishizawa, T. Kimura and T. M. Suzuki, *Bull. Chem. Soc. Jpn.*, **58**, 3271 (1985).
201. R. C. Michaelson, R. E. Palermo and K. B. Sharpless, *J. Am. Chem. Soc.*, **99**, 1990 (1977).
202. K. B. Sharpless and T. R. Verhoeven, *Aldrichim. Acta*, **12**, 63 (1979).
203. S. I. Yamada, T. Mashiko and S. Terashima, *J. Am. Chem. Soc.*, **99**, 1988 (1977).
204. S. Coleman-Kammula and E. T. Duim-Koolstra, *J. Organomet. Chem.*, **246**, 53 (1983).

205. A. Pfenninger, *Synthesis*, 89 (1986).
206. T. Katsuki and K. B. Sharpless, *J. Am. Chem. Soc.*, **102**, 5974 (1980).
207. D. Schinzer, *Nachr. Chem. Tech. Lab.*, **37**, 1294 (1989).
208. Y. Gao, R. M. Hanson, J. M. Klunder, S. Y. Ko, H. Masamune and K. B. Sharpless, *J. Am. Chem. Soc.*, **109**, 5765 (1987).
209. M. J. Farrell, M. Alexis and M. Trecarten, *Nouv. J. Chim.*, **7**, 449 (1983).
210. B. E. Rossiter and K. B. Sharpless, *J. Org. Chem.*, **49**, 3707 (1984).
211. V. S. Martin, S. S. Woodard, T. Katsuki, Y. Yamada, M. Ikeda and K. B. Sharpless, *J. Am. Chem. Soc.*, **103**, 6237 (1981).
212. (a) T. Katsuki and V. S. Martin, *Org. React.*, **48**, 1 (1996).
(b) R. Noyori, in *Asymmetric Catalysis in Organic Synthesis*, Chap. 4, Wiley, New York, 1994.
(c) R. A. Johnson and K. B. Sharpless, in *Catalytic Asymmetric Synthesis* (Ed. I. Ojima), Wiley, New York, 2000, p. 231.
213. N. Murase, Y. Hoshino, M. Oishi and H. Yamamoto, *J. Org. Chem.*, **64**, 338 (1999).
214. Y. Hoshino, N. Murase, M. Oishi and H. Yamamoto, *Bull. Chem. Soc. Jpn.*, **73**, 1653 (2000).
215. Y. Hoshino and H. Yamamoto, *J. Am. Chem. Soc.*, **122**, 10452 (2000).
216. C. Bolm and T. Kühn, *Synlett*, 899 (2000).
217. C. Bolm, O. Beckmann, T. Kuhn, C. Palazzi, W. Adam, P. B. Rao and C. R. Saha-Möller, *Tetrahedron: Asymmetry*, **12**, 2441 (2001).
218. H. L. Wu and B. J. Uang, *Tetrahedron: Asymmetry*, **13**, 2625 (2002).
219. W. Adam, M. N. Korb, K. J. Roschmann and C. R. Saha-Möller, *J. Org. Chem.*, **63**, 3423 (1998).
220. W. Adam and M. N. Korb, *Tetrahedron: Asymmetry*, **8**, 1131 (1997).
221. W. Adam, A. K. Beek, A. Pichota, C. R. Saha-Möller, D. Seebach, N. Vogl and R. Zhang, *Tetrahedron: Asymmetry*, **14**, 1355 (2003).
222. (a) W. Adam, P. L. Alsters, R. Neumann, C. R. Saha-Möller, D. Seebach and R. Zhang, *Org. Lett.*, **5**, 725 (2003).
(b) W. Adam, P. L. Alsters, R. Neumann, C. R. Saha-Möller, D. Seebach, A. K. Beck and R. Zhang, *J. Org. Chem.*, **68**, 8222 (2003).
223. W. Adam, C. M. Mitchell and C. R. Saha-Möller, *Eur. J. Org. Chem.*, 785 (1999).
224. K. Kamata, K. Yamaguchi, S. Hikichi and N. Mizuno, *Adv. Synth. Catal.*, **345**, 1193 (2003).
225. K. B. Sharpless and R. C. Michaelson, *J. Am. Chem. Soc.*, **95**, 6136 (1973).
226. W. Adam and T. Wirth, *Acc. Chem. Res.*, **32**, 703 (1999).
227. B. E. Rossiter, T. R. Verhoeven and K. B. Sharpless, *Tetrahedron Lett.*, **20**, 4733 (1979).
228. W. Adam, R. Kumar, T. I. Reddy and M. Renz, *Angew. Chem., Int. Ed. Engl.*, **35**, 880 (1996).
229. W. Adam and A. K. Smerz, *J. Org. Chem.*, **61**, 3506 (1996).
230. W. Adam, A. Corma, T. I. Reddy and M. Renz, *J. Org. Chem.*, **62**, 3631 (1997).
231. M. Taramasso, G. Perego and B. Notari, US 4,410,501 (1983); G. Perego, M. Taramasso and B. Notari, *Chem. Abstr.*, **95**, 206272k (1981).
232. L. Palombi, F. Bonadies and A. Scettri, *Tetrahedron*, **53**, 11369 (1997).
233. (a) S. Kobayashi and S. Nagayama, *J. Am. Chem. Soc.*, **120**, 4554 (1998).
(b) S. Nagayama, M. Endo and S. Kobayashi, *J. Org. Chem.*, **63**, 6094 (1998).
(c) S. Kobayashi, T. Ishida and R. Akiyama, *Org. Lett.*, **3**, 2649 (2001).
(d) R. Akiyama and S. Kobayashi, *Angew. Chem., Int. Ed.*, **40**, 3469 (2001).
234. A. Lattanzi and N. E. Leadbeater, *Org. Lett.*, **4**, 1519 (2002).
235. (a) W. Adam, K. Peters and M. Renz, *Angew. Chem., Int. Ed. Engl.*, **33**, 1107 (1994).
(b) W. Adam, M. N. Korb and C. R. Saha-Möller, *Eur. J. Org. Chem.*, 907 (1998).
236. W. Adam, K. Peters and M. Renz, *J. Org. Chem.*, **62**, 3183 (1997).
237. A. O. Chong and K. B. Sharpless, *J. Org. Chem.*, **42**, 1587 (1977).
238. H. Mimoun, *J. Mol. Catal.*, **7**, 1 (1980).
239. R. A. Sheldon, *J. Mol. Catal.*, **7**, 107 (1980).
240. R. A. Sheldon and J. A. Vandoorn, *J. Catal.*, **31**, 427 (1973).
241. R. A. Sheldon and J. K. Kochi, in *Metal Catalyzed Oxidations of Organic Compounds*, Academic Press, New York, 1981
242. F. Wattimena and H. P. Wulff (Shell International Research), DE 2015503 [GB 1 249 079] (1971); *Chem. Abstr.*, **74**, 12981m (1971).
243. H. J. Ledon and F. Varescon, *Inorg. Chem.*, **23**, 2735 (1984).

244. C. P. Lau, B. H. Chang, R. H. Grubbs and C. H. Brubaker, *J. Organomet. Chem.*, **214**, 325 (1981).
245. B. Notari, *Catal. Today*, **18**, 163 (1993).
246. (a) J. S. Reddy, R. Kumar and P. Ratnasamy, *Appl. Catal.*, **58**, L1 (1990).
(b) J. S. Reddy and R. Kumar, *J. Catal.*, **130**, 440 (1991).
247. M. A. Camblor, M. Costantini, A. Corma, L. Gilbert, P. Esteve, A. Martínez and S. Valencia, *J. Chem. Soc., Chem. Commun.*, 1339 (1996).
248. C. T. Kresge, M. E. Leonowicz, W. J. Roth, J. C. Vartuli and J. S. Beck, *Nature*, **359**, 710 (1992).
249. (a) W.-H. Zhang, M. Froba, J. L. Wang, P. T. Tanev, J. Wong and T. J. Pinnavaia, *J. Am. Chem. Soc.*, **118**, 9164 (1996).
(b) S. Inagaki, Y. Fukushima and K. Kuroda, *J. Chem. Soc., Chem. Commun.*, 680 (1993).
(c) W. Z. Zhang, J. L. Wang, P. T. Tanev and T. J. Pinnavaia, *J. Chem. Soc., Chem. Commun.*, 979 (1996).
(d) K. A. Koyano and T. Tatsumi, *J. Chem. Soc., Chem. Commun.*, 145 (1996).
250. A. Corma, M. T. Navarro and J. Pérez Pariente, *J. Chem. Soc., Chem. Commun.*, 147 (1994).
251. A. Corma, *Chem. Rev.*, **97**, 2373 (1997).
252. M. A. Roberts, G. Sankar, J. M. Thomas, R. H. Jones, H. Du, J. Chen, W. Pang and R. Xu, *Nature*, **381**, 401 (1996).
253. A. Corma, U. Díaz, V. Fornés, J. L. Jordá, M. Domine and F. Rey, *J. Chem. Soc., Chem. Commun.*, 779 (1999).
254. P. Wu and T. Tatsumi, *J. Phys. Chem. B*, **106**, 748 (2002).
255. S. C. Laha and R. Kumar, *J. Catal.*, **208**, 339 (2002).
256. L. J. Schofield, O. J. Kerton, P. McMorn, D. Bethell, S. Ellwood and G. J. Hutchings, *J. Chem. Soc., Perkin Trans. 2*, 1475 (2002).
257. S. Ikegami, T. Katsuki and M. Yamaguchi, *Chem. Lett.*, 83 (1987).
258. B. H. Chang, R. H. Grubbs and C. H. Brubaker, *J. Organomet. Chem.*, **280**, 365 (1985).
259. E. G. E. Hawkins, *J. Chem. Soc.*, 2169 (1950).
260. C. C. Su, J. W. Reed and E. S. Gould, *Inorg. Chem.*, **12**, 337 (1973).
261. (a) R. D. Bach, G. J. Wolber and B. A. Coddens, *J. Am. Chem. Soc.*, **106**, 6098 (1984).
(b) E. S. Gould, R. R. Hiatt and K. C. Irwin, *J. Am. Chem. Soc.*, **90**, 4573 (1968).
262. H. Mimoun, M. Mignard, P. Brechot and L. Saussine, *J. Am. Chem. Soc.*, **108**, 3711 (1986).
263. G. L. Linden and M. F. Farena, *J. Catal.*, **48**, 284 (1977).
264. S. Bhaduri, A. Ghosh and H. Khwaja, *J. Chem. Soc., Dalton Trans.*, 447 (1981).
265. G. L. Linden and M. F. Farena, *Inorg. Chem.*, **16**, 3170 (1977).
266. K. Zhang, G. S. Kumar and D. C. Neckers, *J. Polym. Sci., Part A: Polym. Chem.*, **23**, 1213 (1985).
267. J. Sala-Pala, J. Roue and J. E. Guerchais, *J. Mol. Catal.*, **7**, 141 (1980).
268. R. Landau, G. A. Sullivan and D. Brown, *Chemtech*, 602 (1979).
269. M. N. Sheng and J. G. Zajacek (Atlantic Richfield), GB 1,136,923 (1968); *Chem. Abstr.*, **70**, 87546z (1969).
270. H. P. Wulff (Shell Oil Company), US 3,829,392 (1975); *Chem. Abstr.*, **84**, 89977d (1976).
271. T. Kratz and W. Zeiß, in *Peroxide Chemistry* (Ed. W. Adam), Chap. B1, Wiley, Weinheim, 2000.
272. T. Szymanska-Buzar and J. J. Ziolkowski, *J. Mol. Catal.*, **11**, 371 (1981).
273. Y. Matoba, H. Inoue, J. Akagi, T. Okabayashi, Y. Ishii and M. Ogawa, *Synth. Commun.*, **14**, 865 (1984).
274. H. J. Ledon, P. Durbut and F. Varescon, *J. Am. Chem. Soc.*, **103**, 3601 (1981).
275. E. T. Marquis, K. P. Keating, J. F. Knifton, W. A. Smith, J. R. Sanderson and J. P. Lustrì (Texaco Development Corporation), EP 0 188 912 A2 (1986); *Chem. Abstr.*, **105**, 135938u (1986).
276. P. Chaumette, H. Mimoun, L. Saussine, J. Fischer and A. Mitschler, *J. Organomet. Chem.*, **250**, 291 (1983).
277. (a) K. B. Sharpless, D. R. Williams and J. M. Townsend, *J. Am. Chem. Soc.*, **94**, 295 (1972).
(b) A. A. Achrem, T. A. Timoschtschuk and D. I. Metelitz, *Tetrahedron*, **30**, 3165 (1974).
(c) H. Arakawa, Y. Morooka and A. Ozaki, *Bull. Chem. Soc. Jpn.*, **47**, 2958 (1974).
278. H. Mimoun, I. S. D. Roch and L. Sajus, *Tetrahedron*, **26**, 37 (1970).

279. C.-S. Chien, T. Kawasaki, M. Sakamoto, Y. Tamura and Y. Kita, *Chem. Pharm. Bull.*, **33**, 2743 (1985).
280. H. Mimoun, in *The Chemistry of Peroxides* (Ed. S. Patai), Chap. 15, Wiley, New York, 1983.
281. D. V. Banthorpe and S. E. Barrow, *Chem. Ind. (London)*, 502 (1981).
282. W. R. Thiel, *J. Mol. Catal. A: Chem.*, **117**, 449 (1997).
283. W. R. Thiel, in *Transition Metals for Organic Synthesis* (Eds. M. Beller and C. Bolm), Chap. 2.7.4, Wiley-VCH, Weinheim, 1998.
284. J. Sobczak and J. J. Ziolkowski, *J. Mol. Catal.*, **3**, 165 (1977/78).
285. Y. Kurusu, Y. Masuyama, M. Saito and S. Saito, *J. Mol. Catal.*, **37**, 235 (1986).
286. J.-H. Ahn and D. C. Sherrington, *J. Chem. Soc., Chem. Commun.*, 643 (1996).
287. M. M. Miller, D. C. Sherrington and S. Simpson, *J. Chem. Soc., Perkin Trans. 2*, 2091 (1994).
288. M. M. Miller and D. C. Sherrington, *J. Chem. Soc., Chem. Commun.*, 55 (1994).
289. Y. Itoi, M. Inoue, S. Enomoto and Y. Watanabe, *Chem. Pharm. Bull.*, **32**, 418 (1984).
290. Y. Itoi, M. Inoue and S. Enomoto, *Chem. Pharm. Bull.*, **33**, 3583 (1985).
291. P.-S. E. Dai and J. H. Lunsford, *J. Catal.*, **64**, 184 (1980).
292. M. B. Ward, K. Mizuno and J. H. Lunsford, *J. Mol. Catal.*, **27**, 1 (1984).
293. J. R. Sohn and J. H. Lunsford, *J. Mol. Catal.*, **32**, 325 (1985).
294. E. Tempesti, L. Giuffre, F. di Renzo, C. Mazzocchia and G. Airoldi, *Appl. Catal.*, **26**, 285 (1986).
295. T. Kamiyama, M. Inoue, H. Kashiwagi and S. Enomoto, *Bull. Chem. Soc. Jpn.*, **63**, 1559 (1990).
296. M. Abrantes, A. Valente, M. Pillinger, I. S. Goncalves, J. Rocha and C. C. Romão, *J. Catal.*, **209**, 237 (2002).
297. J. Ichihara, S. Yamaguchi, T. Nomoto, H. Nakayama, K. Iteya, N. Naitoh and Y. Sasaki, *Tetrahedron Lett.*, **43**, 8231 (2002).
298. Y. Watanabe, M. Inoue and Y. Itoi, *Chem. Pharm. Bull.*, **31**, 1119 (1983).
299. K. Tani, M. Hanafusa and S. Otsuka, *Tetrahedron Lett.*, **20**, 3017 (1979).
300. (a) W. Winter, C. Mark and V. Schurig, *Inorg. Chem.*, **19**, 2045 (1980).
(b) H. B. Kagan, H. Mimoun, C. Mark and V. Schurig, *Angew. Chem., Int. Ed. Engl.*, **18**, 485 (1979).
301. K. S. Kirshenbaum and K. B. Sharpless, *J. Org. Chem.*, **50**, 1979 (1985).
302. G. Amato, A. Arcoria, F. P. Ballistreri, G. A. Tomaselli, O. Bortolini, V. Conte, F. DiFuria, G. Modena and G. Valle, *J. Mol. Catal.*, **37**, 165 (1986).
303. G. G. Allan (du Pont de Nemours and Company), US 3,156,709 (1964); *Chem. Abstr.*, **62**, 2762f (1965).
304. Y. Itoi, M. Inoue and S. Enomoto, *Bull. Chem. Soc. Jpn.*, **58**, 3193 (1985).
305. C. Venturello, E. Alneri and M. Ricci, *J. Org. Chem.*, **48**, 3831 (1983).
306. C. Venturello, R. D'Aloisio, J. J. Bart and M. Ricci, *J. Mol. Catal.*, **32**, 107 (1985).
307. C. Venturello and R. D'Aloisio, *J. Org. Chem.*, **53**, 1553 (1988).
308. Y. Ishii, K. Yamawaki, T. Ura, H. Yamada, T. Yoshida and M. Ogawa, *J. Org. Chem.*, **53**, 3587 (1988).
309. S. Sakaguchi, Y. Nishiyama and Y. Ishii, *J. Org. Chem.*, **61**, 5307 (1996).
310. R. Noyori, M. Aoki and K. Sato, *J. Chem. Soc., Chem. Commun.*, 1977 (2003).
311. K. Sato, M. Aoki, M. Ogawa, T. Hashimoto and R. Noyori, *J. Org. Chem.*, **61**, 8310 (1996).
312. K. Sato, M. Aoki, M. Ogawa, T. Hashimoto, D. Panyella and R. Noyori, *Bull. Chem. Soc. Jpn.*, **70**, 905 (1997).
313. (a) G. Gelbard, F. Raison, E. Roditi-Lachter, R. Thouvenot, L. Ouahab and D. Grandjean, *J. Mol. Catal. A: Chem.*, **114**, 77 (1996).
(b) M. Schulz, J. H. Teles, J. Sundermeyer and G. Wahl (BASF AG), WO 97/32867 A1 (1997); *Chem. Abstr.*, **127**, 287229f (1997).
314. G. Gelbard, *C. R. Acad. Sci. Paris, Ser. IIc: Chim.*, **3**, 757 (2000).
315. K. Kamata, K. Yonehara, Y. Sumida, K. Yamaguchi, S. Hikichi and N. Mizuno, *Science*, **300**, 964 (2003).
316. G. Maayan, R. H. Fish and R. Neumann, *Org. Lett.*, **5**, 3547 (2003).
317. B. Meunier, *Bull. Soc. Chim. Fr.*, 578 (1986); B. Meunier, *Bull. Soc. Chim. Fr.*, II-345 (1983).
318. J.-P. Renaud, P. Battoni, J. F. Bartoli and D. Mansuy, *J. Chem. Soc., Chem. Commun.*, 888 (1985).

319. (a) P. N. Balasubramanian, A. Sinha and T. C. Bruice, *J. Am. Chem. Soc.*, **109**, 1456 (1987).
(b) D. Mansuy, P. Battioni and J.-P. Renaud, *J. Chem. Soc., Chem. Commun.*, 1255 (1984).
320. K. Srinivasan, S. Perrier and J. K. Kochi, *J. Mol. Catal.*, **36**, 297 (1986).
321. P. L. Anelli, S. Banfi, F. Montanari and S. Quici, *J. Chem. Soc., Chem. Commun.*, 779 (1989).
322. P. Battioni, J.-P. Renaud, J. F. Bartoli, M. Reina-Artiles, M. Fort and D. Mansuy, *J. Am. Chem. Soc.*, **110**, 8462 (1988).
323. A. M. d'A. Rocha Gonsalves, R. A. W. Johnstone, M. M. Pereira and J. Shaw, *J. Chem. Soc., Perkin Trans. 1*, 645 (1991).
324. A. Thellend, P. Battioni and D. Mansuy, *J. Chem. Soc., Chem. Commun.*, 1035 (1994).
325. R. Hage, J. E. Iburg, J. Kerschner, J. H. Koek, E. L. M. Lempers, R. J. Martens, U. S. Racherla, S. W. Russell, T. Swarthoff, M. R. P. van Vliet, J. B. Warnaar, L. van der Wolf and B. Krijnen, *Nature*, **369**, 637 (1994).
326. D. E. De Vos and T. Bein, *J. Organomet. Chem.*, **520**, 195 (1996).
327. D. E. De Vos, B. F. Sels, M. Reynaers, Y. V. Subba Rao and P. A. Jacobs, *Tetrahedron Lett.*, **39**, 3221 (1998).
328. Y. V. Subba Rao, D. E. de Vos, T. Bein and P. A. Jacobs, *J. Chem. Soc., Chem. Commun.*, 355 (1997).
329. D. E. De Vos, J. L. Meinershagen and T. Bein, *Angew. Chem., Int. Ed. Engl.*, **35**, 2211 (1996).
330. D. E. De Vos, S. de Wildeman, B. F. Sels, P. J. Grobet and P. A. Jacobs, *Angew. Chem., Int. Ed.*, **38**, 980 (1999).
331. A. Berkessel and C. A. Sklorz, *Tetrahedron Lett.*, **40**, 7965 (1999).
332. C. Bolm, D. Kadereit and M. Valacchi, *Synlett*, 687 (1997).
333. C. Bolm, D. Kadereit and M. Valacchi (Degussa AG), DE 197 20 477 A1 (1998); *Chem. Abstr.*, **130**, 32256g (1999).
334. B. C. Gilbert, J. R. Lindsay Smith, A. Mairata i Payeras, J. Oakes and R. Pons i Prats, *J. Mol. Catal. A: Chem.*, **219**, 265 (2004).
335. T. Katsuki, *Coord. Chem. Rev.*, **140**, 189 (1995).
336. K. Muñoz-Fernandez and C. Bolm, in *Transition Metals for Organic Synthesis* (Eds. M. Beller and C. Bolm), Chap. 2.7.2, Wiley-VCH, Weinheim, 1998.
337. A. Méou, M.-A. Garcia and P. Brun, *J. Mol. Catal. A: Chem.*, **138**, 221 (1999).
338. P. Pietikäinen, *Tetrahedron Lett.*, **35**, 941 (1994).
339. T. Schwenkreis and A. Berkessel, *Tetrahedron Lett.*, **34**, 4785 (1993).
340. P. Pietikäinen, *Tetrahedron*, **54**, 4319 (1998).
341. R. Irie, N. Hosoya and T. Katsuki, *Synlett*, 255 (1994).
342. W. A. Herrmann, R. W. Fischer and D. W. Marz, *Angew. Chem., Int. Ed. Engl.*, **30**, 1638 (1991).
343. (a) F. E. Kühn, R. W. Fischer and W. A. Herrmann, *Chem. unserer Zeit*, **33**, 192 (1999); *Chem. Abstr.*, **132**, 299430 (2000).
(b) C. C. Romão, F. E. Kühn and W. A. Herrmann, *Chem. Rev.*, **97**, 3197 (1997).
344. W. A. Herrmann, F. E. Kühn, M. R. Mattner, G. R. J. Artus, M. R. Geisberger and J. D. G. Correia, *J. Organomet. Chem.*, **538**, 203 (1997).
345. W. A. Herrmann, R. W. Fischer, M. U. Rauch and W. Scherer, *J. Mol. Catal. A: Chem.*, **86**, 243 (1994).
346. W. A. Herrmann, *J. Organomet. Chem.*, **500**, 149 (1995).
347. W. A. Herrmann, R. W. Fischer, W. Scherer and M. U. Rauch, *Angew. Chem., Int. Ed. Engl.*, **105**, 1157 (1993).
348. W. A. Herrmann, R. M. Kratzer and R. W. Fischer, *Angew. Chem., Int. Ed. Engl.*, **36**, 2652 (1997).
349. A. Gansäuer, *Angew. Chem., Int. Ed. Engl.*, **36**, 2591 (1997).
350. W. Adam and C. M. Mitchell, *Angew. Chem., Int. Ed. Engl.*, **35**, 533 (1996).
351. J. Rudolph, K. L. Reddy, J. P. Chiang and K. B. Sharpless, *J. Am. Chem. Soc.*, **119**, 6189 (1997).
352. C. Copéret, H. Adolphsson and K. B. Sharpless, *J. Chem. Soc., Chem. Commun.*, 1565 (1997).
353. W. A. Herrmann, H. Ding, R. M. Kratzer, F. E. Kühn, J. J. Haider and R. W. Fischer, *J. Organomet. Chem.*, **549**, 319 (1997).
354. H. Rudler, J. Ribeiro Gregorio, B. Denise and J.-M. Bregault, *J. Mol. Catal. A: Chem.*, **133**, 255 (1998).

355. W. A. Herrmann, R. M. Kratzer, H. Ding, W. R. Thiel and H. Glas, *J. Organomet. Chem.*, **555**, 293 (1998).
356. M. Nakajima, Y. Sasaki, H. Iwamoto and S. Hashimoto, *Tetrahedron Lett.*, **39**, 87 (1998).
357. H. Adolffson, A. Converso and K. B. Sharpless, *Tetrahedron Lett.*, **40**, 3991 (1999).
358. M. C. A. van Vliet, I. W. C. E. Arends and R. A. Sheldon, *J. Chem. Soc., Chem. Commun.*, 821 (1999).
359. A. K. Yudin and K. B. Sharpless, *J. Am. Chem. Soc.*, **119**, 11536 (1997).
360. A. O. Bouh and J. H. Espenson, *J. Mol. Catal. A: Chem.*, **200**, 43 (2003).
361. M. C. A. van Vliet, I. W. C. E. Arends and R. A. Sheldon, *J. Chem. Soc., Perkin Trans. 1*, 377 (2000).
362. A. Berkessel and M. R. M. Andreae, *Tetrahedron Lett.*, **42**, 2293 (2001).
363. A. Berkessel and J. Adrio, *Adv. Synth. Catal.*, **346**, 275 (2004).
364. A. Berkessel, J. Frey and R. Giernoth, submitted.
365. M. Ochiai, A. Nakanishi and T. Ito, *J. Org. Chem.*, **62**, 4253 (1997).
366. K. S. Ravikumar, J.-P. Bégué and D. Bonnet-Delpon, *Tetrahedron Lett.*, **39**, 3141 (1998).
367. T. Takata and W. Ando, *Bull. Chem. Soc. Jpn.*, **59**, 1275 (1986).
368. (a) S. Colonna, N. Gaggero, A. Manfredi, L. Casella and M. Gullotti, *J. Chem. Soc., Chem. Commun.*, 1451 (1988).
(b) S. Colonna, N. Gaggero, A. Manfredi, L. Casella, M. Gullotti, G. Carrea and P. Pasta, *Biochemistry*, **29**, 10465 (1990).
369. S. Colonna, N. Gaggero, L. Casella, G. Carrea and P. Pasta, *Tetrahedron: Asymmetry*, **3**, 95 (1992).
370. S. G. Allenmark and M. A. Andersson, *Tetrahedron: Asymmetry*, **7**, 1089 (1996).
371. L. Kuhnén, *Angew. Chem., Int. Ed. Engl.*, **5**, 893 (1966).
372. F. Di Furia, G. Modena and R. Curci, *Tetrahedron Lett.*, **17**, 4637 (1976).
373. (a) W. Adam, C. M. Mitchell, C. R. Saha-Möller, T. Selvam and O. Weichold, *J. Mol. Catal. A: Chem.*, **154**, 251 (2000).
(b) W. Adam, A. Corma, H. García and O. Weichold, *J. Catal.*, **196**, 339 (2000).
(c) W. Adam, W. Malisch, K. J. Roschmann, C. R. Saha-Möller and W. A. Schenk, *J. Organomet. Chem.*, **661**, 3 (2002).
374. W. Adam, C. M. Mitchell and C. R. Saha-Möller, *Tetrahedron*, **50**, 13121 (1994).
375. J. M. Brunel, P. Diter, M. Duetsch and H. B. Kagan, *J. Org. Chem.*, **60**, 8086 (1995).
376. S. H. Zhao, O. Samuel and H. B. Kagan, *Tetrahedron*, **43**, 5135 (1987).
377. P. Pitchen, E. Dunach, M. N. Deshmukh and H. B. Kagan, *J. Am. Chem. Soc.*, **106**, 8188 (1984).
378. F. Di Furia, G. Modena and R. Seraglia, *Synthesis*, 325 (1984).
379. J. M. Brunel and H. B. Kagan, *Bull. Soc. Chim. Fr.*, **133**, 1109 (1996).
380. J. M. Brunel and H. B. Kagan, *Synlett*, 404 (1996).
381. N. Komatsu, M. Hashizume, T. Sugita and S. Uemura, *J. Org. Chem.*, **58**, 7624 (1993).
382. F. DiFuria, G. Licini, G. Modena, R. Motterle and W. A. Nugent, *J. Org. Chem.*, **61**, 5175 (1996).
383. S. Superchi and C. Rosini, *Tetrahedron: Asymmetry*, **8**, 349 (1997).
384. Y. Yamanoi and T. Imamoto, *J. Org. Chem.*, **62**, 8560 (1997).
385. R. M. Hanson and K. B. Sharpless, *J. Org. Chem.*, **51**, 1922 (1986).
386. N. Komatsu, M. Hashizume, T. Sugita and S. Uemura, *J. Org. Chem.*, **58**, 4529 (1993).
387. M. I. Donnoli, S. Superchi and C. Rosini, *J. Org. Chem.*, **63**, 9392 (1998).
388. M. A. M. Capozzi, C. Cardellischio, F. Naso and V. Rosito, *J. Org. Chem.*, **67**, 7289 (2002).
389. M. Palucki, P. Hanson and E. N. Jacobsen, *Tetrahedron Lett.*, **33**, 7111 (1992).
390. J. Legros and C. Bolm, *Angew. Chem., Int. Ed.*, **42**, 5487 (2003).
391. A. Lattanzi, F. Bonadies, A. Senatore, A. Soriente and A. Scettri, *Tetrahedron: Asymmetry*, **8**, 2473 (1997).
392. A. Lattanzi, F. Bonadies and A. Scettri, *Tetrahedron: Asymmetry*, **8**, 2141 (1997).
393. A. Scettri, F. Bonadies and A. Lattanzi, *Tetrahedron: Asymmetry*, **7**, 629 (1996).
394. L. Palombi, F. Bonadies, A. Pazienza and A. Scettri, *Tetrahedron: Asymmetry*, **9**, 1817 (1998).
395. A. Lattanzi, P. Iannece and A. Scettri, *Tetrahedron: Asymmetry*, **15**, 413 (2004).
396. (a) M. Hudlický, in *Oxidations in Organic Chemistry*, Chap. 3, American Chemical Society, Washington DC, 1990.

- (b) R. C. Larock, *Comprehensive Organic Transformations*, Wiley VCH, New York, 1999, pp. 487–488 and pp. 604–614.
397. S. E. Jacobson, D. A. Muccigrosso and F. Mares, *J. Org. Chem.*, **44**, 921 (1979).
398. B. M. Trost and Y. Masuyama, *Tetrahedron Lett.*, **25**, 173 (1984).
399. C. Venturello and M. Gambaro, *J. Org. Chem.*, **56**, 5924 (1991).
400. K. Sato, M. Aoki, J. Takagi, K. Zimmermann and R. Noyori, *Bull. Chem. Soc. Jpn.*, **72**, 2287 (1999).
401. K. Sato, J. Takagi, M. Aoki and R. Noyori, *Tetrahedron Lett.*, **39**, 7549 (1998).
402. R. T. Taylor and L. A. Flood, *J. Org. Chem.*, **48**, 5160 (1983).
403. R. A. Sheldon and J. Dakka, *Catal. Today*, **19**, 215 (1994).
404. R. A. Sheldon, *J. Mol. Catal. A: Chem.*, **107**, 75 (1996).
405. (a) W. G. Dauben, M. Lorber and D. S. Fullerton, *J. Org. Chem.*, **34**, 3587 (1969).
(b) M. Nakayama, S. Shinke, Y. Matsushita, S. Ohira and S. Hayashi, *Bull. Chem. Soc. Jpn.*, **52**, 184 (1979).
406. J. Muzart, *Chem. Rev.*, **92**, 113 (1992).
407. S. Boitsov, A. Riahi and J. Muzart, *C.R. Acad. Sci. Paris, Ser. IIc, Chim.*, **3**, 747 (2000).
408. J. D. Chen, J. Dakka, E. Neeleman and R. A. Sheldon, *J. Chem. Soc., Chem. Commun.*, 1379 (1993).
409. (a) R. A. Sheldon, J. D. Chen, J. Dakka and E. Neeleman, *Stud. Surf. Sci. Catal.*, **83**, 407 (1994).
(b) J. D. Chen, M. J. Haanepen, J. H. C. van Hooff and R. A. Sheldon, *Stud. Surf. Sci. Catal.*, **84**, 973 (1994).
410. R. A. Sheldon, J. D. Chen, J. Dakka and E. Neeleman, *Stud. Surf. Sci. Catal.*, **82**, 515 (1994).
411. B. M. Choudary, A. Durgaprasad and V. L. K. Valli, *Tetrahedron Lett.*, **31**, 5785 (1990).
412. G. Rothenberg, L. Feldberg, H. Wiener and Y. Sasson, *J. Chem. Soc., Perkin Trans. 2*, 2429 (1998).
413. G. Ferguson and A. N. Ajjou, *Tetrahedron Lett.*, **44**, 9139 (2003).
414. S. Das and T. Punniyamurthy, *Tetrahedron Lett.*, **44**, 6033 (2003).
415. S. Velusamy and T. Punniyamurthy, *Eur. J. Org. Chem.*, 3913 (2003).
416. C. B. Li, P. W. Zheng, B. Li, H. Zhang, Y. Ciu, Q. Y. Shao, X. J. Ji, J. Zhang, P. Y. Zhao and Y. L. Xu, *Angew. Chem., Int. Ed.*, **42**, 5063 (2003).
417. Y. Kurusu, *J. Inorg. Organomet. Polym.*, **10**, 127 (2000).
418. W. H. Cheung, W. Y. Yu, W. P. Yip, N. Y. Zhu and C.-M. Che, *J. Org. Chem.*, **67**, 7716 (2002).
419. D. Crich and S. Neelamkavil, *Tetrahedron*, **58**, 3865 (2002).
420. P. C. Bulman Page and T. J. McCarthy, in *Comprehensive Organic Synthesis* (Eds. B. M. Trost and I. Fleming), Chap. 2.1, Pergamon Press, Oxford, 1991.
421. J. Muzart, *Bull. Soc. Chim. Fr.*, 65 (1986).
422. (a) M. Kimura and T. Muto, *Chem. Pharm. Bull.*, **27**, 109 (1979).
(b) M. Kimura and T. Muto, *Chem. Pharm. Bull.*, **28**, 1836 (1980).
423. N. Chidambaram and S. Chandrasekaran, *J. Org. Chem.*, **52**, 5048 (1987).
424. J. Muzart, *Tetrahedron Lett.*, **28**, 4665 (1987).
425. A. J. Pearson, Y.-S. Chen, S.-Y. Hsu and T. Ray, *Tetrahedron Lett.*, **25**, 1235 (1984);
A. J. Pearson, Y.-S. Chen, G. R. Han, S.-Y. Hsu and T. Ray, *J. Chem. Soc., Perkin Trans. 1*, 267 (1985).
426. R. A. Miller, W. Li and G. R. Humphrey, *Tetrahedron Lett.*, **37**, 3429 (1996).
427. J. A. R. Salvador, M. L. Sá e Melo and A. S. Campos Neves, *Tetrahedron Lett.*, **38**, 119 (1997).
428. M. A. Umbreit and K. B. Sharpless, *J. Am. Chem. Soc.*, **99**, 5526 (1977).
429. F. W. Sum and L. Weiler, *J. Am. Chem. Soc.*, **101**, 4401 (1979).
430. O. Campos and J. M. Cook, *Tetrahedron Lett.*, 1025 (1979).
431. B. Chabaud and K. B. Sharpless, *J. Org. Chem.*, **44**, 4202 (1979).
432. C. J. Zhang, Y. Ozawa, Y. Hayashi and K. Isobe, *J. Organomet. Chem.*, **373**, C21 (1989).
433. H. E. B. Lempers and R. A. Sheldon, *Appl. Catal. A: General*, **143**, 137 (1996).
434. H. E. B. Lempers and R. A. Sheldon, *Stud. Surf. Sci. Catal.*, **94**, 705 (1995).
435. A. S. Gokhale, A. B. E. Minidis and A. Pfaltz, *Tetrahedron Lett.*, **36**, 1831 (1995).
436. M. B. Andrus, A. B. Argade, X. Chen and M. G. Pamment, *Tetrahedron Lett.*, **36**, 2945 (1995).

437. (a) K. Kawasaki, S. Tsumura and T. Katsuki, *Synlett*, 1245 (1995).
(b) K. Kawasaki and T. Katsuki, *Tetrahedron*, **53**, 6337 (1997).
438. (a) A. DattaGupta and V. K. Singh, *Tetrahedron Lett.*, **37**, 2633 (1996).
(b) G. Sekar, A. DattaGupta and V. K. Singh, *J. Org. Chem.*, **63**, 2961 (1998).
439. C. Zondervan and B. L. Feringa, *Tetrahedron: Asymmetry*, **7**, 1895 (1996).
440. A. V. Malkov, M. Bella, V. Langer and P. Kočovský, *Org. Lett.*, **2**, 3047 (2000).
441. M. J. Södergren and P. G. Andersson, *Tetrahedron Lett.*, **37**, 7577 (1996).
442. A. Levina and J. Muzart, *Tetrahedron: Asymmetry*, **6**, 147 (1995).
443. A. Levina, F. Hénin and J. Muzart, *J. Organomet. Chem.*, **494**, 165 (1995).
444. M. T. Rispens, C. Zondervan and B. L. Feringa, *Tetrahedron: Asymmetry*, **6**, 661 (1995).
445. J. A. R. Salvador and J. H. Clark, *J. Chem. Soc., Chem. Commun.*, 33 (2001).
446. B. M. Choudary, G. V. S. Reddy and K. K. Rao, *J. Chem. Soc., Chem. Commun.*, 323 (1993).
447. J. Muzart, *Tetrahedron Lett.*, **28**, 2131 (1987).
448. S. Velusamy and T. Punniyamurthy, *Tetrahedron Lett.*, **44**, 8955 (2003).
449. A. García Martínez, E. Teso Vilar, A. García Fraile, S. de la Moya Cerero, S. de Oro Osunar and B. Lora Maroto, *Tetrahedron Lett.*, **42**, 7795 (2001).
450. R. Rosenthal and G. A. Bonetti (Atlantic Richfield Company), US 3,755,453 (1973); *Chem. Abstr.*, **79**, 125957e (1973).
451. E. Vedejs and S. Larsen, *Org. Synth.*, **64**, 127 (1985).
452. M. Schulz, R. Kluge, M. Schübler and G. Hoffmann, *Tetrahedron*, **51**, 3175 (1995).
453. W. Adam, M. Müller and F. Prectl, *J. Org. Chem.*, **59**, 2359 (1994).
454. D. Enders and V. Bhushan, *Tetrahedron Lett.*, **29**, 2437 (1988).
455. (a) Y. Zhu, Y. Tu, H. Yu and Y. Shi, *Tetrahedron Lett.*, **39**, 7819 (1998).
(b) W. Adam, R. T. Fell, C. R. Saha-Möller and C.-G. Zhao, *Tetrahedron: Asymmetry*, **9**, 397 (1998).
456. A. Paju, T. Kanger, T. Pehk and M. Lopp, *Tetrahedron*, **58**, 7321 (2002).
457. (a) A. Paju, T. Kanger, T. Pehk, A. M. Muurisep and M. Lopp, *Tetrahedron: Asymmetry*, **13**, 2439 (2002).
(b) A. Paju, T. Kanger, T. Pehk and M. Lopp, *Tetrahedron Lett.*, **41**, 6883 (2000).
458. M. Roussel and H. Mimoun, *J. Org. Chem.*, **45**, 5387 (1980).
459. H. Mimoun, R. Charpentier, A. Mitschler, J. Fischer and R. Weiss, *J. Am. Chem. Soc.*, **102**, 1047 (1980).
460. J. Tsuji, H. Nagashima and K. Hori, *Chem. Lett.*, 257 (1980).
461. K. Weissermel and H.-J. Arpe, *Industrial Organic Chemistry*, VCH, Weinheim, 1997, p. 239.
462. K. Sato, M. Aoki and R. Noyori, *Science*, **281**, 1646 (1998).
463. S. M. Reed and J. E. Hutchison, *J. Chem. Educ.*, **77**, 1627 (2000).
464. M. M. Lakouraj, B. Movassagh and K. Bahrami, *Monatsh. Chem.*, **133**, 1193 (2002).
465. S. O. Lee, R. Raja, K. D. M. Harris, J. M. Thomas, B. F. G. Johnson and G. Sankar, *Angew. Chem., Int. Ed.*, **42**, 1520 (2003).
466. W. L. Dai, H. Chen, Y. Cao, H. X. Li, S. H. Xie and K. N. Fan, *J. Chem. Soc., Chem. Commun.*, 892 (2003).
467. N. I. Moiseeva, A. E. Gekhman and I. I. Moiseev, *J. Mol. Catal. A: Chem.*, **117**, 39 (1997).
468. I. I. Moiseev, A. E. Gekhman and D. I. Shishkin, *New J. Chem.*, **13**, 683 (1989).
469. P. R. Hari Prasad Rao and A. V. Ramaswamy, *J. Chem. Soc., Chem. Commun.*, 1245 (1992).
470. W. A. Herrmann, J. D. G. Correia, F. E. Kühn, G. R. J. Artus and C. C. Romão, *Chem. Eur. J.*, **2**, 168 (1996).
471. W. Adam, W. A. Herrmann, J. Lin, C. R. Saha-Möller, R. W. Fischer and J. D. G. Correia, *Angew. Chem., Int. Ed. Engl.*, **33**, 2475 (1994).
472. (a) D. Bianchi, R. Bortolo, R. Tassinari, M. Ricci and R. Vignola, *Angew. Chem., Int. Ed.*, **39**, 4321 (2000).
(b) D. Bianchi, M. Bertoli, R. Tassinari, M. Ricci and R. Vignola, *J. Mol. Catal. A: Chem.*, **200**, 111 (2003).
473. H. H. Monfared and M. Ghorbani, *Monatsh. Chem.*, **132**, 989 (2001).
474. G. B. Payne, P. H. Deming and P. H. Williams, *J. Org. Chem.*, **26**, 659 (1961).
475. G. A. Tolstikov, U. M. Jemilev, V. P. Jurjev, F. B. Gershanov and S. R. Rafikov, *Tetrahedron Lett.*, 2807 (1971).
476. J. L. Russell and J. Kollar (Halcon International), 1,100,672 (1965); J. L. Russell and J. Kollar, *Chem. Abstr.*, **65**, 8792b (1966).

477. G. R. Howe and R. R. Hiatt, *J. Org. Chem.*, **35**, 4007 (1970).
478. K. Kosswig, *Liebigs Ann. Chem.*, **749**, 206 (1971).
479. M. N. Sheng and J. G. Zajacek, *J. Org. Chem.*, **33**, 588 (1968).
480. R. W. Murray, K. Iyanar, J. X. Chen and J. T. Wearing, *Tetrahedron Lett.*, **37**, 805 (1996).
481. C. Copéret, H. Adolfsson, T.-A. V. Khuong, A. K. Yudin and K. B. Sharpless, *J. Org. Chem.*, **63**, 1740 (1998).
482. C. Copéret, H. Adolfsson, J. P. Chiang, A. K. Yudin and K. B. Sharpless, *Tetrahedron Lett.*, **39**, 761 (1998).
483. D. Döpp and H. Döpp, in *Houben Weyl - Methoden der organischen Chemie* (Eds. D. Klamann and H. Hagemann), Vol. E 14b, part 2, Georg Thieme Verlag, Stuttgart, 1990.
484. S. Cicchi, F. Cardona, A. Brandi, M. Corsi and A. Goti, *Tetrahedron Lett.*, **40**, 1989 (1999).
485. R. S. Varma and K. P. Naicker, *Org. Lett.*, **1**, 189 (1999).
486. R. Joseph, A. Sudalai and T. Ravindranathan, *Synlett*, 1177 (1995).
487. (a) M. R. Prasad, G. Kamalakar, G. Madhavi, S. J. Kulkarni and K. V. Raghavan, *J. Chem. Soc., Chem. Commun.*, 1577 (2000).
(b) M. R. Prasad, G. Kamalakar, G. Madhavi, S. J. Kulkarni and K. V. Raghavan, *J. Mol. Catal. A: Chem.*, **186**, 109 (2002).
488. (a) G. R. Krow, *Org. React.*, **43**, 251 (1993).
(b) M. Renz and B. Meunier, *Eur. J. Org. Chem.*, 737 (1999).
489. G. Strukul, *Angew. Chem., Int. Ed.*, **37**, 1199 (1998).
490. R. D. Chambers and M. Clark, *Tetrahedron Lett.*, **11**, 2741 (1970).
491. A. Lambert, D. J. MacQuarrie, G. Carr and J. H. Clark, *New J. Chem.*, **24**, 485 (2000).
492. C. D. Chang and S. D. Hellring (Mobil Oil Corporation), US 4,870,192 A (1989); *Chem. Abstr.*, **112**, 158077w (1990).
493. J. Fischer and W. F. Hölderich, *Appl. Catal. A: General*, **180**, 435 (1999).
494. S. E. Jacobson, F. Mares and P. M. Zambri, *J. Am. Chem. Soc.*, **101**, 6938 (1979).
495. W. Hölderich, J. Fischer, G.-P. Schindler and D. Arntz (Degussa AG), DE 197 45 442 A1 (1999); *Chem. Abstr.*, **130**, 281989u (1999).
496. R. Gavagnin, M. Cataldo, F. Pinna and G. Strukul, *Organometallics*, **17**, 661 (1998).
497. C. Bolm and O. Beckmann, *Chirality*, 523 (2000).
498. A. M. Faisca Phillips and C. Romão, *Eur. J. Org. Chem.*, 1767 (1999).
499. W. A. Herrmann, R. W. Fischer and J. D. G. Correia, *J. Mol. Catal.*, **94**, 213 (1994).
500. G.-J. ten Brink, J.-M. Vis, I. W. C. E. Arends and R. A. Sheldon, *J. Org. Chem.*, **66**, 2429 (2001).
501. P. A. Grieco, Y. Yokoyama, S. Gilman and Y. Ohfuné, *J. Chem. Soc., Chem. Commun.*, 870 (1977).
502. S. E. Jacobson, R. Tang and F. Mares, *J. Chem. Soc., Chem. Commun.*, 888 (1978).
503. C. Palazzi, F. Pinna and G. Strukul, *J. Mol. Catal. A: Chem.*, **151**, 245 (2000).
504. L. Syper, *Synthesis*, 167 (1989).
505. L. Syper and J. Mlochowski, *Tetrahedron*, **43**, 207 (1987).
506. M. Renz, T. Blasco, A. Corma, V. Fornés, R. Jensen and L. Nemeth, *Chem. Eur. J.*, **8**, 4708 (2002).
507. A. Corma, L. Nemeth, M. Renz and S. Valencia, *Nature*, **412**, 423 (2001).
508. A. Corma, M. T. Navarro, L. Nemeth and M. Renz, *J. Chem. Soc., Chem. Commun.*, 2190 (2001).
509. U. R. Pillai and E. Sahle-Demessie, *J. Mol. Catal. A: Chem.*, **191**, 93 (2003).
510. R. Bernini, E. Mincione, M. Cortese, R. Saladino, G. Gualandi and M. C. Belfiore, *Tetrahedron Lett.*, **44**, 4823 (2003).
511. R. Bernini, A. Coratti, G. Fabrizi and A. Goggiamani, *Tetrahedron Lett.*, **44**, 8991 (2003).
512. (a) C. Bolm, O. Beckmann and T. K. K. Luong, in *Transition Metals for Organic Synthesis: Building Blocks and Fine Chemicals* (Eds. M. Beller and C. Bolm), Wiley VCH, Weinheim, 1998, p. 213.
(b) C. Bolm and O. Beckmann, in *Comprehensive Asymmetric Catalysis* (Eds. E. N. Jacobsen, A. Pfaltz and H. Yamamoto), Chap. 22, Springer, Berlin, 1999.
513. A. Gusso, C. Baccin, F. Pinna and G. Strukul, *Organometallics*, **13**, 3442 (1994).
514. G. Strukul, A. Varagnolo and F. Pinna, *J. Mol. Catal. A: Chem.*, **117**, 413 (1997).
515. C. Paneghetti, R. Gavagnin, F. Pinna and G. Strukul, *Organometallics*, **18**, 5057 (1999).
516. M. Lopp, A. Paju, T. Kanger and T. Pehk, *Tetrahedron Lett.*, **37**, 7583 (1996).

517. A. Berkessel, M. R. M. Andreae, H. Schmickler and J. Lex, *Angew. Chem., Int. Ed.*, **41**, 4481 (2002).
518. (a) C. Bolm, J. P. Hildebrand and K. Muñiz, in *Catalytic Asymmetric Synthesis* (Ed. I. Ojima), Wiley, New York, 2000, p. 399.
(b) R. A. Johnson and K. B. Sharpless, in *Catalytic Asymmetric Synthesis* (Ed. I. Ojima), Wiley, New York, 2000, p. 357.
519. M. Schröder, *Chem. Rev.*, **80**, 187 (1980).
520. K. B. Sharpless and K. Akashi, *J. Am. Chem. Soc.*, **98**, 1986 (1976).
521. K. Akashi, R. E. Palermo and K. B. Sharpless, *J. Org. Chem.*, **43**, 2063 (1978).
522. M. N. Sheng and W. A. Mameniskis (Atlantic Richfield Company), US 4,049,724 (1977); *Chem. Abstr.*, **88**, 22130m (1978).
523. C.-Y. Wu and T. P. Kobylinski (Gulf Research & Development Company), US 4,203,926 (1980); T. P. Kobylinski and C.-Y. Wu, *Chem. Abstr.*, **93**, 167618q (1980).
524. A. Byers and W. J. Hickinbottom, *J. Chem. Soc.*, 1328 (1948).
525. M. Schröder, A. J. Nielson and W. P. Griffith, *J. Chem. Soc., Dalton Trans.*, 1607 (1979).
526. S. G. Hentges and K. B. Sharpless, *J. Am. Chem. Soc.*, **102**, 4263 (1980).
527. H. C. Kolb, M. S. VanNieuwenhze and K. B. Sharpless, *Chem. Rev.*, **94**, 2483 (1994).
528. J. S. M. Wai, I. Marko, J. S. Svendsen, M. G. Finn, E. N. Jacobsen and K. B. Sharpless, *J. Am. Chem. Soc.*, **111**, 1123 (1989).
529. A. Severeys, D. E. de Vos and P. A. Jacobs, *Top. Catal.*, **19**, 125 (2002).
530. (a) H. Adolfsson and F. Stålfors, in *221st National Meeting of the Am. Chem. Soc.*, San Diego, 2001, paper 616.
(b) M. A. Andersson, V. V. Fokin and K. B. Sharpless, in *221st National Meeting of the Am. Chem. Soc.*, San Diego, 2001, paper 609.
531. (a) T. Oishi and M. Hirama, *J. Org. Chem.*, **54**, 5834 (1989).
(b) M. Hirama, T. Oishi and S. Ito, *J. Chem. Soc., Chem. Commun.*, 665 (1989).
(c) K. Tomioka, M. Nakajima and K. Koga, *J. Am. Chem. Soc.*, **109**, 6213 (1987).
(d) E. J. Corey, P. DaSilva Jardine, S. Virgil, P.-W. Yuen and R. D. Connell, *J. Am. Chem. Soc.*, **111**, 9243 (1989).
(e) S. Hanessian, P. Meffre, M. Girard, S. Beaudoin, J.-Y. Sanceau and Y. Bennani, *J. Org. Chem.*, **58**, 1991 (1993).
(f) T. Yamada and K. Narasaka, *Chem. Lett.*, 131 (1986).
(g) K. Fujii, K. Tanaka and H. Miyamoto, *Tetrahedron Lett.*, **33**, 4021 (1992).
(h) M. Nakajima, K. Tomioka, Y. Iitaka and K. Koga, *Tetrahedron*, **49**, 10793 (1993).
(i) K. Tomioka, M. Nakajima and K. Koga, *Tetrahedron Lett.*, **31**, 1741 (1990).
(j) K. Tomioka, M. Nakajima, Y. Iitaka and K. Koga, *Tetrahedron Lett.*, **29**, 573 (1988).
(k) M. Tokles and J. K. Snyder, *Tetrahedron Lett.*, **27**, 3951 (1986).
532. (a) T. Oishi and M. Hirama, *Tetrahedron Lett.*, **33**, 639 (1992).
(b) Y. Imada, T. Saito, T. Kawakami and S.-I. Murahashi, *Tetrahedron Lett.*, **33**, 5081 (1992).
533. G. Cainelli, M. Contento, F. Manescalchi and L. Plessi, *Synthesis*, 45 (1989).
534. W. A. Herrmann, R. M. Kratzer, J. Blümel, H. B. Friedrich, R. W. Fischer, D. C. Apperley, J. Mink and O. Berkesi, *J. Mol. Catal. A: Chem.*, **120**, 197 (1997).
535. (a) P. Salvadori, D. Pini and A. Petri, *J. Am. Chem. Soc.*, **119**, 6929 (1997).
(b) C. Bolm, A. Maischak and A. Gerlach, *J. Chem. Soc., Chem. Commun.*, 2353 (1997).
(c) B. M. Choudary, N. S. Chowdari, K. Jyothi and M. L. Kantam, *J. Am. Chem. Soc.*, **124**, 5341 (2002).
(d) B. M. Choudary, N. S. Chowdari, M. L. Kantam and K. V. Raghavan, *J. Am. Chem. Soc.*, **123**, 9220 (2001).
536. R. C. Michaelson, R. G. Austin and D. A. White (Exxon Research & Engineering Co.), US 4,413,151 (1983); *Chem. Abstr.*, **100**, 34132t (1984).
537. K. Bergstad, S. Y. Jonsson and J.-E. Bäckvall, *J. Am. Chem. Soc.*, **121**, 10424 (1999).
538. S. Y. Jonsson, K. Färnegardh and J.-E. Bäckvall, *J. Am. Chem. Soc.*, **123**, 1365 (2001).
539. S. Y. Jonsson, H. Adolfsson and J.-E. Bäckvall, *Org. Lett.*, **3**, 3463 (2001).
540. A. H. Ell, S. Y. Jonsson, A. Börje, H. Adolfsson and J.-E. Bäckvall, *Tetrahedron Lett.*, **42**, 2569 (2001).
541. B. M. Choudary, N. S. Chowdari, S. Madhi and M. L. Kantam, *Angew. Chem., Int. Ed.*, **40**, 4620 (2001).

542. B. M. Choudary, N. S. Chowdari, S. Madhi and M. L. Kantam, *J. Org. Chem.*, **68**, 1736 (2003).
543. B. M. Choudary, B. Bharathi, C. V. Reddy, M. L. Kantam and K. V. Raghavan, *J. Chem. Soc., Chem. Commun.*, 1736 (2001).
544. Y. Usui, K. Sato and M. Tanaka, *Angew. Chem., Int. Ed.*, **42**, 5623 (2003).
545. M. R. Detty, F. Zhou and A. E. Friedman, *J. Am. Chem. Soc.*, **118**, 313 (1996).
546. C. Francavilla, M. D. Drake, F. V. Bright and M. R. Detty, *J. Am. Chem. Soc.*, **123**, 57 (2001).
547. D. E. Higgs, M. I. Nelen and M. R. Detty, *Org. Lett.*, **3**, 349 (2001).
548. N. Narender, K. V. V. K. Mohan, R. V. Reddy, P. Srinivasu, S. J. Kulkarni and K. V. Raghavan, *J. Mol. Catal. A: Chem.*, **192**, 73 (2003).
549. R. Ben-Daniel, S. P. de Visser, S. Shaik and R. Neumann, *J. Am. Chem. Soc.*, **125**, 12116 (2003).
550. P. V. Vyas, A. K. Bhatt, G. Ramachandraiah and A. V. Bedekar, *Tetrahedron Lett.*, **44**, 4085 (2003).

CHAPTER 7

Analytical and safety aspects of organic peroxides and related functional groups

JACOB ZABICKY

*Institutes for Applied Research and Department of Chemical Engineering, Ben-Gurion
University of the Negev, Beer-Sheva 84105, Israel
Fax: +972 8647 2969; e-mail: zabicky@bgu.ac.il*

I. ACRONYMS	600
II. INTRODUCTION	603
A. Peroxides in Nature and the Technological World	603
1. Environmental issues	604
a. Atmosphere	604
b. Water	605
c. Soil	608
2. Biological and biomedical systems	608
a. Natural products and their analogs	608
b. Reactive oxygen species	610
c. Lipid peroxides	612
d. Miscellaneous oxidation substrates	614
3. The chemical and related industries	617
a. A cautionary note	617
b. Peroxide manufacture	617
c. Applications involving polymerization	622
d. Bleaching and disinfection	622
e. Pharmaceutical preparations	623
f. Etching	623
g. Autoxidation	623
B. Remarks on Modern Analytical Methods	624
C. Scope of the Chapter	624
III. HYDROGEN PEROXIDE	625
A. General	625
B. Detection and Determination	626

The chemistry of peroxides, volume 2

Edited by Z. Rappoport © 2006 John Wiley & Sons, Ltd ISBN: 0-470-86274-2

1. Titration methods	627
2. Ultraviolet-visible spectrophotometry and colorimetry	627
a. Absorption spectrophotometry	627
b. Fluorometry	637
c. Chemiluminescence	643
3. Near-infrared spectrophotometry	649
4. Electrochemical methods	650
a. Classical methods	650
b. Biosensors and their mimics	652
5. Radiometric method	655
IV. OXIDATION INDICES	656
A. General	656
B. Peroxide Value	657
1. Definition	657
2. Direct titration	657
3. Ultraviolet-visible spectrophotometry and colorimetry	658
a. Absorption measurements	658
b. Fluorescence methods	659
4. Infrared spectrophotometry	661
5. Near-infrared spectrophotometry	663
6. Electrochemical methods	663
C. Tests for Stability on Storage under Exposure to Air	664
D. Secondary Oxidation Products	665
1. Anisidine value	666
2. Thiobarbituric acid reactive substances	666
3. Miscellaneous methods for carbonyl compounds	669
4. Conjugated dienes value	671
5. Acid value	672
E. Thermal Analysis	672
V. HYDROPEROXIDES	672
A. General	672
B. Detection and Determination	673
1. Titration methods	673
2. Ultraviolet-visible spectrophotometry and colorimetry	674
a. Absorption UVV spectrophotometry	674
b. Fluorometry	678
c. Chemiluminescence	680
3. Infrared spectrophotometry	683
4. Thermal stability and GLC	684
5. Nuclear magnetic resonance spectroscopy	685
6. Electrochemical methods	685
a. Classical methods	685
b. Biosensors and their mimics	687
7. Flame ionization detection	689
8. Mass spectrometry	689
C. Structural Characterization	690
1. General	690
2. Vibrational spectra	692
3. Mass spectrometry	692
4. Nuclear magnetic resonance	694

5. X-Ray diffraction	695
6. Molecular refraction	696
VI. PEROXYACIDS AND THEIR FUNCTIONAL DERIVATIVES	697
A. General	697
B. Detection and Determination	698
1. General	698
2. Peroxyacids	698
3. Peroxyesters	700
4. Acyl peroxides	701
C. Structural Characterization	701
1. Peroxycarboximidic acids	701
2. Acyl peroxides	702
3. Peroxyesters	705
4. Functional derivatives of peroxycarbonic acid	705
VII. DIALKYL PEROXIDES	705
A. General	705
B. Detection and Determination	707
1. Titration methods	707
2. Ultraviolet-visible spectrophotometry and colorimetry	707
3. Nuclear magnetic resonance spectroscopy	708
4. Flame ionization detection	708
C. Structural Characterization	708
1. General	708
2. Nuclear magnetic resonance	709
3. X-Ray crystallography	711
4. Electron diffraction	713
5. Vibrational spectra	713
6. Mass spectrometry	714
7. Thermal analysis	714
8. Electrochemical analysis	715
VIII. OZONIDES	716
A. General	716
B. Detection and Determination	718
1. Titration methods	718
2. Infrared spectrophotometry	718
3. Chromatography	719
a. Gas-liquid chromatography	719
b. Liquid chromatography	719
4. Nuclear magnetic resonance spectrometry	719
C. Structural Characterization	719
1. Infrared spectroscopy	719
a. Primary ozonides	719
b. Final ozonides	720
2. Microwave spectroscopy	721
a. Primary ozonides	721
b. Final ozonides	721
3. Electron diffraction	723
4. Nuclear magnetic resonance spectroscopy	723
5. Mass spectrometry	726
6. X-Ray crystallography	726

a. Final ozonides	726
b. Final ozonide analogs	729
7. Thermal analysis	730
8. Molecular refraction	731
D. Miscellaneous Ozone Adducts	731
1. π -Complexes with ozone	731
2. Phosphite-ozone adducts	732
3. Ozonide zwitterionic complexes	734
4. Miscellaneous organic ozonides	734
5. Alkali metal and quaternary ammonium ozonides	735
E. Ozonolysis as Analytical Tool	737
IX. MISCELLANEOUS FUNCTIONS BEARING THE O—O GROUP	740
A. Trioxides and Tetroxides	740
B. Peroxynitrite and Peroxynitrous Acid	740
C. Peroxynitrates	742
1. Infrared and Raman spectroscopies	742
2. Ultraviolet spectroscopy	743
3. Nuclear magnetic resonance spectroscopy	743
4. Mass spectrometry	743
5. Gas electron diffraction	743
D. Imine Peroxide	744
E. Peroxysulfates	744
X. SAFETY ISSUES	744
A. General	744
B. Regulatory Agencies	745
1. Transportation	745
2. Environmental hazards	747
3. Occupational hazards	747
XI. ACKNOWLEDGMENTS	749
XIII. REFERENCES	756

I. ACRONYMS

ABTS	2,2'-azinobis(3-ethylbenzothiazoline)-6-sulfonate
ACV	acidity value
ADN	International Carriage of Dangerous Goods by Inland Waterways (agreement of UNECE)
ADR	International Carriage of Dangerous Goods by Road (agreement of UNECE)
ALOHA	areal locations of hazardous atmospheres
ANV	anisidine value
AOAC	Association of Official Analytical Chemists
AOCS	American Oil Chemists' Society
CAMEO	computer-aided managements of emergency operations
CDV	conjugated double bond value
CFR	Code of Federal Regulations (USA)
CHRIS	chemical hazards response information system (USA)
CID	collision induced dissociation
CIS	chemical information system (USA)

CIS-MS	coordination ionspray MS
CL	chemiluminescence
CLD	chemiluminescence detection/detector
COSY	correlation spectroscopy
COTIF	Convention on the International Carriage by Rail
CPE	carbon paste electrode
CRTD	Convention on Civil Liability for Damage Caused During Carriage of Dangerous Goods by Road, Rail and Inland Navigation Vessels {UNECE}
CZE	capillary zone electrophoresis
DA-UVD	diode array ultraviolet-visible detection/detector
DEPT	distortionless enhancement of polarization transfer
DNA	desoxyribonucleic acid
DNP	2,4-dinitrophenylhydrazine or 2,4-dinitrophenylhydrazone
DOC	dissolved organic carbon
DSC	differential scanning calorimetry
DTA	differential thermal analysis
ECD	electron capture detection/detector
ECN	effective carbon number
EHS	extremely hazardous substance
EI-MS	electron-impact mass spectrometry/spectrum
ELD	electrochemical detection/detector
ELISA	enzyme-linked immunosorbent assay
ELSD	evaporative light scattering detection/detector
EOF	electroosmotic flow
EPA	Environmental Protection Agency (USA)
ERG	emergency response guidebook
ESR	electron spin resonance
FD-MS	field desorption mass spectrometry
FIA	flow injection analysis
FID	flame ionization detection/detector
FLD	fluorescence detection/detector
FOX	Xylenol Orange-ferric complex
FOZ	final ozonide
FT...	Fourier transform... , e.g. FTIR, FTNIR, FTNMR
GCE	glassy carbon electrode
GED	gas electron diffraction
GEF	Global Environment Facility
GHS	globally harmonized system of classification and labeling of chemicals
GOX	glucose oxidase
GPC	glycerophosphocholine
GPO	glycerol-3-phosphate oxidase
GSH	glutathione
HDL	high-density lipoprotein
HEHP	1-hydroxyethyl hydroperoxide
HMBC	heteronuclear multiple bond correlation
HMHP	hydroxymethyl hydroperoxide
HMQC	heteronuclear multiple-quantum coherence
HNE	4-hydroxynon-2-enal
HPETE	hydroperoxyeicosatetraenoic acid

HPIC	high-performance ion chromatography
HPLC	high-performance liquid chromatography
HPSEC	high-performance size exclusion chromatography
HPTLC	high-performance thin layer chromatography
HRP	horseradish peroxidase
HRP-C	horseradish peroxidase isoenzyme C
HSQC	heteronuclear single quantum coherence
HVP	high volume production
IATA	International Air Transport Association
ICAO	International Civil Aviation Organization
IDF	International Dairy Federation
ILO	International Labor Organization
IMDG	International Maritime Dangerous Goods Code
IMO	International Maritime Organization
IPCS	International Programme on Chemical Safety
IUPAC	International Union of Pure and Applied Chemistry
LDL	low-density lipoprotein
LDPE	low-density polyethylene
LLDPE	linear low-density polyethylene
LOD	limit(s) of detection
LOQ	limit(s) of quantitation
LSD	light scattering detection/detector
MARPLOT	mapping application for response planning and operational tasks
MAS-NMR	magic-angle spinning NMR
MDA	malondialdehyde
MEKC	micellar electrokinetic chromatography
MHP	methyl hydroperoxide
MLR	multiple linear regression
MOSA	method of standard addition
MSD	α -methylstyrene dimer
NADP ⁺	nicotinamide adenine dinucleotide phosphate
NADPH	nicotinamide adenine dinucleotide phosphate reduced form
NI-MS	negative ion mass spectrometry
NIOSH	National Institute for Occupational Safety and Health (USA)
NIR	near infrared
NOAA	National Oceanic and Atmospheric Administration (USA)
NOESY	nuclear Overhauser enhancement/exchange spectroscopy
NPG	NIOSH pocket guide to chemical hazards
OEL	occupational exposure limits
OSHA	Occupational Safety and Health Administration (USA)
OTIF	Intergovernmental Organisation for International Carriage by Rail
PCA	principal component analysis
PC-OOH	phosphatidylcholine hydroperoxide
PLS	partial least squares
POP	persistent organic pollutants
POV	peroxide value
POZ	primary ozonide
ppbv	parts per billion on a volumetric basis
ppmv	parts per million on a volumetric basis
pptv	parts per trillion on a volumetric basis
PRESS	predicted residual error sum of squares

PS-OOH	phosphatidylserine hydroperoxide
PTFE	poly(tetrafluoroethylene)
PTS	persistent toxic substances
PVDF	poly(vinylidene difluoride)
RBD	refined-bleached-deodorized
RID	refractive index detection/detector or regulations concerning the international carriage of dangerous goods by rail
ROS	reactive oxygen species
SADT	self-accelerated decomposition temperature
SCE	saturated calomel electrode
SCSE	AgCl/Ag electrode
SEDAC	Socioeconomic Data and Applications Center
SFE	supercritical fluid extraction
SIMPLISMA	simple-to-use interactive self-modeling analysis
SIRE	sensors based on injection of the recognition element
SNR	signal-to-noise ratio
SPE	solid-phase extraction
SPME	solid-phase microextraction
SRM	selected reaction monitoring
TBA	thiobarbituric acid
TBARS	thiobarbituric acid reactive substances
TCN	total carbon number
TDG	transport of dangerous goods
TEOS	tetraethyl orthosilicate
TGA	thermogravimetric analysis
TMOS	tetramethyl orthosilicate
TMS	tetramethylsilane
TSCATS	toxic substances control act test submissions
TS-MS	thermospray ionization mass spectrometry
UN	United Nations
UNECE	UN Economic Commission for Europe
UNEP	UN Environmental Programme
UVD	UVV detector/detection
UVV	ultraviolet-visible
VLDL	very low density lipoprotein
VOC	volatile organic compounds
VOHMA	International Vessel Operators Hazardous Materials Association, Inc.
WHO	World Health Organization
XRD	X-ray diffraction

II. INTRODUCTION

A. Peroxides in Nature and the Technological World

The present section is an overview of the varied involvement of peroxides in natural phenomena, ranging from atmospheric chemistry to important physiological systems in all living organisms, and the functions fulfilled by these compounds in industry. All this requires adequate analytical methods to identify, determine and characterize peroxides. This section should not be considered as a comprehensive review on natural and industrially relevant peroxides, but rather as a structured set of examples related to analytical methods described in the sequel.

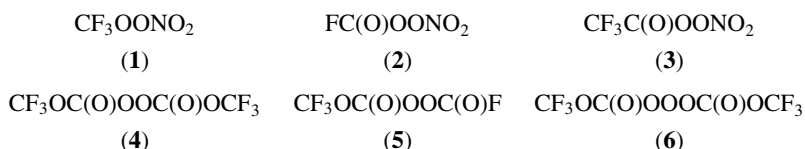
1. Environmental issues

a. Atmosphere. The generation and function of atmospheric peroxides have been reviewed¹⁻⁴. Analysis of peroxides in the atmosphere is a complex endeavor, including the choice of collection method (e.g. a cryotrap or a continuous scrubbing coil, each one with its advantages and pitfalls), the presence of interfering compounds (e.g. SO₂, O₃, N oxides and airborne transition metal ions), decomposition kinetics of the analytes, which becomes especially significant when end analysis is delayed, separation method (e.g., GLC or HPLC) and end determination⁵. The design of sampling devices for peroxides in the atmosphere requires careful consideration of many factors, however two are outstanding: The concentrations are very low and the analytes are quite reactive. The first implies that sufficient sample need be collected to perform the end analysis by the chosen method, whereas the second implies that decomposition of the analyte by itself, or by contact with the sampler, or with other analytes or with reactive impurities should be kept to a minimum. Additional important considerations are the place where the sample is to be collected and whether the end analysis device is incorporated with the sampler⁶⁻⁹.

The presence of H₂O₂ in the atmosphere is the result of photochemical reactions and has an important function in the generation of acid rain from SO₂ and nitrogen oxides. Among the atmospheric trace components are the volatile organic compounds (VOC), many of which are biogenic and others are anthropogenic¹⁰. Methyl hydroperoxide (MHP, MeOOH), hydroxymethyl hydroperoxide (HMHP, HOCH₂OOH) and 1-hydroxyethyl hydroperoxide (HEHP, MeCH(OH)OOH) are among the most abundant organic peroxides in the atmosphere. Their generation can be traced to the action of HO• and O₃ on biogenic VOC such as terpenes. HMHP may also be implicated in generation of acid rain. These peroxides have toxic effects¹¹⁻¹³. Also the hydroperoxy free radical, HOO•, generated from HO•, plays an important role in the trace chemistry of the atmosphere¹⁴. Measurements of H₂O₂ at a site in North Carolina during the summer of 1994 showed variation from 26 to 106 ppb during 1 h. These results were quite similar to those obtained during the summer of 1996, never exceeding the 125 ppb maximum during 1 h, which is the local quality standard⁷. The latitudinal distribution of these peroxides measured over the Atlantic Ocean shows a maximum in the equatorial region and diminution towards the poles¹⁵.

Rain and cloud water collected during the FELDEX campaign in November 1995 were analyzed for H₂O₂, HMHP and HEHP. For a certain location concentrations of these compounds varied from below the LOD to the following values: *ca* 3 μM H₂O₂, *ca* 0.2 μM HMHP and *ca* 0.1 μM HEHP^{16,17}. In southeastern USA the organic peroxides (mainly MHP and HMHP) were found to vary from 20 to 80% of the total peroxide vapors in the gaseous atmosphere¹⁸. A plethora of minor peroxides is generated by photochemical activity on biogenic emissions; of especial environmental significance are those derived from anthropogenic emissions such as the chlorofluorocarbons, that contribute to the ozone depletion in the stratosphere. Chlorinated MHPs are important intermediates in the combustion and atmospheric photochemistry of chlorocarbons. UV irradiation of a low partial pressure mixture of MeCl (33–569 mTorr), H₂ (0–9.6 Torr) and Cl₂ (54–311 mTorr) in air (700 Torr) yields two main intermediate free radicals, ClCH₂O₂• and HOO•, and two main products, formyl chloride (HC(O)Cl) and chloromethyl hydroperoxide (ClCH₂OOH)¹⁹. Hydrofluorocarbons are now being considered as replacement for the chlorofluorocarbons; the main products of their photochemical decomposition are the FC(O)O_x• and CF₃O_x• (*x* = 1, 2) free radicals, which on reaction with minor atmospheric pollutants, such as NO₂ and CO in the presence of O₂, can produce perfluoro derivatives such as peroxy nitrates (e.g. **1** to **3**)²⁰⁻²², peroxy carbonates (e.g. **4** and **5**) and trioxycarbonates (e.g. **6**)^{23,24}. The environmental impact of all these derivatives of hydrofluorocarbons

is still to be assessed before they enter the market in force.



In the atmosphere certain biogenic olefins, such as ethylene, propylene, Z-2-butene and isoprene, react with O_3 and moisture, leading to formation of H_2O_2 , MHP, EtOOH, HMHP and HEHP^{25,26}. In spite of this, VOC of biogenic and anthropogenic origin can be considered as precursors of atmospheric O_3 ^{10,27}. Local ozone concentration in the atmosphere can be determined with an electrochemical concentration cell mounted on an ozonesonde²⁸. The total amounts of O_3 , NO_2 and SO_2 in the atmosphere over a certain point can be determined by the absorption spectrum of the solar radiation in the UV region, using a Brewer spectrophotometer. This instrument may be mounted on ozonesondes for mapping the O_3 concentrations of regions at various altitudes. The complexity of ozonesonde studies may be appreciated by the reports on a campaign carried out in the equatorial upper troposphere²⁹, or the occurrence of *O₃-valley* events, with unusually low O_3 concentrations over certain zones³⁰. A near real time appreciation of the global O_3 distribution in the atmosphere was gained from the *Global Ozone Monitoring Experiment* (GOME), based on a DA-UVD instrument with spectral range from 240 to 790 nm and 0.1 to 0.2 nm resolution, mounted on a satellite with polar orbit, covering the entire Earth surface in 3 days^{31,32}. The total ozone concentration over a location varies during the same day over a broad range of values, however this range shows a yearly periodicity. Measurements over a period of more than four years in a location in the Czech Republic showed minima in December and maxima in May. These variations of O_3 concentration affect the UV spectrum of the light reaching the ground and have, therefore, strong biological effect on plants³³. The stratospheric ozone crisis of the latter decades and its potential dangers have been summarized³⁴. A 9.6 μm pulsed quantum-cascade laser system for determination of O_3 in the atmosphere at ambient pressure was under development at the time this chapter was written³⁵.

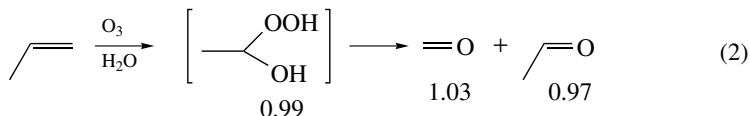
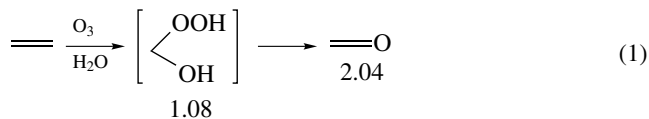
A model was proposed for simulation of atmospheric physical and chemical phenomena, involving anthropogenic and natural emissions, advective and convective transport, vertical diffusion, dry deposition, wet scavenging and photochemistry, taking place in the stratosphere, tropopause and troposphere. The model estimates a total annual flux of 663 million ton O_3 from the stratosphere and a net yearly photochemical production of 161 million ton in the troposphere. These calculations agree with estimates made based on measurements from satellites, ozonesondes and the ground. About 100 chemicals and 300 chemical reactions are considered³⁶. A statistical investigation was carried out linking daily mortality with atmospheric levels of O_3 , based on daily data collected by the meteorological services in Seoul, over the period from 1995 to 1999. Other considerations in this study were pollutants such as particulate matter of aerodynamic diameter under 10 μm (PM_{10}), CO, SO_2 and NO_2 , meteorological parameters (temperature, pressure and moisture) and the seasons. The best fitting model suggests a threshold of about 25 ppb of innocuous atmospheric O_3 , over which exposure becomes harmful, with daily mortality following a nonlinear J-shaped function, as occurs in the summer³⁷.

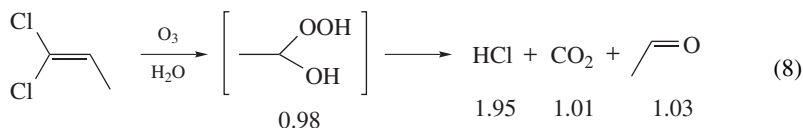
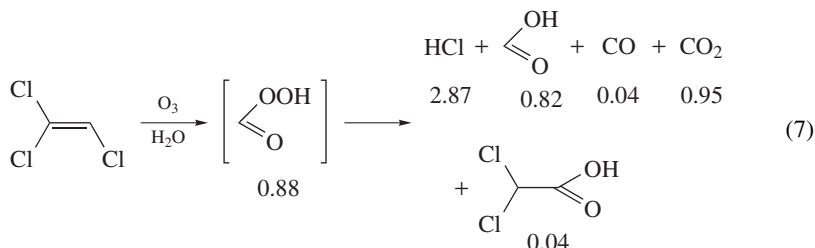
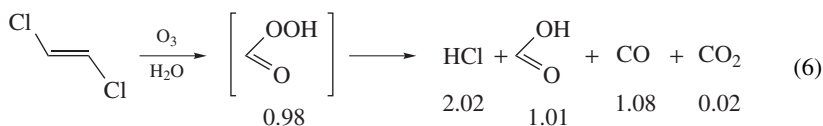
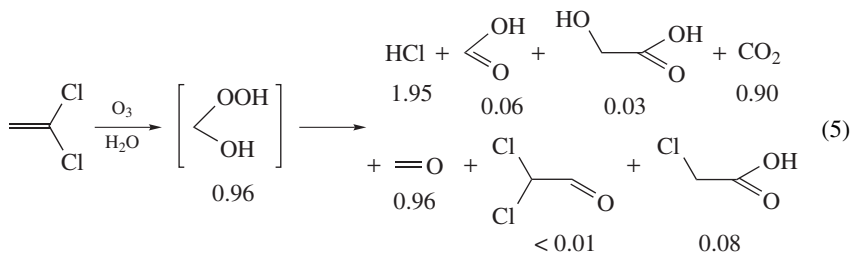
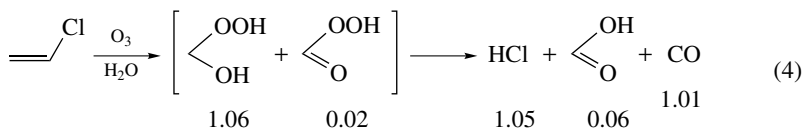
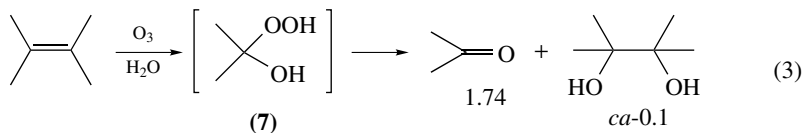
b. Water. All interactions of natural waters and wastewaters with ROS and external physical factors such as UV radiation, ultrasound and abrupt temperature changes have to take into account the presence of suspended and dissolved organic matter. The latter is

usually quantitatively expressed in term of *dissolved organic carbon* (DOC). A complex picture is usually obtained even after ultrafiltration, due to the functional and structural diversity of the DOC. For tracking the fate of various types of DOC it is convenient to separate this material into two groups, hydrophobic and hydrophilic, each of them comprising three fractions, basic neutral and acid. These six fractions are the result of separation of the total DOC on three LC columns, according to a strictly defined procedure³⁸.

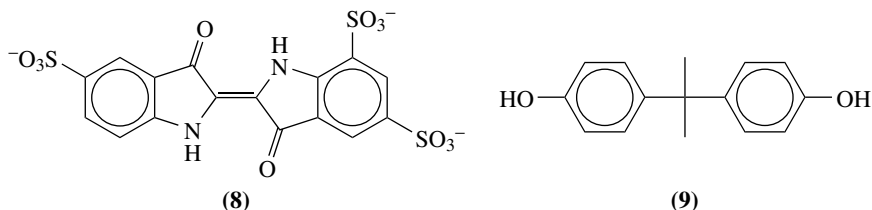
The presence of H₂O₂ in seawater is mainly the result of photochemical activity involving free radicals and DOC³⁹; part is also produced by certain species of phytoplankton⁴⁰. Depth profiles of H₂O₂ are dependent on photogeneration, for example in the West Mediterranean Sea in July measurements showed surface level concentrations from 16 to 154 nM H₂O₂, with rapid decrease below the thermocline. Humic material is more effective than fulvic material or macromolecular acids in promoting H₂O₂ photogeneration⁴¹. H₂O₂ may also be produced in water without the intervention of photochemical or enzyme-catalyzed processes, for example, by sonication. Ultrasound treatment of water leads to H₂O₂ formation, accompanied by light emission, sonoluminescence. The nature of this emission is a matter of debate, as being due to purely thermal phenomena, e.g. black body radiation by the very hot content of cavitating bubbles (up to 25000 K), or CL phenomena. A study with dissolved noble gases shows a correlation between the yield of H₂O₂ and the intensity of sonoluminescence, pointing to the chemical nature of the phenomenon⁴².

The chemical aspects of ozone disinfection of drinking water were reviewed^{43,44}. Ozone has long been used for drinking water disinfection and recycling of wastewaters. Recent interest revival on these methods followed the objections to chlorine disinfection of drinking water, producing trace amounts of chloroform and other toxic compounds. This interest is accompanied by deep concern about the toxicological properties of the ozonolysis products of water micropollutants. Although O₃ reacts readily with double bonds, activated aromatic compounds and amino groups, other reactions are possible with radicals derived from ozone and water, such as HO• and O₂^{-•}, which react faster than O₃ and may attack less reactive moieties. A kinetic study of the reaction of ethylene and variously substituted derivatives, in water solution at ambient temperatures, shows that formation of the primary ozonide (POZ) is rate determining, and no formation of a final ozonide (FOZ) is likely. However, Criegee's mechanism (Scheme 16, Section VIII.A) seems to apply until the step before FOZ formation. The experimentally determined product yields, in mole per mole O₃ consumed, for various substrates are depicted in equations 1 to 8. It should be noted that the chlorine-containing intermediates derived from chlorinated ethylenes all spontaneously decompose or hydrolyze to yield HCl; also, some hydroperoxides are formed as unstable intermediates (in square brackets) that can be determined but ultimately turn into carbonyl compounds or carboxylic acids. In the case of 2-hydroxyisopropyl hydroperoxide (7), its presence can only be assumed because the assay with Allen's reagent used for the other hydroperoxides (Section V.B.2.a) is too slow for its determination⁴⁵.





Multiple-stage ozonization seems to be more effective than single-stage ozonization, both followed by biodegradation, for DOC elimination in treatment of reservoir waters and secondary effluents of a domestic wastewater treatment plant⁴⁶. The fate of O₃ in water ozonization consists of a fast reaction with the DOC and a slow first-order decay of unreacted O₃. A method for optimization of a two-stage water ozonization process is based on control with a FIA unit, where the ozone concentration is continuously measured by oxidation of indigotrisulfonate(**8**)^{47,48}. The various fractions of DOC (in the ppm range) may react with the traces of bromide (sub-ppm) found in natural waters, as this anion

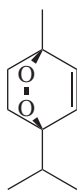


undergoes oxidation by ozone to hypobromite and other reactive species. The products include a variety of aromatic and aliphatic aldehydes, probably stemming from organic ozonides, and the following brominated species: bromoform, mono- and dibromoacetic acid, 2,4-dibromophenol, dibromoacetone and dibromoacetonitrile. The concentration of these species ranges in the ppb levels, depending on the ratio of O_3 to DOC used. The various hydrophobic and hydrophilic fractions of DOC defined above yield different amounts of aldehydes and brominated products⁴⁹. An alternative classification of DOC in industrial and potable waters can be made based on the kinetics of O_3 uptake⁵⁰. Ozonization totally eliminates traces of bisphenol A (9), an endocrine disrupting chemical, in aqueous solutions, over the pH range from 2 to 12. The rate of the process is limited by the rate of mass transfer of O_3 , with no significant influence by the presence of H_2O_2 in the solution⁵¹. Ozonization can be used for decolorizing textile wastewaters. Increasing the pH increases both the efficiency of color removal and oxygen consumption⁵².

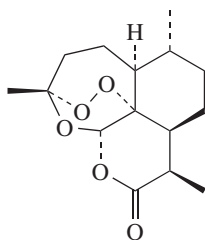
c. Soil. Ozone undergoes reaction with the organic matter in the soil under laboratory conditions, causing an increase of water-soluble organic matter, which is more biodegradable and has increased acidity and optical density in the UV region⁵³. It may be assumed that similar results will be attained by the long-term cumulative action of atmospheric ozone. A model was proposed for evaluation of the ozone risk (ozone absorbed through the stomata) to arable crops and pastures. It takes into account the soil, which happens to be a considerable sink for atmospheric ozone, with an uptake of about 50%, and a minor uptake (about 10%) by the external plant surfaces⁵⁴.

2. Biological and biomedical systems

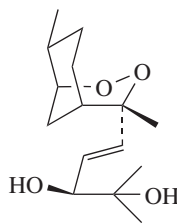
a. Natural products and their analogs. Various natural products bearing the peroxide functional group are known, for example ascaridole (10), the main constituent of the oil of *Chenopodium ambrosioides*, formerly used as an anthelmintic, artemisinin (11) found in *Artemisia annua* L. and yingzhaosu A (12) in *Artrabotrys uncinatum*, two traditional Chinese medicinal herbs. Some cyclic peroxides have potent pharmacological activity, as in the case of the natural products 11 and 12, their semisynthetic derivatives (e.g. 13), some synthetic ozonides (14), 1,2,4-trioxanes (15) and dispiro-1,2,4,5-tetraoxanes (16) that are effective against *Plasmodium falciparum*, a microorganism resistant to treatment with the usual antimalarial drugs⁵⁵⁻⁶⁰. The cytotoxic triterpene (–)-longilene peroxide (17) (for KB cells, $IC_{50} = 5.3 \text{ mg L}^{-1}$) is found in the wood of *Eurycoma longifolia*⁶¹. Stolonoxide A (18a) is a cyclic peroxide isolated from the tunicate *Stolonica socialis*. The structure of its Me ester (18b) can be totally elucidated by NMR spectroscopic techniques (Section VII.C.2)⁶². The ozonides of sunflower oil and of methyl oleate have antimicrobial activity that can be linked to the presence of a stable FOZ moiety (see Section VIII.A)⁶³.



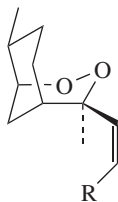
(10)



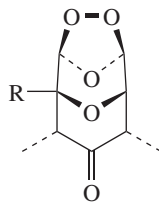
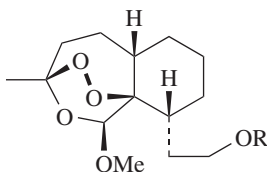
(11)



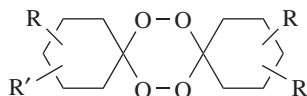
(12)



(13) R = Ar, Het, long alkyl

(14) R = H, Et, *n*-C₇H₁₅

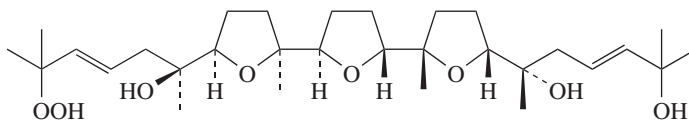
(15) e.g., R = H, alkyl, Ar, acyl etc.



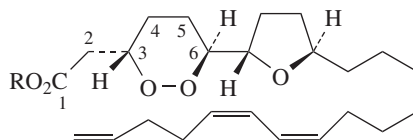
(16) (a) R = 3-Me, R' = 5-Me

(b) R = 4-Me, R' = H

(c) R = 2-Me, R' = H



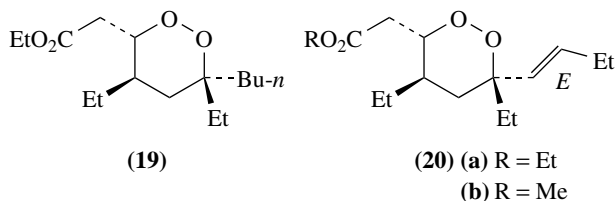
(17)



(18) (a) R = H

(b) R = Me

Ethyl plakortide Z (**19**) and its two didehydro analogs (**20a** and **20b**) are found in the Papuan sponge *Plakortis lita*. These compounds are cytotoxic and show some antitumor activity *in vitro*⁶⁴.



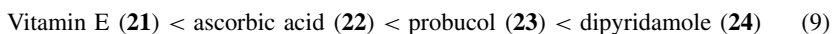
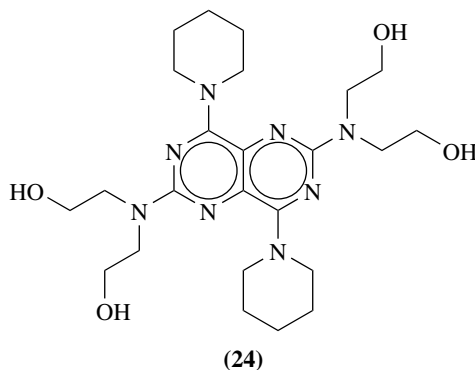
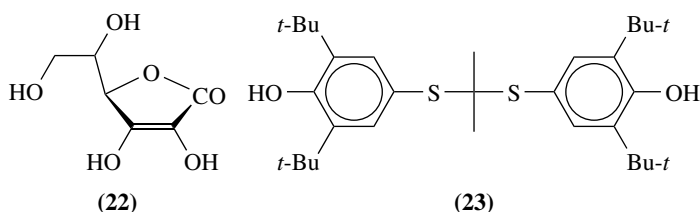
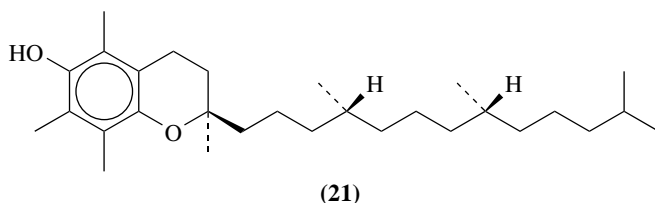
b. Reactive oxygen species. The participation of reactive oxygen species (ROS) in human diseases and aging has been reviewed⁶⁵. The balance between various intracellular ROS, for example $O_2^{\bullet -}$ and H_2O_2 , is a determinant factor for cell survival or apoptosis (process of programmed cell death)⁶⁶. $O_2^{\bullet -}$ is the product of O_2 reduction catalyzed by NADPH oxidase, and is converted to H_2O_2 either spontaneously or in a process catalyzed by superoxide dismutase. H_2O_2 production with NADPH peroxidase mediation is an important process of the phagocyte activity⁶⁷.

The phytopathogenic effects of certain basidiomycetes (e.g. *Sclerotium rolfsii*) may be linked to the oxidative stress caused by their ability to produce H_2O_2 ⁶⁸. *Pseudomonas aureoginosa* develops a protective mechanism which is upregulated in the presence of H_2O_2 with simultaneous downregulation of primary metabolism⁶⁹. A complex of defensive and repair mechanisms against peroxide and superoxide is genetically encoded in *Bacillus subtilis*⁷⁰. The gene expression induced by H_2O_2 in tobacco has been thoroughly analyzed⁷¹.

H_2O_2 is excreted in the urine in concentrations of the order of 0.1 mM⁷². The concentration of H_2O_2 in urine of healthy patients tends to diminish under the influence of exercise and to increase on increasing the level of sodium ion⁷³. An increase of H_2O_2 is observed in the urine of healthy persons immediately after drinking instant coffee, which starts to decline to normal levels within 2 h. It is a moot point whether some of the H_2O_2 contained in the beverage is directly excreted or all stems from metabolism of other ingested components⁷⁴. The ROS seem to have regulatory effects on the renal function^{75,76}. An increase of the H_2O_2 level is observed in the extracellular liquid after impact injury on the spinal chord⁷⁷. The peroxysome organelles present in fruits are an important pool of antioxidant activity and may also function as modulators of signal ROS during fruit maturation⁷⁸.

Besides the adverse effects associated with the formation of lipid hydroperoxides mentioned in Section II.A.2.c, other oxidation paths leading to pathological conditions have been described. A 100-fold concentration level of *o,o'*-dityrosine residues is found in LDL fixed on an atherosclerotic tissue as compared to that in freely circulating LDL. This protein cross-linking feature cannot be directly attained by enzymatic action on protein strands; however, it has been shown *in vitro* that myeloperoxidase, lactoperoxidase and HRP are capable of producing tyrosyl free radicals in the presence of H_2O_2 ; on release of these free radicals to the solution they may cause charge transfer and ultimately dimerization of tyrosyl residues on the protein⁷⁹. This process is analogous to the one shown in equation 34, Section III.B.2.b. The toxic action of 1O_2 involves reaction with cellular lipids, which convert to hydroperoxides and may lead to cellular destruction. Vitamin B₆ (pyridoxine) is all-important in the mechanism of 1O_2 detoxification (see equation 75 in Section VII.C.2)⁸⁰. Oxidation of LDL by various methods, both at

the chemical and cellular levels, can be decreased in the presence of pharmacologically relevant concentrations of natural antioxidants, such as Vitamin E (**21**) and ascorbic acid (**22**), and synthetic antioxidants such as probucol (**23**) and dipyradamole (**24**). The effectiveness of these antioxidants is in the order shown in equation 9⁸¹. Atherogenesis and cardiac hypertrophy are linked with the presence of the nuclear transcription factor PPAR γ in the peroxysome organelles of the arteries and hearts of affected patients⁸².

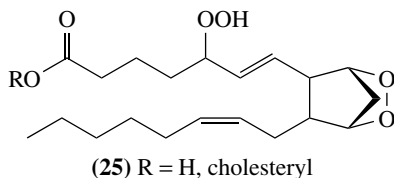


Various reactive oxygen and nitrogen species in the vascular system, including $O_2^{\bullet-}$, H_2O_2 , NO (nitric oxide) and $ONOO^-$ (peroxynitrite), are of central significance for their cell signaling, cytotoxicity and other functions⁸³. Peroxynitrite ($ONOO^-$) and its corresponding acid ($ONOOH$) are very reactive species generated *in vivo* from nitric oxide (NO) and superoxide ($O_2^{\bullet-}$) or the hydroperoxide radical (HOO^{\bullet}), respectively, or by pulse radiolysis in an involved process^{84,85}. The fast reaction with many substrates present in living organisms may cause irreversible damage to cells and tissues; however, in the presence of various reducing agents a detoxification process may take place, leading to NO regeneration and the formation of other compounds that are beneficial to the cardiovascular system. Peroxynitrite, a metabolite of nitric oxide produced in the endothelium of the

vascular system, has both toxic and therapeutic properties of clinical relevance^{86,87}. Thus, for example, both NO and ONOO⁻ inhibit generation of O₂^{-•} by polymorphonuclear leucocytes, stimulated by formyl-methionyl-leucyl-phenylalanine, taking place in conditions such as severe inflammation⁸⁸.

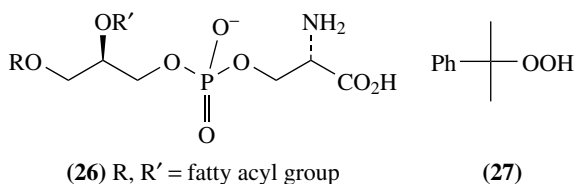
The lactoperoxidase system produces various compounds for antimicrobial protection of milk, the principal one of which is hypothiocyanite (OCNS⁻) as a result of the lactoperoxidase-catalyzed oxidation of thiocyanate (SCN⁻) by H₂O₂. No overheating should take place during the pasteurization process, to avoid damaging lactoperoxidase⁸⁹.

c. Lipid peroxides. Lipid oxidation has been amply reviewed^{90,91}. Lipid oxidation pathways belong to two main groups: Enzymatically catalyzed metabolic processes ultimately resulting in useful compounds for the organism, and free radical processes that may lead to desirable compounds or may cause lipid degradation and possibly production of harmful substances. In certain cases it is possible to deduce the proportion of lipid hydroperoxide that was obtained by enzymatically catalyzed and free radical routes (Section V.C.1)^{92,93}. The mean levels of phosphatidylcholine hydroperoxides and cholesteryl ester hydroperoxides (see Section V.B.2.c) found in normal human plasma are 36.0 ± 4.0 and 12.3 ± 3.1 nM (*n* = 6), respectively⁹⁴. The LDL fraction in plasma shows higher propensity for oxidation than the HDL fraction⁹⁵. H₂-Isoprostane bicyclic endoperoxides (e.g. **25**, R = H) are derived from arachidonic acid and are intermediates in the formation of various classes of isoprostanes, neuroprostanes and isofurans by a combination of reduction, rearrangement and hydrolysis steps. Hydroperoxides of arachidonic acid (see Section VII.C.6) are involved in the formation of prostaglandins, leucotrienes and thromboxanes. The lipids of LDL undergo oxidation to a mixture of hydroperoxides, bicyclic endoperoxides (e.g. **25**), monocyclic peroxides and serial cyclic peroxides^{96,97}.

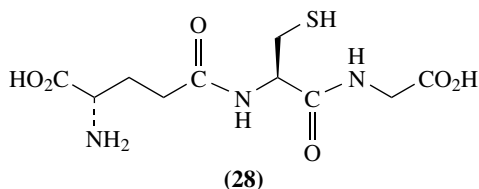


Intense research activity is invested in correlating the presence of lipid peroxides with various physiological and pathological condition of cells, tissues and organs. Some examples of recently published research works follow. Cholesterol hydroperoxides are produced in the skin by attack of singlet oxygen or free radicals, as a result of prolonged exposure to UV irradiation (see Scheme 1 in Section II.A.2.c)⁹⁸. Atmospheric ozone causes formation of lipid hydroperoxides in epithelial cells of the respiratory track⁹⁹. The presence of intravitreal H₂O₂ and hydroperoxides is associated with ophthalmopathological conditions, including various retinal ischemic diseases¹⁰⁰. The ROS (H₂O₂, O₂^{-•}, HO[•], ClO[•]) produced by human spermatozoa and contaminating leucocytes in ejaculated semen contribute to infertility by impairing sperm motility. Lipid peroxidation is involved in this malfunction. Also, the integrity of the sperm genome can be affected by ROS^{101–103}. The presence of peroxidized forms of cholesteryl fatty acid esters (Section V.B.2) carried by LDL in the blood stream is associated with hypercholesterolemia, atherogenesis^{104,105} and myocardial ischemia induced by physical stress and various endothelial conditions, although the cause–effect order in certain cases is unclear^{106,107}. Also in the case of tissue damage in cerebral ischemia, there is controversy about the cause–effect order of the presence of lipid hydroperoxides and the validity of certain analytical methods used for their detection^{108,109}.

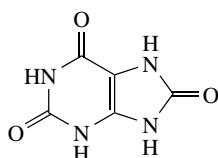
Studies carried out with complete cells *in vivo*, cell membranes and other cell fractions point to the selective oxidation of phosphatidylserine (**26**) to a hydroperoxide (PS-OOH) on oxidative stress caused by toxic agents such as H₂O₂, *t*-BuOOH and cumyl hydroperoxide (**27**). Formation of PS-OOH is observed during apoptosis. These phenomena are important because of the cytotoxic effects of various peroxides used in commercial products coming into direct contact with the human body, as is the case of epidermal keratinocytes in contact with cosmetic formulations^{110, 111}. The toxic effects of *t*-BuOOH are associated with vasoconstriction and damage to the vascular smooth muscles¹¹². Global determination methods for primary lipid oxidation products are discussed in Section IV.B.



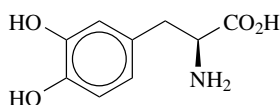
Although lipid hydroperoxide formation seems to be a primary avenue for oxidative stress, subsequent reactions leading to formation of malondialdehyde (MDA) and other aldehydes, such as 2-alkenals and 4-hydroxyalk-2-enals, e.g. 4-hydroxynon-2-enal (HNE), are also important for assessment of both the oxidation degree and the toxic effects of these compounds on the living system. The lysine residues of LDL form adducts with both MDA and HNE. The kinetics of Cu(II)-induced oxidation of LDL passes through various stages. At the inception, lipid hydroperoxides are formed with accelerating rate that reaches a maximum and slows down to a standstill, after which the lipid hydroperoxides start disappearing, leading to degradation products¹¹³. The presence of HNE is linked with various pathological conditions. The HNE contents in both blood plasma and the cerebrospinal fluid of Parkinson's disease patients increases with time over several years; this may also be related to the depletion of glutathione (GSH, **28**) in the *substantia nigra* of these patients, probably caused by condensation with HNE. Biopsy specimens taken from the affected area of patients with inflammatory bowel disease contain significantly more HNE than the same tissue from a control group. The HNE concentration in plasma increases from a healthy control group to a group affected with HIV-1 to a group of AIDS patients. This may also be related to the strong immunosuppressant effects of HNE¹¹⁴. Various chronic liver diseases and pathological conditions are related to the presence of lipid hydroperoxides and their secondary products, MDA and HNE. These aldehydes form adducts with the lysine residues of LDL, for which specific antibodies can be developed and used in immunohistochemical methods (beyond the scope of the present chapter) to ascertain their presence inside and outside cells^{115, 116}. A correlation exists between lipid peroxides in the plasma of patients affected by type 2 diabetes, as determined by a HPLC-FLD method for MDA¹¹⁷, and glycaemic control assessed by HbA1 levels¹¹⁸. Various aldehydes of cytotoxic activity, and HNE in particular, are formed *in vivo* in



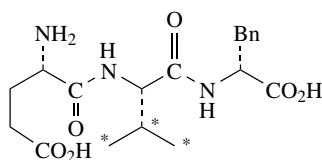
free radicals formed by UV radiation, after eliminating from the system the H_2O_2 , only the aromatic substrates show hydroperoxide formation, probably by a photosensitized mechanism. On the other hand, all five amino acids show significant hydroperoxide yields on exposure to free radicals generated by γ -radiation. The hydroperoxide from **36** undergoes rearrangement to *N*-formylkynurenine (**37**), as shown in equation 10¹⁴⁴. The antioxidant capacity of Vitamin E (**21**), opposing the oxidative action of free radicals derived from lipid hydroperoxides (ROO^\bullet), yields more stable peroxide derivatives (**38**), as shown in equation 11¹⁴⁵.



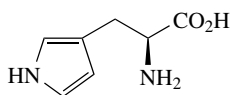
(29)



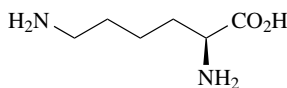
(30)



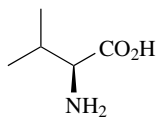
(31)



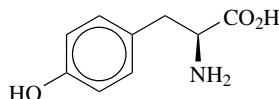
(32)



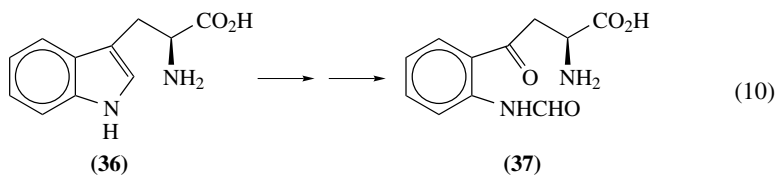
(33)



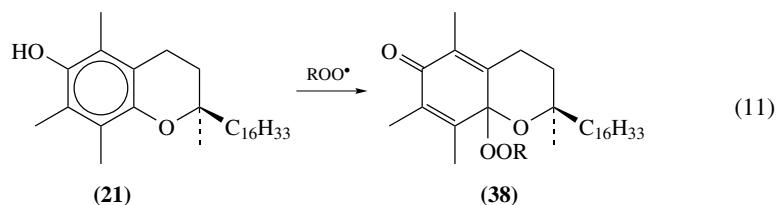
(34)



(35)

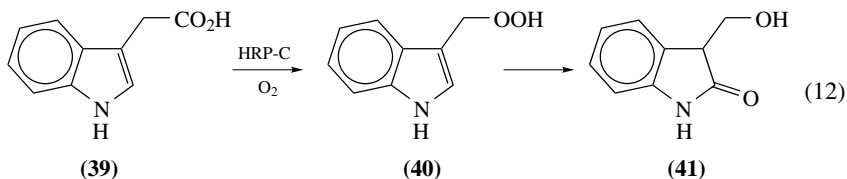


(10)

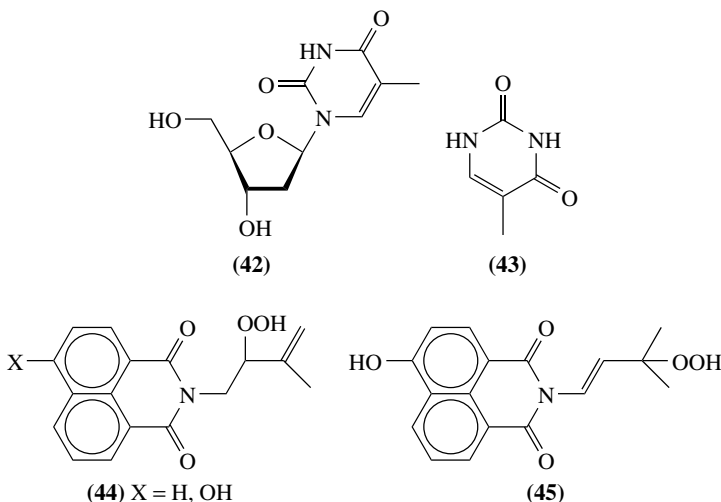


(11)

The mechanism of metabolic degradation of indol-3-ylacetic acid (**39**) is a matter of debate. A possible route demonstrated *in vitro* includes oxidative decarboxylation to skatolyl hydroperoxide (**40**), catalyzed by horseradish peroxidase isoenzyme C (HRP-C), followed by rearrangement to 3-(hydroxymethyl)oxindole (**41**), as shown in equation 12¹⁴⁶.



H₂O₂ damage to endothelial cells is related to inflammatory processes¹⁴⁷. H₂O₂ is suspect of causing *in vitro* mutations by oxidative damage to DNA¹⁴⁸. In fact, about 70% of the damage caused by ionizing radiation to DNA in aqueous solution involves initial hydroperoxide formation¹⁴⁹, which seems to preferentially occur on thymidine (**42**) residues. Similar oxidative action on the thymidine residues of DNA is attributed to therapeutic drugs¹⁵⁰ and the aging process¹⁵¹. The mechanism of ozone disinfection involves damage to the protein, DNA and RNA of bacteria and viruses, which is far from being understood either in its workings or the toxicological implications of its products. The possible effects of ozone on DNA can be appreciated from a model study on the ozonolysis of thymidine (**42**) and thymine (**43**) in aqueous solution, leading to a complex scheme involving hydroperoxides, peroxyacids, peroxyesters and their reduction compounds¹⁵². Similar implications may be assumed for DNA from the photosensitized oxidation products of thymidine mentioned above¹⁴⁰. Resistance to ozone damage by rice is a quantitative genetic trait. The loci of this trait and markers are known, allowing assessment of O₃ resistance of rice germplasm and development of resistant lines in breeding programs¹⁵³.

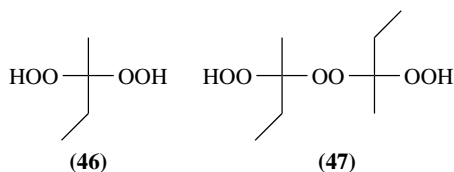


The naphthalimide hydroperoxides **44** and **45** are called artificial photonucleases for their *in vitro* ability of intercalating in the DNA structure and causing photochemically induced cleavage^{154, 155}. Lipid hydroperoxides interfere with the photosynthesis process.

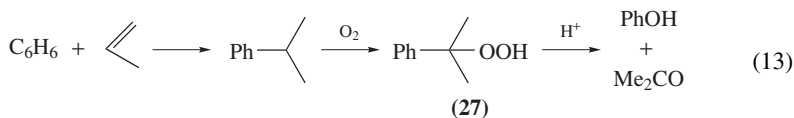
A vesiculation defensive mechanism is in operation to remove peroxidized lipids from the thylakoid membranes¹⁵⁶.

3. The chemical and related industries

a. A cautionary note. When handling peroxides, special attention has to be paid in many cases to avoid excessive concentration, excessive heating and contact with certain materials, lest the intrinsic instability of the peroxide brings about detonation or deflagration. Methods are described for drying hydroperoxides needed for fuel instability studies. These relatively safe procedures are to be carried out in small batches of a few cubic centimeters at most, avoiding contact with materials other than glass, and keeping the temperature under close control¹⁵⁷. Various studies have been carried out on the hazards involved in handling of industrial compounds that have undergone autooxidation on contact with air. For example, the common solvent 2-butanone (methyl ethyl ketone) has several peroxide derivatives, of which a monomeric (**46**) and dimeric species (e.g. **47**) are of special significance in industry. These compounds have been responsible for many explosions caused by thermal exposure of the solvent under various conditions of storage, reaction or conflagration. A thermoanalytical study of these peroxides by DSC revealed that the mechanism of decomposition involves strongly exothermic steps. The onset temperature for these processes in the case of **46** is as low as 40 °C¹⁵⁸. The danger of spontaneous decomposition of peroxidic compounds has induced several regulating agencies to adjudicate a special classification as for the mode of storage and transportation of these compounds and of substances that might inadvertently contain them^{159–163}. Furthermore, some peroxides have peculiar toxicological properties. More about safety measures and regulations can be found in Section X.



b. Peroxide manufacture. The yearly worldwide production of hydrogen peroxide and its organic derivatives is estimated at about 1.5 million ton¹⁶⁴. Only a few organic peroxides are sold in the chemical market, and usually in dilute and stabilized form due to the toxicity, potential explosion, conflagration and environmental hazards involved in handling bulk amounts of these compounds (see Section X). Table 1 lists commercially available organic and inorganic peroxides.



Hydrogen peroxide is by far the leading peroxide in the market among the compounds mentioned in this table, with a wide spectrum of applications, as general oxidizing and reducing agent, synthone for organic peroxides, bleaching agent and disinfectant. However, cumyl hydroperoxide (**27**) takes over H₂O₂ in production tonnage, though not in sales tonnage, as it serves as intermediate stage in the manufacture of phenol and acetone, according to equation 13. Thus, based on recently published statistics for phenol production in USA¹⁶⁵, an estimate of 4.6 million tons per year may be made for **27** in that

TABLE 1. Commercially available peroxidic reagents

Compounds [CAS No.]	Properties ^a	Notes
A. Hydrogen peroxide and complexes		
Hydrogen peroxide [7722-84-1]	SR(3)3293C, MX0887000, UN2015 (H: 5.1; R: 34; S: 3, 28, 36/39, 45; P: I), ICSC0164, O, C, N .	<i>b, c, d, e, f</i>
Percarbamide [124-43-6] (48)	SH3579B, SR(1)939G, YT4850000, UN1511 (H: 5.1; R: 8, 34; S: 15, 17, 26, 36/37/39, 45), O, C .	<i>b, d</i>
Sodium percarbonate [15630-89-4] (49)	SR(3)3403E, FG0750000, UN2457 (H: 5.1; R: 8, 22, 36/38; 5:8, 17, 26, 39).	<i>d, f</i>
B. Hydroperoxides		
<i>t</i> -Butyl hydroperoxide [75-91-2]	EQ4900000, ICSC0842, UN2093, 3102, 3109 (H: 5.2; R: 7, 10, 20/21, 22, 34; S: 3/7, 14.2, 26, 36/37/39, 45 P: II), O, C, N, T .	<i>b, e, f</i>
Cumyl hydroperoxide [80-15-9] (27)	N(2)329C, MX2450000, UN3109 (H: 5.2; R: 7, 11, 20/22, 34; S: 3/7, 17, 36/37/39, 45, 50.3; P: II), ICSC0761, O, C, T .	<i>f, g, h</i>
2,5-Dimethylhexan-2,4-diyl dihydroperoxide [3025-88-5]	UN2174.	<i>f</i>
C. Dialkyl peroxides		
Bis(trifluoromethyl) peroxide [927-84-4]		
<i>t</i> -Butyl peroxide [110-05-4]	SH643D, SR(1)209K, ER2450000, UN2102, O , UN3107 (H: 5.2; R: 7, 11; S: 3/7, 14.2, 16, 36/37/39; P: II), ICSC1019, O, F .	<i>f</i>
Cumyl peroxide [80-43-3]	SD8150000, UN3110 (H: 5.2; R: 7, 36/38, 51/53; S: 3/7, 14.2, 36/37/39, 61; P: II), ICSC1346, O, Xi, N .	<i>f, g</i>
Ethyl 3,3-bis(<i>t</i> -butylperoxy)butyrate [55794-20-2]	UN2598.	<i>g</i>
Ethyl 3,3-bis(<i>t</i> -amylperoxy)butyrate [67567-23-1]		<i>g</i>
Ascaridole [512-85-6] (10)	OT0175000	<i>e</i>
Artemisinin [63968-64-9] (11)	N(1)1163B, SR(1)819K, KD4170000.	
2,2-Bis(<i>t</i> -butylperoxy)butane [2157-23-9]		<i>e, g</i>
2,5-Bis(<i>t</i> -butylperoxy)-2,5-dimethylhexane [78-63-7]	SR(1)213C, MO1835000, UN2155, O .	<i>g</i>
2,5-Bis(<i>t</i> -butylperoxy)-2,5-dimethyl-3-hexyne [1068-27-5]	MQ9750000, UN2158.	<i>g</i>
1,1-Bis(<i>t</i> -butylperoxy)cyclohexane [3006-86-8]	UN2179.	<i>g</i>
1,1-Bis(<i>t</i> -amylperoxy)cyclohexane [15667-10-4]		<i>g</i>
Bis[1-(<i>t</i> -butylperoxy)-1-methylethyl]benzene [25155-25-3] (50)		<i>g, i</i>

TABLE 1. (continued)

Compounds [CAS No.]	Properties ^a	Notes
1,1-Bis(<i>t</i> -butylperoxy)-3,3,5-trimethylcyclohexane [6731-36-8] (51)	UN2146.	<i>f, g</i>
D. 'Ketone peroxides'		
2-Butanone peroxide [1338-23-4] (46 + 47)	EL9450000, UN2550, UN3105 (H: 5.2; R: 7, 11, 22, 23, 34, 41; S: 3/7, 14.2, 17, 26, 36/37/39, 45), O .	<i>e, g, j</i>
2,4-Pentanedione peroxide [37187-22-7] (52)	SA2400000, UN2080, UN3105, UN3106.	<i>e, f, g</i>
Cyclohexanone peroxide [78-18-2] (dimer: 53)	UN2896.	<i>f</i>
E. Peroxides and derivatives		
1. Free acids		
Peracetic acid [79-21-0]	I(1)481C, SH2726B, SD8750000, UN2015, UN3105(H: 5.2; R: 7, 10, 20/21/22, 35; S: 7, 14.2, 36/37/39, 45; P: II), ICSC1031, O, C, N .	<i>b, e</i>
Perpropionic acid [4212-43-5]		<i>f</i>
Decyldipersuccinic acid [87458-73-9] (54, n = 9)		<i>f</i>
Dodecyldipersuccinic acid [87458-70-6] (54, n = 11)		<i>f</i>
Dodecanediperoxoic acid (HO ₃ C(CH ₂) ₁₀ CO ₃ H) [66280-55-5]		<i>f</i>
3-Chloroperbenzoic acid [937-14-4]	I(2)191B, SR(2)1785N, SD9470000, UN2755 (H: 5.2; R: 5, 8, 36/37/38; S: 26, 36).	<i>b, h</i>
Monoperphthalic acid [2311-91-3] (55)		<i>f</i>
2. Esters		
<i>t</i> -Butyl peracetate [107-71-1]	UN2095.	<i>e, g, k</i>
<i>t</i> -Butyl perpivalate [927-07-1]	UN2110.	<i>f</i>
<i>t</i> -Butyl 2-ethylperhexanoate [3006-82-4]	UN2887.	<i>f</i>
<i>t</i> -Amyl 2-ethylperhexanoate [686-31-7]	UN2898.	<i>f</i>
<i>t</i> -Butyl perbenzoate [614-45-9]	I(2)291D, SH644A, SR(2)1899I, SD9450000, UN2097 (H: 5.2; R: 5, 8, 22; S: 23, 24/25, 36/39).	<i>b, g, l</i>
<i>t</i> -Amyl perbenzoate [4511-39-1]		<i>g</i>
<i>t</i> -Butylperoxy isopropyl carbonate [2372-21-6] (56a)	UN2103.	<i>f, g</i>
<i>t</i> -Butylperoxy 3-octyl carbonate [34443-12-4] (56b)		<i>g</i>
<i>t</i> -Amylperoxy 3-octyl carbonate [70833-40-8] (56c)		<i>g</i>
<i>t</i> -Butyl peroxyneodecanoate (<i>neo</i> -C ₉ H ₁₉ CO ₃ Bu- <i>t</i>) [26748-41-4]	UN2177.	<i>f</i>

(continued overleaf)

TABLE 1. (continued)

Compounds [CAS No.]	Properties ^a	Notes
<i>t</i> -Amyl peroxyneodecanoate (<i>neo</i> -C ₉ H ₁₉ CO ₃ Am- <i>t</i>) [68299-16-1]	UN2891.	<i>f</i>
Chlorodifluoromethyl pernitrate (ClCF ₂ OONO ₂) [70490-95-8]		<i>f</i>
3. Diacyl peroxides		
Benzoyl peroxide [94-36-0]	I(2)331B, SH274D, SR(2)1957B, DM8575000, UN2088, UN3102 (H5.2; R: 2, 7, 36, 43; S: 3/7, 14.2, 36/37/39; P: II), ICSC0225, E, Xi .	<i>b, d, f, g, m</i>
Lauroyl peroxide [105-74-8] (57 , <i>n</i> = 10)	N(1)1169A, SH2068A, SR(1)829L, OF2625000, UN2124, UN3106 (H5.2; R: 7; S: 3/7, 14.2, 36/37/39), ICSC0264, O .	<i>f</i>
Succinyl peroxide [123-23-9] (58)	UN2135.	<i>f</i>
Peroxydicarbonic acid bis(2-ethylhexyl) ester [16111-62-9] (59)	UN2123.	<i>f</i>
Chlorodifluoroacetyl peroxyxynitrate [157043-72-6] (60)		<i>f</i>
4. Salt		
Magnesium monoperoxyphthalate [84665-66-7] (61)	SH2475B, SR(2)1865G, UN1479 (H: 5.1; R: 8, 36/37/38; S: 17, 26, 36).	<i>b</i>
F. Miscellaneous inorganic compounds		
1. Metal peroxides		
Lithium peroxide (Li ₂ O ₂) [12031-80-0]	SR(3)3293D, OJ6407500, UN1472 (H: 5.1; R: 8, 14, 34; S: 17, 26, 28.1, 36/37/39, 45), O, C .	
Sodium peroxide (Na ₂ O ₂) [1313-60-6].	WD3450000, UN1404 (H: 5.1; R: 8, 35; S: 8, 27, 39, 45), O, C .	<i>c, n</i>
Magnesium peroxide (MgO ₂) [1335-26-8]	UN1476 (H: 5.1; R: 8, 34; S: 17, 26, 27, 36/37/39, 45).	<i>d</i>
Calcium peroxide (CaO ₂) [1305-79-9]	EW3865000, UN1457, UN3085 (H: 5.1; R: 9, 34; S: 17, 26, 36/37/39, 45), O, C .	
Strontium peroxide (SrO ₂) [1314-18-7]	WL0100000, UN1509, O .	
Barium peroxide (BaO ₂) [1304-29-6]	SR(3)3293F, CR0175000, UN1449 (H: 5.1; R: 8, 20/22; S: 13, 27; P: II), ICSC0381, O, T, Xn .	
Zinc peroxide (ZnO ₂) [1314-22-3]	ZH4865000, UN1518 (H: 5.1; R: 15/29, 28, 32; S: 3/9, 14.3, 30, 36/37, 45), O .	<i>d</i>
2. Superoxide		
Potassium superoxide (KO ₂) [12030-88-5]	SH2909D, SR(3)3293I, TT6053000, UN2466 (H: <i>b</i> 5.1; R: 8, 14, 35; S: 17, 28.1, 36/37/39, 45), O, C .	
3. Salts of peracids		
Sodium perborate (NaOOBO) [10332-33-9, 10486-00-7]	SH3149D, SR(3)3393B, SR(3)3393C, SC7320000, SC7350000, UN1502 (H:5.1; R: 9, 22; S: 13, 22, 27), O, Xn .	<i>b, d</i>
Potassium peroxydiphosphate [15593-49-4] (62)		

TABLE 1. (continued)

Compounds [CAS No.]	Properties ^a	Notes
Ammonium peroxodisulfate [7727-54-0] (63a)	SE0350000, UN1444 (H: 5.1; R: 8, 22, 36/37/38, 42/43; S: 22, 24, 26, 37), O , Xn .	<i>c, g</i>
Sodium peroxodisulfate [7775-27-1] (63b)	I(2)1265B, SH3151C, SR(3)3451A, SE0525000, UN1505 (H: 5.1; R: 8, 22, 36/37/38, 42/43; S: 16, 17, 22, 26, 36/37).	<i>b</i>
Potassium peroxodisulfate [7727-21-1] (63c)	SR(3)3451C, SE0400000, UN1492 (H: 5.1; R: 8, 22, 36/37/38, 42/43; S: 16, 17, 22, 24, 26, 37), O , Xn .	<i>b, c</i>
Potassium monopersulfate triple salt (KHSO ₅ •KHSO ₄ •K ₂ SO ₄) [37222-66-5]	(H: 5.1; R: 8, 34; S: 17, 26, 36/37/39, 45), O , C .	<i>b, f</i>

^a Codes beginning with I and N denote FT-IR spectra in Reference 168 and FT-NMR spectra in Reference 169, respectively. Codes beginning with SH denote data for safety handling in Reference 170, while those beginning with SR are entries on safety regulations in Reference 171. A code of two letters followed by seven digits is a reference to a protocol in RTECS¹⁷² of NIOSH/OSHA. A code starting with UN denotes the UN registration number in the list of dangerous materials. In parentheses appear items discussed in Section X (H: hazard class; R: risk phrases; S: safety phrases; P: packing class). Bold letters denote the distinctive label the packing should carry, as follows: **C**—corrosive, **E**—explosion hazard, **N**—environmental hazard, **O**—oxidant, **T**—toxic, **Xi**—irritant and **Xn**—harmful (see Section X.B).

^b Listed as reagent for organic synthesis in Fieser's series¹⁷³.

^c Analytical reagent.

^d Used in pharmaceutical or personal care preparations¹⁷⁴.

^e Listed in the 49 CFR 172.101 Hazardous Materials Table. Forbidden material for transportation, unless diluted below a stated concentration, sometimes specifically with water, or stabilized by low temperature in an approved manner for the particular compound¹⁷⁵.

^f Compound included in the TSCATS database of EPA¹⁷⁶. Additional organic peroxides in the EPA database not listed in the present table are acetyl peroxide [110-22-5], ethyl peroxide [628-37-5], 1-phenylethyl hydroperoxide [3071-32-7], *t*-amyl hydroperoxide [3425-61-4] and chlorofluoroacetyl peroxide [139702-33-3].

^g Polymerization agent.

^h Epoxidation reagent^{177, 178}.

ⁱ Mixture of isomers.

^j NMAM method 3508 for determination of the vapor of the compound in air¹⁷⁹.

^k Promotes the copper catalyzed acetoxylation of β -lactams at position 4¹⁸⁰.

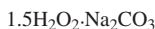
^l Cross-linking agent.

^m NMAM method 5009 for determination of particulates of the compound in air¹⁷⁹.

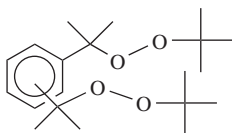
ⁿ Fusion reagent for sample preparation in the analysis of organic and inorganic materials^{181, 182}.



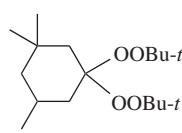
(48)



(49)



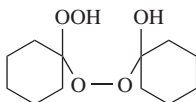
(50)



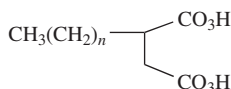
(51)



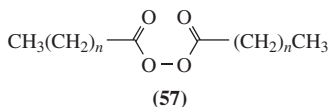
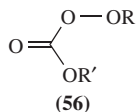
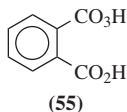
(52)



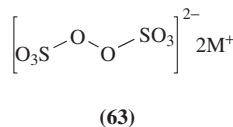
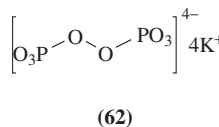
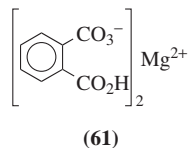
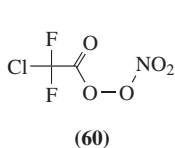
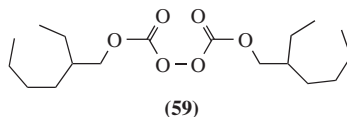
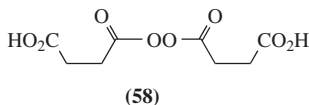
(53)



(54)



- (a) R = *t*-Bu, R' = *i*-Pr
 (b) R = *t*-Bu, R' = CHEtAm-*n*
 (c) R = *t*-Am, R' = CHEtAm-*n*



- (a) M⁺ = NH₄⁺
 (b) M⁺ = Na⁺
 (c) M⁺ = K⁺

country alone—a heavy chemical indeed. This fact entitles cumyl hydroperoxide to be included in the SIDS database¹⁶⁶ of UNEP and EPA for high volume production (HVP) chemicals¹⁶⁷. Other organic peroxides in EPA's HVP list are *t*-butyl hydroperoxide and di-*t*-butyl peroxide.

c. Applications involving polymerization. A review appeared on the methods for evaluating the efficiency of peroxides, hydroperoxides, peroxyesters, diacyl peroxides and peroxy carbonates as polymerization initiating and cross-linking agents¹⁸³. Various criteria were tested and discussed for the efficiency of peroxides and other compounds as initiation or cross-linking agents, such as oxidation of cumene and *n*-decane, effect of inhibitors and model radical polymerizations¹⁸⁴. A most frequent application of organic peroxides is for initiating radical polymerization or cross-linking, as may be observed for the reagents listed in Table 1 carrying notes *g* and *l*. Peroxides are used as cross-linking agents for elastomers¹⁸⁵. Also, ozonides may act as polymerization initiators; of special interest are ozonized polymers acting as macroinitiators and yielding graft polymers¹⁸⁶. An analytical approach to the problem whether a peroxide was used for cross-linking a particular sample of elastomer is based on extraction of fingerprint residues of thermal degradation, followed by chromatographic identification¹⁸⁷. Air sampled in a new car and a newly decorated kitchen showed the presence of peroxides, probably emanating from the plastic materials employed. Among the identified pollutants were *t*-butyl perbenzoate, di-*t*-butyl peroxide and *t*-butyl cumyl peroxide, in the low $\mu\text{g m}^{-3}$ range¹⁸⁸.

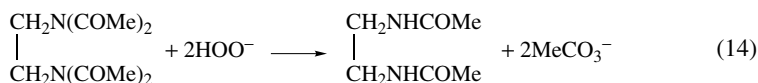
Formation of peroxides by exposure to air and their involvement in polymerization processes is important for surface coating formulations containing polyunsaturated lipids called *drying oils*¹⁸⁹. Also nondrying oils, such as soybean oil, are under development as renewable sources for plastics and resins^{190,191}.

d. Bleaching and disinfection. Peroxides are bleaching agents. Benzoyl peroxide is used for bleaching flour, by oxidation of carotenoid traces left after the milling operation; it slowly disappears as such from the flour as it is converted to benzoic acid^{192,193}.

Hydrogen peroxide is used in the food industry due to its bactericidal action^{67, 194, 195}; it was proposed as the bleaching agent of choice for apple pomace produced in apple juice and cider manufacture¹⁹⁶.

The finishing bleach of pulp for coated paper, by the *alkaline peroxide mechanical pulping process*, using 3.5% NaOH and 3.8% H₂O₂, relative to oven-dry fiber, is energetically economic and produces waste streams that are biodegradable by the conventional activated sludge process¹⁹⁷. Hydrogen peroxide in alkaline solution may cause corrosion of bleaching equipment made of titanium or its alloys¹⁹⁸.

Peracetic acid or its anion, produced *in situ* from *N,N,N',N'*-tetraacetylenediamine, in the presence of hydrogen peroxide, in slightly alkaline solution (equation 14), is an effective bleaching agent used in pulp manufacture and laundering. Household washing solution formulations contain perborate and activators that produce peracetic acid of bleaching effect^{199–203}.



e. Pharmaceutical preparations. Besides the natural products and synthetic compounds of pharmaceutical activity mentioned in Section II.A.2.a and the widespread use of H₂O₂ as disinfectant, several peroxides are of pharmaceutical interest. Benzoyl peroxide is used in formulations against acne and athlete's foot¹⁷⁴. Percarbamide (**48**) and H₂O₂ are used in oral hygiene formulations as teeth whiteners²⁰⁴. Examination by IR and XRD analysis of the effect of **48** on dental enamel lead to the conclusion that formulations containing up to 16% are safe, whereas a 35% formulation affects the enamel²⁰⁵. Occlusion compounds combining **48** and surfactants may find application as preservatives of pharmaceuticals and other technical preparations, due to their wide and balanced spectrum of microbicidal activity²⁰⁶.

f. Etching. Peroxodisulfate (S₂O₈²⁻, **63**) and H₂O₂ are part of modern etching and pickling bath formulations, especially for copper and its alloys²⁰⁷. This operation is used in the electronic industry^{208, 209}.

g. Autoxidation. As opposed to the desirable effects in the coating industry, thermal autoxidation may cause deterioration in other industrial processes. Besides their role as chemical intermediates, peroxides are universally involved in the deterioration of chemicals, organic materials, foodstuffs and other industrial products via autoxidation processes. Excessive oxidation leads to oil degradation during deep fat frying²¹⁰ or a stale taste of beer²¹¹. The mechanism of autoxidation of lipids, an important cause for food deterioration, is shown in Scheme 1 (Section II.A.2.c). The peroxide value and other indices (Section IV) are important in the assessment of exposure of lipids and other organic materials to the effects of autoxidation in industry; various standard procedures have been developed for determination of the extent of this avenue of product quality degradation^{212, 213}.

Autoxidation of polymers involves free radicals and hydroperoxides are the primary decay products²¹⁴. Low-density polyethylene (LDPE) and linear low-density polyethylene (LLDPE) undergo slight thermal oxidation in air (up to 2% oxygen uptake) to yield products bearing various functional groups: keto, *s*- and *t*-alcohols, carboxylic acids, *s*-hydroperoxides and others of lesser abundance. The distribution of these groups is different for the two types of polyethylene. Thus, only LDPE forms peroxides and the *s*-alcohol is the main oxidized functional group, while keto and carboxylic acid groups are preponderant in LLDPE. This is attributed to different branching distributions in these polymers²¹⁵.

Addition of catalytic amounts of a suspension of ZnO in *t*-butyl hydroperoxide to diesel fuel improves the engine performance by increasing the mileage by about 20% and decreasing particle emission by about 50%^{216,217}.

B. Remarks on Modern Analytical Methods

Methods for avoiding analytical interference by peroxides in the analysis of oxygen-containing compounds have been reviewed²¹⁸. Various problems of analytical development are mentioned elsewhere in *The Chemistry of Functional Groups* series²¹⁹. Application of a chemometric approach to the development of analytical methods may largely increase the experimental efficiency. This is important when trying to identify significant variables in complex situations, such as those arising in environmental, biomedical, technological, forensic and other application fields. The bibliography mentioned in this section usually refers to application examples and not to the underlying theory. Thus, for example, a *central composite design* procedure was chosen instead of the *univariate* approach for the optimization of a fluorometric determination method of hydrogen peroxide and organic peroxides in a FIA system, mainly because the former experimental design allows for identification of interaction between variables²²⁰. *Multivariate analysis* and *principal component analysis* of data were used to find correlation between exposure to environmental ozone and the appearance of hydroperoxide signals in a relevant FTIR region⁹⁹ and for ascertaining the determining factors to be measured when following hydroperoxide decomposition of edible oils²²¹. The SIMPLISMA program for multivariate analysis^{222–226} allows resolving complex spectral patterns in the absence of reference spectra and displays intermediate stages of calculation for interactive purposes; it was applied for tracking the kinetics of a reaction involving an unstable peroxide intermediate by FT-Raman spectroscopy, instead of performing tedious chemical analyses²²⁷. Also, *factorial design*^{228,229} was applied in development of analytical methods for peroxides. In one case, screening of critical factors was obtained by a two-level *half-fractional factorial design*, followed by optimization of these variables with a multi-level *central composite design*¹³⁴. Calculation methods such as *multiple linear* (MLR)²³⁰, *forward stepwise multiple linear*²³¹ or *partial least squares* (PLS) regressions^{210,230–236} are frequently used for finding useful analytical correlations. *Back trajectory* and *cluster analysis* were applied in the search of correlations between concentrations of O₃, CO and other pollutants in the lower atmosphere of the Hong Kong area²³⁷. The PRESS technique was used for building reference curves for NIR spectrophotometric determinations with the aid of an independent calibration set²³⁴. *Correlation* and *variance spectra* are used to find the spectral regions where most of the spectral changes take place in calibration sets^{234,235}. The *method of standard addition* (MOA) is often used in validation procedures or with complex matrices^{238,239}.

An important consideration for quality control in industry and commerce relates to the trend of developing faster analytical methods than those described in official standards; the question in such cases is whether a proposed method is acceptable as replacement for the standard. This problem relates to the concepts *fitness for purpose*²⁴⁰ and *measurement uncertainty*²⁴¹, the latter serving for the estimation of the LOD and LOQ parameters of analytical quality²⁴². An example of this dilemma relating to the peroxide value is discussed in Section IV.B.5.

C. Scope of the Chapter

The official methods for determination of peroxides are far from sufficient to cover the needs in the wide range of fields mentioned above. This chapter strives to present a variety of approaches and methods even if sometimes they lack utmost analytical quality,

because often the basic idea involved in a method may inspire a good solution to a difficult analytical problem.

Section III is dedicated to hydrogen peroxide. Although in the traditional sense this compound belongs to the inorganic chemistry realm, it appears here as the model peroxide from which others may be derived on replacing one or both hydrogen atoms with organic moieties. Furthermore, many of the analytical methods for H_2O_2 may apply to other peroxides as such or after slight modification.

Section IV deals with indices for deterioration by the oxidation process. The most important of such indices, the peroxide value (POV) could have been included in Section V dealing with hydroperoxides (ROOH). However, POV is kept separate from hydroperoxides and together with other oxidation indices, as global measures of technological significance. Sections VI to IX are dedicated to diverse functional groups containing the $-\text{OO}-$ moiety, such as dialkyl peroxides, peracids and their functional derivatives, the ozonides and a series of minor organic and inorganic peroxide classes. In Sections IV to IX problems related to detection, determination and structural characterization of these compounds are discussed.

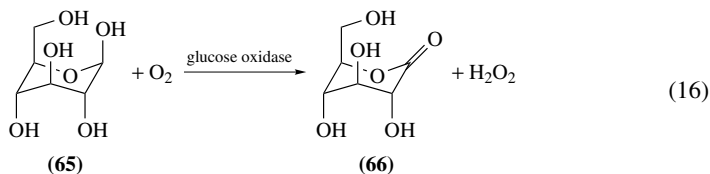
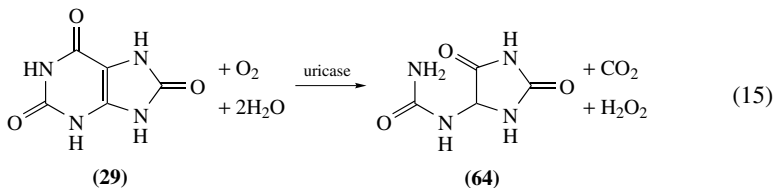
The chapter ends with Section X on safety, dealing with the regulations and recommendations of national and international agencies when handling the type of hazardous chemicals discussed in this volume.

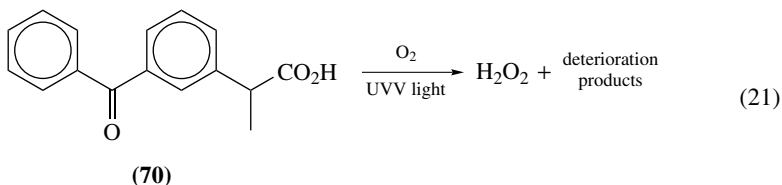
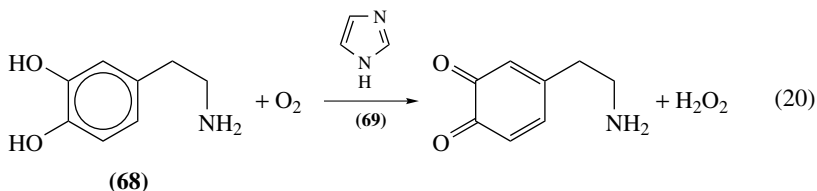
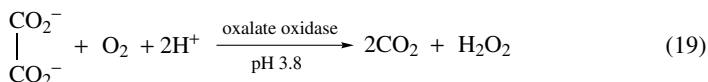
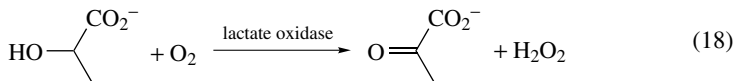
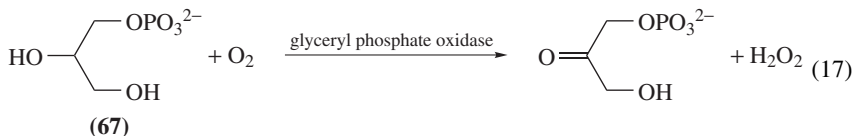
Limits of detection (LOD) and quantitation (LOQ) are reported as published in the literature, either in intensive or extensive units, with no attempt to unify the style. Citation of virtual literature is made to some extent throughout the chapter, and most frequently in Section X. It is hoped that such sources will survive the test of time, especially those originated in official and international organizations.

III. HYDROGEN PEROXIDE

A. General

Some enzymatic and autoxidation processes involve oxygen consumption with concurrent formation of H_2O_2 . Determination of this byproduct is the basis for indirect determination of analytes of clinical significance or for assessment of deterioration of certain compounds. The following are examples of such processes: Enzyme-catalyzed oxidation of uric acid (**29**) to allantoin (**64**, equation 15), D-glucose (**65**) to δ -D-gluconolactone (**66**, equation 16), 1-glycerol phosphate (**67**) to 3-hydroxy-2-oxo-1-propyl phosphate (equation 17), lactate to pyruvate (equation 18), oxalate to CO_2 (equation 19), autoxidation of catecholamines, such as dopamine (**68**) to the corresponding *o*-quinone (equation 20), catalyzed by a base, (**69**), and photochemical deterioration of ketoprofen (**70**, equation 21).



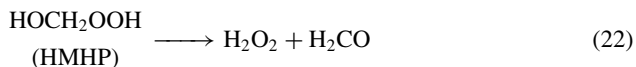


The analytical problems posed by hydrogen peroxide are varied; as a heavy chemical the main question is one of process and quality control; it is also a trace constituent of the atmosphere and environmental waters in all states of aggregation, participating in natural and anthropogenic pollution; and finally, it is present in living organisms, as part of autoxidation, metabolic and pathological processes. Many of the analytical methods for hydrogen peroxide may be applied with slight or no variation to organic peroxides.

B. Detection and Determination

The following reviews are relevant: The main trends in the analytical methods for H_2O_2 ²⁴³; participation of hydrogen peroxide in environmental phenomena and the analytical methods used in this field¹; analytical methods for H_2O_2 related to the vascular system, with special attention given to assays using HRP coupled with fluorogenic or chromogenic reducing substrates, or fluorescence quenching; assays using catalase coupled with various processes; assays involving the Fe(III)-thiocyanate and assays involving dichlorofluorescein⁸³; a critical discussion of various methods for determination of H_2O_2 and organic hydroperoxides, in relation to the chemistry of ozonolysis in aqueous media²⁴⁴.

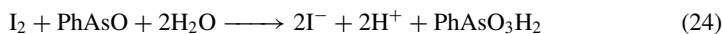
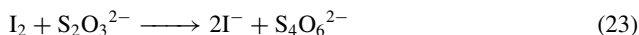
Accurate determination of H_2O_2 in the air is complicated by the presence of organic hydroperoxides; for example, HMHP may undergo a relatively fast decomposition according to equation 22 if the working solution is neutral or alkaline¹³.



It is recommended that all glassware used in sampling and determination of H_2O_2 be passivated by soaking in 35% w/w H_2SO_4 solution, for at least 1 h, followed by rinsing with distilled water and drying. Soiled glassware should be soaked in 10% NaOH solution for 1 h and rinsed with distilled water before passivation²⁴⁵.

1. Titration methods

The Kingzett method for determination of aqueous H_2O_2 consists of reduction with excess I^- in acid solution and titration of the liberated I_2 with standard thiosulfate solution, leading to the formation of tetrathionate (equation 23)²⁴⁶. This venerable method, reported in 1880, is not without complications. Thus, at pH below 2 oxygen of the air oxidizes I^- causing interference. To avoid this, the reaction may be carried out at pH 4; however, it then slows down, requiring the presence of a catalyst such as ammonium molybdate $[(\text{NH}_4)_6\text{Mo}_7\text{O}_{24}]$ ²⁴⁷. Furthermore, as I_2 may react with organic substrates present in natural waters, addition of phenylarsine oxide to the sample will scavenge the I_2 as it is generated²⁴⁸, according to equation 24, and the excess phenylarsine oxide can be titrated with standard I_2 solution to an amperometric endpoint. Good correspondence is observed between the iodometric results using the back titration according to equation 24 and the fluorometric determination using scopoletin (**119**, Section III.2.b), at H_2O_2 concentrations up to $0.5 \mu\text{M}$ in natural waters²⁴⁹. A sample of H_2O_2 diluted with 1:1 H_2SO_4 can be titrated with standard KMnO_4 solution until a pink color persists for 30 s²⁴⁵.

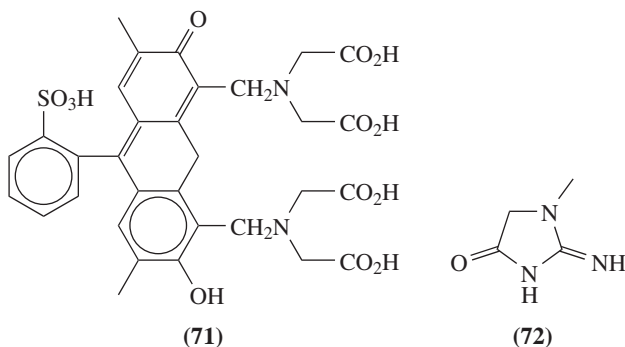


2. Ultraviolet-visible spectrophotometry and colorimetry

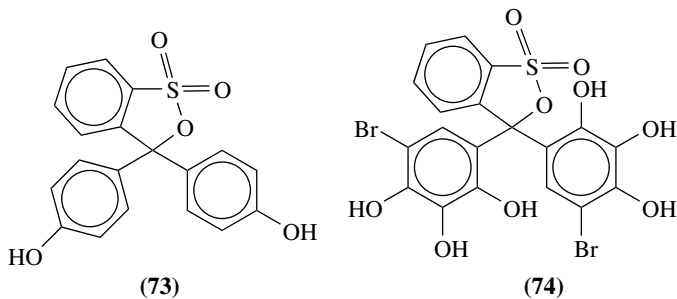
a. Absorption spectrophotometry. H_2O_2 is reduced by excess I^- ions in acidic media to yield I_3^- ions, that can be determined spectrophotometrically ($\lambda_{\text{max}} = 290 \text{ nm}$, $\epsilon = 4.7 \times 10^4 \text{ M}^{-1} \text{ cm}^{-1}$). Exposure to atmospheric oxygen should be avoided by working under N_2 blanketing²⁵⁰. In very dynamic systems, where H_2O_2 may be consumed by other components, the reaction with iodide is considered to be slow; therefore, catalysis with molybdate ions is recommended²⁴⁴. Molybdic acid ($\text{H}_6\text{Mo}_7\text{O}_{24}$) in solution forms a complex with H_2O_2 ($\lambda_{\text{max}} = 330 \text{ nm}$) that may be used for direct determination of the peroxide. To avoid the interference by excess molybdate, measurement should be carried out slightly off the maximum, at 350 nm. The method is linear to about 0.2 mM. It has been applied for determination of H_2O_2 in pulp bleaching liquors. To assist eliminating the interference of lignin, a measurement is also taken at 297 nm where the net analytical system has an isosbestic point²⁵¹. A method was developed for the simultaneous determination of H_2O_2 and hydroperoxides in water, based on kinetic measurements of the reduction with a large excess of I^- in the presence of molybdate, measuring the I_3^- ions at 352 nm ($\epsilon = 26400 \text{ M}^{-1} \text{ cm}^{-1}$). The catalyst accelerates the rate of reduction of H_2O_2 more than 400-fold and of the organic hydroperoxides only about 2- to 3-fold, making the rates of reaction quite distinct at room temperature. It was established that a total peroxide determination by this method proceeds in about 30 min at 60°C , with no thermal decomposition of the peroxides. The LOD is about $5 \mu\text{M}$ of peroxides (see also Section V.B.2.a)²⁵². Oxidation of I^- can be applied to RP-HPLC using dilute aqueous H_3PO_4 as mobile phase, for post-column derivatization in a FIA system, heating to 90°C , and measuring by UVD at 348 nm. These conditions apply for both H_2O_2 and hydroperoxides. LOD for H_2O_2 and MHP are 35 and 50 ppb, respectively²⁵³.

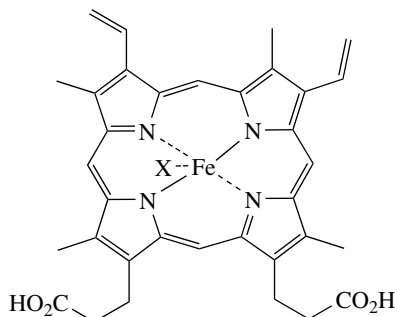
A colorimetric method for determination of H_2O_2 in concentrations down to 1 ppm is based on the intense discoloration of the complex formed on oxidation of Fe(II) to Fe(III) in acid solution, in the presence of thiocyanate ions (SCN^-). The color intensity is compared to that of a calibration curve²⁵⁴. $[\text{Co(II)}\cdot\text{EDTA}]^{2-}$ complex ions undergo oxidation by H_2O_2 to Co(III) that forms colored complexes which can be measured spectrophotometrically near 500 nm, depending on the pH of the solution. At pH *ca* 3 the measured species is the pink complex $[\text{H}\cdot\text{Co(III)}\cdot\text{EDTA}]\cdot\text{H}_2\text{O}$, whereas at pH *ca* 10 $[\text{HO}\cdot\text{Co(III)}\cdot\text{EDTA}]^{2-}$ is the blue species. The method was applied for monitoring H_2O_2 and other oxidants in processes involving lignin and model compounds²⁵⁵.

Various phthalein dyes have been proposed for detection and determination of H_2O_2 , with different operating principles, such as direct measurement of the dye and complex formation. The FOX assay is based on the oxidation of Fe(II) to Fe(III), followed by complex formation of the latter ion with Xylenol Orange (**71**). The concentration of the complex is measured at $\lambda_{\text{max}} = 560 \text{ nm}$ ($\epsilon = 4.3 \times 10^4 \text{ M}^{-1} \text{ cm}^{-1}$)^{256,257}. The linearity of the method holds up to about $30 \mu\text{M}$ ⁴⁵⁸. The FOX assay was applied to detect changes in the H_2O_2 concentration in urine after drinking instant coffee. As liquid ingestion causes urine dilution, the creatinine (**72**) content of urine was taken as reference for the dilution factor⁷⁴. A critical comparison was made for various methods including the FOX assay for the determination of H_2O_2 in urine²⁵⁸.



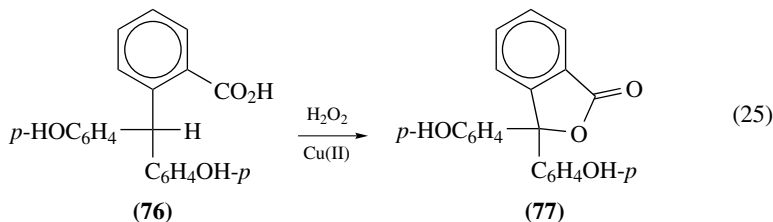
HRP-catalyzed oxidation of Phenol Red (**73**) can be used to track the rate of H_2O_2 production in fungi cultures in liquid nutrient media, measuring the intensity of the developed color at 610 nm. Attention is to be paid to changes of pH induced by the fungi that affect the color of the dye⁶⁸. The Phenol Red assay was used for determination of H_2O_2 produced on free radical generation by UV or γ -irradiation of amino acid solutions¹⁴⁴. Bromopyrogallol Red (**74**) is oxidized by H_2O_2 , catalyzed by hemin (**75a**) as HRP mimic,



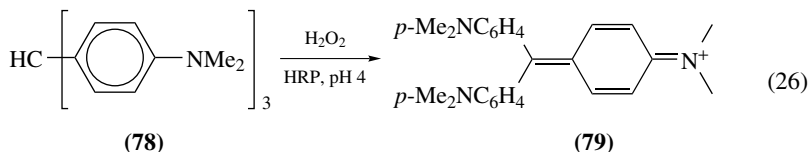


- (75) (a) X = Cl
 (b) X = OH
 (c) no X

in ammonia-ammonium chloride buffer at pH 9.3, measuring the absorbance of the developed dye at 565 nm ($\epsilon = 4.00 \times 10^4 \text{ M}^{-1} \text{ cm}^{-1}$). It should be pointed out that under these conditions no oxidation of hemin takes place. The effect of certain interfering ions, such as Pb(II), Co(II), Cr(III), Al(III), Cu(II), Fe(III), Ag(I), Zn(II), Ni(II), Cd(II), Ba(II), Ca(II) and Mg(II), was investigated; they can be masked by EDTA. The linearity range of the method is 0.32 to 32 μM . The method was applied for water and human serum analysis²⁵⁹. An attempt to use the oxidation of phenolphthalin (76) to phenolphthalein (77), as shown in equation 25, as the basis of a spectrophotometric method for determination of H_2O_2 was discarded due to various technical problems²⁶⁰.

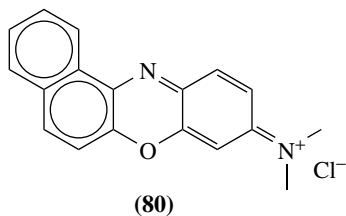


The concentration of H_2O_2 in seawater may be measured following the HRP-catalyzed conversion from Leuco Crystal Violet (78, $\lambda_{\text{max}} = 260 \text{ nm}$) to the colored form (79, $\lambda_{\text{max}} = 592 \text{ nm}$, $\epsilon = 1 \times 10^5 \text{ M}^{-1} \text{ cm}^{-1}$), at pH 4, according to equation 26. LOD is *ca* 0.02 μM , with RSD *ca* 1% at 0.03 μM ^{261, 262}. Equation 26 can be used as the basis for a kinetic method for the simultaneous determination of H_2O_2 and relatively unreactive species, such as *t*-butyl and cumyl hydroperoxides, however, not in the presence of MHP or ethyl hydroperoxide (see also Section V.B.2.a)²⁵².

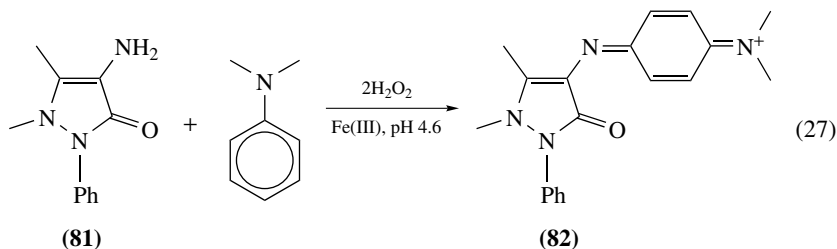


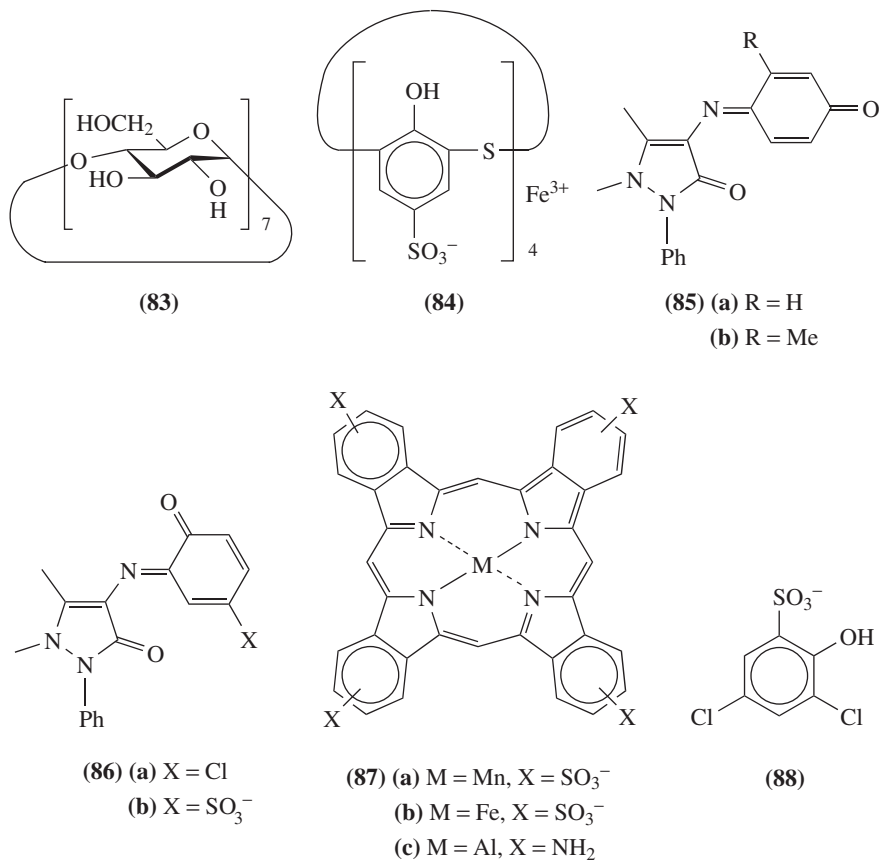
An optode based on Meldola Blue immobilized in tetramethyl orthosilicate gel can be used to evaluate the concentration of H_2O_2 in the pH range from 5 to 12, in the dynamic

range from 10 nM to 0.1 M. The absorbance of the oxidized form (**80**) is measured at 720 nm with a fiber optics spectrophotometer. The reduced form can be restored with a solution of sodium metabisulfite ($\text{Na}_2\text{S}_2\text{O}_5$). No interference by persulfate, urea, tartrate or phosphate can be observed; however, perborate, glucose and oxalate interfere²⁶³.



Many methods are based on the oxidative coupling of 4-aminoantipyrine (**81**) with a phenol or an aromatic amine to yield quinoneimine dyes. A fast kinetic method for determination of H_2O_2 is based on equation 27 in a FIA system, where **81** and *N,N*-dimethylaniline become oxidized, in the presence of Fe(III) ions to catalyze the process, in acetate buffer at pH 4.6. The rate of dye (**82**) formation is measured at 560 nm. LOD is $0.5 \mu\text{M}$ (SNR 2), with linearity in the 1.0 to $600 \mu\text{M}$ range; SRD is 0.8% at $50 \mu\text{M}$ ($n = 30$). Negative interference occurs in the presence of $10 \mu\text{M}$ of Cu(II) , Mo(VI) , Ti(IV) , W(VI) , phosphate and citrate, but 200 g L^{-1} of albumin does not interfere. The sample throughput is 15 h^{-1} . After modification, the method can be applied for determination of uric acid (**19**) and glucose (**65**), following application of reactions 15 and 16, respectively²⁶⁴. A mimic for HRP catalysis of equation 27 is β -CD-hemin, a condensation product between hemin (**75a**) and β -cyclodextrin (**83**), where the carboxy groups of **75a** become esterified by hydroxy groups of **83**. The method is linear up to $86 \mu\text{M}$ ²⁶⁵. A process analogous to equation 27, using phenol instead of dimethylaniline and a thiacalixarene complex of Fe(III) (**84**) immobilized on an anion-exchange resin, in borate buffer at pH 10, leads to the formation of a quinoneimine dye (**85a**), which is measured at 505 nm. The method is linear from 10 to 100 mg L^{-1} ²⁶⁶; the peroxidase-catalyzed color development with phenol was applied for glucose (**65**, equation 16) determination in damaged starch²⁶⁷. Another variant of equation 27 uses *p*-chlorophenol leading to formation of **86a**, when catalyzed by manganese-tetrasulfonatophthalocyanine (**87a**)²⁶⁸, or 3-methylphenol yielding **85b**, with peroxidase catalysis²⁶⁹. The HRP-catalyzed modification of equation 27, using 3,5-dichloro-2-hydroxyphenylsulfonic acid (**88**, Trinder's reagent²⁷⁰) as reductor, is frequently used; for example, this reagent served for determination of 1-glycerol phosphate (**67**) in deproteinized human serum, by measuring the H_2O_2 obtained according to equation 17²⁷¹. In Table 2 are listed commercial kits for determination of H_2O_2 and various analytes mentioned in Section III.A; some of these kits apply color development similar to that in equation 27.





Various ready-to-use reagent solutions and dipping sticks are commercially available for fast determination of H₂O₂, by spectrophotometric measurement or comparison of the developed color with a provided scale. A fast determination of nanomolar concentrations of H₂O₂ consists of the HRP-catalyzed oxidation of *N,N,N',N'*-tetramethyl-*p*-phenylenediamine (**89**) to a colored substance that is determined at 450 nm. The method was applied to measure oxidation level in plasma of persons that underwent trauma and other conditions²⁹³. Commercial kits based on this process are described in Table 2. Variamine Blue (**99**) undergoes oxidation by H₂O₂ to a violet color that can be measured at 550 nm ($\epsilon = 1.8 \times 10^4 \text{ cm}^{-1} \text{ M}^{-1}$). The reaction is catalyzed by HRP immobilized on silica gel by a sol-gel process, using phosphate buffer at pH 6. The reagent solution should be exposed as little as possible to air, as it undergoes slow oxidation. It is important to make the measurement at a fixed time after the sample is mixed with the catalyst, say 10 min, as the color develops fast to a maximum and then decays to colorlessness. In the presence of GOX the method can be applied for determination of glucose (**65**), according to equation 16. The method was applied to determination of glucose in plasma, with good correspondence with an established diagnostic method, based on the peroxidase-catalyzed oxidation of 4-aminoantipyrine with H₂O₂ in the presence of *p*-phenolsulfonic acid, leading to formation of dye **86b**²⁹⁴. The presence of lactoperoxidase activity in

TABLE 2. Commercial kits for determination of peroxides and oxidation indices^a

Trade name	Operating principle	Notes
Nanocolor Peroxid 2	Peroxidase-catalyzed oxidation of <i>N,N,N',N'</i> -tetramethyl- <i>p</i> -phenylenediamine (89) and measurement of the color at 620 nm. Fixed portions of two reagent solutions are added to a sample aliquot ²⁷² .	<i>b</i>
Quantofix Peroxid	Peroxidase-catalyzed oxidation of <i>N,N,N',N'</i> -tetramethyl- <i>p</i> -phenylenediamine (89); best at pH 5–7. The reagents are pasted at the tip of a stick that is dipped into the test sample and after 15 s the developed color is compared with a printed scale ²⁷² .	<i>c</i>
K-Assay–H ₂ O ₂ Assay	CL determination, concentration range from 2.44 to 2500 μg L ⁻¹ in buffer and from 39.06 to 10.000 μg L ⁻¹ in tissue culture medium ²⁷³ .	<i>d</i>
Reflectoquant	A test strip containing peroxidase with an undisclosed redox indicator turns to a yellow-brown product in the presence of H ₂ O ₂ , at pH 2–7. The color intensity is measured with a remission photometer ²⁷⁴ .	
Merckoquant	Test strip containing peroxidase with an undisclosed redox indicator turns to a yellow-brown product in the presence of H ₂ O ₂ that is compared with a printed scale ²⁷⁴ .	
Spectroquant	Titanyl sulfate reacts with H ₂ O ₂ (equation 28) to give a discoloration that is measured photometrically or spectrophotometrically ²⁷⁴ .	
Bioxytech H ₂ O ₂ -560	Spectrophotometric determination of H ₂ O ₂ without interference of peroxidation, based on the FOX assay ²⁷⁵ .	
Bioxytech LPO-560	Colorimetric determination of lipid hydroperoxides based on the FOX assay ²⁷⁶ .	
K-Assay LPO-CC	Oxidation by lipid hydroperoxides of a derivative of the leuco form of Methylene Blue (90) to the colored form (91), catalyzed by hemoglobin, according to equation 29; measurement is at 675 nm ²³⁶ .	<i>e</i>
SafTest System	A set of kits for colorimetric determination of various oxidation indices (POV, ACV, MDA, HNE) with undisclosed reagents ²⁷⁷ .	
Uric acid (29) kits	Commercial kits are based on the enzymatic process shown in equation 15, followed by a chromogenic oxidation process catalyzed by peroxidase, similar to equation 27, involving 4-aminoantipyrin (81) and 3,5-dichloro-2-hydroxybenzenesulfonate (88), measuring at 500 to 520 nm ^{278–281} .	
Glucose (65) kits	Commercial kits are based on the enzymatic process shown in equation 16, followed by a chromogenic oxidation process catalyzed by peroxidase, similar to equation 27, involving 4-aminoantipyrine (81) and a phenol or aniline derivative, leading to a quinoneimine dye. Among the latter aromatic substrates in use are: <i>N</i> -ethyl- <i>N</i> -(2-hydroxy-3-sulfopropyl)-3,5-dimethoxyaniline (92) ²⁸² , phenol ²⁸³ , <i>p</i> -hydroxybenzoic acid ^{284, 285} and <i>p</i> -hydroxybenzenesulfonate ²⁸⁶ ; other chromogenic reactions are peroxidase-catalyzed oxidation of <i>N,N,N',N'</i> -tetramethyl- <i>p</i> -phenylenediamine (89) ²⁸⁶ and <i>o</i> -ditoluidine (93) ²⁸⁷ .	<i>d</i>
Lactate kits	Commercial kits are based on the enzymatic process shown in equation 18, followed by an undisclosed chromogenic oxidation process catalyzed by peroxidase, measuring at 540 nm ²⁸⁸ .	

TABLE 2. (continued)

Trade name	Operating principle	Notes
Triglyceride kits	Commercial kits are based on the lipase-catalyzed total hydrolysis of the triglyceride, followed by glycerol kinase-catalyzed synthesis of 1-glycerol phosphate (67) and GPO-catalyzed oxidation of the latter, as shown in equation 17. The end analysis is by a chromogenic oxidation process catalyzed by peroxidase, similar to equation 27, involving 4-aminoantipyrene (81) and 3,5-dichloro-2-hydroxybenzenesulfonate (88) ²⁸⁹ or <i>N</i> -ethyl- <i>N</i> -(3-sulfopropyl)- <i>m</i> -anisidine (94) ^{289,290} .	
Oxalate kits	Commercial kits are based on the enzymatic process shown in equation 19, followed by a chromogenic oxidation process catalyzed by peroxidase, where 3-methylbenzothiazolinone hydrazone (95) and 3-(dimethylamino)benzoic acid form an indamine dye measured at 590 nm ²⁹¹ .	
Bioxytech MDA-586 K-Assay–Oxidative DNA Damage (qualitative)	Spectrophotometric assay for MDA by the TBARS method ²⁹² . Immunoassay kit, where the antibodies of 8-oxoguanine (96) are conjugated with fluorescein isothiocyanate (97) as fluorophore and combine with the oxidized DNA. Detection of the greenish fluorescence is by fluorescence microscopy for tissues or by fluorescence-activated cell sorting for cell suspensions ²³⁶ .	<i>e</i>
K-Assay–Oxidative DNA Damage (quantitative)	Introduction of biotin markers at abasic aldehyde sites in DNA, resulting from oxidative damage (equation 59, Section IV.D.3), by condensation with <i>N</i> '-aminoxymethylcarbonylhydrazino-D-biotin (98), followed by the avidin-biotin-HRP reaction and UVD ²³⁶ .	
K-Assay Oxidized Low-Density Lipoprotein	Indirect immunoassay by determination in human serum of autoantibodies to oxidized LDL ²³⁶ .	<i>e</i>

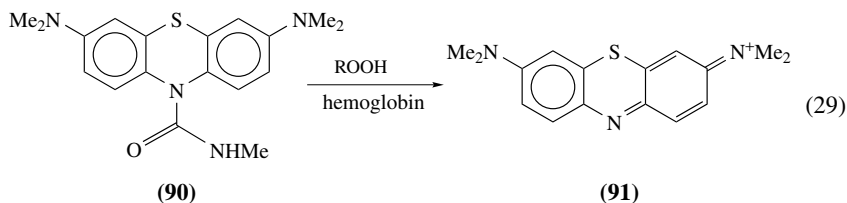
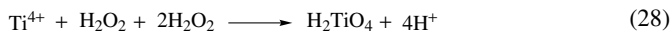
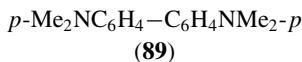
^a The selection of products is random and no specific recommendations are intended. In some cases the manufacturers were kind enough to provide additional data on request.

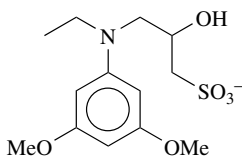
^b May be used for seawater. Strong oxidizing agents interfere. No interference by the following components: up to 100 ppb of CN⁻; up to 10 ppm of Cr(VI), Fe(III), Hg(II) or cationic surfactants; up to 100 ppm of Cu(II), Ni(II), Si, NO₂⁻, PO₄³⁻, SO₄²⁻ or SCN⁻; up to 1000 ppm of NH₄⁺, Ca(II), Cd(II), Mn(II), EDTA, B₂O₇²⁻ or Cl⁻.

^c Various organic hydroperoxides may be determined after wetting the reactive tip with water.

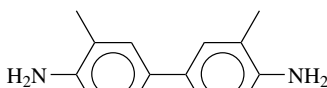
^d Specific determination of D-glucose (65) in plant extracts requires high purity GOX, devoid of β-glucosidase, to avoid interference by hydrolysis of oligo- and polysaccharides that may lead to glucose formation and produce H₂O₂ on autoxidation²⁸⁴.

^e Further details on the method are found in the Kamiya web site²⁷³.

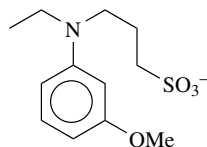




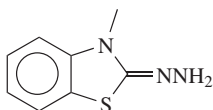
(92)



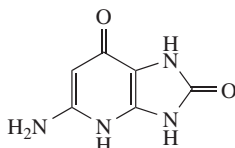
(93)



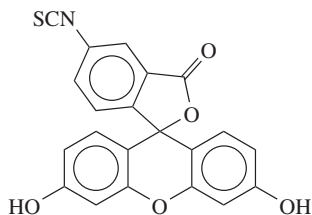
(94)



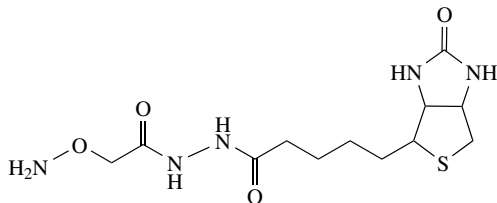
(95)



(96)



(97)



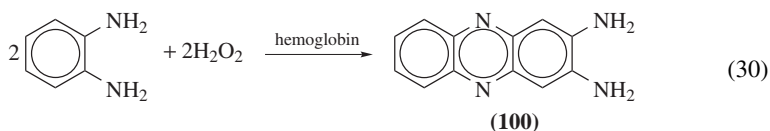
(98)

pasteurized milk is a sign that the pasteurization process was not overdone. A standard method for testing this activity consists of spiking the milk with H_2O_2 and adding *p*-phenylenediamine, which undergoes enzyme-catalyzed oxidation to a purple dye (the Starch test). It was proposed to test the presence of the enzyme, by following the disappearance of H_2O_2 for 1 h after spiking, using testing sticks instead of the potentially dangerous organic reagent⁸⁹.



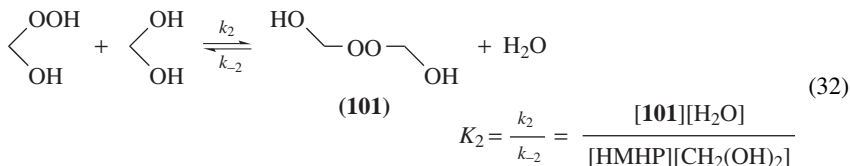
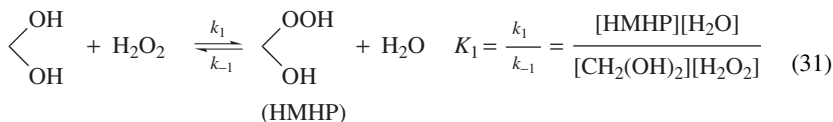
(99)

The hemoglobin-catalyzed oxidation of *o*-phenylenediamine to 2,3-diaminophenazine (**100**), in phosphate-citric acid buffer at pH 5.0, shown in equation 30, is the basis for a kinetic method for determination of H_2O_2 , in a FIA system, measuring at 425 nm by the stopped-flow method. The LOD is 9.2 nM, with RSD 2.08% at 0.5 μM and linearity in the 50 to 3500 nM range²⁹⁵. This colorimetric method was proposed for development as a standard procedure in the Republic of China for determination of H_2O_2 in foodstuffs¹⁹⁵.

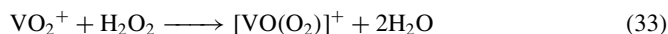


3-Methylbenzothiazolinone hydrazone (**95**) and 3-(dimethylamino)benzoic acid undergo oxidative coupling by H_2O_2 , in the presence of peroxidase, to form an indamine dye ($\lambda_{\text{max}} = 590 \text{ nm}$, $\varepsilon = 47600 \text{ cm}^{-1} \text{ M}^{-1}$). The assay can be applied in the 2 to 20 μM range. This reaction was applied for determination of glucose after oxidation according to equation 16²⁹⁶. Commercial kits (Table 2) for oxalate determination are based on the enzymatic process shown in equation 19, followed by the same chromogenic oxidation process.

Ti(IV) solutions afford titanium peroxyacid in aqueous solution, according to equation 28. The product contains the O–O peroxy moiety which is formed immediately and obeys Beer's law. The concentration can be measured spectrophotometrically at 380 to 430 nm²⁵⁴. A solution of TiCl_4 in aqueous sulfuric acid rapidly forms a 1:1 yellow complex with H_2O_2 , which is measured spectrophotometrically ($\lambda_{\text{max}} = 407 \text{ nm}$, $\varepsilon = 762 \text{ M}^{-1} \text{ cm}^{-1}$). This property can be applied in the design of air samplers for the determination of H_2O_2 vapor in the workplace, by absorption of the analyte on passing an air sample over glass fibers impregnated with a complexing solution. The effect of air pollutants such as AcOOH , NO , NO_2 and SO_2 on the analysis of H_2O_2 was investigated. Of special significance is peracetic acid in places where it is employed, as it hydrolyzes in the aqueous acid reagent, yielding H_2O_2 . Methods for diminishing this possible interference are discussed⁹. Equation 28 was applied to investigate the chemical equilibria of formation of HMHP and bis(hydroxymethyl peroxide (**101**), by reaction of H_2O_2 with hydrated formaldehyde, as depicted in equations 31 and 32. The determination of the various peroxides involved is based on UVV and NMR measurements of the immediate reaction of H_2O_2 with Ti^{4+} , and the different rates of hydrolysis of HMHP and **101** to yield H_2O_2 ²⁹⁷.

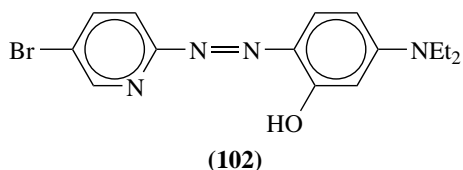


A robust method is based on vanadyl ion forming a colored adduct with H_2O_2 , vanadyl peroxide (equation 33), which can be measured at 520 nm. Although this wavelength is not that of the maximum absorbance of vanadyl peroxide ($\lambda_{\text{max}} = 450 \text{ nm}$), the absorbance is significant and avoids the interference of uranyl nitrate. The method was applied for determining H_2O_2 in solutions of uranyl nitrate. If these solutions were in contact with an organic solvent, e.g. tributyl phosphate-kerosene, the entrained solvent has to be separated by SPE, which also removes Pu(VI). The LOD is 26 μM , with RSD 19.5% at 50 μM and 1.4% at 5 mM²⁹⁸.

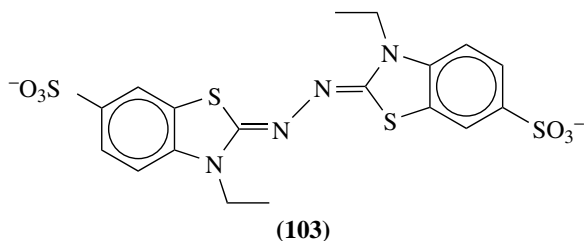


Various metallic ions, for example Ti(IV), V(V), Zr(IV), Nb(V), Mo(VI), Hf(IV), Ta(V), W(VI) and U(VI), form colored triple complexes with H_2O_2 and a dye such as 2-(5-bromo-2-pyridylazo)-5-diethylaminophenol (**102**) as chromogenic agent. These complexes are

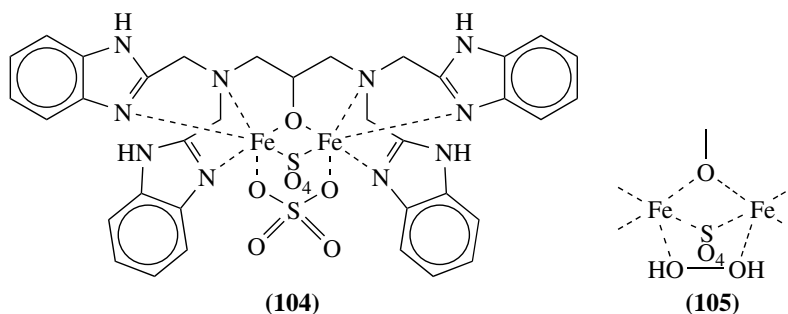
sufficiently stable to undergo RP-HPLC separation from other component in the matrix, however the V(V) complex is the most sensitive. The following numbers of merit are found, respectively, for the complex [Ti(IV)•H₂O₂•**102**] in a Zorbax SB ODS column and [V(V)•H₂O₂•**102**] in a Nucleosil C18 e.c. column: LOD (SNR 3) 0.15 and 0.02 μM, linearity range 0.15 to 5.00 and 0.02 to 5.00 μM. On application of the method with V(V) to environmental and clinical samples, the MOSA technique is preferred over a calibration curve, because it eliminates some of the matrix interferences. This method was applied for determination of the seasonal variation of H₂O₂ in rainwater, formation of H₂O₂ in water during ultrasonic treatment, formation of H₂O₂ on the surface of plant leaves subjected to stress ($7.0 \pm 1.0 \text{ nmol cm}^{-2}$ was detected) and glucose (**65**) in human serum after treatment with GOX (equation 16)²⁴³.



The presence of H₂O₂ can be determined by HRP-catalyzed oxidation of 2,2'-azinobis(3-ethylbenzothiazoline)-6-sulfonate (ABTS, **103**) in acetate buffer at pH 5.5, and measuring at 412 nm the absorbance of the free radical produced. See, however, Section VI.B.2 for selective oxidation of peroxy acids in the presence of H₂O₂. The method has been adapted for detecting the presence of lactoperoxidase in pasteurized milk, after spiking with H₂O₂ and tracking its disappearance²⁹⁹. Multilayer immobilized HRP according to an affinity procedure involving gamma globulin (see Section III.B.4.b) can be used to catalyze the oxidation of **103** by H₂O₂ to a free radical, to be measured at 425 nm³⁰⁰. A peroxidase-catalyzed oxidation of ABTS can serve to determine in a sample either H₂O₂ or the antioxidant capacity (inhibition of oxidation). This procedure was applied for analysis of serum of patients infected with HIV³⁰¹. Some substances are hard to dissolve in aqueous solution. A FIA system for substances dissolved in toluene consists of two trails, one leading directly to the reference cell of a spectrophotometer set at 458 nm, and the other passing through a reactor containing HRP immobilized by adsorption on a pack of controlled-pore glass beads, where the enzyme catalyzes the oxidation of *p*-anisidine dissolved with the analyte, on its way to the sample cell of the spectrophotometer. The system pumps the sample solution simultaneously in both trails. The LOD is 0.9 μM H₂O₂, with linearity in the 0.025 to 0.20 mM range, and a throughput of about 60 h⁻¹. The method was applied to analysis of olive oil and margarine³⁰².

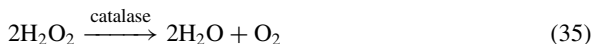
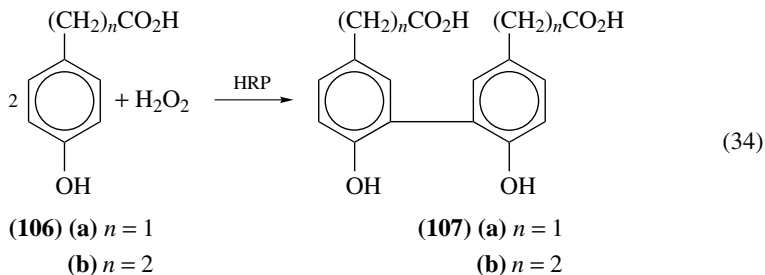


N,N,N',N'-Tetrakis(2-benzimidazolymethyl)-1,3-diaminopropan-2-ol forms dinuclear complexes with Fe(III) ions (**104**). One of the sulfate ligands of this complex is selectively and rapidly displaced by H₂O₂, as shown in the insert **105**, with a significant change of the UVV spectrum, and the absorbance can be measured at 575 nm. Good results are obtained for purely aqueous solutions in the pH range from 3.5 to 7.5, with acetate buffers at pH 3.8 to 5.1 offering the best performance. Formation of **105** is practically immediate and the complex decomposes within 20 min. Great savings in reagents and sample volume are attained on applying the microplate spectrophotometry technique. The method is highly selective, allowing determination of H₂O₂ in the presence of a large excess of other peroxides, such as *t*-BuOOH, cumyl hydroperoxide (**27**) and AcOOH. The LOD is 3 μM and the LOQ is 9 μM, with linearity up to 0.3 mM; for the titanil method (equation 28) the LOD is 20 μM and the LOQ is 60 μM, with linearity up to 2 mM^{239, 303}. The method can be applied in systems where H₂O₂ is derived from the analyte. For example, the determination of glucose in soft drinks by application of the GOX-catalyzed oxidation process shown in equation 16 (Section III.A) can be carried out in a FIA system. The completeness of the latter reaction has to be assured for analytical quality, because formation of **105** is fast. For glucose the LOD is 10 μM and the LOQ is 30 μM, with linearity up to 0.2 mM. For verification, two additional analytical methods involving equation 16 followed by an HRP-catalyzed oxidation process were applied, namely the spectrophotometric determination of the product of a dye derived from **103** (LOD 1 μM and LOQ 3 μM, with linearity up to 0.2 mM) and the fluorimetric determination of the dimerized *p*-hydroxyphenylacetic acid, according to equation 34 (LOD 0.7 μM and LOQ 2 μM, with linearity up to 20 μM)³⁰⁴.



b. Fluorometry. Determination of H₂O₂ in precipitation waters can be carried out based on the fluorescence of product **107a** ($\lambda_{\text{ex}} = 320 \text{ nm}$, $\lambda_{\text{fl}} = 400 \text{ nm}$), obtained from 4-hydroxyphenylacetic acid (**106a**) and H₂O₂ with HRP catalysis, according to equation 34. Blank measurements, attributed to the presence of organic peroxides, are made by adding catalase to the sample to destroy the hydrogen peroxide (equation 35) before adding reagent **106a** and HRP. For H₂O₂, LOD is 12 nM (0.4 ppb), the coefficient of variation being 0.66% at 1.6 μM; linearity is observed up to 18 μM, above which a quadratic calibration curve can be used³⁰⁵. The process depicted in equation 34 with **106a** was adopted for measuring H₂O₂ in rainwater and for testing collection devices of peroxide vapors in the atmosphere⁷. Potential interference by metals or SO₂ can be masked with EDTA or CH₂O, respectively³⁰⁶. The FLD method based on equation 34 with **106a** is comparable to the HRP-catalyzed CLD method based on bis(2,4,6-trichlorophenyl) oxalate (Section III.B.2.c)

for determination of H_2O_2 in rainwater. The LOD for the FL method is 13 nM (0.44 ppb) of H_2O_2 ³⁰⁷.



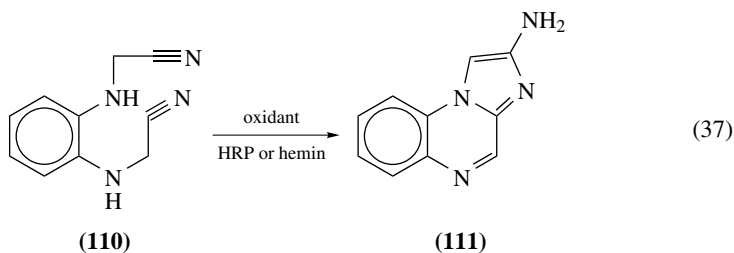
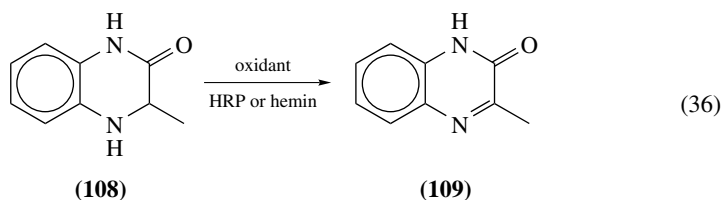
A FIA system was designed for the analysis of H_2O_2 and organic peroxides in air and rain, consisting of a chromatographic C_{18} RP column to separate the components, a long tubular reactor where the peroxide oxidizes reagent **106a** in the presence of HRP, and a fluorescence cell, where the fluorescent dimeric product **107a** is determined at 414 nm on excitation at 301 nm. Only H_2O_2 was detected in coastal air samples, in concentrations from 60 pptv to 1.2 ppbv. The absence of organic peroxides was probably due to their decomposition during sample collection, yielding H_2O_2 . Rain collected in the same site had pH from 4.4 to 5.4, showing H_2O_2 concentrations of the order of 10 μM and concentrations slightly below 1 μM of HMHP and HEHP^{308a}. Similar results were obtained in other field tests using this method²⁶. A chromatographic method with FLD based on equation 34 showed LOD 14 $\mu\text{g L}^{-1}$, linearity in the 42 to 225 $\mu\text{g L}^{-1}$ range and RSD 6.6%^{308b}. A method for determining peroxides in indoor ambients consists in passing the air through an active carbon cartridge, desorbing by SFE with CO_2 containing 2% MeOH, RP-HPLC of an aliquot of the extract, followed by post-column irradiation to convert organic peroxides to H_2O_2 and FLD of the product in equation 34 ($\lambda_{\text{ex}} = 285$ nm, $\lambda_{\text{fl}} = 400$ nm). LOD is 14 $\mu\text{g L}^{-1}$ for H_2O_2 and 34 $\mu\text{g L}^{-1}$ for organic peroxides¹⁸⁸. This method was adapted to the determination of H_2O_2 in rainwater. LOD is 21.5 nM, RSD 3.81% at 0.176 μM and 1.15% at 0.882 μM , with linearity up to 5.0 μM ³⁰⁹; the method was used for post-column derivatization in the RP-HPLC-FLD analysis of H_2O_2 , HMHP and HEHP in rainwater and cloud water¹⁶. RP-HPLC-FLD applying equation 34 with **106a** was used to analyze vapors of H_2O_2 , MHP, EtOOH, HMHP and AcOOH, collected over aqueous solutions of the same compounds, aiming at the determination of their Henry's law constants³¹⁰. An early survey of 25 substrates for fluorometric assays involving peroxidases pointed to **106a** as the indicator of choice, due to the high fluorescent intensity of the oxidation product, its stability to autoxidation and its relatively low price³¹¹.

Ultra-trace analysis of H_2O_2 and other peroxides can be carried out by a combination of chromatographic separation and FLD based on equation 34. Thus, in a FIA system including HPLC, each separated peroxide is treated with a solution containing **106a** and HRP and the fluorescence signal is measured. In a special design, the FIA system is provided with a short column containing the enzyme immobilized on porous glass, which remains active for several months. LOD for H_2O_2 is 0.05 μM , with linearity in the 0.5 to 10.0 μM range and RSD 9.1 to 1.8% ($n = 20$) for the same range^{312, 313}. This technique was used for the determination of hydroperoxide pollutants in air, downwind from Berlin, in the so-called BERLIOZ campaign³¹⁴.

The homolog of **106a**, 3-(4-hydroxyphenyl)propionic acid (**106b**), undergoes a similar oxidation by H_2O_2 to a fluorescent dimer (**107b**, $\lambda_{\text{ex}} = 305 \text{ nm}$, $\lambda_{\text{fl}} = 405 \text{ nm}$), catalyzed by HRP immobilized on chitosan beads ($\varnothing 300 \mu\text{m}$) by cross-linking with glutaraldehyde, using phosphate buffer at pH 7.0, in a FIA system. The LOD is 3 ng L^{-1} (SNR 3). The method was used for determination of H_2O_2 in tap water and rainwater, applying MOSA to improve the analytical quality²³⁸. A similar dimerization takes place on oxidation of *p*-cresol with H_2O_2 , catalyzed by a complex of hemin (**75a**) with β -cyclodextrin (**83**), in phosphate buffer at pH 10.4, yielding 2,2'-dihydroxy-5,5'-dimethylbiphenyl ($\lambda_{\text{ex}} = 322 \text{ nm}$, $\lambda_{\text{fl}} = 410 \text{ nm}$). The LOD is 3.4 nM , with linearity in the range from 30 nM to $8 \mu\text{M}$ ³¹⁵.

Manganese-tetrasulfonatophthalocyanine (**87a**) can serve as mimic for HRP catalysis in the oxidative dimerization of 4-hydroxyphenylacetic acid (**106a**), depicted in equation 34. The reaction is carried out in Tris-HCl buffer at pH 7.77, containing $10 \mu\text{M}$ of Co(II) complexed with EDTA, to avoid interference by other ions. Fluorescence measurements of **107a** ($\lambda_{\text{ex}} = 325 \text{ nm}$, $\lambda_{\text{fl}} = 409 \text{ nm}$) are carried out after filtering any $\text{Mg}(\text{OH})_2$ precipitates that might appear. The LOD is $63 \mu\text{M}$ with linearity range from 80 nM to $5 \mu\text{M}$. The method was used for H_2O_2 determination in seawater³¹⁶. The oxidation of 3-(4-hydroxyphenyl)propionic acid (**106b**) by H_2O_2 to a fluorescent dimer (**107b**, $\lambda_{\text{ex}} = 324 \text{ nm}$, $\lambda_{\text{fl}} = 409 \text{ nm}$), according to equation 34, may be catalyzed by iron-tetrasulfonatophthalocyanine (**87b**), acting as a mimic for HRP. The LOD after a 30 min incubation period is 13 nM , with linearity up to $3.6 \mu\text{M}$ ³¹⁷.

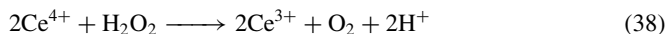
Two substrates, 3-methyl-3,4-dihydroquinoxalin-2(1*H*)-one (**108**) and *N,N'*-bis(cyanomethyl)-*o*-phenylenediamine (**110**), undergo oxidation by H_2O_2 to a fluorogen as depicted in equations 36 and 37, yielding fluorescent products (**109**, $\lambda_{\text{ex}} = 344 \text{ nm}$, $\lambda_{\text{fl}} = 404 \text{ nm}$, and **111**, $\lambda_{\text{ex}} = 360 \text{ nm}$, $\lambda_{\text{fl}} = 454 \text{ nm}$). The sensitivity of these reactions is claimed to be in the nM range, similar to that of equation 34³¹⁸.



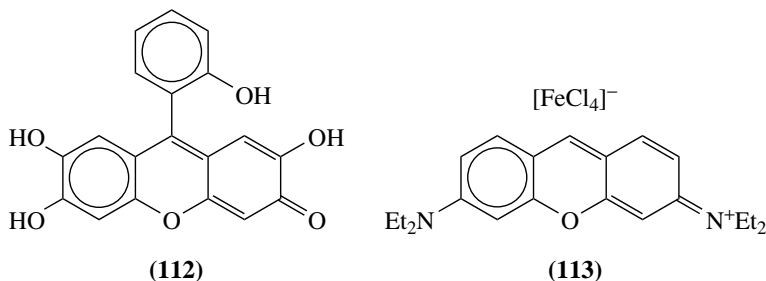
Aluminum tetraaminophthalocyanine (**87c**) was proposed as substrate for the fluorometric HRP-catalyzed determination of H_2O_2 . The method has the advantage of the fluorescence being in the red region of the visible spectrum ($\lambda_{\text{ex}} = 610 \text{ nm}$, $\lambda_{\text{fl}} = 678 \text{ nm}$), while many of the fluorescent reagents proposed for analogous determinations fall in the blue region, where scattered light or background fluorescence may contribute to the analytical error. A modification of the method may be applied for determination of HRP

in solution. The LOD are 0.59 pM for HRP and 1.4 nM for H₂O₂, with linearity up to 39.4 pM for HRP and up to 0.20 μM for H₂O₂³¹⁹.

The oxidation process of H₂O₂ by Ce(IV) depicted in equation 38 may be followed by the change in absorbance of this ion; however, a more sensitive determination is based on the fluorometric measurement of Ce(III) ($\lambda_{\text{ex}} = 260 \text{ nm}$, $\lambda_{\text{fl}} = 360 \text{ nm}$). The reaction should be carried out in acid medium (pH 1–2) and care should be taken that total conversion of Ce(IV) to Ce(III) has been accomplished, lest Ce(IV) absorbs part of the emitted fluorescence. The LOQ of the method is 0.1 ppm³²⁰.

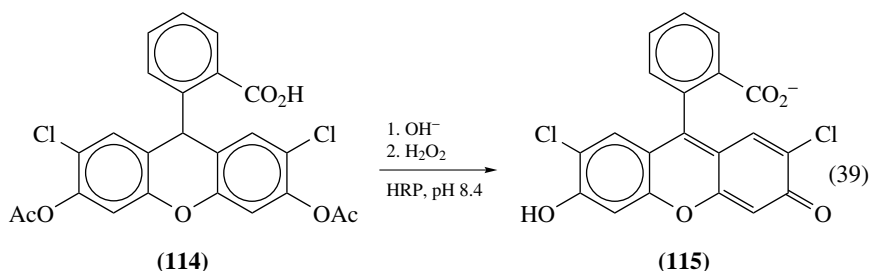


The fluorescent dye *o*-hydroxyphenylfluorone (**112**, $\lambda_{\text{ex}} = 510 \text{ nm}$, $\lambda_{\text{fl}} = 540 \text{ nm}$) is unstable in alkaline solution and can be oxidized to a nonfluorescent product. Fluorescence quenching of **112** can be used to determine the concentration of H₂O₂; however, the reaction is rather slow unless a catalyst such as HRP is present. Iron-tetrasulfonatophthalocyanine (**87b**) can be used as mimetic catalyst instead of HRP. The LOD for H₂O₂ is 0.75 nM, with linearity of $\log(F_0/F)$ up to 0.1 μM, where F and F_0 are the fluorescence intensities of the unquenched and quenched solutions, respectively³²¹. The complex of Mo(VI) with sodium dodecyl sulfate acts as mimic for HRP in fluorescence quenching assays for determination of H₂O₂ and glucose, using pyronin B (**113**) as fluorescent substrate. The linear range is up to about 9 nM and 0.14 μM for H₂O₂ and glucose, respectively. The method was applied for glucose determination in human serum³²².



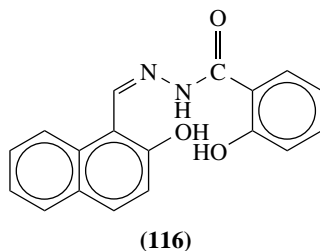
The opposite strategy can also be applied, namely development of a fluorescent dye from a *leuco* form, for example, by subjecting compound **114** to alkaline hydrolysis and converting to fluorescent dichlorofluorescein (**115**) by the action of H₂O₂ catalyzed by HRP, as shown in equation 39. This process was used to develop a FIA system with FLD, based on a long capillary serving as incubating reactor and a fluorescence chamber, where the solution is irradiated by a laser at 488 nm. The FL emission is collected by a microscope focused on the chamber at an angle of 45°, and measured after passing a cutoff filter for 520 nm and shorter wavelengths. The LOD of this method is 0.1 nM H₂O₂ in 25 μL aliquots³²³. A sensitive method for determination of H₂O₂ and lipid hydroperoxides is based on the oxidation depicted in equation 39, by which a fluorescein derivative (**114**) is converted in neutral or basic solution to a strongly fluorescent fluorescein derivative (**115**, $\lambda_{\text{ex}} = 495 \text{ nm}$, $\lambda_{\text{fl}} = 520 \text{ nm}$)³²⁴. A thousandfold improvement of sensitivity may be achieved for this reaction in the presence of hematin (**75b**), acting as a peroxidase mimic. The method was applied for *in vivo* determination of intravitreal H₂O₂ by vitreous photofluorometry, before and after panretinal laser photocoagulation. The measured

concentrations were in the 15 nM to 100 μ M range¹⁰⁰.



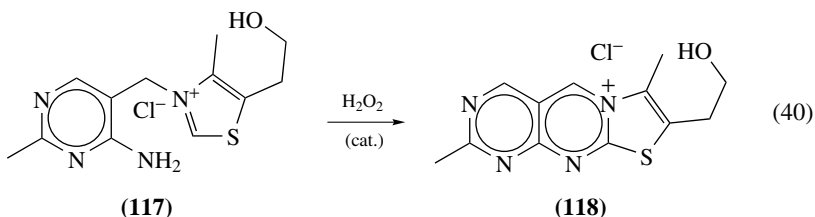
The Fenton method consists of the Fe(II)-catalyzed homolytic scission of H_2O_2 to yield two HO^\bullet radicals, which are scavenged by a substrate present in the solution, which is subsequently determined by an appropriate method^{325, 326}. Sensitive determinations of H_2O_2 can be carried out with benzoic acid in the presence of Fe(II) at pH 1.5. The hydroxylated products can be measured by FLD ($\lambda_{\text{ex}} = 313 \text{ nm}$, $\lambda_{\text{fl}} = 399 \text{ nm}$) and show good correlation with the enzymatically catalyzed method of equation 34³²⁵. Fenton's method was adapted to the determination of H_2O_2 in rainwater. LOD is 1.98 nM, RSD 1.51% at 0.176 μ M and 1.40% at 0.882 μ M, with linearity up to 7.4 μ M³⁰⁹. An automatic sampler for atmospheric hydroperoxides, based on Fenton's reagent (Fe(II) and benzoic acid), for unattended field operation, was designed and tested with satisfactory results⁸. The Fenton reaction is faster for H_2O_2 than for HMHP and can be applied for speciation of atmospheric hydroperoxide gaseous species, as opposed to the method based on equation 34 ($n = 1$) that yields the total peroxide content^{18, 326}. Enhancement of the fluorescence signal is attained on raising the pH to 11 or on adding Al(III) ions at low pH³²⁶. An alternative detection method for the Fenton derivatives is ELD, as shown for equation 47 in Section III.B.4.a.

The HRP-catalyzed oxidation of 2-hydroxy-1-naphthaldehyde salicylhydrazone (**116**) with H_2O_2 , at pH 8.5, is finished in about 10 min, and the fluorescent product ($\lambda_{\text{ex}} = 296 \text{ nm}$, $\lambda_{\text{fl}} = 414 \text{ nm}$) persists for 1 h. The results compare well with those obtained by iodide oxidation. LOD is 0.7 nM and LOQ is 2.5 nM. The influence of various factors on fluorescence development was investigated³²⁷.

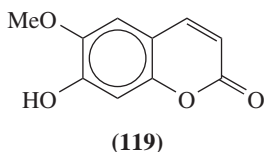


A fluorometric method was developed for determination of atmospheric H_2O_2 simultaneously with other species present at ppbv or lower levels, avoiding chromatographic separation. H_2O_2 is selectively collected by diffusion through a Nafion membrane, and is carried by a water stream into a reactor where it oxidizes thiamine hydrochloride (**117**) to a fluorescent ionic form of thiochrome (**118**), catalyzed by bovine hematin (**75b**) in alkaline solution, as shown in equation 40. The end solution containing **118** is passed through

a cell where it is exposed to pulsed radiation of 370 nm wavelength and the fluorescence is measured at 440 nm. LOD is 8 nM (SNR 3), which under the given operation conditions corresponds to 25 pptv in the gas phase. Various technical considerations attend this method: Nafion readily dissolves H_2O_2 , that diffuses to the water stream, leaving outside species such as MHP and HMHP, which are important atmospheric peroxides; these two compounds can be determined simultaneously with H_2O_2 , as described in Section V.B.2.a. Any HMHP that might have diffused into the water stream is readily hydrolyzed to H_2O_2 and H_2CO in the alkaline solution; the catalyst is hematin (**75b**), a mimic for HRP that has the advantage of higher stability and a much reduced price than the enzyme for the same activity; furthermore, it is a very inefficient catalyst for the oxidation of **117** by MHP, thus improving the selectivity for H_2O_2 ; the pulsed operation allows collecting data in a multi-channel setup for simultaneous measurement of various species, each one demanding a different chemical procedure, but all finally resulting in measurements with a single detector and data processing unit^{328,329}.

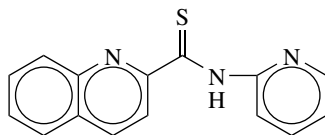


Scopoletin (**119**) undergoes fluorescence decay, taking place on HRP-catalyzed 1:1 oxidation by H_2O_2 in phosphate buffer at pH 7.0. The LOD is 2 nM, with RSD 2%²⁴⁹. The method was applied for tracing the generation of peroxides in river waters under solar radiation²⁴⁹, and for assessing the efficiency of sample collecting devices of peroxide vapors in the atmosphere⁷. As the assay quantizes all the peroxides, a second determination is necessary after adding catalase, to determine H_2O_2 by difference^{7,249}. An adequate procedure for H_2O_2 analysis in marine waters consists of changing the pH to the 8.5 to 9.5 range, adding the **119** reagent and HRP catalyst solutions and measuring the fluorescence quenching ($\lambda_{\text{ex}} = 390$ nm, $\lambda_{\text{fl}} = 460$ nm). If measuring immediately is precluded, the samples may be stored up to four days in the dark, at room temperature³³⁰.



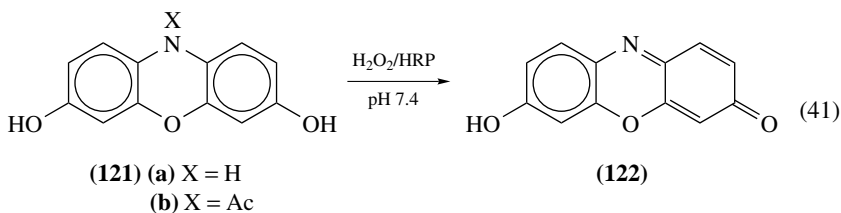
A triple complex is formed between *N*-(α -pyridyl)-2-thioquinaldamide (**120**), vanadate ions and H_2O_2 that becomes fluorescent in acidic solution ($\lambda_{\text{ex}} = 340$ nm, $\lambda_{\text{fl}} = 490$ nm). This reaction, originally developed for determination of V(V) in a FIA system, can be adapted for determination of H_2O_2 and organic peroxides. LOD for H_2O_2 is 0.05 μM , with RSD 2.4% ($n = 3$) at 1 μM , with linearity in the 0.2 to 50 μM range³³⁰.

Hydrogen peroxide causes oxidation of resorufin (**121a**) or its acetylated derivative, Amplex Red (**121b**), according to equation 41. The process takes place in Tris buffer at pH 7.4 and the product **122** is determined by FLD ($\lambda_{\text{ex}} = 563$ nm, $\lambda_{\text{fl}} = 587$ nm). Care has to be paid that the fluorogenic substrate is in excess, lest **122** undergoes further oxidation to a nonfluorescent compound. This assay was proposed for measurement of the



(120)

activity of NADPH oxidase and other oxidases, and for determination of H_2O_2 in food and environmental waters⁶⁷.



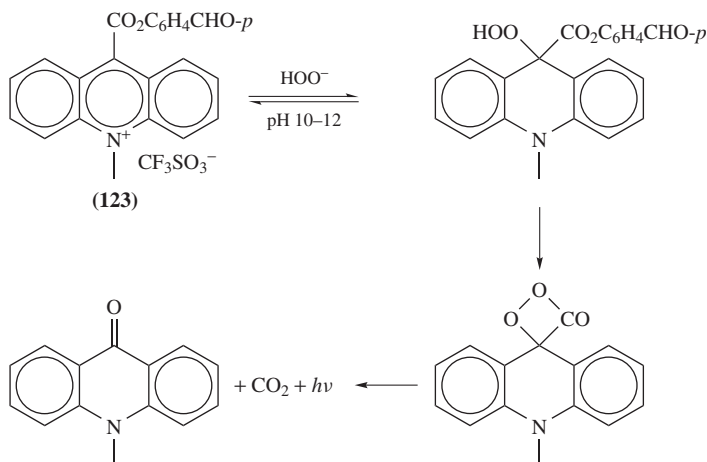
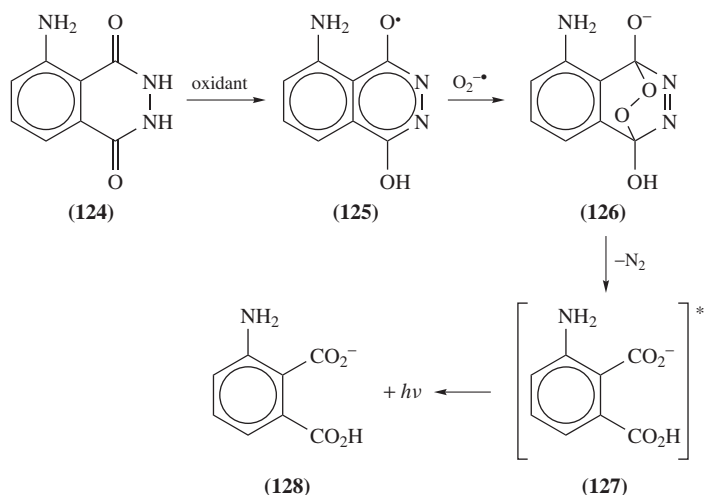
c. Chemiluminescence. CL affords very sensitive methods for determination of H_2O_2 ; however, other oxidants and reducing agents may interfere. CLD may be a good alternative to FLD methods when the sample is fluorescent by itself, or when the fluorescence spectrum overlaps with the spectrum of impurities present in the sample. Reviews have appeared on determination of H_2O_2 in air by CLD methods with emphasis on luminol and oxalate reagents³³¹, applications of peroxalate CL to liquid chromatography³³² and applications of CL to diagnosis¹⁸³.

A selective reaction takes place between H_2O_2 and 10-methyl-9-(*p*-formylphenoxy-carbonyl)acridinium trifluoromethanesulfonate (**123**) in basic solution with CL emission at about 470 nm. A proposed mechanism for CL is depicted in Scheme 2. No catalyst other than an alkali is required for the process to take place. The LOD is about 5 nM, with linearity up to 60 μM . It should be pointed out that the LOD is dictated by the technical capability of obtaining a blank of water devoid of H_2O_2 . The method was applied for H_2O_2 determination in natural waters^{333a}.

A simple and sensitive CL system is afforded by KMnO_4 (<5 mM) in acidic solution (2 M H_2SO_4) in the presence of micelle-forming octylphenyl polyglycol ether (5% v/v). The LOD is 6.0 nM (SNR 3); the linear range depends on the KMnO_4 concentration. Interference occurs from Cr(III), Cr(VI), Nd(III), Fe(II), Co(II), V(VI), S_2^{2-} , S_8^{2-} , ClO_4^- , $\text{C}_2\text{O}_4^{2-}$ and MnO_4^- at 10-fold molar ratio, and other ions only at much higher molar ratios. Interference occurs from a few organic compounds too^{333b}.

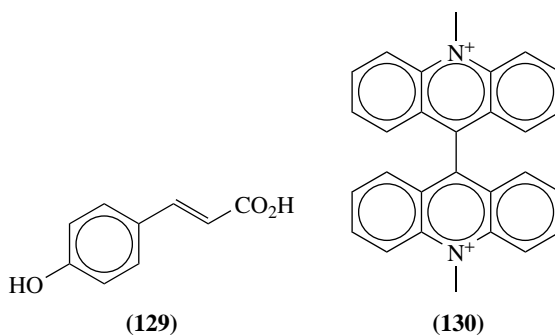
It is generally agreed that the CL obtained with luminol (**124**) is based on the series of transformations shown in Scheme 3, where the analyte (oxidant) as such or in combination with a catalyst produces a free radical (**125**), which in turn captures a superoxide anion to yield an endoperoxide (**126**), which on elimination of N_2 produces an excited intermediate (**127**), which finally settles down to the 3-aminophthalate ion (**128**) on emission of a photon. A linear correlation may be established between the intensity of the CL emission and the concentration of the analyte³³⁴.

HRP-catalyzed oxidation of luminol in a FIA system was used to follow the development of H_2O_2 during forced oxidation of beer²¹¹. A microreactor consisting of immobilized HRP placed in the CL cell, in front of a photomultiplier in a FIA system, is claimed to greatly enhance the CL signal. The CL response for cumyl hydroperoxide (**27**) and *t*-BuOOH is much lower than for H_2O_2 . The method was proposed for clinical

SCHEME 2. CL mechanism of **123** in the presence of hydrogen peroxideSCHEME 3. CL mechanism of luminol (**124**) in the presence of an oxidant

determinations of H_2O_2 in physiological fluids³³⁵. A remote biosensor for determination of H_2O_2 can be obtained based on the enzyme-catalyzed CL of Scheme 3, using HRP immobilized on a gel of TEOS placed at the end of an optical fiber. Furthermore, the LOD may be lowered if a fluorescence enhancer such as *p*-coumaric acid (**129**) is added to the solution. When working in an optical cuvette, without the optical fiber, the reagents and the unbound enzyme may be mixed with the analyte sample. LOD are 16.6 and 1.6 μM , linear ranges are 16.7 to 116.7 μM and 3.3 to 50 μM , with RSD ($n = 5$) 8.0 and 2.4%, for bound and unbound enzyme, respectively³³⁶. A specially designed FIA system, working with immobilized HRP and CLD of luminol (**124**) oxidation in phosphate buffer at pH 6.5, can be applied to measure the H_2O_2 produced in the determination of glucose in serum

according to equation 16³³⁷. A noncracking sol-gel membrane for HRP immobilization was designed for H₂O₂ determination by CLD³³⁸. The CL emission of luminol oxidation can be applied to determine ROS, inclusive H₂O₂, in human semen. **124** is capable of penetrating the spermatozoa membranes, therefore both intra- and extracellular ROS can be evaluated. As the CL of lucigenin (**130**) oxidation is selective for O₂^{-•}, a more detailed analysis can be obtained for the ROS present in the extracellular liquid¹⁰¹.

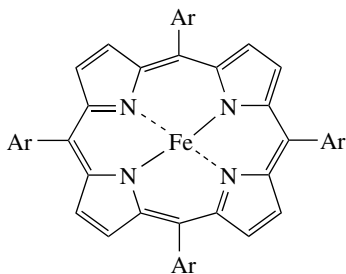


Various transition metal ions can catalyze the CL of the luminol (**124**) oxidation. This reaction may serve as the basis of analytical methods for the determination of such ions³³⁹. A fast and sensitive method for H₂O₂ determination is based on the CL emitted by the Co(II)-catalyzed reaction of luminol (**124**) in a basic medium; the presence of sodium dodecyl sulfate both accelerates and enhances the CL signal. LOD is 0.5 nM (SNR 3), with linearity in the 1 to 105 nM range, with RSD ($n = 11$) 2.8 and 2.3% for 15 and 52 nM of H₂O₂, respectively. The method was tested for rainwater³⁴⁰. A special FIA system design of the Co(II)-luminol CLD method allows sub-nM LOD for the determination of H₂O₂ in seawater. Of the various possible interferences caused by species present in the matrix in the determination at the 50 nM H₂O₂ concentration level, Cr(II), Cr(VI), Cu(II), Fe(III) and Co(II) showed interference at concentrations much higher than the natural ones. Only O₂ and Fe(II) reacted with luminol at their natural concentration levels; however, the half-life time of Fe(II) in seawater is such as to practically disappear after letting the sample rest for 1 h before analysis; as for O₂, it can be eliminated by degassing with He prior to the assay. At the low concentration level of analyte dealt by this method, five possible sources for CL signals have to be carefully evaluated, namely (a) electronic noise and stray light, (b) light emission from seawater, (c) light emission from the reagents, (d) light emission of the reagents in contact with seawater and (e) light emission from the reagents with H₂O₂. The total blank is given from the combination of the first four items. The sampling technique has to be considered in on-board applications, to avoid the effects of light during sample preparation. The LOQ is at least 0.42 nM with precision of 17 pM for a 0.57 nM sample³⁴¹. A FIA system based on Co(II)-catalyzed CL of luminol was used for on-board determination of H₂O₂ in seawater. The throughput was fast; for example, a depth profile of 12 samples could be analyzed in 45 min, keeping in pace with the dynamics of H₂O₂ generation and disappearance in the system⁴¹. An inexpensive CLD setup consists of a liquid core waveguide serving also as reactor, terminating in a conventional, high numerical aperture optical fiber connected to an inexpensive photomultiplier. The instrument was validated by collecting gaseous H₂O₂ through a Nafion membrane and injecting the sample together with luminol and Co(II) at pH 10.8 into the CL cell. The LOD is 25 pptv, with linearity up to at least 100 ppbv. The possible interference of various levels of atmospheric pollutants was assessed: None

for NO₂ up to 200 ppbv; none for SO₂, which cannot significantly traverse the diffusion membrane; and none for O₃ below 50 ppbv³⁴².

In spite of yielding a lower CL intensity, the oxidation of luminol (**124**) by H₂O₂, catalyzed with Cr(II) ions in a FIA system is claimed to be a viable alternative to HPR catalysis, as it avoids the enzyme instability and high price. LOD is 40 nM. The method was tested for determination of H₂O₂ produced *in vitro* by various microalgae species (*Chlamydomonas reinhardtii*, *Chlorella fusca* and *Monoraphidium braunii*)³⁴³.

Manganese-tetrasulfonatophthalocyanine (**87a**) can serve as mimic for HRP catalysis in the oxidation of luminol (**124**) by H₂O₂, in a FIA system, working in phosphate buffer solution at pH 10.7. EDTA masks the interference by traces of transition metal ions. The LOD is 6.8 nM, with linearity in the 40 nM to 20 μM range and RSD 2.4% (*n* = 10) for 1.0 μM H₂O₂³⁴⁴. The CL emission of luminol with H₂O₂ catalyzed by hematin (**75b**) in a FIA system is stabilized if the hematin is immobilized in the bulk of a CPE working at a potential of -0.3 V vs. SCSE, with a Pt auxiliary electrode, in carbonate buffer at pH 10. The LOD is 0.10 μM with linearity from 3.9 μM to 1 mM³⁴⁵. A sensitive determination of oxalate ions in serum can be performed on coupling the oxalate oxidase-catalyzed generation of H₂O₂ shown in equation 19, with CLD of luminol (**124**) oxidation, catalyzed by Fe(III)-*meso*-tetrakis(4-sulfonatophenyl)porphine (**131**). The LOD is 0.2 μM oxalate with a 200 μL sample of serum³⁴⁶.



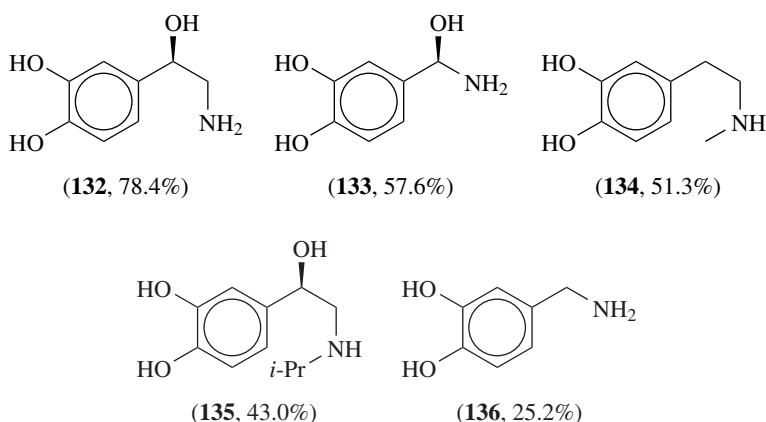
(131) Ar = *p*-C₆H₄SO₃⁻

Various immobilized catalysts and immobilized luminol (**124**) were tried in a FIA system to reduce the number of injection streams. An electrode set at about +0.25 vs. SCSE can serve instead of an oxidizing catalyst to effect the first transformation of **124** to the reactive intermediate **125**, which will proceed to react with the peroxide analyte to yield CL³⁴⁷. A FIA *reagentless* system for determination of H₂O₂ based on Scheme 3 consists of a stream of the sample and a stream of water passing through packs containing MgO and crystalline sublimed luminol (**124**), to provide alkalinity and the luminescent species, respectively. The streams mix before entering the CL cell, where activation of the oxidation is provided by a pair of gold electrodes set at 0.6 V to each other. The determination requires a calibration curve³⁴⁸.

The CLD device mentioned in Section VI.B.4, where the analyte solution is added as microdrops to an alkaline luminol (**124**) solution may be extended to peroxides other than BzOOBz. Optodes based on luminol CL detection of H₂O₂ can be built by immobilizing a peroxidase on a paste made of fume silica, graphite or a LC column fill such as Merck's LCPH-Si or LCPH-NH₂. Covering with electropolymerized *o*-phenylenediamine helps reducing the extent of enzyme elution. After proper conditioning the optode is placed in the CL measuring device. The linear range depends on the solid substrate chosen for the paste, for example 1 to 500 μM for graphite and 80 to 1000 μM for LCPH-Si and LCPH-NH₂. The signal stability of this device needs improvement, by further

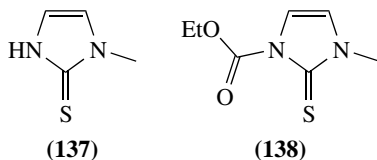
reducing enzyme elution. Additional functionality can be achieved by applying a layer of GOX or lactate oxidase immobilized on hydrogel on top of the poly-*o*-phenylenediamine film, to allow analysis of glucose or lactate, following H₂O₂ production according to equations 16 or 18³⁴⁹.

The CL emission of Scheme 3 catalyzed by HRP can be applied to the quantitative analysis of catecholamines, such as dopamine (**68**), epinephrine (**132**), L-DOPA (**30**), norepinephrine (**133**), deoxyepinephrine (**134**) isoproterenol (**135**) and dihydroxybenzylamine (**136**), in a FIA system, after undergoing the oxidation shown for dopamine (**68**) in equation 20. The mechanism of this process is not totally clear; however, the CL yields of equation 20 depend upon the pH of the system (pH 9 is convenient and is achieved by adjusting the concentration of imidazole), the temperature (60 °C is adequate) and the structure of the analyte (a calibration curve is needed for each one). Taking **68** as reference (100%) the CL yields after 30 min incubation (achieved by controlling the flow through a long capillary tube) are as shown in equation 42^{350, 351}.

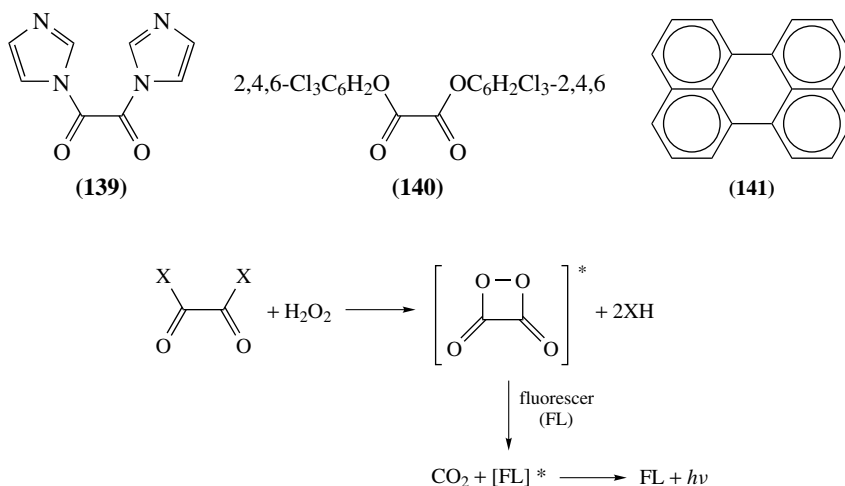


$$\begin{aligned} \mathbf{68}, 100\% > \mathbf{132}, 78.4\% > \mathbf{30}, 62.0\% > \mathbf{133}, 57.6\% > \mathbf{134}, 51.3\% \\ > \mathbf{135}, 43.0\% > \mathbf{136}, 25.2\% \end{aligned} \quad (42)$$

Catalysis quenching can be used for indirect determination of various analytes. A requisite in such analytical schemes is that the catalyst (e.g. a transition metal ion) be in excess of the analyte in the sample, so that CL is always measured. A sigmoidal shape is expected for the dependence of the CL intensity on the logarithm of the analyte concentration in the sample. The LOQ of the inhibiting analyte is determined by the smallest measurable change of the free catalyst ion, whereas the highest allowable concentration of analyte in the sample is that causing the catalyst to drop below its LOD³⁵². Inhibition of CL catalyzed by Cu(II) ions can be applied to the determination of methimazole (**137**) and carbimazole (**138**) in pharmaceutical preparations, using a FIA-CLD system. These antihyperthyroidism drugs form stable 1:1 complexes with Cu(II) ions which have no catalytic action on the oxidation of luminol (**124**). For a set of good working conditions it was found that for **137** and **138** the LOD are 1 and 2 mg L⁻¹, with linearity in the 2 to 100 and 3 to 120 mg L⁻¹, and RSD 1.9 and 2.1 mg L⁻¹ ($n = 10$) for 50 mg L⁻¹ samples, respectively. Although the method seems satisfactory for analysis of pharmaceuticals containing **137** and **138**, application to clinical samples requires avoidance of interference by other possible catalysts and inhibitors^{353, 354}.

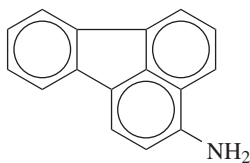


Compounds containing the oxalyl moiety, such as 1,1'-oxalyldiimidazole (**139**) and bis(2,4,6-trichlorophenyl) oxalate (**140**), in the presence of a fluorophore, undergo CL processes involving peroxides. In Scheme 4 is shown a simplified mechanism of CL mediated by oxalic acid derivatives. The HRP-catalyzed CLD method based on **140** is comparable with the FLD method based on equation 34 with **106a**, in Section III.B.2.b, for determination of H_2O_2 in rainwater. The LOD for the CL method is 40 nM (1.36 ppb) of H_2O_2 and the CL response of MHP is only 1.25% of that of H_2O_2 ³⁰⁷. An early example of the problems encountered on development of a CLD-based method is afforded by the determination of glucose in urine, following H_2O_2 generation according to equation 16, using **140** for the peroxalate reaction and perylene (**141**) as fluorescer^{355a}. The peroxalate CL method was applied for determination of H_2O_2 in Antarctic coastal ambient air (average 0.4 ppbv), snow (90 to 480 ppb) and firn cores. No contribution of organic peroxides to the CL signal was detected^{355b}.



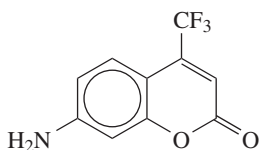
SCHEME 4. Chemiluminescence mechanism of an oxalic acid derivative in the presence of H_2O_2

A method for selective determination of atmospheric H_2O_2 consists of a sampling unit with a diffusion scrubber, a calibration unit for controlled generation of H_2O_2 vapor in a Henry's law device, and a FIA unit where the sample and the reagent solution of 1,1'-oxalyldiimidazole (**139**) are mixed and the analyte is determined. The CL cell consists of a transparent tube with built-in fluorescent 3-aminofluoranthene (**142**) and a photomultiplier. The operation is fast, 120 injections h^{-1} ; the LOD depend on the mode of operation, but are in the 20 to 30 pptv range. The method was applied in the field, in a site where peak H_2O_2 concentrations of about 100 pptv were measured at midday, which descended to the LOD at midnight. Interference by the most abundant organic hydroperoxides in air is minor³⁵⁶.

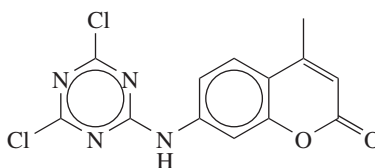


(142)

Various coumarin derivatives were synthesized and tested as blue fluorescers for the peroxyoxalate method of H_2O_2 determination. The most promising one is 7-amino-4-trifluoromethylcoumarin (**143**), as for the speed and the intensity of the fluorescent response³⁵⁷. 7-(4,6-Dichloro-1,3,5-triazinylamino)-4-methylcoumarin (**144**) is specific for H_2O_2 , the CL effect taking place in full a couple of minutes after mixing the analyte solution with the reagent, with no need for a catalyst. A possible mechanism for the CL effect is formation of the excited state on oxidation of **144**, the energy being transmitted to another **144** molecule in the ground state with subsequent emission of a photon. This is supported by the emission spectrum ($\lambda_{\text{max}} = 348 \text{ nm}$) being similar to that of the fluorescence spectrum of **144** in the absence of H_2O_2 ($\lambda_{\text{max}} = 343 \text{ nm}$) and not to the fluorescent spectrum after reaction with H_2O_2 ($\lambda_{\text{ex}} = 338 \text{ nm}$). The sensitivity of the reagent is enhanced in phosphate buffer at pH 11.5, in the presence of cetyldimethylbenzylammonium chloride. The LOD is 40 nM (SNR 3), with linearity from 0.10 μM to 0.40 mM³⁵⁸.

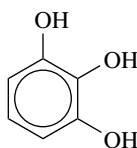


(143)

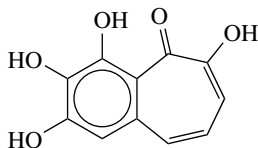


(144)

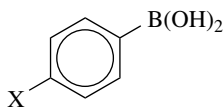
A study on the CL produced by the HRP-catalyzed oxidation of pyrogallol (**145**) and purpurogallin (**146**) shows a 14-fold enhancement of signal intensity for **145** in the presence of 4-boronobenzenepropanoic acid (**147a**) and a 314-fold enhancement for **146** in the presence of 4-biphenylboronic acid (**147b**)³⁵⁹.



(145)



(146)

(147) (a) X = $\text{CH}_2\text{CH}_2\text{CO}_2\text{H}$

(b) X = Ph

3. Near-infrared spectrophotometry

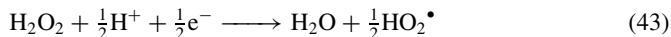
A technically simple method for determination of aqueous H_2O_2 in high concentration is by NIR spectrophotometry, taking advantage of the slight differences in the O–H

stretching vibration overtones of water and H_2O_2 around 1400 nm. Due to the closeness of both spectra, data processing is necessary for the determination of the peroxide concentration. The direct absorption spectrum gives better results than the plausible second derivative spectrum and processing by PLS is somewhat better than by MLR. An obvious advantage of the NIR method is the absence of reagents and minimizing exposure of the analytical operators to the harmful H_2O_2 vapors²³⁰.

4. Electrochemical methods

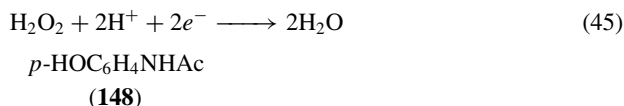
a. Classical methods. A simple amperometric method uses a concentric Pt–Ag electrode pair with a bias voltage of 700 mV across them. H_2O_2 is oxidized at the Pt anode and the released O_2 is reduced at the Ag cathode. This method was applied for measuring the kinetics and equilibria of HMHP and bis(hydroxymethyl) peroxide ($\text{HOCH}_2\text{OOCH}_2\text{OH}$) generation in solutions containing H_2O_2 and CH_2O at constant pH. Interference of the organic peroxides is practically nil¹³. HPLC-ELD using a cation-exchange resin gel column and a Pt working electrode set at +400 mV vs. SCSE can be used for determination of H_2O_2 even when antioxidants are present in the matrix. Thus, investigating the mechanism of H_2O_2 generation during the autoxidation of ascorbic acid (**22**) is a complicated analytical task. However, the process can be easily followed by determining both compounds on the same chromatographic run. The LOD is 0.2 pmol of H_2O_2 (SNR 3). The method was applied to determine H_2O_2 concentration in freshly prepared solutions of freeze-dried instant coffee in boiling water³⁶⁰. A FIA-ELD system is based on amperometric detection of 150 μL samples that flow alternatively through a simple tube or through a microreactor containing catalase immobilized on Amberlite IRA-743. Both samples pass through an electrochemical cell, where the Au–Pt working electrode is set at +0.6 V vs. SCSE, and the H_2O_2 concentration is determined by difference between both measurements. The LOD is 0.29 μM (1.5 ng H_2O_2 in 150 μL sample) with linearity in the 1 to 100 μM range. The method was applied for H_2O_2 determination in automatically collected³⁶¹ samples of rainwater³⁶². A coating can be applied to the working electrode of electrolytically deposited Ir oxide or of a sol-gel layer containing Ir nanoparticles and a further layer of Ir oxide. This can be of advantage in the oxidative determination of H_2O_2 , because of the biocompatibility of the Ir oxide conductive layer and the protection of the supporting metal (e.g. Pt) against poisoning or development of a nonconducting Pt oxide layer. Furthermore, on depositing GOX with the Ir sol, a biosensor is obtained for glucose determination, according to equation 16³⁶³.

Carbon black loaded with perovskite-type oxide ($\text{La}_{0.6}\text{Ca}_{0.4}\text{Ni}_{0.7}\text{Fe}_{0.3}\text{O}_3$) and bonded with PTFE is cast on a Cu screen to form a CPE for potentiometric and amperometric determination of H_2O_2 , using phosphate buffer at pH 7.1 as electrolyte. Both types of measurements are carried out using a SCE as reference electrode; the amperometric measurements use a Pt wire as counterelectrode. While the electrochemical process taking place with a pure CPE is the half-electron reduction of H_2O_2 according to equation 43, the oxide-loaded electrode participates in a 2-electron oxidation of the same substrate, according to equation 44³⁶⁴.



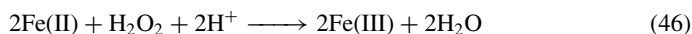
Potentiometric determinations of H_2O_2 can be carried out with a CPE loaded with 4% of MnO_2 and connected to the potentiometer with Cu wire. Measurements are carried out in NH_4^+ - NH_3 buffer, at pH 8.5 vs. SCE, with a Nernstian response of 19.4 mV per concentration decade. The LOD is 0.12 μM , with linear range from 0.300 μM to

0.363 mM³⁶⁵. A similar MnO₂-modified CPE in a FIA system, operating in neutral or slightly alkaline solution, at a potential of +0.46 V vs. SCSE, has LOD of 45 µg L⁻¹ H₂O₂, with linearity between 0.5 and 350 mg L⁻¹. Various oxidants and reductors interfere with the analysis³⁶⁶. Instead of mixing MnO₂ into the CPE, a layer of the oxide can be electrochemically developed on the electrode surface with better results. The LOD for H₂O₂ is 4.7 µg L⁻¹, with linearity from 5 µg L⁻¹ to 450 mg L⁻¹³⁶⁷. An electrode was developed based on colloidal clay on which ruthenium purple (Fe₄[Ru(CN)₆]₃) particles were precipitated. This electrode is claimed to be especially suited for determination of H₂O₂, according to the 2-electron reduction shown in equation 45. Also, ascorbic acid (**22**) can be determined. LOD for both analytes is about 1 ppm at pH 5³⁶⁸. A GCE modified with cobalt(II) hexacyanoferrate, Co₂[Fe(CN)₆], working in optimal conditions, shows fast response to H₂O₂. The LOD is 62.5 nM with linearity up to 1.1 mM. No interference is detected at the 0.20 mM level of ascorbic acid (**22**), dopamine (**68**), catechol, tyrosine (**35**), acetaminophen (**148**) and uric acid (**29**) and at the 50 µM level of polyamines³⁶⁹. Possible irregularities observed when using Ti electrodes for O₂ and H₂O₂ determination are discussed³⁷⁰.



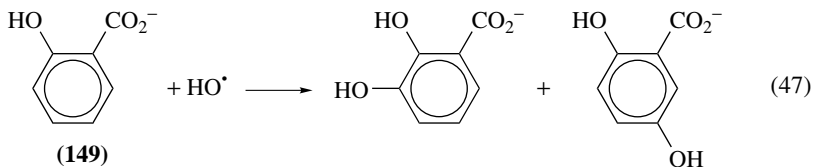
A cell with a small Pt disk working electrode coated with a polyelectrolyte multilayer made of poly(allylamine)-poly(vinyl sulfate), a Pt wire counterelectrode and a reference SCSE may be used for selective amperometric determination of H₂O₂, in the presence of ascorbic acid (**22**), uric acid (**29**) and acetaminophen (**148**). The latter three compounds show a significant response with the bare working electrode at +0.6 V while a practically nil one with the coated electrode. The reason for this selectivity may be an exclusion effect by the coating³⁷¹.

Two methods for H₂O₂ determination are based on the potentiometric determination of the changes caused by the reaction in equation 46 on the potentiometric buffer Fe(III)–Fe(II), measured with a gold electrode vs. SCSE in a FIA system. One of the methods, designed for trace concentrations, is based on a large transient response enlargement (75-fold) achieved when Br⁻ ions are rapidly oxidized to Br₂ in the presence of Mo(VI). Best results are attained using a 0.1 mM Fe(III)–Fe(II) buffer in 1.0 M H₂SO₄, containing 0.4 M NaBr and 0.5% (w/v) (NH₄)₆Mo₇O₂₄. The LOD is 0.4 µM (SNR 3), with RSD 0.6% (*n* = 6) at 4 µM H₂O₂, and a throughput of about 40 h⁻¹. The method can be applied to H₂O₂ determination in rainwater³⁷². The second method is intended for higher concentrations of H₂O₂, compatible with industrial applications such as quality control of the compound or bleaching. The concentration range for the analyte depends on the buffer composition and concentration and the dispersion undergone by the analyte when mixed with the reagents. A molar ratio of 1:1 for Fe(III) to Fe(II) gives a nearly linear response to the analyte concentration. A 1.0 mM solution of each buffer component in 1 M H₂SO₄ is fit for analyte concentrations in the 0.2 to 2 mM range; a 100-fold increase of the buffer concentration raises the analyte concentrations to the 5 to 40 mM range; to analyze 10 M H₂O₂, 30% w/w, the concentration of the buffer components should be about 0.4 M³⁷³.



Determination of H₂O₂ in biological systems can be performed by collecting samples of analyte that diffused from the matrix through a microdialysis membrane, adding Fenton reagents (FeCl₂ and salicylate ions, **149**) and determining the products of equation 47 by

RP-HPLC, using a citric acid–AcONa buffer–MeOH mobile phase and amperometric ELD. The method was used to demonstrate the increase of the H_2O_2 level in the extracellular liquid after impact injury on the spinal chord. The measured H_2O_2 levels were about $1 \mu\text{M}$ ⁷⁷.



A working GCE coated with an electrodeposited film of CuPtCl_6 , together with a reference SCSE and a stainless steel wire as counterelectrode, serve for sensitive amperometric determination of H_2O_2 in phosphate buffer at pH 7.4 in a FIA system. Working at +200 mV on the oxidation of the analyte avoids interference of dissolved oxygen. The response time of the coated electrode is very fast (about 5 s); the LOD is 10 nM, with linearity in the 50 nM to 5 mM range³⁷⁴.

Both O_2 and H_2O_2 can be analyzed in a FIA system consisting of a chemical reactor where the process takes place, a device for sample withdrawal that avoids contact with the atmosphere, injection into a CZE unit, where the analytes become separated in a short time, and an ELD unit for amperometric end analysis. The method was applied for determination of glucose and photochemical deterioration of ketoprofen (70), by measuring the H_2O_2 generated according to equations 16 and 21, respectively^{375, 376}.

An amperometric sensor for gaseous H_2O_2 consists of a Pt anode and a Au cathode embedded in a Nafion plate operating at room temperature, at an applied potential of 0.5 V, below the decomposition voltage of water. On keeping the air moisture constant, the response to H_2O_2 partial pressure is linear up to 200 ppm, however it is not linear at 1400 ppm. Changing the air moisture does not affect much the sensor response. Changing the polarity of the sensor also gives a linear response to concentration in the lower range; however, the current intensity is about 2% of the normal mode³⁷⁷.

A disposable electrode for cyclic voltametry consists of a flexible polypropylene film with a printed layer of silver to serve as wiring and a printed layer of conducting carbon, which after curing and drying is electroplated with a Cu layer. Operating in a FIA system, amperometric measurements can be made with the working electrode at -0.3 V vs. SCSE, with a Pt wire as auxiliary electrode, in phosphate buffer at pH 7.4; the working electrode develops an oxide layer which turns from $\text{Cu(I)}_2\text{O}$ to Cu(II)O on reacting with H_2O_2 in the redox cycles. The electrode may be used repeatedly. The LOD is $0.97 \mu\text{M}$ (SNR 3), with linearity up to $200 \mu\text{M}$ ³⁷⁸.

The concentration of H_2O_2 generated by sodium perborate ($\text{NaBO}_3 \cdot \text{H}_2\text{O}$), present as bleacher in laundering powder formulations, can be determined by polarographic methods³⁷⁹.

b. Biosensors and their mimics. Electrochemical biosensors and their mimics were briefly reviewed. An account was given of the problems encountered on development of a biomimetic sensor for H_2O_2 in water³⁸⁰.

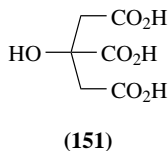
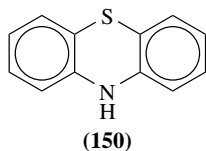
A biosensor electrode developed for the determination of H_2O_2 and other peroxides consists of a disc-shaped GCE incorporating a gel containing HRP and a poly(allylamine) complex with Os(II) ions. The operating principle is based on the Fe(II) of HRP becoming oxidized by the peroxide to Fe(III) and regenerated by Os(II) turning to Os(III). At the appropriate voltage Os(III) becomes reduced by the electrode. This biosensor loses

sensitivity in nonaqueous solvents, due to solvation effects affecting the structure of the enzyme. Therefore, a mimetic biosensor incorporating polymerized Fe-protoporphyrin IX (**75c**) instead of HRP has the advantage of being able to operate both in aqueous and nonaqueous solutions³⁸¹.

Instead of using immobilized enzymes, in the SIRE technique a limited quantity of enzyme solution is injected into the electrochemical chamber and the response of the matrix is measured. This is followed by renewal of the chamber content and measuring the response of the matrix plus analyte without the enzyme, from which the analyte concentration can be calculated. A proposed biosensor based on the SIRE technique for simultaneous measurement of H_2O_2 and ascorbic acid (**22**) in food products consists of a diffusion membrane to introduce these mutually interfering analytes into the electrochemical chamber. Four measurements are carried out after the current has stabilized for a Pt working electrode held at +450 mV vs. a Ag wire reference electrode: at pH 5.8 with and without ascorbate oxidase, and at pH 7.4 with and without catalase. The measurement sequence is fast and may be carried out in a FIA system. The same setup can be used for various analytes and matrix systems, choosing the proper enzymes and working conditions, with no investment in the developing of appropriate immobilizing polymers and electroactive mediators. An added advantage of this system is the possibility of sterilization, which is precluded for immobilized enzymes³⁸².

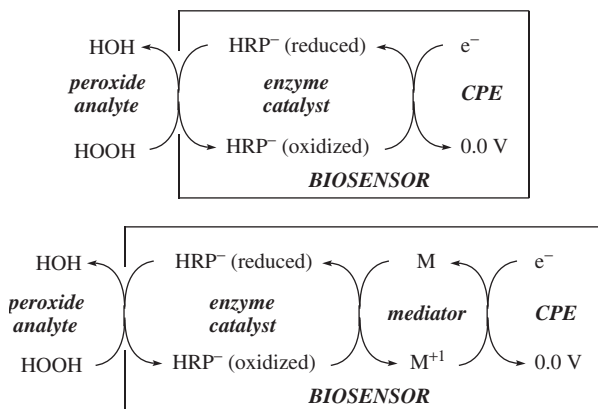
A microsensor system for simultaneous amperometric determination of H_2O_2 and $\text{O}_2^{\cdot-}$ consists of two working electrodes, one Pt counterelectrode and one WO_3 reference electrode. The working electrodes are GCE covered with HRP immobilized in an electrodeposited membrane of polypyrrole; the working electrode for $\text{O}_2^{\cdot-}$ has in addition a layer of immobilized superoxide dismutase. Operation with this system is at pH 5.1, setting both working electrodes at -60 mV. Other operating modes are also possible³⁸³.

A biosensor for amperometric determination of H_2O_2 is made of a CPE incorporating immobilized HRP and a redox mediator, such as phenothiazine (**150**), operating in acetate buffer at pH 4.5, working at a very low potential relative to the reference SCSE, typically 0.0 V. Incorporation of the mediator brings about a considerable acceleration of the electron transfer from the electrode to the reduced enzyme, and a more sensitive amperometric response to the analyte concentration changes, as depicted in Scheme 5. For clinical applications, incorporation of Nafion SAC-13, made of silica nanoparticles coated with Nafion, confers on the biosensor surface an electronegative charge, which is useful to reject interferences such as citric acid (**151**) and fouling by some substances present in the matrix. Under optimal conditions, the LOD (SNR 3) for the various investigated biosensors are 0.8 μM for CPE + HRP, 1 nM for CPE + HRP + **150** and 0.1 nM for CPE + HRP + **150** + Nafion SAC-13; the linear ranges are 1.8 to 40 μM for CPE + HRP and 2 nM to 40 μM for CPE + HRP + **150**³⁸⁴. A variation of this type of amperometric biosensors consists of a GCE covered by a gel film containing immobilized HRP; the mediator is in this case potassium hexacyanoferrate(II), $\text{K}_4[\text{Fe}(\text{CN})_6]$, dissolved in phosphate buffer at pH 7.5, working at -50 mV vs. SCSE. The LOD is 0.5 μM with linearity up to 3.4 mM. Excellent agreement is shown between a spectrophotometric method²⁶⁰ (Section IV.B.2.a) and the biosensor, when applied in a FIA system for determination of H_2O_2 in fresh milk, acid milk and juice³⁸⁵. An amperometric biosensor can be prepared



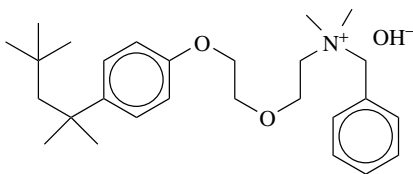
by immobilizing soybean peroxidase in a 4-vinylpyridine-TEOS sol-gel coating of a GCE, working at -0.20 V vs. SCSE and a Pt auxiliary electrode, in biphthalate buffer at pH 5.0, using Methylene Blue (**91**) as mediator. The enzyme shows good stability and the response is fast³⁸⁶.

Several variants of the biosensor in Scheme 5 have been proposed. One is a CPE containing at its tip a paste of graphite powder loaded with HRP and ferrocene ($[\text{Cp}\cdot\text{Fe}(\text{II})\cdot\text{Cp}]$) mediator, which is further covered with a cellulose acetate film coated with Nafion. The biosensor is mounted on a FIA system in a three-electrode setup, as working electrode at a potential of $+100$ mV vs. SCSE and a Pt counterelectrode. The LOD (SNR 6) for H_2O_2 is 200 fmol (20 μL injection of 10 nM solution), with linearity up to 25 μM ³⁸⁷. In another biosensor the immobilizing medium for the enzyme is a TMOS gel containing cetyltrimethylammonium bromide, and the ferrocene mediator is placed in the analyte solution³⁸⁸ or in a sol-gel layer immediately in contact with the CPE³⁸⁹.



SCHEME 5. Mechanism of electrocatalytic reduction of hydrogen peroxide with a biosensor. Top: Direct reduction with enzyme-modified CPE. Bottom: Accelerated reduction with enzyme-modified CPE, incorporating a mediator M (e.g. **150**). The potential is relative to SCSE

A pellet made of graphite and PTFE powder, incorporating HRP and ferrocene, has a fast response as working electrode due to the absence of coatings through which the analyte has to diffuse. Working at 0.00 V vs. SCSE at pH 7.4, the LOD is 0.18 μM and the LOQ is 0.61 μM , with linearity range from 0.4 to 3.6 μM and response of 28 ± 1 nA μM^{-1} . After a few days the response is reduced; however, during two months the electrode can be restored by polishing. If GOX is incorporated during manufacture, the electrode can be used as biosensor for determination of glucose in must and wines (equation 16). Under practical conditions extant in these matrices, selectivity for glucose is high and no interference larger than 10% should be expected from many possible interfering compounds, such as methanol, ethanol, formic, acetic, lactic, succinic, tartaric, malic and citric acids or fructose³⁹⁰. A similar setup uses a GCE coated with a polyionic membrane containing immobilized microperoxidase and ferrocene, working at 0.0 V vs. SCSE, in phosphate buffer at pH 7.0. The membrane may be made of poly-L-lysine or polystyrene sulfonate. Microperoxidase is a low molecular mass (less than 5%) version of peroxidase, showing therefore a corresponding increase of specific activity. The LOD is 0.5 μM with linearity up to 20 μM ³⁹¹.



(153)

IV. OXIDATION INDICES

A. General

The methods for testing the oxidative stability of fats and oils in foodstuffs³⁹⁹ and the assessment of the oxidation state of oils and fats⁴⁰⁰ have been reviewed. A critical review appeared on the FIA methods for edible oils, including various acidity indices⁴⁰¹.

The autoxidation processes of agricultural and chemical produce lead to the formation of many products, part of which have the $-OO-$ moiety, and especially the hydroperoxide group, $-OOH$. However, individual compounds are hard to separate, identify and quantify, given the complexities of the matrix and the profusion of oxygen-enriched and degradation products encountered. Several quality control standards and safety handling procedures are based on the global determinations of oxidizing material, usually expressed as a *peroxide value* (POV) or *active oxygen*, that point to a degree of deterioration or danger in handling, according to a set of relevant specifications. The POV of fats, oils and food products containing these substances is an important parameter in the assessment of their quality and shelf durability, pointing to the concentration of what is considered to be the primary stage of deterioration, namely the formation of hydroperoxides; a high POV is an index of exposure to autoxidation and poor quality of food products such as fats and oils, industrial solvents and fuels (e.g. biodiesel⁴⁰²).

Other indices measure a secondary stage of oxidation, such as the *anisidine value* (ANV), pointing to formation of carbonyl compounds, capable of undergoing condensation reactions with *p*-anisidine, and the *thiobarbituric acid reactive substance* (TBARS) pointing to the presence of malondialdehyde (MDA) in particular. In biological systems, TBARS is of widespread use as a measure for the extent of oxidation damage. Another test for stability of oils to oxidation is based on the development of acidity as secondary product, for example, standards using the Rancimat[®] equipment⁴⁰³ or a similar setup.

Finding the appropriate methods for evaluation of the extent of deterioration requires multiple tests under well-controlled conditions. For example, the effect of storing for 24 h with fluorescent light illumination vs. darkness (the reference state) on the quality of sliced cheese packed with the exclusion of oxygen can be determined by various methods: POV, development of free radicals by trapping and ESR spectroscopy, color development by a tristimulus method, odor changes and determination of secondary oxidation products after SPME, followed by GLC-MS. Only the latter two methods show a clear distinction between samples stored in the dark and under illumination; however, the POV and ESR methods may be improved by adequate modifications⁴⁰⁴. Not all the indices in use are independent of one another; however, each index reflects a different peculiarity of the sample. Thus, in a PCA chemometric investigation, the ANV index was found to be the most adequate for following the kinetic development of the thermal decomposition in the absence of oxygen of the hydroperoxides present in sunflower oil²²¹.

B. Peroxide Value

1. Definition

By definition POV is the number of milliequivalents of active oxygen per kilogram of sample⁴⁰⁵, or in some cases the number of micrograms of active oxygen in one gram of sample, capable of oxidizing iodide to iodine⁴⁰⁰. Many of the methods described in Section V for determination of hydroperoxide classes or individual compounds can also be applied for determination of POV, as *total hydroperoxides*. The iodometric determination of hydroperoxides in lipids and proteins has been reviewed⁴⁰⁶.

2. Direct titration

Although simple in conception and straightforward, the standard methods for POV determination require strict observance of analytical quality to avoid interference of artifacts. For example, according to the AOCS methods⁴⁰⁵, the sample dissolved in AcOH-CHCl₃ (method Cd 8-53) or AcOH-isooctane (method Cd 8b-90) solvent is treated with aqueous KI and the liberated iodine is titrated with standard thiosulfate solution, using starch indicator. Similar standard methods and modifications have been reported in various countries⁴⁰⁰.

A device for POV determination of foodstuffs containing fat is based on the following operations: Extraction of the pulverized sample with a solvent such as isooctane or CHCl₃, drying the extract over anhydrous Na₂SO₄ and filtering; one half of the extract is evaporated to dryness at low pressure, to determine the amount of fat residue; the other half is mixed with AcOH and NaI, and titrated with standard Na₂S₂O₃ solution to the potentiometric end point⁴⁰⁷. A study was carried out on the correlation between POV determined by the AOAC 965.33 method²¹² and the corresponding FTIR spectra (Section IV.B.4) of various oils (safflower, sunflower, rapeseed and olive) exposed to accelerated oxidation (10 g of oil in an 80 mm Petri dish in an oven at 70 °C, in darkness). Olive oil shows a slow linear raise of POV for 10 days and a very fast one until day 13, and the beginning of stabilization by day 14; the other oils start with a fast oxygen uptake, followed by stabilization from day 5 onward. The correlation of these findings with the spectral ones is discussed in Section IV.B.4⁴⁰⁸.

Although the standard iodometric method accounts for the peroxides present in the sample, interference is possible from the action of air that causes liberation of additional I₂, or other moieties present in solution that may react with I₂. Alternative spectroscopic and colorimetric methods have been proposed (Section IV.B.3) that avoid such pitfalls, in addition to being less time-consuming or requiring a smaller sample than the official method⁴⁰⁹. The iodometric titration method was applied for assessment of the damage caused by low dose pulse radiation experiments on thymine (**43**) and DNA in aqueous solution. Due to the concentrations in the μM range of peroxides produced in these experiments, the exclusion of oxygen has to be assured to avoid large interference. A POV for radiation chemistry can be based on the *G* value, defined as the number of molecules of analyte produced per 100 eV of energy absorbed by the solution. Thus, a value of $G = 1$ corresponds to a concentration development of $1.038 \mu\text{M krad}^{-1}$. For the experiments described here, for water (the blank) $G(\text{H}_2\text{O}_2) = 1.68$, for thymine (**43**) $G(\text{total peroxide}) = 2.87$ and for DNA $G(\text{total peroxide}) = 2.18$. This leaves the net values $G(\text{43 hydroperoxide}) = 1.2$ and $G(\text{DNA hydroperoxide}) = 0.5$. The alternative FOX assay (Section III.B.2.a) is inadequate for DNA due to precipitate formation¹³⁹.

3. Ultraviolet-visible spectrophotometry and colorimetry

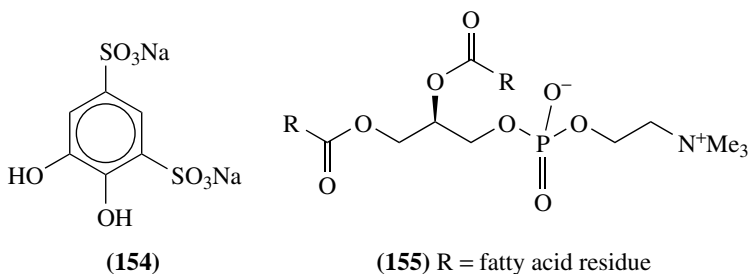
a. Absorption measurements. In the ASTM E 298-91 standard method the sample is dissolved in AcOH–CHCl₃ solvent and mixed with aqueous KI reagent. After 1 h, time necessary for the less reactive peroxides to undergo reduction, the absorbance of the solution is measured at 470 nm, and the POV is determined from a calibration curve. This standard for POV determination is proposed for organic solvents, including saturated and aromatic hydrocarbons, alcohols, ethers, ketones and esters; validity is also claimed for olefinic and α,β -unsaturated solvents. Various peroxide classes can be determined, such as hydroperoxides, diacyl peroxides, diaroyl peroxides, peresters and ketone peroxides. However, di-*t*-alkyl peroxides do not react under the conditions of the analysis⁴¹⁰. A procedure for POV determination of edible oils is based on measuring the I₃⁻ concentration at 290 nm ($\epsilon = 4.7 \times 10^4 \text{ M}^{-1} \text{ cm}^{-1}$)⁴¹⁰. A FIA system for determination of total hydroperoxides and peroxides in lipid pharmaceutical products includes a very long capillary to provide sufficient retention time before the mixture of analyte solution with iodide reagent reaches the UVD. This ensures that a model compound, benzoyl peroxide, is totally reduced without addition of catalyst. An optimization procedure is required to cope with various problems posed by the analyte being a lipid, such as its low solubility in hydrophilic solvents, whereas the reagent, NaI, has low solubility in lipophilic solvents. The method is equivalent to the AOAC standard²¹² and exhibits linearity down to 0.1 nM¹³⁴.

The oxidation extent of alkyd resin coatings containing drying oils can be determined by reduction with I⁻ in boiling *i*-PrOH-AcOH (10:1) solvent, followed by spectrophotometric determination at 357 nm. Oxidation of a typical varnish coating at room temperature starts to be noted about 1 h after application, reaches a maximum (e.g. POV *ca* 500 mmol kg⁻¹) after about 10 h and starts decreasing slowly until the organic layer matures to its final form¹⁸⁹. A FIA system with 10 parallel incubation tracks, with UVD at 360 nm and flow reversion capabilities, allows performing up to 83 POV determinations per hour, allowing 5 min incubation time, and up to 60 determinations per hour when the incubation takes 10 min. The linear range of POV is 2.5 to 80 meq kg⁻¹, with RSD better than 2.0% ($n = 10$). Advantages of the system over the tedious official methods are the small amounts of organic solvents required per analysis (2.0 mL of AcOH and 3.4 mL of *n*-PrOH) and the large throughput. The system was applied to POV determination of edible olive oil samples⁴¹¹.

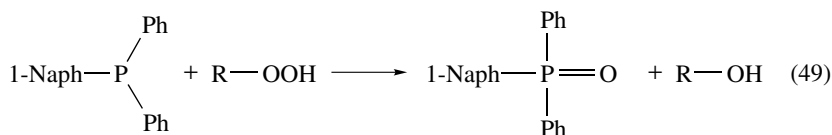
Hydroperoxides cause oxidation of Fe(II) ions to Fe(III) in acid solution. In a modification of the FOX assay (Section III.B.2.a) the oxidized ions form a blue-purple 1:1 complex with Xylenol Orange (**71**) that can be measured at 560 nm^{412–414}. However, it has been found that formation of a 2:1 complex is also possible and some corrections need to be made to obtain a good correlation between this method and POV obtained by the AOCS official method⁴⁰⁹. A modification of the FOX method proposed for determination of POV in beef, chicken, fish, butter and vegetable products correlates well with standard iodometric and FOX assays⁴¹⁵.

Various methods are based on the oxidation of Fe(II) to Fe(III) such as the IDF standard method for POV of fat in dairy products, where a sample of lipid solution is placed in intimate contact with an aqueous solution of Fe(II) ions, a solution of thiocyanate (SCN⁻) is added and the color intensity of the aqueous solution is measured at 505 nm (see also Section III.B.2.a)⁴¹⁶. Another method for colorimetric enhancement of Fe(III) ion uses Tiron (**154**) to form a complex that is measured at 650 nm⁴¹⁷. A modification of the IDF method for materials with a high content of carotenoids consists of performing an extraction of the aqueous solution with Et₂O before adding the thiocyanate complexing agent and measuring at 470 nm. The LOD is POV 0.044 meq kg⁻¹, showing a good correlation with the iodometric AOAC official method⁴¹⁸. Phosphatidylcholine (lecithine, **155**) is a

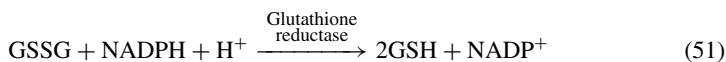
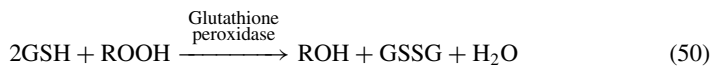
main component of liposomes and other emulsions. Certain modifications of the classical IDF and Tiron methods make them appropriate for determination of hydroperoxides in liposomes. For egg-phosphatidylcholine, the LOQ for the modified IDF and Tiron methods are, respectively, 0.037% (m/m, measuring at 478 nm) and 0.068% (m/m, measuring at 678 nm); the LOQ for the iodometric method is 0.16% (m/m, measuring at 353 nm)⁴¹⁹.



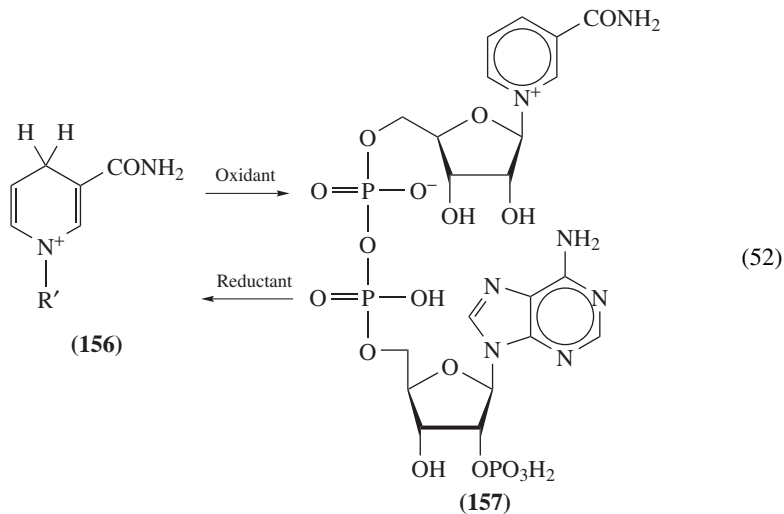
A sensitive method for ultra-trace levels of hydroperoxides is based on equation 49, where a hydroperoxide is reduced to an alcohol by diphenyl-1-naphthylphosphine, which is converted to the corresponding oxide and determined by HPLC-UV. The LOD for cumyl hydroperoxide (**27**) is 10 nM, with linearity up to 50 μ M. The method was applied for determination of hydroperoxides in tissue homogenates⁴²⁰.



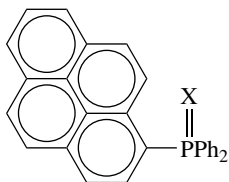
A nonspecific assay for hydroperoxides of all types is based on a two-step enzyme-catalyzed process taking place in one pot, where glutathione (GSH, **28**) is oxidized to the dithio form (GSSG), according to equation 50, and subsequently reduced to the GSH form by NADPH, according to equation 51. The change in absorbance at 340 nm is due to a structural change from a dihydronicotinamide moiety (**156**) of NADPH to the aromatic form of NADP⁺ (**157**), as shown in equation 52. The change in absorbance is correlated to the amount of analyte present in the sample. The method was proposed for biological matrices because it is operative at physiological pH values²⁶⁰.



b. Fluorescence methods. A sensitive method for ultra-trace levels of hydroperoxides in food or biological samples is based on the reduction of the hydroperoxide by diphenyl-1-pyrenylphosphine (**158a**), which is converted to an intensely fluorescent phosphine oxide (**158b**, $\lambda_{\text{ex}} = 352$ nm, $\lambda_{\text{fl}} = 380$ nm), in a process analogous to equation 49 above. The method can be applied for determination of total hydroperoxide content (POV); in batch mode or in a FIA system, of oils, foodstuffs and human plasma or for determination of

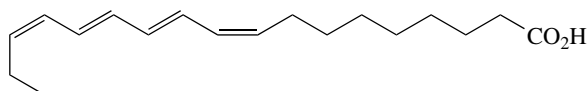


individual species after HPLC separation (Section V.B.2.b). The method was tested for vegetable oils, margarines, butters, mayonnaises and other foodstuffs with POV from 0.09 to 167 meq kg⁻¹ 421, 422.



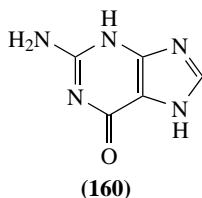
(158) (a) X = nil
(b) X = O

Cells may show a low level of autofluorescence at 413 nm when irradiated at 324 nm. This fluorescence dramatically increases when *cis*-parinaric acid (**159**) is incorporated into the cell membrane, either by intercalation or esterification. Exposure to oxidation stress of cells enriched with the **159** fluorescent probe causes diminution of the fluorescence intensity and is directly correlated with formation of lipid hydroperoxides. Addition of antioxidants, such as Vitamin E (**21**), abates fluorescence diminution. A blank run of cells enriched with **159** but not subjected to oxidation stress is necessary to follow the degradation of **159** when exposed to UV irradiation⁴²³. This method was applied to track lipid oxidation during apoptosis and other phenomena, triggered by toxic compounds such as H₂O₂, *t*-BuOOH and cumyl hydroperoxide (**27**)^{110, 111, 424}.



(159)

Damage to DNA by ROS may affect the thymine (**43**) residues, as mentioned in Section IV.B.2; however, also guanine (**160**) residues of DNA are labile and may yield 8-oxoguanine (**96**). This fact is the basis of a qualitative *in vitro* immunoassay for DNA oxidative damage shown in Table 2²⁷³.

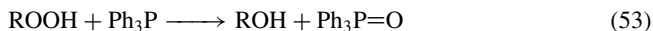


4. Infrared spectrophotometry

Studies of the most significant FTIR bands for assessment of the state of oxidation of edible oils describe their structural origin and form of development in accelerated oxidation tests. Keeping the record of absorbance ratios instead of absolute absorbance values eliminates analytical error due to variance in sample thickness, day-to-day instrumental performance etc. The FTIR spectral features of several edible oils and lard were assigned to various structural features of these lipids, and may serve as a reference state for assessment of autoxidation phenomena in further investigations^{425, 426}. Various stages may be distinguished in an accelerated oxidation run (Section IV.B.2), passing from the fresh oil to well-developed hydroperoxides, to hydroperoxide conversion to other functional groups, to total disappearance of the *cis* double bonds, and possibly polymerization finishing the run. These stages are accompanied by significant changes of certain band intensity ratios. Accelerated oxidation can be useful in forensic investigations, for example, when trying to discover falsification of olive oil by dilution with cheaper oils^{427, 428}. Various regions in the IR spectrum of edible oils are linked to phenomena taking place as autoxidation progresses and may serve for quality assessment and chemical diagnosis. The most significant ones are: a) 3700 to 3150 cm^{-1} , related to the appearance and subsequent disappearance of OOH groups, b) 3030 to 2600 cm^{-1} , mainly related to stretching of vinylic C–H bonds, to keep the record of *cis*- and *trans*-double bonds and other structural features, c) 1800 to 1500 cm^{-1} , related to the glyceryl esters and the appearance of aldehydes, d) 1500 to 1000 cm^{-1} , related to some changes of C–H structure and e) 1000 to 500 cm^{-1} , where particular oils have characteristic bands that change with autoxidation. Three gross stages can be distinguished when following the progress of autoxidation of edible oils under controlled conditions at 70 °C. The most characteristic changes observed in the IR spectra are as follows: During the first stage the intensity of the weak band at 3467 to 3470 cm^{-1} remains unaltered; this may be a short period of 3 to 4 days, as with walnut, safflower and soybean oils, rich in polyunsaturated fatty acids, or a long one up to about 20 days, as with olive oil, rich in monounsaturated fatty acids. During the second period this band becomes wider and more intense, with the maximum ostensibly shifting to lower frequency numbers; this is due to a new strong band of the OOH group being formed by oxidation; this period may last about 1 week for oils rich in polyunsaturated fatty acids to about 3 to 7 weeks for oils rich in monounsaturated fatty acids. When this band ceases to grow and starts receding, the third period sets in, where the hydroperoxides disappear and carbonyl compounds are formed with pronounced variation of the band near 1746 cm^{-1} . This period lasts from 1 to 2 weeks for oils rich in polyunsaturated fatty acids to about 7 to 8 weeks for oils rich in monounsaturated fatty acids. At the end of this period polymerization takes place, precluding determination of FTIR spectra as done for liquids⁴²⁹.

In the comparative study of various edible oils mentioned in Section IV.B.2, several changes in the spectra can be observed as the oxidation of the oil progresses. A weak peak of the fresh oil attributed to an overtone of $\nu(\text{C}=\text{O})$ of the glyceryl ester appears near 3470 cm^{-1} . On primary oxidation of the lipids the $\nu(\text{O}-\text{H})$ stretching mode of the hydroperoxide function appears as a broad band near 3444 cm^{-1} , overlapping with the original peak at 3470 cm^{-1} . The maximum frequency near this peak of olive oil starts wandering toward lower frequencies by the 12th day, reaching a minimum value of *ca* 3440 cm^{-1} by the 24th day, and then back to higher frequencies. The other three oils tested (safflower, sunflower and rapeseed) show a similar behavior; however, the maximum starts its displacement between the 2nd and the 5th day, depending on the oil, reaching the minimum frequency in about one day and returning to nearly the original frequency in 2 to 3 more days. These frequency shifts are concerted with the development of POV described for the same type of oil in Section IV.B.2. A medium strength peak near 3006 cm^{-1} is assigned to the $\nu(\text{C}-\text{H})$ stretching mode of the double bonds of *Z*-configuration; the frequency of this peak increases slightly with the degree of conjugation. After an induction period of about 15 days for olive oil and about 5 to 8 days for the other oils tested, the frequency of this peak starts to decrease toward 3000 cm^{-1} . These frequency shifts are concerted with the development of the ANV and may therefore be associated with the secondary oxidation processes. Also associated with these transformations is the slight decrease of frequency and the peak broadening observed for the $\nu(\text{C}=\text{O})$ of the glyceryl ester near 1746 cm^{-1} , influenced by the overlapping of the $\nu(\text{C}=\text{O})$ near 1728 cm^{-1} of aldehydes and ketones produced at this stage⁴⁰⁸. The integrated band from 3470 to 3082 cm^{-1} shows the highest correlation with POV determined by the AOAC method, according to PLS calculations, for the progressive deterioration of RBD palm olein used for deep frying of potato chips²¹⁰.

Maturation of alkyd resin coating formulations containing drying oils involves hydroperoxide formation as initial step, followed by polymerization and cross-linking reactions. Two main stages are distinguished by IR tracking of the process. First, the solvent evaporates leaving a spectrum mainly expected for drying oils, such as the CH of *Z*-double bonds at 3010 cm^{-1} and alkyl bands at 2950 to 2850 cm^{-1} and 1462 cm^{-1} . Oxidation takes place for 24 h in the *drying* process, by which the 3010 cm^{-1} peak disappears and the absorption increases at 1780 and 1700 cm^{-1} due to formation of γ -lactones or peresters and ketones, respectively^{189,430}. The possibility was investigated of using nondrying oils instead of drying ones for industrial applications where oxidized oil is required. For example, oxidation of rapeseed oil in air shows good PLS linear correlations for the FTIR absorbance at 3340 , 3020 , 1720 and 970 cm^{-1} with POV determined iodometrically or by measuring the absorbance of triphenylphosphine oxide at 542 cm^{-1} , produced according to equation 53²³⁶.



Hydroperoxides undergo reduction with a solution of triphenylphosphine, as shown in equation 53. This process can be used for determination of POV of oils in a FIA system, where the analyte solution and excess reagent solution are mixed together and then passed through a sufficiently long coil to assure quantitative reaction; the solution then passes through the sample cell of an FTIR spectrophotometer, measuring the absorbance at 542 cm^{-1} , taking as baseline the absorbance at 550 cm^{-1} . The method is superior to the standard AOAC method because of the easier implementation, the small amounts of reagents and the higher accuracy and reproducibility⁴³¹. Calibration can be performed with *t*-BuOOH solutions of known concentration. The measured absorbance is linearly correlated with the POV up to 100 meq kg^{-1} ⁴³². A method for POV determination of edible oils based on equation 53 uses commercially available porous polyethylene disposable

membranes on which the reaction mixture is loaded, measuring the Ph_3PO peak height at 542 cm^{-1} and using a calibration curve. Various problems regarding the appropriate loading method and the development of a calibration curve were solved^{2,33}.

5. Near-infrared spectrophotometry

Application of NIR spectroscopy to the analysis of food and especially of oils has been reviewed^{433, 434}. Given a wavenumber ν the corresponding wavelength is calculated by the formula $\lambda[\text{nm}] = 10^7/\nu[\text{cm}^{-1}]$. The overtones of the OO–H stretching frequencies in the IR region mentioned above (3400 to 3600 cm^{-1}) are assigned to peaks in the 1400 to 1560 nm (first overtone) and 950 to 1040 nm (second overtone) in the NIR region⁴³³. It was demonstrated that measuring the NIR absorption spectrum of an oil in the 1350 to 1480 nm region with a single-point baseline at 1514 nm is adequate for determination of POV. These measurements need a calibration curve based on POV determinations by the standard iodometric assay, covering the range of actual application values²³⁴.

The reduction depicted in equation 53 is the basis of a method for determination of POV in the 0 to 10 meq kg^{-1} range by FTNIR. Although the technical procedure is simple, data need PLS analysis because of the overlap of signals in the data acquisition region (4695 to 4553 cm^{-1})^{235, 435}.

A feasibility study on soybean oil showed that estimation of POV and other oxidation indices of oils can be made by measuring the absorbance spectrum and its derivative in the NIR region, at wavelengths in the 1100 to 2200 nm range. Good correspondence is found between POV determined by first derivative measurements at four key wavelengths in this range and POV determined by the Cd 8–53 AOCS⁴⁰⁵ official method in the range from 0.2 to 23 meq kg^{-1} ²³¹.

NIR transmittance spectra in the 1100 to 2200 nm wavelength range, collected at 26°C , are best suited for POV estimation, based on a PLS regression applied on the first derivative spectrum. This method is in excellent agreement with the AOCS official method Cd 8–53⁴⁰⁵ for POV; however, correlation with other oxidation indices such as those determined by the official methods Cd 18–90 for ANV and Ti 1a-64 for CDV⁴⁰⁵ (see Sections IV.D.1 and IV.D.4) is less successful^{436, 437}. The NIR method may report several advantages such as lack of toxic solvents and reagents, having a faster throughput, being nondestructive, and offering the possibility of automation and on-line measurements. A definite disadvantage is the very high cost of the instrument⁴⁰⁹.

6. Electrochemical methods

It was proposed to replace the final titration of I_3^- in the standard method with a redox potentiometric method, which is less laborious, fast and prone to automation. The LOD is 0.16 meq kg^{-1} , allowing determination of POV in fresh oil⁴³⁸. A method based on the potentiometric determination of the equilibrium in equation 54, in aqueous solution containing a large excess of I^- , with a Pt electrode vs. SCSE, was proposed to replace the standard iodometric titrations of Section IV.B.2 for determination of the POV of oils. The proposed method is *fit for purpose*, based on the *measurement uncertainties*, as compared to those of the standards based on iodine titration with thiosulfate solution. The analytical quality of the potentiometric method is similar to that of the standards based on titrations for oils with $\text{POV} > 0.5\text{ meq kg}^{-1}$; however, for fresh oils, with much lower POV, the potentiometric method is better⁴³⁹.



A biosensor was designed for potentiometric determination of hydroperoxides of olive oil and other fatty materials insoluble in hydrophilic solvents. The main advantages of such a device are simplicity (immersion of the electrode in a solution) and speed (<15 min, the response time of the electrode). The biosensor has two main parts: a) an oxygen electrode of the gas diffusion type consisting of a Pt cathode, a reference SCSE acting as anode, both submerged in a phosphate buffer–KCl solution at pH 6.6, with an opening to the surroundings covered by a gas-permeable diffusion membrane; b) a disk of κ -carrageenan gel containing immobilized catalase placed on the diffusion membrane and held there by a dialysis membrane. On submerging the biosensor in a solution of the hydroperoxide in a lipophilic solvent such as toluene, *n*-decane or CHCl_3 , the analyte diffuses through the dialysis membrane, undergoes an enzyme-catalyzed decomposition according to equation 35 (Section III.B.2.b) and the oxygen diffuses through the permeable membrane into the electrode cell to be measured. On accelerated rancidification, extra virgin olive oil in *n*-decane solution shows a progressive increase of POV, from nearly nil at the inception to a maximum of about 50 meq kg^{-1} , with no interference from other types of peroxide, such as benzoyl peroxide⁴⁴⁰.

After placing a pulverized sample in an organic solvent to dissolve the fat, an aliquot of the solution is introduced in a device where the fat content is determined by density analysis. The same solution is subjected to a coulometric titration using iodometry to find the titration value which, together with the fat content value, is used to estimate the POV⁴⁴¹.

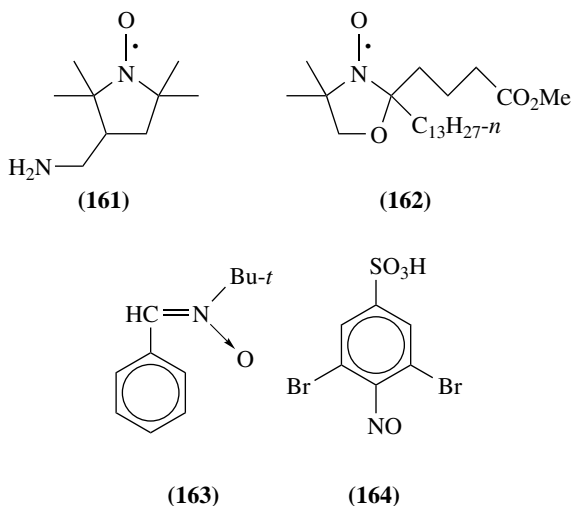
C. Tests for Stability on Storage under Exposure to Air

A widespread method for determining the induction period for autoxidation of oils and fats consists of passing a continuous stream of air through the heated sample and collecting the volatile acids evolved in a water trap, where they are determined on a real time basis. The time plot usually presents a flat appearance for a certain period and then takes off in an accelerated manner. This test is the basis of several national and international standards (e.g. AOCS Cd 12b-92—oil stability index⁴⁰⁵; ISO 6886—accelerated oxidation test for oxidative stability of fats and oils⁴⁴²) and the design of the Rancimat[®] equipment, where the end determination is based on conductivity measurements⁴⁰³. In addition to oxidation stability as determined by the Rancimat method and POV, which negatively affects virgin olive oil stability, other nonstandard properties were proposed for better assessment of the quality of this oil, namely LC determination of Vitamin E (**21**), colorimetric determination of total polar phenols and UVD of total chlorophyll⁴⁴³.

Some procedures for detection and determination of the damage caused by autoxidation are aimed at the determination of rather indefinite substances; for example, the ASTM D-4625-92 standard test for fuel stability on storage consists of tracking the amount of insoluble gums formed by oxidation at a slightly elevated temperature⁴¹⁰.

In the food industry sensorial quality appreciation (taste, odor and discoloration) is an important means for assessment of deterioration, sometimes based on personal experience. The oxidation state of dairy products is traditionally determined by the POV and TBARS methods (Sections IV.B and IV.D.2) or by sensory assessment. Certain ESR techniques have potential for development of oxidation stability tests for dairy products. Free radicals in lipids may be formed during autoxidation, or by decomposition of lipid hydroperoxides, or by scission of H_2O_2 followed by reaction with a lipid. Other free radicals are also produced on exposure of milk to air and UV radiation or high temperature. Three techniques yield significant results, each reporting its own advantages and disadvantages. The direct measurement in solution allows identification of individual species; however, few free radicals are stable in the aqueous solutions prevailing in milk and other dairy products; direct measurements in solids afford broad signals with little information about specific

radicals. *Spin labels* are relatively stable free radicals, such as 3-(aminomethyl)proxyl (**161**) or 5-doxylstearic acid methyl ester (**162**), that are added to the system and their disappearance is followed as they combine with the more reactive radicals formed on autoxidation; wrong results are obtained with spin labels that participate in other redox processes or act as antioxidants. Spin trapping affords stable free radicals by scavenging the original ones with a *spin trap*, usually *N*-oxides or nitroso compounds, such as *N*-*t*-butylphenylnitron (**163**) and 3,5-dibromo-4-nitrosobenzenesulfonic acid (**164**); although identification of the original radicals is difficult and some artifacts may be introduced, this technique seems promising for dairy products. Development of new spin labels and spin traps is necessary to fulfill the special needs of the dairy industry⁴⁴⁴. An accelerated test for oxidative stability based on the spin trap **163** was applied to compare four food-stuffs, namely mayonnaise (enriched with fish oil), rapeseed oil, dairy spread (made of rapeseed oil and cream) and butter. The order of stability increased, as expected from the decreasing order of insaturation, along the given list, as was the induction period for free radical formation⁴⁴⁵.

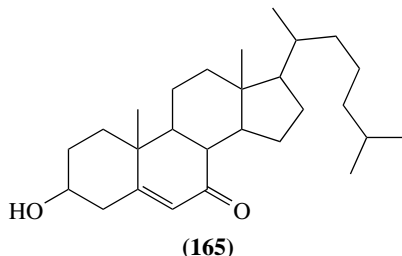


Direct measurement of oxygen uptake can be performed with O₂ sensors in the headspace of a closed system and organic deposition by measuring the weight changes with a quartz microbalance. This method was applied to investigate the dependence of jet fuel autoxidation on temperature and the presence of antioxidants⁴⁴⁶.

D. Secondary Oxidation Products

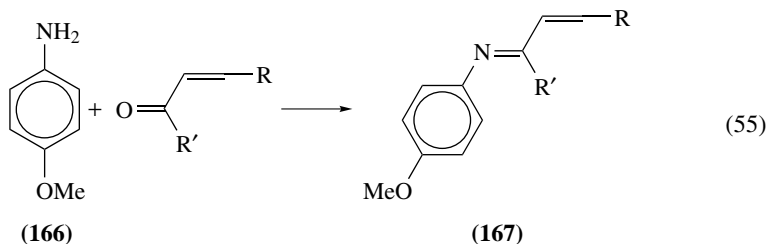
The peroxides resulting from oxidation processes usually act as intermediate stages ultimately turning into more stable compounds, the detection of which is taken as evidence for oxidative damage and the existence of a peroxide precursor in the past. Malondialdehyde (MDA), 4-hydroxyalkenals and alkanals are secondary decomposition products of lipids that underwent primary oxidation to hydroperoxides, their presence denoting a more advanced state of degradation. Various tests are designed to determine these secondary products globally. Among the methods based on UVD, outstanding but not unique are the ANV and TBARS assays. The presence of certain compounds can be taken as oxidation

index; for example, 7-oxocholesterol (**165**) has been proposed for diary products^{447,448}. See also Sections V.B.8 and V.C.3.



1. Anisidine value

According to the Cd 18–90 AOCS⁴⁰⁵ official method, the ANV is 100 times the optical density measured in a 1 cm cell, at 350 nm, of a solution containing 1.00 g of oil in 100 ml of the test solution. The measured absorbance is due to Schiff bases (**167**) formed when *p*-anisidine (**166**) undergoes condensation reaction with carbonyl compounds, according to equation 55. The carbonyl compounds are secondary oxidation products of lipids, such as α,β -unsaturated aldehydes and ketones derived from the hydroperoxides (see Scheme 1 in Section II.A.2.c), and their presence points to advanced oxidation of the oil.



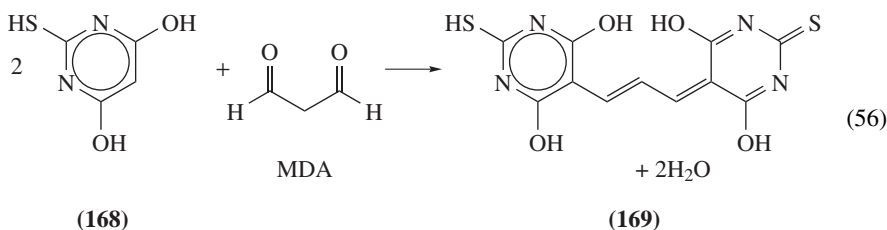
A study was carried out on the correlation between ANV determined by the IUPAC 2504 method⁴⁴⁹ and the corresponding FTIR spectra of various oils (safflower, sunflower, rapeseed and olive) exposed to accelerated oxidation (10 g of oil in an 80 mm Petri dish in an oven at 70 °C, in darkness). All ANV vs. time curves show a typical sigmoid shape; however, the induction period for olive oil is 10 days, after which a moderate growth takes place for two days before the beginning of stabilization by day 13; the ANV of other oils starts to rise after 1 to 4 days and begins stabilization by the 6th day. This points to ANV being a measure of secondary oxidation processes, after the primary ones, as determined by the POV, have taken place to some extent. The correlation of these findings with the spectral ones is summarized in Section IV.B.4.

A good correlation is observed between ANV predicted from the absorbance in the 1100 to 2200 nm NIR region and ANV determined by the Cd 18–90 AOCS⁴⁰⁵ official method, using UVD at 350 nm. The NIR spectroscopic method was applied to determine ANV for oxidized soybean oil⁴⁰⁸.

2. Thiobarbituric acid reactive substances

Thiobarbituric acid (**168**) reacts with carbonyl compounds extracted from foodstuffs or from living tissue giving a measurable discoloration⁴⁵⁰, therefore the denomination

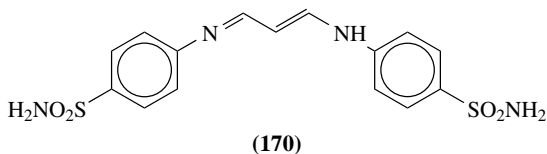
of these compounds as TBARS (thiobarbituric acid reactive substances). This assay was applied long before the nature of the dyestuff was elucidated. A reaction between TBA (**168**) and MDA takes place according to equation 56 producing a cyanine-type dye (**169**) with $\lambda_{\max} = 532 \text{ nm}$ ($\epsilon = 1.56 \times 10^5 \text{ M}^{-1} \text{ cm}^{-1}$)⁴⁵¹⁻⁴⁵³. A TBARS study using RP-HPLC columns of two types, with DA-UVD and supplemented by MS detection and MS-MS analysis, revealed the presence of various products. With one of the columns the main product is a pink dye with $\lambda_{\max} = 532 \text{ nm}$ (**169**) and $m/z = 323$ (M – H) of largest retention time; this product is preceded by a dye with $\lambda_{\max} = 513 \text{ nm}$ and $m/z = 317$ (M – H), attributed to a **169** analog where one of the S atoms is replaced by O, resulting from the 1:1:1 condensation of TBA, MDA and barbituric acid; this product is preceded by a small amount of a dye with $\lambda_{\max} = 490 \text{ nm}$, attributed to the 2:1 condensation of barbituric acid with MDA. These results point to the necessity of purifying the TBA before its use as analytical reagent for TBARS. The second chromatographic column revealed the presence of a yellow dye that was retained by the first column, with $\lambda_{\max} = 455 \text{ nm}$ and $m/z = 297$ (M – H), which may be assigned to the condensation of a saturated aldehyde, propanal in this case, with two molecules of TBA, taking place when TBA is used in excess for the TBARS assay⁴⁵⁴. The method was used for determination of MDA, derived from hydroperoxides produced as a result of oxidative stress, in a suspension of rat liver microsomes exposed to haloalkanes such as CCl_4 and CBrCl_3 . However, it was clear that additional products belong to the TBARS. Independent measurement of various oxidative processes were also carried out (see Section IV.D.3)¹¹⁹⁻¹²³.



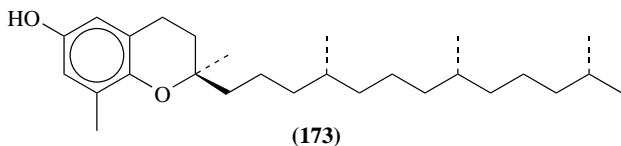
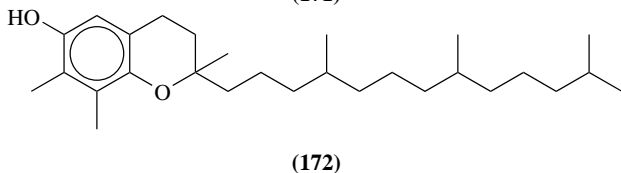
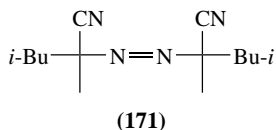
A method for determination of TBARS in the plasma of a 50 μL blood sample is based on FLD of **169**, instead of the usual UVD, with $\lambda_{\text{ex}} = 515 \text{ nm}$ and $\lambda_{\text{fl}} = 553 \text{ nm}$ ⁴⁵⁵. The lipoprotein in human serum can be separated into three fractions, VLDL, LDL and HDL, by a series of precipitation and centrifugation operations, carried out in the presence of EDTA and GSH (**28**) to avoid oxidation. In TBARS measurements carried out for serum by the fluorescence method ($\lambda_{\text{ex}} = 515 \text{ nm}$, $\lambda_{\text{fl}} = 548 \text{ nm}$) it was found that 43% was bound to the lipoproteins, distributed as follows: VLDL + LDL 27% and HDL 16%⁴⁵⁶.

A correlation may be established between the concentration of oxidized lipids and the TBARS value, expressed as MDA equivalents, in nM units. Correction is due in some cases for the interference by dyes or other factors. For example, the presence of anthocyanins in red cabbage leaves⁴⁵⁷ or turbidity⁴⁵⁸ causes overestimation of lipid hydroperoxides in plant tissue by the TBARS method. TBARS was used to assert the level of endogenous peroxides in hypo- and hyperthyroidism, both conditions being characterized by low lipid and lipoprotein plasma levels and enhanced oxidative metabolism⁴⁵⁹. In a procedure for determination of TBARS in edible oils, the sample is placed in a centrifuge at 12000 g before measuring at 532 nm ($\epsilon = 1.56 \times 10^5 \text{ M}^{-1} \text{ cm}^{-1}$)⁴¹³. A usual procedure for determination of TBARS in certain complex matrices involves steam distillation of the aldehydes responsible for the value, instead of extraction. In nitrite-cured meats, excess nitrite may cause nitrosation of MDA, thus interfering with distillation. To avoid this interference sulfanilamide is added, which is converted to a diazonium salt and

ultimately to a dye, thus liberating the MDA for distillation. However, interference is still possible under certain conditions, as MDA forms adducts such as the Schiff base **170**. The structure of MDA adducts such as **169** and **170** was analyzed by UVV, FTIR and NMR spectroscopies and by XRD crystallography⁴⁶⁰.



The correlation between the TBARS assay and MDA during oxidation of edible oils may be complicated by the presence of tocopherols (e.g. Vitamin E, **21**)¹². An evaluation was carried of MDA, determined by an independent method⁴⁶¹, and TBARS as indices for direct oxygen uptake of edible oils and unsaturated fatty acids. The linear increase of MDA and TBARS with oxygen consumption of soybean oil, in a closed vessel at 170 °C, stops when the latter value reaches 500 $\mu\text{mol L}^{-1}$, when both MDA and TBARS start to decrease on further O_2 consumption. The same process carried out at 40 °C, using 2,2'-azobis(2,4-dimethylvaleronitrile) (**171**) as initiator, shows linearity up to 1500 $\mu\text{mol L}^{-1}$ O_2 consumption⁴⁶². A similar behavior is observed for unsaturated fatty acids such as oleic, linoleic and linolenic acids⁴⁶³. On the other hand, depletion of Vitamin E (α -tocopherol, **21**) and its analogs γ - and δ -tocopherol (**172**, **173**) present in the oil show a linear dependence on O_2 consumption of the oil, up to 1800 $\mu\text{mol L}^{-1}$. This points to the consumption of these antioxidants, and especially **21**, as a good index for the O_2 uptake in oils at high temperature. The determination of the tocopherols is carried out by HPLC-FLD ($\lambda_{\text{ex}} = 295 \text{ nm}$, $\lambda_{\text{fl}} = 325 \text{ nm}$)^{12,462}.



Instead of measuring the absorbance of the solution immediately after incubation, it is possible to determine the colored product **169** by HPLC-FLD ($\lambda_{\text{ex}} = 515 \text{ nm}$, $\lambda_{\text{fl}} = 553 \text{ nm}$). This procedure was applied for determination of MDA after oxidation of phospholipids catalyzed by soybean lipoxygenase⁴⁶⁴. Peroxidation in the extracellular liquid of the brain cortex of rats was evaluated *in vivo* by microdialysis followed by reaction

with TBA and HPLC-FLD ($\lambda_{\text{ex}} = 515 \text{ nm}$, $\lambda_{\text{fl}} = 550 \text{ nm}$). A significant increase of MDA takes place following H_2O_2 perfusion⁴⁶⁵. An *in vitro* study showed a clear correlation between lipid oxidation and sperm motility, as attested by the presence of MDA measured by the TBA assay. The presence of 1 mM ascorbic acid (**22**) protects the sperm against loss of motility due to ROS, and lowers the MDA concentration¹⁰³. A fast method for determination of lipid peroxidation in animal tissue, food and feedstuff samples consists of water extraction of MDA from the sample homogenate, generation of the TBA adduct and determination of the absorbance at 532 nm in the third derivative absorption spectrum. The derivative spectrum avoids possible interference by other absorbing substances in this region⁴⁶⁶.

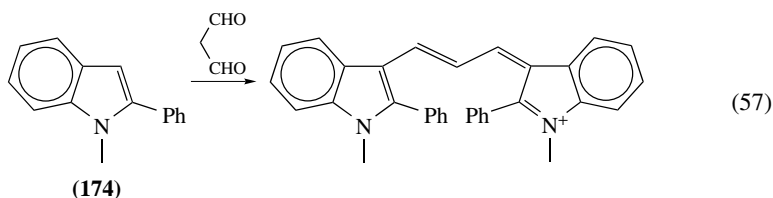
TBARS is not restricted to lipids, as other substrates are capable of producing MDA and react with TBA. For example, amino acids, carbohydrates and DNA are damaged by free radicals in the presence of Fe(III) ions, leading to products that ultimately release MDA⁴⁶⁷.

3. Miscellaneous methods for carbonyl compounds

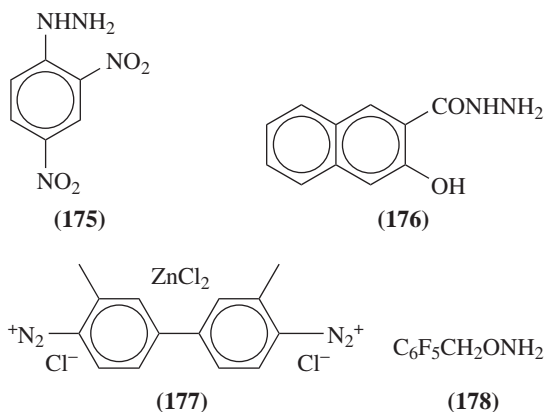
A simple method for assessing lipid oxidation is measuring the headspace concentration of hexanal by capillary GLC. Also, the total volatiles appearing in the chromatogram up to hexanal can be taken as oxidation index. The method was applied to determine the amounts of lipid peroxides present in rat liver cells. Enhancement of the hexanal concentration can be achieved on adding ascorbic acid (**22**), that reduces Fe(III) present in the matrix to Fe(II), which catalyzes decomposition of hydroperoxides to aldehydes. Significant correlations are found between hexanal concentrations and various oxidation indices, such as TBARS (Section IV.D.2)⁴⁶⁸.

An alternative method to TBARS for determination of MDA is formation of the DNP derivative and quantitation by RP-HPLC with DA-UVD, recording in the 195 to 500 nm range. Other carbonyl compounds present in the sample also form the corresponding DNP compounds and are also determined. The method was applied to MDA determination in plasma of rats, after they were subjected to oxidative stress by intraparental injection of a dose of bacterial lipopolysaccharide⁴⁶⁹.

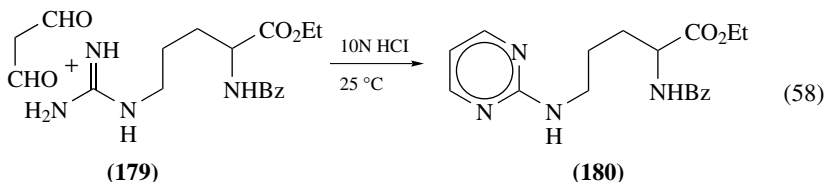
N-Methyl-2-phenylindole (**174**) undergoes condensation in acidic media with MDA or 4-hydroxyalkenals to yield a stable chromophore that is measured at 586 nm, as shown in equation 57 for MDA. It is possible to distinguish between MDA and 4-hydroxyalkenals, and between this pair and other aldehydes. Thus, in the presence of methanesulfonic acid, both malondialdehyde and 4-hydroxyalkenals show chromogenic activity at 586 nm, whereas other aldehydes show negligible activity at this wavelength. On the other hand, 4-hydroxyalkenals and other aldehydes show activity at 505 nm. In the presence of HCl only MDA shows activity at 586 nm. However, 4-hydroxyalkenals show activity at this wavelength in the presence of Fe(III), a frequent component in samples of biological origin; the specificity for MDA at 586 nm in the presence of HCl and Fe(III) may be restored on masking the effect of Fe(III) with probuocol (**23**)^{470,471}. The method can be applied to determine these aldehydes in plasma or tissue homogenates, as an index of oxidative damage. Commercial kits for MDA and HNE determination are mentioned in Table 2.



Detection of nonprotein bound aldehydes can be done by forming hydrazones with reagents such as 2,4-dinitrophenylhydrazine (DNP, **175**) and 3-hydroxy-2-naphthoic acid hydrazide (**176**), which are also applicable as precolumn derivatizing agents for HPLC or TLC. Although UVD is useful for both derivatives, ELD for those of **175** is 10-fold more sensitive allowing sub-pmol detection¹²³. Application of **176** followed by coupling with Fast Blue B (**177**) can be used as a sensitive histochemical means for visualization of regions where lipid peroxidation takes place, by means of microspectrophotometry⁴⁷². Precolumn derivatization with **175** and HPLC-UVD at 360 nm was applied to the carbonyl products obtained in a set of experiments for assessing the effectiveness of lipoxigenase enzymes extracted from various microorganisms⁴⁷³. Aldehyde degradation products of lipid oxidation can be conveniently determined after precolumn derivatization to hydrazones with pentafluorophenylhydrazine^{474,475} or to oximes with *O*-pentafluorobenzylhydroxylamine (**178**)^{124,476} followed by GLC-NI-MS or GLC-ECD. Precolumn derivatization with **178** followed by GLC with NI-MS detection was used for determination of HNE in physiological fluids of patients affected by Parkinson's disease, bowel inflammatory disease, HIV-1 infection and AIDS¹¹⁴.

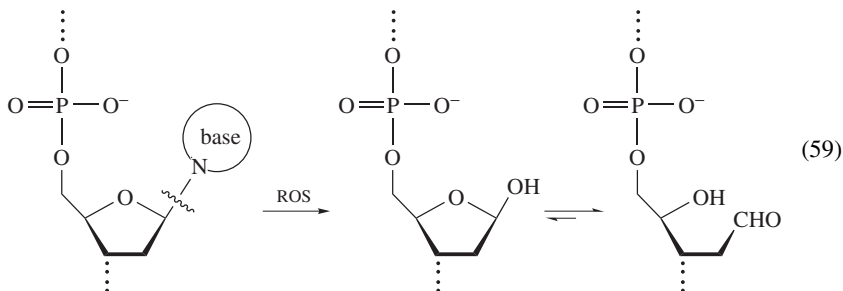


In contrast with the nondiscriminating methods for carbonyl compounds described above, MDA can be selectively determined by acid-catalyzed condensation with α -*N*-benzoyl-L-arginine ethyl ester (**179**), forming a pyrimidine derivative (**180**), according to equation 58. Formation of **180** can be detected at the 1 pmol level by RP-HPLC with UVD at 309 nm. The structure of **180** can be fully characterized by ¹H-¹H COSY^{461,477}.



Besides the direct oxidation products of base residues of DNA, such as the oxidation of thymine (**43**) and guanine (**160**) residues mentioned in Sections IV.B.2 and IV.B.3, ROS and other factors may bring about detachment of base residues from the DNA strand,⁴⁷⁸ leading to formation of aldehyde *abasic sites* on the main chain, as shown in

equation 59. The abasic sites can be quantized by various methods, as a measure of the oxidative damage that took place. Table 2 contains a quantitative method, where the aldehyde moieties undergo condensation to an *O*-alkyloxime bearing a biotin residue (**98**), and are further derivatized by the avitin-biotin-HRP method that lies outside the scope of the present chapter.



4. Conjugated dienes value

Hydroperoxide formation by the ene reaction path may lead to formation of conjugated double bonds in polyunsaturated fatty acids (see Section V.A); this reaction is concurrent with POV increase. An increase of the CDV, as measured from the absorbance at 233 nm, therefore indicates oxidation of polyunsaturated lipids. A strong correlation exists between CDV predicted from the absorbance in the 1100 to 2200 nm NIR region and CDV determined by the Ti Ia-64 AOCS official method⁴⁰⁵, by UV spectrophotometry at 233 nm. The method was applied to determine CDV for oxidized soybean oil²³¹. A secondary absorption maximum of lesser intensity appears in the 260–280 nm range, and is assigned to ketone dienes⁴⁷⁹.

The following spectrophotometric methods are conceptually related to the POV; however, they are intended for other purposes. HPLC-UVD at 234 nm was applied to detect lipid hydroperoxides, obtained in a set of experiments for assessing the effectiveness of lipoxigenase enzymes extracted from various microorganisms⁴⁷³. The absorbance, *A*, measured at three different wavelengths is linearly correlated to the concentrations in μM units of lipid hydroperoxides, C_{LH} , 7-oxocholesterol, C_{OC} , and dienals, C_{DE} , according to the set of simultaneous equations 60. This method was used to track the Cu(II)-induced oxidation of LDL^{113,480}.

$$\begin{aligned}
 A(245 \text{ nm}) &= 0.01485C_{\text{LH}} + 0.01050C_{\text{OC}} + 0.00582C_{\text{DE}} \\
 A(250 \text{ nm}) &= 0.00482C_{\text{LH}} + 0.00707C_{\text{OC}} + 0.01122C_{\text{DE}} \\
 A(268 \text{ nm}) &= 0.00003C_{\text{LH}} + 0.00088C_{\text{OC}} + 0.02898C_{\text{DE}}
 \end{aligned}
 \tag{60}$$

RP-HPLC with nonaqueous solvents and UVD at 246 nm was developed for the determination of low level POVs of vegetable oils. These measurements are specific for conjugated diene peroxides derived from vegetable oils with relatively high linoleic acid content. These measurements may be supplemented by nonspecific UVD at 210 nm and ELSD for detection of all eluted species. The elution sequence of the triglycerides in a nonaqueous RP-HPLC is linearly dependent on the *partition number* of each species, N_p , which is defined as $N_p = N_c - 2N_d$, where N_c is the *carbon number* and N_d is the double bond number. In the case of hydroperoxides $N_p = N_c - 2N_d - N_{\text{hpo}}$, where N_{hpo} is the number of hydroperoxyl groups in the molecule (usually 1 for incipient POV). For

given chromatographic conditions one may determine the elution times for a series of triglyceride standards and their dependence on N_p . This is important as it allows indirect identification of the eluted peaks detected at 246 nm, even in the absence of good hydroperoxide standards, which are difficult to prepare. The area of the relevant peaks can be used to estimate POV_{HPLC} , which is usually several times larger than the POV determined by standard methods⁴⁸¹.

5. Acid value

The ACV is defined as the number of acid equivalents expressed as mg KOH per g of sample. It may be also expressed as percentage (m/m) of a particular fatty acid in a fat or oil. This parameter usually indicates alterations undergone by hydrolysis, and can be determined by direct titration⁴⁰⁰. The ACV is used as a standard, for example, ISO 660⁴⁸² or IUPAC 2.201⁴⁴⁹. The acidity of refined oils is always below 1%, whereas that of virgin oils is higher and variable. In cases of extreme oxidation, free carboxylic acids are produced (Scheme 1, Section II.A.2.c) that contribute to the ACV. This is the operational principle on which the Rancimat[®] equipment⁴⁰³ for POV determination is based.

E. Thermal Analysis

Calorimetric studies have long been used for evaluating the long-term stability of industrial products in a noninvasive and nondestructive manner, and in particular of pharmaceutical products. Isothermal microcalorimetric data may be acquired in a relatively short time (less than 24 h) using modern instrumentation. Data refinement enables one to establish kinetic and thermodynamic parameters of the system under investigation, which need not be a pure compound or a single phase, and may involve complicated processes⁴⁸³. The stability of hydrated benzoyl peroxide, which is the stabilized form handled in the pharmaceutical and food industry, was examined by isothermal microcalorimetry. The collected data can be interpreted as slow decomposition following first-order kinetics, for which the activation energy is estimated from an Arrhenius plot⁴⁸⁴. Examination of the calorimetric behavior of various benzoyl peroxide formulations points to the stabilizing effect of most additives present in the formulation, an important piece of information when developing new commercial presentations⁴⁸⁵.

Oxidation of a typical alkyd resin varnish coating containing drying oils, at room temperature, can be tracked by DSC, following the development of an exothermic peak appearing at about 150 °C, which is attributed to decomposition of peroxides. Although the thermal homolytic decomposition of the peroxide group is endothermic, the subsequent bond reformations are strongly exothermic. On estimating the enthalpy of this process as 320 kJ mol⁻¹ of peroxide groups, a POV value can be calculated as a function of maturation time, that closely resembles the POV development curve determined by I⁻ reduction mentioned in Section IV.B.2¹⁸⁹.

The thermal behavior of peroxides as determined by thermal analysis is an important source of information about the potential dangers of storing and transporting bulk amounts of peroxides or materials that may contain peroxides. For example, thermal analysis is helpful in determining the SADT, a parameter required by storage and transportation regulations of organic peroxides (Section X.B.1), or predicting possible explosive behavior of these compounds, such as the cyclic peroxides mentioned in Section VII.B.2.

V. HYDROPEROXIDES

A. General

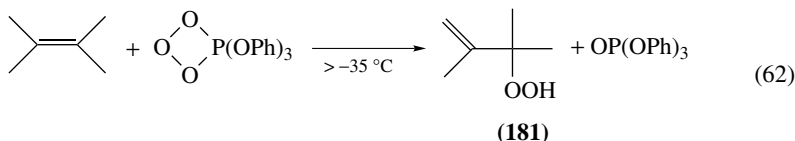
The term *hydroperoxide* can loosely refer to all compounds carrying the -OOH group, as is the case of H₂O₂ and the peroxyacids. However, in the present section and the rest

of this chapter it is usually restricted to compounds with the group attached to a saturated C atom. Many of the methods for detection and determination of hydroperoxides are the same as those described for POV in Section IV.B or slightly modified ones.

Alkyl hydroperoxides can be synthesized from the corresponding alkyl methyl sulfonates, according to equation 61^{486–488}.



Hydroperoxides may be the primary result of autoxidation processes of organic materials exposed to air and ROS (see Section III). Olefins with allylic hydrogen atoms may undergo the 'ene' reaction with singlet oxygen either by photosensitized oxidation^{489–492} (for example, Scheme 10 in Section V.C.1), a mixture of hydrogen peroxide and sodium hypochlorite⁴⁹¹ or with the triphenyl phosphite-ozone adduct, as shown in equation 62⁴⁹³, to yield allylic hydroperoxides (such as **181**). Also, *t*-BuOOH can generate ¹O₂ on treatment with hypochlorite, as demonstrated by the typical red CL emission obtained from this mixture⁴⁹⁴. Alternative routes were investigated for photosensitized oxidation of lipids⁴⁹⁵. Thermal oxidation of polyethylene in air leads to increasing concentration of hydroperoxide (see Section V.B.5), which reaches a maximum and starts to decrease while other derivatives are formed⁴⁹⁶.



Generation of hydroperoxides in the atmosphere by ozonolysis of biogenic olefins was mentioned in Section II.A.1.a. Ozonolysis in aqueous phase, e.g. disinfection of drinking water, may produce hydroperoxides, some of which are only inferred because they are too short-lived for detection⁴⁹⁷. Ozonolysis in a solution containing alcohols can produce a hydroperoxide derivative incorporating the alcohol, as shown, for example, in Scheme 11 (Section V.C.5) for the ozonolysis of cholesteryl acetate in the presence of various alcohols. Reduction of hydroperoxides may be readily accomplished with NaBH₄⁴⁹¹ and other reducing agents, yielding the corresponding alcohols that are easier to handle in analytical procedures involving separation.

B. Detection and Determination

Reviews appeared on the following subjects: Analysis of lipid hydroperoxides⁴⁹⁸, the difficulties encountered for hydroperoxide analysis in a plasma matrix⁴⁹⁹, post-column derivatization after GLC of lipid hydroperoxides¹³² and methods for detection and characterization of hydroperoxy groups in oxidized polyolefins⁵⁰⁰.

1. Titration methods

The iodometric determination of hydroperoxides in lipids and proteins has been reviewed⁴⁰⁶. Although the standard AOCS iodometric method for POV²¹² accounts for the peroxides present in the sample, interference is possible from the action of air that causes liberation of additional I₂, or other moieties present in solution that may react with I₂. Thus, alternative methods have been proposed for the determination of this important parameter, such as the analytical kits in Table 2, other spectrophotometric

methods (Section V.B.2) and IR spectrometric methods (Section V.B.3)⁴⁰⁹. Iodometric titrations using starch indicator can be applied to monitor the development of α -hydroxy hydroperoxides during oxidation of alcohols. As H_2O_2 is also produced in the oxidation process, two titrations are required, one for total oxidative capacity and one after addition of catalase to destroy H_2O_2 ⁵⁰¹. The yield of primary alkyl hydroperoxides according to equation 61 may be determined by refluxing the analyte in AcOH containing KI, followed by thiosulfate titration of the liberated I_2 ⁴⁸⁶.

2. Ultraviolet-visible spectrophotometry and colorimetry

a. Absorption UVV spectrophotometry. A discussion of the problems encountered in the separation of the naturally occurring fatty acids and their hydroperoxide oxidation products proposes MEKC with selected buffers as an effective method for achieving good separation. The method uses DA-UVD, measuring at 195 and 234 nm; the former wavelength serves to detect compounds with isolated double bonds and at the latter wavelength the signal of oxidized compounds containing conjugated double bonds has higher intensity. The LOD is in the μM range⁵⁰².

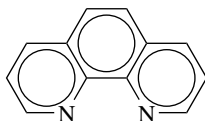
Hydroperoxides may be determined by measuring at 290 nm ($\epsilon = 44100 \text{ M}^{-1} \text{ cm}^{-1}$) or 360 nm ($\epsilon = 28000 \text{ M}^{-1} \text{ cm}^{-1}$) the concentration of I_3^- formed in the presence of a large excess of I^- ions. The reaction may be too slow for practical purposes, unless a catalyst is present. For example, an assay for lipid hydroperoxides conducted without a catalyst may require several measurements every 6 min until the absorbance reaches a maximum. Exclusion of air from the sample cuvette is important. The method is about 1000-fold more sensitive than thiosulfate titration^{250, 458}. The iodometric method with UVD at 360 was adopted for detecting the presence of hydroperoxides derived from protein, peptide or amino acid substrates subjected to γ -radiation, after destroying the generated H_2O_2 with catalase¹⁴³.

HMHP and its dimerization product may be present in the atmosphere together with H_2O_2 . The organic peroxides are determined after scrubbing from air by passing through a MnO_2 column to eliminate H_2O_2 , and measuring the I_3^- absorbance at 352 nm, developed on treatment with aqueous acidic KI ³²⁸. The hydroperoxides present in liposomes can be determined by reduction with excess I^- ions and measuring the I_3^- product at 290 nm ($\epsilon = 4.7 \times 10^4 \text{ M}^{-1} \text{ cm}^{-1}$)²⁵⁷.

Allen's reagent, ammonium molybdate in potassium hydrogen phthalate buffer, can be used to catalyze the oxidation of I^- to I_2 by hydroperoxides ($\lambda = 350 \text{ nm}$, $\epsilon = 25000 \text{ M}^{-1} \text{ cm}^{-1}$)^{503a}. The method has the advantage that no free radical chains are involved in the reduction, as in the case of aqueous Fe(II) species mentioned in Section IV.B.3.a^{503b}. Allen's reagent was used to determine the concentration of unstable hydroperoxide intermediates obtained by ozonolysis of olefins in water (equations 1 to 8, Section II.A.1.b)⁴⁵. The iodide-molybdate method can be used to determine certain species in mixtures of hydroperoxides, because the kinetics of the reduction usually varies from one to the other²⁴⁴. A method was proposed for the simultaneous determination of H_2O_2 and hydroperoxides based on determining the total concentration of peroxides by the iodide-molybdate method, measuring the I_3^- ions at 352 nm ($\epsilon = 26400 \text{ M}^{-1} \text{ cm}^{-1}$), and the organic peroxides by the kinetics of the same reaction, after specific elimination of H_2O_2 with catalase (in neutral solution this is complete after 10 min at 25°C)²⁵².

The oxidation of I^- can proceed with hydroperoxides at a convenient rate without a catalyst, if the solution is heated to 90°C , measuring at 348 nm ²⁵³. A modification of the iodometric method was proposed for determination of hydroperoxides in liposomes, using anhydrous EtOH as solvent in all the operations. A sample of liposome suspension is evaporated to dryness in a vacuum, after adding EtOH in a 4:96 sample-to-solvent proportion.

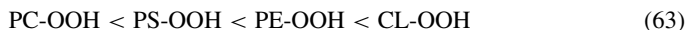
The dry residue is dissolved in EtOH containing AlCl_3 and 1,10-phenanthroline (**182**), an aliquot of fresh solution of KI in EtOH is added, all is incubated in the dark for 15 min at 37°C and the absorbance is measured at 357 nm ($\epsilon = 4.5 \pm 0.2 \times 10^4 \text{ M}^{-1} \text{ cm}^{-1}$). The LOD is $1.4 \mu\text{M}$, with linearity up to $20 \mu\text{M}$. It is important to avoid contact with air during the incubation, that may oxidize I^- ions, and the presence of water in the system, which reduces the analytical result⁵⁰⁴. HPLC with UVD at 234 nm can be applied in the analysis of lipid hydroperoxides in LDL, using a conjugated diene as internal standard⁵⁰⁵.



(182)

Phospholipid classes (see Section V.B.3) may be separated from one another by HPLC-UVD, measuring at 210 nm. Oxidized phospholipids, including hydroperoxide and hydroxy derivatives, can be detected by the same method measuring the signal at 234 nm. This was applied for assessment of the oxidation of phospholipids in human erythrocyte membranes catalyzed by soybean lipoxydase in the presence of various modifiers^{464, 506, 507}.

The hydroperoxides of various phospholipids, such as phosphatidylcholine (PC-OOH, **155**), phosphatidylserine (PS-OOH), phosphatidylethanolamine (PE-OOH), phosphatidylinositol (PI-OOH) and cardiolipin (CL-OOH), can be separated on HPTLC silica gel plates, using as mobile phase a $\text{CHCl}_3/\text{EtOH}/\text{AcOH}/\text{H}_2\text{O}$ mixture (100:75:7:4 by volume). After drying the plate, the various phospholipid hydroperoxides can be detected on spraying with a freshly prepared slightly acidic solution of *N,N,N',N'*-tetramethyl-*p*-phenylenediamine (**89**) under blanketing, by the purple spots on the plate. This procedure can be made quantitative on scanning the plate with a densitometer and comparing the spot intensity with that of a calibration curve prepared with known standards for each type of phospholipid hydroperoxide. The relative mobility for the given chromatographic system is shown in equation 63. The LOD varies from about 0.1 to 1.0 nmol with linearity from about 20 to 40 nmol, depending on the class of phospholipid hydroperoxide⁵⁰⁸.



Some substances are hard to dissolve in aqueous solution. The FIA system described in Section III.B.2.a for determination of H_2O_2 in substances dissolved in toluene, using HRP immobilized by adsorption on a pack of controlled-pore glass beads, where the enzyme catalyzes the oxidation of *p*-anisidine (*p*- $\text{MeOC}_6\text{H}_4\text{NH}_2$) dissolved with the analyte, can also be used with hydroperoxides. However, the throughput has to be lower due to the slower reaction of this type of analyte. The LOD for *t*-BuOOH is $2.6 \mu\text{M}$, with linearity in the 0.4 to 24 mM range, and a throughput of about 30 h^{-1} . The method was applied to analysis of olive oil and margarine³⁰².

Hydroperoxides undergo reduction with aqueous Fe(II), which turns to aqueous Fe(III). The reaction can be followed at 305 nm ($\epsilon = 2095 \text{ M}^{-1} \text{ cm}^{-1}$)⁵⁰⁹. Although the stoichiometry of this process is straightforward, with two Fe(II) ions being consumed per molecule of hydroperoxide, the mechanism involves an alkoxide free radical, RO^\bullet , that may undergo β -elimination, H abstraction from R-H, or a 1,2-H-shift and reaction with other components in the system. A case in point is the determination of *t*-butyl hydroperoxide which consumes under 1 mol of Fe(II) per mol of analyte under inert gas cover, while in the presence of O_2 four mols are consumed, pointing to extensive side reactions of the RO^\bullet free radical, both without and with O_2 in the system²⁴⁴.

A method based on a similar reduction of the hydroperoxide by Fe(II) consists of forming an intensely colored complex of Fe(III) with thiocyanate ions (SCN^-) and measuring the absorbance at 500 nm⁵¹⁰. The same complex can be measured colorimetrically in organic solvents, allowing hydroperoxide determinations in the 10 to 25 ppm active oxygen concentration range. Color development is slower than with hydrogen peroxide (Section III.B.2.a). The method can be used for determination of hydroperoxides in nonvulcanized rubber dissolved in hydrocarbon solvents²⁵⁴. Determination of lipid hydroperoxides by Fe(II) to Fe(III) oxidation with color enhancement by SCN^- is more sensitive than the iodometric assay⁵¹¹. Lipid hydroperoxides are insoluble in the aqueous alcohol media used for other organic hydroperoxides in the latter assay and require more lipophilic solvents, such as a mixture of CHCl_3 and alcohol. Erratic results are sometimes obtained when changing the brand of CHCl_3 solvent, related to the type of stabilizing agent used. Thus, CHCl_3 stabilized with amylene (2-methyl-2-butene) affords unusually high blank readings, as opposed to the ethanol-stabilized solvent, which is the type recommended for this analysis⁵¹². A solution of FeSO_4 and NH_4SCN in aqueous acetone may serve as detection reagent for hydroperoxide spots in TLC. This was applied for measuring the effectiveness of lipoxxygenase enzymes extracted from various microorganisms⁴⁷³.

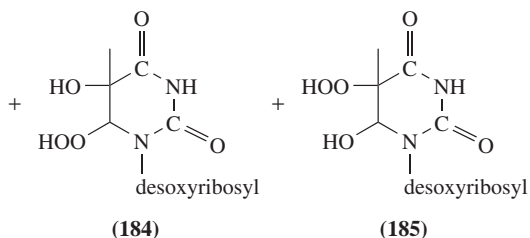
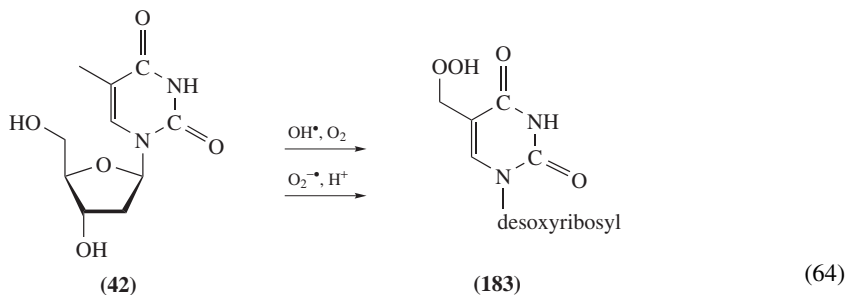
1,10-Phenanthroline (**182**) can be used instead of thiocyanate to form a complex with Fe(III) ions resulting from the oxidation of Fe(II), and the measurement is made at 500 to 510 nm. The use of **182** has the advantage of stability in the presence of air and also of allowing the use of hydrocarbon solvents for increased solubility of certain analytes. The method was applied for determination of hydroperoxides in natural rubber and synthetic elastomers, in the range of 10 to 20 ppm active oxygen. The sensitivity can be improved to less than 1 ppm, depending on the color of the sample solution²⁵⁴.

The FOX assay mentioned in Section III.B.2.a can also be used for determination of organic hydroperoxides; however, the original reagent formulation²⁵⁶ needs modification when applied to lipids, lest the aliphatic side chain undergoes oxidation. The results of the FOX assay are similar to those obtained by the I_3^- spectrophotometric method^{257, 513}. Blank determinations of lipid hydroperoxides are carried out by adding a solution of triphenylphosphine before the FOX assay⁵¹⁴. This method was adapted to the determination of lipid hydroperoxides in plasma⁵¹³, raw and cooked dark chicken meat²²⁹ and plant tissue⁴⁵⁸. Use of perchloric acid instead of sulfuric acid to provide the low pH required in the FOX method is of advantage when determining organic hydroperoxides; however, the kinetics of color development is slower⁵¹⁵. Various classes of lipid hydroperoxides can be obtained on photosensitized oxidation of plasma, including those derived from fatty acids, phosphatidylcholine, triglycerides and cholesterol esters. These can be analyzed by RP-HPLC with post-column application of the FOX method, measuring at 592 nm⁵¹⁶.

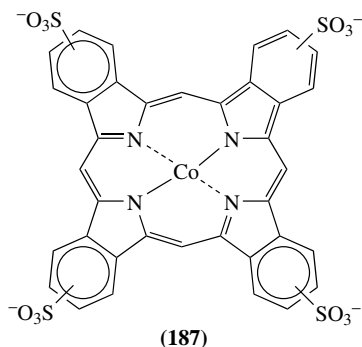
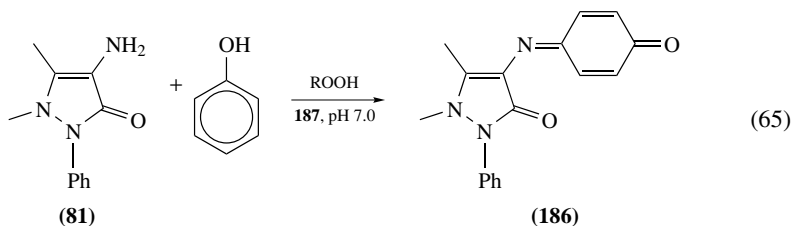
The FOX assay applied to a skatole oxidation product isolated by HPLC gave a positive result, supporting the contention that it is skatolyl hydroperoxide (**40**)¹⁴⁶. Mixtures of **183** and the eight diastereoisomeric hydroperoxides **184** and **185** derived from thymidine (**42**), as shown in equation 64, can be separated and detected by RP-HPLC with UVD at 229 nm. Each isomer is determined by applying the FOX assay using a capillary reactor heated at 60 °C to provide sufficient time for total oxidation of the Fe(II) ions, followed by UVD at 596 nm⁵¹⁷. A commercial kit based on the FOX assay for hydroperoxide determination in plasma, serum and tissue homogenizates appears in Table 2.

A kit in Table 2 is used to determine lipid hydroperoxides by producing Methylene Blue (**91**) according to equation 29 and measuring the absorbance at 675 nm. The assay was applied to determine the concentration of lipid hydroperoxides in serum of patients infected with HIV³⁰¹.

The reduction of hydroperoxides may be coupled with the oxidation of phenol in the presence of 4-aminoantipyrine (**81**) to yield a quinoneimine dye (**186**), determined



at 505 nm, as shown in equation 65. This process is similar to the one depicted in equation 27 (Section III.B.2.a). The reaction is carried out in borate buffer at pH 7.0, catalyzed by Co(III)-phthalocyaninetetrasulfonate (**187**), immobilized on an anion exchange resin. This particular catalyst shows selectivity toward hydroperoxides vs. H_2O_2 , which may be present in the sample. The method is especially selective for the determination of linoleate hydroperoxide⁵¹⁸.



Hydroperoxides on TLC plates may be visualized by immersing the chromatogram in a 1% aqueous solution of *N,N,N',N'*-tetramethyl-*p*-phenylenediamine dihydrochloride (Wurster's reagent), containing 1% (v/v) of AcOH; the colored dye spots that develop after 5 min are scanned at 400–700 nm with an imaging densitometer in transmittance mode⁹⁹. This method was applied to visualize hydroperoxides of steroids on TLC plates⁵¹⁹, for determination of phospholipid hydroperoxides extracted from turkey meat, after separation on a TLC glass plate, and scanning the glass side at 645 nm by means of a photodensitometer⁵²⁰ and for visualizing the hydroperoxides derived from thymidine (**81**, equation 65) after 2D-TLC⁵¹⁷. A method for determination of hydroperoxides and other reactive peroxides in solid matrices consists of SFE of the sample with CO₂, deposition of an initial spot on a TLC plate by direct impingement of the gaseous extract through a capillary restrictor, development and visualization with *N,N*-dimethyl-*p*-phenylenediamine dihydrochloride. The purple spots of the hydroperoxides are different from the spots of Schiff bases formed by carbonyl compounds. The spots can be measured with a scanning densitometer in the remission mode at 554 nm. The method was applied for determination of hydroperoxides in combustion aerosols, such as Diesel engine soot and flame soot collected on fiber-glass filters, with samples as little as 0.1 to 0.4 mg⁵²¹.

The peroxidase-catalyzed oxidation of ABTS (**103**) by H₂O₂ can also be performed by hydroperoxides, yielding a green-colored free radical. This reaction, catalyzed by HRP-C, was applied to the identification of an oxidation product of skatole isolated by HPLC, as a hydroperoxide (**40**). This assignment was confirmed by MS analysis (Section V.C.3)¹⁴⁶.

The kinetics of oxidation of Leuco Crystal Violet, depicted in equation 26 (Section III.B.2.a), can be applied for the determination of organic hydroperoxides after elimination of H₂O₂ with catalase²⁵².

b. Fluorometry. MHP at ppbv levels in the atmosphere can be determined simultaneously with H₂O₂ in a FIA system, by the fluorometric method based on equation 34 with **106a** (Section III.B.2.b). However, a separate channel is required with the following modifications. The diffusion membrane for MHP is made of expanded PTFE that allows penetration of many species to the absorbing water stream. H₂O₂ is eliminated from the aqueous solution by passing through a scavenging column of MnO₂, which barely affects the MHP concentration. HRP is used as catalyst for the oxidation of thiamine hydrochloride (**117**) with MHP, as bovine hematin fails because its response is 25-fold weaker than for equimolar concentrations of H₂O₂, and the atmospheric concentrations of MHP usually are much lower than those of H₂O₂. LOD is 15 pptv in the gas phase. The interference of ozone and SO₂ was investigated³²⁹. HPLC can be applied for the separation of environmental hydroperoxides collected from the air, aerosols and rain. The column effluent is treated according to equation 34 with **106a** and determined by fluorometry ($\lambda_{\text{ex}} = 326$ nm, $\lambda_{\text{fl}} = 420$ nm). Individual hydroperoxide concentrations as low as 0.01 μM and as high as *ca* 5 μM in rain were measured in a field test. The LOD for the fluorometric method is 0.005 μM ²⁶. RP-HPLC with post-column derivatization by a method based on equation 34 with **106a** and FLD can be applied to the analysis of *n*-alkyl hydroperoxides (up to *n*-C₁₈H₃₇OOH was investigated)⁵²² or small peroxide molecules found in the atmosphere⁵²³; the method was used for analysis of H₂O₂, MHP, HMHP and HEHP in rain and cloud water. The LOD is 0.007 μM of peroxide^{16,312}. RP-HPLC-FLD applying equation 34 with **106a** was used to analyze vapors of H₂O₂, MHP, EtOOH, HMHP and AcOOH, collected over aqueous solutions of the same compounds, aiming at the determination of their Henry's law constants³¹⁰.

Although the reaction depicted in equation 34 may be applied also to the simplest hydroperoxides, it fails for bulkier ones, such as *t*-BuOOH, due to the steric requirements of the HRP catalyst. A three step method was proposed for the analysis of mixtures of

hydroperoxides and peroxides, consisting of RP-HPLC separation, photolytic conversion of the emerging hydroperoxide to H_2O_2 , by irradiation with a 254 nm UV lamp and application of the fluorometric technique to determine this analyte. *t*-BuOOH and cumyl hydroperoxide (**27**) show, respectively, LOD 0.9 and 0.7 mg L^{-1} , linearity range 2.7 to 130 and 2.1 to 95 mg L^{-1} and RSD 4.7 and 5.9%^{308b}.

Ultra-trace analysis of H_2O_2 and other peroxidic compounds is carried out in a FIA system by a combination of RP-HPLC separation and fluorometric detection. The method is based on equation 34 with **106a**, effected by the peroxidic compound with enzymatic catalysis by HRP. For the determination of hydroperoxides, several details need to be taken into account. Retention times are longer for the organic compounds than for H_2O_2 , and they increase with the hydrophobic character of the organic molecule; the peak broadening caused by protracted retention times may significantly reduce the SNR, making the method viable only for the more hydrophilic analytes. Among the investigated analytes were alkyl hydroperoxides (**188**) and geminal hydroxyalkyl hydroperoxides (**189**). Compounds **188** give the same response as H_2O_2 , whereas compounds **189** are quantitatively converted to H_2O_2 in the alkaline pH prevalent in the post-column part of the FIA system. LOD for **188d** is *ca* 0.5 μM , one order of magnitude larger than that of H_2O_2 and in accord with its larger retention time in the chromatographic column (about 8-fold)^{312, 313}. RP-HPLC followed by FLD based on equation 34 may be applied in a FIA system for simultaneous determination of mixtures of hydroperoxides including H_2O_2 . Different peroxides have different LOD because the HRP catalyst acts at different rates for each of them⁵²⁴. A mixture containing 2–8 μM of H_2O_2 , **189a**, **189b**, 2-hydroxyethyl hydroperoxide, **188a**, **188b** and **189c** is separated in that order of increasing elution time, on a C_{18} RP-HPLC column, at 1 °C, using a mobile phase of dilute phosphoric acid of pH 3.3. To ensure that the eluted organic compounds undergo the reaction of equation 34 to completion, the emergent solution is heated to 42 °C in a long capillary reactor, on its way to a fluorescence cell, where the concentration is determined at 414 nm, on excitation at 301 nm. The method can be applied to determination of peroxides in atmospheric and rain samples^{308a}.

	ROOH		RCH(OH)OOH
(188)	(a) R = Me (MHP)	(189)	(a) R = H (HMHP)
	(b) R = Et		(b) R = Me (HEHP)
	(c) R = <i>i</i> -Pr		(c) R = Et
	(d) R = <i>n</i> -Pr		(d) R = <i>i</i> -Pr
			(e) R = <i>n</i> -Pr

The HRP-catalyzed oxidation of 2-hydroxy-1-naphthaldehyde salicylhydrazone (**116**) reported for H_2O_2 (Section III.B.2.b) can be applied for the spectrofluorometric determination of polyethyleneglycol hydroperoxides³²⁷. The method involving fluorescence of a triple complex of *N*-(α -pyridyl)-2-thioquinaldamide (**120**) in the presence of V(V) and H_2O_2 (Section III.B.2.b) can also be applied to the determination of organic peroxides, represented by *t*-BuOOH. LOD for *t*-BuOOH is 0.03 μM , with RSD 2% ($n = 3$, 0.5 μM), and linearity in the 0.1 to 2 μM range³³⁰.

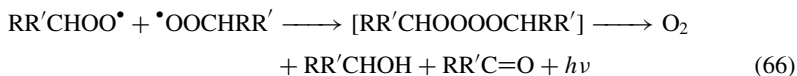
Fatty acid hydroperoxides can be separated from each other and other lipids by MEKC followed by FLD according to equation 34 with **106a**, using as catalyst micropoxidase-11 immobilized on the wall of a small capillary coupled at the end of the electrophoresis track⁵²⁵. MEKC with DA-UVD can be applied for separation of unsaturated fatty acids from the mixture of hydroperoxides obtained on oxidation with $^1\text{O}_2$ ^{526, 527}.

A sensitive method for ultra-trace levels of hydroperoxides in food or biological samples is based on the reduction of the hydroperoxide by a triarylphosphine reagent, in a process analogous to equation 49 in Section IV.B.3.a. The preferred reducing agent, diphenyl-1-pyrenylphosphine (**158a**), is converted to an intensely fluorescent phosphine

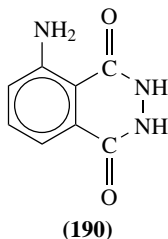
oxide (**158b**, $\lambda_{\text{ex}} = 352 \text{ nm}$, $\lambda_{\text{fl}} = 380 \text{ nm}$). The method can be applied for determination of total hydroperoxide content (POV) in batch mode or in a FIA system (Section IV.B.3.b), or for evaluation of a few picograms of individual hydroperoxides after HPLC, such as those derived from free fatty acids, unsaturated triglycerides, phosphatidylcholine (**155**) or cholesteryl esters, in oils, foodstuffs and human plasma^{421,528-531}. This FLD method was applied in a FIA system as post-column detection method for determination of neutral lipid hydroperoxides, after separation by HPSEC on a series of 100 Å and 50 Å analytical columns with UVD, using CH_2Cl_2 as mobile phase. This method was tested for determination of triglyceride and cholesteryl ester hydroperoxides in mayonnaise reinforced with fish oil⁵³².

A method for revealing lipid hydroperoxides on TLC plates consists of wetting the dry developed plate with a dilute solution of **158a**, covering the plate in succession with a poly(vinylidene difluoride) (PVDF) membrane, a polytrifluoroethylene membrane and a layer of glass fiber filters, heating this composite in a thermal blotter at 180 °C for 1 min, illuminating the PVDF layer with a 150 W projection lamp for 20 min at room temperature and observing the fluorescent spots under UV illumination, due to formation of **158b** at hydroperoxide spots⁵³³. Reaction with **158a** was applied for HPLC-FLD determination of lipid hydroperoxides in seafood⁵³⁴.

c. Chemiluminescence. The kinetics of thermal decomposition of PC-OOH was followed by measuring the CL emitted on thermolysis. A proposed mechanism for CL is shown in equation 66. *s*-Alkylperoxy free radicals derived from the hydroperoxide undergo dimerization to an unstable intermediate tetroxide, which on decomposition leads to formation of oxygen, an alcohol and a ketone in an excited state, with consequent emission on proceeding to the ground state^{535,536}.



The CLD methods for HPLC using isoluminol (**190**) with microperoxidase catalysis, for determination of lipid hydroperoxides in clinical fluids, have been reviewed⁵³⁷. Determination of phospholipids hydroperoxides by luminol (**124**) CL has been reviewed⁵³⁸. A fast RP-HPLC method (retention times 1 to 2 min) for determination of hydroperoxides and other peroxide compounds includes UVD, which is not always effective, and CLD, attained on injection of luminol (**124**), the CL reagent (Scheme 3), hemin (**75a**), a catalyst, and NaOH to raise the pH of the solution. A FLD cell may act as CLD cell if the excitation source is turned off. The selectivity of CLD is of advantage over UVD in industrial analysis; thus, for example, UVD of a sample from a phenol production line based on cumene oxidation (equation 13) shows peaks for cumyl hydroperoxide (**27**), unreacted cumene, cumyl alcohol and acetophenone, whereas CLD shows only the **27** peak. The



method has high sensitivity and a wide linear range, but these vary from compound to compound. Equation 67 presents the LOD found for various types of peroxides for this method under the same experimental conditions¹⁶⁴.

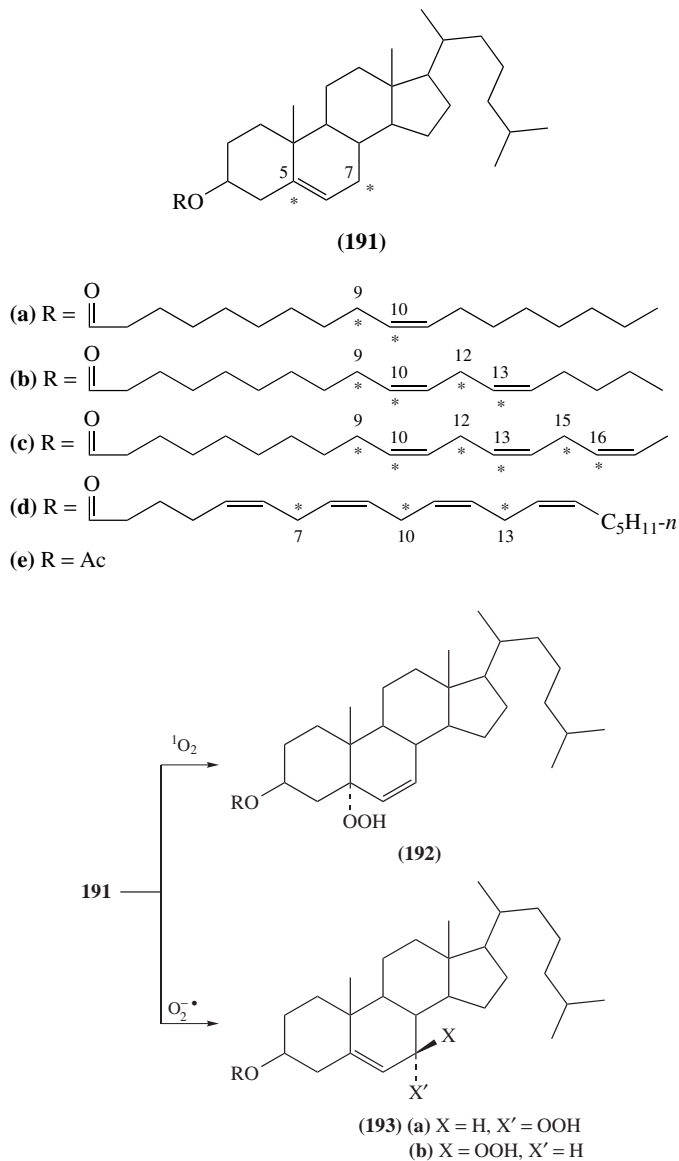
$$\begin{aligned} \text{BzOOBz (0.45 pmol)} &< \text{BzOOH(1.6 pmol)} < \text{PhEtCHOOH(7.2 pmol)} \\ &< \text{PhMe}_2\text{COOH (69 pmol)} < t\text{-BuOOBz (0.11 nmol)} \\ &< t\text{-BuOOH (0.19 nmol)} < \text{PhMe}_2\text{COOC(O)Pr-}i\text{(0.24 nmol)} \\ &< \text{PhMe}_2\text{COOAl (32 nmol)} \end{aligned} \quad (67)$$

The hydroperoxide content of lipoproteins in plasma is low, and therefore subject to error stemming from many factors. A kinetic method designed to avoid some of these pitfalls is based on the measurement of the CL emission during oxidation of luminol (**124**) catalyzed by hemin (**75a**, Scheme 3). A nonlinear correlation is found for the kinetic measurement of CL at a given time and the concentration of hydroperoxide, as a result of the involved mechanism of the luminol CL emission. This raises controversial issues relating to some determination methods based on Scheme 3, claiming linearity ranges after a fixed developing time. There is evidence of the same kinetics for the CL obtained from the hydroperoxides of phospholipids, triglycerides and cholesteryl esters. Furthermore, the CL emission efficiency of these compounds is about two orders of magnitude higher than that of H₂O₂. A possible reason for this is that H₂O₂ undergoes homolytic scission to very reactive HO• radicals, which may combine with other substrates in the matrix before meeting luminol, whereas the organic hydroperoxides decompose into more long-lived free radicals⁴⁹⁹.

A procedure for determination of lipid hydroperoxides in human plasma is based on kinetic measurement of the CL of luminol (**124**) with hemin (**75a**) catalysis⁵³⁹. CLD of microperoxidase-catalyzed oxidation of luminol (**124**) or isoluminol (**190**) was applied to detection and determination of amino acid hydroperoxides after exposure to UV and γ -irradiation^{143, 144}. A method for determination of hydroperoxides in the phospholipids of cultured cells uses isoluminol (**190**) and microperoxidase as catalyst⁵⁰⁵. Simultaneous determination of phosphatidylcholine hydroperoxides and cholesteryl ester hydroperoxides in human serum is carried out by quantitative extraction of the lipids, HPLC separation by column switching and CLD using isoluminol (**190**) with microperoxidase catalysis⁹⁴.

An application of biological significance is the determination of 5-hydroperoxyeicosatetraenoic acid (5-HPETE) extracted from rat basophilic leukemia cells. 5-HPETE (**191d**) is a hydroperoxide intermediate derived from arachidonic acid in the biosynthesis of a specific leucotriene. The procedure consists of liquid extraction of the cells, HPLC-UVD at 235 nm of the extract to separate the various HPETE isomers, followed by injection of luminol reagent and cytochrome C catalyst (a complex of a protein with protoporphyrin IX, **75c**) in borate buffer at pH 10.8, and CLD at 420 nm. A linear log-log correlation is shown between the amounts of 5-HPETE injected and the peak area of the CL response over the range from 0.1 to 100 ng. The extract shows the same behavior after reduction of the HPETEs to corresponding alcohols with NaBH₄⁵⁴⁰.

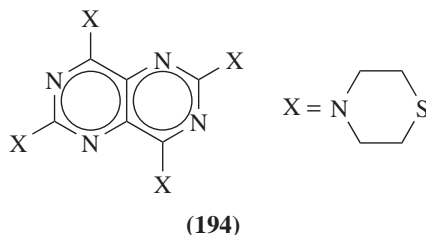
Cholesterol (**191**, R = H) and its esters (**191a-d**) undergo *in vivo* oxidation by ¹O₂ at positions 5 and 7, under the influence of UV irradiation, or by free radicals (e.g. O₂^{-•}), as shown in Scheme 6. This was demonstrated in the laboratory for cholesterol (**191**, R = H), on irradiating rats under controlled conditions and isolating from the skin 5 α -(**192**), 7 α - (**193a**) and 7 β -hydroperoxycholesterol (**193b**), by an involved chromatographic procedure, culminating with HPLC-CLD, using isoluminol (**190**) oxidation catalyzed by microperoxidase. The CL quantitative measurements were corroborated by radioactive tracing of the products derived from ³H-labeled cholesterol⁹⁸.



SCHEME 6. *In vivo* oxidation of cholesterol (R = H) and other lipids (R = fatty acyl group) under the influence of UV radiation, by two different paths

Similarly to the chromatographic three-step method culminating in FLD of H_2O_2 described above, a mixture of peroxide compounds of all types can be analyzed by RP-HPLC, followed by post-column conversion of the peroxide to H_2O_2 by UV light and CLD with bis(2,4,6-trichlorophenyl) oxalate (**140**) in the presence of 2,4,6,8-tetrakis(thiomorpholino)pyrimido[5,4-*d*]pyrimidine (**194**)⁴⁷⁴ as fluorescent enhancer. *t*-BuOOH and cumyl

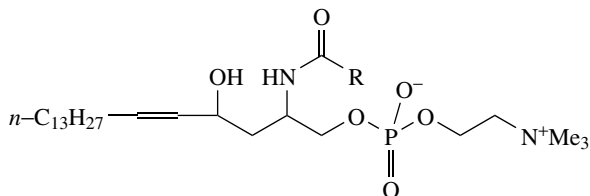
hydroperoxide (**27**) show, respectively, LOD (SNR 3) 31.3 and 1.3 μM and linearity range from 160 to 1600 and from 8 to 80 μM ¹⁹³.



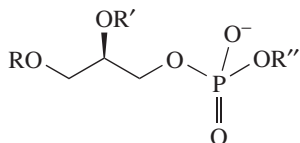
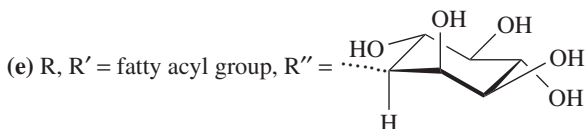
A simple assembly for measuring the CL emitted in the 380–700 nm range, on thermal decomposition of solid samples containing hydroperoxide groups, consists of a sample-holding chamber fitted with controlled heating, inert gas flushing and a transparent quartz window facing a photometer sensitive to single photon detection. A typical pyrolysis profile of photon counts vs. temperature is a bell-shaped curve, the area under which may be integrated for quantitative estimations. Such a device can be used for testing durability of organic surface coatings exposed to the sunlight, which are assumed to undergo long-term chemical degradation via hydroperoxide formation. An accelerated test for surface coatings consists of exposing coated pieces to illumination by fluorescent UV bulbs emitting at 340 nm, and measuring the development of CL for several weeks. Although the use of shorter wavelengths accelerates the oxidation process, the light is considered to be *unnatural* and does not discriminate between formulations of known different durability. The rate constants of hydroperoxide formation in polyester-melamine coatings, as determined by the accelerated test, correlates well with ablation measurements of the same coatings exposed to outdoor conditions for three years⁵⁴¹.

3. Infrared spectrophotometry

A sensitive detection method for lipid hydroperoxides is based on a combination of HPTLC, spot development and FTIR. The placement of spots on the TLC plate can be revealed by immersing in a 10% aqueous solution of $\text{CuSO}_4 \cdot 5\text{H}_2\text{O}$, containing 8% (v/v) of H_3PO_4 , charring for 30 min at 185 °C and scanning at 400–700 nm with an imaging densitometer in reflectance mode. Analysis is performed using FTIR instrumentation equipped with an attenuated total reflection unit. The latter consists of a set of mirrors and a ZnSe prism (transparent between 600 and 17000 cm^{-1}). The TLC plate is pressed on one of the phases of the prism and the spectrum is scanned between 700 and 3000 cm^{-1} . The presence of hydroperoxides can be ascertained by multivariate analysis, from the significant variance observed in the spectrum of an original substrate undergoing oxidation to hydroperoxides. Thus, an *in vitro* experiment was carried out, involving exposure of a tissue culture of healthy human bronchial epithelial cells to several environmental levels of ozone, from 0.1 ppm (low pollution area) to 1 ppm (industrial pollution area) for periods of 4 and 12 h. After extraction of the phospholipid fraction it was resolved by HPTLC. Six phospholipid types were recognized by their R_f value not being far from that of a reference compound, namely sphingomyelin (**195**), lysophosphatidylcholine (**196a**), phosphatidylcholine (**196b**), lysophosphatidylethanolamine (**196c**), phosphatidylethanolamine (**196d**) and phosphatidylinositol (**196e**). As exposure to ozone increased, so new peaks appeared at 892, 882, 871, 864, 855, 846, 839 and 829 cm^{-1} , which were assigned to O–O stretching of hydroperoxides and changes in the 730 to 675 cm^{-1} region, related to *cis* unsaturation



(195) R = fatty acid residue

(196) (a) R or R' = H, R' or R = fatty acyl group, R'' = CH₂CH₂N⁺Me₃(b) R, R' = fatty acyl group, R'' = CH₂CH₂N⁺Me₃(c) R or R' = H, R' or R = fatty acyl group, R'' = CH₂CH₂N⁺H₃(d) R, R' = fatty acyl group, R'' = CH₂CH₂N⁺H₃

(e) R, R' = fatty acyl group, R'' =

in the lipid chain. It should be pointed out that the amounts of hydroperoxide formed were below the LOD of Wurster's test (Section V.B.2.a). However, the FTIR reflection method could discern the presence of these compounds⁹⁹.

The hydroperoxide groups produced by reaction of certain elastomers with ¹O₂ can be characterized by IR spectroscopy. Two such groups may be distinguished in the region of OH stretching, associated hydroperoxides, showing a broad band with maximum at 3420 cm⁻¹, and isolated hydroperoxides, with a relatively sharper band at 3550 cm⁻¹. The progressive increase or decrease of both bands can be observed as the oxidation of the polymer goes on or a reduction of the hydroperoxides with Me₂S, Ph₃P or NO is applied. The first two reducing agents give rise to associated or isolated alcohols, with the bands shifting to 3420 and 3360 cm⁻¹, respectively. Reaction of hydroperoxides with NO yields nitrate esters, RONO₂, with sharp characteristic peaks at 1631, 1276 and 853 cm⁻¹. Also the alcohols obtained on hydroperoxide reduction may be treated with NO; the resulting nitrite esters, RONO, can be identified by a band at 780 cm⁻¹²¹⁴.

4. Thermal stability and GLC

It is frequently the case that organic peroxides, and the hydroperoxides in particular, cannot be analyzed by GLC in the usual way, as they undergo decomposition inside the instrument. A study on the thermal stability of various organic peroxides shows that on using the *cold on-column injection* technique, with the temperatures of the injection port and column as low as practically possible and applying slow heating rates, it is possible to

perform good separations of volatile peroxides, with no decomposition taking place during retention times up to 30 min. The following compounds were included in this study, in the order of emergence from the column and their LOD and linearity ranges in mg L⁻¹ units: *t*-BuOOH (0.7, 2.1 to 110), cumyl hydroperoxide (**27**, 0.9, 2.7 to 100), *t*-BuOOBu-*t* (0.3, 0.9 to 125), PhCO₃Bu-*t* (0.3, 0.9 to 124) and *t*-Bu cumyl peroxide (0.2, 0.6 to 100)⁵⁴².

5. Nuclear magnetic resonance spectroscopy

NMR studies of aging of polymers and model compounds have been briefly reviewed^{543,544}. Various NMR techniques may be applied for detection and quantitation of hydroperoxides formed when organic polymeric materials are subjected to thermal or radiation stress in oxygen-containing atmospheres. The thermal oxidation of pentacosane (C₅₀H₁₀₂) using ¹⁷O-enriched oxygen was studied by a combination of ¹H, ¹³C and especially ¹⁷O NMR solution and solid state techniques. Hydroperoxide formation is detected at the inception of the oxidation process, but at the working temperature (125 °C) it rapidly evolves toward more stable functional groups, such as ketone and aldehyde, carboxylic acid and ester and evolution of CO and CO₂⁵⁴³. On subjecting ¹³C-enriched (99%) polyethylene films to aging under γ -radiation (0.74 kGy h⁻¹) in air, for 4 to 20 days, at 25 and 80 °C, formation of small amounts of oxidation products can be assessed by ¹³C MAS-NMR with high-power ¹H decoupling. The main spectral features of the polymer before aging are the backbone $-\underline{\text{C}}\text{H}_2-$ groups at 30 (amorphous) and 33 (crystalline) ppm and very weak signals (less than 1% of the total intensity) at 14 ppm (end Me groups) and at 11 ppm (Me group of Et side chains). The major aging products include the functional groups hydroperoxide (85 ppm), alcohol (73 ppm), ketone (205 ppm), carboxylic acid and ester (170 to 180 ppm) and the minor ones are dialkyl peroxide (81 ppm), vinyl (99 ppm) and aldehyde (194 ppm). After some aging, a definite line broadening of the polymer backbone signal is observed at 25 °C and a more pronounced one at 80 °C. This is due to slight chemical shift displacements of carbons in β -positions to those bearing oxidized functional groups. The concentrations of the various functional groups are time- and temperature-dependent, and point to hydroperoxide being the primary product, from which the other functions are derived in subsequent steps⁵⁴⁴.

Ozonolysis of *E*-1,2-dichloro-2-butene (**197**) presumably proceeds through a primary ozonide that decomposes according to Criegee's mechanism⁵⁴⁵; however, the intermediate species fail to recombine into a final ozonide (see Scheme 16 in Section VIII.A) and proceed by other paths to a variety of products, as shown in Scheme 7. Thus, normal ozonolysis in CH₂Cl₂ leads to a mixture of *cis*- and *trans*-dichlorodimethyltetroxanes (**199a** and **199b**), of which the latter is unstable at room temperature. Ozonolysis in a wet medium yields a mixture of acetic and peracetic acid, while in a dry medium, in the presence of hydrogen chloride, a mixture of acetyl chloride and 1,1-dichloroethyl hydroperoxide (**198**) is formed. The product mixture slowly undergoes esterification to a prester (**200**). Alternatively, the isolated **198** may be hydrolyzed to a mixture of acetic and hydrochloric acids, or decomposes at room temperature into acetic acid and chlorine. ¹H NMR spectroscopy is an important means for identification and relative quantitation of the products shown in this scheme. Compounds **199a** and **200** were reported to explode when exposed to heat or shock⁵⁴⁶.

6. Electrochemical methods

a. Classical methods. A technical problem often encountered in electrochemical determination of fatty materials is their low solubility in water or hydrophilic solvents, and the requirement of a supporting electrolyte, usually soluble in this type of solvents, to attain electric conductivity.

are 20 and 25 nM, with linearity up to 1.5 and 1.2 μM , for the hydroperoxides of linoleic and linolenic acids, respectively⁵⁴⁹.



CZE-ELD, with a Au microelectrode at -0.6 V vs. SCSE and a Pt wire as auxiliary electrode, using sodium borate buffer and dodecyltrimethylammonium bromide for dynamic coating of the capillary internal surface, can be applied for separation and determination of hydroperoxides in ultra-trace amounts. Thus, various hydroperoxides derived from linoleic acid undergo total dissociation to carboxylates in borate buffer; however, due to their similar molecular masses, in order to resolve the ELD signals, it is necessary to add β -cyclodextrin (**83**) to form complexes with the analytes and reduce their mobility, in accordance with the value of the complexation equilibrium constants²⁰⁷.

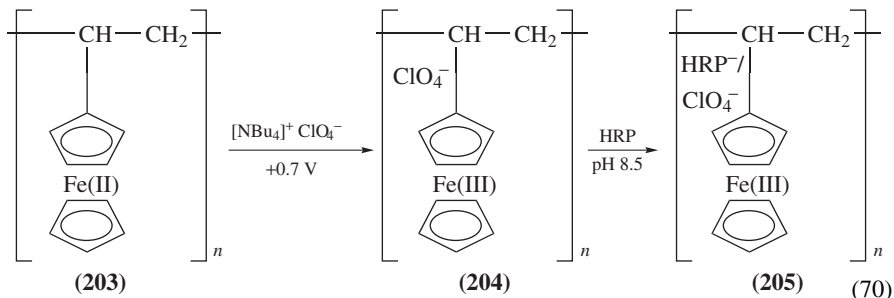
The main disadvantage of GCE or Au electrodes used for ELD after chromatographic separation of lipids is fouling, which gradually impairs the electrode response. This does not apply to the dropping Hg electrode, where the surface is continuously renewed. HPLC-ELD with a dropping Hg electrode can be applied for analysis of biologically relevant lipids, such as cholesterol, cholesteryl unsaturated fatty esters and phosphatidylcholines. To attain good baseline separation the eluting solvent and electrolyte need to be changed for the various classes of compounds, and the ELD carried out cathodically, with the working electrode set at -150 to -300 mV vs. SCSE^{550,551}. This method was applied for analysis of the lipids extracted from L1210 leukemia cells that were exposed to photooxidative stress. The low retention time peaks correspond to various cholestene hydroperoxide isomers. The major fraction corresponds to phospholipid hydroperoxides, especially PC-OOH species, as demonstrated by the retention times compared with authentic samples, the behavior toward reductors such as Ph_3P (formation of phosphine oxide and an alcohol) and GSH (**28**) in the presence of glutathione peroxidase (equation 50, Section IV.B.3.a) and further evidence⁵⁵².

A coulometric method may serve for RP-HPLC-ELD, with enhanced sensitivity over amperometric detection, due to the higher electrochemical efficiency of coulometry. The electrochemical cell is equipped with two working electrodes and a SCSE; the first working electrode is set at -10 mV and is meant to reduce the noise and the second one, set at -50 mV , is for measuring the analytes. This method may be applied to the determination of PC-OOH species in plasma, which gives a chromatographic response quite similar to that of UVD at 235 nm, whereas the reduced PC-OH species has UVD response but no ELD response. For a calibration standard the LOD is about $1\ \mu\text{M}$ of PC-OOH, with linearity in the 2.3 to $50\ \mu\text{M}$ range⁵⁵³. A similar method of separation by RP-HPLC followed by ELD and UVD can be applied for determination of cholesteryl ester hydroperoxides and their derivatives, such as the corresponding hydroxides. The UVD set at 234 nm detects species containing conjugated diene moieties obtained on oxidation of the original lipids to hydroperoxides; the conjugated double bonds are preserved when the hydroperoxides are reduced to the corresponding hydroxides with NaBH_4 . The coulometric cell provided with two working electrodes set at -10 and -50 mV vs. SCSE, as described before, is used for detection of the hydroperoxides alone. Cholesteryl Z-15-tetracosenoate hydroperoxide serves as internal standard. The method was applied for determination of cholesteryl ester hydroperoxides in spiked human plasma⁵⁵⁴.

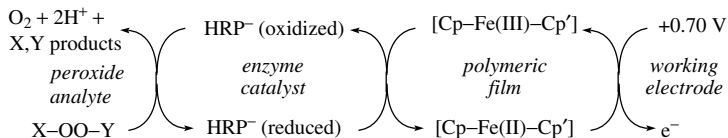
b. Biosensors and their mimics. Biosensors involving immobilized enzymes are in vogue for the determination of hydroperoxides in trace and ultra-trace concentrations. Coating of the working electrode can be achieved by electropolymerization, the enzyme

being immobilized either while the coating is being formed or by subsequent dipping. The technique has the advantage of allowing coating of very small surfaces, with control of the layer thickness by the amount of charge conducted. This type of biosensors has been reviewed^{555,556}.

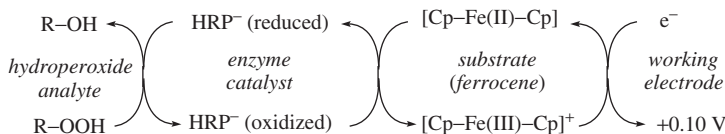
A biosensor can be prepared as shown in equation 70. A Pt electrode immersed in a poly(vinylferrocene) (**203**) solution in CH_2Cl_2 , containing tetrabutylammonium perchlorate, can be coated with a film of poly(vinylferrocenium perchlorate) (**204**), on applying a potential of +0.70 V vs. SCSE. The coated electrode is converted into a biosensor on immersing the film in a solution of HRP in phosphate buffer at pH 8.5. At this pH the enzyme is past its isoelectric point and acts in anionic form, HRP^- , which can exchange perchlorate and become immobilized on the film (**205**). The biosensor can be used for amperometric determination of hydroperoxides, operating at a constant voltage (+0.70 V) and pH 8.5 under inert gas blanketing. The mechanism shown in Scheme 8 consists of an enzyme-catalyzed oxidation of the analyte, followed by recovery of the oxidized state of the enzyme assisted by a ferrocenium residue of the polymeric film and return of the ferrocenium moiety by electron transfer to the electrode. The influence of various factors (temperature, film thickness, concentration, nature of analyte) on the determination of *t*-BuOOH and cumyl hydroperoxide (**27**), 2-butanone peroxide (**46** + **47**) and *t*-butyl peracetate (Section VI.B.3) was investigated⁵⁵⁷.



A biosensor based on HRP immobilized on electropolymerized *N*-methylpyrrole can be used for determination of hydroperoxides. The device is immersed in a solution of the analyte in ethyl acetate, also containing ferrocene, an emulsifier and phosphate buffer at pH 7.4. Reversed micelles are formed, containing the supporting electrolyte. The amperometric determination is carried out on applying a potential of +0.10 V vs. SCSE. The operation of this biosensor is depicted in Scheme 9, which contains the same essential elements as Scheme 8, but the current flows in the reverse direction. The LOD are 0.086 μM for 2-butanone peroxide (**46** + **47**) and 30 μM for *t*-BuOOH and the LOQ are about three times as large⁵⁵⁸. The amperometric biosensor made of graphite and PTFE powder, incorporating HRP and ferrocene described for H_2O_2 in Section III.B.4.b, can also be used for determination of hydroperoxides; however, the sensitivity is considerably



SCHEME 8. Operation of the biosensor based on an electrode coated by a polymeric film containing both immobilized HRP and iron ions. The organic peroxide acts as a reducing agent



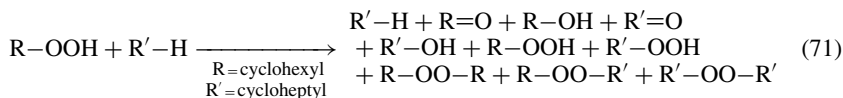
SCHEME 9. Operation of the biosensor based on an electrode coated by a polymeric film containing immobilized HRP. The organic peroxide acts as an oxidizing agent for the ferrocene solute

diminished. For example, the analytical parameters for butanone peroxide (**46** + **47**) and cumyl hydroperoxide (**27**) are, respectively, as follows: LOD 0.47 and 3.7 μM , LOQ 1.6 and 12 μM , with linearity ranges from 1.0 to 40 and 20 to 700 μM and response of 5.1 ± 0.11 and 0.45 ± 0.01 $\text{nA } \mu\text{M}^{-1}$ ³⁹⁰.

A sensitive assay for lipid hydroperoxides is afforded by prostaglandin endoperoxide synthase, that in the presence of hydroperoxides is activated to liberate O_2 , which is measured with an oxygen electrode⁵⁵⁹. Although it may be of advantage in certain cases, the procedure seems too complex to become of widespread application in practical analysis.

7. Flame ionization detection

The relative concentration of organic peroxides in a mixture can be estimated from the corresponding peak intensities after GLC-FID separation, by applying the concepts of *effective carbon number* (ECN) and *relative mass response factor* (f) to a given compound, in the absence of calibration standards, as is frequently the case for organic peroxides. For example, an aliphatic or aromatic C atom bound to C or H atoms contributes 1 to the ECN, whereas a secondary C atom bound to one H and one O atom contributes 0.25. For a given analyte x and a given reference compound r , $f = (M_x/\text{ECN}_x)/(M_r/\text{ECN}_r)$, where M is the corresponding molecular mass. An example for the application of these concepts attains the reaction of cyclohexyl hydroperoxide with cycloheptane, carried out in a sealed tube at 163 °C for 15 min. The products depicted in equation 71 are in their order of appearance during separation by GLC-FID, using a capillary column coated with poly(dimethylsiloxane), with temperature gradient and *p*-xylene as internal reference ($M_r = 106.17$, $\text{ECN} = 8$); the peaks may be independently assigned by MS detection. Products $\text{R}=\text{O}$ and $\text{R}'=\text{O}$ are cyclohexanone and cycloheptanone, respectively; other peaks irrelevant to the present discussion appear in the chromatogram too. The f values for the hydroperoxides $\text{R}-\text{OOH}$ (1.67) and $\text{R}'-\text{OOH}$ (1.57), and the peroxides $\text{R}-\text{OO}-\text{R}$ (1.42), $\text{R}-\text{OO}-\text{R}'$ (1.39) and $\text{R}'-\text{OO}-\text{R}'$ (1.36) allow quantitation of these compounds^{560,561}. See in Section V.B.8 an estimation technique based on the total carbon number (TCN).



8. Mass spectrometry

The elution factors in normal-phase TLC and RP-HPLC, using a fixed set of chromatographic parameters, were determined for a series of saturated triacylglycerides with TCN from C_{30} to C_{60} , serving as reference compounds and various oxidation derivatives of analogous unsaturated triglycerides, including hydroperoxides, peroxides, epoxides, core aldehydes and their DNP derivatives. From these measurements, a series of incremental

factors were calculated for the evaluation of the elution factor. This helps in assessment of the class of compound in the analysis of natural triglyceride mixtures by HPLC with MS detection^{562a}. See in Section V.B.7 an estimation technique based on the ECN. Picomolar amounts of fatty acid hydroperoxides can be analyzed by normal-phase HPLC using tandem electrospray NI-MS detection in multiple reaction monitoring mode, following the specific peaks of each analyte, as discussed in Section V.C.3^{562b}. The hydroperoxides of synthetic phosphatidylcholine, phosphatidylethanolamine and phosphatidylglycerol and their dehydration carbonyl products show the molecular peaks in the ion spray MS, with no further fragmentation. The peak-height ratios relative to an internal standard (2-*O*-benzylphosphatidylcholine) show a linear dependence on the concentration and their LOD are compatible with the determination of glycerophospholipid hydroperoxides present in 1 mL of human plasma⁵⁶³.

The hydroperoxides obtained on thermal oxidation of cholesteryl acetate (**191e**) can be selectively separated by SPE and elution with a polar solvent. After reduction to the corresponding alcohols by NaBH₄ and further derivatization to the trimethylsilyl ether, the products can be subjected to GLC with ion-trap MS detection. It can be thus demonstrated with the aid of standards that under the oxidation conditions (160 °C for 90 min) only the 7-position is attacked, leading to the 7 α - and 7 β -hydroperoxy derivatives, while the plausible 4-position remains unscathed⁵⁶⁴. Treatment of erythrocyte ghosts with *t*-BuOOH causes a manyfold content increase of 5-hydroxyeicosatetraenoic acid (5-HETE), 5-hydroperoxyeicosatetraenoic acid (5-HPETE) and 5-oxoeicosatetraenoic acid (5-oxo-ETE) residues of phospholipids. These acids can be separated by HPLC, identified and quantized by tandem MS⁵⁶⁵.

Temperature-programmed thermal desorption particle beam MS of collected secondary aerosol particles shows that the major ozonization products of normal alkenes in an environmental chamber include organic hydroperoxides, peroxides, final ozonides and monocarboxylic acids. Attempts to analyze these compounds by GC result in their decomposition to simpler molecules¹¹.

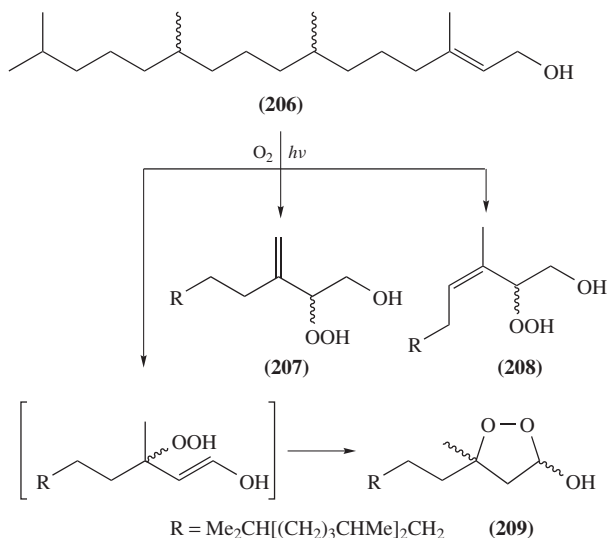
C. Structural Characterization

1. General

The structure of peroxides shows peculiar characteristics often absent in their analogs lacking the –OO–functional group. Theoretical calculations of noncovalent interactions in five peroxides R–OO–R' (R = *t*-Bu, Ac; R' = H, *t*-Bu, Ac) point to the main reasons for such peculiarities. The favored conformations of these compounds are dictated by three factors: (1) Conjugation of the lone electron pairs of peroxide O atoms with the antibonding σ^* orbitals of neighboring O–C or O–H bonds, leading to stable skewed structures, with torsion angles of about 80°; (2) Coulomb repulsion of lone pairs of electrons and (3) steric interactions, both causing destabilization of the molecule and increase of the torsion angle. In the specific case of peracetic acid, the internal H-bond overcomes the destabilization factors and confers a planar conformation⁵⁶⁶.

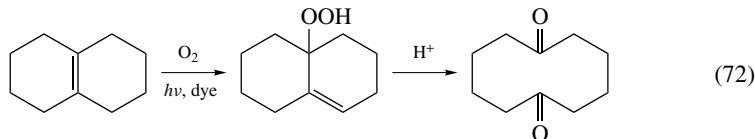
An example of the complex set of spectroscopic information required in natural products research is afforded by the mixture of hydroperoxides **207**, **208**, the endoperoxide **209** and other minor products, obtained by photosensitized addition of O₂ to phytol (**206**), according to Scheme 10. The scheme is complicated by the fact that **208** is a mixture of the *E* and *Z* isomers. After separation by HPLC, each fraction can undergo characterization by FTIR, ¹H and ¹³C NMR, also applying the HSQC, HMBC, ¹H-¹H COSY and NOESY techniques, and EI-MS⁴⁹².

Tertiary hydroperoxides derived from tetrasubstituted olefins containing allylic H atoms undergo scission on acid treatment at the site of the original double bond, yielding



SCHEME 10. Photosensitized oxidation of phytol

keto groups (equation 72)⁴⁸⁹. Characterization of the original olefin or its hydroperoxide derivative may be easier when dealing with the ketone products, especially when chromatographic separation is carried out at relatively high temperature.



Another derivatization approach is reduction of the hydroperoxide, followed by structural characterization of the corresponding alcohol, which is usually easier to handle. Thus, the structure of amino acid hydroperoxides can be characterized more easily if, after having ascertained the hydroperoxide nature of the compound, it is reduced to the alcohol with $NaBH_4$. The structure of three valine hydroperoxides obtained on γ -radiation of bovine serum albumin, a tripeptide (31) or valine (34) was elucidated after reduction, hydrolysis (if necessary), chromatographic separation, and application of the usual MS and NMR methods on the individual hydroxy derivatives of valine¹⁴³.

The absolute configuration of unsaturated fatty acid hydroperoxides obtained either by autoxidation or enzymatic oxidation can be deduced after reduction with $SnCl_2$, derivatization of the alcohol with an asymmetric reagent and chromatographic separation. Assuming that the enzymatic route is stereospecific and the free radical routes are not, then the enantiomeric excess will point to the proportion of the hydroperoxide stemming from either route. Determination of the fate of methyl linoleate under thermal oxidation, leading to a mixture of hydroperoxides, can be attained by reduction with $NaBH_4$ to the corresponding alcohols and a combination of TLC, HPLC and GLC techniques, for both the hydroperoxy and hydroxy species to separate the individual components of the mixture. Elucidation of the substitution site of the OOH or OH group (position 9 or 13) requires GLC-MS, whereas the various possible geometric isomers of the conjugated diene structure (*E,E*-

E,Z-, *Z,E*- or *Z,Z*-) can be assigned with the help of retention time considerations and DA-UVD⁹³. Examples of the analytical process required for the peroxides derived from linoleic acid are shown in Scheme 20, Section VIII.E⁹² and for cholesteryl esters (**191**) in Section VIII.C.3.

2. Vibrational spectra

The hydroperoxide function has characteristic IR and Raman spectral features; for example, *t*-BuOOH has ν OO bands at 845 and 848 cm^{-1} and δ OO bands at 526 and 529 cm^{-1} . The bands assigned to ν OOH at 3371 and 3362 cm^{-1} are in the same region of the OH stretching vibration of alcohols, and therefore devoid of specificity⁵⁶⁷. The IR calculated spectrum of ClCH₂OOH is similar to that of the analogous fluorine compound in all the modes that do not involve the halogen atom. This feature helped to identify ClCH₂OOH among the photolysis products of MeCl, H₂ and Cl₂ when present together in the atmosphere¹⁹. A similar experimental and theoretical study attained the vibrational spectra of FCH₂OOH, with a ν OO band at 822 cm^{-1} (calculated 873 cm^{-1}) and a ν OH band at 3586 cm^{-1} (calculated 3810 cm^{-1}). The corresponding vibrational modes for MHP are ν OO at 821 cm^{-1} (calculated 871 cm^{-1}) and ν OH at 3601 cm^{-1} (calculated 3833 cm^{-1}), which contributed to the assignments of the fluorinated hydroperoxide⁵⁶⁸.

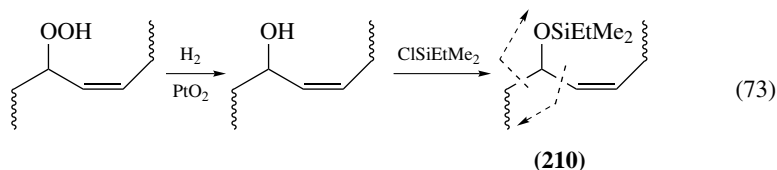
The multiple transformations taking place during the curing process of drying oils can be followed by observing the long-term changes in the FTIR and FT-Raman spectra. Of central importance are formation and subsequent transformations of hydroperoxides. Thus, in linseed and poppyseed oils appearance of a broad band centered at *ca* 3425 cm^{-1} is due to formation of hydroperoxides, accompanied by disappearance of *Z*-double bond bands at 3011 and 716 cm^{-1} and appearance of *E*-double bond bands at 987 and 970 cm^{-1} due to conjugation and *Z* to *E* isomerization. These hydroperoxides in the presence of oxygen turn to alcohols, aldehydes, ketones, carboxylic acids and peresters or γ -lactones, all with characteristic spectral bands. Further curing involves epoxide formation with a characteristic band at 885 cm^{-1} and elimination of volatile molecules⁵⁶⁹.

Hydroperoxide and hydroxide formation by slight thermal oxidation of LDPE can be confirmed by IR spectroscopy, showing bands at 3555 cm^{-1} for OOH and about 3400 cm^{-1} for OH. The band at 3555 cm^{-1} is very weak or absent for the oxidation products of LLDPE²¹⁵. ¹³C FT-NMR is also useful to investigate this process (see Section V.C.4).

3. Mass spectrometry

A study on incipient photosensitized oxidation of the cholesteryl esters of oleic (**191a**), linoleic (**191b**) and linolenic (**191c**) acids demonstrates that hydroperoxide formation is regioselective. The photosensitized oxidation of the corresponding Me esters serves as a guide to the more complex processes expected for the cholesteryl esters **191a-c**. The structural elucidation of the hydroperoxides derived from each of the Me esters proceeds through separation by column chromatography followed by derivatization as shown in equation 73, reduction of each hydroperoxide to the corresponding alcohol either by H₂/PtO₂ or NaBH₄, silylation of the alcohol and structural characterization of each of the resulting derivatives using various spectroscopic techniques. Especially significant is MS of the silylated derivative (**210**), showing fragmentation resulting from the two α -cleavage possibilities. This analysis points to oxidation at allylic positions or by the ene mechanism proceeding at only one of two possible sites, as denoted by the asterisk on the various R groups of **191**. Thus, for example, in the case of oleic acid no oxidation is obtained on the allylic position 12 or the ene position 11. In the case of the cholesteryl

esters **191a–c**, besides regioselective oxidation on the fatty acid residue identical to that obtained for the corresponding Me ester, also positions 5 or 7 of the steroidal structure are regioselectively attacked, however, with lower yields. This study points to possible oxidation paths of cholesteryl fatty acid esters in living organisms⁵⁷⁰.



The tedious analysis and structural assignment of the oxidation products of cholesteryl esters just described may be simplified to some extent, by applying normal-phase HPLC followed CIS-MS detection, using AgBF_4 as coordinating agent. Typical spectrograms show the molecular peak and various homolytic degradation stages associated with $^{107}\text{Ag}^+$ and $^{109}\text{Ag}^+$ ions ($[\text{M} + \text{Ag}]^+$) and loss of water from hydroperoxide groups ($[\text{M} + \text{Ag} - \text{H}_2\text{O}]^+$). Application of SRM and tandem techniques is very useful for these complex analytes. Both cholesteryl linoleate (**191b**) and cholesteryl arachidonate (**191d**) show hydroperoxide formation on position 7 of the ring system and the places marked with asterisks on the fatty acid side⁵⁷¹. The CIS-MS technique using Ag^+ ions was also applied for characterization of isoprostane bicyclic endoperoxides bearing a hydroperoxy substituent (**25**)⁹⁶. A detailed analysis was carried out of the hydroperoxides and other metabolites obtained on enzymatically-catalyzed oxidation of oleic, linoleic and linolenic acids, by HPLC-MS, with ion-trap MS. Consideration of the fragmentation patterns helped in the placement of the oxygen on the fatty acid chain⁵⁷².

The negative ion electrospray MS of fatty acid hydroperoxides exhibits various typical features that may be useful for characterization of this type of compounds, such as loss of small neutral molecules and fragmentation associated with the position of the OOH group. The $[\text{M} - \text{H}]$ and $[\text{M} - \text{H}_2\text{O}]$ peaks are usually most abundant and cleavage of the double bond allylic to the hydroperoxy group is also observed. The features of the fragmentation after loss of H_2O in the MS of a fatty acid hydroperoxide are the same as those observed in the MS of the analogous keto acid⁵⁶².

t-BuOOH is often used as oxidant for lipids. Its action mimics to some extent natural peroxidation; however, various peculiar products are also obtained. The product characterization of various triglyceride derivatives involved RP-HPLC-LSD and RP-HPLC-CIS-MS with NH_4^+ ions, and functional assignment based on the m/z values of $[\text{M} + \text{NH}_4]^+$, the TCN concept and other experimental evidence. For example, the triglyceride **211**, containing one linolenoyl and two stearoyl acyl residues, yields the products summarized in Table 3, showing that the reagent may form peroxide adducts with the substrate and that the primary hydroperoxide products may undergo secondary reactions⁵⁷³. A similar study was carried out with corn oil instead of synthetic triglycerides⁵⁷⁴.

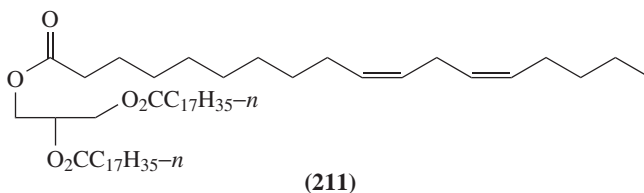


TABLE 3. Structural analysis of the oxidation products of an unsaturated triglyceride (**211**) with *t*-BuOOH

Peak No. ^a	[M + NH ₄] ⁺ <i>m/e</i>	Peak area (%) ^b	Functional groups on the linolenoyl residue				
			C=C	OOH	endo OO	epoxy	<i>t</i> -BuOO
6	1058	0.3	1	1	1	—	1
7	952	0.3	2	1	—	1	—
8	1024	2.0	2	1	—	—	1
9	936	22.1	2	1	—	—	—
10	1114	19.3	1	—	1	—	2
11	918	3.5	3	—	—	1	—
14	1080	1.0	2	—	—	—	2
15 ^c	992	28.5	2	—	—	—	1
15 ^c	1170	2.0	1	—	—	—	3
16 ^d	904	21.0	2	—	—	—	—

^a In order of emergence from the RP-HPLC column.

^b Relative to the total LSD signal area.

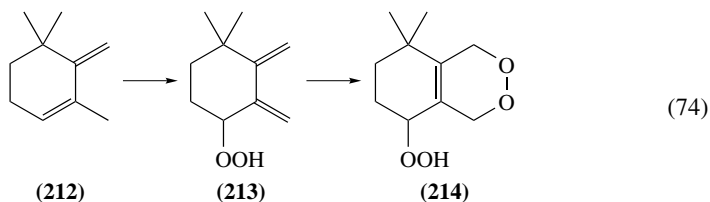
^c A partially resolved peak.

^d Probably the unreacted triglyceride **211**.

The MS of compound **40**, a putative intermediate of the metabolic degradation of indol-3-ylacetic acid (**39**), shows the molecular peak at *m/e* 163 and the parent negative peak at 162. This and other spectral and chemical evidence pointed to the compound being a hydroperoxide¹⁴⁶.

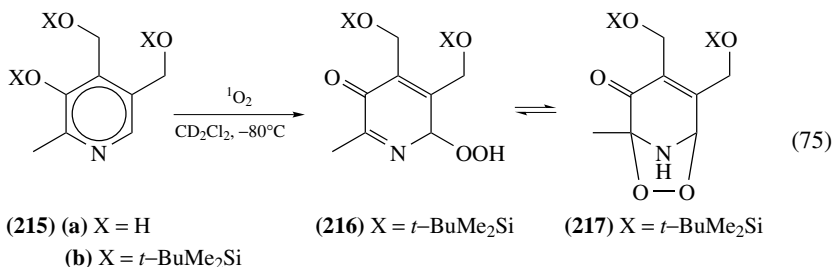
4. Nuclear magnetic resonance

γ -Pyronene (**212**) undergoes selective photosensitized oxidation involving rearrangement of the endocyclic double bond to yield an allylic hydroperoxide (**213**); on a further step the slower 1,4-cycloaddition to the conjugated exocyclic double bonds takes place, yielding compound **214**, as shown in equation 74. The structure of compounds **213** and **214** can be characterized by ¹H and ¹³C NMR spectra and some 2D techniques. For example, the spectral assignments relevant to this chapter (in CDCl₃/TMS, δ in ppm, *J* in Hz); **213** shows δ = 8.06 (1H, s, OOH); 4.45 (1H, t, *J* = 2.4, CHOOH); 85.2 (CHOOH); and **214** shows δ = 8.60 (1H, s, OOH); 4.25–4.35 (1H, m, CHOOH); 78.1 (CHOOH); 68.8 and 70.8 (COOC)⁵⁷⁵; see also the structural assignment of **256** in Section VII.C.2.



The mechanism of singlet oxygen detoxification involves quenching by Vitamin B₆ (**215a**). After silylating this compound to **215b**, in order to make it soluble in CD₂Cl₂ at low temperature, the quenching process proceeds as shown in equation 75. The main product is endoperoxide **217**, probably in equilibrium with hydroperoxide **216**. The structure of **216** can be elucidated from ¹H and ¹³C NMR spectra, e.g. δ_{H} = 4.76 ppm (1H, s, OOH) and δ_{C} = 96.1 ppm (NC(H)OO); see Section VII.C.2 for discussion of the structure

of **217**. The role of Vitamin B₆ (**215a**) as the main guard against singlet oxygen attack on lipids was contested on the grounds of its high reactivity that will cause fast depletion and its low solubility in hydrophobic solvents⁵⁷⁶.

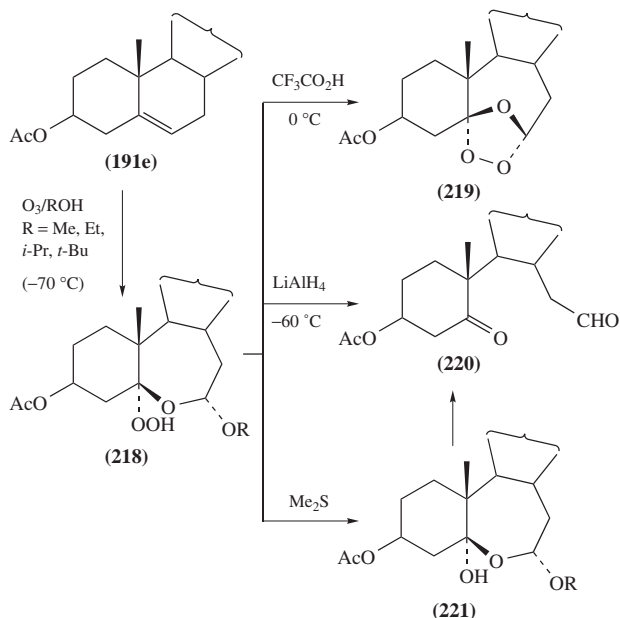


The primary products of free radical oxidation of DNA are hydroperoxides of thymidine moieties. Thymidine (**42**) in aqueous solution leads to oxidation products by various routes involving reaction with CF₃CO₂H in the presence of H₂O₂ or free radicals produced by photosensitized UV radiation, as shown in equation 64 (Section V.B.2.a). Reaction with the peroxide may start with double bond epoxidation followed by H₂O₂ addition to yield **184**; alternatively, a charge transfer to the photosensitizer followed by proton transfer and reaction with the free radicals generated in the medium leads to formation of **183** and **185**. It should be noted that **184** and **185** each has four diastereoisomers. The products may be separated by HPLC and partially characterized by ¹H and ¹³C NMR spectroscopies. For example, in **183**, δ_H = 4.73 ppm (s, CH₂OOH); the only proton on the thymine ring (on C(5)) has δ_H = 8.04 ppm for **183**, as it is on a double bond, whereas in all the eight diastereoisomers of **184** and **185**, 5.20 ≤ δ_H ≤ 5.46 ppm, for a CH₂O-group, irrespectively of whether it is CHOH or CHOOH. The ¹³C NMR spectra are more discriminating about the oxygen substituent on C(5) and C(2) and the ring configuration. For **183**, δ_C = 70.4 ppm (CH₂OOH); for both **184** and **185** the Me group is at a higher field when the configuration is either (5*R*,6*R*) or (5*S*,6*S*) than for the other two diastereoisomers (5*R*,6*S*) or (5*S*,6*R*), namely δ_C = 17.9, *ca* 23.5 ppm for **184** and δ_C = *ca* 14.2, *ca* 18.0 ppm for **185**; 69.0 ≤ δ_C ≤ 69.9 ppm (C(5)HOH) and 88.7 ≤ δ_C ≤ 90.6 ppm (C(6)HOOH) for **184** and 81.7 ≤ δ_C ≤ 81.9 ppm (C(5)HOOH) and 76.0 ≤ δ_C ≤ 77.1 ppm (C(6)HOH) for **185**¹⁴⁰.

The products of thermal oxidation of polyethylene films can be characterized by ¹³C FTNMR; furthermore, using the spin–lattice relaxation technique, quantitative estimates can be made of the oxidized functional groups. Observation of the development progress of the various functional groups leads to the postulation of hydroperoxides as the primary oxidation products, which undergo further transformations to the other derivatives in a complex scheme⁴⁹⁶.

5. X-Ray diffraction

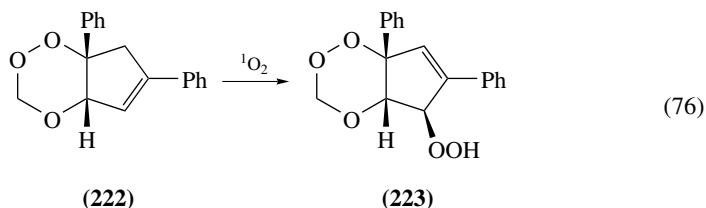
Ozonolysis of cholesteryl acetate (**191e**, Scheme 11) in the presence of an alcohol leads to the formation of a hydroperoxide (**218**), the structure of which was elucidated by XRD analysis for both R = Me and *i*-Pr. However, given the relatively poor crystallographic quality of these compounds, additional chemical and spectroscopic evidence had to be sought. Thus, products **218** show a ¹H NMR signal at δ *ca* 10 and a strong IR band in the range between 3250 and 3315 cm⁻¹, both consistent with the presence of a OOH group. The chemical behavior of the putative hydroperoxides is shown in Scheme 11. Treatment with trifluoroacetic acid leads to formation of a stable ozonide of known structure (**219**),



Scheme 11. Ozonolysis of cholesteryl acetate in alcohol solution and subsequent derivatization

isolated by chromatography in 15% yield. This is consistent with the α -configuration of the hydroperoxide. Reduction of **218** with LiAlH_4 at -60°C leads to the *seco*-form of the steroid at the B ring (**220**). This is the compound expected from normal ozonolysis followed by reduction with Ph_3P . An attempt to convert the hydroperoxide (**218**) to the corresponding alcohol (**221**) with a mild reducing agent such as Me_2S yielded only **220**. This is to be expected, as **221** is an unstable hemiacetal. Nevertheless, spectroscopic analysis of the crude product shows evidence for the presence of **221**⁵⁷⁷.

Treatment of compound **222**, containing a 1,2,4-trioxane ring fused to a cyclopentene ring, with $^1\text{O}_2$ leads to formation of a hydroperoxide (**223**) with ene displacement, as shown in equation 76. The structure of **223** was determined by single-crystal XRD analysis. A contact of the hydroperoxy group with the endocyclic ether O atom of a neighboring molecule (287.4 pm) points to weak H-bonding⁵⁷⁸.



6. Molecular refraction

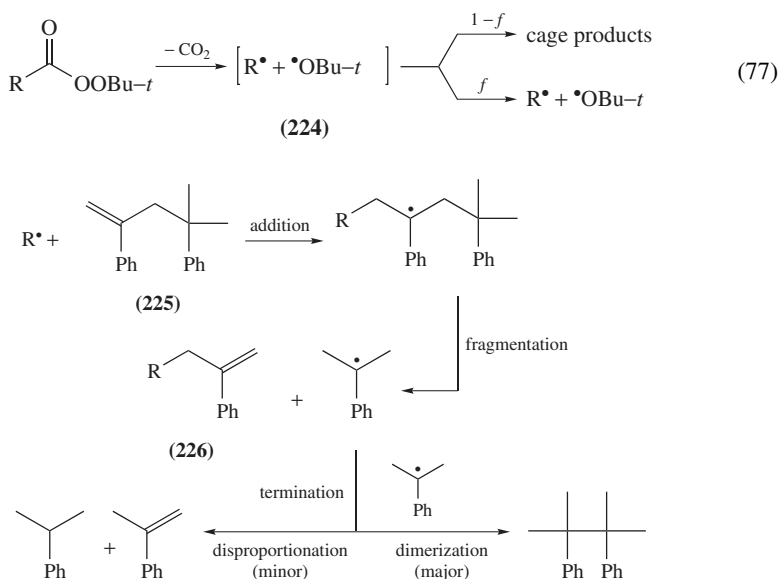
This is an additive constitutive property that is easy to determine experimentally and has theoretical significance, but it has been superseded by spectral methods that offer a deeper

insight to the molecular structure. Good agreement between experimental and calculated values is observed for the molecular refraction of *s*-alkyl hydroperoxides determined at the N_{D} line, on assuming certain average values for the contributions of the C, H and OOH groups. Contributions for the OOH group were found for the molar refraction of secondary alkyl hydroperoxides, ranging from 4.34 for 3-pentyl hydroperoxide to 4.93 for 2-octyl hydroperoxide, on assuming invariable contributions for the hydrocarbon chain⁴⁸⁷.

VI. PEROXYACIDS AND THEIR FUNCTIONAL DERIVATIVES

A. General

A review appeared on the methods for evaluating the efficiency of peroxyesters, peroxy-carbonates and other peroxide compounds as polymerization initiating and cross-linking agents¹⁸³. Esters of peroxy-carboxylic acids are used as initiators in radical polymerization. These esters undergo thermal decomposition as depicted in equation 77, starting with decarboxylation and production of a pair of free radicals. The proximity of these radicals leads to partial recombination into the so-called cage products. The efficiency, f , of the peroxyacid ester as a polymerization initiator is determined by the number of free radicals that diffuse away from the cage (**224**). A method was devised for evaluating f , based on trapping the free radicals with MSD (**225**), as shown in Scheme 12, where the free radical R^{\bullet} undergoes an addition reaction on a double bond of MSD and the intermediate free radical undergoes fragmentation into a stable α -substituted styrene (**226**) and a cumyl free radical; the latter tends to react with other cumyl radicals either by disproportionation or dimerization. The reaction of the *t*-BuO $^{\bullet}$ free radical with MSD may be complicated by side reactions; however, the alkyl free radical proceeds as shown in Scheme 12, yielding **226**, which can be determined by GLC-MS. As the reactivity of MSD toward free radicals is similar to that of styrene, the determination of f according to this scheme is a good evaluation method for initiators of styrene polymerization⁵⁷⁹. See also a similar discussion attaining equation 87 in Section VII.A.

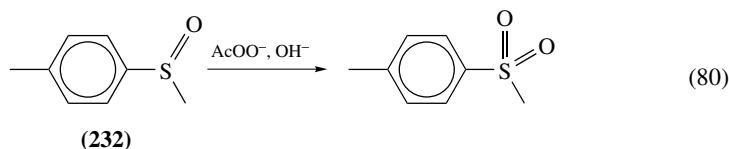
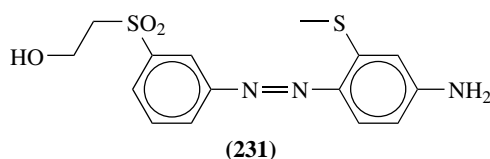
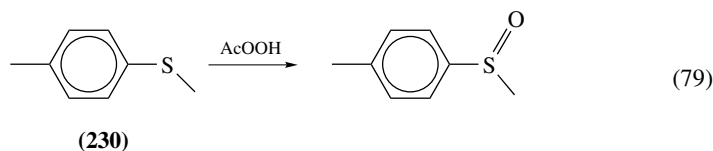


SCHEME 12. Free radical capture by α -methylstyrene dimer (**225**, MSD)

percarboxylic acids, which are totally dissociated into the carboxylate form, move in opposite order to the EOF, *n*-perbutanoic acid appearing first and performic acid last. The LOD for peracetic acid is 10 μM for an injection volume of 0.9 nL. The gradual disappearance of peracetic acid from household detergent solution when used with hot water was conveniently demonstrated by this method²⁰⁷.

The presence of peracetic acid and 1,1-dichloroethyl peracetate, formed by ozonolysis of *E*-2,3-dichloro-2-butene under various conditions (see Scheme 7), can be determined by ^1H NMR spectroscopy⁵⁴⁶. Peracetic acid can be determined in the presence of a large excess of H_2O_2 by a potentiometric method, based on the facts that I^- and I_3^- form a potentiometric buffer, and the rate of reduction of H_2O_2 by I^- at pH 5.6 is much slower than that of the acid. Under such conditions the selectivity of the method is high, and the LOD may be in the μM range, depending upon the H_2O_2 concentration⁵⁸¹. The oxidation of $[\text{Fe}(\text{CN})_6]^{4-}$ ions to $[\text{Fe}(\text{CN})_6]^{3-}$ ions by performic acid (**227**) can be followed at 420 nm ($\epsilon = 1020 \text{ M}^{-1} \text{ cm}^{-1}$)²⁴⁴.

Peracetic acid undergoes reduction with thioethers to yield sulfoxides, as shown in equation 79 for methyl *p*-tolyl thioether (**230**). This process is the basis of a selective method for determination of AcOOH vapor in the presence of a large excess of H_2O_2 . The azo dye **231** undergoes an analogous reaction and is preferred when dealing with peroxide vapors because of its lower volatility. The determination method consists of passing a sample of the gas, typically workplace air, through an absorption device (e.g. an impinger or a packed tube) where contact is made with a solution containing a known amount of **230** or **231**, diluting the absorption solution to a given volume, injecting an aliquot of the solution into a HPLC instrument and measuring the peak area of residual reagent and the derived sulfoxide (at 230 nm for **230** and 410 nm for **231**). The LOD using **231** is 46 ppb, for 5 L of air sampled during 10 min^{582a}. The process in equation 79 followed by HPLC-UVD at 225 nm can be applied for selective determination of AcOOH and other percarboxylic acids in acidic solutions, as used for disinfection. If the concentration of H_2O_2 is also needed, reduction with Ph_3P (analogous to equation 53) may be applied after the reduction with thioether and before the HPLC-UVD analysis^{582b}. If the solution is alkaline (pH 9–12), as in laundering and bleaching, the selective reagent for percarboxylate is the sulfoxide (**232**) turning to a sulfone, as shown in equation 80. Again, this reaction may be combined with subsequent treatment with Ph_3P , before HPLC-UVD⁵⁸³.



A UVV spectrophotometric method for the specific detection of peroxycarboxylic acids in the presence of H_2O_2 is based on direct oxidation of ABTS (**103**) by the analyte in an acidic medium. The spectrum of the resulting green free radical presents five absorption maxima where measurements can be made: 406, 415 (the most intense), 649, 732 and 815 nm. Full color development may be accelerated by traces of iodide. The LOD is $1 \mu\text{M}$ of AcOOH , with linearity in the 2.5 to $100 \mu\text{M}$ range⁵⁸⁴. Note that reaction of **103** with H_2O_2 in Section III.B.2.a requires peroxidase catalysis.

3. Peroxyesters

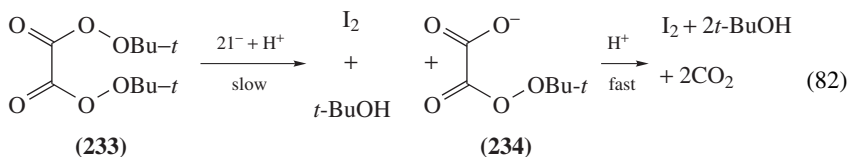
A three-step method can be applied for analysis of mixtures of hydroperoxides and peroxides, consisting of RP-HPLC separation, photolytic conversion of the emerging analyte to H_2O_2 , by irradiation with a 254 nm UV lamp and application of the fluorometric technique depicted in equation 34 ($n = 1$) to determine this analyte. *t*-Butyl perbenzoate has LOD 0.3 mg L^{-1} , linearity range $0.9\text{--}80 \text{ mg L}^{-1}$ and RSD 6.1%^{308b}. See a similar method in Section VI.B.1.

The RP-HPLC method based on the CL reaction of luminol (**124**) catalyzed by Co(II) (Section III.B.2.c) can be applied for determination of peroxycarboxylic acids, esters and diacyl peroxides (see examples of LOD in equation 67, Section V.B.2.c)¹⁶⁴. The biosensor prepared according to equation 70, that is effective in the determination of hydroperoxides (Section V.B.6.b), becomes deactivated after three days of operation when trying to determine *t*-butyl peracetate⁵⁵⁷.

Control of the yields in the synthesis of alkyl peresters from the corresponding hydroperoxide and excess of acyl halide (equation 81) can be realized by RP-HPLC with DA-UVD or RID. The usual components of the analyte mixture are stable in the short retention times of the chromatographic runs (less than 4 min). The method was applied to control the synthesis of cumyl perbenzoate, perbutyrate and pervalerate⁵⁸⁵.

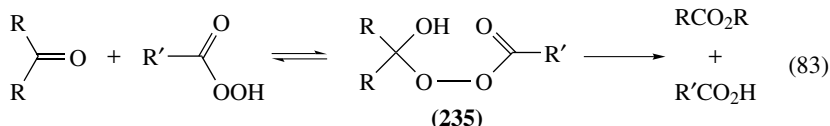


Also, di-*t*-butyl peroxalate (**233**) can be synthesized according to equation 81 from the analogous reagents. The iodometric determination of **233** can be carried out by letting iodide react for about 30 min. The titration shows only half of the expected equivalents. The mechanism of this reduction involves a slow step leading to an anionic intermediate (**234**), which decomposes in a fast step before the second reduction can be accomplished, as shown in equation 82^{586a}. An explosion has been reported when handling wet crystals of **233**, which seem to be extremely friction-sensitive^{586b}.



The Baeyer–Villiger process for conversion of open-chain ketones to esters, or cyclic ketones to lactones by a peracid involves an intermediate α -hydroxyperester (**235**) step, as shown in equation 83. Determination of **235** in the reaction mixture involves selective reduction of the peroxyacid with diphenyl sulfide and reduction of **235** with excess iodide, followed by titration of the liberated iodine. The presence of various transition metal ions may affect the determination by accelerating the final step of the synthetic process, thus

diminishing the analytical result. This effect can be masked by adding EDTA to the analytical sample⁵⁸⁷.



4. Acyl peroxides

According to NMAM method 5009, traces of particulate BzOOBz in the workplace atmosphere are determined by passing an air aliquot through a glass fiber filter, extracting with ether and carrying out the end analysis by RP-HPLC with UVD, measuring at 254 nm. The determination is linear in the range of 0.2 to 1.7 mg per sample, with estimated LOD of 0.1 mg per sample and precision of 2.4%⁵⁸⁸. A method for determination of BzOOBz consists of extraction with EtOH and conversion to BzO⁻ by addition of KOH and sonication for 2 min. End analysis is by HPLC-UVD, measuring at 222 nm. The LOD (SNR 3) is 19 μg L⁻¹ of BzOOBz, with linearity in the 0.12 to 20 mg L⁻¹ range. The method was proposed for the analysis of flour⁵⁸⁹.

The RP-HPLC method based on the CL reaction of luminol (**124**) catalyzed by Co(II) (Section III.B.2.c) can be applied for determination of peroxycarboxylic acids, esters and diacyl peroxides (see examples of LOD in equation 67, Section V.B.2.c)¹⁶⁴. Some substances are hard to dissolve in aqueous solution. The FIA system described in Section III.B.2.a for determination of H₂O₂ in substances dissolved in toluene, using HRP immobilized by adsorption on a pack of controlled-pore glass beads, where the enzyme catalyzes the oxidation of *p*-anisidine (*p*-MeOC₆H₄NH₂) dissolved with the analyte, can also be used with diacyl peroxides. However, the throughput has to be lower due to the slower reaction of these compounds. The LOD for BzOOBz is 2.0 μM, measuring at 466 nm, with linearity in the 1.4 to 17 mM range, and a throughput of about 30 h⁻¹. The method was applied to analysis of olive oil and margarine³⁰². An amperometric biosensor based on the design of Scheme 5, with HRP immobilized on a CPE, using ferrocene as mediator, is effective for determination of diacyl peroxides, e.g. dilauroyl peroxide; however, its response is weaker than with H₂O₂³⁸⁸.

A CLD method for determination of BzOOBz in wheat flour is based on measuring the CL emitted on oxidation with luminol in bicarbonate-hydroxide buffer at pH 11.5, according to Scheme 3 but with no catalyst present other than the base. The analyte solution is added to the reagent solution in the CL cell as microdrops of about 8 μL volume, at a rate allowing each drop to develop an optimal signal. The LOD is 0.14 μg L⁻¹ (SNR 3), with linearity from 0.5 μg L⁻¹ to 1 mg L⁻¹⁵⁹⁰.

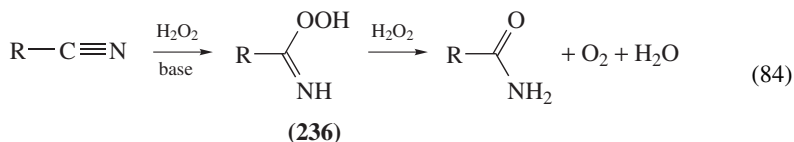
The mimetic biosensor for ELD described in Section III.B.4.b, incorporating polymerized Fe-protoporphyrin IX (**75c**) and Os(II) ions, can be used for determination of diacyl peroxides in organic solution. The electrode was tested for determination of BzOOBz extracted from a pharmaceutical gel³⁸¹.

C. Structural Characterization

1. Peroxycarboximidic acids

An interesting method for the hydrolysis of nitriles to amides involves two redox processes with H₂O₂ and a peroxycarboximidic acid (**236**) intermediate stage, as shown in equation 84. The mechanism of hydrolysis was established for acetonitrile and benzonitrile

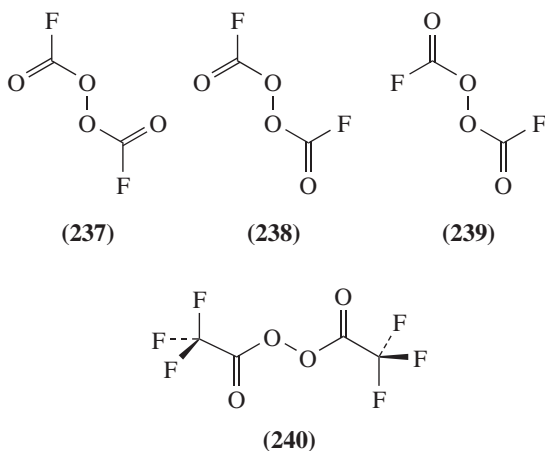
(R=Me, Ph) by kinetic measurements using FT-Raman spectroscopy. Given the instability of intermediates **236**, no reference spectra are available for this type of compound; however, the problem was solved by applying SIMPLISMA, a self-modeling multivariate analysis technique. The method is interactive, requiring decisions by the user about the quality of intermediate stages of the calculation and noise levels. The calculations afforded a reasonable Raman spectrum ($\nu_{\text{O-O}} = 870 \text{ cm}^{-1}$, $\delta_{\text{OOH}} = 1450 \text{ cm}^{-1}$) for the peroxy-carboximidic acid functional group, which is by itself a proof of the existence of such unstable compounds in solution²²⁷.



2. Acyl peroxides

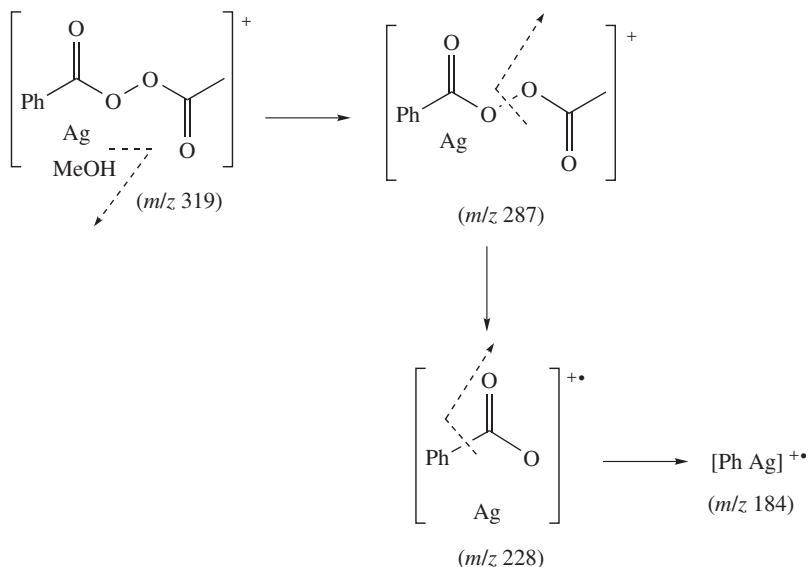
Benzoyl peroxide has clear IR and Raman stretching frequencies at $\nu_{\text{O-O}}$ 846 and 847 cm^{-1} , respectively, whereas for lauroyl peroxide the IR band at 886 cm^{-1} is very weak and only the Raman band at 876 cm^{-1} can be useful for structural assignment⁵⁶⁷.

Of the three possible conformations of fluoroformyl peroxide for a given C–OO–C dihedral angle (**237–239**), the *syn-syn* one (**237**) seems to be the only one present, according to the assignments of $\nu_{\text{as}}\text{C=O}$ at 1929 cm^{-1} and $\nu_{\text{s}}\text{C=O}$ at 1902 cm^{-1} in the IR spectra, both in the gas phase and in a solid matrix. Theoretical calculations support this contention, as the energy of **237** is lower by 13.5 and 26.9 kJ mol^{-1} than that of the *syn-anti* (**238**) and *anti-anti* (**239**) conformations, respectively. GED experiments point to several features of a *gauche-syn-syn* conformation: The O=C–OO chains are coplanar, forming a very small dihedral angle C–OO–C of 83.5° , similar to that of F_2O_2 and Cl_2O_2 ; the O–O distance of 1.419 \AA is short⁵⁹¹. The structure of trifluoroacetyl peroxide can be elucidated using various spectroscopic techniques, which are supported by DFT calculations. GED and the vibrational spectra (gas and Ar matrix FTIR, liquid FT-Raman) point to a *syn-syn* preferred conformation (**240**) of C_2 symmetry, a short O–O distance of 1.426 \AA and dihedral angle C–OO–C of 86.5° , similar to other acyl



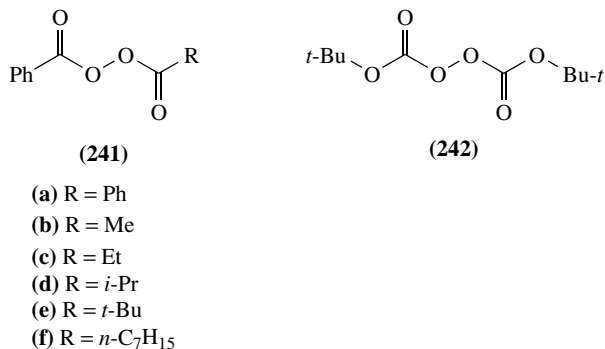
peroxides. For each of the CF_3 groups one of the C–F bonds is eclipsed with the C–OO bond. Compared with nonperoxide analogs, the peroxide function shows a relatively strong absorption in the 200 nm region, besides the $n \rightarrow \pi^*$ transition of the C=O chromophore at ca 220 nm. A cautionary note was given about handling only submillimolar amounts of trifluoroacetyl peroxide, due to unpredictable explosions taking place on the solid-to-liquid and liquid-to-solid phase transitions⁵⁹².

Diacyl peroxides undergo various primary homolytic and heterolytic fragmentation processes in EI-MS, of which only the latter class can be observed, while homolytic splits of the C–OO and the O–O bonds are easily attainable. On carrying out EI-MS of a ca 0.5% (m/v) solution of a diacyl peroxide in MeOH, containing about one-half as much moles of AgBF_4 , the spectrum shows the molecular peak of the peroxide $\text{M}^{+\bullet}$ and also the peaks of complexes of the diacyl peroxide with Ag^+ and the solvent, $[\text{M}-\text{Ag}-\text{MeOH}]^+$, and with Ag^+ and a second peroxide molecule, $[\text{M}-\text{Ag}-\text{M}]^+$. Tandem CIS-MS/MS of the complex ions allows investigation of their homolytic fragmentation track, as one of the fragments contains the silver ion, providing the necessary electric charge. This method shows interesting features when applied to benzoyl acetyl peroxide. For example, the main homolytic dissociation track of the complex involving the solvent takes place as depicted in Scheme 13⁵⁹³.

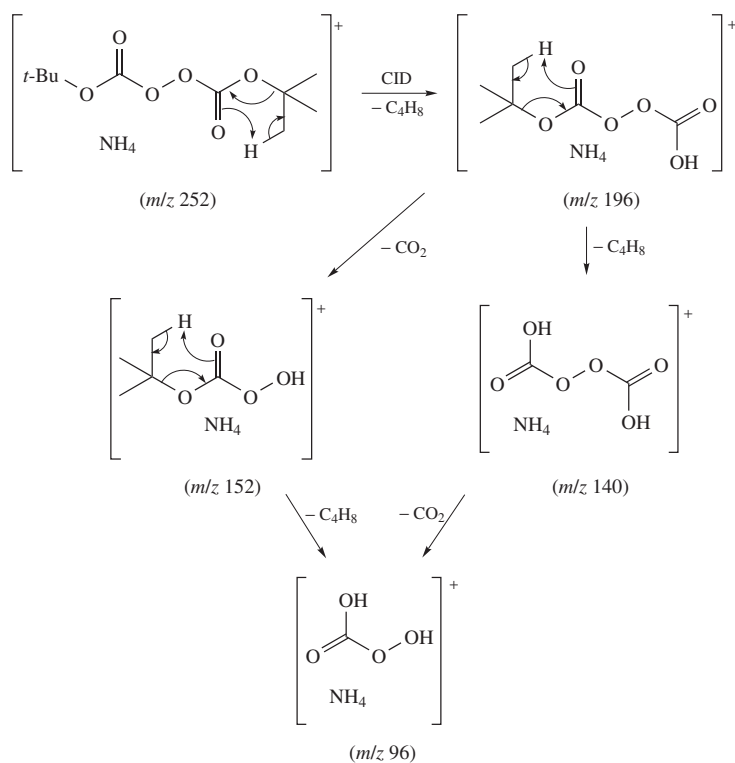


SCHEME 13. Main homolytic fragmentation path of acetyl benzoyl peroxide undergoing CID with $^{107}\text{Ag}^+$ ions

Instructive tandem CIS-MS-MS studies may be carried out using NH_4^+ ions instead of Ag^+ , introducing ammonium acetate together with the analyte. Diacyl peroxides containing at least one benzoyl group (**241a–f**), and various isotopomers containing ^2H and ^{18}O , form ammonium complex ions $[\text{M}-\text{NH}_4]^+$, which appear in the EI-MS spectrum. These ions undergo CID in a tandem mass spectrometer losing NH_3 and leaving $[\text{M}-\text{H}]^+$ ions, which undergo, among other processes, homolytic scission of the O–O bond, leaving the aromatic fraction on the cation radical, in a process analogous to the steps of Scheme 13. *Di-t*-butyl peroxydicarbonate (**242**) undergoes similar fragmentations;



however, the ammonium ion complexes are more stable and partly persist in the CID stages. McLafferty rearrangements are observed for analytes containing branched alkyl residues such as **241d**, **241e** and **242**, yielding ions that may easily lose CO₂, as shown, for example, in Scheme 14 for the CID fragmentation of the primary complex ion formed from **242**⁵⁹⁴.



SCHEME 14. One of the CID fragmentation paths of the primary complex of bis(*t*-butoxycarbonyl) peroxide (**242**) with NH₄⁺, involving McLafferty rearrangements and CO₂ eliminations

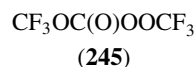
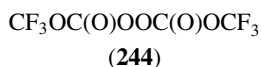
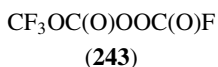
3. Peroxyesters

The IR and Raman spectra of esters derived from peroxy-carboxylic and peroxy-carbonic esters show a band near 860 cm^{-1} , assigned to a stretching mode of the OO group. The band of the carbonyl group in these compounds is shifted to higher frequencies by $30\text{--}40\text{ cm}^{-1}$, as compared to ordinary esters⁵⁶⁷.

4. Functional derivatives of peroxy-carbonic acid

See above the discussion attaining compound **242** and Scheme 14.

Trifluoromethyl fluoroformyl peroxy-carbonate (**243**) is the product of a photochemical process of a mixture of trifluoroacetic anhydride, oxalyl fluoride, CO and O₂ at -15°C . It is quite stable at room temperature. The chemical shifts and coupling constants in the ¹⁹F and ¹³C NMR spectra assigned to the various sites correspond to those of the same groups in similar compounds (**237**, **244**). The stretching modes of the various groups of **243** can be assigned based on the IR and Raman spectra of the vapor and the liquid, respectively, and theoretical calculations resulting in a *syn-syn-syn* preferred conformation, where the first *syn* refers to the conformation of the CF₃ group relative to the closer C=O group, and the other two to those of the C=O groups relative to the O-O group. The Raman spectrum shows a very strong peak at 924 cm^{-1} for O-O stretching, which is weak in the IR. The skeletal modes apparently are coupled and none can be assigned. Theoretical calculations point to some peculiar features that may make difficult the interpretation of spectroscopic evidence. The most stable conformation is that with a *gauche* CF₃-O-C=O, the first *syn*, both C=O groups being *syn* with respect to O-O, thus *syn-syn-syn*, and nearly 90° for the C-O-O-C dihedral angle. The latter feature is typical for peroxides X-O-O-Y, where X and Y are strongly electronegative groups or *sp*²-hybridized substituents, as in the present case. The O-O bond distance calculated for **243** (1.43 \AA) is not far from those experimentally found for other fluorinated peroxides, including **237** (1.436 \AA) and **3** in Section IX.C.1 (1.393 \AA)²⁴. Bis(trifluoromethyl) peroxydicarbonate (**244**), bis(trifluoromethyl) peroxy-carbonate (**245**) and a trioxide (Section IX.A) are obtained on UV irradiation of a mixture of (CF₃CO)₂O, CO and O₂. The vibrational and NMR spectra of compounds **244** and **245** are quite similar to those of **243**, including the very strong Raman peak at 934 cm^{-1} of the O-O stretching mode. Common to these fluorinated peroxy-carbonates is the featureless UV absorption cross-section σ , descending from a few tens of 10^{-20} cm^2 to nearly nil values over the wavelength range from 190 to 300 nm ²³.



VII. DIALKYL PEROXIDES

A. General

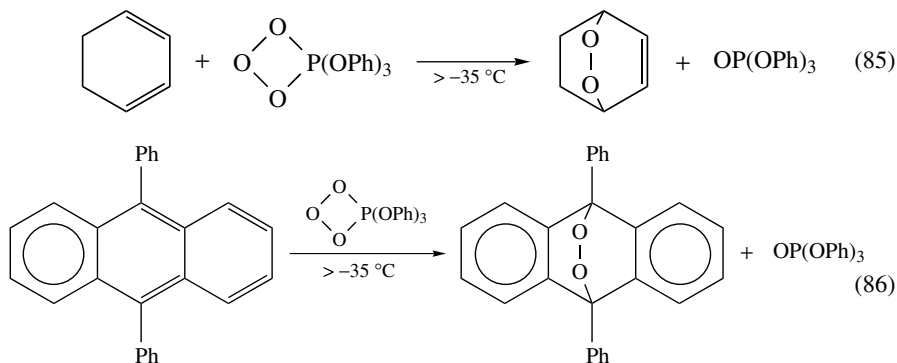
The *dialkyl* denomination also includes cyclic peroxides (endoperoxides). The most significant route for peroxide formation is probably that of autoxidation of organic materials, leading to their gradual degradation. Although hydroperoxides are the main products of this process, also peroxyesters are formed, as is the case, for example, of isoprostane bicyclic endoperoxides (**25**) mentioned in Section II.A.2.c.

Peroxides can be obtained from ozonides in various ways. Dioxirane (**246**), the simplest cyclic peroxide, appears in the microwave spectrum of ethylene-ozone mixtures, in the -115 to -110°C temperature range, probably as a decomposition product of the primary

ozonide of ethylene in the gas phase, by two possible routes⁵⁹⁵. Primary ozonides may transform to peroxides and other products, as shown in Scheme 7 (Section V.B.5). Final ozonides can undergo acid-catalyzed processes, such as oligomerization to various cyclic products or condensation with carbonyl compounds, as illustrated in Section VII.C.3. A well-established route for peroxide synthesis is the photosensitized reaction of oxygen with a pair of conjugated double bonds, yielding the product of a 1,4-cycloaddition, such as ascaridole (**10**)⁵⁹⁶ and the endoperoxide **247**⁵⁹⁷, which are derived from their corresponding cyclodienes (α -terpinene and cyclopentadiene, respectively). The double bond of **10** and **247** can be hydrogenated with thiourea at low temperature preserving the peroxy bridge⁵⁹⁷.



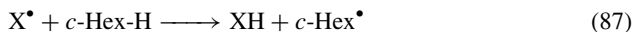
The reaction of singlet oxygen with conjugated double bonds usually is a 1,4-cycloaddition leading to formation of derivatives of the 1,2-diox-4-ene ring system. This can be achieved either by photooxidation or by reaction in the presence of triphenyl phosphite-ozone adduct (Section VIII.D.2), shown in equations 85 and 86⁴⁹³.



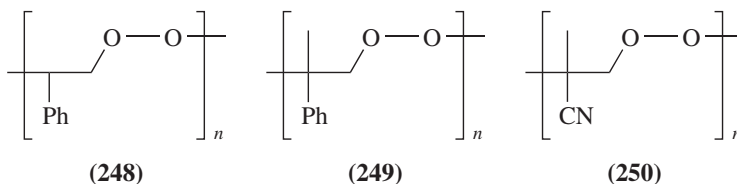
Treatment of variously substituted cyclohexanones with H_2O_2 in acidic medium leads to formation of dispiro-1,2,4,5-tetraoxanes (**16**, Section II.A.2.a). The products obtained in the case of **16a** and **16b** are mixtures of the *meso*, D- and L-stereoisomers, whereas **16c** is a single compound⁵⁸. See also Scheme 7 for the formation of *cis*- and *trans*-3,6-dichloro-1,2,4,5-tetraoxanes, obtained on ozonolysis of 1,2-dichloroethylene⁵⁴⁶.

Methods for detecting whether peroxy compound have been used for cross-linking elastomers have been reviewed¹⁸⁵. An important application of dialkyl peroxides is as initiators of cross-linking and graft polymerization processes. The success of both processes depends on the ability of the peroxide to produce free radicals and the ability of the free radicals for H-abstraction from a relevant donor substrate. A method for evaluating this ability consists of inducing thermal decomposition of the peroxide dissolved in a mixture of cyclohexane and MSD (**225**). The free radical X^\bullet derived from the

peroxide may abstract an H atom from cyclohexane according to equation 87, forming a cyclohexyl free radical. Now, either X^\bullet or $c\text{-Hex}^\bullet$ undergo the process depicted in Scheme 12 (Section VI.A), reacting with **225**, $R^\bullet = X^\bullet$ or $c\text{-Hex}^\bullet$, and the ratio between the two possible products **226**, as determined by GLC-MS, is a measure of the efficiency of the peroxide for H-abstraction⁵⁹⁸.



Radical polymerization carried out with oxygen under pressure brings about formation of alternating peroxy polymers, such as poly(styrene peroxide) (**248**)^{599,600}, poly(α -methylstyrene peroxide) (**249**)⁶⁰¹ and poly(methacrylonitrile peroxide) (**250**)⁶⁰². Another possibility of generating polymeric peroxides is shown in Scheme 18, Section VIII.C.7. The peroxide copolymer **248** can be used with advantage instead of BzOOBz for curing resins in coating and molding formulations, applying either photochemical or thermal processes⁶⁰³. See Section VII.C.2 for various structural characteristics of these polymers.



B. Detection and Determination

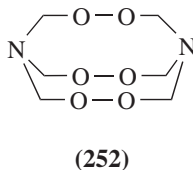
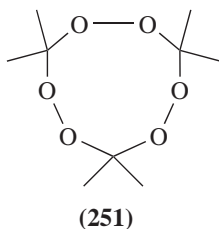
1. Titration methods

The standard iodometric AOCS methods for the evaluation of POV mentioned in Section IV.B.2 are also suitable for determination of dialkyl peroxides²¹².

2. Ultraviolet-visible spectrophotometry and colorimetry

Dialkyl peroxides containing the cumyl group can be determined by RP-HPLC, using MeOH–water mixtures as mobile phase, by applying UVD at 257 nm⁶⁰⁴. RP-HPLC with post-column derivatization by a method based on equation 34 with **106a** and FLD can be applied to the analysis of small peroxide molecules found in the atmosphere, e.g. bis(hydroxymethyl) peroxide⁵²³. A three-step method was proposed for the analysis of mixtures of hydroperoxides and peroxides, consisting of RP-HPLC separation, photolytic conversion of the emerging analyte to H_2O_2 , by irradiation with a 254 nm UV lamp, and application of the fluorometric technique of equation 34 with **106a** to determine this analyte. The identity of a chromatographic peak as belonging to a peroxide depends on its response to post-column irradiation. Di-*t*-butyl peroxide and *t*-butyl cumyl peroxide showed, respectively, LOD 5 and 0.1 mg L^{-1} , linearity range from 15 to 112 and from 0.3 to 75 mg L^{-1} and RSD 3.6 and 5.1%^{308b}.

Inspired by the effective post-column photochemical conversion of hydroperoxides and peroxides to H_2O_2 just described, a method was developed for trace analysis of peroxide explosives, such as triacetone triperoxide (**251**) and hexamethylene triperoxide diamine (**252**). These are powerful explosives with no commercial or military applications because



of their extreme sensitivity to shock, friction and temperature changes on dry storage; however, they seem to be favored by common criminals and terrorists. Thus, their trace analysis has forensic interest, both to discover manufacturing sites or for identification after use. For both **251** and **252** LOD is 2 μM , LOQ 6 μM and RSD ($n = 4$) up to about 4% for concentrations as low as 8 μM . Traces of the diperoxide and tetraperoxide analogs are also present after an explosion of **251**⁶⁰⁵. A simplified version of the proceedings for determination of peroxide explosives consists of treating the sample solution with catalase to destroy any H_2O_2 present, exposing the sample to UV radiation to convert the peroxides into H_2O_2 , addition of the reagent solution, HRP and ABTS (**103**) in acetate buffer at pH 5.5 and measuring at 415 nm the absorbance of the free radical produced. This method was adapted for field use with a portable UVV spectrophotometer. LOD are 8×10^{-6} M for **251** and 8×10^{-7} M for **252**⁶⁰⁶.

The HPLC method with CLD described in Section V.B.2.c for determination of hydroperoxides using luminol (**124**) with hemin (**75a**) catalysis is ineffective with dialkyl peroxides, such as di-*t*-butyl peroxide, cumyl propyl peroxide and cumyl 3-phenylpropyl peroxide. However, for a certain set of experimental conditions, cumyl allyl peroxide can be determined, but the sensitivity is much lower than for hydroperoxides¹⁶⁴.

3. Nuclear magnetic resonance spectroscopy

The 1,2,4,5-tetroxane products **199a** and **199b** in Scheme 7 were identified and their transformation to other products could be followed by ^1H NMR spectroscopy⁵⁴⁶.

4. Flame ionization detection

The discussion on ECN and relative mass response factors attaining equation 71 in Section V.B.7 applies also to quantitation of dialkyl peroxides, such as dicyclohexyl peroxide, cyclohexyl cycloheptyl peroxide and dicycloheptyl peroxide after separation by GLC-FID⁵⁶¹.

C. Structural Characterization

1. General

Certain considerations made for structural analysis of compounds containing OOH groups mentioned in previous sections apply here too; however, the characterization is usually more difficult and requires concurrent evidence from various techniques to ascertain the presence of the C-OO-C moiety. The main characterization tools are NMR, looking for the effects of -OO- on the resonance of nearby atoms and XRD for compounds with single crystals of good crystallographic quality.

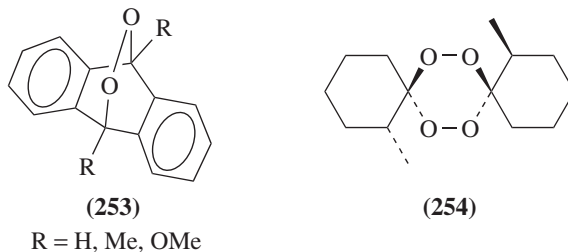
2. Nuclear magnetic resonance

The ^1H NMR spectrum of poly(methacrylonitrile peroxide) (**250**) shows the two expected peaks at $\delta = 1.70$ ppm (3H, s, CH_3CCN) and 4.48 ppm (2H, s, CH_2OO). Due to the relatively low average molecular weights of the peroxide polymers (in the present case $M_{n,\text{av}} = 2190$ Da and $M_{w,\text{av}} = 3670$ Da), two additional small signals can be discerned at $\delta = 9.80$ ppm (s, CH_2OOH) for the beginning of the chain and 5.76 ppm (d, $\text{OOCH}_2\text{CH}(\text{CN})\text{Me}$) for the end of the chain. The ^{13}C NMR signals at $\delta = 76.7$ and 78.1 ppm correspond to the backbone methylene and tertiary carbons, respectively, displaced downfield by $-\text{OO}-$ groups. The flexibility of the polymer chain in solution can be assessed by nuclear spin relaxation measurements, pointing to a higher flexibility of **250** as compared to polymethacrylonitrile⁶⁰². Information about the structure of poly(styrene peroxide) (**248**) can be obtained from ^1H and ^{13}C NMR spectroscopy, including tacticity, chain dynamics and nature of the end groups. When **248** is prepared under oxygen at high pressure, the copolymer is strictly alternating. Analysis of the weak resonances in the normal spectra points to carbonyl and hydroperoxide as the most frequent terminal groups. Molecular dynamics studies of **248** in solution, based on tumbling, segmental reorientation and phenyl group rotation motions, helped to assess its chain flexibility. Besides the clear distinction of the methylene and methyne carbons on the polymer backbone, the styrene-peroxy sequences act as dyads, modifying the magnetic environment of neighboring dyads; NOESY data show that **248** has a larger chain flexibility than polystyrene of similar molecular weight^{599,600}. Also, the structure of poly(methylstyrene peroxide) (**249**) can be characterized by ^1H and ^{13}C NMR spectroscopy, showing the methylene protons shifted to $\delta = 4.20$ ppm by the $-\text{OO}-$ link, as are the methylene and quaternary ^{13}C resonances shifted to $\delta = 77.4$ and 84.5 ppm, respectively. Spin-lattice relaxation spectroscopy also shows a larger chain flexibility in the case of **249** as compared to the usual synthetic polymers⁶⁰¹.

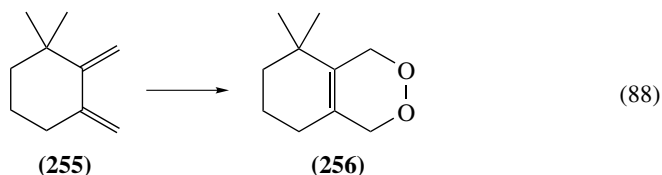
The structure of stolonoxide A (**18a**, Section II.A.2.a) and its Me ester can be totally elucidated by ^1H and ^{13}C NMR techniques. Relevant to the present chapter are the following details: Besides the methoxycarbonyl group, the ^{13}C NMR spectrum shows six olefinic carbons and four oxygen-bearing carbons, suggestive of three double bonds and two oxygen-containing heterocycles; all the other carbon signals are assigned to CH_2 groups. The NOESY spectrum of **18a** in C_6D_6 , showing cross peaks due to 1,3-diaxial interactions between H(3) ($\delta = 4.55$ ppm) and H(5) ($\delta = 1.30$ ppm), and also between H(6) ($\delta = 3.94$ ppm) and H(4) ($\delta = 1.21$ ppm), points to the substituents on the 1,2-dioxane ring being in equatorial positions. The chemical shifts in CDCl_3 of the atoms directly linked to the $-\text{OO}-$ groups of **18b** are also characteristic: H(3) ($\delta = 4.54$ ppm, m), H(6) ($\delta = 4.05$ ppm, m), C(3) ($\delta = 77.6$ ppm, d) and C(6) ($\delta = 83.8$ ppm, d)⁶².

The 9,10-peroxy derivative of 9,10-disubstituted anthracenes (**253**) has the ^1H NMR bands of the aromatic rings at slightly upfield chemical shifts relative to the corresponding signals of the analogous primary ozonide. It was demonstrated that these epoxides are not a decomposition product of the primary ozonides (see Scheme 17 in Section VII.C.4)⁶⁰⁶. The ^{13}C NMR spectrum of the product derived from 2-methylcyclohexanone shows seven peaks, pointing to the unique structure **254**, in accordance with the structure obtained by XRD analysis. The ^{13}C NMR spectra of the tetroxanes **16a** and **16b** before effecting a chromatographic separation show multiple peaks, as expected from a mixture of diastereoisomers. Furthermore, the ^{13}C NMR spectra of all **16** products show chemical shifts downfield of $\delta = 107$ ppm, pointing to the presence of geminal $-\text{O}$ substituents on the spiro C positions⁵⁸.

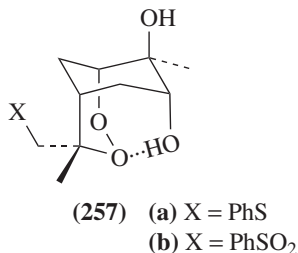
δ -Pyronene (**255**) undergoes photosensitized 1,4-cycloaddition of oxygen to yield the endoperoxide **256**, according to equation 88. The structure of this compound and many



of its derivatives can be elucidated by ^1H and ^{13}C NMR spectroscopy and some of its 2D techniques. For example, the spectral assignments of **256** relevant to this chapter (in CDCl_3 , δ in ppm) are $\delta = 4.40$ to 4.75 (4H, m, CH_2OOCH_2), 68.8 and 70.8 (COOC)⁵⁷⁵; see also the assignments for the derivatives of γ -pyronene **213** and **214** in Section V.C.4.



The presence of an intramolecular H-bond in **257a** and **257b**, synthetic precursors of antimalarial drugs, can be shown by COSY ^1H NMR. The pertinent OH groups ($\delta = 4.09$ and 3.89 ppm, broad d, $J = 13.2$ Hz) on establishing the H-bond with one of the peroxy O atoms are nearly coplanar with the corresponding HCOH atom ($\delta = 3.57$ ppm, ddd, $J = 0.9, 5.4, 13.2$ Hz), thus explaining the unusually large coupling constant. The strength of this H-bond is demonstrated by the coupling being persistent in the presence of D_2O or CD_3OD , disappearing only in the presence of $\text{CD}_3\text{CO}_2\text{D}$ ⁶⁰.



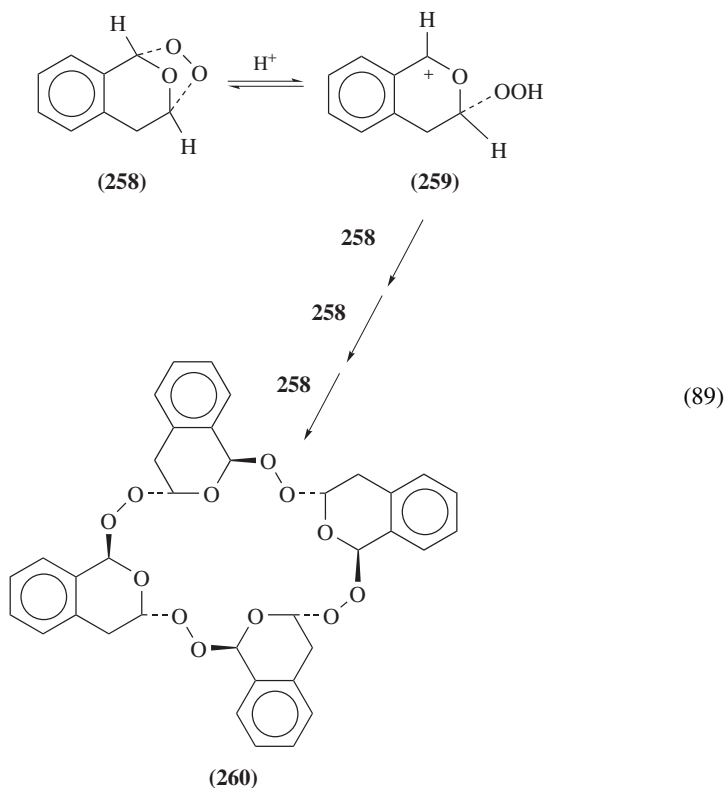
The mechanism of singlet oxygen detoxification involves quenching by Vitamin B₆ (**215a**). After silylating this compound, in order to make it soluble in CD_2Cl_2 to work at low temperature, the quenching process proceeds as shown in equation 75 (Section V.C.4). The main product is endoperoxide **217**, probably in equilibrium with hydroperoxide **216**. The structure of **217** can be established from the ^1H and ^{13}C NMR spectra, e.g. $\delta_{\text{H}} = 6.06$ ppm (1H, d, $J = 4.4$ Hz, HCOO), 4.19 (1H, broad, NH), $\delta_{\text{C}} = 96.8$ ppm (MeCOO), 86.6 ppm (HCOO), and DEPT, phase-sensitive COSY, HMQC and HMBC spectra⁵⁷⁶.

The quenching mechanism of Vitamin E (**21**) toward hydroperoxides is depicted in equation 11 (Section II.A.2.d). The structure of products **38** obtained when quenching hydroperoxides from phosphatidylcholines (**155**) was elucidated by the usual MS and NMR techniques¹⁴⁵.

The ¹H NMR spectra of the compounds **273a** and **274a** as BF₄⁻ salts appearing in equation 92 (Section VII.C.8), show the chemical shifts expected for the aromatic protons in the various types of aromatic systems present in these compounds⁶⁰⁷. NOESY of the macrocyclic compound **262** (equation 90, Section VII.C.3) points to interaction between the Me protons of the *t*-Bu groups and the remote methine protons. This is in accordance with the structure as determined from single crystal XRD of this compound⁶⁰⁸.

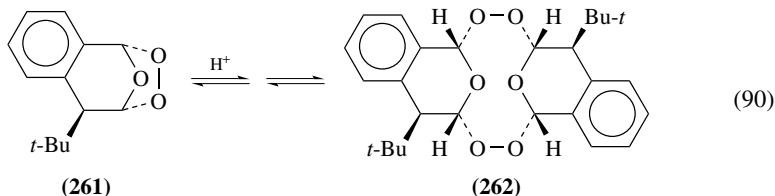
3. X-Ray crystallography

The ozonide of indene (**258**) undergoes the acid-catalyzed oligomerization shown in equation 89, presumably by successive scissions of C–OO bonds, leading to intermediate carbenium ions bearing a hydroperoxide group (**259**) and finally closing to a cyclic tetramer (**260**). The structure of **260** was determined by X-ray crystallography, the molecule having a C₂ axis of symmetry⁶⁰⁸.

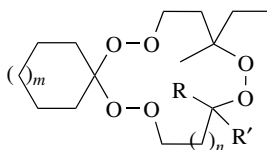


The ozonides of indenenes substituted with bulky alkyl groups in the allylic position (e.g. **261**) undergo acid-catalyzed dimerization to a 10-membered endoperoxide (**262**), as shown in equation 90. Similarly to equation 89, the process involves hydroperoxide

intermediates. Of the possible configurations of the dimer, the molecule with C_{2v} symmetry is obtained, as shown by XRD analysis. This configuration is in accordance with the NOESY results mentioned in Section VII.C.2, regarding the interaction between the Me protons of the *t*-butyl group and the remote methyne protons indicated in **262**⁶⁰⁹.



Macrocyclic compounds containing three peroxy groups were synthesized by different routes. The structure of three such compounds (**263–265**) was determined by single-crystal XRD analysis. The two 13-membered macrocycles (**263** and **264**) adopt a 5-3-5 triangular conformation with a peroxy group on the short leg; the 16-membered one (**265**) adopts a 5-3-5-3 rectangular conformation, as opposed to the 4-4-4-4 square conformation of cyclohexadecane⁶¹⁰.

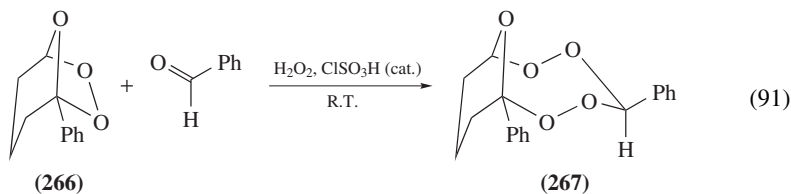


(263) R = Me, R' = OMe, $m = n = 1$

(264) R = R' = Me, $m = 7, n = 1$

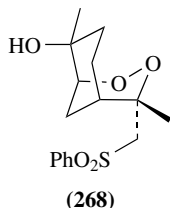
(265) R = R' = H, $m = 7, n = 4$

Acid-catalyzed condensation of bicyclic ozonides with aldehydes and ketones, in the presence of hydrogen peroxide, leads to the formation of bicyclic peroxide analogs of acetals in low yields, as shown in equation 91 for the condensation of the ozonide of 1-phenylcyclopentene (**266**) with benzaldehyde. The structure of compound **267**, with the preferred ring conformation as shown, was determined by XRD analysis⁶¹¹. The same method served to demonstrate that the condensation compound **16c** is unique, with structure **254**⁵⁸.

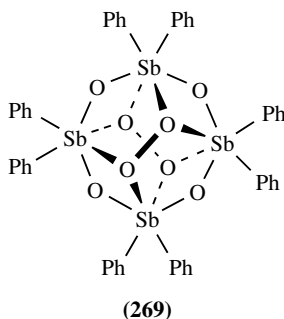


Single-crystal XRD analysis of an endoperoxide precursor in the synthesis of the antimalarial yingzhaosu A (**12**, Section II.A.2.a) points to structure **268**, with the same configuration of the corresponding asymmetric carbons⁶⁰.

Tetraphenyldistibane, $(\text{Ph}_2\text{Sb})_2$, undergoes oxidation with air to form oxides $(\text{Ph}_2\text{Sb})_2\text{O}$ and $(\text{Ph}_2\text{Sb})_4\text{O}_6$. The latter oxide undergoes further oxidation with H_2O_2 to yield $(\text{Ph}_2\text{SbO})_4(\text{O}_2)_2$ (**269**), which is an antimony–oxygen cluster with μ_4 -peroxy ligands. The structure



of the compound was elucidated by XRD. $(\text{SbO})_4$ forms an 8-membered ring of alternating Sb and O atoms at a mean bond distance of 196 pm; the two peroxy pairs have a mean bond distance of 147 pm within themselves and 223 pm to the Sb atoms. Furthermore, each peroxy pair is nearly collinear with a pair of diametrically opposite O atoms of the ring. The eight phenyl groups linked to the Sb atoms form an external shield to the inner Sb–O cage⁶¹².



The compounds appearing in equation 102 (Section VIII.C.6.a), containing a 1,2,4-trioxane ring, were examined by single-crystal XRD analysis. The O–O distances in this ring (143.3, 147.2 and 148.8 pm) are in accord with the mean value (147.0 pm) measured for the $\text{Csp}^3\text{--OO--Csp}^3$ moiety⁵⁷⁸.

Single-crystal XRD analysis of the 9-membered endocyclic peroxide compounds as BF_4^- salts appearing in equation 92 shows torsion angles of 160.8 and 154.6°, and O–O distances of 150.7 and 150.2 pm, respectively. In spite of these bond lengths being among the longest ever reported for endocyclic peroxides, the bond scission shown in equation 92 does not involve splitting of the O–O bond, as discussed in Section VII.C.8⁶⁰⁷.

4. Electron diffraction

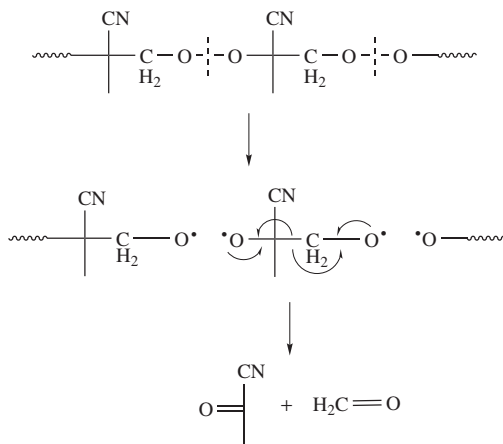
The molecular structure of bis(trifluoromethyl) peroxide can be determined by electron diffraction spectrometry. The following molecular parameters and their estimated standard deviations (3σ) are obtained by this method: Bond distances in pm units are O–O 141.9 ± 2.0 , C–O 139.9 ± 0.9 and C–F 132.0 ± 0.2 ; bond angles are $\angle\text{C–O–O}$ $107.2 \pm 1.2^\circ$, $\angle\text{F–C–F}$ $109.0 \pm 0.5^\circ$ and dihedral angle C–O–O–C $123.3 \pm 14.0^\circ$. A staggered conformation with a small tilt for the group axis is observed for the CF_3 groups. A C_2 molecular structure may be assumed⁶¹³.

5. Vibrational spectra

The stretching modes in the $ca\ 800\ \text{cm}^{-1}$ region give rise to very weak bands in the IR spectrum of dialkyl peroxides, e.g. *t*-BuOOBu-*t*, while the corresponding Raman bands

are much stronger. These peaks can be useful for identification of compounds with known spectra, but are of controversial value for assignments in structural analysis because other features may have bands in the same region, e.g. $\nu\text{C}-\text{C}$ and $\nu\text{C}-\text{O}$ ⁵⁶⁷.

The FTIR spectra at room temperature of poly(methacrylonitrile peroxide) **250** reveal both characteristic structural items and gradual decomposition. Thus, the freshly prepared polymer has, among other features, strong bands at 1040 and 1132 cm^{-1} , assigned to O–O and C–O stretching modes, respectively, a broad peak centered at 3480 cm^{-1} , assigned to terminal H-bonded OH and OOH groups, and a strong peak at 1755 cm^{-1} , assigned to carbonyl groups of structure $\text{O}=\text{CHC}(\text{Me})(\text{CN})-$. After about 20 and 40 min, the 1040 and 1132 cm^{-1} peaks weaken progressively and the OH and carbonyl bands become progressively intensified, producing formaldehyde and pyruvonnitrile, by homolytic scission of the O–O bonds, according to Scheme 15⁶⁰².



SCHEME 15. Thermolysis of poly(methacrylonitrile peroxide) by homolytic scission of the peroxide links

6. Mass spectrometry

The base peak of the EI-MS of the peroxy polymer **250** appears at $m/z = 69$ [$\text{CH}_2\text{C}(\text{O})\text{CN} + 1$]. Other identified peaks appear at $m/z = 43$ [$\text{MeC}=\text{O}$], 54 [$\text{O}=\text{CCN}$], 87 [$\text{CH}_2=\text{C}(\text{Me})\text{OOCH}_2$], 98 [$\text{OOCH}=\text{C}(\text{Me})\text{CN}$] or [$\text{O}=\text{CHC}(\text{Me})(\text{CN})\text{O}$] and 112 [$\text{CH}_2\text{OOCH}=\text{C}(\text{Me})\text{CN}$], all of which are directly related to the structure of the polymer⁶⁰². The CIS-MS technique using Ag^+ ions mentioned in Section V.C.3 was applied for characterization of isoprostane bicyclic endoperoxides (**25**)⁹⁶.

7. Thermal analysis

DSC runs of the peroxide polymer **250**, carried out at various heating rates, typically show one strongly exothermic peak at about 120°C. Concurrent TGA shows a sharp loss in weight and total disappearance of the sample, in accordance with the process depicted in Scheme 15. The enthalpy of the pyrolytic process can be estimated from integration of the DSC curves ($-178 \pm 8 \text{ kJ mol}^{-1}$), in good agreement with theoretical estimations (-166 kJ mol^{-1}), and the activation energy from the slope of a Kissinger plot ($152 \pm 8 \text{ kJ mol}^{-1}$)⁶⁰².

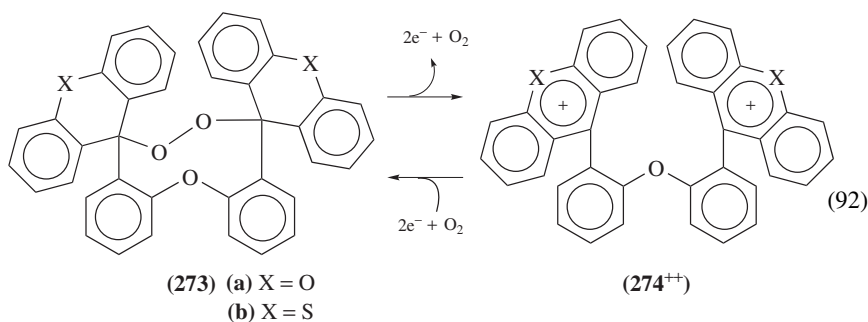
TABLE 4. First decomposition range ($^{\circ}\text{C}$) and weight of residue (% in parentheses) of conjugated diacetylene peroxides of general formula

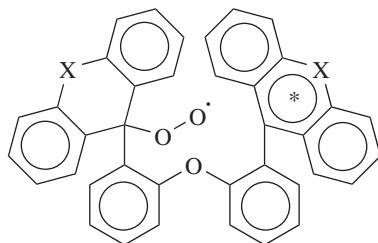
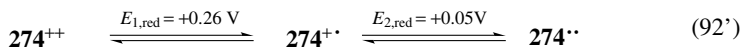
	(270) R = Me	(271) R = Et	(272) R = <i>n</i> -Pr
(a) R' = <i>n</i> -Bu	135–180 (40)	132–175 (53)	128–185 (52)
(b) R' = CH ₂ OH	116–175 (43)	113–182 (36)	115–175 (37)
(c) R' = CO ₂ H	92–138 (81)	84–133 (40)	90–140 (65)
(d) R' = <i>m</i> -C ₆ H ₄ CO ₂ H	143–175 (82)	138–175 (86)	140–180 (80)
(e) R' = <i>p</i> -C ₆ H ₄ CO ₂ H	134–153 (65)	134–165 (73)	131–162 (75)
(f) R' = CH ₂ OAc	128–180 (64)	127–175 (37)	125–175 (38)

Table 4 summarizes the TG and DTA data for the first decomposition range of three series (270–272) of variously substituted conjugated diacetylene peroxides. In this table the columns correspond to members of a homologous series where the R group is varied stepwise, whereas the rows correspond to various functional groups according to the group R'. The starting compounds are liquid or solid at room temperature, and decompose leaving solid residues of self-initiated polymers. The aromatic carboxylic acids (270d to 272d and 270e to 272e) seem to be quite stable thermally, whereas the aliphatic carboxylic acids (270c to 272c) are the least thermally stable among the compounds studied. Slightly more stable are the aliphatic alcohols (270b to 272b), which become stabilized on conversion to acetate esters, to approximately the same stability level as that of the hydrocarbon peroxides (270a to 272a)⁶¹⁴.

8. Electrochemical analysis

Oxidation of the peroxides 273a and 273b leads to oxygen loss and formation of intensely colored divalent cations 274⁺⁺, according to equation 92. Cyclic voltammetry reveals that the ionic form undergoes an easy and reversible two-step reduction under argon blanketing, according to equation 92' (reduction potentials are vs. SCE), to yield long-lived diradical species 274^{••}. However, in the presence of saturated O₂ in the solution, only irreversible reduction takes place, as O₂ readily forms an adduct (275a) with intermediate 274^{••}, which undergoes further reduction to a diradical (275b). The latter species undergoes ready closure to the entropically disfavored 273 species. These redox processes can be followed by UVV spectrophotometry; however, the mechanism of electron transfer and oxygen capture or release is not yet totally elucidated⁶⁰⁷.

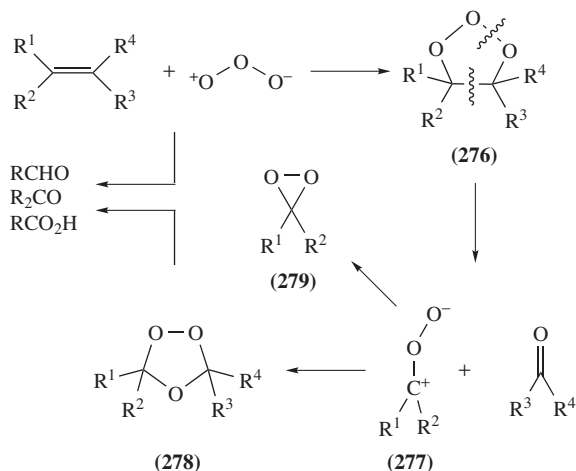


(275) (a)^{*} = + (cation)(b)^{*} = • (free radical)

VIII. OZONIDES

A. General

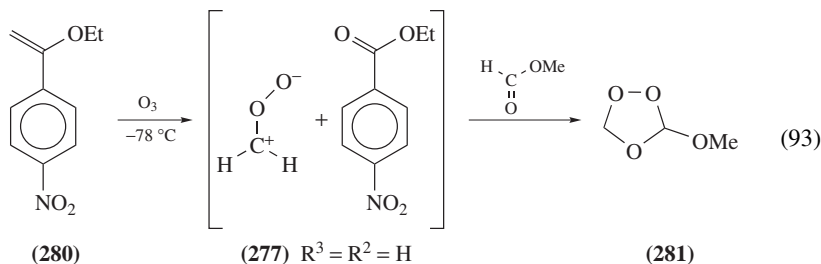
Application of ozonolysis in organic synthesis and the mechanism of the process have been reviewed^{545, 615, 616}. Ozonides are frequently encountered as intermediate stages in the cleavage of carbon–carbon double bonds, using ozone as reagent. The mechanism of ozonide formation was investigated by Criegee and coworkers, who proposed Scheme 16, involving various steps^{617, 618}. First, the so-called *primary ozonide* (POZ) or *molozone* (**276**) is formed in a 1,3-dipolar cycloaddition process. Compounds **276** are rather unstable and undergo a cycloreversion to a stable carbonyl compound and a carbonyl oxide, Criegee's intermediate (**277**), which is isoelectronic with ozone and very reactive. Intermediate **277** either recaptures the nearby carbonyl compound in a 1,3-dipolar cycloaddition to form the relatively stable *secondary ozonide*, *final ozonide* (FOZ) or simply *ozonide* (**278**), or cyclizes to the dioxirane (**279**). Instead of the concerted step involving intermediate



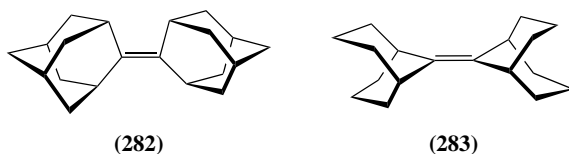
SCHEME 16. Criegee's mechanism of ozonide formation and ozonolysis

277, a two-step mechanism involving a biradical species has also been postulated, based on kinetic measurements of the POZ decomposition⁶¹⁹. In the discussions of the present section, the oxygen atoms of the OO link in the FOZ (the peroxide link) are sometimes denoted by O_p while the other O atom (the ether link) is denoted by O_e .

Mechanistic studies of ozonolysis try to elucidate the regioselectivity of the POZ fragmentation, that determines whether intermediate **277** will carry the R^1 and R^2 or the R^3 and R^4 pair of substituents, and the relative orientation of the R^1 and O^- groups in **277**^{620,621}. The presence of carbonyl groups in the molecule undergoing ozonolysis may strongly influence the course of fragmentation of the POZ, participating in the formation of the FOZ⁶²². The stereochemical courses of the POZ-to-FOZ transformation of vinyl fluoride and the two geometrical isomers of 1,2-difluoroethylene were also theoretically evaluated⁶²³. A nice confirmation of Criegee's mechanism for the FOZ formation is offered by the synthesis of the ozonide of methyl vinyl ether by an indirect route, according to equation 93. Thus, ozonization of α -ethoxy-*p*-nitrostyrene (**280**) in methyl formate solvent yields 3-methoxy-1,2,4-trioxolane (**281**), due to the effect of a large excess of solvent in the presence of Criegee's carbonyl oxide (**277**). The structure of **281** is discussed in Section VIII.C.2.b^{624,625}. In an early study, formation of the POZ of *E*-di-*t*-butylethylene was observed at low temperature, but no analogous structure was detected for the *Z* form; however, both geometric isomers gave the FOZ derivatives⁶²⁶.



The structural elucidation of the ozonide function is not always an easy task. For example, compounds **282** and **283**, carrying stiff substituents on the double bond, each yield on ozonization a stable derivative containing three O atoms, that is hard to characterize as POZ or FOZ by the usual chemical and spectroscopic methods⁶²⁷.



Synthetic operations involving ozonolysis lead to formation of aldehydes, ketones or carboxylic acids, as shown in Scheme 16, or to various peroxide compounds, as depicted in Scheme 7 (Section V.B.5), depending on the nature of the R^1 to R^4 substituents and the prevalent conditions of reaction; no effort is usually made to isolate either type of ozonide, but only the final products. This notwithstanding, intermediates **276** and **278** are prone to qualitative, quantitative and structural analysis. The appearance of a red-brown discoloration during ozonization of an olefin below -180°C was postulated as due to formation of an olefin-ozone complex, in analogy to the π -complexes formed with aromatic compounds⁶²⁸; however, this contention was contested⁶²⁹ (see also Section VII.C.2).

Although addition of ozone to C=C bonds is the main route for synthesis of ozonides, an alternative method is photosensitized singlet oxygen addition, provided other oxygen-carrying functional groups are present in the substrate molecule, as shown in Section VIII.C.7. Ozonization of olefins bearing halogen substituents has been an elusive undertaking until as late as 1976, when the FOZ of a cyclic olefin was isolated and characterized⁶³⁰ (see Section VIII.C.6.a). Other examples are discussed in the sections below. Final ozonides can undergo acid-catalyzed oligomerization to cyclic peroxides, where the —OO—bridges turn to hydroperoxides and serve as links between the monomeric units, as shown in Section VII.C.3.

Handling ozonides even in small amounts demands special care. Thus, various ozonides can be innocuously synthesized, by passing ozone-enriched oxygen through dry solutions of the corresponding olefins at -78°C , followed by low-pressure distillation below 60 to 70°C ⁶³¹. For example, the FOZs of methylenecyclohexene and methylenecyclopentene can be distilled at low pressure, however the FOZ of methylenecyclobutene explodes at *ca* -20°C ⁶³². Attempts to release low molecular weight byproducts from ozonized jojoba oil, a wax with unsaturated fatty acid and fatty alcohol residues, by low-pressure distillation results in very fast, though not explosive, decomposition of the product⁶³³. Mixing ozone and ethylene in the gas phase may be a hazardous undertaking, leading to explosion if the partial pressures exceed a very low threshold⁵⁹⁵.

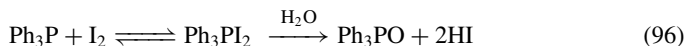
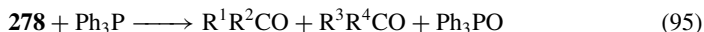
B. Detection and Determination

1. Titration methods

The oxidant properties of compounds **278** are the basis for their determination with reducing agents. In the presence of iodide ions, iodine liberation takes place (equation 94), which can be titrated with standard thiosulfate solution⁶³⁴. This reaction affords quantitative results only when the products are ketones; otherwise, significant departures have been reported⁶³². A method was proposed to avoid this pitfall based on reduction of the FOZ (**278**) with excess Ph_3P under inert atmosphere, according to equation 95. After the solution stands for three days at least in the dark, the excess triphenylphosphine is titrated with standard iodine solution, according to equation 96, until a stable yellow discoloration marks the end point. When using nonpolar solvents for the reduction stage, a small amount of phenol aids in attaining quantitative conversion for the slow process⁶³¹.



(278)



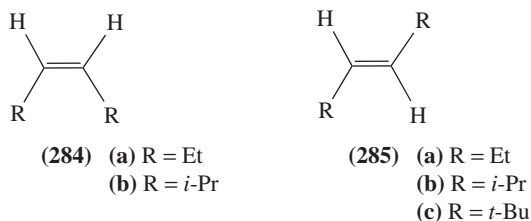
2. Infrared spectrophotometry

The kinetics of conversion of POZ into FOZ and the Arrhenius parameters in solution can be measured by following the disappearance of a characteristic peak of the POZ, generated *in situ* in a solution of the olefin in liquid ethane or CS_2 , at low temperature. The peak at 690 cm^{-1} is the most convenient one because it is relatively free from interference

by the solvent, the olefin and the FOZ⁶³⁵. The course of ozonolysis of the methyl esters of the fatty acids of sunflower oil can be followed by observing in FTIR spectra the gradual disappearance of the olefinic bands and the appearance of the 3,5-dialkyl-1,2,4-trioxolane bands. Formation of a small amount of aldehyde, which at the end of the process turns into carboxylic acid, is also observed⁶³⁶.

3. Chromatography

a. Gas-liquid chromatography. The *cis* to *trans* ratio of the FOZs obtained on ozonization of simple olefins of *Z* and *E* configuration, such as **284a**, **284b**, **285a** and **285b**, can be determined by GLC-FID, maintaining the injector at 70 °C and the column at 65 °C⁶³⁷.



The ozonides of choline and ethanolamine phosphatides subjected to reduction with Ph₃P yield the corresponding core aldehydes. After hydrolysis with phospholipase C to eliminate the polar group and silylation with trimethylsilyl chloride, the core aldehydes can be determined by GLC-FID using temperature programming to high temperatures⁶³⁸.

b. Liquid chromatography. The ozonides of choline and ethanolamine phosphatides and triglycerides can be separated by TLC. The ozonides subjected to reduction with Ph₃P yield the corresponding core aldehydes, which can be separated by TLC and revealed as purple spots with Schiff's reagent⁶³⁸.

4. Nuclear magnetic resonance spectrometry

Protons attached to the C atoms of the 1,2,4-trioxolane moiety of FOZs have chemical shifts at distinctly lower field than alcohols, ethers or esters. For example, the chemical shifts of the ozonide product in equation 100 (Section VIII.C.6.a) are δ (CDCl₃) 5.7 ppm for the H atoms of the trioxolane partial structure, and 4.1 ppm for the protons at the heads of the other ether bridge⁶³⁹. Measurement of the rate of disappearance of these signals can be applied in kinetic studies of modifications in the ozonide structure. The course of ozonization of the methyl esters of the fatty acids of sunflower oil can be followed by observing in ¹H and ¹³C NMR spectra the gradual disappearance of the olefinic peaks and the appearance of the 3,5-dialkyl-1,2,4-trioxolane peaks. Formation of a small amount of aldehyde, which at the end of the process turns into carboxylic acid, is also observed⁶³⁶.

C. Structural Characterization

1. Infrared spectroscopy

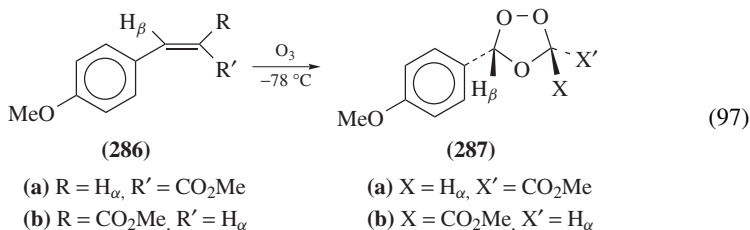
a. Primary ozonides. IR spectroscopy has been applied for the characterization of primary ozonides in solution or in a solid matrix. Tentative assignments were made for the IR bands of the POZs of ethylene, all its derivatives formed by introducing Me

groups on the double bond (from propene to 2,3-dimethyl-2-butene), cyclopentene and cyclohexene, condensed on a CsBr window at low temperatures (about -160°C). These POZs show strong bands in the $650\text{--}730\text{ cm}^{-1}$ region, attributed to O–O–O bending, and in the $950\text{--}1050\text{ cm}^{-1}$ region, assigned to stretching vibrations. The C–O stretching modes appear in the 1100 to 1200 cm^{-1} region. On raising the temperature, these bands disappear and new ones appear that are attributed to the FOZ; however, this does not occur with the POZ of 2,3-dimethyl-2-butene, which yields acetone as the major product⁶⁴⁰. More refined assignments were attained in a frozen Xe matrix for the POZ of ethylene and various ^2H and ^{18}O isotopomers⁶⁴¹. The stability of the POZ of a simple olefin is dependent on the position and configuration of the double bond. Thus, the formation and decomposition of the POZ of Δ^1 -olefins, such as 1-hexene and various symmetrically substituted compounds (**284**, **285**), was followed by the appearance of bands in the 690 , 970 and 1100 cm^{-1} regions and their disappearance with concurrent appearance of new bands, attributed to the corresponding FOZ. The POZ bands of 1-hexene and the *Z*-olefin **284b** could be observed only at -175°C and slightly higher temperatures, while those of the *E*-olefins **285a–c** were stable at -105°C or slightly higher. In all cases, the POZ disappears after a few hours at -78°C or higher temperature⁶³⁵.

In contrast with more richly chlorinated ethylenes, forming π -complexes (Section VIII.D.1), an IR spectroscopic study of the reaction of condensed $\text{CH}_2=\text{CHCl}$ with ozone at low temperature reveals the formation of two primary ozonides, showing peaks of various intensities in the 400 , 700 , 800 , 1000 and 1270 cm^{-1} regions (spectral features similar to those of the POZ of ethylene). On gradually raising the temperature from that of liquid nitrogen (about -196°C) to about -40°C , decomposition of the ozonides sets in, yielding formyl chloride, formic acid, carbon dioxide and hydrogen chloride, also observed in the IR spectrum⁶⁴².

Solid styrene was exposed at -196°C to ozone, in an attempt to discern whether the behavior of the system is similar to that of olefinic compounds, yielding an ozonide, or to that of aromatic compounds, yielding a π -complex. On heating to about -100°C , an adduct is formed that is stable until about -55°C , when benzaldehyde and a peroxidic polymer are slowly obtained. The structure of the adduct is probably that of a POZ, based on the similarity of the IR spectrum with the ozone adduct of vinyl chloride described in the preceding paragraph⁶⁴³.

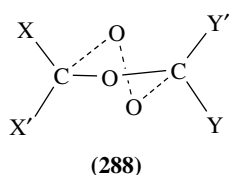
b. Final ozonides. The *Z* (**286a**) and *E* (**286b**) isomers of methyl *p*-methoxycinnamate subjected to ozonization at -78°C yield a mixture of two relatively stable products, namely the FOZ in both *cis* (**287a**) and *trans* (**287b**) configuration (equation 97). The IR spectra of these isomers are quite similar; however, **287b** has a band at 1360 cm^{-1} which is absent in **287a**. On the other hand, the latter isomer has a small shoulder at 855 cm^{-1} and the other one has none. Such features seem to be present also in other pairs of *cis* and *trans* isomers of FOZs. In addition, the *cis* isomer (**287a**) has bands at 685 , 995 and 1015 cm^{-1} , which are absent in the spectrum of the *trans* isomer. The structural characterization of the two **287** isomers is also discussed in Section VIII.C.4⁶⁴⁴.



2. Microwave spectroscopy

a. Primary ozonides. The simplest ozonides are obtained from ethylene. A study was carried out with plain ethylene and its isotopomers $^{13}\text{CH}_2=^{13}\text{CH}_2$, $Z\text{-CDH}=\text{CDH}$, $E\text{-CDH}=\text{CDH}$, $\text{CD}_2=\text{CD}_2$, as well as isotopically enriched ozone, $^{18}\text{O}_3$. The rotational spectra of the gaseous primary ozonides, obtained *in situ* in the waveguide, was determined at temperatures above -175°C . The spectra pointed to the POZ as having a puckered 1,2,3-trioxolane structure (**276**, R^1 to $\text{R}^4 = \text{H}$), of C_s symmetry, with the coplanar $\text{O}-\text{C}-\text{C}-\text{O}$ section of the ring forming a dihedral angle of 50.85° with the $\text{O}-\text{O}-\text{O}$ triangle, the so-called O-envelope, as shown in the top item of Appendix 1. This leads to two distinct conformers of the primary ozonide of $Z\text{-CDH}=\text{CDH}$. Conformational analysis based on microwave spectroscopic data points to a possibility of inversion of the ring puckering without passing through a highly strained planar conformation, by introducing low-energy pseudorotational modes (ring twisting vibrations) instead of the radial modes (ring bending vibrations). The dipole moment of the normal isotopic composition of the POZ can also be estimated. As the temperature of reaction between ethylene and ozone is raised, the presence of species derived from 1,2,3-trioxolane decomposition could be ascertained, such as formaldehyde, dioxirane (**279**, $\text{R}^1 = \text{R}^2 = \text{H}$) and the final ozonide (**278**, R^1 to $\text{R}^4 = \text{H}$)^{595,645}. A theoretical study of the conformations of the POZ of ethylene was centered only on the planar and three possible half-chair conformations⁶⁴⁶, while another study dealt with the molecular structure of POZs and the effects of methyl substituents on the ring conformation⁶¹⁹.

b. Final ozonides. Rotational spectra studies of the FOZ of ethylene point to the structure shown in the bottom item of Appendix 1, where the molecule has one C_2 axis of symmetry. No evidence of pseudorotational modes is found for this species. Microwave spectroscopy of the ozonization products of monodeuteriated ethylene affords support to Criegee's mechanism, proceeding via a separate formaldehyde and intermediate **277**, as all six possible isomers, including stereoisomers (**288a-f**) resulting from their recombination, are formed. In Table 5 are summarized the structural parameters of the **288c** molecule, as derived from microwave spectroscopy⁶⁴⁷ and electron diffraction⁶⁴⁸, showing excellent agreement in most items; the slight discrepancy in the $\text{C}-\text{O}$ bond distances stems from a necessary assumption made in the electron diffraction calculations. Refinement of the calculation methods derived from rotational spectra led to improved estimates of the bond lengths and angles of the FOZ of ethylene and its isotopomers enriched with ^2H and ^{18}O ^{649,650}. A microwave spectral study, carried out with the FOZs of propene, E -2-butene and some of their isotopomers enriched with ^2H , ^{13}C and ^{18}O , affords further insight into the stereochemical control of the course of Scheme 16 during scission of the POZ and recombination of the parts to form the FOZ⁶⁵¹. The half-chair conformation prevalent in the 1,2,4-trioxolane ring of these simple final ozonides in the gas phase, as determined from microwave spectroscopy, is not the only stable one, as was shown by XRD crystallography of larger molecules described in Section VIII.C.6. Theoretical calculations were carried out of the molecular structure of FOZs and the effects of methyl substituents on



- (a) $\text{X} = \text{Y} = \text{X}' = \text{H}$, $\text{Y}' = \text{D}$
- (b) $\text{X} = \text{Y} = \text{Y}' = \text{H}$, $\text{X}' = \text{D}$
- (c) $\text{X} = \text{Y} = \text{X}' = \text{Y}' = \text{H}$
- (d) $\text{X} = \text{Y} = \text{H}$, $\text{X}' = \text{Y}' = \text{D}$
- (e) $\text{X} = \text{Y} = \text{D}$, $\text{X}' = \text{Y}' = \text{H}$
- (f) $\text{X} = \text{Y}' = \text{H}$, $\text{X}' = \text{Y} = \text{D}$

TABLE 5. Comparison of the structural parameters of gaseous 1,2,4-trioxolane determined by microwave spectroscopy⁶⁴⁷ and electron diffraction⁶⁴⁸

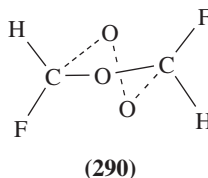
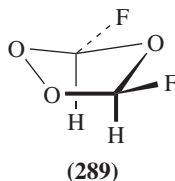
Structural feature	Microwave spectroscopy	Electron diffraction
Bond distances (pm)		
C—O _{peroxide}	139.5	141.4 ^a
C—O _{ether}	143.6	141.4 ^a
O—O	147.0	148.7
C—H	109.4	112.6
Bond angles (°)		
C—O—C	102.8	105.9
O—C—O	106.3	105.3
C—O—O	99.2	99.2
H—C—H	112.9	112.3
H _{equatorial} CO _{peroxide}	107.2	
H _{axial} CO _{peroxide}	111.7	
H _{equatorial} CO _{ether}	109.4	
H _{axial} CO _{ether}	109.1	
Torsional angles (°)		
O—C—O—C	16.6	16.2
O—C—O—O	41.3	40.2
C—O—O—C	50.2	49.1

^a Both C—O distances are assumed to be equal.

the ring conformation. The results support the dipole moments and structural parameters found from rotational spectra. Ring vibrations by pseudorotation are preferred to ring bending modes⁶⁵².

The rotational spectra of the FOZ of fluorinated derivatives of ethylene and various isotopomers have been used to establish their configuration and the preferred conformations. In all cases, abnormally long C—F and short C—O bonds are observed and attributed to anomeric interactions between F and nearby O atoms. The FOZ of vinyl fluoride has a distorted half-chair conformation with F in an axial position. The outstanding bond lengths are C(3)—F (137.5 pm), C(3)—O_e and C(3)—O_p (138.2 pm) as compared to the C(5)—O_e and C(5)—O_p distances (142.6 and 141.1 pm, respectively). The absence of stable F isotopes makes the analysis of the rotational spectra more difficult⁶⁵³. Ozonization in solution of *Z*-1,2-difluoroethylene leads to formation of *cis*-difluoroethylene oxide, *trans*-difluoroethylene FOZ and *cis*-difluoroethylene FOZ, as major components that can be separated by GLC and stored under vacuum in liquid nitrogen. The *cis*-FOZ has an O_e envelope conformation with the F atoms in pseudo-equatorial conformation (**289**) in the ground state. The unusual bond lengths are C—F (137.6 pm), C—O_e (138.5 pm) and C—O_p (137.6 pm). Calculations on pseudorotation point to **289** as the conformation of minimum potential energy⁶⁵⁴. In contrast to the preferred envelope conformation of **289**, the FOZ with *trans*-configuration (**290**) has an average O—O twist ring conformation with C₂ symmetry and the F atoms in pseudo-axial positions. The unusual bond lengths are C—F (136.6 pm), C—O_e (140.1 pm) and C—O_p (136.8 pm)⁶⁵⁵.

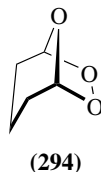
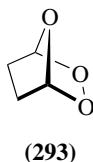
The rotational spectra of 3-methoxy-1,2,4-trioxolane (**281**) and 15 isotopomers containing ²H, ¹³C and ¹⁸O point to a preferred conformation for both the ring and the methyl group and to other structural features. The C(3) atom is bonded to three oxygen atoms, for which the C—OMe bond distance is short (137.7 pm) as compared to C—O_p (141.1 pm)



and C–O_e (140.6 pm). The five-membered ring has an envelope conformation with O(1) folded toward the OMe group, attributed to an anomeric effect. In spite of steric repulsion, the O–Me bond is staggered between the other two O atoms attached to C(3), as shown in the Newman projection **291** and not as in **292**. Conformation **291** illustrates an *exo*-anomeric effect. This interpretation of the rotational spectra is supported by theoretical calculations⁶²⁵.



The structure of the ozonides of the simplest unsaturated cyclic hydrocarbons can be elucidated based on the rotational spectra of the FOZ and its isotopomers, such as species singly enriched with ²H, ¹³C or ¹⁸O or multiply enriched with ¹⁸O. Thus, the FOZ of cyclobutene has structure **293**, of C_s symmetry, with the OO bridge slightly longer than that of the FOZ of ethylene, to accommodate some ring tension⁶⁵⁶. The microwave spectra of the FOZ of cyclopentene point to a ground state of structure **294**, of C_s symmetry, with the OO bridge in the *endo* conformation⁶⁵⁷.



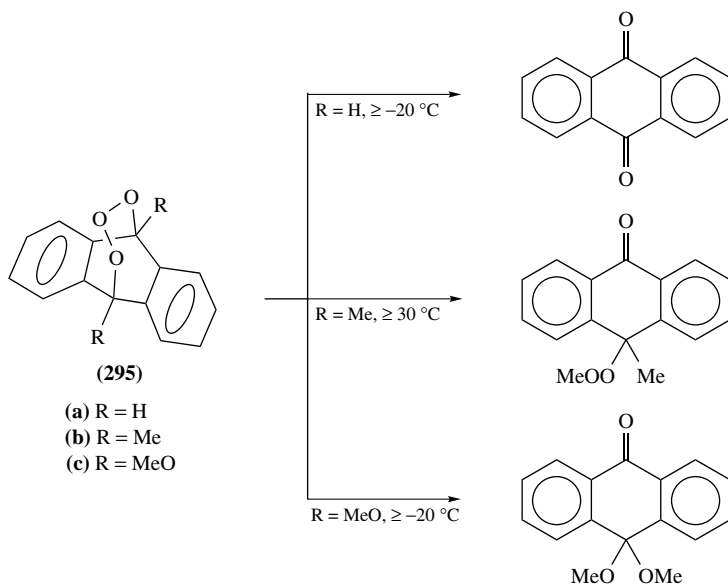
3. Electron diffraction

Electron diffraction measurements of gaseous 1,2,4-trioxolane point to either a C₂ symmetry, as depicted at the bottom of Appendix A, or a C_s symmetry, corresponding to an envelope conformation. However, consideration of steric interactions favors the twisted chair conformation (**288c**) for the molecule. Table 5 presents the structural parameters derived from electron diffraction, assuming that both C–O distances are equal and that the H atoms are symmetrically placed with respect of the neighboring atoms. Assumptions on the vibrational amplitudes of the ring bonds do not affect the calculated values of Table 5, except for the H–C–H angle⁶⁴⁸.

4. Nuclear magnetic resonance spectroscopy

Anthracene and its derivatives yield relatively stable POZs (**295**). Compound **295b** shows an AA'BB' structure for the ¹H NMR spectrum of the aromatic protons, taken

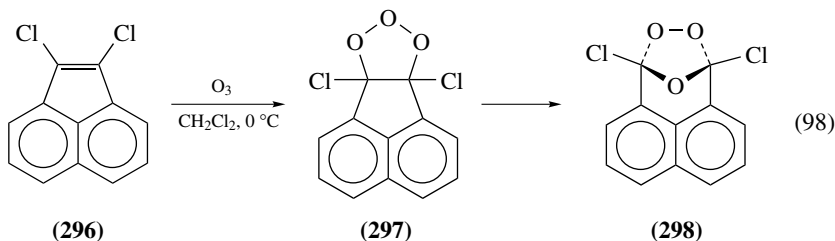
at -50°C . On raising the temperature to 20°C the spectrum turns to AB type. This is interpreted as the OOO bridge having a frozen envelope conformation at low temperature, establishing different environments for the two aromatic rings; at higher temperatures the central O atom flips rapidly between the two equivalent conformations of the bridge, yielding a similar environment for both rings on the NMR time scale. The ^{13}C NMR spectra of **295a** and **295c** in solution can be interpreted in similar terms. The POZs decompose at higher temperatures yielding ketonic compounds, as shown in Scheme 17. These products can also be characterized by their NMR spectra⁶⁰⁶.



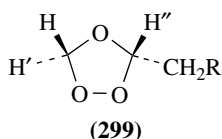
SCHEME 17. Thermal decomposition of the primary ozonides of anthracenes

The presence of halogen substituents on the trioxolane ring has stabilizing effects on the ozonides. Thus after ozone treatment of 1,2-dichloroacene (296, equation 98) even the POZ (297) could be isolated by column chromatography from its fresh mixture, together with the FOZ (298). The relative instability of the POZ is demonstrated by TLC, where the transformation of its spot at $R_f = 0.27$ to that of the FOZ at $R_f = 0.51$ can be revealed on spraying with diphenylamine. A shift from $\delta = 116.39$ ppm to $\delta = 120.42$ ppm is observed in the ^{13}C NMR spectra for the trioxolane C atoms on passing from 297 to 298. Additional techniques for characterizing these ozonides are cryoscopy in benzene, FD-MS showing the characteristic triplets for the molecular ions at m/e 268, due to the presence of two Cl atoms, and IR spectrum of the FOZ, with absorption bands at 1040 and 1090 cm^{-1} , assigned to the C–O stretching in a 1,2,4-trioxolane ring⁶⁵⁸. However, with the simpler chlorinated or brominated ethylenes (e.g. *E*-2,3-dichloro-2-butene) NMR spectroscopy fails to detect an ozonide, whereas the analogous fluorine compounds show at least one⁶⁵⁹ (see also Sections VIII.C.1 and 2).

The FOZ of Δ^1 -alkenes singly substituted on position 3 with an alkyl group or with various open-chain and ring ketones (299) can be structurally characterized by ^1H and ^{13}C NMR spectroscopy. Thus, with one exception the proton denoted as H shows a singlet at $\delta = 4.98$ to 5.04 ppm whereas H' and H'' show a singlet and a triplet, respectively,

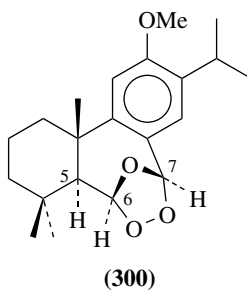


all at 5.12 to 5.20 ppm. It should be pointed out that the coupling constants between the pair of *gem* or the pair of *cis* protons are practically nil. As for the ^{13}C spectrum, the chemical shift of the methine carbon is at $\delta = 101.88$ to 103.53 ppm, while that of the ring methylene carbon is at $\delta 93.56$ to 93.91 ppm⁶⁰.



Downfield chemical shifts of ^{13}C are typical of C atoms bearing two $-\text{O}-$ substituents; e.g. the 1,2,4-trioxane compound **15** with $\text{R} = \text{H}$ has two signals near $\delta = 105$ ppm⁵⁷. The structure of the products of equation 97 (Section VIII.C.1.a) can be characterized by their ^1H NMR spectra; the relevant protons of compounds **286** and **287** for the present discussion are those denoted as H_α and H_β , which have different chemical shifts for the various compounds and their isomers. This allows making an estimate of the yields of both isomers in the ozonization process. Thus, the *E*-cinnamate (**286b**) affords a slightly higher yield of the *trans*-isomer (53%) than for the *cis*-isomer (47%). These yields are almost exactly reversed for the ozonization of the *Z*-cinnamate (**286a**). Another important feature is that the spin-spin coupling of these protons in compounds **286a** and **286b** is absent in the ozonides⁶⁴. The crude ozonization products of sunflower oil and methyl oleate, of tested antimicrobial activity, can be characterized by their ^1H NMR spectra. Especially significant is the $\delta = 5.1$ to 5.5 ppm region relative to TMS, where the protons of the 1,2,4-trioxolane ring and the unreacted olefinic protons appear⁶³.

The structure of the stable ozonide of a diterpene (**300**) was elucidated based on knowledge of the original structure assisted by ^1H and ^{13}C NMR spectroscopies. Thus, a ^{13}C NMR DEPT experiment points to the presence of six quaternary C, six CH, three



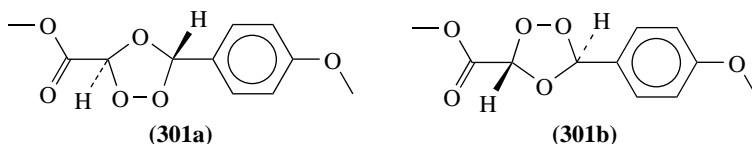
CH₂ and six CH₃ groups. A decision on whether the ether or the peroxy bridge lies on the α -phase of the molecule can be based on the assignment of the relevant δ_{H} (90 MHz, CDCl₃) peaks of the CH groups, as follows: 2.04 (1H, d, *J* 4 Hz, H5), 5.79 (1H, d, *J* 4 Hz, H6) and 6.22 (1H, s, H7). Examination of a model of **300** shows a dihedral angle of about 110° for H(5)–CC–H(6), thus explaining the observed doublets. For the alternative configuration of the ozonide moiety, with O_e on the α -phase, this angle would be nearly orthogonal and the coupling constant would be nearly nil⁶⁶¹.

5. Mass spectroscopy

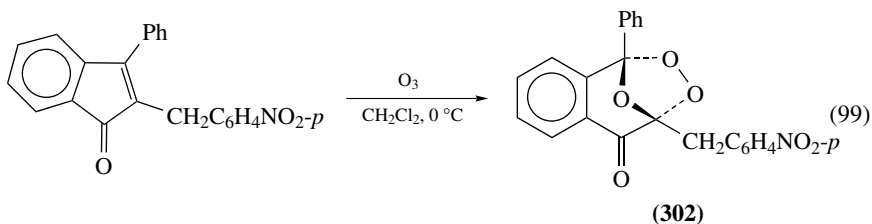
The ozonides of choline and ethanolamine phosphatides and triglycerides can be subjected to reduction with triphenylphosphine to yield the corresponding core aldehydes, and further derivatized to the 2,4-dinitrophenylhydrazones (DNP). The core aldehydes and their DNP derivatives can be separated by HPLC and characterized by various techniques, including EI-MS and TS-MS of positive and negative ions⁶³⁸. See also Section VIII.E.

6. X-Ray crystallography

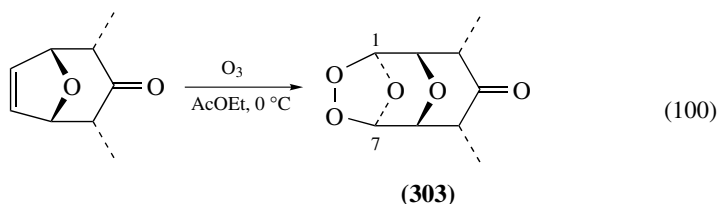
a. Final ozonides. The structural elucidation of the FOZ of methyl *p*-methoxycinnamate is a good example of the difficulties one may encounter in the crystallographic analysis of this type of compounds. Criegee's mechanism depicted in Scheme 16 allows for the formation of *cis*- and *trans*-diastereoisomeric 1,2,4-trioxolane rings, each of them in *R* and *S* enantiomeric configurations. Furthermore, several conformations are possible by free rotation of certain bonds. In the present case the FOZ has *trans*-configuration of which one of the enantiomers is shown in two conformations, **301a** and **301b**. In the crystal at room temperature all the main parts of the ozonide molecule are nearly coplanar, with conformation **301a** being nearly twice as frequent as **301b**. The crystal has 8 molecules in the unit cell, and each site might be occupied by either of the two possible configurations (*R* or *S*) in any of the two conformations, thus making the refinement of the structure of the trioxolane ring especially problematic⁶⁶².



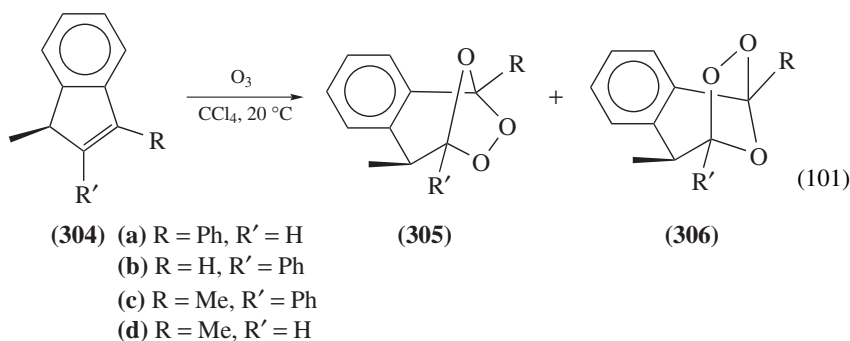
Probably the first unambiguous structural analysis of a FOZ by single-crystal XRD was that of **302**, derived from a substituted indene-1-one, by ozonization, as shown in equation 99⁶⁶³.



The XRD analysis of the FOZ **303**, obtained in equation 100, has the ether bridges in *trans* configuration. An interesting feature of this ozonide is the distortion of the 1,2,4-trioxolane ring caused by the uneven C–O bond distances: C(1)–O_e 140.6 pm, C(1)–O_p 142.6 pm, C(7)–O_e 142.3 pm and C(7)–O_p 139.1 pm⁶³⁹.

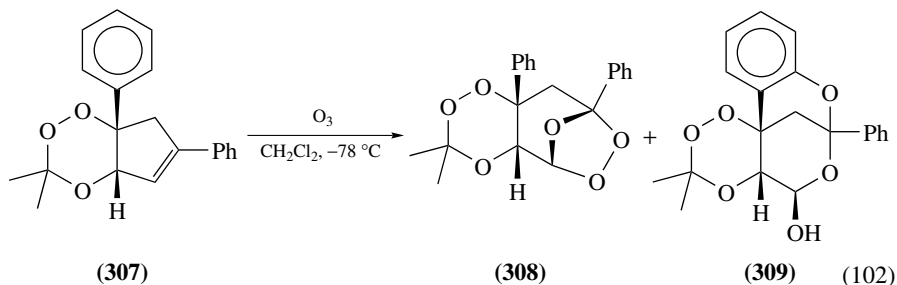


The preferred configuration of the FOZ is strongly dependent on the groups attached to the 1,2,4-trioxolane moiety of the compound and on the solvent. Thus, for example, the ozonization depicted in equation 101 yields both *exo*- (**305**) and *endo*-FOZ (**306**) derivatives from various substituted 1-methylindenes (**304**). The structure of the isomeric ozonides was determined by XRD analysis. The *exo*:*endo* ratio under the conditions of equation 101 varies from nearly 2:1 for **304a** and **304d** to nearly 1:3 for **304b** and **304c**, as determined by HPLC. Various reactions take place when the FOZ isomers are in the presence of an acid catalyst, such as *exo*–*endo* interconversion, the equilibrium being in favor of the *exo*-FOZ, proton exchange on substituent R when R = Me, demonstrated in the presence of AcOD. The kinetics of these reactions may be followed by ¹H NMR spectroscopy⁶⁶⁴.

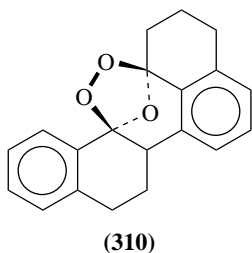


Ozonization of compound **307**, containing a 1,2,4-trioxane ring fused to a cyclopentene ring, proceeds in two directions as shown in equation 102, yielding a stable FOZ (**308**) and a spirocyclic acetal (**309**). Compound **309** is the first reported case where Criegee's carbonyl oxide intermediate (**277**) oxidizes a neighboring phenyl group. The structures of the three compounds in equation 102 were determined by single-crystal XRD. In compound **309**, the contacts between the O atom of the OH group and the nearest heterocyclic O atoms (201.1 and 216.5 pm) point to H-bonding⁵⁷⁸.

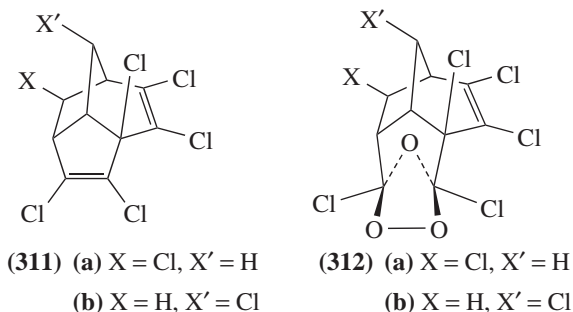
The FOZ **310**, derived from the corresponding hydrocarbon bearing a C=C link, is unusually stable (m.p. 159–161 °C) and resistant to reduction by NaBH₄. Its structure was elucidated by XRD analysis, showing the same O_e envelope conformation of **288**,



and not the theoretically predicted half-chair conformation shown by the ozonides of simpler olefins⁶⁶⁵.

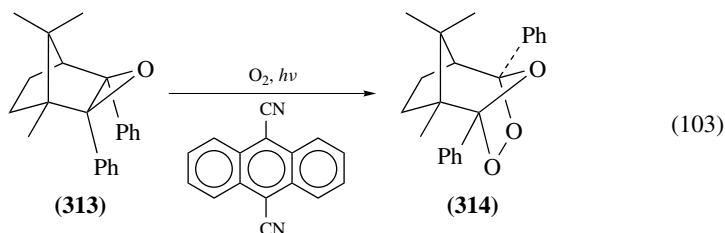


The γ -chloridene isomers (**311a** and **311b**), with two double bonds bearing chlorine substituents, are selectively ozonized in CCl_4 at room temperature on the double bond of the cyclopentene ring. The configuration of the FOZ as shown by XRD analysis is **312**, with the peroxide bridge in the *exo*- and the ether bridge in the *endo*-positions. These FOZs are stable, m.p. 100 to 101 and 141 to 143 $^\circ\text{C}$, respectively, and can undergo separation by GLC at 189 $^\circ\text{C}$. Further evidence for the structure of **312a** and **312b** may be obtained from IR, ^1H and ^{13}C NMR spectroscopies, MS, and structural analysis of the derivatives obtained on reduction with KI^{630, 666, 667}.

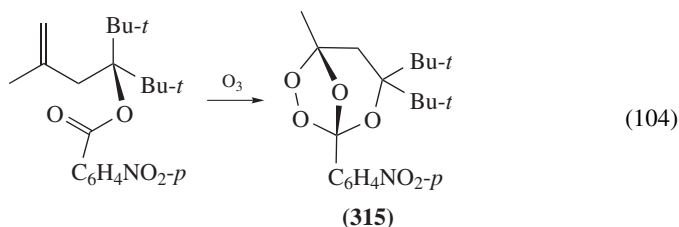


The ozonide of 2,3-diphenyl-2-bornene can be prepared by photosensitized addition of oxygen to the corresponding epoxide (**313**), as shown in equation 103. The structure of product **314** was determined by single-crystal XRD crystallographic analysis. It should be pointed out that both **302** and **314** have O_e envelope conformation for the 1,2,4-trioxolane

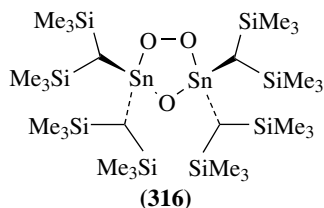
ring, as opposed to the half-chair conformation with a C_2 axis through that oxygen atom reported for **288** and other simpler FOZs. A slight twist for the C–OO–C chain of **314** is nevertheless observed⁶⁶⁸.



b. Final ozonide analogs. Several analogs of the FOZ structure **278** are known, in which a peroxide and ether functions are geminally placed in the molecule, but not necessarily forming a 2,6,7,8-tetraoxabicyclo[3.2.1]octane ring system as in **315**. Such compounds may be formed as an immediate product of the POZ decomposition or as subsequent derivatives of the FOZ, given favorable conditions. The postulated Criegee's intermediates (**277**) may react with a remote carbonyl group, leading to atypical ozonides. The carbonyl group of an ester is generally less reactive in such processes. However, it may be activated by electronegative groups, as shown in equation 104, where Criegee's intermediate **277** reacts with the carbonyl group of the ester function. This is probably also favored by the steric effect of the geminal *t*-Bu groups; when one of the *t*-Bu groups is replaced by Me, no reaction path analogous to equation 104 is observed^{669,670}. The structure of the stable ozonolysis product (**315**) was determined by ¹H NMR and IR spectroscopies and single-crystal XRD crystallography⁶⁷⁰.



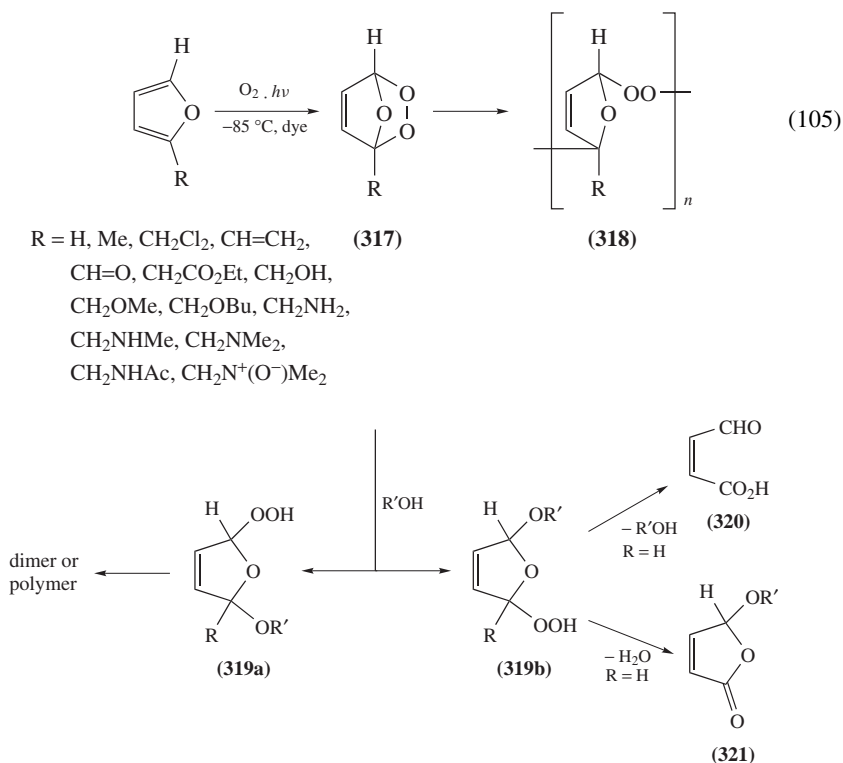
μ -Peroxo- μ -oxo-bis[bis(trimethylsilyl)methyl]tin (**316**) is an organotin analog of the FOZ of a symmetrically tetraalkylated olefin (**278**). It is obtained in low yield by oxidation of the corresponding silylated dialkyltin in the presence of a molybdenum catalyst. The structure was elucidated by XRD analysis and has some characteristic features: (a) The O–O distance is unusually long (154.3 pm) as compared to that of similar transition metal



species (144–149 pm) and H_2O_2 (147 pm); (b) both C–Sn–C angles are unusually large (123.3° and 124.3°); (c) the μ -oxo bridge (Sn–O–Sn) is symmetrical; and (d) a dihedral angle of *ca* 40° between both Sn–O–O planes, conferring the five-membered ring a half-chair conformation, as encountered in some structurally related complexes, such as $[\text{L}_4\text{Co}(\mu\text{-NH}_2)(\mu\text{-O-O})\text{CoL}_4]^{671}$.

7. Thermal analysis

Furan and its derivatives undergo 1,4-addition of singlet oxygen at low temperature to yield ozonides (**317**), as shown in equation 105. A complex scheme of decomposition reaction sets in when products **317**, either alone or in the presence of an alcohol, are subjected to nonisothermal DTA (Scheme 18). Diverse products may be formed, such as oligomers resembling **260** (e.g. **318**), hydroperoxides (**319a** and **319b**), and in the particular case of furan ($\text{R} = \text{H}$), **319b** may undergo elimination to attain either malealdehydic acid (**320**) or the γ -lactone (**321**) derived from the hemiacetal of **320** with the added alcohol. From the kinetic data collected in the DTA runs, parameters may be calculated to help discerning mechanisms of various types, such as single-step, concurrent, consecutive and reversible reactions⁶⁷². The double bond in ozonides obtained from furan derivatives (e.g. **317**) may be reduced by diazene ($\text{HN}=\text{NH}$), generated *in situ* after forming the ozonide by singlet oxygen addition⁶⁷³.



SCHEME 18. Generation of an ozonide (**317**) from a furan derivative in solution and paths for its disappearance, alone or in the presence of an alcohol

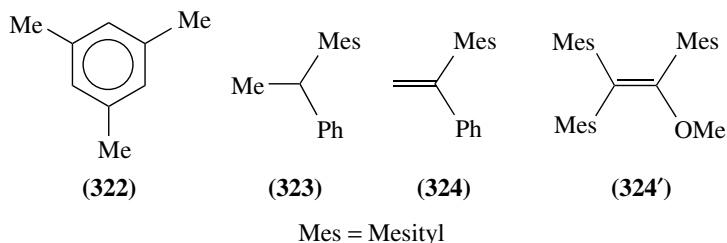
8. Molecular refraction

This is an additive constitutive property that is easy to determine experimentally and has theoretical significance, but it has been superseded by spectral methods that offer a deeper insight into the molecular structure. Nevertheless, it has historical value in the early elucidation of the structure of secondary ozonides as substituted 1,2,4-trioxolanes⁶³².

D. Miscellaneous Ozone Adducts

1. π -Complexes with ozone

A charge-transfer complex structure was postulated for an unstable intermediate observed in the IR spectrum of toluene in the presence of O₃ between -175 to -150 °C. The UV spectrum of this species has a peak at 350 nm that disappears simultaneously with the characteristic IR bands at higher temperatures⁶⁴⁰. Compounds containing aromatic rings (e.g. **322** to **324'**) form a π -complex with ozone at very low temperature. The complex disappears on raising the temperature with recovery of the initial substrate (e.g. **322** and **323**) or a derivative if an olefinic moiety is also present in the molecule, as is the case of **324**, leading to the formation of an epoxy compound. Formation of the π -complex of ozone with **324'** is reversible, probably due to strong steric hindrance by the mesityl substituents to binding of ozone to the C=C moiety. The presence of the π -complex with aromatic compounds can be demonstrated by a distinct discoloration and UVV spectrophotometry. The transition from **324** to the π -complex at -150 °C can be seen by ¹H NMR, where slight upfield shifts of all four types of proton is observed, namely those of the Me groups of Mes, the Mes ring, the phenyl group and the vinyl group. On heating to -135 °C the vinyl protons are converted to protons of an epoxy group with a significant upfield shift^{637,674}. Toluene undergoes a reversible reaction with ozone at -175 to -159 °C, yielding a yellow solid with peculiar IR bands at 2100 and 1030 cm⁻¹ and a UV absorption maximum at 385.0 nm⁶⁴⁰.



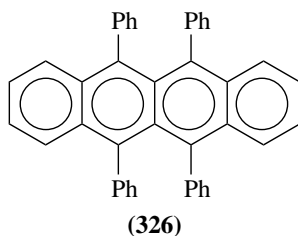
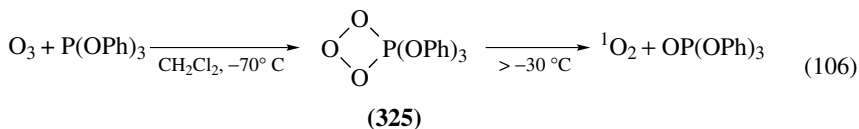
An IR spectroscopic study of the reaction of condensed chlorinated ethylenes with ozone at low temperature reveals a behavior dependent on the degree of chlorination and temperature. At the temperature of liquid nitrogen (about -196 °C) Cl₂C=CCl₂ and Cl₂C=CH₂ show a weak but sharp band at 1030 cm⁻¹, attributed to the formation of a π -complex of ozone with the chlorinated olefin. On raising the temperature to about -120 °C, the π -complex band gradually and reversibly disappears. At -80 °C, Cl₂C=CCl₂ shows formation of phosgene (Cl₂C=O), trichloroacetyl chloride and the corresponding epoxide. In the case of Cl₂C=CH₂, the decomposition products detected at about -90 °C are phosgene and chloroacetyl chloride. The π -complex peak of ozone with *Z*- and *E*-ClCH=CHCl appears only at -150 °C concomitantly with a doublet at 1760 cm⁻¹ and a broad band at 715 cm⁻¹, pointing to formation of formyl chloride. In

the case of $\text{ClCH}=\text{CH}_2$, formation of a π -complex with ozone cannot be ascertained due to the presence of a strong band related to other structural features, but the peaks of formyl chloride and evidence for the independent formation of two different primary ozonides are present at -170°C (Section VIII.C.1.a). Traces of various liquid and gaseous products and formation of explosive polymeric residues are also observed for these chlorinated olefins. The products of condensed-phase ozonolysis of the chlorinated ethylenes resemble those observed for the process carried out in the gas phase⁶⁴².

Formation of a π -complex between 1-hexene or 2,4,4-trimethylpent-1-ene and ozone was tentatively proposed based on the appearance of a sharp band at *ca* 980 cm^{-1} , assigned to one of the ozone vibrations⁶³⁵. However, the existence of olefin-ozone π -complexes has been contested⁶²⁹.

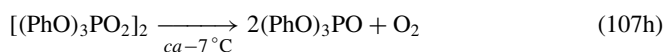
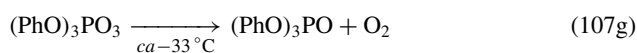
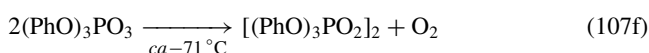
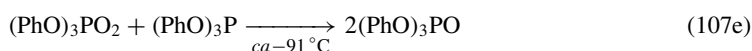
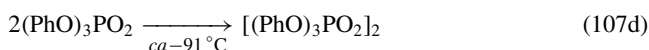
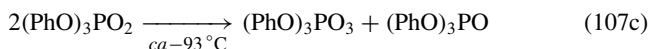
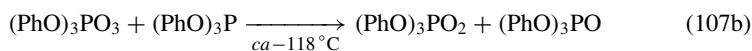
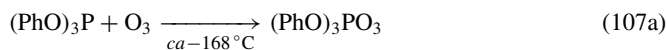
2. Phosphite-ozone adducts

Solutions of triphenyl phosphite at low temperature form a stable adduct with ozone (**325**), which has a structure similar to that of the primary ozonides, as was demonstrated by NMR spectroscopy⁶⁷⁵. The adduct decomposes at higher temperatures yielding singlet oxygen and triphenyl phosphate, as shown in equation 106⁶⁷⁶. The ozone adducts with alkyl phosphites have much lower stability than those with aryl phosphites⁴⁹³. The structure of alkyl and aryl phosphite ozonides in solution is monomeric and no evidence for dimeric or oligomeric species is shown by cryoscopic experiments or ³¹P NMR spectroscopy⁶⁷⁷. The kinetics of decomposition of **325** and its reaction with various substrates (e.g. equations 62 and 85) were studied by DTA. It was found that the principal oxidation products obtained from reaction with **325** are the same as those obtained by photosensitized oxidation^{676,678a}. The decomposition reaction may serve for determination of the **325** concentration, by measuring the evolved oxygen; the presence of **325** can be detected with a dilute solution of rubrene (**326**), which turns from red-orange to colorless on undergoing an addition reaction similar to equation 86⁴⁹³.

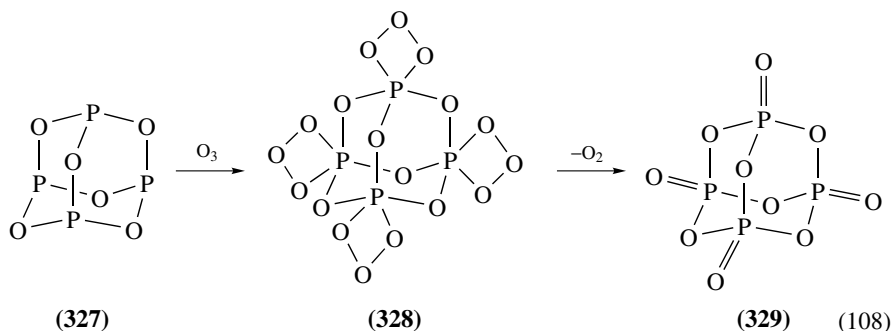


The mechanism of formation and decomposition of **325** was investigated in CClF_3 solution by nonisothermal DTA starting at about -170°C and finishing slightly below 0°C . The thermal analysis data were interpreted in terms of kinetic parameters for the tentative processes depicted in equations 107a–h, taking place in the following approximate order

as the temperature increases^{672,676}.

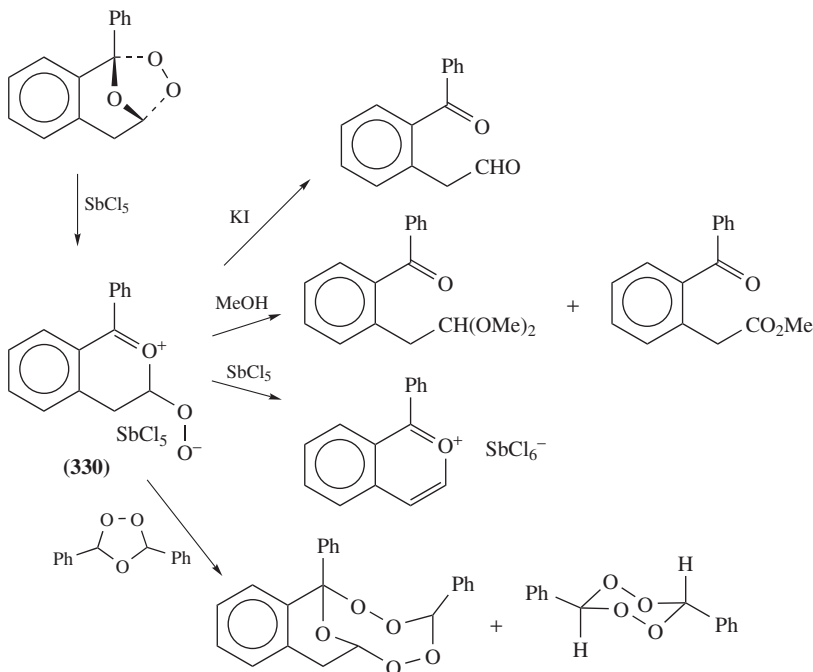


A series of adamantane-like phosphorus oxides takes part in the process depicted in equation 108. Thus, the P(III) oxide (P_4O_6 , **327**) is formed at -78°C , which yields an unstable adduct with ozone (P_4O_{18} , **328**), that starts decomposing in solution or suspension on raising the temperature above -35°C to yield a P(V) oxide (P_4O_{10} , **329**); the decomposition of the dry powder is explosive. The structure of **328** can be characterized by the single ^{31}P NMR signal in CD_2Cl_2 solution at $\delta = -66.3$ ppm, relative to 85% $\text{H}_3^{31}\text{PO}_4$ as external standard; after decomposition of **328**, the known MAS ^{31}P NMR spectrum of **329** is obtained. The Raman spectrum of **328** at -80°C shows the bands attributed to the adamantane cage and three strong bands at 901, 887 and 870 cm^{-1} , assigned to the PO_3 ring; these bands gradually disappear on raising the temperature to -35°C . Compounds containing both P(III) and P(V) on the adamantane-like cage are also present among the products of reaction. The structure of **328** is confirmed by single-crystal XRD, showing the connectivity of **328** but also a distorted symmetry^{678b}.



3. Ozonide zwitterionic complexes

Certain ozonides bearing a phenyl group on position 3 of the 1,2,4-trioxolane ring form very reactive zwitterion complexes with SbCl_5 (e.g. **330**). The structure of these compounds can be assigned based on NMR and UVV spectroscopic evidence and chemical behavior in the presence of various reagents, as shown in Scheme 19. These reactions include reduction with iodide, reduction with an alcohol, reaction with additional Lewis acid and cross-coupling with the same or another ozonide. The decomposition reactions of the zwitterion **330** can be considered as acid-catalyzed processes of the corresponding ozonide⁶⁷⁹.

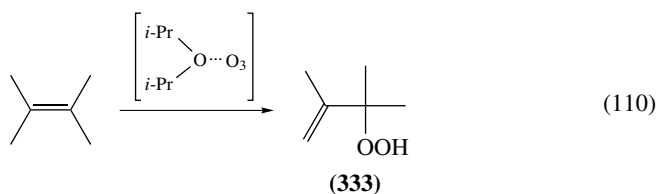
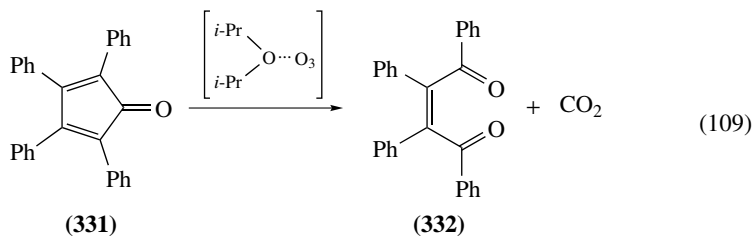


SCHEME 19. Generation and decomposition of a zwitterion species derived from an ozonide

4. Miscellaneous organic ozonides

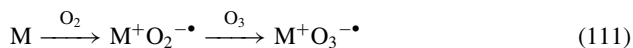
Similarly to the formation of the triphenyl phosphite-ozone adduct described in Section VIII.D.2, other organic substrates, including hydrocarbons, silanes, ethers^{680, 681}, alcohols, amines, aldehydes and diazo compounds, form unstable compounds with ozone. Based on the active oxygen content, the bleaching of certain dyes, the presence of a proton at $\delta = -12.98$ ppm in the low-temperature ^1H NMR spectrum and other evidence, these adducts possibly are hydrotrioxides, containing the $-\text{OOOH}$ group (see Section IX.A). The adducts are potentially capable of releasing $^1\text{O}_2$ on decomposition. For example, the *i*- Pr_2O -ozone adduct yields typical reaction products of $^1\text{O}_2$, such as bleaching of rubrene (**326**) to give the corresponding endoperoxide, similarly to equation 86, bleaching of tetracyclone (**331**) to give *Z*-dibenzoylstilbene (**332**), as shown in equation 109,

and hydroperoxide (**333**) formation by the ene-reaction with an olefin, as shown in equation 110⁶⁸².



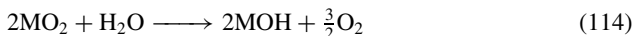
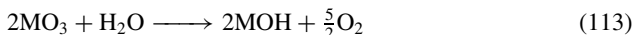
5. Alkali metal and quaternary ammonium ozonides

Ozone forms ionic compounds with alkali metals, M^+O_3^- , which can be synthesized in a gram scale for $\text{M} = \text{K}, \text{Rb}, \text{Cs}$. The basic synthetic process consists of converting the alkali metal to superoxide by exposure to oxygen and then to ozonide by exposure to an O_3/O_2 mixture, as depicted in equation 111. These compounds are thermally unstable and sensitive to moisture and the presence of reducing agents. They are soluble in liquid NH_3 from which intense red single crystals may be obtained. XRD analysis of KO_3 and RbO_3 reveals a CsCl-type structure, with M^+ cations occupying all the corners of a cubic lattice with one O_3^- anion inside each one of these cubes, however, not precisely centered. The structure of the O_3^- anion has interesting features when compared to ozone. The average O—O bond length is larger, 1.35 vs. 1.28 Å, and the average bond angle is slightly reduced, 114 vs. 117°, therefore the distance between the terminal O atoms is also significantly larger, 2.26 vs. 2.18 Å. Although the reason for the structural details is not yet totally understood, an important factor is the extra electron occupying an antibonding orbital, introducing a certain degree of instability that results in the increased bond distances^{683,684}. A reversible phase transition takes place at 8 °C for CsO_3 , from a low-temperature monoclinic structure to a cubic structure of CsCl type, with disordered O atoms. The force constants of the O_3^- anion can be estimated from vibrational frequencies of its ¹⁸O isotopomers and the geometry of the anion⁶⁸⁵.

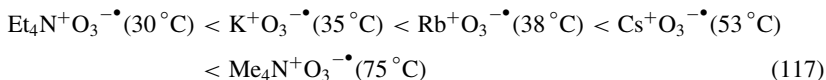
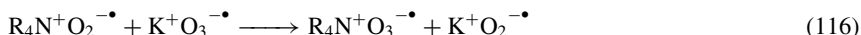
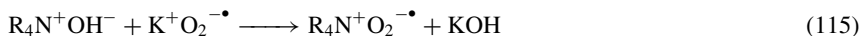


A simple method for determination of metal ozonides is by gasometry of the oxygen liberated on heating, according to equation 112. However, some interference may be expected from small amounts of water possibly present in the system. One of them could be a reaction yielding more oxygen than the thermal decomposition, as in equation 113. Water may also react with other species present in the system, such as superoxide, according to equation 114, or with oxide with no oxygen evolution. To discern the

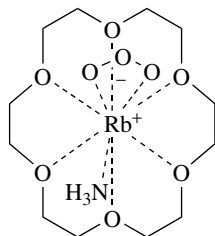
contribution of these reactions and the ozonide content, various analyses have to be carried out besides gasometry, such as a redox titration with standard KMnO_4 and weigh loss at a temperature sufficiently high for equations 112 and 113 to proceed but sufficiently low for equation 114 to stop⁶⁸⁶.



Tetramethylammonium ozonide and tetraethylammonium ozonide cannot be prepared by emulating equation 111. A synthetic method is based on two metathetic reactions, taking advantage of the low solubility of KOH and KO_2 in liquid ammonia, as shown in equations 115 and 116. Equation 115 takes place in the solid state; if no dry tetraalkylammonium hydroxide can be supplied, then for each mole of H_2O two moles of excess KO_2 are required, which are converted to KOH and gaseous O_2 (equation 114). The tetraalkylammonium superoxide is extracted with liquid NH_3 and purified by recrystallization. The process in equation 116 takes place in liquid ammonia where KO_2 precipitates on formation. The tetraalkylammonium ozonide crystallizes on evaporating the solvent, from which it may be recrystallized. The structure of $\text{Me}_4\text{N}^+\text{O}_3^-$ and $\text{Et}_4\text{N}^+\text{O}_3^-$ can be elucidated by XRD crystallography, DTA-TG, IR spectroscopy and MS. The most salient features are disorder of the ions in the solid state and hydrogen bonding between the α -C and the O atoms. The order of thermal stability of the various ozonides is shown in equation 117 with the inception temperature of decomposition. Thermal decomposition of $\text{Me}_4\text{N}^+\text{O}_3^-$ yields NMe_3 , CO , O_2 , H_2O , Me_2O , MeOH and PrNO . The relative thermal instability of $\text{Et}_4\text{N}^+\text{O}_3^-$ is explained by a Hofmann type of elimination catalyzed by the basic O_3^- ion, yielding NEt_3 , C_2H_4 and O_2 ⁶⁸⁷.



Complexes of alkali metal ozonides with cryptand[2.2.2] and various crown ethers have been prepared in order to increase the solubility range of these compounds in solvents other than NH_3 . The first structural analysis reported for such complexes was that of $([18\text{-crown-6}]\text{Rb})\text{O}_3 \cdot \text{NH}_3$ (**334**), carried out by single-crystal XRD. The Rb^+ cation is part of



(334)

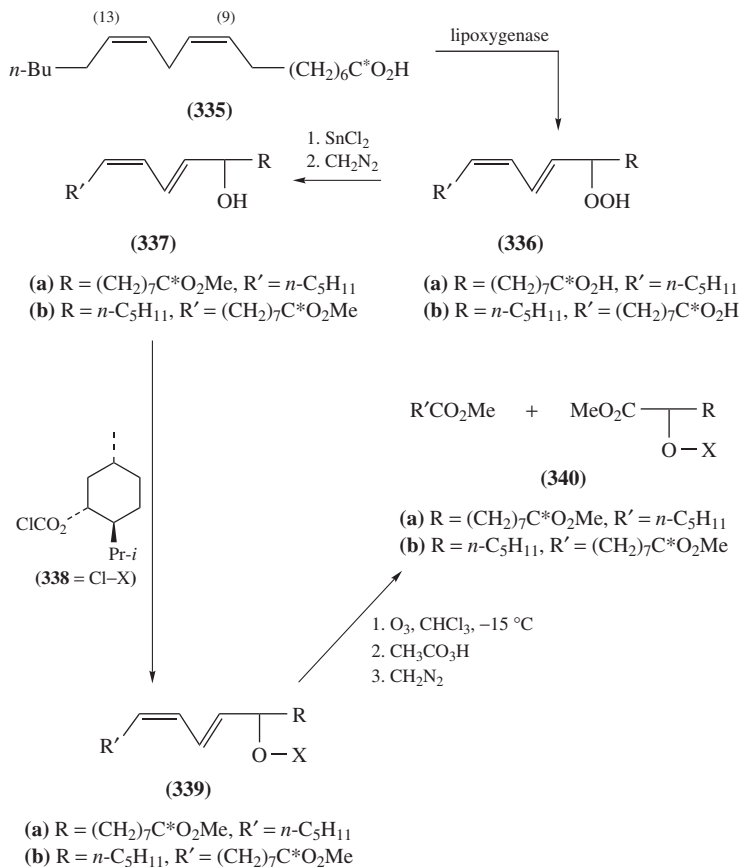
a complex cation of D_{3d} point group symmetry; because of the large size of the Rb^+ cation, it does not fit in the hole and sits slightly off the plane of the crown ether; Rb^+ has also contacts with the two end atoms of the $O_3^{-\bullet}$ anion and the N of the solvating NH_3 molecule. The O—O distance (1.30 Å) and O—O—O angle (117°) are in agreement with those found for $O_3^{-\bullet}$ in metal ozonides; however, this anion shows some disorder. There seems to be weak H-bonding between $O_3^{-\bullet}$ and NH_3 . Also, these complexes need careful handling and long-term storing at low temperature⁶⁸⁸.

E. Ozonolysis as Analytical Tool

Ozonization of unsaturation sites, usually, but not necessarily, followed by hydrolysis or reduction of the FOZ and analysis of the products, has long been applied to structural elucidation of organic molecules. This is especially useful for the characterization of unsaturated lipids, for which the presence of unsaturation may be easily ascertained by IR or 1H NMR spectroscopies. However, the site of unsaturation cannot be established by these methods. Determination of positional isomers of monounsaturated fatty acids, in materials such as partially hydrogenated margarine and shortening, can be accomplished by a protocol including hydrolysis, esterification of the fatty acids to the methyl ester, ozonization at low temperature and reduction with Ph_3P to carbonyl compounds as in equation 95. The mixture of aldehydes and aldehyde-esters thus obtained is then determined by GLC. As unsaturated fatty acids undergo positional isomerization during hydrogenation, the GLC columns have to be capable of operating without crystallizing or bleeding over a large temperature range, to account for normal aldehydes from C_3 to C_{16} or larger and the ester aldehydes^{689–692}. To avoid some problems encountered with the GLC method it is possible to convert the aldehydes into the corresponding DNP, followed by RP-HPLC. The procedure requires previous separation of the derivatives of the simple aldehydes from those of the aldehyde-esters on a silica cartridge, as some species are not well resolved in the RP column. This allows two independent structure assignments of the C_{18} monounsaturated fatty acids. UVD is convenient, due to the high extinction coefficients of the DNP derivatives⁶⁹³.

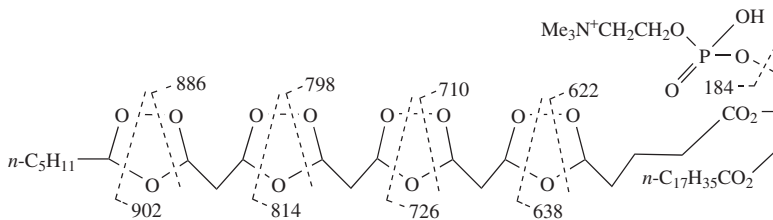
Also, oxidative ozonolysis can be applied for localization of double bonds of unsaturated fatty acids and other compounds, by destroying the FOZ in the presence of peracetic acid. This was applied to determine whether linoleic acid (**335**) is oxidized to hydroperoxide on the 9- or 13-position, according to Scheme 20. Thus, the hydroperoxide (**336**) is reduced to the corresponding alcohol and converted to the Me ester (**337**). Before ozonolysis, it is convenient to protect the OH group; in the present case an asymmetric protective group, X, is introduced, using (–)-menthyl chloroformate (**338**, Cl–X). After oxidative ozonolysis of the carbonate esters (**339**), peracetic acid destruction of the FOZ and conversion of the carboxy groups to the Me esters, GLC may show whether the mixture of esters (**340**) bears the menthyl group on the monocarboxylic or dicarboxylic ester fraction. Introduction of the asymmetric group X allows further insight into the configuration of the hydroperoxides, as discussed at the end of Section V.C.¹⁹².

The location of the double bonds in unsaturated glycerophosphocholine (GPC) lipids is made difficult mainly due to the limited amounts of these compounds isolated from cells. When a thin layer of a GPC lipid is exposed to the action of ozone, partial or total ozonization of the unsaturated fatty acid residues may take place, depending on the particular compound being analyzed. The ozonized lipid is dissolved and analyzed by tandem MS. A typical injection into the instrument may be 5 μL containing 10–20 ng of the lipid. An illustrative example is the ozonized 1-stearoyl-2-arachidonoyl-GPC, showing the systematic fragmentation pattern in Scheme 21, typical of the ozonized GPC lipids. Thus, the molecular peak appears increased by one nominal unit ($M + H$, m/e 1002),



SCHEME 20. Application of oxidative ozonolysis for structural analysis of unsaturated fatty acid hydroperoxides

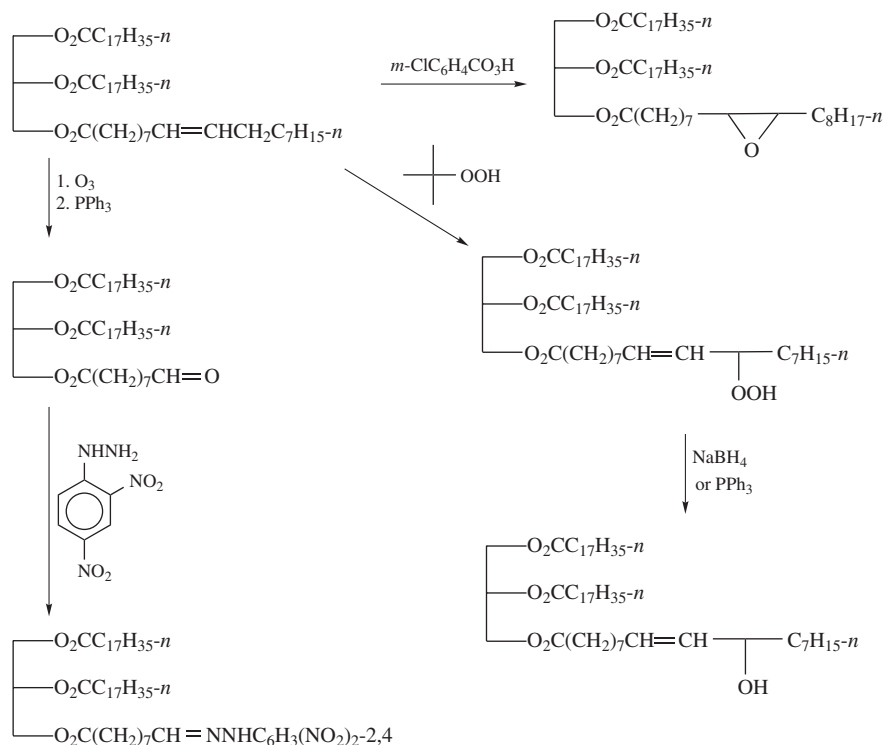
attributed to a proton sticking to the phosphate anion and giving a net positive charge to the species; this feature persists in all the other fragments; a series of remote charge-induced homolytic scissions then takes place, leading to the glycerophosphocholine unit (*m/e* 184), and each of the ozonide moieties breaks into the two possible fractions, namely



SCHEME 21. Fragmentation pattern of the ozonide of an unsaturated glycerophosphocholine lipid in electrospray MS

an acyl free radical (e.g. *m/e* 622, 710 etc.) and a carboxylate free radical (e.g. *m/e* 638, 726 etc.). The presence of a hydroxy group in the unsaturated fatty acid residue disturbs the mode of ozonolysis and fragmentation of the ozonide shown in Scheme 21; however, the products still afford interesting structural information by MS analysis⁶⁹⁴.

Preparation of a series of reference derivatives of unsaturated triglycerides was recommended for determination of elution factors, as an aid in the identification of peroxidized natural triglycerides by RP-HPLC with EI-MS detection. These model compounds are synthesized as shown in Scheme 22 for 1,2-distearoyl-3-oleyl-*sn*-glycerol. Quite distinct R_f values are obtained for the recommended model derivatives, which include mono- and diepoxides, mono- and diallyl alcohols, mono- and dialdehydes prepared by reductive ozonolysis and their DNPs. Under proper LC conditions various positional and regioisomers can be separated. In addition, the core aldehydes may form hemiacetals with MeOH in the eluting MeOH solvent, yielding $[M + 32]$ peaks, and their DNP derivatives show a double chromatographic peak assigned to the *syn* and *anti* isomers⁶⁹⁵.



SCHEME 22. Synthesis of some useful reference derivatives of 1,2-distearoyl-3-oleyl-*sn*-glycerol, as an example of an unsaturated triglyceride

Ozonolysis can be applied for assessing the pollution level of potable and wastewaters, by determining the ozone demand in an apparatus including an ozone generator and UVD for measuring the amount of O₃ supplied. A correlation can be established between the ozone demand and the *chemical oxygen demand*, which is a standard method for pollution evaluation. The advantage of the ozonolysis route is its speed (a few minutes for sample

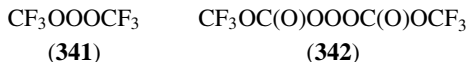
preparation and up to 2 min measurement). Furthermore, it is possible to assess the type of pollutants present in the water sample by measuring the kinetics of O₃ uptake⁵⁰. A similar procedure can be used for establishing the double bond content of slightly unsaturated polyolefins (less than 0.01% by mass) and their average distribution in the polymer. This method correlates well with the iodine number assay and has the advantage of not requiring dissolution of the polymer. The sensitivity is high, with a LOD of about 10⁻⁷ mol of double bonds per gram of polymer⁶⁹⁶.

IX. MISCELLANEOUS FUNCTIONS BEARING THE O—O GROUP

A. Trioxides and Tetroxides

The compounds included in this section are very ephemeral due to the instability of the OOO and OOOO chains at room temperature. In Section VIII.A the primary ozonides were mentioned, and they may be conserved for some time at low temperatures. An example of a compound stable at room temperature (**296**) is mentioned in Section VIII.C.4. A brief review appeared of unstable ozonization products derived from various sources, involving hydrotrioxides⁶⁸².

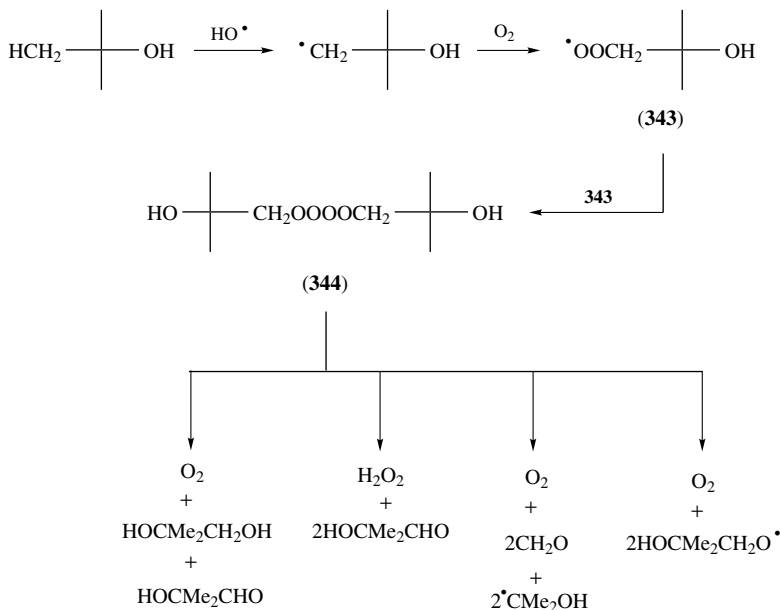
Bis(trifluoromethyl) trioxide (**341**) is a volatile byproduct of the photochemical synthesis of trifluoromethyl fluoroformyl peroxy carbonate (**243**). It may be distinguished from other volatile products by a characteristic IR peak at 1170 cm⁻¹. Bis(trifluoromethyl) trioxydicarbonate (**342**) is obtained as a byproduct of the photochemical synthesis of peroxy carbonates **244** and **245** (see Section VI.C.3) from a mixture of (CF₃CO)₂O, CO and O₂. It cannot be totally separated by distillation from its analogous peroxydicarbonate compound due to their close boiling points and its inherent instability. The main evidence for its presence stems from a ¹³C NMR signal of the crude liquid mixture with **244**, a quartet at δ(CO) = 145.7 ppm, J_{CF} = 2.3 Hz, slightly downfield from the corresponding peak of the peroxide at δ(CO) = 145.5 ppm. The small coupling constant is due to the adjacent CF₃ group²³. The assignment of the peak at 147.7 to the trioxide is supported by a similar trend observed for the pair **341** and CF₃OOCF₃, δ(C) = 123.7 and 122.5 ppm, respectively⁶⁹⁷.



Ozone forms hydrotrioxides ROOOH on reacting with substances with aliphatic C—H groups at low temperature. Thus, for example, isopropyl ether or isopropyl alcohol form such trioxides that are stable at -80 °C. When subjecting these compounds to nonisothermal DTA, a series of unimolecular, bimolecular, parallel and successive reactions can be discerned, depending on their concentration⁶⁷²; see Section VIII.D.4. Also, tetroxides are unstable byproducts of ozonolysis. For example, *t*-butyl alcohol undergoes reaction with HO• free radicals, which are a product of the reaction of ozone with water or organic matter; the peroxy free radical (**343**) thus produced undergoes dimerization to a tetroxide compound (**344**) and subsequently decomposition by various paths, as shown in Scheme 23. These processes are important when using ozone for drinking water disinfection²⁴⁴.

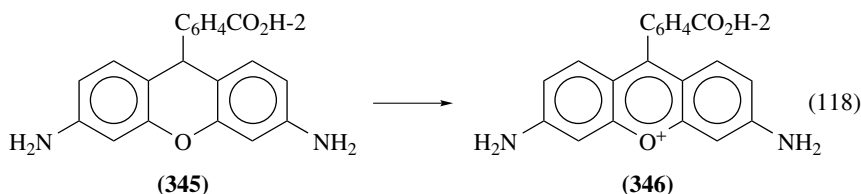
B. Peroxynitrite and Peroxynitrous Acid

Analytical methods for ONOO⁻ related to the vascular system have been reviewed. Special attention is given to assays involving oxidation of dihydrorhodamine 123 (**345**) to yield the fluorescent product rhodamine 123 (**346**, equation 118), luminol (**124**) CL and nitrotyrosine formation⁸³. The reaction of peroxynitrite and carbon dioxide or bicarbonate



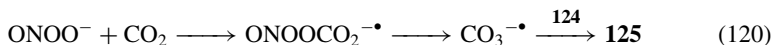
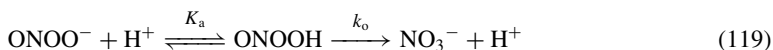
SCHEME 23. Processes taking place during ozonolysis of *t*-butyl alcohol in aqueous media, involving intermediate formation of a tetroxy compound

and its effects as ROS and nitrating agent for tyrosine residues in biological systems was discussed. Tracing nitrotyrosine residues in biological systems as a footprint of peroxynitrite can be carried out by methods outside the scope of this chapter⁶⁹⁸. Solutions of peroxynitrite salts can be prepared and kept in cold storage for relatively long periods. The concentration of such solutions can be checked by UVV spectrophotometry at 302 nm ($\epsilon = 1.67 \times 10^3 \text{ M}^{-1} \text{ cm}^{-1}$)⁶⁹⁹. However, tracking this species at physiological concentrations and in physiological matrices requires more sensitive procedures. A stop flow method with UVD at 290 nm was used to follow the kinetics of formation or disappearance of ONOOH in various systems⁷⁰⁰. The CL process with luminol (**124**) can be catalyzed with Fe(II); however, the mechanisms proposed for this process are rather controversial⁷⁰¹. The presence of CS₂ enhances the intensity and the speed of CL response of luminol in the determination of peroxynitrite in cell cultures⁷⁰².

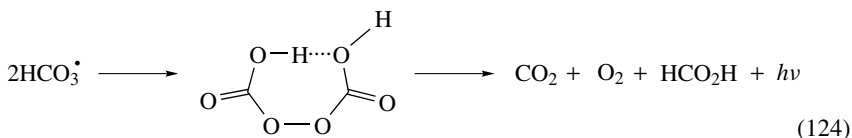
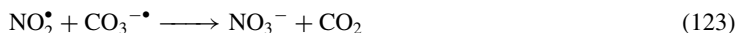
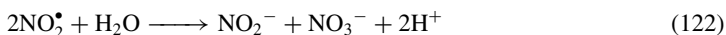
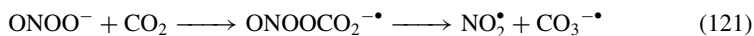


A method for determination of peroxynitrite down to subnanomolar concentrations is based on CL in the presence of luminol (**124**, Scheme 3). The kinetic of decomposition of peroxynitrite according to equation 119 is a function of pH and can be measured in a FIA system. The solution carrying the analyte is mixed in the CL cell with **124** dissolved

in carbonate buffer, where a photomultiplier collects the emitted light. The production of the intermediate luminol free radical (**125**) may proceed directly with peroxyxynitrite in phosphate buffer or with the free radical $\text{CO}_3^{\bullet-}$ in carbonate buffer, according to equation 120. To avoid interference of macromolecular solutes a permselective membrane can be used, only allowing diffusion of small molecules into the analytical system. LOD is about 1×10^{-11} M and about 1×10^{-10} M, without or with the membrane, respectively. Instrumentation for *in vivo* measurements was under development when this chapter was being written³³⁴.



A reaction with CL takes place when ONOOH or ONOO⁻ are mixed with carbonate ions, without any of the known CL reagents mentioned in this chapter. Furthermore, quantum yield enhancement takes place in the presence of a large surface area. Thus, in a FIA system a solution containing the analyte is mixed with carbonate solution at pH 10.3 and passed through a CL cell packed with cotton wool for surface enlargement. The following mechanism was proposed for the CL reaction: At the given pH, carbonate is in equilibrium with bicarbonate and carbon dioxide, which undergoes the fast consecutive reactions depicted in equation 121. Recombination of the free radicals obtained in this equation leads to formation of nitrite and nitrate, as shown in equations 122 and 123. However, the $\text{CO}_3^{\bullet-}$ free radical anion can abstract a proton from the solvent, leading to the neutral HCO_3^{\bullet} free radical, that can recombine to an excited intermediate, which decomposes with photon emission, according to equation 124. The reasons for the surface enhancement effect are moot. The method can be used for determination of nitrite in water by previous conversion of NO_2^- to ONOOH, on addition of H_2O_2 in acid solution⁷⁰³.



C. Peroxynitrates

1. Infrared and Raman spectroscopies

The fundamental vibrations (8 stretching, 10 deformation and 3 torsional modes) of trifluoromethyl peroxyxynitrate (**1**) can be assigned from the FTIR spectrum in the gas phase and FT-Raman spectrum of the liquid. The high-frequency stretching modes are characteristic and easily assigned, except for the $\nu_s(\text{CF}_3)$ and $\nu_s(\text{NO}_2)$ fundamental modes, which overlap in the gas-phase IR spectrum. Near agreement is obtained between the experimental and the theoretically calculated vibrational spectra²². Due to the C_1 symmetry of the molecule, all the fundamental modes (7 stretching, 8 deformation and 3

torsional) are Raman and IR active in the vibrational spectra of gaseous, liquid and solid matrix fluorocarbonyl peroxyxynitrate (**2**). The bending modes can be assigned by analogy to the corresponding modes in other molecules, such as FC(O)OOC(O)F, FC(O)OF and O₂NOF. The NO₂ stretching modes, $\nu_s = 1302 \text{ cm}^{-1}$ and $\nu_{as} = 1763 \text{ cm}^{-1}$, have an average $\nu_{av} = [(\nu_s^2 + \nu_{as}^2)/2]^{1/2} = 1550 \text{ cm}^{-1}$, that points to the presence of a strongly electronegative group (FC(O)O-) attached to the -ONO₂ moiety. The ν_{av} values seem to increase with the electronegativity of the X group in X-ONO₂, for example Cl-ONO₂ ($\nu_{av} = 1533 \text{ cm}^{-1}$) and F-ONO₂ ($\nu_{av} = 1548 \text{ cm}^{-1}$)²⁰. The IR spectrum of trifluoroacetyl peroxyxynitrate (**3**) in an isolated solid matrix points to the presence of only one rotamer, which is expected to be of *gauche* conformation, as is the case of **2**. However, vibrational spectra are incapable of distinguishing between two cases: the carbonyl group being close to the OO bridge (*syn*) or far from it (*anti*); NMR can tell the difference. Due to the low symmetry of **3**, C₁, all the fundamental vibrational modes (10 stretching, 13 deformation and 4 torsional) are active in both Raman and IR, and the assignments may be made²¹.

2. Ultraviolet spectroscopy

The UV absorption spectrum of gaseous trifluoromethyl peroxyxynitrate (**1**) shows a continuous decrease of intensity from 185 nm to 340 nm. The reported absorption cross section ($\sigma/10^{-20} \text{ cm}^2$) ranges from 370 at 190 nm, to 1.0 at 290 nm and to 0.014 at 340 nm. Using published solar flux data in the troposphere at sea level, and assuming a unity quantum yield, a half-life time of about 1 month can be estimated for compound **1**, which makes it a potentially effective carrier of pollutants from industrial zones to remote unpolluted sites^{22,704}.

3. Nuclear magnetic resonance spectroscopy

The ¹⁹F and ¹³C NMR spectra of pure liquid trifluoromethyl peroxyxynitrate (**1**) at -30 °C show a single signal at $\delta = -71.8$ ppm relative to CFCl₃ and a quartet at $\delta = 123.7$ ppm relative to TMS, respectively. Both spectra have identical coupling constants $^1J_{CF} = 269.5$ Hz; in the case of the singlet in the ¹⁹F spectrum, the $^1J_{CF}$ value can be calculated from the position of the ¹³C satellites²². The single ¹⁹F NMR signal of fluorocarbonyl peroxyxynitrate (**2**) at $\delta = -31.0$ to -32.3 ppm relative to CFCl₃, in the temperature range from -90 to +20 °C, points to a conformation where the carbonyl O atom is *syn* to the OO group, in accordance with the chemical shifts of FC(O)OF, but a signal for the *anti* conformation also appears²⁰. Similar considerations also apply for trifluoroacetyl peroxyxynitrate (**3**) and its CH₃ analog, the ¹⁹F and ¹³C chemical shifts and CF coupling constants of which also point to the *syn* conformation²¹.

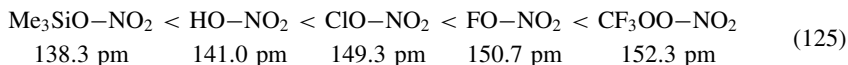
4. Mass spectrometry

The MS of fluorocarbonyl peroxyxynitrate (**2**) and trifluoroacetyl peroxyxynitrate (**3**) both show the base peak at $m/z = 46$, in accord with the high stability of the NO₂⁺ ion, whereas no molecular peak appears, due to the weakness of the O-NO₂ bond^{20,21}.

5. Gas electron diffraction

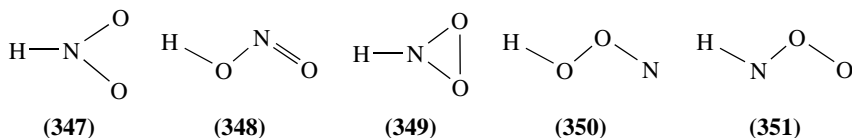
The GED pattern of trifluoromethyl peroxyxynitrate (**1**) can be used to calculate a radial distribution function for the molecule with a few constraints, such as a C_{3v} symmetry for the CF₃ group, a planar configuration for the ONO₂ group and some of the angles taken from the theoretical calculations. The geometric parameters for the molecule, such as interatomic distances, bond angles and twist angles estimated from GED, are in close

accord with the theoretically calculated ones. A special feature of this molecule is the unusually long O–NO₂ bond (152.3 pm). The length of this bond seems to be governed by the electronegativity of the group attached to the O atom, as shown in equation 125, making the CF₃O group more electronegative than F²². The GED pattern of fluorocarbonyl peroxyxynitrate (**2**) affords a radial density distribution function that is in accord with the *syn* conformation for the molecule, also deduced from the ¹⁹F and ¹³C NMR spectra. The bond distances and angular parameters of **2** derived from GED with a few constraints are close to the theoretically estimated values²⁰.



D. Imine Peroxide

Methyl nitrate and its perdeuteriated isotopomer trapped in an Ar matrix at 17 K undergo photolysis on laser irradiation at 266 nm, yielding three main products, one of which is identified from its FTIR spectrum as CH₂O and the other two are isomers of empirical formula HNO₂ (**347**–**351**) or their corresponding ²H isotopomers. The spectrum of the second compound corresponds to that of hydrogen nitril (**347**), a known species of C_{2v} symmetry. The third compound is neither *cis*- nor *trans*-nitrous acid (**348**), of well-known spectra. Quantum chemical calculation for **349** show that this structure does not account for the spectrum of the third compound. Structure **350**, in both the *cis*- and *trans*-configurations, is problematic for the chosen calculation methods; however, they show that both conformations have an exceptionally long O–O bond, of about 200 pm, making this structure look rather like a loosely bound complex of OH and NO species. Structure **351**, imine peroxide in the *cis*- and *trans*-configurations, is the one for which the calculations give the best approximation to the observed vibrational spectrum. The calculations point to the *cis*- as being more stable than the *trans*-isomer by about 13 kJ mol⁻¹ with a very high barrier of > 57 kJ mol⁻¹ separating between them⁷⁰⁵.



E. Peroxysulfates

CZE-ELD, with a Au microelectrode at –0.6 V vs. SSCE and a Pt wire as auxiliary electrode, using sodium borate buffer and dodecyltrimethylammonium bromide for dynamic coating of the capillary internal surface, can be applied for separation and determination of ultra-trace amounts of many oxidizing substances. Thus, the concentration of peroxodisulfate (S₂O₈²⁻) and peroxomonosulfate (SO₅²⁻) ions in pickling baths can be monitored by this method. The faster emergence of the heavier peroxodisulfate ion is attributed to different adsorption of the two analyte ions by the capillary coating²⁰⁷.

X. SAFETY ISSUES

A. General

Contact with hazardous materials is inevitable in modern life. All peroxides are hazardous and some of them are regarded as extremely hazardous substances (EHS). The

word *hazardous* carries many connotations far beyond the dictionary equivalents, based on evaluation of the following interrelated factors: (i) Type of hazard (e.g. explosion, flammability, toxicity); (ii) status (e.g. store, transportation, production line, spill); (iii) time scale (e.g. acute, delayed, chronic); (iv) spatial scale (e.g. immediate vicinity, remote sites); (v) identity of target (e.g. persons, livestock, plants, objects, property, the environment), (vi) extent of danger (how many persons, objects etc. are in danger); (vii) severity scale (e.g. light, maiming, fatal, obliterating). Besides the physical phenomena involved in these considerations, of equal importance are the legal implications of mishandling hazardous materials (e.g. CRTD⁷⁰⁶). Thus, a branched organization has been established dealing with safety, from the safety officers and committees at the workplace up to national and international regulatory agencies, besides infrastructures to aid in emergency cases, such as centers of information, intensive care units, detoxification units etc.

Experience of more than two centuries in organized laboratories and production plants led to the development of general safety instructions, as presented in many laboratory safety manuals⁷⁰⁷. However, peroxides require extra care and knowledge of the risks derived from mishandling. Commercial peroxides, such as those in Table 1, involve several score of chemicals, of which only one in dilute form, H₂O₂, and few others in low concentrations as part of formulations, reach the wide public. All the others are handled only in industry, agriculture, medicine and research. A glossary of terms relating to hazardous materials⁷⁰⁸ includes the term *peroxide* with a concise discussion on safety handling in the laboratory of organic compounds that underwent autoxidation to peroxides⁷⁰⁹. Standards exist for determining the presence of organic peroxides in solvents^{710,711} and for storage of organic peroxide formulations¹⁵⁹.

B. Regulatory Agencies

Handling of chemicals is extensively regulated today, from the global level of the UN, the international level (e.g. UNECE in Europe), down to the national, regional, local and organizational levels. Specialized agencies are concerned with transportation, environmental pollution and occupational hazards, at the global (e.g. UNEP, ILO and WHO) and national (e.g. DOT, EPA, NIOSH and OSHA in USA) levels. Cooperation and cross-pollination between these agencies is extensive; however, redundancy and even rivalry cannot be avoided. The intricacies of the dealings on hazardous materials at the global level may be appreciated from the classification of the hazards involved in maritime transportation of materials as defined in the CHRIS manual⁷¹² or from a document prepared in close cooperation with the UNECE and WHO secretariats, explicitly declared as *not to be cited*⁷¹³.

The TSCATS database of EPA is part of CIS¹⁷⁶, and included when this chapter was written more than 24000 documents about over 8400 substances, usually supplied by big industrial enterprises. They mostly relate to toxicological, environmental and other safety issues. Entries of Table 1 carrying note *f* are included in this database. Queries about TSCATS can be sent to cissupport@nisc.com.

1. Transportation

Perhaps the most involved situation in handling dangerous chemicals concerns transportation, because the professional teams in charge are not trained for dealing with specific hazardous chemicals. The secretariat of UN maintains in continuous operation the *Committee of Experts on the Transport of Dangerous Goods and on the Globally Harmonized System of Classification and Labelling of Chemicals* and its subcommittees on TDG and GHS. Two of their publications are of general relevance, a set of model regulations⁷¹⁴

TABLE 6. UN classification of hazardous materials for transportation

Class	Type of material
1 or 1a	Explosives
2	Gases
3	Flammable liquids
4.1	Flammable solids
4.2	Spontaneously combustible substances
4.3	Substances emitting flammable gases on contact with water
5.1	Oxidants
5.2	Organic peroxides
6.1	Toxic substances
7	Radioactive substances
8	Corrosive substances
9	Miscellaneous dangerous goods

and a set of tests and criteria⁷¹⁵, which serve as basis for international agreements (e.g. ADN⁷¹⁶, ADR⁷¹⁷, COTIF/RID⁷¹⁸ and CRTD⁷⁰⁶), regulations of global transport organizations (e.g. IATA¹⁶⁰, ICAO⁷¹⁹ and IMDG¹⁶³) and national regulations (e.g. the CFR of USA¹⁷⁵).

The criteria for various types of dangerous properties are set in a UN publication⁷¹⁵, however these are not necessarily unique or the most demanding among the various regulatory agencies. For the purposes of TDG the classes of substances shown in Table 6 have been defined. The classes are not necessarily exclusive of one another, and a particular substance may fit two or more of them, but the most demanding class usually applies. The inorganic peroxides belong to class 5.1, the oxidizing substances, whereas the organic peroxides have class 5.2 of their own. According to the UN, a substance containing organic peroxides belongs to class 5.2 if more than 1.0% of the available oxygen stems from organic peroxides. A further subdivision of compounds and formulations belonging to class 5.2 is given, as determined by tests, ranging from type A, which is forbidden for transportation in the tested form, down to type G, for which the restrictions of class 5.2 do not apply. A most important property in this respect is the self-accelerated decomposition temperature (SADT), which should be determined in the same type of package as used in transportation. Organic peroxides with SADT $\leq 55^\circ\text{C}$ are considered as requiring refrigeration from 10 to 20°C below the SADT for safe transportation. Substances with SADT requiring refrigeration are forbidden by IATA in its carriers. DOT in USA is slightly less stringent, setting the SADT limit at 50°C¹⁷⁵.

Appendix 2 shows a poster used by IATA and ICAO regarding the labeling required for TDG in their vessels. Various relevant labels may be used on the same package. Compounds in Table 1 requiring such labels have comments **C** for corrosive, **F** for flammable, **O** for oxidant or organic peroxide or **T** for toxic. Other labels are relevant to environmental and health matters, as discussed below. Besides labeling, also the packaging method is tightly controlled for substances belonging to classes 5.1 and 5.2 (see, for example, the CFR definitions and assignment methods of packaging for oxidants and organic peroxides⁷²⁰).

The governments of the North American continent issued a downloadable guidebook for incidents occurring during inland transportation of hazardous materials, of which guides 140 to 144 refer to oxidizers in general and guides 145 to 148 specifically refer to organic peroxides (see Table 7). Each guide contain concise instructions on action to be taken in case of spills of various sizes, fire or injury, including dos and don'ts, emergency calls and special procedures⁷²¹.

TABLE 7. Relevant guides for emergency procedures for various types of hazardous materials in the Emergency Response Guidebook⁷²¹

Guide number	Type of material
140	Oxidizers
141	Oxidizers—toxic (solid)
142	Oxidizers—toxic (liquid)
143	Oxidizers (unstable)
144	Oxidizers (water reactive)
145	Organic peroxides (heat and contamination sensitive)
146	Organic peroxides (heat, contamination and friction sensitive)
147	Organic peroxides (heat and contamination sensitive—severe irritants)
148	Organic peroxides (heat and contamination sensitive—temperature controlled)

2. Environmental hazards

Of great international concern for their possible environmental damage are the persistent toxic substances (PTS) and, in particular, the persistent organic pollutants (POP)^{722, 723}. The organic peroxides do not belong to either classification, and do not attract special attention from the UNEP. On the other hand, at the national and local levels, various agencies are interested in the possible environmental damage that may cause accidental spills or conflagration of large stocks of chemicals in either static or astatic state or under transportation. Thus, for example, the programs CAMEO⁷²⁴, ALOHA⁷²⁵ and MARPLOT⁷²⁶ allow prediction of possible outcome of major incidents involving chemicals and planning of the appropriate course of action (e.g. evacuation of population or involvement of specialized groups). The guides relating to organic peroxides mentioned in Table 7 contain warnings about runoff waters of firefighting or dilution of spills possibly causing environmental pollution, and advise diking such waters until further treatment can be applied⁷²¹. Relatively few peroxides have been investigated in depth for their potential damage to the environment as toxic materials. Compounds in Table 1 required to carry the *environmental hazard* label, as depicted in Appendix 2, are denoted by comment N.

3. Occupational hazards

Several documents dealing with hazardous chemicals are of particular interest to people coming in direct contact with them, their immediate managers and the safety officers of their institutions or enterprises.

The International Chemical Safety Cards (ICSC)⁷²⁷ are produced within the framework of the International Programme on Chemical Safety (IPCS)⁷²⁸, which is a joint project of WHO, ILO and UNEP. All ICSCs appear as a two-sided card with the same formal structure, as illustrated for peracetic acid in Appendix 3. The front page of the card has a set of identification terms for the compound, a most significant template with four columns relating to the type of hazard, definition of an acute hazard or symptoms, prevention and immediate action to take; the fixed types of hazard defining the rows of the template are *fire*, *explosion* and *exposure*, where the latter entry is subdivided into four varieties, namely *inhalation*, *skin*, *eyes* and *ingestion*. The lower part of the front page carries information on spillage disposal, packaging/labeling, emergency response (call stations for emergencies in transportation) and *storage*. The back page of the card is divided into fields of *important data* (appearance, chemical dangers, routes of exposure, inhalation risk

and effects of short-term exposure), *physical properties, environmental data, notes and additional information*. Available ICSCs appear in the comments of Table 1. As the style of these cards is very concise, it is important to correctly understand the precise meaning of each word. For example, the terms 'flammable' and 'combustible' are dictionary

TABLE 8. Risk and safety phrases frequently used for organic peroxides

Phrase	Comments	Notes
<i>Risk phrases</i>		
R2	Risk of explosion by shock, friction, fire or other sources of ignition.	<i>a</i>
R7	May cause fire.	<i>a</i>
R8	Contact with combustible material may cause fire.	<i>a</i>
R10	Flammable.	<i>a</i>
R11	Highly flammable.	<i>a</i>
R20/21/22	Harmful by inhalation, in contact with skin and if swallowed.	<i>a, b</i>
R20/22	Harmful by inhalation and if swallowed.	<i>a, b</i>
R34	Causes burns.	<i>a, b</i>
R35	Causes severe burns.	<i>a, b</i>
R36	Irritating to eyes.	<i>a, b</i>
R36/38	Irritating to eyes and skin.	<i>a, b</i>
R50	Very toxic to aquatic organisms.	<i>a, b, c</i>
R51/53	Toxic to aquatic organisms, may cause long-term adverse effects in the aquatic environment.	<i>a, b, c</i>
<i>Safety phrases</i>		
S1/2	Keep locked up and out of the reach of children.	
S2	Keep out of the reach of children.	
S3	Keep in a cool place.	
S3/7	Keep container tightly closed in a cool place.	
S13	Keep away from food, drink and animal feeding stuffs.	
S14	Keep away from ... (<i>incompatible materials to be indicated by the manufacturer</i>).	
S27	Take off immediately all contaminated clothing.	
S28	After contact with skin, wash immediately with plenty of ... (<i>to be specified by the manufacturer</i>).	
S36/37/39	Wear suitable protective clothing, gloves and eye/face protection.	
S36/39	Wear suitable protective clothing and eye/face protection.	
S45	In case of accident or if you feel unwell, seek medical advice immediately (<i>show the label where possible</i>).	
S50	Do not mix with ... (<i>to be specified by the manufacturer</i>).	
S61	Avoid release to the environment. Refer to special instructions/safety data sheets.	

^a Certain substances which are susceptible to spontaneous polymerization or decomposition are generally placed on the market in a stabilized form. It is in this form that they are listed in Annex I to the Commission Directive 98/98/EC. However, such substances are sometimes sold in a nonstabilized form. In this case, the manufacturer or any person who places such a substance on the market must state on the label the name of the substance followed by the words 'non-stabilized'.

^b Some substances (acids, bases etc.) are placed on the market in aqueous solutions of various concentrations and therefore require different labeling, since the hazards vary with the concentration. In this case, the manufacturer or any other person who markets such a substance must state the percentage concentration of the solution on the label. Unless otherwise stated, it is assumed that the percentage concentration is calculated on a weight/weight basis. The use of additional data (e.g. specific gravity, degrees Baumé) or descriptive phrases (e.g. fuming or glacial) is permissible.

^c See Section X.B.2. Carrying a special label on the package is applicable together with risk phrases R50 and R51/53.

synonyms; however, flammable materials have a relatively low flash point. The card structure and the terms included are explained in a manual⁷²⁹.

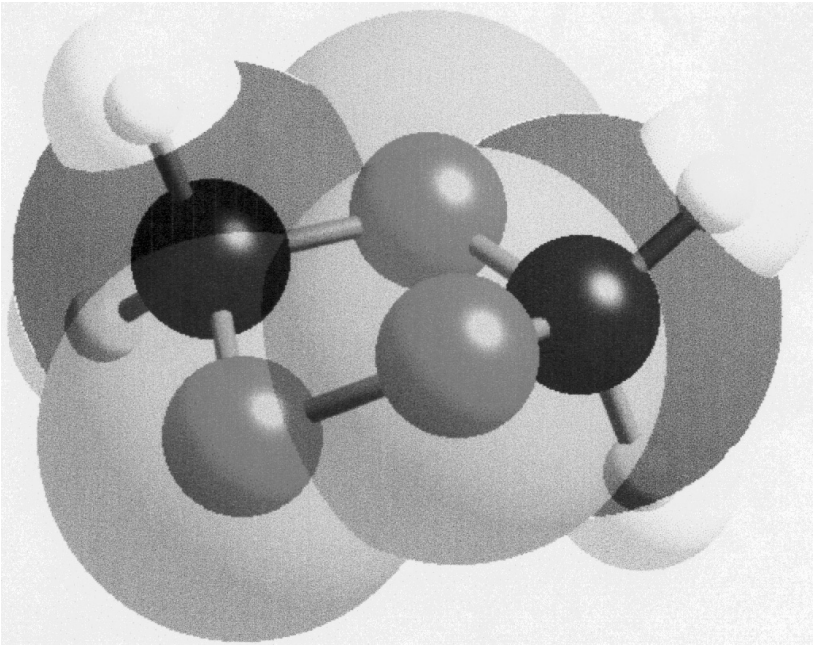
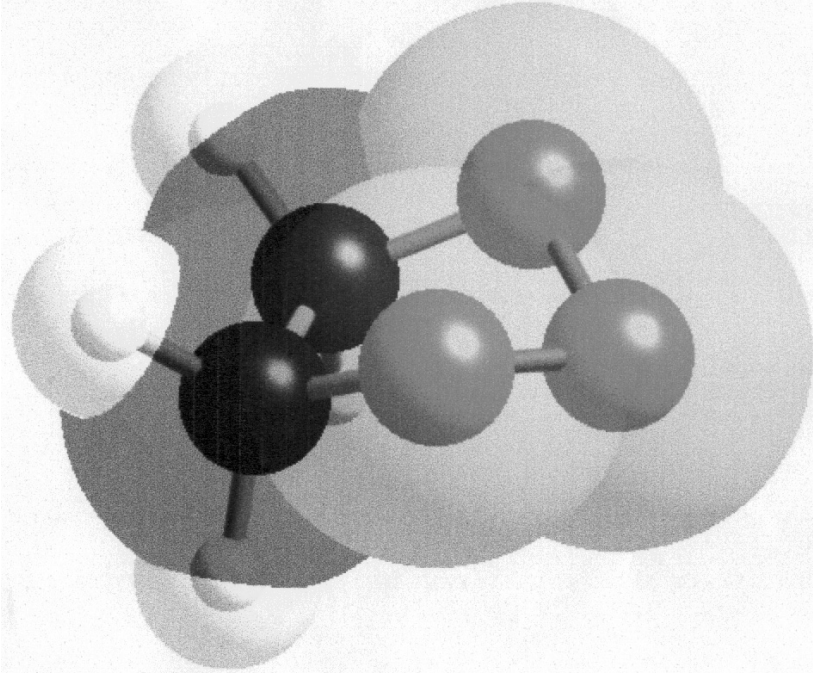
The *NIOSH Pocket Guide to Chemical Hazards (NPG)* is a useful compilation of properties, occupational hazards data and emergency procedures in html, printed and CD-ROM formats. However, only counted peroxides have been incorporated to this database⁷³⁰. The same limitation applies to the collections of analytical methods by NIOSH⁵⁸⁸, OSHA⁷³¹ and EPA^{732,733}. Nevertheless, due to the regulatory character of the occupational exposure limits (OEL) and other provisions by these organizations, the quality of the sampling and analytical methods used in the workplace has to be assured; a valuable series of guidelines may be downloaded from the OSHA site for evaluation of the sampling and analytical methods⁷³⁴.

A large compilation of information on the toxic effects of chemical substances is NIOSH's RTECS, which included in March 2004 about 158000 substances and many of the compounds listed in Table 1^{172,735} (see also note *a* in that table). The regulatory character of the OEL and other provisions of RTECS require precise definition and placement within the complex regulatory system, which is done in a special downloadable guide⁷³⁶. An example of an RTECS document, the one for peracetic acid⁷³⁷, may be downloaded. It contains identification items and the following concise information: (i) synonyms; (ii) skin and eye irritation data; (iii) tumorigenic data; (iv) acute toxicity data; (v) other multiple dose data; (vi) standards and regulations; (vii) NIOSH documentation and surveillance; (viii) status in federal agencies and (ix) references.

The most familiar documentation for hazardous substances is the MSDS. Although the legal value of these documents is limited, they offer concise safety information for many more substances than ICSC or RTECS. MSDSs can be asked from chemical suppliers or may be looked for in the Internet^{738,739}. However, in the latter case the information is not always freely available. The MSDS version for peracetic acid by one supplier of laboratory reagents⁷⁴⁰ may be downloaded. Besides the physical, chemical and toxicological data shown, two items are of special interest, the *risk phrases*⁷⁴¹ and the *safety phrases*⁷⁴², operating as catch phrases to be heeded when handling the substance (see Table 8). Although the general guidelines for presentation of ICSC or RTECS documents are followed, plenty of additional information can be included. Practically everybody can formulate an MSDS, stressing the points that are considered most important⁷⁴³; thus, for example, the MSDS of peracetic acid mentioned above differs from that obtained elsewhere⁷⁴⁴.

XI. ACKNOWLEDGMENTS

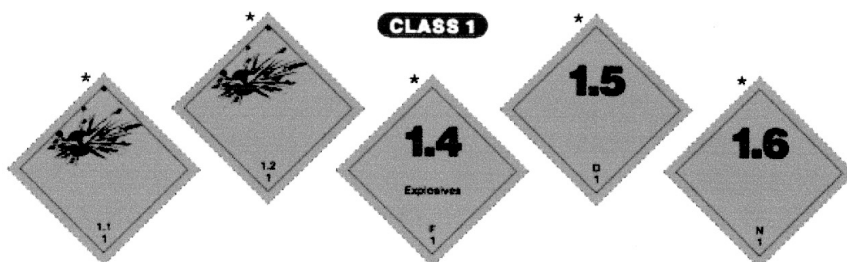
The author wishes to thank the following persons and organizations for helpful information provided: Mr. Emmert Clevestine of International Occupational Safety and Health Information Centre; Mr. David Brennan of International Air Transport Association (IATA); Mr. Bill Earle of National Information Services Corporation (NISC) and the Chemical Information System of NISC; EID technical information of The National Institute for Occupational Safety and Health (NIOSH); Dr. Ronald van der A of the Royal Netherlands Meteorological Institute (KNMI); Dr. Christopher Laursen of The University of Akron; Dr. Tatyana Poznyak of Instituto Politécnico Nacional (Mexico); Ms. Idit Booch of Mercury Scientific & Industrial Products Ltd.; Mr. Lawrence Hassner of Sigma-Aldrich Israel Ltd.; Ms. Kim Brucato of Sigma-Aldrich Corporation; Dr. Chester Duda of Bio-analytical Systems, Inc.; Dr. Virginia Gordon of SafTest, Inc.; Dr. Achim Leitzke of Macherey-Nagel GmbH & Co. KG; Dr. Tatsue Monji of Kamiya Biomedical Company and Dr. Lynsey Smyth of Radox Laboratories Ltd.



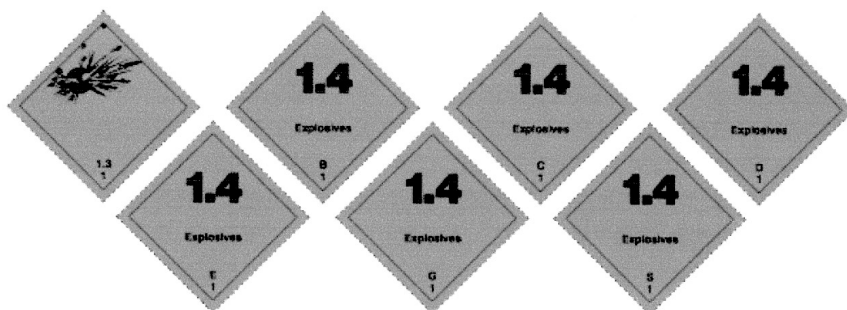
APPENDIX 1 (PLATE 1)

IATA/ICAO HAZARD AND HANDLING LABELS

Except for Radioactive and Handling Labels, text indicating the nature of risk on label is optional.

HAZARD LABELS

* Articles bearing the Explosive labels shown above and falling into Divisions 1.1, 1.2, 1.4F, 1.5 and 1.6 are normally forbidden.

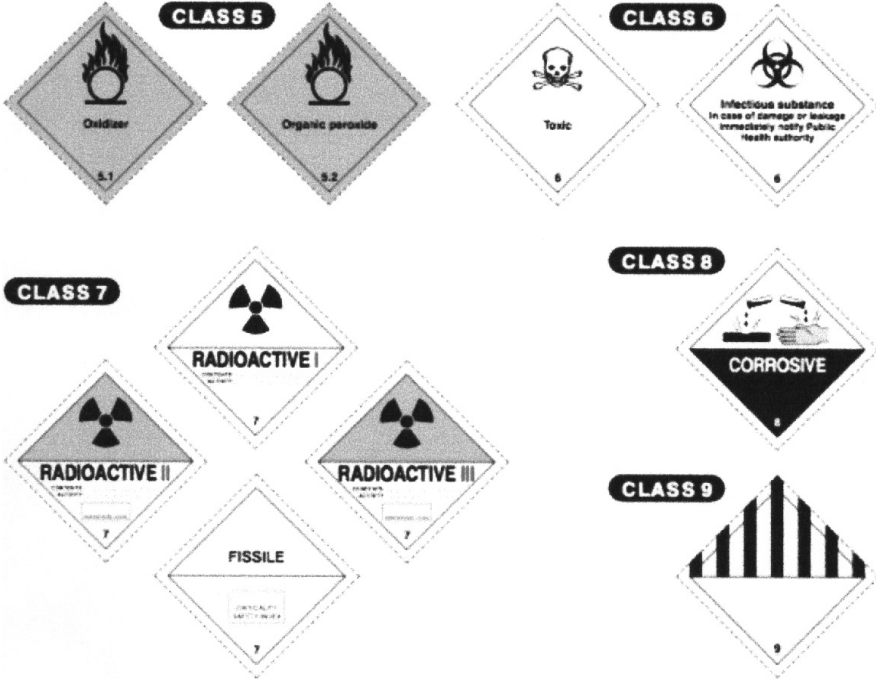


APPENDIX 2 (PLATE 2) Reproduced by permission of the International Air Transport Association (IATA)

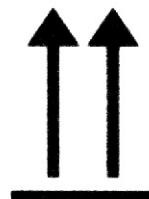
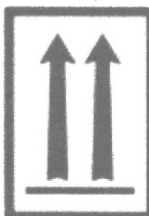
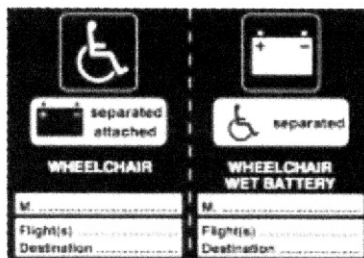
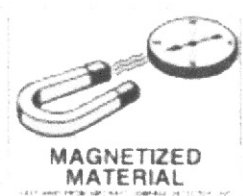
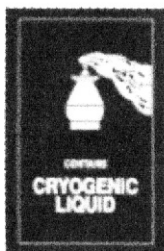
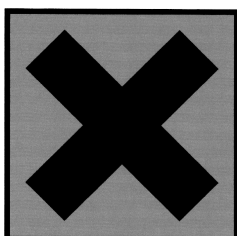
IATA/ICAO HAZARD AND HANDLING LABELS

Except for Radioactive and Handling Labels, text indicating the nature of risk on label is optional.

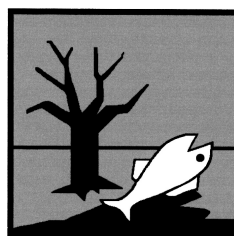
HAZARD LABELS



APPENDIX 2 (PLATE 2) (continued)





HANDLING LABELS**MORE HAZARD LABELS**

HARMFUL (Xn) or
IRRITANT (Xi)



ENVIRONMENTAL
HAZARD

APPENDIX 2 (PLATE 2) (continued)

PERACETIC ACID (stabilized)		1031 October 2000	
CAS No: 79-21-0 RTECS No: SD8750000 UN No: 3105 EC No: 607-094-00-8		Peroxyacetic acid Ethaneperoxyic acid Acetyl hydroperoxide $C_2H_3O_5$ / CH_3COOOH Molecular mass: 76.1	
TYPES OF HAZARD/ EXPOSURE	ACUTE HAZARDS/SYMPTOMS	PREVENTION	FIRST AID/FIRE FIGHTING
FIRE	Flammable. Explosive.	NO open flames. NO sparks, and NO smoking. NO contact with flammable substances. NO contact with hot surfaces.	Water spray.
EXPLOSION	Above 40.5°C explosive vapour/air mixtures may be formed.	Above 40.5°C use a closed system, ventilation, and explosion-proof electrical equipment. Do NOT expose to friction or shock.	In case of fire: keep drums, etc., cool by spraying with water. Combat fire from a sheltered position.
EXPOSURE		AVOID ALL CONTACT!	
Inhalation	Burning sensation. Cough. Laboured breathing. Shortness of breath. Sore throat. Symptoms may be delayed (see Notes).	Ventilation, local exhaust, or breathing protection.	Fresh air, rest. Half-upright position. Refer for medical attention. See Notes.
Skin	MAY BE ABSORBED! Redness. Pain. Blisters. Skin burns.	Protective gloves. Protective clothing.	First rinse with plenty of water, then remove contaminated clothes and rinse again. Refer for medical attention.
Eyes	Redness. Pain. Severe deep burns.	Face shield, or eye protection in combination with breathing protection.	First rinse with plenty of water for several minutes (remove contact lenses if easily possible), then take to a doctor.
Ingestion	Abdominal pain. Burning sensation. Shock or collapse.	Do not eat, drink, or smoke during work.	Rinse mouth. Do NOT induce vomiting. Refer for medical attention.
SPILLAGE DISPOSAL		PACKAGING & LABELLING	
Evacuate danger area! Consult an expert! Collect leaking liquid in covered plastic containers. Absorb remaining liquid in sand or inert absorbent and remove to safe place. Do NOT absorb in saw-dust or other combustible absorbents. Do NOT wash away into sewer. Do NOT absorb in saw-dust or other combustible absorbents. (Extra personal protection, chemical protection suit including self-contained breathing apparatus). Do NOT let this chemical enter the environment.		O Symbol C Symbol N Symbol R: 7-10-20/21/22-35-50 S: (1/2-)/3/7-14-36/37/39-45-61 Note: B, D UN Hazard Class: 5.2 UN Pack Group: II	
EMERGENCY RESPONSE		STORAGE	
Transport Emergency Card: TEC (R)-52G01b NFPA Code: H3; F2; R4; ox		Fireproof. Provision to contain effluent from fire extinguishing. Separated from combustible and reducing substances, incompatible materials. See Chemical Dangers. Cool. Store only if stabilized.	
   		Prepared in the context of cooperation between the International Programme on Chemical Safety and the European Commission © IPCS 2000 SEE IMPORTANT INFORMATION ON THE BACK.	

1031		PERACETIC ACID (stabilized)	
IMPORTANT DATA			
Physical State: Appearance COLOURLESS LIQUID, WITH CHARACTERISTIC ODOUR.		Routes of exposure The substance can be absorbed into the body by inhalation, through the skin and by ingestion.	
Chemical dangers May explosively decompose on shock, friction, or concussion. May explode on heating. The substance is a strong oxidant and reacts violently with combustible and reducing materials. The substance is a weak acid. Attacks many metals including aluminium.		Inhalation risk No indication can be given about the rate in which a harmful concentration in the air is reached on evaporation of this substance at 20°C.	
Occupational exposure limits TLV not established. MAK not established.		Effects of short-term exposure The substance is corrosive to the eyes, the skin and the respiratory tract. Corrosive on ingestion. Inhalation of may cause lung oedema (see Notes).	
PHYSICAL PROPERTIES			
Boiling point: 105°C Melting point: 0°C Relative density (water = 1): 1.2 Solubility in water: miscible Vapour pressure, kPa at 20°C: 2.6		Relative vapour density (air = 1): 2.6 Relative density of the vapour/air-mixture at 20°C (air = 1): 1.04 Flash point: 40.5°C o.c. Auto-ignition temperature: 200°C Explosive limits, vol% in air: see Notes	
ENVIRONMENTAL DATA			
The substance is very toxic to aquatic organisms.			
NOTES			
Explosive limits are unknown in literature, although the substance is combustible and has a flash point 61°C. Rinse contaminated clothes (fire hazard) with plenty of water. The symptoms of lung oedema often do not become manifest until a few hours have passed and they are aggravated by physical effort. Rest and medical observation is therefore essential. An added stabilizer or inhibitor can influence the toxicological properties of this substance, consult an expert.			
ADDITIONAL INFORMATION			
LEGAL NOTICE		Neither the EC nor the IPCS nor any person acting on behalf of the EC or the IPCS is responsible for the use which might be made of this information	
©IPCS 2000			

XIII. REFERENCES

1. W. G. Gunz and M. R. Hoffman, *Atmos. Environ.*, **24A**, 1601 (1990).
2. H. Sakugawa, I. R. Kaplan, W. Tsai and Y. Cohen, *Environ. Sci. Technol.*, **24**, 1452 (1990).
3. A. V. Jackson, *Crit. Rev. Environ. Sci. Technol.*, **29**, 175 (1999).
4. M. Lee, B. G. Heikes and D. W. O'Sullivan, *Atmos. Environ.*, **34**, 3475 (2000).
5. M. Lee, B. C. Noone, D. O'Sullivan and B. G. Heikes, *J. Atmos. Ocean. Technol.*, **12**, 1060 (1995).
6. C. de Serves and H. B. Ross, *Environ. Sci. Technol.*, **27**, 2712 (1993).
7. C. L. Deforest, R. J. Kieber and J. D. Willey, *Environ. Sci. Technol.*, **31**, 3068 (1997).
8. B. Bolarinwa and J. Weinstein-Lloyd, *Book of Abstracts, 216th ACS National Meeting, Boston, August 23–27*, American Chemical Society, Washington, D.C, 1998.
9. C. S. Christensen, S. Brødsgaard, P. Mortensen, K. Egmos and S. A. Linde, *J. Environ. Monit.*, **2**, 339 (2000).
10. C. Badol, A. Borbon, N. Locoge, T. Léonardis and J.-C. Galloo, *Anal. Bioanal. Chem.*, **378**, 1815 (2004).
11. H. J. Tobias, K. S. Ducherty, D. E. Beving, S. Chattopadhyay and P. J. Ziemann, *Int. Symp. Measurement of Toxic and Related Air Pollutants*, Sept. 12–14, 2000, Research Triangle Park, NC, USA.
12. E. Kishida, M. Oribe and S. Kojo, *J. Nutr. Sci. Vitaminol.*, **36**, 619 (1990).
13. X. Zhou and Y.-N. Lee, *J. Phys. Chem.*, **96**, 265 (1992).
14. J. Zheng, S. R. Springston and J. Weinstein-Lloyd, *Anal. Chem.*, **75**, 4696 (2003).
15. F. Slemr and H. G. Tremmel, *J. Atmos. Chem.*, **19**, 371 (1994).
16. F. Sauer, G. Schuster, C. Schäfer and G. K. Moorgat, *Geophys. Res. Lett.*, **23**, 2605 (1996).
17. F. Sauer, G. Schuster, C. Schäfer and G. K. Moorgat, *Geophys. Res. Lett.*, **24**, 827 (1997).
18. J. H. Lee, D. F. Leahy, I. N. Tang and L. Newman, *J. Geophys. Res.*, **98**, 2911 (1993).
19. T. J. Wallington, M. D. Hurley and W. F. Schneider, *Chem. Phys. Lett.*, **251**, 164 (1996).
20. D. Scheffler, I. Schaper, H. Willner, H.-G. Mack and H. Oberhammer, *Inorg. Chem.*, **36**, 339 (1997).
21. R. Kopitzky, M. Beuleke, G. Balzer and H. Willner, *Inorg. Chem.*, **36**, 1994 (1997).
22. R. Kopitzky, H. Willner, H.-G. Mack, A. Pfeiffer and H. Oberhammer, *Inorg. Chem.*, **37**, 6208 (1998).
23. G. A. Argüello, H. Willner and F. E. Malanca, *Inorg. Chem.*, **39**, 1195 (2000).
24. M. A. Burgos Paci, P. García, F. E. Malanca, G. A. Argüello and H. Willner, *Inorg. Chem.*, **42**, 2131 (2003).
25. S. Gäb, E. Hellpointner, W. V. Turner and F. Korte, *Nature*, **316**, 535 (1985).
26. C. N. Hewitt and G. L. Kok, *J. Atmos. Chem.*, **12**, 181 (1991).
27. M. Bell and H. Ellis, *Atmos. Environ.*, **35**, 1879 (2004).
28. W. D. Komhyr, *Ann. Geophys.*, **25**, 203 (1969).
29. M. Fujiwara, Y. Tomikawa, K. Kita, Y. Kondo, N. Komala, S. Saraspriya, T. Manik, A. Suripto, S. Kawakami, T. Ogawa, E. Kelana, B. Suhardi, S. W. B. Harijono, M. Kudsy, T. Sribimawati and M. D. Yamanaka, *Atmos. Environ.*, **37**, 353 (2003).
30. Z. Xiangdong, Z. Xiujia, T. Jie, Q. Yu and C. Chuenyu, *Atmos. Environ.*, **38**, 261 (2004).
31. R. J. van der A, A. J. M. Pijters, R. F. van Oss, P. J. M. Valks, J. H. G. M. van Geffen, H. M. Kelder and C. Zehner, *Near-real time delivery of GOME ozone profiles* (http://www.knmi.nl/gome_fd/doc/373vandera.pdf).
32. R. J. van der A, A. J. M. Pijters, R. F. van Oss and C. Zehner, *Int. J. Remote Sensing*, **24**, 4969 (2003).
33. A. W. Schmalwieser, G. Schaubberger and M. Janouch, *Agric. Forest. Meteorol.*, **120**, 9 (2003).
34. SEDAC, *Environmental Effects of Ozone Depletion 1998 Assessment* (<http://sedac.ciesin.org/ozone/docs/UNEP98/UNEP98p2.html>).
35. R. Jiménez, M. Taslakov, V. Simeonov, B. Calpini, F. Jeanneret, D. Hofstetter, M. Beck, J. Faist and H. van der Bergh, *Appl. Phys. B*, **78**, 249 (2004).
36. D. A. Rotman, C. S. Atherton, D. J. Bergmann, P. J. Cameron-Smith, C. C. Chuang, P. S. Connell, J. E. Dignon, A. Franz, K. E. Grant, D. E. Kinnison, C. R. Molenkamp, D. D. Proctor and J. R. Tannahill, *J. Geophys. Res. Atmos.*, **109**, 42 (2004).
37. S.-Y. Kim, J.-T. Lee, Y.-C. Hong, K.-J. Ahn and H. Kim, *Environ. Res.*, **94**, 113 (2004).
38. J. A. Leenheer, *Environ. Sci. Technol.*, **15**, 578 (1981).

39. D. Price, P. J. Worsfold and R. F. C. Mantoura, *Anal. Chim. Acta*, **298**, 121 (1994).
40. S. E. Stevens, Jr., C. O. P. Patterson and J. Myers, *J. Phycol.*, **9**, 427 (1973).
41. D. Price, R. F. C. Mantoura and P. J. Worsfold, *Anal. Chim. Acta*, **377**, 145 (1998).
42. Y. T. Didenko and S. P. Pugach, *J. Phys. Chem.*, **98**, 9742 (1994).
43. U. von Gunten, *Water Res.*, **37**, 1443 (2003).
44. U. von Gunten, *Water Res.*, **37**, 1469 (2003).
45. P. Dowidiet and C. von Sonntag, *Environ. Sci. Technol.*, **32**, 1112 (1998).
46. Fahmi, W. Nishijima and M. Okada, *J. Water Supply Res. Technol.-AQUA*, **52**, 291 (2003).
47. M. R. Straka, G. Gordon and G. E. Pacey, *Anal. Chem.*, **57**, 1799 (1985).
48. H.-J. Oh, W.-J. Kim, J.-S. Choi, C.-S. Gee, T.-M. Hwang, J.-G. Kang and J.-W. Kang, *Ozone-Sci. Eng.*, **25**, 383 (2003).
49. W.-J. Huang, L.-Y. Chen and H.-S. Peng, *Environ. Int.*, **29**, 1049 (2004).
50. T. I. Poznyak and E. V. Kiseleva, *Fresenius J. Anal. Chem.*, **354**, 233 (1996).
51. J. Lee, H. Park and J. Yoon, *Environ. Technol.*, **24**, 241 (2003).
52. M. F. Sevimli, H. Z. Sarikaya and M. S. Yazgan, *Ozone-Sci. Eng.*, **25**, 137 (2003).
53. H. Jung and H. Choi, *Environ. Eng. Sci.*, **20**, 289 (2003).
54. S. Nussbaum, J. Remund, B. Rihm, K. Miegli, J. Gurtz and J. Fuhrer, *Environ. Int.*, **29**, 385 (2003).
55. A. R. Butler and Y.-L. Wu, *Chem. Soc. Rev.*, 85 (1992).
56. L.-C. de Almeida Barbosa, D. Cutler, J. Mann and G. C. Kirby, *J. Chem. Soc., Perkin Trans. I*, 3251 (1992).
57. G. H. Posner, C. H. Oh, L. Gerena and W. K. Milhous, *J. Med. Chem.*, **35**, 2459 (1992).
58. J. L. Vennerstrom, H. N. Fu, W. Y. Ellis, A. L. Ager, Jr., J. K. Wood, S. L. Andersen, L. Gerena and W. K. Milhous, *J. Med. Chem.*, **35**, 3023 (1992).
59. W. Hofheinz, H. Burgin, E. Gocke, C. Jaquet, R. Masciadri, G. Schmid, H. Stohler and H. Urwyler, *Trop. Med. Parasitol.*, **45**, 261 (1994).
60. E. E. Korshin, R. Hoos, A. M. Szpilman, L. Konstantinovski, G. H. Posner and M. D. Bachi, *Tetrahedron*, **58**, 2449 (2002).
61. Y. Morimoto, T. Iwai and T. Kinoshita, *Tetrahedron Lett.*, **42**, 6307 (2001).
62. A. Fontana, M. Carmen González, M. Gavagnin, J. Templado and G. Cimino, *Tetrahedron Lett.*, **41**, 429 (2000).
63. M. Díaz, I. Lezcano, J. Moleiro and F. Hernández, *Ozone-Sci. Eng.*, **23**, 35 (2001).
64. B. Harrison and P. Crews, *J. Nat. Prod.*, **61**, 1033 (1998).
65. Randox, *Free Radicals*, Randox Laboratories Ltd., Crumlin, Co. Antrim, UK (<http://www.randox.com/freeradicals.asp>).
66. M.-V. Clément and S. Pervaiz, *Redox Rep.*, **6**, 211 (2001).
67. M. Zhou, Z. Diwu, N. Panchuk-Voloshina and R. P. Haugland, *Anal. Biochem.*, **253**, 162 (1997).
68. C. D. Georgiou and M. Sideri, *Mycologia*, **92**, 835 (2000).
69. M. Palma, D. DeLuca, S. Worgall and L. E. N. Quadri, *J. Bacteriol.*, **186**, 248 (2003).
70. J. Mostertz, C. Scharf, M. Hecher and G. Homuth, *Microbiology*, **150**, 497 (2004).
71. S. Vandenebeele, K. Van Der Kelen, J. Dat, I. Gadjev, T. Boonefaes, S. Morsa, P. Rottiers, L. Slooten, M. Van Montagu, M. Zabeau, D. Inzé and F. Van Breusegem, *Plant Biol.*, **100**, 16113 (2003).
72. K. H. Becker, K. J. Brockmann and J. Bechara, *Nature*, **346**, 256 (1990).
73. N. Kuge, M. Kohzuki and T. Sato, *Free Radical Res.*, **30**, 119 (1999).
74. L. H. Long and B. Halliwell, *Free Radical Res.*, **32**, 463 (2000).
75. R. C. Strange, C. Hiley, C. Roberts, P. W. Jones, J. Bell and R. Hume, *Free Radical Res. Commun.*, **7**, 105 (1989).
76. Z. Zhang, X. Y. Yang and D. M. Cohen, *Am. J. Physiol. Renal Physiol.*, **276**, F786 (1999).
77. D. Liu, J. Liu and J. Wen, *Free Radical Biol. Med.*, **27**, 478 (1999).
78. R. M. Mateos, A. M. León, L. M. Sandalio, M. Gómez, L. A. del Río and J. M. Palma, *J. Plant Physiol.*, **160**, 1507 (2003).
79. M. L. McCormick, J. P. Gaut, T.-S. Lin, B. E. Britigan, G. R. Buettner and J. W. Heinecke, *J. Biol. Chem.*, **273**, 32030 (1998).
80. P. Bilski, M. Y. Li, M. Ehrenshaft, M. E. Daub and C. F. Chignell, *Photochem. Photobiol.*, **71**, 129 (2000).

81. L. Iuliano, A. R. Colavita, C. Camastra, V. Bello, C. Quintarelli, M. Alessandrini, F. Piovella and F. Violi, *Brit. J. Pharmacol.*, **119**, 1438 (1996).
82. M. R. Mehrabi, P. Haslmayer, S. Humpeler, G. Strauss-Blasche, W. Marktl, F. Tamaddon, N. Serbecic, G. Wieselthaler, T. Thalhammer, H. D. Glogar and C. Ekmekcioglu, *Eur. J. Heart Failure*, **5**, 733 (2003).
83. M. M. Tarpey and I. Fridovich, *Circ. Res.*, **89**, 224 (2001).
84. S. Goldstein and G. Czapski, *Free Radical Biol. Med.*, **19**, 505 (1995).
85. N. Nalwaya and W. M. Deen, *Chem. Res. Toxicol.*, **16**, 920 (2003).
86. J. S. Beckman and W. H. Koppenol, *Am. J. Physiol.*, **271**, C1424 (1996).
87. R. S. Ronson, M. Nakamura and J. Vinten-Johansen, *Cardiovasc. Res.*, **44**, 47 (1999).
88. M.-C.-i. Lee, H. Shoji, T. Komatsu, F. Yoshino, Y. Ohmori and J. L. Zweier, *Redox Rep.*, **7**, 271 (2002).
89. N. E. Marks, A. S. Grandison and M. J. Lewis, *Int. J. Dairy Technol.*, **54**, 20 (2001).
90. E. N. Frankel, *J. Am. Oil Chem. Soc.*, **61**, 1908 (1984).
91. L. J. Roberts II and J. P. Fessel, *Chem. Phys. Lipids*, **128**, 173 (2004).
92. M. Hamberg, *Anal. Biochem.*, **43**, 515 (1971).
93. T. G. Toschi, F. Stante, P. Capella and G. Lercker, *HRC-J. High Resolut. Chromatogr.*, **18**, 764 (1995).
94. M. Yasuda and S. Narita, *J. Chromatogr. B*, **693**, 211 (1997)
95. J. Nourooz-Zadeh, J. Tajaddini Sarmadi, K. L. E. Ling and S. P. Wolff, *Biochem. J.*, **313**, 781 (1996).
96. H. Yin, C. M. Havrilla, J. D. Morrow and N. A. Porter, *J. Am. Chem. Soc.*, **124**, 7745 (2002).
97. H. Yin, J. D. Morrow and N. A. Porter, *J. Biol. Chem.*, **279**, 3766 (2004).
98. S. Yamasaki, N. Ozawa, A. Hiratsuka and T. Watanabe, *Free Radical Biol. Med.*, **27**, 110 (1999).
99. A. Hemmingsen, J. T. Allen, S. Zhang, J. Mortensen and M. A. Spiteri, *Free Radical Res.*, **31**, 437 (1999).
100. H. Taguchi, Y. Ogura, T. Takanashi, M. Hashizoe and Y. Honda, *Invest. Ophthalmol. Vis. Sci.*, **39**, 358 (1998).
101. K. A. McKinney, S. E. M. Lewis and W. Thompson, *Arch. Androl.*, **36**, 119 (1996).
102. J. Twigg, N. Fulton, E. Gomez, D. S. Irvine and R. J. Aitken, *Human Reprod.*, **13**, 1429 (1998).
103. A. Verma and K. C. Kanwar, *Andrologia*, **30**, 325 (1998).
104. D. Steinberg, S. Parhsarathy, T. E. Carew, J. C. Khoo and J. L. Witztum, *N. Engl. J. Med.*, **320**, 915 (1989).
105. L. Chancharme, F. Nigon, S. Zarev, A. Mallet and E. Bruckert, *J. Lipid Res.*, **43**, 453 (2002).
106. H.-C. Hsu, M.-F. Chen, C.-M. Lee and Y.-T. Lee, *Clin. Sci.*, **94**, 29 (1998).
107. Y. S. Jang, O. Y. Kim, H. J. Ryu, J. Y. Kim, S. H. Song, J. M. Ordovas and J. H. Lee, *J. Lipid Res.*, **44**, 2356 (2003).
108. H. Yoshino, N. Hattori, T. Urabe, K. Uchida, M. Tanaka and Y. Mizuno, *Brain Res.*, **767**, 81 (1997).
109. B. D. Watson, *Cell. Mol. Neurobiol.*, **18**, 581 (1998).
110. A. A. Shvedova, J. Y. Tyurina, K. Kawai, V. A. Tyurin, C. Kommineni, V. Castranova, J. P. Fabisiak and V. E. Kagan, *J. Invest. Dermatol.*, **118**, 1008 (2002).
111. J. Y. Tyurina, K. T. Kawai, A. Vladimirov, S.-X. Liu, V. E. Kagan and J. P. Fabisiak, *Antioxidants & Redox Signaling*, **6**, 209 (2004).
112. S. O. Awe and A. S. O. Adeagbo, *Life Sci.*, **71**, 1255 (2002).
113. I. Pinchuk, E. Schnitzer and D. Lichtenberg, *Biochim. Biophys. Acta*, **1389**, 155 (1998).
114. M. L. Selley, *J. Chromatogr. B*, **691**, 263 (1997).
115. V. Paradis, M. Kollinger, M. Fabre, A. Holstege, T. Poynard and P. Bedossa, *Hepatology*, **26**, 135 (1997).
116. V. Paradis, P. Mathurin, M. Kollinge, F. Imbert-Bismuth, F. Charlotte, A. Piton, P. Opolon, A. Holstege, T. Poynard and P. Bedossa, *J. Clin. Pathol.*, **50**, 401 (1997).
117. I. S. Young and E. R. Trimble, *Ann. Clin. Biochem.*, **28**, 504 (1991).
118. J. R. Lawrence, G. R. Campbell, H. Barrington, E. A. Malcolm, G. Brennan, D. H. Wiles and J. R. Paterson, *Ann. Clin. Biochem.*, **35**, 387 (1998).
119. T. F. Slater, *Biochem. J.*, **106**, 155 (1968).
120. T. F. Slater and B. C. Sawyer, *Biochem. J.*, **111**, 317 (1969).

121. T. F. Slater and B. C. Sawyer, *Biochem. J.*, **123**, 805 (1971).
122. T. F. Slater and B. C. Sawyer, *Biochem. J.*, **123**, 815 (1971).
123. M. Comporti, *Free Radical Res.*, **28**, 623 (1998).
124. L. L. De Zwart, J. Venhorst, M. Groot, J. N. M. Commandeur, R. C. A. Hermanns, J. H. M. Meerman, B. L. M. Van Baar and N. P. E. Vermeulen, *J. Chromatogr. B*, **694**, 277 (1997).
125. R. A. Riemersma, *Eur. J. Lipid Sci. Technol.*, **104**, 419 (2002).
126. R. Wilson, C. E. Fernie, C. M. Scrimgeour, K. Lyall, L. Smyth and R. A. Riemersma, *Eur. J. Clin. Invest.*, **32**, 79 (2002).
127. J. Linseisen and G. Wolfram, *Ann. Nutr. Metab.*, **42**, 221 (1998).
128. F. Ursini, A. Zamburlini, G. Cazzolato, M. Maiorina, G. B. Bon and A. Sevanian, *Free Radical Biol. Med.*, **25**, 250 (1998).
129. T. Y. Aw, *Free Radical Res.*, **28**, 637 (1998).
130. A. Kanazawa, T. Sawa, T. Akaike and H. Maeda, *Eur. J. Lipid Sci. Technol.*, **104**, 439 (2002).
131. K. Robards, A. F. Kerr and E. Patsalides, *Analyst*, 213 (1988).
132. G. C. Yang, *Trends Food Sci. Technol.*, **3**, 15 (1992).
133. J. N. Coupland and D. J. McClements, *Trends Food Sci. Technol.*, **7**, 83 (1996).
134. M. S. Bloomfield, *Analyst*, **124**, 1865 (1999).
135. L. Barrier, G. Page, B. Fauconneau and F. Juin, *Free Radical Res.*, **28**, 411 (1998).
136. J. Diaz, E. Serrano, F. Acosta and L. F. Carbonell, *Clin. Chem.*, **44**, 2215 (1998).
137. S. Steenken, *Chem. Rev.*, **89**, 503 (1989).
138. M. C. Schweibert and M. Daniels, *Int. J. Radiat. Phys. Chem.*, **3**, 353 (1971).
139. H. B. Michaels and J. W. Hunt, *Anal. Biochem.*, **87**, 135 (1978).
140. J. R. Wagner, J. E. van Lier, M. Berger and J. Cadet, *J. Am. Chem. Soc.*, **116**, 2235 (1994).
141. D. D. M. Wayner, G. W. Burton, K. U. Ingold, L. R. C. Barclay and S. J. Locke, *Biochim. Biophys. Acta.*, **924**, 408 (1987).
142. S. Fu, M. X. Fu, J. W. Baynes, S. R. Thorpe and R. T. Dean, *Biochem J.*, **330** (Part 1), 233 (1998).
143. S. Fu, L. A. Hick, M. M. Sheil and R. T. Dean, *Free Radical Biol. Med.*, **19**, 281 (1995).
144. S. Robinson, R. Bevan, J. Lunec and H. Griffiths, *FEBS Lett.*, **430**, 297 (1998).
145. R. Yamauchi, H. Mizuno and K. Kato, *Biosci. Biotechnol. Biochem.*, **62**, 1293 (1998).
146. I. G. Gazarian, L. M. Lagrimini, F. A. Mellon, M. J. Naldrett, G. A. Ashby and R. N. F. Thorneley, *Biochem. J.*, **333**, 223 (1998).
147. H. B. Oral, A. J. T. George and D. O. Haskard, *Endothelium*, **6**, 143 (1998).
148. G. J. S. Jenkins, C. Morgan, J. N. Baxter, E. M. Parry and J. M. Parry, *Mutat. Res. Genet. Toxicol. Environ. Mutagen.*, **498**, 135 (2001).
149. J. Cadet, T. Douki and J.-L. Ravanat, *Oxidative Stress and Disease*, **10**, 145 (2004); *Chem. Abstr.*, **140**, 336635 (2004).
150. P. Powis, *Free Radical Biol. Med.*, **6**, 63 (1989).
151. R. Aldelman, R. L. Saul and B. N. Ames, *Proc. Natl. Acad. Sci. U.S.A.*, **85**, 2706 (1988).
152. R. Flyunt, J. A. Theruvathu, A. Leitzke and C. von Sonntag, *J. Chem. Soc., Perkin Trans. 2*, 1572 (2002).
153. K. M. Kim, Y. S. Kwon, J. J. Lee, M. Y. Eun and J. K. Sohn, *Mol. Cells*, **17**, 151 (2004).
154. Z.-F. Tao, X. Qian and D. Wei, *Dyes Pigments*, **31**, 245 (1996).
155. Z.-F. Tao and X. Qian, *Dyes Pigments*, **43**, 139 (1999).
156. J. D. Bond, C. D. Froese, S. Ghosh, E. B. Dumbroff and J. E. Thompson, *J. Plant Physiol.*, **151**, 541 (1997).
157. G. W. Mushrush, E. J. Beal, D. R. Hardy and S. M. Rosenberg, *Pet. Sci. Technol.*, **15**, 699 (1997).
158. P.-Y. Yeh, C.-M. Shu and Y.-S. Duh, *Ind. Eng. Chem. Res.*, **42**, 1 (2003).
159. NFPA, *432 Code for the Storage of Organic Peroxide Formulations*, National Fire Protection Association, Quincy, MD, USA, 2002 (<http://www.nfpa.org/catalog/home/index.asp>).
160. IATA, *Dangerous Goods Regulations*, 45th edn., International Air Transport Association, Geneva Airport, Switzerland, 2004.
161. UNECE, OTIF, *International Carriage of Dangerous Goods by Rail ("RID")* (http://www.otif.org/html/e/orga_CExp_RID.php, http://www.otif.org/html/e/pres_info_generales.php).
162. UNECE, *International Carriage of Dangerous Goods by Road ("ADR")* (http://www.unece.org/trans/danger/publi/adr/adr_e.html).

163. IMO, *International Maritime Transportation of Dangerous Goods, IMDG-Code* (<http://www.imo.org/home.asp>, <http://www.hazmateam.com/transportation/IMDG.html>, <http://www.epa.gov/fedrgrstr/EPA-IMPACT/2003/January/Day-08/i325.htm>).
164. S. Baj, A. Chrobok, M. Cieřlik and T. Krawczyk, *Anal. Bioanal. Chem.*, **375**, 327 (2003).
165. CMR, *Phenol*, The Innovation Group, Morristown, NJ, USA (<http://www.the-innovation-group.com/ChemProfiles/Phenol.htm>).
166. EPA, *Public Access to Screening Information Data Sets (SIDS)* (<http://www.epa.gov/opptintr/sids/overview.htm>, <http://www.epa.gov/tri/tridata/tri96/pdr/appc.pdf>).
167. EPA, *High Production Volume (HPV) Challenge Program* (<http://www.epa.gov/chemrtk/volchall.htm>).
168. C. J. Pouchert, *The Aldrich Library of FT-IR Spectra*, 2nd edn., Aldrich Chemical, Milwaukee, WI, 1997.
169. C. J. Pouchert, *The Aldrich Library of NMR Spectra*, 2nd edn., Aldrich Chemical, Milwaukee, WI, 1983.
170. R. E. Lenga (Ed.), *The Sigma-Aldrich Data of Chemical Safety Data*, 2nd edn., Sigma-Aldrich, Milwaukee, WI, 1988.
171. R. E. Lenga and K. L. Votoupal (Eds.), *The Sigma-Aldrich Library of Regulatory and Safety Data*, Aldrich Chemical, Milwaukee, WI, 1992.
172. NIOSH, *Registry of Toxic Effects of Chemical Substances (RTECS)* (<http://www.cdc.gov/niosh/rtecs.html>, <http://ccinfoweb.ccohs.ca/rtecs/search.html>).
173. L. F. Fieser, M. Fieser and T.-L. Ho, *Reagents for Organic Synthesis*, Vols. 1–20, Wiley, New York, 1967–2000.
174. J. E. F. Reynolds, *Martindale: The Extra Pharmacopoeia*, 31st edn., Pharmaceutical Press, London, 1996.
175. CFR, *Forbidden Materials listed in the 49 CFR 172.101 Hazardous Materials Table* (http://hazmat.dot.gov/cfr_forbidden.pdf).
176. EPA, *The TSCATS database and the Toxic Substances Control Act* (http://www.nisc.com/cis/TSCATS_Analysis_March_2004.pdf).
177. Y. Iseki, M. Kudo, A. Mori and S. Inoue, *J. Org. Chem.*, **57**, 6329 (1992).
178. A. Debal, G. Rafaralahitsimba and E. Ucciani, *Fett Wiss. Technol.*, **95**, 236 (1993).
179. M. E. Cassinelli and P. F. O'Connor (Eds.), *NIOSH Manual of Analytical Methods*, 4th edn., DHHS (NIOSH), Publication 94–113, Washington, D.C., U. S. A., 1994 (<http://www.cdc.gov/niosh/nmam/method-h.html>).
180. C. J. Easton, S. G. Love and P. Wang, *J. Chem. Soc., Perkin Trans. 1*, 277 (1990).
181. R. Bock, *Aufschlussmethoden der anorganischen und organischen Chemie*, Verlag Chemie, Weinheim, Germany, 1972.
182. Z. Sulcek and P. Povondra, *Methods of Decomposition in Inorganic Analysis*, CRC Press, Boca Raton, FL, 1989.
183. C. Dodeigne, L. Thunus and R. Lejeune, *Talanta*, **51**, 415 (2000).
184. V. L. Antonovskii, *Kinet. Catal.*, **44**, 54 (2003).
185. S. Affolter, *Kautschuk Gummi Kunstst.*, **50**, 216 (1997).
186. T. Fargere, M. Abdennadher, M. Delmas and B. Boutevin, *Eur. Polym. J.*, **31**, 489 (1995).
187. S. Affolter, *Macromol. Symp.*, **165**, 133 (2001).
188. J. Hong, J. Maguhn, D. Freitag and A. Kettrup, *Fresenius J. Anal. Chem.*, **371**, 961 (2001).
189. J. Mallécol, L. Gonon, S. Commereuc and V. Verney, *Prog. Org. Coatings*, **41**, 171 (2001).
190. R. W. Tock, *Proc. 4th Ann. Green Chem. & Eng. Conf. Sustainable Technol.*, June 27–29 Jun, 2000, Washington, DC, USA (http://www.epa.gov/greenchemistry/docs/gc_conference_2000_proceedings.pdf).
191. R. P. Wool, S. N. Khot, J. J. LaScala, G. I. Williams, S. P. Bunker, W. Thielemans, J. Lu and S. S. Morye, in Reference 190.
192. A. I. Saiz, G. D. Manrique and R. Fritz, *J. Agric. Food Chem.*, **49**, 98 (2001).
193. M. Wada, K. Inoue, A. Ihara, N. Kishikawa, K. Nakashima and N. Kuroda, *J. Chromatogr. A*, **987**, 189 (2003).
194. *Standard Methods of Analysis in Food Safety Regulations. Analytical Methods for Food Additives in Food*, Ministry of Health and Welfare, Nihon Shokuin Eisei Kyokai, Tokyo, Japan, 1989, pp. 68–71.
195. S.-C. Su, C.-H. Liu, H.-C. Chen, P.-C. Chang and S.-S. Chou, *J. Food Drug Anal.*, **7**, 131 (1999).

196. C. M. G. C. Renard, Y. Rohou, C. Hubert, G. Della Valle, J.-F. Thibault and J.-P. Savina, *Lebensm. Wiss. Technol.*, **30**, 398 (1996).
197. A. Schnell, M. J. Sabourin, S. Krog and M. Garvie, *Water Sci. Technol.*, **35**, 7 (1997).
198. O. A. Hyökyvirta, *Mater. Corrosion*, **48**, 376 (1997).
199. H. G. Hauthal, H. Schmidt, H. J. Scholz, J. Hofmann and W. Pritzkow, *Tenside Surf. Deterg.*, **27**, 35 (1990).
200. M. M. Sain, C. Daneault and M. Parenteau, *Can. J. Chem. Eng.*, **75**, 62 (1997).
201. R. C. Sun and J. Tomkinson, *Eur. Polym. J.*, **39**, 751 (2003).
202. Borax, *Bibliography* (<http://www.borax.com/detergents/bibliography.html>).
203. Borax, *Borax Detergent Book* (<http://www.borax.com/detergents/bleaching.html>).
204. A. Yarnell, *Chem. Eng. News*, **81** [6], 29 (2003).
205. U. Oltu and S. Gurgan, *J. Oral Rehabil.*, **27**, 332 (2000).
206. W. D. Julich, R. Ohme, N. Alhitari, V. Adrian, T. von Woedtke and A. Kramer, *Pharmazie*, **54**, 8 (1999).
207. H.-H. Rüttinger and A. Radschuweit, *J. Chromatogr. A*, **868**, 127 (2000).
208. D. Sužnjević, S. Blagojević, D. Vučelić and P. Zuman, *Electroanalysis*, **9**, 861 (1997).
209. H. Matschiner and W. Thiele, *Proc. BMBF Conf. Recycling of Pickling Baths*, UTECH, Berlin, 1998.
210. G. Setiowaty, Y. B. Che Man, S. Jinap and M. H. Moh, *Phytochem. Anal.*, **11**, 74 (2000).
211. M. Uchida and M. Ono, *J. Am. Soc. Brew. Chem.*, **57**, 145 (1999).
212. AOAC, *Official Methods of Analysis*, 15th edn., Association of Official Analytical Chemists, Arlington, VA, USA, 1990, Section 965.33.
213. IDF, *International IDF Standards*, International Dairy Federation, Brussels, 1991, Section 74A.
214. S. Chmela, G. Teissèdre and J. Lacoste, *J. Polym. Sci., Part A*, **33**, 743 (1995).
215. L. W. Jelinski, J. J. Dumais, J. P. Luongo and A. L. Cholli, *Macromolecules*, **17**, 1650 (1984).
216. R. W. Tock, Q. Arefeen and J. K. Sanders, *World Refin.*, **9**[2], 53 (1999).
217. J. K. Sanders and R. W. Tock, *PCT Int. Appl.*, 9921941 A1 19990506 (1999); *Chem. Abstr.*, **130**, 314244 (1999).
218. A. L. Perkel and S. G. Voronina, *J. Anal. Chem.*, **53**, 299 (1998).
219. J. Zabicky, in *The Chemistry of Phenols*, Chap. 13 (Ed. Z. Rappoport), Wiley, Chichester, 2003.
220. E. K. Paleologos, D. L. Giokas, S. M. Tzouwara-Karayanni and M. I. Karayannis, *Anal. Chem.*, **74**, 100 (2002).
221. K. Héberger, A. Keszler and M. Gude, *Lipids*, **34**, 83 (1999).
222. W. Windig, J. L. Lippert, M. J. Robbins, K. R. Kresinske and J. P. Twist, *Chemometrics Intel. Lab. Syst.*, **9**, 7 (1990).
223. W. Windig and J. Guilment, *Anal. Chem.*, **63**, 1425 (1991).
224. W. Windig, *Chemometrics Intel. Lab. Syst.*, **16**, 1 (1992).
225. W. Windig and S. Markel, *J. Mol. Struct.*, **292**, 161 (1993).
226. J. Guilment, S. Markel and W. Windig, *Appl. Spectrosc.*, **48**, 320 (1994).
227. V. Vacque, N. Dupuy, B. Sombret, J. P. Huvenne and P. Legrand, *Appl. Spectrosc.*, **51**, 407 (1997).
228. W. A. Alves, M. A. de Almeida Azzellini, R. E. Bruns and A. M. da Costa Ferreira, *Int. J. Chem. Kinet.*, **33**, 472 (2001).
229. A. Grau, R. Codony, M. Rafecas, A. C. Barroeta and F. Guardiola, *J. Agric. Food Chem.*, **48**, 4136 (2000).
230. Y.-A. Woo, H.-R. Lim, H.-J. Kim and H. Chung, *J. Pharm. Biomed. Anal.*, **33**, 1049 (2003).
231. G. Yildiz, R. L. Wehling and S. L. Cuppett, *J. Am. Oil Chem. Soc.*, **78**, 496 (2001).
232. M. P. Fuller, G. L. Ritter and C. S. Drapper, *Appl. Spectrosc.*, **42**, 217 (1988).
233. K. Ma, F. R. van de Voort, A. A. Ismail and J. Sedman, *J. Am. Oil Chem. Soc.*, **75**, 1095 (1998).
234. M. H. Moh, Y. B. Che Man, F. R. van de Voort and W. J. W. Abdullah, *J. Am. Oil Chem. Soc.*, **76**, 19 (1999).
235. H. Li, F. R. van de Voort, A. A. Ismail and R. Cox, *J. Am. Oil Chem. Soc.*, **77**, 137 (2000).
236. H. Zhou, M. Liu, J. Zhang and X. Zhang, *J. Soc. Leather Technol. Chem.*, **86**, 153 (2002).
237. T. J. Wang, K. S. Lam, C. W. Tsang and S. C. Kot, *Adv. Atmos. Sci.*, **21**, 141 (2004).
238. T. Taniai, A. Sakuragawa and T. Okutani, *Anal. Sci.*, **15**, 1077 (1999).

239. D. Harms, R. Than and B. Krebs, *Fresenius J. Anal. Chem.*, **364**, 184 (1999).
240. EURACHEM, *EURACHEM-CITAC Guide. The Fitness for Purpose of Analytical Methods: A Laboratory Guide to Method Validation and Related Topics*, EURACHEM Working Group, Teddington, U. K., 1998 (<http://www.eurachem.ul.pt/index.htm>).
241. EURACHEM, *EURACHEM- CITAC Guide. Quantifying uncertainty in analytical measurement*, 2nd edn., EURACHEM Working Group, Teddington, UK, 2000 (<http://www.measurementuncertainty.org>)
242. I. Kuselman and F. Sherman, *Accred. Qual. Assur.*, **4**, 124 (1999).
243. S. Oszwałdowski, R. Lipka and M. Jarosz, *Anal. Chim. Acta*, **421**, 35 (2000).
244. R. Flyunt, A. Leitzke, G. Mark, E. Mvula, E. Reisz, R. Schick and C. von Sonntag, *J. Phys. Chem. B*, **107**, 7242 (2003).
245. F. J. Welcher (Ed.), *Standard Methods of Chemical Analysis*, Vol. 2, part B, 6th edn., Van Nostrand Reinhold, New York, 1983, p. 1328.
246. C. T. Kingzett, *J. Chem. Soc.*, **37**, 792 (1880).
247. R. H. Smith and J. Kilford, *Int. J. Chem. Kinet.*, **8**, 1 (1976).
248. D. A. Jaworske and G. R. Helz, *J. Environ. Anal. Chem.*, **19**, 189 (1985).
249. R. J. Kieber and G. R. Helz, *Anal. Chem.*, **58**, 2312 (1986).
250. M. Hicks and J. M. Gebicki, *Anal. Biochem.*, **99**, 249 (1979).
251. X.-S. Chai, Q. X. Hou, Q. Luo and J. Y. Zhu, *Anal. Chim. Acta*, **507**, 281 (2004).
252. E. P. Gere, B. Bérczi, P. Simándi, G. Wittmann and A. Dombi, *Int. J. Environ. Anal. Chem.*, **82**, 443 (2002).
253. K. Yamada, S. Matsutani, Y. Horiguchi and T. Hobo, *Bunseki Kagaku*, **49**, 587 (2000); *Chem. Abstr.*, **133**, 316923 (2000).
254. F. D. Snell and C. T. Snell, *Colorimetric Methods of Analysis*, 3rd edn., Van Nostrand, New York, 1949, vol. 2, ch. 67.
255. K. G. McGruther, R. Smit, T. Delagoutte and I. D. Suckling, *Holzforschung*, **52**, 640 (1998).
256. Z.-Y. Jiang, A. C. S. Woollard and S. P. Wolff, *FEBS Lett.*, **268**, 69 (1990).
257. Y. Jiang, A. C. S. Woollard and S. P. Wolff, *Lipids*, **26**, 853 (1991).
258. L. H. Long, P. J. Evans and B. Halliwell, *Biochem. Biophys. Res. Commun.*, **262**, 605 (1999).
259. Z.-X. Guo, H.-X. Shen and L. Li, *Mikrochim. Acta*, **131**, 171 (1999)
260. J. W. Frew, P. Jones and G. Scholes, *Anal. Chim. Acta*, **155**, 139 (1983).
261. H. A. Mottola, B. E. Simpson and G. Gorin, *Anal. Chem.*, **42**, 410 (1970).
262. L.-S. Zhang and G. T. F. Wong, *Talanta*, **41**, 2137 (1994).
263. A. Lobnik and M. Čajlaković, *Sens. Actuators B*, **74**, 194 (2001).
264. N. Maeuchiara, S. Nakano and T. Kawashima, *Anal. Sci.*, **17**, 255 (2001).
265. Y. Huang, R. Cai, L. Mao, Z. Liu and H. Huang, *Anal. Sci.*, **15**, 889 (1999).
266. J. Odo, N. Kawahara, Y. Inomata, A. Inoue, H. Takeya, S. Miyanari and H. Kumagai, *Anal. Sci.*, **16**, 963 (2000).
267. J. J. Karkalas, *J. Sci. Food Agric.*, **36**, 1016 (1985) (<http://www.dps.ufl.edu/hall/NDESCCHPH.pdf>).
268. X.-M. Huang, M. Zhu, L.-Y. Mao and H.-X. Shen, *Anal. Sci.*, **13**, 145 (1997).
269. *Glucose Test*. Faculty of Medicine, Charles University, Praha, Czech Republic (<http://www.lf3.cuni.cz/ustavy/chemie/eng/first/l/s/a4.doc>).
270. P. Trinder, *Ann. Clin. Biochem.*, **6**, 24 (1969).
271. E. R. Kiranas, M. I. Karayannis and S. M. Tzouwara-Karayanni, *Talanta*, **45**, 1015 (1998).
272. Macherey-Nagel, *NANOCOLOR[®] peroxide 2*, Macherey-Nagel GmbH & Co. KG, Düren, Germany (<https://www.mn-net.com/web/MN-WEB-Testenkatalog.nsf/Web/FramesE?Open>).
273. Kamiya Biomedical Co., Seattle, WA, USA (<http://www.kamiyabiomedical.com/04LifeScienceResearchProducts/03Assaykits/043Home.htm>).
274. Merck, *Food & Environmental Analysis Catalogue*, Merck KGaA, Darmstadt, Germany (<http://photometry.merck.de/servlet/PB/menu/1292110/index.html>).
275. OXIS, *Quantitative Hydrogen Peroxide Assay*, OXIS International Inc., Portland, OR, USA (<http://www.oxisresearch.com/products/assays/21024/21024.shtml>).
276. OXIS, *Colorimetric, Quantitative Assay for Lipid Hydroperoxides*, OXIS International Inc., Portland, OR, USA (<http://www.oxisresearch.com/products/products.shtml>).
277. SafTest, *Rapid Standardized Testing for the Food Industry*, Safety Associates, Inc., Temple, AZ, USA (<http://www.safetest.com/index.html>).

278. NHANES, *Uric Acid in Refrigerated Serum—NHANES 2001–2002*, Collaborative Laboratory Services, L.L.C. (www.cdc.gov/nchs/data/nhanes/nhanes_01_02/l40_b_met_uric_acid.pdf).
279. Catachem, *Uric acid*, Catachem, Inc., Bridgeport, CT, USA (http://www.catacheminc.com/index_files/page0043.htm).
280. Cima Scientific, *Uric Acid (Liquid/Uricase) Procedure*, Cima Scientific, Dallas, TX, USA (www.cimascientific.com/4260.htm).
281. TECO, *Clinical Chemistry Reagents—Uric acid*, TECO Diagnostics, Anaheim, CA, USA (<http://www.tecodiag.com/Portal/DesktopDefault.aspx?tabindex=0&tabid=37>).
282. Prestige, *Glucose test strips*, My Pharmacy, Exeter, UK (http://www.mypharmacy.co.uk/health_products/products/p/prestige_smart_system/prestige_smart_system.htm), (<http://www.walgreens.com/store/product.jhtml?CATID=100133&id=prod18882>).
283. J. J. Karkalas, *J. Sci. Food Agric.*, **36**, 1016 (1985) (<http://www.dps.ufl.edu/hall/NDSCCHPH.pdf>).
284. Megazyme, *Glucose assay procedure*, Megazyme International Ireland Ltd., Bray, Wicklow, Ireland (http://www.megazyme.com/p_range2.asp?Submit.x=52&Submit.y=12&search=glucose#tag35).
285. Megazyme, *Starch Damage*, Megazyme International Ireland Ltd., Bray, Wicklow, Ireland (http://www.megazyme.com/p_range2.asp?Submit.x=52&Submit.y=12&search=starch+damage).
286. Macherey-Nagel, *Glucose test Glycaemie V* (<https://www.mn-net.com/web/MN-WEB-Meditestkatalog.nsf/Web/FramesE?Open&showpage=CWIK-4PLJR9>).
287. Macherey-Nagel, *Medi-Test Glucose PN* (<https://www.mn-net.com/web/MN-WEB-Meditestkatalog.nsf/Web/FramesE?Open>).
288. Trinity Biotech, *Lactate reagent*, Trinity Biotech Plc, Bray, Wicklow, Ireland (http://www.trinitybiotech.com/EN/index2.asp?pg=pro_dtls.asp%3Fid%3D815).
289. TECO Diagnostics USA, *Clinical Chemistry Reagents—Triglyceride-GPO reagent set*, TECO Diagnostics, Anaheim, CA, USA (<http://www.tecodiag.com/Portal/DesktopDefault.aspx?tabindex=0&tabid=37>).
290. Catachem, *Triglycerides*, Catachem, Inc., Bridgeport, CT, USA (http://www.catacheminc.com/index_files/page0040.htm).
291. Trinity Biotech, *Oxalate Kit*, Trinity Biotech Plc, Bray, Wicklow, Ireland (http://www.trinitybiotech.com/EN/index2.asp?pg=pro_dtls.asp%3Fid%3D815).
292. OXIS, *Spectrophotometric Assay for Malondialdehyde*, OXIS International Inc., Portland, OR, USA (<http://www.oxisresearch.com/products/assays/21044/21044.shtml>).
293. F. Tatzber, U. Resch and H. Sinzinger, *Shock*, **12**, 15 (1999).
294. F. A. El-Essi, A. Z. Abu Zuhri, S. I. Al-Khalil and M. S. Abdel-Latif, *Talanta*, **44**, 2051 (1997).
295. K. Zhang, L. Mao and R. Cai, *Talanta*, **51**, 179 (2000).
296. T. T. Ngo and H. M. Lenhoff, *Anal. Biochem.*, **105**, 389 (1980).
297. S. Marklund, *Acta Chem. Scand.*, **25**, 3517 (1971).
298. P. Goodall, *J. Radioanal. Nucl. Chem.*, **240**, 5 (1999).
299. N. E. Barrett, A. S. Grandison and M. J. Lewis, *J. Dairy Res.*, **66**, 73 (1999).
300. M. Farooqi, P. Sosniza, M. Saleemuddin, R. Ulber and T. Scheper, *Appl. Microbiol. Biotechnol.*, **52**, 373 (1999).
301. J. L. McLemore, P. Beeley, K. Thorton, K. Morrisroe, W. Blackwell and A. Dasgupta, *Am. J. Clin. Pathol.*, **109**, 268 (1998).
302. G. Piñeiro Avila, A. Salvador and M. de la Guardia, *Analyst*, **122**, 1543 (1997).
303. D. Harms, R. Than, U. Pinkernell, M. Schmidt, B. Krebs and U. Karst, *Analyst*, **123**, 2323 (1998).
304. D. Harms, J. Meyer, L. Westerheide, B. Krebs and U. Karst, *Anal. Chim. Acta*, **401**, 83 (1999).
305. A. L. Lazrus, G. L. Kok, S. N. Gitlin, J. A. Lind and S. E. McLaren, *Anal. Chem.*, **57**, 917 (1985).
306. G. L. Kok, K. Thompson, A. L. Lazrus and S. E. McLaren, *Anal. Chem.*, **58**, 1192 (1986).
307. N. Beltz, W. Jaeschke, G. L. Kok, S. N. Gitlin, A. L. Lazrus, S. McLaren, D. Shakespeare and V. A. Mohnen, *J. Atmos. Chem.*, **5**, 311 (1987).
308. (a) F. Sauer, S. Limbach and G. K. Moortgat, *Atmos. Environ.*, **31**, 1173 (1997).

- (b) J. Hong, J. Maguhn, D. Freitag and A. Kettrup, *Fresenius J. Anal. Chem.*, **361**, 124 (1998).
309. R. M. Peña, S. García, C. Herrero and T. Lucas, *Atmos. Environ.*, **35**, 209 (2001).
310. D. W. O'Sullivan, M. Lee, B. C. Noone and B. G. Heikes, *J. Phys. Chem.*, **100**, 3241 (1996).
311. G. G. Guibault, P. J. Brignac, Jr. and M. Juneau, *Anal. Chem.*, **40**, 1256 (1968).
312. E. Hellpointner and S. Gäb, *Nature*, **337**, 631 (1989).
313. H.-H. Kurth, S. Gäb, W. B. Turner and A. Kettrup, *Anal. Chem.*, **63**, 2586 (1991).
314. G. K. Moortgat, D. Grossmann, A. Boddenberg, G. Dallmann, A. P. Ligon, W. V. Turner, S. Gäb, F. Slemr, W. Wieprecht, K. Acker, M. Kibler, S. Schlomski and K. Bächmann, *J. Atmos. Chem.*, **42**, 443 (2002).
315. Z. Liu, R. Cai, L. Mao, H. Huang and W. Ma, *Analyst*, **124**, 173 (1999).
316. C.-Q. Zhu, D.-H. Li, H. Zheng, Q.-Z. Zhu, Q.-Y. Chen and J.-G. Xu, *Anal. Sci.*, **16**, 253 (2000).
317. Q.-y. Chen, D.-h. Li, Q.-z. Zhu, H. Zheng and J.-G. Xu, *Anal. Chim. Acta*, **381**, 175 (1999).
318. Y.-Z. Li and A. Townshend, *Anal. Chim. Acta*, **340**, 159 (1997).
319. X.-L. Chen, D.-H. Li, H.-H. Yang, Q.-Z. Zhu, H. Zheng and J.-G. Xu, *Anal. Chim. Acta*, **434**, 51 ((2001)).
320. B. Demirata-Öztiirk, G. Özen, H. Filik, I. Tor and H. Afsar, *J. Fluoresc.*, **8**, 185 (1998).
321. Y.-Z. Chen, D.-h. Li, Q.-z. Zhu, H.-h. Yang, H. Zheng and J.-g. Xu, *Anal. Chim. Acta*, **406**, 209 (2000).
322. L.-H. Chen, L.-Z. Liu and H.-X. Shen, *Anal. Lett.*, **37**, 561 (2004).
323. T. A. Kelli and G. D. Christian, *Anal. Chem.*, **53**, 2110 (1981).
324. H. Taguchi, Y. Ogura, T. Takanashi, M. Hashizoe and Y. Honda, *Invest. Ophthalmol. Vis. Sci.*, **37**, 1444 (1996).
325. J. H. Lee, I. N. Tang and J. B. Weinstein-Lloyd, *Anal. Chem.*, **62**, 2381 (1990).
326. J. H. Lee, I. N. Tang, J. B. Weinstein-Lloyd and J. B. Halper, *Environ. Sci. Technol.*, **28**, 1180 (1994).
327. B. Tang, Y. Wang, Y. Sun and H. X. Shen, *Spectrochim. Acta, Part A*, **58**, 141 (2002).
328. J. Li and P. K. Dasgupta, *Anal. Chem.*, **72**, 5338 (2000).
329. J. Li, P. K. Dasgupta and G. A. Tarver, *Anal. Chem.*, **75**, 1203 (2003)
330. L.-S. Zhang and G. T. F. Wong, *Talanta*, **48**, 1031 (1999).
331. M. J. Navas, A. M. Jiménez and G. Galán, *Atmos. Environ.*, **33**, 2279 (1999).
332. P. J. M. Kwakman and U. A. T. Brinkman, *Anal. Chim. Acta*, **266**, 175 (1992).
333. (a) W. J. Cooper, J. K. Moegling, R. J. Kieber and J. J. Kiddle, *Marine Chem.*, **70**, 191 (2000).
- (b) M. Feng, Z. Li, J. Lu and H. Jiang, *Microchim. Acta*, **126**, 73 (1997).
334. K. Dai, A. G. Vlessidis and N. P. Evmiridis, *Talanta*, **59**, 55 (2003)
335. O. Nozaki and H. Kawamoto, *Luminescence*, **15**, 137 (2000).
336. M. C. Ramos, M. C. Torijas and A. Navas Díaz, *Sensors Actuators B*, **73**, 71 (2001).
337. H. Kawamoto and O. Nozaki, *Bunseki Kagaku*, **48**, 471 (1999); *Chem. Abstr.*, **130**, 331973 (1999).
338. J. Li, K. M. Wang, X. H. Yang and D. Xiao, *Anal. Commun.*, **36**, 3 (1999).
339. B. Yan, P. J. Worsfold and K. Robards, *Analyst*, **116**, 1227 (1991).
340. S. H. Fan, B. T. Hart and I. D. McKelvie, *Lab. Robotics Autom.*, **12**, 149 (2000).
341. S. Yuan and A. M. Shiller, *Anal. Chem.*, **71**, 1975 (1999).
342. J. Li and P. K. Dasgupta, *Anal. Chim. Acta*, **442**, 63 (2001).
343. R. Escobar, S. García-Domínguez, A. Guiraúm, O. Montes, F. Galván and F. F. de la Rosa, *Luminescence*, **15**, 131 (2000).
344. Y. Li, C. Zhu, L. Wang, F. Gao, M. Li, L. Wang and Y. Zhu, *Anal. Lett.*, **34**, 1841 (2001).
345. G. Xu and S. Dong, *Electroanalysis*, **11**, 1180 (1999).
346. J. M. Gaulier, J. P. Steghens, G. Lardet, J. J. Vallon and P. Cochat, *J. Biolumin. Chemilumin.*, **12**, 295 (1997).
347. K. Hool and T. A. Nieman, *Anal. Chem.*, **60**, 834 (1988).
348. J. E. Atwater, J. R. Akse, J. DeHart and R. R. Wheeler, Jr., *Anal. Lett.*, **30**, 21 (1997).
349. D. Janasek and U. Spohn, *Sensors Actuators B*, **38-39**, 291 (1997).
350. O. Nozaki, T. Iwaeda and Y. Kato, *J. Biolumin. Chemilumin.*, **11**, 309 (1998).
351. O. Nozaki, T. Iwaeda, H. Moriyama and Y. Kato, *Luminescence*, **14**, 123 (1999).
352. A. MacDonald and T. A. Nieman, *Anal. Chem.*, **57**, 936 (1985).

353. K. Robards and P. J. Worsfold, *Anal. Chim. Acta*, **266**, 147 (1992).
354. A. Economou, P. D. Tzanavaras, M. Notou and D. G. Themelis, *Anal. Chim. Acta*, **505**, 129 (2004).
355. (a) D. C. Williams III, G. F. Huff and W. R. Seltz, *Anal. Chem.*, **48**, 1003 (1976).
(b) P. Jacob and D. Klockow, *Fresenius J. Anal. Chem.*, **346**, 429 (1993).
356. M. Stigbrand, A. Karlsson and K. Irgum, *Anal. Chem.*, **68**, 3945 (1996).
357. M. J. Chaichi, A. R. Karami, A. Shockravi and M. Shamsipur, *Spectrochim. Acta, Part A*, **59**, 1145 (2003).
358. Q. Ma, H. Ma, Z. Wang, M. Su, H. Xiao and S. Liang, *Talanta*, **53**, 983 (2001).
359. O. Nozaki, X. Ji and L. J. Kricka, *J. Biolumin. Chemilumin.*, **10**, 151 (1995).
360. A. Takahashi, K. Hashimoto, S. Kumazawa and T. Nakayama, *Anal. Sci.*, **15**, 481 (1999).
361. A. Fonaro, P. C. Isolani and I. G. R. Gutz, *Atmos. Environ.*, **27**, 307 (1993).
362. R. Camargo Matos, J. J. Pedrotti and L. Angnes, *Anal. Chim. Acta*, **441**, 73 (2001).
363. H. Elzanowska, E. Abu-Irhayem, B. Skrzynecka and V. I. Birss, *Electroanalysis*, **16**, 478 (2004).
364. Y. Shimizu, H. Komatsu, S. Michishita, N. Miura and N. Yamazo, *Sensors Actuators B*, **34**, 493 (1996).
365. X. Zheng and Z. Guo, *Talanta*, **50**, 1157 (2000).
366. K. Schachl, H. Alemu, K. Kalcher, J. Ježkova, I. Švancara and K. Vytřas, *Analyst*, **122**, 985 (1997).
367. K. Schachl, H. Alemu, K. Kalcher, J. Ježkova, I. Švancara and K. Vytřas, *Anal. Lett.*, **30**, 2655 (1997).
368. S.-C. Shyu and C. M. Wang, *J. Electrochem. Soc.*, **144**, 3419 (1997).
369. M. S. Lin and B. I. Jan, *Electroanalysis*, **9**, 340 (1997).
370. T. Clark and D. C. Johnson, *Electroanalysis*, **9**, 273 (1997).
371. T. Hoshi, H. Saiki, S. Kuwazawa, Y. Kobayashi and J.-i. Anzai, *Anal. Sci.*, **16**, 1009 (2000).
372. H. Ohura, T. Imato, S. Yamasaki and N. Ishibashi, *Talanta*, **43**, 943 (1996).
373. T. Imato, H. Ohura, S. Yamasaki and Y. Asano, *Talanta*, **52**, 19 (2000).
374. J. Pei and X.-y. Li, *Electroanalysis*, **11**, 1211 (1999).
375. H.-H. Rüttinger and A. Radschuweit, *J. Chromatogr. A*, **868**, 127 (2000).
376. A. Radschuweit, H.-H. Rüttinger and P. Nuhn, *J. Chromatogr. A*, **937**, 127 (2001).
377. S. Kuwata and Y. Sadaoka, *Sensors Actuators B*, **65**, 325 (2000).
378. J.-M. Zen, H.-H. Chung and A. S. Kumar, *Analyst*, **125**, 1633 (2000).
379. D. Sužnjević, S. Blagojević, D. Vučelić and P. Zuman, *Electroanalysis*, **9**, 861 (1997).
380. T. F. Nagiev, M. T. Abbasova, S. M. Baba-zade, S. A. Kuliev, E. B. Stepanova and L. M. Agamamedova, *Appl. Biochem. Biotechnol.*, **88**, 275 (2000).
381. E. Baldini, V. C. Dall'Orto, C. Danilowicz, I. Rezzano and E. J. Calvo, *Electroanalysis*, **14**, 1157 (2002).
382. K. Kriz, M. Anderlund and D. Kriz, *Biosens. Bioelectron.*, **16**, 363 (2001).
383. V. Lvovich and A. Scheeline, *Anal. Chem.*, **69**, 454 (1967).
384. S. Serradilla Razola, E. Aktas, J.-C. Viré and J.-M. Kauffmann, *Analyst*, **125**, 79 (2000).
385. B. Wang, J. Zhang, G. Cheng and S. Dong, *Anal. Chim. Acta*, **407**, 111 (2000).
386. B. Wang, B. Li, Z. Wang, G. Xu, Q. Wang and S. Dong, *Anal. Chem.*, **71**, 1935 (1999).
387. K. Yamamoto, T. Ohgaru, M. Torimura, H. Kinoshita, K. Kano and T. Ikeda, *Anal. Chim. Acta*, **406**, 201 (2000).
388. J. Li, S. N. Tan and J. T. Oh, *J. Electroanal. Chem.*, **448**, 69 (1998).
389. S. L. Chut, J. Li and S. N. Tan, *Analyst*, **122**, 1431 (1977).
390. M. A. del Cerro, G. Cayuela, A. J. Reviejo, J. M. Pingarrón and J. Wang, *Electroanalysis*, **9**, 1113 (1997).
391. S. Yabuki, F. Mizutani and Y. Hirata, *J. Electroanal. Chem.*, **468**, 117 (1999).
392. A. A. Karyakin and E. E. Karyakina, *Sensors Actuators B*, **57**, 268 (1999).
393. S. Akgöl and E. Dinçkaya, *Talanta*, **48**, 363 (1999).
394. N. Ertuş, S. Timur, E. Akyılmaz and E. Dinçkaya, *Turk. J. Chem.*, **24**, 95 (2000).
395. F. Miyamoto, M. Saeki and T. Yoshizawa, *J. AOAC Int.*, **80**, 681 (1997).
396. S. D. Varma, *Free Radical Res. Commun.*, **5**, 359 (1989).
397. S. D. Varma and P. S. Devamanoharan, *Free Radical Res. Commun.*, **8**, 73 (1990).
398. N. Kuge, M. Kohzaki and T. Sato, *Free Radical Res. Commun.*, **30**, 119 (1999).

399. K. Warner and N. A. M. Eskin, *Methods to Assess Quality and Stability of Oils and Fat-Containing Foods*, AOCS Press, Champaign, USA, 1995.
400. J. L. Perrin, in *Oils and Fats Manual* (Eds. A. Karleskind and J.-P. Wolff), Intercept Limited, Andover, UK, 1996, pp. 1205 ff.
401. N. S. Thomaidis and C. A. Georgiou, *Lab. Autom. Inf. Manag.*, **34**, 101 (1999).
402. P. Bondioli, A. Gasparoli, L. Della Bella and S. Tagliabue, *Eur. J. Lipid Sci. Technol.*, **104**, 777 (2002).
403. Metrohm, 743 *Rancimat*[®], Metrohm Ltd., Herisau, Switzerland (<http://www.metrohm.ch>).
404. G. Mortensen, J. Sørensen and H. Stapelfeldt, *J. Agric. Food Chem.*, **50**, 4364 (2002).
405. AOCS, *Official Methods and Recommended Practices of the American Oil Chemists' Society*, 5th edn., American Oil Chemists' Society, AOCS Press, Champaign, 1998.
406. W. Jessup, R. T. Dean and J. M. Gebicki, in *Oxygen Radicals in Biological Systems, Part C* (Ed. L. Packer), Academic Press, San Diego, *Methods Enzymol.*, **233**, 289 (1994).
407. O. Suzuki, M. Kakuta and N. Kato, *Jpn. Kokai Tokkyo Koho*, JP 2000199759 (2000); *Chem. Abstr.*, **133**, 104186 (2000).
408. M. D. Guillén and N. Cabo, *Food Chem.*, **77**, 503 (2002).
409. G. Yildiz, R. L. Wehling and S. L. Cuppett, *J. Am. Oil Chem. Soc.*, **80**, 103 (2003).
410. ASTM, *ASTM Annual Book of Standards*, Vol. 15.05, American Society for Testing and Materials, Philadelphia, 1995.
411. P. G. Nourros, C. A. Georgiou and M. G. Polissiou, *Anal. Chim. Acta*, **389**, 239 (1999).
412. Z.-Y. Jiang, A. C. S. Woollard and S. P. Wolff, *Lipids*, **26**, 853 (1992).
413. J. Nourooz-Zadeh, J. Tajaddini-Sarmadi and S. P. Wolff, *J. Agric. Food Chem.*, **43**, 17 (1995).
414. Z.-Y. Jiang, J. V. Hunt and S. P. Wolff, *Anal. Biochem.*, **202**, 384 (1992).
415. N. C. Shantha and E. A. Decker, *J. AOAC Int.*, **77**, 421 (1994).
416. IDF, *International IDF Standards*, International Dairy Federation, Brussels, Belgium, 1991, Section 74A.
417. G. Schwarzenbach and A. Willi, *Helv. Chim. Acta*, **34**, 528 (1951).
418. D. Hornero-Méndez, A. Pérez-Gálvez and M. I. Mínguez-Mosquera, *J. Am. Oil Chem. Soc.*, **78**, 1151 (2001).
419. M. Gabriëls, J. Cirunay, M. Alfandy, M. Brisaert, M. de Tavernier, F. Camu and J. Plaizier-Vercammen, *J. AOAC Int.*, **83**, 589 (2000).
420. S. Tokumaru, I. Tsukamoto, H. Iguchi and S. Kojo, *Anal. Chim. Acta*, **307**, 97 (1995).
421. K. Akasaka, *Bunseki Kagaku*, **44**, 681 (1995); *Chem. Abstr.*, **123**, 217334 (1995).
422. K. Akasaka, T. Takamura, H. Ohru, H. Meguro and K. Hashimoto, *Biosci. Biotech. Biochem.*, **60**, 1772 (1996).
423. S. O. McGuire, M. R. James-Krake, G. Y. Sun and K. L. Fritsche, *Lipids*, **32**, 219 (1997).
424. R. M. Johnson, G. Goyette, Jr., Y. Ravindranath and Y. S. Ho, *Blood*, **96**, 1985 (2000).
425. M. D. Guillén and N. Cabo, *J. Am. Oil Chem. Soc.*, **74**, 1281 (1997).
426. M. D. Guillén and N. Cabo, *J. Agric. Food Chem.*, **46**, 1788 (1998).
427. M. D. Guillén and N. Cabo, *Fett/Lipid*, **101**, 71 (1999).
428. M. D. Guillén and N. Cabo, *J. Sci. Food Agric.*, **80**, 2028 (2000).
429. M. D. Guillén and N. Cabo, *J. Agric. Food Chem.*, **47**, 709 (1999).
430. J. Malléol, J.-L. Gardette and J. Lemaire, *J. Am. Oil Chem. Soc.*, **76**, 967 (1999).
431. K. Ma, F. R. van de Voort, J. Sedman and A. A. Ismail, *J. Am. Oil Chem. Soc.*, **74**, 897 (1997).
432. A. Ruíz, M. J. Ayora Cañada and B. Lendl, *Analyst*, **126**, 242 (2001).
433. B. G. Osborne and T. Fearn (Eds.), *Near Infrared Spectroscopy in Food Analysis*, Wiley, New York, 1988.
434. D. A. Burns and E. W. Ciurczak (Eds.), *Handbook of Near-Infrared Analysis*, Dekker, New York, 1990.
435. J. Dong, K. Ma, F. R. van de Voort and A. A. Ismail, *J. AOAC Int.*, **80**, 345 (1997).
436. D. Firestone (Ed.), *Official Methods and Recommended Practices of the AOCS*, 5th edn., American Oil Chemists' Society, Champaign, IL, USA, 1998.
437. G. Yildiz, R. L. Wehling and S. L. Cuppett, *J. Am. Oil Chem. Soc.*, **78**, 495 (2001).
438. E. Kardash-Strochkova, Ya. I. Tur'yan and I. Kuselman, *Talanta*, **54**, 411 (2001).
439. I. Kuselman, E. Kardash-Strochkova and Y. I. Tur'yan, *Acred. Qual. Assur.*, **7**, 13 (2002).

440. L. Campanella, M. P. Sammartino, M. Tomassetti and S. Zannella, *Sensors Actuators B*, **76**, 158 (2001).
441. M. Kondo, S. Iishima and Y. Fukushima, *Jpn. Kokai Tokkyo Koho*, (2002), JP 2002296265 A2 20021009; *Chem. Abstr.*, **137**, 246831 (2002).
442. ISO 6886:1996, *Animal and vegetable fats and oils—Determination of oxidation stability (Accelerated oxidation test)*, International Organization for Standardization, Geneva, Switzerland (<http://www.iso.ch/iso/en/CatalogueListPage.CatalogueList?ICS1=67&ICS2=200&ICS3=10>).
443. E. Psomiadou, K. X. Karakostas, G. Blekas, M. Z. Tsimidou and D. Boskou, *Eur. J. Lipid Sci. Technol.*, **105**, 403 (2003).
444. D. Kristensen, M. V. Kroger-Ohlens and L. H. Skibsted, in *Free Radicals in Food* (Eds. M. J. Morello, F. Shahidi and C.-T. Ho), *ACS Symposium Series*, **807**, 114 (2002).
445. M. K. Thomsen, D. Kristensen and L. H. Skibsted, *J. Am. Oil Chem. Soc.*, **77**, 725 (2000).
446. S. Zabarnick, S. D. Whitacre, M. S. Mick and J. S. Ervin, *Proc. 6th Int. Conf. on Stability and Handling of Liquid Fuels*, Vancouver, B.C., Canada, 13–17 Oct., 1997.
447. J. H. Nielsen, C. E. Olsen, C. Jensen and L. H. Skibsted, *J. Dairy Res.*, **63**, 159 (1996).
448. J. H. Nielsen, C. E. Olsen, J. Lyndon, J. Sørensen and L. H. Skibsted, *J. Dairy Res.*, **63**, 615 (1996).
449. IUPAC, *Standard Methods for the Analysis of Oil, Fats and Derivatives*, International Union of Pure and Applied Chemistry, Blackwell Scientific Publications, Oxford, UK, 1987.
450. F. Bernheim, M. L. C. Bernheim and K. M. Wilbur, *J. Biol. Chem.*, **174**, 257 (1949).
451. R. O. Sinnhuber and T. C. Yu, *Food Technol.*, **12**, 9 (1958).
452. R. O. Sinnhuber, T. C. Yu and T. C. Yu, *Food Res.*, **23**, 626 (1958).
453. V. Nair and G. A. Turner, *Lipids*, **19**, 804 (1984).
454. D. Jardine, M. Antolovich, P. D. Prenzler and K. Robards, *J. Agric. Food Chem.*, **50**, 1720 (2002).
455. K. Yagi, *Biochem. Med.*, **15**, 212 (1976).
456. D. Bonnefont, A. Legrand, J. Peynet, J. Emerit, J. Delattre and A. Galli, *Clin. Chem.*, **35**, 2054 (1989).
457. D. M. Hodges, J. M. DeLong, C. F. Forney and R. K. Prange, *Planta*, **207**, 604 (1999).
458. J. M. DeLong, R. K. Prange, D. M. Hodges, C. F. Forney, M. C. Bishop and M. Quilliam, *J. Agric. Food Chem.*, **50**, 248 (2002).
459. G. Hesel, U. Resch, F. Tatzber and H. Sinzinger, *Shock*, **12**, 16 (1999).
460. R. B. Pegg, F. Shahidi and C. R. Jablonski, *J. Agric. Food Chem.*, **40**, 1826 (1992).
461. E. Kishida, M. Oribe, K. Mochizuki, S. Kojo and H. Iguchi, *Biochim. Biophys. Acta*, **1045**, 187 (1990).
462. E. Kishida, A. Kamura, S. Tokumaru, M. Oribe, H. Iguchi and S. Kojo, *J. Agric. Food Chem.*, **41**, 1 (1993).
463. E. Kishida, S. Tokumaru, Y. Ishitani, M. Yamamoto, M. Oribe, H. Iguchi and S. Kojo, *J. Agric. Food Chem.*, **41**, 1598 (1993).
464. S. Mawatari and K. Murakami, *Anal. Biochem.*, **264**, 118 (1998).
465. C.-S. Yang, P.-J. Tsai, N.-N. Lin, S.-T. Chou and J. S. Kuo, *J. Chromatogr. B*, **693**, 257 (1997).
466. N. A. Botsoglou, D. J. Fletouris, G. E. Papageorgiou, V. N. Vassilopoulos, A. J. Mantis and A. G. Trakatellis, *J. Agric. Food Chem.*, **42**, 1931 (1994).
467. J. M. C. Gutteridge, *Int. J. Biochem.*, **14**, 649 (1982).
468. E. N. Frankel, M.-L. Hu and A. L. Tappel, *Lipids*, **24**, 976 (1989).
469. G. A. Cordis, D. K. Das and W. Riedel, *J. Chromatogr. A.*, **798**, 117 (1998).
470. D. Gérard-Monnier, I. Erdelmeier, K. Régnard, N. Moze-Henry, J.-C. Yadan and J. Chaudière, *Chem. Res. Toxicol.*, **11**, 1176 (1998).
471. I. Erdelmeier, D. Gérard-Monnier, J.-C. Yadan and J. Chaudière, *Chem. Res. Toxicol.*, **11**, 1184 (1998).
472. A. Pompella and M. Comporti, *Histochemistry*, **95**, 255 (1991).
473. B. Bisakowski, X. Perraud and S. Kermasha, *Biosci., Biotech. Biochem.*, **61**, 1262 (1997).
474. M. Tomita, T. Okuyama, Y. Hatta and S. Kawai, *J. Chromatogr. B*, **526**, 174 (1990).
475. H. C. Yeo, H. J. Helbock, D. W. Chyu and B. N. Ames, *Anal. Biochem.*, **220**, 391 (1994).
476. X. P. Luo, M. Yazdanpanah, N. Bhooi and D. C. Lehotay, *Anal. Biochem.*, **228**, 294 (1995).
477. T. P. King, *Biochemistry*, **5**, 3454 (1966).

478. J. Brozmanova, A. Dudas and J. A. Henriques, *Neoplasma*, **48**, 85 (2001).
479. R. O. Recknagel and E. A. Glende, Jr., in *Oxygen Radicals in Biological Systems* (Ed. L. Packer), Academic Press, Orlando, *Methods Enzymol.*, **105**, 331 (1984).
480. I. Pinchuk and D. Lichtenberg, *Free Radical Res.*, **24**, 351 (1996).
481. C. Bauer-Planck and L. Steenhorst-Slikkerveer, *J. Am. Oil Chem. Soc.*, **77**, 477 (2000).
482. ISO 660:1996, *Animal and vegetable fats and oils—Determination of acid value and acidity*, International Organization for Standardization, Geneva, Switzerland (<http://www.iso.ch/iso/en/CatalogueListPage.CatalogueList?ICS1=67&ICS2=200&ICS3=10>).
483. A. E. Beezer, A. C. Morris, M. A. A. O'Neill, R. J. Willson, A. K. Hills, J. C. Mitchell and J. A. Connor, *J. Phys. Chem. B*, **105**, 1212 (2001).
484. F. Zaman, A. E. Beezer, J. C. Mitchell, Q. Clarkson, A. F. Davis and R. J. Wilson, *Int. J. Pharm.*, **227**, 133 (2001).
485. F. Zaman, A. E. Beezer, J. C. Mitchell, Q. Clarkson, J. Elliot, M. Nisbet and A. F. Davis, *Int. J. Pharm.*, **225**, 135 (2001).
486. H. R. Williams and H. S. Mosher, *J. Am. Chem. Soc.*, **76**, 2984 (1954).
487. H. R. Williams and H. S. Mosher, *J. Am. Chem. Soc.*, **76**, 2987 (1954).
488. H. R. Williams and H. S. Mosher, *J. Am. Chem. Soc.*, **76**, 3495 (1954).
489. G. O. Schenck and K.-H. Schulte-Elte, *Ann. Chem.*, **618**, 185 (1958).
490. C. S. Foote and S. Wexler, *J. Am. Chem. Soc.*, **86**, 3879 (1964).
491. C. S. Foote, S. Wexler, W. Ando and R. Higgins, *J. Am. Chem. Soc.*, **90**, 975 (1968).
492. H.-F. Wong and G. D. Brown, *J. Chem. Res. (S)*, 30 (2002).
493. R. W. Murray and M. L. Kaplan, *J. Am. Chem. Soc.*, **91**, 5358 (1969).
494. J. Armhold, O. M. Panasenko, J. Schiller, K. Arnold, Y. A. Vladimirov and V. I. Sergienko, *Z. Naturforsch.*, **51c**, 386 (1996).
495. S. P. Stratton and D. C. Liebler, *Biochemistry*, **36**, 12911 (1997).
496. H. N. Cheng, F. C. Schilling and F. A. Bovey, *Macromolecules*, **9**, 363 (1976).
497. A. Leitzke, E. Reisz, R. Flyunt and C. von Sonntag, *J. Chem. Soc., Perkin Trans. 2*, 793 (2001).
498. M. C. Dobarganes and J. Velasco, *Eur. J. Lipid Sci. Technol.*, **104**, 420 (2002).
499. A. M. Pastorino, M. Maiorino and F. Ursini, *Free Radical Biol. Med.*, **29**, 397 (2000).
500. J. Schiers, D. J. Carlsson and S. W. Bigger, *Polym. Plast. Technol. Eng.*, **34**, 97 (1995).
501. E. I. Buneeva, S. V. Puchkov, O. N. Yarysh and A. L. Perkel, *J. Anal. Chem.*, **53**, 775 (1998).
502. D. Melchior and S. Gäb, *J. Chromatogr. A*, **894**, 145 (2000).
503. (a) A. O. Allen, C. J. Hochanadel, J. A. Ghormley and T. W. Davis, *J. Phys. Chem.*, **56**, 575 (1952).
- (b) R. Flyunt, A. Leitzke and C. von Sonntag, *Radiat. Phys. Chem.*, **67**, 469 (2003).
504. A. Cimato, G. Facorro, F. Aguirre, A. Hager, T. De Paoli, J. Ihlo, H. A. Farach and C. P. Poole Jr., *Spectrochim. Acta, Part A*, **54**, 2001 (1998).
505. G. T. Shwaery, J. M. Samii, B. Frei and J. F. Keaney, Jr., in *Oxidants and Antioxidants—Part B* (Ed. L. Packer), Academic Press, San Diego, *Methods Enzymol.*, **300**, 51 (1999).
506. Y. Yamamoto, *Free Radical Biol. Med.*, **19**, 943 (1995).
507. J.-R. Zhang, B. S. Lutzke and E. D. Hall, *Free Radical Biol. Med.*, **19**, 944 (1995).
508. T. Kriska and A. W. Girotti, *Anal. Biochem.*, **327**, 97 (2004).
509. W. G. Barb, J. H. Baxendale, P. George and K. R. Hargrave, *J. Chem. Soc., Faraday Trans.*, **47**, 462 (1951).
510. I. M. Kolthoff and A. I. Medalia, *Anal. Chem.*, **23**, 595 (1951).
511. B. Mihaljević, B. Katušin-Ražem and D. Ražem, *Free Radical Biol. Med.*, **21**, 53 (1996).
512. M. P. Richards and Y. Feng, *Anal. Biochem.*, **278**, 232 (2000).
513. J. Nourooz-Zadeh, in *Oxidants and Antioxidants, Part B* (Ed. L. Packer), Academic Press, San Diego, *Methods Enzymol.*, **300**, 58 (1999).
514. J. Nourooz-Zadeh, J. Tajaddini-Sarmadi and S. P. Wolff, *Anal. Biochem.*, **220**, 403 (1994).
515. C. A. Gay and J. M. Gebicki, *Anal. Biochem.*, **304**, 42 (2002).
516. K. Sugino, *Biosci. Biotechnol. Biochem.*, **63**, 773 (1999).
517. J. R. Wagner, M. Berger, J. Cadet and J. E. van Lier, *J. Chromatogr.*, **504**, 191 (1990).
518. M. Mifune, T.-a. Tai, A. Iwado, H. Akizawa, J. Oda, N. Motohashi and Y. Saito, *Talanta*, **54**, 319 (2001).
519. L. L. Smith and F. L. Hill, *J. Chromatogr. A*, **66**, 101 (1972).
520. L. Bruun-Jensen, L. Colarow and L. H. Skibsted, *J. Planar Chromatogr.*, **8**, 475 (1995).

521. G. Esser and D. Klockow, *Mikrochim. Acta*, **113**, 373 (1994).
522. P. Heinmöller, H.-H. Kurth, R. Rabong, W. V. Turner, A. Kettrup and S. Gäb, *Anal. Chem.*, **70**, 1437 (1998).
523. G. L. Kok, S. E. McLaren and T. A. Staffelbach, *J. Atmos. Oceanic Technol.*, **12**, 282 (1995).
524. K. Wang and W. H. Glaze, *J. Chromatogr. A*, **822**, 207 (1998).
525. O. Schmitz, D. Melchior, W. Schuhmann and S. Gäb, *J. Chromatogr. A*, **814**, 261 (1998).
526. O. Schmitz and S. Gäb, *J. Chromatogr. A*, **767**, 249 (1997).
527. O. Schmitz and S. Gäb, *J. Chromatogr. A*, **781**, 215 (1997).
528. K. Akasaka, A. Ohata, H. Ohruï and H. Meguro, *J. Chromatogr. B*, **665**, 37 (1995).
529. T. Ohshima, A. Hopia, J. B. German and E. N. Frankel, *Lipids*, **31**, 1091 (1996).
530. K. Akasaka, H. Ohta, Y. Hanada and H. Ohruï, *Biosci. Biotechnol. Biochem.*, **63**, 1506 (1999).
531. K. Akasaka and H. Ohruï, *J. Chromatogr. A*, **881**, 159 (2000).
532. K. Hartvigsen, L. F. Hansen, P. Lund, K. Bukhave and G. Hølmer, *J. Agric. Food Chem.*, **48**, 5842 (2000).
533. J. Terao, M. Miyoshi and S. Miyamoto, *J. Chromatogr. B*, **765**, 199 (2001).
534. T. Ohshima, H. Ushio and C. Koizumi, in *Flavor and Lipid Chemistry of Seafoods* (Eds. F. Shahidi and K. R. Cadwallader), *ACS Symposium Series*, **674**, 198 (1997).
535. S. K. Singh, M. Suurkuusk, C. Eldsäter, S. Karlsson and A. C. Albertsson, *Int. J. Pharm.*, **142**, 199 (1996).
536. S. K. Singh, M. Suurkuusk and C. Eldsäter, *Int. J. Pharm.*, **142**, 215 (1996).
537. Y. Yamamoto, B. Frei and B. N. Ames, in *Oxygen Radicals in Biological Systems, Part B, Oxygen Radicals and Antioxidants* (Eds. L. Packer and A. N. Glazer), Academic Press, San Diego, *Methods Enzymol.*, **186**, 371 (1990).
538. T. Miyazawa, K. Fujimoto, T. Suzuki and K. Yasuda, in *Oxygen Radicals in Biological Systems, Part C* (Ed. L. Packer), Academic Press, San Diego, *Methods Enzymol.*, **233**, 324 (1994).
539. A. M. Pastorino, A. Zamburlini, L. Zenaro, M. Maiorino and F. Ursini, in *Oxidants and Antioxidants—Part B* (Ed. L. Packer), Academic Press, San Diego, *Methods Enzymol.*, **300**, 33 (1999).
540. N. Chiba, H. Imai and Y. Nakagawa, *J. Chromatogr. B*, **728**, 35 (1999).
541. C. A. Lukey, *Prog. Org. Coatings*, **41**, 129 (2001).
542. J. Honga, J. Maguhn, D. Freitag and A. Kettrup, *J. High Resol. Chromatogr.*, **22**, 475 (1999).
543. T. M. Alam, M. Celina, R. A. Assink, R. L. Clough, K. T. Gillen and D. R. Wheeler, *Macromolecules*, **33**, 1181 (2000).
544. R. A. Assink, M. Celina, T. D. Dunbar, T. M. Alam, R. L. Clough and K. T. Gillen, *Macromolecules*, **33**, 4023 (2000).
545. R. L. Kuczowski, *Chem. Soc. Rev.*, **79** (1992).
546. S. Gäb and W. V. Turner, *J. Org. Chem.*, **49**, 2711 (1984).
547. O. Evans, *Analyst*, **123**, 705 (1998).
548. O. Evans, *Analyst*, **124**, 1811 (1999).
549. A. Mulchandani and D. C. Rudolph, *Anal. Biochem.*, **225**, 277 (1995).
550. W. Korytowski, P. G. Geiger and A. W. Girotti, *J. Chromatogr. B*, **670**, 189 (1995).
551. W. Korytowski, P. G. Geiger and A. W. Girotti, in *Oxidants and Antioxidants—Part B* (Ed. L. Packer), Academic Press, San Diego, *Methods Enzymol.*, **300**, 23 (1999).
552. G. J. Bachowski, W. Korytowski and A. W. Girotti, *Lipids*, **29**, 449 (1994).
553. H. Arai, S. Mohri, T. Suzuki, K. Takama and J. Terao, *Biosci. Biotech. Biochem.*, **61**, 191 (1997).
554. H. Arai, J. Terao, D. S. P. Abdalla, T. Suzuki and K. Takama, *Free Radical Biol. Med.*, **20**, 365 (1996).
555. S. A. Emr and A. M. Yacynych, *Electroanalysis*, **7**, 913 (1995).
556. F. Palmisano, P. G. Zambonin and D. Centone, *Fresenius J. Anal. Chem.*, **366**, 586 (2000).
557. M. Gündoğan, S. S. Çelebi, H. Özyörtük and A. Yildiz, *Biosens. Bioelectron.*, **17**, 875 (2002).
558. E. García-Moreno, M. A. Ruiz, C. Barbas and J. M. Pingarrón, *Anal. Chim. Acta*, **448**, 9 (2001).
559. R. J. Kulmacz, J. F. Miller, Jr., R. B. Pendleton and W. E. M. Lands, in *Oxygen Radicals in Biological Systems, Part B, Oxygen Radicals and Antioxidants* (Eds. L. Packer and A. N. Glazer), Academic Press, San Diego, *Methods Enzymol.*, **186**, 431 (1990).
560. J. Polzer and K. Bächmann, *J. Chromatogr. A*, **653**, 283 (1993).

561. P. T. Wierzychowski and L. W. Zatorski, *Chromatographia*, **51**, 83 (2000).
562. (a) O. Sjövall, A. Kuksis, L. Marai and J. J. Myher, *Lipids*, **32**, 1211 (1997).
(b) D. K. MacMillan and R. C. Murphy, *J. Am. Soc. Mass Spectrom.*, **6**, 1190 (1995).
563. N. Baba, H. Daido, T. Kosugi, M. Miyake and S. Nakajima, *Biosci. Biotechnol. Biochem.*, **62**, 160 (1998).
564. R. Bortolomeazzi, L. Pizzale, S. Vichi and G. Lercker, *Chromatographia*, **39**, 577 (1994).
565. L. M. Hall and R. C. Murphy, *J. Am. Soc. Mass Spectrom.*, **9**, 527 (1998).
566. S. L. Khursan and V. L. Antonovskii, *Doklady Phys. Chem.*, **382**, 59 (2002).
567. V. Vacque, B. Sombret, J. P. Huvenne, P. Legrand and S. Such, *Spectrochim. Acta, Part A*, **53**, 55 (1997).
568. T. J. Wallington, M. D. Hurley, W. F. Schneider, J. Sehested and O. J. Nielsen, *Chem. Phys. Lett.*, **218**, 34 (1994).
569. J. Malléol, J.-L. Gardette and J. Lemaire, *J. Am. Oil Chem. Soc.*, **76**, 967 (1999).
570. S.-P. Hui, T. Yoshimura, T. Murai, H. Chiba and T. Kurosawa, *Anal. Sci.*, **16**, 1023 (2000).
571. C. M. Havrilla, D. L. Hachey and N. A. Porter, *J. Am. Chem. Soc.*, **122**, 8042 (2000).
572. E. H. Oliw, C. Su, T. Skogström and G. Benthin, *Lipids*, **33**, 843 (1988).
573. O. Sjövall, A. Kuksis and H. Kallio, *J. Chromatogr. A*, **905**, 119 (2001).
574. O. Sjövall, A. Kuksis and H. Kallio, *Lipids*, **36**, 1347 (2001).
575. M. Campagnole, M.-J. Bourgeois and E. Montaudon, *Tetrahedron*, **58**, 1165 (2002).
576. B. K. Ohta and C. S. Foote, *J. Am. Chem. Soc.*, **124**, 12064 (2002).
577. Z. Paryzek and U. Rychlewska, *J. Chem. Soc., Perkin Trans. 2*, 2313 (1997).
578. G. Bernardinelli, C. W. Jefford, J. Boukouvalas, D. Joggi and S. Kohmoto, *Acta Crystallogr., Sect. C*, **43**, 701 (1987).
579. Y. Watanabe, H. Ishigaki, H. Okada and S. Suyama, *Polym. J.*, **29**, 733 (1997).
580. H. Kubota, T. Kondo, T. Ichikawa and R. Katakai, *Polym. Degrad. Stabil.*, **60**, 425 (1998).
581. M. I. Awad and T. Ohsaka, *J. Electroanal. Chem.*, **544**, 35 (2003).
582. (a) S. Effkemann, S. Brødsgaard, P. Mortensen, S.-A. Linde and U. Karst, *J. Chromatogr. A*, **855**, 551 (1999).
(b) U. Pinkernell, S. Effkemann and U. Karst, *Anal. Chem.*, **69**, 3623 (1997).
583. S. Effkemann, U. Pinkernell and U. Karst, *Anal. Chim. Acta*, **363**, 97 (1998).
584. U. Pinkernell, H.-J. Lüke and U. Karst, *Analyst*, **122**, 567 (1997).
585. S. Baj and A. Chrobok, *J. Liq. Chromatogr. Relat. Technol.*, **23**, 551 (2000).
586. (a) P. D. Bartlett, E. P. Benzing and R. E. Pincock, *J. Am. Chem. Soc.*, **82**, 1762 (1960).
(b) J. L. Courtneidge and M. Bush, *J. Chem. Soc., Perkin Trans. 1*, 1531 (1992).
587. T. F. Shumkina, S. G. Voronina and A. L. Perkel, *J. Anal. Chem.*, **52**, 562 (1997).
588. NIOSH, *NMAM No. 5009* (<http://www.cdc.gov/niosh/nmam/method-h.html>).
589. Q.-C. Chen, S.-F. Mou, X.-P. Hou and Z.-M. Ni, *J. Liq. Chromatogr. Relat. Technol.*, **21**, 705 (1998).
590. W.-P. Yang, Z.-J. Zhang and X. Hun, *Talanta*, **62**, 661 (2004).
591. H. G. Mack, C. O. Della Védova and H. Oberhammer, *Angew. Chem., Int. Ed. Engl.*, **30**, 1145 (1991).
592. R. Kopitzky, H. Willner, A. Hermann and H. Oberhammer, *Inorg. Chem.*, **40**, 2693 (2001).
593. H. Yin, D. L. Hachey and N. A. Porter, *J. Am. Soc. Mass Spectrom.*, **12**, 449 (2001).
594. H. Yin, D. L. Hachey and N. A. Porter, *Rapid Commun. Mass Spectrom.*, **14**, 1248 (2000).
595. J. Z. Gillies, C. W. Gillies, R. D. Suenram and F. J. Lovas, *J. Am. Chem. Soc.*, **110**, 7991 (1988).
596. G. O. Schenck, K. G. Kinkel and H.-J. Mertens, *Ann. Chem.*, **584**, 125 (1953).
597. G. O. Schenck and D. E. Dunlap, *Angew. Chem.*, **68**, 248 (1956).
598. Y. Watanabe, H. Ishigaki, H. Okada and S. Suyama, *Polym. J.*, **29**, 940 (1997).
599. R. E. Cais and F. A. Bovey, *Macromolecules*, **10**, 169 (1977).
600. P. De and D. N. Sathyanarayana, *Macromol. Chem. Phys.*, **203**, 420 (2002).
601. S. Jayanthi and K. Kishore, *J. Polym. Mater.*, **15**, 5 (1998).
602. P. De, D. N. Sathyanarayana, P. Sadasivamurthy and S. Sridhar, *Polymer*, **42**, 8587 (2001).
603. K. Subramanian and K. Kishore, *Eur. Polym. J.*, **33**, 1365 (1997).
604. S. Baj, *Fresenius J. Anal. Chem.*, **350**, 159 (1994).
605. R. Schulte-Ladbeck, P. Kolla and U. Karst, *Anal. Chem.*, **75**, 731 (2003).
606. F. Gobert, S. Altenburger-Combrisson and J. P. Albouy, *Org. Magn. Reson.*, **12**, 202 (1979).
607. T. Suzuki, J.-i. Nishida, M. Ohkita and T. Tsuji, *Angew. Chem., Int. Ed.*, **39**, 1804 (2000).

608. Y. Ushigoe, S.-i. Kawamura, K. Teshima, M. Nojima and K. J. McCullough, *Tetrahedron Lett.*, **37**, 2093 (1996).
609. K. J. McCullough, K. Teshima and M. Nojima, *J. Chem. Soc., Chem. Commun.*, 931 (1993).
610. K. J. McCullough, T. Ito, T. Tokuyasu, A. Masuyama and M. Nojima, *Tetrahedron Lett.*, **42**, 5529 (2001).
611. M. Miura, A. Ikegami, M. Nojima, S. Kasabayashi, K. J. McCullough and M. D. Walkinshaw, *J. Chem. Soc., Perkin Trans. 1*, 1657 (1983).
612. H. J. Breunig, T. Krüger and E. Lork, *J. Organomet. Chem.*, **648**, 209 (2002).
613. C. J. Marsden, L. S. Bartell and F. P. Diodati, *J. Mol. Struct.*, **39**, 253 (1977).
614. E. A. Dikumar, A. P. Yuvchenko, T. D. Zvereva, N. A. Zhukovskaya and K. L. Moiseichuk, *Rus. J. Org. Chem.*, **36**, 1105 (2000).
615. P. S. Bailey, *Ozonization in Organic Chemistry*, Academic Press, New York, Vol. 1, 1978; Vol. 2, 1982.
616. R. L. Kuczkowski, *Acc. Chem. Res.*, **16**, 42 (1983).
617. R. Criegee, *Rec. Chem. Prog.*, **18**, 111 (1957).
618. R. Criegee, *Angew. Chem., Int. Ed. Engl.*, **14**, 745 (1975).
619. D. Cremer, *J. Chem. Phys.*, **70**, 1911 (1979).
620. N. L. Bauld, J. A. Thompson, C. E. Hudson and P. S. Bailey, *J. Am. Chem. Soc.*, **90**, 1822 (1968).
621. D. Cremer, *J. Am. Chem. Soc.*, **103**, 3627 (1981).
622. H.-J. Wu and C.-C. Lin, *J. Org. Chem.*, **61**, 3820 (1996).
623. D. Cremer, *J. Am. Chem. Soc.*, **103**, 3633 (1981).
624. H. Keul and R. L. Kuczkowski, *J. Am. Chem. Soc.*, **106**, 3383 (1984).
625. M. S. LaBarge, H. Keul, R. L. Kuczkowski, M. Wallasch and D. Cremer, *J. Am. Chem. Soc.*, **110**, 2081 (1988).
626. P. S. Bailey, J. A. Thompson and B. A. Shoulders, *J. Am. Chem. Soc.*, **88**, 4098 (1966).
627. H. Keul, *Chem. Ber.*, **108**, 1207 (1975).
628. W. G. Alcock and B. Mile, *Chem. Commun.*, 5 (1976).
629. B. Nelander and L. Nord, *J. Am. Chem. Soc.*, **101**, 3769 (1979).
630. E. Gäb, S. Nitz, H. Parlar and F. Korte, *Angew. Chem., Int. Ed. Engl.*, **15**, 433 (1976).
631. O. Lorentz, *Anal. Chem.*, **37**, 101 (1965).
632. R. Criegee, A. Kerckow and H. Zinke, *Chem. Ber.*, **88**, 1878 (1955).
633. J. Zabicky and M. Mhasalkar, *J. Am. Oil Chem. Soc.*, **63**, 1547 (1986).
634. R. D. Mair and A. J. Graupner, *Anal. Chem.*, **36**, 194 (1964).
635. B. Mile and G. W. Morris, *J. Chem. Soc., Perkin Trans. 2*, 1644 (1979).
636. N. U. Soriano, Jr., V. P. Migo and M. Matsumura, *Chem. Phys. Lipids*, **126**, 133 (2003).
637. P. S. Bailey, J. W. Ward, T. P. Carter, Jr., E. Nieh, C. M. Fischer and A.-I. Khashab, *J. Am. Chem. Soc.*, **96**, 6136 (1974).
638. A. Rivandi, A. Kuksis, J. J. Myher and L. Marai, *J. Biochem. Biophys. Methods*, **30**, 271 (1995).
639. W. J. Cummins, M. G. B. Drew, J. Mann and E. B. Walsh, *J. Chem. Soc., Perkin Trans. 1*, 167 (1983).
640. L. A. Hull, I. C. Hisatsune and J. Heicklen, *J. Am. Chem. Soc.*, **94**, 4856 (1972).
641. C. K. Kohlmeier and L. Andrews, *J. Am. Chem. Soc.*, **103**, 2578 (1981).
642. I. C. Hisatsune, L. H. Kolopajlo and J. Heicklen, *J. Am. Chem. Soc.*, **99**, 3704 (1977).
643. I. C. Hisatsune, K. Shinoda and J. Heicklen, *J. Am. Chem. Soc.*, **101**, 2524 (1979).
644. P. Kolsaker, *Acta Chem. Scand.*, **19**, 223 (1965).
645. J. Zozom, C. W. Gillies, R. D. Suenram and F. J. Lovas, *Chem. Phys. Lett.*, **139**, 64 (1987).
646. P. Rouff, J. Almlöf and S. Sæbø, *Chem. Phys. Lett.*, **72**, 489 (1980).
647. C. W. Gillies and R. L. Kuczkowski, *J. Am. Chem. Soc.*, **94**, 6337 (1972).
648. A. Almenningen, P. Kolsaker, H. M. Seip and T. Willadsen, *Acta Chem. Scand.*, **23**, 3398 (1969).
649. R. L. Kuczkowski, C. W. Gillies and K. L. Gallaher, *J. Mol. Spectrosc.*, **60**, 361 (1976).
650. U. Mazur and R. L. Kuczkowski, *J. Mol. Spectrosc.*, **65**, 84 (1977).
651. R. P. Lattimer, R. L. Kuczkowski and C. W. Gillies, *J. Am. Chem. Soc.*, **96**, 348 (1974).
652. D. Cremer, *J. Chem. Phys.*, **70**, 1928 (1979).
653. K. W. Hillig II, R. P. Lattimer and R. L. Kuczkowski, *J. Am. Chem. Soc.*, **104**, 988 (1982).
654. K. W. Hillig II, R. L. Kuczkowski and D. Cremer, *J. Phys. Chem.*, **88**, 2025 (1984).

655. M. S. Labarge, K. W. Hillig II, R. L. Kuczowski and D. Cremer, *J. Phys. Chem.*, **90**, 3092 (1986).
656. D. G. Borseth, P. Lorenčák, H. M. Badawi, K. W. Hillig II and R. L. Kuczowski, *J. Mol. Struct.*, **190**, 125 (1988).
657. D. G. Borseth and R. L. Kuczowski, *J. Phys. Chem.*, **87**, 5381 (1983).
658. H. Seltzer, S. Gäb and F. Korte, *Angew. Chem., Int. Ed. Engl.*, **19**, 474 (1980).
659. K. Griesbaum, K. Schlindwein and H. Bettinger, *J. prakt. Chem.*, **338**, 307 (1996).
660. Y.-S. Hon, L. Lu, R.-C. Chang and K.-P. Chu, *Heterocycles*, **32**, 437 (1991).
661. J.-M. Fang, S.-T. Jan and Y.-S. Cheng, *J. Chem. Res. (S)*, 350 (1986).
662. P. Groth, *Acta Chem. Scand.*, **24**, 2137 (1970).
663. J. Karban, J. L. McAtee, Jr., J. S. Belew, D. F. Mullica, W. O. Milligan and J. Korp, *Chem. Commun.*, 729 (1978).
664. M. Miura, A. Ikegami, M. Nojima, S. Kasabayashi, K. J. McCullough and S. Nagase, *J. Am. Chem. Soc.*, **105**, 2414 (1983).
665. T. K. Dobbs, A. R. Taylor, J. A. Barnes, B. D. Iscimenler, E. M. Holt and E. J. Eisenbraun, *J. Org. Chem.*, **49**, 1030 (1984).
666. L. Born and E. Gäb, *Z. Kristallog.*, **147**, 197 (1978).
667. E. Gäb, S. Nitz, H. Parlar and F. Korte, *Chem. Ber.*, **111**, 1440 (1978).
668. E. Palomino, A. P. Schaap, A. F. M. Maqsudur Rahman and M. J. Heeg, *Acta Crystallogr., Sect. C*, **46**, 1942 (1990).
669. V. N. Odinokov, O. S. Kokovins, L. M. Khalilov, G. A. Tolstikov, A. Y. Kosnikov, S. V. Lindeman and Y. T. Struchkov, *Tetrahedron Lett.*, **26**, 5843 (1985).
670. W. H. Bunnelle and E. O. Schlemper, *J. Am. Chem. Soc.*, **109**, 612 (1987).
671. C. J. Cardin, D. J. Cardin, M. M. Devereux and M. A. Convery, *J. Chem. Soc., Chem. Commun.*, 1461 (1990).
672. E. Koch, *J. Therm. Anal.*, **6**, 483 (1974).
673. W. Adam, H. J. Eggelte and A. Rodriguez, *Synthesis*, 383 (1979).
674. P. S. Bailey, J. W. Ward and R. E. Hornish, *J. Am. Chem. Soc.*, **93**, 3552 (1971).
675. Q. E. Thompson, *J. Am. Chem. Soc.*, **83**, 846 (1961).
676. E. Koch, *Tetrahedron*, **26**, 3503 (1970).
677. G. D. Mendenhall, R. F. Ressick and M. Dobrzelewski, *J. Photochem.*, **25**, 227 (1984).
678. (a) E. Koch, *Anal. Chem.*, **45**, 2120 (1973).
(b) A. Dimitrov, B. Ziemer, W.-D. Hunnius and M. Meisel, *Angew. Chem., Int. Ed.*, **42**, 2483 (2003)
679. M. Miura, M. Nojima, S. Kusabayashi and S. Nagase, *J. Am. Chem. Soc.*, **103**, 1789 (1981).
680. C. C. Price and A. L. Tumolo, *J. Am. Chem. Soc.*, **86**, 4691 (1964).
681. R. E. Erickson, R. T. Hansen and J. Harkins, *J. Am. Chem. Soc.*, **90**, 6777 (1968).
682. R. W. Murray, W. C. Lumma, Jr. and J. W.-P. Lin, *J. Am. Chem. Soc.*, **92**, 3205 (1970).
683. W. Schnick and M. Jansen, *Angew. Chem., Int. Ed. Engl.*, **24**, 54 (1985).
684. W. Schnick and M. Jansen, *Z. Anorg. Allg. Chem.*, **532**, 37 (1986).
685. M. Jansen and W. Hesse, *Z. Anorg. Allg. Chem.*, **560**, 47 (1988).
686. M. S. Dobrolyubova, T. I. Rogozhnikova and A. B. Tsentsiper, *Zh. Anal. Khim.*, **26**, 2257 (1971); *J. Anal. Chem.*, **26**, Part 2, 2026 (1971).
687. W. Hesse and M. Jansen, *Inorg. Chem.*, **30**, 4380 (1991).
688. N. Korber and M. Jansen, *J. Chem. Soc., Chem. Commun.*, 1654 (1990).
689. V. L. Davison and H. J. Dutton, *Anal. Chem.*, **38**, 1302 (1966).
690. M. Beroza and B. A. Bierl, *Anal. Chem.*, **39**, 1131 (1967).
691. R. Kleiman, G. F. Spencer, F. R. Earle and I. A. Wolff, *Lipids*, **4**, 135 (1969).
692. A. E. Johnston and H. J. Dutton, *J. Am. Oil Chem. Soc.*, **49**, 98 (1972).
693. C. R. Caughman, L. C. Boyd, M. Keeney and J. Sampugna, *J. Lipid Res.*, **28**, 338 (1987).
694. K. A. Harrison and R. C. Murphy, *Anal. Chem.*, **68**, 3224 (1996).
695. O. Sjövall, A. Kuksis, L. Marai and J. J. Myher, *Lipids*, **32**, 1211 (1997).
696. T. I. Poznyak, *Ozone-Sci. Eng.*, **25**, 145 (2003).
697. R. A. DeMarco, W. B. Fox, W. B. Moniz and S. A. Sojka, *J. Magn. Reson.*, **18**, 522 (1975).
698. R. Radi, G. Peluffo, M. N. Alvarez, M. Navillat and A. Cayota, *Free Radical Biol. Med.*, **30**, 463 (2001).
699. R. Radi, A. Denicola and B. A. Freeman, in *Nitric Oxide—Part C: Biological and Antioxidant Activities* (Ed. L. Packer), Academic Press, San Diego, *Methods Enzymol.*, **301**, 353 (1999).

700. G. Merényi, J. Lind, G. Czapski and S. Goldstein, *Inorg. Chem.*, **42**, 3796 (2003).
701. A. L. Rose and T. D. Waite, *Anal. Chem.*, **73**, 5909 (2001).
702. S. L. Chen, L. Jian and H. Q. Lang, *Luminescence*, **18**, 249 (2003).
703. C. Lu, J.-M. Lin, C. W. Huie and M. Yamada, *Anal. Chim. Acta*, **510**, 29 (2004).
704. H. Tanimoto, O. Wild, S. Kato, H. Furutani, Y. Makide, Y. Komazaki, S. Hashimoto, S. Tanaka and H. Akimoto, *J. Geophys. Res. Atmos.*, **107**, 13 (2002).
705. P. Ling, A. I. Boldyrev, J. Simons and C. A. Wight, *J. Am. Chem. Soc.*, **120**, 12327 (1998).
706. UNECE, *Convention on Civil Liability for Damage Cause during Carriage of Dangerous Goods by Road, Rail and Inland Navigation Vessels (CRTD)* (http://www.unece.org/trans/danger/publi/crtd/crtd_f.html).
707. MSDS Writer, *Selected Titles on Chemical Hygiene and Safety* (<http://www.ilpi.com/msds/booklist.html>).
708. ILPI, *The MSDS HyperGlossary* (<http://www.ilpi.com/msds/ref/index.html>).
709. ILPI, *Peroxide* (<http://www.ilpi.com/msds/ref/ Peroxide.html>).
710. ASTM, E298-01 Standard Test Methods for Assay of Organic Peroxides, in Reference 410.
711. ASTM, E299-97(2002) Standard Test Method for Trace Amounts of Peroxides in Organic Solvents, in Reference 410.
712. DOT, *The CHRIS Manual*, United States Department of Transportation (<http://www.chris-manual.com>).
713. UNECE, *Inventory of agreements and legal instruments relevant to transport, environment and health* (<http://www.unece.org/doc/lc/lc.2000.2.e.pdf>).
714. UN, *Recommendations on the Transport of Dangerous Goods—Model Regulations*, 13th edn. (http://www.unece.org/trans/danger/publi/unrec/rev13/13nature_e.html).
715. UN, *Recommendations on the Transport of Dangerous Goods—Manual of Tests and Criteria*, 4th edn. (http://www.unece.org/trans/danger/publi/manual/manual_e.html, www.unece.org/trans/danger/publi/adr/adr2001/English/Part2-2.pdf).
716. UNECE, *ADN—International Carriage of Dangerous Goods by Inland Waterways* (<http://www.unece.org/trans/danger/adn-agree.html>).
717. UNECE, *European Agreement Concerning the International Carriage of Dangerous Goods by Road (ADR)* (http://www.unece.org/trans/danger/publi/adr/adr_e.html).
718. UNECE, *Convention Concerning International Carriage by Rail (COTIF)* (<http://www.unece.org/trade/cotif/Welcome.html>).
719. ICAO, International Civil Aviation Organization in Action (http://www.icao.int/icao/en/m_in-action.html).
720. CFR, *Section 173.127 Class 5, Division 5.1—Definition and assignment of packing groups* (<http://www.setonresourcecenter.com/49CFR/Docs/wcd00009/wcd0095>).
721. DOT, TC and SCT, *2000 Emergency Response Guidebook (ERG 2000)* (http://www.tc.gc.ca/canutecc/erg_gmu/erg2000_menu.htm, <http://www.envecetra.com/env/erg/about.htm>).
722. UNEP, *UNEP Chemicals Programme* (<http://www.chem.unep.ch/>, <http://www.chem.unep.ch/pts/chemintro.htm>).
723. UNEP, *Regionally Based Assessment of Persistent Toxic Substances* (<http://www.chem.unep.ch/pts/>).
724. EPA and NOAA, *CAMEO User's Manual* (<http://www.epa.gov/ceppo/cameo/>).
725. EPA and NOAA, *ALOHA User's Manual* (<http://www.epa.gov/ceppo/cameo/aloha.htm>).
726. EPA and NOAA, *MARPLOT User's Manual* (<http://www.epa.gov/ceppo/cameo/marplot.htm>).
727. WHO, ILO and UNEP, *International Chemical Safety Cards (ICSCs)* (<http://www.ilo.org/public/english/protection/safework/cis/products/icsc/dtasht/intro.htm>).
728. WHO, ILO and UNEP, *International Programme on Chemical Safety (IPCS)* (<http://www.who.int/pcs/index.htm>).
729. ILO, *ICSC Compiler's Guide* (http://www.unitar.org/cwm/ghs_library/Documents/cat5/International/ILO_ICSC_Comp_Guide.pdf).
730. NIOSH, *Pocket Guide to Chemical Hazards (NPG)* (<http://www.cdc.gov/niosh/npg/npg.html>).
731. OSHA, *Index of Sampling and Analytical Methods* (<http://www.osha-slc.gov/dts/sltc/methods/toc.html>).
732. EPA, *Environmental Test Methods and Guidelines* (<http://www.epa.gov/Standards.html>).
733. EPA, *Envirofacts Master Chemical Integrator (EMCI)* (<http://www.epa.gov/enviro/html/emci/chemref/94360.html>).

734. OSHA, *Sampling and Analytical Methods—Protocols for Methods Evaluation* (<http://www.osha-slc.gov/dts/sltc/methods/index.html>).
735. NIOSH, *Detailed Description of the RTECS® Database—Registry of Toxic Effects of Chemical Substances* (http://www.nisc.com/cis/RTECS_Analysis_March_2004.pdf).
736. D. V. Sweet (Ed.), *Comprehensive Guide to the RTECS*, U.S. Department of Health and Human Services, Cincinnati, Ohio, USA, 1997 (<http://ccinfoweb.ccohs.ca/help/rtecs/rtecs-guide.html>).
737. NIOSH, *Peroxyacetic acid* (<http://www.cdc.gov/niosh/rtecs/sd8583b0.html>).
738. *MSDS Databases*, MSDSSEARCH, Inc., Hendersonville, TN., USA (<http://www.msdssearch.com/DBLinksN.htm>).
739. *Where To Find Material Safety Data Sheets On The Internet*, Interactive Learning Paradigms Inc., Lexington, KY, USA (<http://www.ilpi.com/msds/index.html#What>).
740. Sigma-Aldrich, *Peracetic acid—MSDS*, Sigma-Aldrich Co., St. Louis, MO, USA, 2004 (<http://www.sigmaaldrich.com/Brands/Aldrich.html>).
741. *EC Risk phrases*, The Physical and Theoretical Chemistry Laboratory, Oxford University, Oxford, UK (http://ptcl.chem.ox.ac.uk/MSDS/risk_phrases.html).
742. *EC Safety phrases*, The Physical and Theoretical Chemistry Laboratory, Oxford University, Oxford, UK (http://ptcl.chem.ox.ac.uk/MSDS/safety_phrases).
743. *How to interpret MSDS information sheets*, The Physical and Theoretical Chemistry Laboratory, Oxford University, Oxford, UK (<http://ptcl.chem.ox.ac.uk/MSDS/interpretingmsds.html>).
744. *MSDS of peracetic acid*, The Physical and Theoretical Chemistry Laboratory, Oxford University, Oxford, UK (http://ptcl.chem.ox.ac.uk/MSDS/PE/peroxyacetic_acid.html).

CHAPTER 8

Silicon and germanium peroxides

WATARU ANDO

*Department of Chemistry, University of Tsukuba, Tennodai, Tsukuba, Ibaraki
305-8577, Japan
Fax: +81 29 851 4796; e-mail: wataru.ando@aist.go.jp*

I. INTRODUCTION	776
II. PREPARATION OF SILYL PEROXIDES	776
A. Silyl Hydroperoxides	776
B. Bis(organosilyl) Peroxides	777
C. Silyl Peroxyesters	779
D. Silyl Alkyl and Silyl Aryl Peroxides	779
1. From singlet oxygen reaction with silyl enol ethers	779
2. From chlorotriorganosilanes with alkyl and aryl hydroperoxides	779
III. REACTION OF BIS(TRIMETHYLSILYL) PEROXIDES AND SILYL PEROXOSULFATES	784
A. Baeyer–Villiger Oxidations of Ketones	784
B. Oxidation of Alcohols	787
1. Transition metal-catalyzed oxidation	787
2. Isomerization of allylic alcohols	789
C. Olefin Oxidation	790
1. Catalytic epoxidation	790
2. Direct chlorohydrin and acetoxy alcohol synthesis	792
D. Aromatic Compounds	794
E. Reaction with Nucleophiles	795
F. Reaction with Alkynes	800
G. Oxidation of Saturated Hydrocarbons	800
H. Reaction with Heteroatom Compounds	802
1. Oxidation of nitrogen compounds	802
2. Oxidation of phosphorous compounds	803
3. Oxidation of sulfur compounds	805
4. Oxidation of disilanes and hydrosilanes	806
IV. SYNTHESIS OF ALCOHOLS VIA HEXA- AND PENTACOORDINATE SILYL PEROXIDES	808
V. SILANE OZONOLYSIS: SILANE TRIOXIDES	810

The chemistry of peroxides, volume 2

Edited by Z. Rappoport © 2006 John Wiley & Sons, Ltd ISBN: 0-470-86274-2

VI. CYCLIC SILYL PEROXIDES	814
A. Reaction of Disilazanes with Urea-H ₂ O ₂ Complex	814
B. Oxidation of Cyclic Disilanes with Molecular Oxygen	815
1. Disilolanes	816
2. 1,2-Dioxadisilins and germins	819
C. Disiladioxetanes: Oxidation of Disilenes with Molecular Oxygen	819
VII. GERMYL PEROXIDES	822
A. Germyl Hydroperoxides	822
B. Germyl Hydrotrioxides	823
C. Germyl Peroxides	823
D. Peroxide Transfer Reactions	824
E. 1,2-Digermadioxetane and Related Compounds	825
F. Digermolanes	825
VIII. REFERENCES	827

I. INTRODUCTION

The organic peroxides of group IVa, such as silicon, germanium, tin and lead, can be considered as metalloid organic peroxides containing a metal-oxygen bond which is covalent to a large extent. Generally, organosilicon and -germanium peroxides exhibit greater thermal stability than organic carbon peroxides and can be kept at room temperature in the absence of moisture for prolonged periods of time, and therefore they are very useful in organic synthesis¹⁻⁴. Organosilicon and -germanium peroxides are readily soluble in typical organic solvents such as ether, pentane, benzene, chloroform etc. In particular, bis(trimethylsilyl) peroxides, a masked form of 100% hydrogen peroxide, has emerged as a convenient oxidant for numerous oxidations. This chapter deals with the chemistry of organosilicon and germanium peroxides, i.e. of compounds which have a peroxy group linked directly to a silicon or germanium. These compounds are divided into the following main classes: (i) silyl hydroperoxides (SiOOH), (ii) bis(silyl) peroxides (SiOOSi), (iii) silyl alkyl peroxides and silyl aryl peroxides (SiOOR), (iv) silyl peroxyesters (SiOOCR), (v) cyclic silyl peroxides and (vi) linear and cyclic germanium peroxides (GeOGe, GeOOR).

II. PREPARATION OF SILYL PEROXIDES

A. Silyl Hydroperoxides

In 1954, Berry described in a patent⁵ the formation of triethyl and triphenyl hydroperoxides by the reaction of 90% hydrogen peroxide with the corresponding silanol. In 1956, Hahn and Metzinger⁶ prepared trimethylsilyl hydroperoxide by the reaction of trimethyl chlorosilane with hydrogen peroxide in the presence of pyridine. The peroxide was unstable, and readily disproportionated into bis(silyl) peroxide and hydrogen peroxide and decomposed on heating above 35 °C. Silyl hydroperoxides **1** can be readily prepared either by treating 95% hydrogen peroxide with a silylamine or with a chlorosilane in the presence of base as a hydrogen chloride acceptor (equations 1 and 2). Benzyl and triphenyl hydroperoxides can be readily prepared by the reaction of the appropriate chloro(triorgano)silane with hydrogen peroxide in the presence of hydrochloric acid scavenging bases such as pyridine, triethylamine and ammonia (Table 1)⁷.

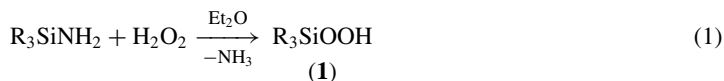


TABLE 1. Preparation of silyl hydroperoxides **1**

R ₃	R ₃ SiOOH (1)	Yield ^a (%)
MePh ₂	MePh ₂ SiOOH	54
(PhCH ₂) ₃	(PhCH ₂) ₃ SiOOH	63
(<i>n</i> -Hexyl) ₃	(<i>n</i> -Hexyl) ₃ SiOOH	83
Ph ₃	Ph ₃ SiOOH	56

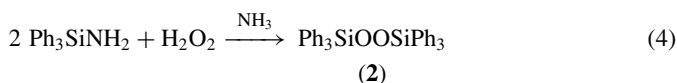
^a In the reaction of silylamines with hydrogen peroxide⁸.



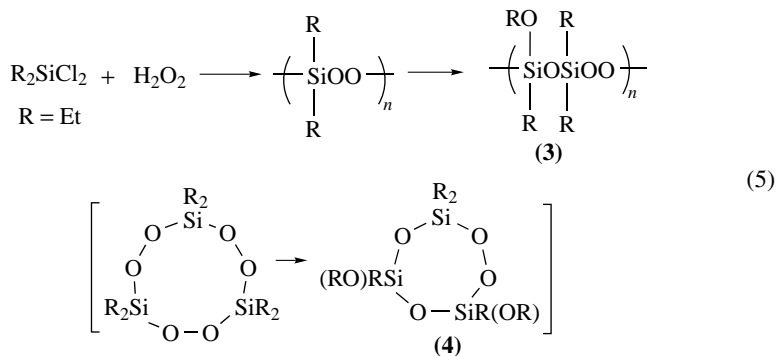
The thermal stability of the silyl hydroperoxides is increased with increasing the steric bulk of the silyl group: triphenylsilyl hydroperoxide with a melting point of 110–112 °C, for example, is indefinitely stable at room temperature⁸.

B. Bis(organosilyl) Peroxides

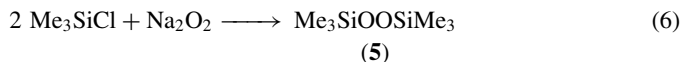
Bis(organosilyl) peroxides are prepared by nucleophilic substitution reactions of hydrogen peroxide with chlorosilanes in the presence of base^{6,9}. Thus, bis(triorganosilyl) peroxide has been prepared from the reaction of 98% hydrogen peroxide and chlorosilane with ammonia as an HCl acceptor (equation 3)⁸. Bis(triphenylsilyl) peroxide **2** can also be prepared by the reaction of hydrogen peroxide and triphenyl silylamine (equation 4).



Condensation of diethyl difluorosilane with 100% hydrogen peroxide in the presence of ammonia results in the formation of ethoxysilane, whereas an analogous condensation with diethyl dichlorosilane produces polymeric peroxides containing ethoxy and siloxane units. The initially formed straight chain or cyclic peroxides probably rearrange to products **3** or **4** containing alkoxy and siloxane moieties (equation 5)¹⁰.



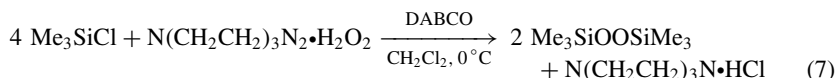
The use of disodium peroxide has been reported for the preparation of bis(trimethylsilyl) peroxide (BTSP) **5** in 80–85% yield (equation 6)¹¹.



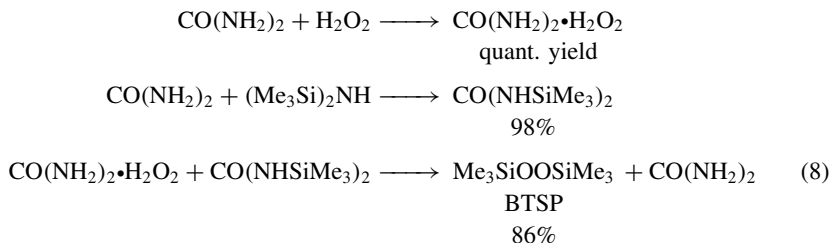
The use of hydrogen peroxide as reagent has been exploited less than it warrants because the anhydrous material is not readily available, and is inconvenient and hazardous to handle.

The most practical procedures may involve the use of stable, preformed hydrogen peroxide–base complexes, such as 1,4-diazabicyclo[2.2.2]octane [DABCO, N(CH₂CH₂)₃N]•2H₂O₂ complex. The reagent DABCO•2H₂O₂ can readily be prepared from aqueous hydrogen peroxide, and it provides a convenient and apparently safe form in which anhydrous hydrogen peroxide can be isolated, stored and handled. Even though this procedure has never caused explosions, it is still advisable to carry out this procedure in safety cupboards and behind blast shields^{12,13}.

BTSP **5** was prepared by adding the appropriate chlorosilane to a slurry of DABCO•2H₂O₂ and DABCO in dichloromethane with ice cooling, when the DABCO•HCl was immediately precipitated (equation 7). The peroxide, as well as analogous peroxides, was generally obtained in high yield (Table 2)¹⁴.



On the other hand, the commonly available urea–hydrogen peroxide complex offers considerable advantage over DABCO•2H₂O₂ for the preparation of BTSP from *N,N'*-bis(trimethylsilyl)urea (equation 8)^{13b}.



Hydrogen peroxide is also complexed with hexamethylenetetramine, industrially prepared from formaldehyde and ammonia, which advantageously replaces DABCO. This

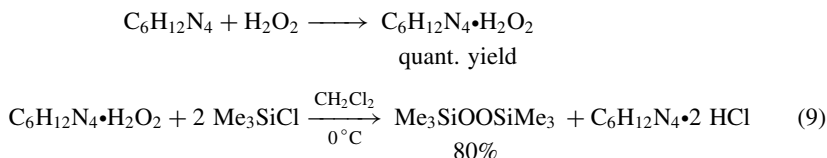
TABLE 2. Preparation of bis(triorganosilyl) peroxides

Peroxide	Yield (%)	
	undistilled	distilled
Me ₃ SiOOSiMe ₃	62 ^a	35
Et ₃ SiOOSiEt ₃	100	71
Pr ₃ SiOOSiPr ₃	100	60
Me ₂ PrSiOOSiPrMe ₂	96	72
Me ₂ (PhCH ₂)SiOOSi(CH ₂ Ph)Me ₂		45
Me ₂ (EtO)SiOOSi(OEt)Me ₂	95	
Et ₃ GeOGeEt ₃ ^b	84	

^a Some peroxide was lost because of its volatility.

^b From triethylchlorogermane.

route is not only cheaper and easier than the urea and DABCO routes, but also faster since both reactions are very quick; indeed, the complexation of hydrogen peroxide is instantaneous and the silylation is fast and exothermic (equation 9)^{13a}.



C. Silyl Peroxyesters

Bis(trimethylsilyl) peroxomonosulfate $\text{Me}_3\text{SiOSO}_2\text{OOSiMe}_3$ **6** and $\text{Me}_3\text{SiOSO}_2\text{OOR}$ ($\text{R} = \text{Pr}, \text{Bu}, n\text{-C}_5\text{H}_{11}$) are obtained by insertion of SO_3 into BTSP and Me_3SiOOR , respectively, at -20 – 30°C in CH_2Cl_2 (equation 10)¹⁵.

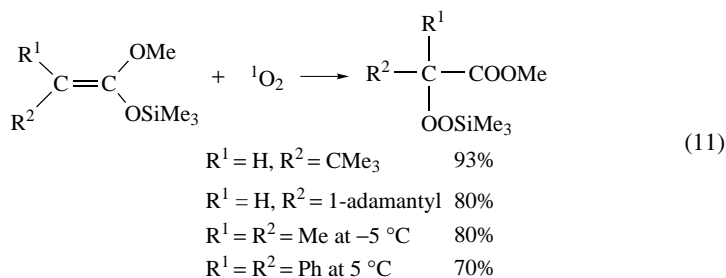


Compound **6** undergoes a slow nucleophilic 1,2-rearrangement, forming the isomer $\text{Me}_3\text{SiOSO}_2\text{OSi}(\text{OMe})\text{Me}_2$.

D. Silyl Alkyl and Silyl Aryl Peroxides

1. From singlet oxygen reaction with silyl enol ethers

When a carbon tetrachloride solution of 1-methoxy-1-trimethylsiloxy-1-alkene in the presence of tetraphenylporphyrin and bubbling oxygen is irradiated with a 400-W Na lamp, α -trimethylsilyl peroxyesters were obtained in good yield (equation 11)^{16,17}.



2. From chlorotriorganosilanes with alkyl and aryl hydroperoxides

Silyl alkyl and silyl aryl peroxides **7** are prepared by reaction of alkyl, aryl or aralkyl hydroperoxides with halosilanes (equation 12). Such reactions are carried out in an inert solvent in the presence of an acid acceptor, such as pyridine, ammonia or a tertiary amine in ether or petroleum ether (Table 3)^{18–22}.

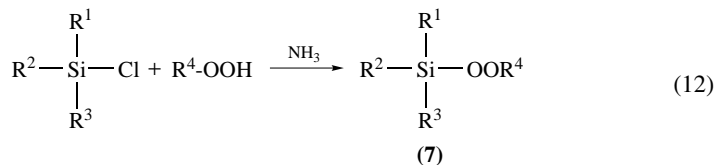


TABLE 3. Silyl alkyl and aryl peroxides $R^1R^2R^3Si-OOR^4$ **7** obtained according to equation 12

R^1	R^2	R^3	R^4	Yield of 7 (%)	Reference
Me	Me	Me	CMe ₂ Et	83	18
Me	Me	Me	CMe ₂ Ph	88	18
Me	Et	vinyl	CMe ₃	59	19
Me	Et	vinyl	CMe ₂ Et	59	20
Me	Et	vinyl	CMe ₂ Ph	43	20
Me	Me	Et	CMe ₃	70	21
Me	Me	<i>n</i> -Pr	CMe ₃	75	21
Me	Me	<i>n</i> -Bu	CMe ₃	65	21
Me	Me	CH ₂ Ph	CMe ₃	72	21
Me	Me	CH ₂ Cl	CMe ₃	70	21
Me	Me	Ph	CMe ₃	—	21
Me	Me	2-Thi	CMe ₃	77	21
Ph	Ph	Ph	CMe ₃	78	18
Ph	Ph	Ph	CMe ₂ Ph	85	22
Ph	Ph	Ph	CPh ₂ Me	80	22
Ph	Ph	Ph	CPh ₃	82	22

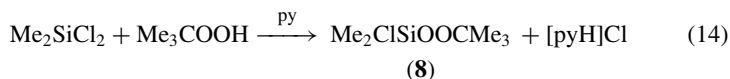
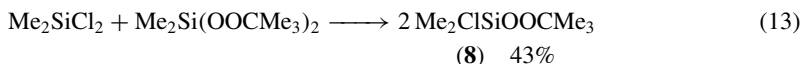
TABLE 4. Silyl alkyl and aryl peroxides $R^1R^2R^3Si-OOR^4$ **7** from chlorotriorganosilane and alkyl peroxide/DABCO adduct²³

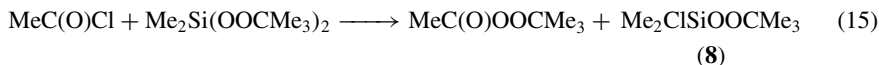
R^1	R^2	R^3	R^4	Yield of 7 (%)
Me	Me	Me	CMe ₃	91
Me	Me	Me	CMe ₂ Ph	75
Me	Me	CH ₂ CH=CH ₂	CMe ₃	95
Me	Me	Ph	CMe ₂ Ph	93
Me	Me	CH ₂ Cl	CMe ₂ Ph	95
Me	Ph	Ph	CMe ₂ Ph	93
Et	Et	Et	CMe ₃	74
Et	Et	Et	CMe ₂ Ph	80
<i>n</i> -Bu	<i>n</i> -Bu	<i>n</i> -Bu	CMe ₃	95
<i>n</i> -Bu	<i>n</i> -Bu	<i>n</i> -Bu	CMe ₂ Ph	95
Vinyl	Ph	Ph	CMe ₂ Ph	92
Ph	Ph	Ph	CMe ₃	95
Ph	Ph	Ph	CMe ₂ Ph	70

Silyl peroxides containing a vinyl group have also been prepared by the same method.

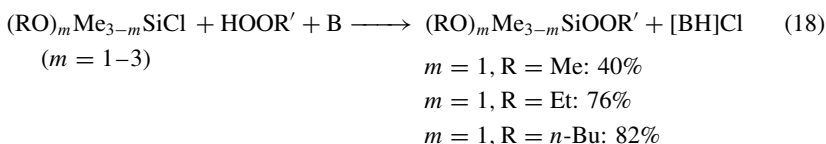
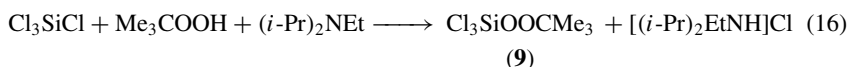
Alkyl hydroperoxides can form 2:1 adducts with DABCO. Both nitrogens of DABCO are involved and the resulting adduct contains 2 mol of hydroperoxide per mol of DABCO²³. Table 4 lists the silyl alkyl peroxides prepared using the DABCO–hydroperoxide adduct techniques.

Alkyl(chloro)silyl peroxides **8** and alkyl alkoxy-silyl peroxides are prepared by the alkyl hydroperoxidation of dichlorodiorganosilane (equations 13–15).

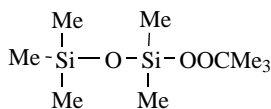




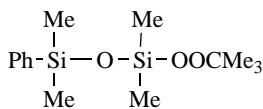
In the presence of diisopropyl(ethyl)amine, tetrachlorosilane reacts with *t*-butyl hydroperoxide to give 1:1 adduct **9** (equation 16). Alkylperoxydiorganoalkoxysilanes are prepared from the reaction of chlorodiorganooxysilane with alkyl hydroperoxides in the presence of ammonia or organic base such as pyridine or triethylamine (equations 17 and 18).



t-Butylperoxy(pentamethyl)disiloxane **10** was prepared in 62% yield by the reaction of chloropentamethyldisiloxane with *t*-butyl hydroperoxide in the presence of ammonia or with *t*-butyl lithium peroxide (85%).



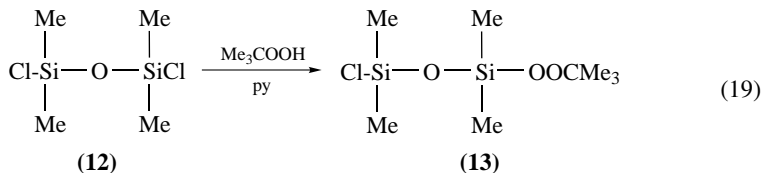
(10)



(11)

Similarly, *t*-butylperoxy(chlorodimethyl)silane reacts with phenyldimethylsilanol in the presence of pyridine to give *t*-butylperoxy-3-phenyltetramethyldisiloxane **11**.

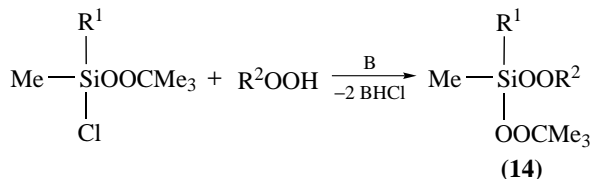
The reaction of 1,3-dichloro(tetramethyl)siloxane **12** with *t*-butyl hydroperoxide in the presence of pyridine in ether gave 1-*t*-butylperoxy-3-chlorotetramethyldisiloxane **13** in 60% yield (equation 19).



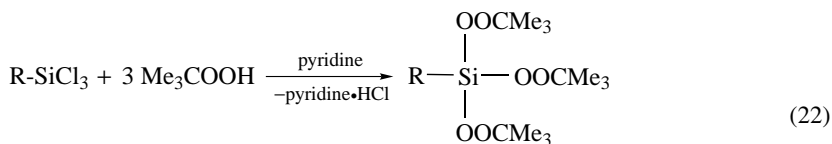
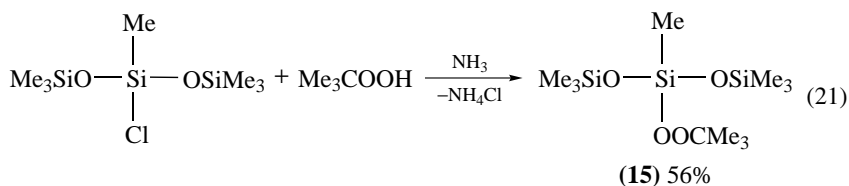
Bis(alkylperoxy)diorganosilanes **14** were prepared by the reaction of alkylperoxy diorganochlorosilane with alkyl hydroperoxides in the presence of ammonia or pyridine (equation 20).

3-Alkylperoxyheptaorganotrisiloxanes **15** are synthesized from the reaction of 3-chloroheptaorganotrisiloxanes with alkyl hydroperoxide in the presence of ammonia or pyridine (equation 21).

Organotris(alkylhydroperoxy)silanes **16** are synthesized from the reaction of organotrichlorosilane with alkyl hydroperoxides in the presence of pyridine (equation 22)¹⁸.



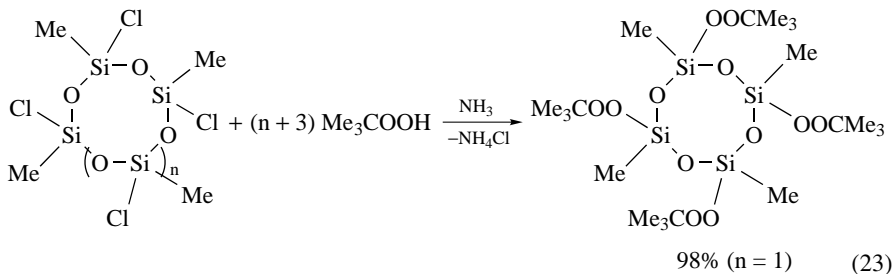
R ¹	R ²	Base	14 (%)
Me	CHMeEt	NH ₃	80
Me	CMe ₂ Et	pyridine	89
Me	CMe ₂ Cy	pyridine	80
Me	CMe ₂ Ph	pyridine	
Ph	CMe ₂ Et	NH ₃	92

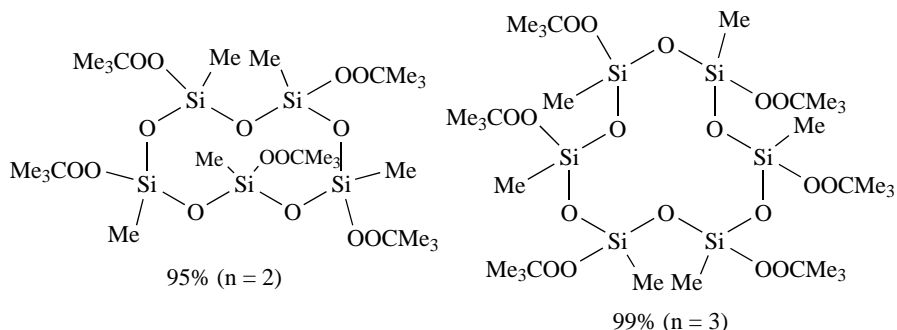


(16) R = Me, 48%

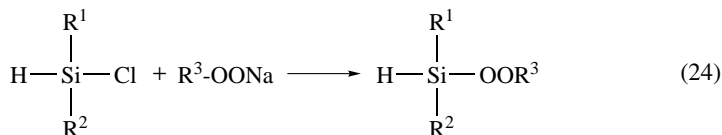
R = CH=CH₂, 48%

Cyclo(alkylperoxyorgano)siloxanes are prepared from the corresponding cyclo(chloroorgano)siloxanes with alkyl hydroperoxide in the presence of ammonia (equation 23)^{18d}.

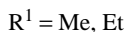
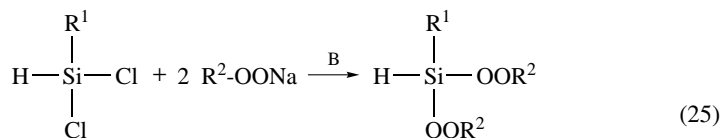




The chlorohydrosilane with alkyl sodium alkyl peroxide or with alkyl hydroperoxide and triethylamine in petroleum ether produced the corresponding alkylperoxy hydrosilane (equation 24)^{18a}.



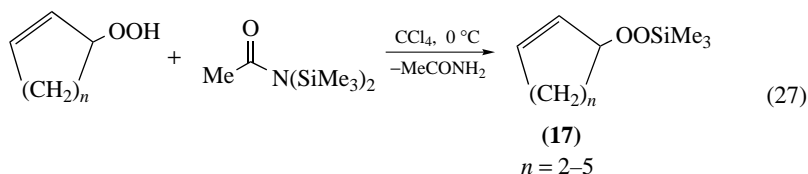
Bis(alkylperoxy)hydrosilanes are obtained from the reaction of dichlorohydrosilane with alkyl hydroperoxide in the presence of base B (equation 25)²⁴.



A less frequently used method involves the condensation of trimethylsilyl alkylamines with *t*-butyl hydroperoxide. A 20% yield of trimethyl(*t*-butylperoxy)silane has been obtained (equation 26)²⁵.



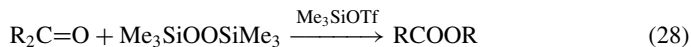
Alkyl hydroperoxides react with *N,N*-bis(trimethylsilyl)acetamide to give alkyl hydroperoxysilanes. For example, 3-hydroperoxycyclopentene, -cyclohexene and -cyclooctene react with *N,N*-bis(trimethylsilyl)acetamide in a 2:1 mole ratio to yield the corresponding trimethylsilyl cycloalkenyl peroxide **17** (equation 27)²⁶.



III. REACTION OF BIS(TRIMETHYLSILYL) PEROXIDES AND SILYL PEROXSULFATES

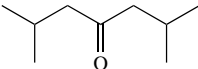
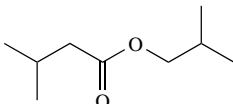
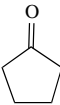
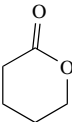
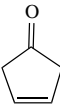
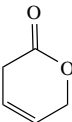
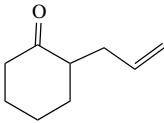
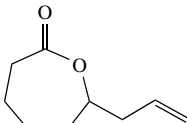
A. Baeyer–Villiger Oxidations of Ketones

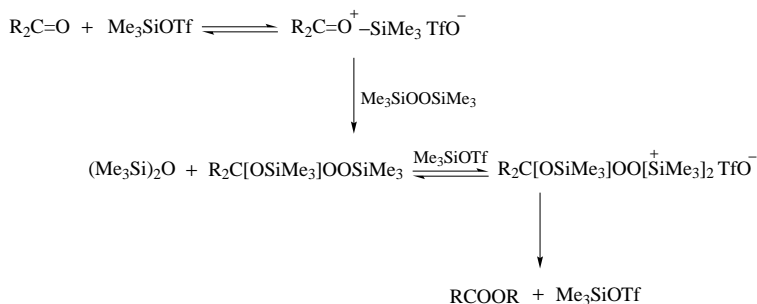
A Baeyer–Villiger type oxidation of ketonic substrates occurs exclusively at the carbonyl function under aprotic conditions by use of BTSP and a catalytic amount of $\text{Me}_3\text{SiO}_3\text{CCF}_3$ (Me_3SiOTf) (equation 28). C–C bonds are not affected (Table 5)²⁷.



The Me_3SiOTf catalyzed oxidation is considered to proceed by the mechanism shown in Scheme 1.

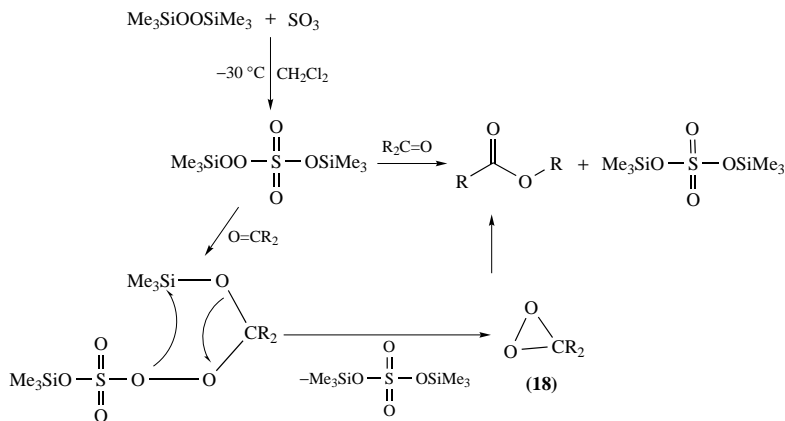
TABLE 5. Oxidation of ketones with BTSP in the presence of trimethylsilyl triflate

	TMSOTf (mol%)	Temp. (°C) (Time, h)	Product	Yield (%)
	10	0 (22)		40
	3.5	-78 (1) and -30 to -20 (8)		58
	10	-78 to -50 (30) 0 (20)		42
	16	-78 (3) and -50 to -10 (4.5)		40

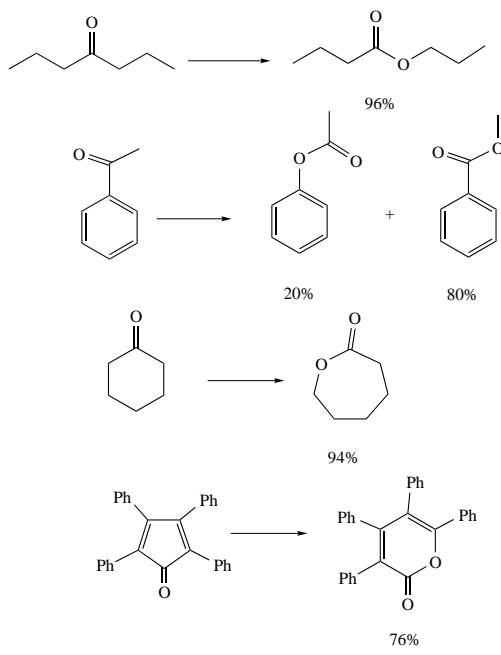


SCHEME 1

Bis(trimethylsilyl)monoperoxysulfate exhibits promise as a Baeyer–Villiger oxidant. Oxidation of the ketones Pr_2CO , Ph_2CO , $p\text{-BrC}_6\text{H}_4\text{Ac}$, fluorenone, adamantanone and tetracyclone gave 74–98% PrCO_2Pr , BzOPh , $p\text{-BrC}_6\text{H}_4\text{OH}$, 2'-hydroxybiphenyl 2-carboxylic acid lactone, 4-oxohomoadamantan-5-one and tetraphenyl- α -pyrone, respectively (Scheme 2 and Table 6)^{28,29}.

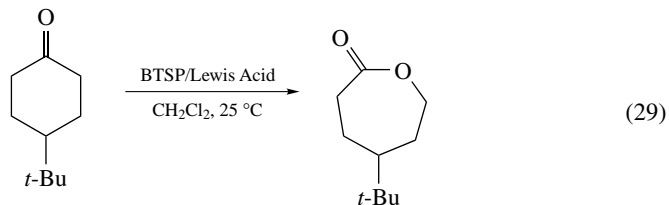


SCHEME 2

TABLE 6. Yields of Baeyer–Villiger product with $\text{Me}_3\text{SiOSO}_2\text{OOSiMe}_3$ 

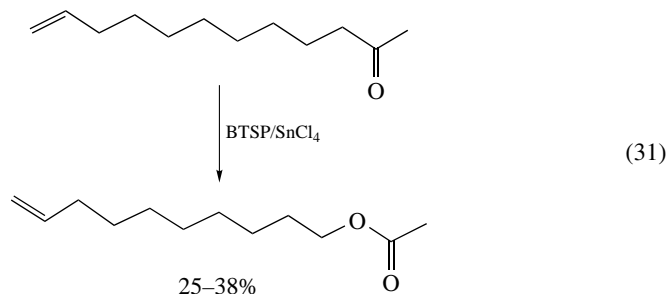
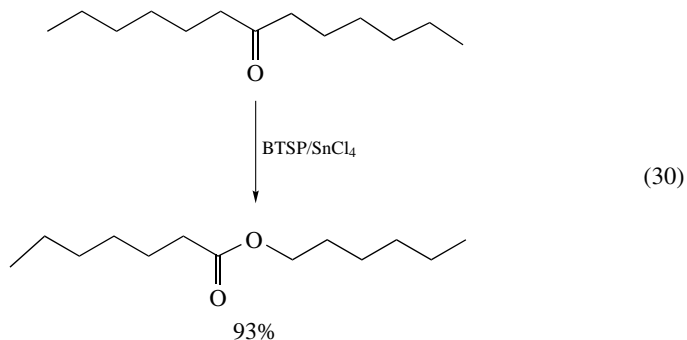
Dioxiranes **18** have been suggested as the reactive intermediates in the oxidation in these reactions.

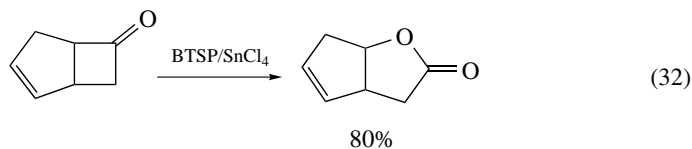
Treatment of ketones with BTSP and a Lewis acid such as SnCl_4 or $\text{BF}_3 \cdot \text{OEt}_2$ in CH_2Cl_2 at room temperature affords esters in fair to excellent yields (equation 29)³⁰.



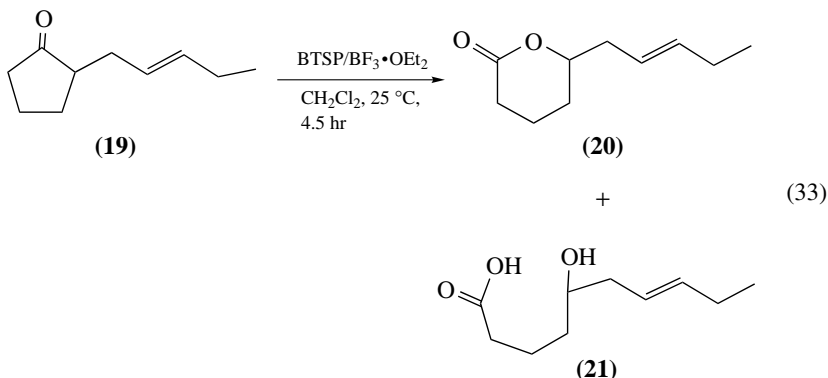
Lewis acid	Yield (%)
SnCl_4	84
$\text{BF}_3 \cdot \text{OEt}_2$	88
FeCl_3	72
AlCl_3	38
ZrCl_4	34
TiCl_4	27
ZnCl_2	<5

The results of the Baeyer–Villiger oxidation with the BTSP– SnCl_4 or $\text{BF}_3 \cdot \text{OEt}_2$ system are summarized in equations 30–32.





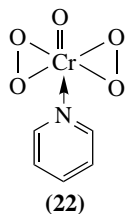
Jasmine lactone **20** is synthesized from 2-[(*Z*)-2-pentenyl]cyclopentanone **19** in several steps (equation 33)^{30b,c} without any protection of the carbon-carbon double bond. The hydroxy acid **21** was formed as a side product.



B. Oxidation of Alcohols

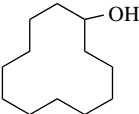
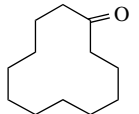
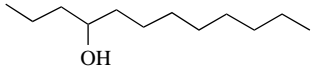
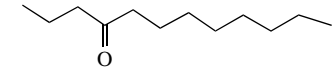
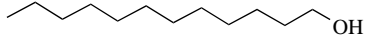
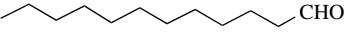
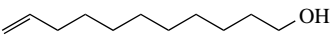
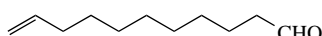
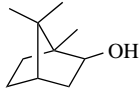
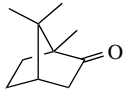
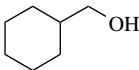
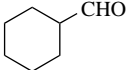
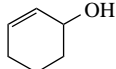
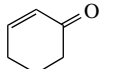
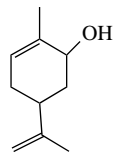
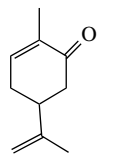
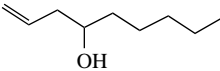
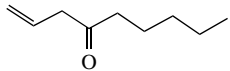
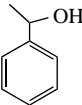
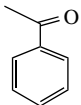
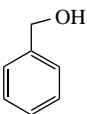
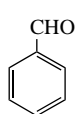
1. Transition metal-catalyzed oxidation

The BTSP-pyridinium dichromate system has proved to be effective for generation of the oxodiperoxychromium complex **22** in dichloromethane. As the peroxy complex decomposed easily, the oxidant BTSP was added dropwise to the reaction mixture using a syringe drive. The BTSP was stable enough even upon contact with the metallic surface of the syringe needle when it was diluted with dichloromethane. Typical results for the conversion of alcohols into carbonyl compounds are summarized in Table 7.



Each substrate was oxidized to the corresponding carbonyl compounds in good yields. Moreover, the coexisting olefin linkage remained intact upon treatment with the oxodiperoxychromium complex and no epoxy compounds were observed in the reaction mixture. Hexavalent chromium reagents such as anhydrous chromium trioxide and pyridinium

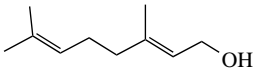
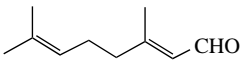
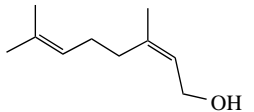
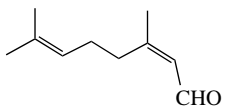
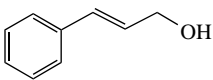
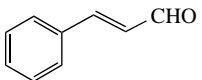
TABLE 7. Oxidation of alcohols with BTSP

Alcohol	Aldehyde or ketone	Yield (%)
		100
		83
		74
		76
		98
		71
		90
		81
		87
		97
		91

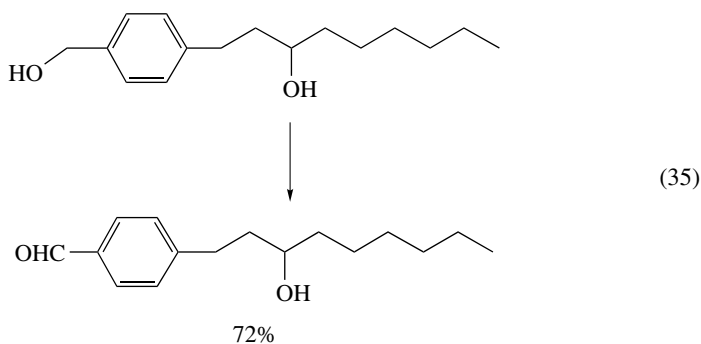
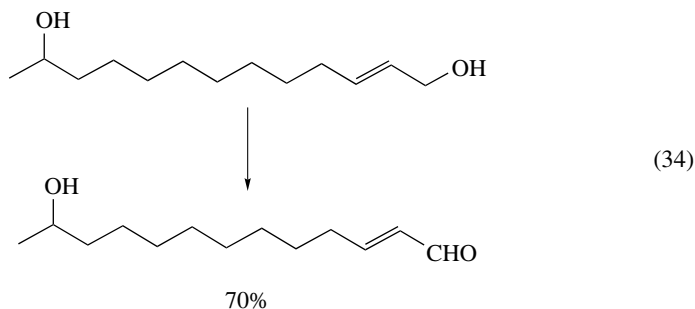
chromate were found to be less effective than pyridinium dichromate³¹. A ruthenium complex, $\text{RuCl}_2(\text{PPh}_3)_3$, is also a popular catalyst for the oxidation of alcohols (Table 8).

It is noteworthy that allylic alcohols are oxidized to products with retained configuration of the olefinic bond. Geraniol and nerol were oxidized to the corresponding (*E*)- and (*Z*)- α -enals, respectively. As expected, primary alcohols were oxidized faster than secondary ones with the $\text{RuCl}_2(\text{PPh}_3)_3/\text{BTSP}$ system with relative rates from 20–40:1. The new system was applicable for the selective oxidation of primary–secondary diols

TABLE 8. Oxidation of alcohols with BTSP in the presence of $\text{RuCl}_2(\text{PPh}_3)_3$

Alcohol	Aldehyde	Yield (%)
		85
		96
		80

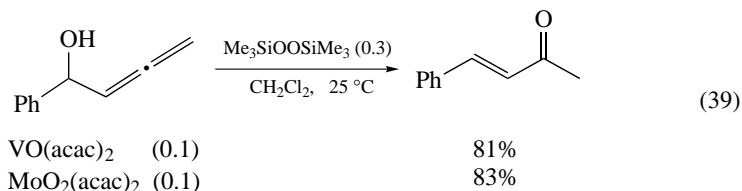
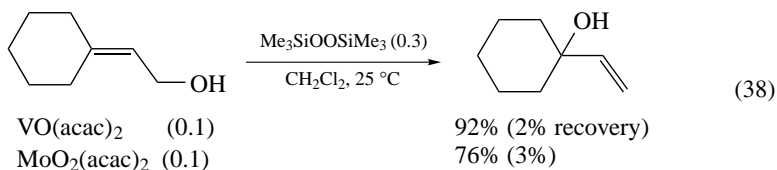
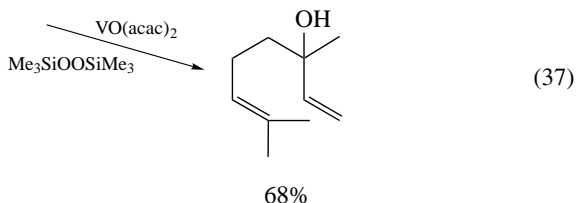
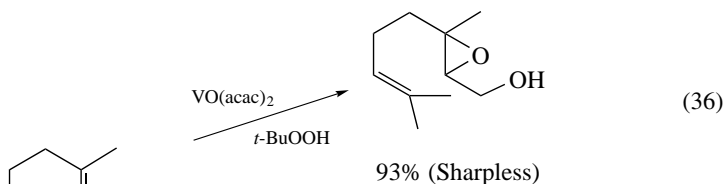
(equations 34 and 35) where only hydroxy aldehyde was obtained in good yield³².



2. Isomerization of allylic alcohols

Isomerization of primary allylic alcohols proceeds in dichloromethane at 25 °C in the presence of a catalyst prepared *in situ* from $\text{VO}(\text{acac})_2$ or $\text{MoO}_2(\text{acac})_2$ and BTSP to give tertiary isomers in good yields. This is in sharp contrast to the well-known Sharpless epoxidation of allylic alcohols³³. The catalysts are also effective for rearrangements of secondary–tertiary allylic alcohols. The isomerization of an allenyl allylic

alcohol, $\text{Me}_2\text{C}:\text{CHCH}(\text{OH})\text{CH}:\text{C}:\text{CH}_2$, gave either (*E*)- $\text{Me}_2\text{C}(\text{OH})\text{CH}:\text{CHCH}:\text{C}:\text{CH}_2$ or (*E*)- $\text{Me}_2\text{C}:\text{CHCH}:\text{CHCOMe}$, selectively, depending on the reaction conditions (equations 36–39)³⁴.



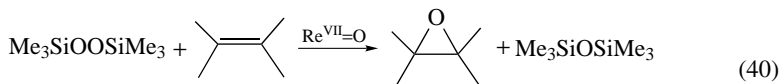
A [3,3] sigmatropic rearrangement of an inorganic ester such as vanadate or molybdate is considered to be involved in one of the reasonable mechanisms.

The reaction of geraniol, nerol and linalool in the presence of $\text{VO}(\text{acac})_2 - \text{Me}_3\text{SiOOSiMe}_3$ in dichloromethane at 25 °C gave α -terpineol as the main product³⁵.

C. Olefin Oxidation

1. Catalytic epoxidation

Conditions were found under which simple inorganic oxorhenium species act as efficient olefin epoxidation catalysts. This has been achieved by simply replacing aqueous H_2O_2 with BTSP as an oxygen atom source in the epoxidation. Representative substrates include fairly unreactive olefins and/or progenitors of sensitive epoxides³⁶. For example, terminal olefins can be efficiently converted to epoxides (equation 40, Table 9).



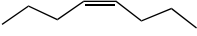
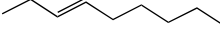
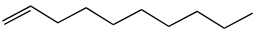
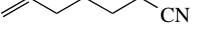
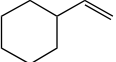
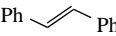
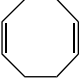
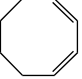
(Effective catalysts include MTO, Re_2O_7 , $\text{ReO}_3(\text{OH})$, ReO_3)

Additives such as pyridines serve to prevent sensitive epoxide ring opening by buffering the highly acidic rhenium species. The amount of ligand necessary to achieve the desired protection is now decreased from 12 to 0.5–1 mol% in both methyltrioxorhenium (MTO) and Re_2O_7 catalyzed epoxidation. In some instances, MTO loadings can be lowered to 0.25 mol% without affecting conversions—a manifestation of prolonged catalyst lifetime. The work-up simply involves destruction of the traces of H_2O_2 with manganese dioxide and evaporation of the hexamethyldisiloxane.

On the basis of these observations, there appears to be a mechanistic role for a trace of water or a similar protic species (e.g. MeOH is also effective) to enable a rapid turnover of the catalytic cycles (Scheme 3)³⁷.

Bis(trimethylsilyl)monoperoxy sulfate **6** is also an excellent agent for oxygen transfer to nucleophilic substrates such as alkenes and heteroatoms. Compound **6** could oxidize alkenes such as 1-methylcyclohexene and *trans*- β -methylstyrene, producing 2-methylcyclohexanone and benzyl methyl ketone, respectively, in high yield, most likely via the

TABLE 9. Epoxidation with BTSP in the presence of Re catalyst

Olefin	Catalyst/solvent ^a	Time (h)	Yield (%)
	{ A B C	15	92
		20	90
		12	88
	{ A D F	9	90
		16	85
		11	79
	{ D D/neat	14	94
		8	83
	D	18	92
	D	7	95
	D	10	96
	E	12	68
	G	10	82
	G	13	78

^aA: MeReO_3 (0.5 mol%), pyridine (1 mol%)/ CH_2Cl_2

B: MeReO_3 (0.25 mol%), pyridine (0.5 mol%)/ CH_2Cl_2

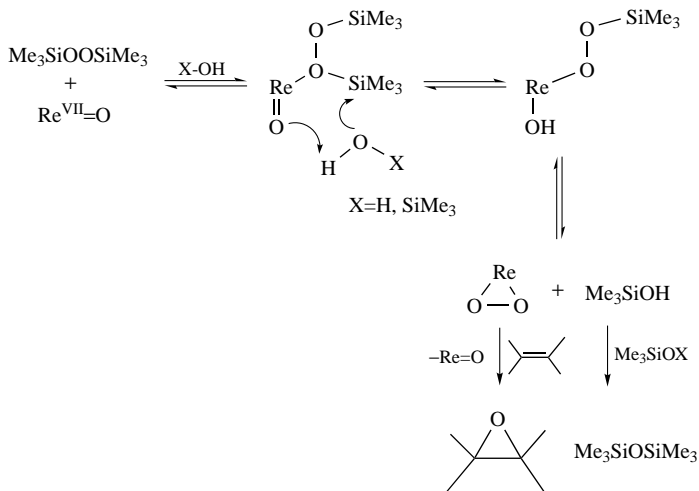
C: Re_2O_7 (0.5 mol%), pyridine (1 mol%)/ CH_2Cl_2

D: Re_2O_7 (0.5 mol%)/ CH_2Cl_2

E: HReO_4 (0.5 mol%)/THF

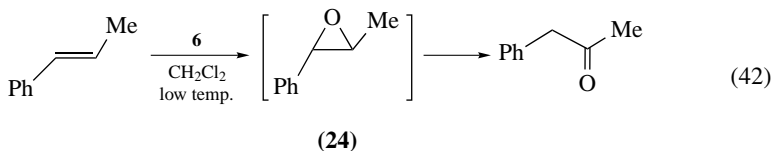
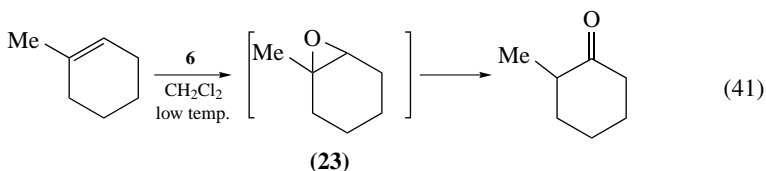
F: ReO_3 (0.5 mol%)/ CH_2Cl_2

G: Re_2O_7 (1 mol%)/THF

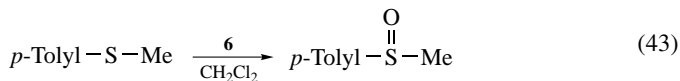


SCHEME 3

parent epoxides **23** or **24** (equations 41 and 42).



The reaction of **6** with *p*-tolyl methyl sulfide is nearly instantaneous even at -30°C , yielding *p*-tolyl methyl sulfoxide (equation 43).

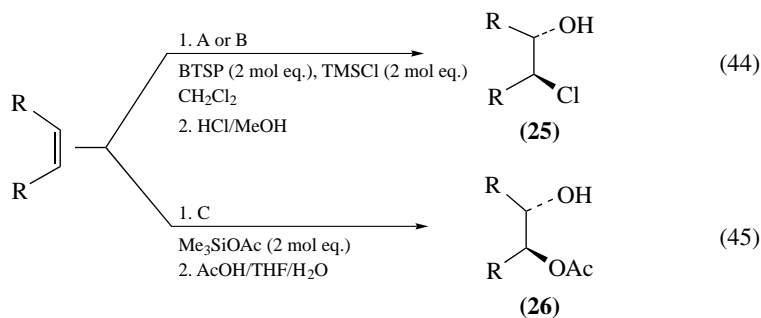


The oxidation of enol acetates of ketones to α -hydroxy (or α -acetoxy) ketones with the BTSP-FeCl₃ system can also be performed³⁰.

2. Direct chlorohydrin and acetoxy alcohol synthesis

Chlorohydrins and acetoxy alcohols were prepared by treating olefins with SnCl₄ (or SnO)/BTSP/Me₃SiCl or Zr(OCHMe₂)₄/BTSP/Me₃SiOAc in -20°C . This is demonstrated by the formation of the chlorohydrin **25** and the acetoxy alcohol **26** in 69% yield.

On the other hand, in the absence of TMSCl, almost quantitative starting material was recovered³⁸. The use of BTSP offers a useful method for direct synthesis of chlorohydrins as shown in equations 44 and 45 and in Table 10.



Catalyst: A) = SnCl_4 (10 mol%), B) = $(\text{SnO})_n$ (10 mol%), C) = $\text{Zr}(\text{OPr-}i)_4$ (10 mol%)

It is noteworthy that the chlorohydrin **27** and acetoxy alcohol **28** can be synthesized in a highly stereocontrolled manner. Zr-catalyzed reaction proceeds, contrasting with the Sn-catalyzed reaction, via an epoxide intermediate to give the acetoxy alcohol.

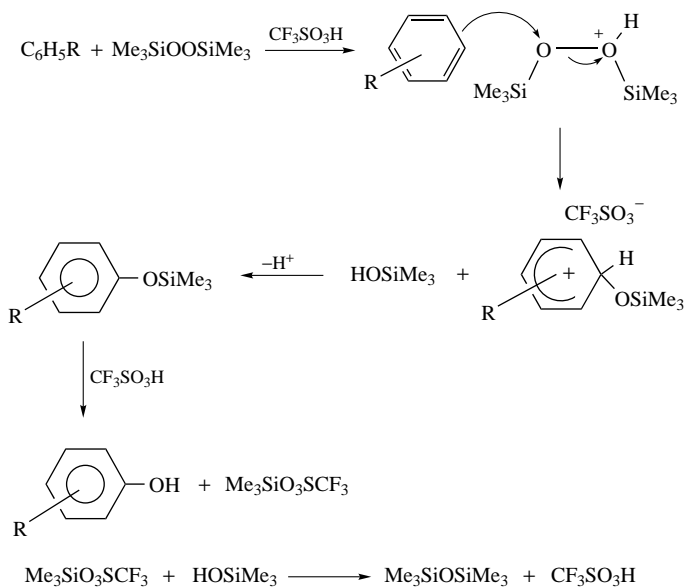
TABLE 10. Chlorohydrin and acetoxy alcohol synthesis from olefins with BTSP, TMSX and Lewis acids

Alkene	Product	X	Catalyst ^a	Yield (%)
		Cl	A	69
		Cl	B	92
		OAc	C	78
		Cl	A	73
		Cl	B	74
		OAc	C	71
		Cl	A	78
		Cl	B	71
		Cl	A	77
			(27)	
		OAc	C	80
			(28)	

^a Catalyst: A = SnCl_4 (10 mol%), B = $(\text{SnO})_n$ (10 mol%), C = $\text{Zr}(\text{OPr-}i)_4$ (10 mol%).

D. Aromatic Compounds

The triflic acid catalyzed electrophilic hydroxylation of aromatics with BTSP gives the corresponding phenols in high yields without apparent polyhydroxylation or secondary oxidation. Thus, treatment of C_6H_6 with CF_3SO_3H followed by BTSP gave 77% PhOH. The isomer distributions are in accord with the electrophilic nature of the reaction. The observed *ortho/para* ratio in the case of toluene agrees with the expected trends (Scheme 4 and Table 11)³⁹.



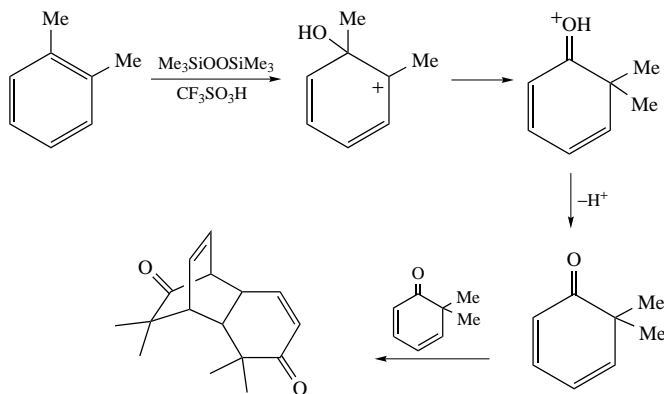
SCHEME 4

The reaction of *o*-xylene showed the formation of dimethylphenols in about 63% yield together with 21% of the dimer of 6,6-dimethyl-2,4-cyclohexadien-1-one, which involves *ipso* attack followed by a methyl shift and cycloadditive dimerization of the intermediate 6,6-dimethyl-2,4-cyclohexadien-1-one catalyzed by the acid (Scheme 5).

Electrophilic hydroxylation of *ortho*- and *para*- $Me_2C_6H_4$ by peroxides including BTSP in the presence of Lewis acids gave mixtures of phenols, including those derived from *ipso* attack followed by rearrangement; *ipso* attack by HO^\bullet leads to dealkylation. For

TABLE 11. Hydroxylation of aromatics with BTSP/ CF_3SO_3H

Substrate	T ($^\circ C$)	Yield (%)	Isomer distribution (%)		
			<i>ortho</i>	<i>meta</i>	<i>para</i>
benzene	0	77			
toluene	0	88	63	10	27
mesitylene	0	94			
<i>o</i> -xylene	-50	63	(2,3-) 48	(2,6-) 22	(3,4-) 30
naphthalene	-50	92	(α -) 67		(β -) 33
chlorobenzene	0	76	63		37



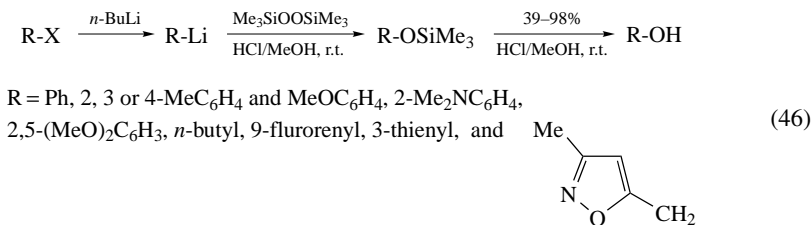
SCHEME 5

example, treatment of *ortho*-Me₂C₆H₄ with a 1:2 mol ratio of BTSP and AlCl₃ gave 18% of a 69:31 mixture of 2,5- and 2,4-Me₂C₆H₃OH, respectively, corresponding to a rate ratio $k = (H/ipso)$ of 1.1⁴⁰.

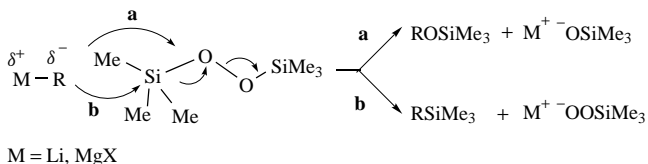
Aromatic compounds are oxidized to quinones by bis(triorganosilyl) peroxides in the presence of a metal acid catalyst. Thus, 2-methylnaphthalene was oxidized with BTSP in the presence of Re₂O₇ and Bu₃PO in the presence of CHCl₃, to a mixture of 59% 2-methyl-1,4-naphthoquinone and 8% 6-methyl-1,4-naphthoquinone⁴¹.

E. Reaction with Nucleophiles

The reactions of BTSP with alkyl, vinyl, alkynyl, aromatic and heteroatom anions show that the two possible reaction pathways take place, i.e. reaction at the electrophilic oxygen and reaction of the carbanion at the silyl group⁴². Alkyl-, aryl- and vinylmagnesium halides react exclusively at oxygen, while vinyl-, aryl- and ethynyllithium reagents react at silicon. Depending on the reaction conditions, the trimethylsiloxy derivatives can be obtained alone or/and together with the corresponding trimethylsilyl derivatives, which are sometimes the major product (equation 46).



Enolates, generated by using magnesium diisopropylamide, give the corresponding hydroxycarbonyl compounds in good yields. An attempt to rationalize the results emphasizes the wide use of BTSP in organic synthesis as an electrophilic hydroxylation reagent. In many cases, the most plausible mechanism involves nucleophilic attack by the substrate at the weak O—O bond of the peroxide (Scheme 6, path a). Path b represents an S_N2-type

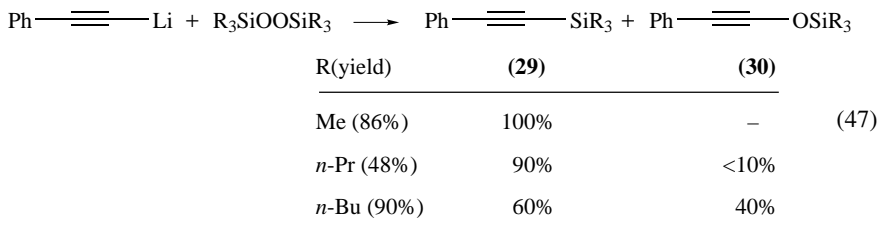


SCHEME 6

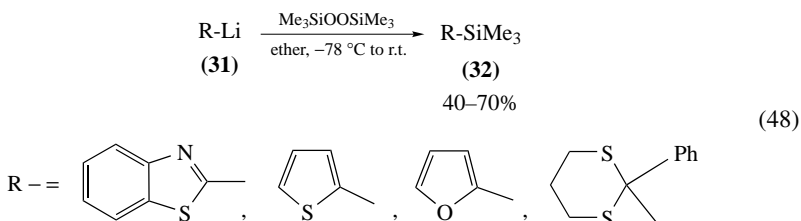
attack at silicon, which is facilitated by the fact that Me_3SiO^- should be a good leaving group⁴³.

The regiospecific introduction of a hydroxy group into aromatic and aliphatic compounds can be performed in good yields by electrophilic hydroxylation of their organometallic derivatives with BTSP. Thus, the reaction of RLi with BTSP gave ROSiMe_3 , which was hydrolyzed with HCl-MeOH to give 39–98% ROH ⁴⁴. The reaction of butyllithium with BTSP proceeds through a radical stage via a one-electron transfer mechanism.

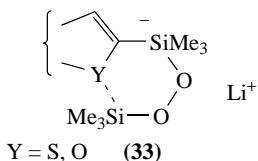
The reaction of phenylethynyllithium with BTSP affords almost exclusively silane **29**, while the reactions with sterically hindered tri(*n*-propyl)silyl and tri(*n*-butyl)silyl peroxides afford mixtures of silanes **29** and silyl ethers **30** (equation 47).



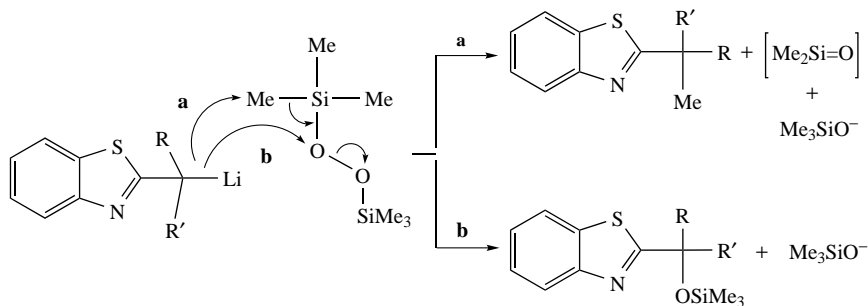
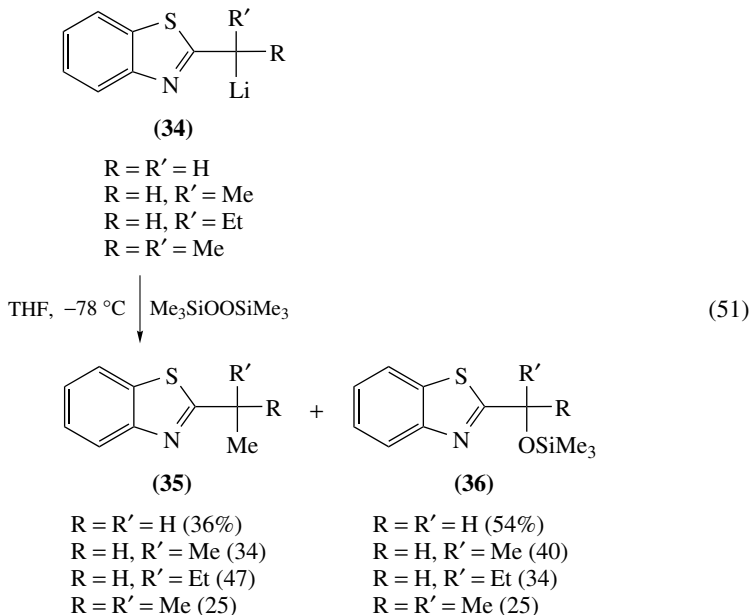
The reaction of BTSP with lithium compounds **31** at the carbanionic center α to a heteroatom affords the corresponding trimethylsilyl derivatives **32** in yield from 40 to 70%. No trace of the expected 2-siloxy or 2-hydroxy derivatives was detected in the reaction mixture (equation 48).



The formation of silyl derivatives **32** might be justified by a reaction mechanism involving a six-membered transition state of the type **33**.



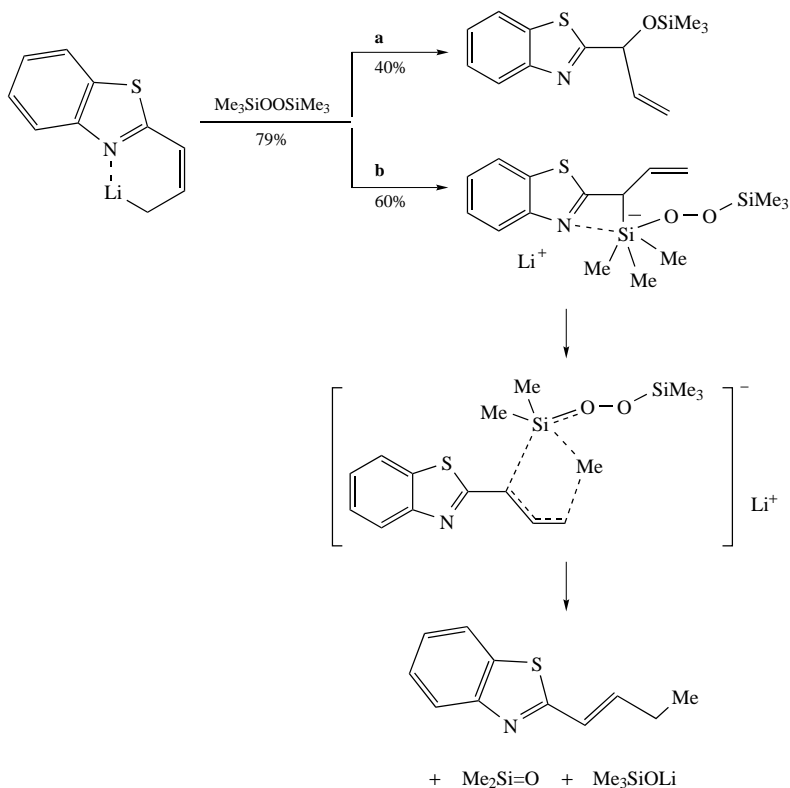
In the reaction of lithiated *alkylbenzothiazoles* with BTSP, the formation of methylated products always competes with the formation of silyl ethers. The *demethylation* of BTSP can tentatively be conceived as being derived from the nucleophilic attack of *alkylbenzothiazole* anion at the methyl group of BTSP with displacement of silanone and silanone anion, while silyl ethers would form by nucleophilic attack of the alkylbenzothiazole anion at the oxygen of BTSP (Scheme 8)⁴⁷.



SCHEME 8

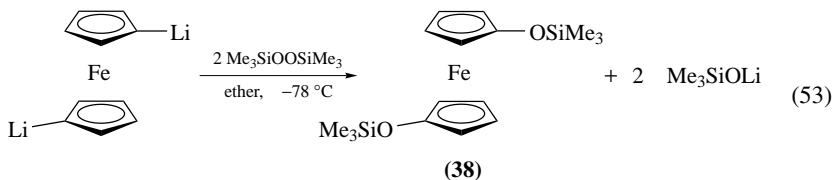
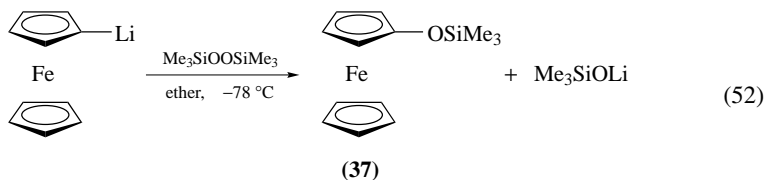
Reaction of BTSP with 2-benzothiazolyl allyl lithium proceeds in a regioselective and stereoselective manner leading to the silyloxylation and the *trans* methylation product (Scheme 9).

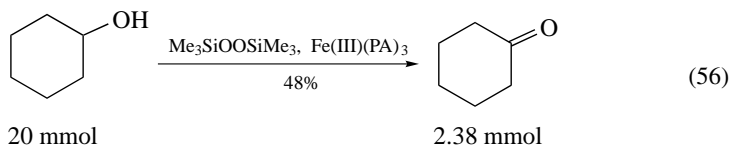
Starting from the alcohols, *ferrocenol* ($\text{Fe}(\text{C}_5\text{H}_5)(\text{C}_5\text{H}_4\text{-OH})$, Fc-OH) and 1,1'-ferrocenediol ($\text{Fe}(\text{C}_5\text{H}_4\text{-OH})_2$, $\text{Fc}(\text{OH})_2$), a series of new ferrocene derivatives has been prepared, in which the oxygen is directly connected with the ferrocene unit. The reactions



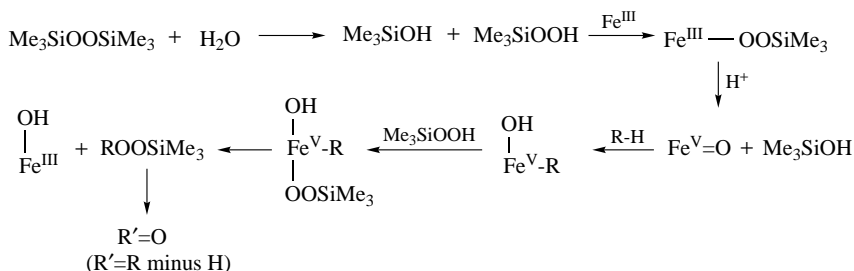
SCHEME 9

with organoelement chlorides such as Me_3SnCl , $t\text{-BuPCl}_2$, $t\text{-Bu}_2\text{PCl}$ and $t\text{-Bu}_2\text{AsCl}$ lead to complexes containing the heteronuclear groups O-Sn, O-P and O-As, respectively. The analogous trimethylsiloxy derivatives, FcOSiMe_3 **37** and $\text{Fc}(\text{OSiMe}_3)_2$ **38**, were obtained by the reaction of the lithiated ferrocenes, FcLi or FcLi_2 , with BTSP (equations 52 and 53).





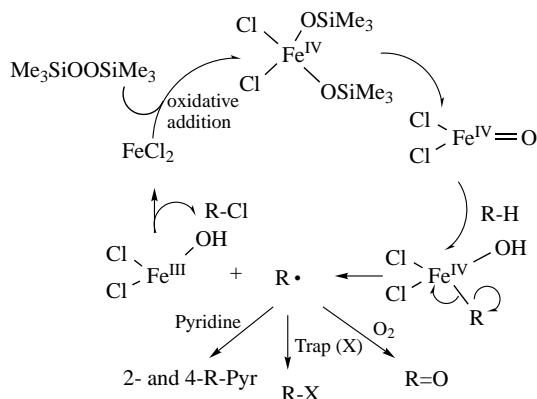
The oxidation of cyclohexane using $\text{Fe}^{\text{III}}(\text{PA})_3$ as catalyst and BTSP in pyridine results in the formation of cyclohexanone as the major product with a small amount of cyclohexanol. The reaction is catalytic, but an increase of $\text{Fe}^{\text{III}}(\text{PA})_3$ from 0.1 mmol to 0.3 mmol did not influence very much the efficiency (51 to 67%). The addition of a small amount of water increased slightly the formation of the ketone and alcohol. A partial hydrolysis of BTSP to trimethylsilyl hydroperoxide could be the explanation for this effect (Scheme 10).



SCHEME 10

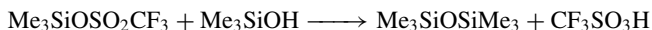
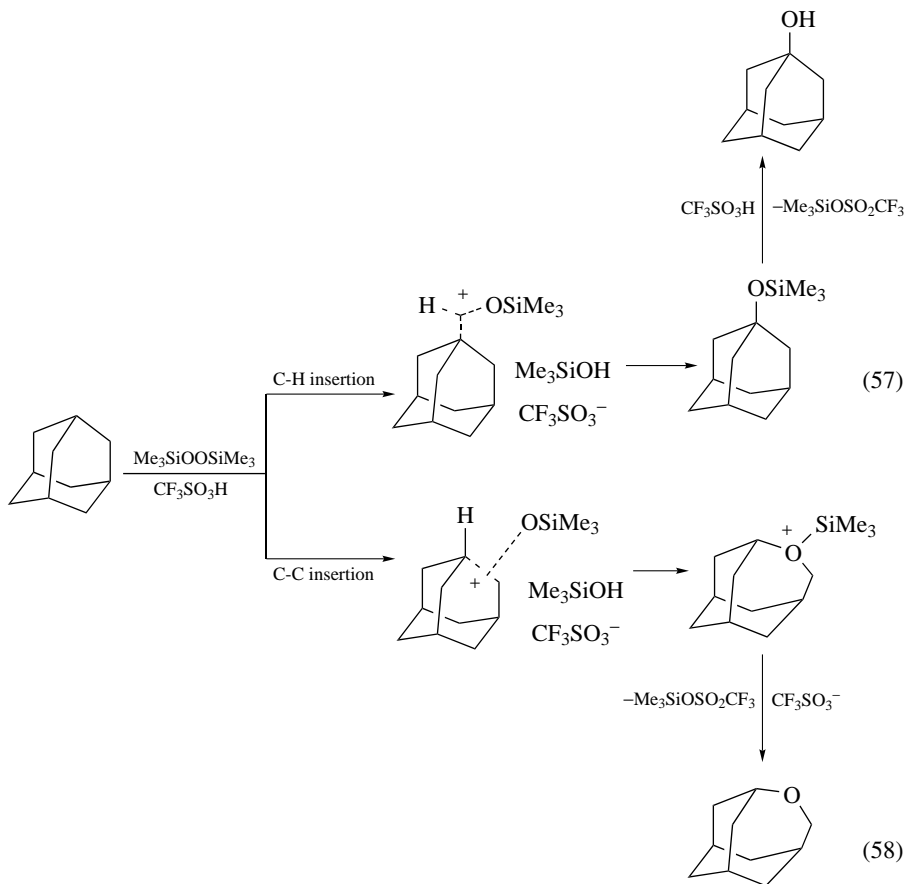
The hydroperoxide could react easily with Fe^{III} , followed by the formation of the oxenoid species $\text{Fe}^{\text{V}}=\text{O}$. The formation of trimethylsilyanol, which dehydrates to hexamethyldisiloxane, is the driving force for the reaction⁵².

A system composed of an $\text{Fe}^{\text{II}}\text{Cl}_2$ and BTSP in a mixture of hydrocarbon, pyridine and oxygen affords alkyl chloride and alkylpyridinium ion by trapping of the radical, in good yields. This system, which involves an $\text{Fe}^{\text{IV}}=\text{O}$, produces a carbon radical (Scheme 11).



SCHEME 11

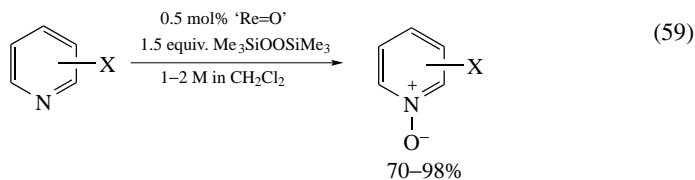
BTSP-CF₃SO₃H is an efficient electrophilic oxygenating agent for adamantane and diamantane. With adamantane, the major reaction product is 4-oxahomoadamantane in isolated yield in 79% through a C-C σ -bond insertion with very little 1-adamantanol, the C-H insertion product (equations 57 and 58)⁵³. In the case of diamantane, two isomeric oxahomodiamantanes were obtained along with two isomeric bridgehead diamantanols corresponding to C-C and C-H σ -bond insertions.



H. Reaction with Heteroatom Compounds

1. Oxidation of nitrogen compounds

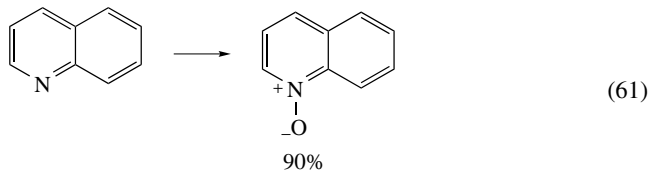
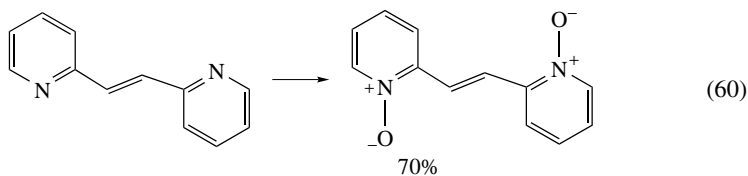
Oxidation of pyridines with BTSP in the presence of catalytic amounts of inorganic rhenium derivatives gives high yields of their analytically pure N-oxides by simple work-ups, typically a filtration or a Kugelrohr distillation (equations 59–61)⁵⁴.



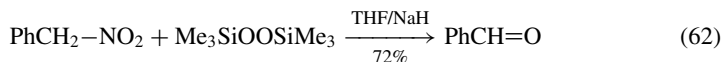
'Re=O': MTO, ReO₃, Re₂O₇, HOREO₃

MTO = methyltrioxorhenium

X = 4-CO₂Me, 3-CO₂Me, 2-CO₂Me, 4-CN, 3-CN, 2-CN,
4-Me, 4-Ph, 3,5-Cl₂, 3,5-Br₂, 3,4,5-Cl₃



Benzylic and secondary nitro compounds are readily converted into the corresponding carbonyl compounds upon treatment with BTSP in the presence of NaH at 0 °C (equation 62 and Table 13)⁵⁵.



2. Oxidation of phosphorous compounds

BTSP can be used for chemo- and stereoselective generation of the P=O group by oxygenation of a P(III) center and transformation of P=S and P=Se groups⁵⁶.

Optically active (+)-(*R*) methylpropylphenyl phosphine oxide **39** was reduced using the Horner method, and then the produced phosphine was oxidized by adding 1.2 molar equivalent of BTSP at room temperature. (-)-(*S*) methylpropylphenyl phosphine oxide **40** was obtained with 95% stereospecificity. Since the reduction step is known to proceed with inversion of the configuration at the phosphorus center⁵⁷, oxidation occurs with retention (equation 63).

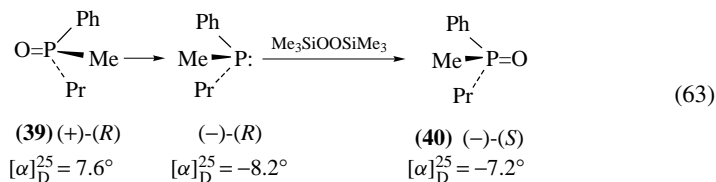
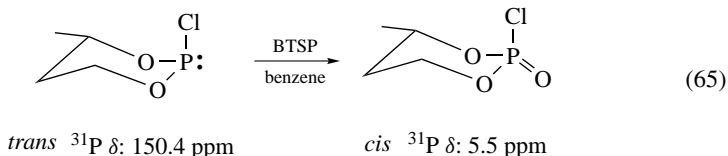
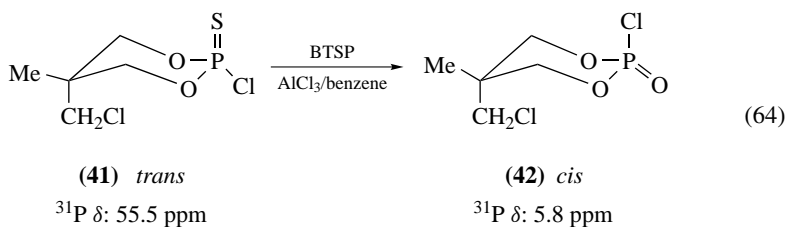


TABLE 13. Base catalyzed oxidation of nitro compounds by BTSP

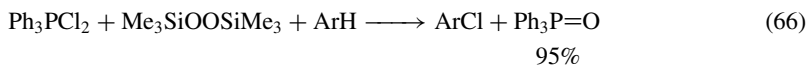
		Yield (%)
		70
		84
		68
		70
		65
		60

BTSP also converts the thioxophosphoryl function to the oxophosphoryl function with inversion of configuration at P. For example, oxidation of *trans*-2-thio-2-chloro-5-methyl-1,3-dioxaphosphorinane **41** by BTSP in the presence of AlCl_3 gives the *cis*-isomer of the corresponding product of the oxygenation accompanied by less than 5% of the *trans*-isomer **42** (equations 64). P(III) esters can also be stereoselectively oxidized by BTSP, as demonstrated by the transformation of 2-chloro-4-methyl-1,3-dioxaphosphorinane to its oxygen derivative (equation 65)⁵⁸.



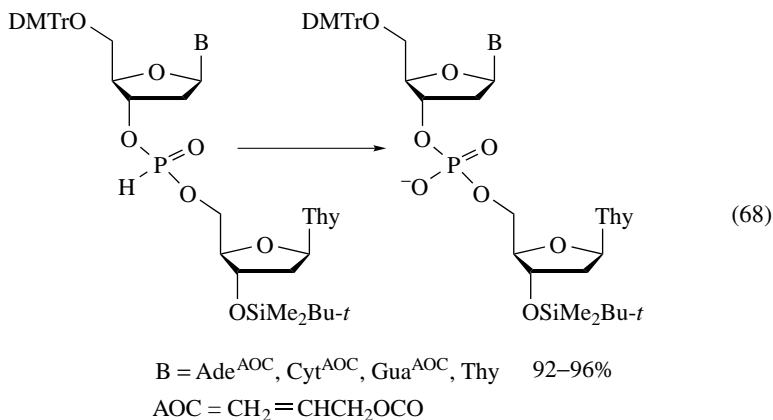
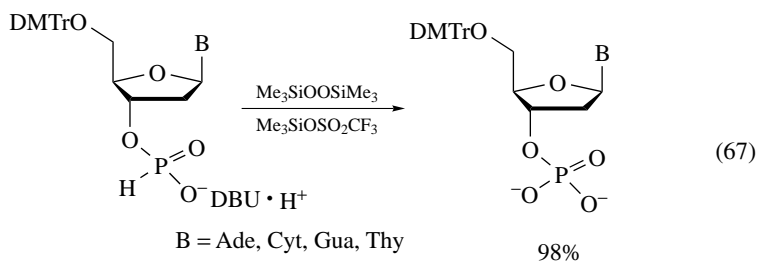
Reactions of dichlorotriphenylphosphorane with BTSP in the presence of some organic compounds give chlorinated products, e.g. *p*-chloroanisole from anisole⁵⁹. Aromatic

hydrocarbons bearing electron-donating substituents give the corresponding monochloroarenes (equation 66) while an enol silyl ether is converted into α -chloroketone.



Ar = 1,3,5-tri- <i>t</i> -butylphenyl	86%
Ar = 1,3,5-trimethylphenyl	44%
Ar = 4-methoxyphenyl	} 61% (<i>p</i> -chloroanisole) 7% (<i>o</i> -chloroanisole)
ArH = diphenyl sulfide	

A facile method for the oxidation of nucleoside H-phosphonates to phosphates has been developed with BTSP and N,O-bis(trimethylsilyl)acetamide, $\text{MeC}(\text{NSiMe}_3)\text{OSiMe}_3$, in the presence of $\text{Me}_3\text{SiOSO}_2\text{CF}_3$ as a catalyst (equations 67 and 68)⁶⁰.

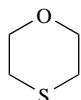


3. Oxidation of sulfur compounds

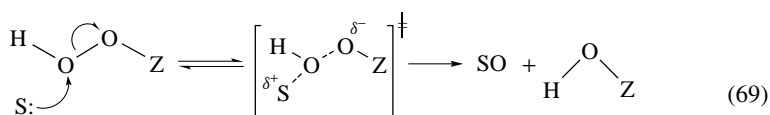
Oxidation of 1,4-thioxane by BTSP and *t*-butyl(trimethylsilyl) peroxide in CHCl_3 at 25 °C is compared to those of the same substrate by the more common oxidants, *t*-butyl hydroperoxide and di-*t*-butyl peroxide, in the same solvent. The two silyl peroxides give similar oxidations rates, which are over 50 times higher than that measured for *t*-BuOOH, while *t*-Bu₂O₂ is almost unreactive under the conditions adopted. Oxidation

TABLE 14. Oxidation rates of thioxane^a and *N,N*-dimethyl-*p*-anisidine by silyl peroxides as compared to analogous carbon peroxide

Substrate	Peroxide	Solvent	10 ⁴ M ⁻¹ s ⁻¹
Thioxane	<i>t</i> -BuOOBu- <i>t</i>	CHCl ₃	0.005
Thioxane	<i>t</i> -BuOOH	CHCl ₃	0.27
Thioxane	<i>t</i> -BuOOH	CHCl ₃	0.30
Thioxane	<i>t</i> -BuOOSiMe ₃	CHCl ₃	14.7
Thioxane	Me ₃ SiOOSiMe ₃	CHCl ₃	24.0
Thioxane	Me ₃ SiOOSiMe ₃	EtOH	0.80
Thioxane	Me ₃ SiOOSiMe ₃	Dioxane	0.15
<i>p</i> -MeOC ₆ H ₄ NMe ₂	Me ₃ SiOOSiMe ₃	CHCl ₃	0.034

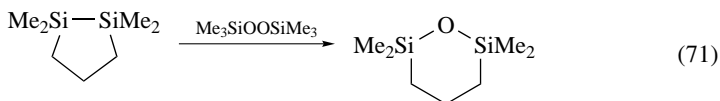
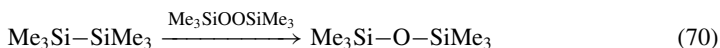
^a Thioxane =

of *N,N*-dimethyl-*p*-anisidine, a nitrogen nucleophile, by silyl peroxide in CHCl₃ is *ca* 1000 times slower than that of the sulfur nucleophile. The results are explained in terms of a mechanism involving nucleophilic attack by the substrate on the peroxide, with the heterolysis of the O–O bond being assisted by the migration of the MeSi group (equation 69 and Table 14)⁶¹.

S = substrate, δ = alkyl, acyl, or inorganic substrate.

4. Oxidation of disilanes and hydrosilanes

Disilanes **43**–**48** are allowed to react with BTSP to give the corresponding disiloxanes (equations 70 and 71), and the results are summarized in Table 15⁶². Compounds **44**–**47** and **48a** react with BTSP exothermally at or below room temperature, while **44** reacted slowly at room temperature, and **48b** and **48c** and hexamethyldisilane required more drastic reaction conditions. The eight-membered ring **48d** does not react with BTSP.



The compounds **43**, **45**, **48b** and **48c** gave the corresponding disiloxanes in quantitative yields, and BTSP is converted into hexamethyldisiloxane, **44**, formed from difluoro-*tert*-butylphenol. The reaction of **44** with BTSP was not inhibited by 2,4,6-tri(*t*-butyl)phenol. Compound **48a** did not react with di-*t*-butyl peroxide, which is the carbon analog of BSTP, suggesting an important role of vacant *d*-orbitals of the silicon atom. The Si–Si oxidation of compound **49** with BSTP proceeds quantitatively and in a stereospecific fashion (equation 72)⁶³.

TABLE 15. Oxidation of disilanes with bis(trimethylsilyl) peroxide

Compounds	Temp. (°C)	Time (h)	Siloxane ^a (yield, %)
Me ₃ SiSiMe ₃	80	42	40 ^b
Me ₃ SiSiMe ₂ F (43)	r.t.	45	100
FMe ₂ SiSiMe ₂ F (44)	r.t.	3.5	92 (trace) ^c
Me ₃ SiSiMeF ₂ (45)	r.t.	4	100
FMe ₂ SiSiMeF ₂ (46)	0	1.5	^d
F ₂ MeSiSiMeF ₂ (47)	-10	1	^e
Me ₂ Si—SiMe ₂ ($\begin{matrix} \text{---} \\ \text{(CH}_2\text{)}_n \\ \text{---} \end{matrix}$)			
(48a), <i>n</i> = 3	r.t.	1.5	95
(48b), <i>n</i> = 4	80	16	98
(48c), <i>n</i> = 5	80	45	64 ^b
(48d), <i>n</i> = 6	80	45	no reaction

^a The corresponding Si—O—Si compound.

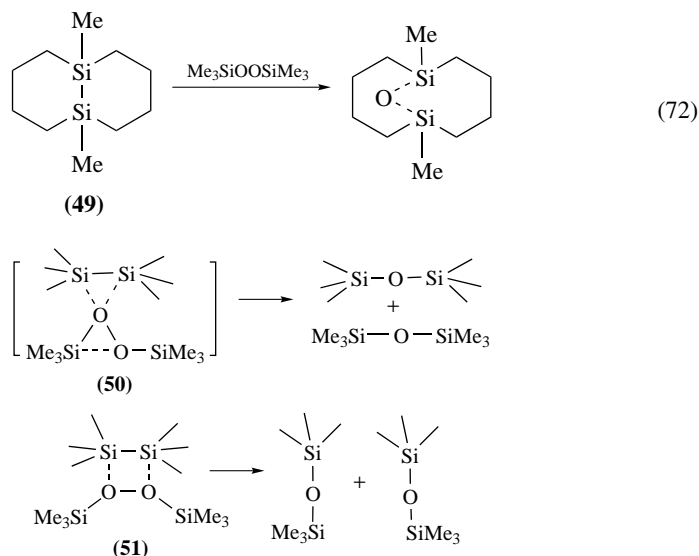
^b Conversion yield.

^c Me₃SiOSiMe₂F.

^d Me₃SiF/FMe₂SiOSiMeF₂/Me₃SiOSiMeF₂ (ratio 0.48/1/0.16); Me₃SiOSiMe₂F (trace).

^e Me₃SiF/Me₃SiOSiMe₂F (= 2/1)

A mechanism involving the intermediate **50** via the nucleophilic attack of the peroxide oxygen atom on the Si—Si bond seems consistent with the results, but intermediate **51** may be formed in a minor reaction path (Scheme 12).



SCHEME 12

The reactions of triethylsilane, phenyldimethylsilane and pentamethyldisilane with BTSP result in the formation of R₃SiOH and R₃SiOSiMe₃ as the primary products. The

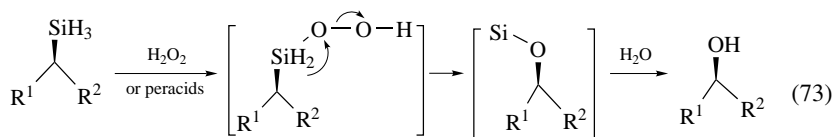
TABLE 16. Oxidation of hydrosilanes with bis(trimethylsilyl) peroxide

Hydrosilane	Temp. (°C)	Time (h)	Conversion (%)	Products (yield, %)
Et ₃ SiH	80	25	100	Et ₃ SiOH (32), Et ₃ SiOSiMe ₃ (40)
Et ₃ SiH	20	40	12	Et ₃ SiOH (trace), Et ₃ SiOSiMe ₃ (6)
PhMe ₂ SiH	80	27	89	PhMe ₂ SiOSiMe ₃ (66), (PhMe ₂ Si) ₂ O (14)
Me ₃ SiSiMe ₂ H	80	23	100	Me(Me ₂ SiO) ₂ SiMe ₃ (31), Me(Me ₂ SiO) ₂ OSiMe ₃ (19), (Me ₅ Si ₂) ₂ O (trace), Me(Me ₂ SiO) ₃ SiMe ₃ (trace)
Me ₃ SiSiMe ₂ H	80	23	47	Me(Me ₂ SiO) ₂ SiMe ₃ (4), Me(Me ₂ Si) ₂ OSiMe ₃ (57)

ratio of SiOH/SiOSi tends to decrease in the order Et₃SiH > PhMe₂SiH > Me₅Si₂H. The symmetrical R₃SiOSiR₃ may be regarded as the secondary condensation product of the former (Table 16)⁶².

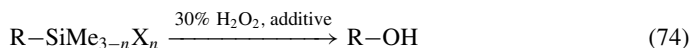
IV. SYNTHESIS OF ALCOHOLS VIA HEXA- AND PENTACOORDINATE SILYL PEROXIDES

The Si–C bonds in certain functionalized silicon compounds, such as alkoxy- and fluoro-silanes, can be oxidatively cleaved by hydrogen peroxide or peracids to form the corresponding alcohols. These transformations proceed via penta- and/or hexacoordinate silyl peroxide intermediates and subsequent intramolecular migration of the organic group from silicon to the adjacent oxygen atom. The oxidation proceeds with complete retention of configuration at the migrating carbon (equation 73)^{64–66}.



Si = functionalized silyl group

Organotrifluorosilanes react quite readily with 3-chloroperoxybenzoic acid⁶⁷. The oxidation of diorganodifluoro- and triorganomonofluorosilanes requires the addition of potassium fluoride. These conditions can also be applied to the oxidation of organoalkoxysilanes and organochlorosilanes. More practically, the Si–C bond in organoalkoxysilanes can be readily cleaved by 30% hydrogen peroxide in the presence of additives such as potassium fluoride, potassium hydrogen fluoride and potassium hydrogen carbonate (equation 74)^{68–70}.

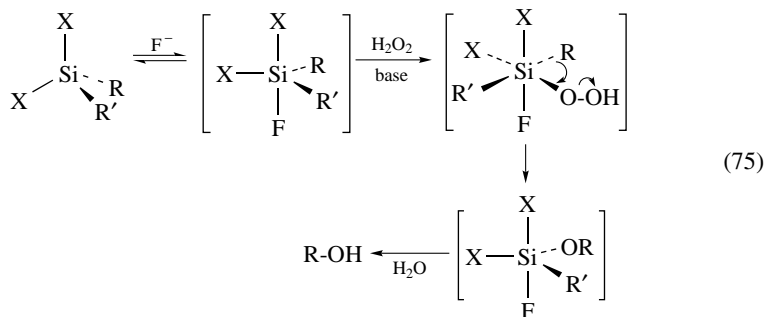


X = H, F, Cl, Br, OR₂, NR₂

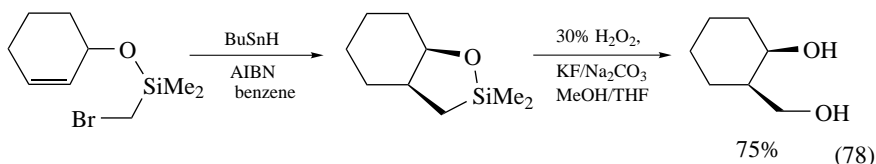
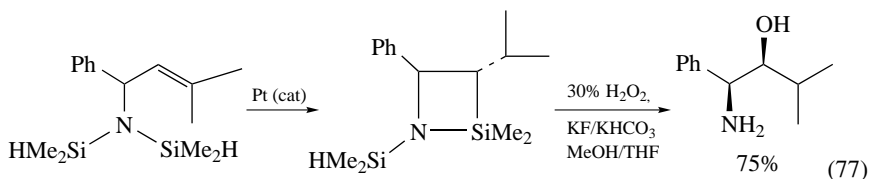
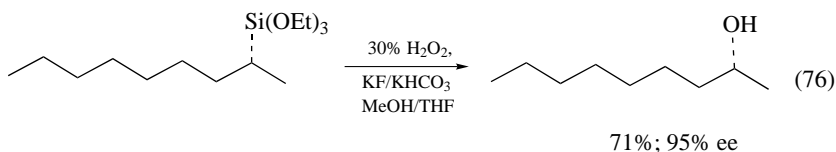
n = 1–3

additive = KF, KHCO₃, KHF₂ in MeOH/THF

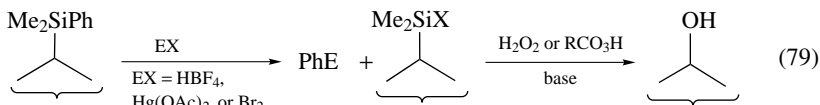
The oxidative cleavage of the Si–C bond requires the presence of at least one heteroatom on silicon. The proposed mechanism involves formation of a pentacoordinate silicon species as the initial key intermediate and a hexacoordinate silicon species in the transition states (equation 75).



The following are selected applications of hydrogen peroxide oxidation of Si–C bonds in stereoselective organic synthesis (equations 76–78)^{71–74}.



Although the Tamao oxidation employs an alkoxy silane, the Fleming protocol converts α -phenylsilane to a fluoro- or carboxysilane before the actual oxidation (equation 79)⁷⁵.



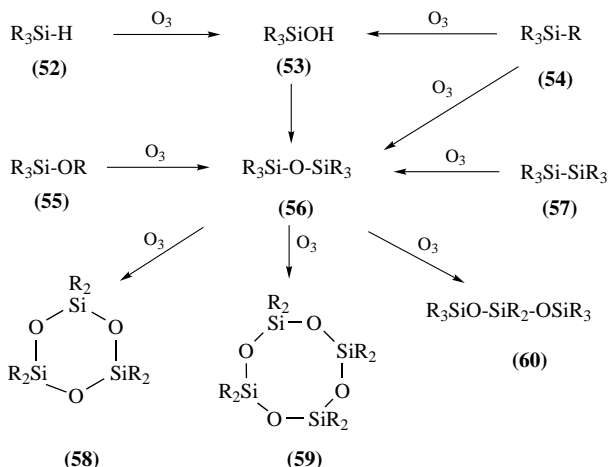
The oxidizing agents most frequently used are hydrogen peroxide, MCPBA or peracetic acid. Additional fluoride (KF and/or KHF₂) is required in many, but not all, existing protocols. Basic conditions (KH, *t*-butyl hydroperoxide and TBAF) have been employed as

well, allowing a wide range of alkyl and aryl substituents on silicon⁷⁶. Silicon substituted with a 2-pyridyl group has been oxidized under Tamao conditions (H_2O_2 , KF), and fluoride was demonstrated to play a critical role in this reaction⁷⁷.

Several mechanisms for the peroxide oxidation of organosilanes to alcohols are compared. Without doubt, the reaction proceeds via anionic, pentacoordinate silicate species, but a profound difference is found between in vacuo and solvated reaction profiles, as expected. In the solvents investigated (CH_2Cl_2 and MeOH), the most favorable mechanism is addition of peroxide anion to a fluorosilane used as starting material or formed in situ, followed by a concerted migration and dissociation of hydroxide anion. In the gas phase, and possibly in very nonpolar solvents, concerted addition-migration of H_2O_2 to a pentacoordinate fluorosilicate is also plausible⁷⁸.

V. SILANE OZONOLYSIS: SILANE TRIOXIDES

The products obtained from ozonolysis of various silanes and derivatives are shown in Scheme 13.

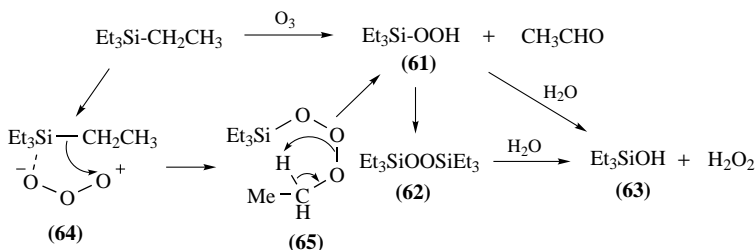


SCHEME 13

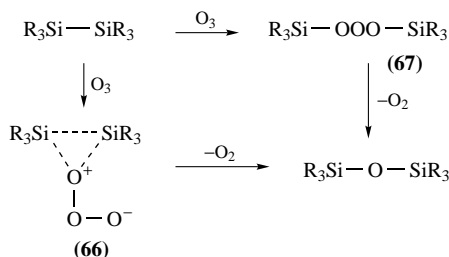
From silanes **52** are obtained, in high yield, the corresponding silanols **53**, which react further to produce disiloxanes **56** and **58–60**. Silanes **54** alkoxy silanes **55** and disilanes **57** give high yields of disiloxanes **56**. Ozonolysis of tetraethylsilane yields initially acetaldehyde and trimethylsilyl hydroperoxide **61**. The latter is partially converted to bis(trimethylsilyl) peroxide **62**, which is hydrolyzed to silanol **63** and hydrogen peroxide. The ozonolysis is of first order, both in regard to the silanes, and to ozone. The ozonolysis starts with formation of **64** followed by formation of the trioxide **65**, which decomposes to acetaldehyde and hydroperoxide **61** (Scheme 14)^{79, 80}.

Silicon–silicon bond cleavage has not been investigated mechanistically. It has been suggested to involve a simple insertion via a triangular transition state **66**, as shown in Scheme 15⁸¹. However, a mechanism involving initial coordination and collapse to a trioxide **67** seems more likely.

Various competitive studies have shown that the ease of bond cleavage is in the order $\text{Si-H} > \text{Si-OR} > \text{Si-OH} > \text{Si-R}$; $\text{Si-Si} > \text{Si-R}$; $\text{Si-Ar} > \text{Si-R}$; $\text{Si-Et} > \text{Si-Me}$ depending upon the nature of substituents on silicon⁸¹.

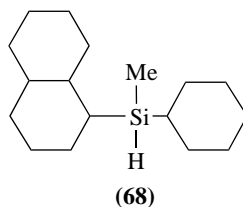


SCHEME 14

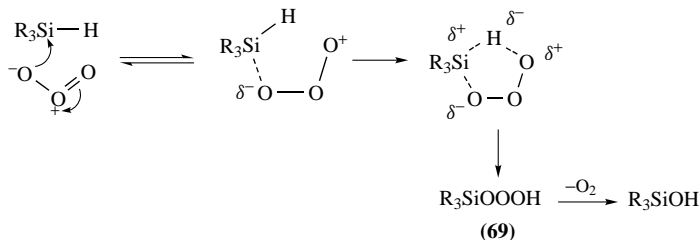


SCHEME 15

The most complete mechanistic studies have been made with trisubstituted silanes, which initially undergo an exclusive silicon–hydrogen bond cleavage. Retention of configuration occurs in the ozonolysis of 1-decahydronaphthylcyclohexylmethylsilane **68** to the corresponding hydroxide^{82,83}.

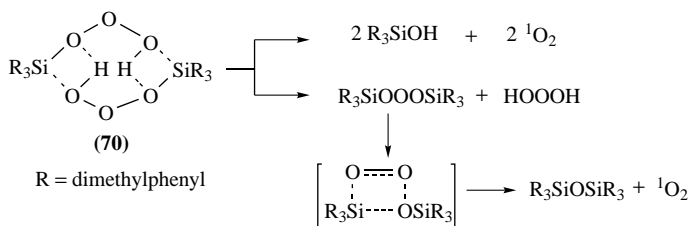


Silane hydrotrioxides **69** were proposed as transient intermediates in the reaction of ozone with various silanols. Hydrotrioxides can lose oxygen to afford silanol (Scheme 16).



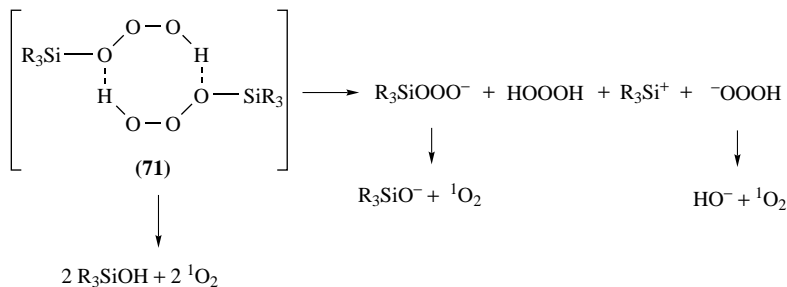
SCHEME 16

NMR spectroscopic evidence for the existence of silyl hydrotrioxides is available. These trioxides exist in basic solvents, probably in the dimeric (or polymeric) form (Scheme 17), whereas stronger bases disrupt the intermolecular hydrogen bonds in the dimers to form the opened hydrotrioxide–oxygen base adducts. Dimethylphenylsilyl hydrotrioxide **70**, $R_3 = \text{Me}_2\text{Ph}$, decomposes in acetone- d_6 to give dimethylphenyl silanol (90%), hydrogen peroxide (9%), dimethylphenyl disiloxane (8%) and singlet oxygen (65% based on 1,3-diphenylisobenzofuran trapping). Dimethylphenylsilyl hydroperoxide (5%) was also detected by NMR spectroscopy in the decomposition mixture below -45°C .⁸⁴



SCHEME 17

The kinetic and activation parameters for the decomposition of dimethylphenylsilyl hydrotrioxide involve large negative activation entropies, a significant substituent effect on the decomposition in ethyl acetate, dependence of the decomposition rate on the solvent polarity (acetone- $d_6 >$ methyl acetate $>$ dimethyl ether) and no measurable effect of the radical inhibitor on the rate of decomposition. These features indicate the importance of polar decomposition pathways. Some of the mechanistic possibilities involving solvated dimeric **71** and/or polymeric hydrogen-bonded forms of the hydrotrioxide are shown in Scheme 18.

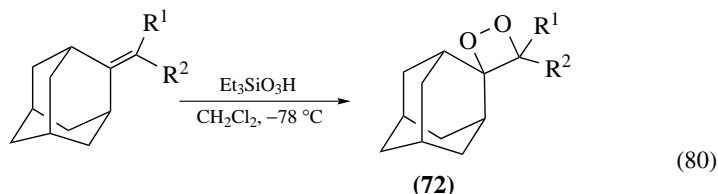


SCHEME 18

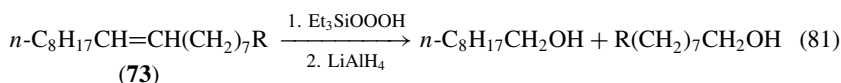
Corey and coworkers have shown that trimethylsilyl hydrotrioxide, produced by the low-temperature (-78°C) ozonization of triethylsilane, decomposes at higher temperatures to give singlet oxygen. The formation of singlet oxygen was confirmed by the change in the IR emission at 1278 nm with time (${}^1\text{O}_2 \rightarrow {}^3\text{O}_2$).⁸⁵

Posner and coworkers reported that triethylsilyl hydrotrioxide is an efficient reagent for direct conversion of electron-rich alkenes to 1,2-dioxetanes **72** (equation 80).⁸⁶

Inactivated alkenes are oxidatively cleaved by the hydrotrioxide to give ketones. For example, methyl oleate **73** reacts with the hydrotrioxide to produce two aldehydes, followed by LiAlH_4 reduction to give 1-nonanol and nonane-1,9-diol in 64 and 74% yields (equation 81).

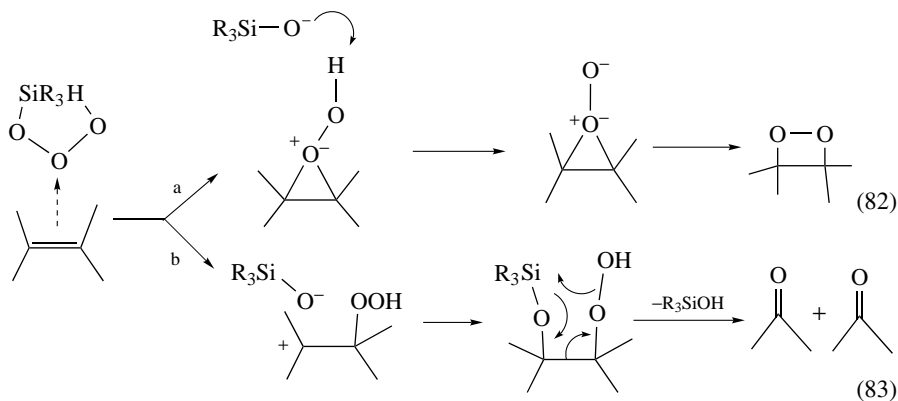


$\text{R}^1 = \text{OMe}; \text{R}^2 = m\text{-HOC}_6\text{H}_4$	46%
$\text{R}^1 = \text{OMe}; \text{R}^2 = \text{H}$	34%
$\text{R}^1 = \text{H}; \text{R}^2 = \text{Ph}$	0



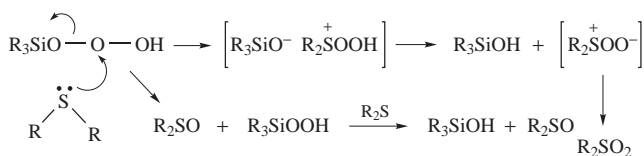
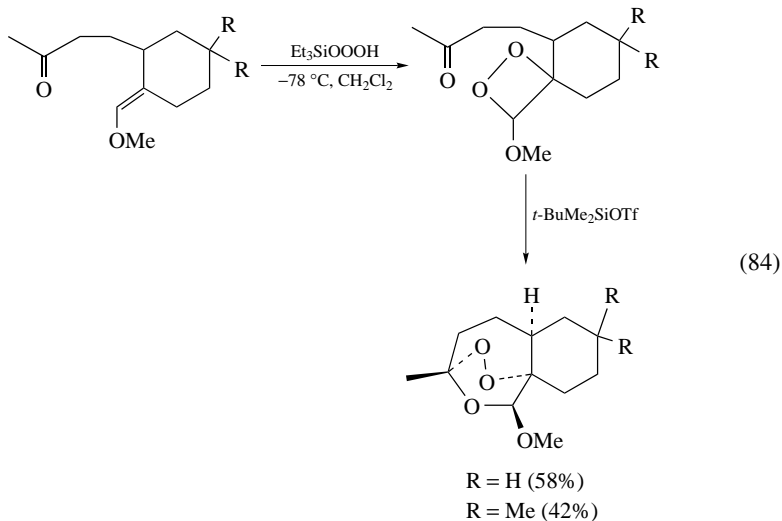
$\text{R} = \text{COOMe}$ (64%), OAc (83%)

A mechanism was proposed to account for the reaction of triethylsilyl hydrotrioxide with electron-rich alkenes as a dioxetane-forming process (route a; equation 82) and with inactivated alkenes as a nondioxetane carbonyl-forming process (route b; equation 83).



The triethylsilyl trioxide reacts smoothly with internal disubstituted olefins to give potent antimalarial 1,2,4-trioxanes, especially when there is oxygen functionality in the molecule (equation 84).

The hydrotrioxides oxidize also simple dialkyl sulfide such as dimethyl and diethyl sulfides to the corresponding sulfoxides and the latter to sulfones in high yields (Scheme 19)⁸⁷.



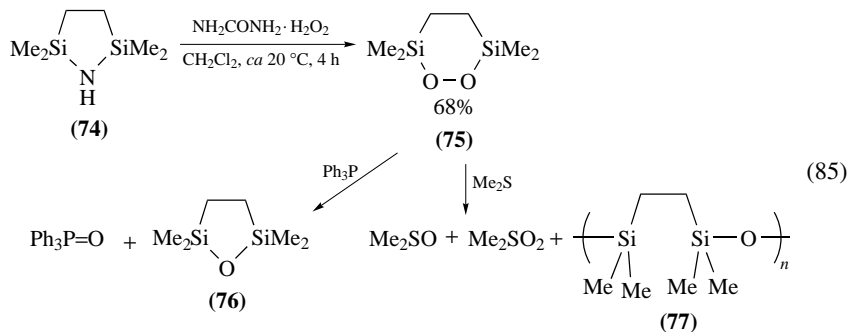
SCHEME 19

VI. CYCLIC SILYL PEROXIDES

Carboxylic peroxides are long known and have been extensively employed in mechanistic and preparative applications⁸⁸. This is also valid for acyclic silyl peroxides, particularly the recently much used BTSP, which as a protected H₂O₂ exhibits marked advantages as oxidizing agent compared to the parent hydrogen peroxide.

A. Reaction of Disilazanes with Urea-H₂O₂ Complex

The simple cyclic silyl peroxide, 1,1,4,4-tetramethyl-1,4-disila-2,3-dioxane, **75**, was prepared by classical synthetic methodology from its corresponding cyclic disilazane **74** and the urea complex of H₂O₂ (equation 85)⁸⁹.

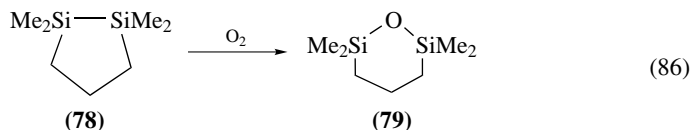


The peroxide **75** reacts with triphenylphosphine to afford the cyclic siloxane **76** and with dimethyl sulfide in petroleum ether at 50 °C to give dimethyl sulfoxide (19%), dimethyl sulfone (15%) and *ca* 50% of a nonperoxidic polymer **77**.

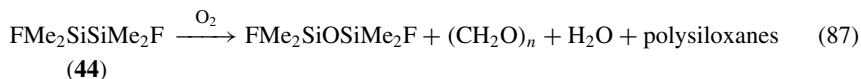
B. Oxidation of Cyclic Disilanes with Molecular Oxygen

An important property of the alkyl polysilanes is their electronic absorption at relatively low energy. This was particularly surprising because such molecules lack π , d or lone pair electrons; they were the first substances containing only bonding σ -electrons to show such long-wavelength absorptions. The unusual electronic properties of the polysilanes have sparked considerable interest in the chemophysical properties of these molecules. The UV spectra of cyclic polysilanes follow a quite different pattern⁹⁰.

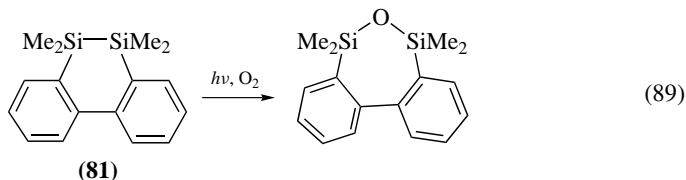
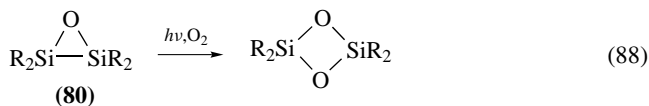
The aerobic oxygenation of organosilicon compounds showed that cyclopentadisilane is gradually oxygenated to produce the corresponding disiloxane. When oxygen was bubbled through the neat liquid at room temperature, compound **78** absorbed 0.8 equivalent of oxygen exothermally to give 2,2,6,6-tetramethyl-1-oxa-2,6-disilacyclohexane **79** in 72% yield (equation 86) and nonvolatile viscous polysiloxanes.



Compound **44** also reacts exothermally with oxygen to give difluorotetramethyl disiloxane in 35% yield and polysiloxanes together with paraformaldehyde (equation 87).

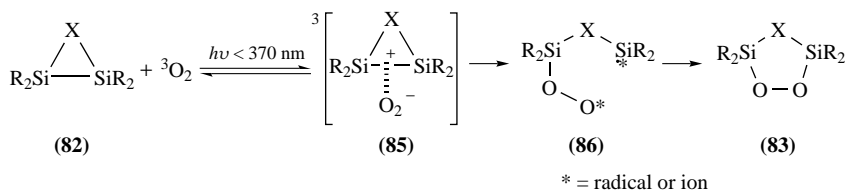


Oxidation of **44** is completely inhibited by the addition of a small amount of 2,4,6-tri-*t*-butylphenol. Consequently, the oxidation of the Si—Si bond with oxygen displays the following features: 1) a Si—Si bond which is either angle-strained or substituted with more than two fluorine atoms is easily oxidized; 2) a radical mechanism is operative; 3) the 'insertion' of oxygen into the Si—Si bond proceeds stereospecifically⁶². Incorporation of molecular oxygen was also observed in the direct photolysis of the cyclopolysilanes **80** and **81** (equations 88 and 89)⁹¹.



These reactions probably occur either by electron transfer (ET) from the silicon–silicon σ -bond to oxygen, or by trapping silyl radicals by oxygen. It was also pointed out that the

The UV absorption spectrum of the disilirane **82a** in oxygen-saturated solvents such as methylene chloride or acetonitrile reveals a weak broad contact CT band with a maximum at 300 nm. Photolysis of **82a** in an oxygen matrix at 16 K resulted in a smooth oxygenation, giving a new species with an intense IR band at 1078 cm⁻¹. When ¹⁸O₂ is employed, the IR band shifts by 39 cm⁻¹ to a lower wave number⁹⁴. Upon subsequent warming of the matrix to a temperature higher than 50 K, the intense band at 1078 cm⁻¹ disappeared and the oxygen matrix became cloudy. The intense band at 1078 cm⁻¹ is ascribable to the characteristic O–O stretching mode of the disilirane–oxygen adduct **85** in the triplet state. Accordingly, the silicon–silicon bond with its low ionizing energy easily donates σ -electrons to the oxygen molecule, thereby forming a CT complex, similar to the CT band observed in the photooxygenation of tetramethylethylene⁹⁵ and sulfides⁹⁶ in cryogenic oxygen matrices. **83** is formed from **85** via **86** (Scheme 21).



SCHEME 21

Irradiation of oxadisilirane **82c** in an acetonitrile–methylene chloride solvent mixture in the presence of 9,10-dicyanoanthracene (DCA) as photosensitizer with a tungsten–halogen lamp under an oxygen flow resulted in the formation of **83c** in 69% yield. In the absence of the sensitizer, no reaction occurred and **82c** was recovered quantitatively. A similar result was also obtained in the reaction of **82c** with ³O₂ in the presence of 10 mol% of tris(*p*-bromophenyl)aminium hexachloroantimonate [*p*-BrC₆H₄]₃N⁺SbCl₆⁻ (BPHA) as the single ET reagent, which gave **83c** in 58% yield (Table 17)⁹⁷.

TABLE 17. Disilirane oxidation with molecular oxygen

Disilirane	Conditions	Product	
		83	84
82			
a	A ^a	75	25
b	A	59	24
c	A	78	15
a	B ^b	15	51
c	B	69	trace
a	C ^c	3	28
c	C	58	0
a	D ^d	92	0
b	D	71	0
c	D	60	0
d	D	40	11
e	D	43	9
f	D	70	0

^a A: $h\nu(\lambda < 370 \text{ nm})/\text{O}_2$ in MeCN.

^b B: $h\nu(\lambda > 400 \text{ nm})/\text{O}_2/\text{DCA}$ in MeCN–CH₂Cl₂.

^c C: BPHA/O₂/-78 °C in CH₂Cl₂.

^d D: $h\nu(\lambda > 400 \text{ nm})/\text{O}_2/\text{TPP}$ in C₆H₆.

TABLE 18. Stereochemical oxidation of disilirane with molecular oxygen

Disilirane 87	Conditions	Product 88 Yield(%)	<i>cis/trans</i> Ratio
<i>cis</i>	$h\nu(\lambda > 400 \text{ nm})/\text{O}_2/\text{CH}_2\text{Cl}_2/\text{DCA}^a$	51	68/32
<i>trans</i>	$h\nu(\lambda > 400 \text{ nm})/\text{O}_2/\text{CH}_2\text{Cl}_2/\text{DCA}^a$	35	41/59
<i>cis</i>	BPHA ^b /O ₂ /-78 °C	88	66/34
<i>trans</i>	BPHA ^b /O ₂ /-78 °C	95	42/58
<i>cis</i>	$h\nu(\lambda > 400 \text{ nm})/\text{O}_2/\text{C}_6\text{H}_6/\text{TPP}^c$	84	100/0
<i>trans</i>	$h\nu(\lambda > 400 \text{ nm})/\text{O}_2/\text{C}_6\text{H}_6/\text{TPP}^c$	91	0/100

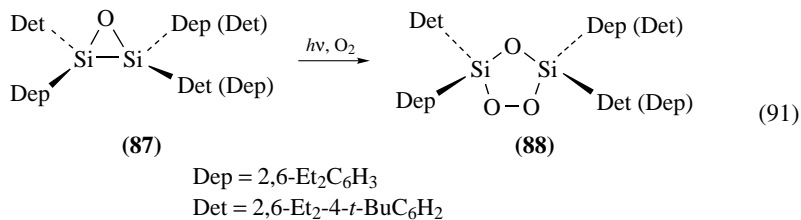
^a DCA = 9, 10-dicyanoanthracene.

^b BPHA = [*p*-BrC₆H₄]₃N⁺SbCl₆⁻.

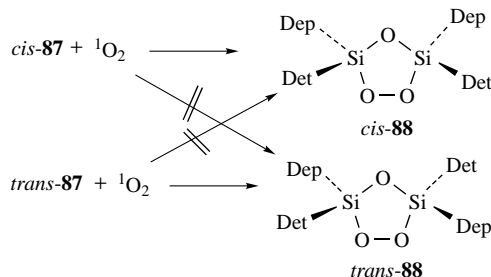
^c TPP = tetraphenylporphyrin.

The singlet oxygenation of disiliranes **82a–f** in benzene with tetraphenylporphyrin (TPP) as sensitizer gave cyclic peroxides **83a–f** in 40–92% yields with a small amount of dioxasiletane **84a–f** (Table 17)^{94,98,99}.

The stereochemistry of the ET oxygenation of both stereoisomers of **87** allows insight into the geometry of the transient intermediate. Thus, DCA-sensitized photooxygenations of *cis*- and *trans*-**87** gave 68:32 and 41:59 mixtures of *cis*- and *trans*-**88**, respectively (equation 91 and Table 18). These results are in agreement with the intermediacy of open intermediate like **86**, and with the fact that rotation around the Si–O bonds is fairly competitive with the collapse to **88**.

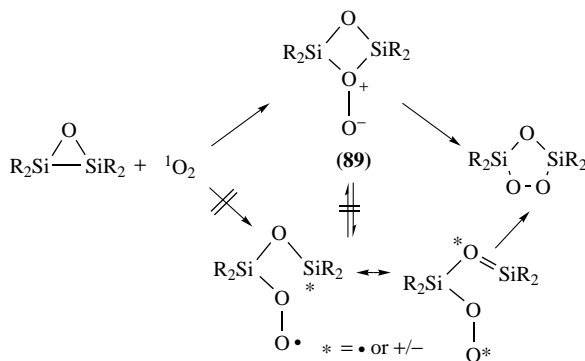


Moreover, singlet oxygenation of *trans*-**87** gave *trans*-**88** as the exclusive product in 84% yield, and that of *cis*-**87** afforded *cis*-**88** in 79% yield (Scheme 22).



SCHEME 22

Clearly, TPP-sensitized oxygenation of disilirane proceeds in a stereospecific manner via peroxonium ion intermediate **89** (Scheme 23). The potential energy surface of the

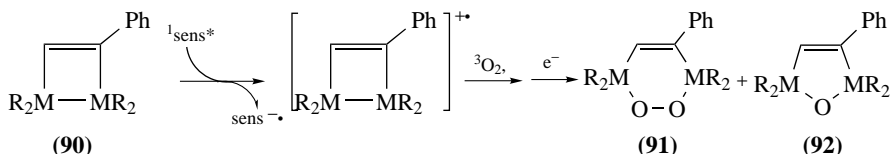


SCHEME 23

optimized geometries showed that the reaction path involves an end-on approach of $^1\text{O}_2$ to the Si–Si bond, and the transition state leads to peroxonium ion, which has C_s symmetry.

2. 1,2-Dioxadisilins and germins

The six-membered-ring cyclic peroxides, 1,2-dioxadisilin and 1,2-dioxadigermin, can be readily prepared by the ET oxygenation of 1,2-disilenes and germetrenes, followed by trapping a M–M σ cation radical with molecular oxygen. Irradiation of 3-phenyl-1,1,2,2-tetramesityl-1,2-disilene **90a** in acetonitrile and methylene chloride in the presence of DCA under bubbling oxygen results in the formation of disilin **91a** in 69% yield (equation 92 and Table 19).



(a) M = Si, R = Mes, $E_{\text{ox}} = 1.2 \text{ V}$ (vs SCE)

(b) M = Ge, R = Mes, $E_{\text{ox}} = 1.34 \text{ V}$ (vs SCE)

(92)

Similarly, oxygenation of 1,2-digermetrene gave the digermin **91b** in 80% yield. Comparable results were also obtained when methylene blue (MB) was employed as the sensitizer^{100–103}. On the other hand, the reaction does not involve singlet oxygen, since **90a** is stable under photooxygenation in the presence of the photosensitizer TPP.

The free-energy changes (ΔG) for ET from **90a** to DCA, MB and 2,4,6-triphenylpyrylium perchlorate (TPPY⁺) are -18.4 , -10.6 and $-32.5 \text{ kcal mol}^{-1}$, respectively, indicative of exothermic electron transfer. The rate of disappearance of **90a** was enhanced by addition of $\text{Mg}(\text{ClO}_4)_2$ (Table 20).

C. Disiladioxetanes: Oxidation of Disilenes with Molecular Oxygen

Although alkenes react rapidly with singlet oxygen, reaction with triplet oxygen is normally slow. Exceptions are very electron-rich alkenes such as tetraaminoethylenes¹⁰⁴, and normal alkenes with low-lying triplet states such as cyclobutadienes¹⁰⁵ and ketenes¹⁰⁶.

TABLE 19. Oxidation of disilenes **90a**

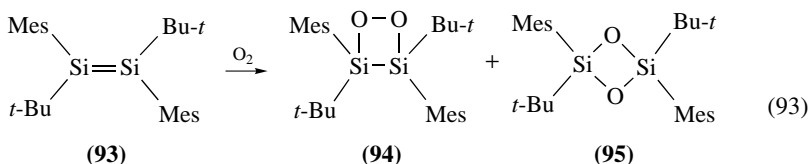
Reaction conditions ^a	Product (%)	
	91a	92a
<i>hν</i> /TPP ^b /O ₂ /C ₆ H ₆ /15 °C	no reaction	
<i>hν</i> /DCA ^c /O ₂ /CH ₃ CN/CH ₂ Cl ₂ /15 °C	69	13
<i>hν</i> /MB ^d /O ₂ /CH ₃ CN/CH ₂ Cl ₂ /15 °C	35	19
<i>hν</i> /TPPY ^e /O ₂ /CH ₃ CN/CH ₂ Cl ₂ /15 °C	51	19
dark/BPHA ^f /O ₂ /CH ₃ CN/CH ₂ Cl ₂ /78 °C	61	39

^a 1.7 × 10⁻² M of **90a**.^b TPP = tetraphenylporphyrin.^c DCA = 9, 10-dicyanoanthracene.^d MB = methylene blue.^e TPPY⁺ = 2,4,6-triphenylpyrylium perchlorate.^f BPHA = [*p*-BrC₆H₄]₃N⁺SbCl₆⁻.TABLE 20. Effect of additives on the disilene **90a** oxidation

Additive	Conversion (%) ^a 91a
TMB(1 eq) ^b /1.5 h	9
DABCO (0.3 eq) ^c /1.5 h	21
TBP(1 eq) ^d /1.5h	39
Mg(ClO ₄) ₂ (0.5 eq)/1h	82

^a Determined by HPLC.^b 1,2,4,6-Tetramethoxybenzene.^c 1,4-Diazabicyclo[2.2.2]octane.^d 2,4,6-Tri-*t*-butylphenol.

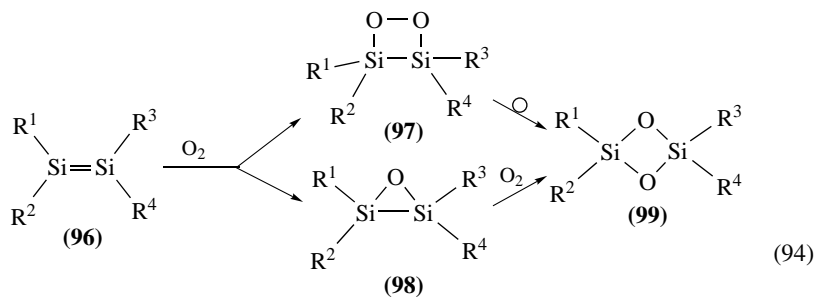
Disilenes have much lower oxidation potentials than olefins¹⁰⁷, and consequently they are much more reactive toward ³O₂. Typically, disilenes **93** react in solution with triplet oxygen to give 1,2-disiladioxetanes **94** as the major product, accompanied at room temperature by a smaller amount of disilaoxirane **95** (equation 93)¹⁰⁸.



Mes = 2,4,6-trimethylphenyl

The four-membered ring in **94** is nearly planar, with a torsional angle of only 8.9 (6)° between the Si–Si and O–O vectors. Theoretical calculations on the parent 1,2-disiladioxetane predict the ring to be planar. 1,2-Disiladioxetanes **97** undergo a remarkably quantitative rearrangement to 1,3-cyclodisiloxanes **99**, either thermally or photochemically (equation 94). Compounds **97** behave very differently from either their germanium or carbon analogs. The organic 1,2-dioxetane does not rearrange, and in fact no carbon analog of the 1,3-cyclodisiloxane is known. Both oxidation of **96** and rearrangement of **97** to 1,3-cyclodisiloxane **99** take place with retention of configuration at silicon. Isotope

labeling studies with ^{18}O showed the rearrangement to be intramolecular in the solid and in solution.



(a) $\text{R}^1 = \text{R}^2 = \text{R}^3 = \text{R}^4 = \text{Mes}$

(b) $\text{R}^1 = \text{R}^2 = \text{R}^3 = \text{R}^4 = \text{Xyl}$

(c) $\text{R}^1 = \text{R}^2 = \text{R}^3 = \text{R}^4 = \text{Dmt}$

(d) $\text{R}^1 = \text{R}^2 = \text{Mes}, \text{R}^3 = \text{R}^4 = \text{Xyl}$

(e) $\text{R}^1 = \text{R}^2 = \text{R}^3 = \text{Xyl}, \text{R}^4 = \text{Mes}$

(f) $\text{R}^1 = \text{R}^3 = \text{Mes}, \text{R}^2 = \text{R}^4 = \text{Xyl}$

(g) $\text{R}^1 = \text{R}^3 = \text{Ad}, \text{R}^2 = \text{R}^4 = \text{Mes}$

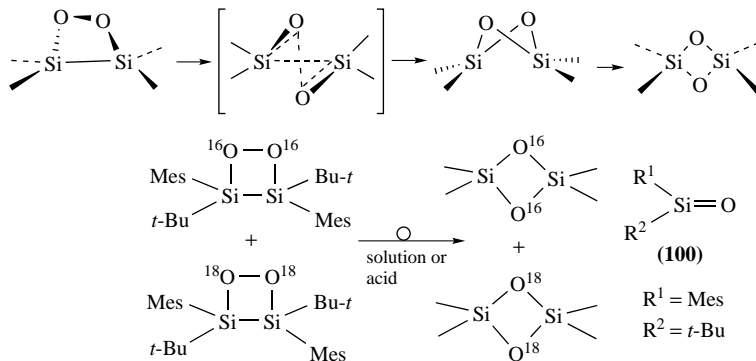
Dmt = 2,6-dimethyl-4-(*t*-butyl)phenyl

Xyl = 2,6-dimethylphenyl

Mes = 2,4,6-trimethylphenyl

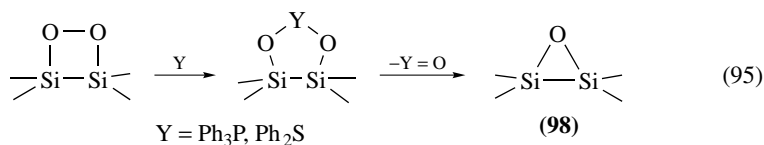
Ad = 1-adamantyl

The rearrangement of silicon compounds **97** does not involve the silanone **100** as an intermediate (Scheme 24).



SCHEME 24

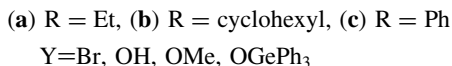
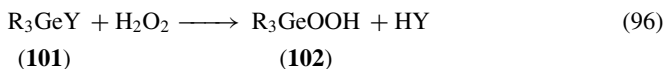
In the presence of phosphines or sulfides, **94** is partially deoxygenated to form disiloxirane **98** (equation 95).



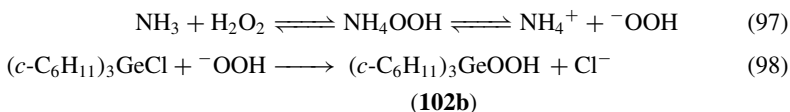
VII. GERMYL PEROXIDES

A. Germyl Hydroperoxides

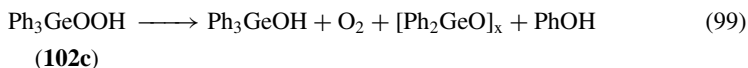
There have been several reports of the synthesis of organogermanium peroxides and organogermanium hydroperoxides¹⁰⁹⁻¹¹³. Triphenylbromogermane **101c**, Y=Br was dissolved in dry ether and 98% H₂O₂ was added. The mixture was stirred and dry ammonia gas was bubbled through the solution for 30 s. The reaction was then quenched by water. The ether layer was separated, and washed with water to give triphenylgermyl hydroperoxide **102c** in 54% yield at mp 135–136°C. The compound does not decompose on melting, and if the molten mass is allowed to solidify, it remelts at mp 135–136°C. The infrared spectrum of the hydroperoxide in CCl₄ has a general qualitative similarity to the spectrum of triphenylsilyl hydroperoxide, including a strong peak at 2.8 μ characteristic of the OH group¹⁰⁴. The hydroperoxide was also obtained from the reaction of 98% H₂O₂ with bis(triphenylgermanium) oxide and with triphenylgermanol **101c**, Y=OH in 65 and 60% yields, respectively (equation 96).

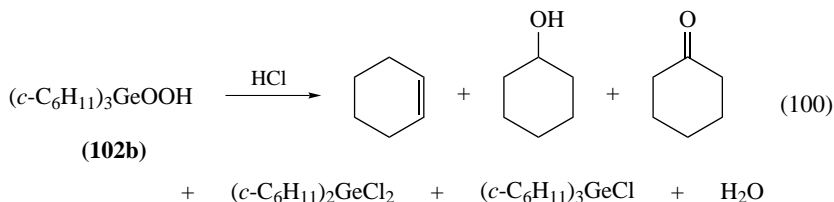


The hydroperoxide is quite stable and can be stored at –20°C without decomposition. When left at room temperature for 30 days, the active oxygen decreased by only 2%. The mechanism of the formation of triarylgermyl hydroperoxides from the corresponding triarylhalogermanes using ammonia as the catalyst is possibly identical with the analogous formation of triorganosilyl hydroperoxides. In the absence of hydrogen peroxide, trigermyl amines are rapidly formed. Displacement of the amide ion by hydrogen peroxide or its anion would lead to the formation of the hydroperoxide. On the other hand, when ammonia was bubbled into an ethereal solution of tricyclohexylgermane at 0°C, the precipitation of ammonium chloride was very slow. However, when the reaction was carried out in the presence of hydrogen peroxide, ammonium chloride precipitates immediately. This indicates that the main reaction sequence involved the nucleophilic displacement of the chloride by hydroperoxide anion according to equations 97 and 98.



Thermal decomposition of the hydroperoxide **102c** in *o*-dichlorobenzene at 160–170°C produced oxygen, water and triphenylgermanol as the major products, and phenol and diphenylgermanium oxide as the minor products (equation 99). The effect of solvents, radical initiators, radical inhibitors and ultraviolet light were consistent with a free-radical mechanism producing these products. Thermal decomposition of tricyclohexylgermyl hydroperoxide **102b** produced cyclohexene, cyclohexanol, tricyclohexylgermanol and dicyclohexylgermanium oxide (equation 100)¹¹⁰.





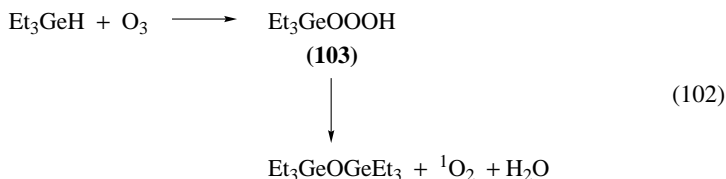
The decomposition products from **102b** differed widely in nature from the products obtained from the triaryl analogs. As no oxygen was evolved, an induced decomposition yielding a peroxyradical must be excluded. The triphenylgermyl hydroperoxide **102c** reacts with hydrogen chloride at 25 °C to produce the corresponding triorganogermanium chloride and hydrogen peroxide in better than 98% yield (equation 101)¹¹¹.



Ph₃GeOOH **102c** also reacts with PhNCO in benzene at 20 °C in the presence of pyridine to give Ph₃GeOGePh₃, PhNH₂, O₂ and CO₂, probably via the Ph₃GeOOCONHPh intermediate¹¹⁴. Cleavage of the Ge–O bond occurred when HNCO was passed through a solution of the compounds in benzene at 10 °C giving Ph₃GeNCO and H₂O₂¹¹⁵. Reaction with Ph₃P in THF at 20 °C yielded benzene and, after hydrolysis, Ph₃P=O, Ph₃GeOGePh₃ and PhOH.

B. Germyl Hydrotrioxides

Germyl hydrotrioxide Et₃GeOOOH **103** was obtained from Et₃GeH and O₃ in toluene or acetone at –78 °C in 10% and 62% yields, respectively. It could not be isolated because it decomposes to (Et₃Ge)₂O above –78 °C (equation 102), and singlet oxygen was trapped by 9,10-diphenylanthracene to give the corresponding *endo*-peroxide.



Kinetic studies on the decomposition of **103** in CD₃COCD₃ at –50 to –35 °C gave the parameters $\Delta H^\ddagger = 13.3 \text{ kcal mol}^{-1}$ and $\Delta S^\ddagger = -17 \text{ cal mol}^{-1} \text{ K}^{-1}$. The stability of the compound in various solvents decreases in the sequence MeCONMe₂ > acetone-*d*₆ > toluene-*d*₈ > Et₃N; ¹H NMR spectrum (at –78 °C): $\delta = 13.70$ (OH) ppm in acetone-*d*₆ and 14.03 ppm in toluene-*d*₈¹¹⁶.

C. Germyl Peroxides

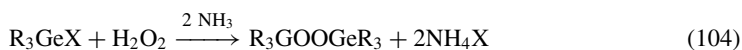
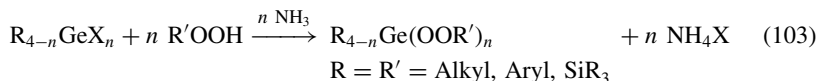
A number of alkylgermanium peroxides have been prepared by treating alkylgermanium halides with the appropriate alkyl hydroperoxide in the presence of base under anhydrous conditions (equations 103 and 104), or with the anhydrous sodium salt of the

TABLE 21. Yields of germyl peroxides

Peroxide	Yield (%)	Reference
Me ₃ GeOOCHMePh	53	117b
Me ₃ GeOOC ₁₀ H ₁₇ ^a		117a
Et ₃ GeOOCHMePh	48	117b
Et ₃ GeOOBu- <i>t</i>	55	117c
Pr ₃ GeOOBu- <i>t</i>		117a
Pr ₃ GeOOC ₁₀ H ₁₇ ^a		117a
Ph ₃ GeOOBu- <i>t</i>	63	117c
Ph ₃ GeOOCPh ₃	54	117c
Et ₃ GeOOSiPh ₃	55	117d
Ph ₃ GeOOSiMe ₃	70	117d
Ph ₃ GeOOSiEt ₃	56	117e
Ph ₃ GeOOSiPr ₃	60	117e
Ph ₃ GeOOSiPh ₃	85	117f
Me ₃ GeOOGeMe ₃	43	118
Et ₃ GeOOGeEt ₃	84	113
Ph ₃ GeOOGePh ₃	60	111
Et ₂ Ge(OOBu- <i>t</i>) ₂	75	117g
EtGe(OOBu- <i>t</i>) ₃	65	117g
PhGe(OOBu- <i>t</i>) ₃	68	117g

^a C₁₀H₁₇ = decahydro-9-naphthyl.

hydroperoxide (equation 105)^{117,118}.



Triphenylgermyl peroxide reacts with triphenylsilylamine to give triphenylsilyl(triphenylgermyl) peroxide¹¹⁹.



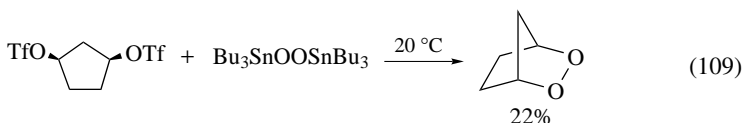
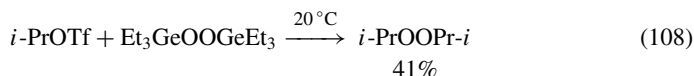
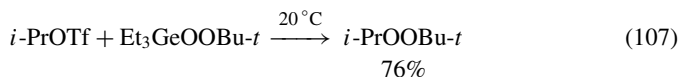
The germanium peroxides are stable up to about 70 °C for short periods, but some decomposition apparently occurs during distillation above this temperature. All peroxides are readily hydrolyzed to give germyl hydroperoxide.

D. Peroxide Transfer Reactions

A new method for synthesis of dialkyl peroxides is based on the novel peroxide transfer reaction between Ge or Sn peroxides and alkyl triflates. Mixed dialkyl peroxides are obtained from the reaction of bis(butyltin)germyl peroxide with alkyl triflates.

Bu₃SnOOSnBu₃ reacts with alkyl triflates to give symmetrical dialkyl peroxides, and with alkyl bistriflates to give 5–8 membered cyclic peroxides¹²⁰, but no dialkyl peroxide is produced from *t*-butylperoxytrimethylsilane. Similarly, symmetrical dialkyl peroxides

are produced by reaction of alkyl triflates with bis(trialkylgermanium) or bis(trialkyltin) peroxides, but not with bis(trialkylsilyl) peroxides (equations 107 and 108).



Prostaglandin endoperoxide, 2,3-dioxabicyclo[2.2.1]heptane, is obtained in 22% yield from the bistriflate of *cis*-1,3-cyclopentane diol and bis(stannyl) peroxide (equation 109).

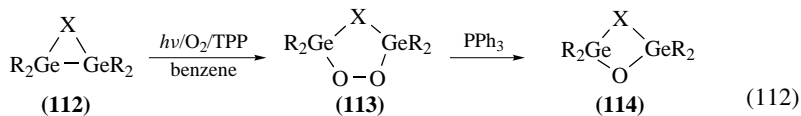
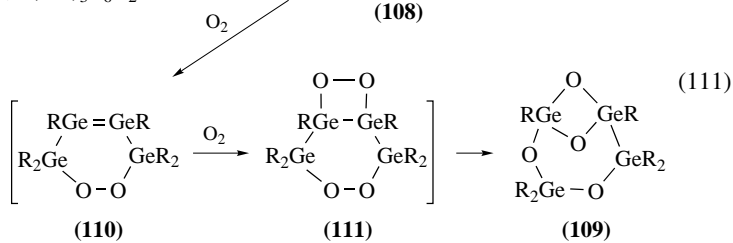
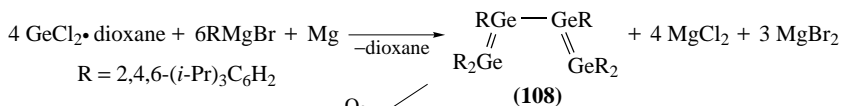
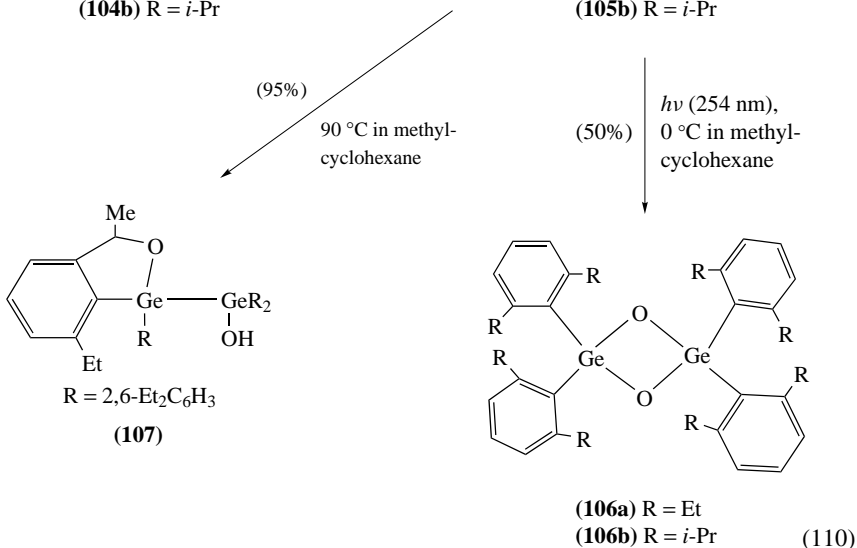
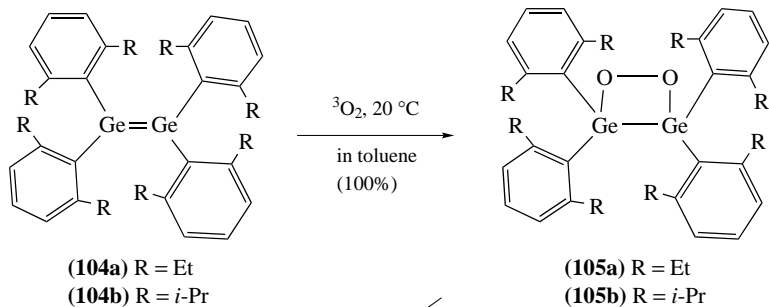
E. 1,2-Digermadioxetane and Related Compounds

Tetrakis(2,6-diethylphenyl)digermene **104a** and tetrakis(2,6-diisopropylphenyl)digermene **104b** undergo oxygenation to provide the corresponding 1,2-digermadioxetanes **105a** and **105b**, and 1,3-cyclodigermoxanes **106a** and **106b** (equation 110)¹²¹. Exposure of **104** in toluene to oxygen at -78°C or 20°C provided **105** quantitatively, which upon heating at 90°C was isomerized to **107**. Photolysis of **105** took an entirely different course to afford **106**. The thermal and photochemical behavior of **105** contrasts with that of **97**, one of the low-temperature (-78°C) oxygenation products of the stable disilene $\text{RR}'\text{Si}=\text{SiRR}'$ (R = mesityl, R' = *tert*-butyl)¹⁰⁸.

Hexakis(2,4,6-triisopropylphenyl)tetragermabuta-1,3-diene **108** is easily accessible by the reaction of the Grignard compound, RMgBr , R = 2,4,6-(*i*-Pr)₃C₆H₂, with $\text{GeCl}_2 \cdot \text{dioxane}$ and magnesium. The reaction of **108** with dry air gave a product isolated in 77% yield, and identified as a 1:2 adduct of the diene and O₂. The pale yellow adduct was identified as having the tetraoxatetragermabicyclo[4.1.1]octane skeleton **109** (equation 111). Compound **109** must be the result of a [2 + 4] cycloaddition of O₂ to the terminal germanium atoms of **108** to afford compound **110**, followed by a 1,2-addition of a second oxygen molecule to the newly formed double bond to give the intermediate **111**. Rearrangement reactions of the two O—O bonds of **111** should then furnish the isolated product **109**¹²².

F. Digermolanes

Photooxygenation of digermirane **112a** and azadigermirane **112b** in dry benzene with TPP as a sensitizer led to the formation of 1,2-dioxa-3,5-digermolanes **113a** and **113b** in 61 and 43% yield, respectively (equation 112). The digermolanes are remarkably stable and, when heated to reflux in benzene, they do not decompose at all. The kinetic stabilization by the sterically demanding 2,6-diethylphenyl and mesityl substituents is probably responsible for this behavior. However, the analogous silicon compound instantaneously undergoes intramolecular rearrangement in refluxing benzene^{123–126}. The structures of **113a** and **113b** were confirmed by their reductions with triphenylphosphine affording **114a** in 95% yield and **114b** in 91% yield, respectively.



(a) R = 2,6-Et₂C₆H₃, X = CH₂, (b) R = 2,4,6-Me₃C₆H₂, X = N-Ph
TPP = tetraphenylporphyrin.

The structure of **113a** was established by single-crystal X-ray analysis. The Ge—O, Ge—C and O—O bond distances are essentially within the range of normal values. The dihedral angle between the O—O bond and the plane containing the Ge(1), C(1) and Ge(2) atoms is 57.7°. These features are comparable to those of the well-known, structurally related organic ozonides¹²⁷.

VIII. REFERENCES

1. A. Ricci, G. C. Secibu, R. Curci and G. L. Larson, in *Advances in Silicon Chemistry* (Ed. G. L. Larson), Vol. 3, JAI Press, Greenwich, CT, 1996, p. 63.
2. (a) K. Tamao, J.-I. Yoshida and K. Itami, in *Science of Synthesis*, Vol. 4, Georg Thieme Verlag, Stuttgart, 2002, p. 413.
(b) L. Huang and T. Hiyama, *Yuki Gosei Kagaku, Kyokaishi*, **48**, 1004 (1990); *Chem. Abstr.*, **114**, 102079x (1991).
3. A. Rieche and J. Dahlmann, *Ann.*, **675**, 19 (1964).
4. G. Sosnovsky and J. H. Brown, *Chem. Rev.*, **66**, 529 (1966).
5. K. L. Berry, U.S. Patent 2,692,887 (Oct. 26, 1954); *Chem. Abstr.*, **49**, 13290g (1955).
6. W. Hahn and L. Metzinger, *Makromol. Chem.*, **21**, 113 (1956).
7. Y. A. Alexandrov, *J. Organomet. Chem.*, **238**, 1 (1982).
8. R. L. Dannley and G. Jalics, *J. Org. Chem.*, **30**, 2417 (1965).
9. A. Simon and H. Arnold, *J. Prakt. Chem.*, **8**, 241 (1959).
10. A. Jenker, *Z. Naturforsch.*, **11b**, 757 (1956).
11. R. A. Pike and L. H. Shaffer, *Chem. Ind.*, 1294 (1957).
12. P. Dembech, A. Ricci, G. Seconi and M. Taddei, *Org. Synth.*, **74**, 84 (1997).
13. (a) P. Rabin, B. Bennetau and J. Dunogues, *Synth. Commun.*, **22**, 2849 (1992).
(b) W. P. Jackson, *Synlett*, **9**, 536 (1990).
14. P. G. Cookson, A. G. Davies and N. Fazal, *J. Organomet. Chem.*, **99**, C31 (1975).
15. (a) A. Blaschette, B. Bressel and U. Wannagat, *Angew. Chem., Int. Ed. Engl.*, **8**, 450 (1969).
(b) A. Blaschette and B. Bressel, *Z. Anorg. Allg. Chem.*, **377**, 182 (1970).
(c) A. Blaschette and H. Safari, *Phosphorus Sulfur*, **17**, 57 (1983).
16. (a) W. Adam and J. del Fierro, *J. Org. Chem.*, **43**, 1159 (1978).
(b) W. Adam and J. C. Liu, *J. Am. Chem. Soc.*, **94**, 2894 (1972).
17. W. Adam, A. Alzerreca, J. C. Liu and F. Vany, *J. Am. Chem. Soc.*, **99**, 5768 (1977).
18. (a) E. Buncel and A. G. Davis, *J. Chem. Soc.*, 1550 (1958).
(b) A. G. Davis and E. Buncel, *Chem. Ind. (London)*, 1052 (1956).
(c) A. G. Davis and E. Buncel, British Patent 827,366 (Feb. 3, 1960); *Chem. Abstr.*, **54**, 14097f (1960).
(d) A. V. Tomadze, V. A. Yablokov, N. V. Yablokova and Yu. A. Aleksandrov, *J. Gen. Chem. USSR (Engl. Transl.)*, **47**, 2328 (1977); *Zh. Obshch. Khim.*, **47**, 2549 (1977).
19. T. I. Yurzhenko and A. K. Litkovets, *Dokl. Akad. Nauk SSSR*, **136**, 1361 (1961); *Chem. Abstr.*, **55**, 18564f (1961).
20. A. K. Litkovets and T. I. Yurzhenko, *Dokl. Akad. Nauk SSSR*, **142**, 1316 (1962); *Chem. Abstr.*, **57**, 2242e (1962).
21. V. P. Sluchevskaya, N. V. Yablokova, V. A. Yablokov and Y. A. Aleksandrov, *Zh. Obshch. Khim.*, **48**, 1136 (1978); *Chem. Abstr.*, **90**, 5673q (1979).
22. V. A. Yablokov, A. P. Tarabarina and D. A. Kreknin, *Zh. Obshch. Khim.*, **40**, 2255 (1970); *Chem. Abstr.*, **74**, 141946c (1971).
23. Y. L. Fan and R. G. Shaw, *J. Org. Chem.*, **38**, 2410 (1973).
24. Y. A. Ol'dekop, F. Z. Livshits and L. B. Beresnevich, *Vestn. Akad. Nauk, B. SSR, Ser. Khim. Nauk*, 113 (1975); *Chem. Abstr.*, **83**, 193430 (1975).
25. R. A. Pike and L. H. Shaffer, *Chem. Ind. (London)*, 1294 (1957).
26. A. J. Bloodworth and H. J. Eggelte, *J. Chem. Soc., Perkin Trans I*, 1375 (1981).
27. M. Suzuki, H. Takada and R. Noyori, *J. Org. Chem.*, **47**, 902 (1982).
28. W. Adam and A. Rodriguez, *J. Org. Chem.*, **44**, 4969 (1979).
29. M. Camporeale, T. Fiorani, L. Troist, W. Adam, R. Curci and J. O. Edward, *J. Org. Chem.*, **55**, 93 (1990).
30. (a) S. Matsubara, K. Takai and H. Nozaki, *Bull. Chem. Soc. Jpn.*, **56**, 2029 (1983).

- (b) E. Demole and M. Winter, *Helv. Chim. Acta*, **45**, 1256 (1962).
(c) A. Ijima, H. Mizuno and K. Kobayashi, *Chem. Pharm. Bull.*, **20**, 197 (1972).
31. S. Kanemoto, K. Oshima, S. Matsubara, K. Takai and H. Nozaki, *Bull. Chem. Soc. Jpn.*, **61**, 3607 (1988).
 32. S. Kanemoto, K. Oshima, S. Matsubara, K. Takai and H. Nozaki, *Tetrahedron Lett.*, **24**, 2185 (1983).
 33. K. B. Sharpless and T. R. Verhoeven, *Aldrichimica Acta*, **12**, 63 (1979) and references cited therein.
 34. S. Matsubara, T. Okazoe, K. Oshima, K. Takai and H. Nozaki, *Bull. Chem. Soc. Jpn.*, **58**, 844 (1985).
 35. S. Matsubara, K. Takai and H. Nozaki, *Tetrahedron Lett.*, **24**, 3741 (1983).
 36. A. K. Yudin and K. B. Sharpless, *J. Am. Chem. Soc.*, **119**, 11536 (1997).
 37. M. Schulz, J. H. Teles, J. Sundermeyer and W. G. Jorg, WO 9732867 A1 12 Sep 1997, 45 pp; *Chem. Abstr.*, **127**, 287229 (1997).
 38. I. Sakurada, S. Yamasaki, R. Göttlich, T. Iida, M. Kanai and M. Shibasaki, *J. Am. Chem. Soc.*, **122**, 1245 (2000).
 39. G. A. Olah and T. D. Ernst, *J. Org. Chem.*, **54**, 1204 (1989).
 40. J. O. Apatu, D. C. Chapman and H. Heaney, *J. Chem. Soc., Chem. Commun.*, 1079 (1981).
 41. J. H. Teles, M. Schulz, J. Sundermeyer and C. Jost, DE 19736428; *Chem. Abstr.*, **130**, 182250 (1999).
 42. L. Camici, P. Dembech, A. Ricci, G. Seconi and M. Taddei, *Tetrahedron*, **44**, 4197 (1988).
 43. R. Curci and J. O. Edwards, in *Organic Peroxides* (Ed. D. Swern), Vol. 1, Chap. IV, Wiley-Interscience, New York, 1970.
 44. M. Taddei and A. Ricci, *Synthesis*, 633 (1986).
 45. P. Dembech, A. Guerrini, A. Ricci, G. Seconi and M. Taddei, *Tetrahedron*, **46**, 2999 (1990).
 46. J. R. Hwu, *J. Org. Chem.*, **48**, 4432 (1983).
 47. S. Florio and L. Troisi, *Tetrahedron Lett.*, **30**, 3721 (1989).
 48. M. Herberhold, H-D. Brendel, A. Hofmann, B. Hofmann and W. Milius, *J. Organomet. Chem.*, **556**, 173 (1998).
 49. A. Ricci, M. Taddei, P. Dembech, A. Guerrini and G. Seconi, *Synthesis*, 461 (1989).
 50. A. Casarini, P. Dembech, G. Reginato, A. Ricci and G. Seconi, *Tetrahedron Lett.*, **32**, 2169 (1991).
 51. D. H. R. Barton and B. M. Chabot, *Tetrahedron*, **53**, 511 (1997).
 52. D. H. R. Barton and B. M. Chabot, *Tetrahedron*, **53**, 487 (1997).
 53. G. A. Olah, T. D. Ernst, C. B. Rao and G. K. S. Prakash, *New J. Chem.*, **13**, 791 (1989).
 54. C. Coperet, H. Adolffson, J. P. Chiang, A. K. Yudin and K. B. Sharpless, *Tetrahedron Lett.*, **39**, 761 (1998).
 55. S. P. Shahi and Y. D. Vankar, *Synth. Commun.*, **29**, 4321 (1999).
 56. J. Kowalski, L. Wozniak and J. Chojnowski, *Phosphorus Sulfur*, **30**, 125 (1987).
 57. L. Horner, *Tetrahedron Lett.*, 1157 (1965).
 58. L. Wozniak, J. Kowalski and J. Chojnowski, *Tetrahedron Lett.*, **26**, 4965 (1985).
 59. K. Shibata, Y. Itoh, N. Tokitoh, R. Okazaki and N. Inamoto, *Bull. Chem. Soc. Jpn.*, **64**, 3749 (1991).
 60. T. Kato and Y. Hayakawa, *Synlett*, 1796 (1999).
 61. R. Curci, R. Mello and L. Troisi, *Tetrahedron*, **42**, 877 (1986).
 62. K. Tamao, M. Kumada and T. Takahashi, *J. Organomet. Chem.*, **94**, 367 (1975).
 63. K. Tamao and M. Kumada, *J. Organomet. Chem.*, **31**, 35 (1971).
 64. K. Tamao, in *Advances in Silicon Chemistry* (Ed. G. L. Larson), Vol. 3, JAI Press, Greenwich, CT, 1996, p. 1.
 65. I. Fleming, *Chemtracks, Org. Chem.*, 1 (1996).
 66. G. R. Jones and Y. Randiais, *Tetrahedron*, **52**, 7559 (1996).
 67. K. Tamao, T. Kakui and M. Kumada, *J. Am. Chem. Soc.*, **100**, 2268 (1978).
 68. K. Tamao, T. Kakui, M. Akita, T. Iwahara, R. Kanatani, J. Yoshida and M. Kumada, *Tetrahedron*, **39**, 983 (1983).
 69. K. Tamao, N. Ishida, T. Tanaka and M. Kumada, *Organometallics*, **2**, 1694 (1983).
 70. K. Tamao and N. Ishida, *J. Organomet. Chem.*, **269**, C37 (1984).
 71. Y. Uozumi and T. Hayashi, *J. Am. Chem. Soc.*, **113**, 9887 (1991).
 72. K. Tamao, Y. Nakagawa and Y. Itoh, *J. Org. Chem.*, **55**, 3438 (1990).

73. H. Nishiyama, T. Kitajima, M. Matsumoto and K. Itoh, *J. Org. Chem.*, **49**, 2298 (1984).
74. G. Stork and M. Kahn, *J. Am. Chem. Soc.*, **107**, 500 (1985).
75. I. Fleming, R. Henning, D. C. Parker, H. E. Plaut and P. E. J. Sanderson, *J. Chem. Soc., Perkin Trans. 1*, 317 (1995).
76. J. H. Smitrovich and K. A. Woepel, *J. Org. Chem.*, **61**, 6044 (1996).
77. K. Itami, K. Mitsudo and J.-I. Yoshida, *J. Org. Chem.*, **64**, 8709 (1999).
78. M. M. Mader and P.-O. Norrby, *J. Am. Chem. Soc.*, **123**, 1970 (2001).
79. Y. A. Aleksandrov and B. I. Tarunin, *Usp. Khim.*, **46**, 1721 (1977); *Russ. Chem. Rev. (Engl. Transl.)*, **46**, 905 (1977).
80. Y. A. Aleksandrov and N. G. Sheyanov, *Zh. Obshch. Khim.* **39**, 141 (1969); *J. Gen. Chem. USSR (Engl. Transl.)*, **39**, 128 (1969).
81. L. Spialter and J. D. Austin, *Inorg. Chem.*, **5**, 1975 (1966).
82. L. Spialter, L. Pazdernik, S. Bernstein, W. A. Swansiger, G. A. Buell and M. E. Freeburger, *Adv. Chem. Ser.*, **112**, 65 (1972).
83. L. Spialter, L. Pazdernik, S. Bernstein, W. A. Swansiger, G. A. Buell and M. E. Freeburger, *J. Am. Chem. Soc.*, **93**, 5682 (1971).
84. B. Plesničar, J. Cerkovnik, J. Koller and F. Kovač, *J. Am. Chem. Soc.*, **113**, 4946 (1991).
85. E. J. Corey, M. M. Mehrotra and A. U. Khan, *J. Am. Chem. Soc.*, **108**, 2472 (1986).
86. (a) G. H. Posner, K. S. Webb, W. H. Nelson, T. Kishimoto and H. H. Seliger, *J. Org. Chem.*, **54**, 3252 (1989).
(b) G. H. Posner, C. H. Oh and W. K. Milhous, *Tetrahedron Lett.*, **32**, 4235 (1991).
87. B. Plesničar, F. Kovač and M. Schara, *J. Am. Chem. Soc.*, **110**, 214 (1988).
88. H. Kropf (Ed.), *Houben-Weyl Methoden Org. Chem.*, Vol. E13, Georg Thieme Verlag, Weinheim, 1988, pp. 217–232.
89. W. Adam and R. Albert, *Tetrahedron Lett.*, **33**, 8015 (1992).
90. R. West, *J. Organomet. Chem.*, **300**, 327 (1986).
91. (a) H. Sakurai, *Symposium on Organosilicon Chemistry*, Horwood, Chichester, UK, 1985, Abstract, p. 87.
(b) C. D. Eley, M. C. A. Rowe and R. Walsh, *Chem. Phys. Lett.*, **126**, 153 (1986).
(c) V. Sandu, A. Jordan, I. Afarik, O. P. Strausz and T. N. Bell, *Chem. Phys. Lett.*, 260 (1987).
92. Y. F. Traven and R. West, *J. Am. Chem. Soc.*, **95**, 6824 (1973).
93. W. Ando, M. Kako, T. Akasaka, S. Nagase, T. Kawai, Y. Nagai and T. Sato, *Tetrahedron Lett.*, **30**, 6705 (1989).
94. T. Akasaka, M. Kako, S. Nagase, A. Yabe and W. Ando, *J. Am. Chem. Soc.*, **112**, 7804 (1990).
95. S. Hashimoto and H. Akimoto, *J. Phys. Chem.*, **90**, 529 (1986).
96. T. Akasaka, Y. Yabe and W. Ando, *J. Am. Chem. Soc.*, **109**, 8085 (1987).
97. W. Ando, M. Kako and T. Akasaka, *Chem. Lett.*, 1679 (1993).
98. W. Ando, M. Kako, T. Akasaka and Y. Kabe, *Tetrahedron Lett.*, **31**, 4117 (1990).
99. W. Ando, M. Kako, T. Akasaka and S. Nagase, *Organometallics*, **12**, 1514 (1993).
100. T. Akasaka, K. Sato, M. Kako and W. Ando, *Tetrahedron*, **48**, 3283 (1992).
101. T. Akasaka, K. Sato, M. Kako and W. Ando, *Tetrahedron Lett.*, **32**, 6605 (1991).
102. W. Ando and T. Tsumuraya, *J. Chem. Soc., Chem. Commun.*, 770 (1989).
103. W. Ando, M. Kako and T. Akasaka, *J. Chem. Soc., Chem. Commun.*, 458 (1992).
104. W. H. Urry and J. Sheeto, *Photochem. Photobiol.*, **4**, 1067 (1965).
105. (a) E. W. Meijer and H. Wynberg, *Tetrahedron Lett.*, 785 (1965).
(b) G. Maier, *Angew. Chem., Int. Ed. Engl.*, **13**, 425 (1974).
106. N. J. Turro, M.-F. Chow and Y. Ito, *J. Am. Chem. Soc.*, **100**, 5580 (1978).
107. B. D. Shepherd and R. West, *Chem. Lett.*, 183 (1988).
108. (a) M. Michalczyk, R. West and J. Michl, *J. Chem. Soc., Chem. Commun.*, 1525 (1984).
(b) K. L. McKillop, G. R. Gillette, D. R. Powell and R. West, *J. Am. Chem. Soc.*, **114**, 5203 (1992).
109. R. L. Dannley and G. Farrant, *J. Am. Chem. Soc.*, **88**, 627 (1966).
110. R. L. Dannley and G. Jalics, *J. Org. Chem.*, **30**, 3848 (1965).
111. R. L. Dannley and G. Jalics, *J. Org. Chem.*, **34**, 2428 (1969).
112. A. Rieche and J. Dahlmann, *Angew. Chem.*, **71**, 194 (1959).
113. A. Rieche and J. Dahlmann, *Liebigs Ann. Chem.*, **675**, 19 (1964).

114. N. E. Tsyganash, N. M. Lapshin and O. S. D'yachkovskaya, *Bull. Acad. Sci. USSR, Div. Chem. Sci.*, 2271 (1973); *Chem. Abstr.*, **80**, 37229j (1974).
115. R. P. Surova, N. P. Muraeva, O. N. Druzhkov, N. M. Lapshin and O. S. D'yachkovskaya, *Bull. Acad. Sci. USSR, Div. Chem. Sci.*, 1516 (1975); *Chem. Abstr.*, **83**, 193459b (1976).
116. M. Koenig, J. Barrau and N. B. Hamida, *J. Organomet. Chem.*, **356**, 133 (1988).
117. (a) A. G. Davis and C. D. Hall, *J. Chem. Soc.*, 3835 (1959).
(b) V. A. Yablokov, N. V. Alkeeva, A. P. Tarabarina, A. V. Tomadze, N. V. Yablokova and Yu. A. Aleksandrov, *J. Gen. Chem.*, **44**, 1756 (1974); *Chem. Abstr.*, **82**, 16911b (1975).
(c) A. Rieche and J. Dahlmann, *Monatsber. Dtsch. Akad. Wiss. Berlin*, **1**, 491 (1959); *Chem. Abstr.*, **55**, 18640g (1961).
(d) A. P. Tarabarina, V. A. Yablokov and N. V. Yablokova, *J. Gen. Chem.* **40**, 1082 (1970); *Chem. Abstr.*, **73**, 66687t (1970).
(e) V. A. Yablokov, A. P. Tarabarina and N. V. Yablokova, *Synth. React. Inorg. Met. Org. Chem.*, **4**, 339 (1974).
(f) N. P. Sluchevskaya, V. A. Yablokov, N. V. Yablokova and Yu. A. Aleksandrov, *J. Gen. Chem.*, **46**, 2559 (1976); *Chem. Abstr.*, **85**, 176625b (1976).
118. N. Hillgärtner, W. P. Neuman, W. Schulten and A. K. Zarkadis, *J. Organomet. Chem.*, **201**, 197 (1980).
119. R. L. Dannley and A. K. Shubber, *J. Org. Chem.*, **36**, 3784 (1971).
120. M. F. Salomon and R. G. Salomon, *J. Am. Chem. Soc.*, **101**, 4290 (1979).
121. S. Masamune, S. A. Batcheller, J. Park, W. M. Davis, O. Yamashita, Y. Ohta and Y. Kabe, *J. Am. Chem. Soc.*, **111**, 1888 (1989).
122. G. Ramaker, A. Schäfer, W. Saak and M. Weidenbruch, *Organometallics*, **22**, 1302 (2003).
123. S. A. Batcheller and S. Masamune, *Tetrahedron Lett.*, **29**, 3383 (1988).
124. T. Tsumuraya and W. Ando, *Organometallics*, **7**, 1882 (1988).
125. T. Tsumuraya, S. Sato and W. Ando, *Organometallics*, **9**, 2061 (1990).
126. M. Kako, T. Akasaka and W. Ando, *J. Chem. Soc., Chem. Commun.*, 457 (1992).
127. P. S. Bailey, *Ozonation in Organic Chemistry*, Vol. I, Academic Press, New York, 1978.

CHAPTER 9

Selective formation of allylic hydroperoxides via singlet oxygen ene reaction

MICHAEL ORFANOPOULOS, GEORGIOS C. VOUGIOUKALAKIS and
MANOLIS STRATAKIS

Department of Chemistry, University of Crete, G-71409 Iraklion, Greece
Fax: +30 281 039 3601; e-mail: orfanop@chemistry.uoc.gr

I. INTRODUCTION	832
II. REGIOSELECTIVE FORMATION OF ALLYLIC HYDROPEROXIDES	833
A. Site Selectivity	833
1. Site selectivity with trisubstituted alkenes	833
2. Site selectivity with allylic alcohols and amines	836
3. Anti 'cis effect' selectivity	836
4. <i>Syn</i> selectivity in phenyl substituted alkenes	839
B. Regioselectivity	842
1. Regioselectivity with <i>cis</i> and <i>trans</i> disubstituted alkenes. The large-group non-bonded effect	842
2. Regioselectivity with geminal dimethyl and diethyl trisubstituted alkenes	844
C. Geminal Regioselectivity	845
1. Effect of a bulky allylic substituent	845
2. Geminal selectivity with respect to a bulky vinyl substituent	849
3. The role of non-bonded interactions between the <i>cis</i> alkyl substituents during the formation of the new double bond in the ene adduct	850
D. Regioselectivity with Olefins Bearing an Electron-withdrawing Group at the α - or β -Position	852
1. Induced geminal regioselectivity from an electron-withdrawing group at the α -position	852
2. Induced geminal regioselectivity from an electron-withdrawing group at the β -position	853
3. Solvent effects on the ene regioselectivity	854

The chemistry of peroxides, volume 2

Edited by Z. Rappoport © 2006 John Wiley & Sons, Ltd ISBN: 0-470-86274-2

E. Regioselectivity with Twisted 1,3-Dienes: Allylic versus Allene Hydroperoxide Formation	856
F. Regioselective Self-sensitized Oxygenation of Fullerene Adducts	857
III. DIASTEREOSELECTIVE FORMATION OF ALLYLIC HYDROPEROXIDES	860
A. Cyclic Hydrocarbons and Hydrocarbons with Heteroatom Substituents	861
1. Monocyclic hydrocarbons	861
2. Bi- and polycyclic hydrocarbons	861
3. Cyclic hydrocarbons with heteroatom substituents	861
B. Diastereoselectivity Induced by a Stereogenic Centre at the α -Position	863
1. Attractive interactions	864
2. Repulsive interactions	867
3. Chiral auxiliaries	868
IV. SELECTIVE FORMATION OF ALLYLIC HYDROPEROXIDES BY DYE-SENSITIZED INTRAZEOLITE PHOTOOXYGENATION	869
A. Structural Features of Zeolites	869
B. Photooxygenation Reactions in Zeolites Na-Y	870
C. Cation- π Interactions within Na-Y	873
D. Regioselectivity in the Intrazeolite Photooxygenation of Trisubstituted Alkenes	874
E. Intrazeolite Photooxygenation of Electron-poor Alkenes	877
F. Intrazeolite Photooxygenation of Isobutenylarenes	878
G. Diastereoselectivity in the Intrazeolite Photooxygenation of Chiral Alkenes	883
V. SYNTHETIC APPLICATIONS	886
VI. PERSPECTIVES	892
VII. ACKNOWLEDGEMENTS	893
VIII. REFERENCES	893

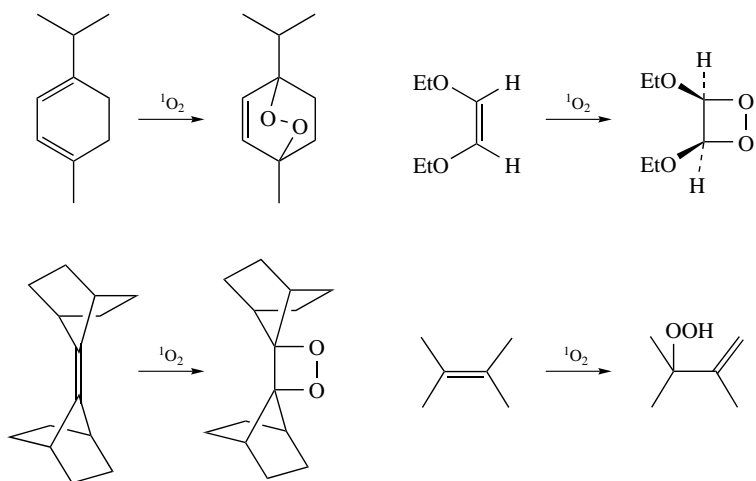
I. INTRODUCTION

The reaction of singlet molecular oxygen ($^1\text{O}_2$, $^1\Delta_g$) with alkenes that bear allylic hydrogen atoms, to form allylic hydroperoxides, is a valuable and environmentally useful methodology in organic synthesis. This chemical transformation, namely the ene reaction of singlet oxygen or the Schenck ene reaction¹⁻⁴, was originally discovered by Schenck and coworkers⁵ in 1943, and revived after the pioneering work of Foote and Wexler⁶ in the early 1960s. Ever since, it has attracted major interest among the singlet oxygen reaction modes, due to its controversial reaction mechanism and fascinating regiochemistry and stereochemistry. The purpose of this chapter is to summarize the fundamental features of the $^1\text{O}_2$ ene reaction, concerning mainly the selective formation of allylic hydroperoxides.

The chemistry of singlet oxygen has received remarkable attention by chemists not only because of its interesting mechanistic and synthetic aspects^{1,2,7,8}, but also because of its large environmental⁹⁻¹¹ and biomedical significance¹²⁻¹⁴. Among the peculiar type of reactions that $^1\text{O}_2$ affords with organic substrates are: [4 + 2], ene and [2 + 2] additions to alkenes (Scheme 1), oxidation of sulphides, phosphines etc.

A great deal of work has been focused on whether the ene reaction proceeds through a concerted or a stepwise mechanism. The initially proposed synchronous pathway¹⁵ was challenged by a biradical¹⁶, zwitterionic¹⁷ or a perepoxide¹⁸ intermediate. Kinetic isotope effects in the photooxygenation of tetrasubstituted¹⁸, trisubstituted¹⁹ and *cis*-disubstituted²⁰ alkenes supported the irreversible formation of an intermediate perepoxide,

9. Selective formation of allylic hydroperoxides via singlet oxygen ene reaction 833



SCHEME 1. [4 + 2], [2 + 2] and ene addition reactions of singlet molecular oxygen to alkenes

while for *trans*-disubstituted alkenes^{21,22} a partial equilibration of the intermediate with the reactants was postulated. Consistent with the perepoxide intermediate is also the observation that the ene reaction proceeds as a highly suprafacial process, in which the conformational arrangement of the allylic hydrogen controls the stereochemistry of the product allylic hydroperoxides²³.

Trapping of the intermediate with sulfoxides²⁴, phosphites²⁵ and sulphenates or sulphinate esters²⁶ in the photooxygenation of adamantylidenoadamantane, and theoretical calculations^{27–31} as well, support the perepoxide as the most possible intermediate. Many authors consider an intermediate exciplex^{32–34} instead of the polar perepoxide. Since the geometry of the intermediate is well defined from the isotope effects and the stereochemical studies, if an intermediate exciplex is formed, its geometrical features must resemble those of a perepoxide. Recent theoretical and experimental work by Singleton and coworkers³⁵, however, proposed a two-step no-intermediate mechanism, with a rate-limiting transition state resembling that for the formation of a perepoxide in the initially proposed stepwise process.

Nevertheless, the mechanistic features of the $^1\text{O}_2$ ene reaction continue to challenge the scientific community, and it is likely that the mechanistic debate will continue in the years to come.

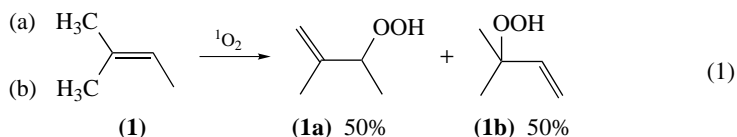
II. REGIOSELECTIVE FORMATION OF ALLYLIC HYDROPEROXIDES

A. Site Selectivity

1. Site selectivity with trisubstituted alkenes

The regioselectivity of the singlet oxygen–olefin reactions went unrecognized throughout more than twenty years of mechanistic study. It was generally recognized that methyl and methylene hydrogens are reactive and that isopropyl C–H and certain conformationally inaccessible hydrogen atoms are not. Photooxidation of trimethylethylene was frequently used as evidence to support or to contradict various mechanistic possibilities for the ene reaction. For example, the equal amounts of photooxidized products **1a** and

1b from olefin **1** (equation 1) led to the conclusion that the ene reaction proceeds without any regioselectivity.



The lack of Markovnikov directing effects in this system has been interpreted as evidence against a biradical or ionic intermediate. Since product **1a** results from H-abstraction from either methyl group (a) or (b) of **1** (equation 1), the relative reactivity of these groups was not known.

The stereospecific deuterium labeling and subsequent photooxidation of olefins **2**, **3** and **4** revealed the hidden regioselectivity of the singlet oxygen ene reaction. A strong preference of H-abstraction from the more substituted side of the double bond (*cis* effect) was found^{36,37}, as illustrated in Table 1. Reviewed in the light of this principle, earlier product distributions, obtained in the photooxidation of a wide variety of olefins, fall into a predictive pattern. Selected examples are shown in Table 1, and demonstrate clearly that the overall reactivity of a given C–H bond is greater on the more crowded side of the trisubstituted olefin (*cis* effect).

The *cis* effect was rationalized by examination of the possible transition states leading to the major and the minor ene adduct (Scheme 2). In transition state 1 (TS₁), the interactions between the incoming oxygen and the two allylic hydrogens are more favourable than those in transition state 2 (TS₂) where only one allylic hydrogen is present (Scheme 2).

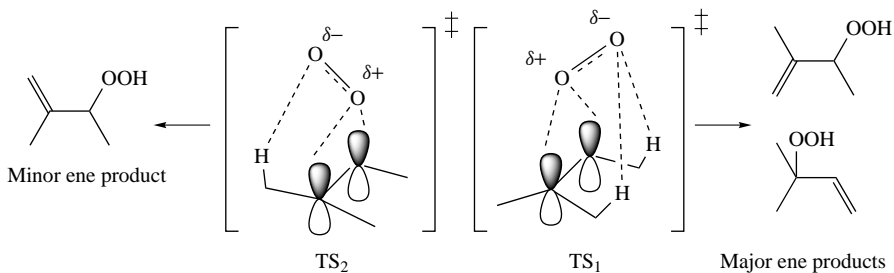
Schuster and coworkers^{38,39} also demonstrated that *trans* olefins show distinctly lower normalized (negative) entropies of activation ΔS^\ddagger for the ene reaction than *cis*, and suggested that a reversible exciplex can be formed, followed by an allylic hydrogen–oxygen interaction in the rate-determining step. In the reaction of *cis*-2-butene, the activation entropy ΔS^\ddagger is less negative by 10 e.u. than that of the *trans*-2-butene, while the activation enthalpies are very similar. The considerable difference in the activation entropies was attributed to the fact that transition states in the case of *cis* olefins require more

TABLE 1. Site selectivity of the photooxygenation of trisubstituted alkenes (*cis* effect)^a

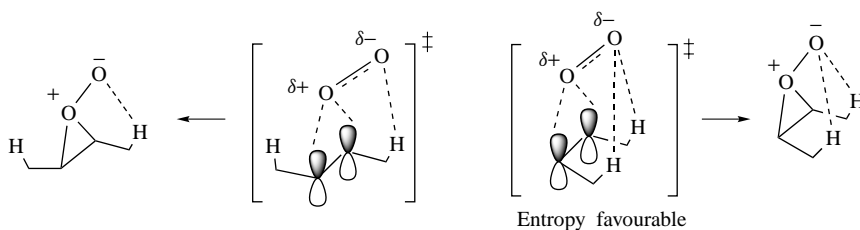
<p>(2)</p>	<p>(3)</p>	<p>(4)</p>	<p>(5)</p>
<p>(6)</p>	<p>(7)</p>	<p>(8)</p>	<p>(9)</p>

^a Numerical values represent percentage of hydrogen abstraction.

9. Selective formation of allylic hydroperoxides via singlet oxygen ene reaction 835



SCHEME 2. Transition states for the reaction of trisubstituted olefins with $^1\text{O}_2$

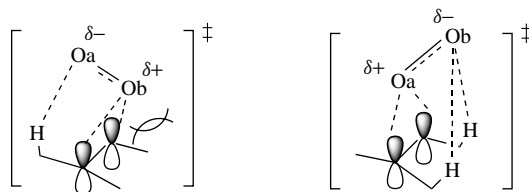


SCHEME 3. Transition states for the reaction of *cis*- and *trans*-2-butenes with $^1\text{O}_2$

organization because of the simultaneous interaction of the incoming oxygen with two allylic hydrogens (Scheme 3).

Gorman and coworkers found^{33,40} that the reactions of singlet oxygen with a variety of substrates have negative activation enthalpies and concluded that a reversible formed exciplex is the intermediate. They pointed out that none of the experiments clearly distinguishes between formation of a peroxide or a geometrically similar exciplex.

A simple way to rationalize the site selectivity is the formation of a peroxide between the olefin and singlet oxygen as the rate-determining step of this reaction. The formation of this intermediate is irreversible, at least within the time scale of the ene reaction. The low activation energy (*ca* 10 kcal mol⁻¹) provides support for the assumption of irreversibility. This complex is formulated in such a way that O_a is over the monosubstituted side and O_b over the disubstituted side of the olefin (Scheme 4).



SCHEME 4. Transition states of $^1\text{O}_2$ -alkene ene reaction

A criss-cross flexibility of $^1\text{O}_2$ in such a complex was reported⁴¹ previously by Bartlett and coworkers. Carbon-oxygen bond formation and C-H bond breaking would then follow such an intermediate. Since the formation of the C-O_a bond requires a closer approach to the olefin than the C-H bond breaking, a transition state favouring C-O_a

bond formation (less-hindered O) over Ob bond formation (more-hindered O) and subsequent C–H bond breaking would be sufficient to rationalize the regioselectivity of the singlet oxygen–trisubstituted olefin reaction. Stephenson suggested⁴² that an interaction between the LUMO orbital of the oxygen and the HOMO orbital of the olefin stabilizes the transition state of peroxide formation. This is particularly evident for the case of *cis*-2-butene where the bonded orbitals of the allylic hydrogen contribute to the HOMO orbital of the olefin, thus generating a system similar to the Ψ_3 state of butadiene. The interaction of this system with the π^* LUMO orbital of the oxygen is favourable. For the *trans* isomer, the contribution of the bonded orbitals of the allylic C–H bonds to the HOMO orbital of the olefin is approximately half, thus making the interaction with the oxygen LUMO less favourable.

The remarkable site selectivity was rationalized by Houk and coworkers⁴³ in terms of rotational-barrier differences within the alkyl groups of the double bond. For example, STO-6G semi-empirical calculations showed that the *cis* methyl groups in 2-methyl-2-butene have lower (approximately by 1 kcal mol⁻¹) rotational barrier than the *trans* methyl group. Therefore, the *cis* allylic hydrogens adopt a perpendicular conformation to the double bond plane more easily than the *trans* allylic hydrogens. According to this postulate, the lower the calculated rotational barrier, the higher the reactivity of the alkyl group. However, this mechanism was challenged later⁴⁴ by experimental results, indicating that rotational barriers do not dictate the regioselectivity of this reaction. This postulate will be discussed in the light of additional experimental results in Section II.B.1.

2. Site selectivity with allylic alcohols and amines

The high diastereoselectivity observed in the photooxygenation of certain chiral allylic alcohols^{45,46}, amines^{47,48} and derivatives, which will be analysed in Section III.B.1, was rationalized in terms of hydroxyl or amino group coordination with the incoming oxygen. The synergy of oxygen–hydroxyl coordination as well as the 1,3-allylic strain provides, in non-polar solvents, high selectivity for the *threo* allylic hydroperoxides. The *syn-anti* regioselectivity in the photooxygenation of deuterium labeled alcohols **10-E** and **10-Z** was controlled by this effect.

The usual site selectivity was observed in non-polar solvents whereas in polar solvents, such as methanol, where hydrogen bonding with the hydroxyl is efficient, the regioselectivity reverses^{49,50} (Table 2). Photooxygenation of **10-E** and **10-Z** in CCl₄ and CH₃CN showed similar *syn* selectivity. This result indicates that the *syn/anti* product selectivity is independent of the specific labeling of the methyl groups. Therefore, the peroxide formation occurs in the rate-determining step.

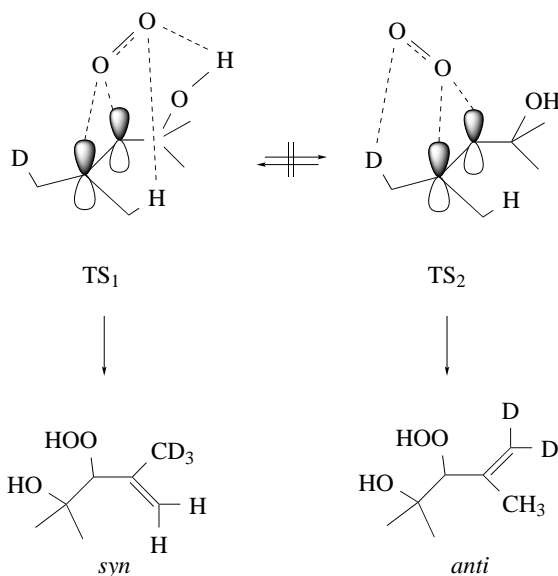
The mechanistic rationalization of the observed regioselectivity derived from examination of the possible reaction transition states is shown in Scheme 5. In TS₁, leading to the major *syn* product, the hydrogen bonding interactions between the hydroxyl functionality and the incoming oxygen in non-polar solvents are stabilizing whereas this interaction in TS₂ is absent. In polar solvents, the hydroxyl functionality of the allyl alcohol interacts with the solvent, rendering the ability to coordinate with the incoming oxygen considerably reduced. In this case, the efficiency of hydroxyl–oxygen coordination depends on solvent polarity. For example, in methanol, where hydroxyl group is fully coordinated by the solvent, the selectivity reverses favouring the *anti* product by 67% (*syn/anti* = 33:67). In this case the selectivity is controlled exclusively by steric factors.

3. Anti 'cis effect' selectivity

In trisubstituted alkenes with highly crowded *cis* alkyl groups, the site selectivity (Section II.A.1) does not apply. In those cases the one and only allylic hydrogen, which

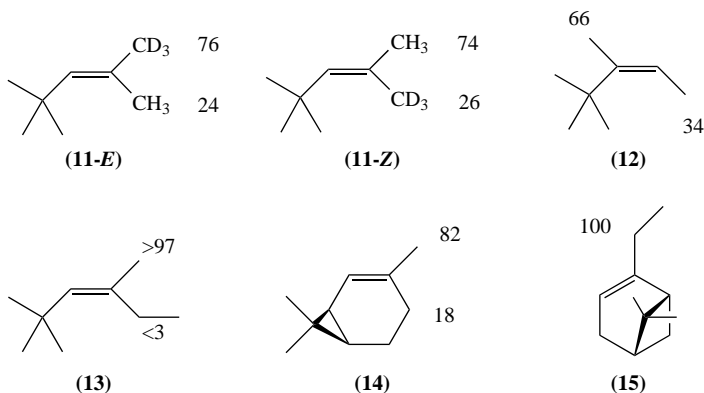
TABLE 2. *Syn/anti* regioselectivity in the photooxygenation of allylic alcohols **10-E** and **10-Z**

Substrate	Solvent	<i>Syn/anti</i> selectivity
10-E	CCl ₄	75/25
10-E	benzene	73/27
10-E	CH ₃ CN	41/59
10-E	MeOH	33/67
10-Z	CCl ₄	72/28
10-Z	CH ₃ CN	40/60

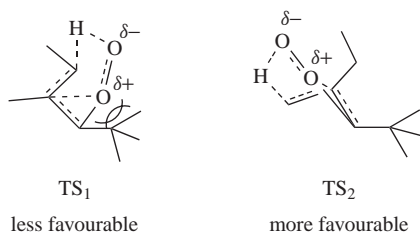
SCHEME 5. Mechanism of the photooxygenation of allylic alcohol **10-E**

is usually available in the more crowded side, is not sufficient to stabilize the proper transition state that could produce *syn* products. Instead, the major product is now produced by abstraction of the allylic hydrogen in the less substituted side of the double bond leading to ‘*anti* selectivity’⁵¹. These results are summarized in Scheme 6.

Photooxygenation of trisubstituted acyclic **11–13**⁵¹ and cyclic **14**⁵² and **15**¹ alkenes illustrates impressively a strong preference for hydrogen abstraction on the less substituted side of the double bond.

SCHEME 6. Numerical values representing percentages of hydrogen abstraction in alkenes **11–15**

Examination of the possible transition states leading to the major (*anti*) and minor (*syn*) allylic hydroperoxide provides reasonable mechanistic rationale into the *anti* selectivity. In TS₁, leading to the minor (*syn*) product, the non-bonded interactions involving the large *tert*-butyl group and the incoming oxygen are expected to be stronger than those in TS₂, where this steric interaction is less significant (Scheme 7).

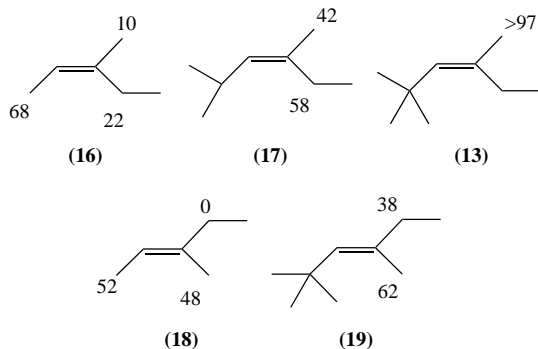
SCHEME 7. Transition states in the ene reaction of ¹O₂ with olefin **11**

The most impressive *anti* selectivity is demonstrated in olefin **13**, where only the *trans* methyl hydrogens react. This can be attributed to the fact that in TS₁, apart from the 1,3 non-bonded interactions of the *tert*-butyl group with oxygen, in the newly forming double bond the methyl groups are *cis* to each other, which is unfavourable.

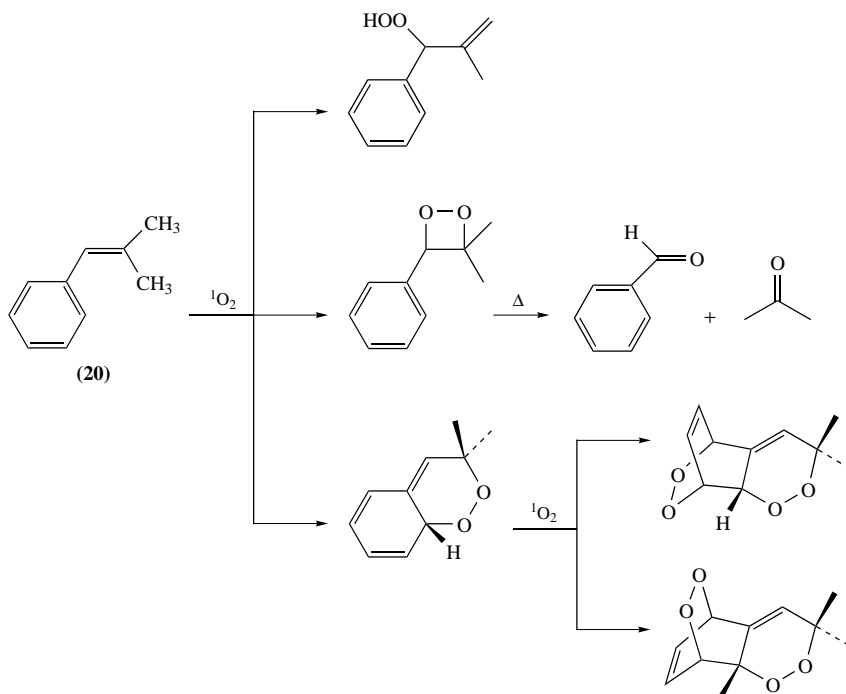
The *anti* selectivity increases as the disubstituted side of the double bond becomes more crowded (Scheme 8). This is illustrated with the trisubstituted alkenes **16**, **17** and **13**⁵¹. Alkene **16** shows the normal '*cis* effect' selectivity where only 10% of the *anti* ene adduct is formed. However, as the size of the *cis* alkyl substituent increases from methyl in **16**, to isopropyl in **17** and *tert*-butyl in **13**, the *anti* selectivity increases from 10% to 42% and to >97%, respectively. The same trend is also noted in substrate **19**. A substantial deviation from '*cis* effect' selectivity is observed by replacing one methyl group in **18** with a *tert*-butyl group in **19**. The totally unreactive methylene hydrogens in **18** (*cis* effect) become reactive in **19**, producing the *exo* ene adduct in 38% yield.

In conclusion, the *anti* selectivity for hydrogen abstraction of the ene reaction of trisubstituted olefins is related: (a) to the degree of crowdedness of the more substituted side of the olefin; (b) to the non-bonded interactions during the new double bond formation; and (c) to the lack of interaction of oxygen with two allylic hydrogens.

9. Selective formation of allylic hydroperoxides via singlet oxygen ene reaction 839



SCHEME 8. Numerical values representing the percentages of hydrogen abstraction in olefins **13** and **16–19**



SCHEME 9. Photooxygenation products of β,β -dimethylstyrene

4. *Syn* selectivity in phenyl substituted alkenes

The phenyl ring of styrene substrates directs a *syn* selectivity in their ene reactions with singlet oxygen⁵³. This effect was demonstrated by the photooxygenation of β,β -dimethylstyrene (**20**). This substrate, apart from the ene product, produces the 1,2-dioxetane and two diastereomeric diendoperoxides^{54,55}, as shown in Scheme 9.

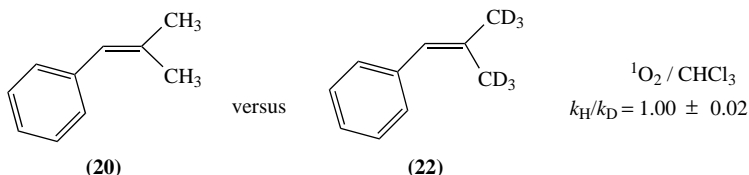
TABLE 3. *Syn/anti* regioselectivity in the ene reaction of $^1\text{O}_2$ with β,β -dimethylstyrene

Solvent	<i>Syn/anti</i> selectivity ^a
CCl_4	56/44
CH_3CN	71/29
MeOH	82/18

^a *syn* = H-abstraction, *anti* = D-abstraction.

The stereospecific labeling of the *anti* methyl by deuterium in compound **20** to produce substrate **21** (Table 3) was required in order to study the *syn/anti* regioselectivity of the ene allylic hydroperoxides. The ene products in different solvents showed a preference for hydrogen abstraction from the methyl *syn* to the phenyl group. The magnitude of this selectivity depends on solvent polarity. On increasing the solvent polarity, a substantial increase in the amount of *syn* product occurs (Table 3).

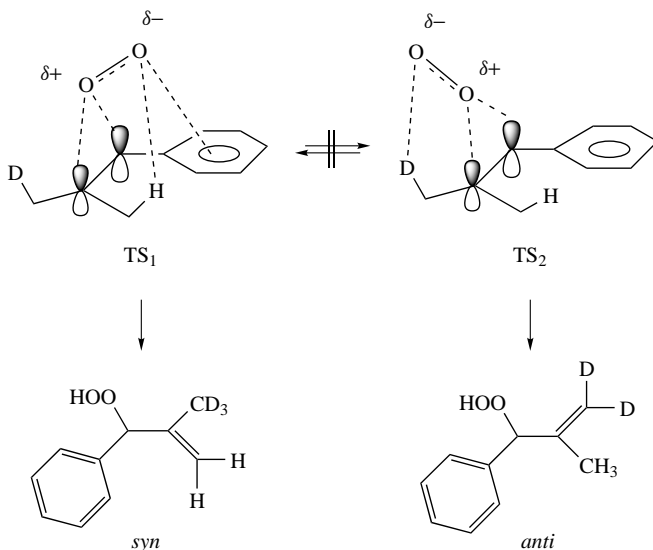
The intermolecular kinetic isotope effect for the competition of **20** with its deuterated analogue **22** in chloroform was negligible (Scheme 10, $k_{\text{H}}/k_{\text{D}} = 1.00 \pm 0.02$)⁵³. Like in other trisubstituted alkenes, this result was interpreted in terms of irreversible formation of a peroxide intermediate.

SCHEME 10. Intermolecular isotope effects in the photooxygenation of alkenes **20** vs **22**

A mechanistic possibility that accounts for the observed *syn* selectivity is shown in Scheme 11. In TS_1 , the incoming oxygen is oriented towards the more substituted side of the double bond, there is only one allylic hydrogen interaction with singlet oxygen and TS_1 leads to the major ene product. In TS_2 , leading to the minor *anti* product, singlet oxygen again interacts with only one allylic hydrogen. Therefore, the extra stabilization of TS_1 leading to the major product versus TS_2 leading to the minor product must arise from 'positive' interactions of singlet oxygen with the phenyl ring. In TS_1 , the electron-donating ability of the phenyl ring stabilizes the partial positive charge, which is developing on the benzylic carbon of the double bond. Simultaneously, the negative charge, which is developing on the oxygen during the formation of the peroxide, is stabilized by the partially positive phenyl group. Thus the overall effect stabilizes better the *syn* transition state TS_1 than the *anti* TS_2 , where this effect is absent.

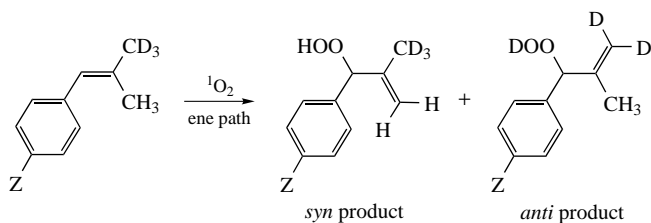
The regioselectivity for the ene pathway, in the photooxidation of several *para*-substituted β,β -dimethylstyrenes, was recently found to depend on the electronic nature of the aryl substituents⁵⁶. Electron-withdrawing substituents, such as *p*- CF_3 or *p*-F,

9. Selective formation of allylic hydroperoxides via singlet oxygen ene reaction 841



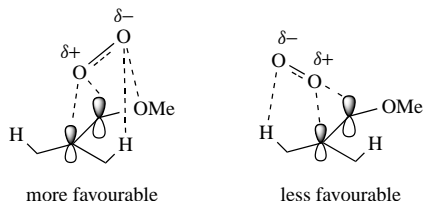
SCHEME 11. Phenyl-group controlling regioselectivity in the photooxygenation of β,β -dimethylstyrene

TABLE 4. *Syn/anti* stereoselectivity in the ene reaction of $^1\text{O}_2$ with *para* substituted β,β -dimethylstyrenes



Substituent (Z)	<i>Syn/anti</i> selectivity
MeO	46/54
Me	55/45
H	63/37
F	68/32
CF ₃	74/26

favour increased reactivity of the allylic hydrogen atoms from the *syn* methyl group, compared to electron-donating substituents, such as *p*-MeO, where the reactivity of the *anti* methyl group increases significantly (Table 4). The mechanistic rationalization presented in Scheme 11 was again used to explain these results. In the case of electron-donating substituents at the *para* position (Me and MeO), the electron density at the aryl group increases and the interaction of oxygen with the aryl ring becomes less favourable. On the other hand, electron-withdrawing substituents, such as F or CF₃, decrease the



SCHEME 12. Transition states in the photooxygenation of trisubstituted enol ethers

electron density of the aryl group, thus the stabilizing interaction of the negatively charged oxygen with the arene is more efficient, leading to 74% *syn* selectivity.

The '*cis* effect', observed also in trisubstituted enol ethers^{57,58}, may as well be rationalized by a similar mechanism (Scheme 12). In this case, the electron-donating group that stabilizes the partially charged double bond carbon of the perepoxide in the *syn* transition state is the alkoxy moiety. Therefore, the favourable interactions of the singlet oxygen with the phenyl or alkoxy substituents direct the orientation of the perepoxide intermediate.

B. Regioselectivity

1. Regioselectivity with *cis* and *trans* disubstituted alkenes. The large-group non-bonded effect

The reaction of singlet oxygen with *cis* and *trans* alkenes shows an unexpected regioselectivity for hydrogen abstraction on the large alkyl group of the double bond⁵⁹.

TABLE 5. Regioselectivity in the photooxygenation of *cis*-alkenes 23–33^a

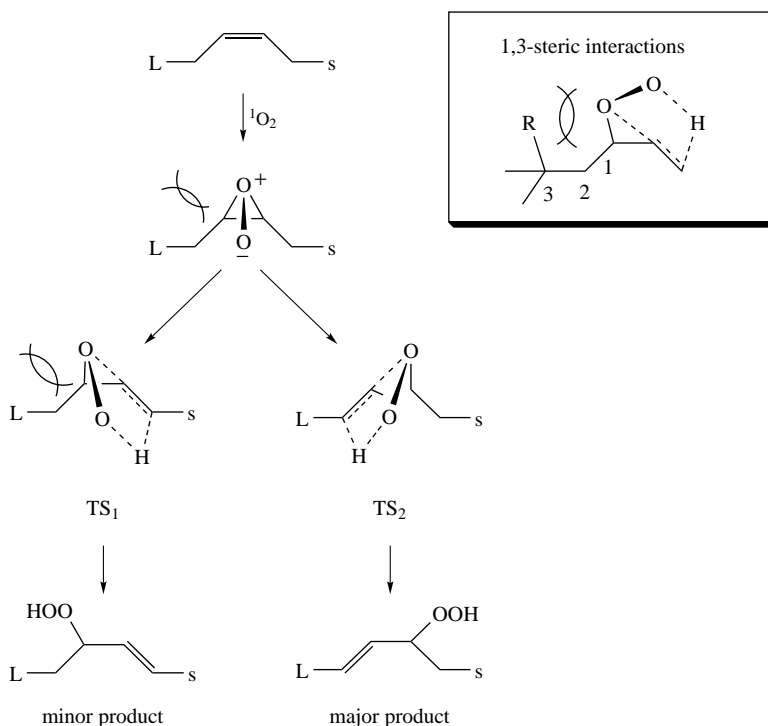
$\text{L}-\text{CH}=\text{CH}-\text{CH}_2-\text{CH}_2-\text{S} \xrightarrow{^1\text{O}_2} \text{L}-\text{CH}=\text{CH}-\text{CH}(\text{OOH})-\text{CH}_2-\text{CH}_2-\text{S} + \text{L}-\text{CH}(\text{OOH})-\text{CH}=\text{CH}-\text{CH}_2-\text{CH}_2-\text{S}$			
L = large substituent	major product		
s = small substituent	minor product		
 (23)	 (24)	 (25)	 (26)
 (27)	 (28)	 (29)	 (30)
 (31)	 (32)	 (33)	

^a Numerical values represent percentage of hydrogen abstraction.

This remarkable and synthetically useful selectivity applies to both *cis* and *trans* non-symmetrically substituted alkenes. The regioselective photooxygenation reaction of some *cis* non-symmetrical alkenes and their regio-limitations are shown in Table 5.

For example, when L (larger group) is isopropyl, *tert*-butyl or phenyl and s (smaller group) is hydrogen, compounds **23**, **25** and **29** respectively, the preferential abstraction of allylic hydrogen adjacent to the larger group is about 70%. In this case the methylene hydrogens are statistically 3.5–4 times more reactive than the s-methyl hydrogens. In substrate **32**, where L = triphenylmethyl group, the regioselectivity is nearly exclusive (95%) on the L substituted side. As the size of the s group becomes larger, the regioselectivity towards the L substituent decreases. This is demonstrated with substrates **28** and **30**, where the preferential hydrogen abstraction is only slightly different on the two sides of the double bond. For example, when L and s are phenyl and isopropyl respectively, substrate **30**, competition for the two allylic sides leads to nearly equal hydrogen abstraction from the two methylene sides. This result indicates further that non-bonding interactions play a more important role than conjugation with the π system of the phenyl ring in the transition state of this reaction.

The regioselectivity was rationalized⁵⁹ mainly in terms of steric interactions in the possible transition states of the photooxygenation reaction (Scheme 13). In the transition state TS₂ leading to the major product, the non-bonding interactions involving the large group are smaller than those of the transition state TS₁ leading to the minor product. Since TS₂ is expected to have lower energy than TS₁, the C–O bond next to the larger substituent should be weakened more than the other C–O bond next to the smaller group.



SCHEME 13. Regioselectivity of the photooxygenation reaction of *cis* alkenes

Trans alkenes show similar regioselectivity on their photooxygenation reactions. However, their reactivity towards singlet oxygen is much less than that of the corresponding *cis* alkenes⁴³.

2. Regioselectivity with geminal dimethyl and diethyl trisubstituted alkenes

The regioselectivity trend in the photooxygenation of geminal dimethyl and diethyl trisubstituted olefins is similar to that observed in *cis* or *trans* disubstituted alkenes, with the allylic hydrogens next to the bulky alkyl substituent being more reactive. The results⁶⁰ are summarized in Table 6. In a representative example (substrate **38**), where L = *t*-Bu and R = H, the methylene hydrogens are statistically 6.5 times more reactive than the hydrogens of the two geminal methyls. Starting from 2-methyl-2-pentene where R = H and L = H and increasing the size of the L substituent, after the ethyl substitution, a significant increase in the percentage of the anti-Markovnikov product is observed. When the L substituent is the very bulky triphenylmethyl (substrate **42**), the reaction becomes highly regioselective (92/8).

The transition states in the hydrogen abstraction step, as seen earlier in Scheme 13, help to explain the observed change in regioselectivity. In a transition state where there is a strengthening of the C–O bond on the tertiary carbon, a release of the 1,3 non-bonded interactions between the oxygen and the L group with respect to the intermediate peroxide occurs. Therefore, this transition state is expected to be lower in energy than the transition state where the non-bonded interactions exist.

When the geminal dimethyl is replaced by a geminal diethyl group (substrates **43** and **44**), a higher degree of regioselectivity is observed. The transition states leading to the

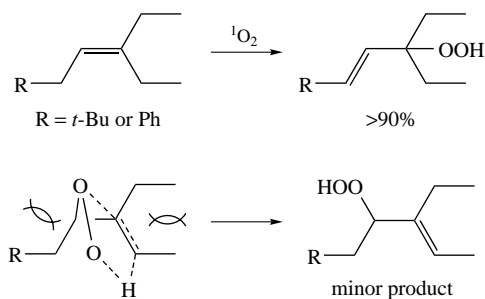
TABLE 6. The percentage of hydrogen abstraction from alkenes **34–44**

L = large substituent R = H, Me			
 (34)	 (35)^a	 (36)	 (37)
 (38)	 (39)^b	 (40)	 (41)
 (42)	 (43)	 (44)	

^a Reference 61.

^b Reference 62.

9. Selective formation of allylic hydroperoxides via singlet oxygen ene reaction 845



SCHEME 14. Repulsive interactions developing between two geminal diethyl groups

minor product are even less favoured not only because of the 1,3 non-bonded interactions between the group L and the oxygen, but because of the repulsions developing when the ethyl group (Scheme 14) adopts a *cis* geometry with a methyl group in the newly forming double bond. We would predict that if the geminal dimethyl group is replaced by a geminal di-*n*-propyl or a longer di-*n*-alkyl group, the reaction would be regioselective (>97% selectivity).

For a series of geminal dimethyl trisubstituted alkenes, the same trend of regioselectivity was earlier recognized by Thomas and Pawlak⁶³ as well as Rautenstrauch and coworkers⁶⁴. By examining molecular models and assuming that the reaction is concerted, Thomas and coworkers proposed that the difference in regioselectivity could be due to the different conformations and steric repulsions in the transition states.

A regioselectivity trend, opposite to what has been described in Table 6, was recently reported for the ene reaction of singlet oxygen with prenylated dihydroxyacetophenones (stabilizing phenolic assistance effect)⁶⁵. In this case, allylic hydrogens of methyl groups were more reactive than the allylic hydrogens next to the phenyl ring due to a stabilizing interaction of the negatively charged oxygen of the perepoxide intermediate with the phenolic hydrogen, *ortho* to the prenyl side chain (Scheme 15).

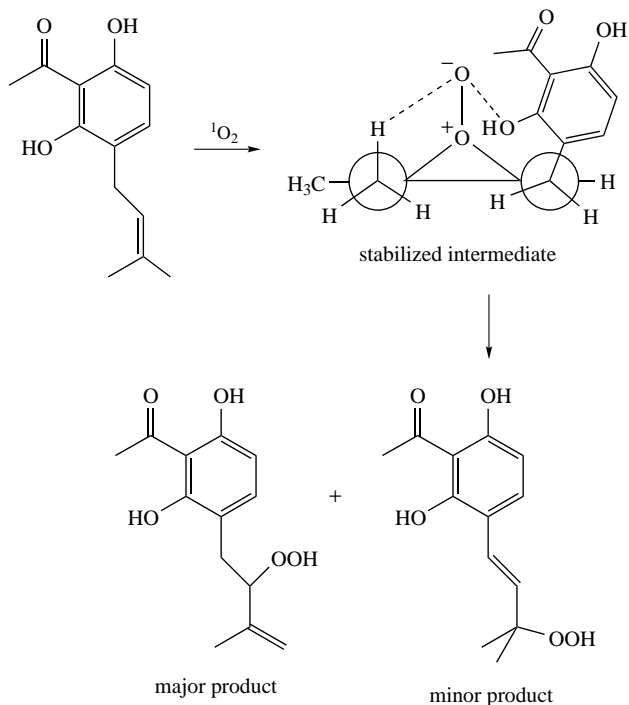
C. Geminal Regioselectivity

1. Effect of a bulky allylic substituent

The reaction of singlet oxygen with alkenes shows a general preference for hydrogen abstraction from the group that is geminal to the larger substituent of the double bond. For example, substrates produced by replacement of an allylic hydrogen in tetramethylethylene with a series of functional groups (sulphides, sulphoxides, sulphones, cyano, halides etc.) undergo selective photooxygenations with a surprising geminal selectivity with respect to the allylic functionality⁶⁶. Some examples are summarized in Table 7.

The various explanations that were provided to rationalize the observed regioselectivity involved: (a) electronic repulsions between the lone pairs of the heteroatoms and the negatively charged oxygen of the perepoxide; (b) anchimeric assistance by the allylic substituent leading to regioselective opening of the possible perepoxide intermediate; (c) rotational barrier differences within the alkyl groups of the double bond.

The geminal selectivity holds even in the reactions of singlet oxygen with simple alkyl substituted alkenes^{67,68}. Photooxygenation of a series of alkyl- and phenyl-substituted olefins shows a strong preference for hydrogen abstraction on the methyl group that is geminal to the larger alkyl or aryl substituent of the alkene. These results are summarized in Table 8.



SCHEME 15. The stabilizing phenolic assistance effect

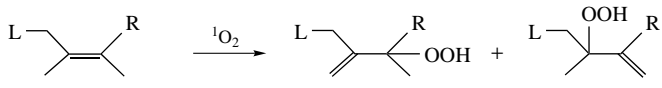
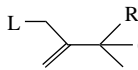
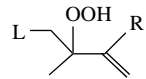
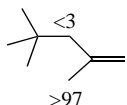
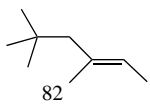
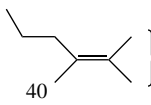
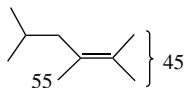
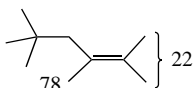
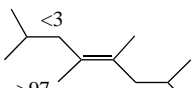
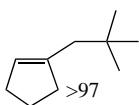
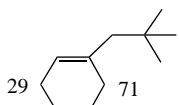
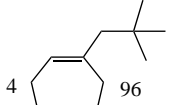
TABLE 7. Geminal selectivity in the photooxygenation of alkenes **45**–**48** bearing an allylic functionality^a

$19 \left\{ \begin{array}{l} \text{SO}_2\text{C}_6\text{H}_4\text{Me-}p \\ \text{81} \end{array} \right.$ (45)	$27 \left\{ \begin{array}{l} \text{SOC}_6\text{H}_4\text{X-}p \\ \text{73} \\ \text{X} = \text{NO}_2, \text{H, Me, MeO} \end{array} \right.$ (46)
$48 \left\{ \begin{array}{l} \text{SC}_6\text{H}_4\text{X-}p \\ \text{52} \\ \text{X} = \text{Me, NO}_2 \end{array} \right.$ (47)	$46 \left\{ \begin{array}{l} \text{Br} \\ \text{54} \end{array} \right.$ (48)

^a Numerical values represent percentage of hydrogen abstraction.

Disubstituted alkene **49** impressively illustrates this point. Similarly tri- and tetrasubstituted alkenes with the bulky alkyl substituent in the allylic position show preferential hydrogen abstraction from the geminal methyl group. Alkenes **50**–**53** give again, as the major product, the ene allylic hydroperoxide with the double bond on the methyl that is geminal to the larger alkyl group. This selectivity is demonstrated once more in symmetrical olefin **54**, where only the methyl hydrogens react. The same trend was also noted in cyclic alkenes **55**–**57**⁶⁹.

TABLE 8. Geminal selectivity in the photooxygenation of alkenes **49–57** bearing a large alkyl substituent at the allylic position^a

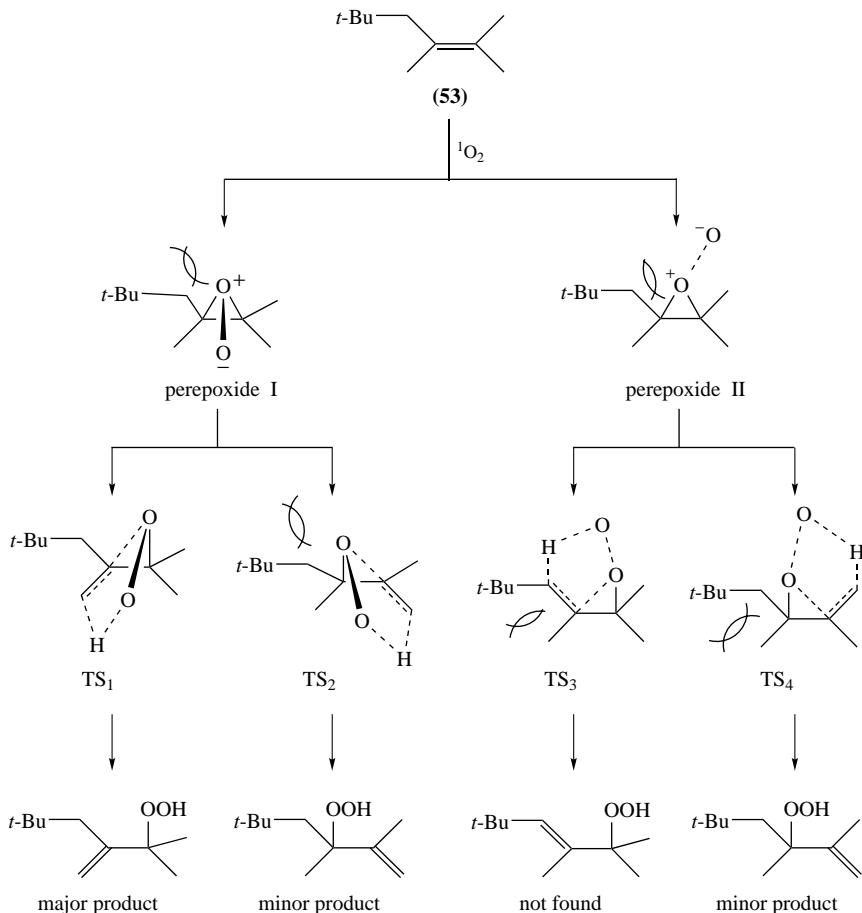
	$^1\text{O}_2$		
L = large alkyl substituent R = H, Me		major product	minor product
 (49)	 (50)	 (51)	
 (52)	 (53)	 (54)	
 (55)	 (56)	 (57)	

^a Numerical values represent percentage of hydrogen abstraction.

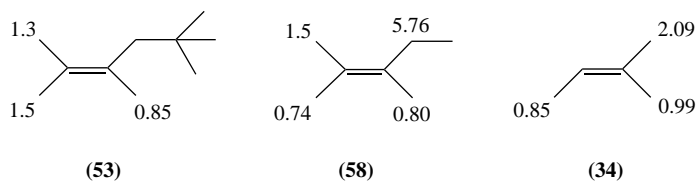
Examination of the possible transition states leading to the major and the minor product in the reaction of $^1\text{O}_2$ with alkene **53** provides a new insight into the geminal selectivity. In transition state TS_3 , leading to the minor or absent product, the non-bonding interactions involving the large *t*-butyl group and the methyl group, which are placed in a *cis* configuration, are expected to be stronger than those in transition states TS_1 , TS_2 and TS_4 where this steric interaction is absent. Because of 1,3 non-bonded interactions, transition state TS_1 leading to the major product is expected to have lower energy than TS_2 and TS_4 .

An alternative explanation of the geminal selectivity (Scheme 16) was based on a computational model proposed by Houk and coworkers⁴³. According to this model, the lower the calculated rotational barrier the higher the reactivity of the alkyl group. For example, molecular mechanics calculations showed that the methyl group geminal to the neopentyl group in 2,3,5,5-tetramethyl-2-hexene (**53**) has the lowest rotational barrier and is the most reactive^{43,68}. Furthermore, the ethyl group in 2,3-dimethyl-2-pentene (**58**) has a much higher rotational barrier (5.76 kcal mol⁻¹) than the methyl groups and is totally inactive to $^1\text{O}_2$. Similar trends hold with 2-methyl-2-butene, **34** (Scheme 17).

However, the barrier to rotation does not always predict the regioselectivity of the ene reaction of $^1\text{O}_2$ with alkenes. As shown later⁴⁴, it is the non-bonded interactions in the isomeric transition states that control product formation and barriers to rotation are rather irrelevant. The calculated rotational barrier values, with the HF-STO-3G method, for the allylic methyls in a series of trisubstituted alkenes, as well as the experimentally observed ene regioselectivity of a series of selective substrates, are shown in Table 9⁴⁴.



SCHEME 16. Mechanism of the geminal selectivity in the photooxygenation of alkenes bearing a large alkyl substituent in allylic position

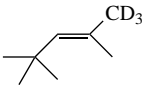
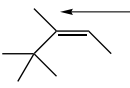
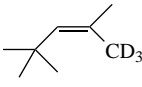
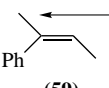
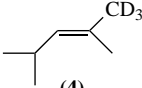


SCHEME 17. Calculated rotational barriers in kcal mol^{-1} by MM2

For alkenes **11-E** and **11-Z**, the *syn* methyl groups have lower rotational barriers than the corresponding *anti* ones by $0.5 \text{ kcal mol}^{-1}$. This is in the opposite direction to the proposed theoretical model. However, for alkene **4** there is a correlation between rotational barriers and ene reactivity. Alkenes **12** and **59** also demonstrate impressively that there is

9. Selective formation of allylic hydroperoxides via singlet oxygen ene reaction 849

TABLE 9. Relative yields of the ene products and rotational barriers of methyl groups

	<i>a</i>	<i>b</i>		<i>a</i>	<i>b</i>
 (11-E)	76	1.63	 (12)	66	2.91
	24	1.11		34	0.91
 (11-Z)	74	1.63	 (59)	64	1.45
	26	1.11		36	1.22
 (4)	14	1.64			
	86	0.40			

^a Numerical values represent percentage of hydrogen abstraction.

^b Barriers to rotation (kcal mol⁻¹).

no correlation between ene reactivity and rotational barriers. Again, in these examples the more reactive *trans* methyl group is the one which shows the higher rotational barrier, in contrast to the predictions of the proposed theoretical model. These results indicate that there is not always a correlation between the reactivity of the methyl groups and their rotational barriers. It was also emphasized⁴⁴ that, according to the Curtin–Hammett principle, the rotational barriers are irrelevant to the product distribution since their values are too small (0.5–2.0 kcal mol⁻¹) compared to the activation energies of the reactions (6–13 kcal mol⁻¹).

2. Geminal selectivity with respect to a bulky vinyl substituent

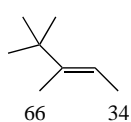
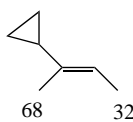
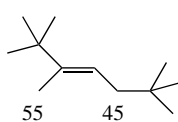
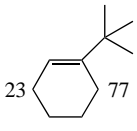
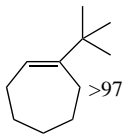
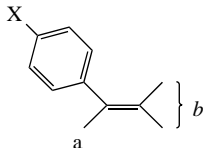
Geminal selectivity is also observed in cases where the bulky substituent is in a vinylic position^{48,67,69}. Examples with compounds **60**–**65** are shown in Table 10.

The presence of a *para*-phenyl substituent does not alter the geminal selectivity. This is demonstrated with substrate **65**, where the selectivity is insensitive to substitution on the phenyl ring. This result indicates that non-bonding interactions play a more important role than electronic effects of the *para*-substituted phenyl ring in determining the stability of the transition state of the product-determining step of the reaction^{48,59}. For these styrene-type substrates (**65**), although the active stereosize of the phenyl group is smaller than that of the *t*-butyl group in **60**, the geminal selectivity is higher. This may be attributed to the fact that the forming double bond is in conjugation with the phenyl group.

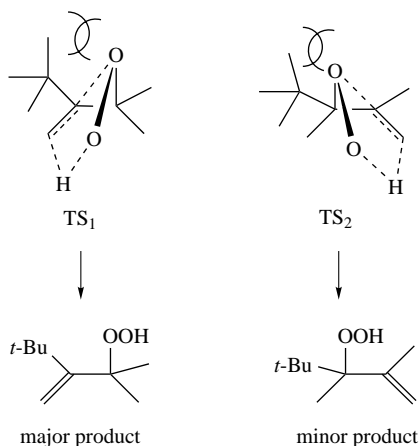
For cycloalkenes, the variation in the percentage of geminal regioselectivity is probably due to the combination of two effects: (a) the different conformational arrangements of the allylic hydrogens in the ring systems as proposed earlier⁷⁰, and (b) the 1,3 non-bonded interactions between the large groups and the oxygen.

On the basis of similar arguments, previously proposed, transition state TS₁ is expected to have lower energy than TS₂ (Scheme 18) and thus account for the geminal selectivity of alkenes with the large L group in the vinyl position.

TABLE 10. Geminal selectivity with respect to a bulky vinyl substituent in **60–65**^a

																		
(60)	(61)	(62)	(63)															
																		
(64)	(65)																	
			<table border="1"> <thead> <tr> <th>X</th> <th>a</th> <th>b</th> </tr> </thead> <tbody> <tr> <td>MeO</td> <td>76</td> <td>24</td> </tr> <tr> <td>Br</td> <td>76</td> <td>24</td> </tr> <tr> <td>CF₃</td> <td>74</td> <td>26</td> </tr> <tr> <td>H</td> <td>74</td> <td>26</td> </tr> </tbody> </table>	X	a	b	MeO	76	24	Br	76	24	CF ₃	74	26	H	74	26
X	a	b																
MeO	76	24																
Br	76	24																
CF ₃	74	26																
H	74	26																

^a Numerical values represent percentage of hydrogen abstraction.



SCHEME 18. Mechanism of the geminal selectivity in the photooxygenation of alkenes bearing a bulky vinyl substituent

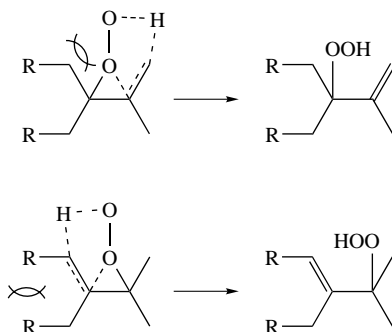
3. The role of non-bonded interactions between the *cis* alkyl substituents during the formation of the new double bond in the *ene* adduct

In the second step of the *ene* reaction, during the formation of the adduct double bond, if two alkyl substituents are forced to adopt a *cis* orientation, the transition state leading to the adduct is highly unfavourable. This can be demonstrated by examining the regioselectivity in the series of substrates⁷¹ of Table 11. For olefin **66**, the methylenic hydrogens are less reactive than the hydrogens of the methyls (ratio 70/30). By increasing the size of the alkyl group (substrate **67**), the methylenic hydrogens become much less reactive (<5%). This remarkable change in regioselectivity can be attributed to higher repulsions between the propyl groups compared to the ethyls, during the formation of the minor allylic hydroperoxide. In the photooxygenation, repulsions exist between an ethyl

9. Selective formation of allylic hydroperoxides via singlet oxygen ene reaction 851

TABLE 11. Numerical values representing percentages of hydrogen abstraction from alkenes **66**–**71**

$30 \left\{ \begin{array}{c} \text{Cyclohexane ring with an exocyclic double bond and a methyl group} \end{array} \right\} 70$ (66)	$<5 \left\{ \begin{array}{c} \text{Cyclohexane ring with an exocyclic double bond and a propyl group} \end{array} \right\} >95$ (67)	$48 \left\{ \begin{array}{c} \text{Cyclohexane ring with an exocyclic double bond and two phenyl groups} \end{array} \right\} 52$ (68)
$49 \left\{ \begin{array}{c} \text{Cyclohexane ring with an exocyclic double bond and two methyl groups} \end{array} \right\} 51$ (69)	$49 \left\{ \begin{array}{c} \text{Cyclohexane ring with an exocyclic double bond and a methyl group} \end{array} \right\} 51$ (70)	$32 \quad 68$ (71)

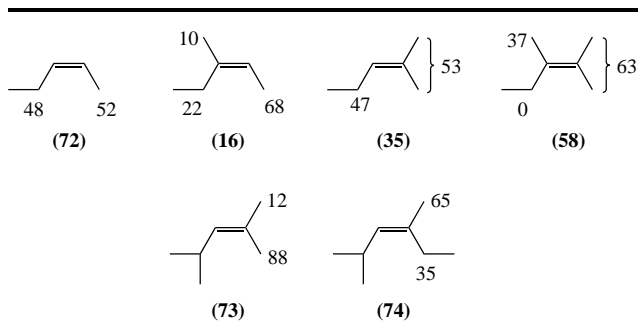
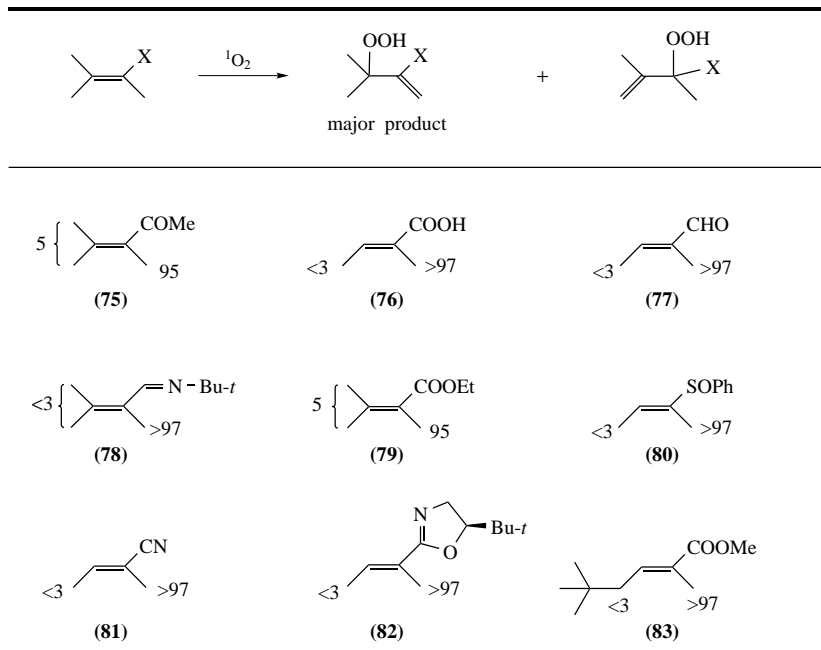


SCHEME 19. The two kinds of steric interactions during the hydrogen abstraction in the reaction of tetrasubstituted alkenes

and a methyl group of **66** and between a propyl and a methyl in **67**. By increasing the size of the alkyl group to phenyl or isopropyl (substrates **68** and **69**, respectively), a reverse regioselectivity trend is found.

For those specific cases there are two equally competing factors in the product-forming transition states which affect the regioselectivity (Scheme 19): (a) the 1,3 non-bonded interactions between the oxygen and the phenyl or isopropyl substituents in the transition state for hydrogen abstraction from the methyl group, and (b) repulsions between the geminal alkyls, due to the formation of the new double bond by methylenic hydrogen abstraction. It is also interesting to note that the stabilizing contribution of the double bond conjugation with the phenyl group in alkene **68** does not affect the regioselectivity, as has been already noticed in the photooxygenation of **29** (Table 5).

Similar arguments can explain the change in regioselectivity of substrates **70** and **71** compared to **23** and **60**, respectively. In **60**, for example, replacement of the geminal methyl by an ethyl group causes a significant drop in geminal selectivity. It is instructive to note in general that the reactivity of the methylene hydrogens is significantly decreasing when a geminal methyl is present. This can be demonstrated by the examples presented in Table 12. For instance, by comparing substrates **73** and **74** it is obvious that the reactivity of the *anti* methyl group increases substantially when a methyl is replaced by an ethyl, leading to *anti* 'cis effect' selectivity⁵¹.

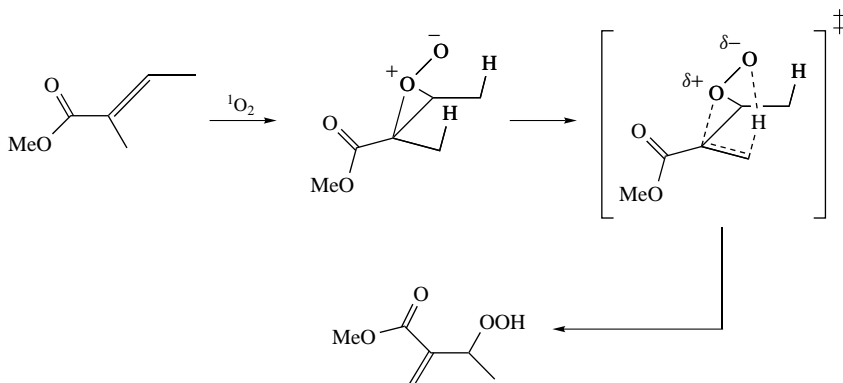
TABLE 12. Percentages of hydrogen abstraction in the reaction of **16**, **35**, **58** and **72–74**TABLE 13. Geminal selectivity^a in the photooxygenation of functionalized alkenes **75–83**.^a Numerical values represent percentage of hydrogen abstraction.

D. Regioselectivity with Olefins Bearing an Electron-withdrawing Group at the α - or β -Position

1. Induced geminal regioselectivity from an electron-withdrawing group at the α -position

For alkenes bearing an electron-withdrawing group at the α -position such as aldehyde⁷², carboxylic acid⁷³, ester⁷⁴, ketone^{75,76}, imine^{77,78}, sulphoxide⁷⁹ and cyano⁸⁰, a high degree of geminal selectivity has been demonstrated. The results are summarized in Table 13.

9. Selective formation of allylic hydroperoxides via singlet oxygen ene reaction 853



Scheme 20. The photooxygenation reaction of methyl tiglate

Many mechanisms had been proposed in the past to rationalize this selectivity (trioxanes, perepoxide, exciplex, dipolar or biradical intermediates); however, it is now generally accepted⁸¹ that the reaction proceeds through an intermediate exciplex which has the structural requirements of a perepoxide. This assumption is supported by: (a) the lack of stereoselectivity in the reactions with chiral oxazolines⁸² and tiglic acid esters⁸³; (b) the comparison of the diastereoselectivity of dialkyl substituted acrylic esters⁸⁴ with structurally similar non-functionalized alkenes; (c) the intermolecular isotope effects⁸⁵ in the photooxygenation of methyl tiglate; and (d) the solvent effects on regioselectivity⁸⁶.

It was proposed that, in the hydrogen abstraction step, the perepoxide opens preferentially at the C–O bond next to the unsaturated moiety. Due to the forthcoming conjugation in the adduct, the corresponding transition state is favourable, as exemplified in the photooxygenation of methyl tiglate in Scheme 20.

The 1,3 non-bonded interactions, which control the regioselectivity in the photooxygenation of non-functionalized alkenes, do not contribute significantly to the geminal selectivity of alkenes bearing an electron-withdrawing group at the α -position. As seen in substrate **83**, no reactivity of the methylene hydrogens next to the *t*-butyl group was found. This result indicates that the non-bonded interactions between the *t*-butyl group and the oxygen atom are less important than the forthcoming double bond–carbonyl conjugation in the ene adduct.

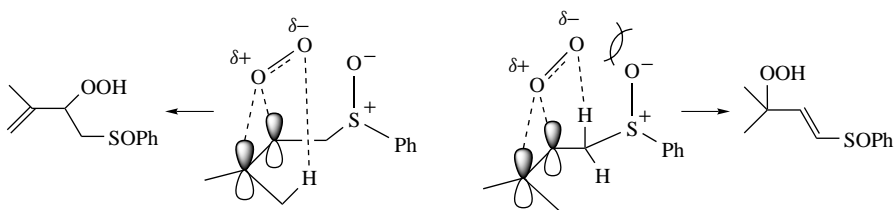
2. Induced geminal regioselectivity from an electron-withdrawing group at the β -position

The presence of an electron-withdrawing substituent at the β -position with respect to the double bond causes various trends in the ene regioselectivity⁸⁷ (Table 14). For example, in the carbonyl derivatives **84–87** the regioselectivity is invariable, and the methylene hydrogen atoms are approximately five times as reactive as those of the methyl groups. The forthcoming conjugation of the double bond with the functionality shows moderate regioselectivity compared to the corresponding α,β -isomers (Table 14).

In substrates **88–91**, where the substituents are sulphoxide, sulphonyl, phosphonate or phosphine oxide, the reactivity next to the allylic substituent decreases significantly, although these substituents are quite bulky. This behaviour was attributed to the electronic repulsions between the highly polarized oxygen atoms of the S–O and P–O bonds and the negative oxygen atom of the perepoxide, which direct the intermediate to abstract a hydrogen from the methyl group (Scheme 21). The electronic repulsions probably do not

TABLE 14. Regioselectivity in the photooxygenation of functionalized alkenes at the β -position^a

38 { (84) ^b	37 { (85)	38 { (86)
35 { (87)	66 { (88) ^c	62 { (89)
53 { (90)	48 { (91)	 (92)

^a Numerical values represent percentage of hydrogen abstraction.^b For previous reports on the regioselectivity, see References 88 and 89.^c See Reference 90.

SCHEME 21. Electronic repulsions in the photooxygenation transition states of sulfoxide-substituted alkenes

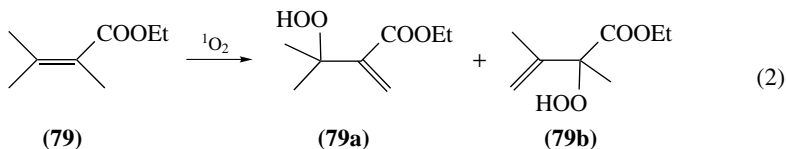
force singlet oxygen to form the intermediate perepoxide on the less substituted side of the olefin, since the *cis* disubstituted β , γ -unsaturated ester **92** exhibits very similar reactivity to the trisubstituted substrate **86**. Analogous unfavourable repulsions have been proposed to control the diastereoselectivity in the photooxygenation of chiral acylated allylic amines, sulfoxides, carbonyl and carboxylic acid derivatives^{91–93}. The electronic control in the stereoselectivity of the electrophilic addition to alkenes is well documented^{94–96}.

3. Solvent effects on the *ene* regioselectivity

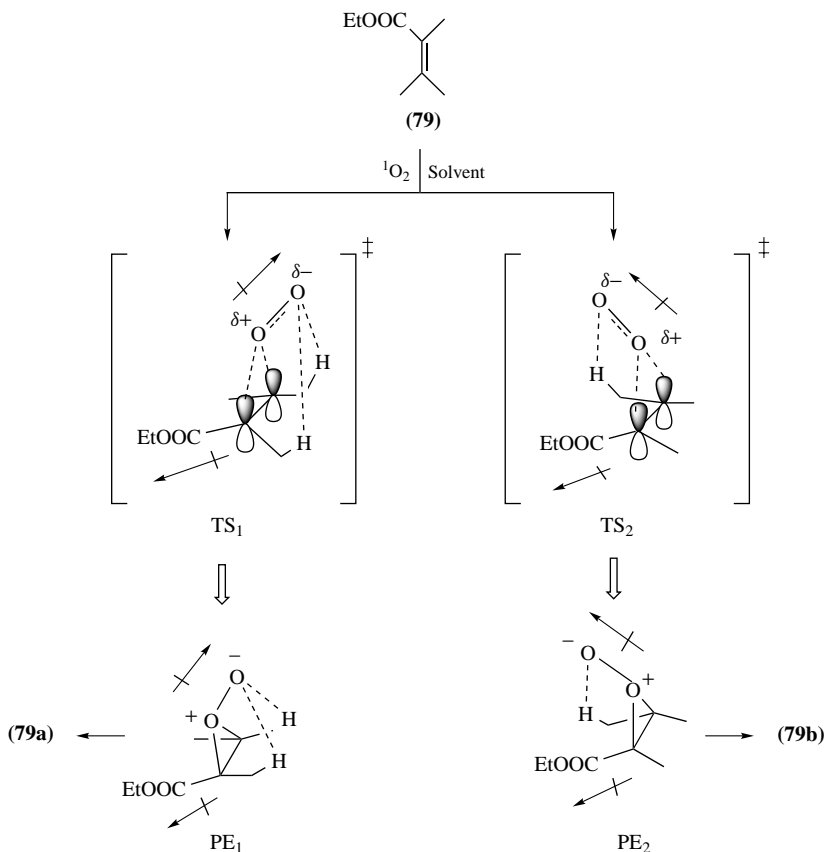
Previous studies have shown that the rate of the ¹O₂ *ene* reaction with alkenes shows negligible dependence on solvent polarity^{97,98}. A small variation in the distribution of the *ene* products by changing solvent was reported earlier^{64,99}. However, no mechanistic explanation was offered to account for the observed solvent effects. It is rather difficult to rationalize these results based on any of the currently proposed mechanisms of singlet oxygen *ene* reactions. Nevertheless, product distribution depends substantially on solvent polarity and reaction temperature only in substrates where both *ene* and dioxetane products are produced^{100–109}.

9. Selective formation of allylic hydroperoxides via singlet oxygen ene reaction 855

In the case of $^1\text{O}_2$ oxidation of α,β -unsaturated esters, there is a small but significant solvent effect on the variation of the ene products⁸⁶. Hydrogen abstraction from the methyl group which is geminal to the ester functionality in compound **79** (equation 2), producing **79a**, decreases substantially as the solvent polarity increases. For example, the ratio of ene products **79a/79b** decreases by a factor of 5 in going from carbon tetrachloride to the more polar solvent DMSO.



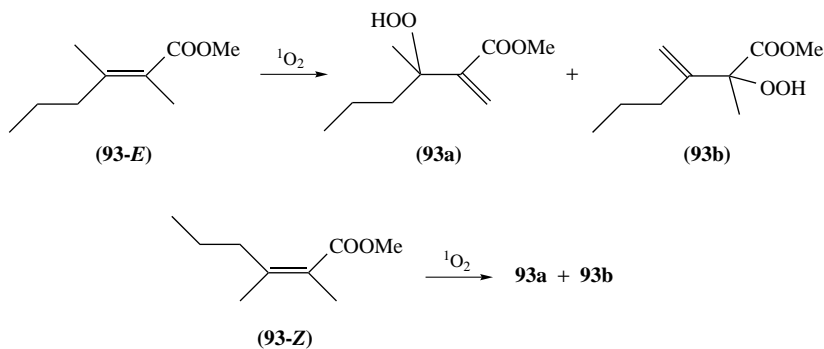
The observed solvent effect on the stereoselectivity of singlet oxygen with ester **79** was rationalized by examination of the possible transition states of this reaction (Scheme 22).



SCHEME 22. Proposed mechanism for the solvent-dependent photooxidation of α,β -unsaturated ester **79**

In transition state TS₂, leading to the minor perepoxide intermediate PE₂ in a limiting step, the oxygen is placed *syn* to the ester group, and the net dipole moment is expected to be larger than that in transition state TS₁ where the oxygen has an *anti* orientation with respect to the ester group. TS₂ is therefore more polar than TS₁, and expected to be stabilized better by polar solvents than TS₁. Consequently, the ratio **79a/79b** decreases with increase of solvent polarity.

To verify this mechanistic possibility, the solvent dependence of the ene products derived from the photooxygenation of the isomeric α,β -unsaturated esters **93-E** and **93-Z** was examined (Scheme 23). For **93-E**, the two ene products are formed from two different perepoxides. When the oxygen atom of the perepoxide intermediate is placed *syn* to the ester group, **93b** is produced, whereas **93a** is formed from the opposite case. For isomer **93-E**, the expected solvent effect was found (**93a/93b** = 85/15 in CCl₄ or benzene, and 70/30 in DMSO). On the other hand, for the isomer **93-Z**, both products are formed from the same intermediate (the perepoxide oxygen is placed *anti* to the ester functionality), and no solvent dependence on the ene products was found (**93a/93b** = 95/5 in CCl₄ and 93/7 in DMSO).



SCHEME 23. The photooxygenation reactions of the isomeric α,β -unsaturated esters **93-E** and **93-Z**

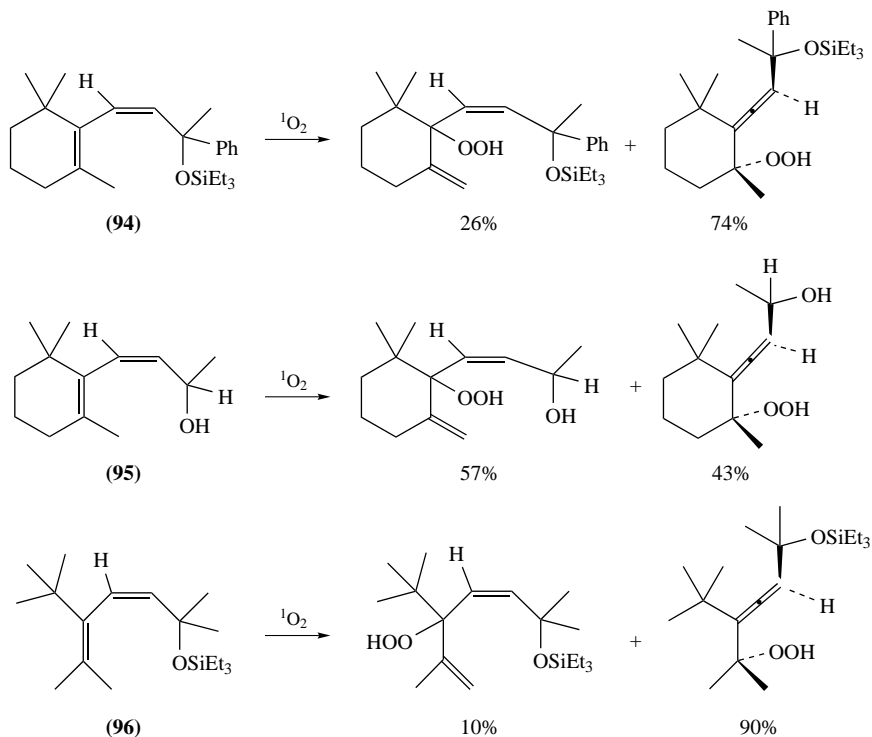
E. Regioselectivity with Twisted 1,3-Dienes: Allylic versus Allene Hydroperoxide Formation

Selectivity was also observed in the photooxygenation of significantly twisted 1,3-dienes which cannot adopt a reactive [4 + 2] conformation. In these substrates, a vinylic hydrogen atom is properly aligned in a perpendicular conformation to the olefinic plane and competes with the allylic hydrogens of the methyl group for ene product formation. Abstraction of the vinylic hydrogen leads to the formation of allene hydroperoxides. Some *trans*- β -ionone derivatives have been reported to afford small amounts of allene hydroperoxides by vinylic hydrogen abstraction^{110–113}. Katsumura and coworkers reported that the twisted 1,3-dienes **94–96** afford allene hydroperoxides in surprising high yields^{114–116} (Scheme 24).

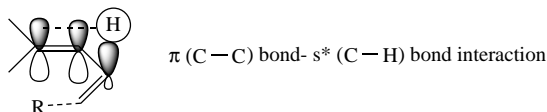
This selectivity was attributed to the perpendicular geometry of the vinylic hydrogen atom to the olefinic plane. In such a conformation, the vinylic hydrogen is ‘activated’ considering the large $\sigma^*-\pi$ interactions between the vinyl C–H bond and the reacting C=C double bond (Scheme 25).

For example, in substrates **94** and **96** the major ene adducts (74% and 90%, respectively) are formed by vinylic hydrogen atom abstraction, whereas the minor ene adducts (26% and 10%, respectively) are produced by allylic hydrogen abstraction. The percentage of

9. Selective formation of allylic hydroperoxides via singlet oxygen ene reaction 857



SCHEME 24. Regioselectivity in the photooxygenation of twisted 1,3-dienes



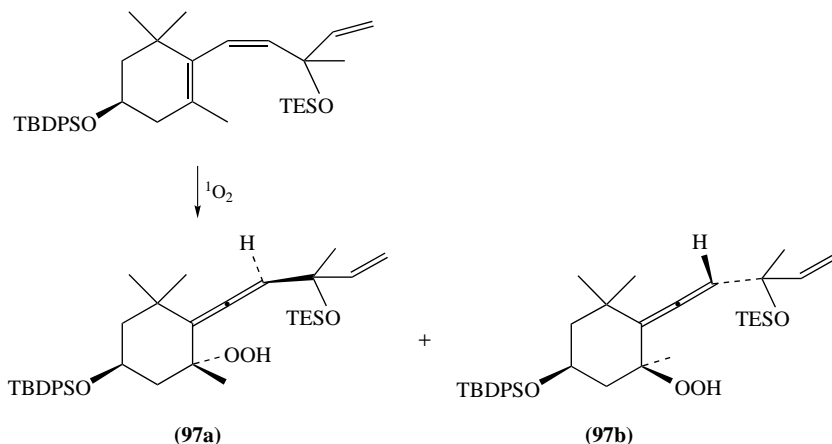
SCHEME 25. $\sigma^*-\pi$ interactions between the vinyl C-H bond and the reacting C=C double bond

allene hydroperoxide is lower (43%) in the photooxidation of **95**. In this substrate, the steric hindrance at the stereogenic centre is lower than in **94** or **96**, and the diene is therefore less twisted and the $\sigma^*-\pi$ interaction less profound, or by analogy, the vinylic hydrogen atom is less perpendicular to the double bond.

By using the same method, Katsumura and coworkers isolated the enantiomerically pure allene segment in **97a** and **97b** (Scheme 26)¹¹⁷. The one-step singlet oxygen ene reaction pathway, to produce the allene moiety from the twisted 1,3,3-trimethylcyclohexenyl-2-vinyl derivatives, was considered as a possible biomimetic route towards the synthesis of carotenoids.

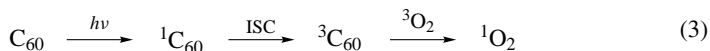
F. Regioselective Self-sensitized Oxygenation of Fullerene Adducts

Fullerene C_{60} is an electron-deficient compound with rich photophysical and photochemical properties. Moreover, the triplet-excited state of C_{60} is formed almost quantitatively and, in the presence of molecular oxygen, energy transfer from the triplet-excited



SCHEME 26. Synthesis of the allene moiety of carotenoids via biomimetic photosensitized oxygenation

state of C_{60} to the ground state oxygen produces singlet oxygen with quantum yield near unity^{118–122} (equation 3). In the case that a fullerene C_{60} adduct bears an oxidizable group, in the presence of oxygen and light, self-sensitized oxidation has been reported^{123–125}. This reaction has been shown to form regioselectively allylic hydroperoxides.

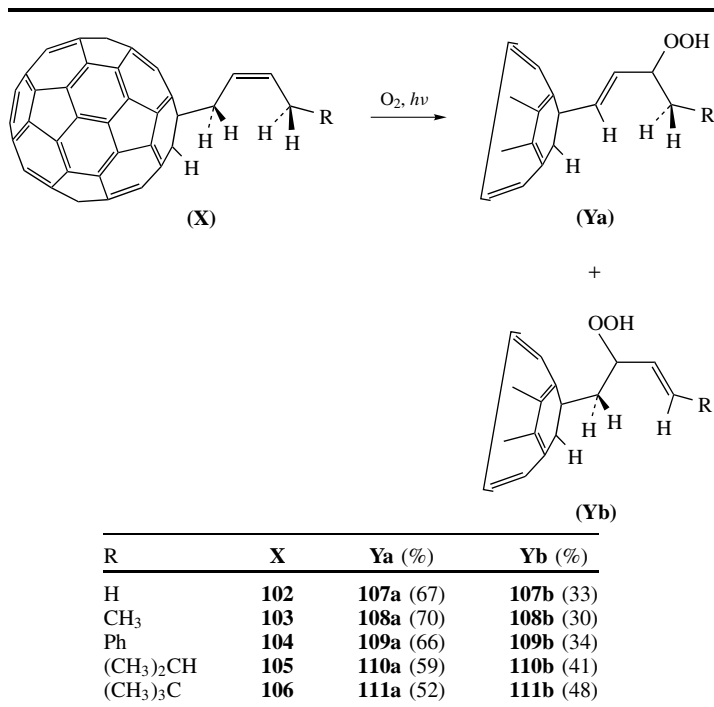


For example, the regioselectivity observed for the ene photooxygenation of two [60]fullerene adducts¹²⁶, prepared by the thermal [4 + 2] cycloaddition of conjugated dienes to C_{60} , is presented in Table 15. For substrates **98** and **100**, the methylene hydrogens next to fullerene are more reactive than the methyls (compare substrates **98** to **99**, and **100** to **101**). The strong preference for the formation of the peroxide *syn* to the fullerene, which leads to the major ene products, was attributed to the ideal interaction of singlet oxygen with the methylene allylic hydrogen atoms during the formation of the *syn* peroxide. The methylene hydrogens adopt the preferable perpendicular conformation to the olefinic double bond⁷⁰. However, additional factors such as favourable electrostatic or electronic interactions between the negative oxygen

TABLE 15. Regioselectivity in the self-sensitized oxygenation of fullerene adducts^a

<p>(98)</p>	<p>(99)</p>	<p>(100)</p>	<p>(101)</p>
--------------------	--------------------	---------------------	---------------------

^a Numerical values represent percentage of hydrogen abstraction.

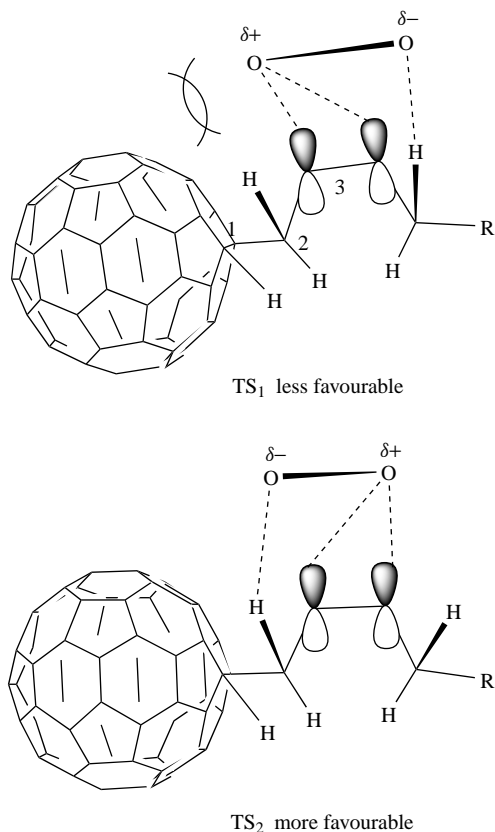
TABLE 16. Regioselective ene photooxygenations of fullerene derivatives **102–106**

of the developing *endo*-peroxide intermediate and the electron-deficient C₆₀ may also contribute to the observed regioselectivity.

The ene reaction of the fullerene C₆₀ substituted alkenes **102–106**¹²⁷ shows a consistent regioselectivity for double bond formation closer to the fullerene substituent, as shown in Table 16 (products **107a–111a** and **107b–111b**). For example, when the R group is hydrogen, methyl or phenyl (compounds **102–104**), the preferential abstraction of hydrogen adjacent to the fullerene group is greater than 66%. This result indicates that non-bonding steric interactions play a more important role than conjugation with the π system of the phenyl ring in the transition state of this reaction.

As the size of the R group becomes larger, the regioselectivity towards the fullerene group decreases. This is demonstrated with substrate **105**, where the preferential hydrogen abstraction is only slightly higher on the fullerene side. When R is *tert*-butyl (compound **106**), competition for the two allylic sides leads to nearly equal hydrogen abstraction from the two methylene sides. It is interesting to note here that photosensitized ene oxidation of 5,5-dimethyl-2-*cis*-hexene (**25**, Table 5) showed similar regioselectivity to that of substrate **102**⁵⁹. This comparison indicates that electrostatic factors from the fullerene group most probably play a negligible role in the transition state of this reaction.

Examination of the possible transition states TS₁ and TS₂, leading to the minor and the major allylic hydroperoxide, respectively, provides an insight into this regioselectivity (Scheme 27). In transition state TS₂ the non-bonding interactions, involving the large fullerene moiety, are smaller than those at the transition state TS₁ leading to the minor product. As the size of the substituents on both sides of the double bond become similar,



SCHEME 27. Transition states leading to the major and the minor allylic hydroperoxides for the self-photooxygenation reactions of [60]fullerene adducts **102–106**

as, for example, in compound **106**, the non-bonding interactions in TS₁ and TS₂ become isoenergetic, leading to equal amounts of the two isomeric ene products. Finally, the regioselectivity observed in this reaction seems to be independent of solvent polarity. Self-photooxygenation of compound **106** in toluene, 1,2-dichlorobenzene and benzonitrile gave similar ratios of the two ene products¹²⁷.

III. DIASTEREOSELECTIVE FORMATION OF ALLYLIC HYDROPEROXIDES

The factors governing π -facial selectivity of the singlet oxygen ene reaction⁴ are usually categorized as: (a) steric, when non-bonding repulsion between a substrate and singlet oxygen makes one π face of the double bond more accessible than the other; (b) electronic, related to electrostatic attractions and repulsions between a substituent of the substrate and singlet oxygen; and (c) conformational, a term that generally deals with the proper alignment of the allylic hydrogens for abstraction. From the above-mentioned factors, only the electrostatic interactions are expected to be sensitive to solvent polarity¹²⁸.

A. Cyclic Hydrocarbons and Hydrocarbons with Heteroatom Substituents

1. Monocyclic hydrocarbons

The factors that influence the diastereoselectivity for the class of monocyclic hydrocarbons, from which monoterpenes are the most studied group, are mainly steric and conformational. Monoterpenes, in general, show relatively low overall *syn/anti* selectivity, usually attributed to the availability of allylic hydrogen atoms in the right alignment for abstraction.

The reaction of singlet oxygen with limonene (**112**), a typical monoterpene, gives a mixture of the 6 isomeric allylic hydroperoxides **113a**–**113c** (Scheme 28)^{129,130}. The overall *syn/anti* selectivity observed is quite low (60/40), in contrast to the relatively higher *syn/anti* preference which was found for **113a**. This selectivity can be attributed to the fact that only the H^a hydrogen atom that leads to the *syn* product is perpendicular to the double bond, as shown in the ground state conformation presented in Scheme 28. Moreover, abstraction from either face of the methyl group (leading to allylic hydroperoxides **113b**), which is conformationally not fixed, is equally possible.

2. Bi- and polycyclic hydrocarbons

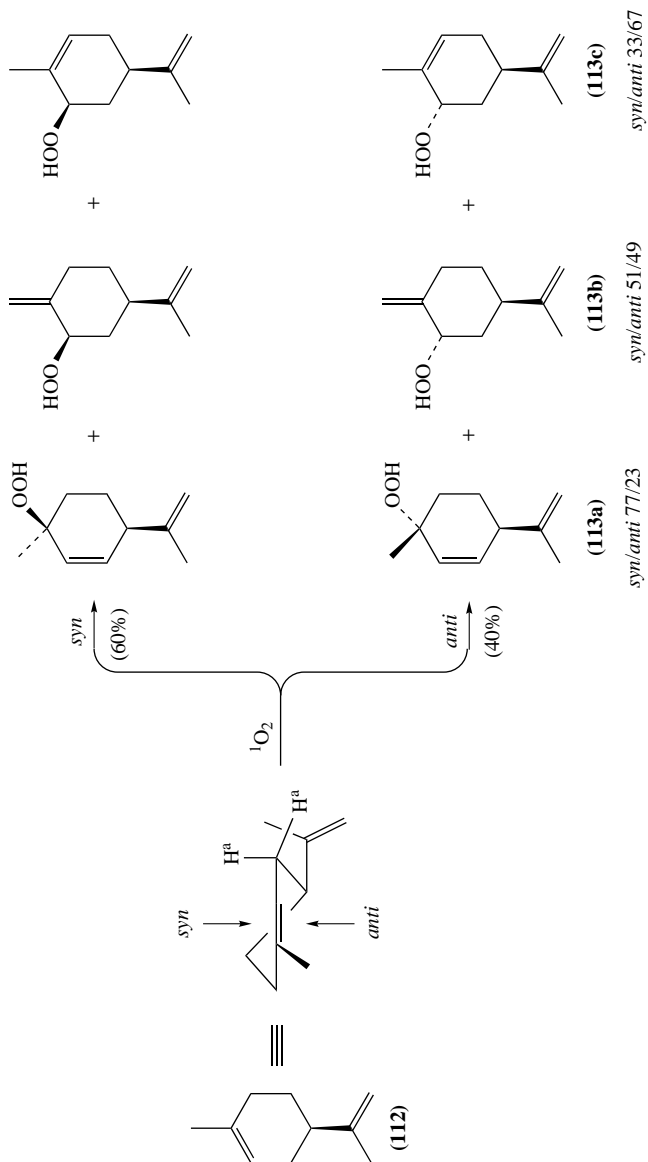
The high π facial selectivity, observed for a number of [2.2.1], [3.1.1] and [4.1.0] rigid bicyclic substrates, such as the monoterpenes presented in Scheme 29, is attributed to the favourable singlet oxygen attack on the sterically less crowded π face. For example, 2-methylnorbornene is strongly *exo*-directing, giving a very small amount of the *endo* products¹³¹. On the contrary, the presence of two methyl groups at the methylene bridge of α -pinene⁵ and *cis*- Δ^2 -carene¹³² lead to a high *endo* selectivity of the allylic hydroperoxide formed as shown in Scheme 29^{133,134}.

Similar steric factors determine the stereoselectivity of the ene reaction of bicyclic octalene **114** presented in Scheme 30. Mostly owing to the methyl group, a significant overall preference for the less crowded π face is found¹³⁵.

3. Cyclic hydrocarbons with heteroatom substituents

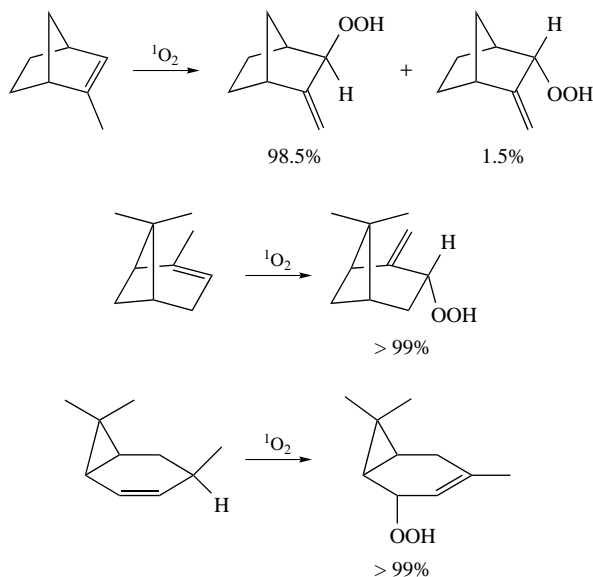
When the carbon framework of the reacting compound is substituted with one or more heteroatom containing functional groups, a direct influence on the electronic environment of the reacting double bond is often induced. 7-Isopropylidenenorbornenes, studied by Okada and Mukai and presented in Scheme 31, are remarkable substrates that clearly demonstrate this issue. Although the electron-withdrawing ester substituents are located relatively far from the reacting double bond to have a direct electrostatic influence on the reaction centre, a great variation of the moderate *anti* selectivity, shown by the parent system, has been found¹³⁶. This observation was initially explained in terms of orbital distortion at the reacting double bond through σ – π mixing due to the perturbation caused by the other double bond. Later on, the importance of π bond assistance in the transition state, through homoconjugative charge delocalization on the side opposite to the incoming singlet oxygen, was acknowledged⁹⁴. Recently, on the basis of theoretical calculations, it was found that the overall electron density in 7-isopropylidenenorbornenes is higher on the less reactive *syn* face, rendering the attack of the oxygen disfavoured due to repulsions¹³⁷.

A moderate to high *anti* selectivity was observed for the singlet oxygen ene reaction with unsaturated systems bearing carboxylic acids, as well as for their anions (Scheme 32)^{91,92}. This selectivity has been rationalized in terms of electrostatic repulsion between the carboxylate group and the partially negatively charged singlet oxygen in the perepoxide

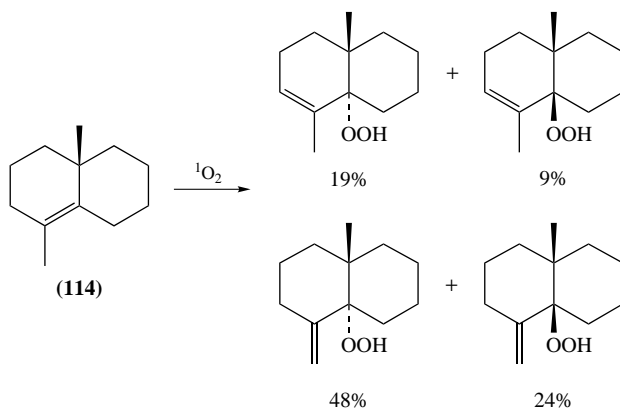


SCHEME 28. Singlet oxygen ene reaction of limonene

9. Selective formation of allylic hydroperoxides via singlet oxygen ene reaction 863



Scheme 29. Singlet oxygen ene reaction of selected bicyclic monoterpenes

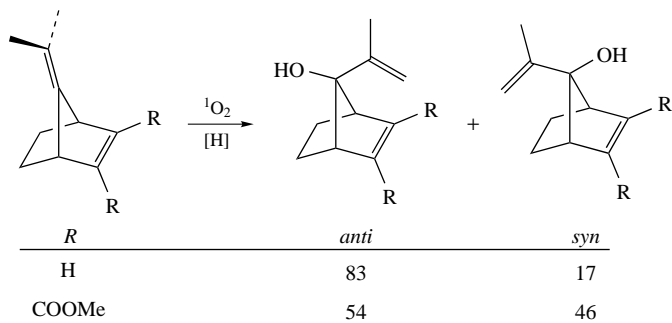


Scheme 30. Singlet oxygen ene reaction of octalene **114**

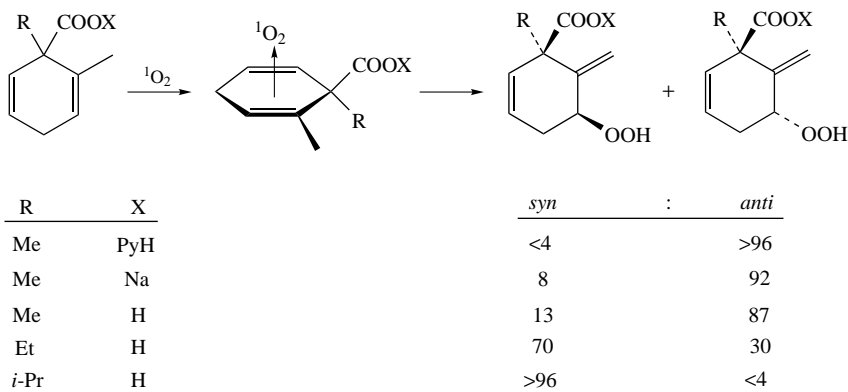
intermediate or exciplex. In the case of a bulky alkyl substituent (*i*-Pr) the diastereoselectivity showed a complete inversion, favouring *syn* attack, obviously due to steric effects.

B. Diastereoselectivity Induced by a Stereogenic Centre at the α -Position

The diastereoselectivity in the ene reaction of $^1\text{O}_2$ with chiral alkenes bearing a stereogenic centre at the α -position with respect to the double bond has been extensively studied⁴. Chiral alkenes which bear a substituent on the asymmetric carbon atom other than the hydroxy or amine functionality afford predominately *erythro* allylic hydroperoxides. The *erythro* selectivity was attributed to steric and electronic repulsions between



SCHEME 31. Diastereoselection in the singlet oxygen ene reaction of 7-isopropylidenenorbornenes

SCHEME 32. *Anti* selectivity for the singlet oxygen ene reaction of unsaturated systems bearing carboxylic acids and their anions

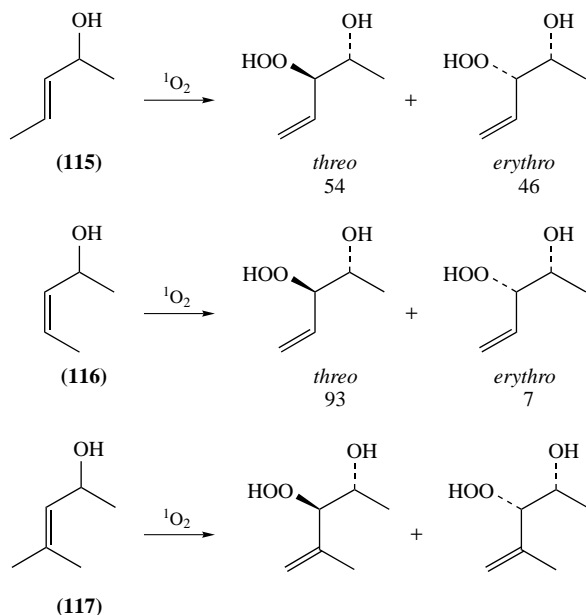
the incoming oxygen and the substituents on the stereogenic carbon atom, and to a preferable conformational arrangement to minimize the 1,3-allylic strain¹³⁸. For allylic alcohols and amines, the *threo* diastereoselectivity was rationalized in terms of an oxygen–hydroxy/amine steering effect.

1. Attractive interactions

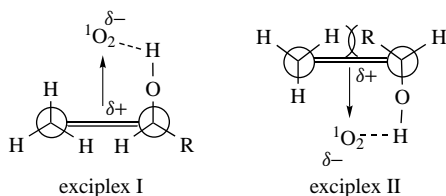
The photooxidation of the *E*-alcohol **115**, in contrast to the highly favoured formation of the *threo*-configured allylic hydroxyhydroperoxide from its isomeric *Z*-alcohol **116**, shows no significant π -facial selectivity^{45,46}, as presented in Scheme 33. Moreover, although the singlet oxygen ene reaction of chiral allylic alcohol **117** displays high *threo* selectivity in non-polar solvents, a substantial decrease in diastereoselectivity is observed in polar ones. An important diastereoselectivity decrease is also induced by protection of the allylic hydroxyl group in **117**.

The proposed mechanistic rationalization, for the interpretation of these stereochemical data, was based on the assumption of hydrogen bonding, between the hydroxyl group of the allylic alcohol and the partially negatively charged singlet oxygen, in the exciplexes visualized in Scheme 34. The stabilizing electronic interaction is effective only in exciplex

9. Selective formation of allylic hydroperoxides via singlet oxygen ene reaction 865

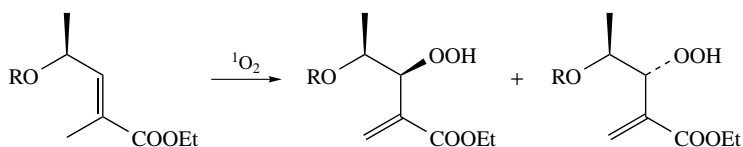


Solvent	<i>threo</i>	<i>erythro</i>
CCl ₄	93	7
CH ₂ Cl ₂	90	10
CH ₃ OH	73	27

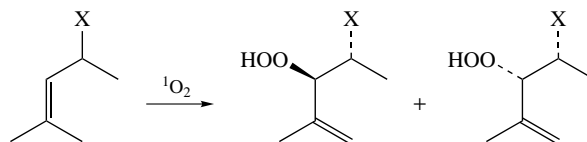
SCHEME 33. *Threo/erythro* diastereoselectivity in the photooxygenation of allylic alcohols **115–117**SCHEME 34. Newman projections for the stabilization of the *threo* exciplex for the reaction of $^1\text{O}_2$ with allylic alcohols

I, leading to the *threo*-configured product, since exciplex II is not operative due to 1,3-allylic strain. Furthermore, according to this mechanistic scheme, coordination of singlet oxygen to the hydroxyl group should exclude hydrogen abstraction at the stereogenic centre. This was found to be true, since alcohol **117** gives products arising from hydrogen abstraction at the stereogenic centre, in less than 4% yield.

Additional studies, concerning the influence of 1,2-allylic strain caused by a geminal substituent near the stereogenic centre of allylic alcohols¹³⁹, showed that it does not effectively compete with 1,3-allylic strain in differentiating the diastereoselectivity of the



<i>R</i>	<i>threo</i>	<i>erythro</i>
H	84	16
CH ₂ Ph	83	17
SiMe ₂ Bu- <i>t</i>	93	7
Si(Pr- <i>i</i>) ₃	>95	<5

SCHEME 35. *Threo/erythro* diastereoselectivity in the photooxygenation of electron-poor allylic alcohols

<i>X</i>	Solvent	<i>threo</i>	:	<i>erythro</i>
NH ₂	CCl ₄	95		5
NH ₂	CD ₃ OD	85		15
NHBoc	CCl ₄	24		76
NBoc ₂	CCl ₄	5		95

SCHEME 36. Diastereoselectivity in the reaction of ¹O₂ with allylic amines

ene reaction. Moreover, the directing effect of the hydroxyl group, leading to high π -facial selectivity, was also found to hold for alkyl groups located *trans* to the stereocontrolling chiral centre¹⁴⁰.

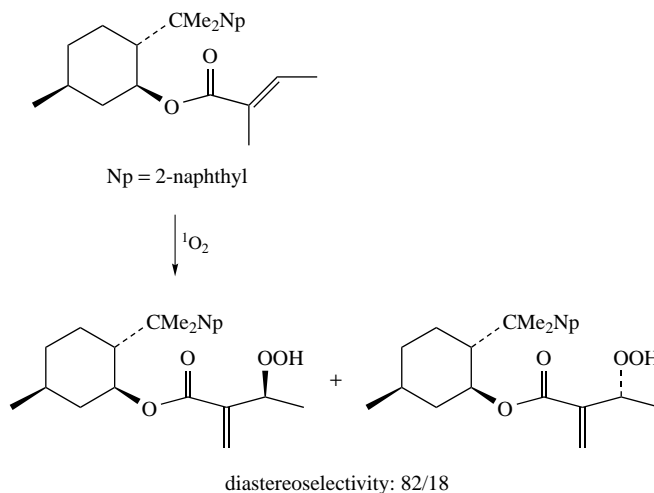
Electron-poor allylic alcohols, studied by Adam and coworkers, were found to react *threo*-selectively, regardless of whether the hydroxy functionality is free or masked by alkyl or silyl groups¹⁴¹ (Scheme 35). This diastereoselectivity, for which the nature of the solvent had no significant influence, was attributed to stereoelectronic effects rather than intramolecular hydrogen bonding or steric strain.

Ene reaction of singlet oxygen with unprotected allylic amines showed high *threo* selectivity in non-polar solvents, whereas in polar protic ones this diastereoselectivity decreased (Scheme 36). On the contrary, monoalkylated and dialkylated amines showed moderate and high *erythro* selectivity, respectively, affording β -hydroperoxy amines in a high diastereoselective manner^{47, 48}. These results were once more rationalized by postulation of hydrogen bonding in the exciplex, in the same fashion as the structurally related allylic alcohols.

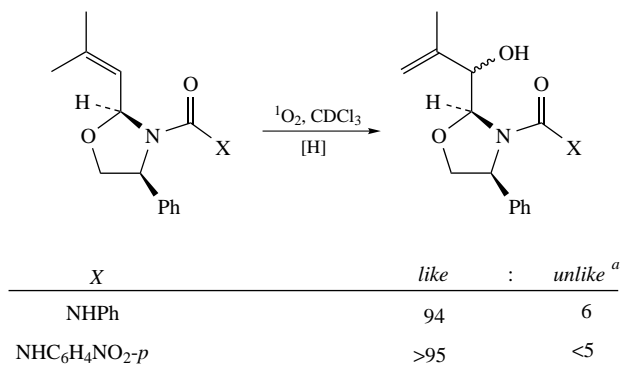
electrostatic repulsion disfavors the approach of singlet oxygen from the π face bearing the previously mentioned electron-withdrawing functional groups.

3. Chiral auxiliaries

Control of the diastereoselectivity in the singlet oxygen ene reaction can be achieved by the use of chiral auxiliaries. Success in this field would open up promising prospects in the preparation of optically active building blocks for asymmetric synthesis, since the oxygenation reaction could be followed by the removal of the chiral auxiliary. Unfortunately,



SCHEME 39. Control of the diastereoselectivity in the singlet oxygen ene reaction by the use of chiral auxiliaries



^a*unlike*: opposite to the urethane group.

SCHEME 40. Diastereoselectivity in the chiral-auxiliary-controlled singlet oxygen ene reaction of optically active oxazolidinones

singlet oxygen is a rather small enophile in size, therefore not sensitive enough to the steric repulsion usually applied by the chiral auxiliaries. Most attempts reported so far in this field have concentrated on the incorporation of an α,β -unsaturated carboxylic acid unit (tiglates) into a chiral environment, though with only low or moderate selectivity^{4, 80, 143-145}. In this context, one of the most satisfying examples is presented in Scheme 39⁸³.

Recently, however, Adam and coworkers reported a high chiral-auxiliary-controlled diastereoselectivity in the singlet oxygen ene reaction in CDCl_3 of the optically active oxazolidines⁹³ presented in Scheme 40. The observed selectivity was attributed to electronic attraction through hydrogen bonding between the NH group of the urea functionality and the attacking singlet oxygen.

IV. SELECTIVE FORMATION OF ALLYLIC HYDROPEROXIDES BY DYE-SENSITIZED INTRAZEOLITE PHOTOXYGENATION

A. Structural Features of Zeolites

Zeolites are crystalline aluminosilicates whose primary structure is formed by SiO_4^{4-} and AlO_4^{5-} tetrahedra sharing the edges¹⁴⁶. Their tertiary structure forms uniform channels and cavities of molecular dimensions that are repeated along the zeolite lattice. Due to the lower valence of the aluminium relative to silicon, the excess negative charge (one per Al atom) is balanced by alkali metal cations, mainly Na^+ . An important class of the zeolite family are the faujasites, known as zeolites X and Y, which have the typical composition for the unit cell as follows:



The faujasite framework consists of two main cages, the supercage, and the sodalites (Figure 1). The supercage results from the assembly of the smaller sodalite cages. The access to the supercages occurs by four 12-membered-ring 'windows', of approximately 7–8 Å in diameter. The 'windows' are tetrahedrally distributed around the centre of the supercages, which are approximately 13 Å in diameter. The charge-compensating cations

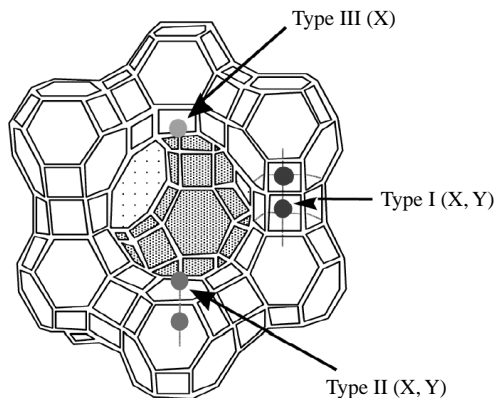


FIGURE 1. Structure of the faujasite supercage (the arrows indicate the positions of the cations)

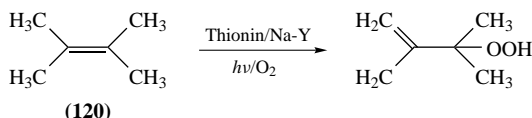
in faujasites occupy three different positions as shown in Figure 1, namely Type I–III¹⁴⁷. Only cations at sites II and III can interact with the host organic compounds. Depending on the size of the cation, the supercages in the alkali metal exchanged Y zeolites (M-Y) have enough net volume to host relatively large organic molecules. For example, Na-Y can adsorb molecules even of the size of a steroid. On the other hand, for type X faujasites, the free volume of the supercages is more limited due to the extra compensating cations, and they find less application in organic chemistry.

The performance of organic reactions in organized media, e.g. by zeolite confinement¹⁴⁸, and the use of zeolites as selective and ‘green’ catalysts¹⁴⁹ for organic transformations, have been popularized in recent years. The main advantage of the zeolites to be tested as media or catalysts for carrying out organic reactions is the so-called ‘shape selectivity’¹⁵⁰.

B. Photooxygenation Reactions in Zeolites Na-Y

The partial exchange of the Na⁺ cations within the zeolite Na-Y supercages by dye molecules that have the structure of organic cations (e.g. methylene blue, thionin etc.)¹⁵¹ triggered interest to examine the dye-sensitized photooxygenation of organic compounds within the confined environment of the faujasite Y cavities. The study of singlet oxygen reactions with alkenes using alternative supramolecular systems as microreactors¹⁵², such as pentasil zeolites¹⁵³, nafion membranes¹⁵⁴ and surfactant vesicles¹⁵⁵, has attracted considerable attention recently, but will not be examined in the present chapter.

For the success of the dye-sensitized singlet oxygen reactions within zeolite Na-Y, the loading level of the dye¹⁵⁶ and the water content¹⁵⁷ in the interior of zeolite are crucial. At increased loading levels, the dye dimerizes and ¹O₂ production is not efficient. At an approximate loading level of 1 thionin cation per 100 zeolite supercages, irradiation under a constant flow of oxygen gas produces singlet oxygen efficiently, leading to rapid oxidation of tri- and tetrasubstituted alkenes to form ene allylic hydroperoxides¹⁵⁸ as shown for the photooxygenation of tetramethylethylene (**120**) in Scheme 41.

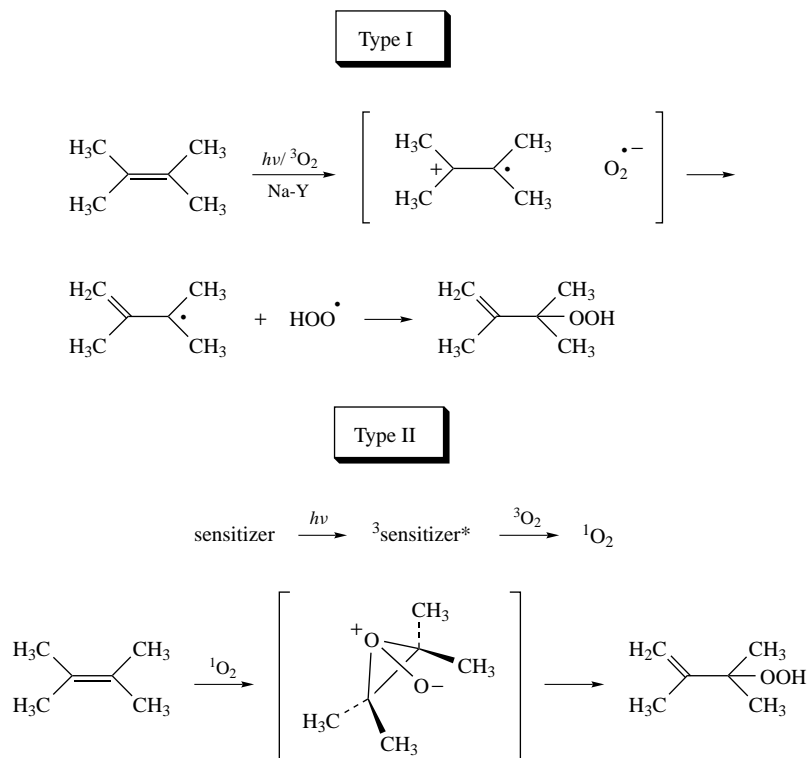


SCHEME 41. Ene hydroperoxidation of tetramethylethylene within thionin-supported Na-Y

For the achievement of mass balances in intrazeolite photooxygenation reaction, >80% loading levels of 0.1–0.3 adsorbed molecules per zeolite supercage have been successfully used in the past. However, the recent observation¹⁵⁹ by Pace and Clennan, that replacing the solvent hexane with perfluorohexane was very crucial for the efficiency of the reaction, allowed the zeolite medium to be used for preparative scale photooxygenation reactions (500 mg of alkene), without loss of the product selectivity or the reduction of the mass balance.

It is well known that faujasites (Na-Y or Na-X) contain a small concentration of both Brønsted¹⁶⁰ and Lewis acid sites¹⁶¹. The acidic sites may cause significant problems, such as the decomposition or rearrangement of product and reactants, giving often poor reaction mass balances. Acid-sensitive alkenes, such as terpenes, upon adsorption within Na-Y undergo isomerization and skeletal rearrangements. Ramamurthy and coworkers have reported such problems in the intrazeolite photooxygenation of limonene¹⁵⁷. In addition, tertiary allylic hydroperoxides, formed in the photooxygenation of trisubstituted alkenes, do not persist within the Na-Y cages¹⁵⁸. The unwanted side-reactions and

9. Selective formation of allylic hydroperoxides via singlet oxygen ene reaction 871

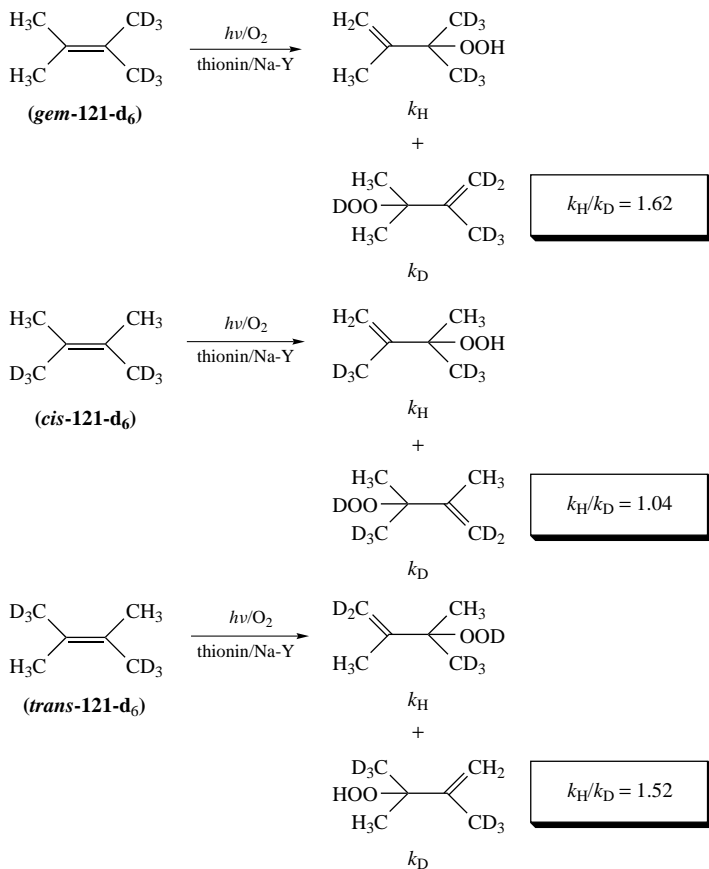
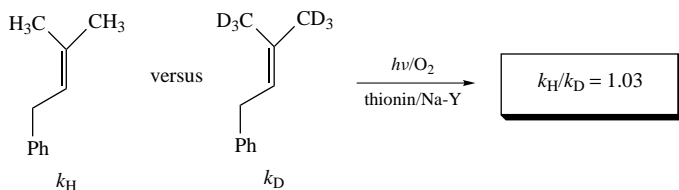


SCHEME 42. Type I and Type II intrazeolite photooxygenation processes

complexities, attributable to acid catalysis, can be minimized or completely suppressed by treatment of the zeolite with bases such as pyridine or triethylamine prior to the photooxygenation reaction.

Type I intrazeolite photooxygenation of alkenes has been also reported^{162, 163} to give mainly allylic hydroperoxides (Scheme 42). In this process, the charge transfer band of the alkene—O₂ complex within Na-Y was irradiated to form the alkene radical cation and superoxide ion. The radical ion pair in turn gives the allylic hydroperoxides via an allylic radical intermediate. On the other hand, for the Type II pathway, singlet molecular oxygen (¹O₂) is produced¹ by energy transfer from the triplet excited state of a photosensitizer to ³O₂.

To clarify the reaction mechanism for the intrazeolite reaction, the photooxygenation of the isomeric *cis*, *trans* and *gem*-tetramethylethylenes-d₆ (**121-d₆**) was examined (Stephenson's isotope effect test)³. *Cis*-**121-d₆** gave a negligible isotope effect of $k_H/k_D = 1.04$ ¹⁶⁴ for the intrazeolite reaction with ¹O₂ within methylene blue-supported Na-Y. In addition, the thionin-sensitized intrazeolite photooxygenation of *trans*-**121-d₆** and *gem*-**121-d₆** gave $k_H/k_D = 1.52 \pm 0.05$ and $k_H/k_D = 1.62 \pm 0.05$, respectively¹⁶⁵ (Scheme 43). The measured intrazeolite isotope effects were very similar to those reported for the photooxygenation in solution³, and therefore, consonant with a Type II photooxygenation process for tetrasubstituted alkenes, in which singlet oxygen forms irreversibly a peroxide or a peroxide-type intermediate in the rate-limiting step of the reaction. A scenario, involving

SCHEME 43. Intrazeolite photooxygenation of the isomeric tetramethylethylenes- d_6 

SCHEME 44. Intermolecular kinetic isotope effect in the intrazeolite photooxygenation of 1-phenyl-3-methyl-2-butene

radical ion pairs as precursors of the ene allylic hydroperoxides, is unlikely to occur upon visible light irradiation within the thionin-supported Na-Y.

Additionally, in order to elucidate the energy reaction profile in the intrazeolite photooxygenation of trisubstituted alkenes, the competing photooxygenation of 1-phenyl-3-methyl-2-butene and its geminal methyl deuteriated analogues (Scheme 44) was studied¹⁶⁵.

A negligible intermolecular isotope effect of $k_H/k_D = 1.03 \pm 0.02$ indicated that also for trisubstituted alkenes, formation of a perepoxide-type transition state is the rate-determining step.

C. Cation- π Interactions within Na-Y

Alkali metal cations have been known to bind strongly to the π face of aromatics¹⁶⁶. The adsorption of alkenes or arenes into the interior of the zeolites is mainly driven by their quadrupolar interaction with the alkali metal cations present in the cages. Haw and coworkers have presented¹⁶⁷ experimental evidence for the Li^+ -benzene interaction within zeolite LiZSM-5 using solid state NMR. The interaction of Na^+ and Li^+ with several alkenes in the gas phase, using the DFT and the MP2 method or *ab initio* calculations, has been recently studied^{168,169} and shed some light on the conformational arrangements of organic substrates upon metal coordination.

Two predominant binding trends were mainly recognized. The first was that for the majority of the alkenes, the cations do not bind on top of the π system, but close to it. Thus, for trisubstituted alkenes, the binding site resides either towards the more or the less substituted side of the olefin. A typical example is trimethylethylene, whose interaction with Li^+ was calculated to give the two almost isoenergetic minima presented in Figure 2. This unexpected type of interaction holds even with highly symmetric alkenes such as tetramethylethylene. The second trend was that there is a relatively strong interaction for both cations (Li^+ or Na^+) to the alkyl chains of the double bond, at the homoallylic position. A typical example is *cis*-3-hexene (Figure 3), in which the structure where the

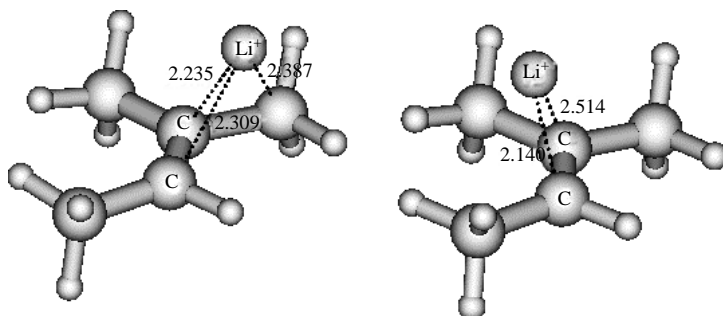


FIGURE 2. Local minima structures of Li^+ binding to trimethylethylene at the B3LYP/6-31G* level of theory

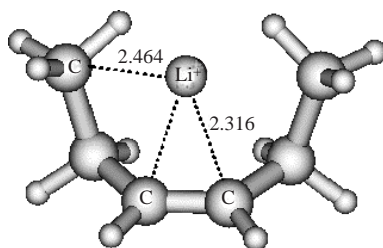


FIGURE 3. Local minimum structure of Li^+ binding to *cis*-3-hexene at the B3LYP/6-31G* level of theory

Li^+ interacts with both alkyl chains is more stable, compared to the structure where it sits at the antiperiplanar position, by $3.0 \text{ kcal mol}^{-1}$. The two binding trends of the alkali metal cations to alkenes were rationalized, taking into account the polarization of the double bond by the cation, polarization of the alkyl chains and steric effects as well. Recently, Gal and coworkers reported a similar alkyl chain– Li^+ attraction in alkylbenzenes, namely the ‘scorpion effect’¹⁷⁰.

D. Regioselectivity in the Intrazeolite Photooxygenation of Trisubstituted Alkenes

For geminal dimethyl trisubstituted alkenes, such as **35** or **39**, photooxygenation in solution gives a nearly solvent independent ratio of secondary to tertiary allylic hydroperoxide of *ca* 1/1¹⁷¹. In addition, for the case of 1-methyl-1-cycloalkenes⁷⁰, such as **123** and **60** (Table 17), the more substituted side of the alkene is the more reactive (‘*cis* effect’ selectivity). Ramamurthy and Li reported¹⁷² that in contrast to the reaction in solution, the thionin-sensitized intrazeolite photooxygenation of trisubstituted alkenes is highly regioselective, giving the secondary allylic hydroperoxide as the major or only product (Table 17). Furthermore, 1-methylcycloalkenes give mainly ene product with hydrogen atom abstraction from the methyl group.

The regioselectivity was significantly affected¹⁷³ by the size of the cation in M-Y (Table 18). For example, in the photooxygenation of **39** within Li-Y, the secondary hydroperoxide **39a** was formed in 100% relative yield, while in Cs-Y, the ratio secondary **39a** to tertiary hydroperoxide **39b** was 66/34, very close to what is found in solution. It was postulated that the cation-dependent change in the regioselectivity is proportional to the magnitude of the cation– π interactions. Li^+ , being the smallest alkali metal cation, in contrast to the larger Cs^+ and Rb^+ , is expected to bind the substrate very strongly and thus to affect the relative energy of the transition states leading to the secondary or tertiary allylic hydroperoxides.

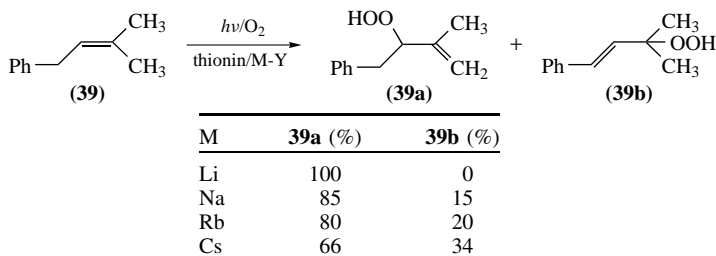
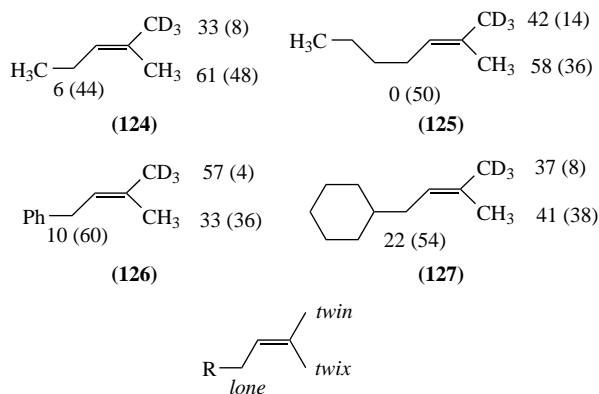
TABLE 17. Intrazeolite photooxygenation of trisubstituted alkenes^a

<p>(34)</p>	<p>(35)</p>
<p>(39)</p>	<p>(60)</p>
<p>(122)</p>	<p>(123)</p>

^a Values in parentheses indicate the relative reactivity in solution.

9. Selective formation of allylic hydroperoxides via singlet oxygen ene reaction 875

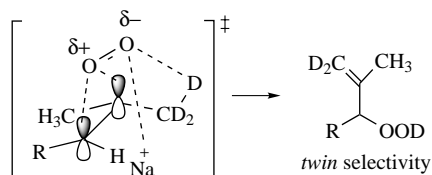
TABLE 18. Cation-dependent regiochemical control in the intrazeolite photooxygenation of 1-phenyl-3-methyl-2-butene

TABLE 19. Regioselectivity in the intrazeolite photooxygenation of deuterium labelled trisubstituted alkenes^a^a Values in parentheses indicate the relative reactivity in solution.

The regioselectivity for the hydrogen atom abstraction from each of two geminal methyl groups (*twin* or *twix*)¹⁷⁴ in trisubstituted alkenes such as **34**, **35**, **39** and **122** (Table 17) was studied by specific deuterium labeling. Independent studies^{175, 176} revealed that the ‘*cis* effect’³⁷ selectivity found in solution no longer operates within the zeolite. As seen in Table 19, for the case of **124–127**, the *twin* methyl group reactivity increases up to 14 times (see substrate **126**) by zeolite confinement.

The enhanced reactivity of the allylic hydrogen atoms at the less substituted side of the trisubstituted alkenes (*twin* position) was realized^{175, 176} in terms of electrostatic interaction between the pendant negatively charged oxygen atom in the intermediate peroxide and the alkali metal cation, which stabilizes the transition state where the oxygen is directed towards the less substituted side of the alkene (Scheme 45). In the absence of the cation-stabilizing interaction, the intermediate in which oxygen can interact only with one allylic hydrogen atom (*twin*-oriented peroxide) is not favourable due to entropic reasons, as has been suggested by Schuster and coworkers³⁹ (*cis*-effect selectivity).

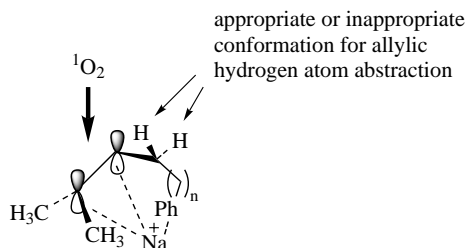
Due to the confined environment and cation- π interactions within the zeolite cavities as well, it is expected that the regioselectivity in the photooxygenation of trisubstituted

SCHEME 45. Cation-directing *twin* regioselectivity in the intrazeolite photooxygenation of trisubstituted alkenesTABLE 20. Substituent effects in the intrazeolite photooxygenation of trisubstituted alkenes^a

<p>(126)</p>	<p>(127)</p>
<p>(128)</p>	<p>(131)</p>
<p>(129)</p>	<p>(132)</p>
<p>(130)</p>	

^a Values in parentheses indicate the relative reactivity in solution.

alkenes might be influenced by remote substituents relative to the reaction centre (alkene double bond), especially if they can strongly bind to the cation. The intrazeolite photooxygenation in a series of deuterium-labeled *gem*-dimethyl trisubstituted alkenes was studied¹⁶⁵, by varying the position of a phenyl or a cyclohexyl substituent at the end of the alkyl chain at the *lone* position. The phenyl and cyclohexyl groups have similar steric demands, but different electronic character. The phenyl group can strongly coordinate to the Na⁺ cations within the Na-Y supercages. The regioselectivity results are presented in Table 20. For the phenyl-substituted alkenes **126** and **128–130**, there is a significant variation of the reactivity at the allylic positions (*twin*, *twix* or *lone*) by changing the length of the phenyl-substituted alkyl chain. For example, the reactivity at the *lone* position is 10% for **126**, slightly drops to 7% for **128**, then increases significantly to 44% in **129** and finally drops to 22% in **130**. Similarly, significant variations were found for the ratio of *twin*/*twix* allylic hydroperoxides. While for **126** *twin*/*twix* = 63/37, by increasing the

SCHEME 46. Possible interaction of Na^+ with phenyl-substituted alkenes within Na-Y

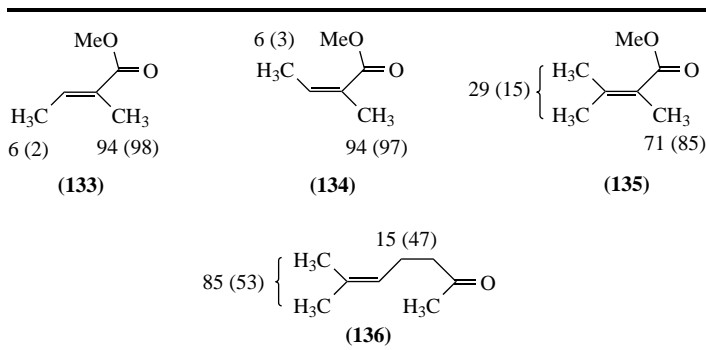
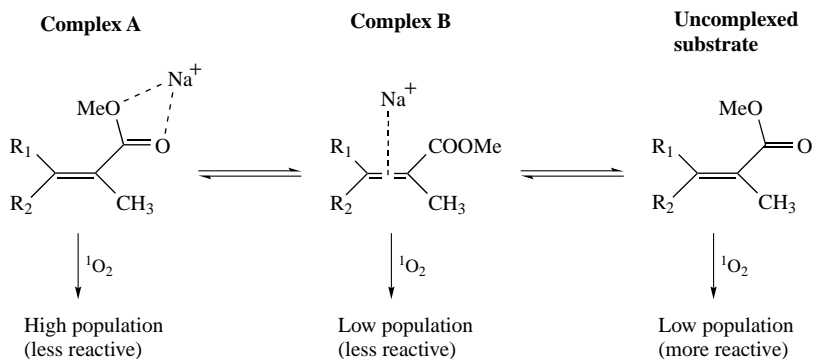
length of the alkyl chain the ratio drops to 30/70 in **128**, to 32/68 in **129**, and finally for alkene **130** it is 50/50. On the contrary, for the cyclohexyl-substituted alkenes **127**, **131** and **132**, the intrazeolite variation of the *lone/twin/twix* reactivity ratio is quite similar (approximately 22/37/41). The novel feature of the intrazeolite regioselectivities for the phenyl-substituted alkenes is that the *lone* and the *twin/twix* reactivity ratios depend significantly on the position of the phenyl group. This effect is absent for the case of the cyclohexyl-substituted alkenes.

It was proposed¹⁶⁵ that the changes in the ene reactivity at the *lone* position for the phenyl-substituted alkenes are controlled by cation- π interactions and conformational effects within the Na-Y supercages. Depending on the remoteness of the phenyl ring from the reaction centre, simultaneous coordination of the Na^+ with the phenyl ring and the alkene double bond probably places the allylic methylene hydrogen atoms in a favourable (perpendicular to the double bond) or unfavourable position for ene reaction (Scheme 46). For the cyclohexyl-substituted alkenes, however, coordination of the Na^+ to the alkene double bond affords similar conformations for the allylic methylene hydrogen atoms and, therefore, they are approximately equally reactive. This is also corroborated by the fact that the *twix/twin* reactivity ratio is the same for all cyclohexyl-substituted alkenes, while for the phenyl-substituted compounds it changes remarkably.

E. Intrazeolite Photooxygenation of Electron-poor Alkenes

Clennan and coworkers reported¹⁷⁷ that the intrazeolite environment is unable to influence the regiochemistry in the photooxygenation of electron-poor alkenes such as α,β -unsaturated carbonyl compounds **133**–**135**, relative to the photooxygenation in solution. The regioselectivity results are presented in Table 21.

To explain the lack of changes in the regioselectivity on going to the zeolite environment, it was suggested that only the alkenes which were not complexed to the cation are reactive, although they are the minor component in a dynamic equilibrium involving uncomplexed and complexed substrates (A and B in Scheme 47, with $[\text{A}] > [\text{B}]$). The Na^+ -bound alkenes are expected to be highly unreactive due to the electron depletion from the double bond. Assuming that the dynamic equilibrium between the Na^+ complexed or uncomplexed species is fast, and applying the Curtin–Hammett principle, the reaction is expected to occur mainly via the uncomplexed alkene; therefore, similar regioselectivity results are expected to those found in solution⁷⁴. On the other hand, if the carbonyl functionality is shifted from the α - to the γ -position with respect to the double bond (substrate **136**, Table 21), the alkenes give the expected regiochemical outcome (predominant formation of the secondary allylic hydroperoxides), as found in the intrazeolite photooxygenation of non-functionalized trisubstituted alkenes¹⁶⁵.

TABLE 21. Regiochemistry in the intrazeolite photooxygenation of electron-poor alkenes **133**–**136**^a^a Values in parentheses indicate the relative reactivity in solution.

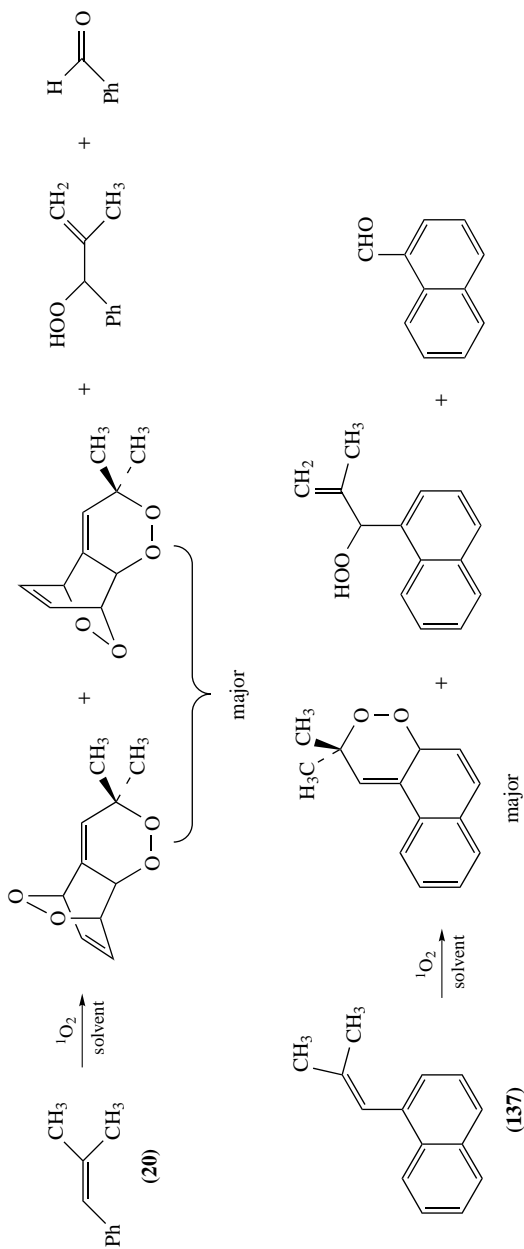
SCHEME 47. Multicomplexation model for the intrazeolite photooxygenation of electron-poor alkenes

F. Intrazeolite Photooxygenation of Isobutenylarenes

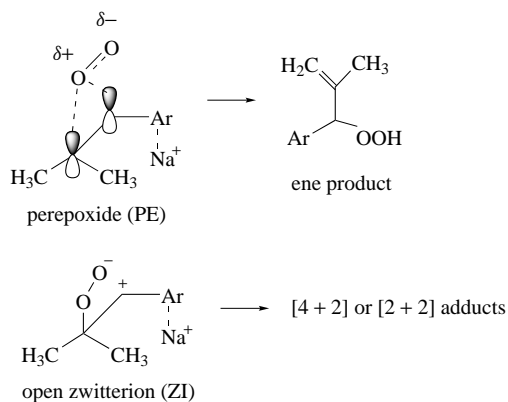
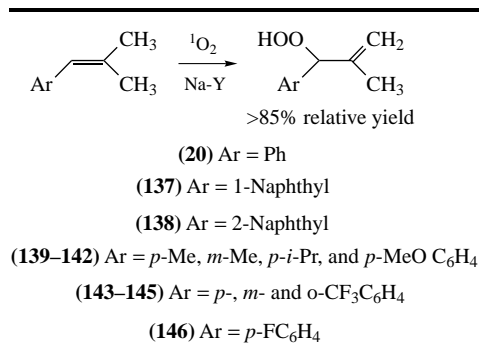
As discussed in Section II.A.4, photooxygenation of 1-aryl-2-methylpropenes in solution proceeds slowly, and affords a complex mixture of products arising mainly from [4 + 2] or [2 + 2] addition to the double bond⁵³. The *ene* pathway is less favourable or even absent. For example, β,β -dimethylstyrene (**20**) affords the *ene* adduct in approximately 20% yield, benzaldehyde (from a [2 + 2] pathway), and mainly two diastereomeric di-endoperoxides (from a [4 + 2] pathway) in a 2/1 ratio (Scheme 48). Similarly, for 1-(2-methylpropenyl)naphthalene (**137**), the 1,4-endoperoxide is mainly formed¹⁷⁸.

The intrazeolite photooxygenation in a series of isobutenylarenes¹⁷⁹ (**20**, **137**–**146**), bearing either electron-withdrawing or electron-deficient substituents on the aryl ring, affords rapidly the *ene* allylic hydroperoxides as the major or even exclusive products (Table 22). The relative yield of the *ene* adduct was always higher than 85%.

To explain the remarkable chemoselectivity, two possible intermediates were invoked; the perepoxide⁵³, that leads to *ene* product, and the open 1,4-zwitterionic intermediate¹⁸⁰, which gives the [4 + 2] or [2 + 2] adducts. Na⁺-binding to the aryl ring within Na-Y destabilizes the open zwitterionic intermediate (ZI), since upon cation complexation the



SCHEME 48. Photooxygenation of isobutenylarenes in solution

TABLE 22. Photooxygenation of isobutenylarenes **20** and **137–146** within the thionin-supported zeolite Na-YSCHEME 49. Destabilization of the zwitterionic intermediate by coordination to the Na⁺

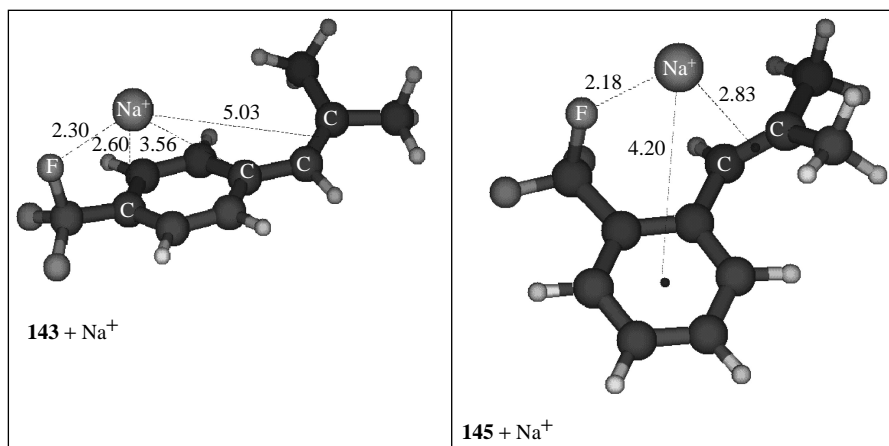
aryl ring is losing electron density and is less capable of stabilizing the positive charge at the benzylic position (Scheme 49). On the other hand, for the perepoxide intermediate, complexation of the aryl ring to the cation is expected to cause significantly less destabilization compared to the open zwitterion.

The intrazeolite photooxygenation of stereoselectively deuterium-labeled 1-aryl-2-methylpropenes **21** and **147–152** revealed that the site selectivity for the ene pathway (*twin/twix* ratio) is significantly affected by cation–arene interactions within the zeolite cavities. The site selectivity for some isobutenylarenes is presented in Table 23¹⁸¹. Remarkable changes in the regioselectivity were found by zeolite confinement relative to the reaction in solution. For example, for the *p*-CF₃ substituted styrene **149**, although in solution the *twin/twix* ratio = 26/74, within Na-Y it becomes 82/18. Similarly, for the *o*-CF₃ substituted styrene **151**, in solution *twin/twix* = 77/23, while within Na-Y, *twin/twix* = 32/68.

The increased reactivity of the *twix* methyl group for the photooxygenation of β,β -dimethylstyrenes, in solution, has been rationalized⁵⁶ in terms of attractive arene–oxygen interactions, in the transition state for the formation of the *twix*-oriented intermediate.

TABLE 23. Site selectivity for the photooxygenation of deuterium-labeled isobutenylarenes **21** and **147–152**

Substrate	Ar	Intrazeolite photooxidation (<i>twin</i> / <i>twix</i>)	Photooxidation in solution (<i>twin</i> / <i>twix</i>)
21	Ph	42/58	37/63
147	<i>p</i> -MeC ₆ H ₄	43/57	45/55
148	1-Naphthyl	61/39	18/82
149	<i>p</i> -CF ₃ C ₆ H ₄	82/18	26/74
150	<i>m</i> -CF ₃ C ₆ H ₄	38/62	30/70
151	<i>o</i> -CF ₃ C ₆ H ₄	32/68	77/23
152	<i>p</i> -FC ₆ H ₄	60/40	32/68

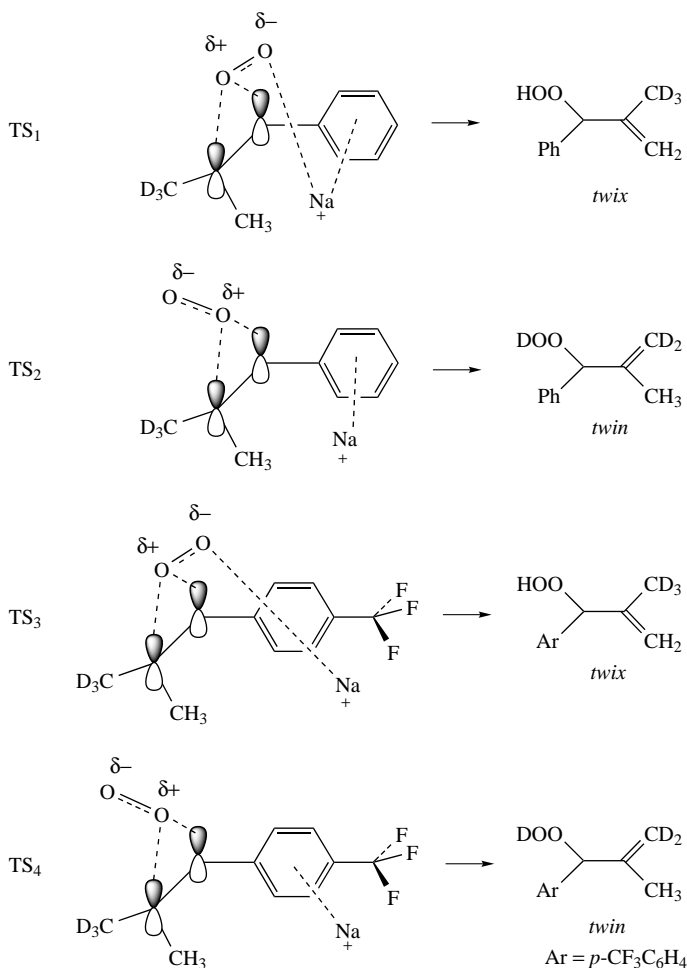
FIGURE 4. Calculated minima structures for the Na⁺ interaction with *p*- and *o*-CF₃ substituted β,β-dimethylstyrenes at the B3LYP/6-31G* level of theory

Cation–π interactions have been primarily invoked as the major reason which dictates the site selectivity for the ene pathway. DFT calculations at the B3LYP/6-31G* level of theory revealed that the binding site of Na⁺ to the substrates of Table 23 is controlled significantly by the presence of substituents capable of interacting with the cation via non-bonded electron pairs (e.g. fluorine or oxygen atoms). The Na⁺–F interaction, for example, is highly exothermic and is the driving force for the facile adsorption of fluorinated compounds within Na-Y¹⁸².

Although for the parent β,β-dimethyl styrene **20**, the cation binds approximately in the middle and on top of the phenyl ring, for the *p*-CF₃ substituted styrene **143**, binding occurs in between the middle of the aryl ring and the fluorine atoms (Figure 4). For the *o*-CF₃ substituted styrene **145**, however, the binding site changes dramatically, and resides closely to the alkene double bond.

It was proposed¹⁸² that the relative reactivity of the *twin* and *twix* methyl groups for allylic hydrogen atom abstraction within Na-Y is controlled: (a) by electrostatic interactions between Na⁺ and the styrenes, and (b) by electrostatic interactions of the negatively charged oxygen of the intermediate perepoxide to the Na⁺. For the parent β,β -dimethylstyrene **20**, the slight preference for the *twix* product formation was attributed to electrostatic interaction between the negatively charged oxygen of perepoxide and the cation (higher stability of TS₁ compared to the TS₂ in Scheme 50).

By placing a CF₃ substituent at the *para*-position of **20**, the interaction of Na⁺ with the highly electronegative fluorine atoms shifts the binding site closer to the CF₃ functionality (see structures in Figure 4). The distance between the Na⁺ and the double bond of the alkene is higher, therefore, and the stabilizing electrostatic interaction between



SCHEME 50. Postulated transition states controlling the site selectivity in the intrazeolite photooxygenation of isobutenylarenes

the incoming oxygen and the cation is less important (transition state TS₃, Scheme 50). Therefore, transition state TS₄ involving *twin* allylic hydrogen atom abstraction predominates. For the case of the *ortho*-substituted CF₃-styrene **151**, binding of Na⁺ to the fluorine atoms shifts the cation very close to the alkene double bond (Figure 4), thus favouring electrostatic interaction between Na⁺ and the negatively charged oxygen atom of the *twix*-oriented peroxide, which essentially leads to *twix* selectivity.

G. Diastereoselectivity in the Intrazeolite Photooxygenation of Chiral Alkenes

It has already been mentioned (Section III) that the study of the diastereoselection in the electrophilic addition of singlet oxygen to the π face of chiral alkenes is of primary interest for the achievement of a selective oxyfunctionalization reaction. Zeolite confinement and cation- π interactions might be expected to affect significantly the diastereoselectivity in the photooxygenation of chiral alkenes.

The diastereoselectivity in the photooxygenation of some chiral alkenes, possessing a phenyl group and an alkyl group (R) of various size on the stereogenic carbon atom (R = methyl, **153**; R = ethyl, **154**; and R = cyclohexyl, **155**), has been recently studied¹⁸³. The reaction of chiral alkenes **153–155** with ¹O₂ in solution is regioselective with preferential formation of the secondary allylic hydroperoxides. Among the secondary hydroperoxides the *erythro* isomer prevails (Table 24). It is notable also that the minor tertiary allylic hydroperoxides has always the (*Z*)-geometrical configuration. By contrast, the thionin-sensitized intrazeolite photooxygenation of **153–155** is highly regioselective, since only the secondary allylic hydroperoxides were formed, however, with an inverse diastereoselection trend (Table 24). The *threo* diastereomer predominates, and the ratio *threo/erythro* increases with the increasing size of the R group. A remarkable

TABLE 24. Regioselectivity and diastereoselectivity in the photooxygenation of chiral alkenes within zeolite Na-Y and in solution (values in parentheses)

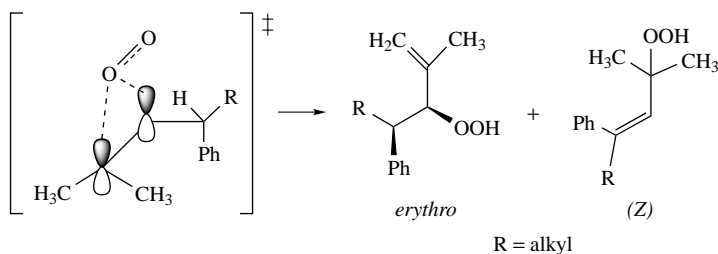
Alkene	R	a (%)	b (%)	c (%)
153	Me	<1 (6)	46 (72)	54 (22)
154	Et	<1 (10)	23 (70)	77 (20)
155	<i>c</i> -C ₆ H ₁₁	<1 (14)	9 (71)	91 (15)

example is substrate **155**, for which the diastereoselection trend was completely reversed (*erythro*/*threo* = 9/91 versus 82/18 in solution).

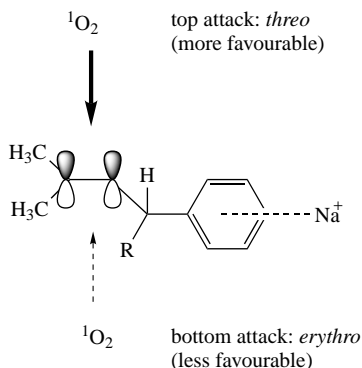
As previously mentioned in Section III.B.2, formation of the major *erythro* diastereomer in the photooxygenation of the chiral alkenes in solution was explained considering the transition state shown in Scheme 51. The phenyl group is placed on the opposite plane of the double bond with respect to the attacking oxygen, due to the unfavourable oxygen–arene electronic repulsions. In addition, a minimal 1,3-allylic strain between the tertiary allylic hydrogen and the *twix* allylic methyl group dictates the preferential $^1\text{O}_2$ approach.

On the other hand, the remarkable change of the diastereoselection on going from the solution to the confined environment of the zeolite was rationalized, taking into account the strong electrostatic interaction of the phenyl ring with the Na^+ within the supercages. The alkene most likely adopts the conformation shown in Scheme 52. Preferential attack of singlet oxygen from the less hindered top phase leads to the major *threo* allylic hydroperoxides. As the size of the R group increases, the energy difference between the *threo* and *erythro* forming transition states is expected to increase, in favour of the *threo* isomer.

For the photooxygenation of chiral alkenes in solution bearing a stereogenic centre at the β - or more remote position with respect to the double bond, low or negligible diastereoselection is expected¹⁸⁴. The photooxygenation of 2-methyl-5-phenyl-2-hexene **156**, a chiral alkene that bears a stereogenic centre at the β -position with respect to the double bond, gave in solution low diastereoselectivity (*ca* 10% *de*)¹⁸⁵. By Na-Y

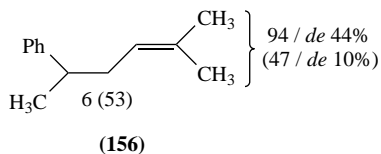


SCHEME 51. *Erythro*-forming transition state for the photooxygenation of phenyl-substituted chiral alkenes in solution



SCHEME 52. *Threo*- and *erythro*-forming direction of approach for the photooxygenation of phenyl-substituted chiral alkenes by zeolite confinement

9. Selective formation of allylic hydroperoxides via singlet oxygen ene reaction 885



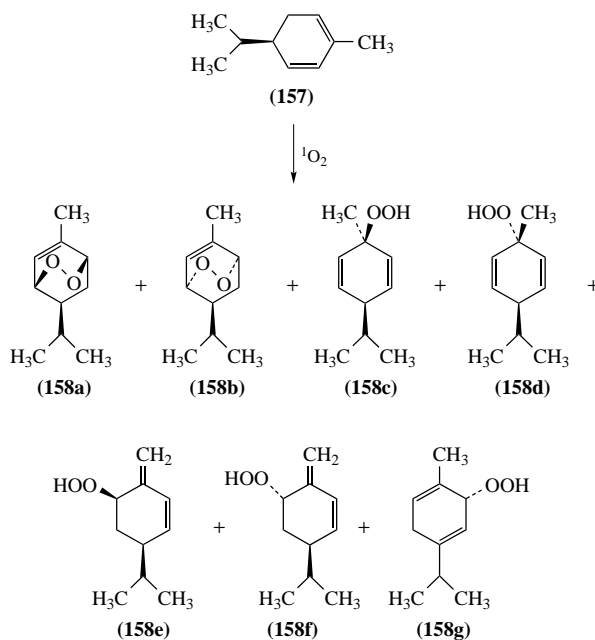
SCHEME 53. Regioselectivity/diastereoselectivity in the photooxygenation of 2-methyl-5-phenyl-2-hexene (values in parentheses: relative reactivity in solution)

confinement, however, the reaction is 94% regioselective in favour of the secondary hydroperoxides and the diastereomeric excess enhances to 44% *de* (Scheme 53). It is likely that, upon interaction of the alkene with a Na^+ within the cage, the substrate folds, and the chirality is 'transferred' close to the reaction centre (double bond). As a result, the distribution of the diastereomeric ene products is significantly affected.

A remarkable enhanced diastereoselection for the ene pathway was also reported in the photooxygenation of (*R*)-(-)- α -phellandrene (**157**)¹⁸⁶. The cycloaddition products for the reaction of **157** with $^1\text{O}_2$ in solution¹⁸⁷ are the two diastereomeric endoperoxides **158a** and **158b** (major products), while five isomeric ene adducts (**158c–g**) are formed in various amounts (Table 25). Within zeolite Na-Y the relative ratio of the overall ene adducts increases (ene/[4 + 2] = 34/66 in solution versus 52/48 in the zeolite). Comparing the Diels–Alder adducts, the diastereomeric ratio of **158a/158b** slightly increases in the zeolite, while for those ene products, where the double bond is formed in the interior of the ring, the predominant diastereomer in solution is also the predominant one in the zeolite. On the other hand, the relative amount of the ene adducts **158e** and **158f** with an exocyclic double bond increases substantially within Na-Y (total 35% in zeolite, versus only 3.5% in solution), with a remarkable change in the diastereoselectivity. The ratio of **158e/158f** is 14/86 in Na-Y versus 58/42 in solution. This interesting example of enhanced diastereoselection found application in organic synthesis, since reduction of the major ene adduct, (1*S*,5*R*)-5-(1-methylethyl)-2-methylidene-3-cyclohexen-1-yl hydroperoxide (**158f**), with triphenylphosphine gave the natural product *trans*-yabunikeol.

For the reaction in solution, the similar stereochemical outcome of the ene and the [4 + 2] adducts (*cis* diastereomers > *trans*) was rationalized in terms of a common peroxide intermediate shown in Scheme 54, which leads either to the ene or to the Diels–Alder products. In that intermediate, singlet oxygen attacks the more reactive trisubstituted double bond of the more stable conformation from the top face and interacts with an axially oriented allylic hydrogen atom. For the intrazeolite reaction, cation binding to the alkene was invoked to explain the stereochemical outcome of the reaction. The major ene adduct was proposed to arise from the transition state shown in Scheme 54. Oxygen attacks from the opposite face of the alkene with regard to the bound cation, and is preferentially oriented towards the less substituted side of the double bond, because in the orientation facing the more substituted side of the alkene, it cannot interact with any axially-oriented allylic hydrogen atom(s).

As indicated earlier, remote substituents with respect to the reaction centre can influence the regiochemistry¹⁶⁵ and the diastereoselection¹⁸⁵ of the intrazeolite singlet oxygen ene reactions. Recent work¹⁸⁸ has shown that a remote substituent with respect to the reacting double bond, suitable for binding to the Na^+ , such as the acetate functionality, can dramatically affect the regiochemistry and the diastereoselectivity of the intrazeolite singlet oxygen ene reaction in the case of 4-substituted 1-methylcyclohexenes. The intrazeolite photooxygenation of limonene (**112**) is highly regioselective¹⁵⁸, with exclusive formation of the ene adducts resulting from allylic hydrogen abstraction from the methyl group, as generally found in the intrazeolite photooxygenation of 1-methylcycloalkenes¹⁷². On the

TABLE 25. Photooxygenation of (*R*)-(-)- α -phellandrene in zeolite and in solution

Conditions	158a	158b	158c	158d	158e	158f	158g
<i>i</i> -PrOH/RB ^a	39	26	14	9	2	1.5	3
Thionin/Na-Y	33	15	12	5	5	30	<1

^a Rose Bengal (photosensitizer).

other hand, limonene (**112**) exhibits little diastereoselectivity. By placing an acetate functionality at the remote 8-position of the limonene skeleton (i.e. α -terpinyl acetate, **159**), the reaction gives mainly one regioisomeric adduct in >90% diastereomeric excess, resulting from allylic hydrogen atom abstraction from the more substituted side of the cycloalkene (Scheme 55). This regiochemistry trend is in contrast to what has been reported for the intrazeolite photooxygenation of 1-methylcycloalkenes.

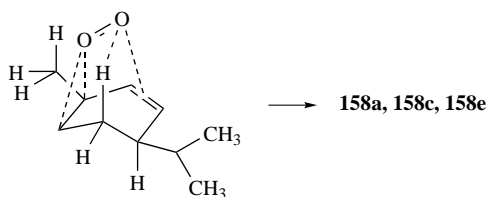
The dramatic change in the regioselectivity can be explained considering attractive singlet oxygen–cation interactions during the formation of the intermediate perepoxide, that direct $^1\text{O}_2$ to abstract preferentially an allylic hydrogen atom from the more substituted side of the alkene (transition state of Scheme 56). Most probably, the Na^+ cation is bound close to the acetate functionality and at the appropriate position to interact electrostatically with $^1\text{O}_2$. The allylic hydrogen at the 3-position has the ideal axial conformation for abstraction, resulting in formation of mainly one diastereomer.

V. SYNTHETIC APPLICATIONS

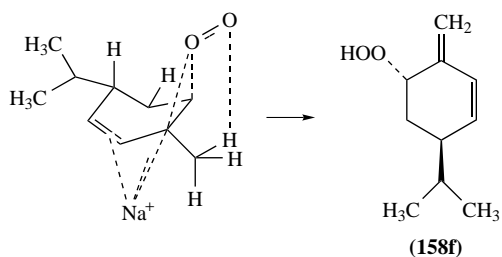
Synthetic applications involving regioselective or diastereoselective photooxygenation ene reactions, as key steps, are very common in the literature and some examples have already been reported in the previous sections. Additionally, the number of natural products

9. Selective formation of allylic hydroperoxides via singlet oxygen ene reaction 887

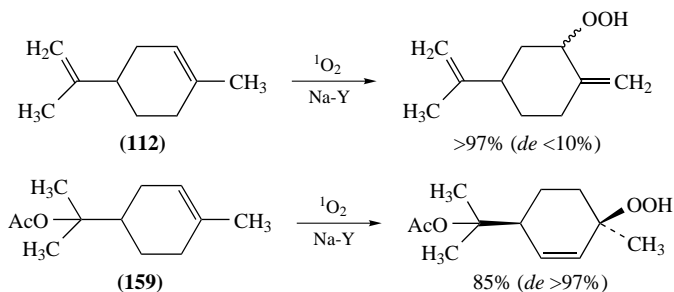
Favourable transition state in solution



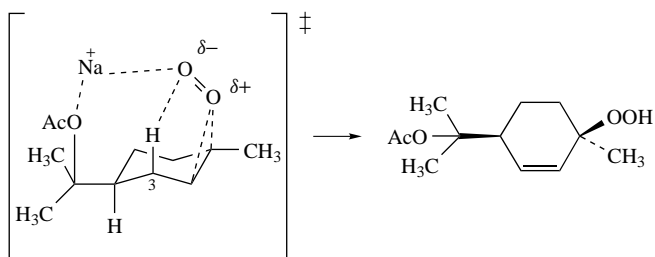
Favourable transition state within zeolite



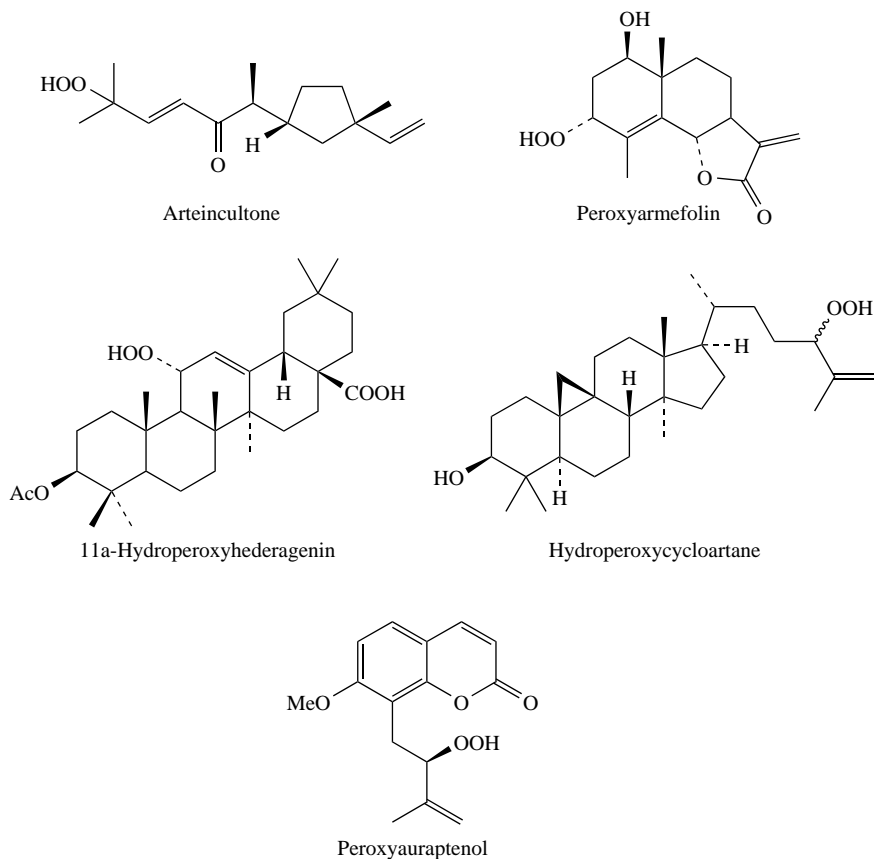
SCHEME 54. Transition states leading the major ene adducts in solution and within Na-Y



SCHEME 55. Changes in the regiochemistry and diastereoselection by zeolite confinement due to a remote substituent



SCHEME 56. Na⁺-directing regioselectivity and diastereoselection in the intrazeolite photooxygenation of α -terpinyl acetate



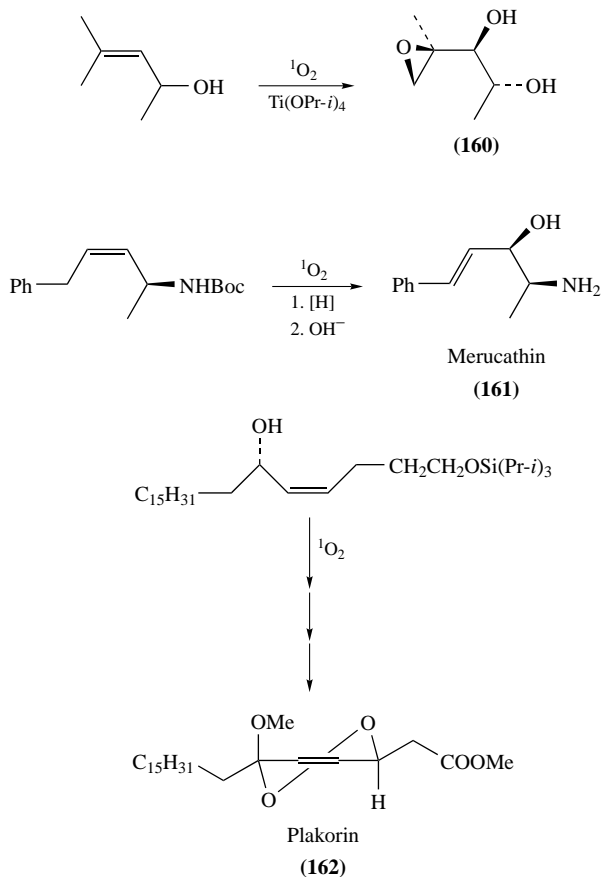
SCHEME 57. Natural products containing the allylic hydroperoxide moiety

containing allylic hydroperoxides, such as steroids, marine metabolites, terpenes, sesquiterpenes, germacranes and germacranolides, eudesmanes and eudesmanolides, guaianes and guaianolides, is huge¹⁸⁹, indicative of the role of singlet oxygen in natural product biosynthesis. Some representative examples of natural products containing the allylic hydroperoxide moiety are presented in Scheme 57.

The hydroperoxy functionality can be introduced into an alkene by a singlet oxygen ene reaction and subsequently reduced quantitatively to an allylic alcohol, by addition of reducing agents such as PPh_3 , Me_2S or NaBH_4 ¹⁹⁰. In addition, the allylic hydroperoxides can be transformed stereospecifically in the presence of $\text{Ti}(\text{OPr-}i)_4$ to an epoxy allylic alcohol, where epoxide and hydroxyl functionalities are *cis* to each other (e.g. substrate **160**, Scheme 58)^{191, 192}.

Singlet oxygen affords a variety of regio and diastereoselective reactions with chiral allylic alcohols^{45, 46, 140}, amines^{47, 48, 193} (e.g. substrate **161**, Scheme 58) and chiral cyclohexadienes^{91, 92} that are useful for synthetic transformations. For example, the photooxygenation of a chiral allylic alcohol was used recently as the key step in the total syntheses of plakorin **162** and *enantio*-chondrilin¹⁹⁴ (Scheme 58). If the photooxidation

9. Selective formation of allylic hydroperoxides via singlet oxygen ene reaction 889



SCHEME 58. Synthetically useful allylic hydroperoxidations via $^1\text{O}_2$ ene reaction

of chiral allylic alcohols and amines is performed in the presence of $\text{Ti(OPr-}i\text{)}_4$, *in situ* epoxidation occurs, affording highly *threo* (ca 95%) diastereoselective ene reactions with respect to the OH or NHR functionality, by generating two new stereogenic centres with high stereoselectivity⁴.

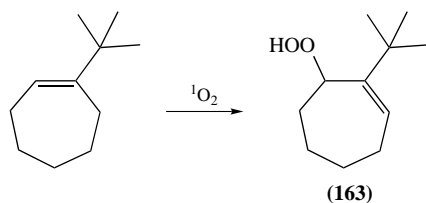
Similarly, regiospecific reactions with vinylic silanes¹⁹⁵, stannanes¹⁹⁶ and sulphoxides¹⁹⁷ afford allylic alcohols, epoxy alcohols or trimethylsilyl enones¹⁹⁸, with high stereospecificity, which are very useful building blocks in organic synthesis. Regiospecific reactions of vinylsilanes with $^1\text{O}_2$ have been used^{199, 200} by Paquette and coworkers for the regiospecific production of trimethylsilyl allylic alcohols whose subsequent desilylation resulted in a novel methodology for carbonyl transposition. Also, the high degree of geminal selectivity in the photooxygenation of α, β -unsaturated carbonyl derivatives was used in the synthesis of novel hydroperoxy heterocycles^{80, 201}.

Highly regioselective ene reactions of singlet oxygen with alkyl-substituted alkenes can also be used for synthetic purposes. For example, in the photooxygenation of 1-*t*-butylcycloheptene only one allylic hydroperoxide, by the exclusive geminal hydrogen

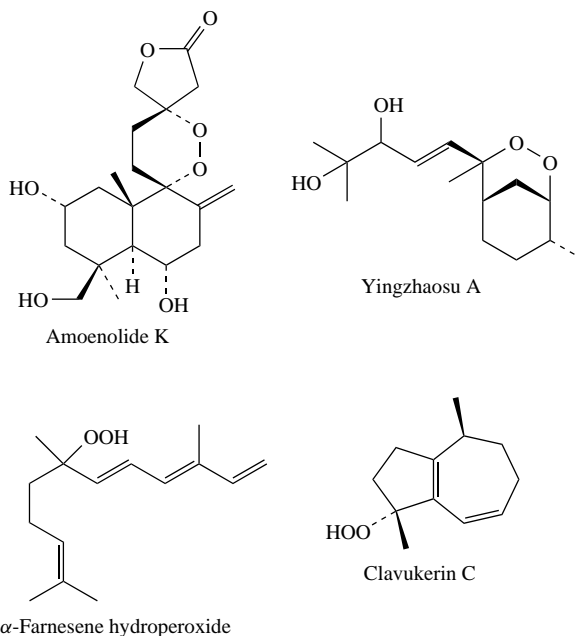
abstraction, is formed⁶⁹. Subsequent reduction of the hydroperoxide with triphenyl phosphine or dimethyl sulphide affords in high yield the allylic alcohol **163**, which is very difficult to prepare regioselectively by the use of conventional allylic hydroxylations methods (Scheme 59).

Several natural products (Scheme 60) have been synthesized *in vitro* via singlet oxygen ene reactions. For example, clavukerin C was prepared²⁰² in racemic form, in a biomimetic synthesis by Kim and Pak, whereas α -farnesene hydroperoxide was obtained²⁰³ starting from geraniol.

Baeckström and coworkers utilized the enhanced selectivity of singlet oxygen towards different types of double bonds, as the key step for the synthesis of *trans*-Sabinene²⁰⁴. By using the method of simultaneous oxidation and reduction (Rose Bengal sensitized photooxidation in the presence of tetrabutylammonium borohydride) they managed to isolate compound **166** by a total conversion of **164** (Scheme 61). Compound **165** remained

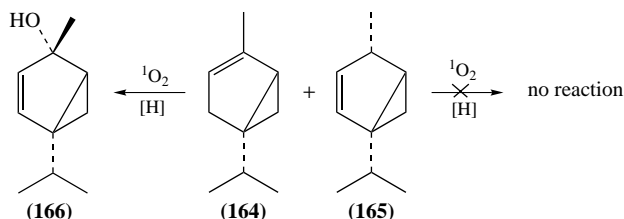


SCHEME 59. Highly regioselective photooxygenation of 1-t-butylcycloheptene

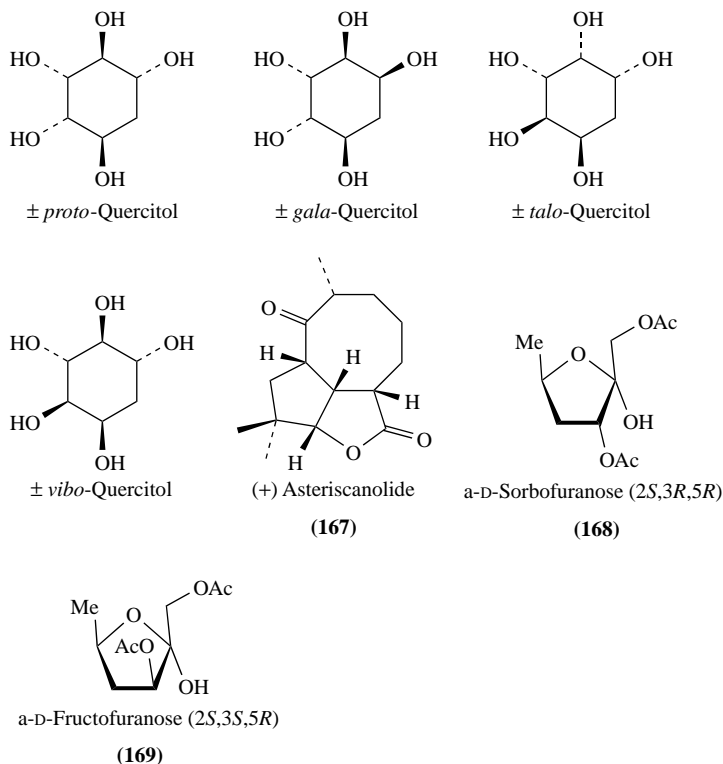


SCHEME 60. *In vitro* synthesized natural products via singlet oxygen ene reactions

9. Selective formation of allylic hydroperoxides via singlet oxygen ene reaction 891



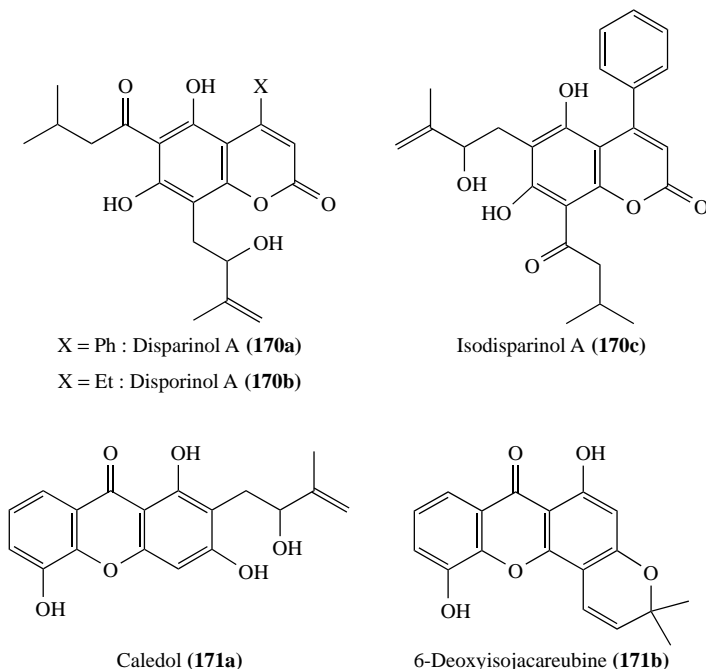
Scheme 61. Synthesis of *trans*-Sabinene via a selective $^1\text{O}_2$ ene reaction as key step



Scheme 62. Compounds synthesized via $^1\text{O}_2$ ene reactions as key steps

intact and isolated in a pure form, since its disubstituted double bond is unreactive with singlet oxygen. The same method can be used to remove undesired isomers from mixtures of olefins.

Balci and coworkers synthesized²⁰⁵ four out of the ten possible diastereomers of quercitols (Scheme 62), some of which are natural products, by using the ene reaction of singlet oxygen as the key step and the commercially available 1,4-cyclohexadiene as starting material. In this fashion, they managed to avoid the use of natural products, or compounds which require many steps to synthesize, employed as starting materials in all previously reported syntheses.

SCHEME 63. Regioselectively synthesized natural products via $^1\text{O}_2$ ene reactions

Regioselective singlet oxygen ene reactions have been also used, as key steps, towards the synthesis of (+)-asteriscanolide (**167**)²⁰⁶, α -D-sorbofuranose (2*S*,3*R*,5*R*) (**168**) and α -D-fructofuranose (2*S*,3*S*,5*R*) (**169**)²⁰⁷ (Scheme 62).

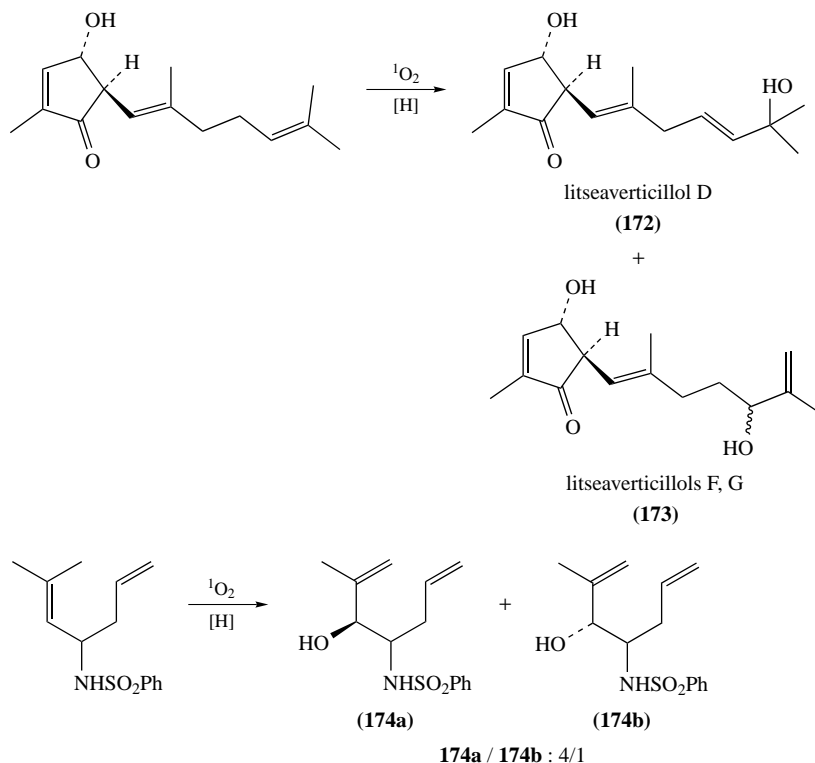
In addition, the synthesis of 2-hydroxy-3-methylbut-3-enyl substituted coumarins **170a**–**170c** and xanthenes **171a** and **171b** (Scheme 63), which are natural products, has been achieved²⁰⁸ by the application of singlet oxygen ene reactions, regioselectively controlled by the competition between the large-group non-bonded effect and the so-called stabilizing phenolic assistance effect⁶⁵ (Section II.B.2). It is interesting to note that pyranoxanthone **171b** is produced quantitatively from the unstable corresponding tertiary alcohol when exposed either to acidic medium or to a slight increase in temperature.

The total synthesis of litseaverticillols D, F and G (**172** and **173**), which are natural products with anti-HIV activity, was achieved²⁰⁹ recently via a singlet oxygen initiated cascade proposed to be biomimetic (Scheme 64). Finally, allylic alcohols **174a** and **174b** (Scheme 64) were isolated²¹⁰ in a 4/1 ratio via a stereoselective singlet oxygen ene reaction. Stereoisomer **174a** is an intermediate in the synthetic route of staurosporine, which is a bioactive alkaloid with hypotensive, antimicrobial and cell cytotoxic properties.

VI. PERSPECTIVES

Selective insertion of the allylic hydroperoxide group in organic substrates will continue to play an important role in chemical and biological systems. The development of new methods for regio-, enantio- and diastereoselective photooxygenations involving singlet oxygen will be of enormous scientific and applied interest. New stereocontrolled processes

9. Selective formation of allylic hydroperoxides via singlet oxygen ene reaction 893



SCHEME 64. Synthesis of the natural products litseaverticillols and staurosporine via selective $^1\text{O}_2$ ene reactions

involving reactive oxygen species in various organized media such as zeolites, vesicles or membranes are highly promising.

VII. ACKNOWLEDGEMENTS

We are grateful to Professor Zvi Rappoport for his kind invitation to contribute this chapter. The financial support from the Greek General Secretariat of Research and Technology (ΠΕΝΕΔ-2001) is also acknowledged. G. C. Vougioukalakis is indebted to the Leonidas Zervas Foundation and the Greek National Scholarships Foundation (IKY) for research fellowships.

VIII. REFERENCES

1. H. H. Wasserman and R. W. Murray, *Singlet Oxygen*, Academic Press, New York, 1979.
2. A. A. Frimer and L. M. Stephenson, in *Singlet Oxygen. Reactions, Modes and Products* (Ed. A. A. Frimer), CRC Press, Boca Raton, 1985.
3. L. M. Stephenson, M. B. Grdina and M. Orfanopoulos, *Acc. Chem. Res.*, **13**, 419 (1980).
4. M. Prein and W. Adam, *Angew. Chem., Int. Ed. Engl.*, **35**, 477 (1996).
5. (a) G. O. Schenck, DE-B 933925, (1943), quoted from ref. 4. (b) G. O. Schenck, H. Eggert and W. Denk, *Justus Liebigs Ann. Chem.*, **584**, 177 (1953).

6. C. S. Foote and S. Wexler, *J. Am. Chem. Soc.*, **86**, 3979 (1964).
7. H. H. Wasserman and J. L. Ives, *Tetrahedron*, **37**, 1825 (1981).
8. C. S. Foote and E. L. Clennan, in *Active Oxygen in Chemistry* (Eds. C. S. Foote, J. S. Valentine, A. Greenberg and J. F. Liebman), Chapman and Hall, London, 1995, pp. 105–140.
9. B. Ranby and J. F. Rabek, *Photodegradation, Photooxidation and Photostabilization of polymers*, Wiley, London, 1975.
10. M. S. A. Abdou and S. Holdcroft, *Macromolecules*, **26**, 2954 (1993).
11. R. D. Scurlock, B. Wang, P. R. Ogilby, J. R. Sheats and R. L. Clough, *J. Am. Chem. Soc.*, **117**, 10194 (1995).
12. K. C. Smith, *The Science of Photobiology*, Plenum Rosetta, New York, 1977.
13. C. S. Foote, *Free Radicals in Biology*, Vol. 2, Academic Press, New York, 1976, pp. 85–133.
14. K. Gollnick and H. Hartmann, *Oxygen and Oxy Radicals in Biology*, Academic Press, New York, 1981, pp. 379–395.
15. A. A. Gorman, *Chem. Soc. Rev.*, **10**, 205 (1981).
16. L. B. Harding and W. A. Goddard, *J. Am. Chem. Soc.*, **102**, 439 (1980).
17. C. W. Jefford, *Tetrahedron Lett.*, 985 (1979).
18. M. B. Grdina, M. Orfanopoulos and L. M. Stephenson, *J. Am. Chem. Soc.*, **101**, 3111 (1979).
19. M. Stratakis, M. Orfanopoulos, J. Chen and C. S. Foote, *Tetrahedron Lett.*, **37**, 4105 (1996).
20. M. Orfanopoulos and C. S. Foote, *J. Am. Chem. Soc.*, **110**, 6583 (1988).
21. M. Orfanopoulos and C. S. Foote, *Free Rad. Res. Commun.*, **2**, 321 (1987).
22. M. Orfanopoulos, I. Smonou and C. S. Foote, *J. Am. Chem. Soc.*, **112**, 3607, (1990).
23. M. Orfanopoulos and L. M. Stephenson, *J. Am. Chem. Soc.*, **102**, 1417 (1980).
24. A. P. Schaap, S. G. Recher, G. R. Falser and S. R. Villasenor, *J. Am. Chem. Soc.*, **105**, 1691 (1983).
25. M. Stratakis, M. Orfanopoulos and C. S. Foote, *Tetrahedron Lett.*, **32**, 863 (1991).
26. E. L. Clennan, M.-F. Chen and G. Xu, *Tetrahedron Lett.*, **37**, 2911 (1996).
27. S. Inagaki and K. Fukui, *J. Am. Chem. Soc.*, **97**, 7480 (1975).
28. M. J. S. Dewar and W. Thiel, *J. Am. Chem. Soc.*, **97**, 3978 (1975).
29. K. Yamaguchi, S. Yabushita, T. Fueno and K. N. Houk, *J. Am. Chem. Soc.*, **103**, 5043 (1981).
30. A. G. Davies and C. H. Schiesser, *Tetrahedron*, **47**, 1707 (1991).
31. Y. Yoshioka, S. Yamada, T. Kawakami, M. Nishino, K. Yamaguchi and I. Saito, *Bull. Chem. Soc. Jpn.*, **69**, 2683 (1996).
32. E. L. Clennan and K. Nagraba, *J. Am. Chem. Soc.*, **105**, 5932 (1983).
33. A. A. Gorman, I. Hamblett, C. Lambert, B. Spencer and M. C. Standen, *J. Am. Chem. Soc.*, **110**, 8053 (1988).
34. J.-M. Aubry, B. Mandard-Cazin, M. Rougée and R. V. Bensasson, *J. Am. Chem. Soc.*, **117**, 9159 (1995).
35. D. A. Singleton, C. Hang, M. J. Szymanski, M. P. Meyer, A. G. Leach, K. T. Kuwata, J. S. Chen, A. Greer, C. S. Foote and K. N. Houk, *J. Am. Chem. Soc.*, **125**, 1319 (2003).
36. K. H. Schulte-Elte, B. L. Muller and V. Rautenstrauch, *Helv. Chim. Acta*, **61**, 2777 (1978).
37. M. Orfanopoulos, M. B. Grdina and L. M. Stephenson, *J. Am. Chem. Soc.*, **101**, 275 (1979).
38. J. R. Hurst, J. D. McDonald and G. B. Schuster, *J. Am. Chem. Soc.*, **104**, 2065 (1982).
39. J. R. Hurst, S. L. Wilson and G. B. Schuster, *Tetrahedron*, **41**, 2191 (1985).
40. A. A. Gorman, I. R. Gould and I. Hamblett, *J. Am. Chem. Soc.*, **104**, 7098 (1982).
41. A. A. Frimer, P. D. Bartlett, A. F. Boschung and J. D. Jewett, *J. Am. Chem. Soc.*, **99**, 7977 (1977).
42. L. M. Stephenson, *Tetrahedron Lett.*, 1005 (1980).
43. K. N. Houk, P. A. Williams, P. A. Mitchell and K. Yamaguchi, *J. Am. Chem. Soc.*, **103**, 949 (1981).
44. M. Orfanopoulos, M. Stratakis, Y. Elemes and F. Jensen, *J. Am. Chem. Soc.*, **113**, 3180 (1991).
45. W. Adam and B. Nestler, *J. Am. Chem. Soc.*, **114**, 6549 (1992).
46. W. Adam and B. Nestler, *J. Am. Chem. Soc.*, **115**, 5041 (1993).
47. W. Adam and H.-G. Brünker, *J. Am. Chem. Soc.*, **115**, 3008 (1993).
48. H.-G. Brünker and W. Adam, *J. Am. Chem. Soc.*, **117**, 3976 (1995).
49. M. Stratakis, M. Orfanopoulos and C. S. Foote, *Tetrahedron Lett.*, **37**, 7159 (1996).

9. Selective formation of allylic hydroperoxides via singlet oxygen ene reaction 895

50. G. Vassilikogiannakis, M. Stratakis, M. Orfanopoulos and C. S. Foote, *J. Org. Chem.*, **64**, 4130 (1999).
51. M. Stratakis and M. Orfanopoulos, *Tetrahedron Lett.*, **36**, 4875 (1995).
52. K. Gollnick and G. Schade, *Tetrahedron Lett.*, 2355 (1966).
53. M. Stratakis, M. Orfanopoulos and C. S. Foote, *J. Org. Chem.*, **63**, 1315 (1998).
54. M. Matsumoto, S. Dobashi and K. Kuroda, *Tetrahedron Lett.*, **33**, 3161 (1977).
55. M. Matsumoto and K. Kuroda, *Synth. Commun.*, **11**, 987 (1981).
56. M. N. Alberti, G. C. Vougioukalakis and M. Orfanopoulos, *Tetrahedron Lett.*, **44**, 903 (2003).
57. G. Rousseau, P. Leperchec and J. M. Conia, *Tetrahedron Lett.*, 2517 (1977).
58. D. Lerdal and C. S. Foote, *Tetrahedron Lett.*, 3227 (1978).
59. M. Orfanopoulos, M. Stratakis and Y. Elemes, *Tetrahedron Lett.*, **30**, 4755 (1989).
60. M. Stratakis, Ph.D. Thesis, University of Crete, 1991.
61. L. E. Manring and C. S. Foote, *J. Am. Chem. Soc.*, **105**, 4710 (1983).
62. T. T. Fujimoto, Ph.D. Dissertation, University of California, Los Angeles, 1972.
63. A. F. Thomas and W. Pawlak, *Helv. Chim. Acta*, **54**, 1822 (1971).
64. V. Rautenstrauch, W. Thommen and K. H. Schulte-Elte, *Helv. Chim. Acta*, **69**, 1638, (1986).
65. J. J. Helsebeux, O. Duval, D. Guilet, D. Seraphin, D. Rondeau and P. Richomme, *Tetrahedron*, **59**, 5091 (2003).
66. E. L. Clennan and X. Chen, *J. Org. Chem.*, **53**, 3124 (1988).
67. M. Orfanopoulos, M. Stratakis and Y. Elemes, *J. Am. Chem. Soc.*, **112**, 6417 (1990).
68. E. L. Clennan, X. Chen and J. J. Koola, *J. Am. Chem. Soc.*, **112**, 5193 (1990).
69. M. Stratakis and M. Orfanopoulos, *Synth. Commun.*, **23**, 425 (1993).
70. K. H. Schulte-Elte and V. Rautenstrauch, *J. Am. Chem. Soc.*, **102**, 1738 (1980).
71. Y. Elemes, M. Stratakis and M. Orfanopoulos, *Tetrahedron Lett.*, **38**, 6437 (1997).
72. W. Adam, L. Catalani and A. Griesbeck, *J. Org. Chem.*, **51**, 5494 (1986).
73. W. Adam and A. Griesbeck, *Angew. Chem., Int. Ed. Engl.*, **24**, 1070 (1985).
74. M. Orfanopoulos and C. S. Foote, *Tetrahedron Lett.*, **26**, 5991 (1985).
75. H. E. Ensley, R. V. C. Carr, R. S. Martin and T. E. Pierce, *J. Am. Chem. Soc.*, **102**, 2836 (1980).
76. B.-M. Kwon, R. C. Kanner and C. S. Foote, *Tetrahedron Lett.*, **30**, 903 (1989).
77. T. Akasaka, T. Kakeushi and W. Ando, *Tetrahedron Lett.*, **28**, 6633 (1987).
78. T. Akasaka, Y. Misawa, M. Goto and W. Ando, *Heterocycles*, **28**, 445 (1989).
79. T. Akasaka, Y. Misawa, M. Goto and W. Ando, *Tetrahedron*, **45**, 6657 (1989).
80. W. Adam and A. Griesbeck, *Synthesis*, 1050 (1986).
81. W. Adam and M. J. Richter, *Tetrahedron Lett.*, **34**, 8423 (1993).
82. W. Adam, H.-G. Brtinker and B. Nestler, *Tetrahedron Lett.*, **32**, 1957 (1991).
83. P. H. Dussalt, K. R. Woller and M. C. Hillier, *Tetrahedron*, **50**, 8929 (1994).
84. W. Adam and B. Nestler, *Justus Liebigs Ann. Chem.*, 1051 (1990).
85. Y. Elemes and C. S. Foote, *J. Am. Chem. Soc.*, **114**, 6044 (1992).
86. M. Orfanopoulos and M. Stratakis, *Tetrahedron Lett.*, **32**, 7321 (1991).
87. M. Stratakis and M. Orfanopoulos, *Tetrahedron Lett.*, **38**, 1067 (1997).
88. N. Furutachi, Y. Nakadaira and K. Nakanishi, *J. Chem. Soc., Chem. Commun.*, 1625 (1968).
89. W. Adam, A. G. Griesbeck and X. Wang, *Justus Liebigs Ann. Chem.*, 193 (1992).
90. E. L. Clennan and X. Cheng, *J. Am. Chem. Soc.*, **111**, 8212 (1989).
91. T. Linker and L. Frohlich, *Angew. Chem., Int. Ed. Engl.*, **33**, 1971 (1994).
92. T. Linker and L. Frohlich, *J. Am. Chem. Soc.*, **117**, 2694 (1995).
93. W. Adam, H.-G. Brtinker, A. S. Kumar, E. M. Peters, K. Peters, U. Schneider and H. G. von Schening, *J. Am. Chem. Soc.*, **118**, 1899 (1996).
94. L. A. Paquette, L. W. Hertel, R. Gleiter, M. C. Bohm, M. A. Beno and G. G. Christoph, *J. Am. Chem. Soc.*, **103**, 7106 (1981).
95. E. L. Clennan and J. J. Koola, *J. Am. Chem. Soc.*, **115**, 3802 (1993).
96. E. L. Clennan, J. J. Koola and M.-F. Chen, *Tetrahedron*, **50**, 8569 (1994).
97. C. S. Foote and R. W. Denny, *J. Am. Chem. Soc.*, **93**, 5168 (1971).
98. K. Gollnick and A. Griesbeck, *Tetrahedron Lett.*, **25**, 725 (1984).
99. L. E. Manring and C. S. Foote, *J. Am. Chem. Soc.*, **105**, 4710 (1983).
100. E. W. H. Asveld and R. M. Kellogg, *J. Am. Chem. Soc.*, **102**, 3644 (1980).
101. W. Ando, K. Watanabe, J. Suzuki and T. Migita, *J. Am. Chem. Soc.*, **96**, 6766 (1974).
102. P. D. Bartlett, G. D. Mendenhall and A. P. Schaap, *Ann. N.Y. Acad. Sci.* **171**, 79 (1970).

103. N. M. Hasty and D. R. Kearns, *J. Am. Chem. Soc.*, **95**, 3380 (1973).
104. C. W. Jefford and S. Kohmoto, *Helv. Chim. Acta*, **65**, 133 (1982).
105. Y.-Y. Chan, C. Zhu and H. K. Leung, *Tetrahedron Lett.*, **27**, 3737 (1986).
106. B.-M. Kwon and C. S. Foote, *J. Org. Chem.*, **54**, 3878 (1989).
107. Y.-Y. Chan, X. Li, C. Zhu, Y. Zhang and H.-K. Leung, *J. Org. Chem.*, **55**, 5497 (1990).
108. K. Gollnick and K. Knutzen-Mies, *J. Org. Chem.*, **56**, 4017 (1991).
109. M. Matsumoto and H. Suganuma, *J. Chem. Soc., Chem. Commun.*, 2449 (1994).
110. S. Isoe, B. S. Hyeon, H. Ichikawa, S. Katsumura and T. Sakan, *Tetrahedron Lett.*, 5561 (1968).
111. M. Mousseron-Canet, J.-P. Dalle and J.-C. Mani, *Tetrahedron Lett.*, 6037 (1968).
112. C. S. Foote and M. Brenner, *Tetrahedron Lett.*, 6041 (1968).
113. S. Isoe, S. Katsumura, B. S. Hyeon and T. Sakan, *Tetrahedron Lett.*, 1089 (1971).
114. H. Mori, K. Ikoma, Y. Masui, S. Isoe, K. Kitaura and S. Katsumura, *Tetrahedron Lett.*, **37**, 7771 (1996).
115. H. Mori, K. Ikoma and S. Katsumura, *J. Chem. Soc., Chem. Commun.*, 2243 (1997).
116. H. Mori, K. Ikoma, S. Isoe, K. Kitaura and S. Katsumura, *J. Org. Chem.*, **63**, 8704 (1998).
117. M. Nakano, N. Furuichi, H. Mori and S. Katsumura, *Tetrahedron Lett.*, **42**, 7307 (2001).
118. J. W. Arbogast and C. S. Foote, *J. Am. Chem. Soc.*, **113**, 8868 (1991).
119. M. Orfanopoulos and S. Kambourakis, *Tetrahedron Lett.*, **35**, 1945 (1994).
120. H. Tokyyama and E. Nakamura, *J. Org. Chem.*, **59**, 1135 (1994).
121. J. L. Anderson, Y.-Z. An, Y. Rubin and C. S. Foote, *J. Am. Chem. Soc.*, **116**, 9763 (1994).
122. T. Hamano, K. Okuda, M. Tadahiko, M. Hirobe, K. Arakane, A. Ryu, S. Mashiko and T. Nagano, *J. Chem. Soc., Chem. Commun.*, 21 (1997).
123. X. Zhang, A. Romero and C. S. Foote, *J. Am. Chem. Soc.*, **115**, 11924 (1993).
124. X. Zhang, A. Fan and C. S. Foote, *J. Org. Chem.*, **61**, 5456 (1996).
125. G. Torre-Garcia and J. Mattay, *Tetrahedron*, **52**, 5421 (1996).
126. Y.-Z. An, A. L. Viado, M.-J. Arce and Y. Rubin, *J. Org. Chem.*, **60**, 8330 (1995).
127. N. Chronakis, G. C. Vougioukalakis and M. Orfanopoulos, *Org. Lett.*, **4**, 945 (2002).
128. A. H. Hoveyda, D. A. Evans and G. C. Fu, *Chem. Rev.*, **93**, 1307 (1993).
129. G. O. Schenck, *Angew. Chem.*, **64**, 12 (1952).
130. G. O. Schenck, K. Gollnick, G. Buchwald, S. Schroeter and G. Ohloff, *Justus Liebigs Ann. Chem.*, **674**, 93 (1964).
131. C. W. Jefford and A. F. Boschung, *Helv. Chim. Acta.*, **57**, 2242 (1974).
132. K. Gollnick, S. Schroeter, G. Ohloff, G. Schade and G. O. Schenck, *Justus Liebigs Ann. Chem.*, **687**, 14 (1965).
133. C. D. Jefford and C. G. Rimbault, *J. Am. Chem. Soc.*, **100**, 6437 (1978).
134. C. D. Jefford and C. G. Rimbault, *J. Org. Chem.*, **43**, 1908 (1978).
135. J. A. Marshall and A. R. Hochstetler, *J. Org. Chem.*, **31**, 1020 (1966).
136. K. Okada and T. Mukai, *J. Am. Chem. Soc.*, **100**, 6509 (1978).
137. Y. D. Wu, Y. Li, J. Na and K. N. Houk, *J. Org. Chem.*, **58**, 4625 (1993).
138. R. W. Hoffmann, *Chem. Rev.*, **89**, 1841 (1989).
139. W. Adam and B. Nestler, *Tetrahedron Lett.*, **34**, 611 (1993).
140. W. Adam, O. Gevert and P. Klug, *Tetrahedron Lett.*, **35**, 1681 (1994).
141. W. Adam, J. Renze and T. Wirth, *J. Org. Chem.*, **63**, 226 (1998).
142. H. Kropf and R. Reichwaldt, *J. Chem. Res. (S)*, 412 (1987).
143. W. Adam and T. Wirth, *Acc. Chem. Res.*, **32**, 703 (1999).
144. W. Adam, T. Wirth, A. Pastor and K. Peters, *Eur. J. Org. Chem.*, **4**, 501 (1998).
145. W. Adam, S. G. Bosio, H.-G. Degen, O. Krebs, D. Stalke and D. Schumaster, *Eur. J. Org. Chem.*, **8**, 3944 (2002).
146. A. Dyer, *An Introduction to Zeolite Molecular Sieves*, Wiley, Bath, 1988.
147. J. Sivaguru, A. Natarajan, L. S. Kaanumalle, J. Shailaja, S. Uppili, A. Joy and V. Ramamurthy, *Acc. Chem. Res.*, **36**, 509 (2003).
148. (a) S. E. Sen, S. M. Smith and K. A. Sullivan, *Tetrahedron*, **55**, 12657 (1999).
(b) N. J. Turro, *Acc. Chem. Res.*, **33**, 637 (2000).
(c) H. Garcia and H. D. Roth, *Chem. Rev.*, **102**, 3947 (2002).
149. A. Corma, *J. Catal.*, **216**, 298 (2003).
150. S. M. Csicsery, *Pure Appl. Chem.*, **58**, 841 (1986).
151. D. Wohrle and G. Schulz-Ekloff, *Adv. Mater.*, **6**, 875 (1994).

9. Selective formation of allylic hydroperoxides via singlet oxygen ene reaction 897

152. C.-H. Tung, L.-Z. Wu, L.-P. Zhang and B. Chen, *Acc. Chem. Res.*, **36**, 39 (2003).
153. C.-H. Tung, H. Wang and Y.-M. Ying, *J. Am. Chem. Soc.*, **120**, 5179 (1998).
154. C.-H. Tung and J.-Q. Guan, *J. Am. Chem. Soc.*, **120**, 11874 (1998).
155. C.-H. Tung, L.-Z. Wu, L. P. Zhang, H. R. Li, X. Y. Yi, K. S. Ming, Z. Y. Yuan, J.-Q. Guan, H. W. Wang, Y.-M. Ying and X. H. Xu, *Pure Appl. Chem.*, **72**, 2289 (2000).
156. W. G. Herkstroeter, P. A. Martic and S. Farid, *J. Am. Chem. Soc.*, **112**, 3583 (1990).
157. J. Shailaja, J. Sivaguru, J. Robbins, V. Ramamurthy, R. B. Sunoj and J. Chandrasekhar, *Tetrahedron*, **56**, 6927 (2000).
158. V. Ramamurthy, P. Lakshminarasimhan, C. P. Grey and L. J. Johnston, *J. Chem. Soc., Chem. Commun.*, 2411 (1998).
159. A. Pace and E. L. Clennan, *J. Am. Chem. Soc.*, **124**, 11236 (2002).
160. V. Jayathirma Rao, D. L. Perlstein, R. J. Robbins, P. H. Lakshminarasimhan, H.-M. Kao, C. P. Grey and V. Ramamurthy, *J. Chem. Soc., Chem. Commun.*, 269 (1998).
161. H. W. G. van Herwijnen and U. H. Brinker, *Tetrahedron*, **58**, 4963 (2002).
162. F. Blatter, H. Sun, S. Vasenkov and H. Frei, *Catal. Today*, **41**, 297 (1998).
163. Y. Xiang, S. C. Larsen and V. H. Grassian, *J. Am. Chem. Soc.*, **121**, 5063 (1999).
164. E. L. Clennan and J. P. Sram, *Tetrahedron Lett.*, **40**, 5275 (1999).
165. M. Stratakis, R. Nencka, C. Rabalakos, W. Adam and O. Krebs, *J. Org. Chem.*, **67**, 8758 (2002).
166. J. C. Ma and D. A. Dougherty, *Chem. Rev.*, **97**, 1303 (1997).
167. D. H. Barich, T. Xu, J. Zhang and J. F. Haw, *Angew. Chem., Int. Ed.*, **37**, 2530 (1998).
168. G. E. Froudakis and M. Stratakis, *Eur. J. Org. Chem.*, **9**, 359 (2003).
169. T. B. McMahon and G. Ohanessian, *Chem. Eur. J.*, **6**, 2971 (2000).
170. O. Mo, M. Yanez, J.-F. Gal, P.-C. Maria and M. Decouzon, *Chem. Eur. J.*, **9**, 4330 (2003).
171. M. Stratakis and M. Orfanopoulos, *Tetrahedron*, **56**, 1595 (2000).
172. X. Li and V. Ramamurthy, *J. Am. Chem. Soc.*, **118**, 10666 (1996).
173. R. J. Robbins and V. Ramamurthy, *J. Chem. Soc., Chem. Commun.*, 1071 (1997).
174. For the terminology *lone*, *twin* and *twix*, see: W. Adam, N. Bottke and O. Krebs, *J. Am. Chem. Soc.*, **122**, 6791 (2000).
175. M. Stratakis and G. Froudakis, *Org. Lett.*, **2**, 1369 (2000).
176. E. L. Clennan and J. P. Sram, *Tetrahedron*, **56**, 6945 (2000).
177. E. L. Clennan, J. P. Sram, A. Pace, K. Vincer and S. White, *J. Org. Chem.*, **67**, 3975 (2002).
178. M. Matsumoto and K. Kondo, *Tetrahedron Lett.*, 3935 (1975).
179. M. Stratakis and C. Rabalakos, *Tetrahedron Lett.*, **42**, 4545 (2001).
180. E. L. Clennan, *Tetrahedron*, **47**, 1343 (1991).
181. M. Stratakis, C. Rabalakos, G. Mpourmpakis and G. E. Froudakis, *J. Org. Chem.*, **68**, 2839 (2003).
182. C. P. Grey, F. I. Poshni, A. F. Gualtieri, P. Norby, J. C. Hanson, D. R. Corbin, K. H. Lim and C. P. Grey, *J. Am. Chem. Soc.*, **119**, 1981 (1997).
183. M. Stratakis, D. Kalaitzakis, D. Stavroulakis, G. Kosmas and C. Tsangarakis, *Org. Lett.*, **5**, 3471 (2003).
184. For the case of homoallylic alcohols, see: W. Adam, C. R. Saha-Möller and K. S. Schmid, *J. Org. Chem.*, **65**, 1431 (2000).
185. M. Stratakis and G. Kosmas, *Tetrahedron Lett.*, **42**, 6007 (2001).
186. M. Stratakis and N. Sofikiti, *J. Chem. Res. (S)*, 374 (2002).
187. R. Matusch and G. Schmidt, *Angew. Chem., Int. Ed. Engl.*, **27**, 717 (1988).
188. M. Stratakis, N. Sofikiti, C. Baskakis and C. Raptis, *Tetrahedron Lett.*, **45**, 5433 (2004).
189. For a recent review, see: D. A. Casteel, *Nat. Prod. Rep.*, **16**, 55 (1999).
190. R. W. Denny and A. Nickon, *Org. React.*, **20**, 133 (1973).
191. W. Adam, A. Griesbeck and E. Staab, *Angew. Chem., Int. Ed. Engl.*, **25**, 269 (1986).
192. W. Adam, M. Braun, A. Griesbeck, V. Lucchini, E. Staab and B. Will, *J. Am. Chem. Soc.*, **111**, 203 (1989).
193. W. Adam and H.-G. Brünker, *Synthesis*, 1066 (1995).
194. P. H. Dussault and K. R. Woller, *J. Am. Chem. Soc.*, **119**, 3824 (1997).
195. W. Adam and P. Klung, *J. Org. Chem.*, **59**, 2695 (1994).
196. W. Adam and M. J. Richter, *J. Org. Chem.*, **59**, 3341 (1994).
197. W. Adam, A. S. Kumar and C. R. Saha-Möller, *Synthesis*, 1525 (1995).
198. W. Adam and M. J. Richter, *Synthesis*, 176 (1994).

199. W. E. Fristad, T. R. Bailey, L. A. Paquette, R. Gleiter and M. C. Bohm, *J. Am. Chem. Soc.*, **101**, 4420 (1979).
200. W. E. Fristad, T. R. Bailey and L. A. Paquette, *J. Org. Chem.*, **45**, 3028 (1980).
201. W. Adam, R. Albert, N. D. Grau, L. Hasemann, B. Nestler, E.-M. Peters, K. Peters, F. Precht and H. G. von Schnering, *J. Org. Chem.*, **56**, 5778 (1991).
202. S. K. Kim and C. S. Pak, *J. Org. Chem.*, **56**, 6829 (1991).
203. S. Fielder, D. D. Rowan and M. S. Sherburn, *Synlett*, 349 (1996).
204. P. Baeckström, B. Koutek, D. Šaman and J. Vrkoč, *Bioorg. Med. Chem.*, **4**, 419 (1996).
205. (a) E. Salamci, H. Seçen, Y. Sütbeyaz and M. Balci, *J. Org. Chem.*, **62**, 2453 (1997).
(b) A. Maraş, H. Seçen, Y. Sütbeyaz and M. Balci, *J. Org. Chem.*, **63**, 2039 (1998).
206. L. A. Paquette, J. Tae, M. P. Arrington and A. H. Sadoun, *J. Am. Chem. Soc.*, **122**, 2742 (2000).
207. W. Adam, C. R. Saha-Möller and K. S. Schmid, *J. Org. Chem.*, **66**, 7365 (2001).
208. J. J. Helsebeux, O. Duval, C. Dartiguelongue, D. Seraphin, J. M. Oger and P. Richomme, *Tetrahedron*, **60**, 2293 (2004).
209. G. Vassilikogiannakis and M. Stratakis, *Angew. Chem., Int. Ed.*, **42**, 5465 (2003).
210. S. Y. Chen, B. J. Uang, F. L. Liao and S. L. Wang, *J. Org. Chem.*, **66**, 5627 (2001).

CHAPTER 10

Polar effects in decomposition of peroxidic compounds and related reactions

SUNG SOO KIM

Department of Chemistry, Inha University, Incheon 402-751, South Korea
Fax: +82 32 867 5604; e-mail: sungsoo@inha.ac.kr

I. INTRODUCTION	899
II. TEMPERATURE STUDIES ON THE RATES OF THE HOMOLYTIC AND RELATED REACTIONS	903
A. Thermolysis of <i>tert</i> -Butyl Phenylperacetates	903
B. Photolysis of Methyl Substituted-benzyl Carbinyl Hypochlorites	907
C. Electron Transfer Reactions (ETR) of <i>tert</i> -Butyl Perbenzoates with Dimethyl Sulfide	909
III. CONCLUSION	911
IV. ACKNOWLEDGMENTS	911
V. REFERENCES	911

I. INTRODUCTION

The polar effect was at first invoked to explain various directive effects observed in aliphatic systems. Methyl radicals^{1,2} attack propionic acid preferentially at the α -position, $k_\alpha/k_\beta = 7.8$ (per hydrogen), whereas chlorine³⁻⁶ prefers to attack at the β -position, $k_\alpha/k_\beta = 0.03$ (per hydrogen). In an investigation of *t*-butyl derivatives, a semiquantitative relationship was observed between the relative reactivity and the polar effect of the substituents, as evidenced by the pK_a of the corresponding acid⁷. In the case of *meta*- and *para*-substituted toluenes, it has been observed that a very small directive effect exists for some atoms or radicals. When treated by the Hammett relation it is observed that $\rho = -0.1$ for H^\bullet ⁸, $C_6H_5^\bullet$ ⁹, $p\text{-CH}_3C_6H_4^\bullet$ and CH_3^\bullet ¹⁰. On the contrary, numerous radicals with an appreciable electron affinity show a pronounced polar effect in the reaction with the toluenes. Compilation of Hammett reaction constants and the type of substituent

The chemistry of peroxides, volume 2

Edited by Z. Rappoport © 2006 John Wiley & Sons, Ltd ISBN: 0-470-86274-2

TABLE 1. Substituent effect for abstraction of benzylic hydrogen by radicals

Abstracting species	ρ or ρ^+ or ρ^*	σ or σ^+ or σ^*	Reference
$(\text{CH}_3\text{CH}_2)_3\text{Si}^\bullet$, 80 °C	+0.3	σ^*	11
H^\bullet , 40 °C	-0.1	—	8
$\text{C}_6\text{H}_5^\bullet$, 60 °C	-0.1	—	9
CH_3^\bullet , 100 °C	-0.1	—	10
$\text{HO}_2\text{CCH}_2^\bullet$, 130 °C	-0.7	σ^+	12
$(\text{CH}_3)_3\text{CO}^\bullet$, 40 °C	-0.4	σ^+	13, 14
$(\text{C}_6\text{H}_5)_3\text{CO}^\bullet$, 22 °C	-1.1	σ^+	15
$(\text{CH}_3)_3\text{COO}^\bullet$, 30 °C	-0.6	σ^+	16
<i>p</i> - $\text{O}_2\text{NC}_6\text{H}_4^\bullet$, 60 °C	-0.6	σ^+	17
Cl^\bullet , CCl_4 , 40 °C	-0.7	—	18
$\text{SO}_2\text{Cl}^\bullet$, CCl_4 , 40 °C	-0.6	σ	19
$\text{SO}_2\text{Cl}^\bullet$, CCl_4 , 40 °C	-0.5 ^a	σ	19
$\text{SO}_2\text{Cl}^\bullet$, CCl_4 , 80 °C	-0.5 ^b	σ	20
$\text{Cl}_3\text{CSO}_2^\bullet$, 80 °C	-0.5 ^b	σ	21
<i>p</i> - $\text{ClC}_6\text{H}_4\text{C(=O)OO}^\bullet$, 30 °C	-0.8 ^b	—	22
$\text{C}_6\text{H}_5\text{CO}_2^\bullet$, 80 °C	-0.6 ^c	σ^+	23
$(\text{CH}_3)_2\text{N}^\bullet$, 136 °C	-1.1	σ^+	24
Br^\bullet , CCl_4 , 80 °C	-1.4	σ^+	25, 26
<i>c</i> - $(\text{CH}_2)_5\text{NH}^{+\bullet}$, 30 °C	-1.4	σ^+	27
CCl_3^\bullet , $\text{C}_6\text{H}_5\text{Cl}$, 50 °C	-1.5	σ^+	28
1- C_N -1- <i>c</i> - $\text{C}_6\text{H}_{11}^\bullet$, 110 °C	-0.4 ^d	—	29

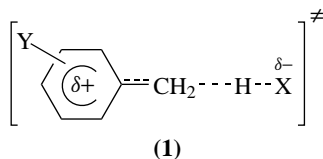
^a Substituted ethylbenzenes.

^b Substituted benzaldehydes.

^c Substituted dibenzyl ethers.

^d Substituted thiophenols.

constant used for various radicals are listed in Tables 1 and 2. Somewhat better correlation with σ^+ than with σ is indicated for numerous reactions. This may clearly demonstrate the importance of the charge separation and the delocalization of the positive charge by the aryl ring as shown in **1**. The effect of bond breaking on the magnitude of the polar effect is shown by the increase in ρ^+ from -0.9 for attack on phenols by *t*-butoxy radicals at 65 °C, to -1.1 for polystyryl radicals (65 °C)⁴⁰, to -1.6 for peroxy radicals (65 °C)³⁷ and to -2.8 (30 °C, benzene)⁴⁷.



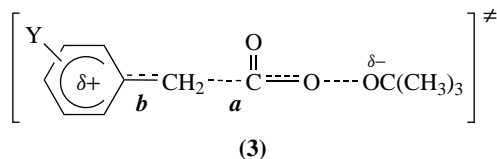
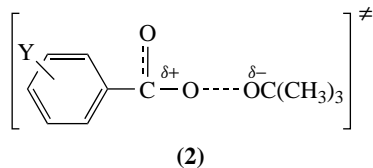
Homolysis of *tert*-butyl peresters involves either one-bond or two-bond cleavage, depending upon the stability of the radical R^\bullet derived from $\text{RCO}_3\text{C}(\text{CH}_3)_3$. The thermal decomposition of *tert*-butyl perbenzoates $\text{YC}_6\text{H}_4\text{CO}_3\text{C}(\text{CH}_3)_3$ in diphenyl ether at 110 °C⁴⁸ gives Hammett value of -1.00 that is better correlated with σ than with σ^+ . This correlation demonstrates that the positive charge does not disperse significantly into the phenyl ring and stays instead on the carboxylate group as with **2**.

Charge-separated two-bond rupture has been observed during thermal decomposition of *tert*-butyl phenylperacetates and related reactions⁴⁹⁻⁵¹. Homolysis of *tert*-butyl phenylperacetates in chlorobenzene⁵¹ shows better correlation with σ^+ to give $\rho^+ = +1.04$ at

TABLE 2. Values of ρ in Hammett $\rho\sigma$ correlations for hydrogen abstraction from various aromatic species by radicals

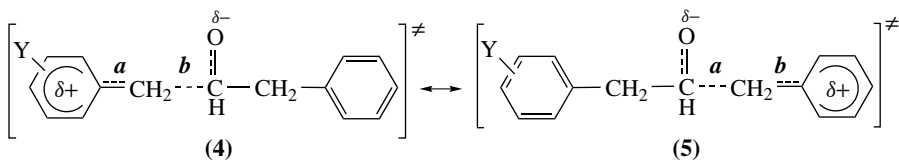
Substrates	ρ or ρ^+	σ or σ^+	Reference
<i>Bromine atom</i>			
Toluenes, 80 °C	-1.4	σ^+	25
Toluenes, 80 °C	-1.3	σ^+	26
Diphenylmethanes, 77 °C	-1.0	σ	30
Neopentylbenzenes, 70 °C	-0.75	σ^+	31
Ethylbenzenes, 80 °C	-0.7	σ^+	32
Allylbenzenes, 70 °C	-0.8	σ^+	33
Deoxybenzoin, 80 °C	-0.9	σ	34
Cumenes, 70 °C	-0.4	σ	35
Benzyl methyl ethers, 80 °C	-0.35	σ^+	36
Benzyl methyl ethers, 40 °C	-0.4	σ^+	19
α,α -Di- <i>t</i> -butylphenols, 80 °C	-0.4	σ^+	36
Dibenzyl ethers, 80 °C	-0.1	σ^+	19
<i>Peroxy radical</i>			
Toluenes, 30 °C	-0.6	σ^+	16
Cumenes, 60 °C	-0.4	σ^+	18
Cumenes, 30 °C	-0.3	σ^+	16
Benzyl phenyl ethers, 60 °C	0	—	18
Phenols, 65 °C	-1.5	σ^+	37
2,6-Di- <i>t</i> -butylphenols, 140 °C	-1.0	σ^+	38
Phenylmethylanilines, 65 °C	-0.6	σ^+	39
Diphenylamines, 65 °C	-0.9	σ^+	39
Benzaldehydes, 30 °C	-0.8	—	22
<i>t-Butoxy radical</i>			
Toluenes, 40 °C	-0.4	σ^+	14
Phenols, 122 °C	-1.2	σ^+	40
Benzyl methyl ethers, 40 °C	-0.4	σ	41
Dibenzyl ethers, 110 °C	-0.5	—	23
Benzaldehydes, 130 °C	-0.32	σ^+	42
<i>N</i> -benzylideneanilines, 130 °C	-0.98	σ^+	43
	-0.72	σ^+	43
<i>Trichloromethyl radical</i>			
Toluenes, 55 °C	-1.5	σ^+	28
Neopentylbenzenes, 70 °C	-0.9	σ^+	31
Ethylbenzenes, 80 °C	-0.5	σ^+	42
Cumenes, 70 °C	-0.7	σ^+	35
Allylbenzenes, 70 °C	-0.6	σ	33, 35
Benzyl methyl ethers, 80 °C	-0.4	σ^+	36
α,α -Dimethoxytoluenes, 80 °C	-0.2	σ^+	44
Benzhydryl methyl ethers, 80 °C	-0.1	σ^+	44
Benzaldehydes, 80 °C	-0.7	σ	45
<i>Benzoyloxy radical</i>			
Thiophenols, 100 °C	-1.19	σ^+	46

100 °C. The better correlation with ρ^+ indicates that the positive charge is delocalized into the benzene ring as in **3**. Both activation enthalpy (ΔH^\ddagger) and activation entropy (ΔS^\ddagger) gradually decrease⁴⁹ when the R in $\text{RCO}_3\text{C}(\text{CH}_3)_3$ is varied in the order C_6H_5 ($\Delta H^\ddagger = 33.5 \text{ kcal mol}^{-1}$, $\Delta S^\ddagger = 7.8 \text{ eu}$), $\text{C}_6\text{H}_5\text{CH}_2$ ($\Delta H^\ddagger = 28.7 \text{ kcal mol}^{-1}$, $\Delta S^\ddagger = -1.0 \text{ eu}$),



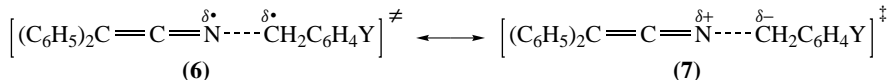
$(\text{C}_6\text{H}_5)_2\text{CH}$ ($\Delta H^\ddagger = 24.3 \text{ kcal mol}^{-1}$, $\Delta S^\ddagger = -1.0 \text{ eu}$) and $\text{C}_6\text{H}_5\text{CH}=\text{CHCH}_2$ ($\Delta H^\ddagger = 23.5 \text{ kcal mol}^{-1}$, $\Delta S^\ddagger = -5.9 \text{ eu}$).

Secondary α -deuterium kinetic isotope effects (KIE) have been studied⁵²⁻⁵⁴. Their values⁵⁴ increase from 1.05 for $\text{Y} = p\text{-NO}_2$ to 1.29 for $\text{Y} = p\text{-OCH}_3$ at 80°C in CDCl_3 . The increase of KIE for the electron-donating group is consistent with more cleavage of bond *a* occurring in **3**, which causes a more vigorous bonding vibration of the methylene. Activation volumes for homolytic scission reactions⁵⁵⁻⁵⁸ in which the primary radical pair cannot return to the starting material reflect the pressure dependence of the bond-breaking process. The value of the activation volume normally falls within the range of +4 to +10 cc mol^{-1} . However, *tert*-butyl phenylperacetates⁵⁸ show significantly lower activation volume than +3 cc mol^{-1} , probably because of the development of double-bond character in bond *b* in **3**. Two-bond homolysis of *tert*-butyl phenylperacetates^{59,60} is also suggested by the viscosity-independent rate of the thermolysis. Two-bond homolysis of *tert*-butyl phenylperacetate produces *tert*-butoxy radical, benzyl radical and one molecule of carbon dioxide. The recombination of three entities to re-generate the *tert*-butyl phenylperacetate may be impossible. Thermolysis of *tert*-butyl phenylperacetates in the presence of thiophenol in CDCl_3 at 80°C ⁶¹ takes place via a dual mechanism. The two-bond homolysis with $\rho^+_{\text{H}} = -1.16$ is accompanied by a single electron transfer (SET) process disclosing $\rho_{\text{ET}} = 1.01$. The photolysis of dibenzylmethyl carbonyl chlorites at 30°C in CCl_4 ⁶² shows an excellent correlation with σ^+ to give $\rho^+ = -1.04$ ($R = 0.999$) whereas a correlation with σ gives $\rho = -1.69$ ($R = 0.973$). The better linear relation with σ^+ again indicates a delocalization of positive charge into the phenyl ring through the formation of transition state (TS) **4** \leftrightarrow **5**.



Thermal isomerization of ketenimines to nitriles⁶³⁻⁶⁵ are known to take place via recombination of the radical pair. Rate constants for the isomerization of diphenyl *N*-(substituted benzyl) ketenimines at several temperatures^{66,67} were measured. The Hammett dual parameters equation ($\log k_{\text{Y}}/k_{\text{H}} = \rho\sigma + \rho^*\sigma^*$)⁶⁸⁻⁷⁰ shows a better correlation than either of the Hammett single correlations ($\log k_{\text{Y}}/k_{\text{H}} = \rho\sigma$ and $\log k_{\text{Y}}/k_{\text{H}} = \rho^*\sigma^*$). This

may indicate that two processes with two TSs for the isomerization reaction are taking place. The *para*-substituents (Y) control the rates mostly by spin delocalization occurring in hybrid **6** with a slight contribution from the inductive effect through hybrid **7** ($\rho^*/\rho \gg 1$). On the other hand, the inductive effect is the major or the sole interaction triggered by *meta*-substituents to give $\rho^*/\rho < 1$.



II. TEMPERATURE STUDIES ON THE RATES OF THE HOMOLYTIC AND RELATED REACTIONS

A. Thermolysis of *tert*-Butyl Phenylperacetates

Hammett relations⁵¹, secondary kinetic isotope effects⁵²⁻⁵⁴, pressure studies⁵⁵⁻⁵⁸ and viscosity-independent rates^{59,60} have all pointed to a two-bond homolysis taking place via TS **3**. The rates are, however, insensitive to change of the solvents ($\rho^+ = -1.18$ in CDCl_3 , $\rho^+ = -1.17$ in CCl_4 and $\rho^+ = -1.0$ in $\text{C}_6\text{H}_5\text{Cl}$ at 80°C). This may indicate that there is little solvent interaction taking place via **3**. The variation of the activation parameters with the substituent can be solely dependent on the formation and cleavage of the bonds *a* and *b* in **3**.

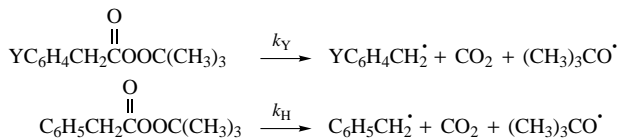
The absolute and relative rates of decomposition of *tert*-butyl phenylperacetates were measured in CDCl_3 at 60, 70, 80, 90, 100 and 110°C and Hammett correlations were obtained (Table 3)⁷¹. An Eyring plot⁷² gave the activation parameters (Table 4).

A differential enthalpy vs. differential entropy plot gives a reasonably linear isokinetic relationship (A in Figure 1) with an isokinetic temperature of $T_k = 230 \text{ K}$ ⁷³. The points of deviation from the isokinetic line are observed with *p*-OMe, *p*-OPh and *p*-NO₂. This raises the possibility of a different activation processes occurring for the substrate with the three substituents. The differential enthalpy and differential entropy are respectively plotted against σ^+ to give the linear relationships (A in Figures 2 and 3). The negative ρ^+ values in Table 3 become more negative on increasing the temperature, from $\rho^+ = -1.13$ at 60°C to $\rho^+ = -1.26$ at 110°C . The increase of ρ^+ with higher temperature is in apparent contradiction to the reactivity/selectivity principle (RSP)⁷⁴. Since the

O
||
C====O----OC(CH₃) part of **3** may be least affected by the substituent Y, alteration of the

$\Delta\Delta H_{\text{Y-H}}^\ddagger$ and $\Delta\Delta S_{\text{Y-H}}^\ddagger$ parameters may solely reflect variations of *a* and *b* occurring in **3**.

Cleavage of bond *a* produces translational entropy while formation of the π -bond *b* reduces the rotational entropy. The almost linear part of the plot with positive slope from *p*-Me to *m*-Cl in A in Figure 1 may indicate that bond cleavage *a* is more important than bond formation *b* and systematically determines the magnitude of activation parameters ($\Delta H_{\text{Y}}^\ddagger$ and $\Delta S_{\text{Y}}^\ddagger$). The isokinetic temperature of 230 K is well below our reaction temperatures and suggests an entropy control of the rates. Therefore, the variable degree of bond cleavage with the change of substituents may be the prime factor in understanding the sign of differential activation parameters $\Delta\Delta H_{\text{Y-H}}^\ddagger = \Delta H_{\text{Y}}^\ddagger - \Delta H_{\text{H}}^\ddagger$ and $\Delta\Delta S_{\text{Y-H}}^\ddagger = \Delta S_{\text{Y}}^\ddagger - \Delta S_{\text{H}}^\ddagger$. The electron-donating group Y causes more bond cleavage than when the substituent is hydrogen, resulting in $\Delta\Delta H_{\text{Y-H}}^\ddagger > 0$. The sign of $\Delta\Delta H_{\text{Y-H}}^\ddagger$ becomes negative when Y is an electron-attracting substituent. The change of $\Delta\Delta H_{\text{Y-H}}^\ddagger$ with σ^+ results in a decent straight line with a slope of -3.50 (A in Figure 2). The entropic change by the substituent Y multiplied by *T* vs. the variation of σ^+ results in

TABLE 3. Relative rates and Hammett correlations for the thermal decompositions of *tert*-butyl phenylperacetates in CDCl₃

Temp (°C)	$k_Y \cdot 10^4 \text{ (s}^{-1}\text{)}, (k_Y/k_H)$								Hammett correlations	
	<i>p</i> -MeO	<i>p</i> -PhO	<i>p</i> -Me	<i>p</i> -Ph	H	<i>p</i> -Cl	<i>m</i> -Cl	<i>p</i> -NO ₂	$\rho^+(R)$	$\rho(R)$
60	1.25 (10.7)	0.47 (3.97)	0.26 (2.22)	0.22 (1.89)	0.12 (1.00)	0.10 (0.86)	0.05 ^a (0.43)	0.02 ^a (0.138)	-1.13 (0.996)	-1.53 (0.913)
70	4.05 (11.04)	1.50 (4.09)	0.82 (2.23)	0.74 (2.03)	0.37 (1.00)	0.32 (0.87)	0.15 (0.41)	0.06 ^a (0.158)	-1.15 (0.996)	-1.56 (0.912)
80	11.90 (11.23)	4.82 (4.55)	2.63 (2.48)	2.29 (2.16)	1.06 (1.00)	0.84 (0.79)	0.42 (0.40)	0.16 (0.156)	-1.18 (0.996)	-1.60 (0.911)
90	35.67 (11.7)	13.9 (4.56)	8.36 (2.74)	7.17 (2.35)	3.05 (1.00)	2.79 (0.91)	1.26 (0.41)	0.44 (0.144)	-1.20 (0.997)	-1.64 (0.919)
100	111.8 ^a (11.95)	45.38 ^a (4.85)	24.98 (2.67)	19.54 (2.09)	9.36 (1.00)	7.60 (0.81)	3.61 (0.39)	1.44 (0.154)	-1.21 (0.997)	-1.63 (0.910)
110	333.9 ^a (12.25)	138.2 ^a (5.07)	78.85 ^a (2.89)	72.06 ^a (2.64)	27.27 (1.00)	22.48 (0.82)	9.77 (0.36)	3.86 (0.141)	-1.26 (0.996)	-1.70 (0.912)

^a The perester decomposition was either too fast or too slow at the temperature to obtain an accurate rate. Therefore, the numbers given were obtained by extrapolations utilizing the relative rates.

TABLE 4. Activation parameters for thermal decomposition of *tert*-butyl phenylperacetates in CDCl₃

Activation parameters	<i>p</i> -MeO	<i>p</i> -PhO	<i>p</i> -Me	<i>p</i> -Ph	H	<i>p</i> -Cl	<i>m</i> -Cl	<i>p</i> -NO ₂
ΔH_Y^\ddagger ^a	27.5	28.1	28.2	28.2	26.8	26.6	26.1	26.2
ΔS_Y^\ddagger ^b	5.9	5.6	4.9	4.4	-0.9	-1.8	-4.8	-6.4
$\Delta\Delta H_{Y-H}^\ddagger$ ^{a,c}	0.7	1.3	1.4	1.3	0	-0.2	-0.7	-0.6
$\Delta\Delta S_{Y-H}^\ddagger$ ^{b,d}	6.8	6.5	5.8	5.3	0	-0.9	-3.9	-5.5
$T\Delta\Delta S_{Y-H}^\ddagger$ ^{a,e}	2.4	2.3	2.0	1.9	0	-0.3	-1.4	-1.9

^a In kcal mol⁻¹.

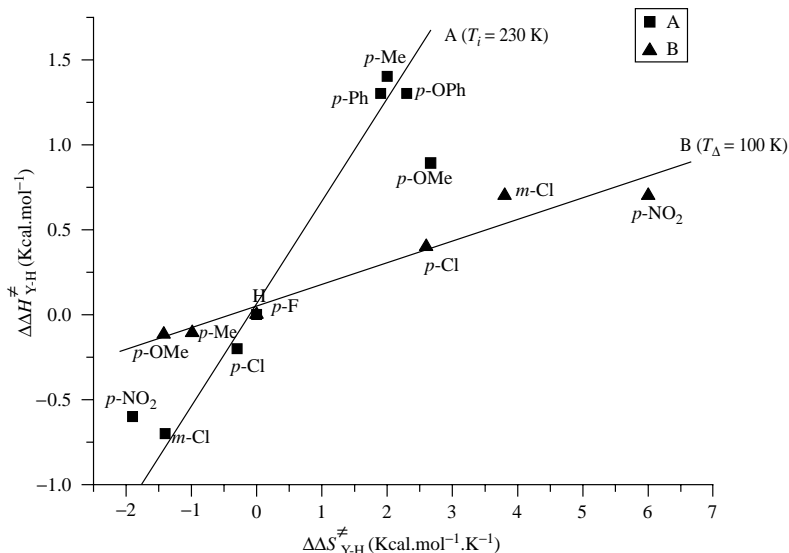
^b In eu.

^c $\Delta\Delta H_{Y-H}^\ddagger = \Delta H_Y^\ddagger - \Delta H_H^\ddagger$, where ΔH_Y^\ddagger and ΔH_H^\ddagger are the activation enthalpies when the substituents are Y and hydrogen, respectively.

^d $\Delta\Delta S_{Y-H}^\ddagger = \Delta S_Y^\ddagger - \Delta S_H^\ddagger$, where ΔS_Y^\ddagger and ΔS_H^\ddagger are similarly related as in the enthalpic terms above.

^e $T = 353 \text{ K}$.

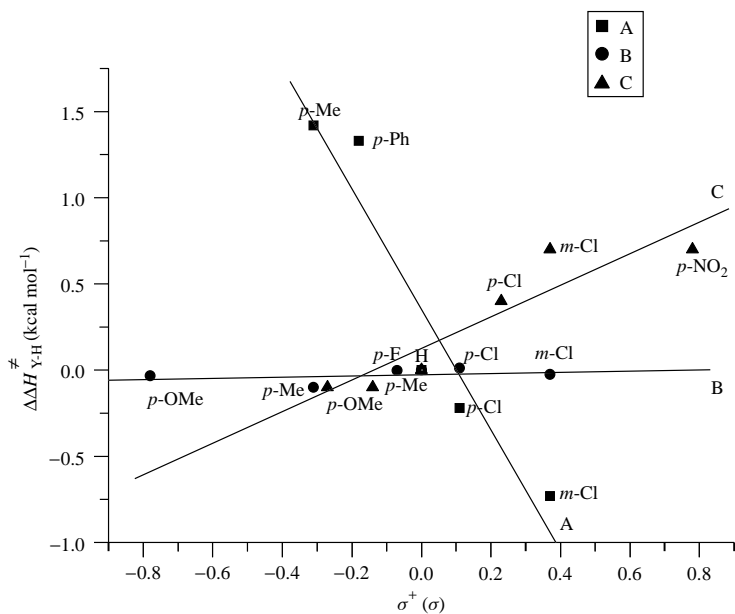
a slope of -5.43 (A in Figure 3). The steeper entropic slope suggests again that substituents influence the rates through entropic contributions. The relative rates of the five substituents (k_Y/k_H) become larger at the higher temperatures, arguing for entropy control of the rates. Such a pattern of relative rates (k_Y/k_H) (see equation 1) violates the RSP, because temperature increase should decrease the selectivity. The variation of substituents on the phenyl ring⁷⁵ can cause much weaker interactions. The contribution of



A. Thermal decomposition of *tert*-butyl phenylperacetates in CDCl₃.

B. Electron transfer reaction of *t*-butyl perbenzoates with dimethyl sulfides.

FIGURE 1. Isokinetic relationship derived from an enthalpy/entropy plot compensation effect

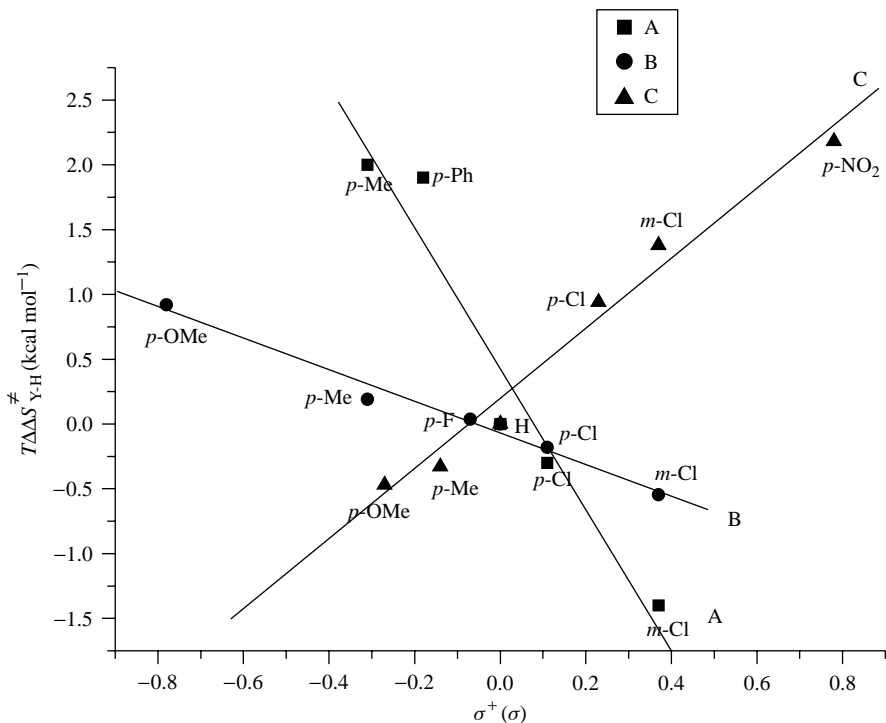


A. Thermal decomposition of *tert*-butyl phenylperacetates in CDCl₃ (slope: -3.50).

B. β -Cleavages of methyl-substituted benzyl carbinoyloxy radicals in CCl₄ (slope: 0.04).

C. Electron transfer reaction of *t*-butyl perbenzoates with dimethyl sulfides (slope: 0.92).

FIGURE 2. Dependence of the activation enthalpy on the substituents



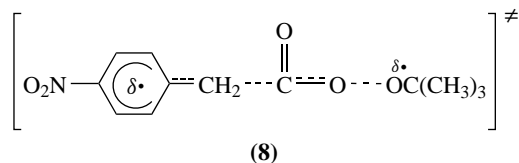
- A. Thermal decomposition of *tert*-butyl phenylperacetates in CDCl_3 (slope: -5.43).
 B. β -Cleavages of methyl-substituted benzyl carbinoyloxy radicals in CCl_4 (slope: -1.21).
 C. Electron transfer reaction of *t*-butyl perbenzoates with dimethyl sulfides (slope: 2.73).

FIGURE 3. Dependence of the activation entropy on the substituents

the $\Delta\Delta S_{Y-H}^\ddagger/R$ term overwhelms the influence of the $\Delta\Delta H_{Y-H}^\ddagger/RT$ term, resulting in an entropy-controlled rate when the difference of bond dissociation energy for the various substituents is small (e.g. $<4 \text{ kcal mol}^{-1}$).

$$S = \text{Log}(k_Y/k_H) = \Delta\Delta S_{Y-H}^\ddagger/R - \Delta\Delta H_{Y-H}^\ddagger/RT \quad (1)$$

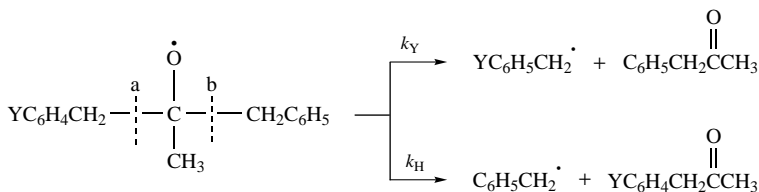
The differential activation parameters of *p*-OMe and *p*-OPh show considerable negative deviations from the linear relationship (A in Figure 1). These substituents are so strongly electron-releasing that π -bond formation by factor **b** becomes large enough to unusually reduce the effect exerted by factor **a**. *p*-NO₂ is a notorious spin delocalizer⁶⁸⁻⁷⁰, and carries a spin delocalization constant of $\sigma_c = 0.57$ ⁶⁹. The plot of k_Y/k_H ⁵⁴ vs. σ^+ also shows a remarkable positive deviation for *p*-NO₂. Accordingly, the *p*-NO₂ substituent may not induce polar TS like **3** but instead may favor homolysis via **8**. The three cage species derived from **8** can undergo recombination when viscosity of the solvents is high enough, not allowing the rotational diffusion in order to keep the coplanarity mentioned by Bartlett and Hiatt⁴⁹. On the other hand, the reactions of other peresters⁷⁶ pass through **3** where the polar character may prevent recombination of the three entities.



B. Photolysis of Methyl Substituted-benzyl Carbinyl Hypochlorites

Combination of the absolute rate theory⁷² with the Bell–Evans–Polanyi principle^{77,78} yields the Leffler–Hammond postulate (LHP)^{79,80} and reactivity/selectivity (RSP)⁷², when the transition state is assumed to be the resonance hybrid of the reactant and the product. When the TS assumes such an intermediate configuration, the substituent effects on the free energy of activation (ΔG^\ddagger_Y) (kinetic substituent effect) and free energy of reaction (ΔG°_Y) (thermodynamic substituent effect) are linearly related to each other. The parallel between the rate and the equilibrium could be eminently accommodated with a two-dimensional reaction profile, whereby the LHP^{79,80} and RSP⁷⁴ successfully predict numerous reactivities. The failures were, however, recognized with many heterolytic reactions. Therefore, the *perpendicular effect*⁸¹ has been proposed and subsequently accommodated in the three-dimensional potential energy surface diagram (PESD)^{82–84}. Alternatively, the outcome of the *perpendicular effect*⁸¹ could be understood in terms of Marcus theory⁸⁵ when the intrinsic barrier is drastically varied by the substituents (Y). The multidimensional reaction profile^{82–84} is further elaborated by the notion of an imbalanced TS⁸⁶ and the Principle of Nonperfect Synchronization (PNS)⁸⁷. The photolytic decomposition of dibenzylmethoxy radicals⁶² proceeds through the polar TS $4 \leftrightarrow 5$. The polar structure is apparently displaced from an intermediate configuration between reactants and products that can be termed imbalanced.

Methyl substituted-benzyl carbinyl radicals⁸⁸ were derived from corresponding hypochlorites at several temperatures (Scheme 1). The relative rates (k_Y/k_H) show a constant value regardless of temperature change (Table 5). Better Hammett constants are obtained in plots against σ^+ and give accordingly the constant figure, $\rho^+ = -0.90$ for all the temperature range. The ρ^+/σ^+ correlation may indicate the polar TS **9** and **10**, where the positive charge is delocalized into the benzene ring. The invariable relative rates (k_Y/k_H) and Hammett ρ^+ with temperature apparently violate RSP. The same invariance is also observed in other solvents such as CCl_4 , $C-\text{C}_6\text{H}_{10}$, C_6H_6 , CH_3CN and $(\text{CH}_3)_3\text{COH}$. This shows that there is no serious solvent interaction taking place with **9** and **10**.

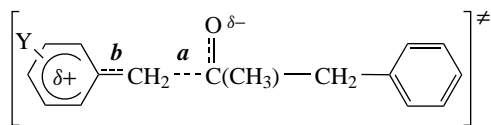


SCHEME 1

Therefore, the variation in differential activation parameters ($\Delta\Delta H^\ddagger_{Y-H}$ and $\Delta\Delta S^\ddagger_{Y-H}$) (Table 6) with substituents is the result of the difference between the degree of bond cleavage **a** in **9** and **10**. The magnitude of the differential activation enthalpies ($\Delta\Delta H^\ddagger_{Y-H} = \Delta H^\ddagger_Y - \Delta H^\ddagger_H$) is close to zero for all the substituents ($Y = p\text{-OCH}_3, p\text{-CH}_3, p\text{-F}, p\text{-Cl}$

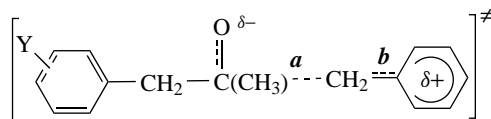
TABLE 5. Relative rates and Hammett correlations for β -cleavages of methyl-substituted benzyl carbinyloxy radicals in CCl_4

Temp $^{\circ}\text{C}$	k_Y/k_H						Hammett Correlations	
	<i>p</i> -MeO	<i>p</i> -Me	<i>p</i> -F	H	<i>p</i> -Cl	<i>m</i> -Cl	ρ^+ (R)	ρ (R)
-20	4.91	1.73	1.07	1	(0.72) ^a	0.42	-0.90 (0.999)	-1.50 (0.946)
-10	4.78	1.64	1.07	1	(0.72) ^a	0.42	-0.89 (0.999)	-1.47 (0.942)
10	4.80	1.63	1.06	1	0.72	0.41	-0.90 (0.998)	-1.42 (0.913)
25	4.74	1.62	1.06	1	0.72	0.41	-0.89 (0.998)	-1.42 (0.943)
40	4.79	1.62	1.07	1	0.73	0.41	-0.89 (0.998)	-1.42 (0.941)
60	4.81	1.63	1.07	1	0.72	0.42	-0.89 (0.998)	-1.42 (0.941)

^a Taken from the value at 10 $^{\circ}\text{C}$.

(9)

or



(10)

TABLE 6. Differential activation parameters for β -cleavages of methyl-substituted benzyl carbinyloxy radicals in CCl_4

Differentials	<i>p</i> -MeO	<i>p</i> -Me	<i>p</i> -F	H	<i>p</i> -Cl	<i>m</i> -Cl
$\Delta\Delta H_{Y-H}^{\ddagger a}$	-0.032	-0.100	-0.002	0	0.012	-0.025
$\Delta\Delta S_{Y-H}^{\ddagger b}$	3.01	0.640	0.123	0	-0.608	-1.83
$T\Delta\Delta S_{Y-H}^{\ddagger c}$	0.92	0.19	0.036	0	-0.181	-0.545

^a $\Delta\Delta H_{Y-H}^{\ddagger} = \Delta H_Y^{\ddagger} - \Delta H_H^{\ddagger}$, where ΔH_Y^{\ddagger} and ΔH_H^{\ddagger} are the activation enthalpies (in kcal mol^{-1}) for the cleavage of substituted and simple benzyl radicals, respectively.^b $\Delta\Delta S_{Y-H}^{\ddagger} = \Delta S_Y^{\ddagger} - \Delta S_H^{\ddagger}$ (in eu), where ΔS_Y^{\ddagger} and ΔS_H^{\ddagger} are similarly related as in the above enthalpic terms.^c $T = 298 \text{ K}$.

and *m*-Cl) (Table 6). Hence, the activation enthalpy due to the bond cleavage **a** in **9** could be almost cancelled out by similar bond cleavage **a** in **10** (B in Figure 2). On the other hand, the difference of translational entropy derived from the cleavage of **a** in **9** minus the rupture of **a** in **10** can be sufficiently significant to give the distinct differential activation entropy value. The differential activation entropy results from the differential substituent effect on the activation entropy between **9** and **10** ($\Delta\Delta S_{Y-H}^{\ddagger} = \Delta S_Y^{\ddagger} - \Delta S_H^{\ddagger}$). The values of $\Delta\Delta S_{Y-H}^{\ddagger}$ keep positive signs for electron-donating substituents but become negative with electron-withdrawing groups. Accordingly, the differential free energy of activation ($\Delta\Delta G_{Y-H}^{\ddagger}$) is seriously influenced by $T\Delta\Delta S_{Y-H}^{\ddagger}$ for the reaction to become entropy-controlled. The reducing trend ($T\Delta\Delta S_{Y-H}^{\ddagger}$ vs. σ^+) shows an excellent straight

line appearing in B of Figure 3. Since the differential enthalpies are close to zero (B in Figure 2), the selectivity S of equation 1 solely depends on $\Delta\Delta S^\ddagger/R$ and remains invariable with temperature.

C. Electron Transfer Reactions (ETR) of *tert*-Butyl Perbenzoates with Dimethyl Sulfide⁸⁹

Hydrogen-atom abstractions from toluenes⁹⁰ and cumenes⁹¹ by bromine atoms, β -scissions of carbinoyloxy radicals⁸⁸ and thermolysis of *tert*-butyl phenylperacetates⁷¹ proceed through a polar TS and reveal entropy control of rates. The relative rates at several temperatures provide differential activation terms ($\Delta\Delta H^\ddagger_{Y-H}$ and $\Delta\Delta S^\ddagger_{Y-H}$) derived from the Eyring equation⁷². The magnitude of differential activation entropies ($\Delta\Delta S^\ddagger_{Y-H}$) outweighs those of differential enthalpies ($\Delta\Delta H^\ddagger_{Y-H}$)^{71,88,90,91}. When the substituent displays a significant electron-donating character, i.e. the value of σ^+ maintains a larger negative value, the $\Delta\Delta S^\ddagger_{Y-H}$ have a much more positive magnitude than $\Delta\Delta H^\ddagger_{Y-H}$. The activation parameters for abstraction of phenolic hydrogen from *p*-methoxyphenol by *tert*-butoxy radical⁹² shows dominance of the entropic term over enthalpy. Triplet δ -hydrogen abstraction by *o-tert*-butyl benzophenones⁹³ shows an entropy-controlled inductive effect. Recently, the rate of hydrogen abstractions by *tert*-butoxy radicals were suggested to involve an entropy-controlled process⁹⁴. *tert*-Butyl peroxybenzoate (TBP) underwent electron transfer reaction (ETR) with dimethyl sulfide⁹⁵.

Absolute and relative rates of ETR of *tert*-butyl perbenzoates with dimethyl sulfide at various temperatures ($T = 80, 90, 100$ and 110°C) were obtained. Hammett correlations at each temperature were also studied (Table 7). The Hammett slopes are positive and the reactions are better correlated with σ rather than with σ^+ . This indicates that a negative charge resides on the benzyloxy group without conjugation with the phenyl

TABLE 7. Absolute rates, relative rates and Hammett correlations for ETR between *tert*-butyl perbenzoates and dimethyl sulfide

$$\text{YC}_6\text{H}_4\text{CO}_2\text{Bu-}t + \text{CH}_3\text{SCH}_3 \xrightarrow{k_{\text{ET}}} \text{YC}_6\text{H}_4\text{CO}_2\text{CH}_2\text{SCH}_3 + t\text{-BuOH}$$

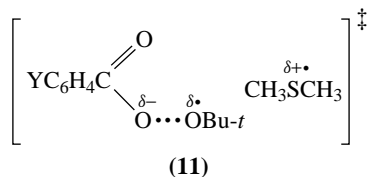
T ($^\circ\text{C}$)/ Substituent	<i>p</i> -OMe	<i>p</i> -Me	H	<i>p</i> -Cl	<i>m</i> -Cl	<i>p</i> -NO ₂	ρ (<i>R</i>)	ρ^+ (<i>R</i>)
	$k_{\text{ET}} \times 10^4, \text{M}^{-1} \text{s}^{-1}{}^a$ ($k_{\text{ET}}^Y/k_{\text{ET}}^H$) ^b							
80	0.0715 ^c (0.585)	0.0931	0.130	0.260	0.343	0.987	1.05	0.72
		(0.716)	(1.00)	(2.00)	(2.64)	(7.52)	(0.998)	(0.949)
90	0.167 (0.603)	0.215 (0.776)	0.277 (1.00)	0.554 (2.00)	0.737 (2.66)	2.27 (8.19)	1.06 (0.998)	0.73 (0.946)
	0.347 (0.595)	0.438 (0.751)	0.583 (1.00)	1.19 (2.04)	1.65 (2.83)	4.76 (8.16)	1.07 (0.998)	0.74 (0.948)
100	0.710 (0.607)	0.837 (0.715)	1.17 (1.00)	2.46 (2.10)	3.29 (2.81)	9.66 (8.26)	1.08 (0.997)	0.74 (0.944)

^a Absolute rate constants of ETR.

^b Relative rate constants of ETR.

^c The value is obtained by extrapolation due to the very slow rate of decomposition.

ring (cf. **11**). This is well compared with the previously mentioned entropy-controlled reactions, where the positive charge is delocalized into a phenyl ring which results in $\rho^+ \sigma^+$ correlations^{71, 88, 90, 91}.



The relative rates of ETR, $k_{\text{ET}}^{\text{Y}}/k_{\text{ET}}^{\text{H}}$, remain nearly invariable irrespective of temperature. This means that the substituent effect is constant at the various temperatures in order to give the identical Hammett ρ value ($\rho = 1.06 \pm 0.02$) (see Table 7). A constant ρ^+ (not ρ), at different temperatures had already been observed in the photobromination of cumenes⁹¹ and the homolytic fragmentation of carbinoyloxy radicals⁸⁸. The Hammett ρ or ρ^+ reaction constant can be regarded as a selectivity parameter and the invariance with temperature apparently violates the reactivity/selectivity principle (RSP)⁷⁴. The activation parameters and their differential values are tabulated in Table 8. An isokinetic relation (Figure 4)⁷⁴, reveals an isokinetic temperature of $\beta = 100 \text{ K} = -173 \text{ }^\circ\text{C}$ which is far below our experimental reaction temperatures. This indicates the significant role of entropy in influencing the rates. The differential activation terms ($\Delta\Delta H_{\text{Y-H}}^\ddagger$ and $T\Delta\Delta S_{\text{Y-H}}^\ddagger$) are plotted against σ in plot C in Figures 2 and 3, respectively. The slopes of the lines suggest that the differential entropy is outweighing the corresponding enthalpy term to give $T\Delta\Delta S_{\text{Y-H}}^\ddagger \gg \Delta\Delta H_{\text{Y-H}}^\ddagger$ in determining the relative reactivities. This implies the rates are controlled by the entropy term for these reactions.

The benzoyloxy group attains partial negative charge and *tert*-butoxy attains a radical character in **11**. The extent of heterolytic O \cdots O bond cleavage into radical and anion is variable, depending upon the substituent (Y). The values of the differential activation terms (Table 8) indicate that electron-withdrawing groups Y boost more bond cleavage than hydrogen. More bond-breaking of **11** requires more energy to raise the activation enthalpy so that $\Delta\Delta H_{\text{Y-H}}^\ddagger > 0$ for electron-attracting Y and $\Delta\Delta H_{\text{Y-H}}^\ddagger < 0$ for electron-releasing Y. Absolute rate theory⁷² suggests that vibration of the O—O bond in *t*-butyl perbenzoate should be replaced by translation during the activation process. The transition from vibration to translation should be accompanied by dramatic entropic increase, since

TABLE 8. Activation parameters and their differential values for ETR between *tert*-butyl perbenzoates and dimethyl sulfide

	<i>p</i> -OMe	<i>p</i> -Me	H	<i>p</i> -Cl	<i>m</i> -Cl	<i>p</i> -NO ₂
$\Delta H_{\text{Y}}^\ddagger$ ^a	18.9	18.9	19.0	19.4	19.7	19.7
$\Delta S_{\text{Y}}^\ddagger$ ^b	-28.7	-28.3	-27.4	-24.8	-23.6	-21.4
$\Delta\Delta H_{\text{Y-H}}^\ddagger$ ^{a,c}	-0.1	-0.1	0	0.4	0.7	0.7
$\Delta\Delta S_{\text{Y-H}}^\ddagger$ ^{b,d}	-1.3	-0.9	0	2.6	3.8	6.0
$T\Delta\Delta S_{\text{Y-H}}^\ddagger$ ^{a,e}	-0.47	-0.33	0	0.94	1.38	2.18

^a In kcal mol⁻¹.

^b In cal mol⁻¹ K⁻¹.

^c $\Delta\Delta H_{\text{Y-H}}^\ddagger = \Delta H_{\text{Y}}^\ddagger - \Delta H_{\text{H}}^\ddagger$, where the subscripts Y and H indicate the substituents Y and H in the perester.

^d $\Delta\Delta S_{\text{Y-H}}^\ddagger = \Delta S_{\text{Y}}^\ddagger - \Delta S_{\text{H}}^\ddagger$, where the subscripts Y and H indicate the substituents Y and H in the perester.

^e $T = 373 \text{ K}$.

vibration occurs in one dimension while translation occurs in three dimensions. Therefore, the increase (decrease) in differential activation entropy multiplied by the absolute temperature term should be much higher than the corresponding differential activation enthalpy ($T\Delta\Delta S_{Y-H}^\ddagger \gg \Delta\Delta H_{Y-H}^\ddagger$). This is shown by comparison of the slope C of Figure 2 (0.92) with C of Figure 3 (2.73). The polarity of **11** is opposite to that of the TSs involved in the previous entropy-dominating reactions. The negative charge is localized on the benzyloxy group to give a $\rho\sigma$ correlation while the positive charge is dispersed into the benzene ring, resulting in the $\rho^+\sigma^+$ relationship^{71, 88, 90, 91}.

The selectivity **S** of a species with competing peresters harboring substituents Y and H, respectively, could be defined as $S = \ln k_{ET}^Y/k_{ET}^H = -(\Delta G_{Y-H}^\ddagger - \Delta G_{Y-H}^\ddagger)/RT = -\Delta\Delta G_{Y-H}^\ddagger$, with k and ΔG^\ddagger being the corresponding rate constant and free energy of activation of the ETR. $S = -\Delta\Delta G_{Y-H}^\ddagger/RT$ can be subdivided into two parts: $-\Delta\Delta G_{Y-H}^\ddagger/RT = \Delta\Delta S_{Y-H}^\ddagger/R - \Delta\Delta H_{Y-H}^\ddagger/RT$. The present ETR involves a $\Delta\Delta H_{Y-H}^\ddagger/RT$ term almost close to zero. Therefore, **S** is mainly controlled by $\Delta\Delta S_{Y-H}^\ddagger/R$, which is temperature-independent and displays a constant value with the substituent (cf. the k_{ET}^Y/k_{ET}^H values in Table 7).

The ETR proceeds through **11** in which the O–O bond is cleaved. The process of the bond-breaking follows isokinetic relations, indicating that $\beta = -173^\circ\text{C}$, which is far below our reaction temperatures. This emphasizes the importance of entropy for the rates. Comparison of the magnitude of $\Delta\Delta H_{Y-H}^\ddagger$ and $\Delta\Delta S_{Y-H}^\ddagger$ shows that the relative rates are controlled by $T\Delta\Delta S_{Y-H}^\ddagger$. The entropic dominance is derived from the translational degree of freedom occurring in the cleavage of the O··O bond.

III. CONCLUSION

When the reactions of peroxidic compounds involve cleavage of the benzylic part in the TS, a benzylic cation character may occur where positive charge is dispersed into the benzene ring. The charge dispersion is reflected in Hammett $\rho^+\sigma^+$ correlations. ETR of *tert*-butyl perbenzoates with dimethyl sulfide proceeds through polar TS, where the benzyloxy group attains negative charge to form benzyloxy anion. This polar TS satisfies Hammett $\rho\sigma$ relations. The rate-determining steps involve cleavage of either benzylic $\text{YC}_6\text{H}_4\text{CH}_2^{\delta+}$ or benzyloxy $\text{YC}_6\text{H}_4\text{CO}_2^{\delta-}$ species. The entropic dominance is also observed for other homolytic reactions in which TS contains a benzylic $\text{YC}_6\text{H}_4\text{CH}_2^{\delta+}$. In such cases, the change of the bond dissociation energy with variation of Y can be less serious. The temperature studies indicate that the bond cleavage is mostly influenced by translational entropy to give entropy-controlled reactions. Accordingly, the relative rates satisfy neither Hammond Postulate nor RSP behavior. The rates are governed by the *perpendicular effect*.

IV. ACKNOWLEDGMENTS

The author is grateful to Professor Cheves Walling and the late Professor Glen A. Russell for scientific advice. Thanks are also due to the author's collaborators without whose help this work would have been impossible. The Korea Science and Engineering Foundation, the Korea Research Foundation, the Korea Federation of Science and Technology Societies and the Korea Institute of Science and Technology Evaluation and Planning are thanked for their financial support during the last 25 years. The author thanks Mr. Sang Hyuck Lee for his work accompanying the preparation of the manuscript.

V. REFERENCES

1. M. S. Kharasch and M. T. Gladstone, *J. Am. Chem. Soc.*, **65**, 15 (1943).
2. C. C. Price and H. Morita, *J. Am. Chem. Soc.*, **75**, 3686 (1953).

3. H. Magritte and A. Bruylants, *Ind. Chim. Belge*, **22**, 547 (1957).
4. A. Bruylants, M. Tits and R. Dandby, *Bull. Soc. Chim. Belg.*, **58**, 210 (1949).
5. A. Bruylants, M. Tits, C. Dieu and R. Gauthier, *Bull. Soc. Chim. Belg.*, **61**, 266 (1952).
6. H. J. Den Hertog, B. de Vries and J. van Brazt, *Recl. Trav. Chim. Pays-Bas*, **74**, 1561 (1955).
7. R. Van Helden and E. C. Kooyman, *Recl. Trav. Chim. Pays-Bas*, **73**, 269 (1954).
8. W. A. Pryor and R. W. Henderson, *J. Chem. Kinet.*, **4**, 325 (1972).
9. R. F. Bridger and G. A. Russell, *J. Am. Chem. Soc.*, **85**, 3754 (1963).
10. W. A. Pryor, U. Tonellato, D. L. Fuller and S. Jumonville, *J. Org. Chem.*, **34**, 2018 (1969).
11. Y. Nagai, I. Yamazaki, N. Shiojima, N. Kobori and M. Mayashi, *J. Organomet. Chem.*, **9**, 25 (1967).
12. E. I. Heiba, R. M. Dessau and W. J. Koehl, *J. Am. Chem. Soc.*, **91**, 138 (1969).
13. C. Walling and A. McGuinness, *J. Am. Chem. Soc.*, **91**, 2053 (1969).
14. H. Sakurai and A. Hosomi, *J. Am. Chem. Soc.*, **89**, 458 (1967).
15. C. Walling and M. J. Gibian, *J. Am. Chem. Soc.*, **87**, 3361 (1965).
16. J. A. Howard, K. U. Ingold and M. Symonds, *Can. J. Chem.*, **46**, 1017 (1968).
17. A. F. Trotman-Dickinson, *Q. Rev. (London)*, **7**, 198 (1953).
18. G. A. Russel and R. C. Williamson, Jr., *J. Am. Chem. Soc.*, **86**, 2357 (1964).
19. K. H. Lee, *Tetrahedron*, **25**, 4357 (1969).
20. K. H. Lee, *Tetrahedron*, **26**, 2041 (1970).
21. K. H. Lee, *Tetrahedron*, **26**, 1503 (1970).
22. C. Walling and E. A. McElhill, *J. Am. Chem. Soc.*, **73**, 2927 (1951).
23. R. L. Huang, K. H. Lee and S. H. Ong, *J. Chem. Soc.*, 3336 (1962).
24. C. J. Michejda and W. P. Hoss, *J. Am. Chem. Soc.*, **92**, 6299 (1970).
25. R. E. Pearson and J. C. Martin, *J. Am. Chem. Soc.*, **85**, 3142 (1963).
26. (a) C. Walling, A. L. Rieger and D. D. Tanner, *J. Am. Chem. Soc.*, **85**, 3129 (1963).
(b) C. Walling and A. L. Rieger, *J. Am. Chem. Soc.*, **85**, 3135 (1963).
27. R. S. Neale and E. Gross, *J. Am. Chem. Soc.*, **89**, 6579 (1967).
28. E. S. Huysen, *J. Am. Chem. Soc.*, **82**, 391, 394 (1960).
29. Y. Schaafsma, A. F. Bickel and E. C. Kooyman, *Recl. Trav. Chim. Pays-Bas.*, **86**, 180 (1967).
30. S. S. Friedrich, L. J. Andrews and R. M. Keefer, *J. Org. Chem.*, **35**, 944 (1970).
31. W. D. Thetherow and G. S. Gleicher, *J. Am. Chem. Soc.*, **91**, 7150 (1969).
32. R. L. Huang and K. H. Lee, *J. Chem. Soc., C*, 935 (1966).
33. M. M. Martin and G. S. Gleicher, *J. Org. Chem.*, **28**, 3266 (1963).
34. T. P. Low and K. H. Lee, *J. Chem. Soc., B*, 535 (1970).
35. G. J. Gleicher, *J. Org. Chem.*, **33**, 332 (1968).
36. R. L. Huang and K. H. Lee, *J. Chem. Soc.*, 5963 (1964).
37. J. A. Howard and K. U. Ingold, *Can. J. Chem.*, **41**, 1744 (1963).
38. K. U. Ingold, *J. Phys. Chem.*, **64**, 1636 (1960).
39. I. H. Brownlie and K. U. Ingold, *Can. J. Chem.*, **45**, 2419 (1967).
40. J. A. Howard and K. U. Ingold, *Can. J. Chem.*, **41**, 2800 (1963).
41. H. Sakurai, A. Hasomi and K. Kumara, *J. Org. Chem.*, **35**, 993 (1970).
42. S. S. Kim, H. M. Koo and S. Y. Choi, *Tetrahedron Lett.*, **26**, 891 (1985).
43. S. S. Kim and S. C. Sohn, *Tetrahedron Lett.*, **23**, 3703 (1982).
44. E. P. Chang, R. L. Huang and K. H. Lee, *J. Chem. Soc., B*, 878 (1969).
45. K. H. Lee, *Tetrahedron*, **24**, 4793 (1968).
46. S. S. Kim, J. S. Seo and M. H. Yoon, *J. Org. Chem.*, **52**, 3691 (1987).
47. J. S. Hogg, D. H. Lohmann and K. E. Russell, *Can. J. Chem.*, **39**, 1588 (1961).
48. A. T. Blomquist and I. A. Berstein, *J. Am. Chem. Soc.*, **73**, 5546 (1951).
49. P. D. Bartlett and R. Hiatt, *J. Am. Chem. Soc.*, **80**, 1398 (1958).
50. P. D. Bartlett and D. M. Simons, *J. Am. Chem. Soc.*, **82**, 1753 (1960).
51. P. D. Bartlett and C. Rüchardt, *J. Am. Chem. Soc.*, **82**, 1756 (1960).
52. T. Koenig and R. Wolf, *J. Am. Chem. Soc.*, **91**, 2574 (1969).
53. T. Koenig, J. Huntington and R. Cruthoff, *J. Am. Chem. Soc.*, **92**, 5413 (1970).
54. S. S. Kim and A. Tuchkin, *J. Org. Chem.*, **64**, 3821 (1999).
55. R. C. Neumann, Jr. and R. J. Bussey, *J. Am. Chem. Soc.*, **92**, 2440 (1970).
56. R. C. Neumann, Jr. and J. V. Behar, *J. Am. Chem. Soc.*, **89**, 4549 (1967).
57. R. C. Neumann, Jr. and J. V. Behar, *J. Am. Chem. Soc.*, **91**, 6024 (1969).
58. R. C. Neumann, Jr. and J. V. Behar, *J. Org. Chem.*, **36**, 654 (1971).

10. Polar effects in decomposition of peroxidic compounds and related reactions 913

59. W. A. Pryor and K. Smith, *J. Am. Chem. Soc.*, **89**, 1741 (1967).
60. W. A. Pryor and K. Smith, *J. Am. Chem. Soc.*, **92**, 5403 (1970).
61. S. S. Kim, A. Tuchkin and C. S. Kim, *J. Org. Chem.*, **66**, 7738 (2001).
62. C. Walling and R. T. Clark, *J. Am. Chem. Soc.*, **96**, 4530 (1974).
63. K. W. Lee, N. Horowitz, J. Ware and L. A. Singer, *J. Am. Chem. Soc.*, **99**, 2622 (1977).
64. R. C. Neumann, Jr. and A. P. Sylwester, *J. Org. Chem.*, **48**, 2285 (1983).
65. L. F. Clarke, A. F. Hegarty and P. O'Neill, *J. Org. Chem.*, **57**, 362 (1992).
66. S. S. Kim, B. Liu, C. H. Park and K. H. Lee, *J. Org. Chem.*, **63**, 1571 (1998).
67. S. S. Kim, Y. Zhu and K. H. Lee, *J. Org. Chem.*, **65**, 2919 (2000).
68. J. M. Dust and D. R. Arnold, *J. Am. Chem. Soc.*, **105**, 1221 (1983).
69. X. Creary, M. E. Mehrsheikh-Mohammadi and S. McDonald, *J. Org. Chem.*, **52**, 3254 (1987).
70. (a) X.-K. Jiang and G.-Z. Ji, *J. Org. Chem.*, **57**, 6051 (1992).
(b) X.-K. Jiang, *Acc. Chem. Res.*, **30**, 283 (1997).
71. S. S. Kim, I. S. Baek, A. Tuchkin and K. M. Go, *J. Org. Chem.*, **66**, 4006 (2001).
72. (a) H. Eyring, *J. Chem. Phys.*, **3**, 107 (1935).
(b) S. Glasstone, K. J. Laidler and H. Eyring, *Theory of Rate Processes*, McGraw-Hill, New York, 1941.
73. The validity of RSP has been discussed by Exner: O. Exner, *J. Chem. Soc., Perkin Trans. 2*, **5**, 973 (1993). For a given reaction series four types of behavior are possible: (i) a valid RSP when the selectivity decreases with reactivity; (ii) anti-RSP when the reverse is true; (iii) indifferent behavior when the change in selectivity is negligible; (iv) a cross-over when RSP is valid in one part of the series and invalid in the other.
74. J. E. Leffler and E. Grunwald, *Rates and Equilibria of Organic Reactions*, Wiley, New York, 1963.
75. Y. Inoue, M. Ikeda, M. Kaneda, T. Sumimura, S. R. L. Everitt and T. Wada, *J. Am. Chem. Soc.*, **122**, 406 (2000).
76. The TS assumes a polar structure. However, the products are neutral species, i.e. $\text{YC}_6\text{H}_4\text{CH}_2^\bullet$, $(\text{CH}_3)_3\text{CO}^\bullet$ and CO_2 so that the reverse recombination to the perester molecule can not take place.
77. (a) M. G. Evans and M. Polanyi, *Trans. Faraday Soc.*, **34**, 11 (1938).
(b) M. G. Evans and E. Warhurst, *Trans. Faraday Soc.*, **34**, 614 (1938).
78. (a) R. P. Bell, *Proc. R. Soc. London, Ser. A*, **154**, 414 (1936).
(b) R. P. Bell, *J. Chem. Soc., Trans. Faraday 2*, **72**, 2088 (1976).
79. G. S. Hammond, *J. Am. Chem. Soc.*, **77**, 334 (1955).
80. J. E. Leffler, *Science*, **117**, 340 (1953).
81. E. R. Thornton, *J. Am. Chem. Soc.*, **89**, 2915 (1967).
82. R. More O'Ferrall, *J. Chem. Soc.*, 274 (1970).
83. W. P. Jencks, *Chem. Rev.*, **72**, 705 (1972).
84. W. J. Albery and M. M. Kreevoy, *Adv. Phys. Org. Chem.*, **16**, 87 (1978).
85. R. A. Marcus, *J. Phys. Chem.*, **72**, 891 (1968).
86. D. A. Jencks and W. P. Jencks, *J. Am. Chem. Soc.*, **99**, 7948 (1977).
87. C. F. Bernasconi, *Acc. Chem. Res.*, **25**, 9 (1992); *Adv. Phys. Org. Chem.*, **27**, 119 (1992).
88. S. S. Kim, H. R. Kim, H. B. Kim, S. J. Youn and C. J. Kim, *J. Am. Chem. Soc.*, **116**, 2754 (1994).
89. S. S. Kim and S. H. Lim, Submitted for publication.
90. S. S. Kim, S. Y. Choi and C. H. Kang, *J. Am. Chem. Soc.*, **107**, 4234 (1985).
91. S. S. Kim and C. S. Kim, *J. Org. Chem.*, **64**, 9261 (1999).
92. P. K. Das, M. V. Encinas, S. Steenken and J. C. Scaiano, *J. Am. Chem. Soc.*, **103**, 4162 (1981).
93. P. J. Wagner, Q. Cao and R. Pabon, *J. Am. Chem. Soc.*, **114**, 346 (1992).
94. M. Finn, R. Friedline, N. K. Suleman, C. J. Wohl and J. M. Tanko, *J. Am. Chem. Soc.*, **126**, 7578 (2004).
95. W. A. Pryor and W. H. Hendrickson Jr., *J. Am. Chem. Soc.*, **105**, 7114 (1983).

CHAPTER 11

Peroxides in biological systems

JEAN CADET

Laboratoire 'Lésions des Acides Nucléiques', LCIB-UMR-E n°3 CEA-UJF, Département de Recherche Fondamentale sur la Matière Condensée, CEA/Grenoble, F-38054 Grenoble Cedex 9, France
Fax: +33 43 878 5090; e-mail: jcadet@cea.fr

and

PAOLO DI MASCIO

Departamento de Bioquímica, Instituto de Química, Universidade de São Paulo, Ar. Prof. Lineu Prestes, 748 CP 26077, CEP 05513-970, São Paulo, SP, Brazil
Fax: +55 113 815 5579; e-mail: pdmascio@iq.usp.br

I. INTRODUCTION	917
II. DNA HYDROPEROXIDES	919
A. Thymine Components	921
1. Characterization	921
a. Base	921
b. Nucleoside	922
2. Mechanism of formation	922
a. Hydroxyl radical reactions	923
b. One-electron oxidation	925
c. Hydrogen atom and solvated electron addition	926
3. Synthesis	927
a. H ₂ O ₂ -mediated peroxidation of the 6-hydroxyl group of 5,6-dihydrothymine derivatives	927
b. H ₂ O ₂ -mediated substitution of the Br atom of thymine and thymidine bromohydrins	927
c. H ₂ O ₂ substitution of the halogen atom of thymidine iodohydrins in acidic solutions	928
d. 2-Methyl-1,4-naphthoquinone photosensitization of thymidine	929
e. Trifluoroacetic acid-H ₂ O ₂ peroxidation of pyrimidine nucleosides	929

The chemistry of peroxides, volume 2

Edited by Z. Rappoport © 2006 John Wiley & Sons, Ltd ISBN: 0-470-86274-2

f. Radiation-induced decomposition of 5,6-dihydrothymine	930
4. Decomposition pathways	930
5. Tandem base modifications	933
B. Uracil Components	933
1. Hydroxyhydroperoxides	933
2. Tandem base modifications	935
C. Cytosine Components	935
1. 6-Hydroxy-5-hydroperoxides	935
2. 5-Hydroxy-6-hydroperoxides	938
D. 5-Methyl-2'-deoxycytidine	939
1. Methyl oxidation products	939
2. Hydroxyhydroperoxides	939
E. Guanine Components	939
1. Radical oxidation reactions	940
2. Singlet oxygen oxidation reactions	941
F. 8-Oxo-7,8-dihydroguanine Components	943
1. Singlet oxygen oxidation reactions	943
2. One-electron oxidation pathways	943
III. LIPID HYDROPEROXIDES	945
A. Lipid Oxidation	945
1. Unsaturated fatty acids	945
a. 'Hock-cleavage' to carbonyl fragments	946
2. Cholesterol	946
B. Photooxidation	947
1. One-electron and hydroxyl radical oxidation	948
2. Singlet oxygen	949
a. Russell mechanism	949
b. Chemical trapping of ¹⁸ O-labeled singlet oxygen	951
c. Light emission of singlet oxygen	951
C. Lipid Peroxides and Nitrogen Species	951
1. Peroxynitrite	951
2. Hydroperoxide and nitrolipids	952
D. Endoperoxides and Dioxetanes	954
IV. PROTEIN HYDROPEROXIDES	954
A. Amino Acids and Peptides	954
1. Hydroxyl radical reactions	954
a. Peroxidation of the protein backbone	955
b. Peroxidation of the amino acid side-chain	955
i. Valine	956
ii. Leucine	956
iii. Lysine	959
iv. Tyrosine	960
v. Tryptophan	960
2. Other radical reactions	960
a. Tryptophan	962
b. Tyrosine	963
3. Singlet oxygen oxidation	966
a. Tryptophan and related compounds	966
b. Tyrosine	968
c. Histidine	968

11. Peroxides in biological systems	917
B. Proteins	970
1. Peroxide formation	970
a. Radical reactions	971
b. Peroxidase-mediated reactions	972
c. Singlet oxygen oxidation	972
2. Secondary reactions mediated by amino acid peroxides	972
a. Transfer within proteins	973
b. Protein cross-links	973
c. Lipid peroxidation	974
d. Nucleic acid–protein cross-links	974
e. Oxidation of DNA and nucleoside	975
V. CELLULAR INDICATORS OF HYDROPEROXIDES	975
A. Stable DNA Oxidation Products Arising from Nucleobase Hydroperoxide Decomposition	975
1. Hydroxyl radical-mediated thymine oxidation products	976
2. Singlet oxygen-induced formation of 8-oxo-7,8-dihydroguanine	976
B. Lipid Hydroperoxides and Related Degradation Products	977
1. Hydroperoxide measurement	977
2. Aldehydes and other breakdown products	977
3. Aldehyde adducts to biomolecules	978
a. DNA adducts	978
b. Protein adducts	984
C. Protein Hydroperoxides and Stable Degradation Products	985
1. Global assessment of hydroperoxides	986
2. Stable decomposition products	986
a. Carbonyl compounds	986
b. Hydroxylated valine and leucine residues as specific markers	987
VI. CONCLUSIONS	988
VII. ACKNOWLEDGMENTS	988
VIII. REFERENCES	988

I. INTRODUCTION

Occurrence of oxidation reactions within cells as the result of aerobic metabolism is now well established¹. In this respect, superoxide radical ($O_2^{\bullet-}$) is generated as a side-product of incomplete reduction of molecular oxygen during electron transport in mitochondria and endoplasmic reticulum². $O_2^{\bullet-}$ is also produced in macrophages and neutrophils as part of the host defense system via NADPH-mediated reduction of O_2 ³. There are other sources of rather unreactive $O_2^{\bullet-}$ including enzymic reactions mediated by, for example, xanthine oxidase, and metabolic activation of xenobiotics such as benz[*a*]pyrene⁴. Most of $O_2^{\bullet-}$ radicals undergo dismutation within cells either enzymatically or chemically, generating H_2O_2 —another reactive oxygen species which by itself exhibits a very low oxidizing activity toward most biomolecules. However, in the presence of reduced transition metals and particularly of Fe^{2+} , H_2O_2 is converted through the so-called Fenton reaction to either the strongly oxidizing $\bullet OH$ radical or a related reactive species⁵. Another possibility to generate $\bullet OH$ radical is provided by X- or gamma-radiolysis of water molecules⁶. It may be added that ionizing radiation as the result of direct interaction, high intensity UV laser pulses and type I photosensitizers are able to generate reactive intermediates, namely radical cations by one-electron oxidation of cellular targets^{6,7}.

Evidence has been accumulated during the last three decades on the strong implication of $\bullet\text{OH}$ radical and one-electron oxidants in the generation of hydroperoxides from several nucleobases, amino acids and unsaturated lipid components. Singlet oxygen ($^1\text{O}_2$) that may be produced among various possibilities by myeloperoxidase⁸, an enzyme implicated in inflammation processes, and by the UVA component⁷ of solar radiation is also a major source of peroxidation of several key cellular components. The breakdown products of the rather unstable hydroperoxide precursors thus produced from exposure to endogenous or exogenous oxidizing agents may be implicated in deleterious biological effects such as cellular lethality, aging, mutagenesis and carcinogenesis (Figure 1). It may be added that oxidative processes to biomolecules are also involved in the etiology of other diseases including arteriosclerosis, arthritis, cataract and diabetes. Emphasis is placed in this chapter on the description of the main peroxidation reactions initiated by $\bullet\text{OH}$ radical, one-electron oxidants and singlet oxygen within key cellular targets including pyrimidine and purine nucleobases, several lipid components and amino acids. In addition, information is provided on the molecular effects of the initial formation of the above hydroperoxides within cellular components. Thus, several stable degradation products of nucleobase hydroperoxides that may be considered as the chemical signature of the formation of the latter unstable compounds were measured within cellular DNA⁹. Indicators of lipid peroxidation that may involve cholesterol hydroperoxides and several degradation products including malondialdehyde (MDA), 4-hydroxy-2-nonenal (4-HNE), 4-hydroxyhexenal (4-HHE) and F(2) isoprostane are also available¹⁰. Increasing interest is now given to the measurement of adducts between amino-substituted nucleobases and reactive aldehydes such as MDA and 4-HNE that may arise from the breakdown of initially generated unstable lipid peroxides¹¹. Evidence has also been provided for the accumulation of oxidatively damaged proteins with age in tissues¹². It was also shown that protein oxidation reactions which often involve initial $\bullet\text{OH}$ radical or $^1\text{O}_2$ -mediated peroxidation of targeted amino acids are implicated in several diseases including advanced human atherosclerotic plaque¹³ and cataractogenesis¹⁴. Measurement of several side-chain altered amino residues

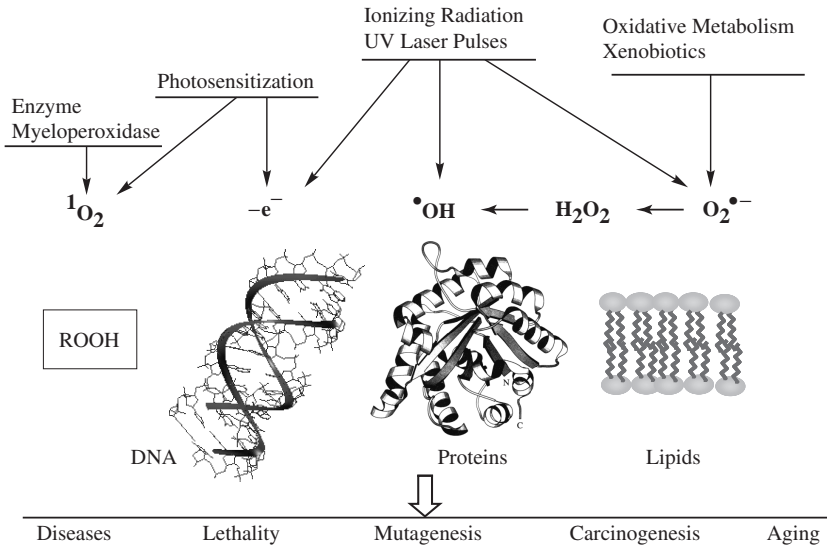
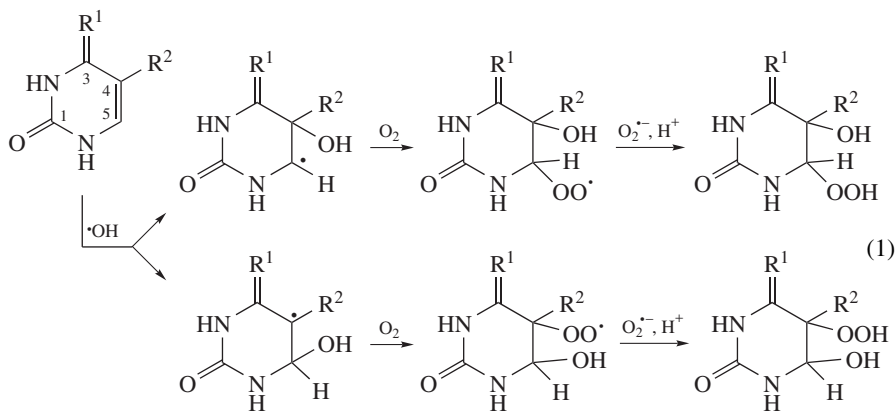


FIGURE 1. Oxidative reactions of biomolecules and biological consequences

that often arise from the fate of initially generated peroxides is used as bio-indicators of protein oxidation within cells¹⁵.

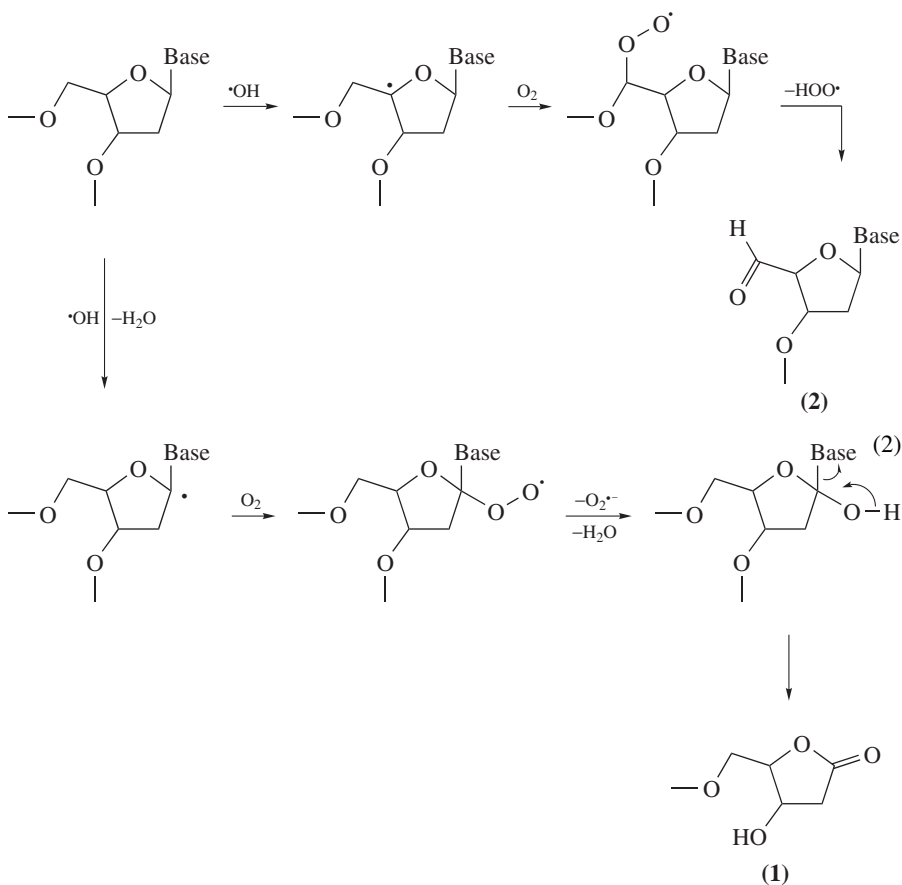
II. DNA HYDROPEROXIDES

First evidence for the radiation-induced formation of organic hydroperoxides within isolated DNA in aerated aqueous solution was provided 50 years ago¹⁶. This was achieved by colorimetric titration. Thus, the formation of H_2O_2 that is also shown to occur by X-ray radiolysis of aerated aqueous solutions of DNA was assessed using titanium sulfate, the so-called Eisenberg reagent¹⁷, whereas the overall amount of hydrogen peroxide and organic peroxides was determined on the basis of KI oxidation and subsequent iodine release as triiodide ion (I_3^-). Subsequently, it was shown using nucleic acid components that pyrimidine bases and in particular thymine were the preferential targets for the radiation-induced formation of relatively stable hydroperoxides¹⁸, at neutral and slightly acidic pH values¹⁹. It may be pointed out that organic peroxides have been also detected upon exposure of uracil to $\cdot OH$ radical in aerated aqueous solutions. However, they are shorter-lived species than the thymine homologues whereas cytosine hydroperoxides are even more labile²⁰. Later on, it was confirmed from the uptake of dioxygen following exposure of naked nucleic acids and their constituents to gamma rays in N_2O/O_2 (4:1) saturated aqueous solutions that pyrimidine bases are the main targets for radiation-induced peroxidation of nucleic acid components²¹. Thus, the yield of consumed oxygen was at least three times higher for the three pyrimidine bases including thymine, cytosine and uracil than for adenine and guanine nucleotides. The formation of the main hydroperoxides for thymine, cytosine and 5-methylcytosine are mostly accounted for by initial $\cdot OH$ radical addition to either C5 or C6 followed by fast O_2 addition to the resulting pyrimidyl radicals. Then, the transient peroxy radicals thus generated are reduced by superoxide (equation 1).



	R ¹	R ²
Thymine	O	CH ₃
Uracil	O	H
Cytosine	NH	H
5-Methylcytosine	NH	CH ₃

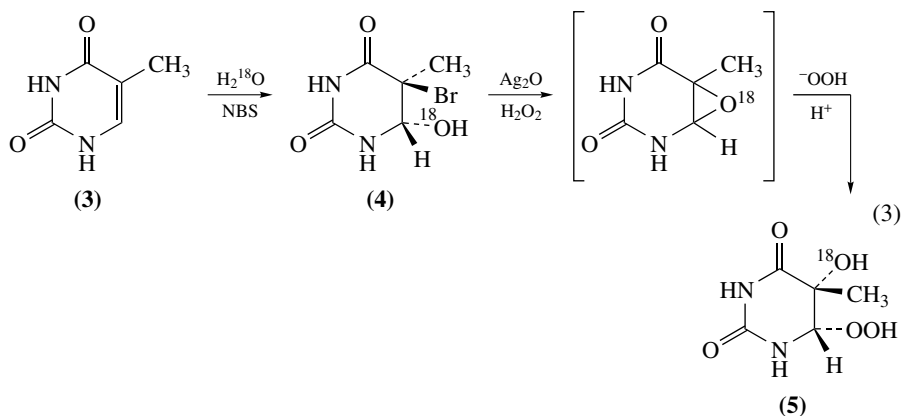
It may be added that radiation-induced carbon-centered radicals within the 2-deoxyribose moiety of DNA are also prone to fast molecular oxygen addition and subsequent formation of peroxy radicals at C1, C3, C4 and C5. However, stable related hydroperoxides have not been detected using the above colorimetric approach upon X-ray irradiation of aerated aqueous solutions of purine and pyrimidine ribonucleotides²². Furthermore, detailed information is now available on the chemical reactions of the C1 and the C5 peroxy radical of the sugar moiety of 2'-deoxyribonucleosides and/or DNA²³. Thus, elimination of superoxide radical from the peroxy group at C1 rather than hydroperoxide formation was inferred from an ¹⁸O-labeling²⁴ and pulse radiolysis²⁵ experiments. The resulting sugar carbocation is likely to undergo nucleophilic addition of water leading to the cleavage of the *N*-glycosidic bond and formation of 2-deoxyribonolactone (1) (equation 2). It may be added that the formation of a 5'-aldehyde function in 2 from the peroxy radical at C5' of nucleosides and DNA may be rationalized in terms of hydroperoxide radical (HO₂•) elimination according to a well-established mechanism for α-hydroxyperoxy radical²¹ as shown in equation 2.



A. Thymine Components

1. Characterization

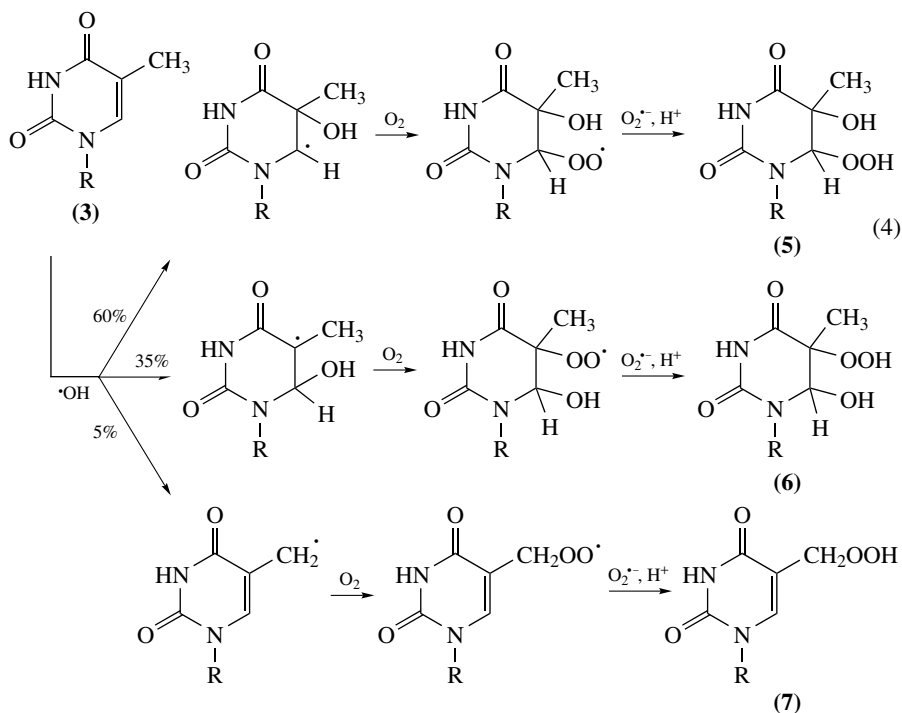
a. Base. The colorimetric detection of radiation-induced organic peroxides in aerated solutions of DNA has been accounted for by the generation of hydroxyhydroperoxides²⁶ involving initial addition of a $\bullet\text{OH}$ radical across the 5,6-ethylenic bond of pyrimidine bases, in fact predominantly thymine (3). This received confirmation from the isolation of two pairs of radiation-induced *cis* and *trans* isomers by paper chromatography²⁷ that were tentatively assigned as 5-hydroperoxy-6-hydroxy-5,6-dihydrothymine and 6-hydroperoxy-5-hydroxy-5,6-dihydrothymine^{27,28}. All the four hydroperoxides were synthesized in a more or less specific way using three synthetic pathways that will be discussed later (Section II.A.3). It may be stressed that the initial assignment of both the stereoconfiguration and the position of the peroxidic group was in error, leading to a confusing situation that was clarified almost 15 years later. First it was shown that the initially proposed *cis* and *trans* configurations have to be inverted²⁹. The determination of the peroxidation site was based on the substitution of the bromine atom of *trans*-5-bromo-6-hydroxy-5,6-dihydrothymine (4) by H_2O_2 in the presence of Ag_2O catalyst. Thus, it was proposed that the substitution reaction gives rise to *trans*-6-hydroperoxy-5-hydroxy-5,6-dihydrothymine. In fact the correct structure for the main product of the reaction that involves a 1,2-shift of the peroxidic group with inversion of configuration at C5 was established as *cis*-6-hydroperoxy-5-hydroxy-5,6-dihydrothymine (5) (equation 3). Subsequently, mass spectrometric studies involving specific ^{18}O -labeling experiments have allowed the complete reassignment of the four *cis* and *trans* isomers of thymine hydroxyhydroperoxides³⁰. Further support for the proposed structures was gained from detailed ^1H ³¹ and ^{13}C NMR³² spectra. As a striking feature, we mention the observation of a ^3J scalar coupling between the C6 hydroxyl group and H6 in the ^1H NMR spectrum of *trans*-5-hydroperoxy-6-hydroxy-5,6-dihydrothymine^{31a} showing that the peroxidic group is located at C5. More recently, the X-ray crystal structure of *cis*-5-hydroperoxy-6-hydroxy-5,6-dihydrothymine was solved providing final unambiguous structural proof. In addition, the electronic properties of the latter hydroperoxide were obtained from *ab initio* theoretical investigations³³ using the crystallographic coordinates as the key parameters.



b. Nucleoside. The main oxidation products of thymidine (**1**, dR = 2-deoxyribose) arising from the reaction of $\bullet\text{OH}$ radical in aerated aqueous solution have been isolated by high performance liquid chromatography analysis and fully characterized^{30b,34}. About 50% of the overall decomposition products are represented by nine hydroperoxides³⁵ that were assigned as the *cis* and *trans* diastereomers of 6-hydroperoxy-5-hydroxy-5,6-dihydrothymidine (**5**) and 5-hydroperoxy-6-hydroxy-5,6-dihydrothymidine (**6**) together with 5-(hydroperoxymethyl)-2'-deoxyuridine (**7**) (equation 4). Interestingly, the structure of thymidine (Thd) hydroperoxides **5–7** that was inferred from extensive ^1H and ^{13}C NMR measurements^{30b,34c,36} was confirmed by chemical synthesis using several approaches (*vide infra*). Thus, the position of the peroxidic group and the stereoconfiguration of the 5,6-substituents was unambiguously assigned by considering the α and γ effects associated with the presence of the electronegative and bulky OOH function. Further support for the stereoconfiguration of the peroxidic group was gained from the stereoselective conversion of each of the 8 diastereomers of hydroxyhydroperoxides into the corresponding 4 diastereomeric 5,6-dihydroxy-5,6-dihydrothymidine (**8**) by reduction of the C–OOH with either KI or H_2S that occurs with retention of configuration at the C–O bond. The NMR features of each of the thymidine diol thus specifically obtained was compared with those of authentic 5,6-dihydroxy-5,6-dihydrothymidine diastereomers (**8**)³⁷ whose absolute configuration was previously established³⁸. This was achieved using a chemical approach which received further confirmation from the determination of the crystal structure of the (+)-*cis*-(5*R*,6*S*) and (–)-*cis*-(5*S*,6*S*) diastereomers of **8**³⁹. Assignment of 5-(hydroperoxymethyl)-2'-deoxyuridine (**7**) was also accomplished by ^1H NMR and ^{13}C NMR spectra. Interestingly, the formation of 5-(hydroperoxymethyl)-2'-deoxyuridine (**7**) was observed within calf thymus DNA upon exposure to gamma rays in aerated aqueous solution at a dose as low as 30 Gy. This was assessed after enzymic digestion of oxidized DNA into nucleosides and subsequent analysis using a sensitive HPLC-tandem mass spectrometry detection method⁴⁰. Evidence was provided that hydroperoxides constitute about 50% of the radiation-induced base damage within DNA using colorimetric measurements based on the reduction of the organic peroxides⁴¹. Two subgroups that differ by the decay kinetics, which in both cases are exponential, were detected. The main component that exhibits the slower decay (half-life of 100 h at 22 °C) is likely to correspond to thymine hydroperoxides. Further work is required to characterize the thymine hydroxyhydroperoxides within DNA, likely by using the accurate and sensitive HPLC-MS/MS method as already applied to the detection of 5-(hydroperoxymethyl)-2'-deoxyuridine (**7**) (*vide supra*).

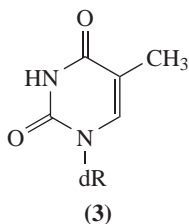
2. Mechanism of formation

An almost complete description of both $\bullet\text{OH}$ radical-mediated and one-electron oxidation reactions of the thymine moiety (**3**) of DNA and related model compounds is now possible on the basis of detailed studies of the final oxidation products and their radical precursors. Relevant information on the structure and redox properties of transient pyrimidine radicals is available from pulse radiolysis measurements that in most cases have involved the use of the redox titration technique⁴². It may be noted that most of the rate constants implicating the formation and the fate of the latter radicals have been also assessed. This has been completed by the isolation and characterization of the main thymine and thymidine hydroperoxides that arise from the fate of the pyrimidine radicals in aerated aqueous solutions. Information is also available on the formation of thymine hydroperoxides as the result of initial addition of radiation-induced reductive species including $\text{H}\bullet$ atom and solvated electron.

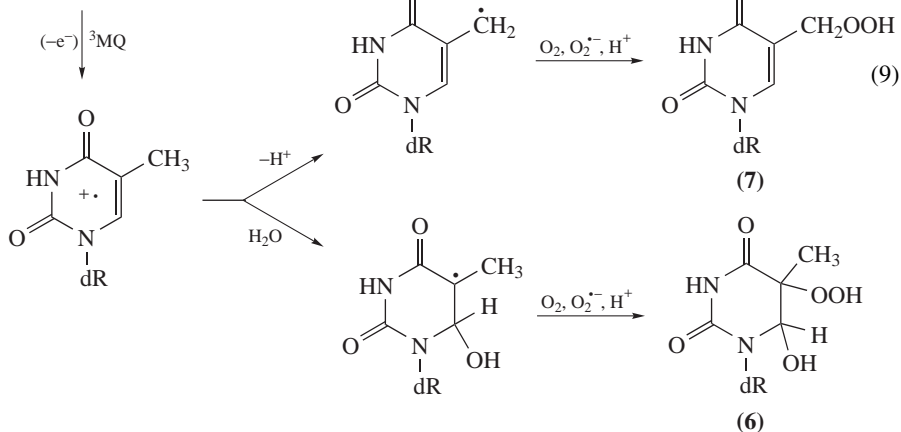


a. Hydroxyl radical reactions. The predominant reaction of $\bullet\text{OH}$ radical with the thymine base (**3**, R = H) has been shown to be addition (60%) at carbon C5^{6,42a} leading to the formation of the reducing 5-hydroxy-5,6-dihydrothym-6-yl radical (equation 4). The oxidizing 6-hydroxy-5,6-dihydrothym-5-yl radical that arises from the addition of the $\bullet\text{OH}$ radical at C6 is generated in a lower yield (35%). The third reaction, which is a minor process (5%), at least for the free base and nucleoside, gives rise to the aromatic 5-(uracilyl)methyl radical. Then, as a common process, the initially generated pyrimidine transient species are converted into the corresponding peroxy radicals by a fast reaction with dioxygen that is controlled by diffusion²¹. About half of the latter peroxy radicals are converted into hydroperoxides **5-7** in γ -irradiated aqueous solutions of thymine (**3**, R = H) or thymidine (**3**, R = 2-deoxyribose) saturated with either air or oxygen. Reduction of the peroxy radical by superoxide radical followed by protonation of the resulting anionic intermediate constitute the sequence of events leading to the corresponding hydroperoxide as suggested earlier^{18c} and confirmed later⁴³. Interestingly, at least, in slightly acidic and neutral aqueous solutions, the formation yield of 5-hydroxy-6-hydroperoxides is higher than that of the isomeric 6-hydroxy-5-hydroperoxides, in agreement with the preferential addition of $\bullet\text{OH}$ radical to the C5 carbon. Another striking feature deals with the predominance of the *trans* isomer for each of the two pairs of 5-(6)-hydroperoxy-6-(5)-hydroxy-5,6-dihydrothymidine, suggesting a preferential *trans*

photosensitization mechanism^{7,47} has been used to efficiently generate the pyrimidine radical cation of thymidine through one-electron oxidation. Two main degradation pathways were inferred from isolation and characterization of the predominant oxidized nucleosides including five hydroperoxides that consist of **7** and four *cis* and *trans* diastereomers of 5-hydroperoxy-6-hydroxy-5,6-dihydrothymidine (**6**) may be rationalized in terms of the specific generation of the oxidizing 6-hydroxy-5,6-dihydrothymid-5-yl radical through hydration of the thymidine radical cation at C6⁴⁸. The competitive deprotonation reaction of the latter intermediate is likely to explain the formation of 5-(hydroperoxymethyl)-2'-deoxyuridine (**7**), which represents about 40% of the total of thymidine hydroperoxides. Interestingly, both the C5 carbon-centered radical and the methyl radical, the respective precursors of hydroperoxides **6** and **7**, have been identified by ESR/spin-trapping experiments⁴⁹.

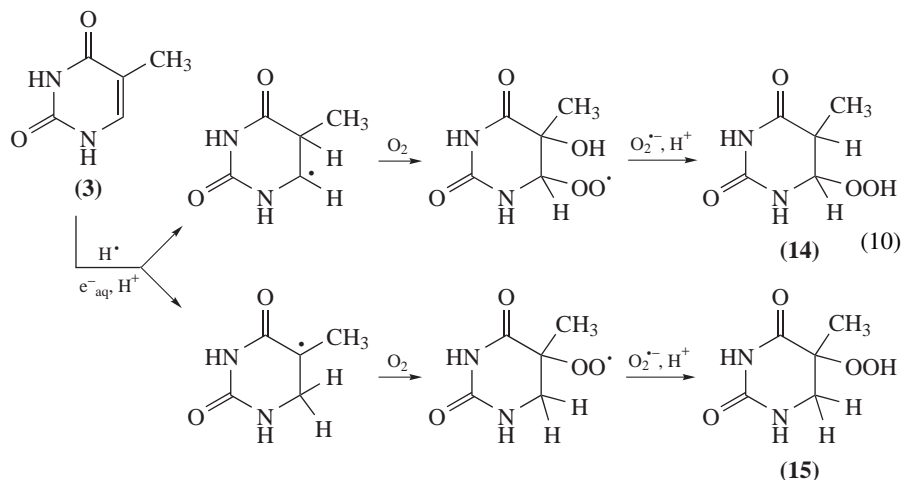


dR = 2-deoxyribose



c. Hydrogen atom and solvated electron addition. Three hydroperoxides, namely 5-hydroperoxy-5,6-dihydrothymine (**15**) together with the *cis* and *trans* isomers of 6-hydroperoxy-5,6-dihydrothymine (**14**), have been isolated and characterized among other hydroperoxides (*vide supra*) in the gamma-irradiated aerated aqueous solution of thymine²⁹ (equation 10). This is accounted for by initial formation of 5,6-dihydrothym-5-yl and 5,6-dihydrothym-6-yl radicals upon addition of H[•] atom and/or solvated electron that have not been fully scavenged by dioxygen. H[•] atom has been shown to mostly add to the C5 atom whereas preferential addition of solvated electron at C6 is followed by protonation, leading to 5,6-dihydrothym-5-yl radical. The formation of the peroxides is likely to be

explained by usual pathways that involve generation of related peroxy radicals and their subsequent reduction.

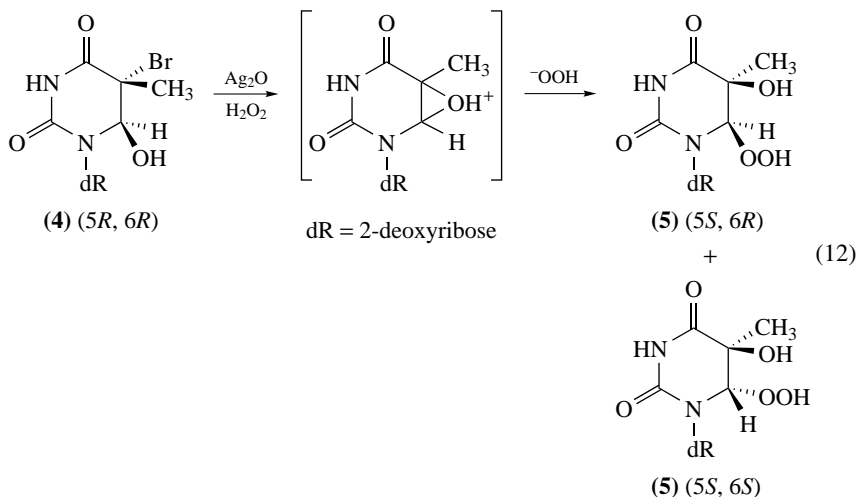
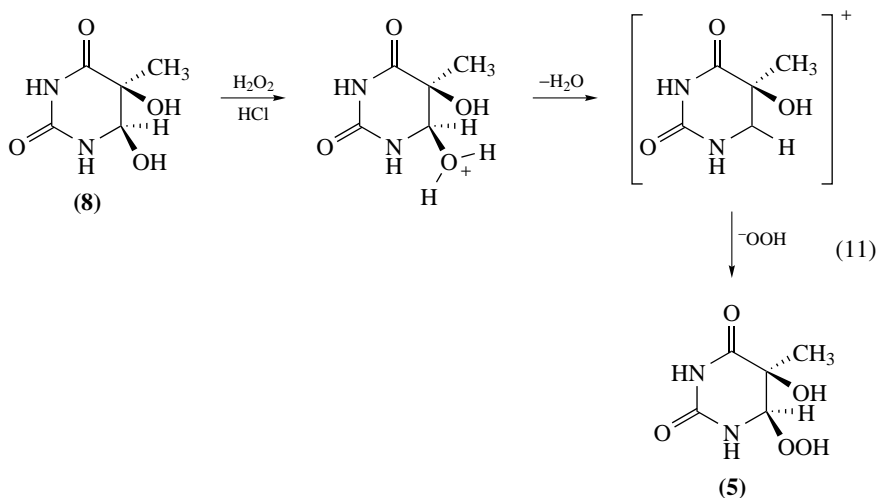


3. Synthesis

a. H₂O₂-mediated peroxidation of the 6-hydroxyl group of 5,6-dihydrothymine derivatives. Incubation of the *cis* isomer of 5,6-dihydroxy-5,6-dihydrothymine **8** in concentrated H₂O₂ solution (15% v/v) in the presence of HCl²⁷ leads to the quantitative formation of the *cis*-6-hydroperoxide **6**^{30a} (equation 11). This may be accounted for by the acid-catalyzed formation of a cationic intermediate^{34a} followed by nucleophilic addition of H₂O₂. The high stereospecificity of the latter reaction may be rationalized in term of steric hindrance provided by the 5-substituent, the HOOH-mediated attack occurring on the side that carries the smaller substituent, namely the OH group⁵⁰. Similar treatment of *cis*-6-hydroxy-5,6-dihydrothymine generates in excellent yields the *cis* and *trans* 6-hydroperoxy-5,6-dihydrothymine (**14**) in the relative ratio 6:4⁵¹. On the other hand, 5-hydroxy-5,6-dihydrothymine is completely unreactive to the latter peroxidation conditions. It may be pointed out that the peroxidation reaction of 6-hydroxylated 5,6-dihydrothymine derivatives is not applicable to related nucleosides due to the occurrence of side-reactions within the 2-deoxyribose moiety.

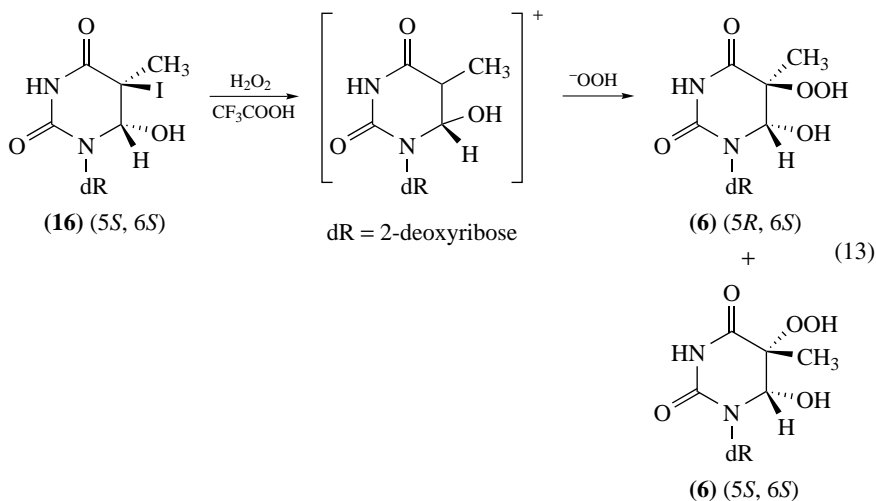
b. H₂O₂-mediated substitution of the Br atom of thymine and thymidine bromohydrins. Substitution of the halogen atom of *trans*-5-bromo-(iodo)-6-hydroxy-5,6-dihydrothymine and related (5*R*,6*R*) and (5*S*,6*S*) *trans* diastereomers of related 2'-deoxyribonucleosides by H₂O₂ in the presence of Ag₂O catalyst has been shown to give rise predominantly to *cis*-5-hydroxy-6-hydroperoxides. Typically, under the latter conditions the conversion of *trans*-(5*R*,6*R*)-5-bromo-6-hydroxy-5,6-dihydrothymidine (**4**, dR = 2-deoxyribose)⁵² leads to the formation of the *cis*-(5*S*,6*R*) and the *trans*-(5*S*,6*S*) diastereomers of 6-hydroperoxy-5-hydroxy-5,6-dihydrothymidine (**5**) in a ratio 4:1 (equation 12). Conversely, the two other 6-hydroperoxides, namely the *cis*-(5*R*,6*S*) and the *trans*-(5*R*,6*R*) diastereomers, are produced in a similar ratio from the *trans*-(5*S*,6*S*)-Thd bromohydrin. The mechanism of formation of the four diastereomers of **5** may be rationalized in terms of an anionotropic rearrangement that implies a concerted loss of the halogen atom and an intramolecular

OH^- group attack with anchimeric assistance. This is likely to lead to a transient bridged intermediate. Since the migrating group is on the opposite side of the pyrimidine ring with respect to the leaving group, the rearrangement displays a strong *anti* character. As a result, an inversion of configuration at C5, the so-called 'migration terminus', is expected whereas the entering nucleophilic OOH group takes place preferentially with retention of the initial stereochemistry. It may be noted that the 1,2-hydroxyl shift from the 6 to the 5 position was previously inferred from mass spectrometry analysis of the *cis* thymine diol upon Ag_2O -mediated substitution of the halogen atom of [^{18}O -6]-labeled 5-bromo-6-hydroxy-5,6-dihydrothymine (**4**) in aqueous solution^{37a}.



c. H_2O_2 substitution of the halogen atom of thymidine iodohydrins in acidic solutions. The synthesis of the two pairs of *cis* and *trans* diastereomers of 6-hydroxy-5-hydroperoxy-5,6-dihydrothymidine (**6**) is based on the lability of the C–I bond of the *trans* diastereomers

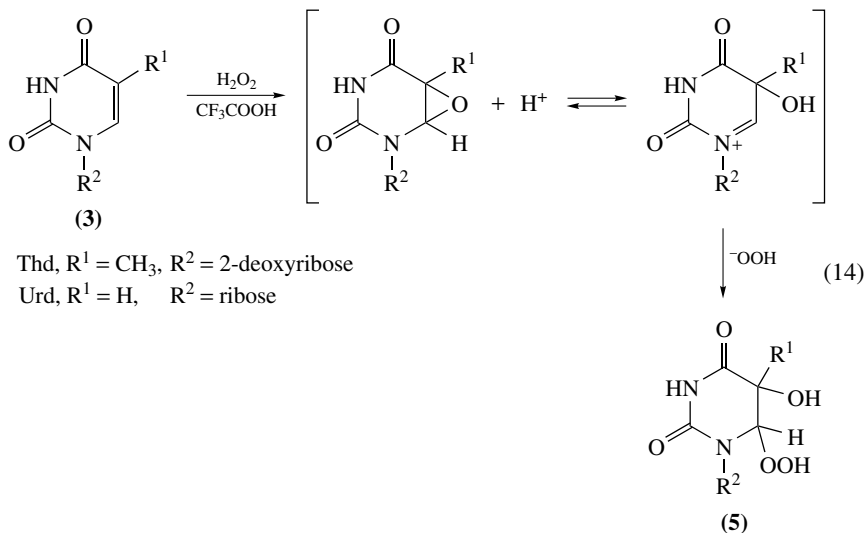
of 6-hydroxy-5-iodo-5,6-dihydrothymidine (**16**) in aqueous acidic solutions. The two latter precursors were prepared by reaction of *N*-iodosuccinimide with Thd in dimethyl sulfoxide before being efficiently separated by HPLC on an ODS column, the *5R,6R* diastereomer being predominant^{36a,53}. Typically, treatment of *trans*-(*5R,6R*)-6-hydroxy-5-iodo-5,6-dihydrothymidine (**16**, dR = 2-deoxyribose) with 15% H₂O₂ in the presence of trifluoroacetic acid for 24 h gives rise to the *trans*-(*5R,6R*) and *cis*-(*5S,6R*) diastereomers of 6-hydroxy-5-hydroperoxy-5,6-dihydrothymidine (**6**) in a ratio 4:1. Similarly, the conversion of the *trans*-(*5S,6S*) diastereomer of Thd iodohydrin **16** was found to generate the other pair of 6-hydroxy-5-hydroperoxides, the *trans*-(*5S,6S*) form being produced in about 4-fold higher yield than the *cis*-(*5R,6S*) diastereomer (equation 13). The observed stereochemistry of the main reaction product that implies preferential retention of the configuration at C5 together with the kinetics of the halogen substitution may be accounted for by a S_N1-type mechanism.



d. 2-Methyl-1,4-naphthoquinone photosensitization of thymidine. As already discussed, the one-electron oxidation of the pyrimidine moiety of thymidine (**3**, dR = 2-deoxyribose) by UVA-excited menadione was found to efficiently generate the four *cis* and *trans* diastereomers of 6-hydroxy-5-hydroperoxy-5,6-dihydrothymidine (**6**) together with 5-(hydroperoxymethyl)-2'-deoxyuridine (**7**) in a ratio 6:4. It may be added that the separation of the five hydroperoxides that represent overall about 50% of the photosensitized decomposition products can be efficiently achieved by HPLC on octadecylsilyl silica gel (ODS) columns, providing easy access to the above precursor compounds.

e. Trifluoroperacetic acid-H₂O₂ peroxidation of pyrimidine nucleosides. Incubation of Thd with trifluoroacetic acid in the presence of 30% (v/v) of H₂O₂ has been found to lead to the formation of the *cis* and *trans* diastereomers of 6-hydroperoxy-5-hydroxy-5,6-dihydrothymidine (**5**) with a preponderance of the former diastereomeric nucleosides^{34c}. A likely mechanism for the specific formation of the 6-hydroperoxides involves initial CF₃CO₃H-mediated generation of an epoxide structure that may exist in a dynamic equilibrium with a zwitterion, followed by a nucleophilic addition of H₂O₂ (equation 14). Interestingly, this leads to a similar product distribution that has been observed for the substitution of thymidine halohydrins by H₂O₂. However, a competitive intramolecular

reaction of the 5' OH group, that provides further support for the transient formation of intermediates **5** and/or **6**, was found to give rise to *O*⁶,5'-cyclo-5-hydroxy-5,6-dihydrothymidine^{34c}. It may be noted that a similar specific hydroxyhydroperoxidation of the base moiety of uridine has also been observed using the same experimental procedure⁵⁴.



f. Radiation-induced decomposition of 5,6-dihydrothymine. 5-Hydroperoxy-5,6-dihydrothymine (**15**) and the *cis* and *trans* isomers of 6-hydroperoxy-5,6-dihydrothymine (**14**) have been shown to be minor radiation-induced decomposition products of thymine (**1**) in aerated aqueous solutions^{29a}. A more efficient way to generate the 5- and 6-hydroperoxides is to expose 5,6-dihydrothymine to $\bullet\text{OH}$ radical in aerated or in $\text{N}_2\text{O}/\text{O}_2$ (75/25 v/v) saturated aqueous solutions⁵⁵. Thus, under the latter conditions^{43,56} where most of initially generated solvated electrons are converted into $\bullet\text{OH}$ radical, 5-hydroperoxy-5,6-dihydrothymine (**15**) and the *cis* and *trans* isomers of 6-hydroperoxy-5,6-dihydrothymine (**14**) are generated in about 4:6:3 ratio, representing overall almost 1/3 of the radiation-induced decomposition products. Hydrogen abstraction by $\bullet\text{OH}$ radical at C5 and C6, followed by fast O_2 addition to the resulting 5-yl and 6-yl pyrimidine radicals, respectively, constitute the first steps of the reaction leading to the formation of **14** and **15**.

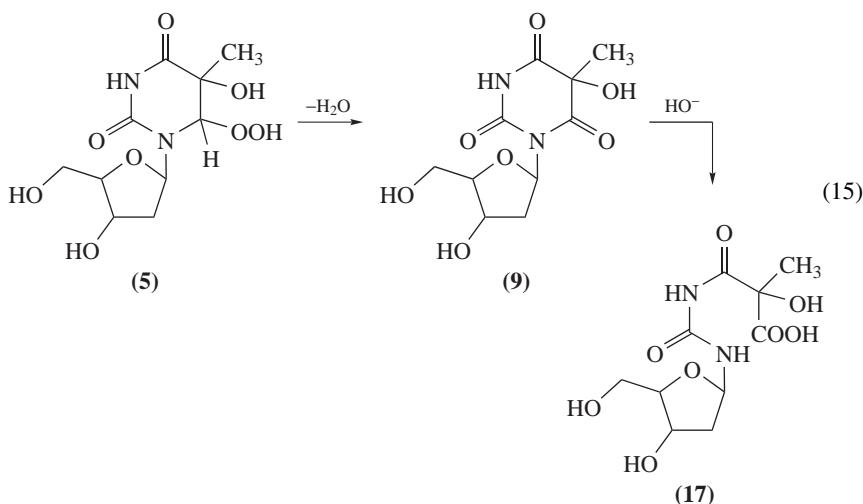
4. Decomposition pathways

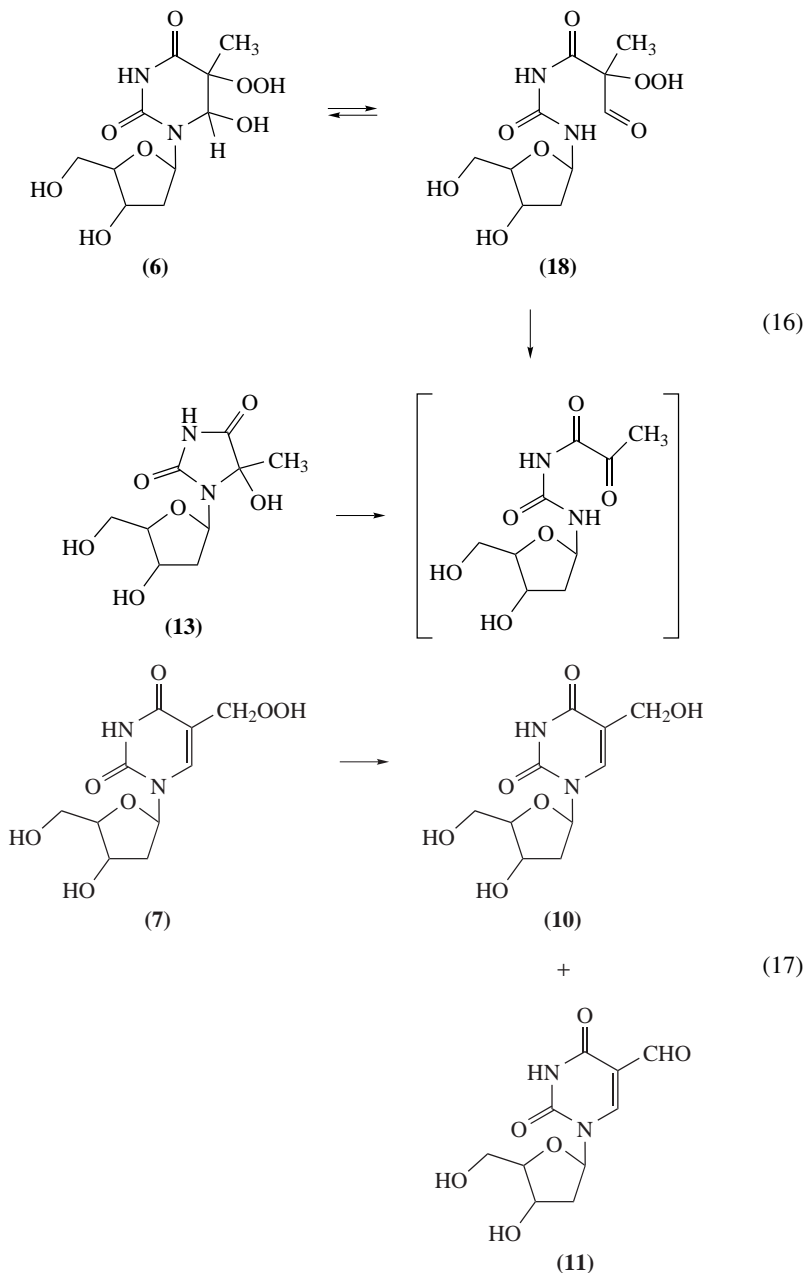
The lifetimes of the 9 main thymidine hydroperoxides **5–7** that were determined in pure aqueous solutions at 37 °C were found to vary from 1 h for the two *trans* diastereomers of 6-hydroperoxides (Table 1) to several weeks for 5-(hydroperoxymethyl)-2'-deoxyuridine. It may be added that the *cis* diastereomers are more stable than the *trans* homologues, irrespective of the pair of diastereomeric hydroperoxides. Interestingly, at neutral or slightly acidic pH values a specific hydrolytic decomposition pathway was observed for the two classes of hydroxyhydroperoxides. Thus, it was found that the *trans* and

TABLE 1. Kinetic and thermodynamic parameters of the 8 *cis* and *trans* diastereomers of 6-hydroperoxy-5-hydroxy-5,6-dihydrothymidine (**5**) and 5-hydroperoxy-6-hydroxy-5,6-dihydrothymidine (**6**)^{34c}

	Half-life (h)		ΔH (kcal mol ⁻¹)	ΔS (cal ⁻¹ mol K ⁻¹)
	22 °C	37 °C		
<i>cis</i> -(5 <i>S</i> ,6 <i>R</i>) 5	66	10.4	22.9 ± 0.6	-7.4 ± 1.9
<i>cis</i> -(5 <i>R</i> ,6 <i>S</i>) 5	66	10.4	22.9 ± 0.3	-7.4 ± 0.9
<i>trans</i> -(5 <i>R</i> ,6 <i>R</i>) 5	7.3	1.0	24.5 ± 0.3	+2.3 ± 1.2
<i>trans</i> -(5 <i>S</i> ,6 <i>S</i>) 5	12	1.6	25.2 ± 0.4	+3.7 ± 1.2
<i>cis</i> -(5 <i>S</i> ,6 <i>R</i>) 6	172	16.4	28.5 ± 1.5	+9.7 ± 4.9
<i>cis</i> -(5 <i>R</i> ,6 <i>S</i>) 6	542	34.6	35.2 ± 1.5	+30.0 ± 4.7
<i>trans</i> -(5 <i>R</i> ,6 <i>R</i>) 6	85	8.5	28.9 ± 0.9	+12.4 ± 2.8
<i>trans</i> -(5 <i>S</i> ,6 <i>S</i>) 6	104	9.6	29.9 ± 0.8	+15.3 ± 2.3

cis diastereomers of 6-hydroperoxide **5** are predominantly converted into *N*¹-(2-deoxy- β -D-*erythro*-pentofuranosyl)-*N*³-tartronylurea (**17**) through intermediacy of hydrolyzable (5*R*^{*})- and (5*S*^{*})-1-(2-deoxy- β -D-*erythro*-pentofuranosyl)-5-hydroxy-5-methylbarbituric acid (**9**) (equation 15). The formation of the latter compounds is explained by elimination of a water molecule, a likely reaction of secondary hydroperoxides. On the other hand, a totally different decomposition pathway is observed for the 5-hydroperoxides **6**, since this leads to the predominant formation of the (5*R*^{*})- and (5*S*^{*})-diastereomers of 1-(2-deoxy- β -D-*erythro*-pentofuranosyl)-5-hydroxy-5-methylhydantoin (**13**) via the ring-opened **18**^{34c}. A likely mechanism for the formation of the latter diastereomeric nucleosides involves opening of the 1,6-bond through ring-chain tautomerism, followed by α -cleavage of the linear hydroperoxide **18** thus generated and subsequent cyclization of the pyruvylurea residue (equation 16). The decomposition of 5-(hydroperoxymethyl)-2'-deoxyuridine (**7**) is also specific, since the corresponding alcohol **10** is generated in more than 90% yield with only traces of 5-formyl-2'-deoxyuridine (**11**) (equation 17).





The situation is completely different when metal ions are added to the solution of 5-(hydroperoxymethyl)-2'-deoxyuridine (7). It was found that Cu^+ and to a lesser extent Fe^{2+} promotes the formation of **11** at the expense of **10** in the metal-induced decomposition

of **7**⁵⁷. The lack of any specificity in the pattern of degradation products of the thymidine hydroperoxides **5** and **7** after chromatographic separation on thin-layer silica gel plates may be explained by the presence of contaminant metal ions that also accelerate the decomposition of the peroxides. This should promote the formation of oxyl radical through an organic Fenton reaction, giving rise to formamide (**12**) and 5-hydroxy-5-methylhydantoin nucleosides (**13**). Another possibility provided by Fe^{2+} is the reduction of the hydroperoxides into the related alcohols.

5. Tandem base modifications

Several lines of evidence support the fact that 5- and 6-hydroperoxyl radicals of pyrimidine bases are able to modify an adjacent guanine either 3' or 5' within oligonucleotides and DNA. This leads to the formation of so-called tandem base lesions, that have been shown to consist of a formamide **12** (Fo) and a 8-oxo-7,8-dihydroguanine (8-oxoGua) residue when the reaction is initiated on the thymine moiety by either addition of a $\bullet\text{OH}$ radical across the 5,6-ethylenic bond or one-electron oxidation of the pyrimidine ring⁵⁸. Interestingly, the formation of both sequence isomers, namely 8-oxoGua/Fo and Fo/8-oxoGua, was assessed as the related dinucleoside monophosphates using a recently designed HPLC-MS/MS assay^{58b}. It was found that both tandem lesions are generated linearly with a low dose range (5–100 Gy), providing further support to the fact that only one radical event hit is involved in their formation. Thus, the radiolytic yield for the induction of 8-oxoGua/Fo, Fo/8-oxoGua and 8-oxoGua was found to be 0.0001, 0.0013 and 0.0130 $\mu\text{mol J}^{-1}$, respectively. A reasonable mechanism to explain the formation of the tandem base lesions involves initial generation of 5-hydroxy- and 6-hydroxy-5,6-dihydrothymyl radicals from the thymine residue of dinucleoside monophosphate **19** (equation 18). This is followed by fast reaction of molecular oxygen with pyrimidyl radicals thus generated, leading to the formation of the corresponding peroxy radicals as previously discussed. Evidence for intramolecular addition of peroxy radicals to the C8 position of vicinal guanine was gained from ¹⁸O-labeled experiments⁵⁹. In a subsequent step, the peroxy adduct would rearrange giving rise to 8-oxoGua on the one hand and an oxyl-type pyrimidine radical on the other hand. As already discussed, the latter alkoxy radical is expected to undergo the scission of the 1,6-pyrimidine bond through a β -scission mechanism with a subsequent formation of the formamide remnant leading to Fo/8-oxoGua **20**.

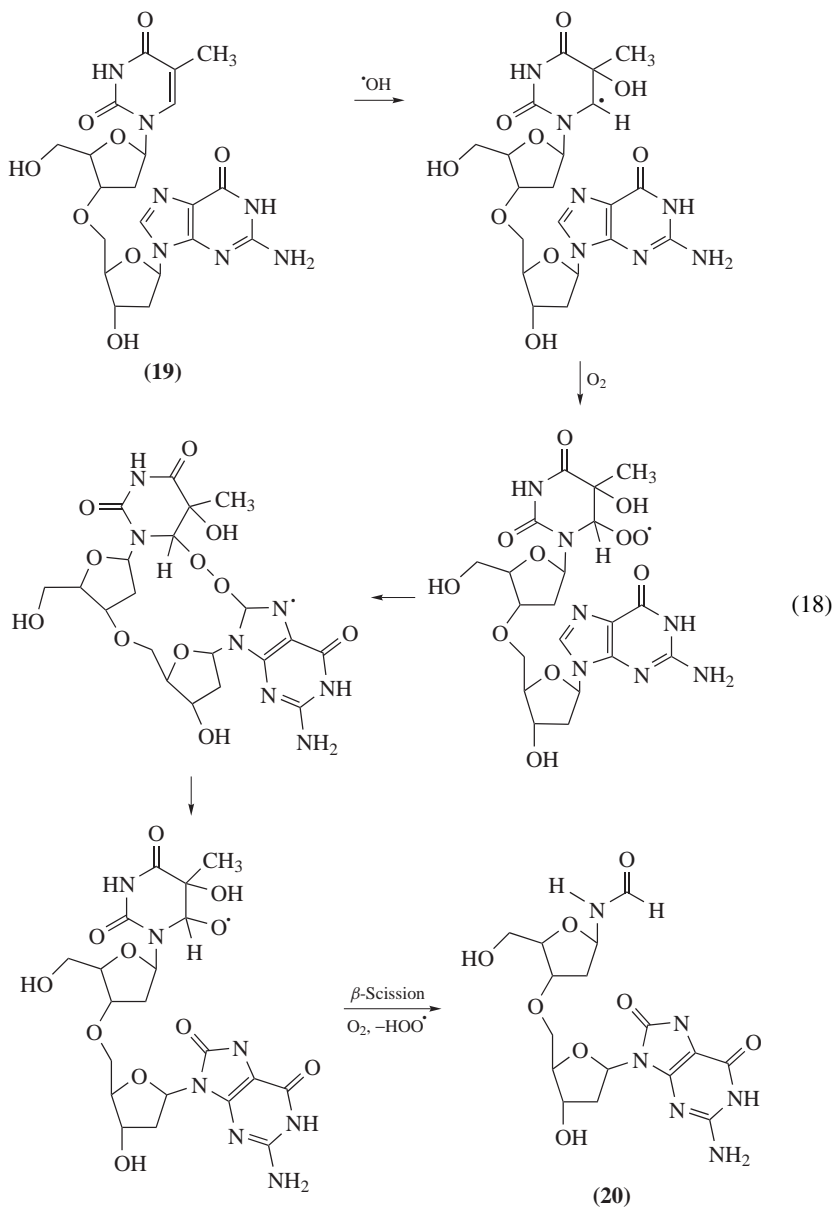
B. Uracil Components

Only limited information is available on uracil hydroperoxides that are likely to be generated in a similar way to thymine analogues by initial $\bullet\text{OH}$ radical addition in aerated aqueous solutions. This is likely due to the higher instability of these peroxides. Evidence has been recently provided for the implication of the 5-peroxy-5,6-dihydrouracil-6-yl radical in the formation of tandem base lesions.

1. Hydroxyhydroperoxides

Pulse radiolysis experiments have shown that $\bullet\text{OH}$ radical adds preferentially at C5 of the uracil moiety, giving rise to the reducing 5-hydroxy-5,6-uracil-6-yl radical. Interestingly, the two *cis* diastereomers of 6-hydroperoxy-5-hydroxy-5,6-dihydrouridine, two of the expected final products of the latter radicals in aerated aqueous solutions, have been prepared by trifluoroacetic acid treatment of uridine (**3**, $\text{R}^1 = \text{H}$, $\text{R}^2 = \text{ribose}$) in the presence of H_2O_2 ⁵⁴ (equation 14). The mechanism of the reaction that involves transient formation of an epoxide-type intermediate followed by nucleophilic attack by a perhydroxyl group at C6 presents similarities with the substitution of thymine bromohydrin by

hydrogen peroxide in the presence of Ag_2O . The two peroxides are stable at acidic pH. However, neutralization of the solutions leads to the decomposition of the hydroperoxides with subsequent formation of the formamide and 5,6-dihydroxy-5,6-dihydrouracil ribonucleosides, which have been shown to be the main radiation-induced degradation products of uridine in aerated aqueous solutions⁶⁰.



2. Tandem base modifications

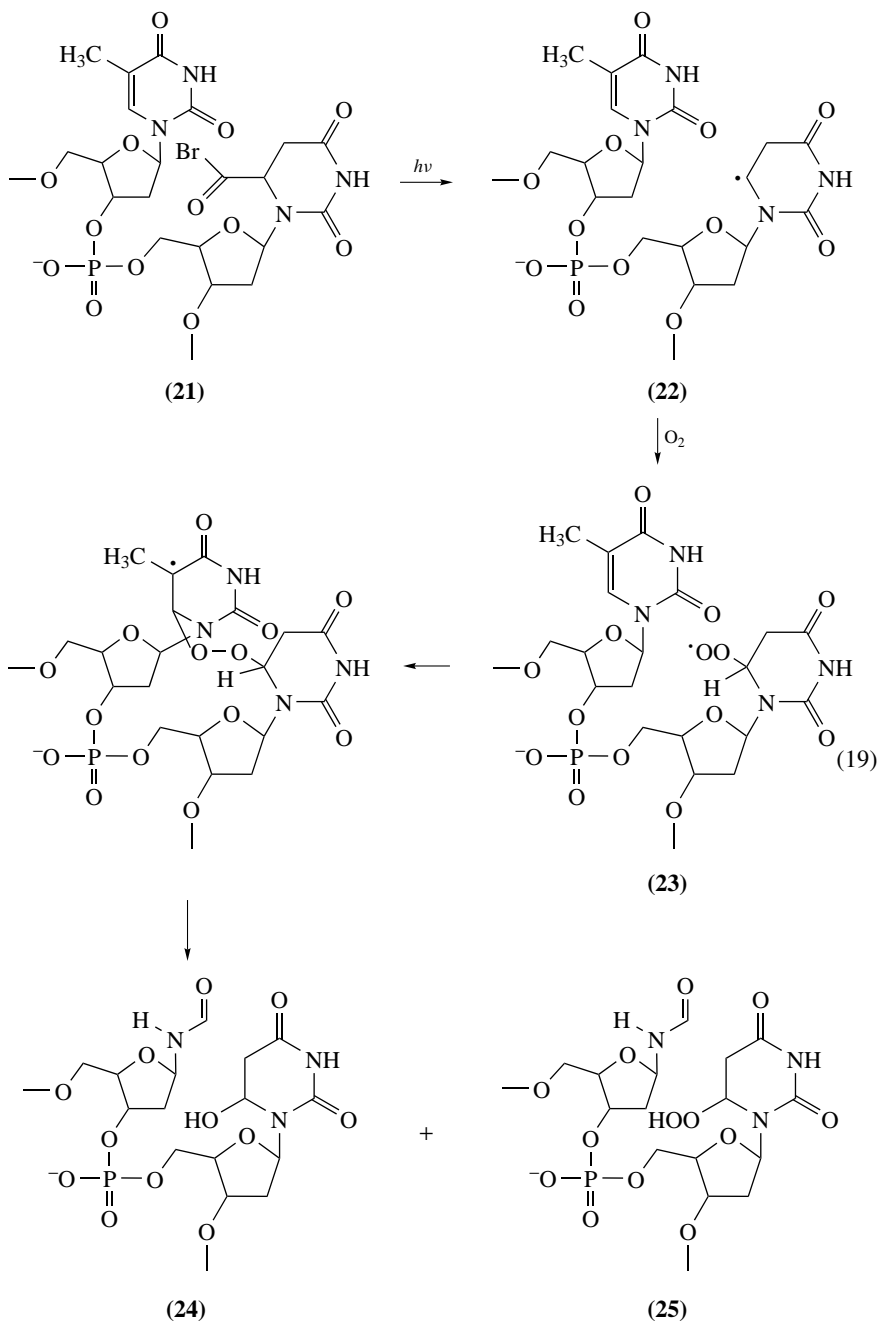
Other examples of tandem base modifications involving a pyrimidine peroxy radical as initiator recently became available. In this respect, 5,6-dihydrouracil-6-yl radical was efficiently generated by UVA-photolysis of a suitable *tert*-butyl ketone precursor⁶¹ that had been site-specifically inserted as a 6-substituted 5,6-dihydro-2'-deoxyuridine **21** into defined sequence oligonucleotides. Thus, it was found by MALDI-TOF mass spectrometric measurement that 6-hydroperoxy-5,6-dihydro-2'-deoxyuridine (**25**) and its related alcohol derivative **24** were formed as one of the degradation products in aerated aqueous solution. The likely reaction pathway for its formation is accounted for by dioxygen addition to the 6-yl radical **22** followed by intramolecular addition of the resulting peroxy radical **23** to C6 of vicinal thymine (equation 19). Subsequent rearrangement of the latter intermediate was proposed to give rise to **24** and **25**, which both contain a formamide remnant as a degradation product of the former thymine base. Interestingly, evidence was provided by mass spectrometric measurements that two 6-hydroperoxy-5,6-dihydrouracil containing tandem base lesions were formed with either a 5-(hydroperoxymethyl)uracil or a 5-(hydroxymethyl)uracil residue on the 3'-side⁶². The formation of the bis-hydroperoxide is likely to be explained by hydroperoxy-5,6-dihydrouracil-6-yl-mediated hydrogen atom abstraction from the methyl of contiguous 3'-thymine. This leads to the formation of the 6-hydroperoxide followed by O₂ addition to the 5-(uracilyl)methyl radical and subsequent formation of the related peroxy radical.

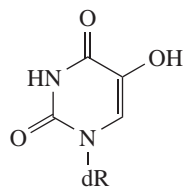
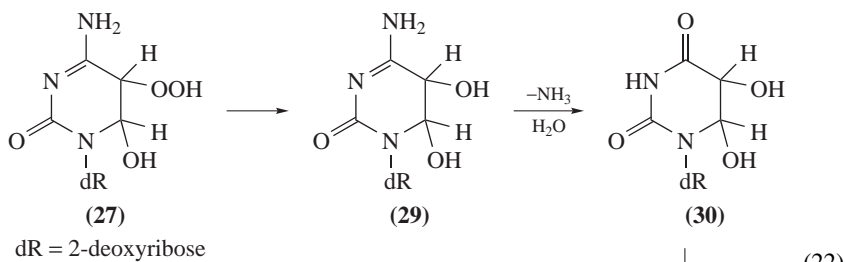
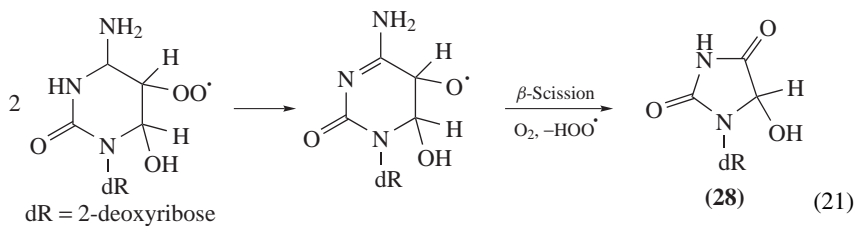
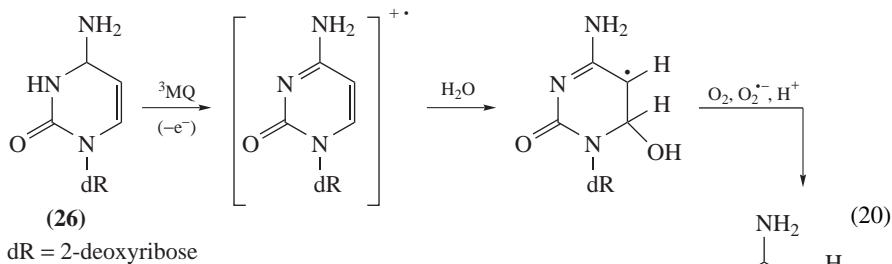
C. Cytosine Components

Cytosine (Cyt) and 2'-deoxycytine (dCyd) hydroxyhydroperoxides generated by either •OH radical or one-electron oxidation have been shown to be highly unstable, so far preventing their isolation and characterization by spectroscopic measurements such as NMR and MS. However, information is available on the chemical transformation of the 5- and 6-hydroperoxides as inferred from the isolation and identification of the main radical oxidation products of Cyt and dCyd.

1. 6-Hydroxy-5-hydroperoxides

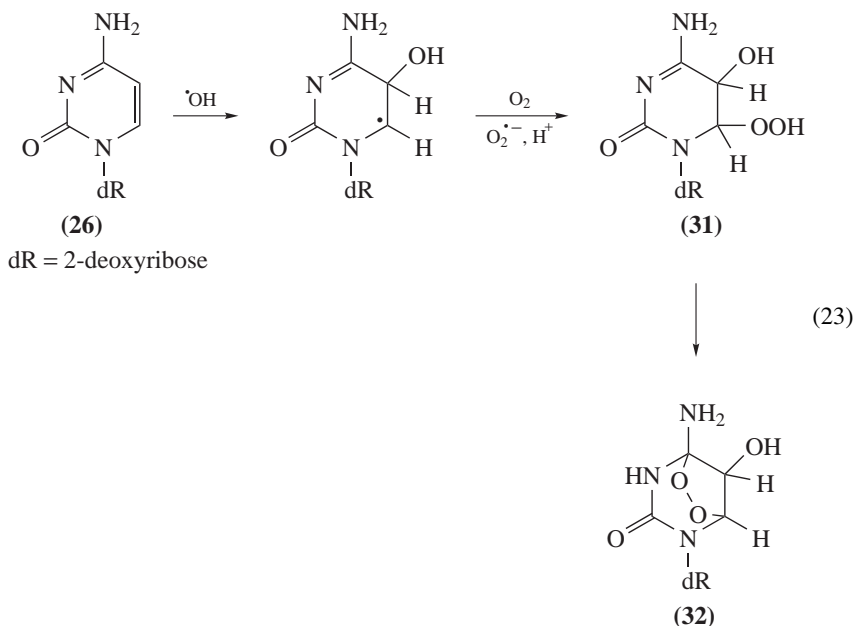
The *cis* and *trans* diastereomers of 5-hydroperoxy-6-hydroxy-5,6-dihydro-2'-deoxycytidine (**27**) were preferentially generated by menadione-mediated photooxidation of the cytosine moiety of **26** (equation 20). Labeling experiments that have involved the use of ¹⁸O-enriched dioxygen have provided support for the occurrence of a specific hydration of the cytosine radical at C6 leading to 6-hydroxy-5,6-dihydro-2'-deoxycytid-5-yl radical. In a subsequent step, fast O₂ addition would give rise to the corresponding peroxy radical that is expected, as observed for other pyrimidine peroxy radicals (*vide supra*), to undergo two competitive reactions. Reduction would lead to unstable hydroxyhydroperoxides whereas dismutation is likely to generate degradation products such as *N*-(2-deoxy- β -D-*erythro*-pentofuranosyl)formamide (**12**) and the (5*R**) and (5*S**) diastereomers of *N*-(2-deoxy- β -D-*erythro*-pentofuranosyl)-5-hydroxyhydantoin (**28**)⁶³ (equation 21). The four *cis* and *trans* diastereomers of 5,6-dihydroxy-5,6-dihydro-2'-deoxyuridine (**30**) that arise from the fast deamination of the initially generated dCyd diols **29**⁶⁴ were also isolated and characterized (equation 22). Dehydration of dUrd and dCyd diols **30** and **29** was found to give rise to 5-hydroxy-2'-deoxyuridine and 5-hydroxy-2'-deoxycytidine, respectively⁶⁵.

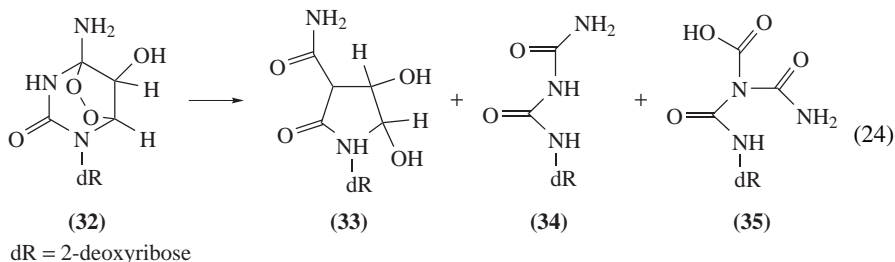




2. 5-Hydroxy-6-hydroperoxides

Hydroxyl radical has been shown to add to the 5,6-ethylenic bond of cytosine with a preference for the C5 carbon⁶ that is even higher (90%) than for thymine (*vide infra*). It is likely that the bimolecular decay of the peroxy radicals that arise from dioxygen addition to the latter 5-hydroxy-5,6-dihydrocytosyl radicals would explain, at least partly, the presence of degradation products **12**, **28** and **30** in aerated solutions of dCyd **26** upon exposure to γ -rays. Interestingly, several \bullet OH-mediated oxidation products of cytosine including biuret⁶⁶, *N*¹-glycolylbiuret⁶⁷, *N*¹-formylbiuret⁶⁸ and 1-carbamoyl-4,5-dihydroxyimidazolidin-2-one⁶⁹, whose formation requires notable rearrangement of the pyrimidine ring, were isolated and characterized. Similar observations were made for the \bullet OH-mediated reactions of dCyd **26** in aerated aqueous solutions that lead to the predominant formation of three classes of specific degradation products of the cytosine moiety (*vide infra*). A reasonable mechanism for the generation of the latter three classes of modified nucleosides involves the transient formation of endoperoxide **32** through intramolecular cyclization of 6-hydroperoxy-5-hydroxy-5,6-dihydro-2'-deoxycytidine (**31**) as a common initial pathway (equation 23). Hydrolytic decomposition of unstable **32** has been proposed to give rise through several competitive rearrangement reactions to the two *trans* diastereomers of *N*-(2-deoxy- β -D-*erythro*-pentofuranosyl)-1-carbamoyl-4,5-dihydroxyimidazolidin-2-one (**33**), the α and β anomers of *N*-(2-deoxy-D-*erythro*-pentosyl)biuret (**34**) together with *N*¹-(2-deoxy- β -D-*erythro*-pentofuranosyl)-*N*⁴-ureidocarboxylic acid (**35**)^{48b,63} (equation 24). The occurrence of such transposition reactions of the pyrimidine ring has been demonstrated by isotopic labeling experiments involving, for example, the incorporation of an ¹⁸O atom from labeled dioxygen into the carbamoyl group of diastereomeric nucleosides **33**⁶³.





D. 5-Methyl-2'-deoxycytidine

1. Methyl oxidation products

5-(Hydroperoxymethyl)-2'-deoxycytidine has been generated as one of the main one-electron oxidation products of the pyrimidine moiety of 5-methyl-2'-deoxycytidine (5-MedCyd) in aerated aqueous solution using photoexcited menadione as the radical oxidant⁷⁰. The hydroperoxide was characterized by extensive analyses including electrospray ionization mass spectrometry together with ¹H and ¹³C NMR spectroscopy. The mechanism of its formation involves initial generation of the base radical cation that undergoes deprotonation of the methyl group as the predominant (60%) of the two main conversion pathways. Subsequently, the resulting 5-(2'-deoxycytidyl)methyl radical is converted upon fast reaction with O₂ into the corresponding peroxy intermediate. Dismutation of the latter radical is expected to give rise to 5-(hydroxymethyl)-2'-deoxycytidine and 5-formyl-2'-deoxycytidine whereas competitive reduction by O₂^{•-} followed by protonation leads to the hydroperoxide. Hydrolytic decomposition of the latter, relatively unstable nucleoside, whose half-life in D₂O at 24 °C has been estimated to be 9.5 ± 0.5 h, leads to the almost exclusive formation of 5-formyl-2'-deoxycytidine.

2. Hydroxyhydroperoxides

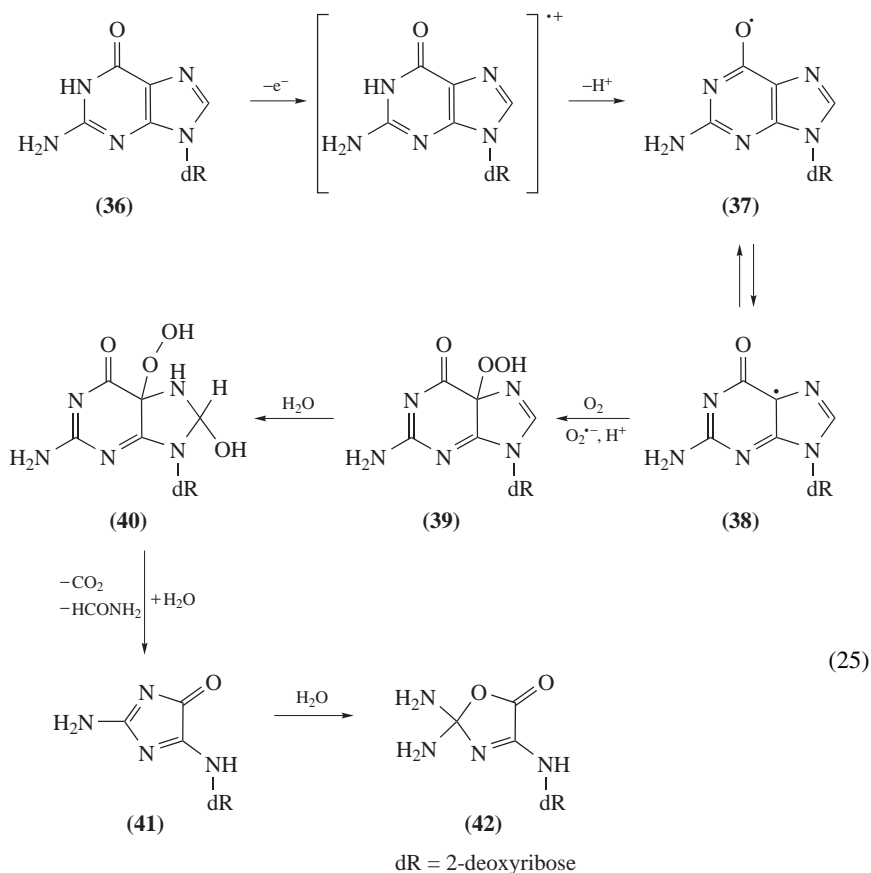
Other hydroperoxides, although not yet identified, have been shown to be generated upon menadione-mediated photooxidation of 5-MedCyd⁷¹. Decomposition of the latter unstable nucleosides that were separated by HPLC analysis was found to lead, among several degradation products, to the formation of the *cis*-(5*R*,6*R*) and (5*S*,6*S*) diastereomers of 5,6-dihydroxy-5,6-dihydro-5-methyl-2'-deoxycytidine. It was shown using ¹⁸O-labeling experiments that dioxygen adds exclusively to the C5 carbon of the transient pyrimidine radical giving rise to the 5-MedCyd diols. This may be rationalized in term of specific hydration reaction at C6 of the initially generated pyrimidine radical cation. The resulting peroxy radical is then likely to be reduced to the corresponding hydroperoxides and/or to be implicated in dismutation reactions. Interestingly, the two *cis* diastereomers of 5-MedCyd diols have been found to be generated upon exposure of 5-MedCyd to γ -rays in aerated aqueous solutions as the result of initial [•]OH addition at C6 and C5 of the base moiety respectively⁷². Interestingly, as observed for cytosine, the 5-hydroxyhydroperoxides of 5-MedCyd were found to generate unstable endoperoxides by intramolecular cyclization at C4^{70b}.

E. Guanine Components

Guanine is a preferential DNA target to several oxidants: it shows the lowest ionization potential among the different purine and pyrimidine nucleobases^{9a} and it is the only nucleic acid component that exhibits significant reactivity toward singlet oxygen (¹O₂) at neutral pH⁷³.

1. Radical oxidation reactions

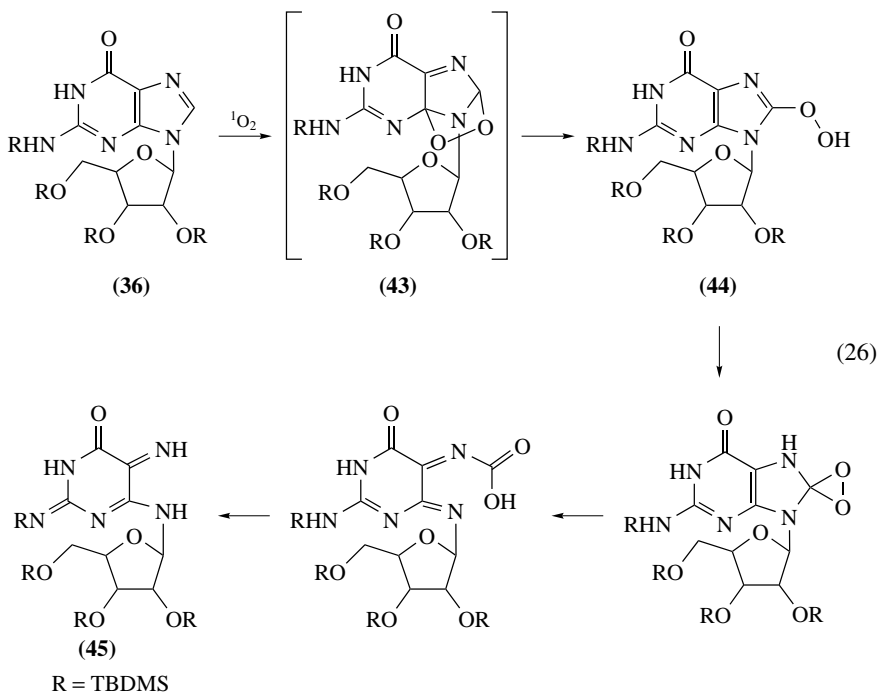
The two overwhelming oxidation products of the purine moiety of 2'-deoxyguanosine (**36**) resulting from either the reaction with $\bullet\text{OH}$ radical or the transformation of guanine radical cation (one-electron oxidation) were isolated and identified as 2,2-diamino-4-[(2-deoxy- β -D-erythro-pentofuranosyl)amino]-5(2*H*)-oxazolone (**42**) and its precursor 2-amino-5-[(2-deoxy- β -D-erythro-pentofuranosyl)amino]-4*H*-imidazol-4-one (**41**)^{74,75}. The mechanism of their production (equation 25) may be rationalized in terms of transient formation of the oxidizing guaninyl radical **37**, which may arise either from dehydration of the $\bullet\text{OH}$ adduct at C4 ($k = 6 \times 10^3 \text{ s}^{-1}$) or deprotonation of the guanine radical cation⁷⁶. The resulting neutral radical dGuo(-H) \bullet **37**, which may exist in several tautomeric forms, is implicated in a rather complicated decomposition pathway. Addition of O_2 to the C5 carbon-centered radical **38** is at best a rather inefficient process, since the rate constant has been found to be lower than $10^3 \text{ M}^{-1} \text{ s}^{-1}$. Evidence has been provided that $\text{O}_2^{\bullet-}$ reacts significantly with a rate constant that has been estimated to be $3 \times 10^9 \text{ M}^{-1} \text{ s}^{-1}$ for the 2'-deoxyribonucleoside⁷⁶. Slightly lower reactivity has been assessed for the related dGMP nucleotide⁷⁷ and short oligonucleotides⁷⁸, the k values being $1.3 \times 10^9 \text{ M}^{-1} \text{ s}^{-1}$ and



$0.47 \times 10^9 \text{ M}^{-1} \text{ s}^{-1}$, respectively. This leads after protonation to the transient formation of a hydroperoxide **39**, which is followed by a nucleophilic addition of a water molecule across the 7,8-ethylenic bond leading to **40**. Then cleavage of the 1,6 bond that is accompanied by the release of formamide⁷⁹ and subsequent rearrangement leads to the formation of oxazolone **42** through the quantitative hydrolysis of unstable imidazolone **41** (half-life = 10 h in aqueous solution at 20 °C)⁷⁴. However, at this stage, the formation of 5-hydroperoxy-8-hydroxy-7,8-dihydro-2'-deoxyguanosine (**40**), the proposed key precursor of the imidazolone and oxazolone nucleosides **41** and **42** that is likely to be highly unstable, remains to be established.

2. Singlet oxygen oxidation reactions

As already mentioned, guanine is the only normal nucleic acid base that significantly reacts with $^1\text{O}_2$ in the $^1\Delta_g$ state ($E = 22.4 \text{ kcal mol}^{-1}$) at neutral pH⁸⁰. The main reaction was found to be a Diels–Alder [4 + 2] cycloaddition of $^1\text{O}_2$ across the 4,8-bond of the imidazole ring of guanine producing unstable 4,8-endoperoxides. Support for the occurrence of the latter mechanism was provided by NMR characterization at low temperature in CD_2Cl_2 of the endoperoxide as arising from type II photosensitization of the 2',3',5'-*O*-*tert*-butyldimethylsilyl derivative of 8-methylguanosine⁸¹. Further support for the formation of transient 8-hydroperoxide **44** was provided by a recent NMR analysis of the content of the photosensitized organic solution of a ^{13}C -8-guanosine derivative **36** ($\text{R} = \text{TBDMS}$) performed at low temperature⁸². Thus an 8C-dioxirane that was proposed to arise from the rearrangement of transient 8-hydroperoxide **44** was assigned by ^{13}C NMR analysis (equation 26). It should, however, be noted that both endoperoxide **43**



in the presence of reducing agents such as thiols or Fe^{2+} ions^{85a}. A similar situation is found in double-stranded DNA since only the formation of 8-oxodGuo **46** has been detected⁸⁶. It has been proposed that initially generated diastereomeric 4,8-endoperoxides **43** are able to rearrange into 8-hydroperoxy-2'-deoxyguanosine (**44**)^{81,83} prior to being reduced into 8-oxodGuo **46**. It may be added that attempts to search for the formation of 2,6-diamino-4-hydroxy-5-formamidopyrimidine (FapyGua) within isolated DNA exposed to a chemical source of $^1\text{O}_2$ were unsuccessful⁸⁶. This rules out the possibility for $^1\text{O}_2$ to act by charge transfer reaction. As a final observation, in contrast to previous reports, it was found that $^1\text{O}_2$ is unable to generate direct strand breaks within both isolated and cellular DNA⁸⁷.

F. 8-Oxo-7,8-dihydroguanine Components

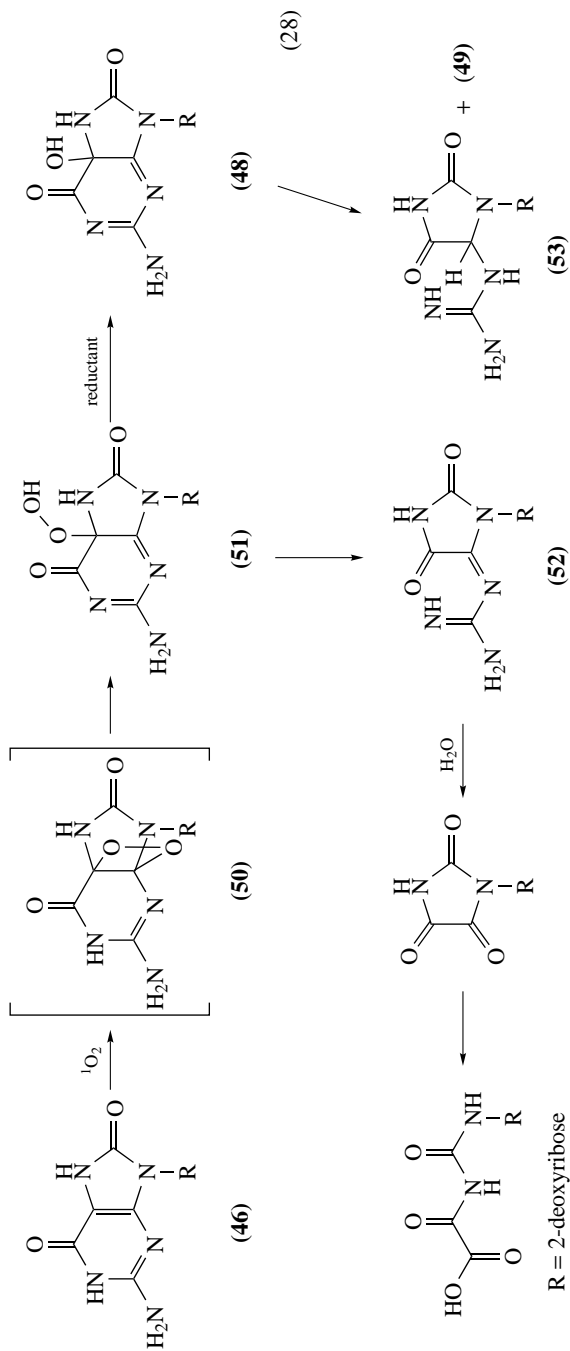
Interestingly, it was shown that 8-oxodGuo **46**, an ubiquitous exposure marker of DNA exposed to most oxidizing agents^{9a}, is a much better substrate than dGuo **36** to further oxidation by $^1\text{O}_2$ ⁸⁸ and one-electron oxidants.

1. Singlet oxygen oxidation reactions

Thus, it was found that the rate of reaction of $^1\text{O}_2$ with 8-oxodGuo **46** is about two orders of magnitude higher than that with dGuo **36**⁸⁹. It is likely that $^1\text{O}_2$ adds across the 4,5-ethylenic bond of 8-oxodGuo **46** to generate a transient dioxetane **50** that decomposes according to two main pathways. This leads to the predominant formation of cyanuric acid⁹⁰ together with 2,2,4-triamino-5-(2*H*)-oxazolone (**42**) and spiroiminodihydantoin nucleosides **49**⁸⁵. The reaction of $^1\text{O}_2$ with an 8-oxo-7,8-dihydro-2'-deoxyguanosine residue (**36**), site-specifically inserted within a single-stranded oligonucleotide, was found to be more specific (equation 28). Thus, the predominant oxidation product in this system was identified as oxaluric acid⁹¹. A likely mechanism for the formation of the latter ureido derivative involves initial formation of the dioxetane **50** by $^1\text{O}_2$ addition across the 5,6-ethylenic bond⁸⁸ which, upon rearrangement, is converted into the unstable 5-hydroperoxide **51**. Cleavage of the 5,6-bond of **51** and subsequent decarboxylation gives rise to a dehydroguanidinohydantoin derivative **52**. Further decomposition of the latter nucleoside leads, by two successive hydrolytic steps, to the formation of oxaluric acid through the parabanic acid precursor. Reduction of **51** is expected to give rise to transient **48** that may undergo conversion to **49** and/or two diastereomers of guanidinohydantoin **53**. Interestingly, the dehydroguanidinohydantoin compound **52** that can be isolated was also found to be generated by two-electron oxidation of the guanine moiety of d(GpT) using the Mn-TMPyp/KHSO₅ oxidizing system⁹².

2. One-electron oxidation pathways

There is a growing body of evidence showing that 8-oxodGuo **46**, whose oxidation potential is about 0.5 eV lower than that of dGuo **36**^{89b}, is a preferential target for numerous one-electron oxidizing agents. These include Na_2IrCl_6 ⁹³, $\text{K}_3\text{Fe}(\text{CN})_6$, $\text{CoCl}_2/\text{KHSO}_5$ ⁹⁴, a high-valent chromium complex⁹⁵, peroxy radicals⁹⁶, triplet ketones, oxyl radicals^{85b}, ionizing radiation through the direct effect⁹⁷ and riboflavin as a type I photosensitizer⁹⁸. Interestingly, the two (*R**) and (*S**) diastereomers of **49** were found to be the predominant one-electron oxidation products of 8-oxodGuo and 8-oxo-7,8-dihydroguanosine (8-oxoGuo) at neutral pH. Formation of the latter oxidized nucleosides was rationalized in terms of the transient generation of 5-hydroxy-8-oxo-7,8-dihydroguanine derivatives (**48**) followed by rearrangement into **49** via an acyl shift. The latter precursors were found to undergo a different decomposition pathway under slightly acidic conditions; this involves



the opening of the 5,6-pyrimidine ring, followed by a decarboxylation reaction with the subsequent formation of the two diastereomers of guanidinohydantoin (Gh) derivatives **53**. The oxazolone nucleoside **42** together with its imidazolone **41** precursor were also found to be one-electron oxidation products of 8-oxodGuo **46**, although generated in lower yields than spiroiminodihydantoin and guanidinohydantoin nucleosides **49** and **53**⁹⁸.

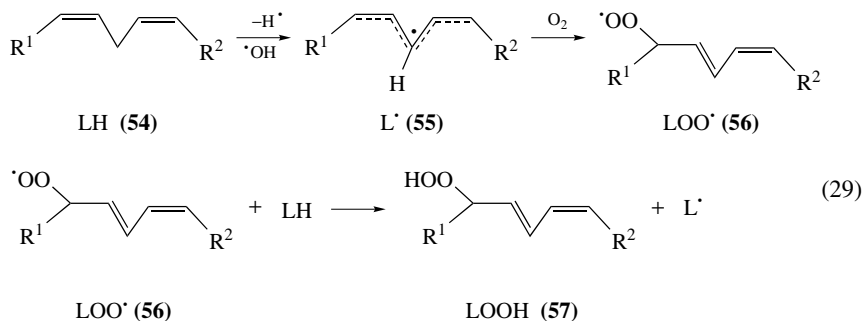
III. LIPID HYDROPEROXIDES

Lipid peroxidation is considered to be a key chemical event of the oxidative stress associated with several inborn and acquired disorders^{99–107}. Lipid peroxidation of polyunsaturated fatty acids such as linoleic acid (**54**) leads to a complex mixture of hydroperoxides^{108,109}. Attention has focused on this process because of its role in destructive biological processes. The oxidation of lipids has been implicated in alterations of membrane structure, DNA damage and protein modification^{110–113}. Disruption of organelle and cell membranes together with calcium homeostasis alterations are the main supramolecular events linked to lipid peroxidation. Not clarified yet, however, is whether the phenomenon constitutes an early, triggering step of the clinical manifestations of the diseases or a terminal consequent process. Lipid hydroperoxides are the primary products of lipid oxidation and it is assumed that their decomposition is involved in the generation of toxic products and in the induction of tissue injury^{105–107}. It is also increasingly recognized that lipid peroxidation that may be initiated by UV and ionizing radiations^{114,115} is associated with the mechanism of tumor initiation^{116–119}, deposition of arterial plaque^{99,120} and aging^{121,122}.

A. Lipid Oxidation

1. Unsaturated fatty acids

Unsaturated membrane lipids are critical targets of oxygen-derived species. Lipid peroxidation starts with the initiation event, in which a hydrogen atom is abstracted from an unsaturated fatty acid (LH) (**54**) containing a methylene ($-\text{CH}_2-$) group, yielding a carbon-centered radical L^\bullet (**55**) (equation 29). Superoxide anion ($\text{O}_2^{\bullet-}$) does not react at significant rates with polyunsaturated fatty acids¹²³ and $\text{O}_2^{\bullet-}$ -mediated damage to membrane has been attributed through the Haber–Weiss reaction (equations 30 and 31), which requires catalysis by transition metal ions^{124,125}. The protonated form of $\text{O}_2^{\bullet-}$, HO_2^\bullet , is more reactive and may abstract H from some fatty acids, such as linoleic acid (**54**) ($-\text{CH}_2- + \text{HO}_2^\bullet \rightarrow -\dot{\text{C}}\text{H}- + \text{H}_2\text{O}_2$). The carbon-centered radical (**55**) tends to be stabilized by a molecular rearrangement to form a conjugated diene.

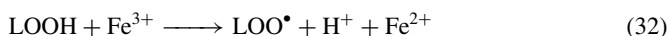


Linoleic acid: $\text{R}^1 = (\text{CH}_2)_4\text{CH}_3$, $\text{R}^2 = (\text{CH}_2)_7\text{COOH}$



The classical mechanism of lipid oxidation by reactive oxygen species may involve initiation by the hydroxyl radical and subsequent propagation reactions using molecular oxygen consumption and formation and reaction of alkyl peroxy radicals (LOO^\bullet) (**56**) (equation 29). For example, radiolysis of aqueous solutions produces $\bullet\text{OH}$, which is well-known to promote the peroxidation of any lipids present. The next step involves propagation reactions, catalyzed by the reaction of peroxy radical intermediates with vicinal unsaturated fatty acids. Reduced metals enter into the reaction scheme by reacting with LOOH (**57**) species and forming the alkoxy radical (LO^\bullet) and epoxyallylic radical species $[\text{L}(\text{O})^\bullet]$, both of which are capable of stimulating lipid oxidation by catalyzing further propagation reaction.

End-products of lipid peroxidation typically include lipid hydroperoxides, aldehydes and other products derived from decomposition of unstable oxidized intermediates. Despite certain stability in organic solutions, lipid hydroperoxides are easily decomposed by reduced metal ions. For example, iron would further participate in lipid peroxidation processes by increasing the chain length of propagation through the induced decomposition of lipid hydroperoxides, forming LOO^\bullet , LO^\bullet or epoxyallylic radical species $[\text{L}(\text{O})^\bullet]$ (equations 32 and 33); both the LOO^\bullet and LO^\bullet being capable of stimulating lipid oxidation by catalyzing further propagation reaction and the generation of toxic compounds^{126a}.

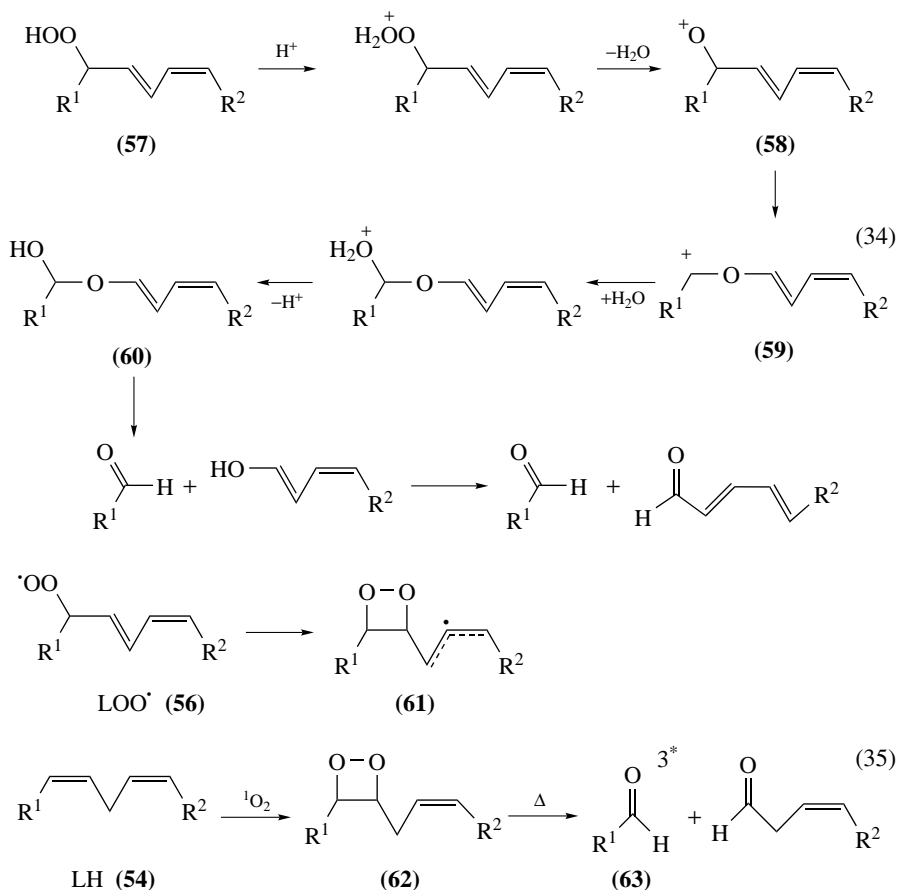


a. 'Hock-cleavage' to carbonyl fragments. Allylic hydroperoxides (**57**) may also undergo acid-catalyzed heterolysis of the peroxide bond generating a positive oxygen fragment (**58**) (equation 34). The instability of the positive oxygen derivative with respect to a carbenium ion would promote the migration of groups to the electron-deficient oxygen concerted with the rearrangement of the carbon skeleton. The resulting oxycarbenium ion (**59**) is nucleophilically attacked by H_2O leading to the corresponding hemiacetal (**60**), which cleaves to two carbonyl fragments, a process called 'Hock-cleavage'^{126b}. It should be noted that such cleavages were reported to occur also in the absence of any added acid^{126c}. The carbonyl fragments (**63**) generated in this mechanism may be the same as obtained from the thermolysis of dioxetanes (**61** and **62**) (equation 35).

2. Cholesterol

Free radical-mediated reaction by a strong oxidant like HO^\bullet or radical-mediated propagation reactions can be initiated directly by hydrogen abstraction at C7 of cholesterol (Ch) (**64**); as a result, cholesterol hydroperoxides (ChOOHs) that include the epimeric pair of 3β -hydroxycholest-5-ene- 7α -hydroperoxide (7α -OOH) (**65**) and 3β -hydroxycholest-5-ene- 7β -hydroperoxide (7β -OOH) (**66**) are produced¹²⁷ (Chart 1). Other non-hydroperoxide compounds corresponding to the diol derivatives (7α -OH, 7β -OH), the 7-ketone (7-one) (**67**), the epimeric 5,6-epoxides (**68**)¹²⁸ and 5α -OH, 6α -OH, 6β -OH derivatives are produced (Chart 1). Singlet oxygen reactions with Ch are characterized by the ene-addition of $^1\text{O}_2$, leading to a different peroxidation pattern that was observed by radical reactions (*vide supra*). The peroxides thus generated are the 3β -hydroxy- 5α -cholest-6-ene-5-hydroperoxide (5α -OOH) (**69**), 3β -hydroxycholest-4-ene- 6α -hydroperoxide (6α -OOH)

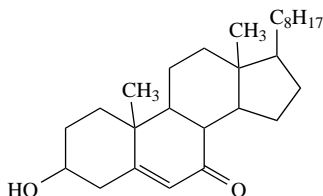
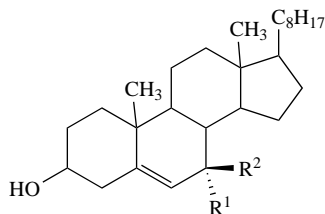
(70) and 3β -hydroxycholest-4-ene-6 β -hydroperoxide (6 β -OOH) (71)¹²⁹ (Chart 1). Nitroso intermediates generated during \cdot NO inhibition of Ch chain peroxidation were proposed¹²⁷.



Linoleic acid: $\text{R}^1 = (\text{CH}_2)_4\text{CH}_3$, $\text{R}_2 = (\text{CH}_2)_7\text{COOH}$

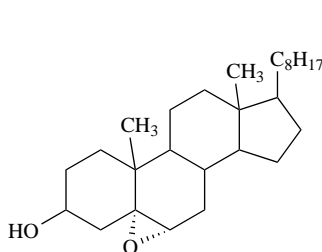
B. Photooxidation

Photooxidative reactions of biomolecules such as unsaturated lipids contribute to the molecular basis of the damage produced by light. The definition of the Type I and Type II (Figure 2) photosensitized oxidation has been described by Foote¹³⁰. These processes are produced via a photosensitizer in its singlet state or, more generally, in its triplet excited state (Sens^*). The Type I process includes the interaction of the Sens^* with the substrate or solvent yielding neutral radicals or radical ions, which can react with oxygen to produce oxygenated products. The Type II process is characteristic of an energy transfer from the Sens^* to triplet oxygen generating exclusively singlet oxygen, followed by reactions of this activated oxygen species with substrates, leading also to oxygenated products¹³⁰.

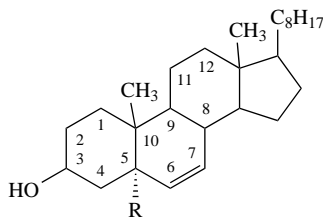


Ch-7-one (67)

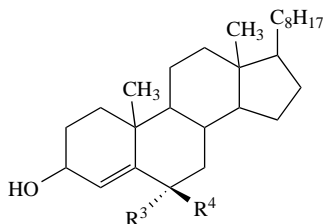
R^1	R^2		
H	H	Ch	(64)
OOH	H	Ch-7 α -OOH	(65)
H	OOH	Ch-7 β -OOH	(66)
OH	H	Ch-7 α -OH	
H	OH	Ch-7 β -OH	



Ch-5,6-epoxide (68)



R		
OOH	Ch-5 α -OOH	(69)
OH	Ch-5 α -OH	



R^3	R^4	
OOH	H	Ch-6 α -OOH (70)
H	OOH	Ch-6 β -OOH (71)
OH	H	Ch-6 α -OH
H	OH	Ch-6 β -OH

CHART 1

1. One-electron and hydroxyl radical oxidation

As exemplified in Figure 2, Type I mechanism, electron transfer from L to $^3\text{sens}^*$ yields two radicals, the substrate radical, L^\bullet , and the sensitizer radical anion ($\text{sens}^{\bullet-}$). In the next step, the lipid radical may induce a chain peroxidation cascade involving propagation reactions^{131,132}. The sensitizer radical anion may also start a sequential one-electron reduction of $^3\text{O}_2$ generating HO^\bullet in the presence of reduced transition metals. As a result, this may lead to abstraction of a lipid allylic hydrogen with subsequent generation of a carbon-centered lipid radical, L^\bullet , that is rapidly oxidized to a peroxy radical (*vide supra*).

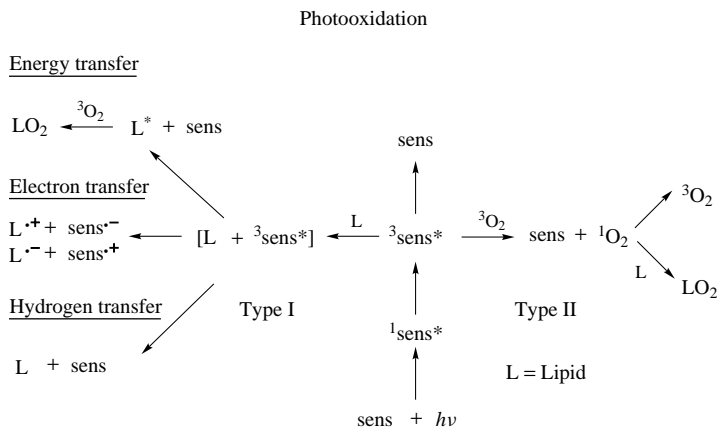
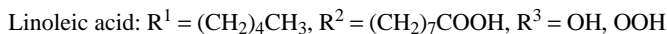
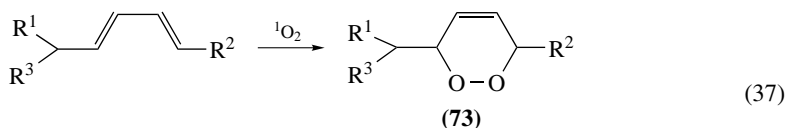
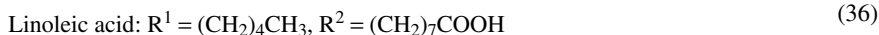
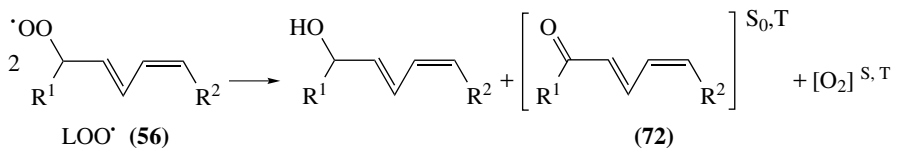


FIGURE 2. Photosensitized oxidation reactions

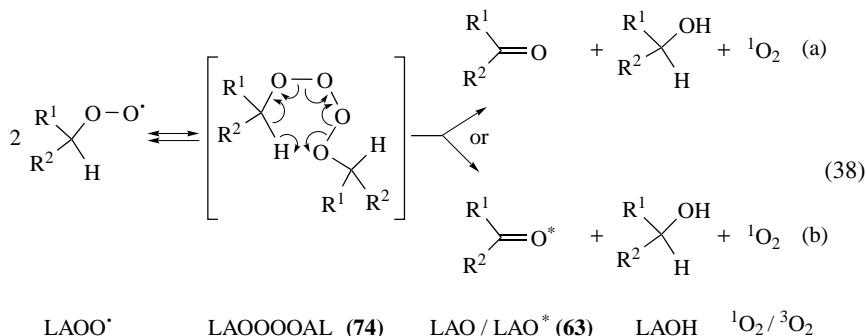
2. Singlet oxygen

Lipid hydroperoxides are also generated in singlet molecular oxygen mediated oxidations^{108,109} and by the action of enzymes such as lipoxygenases¹³³ and cyclooxygenases¹³⁴. Chemiluminescence (CL) arising from lipid peroxidation has been used as a sensitive detector of oxidative stress both *in vitro* and *in vivo*^{135,136}. Several authors have attributed ultra-weak CL associated with lipid peroxidation to the radiative deactivation of $^1\text{O}_2$ and to triplet-excited carbonyls (**63**, **72**) (equations 35 and 36)¹³⁷⁻¹³⁹. It has been proposed that the latter emitters arise from the thermolysis of dioxetane intermediates (**61**, **62**)¹⁴⁰ (equation 35), endoperoxide (**73**) (equation 37) and annihilation of alkoxy¹⁴¹, as well as peroxy radicals^{46, 142-144}.

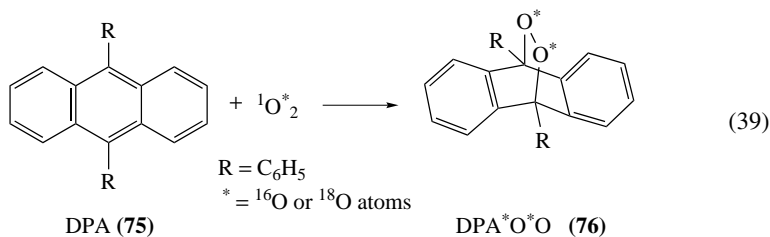


a. Russell mechanism. Following the suggestion of Russell⁴⁶, Howard and Ingold¹⁴² found that the self-reaction of peroxy radicals (linoleic acid peroxy radical, LAOO \cdot) generates $^1\text{O}_2$. Russell proposed the formation of a cyclic transition state from a linear tetraoxide intermediate (LAOOOOAL) (**74**) that decomposes to give an alcohol (LAOH), ketone (LAO) and molecular oxygen (equation 38). It has been postulated that this reaction may generate either an electronically excited oxygen molecule, $^1\text{O}_2$ (equation 38a),

or an electronically excited ketone (**63**) (LAO*) (equation 38b). Indeed, $^1\text{O}_2$ and triplet carbonyls have been identified as the chemiluminescence emitters in the ultra-weak CL associated with lipid peroxidation in biological systems^{145–147}. The generation of $^1\text{O}_2$ during the metal-catalyzed decomposition of alkylhydroperoxides has been studied by several authors^{143, 144, 148–150}. Niu and Mendenhall¹⁴⁹ reported that the yields of $^1\text{O}_2$, in the case of simple alkylhydroperoxides, ranged from 3.9 to 14.0%¹⁴⁹. In contrast, the yields of excited carbonyls (**63**) were 10^3 – 10^4 lower, suggesting that the self-reaction of peroxy radical deriving from fatty acids generates predominantly $^1\text{O}_2$ ¹⁵⁰.

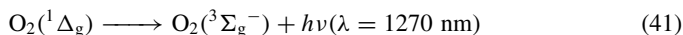
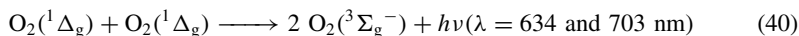


Singlet oxygen displays considerable reactivity toward electron-rich organic molecules including, among others, the guanine moiety of DNA (*vide supra*)^{151, 152}. Evidence has accumulated indicating that $^1\text{O}_2$ is implicated in the genotoxic effect of the UVA component of solar radiation and is likely to play an important role in the cell signaling cascade¹⁵³ and induction of gene expression¹⁵⁴. Various authors have investigated the generation of $^1\text{O}_2$ in biological systems, which have been proposed to occur by a type II photosensitization mechanism¹³⁰ and enzymatic processes of peroxidases and oxidases^{155, 156}. Other chemical reactions are also able to produce $^1\text{O}_2$, such as the reaction of hydrogen peroxide with hypochlorite¹⁵⁷ and the reaction of ONOO⁻ with hydrogen peroxide¹⁵⁸ or *tert*-butyl hydroperoxide¹⁵⁹. Recent studies clearly demonstrate the generation of $^1\text{O}_2$ from lipid hydroperoxides by the mechanism proposed by Russell^{160, 161}. For this purpose, ^{18}O -labeled linoleic acid hydroperoxide (LA $^{18}\text{O}^{18}\text{OH}$) and ceric ion (Ce $^{4+}$) or ferrous ion (Fe $^{2+}$) were used as a mechanistic tool. The study was based on the specific detection and quantification of ^{18}O -labeled singlet oxygen ($^{18}[^1\text{O}_2]$) generated by the combination of two ^{18}O -labeled peroxy radicals, using 9,10-diphenylanthracene (**75**) (DPA) as the chemical trap (equation 39). The corresponding DPA endoperoxide (**76**) containing labeled oxygen (DPA $^{18}\text{O}^{18}\text{O}$) was detected and quantified by high-performance liquid chromatography coupled to tandem mass spectrometry (HPLC-MS/MS).



b. Chemical trapping of ^{18}O -labeled singlet oxygen. Analysis of the products revealed that besides the DPA- ^{18}O (**76**) (equation 39), two other DPA adduct species were also detected: the unlabeled endoperoxide (DPA- ^{16}O), and endoperoxide with one labeled oxygen (DPA- ^{18}O). The quantification of each endoperoxide showed that 70% of the endoperoxide was DPA- ^{16}O , 13% was DPA- ^{18}O and 18% was DPA- ^{18}O . This result showed many interesting features involved in LOO^\bullet and $^1\text{O}_2$ chemistry, which may explain the formation of DPA- ^{16}O and DPA- ^{18}O : for example, (a) exchange of ^{18}O -labeled oxygen of $\text{LA}^{18}\text{O}^{18}\text{O}^\bullet$ with the $^{16}\text{O}_2$, yielding $\text{LA}^{16}\text{O}^{16}\text{O}^\bullet$ ¹⁶²; (b) energy transfer from $^{18}[\text{O}_2]$ to $^{16}\text{O}_2$ yielding $^{16}[\text{O}_2]$ ^{163, 164}, $^{18}\text{O}_2(^1\Delta_g) + ^{16}\text{O}_2(^3\Sigma_g^-) \rightleftharpoons ^{18}\text{O}_2(^3\Sigma_g^-) + ^{16}\text{O}_2(^1\Delta_g)$; and (c) exchange of $\text{LA}^{18}\text{O}^{18}\text{OH}$ with water, yielding $\text{LA}^{18}\text{O}^{16}\text{OH}$ ¹⁶⁵. These experiments indicate that the use of ^{18}O -labeled LOOH associated with HPLC-MS/MS can be a useful tool to clarify mechanistic features involved in the reaction of LOOH in biological media.

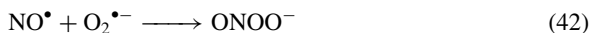
c. Light emission of singlet oxygen. Further evidence for the generation of $^1\text{O}_2$ by self-reaction of peroxy radicals is obtained by direct measurement^{160, 161} of: (i) dimol light emission in the red spectral region ($\lambda > 570$ nm) using a red-sensitive photomultiplier (PMT) (equation 40); (ii) monomol light emission in the near-infrared (IR) region ($\lambda = 1270$ nm) with a liquid-nitrogen-cooled germanium diode detector; and (iii) $^1\text{O}_2$ spectrum in the near-IR region using a specific IR-PMT coupled to a monochromator (equation 41).



C. Lipid Peroxides and Nitrogen Species

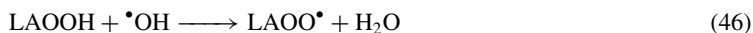
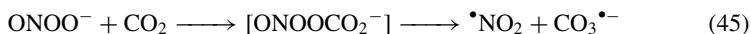
1. Peroxynitrite

Peroxynitrite (oxoperoxonitrate, ONOO^-) (equation 42) and its conjugated acid, peroxynitrous acid (ONOOH , $\text{p}K_a = 6.8$) (equation 43), are strong oxidants of biological importance produced by the reaction of the superoxide anion radical and nitrogen monoxide^{166, 167} (equation 42). Peroxynitrite reacts rapidly ($k = ca\ 10^3\text{--}10^6\ \text{M}^{-1}\ \text{s}^{-1}$) with a number of biological targets, including lipids, thiols, amino acid residues and DNA bases^{168–170}. Among biomolecules, lipids containing polyunsaturated fatty acids are key targets of peroxynitrite oxidation^{171–173}. Studies *in vitro* have shown that the reaction of peroxynitrite with pure lipids generates nitrated oxidized derivatives¹⁷⁴ as well as several lipid oxidation products, including lipid peroxides such as linoleic acid hydroperoxide¹⁷¹. It is known that one-electron oxidation of lipid hydroperoxides mediated by strong oxidants generates peroxy radicals. The reaction of lipid hydroperoxides with peroxynitrite may also promote the generation of peroxy radicals, thus generating $^1\text{O}_2$ as an intermediate oxidant by following the mechanism proposed by Russell⁴⁶.

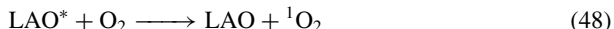


Peroxynitrous acid is a powerful oxidizing agent with estimated one- and two-electron reduction potentials of $E^\circ(\text{ONOOH}, \text{H}^+/\bullet\text{NO}_2, \text{H}_2\text{O}) = 1.6\text{--}1.7\ \text{V}$ and $E^\circ(\text{ONOOH}, \text{H}^+/\text{NO}_2^-, \text{H}_2\text{O}) = 1.3\text{--}1.4\ \text{V}$, respectively¹⁷⁵. In addition, it was reported that, upon protonation, ONOO^- can undergo decomposition via homolytic O–O cleavage to generate nitrogen dioxide radical ($\bullet\text{NO}_2$) and hydroxyl radical ($\bullet\text{OH}$) in approximately 30% yields

(equation 44)^{176,177}. At physiological conditions where normally the concentration of bicarbonate is high, ONOO⁻ reacts with CO₂ ($k = 3 \times 10^4 \text{ M}^{-1} \text{ s}^{-1}$) forming an unstable nitrosoperoxycarbonate anion adduct (ONOOCO₂⁻), which decomposes giving carbonate radical anion (CO₃^{•-}) and •NO₂ in approximately 35% yields (equation 45)¹⁷⁸⁻¹⁸². All these radical species generated from peroxynitrite are highly oxidizing agents. Hydroxyl radical is considered to be one of the most powerful oxidants, with $E^\circ(\text{•OH}, \text{H}^+/\text{H}_2\text{O}) = 2.31 \text{ V}$ at pH 7.0¹⁸³ reacting rapidly with most organic compounds ($ca 10^9 \text{ M}^{-1} \text{ s}^{-1}$). It is well known that •OH stimulates lipid peroxidation by H• abstraction from unsaturated fatty acids. The carbonate radical anion has also a high reduction potential, which is close to that of •OH at pH 7.0, $E^\circ(\text{CO}_3^{\bullet-}/\text{CO}_3^{2-}) = 1.78 \text{ V}$, and therefore is capable of oxidizing a variety of biomolecules^{184,185}. Indeed, CO₃^{•-} is reported to react with thiols by a one-electron oxidation mechanism generating thiol-derived radicals¹⁸⁴. The nitrogen dioxide radical is also a moderately potent oxidant ($E^\circ = 0.99 \text{ V}$) capable of reacting by hydrogen atom abstraction as well^{181,185-187}. On the other hand, the standard reduction potential calculated for ROO•/ROOH is approximately 1.0 V¹⁸⁸. Considering this information, it is thermodynamically probable that the reaction of ONOO⁻ with lipid hydroperoxides generates peroxy radicals. Therefore, we can expect that LAOO• radicals are produced by one-electron oxidation of LAOOH mediated by •OH (equation 46) and CO₃^{•-} (equation 47).



The peroxy radicals formed combine via a tetraoxide intermediate, which decomposes generating ¹O₂ and the corresponding alcohol and a ketone (equation 38a). Alternatively, the tetraoxide intermediate can also decompose, by generating a triplet ketone in the excited state (LAO*, equation 38b), which produces ¹O₂ by energy transfer to the ground state oxygen (equation 48).

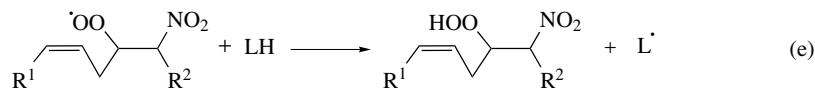
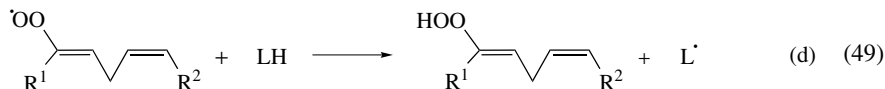
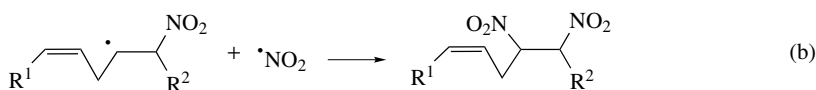
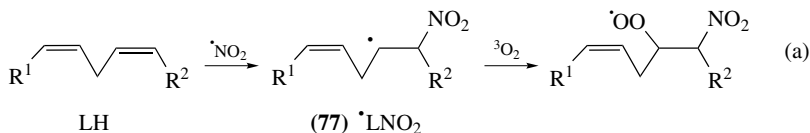


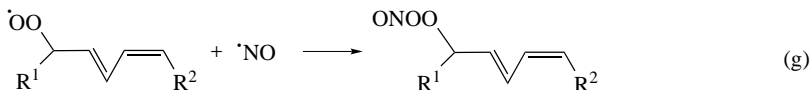
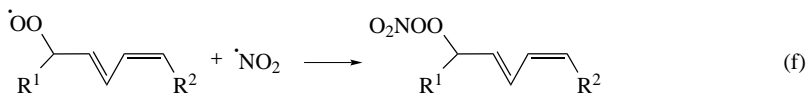
Assuming that lipid hydroperoxides are generated easily in cell membranes, these considerations point to a potential role of ¹O₂ in the cytotoxicity mechanism of LAOOH. Taking into account the longer half-lifetime of peroxy radicals (7 seconds) compared to those of other reactive oxygen species (which for LAO•, LA*, O₂^{•-}, ¹O₂, HO• are 1×10^{-7} , 1×10^{-9} , 1×10^{-6} , 1×10^{-7} , 1×10^{-10} seconds, respectively)¹⁸⁹, this allows for the migration of a fatty acid peroxy radical to other sites, where it can combine with another peroxy radical and generate ¹O₂.

2. Hydroperoxide and nitrolipids

A number of NO-derived reactive species can initiate lipid peroxidation, including nitrogen dioxide and, most notably, ONOO⁻, which displays unique properties as a mediator of lipid oxidation. On a molecular basis, ONOO⁻ is a more potent lipid oxidant than hydrogen peroxide and, unlike H₂O₂, it does not require metal catalysis¹⁷¹. The one-electron oxidants such as metals, as well as heme proteins and peroxynitrite, are assumed to play an important role in many diseases associated with oxidative stress. Heme proteins such as horseradish peroxidase (HRP) can produce alkylperoxy radicals through two sequential

one-electron oxidation reactions of hydroperoxides by compounds I and II, intermediates of HRP. Alternatively, peroxyxynitrite (or its conjugated peroxyxynitrous acid, ONOOH), formed by the reaction of nitric oxide with superoxide anion (equation 42), reacts with the hydroperoxide either directly, by the formation of a hydroxyl radical-like species, or through a CO₂-derived intermediate. Peroxyxynitrite can attack lipids in microenvironments where metals are not present or are bound in catalytically inactive forms. Thus, once formed, ONOO⁻ can bypass lipophilic antioxidant defenses to directly oxidize unsaturated fatty acids. When NO does not exceed local O₂^{•-} concentration, NO will stimulate lipid oxidation via ONOO⁻ formation and reaction. When the concentration of NO is higher in a microenvironment and in 'excess' of O₂^{•-}, it can manifest a predominantly inhibitory role toward lipid peroxidation via termination of LOO[•]. Reaction studies of NO₂[•] with alkene and unsaturated fatty acid solution^{186,187} propose that the reaction proceeds via addition of NO₂[•] to the double bond, forming a nitroalkyl radical (77), which may be scavenged by oxygen or NO₂[•] (equations 49a and 49b). Alkyl radicals and nitrous acid production by internal hydrogen abstraction may occur, leading to the double bond and a corresponding peroxy radical in the presence of oxygen (equations 49c and 49d). The rate constants of the reactions of NO₂[•] with cell membrane constituents such as linoleate and arachidonate are in the order of $1.0 \times 10^6 \text{ M}^{-1} \text{ s}^{-1}$ ¹⁸⁵. In addition to nitrolipids (LNO₂), other compounds such as alkyl nitrites (LONO), LOONO and LOONO₂ are also formed, giving rise to non radical end-products of lipid peroxidation (equations 49e–49g). In fact, in addition to the predominant hydroperoxy derivatives formed after treatment of linolenic acid with peroxyxynitrite, nitrogen-containing lipid species were detected¹⁷². In a membrane which is a milieu of autocatalytic propagation reaction, NO can intervene by avidly reacting with lipid epoxyallylic radical [L(O[•])], alkoxy radical (LO[•]) and LOO[•] species with a rate constant of $ca 2 \times 10^9 \text{ M}^{-1} \text{ s}^{-1}$, yielding both nitrogen oxide- and hydroperoxide-containing products.





Linoleic acid: $\text{R}^1 = (\text{CH}_2)_4\text{CH}_3$, $\text{R}^2 = (\text{CH}_2)_7\text{COOH}$

D. Endoperoxides and Dioxetanes

Because the thermolysis of dioxetanes can produce high yields of triplet carbonyls (**63**, **72**) (10–60%)¹⁸⁹, it has been proposed that the cycloaddition of $^1\text{O}_2$ to unsaturated fatty acids, producing such dioxetanes (**61**, **62**), could provide a plausible mechanism for the chemiluminescence. The excited carbonyl species (n, π^*) can emit phosphorescence in the visible (blue-green) region and $^1\text{O}_2$ in the red and infrared region (equations 40 and 41). In aerated solution, triplet carbonyls are short lived due to their quenching by ground state oxygen¹⁹⁰. $^1\text{O}_2$ was suggested to be formed in the lipid peroxidation process¹⁹¹. However, it has been established that reaction of $^1\text{O}_2$ with linoleic acid results almost exclusively in the formation of hydroperoxides and 1,4-endoperoxides (**73**), not the 1,2-cycloaddition products, dioxetanes (**62**)¹⁹² (equation 35). Nevertheless, the involvement of dioxetanes in lipid peroxidation is worth pursuing as a plausible alternative explanation for the observed chemiluminescence. In fact, dioxetane intermediates may be formed by the cyclization of alkylperoxyl radicals formed either during lipid peroxidation or by the one-electron oxidation of unsaturated fatty acid-derived hydroperoxides, LOOH. The formation of endoperoxides as intermediates in the lipid peroxidation processes or as metabolites in biological systems were also reported^{192c, 193}.

IV. PROTEIN HYDROPEROXIDES

Early efforts have focused on the elucidation of mechanistic aspects of $\cdot\text{OH}$ radical-mediated oxidation reactions of proteins, including peroxidation (for a comprehensive review, see Reference 194). More recently, investigations on peroxidative reactions of proteins have been extended to the action of other oxidizing agents¹⁹⁵. These included the addition of rather relatively unreactive superoxide radical to the tyrosyl radical and the selective singlet oxygen oxidation of aromatic amino acids. Most of the mechanistic information was gained from studies on free amino acids and short peptides whereas evidence of occurrence of propagation reactions from initially generated peroxides was provided within oxidized proteins.

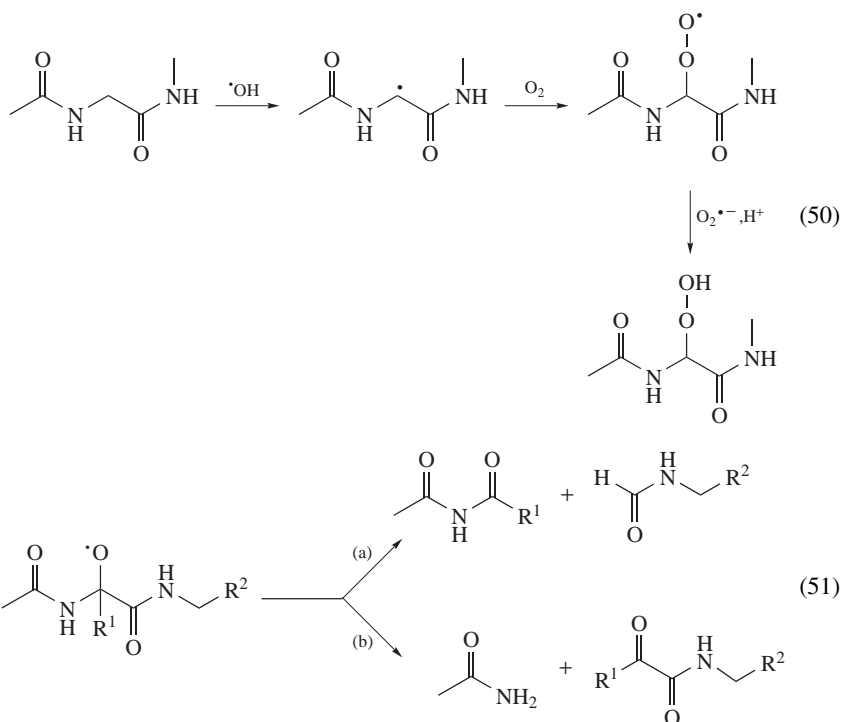
A. Amino Acids and Peptides

1. Hydroxyl radical reactions

Several peroxidative reactions initiated by $\cdot\text{OH}$ radical that may be generated by either γ - and X-radiolysis of aqueous solutions or by transition metal-catalyzed reduction of H_2O_2 have been identified in free amino acids and short peptides. In this respect we may distinguish oxidizing reactions that involve the polypeptide backbone on the one hand

and amino acid side-chains on the other. Evidence for the formation of relatively stable organic peroxides was provided by iodometric measurements of aerated aqueous solutions of amino acids and proteins upon exposure to ionizing radiation- or to chemically-induced $\bullet\text{OH}$ radicals¹⁹⁶. Among the common amino acids it was found that glutamate, isoleucine, leucine and lysine were the most susceptible to peroxidation reactions.

a. Peroxidation of the protein backbone. Hydroxyl radical-mediated abstraction of the α -hydrogen atom of the polypeptide chain gives rise to a carbon-centered radical that subsequently is able to react through several pathways including dismutation and reduction, as already discussed for peroxy radicals derived from radical oxidation of DNA components and unsaturated lipids. Therefore, hydroperoxides are likely to be generated through reduction of the peroxy radical precursors (equation 50) even if the characterization of any of these compounds, which are likely to be quite unstable, has not been so far achieved. It has been proposed that the radiation-induced cleavage of the peptide bond would involve initially produced alkylperoxides on the protein backbone or, more likely, related alkoxy radicals whose formation would result from heterolytic cleavage of the peroxidic bond by metals. Two main reactions, namely the diamide and α -amidation¹⁹⁴ pathways (equation 51), both involving a β -scission cleavage mechanism, would lead to the splitting of the peptide bond with formation of carbonyl compounds¹⁹⁷.

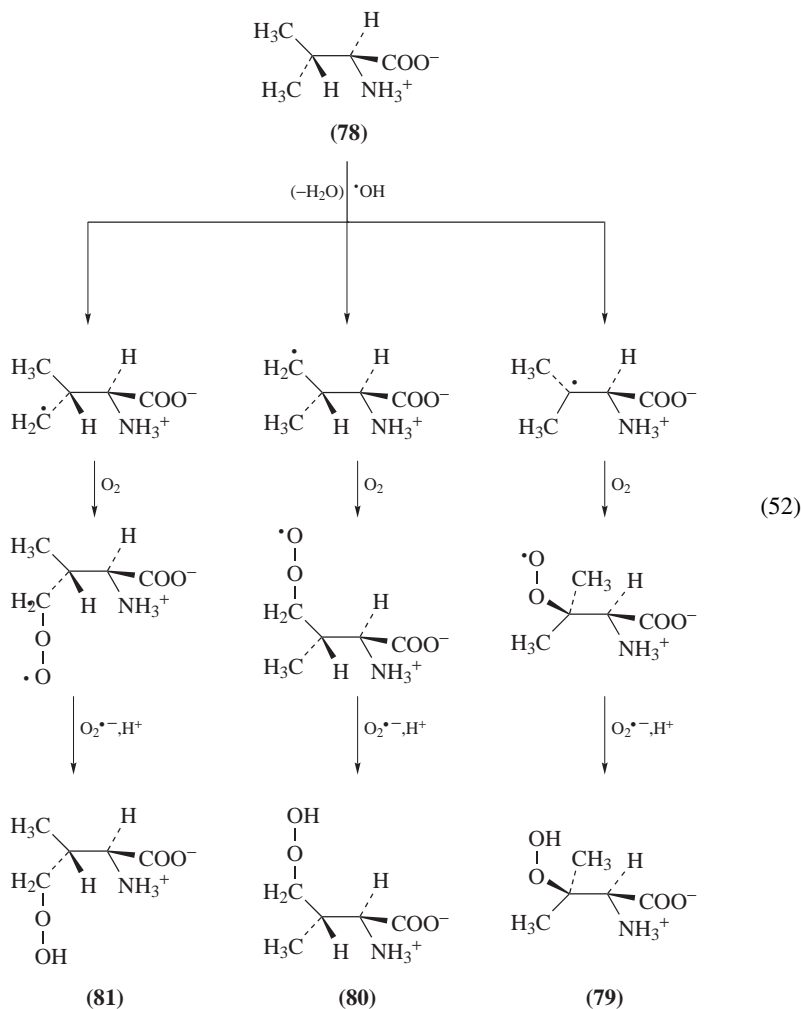


b. Peroxidation of the amino acid side-chain. For most amino acids, the efficiency of the α -hydrogen abstraction pathway (*vide supra*) is relatively low due to a deactivating effect exerted by the vicinal protonated amino group that exhibits strong electron-withdrawing

features or may exert steric effects^{195a,198}. Often, the poor reactivity of α -carbon toward $\bullet\text{OH}$ radical is further accentuated by the presence of stabilizing groups on some side-chains. As a result, formation of side-chain radicals that may involve hydrogen abstraction on hydrocarbon chains and/or $\bullet\text{OH}$ radical addition to aromatic residues predominates. It may be noted that a large body of information is available on the reactivity of $\bullet\text{OH}$ toward amino acids and both kinetic and structural aspects are available for the resulting transient radicals as inferred from pulse radiolysis and ESR measurements (for a comprehensive review, see Reference 199). However, there is still a paucity of available structural data on $\bullet\text{OH}$ -induced amino acid hydroperoxides even if, as already discussed, evidence for peroxidation of amino acids and small peptides in aerated aqueous solutions has been provided on the basis of iodometric measurements^{196b}. In fact, insights into the formation of amino acid hydroperoxides were gained indirectly from the characterization of the stable products that arise upon either reduction or hydrolytic decomposition of the peroxidic precursors. Examples of the first approach are given by detailed characterization studies of related alcoholic derivatives that were obtained by mild reduction of initially generated hydroperoxides of valine, leucine and lysine, whereas formation of stable oxidation products of phenylalanine, tyrosine and tryptophan was rationalized in terms of transient $\bullet\text{OH}$ -mediated generation of ring-derived hydroperoxides and/or related peroxy radicals.

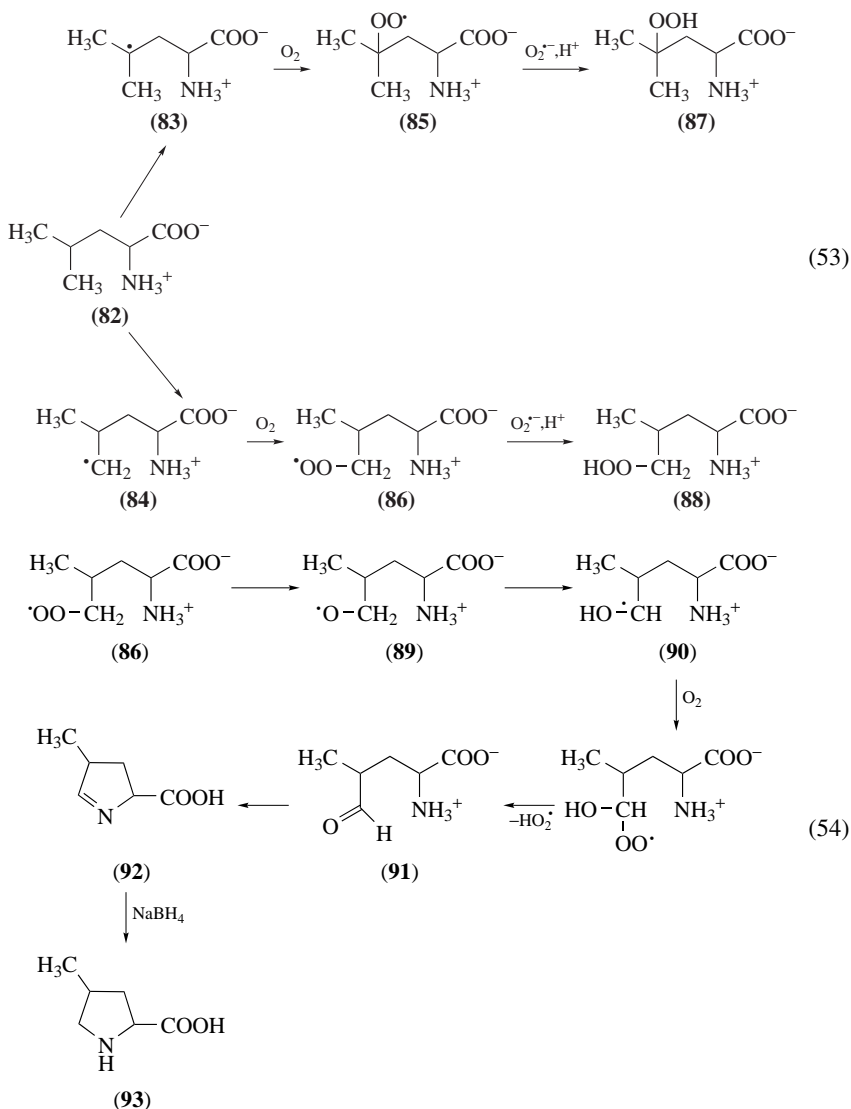
i. Valine. Steady-state gamma radiolysis of aerated aqueous solutions of valine (**78**) has been found to generate significant amounts of hydroperoxides²⁰⁰ as inferred from global colorimetric measurements. Two main peroxide-containing fractions were separated by HPLC on an amino-substituted silica gel column, the specific detection being provided by chemiluminescence using micropoxidase and isoluminol as the post-column reagents²⁰¹. Interestingly, mild NaBH_4 reduction of the hydroperoxides was found to give rise to 3 valine hydroxylated derivatives that were characterized by extensive ^1H and ^{13}C NMR measurements together using electrospray ionization and high-resolution chemical ionization mass spectrometry analyses²⁰⁰. Thus, β -hydroxyvaline and a γ -hydroxyvaline diastereomer were shown to originate from the mixture of hydroperoxides that are eluted in the first HPLC fraction, whereas the second diastereomer of γ -hydroxyvaline arises from the hydroperoxide present in the slowest eluting fraction. Absolute configuration of the two diastereomers of γ -hydroxyvaline was inferred from consideration of steric interactions involving the methyl groups through γ -effects, allowing by deduction the determination of the stereochemistry at C3 of the related hydroperoxides. Thus, the radiation-induced formation of (2*S*)-2-amino-3-hydroperoxy-3-methylbutanoic acid (**79**) and (2*S*,3*S*)- and (2*S*,3*R*)-2-amino-3-hydroperoxymethylbutanoic acids (**80**) and (**81**) may be rationalized in terms of initial $\bullet\text{OH}$ -mediated hydrogen abstraction at C2 and at one of the two methyl groups respectively, followed by fast oxygen addition and subsequent reduction of the resulting peroxy radicals (equation 52).

ii. Leucine. Three main peroxidic HPLC fractions were detected by post-column luminescence detection upon γ -radiolysis of aerated aqueous solutions of L-leucine (**82**). In fact, NaBH_4 reduction of the gamma-irradiated leucine solution was found to give rise to three hydroxylated derivatives, namely (2*S*)- γ -hydroxyleucine and the (2*S**,4*S**) and (2*S**,4*R**) diastereomers of δ -hydroxyproline that were unambiguously characterized²⁰². However, the absolute configuration of the two latter hydroxymethyl derivatives has not been established. The presence of both γ - and δ -hydroxyleucines is strongly suggestive of the $\bullet\text{OH}$ -mediated formation of related hydroperoxides that may be accounted for by initial hydrogen abstraction, which preferentially occurs from the methylene group with respect to any of the two methyl substituents. Fast oxygen addition to the resulting carbon-centered radicals **83** and **84** and subsequent reduction of thus generated peroxy radicals **85**

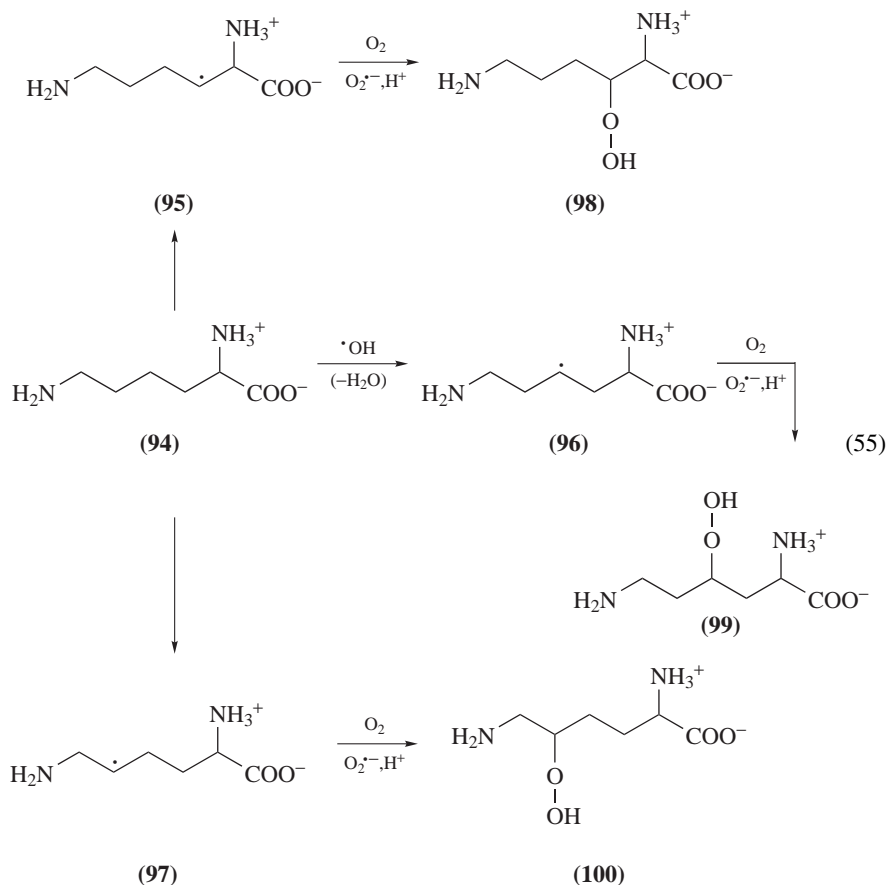


and **86** are the usual steps leading to the formation of two classes of γ -hydroperoxyvaline **87** and the two diastereomers of δ -hydroperoxyvaline **88** (equation 53). It may be noted that, as for valine (**78**), no detectable amount of the α -hydroxylated derivative is formed in agreement with the deactivating effect of the protonated α -amino group on the vicinal carbon site for $\cdot\text{OH}$ -mediated hydrogen atom abstraction. Interestingly, the *trans*-(2*S*,4*R*) and *cis*-(3*S*,4*S*) diastereomers of 4-methyl-L-proline (**93**) were identified as other degradation products in the γ -irradiated solution of L-leucine (**82**) upon NaBH_4 reduction²⁰². The formation of the two rearrangement products is likely to involve in the initial step the hydroperoxymethyl radicals **86** that derive from hydrogen abstraction from the methyl groups. Competitive dismutation of the peroxy radical **86** is expected to generate alkoxy radical **89** which, through 1,2-shift rearrangement, would give rise to carbon-centered radical **90**. Subsequent O_2 addition, followed by $\text{HO}_2\cdot$ elimination, would explain the formation of a leucine aldehyde **91** (equation 54). Another possibility to be considered is

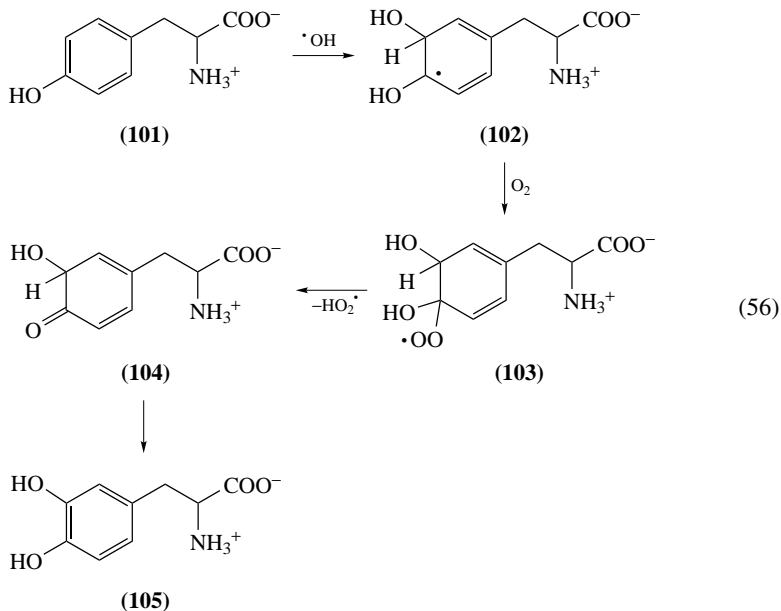
the Russell pathway, which through the intermediacy of a tetraoxide as the result of the bimolecular reaction between two hydroperoxymethyl radicals would give rise to aldehyde **91** together with the related alcohol. It was proposed that the carbonyl group thus generated by either of the two possible pathways is able to undergo intramolecular cyclization, giving rise to the Schiff base **92** before being easily converted to **93** by NaBH_4 reduction. Indirect support for the earlier steps of the latter mechanism of transformation of leucine hydroperoxymethyl radicals **86** is provided by the characterization of valine aldehyde as one of the main radiation-induced degradation products of valine (**78**) in aerated aqueous solutions.



iii. *Lysine*. Gamma radiolysis of aerated aqueous solution of lysine (**94**) has been shown, as inferred from iodometric measurements, to give rise to hydroperoxides²⁰³ in a similar yield to that observed for valine and leucine. However, attempts to isolate by HPLC the peroxidic derivatives using the post-column derivatization chemiluminescence detection approach were unsuccessful. This was assumed to be due to the instability of the lysine hydroperoxides under the conditions of HPLC analysis. Indirect evidence for the $\cdot\text{OH}$ -mediated formation of hydroperoxides was provided by the isolation of four hydroxylated derivatives of lysine as 9-fluoromethyl chloroformate (FMOc) derivatives²⁰⁴. Interestingly, NaBH_4 reduction of the irradiated lysine solutions before FMOc derivatization is accompanied by a notable increase in the yields of hydroxylysine isomers. Among the latter oxidized compounds, 3-hydroxylysine was characterized by extensive ^1H NMR and ESI-MS measurements whereas one diastereomer of 4-hydroxylysine and the two isomeric forms of 5-hydroxylysine were identified by comparison of their HPLC features as FMOc derivatives with those of authentic samples prepared by chemical synthesis. A reasonable mechanism for the formation of the four different hydroxylysines and, therefore, of related hydroperoxides **98–100**, involves initial $\cdot\text{OH}$ -mediated hydrogen abstraction followed by O_2 addition to the carbon-centered radicals **95–97** thus formed and subsequent reduction of the resulting peroxy radicals (equation 55).



iv. *Tyrosine*. Addition of $\cdot\text{OH}$ radical to the aromatic ring of tyrosine (**101**) gives rise to 1-hydroxy-2,4-cyclohexadienyl radical **102**²⁰⁵, which may further react with oxygen to yield peroxy radical **103** (equation 56). Subsequent $\text{HO}_2\cdot$ elimination is expected to generate α -ketol **104**, the likely precursor of 3,4-dihydroxyphenylalanine **105** (DOPA)²⁰⁶. Similar types of reactions have been proposed for the formation of *ortho*-, *meta*- and *para*-tyrosine upon exposure of phenylalanine to $\cdot\text{OH}$ radical²⁰⁴. However, the importance of such oxidation processes and the putative participation of peroxy radicals in the formation of hydroxylated adducts to both tyrosine and phenylalanine remains to be established.

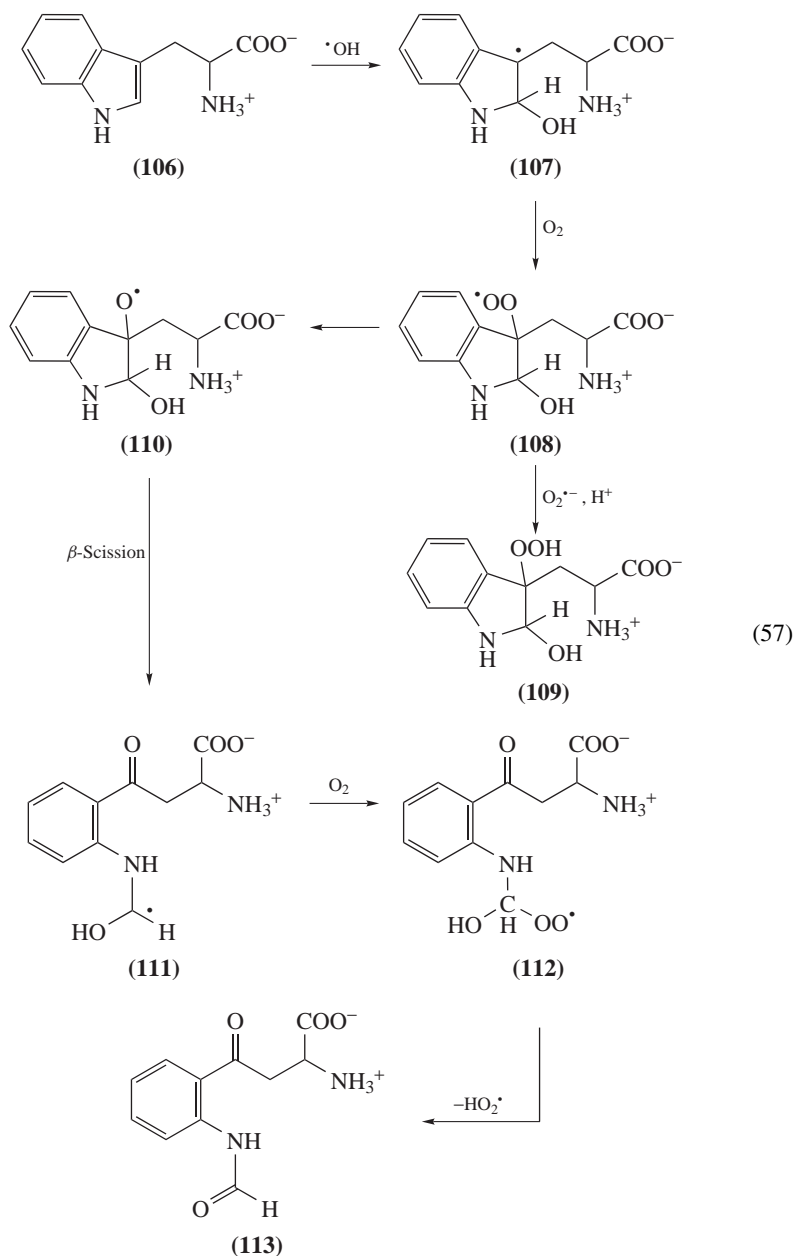


v. *Tryptophan*. Major attention has been given to oxidation reactions of tryptophan (**106**) including those mediated by $\cdot\text{OH}$ radical. Thus, addition of $\cdot\text{OH}$ has been shown to occur both on the benzene ring and the pyrrole moiety of tryptophan (**106**) in a relative ratio 4:6²⁰⁷. One of the main $\cdot\text{OH}$ -induced oxidation products of tryptophan (**106**) has been identified as *N*-formylkynurenine (**113**) (NFKy), whose radiation-induced formation was found to be favored with respect to 4-, 5-, 6- and 7-hydroxytryptophans when oxygen is present in the solution²⁰⁸. The generation of NFKy **113** has been rationalized in terms of initial formation of $\cdot\text{OH}$ radical adduct at C3 of the pyrrole moiety leading to **107**, followed by O_2 addition^{207b, 207c}. Subsequently, the resulting peroxy radical **108** may be reduced to hydroperoxide **109** (*vide infra*) and/or converted to alkoxy radical **110** which, through a β -scission mechanism, would lead to the cleavage of the 2,3-bond of the 5-membered ring. Subsequent addition of O_2 to the resulting α -hydroxyalkyl radical **111** would give rise to hydroxyperoxy radical **112**, the likely precursor of NFKy **113** through a reaction pathway involving $\text{O}_2^{\cdot-}$ elimination (equation 57).

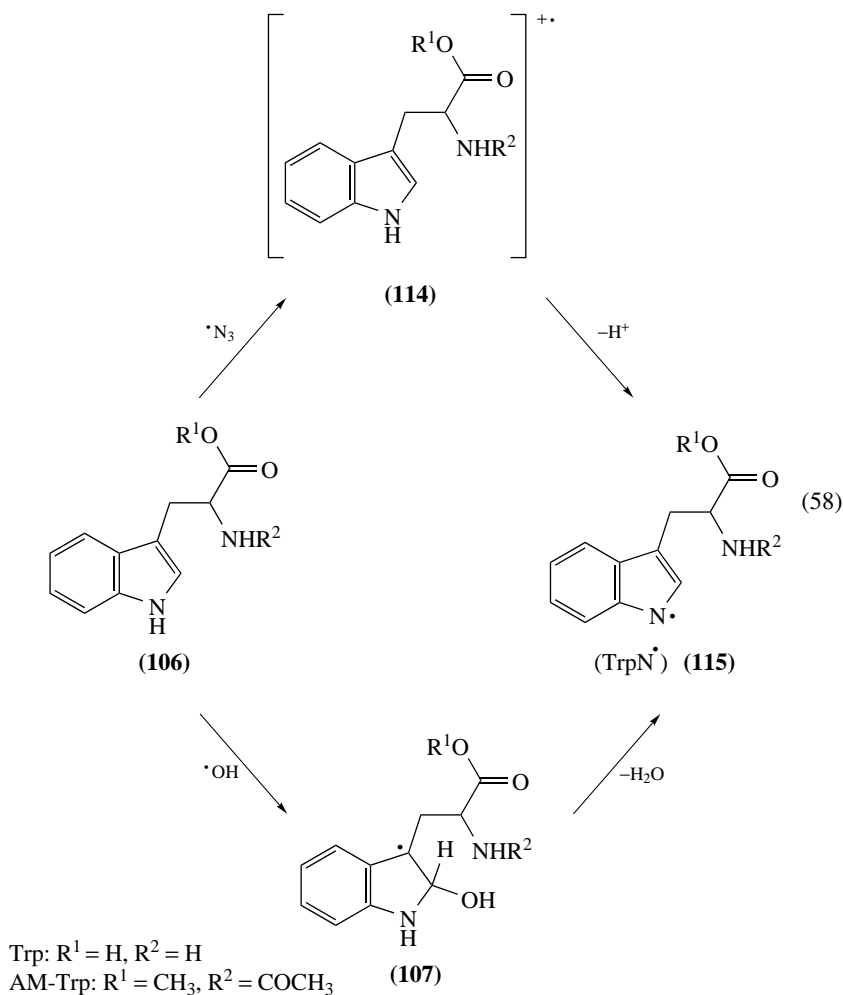
2. Other radical reactions

Aromatic amino acids including tryptophan (Trp) (**106**) and tyrosine (**101**) are highly susceptible to various physical, chemical and biochemical one-electron oxidants; they are

also the targets of enzymic oxidation reactions as discussed below. Evidence is accumulating for the implication of the resulting radicals in reactions with usually the poorly reactive but ubiquitous $O_2^{\bullet-}$, leading to the formation of hydroperoxides.

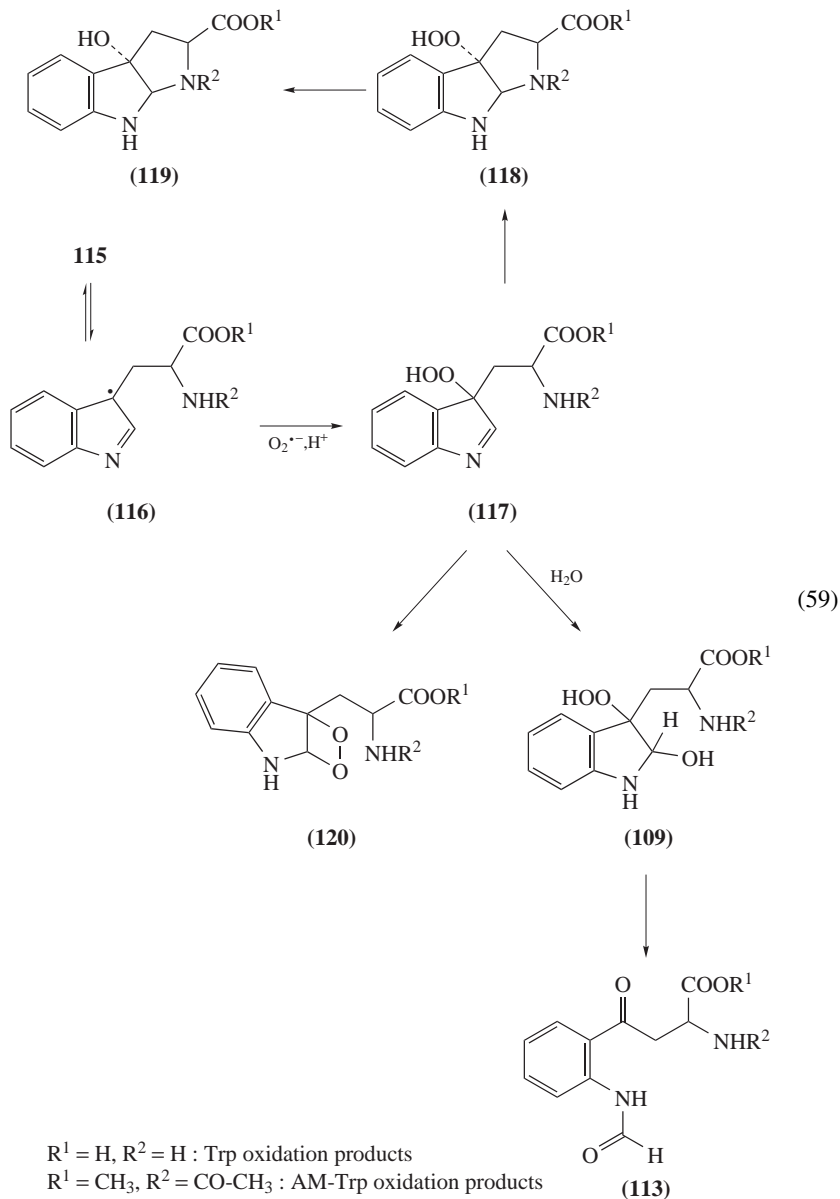


a. Tryptophan. One-electron oxidation of tryptophan (**106**, $R^1 = H$, $R^2 = H$) and its *N*-acetyl methyl ester derivative (AM-Trp) (**106**, $R^1 = CH_3$, $R^2 = CH_3CO$) can be achieved using mild and selective oxidants including azide radical N_3^{\bullet} ²⁰⁹ and type I photosensitizers such as thionine²¹⁰ and tris(2,2'-bipyridyl)ruthenium(II)chloride hexahydrate²¹¹. The resulting radical cation **114** whose pK_a is 4.3²¹² is expected to undergo fast deprotonation at neutral pH, yielding the *N*-centered radical **115** (TrpN $^{\bullet}$). **115** may be also formed by dehydration of **107**, the $\bullet OH$ adduct at C2 within the pyrrole moiety (equation 58). It was found that the decay of **115** and of its methyl ester was not affected by the presence of O_2 as inferred from pulse radiolysis, indicating that the *N*-centered radical would at best react very poorly with oxygen. Interestingly, $O_2^{\bullet -}$ was shown to efficiently react with TrpN $^{\bullet}$, which exhibits a similar reduction potential ($E = +1.0$ V at pH 7) to the phenoxyl radical ($E = +0.93$ V) deriving from tyrosine. The rate constant for the reaction of $O_2^{\bullet -}$



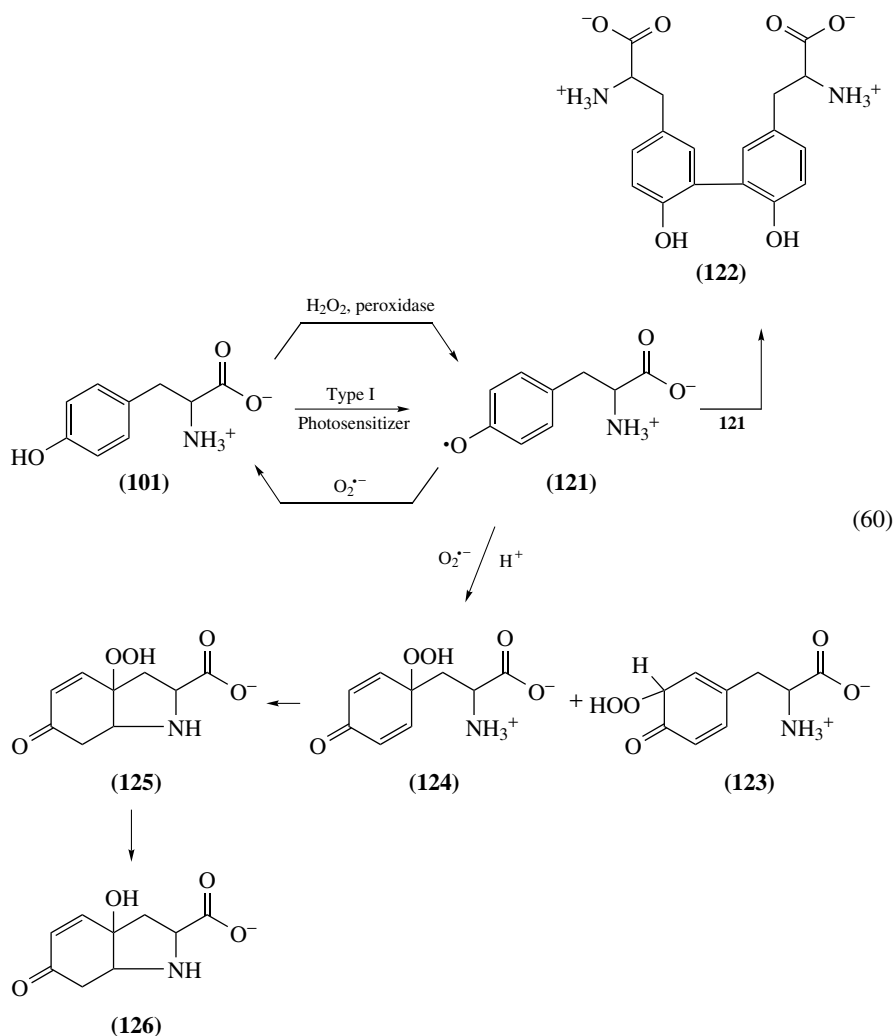
with the methyl ester of the tryptophan radical (AM-TrpN[•]), which consists mostly of an addition process rather than a reduction one, was estimated to be $1.6 \times 10^9 \text{ M}^{-1} \text{ s}^{-1}$ on the basis of pulse radiolysis measurements²⁰⁹. Product analysis, achieved by comparing HPLC features using authentic samples generated by ¹O₂ oxidation²¹³ as reference compounds, shows that the methyl ester of NFKy, and to a lesser extent the *cis* and *trans* isomers of 1-acetyl-2 β -methoxycarbonyl-3 $\alpha\beta$ -hydroxy-1,2,3 α [2,3-*b*]indole (AM-HIP), were the main stable oxidation products. In addition, two peroxidic compounds were detected in the HPLC elution profile. This was achieved using a post-column derivatization method that is based on the oxidation of iodide ions present in the Allen reagent²¹⁴. The formation of the overall AM-Trp oxidation products may be accounted for by the initial generation of diastereomeric hydroperoxides **117** as the result of addition of O₂^{•-} to C3 of **116**, a tautomeric form of AM-TrpN[•] radical **115** (equation 59). The unstable 3 α -hydroperoxyindolenine diastereomers **117** are expected to decay by two competitive pathways. One implies intramolecular Michael-type cyclization reaction yielding a pair of relatively stable diastereomeric hydroperoxides identified as the *cis*- and *trans*-1-acetyl-2 β -methoxycarbonyl-3 $\alpha\beta$ -hydroperoxy-1,2,3 α [2,3-*b*]indole (**118**), which decompose hydrolytically into related alcohol derivatives, namely the two diastereomers of **119**. The other one leads to the formation of AM-NFKy **113** according to a pathway that requires opening of the pyrrole ring at the 2,3-bond. It has been proposed that 2,3-dioxetane **120**, a likely rearrangement product of 3 α -hydroperoxyindolenine **117**, could be the precursor of formylkynurenine²¹⁵. However, this appears to be an unlikely possibility, at least at neutral pH, since usually strong alkaline conditions are required for the formation of dioxetane **120**²¹⁶, which has been postulated to be also a product of the reaction of ¹O₂ with **106** (*vide infra*). There is no evidence of chemiluminescence emission during 2,3-dioxegenase-mediated peroxidation of **106** that could be an indication of the formation of dioxetane **120**, as proposed for the oxidation of indole derivatives by another peroxidase, namely horseradish peroxidase²¹⁷. A more suitable alternative would involve hydration of the 1,2-unsaturated bond of precursor **117** in aqueous solution giving rise to indole 2,3-hydroxyhydroperoxide **109**, which may be independently produced by [•]OH oxidation (*vide supra*). Rearrangement of the latter peroxide into AM-NFKy could be accounted for by the mechanism that has been postulated for explaining the 2,3-bond cleavage of 3-hydroperoxyindolenines²¹⁸. Interestingly, the latter pathway is compatible with the observation that both the formyl and ketone moieties of NFKy **113** are [¹⁸O]-labeled upon enzymic oxidation of Trp **106** by tryptophan 2,3-dioxygenase in ¹⁸O₂-saturated aqueous solutions²¹⁹.

b. Tyrosine. Phenoxyl-type tyrosyl radical **121** (TyrO[•]) that derives from one-electron oxidation of tyrosine (**101**) can be generated by a large range of oxidants including ONOO⁻²²⁰ and inorganic radicals such as CO₃^{•-}^{220,221} and N₃[•]²²². **121** may be also produced by single-excited-state-mediated photoionization²²³ or upon dehydration of [•]OH radical adduct to tyrosine and is a key intermediate in catalytic cycles of prostaglandin synthase and ribonucleotide reductases²²⁴. In addition, **121** has been shown to be generated by several peroxidases²²⁵ that are secreted by eosinophils and neutrophils at inflammation sites and during phagocytosis. **121** does not exhibit any detectable reactivity with O₂²²⁶ but is able to dimerize, leading to the generation of 3,3'-dityrosine (**122**) both in model systems and within cells. Reaction of TyrO[•] with O₂^{•-} has been shown to be an efficient process, since its rate constant ($k = 1.5\text{--}1.7 \times 10^9 \text{ M}^{-1} \text{ s}^{-1}$) is more than three-fold larger²²⁷ than that of the dimerization reaction²²⁶. Initially, it was suggested that O₂^{•-} was mostly acting on **121** by an electron transfer reaction, leading to the regeneration of tyrosine as a result of a chemical repair event. Interestingly, in subsequent radiolysis studies evidence was provided for the occurrence of a much more efficient O₂^{•-} addition to TyrO[•], giving



rise to tyrosine hydroperoxides²²⁷. The latter observation was extended recently to other phenoxy-type radicals including those derived from cresol tyramine and tyrosol²²⁸. Thus, steady-state γ -radiolysis of O_2 -saturated solutions of 0.5 mM Tyr **101** in the presence of 20 mM NaN_3 leads to the generation of TyrO[•] **121** and $O_2^{\bullet-}$, side by side, in a ratio 1.2:1. These conditions were found to disfavor the formation of dityrosine **122**. Instead, two main

stable decomposition products that were assigned as the (2*S*,3*aR*,7*aS*) and (2*S*,3*aS*,7*aR*) diastereomers of 3*a*-hydroxy-6-oxo-2,3,3*a*,6,7,7*a*-hexahydro-1*H*-indole-2-carboxylic acid (**126**) by extensive ¹H NMR analysis of the reaction mixture were shown to be generated. Evidence was also provided for the transient formation of unstable hydroperoxide precursor(s) detected using the Allen reagent²¹⁴, that decay at pH 8 with a half-life of 4.2 h at room temperature with a concomitant release of H₂O₂. The formation of the oxidation products of **101** has been rationalized in term of initial O₂^{•-} addition to the *para* and/or *ortho* positions of the TyrO[•] radical **121**. Subsequent protonation of the resulting anions of 4-alanyl-4-hydroperoxycyclohexa-2,5-dienone and 4-alanyl-2-hydroperoxycyclohexa-3,5-dienone is expected to yield hydroperoxides **123** and **124**, respectively (equation 60). Michael-addition type reaction involving the non substituted amino group of enone **123**



has been proposed to give rise to cyclic hydroperoxide **125** as the precursor of stable compound **126**. Further evidence for the formation of hydroperoxides, the reaction of $O_2^{\bullet-}$ with $TyrO^{\bullet}$ generated by horseradish peroxidase in the presence of H_2O_2 , was provided by the observation of a HPLC peak²²⁹, the content of which gave a positive response with the ferrous oxidation xylene orange (FOX) reagent²³⁰. Peroxidation products that are likely to be **125** and/or a related isomer arising from cyclization of **124** have also been detected as a HPLC peak by the FOX reagent in the myeloperoxidase-mediated oxidation of tyrosine by neutrophils²³¹. Mass spectrometry evidence was also provided for the formation of a peroxidic compound as the result of the addition of $O_2^{\bullet-}$ to $TyrO^{\bullet}$ of the R2 protein of *E. coli* ribonucleotide²³². However, more definite characterization of the latter tyrosine hydroperoxides awaits further experiments that should include NMR analyses.

3. Singlet oxygen oxidation

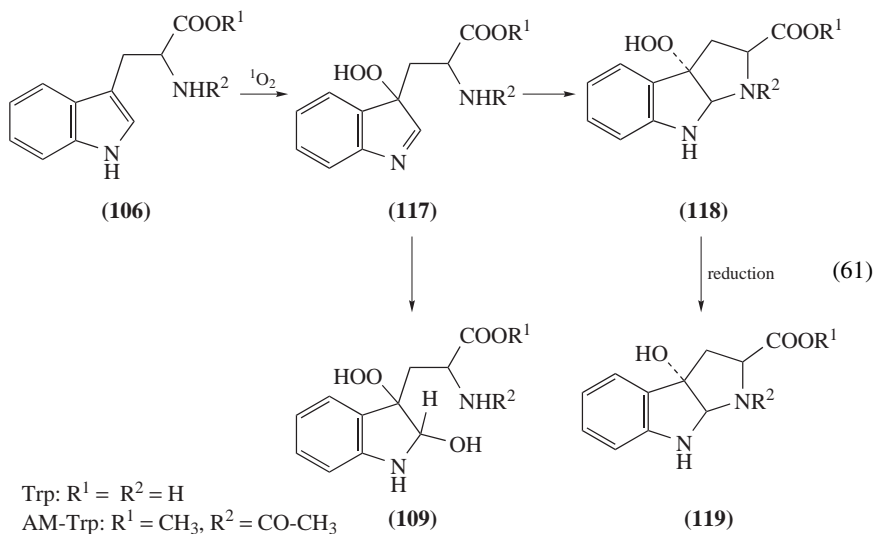
Early studies have shown that tryptophan, tyrosine, histidine, methionine and cysteine, either as free amino acids or as components of peptides, are excellent substrates for 1O_2 oxidation reactions²³³. Usually, reaction of 1O_2 with amino acids is mostly described in terms of chemical quenching with the exception of tryptophan, for which collisional deactivation as the result of physical quenching is not negligible. The rate constants of 1O_2 toward the main reactive amino acids that show a strong solvent dependence are reported in Table 2 for neutral aqueous solutions with values within the range 0.8–3.7 $10^7 M^{-1} s^{-1}$ ²³⁴. In contrast, the rate constants for aliphatic amino acids are much lower, at least by two orders of magnitude. Evidence was provided at least for the three aromatic amino acids that 1O_2 oxidation is able to generate hydroperoxides and/or dioxetanes within the side-chain residues²³⁵. It may be mentioned that 1O_2 -mediated oxidation of Trp has received major attention, already more than 30 years ago.

a. Tryptophan and related compounds. 1O_2 oxidation of Trp **106** ($R^1 = H$, $R^2 = H$) and its *N*-acetyl methyl ester **106** ($R^1 = CH_3$, $R^2 = CH_3CO$) has been shown to generate a similar pattern of degradation products to those resulting from exposure to $\bullet OH$ radical²⁰⁸, incubation with tryptophan 2,3-dioxygenase²¹⁹ or $O_2^{\bullet-}$ addition to one-electron oxidation-induced $TrpN^{\bullet}$ radical²⁰⁹. These include NFKy **113**, 3*a*-hydroperoxy-1,2,3,3*a*,8,8*a*-hexahydropyrrolo[2,3-*b*]indole-2-carboxylic acid **118** and the related alcohol 3*a*-hydroxy-1,2,3,3*a*,8,8*a*-hexahydropyrrolo[2,3-*b*]indole-2-carboxylic acid **119** or the *N*-acetyl methyl ester derivatives as the main oxidation products. Rose-bengal-mediated photosensitization of **106** in aerated 5% ethanol aqueous solution was found to give rise to the predominant formation of the tricyclic hydroperoxide **118**, which was further purified by chromatography on a Sephadex G-10 column. NMR analysis of the colorless powder mixture obtained by lyophilization of the fractions of interest show the presence of

TABLE 2. Rate constants k for the reaction of 1O_2 with the most reactive amino acids in neutral aqueous solutions^{233a, 233c}

Amino acid	$k \times 10^7 (M^{-1} s^{-1})$
Cysteine	3.7
Histidine	3.2
Methionine	1.6
Tryptophan	3.0
Tyrosine	0.8

two diastereomers which can be reduced with Me_2S to the corresponding *cis* and *trans* alcohols **119**. The latter compounds that have been separated by fractional crystallization were characterized by comparison with the 1,2-dicarbomethoxy analogs for which X-ray structure determination was achieved²¹³. It may be added that both *cis* and *trans* diastereomers of **118** and **119**, which were generated by type II photosensitization with sulfonated phthalocyanines²³⁶, were efficiently separated by HPLC analysis on an ODS column. Quantitative conversion of **118** into well-characterized *cis* and *trans* **119**^{213, 215} was achieved by Me_2S and the latter compound was assigned by comparison of the ^1H NMR features with those of reported data²³⁷. This has allowed the assignment of the *trans* configuration to the diastereomer of precursor **118** that exhibited the fastest HPLC elution mobility. However, a more direct characterization of **118** is still lacking. It has been proposed that $^1\text{O}_2$ oxidation of **106** could be rationalized in terms of initial generation of either a 2,3-dioxetane or 3α -hydroperoxyindolenine **117** (equation 61). The first possibility appears quite unlikely since, if this was the case, a higher **113/118** ratio would be expected when **106** is oxidized by $^1\text{O}_2$ compared with a one-electron oxidation process as provided by a type I photosensitizer. In fact, similar ratios were observed using a chemical source of $^1\text{O}_2$, rose bengal as a type II photosensitizer or thionine that operates by both type I and type II mechanisms^{238a}. It has been suggested that enamines could be able to undergo a similar oxidation pathway to the so-called 'ene' reaction²¹⁶, giving rise in the case of **106** to **117**, which may subsequently be involved into two competitive transformation pathways (*vide supra*). These include hydration and Michael-type rearrangement, giving rise to **109** and **118**, respectively. Further work is, however, necessary to gain further insights into this mechanistic proposal. It may be added that the $^1\text{O}_2$ chemical reactions that have been described for **106** are also applicable to a wide variety of indole compounds. Thus, the major oxidation product of an indole-type melatonin compound by $^1\text{O}_2$ was identified as *N*¹-acetyl-*N*²-formyl-5-methoxykynuramine (AFMK)^{238b}. This was achieved using a clean source of $^1\text{O}_2$, namely the endoperoxide of *N,N'*-di(2,3-dihydroxypropyl)-1,4-naphthalenedipropanamide (DHPNO₂)^{238c}. The resulting oxidation product was characterized by high-performance liquid chromatography coupled to tandem mass spectrometry (HPLC-MS/MS) together with ^1H and ^{13}C NMR spectrometry.

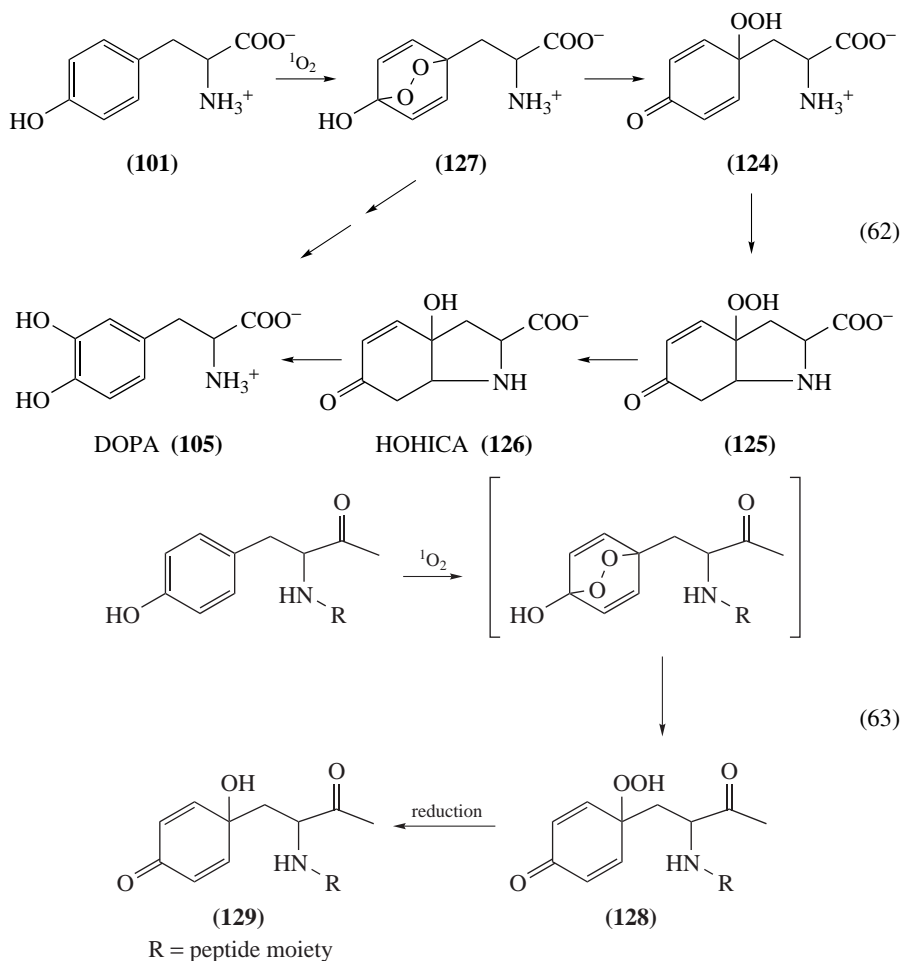


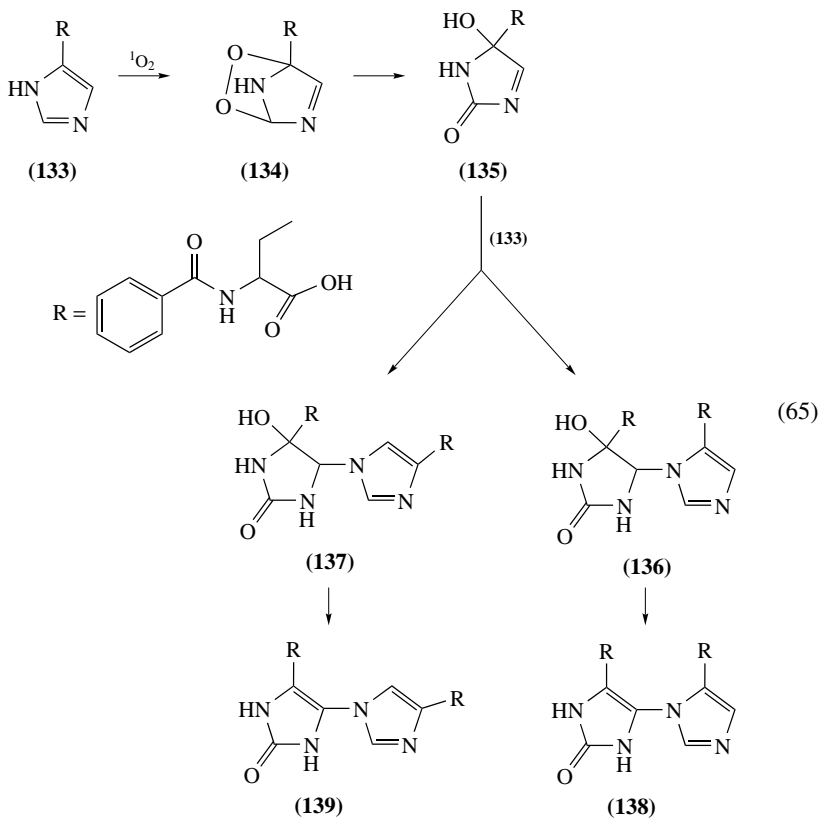
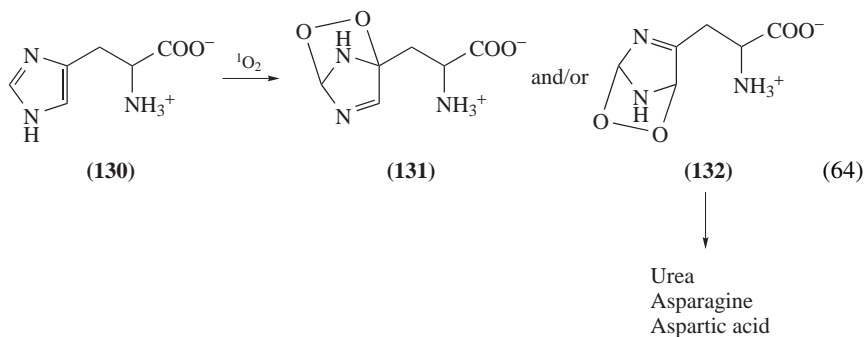
Isotopically labeled DHPN¹⁸O₂ was also used as a source of ¹⁸[¹O₂] to provide further support for the proposed structure. It was thus confirmed that ¹O₂-mediated oxidation of melatonin yields AFMK through the intermediary of a transient endoperoxide as inferred from the fragmentation pattern of the [¹⁸O]-labeled oxidation product. The deformylation product of AFMK, namely *N*¹-acetyl-5-methoxykynuramine, was also shown to be produced.

b. Tyrosine. Attempts were recently made to better assess the ¹O₂-mediated peroxidation reactions of Tyr either as the free amino acid or when inserted into peptides. Early observations²³⁹ that have received further support in recent years²⁴⁰ have shown that the major stable decomposition product of Tyr upon a type II photosensitization mechanism (¹O₂) in aerated aqueous solution is 3*a*-hydroxy-6-oxo-2,3,3*a*,6,7,7*a*-hexahydro-1*H*-indol-2-carboxylic acid **126** (HOHICA). It was proposed that formation of this compound may involve some of the peroxidic intermediates^{239b} that are generated in the reaction of O₂^{•-} with TyrO[•] **121**, giving rise also to **126** (*vide supra*). Evidence for the presence of peroxides in the rose bengal-photosensitized solution of Tyr was provided by global colorimetric measurement using the FOX assay. More interestingly, two main HPLC fractions were shown by ESI-MS analysis to contain peroxidic compounds that have incorporated a molecule of O₂. It was demonstrated that the peroxides with the slowest chromatographic mobility were converted by thermal degradation to **126** through the intermediacy of the fastest eluting peroxidic diastereomers. Relevant structural information on the latter peroxidation products that were characterized as (2*S*,3*aR*,7*aR*)- and (2*S*,3*aS*,7*aS*)-3*a*-hydroperoxy-6-oxo-2,3,3*a*,6,7,7*a*-hexahydro-1*H*-indole-2-carboxylic acids was inferred from extensive ¹H and ¹³C NMR analyses of the photosensitized solution of **101** and further comparison of the NMR features with those of the *cis* and *trans* diastereomers of **126** and their NaBH₄ reduced derivatives. The singlet oxygen oxidation of **101** was rationalized in terms of initial formation of unstable diastereomeric 1,4-endoperoxides **127** as the result of ¹O₂ [4 + 2] cycloaddition. Subsequent opening of the endoperoxides would lead to related indolic hydroperoxides **124** which, through Michael-type reaction, undergo ring closure to yield cyclic peroxides **125**, the precursors of **126** (equation 62). It may be added that decomposition of endoperoxides **127** has been proposed to also give rise to **105**. The cyclization reaction was found to be prevented by the presence of a substituent on the α -amino group, as is the case for *N*-acetyltyrosin and Tyr-containing peptides^{195b, 240, 241}. Thus, the long-lived hydroperoxide **128** derived from Tyr endoperoxide in Gly-Tyr-Gly upon ¹O₂ oxidation is formed and decays only slightly after a several-month incubation period at room temperature, leading to the corresponding alcohol **129**²⁴⁰ (equation 63).

c. Histidine. Evidence for ¹O₂-mediated peroxidation of histidine (His) (**130**) was provided by global measurements using dedicated colorimetric assay. However, attempts to characterize histidine hydroperoxides that are likely to arise from oxidation of the imidazole ring as the result of initial formation of two possible isomeric 2,4- and 2,5-endoperoxides **131** and **132** (equation 64) have been so far unsuccessful due to the instability of the latter compounds. In fact, a complex mixture of degradation products was generated upon rose-bengal-sensitized photooxidation of *N*-benzoylhistidine (**133**)²⁴². Evidence was provided for the presence of dimeric compounds among various oxidation products that were partly characterized. It was postulated that the formation of the **133** degradation products would involve initial generation of two isomeric endoperoxides as the result of 1,4-cycloaddition of ¹O₂ across the 2,4 and 2,5 carbons of the imidazole ring. This is in agreement with the well-established ¹O₂ oxidation reactions of imidazole compounds. Thus, formation of a 2,5-endoperoxide via [4 + 2] cycloaddition was observed upon phthalocyanine-mediated photosensitization at low temperature

of specifically ^{13}C , ^{15}N labeled 4,5-diphenylimidazole used as a model system. This was achieved by careful ^{13}C and ^1H NMR analysis of the main photoproducts present in the irradiated solution. It was shown by warming the solution that the 2,5-endoperoxide formed initially underwent rearrangement, yielding the related 2-hydroperoxide²⁴³. A slightly different pathway is expected for $^1\text{O}_2$ oxidation of **133** as inferred from the formation of a biadduct upon rose bengal photosensitization²⁴⁴. The formation of the latter compound that was characterized by extensive 2D-NMR analysis would involve initial generation of the 2,5-endoperoxide **134**. Subsequently, **134** would undergo splitting of the O–O bond with conversion to **135** rather than rearrange to the hydroperoxide as observed for the 4,5-diphenylimidazole endoperoxide (*vide supra*). Nucleophilic addition of a molecule of **133** at C4 of **135** is expected to lead to the two Bz-His cross-links **138** and **139** resulting from dehydration of **136** and **137**, respectively (equation 65). It is tempting to propose that the latter reaction would be implicated in the formation of photosensitized adducts between His and several amino acids including lysine, cysteine, Trp and Tyr²⁴⁵.





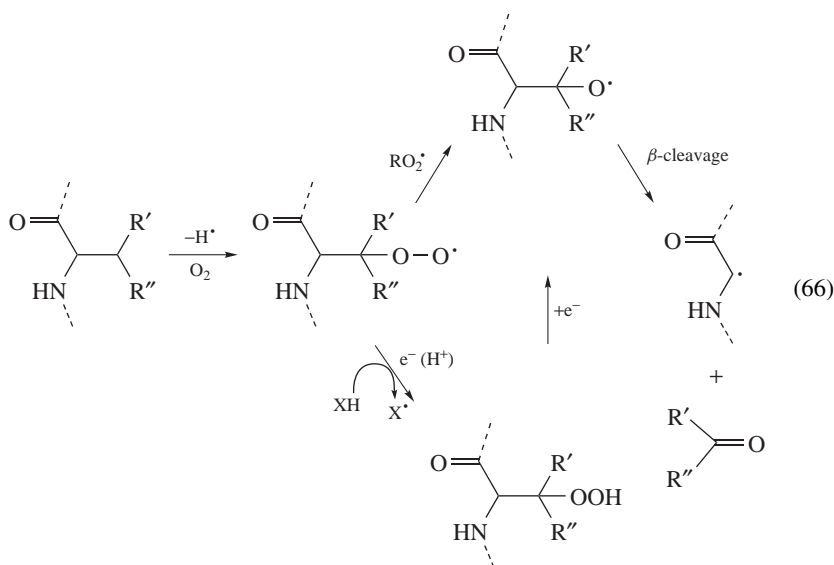
B. Proteins

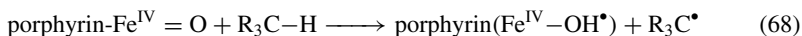
1. Peroxide formation

Various attempts have been made to measure the formation of peroxides in isolated proteins and low density lipoproteins upon exposure to various oxidizing agents including ionizing radiation, transition metals involved in Fenton reaction, peroxy radicals, photosensitizers and enzymatic oxidative systems (for reviews see References 195, 234 and 241).

Most of the measurements were performed using the well-established ferric-xylenol orange (FOX) and iodometric assays that are accurate on isolated proteins, once H_2O_2 has been removed. Assessment of the level of protein hydroperoxides in complex biological systems such as LDL has required improvement of the FOX assay by including a precipitation step with trichloroacetic, metaphosphoric and perchloric acids for eliminating lipids²⁴⁶. These measurements are, however, not informative on the nature of amino acids implicated in the peroxidation reactions. This explains why efforts were made to assess the targets of the oxidation reactions by using exposing dedicated proteins that present peculiar amino acid contents (*vide infra*). Attempts were also made to gain insights into the radical intermediates involved in the latter peroxidizing reactions from the results of ESR-spin trapping experiments (for a recent review, see Reference 199c).

a. Radical reactions. Hydroxyl radical that was generated via γ -radiolysis of aqueous solution has been shown to be an efficient generator of hydroperoxides within bovine serum albumin^{196b, 247}. This may be rationalized in terms of hydrogen atom abstraction from the side-chain carbons of the protein with the exception of α -carbon, leading in the presence of O_2 to peroxy radicals as shown in equation 66. Evidence was provided from ESR-spin trapping measurements and computer simulation of the observed anisotropic signals that $\bullet\text{OH}$ is able to generate peroxy-type radicals within BSA and lysozyme in aerated aqueous solution²⁴⁸. Fenton-type reactions involving copper and ferrous ions²⁴⁹ have been also shown to induce the formation of peroxides that may occur at specific sites as the result of copper ion binding^{249a}. Peroxy radicals that are generated by thermal decomposition of 2,2'-azobis(amidinopropane) dihydrochloride (AAPH) have been shown to produce hydroperoxides in the protein component of LDL²⁵⁰. A relevant example of carbon-centered radicals, likely precursors of hydroperoxides, that were spin-trapped with 5,5-dimethyl-1-pyrroline *N*-oxide (DMPO), is provided by the reaction promoted by *t*-butyl hydroperoxide within methemoglobin and metmyoglobin²⁵¹. The ESR spectra were rationalized in term of generation of valine radicals through hydrogen abstraction at α - and/or β -carbons according to the sequence of reactions 67 and 68 involving the haeme protein in a higher oxidation state:





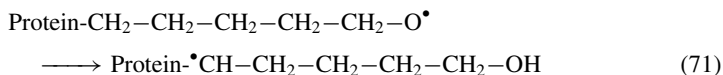
b. Peroxidase-mediated reactions. Utilization of enzymatic reactions could be an approach to generate hydroperoxides within proteins in a more specific way. Various peroxidases including myeloperoxidase and horseradish peroxidase have been shown to produce the phenoxyl radical of tyrosine, which is susceptible to react with $\text{O}_2^{\bullet-}$ to produce a cyclic hydroperoxide in free **101** and on the *N*-terminal Tyr residue within dipeptides²²². However, even if evidence has been provided for the formation of phenoxyl radical from Tyr within proteins, it has not been yet established whether Tyr peroxides can be produced in the latter biomolecules with the exception of ribonuclease reductase²³². In the latter case it has been found that the reaction of TyrO^\bullet with $\text{O}_2^{\bullet-}$ leads to the formation of a hydroperoxide. It may be added that amino acid radicals are assumed to be mostly Tyr phenoxyl radicals that have been detected by ESR within BSA upon reaction with a H_2O_2 -immobilized horseradish peroxidase system²⁵².

c. Singlet oxygen oxidation. $^1\text{O}_2$ has been shown to be much more specific in its oxidation reactions with amino acids than $^\bullet\text{OH}$ radical (*vide supra*). Thus, it has been possible to peroxidize residues of only one amino acid by selecting proteins with a suitable composition^{241b}. Trp peroxides are formed almost exclusively upon type II photosensitization of mellittin, a protein which lacks His, Tyr, methionine and cysteine, four of the five $^1\text{O}_2$ reactive amino acids²³⁴. This also applies to the trypsin inhibitor that exhibits only Tyr residues as the reactive sites²³⁴.

2. Secondary reactions mediated by amino acid peroxides

Most of the peroxides that are generated within proteins upon exposure to $^\bullet\text{OH}$ radical, one-electron oxidants and $^1\text{O}_2$ are relatively stable in neutral aqueous solutions at room temperature in the absence of light, heat and transition metals¹⁹⁶. For example, the half-lifetime of radiation-induced peroxides within bovine serum albumin was found to be about 2 h at 37 °C in the absence of reducing agents²⁴⁷. However, the decomposition of various protein hydroperoxides has been shown to be significantly enhanced by light, heat and the presence of Fe^{2+} or Cu^+ ²⁴⁷, as well as by reducing compounds present in biological fluids and cells^{247,253}. One-electron reduction of peroxides that may have been generated on side-chain sites gives rise to the related alkoxy radicals (equation 66).

The latter radicals may undergo further reactions including hydrogen abstraction from a suitable donor (equation 69) or rearrangement with conversion through either a 1,2- or 1,5-hydrogen shift to alkyl radicals (equations 70 and 71). The latter radicals are able to react with oxygen, thus generating peroxy radicals that, as discussed above, may be either reduced to related hydroperoxides or involved in dismutation reactions with subsequent generation of alkoxy radicals.



Attempts have been made to gain information on these radical intermediates that are likely to exert damaging effects either within the oxidized protein or on other molecules

including a different protein, an unsaturated lipid and DNA. In that respect evidence was inferred from ESR-spin trapping experiments^{197c} that either alkoxy and/or peroxy radicals can be intercepted in peroxidized proteins and oligopeptides^{241,247,248}. This was achieved using mostly 2-methyl-2-nitrosopropane (MNP)²⁴¹ and several cyclic nitrones including 5,5-dimethyl-1-pyrroline *N*-oxide (DMPO)²⁴⁷, *N*-*tert*-butyl- α -phenylnitronone (PBN)²⁴⁷ and 5-diethoxyphosphoryl-5-methylpyrroline *N*-oxide (DEPMPO)²⁴⁸ as spin traps (Chart 2). It was proposed, in agreement with the results of previous experiments on methylperoxy radicals²⁵⁴, that DEMPO is a suitable nitronone to trap peroxy radicals derived from oxidized bovine serum albumin²⁴⁸, whereas evidence was provided that DMPO is more appropriate to scavenge alkoxy radicals²⁵⁵.

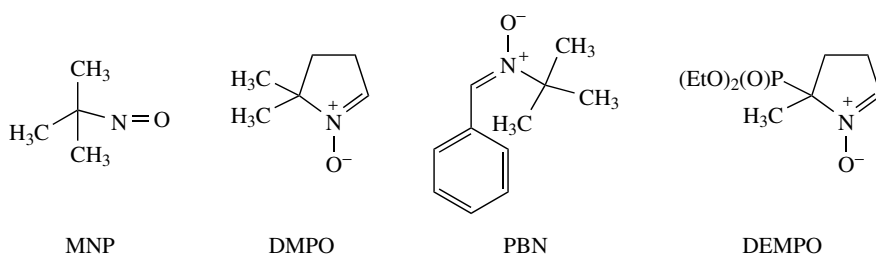
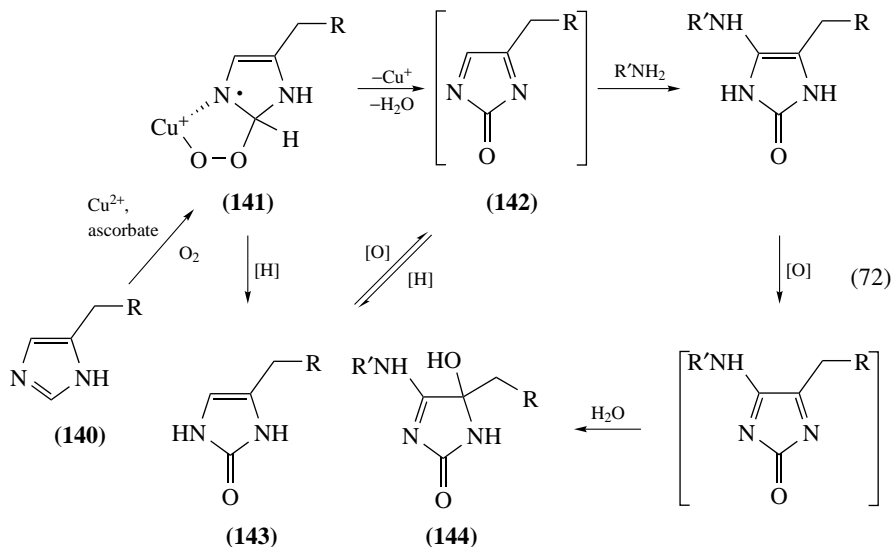


CHART 2

a. Transfer within proteins. Evidence has been provided for the occurrence of amino acid radical-mediated chain reaction up to 7 or even more successive steps within proteins (for a review, see Reference 256). It was suggested that alkoxy radicals that may be generated by transition-metal-induced one-electron reduction of protein hydroperoxides are mostly implicated in these propagation reactions²⁵⁷. Thus radical transfer from a side-chain to the α -carbon is likely to occur via a 1,2-hydrogen shift of the alkoxy radical formed on the C3 carbon. Another possibility to be considered involves an intramolecular 1,5-hydrogen atom shift from remote alkoxy radicals to the C2 carbon in arginine, lysine, leucine and isoleucine. Other reactions including radical transfers from chain to chain and backbone to backbone have been also suggested to take place within peroxidized proteins^{249a}. However, further experiments are required to support the occurrence of such mechanisms.

b. Protein cross-links. ¹O₂-mediated oxidation of histidine-containing proteins has been shown to give rise to aggregates²⁵⁸ that may be rationalized in terms of a covalent nucleophilic attachment of another histidine residue to a reactive intermediate deriving from the thermal rearrangement of an initially generated **134**²⁴⁴ (equation 65). This may also involve the binding of a lysine residue as inferred from a model study²⁵⁹. Another model of oxidative formation of Hist-Lys cross-link that was catalyzed by Cu²⁺ in the presence of ascorbate has recently become available²⁶⁰. Thus, treatment under the latter conditions of a mixture of 4-alkylimidazoles **140** and amines R'NH₂ used as surrogates of histidine and lysine, respectively, was found to give rise to 5-alkyl-5-hydroxy-4-(alkylamino)-1,5-(dihydroimidazol-2-one adducts (**144**). This may be rationalized in terms of initial formation of a cyclic peroxo-Cu²⁺ complex **141** that is susceptible to undergo concomitant dehydration and loss of the copper ion, generating the reactive dehydroimidazolone intermediate **142** that may exist in a dynamic equilibrium with **143**. Subsequent amine

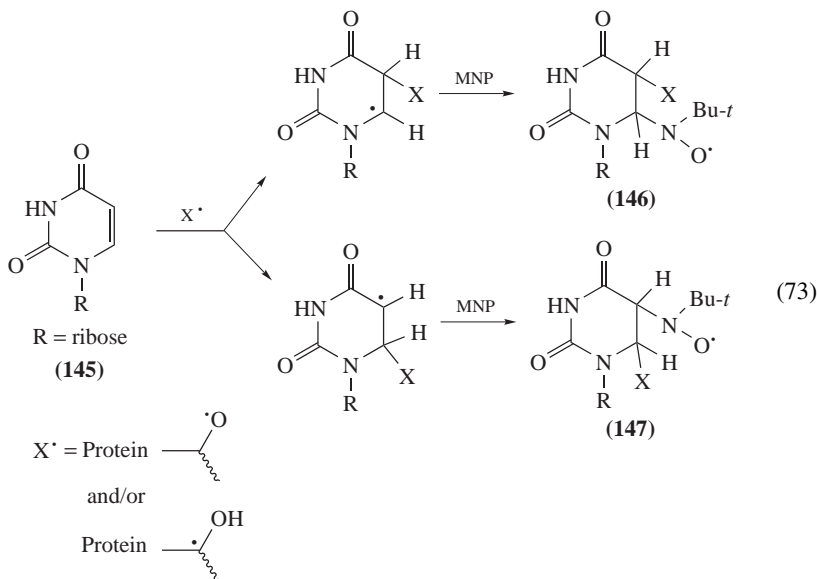
addition to **142** followed by oxidation and hydration are the expected steps leading to the cross-link **144** (equation 72).



c. Lipid peroxidation. It has been reported that oxyl and/or peroxy radicals deriving from one-electron reduction or one-electron oxidation of protein hydroperoxides are able to initiate lipid peroxidation²⁶¹. However, identification of the exact mechanism involved in these propagation reactions is still awaiting further experiments.

d. Nucleic acid–protein cross-links. It was shown from model studies that oxidatively generated DNA–protein cross-links may be produced as the result of initial one-electron oxidation of nucleobases such as guanine²⁶² or 8-oxo-7,8-dihydroguanine²⁶³. Evidence has also been provided for an alternative mechanism that involves protein radicals derived from protein hydroperoxides as the reactive intermediates. This was inferred from the observation that incubation of either linear or plasmid DNA with radiation-induced hydroperoxides of bovine serum albumin, insulin, apotransferrin and α -casein led to cross-link formation²⁶⁴. Alkoxy radicals or secondary rearrangement radicals that may arise from the reduction of the protein hydroperoxides by transition metals such as Fe^{2+} and Cu^+ are the likely reactive intermediates of the latter binding reactions. Several lines of evidence that were provided by ESR-spin trapping measurements would support such hypothesis. Thus, MNP spin-adducts of thymine and uracil radicals that result from the covalent binding of benzoyloxy radicals to the ethylenic 5,6-pyrimidine bond were found to be generated at C5 and C6, respectively²⁶⁵. Further support for the transient formation of pyrimidine radical arising from the binding reaction of amino acid alkoxy radicals to the 5,6-bond of pyrimidine bases was gained from MNP spin trapping experiments. Thus, incubation of uridine (**145**) in oxygen-free aqueous solutions with $\cdot\text{OH}$ -mediated hydroperoxides of lysine, mellittin and histone H1 in the presence of Cu^+ was shown to give rise to both C5 and C6-yl radical adducts **146** and **147**²⁶¹ (equation 73). Similar observations were made when the alkoxy radicals were generated by the reduction of

hydroperoxides of either other individual histones (H2A, H2B, H3 or H4) or histone octamers that consist of 2 molecules of each of them²⁶⁶. Further experiments are, however, required in order to assess whether either alkoxy radicals and/or alkyl radicals that may arise from a 1,2-hydrogen shift of the RO[•] precursors are involved in the binding reaction to pyrimidine bases.



e. Oxidation of DNA and nucleoside. Alkoxy radicals derived from lysine, mellittin and histones have been shown to be able to oxidize the guanine moiety of isolated DNA and 2'-deoxyguanosine, giving rise to 8-oxo-7,8-dihydro-2'-deoxyguanosine^{261, 266} through a mechanism that remains to be determined.

V. CELLULAR INDICATORS OF HYDROPEROXIDES

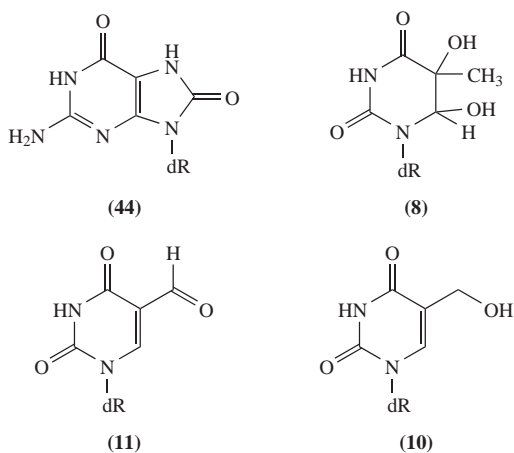
A. Stable DNA Oxidation Products Arising from Nucleobase Hydroperoxide Decomposition

There are no available data on the formation of hydroperoxides derived from DNA within cells. This is likely explained, at least partly, by the fact that DNA is a poorer target than proteins for [•]OH radical as observed upon exposure of mouse myeloma cells to ionizing radiation²⁶⁷. However, indirect evidence for DNA peroxidation within cells may be inferred from the measurement of final degradation products that may derive from thymine and guanine hydroperoxidation as the result of oxidation reactions mediated by [•]OH radical and ¹O₂, respectively (Sections II.A.2 and II.E.2). It may be pointed out that the measurement of oxidized bases and nucleosides within DNA has been the subject of intense research during the last decade and accurate methods are now available²⁶⁸. This includes DNA extraction that involves the chaotropic NaI precipitation step and the use of desferrioxamine to chelate transition metals in order to prevent spurious oxidation of overwhelming nucleobases to occur²⁶⁹. HPLC coupled to electrospray ionization

to tandem mass spectrometry (ESI-MS/MS)²⁷⁰ is a more versatile method than HPLC-electrochemical detection²⁷¹, both assays being much more accurate than the previously utilized CG-MS technique²⁷².

1. Hydroxyl radical-mediated thymine oxidation products

The HPLC-MS/MS method has been recently applied for the measurement of the *cis* and *trans* diastereomers of 5,6-dihydroxy-5,6-dihydrothymidine (**8**), 5-formyl-2'-deoxyuridine (**11**) and 5-(hydroxymethyl)-2'-deoxyuridine (**10**) within cellular DNA exposed to ionizing radiation and heavy particles²⁷³. The two methyl oxidation products **10** and **11** and thymidine glycols **8** (Chart 3) that are produced within the range of 20 to 100 lesions per 10⁹ normal bases and per Gy (Table 3) are likely to be derived from the decomposition of 5-(hydroperoxymethyl)-2'-deoxyuridine (**7**) and 5-(6)-hydroperoxy-6-(5)-hydroxy-5,6-dihydrothymidine **5** and **6**, respectively.



dR = 2-deoxyribose

CHART 3

2. Singlet oxygen-induced formation of 8-oxo-7,8-dihydroguanine

It has been proposed that 8-oxo-7,8-dihydro-2'-deoxyguanosine (**44**) (8-oxodGuo), an ubiquitous DNA oxidation product, is generated through the reduction of ¹O₂-mediated formation of 8-hydroperoxy-2'-deoxyguanosine (**43**) (equation 27). Thus,

TABLE 3. Yields of oxidized nucleosides^a in the DNA of human monocytes THP1 upon exposure to ⁶⁰Co γ -rays and ¹²O⁺⁶ heavy ions^b

Oxidized nucleosides	⁶⁰ Co γ -rays	¹² O ⁺⁶ ions
5,6-Dihydroxy-5,6-dihydrothymidine 8 (4 diastereomers)	97	62
5-(Hydroxymethyl)-2'-deoxyuridine 10	29	12
5-Formyl-2'-deoxyuridine 11	22	11

^a Expressed as number of lesions per 10⁹ normal bases and Gy.

^b From Reference 273.

[^{18}O]-8-oxodGuo has been shown by HPLC-MS/MS measurement to be formed in the DNA of human cells upon exposure to a chemical source of labeled $^{18}\text{O}_2$ ²⁷⁴. In addition, UVA exposure of cells gives rise to 8-oxodGuo that was detected by HPLC-ECD²⁷⁵. Evidence was provided that mostly $^1\text{O}_2$ is involved in the UVA induced formation of 8-oxodGuo as the result of a predominant type II photosensitization mechanism^{275a}.

B. Lipid Hydroperoxides and Related Degradation Products

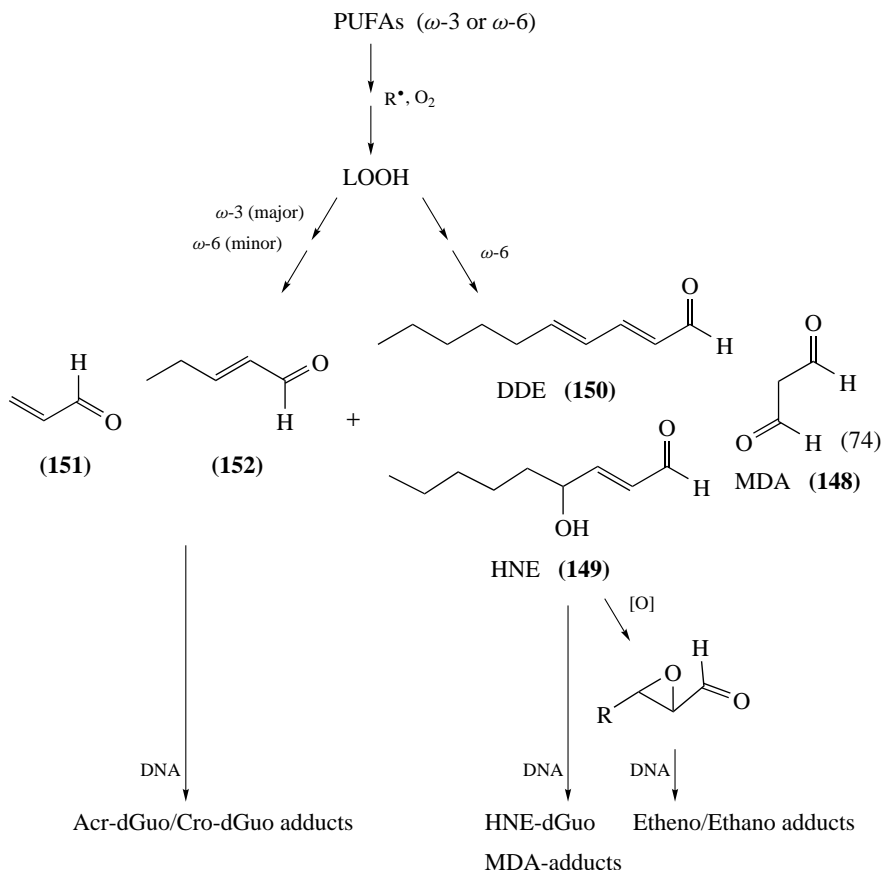
1. Hydroperoxide measurement

Several relatively simple methods of peroxide detection and/or quantification²⁷⁶ with a good degree of sensitivity for monitoring the peroxidation process include (i) the 2-thiobarbituric acid assay, which detects aldehyde by-products of polyunsaturated fatty acids, (ii) absorbance measurement at 234 nm, which detects conjugated diene groups in LOOHs, (iii) the iodometric assay, which detects the LOOH peroxide moiety directly and (iv) formation of the 2',7'-dichlorofluorescein induced by peroxides²⁷⁷. The major disadvantage of the assays is the inability to distinguish between different classes of peroxidized lipids. To separate various LOOH families and the corresponding parent lipids, paper or thin-layer chromatography associated with peroxide-sensitive sprays may be used. These chromatographic approaches allowed different LOOH families to be distinguished from one another, but the disadvantage of this assay is that it is not suitable for quantitative analysis²⁷⁸. Limitations such as these have been overcome by the development of more sophisticated approaches for separating and quantifying LOOHs. High-performance liquid chromatography (HPLC) techniques involving post-column chemiluminescence detection or reductive-mode electrochemical detection were developed with excellent selectivity and very low detection limits for LOOHs²⁷⁹. More recently, powerful approaches including HPLC coupled to a tandem mass spectrometry assembly²⁸⁰ have been widely used for a definitive identification of LOOHs.

2. Aldehydes and other breakdown products

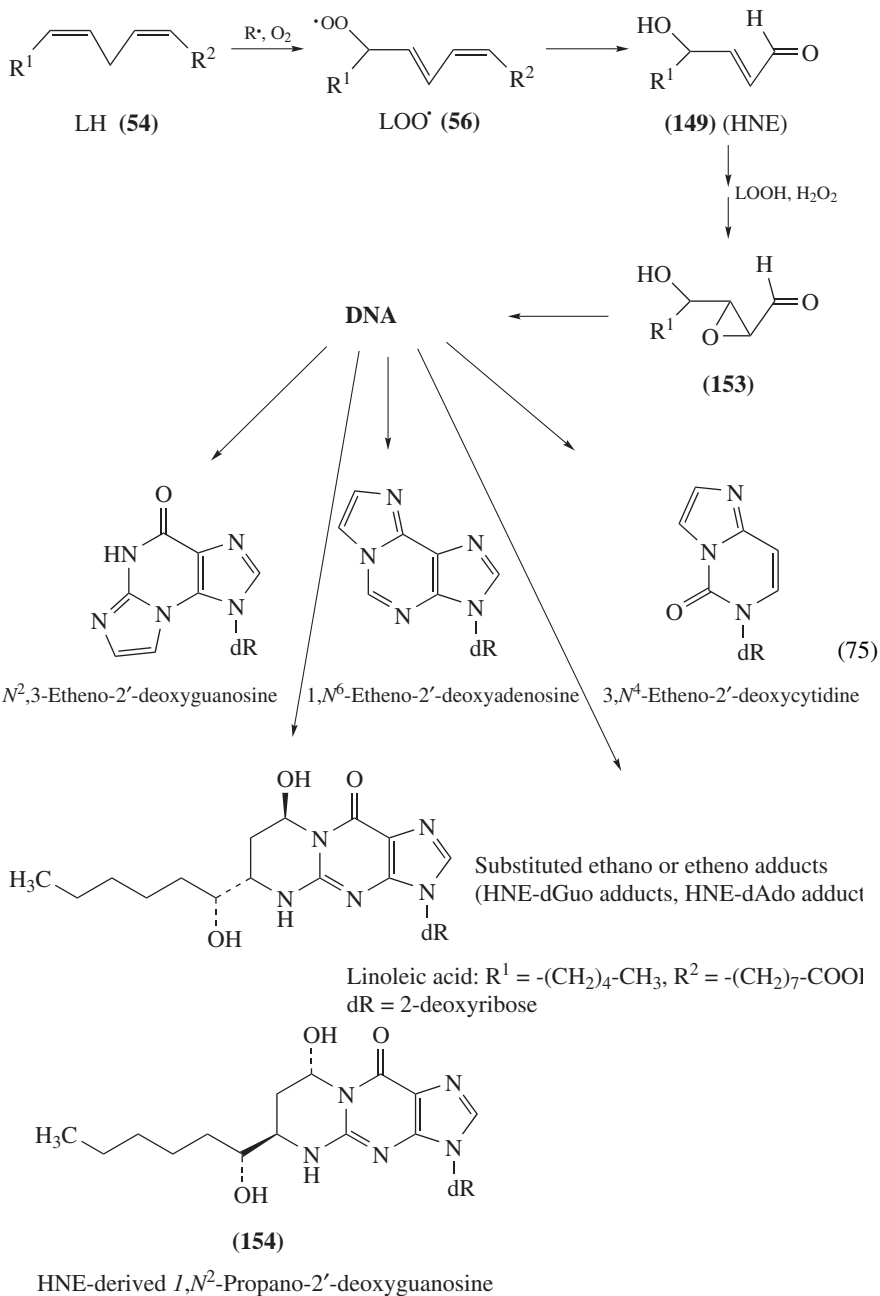
The initial products or primary species of unsaturated fatty acid oxidation, lipid hydroperoxides, may be reduced by glutathione peroxidases to unreactive fatty acid alcohols or react with metals to produce a variety of secondary products which are themselves reactive as epoxides and saturated (e.g. hexanal) and unsaturated aldehydes²⁸¹. The toxicity is largely attributed to α , β -unsaturated aldehydes produced during lipid peroxidation. The decomposition products of lipid hydroperoxides in the presence of air and metals produces compounds that may be trapped with pentafluorobenzylhydroxylamine²⁸². Pentane, ethane and ethylene can be also produced via a β -scission mechanism, a well-known reaction of radicals, especially alkoxy radicals. The major reactive aldehyde products of lipid peroxidation (equation 74) are malondialdehyde (MDA) (**148**), 4-hydroxy-2-nonenal (4-HNE) (**149**), 2,4-decadienal (DDE) (**150**), acrolein (**151**) and crotonaldehyde (**152**). They are highly toxic to mammalian cells due to the direct reaction with biomolecules such as DNA bases or via the corresponding bifunctional epoxides yielding DNA adduct (equation 74). In plants 4-HNE inhibits growth of pathogens²⁸³; 2-alkenals are also genotoxic²⁸⁴ and inhibit growth of fungal cultures²⁸³. Hexanal and other aldehydes decrease seed germination²⁸⁵. Malondialdehyde (malonaldehyde) was the focus of attention in lipid peroxidation for many years due to the use of the 2-thiobarbituric acid test²⁸⁶. In fact, the amount of MDA formed is small during the peroxidation of most lipids but may be larger when microsomes are used in the presence of iron. Peroxidation of polyunsaturated fatty acids (PUFAs) with

more than two double bonds produce a large amount of MDA. Enzymatic reaction during eicosanoid metabolism also generates MDA. The hydroxyalkenal compound 4-HNE, an unsaturated aldehyde and the *trans*-4-hydroxy-2-hexenal (HHE) are extremely toxic²⁸⁷. Their chemical reactivity is due to the aldehyde group, the double bond and the hydroxyl group^{281b}. Another class of toxic products of lipid peroxidation are the isoprostanes, a series of prostaglandin-like compounds formed during the peroxidation of arachidonic acid²⁸⁸. It should be noted that the breakdown products of the primary generated lipid hydroperoxides arise from complex multistep degradation reactions.

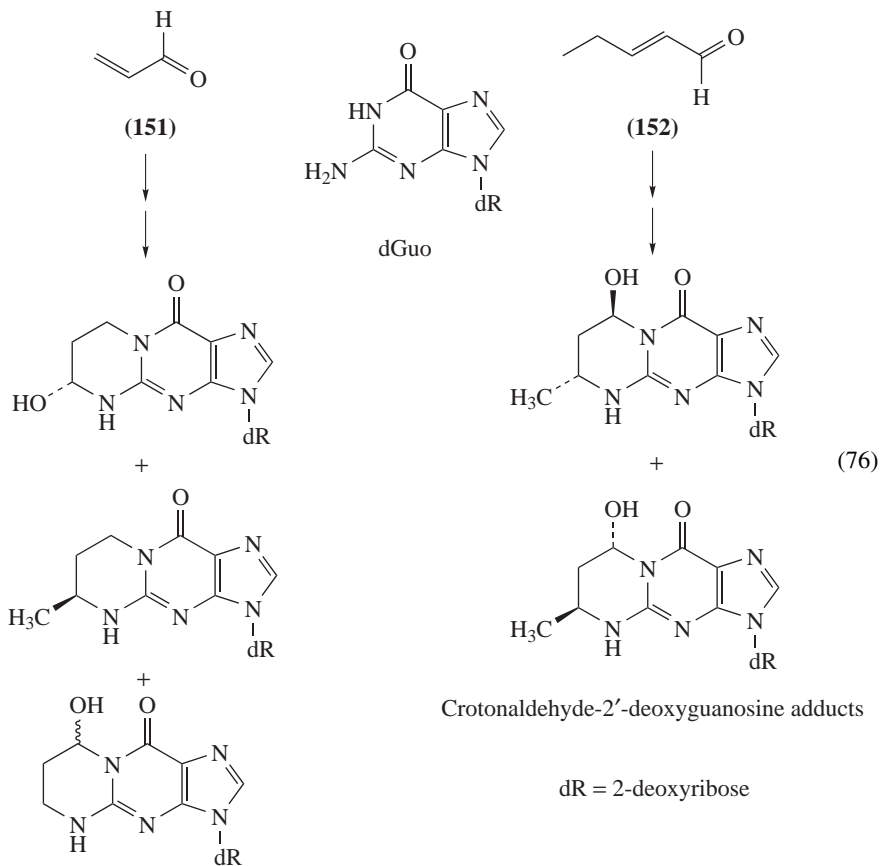


3. Aldehyde adducts to biomolecules

a. DNA adducts. Exocyclic DNA adducts of endogenous origin can be generated by several reactive lipid peroxidation products. Among them, **148–152** have been the most widely studied aldehydes with respect to their chemical and biological activities^{281b}. They have been shown to yield DNA damage either through direct reaction with the DNA bases or through the generation of more reactive electrophilic compounds, such as bifunctional epoxides **153** (equation 75). In the first case, the products generated are the



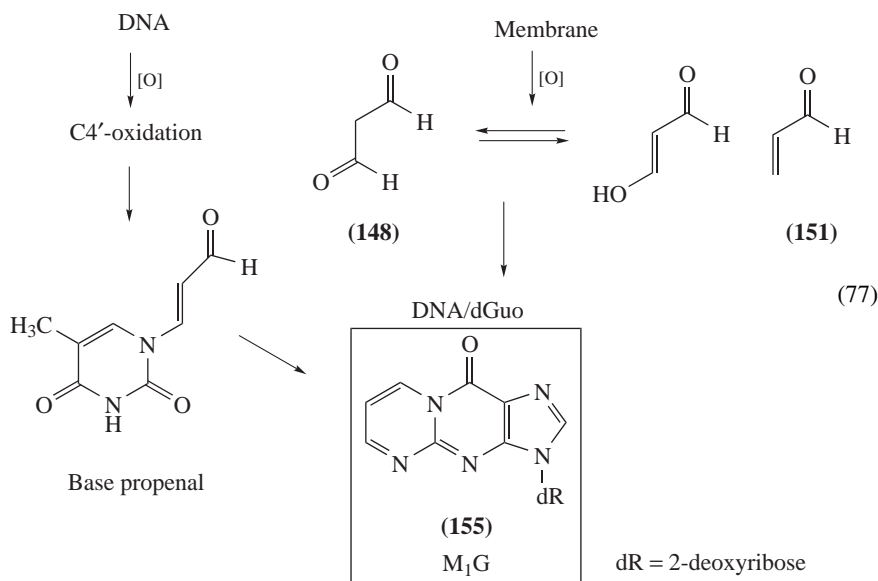
known cyclic substituted propano adducts (equations 75 and 76), mainly 1,*N*²-propano-2'-deoxyguanosine (**154**), for the α , β -unsaturated aldehyde reactions²⁸⁹, and the cyclic pyrimidopurinone (M₁G) (**155**) (M₂G) (equation 77 and Chart 4) and acyclic adducts formed with 2'-deoxyadenosine (M₁dA, M₃dA) and 2'-deoxycytidine (M₁dC, M₃dC) for the MDA (Chart 4) reactions²⁹⁰. The epoxy carbonyl compounds resulting from the oxidation of the α , β -unsaturated aldehydes react with the DNA bases, giving rise to substituted ethano or etheno adducts and unsubstituted etheno adducts^{291,292} (Chart 5). The ability of these reactive electrophiles to alkylate DNA bases, yielding the aforementioned respective promutagenic lesions, has been considered to contribute to the mutagenic and carcinogenic effects associated with the lipid peroxidation process leading to the oxidative stress.



Acrolein-2'-deoxyguanosine adducts

2,4-Decadienal has been reported as one of the most toxic lipid hydroperoxide breakdown products to cells^{281a,293}. Besides 1,*N*⁶-etheno-2'-deoxyadenosine (ϵ dAdo) (**156**)

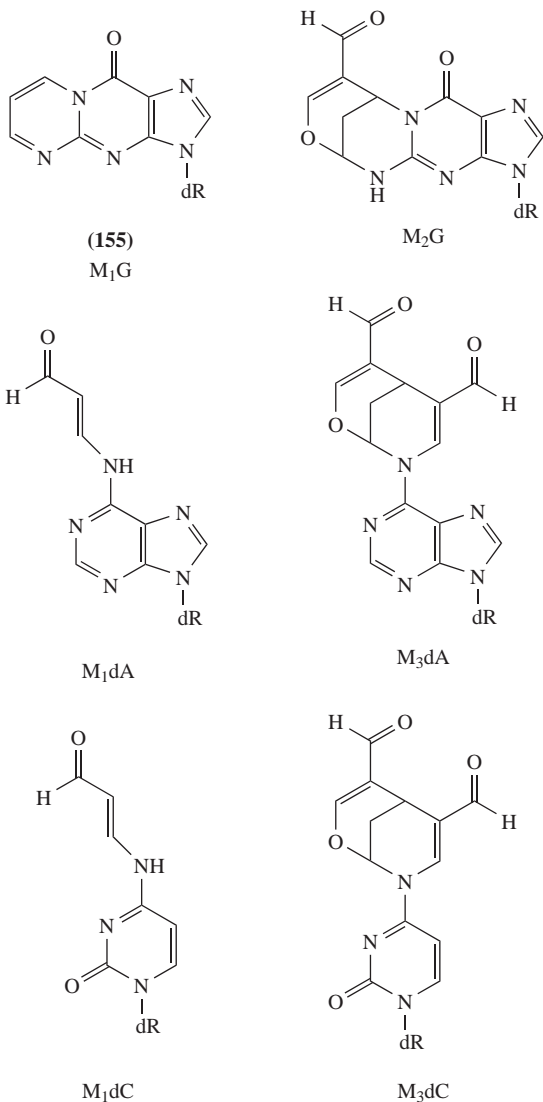
and 1,*N*²-etheno-2'-deoxyguanosine (1,*N*²- ϵ dGuo) (**159**), six different etheno derivative adducts were found to be generated in the reaction of dAdo or dGuo with DDE epoxides²⁹⁴. Recently, 4,5-epoxy-2(*E*)-decenal was shown to be a precursor of ϵ dAdo and 1,*N*²- ϵ dGuo formation²⁹⁵, confirming the proposed reaction mechanism²⁹⁴.



The unsubstituted promutagenic etheno adducts, mainly ϵ dAdo and 3,*N*⁴-etheno-2'-deoxycytidine (ϵ dCyd) (**157**), have been detected as background lesions in rodent and human tissues^{296, 291e, 297}. However, only a few studies have shown the occurrence of *N*²,3-etheno-2'-deoxyguanosine (*N*²,3- ϵ dGuo) (**158**) as a DNA background lesion²⁹⁸. Interestingly, increased levels of ϵ dAdo and ϵ dCyd were observed in clinical situations associated with oxidative stress, such as metal storage diseases²⁹⁹ and chronic infections and inflammation³⁰⁰. These lesions were also shown to be elevated in colon polyps of patients with familial adenomatous polyposis, who later develop carcinomas in the colon³⁰¹, and in white blood cell DNA of women consuming diets rich in polyunsaturated fatty acids³⁰². A correlation between the accumulation of arachidonic acid metabolites and the formation of ϵ dAdo and ϵ dCyd was also observed during the tumor promotion phase of the mouse skin two-stage model of carcinogenesis³⁰³.

In vitro studies have shown that the levels of the four unsubstituted etheno adducts (**156–159**) are increased when nucleosides or DNA are incubated with lipid peroxidation products^{291a–c, 291f, 294a, 294b, 295, 304}. Oxidized α,β -unsaturated aldehydes, such as 4-hydroxynonenal, crotonaldehyde, acrolein and DDE epoxides^{291a–d, 294a, 294b, 305}, are possible endogenous adduct sources. Interestingly, 1,*N*⁶-ethenoadenine was also formed from the reaction of DNA with 2-phosphoglycolaldehyde, a model for the 3'-phosphoglycolaldehyde residue generated by oxidation at C3 of 2-deoxyribose in DNA³⁰⁶. Certain carcinogenic exogenous agents, including mucochloric acid, vinyl chloride and ethyl carbamate (urethane), can also produce etheno adducts^{297h, 307}.

DNA adducts are excellent biomarkers in determining the extent of genetic damage. These markers are useful in understanding the carcinogenesis mechanism and the assessment of cancer risk imposed by several chemical agents. Considering the importance

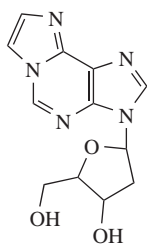
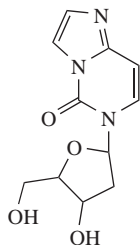
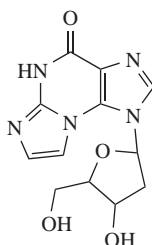
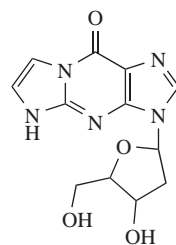


dR = 2-deoxyribose

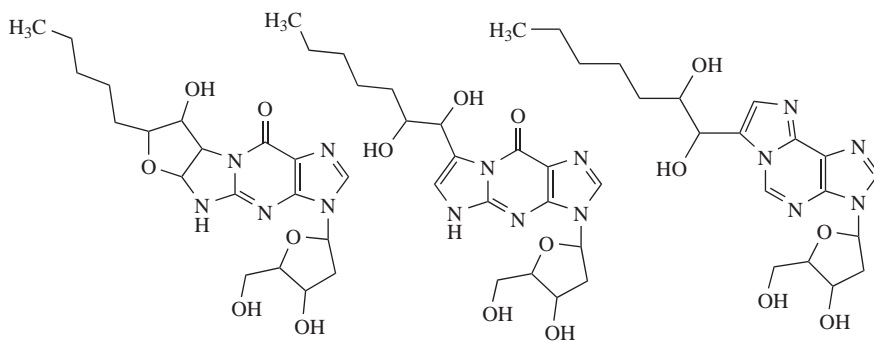
CHART 4

of detection and quantification of these lesions *in vivo*, the development of sensitive and selective methods is necessary. Several methods, such as competitive immunoassay³⁰⁸, the ultra-sensitive, highly specific gas chromatography/electron capture negative chemical ionization high-resolution mass spectrometry^{291g} and liquid chromatography/tandem mass spectrometry (HPLC-ESI-MS/MS) with off-line reversed-phase extraction to purify the adducts from milligram amounts of DNA^{294a, 309}, have been employed. On-line

Unsubstituted etheno adducts

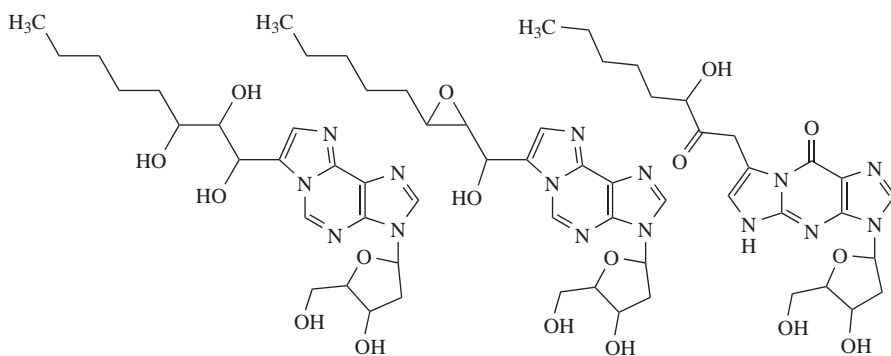
(156)
edAdo(157)
edCyd(158)
*N*²,3-εdGuo(159)
1,*N*²-εdGuo

Substituted ethano or etheno adducts



HNE-dGuo adducts

HNE-dAdo adduct



DDE-dAdo adducts

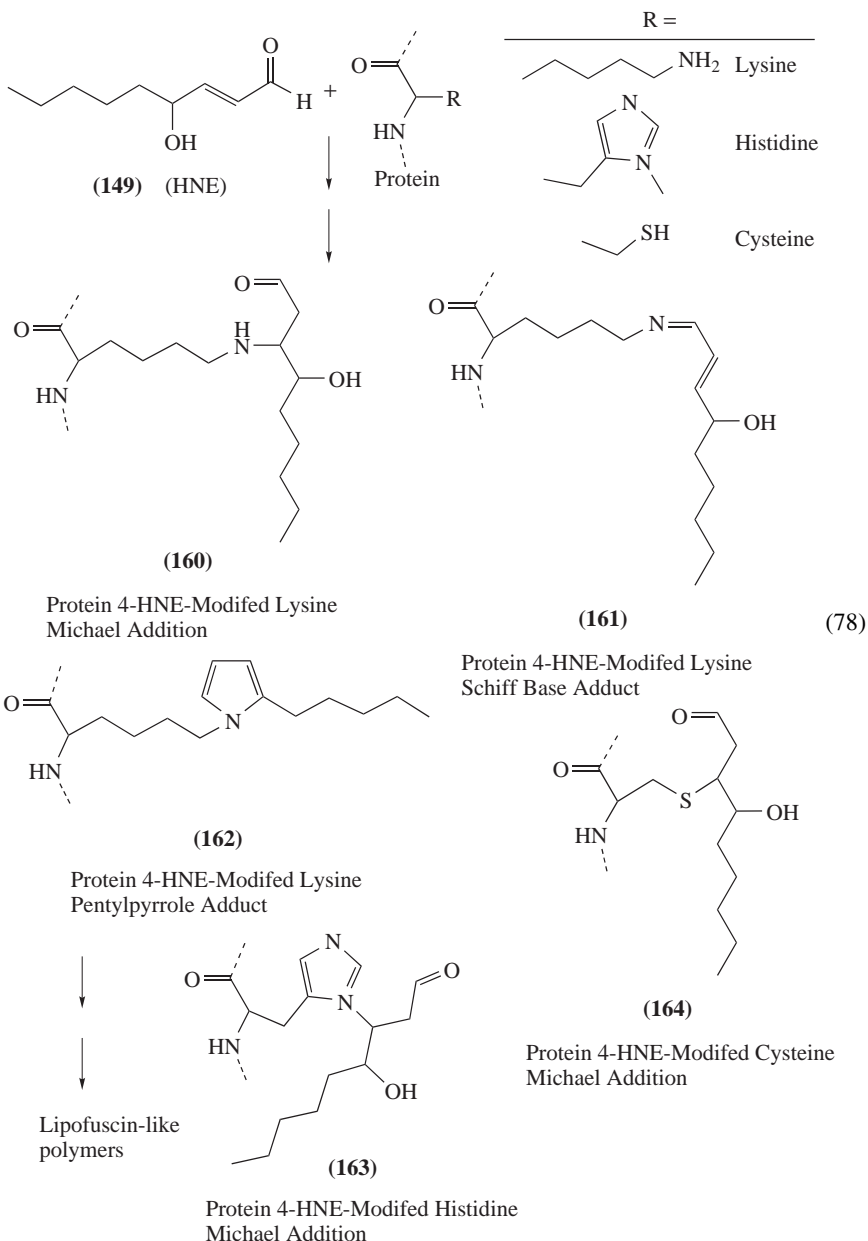
DDE-dGuo adduct

CHART 5

immunoaffinity chromatography coupled with HPLC-ESI-MS/MS has recently been applied for the detection and automated quantification of trace levels of ϵ dCyd in crude DNA hydrolysates^{297g}. The adduct ϵ dAdo was detected using a similar method^{297a}. The good sensitivity of the newly developed techniques and the *in vivo* formation of **159** was only recently demonstrated^{292a}. A method aimed at quantitatively determining **159** in DNA samples using on-line HPLC separation with tandem mass spectrometry detection in the multiple reaction monitoring (MRM) mode was developed. This innovative method improved the analytical assay previously reported for **159** quantification in DNA hydrolysates^{294a}. The major advantage of the method is the on-line adduct separation from normal nucleosides coupled with the accuracy provided by MS/MS detection. It solves the problems involved in off-line pre-purification steps, allowing for the direct analysis of crude DNA hydrolysates. The addition of an isotopically labeled internal standard ($[^{15}\text{N}_5]$ -1, N^2 - ϵ dGuo) prior to DNA hydrolysis improves the confidence level of analyses, since it allows the correction of any possible loss of analyte during the procedure. This methodology enabled the direct quantification of fmol of 1, N^2 - ϵ dGuo in DNA hydrolysate, evidencing the occurrence of **159** as an endogenous basal. This method can be usefully employed to assess the biological levels of **159** under normal and pathological conditions.

The biological relevance of the occurrence of **159** in DNA has been revealed by studies showing the mutagenicity of this adduct. *In vitro* misincorporation studies showed that **159** tends to strongly block replication at and beyond the site of substitution and to favor the misincorporation of dATP and dGTP across it³¹⁰. Another study, in which miscoding opposite this adduct in an *E. coli*/M13MB19-based system was examined, has shown that it is mutagenic in *E. coli* *uvrA*⁻, with more abundant G \rightarrow A mutations, followed by G \rightarrow T mutations³¹¹. **159** also generates deletions, rearrangements, double mutants and base pair substitutions at sites near the 1, N^2 - ϵ dGuo site³¹². Recently, Saparbaev and collaborators³¹³ have reported that 1, N^2 -etheno-guanine (1, N^2 - ϵ Gua) is a primary substrate of *E. coli* mismatch-specific uracil-DNA glycosylase and human alkylpurine-DNA-*N*-glycosylase. These data reinforce the potential biological relevance of this adduct.

b. Protein adducts. Protein adducts of endogenous origin can be generated by several reactive lipid peroxidation products. For example, reactive aldehydes generated in the liver during ethanol metabolism promote aldehyde-derived modification of macromolecules as proteins and has been proposed as a key event leading to liver injury³¹⁴. Aldehyde breakdown products of lipid peroxidation react with biomolecules and contribute to the formation of lipofuscin (equation 78), as seen in aging and in the progression of some degenerative diseases. Oxidative cyclization of lysine-HNE Michael adduct-Schiff (**160** and **161**) base cross-link generates the fluorescence product 2-hydroxy-3-amino-1,2-dihydropyrrole derivative pentylpyrrole adduct (**162**)³¹⁵. The breakdown end-products of lipid peroxidation, such as MDA and α,β -unsaturated aldehydes including 4-oxo-2-nonenal and HNE, cause protein damage by means of reaction with lysine amino groups generating stable carbonyl derivatives³¹⁶ and Michael addition-type reaction, respectively. The sulfhydryl group of cysteine residue (**163**) and the imidazole group of histidine residues (**164**) are also potential targets^{281b,317} (equation 78). Lipid peroxides, which can undergo metal ion-catalyzed conversion to alkoxyl and peroxy radicals, as discussed above, may react directly with side-chains of some amino acid residues to form carbonyl derivative, by mechanisms analogous to those proposed for hydrogen peroxide³¹⁸. Depending on the type of fatty acid and the presence of protein, the presence of pentanal, hexenal, *trans*-2-hexenal, *trans*-2-heptenal and *trans*-2-octenal may be explained by the implication of lipid hydroperoxides or lipid radicals in the observed protein modifications³¹⁹. Beside the secondary lipid peroxidation products, the primary products may also contribute to oxidatively generated damage in proteins leading to age-related diseases³²⁰.



C. Protein Hydroperoxides and Stable Degradation Products

It is now well documented that proteins are efficient cellular targets for peroxidizing agents including $\bullet\text{OH}$ radical, peroxy radical and singlet oxygen^{246,321}. Thus, evidence

was provided by using colorimetric assays, even if the accuracy of the measurements may be questionable (*vide infra*), that protein hydroperoxides are generated upon exposure of cells to ionizing radiation, H_2O_2 or excited photosensitizers. Indirect support for the occurrence of peroxidation processes to cellular proteins was provided by the detection of carbonylated amino acid derivatives as stable degradation products of hydroperoxides or related alkoxy and peroxy radicals. Another example of indirect assessment of protein hydroperoxides in cells is given by the detection of the corresponding alcohol derivatives, the expected reduction products of valine and leucine hydroperoxides.

1. Global assessment of hydroperoxides

As already mentioned (Section IV.B.1), several assays including the ferric-xylenol orange (FOX) and the tri-iodide methods are now available to measure globally hydroperoxides in isolated proteins. The FOX assay has been also applied for monitoring the global formation of hydroperoxides in cells upon exposure to various oxidizing agents. It was shown using the FOX assay that peroxidation of proteins preceded that of lipids in U937 cells upon exposure to peroxy radicals arising from the thermal decomposition of 2,2'-azobis(amidinopropane) dihydrochloride^{321b}. Other relevant features on the formation and the stability of protein peroxides were gained^{321a} from application of the FOX method³²² to THP-1 human monocyte cells that were exposed to photoexcited rose bengal, a well-known 1O_2 generator. Formation of protein peroxides was shown to increase linearly with the time of illumination, leading to a yield of 1.5 nmoles of peroxides per 10^6 cells. It was also observed that the half-lives of the measured protein peroxides in the cells at 37 °C were about 4 h^{321a}.

However, several limitations in the initially proposed protocols²³⁰ that are due to the presence of interfering compounds in the complex cellular media have been more recently identified^{322, 323}. These include lipids that may be subjected to delayed peroxidation, H_2O_2 and ascorbate, that were in a first attempt eliminated by perchloric acid (PCA)-mediated precipitation of proteins followed by washing the resulting solid residue^{322, 323}. It may be added that further improvement of the latter PCA-FOX method has been achieved recently by removing traces of interfering lipids by a subsequent extraction with chloroform. Using this protocol, the formation of protein hydroperoxides was measured in human blood serum and in mouse myeloma Sp20-Ag14 hybrid cells upon exposure to γ -rays²⁴⁶. The induction of protein hydroperoxides in blood serum was linear with the applied dose within the dose-range 0–1000 Gy, whereas the formation of lipid hydroperoxides that was assessed using a modified FOX assay shows a lag response.

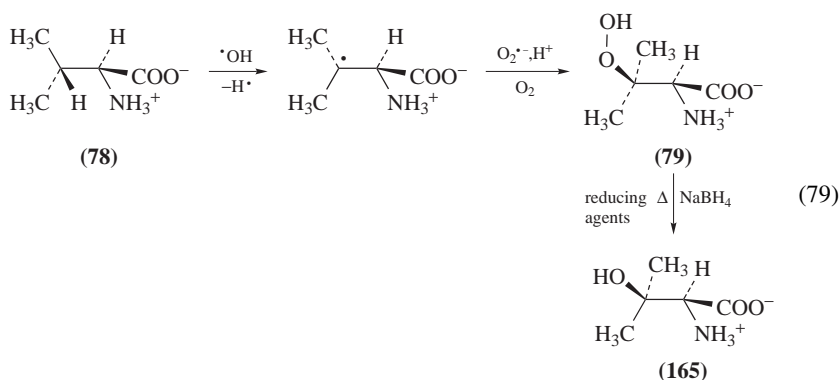
2. Stable decomposition products

Two classes of degradation products that are likely to result at least partly from the decomposition of protein hydroperoxides or related peroxy and alkoxy radicals have been measured in cells as indicators of the occurrence of oxidative reactions.

a. Carbonyl compounds. The latter oxidation products may be generated as discussed earlier by initial hydrogen abstraction on the side-chains of amino acids and subsequent backbone fragmentation of transiently generated oxyl radicals (equations 51 and 66). In isolated proteins both bound and released carbonyls, the latter class including formaldehyde, acetone, isobutyraldehyde and glyoxylic acid³²⁴, may be measured together or separately. However, in cells the measurement of bound carbonyls can be achieved and this allows using them as indicators of aging³²⁵ and pathological situations such as Alzheimer disease³²⁶ and formation of human atherosclerotic plaque³²⁷. Several methods are available to detect the presence of protein-bound carbonyls in cells³²⁸. One approach involves

the reduction of the carbonyl function by NaB^3H_4 that leads to incorporation of tritium atoms allowing radioactive detection of the oxidized proteins³²⁹. Another possibility is to derivatize the carbonyls into 2,4-dinitrophenylhydrazones that may be detected either spectrophotometrically³³⁰ or by immunological methods³³¹. It should be noticed that the measurement of total carbonyls using the latter global methods is likely to suffer from a lack of specificity, since a wide range of oxidized proteins are concerned and most of the latter lesions may not be accounted for by only initial peroxidation processes. Over-estimation of the level of bound-protein carbonyls is expected in most cases, since other aldehyde or ketone residues in other biomolecules such as lipids, sugars or nucleic acids are susceptible to provide a false contribution³²⁵.

b. Hydroxylated valine and leucine residues as specific markers. Hydroperoxides that have been shown to be generated in aliphatic side-chains of amino acid residues upon exposure to $\cdot\text{OH}$ radical are unstable, particularly in the presence of light, metal ions and various reducing agents. The predominant decomposition products of the latter hydroperoxides under conditions of sample homogenization during protein extraction from the cells have been shown to be the corresponding alcohol derivatives. This is the case of (2*S*)-2-amino-3-hydroperoxy-3-methylbutanoic acid (**78**), which is quantitatively converted into 3-hydroxyvaline (**165**) in cell extracts and by NaBH_4 reduction (equation 79). This applies as well to the two diastereomers of δ -hydroperoxyvaline, **87** and **88** (equation 51), that are also quantitatively reduced into related 5-hydroxyvaline diastereomers during sample homogenization. It may be added that the latter alcohols and **165** are not prone to any further reaction and are catabolic products, as is the case for other hydroxylated amino acids such as 4-hydroxyproline and the 4- and 5-hydroxylysine isomers¹⁵. This explains why an assay that involves a two-step HPLC separation together with an *o*-phthalaldehyde derivatization has been designed for the measurement of 3-hydroxyvaline (**165**) and the two diastereomers of 5-hydroxyvaline once released from oxidized proteins by acidic treatment³²⁷. Interestingly, an increase in the levels of the three latter hydroxylated amino acids was observed in advanced plaque points of atherosclerotic patients³²⁷. Another interesting application of the assay is provided by the measurement of 3-hydroxyvaline (**165**) and the two diastereomers of 5-hydroxyvaline in the lens proteins of patients suffering from nuclear cataract³³². The level of oxidized proteins was found to be more elevated under these pathological conditions with about 0.3 3-hydroxyvaline residues per 1000 parent amino acids whereas the relative yields of 5-hydroxyvaline and dityrosine were 0.16 and 0.05, respectively.



VI. CONCLUSIONS

During the last two decades, major effort has been devoted to the elucidation of the mechanisms of peroxidation of major cellular biomolecules including nucleic acids, lipids and proteins. Relevant peroxidation pathways are now available at least for the main components of the key cellular biomolecules although there is still a need of further studies, particularly for isolating and characterizing putative hydroperoxides. Attempts should also be made to validate in the biomolecules themselves the mechanisms of formation of hydroperoxides that were inferred from model studies. Another relevant major topic deals with the search for the molecular signature of the peroxide formation in targeted biomolecules within cells upon exposure to oxidative conditions. It may be anticipated that gentle and sensitive mass spectrometric methods such as ESI-MS/MS in association with HPLC should constitute powerful tools for this purpose.

VII. ACKNOWLEDGMENTS

The authors acknowledge the Brazilian research funding institutions FAPESP (Fundação de Amparo à Pesquisa do Estado de São Paulo), CNPq (Conselho Nacional para o Desenvolvimento Científico e Tecnológico), PRONEX/FINEP (Programa de Apoio aos Núcleos de Excelência) and Fundo Bunka de Pesquisa Banco Sumitomo Mitsui and John Simon Guggenheim Memorial Foundation (PDM Fellowship). In addition, JC acknowledges the support of EU through the research training network CLUSTOXDNA ('Clustered oxidative DNA damage').

VIII. REFERENCES

- (a) H. Sies (Ed.), *Oxidative Stress, Oxidants and Antioxidants*, Academic Press, New York, 1991.
(b) T. Lindahl, *Nature*, **362**, 709 (1993).
(c) B. N. Ames, L. S. Gold and W. C. Willett, *Proc. Natl. Acad. Sci. USA*, **92**, 5258 (1995).
- (a) L. J. Marnett and P. C. Burcham, *Chem. Res. Toxicol.*, **6**, 771 (1993).
(b) S. Loft and H. E. Poulsen, *J. Mol. Med.*, **74**, 297 (1996).
(c) R. A. Floyd, M. West and K. Hensley, *Exp. Gerontol.*, **36**, 619 (2001).
- (a) B. M. Babior, *IUBMB Life*, **50**, 267 (2000).
(b) L. J. Marnett, J. N. Riggins and J. D. West, *J. Clin. Invest.*, **111**, 583 (2003).
- S. Canova, P. Degan, L. D. Peters, D. R. Livingstone, R. Voltan and P. Venier, *Mutat. Res.*, **399**, 17 (1998).
- (a) W. H. Koppenol and J. F. Liebman, *J. Phys. Chem.*, **88**, 99 (1984).
(b) S. Rahhal and H. W. Ritcher, *J. Am. Chem. Soc.*, **110**, 3126 (1988).
(c) W. H. Koppenol, *Free Radic. Biol. Med.*, **15**, 645 (1993).
(d) P. Wardman and L. P. Candeias, *Radiat. Res.*, **145**, 523 (1996).
(e) R. V. Lloyd, P. M. Hanna and R. P. Mason, *Free Radic. Biol. Med.*, **22**, 885 (1997).
- C. von Sonntag, *The Chemical Basis of Radiation Biology*, Taylor and Francis, London, 1987.
- J. Cadet and P. Vigny, in *Bioorganic Photochemistry*, Vol. 1 (Ed. H. Morrison), Chap. 1, Wiley-Interscience, New York, 1990, pp. 1–272.
- (a) J. R. Kanofsky, J. Wright, G. E. Miles-Richardson and A. I. Tauber, *J. Clin. Invest.*, 1489 (1984).
(b) M. J. Steinbeck, A. U. Khan and J. R. Kanofsky, *J. Biol. Chem.*, **267**, 13425 (1992).
(c) H. Tatsuzawa, T. Maruyama, K. Hori, Y. Sano and M. Nakano, *Biochem. Biophys. Res. Commun.*, **262**, 647 (1999).
(d) C. Kiryu, M. Makiuchi, J. Miyazaki, T. Fujinaga and K. Kakinuma, *FEBS Lett.*, **443**, 154 (1999).
- (a) J. Cadet, M. Berger, T. Douki and J.-L. Ravanat, *Rev. Physiol. Biochem. Pharmacol.*, **131**, 1 (1997).

- (b) J. Cadet, T. Delatour, T. Douki, D. Gasparutto, J.-P. Pouget, J.-L. Ravanat and S. Sauvaigo, *Mutat. Res.*, **424**, 9 (1999).
- (c) J. Cadet, T. Douki, D. Gasparutto and J.-L. Ravanat, *Mutat. Res.*, **531**, 5 (2003).
10. M. Guichardant, B. Chantegrel, C. Deshayes, A. Doutheau, P. Morlière and M. Lagarde, *Biochem. Soc. Trans.*, **32**, 139 (2004).
11. (a) L. J. Marnett, *Mutat. Res.*, **424**, 83 (1999).
(b) L. J. Marnett, *Carcinogenesis*, **21**, 361 (2000).
(c) L. J. Marnett, *Toxicol.*, **181–182**, 219 (2002).
12. B. S. Berlett and E. R. Stadtman, *J. Biol. Chem.*, **272**, 20313 (1997).
13. S. Fu, M. J. Davies and R. T. Dean, *Biochem. J.*, **333**, 519 (1998).
14. M. J. Davies and R. J. W. Truscott, *J. Photochem. Photobiol. B: Biol.*, **63**, 114 (2001).
15. M. J. Davies, S. Fu, H. Wang and R. T. Dean, *Free Radic. Biol. Med.*, **27**, 1151 (1999).
16. G. Scholes and J. Weiss, *Biochem. J.*, **56**, C5 (1954).
17. G. M. Eisenberg, *Indust. Eng. Chem. Ed.*, **15**, 327 (1942).
18. (a) G. Scholes, J. Weiss and C. M. Wheeler, *Nature*, **178**, 157 (1956).
(b) M. Daniels, G. Scholes, J. Weiss and C. M. Wheeler, *J. Chem. Soc.*, 226 (1957).
(c) G. Scholes, J. F. Ward and J. Weiss, *J. Mol. Biol.*, **2**, 279 (1960).
(d) J. Weiss, *Progr. Nucleic Acids Res. Mol. Biol.*, **3**, 103 (1964).
(e) G. Scholes, *Progr. Biophys. Mol. Biol.*, **13**, 59 (1963).
19. G. Scholes and J. Weiss, *Radiat. Res. Suppl.*, **1**, 177 (1959).
20. R. Latarjet, B. Ekert and P. Demerseman, *Radiat. Res. Suppl.*, **3**, 247 (1963).
21. M. Isildar, M. N. Schuchmann, D. Schulte-Frohlinde and C. von Sonntag, *Int. J. Radiat. Biol.*, **41**, 525 (1982).
22. (a) M. Daniels, G. Scholes and J. Weiss, *J. Chem. Soc.*, 3771 (1956).
(b) M. Daniels, G. Scholes, J. Weiss and C. M. Wheeler, *J. Chem. Soc.*, 226 (1957).
23. (a) A. P. Breen and J. A. Murphy, *Free Radic. Biol. Med.*, **18**, 1033 (1995).
(b) C. J. Burrows and J. G. Muller, *Chem. Rev.*, **98**, 1109 (1998).
24. K. A. Tallman, C. Tronche, D. J. Yon and M. M. Greenberg, *J. Am. Chem. Soc.*, **120**, 4903 (1998).
25. C. J. Emanuel, M. Newcomb, C. Ferreri and C. Chatgililoglu, *J. Am. Chem. Soc.*, **121**, 2927 (1999).
26. J. Weiss, in *Actions Chimiques et Physiques des Radiations, Les Peroxydes Organiques en Radiobiologie* (Ed. M. Haissinsky), Masson, Paris, 1958, p. 44.
27. B. Ekert and R. Monier, *Nature*, **184**, B. A. 58 (1959).
28. (a) G. Scholes and J. Weiss, *Nature*, **185**, 305 (1960).
(b) R. Latarjet, B. Ekert, S. Alpegot and N. Rebeyrote, *J. Chim. Phys.*, **58**, 1046 (1961).
29. (a) J. Cadet and R. Téoule, *Biochim. Biophys. Acta*, **238**, 8 (1970).
(b) R. Téoule and J. Cadet, *J. Chem. Soc., Chem. Commun.*, 1269 (1971).
30. (a) J. Cadet and R. Téoule, *C. R. Acad. Sci. Paris*, **276C**, 1743 (1973).
(b) J. Cadet and R. Téoule, *Tetrahedron Lett.*, 4245 (1973).
31. (a) J. Cadet and R. Téoule, *Biochem. Biophys. Res. Commun.*, **59**, 1047 (1974).
(b) R. Téoule and J. Cadet, *Z. Naturforsch.*, **29c**, 645 (1974).
32. A. M. Giroud, J. Cadet and R. Ducolomb, *Nouveau J. Chim.*, **4**, 657 (1980).
33. F. Jolibois, C. D'Ham, A. Grand, R. Subra and J. Cadet, *J. Mol. Struct. (Theochem)*, **427**, 143 (1998).
34. (a) J. Cadet and R. Téoule, *Bull. Soc. Chim. Fr.*, 885 (1975).
(b) J. Cadet, R. Nardin, L. Voituriez, M. Remin and F. E. Hruska, *Can. J. Chem.*, **59**, 3313 (1981).
(c) J. R. Wagner, J. E. van Lier, M. Berger and J. Cadet, *J. Am. Chem. Soc.*, **116**, 2235 (1994).
35. (a) J. R. Wagner, J. E. van Lier, C. Decarroz and J. Cadet, *Bioelectrochem. Bioenerg.*, **18**, 155 (1987).
(b) J. R. Wagner, M. Berger, J. Cadet and J. E. van Lier, *J. Chromatogr.*, **504**, 191 (1990).
36. (a) J. Cadet and R. Téoule, *Bull. Soc. Chim. Fr.*, 879 (1975).
(b) M. Bardet, J. Cadet and R. J. Wagner, *Magn. Res. Chem.*, **34**, 577 (1996).
37. (a) J. Cadet, J. Ulrich and R. Téoule, *Tetrahedron*, **31**, 2057 (1975).
(b) J. Cadet, R. Ducolomb and F. E. Hruska, *Biochim. Biophys. Acta*, **563**, 206 (1979).
(c) M. J. Lutsig, J. Cadet, R. J. Boorstein and G. W. Teebor, *Nucleic Acids Res.*, **20**, 4839 (1992).

38. J. Cadet, R. Ducolomb and R. Téoule, *Tetrahedron*, **33**, 1603 (1977).
39. (a) F. E. Hruska, R. Sebastian, A. Grand, L. Voituriez and J. Cadet, *Can. J. Chem.*, **65**, 2618 (1987).
(b) F. Jolibois, L. Voituriez, A. Grand and J. Cadet, *Chem. Res. Toxicol.*, **9**, 298 (1996).
40. J.-L. Ravanat and J. Cadet, unpublished results.
41. (a) M. C. Schweibert and M. Daniels, *Int. J. Radiat. Phys. Chem.*, **3**, 353 (1971).
(b) H. B. Michaels and J. W. Hunt, *Anal. Biochem.*, **87**, 135 (1978).
42. (a) S. Fujita and S. Steenken, *J. Am. Chem. Soc.*, **103**, 2540 (1981).
(b) S. V. Jovanovic and M. G. Simic, *J. Am. Chem. Soc.*, **108**, 5968 (1986).
43. (a) J. Cadet, *C. R. Acad. Sci. Paris.*, **283D**, 725 (1976).
(b) J. Cadet and R. Téoule, *Bull. Soc. Chim. Fr.*, 891 (1975).
(c) J. R. Wagner, J. van Lier and L. J. Johnston, *Photochem. Photobiol.*, **52**, 333 (1990).
44. M. Simic and E. Hayon, *FEBS Lett.*, **44**, 334 (1974).
45. C. von Sonntag and H.-P. Schuchmann, in *Peroxyl Radicals* (Ed. Z. F. Alfassi), Wiley, Chichester, 1997, pp. 173–234.
46. G. A. Russell, *J. Am. Chem. Soc.*, **79**, 3871 (1957).
47. G. J. Fisher and E. J. Land, *Photochem. Photobiol.*, **37**, 27 (1983).
48. (a) C. Decarroz, J. R. Wagner, J. E. van Lier, C. M. Krishna, P. Riesz and J. Cadet, *Int. J. Radiat. Biol.*, **50**, 491 (1986).
(b) J. R. Wagner, J. E. van Lier, C. Decarroz, M. Berger and J. Cadet, *Methods Enzymol.*, **186**, 502 (1990).
49. C. M. Krishna, C. Decarroz, J. R. Wagner, J. Cadet and P. Riesz, *Photochem. Photobiol.*, **46**, 175 (1987).
50. B.-S. Hahn and S. Y. Wang, *Biochem. Biophys. Res. Commun.*, **54**, 1224 (1973).
51. R. Téoule and J. Cadet, *Int. J. Appl. Radiat. Isotop.*, **22**, 273 (1971).
52. J. Cadet and R. Téoule, *Carbohydr. Res.*, **29**, 345 (1973).
53. J. Cadet and R. Téoule, *Tetrahedron Lett.*, 3329 (1972).
54. R. Ducolomb, J. Cadet and R. Téoule, *Z. Naturforsch.*, **29c**, 643 (1974).
55. J. Cadet, *Z. Naturforsch.*, **35b**, 1565 (1980).
56. L. Stelter, C. Von Sonntag and D. Schulte-Frohlinde, *Z. Naturforsch.*, **801**, 609 (1975).
57. S. Tofigh and K. Frenkel, *Free Radic. Biol. Med.*, **4**, 131 (1989).
58. (a) H. C. Box, E. E. Budzinski, J. B. Dawidzik, J. S. Gobey and H. G. Freund, *Free Radic. Biol. Med.*, **23**, 1021 (1997).
(b) A.-G. Bourdat, T. Douki, S. Frelon, D. Gasparutto and J. Cadet, *J. Am. Chem. Soc.*, **122**, 4549 (2000).
59. T. Douki, J. Rivière and J. Cadet, *Chem. Res. Toxicol.*, **15**, 445 (2002).
60. (a) R. Ducolomb, J. Cadet and R. Téoule, *Bull. Soc. Chim. Fr.*, 7 (1979).
(b) R. Ducolomb and J. Cadet, *Bull. Soc. Chim. Fr.*, 81 (1979).
61. K. N. Carter and M. M. Greenberg, *J. Org. Chem.*, **68**, 4275 (2003).
62. K. N. Carter and M. M. Greenberg, *J. Am. Chem. Soc.*, **125**, 13376 (2003).
63. J. R. Wagner, C. Decarroz, M. Berger and J. Cadet, *J. Am. Chem. Soc.*, **121**, 4101 (1999).
64. S. Tremblay, T. Douki, J. Cadet and J. R. Wagner, *J. Biol. Chem.*, **274**, 20833 (1999).
65. J. R. Wagner, C. C. Hu and B. N. Ames, *Proc. Natl. Acad. Sci. USA*, **89**, 3380 (1992).
66. M. Polverelli and R. Téoule, *Z. Naturforsch.*, **29c**, 12 (1974).
67. M. Polverelli, J. Ulrich and R. Téoule, *Z. Naturforsch.*, **39c**, 64 (1984).
68. M. Polverelli, PhD Thesis, University of Grenoble (1983).
69. (a) B. S. Hahn, S. Y. Wang, J. L. Flippen and I. L. Karle, *J. Am. Chem. Soc.*, **95**, 2711 (1973).
(b) N. J. Leonard and D. F. Wiemer, *J. Am. Chem. Soc.*, **98**, 6218 (1976).
70. (a) C. Bienvenu, J. R. Wagner and J. Cadet, *J. Am. Chem. Soc.*, **118**, 11406 (1996).
(b) C. Bienvenu, J. R. Wagner and J. Cadet, unpublished results.
71. C. Bienvenu, C. Lebrun and J. Cadet, *J. Chim. Phys.*, **94**, 300 (1997).
72. C. Bienvenu and J. Cadet, *J. Org. Chem.*, **61**, 2632 (1996).
73. S. Steenken and S. V. Jovanovic, *J. Am. Chem. Soc.*, **119**, 617 (1997).
74. (a) J. Cadet, M. Berger, G. W. Buchko, P. Joshi, S. Raoul and J.-L. Ravanat, *J. Am. Chem. Soc.*, **116**, 7403 (1994).
(b) S. Raoul, M. Berger, G. W. Buchko, P. C. Joshi, B. Morin, M. Weinfeld and J. Cadet, *J. Chem. Soc., Perkin Trans. 2*, 371 (1996).

75. (a) D. Gasparutto, J.-L. Ravanat, O. Gérot and J. Cadet, *J. Am. Chem. Soc.*, **120**, 10283 (1998).
(b) K. Kino, I. Saito and H. Sugiyama, *J. Am. Chem. Soc.*, **120**, 7373 (1998).
76. L. P. Candeias and S. Steenken, *Chem. Eur. J.*, **6**, 475 (2000).
77. V. Shafirovich, J. Cadet, D. Gasparutto, A. Dourandin and N. E. Geacintov. *Chem. Res. Toxicol.*, **14**, 233 (2001).
78. R. Misiaszek, C. Crean, A. Joffe, N. E. Geacintov and V. Shafirovich. *J. Biol. Chem.*, **31**, 32106 (2004).
79. C. Vialas, G. Pratviel, C. Claparols and B. Meunier, *J. Am. Chem. Soc.*, **120**, 11548 (1998).
80. (a) J. Cadet, T. Douki, J.-P. Pouget and J.-L. Ravanat, *Methods Enzymol.*, **319**, 143 (2000).
(b) J.-L. Ravanat, G. R. Martinez, M. H. G. Medeiros, P. Di Mascio and J. Cadet, *Arch. Biochem. Biophys.*, **423**, 23 (2004).
81. C. Sheu and C. S. Foote, *J. Am. Chem. Soc.*, **115**, 10446 (1993).
82. P. Kang and C. S. Foote, *J. Am. Chem. Soc.*, **124**, 4865 (2002).
83. C. Sheu, P. Kang, S. Khan and C. S. Foote, *J. Am. Chem. Soc.*, **124**, 3905 (2002).
84. J.-L. Ravanat and J. Cadet, *Chem. Res. Toxicol.*, **8**, 379 (1995).
85. (a) J. C. Niles, J. S. Wishnok and S. R. Tannenbaum, *Org. Lett.*, **3**, 963 (2001).
(b) W. Adam, M. A. Arnold, M. Grune, W. M. Nau, U. Pischel and C. R. Saha-Möller, *Org. Lett.*, **4**, 37 (2002).
(c) G. R. Martinez, M. H. G. Medeiros, J.-L. Ravanat, J. Cadet and P. Di Mascio, *Biol. Chem.*, **383**, 607 (2002).
86. J.-L. Ravanat, C. Saint-Pierre, P. Di Mascio, G. R. Martinez, M. H. G. Medeiros and J. Cadet, *Helv. Chim. Acta*, **84**, 3702 (2001).
87. J.-L. Ravanat, S. Sauvaigo, S. Caillat, G. R. Martinez, M. H. G. Medeiros, P. Di Mascio, A. Favier and J. Cadet, *Biol. Chem.*, **385**, 17 (2004).
88. C. Sheu and C. S. Foote, *J. Am. Chem. Soc.*, **117**, 474 (1995).
89. (a) F. Prat, K. N. Houk and C. S. Foote, *J. Am. Chem. Soc.*, **120**, 845 (1998).
(b) R. Bernstein, F. Prat and C. S. Foote, *J. Am. Chem. Soc.*, **121**, 464 (1999).
90. S. Raoul and J. Cadet, *J. Am. Chem. Soc.*, **118**, 1982 (1996).
91. V. Duarte, D. Gasparutto, L. F. Yamaguchi, J.-L. Ravanat, G. R. Martinez, M. H. G. Medeiros, P. Di Mascio and J. Cadet, *J. Am. Chem. Soc.*, **122**, 12622 (2000).
92. A. Chworos, Y. Coppel, I. Dubey, G. Pratviel and B. Meunier, *J. Am. Chem. Soc.*, **123**, 5867 (2001).
93. (a) V. Duarte, J. G. Muller and C. J. Burrows, *Nucleic Acids Res.*, **27**, 496 (1999).
(b) W. Luo, J. G. Muller, E. M. Rachlin and C. J. Burrows, *Chem. Res. Toxicol.*, **14**, 927 (2001).
94. W. Luo, J. G. Muller, E. M. Rachlin and C. J. Burrows, *Org. Lett.*, **2**, 613 (2000).
95. K. D. Sugden, C. K. Campo and B. D. Martin, *Chem. Res. Toxicol.*, **14**, 1315 (2001).
96. W. Adam, A. Kurz and C. R. Saha-Möller, *Chem. Res. Toxicol.*, **13**, 1199 (2000).
97. A. Z. Doddridge, P. M. Cullis, G. D. D. Jones and M. E. Malone, *J. Am. Chem. Soc.*, **120**, 10998 (1998).
98. W. Luo, J. G. Muller and C. J. Burrows, *Org. Lett.*, **3**, 2801 (2001).
99. H. Esterbauer, J. Gebicki, H. Puhl and G. Jurgens, *Free Radic. Biol. Med.*, **13**, 341 (1992).
100. J. A. Berliner and J. W. Heinecke, *Free Radic. Biol. Med.*, **20**, 707 (1996).
101. W. R. Markesbery, *Free Radic. Biol. Med.*, **23**, 134 (1997).
102. D. Rowley, J. M. C. Gutteridge, D. Blake, M. Farr and B. Halliwell, *Clin. Sci.*, **66**, 691 (1984).
103. J. W. Baynes, *Diabetes*, **40**, 405 (1991).
104. T. Otamiri and R. Sjordahl, *Cancer*, **64**, 422 (1989).
105. H. Esterbauer, *Am. J. Clin. Nutr.*, **57**, 779S (1993).
106. A. W. Girotti, *J. Lipid Res.*, **39**, 1529 (1998).
107. G. Spiteller, *Chem. Phys. Lipids*, **95**, 105 (1998).
108. E. N. Frankel, W. E. Neff and T. R. Bessler, *Lipids*, **14**, 961 (1979).
109. J. Terao and S. Matsushita, *J. Am. Oil Chem. Soc.*, **54**, 234 (1977).
110. L. J. Marnett, *Carcinogenesis*, **21**, 361 (2000).
111. H. H. F. Refsgaard, L. Tsai and E. R. Stadtman, *Proc. Natl. Acad. Sci. USA*, **97**, 611 (2000).
112. Y. Kato, Y. Mori, Y. Makino, Y. Morimitsu, S. Hiroi, T. Ishikawa and T. Osawa, *J. Biol. Chem.*, **274**, 20406 (1999).

113. M. Moriya, W. Zhang, F. Johnson and A. P. Grollman, *Proc. Natl. Acad. Sci. USA*, **91**, 11899 (1994).
114. G. F. Vile and R. M. Tyrrell, *Free Radic. Biol. Med.*, **18**, 721 (1995).
115. P. Morlière, A. Moysan and I. Tirache, *Free Radic. Biol. Med.*, **19**, 365 (1995).
116. S. P. Fink, G. R. Reddy and L. J. Marnett, *Proc. Natl. Acad. Sci. USA*, **94**, 8652 (1997).
117. F.-L. Chung, H. J. C. Chen and R. G. Nath, *Carcinogenesis*, **17**, 2105 (1996).
118. P. C. Burcham, *Mutagenesis*, **13**, 287 (1998).
119. J. Pan and F.-L. Chung, *Chem. Res. Toxicol.*, **15**, 367 (2002).
120. M. Mayer, *Clin. Chem.*, **46**, 1723 (2000).
121. M. Choe, C. Jackson and B. P. Yu, *Free Radic. Biol. Med.*, **18**, 977 (1995).
122. G. Spitteller, *Exp. Gerontol.*, **36**, 1425 (2001).
123. B. H. Bielski, R. L. Arudi and M. W. Sutherland, *J. Biol. Chem.*, **258**, 4759 (1983).
124. A. W. Girotti, *J. Free Radic. Biol. Med.*, **1**, 87 (1985).
125. W. A. Prutz, H. Monig, J. Butler and E. J. Land, *Arch. Biochem. Biophys.*, **243**, 125 (1985).
126. (a) H. W. Gardner, *Free Radic. Biol. Med.*, **7**, 65 (1989).
(b) H. Hock and O. Schrader, *Angew. Chem.*, **49**, 595 (1936).
(c) A. A. Frimer, *Chem. Rev.*, **79**, 359 (1979).
127. A. W. Girotti and J. Cadet, in *Photobiology for the 21st Century* (Eds. P. P. Coohill and D. P. Valenzano), Valdemar Publishing Company, Overland Park, KS, 2001, pp. 285–309.
128. L. L. Smith, J. I. Teng, M. J. Kulig and F. L. Hill, *J. Org. Chem.*, **38**, 1763 (1973).
129. M. J. Kulig and L. L. Smith, *J. Org. Chem.*, **38**, 3639 (1973).
130. C. S. Foote, *Photochem. Photobiol.*, **54**, 659 (1991).
131. C. S. Foote, *Science*, **162**, 963 (1968).
132. A. W. Girotti, *Photochem. Photobiol.*, **51**, 497, (1990).
133. A. R. Brash, *J. Biol. Chem.*, **274**, 23679 (1999).
134. M. Hamberg and B. Samuelsson, *Biochim. Biophys. Acta*, **617**, 545 (1980).
135. E. Cadenas, A. Boveris and B. Chance, *Biochem. J.*, **188**, 577 (1980).
136. A. Boveris, E. Cadenas, R. Reiter, M. Filipkowski, Y. Nakase and B. Chance, *Proc. Natl. Acad. Sci. USA*, **77**, 347 (1980).
137. A. Boveris, E. Cadenas and B. Chance, *Fed. Proc.*, **40**, 195 (1980).
138. E. A. Lissi, T. Caceres and L. A. Videla, *Free Radic. Biol. Med.*, **4**, 93 (1988).
139. A. G. Prat and J. F. Turrens, *Free Radic. Biol. Med.*, **8**, 319 (1990).
140. K. Briviba, C. R. Saha-Möller, W. Adam and H. Sies, *Biochem. Mol. Biol. Int.*, **38**, 647 (1996).
141. D. Phillips, V. Assimov, O. Karpukhin and V. Shiliapintokh, *Nature*, **215**, 1163 (1967).
142. J. A. Howard and K. U. Ingold, *J. Am. Chem. Soc.*, **90**, 1057 (1968).
143. F. J. Hawco and P. J. O'Brien, *Biochem. Biophys. Res. Commun.*, **76**, 354 (1976).
144. J. R. Kanofsky, *J. Org. Chem.*, **51**, 3386 (1986).
145. M. M. King, E. K. Lai and P. B. McCay, *J. Biol. Chem.*, **250**, 6496 (1975).
146. K. Sugioka and M. Nakano, *Biochim. Biophys. Acta*, **423**, 203 (1976).
147. H. Sies, *Arch. Toxicol.*, **60**, 138 (1987).
148. S. Koga, M. Nakano and K. Uehara, *Arch. Biochem. Biophys.*, **289**, 223 (1991).
149. Q. Niu and G. D. Mendenhall, *J. Am. Chem. Soc.*, **112**, 1656 (1990).
150. G. D. Mendenhall and X. C. Sheng, *J. Am. Chem. Soc.*, **113**, 8976 (1991).
151. J. Cadet, T. Douki, J. P. Pouget and J.-L. Ravanat, *Methods Enzymol.*, **319**, 143 (2000).
152. P. Kang and C. S. Foote, *J. Am. Chem. Soc.*, **124**, 4865 (2002).
153. L. O. Klotz, K. Briviba and H. Sies, *Methods Enzymol.*, **319**, 130 (2000).
154. S. W. Ryter and R. M. Tyrrell, *Free Radic. Biol. Med.*, **24**, 1520 (1998).
155. G. Cilento, in *Chemical and Biological Generation of Excited States* (Eds. V. Adam and G. Cilento), Academic Press, London, 1982, pp. 277–307.
156. E. Cadenas and H. Sies, *Methods Enzymol.*, **319**, 67 (2000).
157. A. U. Khan and M. Kasha, *J. Chem. Phys.*, **39**, 2105 (1963).
158. P. Di Mascio, E. J. H. Bechara, M. H. G. Medeiros, K. Briviba and H. Sies, *FEBS Lett.*, **355**, 287 (1994).
159. P. Di Mascio, K. Briviba, S. T. Sasaki, L. H. Catalani, M. H. G. Medeiros, E. J. H. Bechara and H. Sies, *Biol. Chem.*, **378**, 1071 (1997).
160. S. Miyamoto, G. R. Martinez, M. H. G. Medeiros and P. Di Mascio, *J. Am. Chem. Soc.*, **125**, 6172 (2003).

161. S. Miyamoto, G. R. Martinez, A. P. B. Martins, M. H. G. Medeiros and P. Di Mascio, *J. Am. Chem. Soc.*, **125**, 4510 (2003).
162. H. W. S. Chan, G. Levett and J. A. Matthew, *Chem. Phys. Lipids*, **24**, 245 (1979).
163. I. T. N. Jones and K. D. Bayes, *J. Chem. Phys.*, **2**, 1003 (1972).
164. G. R. Martinez, J.-L. Ravanat, J. Cadet, S. Miyamoto, M. H. G. Medeiros and P. Di Mascio, *J. Am. Chem. Soc.*, **126**, 3056 (2004).
165. A. Loidl-Stahlhofen, K. Hannemann and G. Spitteller, *Biochim. Biophys. Acta*, **1213**, 140 (1994).
166. J. S. Beckman and W. H. Koppenol, *Am. J. Physiol. Cell Physiol.*, **271**, C1424 (1996).
167. R. Radi, A. Denicola, B. Alvarez, G. Ferrer-Sueta and H. Rubbo, in *Nitric Oxide* (Ed. L. Ignarro), Academic Press, London, 2000, pp. 57–82.
168. R. Radi, G. Peluffo, M. N. Alvarez, M. Naviliat and A. Cayota, *Free Radic. Biol. Med.*, **30**, 463 (2001).
169. V. Yermilov, Y. Yoshie, J. Rubio and H. Ohshima, *FEBS Lett.*, **399**, 67 (1996).
170. J. S. Beckman, T. W. Beckman, J. Chen, P. A. Marshall and B. Freeman, *Proc. Natl. Acad. Sci. USA.*, **87**, 1620 (1990).
171. R. Radi, J. S. Beckman, K. M. Bush and B. A. Freeman, *Arch. Biochem. Biophys.*, **288**, 481 (1991).
172. H. Rubbo, R. Radi, M. Trujillo, R. Telleri, B. Kalyanaraman, S. Barnes, M. Kirk and B. A. Freeman, *J. Biol. Chem.*, **269**, 26066 (1994).
173. F. R. Gadelha, L. Thomson, M. M. Fagian, A. D. Costa, R. Radi and A. E. Vercesi, *Arch. Biochem. Biophys.*, **345**, 243 (1997).
174. V. B. O'Donnell, J. P. Eiserich, P. H. Chumley, M. J. Jablonsky, N. R. Krishna, M. Kirk, S. Barnes, V. M. Darley-Usmar and B. A. Freeman, *Chem. Res. Toxicol.*, **12**, 83 (1999).
175. W. V. Koppenol and R. Kissner, *Chem. Res. Toxicol.*, **11**, 87 (1998).
176. R. M. Gatti, B. Alvarez, J. Vásquez-Vivar, R. Radi and O. Augusto, *Arch. Biochem. Biophys.*, **349**, 36 (1998).
177. J. W. Coddington, J. K. Hurst and S. V. Lymar, *J. Am. Chem. Soc.*, **121**, 2438 (1999).
178. M. G. Bonini, R. Radi, G. Ferrer-Sueta, A. M. Ferreira and O. Augusto, *J. Biol. Chem.*, **274**, 10802 (1999).
179. G. Merényi, J. Lind, S. Goldstein and G. Czapski, *Chem. Res. Toxicol.*, **11**, 712 (1998).
180. G. Merényi and J. Lind, *Chem. Res. Toxicol.*, **10**, 1216 (1997).
181. S. V. Lymar and J. K. Hurst, *Inorg. Chem.*, **37**, 294 (1998).
182. S. V. Lymar and J. K. Hurst, *J. Am. Chem. Soc.*, **117**, 8867 (1995).
183. W. H. Koppenol, J. J. Moreno, W. A. Pryor, H. Ishiropoulos and J. S. Beckman, *Chem. Res. Toxicol.*, **5**, 834 (1992).
184. M. G. Bonini and O. Augusto, *J. Biol. Chem.*, **276**, 9749 (2001).
185. O. Augusto, M. G. Bonini, A. M. Amanso, E. Linares, C. C. X. Santos and S. L. Menezes, *Free Radic. Biol. Med.*, **32**, 841 (2002).
186. W. A. Pryor and J. W. Lightsey, *Science*, **214**, 435 (1981).
187. W. A. Pryor, J. W. Lightsey and D. F. Church, *J. Am. Chem. Soc.*, **104**, 6685 (1982).
188. W. H. Koppenol, *FEBS Lett.*, **264**, 165 (1990).
189. W. A. Pryor, in *Free Radical in Molecular Biology, Aging and Disease* (Eds. D. Armstrong, R. S. Sohal, R. G. Cutler and T. F. Slater), Raven Press, New York, 1984, pp. 13–41.
190. L. H. Catalani and E. J. H. Bechara, *Photochem. Photobiol.*, **39**, 823 (1984).
191. K. C. Wu and A. M. Trozzolo, *J. Photochem.*, **10**, 407 (1979).
192. (a) W. Adam and G. Cilento, *Chemical and Biological Generation of Excited States*, Academic Press, New York, 1982.
(b) A. A. Frimer, in *The Chemistry of Peroxides* (Ed. S. Patai), Wiley, Chichester, 1983, pp. 201–234.
(c) A. A. Frimer, *Singlet O₂*, CRC Press, Boca Raton, 1985.
193. (a) I. Saito and S. S. Nittala, in *The Chemistry of Peroxides* (Ed. S. Patai), Wiley, Chichester, 1983, pp. 311–374.
(b) P. Di Mascio, L. H. Catalani and E. J. H. Bechara, *Free Radic. Biol. Med.*, **12**, 471 (1992).
194. W. M. Garrison, *Chem. Rev.*, **87**, 381 (1987).
195. (a) C. L. Hawkins and M. J. Davies, *Biochim. Biophys. Acta*, **1360**, 64 (1997).
(b) M. J. Davies, *Biochem. Biophys. Res. Commun.*, **305**, 761 (2003).

196. (a) J. A. Simpson, S. Narita, S. Giesege, S. Gebicki, J. M. Gebicki and R. T. Dean, *Biochem. J.*, **282**, 621 (1992).
(b) S. Gebicki and J. M. Gebicki, *Biochem. J.*, **289**, 743 (1993).
(c) J. M. Gebicki, *Redox Rep.*, **3**, 99 (1997).
197. (a) E. R. Stadtman, *Ann. Rev. Biochem.*, **62**, 797 (1993).
(b) S. Berlett and E. R. Stadtman, *J. Biol. Chem.*, **272**, 20313 (1997).
198. B. N. Nukuna, M. B. Goshe and V. E. Anderson, *J. Am. Chem. Soc.*, **123**, 1208 (2001).
199. (a) G. V. Buxton, C. L. Greenstock, W. P. Helman and A. B. Ross, *J. Phys. Chem. Ref. Data*, **17**, 513 (1988).
(b) M. J. Davies and R. T. Dean, in *Chemistry to Medicine*, Oxford University Press, Oxford, 1997.
(c) M. J. Davies and C. L. Hawkins, *Free Radic. Biol. Med.*, **36**, 1072 (2004).
200. S. Fu, L. A. Hick, M. M. Sheil and R. T. Dean, *Free Radic. Biol. Med.*, **19**, 281 (1995).
201. (a) B. Frei, Y. Yamamoto, D. Niclas and B. N. Ames, *Anal. Biochem.*, **175**, 120 (1988).
(b) W. Sattler, R. Mohr and R. Stocker, *Methods Enzymol.*, **233**, 469 (1994).
202. S.-L. Fu and R. T. Dean, *Biochem. J.*, **324**, 41 (1997).
203. B. Morin, W. A. Bubb, M. J. Davies, R. T. Dean and S. Fu, *Chem. Res. Toxicol.*, **11**, 1265 (1998).
204. (a) S. Einarsson, B. Josefsson and S. Lagerkvist, *J. Chromatogr.*, **282**, 609 (1983).
(b) J. R. E. Lewis, J. S. Morley and R. F. Venn, *J. Chromatogr.*, **615**, 37 (1993).
205. M. Dizdaroglu and M. G. Simic, *Radiat. Res.*, **83**, 437 (1983).
206. (a) G. L. Fletcher and S. Okada, *Radiat. Res.*, **15**, 349 (1961).
(b) K. R. Lynn and J. W. Purdie, *Int. J. Radiat. Phys. Chem.*, **8**, 685 (1976).
207. (a) R. C. Armstrong and A. J. Swallow, *Radiat. Res.*, **40**, 563 (1969).
(b) R. V. Winchester and K. R. Lynn, *Int. J. Radiat. Biol.*, **17**, 541 (1970).
(c) L. Josimovic, I. Jankovic and S. V. Jovanovic, *Radiat. Phys. Chem.*, **41**, 835 (1993).
208. Z. Maskos, J. D. Rush and W. H. Koppenol, *Arch. Biochem. Biophys.*, **296**, 521 (1992).
209. X. Fang, F. Jin, H. Jin and C. von Sonntag, *J. Chem. Soc., Perkin Trans. 2*, 259 (1998).
210. K. Inoue, T. Matsuura and I. Saito, *Bull. Chem. Soc. Jpn.*, **55**, 2959 (1982).
211. J. Wessels, C. S. Foote, W. E. Ford and M. A. J. Rodgers, *Photochem. Photobiol.*, **65**, 90 (1997).
212. S. V. Jovanovic and M. G. Simic, *Free Radic. Biol. Med.*, **1**, 125 (1985).
213. N. Nakagawa, H. Watanabe, S. Kodato, H. Okajima, T. Hino, J. L. Flippen and B. Witkop, *Proc. Natl. Acad. Sci. USA*, **74**, 4730 (1977).
214. A. O. Allen, C. J. Hochanadel, J. A. Ghormley and T. W. Davis, *J. Phys. Chem.*, **56**, 575 (1952).
215. M. Nakagawa, S. Kato, S. Kataoka and T. Hino, *J. Am. Chem. Soc.*, **101**, 3136 (1979).
216. I. Saito, T. Matsuura, M. Nakagawa and T. Hino, *Acc. Chem. Res.*, **10**, 346 (1977).
217. V. F. Ximenes, A. Campa and L. H. Catalani, *Arch. Biochem. Biophys.*, **387**, 173 (2001).
218. R. J. Sundberg, *The Chemistry of Indoles*, Academic Press, New York, 1970, p. 282.
219. O. Hayaishi, R. Rothberg, A. H. Melhler and Y. Saito, *J. Biol. Chem.*, **229**, 880 (1957).
220. C. X. C. Santos, M. G. Bonini and O. Augusto, *Arch. Biochem. Biophys.*, **377**, 146 (2000).
221. H. Zhang, J. Joseph, C. Felix and B. Kalyanaraman, *J. Biol. Chem.*, **275**, 14038 (2000).
222. (a) C. C. Winterbourn and A. J. Kettle, *Biochem. Biophys. Res. Commun.*, **305**, 729 (2003).
(b) C. C. Winterbourn, H. N. Parsons-Mair, S. Gebicki, J. M. Gebicki and M. J. Davies, *Biochem. J.*, **381**, 241 (2004).
223. F. Jin, J. Leitich and C. von Sonntag, *J. Photochem. Photobiol. A: Chem.*, **92**, 147 (1995).
224. (a) L. C. Hsi, C. W. Hoganson, G. T. Babcock and W. L. Smith, *Biochem. Biophys. Res. Commun.*, **202**, 1592 (1994).
(b) P. Reichard, *Annu. Rev. Biochem.*, **57**, 349 (1988).
225. (a) P. J. O'Brien, *Free Radic. Biol. Med.*, **4**, 169 (1988).
(b) J. W. Heinecke, W. Li, H. L. Daehnke and J. A. Goldstein, *J. Biol. Chem.*, **268**, 4069 (1993).
(c) J. S. Jacob, D. P. Cistola, F. F. Hsu, S. Muzaffar, D. M. Mueller, S. L. Hazen and J. W. Heinecke, *J. Biol. Chem.*, **271**, 19950 (1996).
226. E. P. L. Hunter, M. F. Desrosiers and M. G. Simic, *Free Radic. Biol. Med.*, **6**, 581 (1989).
227. (a) F. Jin, J. Leitich and C. von Sonntag, *J. Chem. Soc., Perkin Trans. 2*, 1583 (1993).
(b) I. Cudina and L. J. Josimovic, *Radiat. Res.*, **109**, 206 (1987).

228. N. d'Alessandro, G. Bianchi, X. Fang, F. Jin, H.-P. Schuchmann and C. von Sonntag, *J. Chem. Soc., Perkin Trans. 2*, 1862 (2000).
229. H. Pichorner, D. Melodiewa and C. C. Winterbourn, *Arch. Biochem. Biophys.*, **323**, 429 (1995).
230. S. P. Wolff, *Methods Enzymol.*, **233**, 182 (1994).
231. C. C. Winterbourn, H. Pichorner and A. J. Kettle, *Arch. Biochem. Biophys.*, **338**, 15 (1997).
232. P. Gaudu, V. Nivière, Y. Petillot, B. Kauppi and M. Fontecave, *FEBS Lett.*, **387**, 137 (1996).
233. (a) F. Wilkinson, W. P. Helman and A. B. Ross, *J. Phys. Chem. Ref. Data*, **24**, 663 (1995).
(b) M. Rougée, R. V. Bensasson, E. J. Land and R. Pariente, *Photochem. Photobiol.*, **47**, 485 (1988).
(c) R. V. Bensasson, E. J. Land and T. G. Truscott, *Excited States and Free Radicals in Biology and Medicine*, Oxford University Press, Oxford, 1993.
(d) B. Monroe, in *Singlet O₂* (Ed. A. A. Frimer), Vol. 1, CRC Press, Boca Raton, 1995, p. 171.
234. M. J. Davies, *Photochem. Photobiol. Sci.*, **3**, 17 (2004).
235. R. C. Straight and J. D. Spikes, in *Singlet O₂* (Ed. A. A. Frimer), Vol. 1, CRC Press, Boca Raton, 1995, p. 91.
236. R. Langlois, H. Ali, N. Brasseur, J. R. Wagner and J. E. van Lier, *Photochem. Photobiol.*, **44**, 117 (1986).
237. M. Nakagawa, S. Kato, S. Kataoka, S. Kodato, H. Watanabe, H. Okajima, T. Hino and B. Witkop, *Chem. Pharm. Bull.*, **29**, 1013 (1981).
238. (a) K. Inoue, T. Matsuura and I. Saito, *Bull. Chem. Soc. Jpn.*, **55**, 2959 (1982).
(b) E. A. Almeida, G. R. Martinez, C. F. Klitzke, M. H. G. Medeiros and P. Di Mascio, *J. Pineal Res.*, **35**, 1 (2003).
(c) G. R. Martinez, J.-L. Ravanat, M. H. G. Medeiros, J. Cadet and P. Di Mascio, *J. Am. Chem. Soc.*, **122**, 10212 (2000).
239. (a) E. Katsuya, K. Seya and H. Hikino, *J. Chem. Soc., Chem. Commun.*, 934 (1988).
(b) F. Jin, J. Leitich and C. von Sonntag, *J. Photochem. Photobiol. A: Chem.*, **92**, 147 (1995).
(c) S. Criado, A. T. Soltermann, J. M. Marioli and N. A. Garcia, *Photochem. Photobiol.*, **68**, 453 (1998).
240. A. Wright, W. A. Bubb, C. L. Hawkins and M. J. Davies, *Photochem. Photobiol.*, **76**, 35 (2002).
241. A. Wright, C. L. Hawkins and M. J. Davies, *Redox Rep.*, **5**, 159 (2000).
242. M. Tomita, M. Irie and T. Ukita, *Biochemistry*, **8**, 5149 (1969).
243. (a) P. Kang and C. S. Foote, *Tetrahedron Lett.*, 9623 (2000).
(b) P. Kang and C. S. Foote, *J. Am. Chem. Soc.*, **124**, 9629 (2002).
244. H.-R. Shen, J. D. Spikes, C. J. Smith and J. Kopeček, *J. Photochem. Photobiol. A: Chem.*, **130**, 1 (2000).
245. (a) M. Verwij and J. van Steveninck, *Photochem. Photobiol.*, **35**, 265 (1982).
(b) T. M. A. R. Dubbelman, A. F. P. M. de Goeij and J. van Steveninck, *Biochim. Biophys. Acta*, **511**, 141 (1978).
246. C. A. Gay and J. M. Gebicki, *Anal. Biochem.*, **315**, 29 (2003).
247. H. A. Headlam and M. J. Davies, *Free Radic. Biol. Med.*, **34**, 44 (2003).
248. J. L. Clement, B. C. Gilbert, A. Rockenbauer and P. Tordo, *Free Radic. Res.*, **36**, 883 (2002).
249. (a) C. L. Hawkins and M. J. Davies, *Biochim. Biophys. Acta*, **1360**, 84 (1997).
(b) H. M. Knott, A. Baoutina, M. J. Davies and R. T. Dean, *Arch. Biochem. Biophys.*, **400**, 223 (2002).
250. S. P. Gieseg, J. Pearson and C. A. Firth, *Free Radic. Res.*, **37**, 983 (2003).
251. J. van der Zee, *Biochem. J.*, **322**, 633 (1997).
252. H. Østdal, M. J. Davies and H. J. Andersen, *Free Radic. Biol. Med.*, **33**, 201 (2002).
253. (a) S. Fu, S. Gebicki, W. Gessup, J. M. Gebicki and R. T. Dean, *Biochem. J.*, **311**, 821 (1995).
(b) M. Soszynski, A. Filipiak, G. Bartosz and J. M. Gebicki, *Free Radic. Biol. Med.*, **20**, 45 (1996).
254. C. Fréjaville, H. Karoui, B. Tuccio, F. Lemoigne, S. Pietri, M. Culcasi, R. Lauricella and P. Tordo, *J. Med. Chem.*, **38**, 258 (1995).
255. (a) S. I. Dikakov and R. P. Mason, *Free Radic. Biol. Med.*, **27**, 864 (1999).
(b) S. I. Dikakov and R. P. Mason, *Free Radic. Biol. Med.*, **30**, 187 (2001).

256. R. T. Dean, S. Fu, R. Stocker and M. J. Davies, *Biochem. J.*, **324**, 1 (1997).
257. M. J. Davies, S. Fu and R. T. Dean, *Biochem. J.*, **305**, 643 (1995).
258. D. Balasubramanian, N. Du and J. S. J. Zigler, *Photochem. Photobiol.*, **52**, 761 (1990).
259. H.-R. Shen, J. D. Spikes, P. Kopecekova and J. Kopecek, *J. Photochem. Photobiol. B: Biol.*, **34**, 203 (1996).
260. Y. Liu, G. Sun, A. David and L. M. Sayre, *Chem. Res. Toxicol.*, **17**, 110 (2004).
261. C. Luxford, B. Morin, R. T. Dean and M. J. Davies, *Biochem. J.*, **344**, 125 (1999).
262. (a) B. Morin and J. Cadet, *Chem. Res. Toxicol.*, **8**, 192 (1995).
(b) B. Morin and J. Cadet, *J. Am. Chem. Soc.*, **117**, 12408 (1995).
(c) K. L. Nguyen, M. Steryo, K. Kurbanyan, M. Nowitzki, S. M. Butterfield, S. R. Ward and E. D. A. Stemp, *J. Am. Chem. Soc.*, **122**, 3585 (2000).
(d) K. Kurbanyan, K. L. Nguyen, P. To, E. V. Rivas, A. M. K. Lueras, C. Kosinski, M. Steryo, A. Gonzalez, D. A. Mah and E. D. A. Stemp, *Biochemistry*, **42**, 10269 (2003).
263. R. P. Hickerson, C. L. Chepanoske, S. D. Williams, S. S. David and C. J. Burrows, *J. Am. Chem. Soc.*, **121**, 9901 (1999).
264. S. Gebicki and J. M. Gebicki, *Biochem. J.*, **338**, 629 (1999).
265. C. Hazlewood and M. J. Davies, *Arch. Biochem. Biophys.*, **332**, 79 (1996).
266. C. Luxford, R. T. Dean and M. J. Davies, *Chem. Res. Toxicol.*, **13**, 665 (2000).
267. J. Du and J. M. Gebicki, *Int. J. Biochem. Cell Biol.*, **36**, 2334 (2004).
268. (a) J. Cadet, C. D'Ham, T. Douki, J.-P. Pouget, J.-L. Ravanat and S. Sauvaigo, *Free Radic. Res.*, **29**, 541 (1998).
(b) J. Cadet, T. Douki, S. Frelon, S. Sauvaigo, J.-P. Pouget and J.-L. Ravanat, *Free Radic. Biol. Med.*, **33**, 441 (2002).
(c) A. R. Collins, J. Cadet, L. Möller, H. E. Poulsen and J. Viña, *Arch. Biochem. Biophys.*, **423**, 57 (2004).
269. (a) H. J. Helbock, K. B. Beckman, M. K. Shigenaga, P. B. Walter, A. A. Woodall, H. C. Yeo and B. N. Ames, *Proc. Natl. Acad. Sci. USA*, **95**, 288 (1998).
(b) J.-L. Ravanat, T. Douki, P. Duez, E. Gremaud, K. Herbert, T. Hofer, L. Lasserre, C. Saint-Pierre, A. Favier and J. Cadet, *Carcinogenesis*, **23**, 1911 (2003).
270. (a) J.-L. Ravanat, B. Duret, A. Guiller, T. Douki and J. Cadet, *J. Chromatogr. B*, **715**, 349 (1998).
(b) Y. Hua, S. B. Wainhaus, Y. Yang, L. Shen, Y. Xiong, X. Xu, F. Zhang, J. L. Bolton and R. B. van Breemen, *J. Am. Soc. Mass Spectrom.*, **12**, 80 (2000).
(c) S. Frelon, T. Douki, J.-L. Ravanat, J. P. Pouget, C. Tornabene and J. Cadet, *Chem. Res. Toxicol.*, **13**, 1002 (2000).
271. R. A. Floyd, J. J. Watson, P. K. Wong, D. H. Altmiller and R. C. Rickard, *Free Rad. Res. Commun.*, **1**, 163 (1986).
272. (a) M. Dizdaroglu, *Free Radic. Biol. Med.*, **10**, 225 (1991).
(b) D. C. Malins, K. E. Hellström, K. M. Anderson, P. M. Johnson and M. A. Vinson, *Proc. Natl. Acad. Sci. USA*, **99**, 5937 (2002).
273. J.-P. Pouget, S. Frelon, J.-L. Ravanat, I. Testard, F. Odin and J. Cadet, *Radiat. Res.*, **157**, 589 (2002).
274. (a) J.-L. Ravanat, P. Di Mascio, G. R. Martinez, M. H. G. Medeiros and J. Cadet, *J. Biol. Chem.*, **275**, 40601 (2000).
(b) J.-L. Ravanat, G. R. Martinez, M. H. G. Medeiros, P. Di Mascio and J. Cadet, *Arch. Biochem. Biophys.*, **423**, 23 (2004).
275. (a) T. Douki, D. Perdiz, P. Grof, Z. Kuluncsics, E. Moustacchi, J. Cadet and E. Sage, *Photochem. Photobiol.*, **70**, 184 (1999).
(b) J.-P. Pouget, T. Douki, M.-J. Richard and J. Cadet, *Chem. Res. Toxicol.*, **13**, 541 (2000).
(c) J. Cadet, E. Sage and T. Douki, *Mutat. Res.*, **571**, 3 (2005).
276. T. Kriska and A. W. Girotti, *Anal. Biochem.*, **327**, 97 (2004).
277. (a) T. F. Slater, *Methods Enzymol.*, **105**, 283 (1984).
(b) A. W. Girotti, *J. Free Radic. Biol. Med.*, **1**, 87 (1985).
(c) H. H. Draper and M. Hadley, *Methods Enzymol.*, **186**, 421 (1990).
(d) R. O. Recknagel and E. A. Glende, *Methods Enzymol.*, **105**, 331 (1984).
(e) J. A. Buege and S. D. Aust, *Methods Enzymol.*, **52**, 302 (1978).
(f) A. W. Girotti, J. P. Thomas and J. E. Jordan, *Arch. Biochem. Biophys.*, **236**, 238 (1985).
(g) R. Cathcart, E. Schwiers and B. N. Ames, *Methods Enzymol.*, **105**, 352 (1984).

278. (a) A. Rieche and M. Schultz, *Angew. Chem.*, **70**, 694 (1958).
(b) J. Sherma, *Anal. Chem.*, **60**, 74 (1988).
(c) L. L. Smith and F. L. Hill, *J. Chromatogr.*, **66**, 101 (1972).
(d) J. Terao, M. Miyoshi and S. Miyamoto, *J. Chromatogr. B*, **765**, 199 (2001).
279. (a) T. Miyazawa, *Free Radic. Biol. Med.*, **7**, 209 (1989).
(b) Y. Yamamoto, B. Frei and B. N. Ames, *Methods Enzymol.*, **186**, 371 (1990).
(c) W. Korytowski, P. G. Geiger and A. W. Girotti, *J. Chromatogr. B*, **670**, 189 (1995).
(d) W. Korytowski, P. G. Geiger and A. W. Girotti, *Methods Enzymol.*, **300**, 23 (1999).
280. (a) C. M. Spickett, N. Rennie, H. Winter, L. Zambonin, L. Landi, A. Jerlich, R. J. Schaur and A. R. Pitt, *Biochem. J.*, **355**, 449 (2001).
(b) G. L. Milne and N. A. Porter, *Lipids*, **36**, 1265 (2001).
(c) J. R. Seal and N. A. Porter, *Anal. Bioanal. Chem.*, **378**, 1007 (2004).
281. (a) T. Kaneko, S. Honda, S. I. Nakano and M. Matsuo, *Chem.-Biol. Interact.*, **63**, 127 (1987).
(b) H. Esterbauer, R. J. Schaur and H. Zollner, *Free Radic. Biol. Med.*, **11**, 81 (1991).
(c) C. Nappetz, S. Battu and J. L. Beneytout, *Cancer Lett.*, **99**, 115 (1996).
282. (a) F. J. G. M. van Kuijk, A. N. Siakotos, L. G. Fong, R. J. Stephens and D. W. Thomas, *Anal. Biochem.*, **224**, 420 (1995).
(b) G. Spiteller, W. Kern and P. Spiteller, *J. Chromatogr. A*, **843**, 29 (1999).
283. S. F. Vaughn and H. W. Gardner, *J. Chem. Ecol.*, **19**, 2337 (1993).
284. U. Dittberner, G. Eissenbrand and H. Zankl, *Mutat. Res.*, **335**, 259 (1995).
285. H. W. Gardner, D. L. Dornbos Jr. and A. E. Desjardins, *J. Agric. Food Chem.*, **38**, 1316 (1990).
286. J. M. C. Gutteridge and G. J. Quinlan, *J. Appl. Biochem.*, **5**, 293 (1983).
287. (a) H. J. Segall, D. W. Wilson, J. L. Dallas and W. F. Haddon, *Science*, **229**, 472 (1985).
(b) B. S. Kristal, B. K. Park and B. P. Yu, *J. Biol. Chem.*, **271**, 6033 (1996).
288. L. J. Roberts and J. D. Morrow, *Biochim. Biophys. Acta*, **1345**, 121 (1997).
289. (a) C. K. Winter, H. J. Segall and W. F. Haddon, *Cancer Res.*, **46**, 5682 (1986).
(b) P. Yi, D. Zhan, V. M. Samokyszyn, D. R. Doerge and P. P. Fu, *Chem. Res. Toxicol.*, **10**, 1259 (1997).
290. (a) H. Seto, T. Okuda, T. Takesue and T. Ikemura, *Bull. Chem. Soc. Jpn.*, **56**, 1799 (1983).
(b) V. Nair, G. A. Turner and R. J. Offerman, *J. Am. Chem. Soc.*, **106**, 3370 (1984).
(c) L. J. Marnett, A. K. Basu, S. M. O'Hara, P. E. Weller, A. F. M. M. Rahman and J. P. Oliver, *J. Am. Chem. Soc.*, **108**, 1348 (1986).
(d) K. Stone, M. Ksebati and L. J. Marnett, *Chem. Res. Toxicol.*, **3**, 33 (1990).
(e) K. Stone, A. Uzieblo and L. J. Marnett, *Chem. Res. Toxicol.*, **3**, 467 (1990).
(f) L. J. Marnett, in *Exocyclic DNA Adducts in Mutagenesis and Carcinogenesis* (Eds. B. Singer and H. Bartsch), IARC Scientific Publication 150, Lyon, 1999, pp. 17–27.
291. (a) B. M. Goldschmidt, T. P. Blazej and B. L. Van Duuren, *Tetrahedron Lett.*, 1583 (1968).
(b) V. Nair and R. J. Offerman, *J. Org. Chem.*, **50**, 5627 (1985).
(c) R. S. Sodum and F.-L. Chung, *Cancer Res.*, **48**, 320 (1988).
(d) B. T. Golding, P. K. Slaich, G. Kennedy, C. Bleasdale and W. P. Watson, *Chem. Res. Toxicol.*, **9**, 147 (1996).
(e) F.-L. Chung, H. J. Chen and R. G. Nath, *Carcinogenesis*, **17**, 2105 (1996).
(f) A. J. Ham, A. Ranasinghe, H. Koc and J. A. Swenberg, *Chem. Res. Toxicol.*, **13**, 1243 (2000).
(g) E. J. Morinello, A. J. Ham, A. Ranasinghe, R. Sangaiah and J. A. Swenberg, *Chem. Res. Toxicol.*, **14**, 327 (2001).
292. (a) A. P. M. Loureiro, S. A. Marques, C. C. M. Garcia, P. Di Mascio and M. H. G. Medeiros, *Chem. Res. Toxicol.*, **15**, 1302 (2002).
(b) A. P. M. Loureiro, P. Di Mascio and M. H. G. Medeiros, *Quim. Nova*, **25**, 777 (2002).
293. T. Kaneko, K. Kaji and M. Matsuo, *Chem.-Biol. Interact.*, **67**, 295 (1988).
294. (a) A. P. M. Loureiro, P. Di Mascio, O. F. Gomes and M. H. G. Medeiros, *Chem. Res. Toxicol.*, **13**, 601 (2000).
(b) V. M. Carvalho, P. Di Mascio, I. P. Arruda-Campos, T. Douki, J. Cadet and M. H. G. Medeiros, *Chem. Res. Toxicol.*, **11**, 1042 (1998).
(c) V. M. Carvalho, F. Asahara, P. Di Mascio, I. P. Arruda-Campos, J. Cadet and M. H. G. Medeiros, *Chem. Res. Toxicol.*, **13**, 397 (2000).
295. S. H. Lee, T. Oe and I. A. Blair, *Chem. Res. Toxicol.*, **15**, 300 (2002).

296. H. Bartsch and J. Nair, *Eur. J. Cancer*, **36**, 1229 (2000).
297. (a) D. R. Doerge, M. I. Churchwell, J. L. Fang and F. A. Beland, *Chem. Res. Toxicol.*, **13**, 1259 (2000).
(b) H. J. C. Chen, L. C. Chiang, M. C. Tseng, L. L. Zhang, J. Ni and F.-L. Chung, *Chem. Res. Toxicol.*, **12**, 1119 (1999).
(c) J. Nair, A. Barbin, Y. Guichard and H. Bartsch, *Carcinogenesis*, **16**, 613 (1995).
(d) R. R. Misra, S. Y. Chiang and J. A. Swenberg, *Carcinogenesis*, **15**, 1647 (1994).
(e) J. Nair, A. Barbin, I. Velic and H. Bartsch, *Mutat. Res.*, **424**, 59 (1999).
(f) W. P. Watson, J. P. Aston, T. Barlow, A. E. Crane, D. Potter and T. Brown, in *Exocyclic DNA Adducts in Mutagenesis and Carcinogenesis* (Eds. B. Singer and H. Bartsch), IARC Scientific Publication 150, Lyon, 1999, pp. 63–73.
(g) D. W. Roberts, M. I. Churchwell, F. A. Beland, J. L. Fang and D. R. Doerge, *Anal. Chem.*, **73**, 303 (2001).
(h) H. Bartsch, A. Barbin, M. J. Marion, J. Nair and Y. Guichard, *Drug Metab. Rev.*, **26**, 349 (1994).
298. (a) N. Fedtke, J. A. Boucheron, V. E. Walker and J. A. Swenberg, *Carcinogenesis*, **11**, 1287 (1990).
(b) T. Y. Yen, N. I. Christova-Gueogueieva, N. Scheller, S. Holt, J. A. Swenberg and M. J. Charles, *J. Mass Spectrom.*, **31**, 1271 (1996).
(c) A. J. L. Ham, A. Ranasinghe, E. J. Morinello, J. Nakamura, P. B. Upton, F. Johnson and J. A. Swenberg, *Chem. Res. Toxicol.*, **12**, 1240 (1999).
299. (a) J. Nair, P. L. Carmichael, R. C. Fernando, D. H. Phillips, A. J. Strain and H. Bartsch, *Cancer Epidemiol. Biomarkers Prev.*, **7**, 435 (1998).
(b) J. Nair, H. Sone, M. Nagao, A. Barbin and H. Bartsch, *Cancer Res.*, **56**, 1267 (1996).
300. J. Nair, A. Gal, S. Tamir, S. R. Tannenbaum, G. N. Wogan and H. Bartsch, *Carcinogenesis*, **19**, 2081 (1998).
301. K. Schmid, J. Nair, G. Winde, I. Velic and H. Bartsch, *Int. J. Cancer*, **87**, 1 (2000).
302. J. Nair, C. E. Vaca, I. Velic, M. Mutanen, L. M. Valsta and H. Bartsch, *Cancer Epidemiol. Biomarkers Prev.*, **6**, 597 (1997).
303. J. Nair, G. Furstemberger, F. Burger, F. Marks and H. Bartsch, *Chem. Res. Toxicol.*, **13**, 703 (2000).
304. F. El Ghissassi, A. Barbin, J. Nair and H. Bartsch, *Chem. Res. Toxicol.*, **8**, 278 (1995).
305. (a) H. J. Chen, L. Zhang, J. Cox, J. A. Cunningham and F.-L. Chung, *Chem. Res. Toxicol.*, **11**, 1474 (1998).
(b) R. S. Sodom and F.-L. Chung, *Cancer Res.*, **51**, 137 (1991).
(c) H. J. Chen and F.-L. Chung, *Chem. Res. Toxicol.*, **9**, 306 (1996).
306. M. Awada and P. C. Dedon, *Chem. Res. Toxicol.*, **14**, 1247 (2001).
307. (a) J. A. Swenberg, N. Fedtke, F. Ciroussel, A. Barbin and H. Bartsch, *Carcinogenesis*, **13**, 727 (1992).
(b) G. Eberle, A. Barbin, R. J. Laib, F. Ciroussel, J. Thomale, H. Bartsch and M. F. Rajewsky, *Carcinogenesis*, **10**, 209 (1989).
308. P. G. Foiles, L. M. Miglietta, A. Nishikawa, J. T. Kusmirek, B. Singer and F.-L. Chung, *Carcinogenesis*, **14**, 113 (1993).
309. M. Müller, F. J. Belas, I. A. Blair and F. P. Guengerich, *Chem. Res. Toxicol.*, **10**, 242 (1997).
310. S. Langouët, M. Müller and F. P. Guengerich, *Biochemistry*, **36**, 6069 (1997).
311. S. Langouët, A. N. Mican, M. Müller, S. P. Fink, L. J. Marnett, S. A. Muhle and F. P. Guengerich, *Biochemistry*, **37**, 5184 (1998).
312. S. Akasaka and F. P. Guengerich, *Chem. Res. Toxicol.*, **12**, 501 (1999).
313. M. Saparbaev, S. Langouët, C. V. Privezentzev, F. P. Guengerich, H. Cai, R. H. Elder and J. Laval, *J. Biol. Chem.*, **277**, 26987 (2002).
314. O. Niemela, S. Parkkila, S. Yla-Herttuala, J. Villanueva, B. Ruebner and C. H. Halsted, *Hepatology*, **22**, 1208 (1995).
315. L. Tsai, P. A. Szweda, O. Vinogradova and L. I. Szweda, *Proc. Natl. Acad. Sci. USA*, **95**, 7975 (1998).
316. P. C. Burcham and Y. T. Kuhan, *Biochem. Biophys. Res. Commun.*, **220**, 996 (1996).
317. (a) K. Uchida and E. R. Stadtman, *Proc. Natl. Acad. Sci. USA*, **89**, 4544 (1992).
(b) L. M. Sayre, P. K. Arora, R. S. Iyer and R. G. Salomon, *Chem. Res. Toxicol.*, **6**, 19 (1993).
(c) B. Friquet, L. I. Szweda and E. R. Stadtman, *Arch. Biochem. Biophys.*, **311**, 168 (1994).

- (d) B. A. Brunner, A. D. Jones and J. B. German, *Chem. Res. Toxicol.*, **8**, 552 (1995).
- (e) W-H. Zhang, J. Liu, G. Xu, Q. Yuan and L. M. Sayre, *Chem. Res. Toxicol.*, **16**, 512 (2003).
318. Y. Kato, K. Uchida and S. Kawakishi, *J. Biol. Chem.*, **267**, 23646 (1992).
319. (a) A. G. Baker, D. Wiesler and M. V. Novotny, *J. Am. Soc. Mass Spectrom.*, **10**, 613 (1999).
(b) H. H. F. Refsgaard, L. Tsai and E. R. Stadtman, *Proc. Natl. Acad. Sci. USA*, **97**, 611 (2000).
320. E. R. Stadtman and B. S. Berlett, in *Reactive Oxygen Species in Biological Systems* (Eds. D. L. Gilbert and C. A. Colton), Kluwer Academic/Plenum Publishers, New York, 1999, pp. 657–675.
321. (a) A. Wright, C. L. Hawkins and M. J. Davies, *Free Radic. Biol. Med.*, **34**, 637 (2003).
(b) S. Gieseg, S. Duggan and J. M. Gebicki, *Biochem. J.*, **350**, 215 (2000).
322. C. Gay, J. Collins and J. M. Gebicki, *Anal. Biochem.*, **273**, 149 (1999).
323. C. Gay and J. M. Gebicki, *Anal. Biochem.*, **304**, 42 (2002).
324. H. A. Headlam and M. J. Davies, *Free Radic. Biol. Med.*, **36**, 1175 (2004).
325. (a) C. N. Oliver, B. W. Ahn, E. J. Moerman, S. Goldstein and E. R. Stadtman, *J. Biol. Chem.*, **262**, 5438 (1987).
(b) R. L. Levine and E. R. Stadtman, *Exp. Gerontol.*, **36**, 1495 (2001).
(c) S. Linton, M. J. Davies and R. T. Dean, *Exp. Gerontol.*, **36**, 1503 (2001).
(d) H. Aguilaniu, L. Gustafsson, M. Rigoulet and T. Nyström, *Science*, **299**, 1751 (2003).
326. I. Dalle-Donne, R. Rossi, D. Giustarini, A. Milazzi and R. Colombo, *Clin. Chim. Acta*, **329**, 23 (2003).
327. S. Fu, M. J. Davies, R. Stocker and R. T. Dean, *Biochem. J.*, **333**, 519 (1998).
328. (a) R. L. Levine, J. A. Williams, E. R. Stadtman and E. Shacter, *Methods Enzymol.*, **233**, 346 (1994).
(b) M. Chevion, E. Bernenshtein and E. R. Stadtman, *Free Radic. Res.*, **33**, 99 (2000).
(c) S. Richert, N. B. Wehr, E. R. Stadtman and R. L. Levine, *Arch. Biochem. Biophys.*, **397**, 430 (2002).
329. (a) A. G. Lenz, U. Costabel, S. Shaltiel and R. L. Levine, *Anal. Biochem.*, **177**, 419 (1989).
(b) M. L. Winter and J. G. Liehr, *J. Biol. Chem.*, **266**, 14446 (1991).
(c) R. L. Levine, D. Garland, C. N. Oliver, A. Amici, I. Climent, A. G. Lenz, B. W. Ahn, S. Shaltiel and E. R. Stadtman, *Methods Enzymol.*, **186**, 464 (1990).
330. J. M. Fagan, B. G. Sleczo and I. Sohar, *Int. J. Biochem. Cell Biol.*, **31**, 751 (1999).
331. (a) A. Nakamura and S. Goto, *J. Biochem. (Tokyo)*, **119**, 768 (1996).
(b) C. E. Robinson, A. Keshavarzian, D. S. Pasco, T. O. Frommel, D. H. Winship and E. W. Holmes, *Anal. Biochem.*, **266**, 48 (1999).
(c) C. C. Winterbourn and H. Buss, *Methods Enzymol.*, **300**, 106 (1999).
332. S. Fu, R. T. Dean, M. Southan and R. Truscott, *J. Biol. Chem.*, **273**, 28603 (1998).

CHAPTER 12

Sulfur and phosphorus peroxides

VIDYADHAR JADHAV, MIN YOUNG PARK and YONG HAE KIM

Center for Molecular Design and Synthesis, Department of Chemistry, Korea Advanced Institute of Science and Technology, Taejeon 305-701, Korea
Fax: +82 42 869 5818; e-mail: kimyh@kaist.ac.kr

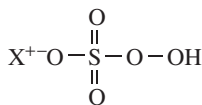
I. INTRODUCTION	1001
II. SULFUR PEROXIDES	1002
A. Persulfonic Acid	1002
B. Sulfonyl Peroxides	1004
C. Peroxydisulfate	1007
D. Organic Salts of Peroxydisulfate	1014
E. Potassium Peroxymonosulfate	1020
F. Organic Salts of Peroxymonosulfate	1030
G. Organic Sulfur Compounds with Superoxide	1032
1. Peroxysulfenate	1033
2. Peroxysulfinate	1033
3. Sulfonylperoxy radical	1035
III. PHOSPHORUS PEROXIDES	1039
A. Monoperoxyphosphoric Acid	1040
B. Symmetrical Phosphorus Peroxides	1041
C. Unsymmetrical Phosphorus Peroxides	1042
D. Peroxyphosphorus Radicals	1044
IV. REFERENCES	1046

I. INTRODUCTION

Numerous sulfur and phosphorus peroxy compounds such as monopersulfuric acid (Caro's acid, **1a**)¹, monopersulfate (Oxone, **1b**)², ammonium monopersulfate **1c**, tetra *n*-butylammonium monopersulfate **1d**³, peroxydisulfates **2a** and **2b**⁴, tetra *n*-butylammonium peroxydisulfate **2c**⁵, symmetrical bisulfonyl peroxide **3**⁶, acyl sulfonyl peroxide **4**⁶, unsymmetrical sulfonyl peroxide **5**⁶, sulfinyl peroxy intermediates **6a**⁷, sulfonyl peroxy intermediate **6b**⁷, sulfonimidoyl peroxy intermediate **7**⁸, bis(diphenyl phosphinyl) peroxide **8**⁹, unsymmetrical phosphorus peroxide **9**¹⁰ and phosphoranyl peroxy intermediate **10**¹¹ are known. Recently, many researchers have shown interest in the preparation and

The chemistry of peroxides, volume 2

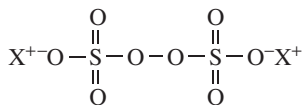
Edited by Z. Rappoport © 2006 John Wiley & Sons, Ltd ISBN: 0-470-86274-2



(1)

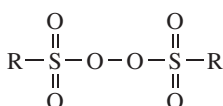
(a) X= H

(b) X= K

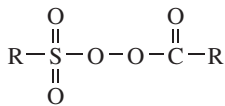
(c) X= NH₄(d) X= *n*-Bu₄N

(2)

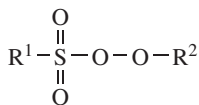
(a) X= K, Na

(b) X= NH₄(c) X= *n*-Bu₄N

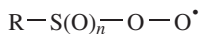
(3)



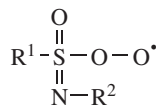
(4)



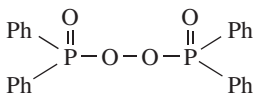
(5)



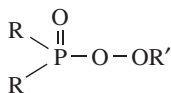
(6)

(a) *n*= 1(b) *n*= 2

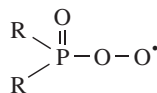
(7)



(8)



(9)



(10)

application of different organic salts of monopersulfate and peroxydisulfate, which are described comprehensively in the respective sections.

Recently, sulfinyl and sulfonyl peroxy radical intermediates **6a** and **6b** have been prepared by the reactions of aryl sulfinyl or sulfonyl chloride with superoxide anion radical, respectively. These peroxy intermediates show strong oxidizing abilities in various oxidations. This chapter will describe the properties and applications of a variety of sulfur and phosphorus peroxy compounds in oxidation reactions. For a more complete picture, readers should consult the original papers cited in the areas that most interest them.

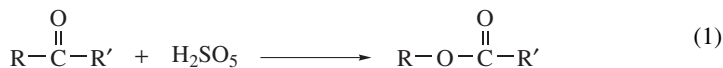
II. SULFUR PEROXIDES

A. Persulfonic Acid

Organic peracids are the most reliable and commonly used oxidizing reagents for various purposes in organic chemistry. Compared to common percarboxylic acids such as performic acid¹², peracetic acid¹³, perbenzoic acid¹⁴ and *m*-chloroperbenzoic acid¹⁵, the first sulfur peroxy acid, i.e. monopersulfuric acid¹⁶, was reported earlier, already in 1891.

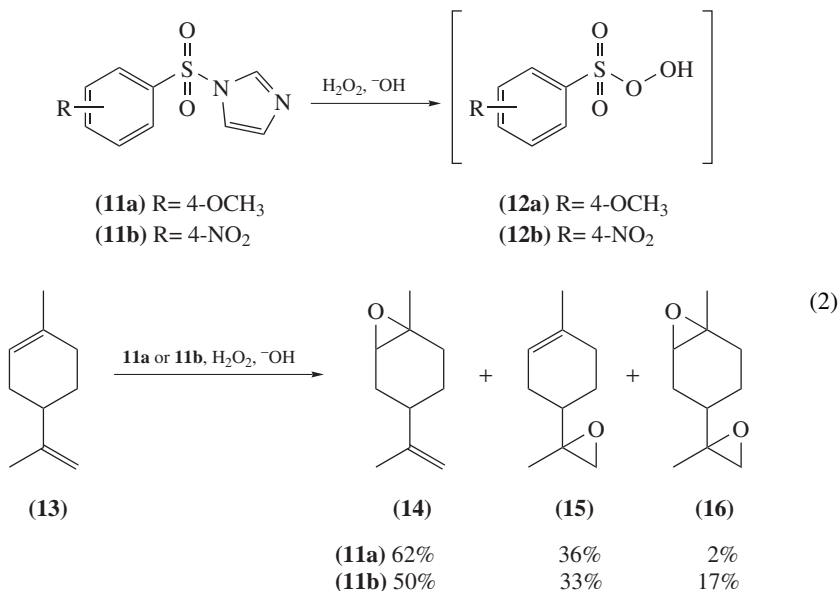
Monopersulfuric acid (monoperoxysulfuric acid, H₂SO₅, Caro's acid) was first detected during electrolysis of sulfuric acid¹⁶. Later, in 1898, Caro found the oxidation of aniline to nitrobenzene with ammonium peroxydisulfate **1c** in H₂SO₄. Later, the oxidizing species was found to be H₂SO₅¹⁷.

Monopersulfuric acid is one of the most powerful oxidizing reagents. Since H_2SO_5 is unstable at room temperature, it is always prepared *in situ* by mixing conc. H_2SO_4 and H_2O_2 or peroxydisulfate ions. The H_2SO_5 is often used as a characteristic oxidizing reagent in the field of organic chemistry. The most common use of H_2SO_5 is in the Baeyer–Villiger reaction for the oxidation of carbonyl compounds to esters (equation 1)^{18,19}.

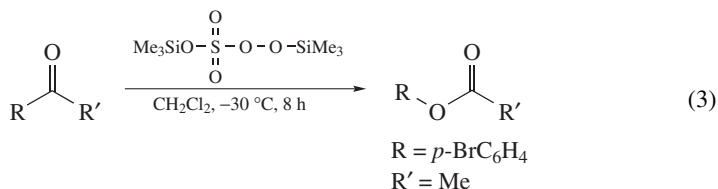


When aldehydes are oxidized with H_2SO_5 in the presence of alcohols, the esters of the corresponding acids are obtained in very high yields²⁰. Mechanistically, it seems plausible that the Baeyer–Villiger reaction occurs first and esterification follows. Thus, the aldehyde is oxidized by H_2SO_5 to the corresponding carboxylic acid, which is esterified immediately with the alcohol.

Various substituted pyrazines have been oxidized by H_2SO_5 to the corresponding *N*-oxides²¹. In this reaction H_2SO_5 was compared with peracetic acid and the difference between H_2SO_5 and peracetic acid oxidations may be mainly due to the different acidities of the solvents. In conc. H_2SO_4 , the ring nitrogens of pyrazine and 2-methylpyrazine were extensively diprotonated, with the outcome that no formation of any *N*-oxide by the H_2SO_5 oxidation took place. The kinetic study of the acetone and cyclohexane catalyzed oxidation of pyridine by HSO_3^- was reported²². The detailed kinetics and mechanistic study of the oxidation of bisulfite ion (HSO_3^-) by monopersulfate ion (HSO_5^-) to form the sulfate ion has been reported²³. Different arylsulfonic peracids **12a** and **12b** were generated *in situ* by the reaction of the corresponding arylsulfonyl imidazolides **11a** and **11b** with H_2O_2 in alkaline medium (equation 2)²⁴. When alkenes having either electron-deficient or electron-rich carbon–carbon double bonds such as **13** were subjected to reaction with these new oxidizing reagents, several products **14–16** were obtained in different ratios (equation 2), indicating that these oxidizing species show electrophilic as well as nucleophilic oxidizing properties.



Bis(trimethylsilyl)monopersulfate (Me_3Si) $_2\text{SO}_5$ is prepared by reacting bis(trimethylsilyl) peroxide and sulfur trioxide in CH_2Cl_2 at -30°C ²⁵. Adam and Rodriguez used (Me_3Si) $_2\text{SO}_5$ for the Baeyer–Villiger oxidation reaction (equation 3)²⁶. It has been found that the (Me_3Si) $_2\text{SO}_5$ mediated oxidation gave purer products and higher yields compared with H_2SO_5 .



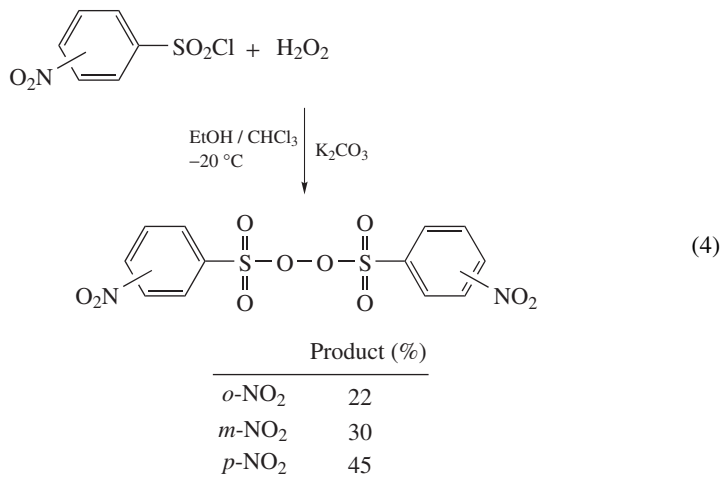
Polymer supported persulfonic acids can be prepared by treating polymer-bound sulfonic acids with H_2O_2 or $\text{K}_2\text{S}_2\text{O}_8$ ²⁷. The resulting resin was found to display an activity of 2.5 mole equivalents per gram of wet resin. This persulfonated resin was successively applied for the oxidation of carboxylic acids, ketones, olefins and for the cleavage of disulfide linkage and of *N*-formylamino acids.

Recently, it has been found that monopersulfonic acid supported on Silica gel gave a free flowing powder of an oxidizing agent, which is stable at 25°C . This new Silica gel supported monopersulfuric acid (Silica gel— H_2SO_5) can be easily prepared by mixing conc. H_2SO_4 , $\text{K}_2\text{S}_2\text{O}_8$ and Silica gel in cold water, stirring for 4 h at -15°C and then, when drying in desiccators, it affords Silica gel— H_2SO_5 . This serves as the best alternative for unstable H_2SO_5 . Silica gel— H_2SO_5 reagent has been successfully used for the oxidation of sulfides to sulfones²⁸, aliphatic thiols to disulfides²⁹ and thioamides to amides³⁰ in good to excellent yields.

Along with the above-mentioned persulfonic acids, some aromatic and aliphatic persulfonic acids are also reported. Peroxytrifluoromethanesulfonic acid prepared *in situ* from H_2O_2 and excess trifluoromethanesulfonic acid is among the powerful oxidants known³¹. It oxidized pentanitroaniline to hexanitrobenzene in 90% yield. Benzoyl monopersulfonic acid which was unstable at 25°C was prepared *in situ* from monopersulfuric acid and benzoyl chloride at 0°C and could be isolated in the form of its solid potassium salt³². Salts of *p*-toluenepersulfonic, β -naphthalenepersulfonic acid and amylnaphthalenesulfonic acid have been prepared from sodium, calcium or silver peroxide and the corresponding arylsulfanyl chlorides^{33,34}.

B. Sulfonyl Peroxides

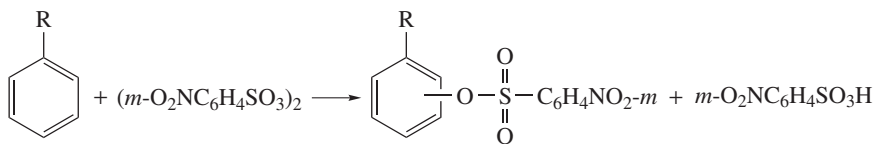
It is generally believed that the attachment of sulfonyl groups at the end of the O—O bond enhances the thermal stability of the peroxide bond, which can be further enhanced by the attachment of phenyl groups containing electron-withdrawing substituents (e.g. 4- $\text{NO}_2\text{C}_6\text{H}_4$, 3- $\text{NO}_2\text{C}_6\text{H}_4$, 3- $\text{CF}_3\text{C}_6\text{H}_4$). These are among the most thermally stable sulfonyl peroxides. Only a few dialkyl peroxides are known. Bis(dimethylsulfonyl) peroxide is stable for one week at 25°C ³⁵. On the other hand, bis(ditrifluoromethylsulfonyl) peroxide is very unstable and decomposes within few minutes at 25°C ³⁶. Sulfonyl peroxides have a rather low active oxygen content of 4–8%, so that the pure materials decompose exothermically but not violently. Mixed sulfonyl acyl peroxides are qualitatively less stable than bissulfonyl peroxides. Sulfonyl alkyl peroxides are somewhat less stable and decompose violently in a few minutes at 25°C . Bissulfonyl peroxides can be prepared by reacting arylsulfonyl chloride with H_2O_2 in aqueous EtOH/ CHCl_3 mixture in the presence of K_2CO_3 at -20°C in high purity (>98%) (equation 4)³⁷.



Thermal decomposition in three different ways, i.e. homolytic, polar and radical induced decomposition, as well as intermolecular reaction of sulfonyl peroxides are the main reactions displayed by sulfonyl peroxides. When bis(arylsulfonyl) peroxides are allowed to decompose at 25–40 °C in chloroform, homolytic O–O bond fission followed by hydrogen abstraction from the solvent results in the formation of the corresponding arylsulfonic acids³⁸. Mixed acyl sulfonyl peroxides undergo complicated thermal decomposition in solution, and have been used commercially as polymerization initiators, since they provide a source of free radicals at a relatively low temperature³⁹.

Although bissulfonyl peroxides can decompose by homolysis of the O–O bond, in the presence of electron donor reagent (π , n and σ donors) they react as electrophiles. Conversely, in the case of an electron-deficient peroxide bond, electron-donating reagents can be regarded as attacking nucleophilically the O–O bond.

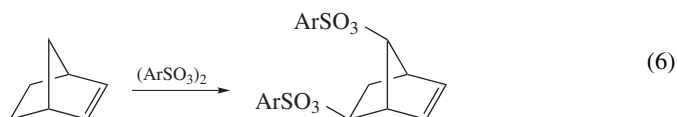
Since benzenesulfonyl peroxide was used as an initiator in polymerization reactions, it was thought that a free radical aromatic substitution of benzene by the benzenesulfonyl radical takes place³⁷. A detailed study by Dannley and Knipple reveals that attachment of the sulfonyl group derived from a bis(arylsulfonyl) peroxide to the aromatic ring occurs by electrophilic aromatic substitution (equation 5)⁴⁰.



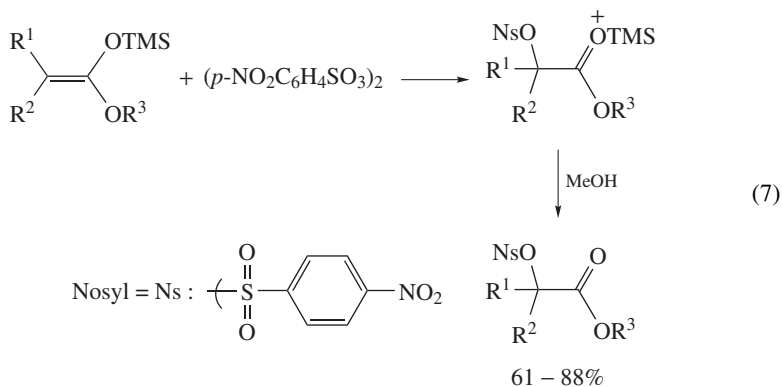
R	Product (%)	Isomer distribution <i>o</i> / <i>m</i> / <i>p</i>
NO ₂	65	24 / 65 / 11
COOMe	70	24 / 67 / 9
OMe	67	14 / – / 86
Br	66	21 / 3 / 76

Electron-donating substituents make the aromatic substrate more reactive than benzene and lead to *o,p*-orientation, while electron-withdrawing substituents decrease the reactivity and give mostly *m*-orientation products. The detailed mechanism of the formation of the σ complex has been studied by oxygen-18 labeling of the sulfonyl oxygen in *p*-nitrobenzenesulfonyl peroxide³⁸. The ionic mechanism for aromatic substitution by sulfonyl peroxides has been confirmed by carrying out the substitution reaction in the presence of redox catalysts such as copper and cobalt salts and aluminum chloride. Small differences in the rate of the products can be found in the presence or absence of these additives, and it has been concluded that the ionic mechanism accounts satisfactorily for these results⁴¹.

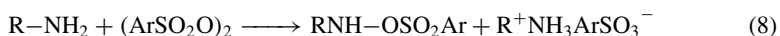
Similarly to aromatic π system, olefinic π -electron donors also readily react with bisulfonyl peroxides. Norbornene, when reacted with bis(arylsulfonyl) peroxides, gives a disubstituted product following Wagner–Meerwein rearrangement (equation 6)⁴².



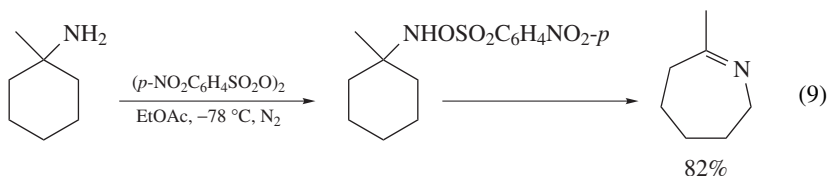
Bis(nitrobenzenesulfonyl) peroxides react with electron-rich alkenes substituted by oxygen or nitrogen in an alcohol to afford the corresponding sulfonylated α -ether adduct in good yield⁶. When a β -diketone reacted with *p*-nitrophenylsulfonyl peroxide, it gave 2-(*p*-nitrophenylsulfonyloxy)- β -keto esters. These compounds can serve as precursors to 2-nosyl ketones by decarbonylation, to 3-hydroxy-2-nosyl esters by reduction and to tricarbonyl compounds by reductive elimination⁴³. *O*-Trimethylsilyl ketene acetals were reacted with *p*-nitrobenzenesulfonyl peroxide and methanol in ethyl acetate at 0 °C to give the nosyl esters in good yields. Methanol was used to trap the oxonium ion produced from the electrophilic addition of *p*-nitrobenzenesulfonyl peroxide to the silyl acetal double bond (equation 7).



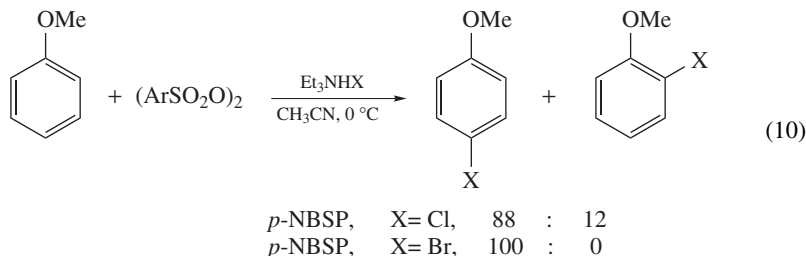
Hoffman and coworkers have extensively studied the reactions between amines and sulfonyl peroxides. When primary amines reacted with arylsulfonyl peroxides at -78 °C in ethyl acetate, *N*-alkyl-*O*-arylsulfonyl hydroxylamine derivatives were obtained (equation 8)⁴⁴, whereas when various primary and secondary amines reacted with sulfonyl peroxides, oxidative deamination was observed⁴⁵.



Aryl alkyl amines gave hydroxylamine *O*-arylsulfonates when reacted with arylsulfonyl peroxide. The products were later decomposed to azomethine and further hydrolysis results in the corresponding amine with one less carbon atom. Thus when *p*-methoxybenzylamine was treated with *p*-nitrophenylsulfonyl peroxide at -78°C in ethyl acetate, *p*-methoxybenzaldehyde and *p*-methoxyaniline were obtained⁴⁶. Cyclic amines with *p*-nitrophenylsulfonyl peroxide were converted to the *N*-(*p*-nitrophenylsulfonyloxy)amine derivatives, which further rearranged to ring-expanded cyclic imines in good yields (equation 9)⁴⁷.



An effective halogenation of anisole on treatment with nitrobenzenesulfonyl peroxides (NBSP) in the presence of ammonium halides was reported (equation 10)⁴⁸. Peroxides react in general as electrophiles in the presence of electron donors. Halide ion may react with a sulfonyl peroxide, which is a good electrophile, to produce hypochlorite. In the sulfonyl hypochlorite, the chlorine should be positively charged owing to the effect of the strong electron-withdrawing nitrobenzenesulfonyl group and may react as an electrophile to be introduced into anisole. Direct halogenations on the methyl carbon of toluene or at the 2-position in thiophene have been shown to afford mixtures of 4- and 2-halogenated benzyl products or solely 2-substituted products in reasonable yields.

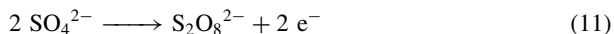


Benzoyl 4-toluenesulfonyl peroxide reacts with triphenylphosphine to give triphenylphosphine oxide and benzoic 4-toluenesulfonic anhydride⁴⁹. A plausible mechanism derived from *O*-labeling experiments has been proposed: the reaction is initiated by phosphorus attack on the peroxide oxygen attached to the carbonyl function. On the other hand, when 4-toluenesulfonyl peroxide is reacted with 4-tolylmagnesium bromide, benzoic acid and 4-tolyl 4-toluenesulfonate are obtained. This reaction appears to be initiated by attack of the Grignard reagent on the peroxide oxygen bond to the sulfonyl moiety. Interaction between magnesium and the carbonyl oxygen of the peroxide probably directs such specificity of attack.

C. Peroxydisulfate

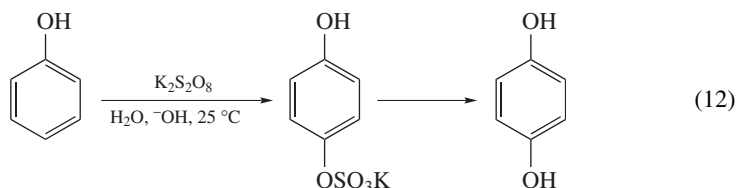
To the best of our knowledge, there is no review about the applications of peroxydisulfates ($\text{S}_2\text{O}_8^{2-}$) and its organic salts. The peroxydisulfate ion is one of the strongest

oxidizing agents known in aqueous solution. The standard oxidation–reduction potential for the reaction shown in equation 11 is estimated to be $-2.01 \text{ V}^{50,51}$.



Commercially available peroxydisulfates are in the form of sodium, potassium or ammonium salts as crystalline solids. The sodium and potassium salts are very stable compared with ammonium salt as dry solids at 25°C . Aqueous solutions undergo slow decomposition even at 25°C^{52} . Kinetic studies of peroxydisulfate mediated oxidation reactions are well documented. Since sodium and potassium peroxydisulfates are water-soluble, their use as an oxidizing reagent in organic chemistry is limited, although some effective oxidations are reported by peroxydisulfate with metal ions in aqueous solution. Mechanistic studies have shown that there are two fundamentally different ways in which these species react. At room temperature (25°C) in the absence of a catalyst the reactions are fast only with strong nucleophiles and proceed by polar mechanisms. At higher temperatures or in the presence of catalysts, rapid radical reactions are taking place. Selectivity can be achieved by careful control of conditions. Peroxydisulfate may be used as a convenient source of peroxymonosulfate, via low temperature acid catalyzed hydrolysis⁵³.

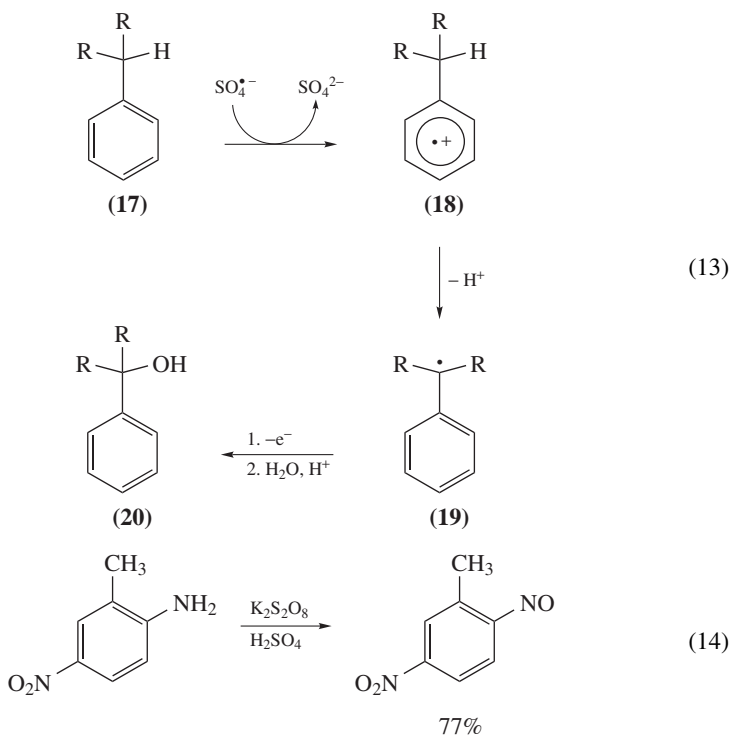
Preparative methods based on oxidations by peroxydisulfate have long been known⁵⁴. Peroxydisulfate ions are capable of oxidizing virtually all functional groups, even hydrocarbons⁵⁵. The oxidation of phenol using potassium peroxydisulfate in alkaline solution, to yield a 1,2- or 1,4-dihydroxybenzene, is called the Elbs reaction and it had been already reported in 1893 (equation 12)⁵⁶.



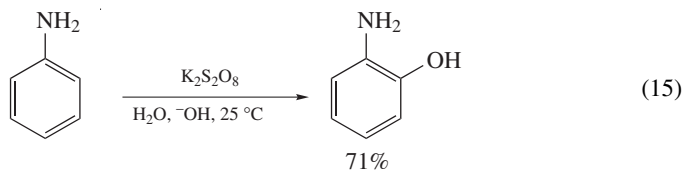
Recently, Behrman and coworkers discussed the mechanism of the Elbs oxidation reaction⁵⁷ and explained why the *para* product predominates over the *ortho* product in this oxidation. According to the authors, semiempirical calculations show that the intermediate formed by the reaction between peroxydisulfate anion and the phenolate ion is the species resulting from reaction of the tautomeric carbanion of the latter rather than by the one resulting from the attack by the oxyanion. This is confirmed by the synthesis of the latter intermediate by the reaction between Caro's acid dianion and some nitro-substituted fluorobenzenes. An example of oxidative functionalization of an aromatic compound is the conversion of alkylated aromatic compound **17** to benzyl alcohols **20**. The initial step in the mechanism of this reaction is the formation of a radical cation **18**, which subsequently undergoes deprotonation. The fate of the resulting benzylic radical **19** depends on the conditions and additives. In aqueous solution, for example, further oxidation and trapping of the cationic intermediate by water lead to the formation of the benzyl alcohols **20** (equation 13)⁵⁸.

Interestingly, persulfate reacts differently with aliphatic and aromatic amines. Aliphatic primary amines are dehydrogenated to imines and further converted to aldehydes when reacted with peroxydisulfate⁵⁹, whereas aromatic primary amines are oxidized to nitroso compounds using potassium persulfate in the presence of H_2SO_4 (equation 14)⁶⁰.

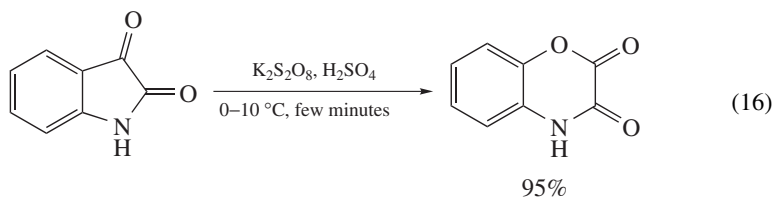
Arylamines are also converted into *o*-aminosulfate esters and the reaction is known as the Boyland–Sims reaction⁶¹.



When aromatic amines react with potassium persulfate in alkaline aqueous solution at room temperature in the absence of a catalyst, they are converted to the corresponding phenol⁶². Behrman has studied the *ortho*–*para* ratio in this reaction and found that the *ortho* product predominates over the *para* product (in contrast with the Elbs reaction) (equation 15)⁶³.

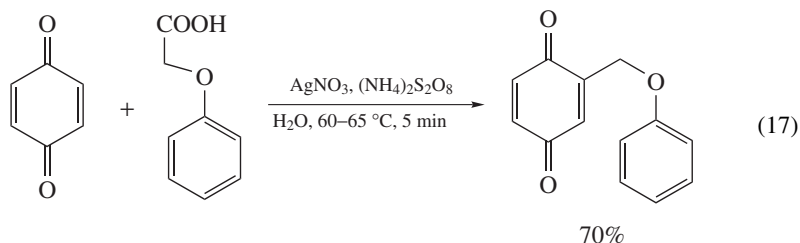


Isatin, a cyclic α -ketoamide, when reacted with potassium peroxydisulfate in the presence of sulfuric acid gave regioselectively an oxidized product, i.e. 2,3-dioxo-1,4-benzoxazine in almost quantitative yield under mild conditions (equation 16). In contrast, when isatin reacted with 30% H_2O_2 in the presence of acetic acid and H_2SO_4 , isoic anhydride was obtained (equation 16)⁶⁴.



Recently, Perumal and coworkers reported aromatization of NAD(P)H model Hantzsch 1,4-dihydropyridines using potassium peroxydisulfate/Co(II)⁶⁵.

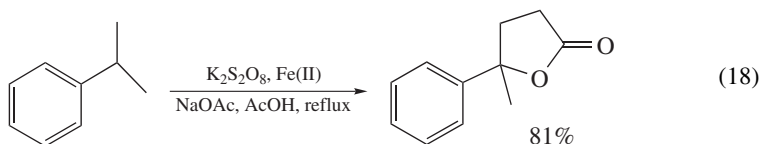
Silver(I) catalyzed oxidative decarboxylation using peroxydisulfate is well studied⁶⁶. Decarboxylated carbon radicals can form a C–C bond with 1,4-benzoquinone or 1,4-naphthoquinone (equation 17)⁶⁷. In the case of 1,4-benzoquinone and phenylacetic acid the yield is 87%, whereas in the case of 2-methyl-1,4-naphthoquinone and cyclopropanecarboxylic acid the yield is as low as 37%.



Carboxylic acids can be converted into the corresponding peroxy acids using peroxydisulfate in the presence of a phase transfer catalyst in good to excellent yields⁶⁸. When *o*-methylbenzoic acid was treated with sodium peroxydisulfate in the presence of Ag(I)/Cu(II), the corresponding lactone was obtained in 56% yield. Acyl radicals were also trapped by quinolines⁶⁹ or alkenes⁷⁰ in the presence of peroxydisulfate to give the products in high yields.

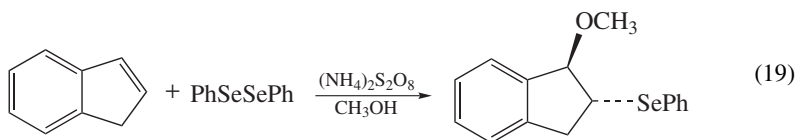
When 2,5-diphenylfuran was treated with potassium peroxydisulfate, 4-methylquinoline was obtained in quantitative yield⁷¹. Peroxydisulfate was also found to be a very efficient reagent for the conversion of thiols to disulfides⁷². Sulfides can be selectively converted into the corresponding sulfoxides in the presence of potassium peroxydisulfate in acetic acid⁷³.

Primary and secondary alcohols are quantitatively oxidized by peroxydisulfate to the corresponding aldehydes and ketones. Thus benzyl alcohols give aldehydes⁷⁴, and in the presence of Ni(II) and ammonia they give nitriles⁷⁵; secondary alcohols give the corresponding ketones⁷⁶. Interestingly, isopropylbenzene reacts with acetates in the presence of peroxy disulfate/Fe(II) to give lactones (equation 18)⁷⁷.



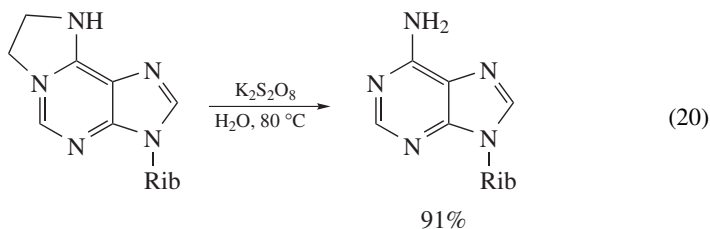
The per(poly)fluoroalkylation of olefins by per(poly)fluoroalkyl chlorides, initiated by ammonium peroxydisulfate and sodium formate, is also reported⁷⁸. The reaction proceeds smoothly in polar aprotic solvents. The presence of functional groups like sodium carboxylate or sulfonate in the polyfluoroalkyl chloride appears to facilitate the reaction. This reaction represents the first example of the reactivity of per(poly)fluoroalkyl chlorides.

The formation and characterization of phenylselenenyl cation by the reaction of diphenyl diselenide with ammonium peroxydisulfate⁷⁹ have been well documented. Various applications of the phenylselenenyl cation in organic synthesis have been reported. Several alkenes can be converted into the corresponding methoxyselenenyl derivatives in good to excellent yields by treatment with diphenyl selenide and $(\text{NH}_4)_2\text{S}_2\text{O}_8$. These reactions are regioselective, following the Markovnikov orientation, and stereospecific by giving *anti* addition (equation 19). Similarly, selenium catalyzed conversion of vinyl halides into α -alkoxyacetals has been reported⁸⁰.



Various alkenes react with diphenyl diselenide/ $(\text{NH}_4)_2\text{S}_2\text{O}_8$, in an aqueous acetonitrile as a solvent in the presence of trifluoromethanesulfonic acid to afford the amidoselenylation products⁸¹. It has been observed that some unsaturated nitriles in dioxane undergo intramolecular cyclization reaction to give the corresponding phenylselenolactones.

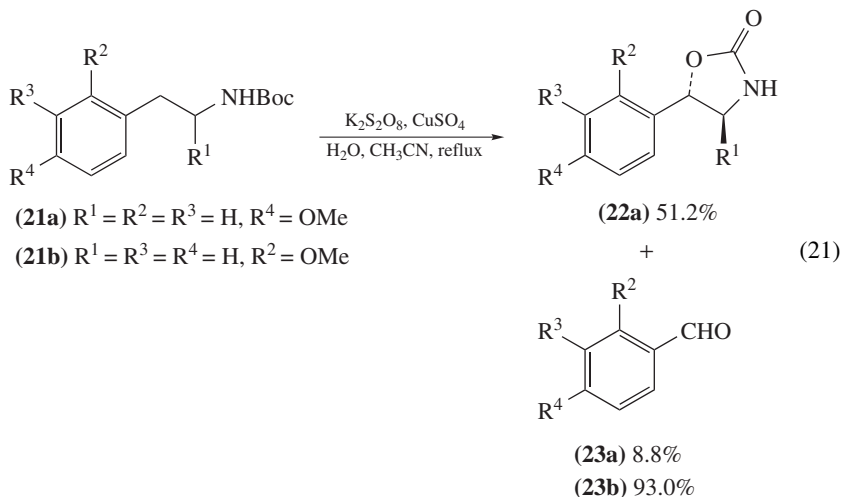
Peroxydisulfate was also reported as a reagent in nucleoside chemistry. Interestingly, the etheno bridge of $1,N^6$ -ethenoadenosine can be smoothly removed by treatment with potassium peroxydisulfate (equation 20)⁸².



Very recently, ammonium peroxydisulfate mediated oxidative hydrolysis of a cyclic $1,N^2$ -propano-2'-deoxyguanosine was also reported by the same research group⁸³. The formation of the guanine ring-opened products in this oxidation reaction seems very interesting and appears to be closely related to the mechanism for the point-mutations of DNA with excessive acetaldehyde and crotonaldehyde.

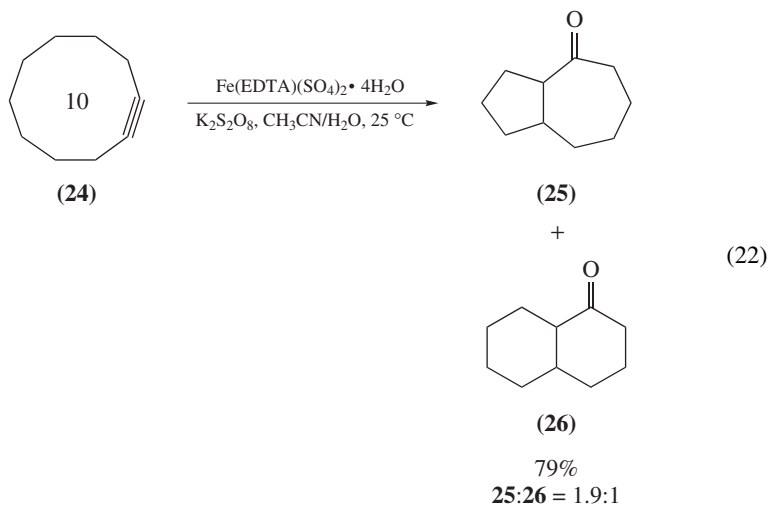
Recently, the reaction between the sulfate radical anion and cyanuric acid, a nondegradable end product of the oxidative degradation of the triazine-based herbicide-atrazine, was reported⁸⁴. The degradation profile indicates that about 76% of the cyanuric acid has been decomposed after an absorbed γ -radiation dose. It is therefore proposed that the reaction of peroxydisulfate could be utilized for the degradation of cyanuric acid in aqueous medium, which is important, since the latter is normally stable to further organic processes.

Irie and coworkers reported a novel oxidation reaction of *N*-Boc-phenethyl amines **21a** and **21b** to the corresponding cyclic carbamate **22** and aldehydes **23a** and **23b** (equation 21)⁸⁵.

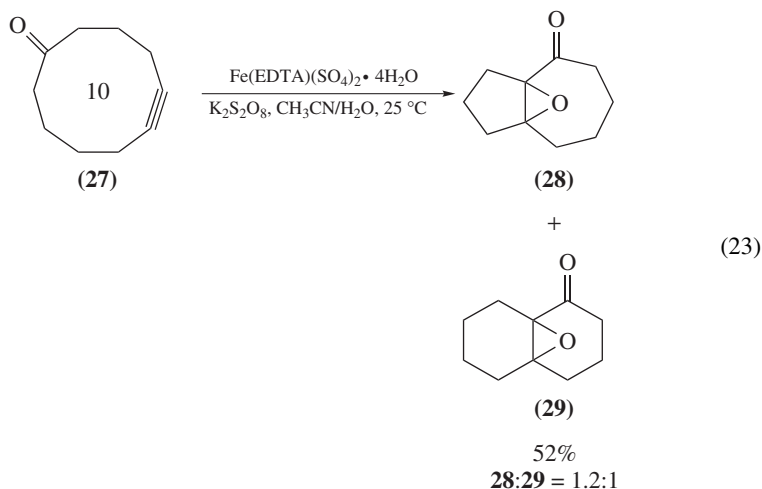


They also reported the oxidation of several ω -phenylalkanoic acid derivatives, e.g. of 4-phenylbutanoic acid to the corresponding lactone in fair yields. When benzoyl aromatics reacted under the same conditions, a mixture containing the two diastereomers, *threo* (*dl*)- and *erythro* (*meso*)-2,3-bis(benzoyl)-1,4-butanedioic acid dimethyl esters, was obtained.

Wille demonstrated recently the utility of $SO_4^{\bullet-}$ as an oxygen atom donor when it was reacted with two different ten-membered alkynes **24** (equation 22) and **27** (equation 23)⁸⁶. This is the first example of transfer of oxygen atom from peroxydisulfate ion.



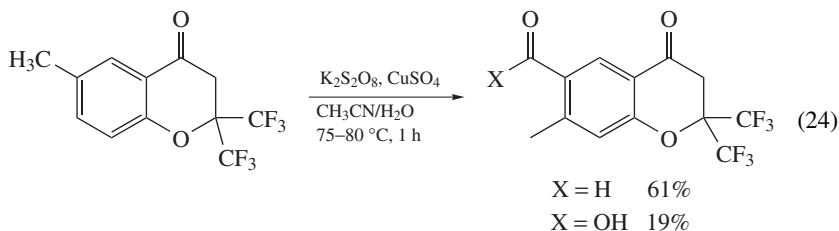
On addition of $\text{SO}_4^{\bullet-}$ to the triple bond in the 10-member cycloalkyne **24** and cycloalkynone **27**, a nonchain, and anionic, self-terminating radical cyclization cascade is induced. In the former reaction (equation 22) the bicyclic ketones **25** and **26** are formed, and in the latter reaction (equation 23) the α,β -epoxy ketones **28** and **29** are formed in good yields. Because of the difficulty of oxidizing isolated triple bonds, $\text{SO}_4^{\bullet-}$ does not react as an electron-transfer reagent in these reactions but acts as a donor of atomic oxygen.



It has been proved that the benzyne intermediate can be easily prepared from *o*-iodobenzoic acid and potassium peroxydisulfate in sulfuric acid⁸⁷. Water-soluble vicinal diols are converted into their corresponding aldehydes in the presence of Ag(I) catalyst⁸⁸.

Polymer-supported persulfonic acid was prepared from potassium persulfate and the cation exchange resin P-SO₃H in water²⁷. The authors reported various applications of this new oxidizing reagent such as epoxidation of olefins, Baeyer-Villiger reaction and cleavage of disulfide and *N*-formylamino acids.

Oxidation of the aromatic methyl group of chromone to the corresponding aldehyde and acid has also been reported recently (equation 24)⁸⁹.



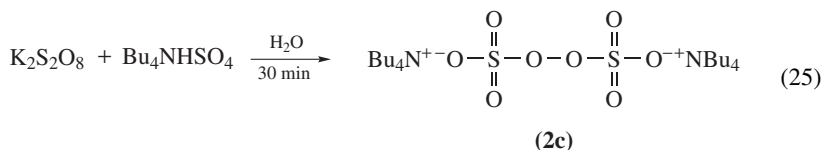
Persulfuric acid ($\text{H}_2\text{S}_2\text{O}_8$) can be prepared *in situ* by reacting H_2O_2 and excess of oleum or 100% H_2SO_4 ³¹. Persulfuric acid oxidizes primary polynitroarylamines and their *N*-acetamido derivatives to polynitro compounds in good to excellent yields. Even though several peracids are reported as reagents for the oxidation of an amine to the nitro functional group, electron-deficient aromatic amines are inert to peracids.

D. Organic Salts of Peroxydisulfate

The reactions using commercially available peroxydisulfate, such as $\text{Na}_2\text{S}_2\text{O}_8$, $\text{K}_2\text{S}_2\text{O}_8$ or $(\text{NH}_4)_2\text{S}_2\text{O}_8$, have been generally carried out in aqueous solutions mostly in the presence of metal catalysts. It was expected that if the peroxydisulfate could be used in anhydrous organic solvents, a clean-cut reaction would take place under mild reaction conditions.

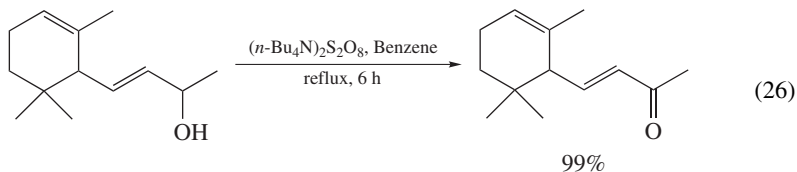
Tetrabutylammonium peroxydisulfate ($n\text{-Bu}_4\text{N}$) $_2\text{S}_2\text{O}_8$ **2c** was already reported in 1978⁹⁰. It was prepared from Bu_4NBF_4 and $\text{K}_2\text{S}_2\text{O}_8$ in 83% yield. Effenberger and Kottmann used ($n\text{-Bu}_4\text{N}$) $_2\text{S}_2\text{O}_8$ for the oxidative phosphorylation of aromatic compounds. Various aryl phosphonates were prepared in good yields by ($n\text{-Bu}_4\text{N}$) $_2\text{S}_2\text{O}_8/\text{AgNO}_3$ in acetic acid⁹¹.

Later, an easy and reliable preparation of ($n\text{-Bu}_4\text{N}$) $_2\text{S}_2\text{O}_8$ was reported just by mixing $\text{K}_2\text{S}_2\text{O}_8$ and Bu_4NHSO_4 (2 eq.) in water and extraction by CH_2Cl_2 . Evaporation of the CH_2Cl_2 afforded pure ($n\text{-Bu}_4\text{N}$) $_2\text{S}_2\text{O}_8$ in quantitative yields (equation 25)⁹².

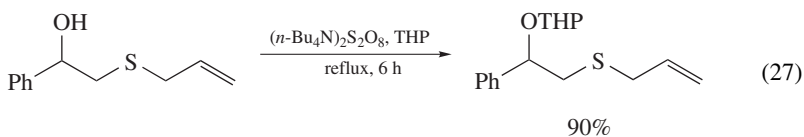


($n\text{-Bu}_4\text{N}$) $_2\text{S}_2\text{O}_8$ is highly soluble in most organic solvents such as CH_2Cl_2 , CHCl_3 , CH_3CN , THF and acetone. Thus, various efficient reactions using ($n\text{-Bu}_4\text{N}$) $_2\text{S}_2\text{O}_8$ have been reported and reviewed⁹³. The salt turned out to be an excellent source for the formation of sulfate ion radical ($\bullet\text{OSO}_3^-$) under anhydrous conditions.

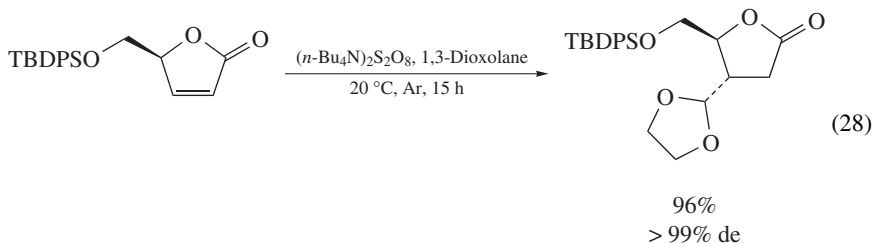
The oxidation of primary benzylic alcohols with $\text{Na}_2\text{S}_2\text{O}_8/\text{Ag(I)}$ gave the corresponding aldehyde and acid in aqueous media⁹⁴. Oxidation of allylic alcohols using $\text{K}_2\text{S}_2\text{O}_8/\text{Ni(II)}$ in H_2O and CH_2Cl_2 gave unsaturated carbonyl compounds⁹⁵. Various allylic and benzylic alcohols were smoothly oxidized selectively to the corresponding carbonyl compounds in almost quantitative yields (90–99%) using ($n\text{-Bu}_4\text{N}$) $_2\text{S}_2\text{O}_8$ in aprotic solvent (equation 26). Under these reaction conditions terminal olefins and a pyridine moiety remain intact⁹⁶.



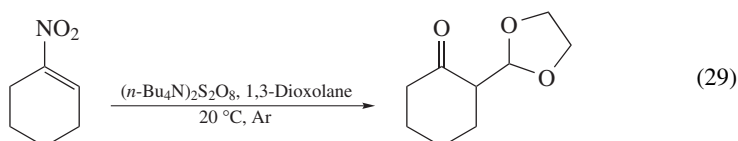
Under anhydrous conditions, side reactions due to hydroxyl or perhydroxyl radical species can be avoided. Tetrahydropyran⁹⁷ and tetrahydrofuran⁹⁸ ethers were prepared in good to excellent yields (85–97%) from the corresponding primary and secondary alcohols and THP and THF as a solvent using ($n\text{-Bu}_4\text{N}$) $_2\text{S}_2\text{O}_8$. Under these reaction conditions the sulfide group and acid-sensitive groups such as allylic hydroxyl or an acetal moiety remain intact (equation 27).



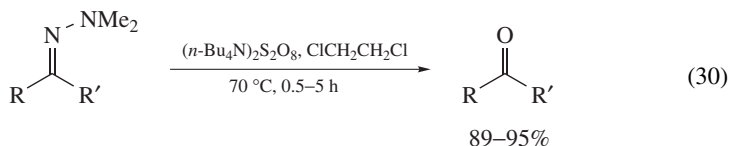
A novel masked β -formylation of electron-deficient olefins with 1,3-dioxolane in the presence of $(n\text{-Bu}_4\text{N})_2\text{S}_2\text{O}_8$ has been observed. Thus when cyclic α,β -unsaturated ketones, esters and sulfonyl alkenes react with $(n\text{-Bu}_4\text{N})_2\text{S}_2\text{O}_8$ in 1,3-dioxolane, the corresponding 1,3-dioxolanyl adducts are obtained in excellent yields (equation 28).



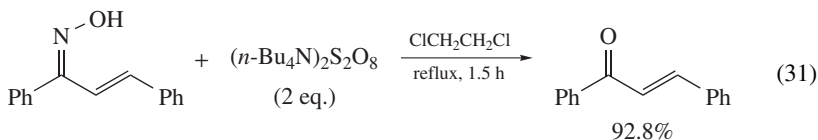
It is possible to introduce a protected formyl group at the α -position of cyclohexanone by reacting 1-nitrocyclohexene with $(n\text{-Bu}_4\text{N})_2\text{S}_2\text{O}_8$ in 1,3-dioxolane (equation 29)⁹⁹.



Highly selective and efficient deprotection of N,N -dimethylhydrazones to ketones in excellent yields using $(n\text{-Bu}_4\text{N})_2\text{S}_2\text{O}_8$ was reported (equation 30)¹⁰⁰.



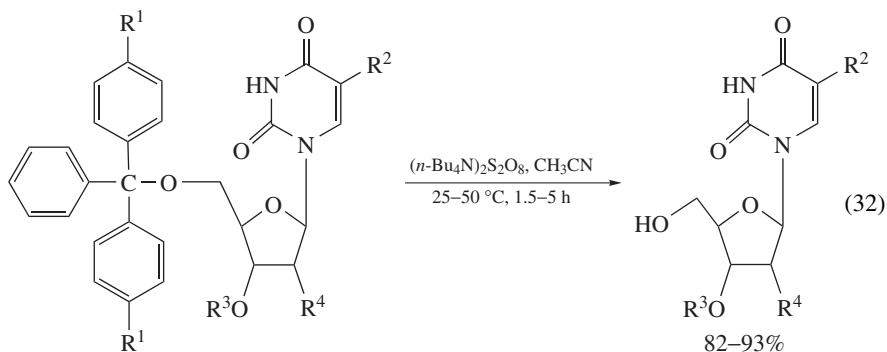
Tosylhydrazones are oxidized with $(n\text{-Bu}_4\text{N})_2\text{S}_2\text{O}_8$ in 1,2-dichloroethane to the corresponding ketones in almost quantitative yields under natural conditions¹⁰¹. Highly selective and efficient oxidative deoxygenation using $(n\text{-Bu}_4\text{N})_2\text{S}_2\text{O}_8$ is also reported¹⁰². Thus various aliphatic and aromatic aldoximes as well as ketoximes reacted with $(n\text{-Bu}_4\text{N})_2\text{S}_2\text{O}_8$ in 1,2-dichloroethane at reflux temperature to afford the corresponding aldehyde and ketone in excellent yields (equation 31). Under these reaction conditions olefinic double bonds remain intact.



In the same way, oxidative cleavage of 2,4-dinitrophenylhydrazones by $(n\text{-Bu}_4\text{N})_2\text{S}_2\text{O}_8$ to the corresponding ketones was also reported¹⁰³.

It was found that when 5'- O -(4,4'-dimethoxytrityl) uridine or thymidine derivatives reacted with $(n\text{-Bu}_4\text{N})_2\text{S}_2\text{O}_8$ in CH_3CN under mild conditions, the corresponding deprotected uridine or thymidine nucleosides were obtained in excellent yields (equation 32)¹⁰⁴.

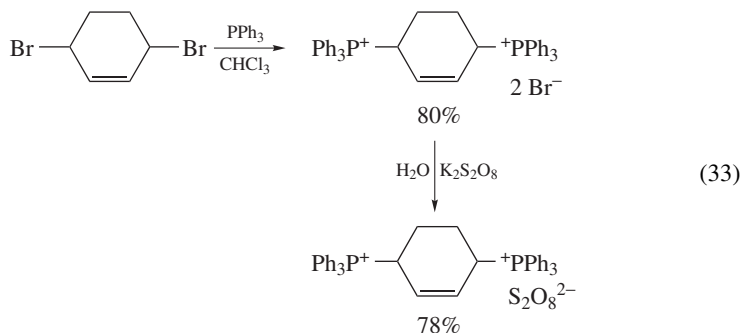
All known methods for the detritylations require organic acids or Lewis acids. The method described in equation 32 proceeds smoothly under mild conditions without the use of any acid at 25–50 °C, and does not cause cleavage of the glycosidic bonds.



$R^1 = \text{H, OMe, } R^2 = \text{H, Me, } R^3 = \text{H, TBDMS, } R^4 = \text{H, OH or } R^3R^4 = \text{ketal}$

Recently, selective oxidation of thiols to disulfate under solvent-free conditions using $(n\text{-Bu}_4\text{N})_2\text{S}_2\text{O}_8$ was reported¹⁰⁵. The main feature of this reaction is that thiol and $(n\text{-Bu}_4\text{N})_2\text{S}_2\text{O}_8$ are mixed in 2:1 ratio, grinded thoroughly in mortar for 5 min, the product is extracted by Et_2O and evaporation of the Et_2O afforded disulfide in good to excellent yields.

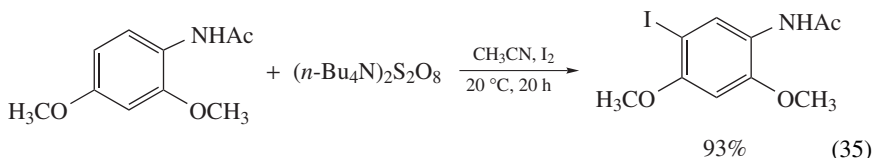
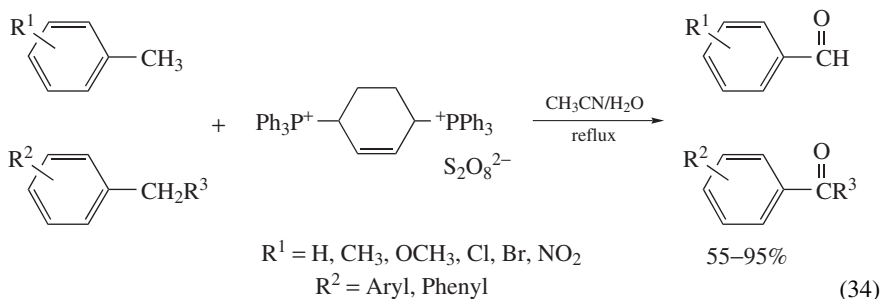
Badri and coworkers recently prepared 3,6-bis(triphenylphosphonium) cyclohexene peroxosulfate (BTPCP) in two steps from 3,6-dibromocyclohexene. (equation 33)¹⁰⁶.



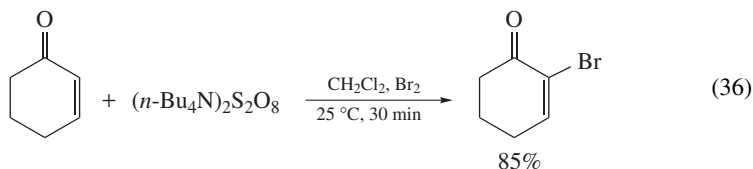
They used this new oxidizing reagent for a rapid and selective oxidation of primary and secondary benzylic alcohols to the corresponding aldehydes and ketones in good to excellent yields. BTPCP was later used for oxidation of various alkylbenzenes under neutral conditions in aqueous CH_3CN to the corresponding carbonyl compounds in good yields (equation 34)¹⁰⁷.

Oxyhalogenation is one of the most efficient halogenation methods. Various oxidizing reagents are reported in combination with different halogenation sources to result in halogenation reactions. Considering these facts, regioselective iodination of aromatic

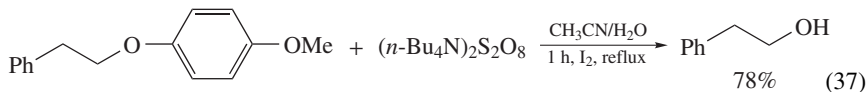
compounds¹⁰⁸ as well as of electron-deficient olefins¹⁰⁹ was also developed with $(n\text{-Bu}_4\text{N})_2\text{S}_2\text{O}_8$ and I_2 in CH_3CN at 25°C and gave very good to excellent yields (equation 35). This reaction has been carried out under mild conditions with very high yield of products and with comparatively cheap reagent.



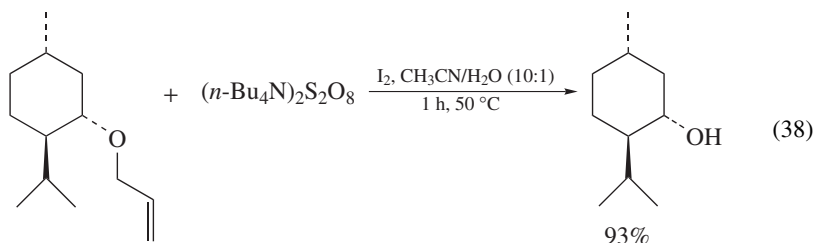
Similarly, bromination of aromatic compounds as well as of electron-deficient olefins was carried out in good to excellent yields using $(n\text{-Bu}_4\text{N})_2\text{S}_2\text{O}_8/\text{Br}_2$ or LiBr at 25°C (equation 36)¹¹⁰.



Interestingly, it was found that $(n\text{-Bu}_4\text{N})_2\text{S}_2\text{O}_8$ is an efficient reagent for the deprotection of a *p*-methoxybenzyl group in the presence of an equimolar amount of I_2 under aqueous conditions ($\text{MeCN}:\text{H}_2\text{O} = 20:1$) in excellent yields (equation 37)¹¹¹. When this reaction was carried out in anhydrous conditions, a low yield of the product was obtained. The reaction of only $(n\text{-Bu}_4\text{N})_2\text{S}_2\text{O}_8$ in the absence of I_2 results in low yield even after prolonged reaction time. Deprotection of the *p*-methoxybenzyl group is found to be easier compared with that of a benzyl group, probably due to the high electron density of the *p*-methoxybenzyl group. Though the deprotection reaction can be carried out under anhydrous conditions, the yields of the deprotected products are poorer compared to those obtained under aqueous conditions.

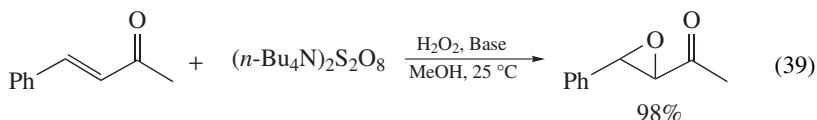


In the same way an allyl ether can be chemoselectively cleaved to the corresponding alcohol by using $(n\text{-Bu}_4\text{N})_2\text{S}_2\text{O}_8/\text{I}_2$ in aqueous acetonitrile under mild conditions in excellent yields (equation 38)¹¹².



A variety of functional groups like benzyl ethers, tetrahydropyranyl ether, benzoate, (*t*-butyldiphenylsiloxy) ether, hemiacetal, lactone and aldehyde remain intact under these reaction conditions.

Epoxidation of electron-deficient olefins has been carried out using $(n\text{-Bu}_4\text{N})_2\text{S}_2\text{O}_8/\text{H}_2\text{O}_2/\text{NaOH}$ in CH_3CN at 25°C in excellent yields¹¹³. It is known that epoxidation of α,β -unsaturated ketones can be carried out with alkaline H_2O_2 alone, but when $(n\text{-Bu}_4\text{N})_2\text{S}_2\text{O}_8$ is used together with $\text{H}_2\text{O}_2/\text{NaOH}$ the reaction yield was increased substantially, and thus a new epoxidation method for electron-deficient olefins was found (equation 39). Compared with K_2CO_3 , NaOH was proved to be the best base for this reaction. Epoxidation of chalcone using only H_2O_2 in alkaline conditions gave the corresponding epoxide in a low yield (30%). As far as the solvent is concerned, CH_3OH and CH_3CN were found to be the best solvents for this reaction compared with benzene, CH_2Cl_2 and CHCl_3 .

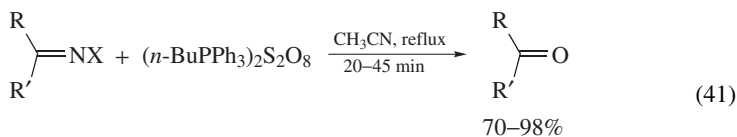
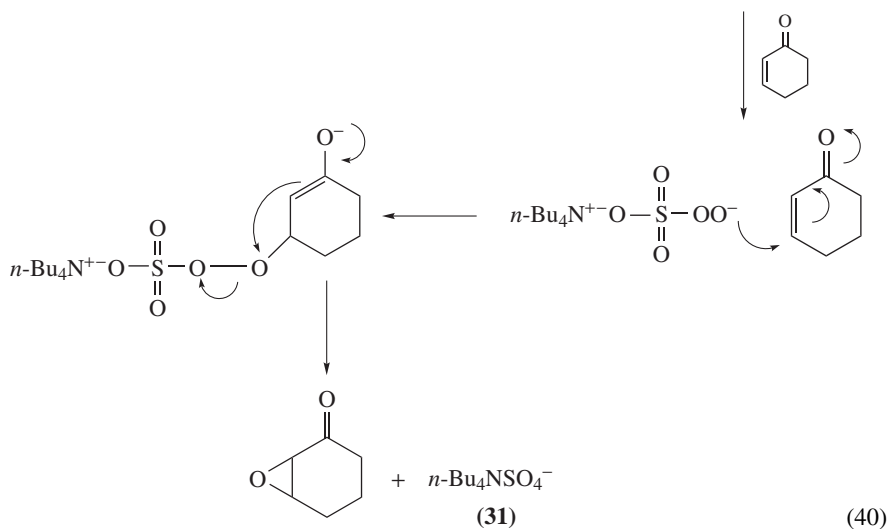
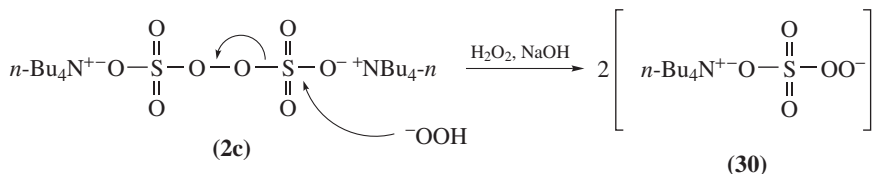


When 0.5 equivalent of $(n\text{-Bu}_4\text{N})_2\text{S}_2\text{O}_8$, H_2O_2 and NaOH were used, the yield of the epoxide was 90%, which indicated that 0.5 equivalent each of $(n\text{-Bu}_4\text{N})_2\text{S}_2\text{O}_8$ and ^-OOH form a stoichiometric amount of **30** with respect to substrate, as shown by a plausible mechanism (equation 40).

In this reaction, the peroxydisulfate $(n\text{-Bu}_4\text{N})_2\text{S}_2\text{O}_8$ (**2c**) is probably converted to the tetra *n*-butylammonium peroxy sulfate anion **30** by attacking ^-OOH ; 1,4-addition of the latter to α,β -unsaturated ketones produces the epoxide product and tetra *n*-butylammonium sulfate **31**. In this reaction **31** was isolated in 80% yield.

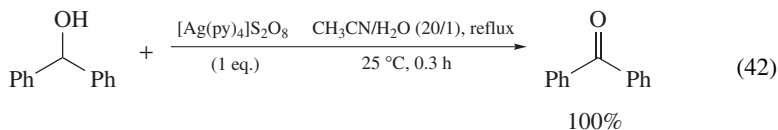
Recently, Baltork and coworkers reported the easy preparation of *n*-butyltriphenyl phosphonium peroxydisulfate $(n\text{-BuPPh}_3)_2\text{S}_2\text{O}_8$ in almost quantitative yield (95%) and used it successfully for the cleavage of carbon–nitrogen double bonds under aprotic conditions¹¹⁴. Thus various oximes, phenyl hydrazones, *p*-nitrophenyl hydrazones and semicarbazones are converted efficiently to the corresponding carbonyl compounds with $(n\text{-BuPPh}_3)_2\text{S}_2\text{O}_8$ in good to excellent yields under neutral conditions (equation 41).

$(n\text{-BuPPh}_3)_2\text{S}_2\text{O}_8$ is also used for the selective oxidative deprotection of trimethylsilyl (TMS) tetrahydropyranyl ethers in the presence of ethylene acetals and ketals to their corresponding carbonyl compounds in excellent yields. Ethylene acetals and ketals were inert in this reaction¹¹⁵.

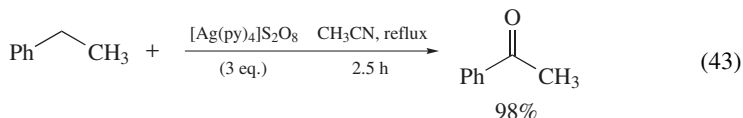


X = OH, NHPh, NHC₆H₄(*p*-NO₂), NHCONH₂

Firouzabadi and coworkers used tetrakis(pyridine) silver(II) peroxodisulfate¹¹⁶ ([Ag(py)₄]S₂O₈) for oxidation of various compounds^{117, 118}. [Ag(py)₄]S₂O₈ can be easily prepared by mixing pyridine, AgNO₃ and K₂S₂O₈ in water. After standing for 30 min at 25 °C, an orange-colored stable solid is formed in a quantitative yield (95%). [Ag(py)₄]S₂O₈ oxidizes various classes of compounds like aldehydes to carboxylic acids, benzylic alcohols to carbonyl compounds, aromatic thiols and allyl aryl thioether to arylsulfonic acids and benzylic carbon-hydrogen bonds to carbonyl groups. α -Hydroxy carboxylic acids and phenylacetic acids are decarboxylated to produce carbonyl compounds (equation 42).



Interestingly, in contrast to the reported $\text{S}_2\text{O}_8^{2-}/\text{Cu}^{2+}$ system, which affects the oxidation of electron-rich benzylic hydrocarbons, nonactivated and deactivated benzylic hydrocarbons are also converted to their corresponding carbonyl compounds with $[\text{Ag}(\text{py})_4]\text{S}_2\text{O}_8$ in moderate to excellent yields (equation 43).

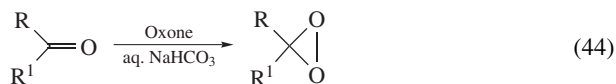


Aniline can react with $(n\text{-Bu}_4\text{N})_2\text{S}_2\text{O}_8$ in the presence of SnCl_4 to give the anilinium salt of $\text{S}_2\text{O}_8^{2-}$. The $(\text{PhNH}_3)_2\text{S}_2\text{O}_8$ can be isolated as a highly hygroscopic white solid. When immediately put into a sealed tube under nitrogen for 10 days at 25°C , it gives dark-colored polyaniline (PANI) which shows very good electrical conductivity¹¹⁹. Treatment of $\text{Fe}(\eta^5\text{-C}_5\text{H}_5)(\eta^1\text{-NC}_4\text{H}_4)(\text{CO})_2$ with $(n\text{-Bu}_4\text{N})_2\text{S}_2\text{O}_8$ in the presence of dodecylbenzenesulfonic acid leads to the formation of a soluble, electrically conducting polymer¹²⁰.

E. Potassium Peroxymonosulfate

Immediately after Caro's report on monopersulfuric acid, Baeyer and Villiger reported 'dry monopersulfuric acid' by mixing H_2SO_4 and $\text{K}_2\text{S}_2\text{O}_8$ in a mortar¹²¹. The best alternative for this is potassium salt of peroxymonosulfuric acid. The stable commercially available triple salt $2\text{KHSO}_5 \cdot \text{KHSO}_4 \cdot \text{K}_2\text{SO}_4$ is prepared by reaction of 85% H_2O_2 with concentrated sulfuric acid, followed by neutralization with K_2CO_3 ¹²². This triple salt is a relatively stable (convenient to handle and store) water-soluble form of peroxymonosulfate also known as potassium caroate or Oxone[®] (trademark of DuPont Co.). Even though Oxone was reported long back in 1957, its use in oxidation reactions became popular only in the last two decades. Since Oxone is insoluble in organic solvents, it is always used in mixtures of ethanol–water, acetic acid–water, methanol–water and ethanol–acetic acid–water as the solvent system. Whenever it is used in organic solvents it is always used with PTC, or as a Silica-supported Oxone.

Various ketones can be converted into the corresponding three-membered cyclic peroxides, i.e. dioxiranes by treatment with buffered aqueous solutions of Oxone (equation 44).



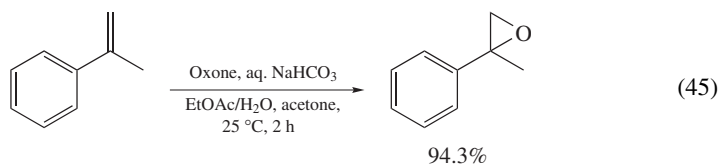
Dioxirane chemistry is well documented¹²³. Extensive kinetic, stereochemical and ^{18}O -labeling data suggested that dimethyldioxirane is the oxygen-atom transfer reagent in the Oxone–acetone system¹²⁴. Murray and Jeyaraman have shown that dialkyl dioxiranes can be isolated by low-temperature distillation from the reaction mixture of oxone and ketone¹²⁵.

Kennedy and Stock reported the first use of Oxone for many common oxidation reactions such as formation of benzoic acid from toluene and of benzaldehyde, of benzophenone from diphenylmethane, of *trans*-cyclohexanediol from cyclohexene, of acetone from 2-propanol, of hydroquinone from phenol, of ϵ -caprolactone from cyclohexanone, of pyrocatechol from salicylaldehyde, of *p*-dinitrosobenzene from *p*-phenylenediamine, of phenylacetic acid from 2-phenethylamine, of dodecylsulfonic acid from dodecyl mercaptan, of diphenyl sulfone from diphenyl sulfide, of triphenylphosphine oxide from triphenylphosphine, of iodoxy benzene from iodobenzene, of benzyl chloride from toluene using NaCl and Oxone and bromination of 2-octene using KBr and Oxone¹²⁶. Thus, they

have covered most of the common oxidation reactions. Many research groups studied these reactions later in more detail.

Several efficient procedures for alkene epoxidation using Oxone were reported, such as Oxone/aqueous NaOH¹²⁷, Oxone/acetone¹²⁸, Oxone/water¹²⁹, Oxone/PTC/benzene/aqueous buffer solution¹³⁰ or Oxone/2-butanone system¹³¹. Thus, sorbic acid can be regioselectively oxidized using Oxone/aqueous NaOH to 4,5-epoxy-2-hexenoic acid in 84% yield¹²⁷. Similarly, cyclooctene is oxidized to cyclooctene oxide in 81% yield, just by stirring it with Oxone in water¹²⁹. 1-Dodecene is epoxidized in good yield by Oxone/PTC in benzene:aqueous buffer solution. It is otherwise difficult to epoxidize 1-dodecene by other oxidizing reagents¹³⁰.

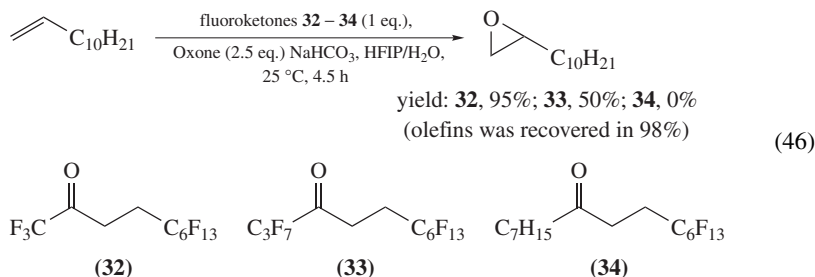
Recently, Hashimoto and Kanda reported a simple and efficient epoxidation using Oxone in a biphasic system of ethyl acetate and water¹³². This reaction is suitable for large-scale preparation of epoxides and does not require any PTC or pH control (equation 45).



Epoxidation reactions have also been performed by the oxidizing reagents, generated *in situ* by reacting Oxone and an iminium salt¹³³, a modified iminium salt¹³⁴, a oxaziridinium salt¹³⁵ or some metals¹³⁶.

Epoxidation of monoterpene olefins and Δ^4 -octalins with dimethyloxirane gives the corresponding epoxides in excellent yields. Some Δ^4 -octalins are oxidized in a much more stereoselective manner than with *m*-CPBA¹³⁷.

Recently, Crousse and coworkers reported that new fluoro ketones serve as efficient catalysts for the epoxidation reactions with Oxone in hexafluoropropan-2-ol (HFIP) (equation 46)¹³⁸.

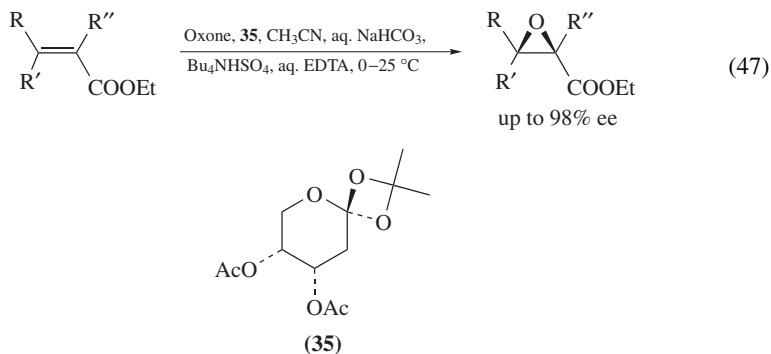


The new fluoroketone **32** is proved to be a better alternative to previously reported expensive and/or volatile fluoroketones.

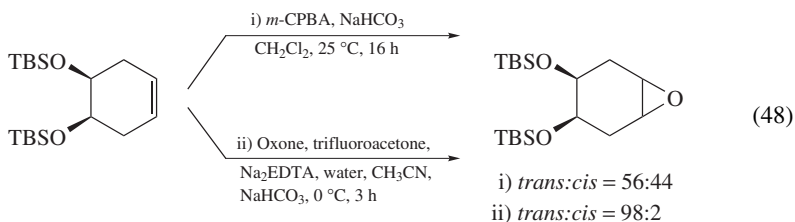
The oxidation of several polycyclic hydrocarbons using Oxone in acetone with PTC was also reported¹³⁹.

Previously, some fluorocyclohexanones were used in a catalytic amount with Oxone for asymmetric epoxidation reaction, but they gave a poor *ee*¹⁴⁰. It was found later that chiral ketones derived from fructose work well as asymmetric epoxidation catalysts and show high enantioselectivity in reactions of *trans*-disubstituted and trisubstituted olefins¹⁴¹. *Cis* and terminal olefins show low *ee* under these reaction conditions. Interestingly, the catalytic efficiency was enhanced dramatically upon raising the pH. Another asymmetric epoxidation was also reported using Oxone with keto bile acids¹⁴².

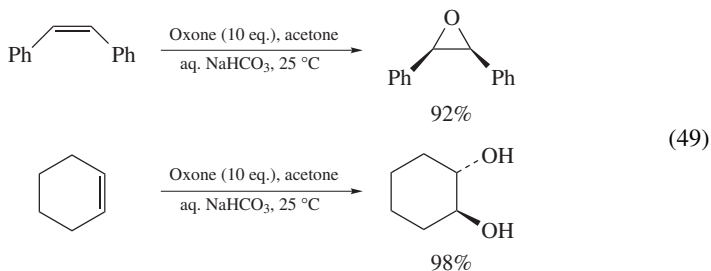
Recently, Shi and coworkers reported high enantioselective asymmetric epoxidation of α,β -unsaturated esters by using the chiral ketone **35** as a catalyst and Oxone as an oxidant (equation 47)¹⁴³.



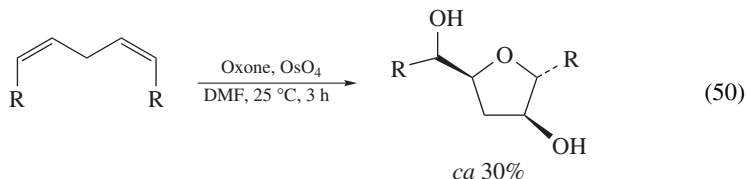
α - and β -Epoxides of cholesterol are the autooxidation products of cholesterol *in vivo* and both are cytotoxic and mutagenic. Yang and Jiao reported highly β -selective epoxidation of Δ^5 -unsaturated steroids catalyzed by ketones¹⁴⁴. Organic oxidants such as *m*-CPBA give α -epoxides as the major epoxidation products for the epoxidation of 3β -substituted Δ^5 -steroids, but they show poor selectivities for the epoxidation of 3α -substituted Δ^5 -steroids. Oxone and trifluoroacetone were found to afford a synthetically useful level of diastereoselectivity comparable to *m*-CPBA¹⁴⁵. A substituted cyclohexene was stereoselectively epoxidized (equation 48).



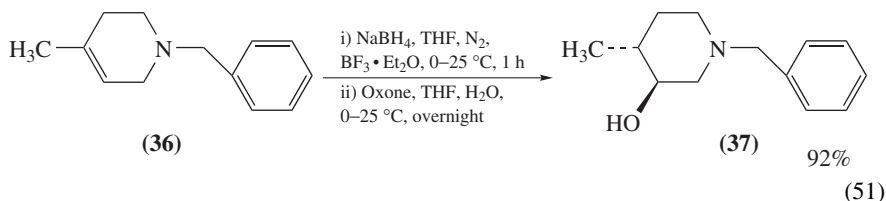
Recently, Rani and Vankar reported dihydroxylation of 1,2-glycols with Oxone in acetone¹⁴⁶. Thus, differently protected glycols were oxidized with Oxone in acetone to 1,2-diols via the opening *in situ* of the corresponding epoxide. Surprisingly, under the reaction conditions, cyclohexene gives the *trans*-1,2-diol and *cis*-stilbene gives the corresponding *cis*-epoxide in almost quantitative yield (equation 49).



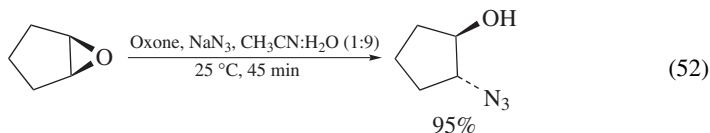
1,4-Dienes undergo oxidative cyclization to substituted tetrahydrofuranol by using Oxone and a catalytic amount of OsO_4 (equation 50)¹⁴⁷. The yield is quite low (30%) owing to cleavage of the double bond to the corresponding carboxylic acid. Later, the same research group reported an OsO_4 catalyzed oxidative cleavage of olefins to the corresponding ketones or carboxylic acids by using Oxone in almost quantitative yields¹⁴⁸. This reaction shows that Oxone is a better alternative than traditional ozonolysis.



A new procedure for the oxidation of carbon–boron bonds to the corresponding alcohols with Oxone was reported by Ripin and coworkers¹⁴⁹. Oxone has been proved to be the best oxidant in this reaction compared with other oxidizing reagents investigated so far. When alkene **36** was reacted with NaBH_4 followed by Oxone oxidation, it gave the corresponding alcohol **37** in highly pure form and high yields (92%) at large scale (100 mmol) (equation 51).



Highly regioselective opening of epoxides and aziridines with sodium azide and Oxone in aqueous acetonitrile in very high yield was reported (equation 52)¹⁵⁰.



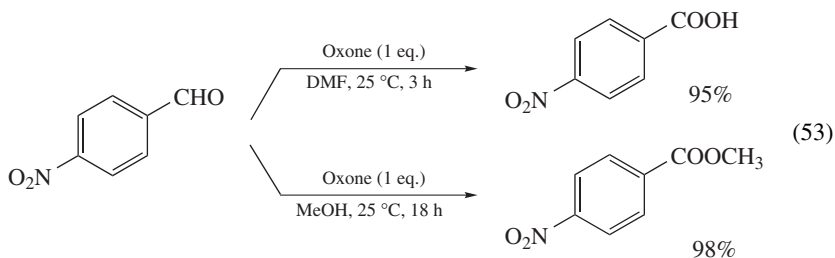
Primary and secondary alcohols were selectively oxidized to the corresponding aldehydes and ketones, respectively, by using Oxone in the presence of a catalytic amount of TEMPO (2,2,6,6-tetramethyl-1-oxypiperidinyl)¹⁵¹. This reaction has been proved to be a highly selective and efficient oxidation reaction, where a catalytic amount of TEMPO plays an important role. Thus TBDMS protected benzyl alcohols were oxidized selectively to benzaldehydes in 81% yield, without affecting the TBDMS moiety.

Oxone has been successfully used in aprotic solvents for oxidation reactions by dispersing it on an alumina surface. Thus, the oxidation of secondary aliphatic, alicyclic and benzylic alcohols using Oxone/wet alumina oxide in CH_2Cl_2 or CH_3CN afforded ketones in good to excellent yields (70–96%).¹⁵² Similarly, the conversion of cycloalkanones to lactones¹⁵³ is also reported.

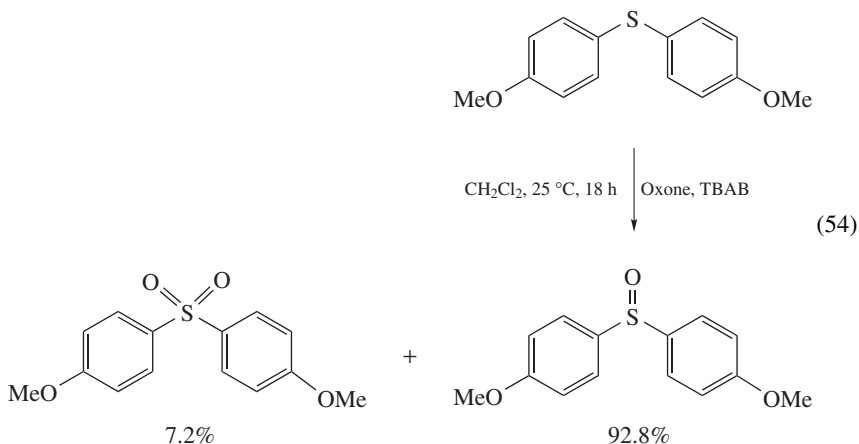
Oxidative cleavage of 1,3-dicarbonyls to carboxylic acids in almost quantitative yields using Oxone was reported¹⁵⁴. The first example of oxidative decarboxylation of α -aminoacids $\text{RCH}(\text{NH}_2)\text{COOH}$, in which a product other than an aldehyde or a carboxylic

acid has been isolated as the major product by using Oxone, was described by Paradkar and coworkers¹⁵⁵. Thus, when 1-aminocyclohexane 1-carboxylic acid was oxidized by Oxone, cyclohexanone oxime and cyclohexanone were obtained in a 3:1 ratio in 88% yield. Similarly, 2-phenylglycine gives benzaldoxime and benzoic acid in 3:1 ratio with 74% yield.

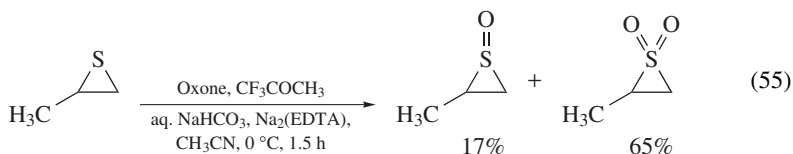
Recently, Borhan and coworkers reported the facile oxidation of aliphatic and aromatic aldehydes to acids and esters in DMF or methanol with Oxone (equation 53)¹⁵⁶. These reactions are considered to be valuable alternatives to traditional metal-mediated oxidations.



It has been shown that a phase-transfer catalyst could control the oxidation of sulfide to the corresponding sulfoxide¹⁵⁷. Thus, the oxidation of diaryl sulfides to sulfoxides using Oxone and PTC (equation 54) is in contrast with the reaction in polar solvents without PTC which gives sulfones as a major product.

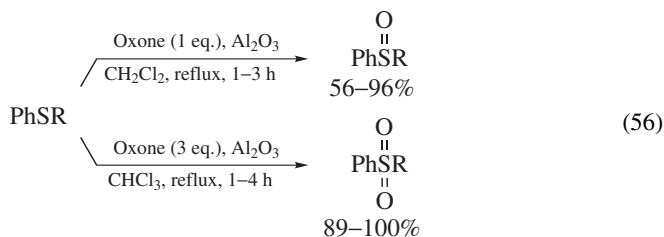


Oxidation of episulfides to episulfones using Oxone/trifluoroacetone was reported for the first time (equation 55)¹⁵⁸.

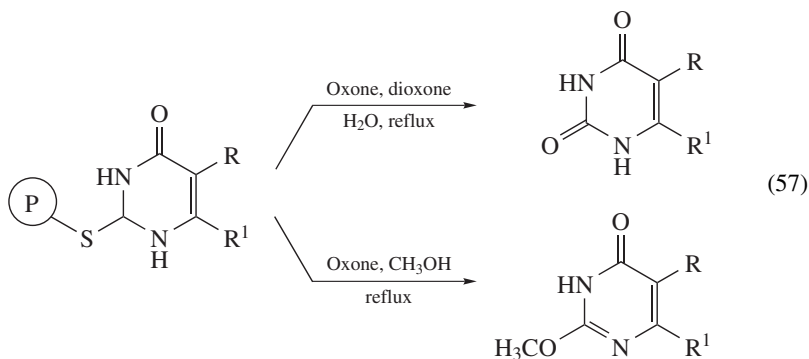


Aromatic sulfides can be selectively converted into sulfoxides or sulfones by using Oxone under solid state conditions¹⁵⁹ or with buffered Oxone in acetonitrile or acetone¹⁶⁰.

Oxidation of sulfides and sulfoxides using Oxone dispersed on silica gel or alumina was reported¹⁶¹. A study of surface mediated reactivity of Oxone compared its reactivity with that of *tert*-butyl hydroperoxide. Oxidation of sulfides to sulfones in aprotic solvents mediated by Oxone on wet montmorillonite¹⁶² or clay minerals¹⁶³ proceeds in high yields. Interestingly, when Oxone on alumina is applied for selective oxidation of sulfides in aprotic solvents, the product distribution is temperature-dependent and sulfoxides or sulfones are obtained in good to excellent yields (equation 56)¹⁶⁴.



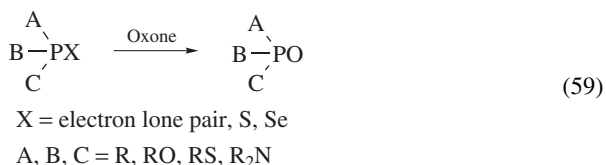
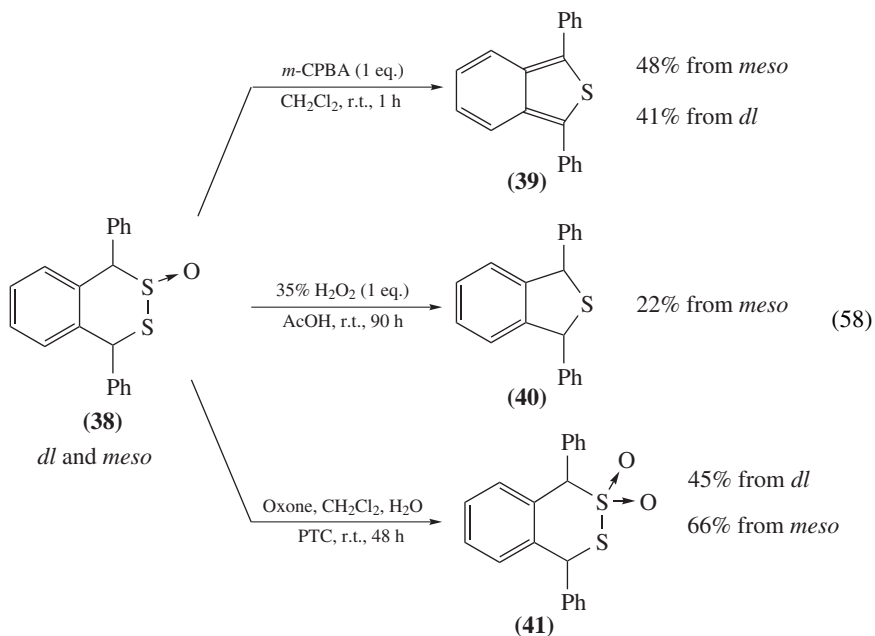
Botta and coworkers recently developed an Oxone cleavage methodology for the solid-phase synthesis of substituted uracils (equation 57)¹⁶⁵. Whereas some common methods of thioether cleavage, such as reduction with Na/NH₃, acid catalyzed hydrolysis, heavy metal ions followed by treatment with hydrogen sulfide and iodotrimethylsilane proved to be unsuccessful for this reduction, Oxone was shown to be an efficient and selective reagent for cleavage of polymer bound thiouracils.



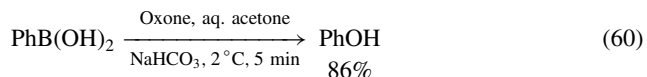
Sato and coworkers reported recently an interesting oxidation reaction of 1,4-dihydro-1,4-diphenyl-2,3-benzodithiin¹⁶⁶. When compound **38** was treated with *m*-CPBA in CH₂Cl₂, ring contraction to 1,3-diphenylbenzo[*c*]thiophene **39** was observed. With H₂O₂ in CH₃COOH, the reaction afforded 1,3-dihydro-1,3-diphenylbenzo[*c*]thiophene **40**, while with Oxone a highly regioselective oxidized product, i.e. 1,4-dihydro-1,4-diphenyl-2,3-benzodithiin 2,2-dioxide **41**, was formed (equation 58).

Oxone has been successfully used for the cleavage of a carbon-sulfur double bond of thiocarbonyl moiety to the corresponding carbonyl compound¹⁶⁷. This method was applied to prepare tricarbonyl compounds.

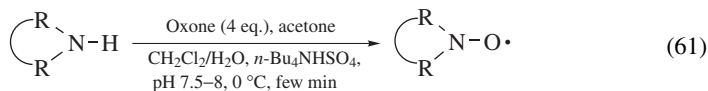
Wozniak and Stec reported for the first time the application of Oxone for chemoselective and stereospecific oxidations of various P(III), phosphothio and phosphoseleno derivatives (equation 59)¹⁶⁸.



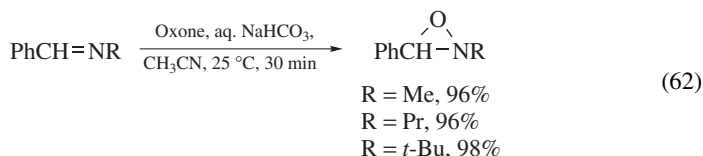
Selenides were oxidized with Oxone in buffered methanol to the corresponding selenones in quantitative yields¹⁶⁹. Webb and Levy showed that several boronic acids and boronic esters can be converted into the corresponding alcohols in excellent yields (equation 60). Oxone had been shown to be a better alternative than alkaline H_2O_2 , which had been used commonly for this conversion¹⁷⁰.



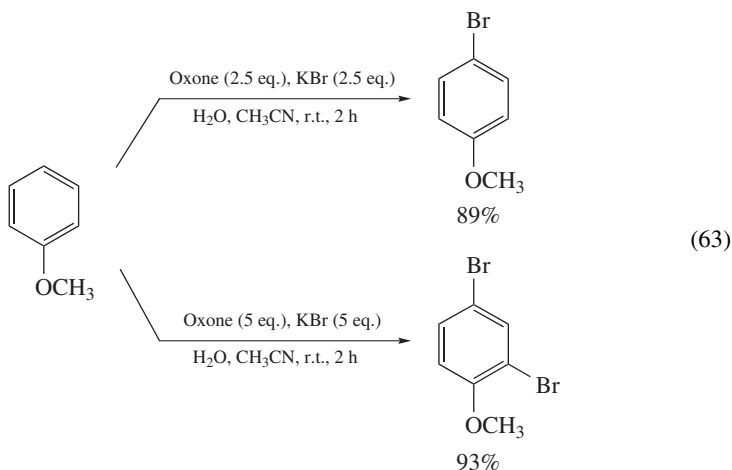
Aliphatic primary amines are known to be oxidized by dimethyl dioxiranes to various products such as oximes, nitroso dimers, nitroalkanes, nitrones and oxaziridines under various conditions depending upon the oxidation reaction¹⁷¹. In contrast, when secondary amines lacking α -hydrogens are allowed to react with Oxone and PTC in buffered acetone solution at 0°C , nitroxides are obtained in good yields in a few minutes (equation 61)¹⁷².



Imines are oxidized by Oxone to oxaziridines in quantitative yields (equation 62)¹⁷³.



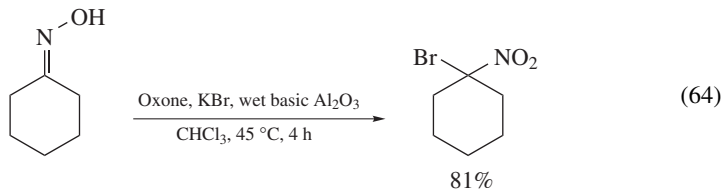
Recently, many researchers reported oxyhalogenation reactions using sodium or potassium halide as a halogen source together with Oxone. Bromination of activated aromatic compounds using potassium bromide and Oxone gives selectively *p*-bromoarene in high yield. When excess of potassium bromide and Oxone are used, the dibromoarene is obtained in high yields (equation 63)¹⁷⁴.



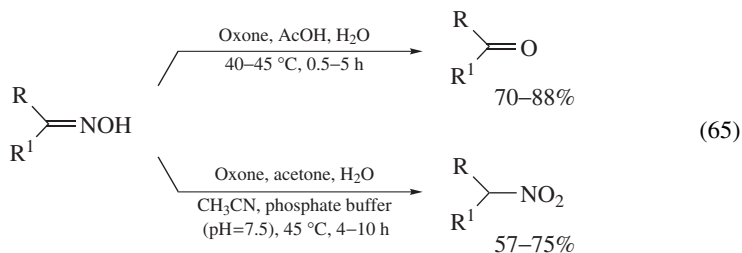
α -Halogenation of aromatic methyl ketones using sodium halide and Oxone was reported¹⁷⁵, but electron-rich heteroatomic methyl ketones undergo ring bromination.

Benzaldehydes and benzoic acids bearing *o*- and *p*-electron-donating substituents having unshared electron pair undergo bromodecarbonylation and bromodecarboxylation on treatment with sodium bromide and Oxone in aqueous methanol¹⁷⁶. Interestingly, whereas chlorodecarbonylation and chlorodecarboxylation using sodium chloride/Oxone occur in acceptable yields, iododecarbonylation or iododecarboxylation using sodium iodide/Oxone did not occur. Addition of chlorine or bromine across the double bond by NaCl or NaBr and Oxone was also reported¹⁷⁷. When NaN_3 and KI with Oxone/wet alumina reacted with alkenes, the corresponding azidoiodinated product was obtained in high yield¹⁷⁸. Selective bromination of pyridine nucleotides in aqueous medium can be easily carried out using Oxone/KBr¹⁷⁹.

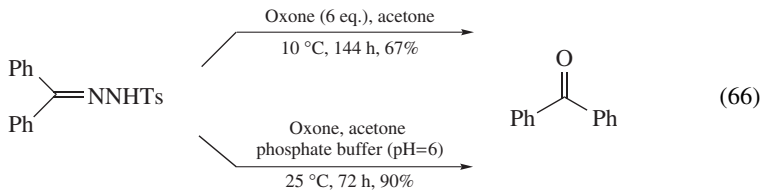
A new method for conversion of oximes to the corresponding *gem*-halonitro derivatives using NaCl or KBr with Oxone and wet basic alumina was reported (equation 64)¹⁸⁰. When the reaction was carried out under the same conditions but by using wet neutral alumina, complex mixtures of compounds in which the parent ketone is the most abundant product (>50%), due to the oxidative deprotection of the oxime, was obtained.



A continuous search for selective and mild reaction conditions for the deprotection of various derivatives for carbonyl group compounds is taking place. Oximes can be readily converted to the corresponding ketones by using Oxone in acetone:aqueous acetic acid¹⁸¹ and aqueous CH_3CN ¹⁸². A solvent-less deoximation using Oxone/wet Al_2O_3 , under microwave irradiation, was also reported¹⁸³. Interestingly, when oximes were treated with Oxone in aqueous acetone in the presence of phosphate buffer (pH = 7.5), they gave the corresponding ketone or nitro compounds, depending on the reaction conditions (equation 65)¹⁸¹.



Regeneration of ketones from tosylhydrazones with Oxone in acetone has been reported. Under controlled pH (pH = 6) the reaction gave very high yield (90%) of the product¹⁸⁴. In this paper we demonstrated that the use of *in situ* formed dimethyldioxirane under controlled pH conditions gives better results (equation 66).



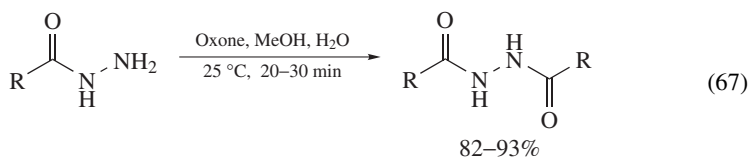
Hydrazones are readily converted to the corresponding ketones in a highly selective way using Oxone¹⁸⁵ and Oxone dispersed on silica¹⁸⁶ under microwave irradiation.

When a variety of aldehydes and *N,N*-dimethylhydrazones are treated with Oxone on wet Al_2O_3 under microwave irradiation in the absence of a solvent, the corresponding nitriles are obtained in good yields¹⁸⁷. Under these reaction conditions high selectivity

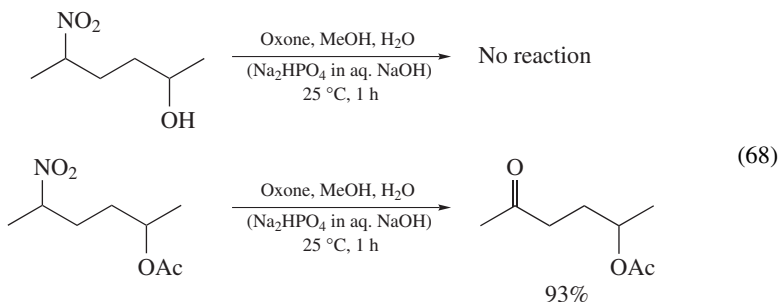
is observed and sulfides, carbon-carbon double bonds, CH_3 , Br, NO_2 and OCH_3 groups remain intact.

Both oxidative deacetalization using Oxone/wet Al_2O_3 ¹⁸⁸ in CHCl_3 and Oxone/ AlCl_3 ¹⁸⁹ in CH_3CN and dethioacetalization with Oxone/wet Al_2O_3 were reported¹⁹⁰. This method is effective for the cleavage of cyclic trimethylene dithioacetal derivatives, which are inert towards the action of a variety of reagents.

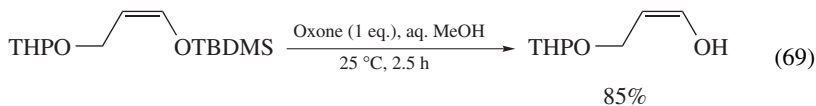
Primary, secondary and tertiary thioamides and thioureas are readily converted to their corresponding oxo analogs with Oxone in refluxing CH_3CN ¹⁹¹. Thiono esters were converted to esters, while thioketones remained intact under these reaction conditions. Hydrazines can be selectively converted to esters and acids in high yields by using Oxone in an alcohol and a water, respectively¹⁹². However, Mane and coworkers showed that hydrazides can be smoothly converted into the corresponding N,N' -diacylhydrazines in excellent yields with Oxone in water (equation 67)¹⁹³.



Mild and convenient oxidative Nef reaction using Oxone was also reported. Primary and secondary nitroalkanes give carboxylic acids and ketones, respectively, in good to excellent yields. Under these conditions 5-nitrohexan-2-ol does not react, probably as a consequence of an intramolecular hydrogen shift from the hydroxyl group to the nitronate carbanion, in a six-membered transition state which prevents the oxidation of the nitro derivative. When the hydroxyl group is protected by an acyl or a *tert*-butyldimethylsilyl (TBDMS) group, the nitro group is oxidized to a carbonyl group in good yield (equation 68)¹⁹⁴.



A highly selective and mild procedure for cleavage of TBDMS ethers to the corresponding alcohols by using Oxone was developed recently. Interestingly, it has been found that *tert*-butyldiphenylsilyl (TBDS) ether and certain acid-labile groups such as tetrahydropyranyl (THP), *N*-Boc or a carbon-carbon double bond remain unaffected under the reaction conditions (equation 69)¹⁹⁵.

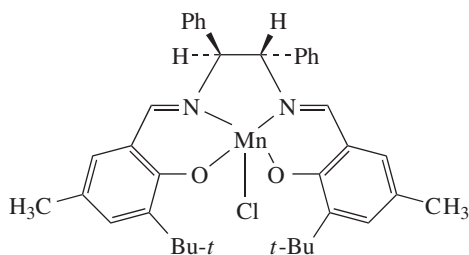
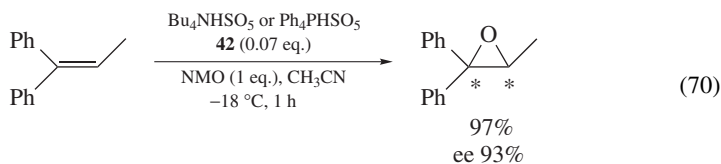


Oxone is a cheap oxidant but contains only about 50% of active oxidant per mol of the triple salt. Some methods¹⁹⁶ have been developed to prepare the pure potassium monoperoxysulfate (KHSO₅), yet this purified oxidant have not been tried in organic synthesis, perhaps due to less convenient procedures for obtaining the pure oxidant. Recently, Borhan and coworkers described a modified, straightforward and stepwise procedure for the preparation of pure KHSO₅•H₂O with 99% activity from Oxone¹⁹⁷. The reactivities of KHSO₅•H₂O and commercially available Oxone were compared in many common reactions. Purified KHSO₅•H₂O was found as effective as Oxone, while requiring only half of the mass of the oxidant, thus making the reaction workup more facile.

F. Organic Salts of Peroxymonosulfate

Generally, Oxone-mediated (2KHSO₅•KHSO₄•K₂SO₄) oxidation reactions are performed in H₂O, CH₃OH, DMF, or a miscible mixture including one of the latter solvents. The need for aqueous and pH-controlled reactions is perhaps the most significant drawback in the use of Oxone in organic chemistry. To overcome the need for aqueous conditions, Oxone can be used with silica gel, alumina or mineral clays in anhydrous organic solvents. In addition, some organic salts of Oxone were prepared and applied for various oxidation reactions. Tetra *n*-butylammonium peroxymonosulfate (Bu₄NHSO₅, TBA-OX) was first prepared by Dehmloew and coworkers¹⁹⁸, and later used for sulfide oxidation by Trost and Braslau³. Bu₄NHSO₅ (also known as Trost salt) can be easily prepared by simply extracting an aqueous solution of Oxone and 5 equivalents of tetra *n*-butylammonium bisulfate with methylene chloride, drying and evaporating the solvent. The white solid obtained has an oxidative activity 37.5% by weight.

Oxidation of hydrocarbons to epoxides, alcohols and/or ketones using Bu₄NHSO₅ in the presence of manganese(III) *meso*-tetraphenylporphyrin catalyst and axial imidazole ligand proceeds in low to very high yields¹⁹⁹. While asymmetric Mn(III)–salen **42** catalyzed epoxidation of trisubstituted alkenes under mild conditions was performed by using Bu₄NHSO₅²⁰⁰ or Ph₄PHSO₅²⁰¹ as the oxidant together with *N*-methylmorpholine *N*-oxide (NMO) as an additive (equation 70), the epoxide was formed in high yields (up to 97%) and good enantiomeric excess (up to 93% ee).



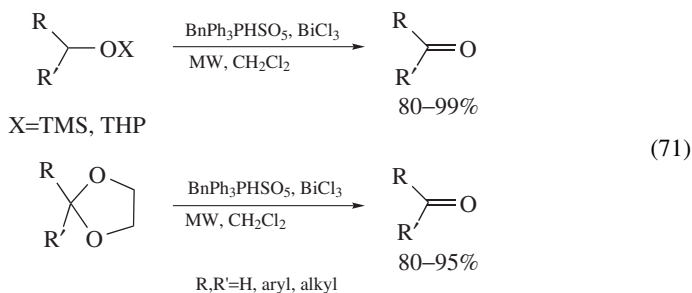
It has been also found that PhIO as an oxidant in the presence of a catalytic amount of sulfonated manganese and iron porphyrin supported on poly(vinylpyridinium) polymers in olefin epoxidation and alkane hydroxylation is a better oxidant than Bu_4NHSO_5 ²⁰². Oxidation of adamantane to 1-adamantanol in good yield using Bu_4NHSO_5 and acetone in the presence of aqueous NaHCO_3 was also reported²⁰³.

Wessel and Crabtree reported that Bu_4NHSO_5 is an effective primary oxidant with a high tendency to promote oxygen transfer rather than to react by a catalyzed radical pathway²⁰⁴. A nonradical hydrocarbon oxidation with Bu_4NHSO_5 and $[\text{Mn}_3\text{O}_4\text{bipy}_4(\text{H}_2\text{O}_2)](\text{ClO}_4)_4$ as catalyst was proved mechanistically, which contrasts the radical pathway followed for the same catalyst with *t*-BuOOH as the primary oxidant.

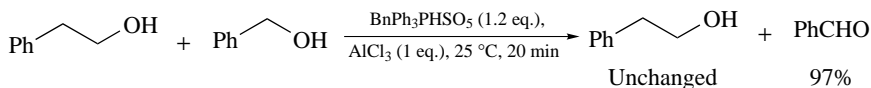
An anionic ligand effect in iron porphyrin complex-catalyzed competitive epoxidations of *cis*- and *trans*-stilbenes by Bu_4NHSO_5 has been studied in detail²⁰⁵. Oxidation of the thiophosphite to the thiophosphate in solid phase oligonucleotide synthesis using Bu_4NHSO_5 was also reported²⁰⁶.

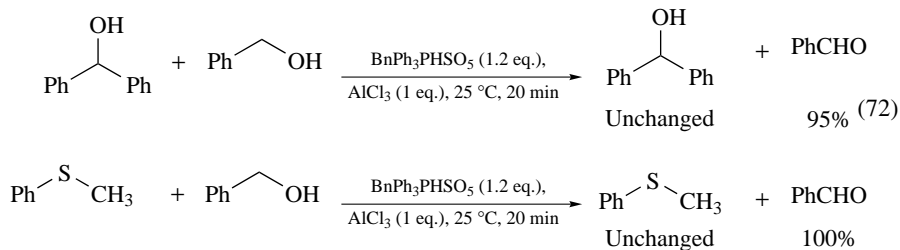
It has been observed that Ph_4PHSO_5 alone does not transfer its oxygen to manganese porphyrin. It is necessary to add either imidazole or pyridine derivatives, i.e. species which act as axial ligands in metalloporphyrins and are known to accelerate also the catalytic oxidation of organic substances²⁰⁷. The kinetics and mechanism of manganese porphyrins oxidation by Ph_4PHSO_5 were well studied²⁰⁸.

Hajipour and coworkers prepared benzyltriphenylphosphonium peroxymonosulfate ($\text{BnPh}_3\text{PHSO}_5$) in a very high yield (95%) and purity (99%). This new oxidizing reagent was applied successfully in various deprotection reactions such as the conversion of oximes, phenylhydrazones, 2,4-dinitrophenylhydrazones and semicarbazones to the corresponding carbonyl compounds in the presence of bismuth chloride under nonaqueous conditions²⁰⁹. Oxidative deprotection of trimethylsilyl ethers, tetrahydropyranyl ethers and ethylene acetals with $\text{BnPh}_3\text{PHSO}_5$ under microwave irradiation²¹⁰ affords the corresponding carbonyl compounds in very high yields (equation 71). The same reaction also proceeds under nonaqueous conditions²¹¹.



Allylic and benzylic alcohols were oxidized to aldehydes or ketones with $\text{BnPh}_3\text{PHSO}_5$ in refluxing CH_3CN ²¹². The yield increased in the presence of bismuth chloride in a catalytic amount. Selective oxidation of various alcohols under solvent free conditions was also reported²¹³. Interestingly, benzyl alcohols were oxidized selectively to benzaldehydes in very high yield (95–100%) when reacted with $\text{BnPh}_3\text{PHSO}_5$ (1.2 eq.) and AlCl_3 (1 eq.) in the presence of an equimolar amount of 2-phenethyl alcohol, diphenyl carbinol or methyl phenyl sulfide (equation 72).





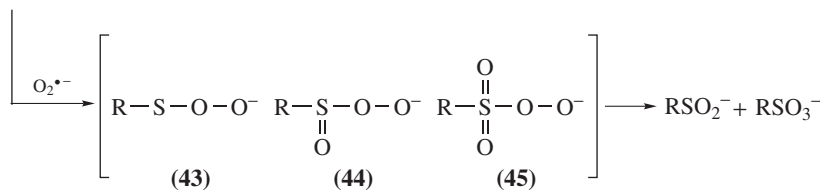
$\text{BnPh}_3\text{PHSO}_5$ was used for deprotection of oximes and semicarbazones to their parent carbonyl compounds under microwave irradiation.²¹⁴ Similarly, dethioacetalization of 1,3-dithiolanes and 1,3-dithianes by $\text{BnPh}_3\text{PHSO}_5$ in aprotic solvents was also reported²¹⁵. In both these reactions a catalytic amount of bismuth chloride was necessary.

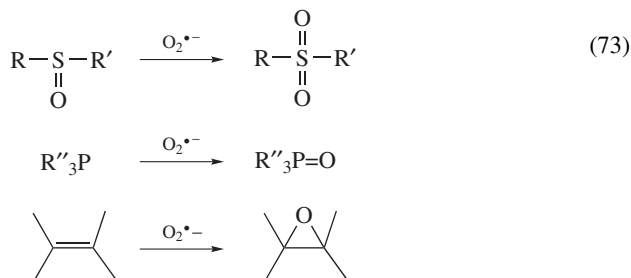
G. Organic Sulfur Compounds with Superoxide

Superoxide ($\text{O}_2^{\bullet-}$), which is an anion radical and one of the activated oxygen species, is an important reactant in biological systems. It characteristically performs various functions such as reduction, oxidation, nucleophilic reactions and deprotonation^{6,216}. Potassium superoxide (KO_2) is the commercial source of $\text{O}_2^{\bullet-}$, but unfortunately it decomposes in water and is only slightly soluble in a highly polar solvent like DMSO. Valentine and Curtis observed that KO_2 could be dissolved appreciably in aprotic solvents, by complexation with crown ethers²¹⁷. Later, it was found by us that KO_2 is soluble enough in aprotic solvents such as CH_3CN , CH_3NO_2 and DMF even without using crown ether catalysts. However, some reports indicate that KO_2 is relatively inactive and has limited use in organic synthesis²¹⁸.

Organic sulfur compounds such as disulfide, thiosulfinic S-ether, thiosulfonic S-ester or thiolate and sulfinate were found to be oxidized by KO_2 to the corresponding sulfinic and sulfonic acids via the peroxy-sulfenate **43**, -sulfinic **44**, and -sulfonate **45** intermediates (equation 73). These intermediates are capable of oxidizing sulfoxides, phosphines and olefins to the corresponding sulfones, phosphine oxides and epoxides, respectively²¹⁹. The formation, characterization and application of peroxysulfur intermediates were reviewed^{3,220}. Various useful organic syntheses using peroxysulfur intermediates formed by reacting sulfur compounds and KO_2 were introduced, with special emphasis on the reaction mechanism and character of peroxy intermediates.

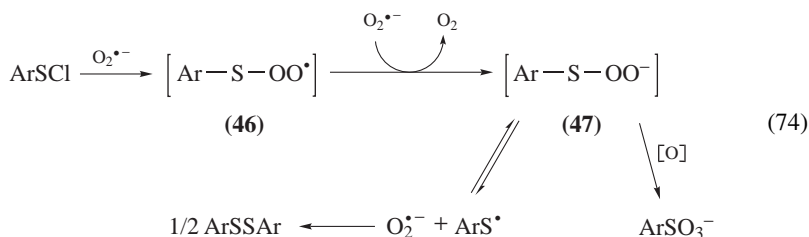
Sulfur compounds



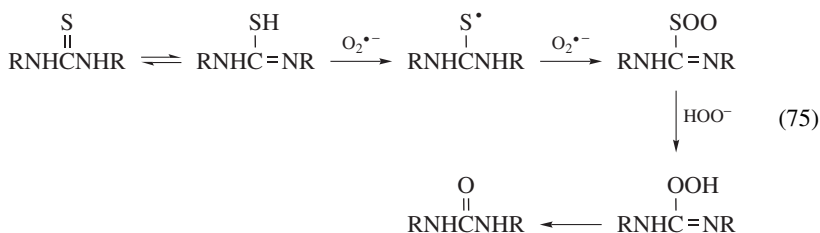


1. Peroxysulfenate

Treatment of arylsulfenyl chlorides with KO_2 in THF or CH_3CN at low temperature (-30°C) gave the corresponding disulfides and arylsulfonates as the major products^{220, 221}. In the case of 2,4-dinitrobenzenesulfenyl chloride, the corresponding disulfide was the major product. The reaction is probably initiated by a nucleophilic attack of $\text{O}_2^{\bullet-}$ on the sulfenyl sulfur atom to form a peroxysulfenate radical **46**, which may be readily converted to the peroxysulfenate anion **47** in the presence of excess $\text{O}_2^{\bullet-}$ (equation 74).



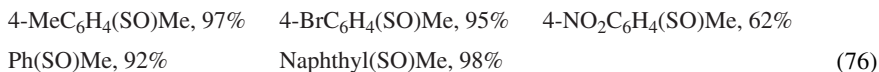
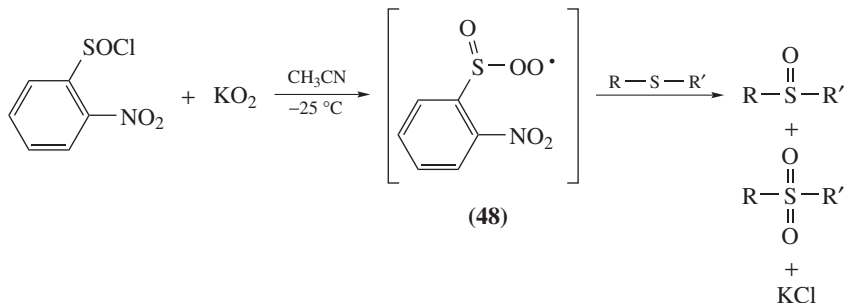
Desulfurization of 1,3-disubstituted thioureas to the corresponding ureas with KO_2 at room temperature in DMSO takes place in good to excellent yields²²⁰. It is believed that this reaction proceeds by formation of a peroxysulfenate intermediate (equation 75).



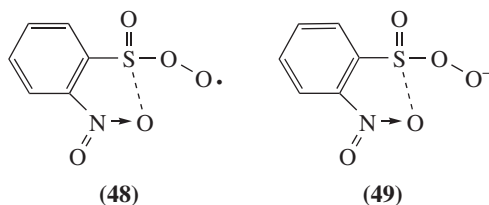
2. Peroxysulfinate

Treatment of 2-nitrobenzenesulfinyl chloride with excess KO_2 at -25°C in CH_3CN generates *in situ* 2-nitrobenzenesulfinylperoxy intermediate, which was successively applied

for the selective oxidation of sulfides to the corresponding sulfoxides in almost quantitative yields (equation 76)²²². Almost all electron-rich sulfides gave the corresponding sulfoxides in very high yield (93–97%), whereas sulfides carrying electron-withdrawing substituents on the phenyl ring, e.g. methyl *p*-nitrophenyl sulfide, gave a moderate yield of sulfoxide (62%) along with the sulfone (12%).



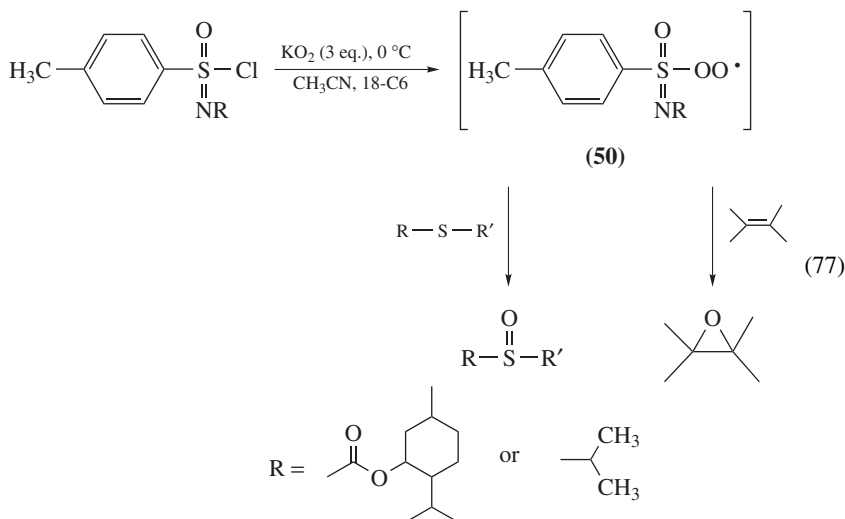
It was found that when 4-tolylsulfinyl and 4-nitrophenylsulfinyl chloride reacted with KO₂ to give the corresponding sulfinylperoxy intermediate, poorer yields of the sulfoxides were obtained compared to the reaction with 2-nitrobenzenesulfinylperoxy intermediate **48** (or **49**). Thus, the presence of the nitro group at the *o*-position of **48** or **49** appears to play an important role in accelerating the substitution of the chlorine with O₂^{-•} and also in stabilizing the intermediate **48** (or **49**).



Oxidation of a sulfide to sulfoxide is known to be an electrophilic reaction, in contrast with nucleophilic oxidation of sulfide to sulfone. Since 2-nitrobenzenesulfinyl chloride/KO₂ oxidizes sulfides to sulfoxides selectively, intermediate **48** must be the actual active intermediate. Moreover, in the presence of 1,4-diazabicyclo[2.2.2]octane (DABCO), which is a radical capturing reagent, the oxidation of methyl phenyl sulfide to the sulfoxide was inhibited. In order to further detect the intermediate **48**, pure 5,5-dimethyl-1-pyrroline-1-oxide (DMPO) was used as a trapping reagent and spin adduct was obtained²²³. The ESR spectrum of the DMPO spin adduct was obtained by the reaction of O₂^{-•} with 2-nitrobenzenesulfinyl chloride (hyperfine coupling constants, *aH* = 10.0 G and *aN* = 12.8 G).

Optically pure (+)-(*S*)-*N*-carbo(-)-menthyl-4-tolylsulfonimidoyl chloride was prepared²²⁴ and reacted with O₂^{-•} at 0 °C in CH₃CN to give the expected optically active sulfonimidoylperoxy intermediate **50**, which oxidizes alkenes to epoxides and sulfides to

sulfoxides in good to excellent yield. However, oxidation of methyl 4-tolyl sulfide by using peroxy-sulfonimidoyl intermediate **50** resulted in the corresponding optically active sulfoxide with poor ee (equation 77)²²⁵.



3. Sulfonylperoxy radical

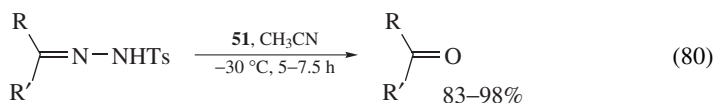
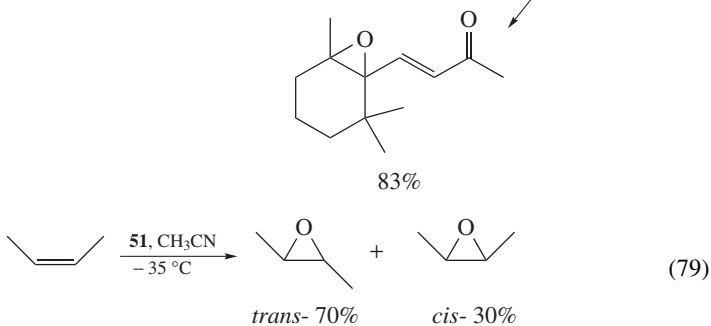
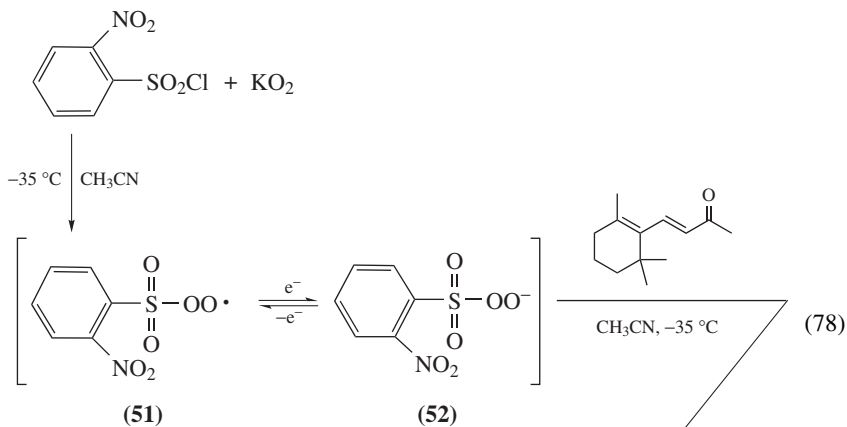
Various arylsulfonyl chlorides reacted with $\text{O}_2^{\bullet-}$ to form peroxy intermediates. 2-Nitrobenzenesulfonylperoxy intermediate **51** had shown a larger oxidizing ability towards olefins compared with the 4-nitrobenzenesulfonylperoxy intermediate. When 2-nitrobenzenesulfonyl chloride reacts with $\text{O}_2^{\bullet-}$ at low temperature (-20 to -35°C) in CH_3CN , the corresponding sulfonylperoxy radical **51** or anion **52** is generated. The radical character of the sulfonylperoxy intermediate **51** was further confirmed by the electrophilic oxidizing nature of a 2-nitrobenzenesulfonyl chloride/ KO_2 mixture.

Various mono- or di-olefins were oxidized regioselectively to their epoxides in high yield with the 2-nitrobenzenesulfonylperoxy intermediate **51** generated *in situ* from 2-nitrobenzenesulfonyl chloride and KO_2 at -35°C in CH_3CN (equation 78)²²⁶. Thus β -ionone was oxidized using **51** to the corresponding mono epoxide product in high yield (83%). That the electron-deficient double bonds remain intact under the reaction conditions shows the electrophilic character of **51**.

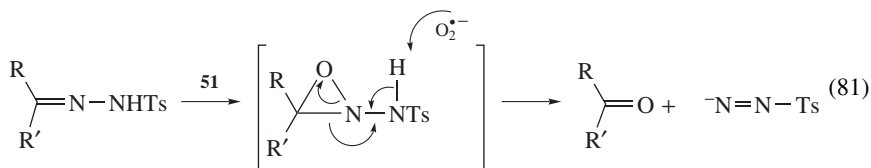
Acenaphthene oxide is known to be unstable under acidic conditions²²⁷ and is therefore isolated in low yields when prepared by common methods²²⁸. The highly strained acenaphthene was smoothly epoxidized in quantitative yield at -30°C in CH_3CN by using **51**²²⁹. *Cis*-stilbene was epoxidized with **51** at -35°C in CH_3CN to a mixture of the *trans*- (70%) and *cis*-epoxides (30%) (equation 79). This result shows that the peroxy-sulfonyl intermediate must be a radical like the acylperoxy radical $\text{ArC}(\text{O})\text{OO}\cdot$ ²³⁰ and the phenyl nitroso oxide radical $\text{PhNO}\cdot$ ²³¹.

Polyaromatic compounds such as phenanthrene and pyrene, which are inert to $\text{O}_2^{\bullet-}$ itself, were readily oxidized to the corresponding K-region arene oxides by treating with **51**²²⁹.

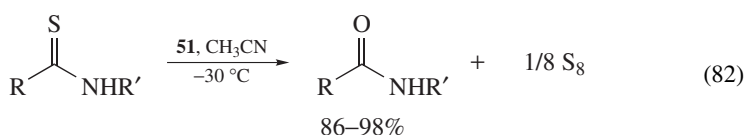
Various alkyl aryl and dialkyl tosylhydrazones react readily with **51** to give the corresponding carbonyl compounds in almost quantitative yields at -30°C in CH_3CN (equation 80)²³².



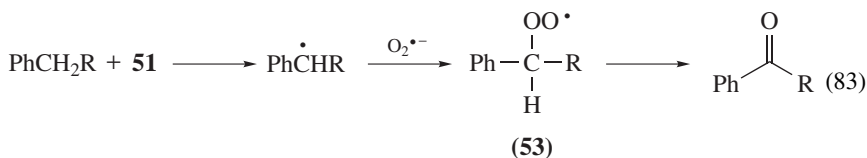
A plausible reaction mechanism is that oxidative cleavage of tosylhydrazones is initiated by oxidation of the imino double bond of the tosylhydrazones with **51** to an oxaziridine derivative, which may be immediately converted to the carbonyl compound by a fragmentation reaction induced by $\text{O}_2^{\bullet-}$ (equation 81).



Oxidative desulfurization of the thiourea moiety is known to occur by an *in vivo* metabolism which forms the corresponding carbonyl compound, although there is no direct evidence for involvement of any activated oxygen species like superoxide, which is distributed widely in living cells²³³. It was found that various thiocarbonyl derivatives such as thioureas, thioamides and thiocarbamates were readily desulfurized with **51** to the corresponding carbonyl compounds in almost quantitative yields at -35°C in CH_3CN (equation 82)²³⁴. Desulfurization of thiourea with $\text{O}_2^{\bullet-}$ was previously reported but the yields were comparatively low²³⁵.



Oxidation of active methylene compounds is important in the *in vivo* metabolic process catalyzed by oxygenase as well as in organic synthesis²³⁶. Various substrates containing a benzylic methylene group were readily reacted with **51** at -35°C to give the corresponding carbonyl compounds in excellent yields. A plausible reaction mechanism initiates by abstraction of one of the hydrogen atoms of the benzylic methylene group by **51**. The resulting benzylic radical **53** may couple with molecular oxygen or with $\text{O}_2^{\bullet-}$ to form a peroxy radical, which is then converted to the corresponding carbonyl group (equation 83).

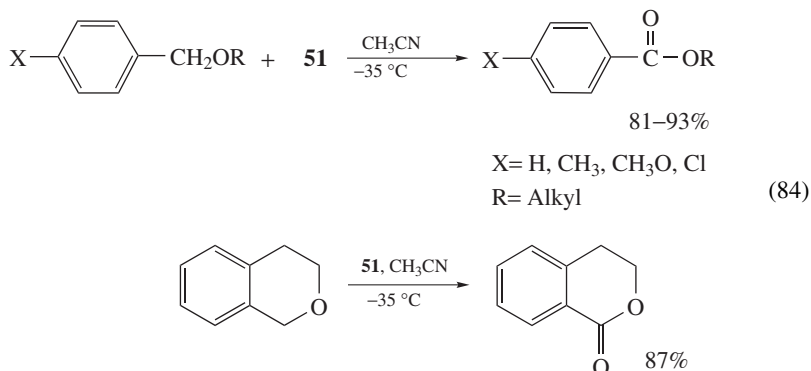


In order to confirm the radical character of **51** and to extend its utility, oxidations of arylacetic acids to the corresponding ketones, aldehydes or alcohols have been conducted²³⁷. Competitive decarboxylation reactions of phenylacetic acid and *p*-substituted phenylacetic acids were carried out. The ratio of the rate constants for the decarboxylation of various substituted phenylacetic acids relative to that of phenylacetic acid was found to decrease on decreasing the electron density at the benzylic carbon. Consequently, compound **51** shows an electrophilic oxidation ability towards arylacetic acids, giving a Hammett ρ^+ value of -0.408 .

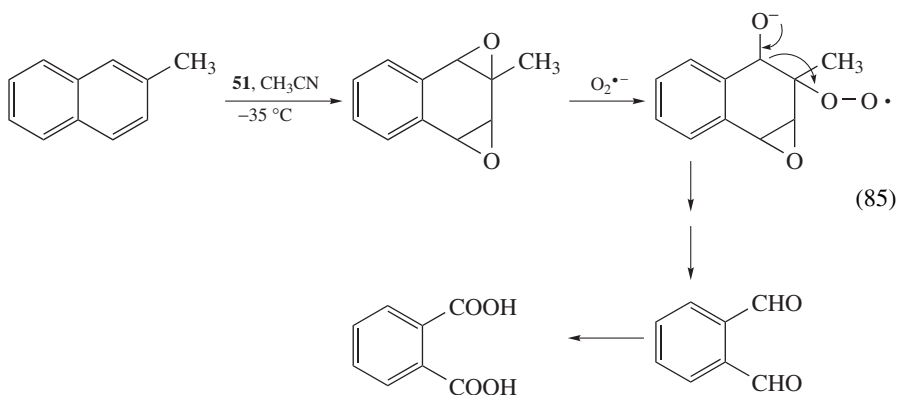
A number of substrates having a benzylic ether moiety were reacted with **51** to afford the corresponding benzylic esters in good yields (equation 84)²³⁸. For evaluating the effects of *p*-substituents on the oxidation of a series of benzylic ethers, a competitive oxidation of *p*-substituted benzylic propyl ethers with **51** was carried out. The Hammett correlation plot for the oxidation reaction gave a better correlation of the relative ratio factors with the σ rather than with the σ^+ substituent constants and afforded a reaction constant $\rho^+ = -0.57$ ($r = 0.99$). This ρ^+ value shows that **51** is an electrophilic species and appears to be comparable to the ρ^+ value of -0.65 for benzylic hydrogen abstraction from dibenzyl ethers by the benzoyloxy radical²³⁹.

Metabolic degradation of polyaromatic hydrocarbons is believed to involve oxidation with an activated oxygen species by an enzyme in all aerobic organisms and also in

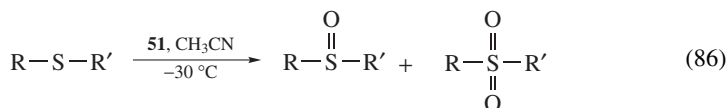
soil bacteria²⁴⁰. 2-Methylnaphthalene is oxidized to phthalic acid along with unidentified products by **51** at -30°C in CH_3CN ²⁴¹.



This oxidation is considered to be initiated by epoxidation of an aromatic ring, followed by fragmentations to the carbonyl compound (equation 85). It is interesting that the aromatic ring can be readily destroyed at low temperature, a reaction which otherwise always requires high energy and drastic conditions.

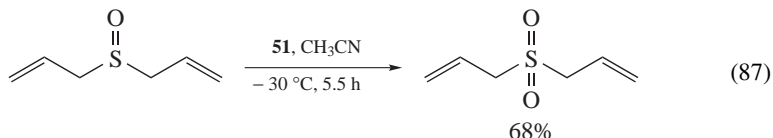


Various alkyl aryl and diaryl sulfides were oxidized selectively to the corresponding sulfoxides in high yields as the major products using sulfonylperoxy intermediate **51** (equation 86)²⁴².



Various dialkyl, alkyl aryl and diaryl sulfoxides were readily oxidized to the corresponding sulfone in excellent yields under mild conditions at -30°C by **51**²⁴³. Interestingly,

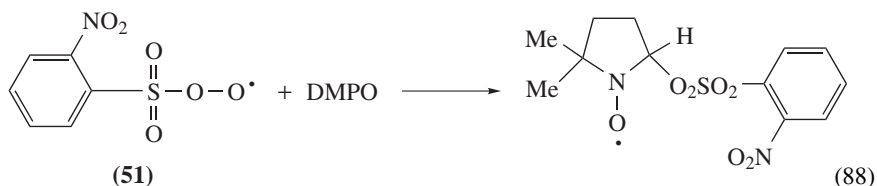
allyl sulfoxide is oxidized chemoselectively to the corresponding sulfone in 68% yield by **51** without formation of epoxide (equation 87).



It was reported earlier that the oxidation of a sulfoxide to a sulfone involves either an initial nucleophilic attack of the nucleophilic oxidant²⁴⁴ or an electrophilic attack by an electrophilic oxidant²⁴⁵. It is noteworthy that the oxidation of *p*-tolyl methyl, phenyl methyl and *p*-chlorophenyl methyl sulfoxides to the sulfones using the sulfonylperoxy intermediate **51** appears to be electrophilic, namely the relative reactivity order was *p*-tolyl methyl > phenyl methyl > *p*-chlorophenyl methyl sulfoxide based on competitive oxidations.

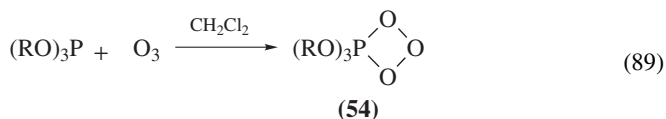
As described in equation 78, the relatively electron-rich ring double bond of α - or β -ionone was regioselectively epoxidized, whereas the electron-deficient double bond was not oxidized at all. This result also supports the radical rather than the anionic character of **52**.

Spectroscopic evidence for peroxy radical **51** was obtained from ESR. Spin trapping studies monitored by ESR have demonstrated that $\text{O}_2^{\bullet-}$ reacts efficiently with 2-nitrobenzenesulfonyl chloride and results in the formation of the peroxy radical intermediate **51** (equation 88)²²³. The 5,5-dimethyl-1-pyrroline-1-oxide (DMPO) spin adduct of **51** shows the hyperfine coupling constants, $aN = 1.8\text{ G}$ and $aH = 10.1\text{ G}$.

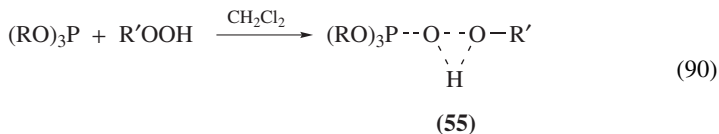


III. PHOSPHORUS PEROXIDES

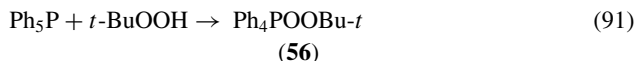
Compared with peroxysulfur compounds, very few peroxyphosphorus compounds are reported. Phosphorus peroxide derivatives have been postulated as possible intermediates in certain biological transformations, although they have never been isolated in such systems²⁴⁶. Monoperoxyphosphonic acid can be prepared *in situ* and applied for some common oxidation reactions²⁴⁷. Only one example of phosphorus peroxide, i.e. bis(phenylphosphinyl) peroxide, has been studied⁹. It is believed that when trivalent phosphorus compounds are allowed to react with ozone and a source of singlet oxygen, phosphorus ozonides **54** are obtained (equation 89)²⁴⁸.



Similarly, the reaction of trialkyl phosphites with hydroperoxides was proposed to give the intermediate **55** (equation 90)²⁴⁹.



Some unstable peroxy esters are also reported. The reaction of pentaphenylphosphine with *tert*-butylhydroperoxide or silicon and germanium hydroperoxides gave the corresponding peroxy derivatives **56**, which cannot be isolated (equation 91).

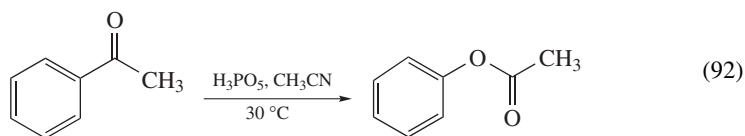


Some peroxyphosphorus radical intermediates such as tetraalkoxy phosphoranyl peroxy radical²⁵⁰, tetrachlorophosphoranyl peroxy radical⁹, phenylphosphorus peroxy radical²⁵¹ and diphenyl phosphinic peroxy radical²⁵² have been reported.

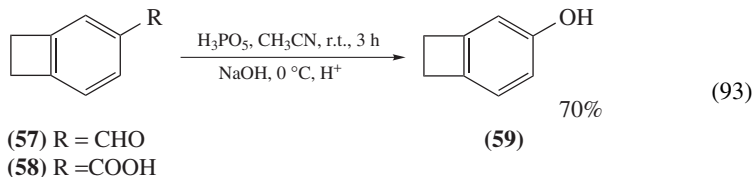
A. Monoperoxyphosphoric Acid

Monoperoxyphosphoric acid (H_3PO_5), which can be prepared *in situ* by reacting phosphorus(V) oxide with 87% H_2O_2 ²⁴⁷, should be used immediately after preparation. H_3PO_5 shows electrophilic oxidizing behavior and is capable of reacting with many functional groups such as alkenes²⁵³, alkynes²⁵⁴, arenes²⁵⁵ and amines²⁵⁶. Oxidation of *trans*-stilbene and diphenylacetylene with H_3PO_5 furnishes *trans*-stilbene oxide (74%)²⁵³ and benzil (48%)²⁵⁴, respectively. H_3PO_5 is an effective reagent for aromatic hydroxylation, the reactivity being comparable to that of trifluoroperacetic acid. Oxidation of mesitylene at room temperature gives mesitol in 77% yield²⁵⁵.

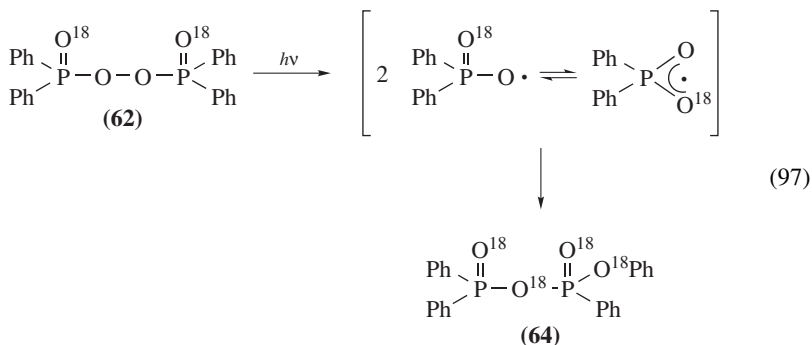
Acetophenone is oxidized efficiently with H_3PO_5 to phenyl acetate in 91% yield (equation 92). Baeyer–Villiger reaction of acetophenones with H_3PO_5 is nearly 100-fold faster than that with perbenzoic acid²⁵⁷.



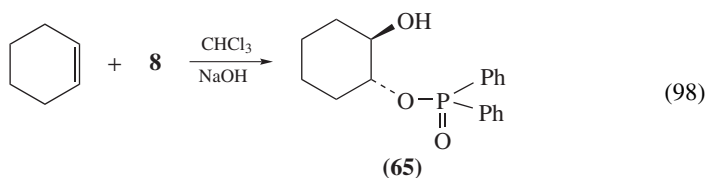
Baeyer–Villiger reaction of **57** with H_3PO_5 gives the phenol **59**. However, the peracetic acid or trifluoroperacetic acid gives the carboxylic acid **58** (equation 93)²⁵⁸. Oxidation of *N,N*-dimethylaniline in aqueous CH_3CN at 30 °C affords the *N*-oxide in 82% yield²⁵⁶.



Photolysis of the peroxide **62** gives the same product with complete oxygen scrambling **64**, presumably via a free radical intermediate (equation 97).

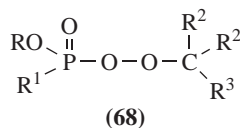
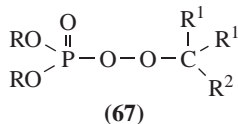
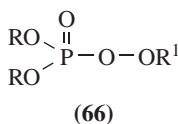


Decomposition of **8** in CHCl_3 in the presence of excess cyclohexene and a catalytic sodium hydroxide results in *trans*-2-hydroxycyclohexyldiphenyl phosphinate **65** in 16% yield (equation 98)⁹. Various sulfides react readily with **8** to give selectively the corresponding sulfoxides in excellent yields²⁵¹.

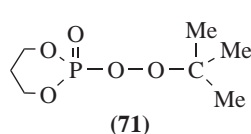
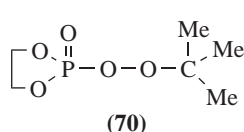
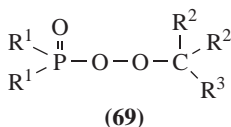


C. Unsymmetrical Phosphorus Peroxides

Since the first synthesis of the peroxyphosphorus ester **66**²⁶⁰, considerable efforts have been made to characterize the expanding chemistry of organophosphorus peroxy esters²⁶¹. Later, unsymmetrical phosphorus peroxides, such as peroxyphosphates **67**²⁶², peroxyphosphonates **68**²⁶³ and peroxyphosphinates **69**²⁶³, were reported. They can be prepared by the reactions of the chlorides and a tertiary carboxylic acid in the presence of base.

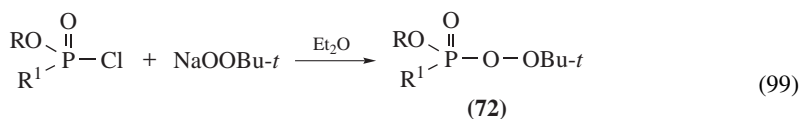


R=Me, Et; R¹=*t*-Bu



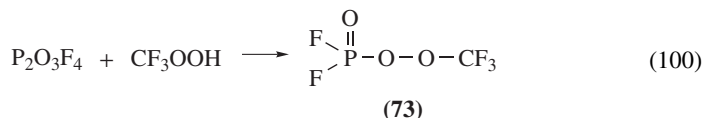
Peroxy esters **67** were prepared *in situ* by the reaction of phosphonochloridate and *tert*-butyl hydroperoxide in diethyl ether. The peroxy ester **67** (R = Ph) is stable for several days at 5 °C in diethyl ether. Most peroxyphosphates **67** with an RO group other than *tert*-butylperoxy are unstable even for short periods²⁶⁴. This synthetic method was successfully applied for synthesis of ring peroxyphosphates **70** and **71** as colorless oils. They are very unstable and decompose at 25 °C to yield polymeric products and volatile side products²⁶⁴.

The first synthesis of a peroxyphosphonate **68**, i.e. *tert*-butyl alkyl peroxyphosphonate **72**, was performed by the condensation of the corresponding alkyl alkylphosphonochloridate with the sodium salt of *tert*-butyl hydroperoxide in anhydrous diethyl ether (equation 99)²⁶³.



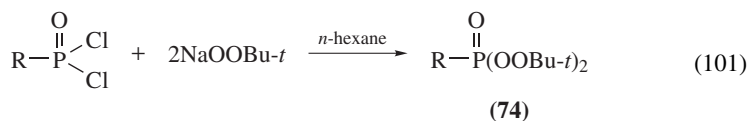
Peroxyphosphonate can be prepared by a similar reaction in the presence of pyridine²⁶⁵ instead of the sodium salt of the hydroperoxide. Peroxyphosphonates **72** are generally synthesized by the condensation of the corresponding phosphinic chloride with the sodium salt of *tert*-butyl hydroperoxidate in a neutral solvent in the presence of sodium sulfate, or alternatively, by the reaction of *tert*-butyl hydroperoxide with phosphinic chloride in the presence of pyridine²⁶⁶.

Interestingly, the fluorine-containing peroxy ester of phosphorus **73** was prepared in 87% yield by the condensation of μ -oxo-bis(phosphonyl difluoride) (P₂O₃F₄) and trifluoromethyl hydroperoxide (equation 100)²⁶⁷.



The fluoroperester **73** is a liquid and was purified by distillation under vacuum and studied extensively as a synthetic intermediate.

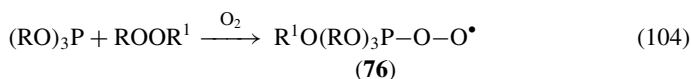
The preparation of the diperoxy esters **74** has been examined and several of them have been isolated in low yields (equation 101)²⁶⁸.



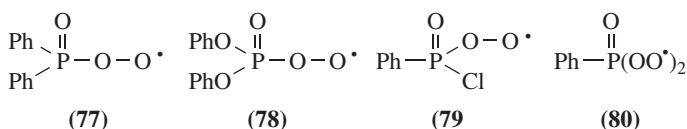
Dialkyl peroxyphosphates **67**²⁶⁹ or monoperoxy phosphates **68**²⁷⁰ react with phenylmagnesium bromide to afford *tert*-butyl phenyl ether in high yield together with dialkylphosphoric acid or alkylphosphoric acid in moderate yields (equation 102).

The peroxyphosphates **67** or the peroxyphosphonates **68** also react with cyclohexene in the presence of copper(I) ion thermally or photochemically to give the corresponding

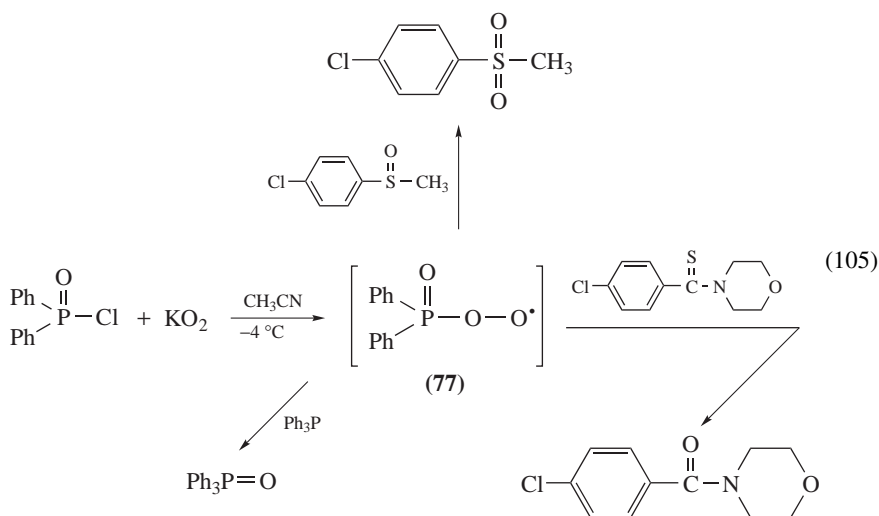
but without any detailed experimental evidence (equation 104)^{250,259}.



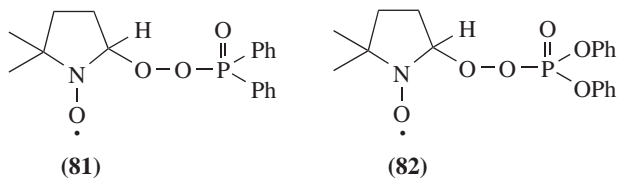
Various peroxyphosphorus radicals **10**, such as the diphenylphosphinic peroxy radical **77**, the diphenylphosphoryl peroxy radical **78** and the phenylchlorophosphinic peroxy radical **79** or the biradical **80**, have been characterized.



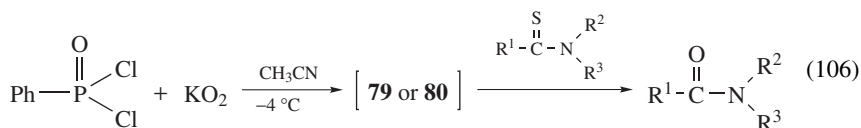
Diphenylphosphinic chloride reacts with the superoxide anion radical ($\text{O}_2^{\bullet-}$) in CH_3CN under mild conditions to form the diphenylphosphinic peroxy radical intermediate **77**, which shows strong oxidizing abilities in the epoxidation of alkenes, oxidation of sulfoxides to sulfones, desulfurization of thioamides to amides and oxidation of triphenylphosphines to triphenylphosphine oxide in good to excellent yields (equation 105)²⁵².



Radical **77** is trapped with 2,2-dimethylpyrrolidine *N*-oxide (DMPO) to form a radical adduct **81**. In the same way, the diphenylphosphoryl peroxy radical **78** is also trapped to give **82**²⁷⁶.



A peroxyphosphorus intermediate **79** or **80** generated from phenylphosphinic dichloride and superoxide at -4°C desulfurizes thioamides to amides in excellent yields (equation 106)²⁷⁷.



IV. REFERENCES

1. G. B. Payne, *Org. Synth., Collect. Vol.*, **5**, 805 (1973).
2. B. M. Trost and D. P. Curran, *Tetrahedron Lett.*, **22**, 1287 (1981).
3. B. M. Trost and R. Braslau, *J. Org. Chem.*, **53**, 532 (1988).
4. F. M. Hause and S. R. Ellenberger, *Synthesis*, 723 (1987); C. S. Foote and S. Wexler, *J. Am. Chem. Soc.*, **86**, 3879 (1964).
5. Y. H. Kim and S. G. Yang, *Heteroatom Chem. Rev.*, **20**, 69 (1999).
6. R. V. Hoffman, in *The Chemistry of Peroxides* (Ed. S. Patai), Wiley, Chichester, 1983, p. 259.
7. Y. H. Kim and K. S. Kim, in *Reviews on Heteroatom Chemistry* (Ed. S. Oae), MYU, Tokyo, 1990, p. 287.
8. Y. H. Kim and D. C. Yoon, *Synth. Commun.*, **19**, 1569 (1989).
9. R. L. Dannley and K. Karbe, *J. Am. Chem. Soc.*, **87**, 4805 (1965).
10. Y. H. Kim, in *Organic Peroxide* (Ed. W. Ando), Wiley, New York, 1992, p. 387.
11. Y. H. Kim, S. C. Lim and H. S. Chang, *J. Chem. Soc., Chem. Commun.*, **36** (1990).
12. J. D'Ans, German Patent, DE 251802 (1911); *Chem. Abstr.*, **7**, 2671 (1913).
13. J. D'Ans and W. Friderich, German Patent, DE 236768 (1910); *Chem. Abstr.*, **5**, 21029 (1911).
14. A. Baeyer and V. Villiger, *Ber.*, **33**, 858 (1900).
15. Anon, *Chem. Week*, **92**, 55 (1963).
16. H. Marshall, *J. Chem. Soc.*, 771 (1891).
17. H. Caro, *Angew. Chem.*, **11**, 845 (1898).
18. C. H. Hassall, *Org. React.*, **9**, 73 (1959).
19. M. Rnez and B. Meunier, *Eur. J. Org. Chem.*, 737 (1999).
20. A. Nishihara and I. Kubota, *J. Org. Chem.*, **33**, 2525 (1968).
21. N. Sato, *J. Org. Chem.*, **43**, 3367 (1978).
22. A. R. Gallopo and J. O. Edwards *J. Org. Chem.*, **46**, 1684 (1981).
23. R. E. Connick, S. Lee and R. Adanic, *Inorg. Chem.*, **32**, 565 (1993).
24. M. Schulz, R. Kluge and M. Lipke, *Synlett*, 915 (1993).
25. B. Bressel and A. Blaschette, *Z. Anorg. Allg. Chem.*, **377**, 182 (1970).
26. W. Adam and A. Rodriguez, *J. Org. Chem.*, **44**, 4969 (1979).
27. C. S. Pande and N. Jain, *Synth. Commun.*, **19**, 1271 (1989).
28. B. Movassagh, M. M. Lakouraj and K. Ghodrati, *Synth. Commun.*, **32**, 847 (2002).
29. B. Movassagh, M. M. Lakouraj and K. Ghodrati, *Synth. Commun.*, **32**, 3597 (2002).
30. B. Movassagh, M. M. Lakouraj and K. Ghodrati, *Synth. Commun.*, **30**, 2353 (2000).
31. A. T. Nielsen, R. L. Atkins, W. P. Novis, C. L. Coon and M. E. Sitzmann, *J. Org. Chem.*, **45**, 2341 (1980).
32. R. Willstätter and E. Hauenstein, *Ber.*, **42**, 1839 (1909).
33. D. O. Handelsgesellschaft and G. C. Fleisch, German Patent, DE 561521 (1930); *Chem. Abstr.*, **27**, 10199 (1933).
34. W. Machu, in *Das Wasserstoffperoxyd und die Perverbindungen*, Springer, Vienna, 1937, p. 408.
35. C. J. Myall and D. Pleacher, *J. Chem. Soc., Perkin Trans. I*, 953 (1975).
36. R. E. Nofle and G. H. Cady, *Inorg. Chem.*, **4**, 1010 (1965).
37. R. L. Dannley and G. E. Corbett, *J. Org. Chem.*, **31**, 153 (1966).
38. Y. Yokoyama, H. Wada, M. Kobayashi and H. Minato, *Bull. Chem. Soc. Jpn.*, **44**, 2497 (1971).
39. J. A. Manner, U.S. Patent, US 3998888 (1976); *Chem. Abstr.*, **86**, 139498 (1977).

40. R. L. Dannley and W. R. Knipple, *J. Org. Chem.*, **38**, 6 (1973).
41. E. M. Levi, P. Kovacic and J. F. Gormish, *Tetrahedron*, **26**, 4537 (1970).
42. J. Bolte, A. Kergomard and S. Vincent, *Bull. Chem. Soc. Fr.*, 301 (1972).
43. R. V. Hoffman, A. L. Willson and H. O. Kim, *J. Org. Chem.*, **55**, 1267 (1990).
44. R. V. Hoffman and E. L. Belfoure, *Synthesis*, 34 (1983).
45. R. V. Hoffman, *J. Am. Chem. Soc.*, **98**, 6702 (1976).
46. R. V. Hoffman, R. Cadena and D. J. Poelker, *Tetrahedron Lett.*, 203 (1978).
47. R. V. Hoffman and G. A. Buntain, *J. Org. Chem.*, **53**, 3316 (1988).
48. M. Yoshida, H. Mochizuki and N. Kamigata, *Chem. Lett.*, 2017 (1988).
49. R. Hisada, M. Kobayashi and H. Minato, *Bull. Chem. Soc. Jpn.*, **45**, 2035 (1972).
50. D. A. House, *Chem. Rev.*, **62**, 185 (1962).
51. F. Minisci, A. Citterio and C. Giordano, *Acc. Chem. Res.*, **16**, 27 (1983).
52. E. J. Behrman and J. O. Edwards, *Rev. Inorg. Chem.*, **2**, 179 (1980).
53. M. Lin and A. Sen, *J. Chem. Soc., Chem. Commun.*, 892 (1992).
54. G. Sosnovsky, in *Organic Peroxides Vol. II* (Ed. D. Swern), Wiley, New York, 1974, p. 57.
55. T. H. Parliment, M. W. Parliment and I. S. Fagerson, *Chem. Ind. (London)*, 1845 (1966); D. N. Dhar and R. C. Munjal, *Synthesis*, 542 (1973).
56. K. Elbs, *J. Prakt. Chem.*, **48**, 179 (1893).
57. E. C. Behrman, S. Chen and E. J. Behrman, *Tetrahedron Lett.*, **43**, 3221, (2002).
58. C. Walling and D. M. Camaioni, *J. Am. Chem. Soc.*, **97**, 1603, (1975).
59. R. G. R. Bacon, W. J. W. Hanna, D. J. Munro and D. Stewart, *Proc. Chem. Soc.*, 113 (1962).
60. W. D. Langley, *Org. Synth., Collect. Vol.*, **3**, 334 (1955).
61. E. J. Behrman, *Org. React.*, **35**, 421 (1988).
62. E. Boyland, P. Sims and D. C. Williams, *Biochem. J.*, **62**, 546 (1956).
63. E. J. Behrman, *J. Org. Chem.*, **57**, 2266 (1992).
64. G. Reissenweber and D. Mangold, *Angew. Chem.*, **92**, 196 (1980).
65. M. Anniyappan, D. Muralidharan and P. T. Perumal, *Tetrahedron*, **58**, 5069 (2002).
66. J. M. Anderson and J. K. Kochi, *J. Am. Chem. Soc.*, **92**, 1651 (1970).
67. N. Jacobsen, *Org. Synth., Collect. Vol.*, **6**, 890 (1988).
68. C. S. Pande and N. Jain, *Synth. Commun.*, **18**, 2123 (1988).
69. A. Citterio, A. Gentile, M. Serravalle, L. Tinucci and E. Vismara, *J. Chem. Res. (S)*, 272 (1982).
70. A. Citterio, F. Ferrario and S. De Bernardinis, *J. Chem. Res. (S)*, 310 (1983).
71. W. Buratti, G. P. Gardini, F. Minisci, F. Bertini, R. Galli and M. Perchinunno, *Tetrahedron*, **27**, 3655 (1971).
72. I. M. Kolthoff and I. K. Miller, *J. Am. Chem. Soc.*, **73**, 5118 (1951).
73. C. Srinivasan, P. Subramaniam and S. Radha, *Ind. J. Chem.*, **26(B)**, 193 (1987).
74. Z. I. Horii, K. Sakurai, K. Tomino and T. Konishi, *Yakugaku Zasshi*, **76**, 1101 (1956); *Chem. Abstr.*, **51**, 17222 (1957).
75. S. Yamazaki and Y. Yamazaki, *Chem. Lett.*, 571 (1990).
76. K. B. Wiberg, *J. Am. Chem. Soc.*, **81**, 252 (1959).
77. C. Giordano, A. Belli, A. Citterio and F. Minisci, *Tetrahedron*, **36**, 3559 (1980).
78. C. Hu and F. Qing, *J. Org. Chem.*, **56**, 6348 (1991).
79. M. Tiecco, L. Testaferri, M. Tingoli, D. Chianelli and D. Bartoli, *Tetrahedron Lett.*, **30**, 1417 (1989).
80. M. Tiecco, L. Testaferri, M. Tingoli, D. Chianelli and D. Bartoli, *Tetrahedron*, **44**, 2273 (1988).
81. M. Tiecco, L. Testaferri, M. Tingoli, D. Chianelli and D. Bartoli, *Tetrahedron*, **45**, 6819 (1989).
82. M. Sako, T. Hayashi, K. Hirota and Y. Maki, *Chem. Pharm. Bull.*, **40**, 1656 (1992).
83. M. Sako, S. Inagaki, Y. Esaka and D. Yoshihiro, *Tetrahedron Lett.*, **44**, 7303 (2003).
84. P. Manoj, R. Varghese, V. M. Manoj and C. T. Aravindakumar, *Chem. Lett.*, 74 (2002).
85. H. Irie, J. Maruyama, M. Shimada, Y. Zhyan, I. Kouno, K. Shimamoto and Y. Ohfune, *Synlett*, 421 (1990).
86. U. Wille, *Org. Lett.*, **2**, 3485 (2000).
87. F. M. Beringer and I. Lillien, *J. Am. Chem. Soc.*, **82**, 725 (1960).
88. F. P. Greenspan and H. M. Woodburn, *J. Am. Chem. Soc.*, **76**, 6345 (1954).

89. V. P. Kamat, R. N. Asolkar and J. K. Kirtany, *J. Chem. Res. (S)*, 41 (2001); V. Y. Sosnovskikh, D. V. Sevenard, B. I. Usachev and G. V. Roschenthaler, *Tetrahedron Lett.*, **44**, 2097 (2003).
90. H. Kobler, R. Munz, G. Al Gasser and G. Simchen, *Justus Liebigs Ann. Chem.*, 1937 (1978).
91. F. Effenberger and H. Kottmann, *Tetrahedron*, **41**, 4171 (1985).
92. J. C. Jung, H. C. Choi and Y. H. Kim, *Tetrahedron Lett.*, **34**, 3581 (1993).
93. Y. H. Kim, J. C. Jung and H. C. Choi, *Phosphorus, Sulfur and Silicon*, **95–96**, 431 (1994); Y. H. Kim, J. C. Jung, H. C. Choi and S. G. Yang, *Pure Appl. Chem.*, **71**, 4 (1999).
94. R. G. R. Bacon and J. R. Doggant, *J. Chem. Soc., Abstr.*, 1332 (1960); R. G. R. Bacon and D. J. Munro, *J. Chem. Soc., Abstr.*, 1339 (1960).
95. S. Yamazaki and Y. Yamazaki, *Chem. Lett.*, 1361 (1989).
96. J. C. Jung, H. C. Choi, S. G. Yang and Y. H. Kim, unpublished data.
97. J. C. Jung, H. C. Choi and Y. H. Kim, *Tetrahedron Lett.*, **34**, 3581 (1993).
98. H. C. Choi, K. I. Cho and Y. H. Kim, *Synlett*, 207 (1995).
99. J. C. Jung, H. C. Choi and Y. H. Kim, unpublished data.
100. C. H. Choi and Y. H. Kim, *Synth. Commun.*, **24**, 2307 (1994).
101. F. N. Chen, J. Yang, H. Zhang, C. Guan and J. Wan, *Synth. Commun.*, **25**, 3163 (1995).
102. F. N. Chen, A. Liu, Q. Yan, M. Liu, D. Zhang and L. Shas, *Synth. Commun.*, **29**, 1049 (1999).
103. F. E. Chen, Q. J. Yan, Z. Z. Peng, D. M. Zhang, H. Fu and J. D. Liu, *Chin. J. Org. Chem.*, **20**, 116 (2000).
104. S. G. Yang, D. H. Lee and Y. H. Kim, *Heteroatom Chem.*, **8**, 435 (1997).
105. F. E. Chen, Y. W. Lu, Y. P. He, Y. F. Luo and M. G. Yan, *Synth. Commun.*, **32**, 3487 (2002).
106. R. Badri, H. Shalhaf and M. A. Heidary, *Synth. Commun.*, **31**, 3473 (2001).
107. R. Badri and M. Soleymani, *Synth. Commun.*, **32**, 2385 (2002); **33**, 1325 (2003).
108. S. G. Yang and Y. H. Kim, *Tetrahedron Lett.*, **40**, 6051 (1999).
109. J. P. Hwang, S. G. Yang and Y. H. Kim, *J. Chem. Soc., Chem. Commun.*, 1355 (1997).
110. M. Y. Park, S. G. Yang and Y. H. Kim, unpublished data.
111. S. G. Yang and Y. H. Kim, unpublished data.
112. S. G. Yang, M. Y. Park and Y. H. Kim, *Synlett*, 492 (2002).
113. S. G. Yang, M. Y. Park and Y. H. Kim, *Tetrahedron Lett.*, **38**, 3009 (1997).
114. I. M. Baltork, A. R. Hajipour and R. Haddadi, *J. Chem. Res. (S)*, 102 (1999).
115. I. M. Baltork, A. R. Hajipour and M. Aghajari, *Synth. Commun.*, **32**, 1311 (2002).
116. R. J. Angelici, in *Synthesis and Technique in Inorganic Chemistry*, 2nd edn., Saunders, Philadelphia, 1977, p. 237.
117. H. Firouzabadi, P. Salehi, A. R. Sardarian and M. Seddighi, *Synth. Commun.*, **21**, 1121 (1991).
118. H. Firouzabadi, P. Salehi and I. M. Baltork, *Bull. Chem. Soc. Jpn.*, **65**, 2878 (1992).
119. G. E. Matsubayash and T. Doi, *Synth. Metals*, **33**, 99 (1989).
120. K. F. Martin and T. W. Hanks, *Organometallics*, **16**, 4857 (1997).
121. A. Baeyer and V. Villiger, *Ber.*, **32**, 3625 (1899); A. Baeyer and V. Villiger, *Ber.*, **33**, 1569 (1900).
122. A. A. D'Addieco and D. B. Lake, U.S. Patent, US 3041139 (1962); *Chem. Abstr.*, **57**, 61068 (1962); S. E. Stephanon, U.S. Patent, US 2802722 (1957); *Chem. Abstr.*, **51**, 102589 (1957).
123. W. Adam, R. Curci and J. O. Edwards, *Acc. Chem. Res.*, **22**, 205 (1989); R. W. Murray, *Chem. Rev.*, **89**, 1187 (1989).
124. J. O. Edwards, R. H. Pater, R. Curci and F. Di Furia, *Photochem. Photobiol.*, **30**, 63 (1979).
125. R. W. Murray and R. Jeyaraman, *J. Org. Chem.*, **50**, 2847 (1985).
126. R. J. Kennedy and A. M. Stock, *J. Org. Chem.*, **25**, 1901 (1960).
127. R. Bloch, J. Abecassis and D. Hassan, *J. Org. Chem.*, **50**, 1544 (1985).
128. P. F. Corey and F. E. Ward, *J. Org. Chem.*, **51**, 1925 (1986).
129. W. T. Ford and W. Zhu, *J. Org. Chem.*, **56**, 7022 (1991).
130. M. Curci Fiorentina, L. Troisi, J. O. Edwards and R. H. Pater, *J. Org. Chem.*, **45**, 4758 (1980).
131. W. Adam, L. Hadjiara Poglou and A. Smerz, *Chem. Ber.*, **124**, 227 (1991).
132. N. Hashimoto and A. Kanda, *Org. Process Res. Dev.*, **6**, 405 (2002).
133. G. Hanquet, X. Lusinchii and P. Millet, *Tetrahedron Lett.*, **29**, 3941 (1988); A. Armstrong, G. Ahmed, L. Garnett, K. Goacolou and J. S. Wailes, *Tetrahedron*, **55**, 2341 (1999).
134. S. E. Denmark and Z. Wu, *J. Org. Chem.*, **63**, 2810 (1998).
135. L. Bohe and M. Kammoun, *Tetrahedron Lett.*, **43**, 803 (2002).
136. B. Meunier, *New J. Chem.*, **16**, 203 (1992).

137. H. M. Ferraz, R. M. Muzzi, T. deO. Vieira and H. Viertler, *Tetrahedron Lett.*, **41**, 5021 (2000).
138. J. Legros, B. Crousse, D. B. Delpont and J. P. Begue, *Tetrahedron*, **58**, 3993 (2002).
139. R. Jeyaraman and R. W. Murray, *J. Am. Chem. Soc.*, **106**, 2462 (1984).
140. S. E. Denmark, Z. Wu, E. M. Crudden and H. Matsuhashi, *J. Org. Chem.*, **62**, 8288 (1997).
141. Z. X. Wang, Y. Tu, M. Frohn, J.-R. Zhang and Y. Shi, *J. Am. Chem. Soc.*, **119**, 11224 (1997).
142. O. Bortolini, G. Fantin, M. Fogagnolo, R. Forlani, S. Maietti and P. Pedrini, *J. Org. Chem.*, **67**, 5802 (2002).
143. X.-Y. Wu, X. She and Y. Shi, *J. Am. Chem. Soc.*, **124**, 8792 (2002).
144. D. Yang and G. S. Jiao, *Chem. Eur. J.*, **6**, 3517 (2000).
145. S. E. Desousa, P. O'Brien, C. D. Pilgram, D. Roder and T. D. Towers, *Tetrahedron Lett.*, **40**, 391 (1999).
146. S. Rani and V. D. Vankar, *Tetrahedron Lett.*, **44**, 907 (2003).
147. B. R. Travis and B. Borhan, *Tetrahedron Lett.*, **42**, 741 (2001).
148. B. R. Travis, R. S. Narayan and B. Borhan, *J. Am. Chem. Soc.*, **124**, 3824 (2002).
149. D. H. B. Ripin, W. Cai and S. J. Brenek, *Tetrahedron Lett.*, **41**, 5817 (2000).
150. G. Sabitha, R. S. Babu, M. S. K. Reddy and J. S. Yadav, *Synthesis*, 2254 (2002).
151. C. Bolm, A. S. Magnus and J. P. Hildebrand, *Org. Lett.*, **2**, 1173 (2000).
152. M. Hirano, M. Oose and T. Morimoto, *Bull. Chem. Soc. Jpn.*, **64**, 1046 (1991).
153. M. Hirano, M. Oose and T. Morimoto, *Chem Lett.*, 331 (1991).
154. S. W. Ashford and K. C. Grega, *J. Org. Chem.*, **66**, 1523 (2001).
155. V. M. Paradkar, T. B. Latham and D. M. Demko, *Synlett*, 1059 (1995).
156. B. R. Travis, M. Sivakumar, G. O. Hollist and B. Borhan, *Org. Lett.*, **5**, 1031 (2003).
157. T. L. Evans and M. M. Grade, *Synth. Commun.*, **16**, 1207 (1986).
158. P. Johnson and R. J. K. Taylor, *Tetrahedron Lett.*, **38**, 5873 (1997).
159. A. R. Hajipour, *Ind. J. Chem.*, **36B**, 1069 (1997).
160. A. R. Hajipour, *Iran. J. Sci. Technol.*, **22**, 205 (1998).
161. P. J. Kropp, G. W. Breton, J. D. Fields, J. C. Tung and B. R. Loomis, *J. Am. Chem. Soc.*, **122**, 4280 (2000).
162. M. Hirano, J. Tomaru and T. Morimoto, *Chem. Lett.*, 523 (1991).
163. M. Hirano, J. Tomaru and T. Morimoto, *Bull. Chem. Soc. Jpn.*, **64**, 3752 (1991).
164. R. P. Greenhalgh, *Synlett*, 235 (1992).
165. E. Petricci, M. Renzulli, M. Radi, F. Corelli and M. Botta, *Tetrahedron Lett.*, **43**, 9667 (2002).
166. R. Sato, E. Takeda, S. Nakajo, R. Kimura, S. Ogawa and Y. Kawai, *Heteroatom Chem.*, **12**, 209 (2001).
167. H. H. Wasserman and C. B. Vu, *Tetrahedron Lett.*, **31**, 5205 (1990).
168. L. A. Wozniak and W. J. Stec, *Tetrahedron Lett.*, **40**, 2637 (1999).
169. P. Ceccherelli, *J. Org. Chem.*, **60**, 8412 (1995).
170. K. S. Webb and D. Levy, *Tetrahedron Lett.*, **36**, 5117 (1995).
171. J. K. Crandall and T. Reix, *J. Org. Chem.*, **57**, 6759 (1992).
172. M. E. Brik, *Tetrahedron Lett.*, **36**, 5519 (1995).
173. A. R. Hajipour and S. G. Pyne, *J. Chem. Res. (S)*, 388 (1992).
174. B. Tamhankar, U. V. Desai, R. B. Mane, P. P. Wadgaonkar and A. V. Bedekar, *Synth. Commun.*, **31**, 2021 (2001).
175. E. H. Kim, B. S. Koo, C. E. Song and S. J. Lee, *Synth. Commun.*, **31**, 3627 (2001).
176. B. S. Koo, E. H. Kim and K. J. Lee, *Synth. Commun.*, **32**, 2275 (2002).
177. R. K. Dieter, L. E. Nice and S. E. Velu, *Tetrahedron Lett.*, **37**, 2377 (1996).
178. M. Curini, F. Epifano, M. C. Marcotullio and O. Rosati, *Tetrahedron Lett.*, **43**, 1201 (2002).
179. S. A. Ross and C. J. Burrows, *Tetrahedron Lett.*, **38**, 2805 (1997).
180. M. Curini, F. Epifano, M. C. Marcotullio, O. Rosati and M. Rossi, *Tetrahedron Lett.*, **55**, 6211 (1999).
181. D. S. Bose and P. Srinivas, *Synth. Commun.*, **27**, 3835 (1997).
182. A. R. Hajipour and N. Mahboubghah, *Org. Prep. Proced. Int.*, **31**, 112 (1999).
183. M. A. Bigdeli, M. M. A. Nikje and M. M. Heravi, *Phosphorus Sulfur Silicon Relat. Elem.*, **177**, 15 (2002).
184. Y. H. Kim, J. C. Jung and K. S. Kim, *Chem. Ind.*, 31 (1992); J. C. Jung, K. S. Kim and Y. H. Kim, *Synth. Commun.*, **22**, 1583 (1992).
185. D. S. Bose, G. Vanajatha and P. Srinivas, *Ind. J. Chem.*, **38B**, 835 (1999).

186. D. S. Bose, A. V. Narsaiah and V. Lakshminarayana, *Synth. Commun.*, **30**, 3121 (2000).
187. T. Ramalingam, B. V. S. Reddy, R. Srinivas and J. S. Yadav, *Synth. Commun.*, **30**, 4507 (2000).
188. M. Curini, F. Epifano, M. C. Marcotullio and O. Rosati, *Synlett*, 777 (1999).
189. B. F. Mirjalili, M. A. Zolfigol and A. Bamoniri, *Russ. J. Org. Chem.*, **38**, 761 (2002).
190. P. Ceccherelli, M. Curini, M. C. Marcotullio, F. Epifano and O. Rosati, *Synlett*, 767 (1996).
191. L. Mohammadpoor-Baltork, M. M. Sadeghi and K. Esmayilpour, *Phosphorus Sulfur Silicon Relat. Elem.*, **178**, 61 (2003).
192. R. Srinivas, B. V. SubbaReddy, J. S. Yadav and T. Ramalingam, *J. Chem. Res. (S)*, 376 (2000).
193. P. P. Kulkarni, A. J. Kadam, U. V. Desai, R. B. Mane and P. P. Wadgaonkar, *J. Chem. Res. (S)*, 184 (2000).
194. P. Ceccherelli, M. Curini, M. C. Marcotullio, F. Epifano and O. Rosati, *Synth. Commun.*, **28**, 3057 (1998).
195. G. Sabitha, M. Syamala and J. S. Yadav, *Org. Lett.*, **1**, 1701 (1999).
196. E. H. Appelman, L. J. Basile, H. Kim and J. R. Ferraro, *Spectrochim. Acta, Part A*, **41**, 1295 (1985); E. O. Schlemper, R. C. Thompson, C. K. Fair, F. K. Ross, E. H. Appelman and L. J. Basile, *Acta Crystallogr., Sect. C*, **40**, 1781 (1984); R. E. Connick, S. Y. Lee and R. Adamic, *Inorg. Chem.*, **32**, 565 (1993).
197. B. R. Travis, B. P. Ciaramitaro and B. Borhan, *Eur. J. Org. Chem.*, **3429** (2002).
198. E. V. Dehmlow, B. Vehre and J. K. Makrand, *Z. Naturforsch., Teil B*, **40**, 1583 (1985).
199. D. Mohajer and A. Rezaeifard, *Tetrahedron Lett.*, **43**, 1881 (2002).
200. P. Pietikainen, *Tetrahedron Lett.*, **40**, 1001 (1999).
201. P. Pietikainen, *Tetrahedron*, **56**, 417 (2000).
202. S. Campestrini and B. Meunier, *Inorg. Chem.*, **31**, 1999 (1992).
203. R. Kumarathasan and N. R. Hunter, *Org. Prep. Proced. Int.*, **23**, 651 (1991).
204. J. Wessel and R. H. Crabtree, *J. Mol. Catal. A, Chem.*, **113**, 13 (1996).
205. W. Nam, S. W. Jin, M. H. Lim, J. Y. Ryu and C. Kim, *Inorg. Chem.*, **41**, 3647 (2002).
206. R. Cosstick and J. S. Vyle, *Tetrahedron Lett.*, **30**, 4693 (1989).
207. S. Campestrini, F. Di Furia, P. Ghiotti, F. Novello and C. Travaglini, *J. Mol. Catal. A, Chem.*, **105**, 17 (1996).
208. S. Campestrini, F. Di Furia, G. Labat and F. Navello, *J. Chem. Soc., Perkin Trans. 2*, 2175 (1994).
209. A. R. Hajipour, S. E. Mallakpour, I. M. Baltork and H. Adibi, *Synth. Commun.*, **31**, 3401 (2001).
210. A. R. Hajipour, S. E. Mallakpour, I. M. Baltork and H. Adibi, *Synth. Commun.*, **31**, 1625 (2001).
211. A. R. Hajipour, S. E. Mallakpour, I. M. Baltork and H. Adibi, *Phosphorus Sulfur Silicon Relat. Elem.*, **165**, 155 (2000).
212. A. R. Hajipour and S. E. Mallakpour, *Phosphorus Sulfur Silicon Relat. Elem.*, **175**, 71 (2000).
213. A. R. Hajipour, S. E. Mallakpour and H. Adibi, *Chem. Lett.*, 460 (2000).
214. A. R. Hajipour, S. E. Mallakpour, I. Mohammadpoor-Baltork and H. Adibi, *Monatsh. Chem.*, **134**, 45 (2003).
215. A. R. Hajipour, S. E. Mallakpour, I. Mohammadpoor-Baltork and H. Adibi, *Phosphorus Sulfur Silicon Relat. Elem.*, **177**, 2805 (2002).
216. D. T. Sawyer and J. S. Valentine, *Acc. Chem. Res.*, **14**, 393 (1981).
217. J. S. Valentine and A. B. Curtis, *J. Am. Chem. Soc.*, **97**, 224 (1975).
218. T. Takata, Y. H. Kim and S. Oae, *Tetrahedron Lett.*, **20**, 821 (1979); S. Oae, T. Takata and Y. H. Kim, *Tetrahedron*, **37**, 37 (1981); S. Oae, T. Takata and Y. H. Kim, *Bull. Chem. Soc. Jpn.*, **54**, 2712 (1981).
219. Y. H. Kim, S. C. Lim and K. S. Kim, *Pure Appl. Chem.*, **65**, 661 (1993); Y. H. Kim, in *Modern Methodology in Organic Synthesis* (Ed. T. Shono), VCH, Cambridge and Kodansha, Kyoto, 1992, p. 303.
220. Y. H. Kim, G. H. Yon and H. J. Kim, *Chem. Lett.*, 309 (1984).
221. B. C. Chung and Y. H. Kim, *Bull. Korean Chem. Soc.*, **5**, 266 (1984).
222. Y. H. Kim and D. C. Yoon, *Tetrahedron Lett.*, **29**, 6453 (1988).
223. Y. H. Kim, S. C. Lim, M. Hoshino, Y. Ohtsuka and T. Ohishi, *Chem. Lett.*, 167 (1989).
224. M. R. Jones and D. J. Cram, *J. Am. Chem. Soc.*, **96**, 2183 (1974).

225. Y. H. Kim and D. C. Yoon, *Synth. Commun.*, **19**, 1569 (1989).
226. Y. H. Kim and B. C. Jung, *J. Org. Chem.*, **48**, 1562 (1983).
227. K. Ishikawa, H. C. Charles and G. W. Griffin, *Tetrahedron Lett.*, **18**, 427 (1977).
228. S. Krishnan, D. G. Kuhn and G. A. Hamilton, *J. Am. Chem. Soc.*, **99**, 8121 (1977); T. H. Kinstle and P. J. Ihrig, *J. Org. Chem.*, **35**, 257 (1970).
229. H. K. Lee, K. S. Kim, J. C. Kim and Y. H. Kim, *Chem. Lett.*, 561 (1988).
230. Y. Sawaki and Y. Ogata, *J. Org. Chem.*, **49**, 3344 (1984).
231. Y. Sawaki, S. Ishikawa and H. Lwamura, *J. Am. Chem. Soc.*, **109**, 584 (1987).
232. Y. H. Kim, H. K. Lee and H. S. Chang, *Tetrahedron Lett.*, **28**, 4285 (1987).
233. E. Spector and F. E. Shideman, *Biochem. Pharmacol.*, **2**, 182 (1959).
234. Y. H. Kim, B. C. Chung and H. S. Chang, *Tetrahedron Lett.*, 1079 (1985).
235. Y. H. Kim and G. H. Yon, *J. Chem. Soc., Chem. Commun.*, 715 (1983).
236. J. Bland, *J. Chem. Educ.*, **55**, 151 (1978).
237. Y. I. Kim and Y. H. Kim, *Tetrahedron Lett.*, **39**, 639 (1998).
238. Y. H. Kim, Y. I. Kim and J. Y. Kim, *J. Chem. Soc., Perkin Trans. 1*, 633 (1998).
239. G. A. Russell and R. C. Williamson, *J. Am. Chem. Soc.*, **86**, 2357 (1964).
240. M. H. Rogoff, *J. Bacteriol.*, **83**, 998 (1966).
241. Y. H. Kim and B. C. Jung, unpublished data.
242. H. K. Lee and Y. H. Kim, *Sulfur Lett.*, **7**, 1 (1987).
243. Y. H. Kim and H. K. Lee, *Chem. Lett.*, 1499 (1987).
244. R. Curci, F. Di Furia, R. Testi and G. Modena, *J. Chem. Soc., Perkin Trans. 2*, 752 (1974).
245. R. Curci, R. A. Goirine and G. Modena, *Tetrahedron*, **22**, 1235 (1966).
246. E. Boyland and D. Manson, *J. Chem. Soc.*, 4689 (1957).
247. E. W. Heiderich, U.S. Patent, US 2765216 (1956); *Chem. Abstr.*, **51**, 23352 (1957).
248. R. W. Murray and M. Kalan, *J. Am. Chem. Soc.*, **91**, 5358 (1969).
249. D. B. Denny, W. F. Goodyear and B. Goldstein, *J. Am. Chem. Soc.*, **82**, 1393, (1960).
250. R. L. Dannley, R. L. Waller, R. V. Hoffmann and R. F. Hudson, *J. Org. Chem.*, **37**, 418 (1972).
251. Y. H. Kim, S. C. Lim and H. C. Choi, unpublished data.
252. S. C. Lim and Y. H. Kim, *Heteroatom Chem.*, **1**, 261 (1990).
253. Y. Ogata, K. Tomizawa and T. Ikeda, *J. Org. Chem.*, **44**, 2362 (1979).
254. Y. Ogata, Y. Sawaki and T. Ohno, *J. Am. Chem. Soc.*, **104**, 216 (1982).
255. Y. Ogata, Y. Sawaki, K. Tomizawa and T. Ohno, *Tetrahedron*, **37**, 1485 (1981).
256. Y. Ogata, K. Tomizawa and T. Morikawa, *J. Org. Chem.*, **44**, 352 (1979).
257. Y. Ogata, K. Tomizawa and T. Ikeda, *J. Org. Chem.*, **43**, 2417 (1978).
258. P. J. Thomas and R. G. Pews, *Synth. Commun.*, **21**, 2335 (1991).
259. R. L. Dannley, R. L. Waller, R. V. Hoffmann and R. F. Hudson, *J. Chem. Soc., Chem. Commun.*, 1362 (1971).
260. A. Rieche, G. Hilgetag and G. Schramm, *Angew. Chem.*, **71**, 285 (1959).
261. A. Rieche, G. Hilgetag and G. Schramm, *Chem. Ber.*, **95**, 381 (1962); G. Sosnovsky and J. H. Brown, *Chem. Rev.*, **66**, 529 (1966).
262. G. Sosnovsky and E. H. Zaret, *J. Org. Chem.*, **34**, 968 (1969).
263. T. I. Yurzhenko and B. I. Kaspruk, *Zh. Obshch. Khim.*, **41**, 1644 (1971); *Chem. Abstr.*, **75**, 98637 (1971).
264. G. Sosnovsky and E. H. Zaret, *Z. Naturforsch., Teil B*, **33**, 732 (1975).
265. V. P. Maslennikov and V. P. Sergeeva, *Zh. Obshch. Khim.*, **40**, 2529 (1970); *Chem. Abstr.*, **74**, 125024 (1971).
266. V. P. Maslennikov, V. P. Sergeeva and N. G. Sukhikh, *Zh. Obshch. Khim.*, **40**, 2019 (1970); *Chem. Abstr.*, **74**, 140616 (1971); V. P. Maslennikov and V. P. Sergeeva, *Zh. Obshch. Khim.*, **40**, 1906 (1970); *Chem. Abstr.*, **74**, 125786 (1971).
267. P. A. Bernstein and D. D. Desmarreau, *J. Fluorine Chem.*, **2**, 315 (1973).
268. T. I. Yurzhenko and B. I. Kaspruk, *Dokl. Akad. Nauk SSSR*, **168**, 113 (1966); *Chem. Abstr.*, **65**, 38611 (1966).
269. G. Sosnovsky, E. H. Zaret and M. Konieczny, *J. Org. Chem.*, **37**, 2267 (1972).
270. K. D. Berlin and M. E. Perterson, *J. Org. Chem.*, **32**, 125 (1967).
271. G. Sosnovsky and G. Karas, *Z. Naturforsch., Teil B*, **33**, 1165 (1978); G. Sosnovsky and G. Karas, *Z. Naturforsch., Teil B*, **33**, 1177 (1978).
272. M. Von Itzstein and I. D. Jenkins, *J. Chem. Soc., Chem. Commun.*, 164 (1983).

273. S. Tsuji, M. Kondo, K. Ishiguro and Y. Sawaki, *J. Org. Chem.*, **58**, 5055 (1993).
274. T. Akasaka and W. Ando, *Phosphorous Sulfur Silicon Relat. Elem.*, **95–96**, 437 (1994);
K. Nahm, Y. Li, J. D. Evanseck, K. N. Houk and C. S. Foote, *J. Am. Chem. Soc.*, **115**, 4879 (1993).
275. M. Nakomoto and K.-Y. Akiba, *J. Am. Chem. Soc.*, **121**, 6958 (1999).
276. Y. H. Kim, S. C. Lim, M. Hoshino, Y. Ohtsuka and T. Ohishi, *Chem. Lett.*, 167 (1989).
277. Y. H. Kim, S. C. Lim and H. S. Chang, *J. Chem. Soc., Chem. Commun.*, 36 (1990).

CHAPTER 13

Transition metal peroxides. Synthesis and role in oxidation reactions*

VALERIA CONTE

*Dipartimento di Scienze e Tecnologie Chimiche, Università di Roma "Tor Vergata",
via della Ricerca Scientifica, I-00133 Roma, Italy
Fax: +39 067 259 4328; e-mail: valeria.conte@uniroma2.it*

and

OLGA BORTOLINI

*Dipartimento di Chimica, Università della Calabria, Via Bucci, cubo 12C, I-87036
Rende (CS), Italy
Fax: +39 098 449 3307; e-mail: o.bortolini@unical.it*

I. INTRODUCTION	1054
A. Abbreviations	1054
B. Historical Background	1055
II. LIMITATIONS AND SCOPE	1057
III. SYNTHESIS AND STRUCTURAL CHARACTERIZATION	1057
A. Synthesis of Peroxo Complexes	1057
B. Synthesis of μ -Peroxo Complexes	1059
C. Solid State Structures	1061
1. Peroxo complexes	1061
2. μ -Peroxo complexes	1064
D. Characterization in Solution	1068
IV. REACTIVITY	1072
A. Mechanistic Aspects	1072

*Dedicated, on the occasion of his 80th birthday, to our '*vitae ac studiorum magister in secunda et in adversa fortuna*' Emeritus Professor Giorgio Modena, Padova University, who showed us the way toward Chemistry.

The chemistry of peroxides, volume 2

Edited by Z. Rappoport © 2006 John Wiley & Sons, Ltd ISBN: 0-470-86274-2

1. Oxidation of electrophilic substrates	1072
2. Oxidation of nucleophilic substrates	1074
3. Radical oxidations	1076
B. Oxidation of Alkenes	1079
1. Unfunctionalized alkenes	1079
2. Electron-poor alkenes	1087
3. Allylic and homoallylic alcohols	1089
4. Cleavage	1094
C. Oxidation of Heteroatoms	1095
1. Sulfides	1095
2. Amines	1101
D. Oxidation of Alcohols	1105
E. Oxidation of Ketones	1108
F. Oxidation of Hydrocarbons	1114
V. CONCLUSIONS	1118
VI. ACKNOWLEDGMENTS	1118
VII. REFERENCES	1118

I. INTRODUCTION

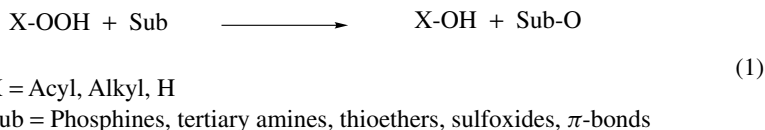
A. Abbreviations

acac	acetylacetonate anion
bbp ⁻	2,6-bis[bis(2-pyridylmethyl)aminomethyl]-4- <i>tert</i> -butylphenolate
DCE	dichloroethane
CHP	cumyl hydroperoxide
<i>m</i> -CPBA	<i>meta</i> -chloroperbenzoic acid
DET	diethyl tartrate
dmpz	3,5-dimethylpyrazole
dppe	ethane-1,2-diylbis(diphenylphosphine) or 1,2-bis(diphenylphosphino)ethane
dipic	pyridine-2,6-dicarboxylate
emim	<i>N</i> -ethyl- <i>N'</i> -methyl imidazolium
ESI	Electrospray Ionization
HB(Pz') ₃	hydrotris(3,5-diisopropylpyrazolyl)borate
HPCA	4-(3-heptyl)pyridine-2-carboxylic acid
Hpz	pyrazole
<i>N</i> -Et-hptb	<i>N,N,N',N'</i> -tetrakis[2'-(1'-ethylbenzimidazolyl)-1,3-diamino-2- hydroxypropane
MTO	methyltrioxorhenium
oxapymeH ₂	2-(bis-pyridin-2-ylmethylamino)- <i>N</i> -[2-(5-{2-[2-(<i>N</i> -methyl- <i>N</i> -pyridin-2- ylmethylamino)acetylamino]phenyl}-[1,3,4]oxadiazol-2- yl)phenyl]acetamide
Ph-bimp	2,6-bis[bis{2-(1-methyl-4,5-diphenylimidazolyl)methyl}aminomethyl]-4- methylphenolate
pic	picolinic acid
PICO	picolinate- <i>N</i> -oxido
POM	polyoxometallates
Py	pyridine
Q ⁺ X ⁻	lipophilic tetraalkylammonium salt
salen	salicylideneaminato ligand
TBHP	<i>t</i> -butyl hydroperoxide

TMSP	transition metal substituted polyoxometalate
TPA	tris(2-pyridylmethyl)amine
trispicMeen	<i>N</i> -methyl- <i>N,N',N'</i> -tris(2-pyridylmethyl)ethane-1,2-diamine
TS-1	titanium silicalite
UHP	urea-H ₂ O ₂ adduct

B. Historical Background

Functionalization of organic and inorganic substrates can be selectively achieved, generally in mild conditions with good to high yields by means of oxidation reactions with peroxides^{1,2}. In the early years of research in this field, organic peracids, hydrogen peroxide and alkyl hydroperoxides were used for performing the reactions indicated below³ (equation 1). From a practical point of view, however, only organic peracids were of synthetic interest because of their much higher reactivity in comparison with that of other peroxidic species (i.e. hydrogen peroxide or *t*-butyl hydroperoxide etc.)⁴.

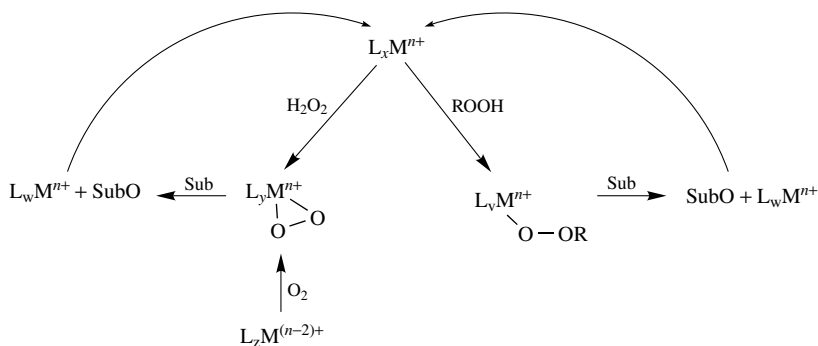


H₂O₂ and alkyl hydroperoxides are in fact quite weak oxidants, so in order to be synthetically attractive they need to be activated. The most used catalysts, excluding bases or Brønsted acids, are derivatives of some transition metal ions. Very active are metals included in the 4–7 groups, i.e. Ti, V, Cr, Mo, W and Re. Recognition of the catalytic activity of some of these metals in oxidation reactions with hydrogen peroxide, conducted by Milas and coworkers, dates back to the mid-'30s of the last century^{5–8}. Subsequently, it was also discovered^{9,10} that the same metals could be used in oxidation reactions with alkyl hydroperoxides. Interestingly, the observed reactivity often approached that of organic peracids.

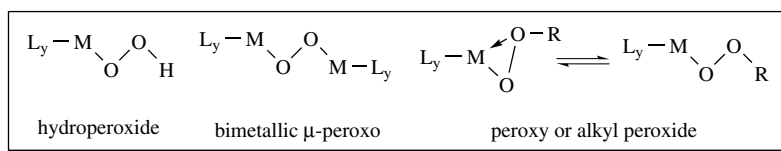
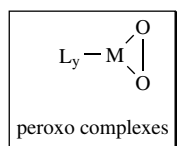
Indeed, several interesting procedures based on three families of active catalysts: organometallic complexes, phase-transfer compounds and titanium silicalite (TS-1), and peroxides have been settled and used also in industrial processes¹¹ in the last decades of the 20th century. The most impressive breakthrough in this field was achieved by Katsuki and Sharpless¹², who obtained the enantioselective oxidation of prochiral allylic alcohols with alkyl hydroperoxides catalyzed by titanium tetra-alkoxides in the presence of chiral nonracemic tartrates. In fact Sharpless was awarded the Nobel Prize in 2001.

The accepted mechanistic scheme for metal catalyzed oxidations with peroxides is sketched in Scheme 1. The features of the active oxidant depend on the nature of the oxygen donor and on its interaction with the metal precursor; in several examples high-valent peroxo metal species have been recognized as competent intermediates^{4,13,14}.

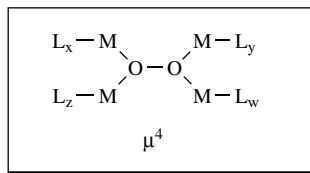
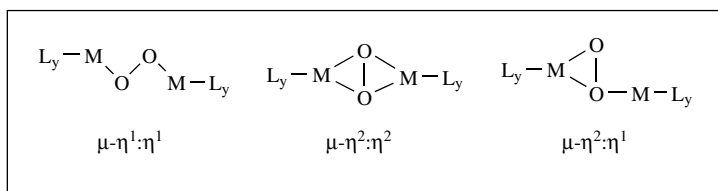
The reactivity of the peroxo metal complexes indicated in Scheme 1 is much higher than that of the peroxidic precursor, either H₂O₂ or ROOH. This fundamental feature is the direct link between the chemistry of metal catalyzed oxidations and that of peroxo metal complexes^{4,14,15}. These are in fact, in the majority of the systems, well defined species in solutions and in numerous cases they can be isolated and fully characterized⁴ also in the solid state. As far as the structure of the active complexes indicated in Scheme 1 is concerned, both in the solid state and/or in solution, several pieces of evidence indicate that most of them share a η^2 triangular arrangement of the peroxo moiety around the metal center (see below). In principle, all the μ -peroxo complexes structures, named following



SCHEME 1

 μ -peroxo complexes

SCHEME 2



SCHEME 3

the definition made by Vaska¹⁶ quite a long time ago, indicated in Scheme 2, are possible and have been found in numerous cases for different metals^{14,17}.

It should be noted that coordination to the metal center of more than one peroxidic moiety is also possible. Up to four O_2^{2-} groups have been observed, for example, with

Cr, Mo and W derivatives¹⁸. V(V) poly peroxy and polynuclear peroxy species have been characterized both in solution and in the solid state^{19,20}, while triperoxy-type vanadium compounds have been isolated and characterized as well²¹; their chemistry has been also accurately analyzed²².

An O_2^{2-} ligand can bind the two metals in bimetallic μ -peroxy complexes in a variety of coordination modes (Scheme 3). Also, tetranuclear μ -peroxy derivatives of the type indicated in Scheme 3 are known.

II. LIMITATIONS AND SCOPE

In the earlier volume of this book, the chapter dedicated to transition metal peroxides, written by Mimoun¹⁴, gave a detailed description of the features of the identified peroxy species and a survey of their reactivity toward hydrocarbons. Here we begin from the point where Mimoun ended, thus we shall analyze the achievements made in the field in the last 20 years. In the first part of our chapter we shall review the newest species identified and characterized; as an example we shall discuss in detail an important breakthrough, made more than ten years ago by Herrmann and coworkers²³ who identified mono- and di-peroxy derivatives of methyl-trioxorhenium. With this catalyst, as we shall see in detail later on in the chapter, several remarkable oxidative processes have been developed. Attention will be paid to peroxy and hydroperoxide derivatives, very uncommon species in 1982. Interesting aspects of the speciation of peroxy and peroxy complexes in solution, made with the aid of spectroscopic and spectrometric techniques, will be also considered. The mechanistic aspects of the metal catalyzed oxidations with peroxides will be only shortly reviewed, with particular attention to some achievements obtained mainly with theoretical calculations. Indeed, for quite a long time there was an active debate in the literature regarding the possible mechanisms operating in particular with nucleophilic substrates. This central theme has been already very well described and discussed, so interested readers are referred to published reviews and book chapters^{2, 4, 17, 24–26}.

Bio-related aspects of these peroxy metal complexes will not be considered due to space limitation. A thematic issue of Chemical Reviews contains the most relevant literature in this field²⁷.

The ample field of transition metal substituted polyoxometallates (POM), which are often other precursors for peroxy derivatives in catalytic processes, will be discussed in brief.

The second part of the chapter will be dedicated to the reactivity of transition metal peroxides, either isolated or formed in solution in catalytic processes, toward several classes of substrates. Hopefully this survey, where particular emphasis is placed on the selectivity aspects of these reactions, will present to the readers the potential of metal catalyzed oxidations with peroxides and highlight the perspective for researchers in the field.

The coverage of the relevant literature is up to the end of 2003, but it is beyond the scope of this chapter to present an exhaustive review of the very many and often important works that have appeared in the field since 1983.

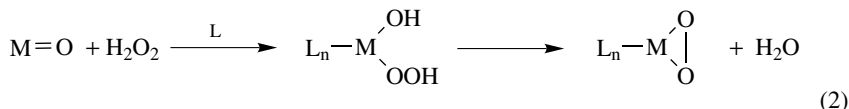
III. SYNTHESIS AND STRUCTURAL CHARACTERIZATION

A. Synthesis of Peroxo Complexes

Synthesis of peroxy metal complexes can be easily obtained by using hydrogen peroxide or dioxygen. Generally, the use of one of the two sources of the peroxidic moiety is determined by the nature of the metal involved.

When early transition metals are considered, the synthesis is essentially accomplished by dissolving the appropriate metal oxide in aqueous solutions of hydrogen peroxide.

The metal peroxy species is thus formed in solution and, in general, it can be isolated by adding to the reaction mixture a suitable ligand (equation 2). This procedure does not vary much with the metal or with the nature of the ligand and it is still based on the old method reported by Mimoun and coworkers^{28,29} about 30 years ago. The intermediate formation of a hydroperoxy species has been postulated and in some cases observed (see below).



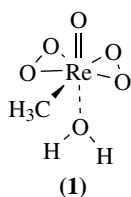
M = Ti(IV), Zr (IV), V(V), Nb(V), Ta(V), Cr(VI), Mo(VI), W(VI), U(VI), etc.

L = aromatic amines, picolinic acids, picolinate N-oxido anions, dicarboxylic acids, O and N containing polydentate ligands etc.

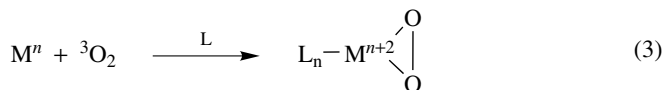
A collection of features for several peroxy species synthesized with this procedure can be found in two books that appeared about ten years ago^{4,26}. With reference to composition and structure of peroxy vanadium derivatives, a meticulous compilation appeared in a 1998 book²⁰. Several other metal peroxy species have been prepared until now and contain in the coordination sphere a plethora of ligands^{15,30-37}; references will be also indicated in the appropriate following paragraphs.

In specific examples, a preliminary coordination of the ligand to the metal is required before addition of the hydrogen peroxide solution. This is the case of cyclopentadienyl Nb, or Ti and Mo porphyrins derivatives²⁶, or for the dinuclear Ti(IV) peroxy citrate complexes³⁸.

One of the most important peroxy complexes synthesized after 1983 is the rhenium species formed from methyltrioxorhenium (MTO) precursor. The synthesis of this complex is achieved in the way indicated in equation 2, by reacting hydrogen peroxide with MTO³⁹. The isolated peroxy complex **1** contains in the coordination sphere two η^2 -peroxide bridges, a direct metal carbon bond and a molecule of water. The crystal structure of the peroxy rhenium derivative, however, was obtained by substitution of the water molecule with other ligands^{39,40}; more details on this aspect are enclosed in the structural characterization paragraph.

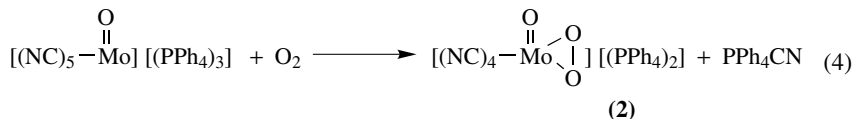


When late transition metals are used, interaction of dioxygen with low-valent precursors to form high-valent peroxy complexes (equation 3) is the key synthetic step¹⁴.



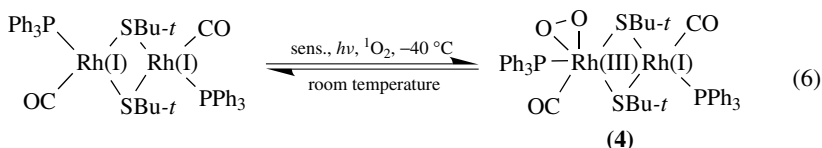
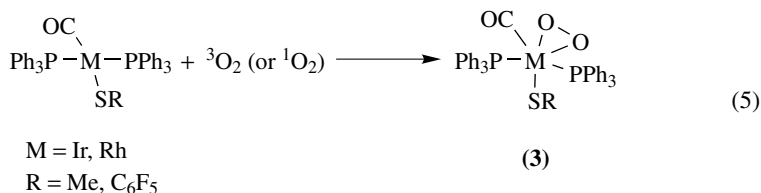
Mimoun has already pointed out clearly that dioxygen carriers, even when reversibly formed, are not different from peroxy complexes prepared from hydrogen peroxide. As a

matter of fact, with some metals, the same peroxy complex may be synthesized, by means of both O_2^{2-} sources¹⁴. In 1988 Arzoumanian and coworkers⁴¹ reported that the cyano oxo monoperoxy molybdenum(VI) compound **2** may be obtained from the corresponding Mo(IV) derivative by dioxygen oxidation (equation 4); the crystal structure of the complex was also solved.



Similarly, peroxy Rh(III) and ethene-peroxy Ir(III) have been prepared by reaction of dioxygen and reduced metal precursor⁴².

Ir(III) and Rh(III) peroxy complexes, species **3**, may be obtained by reaction of 3O_2 or 1O_2 with Ir(I) and Rh(I) thiolato complexes⁴³ (equation 5). An analogous reaction was observed also with a dimeric Rh(I) species and singlet oxygen that produces **4**⁴³ (equation 6).



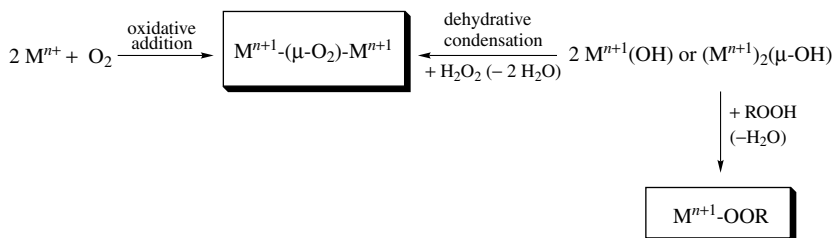
B. Synthesis of μ -Peroxo Complexes

μ -Peroxo complexes are less common than their peroxy analogues and show the different structures indicated in Scheme 2. As far as their synthesis is concerned, few methods are available^{14,26}. Hydroperoxides may be prepared by reaction of H_2O_2 with hydroxo complexes as is the case of Pt species. For Co, Rh, Ir and Pt hydroperoxide complexes, insertion of dioxygen into a metal hydride bond is a viable synthetic procedure as well. Protonation of a preformed metal dioxygen species is also possible for Pd and Pt derivatives.

In the last decade several reports have appeared concerning the preparation of hydroperoxy iron derivatives, which can be in equilibrium with their μ^2-O_2 counterpart⁴⁴⁻⁵⁰. The general synthetic method for in situ preparation of these species is again the addition of a large excess of hydrogen peroxide to a suitable precursor.

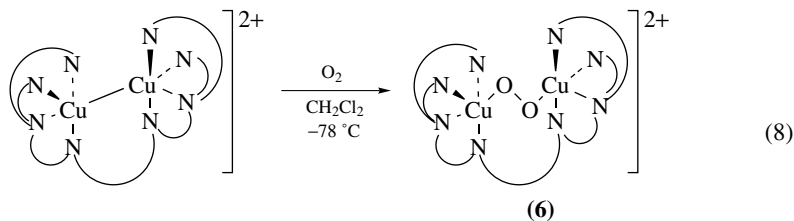
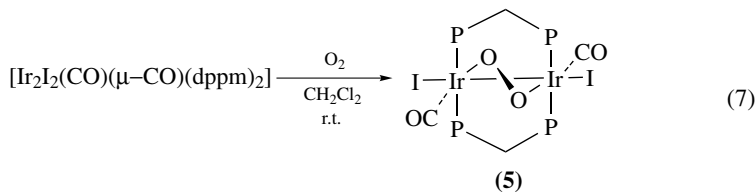
Synthesis of bimetallic μ -peroxy complexes has been described by Mimoun¹⁴. In particular, for Co species reaction between a superoxo complex with a reduced metal is a feasible method, for Pt species acid catalyzed hydrolysis of peroxy complex may be used and for Rh or Pd the protocol implies reaction of potassium superoxide with appropriate precursors.

Akita and coworkers^{51,52} established a *dehydrative condensation* procedure, starting from hydroxo metal precursors containing the hydrotris(3,5-diisopropylpyrazolyl) borato ligand, and they were able to obtain dinuclear (μ -peroxo)Pd complexes, as indicated in Scheme 4. With the same procedure peroxo and hydroperoxo species (for Pd and Rh) and alkyl peroxides (for Mn, Co, Ni and Pd) complexes may be obtained.



SCHEME 4

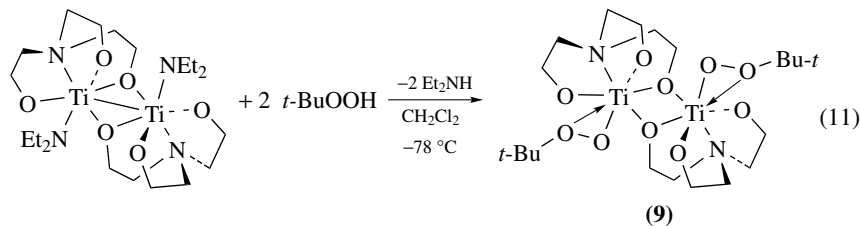
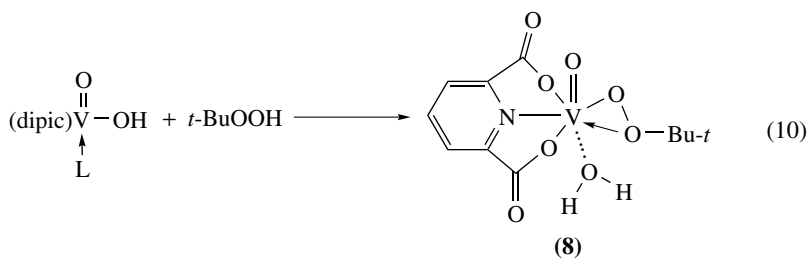
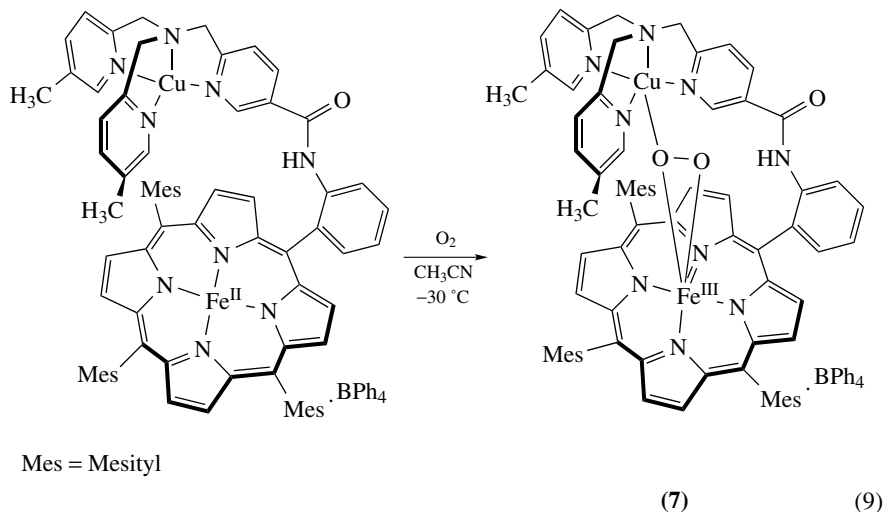
Several other peroxo bridged complexes have been lately synthesized^{53,54} simply by reacting appropriate precursors and dioxygen, as shown in equation 7 for di-Ir(II) complex **5**, with bis(diphenylphosphinomethane) dppm, and in equation 8 for a dicopper(II) species **6**. The same procedure has been also applied to obtain a peroxo bridged μ - η^2 : η^1 heme-copper complex **7**⁵⁵ (equation 9).



ligand = 2,7-bis[bis(2-pyridylmethyl)aminomethyl]-1,8-naphthyridine

The intermediate formation of alkyl peroxide complexes has been postulated, and in several cases observed with spectroscopic and spectrometric techniques in several selective procedures based on metal catalyzed oxidation with hydroperoxides, Ti and V ions being among the transition metals most widely used for this purpose. However, to date the few examples of alkyl peroxide complexes isolated and characterized in the solid state refer to a dimeric VO(OOBu-*t*)(H₂O) **8**, synthesized by Mimoun and coworkers⁵⁶ in 1983, and to a dimeric Ti complex [(η^2 -OOBu-*t*)(titanatrane)₂(CH₂Cl₂)₃] **9**, synthesized by Boche and coworkers⁵⁷.

Complex **8** is obtained by anion exchange between V(V) dipicolinato oxo hydroxo complex and *t*-butyl hydroperoxide^{56,58} (equation 10).



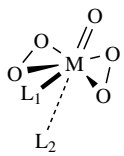
Synthesis of complex **9** is obtained by reacting the diethylamino-titanatrane precursor with the peroxide in CH_2Cl_2 at low temperature⁵⁷ (equation 11).

C. Solid State Structures

1. Peroxo complexes

The η^2 -peroxo complexes are the most common metal peroxides, particularly when mono- and di-peroxo complexes are considered. They have been prepared and characterized

TABLE 1. Structural and selected spectroscopic features for diperoxo metal complexes

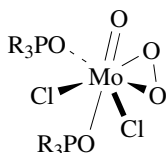
	Bond type	Distances (Å)	ν (cm^{-1})	δ ^{17}O -NMR (ppm)
M=O	1.6–1.7	930–1000	650–1350 ^a	
M–O	1.8–2.2	500–650		
O–O	1.35–1.55	800–950	350–800 ^a	
M–L ₁	1.9–2.2			
M–L ₂	2.2–2.6			

^a Depending on the metal; higher field resonances are observed for Re, W and Mo derivatives.

also at crystallographic level from a large number of transition metals, as has been well summarized by Mimoun¹⁴ and by other authors^{4, 18, 26, 59–61}.

The bipyramidal pentagonal structure is the most frequently found for early transition metals. However, the seventh position, usually the one *trans* to the oxo ligand, is looser as compared with the sixth one. In Table 1 some selected structural and spectroscopic features for diperoxo complexes are collected; more detailed information can be found in the appropriate literature^{4, 14, 15}.

$\text{MoOCl}_2(\text{O}_2)(\text{OPR}_3)_2$, **10**, one of the few examples of mono-peroxo molybdenum derivatives, has been isolated and characterized in the solid state⁶². These derivatives are fairly unstable and the crystal structures obtained derive from a mixture with their reduction products $\text{MoO}_2(\text{Cl}_2)(\text{OPR}_3)_2$.

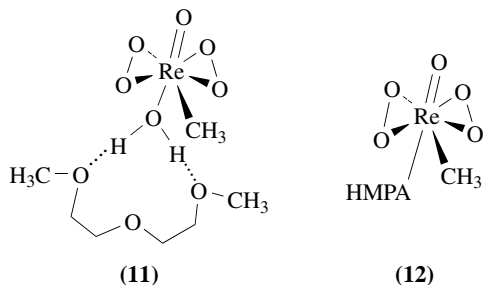


(10)

As anticipated beforehand, bis(η^2 -peroxo)-rhenium complexes have been characterized in the solid state^{39, 40}. The noticeable feature is that the active catalyst $(\text{CH}_3)\text{ReO}(\text{O}_2)_2\text{H}_2\text{O}$ (**1**) does not crystallize as it is, but a modification of the seventh apical ligand is required, as indicated in compounds **11** and **12**. The molecular structure of these peroxo rhenium complexes is yet again a pentagonal bipyramid, and the bond lengths are in the expected range.

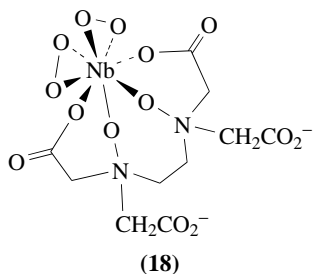
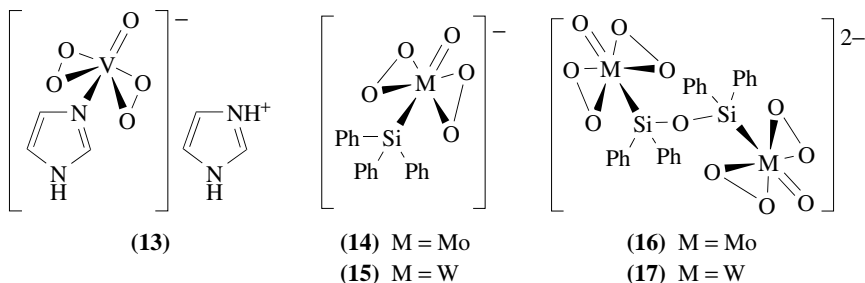
Also, Ir(III) and Rh(III) ethene-peroxo complexes belong to the family of species with the bipyramidal pentagonal structure⁴².

In some instances a pentagonal pyramidal geometry has been detected, even though on these occasions the oxo ligand of another molecule may act as seventh ligand as a long axial bond⁵⁹. In the case of vanadium, the bisperoxovanadium imidazole monoanion **13** was synthesized by Crans and coworkers⁶³.



The solid state structure of **13** is very similar to that reported for $[\text{NH}_4^+][\text{VO}(\text{O}_2)_2\text{NH}_3^-]^{59}$ and for $\text{CrO}(\text{O}_2)_2\text{Py}^{18}$.

The distorted pentagonal–pyramidal coordination has been identified also in Mo and W oxo diperoxo siloxane complexes⁶⁴ (**14**–**17**). Crystal structures for species **14**, **15** and **16** have been solved, while for the tungsten dinuclear compound, structural identification was suggested on the basis of similar IR and Raman spectra obtained for complexes **16** and **17**⁶⁴.

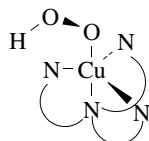
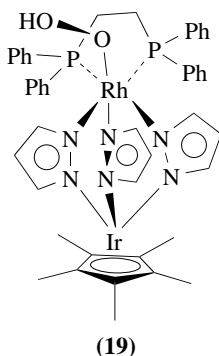


Diperoxo Nb(V) complexes have been synthesized and, in some cases, structurally characterized in the presence of oxidized polyaminocarboxylato ligands⁶⁵. With this metal, the distorted dodecahedral geometry is common for the few species known^{14,65}; **18** is an example.

The synthesis of peroxy Nb species may be obtained with the general method indicated in equation 2, and also by replacing peroxy groups with polyaminocarboxylato ligands from a tetraperoxoniobate anion.

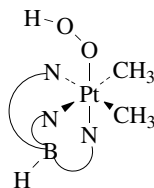
2. μ -Peroxo complexes

Solid state structures for transition metal hydroperoxo complexes are very few. Apart from two old examples concerning Co⁶⁶ and Mo⁶⁷, a rhodium derivative⁶⁸ $[(\eta^5\text{-C}_5\text{Me}_5)\text{Ir}(\mu\text{-pz})_3\text{Rh}(\text{OOH})(\text{dppe})^+][\text{BF}_4^-]$ **19** (Hpz = pyrazole and dppe = 1,2-bis(diphenylphosphino)ethane) with Rh atom in slightly distorted octahedral coordination, a Cu(II) complex⁶⁹ with tripodal pyridylamine ligands having the metal with an axially compressed trigonal bipyramid geometry, **20**, an octahedral Pt(IV) species⁷⁰, **21**, $\text{Tp}^{\text{Me}_2}\text{PtMe}_2(\text{OOH})$ (Tp^{Me_2} = hydrottris(3,5-dimethylpyrazolyl)borate) and a macrocyclic containing octahedral Co(III) hydroperoxo derivative⁷¹ $[(\text{L}^2(\text{CH}_3\text{CN})\text{CoOOH})^+][\text{ClO}_4^-]$ (L^2 = *meso*-5,7,7,12,12,14,14-Me₆-[14]aneN₄), **22**, are known.



N N ligand = bis(6-pivalamide-2-pyridylmethyl)-(2-pyridylmethyl)amine

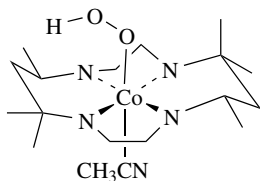
(20)



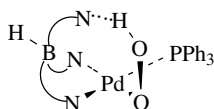
B N ligand = hydrottris(3,5-dimethylpyrazolyl)borate

(21)

Square-planar Pd (**23**) and octahedral Rh (**24**) hydroperoxide complexes containing hydrottris(3,5-diisopropylpyrazolyl)borate ligand^{51,52} have been prepared as well and characterized in the solid state. Strong hydrogen-bond interaction between -OOH moiety and ligands has been detected in these complexes.

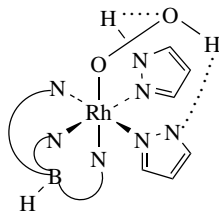
ligand = *meso*-5,7,7,12,12,14,14-Me₆-[14]aneN₄

(22)



B N ligand = hydrotris(3,5-diisopropylpyrazolyl)borate

(23)

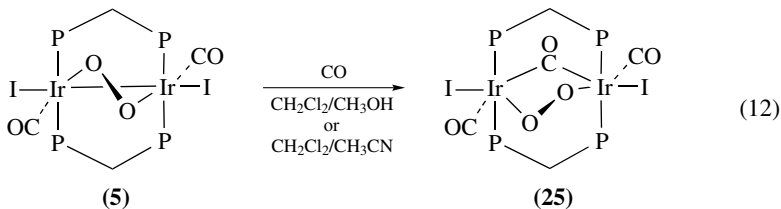


N N ligand = hydrotris(3,5-diisopropylpyrazolyl)borate

(24)

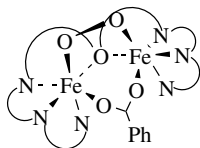
Solid state structures for bimetallic μ -peroxo complexes have been obtained for all the coordination modes of O_2^{2-} moiety indicated in Scheme 3. Several examples can be found in a special issue of Chemical Reviews¹⁵.

The case of the iridium derivative **5**, reported in equation 7, is typical of the μ - $\eta^1:\eta^1$ coordination mode, even though in this specific complex a metal-metal bond is also present⁵³. The two metals have an octahedral arrangement and the bond lengths for the peroxidic moiety are all in the expected range. This di-iridium complex also reacts with CO giving rise to the formation of a new complex, **25**, whose structure was solved, showing the $(\mu$ - $\eta^1:\eta^1$ -O₂) group intact together with a $(\mu$ -CO) ligand⁵³ (equation 12).



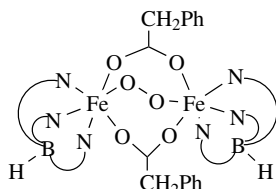
Subsequently, nice examples of di-iron (μ - $\eta^1:\eta^1$ -peroxo) derivatives were published by Suzuki and coworkers⁷², **26** $[Fe_2(\mu-O_2)(Ph-bimp)(\mu-PhCO_2)]^{2+}$, with a hindered bis-

tetradentate ligand; by Kim and Lippard⁷³, **27** $[\text{Fe}_2(\mu\text{-O}_2)(\mu\text{-O}_2\text{CCH}_2\text{Ph})_2\{\text{HB}(\text{Pz}')_3\}_2]$; and by Que and coworkers⁷⁴, **28** $[\text{Fe}_2(\mu\text{-O}_2)(\text{N-Et-hptb})(\text{Ph}_3\text{PO})_2]^{3+}$. All those complexes, used as models for some important classes of enzymes like methane monooxygenases and hemerythrin, have the iron centers in a distorted octahedral arrangement.



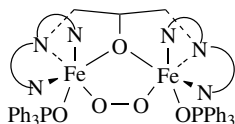
N N ligand = Ph-bimp = 2.6-bis[bis{2-(1-methyl-4,5-diphenyl-imidazolyl)-methyl}aminomethyl]-4-methylphenolate

(26)



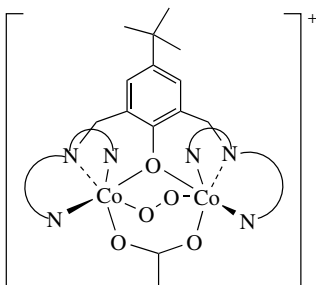
N N ligand = $\text{HB}(\text{Pz}')_3$ = hydrotris(3,5-diisopropylpyrazolyl)borate

(27)



N N ligand = N-Et-hptb = *N,N,N',N'*-tetrakis 2'-(1'-ethylbenzimidazolyl)-1,3-diamino-2-hydroxypropane

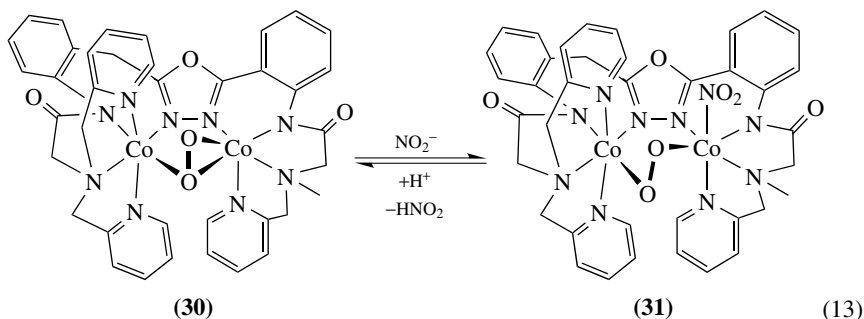
(28)



N N ligand = bpbp⁻ = 2,6-bis[bis(2-pyridylmethyl)aminomethyl]-4-*tert*-butylphenolate

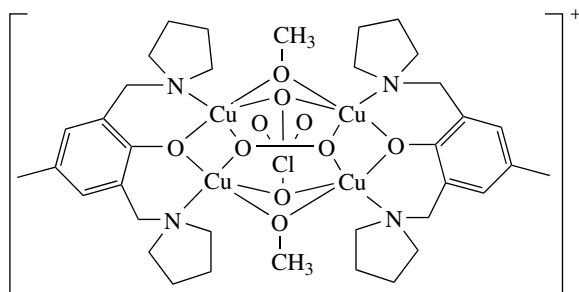
(29)

Dicobalt μ -peroxo complexes have been synthesized: di-Co(III) species, $[\text{Co}_2(\text{bpmp})(\mu\text{-O}_2)(\mu\text{-CH}_3\text{CO}_2)](\text{ClO}_4)$ **29**, was reported by Kofod and coworkers⁷⁵. Di-Co(II) complex, **31** $[\text{Co}_2(\mu\text{-O}_2)(\text{oxapyme}(\text{NO}_2))^+]$, has been prepared starting from the corresponding $[\text{Co}_2(\mu\text{-}\eta^1:\eta^2\text{-O}_2)(\text{oxapyme})]^+$ species **30**, as indicated in equation 13⁷⁶. Both species were characterized in the solid state and interesting aspects of transformation of dioxygen ligand in bimetallic species were therefore explored.



Another interesting example of $(\mu\text{-}\eta^1:\eta^2\text{-O}_2)$ -complex is the heme-copper derivative **755** (equation 9).

The μ^4 -coordination mode of dioxygen is very unusual, as is pointed out by Krebs and coworkers⁷⁷ who in 1998 synthesized the μ^4 -peroxocopper(II) complex, **32**, $[\text{Cu}_4(\text{L}^1)_2(\text{O}_2)(\text{OMe})_2(\text{ClO}_4)]\text{ClO}_4$.



ligand = $\text{L}^1 = 2,6\text{-bis}(\text{pyrrolidinomethyl})\text{-4-methylphenol}$

(32)

Previous examples of this particular type of coordination mode adopted by dioxygen in polynuclear species refer to molybdenum⁷⁸, $\text{K}_4[\text{Mo}_4\text{O}_{12}(\text{O}_2)_2]$, iron^{79,80}: $[\text{Fe}_6(\text{O})_2(\text{O}_2)(\text{O}_2\text{CPh})_{12}(\text{OH}_2)_2]$ and $[\text{Fe}_6(\text{O})_2(\text{O}_2)_3(\text{OAc})_9]^-$, and antimony⁸¹, $[(o\text{-Tol}_2\text{-SbO})_4(\text{O}_2)_2]$, derivatives.

In 1983, Mimoun and coworkers published the first crystal structure of an alkylperoxidic vanadium derivative⁵⁶, $(\text{dipic})\text{VO}(\text{OOBu-}t)(\text{H}_2\text{O})$, **8**, which contains 2,6-dipicolinic acid in the coordination sphere of the metal. This species, together with the Boche⁵⁷ complex $[\text{((}\eta^2\text{-OOBu-}t)\text{titanatrane})_2(\text{CH}_2\text{Cl}_2)_3]$, **9**, are actually, to the best of our knowledge, the only examples of alkylperoxidic species characterized in the solid state. Both species share the $(\eta^2\text{-OOBu-}t)$ group with bond lengths between the metal and the two peroxidic oxygens in the range typical of peroxo derivative (see Table 1), clear evidence of the

η^2 coordination mode. The length of the peroxidic bond is also in the normal range expected for peroxy derivatives (1.436 Å for the vanadium complex and 1.469 Å for the titanium species).

These species, and in particular the Ti derivative, have a fundamental significance, being related to the Sharpless epoxidation reaction¹². In fact, despite the many attempts made in order to isolate and characterize the titanium tartrate peroxide derivative involved in that enantioselective process, only indirect evidence in solution and theoretical calculation clues have been obtained so far^{82,83}.

D. Characterization in Solution

In the previous sections it has been shown that for a large variety of peroxy metal complexes only few types of solid state structures come across. Moreover, the structural motifs (bond lengths, bond angles etc.) are very similar also for very diverse species and only poor relationships with reactivity have been recognized^{4,14,84}.

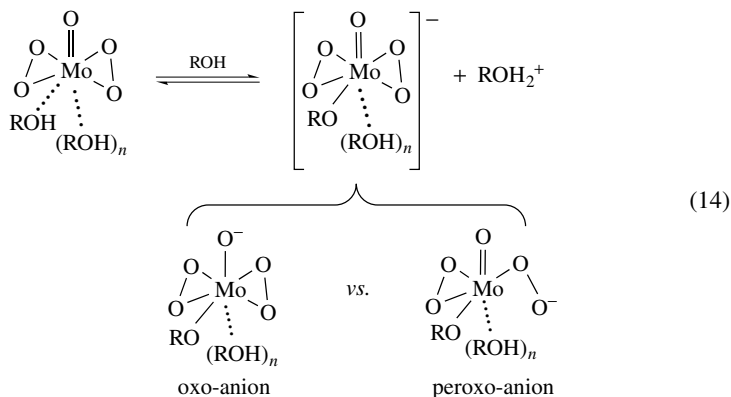
In fact, as we shall see in more detail later in the chapter, peroxy metal complexes are very versatile oxidants capable of reacting with a variety of substrates through different reaction mechanisms, either polar or radical^{4,14,26,85}. Thus, it would be of great help to be able to predict the reactivity of a given peroxy metal complex on the basis of a measurable property⁸⁶. This becomes an even more difficult task when it is considered that the reactivity is related to the structure in solution and a metal peroxy species not necessarily retains in solution its solid state structure. In this context, physico-chemical studies aimed at clarifying the structures of these complexes in solution are fundamental, and in the last decades several papers have appeared and in some cases correlations with reactivity have been established; two examples may be noteworthy^{87,88}. The first one⁸⁷ refers to a correlation found between the ability of peroxy metal complexes to act as one-electron acceptors, measured by cyclic voltammetry, and their O—O bond strength, measured by IR spectroscopy. Different metals with different ligands have been compared and it has been recognized that the nature of the ligand plays a more important role than the nature of the metal in determining the one electron acceptor ability of the peroxy derivative.

The second correlation⁸⁸ shows that peroxy complexes with λ_{\max} values below 400 nm, stretching frequencies below 900 cm^{-1} and ¹⁷O-NMR chemical shifts for peroxy moiety below 600 ppm are more efficient oxidants of nucleophilic substrates.

d^0 metal peroxy complexes usually behave as fairly strong protic acids: two quite old papers report this aspect in detail for vanadium derivatives^{89,90}. This behavior obviously has a major influence on their reactivity. This particular issue has been extensively treated⁴ and will be not repeated here, however a facet appears to be worthy of note. As an example, the acid–base equilibria for molybdenum diperoxy derivatives in alcoholic media may be indicated as in equation 14. The anionic species formed may have the charge localized either on the oxo-oxygen or on one peroxy-oxygen, thus forming a peroxy-anion. Potentiometric titration⁹¹, spectroscopic data⁹² and absence of reactivity toward electrophilic substrates strongly suggest that the anionic charge is localized on the oxo-oxygen.

Several pieces of evidence show that a desired kind of reactivity/selectivity for peroxy metal complexes can be obtained by careful design of the coordination sphere; however, equilibria involving the ligands and solvent molecules must be taken into consideration. This point is essential when asymmetric oxidations are considered. Ti(IV) and V(V) catalyzed enantioselective oxidations with hydrogen peroxide or alkyl hydroperoxide are representative examples of this situation, and have been already carefully described⁴.

Interestingly, solution studies on the nature of the active catalyst, carried out in the case of Ti(IV)-tartrate catalysts proposed by Katsuki and Sharpless for the enantioselective oxidation of allylic alcohols¹², opened routes to enantioselective oxidations of thioethers^{93–98}.



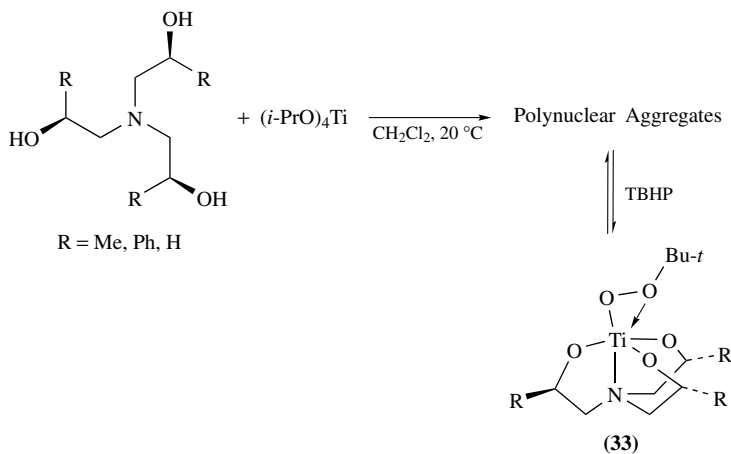
Over the past decades several techniques have been used to obtain direct experimental information on the speciation of peroxo metal complexes: heteronuclear NMR, IR and Raman spectroscopy, potentiometry and electrospray ionization mass spectrometry (ESI-MS). Often, more than one technique was used at the same time for acquiring complementary evidence. A significant, although nonexhaustive, list of examples related to several metals is given in Table 2. They include cases with hydrogen peroxide or alkyl

TABLE 2. Techniques used in the speciation of selected peroxo metal derivatives in solution

Metal	Techniques	Reference
Ti	¹ H-NMR, ESI-MS	99, 100
V	⁵¹ V-NMR, Raman	101
	⁵¹ V-NMR	102–104
	⁵¹ V-NMR, potentiometry	105, 106
	EPR, IR, UV-Vis	107
	⁵¹ V-NMR, ESI-MS	22, 108–111
Nb	Raman	101
	¹ H-, ¹³ C-, ¹⁵ N- NMR, IR	65
Ta	Raman	101
Mo	³¹ P-NMR, IR, Raman	112
	⁹⁵ Mo-, ¹⁷ O-, ¹ H-NMR, EPR	113
	⁹⁵ Mo-, ¹⁷ O-, ¹ H-NMR,	114
	¹ H-NMR, ¹³ C CPMAS	115
	¹⁷ O-NMR, potentiometry, ESI-MS,	116
W	³¹ P-NMR, IR, Raman	112
	³¹ P-, ¹⁸³ W-NMR, IR, Raman	117
	¹⁷ O-NMR, potentiometry, ESI-MS,	116
Fe	UV-Vis, ESI-MS	44, 46
	¹ H-NMR, UV-Vis, ESI-MS	45
	UV-Vis, EPR, ESI-MS	47
	Raman	48
	ESI-MS	118
	EPR, Mössbauer	49
	Raman, EPR, Mössbauer, EXAFS	50
Cu	UV-Vis, Raman, EXAFS	54
	UV-Vis, EPR, IR	119

hydroperoxides, lack or occurrence of ligands and also heteropolyperoxo derivatives. From the systems quoted in Table 2, three examples are, in our opinion, worthy of more detailed description.

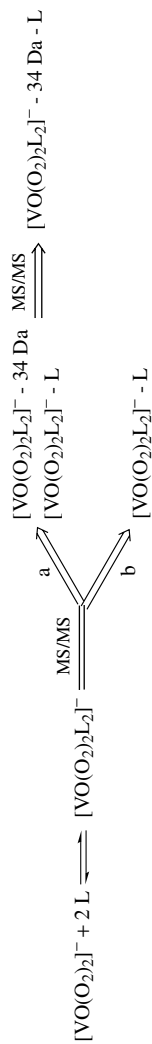
The first example refers to the Ti-trialkanolamine catalyst for enantioselective sulfoxidation reaction^{99,100}. In this system, the catalyst precursor is formed in situ by interaction of titanium(IV) isopropoxide and enantiopure trialkanolamine ligands. Such tetradentate ligand binds the metal, forming a robust titanatrane core, which maintains its structure also in hydroxylic solvents or in the presence of acid. Depending on the relative concentration of metal and ligand, several polynuclear aggregates may be formed in solution. By subsequent addition of *t*-butyl hydroperoxide, all the precatalysts are converted into the mononuclear active species, as indicated in Scheme 5. The nature of the active species **33** was elucidated by joining ESI-MS and conventional low-temperature NMR techniques.



SCHEME 5

In the case of vanadium peroxo derivatives, the combined use of ^{51}V -NMR with ESI-MS, with the further support of *ab initio* calculations, has been proved to be a powerful tool for obtaining direct information about the structure and the chemistry of peroxo vanadates in solutions^{22, 108–111}.

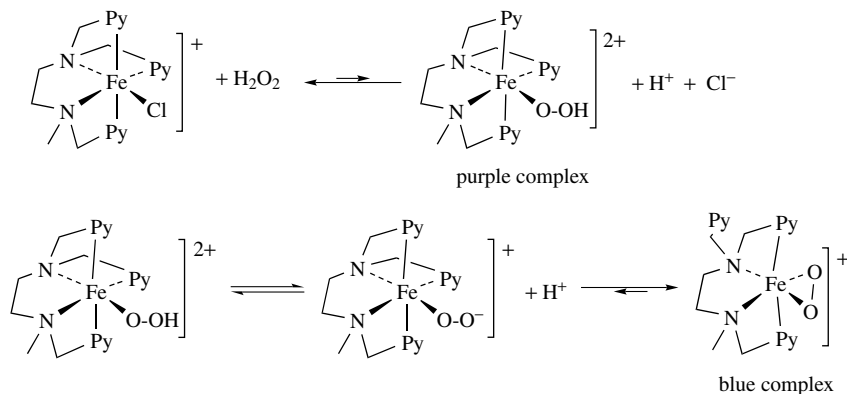
Bisperoxo vanadates have been analyzed with the above-cited methodology in aqueous alcoholic solutions in the presence of a number of histidine and histidine-like ligands¹⁰⁹. Coordination of one or two ligands to the metal center has been observed. Characterization of the two species $[\text{VO}(\text{O}_2)_2\text{L}]^-$ and $[\text{VO}(\text{O}_2)_2\text{L}_2]^-$ was obtained. In particular, with MS/MS (tandem) experiments, specific fragmentation of the peroxidic moiety were distinguished as a function of the nature and the number of the ligands (Scheme 6). The approach used allowed one, *inter alia*, to obtain further evidence on the occurrence of the protonation of the peroxidic moiety as a crucial step in the activation of vanadium peroxo compounds; this is a step with biochemical implication in the reactivity of vanadium haloperoxidase enzymes¹²⁰. Several non-heme hydroperoxo iron(III) complexes have been prepared to model the reactivity of activated Bleomycin or heme-oxygenases. Formation of η^2 -peroxo iron intermediates has been observed in some cytochrome P450 mutants. In this respect, switch between hydroperoxo and η^2 -peroxo iron complexes is an important mechanism that has been studied with a variety of techniques (Table 2). One example refers to the combination of UV-Vis, EPR and ESI-MS experiments⁴⁷ to



a: Decomposition pattern in the presence of ImiCO₂H, ImiCH₂CO₂H, His, HisNHZ, HisGly, HisSer, GlyHis
 b: Decomposition pattern in the presence of HisCO₂Me, HisCO₂Me(HCl)

SCHEME 6

elucidate the equilibria depicted in Scheme 7 for an iron derivative containing as pentadentate ligand trispicMeen, *N*-methyl-*N,N',N'*-tris(2-pyridylmethyl)ethane-1,2-diamine. The colored species were detected by UV-Vis spectra, and combination with EPR spectroscopy allowed the authors to propose the formation of the η^2 -peroxo iron complexes, considering that it is a high-spin iron(III) derivative. The corresponding pentacoordinated η^1 -peroxo complexes should be in fact low-spin. Further support to the suggestion was acquired with ESI-MS.



ligand = trispicMeen = *N*-methyl-*N,N',N'*-tris(2-pyridylmethyl)ethane-1,2-diamine

SCHEME 7

IV. REACTIVITY

A. Mechanistic Aspects

The transition metal based catalytic species derived from hydrogen peroxide or alkyl hydroperoxides are currently regarded as the most active oxidants for the majority of inorganic and organic substrates^{1,2,4,13,26}. An understanding of the mechanism of these processes is therefore a crucial point in the chemistry of catalytic oxidations. This knowledge allows one to predict not only the nature of the products in a given process, but also the stereochemical outcome in asymmetric reactions.

Book chapters^{2,4} and reviews^{17,24,25} have already compiled the numerous indications that, depending on the nature of the substrate and the oxidant, different types of mechanisms operate in transition metal catalyzed oxidations.

1. Oxidation of electrophilic substrates

The reactivity of peroxo metal complexes as nucleophilic oxidants is a known process¹⁴. To visualize this type of reactivity one has to refer to peroxo metal complexes as a 1,3-dipolar reagent M^+-O-O^- interacting in a bimolecular fashion with electrophilic dipolarophiles such as electron-poor olefins^{14,26} (equation 15), to form peroxymetallacycle intermediates.

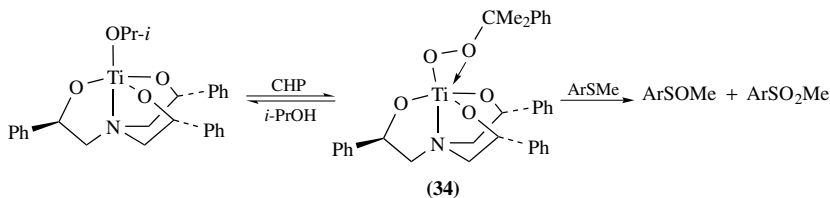
A detailed discussion concerning this type of mechanism has been organized by Strukul in his book²⁶. In particular, kinetic studies concerning Pt hydroxo derivatives indicate that the metal plays two different roles: activation of hydrogen peroxide by increasing its nucleophilicity and activation of the substrate toward nucleophilic attack by coordination to the metal center (Scheme 8).

the importance of coordination of the carbonyl function to the metal center in order to reduce the rate-determining activation barrier for rearrangement of the intermediate to form the products.

Bisperoxo methyltrioxorhenium complex is one of the most powerful oxidants in Baeyer–Villiger reactions¹²⁵. In the same paper, oxidation of Adam probe¹²⁶ was performed in order to provide evidence for the nucleophilic character of this complex.

Reports have appeared^{21,127} claiming that triperoxo vanadates behave as nucleophilic oxidants. In particular, triperoxo vanadium complexes, $A[V(O_2)_3]3H_2O$ ($A=Na$ or K), are proposed^{21,128} as efficient oxidants of α,β -unsaturated ketones to the corresponding epoxide, benzonitrile to benzamide and benzil to benzoic acid, reactions which are usually carried out with alkaline hydrogen peroxide. Subsequent studies²² concerning the oxidation of cyclobutanone to 4-hydroxybutanoic acid, carried out with the above-cited triperoxo vanadium compound, in alcohol/water mixtures, clearly indicated that such a complex does not act as nucleophilic oxidant, but only as a source of HOO^- anion.

Licini and coworkers^{129,130} have demonstrated with detailed kinetic studies that Ti(IV)–trialkanolamines–alkylperoxo complexes behave as biphlic oxidants toward thioethers and sulfoxides (Scheme 10). In particular, by using Hammett-type correlations, they provided evidence that **34** oxidizes aryl methyl thioethers with an electrophilic oxygen transfer reaction, while a nucleophilic pathway dominates in the oxidation of sulfoxides. This alteration of the reactivity is likely generated by coordination of the sulfoxide to the metal center that causes an ‘*umpolung*’ of the oxygen transfer step. The authors also obtained further support for their suggestion by performing *ab initio* calculations that showed a lower HOMO–LUMO gap for a DMSO containing a Ti–alkylperoxo complex. On this basis, an intramolecular oxygen transfer pathway is a favorable process. A similar mechanistic pattern has been observed by the same authors with a partially hydrolyzed Zr catalyst bearing the same polydentate ligand as in **34**¹³¹.



SCHEME 10

In studying asymmetric oxidation of methyl *p*-tolyl sulfide, employing $Ti(OPr-i)_4$ as catalyst and optically active alkyl hydroperoxides as oxidants, Adam and coworkers¹³² collected experimental evidence on the occurrence of the coordination of the sulfoxide to the metal center. Therefore, also in this case the incursion of the nucleophilic oxygen transfer as a mechanism can be invoked. The authors also used thianthrene 5-oxide as a mechanistic probe¹²⁶ to prove the nucleophilic character of the oxidant.

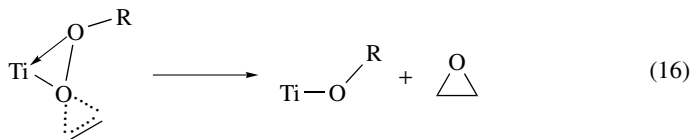
In this respect, care must be exercised in the use of such a mechanistic probe with peroxo metal complexes. In fact, on some occasions incursion of radical mechanisms may give rise to contrasting findings^{133,134}.

2. Oxidation of nucleophilic substrates

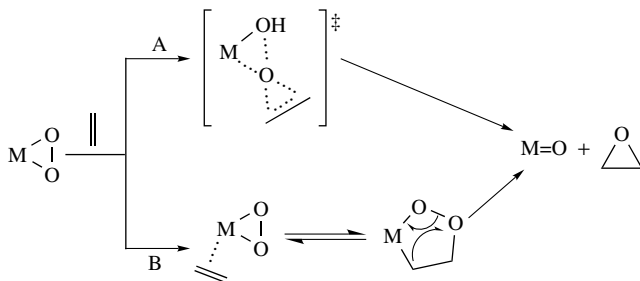
The most active d^0 metal peroxo complexes toward nucleophilic substrates, like amines, phosphines, thioethers, double bonds etc., are molybdenum, tungsten and rhenium derivatives^{2,4,26}; vanadium^{135–137} and titanium^{12,82} catalysis is also important, in particular when

enantioselective processes are carried out. Numerous studies have been performed in the last decades to clarify the mechanism of the oxygen transfer step and also to understand the transfer of chirality in enantioselective processes.

As far as the epoxidation of allylic alcohols with chiral titanium derivatives is concerned, there is agreement in the literature that the oxygen transfer step can be described as in equation 16¹³⁸. An η^2 -bound alkylperoxy moiety is present in the coordination sphere of the metal, and a preliminary coordination of the substrate through its hydroxylic function to the titanium center is required.

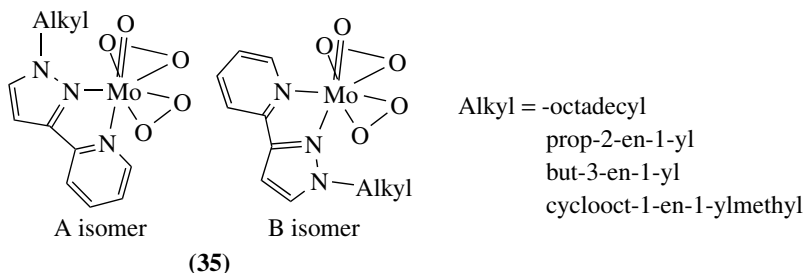


In analogy with this proposal, a similar mechanism has been proposed by Sharpless and coworkers^{139,140} also for oxygen transfer from an η^2 -peroxy metal complex. Here, a direct attack of the substrate by the electrophilic peroxy oxygen is considered (in close relation to the 'butterfly mechanism' accepted in peracids oxidation⁴); no intermediates are thus present but only a spirocyclic transition state (path A of Scheme 11). A different mechanism was proposed by Mimoun and coworkers^{141,142}, where a preliminary coordination of the substrate to a vacant or labile site of the metal is required. As a consequence of this coordination, the nucleophilic character of the substrate is strongly reduced. The subsequent step is the formation of a five-membered peroxymetallacycle intermediate, by an intramolecular 1,3-dipolar cycloaddition of the peroxy group to the coordinated alkene (path B of Scheme 11). Peroxymetallacycle intermediate has been in some cases isolated, but only with Pt and Pd peroxy complexes; no direct evidence on it has been obtained with d^0 peroxy species⁴. For quite a long time a strong debate has been active in the literature concerning the two mechanisms proposed in Scheme 11. A detailed discussion on this topic has been previously presented by several authors and interested readers are referred to those accounts^{4,17,25,26,59,143,144}.

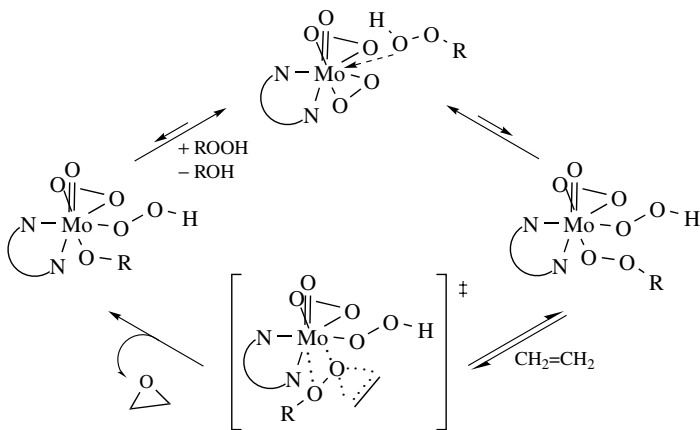


We point out that the mechanism sketched in path A of Scheme 11 is in agreement with the kinetic and spectroscopic data collected from several research groups. On the other hand, a series of contradictions was encountered in fitting the experimental data into the mechanism proposed in path B. Furthermore, several other papers have appeared in the last decade, based on both experimental results and theoretical calculations, supporting an epoxidation mechanism involving a direct oxygen atom transfer to olefins. For selected examples, see References 34, 145–155.

To finish this section, a particular type of Mo(VI) bisperoxo complex deserves consideration. Thiel and collaborators¹⁵⁶ have prepared several seven coordinated species, **35**, containing pyrazolylpyridine ligands bearing long alkyl side chains, which are therefore highly soluble in non-polar organic solvents.



These complexes are effective catalysts in epoxidation reactions with H_2O_2 and alkyl hydroperoxides. Several detailed mechanistic studies have been carried out; in particular, it has been shown that, when the alkyl chain contains a double bond, no autoepoxidation is observed both in the solid state and in solution. Nevertheless, if *t*-BuOOH is added, the epoxidation of the olefinic moiety immediately takes place. Therefore, it has been suggested that these complexes are not the active species in the oxygen transfer step to the substrate, but they behave as catalysts for the primary peroxidic oxidant. On the basis of kinetic, spectroscopic and theoretical studies, the authors provided a mechanism, whose key steps are sketched in Scheme 12. In this context a major role appears to be played by the fluxionality of the particular ligands used¹⁵⁷.



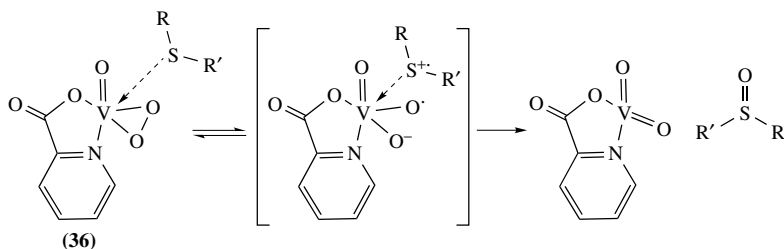
SCHEME 12

3. Radical oxidations

Radical reactions^{133, 158, 159} of peroxy metal complexes have been observed in the oxidation of thioethers¹⁶⁰, alkenes¹⁶¹, aromatics¹⁶¹⁻¹⁶³ and alcohols¹⁶⁴. Vanadium peroxy derivatives, in particular those containing picolinic acid derivatives as ligands, are usually

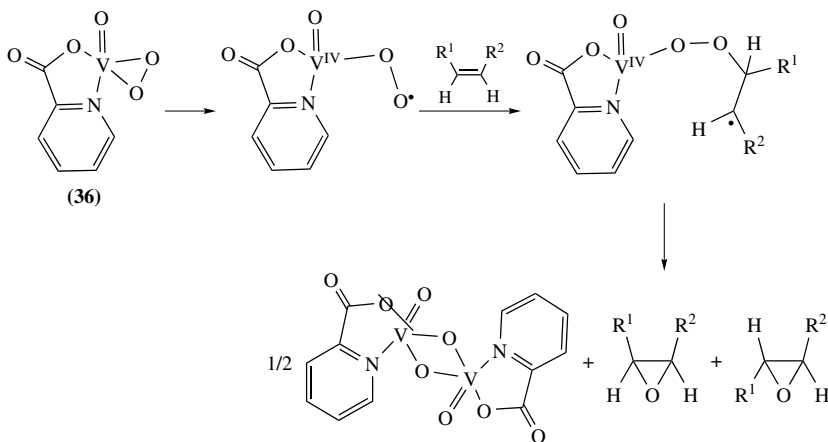
the most characteristic radical oxidants. In fact, the mechanistic studies carried out in this context are typically related to the chemistry of $\text{VO}(\text{O}_2)\text{pic}(\text{H}_2\text{O})_2$, **36** (for simplification, the H_2O is not shown in the structure), synthesized by Mimoun and coworkers in 1983¹⁶¹. An accurate survey of the reactivity of vanadium peroxides in general, and in particular of **36**, has been already presented by Butler and coworkers⁵⁹; therefore, here only the most peculiar aspects of the radical mechanisms will be mentioned.

On the basis of kinetic studies, a mechanism for the radical oxidation of thioether with **36** has been proposed and is indicated in Scheme 13¹⁶⁰. The key step involves the formation of a radical cation–anion pair within the solvent cage. The presence of the pic ligand in the coordination sphere of the metal reduces the electrophilicity of the peroxo complex, thus allowing the competitive radical process to take place.



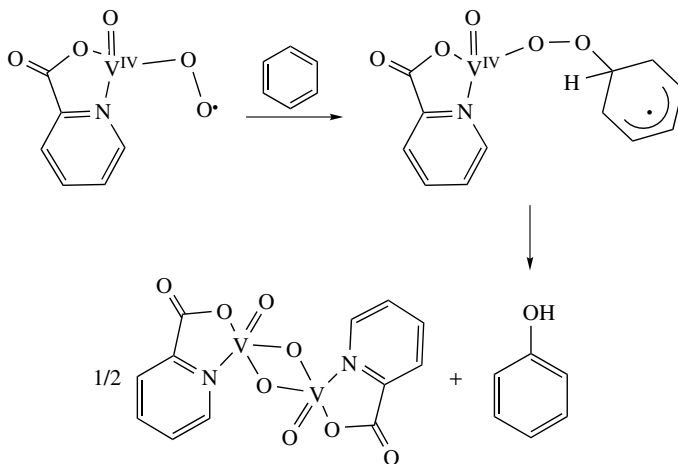
SCHEME 13

At odds with other similar peroxo metal complexes, $\text{VO}(\text{O}_2)\text{pic}(\text{H}_2\text{O})_2$, **36**, performs non-selective epoxidation reactions. On this occasion Mimoun proposed a mechanism¹⁶¹ where a homolytic rupture of one metal-peroxo oxygen bond produces the active oxidant (Scheme 14). When aromatic substrates are allowed to react with **36**, hydroxylation reaction takes place by way of the same active species¹⁶¹ as indicated in Scheme 15.

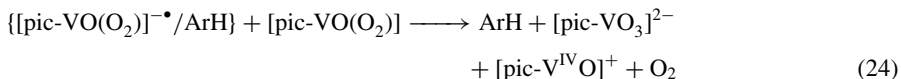
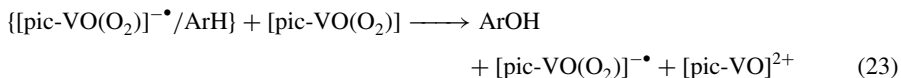
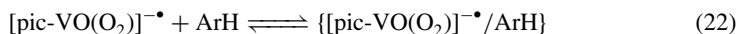
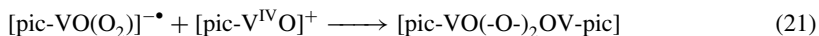
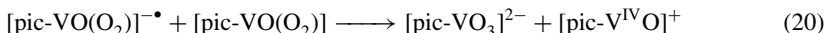
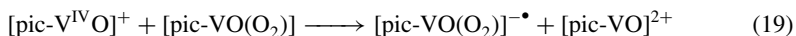
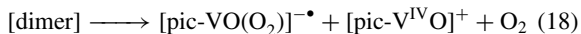


SCHEME 14

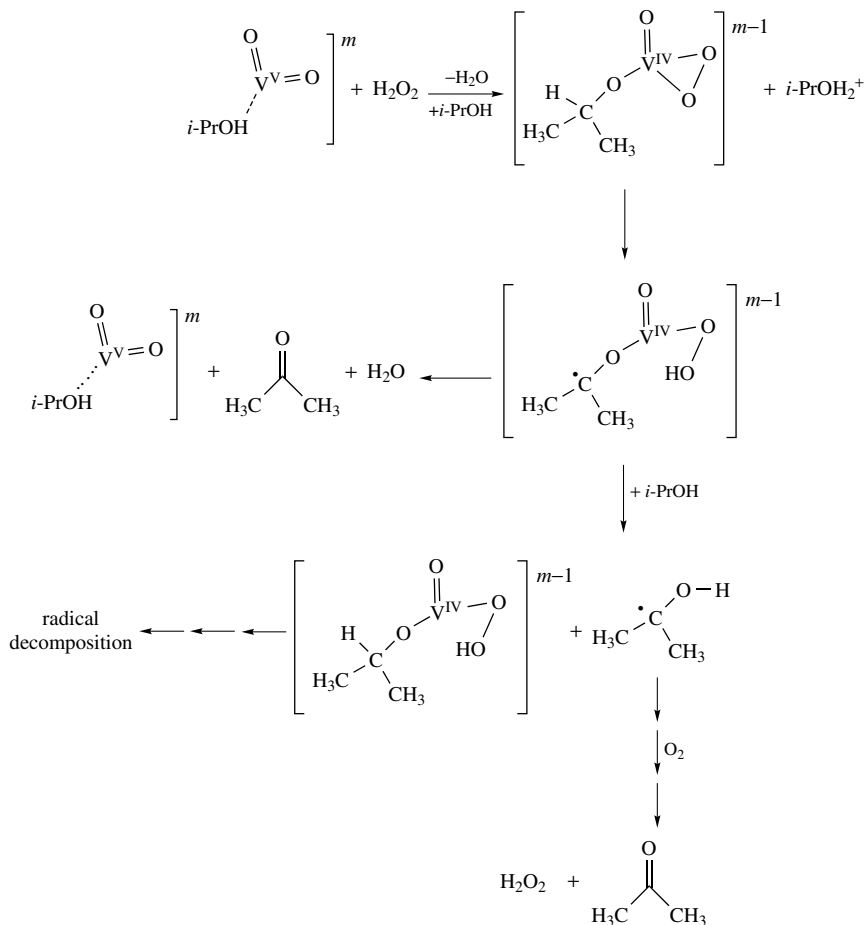
It is important for the definition of the mechanism to stress that these oxidations are always accompanied by decomposition of the peroxidic species to form dioxygen.



Subsequent detailed kinetic studies revealed that the reaction mechanism for the hydroxylation of arenes is much more complicated than that indicated above^{163, 165}. Furthermore, the active intermediate is likely an anion radical species formed upon interaction of two molecules of the vanadium peroxo complex. The sequence of the various steps is indicated in equations 17–24. The steps indicated in equations 17–21 refer to a radical chain which accounts for decomposition of the peroxo complex to form dioxygen, whereas the subsequent steps are those required for the functionalization of the substrate.



Alkoxy monoperoxo vanadium complexes are also efficient radical oxidants of the alcoholic function^{164, 166, 167} again with a radical chain mechanism whose details are indicated in Scheme 16 in the case of 2-propanol. Similar radical peroxo species have been indicated as competent oxidant also in the oxidation of alcohols with bis-peroxo chromium complexes¹⁵⁹.



SCHEME 16

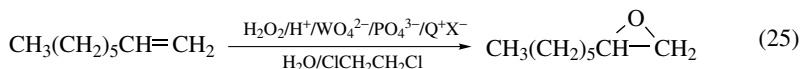
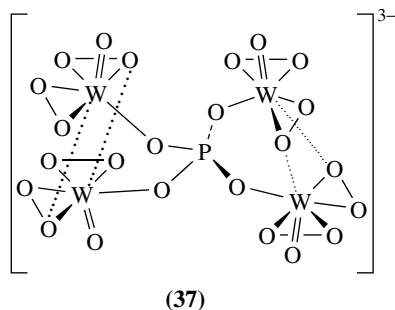
B. Oxidation of Alkenes

1. Unfunctionalized alkenes

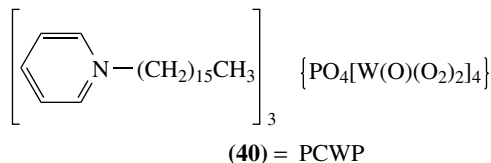
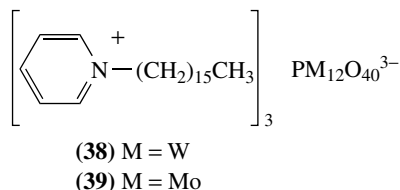
The direct epoxidation of simple alkenes by hydrogen peroxide or alkyl hydroperoxides is a longstanding goal in oxidation chemistry. The reaction is usually catalyzed by suitable high-valent metals, mainly belonging to group 5 and 6, through formation of metal peroxo species¹³.

Hydrogen peroxide may be efficiently employed for the epoxidation of unfunctionalized alkenes in the presence of polyoxo complexes of tungsten and molybdenum¹⁶⁸. Venturello and coworkers first developed a phosphotungstate catalyst¹⁶⁹, with particular emphasis on the tetrakis(diperoxotungsto)phosphate anion $\{\text{PO}_4[\text{W}(\text{O})(\text{O}_2)_2]_4\}^{3-}$, **37**^{170, 171}, that in conjunction with H_2O_2 and a lipophilic tetra-alkylammonium salt Q^+X^- as phase transfer

cocatalyst provided epoxidation of terminal and internal, open-chain or cyclic double bonds, in high yields (88% for 1-octene, up to 94% for other alkenes) and short reaction times (equation 25).



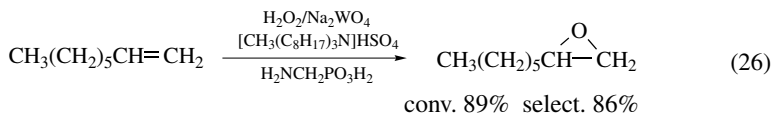
An analogous phase-transfer oxidation method was developed by Ishii and collaborators¹⁷² using 30% hydrogen peroxide in the presence of heteropoly acid anions $\text{PM}_{12}\text{O}_{40}^{3-}$ in combination with cetylpyridinium chloride (**38**, $\text{M}=\text{W}$; **39**, $\text{M}=\text{Mo}$). Both the Mo derivative **39**, when pre-treated with H_2O_2 ¹⁷³, and **37**¹⁷⁰ may act also as stoichiometric oxidants. A further modified catalyst named PCWP, **40**¹⁷⁴, derived by the association of the Ishii cetylpyridinium cation with the Venturello tetrakis(diperoxotungsto) phosphate anion $\{\text{PO}_4[\text{W}(\text{O})(\text{O}_2)_2]_4\}^{3-}$, allowed the selective oxidation of monoterpenes under mild conditions. As an example, the selective almost quantitative epoxidation of the cyclohexene double bond of limonene was achieved by using H_2O_2 (1.1 equivalents) in the presence of catalytic amounts of PCWP, in biphasic conditions $\text{CHCl}_3/\text{H}_2\text{O}$.



The major limitation of the potential value of the Venturello–Ishii systems, however, is related to the use of toxic and industrially undesirable chlorinated solvents^{168, 171}, defeating the environmental advantages of H_2O_2 as primary oxygen source¹⁷⁵. In this respect, the PCWP catalytic system was modified by using *t*-butyl alcohol as solvent and by

treating the H_2O_2 solutions with MgSO_4 prior to use, to remove the water. Following this procedure limonene and 1-octene were oxidized to the corresponding cyclohexane and 1,2-octane epoxides in 80 and 76% yields, respectively¹⁷⁴. More recently, the Venturello catalyst $\text{Q}_3\{\text{PO}_4[\text{W}(\text{O})(\text{O}_2)_2]_4\}$ was employed for the epoxidation of 1-octene with H_2O_2 in a water-in-oil microemulsion. An almost quantitative epoxide yield was obtained (1 h) in the presence of a biodegradable monoalkyl ether of polyethylene glycol, used as non-ionic surfactant¹⁷⁶.

The most important breakthrough from an environmental point of view, however, was disclosed by Noyori and coworkers^{177, 178} who found a completely halide-free procedure, even without an organic solvent, for the epoxidation of several double-bond typologies, including terminal, di-, tri- and tetrasubstituted olefins and cyclic alkenes (equation 26). The presence of lipophilic ammonium hydrogen sulfate, which replaces the conventional chloride, and an (α -aminoalkyl)phosphoric acid are crucial for the high reactivity. In general, the epoxidations performed according to this protocol exhibit unique selectivities not observed in conventional oxidations. The method, however, is not applicable to styrene derivatives.

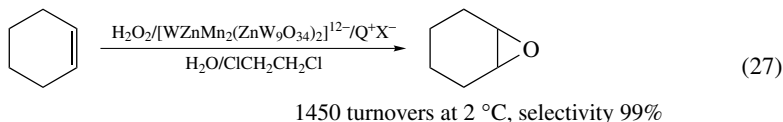


Alternative to the Venturello–Ishii systems, employing anionic heteropolyoxo metalates of Mo and W, is the biphasic approach based on neutral Mimoun-type molybdenum and tungsten peroxo complexes of general formula $[\text{MO}(\text{O}_2)_2\text{L}(\text{H}_2\text{O})]$. Alkyl substituted pyridine N-oxides, phosphoric acid amides¹⁷⁹ or OE(*n*-dodecyl)₃ (E = N, P, As)^{2, 149} have been used as (L) phase transfer agent mediators for the epoxidation of different alkenes with H_2O_2 . In the latter case, the catalytic activity was reported to be comparable to the homogeneous MTO/ H_2O_2 /BuOH-*t* (see below) or the Venturello–Ishii strategies.

Recently, Mizuno and coworkers¹⁸⁰ reported the high catalytic performance exhibited by $[\gamma\text{-SiW}_{10}\text{O}_{34}(\text{H}_2\text{O})_2]^{4-}$ for the epoxidation of various olefins with hydrogen peroxide at 305 K, in CH_3CN . The new catalyst exhibited a 99% selectivity, 99% efficiency of H_2O_2 utilization, high stereospecificity and recovered-reuse of the catalyst. For the oxygenation of *cis*- and *trans*-2-octenes, the configuration around the double bond was retained in the corresponding epoxides. The catalytic activity of this system is reported to be superior to other polyoxometalate-based procedures.

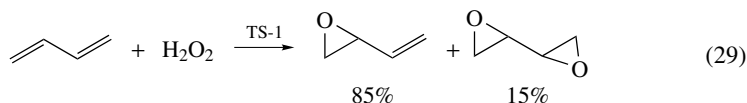
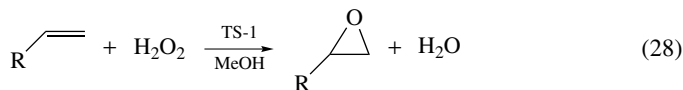
Transition metal substituted polyoxometalates (TMSPs)^{181, 182}, where either the heteroatom or one (or more) addenda are substituted by low-valent transition metals, especially Mn (II), Co (II), Fe(III) or Ru(III), have shown themselves to be effective catalysts for oxygen transfer reactions, as in the epoxidation of alkenes. The most common class of TMSPs are those based on the mono-substituted Keggin and Well–Dawson structures, characterized however by solvolytic and oxidative instability toward aqueous H_2O_2 ¹⁷¹. In this context a new subclass of TMSPs, named sandwich-type polytungstometalates $[\text{WXM}_2(\text{XW}_9\text{O}_{34})_2]^{12-}$, with X = Zn(II), Co(II) and M = Mn(II), Pd(II), Pt(II) etc., originally reported by Tourné and coworkers¹⁸³, have been shown to possess higher resistance toward degradation and remarkable catalytic activity. Neumann and collaborators found that the manganese-containing derivative $[\text{WZnMn}_2(\text{ZnW}_9\text{O}_{34})_2]^{12-}$ was highly active in biphasic oxidation of alkenes with H_2O_2 , achieving high epoxide selectivity and hundreds of thousands of catalytic turnovers^{184, 185} (equation 27). The reactivity, which increased as a function of the nucleophilicity of the alkene double bond but decreased as a function of the steric crowding¹⁸⁶, was related to the formation of a tungsten-peroxo intermediate activated by an adjacent manganese atom.

The same $[\text{WZnMn}_2(\text{ZnW}_9\text{O}_{34})_2]^{12-}$ based epoxidation may be carried out in the absence of solvent by immobilizing the catalyst on a silicate xerogel covalently modified with phenyl and quaternary ammonium groups¹⁸⁷. Other isostructural noble-metal derivatives of $[\text{WXM}_2(\text{XW}_9\text{O}_{34})_2]^{12-}$ [$\text{M} = \text{Rh(III)}$, Pd(II) , Pt(II) and Ru(III)] exhibited catalytic activity both using H_2O_2 or TBHP^{188,189}. The reaction is tungsten centered, not noble-metal centered, with formation of a peroxo tungstate intermediate.



The Hill group^{190–194} reported a H_2O_2 -based epoxidation procedure catalyzed by sandwich polyoxometalates of the type $[\text{Fe}_4(\text{PW}_9\text{O}_{34})_2]^{6-}$, $[\text{Fe}_4(\text{H}_2\text{O})_2(\text{P}_2\text{W}_{15}\text{O}_{56})_2]^{12-}$, $[\text{MFe}_2(\text{P}_2\text{W}_{15}\text{O}_{56})(\text{P}_2\text{M}_2\text{W}_{13}\text{O}_{52})]^{16-}$ ($\text{M} = \text{Cu}$, Co) and $[\text{Fe}_2(\text{NaOH}_2)_2(\text{P}_2\text{W}_{15}\text{O}_{56})_2]^{16-}$ which, as tetraalkylammonium salts, exhibited from reasonable to good rates, selectivities and stabilities. In particular, the selectivities observed with the latter compound (90–99%) rule out homolytic mechanisms including Fenton-type chemistry and compare well with the results obtained by Mizuno and coworkers^{195,196} using $[\gamma\text{-SiW}_{10}(\text{Fe}(\text{OH}_2))_2\text{O}_{38}]^{6-}$. The formation of a peroxo derivative as active intermediate in these systems is not yet proved. Examples of X-ray structures of TMSPs containing peroxo moieties have been reported^{197,198}.

A number of heterogeneous systems have been developed for oxidation reactions using H_2O_2 as oxygen source^{168,199}. In 1981, Taramasso, Notari and collaborators at Enichem opened new perspectives in this field with the discovery of the Ti-silicalite (TS-1)²⁰⁰, a new synthetic zeolite of the ZSM family. In the TS-1 zeolite, titanium atoms are located in vicariant positions in the place of Si atoms in the crystalline framework²⁰¹. The remarkable reactivity of TS-1 is likely ascribable to the site-isolation of tetrahedral Ti(IV) in a hydrophobic environment. TS-1 has proved to be an efficient catalyst for the epoxidation of unfunctionalized short-chain olefins, especially terminal ones (equation 28). In addition, polyunsaturated compounds are mainly converted into the mono epoxides (equation 29).

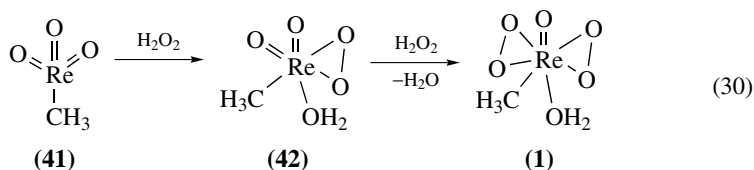


The nature of the titanium-containing active site has been investigated with different techniques, including theoretical calculations. The formation of a hydroperoxidic species²⁰² or of a bidentate side-on titanium peroxo structure was suggested by many authors^{147,203}. Alternatively, some DFT calculations indicated an undissociated molecule of H_2O_2 weakly interacting with Ti centers²⁰⁴ or an active Ti-O-O-Si peroxo moiety as a reactive site²⁰⁵. Recently, Lin and Frei reported the first direct detection, obtained using in situ FT-infrared spectroscopy, of a Ti-OOH moiety as active species in the oxidation of small olefins like ethylene or propylene²⁰⁶.

A serious disadvantage of TS-1 is its limited pore size, which limits the number of substrates suitable for oxidation^{207,208}. This problem has been circumvented with the synthesis

of titanium-containing zeolites having larger pores such as Ti- β ²⁰⁹, Ti-MCM-41²¹⁰ or Ti-MWW²¹¹. The recent development of new silicalite catalysts containing Sn(IV), Zr(IV) and Cr(VI), among other metals, is beyond the scope of this chapter and may be found in the specific literature^{199, 207, 208, 212}.

In 1991, Herrmann's research group reported that methyltrioxorhenium(VII) (MTO) **41** serves as highly efficient catalyst for the oxidation of several classes of organic compounds by H₂O₂²³. In the presence of hydrogen peroxide MTO is stepwise converted into the mono- **42** and bis(peroxo)rhenium complex **1**, the latter isolated and fully characterized^{213, 214} (equation 30). The epoxidations of a wide variety of alkenes were performed at room temperature or below, in the presence of 0.1–1% MTO with respect to olefin using *t*-butyl alcohol as solvent. Depending on the epoxide, ring opening to 1,2-diol and further rearrangement reactions²¹⁵ were observed in most cases, likely catalyzed by MTO. Several additives including tertiary nitrogen bases, urea and NaY zeolite have been reported to limit or suppress this problem (Table 3).



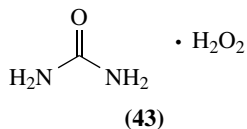
For nitrogen-donor adducts, the selectivity was found to be dependent on the pK_b value of the N-base^{213, 216}. Among this class of additives pyridine or pyrazole, if present in appropriate concentration (12% mol), were reported to have a remarkable acceleration effect on the epoxidation rate, preventing decomposition and increasing the catalyst lifetime^{217–220}.

Another possibility of enhancing the selectivity toward epoxides is the use of urea–H₂O₂ (UHP) adducts **43**, enabling the epoxidation to be carried out in non-aqueous media^{221, 222} or the use of additives like the zeolite NaY^{17, 223, 224}. Polymeric^{225, 226} or oxide-supported (niobia)²²⁷ materials have also been reported as cocatalysts for the heterogeneous epoxidations catalyzed by MTO. A significant modification of the MTO–H₂O₂ system was proposed by Sheldon and coworkers²²⁸ by conducting the epoxidation reactions in 2,2,2-trifluoroethanol as solvent, thus avoiding heterogeneous conditions and the use of chlorinated media. In this frame, noteworthy is the observation that ionic liquids like [emim]BF₄ are suitable solvents for the MTO-catalyzed epoxidation of olefins using UHP^{229, 230}. Ionic liquids have received much attention in recent years as alternative reaction media in light of their negligible vapor pressure and capability to dissolve a wide range of inorganic and organic materials.

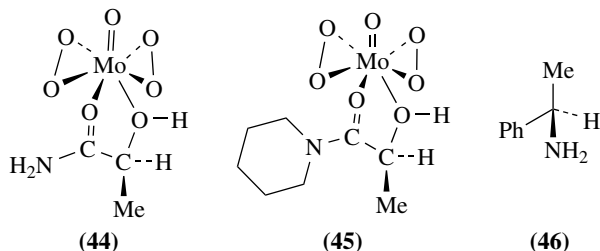
TABLE 3. Additives used in the epoxidation of cyclohexene catalyzed by MTO

Oxidant	Conditions	Epoxide yield (%)	Reference
H ₂ O ₂	0.1–1 mol% MTO, <i>t</i> -BuOH, 10 °C, 5 h	90	23
UHP	0.1 mol% MTO, CDCl ₃ , 20 °C, 18 h	98	221
H ₂ O ₂	0.5 mol% MTO, 12% mol pyridine, CH ₂ Cl ₂ , 20 °C, 6 h	96	217
H ₂ O ₂	0.5 mol% MTO, 12% mol pyrazole, CH ₂ Cl ₂ , 20 °C, 1 h	99	219
H ₂ O ₂	0.1 mol% MTO, 10% mol pyrazole, CF ₃ CH ₂ OH, 5 °C, 0.5 h	99	228
UHP	2% MTO, [emim]BF ₄ , 20 °C, 8 h ^a	95	229

^a *N*-ethyl-*N'*-methylimidazolium.

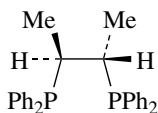


Terminal olefins like 1-octene are oxidized to the corresponding epoxides with 35% H_2O_2 in the presence of $\text{P}_2\text{Pt}(\text{R}_x)(\text{OH})$ complexes (P_2 = mono or diphosphine, R_x = activated alkyl or aryl groups) in both mono- and biphasic media²³¹. Chiral phosphines coordinated to Pt(II) derivatives allowed asymmetric epoxidation, as discussed in subsequent paragraphs. The reports on enantioselective epoxidation of prochiral simple alkenes with metal-peroxide based reagents are limited, due to the scarcity of chiral non-racemic epoxidizing derivatives. In 1979, Kagan, Mimoun and collaborators²³² described the first example of the use of Mo(VI) oxo-diperoxo complexes containing chiral bidentate ligands for asymmetric epoxidations. Complex **44**, with (*S*)-*N,N*-dimethyl lactamide as optically active ligand, was reported to perform the stoichiometric epoxidation of simple olefins like propene, 1-butene and (*E*)-2-butene with enantiomeric excesses in the range 30–35%. Similar complexes containing (*S*)-piperidine lactamide **45**, (*S*)-*N*-acetylprolinol etc. showed asymmetric induction with ee values up to 55%²³³. For the same system, enantiomeric excesses higher than 90% were found for the epoxidation of (*E*)-2-butene, in the presence of chiral diols as additives, likely via kinetic resolution of the epoxides formed. More recently, molybdenum peroxo complexes $\text{MoO}(\text{O}_2)_2$ bonded to chiral phosphinoalcohol ligands have been shown to perform the enantioselective epoxidation of small-chain alkenes like 1-pentene with ee values of about 40%²³⁴. The observation that nitrogen-donor adducts are particularly beneficial for avoiding epoxide ring-opening reaction in the MTO- H_2O_2 oxidation system²¹³ prompted Corma and coworkers²³⁵ to perform this epoxidation in the presence of different chiral amines like **46**. In general, the level of chiral induction was low, although (*E*)- and (*Z*)- β -methylstyrene afforded the corresponding epoxides in 35 and 36% ee, respectively.

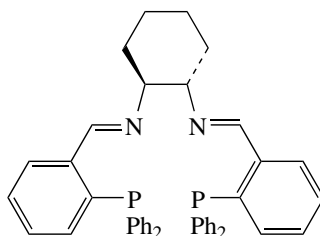


Platinum(II) and ruthenium(II) complexes with chiral modified diphosphines like **47** or tetradentate P_2N_2 ligands like **48** have been used for the asymmetric epoxidation of olefins with hydrogen peroxide with ee values of 18–23%, which increased up to 41% when cationic solvato derivatives such as $\text{P}_2^*\text{Pt}(\text{CF}_3)(\text{CH}_2\text{Cl}_2)(\text{BF}_4)$ are used²³⁶. Similar chiral inductions were reported for Ru derivatives, although the nature of the active intermediate was still in question²³⁷.

t-Butyl hydroperoxide (TBHP)²³⁸ was first reported by Milas and coworkers in 1938²³⁹. However, the real potential of this oxidant is connected with the development of the so-called oxirane process^{240,241} in which propylene is epoxidized by TBHP in the presence of a molybdenum catalyst and it represents one of the most widespread applications of peroxide chemistry (equation 31). Today, ARCO is running the process using a homogeneous

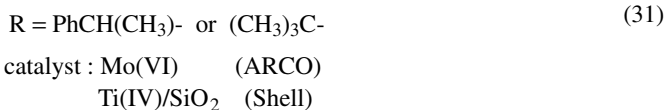
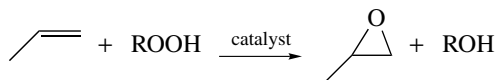


(47)



(48)

Mo catalyst and Shell is using ethylbenzene hydroperoxide as oxidant in the presence of the heterogeneous Ti(IV)/SiO₂ catalyst^{2,207,242}. The adaptation of the oxirane process to laboratory scale was first reported by Sharpless and Verhoeven²⁴³ for the oxidation of different substrates including functionalized and unfunctionalized olefins and acetylenes. The epoxidation of isolated double bonds can be carried out using Mo(CO)₆ and TBHP, in unreactive solvents like benzene, DCE or CH₂Cl₂. Moderately anhydrous conditions and the presence of Na₂HPO₄ are beneficial to reduce byproducts formation. Following this procedure, 1-decene (86% yield) as well as other isolated olefins are epoxidized in 85–95% distilled yield.

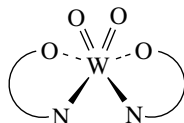
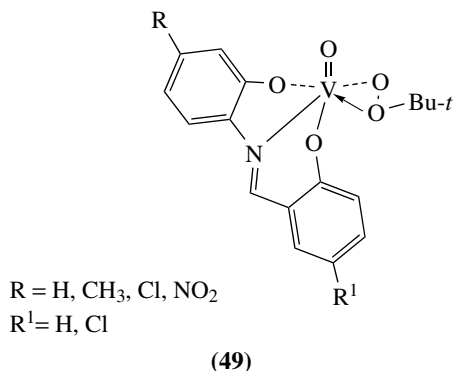


Long-chain derivatives of pyrazolyl pyridines coordinated to MoO(O₂)₂ as **35** may efficiently replace the conventional Mo(CO)₆ in the oxidation of several double-bond typologies with TBHP, in non-polar hydrocarbon solvents^{244,245}. The epoxidation of cyclopentene and 2,3-dimethyl-2-butene led to the corresponding epoxides, notoriously sensitive to ring opening, in 100% and 87% yield respectively, in isooctane, with 1 hour reaction time. Recent advances in the epoxidation of α -pinene and other terpenes using the Mo–TBHP system have been reported².

Mimoun and coworkers¹⁴² described the first well-defined example of a d⁰ metal alkylperoxidic species **49** which epoxidized simple olefins with high selectivity. Several features of the epoxidation performed by **49** resemble those of the Halcon catalytic epoxidation process²⁴⁰. Novel tungsten complexes containing 2'-pyridyl alcoholate ligands like **50** have been synthesized and tested as catalysts in the epoxidation of *cis*-cyclooctene with TBHP in the absence of solvent²⁴⁶. The system displayed modest catalytic activity (100% conversion in 60 h) but excellent product selectivity.

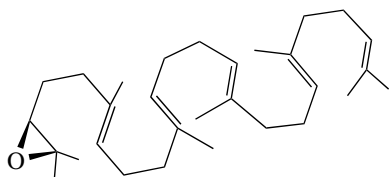
As discussed in previous paragraphs, a disadvantage of TS-1 catalyst is its limited pore size, which restricts the number of oxidants that can be employed^{207,208}. By using larger pore molecular sieves this restriction could be overcome. Titanium-substituted MCM-41²¹⁰ and titanium-grafted MCM-41²⁴⁷ were shown to be particularly active in the epoxidation of bulky olefins like pinene and norbornene with TBHP. In the case of Ti-MCM-41 silicas, the importance of hydrophobicity in the system was demonstrated by the faster reaction rate observed with 2-methyl-1-phenyl-2-propyl hydroperoxide as the oxygen atom

donor^{248,249}. In the field of asymmetric epoxidation with alkyl hydroperoxides in the presence of metal derivatives, important results have been obtained with olefins bearing a pre-coordinating functional groups, i.e. allylic alcohols, while epoxidation of isolated double bonds is rather slow, affording products in modest enantiomeric excesses (*ca* 10–30%). For example, the reaction of squalene with TBHP in the presence of MoO₂(*acac*)₂/(+)-diisopropyl tartrate affords 2,3-epoxysqualene **51** in 31% yield and 14% ee²⁵⁰. More recent selected reports were based on the use of optically active non-racemic 2'-pyridinyl alcoholate ligands coordinated to Mo or W metal centers like **50** (ee ≤ 25%)²⁵¹ and chiral phosphinoyl alcohols bound to molybdenum peroxy complexes MoO(O₂)₂²³⁴. Mo-dioxo derivatives containing chiral organic bidentate O,O- as **52**, O,N- and O,S-ligands have been investigated for enantioselective alkene epoxidation²⁵². The optical values are in the range of those mentioned above. Attempts to immobilize these complexes within the channels of MCM-41 mesoporous silica by using a tethering ligand were unsuccessful.

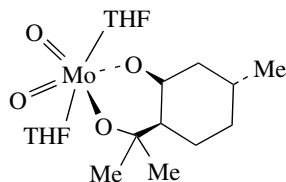


Ligand = N O = 2-(2'-pyridyl)propan-2-ol
di[4'',4''-di(methoxy)phenyl](2'-pyridyl)met hanol
9-(2'-pyridyl)fluoren-9-ol
5-(2'-pyridyl)-10,11-dihydrodibenzo[a,d]cyc loheptan-5-ol

(50)



(51)

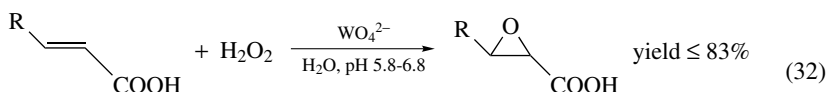


(52)

2. Electron-poor alkenes

Most of the methods for the epoxidation of electron-poor olefins are applications or variants of the Weitz–Scheffer reaction using alkaline H_2O_2 ²⁵³. The requirement of a nucleophilic peroxy oxygen and the efficiency of the purely organic systems appear to be the main reasons why metal peroxides have been moderately used for this reaction.

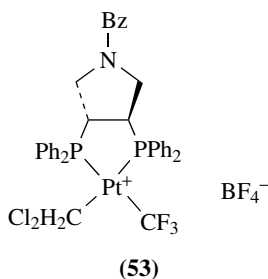
In 1985, Kirshenbaum and Sharpless²⁵⁴ reported a modified Payne–Williams procedure²⁵⁵ for the epoxidation of α,β -unsaturated carboxylic acids by hydrogen peroxide in the presence of WO_4^{2-} (equation 32). The same $\text{WO}_4^{2-}/\text{H}_2\text{O}_2$ catalytic system associated with a lipophilic ammonium hydrogen sulfate and an (α -aminoalkyl) phosphoric acid was active in the epoxidation of α,β -unsaturated ketones and esters, even in the absence of solvent (equation 26)¹⁷⁸. The evidence that tungsten derivatives are suitable catalysts for the epoxidation of electron-poor olefins is also confirmed by the results of Ishii, Oguchi and their coworkers^{256, 257}. Cetylpyridinium 12-tungstophosphate **38** in association with H_2O_2 was found to carry out the epoxidation of α,β -unsaturated carboxylic acids in water at almost neutral pH (6–7), with conversions and selectivities in the range 56–93% and 80–98%, respectively.



R = Me, *i*-Pr, or a double bond inserted in a cyclohexene ring

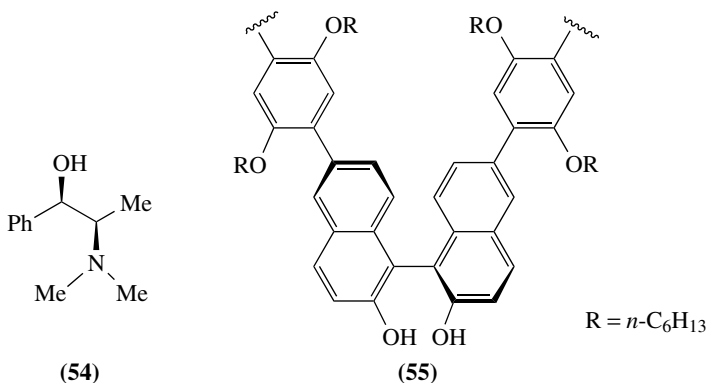
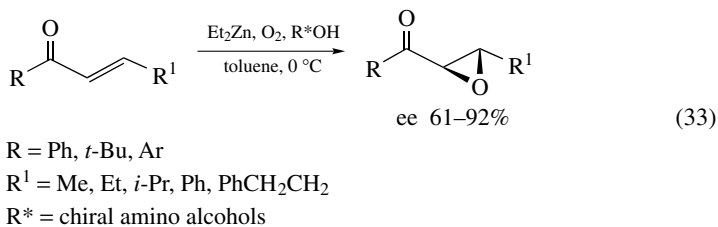
Peroxo Fe(III), Mn(III) and Ti(IV) porphyrins were reacted with a variety of electron-poor organic substrates in order to compare their activity with that of different metalloperoxide complexes. Epoxidation of 2-cyclohexen-1-one and 2-methyl-1,4-naphthoquinone was observed, in 25 and 75% yield respectively, with the extremely nucleophilic Fe(III) complex^{258, 259}. These results opened new perspectives in the oxidation mechanisms of some enzymatic reactions.

Strukul and coworkers have carried out the catalytic epoxidation of α,β -unsaturated ketones with H_2O_2 mediated by a series of platinum diphosphine based complexes, that confirm the ability of the Pt(II) center to increase the nucleophilicity of hydrogen peroxide²⁶⁰. Interestingly, this transformation may be accomplished in enantioselective fashion when chiral diphosphines such as those in **53** are used (ee up to 63%).

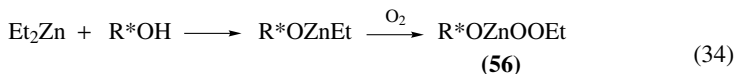


Several methods for the asymmetric epoxidation of electron-poor alkenes rely on the use of metal peroxides associated with chiral ligands²⁶¹. Enders and coworkers reported that (*E*)- α,β -unsaturated ketones may be epoxidized using stoichiometric quantities of diethylzinc and a chiral alcohol, in the presence of molecular oxygen (equation 33). The best enantioselectivities were found using (*R,R*)-*N*-methylpseudoephedrine **54** as R*OH

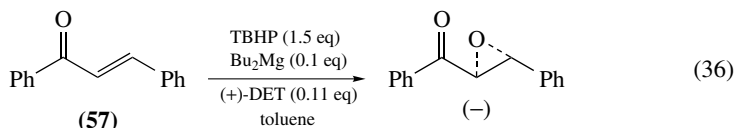
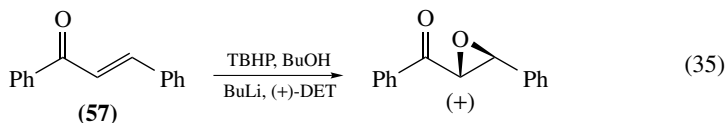
chiral aminoalcohol, which may be almost quantitatively recovered from the reaction mixture²⁶². The same system has been used for the epoxidation of some β -alkylidene- α -tetralones²⁶³ and (*E*)-nitroalkenes²⁶⁴ with enantiomeric excesses in the range 36–82%. The replacement of **54** with the chiral binaphthyl polymer **55**, in otherwise identical conditions, gave unsatisfactory results and prompted Pu and coworkers to investigate TBHP as oxidant in place of molecular oxygen²⁶⁵. The modified system may operate also under catalytic conditions using 10 mol% of Et₂Zn and 5 mol% of the binaphthyl polymer in CH₂Cl₂. Both Enders and Pu have proposed similar reaction pathways with the formation of a chiral zinc peroxide **56** as active species for the reaction with O₂ (equation 34), and of R*OZnOOBu-*t* for the reaction with TBHP.



Chirally modified lithium and magnesium *t*-butyl peroxides, strictly not transition-metal derivatives, have been investigated for the asymmetric epoxidation of chalcone **57** and chalcone derivatives²⁶⁶. Initial work, based on Li-peroxides, was developed on the bases of stoichiometric conditions and (+)-diethyl tartrate was the most effective ligand. For the catalytic system the magnesium derivative was employed in 5–10 mol%, affording the epoxide in 60% yield and 94% ee. It is noteworthy that the Li- and Mg-based procedures provided opposite enantiomeric epoxides, as shown in equations 35 and 36. More recently, the same authors applied the magnesium-derived catalytic procedure to the asymmetric epoxidation of aliphatic α,β -unsaturated ketones²⁶⁷. The original reaction protocol, shown in equation 36, was partially modified by drying TBHP over molecular sieves prior to use and by employing (+)-di-*t*-butyl tartrate as chiral ligand. The enantiomeric excesses for the epoxidation of different substrates are in the range 71–93%. It has been suggested that the chiral ligand tightly binds the magnesium peroxide center, causing a reduction of the reactivity but an activation of the asymmetric induction. A similar lithium-catalyzed epoxidation in the presence of chiral tridentate aminodiether ligands has been recently described²⁶⁸.

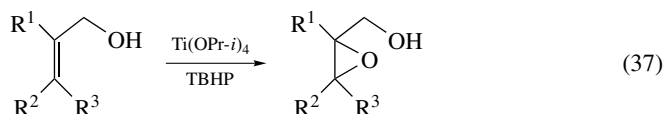


$\text{R}^* = (R,R)\text{-}N\text{-methylpseudoephedrine}$

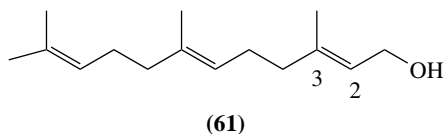
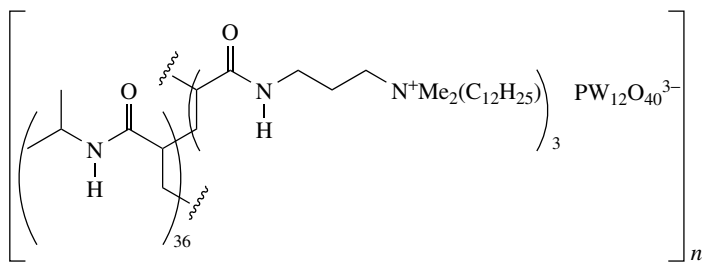
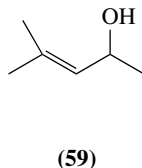
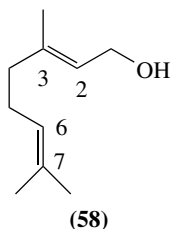


3. Allylic and homoallylic alcohols

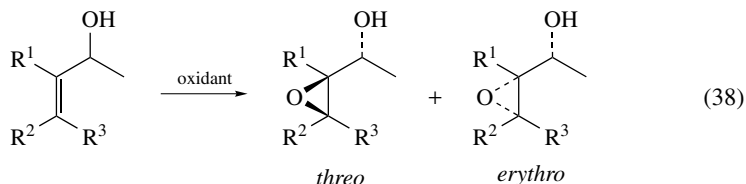
The Ti-catalyzed epoxidation of allylic and homoallylic alcohols using TBHP (equation 37) represents the easiest access for the preparation of epoxy alcohols²⁵, important building blocks for the synthesis of biologically active compounds. From a historical point of view, however, the same transformation carried out by using metal-peroxo derivatives formed from VO(acac)₂/TBHP, Mo(CO)₆/TBHP²⁴³ and H₂WO₄/H₂O₂^{269, 270} is worthy of mention. In 1984, Ishii and coworkers²⁷¹ reported that cetylpyridinium 12-molybdophosphate **39** catalyzed the epoxidation of allylic alcohols with H₂O₂ under phase-transfer conditions. The epoxidation of geraniol **58** proceeded regioselectively, both with the Mo-derivative **39** as well as with the 12-tungstophosphate homologue **38**, affording the 2,3-epoxide almost quantitatively¹⁷². A high stereoselectivity was observed with many substrates like 4-methyl-3-penten-2-ol **59**, which showed a *threo:erythro* epoxide composition of 94:6, similar to that observed with V/TBHP²⁴³ and W-catalyzed²⁷² systems. More recently, the 12-tungstophosphoric acid (H₃PW₁₂O₄₀) was used to prepare a new triphase catalyst **60**, derived from the self-assembly of this inorganic species with an amphiphilic poly(*N*-isopropylacrylamide)-derived polymer²⁷³. Catalyst **60** was successfully applied to the epoxidation of allylic alcohols with 30% H₂O₂ in the absence of an organic solvent, with a turnover number of 35000, much higher than that of other polymer-supported tungsten catalysts. In particular, the oxidation of farnesol **61** and of **58** occurs on the allylic double bond, affording the 2,3-epoxy alcohols in 84 and 80% isolated yield, respectively. Epoxidation of allylic alcohols in the absence of solvent is equally successful either by applying the Noyori catalytic system of equation 26 (conversions 61–99%, yields 42–85%)¹⁷⁸ or by using tungstic acid dispersed on fluoroapatite, in the presence of UHP as oxygen donor²⁷⁴.



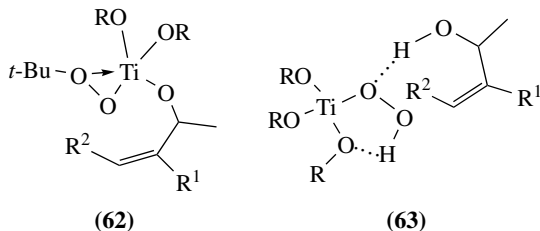
Adam and coworkers have carried out several studies aimed at elucidating the geometry of the transition-state structure for the allylic alcohol epoxidation using chiral substrates as stereochemical probe^{17, 275–277} (equation 38). The *threo:erythro* diastereoselectivities for the epoxidation of a set of methyl-substituted chiral allylic alcohols with A^{1,2}



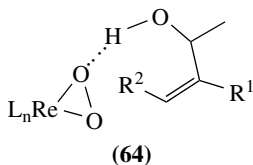
and A^{1,3} strain, using Ti(OPr-*i*)₄/TBHP, VO(acac)₂/TBHP, Mo(CO)₆/TBHP, TS-1/UHP, Ti-β/H₂O₂ oxidizing systems, have been measured and compared. For most of the systems performing this oxidation [VO(acac)₂/TBHP, Ti(OPr-*i*)₄/TBHP, Mo(CO)₆/TBHP], the generally accepted mechanism involves the formation of a metal alcoholate complex such as **62**, depicted for titanium, where the oxygen donor and the allylic alcohol are simultaneously bound to the metal center. For the heterogeneous Ti-containing zeolites TS-1/UHP and Ti-β/H₂O₂ systems, the good correspondence of the data with the *m*-CPBA epoxidation results excluded a metal alcoholate binding in favor of a hydrogen bonding between the allylic alcohol and the Ti-OOH species, as in **63**. For epoxidations catalyzed by Ti-containing zeolites, the epoxy alcohols were obtained without any rearrangement when 30% aqueous H₂O₂ is replaced by its concentrated form (85%) in the presence of MgSO₄ or when the urea adduct (UHP) is used²⁷⁶.



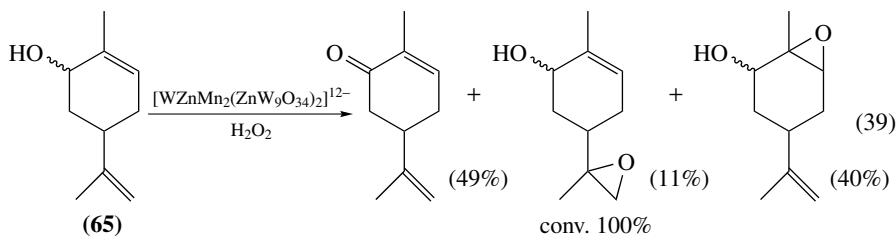
Methyltrioxorhenium-based oxidants, i.e. MTO/H₂O₂²³, MTO/H₂O₂/substituted pyridines²¹⁸ and MTO/UHP^{221, 222}, are active in the epoxidation of many double-bond typologies, including allylic alcohols. Regiochemical and stereochemical probes have been



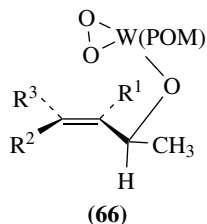
applied in order to elucidate the mechanism of this epoxidation with different oxidizing systems²⁷⁸. Polyunsaturated systems like **58** are preferentially epoxidized at the unfunctionalized 6,7-double bond^{222, 278}. For the stereochemical probes, using chiral allylic alcohols, the observed *threo:erythro* diastereoselectivity (equation 38) is in good correspondence with that of *m*-CPBA and Ti-containing zeolites systems, thus suggesting, also in this case, that hydrogen bonding between the hydroxy functionality and the rhenium catalyst **64** is the decisive electronic feature.



Sandwich-type polyoxometalates, in particular $\{WZn[M(H_2O)]_2(ZnW_9O_{34})_2\}^{q-}$ [$M=Mn(II)$, $Ru(III)$, $Fe(III)$, $Pd(II)$, $Pt(II)$, $Zn(II)$; $q=10-12$], are shown to catalyze the epoxidation of allylic alcohols with H_2O_2 in an aqueous-organic biphasic system²⁷⁹. Neumann and coworkers reported that $[WZnMn_2(ZnW_9O_{34})_2]^{12-}$ was particularly active in this oxidation^{186, 280}. The reactivity trend for the different substrate typologies is allylic alcohols > homoallylic alcohols \approx ω -alkenols and *cis* > *trans*. Contrasting regioselectivities were found with polyunsaturated allylic alcohols. Geraniol **58** is almost exclusively epoxidized at the 2,3-double bond, whereas linalool and carveol **65** afforded a mixture of products as shown in equation 39.



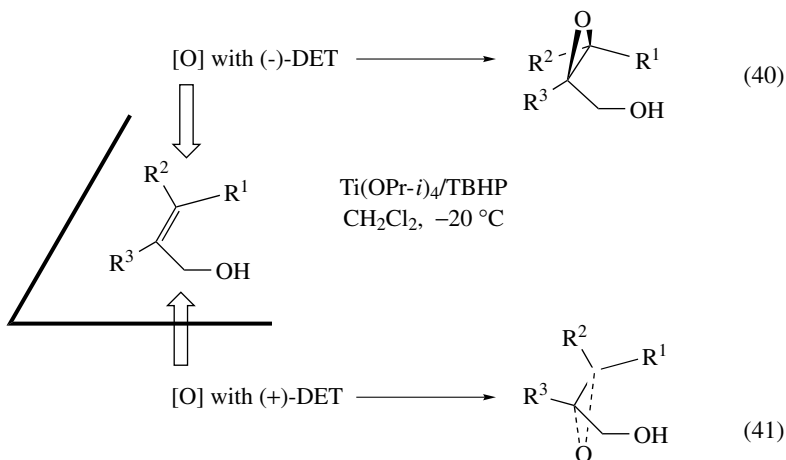
Stereochemical and regiochemical probes have been used to elucidate the mechanism of the $\{WZn[M(H_2O)]_2(ZnW_9O_{34})_2\}^{q-}$ [$M=Mn(II)$, $Ru(III)$, $Fe(III)$, $Pd(II)$, $Pt(II)$, $Zn(II)$; $q=10-12$] catalyzed epoxidation of allylic alcohols with H_2O_2 ²⁷⁹. The transition metals M in the central ring of the TMSPs do not affect the chemo- or stereoselectivity of the reaction. A high regioselective preference for the allylic alcohol double bond in **58** and in 1-methylgeraniol is observed. As in previous cases, the stereochemical probe was applied by using chiral allylic alcohols as substrates. A template effect, in which the



allylic substrate is ligated through metal–alcoholate bonding and H_2O_2 is activated in the form of a peroxotungsten complex like **66**, is proposed for this epoxidation.

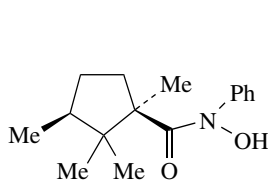
Nickel-containing polyfluorometalated $[\text{Ni}(\text{H}_2\text{O})\text{H}_2\text{F}_6\text{NaW}_{17}\text{O}_{55}]^{9-}$ was capable of catalytic activation of hydrogen peroxide for allylic alcohol oxidation in biphasic conditions (catalyst substrate ratio 1:1000)²⁸¹. Homoallylic alcohols are significantly less reactive than allylic homologues and *cis* > *trans* reactivity is found also in this case.

In 1980, Katsuki and Sharpless¹² described the first really efficient asymmetric epoxidation of allylic alcohols with very high enantioselectivities (ee 90–95%), employing a combination of $\text{Ti}(\text{OPr-}i)_4$ -diethyl tartrate (DET) as chiral catalyst and TBHP as oxidant^{82,83}. Stoichiometric conditions were originally described for this system, however the addition of molecular sieves (which trap water traces) to the reaction allows the epoxidation to proceed under catalytic conditions²⁸². The stereochemical course of the reaction may be predicted by the empirical rule shown in equations 40 and 41. With (–)-DET, the oxidant approaches the allylic alcohol from the top side of the plane, whereas the bottom side is open for the (+)-DET based reagent, giving rise to the opposite optically active epoxide¹². Various aspects of this reaction including the mechanism⁸³, theoretical investigations²⁸³ and synthetic applications of the epoxy alcohol products²⁸⁴ have been reviewed and details may be found in the specific literature^{285,286}.

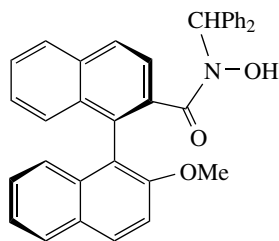


Prior to the usage of the Ti-based catalytic system¹³⁶, the Sharpless group had reported their first asymmetric epoxidation of allylic alcohols using a combination of $\text{VO}(\text{acac})_2/\text{TBHP}$ and the chiral hydroxamic acid **67** (ee $\leq 50\%$)²⁸⁷ or derivatives (ee 80%)²⁴³. In 1999, Yamamoto and coworkers described an improvement of this oxidation protocol, ee values up to 94%, by using hydroxamic acids derived from binaphthol, **68** being the

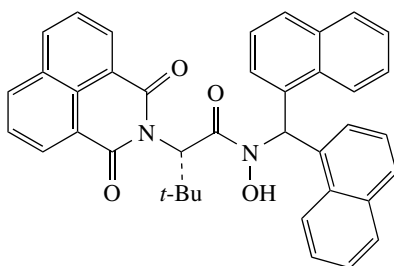
most efficient^{288,289}. This reaction required 5 mol% of VO(OPr-*i*)₃ precursor, only a small excess (7.5 mol%) of ligand and triphenylmethyl hydroperoxide as oxygen source. More recently, the same group introduced a novel α -amino acid-based hydroxamic acid **69** and demonstrated its applicability in the V-catalyzed epoxidation reaction²⁹⁰. Enantiomeric excesses as high as 96% were obtained under mild reaction conditions (0 °C), low degree of catalyst (1 mol%) and ligand (1.5 mol%) loading, using halogen-free solvents. Higher catalyst and ligand concentrations are required to obtain epoxy allylic alcohols (ee up to 95%) in the presence of **70** as chiral inducer (R=Me) and TBHP as oxidant²⁹¹. The steric and electronic properties of substituent R had little effect on the enantioselectivity.



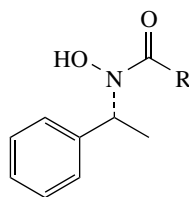
(67)



(68)

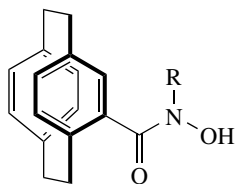


(69)

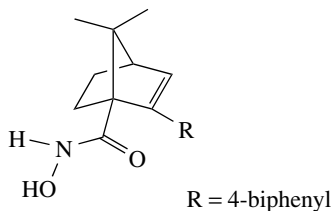


(70)

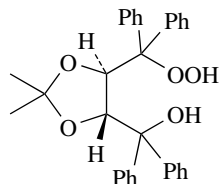
Bolm and coworkers investigated a new class of planar-chiral ligands having a [2.2]paracyclophane backbone^{136,292}. Optimized conditions and the use of **71** as chiral mediator (R = adamantyl) afforded epoxides in good yields, ee values in the range 41–71%, although in long reaction times (3 days). More recently, Wu and Uang reported the use of camphor-based hydroxamic acids in the epoxidation of allylic alcohols²⁹³. Chiral ligands lacking N-substituents and with bulkier aryl groups like **72** afforded the best results (ee \leq 89%).



(71)



(72)



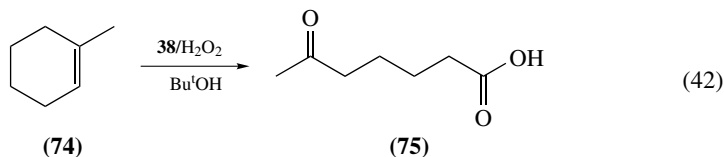
(73)

The metal-catalyzed asymmetric epoxidation of allylic alcohols with various enantiomerically pure hydroperoxides has been studied by several groups. This approach has been employed in the Ti- and V-mediated epoxidation of this class of substrates, in the presence of different achiral additives with modest enantioselectivities ($ee \leq 34\%$ ²⁹⁴, $ee \leq 46\%$ ²⁹⁵), which turned satisfactory ($ee 72\%$)^{17, 296} in the presence of the TADDOL-derived hydroperoxide TADOOH **73**²⁹⁷. This oxidant has been recently employed in the oxovanadium sandwich-type POM $[\text{ZnW}(\text{VO})_2(\text{ZnW}_9\text{O}_{34})_2]^{12-}$ catalyzed epoxidation of various allylic alcohols with very high catalytic efficiency (42000 turnovers) and enantiomeric ratios up to 95:5²⁹⁸.

Different approaches have been used in the preparation of heterogeneous Sharpless-type catalytic systems for the asymmetric epoxidation of allylic alcohols, although in most cases the chiral induction was modest (50–60%). Li and coworkers described the preparation of an organic–inorganic hybrid chiral catalyst grafted onto the surface of silica and in mesopores of MCM-41, and its successful application in asymmetric epoxidation²⁹⁹. Enantiomeric excesses were higher than 80% with conversions in the range 22–76%.

4. Cleavage

Oxidative cleavage of alkenes to aldehydes, ketones or carboxylic acids is an important transformation usually carried out by ozonolysis or oxidation with stoichiometric oxidants, i.e. OsO_4 , MnO_4^- etc.¹⁹⁹. The serious drawbacks of most of these reagents, however, prompt many research groups to investigate this transformation using H_2O_2 in the presence of metal catalysts. Ishii, Ogawa and their coworkers showed that either open chain or cyclic alkenes undergo oxidative cleavage to carboxylic acids with 35% H_2O_2 in the presence of cetylpyridinium 12-tungstophosphate **38**, peroxotungstophosphate **40** or H_2WO_4 in BuOH as solvent^{172, 300, 301}. Thus the oxidation of 1- and 2-octene gave heptanoic and hexanoic acids in 45% and 72% yield, respectively, cyclohexene afforded adipic acid in 81% yield and methylcyclohexene **74** was cleaved to the corresponding keto acid **75** (equation 42). Similarly, hydrogen peroxide may be used in the presence of heteropolyacids like $\text{H}_3\text{PMo}_{10}\text{W}_2\text{O}_{40}$ for the oxidative cleavage of cyclopentene to glutaraldehyde³⁰². 12-Molybdophosphoric, 12-tungstophosphoric and 6-molybdo-6-tungstophosphoric acids, supported onto aluminum, zinc or magnesium oxides and calcinated, showed good catalytic efficiency for the heterogeneously catalyzed olefin cleavage to carboxylic acid with H_2O_2 . The longevity of the catalyst was demonstrated to be maintained up to five or more runs³⁰³. The titanium silicate molecular sieve TS-1 was much less efficient for this heterogeneously mediated transformation, affording oxidative cleavage products in 10–20% yield, depending on reaction conditions³⁰⁴.



Venturello and coworkers³⁰⁵ applied their two-phase catalytic system, based on the tetrakis(diperoxotungsto)phosphate anion $\{\text{PO}_4[\text{W}(\text{O})(\text{O}_2)_2]_4\}^{3-}$ **37** in association with $[(\text{C}_8\text{H}_{17})_3\text{NCH}_3]^+$, to the olefin-to-carboxylic acid oxidation in the absence of organic solvents. Even-number linear-chain α -olefins were easily converted into the respective one less carbon carboxylic acids in 80% yields. Internal and cyclic olefins are equally cleaved with yields in the range 77–87%. A detailed mechanistic investigation of the reaction established, in agreement with most of the studies cited in this section, that the oxidation

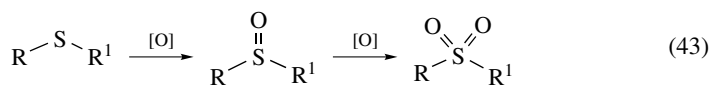
proceeds via epoxidation of the alkene followed by acid hydrolysis or perhydrolysis. Support to this proposal may be found in the studies of Modena and coworkers who found that Mo(VI) peroxo complexes are able to cleave epoxides to carbonyl derivatives, both stoichiometrically and catalytically³⁰⁶, and of Shimizu and coworkers reporting that a number of *vic*-diols have been efficiently cleaved employing heteropolyacid/H₂O₂ systems³⁰⁷. Vanadium compounds have been used for the cleavage of arylalkenes with hydrogen peroxide. Interestingly, the aromatic aldehydes formed (50–98% yield) are not over-oxidized to the corresponding acids³⁰⁸.

The carbon–carbon double-bond cleavage is accessible also with the MTO/H₂O₂ system^{215,309}. By tuning the reaction conditions it was possible to obtain, for a given substrate, either the aldehyde or the carboxylic acid³⁰⁹.

C. Oxidation of Heteroatoms

1. Sulfides

The oxidation of organic sulfur compounds is a broad subject intensively investigated, owing to the importance of sulfoxides as intermediates in organic synthesis³¹⁰. The oxidation of a sulfide affords a sulfoxide as the first product, which may be further oxidized to sulfone (equation 43). Sulfides are oxidized to sulfoxides only by electrophilic oxidants, while sulfoxides are oxidized to sulfones by both electrophilic and nucleophilic oxidants³¹¹. Peroxo complexes of d⁰ transition metals such as Ti(IV), V(V), Mo(VI) and W(VI) are strong electrophiles exhibiting a remarkably high selectivity in the oxidation of dialkyl and alkyl aryl sulfides^{4,13,312}. Homogeneous, two-phase and heterogeneous conditions have been used for this transformation. VO(acac)₂ and MoO₂(acac)₂ catalysts are active in the oxidation of sulfides to sulfoxides with H₂O₂ in EtOH/H₂O^{313,314} or dioxane⁸⁸. The V(V) catalyzed process is 2–3-fold faster than the Mo(VI) analog and both systems are scarcely sensitive to the steric hindrance of the sulfur atom substituents (Bu₂S, BuSBu-*t*, PhSMe, PhSBu-*t*)^{313,315}. The sulfide to sulfoxide oxidation was used to compare the reactivity of the neutral Mimoun-type peroxo complex Mo(O)(O₂)₂HMPT with the anionic peroxo and tetrakisperoxo derivatives Q{Mo(O)(O₂)₂PICO} (Q=R₄N⁺, PICO = picolinate N-oxide anion), **39** and Q₃{PO₄[Mo(O)(O₂)₂]₄} in CHCl₃³¹⁶. The sulfoxide was the sole product observed in the oxidation of substituted methyl phenyl sulfides, the neutral complex Mo(O)(O₂)₂HMPT being the most reactive.

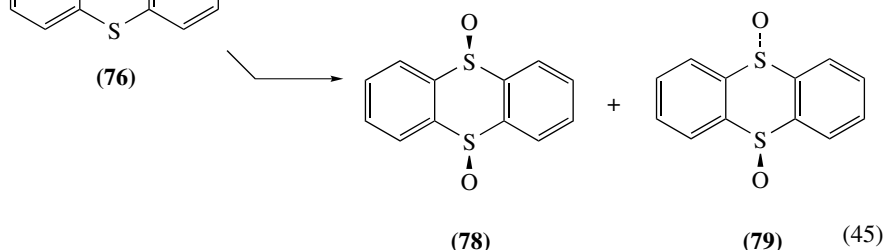
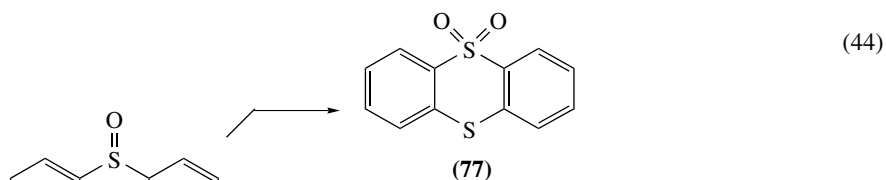


Two-phase procedures have been used for the Mo(VI) and W(VI) catalyzed oxidation of sulfides with aqueous H₂O₂. Both systems involved the formation of an oxidiperoxo complex [MO(O₂)₂] that is transferred into the organic phase either as neutral species or as anion. In the former case neutral ligands like lipophilic phosphoric amides are used as phase-transfer agents¹⁷⁹. The results showed a high degree of selectivity especially with the molybdenum catalyst, the sulfone being often present in traces. In the latter procedure³¹⁷ the use of acidic hydrogen sulfate ion and the ligation of phenylphosphate C₆H₅PO₃H₂ to the W center causes the formation of an anionic [WO(O₂)₂OP(O)(C₆H₅)OH][−] oxidant, transferred into the organic phase by a lipophilic ammonium ion. This peroxo derivative efficiently promotes the oxidation of aromatic and aliphatic sulfides under organic solvent and halogen-free conditions. Oxidation of the sulfide to either sulfoxide or sulfone may be switched depending on conditions. On the contrary, the sulfone was the major product

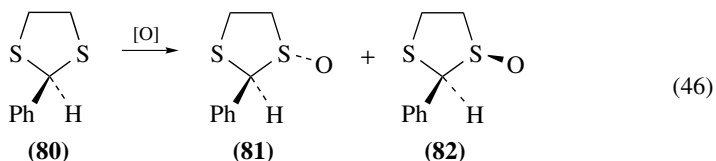
in the oxidation of sulfides with H_2O_2 catalyzed by $\text{PW}_{12}\text{O}_{40}^{3-}$ and a non-cross-linked amphiphilic polymer like **60**, under organic solvent-free conditions³¹⁸.

Methyltrioxorhenium **41** has been established as a good catalyst for the selective oxidation of sulfides to sulfoxides by H_2O_2 ^{319,320}. Both mono **42** and diperoxo species **1** (equation 30) are reactive in this oxidation. High selectivity of sulfoxide over sulfone has been reported, except in the presence of large contents of water in the reaction mixture³¹⁹.

Sulfides may be oxidized to sulfoxides in heterogeneous conditions using Ti-containing zeolites and H_2O_2 or TBHP as oxygen source^{321,322}. Thianthrene 5-oxide **76** has been used as a mechanistic probe to assess the electronic character of the oxidants³²³. Nucleophilic oxidants oxidized the sulfoxide moiety to sulfone **77** (equation 44), while electrophilic species usually afford the *cis*- and *trans*-disulfoxides **78** and **79** (equation 45). For Ti-containing zeolites the latter oxidation pathway prevails³²¹. The same mechanistic probe applied to the homogeneous Ti(IV)/ROOH oxidizing system gave evidence for a coordination of the sulfoxide oxygen to titanium center (template effect), coordination suggested also in previous studies¹³⁰.

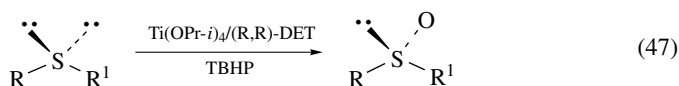


V(V), Mo(VI) and Ti(IV) derivatives proved to be both effective and selective in the oxidation of sulfides with alkyl hydroperoxides³²⁴. As for H_2O_2 , vanadium is at least two-fold more efficient than molybdenum in oxidation and much more selective, as proved by the data obtained with the cyclic disulfide 2-aryl-1,3-dithiolane **80**. A large predominance of the *trans*-S-oxide **81** over the *cis*-derivative **82** is obtained for all the systems investigated (equation 46). However, the diastereoselectivity exhibited by V(V)/TBHP is remarkable^{315,325}.

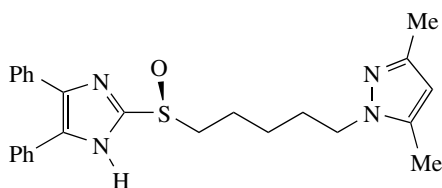


The asymmetric oxidation of prochiral sulfides has become the method of choice for the synthesis of optically active sulfoxides²⁸⁵. The first examples of a really efficient asymmetric oxidation of sulfides to sulfoxides were independently reported by Pitchen

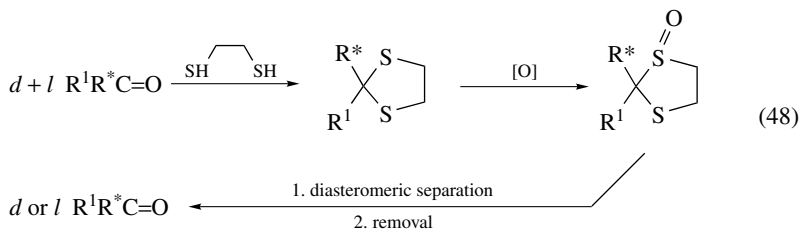
and Kagan⁹⁴ and Modena and coworkers in 1984⁹³ by using a modified Sharpless reagent $\text{Ti}(\text{OPr-}i)_4/\text{DET}/\text{TBHP}$ (equation 47, ee up to 88%)¹². In the oxidation protocol described by Pitchen and Kagan [$\text{Ti}(\text{OPr-}i)_4:\text{DET}:\text{H}_2\text{O}$ 1:2:1], the addition of water significantly increased the enantioselectivity of the reaction. In the experimental conditions reported by Modena and coworkers, a similar enantioselectivity enhancement was found in the presence of an excess of the chiral ligand [$\text{Ti}(\text{OPr-}i)_4:\text{DET}$ 1:4]. The original water-modified oxidation protocol was further optimized (ee values over 99%) by a careful control of the reagent preparation³²⁶, by replacing the oxidant with cumyl hydroperoxide CHP and by reducing catalyst and ligand concentrations³²⁷.



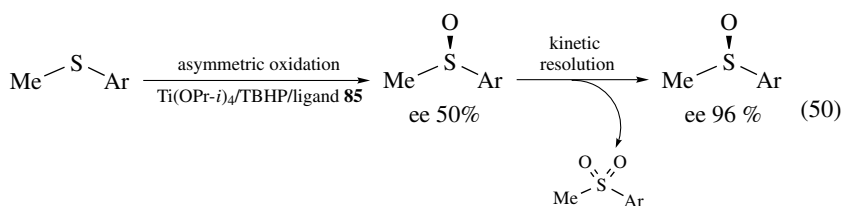
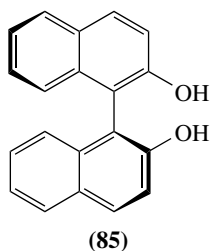
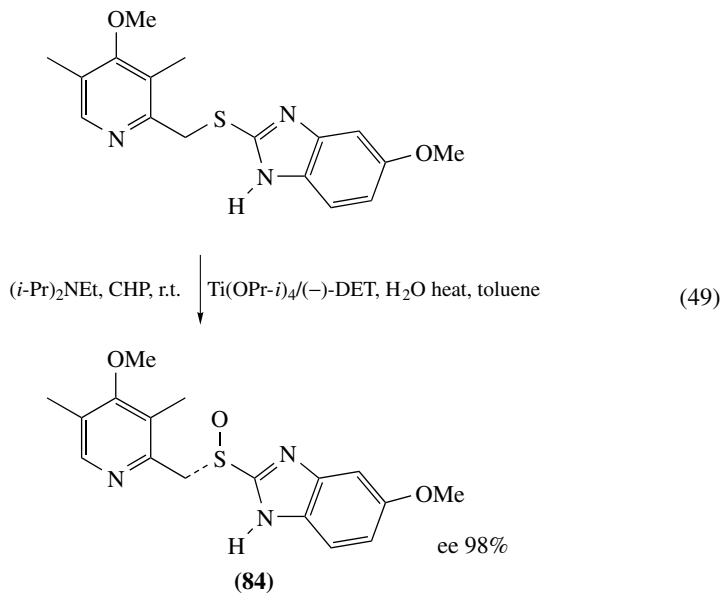
The Kagan and Modena reagents have been successfully applied to a large-scale asymmetric synthesis of biologically active sulfoxides like RP 73163 **83**³²⁸ or for the optical resolution of ketones in the absence of resolving agents³²⁹ (equation 48). More recently, this procedure has been partially modified by addition of diisopropylethylamine (Hunig's base) to the known reagents and applied to the full-scale synthesis of esomeprazole **84**, a drug used in the treatment of acid-related disorders (equation 49)³³⁰.



(83) RP 73163



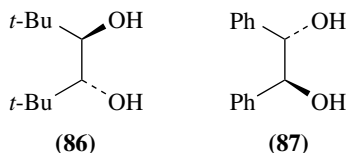
Uemura and coworkers^{331,332} utilized (*R*)-binaphthol **85** as chiral ligand in place of DET in association with $\text{Ti}(\text{IV})/\text{TBHP}$, which not only mediated the oxidation of sulfides to (*R*)-configured sulfoxides, but also promoted the kinetic resolution of sulfoxides (equation 50). In this latter process the two enantiomers of the sulfoxide are oxidized to sulfone by the chiral reagent at different rates, with decrease of the chemical yield, but increase of the ee values³³³. Interestingly, the presence of *ortho*-nitro groups on the binaphthol ligand lead to the reversal of enantioselectivity with formation of the (*S*)-configured sulfoxide³³⁴. Non-racemic amino triols and simple 1,2-diols have been successfully used as chiral mediators.



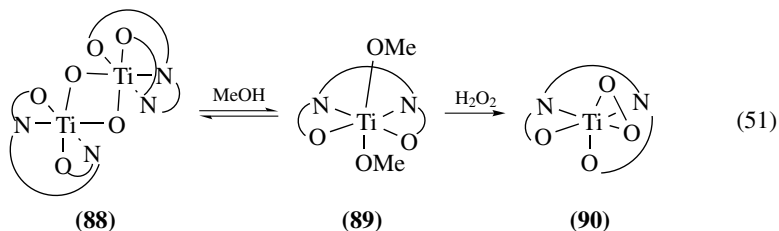
Licini, Bonchio and coworkers^{99,129} utilized trialkanol amines as a new class of ligands for the Ti-based catalytic conversion of sulfides to sulfoxides by TBHP or CHP, as shown in Schemes 5 and 10. Only 0.01 equivalent of catalyst is required to reach ee values up to 84% for (*S*)-sulfoxides. Opposite configured sulfoxides may be obtained using the Zr(IV)/trialkolanol amine combination with ee values in the range 80–90%¹³¹. The occurrence of a Ti-peroxy derivative oxidizing agent **33** for these transformations has been confirmed also by ESI-MS and NMR techniques^{99,100}.

Simple 1,2-diols (*R,R*)-**86** and (*S,S*)-**87** have been used by Yamonai and Imamoto³³⁵ and Rosini and coworkers^{336,337}, respectively, in association with Ti(OPr-*i*)₄ and CHP

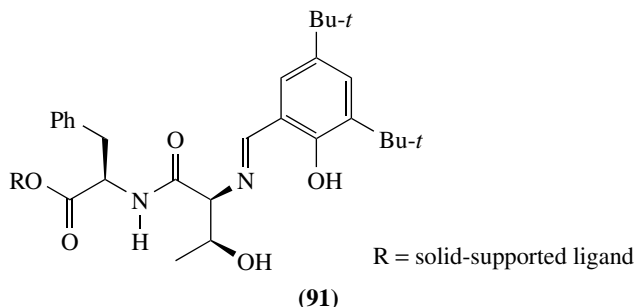
or TBHP as oxidants for sulfide enantioselective oxidation. Kinetic resolution to some extent contributed to the observed ee values, up to 95% and 99% for the two cases. As expected, use of the ligand **87** in opposite configuration, i.e. (*R,R*), afforded the opposite enantiomeric sulfoxide.



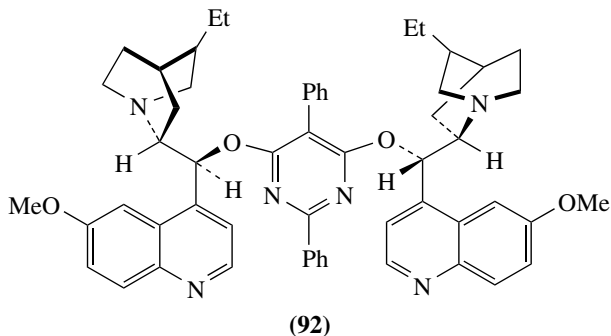
Katsuki³³⁸ reported that di- μ -oxo Ti(salen) complex **88** was an excellent catalyst for asymmetric sulfoxidation with UHP adduct as oxidant in methanol (ee 92–99%)³³⁹. The same group found that **88** dissolved in MeOH rapidly dissociated into a monomeric Ti(salen) complex **89**, which reacted with H₂O₂ to give rise to the corresponding peroxy species **90**, active in the oxidation process³⁴⁰ (equation 51).



A solid-phase sulfur oxidation catalyst has been described in which the chiral ligand is structurally related to Schiff-base type compounds (see also below). A 72% ee was found using Ti(OP*r*-i)₄, aqueous H₂O₂ and solid-supported ligand **91**³⁴¹. More recently, a heterogeneous catalytic system based on WO₃, 30% H₂O₂ and cinchona alkaloids has been reported for the asymmetric oxidation of sulfides to sulfoxides and kinetic resolution of racemic sulfoxides. In this latter case 90% ee was obtained in the presence of **92** as chiral mediator³⁴².

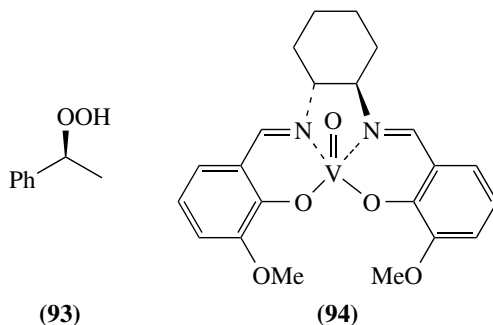


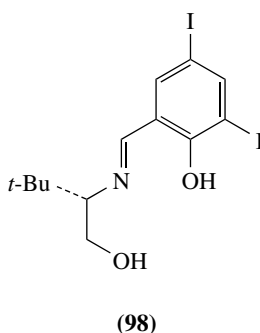
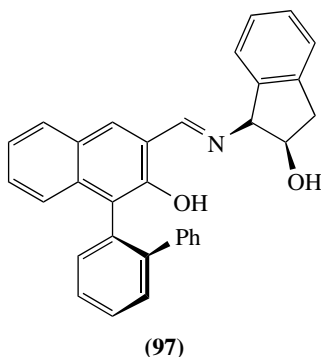
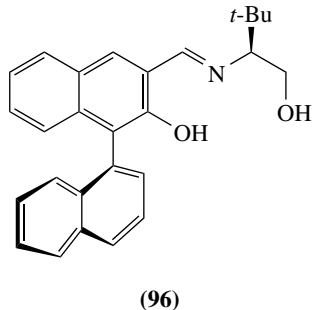
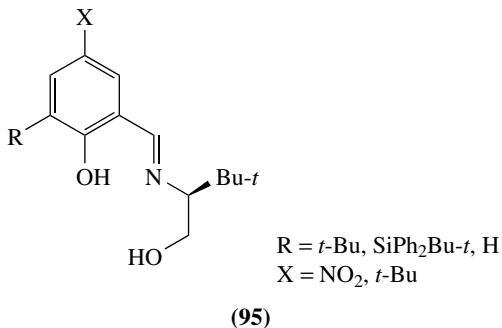
A different approach to the metal peroxy-mediated asymmetric oxidations of sulfides was proposed by Chmielewski and coworkers³⁴³ and more recently by Korb, Adam and coworkers¹³² based on the use of optically active hydroperoxides. First attempts to use



optically active sugar-derived hydroperoxides in the presence of MoO_3 were moderately successful with a maximum ee value of 26%. Higher enantiomeric excesses (*ca* 80%) were reported in the oxidation of methyl *p*-tolyl sulfide, using (*S*)-1-phenylethyl hydroperoxide **93** in CCl_4 ¹³². The enantioselectivity is significantly enhanced by kinetic resolution, through sulfoxide coordination to titanium, as found previously for many Ti-mediated oxidations.

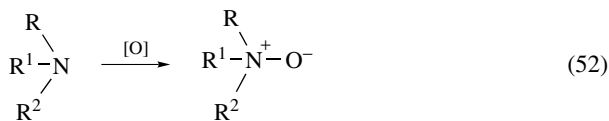
Asymmetric sulfoxidations with vanadium complexes have been extensively investigated by many authors and the most relevant results were achieved using chiral Schiff base complexes¹³⁶. In 1986, Nakajima and collaborators described the application of the tetradentate oxovanadium(IV) complex **94** as catalyst for the sulfoxidation of methyl phenyl sulfide with CHP in 42% ee³⁴⁴. A few years later Bolm and Bienewald reported a very promising and efficient catalyst formed in situ from the Schiff bases **95** and $\text{VO}(\text{acac})_2$, using H_2O_2 as oxygen source³⁴⁵. With the new system a low catalyst amount, in the range 1–0.01 mol%, was sufficient to give optically active sulfoxides with ee values up to 85%. The oxidations are not affected by oxygen or water and the chiral ligands are readily available from salicyl aldehydes and amino alcohols³⁴⁶. Improvements in the selectivity were later achieved using more complex Schiff bases bearing extra chirality on the substituents. Binaphthyl-derived ligands **96**³⁴⁷ and **97**³⁴⁸ in place of **95** afforded methyl phenyl sulfoxide in 78% and 88% ee, respectively, and very high chemical yields. On the contrary, Anson and coworkers demonstrated that high enantioselectivities may be achieved with simple and readily available chiral Schiff bases bearing only one chiral center like **98**³⁴⁹. Enantiomeric excesses from 89 to 97% are found for the different alkyl aryl sulfides investigated.

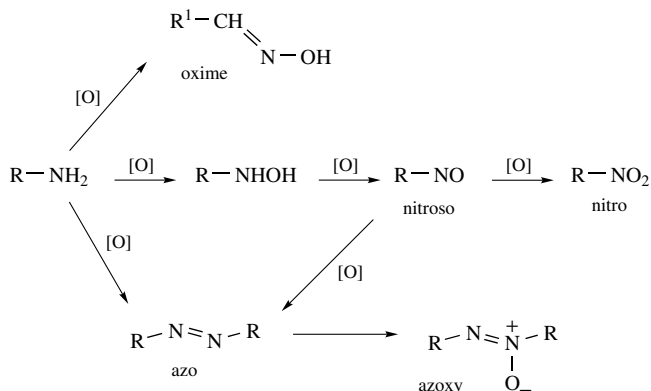




2. Amines

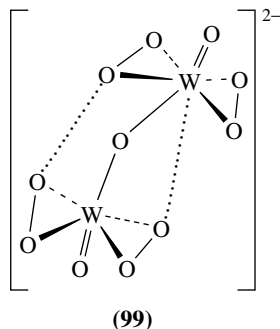
Oxidation of organonitrogen compounds is an important process from both industrial and synthetic viewpoints^{13,199}. N-oxides are obtained by oxidation of tertiary amines (equation 52), which in some cases may undergo further reactions like Cope elimination and Meisenheimer rearrangement¹⁹⁹. The oxygenation products of secondary amines are generally hydroxylamines, nitroxides and nitrones (equation 53), while oxidation of primary amines usually afforded oxime, nitro, nitroso derivatives and azo and azoxy compounds through coupling, as shown in Scheme 17. Product composition depends on the oxidant, catalyst and reaction conditions employed.



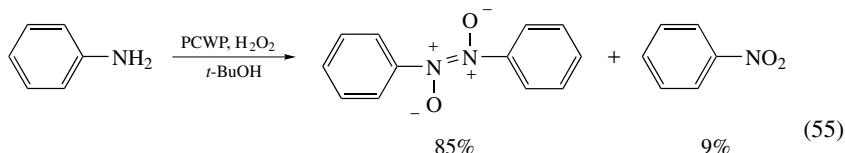
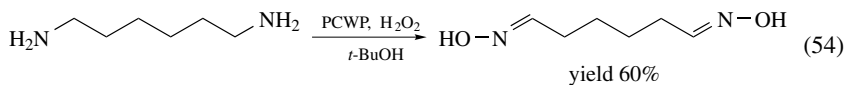


SCHEME 17

Aliphatic tertiary amines can be oxidized to N-oxides by aqueous H_2O_2 ; however, it is possible to increase the system efficiency by adding W- or Mo-based catalysts^{350, 351}. The Venturello catalyst $\{\text{PO}_4[\text{W}(\text{O})(\text{O}_2)_2]_4\}^{3-}$ **37**, the As-analogue $\{\text{AsO}_4[\text{W}(\text{O})(\text{O}_2)_2]_4\}^{3-}$ and the dimeric complex $[\text{W}_2\text{O}_3(\text{O}_2)_4]^{2-}$, in association with the tetrahexylammonium cation $[\text{N}(\text{C}_6\text{H}_{13})_4]^+$, were shown to catalyze the oxidation of tertiary amines to N-oxides with H_2O_2 in toluene–15% water at 85°C ³⁵². Similar efficiencies were found for the three systems, with turnover numbers higher than 200. For the derivative $[\text{W}_2\text{O}_3(\text{O}_2)_4]^{2-}$, an isopolyperoxo structure like **99** has been suggested.

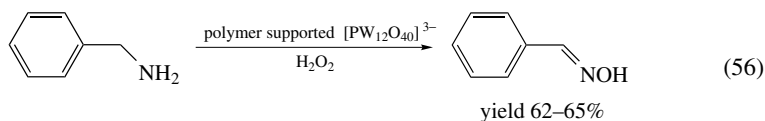


The Venturello–Ishii catalyst PCWP **40** was found to efficiently catalyze the oxidation of primary and secondary amines with H_2O_2 in two-phase or homogeneous conditions³⁵³. Aliphatic cyclic and acyclic primary amines (including benzylamine) are converted into oximes (56–81% yield) and the 1,6-hexadiazine afforded the corresponding dioxime (equation 54). Secondary amines are oxidized to nitrones in very good yields and aromatic amines afforded the corresponding nitroso dimers and nitrobenzenes (equation 55). More recently, the PCWP catalyst and the Mo homologue $\{\text{PO}_4[\text{Mo}(\text{O})(\text{O}_2)_2]_4\}^{3-}$ in association with $[\text{N}(\text{C}_6\text{H}_{13})_4]^+$ or the cetylpyridinium cation were used for the stoichiometric oxidation of *N,N*-benzylalkylamines that are quantitatively converted to nitrones³⁵⁴. Similar results are obtained by employing both anionic and neutral Mo- and W-oxodiperoxo oxidants³⁵⁵.

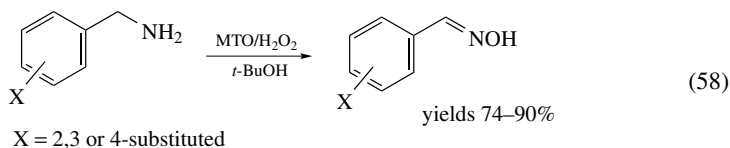
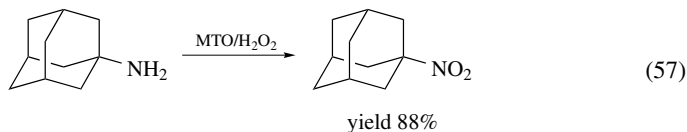


Oxidation of secondary amines with H_2O_2 in the presence of Na_2WO_4 gave the corresponding nitrones in good to excellent yields (40–90%)³⁵⁶. Cyclic and acyclic amines are converted in mild conditions, room temperature, 3 h, using MeOH or H_2O as solvents.

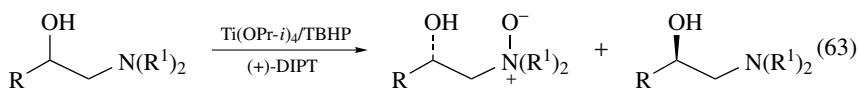
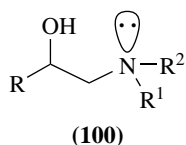
The heteropolyacid anion $[\text{PW}_{12}\text{O}_{40}]^{3-}$ assembled with a non-cross-linked amphiphilic polymer similar to **60** was used as catalyst for the oxidation of amines with H_2O_2 under organic solvent-free conditions³¹⁸. Primary amines are converted into the corresponding oximes (equation 56) and secondary amines are oxidized to nitrones in good yields (70–94%). It is noteworthy that the catalyst can be reused five times with the turnover number up to 500. Cyclic and acyclic secondary amines may be readily oxidized to the corresponding nitrones using UHP **43** and Mo(VI) or W(VI) catalyst³⁵⁷. The reactions, conveniently performed at room temperature in MeOH, indicated Na_2WO_4 as the most effective catalyst.



In 1995, Zhu and Espenson reported on the MTO **41** catalyzed oxidation of aniline to nitrosobenzene and of substituted *N,N*-dimethylanilines to the corresponding *N*-oxides using H_2O_2 as oxygen source³⁵⁸. Similarly and shortly later, Murray and coworkers published their results on the oxidation of primary³⁵⁹, secondary³⁶⁰ and tertiary organonitrogen compounds with the MTO– H_2O_2 system. Anilines and aliphatic primary amines with no α -hydrogens (equation 57) are oxidized to nitro derivatives³⁵⁹, secondary amines are converted into nitrones in very good chemical yields ($\leq 95\%$)³⁶⁰, pyridine is oxidized to *N*-oxide and azobenzene to azoxybenzene³⁵⁹. The MTO– H_2O_2 oxidation of primary amines possessing α -hydrogens was investigated by Yamazaki³⁶¹. Benzylamines were selectively oxidized to oximes (equation 58), whereas primary alkylamines were oxygenated to a mixture of oximes, nitroso dimers and azoxy compounds (equation 59). With the same system secondary amines were converted into nitrones^{361,362}.

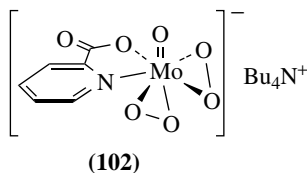
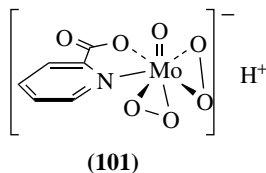


Few reports may be found in the literature concerning the asymmetric oxidation of organonitrogen compounds using metal peroxo derivatives. The most successful examples refer to N-containing substrates having a hydroxyl group able to coordinate the chiral metal centers as in β -hydroxyamine of general formula **100**. In order to have enantioselective oxidation, a slightly modified Sharpless oxidation protocol must be applied to this class of derivatives³⁸⁵. The general procedure consists in the kinetic resolution of the racemic substrate with selective oxidation of one enantiomer to N-oxide using the $\text{Ti}(\text{OPr-}i)_4/\text{TBHP}/(+)\text{diisopropyl tartrate (DIPT)}$ combination, followed by separation from the unreacted optically active amino alcohol, as shown in equation 63^{368, 369}. Except for few substrates, the amino alcohols are obtained in ee values higher than 90% when two important changes are made in the reaction procedure³⁶⁹. The first variation refers to the titanium:tartrate ligand ratio, originally 2:2, optimized to values close to 2:1, depending on substrate^{368, 370}. The second change named 'aging period' consists in the mixing of the amino alcohol with dialkyl tartrate and $\text{Ti}(\text{OPr-}i)_4$ in CH_2Cl_2 for 30 min at room temperature. The solution is then cooled and TBHP is added to perform the N-oxidation.

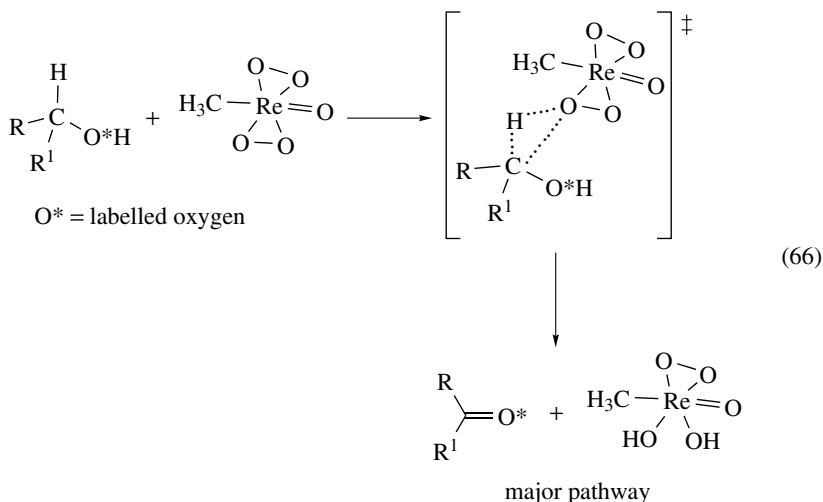


D. Oxidation of Alcohols

The selective oxidation of alcohols to the corresponding carbonyl compounds using peroxometal species is an important transformation in organic synthesis. This kind of reaction is usually observed with early transition metal ions having a d^0 configuration, namely Mo(VI), W(VI), Ti(IV) and Re(VII), and is performed under both homogeneous and heterogeneous conditions in the presence of H_2O_2 (or ROOH) as primary oxidant³⁷¹. Anionic W(VI) and Mo(VI) peroxo complexes, containing either H^+ **101**³⁷² or a lipophilic cation **102**^{373, 374}, have been employed as effective oxidants of primary and secondary alcohols to carbonyl compounds. Using stoichiometric amounts of **102** in non-polar solvents, no competition with double-bond epoxidation or aldehyde over-oxidation is observed³⁷⁴ (equation 64). Trost and Masuyama found that ammonium molybdate $(\text{NH}_4)_6\text{Mo}_7\text{O}_{24} \cdot 4\text{H}_2\text{O}$ in combination with Bu_4NCl and a base (K_2CO_3) catalyzed the oxidation of secondary alcohols with hydrogen peroxide³⁷⁵. Alcohol oxidation prevailed over olefin epoxidation and more hindered hydroxy functions can be oxidized in preference to less hindered ones, although in very long reaction times (1–7 days).

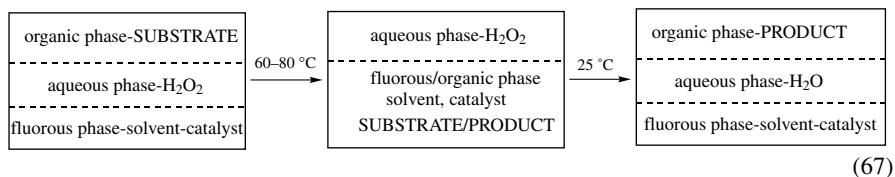


corresponding aldehydes and ketones, respectively. A mechanistic feature involving hydride abstraction is proposed for this reaction for the first time (equation 66) on the basis of kinetic data and labeling experiments. The addition of a catalytic quantity of bromide ions, as HBr or NaBr, greatly enhances the oxidation rates^{382,383}.



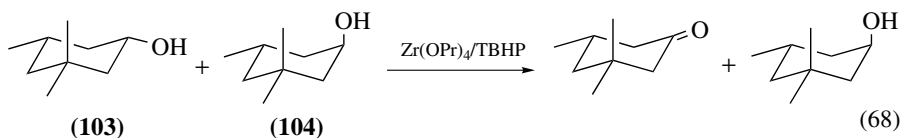
An inner-sphere hydrogen atom abstraction from the alcohol by a peroxo metal complex, thus forming a coordinated ketyl radical $[(\text{CH}_3)_2-\text{C}^\bullet-\text{O}-\text{V}(\text{O})(\text{OOH})]^{m-1}$, has been proposed for the aerobic oxidation of alcohols catalyzed by peroxidic molybdenum and vanadium derivatives^{164,166,167} (Scheme 16). While in the case of Mo-catalyzed reaction the H_2O_2 produced is quantitatively converted to products (ketone and H_2O), in the vanadium mediated process, hydrogen peroxide accumulates^{166,167}. In this latter case, the direct involvement of a vanadium monoperoxo species has been substantiated by ESI-MS data.

Polyoxometalates have been used as catalysts for the oxidation of different alcohol typologies with hydrogen peroxide in biphasic conditions. Neumann and Gara showed that $[\text{WZnMn}_2(\text{ZnW}_9\text{O}_{34})_2]^{12-}$ dissolved in an organic solvent (DCE) by a quaternary ammonium ion may be used as effective catalysts for the oxidation of secondary alcohols with 30% H_2O_2 ¹⁸⁵. Neumann and coworkers prepared a water-soluble derivative, $[\text{WZnZn}_2(\text{H}_2\text{O})_2(\text{ZnW}_9\text{O}_{34})_2]^{12-}$, particularly efficient in the oxidation of various alcohols with H_2O_2 , in the absence of added organic solvents³⁸⁴. Primary and benzylic alcohols are oxidized to the corresponding carboxylic acids. In a further paper, these authors described a remarkable improvement of their methodology based on the use of polyfluorinated quaternary ammonium salts, i.e. $[\text{CF}_3(\text{CF}_2)_7(\text{CH}_2)_3\text{N}^+\text{CH}_3$ or $\text{R}_\text{F}\text{N}^+$, as counteractions for the $[\text{WZnM}_2(\text{H}_2\text{O})_2(\text{ZnW}_9\text{O}_{34})_2]^{12-}$ ($\text{M}=\text{Mn}, \text{Zn}$) catalyst³⁸⁵. The procedure is based on the thermomorphic properties of the fluorous biphasic catalysts $(\text{R}_\text{F}\text{N})_{12}[\text{WZnM}_2(\text{H}_2\text{O})_2(\text{ZnW}_9\text{O}_{34})_2]$ with or without fluorous solvents. At room temperature, the catalyst is freely soluble in perfluorohydrocarbons and insoluble in common organic solvents, but soluble upon heating to 60–80 °C. The temperature-dependent overall process is shown in equation 67 and represents a practical example of separation of the catalyst from the remaining components and its reuse for other reaction cycles.



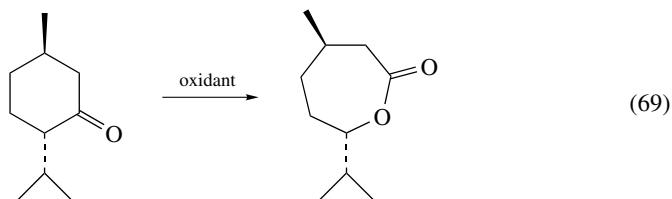
In the field of heterogeneous catalysis using H₂O₂ as oxygen source, examples of the use of titanium-silicalite (TS-1)³⁸⁶ or Ti-beta³⁸⁷ in the oxidation of selected alcohols, with formation of a Ti-peroxo species, have been reported³⁷¹.

Oxidation of primary, secondary and benzylic alcohols with TBHP or CHP, mainly catalyzed by Mo and Zr derivatives, were performed by different authors. As an example, Ishii, Ogawa and coworkers reported the conversion of secondary alcohols such as 2-octanol to ketones mediated by catalyst **39** and TBHP. The oxidation of cyclic alcohols depended on steric factors³⁸⁸. Zirconium alkoxides may act as catalysts in the conversion of different alcohol typologies with alkyl hydroperoxides³⁸⁹. Secondary alcohols, if not severely hindered, are quantitatively converted to the corresponding ketones. The selectivity for equatorial alcohols is a general feature of the system, as confirmed by the oxidation of the sole *cis* isomer **103** of a mixture **103**+**104** (equation 68). Esters and acids could be the by-products in the oxidation of primary alcohols.



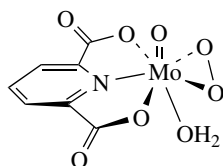
E. Oxidation of Ketones

Acyclic and cyclic ketones may be oxidized to esters or lactones, respectively, by a variety of oxidants including peracids or peroxides associated with suitable catalysts. This reaction is known as Baeyer–Villiger (BV) oxidation³⁹⁰ and it was originally applied to the oxidation of menthone and tetrahydrocarvone with monopersulfuric acid (equation 69). With the increase of environmental concern, much research has focused on the development of catalytic BV processes based on green and cheap oxidants like hydrogen peroxide and relatively non-toxic metals (Re, Pt, Ti)¹²¹.

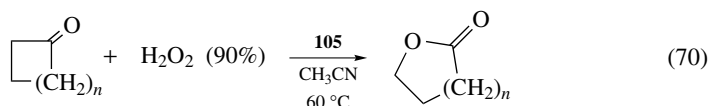


The first report of transition-metal peroxides active in the BV oxidation of cyclic ketones was due to Mares and coworkers in 1978³⁹¹. These authors found that Mo-peroxo complexes, containing picolinato **101** and especially dipicolinato ligands **105**, are able to mediate the transformation of some cyclopentanones and cyclohexanones to the corresponding lactones by concentrated H₂O₂ (equation 70) with yields in the range

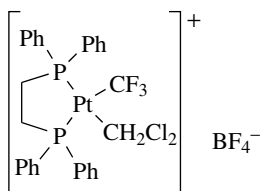
10–87%, although with poor turnovers³⁹¹. This reaction has been revisited by Campestrini and Di Furia, who provided strong evidence that Mo-peroxo complexes are unable to act as nucleophilic oxidants of ketones, hydrogen peroxide being the real active species for this transformation³⁹². The indirect role played by metal peroxo complexes in this kind of oxidation has been also reported by Bortolini and Conte, who found that the vanadium triperoxo complex $[V(O_2)_3]^-$, expected to mediate the BV oxidation of cyclobutanone to γ -butyrolactone²¹, acts uniquely as a source of HOO^- ²².



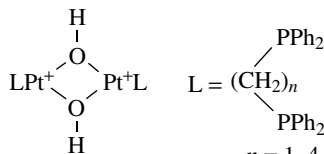
(105)



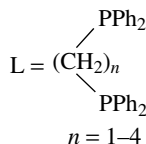
The first unambiguous example of transition-metal catalysis for this reaction is represented by platinum derivatives, in particular complex **106**, successfully tested in the BV oxidation of several cyclic ketones using 35% H_2O_2 at room temperature³⁹³. Simple ketones as well as more complex substrates are oxidized under mild conditions; however, catalyst deactivation, due to the hydroxy acids formed from lactone hydrolysis, limits the turnover of the system. Subsequent studies on the evolution of Pt(II) compounds under acidic condition led to the identification of a class of dimeric hydroxy complexes **107**, efficient in the BV oxidation of ketones using H_2O_2 as primary oxidant^{394, 122}. The ability of **107** to promote the oxidation was investigated using methylcyclohexanone as a model substrate (equation 71). In all cases the selectivity of the reaction was $>99\%$ and ϵ -heptanelactone was the only product observed¹²². The reactivity increased as the size of the diphosphane-Pt ring is enlarged, allowing for **108** the oxidation of a series of acyclic ketones to the corresponding esters (equation 72). Attempts to immobilize the platinum complex **108** into ion-exchange resins resulted in a significant loss of catalytic activity³⁹⁵. The proposed mechanism for this reaction is shown in Scheme 19. A fast dissociation of the dimeric complex is followed by the rate-determining step of an intramolecular nucleophilic attack of the hydroperoxy ligand on the coordinated ketone.

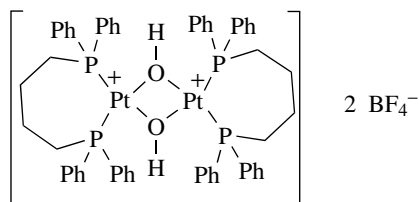


(106)

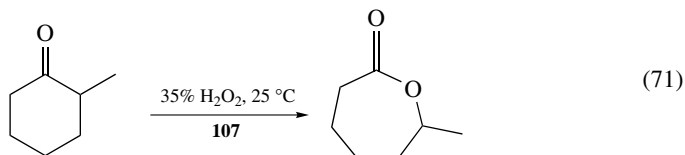


(107)

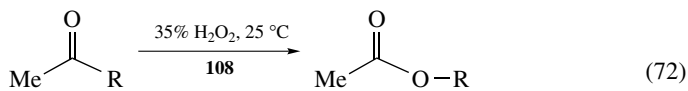




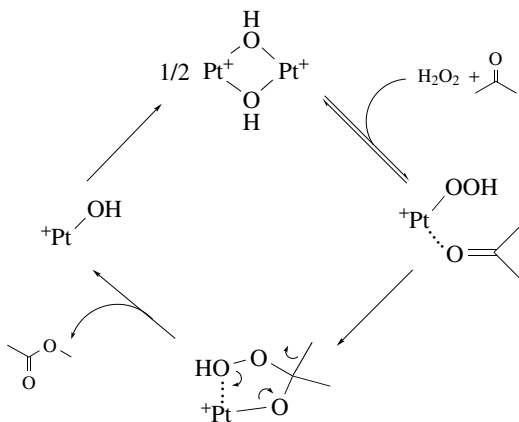
(108)



(71)



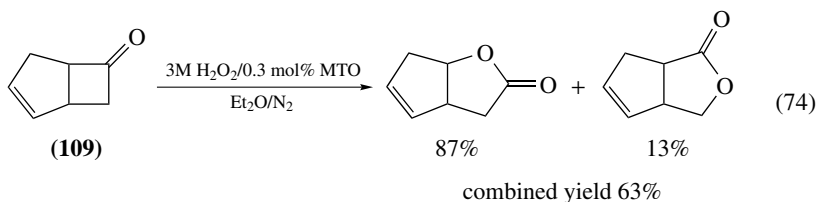
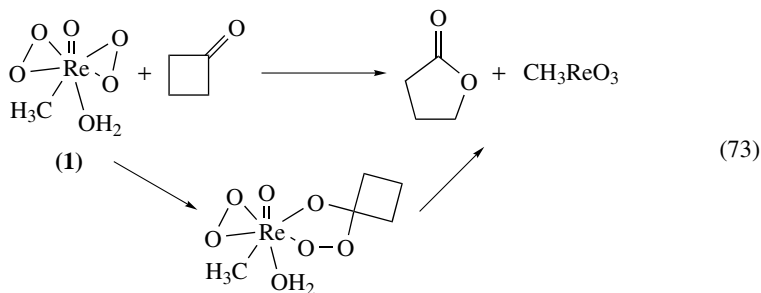
(72)

R = *n*-Bu, *t*-Bu, *s*-Bu, Ph, vinyl

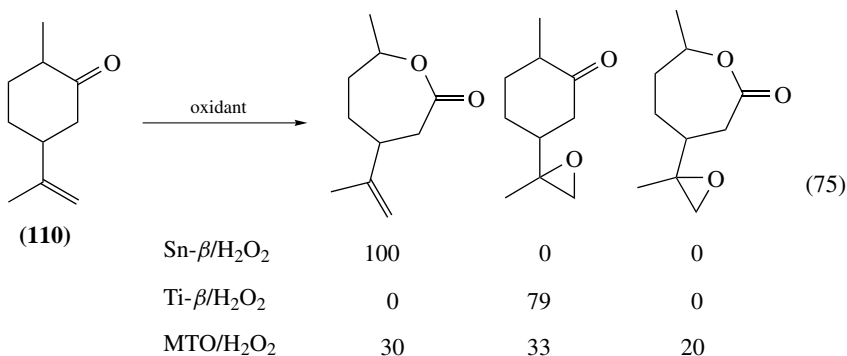
SCHEME 19

The possibility of performing BV oxidations using the MTO/H₂O₂/*t*-BuOH combination^{213,214} was reported by Herrmann and coworkers in their first paper on this oxidizing system²³. Cyclic ketones are converted into lactones (yields in the range 5–80%) with the ring-strained cyclobutanone being the most active³⁹⁶. In contrast with previous studies on other systems^{22,392}, the diperoxorhenium complex **1** reacts with cyclobutanone also under stoichiometric conditions to yield γ -butyrolactone (equation 73). As soon as the ketone has been added to the solution of **1**, the formation of an intermediate, likely peroxometalocyclic^{121,396,397}, can be observed and characterized by means of different techniques. The oxidation of a series of cyclobutanones has been investigated also by Faisca, Philips and Romao, who found lactonization of the cyclic ketones also in the

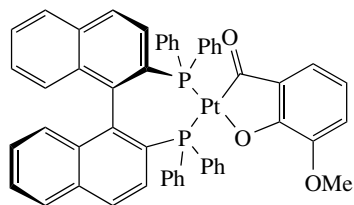
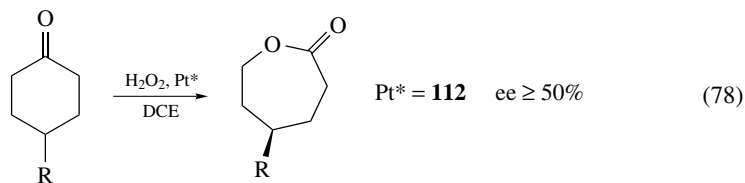
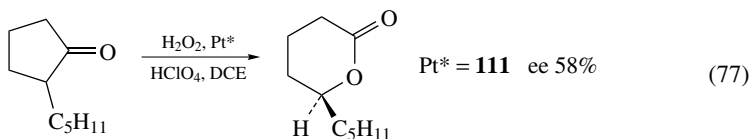
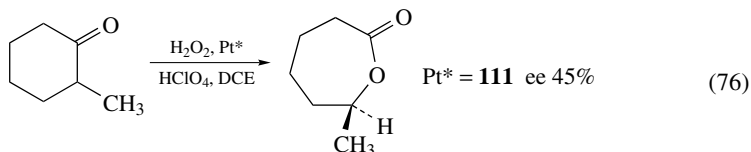
presence of double bonds, aromatic rings and chlorine substituents³⁹⁷. As an example, the oxidation of the bicycloheptenone **109**, in which epoxidation of the double bond could compete with the BV reaction, afforded the bicyclic lactones in 63% combined yield, with only 5% by-product formation (equation 74). Synthetic applications of the MTO/H₂O₂ catalytic system for the BV oxidation of pharmaceutically important flavonone derivatives^{398, 399} or in non-conventional media like ionic liquids have been reported⁴⁰⁰.



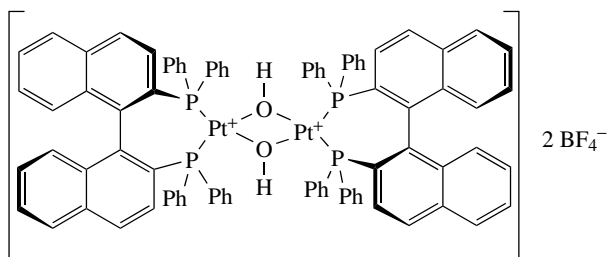
TS-1 zeolites have been used in the presence of H₂O₂ to perform the BV reaction on cyclic and aromatic ketones⁴⁰¹. Cyclohexanone and acetophenone can be oxidized at 80 °C with selectivities lower than 60%, due to the formation of α -hydroxyketones and other undesired products. The observed modest results seem to be associated with the poor selectivity of the active Ti-peroxo species. In this respect, Corma and coworkers developed new Sn-based heterogeneous catalysts able to selectively activate the ketone instead of H₂O₂^{402–404}. Cyclic ketones are transformed into the corresponding lactones and unsaturated cyclic ketones like **110** are oxidized to unsaturated lactones in very high chemoselectivity⁴⁰³, unusual for other oxidizing systems (equation 75). As expected, the authors failed to detect the presence of metal-peroxo derivatives in their systems⁴⁰⁵.



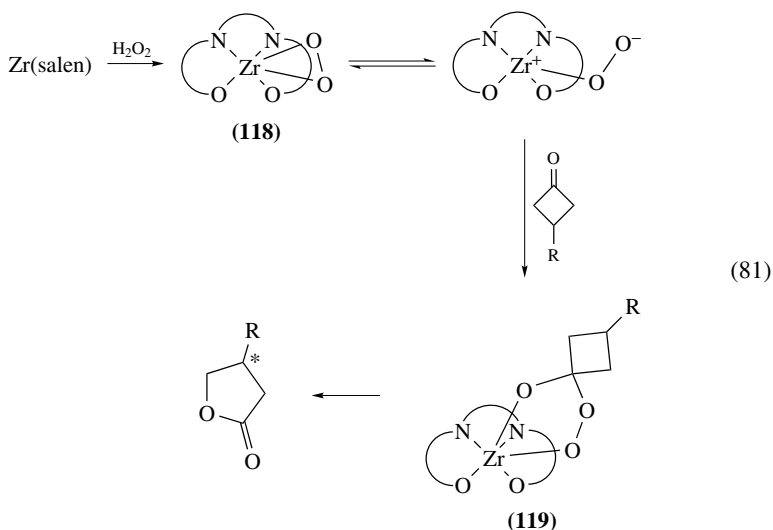
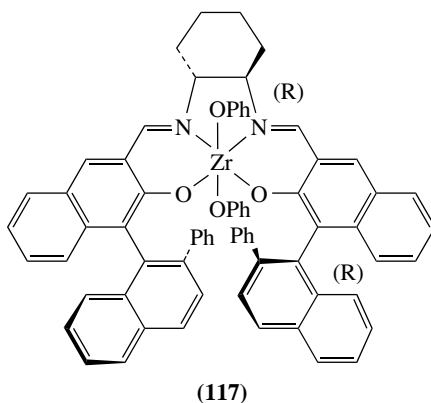
The first example of metal-catalyzed enantioselective BV oxidation using H_2O_2 was published by the group of Strukul in 1994⁴⁰⁶. The kinetic resolution of racemic ketones like 2-methylcyclohexanone (ee 45%, equation 76) and 2-pentylcyclopentanone (ee 58%, equation 77), through enantiospecific conversion into chiral lactones, were obtained using the chiral [(*R*)-binap]Pt(2-van) **111** as metal catalyst. The same catalytic system has been applied to the disymmetrization of *meso* cyclohexanones (equation 78) using 35% H_2O_2 and chiral **107**-type platinum derivatives¹²³. The best results, with ee values higher than 50%, are obtained with Pt complexes coordinated to (*R*)-binap ligands **112**.



(111)



(112)



F. Oxidation of Hydrocarbons

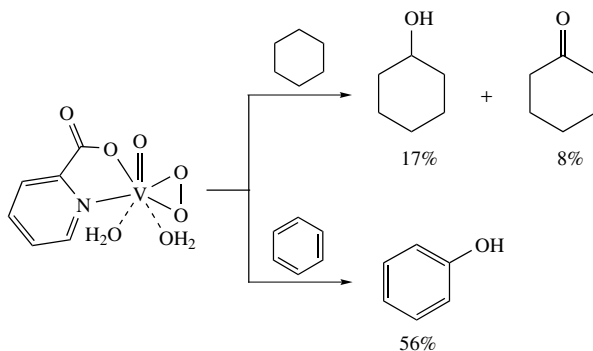
Oxidative functionalization of aliphatic and aromatic hydrocarbons is a somewhat difficult chemical transformation, in particular when a suitable degree of chemoselectivity is required. Until the last decades of the last century, metal-catalyzed functionalization of hydrocarbons with peroxides were basically limited to Fenton and Fenton-like systems⁴¹¹.

The involvement of transition metal peroxo species in the oxidative functionalization of alkanes and arenes has been postulated for several metals with both hydrogen peroxide and alkyl hydroperoxides.

Typical examples referring to titanium derivatives are alkoxides with TBHP⁴¹² and titanosilicate (in particular TS-1) in the presence of H₂O₂⁴¹³. Based on this latter system, ENICHEM¹¹ commercialized a procedure for hydroxylation of phenol to catechol and hydroquinone. Other activated arenes are also hydroxylated by TS-1 and hydrogen peroxide¹¹. Interestingly, for TS-1 catalysis a mechanism similar to that proposed

for vanadium, and reported in Scheme 15, explains the experimental results⁴¹³. In other cases⁴¹² the role of the peroxy metal species is quite unclear.

One of the breakthroughs in the field was reported in 1983 by Mimoun and coworkers¹⁶¹. On that occasion they reported the synthesis, characterization and radical reactivity of a class of vanadium peroxy complexes representative of which is the species $\text{VO}(\text{O}_2)\text{pic}(\text{H}_2\text{O})_2$, **36**. The oxidative ability of this complex has been tested with several aliphatic and aromatic hydrocarbons and the synthetic results obtained can be summarized as in Scheme 20.



SCHEME 20

Subsequently, the reaction has been studied in depth not only from the mechanistic point of view, as has already been discussed in the mechanistic aspects paragraph, but also from a synthetic approach. Details on these studies have been collected and discussed³¹⁵. Indeed, catalytic processes have been settled by using two different methodologies, first by slow or stepwise addition of excess hydrogen peroxide in a homogeneous system⁴¹⁴ (the most important results are collected in Table 4), and second by using the two-phase procedure depicted in Scheme 21. In both cases, acid catalysis is beneficial as far as yields of hydroxylated products and rates of reactions are concerned. With the two-phase procedure and stepwise addition of the peroxide, a 42% yield of phenol was obtained by using only 0.055 mmol of benzene dissolved in 5 mL of the organic phase.

TABLE 4. $\text{C}_6\text{H}_5\text{X}$ hydroxylation reaction (2 mmol) with **36** (0.048 mmol) with or without added H_2O_2 in CH_3CN (10 mL, $\text{CH}_3\text{SO}_3\text{H}$ 0.048 mmol)

X	H_2O_2 , mmol	T^a ($^\circ\text{C}$)	$\text{XC}_6\text{H}_4\text{OH}$, mmol	Yield ^b (%)
CH_3	—	40	2.7	68 ^d
CH_3	0.048 ^c	40	35.9	68 ^d
H	—	25	3.5	70
H	0.025 ^e	40	20.4	69
F	—	40	3.2	67
Cl	—	40	2.8	59
Cl	0.034	40	24.8	63
NO_2	—	40	2.9	62

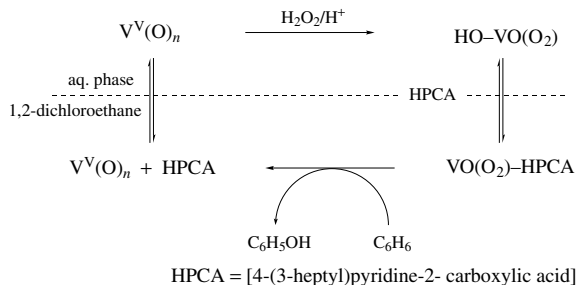
^a Reaction time *ca* 120 min.

^b Measured as $(\text{mol C}_6\text{H}_5\text{OH}/\text{mol}(\mathbf{36} + \text{H}_2\text{O}_2) \times 100)$.

^c Slow addition of peroxide through a syringe pump.

^d About 10% of products derived from methyl oxidation.

^e Stepwise addition of the peroxide.



SCHEME 21

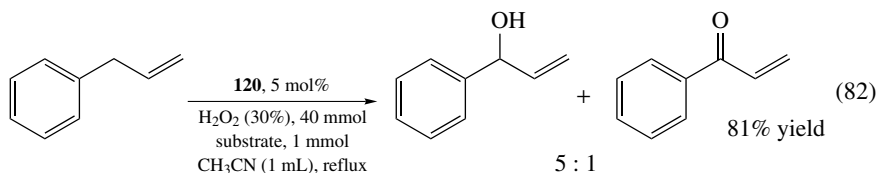
We note that the vanadium alkylperoxidic complex **8** hydroxylates aliphatic and aromatic molecules in a similar manner⁵⁶.

Shul'pin and coworkers have demonstrated, in several papers, that other peroxy vanadium complexes closely related to **36**, containing in the coordination sphere amino acids, nitrogen-containing bases or weak carboxylic acids, are effective oxidants of saturated and aromatic hydrocarbons. An accurate account containing this work, together with results related to the use of other transition metals, has appeared⁴¹⁵ and all the relevant literature can be found there.

Vanadium-catalyzed hydrocarbon oxidation with peroxides can be carried out also by supporting the catalyst with the appropriate ligand on polymers⁴¹⁶, on silica⁴¹⁷ or encapsulating it in zeolites⁴¹⁸. Similar activity has been obtained with vanadium-containing polyoxometalates^{419, 420}.

Vanadium-catalyzed hydroxylation of benzene and cyclohexane has also been obtained with in situ generation of hydrogen peroxide from H_2/O_2 in the presence of palladium⁴²¹. A similar process has been settled for methane oxygenation to methyl trifluoroacetate and formic acid⁴²². Monoperoxovanadate, as well as copper hydroperoxides, have been indicated as the active species for the activation of the C–H bond of methane.

$\text{MoO}(\text{O}_2)_2(\text{dmpz})_2$, **120**, containing 3,5-dimethylpyrazole (dmpz) in the coordination sphere, in the presence of H_2O_2 , selectively oxidizes benzylic C–H bonds of several alkylbenzenes to the corresponding alcohols and ketones⁴²³ (see, e.g., equation 82).

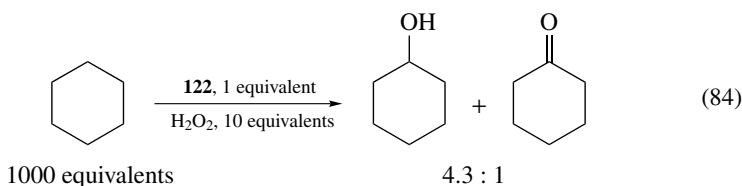
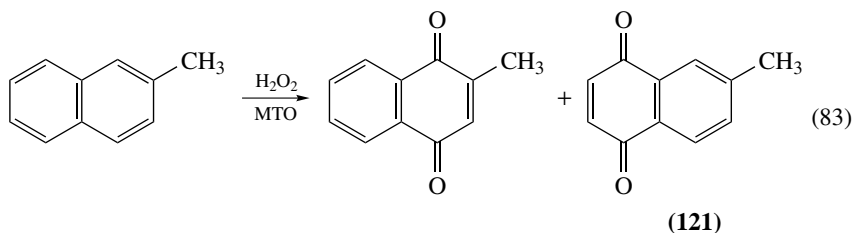


MTO in the presence of H_2O_2 produces complex **1**, which has been used for catalytic oxidations of electron-rich arenes^{424, 425}. An interesting example is the synthesis of vitamin K₃ compound **121** (equation 83), where the two isomeric 2-methylnaphthoquinones are formed in a 7:1 ratio and a chemical yield of **121** of 85%.

Analogously, alkanes have been oxidized with anhydrous hydrogen peroxide and catalytic amounts of MTO in CH_3CN ⁴²⁶. With these substrates, the main products are alkyl hydroperoxides together with alcohols and ketones.

Iron catalysis in oxidation reactions with peroxides, both hydrogen peroxide and alkyl hydroperoxides, is frequently regarded as just a Haber–Weiss-type system¹³ where hydroxyl

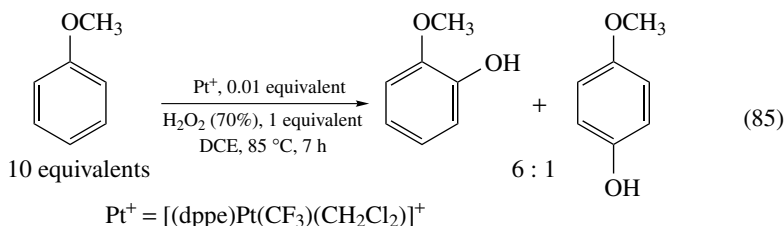
and alkoxy radicals that are responsible for radical chain autoxidation reactions are generated^{427–429}. These oxidations are, however, characterized by a low degree of selectivity, particularly when alkanes are considered. Nevertheless, in few cases peroxy iron intermediates have been invoked as reactive species. For example, complex $[\text{Fe}(\text{TPA})(\text{CH}_3\text{CN})_2](\text{ClO}_4)_2$, **122**, in the presence of excess of H_2O_2 reacts with cyclohexane to give cyclohexanol with a significant selectivity⁴³⁰ (equation 84).



The peroxy iron species reported in Scheme 7 have been used in preliminary studies for oxidative degradation of aromatic pollutants⁴³¹.

Oxygenation of alkanes with hydrogen peroxide in homogeneous reactions¹⁹⁵ can be obtained also with Keggin-type iron-substituted polyoxometalates. Evidence against radical reactions has been offered.

Co(III) alkyl peroxides have been prepared and used by Mimoun and coworkers⁴³² in the hydroxylation of hydrocarbons; with this metal a Haber–Weiss type of reactivity is suggested. Square-planar Pt(II) complexes¹²¹, of the type $[(\text{dppe})\text{Pt}(\text{CF}_3)(\text{sol})]^\dagger$, used by Strukul in the epoxidation of alkenes and in Baeyer–Villiger oxidations of ketones (Schemes 8 and 9), are effective catalysts also in the direct hydroxylation of aromatics with hydrogen peroxide⁴³³. The reactivity increases in the presence of electron releasing substituents in the aromatic ring. *Ortho* and *para* derivatives are practically the only products observed and interesting selectivity toward the *ortho* products has been detected (equation 85).



Intervention of $\mu\text{-}\eta^2\text{:}\eta^2$ -peroxy dicopper cores in hydroxylation of arenes has been postulated during studies aimed at mimicking the activity of tyrosinase enzymes⁴³⁴.

V. CONCLUSIONS

With this chapter we hope that newcomers to the field have received a taste of how active is the research in metal-catalyzed oxidation with peroxides, and also in future perspectives of greener and more efficient oxidative protocols. Additionally, we hope that people deeply involved in this area will appreciate the collection of the main literature that has been published in these last 20 years.

VI. ACKNOWLEDGMENTS

The friendly help in reading and offering valuable suggestions and comments from Prof. Barbara Floris, Roma Tor Vergata University, is gratefully acknowledged. V.C. also thanks the priceless help of Dr. P. Galloni, Roma Tor Vergata University, for literature search.

VII. REFERENCES

1. S. Patai (Ed.), *The Chemistry of Functional Groups. Peroxides*, Wiley, Chichester, 1983.
2. W. Adam (Ed.), *Peroxide Chemistry. Mechanistic and Preparative Aspects of Oxygen Transfer*, Wiley-VCH Verlag GmbH, Weinheim, 2000.
3. D. Swern, in *Organic Peroxides*, Vol. II (Ed. D. Swern), Wiley-Interscience, New York, 1971.
4. V. Conte, F. Di Furia and G. Modena, in *Organic Peroxides* (Ed. W. Ando), Chap. 11.2, Wiley, Chichester, 1992, pp. 559–598 and references cited therein.
5. N. A. Milas and S. Saussman, *J. Am. Chem. Soc.*, **58**, 1302 (1936).
6. N. A. Milas and S. Saussman, *J. Am. Chem. Soc.*, **59**, 342 (1937).
7. N. A. Milas, S. Saussman and H. S. Mason, *J. Am. Chem. Soc.*, **61**, 1844 (1939).
8. N. A. Milas and L. S. Malorey, *J. Am. Chem. Soc.*, **62**, 1841 (1940).
9. W. F. Brill and N. Indictor, *J. Org. Chem.*, **29**, 710 (1964).
10. N. Indictor and W. F. Brill, *J. Org. Chem.*, **30**, 2074 (1965).
11. M. G. Clerici, in *Heterogeneous Catalysis and Fine Chemicals III, Stud. Surf. Sc. Catal.*, Vol 78 (Eds. M. Guisnet, J. Barbier, J. Barrault, C. Bouchoule, D. Dupres, G. Pérot and C. Montassier), Elsevier, Amsterdam, 1993.
12. T. Katsuki and K. B. Sharpless, *J. Am. Chem. Soc.*, **102**, 5974 (1980).
13. R. A. Sheldon and J. K. Kochi, *Metal Catalyzed Oxidations of Organic Compounds*, Academic Press, New York, 1981.
14. H. Mimoun, in Reference 1, Chap. 15, pp. 463–482.
15. Thematic Issue: Metal–Dioxygen Complexes, *Chem. Rev.*, **94**, 567–856 (1994).
16. L. Vaska, *Acc. Chem. Res.*, **9**, 175 (1976).
17. W. Adam, W. Malisch, K. J. Roschmann, C. R. Saha-Möller and W. A. Schenk, *J. Organomet. Chem.*, **661**, 3 (2002).
18. M. H. Dickman and M. T. Pope, *Chem. Rev.*, **94**, 569 (1994) and references cited therein.
19. For example: N. J. Campbel, A. C. Dengel and W. P. Griffith, *Polyhedron*, **8**, 1379 (1989).
20. P. Schwendt and M. Sivák, in *Vanadium Compounds: Chemistry, Biochemistry and Therapeutic Applications*, ACS series book 711 (Eds. D. C. Crans and A. Tracey), Chap. 8, American Chemical Society, Washington D.C., 1998, pp. 136–145.
21. M. Bhattacharjee, S. K. Chettri, M. K. Chaudhuri, N. S. Islam and S. R. Barman, *J. Mol. Catal.*, **78**, 143 (1993).
22. M. Bonchio, O. Bortolini, V. Conte and S. Moro, *Eur. J. Inorg. Chem.*, 2913 (2001).
23. W. A. Herrmann, R. W. Fischer and D. W. Marz, *Angew. Chem., Int. Ed. Engl.*, **30**, 1638 (1991).
24. F. Di Furia and G. Modena, *Pure Appl. Chem.*, **54**, 1853 (1982).
25. K. A. Jørgensen, *Chem. Rev.*, **89**, 431 (1989).
26. G. Strukul, in *Catalytic Oxidations with Hydrogen Peroxide as Oxidant* (Ed. G. Strukul), Chap. 6, Kluwer Academic, Dordrecht, 1992, pp. 177–221.
27. Thematic Issue: Biomimetic Inorganic Chemistry, *Chem. Rev.*, **104**, 347–1200 (2004).
28. H. Mimoun, I. Seree de Roch and L. Sajus, *Bull. Soc. Chim. Fr.*, 1481 (1969).
29. H. Mimoun, I. Seree de Roch and L. Sajus, *Tetrahedron*, **26**, 37 (1970).

30. W. P. Griffith, B. C. Parkin, A. J. P. White and D. J. Williams, *J. Chem. Soc., Chem. Commun.*, 2183 (1995).
31. W. R. Thiel and J. Eppinger, *Chem. Eur. J.*, **3**, 696 (1997).
32. M. R. Maurya and N. Bharti, *Trans. Met. Chem.*, **24**, 389 (1999).
33. S. Kapoor and M. S. Sastry, *Proc. Indian Acad. Sci.*, **112**, 459 (2000).
34. J. M. Mitchell and N. S. Finney, *J. Am. Chem. Soc.*, **123**, 862 (2001).
35. T. T. Bhengu and D. K. Sanyal, *Thermochim. Acta*, **397**, 181 (2003).
36. S.-Y. Hou, Z.-H. Zhou, H.-L. Wan and S.-W. Ng, *Inorg. Chem. Commun.*, **6**, 1246 (2003).
37. V. V. Sharutin, A. P. Pakusina, O. V. Subacheva, O. K. Sharutina and A. V. Gerasimenko, *Russ. J. Coord. Chem.*, **29**, 395 (2003).
38. M. Dakanali, E. T. Kefala, C. P. Raptopoulou, A. Terzis, G. Voyiatzis, I. Kyrikou, T. Mavroustakos and A. Salifoglou, *Inorg. Chem.*, **42**, 4632 (2003).
39. W. A. Herrmann, R. W. Fischer, W. Scherer and M. U. Rauch, *Angew. Chem., Int. Ed. Engl.*, **32**, 1157 (1993).
40. W. A. Herrmann, J. D. G. Correia, G. R. J. Artus, R. W. Fischer and C. C. Romao, *J. Organomet. Chem.*, **520**, 139 (1996).
41. H. Arzoumanian, J.-F. Pétrignani, M. Pierrot, F. Ridouane and J. Sanchez, *Inorg. Chem.*, **27**, 3377 (1988).
42. B. de Bruin, T. P. J. Peters, J. B. M. Wilting, S. Thewissen, J. M. M. Smits and A. W. Gal, *Eur. J. Inorg. Chem.*, 2671 (2002).
43. D. G. Ho, R. Ismail, N. Franco, R. Gao, E. P. Leverich, I. Tsyba, N. N. Ho, R. Bau and M. Selke, *Chem. Commun.*, 570 (2002).
44. M. E. de Vries, R. M. La Crois, G. Roelfes, H. Kooijman, A. L. Spek, R. Hage and B. L. Feringa, *Chem. Commun.*, 1549 (1997).
45. P. Mialane, A. Nivorojkine, G. Pratviel, L. Azéma, M. Slany, F. Godde, A. Simaan, F. Banse, T. Kargar-Grisel, G. Bouchoux, J. Sainon, O. Horner, J. Guilhem, L. Tchertanova, B. Meunier and J.-J. Girerd, *Inorg. Chem.*, **38**, 1085 (1999).
46. K. B. Jensen, C. J. McKenzie, L. P. Nielsen, J. Z. Pedersen and H. M. Svendsen, *Chem. Commun.*, 1313 (1999).
47. A. J. Simaan, F. Banse, P. Mialane, A. Boussac, S. Un, T. Kargar-Grisel, G. Bouchoux and J.-J. Girerd, *Eur. J. Inorg. Chem.*, 993 (1999) and references cited therein.
48. R. Y. N. Ho, G. Roelfes, R. Hermant, R. Hage, B. L. Feringa and L. Que Jr., *Chem. Commun.*, 2161 (1999).
49. O. Horner, C. Jeandey, J. L. Oddou, P. Bonville, C. McKenzie and J.-M. Latour, *Eur. J. Inorg. Chem.*, 3278 (2002).
50. G. Roelfes, V. Vrajimasu, K. Chen, R. Y. N. Ho, J.-U. Rohde, C. Zondervan, R. M. la Crois, E. P. Schudde, M. Lutz, A. L. Spek, R. Hage, B. L. Feringa, E. Munch and L. Que Jr., *Inorg. Chem.*, **42**, 2639 (2003).
51. M. Akita and S. Hikichi, *Bull. Chem. Soc. Jpn.*, **75**, 1657 (2002).
52. T. Miyaji, M. Kujime, S. Hikichi, Y. Moro-Oka and M. Akita, *Inorg. Chem.*, **41**, 5286 (2002).
53. J. Xiao, B. D. Santarsiero, B. A. Vaartstra and M. Cowie, *J. Am. Chem. Soc.*, **115**, 3212 (1993).
54. C. He, J. L. DuBois, B. Hedman, K. O. Hodgson and S. J. Lippard, *Angew. Chem., Int. Ed.*, **40**, 1484 (2001).
55. T. Chishiro, Y. Shimazaki, F. Tani, Y. Tachi, Y. Naruta, S. Karasawa, S. Hayami and Y. Maeda, *Angew. Chem., Int. Ed.*, **42**, 2788 (2003).
56. H. Mimoun, P. Chaumette, M. Mignard, L. Saussine, J. Fischer and R. Weiss, *Nouv. J. Chim.*, **7**, 467 (1983).
57. G. Boche, K. Möbus, K. Harms and M. Marsch, *J. Am. Chem. Soc.*, **118**, 2770 (1996).
58. H. Mimoun, *Isr. J. Chem.*, **23**, 451 (1983).
59. A. Butler, M. J. Claugue and G. E. Meister, *Chem. Rev.*, **94**, 625 (1994) and references cited therein.
60. G. J. Colpas, B. J. Hamstra, J. W. Kampf and V. L. Pecoraro, *J. Am. Chem. Soc.*, **118**, 3469 (1996).
61. K. Kanamori, K. Nishida, N. Miyata, K. Okamoto, Y. Miyoshi, A. Tamura and H. Sakurai, *J. Inorg. Biochem.*, **86**, 649 (2001).
62. F. R. Fronczek, R. L. Luck and G. Wang, *Inorg. Chem. Commun.*, **5**, 384 (2002).

63. D. C. Crans, A. D. Keramidas, H. Hoover-Litty, O. P. Anderson, M. M. Miller, L. M. Lemoine, S. Pleasic-Williams, M. Vandenberg, A. J. Rossomando and L. J. Sweet, *J. Am. Chem. Soc.*, **119**, 5447 (1997).
64. J.-Y. Piquemal, S. Halut and J.-M. Bregeault, *Angew. Chem., Int. Ed.*, **37**, 1146 (1998).
65. D. Bayot, B. Tinant, B. Mathieu, J.-P. Declercq and M. Devillers, *Eur. J. Inorg. Chem.*, 737 (2003) and references cited therein.
66. U. Thewalt and R. Marsh, *J. Am. Chem. Soc.*, **89**, 6364 (1967).
67. J.-M. Le Carpentier, A. Mitschler and R. Weiss, *Acta Crystallogr., Sect. B*, **28**, 1288 (1972).
68. D. Carmona, M. P. Lamata, J. Ferrer, J. Modrego, M. Perales, F. J. Lahoz, R. Atencio and L. A. Oro, *J. Chem. Soc., Chem. Commun.*, 575 (1994).
69. A. Wada, M. Harata, K. Hasegawa, K. Jitsukawa, H. Masuda, M. Mukai, T. Kitagawa and H. Einaga, *Angew. Chem., Int. Ed.*, **37**, 798 (1998).
70. D. D. Wick and K. I. Goldberg, *J. Am. Chem. Soc.*, **121**, 11900 (1999).
71. I. A. Guzei and A. Bakac, *Inorg. Chem.*, **40**, 2390 (2001).
72. T. Ookubo, H. Sugimoto, T. Nagayama, H. Masuda, T. Sato, K. Tanaka, Y. Maeda, H. Okawa, Y. Hayashi, A. Uehara and M. Suzuki, *J. Am. Chem. Soc.*, **118**, 701 (1996).
73. K. Kim and S. J. Lippard, *J. Am. Chem. Soc.*, **118**, 4914 (1996).
74. Y. Dong, S. Yan, V. G. Young Jr. and L. Que Jr., *Angew. Chem., Int. Ed. Engl.*, **35**, 618 (1996).
75. M. Ghiladi, J. T. Gomez, A. Hazell, P. Kofod, J. Lumtscher and C. J. McKenzie, *Dalton Trans.*, 1320 (2003).
76. A. L. Gavrilova, C. J. Qin, R. D. Sommer, A. L. Rheingold and B. Bosnich, *J. Am. Chem. Soc.*, **124**, 1714 (2002).
77. J. Reim, R. Werner, W. Haase and B. Krebs, *Chem. Eur. J.*, **4**, 289 (1998).
78. R. Stomberg, L. Trysberg and I. Larkin, *Acta Chem. Scand.*, **24**, 2678 (1970).
79. W. Micklitz, S. G. Bott, J. G. Bentsen and S. J. Lippard, *J. Am. Chem. Soc.*, **111**, 372 (1989).
80. I. Shweky, L. E. Pence, G. C. Papaefthymiou, R. Sessoli, J. W. Yun, A. Bino and S. J. Lippard, *J. Am. Chem. Soc.*, **119**, 1037 (1997).
81. H. J. Breunig, T. Krüger and E. Lork, *Angew. Chem., Int. Ed. Engl.*, **36**, 615 (1997).
82. K. B. Sharpless Nobel Lecture <http://www.nobel.se/chemistry/laureates/2001/>
83. M. G. Finn and K. B. Sharpless, in *Asymmetric Synthesis*, Vol. 5, Chap. 8 (Ed. J. D. Morrison), Academic Press, New York, 1985.
84. A. F. Ghiron and R. C. Thompson, *Inorg. Chem.*, **29**, 4457 (1990).
85. V. Conte, F. Di Furia and S. Moro, *J. Phys. Org. Chem.*, **9**, 329 (1996).
86. For example: V. Conte, F. Di Furia and S. Moro, *J. Mol. Catal. A: Chem.*, **104**, 159 (1995).
87. M. Bonchio, V. Conte, F. Di Furia, G. Modena, S. Moro, T. Carofiglio, F. Magno and P. Pastore, *Inorg. Chem.*, **32**, 5797 (1993).
88. M. S. Reynolds and A. Butler, *Inorg. Chem.*, **35**, 2378 (1996).
89. O. Bortolini, F. Di Furia, P. Scrimin and G. Modena, *J. Mol. Catal.*, **7**, 59 (1980).
90. O. Bortolini, F. Di Furia, P. Scrimin and G. Modena, *J. Mol. Catal.*, **9**, 323 (1980).
91. A. Arcoria, F. P. Ballistreri, G. A. Tomaselli, F. Di Furia and G. Modena, *J. Mol. Catal.*, **24**, 189 (1984).
92. V. Conte, F. Di Furia, G. Modena and O. Bortolini, *J. Org. Chem.*, **53**, 4581 (1988).
93. F. Di Furia, G. Modena and R. Seraglia, *Synthesis*, 325 (1984).
94. P. Pitchen and H. B. Kagan, *Tetrahedron Lett.*, **25**, 1049 (1984).
95. P. Pitchen, E. Duñach, M. N. Deshmukh and H. B. Kagan, *J. Am. Chem. Soc.*, **106**, 8188 (1984).
96. O. Samuel, B. Ronan and H. B. Kagan, *J. Organomet. Chem.*, **370**, 43 (1989).
97. F. Di Furia, G. Licini, G. Modena and G. Valle, *Bull. Soc. Chim. Fr.*, **127**, 734 (1990).
98. V. Conte, F. Di Furia, G. Licini, G. Modena and G. Sbampato, in *Dioxygen Activation and Homogeneous Catalytic Oxidations* (Ed. L. I. Simandi), Elsevier, Amsterdam, 1991, pp. 385–394.
99. M. Bonchio, G. Licini, G. Modena, S. Moro, O. Bortolini, P. Traldi and W. A. Nugent, *Chem. Commun.*, 869 (1997).
100. M. Bonchio, G. Licini, G. Modena, O. Bortolini, S. Moro and W. A. Nugent, *J. Am. Chem. Soc.*, **121**, 6258 (1999).
101. N. J. Campbell, A. C. Dengel and W. P. Griffith, *Polyhedron*, **8**, 1379 (1989).
102. J. S. Jaswal and A. S. Tracey, *Inorg. Chem.*, **30**, 3718 (1991).

103. V. Conte, F. Di Furia and S. Moro, *J. Mol. Catal.*, **94**, 323 (1994).
104. C. Slebodnick and V. L. Pecoraro, *Inorg. Chim. Acta*, **283**, 37 (1998).
105. I. Andersson, S. Angus-Dunne, O. Howarth and L. Pettersson, *J. Inorg. Biochem.*, **80**, 51 (2000).
106. H. Schmidt, I. Andersson, D. Rehder and L. Pettersson, *Chem. Eur. J.*, **7**, 251 (2001).
107. R. Ando, M. Nagai, T. Yagyu and M. Maeda, *Inorg. Chim. Acta*, **351**, 107 (2003).
108. O. Bortolini, V. Conte, F. Di Furia and S. Moro, *Eur. J. Inorg. Chem.*, 1193 (1998).
109. O. Bortolini, M. Carraro, V. Conte and S. Moro, *Eur. J. Inorg. Chem.*, 1489 (1999).
110. V. Conte, O. Bortolini, M. Carraro and S. Moro, *J. Inorg. Biochem.*, **80**, 41 (2000).
111. O. Bortolini, M. Carraro, V. Conte and S. Moro, *Eur. J. Inorg. Chem.*, 42 (2003).
112. A. C. Dengel, W. P. Griffith and B. C. Parkin, *J. Chem. Soc., Dalton Trans.*, 2683 (1993).
113. E. P. Talsi, O. V. Klimov and K. I. Zamaraev, *J. Mol. Catal.*, **83**, 329 (1993).
114. E. P. Talsi, K. V. Shalyaev and K. I. Zamaraev, *J. Mol. Catal.*, **83**, 347 (1993).
115. H. Glas, M. Spiegler and W. R. Thiel, *Eur. J. Inorg. Chem.*, 275 (1998) and references cited therein.
116. O. Howarth, L. Pettersson and I. Andersson, in *Polyoxometalate Chemistry* (Eds. M. T. Pope and A. Müller), Kluwer Academic, Dordrecht, 2001, pp. 145–159.
117. L. Salles, C. Aubry, R. Thouvenot, F. Robert, C. Dorémieux-Morin, G. Chottard, H. Ledon, Y. Jeannin and J.-M. Brégeault, *Inorg. Chem.*, **33**, 871 (1994).
118. T. Kobayashi, S. Nishino, H. Masuda, H. Einaga and Y. Nishida, *Inorg. Chem. Commun.*, **3**, 608 (2000).
119. G. L. Elizarova, G. V. Odegova, L. G. Matvienko, E. P. Talsi, V. N. Kolomiichuk and V. N. Parmon, *Kinet. Catal.*, **44**, 211 (2003).
120. D. Rehder, *Inorg. Chem. Commun.*, **6**, 604 (2003) and references cited therein.
121. G. Strukul, *Angew. Chem., Int. Ed.*, **37**, 1198 (1998).
122. R. Gavagnini, M. Cataldo, F. Pinna and G. Strukul, *Organometallics*, **17**, 661 (1998).
123. C. Paneghetti, R. Gavagnini, F. Pinna and G. Strukul, *Organometallics*, **18**, 5057 (1999).
124. R. R. Sever and T. W. Root, *J. Phys. Chem. B*, **107**, 10521 (2003).
125. W. A. Herrmann, R. W. Fischer and J. D. G. Correia, *J. Mol. Catal.*, **94**, 213 (1994).
126. W. Adam, W. Haas and G. Sieker, *J. Am. Chem. Soc.*, **106**, 5020 (1984).
127. M. N. Bhattacharjee, M. K. Chaudhuri and N. S. Islam, *Inorg. Chem.*, **28**, 2420 (1989).
128. M. K. Chaudhuri, S. K. Ghosh and N. S. Islam, *Inorg. Chem.*, **24**, 2706 (1985).
129. F. Di Furia, G. Licini, G. Modena, R. Motterle and W. A. Nugent, *J. Org. Chem.*, **61**, 5175 (1996).
130. M. Bonchio, S. Calloni, F. Di Furia, G. Licini, G. Modena, S. Moro and W. A. Nugent, *J. Am. Chem. Soc.*, **119**, 6935 (1997).
131. M. Bonchio, G. Licini, F. Di Furia, S. Mantovani, G. Modena and W. A. Nugent, *J. Org. Chem.*, **64**, 1326 (1999).
132. W. Adam, M. N. Korb, K. J. Roschmann and C. R. Saha-Möller, *J. Org. Chem.*, **63**, 3423 (1998).
133. F. P. Ballistreri, G. A. Tomaselli, R. M. Toscano, V. Conte and F. Di Furia, *J. Am. Chem. Soc.*, **113**, 6209 (1991).
134. M. Bonchio, V. Conte, M. A. De Concillis, F. Di Furia, F. P. Ballistreri, G. A. Tomaselli and R. M. Toscano, *J. Org. Chem.*, **60**, 4475 (1995).
135. A. G. J. Ligtenberg, R. Hage and B. L. Feringa, *Coord. Chem. Rev.*, **237**, 89 (2003).
136. C. Bolm, *Coord. Chem. Rev.*, **237**, 245 (2003).
137. J. Hartung and M. Greb, *J. Organomet. Chem.*, **661**, 67 (2002).
138. D. J. Berrisford, C. Bolm and K. B. Sharpless, *Angew. Chem., Int. Ed. Engl.*, **34**, 1059 (1995).
139. K. B. Sharpless, J. M. Townsend and D. R. Williams, *J. Am. Chem. Soc.*, **94**, 295 (1972).
140. A. O. Chong and K. B. Sharpless, *J. Org. Chem.*, **42**, 1587 (1977).
141. H. Mimoun, *Angew. Chem., Int. Ed. Engl.*, **21**, 734 (1982).
142. H. Mimoun, M. Mignard, P. Brechot and L. Saussine, *J. Am. Chem. Soc.*, **108**, 3711 (1986).
143. J. Sundermeyer, *Angew. Chem., Int. Ed. Engl.*, **32**, 1144 (1993).
144. C. K. Sams and K. A. Jørgensen, *Acta Chem. Scand.*, **49**, 839 (1995).
145. M. J. Filatov, K. V. Shalyaev and E. P. Talsi, *J. Mol. Catal.*, **87**, L5 (1994).
146. Y.-D. Wu and D. K. W. Lai, *J. Org. Chem.*, **60**, 673 (1995).
147. D. Tantanak, M. A. Vincent and I. H. Hillier, *Chem. Commun.*, 1031 (1998).
148. I. V. Yudanov, P. Gisdakis, C. Di Valentin and N. Rösch, *Eur. J. Inorg. Chem.*, 2135 (1999).

149. G. Wahl, D. Kleinhenz, A. Schorm, J. Sundermeyer, R. Stowasser, C. Rummey, G. Bringmann, C. Fickert and W. Kiefer, *Chem. Eur. J.*, **5**, 3237 (1999).
150. C. Di Valentin, P. Gisdakis, I. V. Yudanov and N. Rösch, *J. Org. Chem.*, **65**, 2996 (2000).
151. I. V. Yudanov, C. Di Valentin, P. Gisdakis and N. Rösch, *J. Mol. Catal. A: Chem.*, **158**, 189 (2000).
152. D. V. Deubel, J. Sundermeyer and G. Frenking, *Inorg. Chem.*, **39**, 2314 (2000).
153. D. V. Deubel, J. Sundermeyer and G. Frenking, *Org. Lett.*, **3**, 329 (2001).
154. P. Macchi, A. J. Schultz, F. K. Larsen and B. B. Iversen, *J. Phys. Chem. A*, **105**, 9231 (2001).
155. F. R. Sensato, R. Custodio, E. Longo, V. S. Safont and J. Andrei, *J. Org. Chem.*, **68**, 5870 (2003).
156. W. R. Thiel, M. Barz, H. Glas and A.-K. Pleier, in Reference 2, Chap. 7, pp. 433–453 and references cited therein.
157. A. Hroch, G. Gemmecker and W. R. Thiel, *Eur. J. Inorg. Chem.*, 1107 (2000) and references cited therein.
158. R. Curci, S. Giannattasio, O. Sciacovelli and L. Troisi, *Tetrahedron*, **40**, 2763 (1984).
159. E. Daire, H. Mimoun and L. Saussine, *Nouv. J. Chim.*, **8**, 271 (1984).
160. M. Bonchio, V. Conte, F. Di Furia, G. Modena, C. Padovani and M. Sivák, *Res. Chem. Intern.*, **12**, 111 (1989).
161. H. Mimoun, L. Saussine, E. Daire, M. Postel, J. Fischer and R. Weiss, *J. Am. Chem. Soc.*, **105**, 3101 (1983).
162. M. Bonchio, V. Conte, F. Di Furia and G. Modena, *J. Org. Chem.*, **54**, 4368 (1989).
163. M. Bonchio, V. Conte, F. Di Furia, G. Modena and S. Moro, *J. Org. Chem.*, **59**, 6262 (1994) and references cited therein.
164. V. Conte, F. Di Furia and G. Modena, *J. Org. Chem.*, **53**, 1665 (1988).
165. M. Bonchio, V. Conte, F. Di Furia, G. Modena, S. Moro and J. O. Edwards, *Inorg. Chem.*, **33**, 1631 (1994).
166. M. Bonchio, O. Bortolini, M. Carraro, V. Conte and S. Primon, *J. Inorg. Biochem.*, **80**, 191 (2000).
167. M. Bonchio, O. Bortolini, V. Conte and S. Primon, *J. Chem. Soc., Perkin Trans. 2*, 763 (2001).
168. B. S. Lane and K. Burgess, *Chem. Rev.*, **103**, 2457 (2003).
169. C. Venturello, E. Alneri and M. Ricci, *J. Org. Chem.*, **48**, 3831 (1983).
170. C. Venturello and R. D'Aloisio, *J. Org. Chem.*, **53**, 1553 (1988).
171. D. C. Duncan, R. C. Chambers, E. Hecht and C. L. Hill, *J. Am. Chem. Soc.*, **117**, 681 (1995).
172. Y. Ishii, K. Yamawaki, T. Ura, H. Yamada, T. Yoshida and M. Ogawa, *J. Org. Chem.*, **53**, 3587 (1988).
173. Y. Ishii, K. Yamawaki, T. Yoshida, T. Ura and M. Ogawa, *J. Org. Chem.*, **52**, 1868 (1987).
174. S. Sakaguchi, Y. Nishiyama and Y. Ishii, *J. Org. Chem.*, **61**, 5307 (1996).
175. G. Grigoropoulou, J. H. Clark and J. A. Elings, *Green Chem.*, **5**, 1 (2003).
176. A. Lambert, P. Plucinski and I. V. Kozhevnikov, *Chem. Commun.*, 714 (2003).
177. K. Sato, M. Aoki, M. Ogawa, T. Hashimoto and R. Noyori, *J. Org. Chem.*, **61**, 8310 (1996).
178. K. Sato, M. Aoki, M. Ogawa, T. Hashimoto, D. Panyella and R. Noyori, *Bull. Chem. Soc. Jpn.*, **70**, 905 (1997).
179. O. Bortolini, F. Di Furia, G. Modena and R. Seraglia, *J. Org. Chem.*, **50**, 2688 (1985).
180. K. Kamata, K. Yonehara, Y. Sumida, K. Yamaguchi, S. Hikichi and N. Mizuno, *Science*, **300**, 964 (2003).
181. C. L. Hill and C. M. Prosser-McCartha, *Coord. Chem. Rev.*, **143**, 407 (1995).
182. I. V. Kozhevnikov, *Chem. Rev.*, **98**, 171 (1998).
183. C. M. Tourné, G. F. Tourné and F. Zonnevillje, *J. Chem. Soc., Dalton Trans.*, 143 (1991).
184. R. Neumann and M. Gara, *J. Am. Chem. Soc.*, **116**, 5509 (1994).
185. R. Neumann and M. Gara, *J. Am. Chem. Soc.*, **117**, 5066 (1995).
186. R. Neumann, A. M. Khenkin, D. Juwiler, H. Miller and M. Gara, *J. Mol. Catal. A: Chem.*, **117**, 169 (1997).
187. R. Neumann and H. Miller, *J. Chem. Soc., Chem. Commun.*, 2277 (1995).
188. R. Neumann and A. M. Khenkin, *Inorg. Chem.*, **34**, 5753 (1995).
189. R. Neumann and A. M. Khenkin, *J. Mol. Catal. A: Chem.*, **114**, 169 (1996).
190. A. M. Khenkin and C. L. Hill, *Mendeleev Commun.*, 140 (1993).
191. X. Zhang, Q. Chen, D. C. Duncan, R. J. Lachicotte and C. L. Hill, *Inorg. Chem.*, **36**, 4381 (1997).

192. X. Zhang, Q. Chen, D. C. Duncan, C. F. Campana and C. L. Hill, *Inorg. Chem.*, **36**, 4208 (1997).
193. T. M. Anderson, K. I. Hardcastle, N. Okun and C. L. Hill, *Inorg. Chem.*, **40**, 6418 (2001).
194. X. Zhang, T. M. Anderson, Q. Chen and C. L. Hill, *Inorg. Chem.*, **40**, 418 (2001).
195. N. Mizuno, C. Nozaki, I. Kiyoto and M. Misono, *J. Am. Chem. Soc.*, **120**, 9267 (1998).
196. N. Mizuno, C. Nozaki, I. Kiyoto and M. Misono, *J. Catal.*, **182**, 285 (1999).
197. D. A. Judd, Q. Chen, C. F. Campana and C. L. Hill, *J. Am. Chem. Soc.*, **119**, 5461 (1997).
198. M. K. Harrup, G. S. Kim, H. Zeng, R. P. Johnson, D. VanDerveer and C. L. Hill, *Inorg. Chem.*, **37**, 5550 (1998).
199. C. W. Jones, in *Applications of Hydrogen Peroxide and Derivatives* (Ed. J. H. Clark), RCS, Cambridge, UK, 1999.
200. G. Perego, M. Taramasso and B. Notari, BE Patent No 886812 (1981); *Chem. Abstr.*, **95**, 606272 (1981) (to Snamprogetti).
201. U. Romano, A. Esposito, F. Maspero, C. Neri and M. G. Clerici, *Chim. Ind.*, **72**, 610 (1990); *Chem. Abstr.*, **113**, 233670 (1990).
202. G. Tozzola, M. A. Mantegazza, G. Ranghino, G. Petrini, S. Bordiga, G. Ricchiardi, C. Lamberti, R. Zulian and A. Zecchina, *J. Catal.*, **179**, 64 (1998).
203. J. Sankar, J. M. Thomas, C. R. A. Catlow, C. M. Barker, D. Gleeson and N. Kaltsoyannis, *J. Phys. Chem. B*, **105**, 9028 (2001).
204. G. N. Vayssilov and R. A. Van Santen, *J. Catal.*, **175**, 170 (1998).
205. H. Munakata, Y. Oumi and A. Miyamoto, *J. Phys. Chem. B*, **105**, 3493 (2001).
206. W. Lin and H. Frei, *J. Am. Chem. Soc.*, **124**, 9292 (2002).
207. R. A. Sheldon, M. Wallau, I. W. C. E. Arends and U. Schuchardt, *Acc. Chem. Res.*, **31**, 485 (1998).
208. R. A. Sheldon, I. W. C. E. Arends and H. E. B. Lempers, *Catal. Today*, **41**, 387 (1998).
209. M. A. Cambor, A. Corma, A. Martinez and J. Pérez Pariente, *J. Chem. Soc., Chem. Commun.*, 589 (1992).
210. A. Corma, M. T. Navarro and J. Pérez Pariente, *J. Chem. Soc., Chem. Commun.*, 147 (1994).
211. D. Nuntasri, P. Wu and T. Tatsumi, *Chem. Lett.*, **32**, 326 (2003).
212. M. G. Clerici and P. Ingallina, *Catal. Today*, **41**, 351 (1998).
213. W. A. Herrmann, *J. Organomet. Chem.*, **500**, 149 (1995).
214. C. C. Romao, F. E. Kuhn and W. A. Herrmann, *Chem. Rev.*, **97**, 3197 (1997).
215. A. M. Al-Ajlouni and J. H. Espenson, *J. Am. Chem. Soc.*, **117**, 9243 (1995).
216. W. A. Herrmann, F. E. Kuhn, M. R. Mattner, G. R. J. Artus, M. R. Geisberger and J. D. G. Correia, *J. Organomet. Chem.*, **538**, 203 (1997).
217. J. Rudolph, K. L. Reddy, J. P. Chiang and K. B. Sharpless, *J. Am. Chem. Soc.*, **119**, 6189 (1997).
218. C. Coperet, H. Adolfsson and K. B. Sharpless, *Chem. Commun.*, 1565 (1997).
219. W. A. Herrmann, R. M. Kratzer, H. Ding, W. R. Thiel and H. Glas, *J. Organomet. Chem.*, **555**, 293 (1998).
220. H. Adolfsson, A. Converso and K. B. Sharpless, *Tetrahedron Lett.*, **40**, 3991 (1999).
221. W. Adam and C. M. Mitchell, *Angew. Chem., Int. Ed. Engl.*, **35**, 533 (1996).
222. T. R. Boehlow and C. D. Spilling, *Tetrahedron Lett.*, **37**, 2717 (1996).
223. W. Adam, C. R. Saha-Möller and O. Weichold, *J. Org. Chem.*, **65**, 2897 (2000).
224. W. Adam, C. R. Saha-Möller and O. Weichold, *J. Org. Chem.*, **65**, 5001 (2000).
225. R. Saladino, V. Neri, A. R. Pelliccia, R. Caminiti and C. Sadun, *J. Org. Chem.*, **67**, 1323 (2002).
226. R. Saladino, V. Neri, A. R. Pelliccia and E. Mincione, *Tetrahedron*, **59**, 7403 (2003).
227. A. O. Bouh and J. H. Espenson, *J. Mol. Catal. A: Chem.*, **200**, 43 (2003).
228. M. C. A. van Vliet, I. W. C. E. Arends and R. A. Sheldon, *Chem. Commun.*, 821 (1999).
229. G. S. Owens and M. Abu-Omar, *Chem. Commun.*, 1165 (2000).
230. G. S. Owens, A. Durazo and M. Abu-Omar, *Chem. Eur. J.*, **8**, 3053 (2002).
231. G. Strukul and R. A. Michelin, *J. Am. Chem. Soc.*, **107**, 7563 (1985).
232. H. B. Kagan, H. Mimoun, C. Mark and V. Schurig, *Angew. Chem., Int. Ed. Engl.*, **18**, 485 (1979).
233. V. Schurig, K. Hintzer, U. Leyrer, C. Mark, P. Pitchen and H. B. Kagan, *J. Organomet. Chem.*, **370**, 81 (1989).

234. R. J. Cross, P. D. Newman, R. D. Peacock and D. Stirling, *J. Mol. Catal. A: Chem.*, **144**, 273 (1999).
235. M. J. Sabater, M. E. Domine and A. Corma, *J. Catal.*, **210**, 192 (2002).
236. R. Sinigaglia, R. A. Michelin, F. Pinna and G. Strukul, *Organometallics*, **6**, 728 (1987).
237. R. M. Stoop, S. Bachmann, M. Valentini and A. Mezzetti, *Organometallics*, **19**, 4117 (2000).
238. R. A. Sheldon, in Reference 1, Chap. 6, pp. 161–200 and references cited therein.
239. N. A. Milas and S. A. Harris, *J. Am. Chem. Soc.*, **60**, 2434 (1938).
240. J. Kollar, U. S. Patent No. 3350422 (1967); *Chem. Abstr.*, **68**, 2922e (1967) (to Halcon).
241. M. Sheng and J. G. Zajacek, GB. Patent No. 1136923 (1968); *Chem. Abstr.*, **70**, 87546 (1969) (to Atlantic Richfield).
242. J.-M. Bregeault, *Dalton Trans.*, 3289 (2003).
243. K. B. Sharpless and T. R. Verhoeven, *Aldrichim. Acta*, **12**, 63 (1979).
244. W. R. Thiel, M. Angstl and N. Hansen, *J. Mol. Catal. A: Chem.*, **103**, 5 (1995).
245. W. R. Thiel, *J. Mol. Catal. A: Chem.*, **117**, 449 (1997).
246. W. A. Herrmann, J. Fridgen, G. M. Lobmaier and M. Spiegler, *New J. Chem.*, **23**, 5 (1999).
247. T. Maschmeyer, F. Rey, G. Sankar and J. M. Thomas, *Nature*, **378**, 159 (1995).
248. R. D. Oldroyd, J. M. Thomas, T. Maschmeyer, P. A. MacFaul, D. W. Snelgrove, K. U. Ingold and D. D. M. Wayner, *Angew. Chem., Int. Ed. Engl.*, **35**, 2787 (1996).
249. K. U. Ingold, D. W. Snelgrove, P. A. MacFaul, R. D. Oldroyd and J. M. Thomas, *Catal. Lett.*, **48**, 21 (1997).
250. K. Tani, M. Hanafusa and S. Otsuka, *Tetrahedron Lett.*, **20**, 3017 (1979).
251. W. A. Herrmann, J. J. Haider, J. Fridgen, G. M. Lobmaier and M. Spiegler, *J. Organomet. Chem.*, **603**, 69 (2000).
252. I. S. Goncalves, A. M. Santos, C. C. Romao, A. D. Lopes, J. E. Rodriguez-Borges, M. Pillinger, P. Ferreira, J. Rocha and F. E. Kuhn, *J. Organomet. Chem.*, **626**, 1 (2001).
253. E. Weitz and A. Scheffer, *Ber. Dtsch. Chem. Ges.*, **54**, 2327 (1921).
254. K. S. Kirshenbaum and K. B. Sharpless, *J. Org. Chem.*, **50**, 1979 (1985).
255. G. B. Payne and P. H. Williams, *J. Org. Chem.*, **24**, 54 (1959).
256. Y. Ishii and Y. Sakata, *J. Org. Chem.*, **55**, 5545 (1990).
257. T. Oguchi, Y. Sakata, N. Takeuchi, K. Kaneda, Y. Ishii and M. Ogawa, *Chem. Lett.*, 2053 (1989).
258. M. Selke, M. F. Sisemore and J. S. Valentine, *J. Am. Chem. Soc.*, **118**, 2008 (1996).
259. M. F. Sisemore, M. Selke, J. N. Burstyn and J. S. Valentine, *Inorg. Chem.*, **36**, 979 (1997).
260. C. Baccin, A. Gusso, F. Pinna and G. Strukul, *Organometallics*, **14**, 1161 (1995).
261. M. J. Porter and J. Skidmore, *Chem. Commun.*, 1215 (2000).
262. D. Enders, J. Zhu and G. Raabe, *Angew. Chem., Int. Ed. Engl.*, **35**, 1725 (1996).
263. D. Enders, J. Zhu and L. Kramps, *Liebigs Ann./Recueil*, 1101 (1997).
264. D. Enders, L. Kramps and J. Zhu, *Tetrahedron: Asymmetry*, **9**, 3959 (1998).
265. H. B. Yu, X. F. Zheng, Z. M. Lin, Q. S. Hu, W. S. Huang and L. Pu, *J. Org. Chem.*, **64**, 8149 (1999).
266. C. L. Elston, R. F. W. Jackson, S. J. F. MacDonald and P. J. Murray, *Angew. Chem., Int. Ed. Engl.*, **36**, 410 (1997).
267. O. Jacques, S. J. Richards and R. F. W. Jackson, *Chem. Commun.*, 2712 (2001).
268. Y. Tanaka, K. Nishimura and K. Tomioka, *Tetrahedron*, **59**, 4549 (2003).
269. J. Prandi, H. B. Kagan and H. Mimoun, *Tetrahedron Lett.*, **27**, 2617 (1986).
270. D. Prat and P. Lett, *Tetrahedron Lett.*, **27**, 707 (1986).
271. Y. Matoba, H. Inoue, J. Akagy, T. Okabayashi, Y. Ishii, K. Yamawaki and M. Ogawa, *Synth. Commun.*, **14**, 865 (1984).
272. D. Prat, B. Delpéch and P. Lett, *Tetrahedron Lett.*, **27**, 711 (1986).
273. Y. M. A. Yamada, M. Ichinohe, H. Takahashi and S. Ikegami, *Org. Lett.*, **3**, 1837 (2001).
274. J. Ichihara, *Tetrahedron Lett.*, **42**, 695 (2001).
275. W. Adam, A. Corma, T. I. Reddy and M. Renz, *J. Org. Chem.*, **62**, 3631 (1997).
276. W. Adam, A. Corma, A. Martínez, C. M. Mitchell, T. I. Reddy, M. Renz and A. K. Smerz, *J. Mol. Catal. A: Chem.*, **117**, 357 (1997).
277. W. Adam and T. Wirth, *Acc. Chem. Res.*, **32**, 703 (1999).
278. W. Adam, C. M. Mitchell and C. R. Saha-Möller, *J. Org. Chem.*, **64**, 3699 (1999).
279. W. Adam, P. L. Alsters, R. Neumann, C. R. Saha-Möller, D. Sloboda-Rozner and R. Zhang, *J. Org. Chem.*, **68**, 1721 (2003).

280. R. Neumann and D. Juwiler, *Tetrahedron*, **52**, 8781 (1996).
281. R. Ben-Daniel, A. M. Khenkin and R. Neumann, *Chem. Eur. J.*, **6**, 3722 (2000).
282. Y. Gao, R. M. Hanson, J. M. Klunder, S. Y. Ko, H. Masamune and K. B. Sharpless, *J. Am. Chem. Soc.*, **109**, 5765 (1987).
283. K. A. Jørgensen, R. A. Wheeler and R. Hoffmann, *J. Am. Chem. Soc.*, **109**, 3240 (1987).
284. A. Pfenninger, *Synthesis*, 89 (1986).
285. T. Katsuki (Ed.), *Asymmetric Oxidation Reactions*, Oxford University Press, 2001.
286. T. Katsuki, in *Comprehensive Asymmetric Catalysis*, Vol. 2 (Eds. E. N. Jacobsen, A. Pfaltz and H. Yamamoto), Springer, Berlin, 1999.
287. R. C. Michaelson, R. E. Palermo and K. B. Sharpless, *J. Am. Chem. Soc.*, **99**, 1990 (1977).
288. N. Murase, Y. Hoshino, M. Oishi and H. Yamamoto, *J. Org. Chem.*, **64**, 338 (1999).
289. Y. Hoshino, N. Murase, M. Oishi and H. Yamamoto, *Bull. Chem. Soc. Jpn.*, **73**, 1653 (2000).
290. Y. Hoshino and H. Yamamoto, *J. Am. Chem. Soc.*, **122**, 10452 (2000).
291. B. Traber, Y. G. Jung, T. K. Park and J. I. Hong, *Bull. Korean Chem. Soc.*, **22**, 547 (2001).
292. C. Bolm and T. Kuhn, *Synlett*, **6**, 899 (2000).
293. H. L. Wu and B. J. Uang, *Tetrahedron: Asymmetry*, **13**, 2625 (2002).
294. W. Adam and M. N. Korb, *Tetrahedron: Asymmetry*, **8**, 1131 (1997).
295. A. Lattanzi, P. Iannece, A. Vicinanza and A. Scettri, *Chem. Commun.*, 1440 (2003).
296. W. Adam, A. K. Beck, A. Pichota, C. R. Saha-Möller, D. Seebach, N. Vogl and R. Zhang, *Tetrahedron: Asymmetry*, **14**, 1355 (2003).
297. M. Aoki and D. Seebach, *Helv. Chim. Acta*, **84**, 187 (2001).
298. W. Adam, P. L. Alsters, R. Neumann, C. R. Saha-Möller, D. Seebach and R. Zhang, *Org. Lett.*, **5**, 725 (2003).
299. S. Xiang, Y. Zhang, Q. Xin and C. Li, *Angew. Chem., Int. Ed.*, **41**, 821 (2002).
300. T. Oguchi, T. Ura, Y. Ishii and M. Ogawa, *Chem. Lett.*, 857 (1989).
301. Y. Sakata, Y. Katayama and Y. Ishii, *Chem. Lett.*, 671 (1992).
302. H. Furukawa, T. Nakamura, H. Inagaki, E. Nishikawa, C. Imai and M. Misono, *Chem. Lett.*, 877 (1988).
303. C. D. Brooks, L. C. Huang, M. McCarron and R. A. W. Johnstone, *Chem. Commun.*, 37 (1999).
304. S. B. Kumar, S. P. Mirajkar, G. C. G. Pais, P. Kumar and R. Kumar, *J. Catal.*, **156**, 163 (1995).
305. E. Antonelli, R. D'Aloisio, M. Gambaro, T. Fiorani and C. Venturello, *J. Org. Chem.*, **63**, 7190 (1998).
306. M. Bonchio, V. Conte, F. Di Furia and G. Modena, *J. Mol. Catal.*, **79**, 159 (1991).
307. M. Shimizu, H. Orita, K. Suzuki, T. Hayakawa, S. Hamakawa and K. Takehira, *J. Mol. Catal. A: Chem.*, **114**, 217 (1996).
308. B. M. Choudary and P. N. Reddy, *J. Mol. Catal. A: Chem.*, **103**, L1 (1995).
309. W. A. Herrmann, T. Weskamp, J. P. Zoller and R. W. Fischer, *J. Mol. Catal. A: Chem.*, **153**, 49 (2000).
310. M. C. Careno, *Chem. Rev.*, **95**, 1717 (1995).
311. M. Bonchio, S. Campestrini, V. Conte, F. Di Furia and S. Moro, *Tetrahedron*, **51**, 12363 (1995).
312. V. Conte and F. Di Furia, in *Catalytic Oxidation with Hydrogen Peroxide as Oxidant* (Ed. G. Strukul), Chap. 7, Kluwer Academic, Dordrecht, 1992, pp 223–252.
313. O. Bortolini, F. Di Furia and G. Modena, *J. Mol. Catal.*, **16**, 61 (1982).
314. O. Bortolini, F. Di Furia, G. Modena, C. Scardellato and P. Scrimin, *J. Mol. Catal.*, **11**, 107 (1981).
315. V. Conte, F. Di Furia and G. Licini, *Appl. Catal. A: Gen.*, **157**, 335 (1997).
316. F. P. Ballistreri, A. Bazzo, G. A. Tomaselli and R. M. Toscano, *J. Org. Chem.*, **57**, 7074 (1992).
317. K. Sato, M. Hyodo, M. Aoki, X. Q. Zheng and R. Noyori, *Tetrahedron*, **57**, 2469 (2001).
318. Y. M. A. Yamada, H. Tabata, H. Takahashi and S. Ikegami, *Synlett*, 2031 (2002).
319. W. Adam, C. M. Mitchell and C. R. Saha-Möller, *Tetrahedron*, **50**, 13121 (1994).
320. K. A. Vassell and J. H. Espenson, *Inorg. Chem.*, **33**, 5491 (1994).
321. W. Adam, C. M. Mitchell, C. R. Saha-Möller, T. Selvam and O. Weichold, *J. Mol. Catal. A: Chem.*, **154**, 251 (2000).
322. A. Corma, *Chem. Rev.*, **97**, 2373 (1997).

323. W. Adam and D. Golsch, *Chem. Ber.*, **127**, 1111 (1994).
324. F. Di Furia, G. Modena, R. Curci and J. O. Edwards, *Gazz. Chim. Ital.*, **109**, 571 (1979).
325. F. Di Furia, G. Licini and G. Modena, *Gazz. Chim. Ital.*, **120**, 165 (1990).
326. J. M. Brunel, P. Diter, M. Duetsch and H. B. Kagan, *J. Org. Chem.*, **60**, 8086 (1995).
327. J. M. Brunel and H. B. Kagan, *Synlett*, 404 (1996).
328. P. Pitchen, C. J. France, I. M. McFarlane, C. G. Newton and D. M. Thompson, *Tetrahedron Lett.*, **35**, 485 (1994).
329. O. Bortolini, F. Di Furia, G. Licini, G. Modena and M. Rossi, *Tetrahedron Lett.*, **27**, 6257 (1986).
330. H. J. Federsel, *Chirality*, **15**, S142 (2003).
331. N. Komatsu, M. Hashizume, T. Sugita and S. Uemura, *J. Org. Chem.*, **58**, 4529 (1993).
332. N. Komatsu, M. Hashizume, T. Sugita and S. Uemura, *J. Org. Chem.*, **58**, 7624 (1993).
333. A. Lattanzi, F. Bonadies, A. Senatore, A. Soriente and A. Scettri, *Tetrahedron: Asymmetry*, **8**, 2473 (1997).
334. M. T. Reetz, C. Merk, G. Naberfeld, J. Rudolph, N. Griebenow and R. Goddard, *Tetrahedron Lett.*, **38**, 5273 (1997).
335. Y. Yamanoi and T. Imamoto, *J. Org. Chem.*, **62**, 8560 (1997).
336. S. Superchi and C. Rosini, *Tetrahedron: Asymmetry*, **8**, 349 (1997).
337. M. I. Donnoli, S. Superchi and C. Rosini, *J. Org. Chem.*, **63**, 9392 (1998).
338. T. Katsuki, *Synlett*, 281 (2003).
339. B. Saito and T. Katsuki, *Tetrahedron Lett.*, **42**, 3873 (2001).
340. B. Saito and T. Katsuki, *Tetrahedron Lett.*, **42**, 8333 (2001).
341. S. D. Green, C. Monti, R. F. W. Jackson, M. S. Anson and S. J. F. Macdonald, *Chem. Commun.*, 2594 (2001).
342. V. V. Thakur and A. Sudalai, *Tetrahedron: Asymmetry*, **14**, 407 (2003).
343. H.-J. Hamann, E. Höft, D. Mostowicz, A. Mishnev, Z. Urbanczyk-Lipkowska and M. Chmielewski, *Tetrahedron*, **53**, 185 (1997).
344. K. Nakajima, M. Kojima and J. Fujita, *Chem. Lett.*, 1483 (1986).
345. C. Bolm and F. Bienewald, *Angew. Chem., Int. Ed. Engl.*, **34**, 2640 (1995).
346. C. Bolm, G. Schlingloff and F. Bienewald, *J. Mol. Catal. A: Chem.*, **117**, 347 (1997).
347. A. H. Vetter and A. Berkessel, *Tetrahedron Lett.*, **39**, 1741 (1998).
348. C. Ohta, H. Shimizu, A. Kondo and T. Katsuki, *Synlett*, 161 (2002).
349. B. Pelotier, M. S. Anson, I. B. Campbell, S. J. F. Macdonald, G. Priem and R. F. W. Jackson, *Synlett*, 1055 (2002).
350. H. E. Albert and P. G. Haines, U.S. Patent No. 3274252 (1966); *Chem. Abstr.*, **65**, 107611 (1966) (to Pennsalt).
351. A. Terajima and M. Suzuki, JP Patent No. 62/263164 (1987); *Chem. Abstr.*, **109**, 37836 (1988) (to Sagami).
352. A. J. Bailey, W. P. Griffith and B. C. Parkin, *J. Chem. Soc., Dalton Trans.*, 1833 (1995).
353. S. Sakaue, Y. Sakata, Y. Nishiyama and Y. Ishii, *Chem. Lett.*, 289 (1992).
354. F. P. Ballistreri, E. Barbuzzi, G. A. Tomaselli and R. M. Toscano, *J. Mol. Catal. A: Chem.*, **114**, 229 (1996).
355. F. P. Ballistreri, E. Barbuzzi, G. A. Tomaselli and R. M. Toscano, *J. Org. Chem.*, **61**, 6381 (1996).
356. S. I. Murahashi, H. Mitsui, T. Shiota, T. Tsuda and S. Watanabe, *J. Org. Chem.*, **55**, 1736 (1990).
357. E. Marcantoni, M. Petrini and O. Polimanti, *Tetrahedron Lett.*, **36**, 3561 (1995).
358. Z. Zhu and J. H. Espenson, *J. Org. Chem.*, **60**, 1326 (1995).
359. R. W. Murray, K. Iyanar, J. Chen and J. T. Wearing, *Tetrahedron Lett.*, **37**, 805 (1996).
360. R. W. Murray, K. Iyanar, J. Chen and J. T. Wearing, *J. Org. Chem.*, **61**, 8099 (1996).
361. S. Yamazaki, *Bull. Chem. Soc. Jpn.*, **70**, 877 (1997).
362. A. Goti and L. Nannelli, *Tetrahedron Lett.*, **37**, 6025 (1996).
363. M. N. Sheng and J. G. Zajacek, *J. Org. Chem.*, **33**, 588 (1968).
364. K. Krohn and J. Kupke, *Eur. J. Org. Chem.*, 679 (1998).
365. K. Krohn, J. Kupke and H. Rieger, *J. Prakt. Chem.*, **339**, 335 (1997).
366. K. Krohn and J. Kupke, *J. Prakt. Chem.*, **341**, 509 (1999).
367. W. R. Thiel and K. Krohn, *Chem. Eur. J.*, **8**, 1049 (2002).
368. S. Miyano, L. D. L. Lu, S. M. Viti and K. B. Sharpless, *J. Org. Chem.*, **48**, 3608 (1983).

369. S. Miyano, L. D. L. Lu, S. M. Viti and K. B. Sharpless, *J. Org. Chem.*, **50**, 4350 (1985).
370. M. Hayashi, F. Okamura, T. Toba, N. Oguni and K. B. Sharpless, *Chem. Lett.*, 547 (1990).
371. R. A. Sheldon, I. W. C. E. Arends and A. Dijkstra, *Catal. Today*, **57**, 157 (2000).
372. S. E. Jacobson, D. A. Muccigrosso and F. Mares, *J. Org. Chem.*, **44**, 921 (1979).
373. O. Bortolini, L. Bragante, F. Di Furia, G. Modena and L. Cardellini, *Chimica Oggi*, 69 (1986); *Chem. Abstr.*, **105**, 202021 (1986).
374. O. Bortolini, S. Campestrini, F. Di Furia, G. Modena and G. Valle, *J. Org. Chem.*, **52**, 5467 (1987).
375. B. M. Trost and Y. Masuyama, *Tetrahedron Lett.*, **25**, 173 (1984).
376. O. Bortolini, V. Conte, F. Di Furia and G. Modena *J. Org. Chem.*, **51**, 2661 (1986).
377. C. Venturello and M. Gambaro, *J. Org. Chem.*, **56**, 5924 (1991).
378. K. Sato, M. Aoki, J. Takagi and R. Noyori, *J. Am. Chem. Soc.*, **119**, 12386 (1997).
379. K. Sato, M. Aoki, J. Takagi, K. Zimmermann and R. Noyori, *Bull. Chem. Soc. Jpn.*, **72**, 2287 (1999).
380. K. Sato, J. Takagi, M. Aoki and R. Noyori, *Tetrahedron Lett.*, **39**, 7549 (1998).
381. R. W. Murray, K. Iyanar, J. Chen and J. T. Wearing, *Tetrahedron Lett.*, **36**, 6415 (1995).
382. T. H. Zauche and J. H. Espenson, *Inorg. Chem.*, **37**, 6827 (1998).
383. J. H. Espenson, Z. Zhu and T. H. Zauche, *J. Org. Chem.*, **64**, 1191 (1999).
384. D. Slobods-Rozner, P. L. Alsters and R. Neumann, *J. Am. Chem. Soc.*, **125**, 5280 (2003).
385. G. Maayan, R. H. Fish and R. Neumann, *Org. Lett.*, **5**, 3547 (2003).
386. F. Maspero and U. Romano, *J. Catal.*, **146**, 476 (1994).
387. N. Jappar, Q. Xia and T. Tatsumi, *J. Catal.*, **180**, 132 (1998).
388. K. Yamawaki, T. Yoshida, H. Nishihara, Y. Ishii and M. Ogawa, *Synth. Commun.*, **16**, 537 (1986).
389. K. Krohn, I. Vinke and H. Adam, *J. Org. Chem.*, **61**, 1467 (1996).
390. G. C. Krow, *Org. React.*, **43**, 251 (1993).
391. S. E. Jacobson, R. Tang and F. Mares, *J. Chem. Soc., Chem. Commun.*, 888 (1978).
392. S. Campestrini and F. Di Furia, *J. Mol. Catal.*, **79**, 13 (1993).
393. M. Del Todesco, L. Frisone, F. Pinna and G. Strukul, *Organometallics*, **12**, 148 (1993).
394. G. Strukul, A. Varagnolo and F. Pinna, *J. Mol. Catal. A: Chem.*, **117**, 413 (1997).
395. C. Palazzi, F. Pinna and G. Strukul, *J. Mol. Catal. A: Chem.*, **151**, 245 (2000).
396. W. A. Herrmann, R. W. Fischer and J. D. G. Correia, *J. Mol. Catal.*, **94**, 213 (1994).
397. A. M. Faisca Phillips and C. Romao, *Eur. J. Org. Chem.*, 1767 (1999).
398. R. Bernini, E. Mincione, M. Cortese, G. Aliotta, A. Oliva and R. Saladino, *Tetrahedron Lett.*, **42**, 5401 (2001).
399. R. Bernini, E. Mincione, M. Cortese, R. Saladino, G. Gualandi and M. C. Belfiore, *Tetrahedron Lett.*, **44**, 4823 (2003).
400. R. Bernini, A. Coratti, G. Fabrizi and A. Goggiamani, *Tetrahedron Lett.*, **44**, 8991 (2003).
401. A. Bhaumik, P. Kumar and R. Kumar, *Catal. Lett.*, **40**, 47 (1996).
402. A. Corma, M. T. Navarro, L. Nemeth and M. Renz, *Chem. Commun.*, 2190 (2001).
403. M. Renz, T. Blasco, A. Corma, V. Fornes, R. Jensen and L. Nemeth, *Chem. Eur. J.*, **8**, 4708 (2002).
404. A. Corma, M. T. Navarro and M. Renz, *J. Catal.*, **219**, 242 (2003).
405. A. Corma, L. Nemeth, M. Renz and S. Valencia, *Nature*, **412**, 423 (2001).
406. A. Gusso, C. Baccin, F. Pinna and G. Strukul, *Organometallics*, **13**, 3442 (1994).
407. M. Lopp, A. Paju, T. Kanger and T. Pehk, *Tetrahedron Lett.*, **37**, 7583 (1996).
408. T. Kanger, K. Kriis, A. Paju, T. Pehk and M. Lopp, *Tetrahedron: Asymmetry*, **9**, 4475 (1998).
409. C. Bolm and O. Beckmann, *Chirality*, **12**, 523 (2000).
410. A. Watanabe, T. Uchida, K. Ito and T. Katsuki, *Tetrahedron Lett.*, **43**, 4481 (2002).
411. J. O. Edwards and R. Curci, in *Catalytic Oxidations with Hydrogen Peroxide as Oxidant* (Ed. G. Strukul), Chap. 4, Kluwer Academic, Dordrecht, 1992, pp. 97–151.
412. M. Fujiwara, Q. Xu, Y. Souma and T. Kobayashi, *J. Mol. Catal. A: Chem.*, **142**, 77 (1999) and references cited therein.
413. M. G. Clerici, *Top. Catal.*, **15**, 257 (2001) and references cited therein.
414. M. Bianchi, M. Bonchio, V. Conte, F. Coppa, F. Di Furia, G. Modena, S. Moro and S. Standen, *J. Mol. Catal.*, **83**, 107 (1993).
415. G. B. Shul'pin, *C.R. Chimie*, **6**, 163 (2003).
416. S. K. Das, A. Kumar Jr., S. Nandrajog and A. Kumar, *Tetrahedron Lett.*, **36**, 7909 (1995).

417. C.-H. Lee, T.-S. Lin and C.-Y. Mou, *J. Phys. Chem. B*, **107**, 2543 (2003).
418. A. Kozlov, A. Kozlova, K. Asakura and Y. Iwasawa, *J. Mol. Catal. A: Chem.*, **137**, 223 (1999).
419. N. A. Alekar, V. Indira, S. B. Halligudi, D. Srinivas, S. Gopinathan and G. Gopinathan, *J. Mol. Catal. A: Chem.*, **164**, 181 (2000).
420. G. Süss-Fink, L. Gonzalez and G. B. Shul'pin, *Appl. Catal. A: Gen.*, **217**, 111 (2001).
421. J. E. Remias, T. A. Pavlosky and A. Sen, *J. Mol. Catal. A: Chem.*, **203**, 179 (2003).
422. E. D. Park, Y.-S. Hwang, C. W. Lee and J. S. Lee, *Appl. Catal. A: Gen.*, **247**, 269 (2003).
423. S. Das, T. Bhowmick, T. Punniyamurthy, D. Dey, J. Nath and M. K. Chaudhuri, *Tetrahedron Lett.*, **44**, 4915 (2003).
424. W. Adam, W. A. Herrmann, J. Lin, C. R. Saha-Möller, R. W. Fischer and J. D. G. Correia, *Angew. Chem., Int. Ed. Engl.*, **33**, 2475 (1994).
425. W. Adam, W. A. Herrmann, C. R. Saha-Möller and M. Shimizu, *J. Mol. Catal. A: Chem.*, **97**, 15 (1995).
426. U. Schuchardt, D. Mandelli and G. B. Shul'pin, *Tetrahedron Lett.*, **37**, 6487 (1996).
427. C. Nguyen, R. R. J. Guajardo and P. K. Mascharak, *Inorg. Chem.*, **35**, 6237 (1996).
428. D. D. LeCloux, A. M. Barrios and S. J. Lippard, *Bioorg. Med. Chem.*, **7**, 763 (1999).
429. G. V. Nizova, B. Krebs, G. Süss-Fink, S. Schindler, L. Westerheide, L. Gonzalez Cuervo and G. B. Shul'pin, *Tetrahedron*, **58**, 9231 (2002).
430. C. Kim, K. Chen, J. Kim and L. Que Jr., *J. Am. Chem. Soc.*, **119**, 5964 (1997).
431. N. Raffard, V. Bolland, J. Simaan, S. Létard, M. Nierlich, K. Miki, F. Banse, E. Anxolabéhère-Mallart and J.-J. Girerd, *C.R. Chimie*, **5**, 99 (2002).
432. L. Saussine, E. Brazi, A. Robine, H. Mimoun, J. Fischer and R. Weiss, *J. Am. Chem. Soc.*, **107**, 3534 (1985).
433. A. Marsella, S. Agapakis, F. Pinna and G. Strukul, *Organometallics*, **11**, 3578 (1992).
434. For example: P. L. Holland and W. B. Tolman, *Coord. Chem. Rev.*, **190–192**, 855 (1999) and references cited therein.

CHAPTER 14

Contemporary dioxirane chemistry: Epoxidations, heteroatom oxidations and CH insertions*

WALDEMAR ADAM

*Institute of Organic Chemistry, University of Würzburg, am Hubland, D-97094
Würzburg, Germany and Department of Chemistry, University of Puerto Rico, Rio
Piedras, Puerto Rico 00931, USA*
Fax: +1 787 807 0389; e-mail: wadam@chemie.uni-wuerzburg.de

and

CONG-GUI ZHAO

*Department of Chemistry, University of Texas at San Antonio, San Antonio, TX 78249,
USA*
Fax: +1 210 458 7428; e-mail: cong.zhao@utsa.edu

I. INTRODUCTION	1130
A. Historical Overview	1130
B. Generation and Isolation	1130
C. Spectral Characterization	1132
D. Mechanistic Aspects as Explored by Computations	1134
II. CHEMICAL REACTIVITY	1139
A. Epoxidations	1139
B. Heteroatom Oxidations	1150
1. Nitrogen and phosphorus	1151
2. Oxygen, sulfur and selenium	1155
3. Halogens	1157
C. Insertions	1158
III. CONCLUSIONS	1163

* Dedicated to Professor George R. Negrete of the University of Texas at San Antonio (UTSA).

The chemistry of peroxides, volume 2

Edited by Z. Rappoport © 2006 John Wiley & Sons, Ltd ISBN: 0-470-86274-2

IV. ACKNOWLEDGMENTS	1164
V. REFERENCES	1164

I. INTRODUCTION

During the past two decades, dioxiranes have become a favorite of the synthetic chemist as a powerful and selective oxygen-transfer agent. It is efficient and catalytic in transferring the oxygen atom, selective in its reactivity, mild toward the substrate as well as the oxidized product, conveniently prepared from commercially available materials, and environmentally acceptable. To date well over a thousand papers have been published on dioxiranes. In view of the numerous reviews on this subject¹, the present sequel will focus on the most recent developments of dioxirane chemistry, with emphasis on reactivity and selectivity (Section II). Since the historical developments (Section I.A), the preparation and isolation (Section I.B), the spectral characterization (Section I.C), and the mechanistic features (Section I.D) have been extensively treated in the previous reviews, we shall cover them in this introduction (Section I) curtly. Moreover, although impressive progress has been made during the last decade on the theoretical aspects through high-level computations, this topic is combined in brief form with the mechanistic material (Section I.D); these achievements are expertly presented in detail in Chapter 1.

A. Historical Overview

The important and significant events in dioxirane chemistry have for convenience been collected in Table 1. These *highlights* have been selected on the basis of the impact they have played during the last few decades in the development of dioxiranes as popular practical oxidants for synthetic applications, but also from the point of view of their value in the elucidation of oxygen-transfer mechanisms. Precisely the detailed study of the mechanistic aspects of such oxidation processes has furnished the necessary insight and understanding in developing the desired selective methods for synthesis. The impressive achievements speak for themselves and do not require any further elaboration, although some of these shall be considered in more detail in the appropriate sections.

B. Generation and Isolation

The synthetically most useful method for the preparation of dioxiranes is the reaction of appropriate ketones (acetone, trifluoroacetone, 2-butanone, cyclohexanone etc.) with Caroate, commercially available as the triple salt of potassium monoperoxysulfate (KHSO₅)²⁴. The catalytic cycle of the dioxirane formation and oxidation is shown in Scheme 1 in general form. For acetone as the ketone, by simple distillation at a slightly reduced pressure (*ca* 100 torr) at room temperature (*ca* 20 °C), Jeyaraman and Murray⁹ successfully isolated dimethyldioxirane (DMD) as a pale yellow solution in acetone (maximally *ca* 0.1 M). This pivotal achievement in 1985 fomented the subsequent intensive research activity in dioxirane chemistry, mainly the synthetic applications but also the mechanistic and theoretical aspects. The more reactive (up to a thousandfold!²⁵) fluorinated dioxirane, methyl(trifluoromethyl)dioxirane (TFD), was later isolated in a similar manner by Curci, Mello and coworkers^{11a}. For dioxirane derived from less volatile ketones, e.g. cyclohexanone, the salting-out technique has been developed by Murray and coworkers¹⁰ to obtain the corresponding dioxirane solution.

The benefit of using isolated dioxirane solutions for oxidation purposes is that the reaction may be conducted under neutral and water-free conditions, which is advantageous for the preservation of sensitive substrates and oxidation products. Moreover, the process

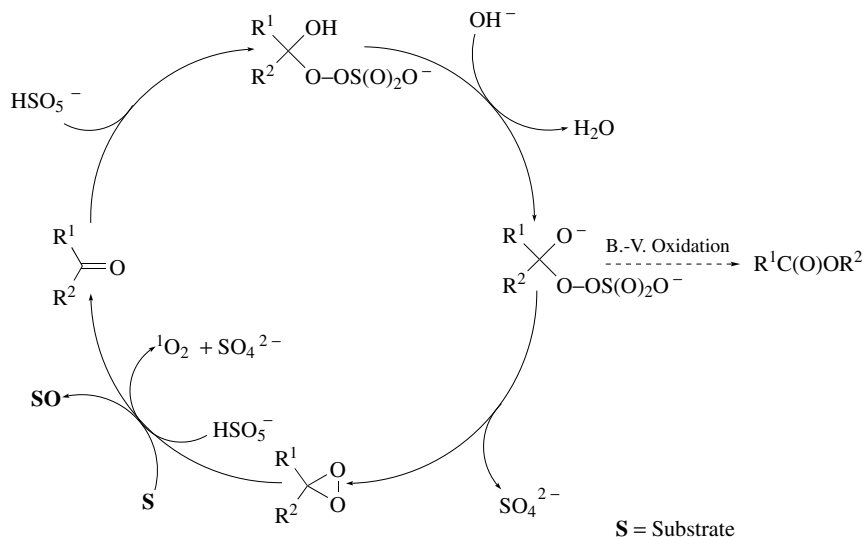
TABLE 1. Chronology of highlights in dioxirane chemistry

1899	The dioxirane structure was postulated by Baeyer and Villiger as a reactive intermediate in the Caroate oxidation of menthone ² .
1972	Talbot and Thompson patented the synthesis of perfluorodimethyldioxirane ³ .
1974	The in-situ generation of dioxiranes was achieved by Montgomery ⁴ .
1978	The parent dioxirane (DO) was synthesized by gas-phase ozonolysis and characterized by Suenram and Lovas ⁵ .
1979	The in-situ oxidation method for dimethyldioxirane (DMD) was developed by Curci and coworkers ⁶ .
1979	The DMD epoxidation of alkenes was reported by Curci and coworkers ⁶ .
1984	The catalytic enantioselective epoxidation was reported by Curci and coworkers ⁷ .
1984	Polycyclic aromatic hydrocarbons were epoxidized by DMD to arene oxides by Jeyaraman and Murray ⁸ .
1985	DMD was isolated as its acetone solution by means of distillation by Jeyaraman and Murray ⁹ .
1986	Cyclohexanone dioxirane was isolated as cyclohexanone solution by means of salting out by Murray and coworkers ¹⁰ .
1988	Methyl(trifluoromethyl)dioxirane (TFD) was isolated by Curci and coworkers ^{11a} .
1989	The enantioselective oxidation of heteroatom substrates (sulfides) was developed by Colonna and Gaggero ¹² .
1989	The oxidation of cyclohexane to cyclohexanone by TFD at $-18\text{ }^{\circ}\text{C}$ in 95% yield within 20 min was achieved by Curci and coworkers ¹³ .
1991	Ketone-free TFD was prepared by selective water extraction of trifluoroacetone by Adam and coworkers ¹⁴ .
1993	The activation energy for the thermal decomposition of DMD was determined to be $24.9\text{ kcal mol}^{-1}$ by Hull and Lalbachan ¹⁵ .
1994	A crystalline dioxirane was isolated and characterized by Sander and coworkers ^{16b} .
1996	The efficient enantioselective epoxidation was reported independently by Yang and coworkers ¹⁷ and Shi and coworkers ¹⁸ .
1997	Ketone-free DMD was prepared by selective water extraction of acetone by Messeguer and coworkers ¹⁹ .
1998	The activation energy for the thermal decomposition of DMD was calculated to be 23 kcal mol^{-1} by Cremer and coworkers ²⁰ .
1998	The enantioselective CH oxidation of diols was reported by Adam and coworkers ²¹ .
2002	The strain energy in DMD was calculated to be only 11 kcal mol^{-1} by Bach and Dmitrenko ²² .
2003	The enantioselective epoxidation of prochiral alkenes with an aldehyde dioxirane was achieved by Bez and Zhao ²³ .

may be carried out at low temperature in a variety of solvents and a wide range of concentrations. The workup is particularly simple, since after all the dioxirane has been consumed (monitored by the peroxide test or spectrophotometrically by following the characteristic yellow color of the dioxirane), the solvent is evaporated and the oxidation product purified according to needs.

Recently, the so-called 'ketone-free' DMD¹⁹ and TFD¹⁵ solutions in CH_2Cl_2 or CCl_4 have been made available by mixing the original dioxirane solution with the appropriate volume of CH_2Cl_2 or CCl_4 and extracting the parent ketone through washing several times with phosphate buffer or water. In this way, the parent ketone is selectively removed and the DMD and TFD concentration is augmented, but at the expense of losing some of the dioxirane.

Should the substrate to be oxidized and its oxidation product be hydrolytically resistant and thermally persistent, the oxidation with in-situ-generated dioxirane is recommended¹ⁿ. The advantages include that more ketone catalyst is available, the generation of the



SCHEME 1. The catalytic cycle for dioxirane formation and its oxidation of the substrate (S)

dioxirane is more efficient, and larger-scale reactions as well as catalytic operation may be conducted. The latter fact is necessary for asymmetric oxidations with dioxiranes derived from chiral ketones and generated under in-situ conditions^{1k-n}.

The following miscellaneous facts must be mentioned in regard to the synthetic efforts in preparing dioxiranes: An organomonoperoxysulfonic acid²⁶ and an organoperoxyimidic acid,²⁷ in situ generated from H_2O_2 , have been used in place of Caroate as peroxide source; other reagents which generate dioxiranes from ketones include peroxynitrite²⁸, HO_2-CH_3CN ²⁹ and peroxycarboxylic acids³⁰. Some preparatively less useful methods include the ozonolysis of alkenes⁵, the oxidation of diazo compounds with singlet oxygen³¹ and the reaction of carbenes with triplet oxygen¹⁶. By using the ozonolysis strategy, the parent dioxirane (H_2CO_2 , DO) was successfully made and spectroscopically characterized, which constitutes the first rigorous experimental evidence for the existence of this fascinating class of peroxide-based oxidants⁵. With the carbene method, for the first time a crystalline dioxirane was isolated as pure substance and its structure determined by X-ray analysis¹⁶.

C. Spectral Characterization

Through the low-temperature ozonolysis of ethylene under low pressure, the parent dioxirane was prepared and characterized by means of microwave spectroscopy^{11a}. The acute bond angle of 66.2° and peroxide bond length of 1.516 \AA unequivocally confirm the three-membered-ring cyclic structure in Figure 1. Furthermore, from this microwave-spectral data a dipole moment was experimentally determined, which is slightly more than that of its carbonyl precursor, namely formaldehyde ($\mu = 2.332 \text{ D}$)^{11b}; thus, this finding implies that the parent dioxirane is slightly more polar than formaldehyde. Subsequently, isolated dioxiranes were fully characterized on the basis of their NMR-spectral chemical shifts (δ), exemplarily shown for methyl(trifluoromethyl)dioxirane (TFD) in Figure 1¹⁰. This example constitutes a particularly informative NMR-spectral case, since four distinct

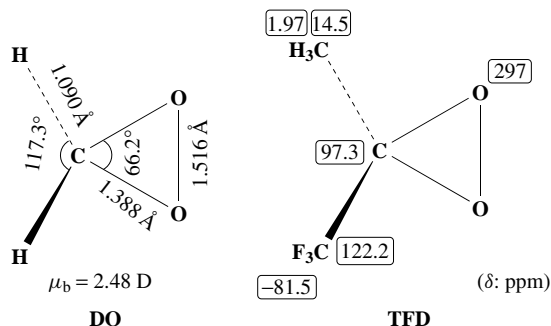
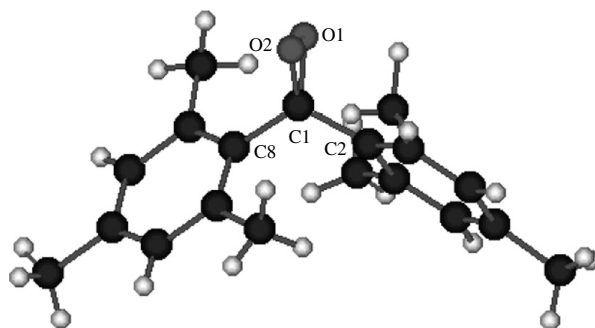


FIGURE 1. Microwave-structural and NMR-spectral data of dioxiranes



Bond	Length (Å)	Bond / Dihedral angle (deg)	
O1-O2	1.503	O1-C1-O2	64.2
C1-O2	1.414	C2-C1-C8	119.2
C1-O1	1.413	Mes ^a -Mes	64.6
C1-C2	1.518	Mes(left) out of COO plane	53.7
C1-C8	1.506	Mes(right) out of COO plane	61.6

^aMes = Mesityl

FIGURE 2. Structural data of the crystalline dimesityldioxirane as determined by X-ray analysis. (Courtesy of Prof. Dr. Wolfram Sander, Reference 16b)

nuclei within this molecule have been characterized, that is, ^{13}C , ^{19}F , ^1H and ^{17}O . Their chemical shifts are given.

Dimesityldioxirane, the first isolated crystalline derivative, offered the opportunity to conduct a structure determination by means of X-ray analysis¹⁶. Clearly, the structural data of the X-ray analysis (Figure 2) match well those obtained by microwave spectroscopy (Figure 1)¹¹. One striking feature of the dioxirane structure is the long oxygen–oxygen

bond (over 1.5 Å), one of the longest known in organic peroxides, which might account for the high reactivity (cf. Section II) of this unusual class of cyclic peroxides.

Solutions of isolated dioxiranes, characteristically dimethyldioxirane (DMD) in acetone, possess a pale yellow color, which serves as a convenient analytical index for monitoring the dioxirane consumption in oxidation reactions³² and kinetic studies¹². For DMD, the absorption maximum ($n-\pi^*$ transition^{1a}) centers at *ca* 325 nm, with a molar extinction coefficient (ϵ) of $12.5 \pm 0.5 \text{ M}^{-1} \text{ cm}^{-1}$ in acetone³². The alternative and more rigorous analytical method for dioxirane quantification utilizes iodometry (KI/starch).

D. Mechanistic Aspects as Explored by Computations

With the recent advances in computational chemistry that allow one to calculate quite accurately reaction trajectories even of complex chemical transformation³³, much progress has been made on the theoretical front in understanding the mechanistic intricacies of the oxygen-transfer process. Specifically for the dioxiranes, much computational activity has been registered, in view of the unusual electronic nature and high oxidative power of these intriguing three-membered-ring cyclic peroxides, which are of mechanistic challenge and a synthetic delight. For the purpose of the present chapter, we have limited ourselves to the essential facets of the theoretical work that relate to the mechanism of the oxygen transfer by these highly effective oxidants and have selected the most relevant contributions of the last handful of years. Fortunately, a detailed account of the theoretical work on peroxides, which includes the dioxiranes, is being featured in Chapter 1 of this volume by Bach.

The structural features, physical and spectral properties, and electronic aspects of the parent dioxirane (DO) and of its simple dimethyl and methyl(trifluoromethyl) derivatives, DMD and TFD, have been well reproduced (actually, from the very beginning of the theoretical work on these cyclic peroxides) by modern computational methods to match experimental data; a recent account is given in the elaborate computations by Cremer and colleagues²⁰. In regard to the thermal persistence of dioxiranes, it has been convincingly concluded in this study that the activation energy (E_a) for the decomposition of unsubstituted DO is only about 18 kcal mol^{-1} and, thus, it is too labile for isolation (indeed, DO could to date be merely detected spectroscopically in the gas-phase ozonolysis of ethylene). In contrast, the E_a value for ring-opening of the dimethyl-substituted DMD was calculated to be *ca* 23 kcal mol^{-1} , which compares quite well with the experimental data of $24.9 \text{ kcal mol}^{-1}$ for its thermolysis in acetone¹⁵. Therewith, DMD is sufficiently persistent at room temperature to be handled in isolated form, as has been amply demonstrated in practice^{1p}.

Relevant for the chemical reactivity of dioxiranes, in Cremer's work²⁰, a strain energy of approximately 26 kcal mol^{-1} has been estimated from desmotic considerations, which makes the parent dioxirane about as strained as cyclopropane ($26.5 \text{ kcal mol}^{-1}$) or the unsubstituted oxirane ($27.6 \text{ kcal mol}^{-1}$). On the basis of more recent computations by Bach and Dmitrenko²², however, it was concluded that DO is much less strained, since a value of only 18 kcal mol^{-1} was obtained when a much larger basis set was employed. Still more astounding, a strain energy of as little as *ca* 11 kcal mol^{-1} was determined for DMD (six diverse methods were utilized to estimate the strain energy!), which makes this dioxirane a relatively unstrained, three-membered-ring structure, certainly much less strained than the parent cyclopropane or oxirane. These authors attribute the low strain energy of DMD to the geminal dimethyl and dioxa substitution, as well as the relatively strong C-CH₃ bonds in this heterocycle. Consequently, they emphatically caution against interpreting the high reactivity of DMD on account of the release of ring strain during

the oxygen-transfer process. Until now, the latter argumentation became established as a paradigm in the mechanistic rationalization of the high oxidation power of dioxiranes, but must be forfeited in view of these recent computational results; conspicuously, factors other than the release of strain are responsible for the high reactivity of dioxiranes.

In regard to the chemical reactivity of dioxiranes, another controversial issue is the so-called *electronic character of the oxygen transfer*, that is, are dioxiranes electrophilic or nucleophilic oxidants, or possibly both? The answer to this challenging question of mechanistic import was provided a few years ago by Deubel, who calculated by advanced quantum-chemical methods the donor–acceptor interactions in the transition structures for the parent-dioxirane (DO) and peroxyformic-acid (PFA) epoxidation of alkenes, substituted by electron-donating (ED) and electron-accepting (EA) substituents³⁴. The conclusion is that the electronic character depends on the substituents on the CC double bond of the alkene: All examined substituents portray PFA as an electrophilic epoxidant (a longstanding intuitive notion), whereas ED groups (methyl, vinyl and amino) reveal the DO as an electrophilic but EA groups (cyano and carbaldehyde) as a nucleophilic oxygen-transfer agent. This means that dioxiranes are biphilic in their electronic character, a novel feature that was hitherto not recognized. Deubel adverts that this unusual feature of dioxiranes is not evident from the inherent electronic and structural properties of the dioxirane itself, but comes to fruition in the transition structure for the dioxirane/alkene pair, akin to the well-known case of the ED/EA effects in Diels–Alder cycloadditions.

One mechanistic matter that has caused quite a bit of general consternation about a decade ago concerns the experimental evidence for the involvement of diradical intermediates (proposed as sources for the observed radical products) in dioxirane epoxidations, which were thought to be formed through induced peroxide-bond homolysis by the alkene³⁵. Nonetheless, rigorous experimental^{1k} and high-level theoretical³⁶ work disposed such radical chemistry in the epoxidation of alkenic substrates. The latter computations unequivocally confirm the established concerted mechanism, in which both CO single bonds in the incipient epoxide are concurrently formed by way of an asynchronous, spiro-structured transition state for the oxygen transfer.

With this brief preamble on the more important current theoretical results for the general structural and electronic characteristics of dioxiranes, we shall now examine the computed transition structures of the oxygen transfer in epoxidations, heteroatom oxidations and CH insertions. Since each reaction type exhibits its individual mechanistic features, these oxyfunctionalizations shall be presented separately.

Numerous computations have been conducted on the reaction trajectories for the dioxirane epoxidations, such that in the context of this subsection, it is necessary to be selective and brief^{37–41}. The newest and to date most complete computations³⁷ on this subject confirm previous conclusions^{38–41} that the π bond in the alkene nucleophile attacks the peroxide bond of the dioxirane electrophile along the conventional S_N2 -type coordinate. In the resulting transition structure **A** for the oxygen transfer (Figure 3), the incipient epoxide and the dioxirane cycles favor (by a couple of kcal mol⁻¹) the spiro geometry (analogous to the Bartlett ‘butterfly’ mechanism⁴²), with the two rings perpendicular to one another. This molecular arrangement allows the dioxirane substituents to point away from the alkene groups (e.g. as shown in the *cis*-configured derivative of the **A** structure in the Figure 3), to minimize steric repulsion in the resulting transition state. This preference was recognized experimentally by Baumstark and McCloskey long before the computations⁴³, but it took some time to put it on firm theoretical grounds⁴⁴.

The mechanistic quintessence of the most recent study by Bach’s group³⁷, in which the oxygen-transfer trajectories for the DMD and TFD epoxidations of the largest set of alkene substrates ever to have been computed are compared with the theoretical results

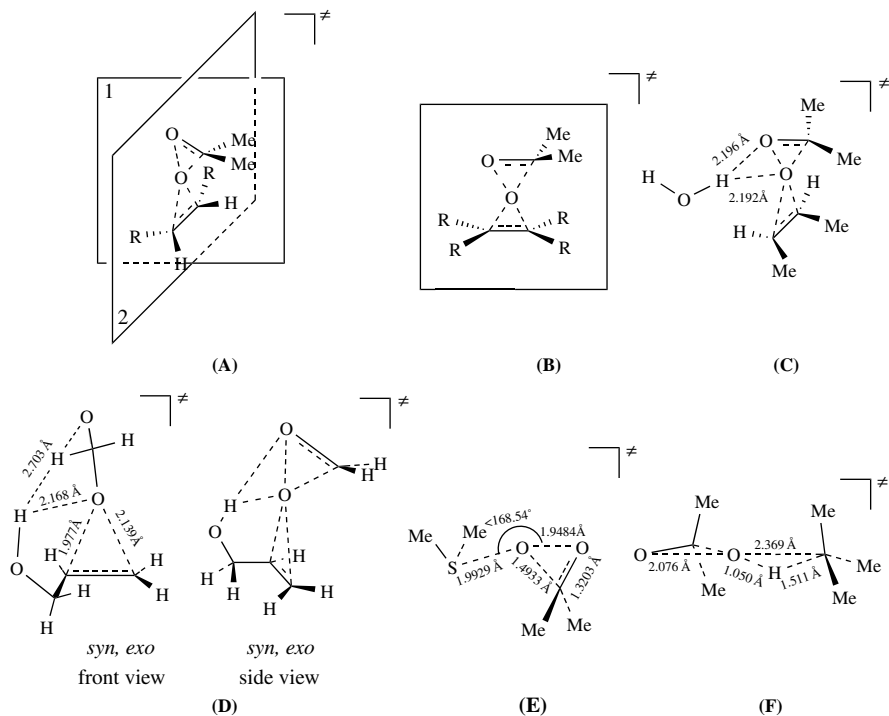


FIGURE 3. Preferred transition structures for the oxygen transfer in the reaction of alkenes, sulfides and alkanes with dioxiranes

obtained for the peroxyformic-acid (PFA) epoxidation, is as follows: (i) In the gas phase the oxidative reactivity of DMD and PFA are essentially the same; the higher reactivity of DMD in acetone solution (about a hundredfold!) is the consequence of polar stabilization of the transition state, whereas PFA is quite insensitive to such polar effects. (ii) Hydrogen bonding is still more effective in differentiating the epoxidation power between DMD and PFA, since the former benefits from stabilization of the polarized transition structure by hydrogen bridging (more on that later), but the latter provides inherently its own hydrogen bonding, and is again relatively insensitive to such external influences; for DMD, however, such hydrogen-bonded stabilization may be dramatic (for *E*-2-butene, a drop in the E_a value from 14.8 to 8.7 kcal mol⁻¹ is calculated, or a stabilization by *ca* 6 kcal mol⁻¹), when an acetic acid molecule is incorporated in the transition structure **B** (Figure 3), as the experimental rate enhancement confirms⁴⁵; similarly, the incorporation of one water molecule in the transition structure for the epoxidation of cyclohexene by DMD lowers the E_a value from 12.6 to 8.5 kcal mol⁻¹ (a lowering of 4.1 kcal mol⁻¹), whereas for two H₂O molecules the stabilization amounts to 6.3 kcal mol⁻¹, which nicely accounts for the experimentally observed water catalysis in the DMD epoxidation⁴⁶. (iii) Unquestionably, the more provocative finding in these calculations is that DMD possesses a relatively unstrained three-membered ring (strain energy of *ca* 11 kcal mol⁻¹!), such that

its epoxidative reactivity must not be attributed to the release of strain during the oxygen-transfer process, as has been the dogma since the discovery of dioxiranes some 30 years ago⁴; instead, the high oxygen-transfer propensity of the electrophilic DMD relates to its relatively low-lying σ^* orbital for the peroxide bond, whereas for TFD, additionally the large inductive effect of the CF_3 group helps.

As for the already briefly mentioned³⁷ polarity effects and hydrogen bonding in dioxirane epoxidations, these aspects have been examined in detail in earlier computational work on simple alkenes^{39–41}. For example, the perplexing water catalysis⁴⁶ was scrutinized by Houk and colleagues for the DMD epoxidation of the *cis* and *trans* 2-butenes³⁹. Besides an adequate account of the substrate *cis/trans* effect (*cis* reacts about tenfold faster than *trans*)⁴³, the salient feature of these calculations is the finding that the hydrogen bonding with a single water molecule (similar results were also obtained with methanol as the hydrogen-bonding entity) engages both oxygen atoms of the dioxirane peroxide bond (structure **C** in Figure 3). This is contrary to the intuitive notion based on experimental data that the stabilization derives only from hydrogen bonding with the distal oxygen atom⁴⁷. The calculated faster rate in the polar solvents is reconciled in terms of the better solvation of the larger dipole moment in the transition structure relative to the reactants.

Similar results were computed for the intermolecular and intramolecular hydrogen bonding in allylic alcohols, in particular 3-methyl-2-buten-1-ol vs. 2-methyl-2-butene⁴⁰, the two distinct double-bond components in geraniol; the regioselectivity of the DMD epoxidation has been experimentally well documented⁴⁸. The results concord with the previous ones³⁹ in regard to the hydrogen bonding to both dioxirane oxygen atoms with an external methanol molecule, as well as with the internal hydroxy functionality of the allylic alcohol, and the stabilization of the larger dipole moment in the transition structure by a polar solvent; however, the electronic effect (the expected inductive electron withdrawal by the allylic hydroxy group) on the reactivity of the π bond in the substrate is questioned in this theoretical work. A much lower activation barrier was calculated for the DMD epoxidation of the allylic alcohol versus the alkene in the gas phase, which is argued to be a consequence of the stabilizing hydrogen bonding in the transition state for the oxygen transfer. In solution, however, particularly in a hydrogen-bonding solvent such as methanol and to a lesser extent in a polar solvent such as acetone (an inevitable component in the oxidations with acetone solutions of DMD!), the increased reactivity of the alkene versus the allylic alcohol derives from more effective stabilization of the transition structures relative to the reactants. This is despite the fact that the transition state for the alkene is less polar than that for the allylic alcohol (e.g. the computed dipole moments for the alkene and allylic alcohol transition structures are 4.22 D and 5.23 D, whereas for the 2-methyl-2-butene and 3-methyl-2-buten-1-ol they are 0.18 D and 1.63 D). Nevertheless, this theoretical work discloses that the activation energy for the oxygen transfer to the alkene is a sensitive function of the solvent polarity (a drop from *ca* 13.6 kcal mol⁻¹ in the gas phase to *ca* 9.3 kcal mol⁻¹ in acetonitrile), but not for the allylic alcohol (the E_a values are correspondingly within 6.8 to 6.4 kcal mol⁻¹). This unexpected medium effect is attributed to the stronger substrate solvation of the allylic alcohol relative to the alkene.

A more extensive and detailed theoretical analysis of the parent dioxirane epoxidation of allylic alcohols was conducted by Sarzi-Amade's group⁴¹. With 2-propen-1-ol as the allylic-alcohol substrate and propene as the model alkene, they located the so-called *syn/exo* transition structure **D** as the lowest-energy one, which is displayed in the form of its *front* and *side* views in Figure 3. Clearly, the hydrogen bonding by the allylic hydroxyl functionality extends to both dioxirane oxygen atoms, in which actually the association is stronger (shorter distance) to the proximal (the oxygen atom that is being transferred) than

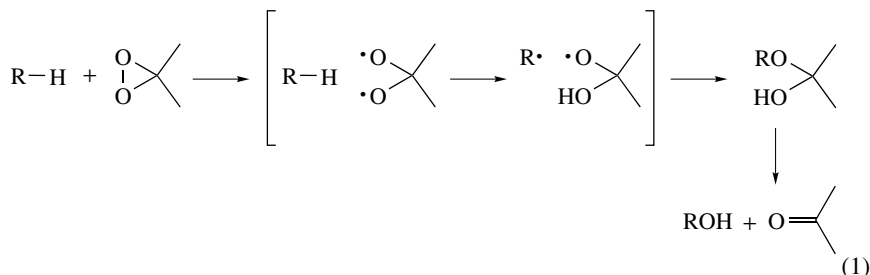
to the distal one; thus, this structural feature in the dioxirane-mediated epoxidation assisted by hydrogen bonding seems to be general^{39,40}. It is gratifying that the computed bond angle of about 136° for optimal hydrogen bonding in the lowest-energy *syn/exo* transition structure **C** matches well the previously reported one of 137–139°, estimated from PM3 calculation⁴⁷. The medium effects of polar solvents on the epoxidation reactivity are in accord with those presented above for the 3-methyl-2-buten-1-ol/2-methyl-2-butene pair⁴⁰, and shall not be further elaborated here.

Considerably fewer computations have been conducted on heteroatom (N, P, S) oxidations by dioxiranes; the new theoretical work on this subject is by Deubel³⁴ and by Bach and coworkers^{44,49,50}. Deubel's paper has already been discussed from the point of view of the *electronic character of oxygen transfer*³⁴, so that we shall concentrate briefly on the results from Bach's group^{49,50}. For DMD, the reaction profiles with the heteroatom nucleophiles Me₃N, Me₃P, Me₂S and Me₂SO have been computed, and in all cases the classical concerted S_N2 mechanism was obtained⁴⁹. The calculated transition state for the oxygen transfer from DMD to Me₂S is exemplarily exhibited by structure **E** in Figure 3; the transition states for the other heteroatom nucleophiles are similarly structured. Thus, in structure **E**, the lone pair of the heteroatom (the sulfide sulfur atom in this case) attacks the peroxide bond of the dioxirane in almost a straight line (the S–O–O bond angle is *ca* 170°), with concurrent displacement of the acetone product.

The computed gas-phase reactivities for the various heteroatom nucleophiles are Me₂S ≈ Me₂SO and Me₃N < Me₃P, whereas in chloroform solution the orders are Me₂S ≈ Me₂SO and Me₃N ≈ Me₃P. Evidently, these do not reproduce well the experimental trends, since the oxidation may be perfectly well stopped at the sulfoxide stage under the appropriate reaction conditions⁵¹. The problem of this lack of chemoselectivity in the computational results is again due to solvation effects in the liquid medium, since the transition structures are highly polarized, as indicated by the very large calculated dipole moments. As yet, the available quantum-chemical methods do not adequately handle such complex solvent effects.

To be considered still in this subsection is the theoretical treatment of the oxygen insertion into the CH bond of an unactivated alkane, unquestionably the most amazing and preparatively more valuable oxyfunctionalization performed by dioxiranes, but also the most complex one from the computational point of view. Unlike the S_N2-type dioxirane oxidations discussed so far, namely the epoxidation (π -bond nucleophiles) and the heteroatom oxyfunctionalization (lone-pair nucleophiles), the insertion of one of the dioxirane oxygen atoms into a σ_{CH} bond of an alkane requires the rupture of the O–O bond, formation of the C–O bond and the transfer of a hydrogen atom. The mechanistically simplest scenario would be abstraction of a hydrogen atom by a dioxy radical to generate a hydroxyl/carbon-centered radical pair, which subsequently collapses to the insertion product, namely the alcohol (equation 1). This sequence of events would be akin to the so-called enzymatic *oxygen-rebound* mechanism, proposed to operate in the cytochrome P-450 oxidation of saturated hydrocarbons⁵². Such a mechanism was also proposed by Minisci's group on the basis of the observed radical-type products³⁵, but shown to be an artifact^{1k}. Indeed, elaborate quantum-chemical calculations confirm the established oxenoid-type mechanism, as exemplified in the concerted diradicaloid transition state for this oxygen-atom insertion into the tertiary CH bond in isobutane by DMD (structure **F** in Figure 3)^{33,53}. Effectively, the spin-paired transition structure consists of an incipient hydroxyl species, which is sandwiched between the developing *tert*-butyl fragment and the departing acetone molecule. At no time is a bona fide radical site generated in this concerted process. Expectedly, appreciable electron spin density accumulates

at the tertiary carbon atom of the *t*-Bu fragment and the oxygen atom of the developing acetone molecule, but negligibly at the hydroxyl fragment. Final collapse of the hydroxyl and *tert*-butyl fragments affords the *tert*-butyl alcohol as insertion product, with departure of the acetone.



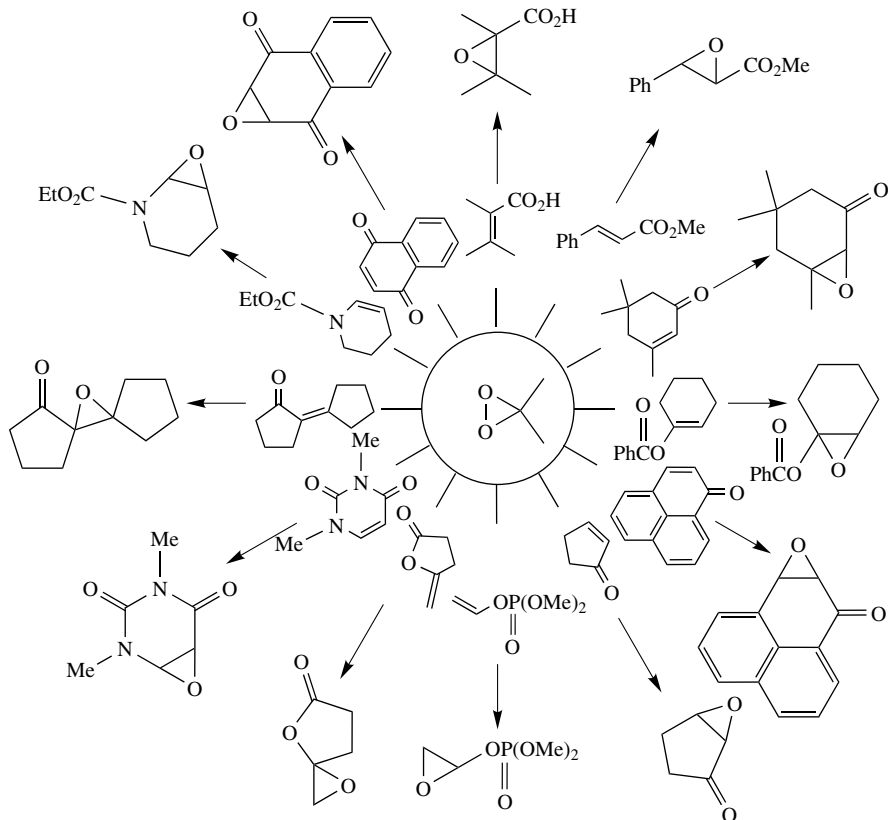
II. CHEMICAL REACTIVITY

Through the efforts of the last two decades, the reactivity and selectivity of dioxirane-mediated oxidations have been thoroughly studied¹. Epoxidations, heteroatom oxidations and sigma-bond insertions constitute the most thoroughly investigated oxyfunctionalizations by dioxiranes¹. In view of the distinct nature of each of these three oxidation types, we will present them separately, while the vast number of examples in each category oblige us to be selective; for more detailed information, the reader is referred to previous reviews¹. Thus, the emphasis will be placed on recent advances on these oxygen-transfer processes.

A. Epoxidations

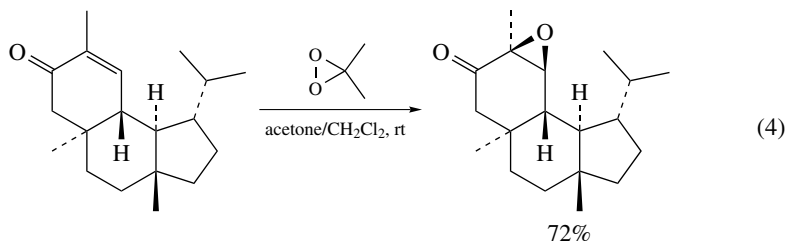
The epoxidation is the most-studied reaction of dioxiranes^{1p}. With the isolated and/or in-situ-generated dioxiranes, numerous examples of all types (electron-rich, unfunctionalized and electron-poor) of alkenes have been successfully epoxidized, whereas the oxidation of the π bonds in arenes and in alkynes is much less abundant^{1p}. In those cases in which the in-situ-generated dioxiranes are used, it should be realized that KHSO_5 possesses some epoxidation power itself, such that in this mode some direct epoxidation by KHSO_5 may take place, especially with electron-rich substrates⁶. For electron-deficient substrates, the competitive oxidation by KHSO_5 is minimal at neutral pH, but at $\text{pH} > 10$, direct epoxidation by KHSO_5 may occur through the Weitz–Scheffer reaction⁵⁴. Such background oxidation by KHSO_5 should be particularly worrying when diastereoselective or enantioselective applications are being conducted^{11-p}.

Electron-rich alkenes are the more reactive π -bond substrates towards epoxidation by the electrophilic dioxiranes^{1a-f,p}. Some typical examples of these oxidations are summarized in Scheme 2. Since the resulting epoxides are usually hydrolytically and thermolytically quite labile, such oxidations are best carried out with isolated dioxiranes. For example, the 8,9 epoxide of the well-known *aflatoxin B*₁, postulated as potent carcinogen in the oxidative metabolism of this natural product⁵⁵, escaped numerous efforts to prepare it by conventional epoxidations because of its sensitivity towards hydrolysis⁵⁶. The synthesis of this labile epoxide was readily accomplished by employing a solution of the isolated DMD at room temperature (equation 2), and its mutagenicity unequivocally

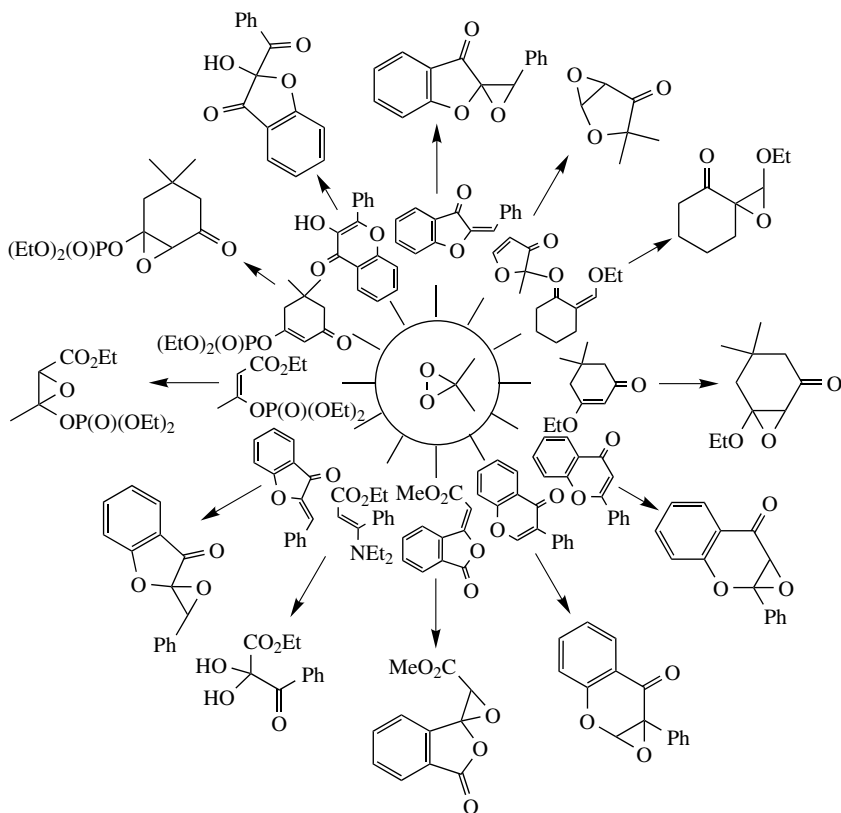


SCHEME 4. Dioxirane oxidation of electron-poor alkenes

access to the corresponding epoxides, which are usually difficult to prepare with peracids as electrophilic oxidants; alternatively, the nucleophilic conditions of the Weitz–Scheffer reaction may be used⁶¹. For example, this strategy has been employed to obtain in good yield and under mild conditions the key intermediate for the total synthesis of the natural products verrucosan-2 β -ol and homoverrucosan-5 β -ol, as displayed in equation 4⁶².



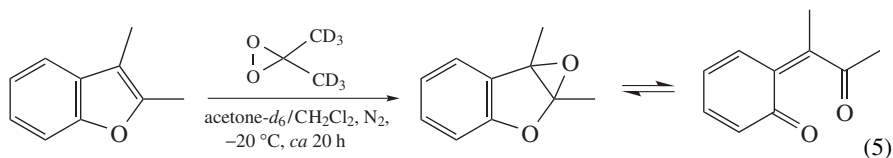
Alkenes with both electron-donating and electron-accepting groups on the π bond behave like electron-poor substrates in reactivity, such that longer (up to days) reaction

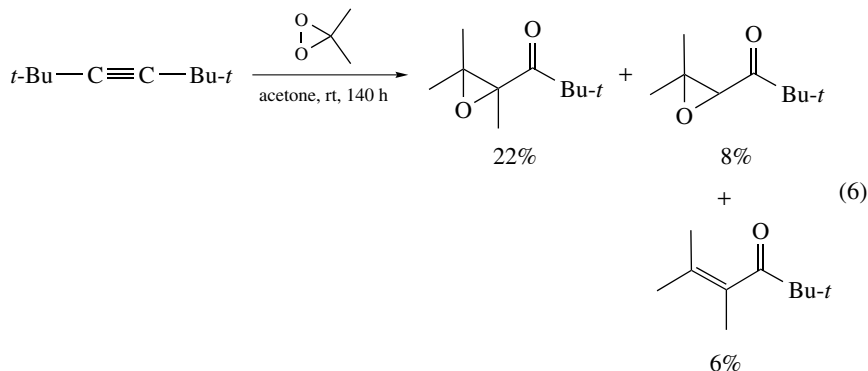


SCHEME 5. Dioxirane oxidation of alkenes with both electron-donor and electron-acceptor groups

times, a large (up to tenfold) excess of DMD, and elevated (up to 60°C) temperatures, or the more powerful TFD, may be required for complete conversion⁶⁰. Scheme 5 summarizes some typical examples of these epoxidations.

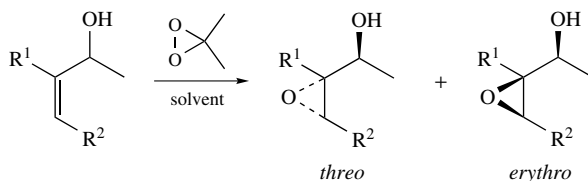
The epoxidation of heteroarenes such as furans and indoles generates very labile products, such that the reaction needs to be carried out at subambient temperature. For example, even at -20°C , the epoxide of 2,3-dimethylbenzofuran rearranges to the *ortho*-quinomethide (equation 5)⁶³. To characterize this epoxide by $^1\text{H-NMR}$ spectroscopy, the fully deuteriated DMD- d_6 solution, prepared in acetone- d_6 , was employed for the oxidation and the epoxide was detected at -78°C ⁶³. Alkynes lead on epoxidation to a multitude of oxidation products (equation 6); thus, the reaction is synthetically hardly useful and, therefore, has been little studied⁶⁴.





As already mentioned, the dioxirane epoxidation of an alkene is a stereoselective process, which proceeds with complete retention of the original substrate configuration. The dioxirane epoxidation of chiral alkenes leads to diastereomeric epoxides, for which the diastereoselectivity depends on the alkene and on the dioxirane structure. A comparative study on the diastereoselectivity for the electrophilic oxidants DMD versus *m*CPBA has revealed that DMD exhibits consistently a higher diastereoselectivity than *m*CPBA; however, the difference is usually small. An exception is 3-hydroxycyclohexene, which displays a high *cis* selectivity for *m*CPBA, but is unselective for DMD⁶⁵.

The results of the dioxirane epoxidation of some 3-alkyl-substituted cyclohexenes and of 2-menthene indicate that the diastereoselectivity control is subject to the steric interactions of the dioxirane with the substituents of the substrate, while the size of the dioxirane substituents has only a minimal effect⁶⁵. In the favored transition structure, the alkyl groups of the dioxirane cannot interact effectively with the substituents at the stereogenic center of the chiral alkene⁶⁵.



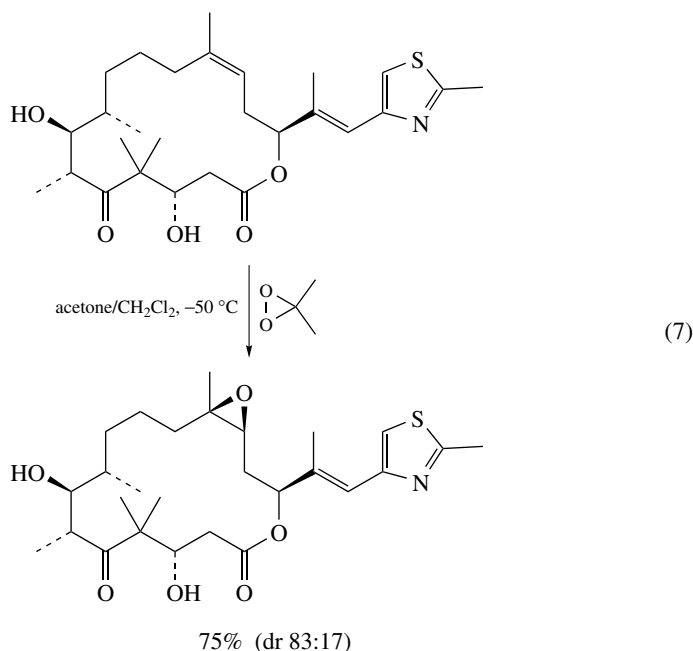
R ¹	R ²	Solvent	<i>threo</i> : <i>erythro</i>
Me	H	9:1 CCl ₄ /acetone	70 : 30
H	Me	9:1 CCl ₄ /acetone	85 : 15
Me	Me	9:1 CCl ₄ /acetone	91 : 9
Me	Me	9:1 MeOH/acetone	82 : 18

SCHEME 6. Hydroxy-group directivity in the *threo*-diastereoselective epoxidation of chiral allylic alcohols by DMD

In the epoxidation of acyclic allylic alcohols (Scheme 6), the diastereoselectivity depends significantly on the substitution pattern of the substrate⁴⁸. The control of the *threo* selectivity is subject to the *hydroxyl-group directivity*^{48,66}, in which conformational preference on account of the steric interactions and the hydrogen bonding between the dioxirane oxygen atoms and the hydroxy functionality of the allylic substrate steer the favored π -facial

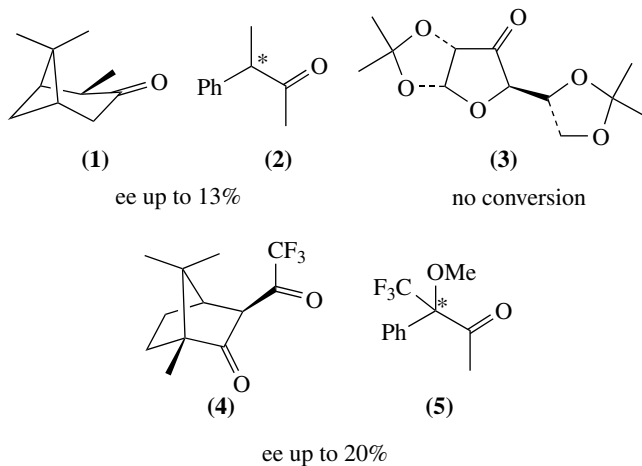
attack on account of $A^{1,2}$ strain. When CCl_4 is used as cosolvent for the substrate, which possesses only a 1,2-allylic strain ($A^{1,2}$), namely when $R^1 = \text{Me}$ and $R^2 = \text{H}$, the *threo* selectivity is moderately preferred (70:30), whereas for the substrate only with 1,3-allylic strain ($A^{1,3}$), namely $R^1 = \text{H}$ and $R^2 = \text{Me}$, effective control (85:15) is observed. When both $A^{1,2}$ and $A^{1,3}$ strain are present in the substrate, as in $R^1 = R^2 = \text{Me}$, the π -facial diastereoselectivity is augmented to 91:9 in favor of *threo* selection. The importance of hydrogen bonding is witnessed in the latter case, since the *threo* diastereoselectivity drops from 91:9 in CCl_4 to 82:18 in MeOH as cosolvent. Evidently, the protic MeOH solvent competes with the hydroxy functionality of the allylic alcohol in the hydrogen bonding with the attacking dioxirane^{48,66}. These results provide valuable mechanistic insight into the stereoselective oxygen-transfer process.

Highly diastereoselective dioxirane epoxidations have been widely employed in organic synthesis^{1p}. For example, in the total synthesis of epothilone B, an important antitumor agent⁶⁷, the required epoxide was obtained in good yield and diastereoselectivity by DMD oxidation (equation 7)⁶⁸.

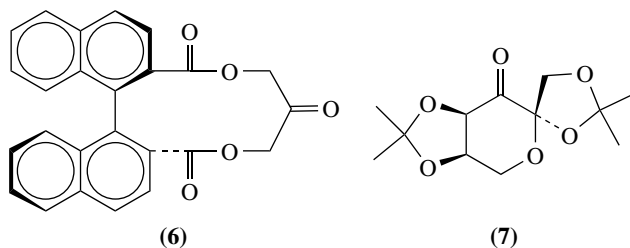


The dioxirane epoxidation of a prochiral alkene will produce an epoxide with either one new chirality center for terminal alkenes, or two for internal alkenes. When an optically active dioxirane is used as the oxidant, expectedly, prochiral alkenes should be epoxidized asymmetrically. This attractive idea for preparative purposes was initially explored by Curci and coworkers in the very beginning of dioxirane chemistry⁷. The optically active chiral ketones **1** and **2** were employed as the dioxirane precursors, but quite disappointing enantioselectivities were obtained. Subsequently, the glucose-derived ketone **3** was used, but unfortunately, this oxidatively labile dioxirane precursor was quickly consumed without any conversion of the alkene⁶⁹. After a long pause (11 years) of activity in this challenging area, the Curci group reported work on the much more reactive ketone

catalysts **4** and **5**, but the enantioselectivity was still low⁷⁰; however, it was pointed out that C_2 -symmetric ketones should be more propitious in increasing the stereocontrol of such asymmetric epoxidations⁷⁰.

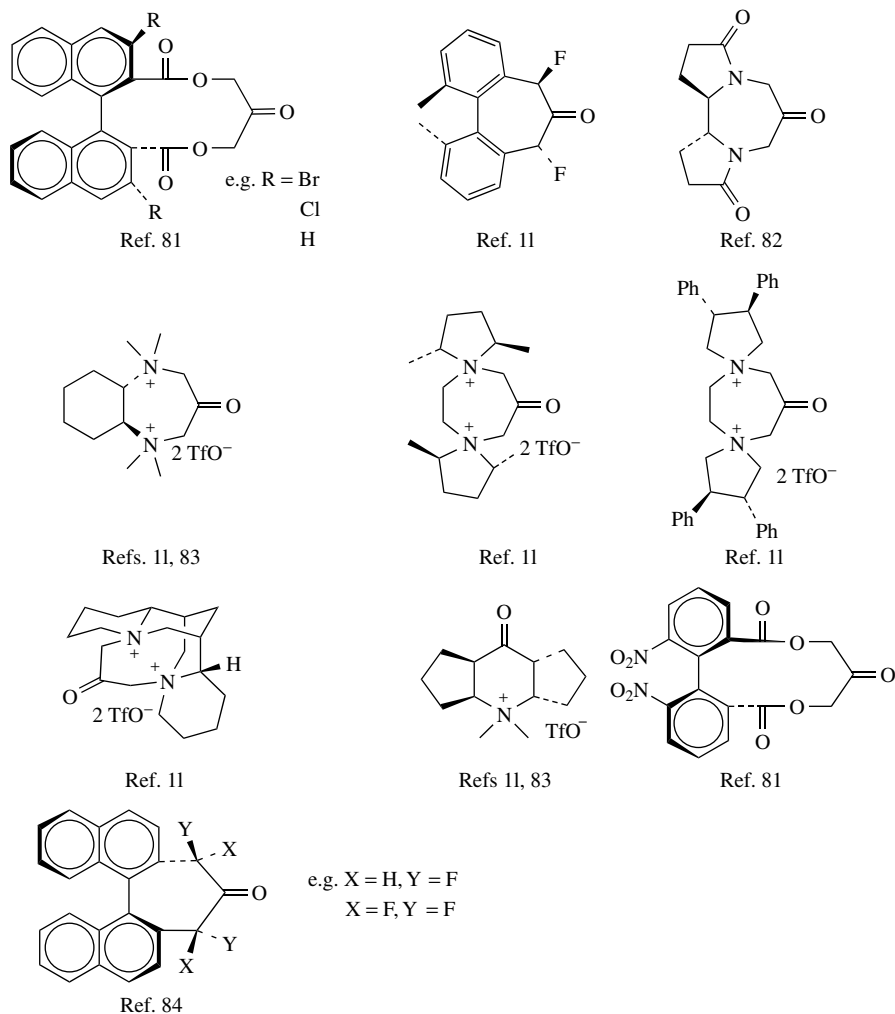


The breakthrough came already in 1996, one year after Curci's prediction, when Yang and coworkers reported the C_2 -symmetric binaphthalene-derived ketone catalyst **6**, with which ee values of up to 87% were achieved¹⁷. A few months later, Shi and coworkers reported the fructose-derived ketone **7**, which is to date still one of the best and most widely employed chiral ketone catalysts for the asymmetric epoxidation of nonactivated alkenes¹⁸. Routinely, epoxide products with ee values of over 90% may be obtained for *trans*- and trisubstituted alkenes. Later on, a catalytic version of this oxygen-transfer reaction was developed by increasing the pH value of the buffer⁷¹. The shortcoming of such fructose-based dioxirane precursors is that they are prone to undergo oxidative decomposition, which curtails their catalytic activity.

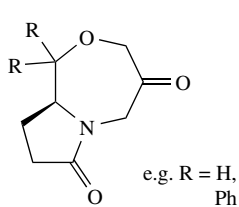


Essentially concurrently, the C_2 -symmetric ketone catalysts **8–10** were reported^{72,73}. In regard to the enantioselectivity, the TADDOL ($\alpha,\alpha',\alpha',\alpha'$ -tetraaryl-1,3-dioxolane-4,5-dimethanol)-derived ketone **10** performs better than the binaphthalene-based ketone **6**, but not as well as the fructose-modified ketone **7**, whereas **10** is more resistant than **7** in regard to oxidative degradation⁷³.

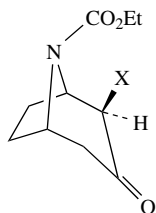
These encouraging results have led to a surge of activity in this promising area, such that numerous ketone catalysts have been developed for asymmetric epoxidations. A

SCHEME 8. C_2 -symmetric ketones as catalysts for asymmetric alkene epoxidation

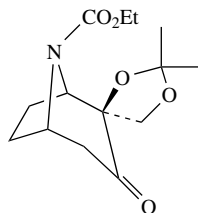
While the above-mentioned ketone catalysts are effective for *trans*- and trisubstituted alkenes, they usually deliver a poor enantioselectivity when terminal and prochiral *cis*-alkenes are used as substrates. Shi's group prepared the optically active ketone **11** (a modification of ketone **7** in which the oxygen atom of the spiro-annulated ring was replaced by a nitrogen functionality), an excellent catalyst for the enantioselective epoxidation of *cis*-configured and terminal alkenes; its efficacy of π -facial stereocontrol depends on the nature of the nitrogen substituent^{79,89}. In contrast, the enantioselectivity dropped dramatically when the annulated dioxolane ring was removed to afford the chiral ketone **12**⁸⁹. Also, the ketone **13** with the fructose backbone was developed for the highly enantioselective epoxidation of electron-poor alkenes⁹⁰.



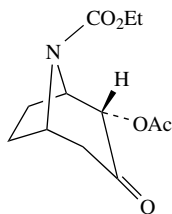
Ref. 82



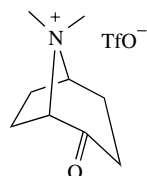
Ref. 85



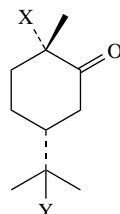
Ref. 85



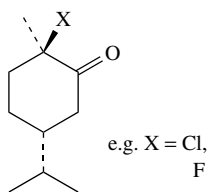
Ref. 85



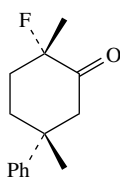
Ref. 86



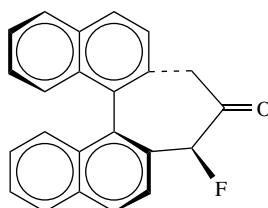
Refs. 87, 88



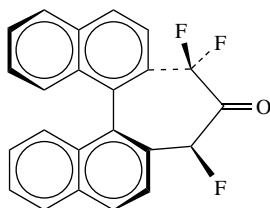
Refs. 87, 88



Ref. 88

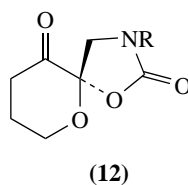
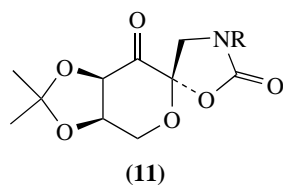


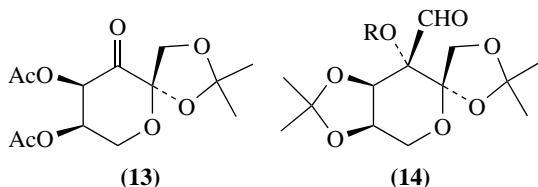
Ref. 84



Ref. 84

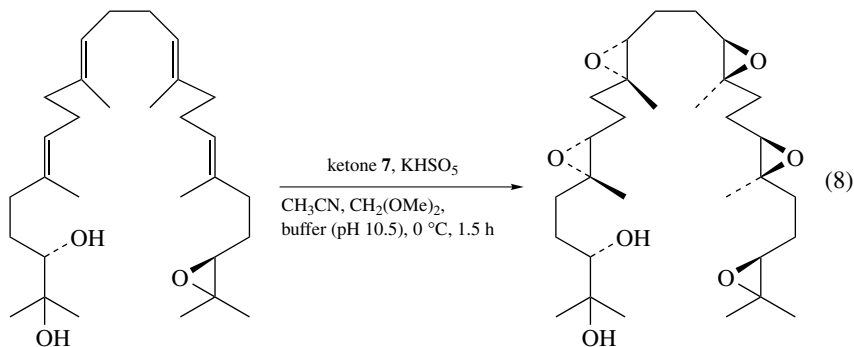
SCHEME 9. Miscellaneous chiral ketones as catalysts for asymmetric alkene epoxidation





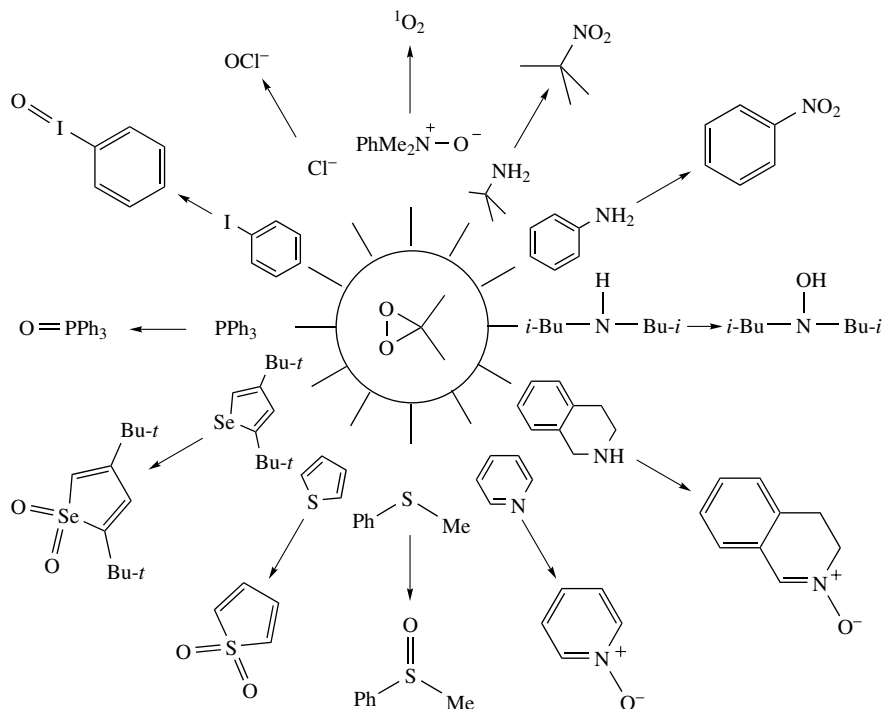
Although the parent formaldehyde-derived dioxirane (H_2CO_2) was the first of this intriguing class of cyclic peroxides to be prepared and spectrally characterized in 1976, the conversion of aldehydes into the corresponding dioxiranes by treatment with Caroate was deemed difficult because of the expectedly facile Baeyer–Villiger oxidation of the aldehydes to their carboxylic acids. Most gratifyingly, however, it was recently demonstrated that optically active aldehydes may also serve as promising catalysts for asymmetric epoxidations²³. For example, ee values up to 94% were obtained with the aldehyde **14** as dioxirane precursor.

The dioxirane-mediated enantioselective oxidation has proven to be an attractive and useful method in organic synthesis. For example, the asymmetric epoxidation of silyl enol ethers^{27,91,92}, enol esters⁹¹, dienes⁹³ and enynes⁹⁴ has been achieved in high enantioselectivity, as well as chemoselectivity and regioselectivity, by employing the in-situ-generated dioxirane of ketone **7**. Moreover, the first kinetic resolution of racemic enol acetates has also been accomplished by means of the stereoselective epoxidation with the ketone **7** catalyst⁹⁵. A highlight in the synthetic application of an in-situ-generated dioxirane from ketone **7** is the preparation of the glabrescol analogue⁹⁶. Finally, the highly enantioselective oxyfunctionalization of the chiral tetraene in equation 8 generates the four epoxide rings in an efficient one-pot process⁹⁶.



B. Heteroatom Oxidations

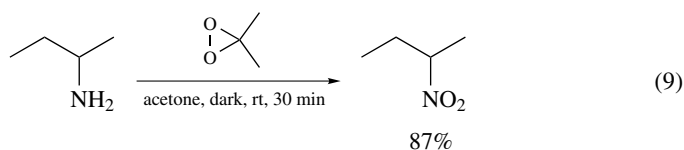
Since dioxiranes are electrophilic oxidants, heteroatom functionalities with lone pair electrons are among the most reactive substrates towards oxidation. Among such nucleophilic heteroatom-type substrates, those that contain a nitrogen, sulfur or phosphorus atom, or a $\text{C}=\text{X}$ functionality (where X is N or S), have been most extensively employed, mainly in view of the usefulness of the resulting oxidation products. Some less studied heteroatoms include oxygen, selenium, halogen and the metal centers in organometallic compounds. These transformations are summarized in Scheme 10. We shall present the substrate classes separately, since the heteroatom oxidation is quite substrate-dependent.



SCHEME 10. Dioxirane oxidation of substrates with heteroatom functionalities

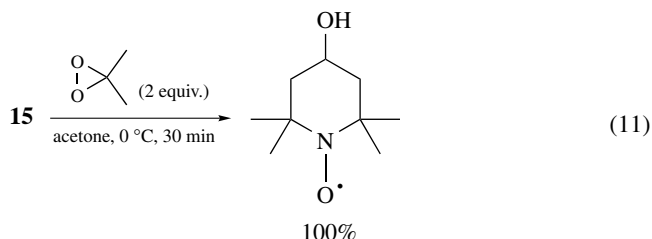
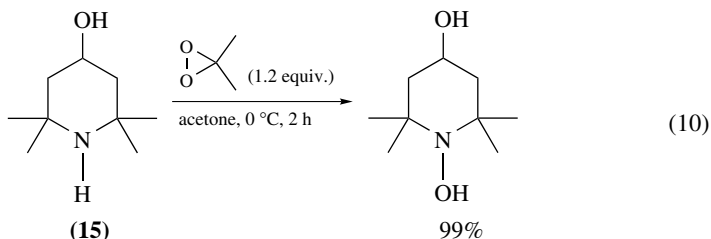
1. Nitrogen and phosphorus

The oxidation of nitrogen-containing compounds, in particular amines, depends on the degree of alkylation of the nitrogen atom and its hybridization state. For example, the oxidation of primary amines usually gives a mixture of products, which includes hydroxylamine, oxime, nitroso, nitro and sometimes even an azoxy compound⁹⁷. To assure chemoselectivity, an appropriate oxidant and adequate reaction conditions must be chosen. Indeed, a preparatively valuable method is the DMD oxidation of aliphatic and aromatic amines to the corresponding nitro compounds. Thus, the 2-aminobutane was oxidized by isolated DMD at room temperature to 2-nitrobutane in high yield (equation 9)⁹⁸. Similarly, also the oxidation with in-situ-generated DMD constitutes a convenient and effective method to convert primary aromatic amines into the corresponding nitro compounds⁹⁹.



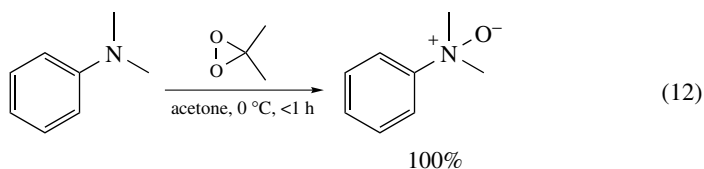
The oxidation of secondary amines with no α -hydrogen atoms leads to hydroxylamines, but excessive dioxirane may further oxidize the hydroxylamines to the corresponding nitroxyl radical. For example, when a slight excess of isolated DMD is employed, 2,2,6,6-tetramethylpiperidin-4-ol (**15**) is quantitatively transformed into the hydroxylamine

(equation 10)¹⁰⁰; however, with two equivalents of DMD under the same conditions, the corresponding nitroxyl radical is produced (equation 11)¹⁰⁰. In contrast, the oxidation of



secondary amines carrying an α -hydrogen affords a complex product mixture of the corresponding nitrones, hydroxylamines or hydroxamic acids, whose composition depends on the reaction conditions^{10, 101}.

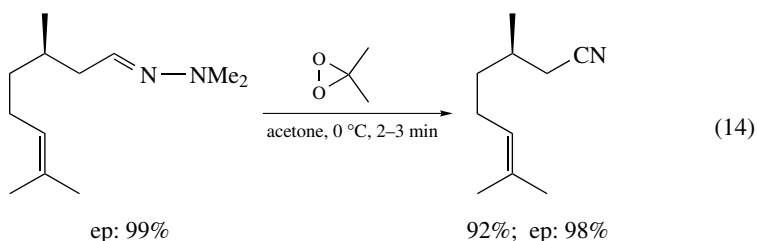
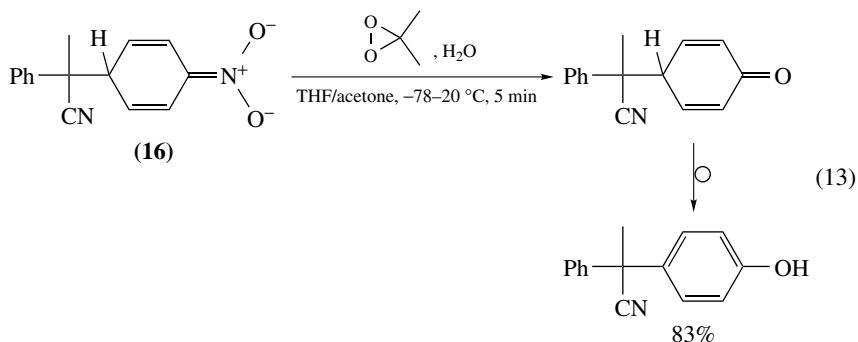
In the case of tertiary amines, the DMD treatment produces cleanly the *N*-oxides; thus, from *N,N*-dimethylaniline the *N*-oxide is quantitatively obtained (equation 12)¹⁹. In this context, it must be pointed out that the *N*-oxide may catalyze the decomposition of the dioxirane (vide infra), so that complete conversion of the amine is not always possible even with an excess of DMD.



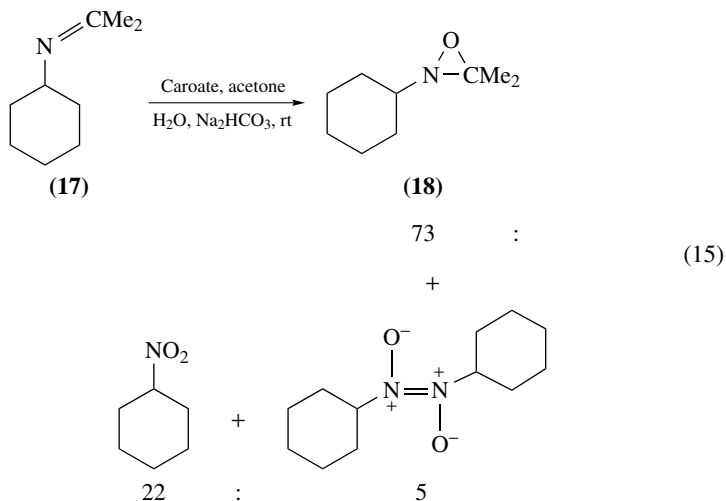
From the aforementioned, it should be evident that the amino group is one of the most reactive functionalities towards dioxirane oxidation; consequently, to achieve a chemoselective oxidation of a multi-functionalized substrate that possesses an amino group, the latter must be protected. This may be accomplished by masking the amino substituent in the form of its ammonium salt¹⁰², or BF_3 complex¹⁰³, even better as an amide functionality (*N*-phenylacetamide resists TFD oxidation at room temperature¹⁰⁴). This will reduce sufficiently the oxidative reactivity of the amino group, such that another less reactive group may be selectively oxidized^{103, 105}.

Substrates with doubly bonded nitrogen-atom functionalities, e.g. the $\text{C}=\text{N}-\text{R}$ (imino, oxime) group, are usually cleaved by dioxirane to give the corresponding carbonyl product¹⁰⁶. A particular case represents the DMD oxidation of the nitronate ions, generated from nitroalkanes¹⁰⁷ or nitroarenes¹⁰⁸. For example, the nitronate anion **16** (equation 13) affords initially the cyclohexadienone on oxidation with DMD, which subsequently tautomerizes to the phenol as the final product¹⁰⁸. An exception is the DMD oxidation of an

N,N-dimethylhydrazone at 0 °C (equation 14), which produces the corresponding nitrile instead¹⁰⁹.



The cycloaddition of an oxygen atom to the CN double bond, analogous to the epoxidation of CC double bonds, is rare. For example, when the imine **17** is oxidized with in-situ-generated dioxirane (equation 15), the oxaziridine **18** is obtained as the major product^{97a}.



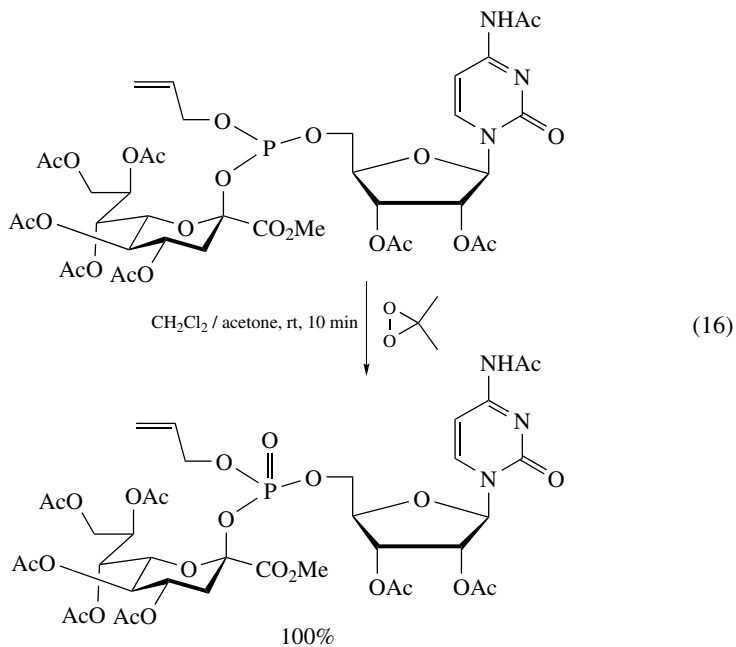
When the nitrogen atom is a part of an aromatic ring, i.e. a nitrogen heteroarene, usually the corresponding *N*-oxide is obtained. For example, pyridine *N*-oxide is the only

product obtained quantitatively in the DMD oxidation of pyridine^{9,19,110}. In contrast, the oxidation of pyrrole and imidazole by DMD leads to a more complex product mixture, because epoxidation of the π system takes place, to afford labile oxidation products.

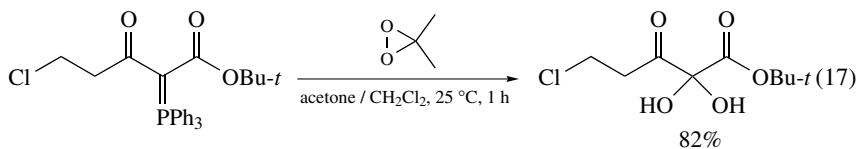
A triple-bonded nitrogen functionality (a *sp*-hybridized nitrogen atom), namely the cyano group, is resistant towards dioxirane oxidation. The fact that acetonitrile is widely used as a solvent for dioxirane oxidations¹¹¹ amply substantiates the lack of oxidative reactivity of cyano compounds.

Trivalent phosphorus compounds are more readily oxidized than the corresponding nitrogen derivatives on account of their higher nucleophilicity; however, the oxidation of such highly reactive substrates by dioxiranes has been sparsely studied. Only about a handful of examples are available in the literature, such that little may be said about the general trends in reactivity and selectivity.

The trivalent phosphorus atom in triphenylphosphine is quantitatively oxidized by in-situ-generated or isolated DMD, to afford triphenylphosphine oxide under a variety of conditions^{9,16a,112}. Recently, the selective oxidation of the phosphite functionality in nucleosides was reported to produce the corresponding nucleotides in nearly quantitative yields¹¹³. One example of such an oxidation is shown in equation 16, to illustrate that this phosphorus oxidation may offer an expedient way of preparing unusual nucleotides.



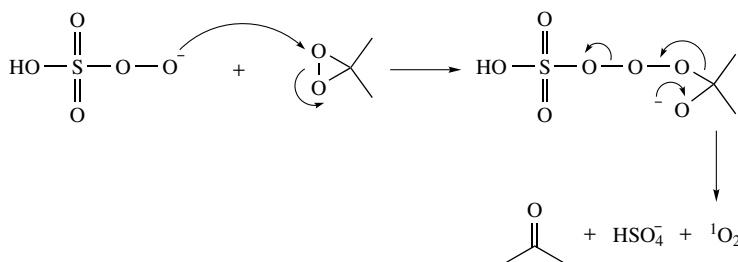
A case of a pentavalent phosphorus-atom oxidation is documented for α,α -dicarbonylphosphoranes (equation 17)¹¹⁴. When treated with DMD, the corresponding α tricarbonyl



product (as its hydrate) is obtained in excellent yields. These results are analogous to the DMD oxidation of related diazo compounds^{106b,c}.

2. Oxygen, sulfur and selenium

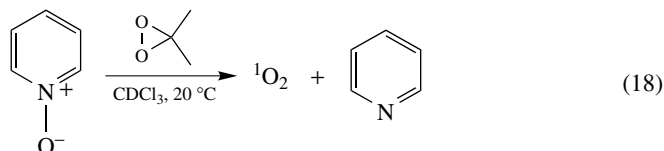
Dioxiranes oxidize only special types of oxygen functionalities, which include peroxides, *N*-oxides and *N*-oxyl radicals. In most of these oxidations, molecular oxygen is produced, mechanistically most significant, in its electronically excited state, namely singlet oxygen (¹O₂). A now classical case, but that required almost two decades to become recognized after its discovery⁴, is the reaction of dioxiranes with Caroate (KHSO₅), the most effective peroxide reagent employed in the preparation of dioxiranes⁴. In this intriguing process, the in-situ-generated DMD reacts with the Caroate to liberate singlet oxygen, KHSO₄ and acetone as products¹¹⁵. The mechanism in Scheme 11 discloses why the released dioxxygen is formed in its singlet-excited state. During the act of dioxxygen release, the electrons involved are all paired and, inevitably, also in the resulting oxygen molecule the electrons must be paired (spin conservation), which corresponds to singlet oxygen.



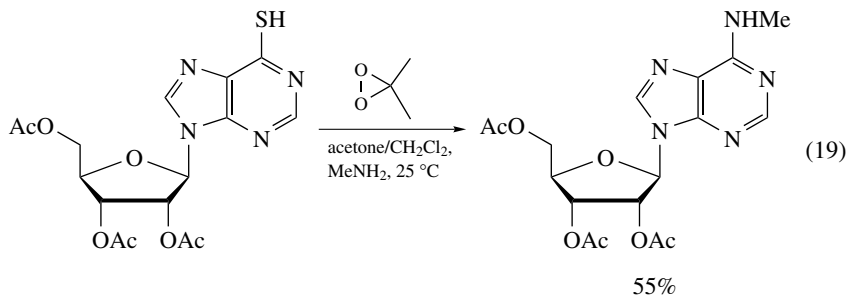
SCHEME 11. Mechanism for the singlet-oxygen formation in the catalytic decomposition of Caroate by ketones

Also, potassium superoxide (KO₂) decomposes DMD in acetone solution to release singlet oxygen, as has been detected by the characteristic infrared chemiluminescence¹¹⁶. Furthermore, a catalytic amount of *n*-Bu₄NI decomposes TFD into oxygen gas and trifluoroacetone in high yield¹¹⁷. Analogous to the Caroate decomposition by ketones, also the catalytic decomposition of peroxyxynitrite by ketones, e.g. methyl pyruvate, is rationalized in terms of peroxyxynitrite oxidation by in-situ-generated dioxirane²⁸.

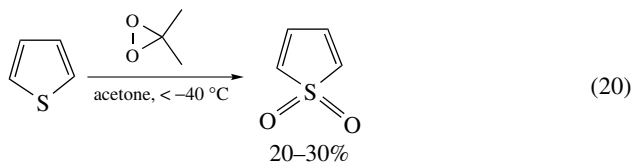
In all of the previous cases that have been presented, the oxygen source for the liberation of singlet oxygen in its reaction with the dioxirane has been a peroxide species. Contrary cases are the *N*-oxides of aliphatic and aromatic tertiary amines, which have been shown to react with dioxiranes to regenerate the free amines and release molecular oxygen in the form of singlet oxygen¹¹⁸. A typical example is shown for the deoxygenation of pyridine *N*-oxide by DMD (equation 18)^{118a}. The mechanism is the same as the one shown in Scheme 11, except that the nucleophile that attacks the peroxide bond in the dioxirane is the *N*-oxide. Finally, *N*-oxyl radicals are also oxidized by dioxiranes, an oxidation that follows a complex radical mechanism to give *O*-alkylated products¹¹⁹.



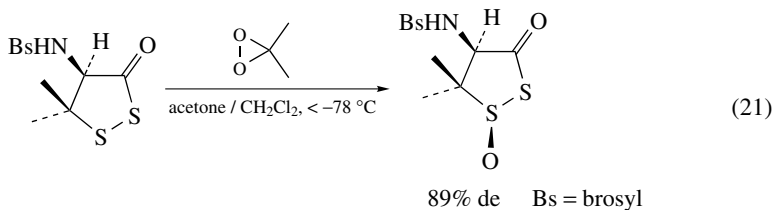
Sulfur compounds with divalent sulfur functionalities are much more prone to dioxirane oxidation on account of their higher nucleophilicity compared to the above-presented oxygen-type nucleophiles. Examples of this type of dioxirane oxidation abound in the literature¹. Such a case is the oxidation of thiols, which may be quite complex and afford a complex mixture of oxidation products, e.g. sulfinic acids, sulfonic acids, disulfides, thiosulfonates and aldehydes¹²⁰, and is, therefore, hardly useful in synthesis. Nevertheless, the oxidation of some 9*H*-purine-6-thiols in the presence of an amine nucleophile produces *ribo*-nucleoside analogs in useful yields (equation 19)¹²¹. This reaction also displays the general chemoselectivity trend that divalent sulfur functionalities are more reactive than trivalent sp³-hybridized nitrogen compounds^{1P}.



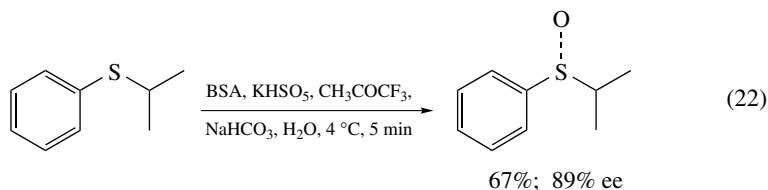
The by far more common and preparatively valuable dioxirane oxidation of divalent sulfur substrates is that of sulfides, to produce either sulfoxides or sulfones^{1,122}. Since sulfoxides are considerably less reactive than sulfides, the reaction outcome may be conveniently controlled by the stoichiometry of the oxidant^{9,123}. For example, in the low-temperature oxidation of thiophene by an excess of DMD, the corresponding 1,1-dioxide (sulfone) has been obtained, albeit in low yield (equation 20)¹²⁴. This is the first preparatively useful method for isolating this elusive sulfone, which also accentuates the importance of the neutral and anhydrous conditions under which the oxidations with the isolated DMD may be conducted.



When a prochiral sulfide is submitted to the oxidation by DMD or TFD, the corresponding racemic sulfoxide is produced, whereas in the case of a chiral sulfide, diastereoselective oxidation is feasible. For example, a good diastereoselectivity was obtained with the chiral cyclic disulfide in equation 21¹²⁵.

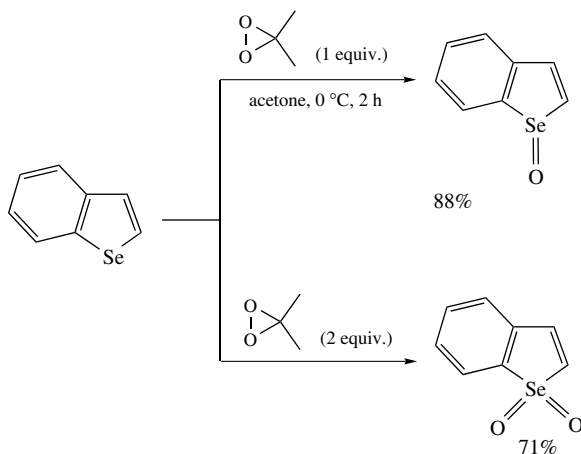


The enantioselective oxidation of prochiral sulfides with DMD has been achieved by using bovine serum albumin (BSA) as the chiral inductor^{12, 126}. Moderate to good enantioselectivities have been reported in the presence of this protein, for which a typical example is shown in equation 22¹²⁶. As yet, however, no enantioselective oxidation of a prochiral sulfide has been documented by employing an optically active dioxirane. We have tried the enantioselective oxidation of methyl phenyl sulfide with the dioxirane generated from the ketone **7** (Shi's ketone), but an ee value of only *ca* 5% was obtained. One major hurdle that needs to be overcome with such enantioselective dioxirane oxidations is the suppression of the background oxidation of the sulfide substrate by Carote, an unavoidable feature of the in-situ mode.



The dioxirane oxidation of the C=S¹²⁷ and N=S¹²⁸ double bonds usually leads to the corresponding *S*-oxides. In the latter case, *N*-oxidation may compete with *S*-oxidation¹²⁹, and the experimental results indicate that the chemoselectivity depends on the electron density of these heteroatoms¹²⁹.

Little has been reported on the oxidation of selenium functionalities by dioxiranes. One case is the oxidation of selenophenes by DMD¹³⁰ at subambient temperatures. Good yields of either the selenophene 1-oxide or 1,1-dioxide may be achieved, which depends on the amount of DMD used (Scheme 12)^{130a}. These results are similar to those already presented for the sulfur congeners¹²⁴.



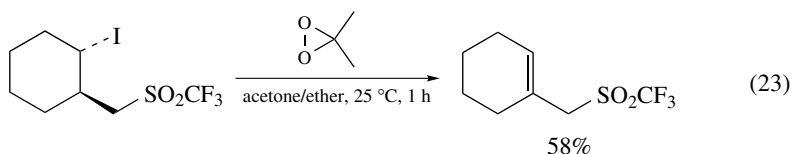
SCHEME 12. The chemoselective DMD oxidation of benzoselenophene

3. Halogens

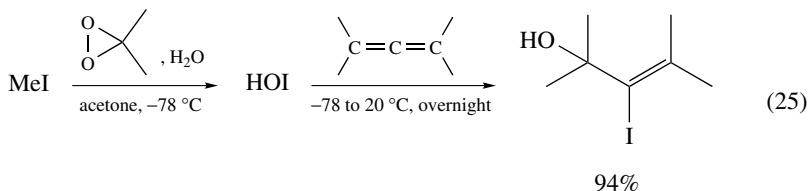
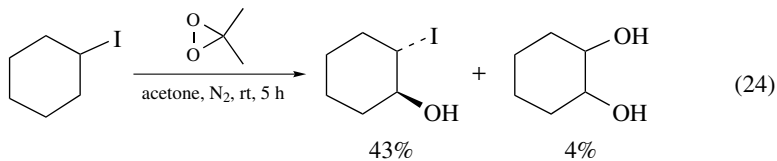
There are only a few reports on the dioxirane oxidation of halogen-containing compounds. The oxidation of the chloride to the hypochlorite anion by DMD (in situ) is one

of the very first examples of dioxirane oxidation known in chemistry⁴. For analytical purposes, in iodometry^{9,32} the iodide ion is oxidized under acidic conditions to elemental iodine, which serves for the quantitative determination of the dioxirane concentration.

Of the organohalides, only the iodides are prone to oxidation by dioxirane; for example, iodobenzene is oxidized by DMD to a mixture of iodobenzene and iodylbenzene^{35c}. In contrast, alkyl iodides afford labile primary oxidation products, which eliminate the oxidized iodine functionality to result in alkenes (equation 23)¹³¹. In such a dioxirane oxidation, the subsequent in-situ reaction of the alkene affords the corresponding epoxides¹³¹.



Similarly, the oxidation of iodocyclohexane by DMD under a nitrogen-gas atmosphere leads to the iodohydrin and diol as unexpected products (equation 24)^{35c}. The iodohydrin, formed as the major product, clearly reveals that hypoiodous acid (HOI) is generated in situ, which adds to the liberated cyclohexene. Indeed, when methyl iodide (MeI) is oxidized by DMD at subambient temperature in the presence of cyclohexene, the corresponding iodohydrin is obtained in very good yield¹³². The latter method may be utilized for the preparation of allylic alcohols with a vinylic iodo functional group from allenes (equation 25)¹³³.

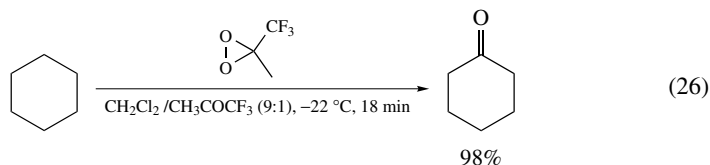


C. Insertions

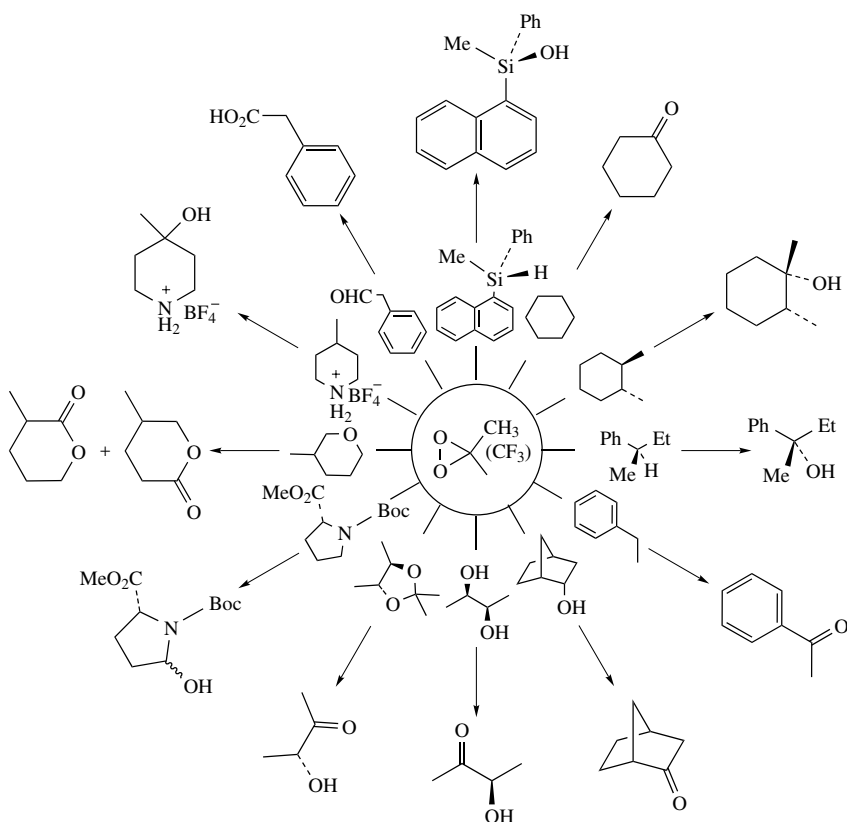
Direct insertion into an X–H σ bond constitutes the highlight of dioxirane chemistry¹. Besides the insertion of a dioxirane oxygen atom into an alkane σ_{CH} bond, for practical purposes a most valuable oxyfunctionalization, also the more facile insertion into the σ_{SiH} bond is known, a convenient and chemoselective method of preparing silanols.

Among the CH oxidations, a most impressive case, for example, concerns the quantitative TFD oxidation of cyclohexane to cyclohexanone at -22°C in only 18 min (equation 26)^{11,134}! There exists no other chemical oxidant, even metal-catalyzed systems, that may compete with this astounding oxidative reactivity of TFD. Whether the oxidation of an amine to a hydroxylamine involves the direct insertion of an oxygen atom into the N–H bond is mechanistically still uncertain, since alternatively (more probably the case on

account of the high electrophilicity of dioxiranes) the reaction may proceed through the oxidation of the nitrogen lone pair, followed by a hydrogen-atom shift^{100a, 135}.



Through the extensive efforts of the past two decades, the C–H oxyfunctionalization of numerous organic compounds has been accomplished under quite mild reaction conditions, that is, at subambient temperature and in acetone solvent (isolated dioxirane) or in aqueous media (in-situ generation)¹. Some of the typical examples are summarized in Scheme 13.

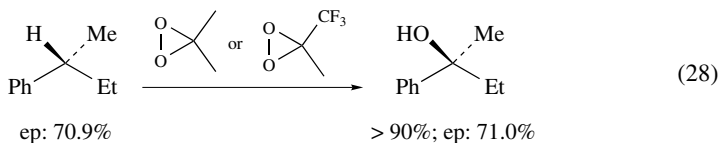
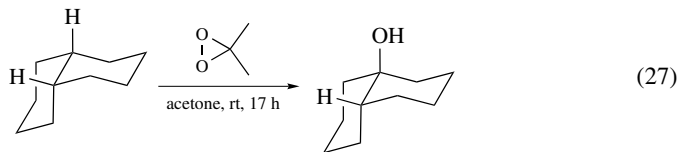


SCHEME 13. Dioxirane oxidation of C–H and Si–H bonds

For the oxidation of alkanes, the reactivity order follows the sequence primary < secondary < tertiary < benzylic < allylic C–H bonds¹. The readily accessible and economical DMD is suitable for most substrates, although this oxyfunctionalization may

sometimes be quite slow. In such a case, the much more reactive but rather expensive TFD is a better choice. For primary and secondary alkanes, the initial alcohol product of the insertion may be subsequently oxidized to its carbonyl compound, since the α -hydrogen atom next to the hydroxy group in the alcohol is more prone to further oxidation by the dioxirane than the starting alkane^{11, 134, 136}; such overoxidation is especially acute in the case of an allylic C–H bond^{47, 137}. Of course, this undesirable further oxidation of the initially formed alcohol is not possible when the insertion is carried out on tertiary C–H bonds, since then tertiary alcohols are produced. Moreover, the overoxidation problem may be circumvented by in-situ protection of the newly formed hydroxy functionality through acylation with trifluoroacetic anhydride¹³⁸. In this context, it is for practical purposes significant to mention that the α -hydrogen atoms in the alkoxy part of esters and ethers are quite difficult to be oxidized by DMD¹³⁹. Additionally, the C–H bonds adjacent to aldehydes, ketones, carboxylic acid, esters, amides, nitriles, sulfonic acids, sulfonates and sulfones are unreactive towards CH insertion even by TFD.

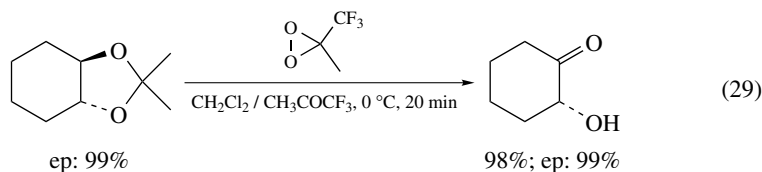
In regard to the stereoselectivity of the insertion process, Murray and coworkers have shown that the CH oxidation of substituted cyclohexanes by dioxiranes is, like the already discussed epoxidation, highly stereo-controlled¹⁴⁰. A specific case is *cis*-decalin, which gives only the *cis* alcohol, as exemplarily displayed in equation 27. A similar stereoselective retention of configuration was also obtained for *trans*-decalin and *cis*- and *trans*-dimethylcyclohexanes¹⁴⁰. In fact, complete retention of configuration was demonstrated in the CH oxidation of chiral alkanes^{1k, 141}. For example, the optically active (*R*)-2-phenylbutane was converted by either DMD^{1k} or TFD¹⁴¹ to (*S*)-2-phenylbutan-2-ol (equation 28) without any loss of the enantiomeric purity (ep) in the product.



These results, as well as rate studies¹⁴² and kinetic isotope effects¹³⁴, support a concerted, *spiro*-structured oxenoid-type transition state for the CH oxidations^{1k}. The original ‘oxygen-rebound’ mechanism¹⁴³ has been discounted (see the computational work in Section I.D). Recently, however, the stepwise radical mechanism was revived in terms of the so-called ‘molecule-induced homolysis’³⁵, but such radical-type reactivity was severely criticized on the basis of experimental^{1k} and theoretical^{33, 53} grounds.

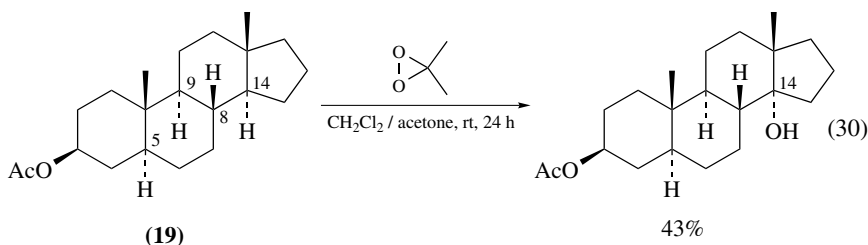
When the C–H bond to be oxidized is proximate to a functional group, as we have stated already, its reactivity depends on the type of functional group. In the case of the hydroxy group, especially in secondary alcohols, these are more prone to dioxirane oxidation than their alkane precursors and, consequently, usually carbonyl products are obtained as the final product¹. Primary alcohols are less reactive, but may still be converted slowly to the corresponding aldehydes or carboxylic acids (due to the facile further oxidation of aldehydes)¹⁴². The functional-group transformation of the alcohols to ethers or acetals reduces the oxidative reactivity^{144, 145}, but these C–H bonds are still more reactive than unfunctionalized ones. Thus, dioxirane oxidation of benzyl ether or acetal may

be used as a neutral and mild oxidative strategy for deprotection. For example, (*R,R*)-1,2-cyclohexanediol acetal is stereoselectively cleaved by means of TFD oxidation to the optically active α -hydroxy ketone in excellent chemical yield and complete preservation of its optical purity (ep) under neutral conditions (equation 29)¹⁴⁵.

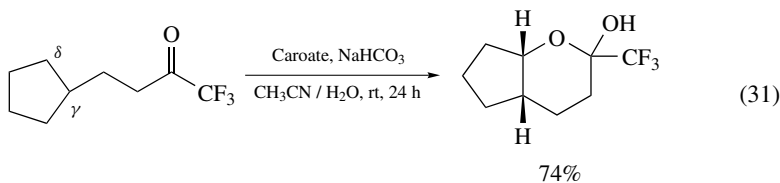


The direct oxidation of a C–H bond next to an amino functionality is not feasible, because the nitrogen atom is much more reactive towards the dioxirane than the C–H bond. To reverse this chemoselectivity, the amino group needs to be protected in the form of its ammonium salt¹⁰², its BF_3 complex¹⁰³ or its amide functionality by acylation¹⁰⁴, prior to the oxidation^{105, 146}.

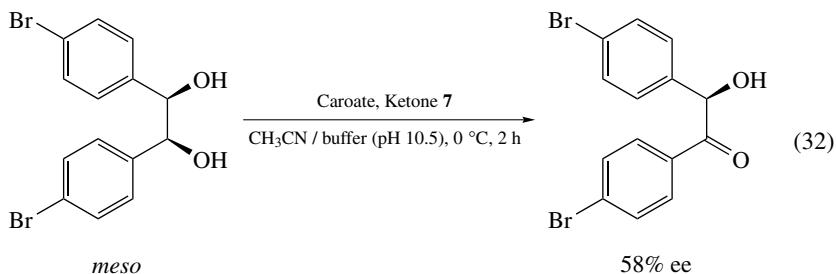
Recently, substantial progress has been registered in regard to the regioselective CH oxidations by dioxiranes. Usually, the regioselectivity of the CH oxidation is mainly governed by the reactivity of the C–H bond; for example, in the above-mentioned oxidation of *cis*-decalin¹⁴⁰, the tertiary C–H bond is selectively oxidized in the presence of the secondary C–H bonds. When the reactivities are similar, the regioselectivity is determined by steric factors¹⁴⁷. For example, the preferential oxyfunctionalization of the tertiary C–H bond at the C-14 position of the steroid **19** by DMD in the presence of the other tertiary C–H bonds at the C-5, C-8 and C-9 positions is due to steric reasons (equation 30)¹⁴⁷.



A novel approach to achieve high regioselectivity was recently developed by Yang and coworkers, in which the in-situ-generated dioxirane functionality, contained within the substrate, oxidizes the secondary $\delta_{\text{C-H}}$ bond rather than the more reactive tertiary $\gamma_{\text{C-H}}$ bond, due to a favorable concerted transition state (equation 31)¹⁴⁸. A limitation of this method, however, is that the ketone unit has to be incorporated into the substrate molecule at the appropriate position, normally a rather impractical and cumbersome task. Moreover, such a process is necessarily stoichiometric in practice and, thereby, it lacks appeal since nowadays catalytic enantioselective oxyfunctionalizations are in vogue^{122, 149}.

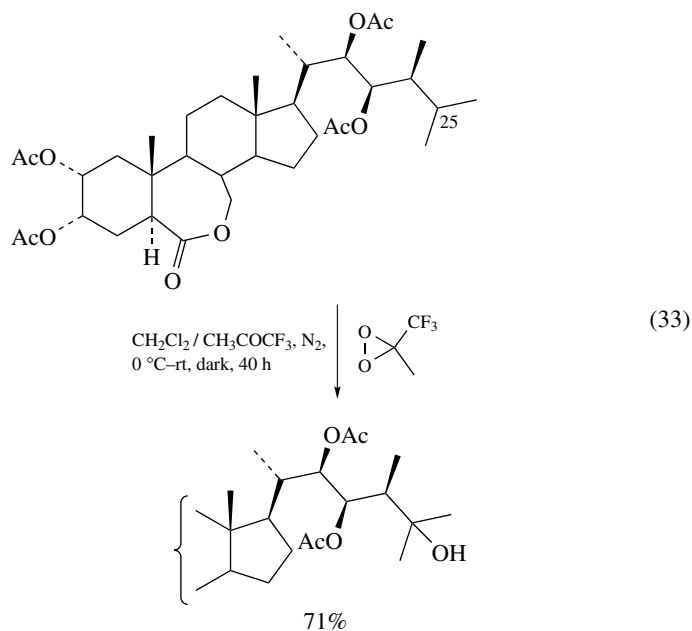


Unlike epoxidations, the enantioselective CH oxidation is still a virgin field in dioxirane chemistry. The first (and to date only!) enantioselective C–H oxidation has been reported for *vic*-diols. Thus, the oxidation with the fructose-derived dioxirane of ketone **7** (Shi's ketone) yields the optically active α -hydroxy ketones in ee values of up to 75%^{21,150}. A typical example of this asymmetric CH oxidation is shown in equation 32¹⁵⁰.

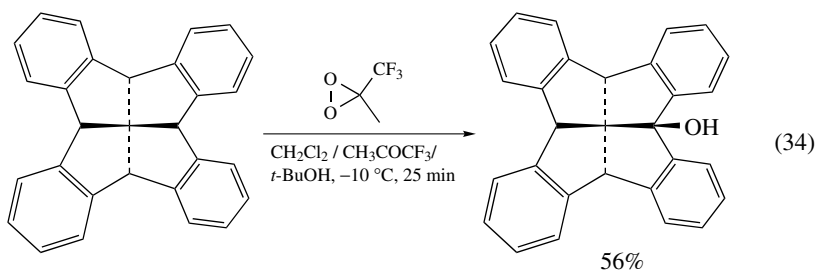


These few cases indisputably illustrate the synthetic value of such enantioselective CH insertions, a challenging area of dioxirane chemistry that demands more intensive research activity. For that purpose more reactive and more effective chiral dioxiranes must be designed.

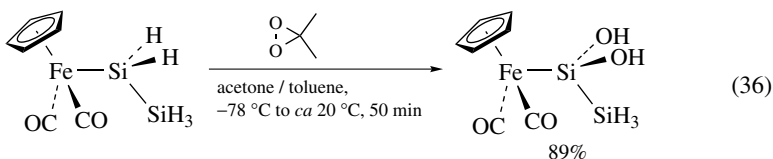
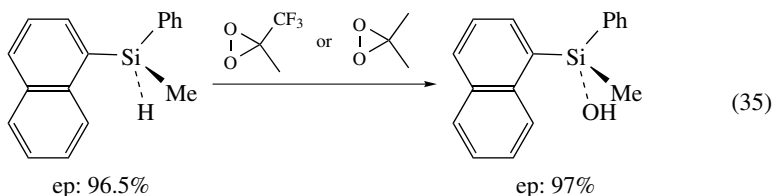
Be this as it may, the CH oxidation has become an attractive and promising preparative method in natural-product synthesis. For example, dioxiranes have been used to introduce selectively a hydroxy group at the C-25 position of steroids, a challenging task not readily achieved with other oxidants¹⁵¹. A specific case is the TFD oxidation of brassinosteroid (equation 33)^{151a}.



The CH oxidation is also useful in the synthesis of special synthetic targets that are difficult to be achieved by means of conventional oxidants. An early example is the conversion of adamantane to its tetrahydroxy derivative by the exhaustive and selective oxyfunctionalization of all four tertiary C–H bonds, which are contained within the adamantane skeleton²⁵. More recently, Curci and coworkers prepared fenestrindane monoalcohol from fenestrindane in good yield by direct TFD oxidation (equation 34), unquestionably a valuable oxyfunctionalization in view of the mild oxidation conditions¹⁵².



As already briefly mentioned, the oxygen-atom insertion into Si–H bonds of silanes constitutes a selective method for the chemoselective preparation of silanols, which has been much less studied compared to the CH oxidation. This unique oxyfunctionalization of silanes is also highly stereoselective (equation 35) since, like the CH insertions, it proceeds with complete retention of configuration¹⁵³. A novel application of the SiH insertion process is the synthesis of the unusual iron complex with a silanediol functionality, in which selectively both Si–H bonds of the silicon atom proximate to the iron ligand are oxidized in the silane substrate (equation 36)^{154a}.



III. CONCLUSIONS

This sequel on contemporary dioxirane chemistry should leave little if any doubt in the interested reader's mind that these fascinating and entertaining three-membered-ring cyclic peroxides are very popular oxidants and still in much demand, as witnessed by the current intensive research activities. Since the last Patai volume on 'Organic Peroxides' some twenty years ago¹⁵⁵, which could have hardly featured a chapter on this subject since it was then in its infancy, dioxirane chemistry has literally exploded and become established as a prominent field in peroxide chemistry, as manifested by the now well over a thousand publications on this subject¹.

The synthetic value of this unusual class of cyclic peroxides in selective oxyfunctionalizations is undisputable, the mechanistic complexity of the oxygen transfer a formidable challenge, and the intricate structural and electronic features a theoretical delight. While we know already much about the reactivity and selectivity of this powerful oxidant, there is conspicuous demand in solving the following problems:

- (i) More resistant carbonyl precursors towards self-oxidation need to be developed to achieve high catalytic activity in the in-situ mode of operation.
- (ii) More powerful dioxiranes are required to conduct sluggish oxidations such as the insertion reactions and the oxidative transformation of electron-poor functionalities.
- (iii) More chemoselective and regioselective oxidations of multifunctionalized substrates are urgently needed, since these are the real-life chores in synthesis, particularly in industrial applications.
- (iv) More effective ketone precursors must be designed for the efficacious enantioselective oxidation of π bonds (epoxidations), of lone pairs (heteroatom oxidations), and of σ bonds (CH/XH insertions).

Much dioxirane work lies still ahead of us and this chapter will have fulfilled its purpose and incentive, if more colleagues would join us in tackling this demanding challenge. *The fun has just begun!*

IV. ACKNOWLEDGMENTS

Our own work in this field has been generously sponsored by the NIH-MBRS SCORE program (Grant No. S06 GM 09148), the University of Texas at San Antonio (UTSA), the Deutsche Forschungsgemeinschaft (DFG), the Deutscher Akademischer Austauschdienst (DAAD), the Alexander von Humboldt-Stiftung, the Fonds der Chemischen Industrie, and the Welch Foundation (Grant No. AX-1593), for which we are most grateful. We express our appreciation and thanks to the numerous coworkers, who have with diligence, dedication and bright ideas contributed in our contributions of dioxirane chemistry; their names are given in the references cited herein.

V. REFERENCES

1. (a) W. Adam, R. Curci and J. O. Edwards, *Acc. Chem. Res.*, **22**, 205 (1989).
- (b) R. W. Murray, *Chem. Rev.*, **89**, 1187 (1989).
- (c) R. Curci, in *Advances in Oxygenated Process* (Ed. A. L. Baumstark), Vol. 2, Chap. I, JAI, Greenwich CT, 1990, pp. 1–59.
- (d) W. Adam, L. P. Hadjirapoglou, R. Curci and R. Mello, in *Organic Peroxides* (Ed. W. Ando), Chap. 4, Wiley, New York, 1992, pp. 195–219.
- (e) W. Adam and L. Hadjirapoglou, *Top. Curr. Chem.*, **164**, 45 (1993).
- (f) R. Curci, A. Dinoi and M. F. Rubino, *Pure Appl. Chem.*, **67**, 811 (1995).
- (g) A. Lévai, W. Adam, J. Halász, C. Nemes, T. Patonay and G. Tóth, *Chem. Heterocycl. Compd. (Engl. Trans.)*, **10**, 1345 (1995).
- (h) W. Adam and A. K. Smerz, *Bull. Soc. Chim. Belg.*, **105**, 581 (1996).
- (i) R. W. Murray and M. Singh, in *Comprehensive Heterocyclic Chemistry II* (Ed. A. Padwa), Vol. 1A, Elsevier, Oxford, 1996, pp. 429–456.
- (j) W. Adam, A. K. Smerz and C.-G. Zhao, *J. Prakt. Chem.*, **339**, 298 (1997).
- (k) W. Adam, R. Curci, L. D'Accolti, A. Dinoi, C. Fusco, F. Gasparini, R. Kluge, R. Paredes, M. Schulz, A. K. Smerz, L. A. Veloza, S. Weinkötz and R. Winde, *Chem. Eur. J.*, **3**, 105 (1997).
- (l) S. E. Denmark and Z. Wu, *Synlett*, 847 (1999).

- (m) W. Adam, H.-G. Degen, A. Pastor, C. R. Saha-Möller, S. B. Schambony and C.-G. Zhao, in *Peroxide Chemistry: Mechanistic and Preparative Aspects of Oxygen Transfer* (Ed. W. Adam), Wiley-VCH, Weinheim, 2000, pp. 78–112.
- (n) M. Frohn and Y. Shi, *Synthesis*, 1979 (2000).
- (o) Y. Shi, *Yuki Gosei Kagaku Kyokaiishi*, **60**, 342 (2002); *Chem. Abstr.*, **137**, 64818 (2002).
- (p) W. Adam, C. R. Saha-Möller and C.-G. Zhao, *Org. React.*, **61**, 219 (2002).
2. A. Baeyer and V. Villiger, *Chem. Ber.*, **32**, 3652 (1899).
 3. R. I. Talbott and P. G. Thompson, US Patent 3632.606 (1972); *Chem. Abstr.*, **76**, P99638t (1972).
 4. R. E. Montgomery, *J. Am. Chem. Soc.*, **96**, 7820 (1974).
 5. R. D. Suenram and F. J. Lovas, *J. Am. Chem. Soc.*, **100**, 5117 (1978).
 6. J. O. Edwards, R. H. Pater, R. Curci and F. Di Furia, *Photochem. Photobiol.*, **30**, 63 (1979).
 7. R. Curci, M. Fiorentino and M. R. Serio, *J. Chem. Soc., Chem. Commun.*, 155 (1984).
 8. R. Jeyaraman and R. W. Murray, *J. Am. Chem. Soc.*, **106**, 2462 (1984).
 9. R. W. Murray and R. Jeyaraman, *J. Org. Chem.*, **50**, 2847 (1985).
 10. R. W. Murray, R. Jeyaraman and L. Mohan, *J. Am. Chem. Soc.*, **108**, 2470 (1986).
 11. (a) R. Mello, M. Fiorentino, O. Sciacovelli and R. Curci, *J. Org. Chem.*, **53**, 3890 (1988).
(b) P. H. Vaccaro, J. L. Kinsey, R. W. Field and H. L. Dai, *J. Chem. Phys.*, **78**, 3659 (1983).
 12. S. Colonna and N. Gaggero, *Tetrahedron Lett.*, **30**, 6233 (1989).
 13. R. Mello, M. Fiorentino, C. Fusco and R. Curci, *J. Am. Chem. Soc.*, **111**, 6749 (1989).
 14. W. Adam, R. Curci, M. E. González-Nuñez and R. Mello, *J. Am. Chem. Soc.*, **113**, 7654 (1991).
 15. L. A. Hull and B. Lalbachan, *Tetrahedron Lett.*, **34**, 5039 (1993).
 16. (a) A. Kirschfeld, S. Muthusamy and W. Sander, *Angew. Chem.*, **106**, 2261 (1994); *Angew. Chem., Int. Ed. Engl.*, **33**, 2212 (1994).
(b) W. Sander, personal communications.
 17. D. Yang, Y.-C. Yip, M.-W. Tang, M.-K. Wong, J.-H. Zheng and K.-K. Cheung, *J. Am. Chem. Soc.*, **118**, 491 (1996).
 18. Y. Tu, Z.-X. Wang and Y. Shi, *J. Am. Chem. Soc.*, **118**, 9806 (1996).
 19. M. Ferrer, F. Sánchez-Baeza and A. Messeguer, *Tetrahedron*, **53**, 15877 (1997).
 20. D. Cremer, E. Kraka and P. G. Szalay, *Chem. Phys. Lett.*, **292**, 97 (1998).
 21. W. Adam, C. R. Saha-Möller and C.-G. Zhao, *Tetrahedron: Asymmetry*, **9**, 4117 (1998).
 22. R. D. Bach and O. Dmitrenko, *J. Org. Chem.*, **67**, 3884 (2002).
 23. G. Bez and C.-G. Zhao, *Tetrahedron Lett.*, **44**, 7403 (2003).
 24. Caroate is also known as Oxone® (DuPont) and Curox® (Peroxidchemie).
 25. R. Mello, L. Cassidei, M. Fiorentino, C. Fusco and R. Curci, *Tetrahedron Lett.*, **31**, 3067 (1990).
 26. M. Schulz, S. Liebsch, R. Klug and W. Adam *J. Org. Chem.*, **62**, 188 (1997).
 27. L. Shu and Y. Shi, *Tetrahedron Lett.*, **40**, 8721 (1999).
 28. D. Yang, Y.-C. Tang, J. Chen, X.-C. Wang, M. D. Bartberger, K. N. Houk and L. Olson, *J. Am. Chem. Soc.*, **121**, 11976 (1999).
 29. S. Rozen, Y. Bareket and M. Kol, *Tetrahedron*, **49**, 8169 (1993).
 30. N. A. Porter, H. Yin and D. A. Pratt, *J. Am. Chem. Soc.*, **122**, 11272 (2000).
 31. H. L. Casal, S. E. Sugamori and J. C. Scaiano, *J. Am. Chem. Soc.*, **106**, 7623 (1984).
 32. W. Adam, J. Bialas and L. Hadjirapoglou, *Chem. Ber.*, **124**, 2377 (1991).
 33. R. D. Bach, in *Peroxide Chemistry: Mechanistic and Preparative Aspects of Oxygen Transfer* (Ed. W. Adam), Wiley-VCH, Weinheim, 2000, pp. 569–600.
 34. D. V. Deubel *J. Org. Chem.*, **66**, 3790 (2001).
 35. (a) F. Minisci, L. Zhao, F. Fontana and A. Bravo, *Tetrahedron Lett.*, **36**, 1895 (1995).
(b) F. Minisci, L. Zhao, F. Fontana and A. Bravo, *Tetrahedron Lett.*, **36**, 1697 (1995).
(c) A. Bravo, F. Fontana, G. Fronza, F. Minisci and A. Serri, *Tetrahedron Lett.*, **36**, 6945 (1995).
(d) A. Bravo, F. Fontana, G. Fronza, A. Mele and F. Minisci, *J. Chem. Soc., Chem. Commun.*, 1573 (1995).
(e) A. Bravo, F. Fontana, G. Fronza, F. Minisci and L. Zhao, *J. Org. Chem.*, **63**, 254 (1998).
 36. J. Liu, K. N. Houk, A. Dinioi, C. Fusco and R. Curci, *J. Org. Chem.*, **63**, 8565 (1998).
 37. R. D. Bach, O. Dmitrenko, W. Adam and S. Schambony, *J. Am. Chem. Soc.*, **125**, 924 (2003).

38. K. N. Houk, J. Liu, N. C. DeMello and K. R. Condroski, *J. Am. Chem. Soc.*, **119**, 10147 (1997).
39. C. Jenson, J. Liu, K. N. Houk and W. L. Jorgensen, *J. Am. Chem. Soc.*, **119**, 12982 (1997).
40. K. Miaskiewicz and D. A. Smith, *J. Am. Chem. Soc.*, **120**, 1872 (1998).
41. M. Freccero, R. Gandolfi, M. Sarzi-Amade and A. Rastelli, *Tetrahedron*, **54**, 12323 (1998).
42. (a) P. D. Bartlett, *Rec. Chem. Progr.*, **47** (1950).
(b) A. A. Roof, M. W. J. Winter and P. D. Bartlett, *J. Org. Chem.*, **50**, 4093 (1985).
43. A. L. Baumstark and C. J. McCloskey, *Tetrahedron Lett.*, **28**, 3311 (1987).
44. R. D. Bach, J. L. Andrés, A. L. Owensby, H. B. Schlegel and J. J. W. McDouall, *J. Am. Chem. Soc.*, **114**, 7207 (1992).
45. R. W. Murray and D. Gu, *J. Chem. Soc., Perkin Trans. 2*, 2203 (1993).
46. A. L. Baumstark and P. C. Vasquez, *J. Org. Chem.*, **53**, 3437 (1988).
47. W. Adam and A. K. Smerz, *Tetrahedron*, **51**, 13039 (1995).
48. W. Adam and A. K. Smerz, *J. Org. Chem.*, **61**, 3506 (1996).
49. A. G. Baboul, H. B. Schlegel, M. N. Glukhovtsev and R. D. Bach, *J. Comput. Chem.*, **19**, 1353 (1998).
50. R. D. Bach, M. N. Glukhovtsev and C. Canepa, *J. Am. Chem. Soc.*, **120**, 775 (1998).
51. W. Adam, W. Haas and B. B. Lohray, *J. Am. Chem. Soc.*, **113**, 6202 (1991).
52. (a) S. Shaik, S. Cohen, S. P. de Visser, P. K. Sharma, D. Kumar, S. Kozuch, F. Ogliaro and D. Danovich, *Eur. J. Inorg. Chem.*, 207 (2004).
(b) F. S. Vinhado, P. R. Martins and Y. Iamamoto, *Curr. Top. Catal.*, **3**, 199 (2002).
(c) M. J. Cryle, J. E. Stok and J. J. De Voss, *Austr. J. Chem.*, **56**, 749 (2003).
(d) F. P. Guengerich and T. L. MacDonald, *Acc. Chem. Res.*, **17**, 9 (1984).
53. M. N. Glukhovtsev, C. Canepa and R. D. Bach, *J. Am. Chem. Soc.*, **120**, 10528 (1998).
54. W. Adam and C.-G. Zhao, unpublished results.
55. (a) C. N. Martin and R. C. Garner, *Nature (London)*, **267**, 863 (1977).
(b) G. Büchi, K. W. Fowler and A. M. Nadzan, *J. Am. Chem. Soc.*, **104**, 544 (1982).
(c) B. F. Coles, A. M. Welch, P. J. Hertzog, J. R. Lindsay Smith and R. C. Garner, *Carcinogenesis*, **1**, 79 (1980).
56. (a) C. P. Gorst-Allman, P. S. Steyn and P. L. Wessels, *J. Chem. Soc., Perkin Trans. 1*, 1360 (1977).
(b) B. F. Cola, J. R. Lindsay Smith and R. C. Garner, *J. Chem. Soc., Perkin Trans. 1*, 2664 (1979).
(c) R. C. Garner, C. N. Martin, J. R. Lindsay, B. F., Coles and M. R. Tolson, *Chem. Biol. Interact.*, **26**, 57 (1979).
(d) J. A. Miller, *Cancer Res.*, **30**, 559 (1970).
57. S. W. Baertschi, K. D. Raney, M. Stone and T. M. Harris, *J. Am. Chem. Soc.*, **110**, 7929 (1988).
58. Z.-X. Wang and Y. Shi, *J. Org. Chem.*, **63**, 3099 (1998).
59. A. Hofland, H. Steinberg and T. J. de Boer, *Recl. Trav. Chim. Pays-Bas*, **104**, 350 (1985).
60. W. Adam, D. Golsch, L. Hadjjarapoglou, A. Lévai, C. Nemes and T. Patonay, *Tetrahedron*, **50**, 13113 (1994).
61. S. Patai and Z. Rappoport, in *The Chemistry of Alkenes* (Ed. S. Patai), Vol. 1, Wiley, New York, 1964, pp 512–517.
62. E. Piers and S. L. Boulet, *Tetrahedron Lett.*, **38**, 8815 (1997).
63. (a) W. Adam, K. Peters and M. Sauter, *Synthesis*, 111 (1994).
(b) W. Adam and M. Sauter, *Tetrahedron*, **50**, 11441 (1994).
(c) M. Sauter and W. Adam, *Acc. Chem. Res.*, **28**, 289 (1995).
64. R. W. Murray and M. Singh, *J. Org. Chem.*, **58**, 5076 (1993).
65. W. Adam, R. Paredes, A. K. Smerz and L. A. Veloza, *Liebigs Ann./Recl.*, 547 (1997).
66. W. Adam and T. Wirth, *Acc. Chem. Res.*, **32**, 703 (1999).
67. (a) M. R. Grever, S. A. Schepartz and B. A. Chabner, *Semin. Oncol.*, **19**, 622 (1992).
(b) D. M. Bollag, P. A. McQueney, J. Zhu, O. Hensens, L. Koupal, J. Liesch, M. Goetz, E. Lazarides and C. M. Woods, *Cancer Res.*, **55**, 2325 (1995).
(c) K. Gerth, N. Bedorf, G. Höfle, H. Irschik and H. Reichenbach, *J. Antibiot.*, **49**, 560 (1996).
(d) G. Höfle, N. Bedorf, H. Steinmetz, D. Schomburg, K. Gerth and H. Reichenbach, *Angew. Chem., Int. Ed. Engl.*, **35**, 1567 (1996).
(e) R. J. Kowalski, P. Giannakakou and E. Hamel, *J. Biol. Chem.*, **272**, 2534 (1997).

68. K. C. Nicolaou, S. Ninkovic, F. Sarabia, D. Vourloumis, Y. He, H. Vallberg, M. R. V. Finlay and Z. Yang, *J. Am. Chem. Soc.*, **119**, 7974 (1997).
69. W. Adam and E. Staab, unpublished results.
70. R. Curci, L. D'Accolti, M. Fiorentino and A. Rosa, *Tetrahedron Lett.*, **36**, 5831 (1995).
71. Z.-X. Wang, Y. Tu, M. Frohn and Y. Shi, *J. Org. Chem.*, **62**, 2328 (1997).
72. C. E. Song, Y. H. Kim, K. C. Lee, S.-G. Lee and B. W. Jin, *Tetrahedron: Asymmetry*, **8**, 2921 (1997).
73. W. Adam and C.-G. Zhao, *Tetrahedron: Asymmetry*, **8**, 3995 (1997).
74. Y. Tu, Z.-X. Wang, M. Frohn, M. He, H. Yu, Y. Tang and Y. Shi, *J. Org. Chem.*, **63**, 8475 (1998).
75. Z.-X. Wang, Y. Tu, M. Frohn, J.-R. Zhang and Y. Shi, *J. Am. Chem. Soc.*, **119**, 11224 (1997).
76. W. Adam, C. R. Saha-Mölller and C.-G. Zhao, *Tetrahedron: Asymmetry*, **10**, 2749 (1999).
77. (a) Z.-X. Wang and Y. Shi, *J. Org. Chem.*, **62**, 8622 (1997).
(b) Z.-X. Wang, S. M. Müller, O. P. Anderson and Y. Shi, *J. Org. Chem.*, **64**, 6443 (1999).
78. T. K. M. Shing, Y. C. Leung and K. W. Yeung, *Tetrahedron*, **59**, 2159 (2003).
79. (a) H. Tian, X. She and Y. Shi, *Org. Lett.*, **3**, 715 (2001).
(b) H. Tian, X. She, J. Xu and Y. Shi, *Org. Lett.*, **3**, 1929 (2001).
(c) L. Shu, P. Wang, Y. Gan and Y. Shi, *Org. Lett.*, **5**, 293 (2003).
(d) H. Tian, X. She, H. Yu, L. Shu and Y. Shi, *J. Org. Chem.*, **67**, 2435 (2002).
80. W.-K. Chan, W.-Y. Yu, C.-M. Che and M.-K. Wong, *J. Org. Chem.*, **68**, 6576 (2003).
81. (a) D. Yang, M.-K. Wong, Y.-C. Yip, X.-C. Wang, M.-W. Tang, J.-H. Zheng and K.-K. Cheung, *J. Am. Chem. Soc.*, **120**, 5943 (1998).
(b) D. Yang, X.-C. Wang, M.-K. Wong, Y.-C. Yip and M.-W. Tang, *J. Am. Chem. Soc.*, **118**, 11311 (1996).
82. K. Matsumoto and K. Tomioka, *Tetrahedron Lett.*, **43**, 631 (2002).
83. S. E. Denmark and Z. Wu, *J. Org. Chem.*, **63**, 2810 (1998).
84. C. J. Stearman and V. Behar, *Tetrahedron Lett.*, **43**, 1943 (2002).
85. (a) A. Armstrong and B. R. Hayter, *J. Chem. Soc., Chem. Commun.*, 621 (1998).
(b) A. Armstrong, G. Ahmed, B. Dominguez-Fernandez, B. R. Hayter and J. S. Wailes, *J. Org. Chem.*, **67**, 8610 (2002).
86. S. E. Denmark, Z. Wu, C. M. Crudden and H. Matsuhashi, *J. Org. Chem.*, **62**, 8288 (1997).
87. D. Yang, Y.-C. Yip, J. Chen and K.-K. Cheung, *J. Am. Chem. Soc.*, **120**, 7659 (1998).
88. A. Solladié-Cavallo, L. Bouérat and L. Jierry, *Eur. J. Org. Chem.*, 4557 (2001).
89. H. Tian, X. She, L. Shu, H. Yu and Y. Shi, *J. Am. Chem. Soc.*, **122**, 11551 (2000).
90. X.-Y. Wu, X. She and Y. Shi, *J. Am. Chem. Soc.*, **124**, 8792 (2002).
91. W. Adam, R. T. Fell, C. R. Saha-Mölller and C.-G. Zhao, *Tetrahedron: Asymmetry*, **9**, 397 (1998).
92. A. Solladié-Cavallo, P. Lupattelli, L. Jierry, P. Bovicelli, F. Angeli, R. Antonioletti and A. Klein, *Tetrahedron Lett.*, **44**, 6523 (2003).
93. M. Frohn, M. Dalkiewicz, Y. Tu, Z.-X. Wang and Y. Shi, *J. Org. Chem.*, **63**, 2948 (1998).
94. Z.-X. Wang, G.-A. Cao and Y. Shi, *J. Org. Chem.*, **64**, 7646 (1999).
95. X. Feng, L. Shu and Y. Shi, *J. Am. Chem. Soc.*, **121**, 11002 (1999).
96. Z. Xong and E. J. Corey, *J. Am. Chem. Soc.*, **122**, 4831 (2000).
97. (a) J. K. Crandall and T. Reix, *J. Org. Chem.*, **57**, 6759 (1992).
(b) R. W. Murray, M. Singh and N. Rath, *Tetrahedron: Asymmetry*, **7**, 1611 (1996).
98. R. W. Murray, R. Jeyaraman and L. Mohan, *Tetrahedron Lett.*, **27**, 2335 (1986).
99. (a) D. L. Zabrowski, A. E. Moorman and K. R. Beck, Jr., *Tetrahedron Lett.*, **29**, 4501 (1988).
(b) K. S. Webb and V. Seneviratne, *Tetrahedron Lett.*, **36**, 2377 (1995).
100. (a) R. W. Murray and M. Singh, *Synth. Commun.*, **19**, 3509 (1989).
(b) R. W. Murray and M. Singh, *Tetrahedron Lett.*, **29**, 4677 (1988).
101. S. M. Neset, T. Benneche and K. Undheim, *Acta. Chem. Scand.*, **47**, 1141 (1993).
102. R. W. Murray, S. N. Rajadhyaksha and L. Mohan, *J. Org. Chem.*, **54**, 5783 (1989).
103. M. Ferrer, F. Sánchez-Baeza, A. Messeguer, A. Diaz and M. Rubiralta, *J. Chem. Soc., Chem. Commun.*, 293 (1995).
104. W. Adam and C.-G. Zhao, unpublished results.
105. G. Asensio, M. E. González-Núñez, C. Biox Bernadini, R. Mello and W. Adam, *J. Am. Chem. Soc.*, **115**, 7250 (1993).

106. (a) D. R. Boyd, P. B. Coulter, M. R. McGuckin, N. D. Sharma, W. B. Jennings and V. E. Wilson, *J. Chem. Soc., Perkin Trans. 1*, 301 (1990).
(b) H. Ihmels, M. Maggini, M. Prato and G. Scorrano, *Tetrahedron Lett.*, **32**, 6215 (1991).
(c) A. Saba, *Synth. Commun.*, **24**, 695 (1994).
(d) W. Adam, L. Hadjiarapoglou, K. Mielke and A. Treiber, *Tetrahedron Lett.*, **35**, 5625 (1994).
107. W. Adam, M. Mąkosza, C. R. Saha-Möller and C.-G. Zhao, *Synlett*, 1335 (1998).
108. (a) W. Adam, M. Mąkosza, C.-G. Zhao and M. Surowiec, *J. Org. Chem.*, **65**, 1099 (2000).
(b) W. Adam, M. Mąkosza, K. Staliński and C.-G. Zhao, *J. Org. Chem.*, **63**, 4390 (1998).
109. A. Altamura, L. D'Accolti, A. Detomaso, A. Dinoi, M. Fiorentino, C. Fusco and R. Curci, *Tetrahedron Lett.*, **39**, 2009 (1998).
110. W. Adam and D. Golsch, *Angew. Chem.*, **105**, 771 (1993); *Angew. Chem., Int. Ed. Engl.*, **32**, 737 (1993).
111. D. Yang, M.-K. Wong and Y.-C. Yip, *J. Org. Chem.*, **60**, 3887 (1995).
112. W. Sander, K. Schröder, S. Muthusamy, A. Kirschfeld, W. Kappert, R. Boese, E. Kraka, C. Sosa and D. Cremer, *J. Am. Chem. Soc.*, **119**, 7265 (1997).
113. M. D. Chappell and R. L. Halcomb, *Tetrahedron Lett.*, **40**, 1 (1999).
114. H. H. Wasserman, C. Baldino and S. J. Coates, *J. Org. Chem.*, **60**, 8231 (1995).
115. L. Cassidei, M. Fiorentino, R. Mello, O. Sciacovelli and R. Curci, *J. Org. Chem.*, **52**, 699 (1987).
116. D. V. Kazakov, G. Y. Maistrenko, N. P. Polyakova, V. P. Kazakov, W. Adam, A. Trofimov, C.-G. Zhao, W. Kiefer and S. Schlücker, *Luminescence*, **17**, 293 (2002).
117. W. Adam, G. Asensio, R. Curci, M. E. González-Núñez and R. Mello, *J. Am. Chem. Soc.*, **114**, 8345 (1992).
118. (a) W. Adam, K. Briviba, F. Duschek, D. Golsch, W. Kiefer and H. Sies, *J. Chem. Soc., Chem. Commun.*, 1831 (1995).
(b) M. Ferrer, F. Sánchez-Baeza, A. Messegue, W. Adam, D. Golsch, F. Görth, W. Kiefer and V. Nagel, *Eur. J. Org. Chem.*, 2527 (1998).
119. (a) W. Adam, S. E. Bottle and R. Mello, *J. Chem. Soc., Chem. Commun.*, 771 (1991).
(b) A. Dinoi, R. Curci, P. Carloni, E. Damiani, P. Stipa and L. Greci, *Eur. J. Org. Chem.*, 871 (1998).
120. D. Gu and D. N. Harpp, *Tetrahedron Lett.*, **34**, 67 (1993).
121. (a) P. Lupattelli, R. Saladino and E. Mincione, *Tetrahedron Lett.*, **34**, 6313 (1993).
(b) R. Saladino, C. Crestini, R. Bernini and E. Mincione, *Tetrahedron Lett.*, **34**, 7785 (1993).
(c) R. Saladino, C. Crestini, R. Bernini, E. Mincione and R. Ciafrino, *Tetrahedron Lett.*, **36**, 2665 (1995).
(d) R. Saladino, R. Bernini, L. Crestini, E. Mincione, A. Bergamini, S. Marini and A. T. Palamara, *Tetrahedron*, **51**, 7561 (1995).
122. W. Adam, C. R. Saha-Möller and P. A. Ganeshpure, *Chem. Rev.*, **101**, 3499 (2001).
123. (a) T. E. Gunda, L. Tamás, S. Sályi, C. Nemes and F. Sztaricskai, *Tetrahedron Lett.*, **36**, 7111 (1995).
(b) A. Ishii, C. Tsuchiya, T. Shimada, K. Furusawa, T. Omata and J. Nakayama, *J. Org. Chem.*, **65**, 1799 (2000).
124. J. Nakayama, H. Nagasawa, Y. Sugihara and A. Ishii, *J. Am. Chem. Soc.*, **119**, 9077 (1997).
125. R. S. Glass and Y. Liu, *Tetrahedron Lett.*, **35**, 3887 (1994).
126. S. Colonna, N. Gaggero and M. Leone, *Tetrahedron*, **47**, 8385 (1991).
127. (a) T. Tabuchi, M. Nojima and S. Kusabayashi, *J. Chem. Soc., Chem. Commun.*, 625 (1990).
(b) T. Tabuchi, M. Nojima and S. Kusabayashi, *J. Chem. Soc., Perkin Trans. 1*, 3043 (1991).
(c) S. Watanabe, T. Yamamoto, T. Kawashima, N. Inamoto and R. Okazaki, *Bull. Chem. Soc. Jpn.*, **69**, 719 (1996).
128. N. Gaggero, L. D'Accolti, S. Colonna and R. Curci, *Tetrahedron Lett.*, **38**, 5559 (1997).
129. M. D. Coburn, *J. Heterocycl. Chem.*, **26**, 1883 (1989).
130. (a) J. Nakayama, T. Matsui, Y. Sigihara, A. Ishii and S. Kumakura, *Chem. Lett.*, 269 (1996).
(b) T. Matsui, J. Nakayama, N. Sato, Y. Sugihara, A. Ishii and S. Kumakura, *Phosphorus Sulfur Silicon*, **118**, 227 (1996).
(c) T. Umezawa, Y. Sugihara, A. Ishii and J. Nakayama, *J. Am. Chem. Soc.*, **120**, 12351 (1998).
131. A. Mahadevan and P. L. Fuchs, *J. Am. Chem. Soc.*, **117**, 3272 (1995).

132. G. Asensio, C. Andreu, C. Boix-Bernardini, R. Mello and M. E. González- Nuñez, *Org. Lett.*, **1**, 2125 (1999).
133. A. Studley and C.-G. Zhao, unpublished results.
134. R. Mello, M. Fiorentino, C. Fusco and R. Curci, *J. Am. Chem. Soc.*, **111**, 6749 (1989).
135. (a) R. W. Murray and M. Singh, *Tetrahedron Lett.*, **29**, 4677 (1988).
(b) K. Miaskiewicz, N. Teich and D. A. Smith, *J. Org. Chem.*, **62**, 6493 (1997).
136. P. Bovicelli, P. Lupattelli, A. Sanetti and E. Mincione, *Tetrahedron Lett.*, **35**, 8477 (1994).
137. R. W. Murray, M. Singh, B. L. Williams and H. M. Moncrieff, *J. Org. Chem.*, **61**, 1830 (1996).
138. G. Asensio, R. Mello, M. E. González-Núñez, G. Castellano and J. Corral, *Angew. Chem.*, **108**, 196 (1996); *Angew. Chem., Int. Ed. Engl.*, **35**, 217 (1996).
139. (a) R. Curci, L. D'Accolti, M. Fiorentino, C. Fusco, W. Adam, M. E. González-Núñez and R. Mello, *Tetrahedron Lett.*, **33**, 4225 (1992).
(b) G. Asensio, G. Castellano, R. Mello and M. E. González-Núñez, *J. Org. Chem.*, **61**, 5564 (1996).
140. R. W. Murray, R. Jeyaraman and L. Mohan, *J. Am. Chem. Soc.*, **108**, 2470 (1986).
141. W. Adam, G. Asensio, R. Curci, M. E. González-Nuñez and R. Mello, *J. Org. Chem.*, **57**, 953 (1992).
142. R. Mello, L. Cassidei, M. Fiorentino, C. Fusco, W. Hümmmer, V. Jäger and R. Curci, *J. Am. Chem. Soc.*, **113**, 2205 (1991).
143. R. Curci, A. Dinoi, C. Fusco and M. A. Lillo, *Tetrahedron Lett.*, **37**, 249 (1996).
144. A. L. Baumstark, F. Kovac and P. C. Vasquez, *Can. J. Chem.*, **77**, 308 (1999).
145. R. Curci, L. D'Accolti, A. Dinoi, C. Fusco and A. Rosa, *Tetrahedron Lett.*, **37**, 115 (1996).
146. R. Saladino, M. Mezzetti, E. Mincione, I. Torrini, M. P. Paradisi and G. Masteropietro, *J. Org. Chem.*, **64**, 8468 (1999).
147. P. Bovicelli, P. Lupattelli, V. Fiorini and E. Mincione, *Tetrahedron Lett.*, **34**, 6103 (1993).
148. (a) M.-K. Wong, N.-W. Chung, L. He, X.-C. Wang, Z. Yan, Y.-C. Tang and D. Yang, *J. Org. Chem.*, **68**, 6321 (2003).
(b) D. Yang, M.-K. Wong, X.-C. Wang and Y.-C. Tang, *J. Am. Chem. Soc.*, **120**, 6611 (1998).
149. (a) K. B. Sharpless, *Angew. Chem., Int. Ed.*, **41**, 2024 (2002).
(b) C. Bonini and G. Righi, *Tetrahedron*, **58**, 4981 (2002).
150. W. Adam, C. R. Saha-Möller and C.-G. Zhao, *J. Org. Chem.*, **64**, 7492 (1999).
151. (a) B. Voigt, A. Porzei, D. Golsch, W. Adam and G. Adam, *Tetrahedron*, **52**, 10653 (1996).
(b) P. Bovicelli, P. Lupattelli, E. Mincione, T. Prencipe and R. Curci, *J. Org. Chem.*, **57**, 5052 (1992).
(c) P. Bovicelli, A. Gambacoirta, P. Lupattelli and E. Mincione, *Tetrahedron Lett.*, **33**, 7411 (1992).
152. (a) C. Fusco, M. Fiorentino, A. Dinoi, R. Curci, R. A. Krause and D. Kuck, *J. Org. Chem.*, **61**, 8681 (1996).
(b) D. Kuck, A. Schuster, C. Fusco, M. Fiorentino and R. Curci, *J. Am. Chem. Soc.*, **116**, 2375 (1994).
153. W. Adam, R. Mello and R. Curci, *Angew. Chem.*, **102**, 916 (1990); *Angew. Chem., Int. Ed. Engl.*, **29**, 890 (1990).
154. (a) W. Malisch, H. Jehle, S. Möller, C. R. Saha-Möller and W. Adam, *Eur. J. Inorg. Chem.*, 1585 (1998).
(b) W. Adam, U. Azzena, F. Prechtel, K. Hindahl and W. Malisch, *Chem. Ber.*, **125**, 1409 (1992).
(c) W. Malisch, R. Lankat, S. Schmitzer and J. Reising, *Inorg. Chem.*, **23**, 5701 (1995).
(d) S. Möller, O. Fey, W. Malisch and W. Seelbach, *J. Organomet. Chem.*, **507**, 239 (1996).
(e) W. Malisch, K. Hindahl, H. Käb, J. Reising, W. Adam and F. Prechtel, *Chem. Ber.*, **128**, 963 (1995).
(f) W. Malisch, R. Lankat, O. Fey, J. Reising and S. Schmitzer, *J. Chem. Soc., Chem. Commun.*, 1917 (1995).
(g) W. Malisch, S. Schmitzer, R. Lankat, M. Neumayer, F. Prechtel and W. Adam, *Chem. Ber.*, **128**, 1251 (1995).
155. S. Patai (Ed.), *The Chemistry of Peroxides*, Wiley, Chichester, 1983.

CHAPTER 15

Contemporary trends in dioxetane chemistry*

WALDEMAR ADAM

Institute of Organic Chemistry, University of Würzburg, am Hubland, D-97094 Würzburg, Germany and Department of Chemistry, University of Puerto Rico, Rio Piedras, Puerto Rico 00931, USA

Fax: +1 787 807 0389; e-mails: wadam@chemie.uni-wuerzburg.de and wadam@adam.uprr.pr

and

ALEXEI V. TROFIMOV

Institute of Biochemical Physics, Russian Academy of Sciences, ul. Kosygina 4, Moscow 119991, Russian Federation and Institute of Organic Chemistry, University of Würzburg, am Hubland, D-97094 Würzburg, Germany

Fax: +7 495 137 4101; e-mail: avt_2003@mail.ru

I. INTRODUCTION	1172
A. Historical Developments	1172
B. Contemporary Trends	1172
II. STEREOSELECTIVE SYNTHESIS OF CHIRAL DIOXETANES AND THEIR TRANSFORMATIONS	1173
III. α -PEROXY LACTONE AS OXIDANT	1178
IV. CHEMILUMINESCENT DECOMPOSITION OF 1,2-DIOXETANES . . .	1181
A. Computational Studies on the Thermal Decomposition	1181
B. Electron-transfer-induced Decomposition: Chemically Initiated Electron-exchange Luminescence (CIEEL)	1182

* This chapter is dedicated to our appreciated friend and esteemed colleague, Professor Rostislav F. Vasil'ev, for his pioneering work on the chemical generation of electronically excited states

C. Dioxetane Intermediates in the Peroxy-oxalate Chemiluminescence . . .	1188
D. Metal-catalyzed Dioxetane Decomposition	1189
V. BIOANALYTICAL APPLICATION OF THE DIOXETANE CHEMILUMINESCENCE	1191
A. Firefly Bioluminescence as a Prototype for a Dioxetane-based Triggered Chemiluminescence (CIEEL) in Bioassays	1191
B. Alkaline-phosphatase-triggered CIEEL	1193
C. Dioxetane Substrates for Molecular Biology and Clinical Assays	1198
VI. PHOTOOXIDATION OF DNA BY 1,2-DIOXETANES	1200
VII. CONCLUSIONS	1205
VIII. ACKNOWLEDGMENT	1205
IX. REFERENCES	1205

I. INTRODUCTION

A. Historical Developments

Dioxetanes and dioxetanones (α -peroxy lactones), four-membered-ring cyclic peroxides, are of particular interest among high-energy molecules. As it has been noticed by Kopecky¹, the beginning of the dioxetane chemistry dates back to Blitz², who had proposed the formation of a dioxetane in the oxidation of tetrakis(4-nitrophenyl)ethylene with chromic acid. Sporadically after this, a number of reports appeared on the intermediacy of dioxetanes in chemical oxidations, which fomented particular interest in these thermally labile substances. For example, dioxetanes were proposed as crucial intermediates in the chemiluminescent oxidations of lophines³, acridines⁴, aminoethylenes⁵, indoles⁶, peroxy oxalates⁷ and firefly luciferin⁸. Nonetheless, before the seminal work by Kopecky and Mumford⁹, all the attempts to isolate these cyclic peroxides failed. The latter work entails the fortuitous preparation of the first authentic 1,2-dioxetane, namely trimethyl-1,2-dioxetane, in the base-catalyzed dehydrobromination of the appropriate β -bromo hydroperoxide. The isolated dioxetane product has proved to be thermally quite persistent (half-life of *ca* 20 h at 60°C). Shortly after this, other dioxetanes were prepared by the direct [2 + 2] cycloaddition of singlet oxygen with alkenes¹⁰. Once the isolation of 1,2-dioxetanes was realized, there followed a burst of activity in this fascinating area of cyclic peroxide chemistry. The interested reader may find the pertinent historical details in preceding reviews¹¹. In the present chapter, we give an overview of the *recent* developments and contemporary trends in dioxetane work.



1,2-Dioxetane

 α -Peroxy Lactone

B. Contemporary Trends

The contemporary trends of dioxetane chemistry include a number of fundamental and applied aspects. The fundamental aspects encompass the stereoselective synthesis and the transformations of novel chiral dioxetanes, as well as the mechanistic studies on the thermal, electron-transfer-induced and catalytic dioxetane decomposition. The emphasis lies on the elucidation of the excited-state generation in these chemiluminescent processes,

both for the thermally persistent and the intermediary dioxetanes, the latter especially in the peroxy oxalate reactions. The applications of the dioxetane chemiluminescence will concentrate on modern bioassay techniques. In particular, chemiluminescence immunoassays and reporter gene assays will be covered in detail for the various needs in clinical chemistry and molecular biology. In subsequent subsections, these current and timely topics will be surveyed separately.

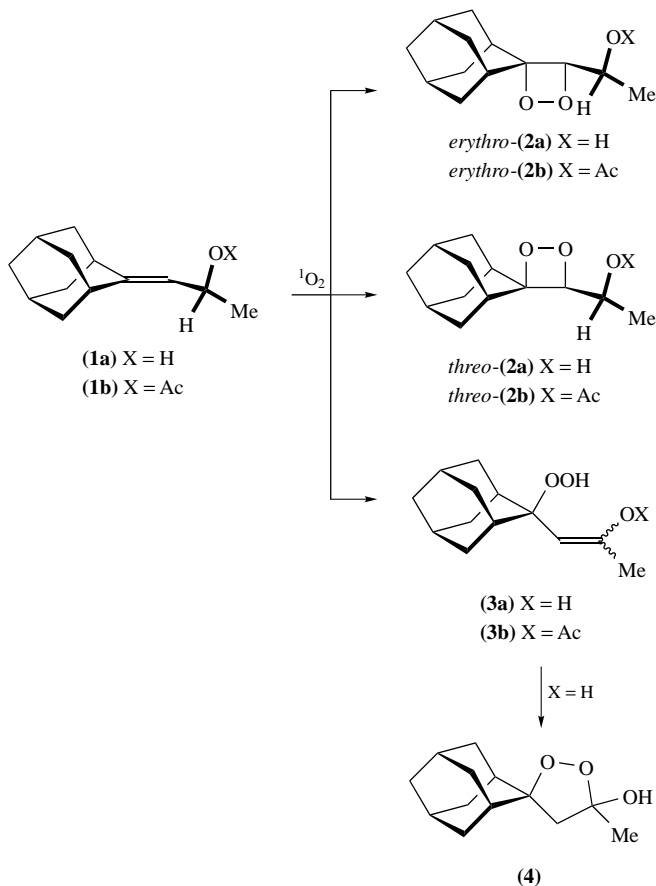
II. STEREOSELECTIVE SYNTHESIS OF CHIRAL DIOXETANES AND THEIR TRANSFORMATIONS

The past decade has seen significant achievements in stereoselective synthesis¹², with some pertinent developments also in dioxetane chemistry. Herein, we consider the most recent and prominent advances in the stereoselective preparation of chiral dioxetanes and their transformation into building blocks for asymmetric synthesis.

A novel aspect pertains to the diastereoselective formation of chiral dioxetanes in the [2 + 2] cycloaddition of singlet oxygen (¹O₂) to appropriate allylic alcohols. The basic strategy utilizes the directing property of the allylic hydroxy functionality in the substrate to steer the attacking singlet oxygen toward the conformationally preferred π face of the C–C double bond. Such a mechanistic phenomenon, coined the hydroxy-group directivity¹², is well known for the ene-reaction¹³ and [4 + 2]-cycloaddition¹⁴ modes of ¹O₂, but as yet not for the [2 + 2] cycloaddition. To test whether this stereocontrol also applies to the formation of chiral dioxetanes, the asymmetric adamantylidene-substituted allylic system **1** (Scheme 1) was chosen as substrates¹⁵. The reason for this selection resides in the fact that the allylic hydrogen atoms at the bridgehead positions of the adamantane ring are not abstractable; therefore, the undesired ene reaction is limited only to the allylic hydrogen atom at the chirality center. Moreover, spiroadamantane substitution stabilizes the resulting 1,2-dioxetanes and makes these usually thermally labile four-membered-ring cyclic peroxides better to handle¹⁶.

It has been shown¹⁵ that the chiral adamantylidene-substituted allylic alcohol **1a** reacts diastereoselectively with ¹O₂ in CDCl₃ to yield the *threo*-**2a** dioxetane through the [2 + 2] cycloaddition. The hydroperoxide **3a** is formed as well by the ene reaction with singlet oxygen at the chirality center of the double bond, which was observed in the form of its cyclic hydroxydioxolane **4** tautomer. Thus, the [2 + 2] versus ene mode selectivity amounts to 47:53 in CDCl₃, whereas in a 7:2 CD₃OD:CCl₄ mixture, the dioxetane product is formed exclusively. The diastereoselectivity for the dioxetane formation dropped, however, from >95:<5 in CDCl₃ to 89:11 in 7:2 CD₃OD:CCl₄ mixture¹⁵. In contrast, in the reaction of ¹O₂ with the acetate derivative **1b**, only the hydroperoxide **3b** was obtained (Scheme 1); not even traces of the desired dioxetane **2b** were detected in both CDCl₃ and CD₃OD¹⁵.

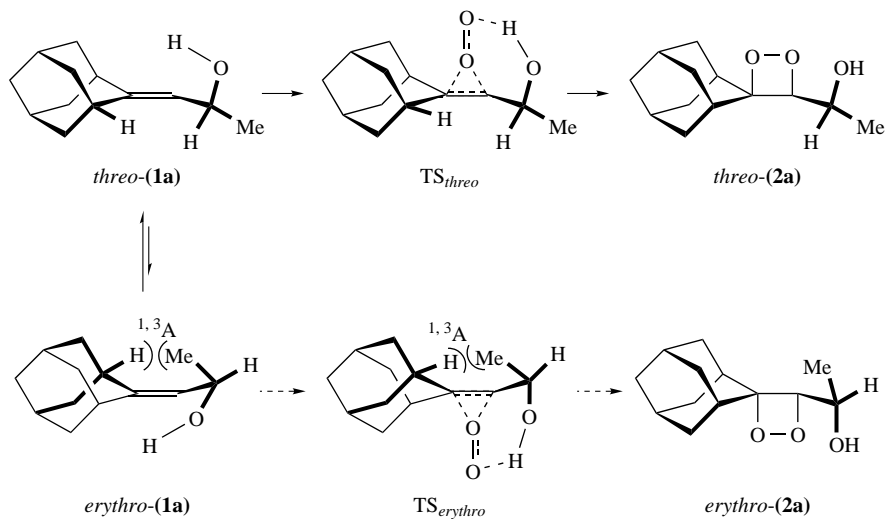
The very high *threo* selectivity (>95:<5) observed for the dioxetane **2a** in the non-polar CDCl₃ unequivocally establishes the hydroxy-directing effect also for the [2 + 2] cycloaddition of singlet oxygen¹⁵. Since experimental^{17a} and computational^{17b} studies favor a two-step mechanism for the [2 + 2] cycloaddition and the ene reaction of ¹O₂, with a common exciplex intermediate¹⁷, similar hydrogen-bonded transition structures must apply for both reaction modes. The 1,3-allylic strain (^{1,3}A) between the methyl group at the chirality center and the allylic hydrogen atom of the adamantylidene skeleton (Scheme 2) aligns the molecule conformationally in such a way that the *threo* transition state (TS_{*threo*}) is favored in energy over the *erythro* (TS_{*erythro*}) one¹⁵. Evidently, already in the developing exciplex, the incoming singlet oxygen is attracted through hydrogen bonding with the hydroxy functionality of the **1a** (*threo*) conformer, to afford exclusively



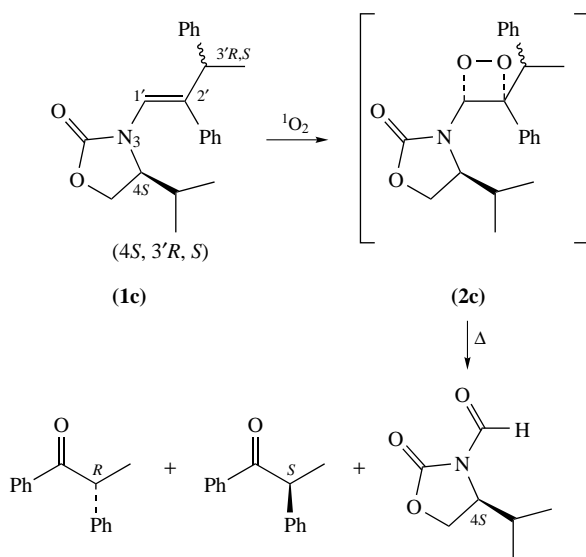
SCHEME 1

the *threo*-**2a** dioxetane. Expectedly, in a protic medium such as methanol, the diastereomeric ratio drops significantly on account of reduced hydrogen bonding between the incoming singlet oxygen and the allylic hydroxy group in the substrate due to competitive intermolecular hydrogen bonding by the methanol¹⁵.

The *threo*-selective [2 + 2] cycloaddition of $^1\text{O}_2$ to afford dioxetanes establishes the hydroxy-group directivity as a general phenomenon, since it applies to all three pericyclic reaction modes of singlet oxygen, namely the ene reaction and [2 + 2] as well as [2 + 4] cycloadditions. A common hydrogen-bonded exciplex is traversed^{13–15}, in which the lower-energy *threo* transition structure intervenes and thus accounts for the observed π -facial diastereoselectivity. The impressive solvent effect on the mode selectivity, i.e. in CDCl_3 about equal amounts of the [2 + 2] and ene products are obtained versus the formation of only the dioxetane **2a** in methanol, may be rationalized in terms of the well-known fact that the [2 + 2] cycloaddition of $^1\text{O}_2$ is preferred in alcoholic solvents due to the more polar transition state for the dioxetane generation¹⁸. The exclusive formation of the dioxetane **2a** in methanol furnishes to date the most dramatic case¹⁵.

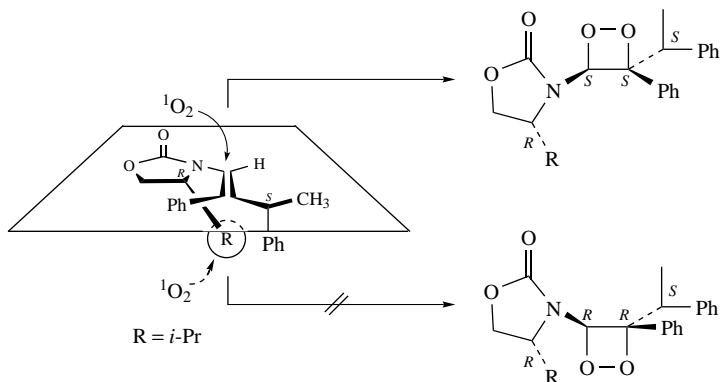


SCHEME 2



SCHEME 3

The oxazolidinone-substituted olefin **1c** (Scheme 3) constitutes another fortunate substrate for the diastereoselective synthesis of a chiral dioxetane¹⁹, which is of preparative value for the enantiomeric synthesis of 1,2 diols^{19c}. For example, the photooxygenation of the encarbamate **1c** produces the asymmetric dioxetane **2c** in >95% π -facial diastereoselectivity. The attack of the 1O_2 occurs from the π face *anti* to the isopropyl

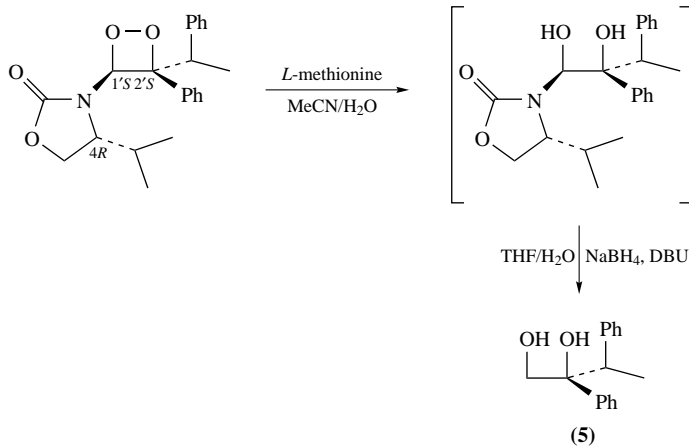


SCHEME 4

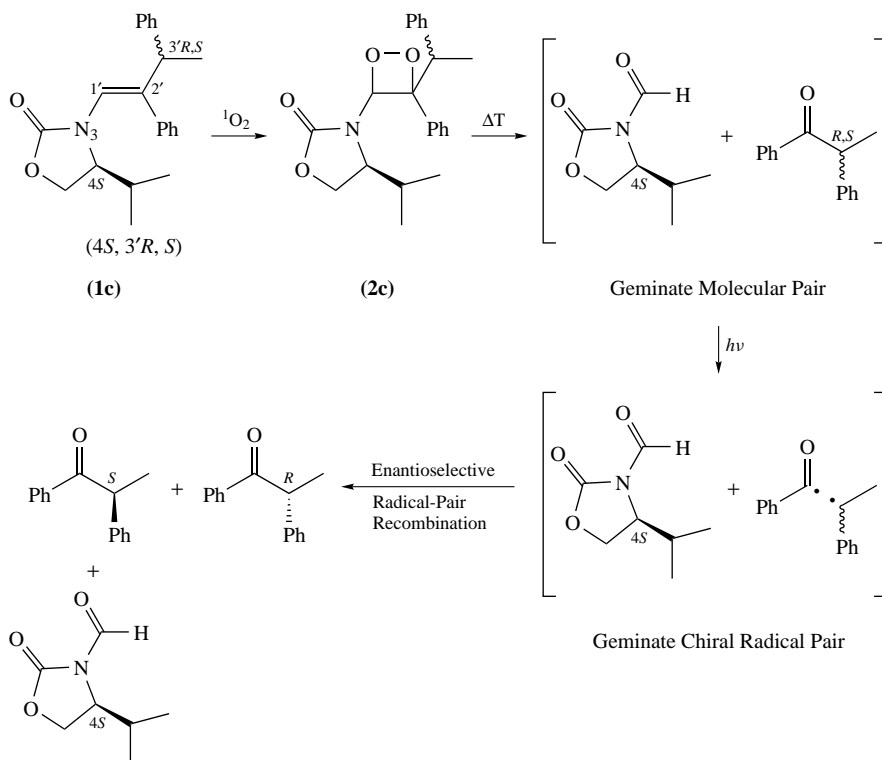
substituent at the C-4 oxazolidinone stereocenter (from below the paper plane). This π -facial diastereoselectivity is imposed by the steric shielding of the $^1\text{O}_2$ attack on behalf of the isopropyl group at C-4 chirality site in the oxazolidinone auxiliary, as shown for the $4R,3'S$ enantiomer in Scheme 4. In fact, a methyl group at this stereogenic position is sterically sufficiently obstructive to effect absolute π -facial stereocontrol^{19d}. Moreover, the chiral enecarbamate **1c** possesses also a second stereogenic center in the alkenyl side chain at the C-3' position, and in view of its proximity to the oxazolidinone C-4 chirality site, both asymmetric centers might influence the stereochemical outcome of the dioxetane formation. It has been shown, however, that only the isopropyl group at the C-4 position controls the diastereofacial attack on the double bond of the enecarbamate **1c**, whereas the configuration at the C-3' position in the alkenyl side chain plays no role in the stereoselectivity^{19d,e}. This is to say, in the chiral enecarbamate **1c** there is no stereochemical *match–mismatch* effect in the [2 + 2] cycloaddition of singlet oxygen, which contrast the recent findings on the epoxidation of this substrate by *m*-chloroperbenzoic acid and by dimethyldioxirane^{19c}.

As already hinted at above, chiral dioxetanes, obtained through the highly stereoselective [2 + 2] cycloaddition of singlet oxygen to the chiral enecarbamate, provide a convenient preparation of optically active 1,2 diols as building blocks for asymmetric synthesis (Scheme 5)^{19c}. Reduction of the dioxetane **2c** by L-methionine, followed by release of the oxazolidinone auxiliary by NaBH_4/DBU reduction, affords the enantiomerically pure *like-5* diol (for additional cases, see Table 4 in Reference 19e).

A promising unprecedented application of the chiral enecarbamates **1c** in asymmetric synthesis is based on the *ship-in-the-bottle* strategy, which entails the oxidation of these substrates in zeolite supercages^{19c}. In this novel concept, presumably dioxetanes intervene as intermediates, as illustrated for the oxidation of the chiral enecarbamate **1c** in the NaY zeolite (Scheme 6). By starting with a 50:50 mixture of the diastereomeric enecarbamates $(4S,3'R)$ -**1c** and $(4S,3'S)$ -**1c**, absorbed by the NaY zeolite, its oxidation furnishes the enantiomerically enriched (ee ca 50%) *S*-methyldeoxybenzoin, whereas the $(4R,3'R)$ -**1c** and $(4R,3'S)$ -**1c** diastereomeric mixture affords preferentially (ee ca 47%) the *R* enantiomer; however, racemic methylbenzoin is obtained when the chirality center at the C-4 position in the oxazolidinone is removed. Evidently, appreciable asymmetric induction is mediated by the optically active oxazolidinone auxiliary.



SCHEME 5



SCHEME 6

Still more impressive, when the 'geminate molecular pair' derived from the (4*S*,3'*R*)-**1c**/(4*S*,3'*S*)-**1c** mixture is irradiated for one hour, the enantio-enriched *S*-methyldeoxybenzoin (ee 50%) is inverted to the *R*-methyldeoxybenzoin (ee 40%). Analogous results are found in the irradiation of the (4*R*,3'*R*)-**1c**/(4*R*,3'*S*)-**1c** mixture, except that the initially formed enantio-enriched *R*-methyldeoxybenzoin (ee 47%) is inverted to *S*-methyldeoxybenzoin (ee 40%). Clearly, nearly complete inversion of the ketone configuration is achieved through the asymmetric induction by the oxazolidinone auxiliary. This constitutes to date the highest enantiomerically selective recombination of geminate radical pairs, produced through the photolytic α cleavage of chiral ketones^{19c}.

Unquestionably, the advantage of the present methodology is that the intermediary dioxetane serves as a vehicle to place the chiral inductor (the oxazolidinone auxiliary) and the racemic substrate to be resolved (the methyldeoxybenzoin) in one and the same zeolite supercage. These represent optimal conditions for efficacious asymmetric induction, a novel application of chiral dioxetanes which merits further elaboration.

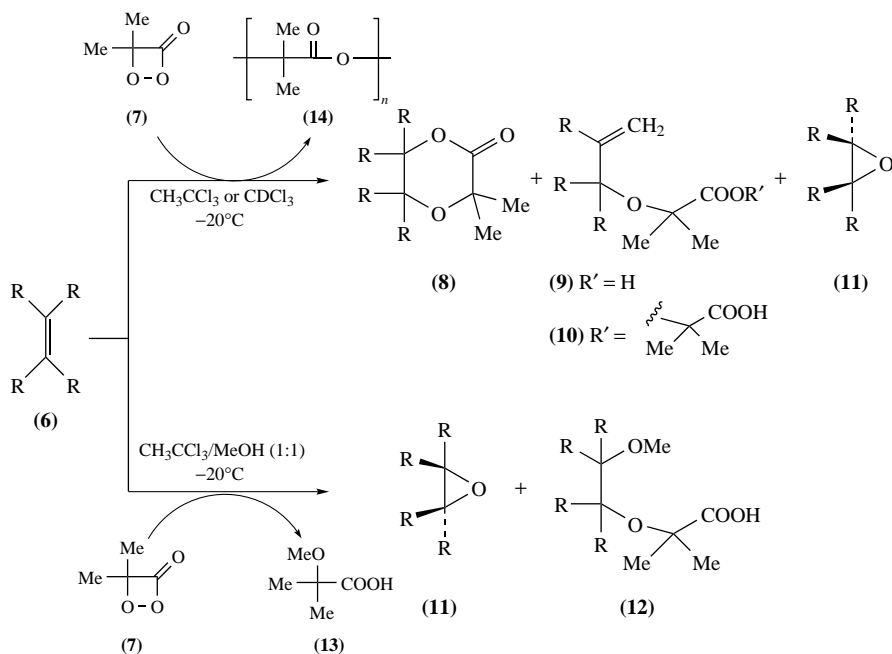
III. α -PEROXY LACTONE AS OXIDANT

The oxidation of organic substances by cyclic peroxides has been intensively studied over the last decades²⁰, from both the synthetic and mechanistic points of view. The earliest mechanistic studies have been carried out with cyclic peroxides such as phthaloyl peroxide^{20a}, and more recently with α -methylene β -peroxy lactones^{20b} and 1,2-dioxetanes^{20c}. During the last 20 years, the dioxiranes (remarkable three-membered-ring cyclic peroxides)^{20d} have acquired invaluable importance as powerful and mild oxidants, especially the epoxidation of electron-rich as well as electron-poor alkenes, heteroatom oxidation and CH insertions into alkanes (cf. the chapter by Adam and Zhao in this volume). The broad scope and general applicability of dioxiranes has rendered them as indispensable oxidizing agents in synthetic chemistry; this is amply manifested by their intensive use, most prominently in the oxyfunctionalization of olefinic substrates.

In contrast to dioxiranes, their four-membered-ring cyclic congeners, namely the 1,2-dioxetanes, are relatively ineffective as oxidizing agents of alkenes. Instead of epoxidation, cycloaddition and ene-type products are mainly observed^{11g}. The latter arise from the S_N2 attack of the alkene double bond on the dioxetane peroxide bond. The mechanistic intricacies and also the synthetic potential of these oxidative transformations have been comprehensively surveyed in preceding reviews¹¹, most extensively in the more recent chapters^{11f,g}. The oxygen transfer by the dioxetane is controlled predominantly by steric factors; the nucleophilic attack on the peroxide bond takes place at the oxygen atom adjacent to the less substituted dioxetane carbon atom. Thus, in tetrasubstituted 1,2-dioxetanes, the steric hindrance of the peroxide bond is so severe that these derivatives are unreactive toward nucleophiles, except triphenylphosphine²¹ and hydride ions (LiAlH₄)²².

In contrast, the α -peroxy lactones, also members of the dioxetane family, display a higher reactivity toward nucleophiles, in view of the inherent polarization of the peroxide bond by the carbonyl functionality. Consequently, the nucleophilic attack is expected to take place at the more sterically hindered but more electrophilic alkoxy-type oxygen atom of the peroxide bond. A recent detailed study of the oxidation of various di-, tri- and tetrasubstituted alkenes **6** with dimethyl α -peroxy lactone (**7**) revealed, however, much complexity, as illustrated in Scheme 7²³ for R = CH₃, since cycloaddition (**8**), ene-reaction (**9** and **10**) and epoxidation (**11**) products were observed²³. In the presence of methanol, additionally the trapping products **12** and **13** were obtained, at the expense of the polyester **14**. The preferred reaction mode is a sensitive function of the steric demand imposed by the attacking alkene nucleophile.

The observed complexity in the product composition may be accounted for in terms of two distinct reaction paths (Scheme 8, R = CH₃), namely one that traverses through



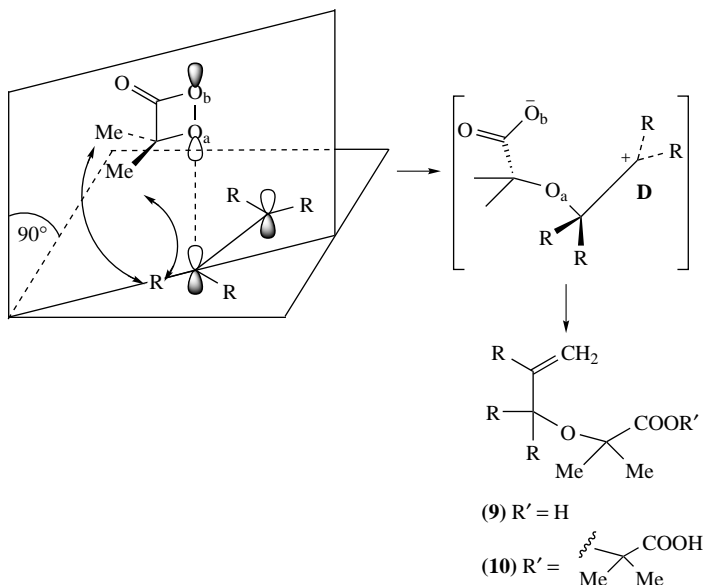
SCHEME 7

the open, 1,6-dipole **D** (upper route) and the other one entails epoxidation by means of direct oxygen transfer (lower route)²³. Both trajectories arise from an $\text{S}_{\text{N}}2$ attack of the double bond in the alkene **6** on the peroxide bond of the α -peroxy lactone **7**, of which the *unsymmetrical, end-on* attack leads to the 1,6-dipole **D**, whereas the *symmetrical, central* attack corresponds to epoxidation (Scheme 8). The 1,6-dipole **D** is postulated to afford the adduct **9**, for which the thermodynamically favored diastereomers are formed, and the ene product **10**²³. In the epoxidation pathway, the α -lactone released after oxygen transfer oligomerizes to the polyester **14**, whereas in the presence of methanol it is trapped in the form of the α -methoxycarboxylic acid **13**.

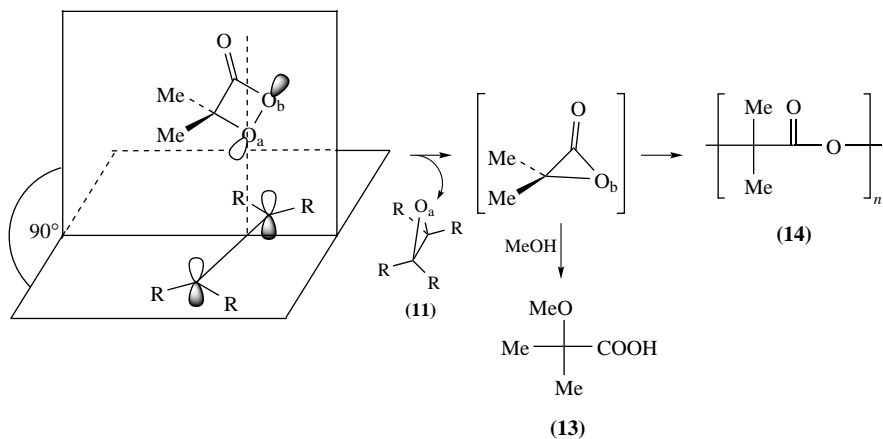
In the case of an unsymmetrical alkene, the oxygen-transfer reaction is regioselective both with respect to the attacking carbon atom of the alkenyl double bond as well as the attacked peroxide bond²³. The regioselectivity in the α -peroxy lactone is dictated by the inherent polarization of the peroxide bond due to the carbonyl group, which makes the alkoxy oxygen atom the more electrophilic one toward nucleophilic attack, whereas the regioselectivity in the alkene is determined by the stabilization of the incipient positive charge in the open 1,6-dipole **D**, i.e. the more substituted carbon atom of the end-on-attacking unsymmetrical alkene.

The preferred reaction mode has been found to be sensitive to the structure of the alkene and the difference in the reactivity has been explained in terms of steric and stereoelectronic factors. Therefore, in the case of the sterically less hindered disubstituted *cis* alkenes, the pathway along the open 1,6-dipole **D** is favored (stereoelectronic control), while the more space-demanding disubstituted *trans* alkenes react by the epoxidation mode (steric control); a similar situation applies to trisubstituted versus tetrasubstituted alkenes²³. This remarkable but complex product dichotomy in the oxidation of alkenes

Unsymmetrical, End-On Nucleophilic Attack



Symmetrical, Central Nucleophilic Attack



SCHEME 8

by α -peroxy lactones combines the characteristic features of the dioxiranes (epoxidation) and of the 1,2-dioxetanes (addition). Unlike the latter, the regioselectivity as to which oxygen atom of the peroxide bond is nucleophilically attacked is not controlled by steric factors but by the inherent polarization of the O—O bond in the α -peroxy lactone.

IV. CHEMILUMINESCENT DECOMPOSITION OF 1,2-DIOXETANES

The cleavage of 1,2-dioxetanes constitutes the model chemiluminescent process, which may be initiated thermally, by electron transfer or in catalytic reactions (e.g. in complexes formed between dioxetanes and transition metals). In the subsequent subsections, we review the most recent significant developments in this area.

A. Computational Studies on the Thermal Decomposition

A wealth of experimental data on the thermal dioxetane decomposition and the excited-state generation in the thermolysis process has been comprehensively surveyed in previous reviews¹¹. During the last decade, computational elucidation of the thermal cleavage received major attention and in the present subsection we consider the relevant studies. Computations on the dioxetane thermolysis were conducted by both *ab initio*²⁴ and semiempirical²⁵ methods at different levels of sophistication.

Inspection of the literature reveals that the computational results of studies on the cleavage of even the simplest 1,2-dioxetane, namely the parent one, depend to a large extent on the method used. Thus, the MCSCF calculations^{24a} give different activation energies for the dioxetane cleavage on the ground-state (S_0) and triplet-state (T_1) Potential Energy Surfaces (PES). While the value of the triplet activation energy (*ca* 20 kcal mol⁻¹) for the parent dioxetane accords with the experimental data^{24a}, the ground-state barrier of only 2 kcal mol⁻¹ is unrealistically low. The subsequent *ab initio* study^{24b}, which engaged CASSCF active space with MP2 correction, has provided an energy barrier consistent with the experimental data. According to the latter computational work, the reaction starts with the rupture of the O–O bond as the first transition state on the S_0 energy surface. The formation of the $\cdot\text{OC}(\text{H}_2)\text{--C}(\text{H}_2)\text{O}\cdot$ diradical is concomitant with the $S_0\text{--}T_1$ intersystem crossing^{24b}, and after transition onto the T_1 energy surface, the second transition state corresponds to C–C bond rupture in the triplet dioxy radical^{24b}. The most recent computational study^{24c} employed the novel Difference-Dedicated-Configuration-Interaction (DDCI) method, which has given a qualitatively similar reaction profile with two transition states, but the energy ordering differed: In contrast to the former case^{24b}, for which the first transition was found to be lower than the second one, the reversed ordering was obtained in the latter case^{24c}.

In parallel with the *ab initio* calculations, also semiempirical studies on the thermolysis of 1,2-dioxetane were performed²⁵. Most computations have been conducted by the PM3 method because it is the best semiempirical method for describing lone electron pairs on adjacent atoms²⁶. As an illustration, only the PM3 method reveals that in the dioxetane molecule the O–O bond is longer and weaker compared with the C–C one, as manifested by the computed values of bond lengths [$d(\text{O--O}) = 1.600 > d(\text{C--C}) = 1.522$ Å] and bond orders [$n(\text{O--O}) = 0.973 < n(\text{C--C}) = 0.989$]^{25f,g}. In contrast, the AM1 and MNDO semiempirical methods exhibit the opposite trends, i.e. AM1 gives $d(\text{O--O}) = 1.334$ Å, $d(\text{C--C}) = 1.539$ Å, $n(\text{O--O}) = 0.995$ and $n(\text{C--C}) = 0.976$, whereas MNDO furnishes $d(\text{O--O}) = 1.316$ Å, $d(\text{C--C}) = 1.558$ Å, $n(\text{O--O}) = 0.996$ and $n(\text{C--C}) = 0.962$ ^{25f,g}. Nevertheless, despite the quantitative differences in the computed bond lengths, bond orders and bond angles, both the AM1 and PM3 methods disclosed qualitatively similar reaction trajectories^{25b}.

The PM3 calculations of the S_0 and the vertical (Franck–Condon) T_1 energies as a function of the O–O bond length [$d(\text{O--O})$] have successfully reproduced the experimental activation energy for the dioxetane thermolysis^{25a}. However, an unusual shape has been found for the energy profile: A flat plateau, in which the ground-state energy

surface merges with the T_1 PES by weakening of the O–O bond, is followed by an abrupt energy drop of 80 kcal mol⁻¹^{25a}. This peculiar break in the reaction profile was originally considered as evidence for a *diradical*-type dioxetane cleavage^{25a}, but subsequent PM3 studies^{25b–c} revealed a computational artifact: Once the first transition state for the O–O bond cleavage has been reached, the O–O distance is no longer a proper reaction coordinate; indeed, in this region the computed O–O bond order tends toward zero^{25b}! When the C–C bond in the resulting dioxy diradical is allowed to elongate simultaneously in the transition-state region, no abrupt energy drop appears along the reaction pathway, as manifested in the three-dimensional energy surface [energy versus $d(\text{O–O})$ and $d(\text{C–C})$]^{23d,e}. Thus, to obtain a valid energy profile, concurrent stretching of both the O–O and C–C bonds must be implemented. It is noteworthy that the three-dimensional energy profile obtained by the simple PM3 method looks qualitatively similar to that computed by the more elaborate DFT (uB3LYP/uB3P86) procedure. Participation of simultaneous C–C bond stretching along the reaction coordinate is consistent with the intuitively assessed *merged* dioxetane cleavage mechanism²⁷, which predicted that O–O bond breaks to result in the $\bullet\text{OC}(\text{H}_2)\text{–C}(\text{H}_2)\text{O}\bullet$ diradical with elongation of the C–C bond.

An additional point to emphasize is that the three-dimensional energy profile does not give a comprehensive account of the reaction mechanism; indeed, the exact reaction PES constitutes a $(n + 1)$ -dimensional hypersurface, i.e. energy plus n internal mutually orthogonal coordinates. For a molecule composed of N atoms, the degrees of freedom are given by $n = 3N - 6$, which in the case of the simplest 1,2-dioxetane with $N = 8$ means that the complete PES is, in fact, 19-dimensional! Of course, some of the molecular degrees of freedom contribute only nominally to the reaction coordinate, but some of them may be important. For instance, CASSCF^{24b} and DDCI^{24c} computations revealed the contribution of the rotation about the C–C bond, i.e. enlarging the O–C–C–O dihedral angle, as an essential variable in understanding the mechanistic details of the thermal decomposition.

In summary, although the computed structural details of the reaction profile depend on the method used for calculations, the general salient mechanistic conclusion^{22, 23} is that the dioxetane thermolysis starts with the O–O bond rupture to generate the $\bullet\text{OC}(\text{H}_2)\text{–C}(\text{H}_2)\text{O}\bullet$ triplet diradical, which is followed by C–C bond cleavage to afford the final ketone products; one of them is formed preferentially in its triplet excited state. Since even simple 1,2-dioxetanes still present a computational challenge to resolve the controversial thermolysis mechanism, the theoretical elucidation of complex dioxetanes constitutes to date a formidable task.

B. Electron-transfer-induced Decomposition: Chemically Initiated Electron-exchange Luminescence (CIEEL)

The electron-transfer-induced cleavage of dioxetanes constitutes a much more efficient way of generating chemiluminescence compared to the thermal decomposition of dioxetanes. This mode of light generation is known as Chemically Initiated Electron-Exchange Luminescence (CIEEL)²⁸, whose biological prototype is the firefly bioluminescence²⁹, the most efficient of the known chemiluminescence processes³⁰. Since numerous commercial applications are based on this CIEEL phenomenon, most prominently modern chemiluminescence bioassays³⁰, the elucidation of the CIEEL process in regard to the chemiexcitation mechanism is of prime importance for the rational design of efficient chemiluminescent probes.

To assess the role of *electron transfer* in the dioxetane decomposition, a comparison of the reaction pathways for the neutral dioxetane and its negatively charged ion is relevant (cf. Figure 1). The energy profiles for the cleavage of a 1,2-dioxetane and its 1,2-dioxetane radical anion as a function of stretching the O–O bond, as calculated by the PM3 method,

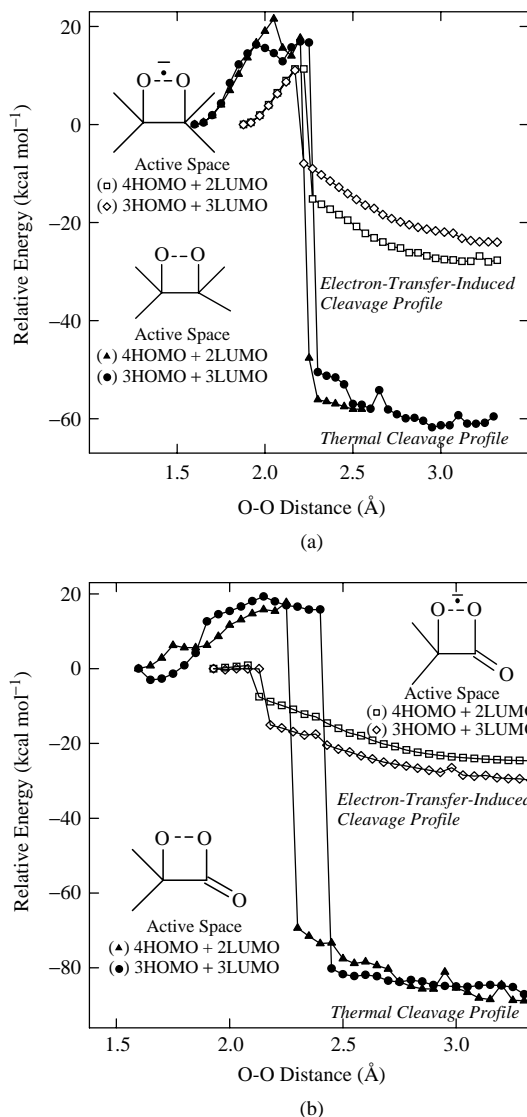


FIGURE 1. (a) Energy profiles for the cleavage of the 1,2-dioxetane (filled symbols) and its anion (open symbols), as calculated by the PM3/MECI method with the active space of six molecular orbitals; (b) the same for α -peroxy lactone (filled symbols) and its anion (open symbols). Reproduced by permission of Schweda-Werbedruck GmbH from Reference 25f

are displayed in Figure 1a. As explained in Section IV.A, the abrupt energy drop beyond the activation barrier is of computational origin. Once the transition state is reached, the O—O distance is no longer a proper reaction coordinate, as suggested by the *merged* cleavage mechanism²⁷. Before the energy drop, the reaction coordinate for the cleavage

of the dioxetane molecule entails mainly elongation of the weak O—O bond^{25b-e}, which reflects the actual activation barrier for the thermal decomposition of dioxetanes. Comparison of the thermal and electron-transfer-induced reaction profiles (Figure 1a) discloses two significant mechanistic features for the CIEEL process: The electron transfer to the dioxetane moiety is initiated by elongation of the O—O bond, which lowers substantially the activation energy for the cleavage of the dioxetane ring, but a small energy barrier still applies. This induced electron transfer is even more pronounced for the α -peroxy lactones, as manifested by the *complete* disappearance of its cleavage barrier (Figure 1b). These mechanistic features of the electron-transfer-induced decomposition profiles are important and require rationalization.

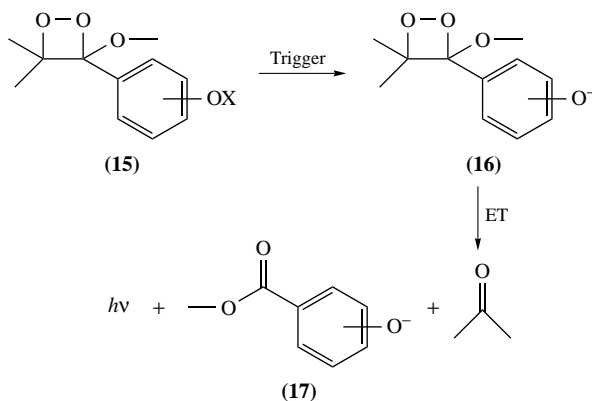
First, the original mechanism of the intermolecular CIEEL process involves, as a key tenet, the chemically *activated* transfer of the electron from the donor (activator) to the peroxide acceptor functionality^{31,32}. Indeed, as estimated from electrochemical data, the electron transfer from an activator is endothermic at the equilibrium geometry of the peroxide bond. For example, the experimental activation energy for the intermolecular electron transfer from the perylene donor to the α -peroxy lactone acceptor was estimated to be 16 kcal mol⁻¹³². It was suggested that this chemical activation process involves most likely stretching of the oxygen—oxygen bond to accommodate the transferred electron³², which is consistent with the semiempirical results shown in Figure 1. Indeed, the O—O bond in the radical anion is markedly elongated relative to the neutral dioxetane (cf. Figure 1).

Second, whereas the cleavage barrier for the dioxetane is reduced on electron transfer (Figure 1a), for the α -peroxy lactone it disappears completely (Figure 1b); presumably, the O—O bond is *irreversibly* cleaved for the α -peroxy-lactone radical anion^{21,32}. This finding is consistent with the experimental observation that the α -peroxy lactones are considerably more efficient in the electron-transfer-induced chemiluminescence than the corresponding dioxetanes³⁰. Thus, if persistent α -peroxy lactones were readily accessible, they should be reagents of choice for commercial applications of chemiluminescence.

During the last years, the intramolecular CIEEL process has been the focus of attention, particularly 1,2-dioxetanes with substituents of low oxidation potentials such as the ArO⁻ functionality³⁰. The chemiexcitation process of such functionalized dioxetanes consists of cleaving the intermediary dioxetane phenolate anion, which is initiated by the intramolecular electron transfer (ET) from the oxidizable phenoxide functionality to the antibonding σ^* orbital of the peroxide bond. To prevent the uncontrolled cleavage of phenolate-substituted dioxetanes, the phenolate functionality must be masked by a readily removable group. For such protected dioxetanes, e.g. **15**, the CIEEL process may be initiated at will on treatment with an appropriate reagent (trigger) to release the phenolate anion **16**, as shown in the general Scheme 9^{30,33}. The choice of a trigger depends on the nature of the protective group (X in Scheme 9). This phenolate-initiated intramolecular CIEEL process provides the basis for numerous commercial applications, most prominently in chemiluminescent bioassay techniques (immunoassays and reporter gene assay)^{30,33}.

Clearly, a detailed knowledge of the electron-transfer process is required if more effective CIEEL-triggerable chemiluminescent systems are to be rationally designed, rather than engage in an empirical trial-and-error hunt. To understand the excited-state generation process, the nature of the CIEEL emitter and the chemiexcitation mechanism should be established.

Figure 2 displays the CIEEL spectra of the monocyclic (*m*-**15a**) and bicyclic (*m*-**15b**) dioxetanes and the fluorescence spectra of the corresponding methyl *m*-oxybenzoate ions *m*-**17a** and *m*-**17b**, generated by the electron-transfer-induced cleavage of these dioxetanes³⁴. The coincidence of the fluorescence and the CIEEL spectra (Figure 2) conspicuously demonstrates that in both cases the same methyl *m*-oxybenzoate chromophore



SCHEME 9

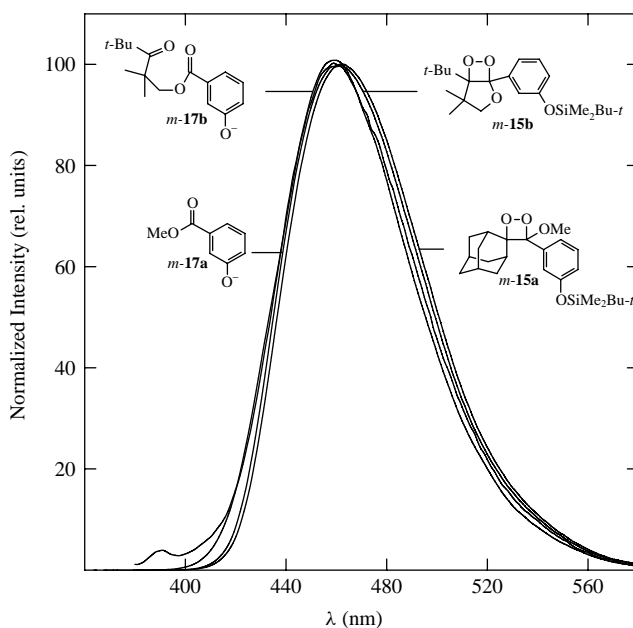


FIGURE 2. Normalized spectra of the CIEEL emission in the fluoride-ion-triggered ($[n\text{-Bu}_4\text{NF}] = 6.3 \times 10^{-4} \text{ M}$) decomposition of the dioxetanes (10^{-4} M) *m*-15a and *m*-15b at *ca* 20°C in MeCN and of the fluorescence emission ($\lambda_{\text{ex}} = 330 \text{ nm}$) for the corresponding methyl *m*-oxybenzoate ions (10^{-5} M) *m*-17a and *m*-17b under the same conditions. Reprinted with permission from Reference 34a. Copyright (1998) American Chemical Society

is responsible for the CIEEL emission. This is consistent with the computational results³⁴ shown in Figure 3. The pertinent molecular orbitals for the excitation of the authentic CIEEL emitters look very similar; in fact, the CIEEL emission derives *exclusively* from $\pi \rightarrow \pi^*$ excitation of the methyl *m*-oxybenzoate ion. Thus, contrary to the thermal

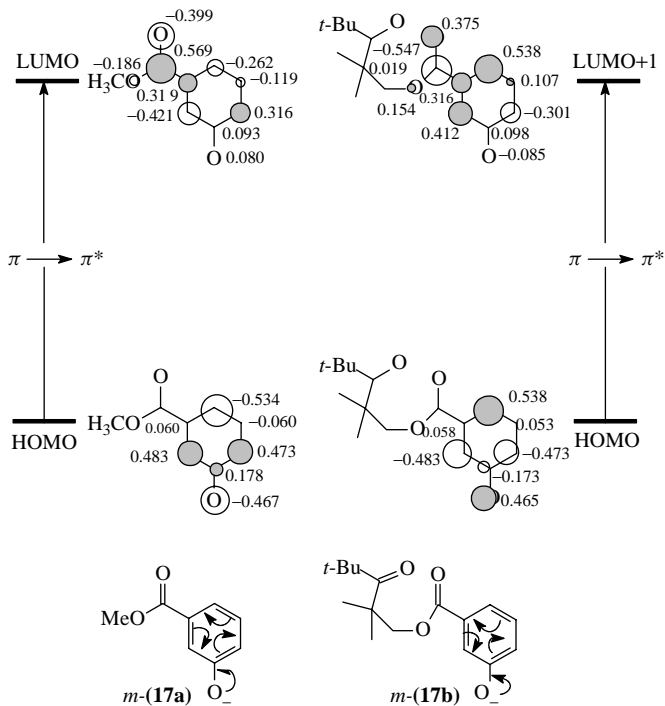
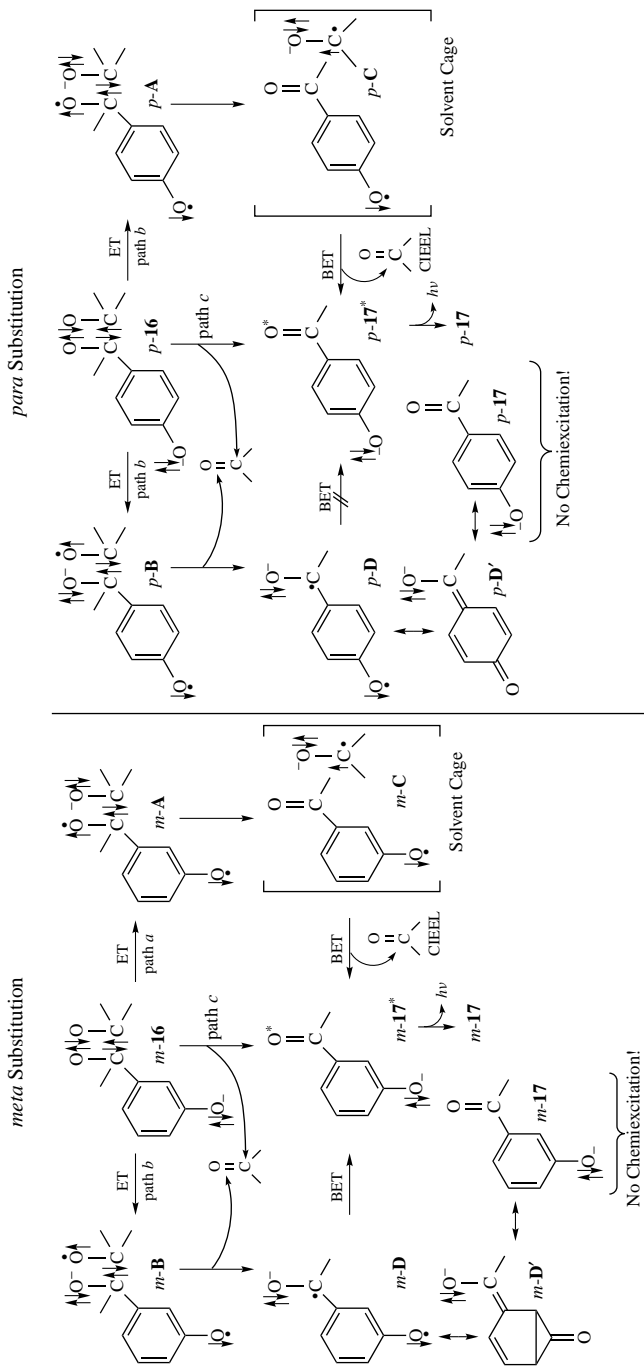


FIGURE 3. Pertinent molecular orbitals for the electronic excitation by the CIEEL process of the crossed-conjugated oxyanions *m*-**17a** and *m*-**17b** derived from the monocyclic (*m*-**15a**) and bicyclic (*m*-**15b**) dioxetane, as calculated by the AM1 method. Reprinted with permission from Reference 34b. Copyright (2000) American Chemical Society

dioxetane decomposition, in which either one of the two carbonyl products or even both may become electronically excited, in the electron-transfer-induced process exclusively the resulting phenolate fragment is the emitting species.

The chemiexcitation efficiency in the CIEEL cleavage process depends dramatically on the position of the triggerable functionality: In the case of *meta* substitution, excited-state generation proceeds more efficiently than in the *para* case by *ca* two orders of magnitude³⁵. What is the origin of these very different chemiexcitation efficiencies? Scheme 10 displays the detailed electronic analysis³⁶ of the mechanistic alternatives for the CIEEL generation of the regioisomeric dioxetane phenolates. The direct process (path *c*) constitutes the concerted chemiexcitation of the CIEEL emitters *m,p*-**17** without intermediates in the cleavage of the dioxetane phenolates *m,p*-**16**. For the stepwise electron back-transfer (BET) channel, two possibilities may be considered, which differ in the distribution of the electrons among the two oxygen atoms of the ring-opened dioxetane during the electron transfer from the phenolate functionality. In path *a*, the unpaired electron is localized on the dioxetane oxygen atom proximate to the phenolate functionality (structures *m*-**A** and *p*-**A**), while in path *b* it is placed onto the remote dioxetane oxygen atom (structures *m*-**B** and *p*-**B**). Subsequent cleavage of the dioxetane C–C bond in the diradical anions *m*-**A** and *p*-**A** affords the caged radical pairs *m*-**C** and *p*-**C**, while *m*-**B** and *p*-**B** generate the diradical ketyl structures *m*-**D** and *p*-**D**. Closer



SCHEME 10

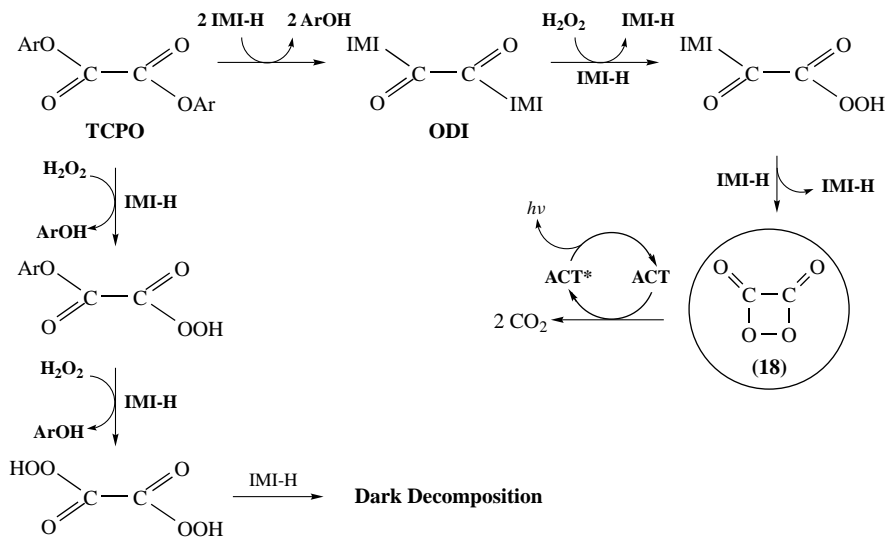
inspection of the *m,p*-**17** in Scheme 10 reveals a significant structural difference in the two emitters, namely the *m*-**17** species is a crossed-conjugated but the *p*-**17** one is an extended-conjugated system. The consequence of this may be found in path *b*: From the extended-conjugated, *para*-patterned anion-diradical intermediate *p*-**D**, spin annihilation leads directly to the resonance-stabilized mesomeric structure *p*-**D'**, which is equivalent to the *ground state* of the methyl oxybenzoate ion *p*-**17**; in contrast, for the crossed-conjugated, *meta*-patterned anion-diradical intermediate *m*-**D**, the high-energy spin-paired *m*-**D'** structure connects with the *m*-**17** ground state. The *intramolecular* BET process in path *b* would be expected to afford the electronically excited *m*-**17*** emitter, which should compete efficiently with the deactivation of the *m*-**D** intermediate to its ground state *m*-**17**. Compared to the *para* regioisomer *p*-**15**, chemiexcitation is expected to be more effective for *m*-**D**. This intuitive rationale may qualitatively account for the higher CIEEL efficiency of the *meta*-substituted dioxetane in comparison with *para* regioisomer³⁶. The intramolecular BET chemiexcitation process in Scheme 10 corresponds to the by now classical Schuster CIEEL mechanism²⁸.

The CIEEL process in both the *meta* and *para* cases is subject to a solvent-cage effect, which is manifested by a viscosity dependence of the excited-state generation^{35b,37}: The more viscous medium retards cage escape, with the consequence that the chemiexcitation yield increases at increasing viscosity (a 4-fold viscosity increase causes *ca* 2.5-fold enhancement of the chemiexcitation efficiency)^{35b,37}. The dramatic difference in the chemiexcitation efficiencies for the *m*-**15** and *p*-**15** dioxetanes may be accounted for in terms of energy considerations: The excited state of the crossed-conjugated methyl oxybenzoate ion *m*-**17** is by *ca* 12 kcal mol⁻¹ lower in energy than its extended-conjugated regioisomer *p*-**17**^{35b}, whereas the corresponding ground states do not display such an energy differentiation. Since the energy for the singlet excited state of the extended-conjugated emitter *p*-**17** is significantly higher than that for its crossed-conjugated isomer *m*-**17**, the BET process to generate the excited *p*-**17** emitter should be more endothermic and, thus, less efficient. Consequently, the experimental observation that the chemiexcitation efficiency is much lower for the *para* than for the *meta* regioisomer is therewith adequately accounted for.

Besides the impressive difference in the chemiexcitation efficiency, also the fluorescence yield of the *meta*-patterned emitter *m*-**17** is by more than an order of magnitude (!) higher than that of the *para* regioisomer *p*-**17**^{34a}. Evidently, crossed-conjugated emitters are advantageous for the design of efficient intramolecular CIEEL systems. In Sections V.A–V.C we shall consider additional internal (substrate structural effects) and external (medium influence) factors, which play an essential role in the development of efficient dioxetane-based analytical probes.

C. Dioxetane Intermediates in the Peroxy-oxalate Chemiluminescence

Since its discovery by Chandross³⁸ and to this day, peroxy-oxalate chemiluminescence has been controversial because of its enormous complexity in view of the many alternative steps involved in this process. The principal mechanistic feature of the peroxy-oxalate chemiluminescence pertains to the base-catalyzed (commonly imidazole) reaction of an activated aryl oxalate with hydrogen peroxide in the presence of a chemiluminescent activator, usually a highly fluorescent aromatic hydrocarbon with a low oxidation potential³⁹. A variety of putative high-energy peroxide intermediates have been proposed for the generation of the excited states⁴⁰. In the context of the present chapter, it is of import to mention that recent work⁴¹ provides experimental evidence for the intervention of the 1,2-dioxetanedione **18** (Scheme 11) as the high-energy species responsible for the chemiexcitation. Furthermore, clear-cut experimental data favor the CIEEL mechanism as a rationalization of the peroxy-oxalate chemiluminescence^{41d}.



Ar = 2,4,6-trichlorophenyl

IMI-H = imidazole

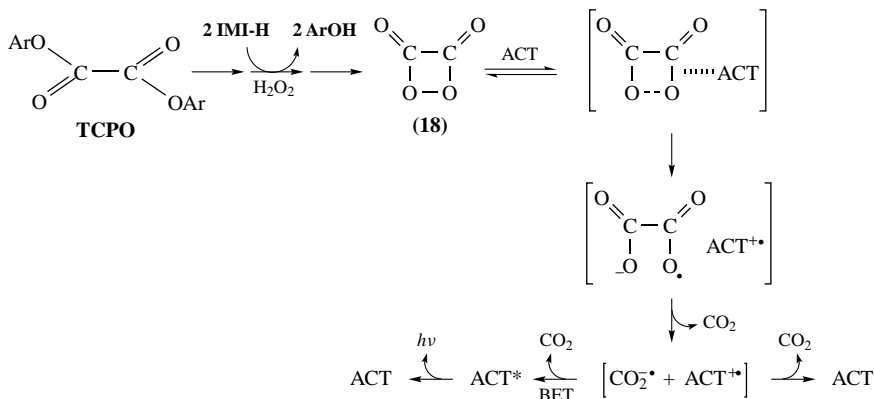
ACT = anthracene, 9,10-diphenylanthracene, 2,5-diphenyloxazole, perylene, rubrene

SCHEME 11

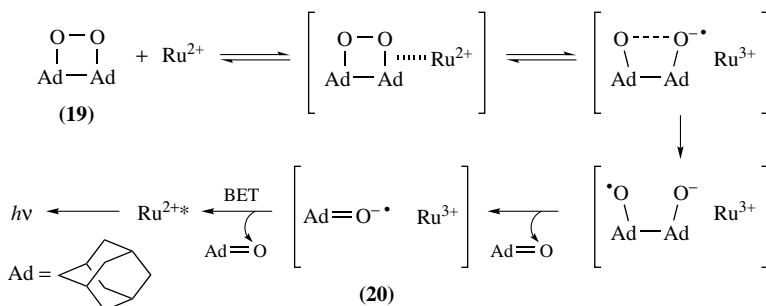
The main features of the chemiluminescence mechanism are exemplarily illustrated in Scheme 11 for the reaction of bis(2,4,6-trichlorophenyl)oxalate (TCPO) with hydrogen peroxide in the presence of imidazole (IMI-H) as base catalyst and the chemiluminescent activators (ACT) anthracene, 9,10-diphenylanthracene, 2,5-diphenyloxazole, perylene and rubrene. In this mechanism, the replacement of the phenolic substituents in TCPO by IMI-H constitutes the slow step, whereas the nucleophilic attack of hydrogen peroxide on the intermediary 1,1'-oxalyl diimidazole (ODI) is fast. This rate difference is manifested by a two-exponential behavior of the chemiluminescence kinetics. The observed dependence of the chemiexcitation yield on the electrochemical characteristics of the activator has been rationalized in terms of the intermolecular CIEEL mechanism (Scheme 12), in which the free-energy balance for the electron back-transfer (BET) determines whether the singlet-excited activator, the species responsible for the light emission, is formed^{41d}.

D. Metal-catalyzed Dioxetane Decomposition

Like other peroxides, also dioxetanes are sensitive to the presence of metal ions and their complexes, which catalyze the decomposition of the dioxetane molecule. In most cases, this decomposition is dark, i.e. no chemiluminescence is generated in such a catalytic cleavage⁴². An informative exception, for instance, constitutes the chemiluminescent decomposition of the dioxetane **19** in Scheme 13, initiated by the ruthenium complex $\text{Ru}(\text{bipy})_3\text{Cl}_2$ ⁴³. It has been shown that this chemiexcitation derives from the valence change of the ruthenium ion in the process $\text{Ru}^{3+} + e^- \rightarrow \text{Ru}^{2+*}$, for which the efficiency of the excited-state generation may be as much as 40%⁴⁴. Hence, when the radical anion of the carbonyl cleavage fragment from the dioxetane and the Ru^{3+} ion are formed in



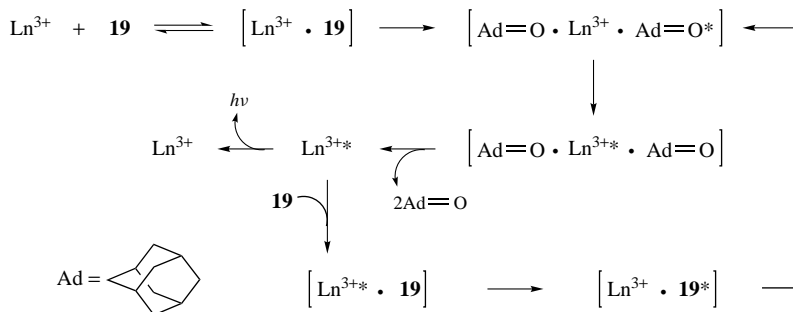
SCHEME 12



SCHEME 13

close proximity, i.e. the radical-ion pair **20** in Scheme 13, the formation of the electronically excited Ru^{2+*} species is plausible. Indeed, experimental evidence for such an intermolecular CIEEL process has been provided for the reaction of $\text{Ru}(\text{bipy})_3\text{Cl}_2$ with the thermally persistent dioxetane **19** (Scheme 13)⁴³.

An alternative case of metal-catalyzed chemiluminescence not based on the CIEEL mechanism has been recently reported for the reaction of the dioxetane **19** with the lanthanide chelates $\text{Eu}(\text{fod})_3$, $\text{Pr}(\text{fod})_3$, $\text{Eu}(\text{btfa})_3$, $\text{Tb}(\text{btfa})_3$, $\text{Eu}(\text{ClO}_4)_3$, $\text{Tb}(\text{ClO}_4)_3$, $\text{Gd}(\text{ClO}_4)_3$, $\text{Sm}(\text{ClO}_4)_3$, $\text{Dy}(\text{ClO}_4)_3$, $\text{Yb}(\text{ClO}_4)_3$ and $\text{Nd}(\text{ClO}_4)_3$ [fod = tris(6,6,7,7,8,8,8-heptafluoro-2,2-dimethyl-3,5-octanedionate, btfa = 4,4,4-trifluoro-1-phenyl-1,3-butanedi-one)]⁴⁵. When the dioxetane **19** was treated with such a lanthanide complex, the electronically excited Ln^{3+*} species was formed, followed by the light emission process $\text{Ln}^{3+*} \rightarrow \text{Ln}^{3+} + h\nu$ (Scheme 14). The generation of the excited Ln^{3+*} emitter does not merely derive from energy transfer between the electronically excited $\text{Ad}=\text{O}^*$ product of the dioxetane decomposition and the Ln^{3+} ions. Instead, the mechanistic intricacies involve the so-called quantum-chain process⁴⁶ (cf. Scheme 14) in the ligand sphere of the Ln^{3+} ion, followed by the dioxetane cleavage to the excited ketone ($\text{Ad}=\text{O}^*$); the latter initiates this complex sequence of events again with the regeneration of electronic excitation. In this quantum-chain process, the electronic excitation migrates from $\text{Ad}=\text{O}^*$ to Ln^{3+} to generate the excited Ln^{3+*} ion. The latter species not only emits light, but also transfers its energy to produce the excited dioxetane **19**^{*}, which cleaves into the



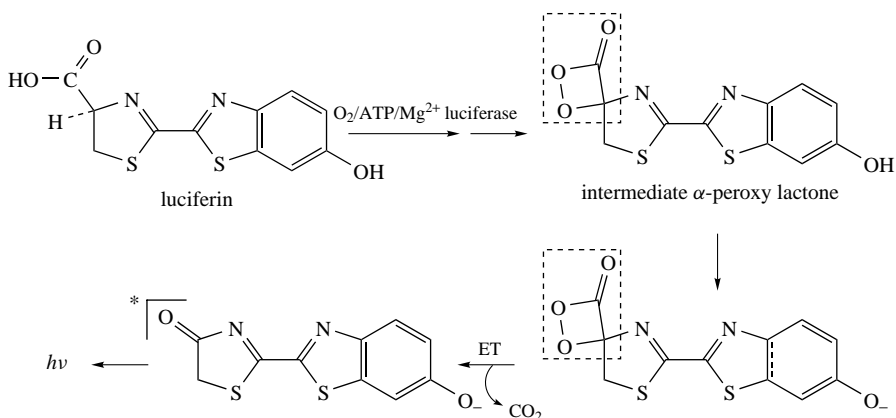
SCHEME 14

electronically excited ketone ($\text{Ad}=\text{O}^*$) and the chain process propagates until all of the dioxetane is consumed. It should be recalled that the quantum-chain process was discovered already in the early 1970s⁴⁶, first for the thermal decomposition of the *cis*-diethoxydioxetane^{46a} and subsequently for the tetramethyldioxetane^{46b,c}.

V. BIOANALYTICAL APPLICATION OF THE DIOXETANE CHEMILUMINESCENCE

A. Firefly Bioluminescence as a Prototype for a Dioxetane-based Triggered Chemiluminescence (CIEEL) in Bioassays

Of the many types of bioluminescence in nature, that of the firefly represents the most thoroughly studied and best understood biological luminescent process. The molecular mechanism of light emission by the firefly was elucidated in the 1960s⁸ in which a dioxetanone (α -peroxy lactone) was proposed as an intermediate, formed by the luciferase-catalyzed enzymatic oxidation of the firefly luciferin with molecular oxygen (Scheme 15). This biological reaction constitutes one of the most efficient luminescent processes known to date³⁰. Hence, it is not surprising that the luciferin–luciferase system finds wide use

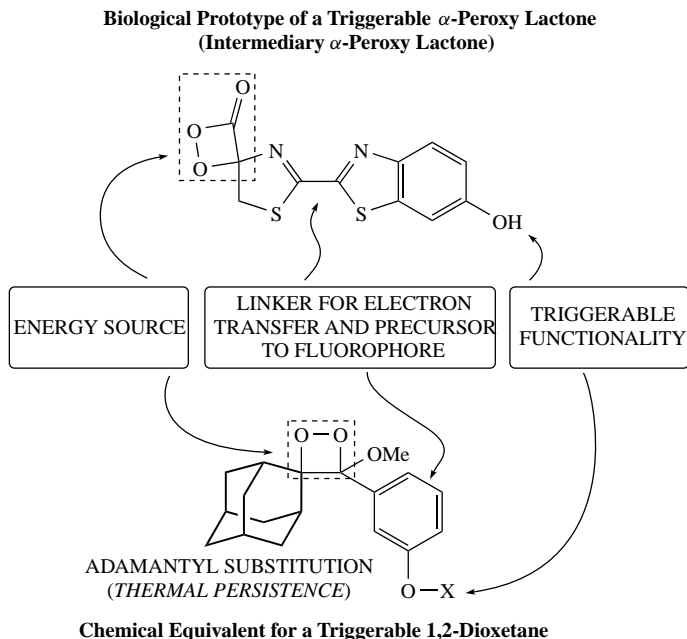


SCHEME 15

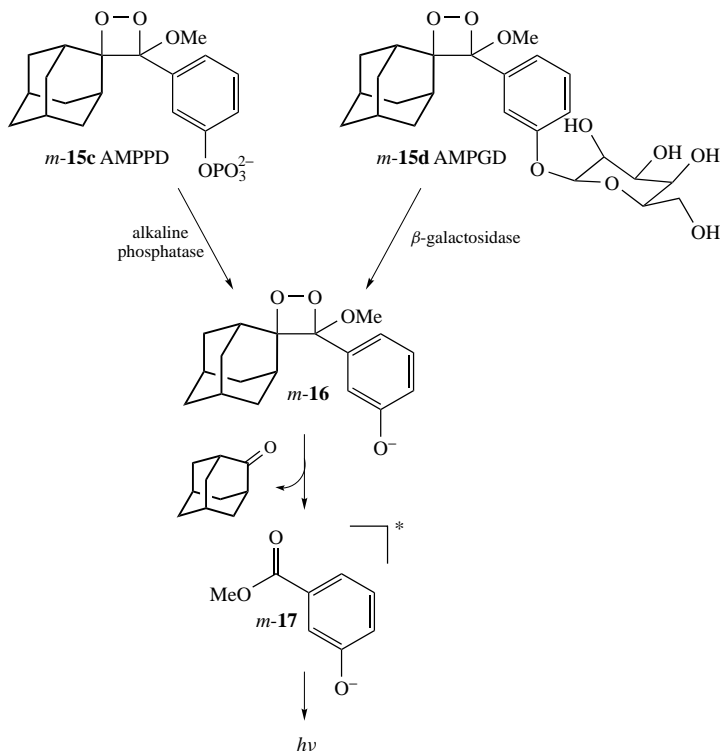
in bioanalytic applications, most prominently in the ATP-based bioassays⁴⁷. The ATP concentration serves to characterize the activity of living cells in the analyte samples and, thus, ATP-based methods constitute an efficient tool for rapid microbiological testing. In this context, it should be mentioned that the generous financial support by USA granting agencies of the research on the firefly bioluminescence in the 1960s rests on the incentives to discover ATP-based life on other planets!

Once the main molecular details of the firefly bioluminescence were understood, a chemical equivalent was designed (for the general case, see Scheme 9) which possesses the essential features of the biological model system for the efficient generation of light, as illustrated in Scheme 16. This scheme portrays the necessary molecular components in an artificial triggerable dioxetane as chemical equivalent of the biological prototype: (i) The energy source (dioxetane ring), (ii) the conjugating aromatic functionality, which serves both as the linker for the intramolecular electron transfer (ET) to the dioxetane cycle as well as the precursor for the fluorophore, and (iii) the triggerable group, namely the X-protected phenolate ion, to prevent spontaneous decomposition of the dioxetane. Besides these three essential components of the triggerable dioxetane as chemical equivalent (Scheme 16, bottom), which are akin to the biological prototype (Scheme 16, top), the substitution provides a practical structural feature, namely the necessary thermal persistence of the dioxetane molecule for ease of handling^{16a}. As has been stressed in Section IV.B it is advantageous for efficient chemiexcitation to place the triggerable functionality at the *meta* position of the aromatic linker. For that reason, such crossed-conjugated dioxetanes are tenable as effective chemiluminescent bioassay probes.

In bioanalytical techniques based on triggerable dioxetanes, the chemiluminescence emission is generated on command by treating the dioxetane solution with an analyte,



SCHEME 16



SCHEME 17

which contains an enzyme that is reactive toward the protecting X group. The choice of the X group depends on the active enzyme in the analyte sample to be assayed. Alkaline phosphatase and β -galactosidase furnish prominent examples of such enzymes, which are used most frequently in chemiluminescent bioassays (immunoassays, reporter gene assays etc.)⁴⁸. For the phosphatase enzyme, a phosphate-ester functionality must be chosen as the triggerable protecting X group, whereas a galactose-based substituent serves as the triggerable functionality for the β -galactosidase case (Scheme 17). Thus, the phosphate-protected dioxetane *m-15c*, namely **AMPPD**, is a selective chemiluminescent probe for alkaline phosphatase, whereas the galactose-protected dioxetane *m-15d*, namely **AMPGD**, is used for the detection of β -galactosidase. There exist other chemiluminescent methods to monitor such enzymes⁴⁹, but the triggerable dioxetanes **AMPPD** and **AMPGD** are the most frequently employed for bioanalytical purposes.

The rational design of effective and efficient dioxetane-based bioanalytical probes requires the in-depth mechanistic understanding of the enzymatically triggered chemiluminescence. In this context, alkaline-phosphatase-triggered CIEEL furnishes a textbook example⁵⁰, which will be examined below in detail.

B. Alkaline-phosphatase-triggered CIEEL

In Section IV.B we discussed the main internal (substrate) structural effects, which are essential for the efficient CIEEL generation. A judicious choice of the proper conditions,

however, for optimal chemiluminescence requires one to know also the external (medium) influence on the enzymatic CIEEL triggering. Accordingly, we consider herein the medium effects on the spectral characteristics, the chemiluminescence yield, and the emission intensity for the practically important case of the CIEEL process, triggered from the **AMPPD** by the alkaline phosphatase.

A noteworthy feature of the CIEEL phenomenon is the fact that the emission spectrum of the alkaline-phosphatase-triggered dioxetane *m-15c* coincides with that of the NaOH-triggered, hydroxy-substituted dioxetane *m-15e* in the absence of enzyme (Figure 4)^{35a}.

Such an observation speaks against the possibility that any specific enzyme-type environmental effects are involved in the generation of the excited CIEEL emitter (*m-17**). This behavior of the CIEEL emission differs from that of its biological prototype, i.e. firefly bioluminescence. Indeed, for the biological process, recently the dependence of the spectral emission characteristics on the enzyme (luciferase) microenvironment has been documented⁵¹. What is the origin of this discrepancy? The answer is the large difference in the lifetimes of the dioxetane precursors for the light emitters: In the case of the firefly bioluminescence, the intermediary α -peroxy lactone (Scheme 15) is so labile³⁰ (lifetimes probably $< 1 \mu\text{s}$) that it decomposes to the bioluminescence emitter immediately within the enzyme vicinity where it has been produced, such that specific environmental effects of the protein should manifest themselves, whereas the intermediary phenolate ion *m-16* of the **AMPPD** as the emitter's precursor is a rather long-lived species (lifetime of *ca* 1 min in the aqueous medium at 37 °C!)⁵⁰, and thus it may exit the enzyme pocket *before*

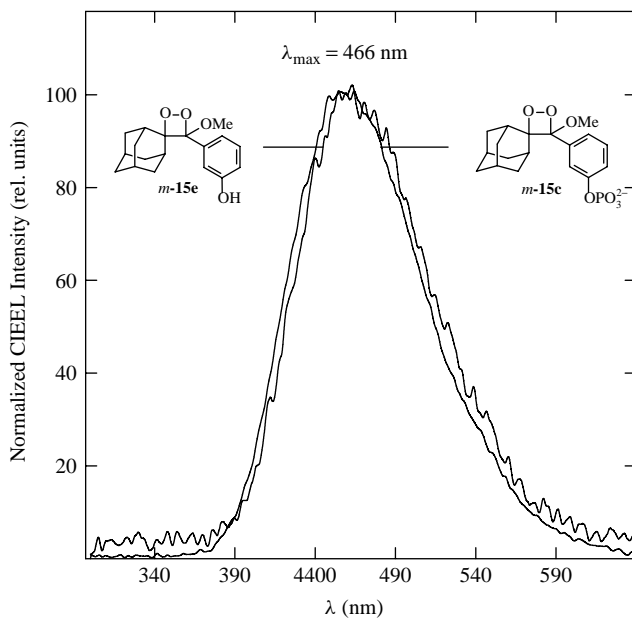


FIGURE 4. Normalized CIEEL spectrum of the alkaline-phosphatase-triggered ([alkaline phosphatase] = 2×10^{-7} M) dioxetane *m-15c* (1.7×10^{-7} M) in 0.05 M carbonate buffer (pH 9.5), and that of the NaOH-triggered, hydroxy-substituted dioxetane *m-15e* (3.4×10^{-3} M, pH 12.7), both at 20 °C. Reprinted with permission from Reference 34b. Copyright (2000) American Chemical Society

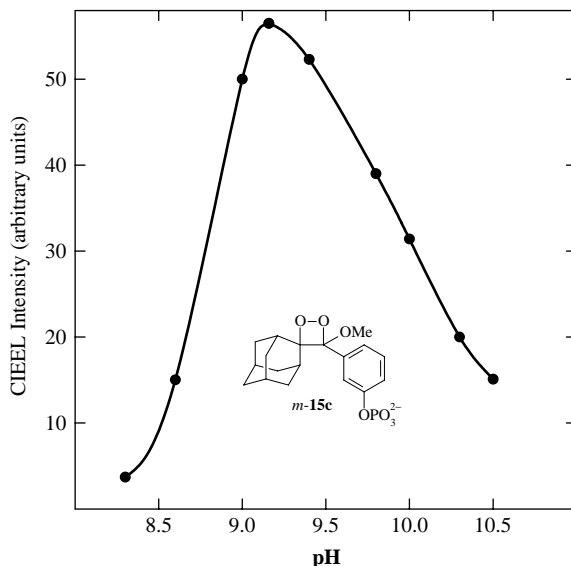


FIGURE 5. CIEEL intensity as a function of pH for the alkaline-phosphatase-triggered ([alkaline phosphatase] = 4.7×10^{-13} M) dioxetane *m*-**15c** (1 mM) in 0.05 M carbonate buffer at 37 °C. Reprinted with permission from Reference 50. Copyright (1996) American Chemical Society

its cleavage to the chemiexcited emitter *m*-**17***. An additional feature to note is that the coincident spectra in Figure 4 have been obtained at quite different alkaline pH values (pH 9.5 and 12.7), which means that under alkaline conditions the CIEEL spectra are independent of pH.

In contrast, the CIEEL intensity depends on pH (Figure 5)⁵⁰. To elucidate the reason of this pH dependence, we need to consider in detail the kinetics of this enzymatic process. Since the CIEEL intensity (I_{CIEEL}) is defined by the product of the rate of the enzymatic catalysis (v_{cat}) and the CIEEL yield (Φ_{CIEEL}) (equation 1), the pH dependence of I_{CIEEL} (Figure 5) resides either in the $v_{\text{cat}}(\text{pH})$ or in the $\Phi(\text{pH})$ term. In view of the fact that the CIEEL yield ($\Phi_{\text{CIEEL}} = 7.5 \times 10^{-6}$) has been found to be independent of pH within the pH range from 8 to 10.5⁵⁰, the observed pH dependence of the CIEEL intensity (Figure 5) is exclusively determined by the pH dependence of the enzymatic dephosphorylation (v_{cat}) of the **AMPPD** substrate, which is the rate-limiting step of the overall CIEEL process (Scheme 17). At low concentration of the enzyme (e_0), v_{cat} is expressed by the Michaelis–Menten rate law (equation 2), in which k_{cat} is the turnover number, K_{M} the Michaelis constant and [**AMPPD**] the substrate concentration, which allows us to scrutinize the details of the pH dependence of the v_{cat} term.

$$I_{\text{CIEEL}} = \Phi_{\text{CIEEL}} v_{\text{cat}} \quad (1)$$

$$v_{\text{cat}} = \frac{k_{\text{cat}} e_0 [\text{AMPPD}]}{[\text{AMPPD}] + K_{\text{M}}} \quad (2)$$

A priori, the pH effect on v_{cat} may derive from the pH dependence of both the $K_{\text{M}}(\text{pH})$ and the $k_{\text{cat}}(\text{pH})$. Figure 6 displays the variation of the catalytic parameters K_{M} and k_{cat} as a function of pH. As seen from Figure 6, at pH > 9 the k_{cat} is independent of pH, whereas

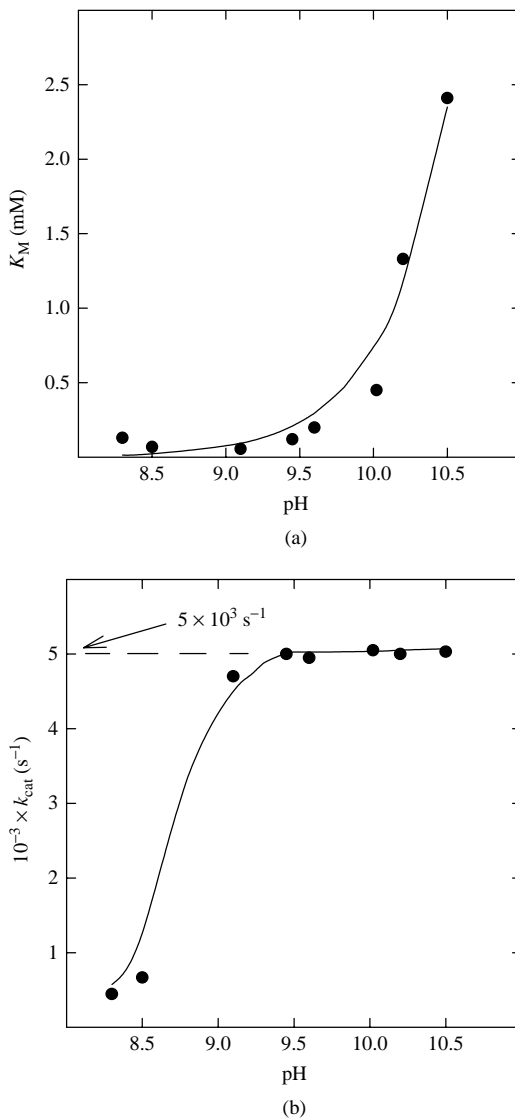
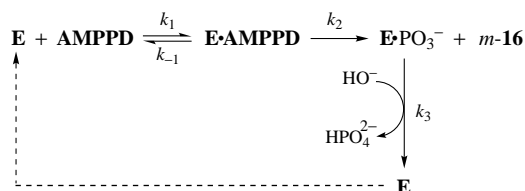


FIGURE 6. (a) The pH dependence of the Michaelis constant (K_M) for the alkaline-phosphatase-catalyzed decomposition of AMPPD in 0.05 M carbonate buffer at 37 °C; (b) the same pH dependence for the turnover number (k_{cat}). Reprinted with permission from Reference 50. Copyright (1996) American Chemical Society

the K_M increases with increasing pH. In contrast, at $\text{pH} < 9$, k_{cat} decreases markedly with decreasing pH, whereas K_M changes only slightly. According to equation 2, the origin of the pH variation of v_{cat} in these two pH regions differs: At $\text{pH} < 9$, the decrease of v_{cat} as the pH is lowered derives from the decrease of the turnover number (k_{cat}), but at $\text{pH} > 9$,



SCHEME 18

the decrease of v_{cat} as the pH is increased relates to the increase of K_M ; the overall effect is the bell-shaped appearance of the pH profile in Figure 5.

The simplified mechanism of the dephosphorylation of the **AMPPD** substrate is illustrated in Scheme 18⁵⁰, in which the enzyme (alkaline phosphatase) is codified by **E**, **E**·**AMPPD** is the Michaelis complex, **E**·**PO₃⁻** represents the phosphorylated enzyme and *m*-**16** designates the deprotected (dephosphorylated) phenolate ion of **AMPPD** (Scheme 17). On the basis of the mechanism depicted in Scheme 18, a kinetic analysis allows one to express k_{cat} by equation 3 and K_M by equation 4⁵⁰, in which K_{a_1} and K_{a_2} represent the ionization constants for the catalytically active form of the enzyme^{50,52}. These equations account for the observed pH dependence of the catalytic parameters K_M and k_{cat} (Figure 6)⁵⁰. Evidently, the lack of pH dependence of the k_{cat} at pH > 9 suggests that the rate-limiting step at high pH is the phosphorylation of alkaline phosphatase (k_2), but the regeneration of the free enzyme **E** through the pH-controlled dephosphorylation of **E**·**PO₃⁻** is fast since $k_3[\text{HO}^-]$ is high enough. This simplifies equation 3 to its limiting form as given by equation 5, which is valid at pH > 9, i.e. at high $[\text{HO}^-]$. Therefore, the turnover number k_{cat} is affected only at pH < 9 (Figure 6), which reflects a switchover of the rate-determining step of the enzyme dephosphorylation to its phosphorylation at increasing pH (increasing $[\text{HO}^-]$; cf. equation 3). Similarly, the Michaelis constant (K_M) in equation 4 simplifies to equation 6 as the limiting case, because at pH > 9, the $k_3[\text{HO}^-]$ term is high.

$$k_{\text{cat}} = \frac{k_2}{1 + \frac{k_2}{k_3[\text{HO}^-]}} \quad (3)$$

$$K_M = \frac{k_{-1} + k_2}{k_1 \left(1 + \frac{k_2}{k_3[\text{HO}^-]}\right)} \left\{ 1 + \frac{[\text{H}^+]}{K_{a_1}} + \frac{K_{a_2}}{[\text{H}^+]} \right\} \quad (4)$$

$$k_{\text{cat}} \approx k_2 \quad (5)$$

$$K_M \approx \frac{k_{-1} + k_2}{k_1} \left\{ 1 + \frac{[\text{H}^+]}{K_{a_1}} + \frac{K_{a_2}}{[\text{H}^+]} \right\} \quad (6)$$

The pH dependence of K_M is thereby determined by the relative importance of the $[\text{H}^+]/K_{a_1}$ and $K_{a_2}/[\text{H}^+]$ ratios in equation 6. The shape of the pH dependence in Figure 6 suggests that in the alkaline pH range the $K_{a_2}/[\text{H}^+]$ ratio contributes mainly to K_M , since it is this term that accounts for the steady increase of K_M with increasing pH (decreasing $[\text{H}^+]$). This fact is associated with the lower concentration of the catalytically active enzyme form through its deprotonation at higher pH⁵⁰.

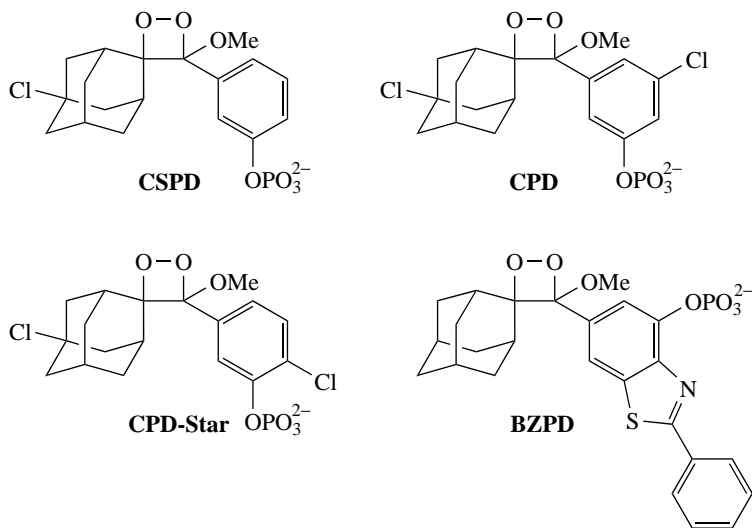
From this detailed kinetic analysis of the complex pH dependence for the chemiluminescence intensity we conclude that only the enzymatic dephosphorylation of **AMPPD**

depends on pH in the alkaline-phosphatase-triggered CIEEL process. The superposition of the pH effects on the catalytic parameters K_M and k_{cat} determines the position of the pH maximum (*ca* 9), at which the optimal CIEEL intensity may be attained. When the target molecule (a protein or nucleic acid) is attached to the enzyme, however, the catalytic properties of the modified enzyme should be affected on account of the pH dependence of both the turnover number and the Michaelis constant compared to the free enzyme. Therefore, the pH conditions should be optimized for every particular enzyme-triggered chemiluminescent probe, especially when enzymes immobilized on membranes or on water-soluble polymers are employed.

C. Dioxetane Substrates for Molecular Biology and Clinical Assays

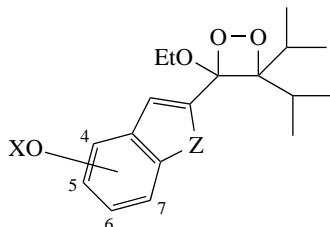
1,2-Dioxetanes, labeled with triggers sensitive to the alkaline-phosphatase enzyme, serve as highly sensitive chemiluminescent probes in numerous bioassays. Current applications include immunoassays, membrane-based detection of proteins and nucleic acids, and microplate-based and array-based nucleic-acid detection⁵³.

At present, a family of the **AMPPD**-type dioxetanes (e.g. **AMPPD**, **CSPD**, **CDP**, **CDP-Star**, **BZPD**) is commercially available for the detection of the alkaline-phosphatase-based labels. The replacement of the phosphate protective group by the galactose functionality (cf. Scheme 17) in these dioxetanes makes them suitable for β -galactosidase monitoring, a second important class of bioassays^{53,54}. After enzymatic deprotection of the β -galactose group, the resulting dioxetane phenolate anion breaks down with exactly the same spectral and kinetic performance as displayed by the related alkaline-phosphatase-sensitive series⁵³.



Of great promise and formidable challenge is the application of triggerable dioxetanes in multiplex-detection assays^{33e,53} in which several enzymes are simultaneously monitored. To realize this goal, chemiluminescent probes are required which emit at distinct wavelengths, i.e. a separate wavelength for each specific enzyme. Since the **AMPPD**-type *m*-15 dioxetane emits on chemical and enzymatic triggering relatively short-wavelength (blue) light, i.e. in the 460–480 nm spectral region, triggerable dioxetanes are needed,

which emit long-wavelength (red) chemiluminescence. For that purpose, benzofuran- and benzothiophene-substituted dioxetanes **21a–f** were developed, which on chemical triggering in DMSO emit red light in the 615–628 nm range⁵⁵. For biological use, it would merely be necessary to replace the protective X group by phosphate (for alkaline phosphatase) or sugar (for β -galactosidase) functionalities.



(21a) Z = O, X = 5-*t*-BuMe₂Si

(21b) Z = O, X = 6-*t*-BuMe₂Si

(21c) Z = O, X = 7-*t*-BuMe₂Si

(21d) Z = S, X = 5-*t*-BuMe₂Si

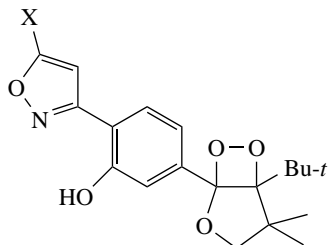
(21e) Z = S, X = 6-*t*-BuMe₂Si

(21f) Z = S, X = 7-*t*-BuMe₂Si

As for improving the chemiluminescence efficiency^{48,53,56} the addition of macromolecular enhancers helps significantly. Normally, the CIEEL efficiency of the triggerable dioxetanes in aqueous media is by a few orders of magnitude lower in organic solvents. For example, the water-soluble quaternary amine polymers provide at least a 100-fold amplification of the light emission in aqueous media. Similar enhancement may be achieved with the use of natural macromolecules (e.g. bovine serum albumin)^{48,53}. The nature of this effect resides in the formation of an aprotic microenvironment around the reaction site: The hydrophobic domains of water-soluble macromolecules exclude the water from the vicinity of the deprotected dioxetane phenolate ion and thereby reduce the influence of hydrogen bonding on the CIEEL generation. Polymer formulations with fluorescein as the energy-transfer acceptor further increase the light yield substantially and shift the wavelength maximum of emission up to 540 nm. For instance, a fluorescent micelle-enhancer system that is formed from cetyltrimethylammonium bromide and fluorescein enhances the chemiluminescence yield about 400-fold^{56a}. Such changes of the microenvironment may be achieved by attaching surfactants or tethered fluoroscens to the triggerable dioxetanes^{48,53,56} which also enhances considerably the chemiluminescence yield in aqueous media.

Recently, the synthesis has been reported of the novel bicyclic dioxetanes **22a–c**⁵⁷, which possess a remarkable chemiluminescence efficiency in aqueous media. Of the dioxetanes **22a–c** with the 3-hydroxy-4-isoxazolylphenyl functionality, the derivative **22a** is the most suitable: On triggering by NaOH in water, the dioxetane **22a** displays the highest CIEEL yield (0.24 at 25 °C)⁵⁷, whereas the efficiency of compounds **22b** and **22c** is much lower (0.064 and 0.015, respectively)⁵⁷. Nevertheless, the latter are still sufficiently efficient triggerable dioxetanes and quite adequate for their use in aqueous media. Such unprecedented results definitely merit further exploration.

In the application of alkaline-phosphatase-sensitive, triggerable 1,2-dioxetanes, the nucleic-acid hybridization assay is nowadays quite popular⁵³. Such techniques include viral load assays for hepatitis B and C and for human immunodeficiency viruses (HBV,



(22a) X = CF₃

(22b) X = H

(22c) X = *t*-Bu

HCV and HIV-1). The bDNA assay⁵³ is being much employed for the quantification of messenger RNA. Moreover, for the detection of viral and pathogenic disorders based on alkaline-phosphatase-sensitive dioxetanes, several assay methods are available; these include the Polymerase-Chain-Reaction (PCR) amplification, probe ligation, strand-displacement amplification and the ligase chain reaction⁵³.

Drug discovery and high-efficiency pharmaceutical screening constitute currently important applications of the chemiluminescent methods based on triggerable 1,2-dioxetanes. These dioxetanes are also being increasingly employed in functional assays for genomic and proteomic studies⁵³. Applications include reporter-gene assays to monitor gene expression, second-messenger quantification, protein kinase assays and protein–protein interaction analysis.

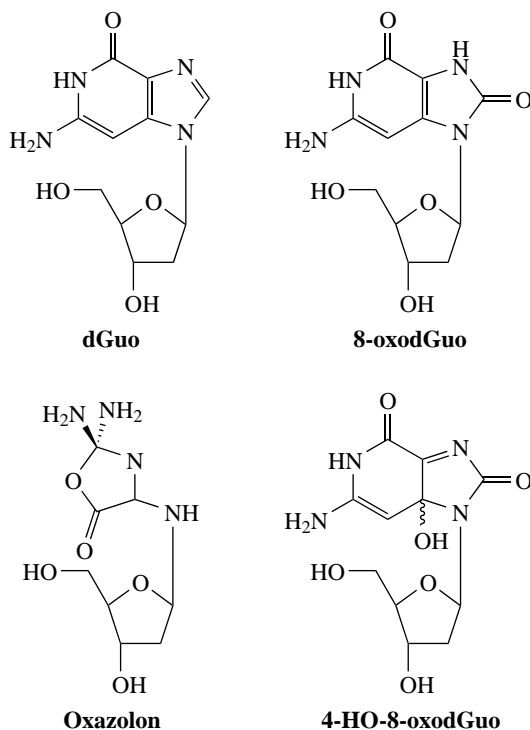
It should have become evident from this brief overview of the chemiluminescent bioassays that triggerable dioxetanes play a central role in the development of such modern technology. It is anticipated that these timely chemiluminescent systems will receive in the future much more attention in clinical diagnostics, drug discovery and biological needs. The ultimate success in such applications will rely on the design of triggerable dioxetane molecules with distinct spectral emission properties to make available efficacious multiplex multichannel chemiluminescent assays. Be this as it may, it must be emphasized that nature has offered through its firefly bioluminescence an inspiring and challenging phenomenon for the conceptualization, design and realization of the novel bioanalytical probes presented in this subsection.

VI. PHOTOOXIDATION OF DNA BY 1,2-DIOXETANES

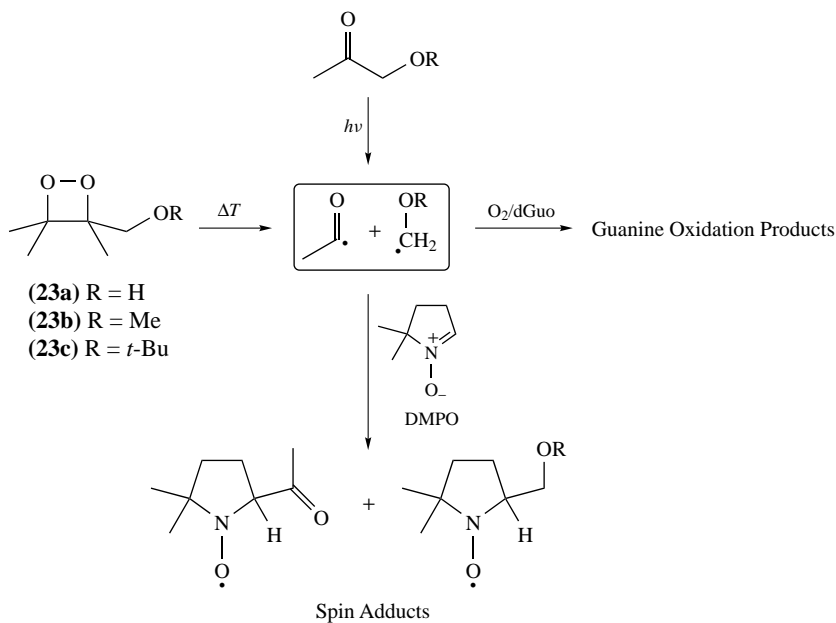
1,2-Dioxetanes have been postulated as labile intermediates in a variety of biologically relevant processes⁵⁸. Most attention was given to their involvement in the enzymatic generation of electronically excited states, particularly in oxidative stress and in the induction of spontaneous mutations⁵⁹. Due to the fact that dioxetanes are efficient thermal sources for the generation of electronically excited carbonyl fragments, these high-energy cyclic peroxides have been extensively used in the past to study the genotoxicity of excited carbonyl compounds in the dark⁵⁸. The thermal generation of excited states from dioxetanes has the advantage that it circumvents the direct exposure of biological systems, in particular cells, to UV radiation. Thereby, valuable mechanistic insight may be gained into the complex photooxidative processes associated with genotoxicity and carcinogenicity, but without the direct use of radiation. This paved the way for the extensive studies on *photobiology without light*, an important and timely topic in bioorganic chemistry⁶⁰. It has been

demonstrated that dioxetanes are convenient and efficient thermal sources of triplet-excited ketones, which are used for the damage of DNA in cell-free and cellular systems⁶¹.

The purine base guanine (the structure of its nucleoside is shown below) is oxidatively the most vulnerable target in the chemical alteration of DNA⁶¹. The highly mutagenic 8-oxo-7,8-dihydro-2'-deoxyguanosine (**8-oxodGuo**)⁶², the 2,2-diamino-[(2-deoxy- β -D-*erythro*-pentofuranosyl)-4-amino]-5(2*H*)-oxazolone (commonly referred to simply as oxazolone and results from the hydrolysis of the corresponding imidazolone precursor⁶³) and the 4-hydroxy-8-oxo-4,8-dihydro-2'-deoxyguanosine (**4-HO-8-oxodGuo**)⁶⁴ constitute the major photooxidation products of **dGuo**. These guanine-derived products have been extensively used as chemical markers to quantify the oxidative damage of DNA. To assess the oxidative propensity of 1,2-dioxetanes, most of the chemical model studies have been carried out on the nucleoside 2'-deoxyguanosine (**dGuo**) and calf thymus DNA⁶⁴.



The major mechanisms of the dioxetane-induced, photooxidative damage of DNA recognized to date^{64,65} are displayed in Scheme 19. The type-I damage consists of hydrogen-atom abstraction and electron transfer, while the type-II process is caused by singlet-oxygen oxidation⁶⁴. The channel which involves α cleavage of the triplet-excited carbonyl products generated in the dioxetane thermolysis and is relevant to radical-type DNA modification constitutes the most recently studied case (Scheme 19, right)⁶⁵. In this context, the simple alkyl-substituted 1,2-dioxetanes damage DNA by both the type-I and type-II mechanisms. Therewith, **8-oxodGuo** is formed either directly through the type-I channel or indirectly through the type-II process, whereas the oxazolone derives principally from the type-I oxidation, and the **4-HO-8-oxodGuo** usually from the type-II reaction⁶⁴.



SCHEME 20

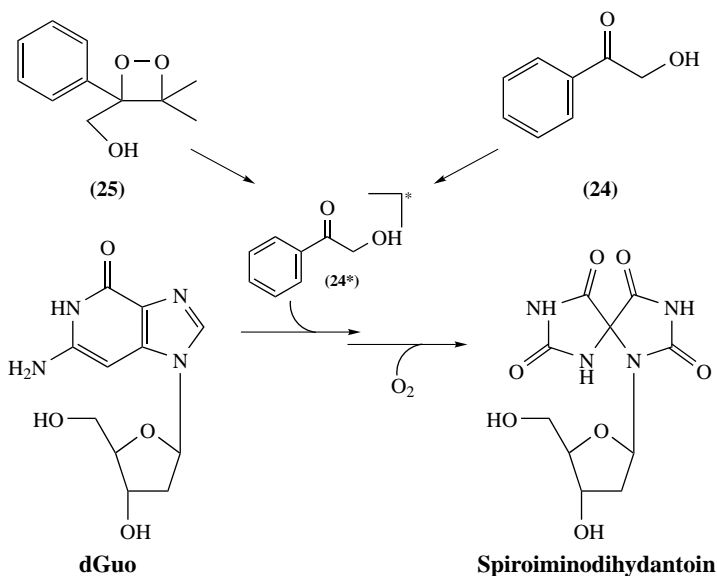
by EPR spectroscopy of the spin-trapped products; cf. Scheme 20) with 5,5-dimethyl-1-pyrroline N-oxide (**DMPO**) and by laser-flash photolysis⁶⁵. Subsequently, comparative studies on the guanine oxidation by the thermolysis of the dioxetanes **23a–c** and the photolysis of the corresponding ketones (primary dioxetane thermolysis products) substantiated the radical nature of this DNA damage^{65b}. Specifically, it was established that the oxidative reactivity order in the dioxetane thermolysis and in the ketone photolysis parallels the ability of the electronically excited ketones to release radicals upon α cleavage. In the presence of molecular oxygen, the carbon-centered radicals are efficiently scavenged by O_2 to afford peroxy radicals, which initiate a complex sequence of oxidative DNA modifications. As a result, oxazolone and **4-HO-8-oxodGuo** are the major products in the oxidation of **dGuo** by the peroxy radicals, while **8-oxodGuo** is produced in minor amounts. It is noteworthy that the observed yield of **4-HO-8-oxodGuo**^{65b} (usually considered as a characteristic product of the **dGuo** oxidation by singlet oxygen alone⁶⁶) cannot be attributed alone to singlet oxygen, since it was shown that insufficient amounts of the latter are being generated during the thermolysis of dioxetanes **23a–c**.

In contrast to **dGuo**, the oxidation of DNA affords the **8-oxoGua** as the major product, but also significant amounts of the guanidine-released oxazolone were found^{65b}. As for **4-HO-8-oxoGua**, only little is formed of this oxidation product in DNA^{65b} and thus it is difficult to quantify. It is a general fact that in the oxidation of DNA, **8-oxoGua** is found in substantial amounts, whereas in **dGuo** only in traces^{65b,67}. This reactivity trend applies also in the case of one-electron oxidants, which has been rationalized in terms of the intermediacy of the guanine radical cation, a labile species that is stabilized in the DNA matrix; subsequently, the radical cation is selectively transformed into **8-oxoGua** through a complex sequence of hydrolytic events. Under the experimental conditions of the dioxetane-induced DNA damage^{65b}, the **8-oxoGua** accumulates in the DNA, but in the **dGuo**, the corresponding **8-oxodGuo** is rapidly consumed by oxidative destruction;

hence the high levels of **8-oxoGua** observed in DNA are due to its protection in the DNA matrix against further oxidation.

A timely point to note is that recently the **4-HO-8-oxodGuo** structure has been questioned⁶⁸. By means of careful HPLC analysis, it was shown that the so-called 'established' 4-hydroxy-8-oxo structure is actually spiroiminodihydantoin (Scheme 21). The latter was prepared by the one-electron oxidation of **8-oxodGuo** and characterized on the basis of mass-spectral and NMR-spectral analyses^{68,69}. Since the authentic **4-HO-8-oxodGuo** is not available, a definitive differentiation from the spiroiminodihydantoin had to be indirect. Thus, the unequivocal assignment rests on the distinct connectivities in the spiroiminodihydantoin and **4-HO-8-oxodGuo** structures, which was achieved with the SELINQUATE⁷⁰ NMR technique. In this context, when the triplet-excited 2-hydroxyacetophenone **24** was chosen for the oxidation of **dGuo**, generated photochemically by the direct excitation of the ketone and thermally by the decomposition of the dioxetane **25** (Scheme 21)⁷¹, these most recent studies confirmed that the major **dGuo** oxidation product is, indeed, the spiroiminodihydantoin rather than **4-HO-8-oxodGuo**⁷¹. Presumably, the spiroiminodihydantoin is an ubiquitous oxidation product of **dGuo** by metal-based one-electron oxidants, triplet ketones, singlet oxygen and oxyl radicals, but this claim still needs to be unequivocally established.

It is known that the triplet-excited **24** cleaves exclusively into benzoyl and hydroxymethyl radicals⁷², which on trapping with O₂ afford peroxy radicals for the oxidation of **dGuo**. Photomechanistically relevant and practically advantageous is that, due to the benzoyl chromophore, the **24** triplet state, in contrast to ketone cleavage products of **23**, enables transient spectroscopy. Consequently, it was possible to assess the relative importance of the direct photooxidation of the nucleoside **dGuo** by the triplet-excited **24** (electron transfer, hydrogen abstraction) vs. the oxidative damage by the radicals generated through the α cleavage of the excited **24**⁷¹. This study disclosed that the direct photooxidation of guanine in **dGuo** takes place by the **24** triplets (presumably through



SCHEME 21

electron transfer) as well as by radicals generated thereof; the latter dominate at low **dGuo** concentration in the presence of molecular oxygen.

It should be evident from this discussion that the dioxetane **25** represents an example par excellence for photobiological studies in the dark (photobiology without light⁶⁰). It generates efficiently electronically excited ketones, which may be directly viewed by transient spectroscopy and which are convenient sources of active radical species through their facile α cleavage.

VII. CONCLUSIONS

In the present chapter, we have considered the main recent developments in dioxetane studies. Our incentive to concentrate on the contemporary facets of dioxetane chemistry was to assure the reader that interest in these unique cyclic peroxides has not subsided since their discovery about 35 years ago. Particularly the last decade has witnessed impressive advances in this fascinating field, from both the mechanistic and applied points of view. Moreover, a novel feature of dioxetane chemistry pertains to harnessing them as building blocks in asymmetric synthesis, hardly thought feasible about a decade ago.

The remarkable propensity of dioxetanes to generate electronically excited states still constitutes the overriding interest in these high-energy molecules, currently most prominently for clinical and biological purposes. This concerns their applications as bioanalytical tools (e.g. immunoassays, in which the chemiluminescence of enzyme-triggerable dioxetanes is utilized) and their studies in the photobiology of DNA (e.g. photogenotoxicity). As to the clinical benefits of dioxetane-based bioassays, these modern chemiluminescent techniques enable the detection of analytes at the attomol (10^{-18}) and even zeptomol (10^{-21}) levels, which is about 10000 times (!) below the detection limit possible with the conventional radioactive assays.

VIII. ACKNOWLEDGMENT

We express our sincere gratitude to all our colleagues who have participated in the experimental and theoretical work, which promoted current progress in dioxetane chemistry; their names are cited in the original publications. The generous financial support from the Deutsche Forschungsgemeinschaft (SFB-172 Research Program), the Volkswagen Stiftung and the Fonds der Chemischen Industrie is gratefully appreciated; AVT thanks also the Russian Foundation for Basic Research and the Russian Academy of Sciences (Research Program 'Fundamentals of Chemical Bonding and Structure').

IX. REFERENCES

1. K. R. Kopecky, in *Chemical and Biological Generation of Excited States* (Eds. W. Adam and G. Cilento), Academic Press, New York, 1982, pp. 85–114.
2. H. Blitz, *Justus Liebigs Ann. Chem.*, **296**, 238 (1897).
3. E. H. White and M. J. C. Harding, *J. Am. Chem. Soc.*, **86**, 5686 (1964).
4. (a) F. McCapra and D. G. Richardson, *Tetrahedron Lett.*, 3167 (1964).
(b) F. McCapra, D. G. Richardson and Y. C. Chang, *Photochem. Photobiol.*, **4**, 1111 (1965).
5. W. H. Urry and J. Sheeto, *Photochem. Photobiol.*, **4**, 1067 (1965).
6. F. McCapra and Y. C. Chang, *J. Chem. Soc., Chem. Commun.*, 522 (1966).
7. M. M. Rauhut, *Acc. Chem. Res.*, **2**, 80 (1969).
8. (a) A. H. Thomas, H. H. Seliger, E. H. White and M. W. Cass, *J. Am. Chem. Soc.*, **89**, 7148 (1967).
(b) F. McCapra, Y. C. Chang and V. P. François, *J. Chem. Soc., Chem. Commun.*, 22 (1968).
9. K. R. Kopecky and C. Mumford, *Can. J. Chem.*, **47**, 709 (1969).
10. (a) P. D. Bartlett and A. P. Schaap, *J. Am. Chem. Soc.*, **92**, 3223 (1970).
(b) S. Mazur and C. S. Foote, *J. Am. Chem. Soc.*, **92**, 3225 (1970).

11. (a) W. Adam and G. Cilento, *Angew. Chem., Int. Ed. Engl.*, **22**, 529 (1983).
(b) W. Adam, in *The Chemistry of Functional Groups. The Chemistry of Peroxides* (Ed. S. Patai), Chap. 24, Wiley, Chichester, 1983, pp. 830–920.
(c) W. Adam, W. J. Baader, C. Babatsikos and E. Schmidt, *Bull. Soc. Chim. Belges*, **93**, 605 (1994).
(d) W. Adam and F. Yany, in *Small Ring Heterocycles*, Part 3 (Ed. A. Hassner), Chap. 4, Wiley, New York, 1985, pp. 351–429.
(e) W. Adam and A. Beinhauer, in *CRC Handbook of Organic Photochemistry* (Ed. J. C. Scaiano), Vol. 2, CRC Press, Boca Raton, 1989, pp. 271–327.
(f) W. Adam, M. Heil, T. Mosandl and C. R. Saha-Möllner, in *Organic Peroxides* (Ed. W. Ando), Wiley, Chichester, 1992, pp. 221–254.
(g) C. R. Saha-Möllner and W. Adam, in *Comprehensive Heterocyclic Chemistry, Second Edition* (Eds. A. R. Katritzky, C. W. Rees and E. F. V. Scriven), Vol. 1B, Chap. 1.33, Pergamon Press, Oxford, 1996, pp. 1041–1082.
(h) T. Wilson, *Photochem. Photobiol.*, **62**, 601 (1995).
(i) G. L. Sharipov, V. P. Kazakov and G. A. Tolstikov, in *Chemistry and Chemiluminescence of 1,2-Dioxetanes* (Ed. R. F. Vasil'ev), Nauka, Moscow, 1990 (in Russian); *Chem. Abstr.*, **114**, 143390 (1991).
12. (a) W. S. Knowles, *Angew. Chem., Int. Ed.*, **41**, 1998 (2002).
(b) R. Noyori, *Angew. Chem., Int. Ed.*, **41**, 2008 (2002).
(c) K. B. Sharpless, *Angew. Chem., Int. Ed.*, **41**, 2024 (2002).
13. (a) W. Adam and B. Nestler, *J. Am. Chem. Soc.*, **114**, 6549 (1992).
(b) W. Adam and B. Nestler, *J. Am. Chem. Soc.*, **115**, 5041 (1993).
(c) W. Adam and M. Prein, *Angew. Chem., Int. Ed. Engl.*, **35**, 477 (1996).
14. (a) W. Adam and M. Prein, *J. Am. Chem. Soc.*, **115**, 3766 (1993).
(b) W. Adam, E.-M. Peters, K. Peters and M. Prein, *J. Am. Chem. Soc.*, **117**, 6686 (1995).
(c) W. Adam and M. Prein, *Acc. Chem. Res.*, **29**, 275 (1996).
15. W. Adam, C. R. Saha-Möllner and S. B. Schambony, *J. Am. Chem. Soc.*, **121**, 1834 (1999).
16. (a) W. Adam, L. A. Arias Encarnación and K. Zinner, *Chem. Ber.*, **116**, 839 (1983).
(b) M. Matsumoto, N. Watanabe, N. C. Kasuga, F. Hamada and K. Tadokoro, *Tetrahedron Lett.*, **38**, 2863 (1997).
17. (a) M. Stratakis, M. Orfanopoulos and C. S. Foote, *Tetrahedron Lett.*, **37**, 7159 (1996).
(b) Y. Yoshioka, S. Yamada, T. Kawakami, M. Nishino, K. Yamaguchi and I. Saito, *Bull. Chem. Soc. Jpn.*, **69**, 2683 (1996).
18. (a) P. D. Bartlett and A. A. Frimer, *Heterocycles*, **11**, 419 (1978).
(b) E. W. H. Asveld and R. M. Kellog, *J. Am. Chem. Soc.*, **102**, 3644 (1980).
19. (a) W. Adam, S. G. Bosio and N. J. Turro, *J. Am. Chem. Soc.*, **124**, 8814 (2002).
(b) W. Adam, S. G. Bosio and N. J. Turro, *J. Am. Chem. Soc.*, **124**, 14004 (2002).
(c) T. Poon, N. J. Turro, J. Lakshminarasimhan, X. Lei, W. Adam and S. G. Bosio, *Org. Lett.*, **5**, 2025 (2003).
(d) T. Poon, N. J. Turro, J. Chapman, J. Lakshminarasimhan, X. Lei, S. Jockusch, R. Franz, I. Washington, W. Adam and S. G. Bosio, *Org. Lett.*, **5**, 4951 (2003).
(e) W. Adam, S. G. Bosio, N. J. Turro and B. T. Wolff, *J. Org. Chem.*, **69**, 1704 (2004).
20. (a) F. D. Greene and W. W. Rees, *J. Am. Chem. Soc.*, **80**, 3432 (1958).
(b) W. Adam, A. Griesbeck and D. Kappes, *J. Org. Chem.*, **51**, 4479 (1986).
(c) W. Adam, S. Andler and M. Heil, *Angew. Chem., Int. Ed. Engl.*, **30**, 1365 (1991).
(d) W. Adam, L. Hadjiarapoglou, R. Curci and R. Mello, in *Organic Peroxides* (Ed. W. Ando), Wiley, Chichester, 1992, pp. 195–220.
21. P. D. Bartlett, A. L. Baumstark, M. E. Landis and C. L. Lerman, *J. Am. Chem. Soc.*, **96**, 5268 (1974).
22. K. R. Kopecky, J. E. Filby, C. Mumford, P. A. Lockwood and J.-Y. Ding, *Can. J. Chem.*, **53**, 1103 (1975).
23. W. Adam and L. Blancafort, *J. Am. Chem. Soc.*, **118**, 4778 (1996).
24. (a) M. Reguero, F. Bernardi, A. Bottoni, M. Olivucci and M. A. Robb, *J. Am. Chem. Soc.*, **113**, 1566 (1991).
(b) S. Wilsey, F. Bernardi, M. Olivucci, M. A. Robb, S. Murphy and W. Adam, *J. Phys. Chem. A*, **103**, 1669 (1999).

- (c) Y. Takano, T. Tsunesada, H. Isobe, Y. Yoshioka, K. Yamaguchi and I. Saito, *Bull. Chem. Soc. Jpn.*, **72**, 213 (1999).
- (d) C. Tanaka and J. Tanaka, *J. Phys. Chem. A*, **104**, 2078 (2000).
- (e) E. Rodriguez and M. Reguero, *J. Phys. Chem. A*, **106**, 504 (2002).
25. (a) T. Wilson and A. M. Halpern, *J. Phys. Org. Chem.*, **8**, 359 (1995).
- (b) R. F. Vasil'ev, *Dokl. Phys. Chem. (Engl. Transl.)*, **353**, 151 (1997).
- (c) R. F. Vasil'ev, *J. Biolumin. Chemilumin.*, **13**, 69 (1998).
- (d) R. F. Vasil'ev and A. V. Trofimov, in *Bioluminescence and Chemiluminescence: Perspectives for 21st Century* (Eds. A. Roda, M. Pazzagli, L. J. Kricka and P. E. Stanley), Wiley, Chichester, 1999, pp. 13–16.
- (e) R. F. Vasil'ev, *Kinet. Catal. (Engl. Transl.)*, **40**, 172 (1999).
- (f) W. Adam, A. V. Trofimov and R. F. Vasil'ev, in *Chemiluminescence at the Turn of the Millenium. An Indispensable Tool in Modern Chemistry, Biochemistry and Medicine* (Eds. S. Albrecht, T. Zimmermann and H. Brandl), Schweda-Werbedruck GmbH, Druckerei & Verlag, Dresden, 2001, pp. 11–14.
- (g) R. F. Vasil'ev, *High Energy Chem. (Engl. Transl.)*, **36**, 170 (2002).
26. T. Clark, in *Recent Experimental and Computational Advances in Molecular Spectroscopy* (Ed. R. Fausto), Kluwer Academic, Dordrecht, 1993, pp. 369–380.
27. W. Adam and W. J. Baader, *J. Am. Chem. Soc.*, **107**, 410 (1985).
28. G. B. Schuster, *Acc. Chem. Res.*, **12**, 366 (1979).
29. J.-Y. Koo, S. P. Schmidt and G. B. Schuster, *Proc. Natl. Acad. Sci. U.S.A.*, **75**, 30 (1978).
30. W. Adam, D. Reinhardt and C. R. Saha-Möller, *Analyst*, **121**, 1527 (1996).
31. G. B. Schuster, *J. Am. Chem. Soc.*, **101**, 5851 (1979).
32. S. P. Schmidt, M. A. Vicent, C. E. Dykstra and G. B. Schuster, *J. Am. Chem. Soc.*, **103**, 1292 (1981).
33. (a) A. P. Schaap, T.-S. Chen, R. S. Handley, R. DeSilva and B. P. Giri, *Tetrahedron Lett.*, **28**, 1155 (1987).
- (b) A. P. Schaap, R. S. Handley and B. P. Giri, *Tetrahedron Lett.*, **28**, 935 (1987).
- (c) I. Bronstein, B. Edwards, A. Sparks and J. C. Voyta, *J. Biolumin. Chemilumin.*, **2**, 186 (1988).
- (d) I. Bronstein, B. Edwards, A. Sparks and J. C. Voyta, *J. Biolumin. Chemilumin.*, **4**, 99 (1989).
- (e) B. Edwards, A. Sparks, J. C. Voyta and I. Bronstein, *J. Biolumin. Chemilumin.*, **5**, 1 (1990).
- (f) B. Edwards, A. Sparks, J. C. Voyta, R. Strong, O. Murphy and I. Bronstein, *J. Org. Chem.*, **55**, 6225 (1990).
34. (a) W. Adam, I. Bronstein and A. V. Trofimov, *J. Phys. Chem. A*, **102**, 5406 (1998).
- (b) W. Adam, M. Matsumoto and A. V. Trofimov, *J. Org. Chem.*, **65**, 2078 (2000).
35. (a) F. McCapra, *Tetrahedron Lett.*, **34**, 6941 (1993).
- (b) W. Adam and A. V. Trofimov, *J. Org. Chem.*, **65**, 6474 (2000).
36. W. Adam and A. V. Trofimov, in *Chemiluminescence at the Turn of the Millenium. An Indispensable Tool in Modern Chemistry, Biochemistry and Medicine* (Eds. S. Albrecht, T. Zimmermann and H. Brandl), Schweda-Werbedruck GmbH, Druckerei & Verlag, Dresden, 2001, pp. 7–10.
37. (a) W. Adam, I. Bronstein, A. V. Trofimov and R. F. Vasil'ev, *J. Am. Chem. Soc.*, **121**, 958 (1999).
- (b) A. I. Burstein, *Chem. Phys.*, **289**, 251 (2003).
38. E. A. Chandross, *Tetrahedron Lett.*, 761 (1963).
39. C. L. R. Catherall, T. F. Palmer and R. B. Cundall, *J. Biolumin. Chemilumin.*, **3**, 147 (1989).
40. (a) C. L. R. Catherall, T. F. Palmer and R. B. Cundall, *J. Chem. Soc., Faraday Trans. 2*, **80**, 823 (1984).
- (b) C. L. R. Catherall, T. F. Palmer and R. B. Cundall, *J. Chem. Soc., Faraday Trans. 2*, **80**, 837 (1984).
- (c) F. J. Alvarez, N. J. Parekh, B. Matuszewski, R. S. Givens, T. Higuchi and R. L. Schowen, *J. Am. Chem. Soc.*, **108**, 6435 (1986).
- (d) M. Orlovic, R. L. Schowen, R. S. Givens, F. Alvarez, B. Matuszewski and N. Parekh, *J. Org. Chem.*, **54**, 6435 (1989).
- (e) G. Orosz, *Tetrahedron*, **45**, 3493 (1989).
- (f) R. E. Milofsky and J. W. Birks, *J. Am. Chem. Soc.*, **113**, 9715 (1991).

41. (a) C. V. Stevani, D. F. Lima, V. G. Toscano and W. J. Baader, *J. Chem. Soc., Faraday Trans. 2*, 989 (1996).
(b) C. V. Stevani, I. P. de Arruda Campos and W. J. Baader, *J. Chem. Soc., Faraday Trans. 2*, 1645 (1996).
(c) C. V. Stevani and W. J. Baader, *J. Phys. Org. Chem.*, **10**, 593 (1997).
(d) C. V. Stevani, S. M. Silva and W. J. Baader, *Eur. J. Org. Chem.*, 4037 (2000).
42. N. J. Turro and P. Lechtken, *J. Am. Chem. Soc.*, **95**, 264 (1973).
43. A. I. Voloshin, G. L. Sharipov, V. P. Kazakov and G. A. Tolstikov, *Bull. Acad. Sci. USSR, Div. Chem. Sci. (Engl. Transl.)*, **40**, 1158 (1991).
44. (a) J. E. Martin, E. J. Hart, A. W. Adamson, H. Gafney and J. Halpern, *J. Am. Chem. Soc.*, **94**, 9238 (1972).
(b) C. D. Jonah, M. S. Matheson and D. Meisel, *J. Am. Chem. Soc.*, **100**, 1449 (1978).
45. (a) V. P. Kazakov, A. I. Voloshin and S. S. Ostakhov, *Opt. Spectrosc. (USSR)*, **83**, 860 (1997).
(b) V. P. Kazakov, A. I. Voloshin, S. S. Ostakhov, I. A. Khusainova and E. V. Zharinova, *Russ. Chem. Bull.*, **46**, 699 (1997).
(c) V. P. Kazakov, A. I. Voloshin and N. M. Shavaleev, *Mendeleev Commun.*, **8**, 110 (1998).
46. (a) P. Lechtken, A. Yekta and N. J. Turro, *J. Am. Chem. Soc.*, **95**, 3027 (1973).
(b) N. J. Turro, N. E. Schore, H.-C. Steinmetzer and A. Yekta, *J. Am. Chem. Soc.*, **96**, 3027 (1974).
(c) P. Lechtken, A. Yekta, N. E. Schore, H. C. Steinmetzer, W. H. Waddell and N. J. Turro, *Z. Phys. Chem.*, **101**, 79 (1976).
47. (a) P. E. Stanley, B. J. McCarthy and R. Smiter (Eds.), *ATP Luminescence. Rapid Methods in Microbiology*, Blackwell Scientific Publications, Oxford, 1989.
(b) N. Yu. Filippova, A. F. Dukhnovich and N. N. Ugarova, *J. Biolumin. Chemilum.*, **4**, 419 (1989).
(c) E. Schram, in *Bioluminescence and Chemiluminescence. Current Status* (Eds. P. E. Stanley and L. J. Kricka), Wiley, Chichester, 1990, pp. 407–412.
(d) A. Lundin, in *Bioluminescence and Chemiluminescence. Perspectives for the 21st Century* (Eds. A. Roda, M. Pazzagli, L. J. Kricka and P. E. Stanley), Wiley, Chichester, 1999, pp. 145–148.
(e) F. Brau, P. Helle and J. C. Bernengo, in *Bioluminescence and Chemiluminescence. Perspectives for the 21st Century* (Eds. A. Roda, M. Pazzagli, L. J. Kricka and P. E. Stanley), Wiley, Chichester, 1999, pp. 149–152.
48. I. Bronstein, J. J. Fortin, J. C. Voyta, R.-R. Juo, B. Edwards, C. E. M. Olesen, N. Lijam and L. J. Kricka, *BioTechniques*, **17**, 172 (1996).
49. (a) R. Geiger and W. Miska, *J. Clin. Chem. Clin. Biochem.*, **15**, 31 (1987).
(b) V. F. Ximenes, A. Campa, W. J. Baader and L. H. Catalani, *Anal. Chim. Acta*, **402**, 99 (1999).
50. W. Adam, I. Bronstein, B. Edwards, T. Engel, D. Reinhardt, F. W. Schneider, A. V. Trofimov and R. F. Vasil'ev, *J. Am. Chem. Soc.*, **118**, 10400 (1996).
51. N. N. Ugarova and L. Yu. Brovko, *Russ. Chem. Bull.*, **50**, 1752 (2001).
52. C. K. Mathews and K. E. van Holde, *Biochemistry*, The Benjamin Cummings, Redwood City, 1990.
53. (a) C. E. M. Olesen, C. S. Martin, J. C. Voyta, B. Edwards and I. Bronstein, *J. Clin. Ligand Assay*, **22**, 129 (1999).
(b) C. E. M. Olesen, L. J. Kricka, B. Edwards, R.-R. Juo, J. C. Voyta and I. Bronstein, *IVD Technology*, 45 (2001).
54. C. S. Martin, P. A. Wight, A. Dobretsova and I. Bronstein, *BioTechniques*, **21**, 520 (1996).
55. M. Matsumoto, T. Hiroshima, S. Chiba, N. Watanabe and H. Kobayashi, *Luminescence*, **14**, 345 (1999).
56. (a) A. P. Schaap, H. Akhavan and L. J. Romano, *Clin. Chem.*, **35**, 1863 (1989).
(b) A. Mayer and S. Neuenhofer, *Angew. Chem., Int. Ed. Engl.*, **33**, 8535 (1994).
57. M. Matsumoto, T. Sakuma and N. Watanabe, *Tetrahedron Lett.*, **43**, 8955 (2002).
58. (a) G. Cilento and W. Adam, *Photochem. Photobiol.*, **48**, 361 (1988).
(b) D. T. Gibson, G. E. Cardini, F. C. Maseles, R. E. Kallio and E. Reino, *Biochemistry*, **9**, 1631 (1970).
(c) D. R. Boyd, N. D. Sharma, R. Boyle, R. A. S. McMordie, J. Chima and H. Dalton, *Tetrahedron Lett.*, **33**, 1241 (1992).

59. (a) H. Sies, *Angew. Chem., Int. Ed. Engl.*, **25**, 1058 (1986).
(b) K. C. Smith, *Mutat. Res.*, **277**, 139 (1992).
60. (a) W. Adam, A. Beinhauer, T. Mosandl, C. R. Saha-Möller, F. Vargas, B. Epe, E. Müller, D. Schiffmann and D. Wild, *Environ. Health Perspect.*, **88**, 89 (1990).
(b) W. Adam, M. Ahrweiler, C. R. Saha-Möller, M. Sauter, A. Schönberger, B. Epe, E. Müller, D. Schiffmann, H. Stopper and D. Wild, *Toxicol. Lett.*, **67**, 41 (1993).
61. (a) S. Steenken, *Chem. Rev.*, **89**, 503 (1989).
(b) L. P. Candeias and S. Steenken, *J. Am. Chem. Soc.*, **111**, 1094 (1989).
62. (a) H. Kasai, S. Nishimura, in *Oxidative Stress, Oxidants and Antioxidants* (Ed. H. Sies), Academic Press, New York, 1991, pp. 99–116.
(b) B. N. Ames, *Science*, **221**, 1256 (1983).
(c) R. A. Floyd, *Carcinogenesis*, **11**, 1447 (1990).
(d) S. Shibutani, M. Takeshita and A. P. Grollman, *Nature*, **349**, 431 (1991).
63. (a) J. Cadet, M. Berger, G. W. Buchko, P. C. Joshi, S. Raoul and J.-L. Ravanat, *J. Am. Chem. Soc.*, **116**, 7403 (1994).
(b) S. Raoul, M. Berger, G. W. Buchko, P. C. Joshi, B. Morin and J. Cadet, *J. Chem. Soc., Perkin Trans. 2*, 371 (1996).
(c) H. Kasai, Z. Yamaizumi, M. Berger and J. Cadet, *J. Am. Chem. Soc.*, **114**, 9692 (1992).
64. (a) W. Adam and A. Treiber, *J. Am. Chem. Soc.*, **117**, 2686 (1995).
(b) W. Adam, C. R. Saha-Möller, A. Schönberger, M. Berger and J. Cadet, *Photochem. Photobiol.*, **62**, 231 (1995).
(c) W. Adam, C. R. Saha-Möller and A. Schönberger, *J. Am. Chem. Soc.*, **118**, 9233 (1996).
(d) W. Adam, C. R. Saha-Möller and A. Schönberger, *J. Am. Chem. Soc.*, **119**, 719 (1997).
65. (a) W. Adam, S. Andler, W. M. Nau and C. R. Saha-Möller, *J. Am. Chem. Soc.*, **120**, 3549 (1998).
(b) W. Adam, M. A. Arnold and C. R. Saha-Möller, *J. Org. Chem.*, **66**, 597 (2001).
66. C. Sheu and C. S. Foote, *J. Am. Chem. Soc.*, **117**, 474 (1995).
67. (a) S. D. Wetmore and R. J. Boyd, *J. Phys. Chem. B*, **102**, 9332 (1998).
(b) J. Cadet, T. Delatour, T. Douki, D. Gasparutto, J.-P. Pouget, J.-L. Ravanat and S. Sauvaigo, *Mutat. Res.*, **424**, 9 (1999).
68. J. C. Niles, J. S. Wishnok and S. R. Tannenbaum, *Org. Lett.*, **3**, 963 (2001).
69. (a) W. Luo, J. G. Muller, E. M. Rachlin and C. J. Burrows, *Org. Lett.*, **2**, 613 (2000).
(b) W. Luo, J. G. Muller and C. J. Burrows, *Org. Lett.*, **3**, 2801 (2001).
(c) W. Luo, J. G. Muller, E. M. Rachlin and C. J. Burrows, *Chem. Res. Toxicol.*, **14**, 927 (2001).
70. S. Berger, *Angew. Chem., Int. Ed. Engl.*, **27**, 1196 (1988).
71. W. Adam, M. A. Arnold, M. Grüne, W. M. Nau, U. Pischel and C. R. Saha-Möller, *Org. Lett.*, **4**, 537 (2002).
72. (a) W. U. Palm and H. Dreeskamp, *J. Photochem. Photobiol. A*, **52**, 439 (1990).
(b) S. Grimme, *Chem. Phys.*, **163**, 313 (1992).

CHAPTER 16

Chemiluminescence of organic peroxides*

WILHELM J. BAADER, C. V. STEVANI and ERICK L. BASTOS

*Instituto de Química, Universidade de São Paulo-Av. Prof. Lineu Prestes, 748 Bl.,
12S CEP 05508-900, São Paulo – SP, Brazil*
Fax: +55 113 815 5579; e-mail: wjbaader@iq.usp.br

I. HISTORICAL INTRODUCTION	1212
II. BASIC PRINCIPLES OF CHEMILUMINESCENCE	1215
III. CLASSIFICATION OF CHEMILUMINESCENT REACTIONS	1218
IV. METHODS IN CHEMILUMINESCENCE RESEARCH	1221
A. Rate Constants and Activation Parameters	1221
B. Quantum Yields	1222
C. Calibration of Light Emission Intensities	1224
V. GENERAL MECHANISMS IN ORGANIC CHEMILUMINESCENCE	1227
A. Unimolecular Peroxide Decomposition	1227
B. Catalyzed Peroxide Decomposition	1231
1. Intermolecular electron transfer initiated peroxide decomposition	1231
2. Intramolecular electron transfer initiated peroxide decomposition	1236
VI. HIGH-EFFICIENCY ORGANIC CHEMILUMINESCENT REACTIONS INVOLVING PEROXIDE INTERMEDIATES	1238
A. Chemiluminescence in Luminol Oxidation	1239
1. General reaction mechanism	1239
2. Chemiexcitation mechanism	1244
B. Chemiluminescence from Lucigenin and Related Compounds	1248
1. Lucigenin	1248
2. Acridinium salts and acridans	1251
C. Peroxyoxalate Chemiluminescence	1256

*The authors dedicate this chapter to the late Prof. Dr. Giuseppe Cilento (Universidade de São Paulo), whose untimely demise ten years ago saddened everyone who knew him as an excellent scientist and outstanding human being. This chapter is also dedicated to Prof. Waldemar Adam (Universität Würzburg, now 'retired' in Puerto Rico), who was directly or indirectly responsible for the research interests of the authors.

The chemistry of peroxides, volume 2

Edited by Z. Rappoport © 2006 John Wiley & Sons, Ltd ISBN: 0-470-86274-2

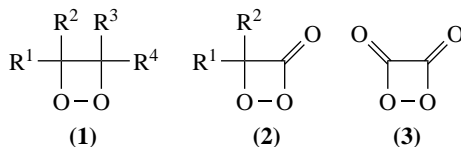
1. Mechanistic studies on the steps prior to chemiexcitation	1258
2. Nature of the high-energy intermediate	1261
3. Mechanistic studies on the chemiexcitation step	1266
VII. ACKNOWLEDGMENTS	1270
VIII. REFERENCES	1270

I. HISTORICAL INTRODUCTION

Bioluminescence (BL), the emission of visible light by living organisms, and chemiluminescence (CL), light emission caused by a chemical reaction, are long-known phenomena that have attracted the interest of researchers of different areas for many decades. Although bioluminescence was already described by Aristotle (384 – 322 BC)¹, the first clear-cut definition of chemiluminescence was given by Wiedemann in 1888², ‘Das bei chemischen Prozessen auftretende Leuchten würde Chemilumineszenz genannt’, which translates into: ‘The emission observed during chemical processes should be called chemiluminescence’. This definition was based on the experimental observation made by Radziszewski in 1887, who found that lophine (2,4,6-triphenylimidazole) does not emit light when heated in the absence of oxygen, but produces intense light emission upon its autoxidation³. Albrecht described the first well-defined CL system in 1928, the transition metal catalyzed oxidation of luminol (5-amino-2,3-dihydrophthalazin-1,4-dione) by hydrogen peroxide⁴. A few years later, the CL reaction of lucigenin (*N,N'*-dimethyl-9,9'-biacridine) was reported by Gleu and Petsch⁵. Another organic CL system which proved to be of outstanding importance, peroxyoxalate CL, was discovered by Chandross, who observed visible light emission upon mixing oxalyl chloride and hydrogen peroxide in the presence of the polycondensed aromatic hydrocarbon rubrene⁶. Subsequent studies by Rauhut⁷ on this system have led to the elucidation of several mechanistic aspects of these transformations, contributing, moreover, to establish general concepts of organic CL but also, and perhaps more importantly, to a wide variety of practical and analytical applications⁸.

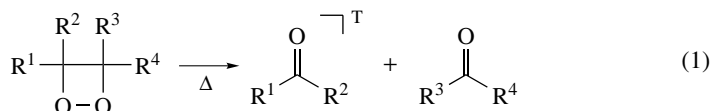
A common feature of the above-mentioned ‘classical’ CL systems is that they all involve a complex reaction sequence which ultimately leads to the formation of an electronically excited product and subsequent CL emission. The reaction sequence can be divided operationally into three parts: (i) ‘chemical’ transformations, occurring only on the ground-state energy surface and leading to the formation of one or several high-energy intermediates (HEI), which are peroxides, in every case of highly efficient CL reaction; (ii) the ‘excitation step’, in which the HEI is transformed into the excited-state product by unimolecular reaction or interaction with another reactant; and (iii) the emission of CL, which may be fluorescence or phosphorescence, depending upon the multiplicity of the excited state formed. The first part, ground-state chemical transformation, is the rate-limiting step, and therefore any kinetic investigations into these complex CL reactions will provide insights only on this part and not on the excitation step, in which the chemical energy is transformed into electronic excitation. It is this step which is of interest in mechanistic investigations on CL.

A qualitative leap in mechanistic CL research was achieved in the late sixties and early seventies of last century with the synthesis of the first 1,2-dioxetanes (**1**)⁹ and 1,2-dioxetanones (**2**)¹⁰. These four-membered ring peroxides constitute isolable HEI and kinetic studies on these compounds provided direct evidence of the mechanism of the excitation step, since there are no former slow ‘chemical’ transformations involved in their CL reactions. Since then, several hundred 1,2-dioxetanes, including the unsubstituted derivative¹¹, have been synthesized and studied, as well as more than a dozen 1,2-dioxetanones^{12–16}. The third class of four-membered cyclic peroxides comprises only one compound, 1,2-dioxetanedione (**3**), the cyclic peroxidic dimer of carbon dioxide. This

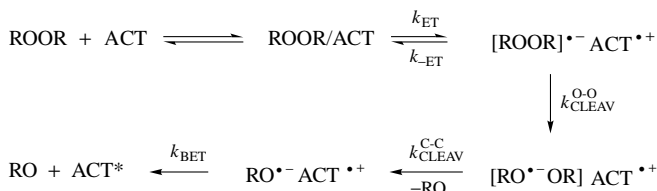


compound has been proposed as the HEI occurring in peroxyoxalate CL in the early work of Rauhut⁷; however, its existence is still a matter of discussion^{17,18}.

On the basis of mechanistic studies, mainly on these isolable cyclic four-membered peroxides (1 and 2), two main efficient chemiexcitation mechanisms can be defined in organic peroxide decomposition: (i) the unimolecular decomposition or rearrangement of high-energy compounds leading to the formation of excited-state products, exemplified here in the case of the thermal decomposition of 1,2-dioxetane (equation 1)^{11,15,19}; and (ii) the decomposition of a peroxide, catalyzed by the interaction with a second compound, which is ultimately formed in its electronically excited state.



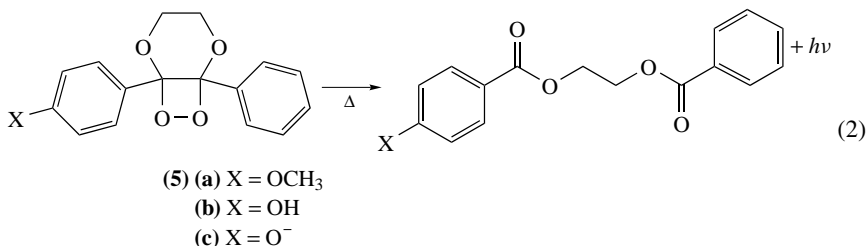
This second chemiexcitation mechanism was formulated by Schuster as the Chemically Initiated Electron Exchange Luminescence (CIEEL) mechanism and involves an initial electron-transfer (k_{ET}) from the catalyst, known as activator (ACT), to the peroxide and chemiexcitation is achieved by a back-electron transfer (k_{BET}), after peroxide oxygen-oxygen and carbon-carbon bond cleavage ($k_{\text{CLEAV}}^{\text{O-O}}$ and $k_{\text{CLEAV}}^{\text{C-C}}$, respectively, Scheme 1)²⁰.



SCHEME 1

This mechanism has been formulated in analogy to the known electrochemiluminescence, in which radical-ion annihilation generated at opposite electrodes leads to the formation of the electronically excited state (Scheme 2)²¹. The difference between the CIEEL mechanism and electrochemiluminescence is that, in the former, the radical ions—whose annihilation is responsible for the formation of the excited state—are formed ‘chemically’ by electron transfer to high-energy peroxides and subsequent bond cleavage or rearrangements.

The CIEEL mechanism has been utilized to explain the catalyzed decomposition of several cyclic and linear peroxides, including diphenoyl peroxide (4), peroxyesters and 1,2-dioxetanones²². Special interest has focused on this mechanism when it was utilized to explain the efficient excited state formation in the chemiexcitation step of the firefly’s luciferin/luciferase bioluminescence²³. However, doubts have been voiced more recently about the validity of this mechanistic scheme, due to divergences about the

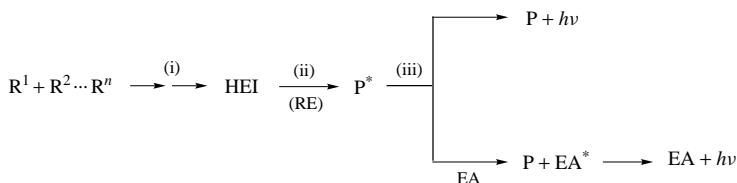


In subsequent studies, the same research group developed stable dioxetane derivatives containing trialkylsilyloxyaryl groups, which, upon fluoride-induced deprotection, become unstable and yield singlet excited decomposition products in high yields³²⁻³⁴. These phenolate-initiated intramolecular CIEEL processes, using mainly phosphate ester protecting groups, provide the basis for numerous commercial applications, most prominently in chemiluminescence immunoassays³⁵⁻³⁹.

II. BASIC PRINCIPLES OF CHEMILUMINESCENCE

Chemiluminescence is the phenomenon of visible light emission promoted by a chemical transformation. However, why should any highly exothermal chemical reaction generate electronically excited state products, necessary for the observed emission, when the same species can be formed in its electronic ground state in an energetically much more favorable pathway? This apparently simple question has not yet been answered in a general way, although much effort has been dedicated to it. Over the last four decades, highly detailed studies have focused on several CL systems and the mechanistic question of the formation of excited states by chemical reactions has been addressed by various research groups. In this part of the chapter, we will give a brief introduction to the basic principles that govern the efficiency of excited-state formation by chemical reactions.

Chemical transformations that are accompanied by light emission can be divided generally into three main reaction steps: (i) a ground-state chemical reaction of one or more reagents (R^n), in one or more reaction steps, which leads to the formation of an intermediate possessing a high amount of energy (high-energy intermediate—HEI); (ii) a reaction of this HEI, in an unimolecular fashion, or by interaction with another reagent (RE), in a single elementary step yielding one of the products in an electronically excited state (P^*), and; (iii) light emission from the excited product yielding the ground-state product (P), or energy transfer from P^* to an appropriate energy acceptor (EA) yielding P and the excited EA (EA^*), which is now responsible for the CL emission (Scheme 3).



SCHEME 3

The basic requirements for the formation of excited states by chemical reactions have been widely discussed in several review articles dating mainly from the late 1970s and early 1980s, and more recent research has not made further fundamental contributions to

these principles. Therefore, we will summarize these principles only briefly here and refer to the corresponding earlier reviews^{12-16, 40, 41}.

Possibly the most obvious requirement for CL is that one of the products possess an energetically accessible excited state that can receive the chemical excitation energy. For CL reactions of organic molecules in solution, two classes of product molecules appear to be adequate: carbonyl compounds and aromatic hydrocarbons⁴¹. The first class of compounds is the one involved in most of the efficient CL reactions of organic peroxides known so far. Once formed, the electronically excited state must be capable of emitting excitation energy in the form of light so that proper CL can be observed. This criterion is not well-fulfilled for the singlet state of simple carbonyl compounds and certainly not for triplet states of carbonyl compounds in oxygenated solutions. In these cases, the addition of an appropriate energy acceptor, which is excited by energy transfer from the originally formed excited-state product, can lead to efficient CL emission⁴⁰.

Undoubtedly the most important requirement for efficient chemiexcitation is the 'energy sufficiency criterion', which means that the chemical reaction must be able to liberate sufficient energy to populate the excited state of the product. This places the exothermicity required for a CL reaction in the range of 50 to 100 kcal mol⁻¹, the excitation energies of common organic chromophores. Furthermore, and equally important, this energy must be released in a single step, since the electronic excitation step must be instantaneous. However, although the main contribution for excitation is the reaction enthalpy, the activation enthalpy may also contribute to the feasibility of CL reactions in cases in which the energy of the observed photon is greater than the reaction enthalpy (equation 3, Figure 1)⁴¹.

$$E^* \leq -\Delta H_0 + \Delta H^{\ddagger*} \quad (3)$$

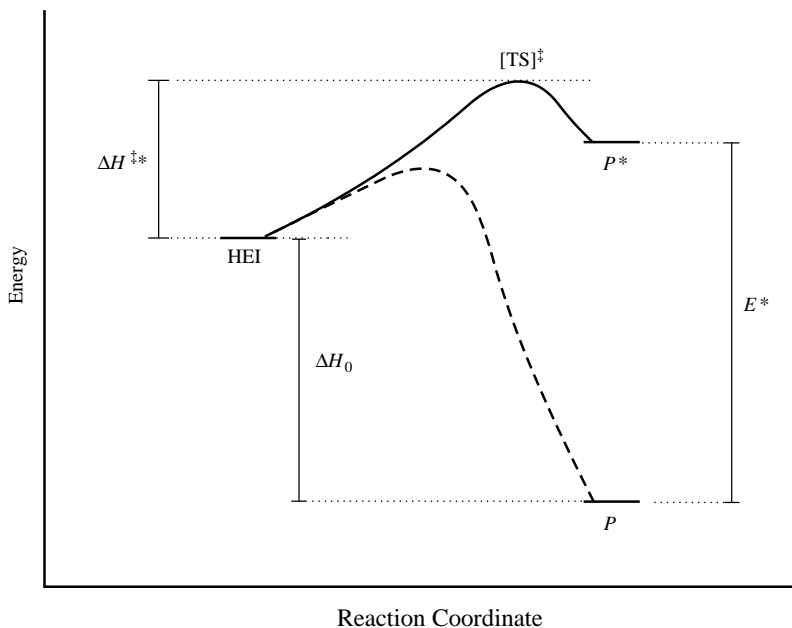


FIGURE 1. Potential energy diagram for excited- and ground-state formation in a highly exothermic reaction, illustrating the 'energy sufficiency requirement' (equation 3). (—) excited-state formation; (---) ground-state formation

Considering only the energetic aspects, a given transformation can be expected to lead to the formation of electronically excited states when the activation enthalpy (ΔH^\ddagger) of the excitation step, added to the negative reaction enthalpy (ΔH_0), leads to an energy difference higher than or equal to the excitation energy (E^*) of the lowest accessible electronically excited state of one of the reaction products (equation 3, Figure 1). However, even if the 'energy sufficiency requirement' is fulfilled for a given transformation, that does not necessarily mean it will lead to the formation of the excited state, since there is always an energetically more favorable pathway for the formation of ground-state products (Figure 1, dashed line).

Although the energy requirement is absolutely essential for the CL reaction to occur, it is certainly not sufficient and there are other factors that determine whether CL can occur in a given chemical reaction and whether this CL emission will be of high efficiency. These 'other' factors can generally be called 'geometric requirements' for efficient excited-state formation and they relate to the well known Franck–Condon Principle⁴². This photo-physical principle is based on the fact that electronic transitions occur on a much shorter time scale (10^{-16} to 10^{-14} s) than nuclear motions (10^{-13} to 10^{-12} s) and states 'for the classical electronic transition of a vibrating molecule. Since electronic motions are much faster than nuclear motion, electronic transitions occur most favorably when the nuclear structure of the initial and final states are most similar'⁴². Therefore, conversion between electronic states occurs without a change in the geometry of the species involved. In other words, the nuclear positions and, hence, the geometry of a molecule can change only on a much longer time scale than the time scale required for electronic state transition and for electron-transfer reactions. This principle can be applied qualitatively to rationalize the probability of a reaction being chemiluminescent and the efficiency of that chemiluminescence. A chemical transformation, in which the transition state of the excitation step has a geometry similar to that of the excited-state product, can be expected to lead to the formation of this excited-state. Furthermore, the efficiency of the excited-state formation will be greater if the geometry of the ground-state product is considerably different from that of the transition state and also from the excited-state product, reducing the probability of ground-state product formation.

An alternative model which can be applied to understand the occurrence of excited-state formation in a chemical reaction is based on the Marcus Theory^{43–45} of electron-transfer reactions. However, this model can also be used qualitatively for other types of CL reactions, as discussed by Hercules⁴⁶. The theory considers the relative probabilities for ground-state and excited-state product formation in an electron-transfer reaction in relation to the accessibility of crossing points on the potential energy surface, and correlates the activation enthalpy to the reaction enthalpy. For an endothermic reaction to a certain electronic state, the activation barrier will initially decrease as ΔH_0 becomes less positive and subsequently increasingly negative. However, and this is the important point, for highly negative ΔH_0 values, the activation barrier can actually increase as ΔH_0 continues to become more negative⁴⁶. This increase in the activation energy with increasing exothermicity may cause the velocity of the *less exothermic* transformation to an *excited-state product* to *exceed* that of the *more exothermic* transformation to *ground-state products*. This situation can be illustrated by a simplified and qualitative reaction coordinate diagram of the reaction of reagents *A* and *B* to products *C* and *D*, in a nonchemiluminescent reaction, or to products *C*^{*} and *D* in the chemiluminescent transformation (Figure 2)⁴⁶.

In the nonchemiluminescent reaction (I), the activation energy for ground-state product formation (ΔH^\ddagger) is *lower* than the energy barrier for excited product formation ($\Delta H^{\ddagger*}$); hence, the ground-state reaction is kinetically favorable. In contrast, in the chemiluminescent reaction (II), the activation energy for ground-state product formation (ΔH^\ddagger) is *higher* than the energy barrier for excited product formation ($\Delta H^{\ddagger*}$); thus, the excited-state reaction should occur at a higher rate constant, leading to efficient excited-state

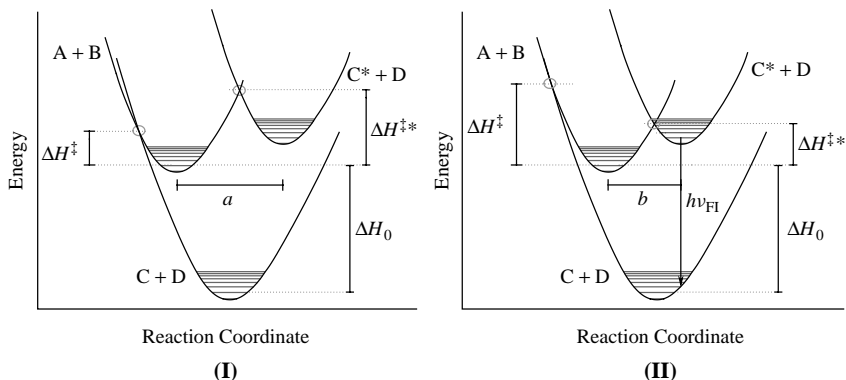


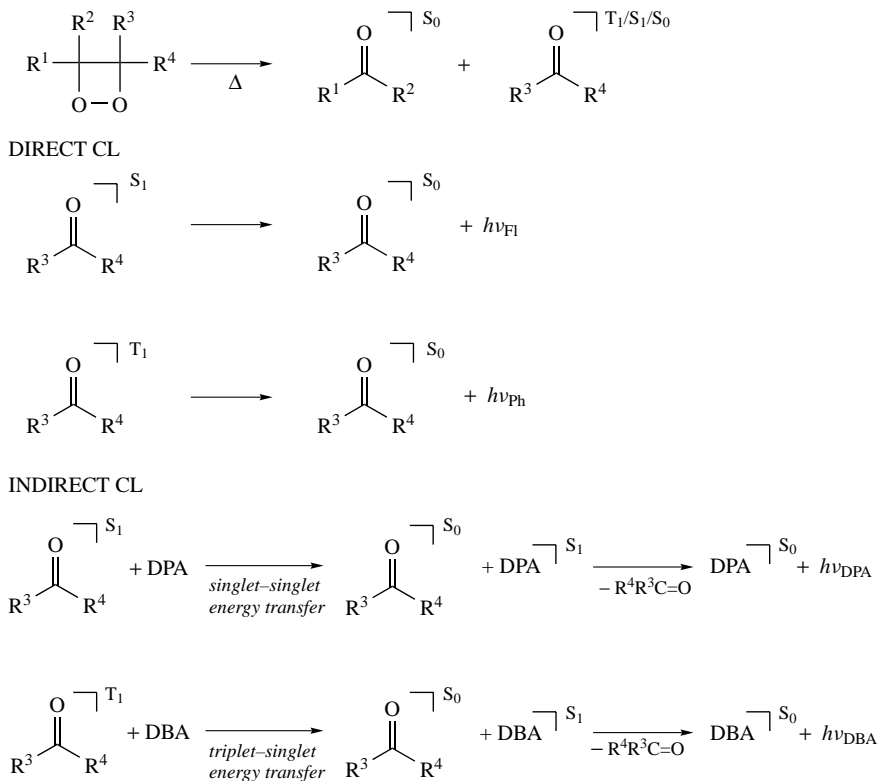
FIGURE 2. Reaction coordinate diagram for a nonchemiluminescent (I) and a chemiluminescent (II) transformation of the reactants ($A + B$) to products in the ground ($C + D$) or the excited state ($C^* + D$). The distances of the equilibrium geometries for $A + B$ and $C^* + D$ in I and II are indicated by a and b , respectively

formation and subsequent CL emission. Note that, for both examples I and II, we have chosen a reaction in which the 'energy sufficiency requirement' is only fulfilled when the activation enthalpy is also considered available to provide the necessary excitation energy. The ultimate difference between the two situations illustrated in Figure 2 is the relative position of the potential curves for $A + B$ and $C^* + D$ on the reaction coordinate. In the chemiluminescent transformation, both potential curves are close together on the reaction coordinate, whereas in the nonchemiluminescent reaction they are more distant (Figure 2, $a > b$). Therefore, the probability of excited-state formation is associated with the geometrical similarity between the reactant ($A + B$) and the excited-state products ($C^* + D$) and the application of the Marcus Theory allows one to combine the consideration regarding energy with the 'other' factors that influence the excitation efficiency, loosely termed geometric requirements. A highly exothermic transformation to ground-state products can become slower than the transformation to the corresponding excited-state product, especially when the excited-state product is structurally similar to the reactants. Additionally, the efficiency of excited-state formation should increase if the ground-state products are structurally unlike the reactants.

III. CLASSIFICATION OF CHEMILUMINESCENT REACTIONS

In this part of the chapter, we will briefly outline the main types of CL reactions which can be functionally classified by the nature of the excitation process that leads to the formation of the electronically excited state of the light-emitting species. *Direct chemiluminescence* is the term employed for a reaction in which the excited product is formed directly from the unimolecular reaction of a high-energy intermediate that has been formed in prior reaction steps. The simplest example of this type of CL is the unimolecular decomposition of 1,2-dioxetanes, which are isolated HEI. Thermal decomposition of 1,2-dioxetanes leads mainly to the formation of triplet-excited carbonyl compounds. Although singlet-excited carbonyl compounds are produced in much lower yields, their fluorescence emission constitutes the direct chemiluminescence emission observed in these transformations under normal conditions in aerated solutions^{1, 13, 14, 16, 26, 40, 41}.

Phosphorescence emission from triplet states of carbonyl compounds formed through dioxetane decomposition can only be observed under specific conditions in the absence



SCHEME 4

of oxygen (Scheme 4)^{40,42,47}. Other examples of direct chemiluminescence are the well-known reactions of luminol and lucigenin with hydrogen peroxide (see Section VI)¹.

In the presence of appropriate energy acceptors with high fluorescence quantum yields, the direct CL emission in thermal dioxetane decomposition can be considerably enhanced and the emission now observed corresponds to the fluorescence of the added energy acceptor. This type of CL is called *indirect* or *enhanced chemiluminescence*¹. 9,10-Diphenylanthracene (DPA) is the most commonly used energy acceptor. This highly fluorescent compound can be excited by energy transfer from singlet excited carbonyl compounds and an enhancement of the emission intensity is observed upon addition of DPA in dioxetane decomposition (Scheme 4). However, the addition of another anthracene derivative, 9,10-dibromoanthracene (DBA), exerts a much more pronounced effect on the emission intensity observed in dioxetane decomposition. This greater enhancement effect of DBA on the emission intensity can be explained by the occurrence of a formal triplet-to-singlet energy transfer from the triplet carbonyl compound (formed in higher yields during dioxetane decomposition) to DBA, facilitated by the heavy-atom effect of the bromine substituents⁴⁰, and DBA is formed in its first singlet-excited state (Scheme 4). The more pronounced emission intensity enhancement during the decomposition of 1,2-dioxetane upon addition of the triplet energy acceptor DBA, when compared with the singlet energy acceptor DPA, is a nice practical way of illustrating the much higher yields

in the peroxyoxalate reaction and, for comparison, in tetramethyl-1,2-dioxetane (TMD) decomposition. In the dioxetane system, energy acceptors with singlet energies lower than $E_s = 84 \text{ kcal mol}^{-1}$ (E_s of acetone) show essentially constant CL emission intensities, corrected by the fluorescence quantum yields. A sharp decrease in the corrected CL intensity is observed when energy acceptors with higher singlet energies are utilized. This behavior is typical of the occurrence of an energy transfer process from singlet-excited acetone to the energy acceptor. In contrast, in the peroxyoxalate system, a continuous decrease of the corrected CL intensities with increasing singlet energies of the acceptors is observed, excluding the occurrence of an electronic energy transfer to the acceptor⁴⁸.

To summarize this section, the difference between indirect and activated CL should be pointed out again. In *indirect* or *energy transfer CL*, the ultimate emitting species is excited by an electronic energy transfer from an excited product formed during the reaction, and the energy acceptor does not participate in the excitation step. In contrast, in the activated CL, the activator is not excited by electronic energy transfer but participates in the excitation step, being formed in its electronically excited state by a chemical interaction with the high-energy intermediate produced in prior reaction steps. Although the definition is simple and clear-cut, experimental differentiation between the two cases is not an easy task in some complex reaction systems and mechanistic conclusions may sometimes be inaccurate if this differentiation is not performed correctly.

IV. METHODS IN CHEMILUMINESCENCE RESEARCH

The physicochemical parameters commonly determined in mechanistic CL research are the *rate constants*, the *activation parameters* and the *CL emission quantum yields* (Φ_{CL}), as well as the *electronic excitation yields* (Φ_*), which can be *singlet* (Φ_s) or *triplet* *quantum yields* (Φ_T)^{12,40}.

A. Rate Constants and Activation Parameters

For isolated HEI such as dioxetanes and other cyclic and linear peroxides that act directly as reagents in the excitation step, kinetic studies lead to *rate constants* and *activation parameters* for this excitation step and conclusions with respect to the mechanism of chemiexcitation can be obtained from the structural and conditional dependence of these parameters. For complex CL systems, in which the HEI is formed in rate-limiting steps prior to the excitation step, the kinetic parameters of this essential reaction step can only be obtained indirectly (see below).

The kinetics of CL reactions can most conveniently be followed by measuring the time course of the emission intensity. The emission intensity at any time of the reaction corresponds to the velocity of excited-state formation and therefore to the velocity of the excitation step (electronic transitions and energy transfer processes should certainly be faster than the excitation step⁴²). Therefore, the emission intensity (I_{em}) is determined by the rate constant of the excitation step (k_{ex}), the concentration of the HEI and, in the case of activated CL, the concentration of the ACT, as well as the Φ_* and the emission quantum yield of the emitting species (Φ_*^{em}) (equation 4).

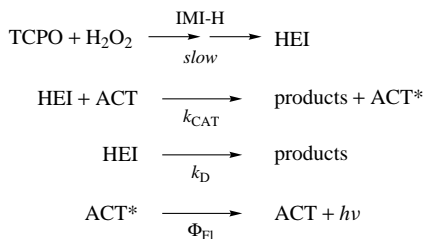
$$I_{\text{em}} = k_{\text{ex}}[\text{HEI}][\text{ACT}]\Phi_*\Phi_*^{\text{em}} \quad (4)$$

The time course of the emission intensity is proportional to the concentration of the HEI and, in the case of isolated HEIs, the rate constant for its decomposition is obtained from the CL emission curves. Isothermal kinetic measurements give rise to the activation parameters for the whole transformation and can be used for mechanistic discussion in the case of isolated HEI^{40,49}. Specific CL methods have also been used to determine

activation parameters, for which the emission intensities rather than rate constants are used. The temperature dependence of the emission intensities, measured by isothermal kinetics^{50,51}, temperature jump techniques^{40,49,52}, as well as by a continuous temperature change method⁵³, leads to the chemiluminescence activation parameter, which corresponds only to the 'light-generation pathway', eliminating possible 'dark catalytic reaction pathways'^{40,49}.

An indirect method has been used to determine relative rate constants for the excitation step in peroxyoxalate CL from the imidazole (IM-H)-catalyzed reaction of bis(2,4,6-trichlorophenyl) oxalate (TCPO) with hydrogen peroxide in the presence of various ACTs¹⁸. In this case, the HEI is formed in slow reaction steps and its interaction with the ACT is not observed kinetically. However, application of the steady-state approximation to the reduced kinetic scheme for this transformation (Scheme 6) leads to a linear relationship of $1/\Phi_S$ vs. $1/[ACT]$ (equation 5) and to the ratio of the chemiluminescence parameters k_{CAT}/k_D , which is a direct measure of the rate constant of the excitation step. Therefore, this method allows for the determination of relative rate constants for the excitation step in a complex reaction system, where this step cannot be observed directly by kinetic measurements¹⁸. The singlet quantum yield at infinite activator concentrations (Φ_S^∞), where all high-energy intermediates formed interact with the activator, is also obtained from this relationship (equation 5).

$$\frac{1}{\Phi_S} = \frac{1}{\Phi_S^\infty} + \frac{k_D}{k_{CAT} \Phi_S^\infty} \frac{1}{[ACT]} \quad (5)$$



SCHEME 6

B. Quantum Yields

The methods for determining quantum yields in CL reactions, particularly the unimolecular decomposition of 1,2-dioxetanes^{1,13-16,40,54,55}, have been extensively reviewed by various authors. Therefore, we will give only a brief outline of the basic methodological principles here. The simplest and most direct quantum yield characterizing a CL reaction is the *CL emission quantum yield* (Φ_{CL}), which is simply the yield of photons obtained in relation to the number of molecules of the limiting reagent, normally expressed in Einstein per mol (E mol^{-1}). The quantity of emitted photons is determined by the area under the emission curve; however, calibration of the detection instrument is necessary (see below). In direct CL reactions, in which the emitting species is the initially formed excited product, the Φ_{CL} is composed of the *electronic excitation quantum yields* (Φ_*), and the emission quantum yield of the excited species (Φ_*^{em}). If the nature of the emitting species and its Φ_*^{em} are known, the excitation quantum yields can be obtained from the CL quantum yields determined (equation 6).

$$\Phi_{CL} = \Phi_* \Phi_*^{\text{em}} \quad (6)$$

However, in many complex CL reactions, the emitting species is unknown, in which case the excitation quantum yields must be determined by indirect methods, utilizing energy transfer to appropriate acceptors. The excited energy acceptor may lead to light emission which is quantified (*photophysical method*) or give rise to a chemical reaction (*photochemical method*). The *photophysical* method has been widely utilized to determine excitation quantum yields in 1,2-dioxetane decomposition, using DPA for singlet quantum yield determination and DBA for triplet quantum yield determination^{13-16,40,50,51,54,55}. The energy transfer CL quantum yield ($\Phi_{\text{CL}}^{\text{ET}}$) is determined, in this case, by Φ_* , the emission quantum yield of the energy acceptor (Φ_*^{EA}) and by the energy transfer quantum yield (Φ^{ET}), and Φ_* can be calculated from the measured $\Phi_{\text{CL}}^{\text{ET}}$, provided the other two yields are known (equation 7).

$$\Phi_{\text{CL}}^{\text{ET}} = \Phi_* \Phi_*^{\text{EA}} \Phi^{\text{ET}} \quad (7)$$

Because the energy transfer efficiency at a certain energy acceptor concentration cannot be determined easily, $\Phi_{\text{CL}}^{\text{ET}}$ is determined experimentally at different energy acceptor concentrations and the intercept of the linear correlation between the reciprocal energy acceptor concentration ($1/[\text{EA}]$) and the reciprocal quantum yields ($1/\Phi_{\text{CL}}^{\text{ET}}$) corresponds to $\Phi_{\text{CL}}^{\text{ET}}$ at infinite energy acceptor concentrations. Under these conditions, the energy transfer efficiency $\Phi^{\text{ET}} = 1.0$ and each excited product formed is intercepted by the energy acceptor. The excitation quantum yield (Φ_*) can now be calculated, providing the emission quantum yield of the energy acceptor (Φ_*^{EA}) is known⁴⁰.

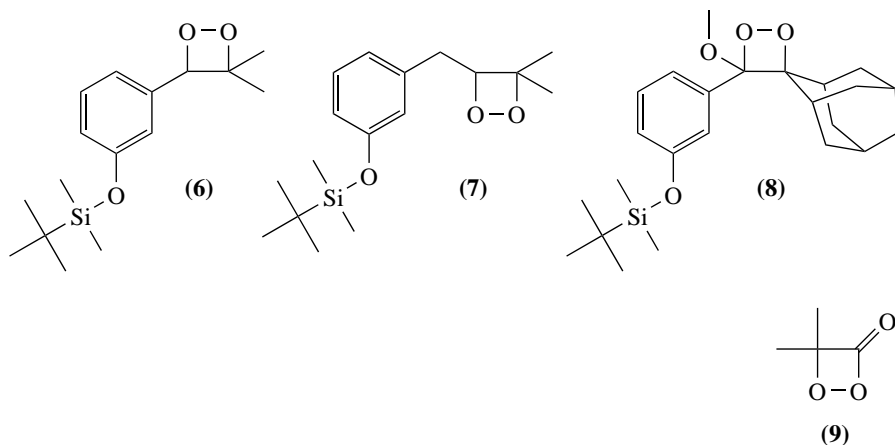
It should be pointed out that the experimental approach described here to determine Φ_* by energy transfer to acceptors is very similar to that described for the determination of relative rate constants in the excitation step of the peroxyoxalate reaction. However, although the kinetic approach is similar, the excitation mechanism operating is distinct inasmuch as the energy acceptor (activator) in the peroxyoxalate reaction participates in the chemical excitation step (activated CL), whereas, in the above-described methodology, the acceptor receives electronic excitation energy from the excited-state product. This represents a possible complication in the use of the energy acceptor to determine excitation quantum yields when the energy acceptor can act as an activator, participating in the excitation step and not simply functioning as an electronic energy acceptor¹⁵. This is usually of little importance in 1,2-dioxetane decomposition; however, activated CL can become the major chemiexcitation mechanism in 1,2-dioxetanone (α -peroxylactone) decomposition in the presence of energy acceptors. In the case of isolated HEI, the occurrence of an activated CL can be deduced from kinetic measurements as the ACT accelerates peroxide decomposition. For complex systems, a simple approach is the use of DPA and rubrene as energy acceptors under identical experimental conditions. If an indirect CL occurs, the emission intensities observed should be nearly identical with the two energy acceptors, since they both possess almost unit fluorescence quantum yields. However, the occurrence of an activated CL is indicated if the emission intensity of rubrene is considerably higher than that of DPA. This fact is due to the low oxidation potential of rubrene, which allows it to be a more efficient activator in the excitation step than DPA¹⁵.

Energy transfer to photoreactive acceptors has also been widely utilized for excitation quantum yield determination (chemical titration), mainly in the decomposition of dioxetanes^{13-16,40,42,54,55}. The quantum yields are calculated from the photoproduct yield obtained at 'infinite' energy acceptor concentrations ($\Phi^{\text{ET}} = 1.0$) by extrapolation of the double-reciprocal relationship between the photochemically active energy acceptor concentration and the photoproduct yield (Φ^{prod}). If the quantum yield of the photochemical reaction (Φ^{photo}) is known, the excitation quantum yield (Φ_*) can be calculated (equation 8)^{15,54,55}.

$$\Phi^{\text{prod}} = \Phi_* \Phi^{\text{photo}} \Phi^{\text{ET}} \quad (8)$$

peroxide in the presence of various activators, using a specially constructed spectro-radiometer–luminometer⁷⁰. Absolute light intensities were obtained by calibration with the fluorescence quantum yield of quinine sulfate and by ferrioxalate actinometry of the exciting light⁷¹. The quantum yields obtained for the more efficient peroxyoxalate systems are in the range of 10 to 30%^{7,71}. More recently, another absolute determination of the CL quantum yields has been reported for the peroxyoxalate reaction with bis(pentachlorophenyl) oxalate (PCPO), using sodium salicylate as base catalyst and DPA as activator, in chlorobenzene as solvent⁷². Under certain experimental conditions the quantum yield appeared to be independent of the substrate and hydrogen peroxide concentrations and CL quantum yields of $\Phi_{\text{CL}} = 0.16 \pm 0.01 \text{ E mol}^{-1}$ were obtained, using a DPA concentration of $5.0 \times 10^{-3} \text{ mol L}^{-1}$. This value is in good agreement with the quantum yields determined earlier by the Rauhut group^{7,71}.

We have recently described¹⁸ a calibration procedure for the determination of excitation quantum yields on commercial fluorimeters, utilizing the luminol standard⁶⁴, and have thereby determined singlet excitation quantum yields for the peroxyoxalate reaction with bis(2,4,6-trichlorophenyl) oxalate (TCPO), hydrogen peroxide and imidazole, using various activators^{18,73}. The same calibration method has been utilized to determine the singlet quantum yields obtained in the induced decomposition of protected phenoxy-substituted 1,2-dioxetanes **6** and **7**^{74–76}, and compared them to the well-investigated spiroadamantyl-substituted 1,2-dioxetane **8**³³. Furthermore, triplet and singlet quantum yields in the uncatalyzed, unimolecular decomposition of **6** and **7** have been determined using this luminol standard⁷⁷. Most recently, this calibration method was applied to determine singlet excitation yields in the catalyzed decomposition of α -peroxylactone, dimethyl-1,2-dioxetanone (**9**), using rubrene as activator (Table 1)⁷⁸.



The quantum yields we obtained for the peroxyoxalate reaction with two representative activators are in general agreement with the early results published by the Rauhut group^{7,71}, as well as with the results of a more recent absolute calibration⁷², especially considering the different experimental conditions used (Table 1). The high value obtained for rubrene using the modified luminol standard (Φ_{S} ca 0.7) can be considered as a validation for this calibration. Since the quantum yield obtained is close to the maximum value of 1.0, the calibration method can, at the most, underestimate the quantum yield by a factor of 1.5. Although the value reported for rubrene in Table 1 is extrapolated to 'infinite' activator concentrations, it should be noted that, when using a rubrene concentration of

TABLE 1. Quantum yield determination for several representative CL systems

CL system	Condition ^a	Reagent	$\Phi_{\text{CL}} \times 10^2$ (E mol ⁻¹)	$\Phi_{\text{S}} \times 10^2$ (E mol ⁻¹)	$\Phi_{\text{T}} \times 10^2$ (E mol ⁻¹)	Calibration method ^b	Reference
Peroxyoxalate	A	TCPO	5.7 ± 0.8	6.0 ± 0.8	—	I	18
	B	TCPO	67 ± 5	68 ± 5	—	I	18
	C	PCPO	15	15.8	—	II	72
Induced 1,2-dioxetane decomposition	D	6 (THF)	3.7 ± 0.8	100 ± 30	—	I	75
	E	7 (THF)	0.0074 ± 0.0018	1.0 ± 0.3	—	I	75
	F	8 (ACN)	11.6 ± 1.5	55 ± 7	—	III	79
	G	8 (DMSO)	29.0 ± 4.0	66 ± 9	—	III	79
	H	8 (ACN)	9.4	45	—	IV	33
	I	8 (DMSO)	25	57	—	IV	33
Unimolecular 1,2-dioxetane decomposition	J	6	—	0.36 ± 0.01	6.8 ± 1.8	I	75
	K	7	—	0.022 ± 0.001	6.6 ± 0.6	I	75
	L	TMD	—	0.25 ± 0.14	35 ± 5	V	55
Dimethyl- 1,2- dioxetanone (9)	M	9	—	10 ± 5	—	V	80
	N	9	—	0.10 ± 0.02	—	I	78
Diphenoyl peroxide (4)	O	4	—	10 ± 5	—	VI	81
	P	4	—	0.002 ± 0.001	—	III	24

^a Experimental conditions: A: TCPO: 10⁻³ M, H₂O₂: 10⁻² M, imidazole: 10⁻³ M, DPA, in ethyl acetate, 25 °C, value obtained by extrapolation to 'infinite' activator concentrations; B: TCPO 10⁻³ M, H₂O₂: 10⁻² M, imidazole: 10⁻³ M, rubrene, in ethyl acetate, 25 °C, value obtained by extrapolation to 'infinite' activator concentrations; C: PCPO 5 × 10⁻⁴ M, H₂O₂: 5 × 10⁻⁵ M, sodium salicylate: 1.2 × 10⁻⁴ M, DPA: 5 × 10⁻³ M, in chlorobenzene; D: **6**: 2 × 10⁻⁵ M, tetra-*n*-butyl ammonium fluoride (TBAF): 3 × 10⁻² M, in tetrahydrofuran (THF), 25 °C; E: **7**: 4 × 10⁻⁵ M, TBAF: 3 × 10⁻² M, in tetrahydrofuran, 25 °C; F: **8**: 10⁻⁷ M, TBAF: 3.3 × 10⁻³ M, in acetonitrile (ACN), 25 °C; G: **8**: 10⁻⁷ M, TBAF: 3.3 × 10⁻³ M, in dimethyl sulfoxide, 25 °C; H: **8**: 10⁻⁷ M, TBAF: 10⁻³ M, in acetonitrile, 25 °C; I: **8**: 10⁻⁷ M, TBAF: 10⁻³ M, in dimethyl sulfoxide, 25 °C; J: **6**: 5 × 10⁻⁵ M, in toluene; 80 °C, singlet yields with DPA (1.7 × 10⁻³ to 1.0 × 10⁻² M), triplet yields with DBA (1.7 × 10⁻³ to 1.0 × 10⁻² M); K: **7**: 5 × 10⁻⁵ M, in toluene; 80 °C, singlet yields with DPA (1.7 × 10⁻³ to 1.0 × 10⁻² M), triplet yields with DBA (1.7 × 10⁻³ to 1.0 × 10⁻² M); L: mean literature values for tetramethyl-1,2-dioxetane (TMD), obtained under different experimental conditions⁵⁵; M: **9**: 10⁻³ M, rubrene: 5 × 10⁻⁵ M, in dichloromethane at 24.5 °C, value calculated by considering only the bimolecular reaction of **9** with rubrene; N: **9**: 10⁻⁴ M, rubrene: 10⁻³ M, in dichloromethane at 25 °C, value calculated by considering only the bimolecular reaction of **9** with rubrene; O: **4**: 5 × 10⁻⁵ M, pyrene, in dichloromethane at 32 °C, value obtained by extrapolation to 'infinite' activator concentrations; P: **4**: 4 × 10⁻⁴ M, pyrene, in dichloromethane at 32.5 °C, value calculated by considering only the bimolecular reaction of **4** with pyrene.

^b Calibration methods: I: modified luminol standard¹⁸; II: absolute calibration⁷²; III: Hastings–Weber light standard⁶⁵; IV: luminol standard^{63,69}; V: mean value obtained by different determination methods, including chemical titrations⁵⁵; VI: triplet yield of 0.3 E mol⁻¹ for TMD, obtained with DBA.

10⁻³ M, the experimental value for the singlet quantum yield is $\Phi_{\text{S}} = 0.5 \pm 0.1$ E mol⁻¹, which also corresponds, in this case, to the CL emission quantum yield, since the fluorescence quantum yield for rubrene is close to one, showing the high emission efficiency of the peroxyoxalate reaction in these conditions¹⁸. The values we obtained in the unimolecular and induced 1,2-dioxetane decomposition are also in agreement with representative values in the literature (Table 1)^{32,55,79}. The results with dioxetanes **6–8** clearly indicate the extremely high singlet chemiexcitation efficiency in the induced decomposition of these phenoxy-substituted cyclic peroxides; the emission quantum yields for **6** and **7** are lower than that obtained for **8** due to the low fluorescence quantum yields of the carbonyl products of **6** and **7**, although the chemiexcitation yield for **6** ($\Phi_{\text{S}} = 1.0 \pm 0.3$ E mol⁻¹) is the highest possible. Although the quantum yields for the unimolecular decomposition of **6** and **7** are considerably lower than the mean values reported in the literature for TMD, they are in agreement with the yields commonly obtained for trisubstituted 1,2-dioxetanes utilizing the photophysical method with DPA and DBA⁵⁵.

Interestingly, the quantum yield obtained recently by our research group for the catalyzed decomposition of dimethyl-1,2-dioxetanone (**9**)⁷⁸ is two orders of magnitude lower

than the one obtained originally⁸⁰. However, a discrepant result was also obtained by Catalani and Wilson²⁴ for the diphenoyl peroxide (**4**) system, although, in this case, the difference is four orders of magnitude. Finally, it should be pointed out again that, for the peroxyoxalate system, we have obtained the expected high quantum yields, using the same calibration method (Table 1).

V. GENERAL MECHANISMS IN ORGANIC CHEMILUMINESCENCE

In this part of the chapter we briefly outline the main classes of mechanisms occurring in chemiluminescent transformations of organic peroxides. The transformations involving isolated 1,2-dioxetanes and related species will not be extensively discussed, since a specific chapter is dedicated to these compounds. We therefore limit ourselves to describing the general decomposition mechanisms of these peroxides, as these are important in the context of the more complex CL systems that we will describe in the last part of this chapter.

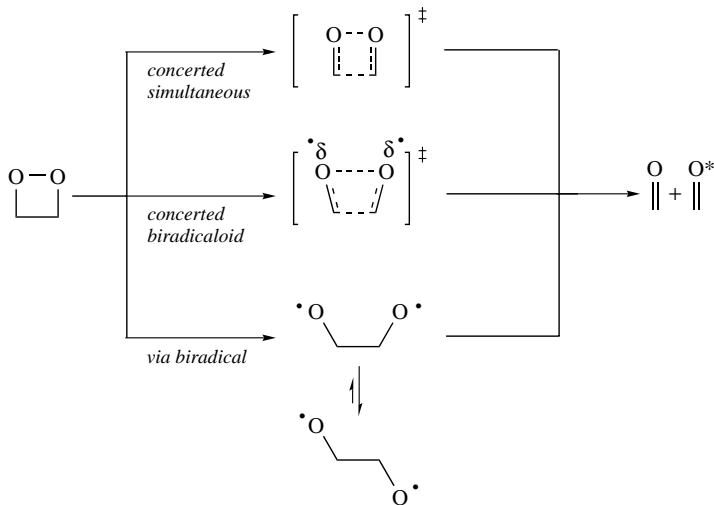
A. Unimolecular Peroxide Decomposition

The unimolecular decomposition of 1,2-dioxetanes and 1,2-dioxetanones (α -peroxylactones) is the simplest and most exhaustively studied example of a thermal reaction that leads to the formation, in this case in a single elementary step, of the electronically excited state of one of the product molecules. The mechanism of this transformation was studied intensively in the 1970s and early 1980s and several hundreds of 1,2-dioxetane derivatives and some 1,2-dioxetanones were synthesized and their activation parameters and CL quantum yields determined. Thermal decomposition of these cyclic peroxides leads mainly to the formation of triplet-excited carbonyl products in up to 30% yields. However, formation of singlet excited products occurs in significantly lower yields (below 1%)^{12-16, 20, 25, 26, 40, 41, 50, 51, 54, 55}.

Two extreme mechanisms have been proposed for the unimolecular dioxetane decomposition: the concerted mechanism^{82,83}, whereby cleavage of the peroxide and the ring C—C bond occurs simultaneously, and the biradical mechanism^{84,85}, whereby the initial cleavage of the O—O bond leads to the formation of a 1,4-dioxy biradical whose subsequent C—C bond cleavage leads to the formation of the two carbonyl fragments (Scheme 8). Although the biradical mechanism adequately explains the activation parameters obtained for most of the dioxetanes studied, it appears not to be the appropriate mechanistic model for the rationalization of singlet and triplet quantum yields. Therefore, an intermediate mechanism has been proposed, whereby the C—C and O—O bonds cleave in a concerted, but not simultaneous, manner (Scheme 8)⁸⁶.

This biradical-like concerted mechanism, in which the kinetic features reflect the biradical character and the formation of excited-state products can best be rationalized by the concerted nature of the complex reaction coordinate, was proposed to optimally reconcile the experimentally determined activation and excitation parameters of most 1,2-dioxetanes studied and has been called the 'merged' mechanism^{51,87}. Specifically, both thermal stability and singlet and triplet quantum yields in the series of methyl-substituted 1,2-dioxetanes, including the parent 1,2-dioxetane^{11,50,51}, could be readily rationalized on the basis of the merged mechanism and qualitative quantum mechanics considerations⁸⁶.

Although the activation parameters obtained from the thermal decomposition of a great number of diverse dioxetane derivatives have been interpreted on the basis of the biradical mechanism, no general interpretation of the excitation efficiencies has been given on the basis of this mechanism^{13-16, 40, 41, 54, 55, 88-91}. Furthermore, most theoretical



SCHEME 8

semiempirical and *ab initio* calculations have been performed on the basis of the biradical mechanism^{92–100}. Even though most calculations are well able to explain the activation parameters in dioxetane decomposition, to the best of our knowledge, so far no general theoretical rationalization for quantum yield trends in dioxetane derivatives has been put forward.

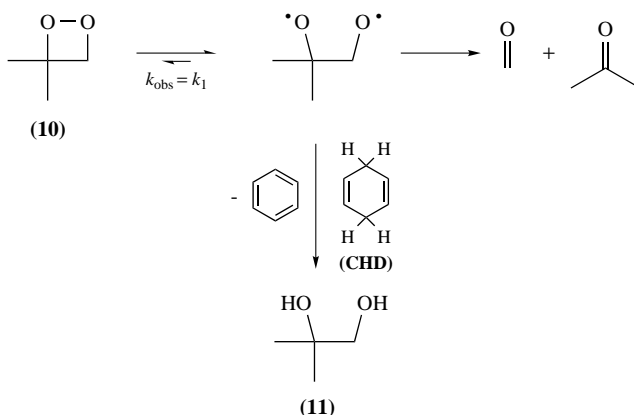
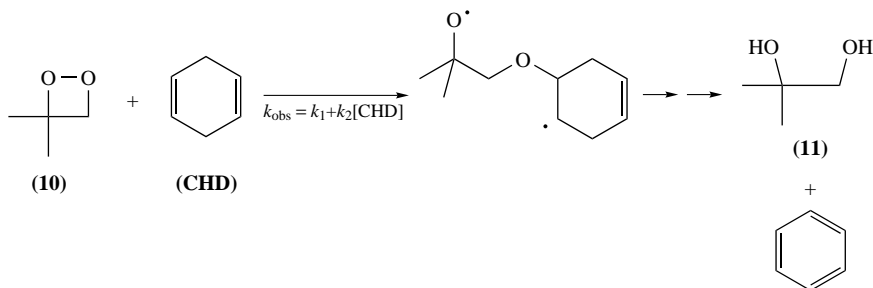
The experimentally observed substituent effect on the triplet and singlet quantum yields in the complete series of methyl-substituted dioxetanes, as well as the predicted C–C and O–O bond strength for the four-membered peroxidic rings¹⁰¹, have led to the hypothesis that a more concerted, almost synchronized, decomposition mechanism should lead to high excitation quantum yields (as in the case of tetramethyl-1,2-dioxetane), whereas the biradical pathway presumably leads to low quantum yields (as in the case of the unsubstituted 1,2-dioxetane)^{11,50,51}. However, it appears that this criterion of ‘concertedness’ is difficult to apply generally to structurally dissimilar dioxetane derivatives.

On the basis of the biradical mechanism, Richardson’s research group has suggested an alternative explication to rationalize excitation quantum yields in the decomposition of a series of asymmetrically substituted phenyl and aryl dioxetanes^{102–104}. The triplet quantum yields were shown to depend critically on the difference between the triplet energies in the two carbonyl products, leading to the suggestion of exciplex formation between the dissimilar carbonyl products, initially formed upon dioxetane ring cleavage. The exciplex stability is presumably related with the difference in the triplet energies (which relate to the redox properties of the carbonyl compounds, and therefore a greater difference in the triplet energies leads to a more pronounced stabilization of the exciplex by the involvement of charge-transfer structures) and a more efficient exciplex formation leads to lower excitation yields due to energy dissipation in the exciplex^{102–104}.

The $n-\pi^*$ state selectivity observed in the decomposition of 1,2-dioxetanes, even in cases in which the $\pi-\pi^*$ excited state of the carbonyl product possesses lower energy^{105–108}, appears to be best explained by the concerted biradicaloid decomposition of the dioxetanes, or by the intermediacy of an extremely short-lived biradical⁶⁰. These studies provide strong evidence for the asynchronous, concerted mechanism because a

biradical intermediate with appreciable lifetime would lose the memory of its orbital symmetry and the preferential formation of $n-\pi^*$ triplet states would not be expected.

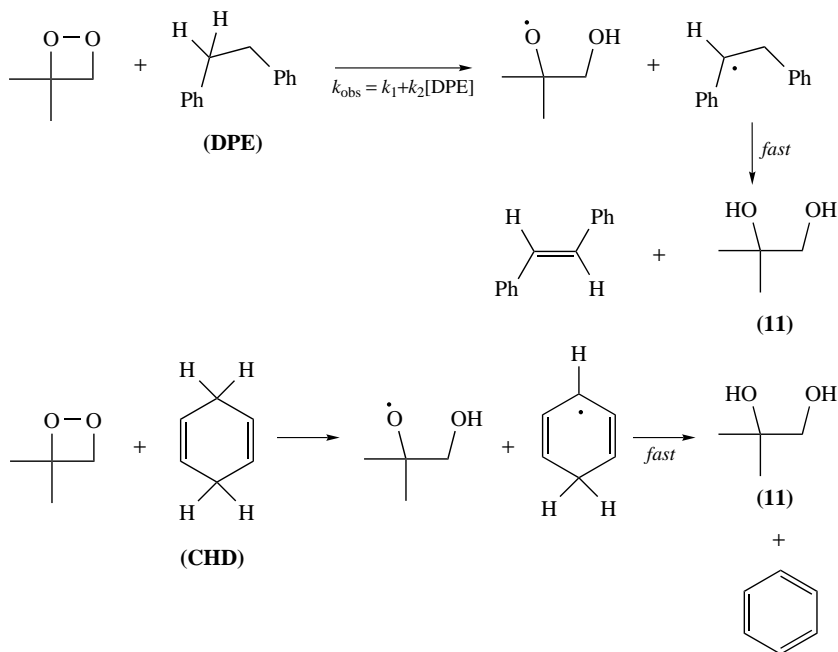
Experimental evidence of the involvement of a biradical intermediate in the decomposition of 3,3-dimethyl-1,2-dioxetane (**10**) has been obtained by radical trapping with 1,4-cyclohexadiene (CHD). Decomposition of **10** in neat CHD was shown to result in the formation of the expected 1,4-dioxy biradical trapping product, 2-methyl-1,2-propanediol (**11**)¹⁰⁹. However, more recently, it has been shown that the previously observed 'trapping product' **11** was formed by induced decomposition of the dioxetane, initiated by the attack of the C=C double bond of the diene on the strained O-O bond of the cyclic peroxide (Scheme 9)¹¹⁰.

1,4-DIOXYBIRADICAL TRAPPING¹⁰⁹INDUCED 1,2-DIOXETANE DECOMPOSITION¹¹⁰

SCHEME 9

The results obtained by Murphy and Adam¹¹⁰ were independently confirmed by another research group, which determined a bimolecular rate constant for the interaction of CHD with the dioxetane **10** of $k_2 = (5.5 \pm 0.2) 10^{-4} \text{ M}^{-1} \text{ s}^{-1}$ at 70°C , whereas a rate constant for the unimolecular dioxetane decomposition at this temperature of $k_1 = (5.5 \pm 0.2) 10^{-4} \text{ s}^{-1}$ has been obtained. Therefore, in neat CHD (10.6 M), half of the dioxetane decomposes by the induced pathway, leading to the formation of **11**, and the amounts of the diol **11** obtained should therefore be due only to diene-induced decomposition of the dioxetane and not to 1,4-dioxy biradical trapping¹¹¹. Additionally, it was shown in this

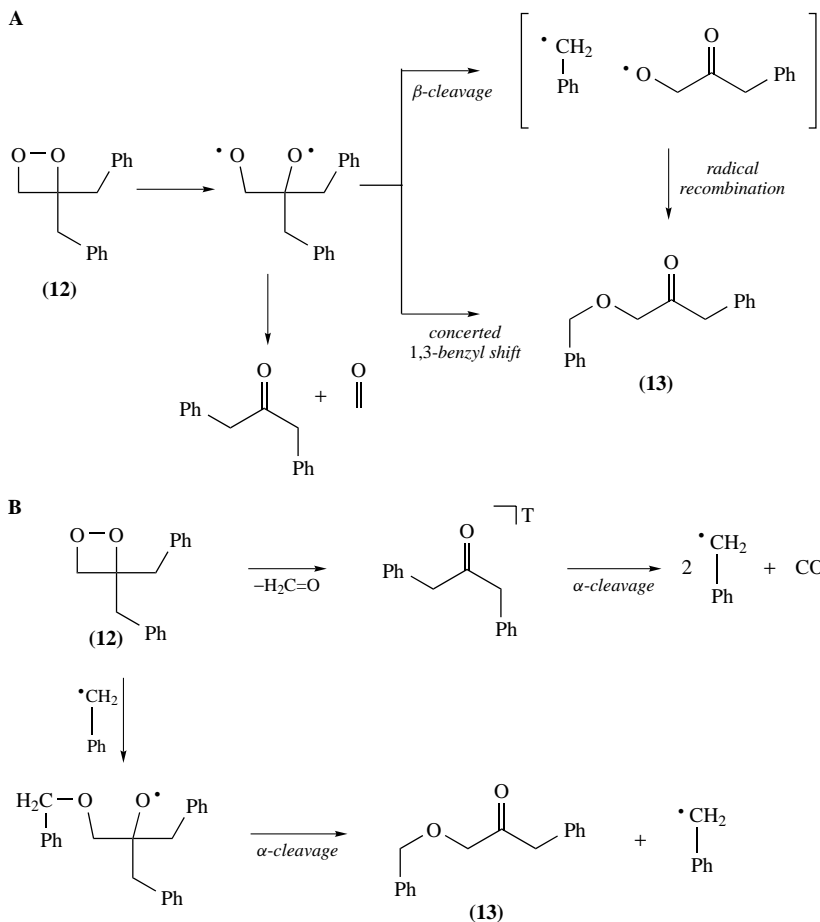
work that, in the presence of 1,2-diphenylethane, which contains no reactive double bond, diol **11** is also formed in considerable amounts from **10** and that induced 1,2-dioxetane decomposition occurs. Therefore, it appears that the mechanism of induced dioxetane decomposition involves a direct hydrogen atom transfer from the active hydrogen donor (CHD or 1,2-diphenylethane) to the O–O bond of the dioxetane and is not initiated by C–C double bond attack (Scheme 10)¹¹¹.



SCHEME 10

Experimental evidence of the occurrence of a 1,4-dioxy biradical intermediate was initially obtained in the thermal decomposition of 3,3-dibenzyl-1,2-dioxetane (**12**) by the observation of the rearrangement product 1-(benzyloxy)-3-phenyl-2-propanone (**13**). This product was believed to be formed by β -cleavage of the initially generated 1,4-dioxy biradical, followed by in-cage radical recombination, or alternatively by a concerted 1,3-shift of the benzyl group (Scheme 11, A)¹¹². However, this experimental evidence on the 1,4-dioxy biradical was subsequently revised in an elaborate mechanistic study by the same research group, which demonstrated that the rearrangement product **13** resulted from a complex radical-chain mechanism initiated by attack of a benzyl radical on the oxygen atom of the dioxetane peroxide bond. The benzyl radical was presumably generated by α -cleavage of triplet 1,3-diphenylpropanone, formed in the unimolecular cleavage of dioxetane **12** (Scheme 11, B)¹¹³.

In view of the above exposed facts, to date there is no direct experimental evidence of the intermediary 1,4-dioxy biradical in the decomposition of 1,2-dioxetanes. Therefore, it appears that the asynchronous (biradicaloid or biradical-like) concerted mechanism (merged mechanism) is the one consistent with all the experimental and theoretical data currently available.



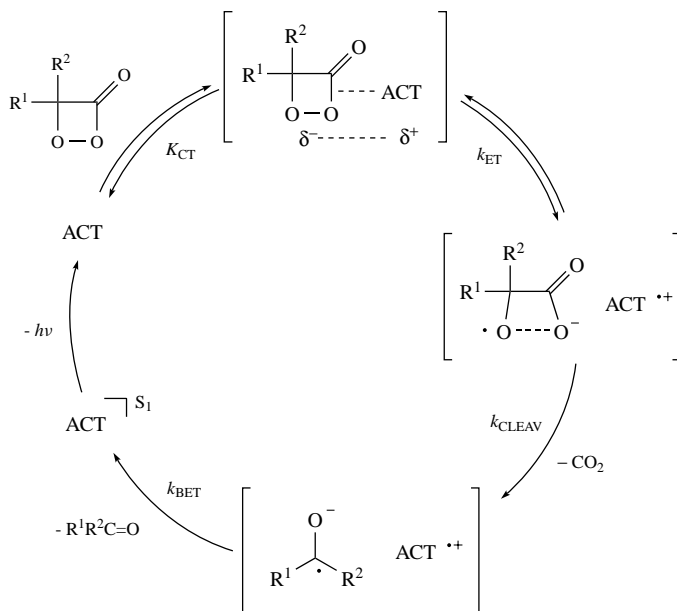
SCHEME 11

B. Catalyzed Peroxide Decomposition

1. Intermolecular electron transfer initiated peroxide decomposition

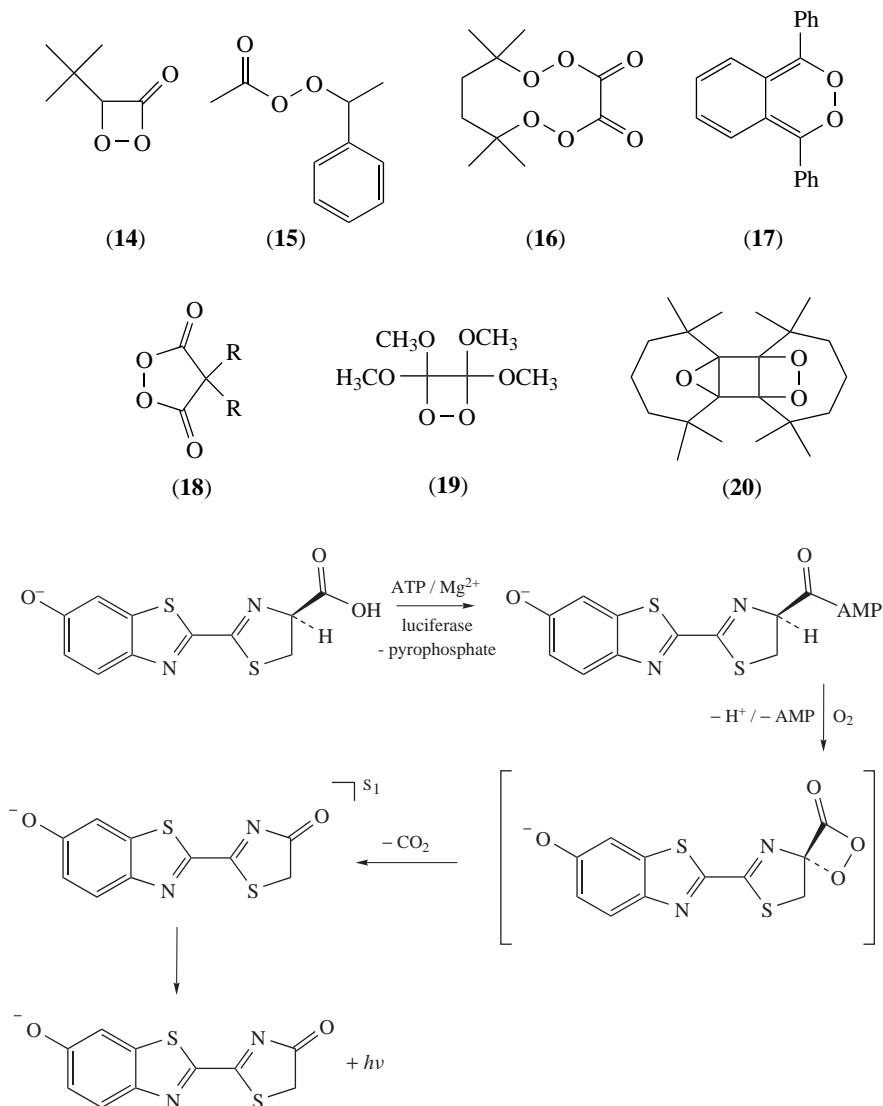
In the course of the mechanistic studies on the CL of organic peroxides, the important observation that the decomposition of certain peroxides can be catalyzed by polycondensed aromatic hydrocarbons led to the formulation of the Chemically Initiated Electron Luminescence (CIEEL) mechanism. This mechanism was first proposed by Schuster and coworkers^{20, 22, 41}, based mainly on the study of isolable cyclic and linear peroxides. The decomposition rates of these peroxides, monitored by the decay of light emission, increased in the presence of polycondensed aromatic hydrocarbons of low oxidation potential and high fluorescence quantum yield (Φ_{Fl}), the so-called activators (ACT), and the emission intensities were strongly enhanced. Furthermore, rate constants and emission intensities were shown to depend on the oxidation potential of the activator utilized, indicating the occurrence of an electron-transfer process in the rate-limiting step. The CIEEL sequence, as proposed by Schuster and shown here for the catalyzed

reaction of 1,2-dioxetanone, is initiated by charge transfer complex formation between the peroxide and the activator, followed by electron transfer from the activator to the peroxide, probably simultaneously with O—O bond cleavage^{114,115}. Cleavage of the C—C bond and the formation of carbon dioxide leave a pair of radical ions, still in contact within the solvent cage (radical cation of the activator and radical anion of acetone). The back-electron transfer between these two radical ions can release enough energy to form the activator in its first singlet-excited state (Scheme 12)^{20,41}.



SCHEME 12

Intensive studies in the field of mechanistic CL by several research groups have resulted in the description of a large variety of peroxides which, in the presence of appropriate activators, show decomposition in an activated CL process and might involve the CIEEL mechanism^{25,26,116}. Even before the formulation of the CIEEL mechanism, Rauhut's research group obtained evidence of the involvement of electron-transfer processes in the excitation step of the peroxyoxalate CL⁷. Results obtained in the activated CL of diphenoyl peroxide (**4**) led to the formulation of this chemiexcitation mechanism^{20,41,81,117}, and several 1,2-dioxetanones (α -peroxylactones), such as 3,3-dimethyl-1,2-dioxetanone (**9**) and the first α -peroxylactone synthesized, 3-*tert*-butyl-1,2-dioxetanone (**14**), have been shown to possess similar CL properties, compatible with the CIEEL mechanism^{80,118–121}. Furthermore, the CL properties of secondary peroxyesters, such as 1-phenethylperoxy acetate (**15**)^{122,123}, peroxyates (**16**)¹²⁴, *o*-xylylene peroxide (**17**)¹²⁵, malonyl peroxides (**18**)^{126,127}, as well as some especially substituted 1,2-dioxetanes, like tetramethoxy-1,2-dioxetane (**19**)¹²⁸ and the sterically stabilized highly strained 1,2-dioxetane **20**¹²⁹, are in agreement with the occurrence of an intermolecular CIEEL mechanism during the chemiluminescent decomposition of these peroxides, activated by appropriate additives. Furthermore, the CIEEL mechanism was postulated to occur in the chemiexcitation step of firefly luciferin/luciferase bioluminescence (Scheme 13)²³.



SCHEME 13

The CIEEL mechanism, as initially proposed by Schuster^{20,22,41,114,115}, has been applied to a wide variety of CL systems^{12-15,17,22,25,26,41} but this hypothesis has also been controversially discussed, mainly by Wilson^{25,130} and McCapra^{131,132}. Here, we will but briefly point out the most important experimental evidence upon which the mechanistic proposal is based and indicate some as yet unresolved problems relating to the CIEEL mechanism.

The most clear-cut experimental evidence is presented with respect to the initial parts of the mechanistic sequence. Evidence, also indirect, for the formation of a charge-transfer

complex between the peroxide and the ACT has been obtained for metalloporphyrins, which are highly efficient activators for dimethyl-1,2-dioxetanone decomposition. The possibility of complex formation between these activators and cyclic organic peroxides has been verified with tetramethyl-1,2-dioxetane, which does not undergo induced decomposition by these activators. The metalloporphyrins studied showed a shift in the absorption maximum of the Soret band, indicating complex formation^{22,133}. The second step in the reaction sequence (Scheme 12) is the rate-limiting step and undoubtedly the one which is best supported by experimental data. The observed dependence of the reaction rates and CL emission intensities on the activator's oxidation potential indicates the occurrence of an electron transfer from the ACT to the peroxide or, at least, the involvement of a charge transfer interaction between the two reactants^{20,22,114,130}. This step is assumed to be endergonic and can only occur if the O—O bond is stretched by thermal activation, as indicated by self-consistent field calculations on the unsubstituted 1,2-dioxetanone¹³⁴. Therefore, the initial electron-transfer step should be irreversible and accompanied by cleavage of the peroxide's oxygen—oxygen bond in order to prevent fast exothermic back-electron transfer. The linear free-energy relationship between the rate constants (k_{ET}) and the oxidation potentials (E_{ox}) of the activators (equation 9, where k_{ET} is the rate-limiting electron transfer rate constant, K the constant incorporating the equilibrium constant for charge-transfer complex formation (K_{CT}), E_{red} the reduction potential of the peroxide, which is unknown, E_{ox} the oxidation potential of the activator, known from electrochemical measurements, and α the proportionality constant indicating the sensitivity of the reaction to potential changes)⁴¹ leads to straight-line plots and the slope of these plots to correlation constants of $\alpha = 0.3$ for most CIEEL systems studied²⁵. It has been argued that values of $\alpha < 1.0$ can be congruent with the occurrence of a full electron transfer^{114,115}; however, as pointed out by Wilson²⁵, they are also fully compatible with the involvement of partial charge-transfer mechanisms.

$$\ln k_{ET} = \ln K + \frac{\alpha(E_{red} + E_{coul})}{RT} - \frac{\alpha E_{ox}}{RT} \quad (9)$$

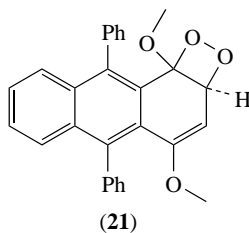
No direct experimental evidence has so far been obtained regarding any of the subsequent steps in the CIEEL sequence. It is assumed that these steps should be extremely fast and occur within the solvent cage, so that they can result in excited-state formation upon back-electron transfer. Carbon—carbon bond cleavage in the anion radical (k_{CLEAV}) releases a neutral species and results in a new ion radical pair, containing a better reducing species than the original one. In the case of dimethyl-1,2-dioxetanone, the radical ion pair formed may contain either the acetone anion radical or the carbon dioxide anion radical and, to the best of our knowledge, there is no evidence favoring either one of these possibilities^{25,130}. Nevertheless, Catalani and Wilson²⁴ argue that, in the case of dioxetanone, the radical anion formed should be the carbon dioxide radical anion due to its slightly lower reduction potential^{135,136}.

The back-electron transfer from the radical anion (of acetone or carbon dioxide, in this case) to the activator radical cation is 'energy sufficient' to form the activator in an excited state. Provided the processes following the initial electron transfer are sufficiently rapid to prevent spin inversion and the electrons remain correlated (the radical ion pair remains in the initially formed singlet state), singlet-excited states should be formed. This is the most important difference between the CIEEL sequence and electrochemiluminescence, where the partitioning between singlet and triplet states is expected to be statistical²¹. There is no evidence for the formation of triplet-excited activators in peroxide decomposition, although it appears to be quite difficult to design an experiment which can completely rule out the occurrence of triplet products¹³⁰.

Indications of the involvement of activator radical cations in the CIEEL sequence have been obtained from a laser flash-photolysis study using singlet-excited pyrene and some triplet-excited anthracene derivatives as activators. The radical cation of pyrene, corresponding to the fraction that has escaped the solvent cage, has been identified by its absorption spectrum^{22, 137, 138}. However, the interpretation of these results has been questioned more recently¹³⁰. Other indications of the validity of the CIEEL hypothesis have been obtained in studies of energy-deficient systems. For example, the final back-electron transfer in the 1-phenethylperoxy acetate system with dimethyldihydrophenazine as activator should not release sufficient energy for the formation of the activator's singlet-excited state, congruent with the low excitation efficiency observed experimentally^{122, 123}. However, the interpretation of these results has been questioned due to the uncertainty involved in the calculation of the energy available for excitation caused by considerable differences in reported redox-potential and its correction for solvent polarity¹³⁰. Nonetheless, a specially substituted malonyl peroxide was proved to constitute a low-efficient CL system and this low excitation efficiency has been explained on the basis of the CIEEL mechanism and the occurrence of two competitive pathways in the electron transfer initiated decomposition of this peroxide¹³⁹.

We have recently been able to correlate the experimentally obtained singlet excitation yields in the peroxyoxalate reaction, using two different sets of activators, with the free energy change of the back-electron transfer, calculated on the basis of the CIEEL mechanism, thereby contributing to the validation of this hypothesis^{18, 140}. Furthermore, we have investigated the dependence of the singlet quantum yields in the peroxyoxalate reaction on the solvent viscosity, utilizing mixtures of toluene and diphenylmethane which possess very similar Marcus solvent parameters^{141, 142}. The singlet quantum yields obtained in diphenylmethane ($\eta = 2.6$ cP) are up to tenfold higher than in toluene ($\eta = 0.5$ cP), demonstrating the importance of the solvent-cage effect for efficient chemiexcitation¹⁴³. This finding also contributes to the validation of the CIEEL sequence as initially proposed by Schuster and appears to rule out alternative proposals which favor concerted charge-transfer interactions^{25, 130-132}.

However, the most severe criticism of the CIEEL hypothesis relates to the chemiexcitation efficiency experimentally obtained for the standard CIEEL systems, diphenoyl peroxide (**4**) and 1,2-dioxetanone (**2**)^{24, 25}. In a study on the electron transfer catalyzed decomposition of 1,4-dimethoxy-9,10-diphenylanthracence peroxide (**21**), Catalani and Wilson²⁴ obtained very low chemiexcitation quantum yields with various commonly utilized activators ($\Phi_S = 2 \cdot 10^{-5} \text{ E mol}^{-1}$) and reinvestigated the CL of diphenoyl peroxide (**4**), determining quantum yields in the same order of magnitude ($\Phi_S = (2 \pm 1) \cdot 10^{-5} \text{ E mol}^{-1}$) as those obtained by **21** (Table 1). We have more recently determined the quantum yields in the rubrene-catalyzed decomposition of dimethyl-1,2-dioxetanone (**9**)⁷⁸ and also found a much lower value than the one initially reported (Table 1)⁸⁰. Since the diphenoyl peroxide and the 1,2-dioxetanone systems are the two prototype CIEEL systems, the validity of this hypothesis itself might be questioned due to its low efficiency in excited-state formation²⁵.

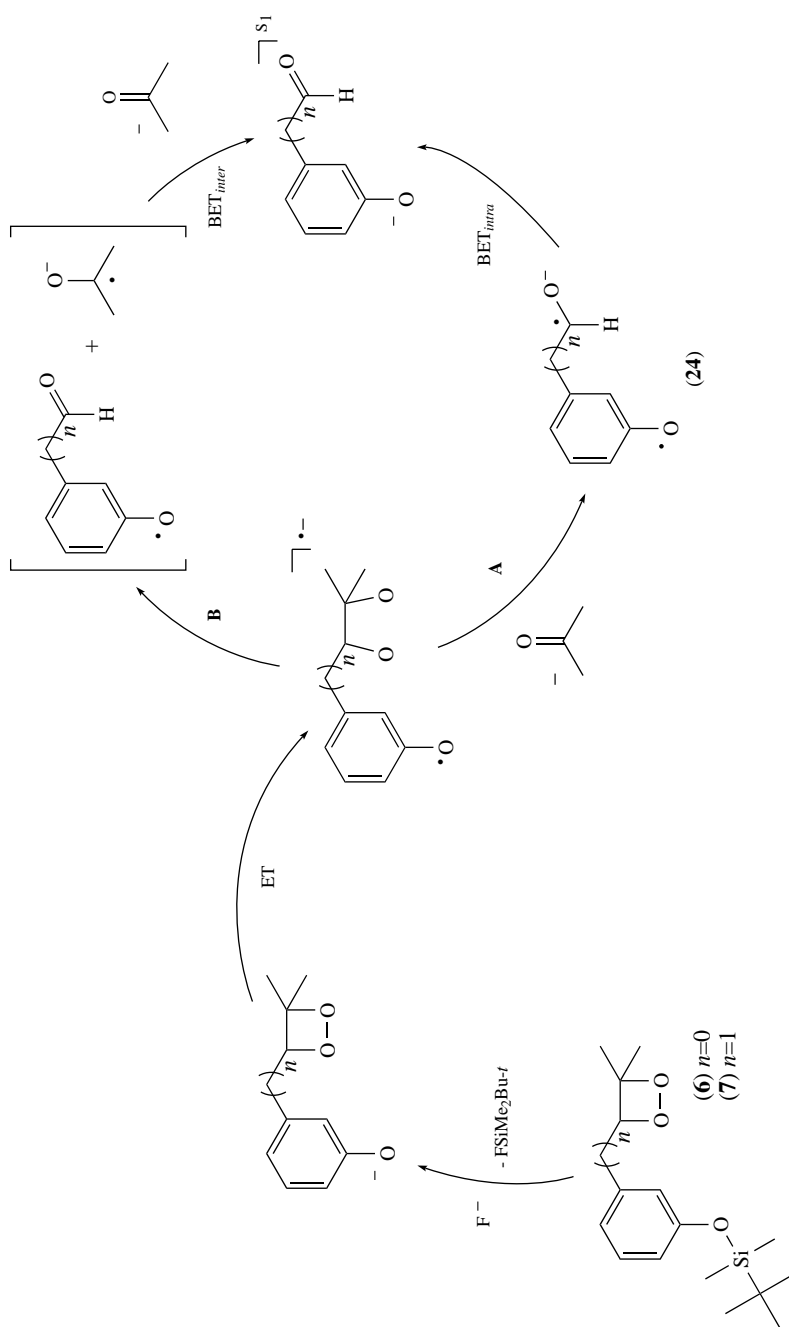


Nevertheless, there are two highly efficient CL systems which are believed to involve the CIEEL mechanism in the chemiexcitation step, i.e. the peroxyoxalate reaction and the electron transfer initiated decomposition of properly substituted 1,2-dioxetanes (Table 1)^{17,26}. We have recently confirmed^{18,73,140} the high quantum yields of the peroxyoxalate system^{7,72} and obtained experimental evidence for the validity of the CIEEL hypothesis as the excitation mechanism in this reaction. The catalyzed decomposition of protected phenoxy-substituted 1,2-dioxetanes is believed to be initiated by an intramolecular electron transfer, analogously to the intermolecular CIEEL mechanism¹⁴⁴. Therefore, these two highly efficient systems demonstrate the feasibility of efficient excited-state formation by subsequent electron transfer, chemical transformation (cleavage) and back-electron transfer steps, as proposed in the CIEEL hypothesis.

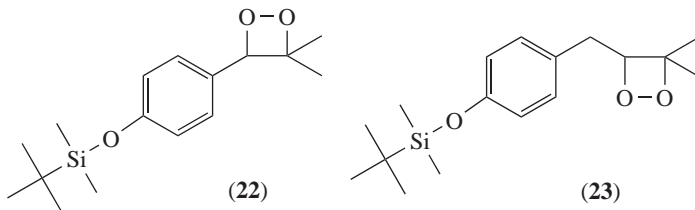
2. Intramolecular electron transfer initiated peroxide decomposition

As outlined above, the thermal cleavage of 1,2-dioxetanes generates two carbonyl fragments, one of which can be formed in an electronically excited state, predominantly in the triplet state. However, when these high-energy molecules bear an electron-rich substituent, singlet states are obtained predominantly and it is believed that an intramolecular CIEEL mechanism is operating. Thus, 1,2-dioxetanes containing substituents with low oxidation potentials prove to be quite labile, decomposing by this intramolecular CIEEL. The most successful design of an intramolecular CIEEL system is based on spiroadamantane-substituted dioxetanes with a protected phenolate ion³²⁻³⁴. The advantage of such dioxetanes is their thermal persistence and their convenient synthesis through photooxygenation¹⁴⁴. The decomposition of these dioxetanes can be achieved by treatment with an appropriate reagent (trigger) to induce phenolate ion release. These phenolate-initiated intramolecular CIEEL processes provide the basis for numerous commercial applications, most prominently in chemiluminescence immunoassays^{35-38,145,146}. Thus, the search for other triggerable CIEEL-active dioxetanes continues attracting the interest of many research groups¹⁴⁴; however, the efficiency of the light emission from these systems is often very low¹⁴⁷⁻¹⁵⁵. Recent work in this field has been devoted mainly to the synthesis of stable dioxetanes with triggering functionalities, in the search for efficient chemiluminescent systems useful in analytical applications^{151,156-158}.

Recent mechanistic studies have been performed chiefly using the spiroadamantyl-substituted dioxetane (**8**) and similar derivatives^{79,159-162}. Furthermore, mechanistic discussions on the induced dioxetane decomposition have focused mainly on the explication of the influence of the substitution pattern in the aromatic ring, containing the trigger function, on the chemiexcitation quantum yields, the so-called 'meta-effect'^{26,33} or odd/even substituent rule¹⁶³. The experimental observation that phenyl-substituted dioxetanes, containing the trigger function in *meta* position to the peroxidic ring, are more stable and possess higher excitation yields has been explained through the qualitative concept of extended conjugation and cross-conjugation¹⁴⁴ and through the use of molecular orbital calculations¹⁶². In a study on the CL properties of the *meta*-substituted dioxetanes **6** and **7** and the corresponding *para*-substituted derivatives **22** and **23**, the much higher quantum yields obtained for the *meta*-substituted derivatives has been explained by the structural and electronic similarity of the excited *meta*-substituted benzaldehyde derivatives (in the case of **6**) with the intermediary biradical anion **24**, formally obtained by the intramolecular CIEEL sequence (Scheme 14). In contrast, in the *para*-substituted derivatives, the biradical anion corresponding to **24** shows direct conjugation with the ground state of the carbonyl product, thus leading to low excitation efficiencies^{26,74,75,77,164}. This interpretation has been made in analogy to the *meta*-effect observed in the photosolvolysis of benzyl halides and related compounds¹⁶⁵⁻¹⁶⁷.



SCHEME 14



This qualitative interpretation of structural and electronic similarity has also been employed to rationalize the fact that the quantum yield for the dioxetane derivative **6**, in which the phenoxy substituent is directly linked to the peroxidic ring, is two orders of magnitude higher than for the dioxetane **7**, in which the trigger function is separated by a methylene bridge. Furthermore, the different quantum yields were rationalized in terms of a competition between the intramolecular (pathway A) and intermolecular back-electron transfer (pathway B) in the decomposition of **7**, whereas the intramolecular back-electron transfer was believed to occur exclusively in the decomposition of **6**, due to the higher stability of the radical anion of the benzaldehyde derivative, as compared with the radical anion of acetone (Scheme 14).

However, this interpretation of different back-electron transfer pathways for the dioxetanes **6** and **7** can no longer be maintained due to the findings of recent studies by Adam's research group on the solvent-cage effect in the induced decomposition of spiroadamantyl dioxetane **8** and other derivatives. Adam and coworkers reported that a viscosity variation from 0.6 (benzene) to 2.5 cP (diphenylmethane) results in a 2.5-fold increase in the singlet quantum yields (Φ_S) in the induced decomposition of **8**¹⁶⁸. Using the same methodology, this research group also reported similar results for the corresponding *para*-substituted derivative of **8**¹⁶⁹, additionally showing that the quantum efficiency increases to a much smaller extent in the induced decomposition of a bicyclic furan-annelated dioxetane derivative¹⁷⁰. We have independently confirmed the findings of Adam's group for the dioxetanes **6** and **7** as well as **8**, using the binary solvent systems toluene/diphenylmethane and acetonitrile/propylene carbonate⁷⁶.

The results on the viscosity dependence of the singlet quantum yields in the induced decomposition of 1,2-dioxetane clearly indicate the occurrence of an intermolecular electron transfer in the excitation step of this transformation (Scheme 14, pathway B). However, this conclusion again brings up the question of the efficiency of chemiexcitation in various CIEEL systems. Whereas the *intramolecular* induced 1,2-dioxetane decomposition leads to high singlet excitation quantum yields in many of the known examples, most of the examples for the *intermolecular* induced peroxide decomposition have been shown to possess quite low quantum yields (Table 1). A noteworthy exception to this rule is the peroxyoxalate system, in which the intermolecular nature of the excitation step has been clearly demonstrated, showing, however, extremely high singlet quantum yields comparable only to bioluminescence systems.

VI. HIGH-EFFICIENCY ORGANIC CHEMILUMINESCENT REACTIONS INVOLVING PEROXIDE INTERMEDIATES

In this part of the chapter we will give a more detailed description of some highly efficient organic chemiluminescence systems, which occur with the involvement of peroxide intermediates. We have chosen to begin the subject with the well-known and widely applied luminol oxidation and will show that, even though this reaction has been exhaustively studied, several critical points in its mechanism remain unclear and are still the subject of

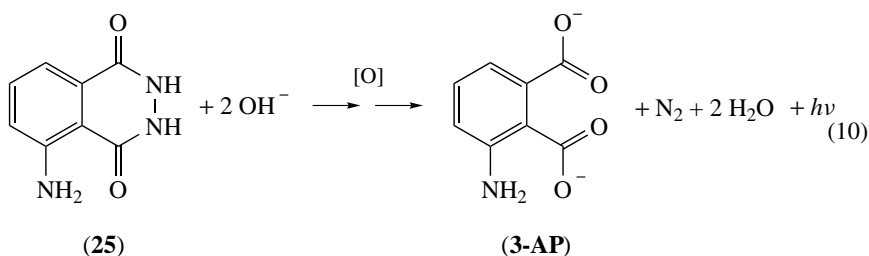
controversial discussion. This applies especially to the high-energy intermediate structure responsible for chemiexcitation and the mechanism of this chemiexcitation step.

The second system to be described is the CL obtained in the transformation of lucigenin and related derivatives; here, too, the mechanisms which lead to chemiexcitation are still discussed in the literature. Finally, we will concentrate our discussion on one of the most efficient CL systems known, the peroxyoxalate reaction. After a brief discussion of kinetic results obtained with the different peroxyoxalate substrates, we will focus mainly on studies which attempt to elucidate the structure of the high-energy intermediate in these reactions and describe the experimental evidence obtained with respect to the mechanism of the excitation step.

A. Chemiluminescence in Luminol Oxidation

1. General reaction mechanism

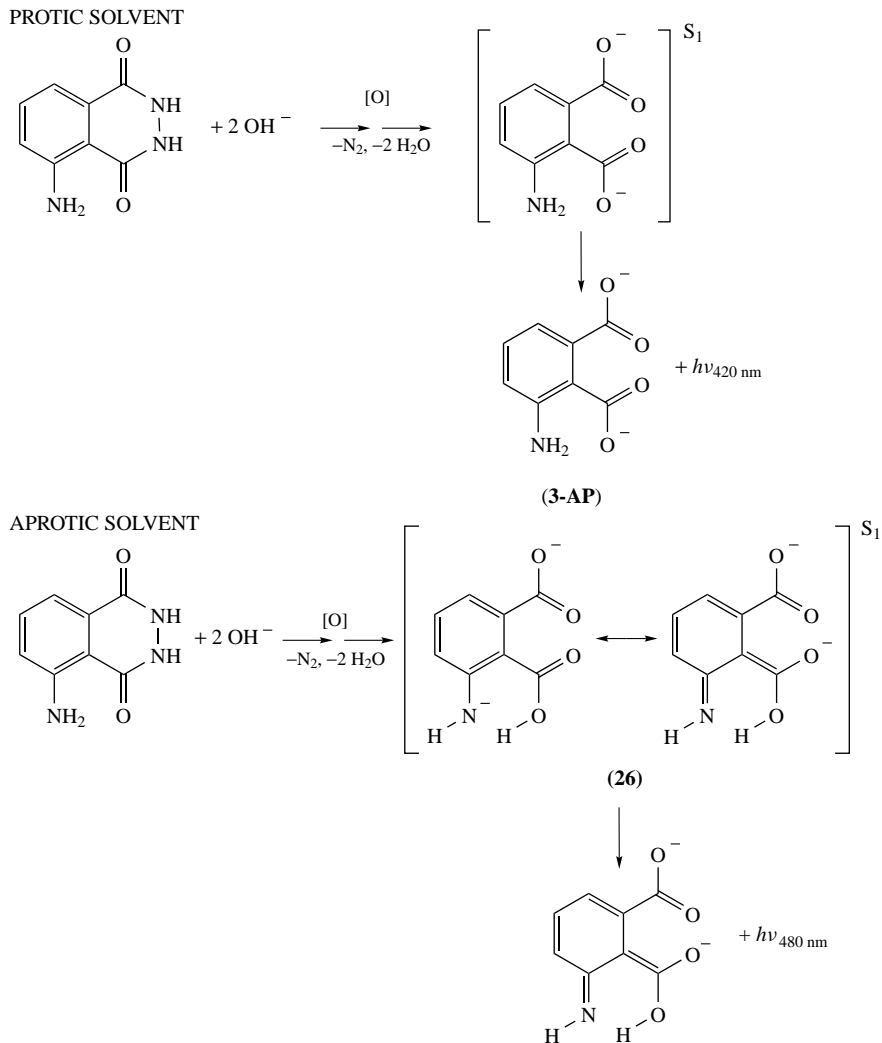
The chemiluminescence emission resulting from the oxidation of luminol (5-amino-2,3-dihydro-1,4-phthalazinedione) has been extensively studied since its discovery by Albrecht in 1928⁴. Although luminol oxidation is one of the most commonly applied chemiluminescent reactions, to date no definitive mechanism is known¹⁷¹⁻¹⁷⁴. Efficient chemiluminescence emission is only observed when luminol (**25**) is oxidized under alkaline conditions. Depending on the medium, co-oxidants are required in addition to molecular oxygen for the observation of light emission, but under any condition, 3-aminophthalate (**3-AP**) and molecular nitrogen are the main reaction products (equation 10).



The emitting species was found to be the singlet-excited state of 3-aminophthalate ion in both protic and aprotic solvents. This identification was made based on the equivalence of the chemiluminescence spectrum of luminol and the fluorescence spectrum of **3-AP** ion¹⁷⁵⁻¹⁷⁹. In different reaction media, slightly different maximum chemiluminescence wavelengths are observed (Table 2). The spectral shift observed when the system changes from aqueous media to DMSO or other aprotic solvents can be ascribed to a quinoidal form of 3-aminophthalate (**26**) formed in aprotic solvents (Scheme 15)¹⁷⁵.

TABLE 2. Chemiluminescence maxima of luminol and fluorescence maxima of 3-aminophthalate ($\text{Fl}_{3-\text{AP}}$)¹⁷⁸

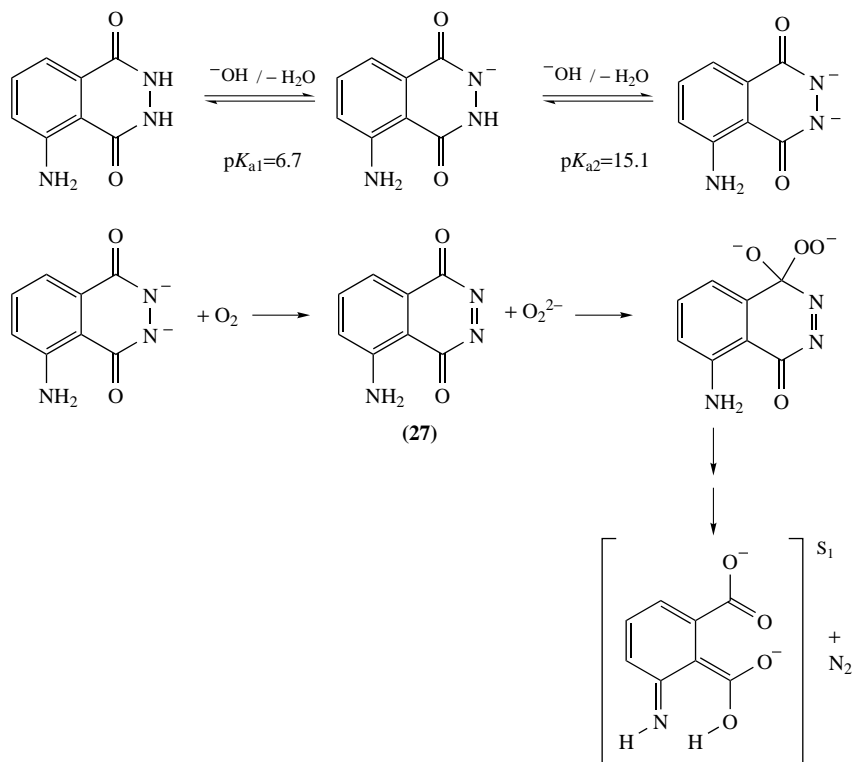
Solvent	λ_{MAX}	$\text{CL}_{\text{luminol}}$ (nm)	λ_{MAX}	$\text{Fl}_{3-\text{AP}}$ (nm)
Water		431		431
DMSO		502		495
DMF		499		497
MeCN		500		500
THF		496		500



SCHEME 15

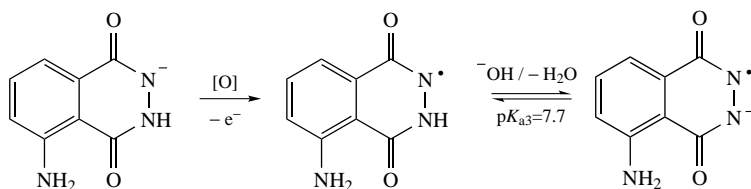
In aprotic media, only molecular oxygen and a strong base are needed to produce chemiluminescence from luminol¹⁷⁵⁻¹⁷⁷. In such media, an important intermediate in the reaction is the dianion of luminol, which can be oxidized by oxygen, resulting in the formation of the diazaquinone **27** and deprotonated hydrogen peroxide. The subsequent nucleophilic attack by hydrogen peroxide dianion to one of the diazaquinone carbonyls gives rise to the formation of a metastable peroxidic intermediate that, by several steps, results in chemiexcited 3-aminophthalate (Scheme 16)^{173, 174, 180}.

Apparently, the mechanisms in protic and aprotic conditions only differ in their early steps, in which the protic system requires additional oxidants to convert luminol to



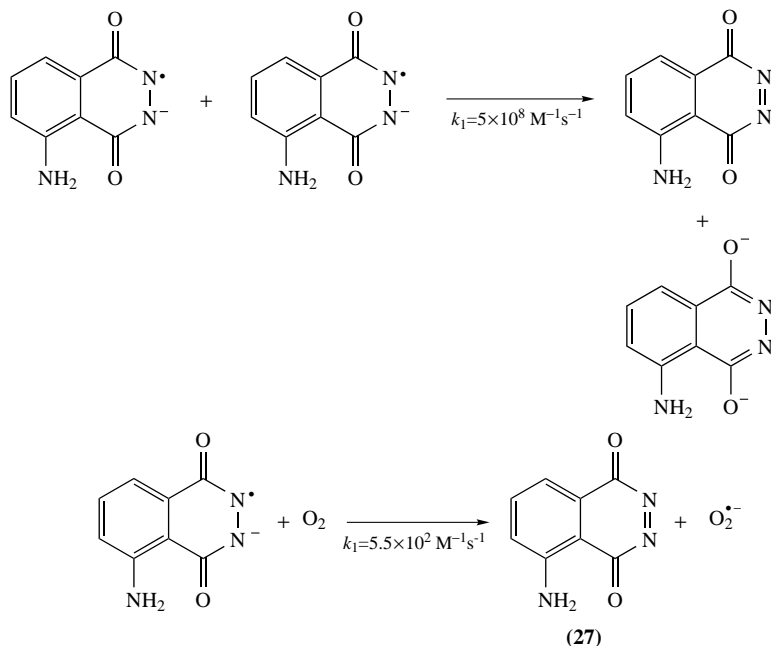
SCHEME 16

diazaquinone **27**, since the luminol dianion is not present in significant quantities. The formation of luminol radical anion depends on the presence of an oxidant and a catalyst that can act as a co-oxidant (Scheme 17). The rate of one-electron oxidation of luminol anion varies with the oxidant and must be determined independently for each particular system. Among the most commonly employed primary oxidants are horseradish peroxidase (HRP)^{180,181}, transition metals such as cobalt, copper, chromium, manganese, and iron and their complexes, and many free-radical species such as N_3^\bullet , $CO_3^{\bullet-}$, $Br_2^{\bullet-}$, ClO_2^\bullet and HO^\bullet ^{178,182}. The kinetics of the oxidation can be determined from the decay of the chemiluminescence emission intensity, as the abstraction of one electron is the rate-limiting step.



SCHEME 17

The diazaquinone **27** can be obtained by disproportionation of two luminol radical anions or by its oxidation by molecular oxygen, yielding superoxide radical anion (Scheme 18). The rate constants for these two pathways indicate that the disproportionation is kinetically favored¹⁸⁰. Although luminol diazaquinone can be generated by potassium persulfate or hypochlorous acid, its lifetime in aqueous media is very short and chemiluminescence is only observed in the presence of hydrogen peroxide^{183, 184}. Hence, although hydrogen peroxide itself is unable to oxidize luminol, it greatly enhances the luminescence of luminol, competing successfully with water for the diazaquinone intermediate^{185–187}. The diazaquinone **27** has never been isolated; however, it was trapped as the Diels–Alder adduct with cyclopentadiene in a reaction of luminol with H_2O_2 catalyzed by $\text{K}_3\text{Fe}(\text{CN})_6$ ¹⁸⁸.



SCHEME 18

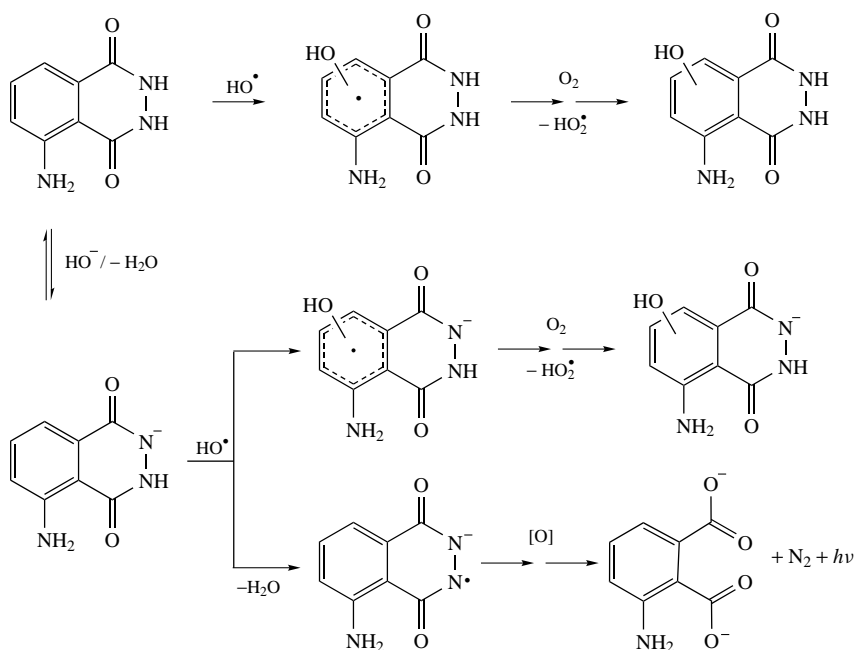
Several one-electron oxidants play a fundamental role in biological systems. Because these species react with luminol and result in chemiluminescence, luminol and derivatives are widely used in analytical assays^{171, 172, 174}. The effect of free radicals as oxidants of luminol has been extensively applied to studies of oxidative stress^{189–191} and, more recently, to the evaluation of the antiradical capacity of compounds used as antioxidants^{190, 192, 193}. In this context, the role of $\text{O}_2^{\bullet-}$ in luminol oxidation has been extensively investigated^{63, 178, 180, 194–196}. The suggestion that superoxide ions might be involved in luminol chemiluminescence was first made by Lee and Seliger⁶³. Merényi and collaborators have shown that luminol chemiluminescence depends on the recombination of luminol radical anion and superoxide ion¹⁷⁸. A variety of evidence indicates the importance of the superoxide ion for light generation during luminol oxidation. As oxygen is removed, or superoxide dismutase (SOD) is added to the reaction media, the light emission intensity decreases significantly¹⁹⁷. Even if $\text{O}_2^{\bullet-}$ is initially absent, it will still be generated by

redox reaction between luminol radical anion and molecular oxygen (Scheme 18) and by decomposition of hydrogen peroxide catalyzed by transition metal ions¹⁹⁵. However, $O_2^{\bullet-}$ alone cannot promote the one-electron oxidation required to generate luminol radical anion. Consequently, the chemiluminescence quantum yields are three orders of magnitude higher when superoxide is accompanied by a stronger oxidant¹⁹⁶. Table 3 shows the chemiluminescence quantum yields measured with several oxidizing agents under different conditions.

The effect of the hydroxyl radical (HO^{\bullet}) on luminol chemiluminescence has also been intensively studied^{178, 187, 198, 199}. Although detailed mechanisms for the reaction of hydroxyl radicals with hydrazides remain unknown, two different processes are assumed to be involved: oxidation of the hydrazide group and addition of hydroxyl radical to the aromatic ring (Scheme 19)^{180, 199}.

TABLE 3. Luminol chemiluminescence quantum yields in different solvents with some oxidative systems^{63, 178, 195, 197}

[Luminol] (M)	Solvent	<i>T</i> (°C)	pH	Oxidant	Φ_{CL} ($/10^{-2}$)
10^{-3}	Water	20	11.6	H_2O_2 /Hemin	1.24
10^{-3}	DMSO	25	—	O_2/t -BuOK	1.24
10^{-5}	Water	20	12.2	$K_3Fe(CN)_6$	0.01
10^{-5}	Water	20	11.6	NaOCl	0.40
10^{-3}	Water	20	11.6	$K_2S_2O_8$	0.70
10^{-5}	Water	20	11.6	$h\nu$ /methylene blue/ O_2	0.30
10^{-4}	Water	25	9.3	$O_2^{\bullet-}$	0.0004



SCHEME 19

The reaction between hydroxyl radical and luminol results in the quantitative formation of hydroxylated products, which are known to be radical scavengers (Scheme 19)¹⁸⁰. The reduction of luminol radical anion by these species decreases the emission intensity, unless HO• is generated rapidly in high concentrations¹⁸⁰. The emission observed under these conditions may be attributed to one-electron oxidation of luminol by hydroxyl radicals, yielding luminol radical anion, or by hydroxyl-mediated generation of potent one-electron oxidants from its reaction with bases¹⁷⁸. Moreover, the addition of HO• to luminol or its monoanion results in an adduct able to react very rapidly with O₂, yielding, in addition to hydroxylated luminol, superoxide (Scheme 19)¹⁸⁰.

Schiller and collaborators have shown that, while radiolysis-generated HO• reacts with luminol to yield hydroxylation, only small amounts of hydroxylated products are obtained for phthalic hydrazide¹⁹⁹. This difference is likely attributable to the electron-donating effect of the amino group, activating the aromatic ring and influencing its reactivity¹⁹⁹. In addition, the oxidation of luminol anion to its semidiazquinone radical by half of the HO• generated was confirmed and it was proposed that the formation of the semidiazquinone is favored in the presence of low concentrations of ferric ions and hydroxyl radicals, resulting in an increase of chemiluminescence quantum yields¹⁹⁹.

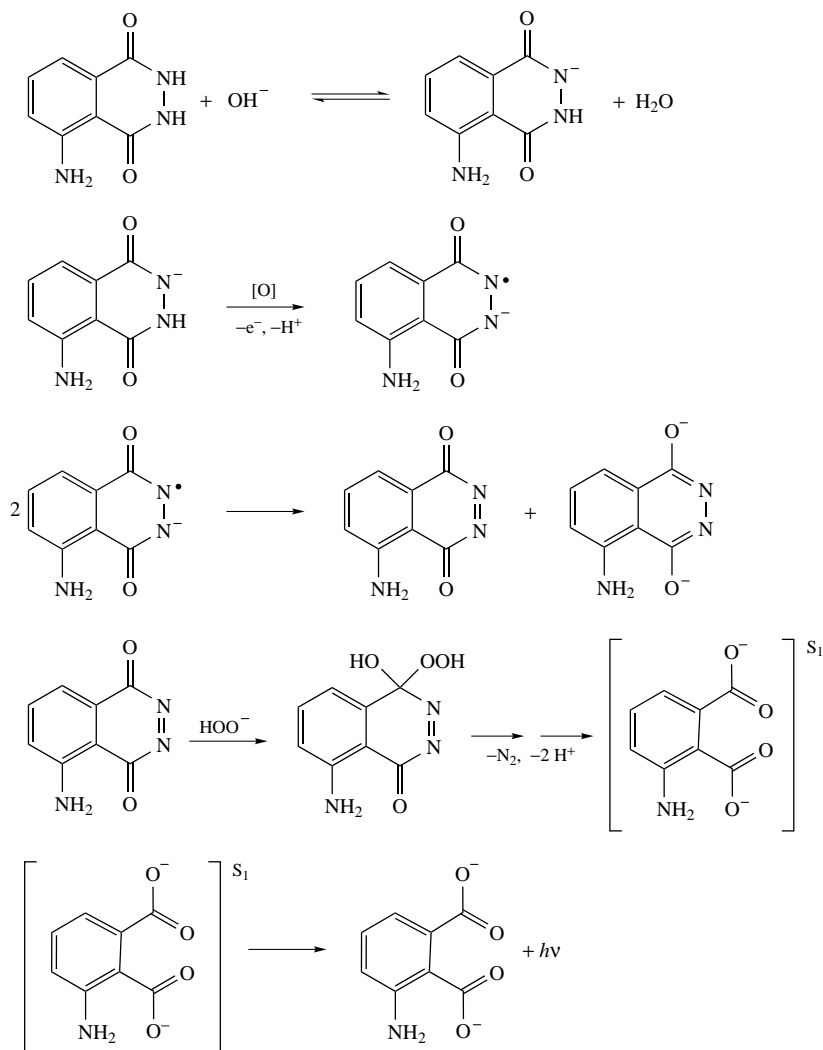
Briefly, the well-established mechanism for luminol oxidation by hydrogen peroxide and a catalyst in alkaline aqueous media involves the formation of a luminol radical anion that is further oxidized to a diazaquinone, which, upon reaction with hydrogen peroxide, undergoes nitrogen elimination with ring opening to yield **3-AP** in its singlet excited state. The latter's decay is responsible for the emission of light observed^{178,180} (Scheme 20). However, the mechanism of chemiexcitation is still unknown and several proposals have been made over the years.

2. Chemiexcitation mechanism

In the first proposal of a mechanism for chemiluminescent luminol oxidation, Albrecht postulates a bicyclic endoperoxide as the high-energy intermediate⁴. The endoperoxide is presumably formed by nucleophilic attack of hydrogen peroxide monoanion on one of the diazaquinone **27** carbonylic groups to form **28**, followed, after deprotonation to **29**, by ring closure to **30** (Scheme 21)^{177,200}.

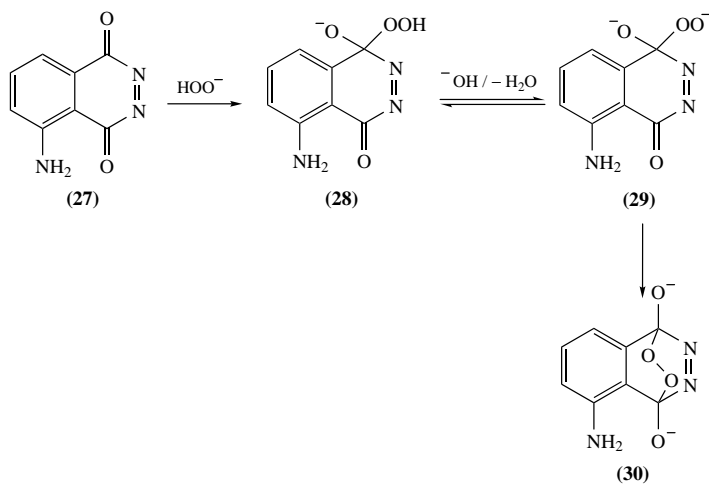
Decomposition of the endoperoxide **30** releasing a N₂ molecule, concomitantly with 3-aminophthalate excitation, can be viewed as an allowed [2 + 2 + 2] pericyclic reaction; therefore, this transformation should not lead to excited-state formation²⁰¹. However, the mechanism proposed by Flynn and Michl for chemiexcitation postulates that the first step, involving the endoperoxide **30**, would be analogous to the retro-Diels–Alder reaction of 1,4-dihydrophthalazine (Scheme 22)²⁰². In this way, the energy-rich peroxide dianion **31** is not converted to a much more stable aminophthalate dianion product in the ground state, as the 18 π electron ground state of peroxide **31** correlates with a doubly excited n,n – π^* , π^* state of aminophthalate product and not with the 16 π electron ground state²⁰¹. Since both species are totally symmetrical, the crossing of two states is avoided. However, it is likely that an S₁-S₀ conical intersection can be reached when the symmetry is lowered, and this ought to provide a facile radiationless crossing between surfaces, resulting in the chemiexcited **3-AP**²⁰¹.

The attempt to prepare a compound analogous to endoperoxide **30** from the reaction of 1,4-dimethoxyphthalazines with singlet oxygen resulted in the formation of the corresponding phthalate by elimination of N₂, albeit no chemiluminescence was observed²⁰³. Even though no experimental evidence indicates its existence, the endoperoxide intermediate **30** is one of the most well-accepted HEI postulated for the chemiexcitation step in luminol chemiluminescence.

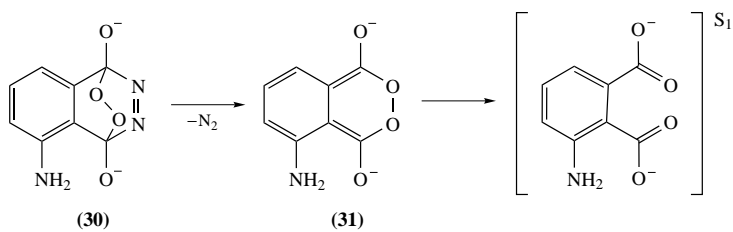


SCHEME 20

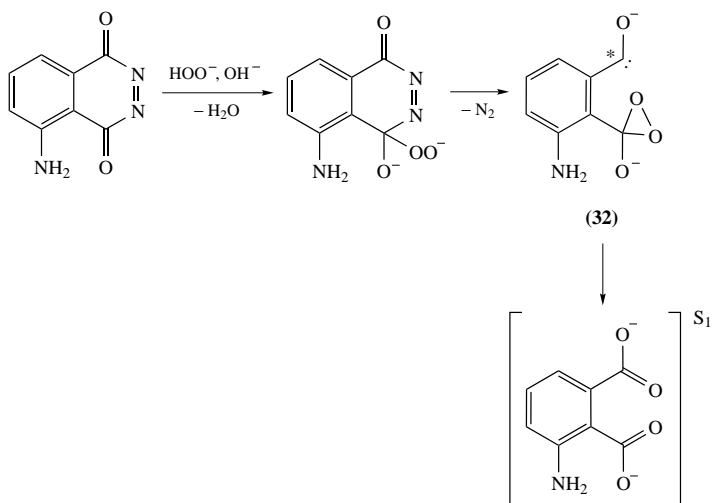
Steinfatt proposed an alternative mechanism for the formation of excited aminophthalate, based on the concept of dioxirane-carbene mediated chemiexcitation, which is also attributed to other chemiluminescent systems^{204–208}. After the attack of hydrogen peroxide on the diazaquinone **27** carbonyl carbon, a perhydrolysis step is postulated to result in the intramolecular dioxirane-carbene system (**32**) in the excited state^{207,209}. This species presumably rearranges to 3-aminophthalate dianion while still in the singlet-excited state (Scheme 23). Although this is a very interesting mechanistic proposal, it is based on experimental evidence obtained with indirect phthaloyl peroxide chemiluminescence^{210–212} and no further evidence corroborates this proposal.



SCHEME 21

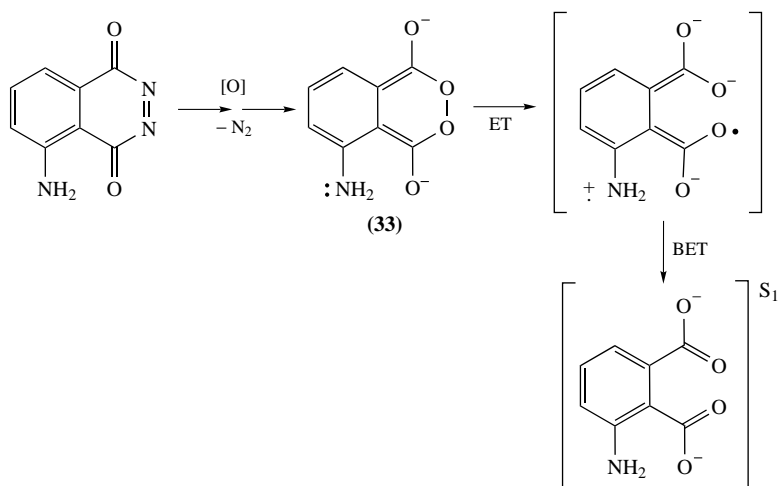


SCHEME 22

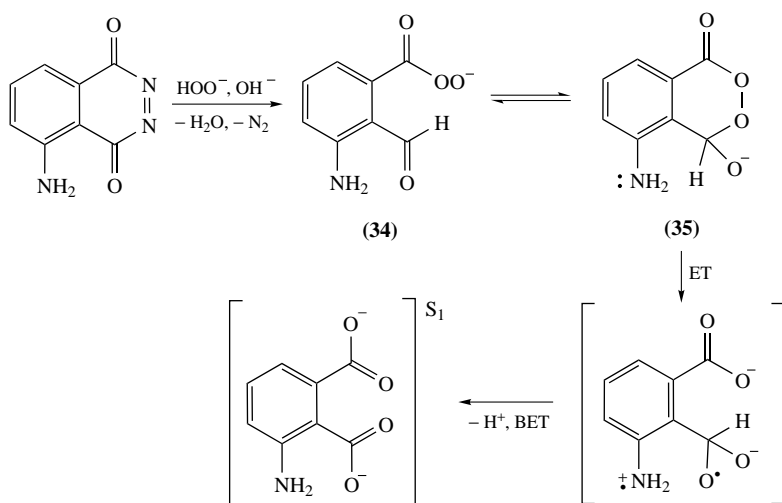


SCHEME 23

A CIEEL approach can also be used to explain chemiexcitation in luminol chemiluminescence^{213,214}. Two possibilities arise: (i) an electron transfer from the amino group to the peroxidic moiety in the antiaromatic peroxide **33**, resulting in bond cleavage followed by intramolecular back-electron transfer and formation of excited 3-aminophthalate (Scheme 24)^{213,214}; (ii) the equilibrium between the peroxy-carboxylic aldehyde **34**, formed after elimination of nitrogen, and the cyclic peroxy semiacetal **35** is shifted in the direction of **35**, as the result of an electron transfer from the amino group to the cyclic peroxide moiety, followed by O–O bond cleavage^{213,214}. Back-electron transfer would result in chemiexcitation (Scheme 25).



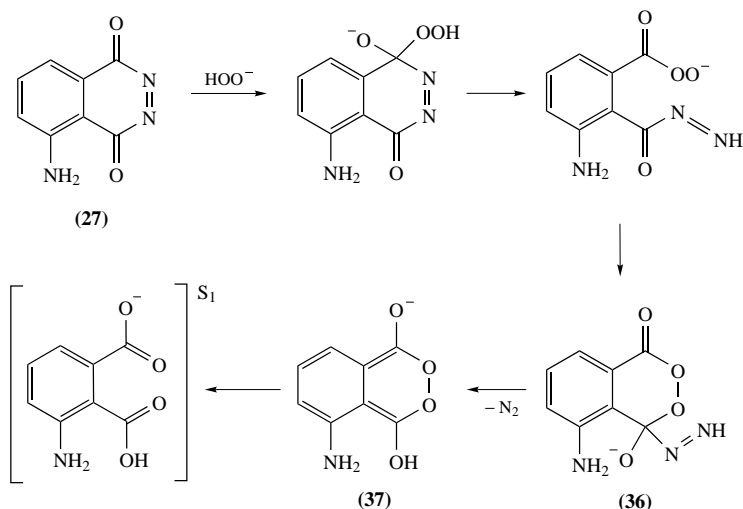
SCHEME 24



SCHEME 25

It must be pointed out that, despite the lack of direct experimental support for this hypothesis, the involvement of the electron transfer in luminol chemiexcitation is related to the chemiexcitation steps proposed for several highly efficient chemi- and bioluminescent systems, such as activated peroxyoxalate chemiluminescence and the firefly luciferin/luciferase system (Section VI.C)^{41,215}.

An alternative mechanistic proposal has been made involving opening of the cyclic hydrazide after the initial nucleophilic attack of H₂O₂. Investigations of the reaction of several nucleophiles with diazaquinone **27** show that nucleophilic attack occurs on the carbonyl group, followed by ring opening²¹⁶. The steps following the rupture of the C–N bond of luminol hydroperoxide are too fast to be detected. The subsequent intramolecular nucleophilic peracid attack on the carbonyl hydrazide results in the formation of compound **36** (Scheme 26). The breakdown of this cyclic tetrahedral intermediate through the expulsion of N₂ generates the antiaromatic endoperoxide **37**, which is transformed into excited phthalate in a pericyclic process (Scheme 26).



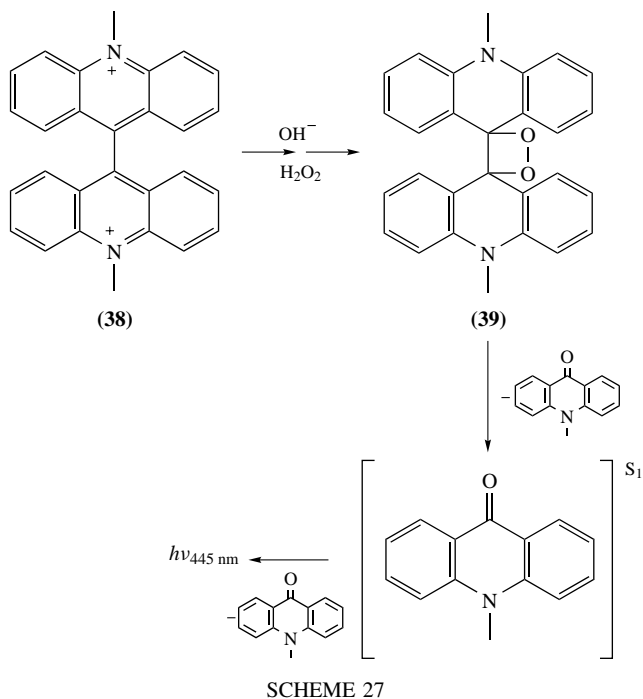
SCHEME 26

Semiempirical calculations indicate that there is a local energy minimum for the endoperoxide **37** with a barrier height of 6 kcal mol⁻¹ corresponding to a lifetime of *ca* 10⁻⁹ s, in agreement with experimental results^{178,217}. However, the most important result, which corroborates the hypothesis of **37** as the HEI in luminol chemiluminescence, is the state correlation between the ground state of **37** and the excited state of **3-AP**²¹⁷.

B. Chemiluminescence from Lucigenin and Related Compounds

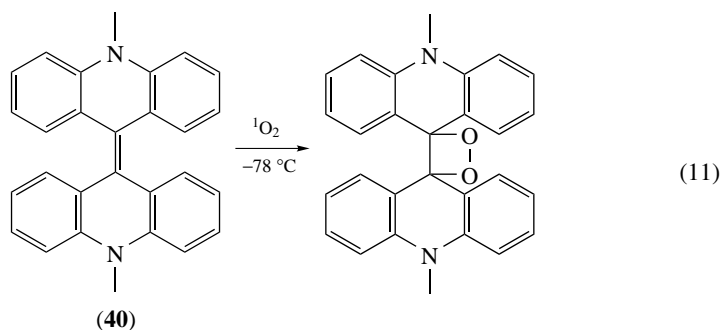
1. Lucigenin

Lucigenin (10,10'-dimethyl-9,9'-biacridinium or bis-*N*-methylacridinium (**38**)), in the presence of hydrogen peroxide in alkaline media, exhibits chemiluminescence with a maximum emission wavelength at 445 nm²¹⁸. Lucigenin chemiluminescence was first reported in 1935 by Gleu and Petsch, and the 1,2-dioxetane **39** was postulated as a key intermediate⁵. Nevertheless, the mechanism of lucigenin chemiluminescence was only elucidated by McCapra and Richardson, who also proposed the thermal decomposition



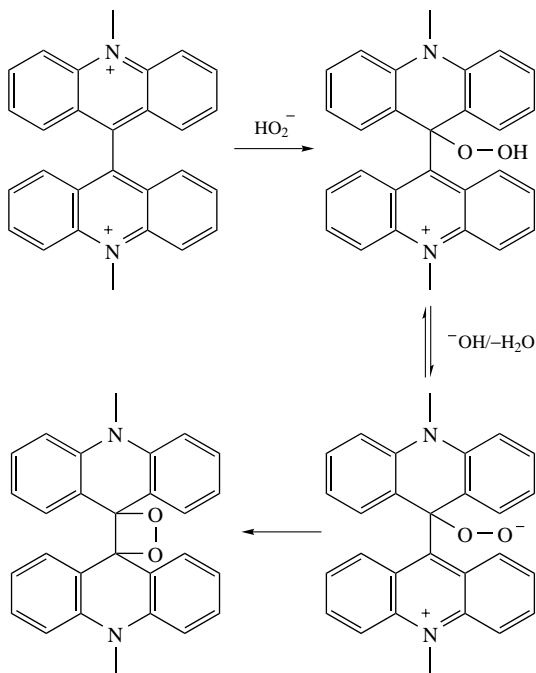
of a 1,2-dioxetane as the energy source for *N*-methylacridane electronic excitation²¹⁸ (Scheme 27).

The 1,2-dioxetane postulated as intermediate was never isolated²¹⁹. However, indirect evidence of a 1,2-dioxetane as a reaction intermediate was obtained by chemiluminescence resulting from the reaction of 10,10'-dimethyl-9,9'-biacridene (**40**) with singlet oxygen^{219,220} (equation 11). Several sources of singlet oxygen were used and, in each case, the reaction resulted in chemiexcitation of *N*-methylacridane.



The mechanism of 1,2-dioxetane formation in the reaction of lucigenin with hydrogen peroxide suggests a nucleophilic attack of peroxide anion on position 9 of the acridinium ring, followed by deprotonation and subsequent formation of 1,2-dioxetane ring

(Scheme 28)^{219, 220}. Quantum yields of lucigenin oxidation by hydrogen peroxide in alkaline media are comparable with the values obtained in luminol oxidation ($1.24 \times 10^{-2} \text{ E mol}^{-1}$)²²⁰⁻²²². However, the use of other peroxides, such as *tert*-butyl hydroperoxide, results in a decrease of chemiluminescence quantum yields of two orders of magnitude, confirming the hypothesis that a 1,2-dioxetane is the HEI, since its formation would be impossible with alkyl peroxides²²⁰.

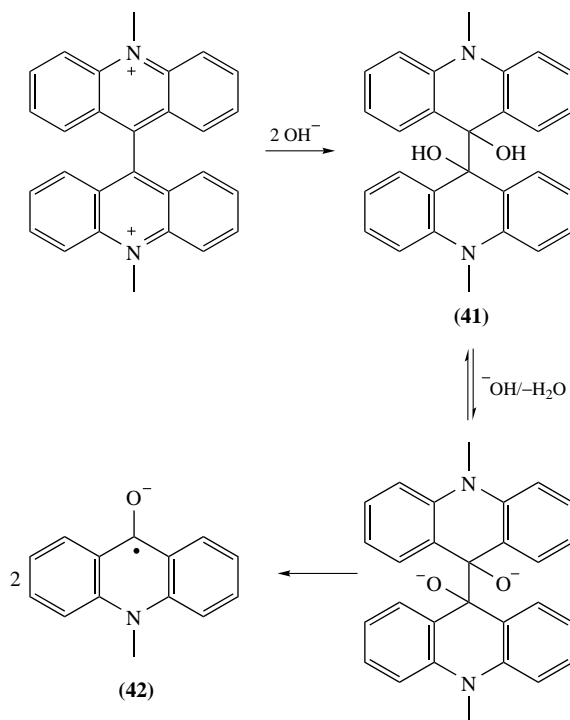


SCHEME 28

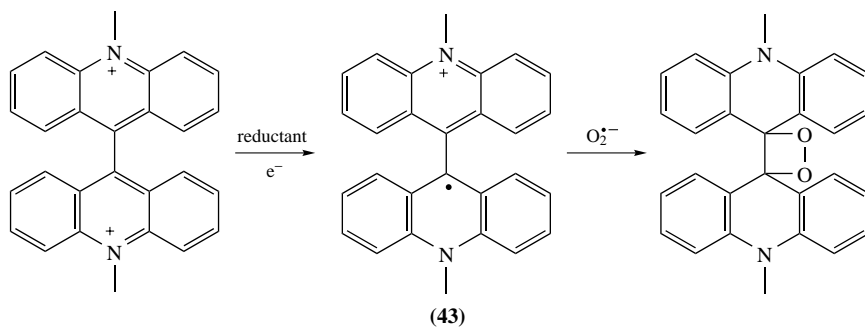
The reaction of lucigenin and different nucleophiles was first studied by Janzen and collaborators²²³. In highly alkaline media, the formation of lucigenin pinacol (**41**) resulting from the nucleophilic attack of hydroxyl ion at position 9 of lucigenin is observed^{218, 221, 223}. Other nucleophiles, like cyanide, trifluoroethoxide and triethylamine, have been investigated in DMSO as solvent and *N*-methylacridone was consistently formed as the final product, presumably via oxidation of a *N*-methylacridone radical anion (**42**). Although this radical was never observed in EPR experiments²²³, homolytic cleavage of a pinacol dianion is assumed to be likely²²⁴ (Scheme 29).

Legg and Hercules have shown that the reaction of superoxide with lucigenin results in chemiluminescence²²⁵. A similar conclusion was reached by Fridovich and coworkers, who observed chemiluminescence upon the addition of lucigenin to the xanthine-xanthine oxidase system, which is known to produce $\text{O}_2^{\cdot-}$ ²²⁶. In order to emit chemiluminescence, lucigenin must first be reduced by one electron to produce the radical cation **43**²²⁷ (Scheme 30). This species reacts with superoxide ion, producing the intermediate 1,2-dioxetane, whose decomposition is responsible for luminescence²²⁸.

In addition, Bruice and collaborators have found that the addition of superoxide dismutase to a solution of lucigenin in aerated carbonate buffer (pH 10.7) decreases the intensity



SCHEME 29



SCHEME 30

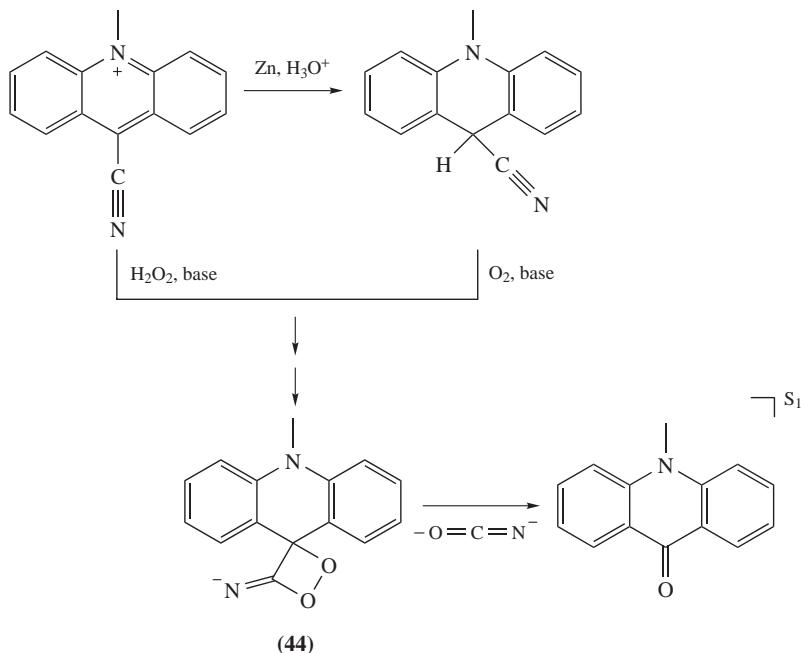
of light emission^{220,221}. Hence, lucigenin is widely used as a chemiluminescent probe for detecting superoxide ions, especially in biological systems²²⁹⁻²³¹.

2. Acridinium salts and acridans

Acridinium derivatives can be oxidized with hydrogen peroxide²³²⁻²³⁵ and other peroxides²³⁶, persulfates²³⁷ or molecular oxygen²³⁸⁻²⁴⁰ in neutral or alkaline media, resulting

in chemiluminescence²⁴¹. It has been shown that the chemiluminescence efficiency is correlated with the pK_a of a leaving group linked to the 9-carboxylic function of the acridinium rings^{218, 232}. Several classes of chemiluminescent acridinium derivatives, using phenols, thiols, sulfonamides and fluoroalcohols as leaving groups, have been described²³⁴. Ring substitution, as well as replacement of the *N*-methyl group by an alkyl chain or a carboxymethyl group, has little effect on either the quantum yield or the chemical stability¹⁷⁴. Higher applicability can be obtained, however, by using groups that can maintain the emitting species linked to biomolecules²⁴²⁻²⁴⁵.

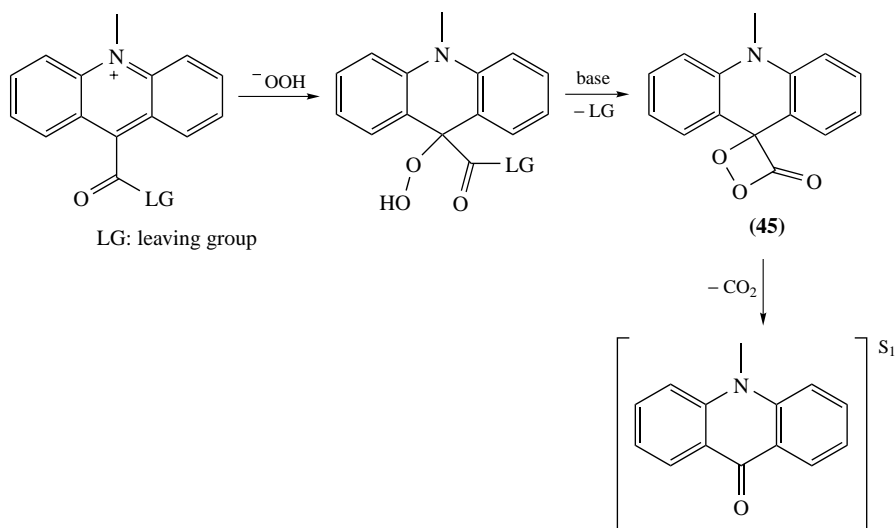
In the presence of hydrogen peroxide and base, acridinium salts lead to chemiluminescence emission. Acridans, in their reduced forms, are able to react directly with oxygen in aprotic solvents with Φ_{CL} up to 10%²⁴⁶. Scheme 31 shows the proposed mechanism for chemiluminescence of 9-cyano-10-methylacridan and 9-cyano-10-methylacridinium salt in the presence of oxidant and base, which postulates the cyclic peroxidic intermediate **44**.



SCHEME 31

Analogously to the firefly luciferin/luciferase system, the general chemiluminescence mechanism postulated for 9-carboxyacridinium derivatives proposes the 1,2-dioxetanone **45** as high-energy intermediate^{218, 232, 247}. However, this 1,2-dioxetanone is the only intermediate that has not yet been isolated¹⁷⁴. The cleavage of the peroxidic ring presumably results in the release of CO₂ and the formation of an acridan residue in its electronically excited state (Scheme 32).

Acridinium derivatives, specifically the 9-carboxyacridinium phenyl esters, are one of the most efficient chemiluminescent labels used in immunoassays since 1980^{172, 174}.



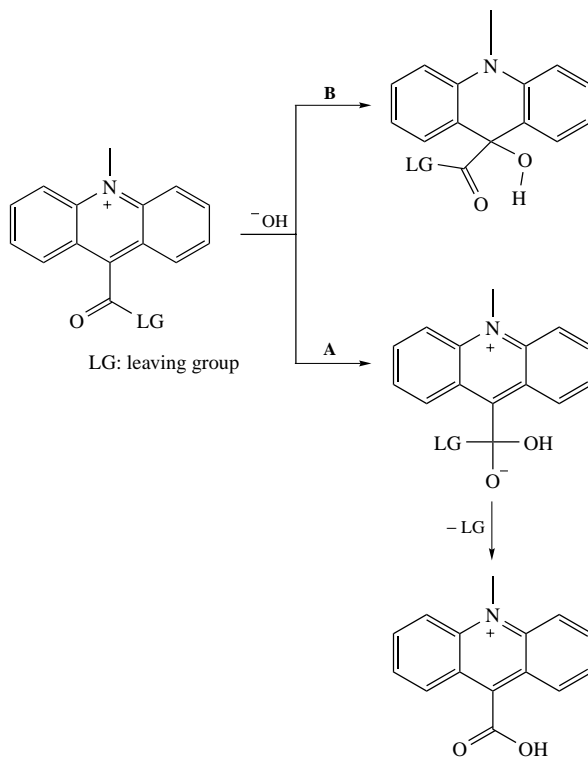
SCHEME 32

Hydrolysis resulting from nucleophilic attack of HO^- on carbonyl carbon is the main source of loss of efficiency, since the carboxylic acid derivative is nonchemiluminescent (Scheme 33, A). However, nucleophilic attack of the hydroxide anion on position 9 of the acridinium ring is preferred and also results in loss of chemiluminescence (Scheme 33, B)²³⁵.

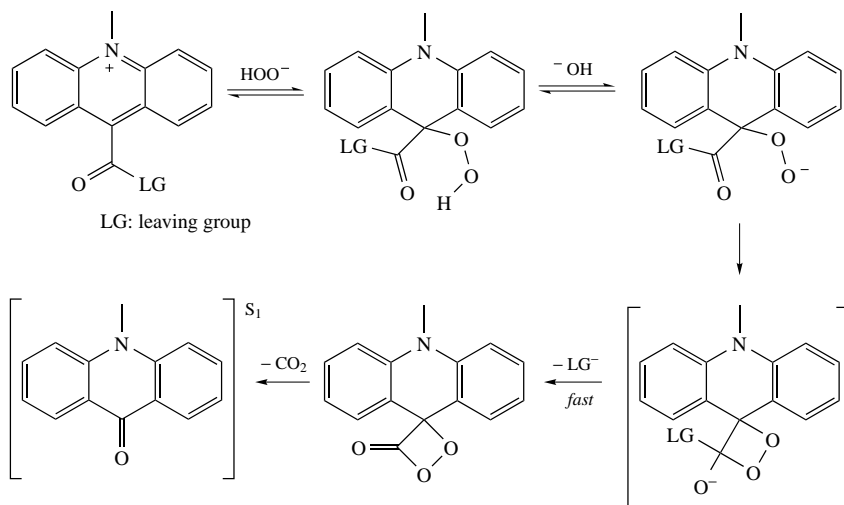
Blazejowski and collaborators have studied the chemiluminescence of 9-carboxy and 9-cyano-10-methylacridinium, in the presence of hydrogen peroxide, using theoretical methods^{235,241}. For both compounds, attack of HOO^- on carbon atom 9 of the acridinium derivative was confirmed to be favorable compared to a base attack on the same position. After the deprotonation of the hydroperoxyl group, an intramolecular nucleophilic attack leads to an intermediate which might, in the case of 9-carboxyacridines, eliminate the leaving group (LG), resulting in 1,2-dioxetanone, the postulated HEI of this system (Scheme 34). In the case of 9-cyano derivatives, the analogous pathway would lead to the formation of the cyclic peroxidic intermediate **44**, which would yield an electronically excited acridane upon thermal decomposition (Scheme 35).

The most widely accepted mechanism for chemiluminescent oxidation of acridinium derivatives proposes that chemiexcitation can originate from intermediates analogous to **45** and **46**. Theoretical calculations indicate that the preferential pathway, in the case of 9-carboxy derivatives, may be the cleavage of the peroxidic ring in compound **46**, with release of a carboxylic fragment containing the leaving group, instead of cleavage of a 1,2-dioxetanone. (Scheme 36)²³⁵. This may be reaffirmed by a concerted chemiexcitation of the 9-cyano derivatives instead of cleavage of intermediate **44**. However, the results obtained using the PM3 semiempirical method are still inconclusive and experimental evidence is certainly necessary to confirm one or the other possibility for the HEI responsible for chemiexcitation in these transformations²⁴¹.

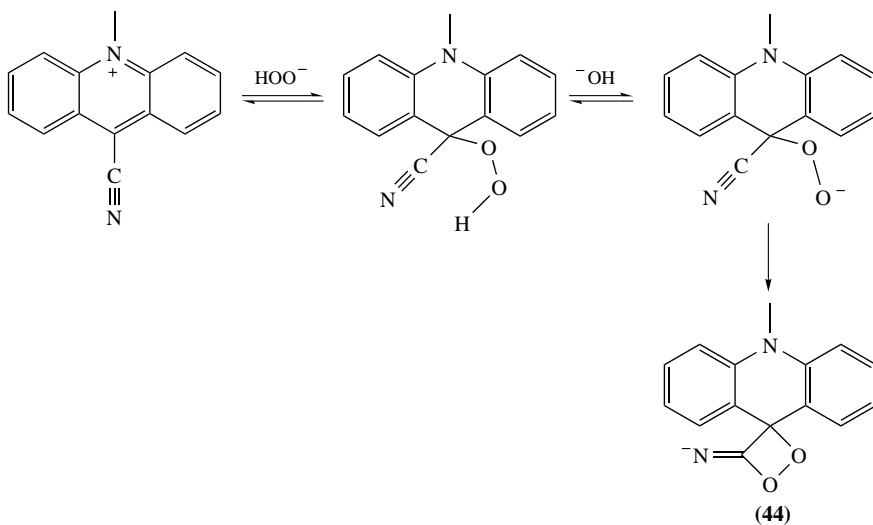
The synthesis of *N*-methylacridan dioxetane derivatives would be very promising for analytical application as chemiluminescence probes. Despite the high quantum yields



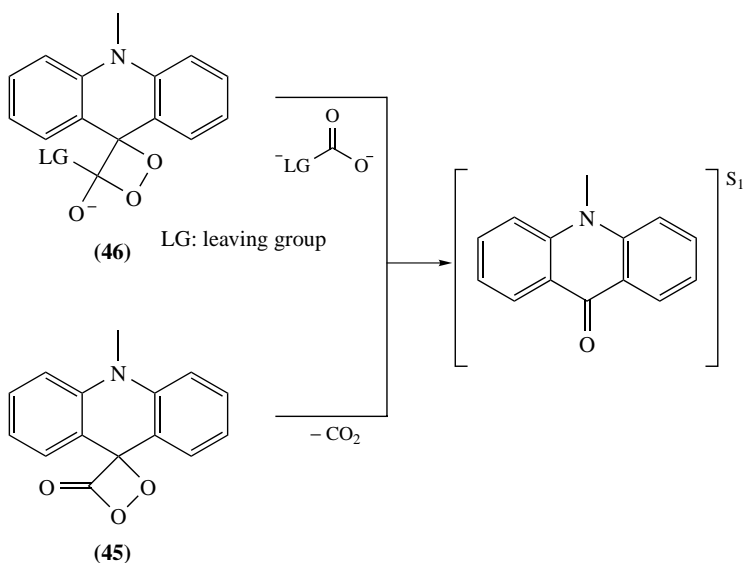
SCHEME 33



SCHEME 34



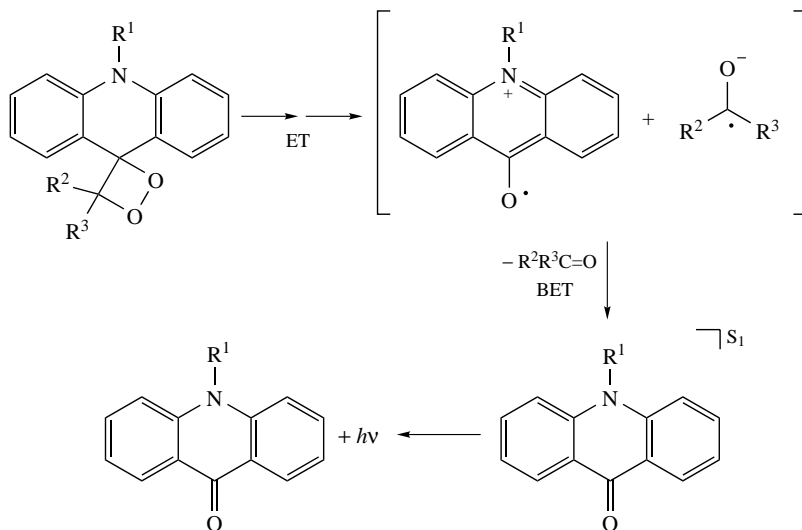
SCHEME 35



SCHEME 36

deriving from its decomposition (*ca* 25%), these compounds are highly unstable and only adamantyl-substituted dioxetanes were isolated^{38,248}. The intramolecular decomposition of *N*-methylacridan dioxetanes is in agreement with the proposed electron transfer in *Cypridina*, *Renilla*, and firefly bioluminescence²⁷. McCapra and coworkers associated the high chemiluminescent quantum yields observed in the decomposition of 10-methylacridan

dioxetanes with a mechanism that postulates the involvement of radical-ion intermediates (Scheme 37). This hypothesis is supported by the electron-donating nature of the nitrogen atoms in these acridinium substituted 1,2-dioxetanes, which should facilitate the initial electron transfer (Scheme 37, ET)²⁷.



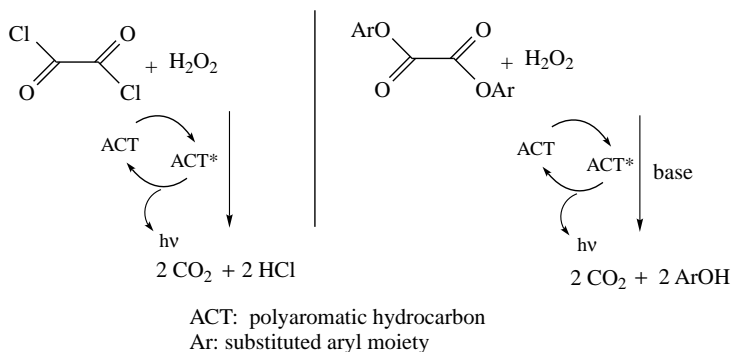
SCHEME 37

Several other examples of 1,2-dioxetane derivatives containing easily oxidizable groups have been reported and the high singlet quantum yield observed in their decomposition was attributed to the occurrence of the intramolecular CIEEL sequence^{28,144}. Based on this concept, Schaap and coworkers have introduced the concept of induced chemiluminescence, which is very relevant for investigations into firefly luciferin bioluminescence^{29,31} and has led to the development of chemiluminescent probes widely used in immunoassays (Section V.B.2)^{233,249-253}.

C. Peroxyoxalate Chemiluminescence

In the early 1960s, Chandross⁶ observed the emission of visible light during the reaction between oxalyl chloride and hydrogen peroxide in the presence of rubrene. This was considered a milestone in the discovery of a new chemiluminescent reaction, which was named the peroxyoxalate system. Rauhut's group replaced oxalyl chloride by electron withdrawing substituted phenolic esters of oxalic acid^{7,254,255}, thereby obtaining more adequate reagents for the practical application of chemiluminescence. The reaction of either oxalyl chloride or these esters with hydrogen peroxide catalyzed by a nucleophilic base (usually salicylates or imidazole), in the presence of suitable polyaromatic hydrocarbons with low oxidation potential, the so-called activators (ACT), is accompanied by a strong light emission (Scheme 38).

This chemiluminescent reaction is responsible for the bright light emission in the light-sticks used as a source of cold light in entertainment, fishing, diving and mining, where nonflammable cold light is desirable. In order to increase the emission intensity and lifetime of light-sticks, it is necessary to use very soluble oxalic ester derivatives and to



SCHEME 38

optimize the concentration of hydrogen peroxide, activator and catalyst. It is worth noting that, although light-sticks are considered nontoxic and used by children, to the best of our knowledge, no systematic approach has been proposed to evaluate the toxicity of oxalic esters and activators. As can be inferred from the known toxicity of polyaromatic hydrocarbons (activators), chlorophenols and oxalic acid, it is highly unlikely that light-sticks are nontoxic.

Apart from the practical and leisure-related uses of the peroxyoxalate system, it is also widely utilized as a highly sensitive analytical tool for the quantification of fluorescent substances^{256–260}, metals^{261,262} and hydrogen peroxide^{263–269}. Since Chandross first reported this chemiluminescent reaction, many articles have appeared in the literature reporting on the development of efficient and reproducible systems for analytical purposes. These studies generally concern the synthesis of suitable oxalic ester derivatives^{270–273} or analyte quantification using high-pressure liquid chromatography and capillary electrophoresis with direct detection^{274–286} or with post-column derivatization^{259,267,287–295}. A particularly attractive feature many researchers have been seeking is the synthesis of designed oxalic esters that are more soluble and stable in an aqueous medium^{266,296–300}. To circumvent the problem of lower water solubility and fast hydrolysis by water, some authors have investigated peroxyoxalate emission in micellar environments^{301–303}.

Due either to the appeal of analytical applications or the complex mechanistic pathways, one can envisage why most articles on peroxyoxalate in the literature involve analytical subjects while only a fraction focus on the mechanistic aspects of this transformation. Even so, it is obvious that unequivocal knowledge about the mechanism involved in the generation of electronically excited states in this complex transformation is of fundamental importance, not only from the academic point of view but also, and far more, for the rational design of analytical application and the interpretation of analytical results^{73,301–304}.

In this part of the chapter, we will focus essentially on mechanistic aspects of the peroxyoxalate reaction. For the discussion of the most important advances in mechanistic aspects of this chemiluminescent system, covering mainly literature reports published in the last two decades, we will divide the sequence operationally into three main parts: (i) the kinetics of chemical reactions that take place before chemiexcitation, which ultimately produce the high-energy intermediate (HEI); (ii) the efforts to elucidate the structure of the proposed HEIs, either attempting to trap and synthesize them, or by indirect spectroscopic studies; and lastly, (iii) the mechanism involved in chemiexcitation, whereby the interaction of the HEI with the activator leads to the formation of the electronically excited state of the latter, followed by fluorescence emission and decay to the ground state.

1. Mechanistic studies on the steps prior to chemiexcitation

The mechanism of the peroxyoxalate reaction can be investigated either by changes in absorbance caused by the release of phenolic moieties from the oxalic ester or by light-emission measurements. In a typical light emission experiment (Figure 3A) using, for example, bis(2,4,6-trichlorophenyl) oxalate (TCPO), H_2O_2 and imidazole (as catalyst) in the presence of the activator 9,10-diphenylanthracene (DPA), one can observe an initial increase in light emission (k_{obs2} , formation rate constant), followed by light intensity decay (k_{obs1} , decay rate constant). The rate constant k_{obs1} obtained in emission experiments corresponds to the rate constant determined from absorption experiments (k_{obs} , Figure 3B), indicating that these rate constants correspond to the same reaction step. The observed rate constants k_{obs1} and k_{obs2} are related to the slow initial reaction steps and attributions can be made from the dependence of these constants on the reagent concentrations (H_2O_2 and imidazole). Because the chemiexcitation step is undoubtedly faster than the preceding ones, it cannot be observed by conventional kinetic methods.

Although kinetic results obtained from the peroxyoxalate system have been interpreted in different ways, it is possible to group the convergent results and interpretations in order to formulate a consensual and more general mechanism for the steps that lead to HEI formation. In the presence of a nucleophilic base, the foremost pathway for the chemiluminescent reaction is the replacement of two phenolic moieties by the nucleophile, followed by the reaction of the formed intermediate with hydrogen peroxide, which subsequently leads to the HEI formation and, hence, light emission in the presence of an activator. In the absence of a nucleophilic base, the mechanistic pathway is simpler, involving the initial replacement of a single phenolic moiety by hydrogen peroxide, probably followed by cyclization and HEI formation (Scheme 39).

Rauhut and coworkers^{7,305-307} were the first to obtain rate constants from emission kinetic studies and to verify the dependence of k_{obs1} and k_{obs2} on the concentration of the base catalyst and on hydrogen peroxide, respectively. Schowen and coworkers³⁰⁸, using TCPO, H_2O_2 and DPA, with triethylamine as catalyst, observed an oscillatory behavior in emission experiments and proposed a mechanism involving the formation of two HEIs (involved in parallel chemiluminescent reactions) to explain it. Other authors have also observed a similar oscillating behavior^{309,310}, but have explained it as a complex

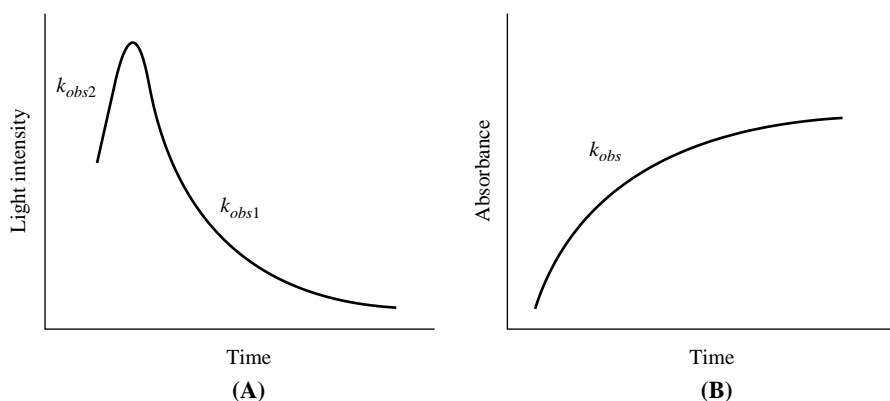
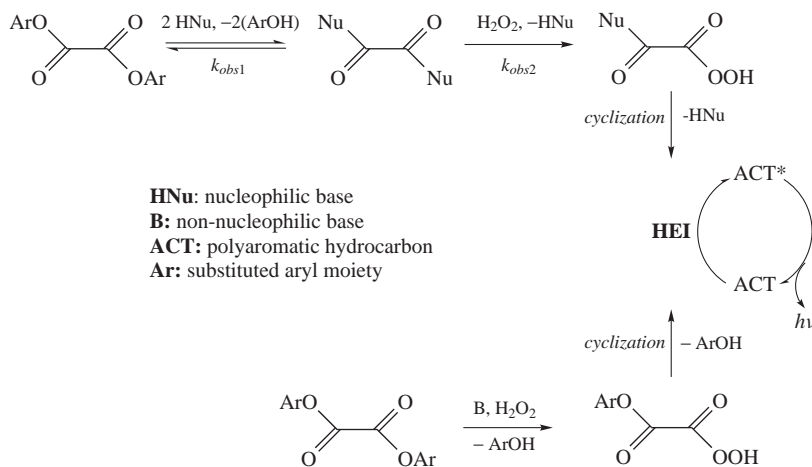


FIGURE 3. Typical emission (A) and absorbance (B) profiles observed in kinetic experiments with the peroxyoxalate system of oxalic esters reacting with base. A: Light emission in the presence of ACT. B: Absorption change due to phenol release in the absence of ACT



SCHEME 39

competition between the preceding steps of the HEI formation at low catalyst concentration, without the necessary postulation of two HEIs. It should be pointed out here that the oscillatory or chaotic behavior is observed when either low nucleophilic base concentrations or no base at all is used and it can be prevented by using any base in higher concentrations.

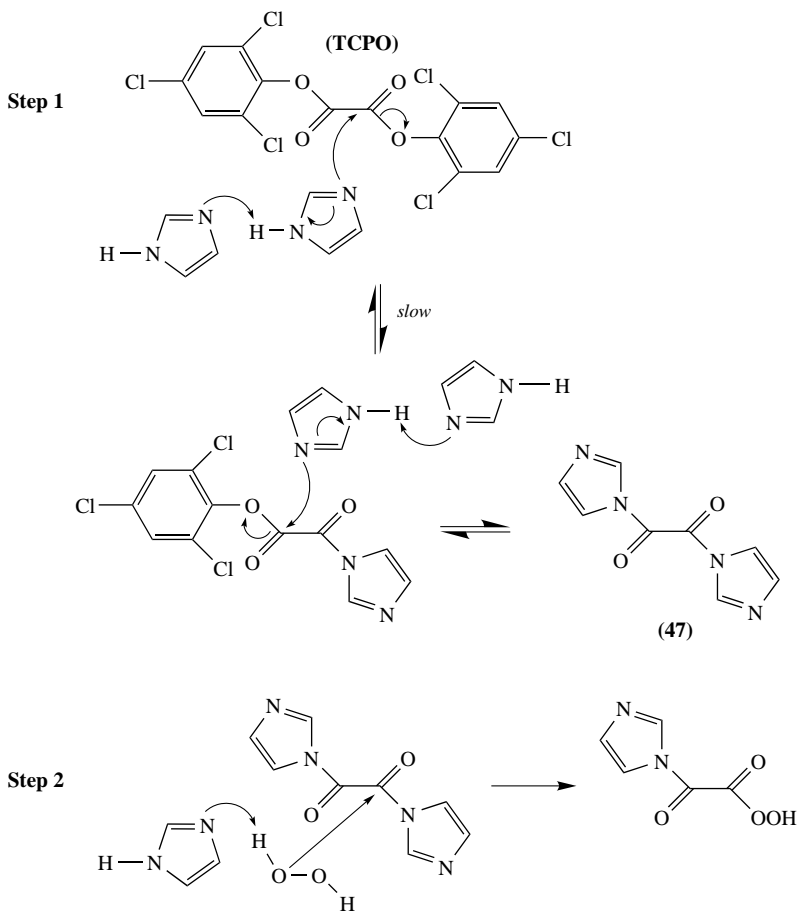
Schowen and coworkers³¹¹ concluded that a simplified kinetic behavior can be obtained only in the presence of substantial amounts of water ($\text{CH}_3\text{CN}/\text{H}_2\text{O}$, 3:1). The authors assigned k_{obs2} to a sum of two rate constants associated with the competitive nucleophilic attack of H_2O_2 and imidazole on the carbonyl carbons of TCPO. In addition, k_{obs1} was assigned to a nonchemiluminescent decomposition step of a peracid intermediate and the cyclization rate of the latter to the HEI. Nevertheless, as was later shown independently by two research groups^{309,312}, k_{obs2} is related to the nucleophilic attack of hydrogen peroxide assisted by the base on the carbonyl function of 1,1'-oxalyldiimidazole (**47**), a key intermediate formed by replacement of the two TCPO phenolic moieties by imidazole. Furthermore, k_{obs1} was shown to correspond to the nucleophilic replacement of the first phenolic unit by imidazole (the slowest step in the reaction); the replacement of the second 2,4,6-trichlorophenol by imidazole appears to occur in a much faster step not observed kinetically³⁰⁹.

Imidazole is currently the most commonly used catalyst in kinetic studies on the peroxyoxalate reaction, because it leads to reproducible kinetic results and is highly soluble in organic solvents as well as in water. (Although it is a mere coincidence and not the cause of its use in the peroxyoxalate reaction, it is interesting to mention that the catalytic site of some hydrolytic enzymes and luciferin, the enzyme associated with the bioluminescence in fireflies, contain imidazole moieties from the amino acid histidine.) It has already been used in mechanistic investigations on this reaction in the early 1980s³¹³ and still appears to be the nucleophilic and base catalyst producing one of the highest total quantum yields of light emission, although other catalysts have been shown to be useful and can lead to faster reaction kinetics³¹⁴.

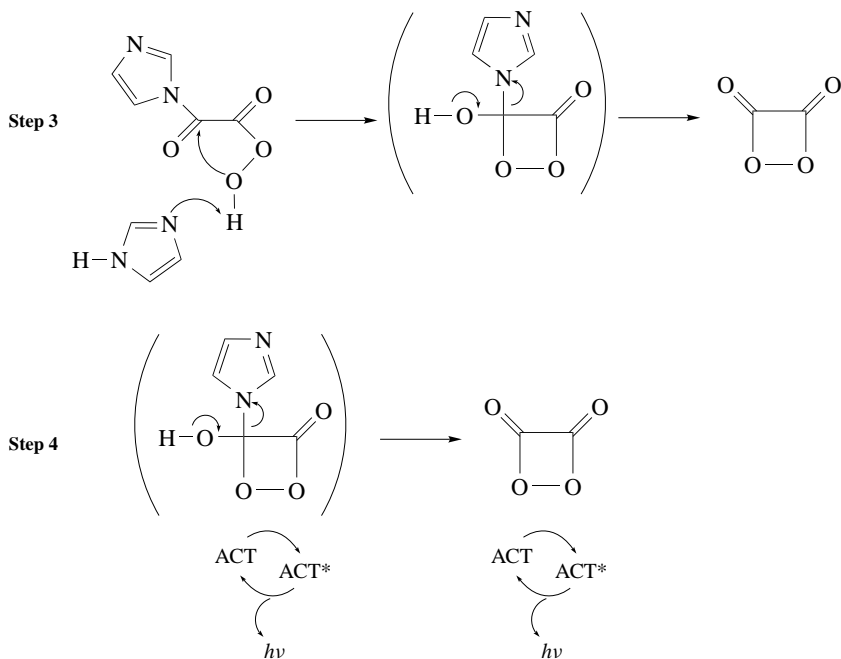
The reliability and reproducibility of kinetic experiments performed with imidazole as nucleophilic base catalyst have allowed mechanistic information to be obtained on the initial reaction steps. The observation of second-order dependencies of k_{obs1} ^{309,312} on the imidazole concentration supported the conclusion that two imidazole molecules

are involved in the transition state and can be rationalized on basis of the 'imidazole catalyzed nucleophilic attack of imidazole'³¹⁵. As mentioned earlier, the rate-determining step in the peroxyoxalate chemiluminescent reaction in the presence of imidazole is the replacement of the first phenolic moiety of the oxalic ester by this base, followed by the faster replacement of the second phenol, leading to 1,1'-oxalyldiimidazole formation. However, at high concentrations of hydrogen peroxide, the direct attack on the ester can also be observed^{309,310,316,317}. In fact, k_{obs1} does not depend on hydrogen peroxide (at least in concentrations below 20 mM). A linear correlation of k_{obs2} with the peroxide concentration is observed, indicating that this rate constant corresponds to the nucleophilic attack of hydrogen peroxide on 1,1'-oxalyldiimidazole^{309,317}.

On the basis of the results discussed above, it is possible to propose a detailed mechanistic scheme for the occurrence of the chemiluminescent reaction of oxalic esters and hydrogen peroxide in the presence of imidazole as base and an ACT (Scheme 40). The oxalic ester (exemplified with TCPO) reacts in the rate-determining step with imidazole, catalyzed by



SCHEME 40



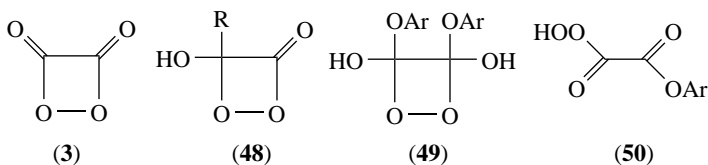
another imidazole molecule, leading to the formation of 1,1'-oxalyldiimidazole (**47**) (step 1). The latter reacts with hydrogen peroxide, yielding a peracid derivative (step 2) which, in turn, can cyclize, probably after a proton abstraction by imidazole, leading to the HEI formation (step 3). The interaction of this reactive intermediate with the ACT leads to the formation of the excited state of the ACT and consequent light emission (step 4).

The reaction of **47** with hydrogen peroxide should lead to the formation of the corresponding peracid derivative^{312,318,319}. Although peracid derivatives were initially seen as possible HEIs, they were unequivocally excluded as HEI by Stevani and coworkers³²⁰. Nevertheless, **47** as well as peracid derivatives are key intermediates in the formation of the extremely sensitive and elusive HEI.

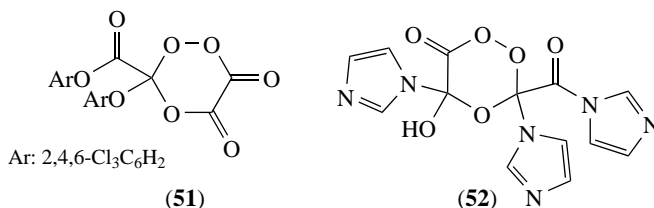
2. Nature of the high-energy intermediate

Chandross⁶ was also the first to observe the 'volatile' nature of the HEI, probably 1,2-dioxetane-3,4-dione (1,2-dioxetanedione, **3**), involved in the peroxyoxalate reaction, reporting that vapors evolving from the chemical reaction of oxalyl chloride with 30% hydrogen peroxide in dioxane '... have the unusual property of inducing the fluorescence of suitable indicators, e.g., a filter paper impregnated with anthracene'. Rauhut and coworkers³⁰⁵ also reported the observation of a volatile HEI using a system in which a strong flux of argon, nitrogen or oxygen was passed through a solution containing bis(2,4-dinitrophenyl) oxalate (DNPO) and hydrogen peroxide in dimethyl phthalate as solvent. The evolving gas produced chemiluminescence in the presence of DPA or rubrene. Unfortunately, further attempts to characterize the volatile HEI using either gas-phase infrared spectroscopy or mass spectrometry have failed^{321,322}, probably due to the

thermal instability of this intermediate. It should be pointed out here that confirmation of the volatile nature of the HEI would provide important evidence regarding its structure since **3** is the only HEI structure, which should certainly be volatile.



R: aryl or imidazolyl group



Catherall and coworkers³²³ studied the reaction kinetics of bis(pentachlorophenyl) oxalate and H_2O_2 catalyzed by salicylate in the presence of DPA and verified that the delayed addition of DPA did not alter the reaction kinetics. The authors also conducted several kinetic studies on the peroxyoxalate system and proposed the participation of 4-hydroxy-4-(pentachlorophenoxy)-1,2-dioxetan-3-one (**48**, $\text{R} = \text{Cl}_5\text{C}_6\text{O}$) as the HEI in the reaction^{72,323}.

Schowen and coworkers³⁰⁸ postulated a mechanistic pathway in which at least two HEIs (**X** and **Y**) interconnected with a nonchemiluminescent intermediate (**Z**) were involved. Possibly, **X** is a peracid intermediate, like either $\text{ArOC(OH)(OOH)CO}_2\text{Ar}$ ($\text{Ar} = 2,4,6\text{-Cl}_3\text{C}_6\text{H}_2$) or **50** ($\text{Ar} = 2,4,6\text{-Cl}_3\text{C}_6\text{H}_2$), while **Y** may be **3** or **48** ($\text{R} = 2,4,6\text{-Cl}_3\text{C}_6\text{H}_2\text{O}$) and **Z** the 3,4-bis(2,4,6-trichlorophenoxy)-1,2-dioxetane-3,4-diol (**49**, $\text{Ar} = 2,4,6\text{-Cl}_3\text{C}_6\text{H}_2$). Schowen and coworkers³¹¹ likewise considered **48** ($\text{R} = 2,4,6\text{-Cl}_3\text{C}_6\text{H}_2\text{O}$) the most probable structure for the HEI.

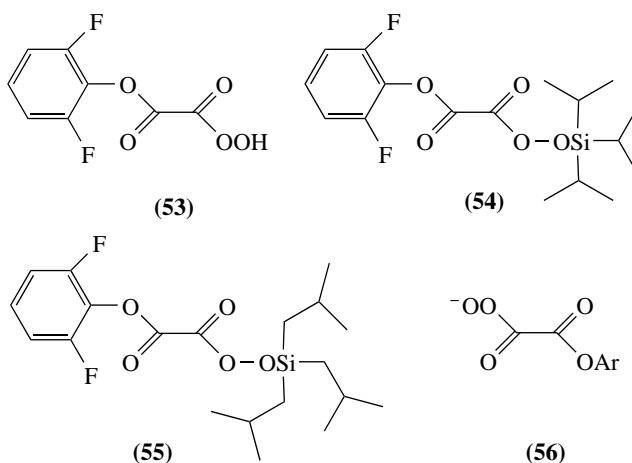
Based on the kinetic results of experiments with photoinitiated peroxyoxalate chemiluminescence³²⁴, Milofsky and Birks³²⁵ proposed, for the first time, the involvement of a six-membered cyclic peroxide (**51**) as HEI. On the basis of this suggestion, Hadd and coworkers³¹⁸, using conventional chemiluminescent kinetic studies with **47**, also proposed the involvement of two HEIs, **48** and another six-membered cyclic peroxide **52** similar to **51**.

Lee and coworkers³²⁶ postulated the involvement of **50** and **51** ($\text{Ar} = 2,4\text{-dinitrophenyl}$) as two HEIs formed in parallel in the uncatalyzed reaction of DNPO and hydrogen peroxide in the presence of perylene. Due to the experimental observations of light emission from the reaction of DNPO and TCPO also in the absence of hydrogen peroxide, Lee and coworkers³²⁷ postulated the involvement of a nonperoxidic HEI (additionally to **51** and **3**, **48** or **52**) under these conditions. However, neither chemiluminescence quantum yields nor even relative emission intensities have been reported. Furthermore, it was shown¹⁴³ that the intensities and the chemiluminescence quantum yields in the absence of hydrogen peroxide are five orders of magnitude lower than in the presence of 10^{-2} M H_2O_2 , indicating that the proposed additional pathway is of extremely low efficiency for excited-state

formation, if it exists at all. Furthermore, it was proposed that the observed chemiluminescence emission in the absence of added hydrogen peroxide might be due to peroxide traces present in ethyl acetate used as solvent¹⁴³.

Chokshi and coworkers³²⁸ reported the first attempt to obtain more direct evidence of the HEI structure. Using the reaction of hydrogen peroxide and bis(2,6-difluorophenyl) oxalate in acetonitrile/water (3:1), monitored by ¹⁹F NMR, the authors observed a peak (different from those of the reagent or the released 2,6-difluorophenol) assigned putatively to a 2,6-difluorophenyl-containing peracid (**53**), whose intensity decreased in the presence of the activator. Considering that peracid derivatives like **50** were later excluded as possible HEIs³²⁰, another HEI structure accountable for the observed NMR peak could be 4-hydroxy-4-(2,6-difluorophenoxy)-1,2-dioxetan-3-one, a derivative of **48**.

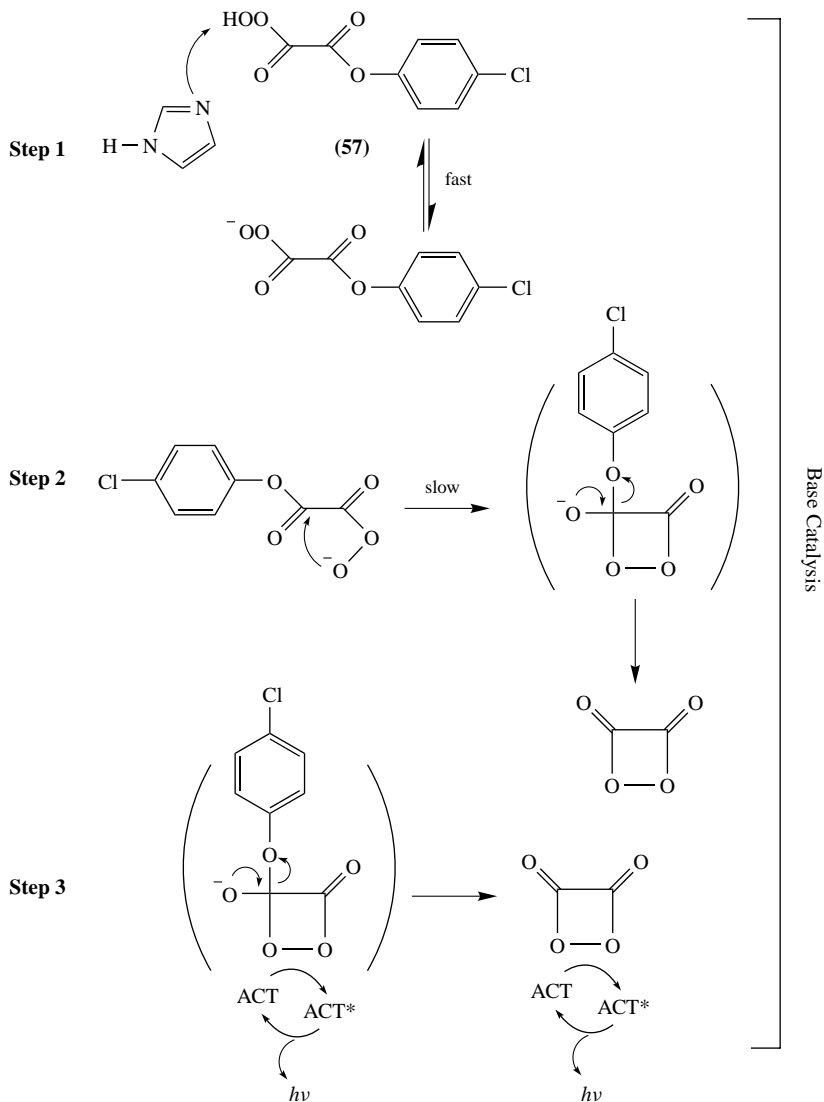
Hohman and coworkers³¹⁶ prepared silyl-protected peracid derivatives, 2,6-difluorophenyl-*O,O*-triisopropylsilyl monoperoxalate (**54**) and 2,6-difluorophenyl-*O,O*-triisobutylsilyl monoperoxalate (**55**) in order to confirm the involvement of peracid derivatives as HEIs. Kinetic experiments using the protected peracids and tetrabutylammonium fluoride in the presence of DPA show that light emission only occurs after deprotection of the silyl group by fluoride. The authors interpreted these results as indication of the percarboxylate (**56**) as the HEI, but here, again, one might alternatively suggest the cyclization products **3** or **48** (Ar = 2,4-F₂C₆H₃).



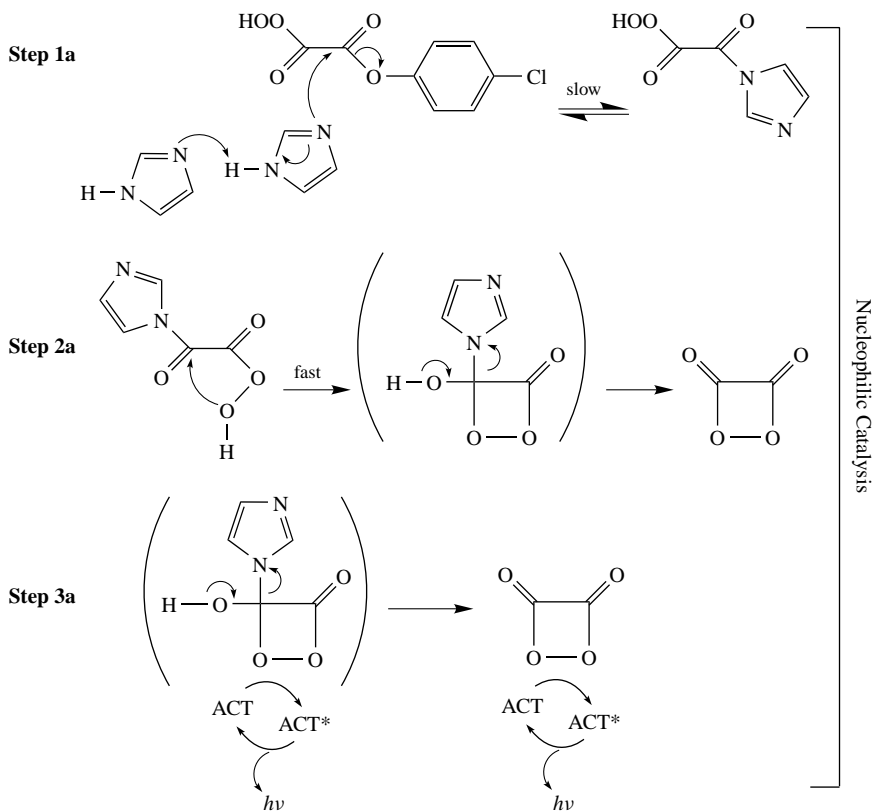
Stevani and coworkers³²⁰ prepared and characterized a peracid intermediate, 4-chlorophenyl-*O,O*-hydrogen monoperoxalate (**57**) and found that no chemiluminescence was observed in the presence of activators (i.e. rubrene, perylene and DPA) and the absence of a base. Based on this result, the authors excluded **57** and similar peracid derivatives as HEI in the peroxyoxalate system. Moreover, **57** only emits light in the presence of an activator and a base with $pK_a > 6$, suggesting that a slow chemical transformation must still occur prior to the chemiexcitation step. Kinetic experiments with **57**, using mainly imidazole, but also in the presence of other bases such as potassium 4-chlorophenolate, *t*-butoxide and 1,8-bis(dimethylamino)naphthalene³²⁹, showed that imidazole can act competitively as base and nucleophilic catalyst (Scheme 41). At low imidazole concentrations, base catalysis is the main pathway (steps 1 and 2); however, increasing the base concentration causes nucleophilic attack of imidazole catalyzed by imidazole to become the main pathway (steps 1a and 2a). Contrary to the proposal of Hohman and coworkers³¹⁶, the

authors suggested **3**, instead of a percarboxylate-like molecules (**56**), as HEI. As mentioned above, a slow chemical transformation of the peracid occurs prior to the HEI formation. This transformation should be the cyclization (Scheme 41, step 2), since it is well known that proton transfer reactions between heteroatom proton donor–acceptor are extremely fast³³⁰.

More recently, using rate constants obtained at low imidazole concentrations (base catalysis) with peracid derivatives containing different substituents on the aromatic ring



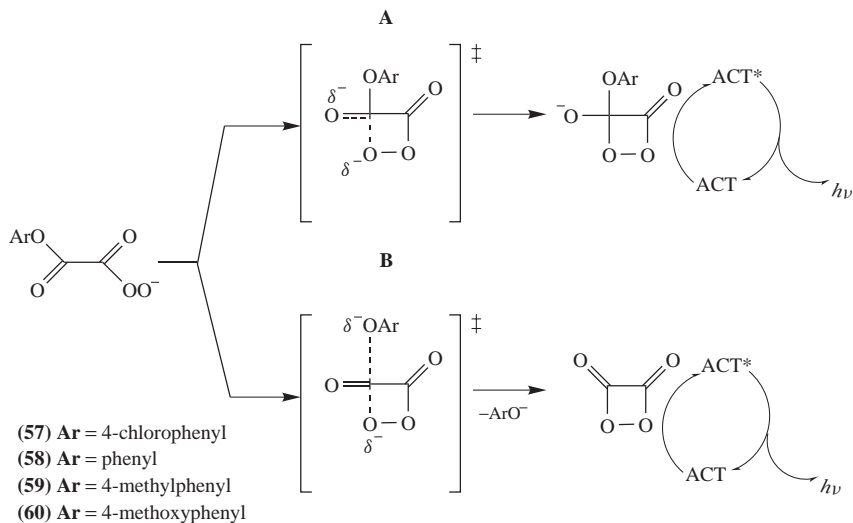
SCHEME 41



SCHEME 41. (continued)

57–60, Silva obtained more detailed information about the cyclization step¹⁴³ (Scheme 41, step 2), which probably leads to HEI formation. This transformation could occur in a stepwise process, leading to the formation of a 1,2-dioxetanone derivative, which might act as the HEI (Scheme 42, path A), or in a concerted way, where the leaving group departure accompanies the nucleophilic percarboxylate attack, leading to 1,2-dioxetanedione (**3**) as the only possible HEI (Scheme 42, path B). Hammett correlations of the rate constants with the substituent parameters ($\rho^- = 1.9$) and determination of the β value ($\beta = 0.79$) for the extension of the carbon–phenolic oxygen bond both indicate that the cyclization of the peracid derivatives to a cyclic peroxide occurs with simultaneous expulsion of the phenolic leaving group (Scheme 42, path B). Therefore, these results confirm the participation of **3** as high-energy intermediate in the peroxyoxalate chemiluminescence.

Stevani and Baader³³¹ attempted, unsuccessfully, to trap the volatile intermediate with triphenylantimony. Unfortunately, poly(triphenylstibine) oxide³³² was formed instead of the expected insertion product, 2,2,2-triphenyl-2 λ^5 -1,3,2-dioxastibolane-4,5-dione, probably by the reaction of triphenylantimony with hydrogen peroxide, carried by the gas stream to the flask containing triphenylantimony. Although it was impossible to detect the trapping product of 1,2-dioxetanedione by triphenylantimony, that does not necessarily mean that this substance is not formed during the reaction. This intermediate might



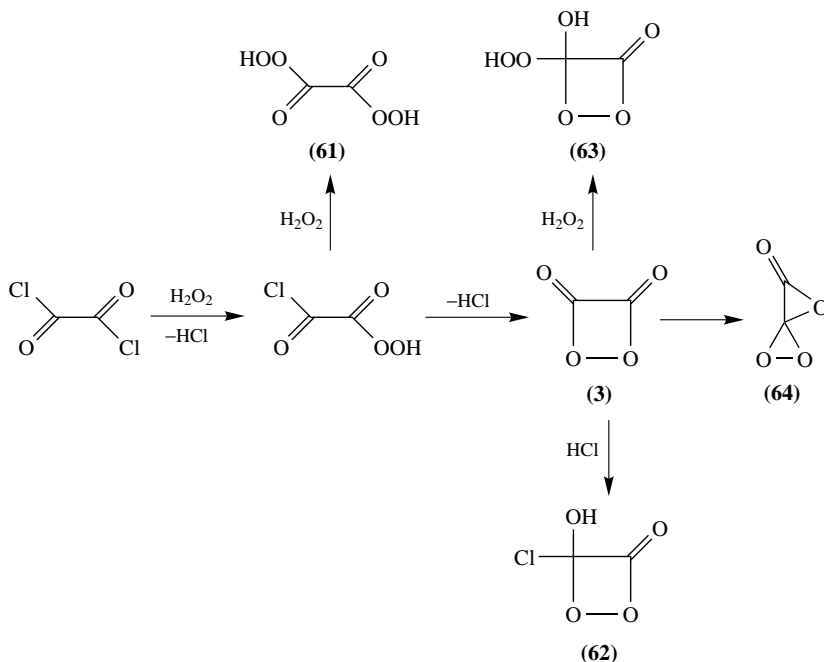
SCHEME 42

not be sufficiently stable to persist for the time required to reach the flask containing triphenylantimony, or else the main reaction of this cyclic peroxide may be catalytic decomposition³³³.

Bos and coworkers³³⁴ conducted a very interesting ¹³C NMR experiment of the reaction of doubly labeled oxalyl chloride with hydrogen peroxide at low temperature in the presence of DPA as activator, in order to garner direct evidence of the high-energy intermediate structure. Based on the experimental and calculated ¹³C NMR shift data, the authors were able to attribute the NMR signals to postulated intermediates in the reaction (Scheme 43). A small singlet observed at 154.5 ppm was assigned to **3**, in agreement with calculated chemical shift values and as the only possible symmetrical species apart from oxalic acid. It should be pointed out here that the experiment was performed in the presence of DPA, which is known to react rapidly with the HEI and should prevent the accumulation of the latter, even at low temperature. Moreover, apparently (no experimental conditions are given) the reaction was carried out in the presence of an excess of anhydrous hydrogen peroxide; hence, the formation of peroxyoxalic acid (**61**) should be considered, and this compound could be responsible for the singlet observed and assigned to **3**, since it is another symmetrical species possibly formed in the reaction system. Finally, **3** presumably has a very short lifetime and its reaction with hydrochloric acid or hydrogen peroxide, leading to the formation of compounds **62** and **63**, is hardly possible. It is also very interesting to note that structure **64** was first proposed by Steinfatt in 1985²⁰⁶ as the HEI in the peroxyoxalate system, albeit based on rather indirect kinetic evidence.

3. Mechanistic studies on the chemiexcitation step

Rauhut and coworkers^{7,305,306} proposed the occurrence of a charge transfer complex between the HEI and the ACT in order to explain the electronically excited-state generation in the peroxyoxalate system. Chemiluminescence quantum yield (Φ_{CL}) measurements with different activators have shown that the lower the ACT half-wave oxidation potential ($E_{1/2}^{ox}$) or singlet energy (E_s), the higher the electronically excited-state formation rate and Φ_{CL} . According to the mechanistic proposal of Schuster and coworkers for the CIEEL



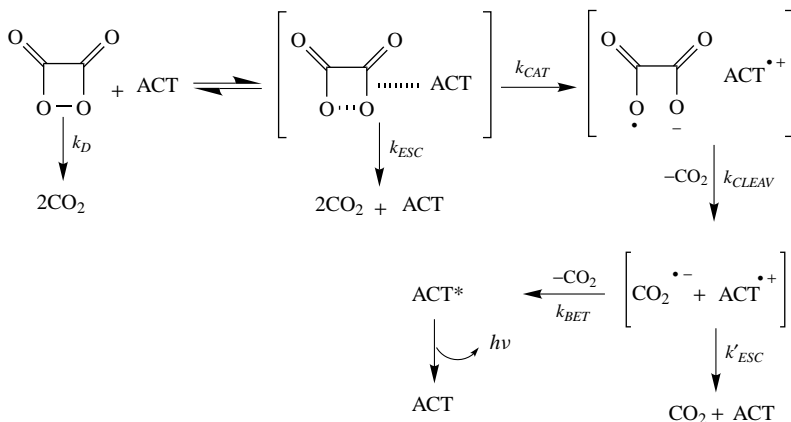
SCHEME 43

sequence^{20,115} and based on the results of Rauhut's group, the peroxyoxalate system was assumed to involve electron transfer, as predicted by this mechanism.

Catherall and coworkers³²³ measured the Φ_{CL} in the presence of several ACTs and reported chemiluminescent quantum yields of up to 30%. They did not observe chemiluminescence when using anisole ($E_s = 102 \text{ kcal mol}^{-1}$) as ACT nor did they find any correlation between Φ_{CL} and the singlet energy of the ACT in the peroxyoxalate reaction. These results are reasonably congruent with Lechtken and Turro's⁴⁸ observation that the peroxyoxalate system can generate electronically excited states using ACTs with E_s up to $105 \text{ kcal mol}^{-1}$ (Section III). The authors did, however, observe a linear correlation between the logarithms of the Φ_{CL} and $E_{1/2}^{\text{ox}}$, using the ACTs 2,5-diphenyloxazole (PPO), 9,10-dibromoanthracene, 1,4-bis(5-phenyl-2-oxazolyl)benzene, anthracene and 9,10-diphenylanthracene, indicating the importance of electron transfer for excited-state formation.

The peroxyoxalate system is the only intermolecular chemiluminescent reaction presumably involving the CIEEL sequence (Scheme 44), which shows high singlet excitation yields (Φ_S), as confirmed independently by several authors^{7,18,71,72}. Moreover, Stevani and coworkers¹⁸ reported a correlation between the singlet quantum yields, extrapolated to infinite activator concentrations (Φ_S^∞), and the free energy involved in back electron-transfer (ΔG_{BET}^*), as well as between the catalytic electron-transfer/deactivation rate constants ratio, $\ln(k_{\text{CAT}}/k_{\text{D}})$, and $E_{1/2}^{\text{ox}}$ (see Section V). A linear correlation of $\ln(k_{\text{CAT}}/k_{\text{D}})$ and $E_{1/2}^{\text{ox}}$ was obtained for the peroxyoxalate reaction with TCPO and H_2O_2 catalyzed by imidazole and for the imidazole-catalyzed reaction of **57**, both in the presence of five activators commonly used in CIEEL studies (anthracene, DPA, PPO, perylene and rubrene). A further confirmation of the validity of the CIEEL mechanism in the excitation step of

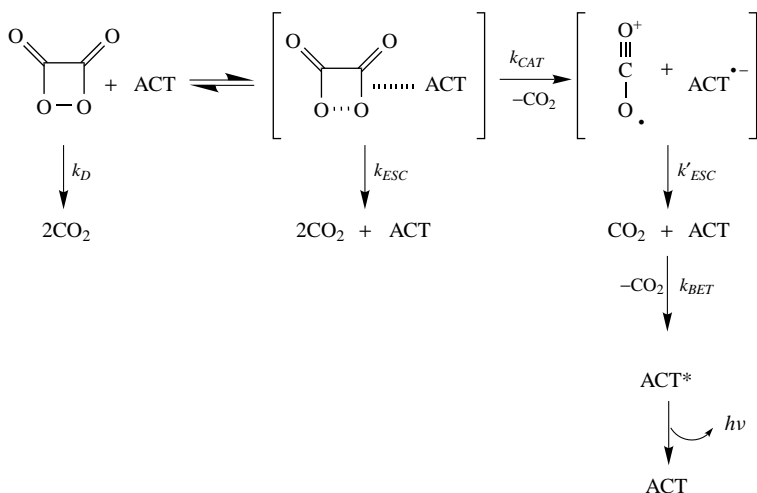
the peroxyoxalate system was obtained more recently in a study using steroid-substituted oxazolinylidenes as activators where, in accordance with this excitation mechanism, the same relationships mentioned above were observed¹⁴⁰.



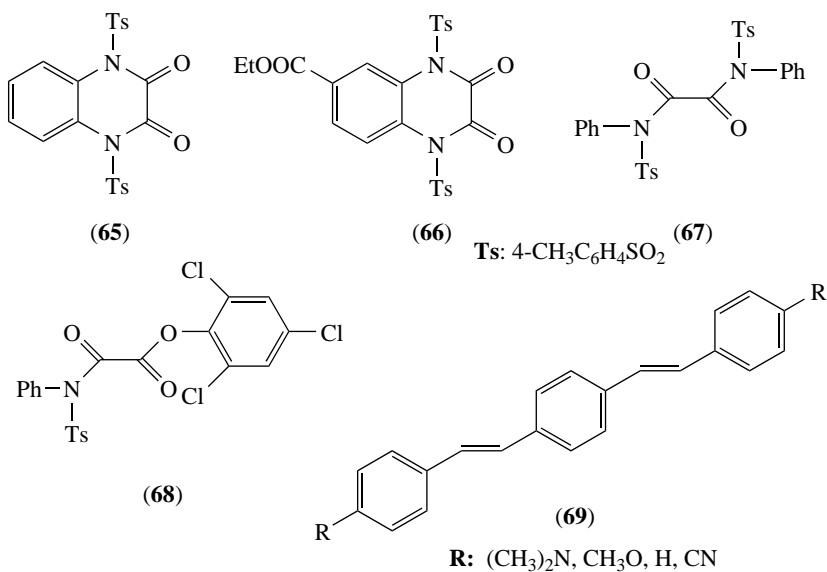
Furthermore, the authors were the first to garner evidence that the Φ_S^∞ values are determined by the energetics of back electron-transfer (BET) from the CO_2 anion-radical to the cation-radical of the ACT, leading to the formation of the activator's excited singlet state. The ΔG_{BET}^* values were calculated on the basis of the CIEEL sequence (Scheme 44), so this finding contributes further to confirm this mechanism. However, data obtained on two less commonly used activators 9,10-dimethoxyanthracene and, particularly, 9,10-dicyanoanthracene do not fit into the correlations obtained for the other activators, implying that details of this mechanism still require clarification. A putative explanation for the fact that 9,10-dimethoxyanthracene and 9,10-dicyanoanthracene do not correlate as predicted by CIEEL is the involvement of an alternative pathway, in which CO_2 cation radical and the anion radical of the activator are formed by initial electron transfer from the peroxide to the activator (Scheme 45)³³⁵.

Clear-cut evidence on the intermolecular nature of the excitation step and the need for 'in-cage' radical annihilation has been gained from a study on the solvent-cage effect in the peroxyoxalate reaction¹⁴³. The viscosity effect on the singlet quantum yields was verified using the binary solvent system toluene–diphenylmethane. A rise in solvent viscosity from 0.50 cP (toluene) to 2.67 cP (diphenylmethane) leads to an up to tenfold increase in the quantum yields, demonstrating the intermolecular nature of the excitation step.

More recently, Motoyoshiya and coworkers³³⁶ reported on a comparison of chemiluminescence quantum yields for the reaction of four α -oxoamides (**65**–**68**) or TCPO with hydrogen peroxide in the presence of perylene. Furthermore, using the reaction of **65** and hydrogen peroxide in the presence of *para-para'*-disubstituted distyrylbenzenes (**69**) as activator, the authors observed a Hammett relationship between the logarithms of the relative Φ_S and the σ_p^+ substituent parameters of the activators. The ρ value (–0.98) indicates that the chemiluminescent reaction is favored by electron-donating groups present in the ACT. These results and an additional linear correlation of the logarithms of Φ_{CL} with $E_{1/2}^{\text{ox}}$, for the reaction of **65** or TCPO with hydrogen peroxide in the presence of naphthalene, perylene, rubrene and 9,10-diphenylanthracene, support the postulation that the CIEEL mechanism is also involved with these derivatives.



SCHEME 45



As discussed herein, it can be concluded that the mechanistic pathways of the peroxyoxalate system in the presence of imidazole are well described and that there is a consensus at least in regard to the steps prior to the formation of the HEI. Conventional kinetic studies on this complex transformation, with various consecutive and parallel reaction steps, permit the formulation of a mechanistic scheme, containing the important steps in the 'light-producing' pathways, for which rate constants have been determined. Even so, the studies concerning the HEI structure are still controversial. Many authors favor **3** and/or **48** as the most probable candidates for the HEI, while others have suggested

either six-membered cyclic peroxides or oxalic ester percarboxylates. However, unlike dioxetanes, six-membered peroxides have not, to date, been shown to be involved in efficient chemiluminescence transformations. Percarboxylates are also less probable candidates, as it was shown that isolated peracid derivatives must undergo a slow chemical transformation prior to chemiexcitation. Recently, several groups independently found that the chemiexcitation step occurs via CIEEL mechanism with high chemiluminescence yields. The importance of in-cage radical-ion annihilation has been demonstrated by the solvent viscosity effect on the quantum yields, indicating the intermolecular nature of the back-electron transfer in the chemiexcitation steps of the peroxyoxalate system.

VII. ACKNOWLEDGMENTS

The authors thank the 'Fundação de Amparo à Pesquisa do Estado de São Paulo' (FAPESP) for its generous financial support. Without the funding of this foundation, research in the State of São Paulo would be impossible. We also thank the Brazilian federal agencies CNPq and CAPES for partial financial support, mainly in the form of grants for graduate students. In addition, we are indebted to Prof. Etelvino J. H. Bechara for his critical reading of the manuscript, to Ms. Beatrice Allain for proofreading it, and to Prof. Zvi Rappoport for his kind invitation to write this chapter.

VIII. REFERENCES

1. A. K. Campbell, *Chemiluminescence: Principles and Applications in Biology and Medicine*, Ellis Horward Ltd., Chichester, 1988.
2. E. Wiedemann, *Ann. Phys. Chem.*, **24**, 446 (1888).
3. B. Radziszewski, *Ber. Chem. Ges.*, **10**, 70 (1877).
4. H. O. Albrecht, *Z. Phys. Chem. (Muenchen, Ger.)*, **136**, 321 (1928).
5. K. Gleu and W. Petsch, *Angew. Chem.*, **48**, 57 (1935).
6. E. A. Chandross, *Tetrahedron Lett.*, 761 (1963).
7. M. M. Rauhut, *Acc. Chem. Res.*, **2**, 80 (1969).
8. M. M. Rauhut, B. G. Roberts, D. R. Maulding, W. Bergmark and R. Coleman, *J. Org. Chem.*, **40**, 330 (1975).
9. K. R. Kopecky and C. Mumford, *Can. J. Chem.*, **47**, 709 (1969).
10. W. Adam and J. C. Liu, *J. Am. Chem. Soc.*, **94**, 2894 (1972).
11. W. Adam and W. J. Baader, *Angew. Chem., Int. Ed. Engl.*, **23**, 166 (1984).
12. W. Adam and G. Cilento, *Chemical and Biological Generation of Excited States*, Academic Press, New York, 1982.
13. W. Adam and G. Cilento, *Angew. Chem., Int. Ed. Engl.*, **22**, 529 (1983).
14. W. Adam, M. Heil, T. Mosandl and C. R. Saha-Möllner, in *Organic Peroxides* (Ed. W. Ando), Wiley, Chichester, 1992, p. 221.
15. W. Adam, in *The Chemistry of Peroxides* (Ed. S. Patai), Wiley, Chichester, 1983, p. 829.
16. A. L. Baumstark, in *Advances in Oxygenated Processes* (Ed. A. L. Baumstark), JAI Press Inc., Greenwich, 1988, p. 31.
17. C. V. Stevani and W. J. Baader, *Quim. Nova*, **22**, 715 (1999).
18. C. V. Stevani, S. M. Silva and W. J. Baader, *Eur. J. Org. Chem.*, 4037 (2000).
19. W. Adam, W. J. Baader, C. Babatsikos and E. Schmidt, *Bull. Soc. Chim. Belg.*, **93**, 605 (1984).
20. G. B. Schuster, *Acc. Chem. Res.*, **12**, 366 (1979).
21. K. Faulkner and R. S. Grass, in *Chemical and Biological Generation of Excited States* (Eds. W. Adam and G. Cilento), Academic Press, New York, 1982, p. 191.
22. G. B. Schuster and K. A. Horn, in *Chemical and Biological Generation of Excited States* (Eds. W. Adam and G. Cilento), Academic Press, New York, 1982, p. 229.
23. J.-Y. Koo, S. P. Schmidt and G. B. Schuster, *Proc. Natl. Acad. Sci. U.S.A.*, **75**, 30 (1978).
24. L. H. Catalani and T. Wilson, *J. Am. Chem. Soc.*, **111**, 2633 (1989).
25. T. Wilson, *Photochem. Photobiol.*, **62**, 601 (1995).

26. A. L. P. Nery and W. J. Baader, *Quim. Nova*, **24**, 626 (2001).
27. F. McCapra, I. Beheshti, A. Burford, R. A. Hann and K. A. Zaklika, *J. Chem. Soc., Chem. Commun.*, **24**, 944 (1977).
28. C. Lee and L. A. Singer, *J. Am. Chem. Soc.*, **102**, 3823 (1980).
29. K. A. Zaklika, T. Kissel, A. L. Thayer, P. A. Burns and A. P. Schaap, *Photochem. Photobiol.*, **30**, 35 (1979).
30. H. Nakamura and T. Goto, *Chem. Lett.*, 1231 (1979).
31. A. P. Schaap and S. D. Gagnon, *J. Am. Chem. Soc.*, **104**, 3504 (1982).
32. A. P. Schaap, R. S. Handley and B. P. Giri, *Tetrahedron Lett.*, **28**, 935 (1987).
33. A. P. Schaap, T. S. Chen, R. S. Handley, R. Desilva and B. P. Giri, *Tetrahedron Lett.*, **28**, 1155 (1987).
34. A. P. Schaap, M. D. Sandison and R. S. Handley, *Tetrahedron Lett.*, **28**, 1159 (1987).
35. I. Bronstein, J. C. Voyta, O. J. Murphy, L. Bresnick and L. J. Kricka, *Biotechniques*, **12**, 748 (1992).
36. I. Nishizono, S. Iida, N. Suzuki, H. Kawada, H. Murakami, Y. Ashihara and M. Okada, *Clin. Chem.*, **37**, 1639 (1991).
37. T. Lim, Y. Komoda, N. Nakamura and T. Matsunaga, *Anal. Chem.*, **71**, 1298 (1999).
38. S. Beck and H. Koster, *Anal. Chem.*, **62**, 2258 (1990).
39. S. Beck, *Methods Enzymol.*, **216**, 143 (1992).
40. T. Wilson, *Int. Rev. Sci. Phys. Chem. Ser. Two*, **9**, 266 (1976).
41. G. B. Schuster and S. P. Schmidt, *Adv. Phys. Org. Chem.*, **18**, 187 (1982).
42. N. J. Turro, *Molecular Photochemistry*, The Benjamin/Cummings Publishing Co. Inc., Menlo Park, 1978.
43. R. A. Marcus, *J. Chem. Phys.*, **43**, 2654 (1965).
44. R. A. Marcus and P. Siders, *J. Phys. Chem.*, **86**, 622 (1982).
45. R. A. Marcus, in *Electron Transfer: From Isolated Molecules to Biomolecules, Pt 1* (Eds. J. Jortner and M. Bixon), Wiley, Chichester, 1999, p. 1.
46. D. M. Hercules, *Acc. Chem. Res.*, **2**, 301 (1969).
47. N. J. Turro, H. C. Steinmetzer and A. Yekta, *J. Am. Chem. Soc.*, **95**, 6468 (1973).
48. P. Lechtken and N. J. Turro, *Mol. Photochem.*, **6**, 95 (1974).
49. W. Adam and K. Zinner, in *Chemical and Biological Generation of Excited States* (Eds. W. Adam and G. Cilento), Academic Press, New York, 1982, p. 153.
50. W. J. Baader, Doctoral Dissertation, Bayerischen Julius-Maximilians-Universität Würzburg, Würzburg, 1983.
51. W. Adam and W. J. Baader, *J. Am. Chem. Soc.*, **107**, 410 (1985).
52. H. C. Steinmetzer, A. Yekta and N. J. Turro, *J. Am. Chem. Soc.*, **96**, 282 (1974).
53. P. Lechtken, *Chem. Ber.*, **109**, 2862 (1976).
54. W. Adam, *Pure Appl. Chem.*, **52**, 2591 (1980).
55. W. Adam, in *Chemical and Biological Generation of Excited States* (Eds. W. Adam and G. Cilento), Academic Press, New York, 1982, p. 115.
56. N. J. Turro and P. Lechtken, *J. Am. Chem. Soc.*, **94**, 2886 (1972).
57. N. J. Turro, P. Lechtken, N. E. Schore, G. Schuster, H. C. Steinmetzer and A. Yekta, *Acc. Chem. Res.*, **7**, 97 (1974).
58. W. Adam and K. Hannemann, *J. Am. Chem. Soc.*, **105**, 714 (1983).
59. W. H. Richardson, M. B. Lovett, M. E. Price and J. H. Anderegg, *J. Am. Chem. Soc.*, **101**, 4683 (1979).
60. W. H. Richardson, G. Batinica, K. Janotapperret, T. Miller and D. M. Shen, *J. Org. Chem.*, **56**, 6140 (1991).
61. P. E. Stanley, *J. Biolumin. Chemilumin.*, **12**, 61 (1997).
62. J. Lee and H. H. Seliger, *Photochem. Photobiol.*, **4**, 1015 (1965).
63. J. Lee and H. H. Seliger, *Photochem. Photobiol.*, **15**, 227 (1972).
64. J. Lee, A. S. Wesley, J. F. Ferguson III and H. H. Seliger, in *Bioluminescence in Progress* (Eds. F. H. Johnson and Y. Haneda), Princeton University Press, Princeton, 1966, p. 35.
65. J. W. Hastings and G. Weber, *J. Opt. Soc. Am.*, **53**, 1410 (1963).
66. J. W. Hastings and G. Weber, *Photochem. Photobiol.*, **4**, 1049 (1965).
67. J. W. Hastings and G. T. Reynolds, in *Bioluminescence in Progress* (Eds. F. H. Johnson and Y. Haneda), Princeton University Press, Princeton, 1966, p. 45.
68. D. K. Dunn, *Biochemistry*, **12**, 4911 (1973).

69. P. R. Michael and L. R. Faulkner, *Anal. Chem.*, **48**, 1188 (1976).
70. B. G. Roberts and R. C. Hirt, *Appl. Spectrosc.*, **21**, 250 (1967).
71. S. S. Tseng, A. G. Mohan, L. G. Haines, L. S. Vizcarra and M. M. Rauhut, *J. Org. Chem.*, **44**, 4113 (1979).
72. C. L. R. Catherall, T. F. Palmer and R. B. Cundall, *J. Biolumin. Chemilumin.*, **3**, 147 (1989).
73. C. V. Stevani, Doctoral Thesis, Universidade de São Paulo, São Paulo, 1997.
74. A. L. P. Nery, S. Ropke, L. H. Catalani and W. J. Baader, *Tetrahedron Lett.*, **40**, 2443 (1999).
75. A. L. P. Nery, D. Weiss, L. H. Catalani and W. J. Baader, *Tetrahedron*, **56**, 5317 (2000).
76. E. L. Bastos, Doctoral Thesis, Universidade de São Paulo, São Paulo, 2004.
77. A. L. P. Nery, Doctoral Thesis, Universidade de São Paulo, São Paulo, 1997.
78. M. A. Oliveira and W. J. Baader, Unpublished results.
79. A. V. Trofimov, K. Mielke, R. F. Vasilev and W. Adam, *Photochem. Photobiol.*, **63**, 463 (1996).
80. S. P. Schmidt and G. B. Schuster, *J. Am. Chem. Soc.*, **102**, 306 (1980).
81. J.-Y. Koo and G. B. Schuster, *J. Am. Chem. Soc.*, **100**, 4496 (1978).
82. F. McCapra, *Chem. Commun.*, 155 (1968).
83. N. J. Turro and P. Lechtken, *Pure Appl. Chem.*, **33**, 363 (1973).
84. W. H. Richardson and H. E. O'Neal, *J. Am. Chem. Soc.*, **92**, 6553 (1970).
85. W. H. Richardson and H. E. O'Neal, *J. Am. Chem. Soc.*, **94**, 8665 (1972).
86. N. J. Turro and A. Devaquet, *J. Am. Chem. Soc.*, **97**, 3858 (1975).
87. W. Adam, *Adv. Heterocycl. Chem.*, **21**, 437 (1977).
88. E. J. H. Bechara and T. Wilson, *J. Org. Chem.*, **45**, 5261 (1980).
89. A. L. Baumstark, C. A. Retter, K. Tehrani and C. Kellogg, *J. Org. Chem.*, **52**, 3308 (1987).
90. A. L. Baumstark and P. C. Vasquez, *J. Org. Chem.*, **51**, 5213 (1986).
91. A. L. Baumstark, M. Moghaddari and M. L. Chamblee, *Heteroat. Chem.*, **1**, 175 (1990).
92. W. H. Richardson, *J. Org. Chem.*, **54**, 4677 (1989).
93. M. Reguero, F. Bernardi, A. Bottoni, M. Olivucci and M. A. Robb, *J. Am. Chem. Soc.*, **113**, 1566 (1991).
94. T. Wilson and A. M. Halpern, *J. Phys. Org. Chem.*, **8**, 359 (1995).
95. R. F. Vasil'ev, *J. Biolumin. Chemilumin.*, **13**, 69 (1998).
96. Y. Takano, T. Tsunesada, H. Isobe, Y. Yoshioka, K. Yamaguchi and I. Saito, *Bull. Chem. Soc. Jpn.*, **72**, 213 (1999).
97. R. F. Vasil'ev, *Kinet. Catal.*, **40**, 172 (1999).
98. S. Wilsey, F. Bernardi, M. Olivucci, M. A. Robb, S. Murphy and W. Adam, *J. Phys. Chem. A*, **103**, 1669 (1999).
99. C. Tanaka and J. Tanaka, *J. Phys. Chem. A*, **104**, 2078 (2000).
100. E. Rodriguez and M. Reguero, *J. Phys. Chem. A*, **106**, 504 (2002).
101. P. Lechtken, *Chem. Ber.*, **111**, 1413 (1978).
102. W. H. Richardson, D. L. Stiggallstberg, Z. P. Chen, J. C. Baker, D. M. Burns and D. G. Sherman, *J. Org. Chem.*, **52**, 3143 (1987).
103. W. H. Richardson and S. A. Thomson, *J. Org. Chem.*, **50**, 1803 (1985).
104. W. H. Richardson and D. L. Stiggallstberg, *J. Am. Chem. Soc.*, **104**, 4173 (1982).
105. H. E. Zimmerman, G. E. Keck and J. L. Pfederer, *J. Am. Chem. Soc.*, **98**, 5574 (1976).
106. H. E. Zimmerman and G. E. Keck, *J. Am. Chem. Soc.*, **97**, 3527 (1975).
107. M. J. Mirbach, A. Henne and K. Schaffner, *J. Am. Chem. Soc.*, **100**, 7127 (1978).
108. T. J. Ekersley and N. A. Roger, *Tetrahedron*, **40**, 3759 (1984).
109. W. H. Richardson, M. B. Lovett and L. Olson, *J. Org. Chem.*, **54**, 3523 (1989).
110. S. Murphy and W. Adam, *J. Am. Chem. Soc.*, **118**, 12916 (1996).
111. D. F. Lima, Master Dissertation, Universidade de São Paulo, São Paulo, 1996.
112. W. Adam and M. Heil, *J. Am. Chem. Soc.*, **114**, 8807 (1992).
113. W. Adam and S. Andler, *J. Am. Chem. Soc.*, **116**, 5674 (1994).
114. F. Scandola, V. Balzani and G. B. Schuster, *J. Am. Chem. Soc.*, **103**, 2519 (1981).
115. G. B. Schuster, in *Advances in Electron Transfer Chemistry* (Ed. P. S. Mariano), JAI Press Inc., Greenwich, 1991, p. 163.
116. G. B. Schuster, B. Dixon, J. Y. Koo, S. P. Schmidt and J. P. Smith, *Photochem. Photobiol.*, **30**, 17 (1979).
117. J.-Y. Koo and G. B. Schuster, *J. Am. Chem. Soc.*, **99**, 5403 (1977).

118. S. P. Schmidt and G. B. Schuster, *J. Am. Chem. Soc.*, **100**, 1966 (1978).
119. W. Adam, G. A. Simpson and F. Yany, *J. Phys. Chem.*, **78**, 2559 (1974).
120. W. Adam and O. Cueto, *J. Am. Chem. Soc.*, **101**, 6511 (1979).
121. N. J. Turro and M.-F. Chow, *J. Am. Chem. Soc.*, **102**, 5058 (1980).
122. B. G. Dixon and G. B. Schuster, *J. Am. Chem. Soc.*, **101**, 3116 (1979).
123. B. G. Dixon and G. B. Schuster, *J. Am. Chem. Soc.*, **103**, 3068 (1981).
124. W. Adam, C. Cadilla, O. Cueto and L. O. Rodriguez, *J. Am. Chem. Soc.*, **102**, 4802 (1980).
125. J. P. Smith, A. K. Schrock and G. B. Schuster, *J. Am. Chem. Soc.*, **104**, 1041 (1982).
126. M. J. Darmon and G. B. Schuster, *J. Org. Chem.*, **47**, 4658 (1982).
127. J. E. Porter and G. B. Schuster, *J. Org. Chem.*, **48**, 4944 (1983).
128. T. Wilson, *Photochem. Photobiol.*, **30**, 177 (1979).
129. W. Adam, K. Zinner, A. Krebs and H. Schmalstieg, *Tetrahedron Lett.*, **22**, 4567 (1981).
130. T. Wilson, in *Singlet Oxygen* (Ed. A. A. Frimer), CRC Press, Inc., Boca Raton, 1985, p. 37.
131. F. McCapra, *J. Photochem. Photobiol., A*, **51**, 21 (1990).
132. F. McCapra, in *Bioluminescence and Chemiluminescence: Molecular Reporting with Photons* (Eds. J. W. Hastings, L. J. Kricka and P. E. Stanley), Wiley, Chichester, 1997.
133. S. P. Schmidt and G. B. Schuster, *J. Am. Chem. Soc.*, **102**, 7100 (1980).
134. S. P. Schmidt, M. A. Vincent, C. E. Dykstra and G. B. Schuster, *J. Am. Chem. Soc.*, **103**, 1292 (1981).
135. M. M. Chang, T. Saji and A. J. Bard, *J. Am. Chem. Soc.*, **99**, 5399 (1977).
136. R. O. Loufty and R. O. Loufty, *J. Phys. Chem.*, **77**, 336 (1973).
137. K. A. Horn and G. B. Schuster, *J. Am. Chem. Soc.*, **101**, 7097 (1979).
138. K. A. Horn and G. B. Schuster, *Tetrahedron*, **38**, 1095 (1982).
139. J. E. Porter and G. B. Schuster, *J. Org. Chem.*, **50**, 4068 (1985).
140. S. M. Silva, K. Wagner, D. Weiss, R. Beckert, C. V. Stevani and W. J. Baader, *Luminescence*, **17**, 362 (2002).
141. R. A. Marcus, *J. Chem. Phys.*, **24**, 966 (1956).
142. L. E. Ebersson, *Electron Transfer Reactions in Organic Chemistry*, Springer-Verlag, Berlin, 1987.
143. S. M. Silva, Doctoral Thesis, Universidade de São Paulo, São Paulo, 2004.
144. W. Adam, D. Reinhardt and C. R. Saha-Möller, *Analyst*, **121**, 1527 (1996).
145. S. Albrecht, H. Brandl, C. Schönfels and W. Adam, *Chem. unserer Zeit*, **26**, 63 (1992).
146. A. Mayer and S. Neuenhofer, *Angew. Chem., Int. Ed. Engl.*, **33**, 1044 (1994).
147. M. Matsumoto and M. Azami, *Tetrahedron Lett.*, **38**, 8947 (1997).
148. M. Matsumoto, N. Watanabe, T. Shiono, H. Suganuma and J. Matsubara, *Tetrahedron Lett.*, **38**, 5825 (1997).
149. M. Matsumoto, T. Hiroshima, S. Chiba, R. Isobe, N. Watanabe and H. Kobayashi, *Luminescence*, **14**, 345 (1999).
150. M. Matsumoto, T. Sakuma and N. Watanabe, *Luminescence*, **16**, 275 (2001).
151. M. Matsumoto, *J. Synth. Org. Chem. Jpn.*, **61**, 595 (2003).
152. N. Watanabe, H. Suganuma, H. Kobayashi, H. Mutoh, Y. Katao and M. Matsumoto, *Tetrahedron*, **55**, 4287 (1999).
153. N. Watanabe, H. Kobayashi, M. Azami and M. Matsumoto, *Tetrahedron*, **55**, 6831 (1999).
154. W. Adam and D. Reinhardt, *Justus Liebigs Ann. Chem.*, 1359 (1997).
155. T. Imanishi, Y. Ueda, R. Tainaka, K. Miyashita and N. Hoshino, *Tetrahedron Lett.*, **38**, 841 (1997).
156. M. Matsumoto, T. Mizuno and N. Watanabe, *Chem. Commun.*, 482 (2003).
157. M. Matsumoto, J. Murayama, M. Nishiyama, Y. Mizoguchi, T. Sakuma and N. Watanabe, *Tetrahedron Lett.*, **43**, 1523 (2002).
158. M. Matsumoto, T. Sakuma and N. Watanabe, *Tetrahedron Lett.*, **43**, 8955 (2002).
159. A. V. Trofimov, R. F. Vasil'ev, K. Mielke and W. Adam, *Photochem. Photobiol.*, **62**, 35 (1995).
160. W. Adam, I. Bronstein, B. Edwards, T. Engel, D. Reinhardt, F. W. Schneider, A. V. Trofimov and R. F. Vasil'ev, *J. Am. Chem. Soc.*, **118**, 10400 (1996).
161. W. Adam, *J. Phys. Chem. A*, **102**, 5406 (1996).
162. W. Adam, M. Matsumoto and A. V. Trofimov, *J. Org. Chem.*, **65**, 2078 (2000).
163. B. Edwards, A. Sparks, J. C. Voyta and I. Bronstein, *J. Biolumin. Chemilumin.*, **5**, 1 (1990).
164. S. Röpke, Master Dissertation, Universidade de São Paulo, São Paulo, 2000.

165. H. E. Zimmerman, *J. Am. Chem. Soc.*, **85**, 922 (1963).
166. J. A. Pincock and P. J. Wedge, *J. Org. Chem.*, **59**, 5578 (1994).
167. S. A. Fleming and A. W. Jensen, *J. Org. Chem.*, **61**, 7040 (1996).
168. W. Adam, I. Bronstein, A. V. Trofimov and R. F. Vasil'ev, *J. Am. Chem. Soc.*, **121**, 958 (1999).
169. W. Adam and A. V. Trofimov, *J. Org. Chem.*, **65**, 6474 (2000).
170. W. Adam, M. Matsumoto and A. V. Trofimov, *J. Am. Chem. Soc.*, **122**, 8631 (2000).
171. S. Albrecht, H. Brandl and T. Zimmermann, *Chemilumineszenz*, Huethig GmbH, Heidelberg, 1996.
172. A. M. Jiménez and M. J. Navas, *Grasas Aceites (Seville)*, **53**, 64 (2002).
173. A. M. García-Campana, W. R. G. Baeyens, L. Cuadros-Rodríguez, F. A. Barrero, J. M. Bosque-Sendra and L. Gamiz-Gracia, *Curr. Org. Chem.*, **6**, 1 (2002).
174. C. Dodeigne, L. Thunus and R. Lejeune, *Talanta*, **51**, 415 (2000).
175. E. H. White and M. M. Bursey, *J. Am. Chem. Soc.*, **86**, 941 (1964).
176. E. H. White, E. G. Nash, D. R. Roberts and O. C. Zafiriou, *J. Am. Chem. Soc.*, **90**, 5932 (1968).
177. D. Kearns and S. Ehrenson, *J. Am. Chem. Soc.*, **84**, 739 (1962).
178. J. Lind, G. Merényi and T. E. Eriksen, *J. Am. Chem. Soc.*, **105**, 7655 (1983).
179. D. F. Rosewell and E. H. White, *Methods Enzymol.*, **57**, 409 (1978).
180. G. Merenyi, J. Lind and T. E. Eriksen, *J. Biolumin. Chemilumin.*, **5**, 53 (1990).
181. M. Nakamura and S. Nakamura, *Free Radical Biol. Med.*, **24**, 537 (1998).
182. A. L. Rose and T. D. Waite, *Anal. Chem.*, **73**, 5909 (2001).
183. J. H. Baxendale, *J. Chem. Soc., Faraday Trans.*, **69**, 1665 (1973).
184. M. M. Rauhut, A. M. Semsel and B. G. Roberts, *J. Org. Chem.*, **31**, 2431 (1966).
185. I. Isacson and G. Wettermark, *Anal. Chim. Acta*, **83**, 227 (1976).
186. E. P. Brestel, *Biochem. Biophys. Res. Commun.*, **126**, 482 (1985).
187. J. Arnhold, S. Mueller, K. Arnold and E. Grimm, *J. Biolumin. Chemilumin.*, **6**, 189 (1991).
188. Y. Omote, T. Miyake and N. Sugiyama, *Bull. Chem. Soc. Jpn.*, **40**, 2446 (1967).
189. P. M. Abuja and R. Albertini, *Clin. Chim. Acta*, **306**, 1 (2001).
190. E. Lissi, M. Salimhanna, C. Pascual and M. D. Delcastillo, *Free Radical Biol. Med.*, **18**, 153 (1995).
191. W. J. Baader, A. Hatzelmann and V. Ullrich, *Biochem. Pharmacol.*, **37**, 1089 (1988).
192. T. P. Whitehead, G. H. G. Thorpe and S. R. J. Maxwell, *Anal. Chim. Acta*, **266**, 265 (1992).
193. E. L. Bastos, P. Romoff, C. R. Eckert and W. J. Baader, *J. Agric. Food Chem.*, **51**, 7481 (2003).
194. G. Merenyi and J. S. Lind, *J. Am. Chem. Soc.*, **102**, 5830 (1980).
195. G. Merenyi, J. Lind and T. E. Eriksen, *J. Phys. Chem.*, **88**, 2320 (1984).
196. G. Merenyi, J. Lind and T. E. Eriksen, *Photochem. Photobiol.*, **41**, 203 (1985).
197. E. K. Miller and I. Fridovich, *J. Free Rad. Biol. Med.*, **2**, 107 (1986).
198. T. E. Eriksen, J. Lind and G. Merenyi, *J. Chem. Soc., Faraday Trans.*, **79**, 1503 (1983).
199. J. Schiller, J. Arnhold, J. Schwinn, H. Sprinz, O. Brede and J. Arnhold, *Free Radical Res.*, **30**, 45 (1999).
200. W. R. Seitz, *J. Phys. Chem.*, **79**, 101 (1975).
201. J. Michl, *Photochem. Photobiol.*, **25**, 141 (1977).
202. C. R. Flynn and J. Michl, *J. Am. Chem. Soc.*, **96**, 3280 (1974).
203. T. Goto, I. Kubota, N. Suzuki, Y. Kishi and K. Inoue, in *Chemiluminescence and Bioluminescence* (Eds. M. J. Cormier, D. M. Hercules and J. Lee), Plenum Press, New York, 1973, p. 325.
204. M. F. D. Steinfatt, *J. Chem. Res., Synop.*, 211 (1984).
205. M. F. D. Steinfatt, *J. Chem. Res., Synop.*, 111 (1984).
206. M. F. D. Steinfatt, *Bull. Soc. Chim. Belg.*, **94**, 85 (1985).
207. M. F. D. Steinfatt, *Bull. Soc. Chim. Belg.*, **94**, 407 (1985).
208. M. F. D. Steinfatt, *J. Chem. Res., Synop.*, 140 (1985).
209. H. Brandl, in *Photochemie* (Eds. D. Wöhrle, M. W. Tausch and W. Stohrer), Wiley-VCH, Weinheim, 1998, p. 231.
210. K. D. Gundermann, M. Steinfatt and H. Fiege, *Angew. Chem., Int. Ed. Engl.*, **10**, 67 (1971).
211. K. D. Gundermann and M. Steinfatt, *Angew. Chem., Int. Ed. Engl.*, **14**, 560 (1975).

212. K. D. Gundermann, M. Steinfatt, P. Witt, C. Paetz and K. L. Poppel, *J. Chem. Res., Synop.*, 195 (1980).
213. F. McCapra, *J. Chem. Soc., Chem. Commun.*, 946 (1977).
214. F. McCapra and P. D. Leeson, *J. Chem. Soc., Chem. Commun.*, 114 (1979).
215. G. Orlova, J. D. Goddard and L. Y. Brovko, *J. Am. Chem. Soc.*, **125**, 6962 (2003).
216. G. Merenyi, J. Lind and T. E. Eriksen, *J. Am. Chem. Soc.*, **108**, 7716 (1986).
217. S. Ljunggren, G. Merenyi and J. Lind, *J. Am. Chem. Soc.*, **105**, 7662 (1983).
218. F. McCapra and D. G. Richardson, *Tetrahedron Lett.*, 3167 (1964).
219. F. McCapra and R. A. Hann, *J. Chem. Soc., Chem. Commun.*, 442 (1969).
220. R. Maskiewicz, D. Sogah and T. C. Bruice, *J. Am. Chem. Soc.*, **101**, 5347 (1979).
221. R. Maskiewicz, D. Sogah and T. C. Bruice, *J. Am. Chem. Soc.*, **101**, 5355 (1979).
222. J. R. Totter, *Photochem. Photobiol.*, **3**, 231 (1964).
223. E. G. Janzen, J. B. Pickett, J. W. Happ and W. DeAngelis, *J. Org. Chem.*, **35**, 88 (1970).
224. K. Gundermann and F. McCapra, in *Chemiluminescence in Organic Chemistry* (Eds. K. Hafner, J. M. Lehn, C. W. Rees, F. R. S. Hofmann, P. v. R. Schleyer, B. M. Trost and R. Zahradnik), Springer-Verlag, Berlin, 1987, p. 77.
225. K. D. Legg and D. M. Hercules, *J. Am. Chem. Soc.*, **91**, 1902 (1969).
226. L. Greenlee, I. Fridovich and P. Handler, *Biochemistry*, **1**, 779 (1962).
227. K. Faulkner and I. Fridovich, *Free Radical Biol. Med.*, **15**, 447 (1993).
228. O. Myhre, J. M. Andersen, H. Aarnes and F. Fonnum, *Biochem. Pharmacol.*, **65**, 1575 (2003).
229. T. Okajima and T. Ohsaka, *Luminescence*, **18**, 49 (2003).
230. I. Lenaerts, B. P. Braeckman, F. Matthijssens and J. R. Vanfleteren, *Anal. Biochem.*, **311**, 90 (2002).
231. Z. H. Bai, L. M. Harvey and B. McNeil, *Biotechnol. Bioeng.*, **75**, 204 (2001).
232. F. McCapra, *Acc. Chem. Res.*, **9**, 201 (1976).
233. I. Weeks, I. Beheshti, F. McCapra, A. K. Campbell and J. S. Woodhead, *Clin. Chem.*, **29**, 1474 (1983).
234. G. Zomer, J. F. C. Stavenuier, R. H. van den Berg and E. H. J. M. Janzen, *Pract. Spectrosc.*, **12**, 505 (1991).
235. J. Rak, P. Skurski and J. Blazejowski, *J. Org. Chem.*, **64**, 3002 (1999).
236. K. Sakanishi, Y. Kato, E. Mizukoshi and K. Shimizu, *Tetrahedron Lett.*, **35**, 4789 (1994).
237. M. W. Cass, E. Rapaport and E. H. White, *J. Am. Chem. Soc.*, **94**, 3168 (1972).
238. J. W. Happ and E. G. Jansen, *J. Org. Chem.*, **35**, 3396 (1970).
239. J. W. Happ, E. G. Jansen and B. C. Rudy, *J. Org. Chem.*, **35**, 3382 (1970).
240. E. Rapaport, M. W. Cass and E. H. White, *J. Am. Chem. Soc.*, **94**, 3160 (1972).
241. A. Wróblewska, O. M. Huta, S. V. Midyanyj, I. O. Patsay, J. Rak and J. Blazejowski, *J. Org. Chem.*, **69**, 1607 (2004).
242. G. Zomer and J. F. C. Stavenuier, *Anal. Chim. Acta*, **227**, 11 (1989).
243. G. Sarlet, R. Renotte, J. L. Cloux and R. Lejeune, *Clin. Chem.*, **42**, 95 (1996).
244. M. Adamczyk, P. G. Mattingly, J. A. Moore and Y. Pan, *Org. Lett.*, **1**, 779 (1999).
245. M. Becker, V. Lerum, S. Dickson, N. C. Nelson and E. Matsuda, *Biochemistry*, **38**, 5603 (1999).
246. K. Gundermann and F. McCapra, in *Chemiluminescence in Organic Chemistry* (Eds. K. Hafner, J. M. Lehn, C. W. Rees, F. R. S. Hofmann, P. v. R. Schleyer, B. M. Trost and R. Zahradnik), Springer-Verlag, Berlin, 1987, p. 109.
247. E. H. White, D. F. Roswell, A. C. Dupont and A. A. Wilson, *J. Am. Chem. Soc.*, **109**, 5189 (1987).
248. A. P. Schaap, *Photochem. Photobiol.*, **47S**, 50S (1988).
249. I. Bronstein, J. C. Voyta and B. Edwards, *J. Biolumin. Chemilumin.*, **2**, 186 (1988).
250. A. P. Schaap, *J. Biolumin. Chemilumin.*, **2**, 252 (1988).
251. A. P. Schaap, *J. Biolumin. Chemilumin.*, **2**, 253 (1988).
252. A. K. Campbell, C. J. Davies, R. Hart, F. McCapra, A. Patel, A. Richardson, M. E. T. Ryall, J. S. A. Simpson and J. S. Woodhead, *J. Physiol. (London)*, **306**, P3 (1980).
253. S. Sabelle, P. Y. Renard, K. Pecorella, S. de Suzzoni-Dezard, C. Creminon, J. Grassi and C. Mioskowski, *J. Am. Chem. Soc.*, **124**, 4874 (2002).
254. L. J. Bollyky, R. H. Whitman, B. G. Roberts and M. M. Rauhut, *J. Am. Chem. Soc.*, **89**, 6523 (1967).

255. M. M. Rauhut, D. Sheehan, R. A. Clarke and A. M. Semsel, *Photochem. Photobiol.*, **4**, 1097 (1965).
256. D. Salerno and J. R. Daban, *J. Chromatogr., B*, **793**, 75 (2003).
257. B. W. Sandmann and M. L. Grayeski, *J. Chromatogr., B: Anal. Technol. Life Sci.*, **653**, 123 (1994).
258. P. J. M. Kwakman, D. A. Kamminga, U. A. T. Brinkman and G. J. Dejong, *J. Pharm. Biomed. Anal.*, **9**, 753 (1991).
259. P. J. M. Kwakman, D. A. Kamminga, U. A. T. Brinkman and G. J. Dejong, *J. Chromatogr.*, **553**, 345 (1991).
260. M. Tod, J. Y. Legendre, J. Chalom, H. Kouwatli, M. Poulou, R. Farinotti and G. Mahuzier, *J. Chromatogr.*, **594**, 386 (1992).
261. M. M. Nakamura, S. A. Saraiva and N. Coichev, *Anal. Lett.*, **33**, 391 (2000).
262. O. M. Steijger, P. H. M. Rodenburg, H. Lingeman, U. A. T. Brinkman and J. J. M. Holthuis, *Anal. Chim. Acta*, **266**, 233 (1992).
263. D. C. Williams, G. F. Huff and W. R. Seitz, *Anal. Chem.*, **48**, 1003 (1976).
264. G. Scott, W. R. Seitz and J. Ambrose, *Anal. Chim. Acta*, **115**, 221 (1980).
265. P. Vanzoonen, D. A. Kamminga, C. Gooijer, N. H. Velthorst and R. W. Frei, *Anal. Chim. Acta*, **167**, 249 (1985).
266. M. L. Grayeski, E. J. Woolf and P. J. Helly, *Anal. Chim. Acta*, **183**, 207 (1986).
267. J. R. Poulsen, J. W. Birks, G. Gubitza, P. Vanzoonen, C. Gooijer, N. H. Velthorst and R. W. Frei, *J. Chromatogr.*, **360**, 371 (1986).
268. K. Nakashima, N. Kuroda, S. Kawaguchi, M. Wada and S. Akiyama, *J. Biolumin. Chemilumin.*, **10**, 185 (1995).
269. O. Nozaki, T. Iwaeda and Y. Kato, *J. Biolumin. Chemilumin.*, **10**, 339 (1995).
270. K. Nakashima, K. Maki, S. Akiyama, H. W. Wei, Y. Tsukamoto and K. Imai, *Analyst*, **114**, 1413 (1989).
271. M. Shamsipur and M. J. Chaichi, *Spectrosc. Lett.*, **34**, 459 (2001).
272. K. Imai, H. Nawa, M. Tanaka and H. Ogata, *Analyst*, **111**, 209 (1986).
273. N. W. Barnett, R. Bos, R. N. Evans and R. A. Russell, *Anal. Chim. Acta*, **403**, 145 (2000).
274. K. Imai, A. Nishitani and Y. Tsukamoto, *Chromatographia*, **24**, 77 (1987).
275. W. Baeyens, J. Bruggeman, C. Dewaele, B. Lin and K. Imai, *J. Biolumin. Chemilumin.*, **2**, 177 (1988).
276. C. Gooijer, P. Vanzoonen, N. H. Velthorst and R. W. Frei, *J. Biolumin. Chemilumin.*, **2**, 207 (1988).
277. K. Tsukagoshi, M. Otsuka, M. Hashimoto, R. Nakajima and H. Kimoto, *Chem. Lett.*, **98** (2000).
278. C. Gooijer, P. Vanzoonen, N. H. Velthorst and R. W. Frei, *J. Biolumin. Chemilumin.*, **4**, 479 (1989).
279. W. Baeyens, J. Bruggeman, C. Dewaele, B. Lin and K. Imai, *J. Biolumin. Chemilumin.*, **5**, 13 (1990).
280. S. Uzu, K. Imai, K. Nakashima and S. Akiyama, *J. Pharm. Biomed. Anal.*, **10**, 979 (1992).
281. S. Higashidate, K. Imai, P. Prados, S. Adachiakahane and T. Nagao, *Biomed. Chromatogr.*, **8**, 19 (1994).
282. P. Prados, S. Higashidate and K. Imai, *Biomed. Chromatogr.*, **8**, 1 (1994).
283. H. Yamada, Y. Kuwahara, Y. Takamatsu and T. Hayase, *Biomed. Chromatogr.*, **14**, 333 (2000).
284. K. Imai, R. Gohda, T. Fukushima, T. Santa and H. Homma, *Biomed. Chromatogr.*, **11**, 73 (1997).
285. A. Nishitani, S. Kanda and K. Imai, *Biomed. Chromatogr.*, **6**, 124 (1992).
286. G. Orosz, R. S. Givens and R. L. Schowen, *Crit. Rev. Anal. Chem.*, **26**, 1 (1996).
287. M. Wada, K. Inoue, A. Ihara, N. Kishikawa, K. Nakashima and N. Kuroda, *J. Chromatogr., A*, **987**, 189 (2003).
288. A. M. Garcia-Campana, L. Gamiz-Gracia, W. R. G. Baeyens and F. A. Barrero, *J. Chromatogr., B: Anal. Technol. Biomed. Life Sci.*, **793**, 49 (2003).
289. N. Hanaoka, *J. Chromatogr.*, **503**, 155 (1990).
290. K. Hayakawa, N. Imaizumi and M. Miyazaki, *Biomed. Chromatogr.*, **5**, 148 (1991).
291. B. Mann and M. L. Grayeski, *Biomed. Chromatogr.*, **5**, 47 (1991).
292. N. W. Barnett, R. Bos, S. W. Lewis and R. A. Russell, *Anal. Commun.*, **34**, 17 (1997).

293. P. Appelblad, T. Jonsson, T. Backstrom and K. Irgum, *Anal. Chem.*, **70**, 5002 (1998).
294. A. Carr, J. Dickson, M. Dickson and R. Milofsky, *Chromatographia*, **55**, 687 (2002).
295. B. W. Sandmann and M. L. Grayeski, *Chromatographia*, **38**, 163 (1994).
296. S. Kojo, S. Tokumaru, E. Kishida and I. Tsukamoto, *Clin. Chem.*, **38**, 788 (1992).
297. M. Emteborg, K. Irgum, C. Gooijer and U. A. T. Brinkman, *Anal. Chim. Acta*, **357**, 111 (1997).
298. N. W. Barnett, R. Bos, S. W. Lewis and R. A. Russell, *Analyst*, **123**, 1239 (1998).
299. P. Vanzoonen, H. Bock, C. Gooijer, N. H. Velthorst and R. W. Frei, *Anal. Chim. Acta*, **200**, 131 (1987).
300. E. J. Woolf and M. L. Grayeski, *J. Lumin.*, **39**, 19 (1987).
301. L. Gamiz-Gracia, A. M. Garcia-Campana, F. A. Barrero and L. C. Rodriguez, *Anal. Bioanal. Chem.*, **377**, 281 (2003).
302. N. Dan, M. L. Lau and M. L. Grayeski, *Anal. Chem.*, **63**, 1766 (1991).
303. M. S. Abdel-Latif and G. G. Guilbault, *Anal. Chem.*, **60**, 2671 (1988).
304. P. A. Sherman, J. Holzbecher and D. E. Ryan, *Anal. Chim. Acta*, **97**, 21 (1978).
305. M. M. Rauhut, L. J. Bollyky, B. G. Roberts, M. Loy, R. H. Whitman, A. V. Iannotta, A. M. Semsel and R. A. Clarke, *J. Am. Chem. Soc.*, **89**, 6515 (1967).
306. M. M. Rauhut, D. Sheehan, R. A. Clarke, B. G. Roberts and A. M. Semsel, *J. Org. Chem.*, **30**, 3587 (1965).
307. M. M. Rauhut, B. G. Roberts and A. M. Semsel, *J. Am. Chem. Soc.*, **88**, 3604 (1966).
308. F. J. Alvarez, N. J. Parekh, B. Matuszewski, R. S. Givens, T. Higuchi and R. L. Schowen, *J. Am. Chem. Soc.*, **108**, 6435 (1986).
309. C. V. Stevani, D. F. Lima, V. G. Toscano and W. J. Baader, *J. Chem. Soc., Perkin Trans. 2*, 989 (1996).
310. H. Neuvonen, *J. Chem. Soc., Perkin Trans. 2*, 945 (1995).
311. M. Orlovic, R. L. Schowen, R. S. Givens, F. Alvarez, B. Matuszewski and N. Parekh, *J. Org. Chem.*, **54**, 3606 (1989).
312. H. Neuvonen, *J. Biolumin. Chemilumin.*, **12**, 241 (1997).
313. W. J. Baader, Diplomarbeit, Bayerischen Julius-Maximilians-Universität Würzburg, Würzburg, 1980.
314. T. Jonsson and K. Irgum, *Anal. Chem.*, **72**, 1373 (2000).
315. J. F. Kirsch and W. P. Jencks, *J. Am. Chem. Soc.*, **86**, 833 (1964).
316. J. R. Hohman, R. S. Givens, R. G. Carlson and G. Orosz, *Tetrahedron Lett.*, **37**, 8273 (1996).
317. S. M. Silva, F. Casallanovo, K. H. Oyamaguchi, L. Ciscato, C. V. Stevani and W. J. Baader, *Luminescence*, **17**, 313 (2002).
318. A. G. Hadd, A. Seeber and J. W. Birks, *J. Org. Chem.*, **65**, 2675 (2000).
319. A. G. Hadd, A. L. Robinson, K. L. Rowlen and J. W. Birks, *J. Org. Chem.*, **63**, 3023 (1998).
320. C. V. Stevani, I. P. D. Campos and W. J. Baader, *J. Chem. Soc., Perkin Trans. 2*, 1645 (1996).
321. J. J. DeCorpo, A. Baronavski, M. V. McDowell and F. E. Saafeld, *J. Am. Chem. Soc.*, **94**, 2879 (1972).
322. H. F. Cordes, H. P. Richter and C. A. Heller, *J. Am. Chem. Soc.*, **91**, 7209 (1969).
323. C. L. R. Catherall, T. F. Palmer and R. B. Cundall, *J. Chem. Soc., Faraday Trans.*, **80**, 823 (1984).
324. R. E. Milofsky and J. W. Birks, *Anal. Chem.*, **62**, 1050 (1990).
325. R. E. Milofsky and J. W. Birks, *J. Am. Chem. Soc.*, **113**, 9715 (1991).
326. J. H. Lee, J. C. Rock, M. A. Schlautman and E. R. Carraway, *J. Chem. Soc., Perkin Trans. 2*, 1653 (2002).
327. J. H. Lee, J. C. Rock, S. B. Park, M. A. Schlautman and E. R. Carraway, *J. Chem. Soc., Perkin Trans. 2*, 802 (2002).
328. H. P. Chokshi, M. Barbush, R. G. Carlson, R. S. Givens, T. Kuwana and R. L. Schowen, *Biomed. Chromatogr.*, **4**, 96 (1990).
329. C. V. Stevani and W. J. Baader, *J. Phys. Org. Chem.*, **10**, 593 (1997).
330. M. Eigen, *Angew. Chem., Int. Ed. Engl.*, **3**, 1 (1964).
331. C. V. Stevani and W. J. Baader, *J. Chem. Res., Synop.*, 430 (2002).
332. D. L. Venezky, C. W. Sink, B. A. Nevett and W. F. Fortescue, *J. Organomet. Chem.*, **35**, 131 (1972).
333. A. L. Baumstark, M. E. Landis and P. J. Brooks, *J. Org. Chem.*, **44**, 4251 (1979).

334. R. Bos, N. W. Barnett, G. A. Dyson, K. F. Lim, R. A. Russell and S. P. Watson, *Anal. Chim. Acta*, **502**, 141 (2003).
335. W. J. Baader, S. M. Silva, K. H. Oyamaguchi, L. F. L. M. Ciscato and C. V. Stevani, in *Chemiluminescence at the Turn of the Millennium* (Eds, S. Albrecht, T. Zimmermann and H. Brandl), Schweda-Werbedruck GmbH, Dresden, 2001.
336. J. Motoyoshiya, N. Sakai, M. Imai, Y. Yamaguchi, R. Koike, Y. Takaguchi and H. Aoyama, *J. Org. Chem.*, **67**, 7314 (2002).

CHAPTER 17

Biomimetic Fe(II) chemistry and synthetic studies on antimalarial and antitumour endoperoxides

PAUL M. O'NEILL, JAMES CHADWICK and SARAH L. RAWE

Department of Chemistry, The Robert Robinson Laboratories, University of Liverpool, Liverpool, L69 7ZD, UK

Fax: +44 151 794 3553; e-mail: P.M.oneill01@liv.ac.uk

I. INTRODUCTION	1280
A. Malaria and Parasite Haemoglobin Degradation	1281
II. ENDOPEROXIDE-CONTAINING ANTIMALARIALS	1282
III. THE ROLE OF IRON	1283
A. Generation of C-centred Radicals	1283
1. Evidence for involvement of a secondary C-centred radical—The 'O ₂ route'	1284
2. Evidence for involvement of primary C-centred radical—The 'O ₁ route'	1292
B. Involvement of Non-heme Iron	1299
C. Heterolytic Cleavage of Peroxide Bond	1301
D. Iron(II) Degradation of Arteflene	1304
E. Summary	1309
IV. THE BIOLOGICAL TARGETS OF ANTIMALARIAL ENDOPEROXIDES	1311
A. Lipid Membranes	1311
1. Heme	1311
2. Enzymes as targets	1313
V. SEMI-SYNTHETIC ARTEMISININ DERIVATIVES	1313
A. Improved Semi-synthetic Artemisinin Analogues	1313
1. Artemisinin chemistry	1314
VI. SYNTHETIC ENDOPEROXIDES	1317
A. Drug Hybrids and Pro-drugs	1320
B. Chemistry for the Synthesis of Lead Synthetic Endoperoxides	1323
C. Fenozan B0-7 (4 + 2 Cycloaddition of ¹ O ₂ to a Diene)	1324

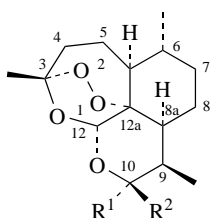
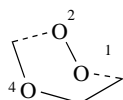
The chemistry of peroxides, volume 2

Edited by Z. Rappoport © 2006 John Wiley & Sons, Ltd ISBN: 0-470-86274-2

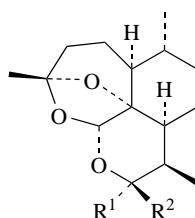
D. Arteflene (Ene Reaction of $^1\text{O}_2$)	1324
E. C3-Aryl 1,2,4-Trioxanes (2 + 2 Cycloaddition of $^1\text{O}_2$ to a Vinyl Ether)	1325
F. Spiro 1,2,4-Trioxanes (Ene Reaction)	1326
G. Synthesis of Tetraoxanes (Use of Hydrogen Peroxide)	1326
H. Spirotrioxanes via Mukaiyama Co(II) Mediated Aerobic Hydroperoxysilylation of Allylic Alcohols (Use of Triplet Oxygen)	1330
I. Synthesis of Endoperoxides via Thiol Olefin Co-oxidation Methodology (Use of Triplet Oxygen)	1330
J. Synthesis of 1,2,4-Trioxolanes via Griesbaum Co-ozonolysis (Use of Ozone)	1331
VII. ANTIMALARIAL ACTIVITIES OF SYNTHETIC ENDOPEROXIDE ANTIMALARIALS	1332
VIII. ENDOPEROXIDE CONTAINING COMPOUNDS WITH ANTITUMOUR ACTIVITY	1333
A. Marine Metabolites	1333
B. Steroidal Endoperoxides	1334
C. Synthetic Endoperoxides with Antitumour Activity	1335
D. Suspected Mechanisms of Antitumour Action	1335
E. Artemisinins as Antitumour Agents	1336
F. Summary and Conclusion	1338
IX. REFERENCES	1342

I. INTRODUCTION

In 1972, Chinese researchers isolated, by extraction at low temperature from a plant, a crystalline compound that they named *qinghaosu* [the name artemisinin (**1a**) is preferred by *Chemical Abstracts*, RN 63968-64-9]¹. The plant source of artemisinin is a herb, *Artemisia annua* (Sweet wormwood), and the fact that artemisinin is a stable, easily crystallizable compound renders the extraction and purification processes reasonably straightforward². The key pharmacophore of this natural product is the 1,2,4-trioxane unit (**2**) and, in particular, the endoperoxide bridge. Reduction of the peroxide bridge to an ether provides an analogue, deoxyartemisinin **3**, that is devoid of antimalarial activity³.

(1a) $\text{R}^1\text{R}^2 = \text{O}$ (1b) $\text{R}^1 = \text{H}, \text{R}^2 = \text{OH}$ (1c) $\text{R}^1 = \text{H}, \text{R}^2 = \text{OMe}$ (1d) $\text{R}^1 = \text{H}, \text{R}^2 = \text{OEt}$ (1e) $\text{R}^1 = \text{OCOCH}_2\text{CH}_2\text{CO}_2\text{Na}, \text{R}^2 = \text{H}$ (1f) $\text{R}^1 = \text{R}^2 = \text{H}$ 

(2) 1,2,4-trioxane

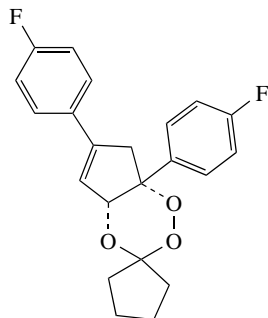
(3) $\text{R}^1\text{R}^2 = \text{O}$

Although artemisinin (**1a**, qinghaosu) has been used clinically in China for the treatment of multidrug-resistant *Plasmodium falciparum* malaria, the therapeutic value of **1a** is limited to a great extent by its low solubility in both oil and water. Consequently, in the search for more effective and soluble drugs, many researchers have prepared a number of derivatives of the parent drug^{4,5}. Reduction of the C10 lactone of artemisinin produces dihydroartemisinin (**1b**), which exists in solution as a mixture of α and β anomers. Dihydroartemisinin has been used for the preparation of a series of semi-synthetic first-generation analogues that include artemether (**1c**) and arteether (**1d**). Both of these compounds express activity in the low, single nanomolar range versus chloroquine-resistant Plasmodia. For treatment of advanced cases of *P. falciparum* malaria, a water-soluble derivative, sodium artesunate (**1e**) is usually preferred since this drug can be delivered faster than by intramuscular (i.m.) injection⁶.

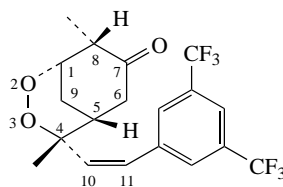
In spite of the fact that artemisinins have been used to treat over a million patients infected with malaria, the mechanism of bioactivation remains an area of intense research and several theories have been put forward to explain the phenomenal parasite selective antimalarial activity of this class of drug^{7,8}. In this chapter, we will examine the biomimetic iron-mediated degradation chemistry of artemisinin and its synthetic trioxane analogues, and the results will be compared with analogous studies on antimalarially active endoperoxides. The chapter will also contain a brief summary of the structures and chemistry for the synthesis of lead peroxide antimalarials that are undergoing preclinical development and we will also describe current research into hybrid analogues that have the capacity to kill parasites by more than one mechanism. We present studies on the mechanism of action of the endoperoxides prior to dealing with the syntheses of analogues, simply due to the fact that some of these mechanistic studies have provided the basis for rationale antimalarial drug design. The chapter will conclude with a brief look at research that suggests that trioxane analogues may also have use as antitumour agents and the current status of this research will be critically assessed.

A. Malaria and Parasite Haemoglobin Degradation

A human becomes infected with malaria parasites by inoculation of sporozoites during the bite of a parasite-infected female anopheline mosquito. Several phases of its asexual life cycle occur within its mammalian host either in the liver or in the red blood cells (erythrocytes). Most antimalarial drugs, including chloroquine-type antimalarials and endoperoxides, are blood schizontocides (i.e. they act to kill the parasite schizonts during the blood phase of the parasitic life cycle)⁹. Within the erythrocytes the parasite uses host haemoglobin as a source of essential amino acids for its development. As a result of haemoglobin catabolism, parasite-infected cells contain high concentrations of iron(II)/iron(III) in the form of heme/hematin^{10,11} and it was proposed by several workers in the field that ferrous heme is the target for endoperoxide-containing antimalarials ensuring their selective cytotoxicity¹². Consequently, investigations into the mechanism of action have centred round the role of iron(II). However, it is important to note that although our mechanistic understanding of the bioactivation of the endoperoxide bridge of the artemisinins is now well understood, the exact antimalarial molecular mechanism of action of these systems has yet to be fully elucidated, although there are several groups working in the area and their progress is reviewed below. An understanding is essential because it would lead to rational design of this class of drugs, which is becoming increasingly urgent with growing resistance of the malaria parasite to traditional alkaloidal antimalarials, such as chloroquine.



(4) fenozan B0-7

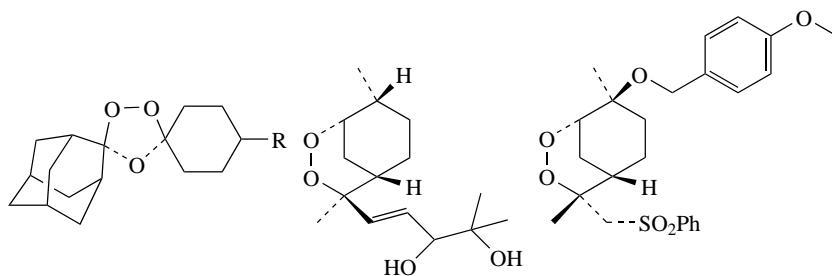


(5) arteflene

II. ENDOPEROXIDE-CONTAINING ANTIMALARIALS

In addition to artemisinin, other synthetic trioxanes and endoperoxides (fenozan B0-7 **4**¹³ and arteflene **5**¹⁴) have enjoyed some success; arteflene reached Phase II pre-clinical trials. More recently, Vennerstrom and coworkers have reported on the outstanding antimalarial properties of several 1,2,4-trioxolanes, one of which, OZ 277 (**6**), has entered clinical trials in man^{15,16}. These exciting, easily prepared drugs will be discussed in detail later in this chapter. In order to determine the parasitocidal action of this class of antimalarial, many research groups have focused their efforts on artemisinin and its semi-synthetic derivatives (artemether, arteether and artesunate **1c**, **1d** and **1e**), and this is the point where our discussion will begin.

Posner and coworkers^{17,18} have developed versatile methodology for the synthesis of novel 1,2,4-trioxanes that has allowed detailed investigation of their Structure–Activity Relationships (SAR)¹⁹, while Jefford and coworkers²⁰ first synthesized fenozan B0-7, so naturally some of their work has centered on its mechanism of action. Avery and coworkers have also contributed significantly to the area by the syntheses^{21–24} and QSAR (Quantitative SAR)^{25–26} studies of many artemisinin analogues.



(6) OZ 277



(7) yingzhaosu A

(8)

Bicyclic endoperoxide antimalarials, such as arteflene (**5**) and naturally occurring yingzhaosu A (**7**)²⁷ and endoperoxide **8**²⁸, share a unique feature of this class of compounds in their peroxide bond. As mentioned earlier, the peroxide bond of artemisinin has

been shown to be essential for bioactivity (deoxyartemisinin (**3**) does not possess any antimalarial activity) and so it has been assumed that all endoperoxide-containing antimalarials have a similar mechanism of action.

III. THE ROLE OF IRON

As free heme is released during the parasite's degradation of haemoglobin, it is oxidized to its ferric form, namely hematin. Hematin can be reduced to its iron(II) state intracellularly (by a thiol, *N*-acetylcysteine or glutathione, for example) and the presence of this redox active ferrous heme can result in toxicity to the parasite. Hematin is biocrystallized to hemozoin, a microcrystalline black-brown iron(III) pigment that is excreted into the cell cytosol^{29,30}. The hematin aggregation process is unique to the parasite; it is known that traditional alkaloidal antimalarials, such as chloroquine, act by binding to free hematin and prevent detoxification by inhibiting formation of a hematin dimer, the unit cell of crystalline hemozoin³¹.

Iron(II) is known to decompose hydrogen and dialkyl peroxides to free radicals by reductive cleavage of the O—O bond and early investigations established the parasite's sensitivity to these species. When treated with radiolabelled ¹⁴C-artemisinin, the hemin-hemozoin fraction of the lysed malaria-infected erythrocytes was shown to contain a radiolabel, though the mechanism of incorporation is not clear. Meshnick and coworkers demonstrated that uninfected cells did not contain radiolabelled proteins whereas six radiolabelled proteins were isolated from cells infected with the *Plasmodium falciparum* (*P. falciparum*) strain of the parasite³². It was suspected that one of the alkylated proteins was the Histidine Rich Protein (HRP) that was known to bind multiple heme monomers and therefore thought to be instrumental to the parasite's detoxification process³³. Moreover, iron chelators were found to inhibit the lethal effects of peroxides on the parasite³⁴.

Elucidating the mechanism of action of endoperoxide-containing antimalarials is not trivial; the active species is not the intact endoperoxide but one or more transient intermediates. Posner and Oh were the first chemists to confront the problem and they focused on the role of iron(II)³⁵. In order to determine the 'killing species' responsible for the parasitocidal action, the products of iron(II)-initiated degradation were identified in the hope that one or more of these was responsible for the parasite's death. The following sections will describe the proposed intermediates and their possible role in the pharmacological activity of these drugs. The reductive cleavage of the peroxide bond leads to isomerization of the artemisinin backbone, via carbon-centred radicals and other highly reactive species (see Sections III.A, III.A.1 and III.A.2) capable of alkylating parasite biomolecules. However, more recently, it has been proposed that Lewis or protic acid catalysed heterolysis of the peroxide bond could also afford alkoxy or hydroxyl radicals that may be responsible for the parasitocidal action (Section III.C). Both proposals will be discussed below. Finally, recent publications have implicated the role of non-heme iron. It has been proposed that exogenous iron(II) can be activated by complexation with amino acid residues and cause reductive cleavage of the peroxide bond of artemisinin (Section III.B).

A. Generation of C-centred Radicals

Posner and Oh³⁵, and later Jefford and coworkers^{36,37}, led the earliest investigations by synthetic chemists into the mechanism of action of 1,2,4-trioxane antimalarials. Both proposed that formation of a C-centred radical was essential for activity but the nature of the radical (primary or secondary) and the mechanistic pathways put forward were not identical. The iron degradation studies of Posner and coworkers implicated a role for the

secondary C-centred radical, while Jefford and coworkers preferred a primary C-centred radical. Several groups have attempted to resolve the issue and evidence for both species has now been provided in the literature.

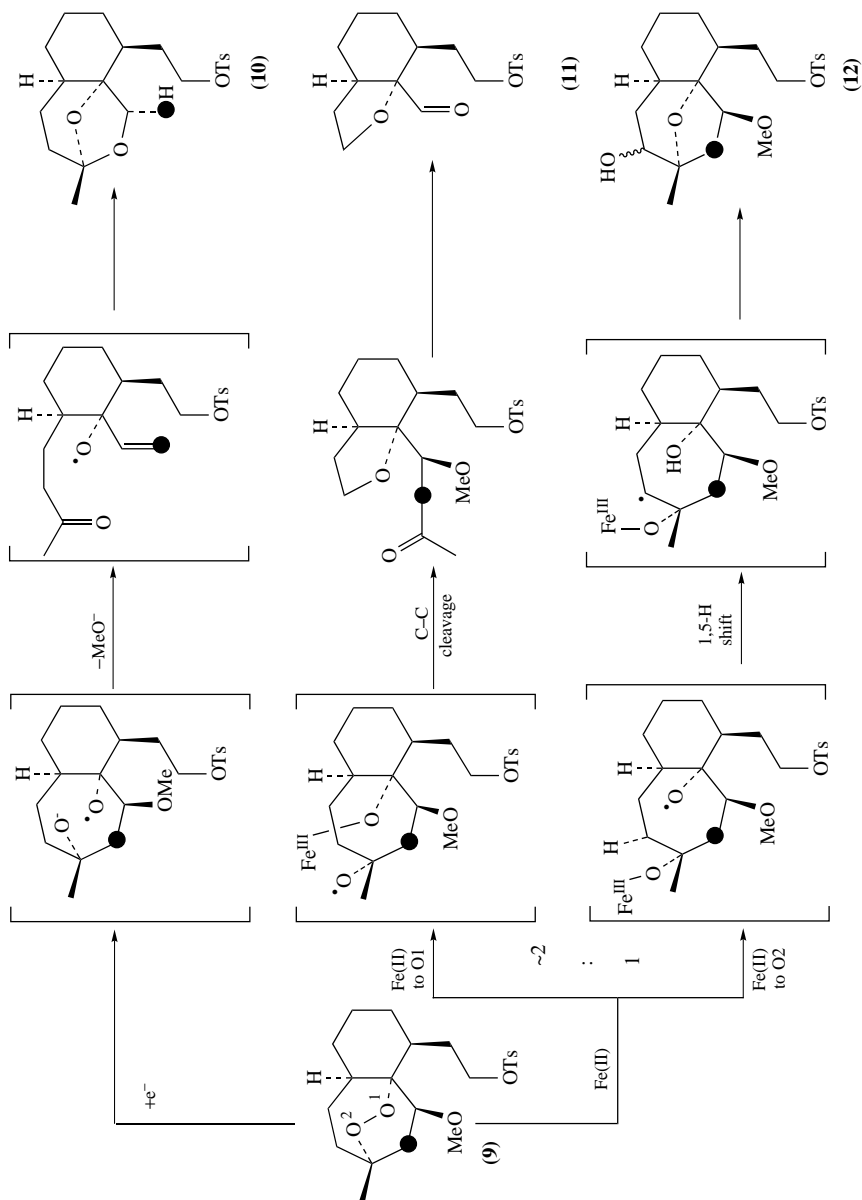
1. Evidence for involvement of a secondary C-centred radical – The 'O₂ route'

Regiospecific oxygen-18 labelling of a simplified trioxane **9** at O4 (marked with a black circle), structurally related to artemisinin, allowed Posner and Oh³⁵ to provide the first mechanistic evidence that iron(II) ions (ferrous bromide or hemin with benzyl mercaptan) displayed different reactivity towards a trioxane than other reducing agents. Zinc, samarium diiodide, tributyltin hydride with AIBN and trityllithium afforded only the deoxygenated product **10**, whereas iron(II)-mediated rupture of the O–O bond led to a mixture of products via a cascade of subsequent rearrangements of the initially generated oxygen (O-) centred radical (Scheme 1). Association of reducing ferrous iron with O1 leads to the formation of an O-centred radical that subsequently generates a primary carbon-centred radical species. This species reacts in an intramolecular sense to produce the ring-contracted tetrahydrofuran derivative that upon hydrolysis produces the aldehyde **11**. The alternative pathway involves association of O₂ with ferrous iron—the resulting O-centred radical can abstract, via a 1,5-H shift, an α -hydrogen on the carbocyclic ring to produce a secondary carbon-centred radical **12**. This pathway will be referred to as the 'O₂ route' and it was proposed that this pathway may be more important for expression of high levels of antimalarial activity.

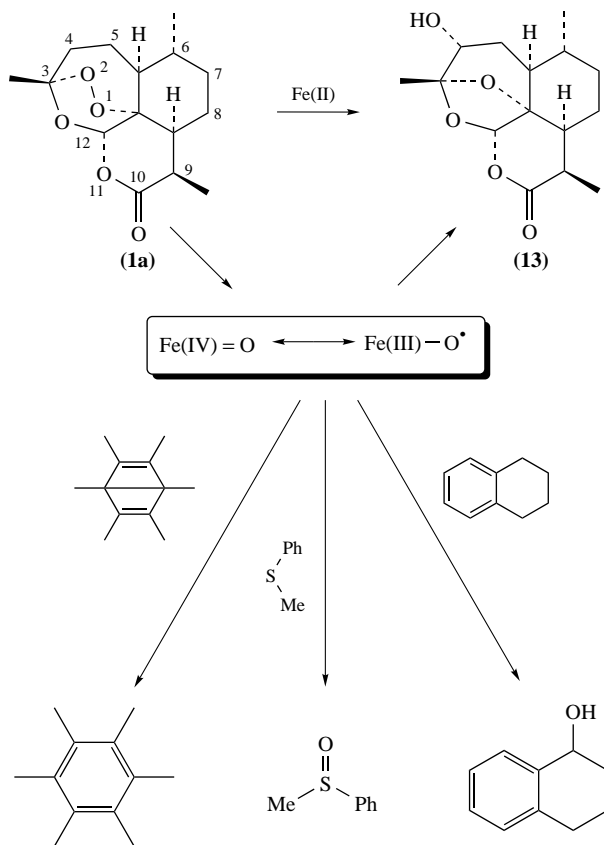
Monoxygenase metalloenzymes are known to cause oxidative damage and Posner postulated that a high-valent iron(IV) oxo species (formed by oxygen atom transfer from the peroxide bridge to the iron centre) was formed as a reactive intermediate of the degradation reaction. Posner and coworkers³⁸ observed that when the iron(II) degradation of artemisinin was carried out in the presence of (a) Dewar benzene, (b) methyl phenyl sulphide and (c) tetralin, dewar benzene was rearranged in 40% yield to hexamethylbenzene, while oxidation to the corresponding sulphoxide and to hydroxytetralin was observed for (b) and (c), respectively (Scheme 2). Later, they observed the same result during the degradation of other antimalarial synthetic trioxanes, but not in the cases of inactive trioxanes, providing additional evidence for the iron(IV) oxo species^{18,39}.

The isolation and identification of artemunin D **13** as a product of the degradation experiments prompted Posner to suggest a pathway for the iron(II)-induced isomerization of artemisinin similar to what had been seen earlier for the synthetic trioxane **9** (Scheme 1). It was proposed that the peroxide bond was broken by a single electron transfer (SET) from iron(II) (to O₂) to afford an O-centred radical at O1 (Scheme 3). A subsequent 1,5-H shift generated a secondary C4-centred radical **14**, which was followed either by β -scission of C3–O₂ bond (and extrusion of high-valent iron(IV) oxo species) affording the enol ether **15** or by loss of iron(II) to afford the epoxide **16**. Rebound epoxidation of **15** by the iron(IV) oxo intermediate also afforded **16** while ring opening of the epoxide by the internal hydroxyl group afforded artemunin D **13**.

Posner and coworkers proposed that the highly electrophilic epoxide could not be isolated due to its 'inherent instability' but was a potent alkylating agent responsible for parasite death. However, Wu and coworkers have isolated a small quantity (1–2% yield) of the epoxide **16** in their iron(II) degradations of artemisinin using iron(II) sulphate in aqueous acetonitrile⁴⁰. These authors conclude that it is not the active 'killing species' since any external nucleophiles would have to compete with the in-built nucleophile (the OH moiety). Moreover, Avery and coworkers also concluded that the epoxide could not



SCHEME 1

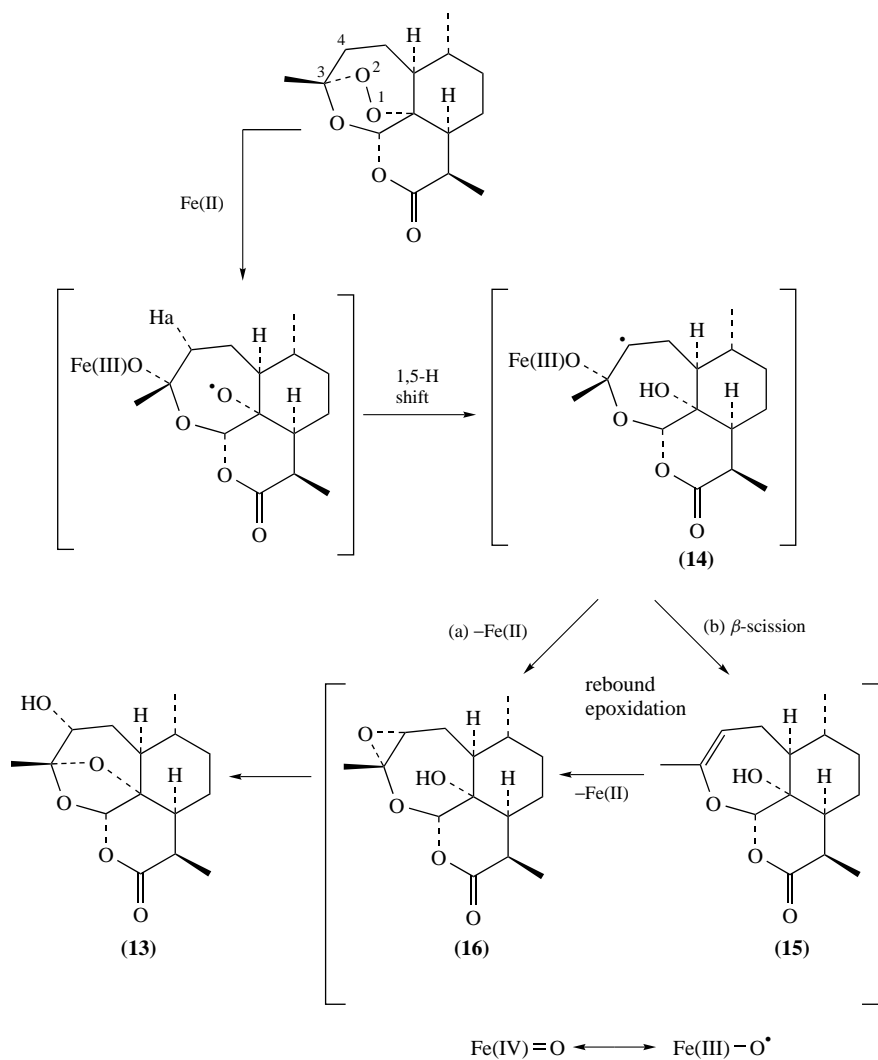


SCHEME 2

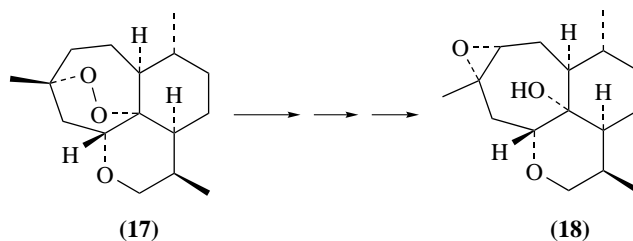
be essential for the activity by preparing the carba-analogues **17** and **19** of artemisinin and testing for their antimalarial activity⁴¹. It was found that **19** was more potent than **17**, even though the epoxide **18** (proposed as an intermediate of iron(II) degradation of **17**) should be more reactive to nucleophilic attack at the C3 position than the epoxide **20** isolated from the degradation of **19**. The epoxide **20** was itself inert.

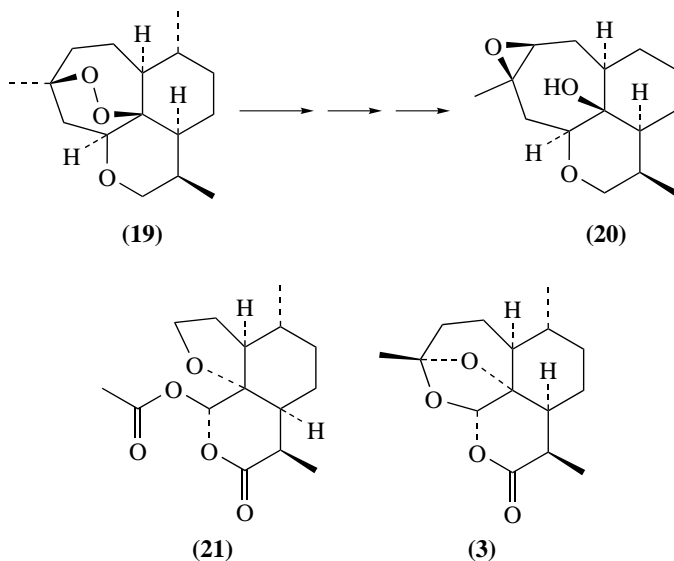
It should be noted that, in addition to the product shown in Scheme 3, the ring-contracted THF product **21** was also observed. Indeed, significant quantities of both **21** and deoxyartemisinin **3** (using iron(II) bromide in THF) were observed in a ratio **13:21:3** of 1:6:3, determined from the proton NMR spectrum. A second pathway (in which SET occurs from iron(II) to O1; the 'O1 route') leading to formation of a similar THF product was suggested in 1992 when investigating the degradation of an ¹⁸O-labelled trioxane (Scheme 1)³⁵.

In the presence of 1,4-cyclohexadiene (CHD) the C4-centred radical pathway was diverted from formation of artemunin D, **13**, to afford significantly more deoxyartemisinin **3** (by the secondary C4 radical abstracting a H-atom from CHD) while the proportion of **21** remained the same. The authors proposed that the O2 pathway (Scheme 3) contributed most to the activity and that the C4 secondary radical intermediate (generated by

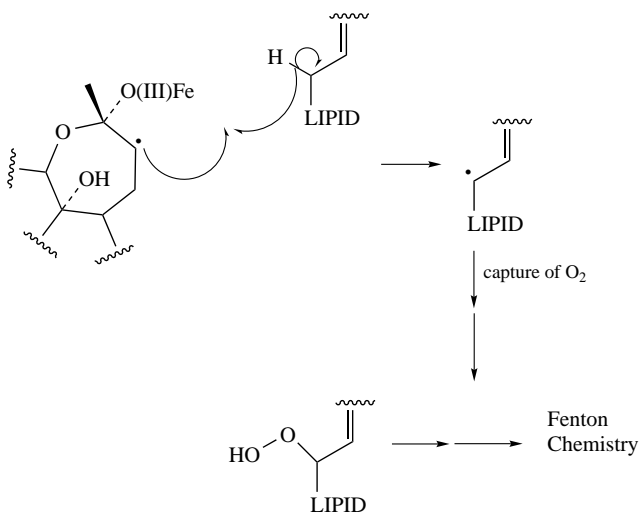


SCHEME 3



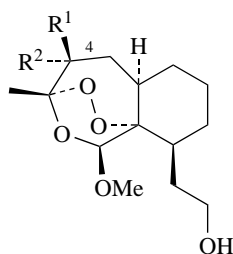


the 1,5-H shift) or subsequent intermediates along the same pathway were essential for antimalarial potency. The increased yield of deoxyartemisinin observed with increasing concentrations of 1,4-cyclohexadiene suggests that the secondary C4 radical is able to efficiently abstract allylic hydrogen atoms to produce lipid-based C-radicals. It is possible that this radical species is also able to mediate lipid peroxidation of the parasite's cell membranes (Scheme 4)⁴².



SCHEME 4

In order to determine the significance of the 1,5-H shift and the secondary radical species for antimalarial activity, the trioxanes **22a–c** were synthesized and tested¹⁸. The diastereomeric trioxanes **22a** and **22b** possessed very different antimalarial activity against both chloroquine-resistant and chloroquine-sensitive strains of the parasite; the 4- β isomer was approximately twice as active as artemisinin while the 4- α isomer and the disubstituted trioxane were more than sixty times less potent. The authors proposed that the α -substituent prevented the suprafacial 1,5-H shift and therefore suppressed the activity of these compounds.



(**22a**) $R^1 = H, R^2 = Me$

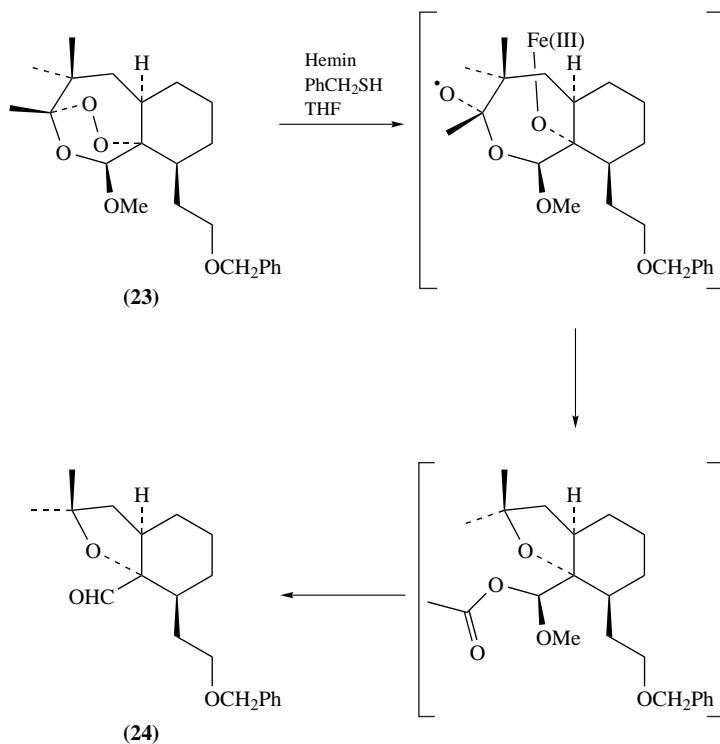
(**22b**) $R^1 = Me, R^2 = H$

(**22c**) $R^1 = R^2 = Me$

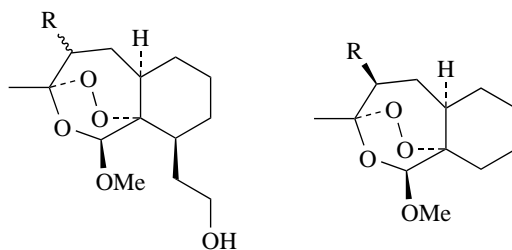
In addition, in the benzyl ether of the inactive trioxane **23**, the geminally substituted C4 position was degraded using heme (generated from hemin in the presence of benzyl mercaptan) and was found to decompose to the ring contracted THF product **24** as the major product via the O1 route (Scheme 5), which suggested that intermediates of this second route were not important for pharmacological activity¹⁸. Moreover, this result is significant because Meunier and coworkers⁴³ have suggested that the inactivity of C4 α -substituted trioxanes arises from their inability to dock closely with heme, preventing SET from the iron(II) centre to the peroxide bridge. The fact that this geminally disubstituted trioxane is completely isomerized by heme demonstrates that this is not the case^{44,45}.

Introduction of a methyl group at the 4- β position actually resulted in increased activity, because of the additional stabilization of the secondary C4 radical. A series of trioxanes **25–32** were prepared to determine the effect of C4 substitution on antimalarial activity. The functionalities introduced included radical stabilizing groups (methyl, phenyl, benzyl, CH_2TMS)⁴⁶ and CH_2SnR_3 ($R = Me, Bu$) designed to intercept the C4 radical. As previously observed, for all compounds with measurable antimalarial activity the β -isomers were more antimalarially active than the α -isomers.

Introduction of C4 benzyl and methyl substituents increased antimalarial activity relative to the unsubstituted trioxanes, which the authors concluded was due to stabilization of the C4 radical^{18,47}. A powerfully stabilizing group at C4 (for example, Ph or CH_2TMS , **28** and **29**) was found to decrease the antimalarial potency relative to the unsubstituted analogues. The authors did not feel that the steric bulk was responsible for the lowered activity since the α -orientated peroxide bridge was remote from the β -orientated substituents. Therefore, they investigated the iron(II) degradation of **28** and observed that the major product resulted from a ring-contracted THF species formed via the O1 route. They concluded that too much stabilization reduced the reactivity of the C4 radical and therefore reduced the antimalarial potency.



SCHEME 5



(25) R = H

(26) R = Me

(27) R = CH₂Ph

(28) R = Ph

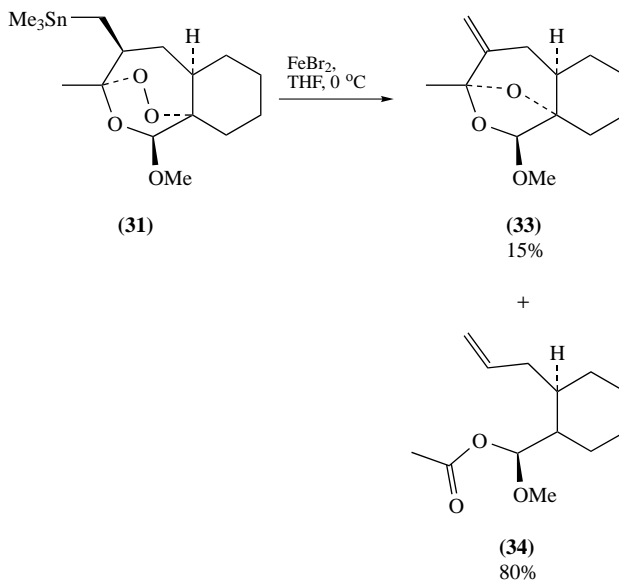
(29) R = CH₂TMS

(30) R = H

(31) R = CH₂SnMe₃(32) R = CH₂SnBu₃

It was anticipated that a C4 β -trialkylstannyl group would intercept the C4 radical and result in loss of antimalarial activity. Indeed, **31** and **32** were inactive and iron(II) degradation afforded two major products in which the stannyl group had been eliminated (Scheme 6). They proposed that the deoxo derivative **33** was produced by elimination of a

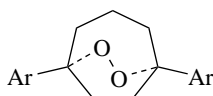
trimethyltin radical following 1,5-H shift (O2 route), while **34** was afforded by elimination following C3–C4 bond scission (O1 route).



SCHEME 6

Posner and coworkers⁴⁷ concluded that the low activity of the stannyl-substituted trioxanes indicated that the 'killing species' must be an intermediate somewhere along the route after the 1,5-H shift has generated a C4-centred radical.

Based on this mechanistic insight, Posner and coworkers prepared the simple bicyclic endoperoxides⁴⁸, **35** and **36**, compounds able to undergo a facile 1,5-H shift. They were shown to possess significant antimalarial activity *in vitro*, but unfortunately the plasma half-life of **35** in rodents was too short for these easily prepared endoperoxides to be developed as antimalarial drugs⁴⁵. However, Kamata and coworkers⁴⁹ have recently investigated the iron degradation of these endoperoxides (using iron(II) bromide in dichloromethane) and have observed multifaceted reactivity resulting from reductive and heterolytic cleavage of the O–O bond.



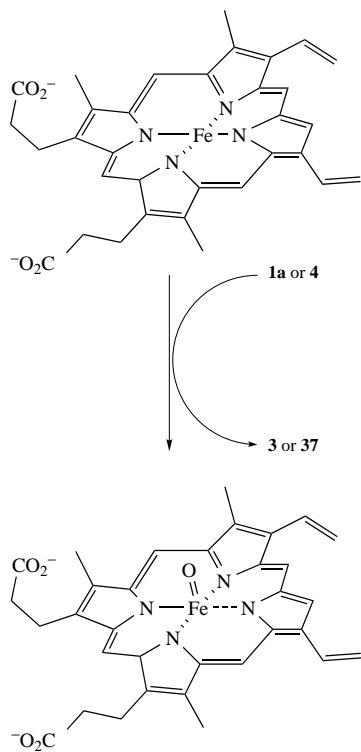
(35) Ar = Ph

(36) Ar = 4-MeOC₆H₄

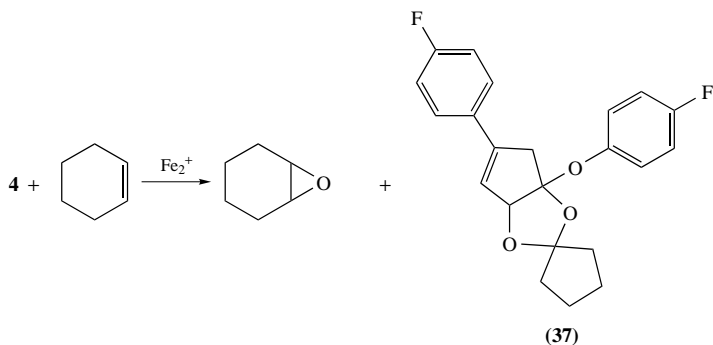
Wu and coworkers provided the first direct evidence for the formation of a secondary radical intermediate from artemisinin⁴⁰. By degrading artemisinin in the presence of a spin-trapping agent, 2-methyl-2-nitrosopropane, they were able to observe an ESR spectrum characteristic of a secondary radical⁴⁰. In addition, they have recently reported isolation of a cysteine–artemisinin adduct derived from the C4 secondary radical, *vide infra*⁵⁰.

2. Evidence for involvement of primary C-centred radical – The 'O1 route'

Jefford and coworkers have investigated the iron(II) degradation of fenoan B0-7 (**4**) and have proposed that a primary radical must be implicated in the mechanism of action of 1,2,4-trioxane antimalarials³⁶. Fenoan was degraded using iron(II) chloride in aqueous



SCHEME 7



SCHEME 8

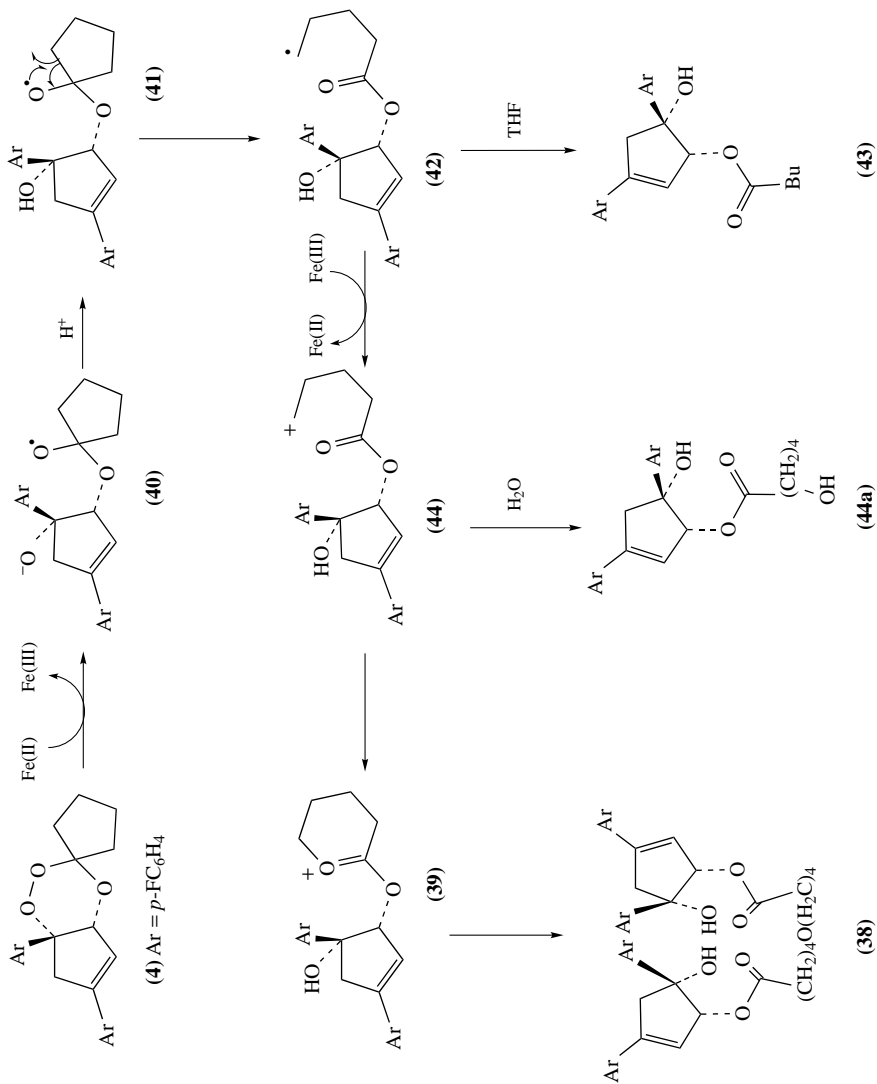
acetonitrile in the presence of cyclohexene. Jefford anticipated that the trioxane could act *in vivo* by transfer of an oxygen atom to heme, generating an iron(IV) oxo species (with concomitant formation of the dioxalone **37**) able to kill the parasite (Scheme 7). If an analogous iron(IV) oxo species was generated during degradation of fenoan B0-7, he proposed that it would transfer an oxygen atom to cyclohexene, affording the epoxide (Scheme 8)^{36,51}. As noted earlier, Posner had proposed that an iron(IV) oxo intermediate is important for the activity (Section III.A.1). Neither the epoxide nor the dioxalone **37** were observed, indicating that oxygen atom transfer did not occur; instead, **38** was obtained as the major product under most of the reaction conditions (acetonitrile or acetic acid, -40 °C to room temperature, 45 minutes to 24 hours) and a second product **39** was also observed (Scheme 9).

Jefford and coworkers proposed that the mechanism for their formation began with rupture of the peroxide bond and SET from iron(II) to afford radical **40** that was protonated under the reaction conditions to give **41**. C-C bond scission gave the C-centred primary radical **42**, which was able to follow one of two pathways. In the first pathway, this species was quenched by H-transfer from the reaction medium affording **43**. The second pathway resulted in the major product and was catalytic with respect to iron(II); a second SET to iron(III) generated the carbocation **44** (and recycled iron(II)), which underwent nucleophilic attack by **39** to afford dimer **38** or reaction with water to give **44a**. The mechanism proposed is similar to that suggested by Posner for artemisinin; the peroxide bond is cleaved to generate an oxygen-centred radical, which subsequently rearranges to a C-centred radical that initiates isomerization of the trioxane's carbon atom backbone; however, in this instance only a primary radical is implicated. Products that could be derived from a 1,5-H shift were not observed. Jefford also commented that the reaction conditions significantly affected the product distribution; in THF **38** was not formed, although it was the major product in acetonitrile.

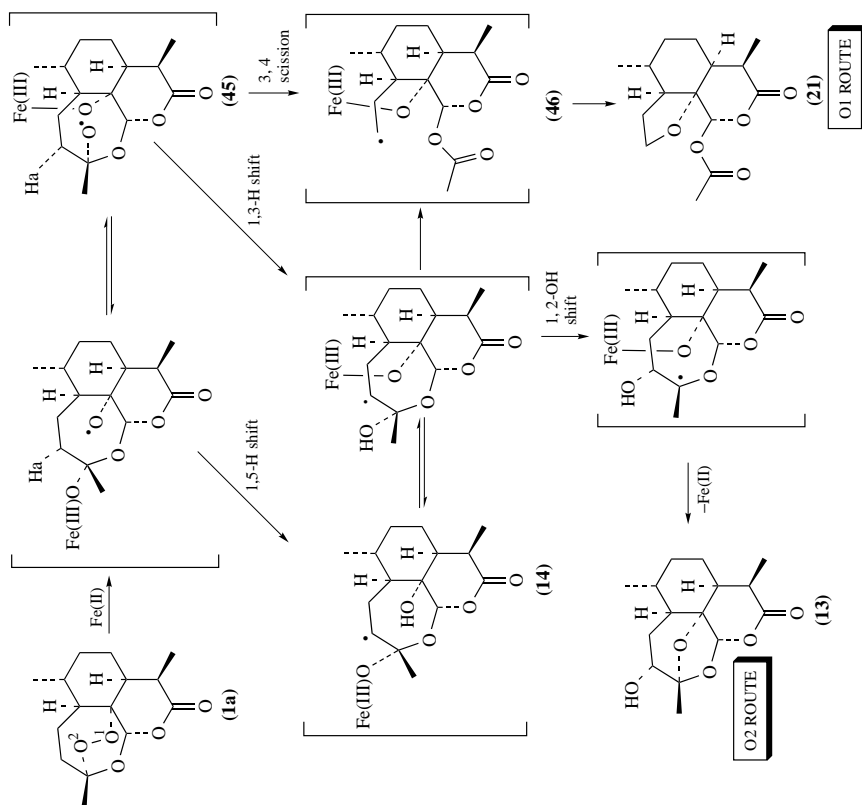
Before proceeding with the current discussion, it is worth noting that there is growing evidence that carbocation intermediates, such as **44**, are one of the species responsible for bioactivity⁵². There is very little in the literature concerning the alkylation of proteins by C-centred radicals, although they are potent hydrogen atom abstractors and are likely to promote lipid peroxidation (Scheme 4). On the other hand, carbocations are potent alkylating agents and should probably be regarded as good candidates for the alkylation of parasite proteins⁴⁴.

The results prompted Jefford and coworkers to re-examine the iron(II) degradation of artemisinin in aqueous acetonitrile with iron(II) chloride (Scheme 10), a system they suggested was closer to the physiological conditions than iron(II) bromide in THF³⁷. They reported that iron(II) chloride catalysed isomerization of artemisinin to afford the same products identified by Posner (**13** and **21**), except that deoxyartemisinin **3** was not observed. When the reaction was carried out in the presence of cyclohexene, none of the expected epoxide was produced, which suggested (in sharp contrast to Posner's results) that a high-valent metal oxo species was not involved.

The mechanism of the iron degradation proposed by Jefford (Scheme 10) again is similar to Posner's (Scheme 1) in that it is initiated by SET to the peroxide bond, resulting in its reductive cleavage to give an O-centred radical that rearranges to afford the two products. (It was also proposed that the initially formed oxyl radical can reversibly produce **45**.)³⁷ However, since these results did not support the involvement of an iron(IV) oxo species, the proposed route to product **13** differs markedly and involves an unlikely 1,2-OH shift. Moreover, Jefford suggested that the rearrangement of Dewar benzene and the oxidation of 'easily oxidizable addends' were 'artefacts of workup or due to adventitious oxidation'. Jefford proposed that intermediates of the O1 route (in which the initial O-radical is centred on O2) predominated the parasiticidal action of trioxanes. He postulated



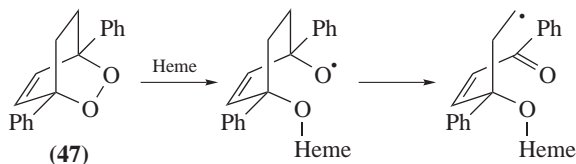
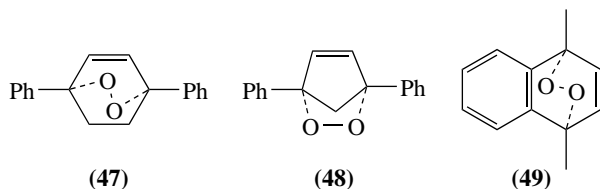
SCHEME 9



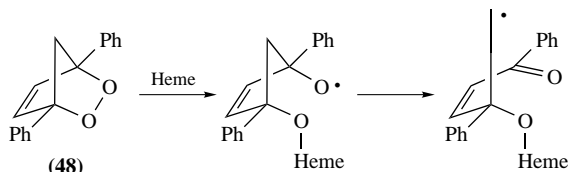
SCHEME 10

that the 'pendent' C-centred radical **46** could alkylate parasitic protein with formation of the ester group in **21**, providing the thermodynamic driving force.

Jefford and coworkers proposed that the difference of *in vitro* antimalarial activity of endoperoxides **47**, **48** and **49** could be explained in terms of their ability to form a pendent primary radical⁵³. The endoperoxide **47** possessed 50 to 100 times lower activity than artemisinin, while the lower homologue **48** was much less active. He suggested that the 'rigid bicyclic skeleton of **47** was perfectly set up for...scission to the key ethyl radical' with the formation of an enone moiety providing the thermodynamic driving force (Scheme 11). For the lower homologue **48** they postulated that the activity was reduced, since the resulting methyl radical was more sterically hindered and therefore was a less efficient alkylating agent (Scheme 12). The endoperoxide of 1,4-dimethylnaphthalene **49** was unable to afford the required pendent radical and was inactive.



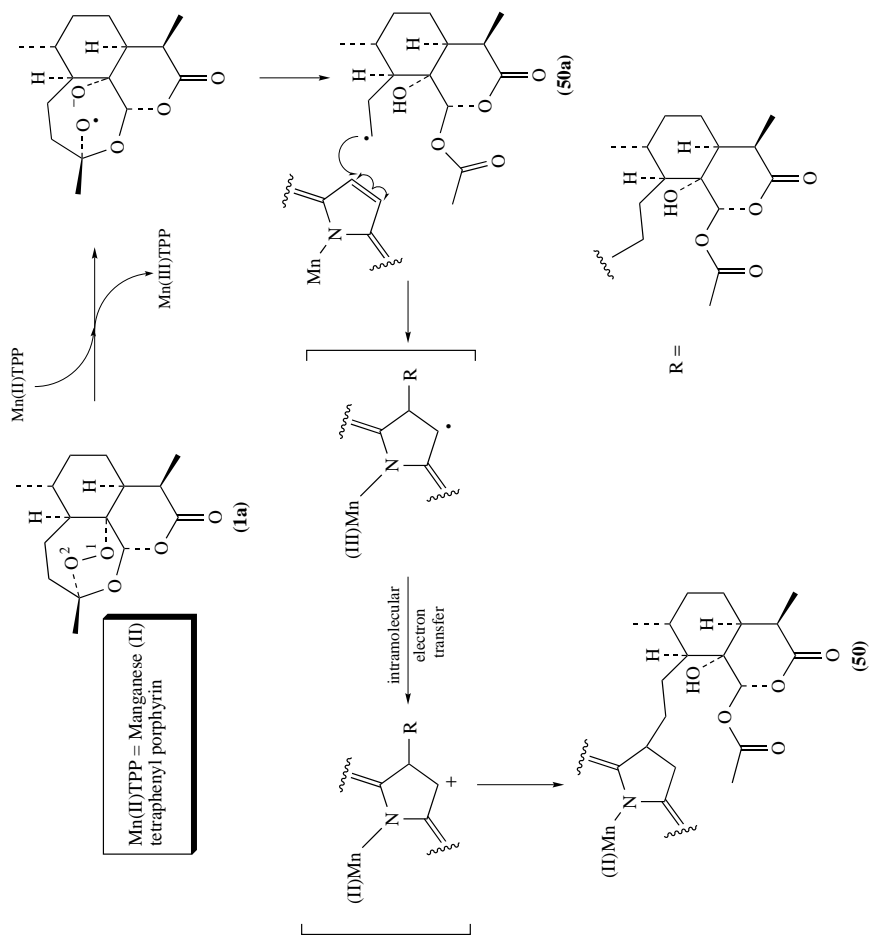
SCHEME 11



SCHEME 12

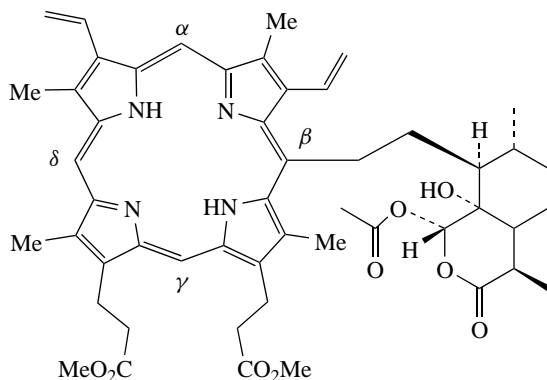
Robert and Meunier⁵⁴ have isolated and characterized covalent adducts of metalloporphyrins with artemisinin. Initial attempts using an iron(II) heme model were inconclusive, since the strong paramagnetism of the iron did not allow detailed characterization of the adduct and attempts at demetallation resulted in its degradation. Therefore, manganese(II) tetraphenylporphyrin (TPP) was used since it required milder demetallation conditions and the adduct **50a** was formed. The suggested mechanism for the alkylation involves a pendent ethyl radical **50** (Scheme 13).

The analogous adducts of artemether **1c** and fenozan **4** were also obtained and characterized; in each case porphyrin adducts were isolated in 20–30% yield. When artemisinin was treated with manganese(II) TPP in the presence of cyclohexene, Robert and Meunier also failed to observe any of the corresponding epoxide⁵⁵. The authors suggest that the Dewar benzene rearrangement and the oxidation reactions observed by Posner



SCHEME 13

were as a result of a SET process. More recently, Meunier and coworkers have isolated artemisinin-heme adducts using iron(III) protoporphyrin-IX dimethyl ester (in the presence of a hydroquinone derivative or a thiol to generate iron(II) *in situ*) in high yields⁵⁶. Heme was alkylated at the α -, β - and δ -positions to provide **51**–**53**, although only the monoalkylated products were obtained even when an excess of the drug was employed. They reported that the stereochemistry of artemisinin-derived chiral centres was maintained in the products and concluded that alkylation (subsequent to radical generation) must be a fast process. In addition, they suggested that the reactive radical species would be able to escape and alkylate parasite proteins that were located close to heme (see Sections IV.A.1 and IV.A.2).

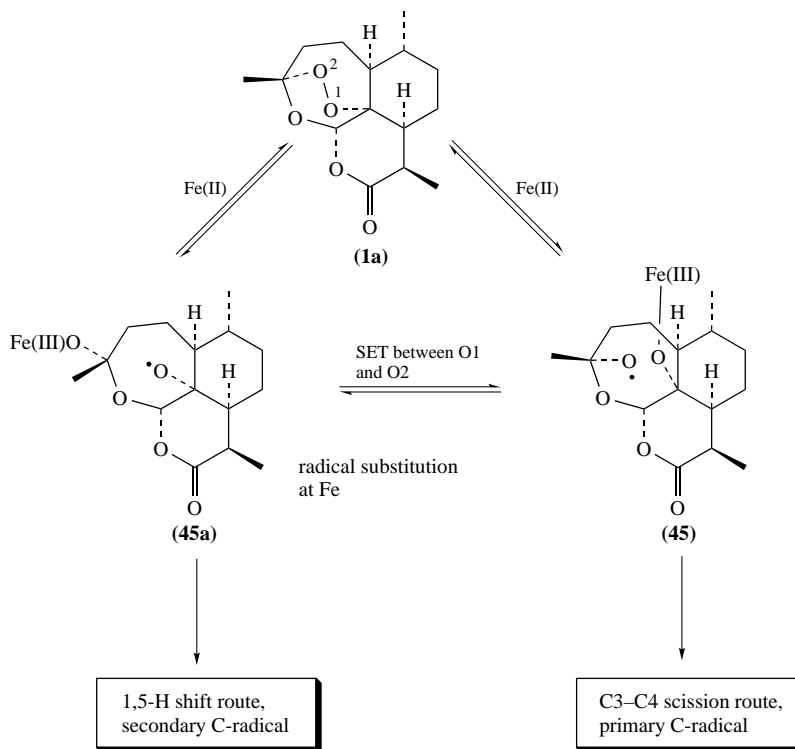


(**51**) substitution at α -position
 (**52**) substitution at β -position
 (**53**) substitution at δ -position

Robert and Meunier also observed that the most promising leads for antimalarial drug development are all lipophilic (allowing rapid diffusion through cell membranes) and all adopt a boat conformation of the peroxide ring, allowing the peroxide bond to 'dock' closely with heme and initiate alkylation.

As noted earlier, Wu and coworkers published the results of their iron(II) degradation of artemisinin using iron(II) sulphate and attempted to provide a unified mechanism⁴⁰. They concluded that the choice of counterion and solvent influences the yields and product distributions observed. Apparently contradictory results were explained by their unified mechanism in which the radicals **45** and **46** were freely interconvertable (Scheme 14, either by reversible cleavage or by a SET between the two oxygen atoms). It should be noted that both Posner and Jefford reported and commented on the varying product distributions and yields observed under varying reaction conditions. In a recent review by Meunier and coworkers, the authors observed that when using iron(II) chloride in acetonitrile or hemin and a thiol in THF the O1 pathway predominates, whereas the O2 pathway predominates when iron(II) bromide in THF is employed⁴³. As mentioned above⁴⁵, Kamata and coworkers also reported large effects on the reaction pathway (for the degradation of endoperoxides **35** and **36**) with solvent and even observed products resulting from heterolytic cleavage of the peroxide bond when the reactions were performed in dichloromethane.

As mentioned earlier, Posner and coworkers have provided evidence that the ability to undergo a 1,5-H shift is essential for antimalarial potency (Section III.A.1)¹⁸. Jefford and



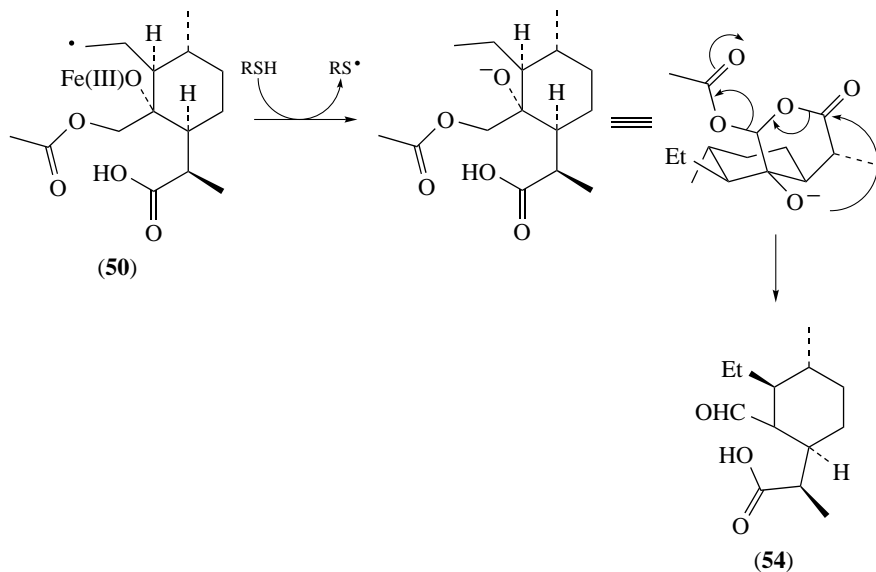
SCHEME 14

coworkers have argued that this process was not possible since the 'pertinent interatomic distances... appear too great' and suggested a 1,3-H shift as an alternative (Scheme 10). Wu and coworkers countered that the critical distance of 2.1 Å required for a 1,5-H shift could be met in artemisinin by conformational adjustments⁴⁰. Following the formation of the interconvertible intermediates (Scheme 13), the mechanism of the degradation proposed by Wu was largely a composite of the O2 route proposed by Posner and the O1 route suggested by Jefford. They concluded only that they believed C-centred radicals were responsible for the lethal effects of artemisinin on the parasite.

B. Involvement of Non-heme Iron

More recently, Wu and coworkers proposed that heme may not be the only iron containing species capable of initiating degradation of the peroxide bond but free iron(II) could form complexes with amino acids and be 'greatly activated'. They examined the iron(II) degradation of artemisinin in the presence of non-heme iron chelates such as cysteine^{50,57}.

When artemisinin was degraded in the presence of cysteine, they observed that the reaction was rapid and, in addition to the usual products (*vide supra*), an aldehyde **54** was formed. They concluded that **54** could only arise from a pendent ethyl radical **50** (Scheme 15) and therefore provided unequivocal evidence for its involvement as a 'killing species'.

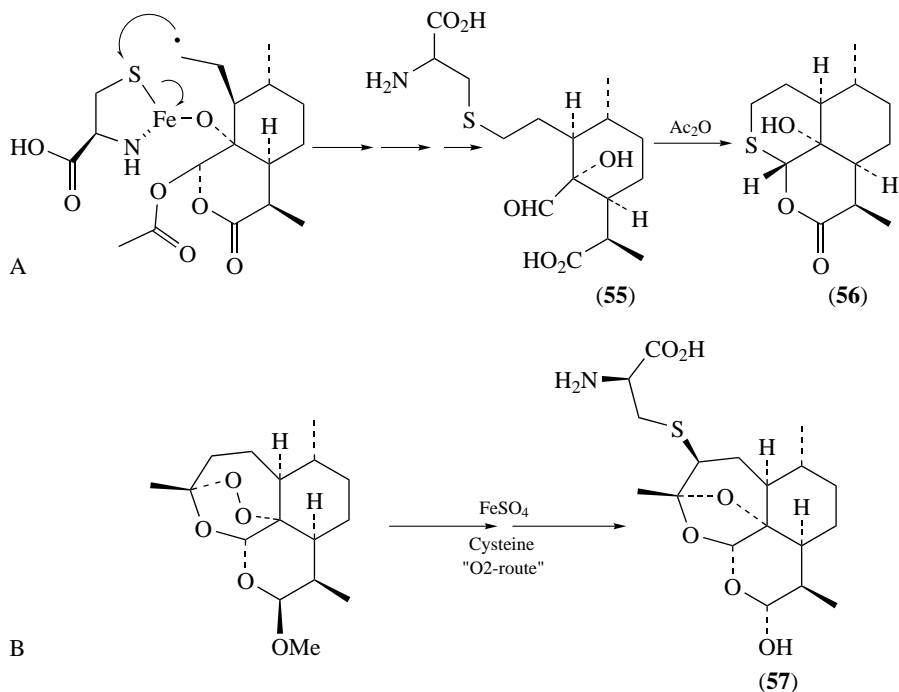


SCHEME 15

Perhaps more significantly they were also able to isolate a polar, water-soluble compound that they believed was **55** in which the cysteine residue had been incorporated into the artemisinin backbone. The broadness of the signals in the proton NMR spectrum made characterization problematic, but treatment of **55** with acetic anhydride afforded **56**, which was fully characterized (Scheme 16A). More recently, the same group has isolated and characterized another product from artemether. Adduct **57** was derived from the C4 secondary radical and cysteine (Scheme 16B).

They concluded that the parasiticidal action of trioxanes involved reductive cleavage of the peroxide bond by intracellular iron–sulphur redox centres (rather than heme) and subsequent alkylation of the redox centre. This type of redox centre is known to exist in many enzymes and Wu and coworkers proposed that structural differences between those in the parasite and those in mammalian systems could account for the high selective cytotoxicity of artemisinin.

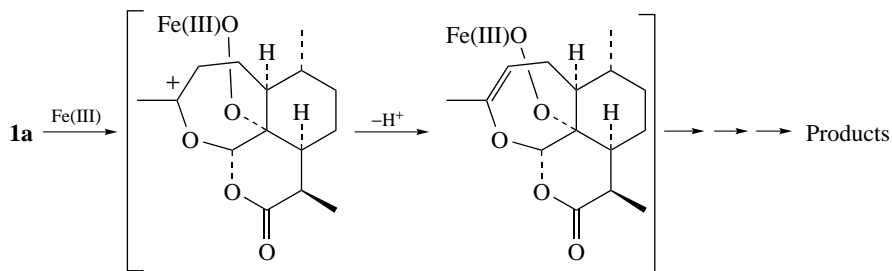
In a later review, Wu has questioned whether heme can be involved in the mechanism of action of peroxide-containing antimalarials at all⁵⁸. He notes that the effect of alkylation of heme would be the accumulation of redox active alkylated free heme, leading to molecular oxygen-derived radical species able to cause the parasite's death. He argued that if that was the case, simple peroxides would also be potent antimalarials since the efficacy of the drug would be proportional to the amount of radicals generated. In addition, he argued that the parasite's intracellular radical scavenging system should be able to cope with the free radicals generated, including an iron(IV) oxo species. Therefore, he concluded that free heme and simple iron chelates were not important for the mechanism of action of these compounds and that the receptors for these drugs are the iron–sulphur redox centres of functional proteins. Alkylation would prevent the essential function of these proteins and so lead to parasite death. In spite of these assertions, to date, there is no supportive biochemical evidence to support this mechanism of action.



SCHEME 16

C. Heterolytic Cleavage of Peroxide Bond

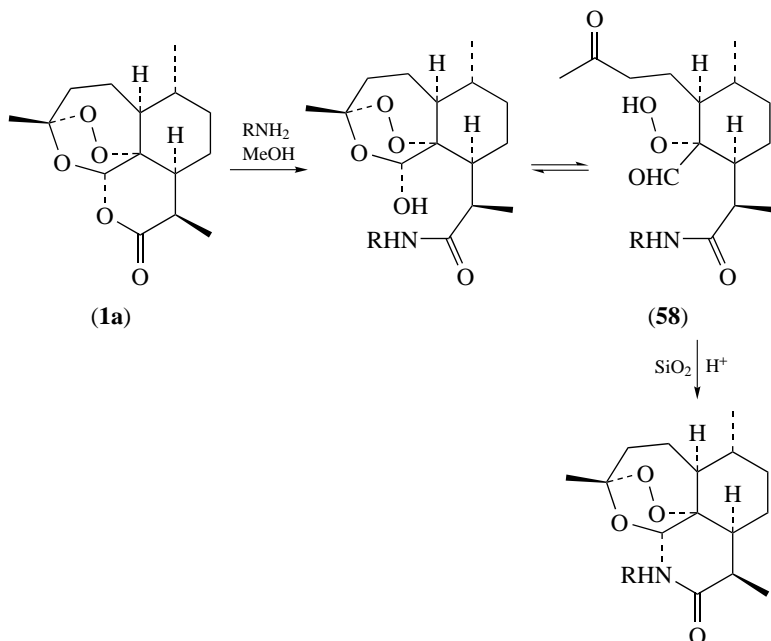
Haynes and Vonwiller reported that artemisinin displayed multifarious reactivity in the presence of heme and non-heme iron(II) and also iron(III)^{59,60}. The THF product **21** and artemunin D **13** were generally observed in varying ratios that were dependent upon the conditions used. Other products were also formed and the authors concluded that it was not possible to assign the parasiticidal species. However, they proposed an alternative mechanism of action that did not involve reductive ring opening of the peroxide bridge (Scheme 17).



SCHEME 17

They suggested that heterolytic ring opening by cleavage of the C3–O2 bond resulted in the hydroperoxide or metal peroxide and a carbocation. These intermediates could cause parasite death by oxygen transfer to oxidizable substrates or by generating damaging O-centred radicals. The carbocation could be intercepted by intracellular nucleophiles (water, thiols and amines, for example) to give a neutral species. Tertiary peroxides are able to undergo Lewis and protic acid catalysed ring opening and, moreover, all active compounds possess a moiety (alkoxy, aryl or alkyl) capable of stabilizing the resulting carbocation. However, Wu has argued that the O-centred radicals generated from the free hydroperoxide would not be toxic to the parasite because they would be mopped up by the intraparasitic system against oxidative stress, although this would depend upon their cellular location when generated⁵⁸.

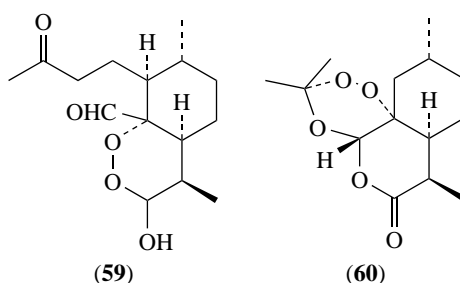
Following the synthesis of 11-azaartemisinin derivatives by Torok, Ziffer and coworkers in which the 11-azadeoxoartemisinin derivatives were observed as a by-product (Scheme 18)⁶¹, Haynes and coworkers were able to demonstrate that the open hydroperoxide **58** (detected by proton NMR spectroscopy) could act as an electrophilic oxygenating species⁶². In the presence of tertiary amines (for example, *N*-methylmorpholine and triethylamine), *N*-oxide formation occurred with concomitant formation of the 11-aza deoxoartemisinin as the only other major product. They concluded that the *N*-oxide was formed by oxygen atom transfer (which could occur *in vivo* in the presence of oxidizable substrates) from the open hydroperoxide, a process that would be facilitated in the presence of Lewis or protic acids. It was proposed that the 'key to the general activity [of artemisinin] is in the unique electronic ability of the trioxane to provide hydroperoxide. . . upon *heterolysis* of the C3–O2 bond'. The authors also proposed that the antimalarial activity of arteflene **5** arises from its ability to undergo heterolytic cleavage of its peroxide



SCHEME 18

bond by a retro-Michael addition, but the iron degradation studies of **5**, performed within the O'Neill group, have shown that this was unlikely (see Scheme 19, *vide infra*) since a C-centred radical is generated⁶³.

The 1,2,4-trioxane pharmacophore results in optimal activity of peroxide-containing antimalarials (arteflene **5** and other simple endoperoxides are somewhat less potent). Replacement of the non-peroxidic oxygen of artemisinin with a carbon atom results in a huge drop in potency, although the three-dimensional structure of the carba-analogue is almost identical to that of artemisinin⁶⁴. Olliario and coworkers⁷ have suggested that the non-peroxidic oxygen provides efficient stabilization of the carbocation intermediate generated following heterolytic C3–O2 bond cleavage and therefore facilitates ring opening. They disputed the involvement of C4-centred radicals, since **59** and **60** were found to possess antimalarial activity despite their inability to afford stable radical species such as those discussed earlier. However, we might expect **59** to unzip in the presence of protic acid and recyclyze to produce dihydroartemisinin, a process that is observed *in vitro*⁴⁴.

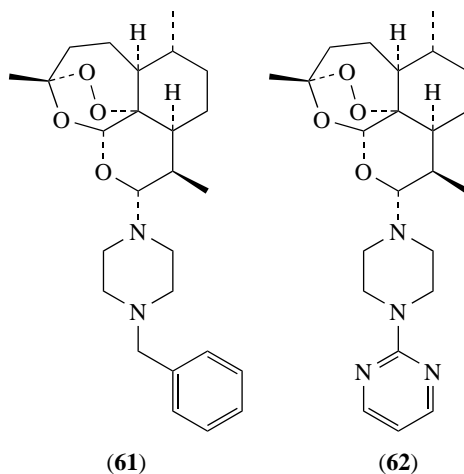


Olliario and coworkers suggested that the introduction of large radical stabilizing groups at C4 and C3 suppressed the bioactivity by sterically hindering the complexation of the peroxide bridge with the redox centre, rather than by preventing the 1,5-H shift (Meunier and coworkers⁴³ also proposed that close docking of the O–O bond with the iron(II) centre of heme was essential for antimalarial activity). Zouhri and coworkers have observed that C5 α -substitution diminished antimalarial potency and concluded that the substituent sterically hindered formation of a heme–drug complex⁶⁵. Olliario and coworkers⁷ have also questioned the evidence for the intermediacy of a high-valent iron(IV) oxo species, though it has been observed spectroscopically using resonance Raman spectroscopy⁶⁶.

Olliario and Haynes⁷ observed that the ability of this class of compounds to generate C-centred radicals leading to epoxides and carbonyl compounds was general to peroxides and was not indicative of antimalarial activity. They suggested that the ability of artemisinin to form adducts with heme models implied that any radicals formed would not have a sufficient lifetime to migrate from heme and react with biomolecules. The assumption that heme is the receptor for artemisinin has also been questioned by Wu and Liu⁶⁷; Olliario and coworkers observed that the ability of iron chelators to suppress activity indicated the involvement of exogenous non-heme iron, since heme iron cannot be complexed by these chelators⁷. In addition, it has recently been demonstrated that protease inhibitors, which prevent hemoglobin catabolism and therefore free heme generation, do not antagonize the action of artemisinin.

In line with the above discussion, a very recent paper by Haynes and coworkers again questions the involvement of heme Fe(II) and free ferrous iron in the mode of action of artemisinin and its derivatives⁶⁸. They were able to demonstrate that several highly potent analogues, such as **61** and **62**, reacted poorly with FeSO₄ in aqueous acetonitrile. Compound **61** was also relatively inert to cleavage by heme with 62% recovered after

24 h. They suggested that complexation of the piperazinyl group with free ferrous iron may act to prevent approach of a second equivalent of iron to the endoperoxide bridge. This piece of work provides additional evidence against the 'heme-activation' theory, but the results taken alone are not sufficient to rule out iron altogether in the mechanism of action of antimalarial endoperoxides; the main reason for this is that we are still not completely clear as to the definitive parasitic environment of 'endoperoxide bioactivation'—indeed, if bioactivation occurs within a hydrophobic environment of a lipid membrane or hydrophobic pocket of an enzyme, ferrous sulphate in aqueous acetonitrile may be a poor biological mimic. Indeed, ferrous-mediated cleavage of endoperoxides is very much more rapid under aprotic conditions.

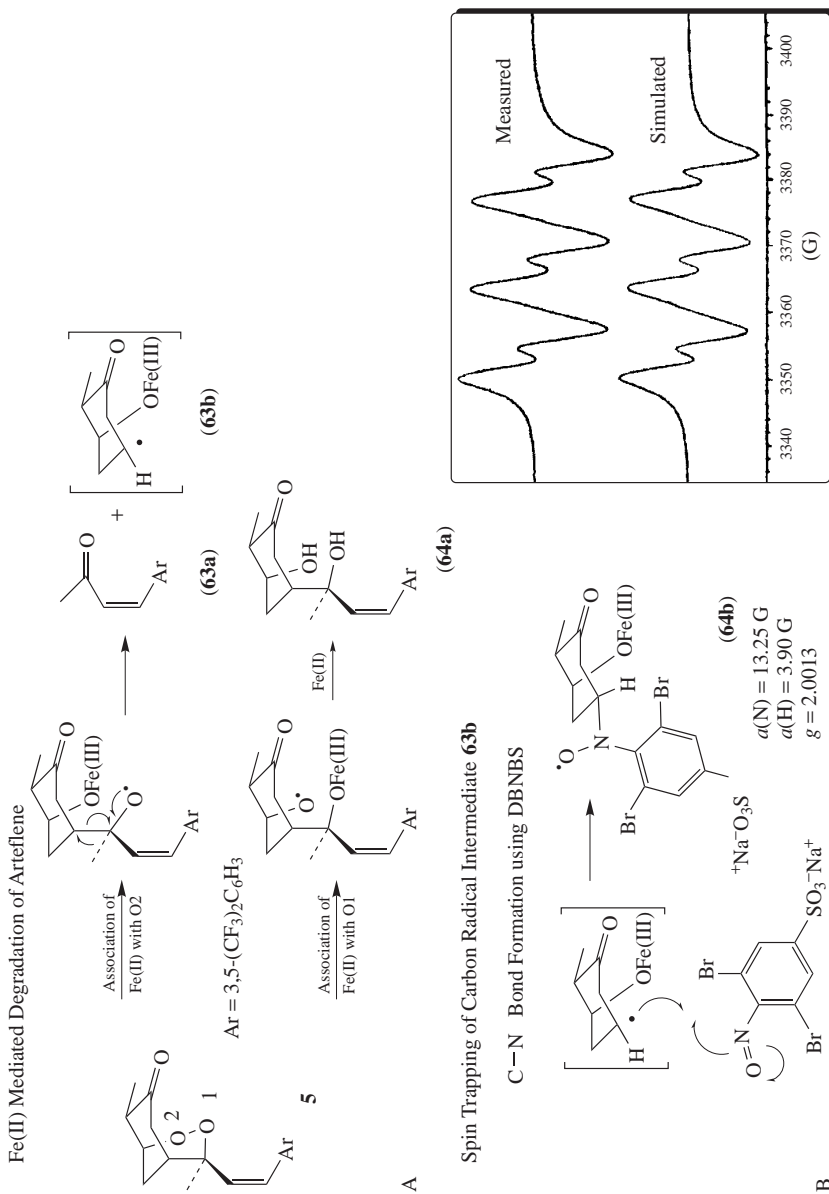


D. Iron(II) Degradation of Arteflene

Although arteflene **5** is not a 1,2,4-trioxane, its mechanism of action is believed to be very similar to trioxanes due to the presence of the peroxide bond. Indeed, when radioactive ¹⁴C-arteflene was incubated with *P. falciparum*, several alkylated parasitic proteins were identified^{69,70}. The O'Neill group carried out the first iron(II) degradation studies of arteflene using iron(II) chloride in aqueous acetonitrile; they isolated enone **63a** (in tandem with radical **63b**) and diol **64a** (Scheme 19A)⁷¹. The degradation with heme (generated from hemin chloride by *N*-acetylcysteine) was observed to be slower, but afforded the same products although in different ratio.

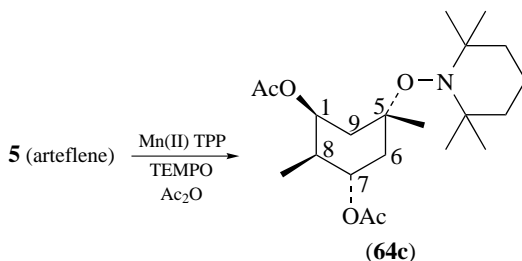
The proposed mechanism for the degradation involves SET to the peroxide resulting in homolytic cleavage of the O–O bond. An O1-centred radical led to the formation of the enone, while an O2-centred radical afforded the diol.

O'Neill and coworkers⁶³ were also able to spin-trap the previously proposed C-centred radical **63b** with sodium 3,5-dibromo-4-nitrosobenzenesulphonate (DBNBS) and the EPR of the adduct **64b** was characteristic of a secondary radical (Scheme 19B). It was suggested that the parasiticidal action of arteflene stems from the alkylating properties of the radical intermediate or possibly from the enone **63a**, which may be able to react with intracellular nucleophiles by a Michael addition. The enone itself did not exhibit antimalarial activity, possibly due to extracellular detoxification by glutathione before reaching its intraparasitic site of action.



SCHEME 19

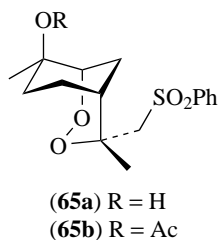
Meunier and coworkers investigated the degradation of arteflene using manganese(II) TPP as a heme model. They were able to spin-trap the secondary C-centred radical with the piperidyl radical (TEMPO) and the adduct **64c** was fully characterized following acetylation of the crude reaction mixture (Scheme 20)⁷². An arteflene-heme adduct was not observed and the authors suggest that this is attributable to steric hindrance factors. However, this could be further evidence that endoperoxide antimalarials do not target heme.



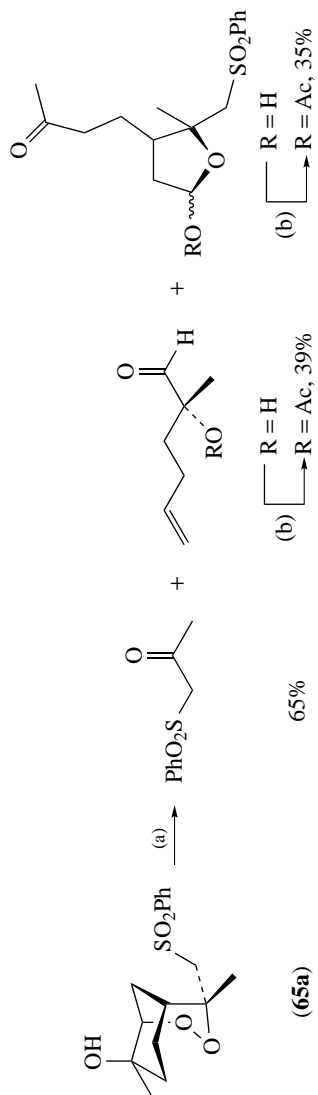
SCHEME 20

They proposed that the mechanism of action of arteflene could involve alkylation of biomolecules by the secondary radical, although ¹⁴C-radiolabelling of arteflene at C11 had resulted in incorporation of the radiolabelled fragment into the protein–drug adducts. Since C11 was not present in the radical fragment, they conclude that this fragment was probably not the ‘killing species’ and also suggest that the enone **63a** (unmasked intracellularly by reductive cleavage of peroxide bond by iron(II)) may undergo 1,4-addition reactions with nucleophilic side chains of amino acid residues.

Based on the potent activity of arteflene and yingzhaosu A, Bachi and coworkers developed a very efficient synthesis of bicyclic β -sulphonyl endoperoxides (**65a** and **65b**) (described in more detail later)⁷³. In order to gain insight into the potential mechanism of action of analogues in this class, Bachi and coworkers investigated the iron(II)-induced as used previously by degradation of **65a** and **65b**. The conditions used were based on those used previously by Posner and coworkers³⁸ and Avery and coworkers⁷⁴.

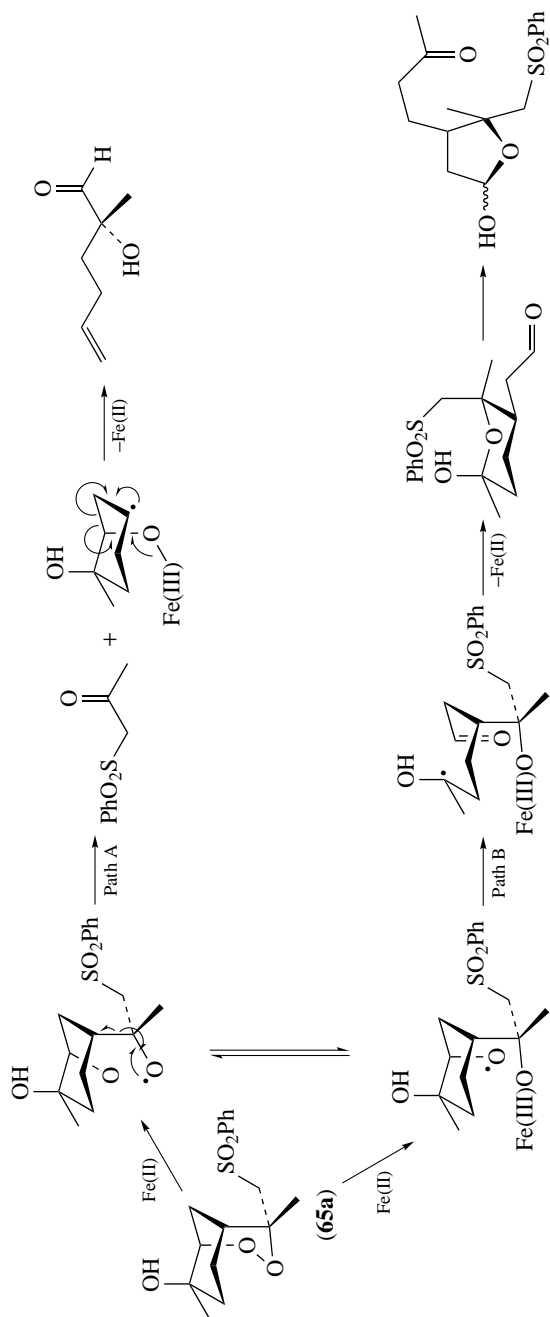


The results for sulphonyl endoperoxide **65a** are shown in Scheme 21 with the products acylated for characterization purposes. A full rationalization via an all-homolytic mechanism is depicted in Scheme 22.



(a) 0.2 eq. FeBr₂, THF, 0 °C; (b) 6 eq. Ac₂O, 0.25 eq. DMAP, pyridine, r.t.

SCHEME 21



SCHEME 22

This review has highlighted strong evidence that carbon-centred radicals may kill the parasite through alkylation of essential parasite biomolecules or heme. Such a pathway could easily be envisaged when looking at Scheme 22. However, an alternative, efficient alkylating process would result from the involvement of carbocations and a corresponding mechanism accounting for the formation of the compounds reported in Scheme 23.

It is suggested that carbocation **66a** and iron(II) are formed through single-electron transfer from carbon-centred radical to iron(III) in **66b**. Therefore, an analogous process would account for the generation of carbocation **67** from radical **68**. Oxidation of carbon-centred radicals by iron(III) salts to carbocations is well documented. Due to the lack of an effective nucleophile, carbocation **66a** should undergo β -cleavage to give the unsaturated hydroxyaldehyde product via a thermodynamically favoured Grob-type fragmentation, whereas in path B instantaneous proton shift in carbocation **67** followed by spontaneous acid-catalysed cyclization would yield the five-membered lactol product⁵².

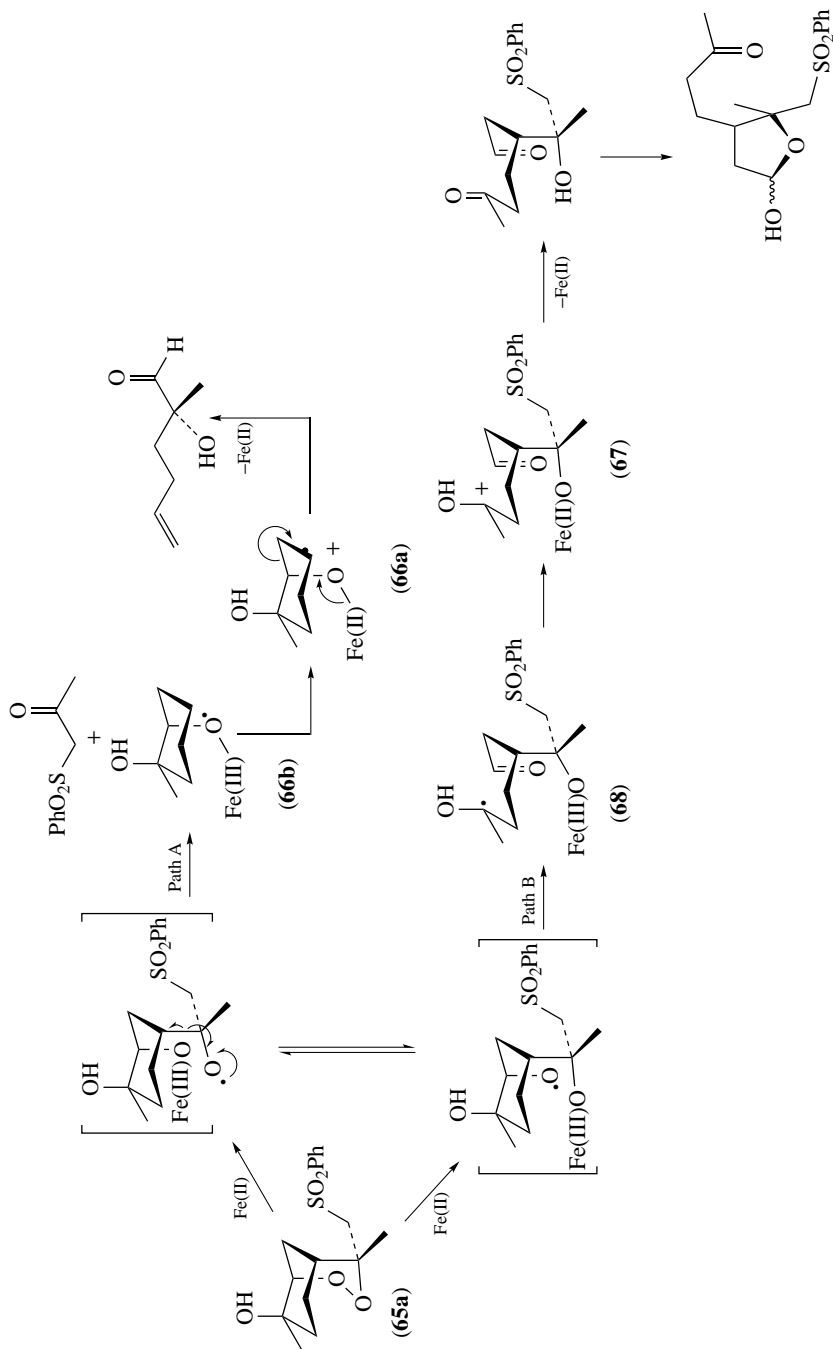
The Bachi group then performed an additional comprehensive set of experiments on **65a** and **65b**. Variations included the equivalents of FeBr₂, the solvents, and the inclusion or absence of 2,6-lutidine and tetrabutylammonium acetate. The conclusion from this work is that the first step in which oxygen-centred radicals are generated through iron(II)-induced reductive cleavage of the peroxide bonds is common to all peroxides; it was proposed that subsequent events are highly dependent on the structural characteristics of individual molecules. Bachi and coworkers believe these results provide strong evidence in favour of major involvement of carbocations in the parasiticidal activity of β -sulphonyl peroxides and possibly artemisinin and other structurally related analogues.

E. Summary

The precise identity of the parasite killing species derived from artemisinin and other peroxide containing antimalarials is not yet fully known, although several possibilities have been suggested:

- Involvement of alkylating C-centred radicals.
- Involvement of high-valent iron(IV) oxo intermediates.
- Direct oxygen transfer from an open hydroperoxide.
- Involvement of O-centred radicals formed from open hydroperoxide.
- Nucleophilic attack of intracellular residues on a carbocationic species generated by heterolytic ring opening of the peroxide C–O bond.
- Transformation of carbon radicals to carbocation species that can function as efficient alkylating agents.

It should be emphasized that virtually all of the above discussion is based on **biomimetic chemistry**, where the Fe(II) source varies from salts such FeSO₄ to the more reactive FeCl₂·4H₂O as well as heme mimetics (TPP) and ester hematin variants. When heme models are used, since porphyrin alkylation is a favoured process, end-product distributions of products can be very different from when a free ferrous ion source is employed. Furthermore, solvent has been shown to have a profound effect on the rate of reaction and product distributions obtained in iron-mediated endoperoxide degradation. Thus all of these studies are truly only approximate models of the actual events within the malaria parasites. Future work is needed to correlate the results of biomimetic chemistry with the actual situation within the parasite. In general, most workers do accept the role of carbon-centred radicals in mediating the antimalarial activity of the endoperoxides, but the key information defining (a) the chemical mechanism by which these species alkylate proteins and (b) the basis for the high parasite selectivity remains to be unequivocally established.



SCHEME 23

IV. THE BIOLOGICAL TARGETS OF ANTIMALARIAL ENDOPEROXIDES

The previous section dealt with the mechanisms behind the bioactivation of 1,2,4-trioxanes and endoperoxides. In this section we will examine briefly the suggested targets of the artemisinins. Since the original proposal by Meshnick and coworkers¹² it is still believed by many researchers in the field that heme liberated from the haemoglobin proteolysis process is the species responsible for the bioactivation of the endoperoxide bridge to potentially toxic free radicals in the food vacuole of the parasite (see above).

A. Lipid Membranes

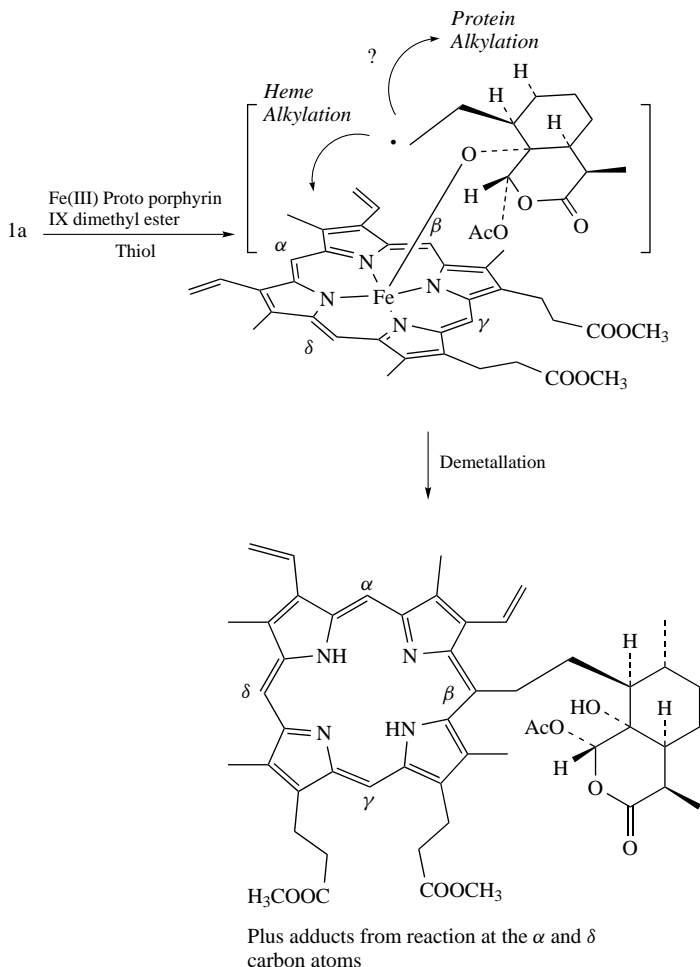
Consistent with this proposal, biomimetic studies by Berman and Adams have clearly demonstrated that artemisinin can effect a six-fold increase in heme-mediated lipid membrane damage⁴². Of importance to this observation are the findings of Fitch, who has recently demonstrated that unsaturated lipids co-precipitate with heme in the parasite's acidic food vacuole and also dissolve sufficient monomeric heme to allow efficient crystallization⁷⁵. A possible mechanism of artemisinin induced lipid peroxidation was described in Scheme 4 and provides downstream access to typical reactive oxygen species such as oxyl radicals and the superoxide anion. Interaction of lipid solubilized heme with artemisinin followed by ferrous-mediated generation of oxyl and carbon radicals places these reactive intermediates in the vicinity of target allylic hydrogens of unsaturated lipid bilayers. Hydrogen abstraction and allylic carbon radical formation with subsequent triplet ground state oxygen capture results ultimately in the formation of lipid hydroperoxides. The explicit mechanism depicted in Scheme 4 is supported by the work of Berman and Adams and others, and it was proposed that the damage caused to the parasite's FV membrane leads to vacuolar rupture and parasite autodigestion. The biological significance of hydroperoxides in relation to biological hydroxylation and autoxidation of, for example, lipids and membrane bilayers is well established. The generation of unsaturated lipid hydroperoxides provides a means of initiation of such processes.

In contrast to these proposals, other workers in the field have suggested that membrane bound heme may have a role to play in reducing the effectiveness of endoperoxides such as dihydroartemisinin⁷⁶. Further work is required to clarify the role of vacuolar membrane bound heme in the mechanism of action of endoperoxide antimalarials. Although the above scheme would appear chemically plausible, several workers have proposed that parasite death in the presence of artemisinin is probably not due to non-specific or random cell damage caused by freely diffusing oxygen radical species, but might involve specific radicals and targets, some of which are described below.

When artemisinin or other active trioxanes were incubated at pharmacologically relevant concentrations within human red blood cells infected by *P. falciparum*, a heme-catalysed cleavage of the peroxide bond was reported to be responsible for the alkylation of heme and a small number of specific parasite proteins, one of which has a molecular size similar to that of a histidine-rich protein (42 kDa)⁶⁹. Another possible target protein is the *P. falciparum* translationally controlled tumour protein (TCTP)⁷⁷. *In vitro*, dihydroartemisinin reacts covalently with recombinant TCTP in the presence of heme. The association between drug and protein increases with increasing drug concentrations until it reaches a stoichiometry of 1 drug/TCTP molecule. The function of TCTP is unknown and thus the role of heme-mediated artemisinin alkylation in the mode of action of this drug awaits further biochemical elucidation.

1. Heme

As mentioned earlier, alkylation of heme by artemisinin was first reported by Meshnick and coworkers after identification of heme–drug adducts by mass spectrometry, but no



SCHEME 24

structures were proposed for the resulting covalent adducts⁷⁸. As described in Scheme 24, they were able to demonstrate that the α , β and δ *meso* carbons of heme were alkylated by artemisinin; such results prompted Meunier and coworkers to suggest that the low and transient concentration of free heme generated by haemoglobin degradation *in vivo* may be responsible for the reductive activation of the endoperoxide function of active trioxanes⁷⁹. This pathway generates alkylating species, such as the primary carbon radical, which are likely to disrupt vital biochemical processes of the parasite via alkylation of biomolecules located in the close vicinity of the free heme. This proposal is based on the assumption that the primary C-radical has sufficient life-time to migrate from the face of the porphyrin metallocycle and subsequently to interact with its biological target (Scheme 24).

Although it is clear in model systems that artemisinin can efficiently alkylate heme-based models, the role of this event in the mechanism of action of artemisinin has

been questioned. Haynes and coworkers have ruled out this potential mechanism by demonstrating clearly that although artemisinin (**1a**) and dihydroartemisinin (**1b**) have the ability to inhibit β -hematin formation *in vitro*, the closely related and antimalarially potent **3** has no effect on crystallization⁸⁰. Thus, it was proposed that the observed inhibitory activities in the heme polymerization inhibitory assay (HPIA) for **1a** and **1b** are a reactivity or property not related to the inherent antimalarial mode of action of this class of drugs.

2. Enzymes as targets

As described earlier, erythrocytic malaria parasites degrade haemoglobin to acquire amino acids for protein synthesis. Falcipain 2 (FP-2)⁸¹ is a papain family cysteine protease that appears to act in concert with other enzymes, including two aspartic proteases, to degrade haemoglobin. Incubation of erythrocytic parasites with inhibitors of FP-2 blocks haemoglobin degradation and parasite development. Pandey and coworkers have demonstrated that, in purified digestive vacuoles from *P. yoelli*, cysteine protease activity can be inhibited by artemisinin in a similar manner to the potent cysteine protease inhibitor E-64⁸². Inhibition of falcipain mediated cleavage of the fluorogenic peptide substrate benzyloxycarbonyl-Phe-Arg 7-amino-4-methylcoumarin (Z-Phe-Arg-AMC) was also demonstrated in a continuous fluorometric assay, and surprisingly protease inhibition was increased in the presence of heme (surprising in the sense that strong arguments have been made that the heme-generated radical species cannot escape the porphyrin macrocycle and hit biological targets, post endoperoxide cleavage). To fully validate falcipain 2 and 3 as targets for endoperoxide drugs, it is essential that these studies be expanded to human forms of the parasite. In addition, it would be of great interest to compare the efficiency of falcipain inhibition with the known antimalarial activities of a series of artemisinin analogues of varying potency.

Krishna and coworkers have very recently provided compelling evidence that artemisinins act by inhibiting PfATP6, the Sarco/Endoplasmic reticulum Ca^{2+} -ATPase (SERCA) orthologue of *Plasmodium falciparum*³⁴. When expressed in *Xenopus* oocytes, Ca^{2+} -ATPase activity of PfATP6 is inhibited by artemisinin with similar potency to thapsigargin (another sesquiterpene lactone and highly specific SERCA inhibitor), but not by quinine or chloroquine. As predicted from this observation, thapsigargin antagonizes the parasitocidal activity of artemisinin. Deoxyartemisinin is ineffective as an antimalarial and was shown not to inhibit PfATP6 activity. Chelation of iron by desferrioxamine abrogates the antiparasitic activity of artemisinins and correspondingly attenuates inhibition of PfATP6. Single-cell imaging of living parasites with BODIPY-thapsigargin demonstrates cytosolic labelling that is competed with an excess of artemisinin. Furthermore, similar labelling is observed with a novel fluorescent artemisinin derivative. These studies support PfATP6 as a target of artemisinins operating via an Fe^{2+} -dependent activation mechanism.

V. SEMI-SYNTHETIC ARTEMISININ DERIVATIVES

The following section will highlight the chemistry that has been carried out on the artemisinin framework in pursuit of analogues with improved pharmacological profiles.

A. Improved Semi-synthetic Artemisinin Analogues

The first generation C10 acetal derivatives artemether (**1c**) and arteether (**1d**) both have a short half-life as a consequence of cytochrome P450 catalysed transformation to DHA (**1b**), which in turn is an efficient substrate for Phase II clearance through

glucuronidation⁸³. In addition to metabolism, other first generation analogues such as artesunate are chemically unstable and hydrolyse rapidly to DHA in plasma. Based on these observations, medicinal chemists have made significant efforts to design more potent and stable analogues of the first generation semi-synthetic derivatives using the chemistry depicted below in Scheme 25⁸⁴. The metabolically more robust C10 carba analogues **69a**⁸⁵ and C10 aryl analogues of DHA **69b**⁸⁶ (Chart 1) have been the focus of medicinal chemists for ten years. Of note are the C10 alkyl deoxo analogues prepared by Haynes and coworkers⁸⁷ and the C10 aryl or heteroaromatic derivatives **69c** prepared by the group of Haynes⁸⁸. Equally impressive are the C14-modified analogues **69d** prepared by the Avery⁸⁹ and Jung groups^{90,91}.

Recently, a C10 carba analogue (TDR 40292) **70** has been compared with artemether⁹². This compound cannot form DHA as a metabolite and contains a side-chain that can be formulated as a water-soluble salt. In addition, this compound has superior activity to artemether and artesunate, both *in vitro* and *in vivo*. From initial pharmacokinetic data, **70** has a higher volume of distribution than artemether and is considerably more orally bioavailable (16% versus 1.5% for artemether)⁹².

An important factor in the design of any new peroxide analogue is the concern about potential neurotoxicity. Any analogue with a higher log *P* than artemether (3.3–3.5) is likely to cross the blood brain barrier⁸⁸. Haynes and coworkers have prepared new analogues (see the C10 hemi-aminals depicted below in Scheme 25) with reduced neurotoxicity by considering the absorption, distribution, metabolism and excretion profiles of analogues (ADME paradigm). By considering physicochemical properties, it is possible to enhance efficacy through chemical substitution designed to increase drug absorption (coupled with a reduction in the ability of the new analogue to cross the blood brain barrier). Artemisone (undergoing development by Bayer) is a hemi-aminal⁶⁸ with much improved properties and represents the success of the ADME approach to drug design.

An alternative approach to preventing the formation of dihydroartemisinin by simple P450 metabolism is to replace the methyl function in artemether with an aryl function. Phenoxy analogues of DHA can easily be prepared in a one-step synthesis from dihydroartemisinin in a manner similar to the preparation of **1c** and **1d**. In addition to having superior *in vivo* activity to artesunate and artemether, analogues substituted with a *p*-fluoro (**71a**) or trifluoromethyl group (**71b**), in the phenoxy ring, resist metabolism to DHA⁹³.

The Avery group has produced a large number of artemisinin analogues by semi-syntheses and elegant total synthesis^{21,22,24,64,89,94–96}. This has enabled Avery to develop predictive 3-D QSAR (CoMFA)⁹⁷ analyses for the artemisinin class of antimalarial. This information coupled with the ADME approach described above should permit highly potent and orally bioavailable semi-synthetic analogues to be designed by a truly rational approach.

The main challenge for chemists in this area is to provide an analogue from DHA in the shortest number of chemical steps to make the drug economically viable for the treatment of malaria. The following section will describe the chemistry behind the synthesis of semi-synthetic analogues of the natural product, some of which have much improved pharmacological profiles.

1. Artemisinin chemistry

A remarkable feature of the chemistry of artemisinins is the fact that the peroxide bond withstands a whole range of organic reagents including organometallics and reducing agents. Treatment of artemisinin with sodium borohydride in ethanol provides dihydroartemisinin (**1b**) by reduction of the D-ring lactone function⁹⁸. Dihydroartemisinin

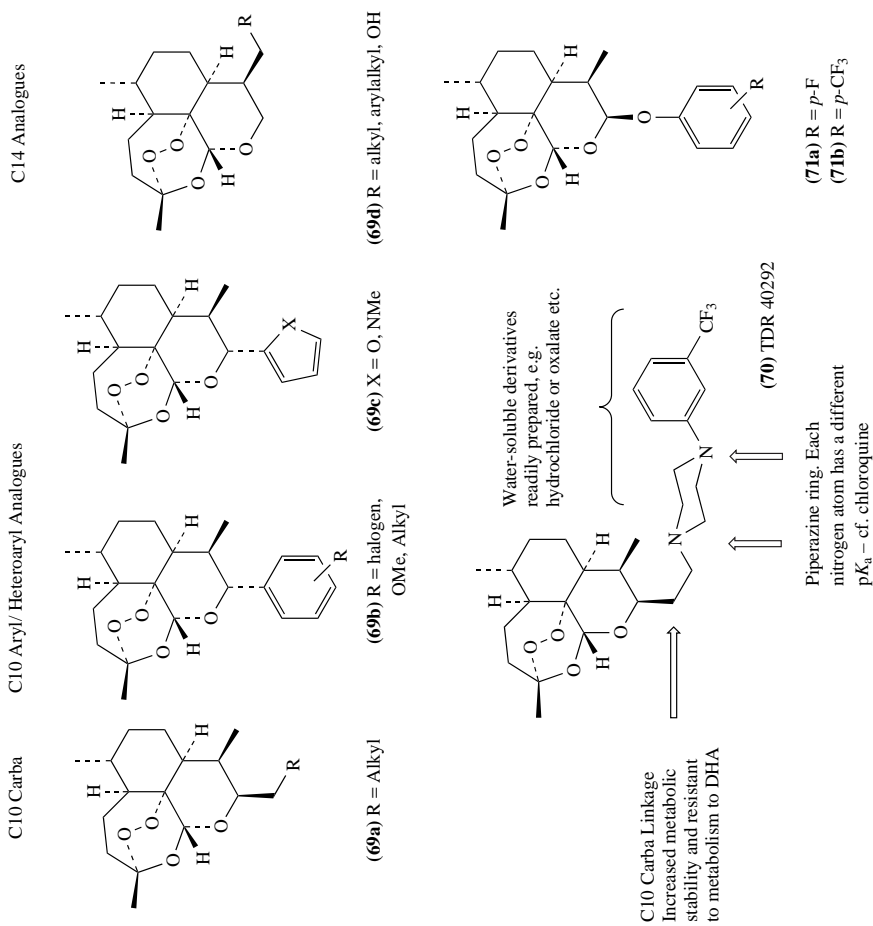
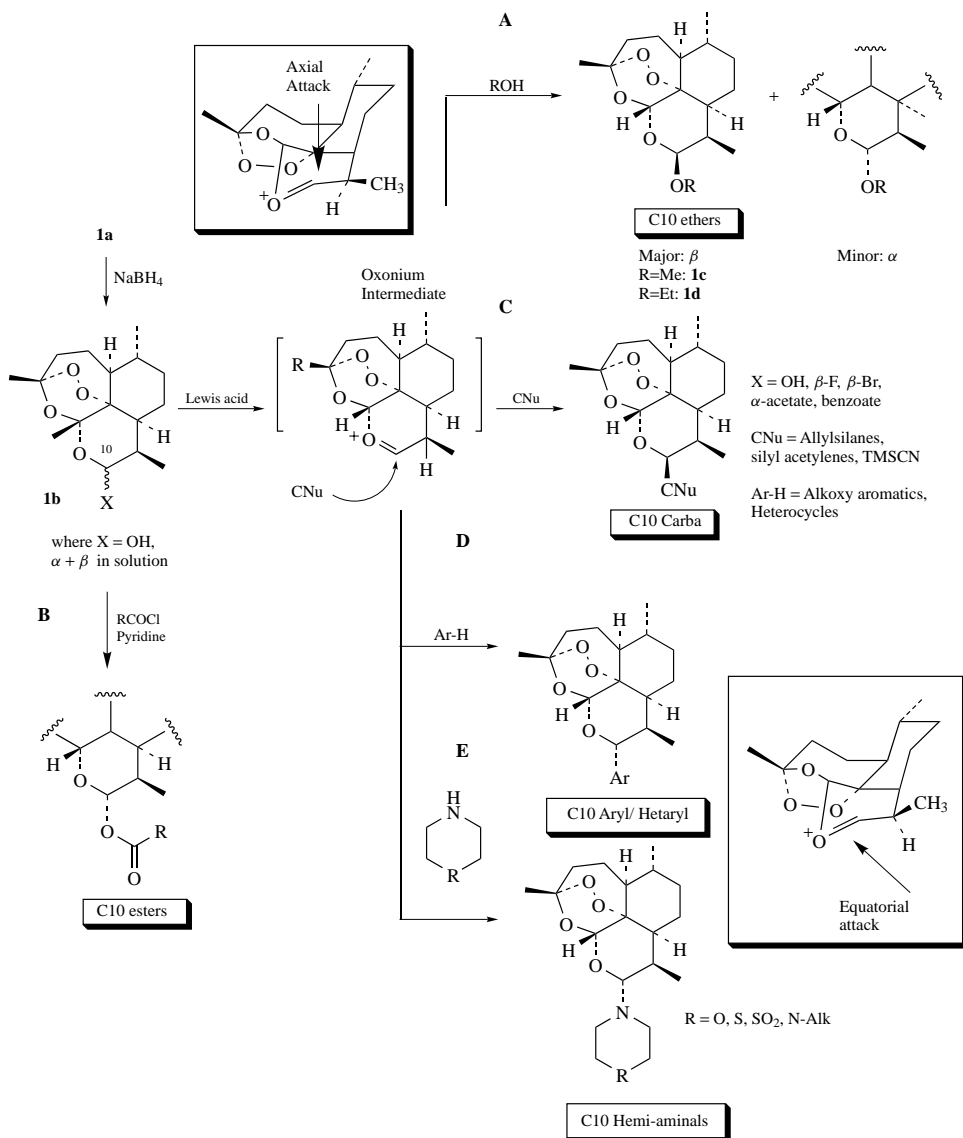


CHART 1. Second generation artemisinin analogues



SCHEME 25

exists as a mixture of α and β anomers at room temperature. Treatment of DHA with a Lewis acid such as $\text{BF}_3 \cdot \text{Et}_2\text{O}$ in an ethereal solvent generates an oxonium species that can be intercepted by an oxygen-based nucleophile (Scheme 25A)⁹⁹. The synthesis of **1c** and **1d** proceeds in this manner—axial attack of the nucleophile provides the anomericly

stabilized C10 β -ether products. For the synthesis of esters such as artesunate **1e**, dihydroartemisinin is treated with a base such as pyridine and an acid chloride. In this case the major product is the equatorial α anomer as shown (Scheme 25B)¹⁰⁰.

For the synthesis of C10 carba derivatives, a better leaving group than hydroxyl is usually preferred. The anomeric fluoride⁸⁶, bromide⁸⁷, acetate, benzoate¹⁰¹ and phenylsulphonyl groups¹⁰² have all been used and some of the chemistry that has been achieved is shown in Scheme 25. Allylsilanes tend to provide β -configured products by axial attack on the oxonium ion species (Scheme 25C) whereas larger nucleophiles such as electron-rich aromatics add by attack on the α face (Scheme 25D). For nitrogen nucleophiles, Haynes and coworkers have employed the C10 anomeric bromide intermediate that gives the C10- α hemi-aminal products (Scheme 25E), some of which exhibit remarkable stability (Chart 1)⁶⁸.

VI. SYNTHETIC ENDOPEROXIDES

The disadvantage of all the semi-synthetic compounds is that their production requires **1a** as starting material. Artemisinin is extracted from the plant *Artemisia annua* in low yield (0.01–0.8% yield)¹⁰³. To circumvent this problem, a number of groups have produced totally synthetic peroxide analogues, some of which demonstrate remarkable antimalarial activity. These include the synthetic 1,2,4-trioxane, fozan BO-7 (**4**)¹⁰⁴, the dispiro tetraoxanes (**72**, **73a**, **73b**)^{105–107} and the endoperoxide analogues such as arteflene (**5**)¹⁴. More recently, tetraoxane (**74**)¹⁰⁸ with an IC₅₀ as low as 3 nM has been discovered (artemisinin IC₅₀ = 10 nM) and analogues in this class have been shown to be effective when given orally in mice infected with *Plasmodium berghei* with no observable toxic side effects.

Other synthetic candidates worthy of mention include the C3 aryl trioxanes (**75a** and **75b**)^{109,110} and the endoperoxide analogue (**76**)¹¹¹. These latter compounds have oral activity (ED₅₀) as low as 0.5 mg kg⁻¹ in mice infected with *Plasmodium berghei*.

Vennerstrom and coworkers have recently described how by iterative drug design, a new class of endoperoxide antimalarial has been discovered with superior properties to the available semi-synthetic artemisinins (Chart 2)¹⁵. The first stage of their drug discovery process involved a systematic examination of a series of 1,2,4-trioxolanes (or 2° ozonides) (Scheme 26). This class of compounds is well known to organic chemists as unstable intermediates obtained from the exposure of alkenes to ozone—hardly the starting point for the discovery of a new antimalarial drug, one might think. In line with the known chemical instability of such compounds, some of the initial ozonides tested turned out to be very poor antimalarials. The first breakthrough was made when an adamantane ring was fused onto the ozonide ring system (Scheme 26). Remarkably, not only were these structurally simple compounds stable (**77a** and **77b**), but when tested against human strains of the malaria parasite, they were shown to have superior parasite-killing properties than the clinically used artemisinins such as artesunate and artemether¹⁶.

Since the first series of compounds were poorly soluble in water, the next crucial phase of the project set out to increase the water solubility of the drug candidates in order to increase absorption from the gastrointestinal tract. Further refinements led to a candidate that was not only well absorbed when administered orally to animals, but also had outstanding antimalarial profiles both *in vitro* and *in vivo*. In comparison to available semi-synthetic artemisinins, the drug candidate OZ 277 (Scheme 27) exhibits structural simplicity, an economically feasible and scalable synthesis, superior antimalarial activity and an improved pharmaceutical profile. The toxicological profiles are also acceptable and this drug candidate entered 'first into man' studies during 2004.

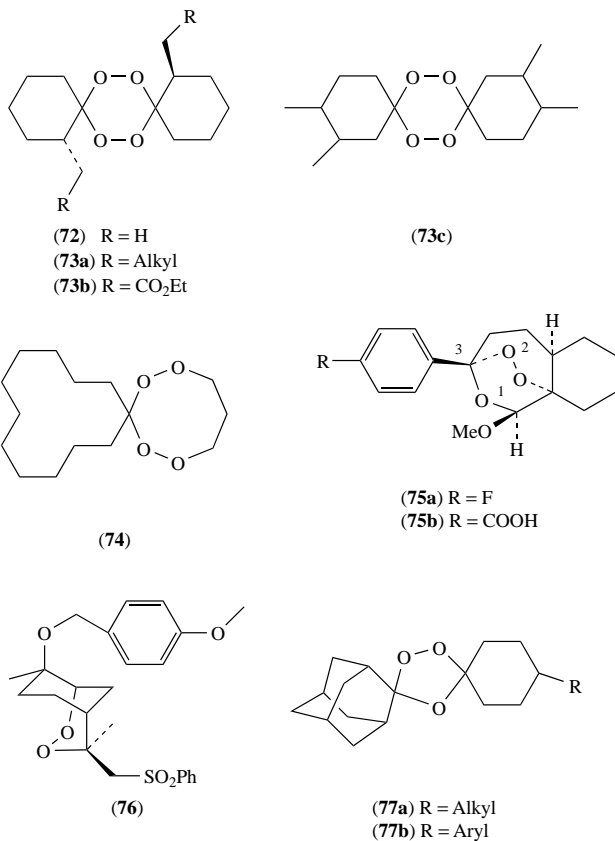
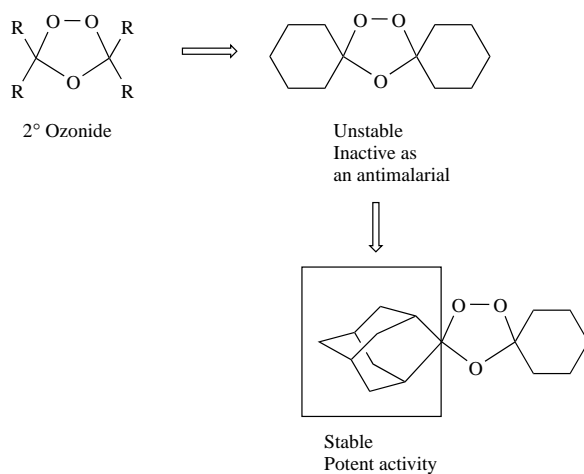
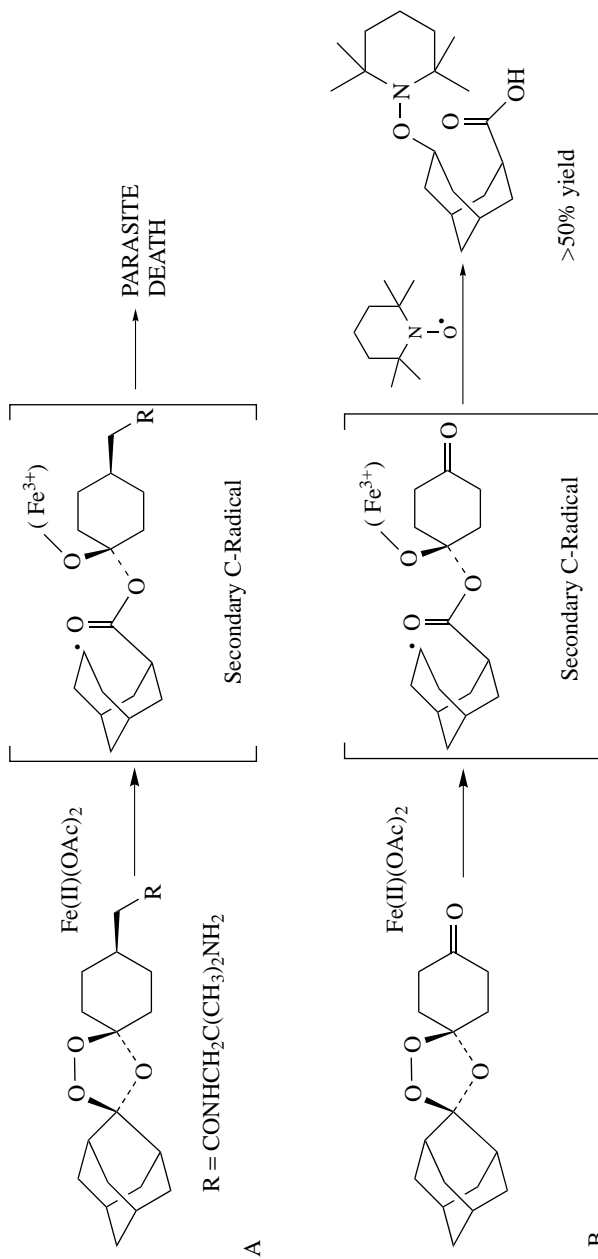


CHART 2. Synthetic antimalarial endoperoxides



SCHEME 26



It seems likely that these new peroxides share a common mechanism of action with the artemisinins. Using spin-trapping techniques, the authors provide evidence that trioxolanes, when exposed to reducing Fe^{2+} , can smoothly generate a secondary carbon-centred radical species in a manner reminiscent of carbon radical production from the artemisinins (Scheme 27). For artemisinin, there is evidence that there are several different protein targets for such 'noxious free-radicals', one of which is an enzyme known as PfATP6. In future studies, it will be fascinating to see if these compounds target the same proteins (enzymes) as the semi-synthetic artemisinins. The logic that has enabled a chemically unstable entity such as a 2° ozonide to be rationally redesigned to not only increase chemical and metabolic stability but also to provide a class of compound that has phenomenal antimalarial properties is extremely noteworthy. The tailoring of the 'ozonide' molecule to enhance bioavailability has been extremely successful—these synthetic analogues are superior to the clinically used semi-synthetic artemisinin derivatives artemether and artesunate by some margin. As such, when combined with a second antimalarial, this new class may offer the best solution we have seen to date for treating drug-resistant malaria parasites.

A. Drug Hybrids and Pro-drugs

Trioxaquinines and Trioxoloquinines. The haemoglobin degradation pathway in *P. falciparum* is a specialized parasite process with a proven history as an exploitable therapeutic target, as exemplified by the 4-aminoquinolines and the endoperoxide derivatives. Meunier and coworkers recently prepared new chimeric molecules by covalent attachment of a trioxane moiety to a 4-aminoquinoline entity^{112, 43, 113}. These molecules, named trioxaquinines (**78a** and **78b**), were designed according to the current knowledge of the mechanism of action of artemisinin derivatives: they combine in a single molecule a peroxidic entity, which can function as a potential alkylating agent, and an aminoquinoline, known to easily penetrate within infected erythrocytes. It was proposed that this 'covalent bitherapy' would be expected to considerably reduce the risk of drug-resistant antimalarial compounds. The first synthesized trioxaquinines demonstrated potent activity *in vitro* against a variety of chloroquine-resistant parasites. Preliminary results indicated that some trioxaquinines are active by oral administration to infected mice (Chart 3). The main drawback with these first generation chimeras is the fact that diastereomers are formed in the synthetic approaches used and that antimalarial testing has been done thus far using such diastereomeric mixtures of the trioxaquinines. Singh and coworkers have also investigated the utility of this approach and several spiro trioxanes (**79a–79b**) were prepared and assayed for *in vivo* activity¹¹⁴.

More recently, and based on the same concept, O'Neill and coworkers have prepared a series of related systems (**80a–c**) based on Vennerstrom's adamantyl trioxolane unit¹¹⁵. These derivatives, which are synthesized in only three steps from adamantan-2-one, have activity in the low nanomolar region (<3 nM versus K1 *P. falciparum*). Like the prototypes synthesized by the groups of Meunier¹¹² and Singh¹¹⁴, these compounds can be formulated as water-soluble salts and it is anticipated that these agents may have the capacity to hit the parasite by two distinctive mechanisms. Indeed, any chemical or metabolic degradation of the endoperoxide bridge in these compounds will result in metabolites that may still have the ability to function as inhibitors of heme polymerization provided that they do not become covalently attached to proteins in the bioactivation process.

A particularly attractive feature of acridine (**80d**) is that this compound can be tracked through the parasite using confocal microscopy and this has enabled O'Neill and coworkers to determine intraparasitic sites of protein alkylation¹¹⁵.

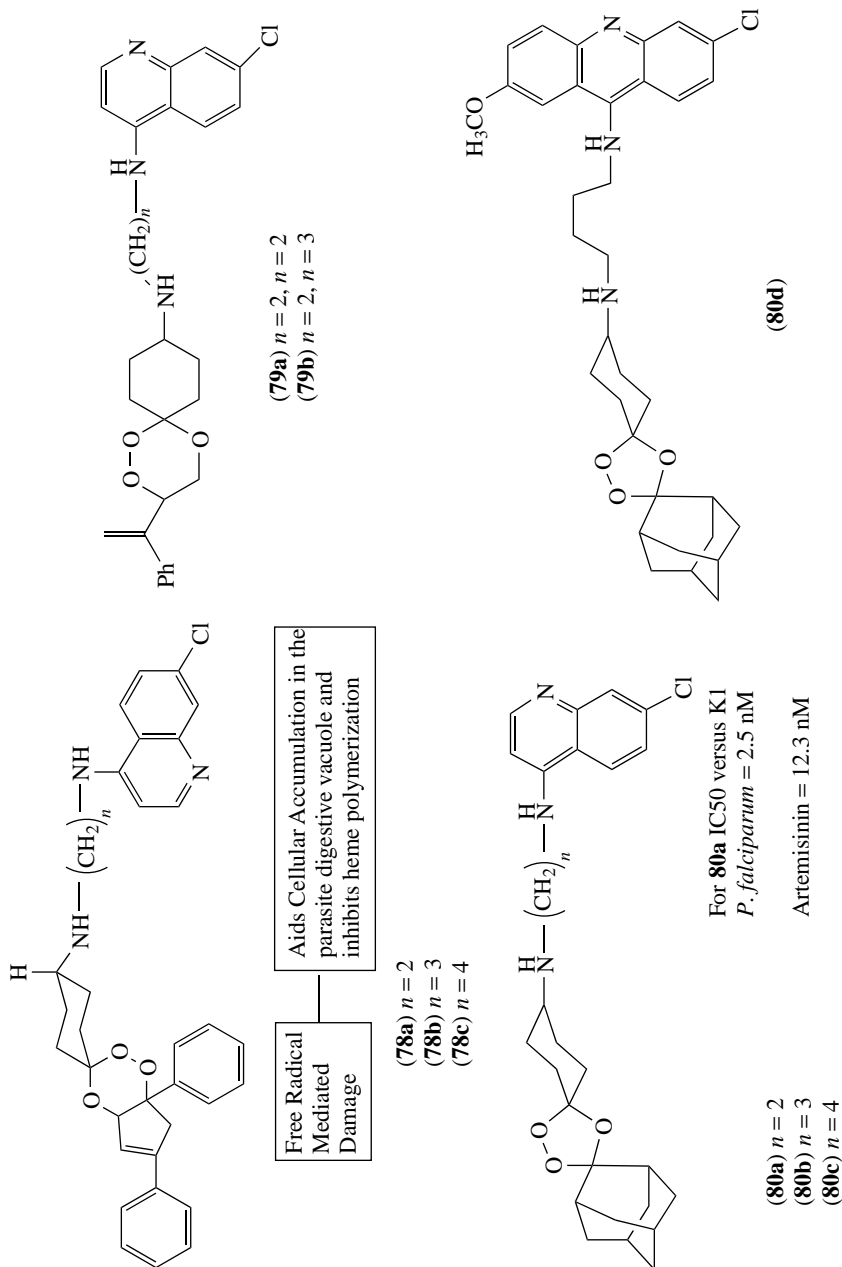
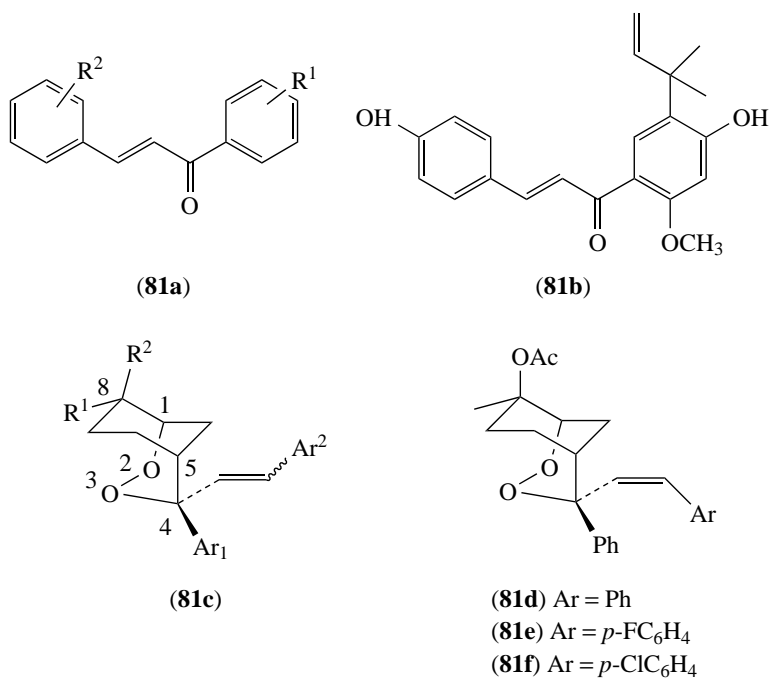
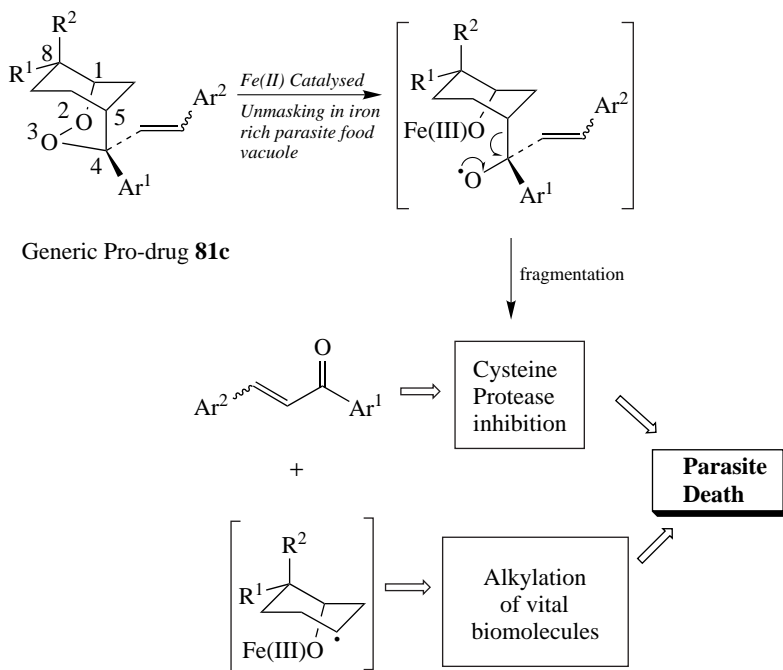


CHART 3. Trioxaquinones and trioxolaquinones

Endoperoxide Cysteine Protease Inhibitor (ECPI) Pro-drugs. Among new targets for antimalarial drugs is the digestive vacuole (DV) *Plasmodium falciparum* haemoglobinase falcipains 2 and 3^{81,116}. Molecular modelling studies using the ligand identification algorithm DOCK and homology-based models of the trophozoite malaria cysteine protease have identified several novel antimalarial cysteine protease inhibitors that include the chalcones **81a**^{117,118}. At about the same time as this research, a paper was published on the potent antimalarial activity of the natural product licochalcone A **81b**¹¹⁹. These derivatives have good antimalarial potency both *in vitro* against chloroquine resistant *P. falciparum* and *in vivo* versus *Plasmodium berghei* in mice. In spite of the promising antimalarial activities of these derivatives, a potential concern with the chalcone class of drug is that they might be expected to react with host proteins, thereby causing toxicity. In line with this, researchers have shown that, *in vitro*, **81b** readily reacts with sulphur-based biological nucleophiles¹²⁰. Therefore, a masked pro-drug-based approach to delivering the chalcone selectively to the parasite would be desirable.



As described earlier, O'Neill and coworkers have recently defined the mechanism of action of the second-generation peroxide arteflene (**5**), which involves ferrous-mediated fragmentation to a stable enone system and a cyclohexyl carbon-centred radical. Based on this knowledge, they designed a novel class of endoperoxide–chalcone-based pro-drugs **81c** and have recently completed the synthesis of several prototypes **81d–f**¹²¹. It was proposed that these pro-drugs would selectively deliver the chalcone-based cysteine protease inhibitor to its site of action by means of ferrous-catalysed unmasking in the parasite digestive vacuole. This represents an exciting and totally new approach to antiparasitic drug design, in that besides the selective generation of C-centred radicals in the parasite,



SCHEME 28

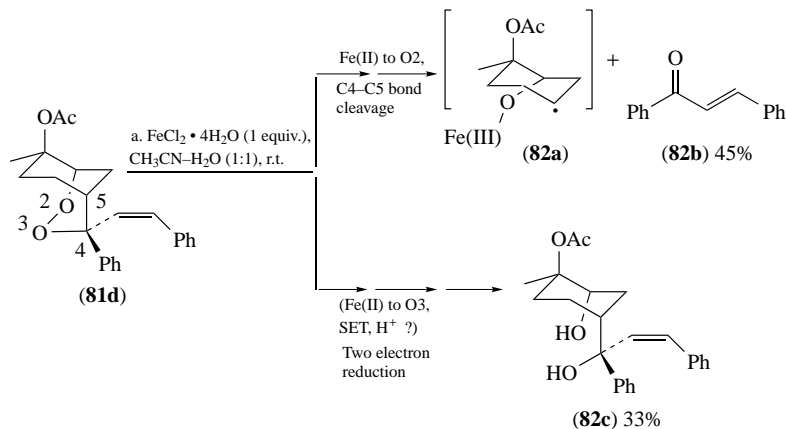
a second drug molecule with a different mechanism of drug action will be produced (Scheme 28)¹²¹.

In effect, antimalarial ‘trojan horse’ drugs of this type should deliver a double blow to the parasite by exploiting the presence of high concentrations of ferrous ion present in the parasite food vacuole as the trigger for protease inhibitor release. In model studies with prototype **81d**, in the presence of ferrous ions, these systems readily degrade to produce the desired chalcone (**82b**, R = H, in 45% yield from **81d**), in tandem with secondary carbon-centred radical **82a** (Scheme 29). Furthermore, analogues **81d–f** have superior *in vitro* antimalarial activity to that of arteflene (<25 nM *in vitro* versus *Plasmodium falciparum*, arteflene >50 nM). The other product obtained is the diol (**82c**), a product of two-electron reduction of the endoperoxide bridge.

This ‘pro-drug’ approach provides a paradigm for future antimalarial drug discovery efforts in the sense that this approach can be extended to any protease inhibitor that contains a carbonyl group as the reactive protease inhibitor ‘warhead’. Simply masking the carbonyl group within a trioxane or endoperoxide provides a unique and selective mechanism for targeting the malaria parasite by two different mechanisms⁴⁴.

B. Chemistry for the Synthesis of Lead Synthetic Endoperoxides

In this section, we will consider the chemistry that has been employed in the synthesis of lead synthetic analogues. There is a large amount of literature in this area and for the purposes of this chapter we will focus on compounds that have been fully assessed both *in*



SCHEME 29

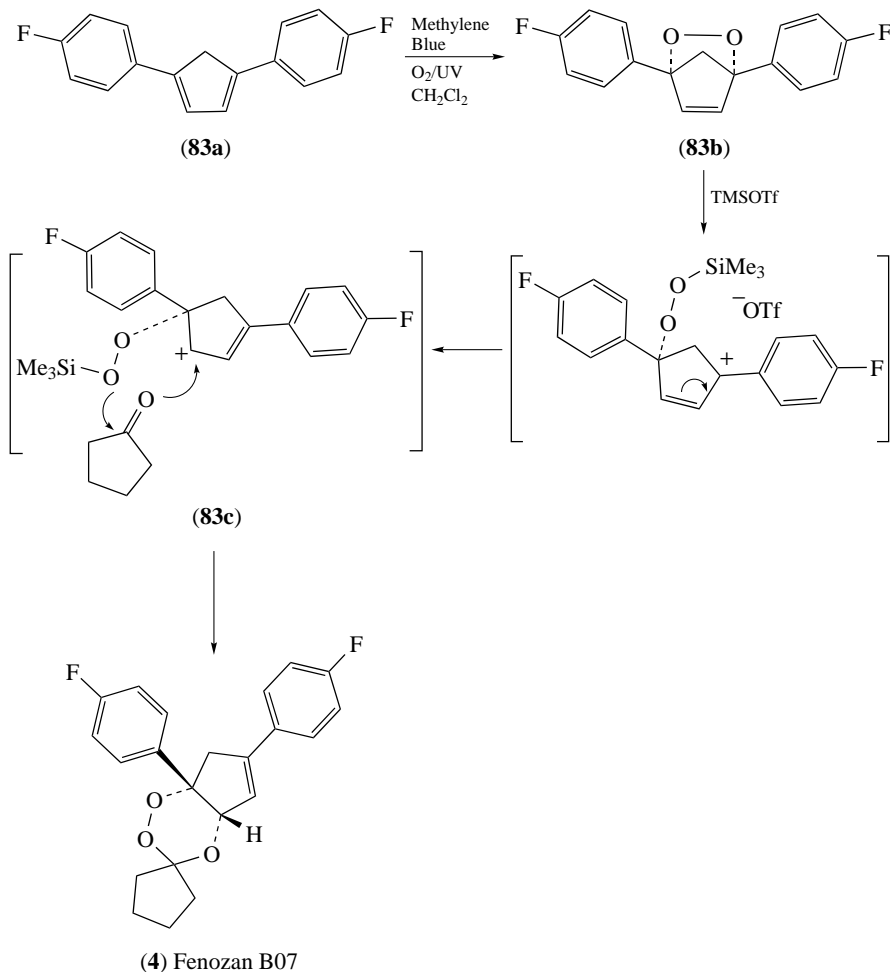
vitro and *in vivo* and have antimalarial activities close to the natural product artemisinin. The sections are sub-divided depending on the method employed for 'O₂' incorporation. The outstanding utility of singlet oxygen for the synthesis of endoperoxides is illustrated in the following section. We will see that singlet oxygen has been employed for the synthesis of both trioxanes and endoperoxides.

C. Fozan B0-7 (4 + 2 Cycloaddition of ¹O₂ to a Diene)

The synthesis of fozan B0-7 **4** involves two key steps, the first of which employs a 4 + 2 cycloaddition of singlet oxygen to the diene **83a**^{122, 20, 123}. This provides the endoperoxide **83b** that can be transformed into the target *cis*-fused 1,2,4-trioxane by treatment with the Lewis acid, TMSOTf, in the presence of a carbonyl compound. The reaction proceeds by Lewis acid promoted heterolysis of the C–O bond to give an intermediate peroxy allyl cation **83c** that is captured by the carbonyl compound (in this case, cyclopentanone) to give the product (Scheme 30). A number of different carbonyls have been used in this reaction along with a number of different endoperoxide templates and detailed SAR have been developed (Scheme 30).

D. Arteflene (Ene Reaction of ¹O₂)

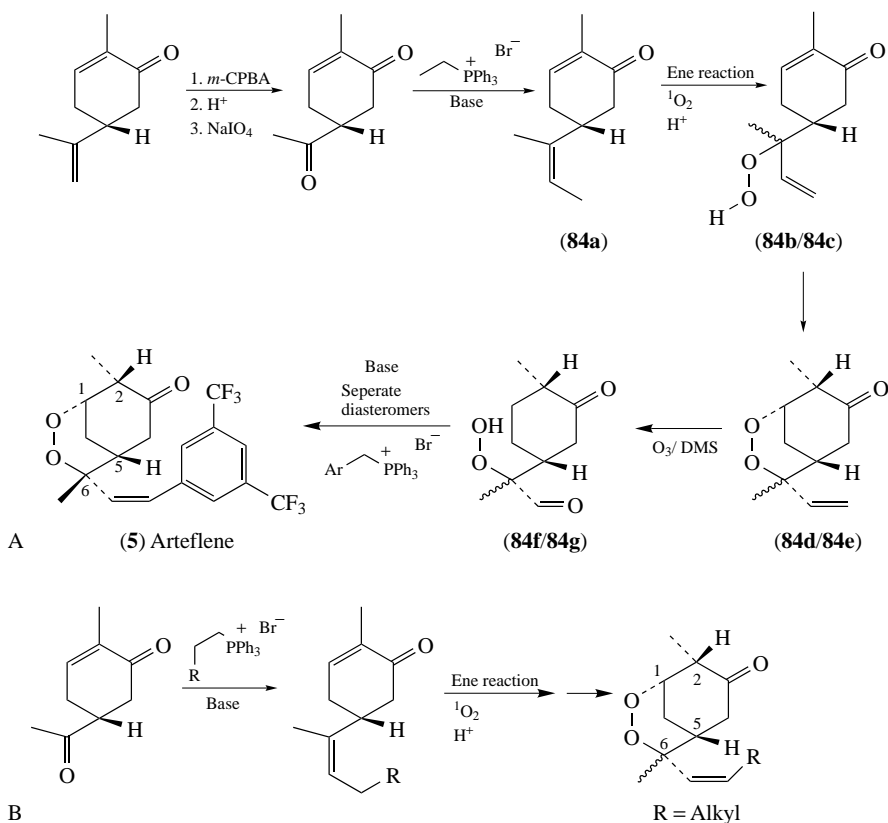
The key step in the synthesis of arteflene **5** involves the ene reaction of photochemically generated singlet oxygen with the *R*-(-)-carvone derived alkene **84a** to give a mixture of allylic peroxide **84b** and **84c**^{124, 14, 125}. Intramolecular conjugate addition of the hydroperoxide to the α,β -unsaturated enone provides a mixture of diastereomeric endoperoxides **84d** and **84e**. Ozonolysis of the mixture provides the aldehydes **84f** and **84g** which can be subjected to a Wittig *cis*-olefination to provide a mixture of diastereomers, that can be readily separated by chromatography to give the desired product **5** (Scheme 31A). Variations on this synthesis include carrying out the ene reaction on a mixture of alkenes at stage 5 (Scheme 31B) of the synthesis and approaches to producing a single diastereomeric endoperoxide aldehyde with the desired *R*-configuration at the C6 position of the bicyclic framework.



SCHEME 30

E. C3-Aryl 1,2,4-Trioxanes (2 + 2 Cycloaddition of $^1\text{O}_2$ to a Vinyl Ether)

Following seminal work by Jefford and coworkers on the generation and rearrangement of dioxetanes²⁰, Posner and coworkers applied this chemistry in the synthesis of a series of C3-aryl 1,2,4-trioxanes **75a** and **75b** as depicted in Scheme 32¹⁰⁹. The rationale for these compounds was the proposal that the aryl group at the C3 position would promote formation of a high-valent iron-oxo species (see Scheme 2). The key step in the synthesis involves a dye-sensitized [2 + 2] cycloaddition of singlet oxygen to the methoxy vinyl ether **85a**. The unstable dioxetane **85b**, upon exposure to Lewis acids, ruptures to produce a cationic intermediate that can cyclize to produce the tricyclic artemisinin analogue in good yields. A drawback with this approach is the formation of both α and β diastereomers



SCHEME 31

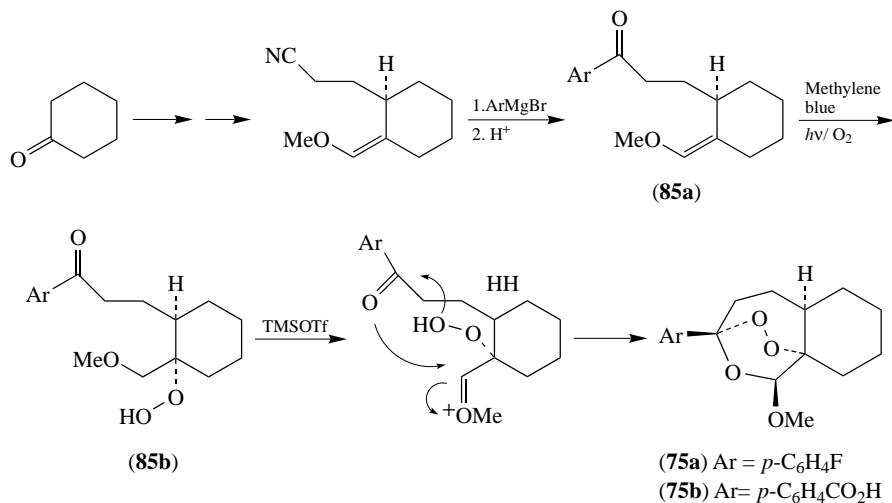
at the anomeric C12 position. Water-soluble derivatives have recently been produced and shown to have superior therapeutic indices to sodium artesunate¹²⁶.

F. Spiro 1,2,4-Trioxanes (Ene Reaction)

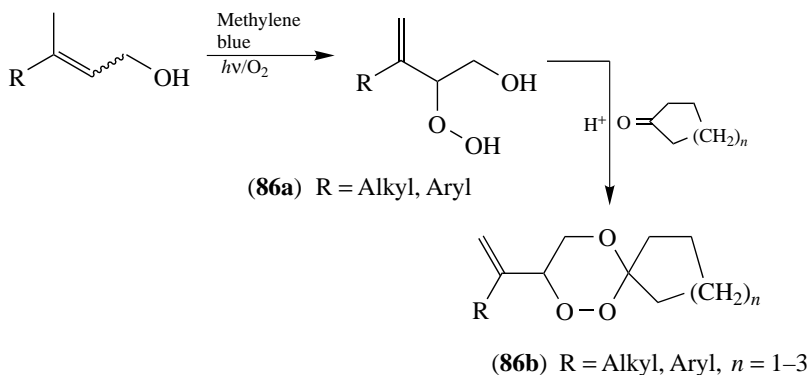
Singh and coworkers have carried out a large amount of work on the synthesis of spiro 1,2,4-trioxanes by employing the ene reaction of singlet oxygen with substituted allylic alcohols^{127–129}. The resulting hydroperoxy alcohols **86a** can be condensed with a variety of different carbonyl compounds including cyclic ketones (Scheme 33). Some of these trioxanes **86b** have excellent *in vivo* activity (see Table 1).

G. Synthesis of Tetraoxanes (Use of Hydrogen Peroxide)

As noted in the previous section, Vennerstrom and coworkers have carried out a large amount of research into the synthesis of tetraoxanes, e.g. **72**, **73a** and **73b**, some of which have proven to be highly potent *in vitro*^{105,106}. For the synthesis of symmetrical

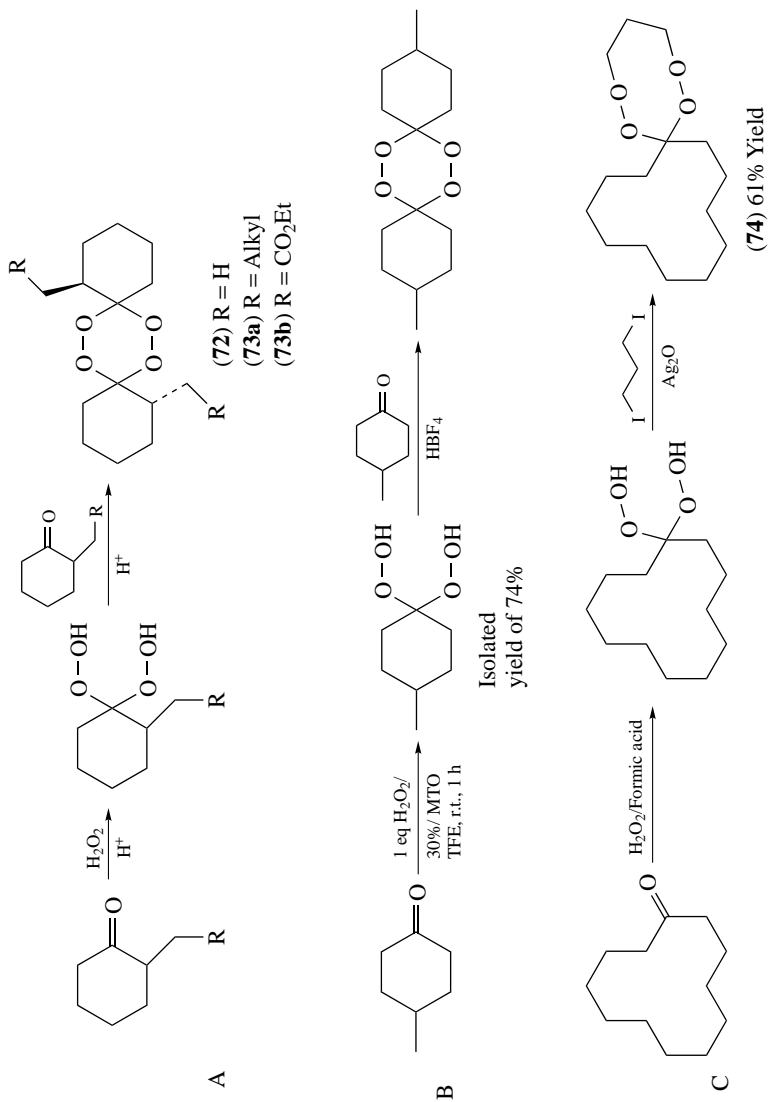


SCHEME 32

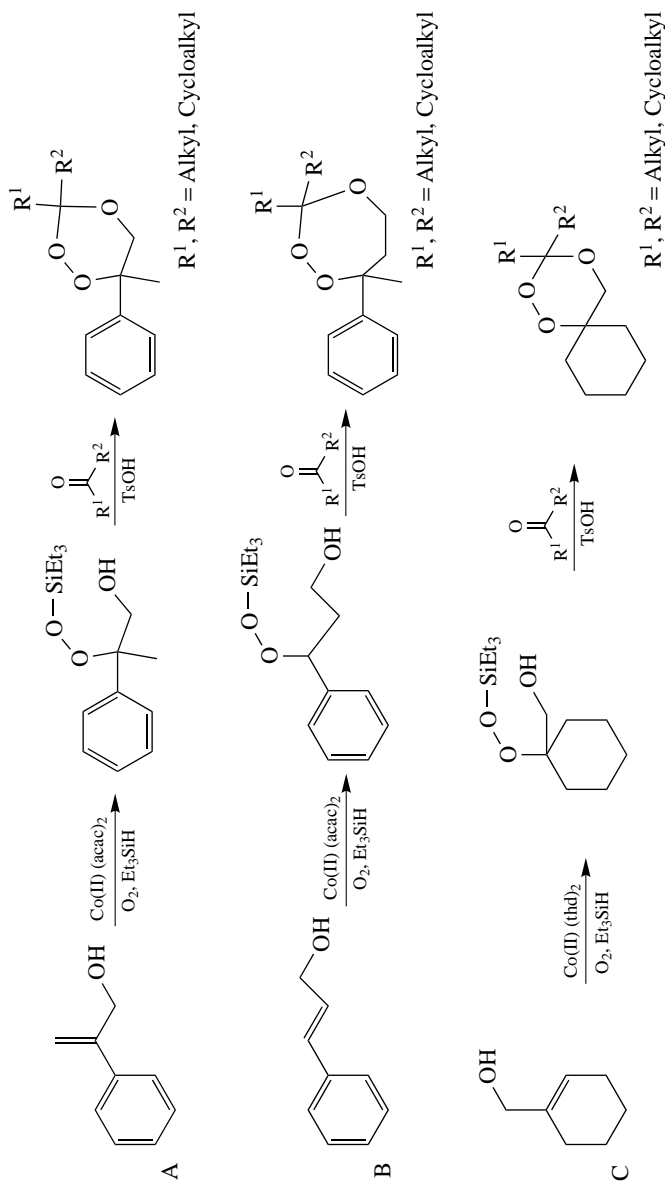


SCHEME 33

systems, carbonyl compounds can be allowed to react with aqueous solutions of hydrogen peroxide in the presence of acids¹²⁵. The reaction proceeds through the intermediacy of the *gem*-dihydroperoxy intermediate (Scheme 34A). The yields are usually low for this process and an improved procedure has recently been developed by employing fluoruous solvents and a methyltrioxorhenium (MTO) to provide the hemiacetal and HBF₄ catalyst/ketone to provide the desired products (Scheme 34B)¹³⁰. More recently, Kim and coworkers have prepared **74** by a two-step procedure¹⁰⁸. This involves the preparation of the *gem*-dihydroperoxy intermediate from cyclododecanone followed by alkylation with a 1,3-diiodopropane in the presence of silver oxide. Yields of 61% were reported for the preparation of orally active tetraoxane **74** (Scheme 34C).



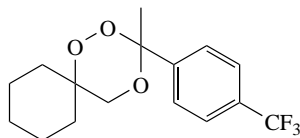
SCHEME 34



SCHEME 35

H. Spirotrioxanes via Mukaiyama Co(II) Mediated Aerobic Hydroperoxysilylation of Allylic Alcohols (Use of Triplet Oxygen)

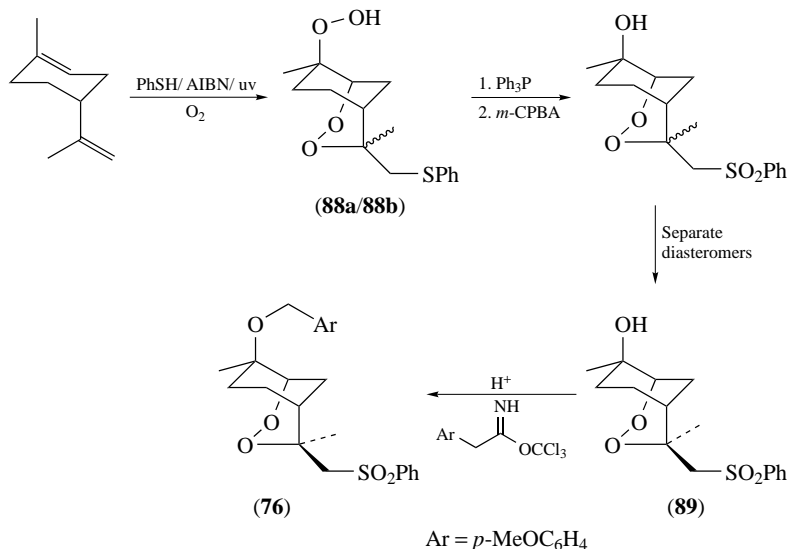
Aerobic Co(II) catalysed hydroperoxysilylation of allylic alcohols provides silyl peroxides that can be condensed with ketones to produce 1,2,4-trioxanes^{131,132} or 1,2,4-trioxepanes¹³³ by a simple one-pot procedure (Scheme 35A). A recent improvement in the use of Co(acac)₂ is the use of Co(thd)₂ (thd = bis (2,2,6,6-tetramethyl-3,5-heptanedionato)). This more reactive catalyst allows cyclic allylic alcohols to be oxygenated and the resulting peroxysilyl alcohol can be transformed to spiro trioxanes, some of which have potent *in vitro* antimalarial activity (Scheme 35B). For example, compound **87** expresses activity around 20 nM (artemisinin = 10 nM).



(87)

I. Synthesis of Endoperoxides via Thiol Olefin Co-oxidation Methodology (Use of Triplet Oxygen)

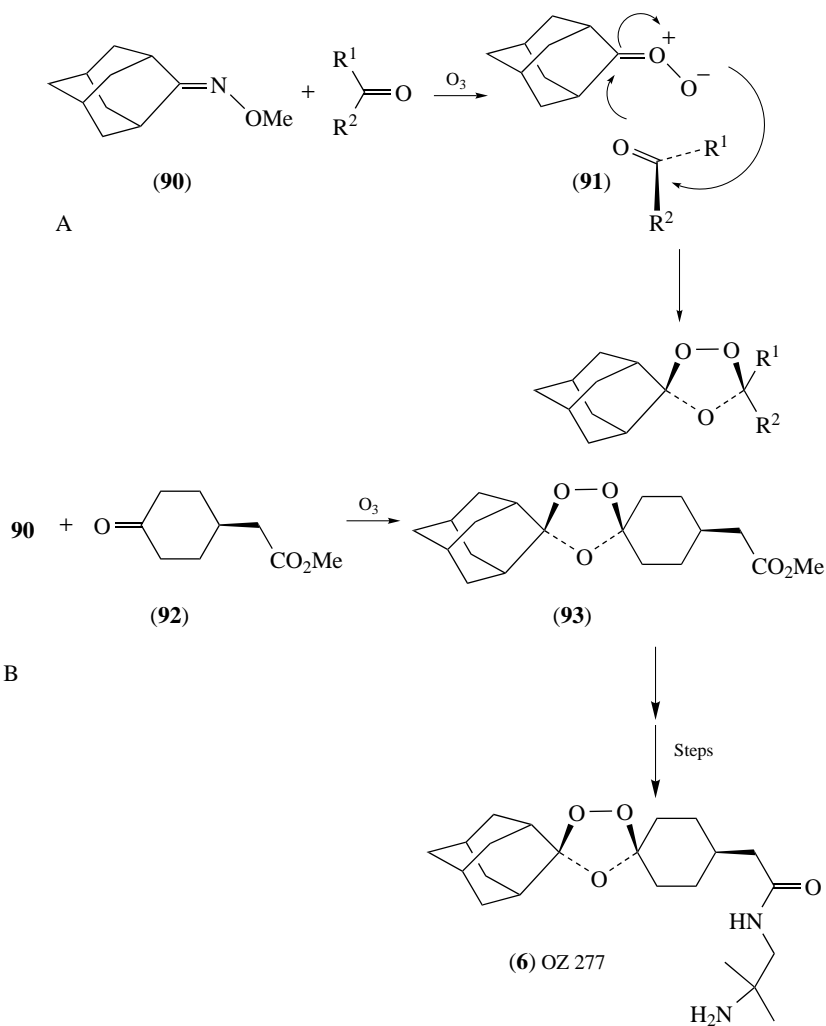
Endoperoxide **76** was prepared by a very efficient four-component thiol olefin co-oxidation of limonene as depicted in Scheme 36^{134,73}. The mixture of hydroperoxy endoperoxides (**88a** and **88b**) that are produced in this process is reduced by triphenylphosphine and then oxidized to the corresponding sulphones. The resultant diastereomers are separated using silica gel chromatography. Alkylation of diastereomer **89** provides **76** in excellent yield. As described earlier, this compound has an excellent pharmacological profile¹¹¹.



SCHEME 36

J. Synthesis of 1,2,4-Trioxolanes via Griesbaum Co-ozonolysis (Use of Ozone)

The final synthetic analogues we consider are the trioxolanes prepared by Vennerstrom and coworkers¹⁵. These are prepared by a very efficient co-ozonolysis procedure from oxime **90** and a carbonyl compound **91** (Scheme 37A). This provides the 1,2,4-trioxolane in yields of greater than 50%. Further studies on 4-substituted cyclohexanones (e.g. **92**) revealed that this reaction proceeds with very good *cis/trans* selectivity to produce the ester **93**, which was derivatized to produce a clinical candidate OZ 277 (**6**) as shown. The chemistry for the synthesis of this compound has been scaled up beyond 30 kg (Scheme 37B).



SCHEME 37

VII. ANTIMALARIAL ACTIVITIES OF SYNTHETIC ENDOPEROXIDE ANTIMALARIALS

Table 1 summarizes the synthetic and antimalarial profiles of selected endoperoxides. Clearly, synthetic organic chemistry has enabled several excellent potential drug candidates to be prepared, some of which have outstanding antimalarial properties. At the forefront of these efforts are the trioxolanes prepared by Vennerstrom and colleagues. The challenge in this field in future years will be to construct additional endoperoxide templates that can be prepared in a few steps using scalable synthesis and have similar pharmacological profiles to lead semi-synthetic artemisinins and trioxolanes (e.g. **6**).

TABLE 1. Lead synthetic endoperoxide antimalarials (The table compares the antimalarial activities, the method of synthesis and the number of synthetic steps required for drug synthesis)

Endoperoxide analogue	Number of synthetic steps/Non-racemic (NR), Achiral (A) or Racemic (R)	Method of O ₂ incorporation	<i>In Vitro</i> IC50 (nM) ^a / <i>In vivo</i> ED50 (oral) (mg kg ⁻¹) ^b	Metabolism/Toxicity studies	References
Fenozan B07 (4)	4 steps (R)	Dye-sensitized photo-oxygenation [4 + 2 cycloaddition]	4 nM (K1) 2.7 mg kg ⁻¹	Not reported	13
Arteflene (5)	>7 steps (A)	Dye-sensitized photo-oxygenation (Ene reaction)	35 nM (K1) 20 mg kg ⁻¹	Metabolism and toxicity studies completed prior to phase 2 clinical trials	14
C3 Aryl trioxanes (75a , 75b)	5 steps (R)	Dye-sensitized photo-oxygenation	30 nM (NF54) 10 mg kg ⁻¹	Toxicity studies reveal that 11b has a similar therapeutic index to artelinic acid	109, 110
Sulphonyl endoperoxides (76)	4 steps (NR)	Molecular oxygen (TOCO) reaction	9.4 nM (NF54) 0.43 mg kg ⁻¹	Initial toxicity studies for 76 reveal no observable toxicity in mice at doses up to 200 mg kg ⁻¹	111
Dispirotrioxanes (86a , 86b)	4 steps (R)	Dye-sensitized photo-oxygenation	<i>In Vitro</i> data not recorded 10 mg kg ⁻¹	Not recorded	105
Tetraoxane (74)	3 steps (A)	Hydrogen peroxide/Ozone	25 nM (FCR-3) 20 mg kg ⁻¹	No toxicity reported at doses of up to 1600 mg kg ⁻¹ in mice	108
Trioxolanes (77a–b , 6)	2 steps (A)	Ozone	3–10 nM (K1) 1–3 mg kg ⁻¹	Ongoing in a project sponsored by Medicines for Malaria Venture (MMV)	15

^a *In Vitro* assays were performed as reported in References 92 and 93.

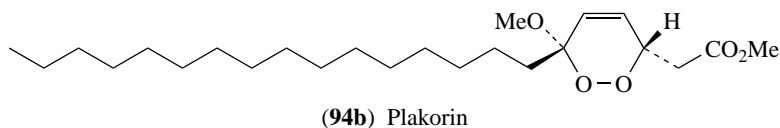
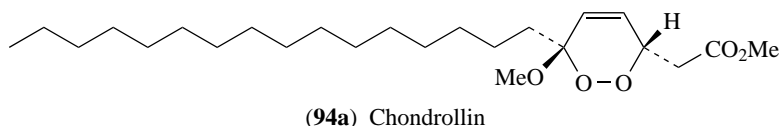
^b *In vivo* assays were performed using the standard Peters 4-day test. The activity refers to oral antimalarial activity and reflects the concentration of drug required to reduce parasitaemia, in mice infected with *Plasmodium berghei*, by 50% of the control.

VIII. ENDOPEROXIDE CONTAINING COMPOUNDS WITH ANTITUMOUR ACTIVITY

In the final part of this chapter, we will look at studies where endoperoxides have been investigated for their antitumour potential. There have been a large number of endoperoxide-containing natural products isolated and this has been the focus of some excellent review articles. Countless peroxy natural products have been assayed for various biological properties and many have been found to be cytotoxic to tumour cell lines.

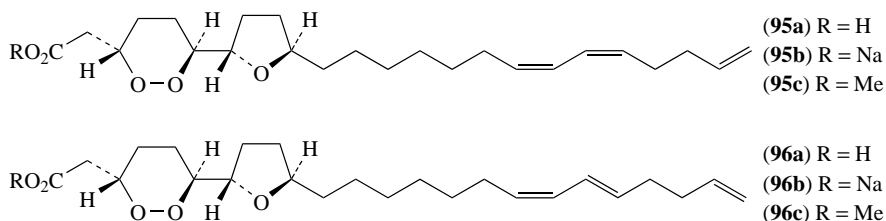
A. Marine Metabolites

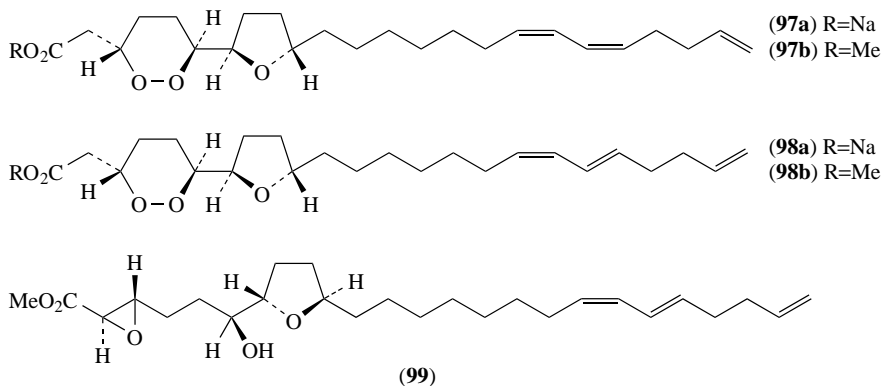
Marine metabolites provide a rich source of peroxide containing natural products with cytotoxic properties^{135,136}. The peroxy ketal chondrillin **94a**, isolated from a sponge of the genus *Chondrilla*, was the first peroxy marine metabolite to be found¹³⁷. Chondrillin has been shown to be cytotoxic to P388 tumour cells with an IC_{50} of $5 \mu\text{g ml}^{-1}$ ¹³⁸. The epimer of Chondrillin, plakorin **94b**, isolated from a *Plakortis* sponge¹³⁹, also exhibited *in vitro* antitumour activity against murine lymphoma L1210 cells ($IC_{50} = 0.85 \mu\text{g ml}^{-1}$) and human epidermoid carcinoma KB cells ($IC_{50} = 1.8 \mu\text{g ml}^{-1}$)¹⁴⁰.



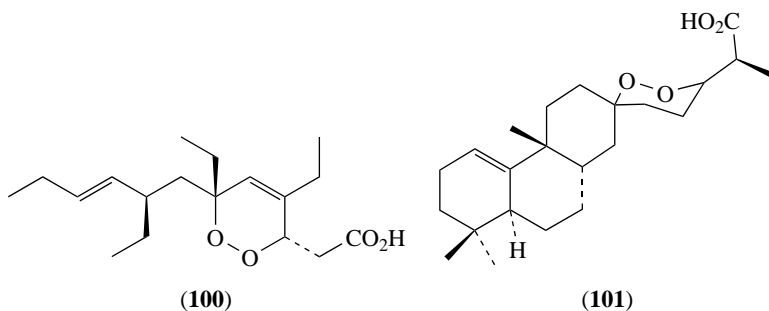
Recently a bioassay guided screening approach has led to the isolation of a series of cyclic peroxides from *Stolonica socialis*¹⁴¹. Crude and purified mixtures of stolonoxides **95a–95c**, **96a–96c**, **97a,b** and **98a,b** were reported to have strong cytotoxicity ($IC_{50} \leq 0.1 \mu\text{g ml}^{-1}$) against several mammalian tumour cell lines. Interestingly, a synthetic epoxide derivative **99** of the stolonoxides was completely inactive against the tumour cell lines tested. This result states the importance of the presence of the peroxide ring for cytotoxic activity. The activity of these compounds may be due to their potent inhibitory effect on mitochondrial electron transfer¹⁴².

Haterumadioxins A and B were isolated from the Okinawan sponge *Plakortis lita*. Haterumadioxin A **100** was evaluated against a human cancer cell line panel and found to be effective against a melanoma cancer cell line. An analysis of the results obtained





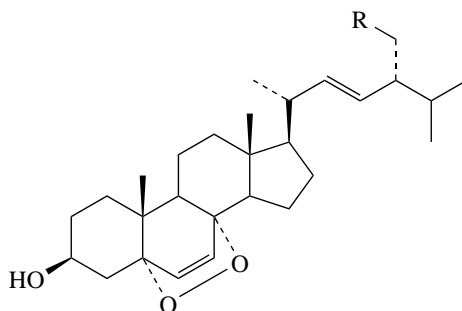
indicated that Haterumadioxin A is an antimetabolite, since its spectrum of activity correlates with that of doxifluridine, a known antimetabolite¹⁴³. Secondary screening with a panel of nude mice xenografts is underway. Mycaperoxide H **101**, a cyclic norsesterterpene peroxide, has recently been isolated from a Thai marine sponge *Mycale* sp.¹⁴⁴. Its structure was deduced by spectroscopic and chemical analysis. Mycaperoxide H was found to be cytotoxic against HeLa cells with an IC₅₀ value of 0.8 $\mu\text{g ml}^{-1}$.



These examples represent only a fraction of the endoperoxide-containing marine metabolites and the number of peroxide metabolites discovered with cytotoxic properties is likely to continue to expand.

B. Steroidal Endoperoxides

Peroxy derivatives of steroids have been isolated from both marine and terrestrial sources. They are most commonly 5α , 8α -endoperoxides with variations in the side-chains. The ergosterol peroxide **102** is the most ubiquitous endoperoxide-containing natural product and is isolated from a large number of sources. Ergosterol peroxide **102** was found to have antitumour activity against breast cancer and carcinosarcoma cell lines¹⁴⁵. A number of other steroidal endoperoxides have been reported which differ in the nature of the side-chain. Compound **103** was found to be an inhibitor of tumour promotion in mouse studies¹⁴⁶.

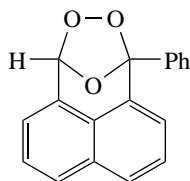


(102) R=H

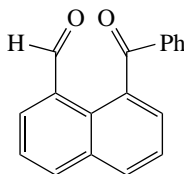
(103) R=CH₃

C. Synthetic Endoperoxides with Antitumour Activity

There are several examples of entirely synthetic endoperoxides with antitumour activity. There is a recent report of ozonides, which contain a cyclic peroxide group, inhibiting angiogenesis and possessing antitumour activity¹⁴⁷. The lead compound in this study, ANO2 **104**, was capable of inhibiting angiogenesis *in vivo* and *in vitro*. In addition, ANO2 also suppressed primary tumour growth and reduced the number of pulmonary metastases caused by Lewis lung carcinoma cells in mice. Reduction of ANO2 gives a compound **105** that has very weak anti-angiogenic activity and no effect on tumour growth or metastasis.



(104)



(105)

D. Suspected Mechanisms of Antitumour Action

As has been discussed, the artemisinin class of antimalarials exerts their effect by iron-mediated cleavage of the endoperoxide bridge and subsequent formation of free radicals. Recent studies have reported on the cytotoxic activity of artemisinin derivatives against tumour cells. The iron content of tumour cells is generally higher than that of normal cells, and since ferrous iron is required for the bioactivation of artemisinin this provides a strategy for the use of artemisinins against tumour cells.

The increased iron content of tumour cells is a consequence of the overexpression of transferrin receptors. Transferrin is an endogenous protein that transports iron from the circulation into cells¹⁴⁸. Many tumour cell lines have a high metabolic requirement for iron and as such overexpress transferrin receptors and have higher rates of iron influx than normal cells^{149, 150}.

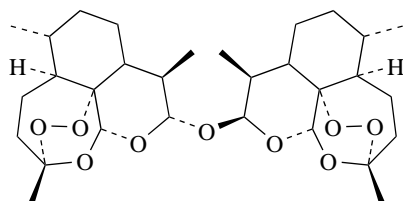
The role of iron in the toxicity of artemisinins towards tumour cells is not completely understood. However, there have been several reports on the benefits of administering artemisinins in combination with either ferrous salts or holotransferrin (iron-loaded transferrin). It has been reported that artemisinin selectively killed molt-4-lymphoblastoid cells (a human leukaemia cell line) after incubation with holotransferrin, whereas the same treatment had appreciably less effect on normal lymphocytes¹⁵¹. Similar results were also found in a study examining the selective cytotoxicity of dihydroartemisinin and holotransferrin towards human breast cancer cells¹⁵². The authors assert that administration of artemisinin-like drugs and intracellular iron-enhancing compounds may provide a simple, effective and economical treatment for cancer. An *in vivo* study showed that oral administration of dihydroartemisinin and ferrous sulphate significantly retarded the growth of implanted fibrosarcoma in rats¹⁵³. No significant tumour growth reduction was observed in rats treated with either dihydroartemisinin or ferrous sulphate alone.

Attempts have been made to correlate the response of tumour cells to the artemisinins with genetic pathways. mRNA response profiles associated with the response of tumour cells to artesunate, arteether and artemether were investigated and point towards a common mechanism of tumour inhibition by all three drugs in which genes affecting cellular proliferation play an important role^{154,155}. The same researchers also looked at the role of antioxidant genes for the activity of artesunate against tumour cells and found that oxidative stress plays an important part in the mechanism of action of artesunate, which suggests that antioxidant defences act in combination with artesunate to affect the cellular response¹⁵⁶.

Angiogenesis, the formation of new blood vessels from pre-existing ones, is essential for a number of physiological processes such as wound healing and during the female reproductive cycle. Without the production of new blood vessels, the distance that oxygen and other nutrients can diffuse through tissues limits tumour growth. Consequently, anti-angiogenic therapy might be clinically useful for the treatment of tumours. Artemisinin derivatives have been shown to inhibit angiogenesis both *in vitro* and *in vivo*¹⁵⁷⁻¹⁵⁹. A problem with angiostatic therapy is that tumour hypoxia activates the transcription factor, hypoxia-inducible factor-1 α (HIF-1 α), which increases tumour angiogenesis and leads to resistance to angiostatic therapy. However, HIF-1 α also up-regulates the expression of transferrin receptors so it has been suggested that treatment with artemisinin derivatives may provide a way to circumvent the problem of resistance¹⁶⁰.

E. Artemisinins as Antitumour Agents

Woerdenbag and coworkers reported on the cytotoxicity of artemisinin endoperoxides to Ehrlich ascites tumour cells¹⁶¹. Artemisinin had an IC₅₀ of 29.8 μ M, whereas arteether, artemether, artelinic acid and sodium artesunate all had more potent activities, ranging from 12.2 to 19.9 μ M. It was found that opening of the lactone ring of artemisinin dramatically reduced the cytotoxicity. An ether dimer of dihydroartemisinin **106**, prepared by

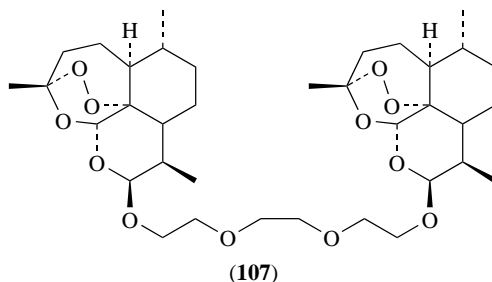


(106)

treatment of dihydroartemisinin with $\text{BF}_3 \cdot \text{Et}_2\text{O}$, was the most potent compound assayed, with an IC_{50} of 1.4 μM . It was noted that the variations in cytotoxicity correlated with the capacity for radical formation and stabilization and in some cases the lipophilicity had an influential effect on activity.

Further studies by the same researchers suggested that these compounds exert their effect on tumour cells by growth inhibition and that the endoperoxide bridge is essential for activity. They also investigated the influence that the stereochemistry of the ether bridge had on cytotoxicity towards EN2 tumour cells and found that the non-symmetrical dimer was more cytotoxic than the symmetrical one.

Posner and coworkers have prepared a series of semi-synthetic and synthetic ether and ester-linked dimers that were found to have potent anti-proliferative and antitumour activities *in vitro*¹⁶². Some of these trioxane dimers were found to be as antiproliferative as calcitriol, the hormonally active form of vitamin D, which is used to treat psoriasis, a skin disorder characterized by uncontrolled cell proliferation. Of the semi synthetic dimers, a polyethylene glycol-linked dimer **107**, with β -stereochemistry at both of the lactol acetal positions, was found to be very anti-proliferative and showed activity against leukaemia and colon cancer cell lines in the National Cancer Institute (NCI), USA 60-cell line assay.

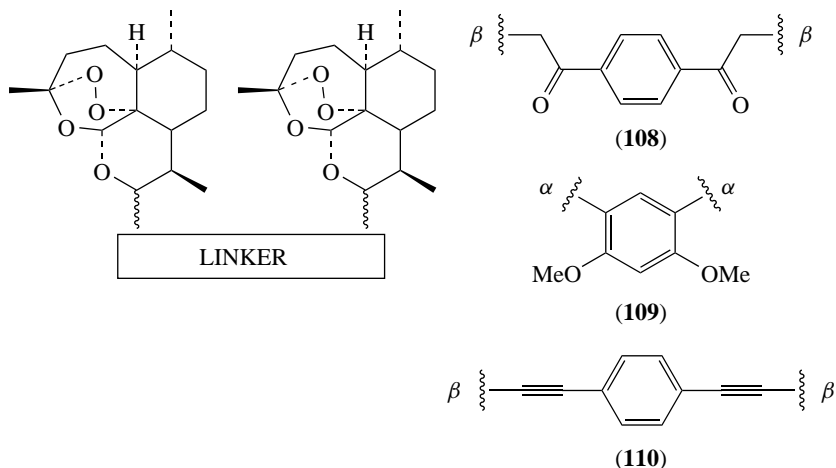


The problem with the ether and ester linkage is that they are often hydrolytically unstable, and so there have been approaches to replace the C10 acetal linkage with more chemically robust linkages. Posner's group prepared a series of C10 olefinic non-acetal dimers and C10 saturated dimers that showed good antiproliferative activities¹⁶³. Dimers **108–110** were all especially potent and selective at inhibiting leukaemia and colon cancer in the NCI assay (Scheme 38)¹⁶⁴.

Posner and coworkers have recently reported on the preparation of a number of orally active trioxane dimers with high stability and efficacy. In only a few chemical steps from naturally occurring artemisinin they are able to synthesize a number of compounds that show potent activity in an *in vivo* murine model of prostate cancer.

The dimer **111** was easily prepared in two steps from artemisinin. Hydroboration–oxidation produced alcohol **112**, which was easily oxidized to give the carboxylic acid **113** or it could be esterified in high yield to give the N-oxide **114** (Scheme 39). Four TRAMP (TRAnsgenic Adenocarcinoma of Mouse Prostate) cell lines were used to test the anticancer activity of the trioxane dimers. The alcohol dimer **112** and the N-oxide dimer **114** strongly inhibit the growth of prostate cancer cells.

O'Neill and coworkers have also sought to address the problem of the metabolically susceptible C10 acetal linkage¹⁶⁵. A series of C10 carba dimers were prepared and assayed for antitumour activity. The two most potent compounds that were prepared are two phosphate ester linked dimers **115** and **116** (Scheme 40). They are principally active against leukaemia, colon and certain melanoma and breast cancer cell lines in the NCI 60-cell line assay.



SCHEME 38

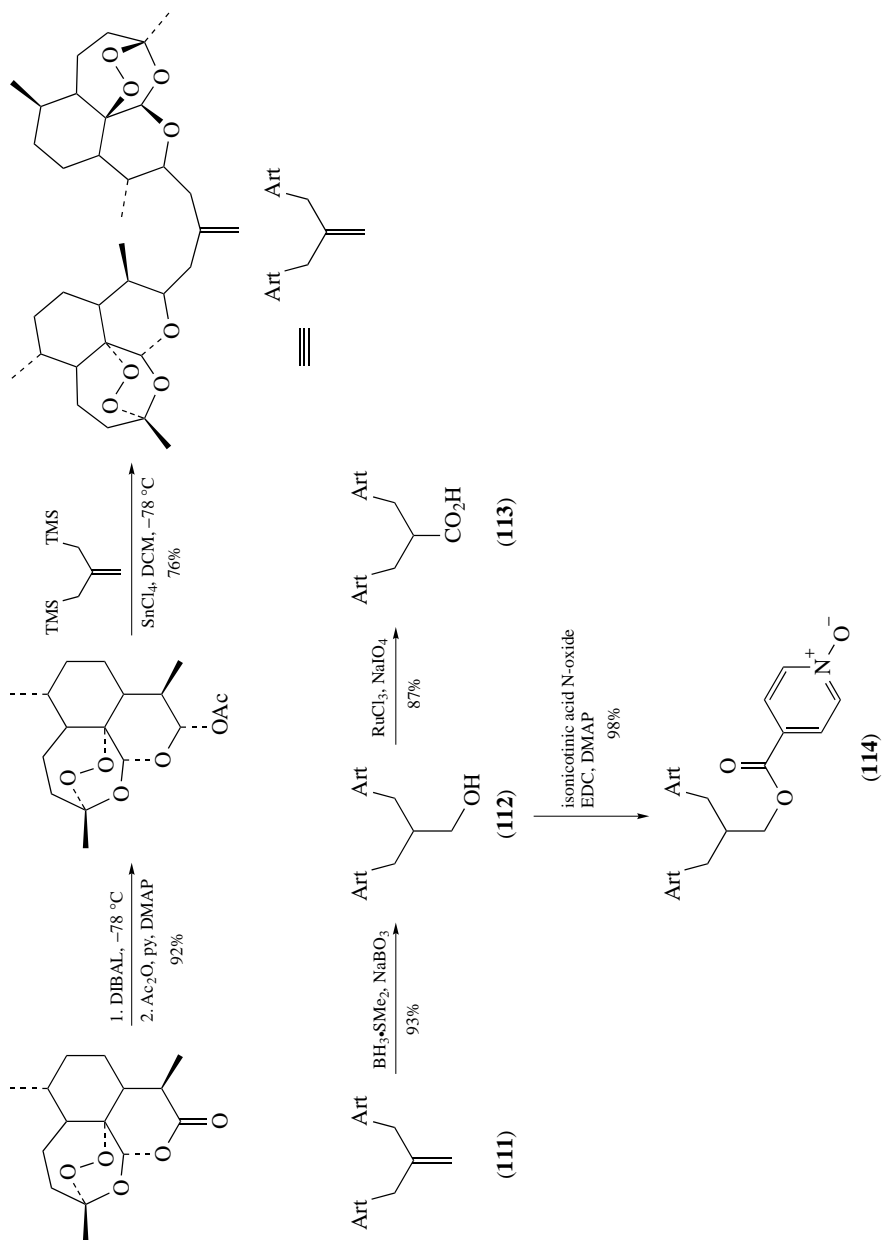
The dimers were studied more closely in HL-60 leukaemia and Jurkat cell lines, and it was found that they have activities comparable to the clinically used anticancer drug doxorubicin. In terms of general toxicity to normal cells, it was observed that dimers **115** and **116** were not toxic to lymphocytes at doses approaching 100 μM . In preliminary studies, apoptotic cell death was observed on exposure to these compounds and further studies are ongoing to elucidate the underlying mechanism of apoptosis. For purposes of comparison, the corresponding phosphate ester monomers **117** and **118** were prepared and proved to have no antitumour activity in the cell lines examined. This result is important, because it rules out any role of the phosphate ester functionality in mediating the observed cytotoxic effects and emphasizes the necessity for a bivalent unit.

Jung and coworkers have synthesized a series of monomers, dimers and a trimer possessing antitumour activity¹⁶⁶. Since artemisinin is much more expensive than artemisinic acid and because the direct introduction of a C–C bond at the C10 position of artemisinin in their derivatives may cause destruction of the endoperoxide bridge, they applied a photoxygenative cyclization of artemisinic acid as a key step. The most potent compounds from this study are dimers **119–121** and trimer **122**. These compounds were particularly potent and selective at inhibiting the growth of certain tumour cell lines and were comparable to clinically used anticancer drugs. In this study it was found that the dimers and trimer have much greater activity than any of the monomers that were prepared. It is also noted that the anticancer activities of the dimeric compounds are dependent on the length of the linkage between the endoperoxide-containing units.

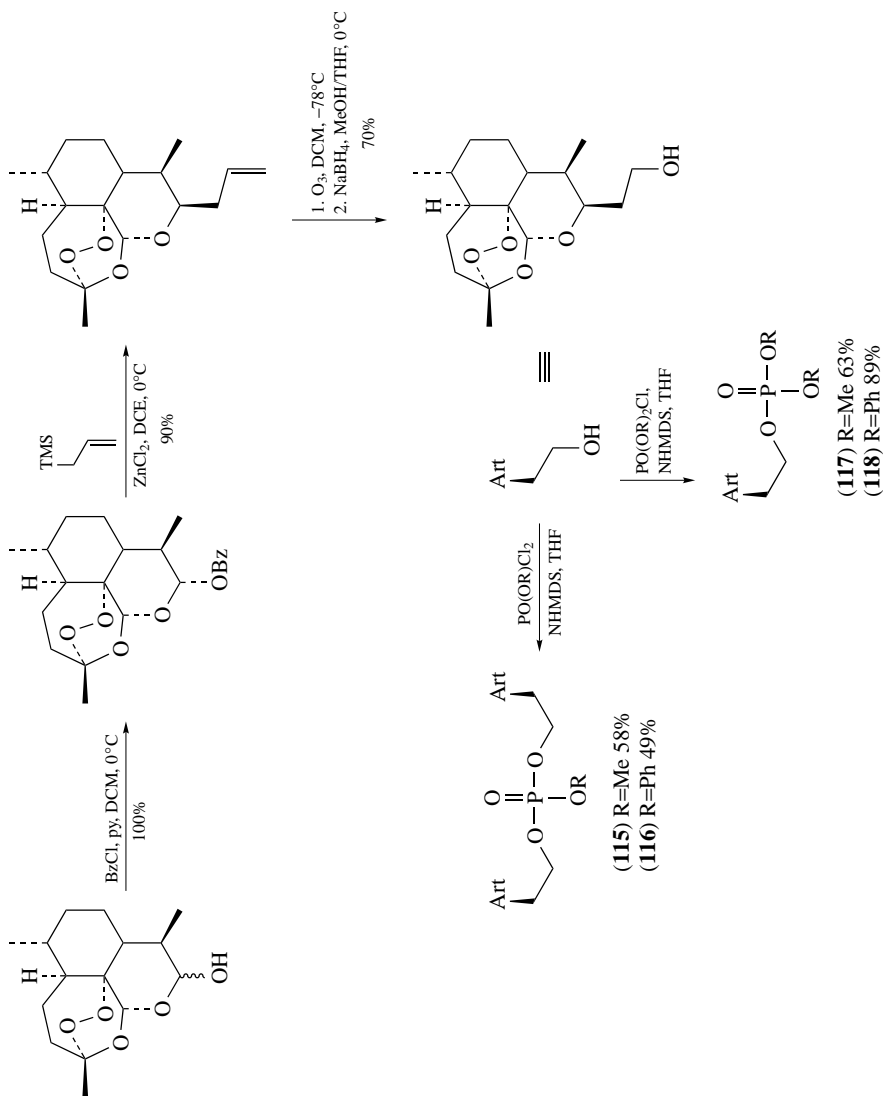
It is noteworthy that the most potent compounds prepared by O'Neill's and Jung's groups have similar linker chain lengths and hydrogen bond acceptors in the side chain. Both studies also found that longer side chains led to poor activity.

F. Summary and Conclusion

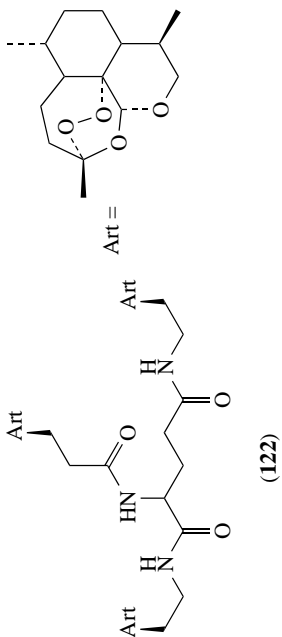
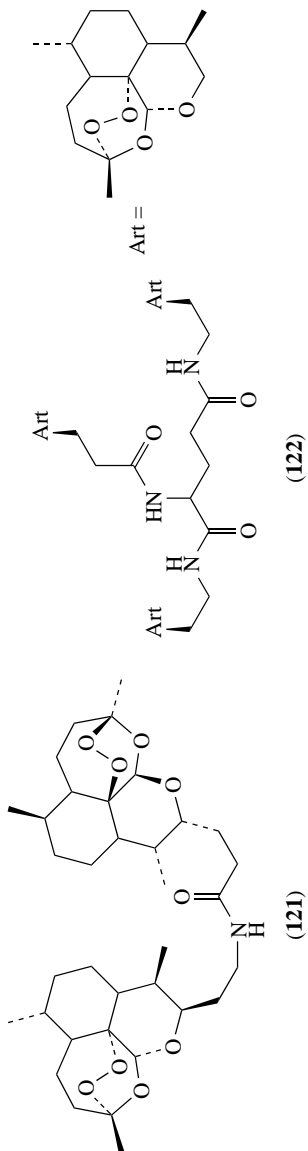
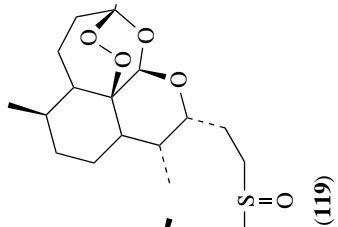
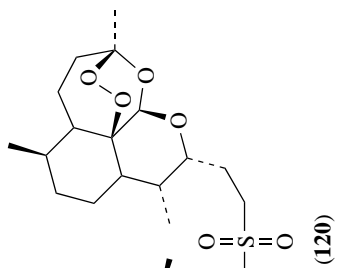
As described in this chapter, significant progress has been made in the elucidation of the chemical mechanisms of bioactivation and identification of potential biological targets of the antimalarial endoperoxide class of drug. Equally, medicinal chemists have had success in the preparation of both semi-synthetic artemisinin analogues and simplified



SCHEME 39



SCHEME 40



cyclic peroxides: new design strategies encompassing hybrid drugs and identification of chemically and metabolically stable artemisinin derivatives have been explored. These efforts are now producing candidates undergoing preclinical evaluation. Future efforts on establishing lead compounds should focus on *in vivo* efficacy, pharmacokinetics, neurotoxicity, *in vivo* toxicity and direct head to head comparisons of the most promising drug candidates. In addition, it is also clear that endoperoxides have considerable potential as antitumour agents and, with the advent of high through-put screening techniques, screening of a diverse range of synthetic and natural endoperoxide-containing compounds should be encouraged.

IX. REFERENCES

1. D. L. Klayman, *Science*, **228**, 1049 (1985).
2. D. L. Klayman, A. J. Lin, N. Acton, J. P. Scovill, J. M. Hoch, W. K. Milhous and A. D. Theoharides, *J. Nat. Prod.*, **47**, 715 (1984).
3. D. R. Wang, X. Y. Lin and H. Z. Zhang, *Acta Pharmacol. Sin.*, **8**, 355 (1987).
4. Y. P. Zhu and H. J. Woerdenbag, *Pharm. World Sci.*, **17**, 103 (1995).
5. M. J. Shmuklarsky, D. L. Klayman, W. K. Milhous, D. E. Kyle, R. N. Rossan, A. L. Ager, D. B. Tang, M. H. Heiffer, C. J. Canfield and B. G. Schuster, *Am. J. Trop. Med. Hyg.*, **48**, 377 (1993).
6. L. B. Barradell and A. Fitton, *Drugs*, **50**, 714 (1995).
7. P. L. Olliaro, R. K. Haynes, B. Meunier and Y. Yuthavong, *Trends Parasitol.*, **17**, 122 (2001).
8. G. H. Posner and S. R. Meshnick, *Trends Parasitol.*, **17**, 266 (2001).
9. D. C. Warhurst and S. C. Thomas, *Biochem. Pharmacol.*, **24**, 2047 (1975).
10. T. J. Egan, *S. Afr. J. Sci.*, **98**, 411 (2002).
11. E. Hempelmann and T. J. Egan, *Trends Parasitol.*, **18**, 11 (2002).
12. S. R. Meshnick, A. Thomas, A. Ranz, C. M. Xu and H. Z. Pan, *Mol. Biochem. Parasitol.*, **49**, 181 (1991).
13. W. Peters, B. L. Robinson, G. Tovey, J.-C. Rossier and C. W. Jefford, *Ann. Trop. Med. Parasitol.*, **87**, 111 (1993).
14. W. Hofheinz, H. Burgin, E. Gocke, C. Jaquet, R. Masciadri, G. Schmid, H. Stohler and H. Urwyler, *Trop. Med. Parasitol.*, **45**, 261 (1994).
15. J. L. Vennerstrom, S. Arbe-Barnes, R. Brun, S. A. Charman, F. C. K. Chiu, J. Chollet, Y. X. Dong, A. Dorn, D. Hunziker, H. Matile, K. McIntosh, M. Padmanilayam, J. S. Tomas, C. Scheurer, B. Scorenaux, Y. Q. Tang, H. Urwyler, S. Wittlin and W. N. Charman, *Nature*, **430**, 900 (2004).
16. P. M. O'Neill, *Nature*, **430**, 838 (2004).
17. J. N. Cumming, D. S. Wang, S. B. Park, T. A. Shapiro and G. H. Posner, *J. Med. Chem.*, **41**, 952 (1998).
18. G. H. Posner, C. H. Oh, D. S. Wang, L. Gerena, W. K. Milhous, S. R. Meshnick and W. Asawamahasadka, *J. Med. Chem.*, **37**, 1256 (1994).
19. P. Ploypradith and G. H. Posner, *Adv. Pharmacol.*, **37**, 253 (1997).
20. C. W. Jefford, J. A. Velarde, G. Bernardinelli, D. H. Bray, D. C. Warhurst and W. K. Milhous, *Helv. Chim. Acta*, **76**, 2775 (1993).
21. M. A. Avery, C. Jenningswhite and W. K. M. Chong, *Tetrahedron Lett.*, **28**, 4629 (1987).
22. M. A. Avery, C. Jenningswhite and W. K. M. Chong, *J. Org. Chem.*, **54**, 1789 (1989).
23. M. A. Avery, W. K. M. Chong and J. E. Bupp, *J. Chem. Soc., Chem. Commun.*, 1487 (1990).
24. M. A. Avery, W. K. M. Chong and C. Jenningswhite, *J. Am. Chem. Soc.*, **114**, 974 (1992).
25. J. R. Woolfrey, M. A. Avery and W. M. Doweyko, *J. Comput. Aided Mol. Des.*, **12**, 165 (1998).
26. M. A. Avery, M. Alvim-Gaston, C. R. Rodrigues, E. J. Barreiro, F. E. Cohen, Y. A. Sabnis and J. R. Woolfrey, *J. Med. Chem.*, **45**, 292 (2002).
27. H. S. Kim, H. Begum, N. Ogura, Y. Wataya, T. Tokuyasu, A. Masuyama, M. Nojima and K. J. McCullough, *J. Med. Chem.*, **45**, 4732 (2002).
28. W. S. Zhou and X. X. Xu, *Acc. Chem. Res.*, **27**, 211 (1994).
29. I. Harvey and T. J. Egan, *J. Inorg. Biochem.*, **86**, 252 (2001).

30. T. J. Egan, W. W. Mavuso and K. K. Ncokazi, *Biochemistry*, **40**, 204 (2001).
31. P. M. O'Neill, P. G. Bray, S. R. Hawley, S. A. Ward and B. K. Park, *Pharmacol. Ther.*, **77**, 29 (1998).
32. S. R. Meshnick, T. E. Taylor and S. Kamchonwongpaisan, *Microbiol. Rev.*, **60**, 301 (1996).
33. R. Kannan, D. Sahal and V. S. Chauhan, *Chem. Biol.*, **9**, 321 (2002).
34. U. Eckstein-Ludwig, R. J. Webb, I. D. A. van Goethem, J. M. East, A. G. Lee, M. Kimura, P. M. O'Neill, P. G. Bray, S. A. Ward and S. Krishna, *Nature*, **424**, 957 (2003).
35. G. H. Posner and C. H. Oh, *J. Am. Chem. Soc.*, **114**, 8328 (1992).
36. C. W. Jefford, F. Favarger, M. D. Graca, H. Vicente and Y. Jacquier, *Helv. Chim. Acta*, **78**, 452 (1995).
37. C. W. Jefford, M. G. H. Vicente, Y. Jacquier, F. Favarger, J. Mareda, P. Millasson-Schmidt, G. Brunner and U. Burger, *Helv. Chim. Acta*, **79**, 1475 (1996).
38. G. H. Posner, J. N. Cumming, P. Ploypradith and H. O. Chang, *J. Am. Chem. Soc.*, **117**, 5885 (1995).
39. G. H. Posner, S. B. Park, L. Gonzalez, D. S. Wang, J. N. Cumming, D. Klinedinst, T. A. Shapiro and M. D. Bachi, *J. Am. Chem. Soc.*, **118**, 3537 (1996).
40. W. M. Wu, Y. K. Wu, Y. L. Wu, Z. J. Yao, C. M. Zhou, Y. Li and F. Shan, *J. Am. Chem. Soc.*, **120**, 3316 (1998).
41. M. A. Avery, P. Fan, J. M. Karle, J. D. Bonk, R. Miller and D. K. Goins, *J. Med. Chem.*, **39**, 1885 (1996).
42. P. A. Berman and P. A. Adams, *Free Radic. Biol. Med.*, **22**, 1283 (1997).
43. A. Robert, O. Dechy-Cabaret, J. Cazelles and B. Meunier, *Acc. Chem. Res.*, **35**, 167 (2002).
44. P. M. O'Neill and G. H. Posner, *J. Med. Chem.*, **47**, 2945 (2004).
45. G. H. Posner and P. M. O'Neill, *Acc. Chem. Res.*, **37**, 397 (2004).
46. G. H. Posner, D. S. Wang, J. N. Cumming, C. H. Oh, A. N. French, A. L. Bodley and T. A. Shapiro, *J. Med. Chem.*, **38**, 2273 (1995).
47. G. H. Posner, D. J. McGarvey, C. H. Oh, N. Kumar, S. R. Meshnick and W. Asawama-hasadka, *J. Med. Chem.*, **38**, 607 (1995).
48. G. H. Posner, D. S. Wang, L. Gonzalez, X. L. Tao, J. N. Cumming, D. Klinedinst and T. A. Shapiro, *Tetrahedron Lett.*, **37**, 815 (1996).
49. M. Kamata, M. Ohta, K. Komatsu, H. S. Kim and Y. Wataya, *Tetrahedron Lett.*, **43**, 2063 (2002).
50. Y. Wu, Z.-Y. Wu and Y.-L. Wu, *Angew. Chem., Int. Ed.*, **38**, 2580 (1999).
51. C. W. Jefford, M. G. H. Vicente, Y. Jacquier, F. Favarger, J. Mareda, P. Millasson-Schmidt, G. Brunner and U. Burger, *Helv. Chim. Acta*, **79**, 1473 (1996).
52. A. M. Szpilman, E. E. Korshin, R. Hoos, G. H. Posner and M. D. Bachi, *J. Org. Chem.*, **66**, 6531 (2001).
53. C. W. Jefford, J.-C. Rossier and W. K. Milhous, *Heterocycles*, **52**, 1345 (2000).
54. A. Robert and B. Meunier, *J. Am. Chem. Soc.*, **119**, 5968 (1997).
55. A. Robert and B. Meunier, *Chem. Soc. Rev.*, **27**, 273 (1998).
56. J. Cazelles, A. Robert and B. Meunier, *J. Org. Chem.*, **67**, 609 (2002).
57. Y. K. Wu, Z. Y. Yue and H. H. Liu, *Helv. Chim. Acta*, **84**, 928 (2001).
58. Y. K. Wu, *Acc. Chem. Res.*, **35**, 255 (2002).
59. R. K. Haynes and S. C. Vonwiller, *Tetrahedron Lett.*, **37**, 253 (1996).
60. R. K. Haynes and S. C. Vonwiller, *Tetrahedron Lett.*, **37**, 257 (1996).
61. D. S. Torok, H. Ziffer, S. R. Meshnick, X. Q. Pan and A. Ager, *J. Med. Chem.*, **38**, 5045 (1995).
62. R. K. Haynes, H. H. O. Pai and A. Voerste, *Tetrahedron Lett.*, **40**, 4715 (1999).
63. P. M. O'Neill, L. P. D. Bishop, N. L. Searle, J. L. Maggs, R. C. Storr, S. A. Ward, B. K. Park and F. Mabbs, *J. Org. Chem.*, **65**, 1578 (2000).
64. M. A. Avery, P. C. Fan, J. M. Karle, J. D. Bonk, R. Miller and D. K. Goins, *J. Med. Chem.*, **39**, 1885 (1996).
65. F. Zouhiri, D. Desmaële, J. d'Angelo, C. Riche, F. Gay and L. Cicéron, *Tetrahedron Lett.*, **39**, 2969 (1998).
66. S. Kapetanaki and C. Varotsis, *J. Med. Chem.*, **44**, 3150 (2001).
67. Y. K. Wu and H. H. Liu, *Chem. Res. Toxicol.*, **16**, 1202 (2003).
68. R. K. Haynes, W. Y. Ho, H. W. Chan, B. Fugmann, J. Stetter, S. L. Croft, L. Vivas, W. Peters and B. L. Robinson, *Angew. Chem., Int. Ed.*, **43**, 1381 (2004).

69. Y. Z. Yang, B. Little and S. R. Meshnick, *Biochem. Pharmacol.*, **48**, 569 (1994).
70. S. R. Meshnick, *Trans. Ry. Soc. Trop. Med. Hyg.*, **88**, 31 (1994).
71. P. M. O'Neill, L. P. Bishop, N. L. Searle, J. L. Maggs, S. A. Ward, P. G. Bray, R. C. Storr and B. K. Park, *Tetrahedron Lett.*, **38**, 4263 (1997).
72. J. Cazelles, A. Robert and B. Meunier, *J. Org. Chem.*, **64**, 6776 (1999).
73. E. E. Korshin, R. Hoos, A. M. Szpilmann, L. Konstantinovski, G. H. Posner and M. D. Bachi, *Tetrahedron*, **58**, 2449 (2002).
74. M. A. Avery, P. C. Fan, J. M. Karle, R. Miller and K. Goins, *Tetrahedron Lett.*, **36**, 3965 (1995).
75. C. D. Fitch, *Life Sci.*, **74**, 1957 (2004).
76. P. Vattanaviboon, N. Siritanaratkul, J. Ketpirune, P. Wilairat and Y. Yuthavong, *Biochem. Pharmacol.*, **64**, 91 (2002).
77. S. R. Meshnick, *Int. J. Parasit.*, **32**, 1655 (2002).
78. F. Zhang, D. K. Gosser and S. R. Meshnick, *Biochem. Pharmacol.*, **43**, 1805 (1992).
79. A. Robert, J. Cazelles and B. Meunier, *Angew. Chem., Int. Ed.*, **40**, 1954 (2001).
80. R. K. Haynes, D. Monti, D. Taramelli, N. Basilico, S. Parapini and P. Olliaro, *Antimicrob. Agents Chemother.*, **47**, 1175 (2003).
81. M. Dua, P. Raphael, P. S. Sijwali, P. J. Rosenthal, A. H. Chishti and M. Hanspal, *Blood*, **96**, 946 (2000).
82. A. V. Pandey, B. L. Tekwani, R. L. Singh and V. S. Chauhan, *J. Biol. Chem.*, **274**, 19383 (1999).
83. P. M. O'Neill, F. Scheinmann, A. V. Stachulski, J. L. Maggs and B. K. Park, *J. Med. Chem.*, **44**, 1467 (2001).
84. K. Borstnik, I. H. Paik, T. A. Shapiro and G. H. Posner, *Int. J. Parasit.*, **32**, 1661 (2002).
85. Y. M. Pu and H. Ziffer, *J. Med. Chem.*, **38**, 613 (1995).
86. S. H. Woo, M. H. Parker, P. Ploypradith, J. Northrop and G. H. Posner, *Tetrahedron Lett.*, **39**, 1533 (1998).
87. R. K. Haynes, H. W. Chan, M. K. Cheung, S. T. Chung, W. L. La, H. W. Tsang, A. Voerste and I. D. Williams, *Eur. J. Org. Chem.*, 2098 (2003).
88. R. K. Haynes, *Curr. Opin. Infect. Dis.*, **14**, 719 (2001).
89. J. A. Vroman, M. Alvim-Gaston and M. A. Avery, *Curr. Pharm. Design*, **5**, 101 (1999).
90. M. Jung, K. Lee and H. Jung, *Tetrahedron Lett.*, **42**, 3997 (2001).
91. M. Jung, K. Lee, H. Jung, H. Kendrick, V. Yardley and S. L. Croft, *Bioorg. Med. Chem. Lett.*, **14**, 2001 (2004).
92. S. Hindley, S. A. Ward, R. C. Storr, N. L. Searle, P. G. Bray, B. K. Park, J. Davies and P. M. O'Neill, *J. Med. Chem.*, **45**, 1052 (2002).
93. P. M. O'Neill, A. Miller, L. P. D. Bishop, S. Hindley, J. L. Maggs, S. A. Ward, S. M. Roberts, F. Scheinmann, A. V. Stachulski, G. H. Posner and B. K. Park, *J. Med. Chem.*, **44**, 58 (2001).
94. M. A. Avery, C. Jenningswhite and W. K. M. Chong, *J. Org. Chem.*, **54**, 1792 (1989).
95. M. A. Avery, F. G. Gao, W. K. M. Chong, S. Mehrotra and W. K. Milhous, *J. Med. Chem.*, **36**, 4264 (1993).
96. M. A. Avery, J. D. Bonk, W. K. M. Chong, S. Mehrotra, R. Miller, W. Milhous, D. K. Goins, S. Venkatesan, C. Wyandt, I. Khan and B. A. Avery, *J. Med. Chem.*, **38**, 5038 (1995).
97. M. A. Avery, K. M. Muraleedharan, P. V. Desai, A. K. Bandyopadhyaya, M. M. Furtado and B. L. Tekwani, *J. Med. Chem.*, **46**, 4244 (2003).
98. A. J. Lin, M. Lee and D. L. Klayman, *J. Med. Chem.*, **32**, 1249 (1989).
99. R. A. Vishwakarma, *J. Nat. Prod.*, **53**, 216 (1990).
100. R. K. Haynes, H. W. Chan, M. K. Cheung, W. L. Lam, M. K. Soo, H. W. Tsang, A. Voerste and I. D. Williams, *Eur. J. Org. Chem.*, 113 (2002).
101. P. M. O'Neill, M. Pugh, A. V. Stachulski, S. A. Ward, J. Davies and B. K. Park, *J. Chem. Soc., Perkin Trans. 1*, 2682 (2001).
102. S. Lee and S. Oh, *Tetrahedron Lett.*, **43**, 2891 (2002).
103. C. Z. Liu, C. Guo, Y. C. Wang and O. Y. Fan, *World J. Microbiol. Biotechnol.*, **19**, 535 (2003).
104. S. L. Fleck, B. L. Robinson and W. Peters, *Ann. Trop. Med. Parasitol.*, **91**, 33 (1997).
105. Y. X. Dong, H. Matile, J. Chollet, R. Kaminsky, J. K. Wood and J. L. Vennerstrom, *J. Med. Chem.*, **42**, 1477 (1999).

106. J. L. Vennerstrom, Y. X. Dong, S. L. Andersen, A. L. Ager, H. N. Fu, R. E. Miller, D. L. Wesche, D. E. Kyle, L. Gerena, S. M. Walters, J. K. Wood, G. Edwards, A. D. Holme, W. G. McLean and W. K. Milhous, *J. Med. Chem.*, **43**, 2753 (2000).
107. J. L. Vennerstrom, A. L. Ager, S. L. Andersen, J. M. Grace, V. Wongpanich, C. K. Angerhofer, J. K. Hu and D. L. Wesche, *Am. J. Trop. Med. Hyg.*, **62**, 573 (2000).
108. H. S. Kim, Y. Shibata, Y. Wataya, K. Tsuchiya, A. Masuyama and M. Nojima, *J. Med. Chem.*, **42**, 2604 (1999).
109. G. H. Posner, J. N. Cumming, S. H. Woo, P. Ploypradith, S. J. Xie and T. A. Shapiro, *J. Med. Chem.*, **41**, 940 (1998).
110. G. H. Posner, H. B. Jeon, M. H. Parker, M. Krasavin, I. H. Paik and T. A. Shapiro, *J. Med. Chem.*, **44**, 3054 (2001).
111. M. D. Bachi, E. E. Korshin, R. Hoos, A. M. Szpilman, P. Ploypradith, S. J. Xie, T. A. Shapiro and G. H. Posner, *J. Med. Chem.*, **46**, 2516 (2003).
112. L. K. Basco, O. Dechy-Cabaret, M. Ndounga, F. S. Meche, A. Robert and B. Meunier, *Antimicrob. Agents Chemother.*, **45**, 1886 (2001).
113. O. Dechy-Cabaret, A. Robert and B. Meunier, *C. R. Chim.*, **5**, 297 (2002).
114. C. Singh, H. Malik and S. K. Puri, *Bioorg. Med. Chem.*, **12**, 1177 (2004).
115. N. C. Araujo, S. A. Ward, J. Davies, P. G. Bray and P. M. O'Neill, unpublished results.
116. P. S. Sijwali, B. R. Shenai, J. Gut, A. Singh and P. J. Rosenthal, *Biochem. J.*, **360**, 481 (2001)
117. R. S. Li, G. L. Kenyon, F. E. Cohen, X. W. Chen, B. Q. Gong, J. N. Dominguez, E. Davidson, G. Kurzban, R. E. Miller, E. O. Nuzum, P. J. Rosenthal and J. H. McKerrow, *J. Med. Chem.*, **38**, 5031 (1995).
118. R. S. Li, X. W. Chen, B. Q. Gong, P. M. Selzer, Z. Li, E. Davidson, G. Kurzban, R. E. Miller, E. O. Nuzum, J. H. McKerrow, R. J. Fletterick, S. A. Gillmor, C. S. Craik, I. D. Kuntz, F. E. Cohen and G. L. Kenyon, *Bioorg. Med. Chem.*, **4**, 1421 (1996).
119. M. Chen, T. G. Theander, S. B. Christensen, L. Hviid, L. Zhai and A. Kharazmi, *Antimicrob. Agents Chemother.*, **38**, 1470 (1994).
120. L. Nadelmann, J. Tjornelund, S. H. Hansen, C. Cornett, U. G. Sidelmann, U. Braumann, E. Christensen and S. B. Christensen, *Xenobiotica*, **27**, 667 (1997).
121. P. M. O'Neill, P. A. Stocks, M. D. Pugh, N. C. Araujo, E. E. Korshin, J. F. Bickley, S. A. Ward, P. G. Bray, E. Pasini, J. Davies, E. Verissimo and M. D. Bachi, *Angew. Chem., Int. Ed.*, **43**, 4193 (2004).
122. C. W. Jefford, S. Kohmoto, D. Jaggi, G. Timari, J.-C. Rossier, M. Rudaz, O. Barbuzzi, D. Gerard, U. Burger, P. Kamalaprija, J. Mareda, G. Bernardinelli, I. Manzanares, C. J. Canfield, S. L. Fleck, B. L. Robinson and W. Peters, *Helv. Chim. Acta*, **78**, 647 (1995).
123. C. W. Jefford, S. J. Jin, J.-C. Rossier, S. Kohmoto and G. Bernardinelli, *Heterocycles*, **44**, 367 (1997).
124. P. M. O'Neill, N. L. Searle, K. J. Raynes, J. L. Maggs, S. A. Ward, R. C. Storr, B. K. Park and G. H. Posner, *Tetrahedron Lett.*, **39**, 6065 (1998).
125. K. J. McCullough and M. Nojima, *Curr. Org. Chem.*, **5**, 601 (2001).
126. G. H. Posner, H. B. Jeon, P. Ploypradith, I. H. Paik, K. Borstnik, S. J. Xie and T. A. Shapiro, *J. Med. Chem.*, **45**, 3824 (2002).
127. C. Singh, D. Misra, G. Saxena and S. Chandra, *Bioorg. Med. Chem. Lett.*, **2**, 497 (1992).
128. C. Singh, H. Malik and S. K. Puri, *Bioorg. Med. Chem. Lett.*, **14**, 459 (2004).
129. C. Singh, N. Gupta and S. K. Puri, *Bioorg. Med. Chem. Lett.*, **13**, 3447 (2003).
130. J. Iskra, D. Bonnet-Delpon and J. P. Begue, *Tetrahedron Lett.*, **44**, 6309 (2003).
131. P. M. O'Neill, M. Pugh, J. Davies, S. A. Ward and B. K. Park, *Tetrahedron Lett.*, **42**, 4569 (2001).
132. P. M. O'Neill, S. Hindley, M. D. Pugh, J. Davies, P. G. Bray, B. K. Park, D. S. Kapu, S. A. Ward and P. A. Stocks, *Tetrahedron Lett.*, **44**, 8135 (2003).
133. C. H. Oh and J. H. Kang, *Tetrahedron Lett.*, **39**, 2771 (1998).
134. M. D. Bachi, E. E. Korshin, P. Ploypradith, J. N. Cumming, S. J. Xie, T. A. Shapiro and G. H. Posner, *Bioorg. Med. Chem. Lett.*, **8**, 903 (1998).
135. D. A. Casteel, *Nat. Prod. Rep.*, **9**, 289 (1992).
136. D. A. Casteel, *Nat. Prod. Rep.*, **16**, 55 (1999).
137. R. J. Wells, *Tetrahedron Lett.*, 2637 (1976).
138. S. Sakemi, T. Higa, U. Anthoni and C. Christophersen, *Tetrahedron*, **43**, 263 (1987).

139. T. Murayama, Y. Ohizumi, H. Nakamura, T. Sasaki and J. Kobayashi, *Experimentia*, **45**, 898 (1989).
140. J. Kobayashi, T. Murayama and Y. Oizumi, *Chem. Abstr.*, **114**, 49563x.
141. R. Duran, E. Zubia, M. J. Ortega, S. Naranjo and J. Salva, *Tetrahedron*, **56**, 6031 (2000).
142. A. Fontana, G. Cimino, M. Gavagnin, M. C. Gonzalez and E. Estornell, *J. Med. Chem.*, **44**, 2362 (2001).
143. N. Takada, M. Watanabe, A. Yamada, K. Suenaga, K. Yamada, K. Ueda and D. Uemura, *J. Nat. Prod.*, **64**, 356 (2001).
144. P. Phuwapraisirisan, S. Matsunaga, N. Fusetani, N. Chaitanawisuti, S. Kritsanapuntu and P. Menasveta, *J. Nat. Prod.*, **66**, 289 (2003).
145. K. Kahlos, L. Kangas and R. Hiltunen, *Planta Med.*, 389 (1989).
146. K. Yasukawa, T. Akihisa, H. Kanno, T. Kaminaga, M. Izumida, T. Sakoh, T. Tamura and M. Takido, *Biol. Pharmacol. Bull.*, **19**, 573 (1996).
147. K. Arakawa, Y. Endo, M. Kimura, T. Yoshida, T. Kitaoka, T. Inakazu, Y. Nonami, M. Abe, A. Masuyama, M. Nojima and T. Sasaki, *Int. J. Cancer*, **100**, 220 (2002).
148. W. S. May and P. Cuatrecasas, *J. Membr. Biol.*, **88**, 205 (1985).
149. K. C. Gatter, G. Brown, I. S. Trowbridge, R. E. Woolston and D. Y. Mason, *J. Clin. Pathol.*, **36**, 539 (1983).
150. N. Shterman, B. Kupfer and C. Moroz, *Pathobiology*, **59**, 19 (1991).
151. H. Lai and N. P. Singh, *Cancer Lett.*, **91**, 41 (1995).
152. N. P. Singh and H. Lai, *Life Sci.*, **70**, 49 (2001).
153. J. C. Moore, H. Lai, J. R. Li, R. L. Ren, J. A. McDougall, N. P. Singh and C. K. Chou, *Cancer Lett.*, **98**, 83 (1995).
154. T. Efferth, R. Bauer, J. O. Funk, M. Davey, M. Volm and R. Davey, *Eur. J. Cancer*, **38**, 329 (2002).
155. T. Efferth, A. Olbrich and R. Bauer, *Biochem. Pharmacol.*, **64**, 617 (2002).
156. T. Efferth, M. M. Briehl and M. E. Tome, *Int. Journal of Oncol.*, **23**, 1231 (2003).
157. H.-H. Chen, H. J. Zhou and X. Fan, *Pharmacol. Res.*, **48**, 231 (2003).
158. M. Wartenberg, S. Wolf, P. Budde, F. Grunheck, H. Acker, J. Hescheler, G. Wartenberg and H. Sauer, *Lab. Invest.*, **83**, 1647 (2003).
159. H.-H. Chen, H. J. Zhou, W. Q. Wang and G. D. Wu, *Cancer Chemother. Pharmacol.*, **53**, 423 (2004).
160. M. F. McCarty, *Med. Hypotheses*, **61**, 509 (2003).
161. H. J. Woerdenbag, T. A. Moskal, N. Pras, T. M. Malingre, F. S. Elferaly, H. H. Kampinga and A. W. T. Konings, *J. Nat. Prod.*, **56**, 849 (1993).
162. G. H. Posner, P. Ploypradith, W. Hapangama, D. S. Wang, J. N. Cumming, P. Dolan, T. W. Kensler, D. Klinedinst, T. A. Shapiro, Q. Y. Zheng, C. K. Murray, L. G. Pilkington, L. R. Jayasinghe, J. F. Bray and R. Daughenbaugh, *Bioorg. Med. Chem.*, **5**, 1257 (1997).
163. G. H. Posner, P. Ploypradith, M. H. Parker, H. O'Dowd, S. H. Woo, J. Northrop, M. Krasavin, P. Dolan, T. W. Kensler, S. J. Xie and T. A. Shapiro, *J. Med. Chem.*, **42**, 4275 (1999).
164. G. H. Posner, A. J. McRiner, I. H. Paik, S. Sur, K. Borstnik, S. J. Xie, T. A. Shapiro, A. Alagbala and B. Foster, *J. Med. Chem.*, **47**, 1299 (2004).
165. J. P. Jeyadevan, P. G. Bray, J. Chadwick, A. E. Mercer, A. Byrne, S. A. Ward, B. K. Park, D. P. Williams, R. Cosstick, J. Davies, A. P. Higson, E. Irving, G. H. Posner and P. M. O'Neill, *J. Med. Chem.*, **47**, 1290 (2004).
166. M. Jung, S. Lee, J. Ham, K. Lee, H. Kim and S. K. Kim, *J. Med. Chem.*, **46**, 987 (2003).

Author Index

This author index is designed to enable the reader to locate an author's name and work with the aid of the reference numbers appearing in the text. The page numbers are printed in normal type in ascending numerical order, followed by the reference numbers in parentheses. The numbers in *italics* refer to the pages on which the references are actually listed.

- A1-Khalil, S. I. 631(294), 763
Aarnes, H. 1250(228), 1275
Abbasova, M. T. 652(380), 765
Abdalla, D. S. P. 687(554), 769
Abdel-Latif, M. S. 631(294), 763, 1257(303), 1277
Abdennadher, M. 622(186), 760
Abdou, M. S. A. 832(10), 894
Abdullah, W. J. W. 663(234), 761
Abecassis, J. 1021(127), 1048
Abe, M. 192(62), 225(220), 293, 296, 1335(147), 1346
Abrahams, S. C. 95(16), 96(24), 139
Abrantes, M. 471(296), 589
Abu Zuhri, A. Z. 631(294), 763
Abu-Irhayem, E. 650(363), 765
Abu-Omar, M. 1083(229, 230), 1123
Abuja, P. M. 1242(189), 1274
Achrem, A. A. 426(277b), 588
Acker, H. 1336(158), 1346
Acker, K. 638(314), 764
Acosta, F. 614(136), 759
Acree, W. E. 155(22), 160(38), 168, 169
Acton, N. 288(562–564, 573), 305, 1280(2), 1342
Adachiakahane, S. 1257(281), 1276
Adachi, K. 50(50b), 87
Adamczyk, M. 1252(244), 1275
Adamic, R. 1030(196), 1050
Adamo, C. 12(7), 85
Adamson, A. W. 1189(44a), 1208
Adams, C. M. 267(408), 301
Adams, P. A. 1311(42), 1343
Adam, G. 1162(151a), 1169
Adam, H. 1108(389), 1127
Adam, V. 950(155), 992
Adam, W. 47(103), 65(137a, 139), 73(19d), 78(20), 86, 89, 90, 94(2), 112(84), 138, 141, 161(45), 169, 192(62), 193(58, 61, 65, 68), 195(69), 196(64, 71, 72), 235(235), 253(330, 333), 255(355), 259(368), 260(371, 372), 263(386), 267(411–413), 269(399), 271(331, 332, 433), 272(432, 434–436), 273(474), 291(593), 293, 297, 299–302, 305, 324(51a), 326(59), 337(74, 75), 338(76), 339(78, 79), 343(89, 90), 345(93, 95), 346(94), 352(17, 50, 72), 363(137), 373(152), 408(86, 220–222, 222b), 410(223, 226, 229), 411(230), 414(228), 416(235, 235b, 236), 468(271), 469(350), 475(70, 73), 477(373a–c), 478(374), 493(66, 219), 520(453, 455b), 529(471), 539(20), 560(39), 561(217), 582–585, 587, 588, 590, 591, 593, 730(673), 772, 779(16a, b, 17), 785(28, 29), 814(89), 827, 829, 852(72, 73), 853(81, 82, 84), 854(89), 865(139), 866(141), 869(93, 143–145), 875(174), 884(184), 885(165), 888(45–48, 140, 191–193), 889(4, 80, 195–198, 201), 892(207), 893–898, 943(85b, 96), 949(140), 954(192a), 991–993, 1004(26), 1020(123), 1021(131), 1046, 1048, 1074(126), 1083(223, 224), 1089(275, 277), 1090(221, 276), 1091(278, 279), 1094(17, 294, 296, 298), 1096(319, 321, 323), 1100(132), 1113(2), 1116(424, 425), 1118, 1121, 1123–1126, 1128, 1140(14, 26, 37, 51, 54, 76), 1143(60, 63a–c), 1144(65), 1145(48, 66, 69), 1146(73), 1150(91), 1152(107, 108a, b), 1154(110), 1155(106d, 116, 117,

- 118a, b, 119a), 1158(32), 1160(33, 47, 139a, 141), 1161(104, 105, 122), 1162(21, 150, 151a), 1163(1a, 1d, e, 1g, h, 1j, k, 1m, 1p, 153, 154a, b, 154e, 154g), 1164–1169, 1172(1), 1174(13a–c, 14a–c, 15), 1178(19a–e, 20b–d), 1181(11a–g), 1182(23, 24b), 1184(25f, 27), 1188(34a, b, 36, 37a), 1192(16a), 1194(30, 35b), 1197(50), 1200(58a), 1202(64a–d), 1203(65a, b), 1204(71), 1205(60a, b), 1205–1209, 1212(10), 1213(19), 1222(49), 1224(58), 1227(54, 55, 87), 1228(11, 51, 98), 1229(110), 1230(112, 113), 1232(119, 120, 124, 129), 1233(12–15), 1234(21), 1235(22), 1236(79, 145, 154, 159–162), 1238(168–170), 1256(144), 1270–1274
- Adam, Waldemar 1172(10b), 1188(40f), 1206, 1208
- Adanic, R. 1003(23), 1046
- Adeagbo, A. S. O. 613(112), 758
- Adebodun, F. 185(38), 187
- Adger, B. M. 381(159), 585
- Adibi, H. 1031(209–211, 213), 1032(214, 215), 1050
- Adolfsson, H. 467(352), 468(357), 534(481, 482), 567(530a), 574(539, 540), 590, 591, 594, 595, 802(54), 828, 1083(220), 1090(218), 1123
- Adrian, V. 623(206), 761
- Adrio, J. 471(363), 591
- Aeschliman, S. M. 77(152b), 91
- Afarik, I. 815(91c), 829
- Afeefy, H. Y. 160(3, 36), 167, 169
- Affolter, S. 622(187), 706(185), 760
- Afri, M. 285(285), 298
- Afsar, H. 640(320), 764
- Agamamedova, L. M. 652(380), 765
- Agapakis, S. 1117(433), 1128
- Ager, A. L. 712(58), 757, 1281(5), 1317(107), 1326(106), 1342, 1345
- Ager, A. 276(501), 303, 1302(61), 1343
- Aggarwal, V. K. 386(190b), 586
- Aghajari, M. 1018(115), 1048
- Agosta, W. C. 250(295), 298
- Agrios, K. A. 259(362–364), 300
- Aguilaniu, H. 987(325d), 999
- Aguirre, F. 675(504), 768
- Ahmed, G. 1021(133), 1048, 1140(85b), 1167
- Ahn, B. W. 987(325a, 329c), 999
- Ahn, J.-H. 428(286), 589
- Ahn, K.-J. 605(37), 756
- Ahrweiler, M. 259(368), 300, 1205(60b), 1209
- Airoldi, G. 428(294), 589
- Aitken, R. J. 612(102), 758
- Ajjou, A. N. 511(413), 592
- Akagi, J. 434(273), 588
- Akagy, J. 1089(271), 1124
- Akaïke, T. 614(130), 759
- Akasaka, K. 660(422), 680(421, 528, 530, 531), 766, 769
- Akasaka, S. 984(312), 998
- Akasaka, T. 246(286), 298, 816(93), 817(96, 97), 818(94, 98, 99), 819(100, 101, 103), 825(126), 829, 830, 852(77–79), 895, 1044(274), 1052
- Akashi, K. 574(521), 575(520), 595
- Akbulut, N. 264(391), 267(407, 409), 300, 301
- Akeshch, T. S. 166(58), 169
- Akgöl, S. 655(393), 765
- Akhavan, H. 1199(56a), 1208
- Akhrem, A. A. 278(278), 298
- Akiba, K.-Y. 1044(275), 1052
- Akiba, K. 118(139), 142
- Akihisa, T. 1334(146), 1346
- Akimoto, H. 743(704), 773, 817(95), 829
- Akinaga, T. 129(171), 143
- Akita, M. 118(126), 133(133), 142, 808(68), 828, 1064(51, 52), 1119
- Akiyama, K. 206(121, 122), 294
- Akiyama, R. 413(233c, d), 587
- Akiyama, S. 1257(268, 270, 280), 1276
- Akiya, N. 97(29), 139
- Akizawa, H. 677(518), 768
- Aki, M. 129(171), 143
- Akse, J. R. 646(348), 764
- Aktas, E. 653(384), 765
- Akutagawa, M. 285(551), 304
- Akyilmaz, E. 655(394), 765
- Al Gasser, G. 1014(90), 1048
- Al-Ajlouni, A. M. 1095(215), 1123
- Al-Laham, M. A. 12(7), 85
- Al-Yahya, M. A. 134(197), 144
- Alagbala, A. 1337(164), 1346
- Alam, T. M. 685(543, 544), 769
- Albertini, R. 1242(189), 1274
- Alberti, M. N. 880(56), 895
- Albertsson, A. C. 680(535), 769
- Alberts, I. L. 12(7e), 85
- Albert, H. E. 1102(350), 1126
- Albert, R. 814(89), 829, 889(201), 898
- Albery, W. J. 907(84), 913
- Albouy, J. P. 724(606), 770
- Albrecht, H. O. 1244(4), 1270
- Albrecht, S. 1184(25f), 1188(36), 1207, 1236(145), 1242(171), 1268(335), 1273, 1274, 1278
- Albright, J. O. 318(9), 352(10), 582
- Alcock, N. W. 118(132), 142
- Alcock, W. G. 717(628), 771
- Aldelman, R. 616(151), 759
- Alekar, N. A. 1116(419), 1128
- Aleksandrov, Yu. A. 783(18d), 827
- Aleksandrov, Y. A. 780(21), 810(79, 80), 827, 829
- Aleksandrov, Yu. A. 824(117b, 117f), 830
- Alemu, H. 651(366, 367), 765

- Alessandroni, M. 611(81), 758
 Alexandrov, Y. A. 776(7), 827
 Alexis, M. 396(209), 587
 Alfandy, M. 659(419), 766
 Alfassi, Z. F. 924(45), 990
 Alford, J. A. 177(17), 187
 Alhitari, N. 623(206), 761
 Alini, S. 107(89), 141
 Aliotta, G. 1111(398), 1127
 Ali, A. E. 233(13), 292
 Ali, H. 967(236), 995
 Alkeeva, N. V. 824(117b), 830
 Allan, D. S. 174(9), 186
 Allan, G. G. 432(303), 589
 Allenmark, S. G. 475(370), 591
 Allen, A. O. 674(503a), 768, 965(214), 994
 Allen, F. H. 105(66), 140
 Allen, J. T. 684(99), 758
 Allen, J. V. 379(163), 380(162, 171), 585, 586
 Allinger, N. L. 155(23), 168
 Almeida, E. A. 967(238b), 995
 Almenningen, A. 723(648), 771
 Almlöf, J. 721(646), 771
 Alneri, E. 444(305), 589, 1079(169), 1122
 Alpegot, S. 921(28b), 989
 Alstad, R. 263(387), 300
 Alsters, P. L. 408(222, 222b), 587, 1091(279),
 1094(298), 1107(384), 1124, 1125, 1127
 Altamura, A. 1153(109), 1168
 Altenburger-Combrisson, S. 724(606), 770
 Altmiller, D. H. 976(271), 996
 Alvarez, A. 375(156), 585
 Alvarez, B. 951(167), 952(176), 993
 Alvarez, F. J. 1188(40c), 1207, 1262(308),
 1277
 Alvarez, F. 1188(40d), 1207, 1262(311), 1277
 Alvarez, M. N. 741(698), 772, 951(168), 993
 Alvarez, R. A. 31(80), 88
 Alves, W. A. 624(228), 761
 Alvim-Gaston, M. 273(40), 276(501), 292,
 303, 1282(26), 1314(89), 1342, 1344
 Alzerreca, A. 779(17), 827
 Amanso, A. M. 953(185), 993
 Amato, G. 432(302), 589
 Ambrose, J. 1257(264), 1276
 Ames, B. N. 616(151), 670(475), 680(537),
 759, 767, 769, 917(1c), 935(65), 956(201a),
 975(269a), 977(277g, 279b), 988, 990, 994,
 996, 997, 1201(62b), 1209
 Amici, A. 987(329c), 999
 Amirabadi, H. M. 357(117), 584
 Amos, R. D. 12(7d, e), 85
 Amstrong, R. C. 960(207a), 994
 Anderegg, J. H. 1224(59), 1271
 Anderlund, M. 653(382), 765
 Andersen, H. J. 972(252), 995
 Andersen, J. M. 1250(228), 1275
 Andersen, S. L. 712(58), 757, 1317(107),
 1326(106), 1345
 Anderson, J. L. 858(121), 896
 Anderson, J. M. 1010(66), 1047
 Anderson, K. M. 976(272b), 996
 Anderson, O. P. 1062(63), 1120, 1140(77b),
 1167
 Anderson, R. F. 82(162), 91
 Anderson, T. M. 1082(193, 194), 1123
 Anderson, V. E. 956(198), 994
 Andersson, I. 1069(105, 106, 116), 1121
 Andersson, M. A. 475(370), 567(530b), 591,
 595
 Andersson, P. G. 514(441), 593
 Andersson, S. 84(84), 88
 Andler, S. 1178(20c), 1203(65a), 1206, 1209,
 1230(113), 1272
 Ando, M. 209(136, 139, 143), 295
 Ando, R. 1069(107), 1121
 Ando, W. 13(13d), 86, 233(155), 246(286),
 269(52), 293, 295, 298, 309(1), 340(85a, b),
 351(107), 493(367), 581, 583, 584, 591,
 673(491), 768, 816(93), 817(96, 97),
 818(94, 98, 99), 819(100–103),
 825(124–126), 829, 830, 852(77–79),
 854(101), 895, 1001(10), 1044(274), 1046,
 1052, 1095(4), 1118, 1163(1d), 1164,
 1178(20d), 1181(11f), 1206, 1233(14), 1270
 Andre-Barres, C. 201(91, 92), 294
 Andreea, M. R. M. 556(517), 558(362), 591,
 595
 Andrei, J. 1075(155), 1122
 Andrés, J. L. 12(7), 29(63), 56(48b, c), 85, 87,
 88, 97(32b), 139, 1140(44), 1166
 Andreu, C. 1158(132), 1169
 Andrews, J. S. 12(7e), 85
 Andrews, L. J. 901(30), 912
 Andrews, L. 720(641), 771
 Andrus, M. B. 516(436), 592
 Andzelm, J. 101(52b), 140
 Anelli, P. L. 531(321), 590
 Angelici, R. J. 1019(116), 1048
 Angeli, F. 1150(92), 1167
 Angenot, L. 190(42), 292
 Angerhofer, C. K. 1317(107), 1345
 Anglada, J. M. 36(87), 65(65), 77(77b), 88
 Anglada, J. 32(85b), 77(77a), 88
 Angnes, L. 650(362), 765
 Angstl, M. 1085(244), 1124
 Angus-Dunne, S. 1069(105), 1121
 Anniyappan, M. 1010(65), 1047
 Annunziata, R. 380(155), 383(184), 585, 586
 Anson, M. S. 1099(341), 1100(349), 1126
 Anthoni, U. 190(25), 292, 1333(138), 1345
 Antipin, M. Y. 103(47), 110(70), 122(152),
 128(50), 140, 142
 Antolini, L. 130(174), 143
 Antolovich, M. 667(454), 767

- Antonelli, E. 1094(305), *1125*
 Antonello, S. 96(20), 123(162), 129(172), *139*,
143
 Antonioletti, R. 1150(92), *1167*
 Antonovskii, V. L. 103(47, 48), 118(140),
 122(158), 123(104), 130(185), 131(180),
140–143, 156(27), *168*, 622(184), 690(566),
760, *770*
 Antonovsky, V. L. 105(62a), 119(9), *139*, *140*
 Anxolabéhère-Mallart, E. 1117(431), *1128*
 Anzai, J.-i. 651(371), *765*
 An, Y.-Z. 858(121, 126), *896*
 Aoki, M. 106(67), *140*, 444(310, 311),
 445(312), 496(400), 506(401), 525(462),
 562(98), *584*, *589*, *592*, *593*, 1081(177),
 1089(178), 1095(317), 1106(378–380),
 1113(297), *1122*, *1125*, *1127*
 Aoki, T. 209(144), *295*
 Aoyama, H. 255(350), 285(551), *300*, *304*,
 1268(336), *1278*
 Apatu, J. O. 795(40), *828*
 Apblett, A. W. 136(136), *142*
 Aplincourt, P. 82(82b), *88*
 Appelblad, P. 1257(293), *1277*
 Appelman, E. H. 1030(196), *1050*
 Appendino, G. 106(78), 125(150), 129(175),
140, *142*, *143*
 Apperley, D. C. 569(534), *595*
 Arain, M. F. 212(148, 151), *295*
 Arai, H. 687(553, 554), *769*
 Arai, S. 374(150), 375(149), *585*
 Arai, T. 390(197), 392(195, 196), *586*
 Arakaki, T. L. 202(95), *294*
 Arakane, K. 858(122), *896*
 Arakawa, H. 426(277c), *588*
 Arakawa, K. 1335(147), *1346*
 Araujo, N. C. 223(207), 296, 1320(115),
 1323(121), *1345*
 Aravindakumar, C. T. 1011(84), *1047*
 Arbe-Barnes, S. 1332(15), *1342*
 Arbogast, J. W. 858(118), *896*
 Arce, M.-J. 858(126), *896*
 Arciniegas, A. 134(198), *144*
 Arcoria, A. 432(302), 589, 1068(91), *1120*
 Arefeen, Q. 624(216), *761*
 Arends, I. W. C. E. 368(142), 462(361),
 468(358), 560(500), 585, *591*, *594*,
 1083(228), 1085(207, 208), 1108(371),
1123, *1127*
 Argade, A. B. 516(436), *592*
 Argiuello, G. A. 705(24), 740(23), *756*
 Arias Encarnación, L. A. 1192(16a), *1206*
 Armstrong, A. 40(96), 89, 1021(133), *1048*,
 1140(85a, b), *1167*
 Armstrong, D. 954(189), *993*
 Arnau, J. L. 133(189), *143*
 Arnold, J. 673(494), 768, 1243(187),
 1244(199), *1274*
 Arnold, D. R. 906(68), *913*
 Arnold, E. 263(381), *300*
 Arnold, H. 777(9), *827*
 Arnold, K. 673(494), 768, 1243(187), *1274*
 Arnold, M. A. 943(85b), *991*, 1203(65b),
 1204(71), *1209*
 Arntz, D. 539(495), *594*
 Arora, P. K. 984(317b), *998*
 Arpe, H.-J. 525(461), *593*
 Arrington, M. P. 892(206), *898*
 Arruda-Campos, I. P. 984(294b, c), *997*
 Artus, G. R. J. 466(344), 529(470), *590*, *593*,
 1062(40), 1083(216), *1119*, *1123*
 Arudi, R. L. 945(123), *992*
 Arzoumanian, H. 1059(41), *1119*
 Asahara, F. 984(294c), *997*
 Asakura, K. 1116(418), *1128*
 Asano, Y. 651(373), *765*
 Asawamahasadka, W. 1291(47), *1343*
 Asawamahasadka, W. 280(518), *304*,
 1298(18), *1342*
 Asensio, G. 1155(117), 1158(132), 1160(138),
 139b, 141, 1161(105), *1167–1169*
 Ashby, G. A. 694(146), *759*
 Ashford, R. D. 253(340), *299*
 Ashford, S. W. 1023(154), *1049*
 Ashihara, Y. 1236(36), *1271*
 Asolkar, R. N. 1013(89), *1048*
 Assimov, V. 949(141), *992*
 Assink, R. A. 685(543, 544), *769*
 Aston, J. P. 984(297f), *998*
 Asveld, E. W. H. 854(100), 895, 1174(18b),
1206
 Atassi, G. 273(458), *302*
 Atencio, R. 1064(68), *1120*
 Atherton, C. S. 605(36), *756*
 Atkins, R. L. 1013(31), *1046*
 Atsumi, T. 109(119), *142*
 Atwater, J. E. 646(348), *764*
 Aubry, C. 1069(117), *1121*
 Aubry, J.-M. 269(421), *301*, 833(34), *894*
 Aubry, J. M. 253(343), 269(329, 425, 426),
299, *301*
 Augusto, O. 952(176, 178, 184), 953(185),
 963(220), *993*, *994*
 Augustyn, J. A. N. 379(168), *585*
 Austin, J. D. 810(81), *829*
 Austin, R. G. 569(536), *595*
 Aust, S. D. 977(277e), *996*
 Avery, B. A. 276(498), *303*, 1314(96), *1344*
 Avery, M. A. 273(40, 444), 275(492),
 276(441, 493–502), 288(574–576), *292*,
302, *303*, *305*, 1282(23, 25, 26), 1286(41),
 1306(74), 1314(21, 22, 24, 64, 89, 94–97),
1342–1344
 Aviyente, V. 29(74), *88*
 Awada, M. 981(306), *998*
 Awad, M. I. 699(581), *770*

- Awe, S. O. 613(112), 758
 Aw, T. Y. 614(129), 759
 Ayala, P. Y. 4(11a), 12(7), 60(16a), 85, 86, 96(8a), 138
 Ayalp, A. 134(197), 144
 Ayora Cañada, M. J. 662(432), 766
 Azami, M. 1236(147, 153), 1273
 Azéma, L. 1069(45), 1119
 Azman, A. 49(118), 89
 Azzena, U. 1163(154b), 1169
 Baader, W. J. 1181(11c), 1184(27), 1189(41a–d), 1193(49b), 1206–1208, 1213(19), 1228(11, 50, 51), 1235(78), 1236(17, 26, 74, 75), 1242(191, 193), 1259(313), 1260(309, 317), 1263(320, 329), 1265(331), 1267(18), 1268(140, 335), 1270–1274, 1277, 1278
 Baars, S. 378(166), 585
 Baba-zade, S. M. 652(380), 765
 Babatsikos, C. 1181(11c), 1206, 1213(19), 1270
 Baba, N. 339(84), 374(148), 583, 585, 690(563), 770
 Babcock, G. T. 963(224a), 994
 Babior, B. M. 917(3a), 988
 Baboul, A. G. 56(12b, 48d), 58(124), 86, 87, 90, 1140(49), 1166
 Babushkin, D. E. 186(43), 187
 Babu, R. S. 277(507), 303, 1023(150), 1049
 Baccin, C. 558(513), 594, 1087(260), 1112(406), 1124, 1127
 Bachi, M. D. 223(205–212), 275(487), 280(527), 296, 303, 304, 712(60), 757, 1284(39), 1309(52), 1323(121), 1330(73, 134), 1332(111), 1343–1345
 Bächmann, K. 638(314), 689(560), 764, 769
 Bachmann, S. 1084(237), 1124
 Bachowski, G. J. 687(552), 769
 Bach, R. D. 29(63), 43(38), 46(27a, b), 47(107), 50(122), 56(12a, b, 48, 48b–d), 57(52, 131), 58(124, 128a, b, 133, 134), 60(16a, b), 65(97, 139), 66(138), 67(140), 68(119, 141), 73(19a–d), 75(147), 78(20, 20b, c), 79(17a–c), 82(156), 84(166), 86(21b), 86–91, 94(11b), 96(8a), 97(32a, b), 138, 139, 423(261a), 588, 1140(22, 37, 44, 49, 50), 1160(33, 53), 1165, 1166
 Backstrom, T. 1257(293), 1277
 Bäckvall, J.-E. 574(537–540), 595
 Bacon, R. G. R. 1008(59), 1014(94), 1047, 1048
 Baczynskyj, L. 233(10), 292
 Badawi, H. M. 723(656), 772
 Badol, C. 605(10), 756
 Badri, R. 1016(106, 107), 1048
 Baeckström, P. 890(204), 898
 Baeck, K. K. 12(7c), 85
 Baek, I. S. 911(71), 913
 Baertschi, S. W. 1140(57), 1166
 Baeyens, W. R. G. 1240(173), 1257(288), 1274, 1276
 Baeyens, W. 1257(275, 279), 1276
 Baeyer, A. 1002(14), 1020(121), 1046, 1048, 1140(2), 1165
 Bae, J. 290(585), 305
 Bagryanskaya, I. Y. 123(164), 143
 Bahrami, K. 368(144), 525(464), 585, 593
 Bailey, A. J. 1102(352), 1126
 Bailey, P. L. 366(139), 585
 Bailey, P. S. 716(615), 717(620, 626), 731(637, 674), 771, 772, 827(127), 830
 Bailey, S. M. 154(21), 168
 Bailey, T. R. 889(199, 200), 898
 Bai, Z. H. 1251(231), 1275
 Baj, S. 329(64), 583, 700(585), 707(604), 708(164), 760, 770
 Bakac, A. 1064(71), 1120
 Bakasov, A. 97(27b), 139
 Baker, A. G. 984(319a), 999
 Baker, J. C. 1228(102), 1272
 Bakken, V. 84(165b), 91
 Bakker, B. H. 199(87), 293
 Bakus, G. J. 190(24), 292
 Balasubramanian, D. 973(258), 996
 Balasubramanian, P. N. 443(319a), 590
 Balch, A. L. 138(138), 142
 Balci, M. 262(230), 264(391–398, 400, 401), 267(407, 409–415), 269(399), 297, 300, 301, 891(205a, b), 898
 Baldini, E. 701(381), 765
 Baldino, C. 1154(114), 1168
 Baldrige, K. K. 12(7b), 85
 Baldwin, A. C. 13(13), 86
 Balková, A. 12(7c), 85
 Balland, V. 1117(431), 1128
 Ballistreri, F. P. 185(41), 187, 432(302), 589, 1068(91), 1074(134), 1076(133), 1095(316), 1102(354, 355), 1120, 1121, 1125, 1126
 Ballou, D. P. 77(152b), 82(161), 91
 Ball, M. 357(120), 584
 Ball, S. 79(153a–c), 91
 Ball, V. 175(11), 183(10), 186
 Baltas, M. 201(91, 92), 294
 Baltork, I. M. 1018(114, 115), 1019(118), 1031(209–211), 1048, 1050
 Balzani, V. 1234(114), 1272
 Balzer, G. 743(21), 756
 Bamoniri, A. 1029(189), 1050
 Bandyopadhyaya, A. K. 1314(97), 1344
 Banfi, S. 375(156), 381(154), 531(321), 585, 590
 Banse, F. 1069(45), 1070(47), 1117(431), 1119, 1128
 Banthorpe, D. V. 427(281), 589
 Baouina, A. 973(249b), 995
 Baratti, J. 339(82), 583

- Barbara, C. 259(361), 300
 Barbas, C. 688(558), 769
 Barbier, J. 1114(11), 1118
 Barbin, A. 981(299b, 304, 307a, b), 984(297c, 297e, 297h), 998
 Barbush, M. 1263(328), 1277
 Barbuzzi, E. 1102(354, 355), 1126
 Barbuzzi, O. 284(540), 304, 1324(122), 1345
 Barb, W. G. 675(509), 768
 Barclay, L. R. C. 614(141), 759
 Bardet, M. 929(36b), 989
 Bard, A. J. 1234(135), 1273
 Bareket, Y. 1140(29), 1165
 Barentsen, A. R. W. 273(465), 302
 Barich, D. H. 873(167), 897
 Barieux, J. J. 183(29), 187
 Barker, C. M. 1082(203), 1123
 Barker, J. R. 18(18b), 45(45), 86, 87, 100(44), 140
 Barker, P. A. 221(204), 296
 Barkley, J. V. 381(159), 585
 Barlow, T. 984(297f), 998
 Barman, S. R. 1109(21), 1118
 Barnes, C. L. 290(592), 305
 Barnes, J. A. 728(665), 772
 Barnes, S. 951(174), 953(172), 993
 Barnette, W. E. 190(14), 292
 Barnett, N. W. 1257(273, 292, 298), 1266(334), 1276–1278
 Baronavski, A. 1261(321), 1277
 Barone, V. 12(7), 41(41), 44(102), 85, 87, 89
 Barrabee, E. B. 134(200), 144
 Barradell, L. B. 1281(6), 1342
 Barrault, J. 1114(11), 1118
 Barrau, J. 823(116), 830
 Barreiro, E. J. 1282(26), 1342
 Barrero, F. A. 1240(173), 1257(288, 301), 1274, 1276, 1277
 Barrett, A. G. M. 252(321), 299
 Barrett, C. S. 95(17a), 139
 Barrett, N. E. 636(299), 763
 Barrier, L. 614(135), 759
 Barrington, H. 613(118), 758
 Barrios, A. M. 1117(428), 1128
 Barroeta, A. C. 676(229), 761
 Barron, A. R. 118(137), 136(136), 142
 Barrow, S. E. 427(281), 589
 Bartberger, M. D. 37(37d), 55(55), 87, 1155(28), 1165
 Bartell, L. S. 102(54, 55), 140, 713(613), 771
 Bartlett, P. D. 48(117a, 117c), 89, 211(104), 213(159), 294, 295, 700(586a), 770, 835(41), 854(102), 894, 895, 900(50), 903(51), 906(49), 912, 1140(42a, b), 1166, 1172(10a), 1174(18a), 1184(21), 1205, 1206
 Bartlett, R. J. 8(8b), 12(7c), 85
 Bartoli, D. 1011(79–81), 1047
 Bartoli, J. F. 455(318), 531(322), 589, 590
 Barton, A. E. 318(9), 582
 Barton, D. H. R. 211(109, 110), 294, 324(36b), 582, 800(51), 801(52), 828
 Bartoschek, A. 252(322), 253(333), 299
 Bartosz, G. 972(253b), 995
 Bartsch, H. 980(290f), 981(296, 299a, b, 300–304, 307a, b), 984(297c, 297e, f, 297h), 997, 998
 Bart, J. J. 444(306), 589
 Barua, N. C. 273(56), 293
 Barusch, M. R. 356(119), 584
 Barz, M. 1076(156), 1122
 Bascetta, E. 254(254), 297, 310(7a), 581
 Basco, L. K. 1320(112), 1345
 Basile, L. J. 1030(196), 1050
 Basilico, N. 1313(80), 1344
 Baskakis, C. 885(188), 897
 Bastos, E. L. 1238(76), 1242(193), 1272, 1274
 Basu, A. K. 980(290c), 997
 Batcheller, S. A. 825(121, 123), 830
 Batinica, G. 1228(60), 1271
 Batten, R. J. 213(157, 163), 295
 Battioni, P. 443(319b), 457(324), 531(322), 590
 Battistuzzi, G. 370(146), 585
 Battoni, P. 455(318), 589
 Battu, S. 984(281c), 997
 Bauder, A. 101(46), 104(58), 140
 Bauer-Planck, C. 672(481), 768
 Bauer, R. 273(460), 302, 1336(154, 155), 1346
 Bauld, N. L. 717(620), 771
 Baumel, S. D. 285(285), 298
 Baumstark, A. L. 14(14b), 40(94b), 86, 89, 177(13), 183(12), 184(2), 186, 221(198, 199), 296, 1140(43, 46), 1160(144), 1163(1c), 1164, 1166, 1169, 1184(21), 1206, 1227(16, 89–91), 1266(333), 1270, 1272, 1277
 Baumstark, A. 352(28), 582
 Baum, G. 128(128), 142
 Bau, R. 1059(43), 1119
 Baxendale, J. H. 675(509), 768, 1242(183), 1274
 Baxter, J. N. 616(148), 759
 Bayer, O. 355(121), 584
 Bayes, K. D. 951(163), 993
 Baynes, J. W. 614(142), 759, 945(103), 991
 Bayot, D. 1069(65), 1120
 Bazhanov, A. V. 122(152), 142
 Bazzo, A. 1095(316), 1125
 Beak, P. 52(127), 90
 Beal, E. J. 617(157), 759
 Beaudoin, S. 567(531e), 595
 Bechara, E. J. H. 950(158, 159), 954(190, 193b), 992, 993, 1227(88), 1272
 Bechara, J. 610(72), 757
 Beckert, R. 1268(140), 1273
 Becker, C. 198(83), 293

- Becker, H.-D. 112(81), 113(82), *141*, 322(37), 326(38), 582
 Becker, K. H. 610(72), 757
 Becker, M. 1252(245), *1275*
 Beckhaus, H.-D. 161(44), 165(62), *169*
 Beckmann, O. 549(512a, b), 561(217), 562(497), 587, 594, 1113(409), *1127*
 Beckman, J. S. 22(22a, b), 25(25), 31(31), 34(34), 35(35), 86, 87, 612(86), 758, 951(166, 170), 952(171, 183), 993
 Beckman, K. B. 975(269a), *996*
 Beckman, T. W. 22(22a), 86, 951(170), 993
 Beckwith, A. L. J. 221(202–204), 296
 Beck, A. K. 408(222b), 587, 1094(296), *1125*
 Beck, J. S. 418(248), 588
 Beck, K. R. 1151(99a), *1167*
 Beck, M. 605(35), 756
 Beck, S. 12(7c), 85, 1215(39), 1255(38), *1271*
 Bedekar, A. V. 580(550), 596, 1027(174), *1049*
 Bedorf, N. 1145(67c, d), *1166*
 Bedossa, P. 613(115, 116), 758
 Beekman, A. C. 273(465, 466), 302
 Beek, A. K. 408(221), 587
 Beeley, P. 676(301), 763
 Beerthuis, R. K. 190(5), 292
 Beezer, A. E. 672(483–485), 768
 Bégué, J.-P. 473(366), 591
 Begue, J. P. 1021(138), *1049*, 1327(130), *1345*
 Begum, H. 267(267), 298, 1282(27), *1342*
 Begum, K. 225(220), 296
 Behar, J. V. 903(56–58), 912
 Behar, V. 1140(84), *1167*
 Beheshti, I. 1256(27, 233), *1271*, *1275*
 Behrman, E. C. 1008(57), *1047*
 Behrman, E. J. 1008(52, 57), 1009(61, 63), *1047*
 Beiler, T. W. 319(21), 582
 Beinhauer, A. 1181(11e), 1205(60a), *1206*, *1209*
 Bein, T. 446(328), 455(326, 329), 590
 Beland, F. A. 984(297a, 297g), 998
 Belas, F. J. 982(309), 998
 Belwe, J. S. 726(663), 772
 Belfiore, M. C. 560(510), 594, 1111(399), *1127*
 Belfoure, E. L. 1006(44), *1047*
 Belitskus, D. 105(64), *140*
 Bella, M. 514(440), 593
 Beller, M. 434(283), 449(336), 549(512a), 589, 590, 594
 Belli, A. 1010(77), *1047*
 Bello, V. 611(81), 758
 Bell, I. M. 338(81), 583
 Bell, J. 610(75), 757
 Bell, M. 605(27), 756
 Bell, R. P. 907(78a, b), 913
 Bell, T. N. 815(91c), 829
 Beltz, N. 648(307), 763
 Bemis, A. G. 360(132), 584
 Ben-Daniel, R. 579(549), 596, 1092(281), *1125*
 Benassi, R. 105(62b), 130(174), *140*, *143*
 Beneytout, J. L. 984(281c), 997
 Benigni, D. A. 112(74), *140*
 Bennani, Y. 567(531e), 595
 Benneche, T. 1152(101), *1167*
 Bennetau, B. 779(13a), 827
 Benoit-Vical, F. 284(541, 548), 286(557), *304*, *305*
 Beno, M. A. 861(94), 895
 Bensasson, R. V. 253(343), 299, 833(34), 894, 966(233b, c), 995
 Benson, S. W. 18(18b), 86, 100(44), *140*
 Benthin, G. 693(572), 770
 Bentley, P. A. 380(160), 381(175, 176), 382(178b), 585, 586
 Bentsen, J. G. 1067(79), *1120*
 Benzing, E. P. 213(159), 295, 700(586a), *770*
 Bercaw, J. E. 125(125), *142*
 Bérczi, B. 678(252), 762
 Beresnevich, L. B. 783(24), 827
 Bergamini, A. 1156(121d), *1168*
 Bergeron, S. 380(160, 162), 381(159), 585
 Berger, M. 678(517), 695(140), 759, 768, 922(35b), 931(34c), 938(48b, 63), 941(74a, b), 943(9a), 988–990, 1201(63a–c), 1202(64b), *1209*
 Berger, S. 177(15), 182(3, 27), *186*, *187*, *1204*(70), *1209*
 Bergmann, D. J. 605(36), 756
 Bergmark, W. 1212(8), *1270*
 Bergstad, K. 574(537), 595
 Beringer, F. M. 1013(87), *1047*
 Berkesi, O. 569(534), 595
 Berkessel, A. 382(179), 456(339), 471(363, 364), 509(331), 556(517), 558(362), 586, 590, 591, 595, 1100(347), *1126*
 Berlett, B. S. 918(12), 984(320), 989, 999
 Berlett, S. 973(197b), 994
 Berliner, J. A. 945(100), 991
 Berlin, K. D. 1043(270), *1051*
 Berman, P. A. 1311(42), *1343*
 Bernardinelli, G. 113(75), 122(159), *140*, *143*, 280(513, 514), 284(535, 537, 538, 540, 543–547), 285(550), 303, 304, 727(578), 770, 1324(122, 123), 1325(20), *1342*, *1345*
 Bernardi, F. 1182(24a, b), *1206*, 1228(93, 98), *1272*
 Bernasconi, C. F. 907(87), 913
 Bernengo, J. C. 1192(47e), *1208*
 Bernenshtein, E. 986(328b), 999
 Bernhardsson, A. 12(7d), 30(75a), 85, 88
 Bernheim, F. 666(450), 767
 Bernheim, M. L. C. 666(450), 767
 Bernholdt, D. E. 12(7c), 85

- Berning, A. 12(7d), 85
 Bernini, R. 370(146), 560(510, 511), 585, 594,
 1111(398–400), 1127, 1156(121b–d), 1168
 Bernstein, P. A. 1043(267), 1051
 Bernstein, R. 943(89b), 991
 Bernstein, S. 811(82, 83), 829
 Beroza, M. 737(690), 772
 Berrien, J.-F. 249(249), 297
 Berrien, J. F. 217(191), 296
 Berrisford, D. J. 1075(138), 1121
 Berry, K. L. 776(5), 827
 Berstein, I. A. 900(48), 912
 Berthelot, M. 111(22), 139
 Bertini, F. 1010(71), 1047
 Bertoli, M. 529(472b), 593
 Besseau, F. 111(22), 139
 Bessler, T. R. 949(108), 991
 Betancor, C. 230(223, 224, 227, 228), 297
 Bethell, D. 130(177–179, 186), 143, 422(256),
 588
 Bettinger, H. 724(659), 772
 Betzemeier, B. 384(187), 560(39), 582, 586
 Beuleke, M. 104(58), 140, 743(21), 756
 Beusen, D. D. 106(80), 140
 Bevan, R. 681(144), 759
 Beveridge, D. 6(6), 85
 Beving, D. E. 690(11), 756
 Bezuidenhout, B. C. B. 379(168), 585
 Bez, G. 273(56), 293, 1150(23), 1165
 Bhaduri, S. 425(264), 588
 Bharathi, B. 571(543), 596
 Bharti, N. 1058(32), 1119
 Bhattacharjee, M. N. 1074(127), 1121
 Bhattacharjee, M. 1109(21), 1118
 Bhattacharya, A. K. 273(55), 293
 Bhatt, A. K. 580(550), 596
 Bhatt, R. K. 379(169), 586
 Bhaumik, A. 1111(401), 1127
 Bhengu, T. T. 1058(35), 1119
 Bhooi, N. 670(476), 767
 Bhowmick, T. 1116(423), 1128
 Bhushan, V. 520(454), 593
 Biagini, G. A. 273(454), 302
 Bialas, J. 1158(32), 1165
 Bianchi, D. 362(134c), 529(472a, b), 585, 593
 Bianchi, G. 964(228), 995
 Bianchi, M. 1115(414), 1127
 Bickelhaupt, F. 199(85), 293
 Bickel, A. F. 900(29), 912
 Bickley, J. F. 223(207), 275(487), 280(526),
 296, 303, 304, 1323(121), 1345
 Bielski, B. H. J. 131(187), 143
 Bielski, B. H. 945(123), 992
 Bienewald, F. 1100(345, 346), 1126
 Bienvenu, C. 939(70a, b, 71, 72), 990
 Bierl, B. A. 737(690), 772
 Biermann, M. 196(73), 293
 Bigdeli, M. A. 1028(183), 1049
 Bigger, S. W. 673(500), 768
 Biggs, P. 138(210b), 144
 Billeter, S. R. 82(160), 91
 Bilski, P. 610(80), 757
 Bil, A. 84(164), 91
 Bino, A. 1067(80), 1120
 Biox Bernadini, C. 1161(105), 1167
 Birke, A. 235(235), 297, 352(17), 582
 Birks, J. W. 1188(40f), 1207, 1257(267),
 1261(319), 1262(318, 324, 325), 1276, 1277
 Birss, V. I. 650(363), 765
 Bisakowski, B. 676(473), 767
 Bischoff, C. 316(4), 354(115, 116), 581, 584
 Bischof, P. 72(72a), 88
 Bishop, C. E. 177(18), 187
 Bishop, L. P. D. 1304(63), 1332(93), 1343,
 1344
 Bishop, L. P. 1304(71), 1344
 Bishop, M. C. 676(458), 767
 Bixon, M. 1217(45), 1271
 Blackwell, W. 676(301), 763
 Blagojević, S. 623(208), 652(379), 761, 765
 Blair, I. A. 981(295), 982(309), 997, 998
 Blair, R. A. 95(13a), 139
 Blake, D. 945(102), 991
 Blancafort, L. 1182(23), 1206
 Blanchette, P. E. 65(97), 89
 Bland, J. 1037(236), 1051
 Blaschette, A. 779(15a–c), 827, 1004(25),
 1046
 Blasco, T. 564(506), 594, 1111(403), 1127
 Blatter, F. 871(162), 897
 Blat, E. J. 163(5), 167
 Blazejowski, J. 1253(235, 241), 1275
 Blazej, T. P. 982(291a), 997
 Bleasdale, C. 982(291d), 997
 Blekas, G. 664(443), 767
 Blitz, H. 1172(2), 1205
 Bloch, R. 1021(127), 1048
 Blomquist, A. T. 900(48), 912
 Blom, C. E. 101(46), 140
 Bloodworth, A. J. 238(165, 221, 238, 251),
 240(261), 250(250), 252(252), 256(256),
 259(259), 260(260), 262(262), 270(270),
 273(325), 285(552–554), 286(555, 556),
 295, 297–299, 304, 305, 317(26), 324(36a),
 358(127, 128), 582, 584, 783(26), 827
 Bloomfield, M. S. 658(134), 759
 Blümel, J. 569(534), 595
 Boatz, J. A. 12(7b), 85
 Bobrowski, M. 253(337), 299
 Bocelli, G. 122(101), 141
 Boche, G. 118(122), 124(124), 142, 1067(57),
 1119
 Bockhorn, H. 103(57), 140
 Bock, H. 1257(299), 1277
 Bock, R. 621(181), 760
 Boddenberg, A. 638(314), 764

- Bodin, A. 326(60), 583
 Bodley, A. L. 1289(46), 1343
 Boehlow, T. R. 1091(222), 1123
 Boese, R. 1154(112), 1168
 Bofill, J. M. 36(87), 77(77a), 88
 Boggs, J. E. 100(28b), 139
 Bohe, L. 1021(135), 1048
 Bohm, M. C. 861(94), 889(199), 895, 898
 Bohm, M. 267(420), 301
 Boitsov, S. 518(407), 592
 Boix-Bernardini, C. 1158(132), 1169
 Bolarinwa, B. 641(8), 756
 Boldyrev, A. I. 744(705), 773
 Bolland, D. M. 1145(67b), 1166
 Bollyky, L. J. 1256(254), 1266(305), 1275, 1277
 Bolm, C. 434(283), 447(333), 449(336), 458(332), 487(390), 542(216), 549(512a, b), 556(518a), 561(217), 562(497), 569(535b), 587, 589–591, 594, 595, 1023(151), 1049, 1075(138), 1093(292), 1100(136, 345, 346), 1113(409), 1121, 1125–1127
 Bolte, J. 1006(42), 1047
 Bolte, M. L. 199(89), 294
 Bolton, J. L. 976(270b), 996
 Bonadies, F. 414(232), 488(392), 493(391, 393, 394), 587, 591, 1097(333), 1126
 Bonchio, M. 1068(87), 1074(134), 1076(162), 1077(160), 1078(163, 165), 1095(306, 311), 1096(130), 1098(99, 100, 131), 1107(166, 167), 1110(22), 1115(414), 1118, 1120–1122, 1125, 1127
 Bondioli, P. 656(402), 766
 Bondi, A. 118(65), 140
 Bond, J. D. 617(156), 759
 Bonetti, G. A. 520(450), 593
 Bonhoure, A. 284(548), 304
 Bonini, C. 1161(149b), 1169
 Bonini, M. G. 952(178, 184), 953(185), 963(220), 993, 994
 Bonk, J. D. 276(498–500), 303, 1286(41), 1314(64, 96), 1343, 1344
 Bonnefont, D. 667(456), 767
 Bonnet-Delpon, D. 473(366), 591, 1327(130), 1345
 Bonville, P. 1069(49), 1119
 Bon, G. B. 614(128), 759
 Boonefaes, T. 610(71), 757
 Boorstein, R. J. 928(37c), 989
 Boothe, R. 196(60), 293
 Borbon, A. 605(10), 756
 Bordiga, S. 1082(202), 1123
 Borhan, B. 1023(147, 148), 1024(156), 1030(197), 1049, 1050
 Börje, A. 574(540), 595
 Bornaz, C. 163(51), 169
 Born, L. 124(147), 142, 728(666), 772
 Borseth, D. G. 723(656, 657), 772
 Borstnik, K. 273(37, 447, 468, 469), 283(524), 292, 302, 304, 1314(84), 1326(126), 1337(164), 1344–1346
 Bortolini, O. 432(302), 589, 1021(142), 1049, 1068(89, 90, 92), 1070(108–111), 1095(179, 313, 314), 1097(329), 1098(99, 100), 1105(373, 374), 1106(376), 1107(166, 167), 1110(22), 1118, 1120–1122, 1125–1127
 Bortolomeazzi, R. 690(564), 770
 Bortolo, R. 362(134c), 529(472a), 585, 593
 Boschung, A. F. 835(41), 861(131), 894, 896
 Bose, D. S. 1028(181, 185, 186), 1049, 1050
 Böse, R. 72(72e), 88
 Bosio, S. G. 112(84), 141, 260(372), 300, 869(145), 896, 1178(19a–e), 1206
 Bosio, S. 253(333), 299
 Boskou, D. 664(443), 767
 Bosnich, B. 1067(76), 1120
 Bosque-Sendra, J. M. 1240(173), 1274
 Boss, B. 339(78), 583
 Bos, R. 1257(273, 292, 298), 1266(334), 1276–1278
 Bothwell, B. D. 270(270), 298
 Boto, A. 230(223, 224, 226–228), 297
 Botsoglou, N. A. 669(466), 767
 Botta, M. 1025(165), 1049
 Bottke, N. 875(174), 897
 Bottle, S. E. 193(68), 293, 1155(119a), 1168
 Bottoni, A. 1182(24a), 1206, 1228(93), 1272
 Bott, S. G. 1067(79), 1120
 Boucheron, J. A. 981(298a), 998
 Bouchoule, C. 1114(11), 1118
 Bouchoux, G. 1069(45), 1070(47), 1119
 Bouchy, A. 30(75b), 88
 Bouérat, L. 1140(88), 1167
 Bougauchi, M. 390(197), 392(195, 196), 586
 Bouh, A. O. 466(360), 591, 1083(227), 1123
 Bouillon, G. 13(13b), 86
 Boukouvalas, J. 113(75), 140, 213(156), 217(190), 229(222), 278(509), 284(508), 510, 537, 539, 549, 285(550), 295–297, 303, 304, 727(578), 770
 Boulet, S. L. 1142(62), 1166
 Bourdat, A.-G. 933(58b), 990
 Bourgeois, M.-J. 710(575), 770
 Bourne, S. A. 264(395), 300
 Boussac, A. 1070(47), 1119
 Boutevin, B. 622(186), 760
 Boveris, A. 949(135–137), 992
 Bovey, F. A. 695(496), 709(599), 768, 770
 Bovicelli, P. 1150(92), 1160(136), 1161(147), 1162(151b, c), 1167, 1169
 Bowes, C. M. 198(78), 293
 Bowry, V. W. 10(24a), 86
 Bowyer, K. J. 358(128), 584
 Box, H. C. 933(58a), 990
 Boyd, D. R. 1155(106a), 1168, 1200(58c), 1208

- Boyd, L. C. 737(693), 772
 Boyd, R. J. 1203(67a), 1209
 Boykin, D. W. 177(13), 183(12), 184(2), 186
 Boyland, E. 1009(62), 1039(246), 1047, 1051
 Boyle, R. 1200(58c), 1208
 Bozzelli, J. W. 103(57), 140
 Braeckman, B. P. 1251(230), 1275
 Bragante, L. 1105(373), 1127
 Brandi, A. 536(484), 594
 Brandl, H. 1184(25f), 1188(36), 1207, 1236(145), 1242(171), 1245(209), 1268(335), 1273, 1274, 1278
 Brash, A. R. 949(133), 992
 Braslau, R. 1032(3), 1046
 Brasseur, N. 967(236), 995
 Braumann, U. 1322(120), 1345
 Braun, A. M. 184(33), 187
 Braun, M. 888(192), 897
 Braun, S. 182(3, 27), 186, 187
 Brau, F. 1192(47e), 1208
 Bravo, A. 45(92, 106a–d), 89, 1160(35a–e), 1165
 Bray, D. H. 280(514), 303, 1325(20), 1342
 Bray, J. F. 283(471), 302, 1337(162), 1346
 Bray, P. G. 223(207), 273(453, 454, 467), 275(489), 296, 302, 303, 1283(31), 1304(71), 1313(34), 1320(115), 1323(121), 1330(132), 1332(92), 1337(165), 1343–1346
 Bray, R. C. 80(151), 91
 Brazzi, E. 131(131), 142, 1117(432), 1128
 Brechot, P. 423(262), 588, 1085(142), 1121
 Brecht, R. 267(418–420), 301
 Brede, O. 316(25), 582, 1244(199), 1274
 Breen, A. P. 920(23a), 989
 Bregeault, J.-M. 470(354), 590, 1063(64), 1085(242), 1120, 1124
 Brégeault, J.-M. 1069(117), 1121
 Breitenbach, J. W. 163(46), 169
 Breitmaier, E. 134(199), 144
 Brendel, H.-D. 800(48), 828
 Brenek, S. J. 1023(149), 1049
 Brennan, G. 613(118), 758
 Brenner, M. 856(112), 896
 Bresnick, L. 1236(35), 1271
 Bressel, B. 779(15a, b), 827, 1004(25), 1046
 Brestel, E. P. 1242(186), 1274
 Breton, G. W. 1025(161), 1049
 Breuckmann, R. 196(74), 293
 Breunig, H. J. 713(612), 771, 1067(81), 1120
 Brickwood, A. C. 256(358), 300
 Bridger, R. F. 900(9), 912
 Briehl, M. M. 1336(156), 1346
 Briggs, A. D. 367(140), 585
 Bright, F. V. 576(546), 596
 Brignac, P. J. 638(311), 764
 Brik, M. E. 1026(172), 1049
 Brill, W. F. 1055(9, 10), 1118
 Briner, E. 165(55), 169
 Bringmann, G. 1081(149), 1122
 Bringmann, G. 123(163), 143
 Brinker, U. H. 870(161), 897
 Brinkman, U. A. T. 643(332), 764, 1257(258, 259, 262, 297), 1276, 1277
 Briones, J. A. 118(127), 142
 Brisaert, M. 659(419), 766
 Britigan, B. E. 610(79), 757
 Briviba, K. 269(421), 301, 949(140), 950(153, 158, 159), 992, 1155(118a), 1168
 Brizuela, C. L. 273(475), 303, 319(19), 582
 Broucker, U. 269(424), 301
 Brockmann, K. J. 610(72), 757
 Brødsgaard, S. 635(9), 699(582a), 756, 770
 Bronstein, I. 1188(34a, 37a), 1197(50), 1198(33c–f, 54), 1199(48), 1200(53a, b), 1207, 1208, 1236(35, 160, 163), 1238(168), 1256(249), 1271, 1273–1275
 Brooks, C. D. 1094(303), 1125
 Brooks, P. J. 1266(333), 1277
 Brossi, A. 273(440), 301
 Brovko, L. Y. 1248(215), 1275
 Brovko, L. Yu. 1194(51), 1208
 Brownlie, I. H. 901(39), 912
 Brown, D. 425(268), 588
 Brown, G. D. 133(196a, b), 144, 288(567–569), 305, 690(492), 768
 Brown, G. 1335(149), 1346
 Brown, J. H. 776(4), 827, 1042(261), 1051
 Brown, P. A. 367(140), 585
 Brown, R. S. 57(51a), 87
 Brown, T. 984(297f), 998
 Broxterman, Q. B. 123(162), 143
 Brozmanova, J. 670(478), 768
 Brubaker, C. H. 419(258), 425(244), 588
 Bruckert, E. 612(105), 758
 Bruggeman, J. 1257(275, 279), 1276
 Brugger, R. 94(6), 138
 Bruice, T. C. 79(153a–d), 80(151), 91, 443(319a), 590, 1251(220, 221), 1275
 Brumer, J. G. 262(377), 300
 Brunel, J. M. 480(375), 487(379, 380), 591, 1097(326, 327), 1126
 Brunken, J. 253(2), 292
 Brünker, H.-G. 853(82), 869(93), 888(47, 48, 193), 894, 895, 897
 Brünker, H. G. 343(90), 345(95), 583, 584
 Brunner, B. A. 984(317d), 999
 Brunner, G. 1293(37, 51), 1343
 Bruns, R. E. 624(228), 761
 Bruns, R. 130(170), 143
 Brun, P. 449(337), 590
 Brun, R. 274(484), 303, 1332(15), 1342
 Bruun-Jensen, L. 678(520), 768
 Bruylants, A. 899(3–5), 912
 Bubb, W. A. 959(203), 968(240), 994, 995
 Büchi, G. 1140(55b), 1166

- Buchko, G. W. 941(74a, b), 990, 1201(63a, b), 1209
- Buchs, P. 273(440), 301
- Buchwald, G. 861(130), 896
- Budde, P. 1336(158), 1346
- Budzinski, E. E. 933(58a), 990
- Buege, J. A. 977(277e), 996
- Buell, G. A. 811(82, 83), 829
- Buettner, G. R. 610(79), 757
- Bui, T. T. T. 382(181), 586
- Bukhave, K. 680(532), 769
- Bulman Page, P. C. 503(420), 592
- Buncel, E. 783(18a–c), 827
- Buneeva, E. I. 674(501), 768
- Bunker, S. P. 622(191), 760
- Bunnage, M. E. 259(364), 300
- Bunnelle, W. H. 71(71), 88, 290(592), 305, 729(670), 772
- Buntain, G. A. 1007(47), 1047
- Bunting, S. 214(166), 295
- Bunton, C. A. 362(136a), 585
- Buono, G. 339(82), 583
- Bupp, J. E. 276(493), 303, 1282(23), 1342
- Burant, J. C. 12(7), 85
- Buratti, W. 1010(71), 1047
- Burcham, P. C. 917(2a), 945(118), 984(316), 988, 992, 998
- Burdett, J. K. 101(53), 140
- Burd, V. N. 283(283), 298
- Burford, A. 1256(27), 1271
- Burger, F. 981(303), 998
- Burger, U. 284(508, 540), 303, 304, 1293(37, 51), 1324(122), 1343, 1345
- Burgess, J. R. 177(17, 18), 187
- Burgess, K. 1082(168), 1122
- Burgin, H. 273(273), 298, 608(59), 757, 1332(14), 1342
- Burgos Paci, M. A. 705(24), 756
- Burnett, M. N. 196(60), 293
- Burns, D. A. 663(434), 766
- Burns, D. M. 1228(102), 1272
- Burns, P. A. 1256(29), 1271
- Burrows, C. J. 920(23b), 943(93a, b, 94), 945(98), 974(263), 989, 991, 996, 1027(179), 1049, 1204(69a–c), 1209
- Burse, M. M. 1240(175), 1274
- Burstein, A. I. 1188(37b), 1207
- Burstyn, J. N. 1087(259), 1124
- Burton, G. W. 614(141), 759
- Bush, K. M. 952(171), 993
- Bush, M. 255(255), 297, 700(586b), 770
- Busing, W. R. 101(15), 139
- Bussey, R. J. 903(55), 912
- Buss, H. 987(331c), 999
- Bustos, D. A. 289(578), 290(582), 305
- Bustos, D. 290(589, 590), 305
- Butler, A. R. 273(31), 292, 608(55), 757
- Butler, A. 1077(59), 1095(88), 1119, 1120
- Butler, J. 945(125), 992
- Butterfield, S. M. 974(262c), 996
- Buttner, F. 267(420), 301
- Buxton, G. V. 971(199a), 994
- Byers, A. 556(524), 595
- Byers, J. D. 233(11–13), 292
- Byriel, K. A. 136(202), 144
- Byrne, A. 273(467), 302, 1337(165), 1346
- Cabo, N. 661(425–429), 666(408), 766
- Caceres, T. 949(138), 992
- Cadenas, E. 949(135–137), 950(156), 992
- Cadena, R. 1007(46), 1047
- Cadet, J. 269(423), 301, 616(149), 678(517), 695(140), 759, 768, 921(31a, b, 32, 33), 922(35a, b, 38, 39a, b, 40), 926(7, 49), 927(30a, b, 51, 52), 928(37a–c), 929(36a, b, 53), 930(29a, b, 43a, b, 55), 931(34a–c), 933(54, 58b, 59), 934(60a, b), 935(64), 938(48a, b, 63), 939(70a, b, 71, 72), 940(75a, 77), 941(74a, b, 80a, b), 942(84), 943(9a–c, 85c, 86, 87, 90, 91), 947(127), 950(151), 951(164), 967(238c), 974(262a, b), 975(268a–c, 269b), 976(270a, 270c, 273), 977(274a, b, 275a–c), 984(294b, c), 988–993, 995–997, 1201(63a–c), 1202(64b), 1203(67b), 1209
- Cadilla, C. 1232(124), 1273
- Cadiz, C. 235(235), 297
- Cádiz, C. 352(17), 582
- Cadwallader, K. R. 680(534), 769
- Cady, G. H. 1004(36), 1046
- Cafferro, T. 283(530), 304
- Cafferata, L. F. R. 165(54), 169
- Caignard, D. H. 273(458), 302
- Caillat, S. 943(87), 991
- Cainelli, G. 575(533), 595
- Cais, R. E. 709(599), 770
- Cai, H. 984(313), 998
- Cai, J. 286(558), 305
- Cai, R. 630(265), 634(295), 639(315), 762–764
- Cai, W. 1023(149), 1049
- Čajlaković, M. 630(263), 762
- Caldwell, S. E. 217(169, 181, 182), 295, 296
- Calleri, M. 106(78), 125(150), 140, 142
- Calloni, S. 1096(130), 1121
- Calpini, B. 605(35), 756
- Calvo, E. J. 701(381), 765
- Camaioni, D. M. 1008(58), 1047
- Camargo Matos, R. 650(362), 765
- Camastra, C. 611(81), 758
- Cambolor, M. A. 418(247), 588, 1083(209), 1123
- Cambrissin, S. 254(347), 299
- Camerman, A. 112(88), 141
- Camerman, N. 112(88), 141
- Cameron-Smith, P. J. 605(36), 756
- Camici, L. 797(42), 828

- Caminiti, R. 1083(225), *1123*
 Cammi, R. 12(7), 85
 Campagnole, M. 710(575), *770*
 Campana, C. F. 1082(192, 197), *1123*
 Campanella, L. 664(440), *767*
 Campa, A. 963(217), *994*, 1193(49b), *1208*
 Campbell, A. K. 1222(1), 1256(233, 252),
1270, *1275*
 Campbell, G. R. 613(118), *758*
 Campbell, I. B. 1100(349), *1126*
 Campbell, N. J. 1069(101), *1120*
 Campbel, N. J. 1057(19), *1118*
 Campestrini, S. 1031(202, 207, 208), *1050*,
 1095(311), 1105(374), 1110(392), *1125*,
1127
 Camporeale, M. 785(29), *827*
 Campos Neves, A. S. 516(427), *592*
 Campos, I. P. D. 1263(320), *1277*
 Campos, O. 512(430), *592*
 Campo, C. K. 943(95), *991*
 Camuzat-Dedenis, B. 283(534), *304*
 Camu, F. 659(419), *766*
 Candeias, L. P. 917(5d), 940(76), 988, *991*,
 1201(61b), *1209*
 Canepa, C. 43(38), 47(107), 65(97), 73(19c),
 78(20c), 86, 87, 89, 1140(50), 1160(53),
1166
 Canfield, C. J. 284(540, 546), *304*, 1281(5),
 1324(122), *1342*, *1345*
 Canosamas, C. E. 138(210b), *144*
 Canova, S. 917(4), *988*
 Cantos, M. 29(64), *88*
 Cao, G.-A. 1150(94), *1167*
 Cao, Q. 909(93), *913*
 Cao, Y. 527(466), *593*
 Capdevielle, P. 254(347), *299*
 Capella, P. 692(93), *758*
 Capozzi, M. A. M. 487(388), *591*
 Cappi, M. W. 380(160, 171), 381(159, 176),
 585, *586*
 Carbonell, L. F. 614(136), *759*
 Cardellicchio, C. 487(388), *591*
 Cardellini, L. 1105(373), *1127*
 Carde, L. 381(174), *586*
 Cardini, G. E. 1200(58b), *1208*
 Cardin, C. J. 730(671), *772*
 Cardin, D. J. 730(671), *772*
 Cardona, F. 536(484), *594*
 Careno, M. C. 1095(310), *1125*
 Carew, T. E. 612(104), *758*
 Carey, F. A. 79(155), *91*
 Carless, H. A. J. 213(157, 163), *295*
 Carloni, P. 1155(119b), *1168*
 Carlson, R. G. 1263(316, 328), *1277*
 Carlsson, D. J. 673(500), *768*
 Carmen González, M. 709(62), *757*
 Carmichael, P. L. 981(299a), *998*
 Carmona, D. 1064(68), *1120*
 Carnduff, J. 323(46), *582*
 Carnell, A. J. 110(99), *141*
 Caroff, E. 382(181), *586*
 Carofiglio, T. 1068(87), *1120*
 Caro, H. 1002(17), *1046*
 Carpenter, B. K. 262(378), *300*
 Carpenter, J. E. 95(13b), *139*
 Carraro, M. 1070(109–111), 1107(166), *1121*,
1122
 Carraway, E. R. 1262(326, 327), *1277*
 Carrea, G. 75(146), 90, 384(185), 476(368b,
 369), 586, *591*
 Carrell, H. L. 106(80), *140*
 Carroll, F. I. 291(595), *305*
 Carr, A. 1257(294), *1277*
 Carr, G. 558(491), *594*
 Carr, R. V. C. 263(381), 284(284), 298, *300*,
 343(92), 584, 852(75), 895
 Carson, A. S. 163(48, 49), *169*
 Carter, K. N. 935(61, 62), *990*
 Carter, R. L. 217(183), *296*
 Carter, T. P. 731(637), *771*
 Carté, B. 134(200), *144*
 Carvalho, V. M. 984(294b, c), *997*
 Casallanovo, F. 1260(317), *1277*
 Casal, H. L. 1140(31), *1165*
 Casarini, A. 800(50), *828*
 Casella, L. 384(185), 476(368a, b, 369), 586,
591
 Časný, M. 186(42), *187*
 Caspar, A. 270(431), *301*
 Cassidei, L. 1155(115), 1160(142), 1163(25),
1165, *1168*, *1169*
 Cassinelli, M. E. 621(179), *760*
 Cass, M. W. 1191(8a), *1205*, 1251(237, 240),
1275
 Casteel, D. A. 94(3b), *138*, 190(17, 18), *292*,
 888(189), 897, 1333(135, 136), *1345*
 Castellanos, M. G. 165(54), *169*
 Castellano, G. 1160(138, 139b), *1169*
 Castranova, V. 660(110), *758*
 Castro, E. A. 164(53), 165(54), *169*
 Catalani, L. H. 950(159), 954(190, 193b),
 963(217), 992–994, 1193(49b), *1208*,
 1235(24), 1236(74, 75), *1270*, *1272*
 Catalani, L. 852(72), *895*
 Cataldo, M. 539(496), *594*, 1109(122), *1121*
 Cathcart, R. 977(277g), *996*
 Catherall, C. L. R. 1188(39, 40a, b), *1207*,
 1267(72, 323), *1272*, *1277*
 Cativiela, C. 245(281), *298*
 Catlow, C. R. A. 1082(203), *1123*
 Caughman, C. R. 737(693), *772*
 Cayota, A. 741(698), *772*, 951(168), *993*
 Cayuela, G. 689(390), *765*
 Cazelles, J. 273(452), 283(534), *302*, *304*,
 1298(56), 1306(72), 1312(79), 1320(43),
1343, *1344*

- Cazzolato, G. 614(128), 759
 Ceccherelli, P. 1026(169), 1029(190, 194),
 1049, 1050
 Celani, P. 12(7d), 85
 Çelebi, S. S. 700(557), 769
 Celik, M. 264(401), 267(407), 301
 Celina, M. 685(543, 544), 769
 Centone, D. 688(556), 769
 Cerfontain, H. 183(31), 187, 199(87), 293
 Cerioni, G. 183(32), 186(44), 187
 Cerkovnik, J. 131(192a), 132(193), 144,
 182(20–25), 187, 812(84), 829
 Cermola, F. 108(100), 112(103), 118(118),
 141, 142, 259(367), 273(438), 300, 301
 Chabaud, B. 513(431), 592
 Chabner, B. A. 1145(67a), 1166
 Chabot, B. M. 800(51), 801(52), 828
 Chadha, R. 259(363), 300
 Chadwick, D. J. 130(177–179, 186), 143
 Chadwick, J. 273(467), 302, 1337(165), 1346
 Chadwick, James 1268(336), 1317(68), 1342,
 1344
 Chaichi, M. J. 649(357), 765, 1257(271), 1276
 Chaitanawisuti, N. 1334(144), 1346
 Chai, X.-S. 627(251), 762
 Challacombe, M. 12(7), 85
 Chalom, J. 1257(260), 1276
 Chambers, R. C. 1081(171), 1122
 Chambers, R. D. 539(490), 594
 Chamblee, M. L. 1227(91), 1272
 Chance, B. 949(135–137), 992
 Chancharme, L. 612(105), 758
 Chandrasekaran, S. 503(423), 592
 Chandrasekhar, J. 267(416), 301, 870(157),
 897
 Chandra, S. 274(479, 480), 303, 1326(127),
 1345
 Chandross, E. A. 1188(38), 1207, 1261(6),
 1270
 Chang, B. H. 419(258), 425(244), 588
 Chang, C. D. 539(492), 594
 Chang, E. P. 901(44), 912
 Chang, H. M. 273(28), 292
 Chang, H. O. 280(526), 304, 1306(38), 1343
 Chang, H. S. 1001(11), 1036(232), 1037(234),
 1046(277), 1046, 1051, 1052
 Chang, M. M. 1234(135), 1273
 Chang, P.-C. 634(195), 760
 Chang, R.-C. 725(660), 772
 Chang, Y. C. 1172(4b, 6), 1191(8b), 1205
 Chanon, F. 204(101), 294
 Chanon, M. 204(101), 294
 Chantegrel, B. 918(10), 989
 Chan, H. W. S. 951(162), 993
 Chan, H. W. 273(450), 302, 1317(68, 87,
 100), 1343, 1344
 Chan, W.-K. 1140(80), 1167
 Chan, Y.-Y. 854(105, 107), 896
 Chapman, D. C. 795(40), 828
 Chapman, J. 1178(19d), 1206
 Chappell, M. D. 1154(113), 1168
 Charles, H. C. 1035(227), 1051
 Charles, M. J. 981(298b), 998
 Charlotte, F. 613(116), 758
 Charman, S. A. 1332(15), 1342
 Charman, W. N. 1332(15), 1342
 Charman, W. 276(501), 303
 Charpentier, R. 523(459), 593
 Chase, M. W. 15(15), 86
 Chassagnard, C. 270(431), 301
 Chatgılıaloglu, C. 920(25), 989
 Chattopadhyay, S. 690(11), 756
 Chaudhuri, M. K. 1074(127, 128), 1109(21),
 1116(423), 1118, 1121, 1128
 Chaudière, J. 669(470), 767
 Chaudière, J. 669(471), 767
 Chauhan, V. S. 1283(33), 1313(82), 1343,
 1344
 Chaumette, P. 426(276), 588, 1116(56), 1119
 Chavez, F. A. 118(127), 130(130), 142
 Che Man, Y. B. 662(210), 663(234), 761
 Cheeseman, J. R. 12(7), 85
 Chelli, M. 107(87), 141
 Cheng, G. 653(385), 765
 Cheng, H. N. 695(496), 768
 Cheng, X. 854(90), 895
 Cheng, Y.-S. 726(661), 772
 Chen, B.-Z. 77(77b), 88
 Chen, B. 870(152), 897
 Chen, F. E. 1015(103), 1016(105), 1048
 Chen, F. N. 1015(101, 102), 1048
 Chen, H.-C. 634(195), 760
 Chen, H.-H. 1336(157, 159), 1346
 Chen, H. J. C. 945(117), 984(297b), 992, 998
 Chen, H. J. 981(305a, 305c), 982(291e), 997,
 998
 Chen, H. 527(466), 593
 Chen, J. D. 512(408), 514(409a, b), 526(410),
 592
 Chen, J. S. 833(35), 894
 Chen, J. X. 534(480), 594
 Chen, J. 22(22a, b), 86, 418(252), 588,
 832(19), 894, 951(170), 993, 1103(359,
 360), 1106(381), 1126, 1127, 1140(87),
 1155(28), 1165, 1167
 Chen, K. 1069(50), 1117(430), 1119, 1128
 Chen, L.-H. 640(322), 764
 Chen, L.-Y. 608(49), 757
 Chen, M.-F. 612(106), 758, 833(26), 854(96),
 894, 895
 Chen, M. 1322(119), 1345
 Chen, Q.-C. 701(589), 770
 Chen, Q.-Y. 639(316, 317), 640(321), 764
 Chen, Q. 1082(191, 192, 194, 197), 1122,
 1123
 Chen, S. L. 741(702), 773

- Chen, S. Y. 892(210), 898
 Chen, S. 1008(57), 1047
 Chen, T.-S. 1198(33a), 1207
 Chen, T. S. 1236(33), 1271
 Chen, W. P. 380(170), 586
 Chen, W. 12(7), 85
 Chen, X.-L. 640(319), 764
 Chen, X. W. 1322(117, 118), 1345
 Chen, X. 516(436), 592, 845(66), 847(68), 895
 Chen, Y.-S. 503(425), 592
 Chen, Z. P. 1228(102), 1272
 Chepanoske, C. L. 974(263), 996
 Chern, C.-I. 315(32b), 582
 Chettri, S. K. 1109(21), 1118
 Cheung, K.-K. 1140(81a, 87), 1146(17), 1165, 1167
 Cheung, M. K. 1317(87, 100), 1344
 Cheung, W. H. 511(418), 592
 Chevion, M. 986(328b), 999
 Chew, S. Y. 288(571), 305
 Che, C.-M. 511(418), 592, 1140(80), 1167
 Chianelli, D. 1011(79–81), 1047
 Chiang, J. P. 468(351), 534(482), 590, 594, 802(54), 828, 1083(217), 1123
 Chiang, L. C. 984(297b), 998
 Chiang, S. Y. 984(297d), 998
 Chiari, G. 106(78), 125(150), 129(175), 140, 142, 143
 Chiaroni, A. 280(529), 304
 Chiba, H. 693(570), 770
 Chiba, N. 681(540), 769
 Chiba, S. 1199(55), 1208, 1236(149), 1273
 Chickos, J. S. 155(22), 160(38), 165(17), 167–169
 Chidambaram, N. 503(423), 592
 Chien, C.-S. 426(279), 589
 Chignell, C. F. 610(80), 757
 Chima, J. 1200(58c), 1208
 Chishiro, T. 1067(55), 1119
 Chishtii, A. H. 1322(81), 1344
 Chitambar, C. R. 273(461), 302
 Chiu, F. C. K. 1332(15), 1342
 Chmela, S. 684(214), 761
 Chmielewski, M. 348(18), 493(100, 101), 582, 584, 1099(343), 1126
 Choe, M. 945(121), 992
 Choi, C. H. 1015(100), 1048
 Choi, H. C. 1014(92, 93, 96–98), 1015(99), 1042(251), 1048, 1051
 Choi, H. 608(53), 757
 Choi, J.-S. 607(48), 757
 Choi, S. Y. 44(104), 89, 901(42), 911(90), 912, 913
 Chojnowski, J. 803(56), 804(58), 828
 Chokshi, H. P. 1263(328), 1277
 Chollet, J. 277(277), 298, 1332(15, 105), 1342, 1344
 Cholli, A. L. 692(215), 761
 Chong, A. O. 423(237), 587, 1075(140), 1121
 Chong, W. K. M. 275(492), 276(441), 493–498, 302, 303, 1282(23), 1314(21, 22, 24, 94–96), 1342, 1344
 Chottard, G. 1069(117), 1121
 Choudary, B. M. 512(411), 518(446), 569(535c, d), 571(542, 543), 573(541), 592, 593, 595, 596, 1095(308), 1125
 Chou, C.-H. 198(80), 293
 Chou, C. K. 1336(153), 1346
 Chou, S.-S. 634(195), 760
 Chou, S.-T. 669(465), 767
 Chou, W.-S. 273(29), 292
 Chowdari, N. S. 569(535c, d), 571(542), 573(541), 595, 596
 Chowdhury, F. A. 252(312, 314, 315), 299
 Chow, M.-F. 167(64), 169, 269(427), 301, 819(106), 829, 1232(121), 1273
 Cho, K. I. 1014(98), 1048
 Christensen, C. S. 635(9), 756
 Christensen, E. 1322(120), 1345
 Christensen, S. B. 1322(119, 120), 1345
 Christen, D. 94(11a), 104(58), 139, 140
 Christiansen, P. A. 3(3b), 85
 Christian, G. D. 640(323), 764
 Christophersen, C. 190(25), 292, 1333(138), 1345
 Christoph, G. G. 861(94), 895
 Christova-Gueogueieva, N. I. 981(298b), 998
 Christ, H. A. 172(6), 183(4), 186
 Chrobok, A. 329(64), 583, 700(585), 708(164), 760, 770
 Chronakis, N. 860(127), 896
 Chuang, C. C. 605(36), 756
 Chubb, F. L. 166(63), 169
 Chuchmarev, S. K. 148(6), 156(7, 26), 162(35), 167–169
 Chuda, K. 129(171), 143
 Chuenyu, C. 605(30), 756
 Chumakov, Y. M. 122(101), 141
 Chumley, P. H. 951(174), 993
 Chung, B. C. 1033(221), 1037(234), 1050, 1051
 Chung, F.-L. 945(117, 119), 981(305a–c), 982(291c, 291e, 308), 984(297b), 992, 997, 998
 Chung, H.-H. 652(378), 765
 Chung, H. 650(230), 761
 Chung, J. 185(38), 187
 Chung, N.-W. 1161(148a), 1169
 Chung, S. T. 1317(87), 1344
 Churchwell, M. I. 984(297a, 297g), 998
 Church, D. F. 953(187), 993
 Churney, K. L. 154(21), 168
 Chut, S. L. 654(389), 765
 Chu, J.-W. 71(148), 90
 Chu, K.-P. 725(660), 772
 Chworos, A. 943(92), 991

- Chyu, D. W. 670(475), 767
 Ciafrino, R. 1156(121c), 1168
 Ciaramitaro, B. P. 1030(197), 1050
 Cicchi, S. 536(484), 594
 Ciceron, L. 249(249), 297
 Cicéron, L. 1303(65), 1343
 Cieślak, M. 708(164), 760
 Cilento, G. 950(155), 954(192a), 992, 993,
 1172(1), 1181(11a), 1200(58a), 1205, 1206,
 1208, 1222(49), 1227(55), 1233(12, 13),
 1234(21), 1235(22), 1270, 1271
 Cimato, A. 675(504), 768
 Cimino, G. 709(62), 757, 1333(142), 1346
 Cingolani, A. 112(115), 141
 Ciocazan, I. 163(51), 169
 Cioslowski, J. 12(7), 85
 Ciroussel, F. 981(307a, b), 998
 Cirunay, J. 659(419), 766
 Ciscoato, L. F. L. M. 1268(335), 1278
 Ciscoato, L. 1260(317), 1277
 Cistola, D. P. 963(225c), 994
 Citterio, A. 107(89), 141, 1008(51), 1010(69,
 70, 77), 1047
 Ciurczak, E. W. 663(434), 766
 Ciu, Y. 511(416), 592
 Cizek, J. 8(8a), 85
 Claparols, C. 941(79), 991
 Clardy, J. J. 263(381), 300
 Clardy, J. 190(49, 50), 293
 Clarke, L. F. 902(65), 913
 Clarke, R. A. 1256(255), 1266(305, 306),
 1276, 1277
 Clarkson, Q. 672(484, 485), 768
 Clark, E. 196(60), 293
 Clark, J. H. 517(445), 558(491), 593, 594,
 1080(175), 1101(199), 1122, 1123
 Clark, M. 539(490), 594
 Clark, R. T. 907(62), 913
 Clark, T. 651(370), 765, 1184(26), 1207
 Claugue, M. J. 1077(59), 1119
 Cleaver, W. M. 118(137), 136(136), 142
 Clegg, W. 110(99), 141, 366(139), 367(140),
 585
 Clement, J. L. 973(248), 995
 Clément, M.-V. 610(66), 757
 Clennan, E. L. 174(9), 186, 262(323),
 263(380), 269(52), 273(477), 293, 299, 300,
 303, 832(8), 833(26, 32), 845(66), 847(68),
 854(90, 95, 96), 870(159), 871(164),
 875(176), 877(177), 878(180), 894, 895, 897
 Clerici, M. G. 1082(201), 1083(212),
 1114(11), 1115(413), 1118, 1123, 1127
 Clifford, S. 12(7), 85
 Climent, I. 987(329c), 999
 Clough, R. L. 685(543, 544), 769, 832(11),
 894
 Cloux, J. L. 1252(243), 1275
 Coates, S. J. 1154(114), 1168
 Coburn, M. D. 1157(129), 1168
 Cochot, P. 646(346), 764
 Coddens, B. A. 423(261a), 588
 Coddington, J. W. 952(177), 993
 Codony, R. 676(229), 761
 Cohen, D. M. 610(76), 757
 Cohen, F. E. 1282(26), 1322(117, 118), 1342,
 1345
 Cohen, S. 1140(52a), 1166
 Cohen, Y. 604(2), 756
 Coichev, N. 1257(261), 1276
 Coiteaux, L. 217(191), 249(249), 296, 297
 Colarow, L. 678(520), 768
 Colavita, A. R. 611(81), 758
 Cola, B. F. 1140(56b), 1166
 Coleman-Kammula, S. 394(204), 586
 Coleman, M. C. 214(172, 173), 295
 Coleman, R. 1212(8), 1270
 Coles, B. F. 1140(55c, 56c), 1166
 Coles, S. J. 122(145), 142
 Cole, R. J. 190(50), 293
 Collins, A. N. 270(270), 298
 Collins, A. R. 975(268c), 996
 Collins, J. 986(322), 999
 Collin, R. L. 96(24), 139
 Colombo, R. 986(326), 999
 Colonna, S. 375(156), 380(155), 381(154),
 383(183, 184), 384(185, 186), 476(368a, b,
 369), 585, 586, 591, 1157(12, 126, 128),
 1165, 1168
 Colpas, G. J. 1062(60), 1119
 Colton, C. A. 984(320), 999
 Colussi, A. J. 138(209a), 144
 Colwell, S. M. 12(7e), 85
 Commandeur, J. N. M. 670(124), 759
 Commereuc, S. 672(189), 760
 Comporti, M. 670(123, 472), 759, 767
 Condroski, K. R. 37(37e), 56(90a), 87, 88,
 1140(38), 1166
 Conia, J. M. 842(57), 895
 Connell, P. S. 605(36), 756
 Connell, R. D. 567(531d), 595
 Connick, R. E. 1003(23), 1030(196), 1046,
 1050
 Connor, J. A. 672(483), 768
 Contento, M. 575(533), 595
 Conte, V. 185(41), 186(42), 187, 432(302),
 589, 1068(85–87, 92, 98), 1069(103),
 1070(108–111), 1074(134), 1076(133, 162),
 1077(160), 1078(163, 165), 1095(4, 306,
 311, 312), 1106(376), 1107(164, 166, 167),
 1110(22), 1115(315, 414), 1118,
 1120–1122, 1125, 1127
 Contreras, J. L. 134(198), 144
 Converso, A. 468(357), 591, 1083(220), 1123
 Convery, M. A. 730(671), 772
 Coohill, P. P. 947(127), 992
 Cookson, P. G. 351(5), 581, 778(14), 827

- Cook, J. M. 512(430), 592
 Coon, C. L. 1013(31), 1046
 Copéret, D. L. 12(7d), 85
 Cooper, W. J. 643(333a), 764
 Coops, J. 161(43), 169
 Coperet, C. 802(54), 828, 1090(218), 1123
 Copéret, C. 467(352), 534(481, 482), 590, 594
 Cope, A. C. 56(56a), 87
 Coppa, F. 1115(414), 1127
 Coppel, Y. 943(92), 991
 Coratti, A. 370(146), 560(511), 585, 594, 1111(400), 1127
 Corbett, G. E. 1005(37), 1046
 Corbett, R. M. 112(77), 140
 Corbin, D. R. 882(182), 897
 Cordes, H. F. 1261(322), 1277
 Cordis, G. A. 669(469), 767
 Corelli, F. 1025(165), 1049
 Coretsopoulos, C. 185(38), 187
 Corey, E. J. 214(176), 233(231), 238(174, 175), 295, 297, 315(32a), 318(9), 352(10), 567(531d), 582, 595, 812(85), 829, 1150(96), 1167
 Corey, P. F. 1021(128), 1048
 Corma, A. 411(230), 418(247, 251), 421(253), 422(250), 477(373b), 560(508), 561(507), 564(506), 587, 588, 591, 594, 870(149), 896, 1083(209), 1084(235), 1085(210), 1089(275), 1090(276), 1096(322), 1111(402–405), 1123–1125, 1127
 Cormier, M. J. 1244(203), 1274
 Cornett, C. 1322(120), 1345
 Cornman, C. R. 138(138), 142
 Corral, J. 1160(138), 1169
 Correia, J. D. G. 466(344), 590
 Correia, J. D. G. 529(470, 471), 558(499), 593, 594, 1062(40), 1074(125), 1083(216), 1110(396), 1116(424), 1119, 1121, 1123, 1127, 1128
 Corsi, M. 536(484), 594
 Cortese, M. 560(510), 594, 1111(398, 399), 1127
 Cossi, M. 12(7), 41(41), 44(102), 85, 87, 89
 Cosstick, R. 273(467), 302, 1031(206), 1050, 1337(165), 1346
 Costabel, U. 987(329a), 999
 Costantini, M. 418(247), 588
 Costa, A. D. 951(173), 993
 Coulter, P. B. 1155(106a), 1168
 Coupland, J. N. 614(133), 759
 Courtneidge, J. L. 255(255), 262(262), 297, 358(127), 584, 700(586b), 770
 Covey, D. F. 106(80), 140
 Cowie, M. 1065(53), 1119
 Cox, J. D. 160(14), 167
 Cox, J. 981(305a), 998
 Cox, R. A. 138(209b), 144
 Cox, R. 663(235), 761
 Crabtree, R. H. 1031(204), 1050
 Craik, C. S. 1322(118), 1345
 Cram, D. J. 1034(224), 1050
 Crandall, J. K. 1026(171), 1049, 1153(97), 1167
 Crane, A. E. 984(297f), 998
 Crans, D. C. 1058(20), 1062(63), 1118, 1120
 Crean, C. 940(78), 991
 Creary, X. 219(196), 296, 906(69), 913
 Crehuet, R. 32(85b), 36(87), 88
 Cremer, D. 32(83, 85a, b), 36(87), 40(94a), 67(1, 67), 70(70), 72(72a–f), 78(78), 82(82a), 84(84), 85, 88, 89, 94(12a, b), 131(192a, b), 139, 144, 182(23, 24), 185(35), 187, 717(621, 623), 721(619), 722(652, 654, 655), 723(625), 771, 772, 1140(20), 1154(112), 1165, 1168
 Creminon, C. 1256(253), 1275
 Crestini, C. 1156(121b, c), 1168
 Crestini, L. 1156(121d), 1168
 Crews, P. 190(24), 276(494), 292, 303, 610(64), 757
 Criado, S. 968(239c), 995
 Crich, D. 324(36a, b), 501(419), 582, 592
 Criegee, R. 29(68), 88, 177(16), 187, 716(617, 618), 731(632), 771
 Crisma, M. 123(162), 129(172), 143
 Croft, S. L. 273(450), 290(580, 584), 302, 305, 1314(91), 1317(68), 1343, 1344
 Cross, R. J. 1086(234), 1124
 Crousse, B. 1021(138), 1049
 Crow, J. P. 22(22b), 86
 Crow, W. D. 199(89), 294
 Crudden, C. M. 1140(86), 1167
 Crudden, E. M. 1021(140), 1049
 Cruthoff, R. 903(53), 912
 Cryle, M. J. 1140(52c), 1166
 Csiscery, S. M. 870(150), 896
 Csizmadia, I. C. 56(48), 87
 Cuadros-Rodriguez, L. 1240(173), 1274
 Cuatrecasas, P. 1335(148), 1346
 Cuchmarev, S. K. 154(11), 167
 Cudd, M. A. 241(258), 263(263), 297
 Cudina, I. 964(227b), 994
 Cueto, O. 324(51a), 582, 1232(120, 124), 1273
 Cueto, R. 14(46), 87
 Cui, Q. 12(7), 85
 Culcasi, M. 973(254), 995
 Cullis, P. M. 943(97), 991
 Cumming, J. N. 202(96), 209(140, 141), 223(209), 273(35, 446), 280(521, 522, 527), 283(471, 530), 292, 294–296, 302, 304, 1282(17), 1284(39), 1289(46), 1291(48), 1306(38), 1330(134), 1332(109), 1337(162), 1342, 1343, 1345, 1346
 Cummins, W. J. 727(639), 771
 Cundall, R. B. 1188(39, 40a, b), 1207, 1267(72, 323), 1272, 1277

- Cunningham, J. A. 981(305a), 998
 Cuppett, S. L. 663(437), 671(231), 674(409), 761, 766
 Curci Fiorentina, M. 1021(130), 1048
 Curci, R. 14(14, 14b), 32(59), 40(98), 41(93), 47(103), 73(149), 74(150), 86, 88–90, 183(30), 184(34), 187, 477(372), 591, 776(1), 785(29), 796(43), 806(61), 827, 828, 1020(123, 124), 1039(244, 245), 1048, 1051, 1076(158), 1096(324), 1114(411), 1122, 1126, 1127, 1140(6, 13, 14, 36), 1145(7), 1146(70), 1153(109), 1155(115, 117, 119b), 1157(128), 1160(11a, 134, 139a, 141–143), 1161(145), 1162(151b), 1163(1a, 1c, d, 1f, 1k, 25, 152a, b, 153), 1164, 1165, 1167–1169, 1178(20d), 1206
 Curini, M. 1027(178), 1028(180), 1029(188, 190, 194), 1049, 1050
 Curran, D. P. 213(162), 295, 1001(2), 1046
 Currie, J. 274(486), 303
 Curtis, A. B. 1032(217), 1050
 Curtis, R. J. 238(165, 221), 256(256), 262(262), 295, 297
 Custodio, R. 1075(155), 1122
 Cutler, D. 608(56), 757
 Cutler, R. G. 954(189), 993
 Cynn, H. 96(25), 139
 Czapski, G. 131(187), 143, 611(84), 741(700), 758, 773, 952(179), 993
 d'A. Rocha Gonsalves, A. M. 457(323), 590
 D'Accolti, L. 47(103), 89, 1146(70), 1153(109), 1157(128), 1160(139a), 1161(145), 1163(1k), 1164, 1167–1169
 D'Addieco, A. A. 1020(122), 1048
 d'Alessandro, N. 964(228), 995
 D'Aloisio, R. 362(134c), 437(307), 444(306), 585, 589, 1080(170), 1094(305), 1122, 1125
 d'Angelo, J. 1303(65), 1343
 D'Ans, J. 1002(12, 13), 1046
 D'Ham, C. 921(33), 975(268a), 989, 996
 D'yachkovskaya, O. S. 823(114, 115), 830
 da Costa Ferreira, A. M. 624(228), 761
 Daban, J. R. 1257(256), 1276
 Daehnke, H. L. 963(225b), 994
 Dagdagan, O. A. 155(23), 168
 Dahlmann, J. 776(3), 822(112), 824(113, 117c), 827, 829, 830
 Dahn, H. 183(4), 184(33), 186, 187
 Daido, H. 690(563), 770
 Daikai, K. 392(198), 586
 Daire, E. 1078(159), 1115(161), 1122
 Dai, H. L. 1160(11b), 1165
 Dai, K. 742(334), 764
 Dai, P.-S. E. 428(291), 589
 Dai, W. L. 527(466), 593
 Dakanali, M. 1058(38), 1119
 Dakka, J. 497(403), 512(408), 514(409a), 526(410), 592
 Dalkiewicz, M. 1150(93), 1167
 Dall'Orto, V. C. 701(381), 765
 Dallas, J. L. 978(287a), 997
 Dalle-Donne, I. 986(326), 999
 Dalle, J.-P. 856(111), 896
 Dallmann, G. 638(314), 764
 Dallwigk, E. 165(55), 169
 Dalton, H. 1200(58c), 1208
 Damiani, E. 1155(119b), 1168
 Dandby, R. 899(4), 912
 Daneault, C. 623(200), 761
 Dang, H.-S. 236(244), 245(245), 246(246), 297
 Dang, H. S. 346(96a–c), 584
 Daniels, A. D. 12(7), 85
 Daniels, M. 614(138), 759, 920(22a, b), 922(41a), 923(18b), 989, 990
 Danilowicz, C. 701(381), 765
 Danis, M. 249(249), 297
 Dankleff, M. A. P. 73(149), 90
 Dannley, R. L. 777(8), 822(109, 110), 824(111, 119), 827, 829, 830, 1005(37, 40), 1044(9), 1045(250, 259), 1046, 1047, 1051
 Danovich, D. 1140(52a), 1166
 Dan, N. 1257(302), 1277
 Dapprich, S. 12(7), 85
 Darley-USmar, V. M. 951(174), 993
 Darmograi, M. I. 161(34), 169
 Darmon, M. J. 1232(126), 1273
 Dartiguelongue, C. 892(208), 898
 Dasgupta, A. 676(301), 763
 Dasgupta, P. K. 646(342), 674(328), 678(329), 764
 DaSilva Jardine, P. 567(531d), 595
 Dastan, A. 267(410), 301
 Das, D. K. 669(469), 767
 Das, P. K. 909(92), 913
 Das, S. K. 1116(416), 1127
 Das, S. 510(414), 592, 1116(423), 1128
 DattaGupta, A. 516(438a, b), 593
 Dat, J. 610(71), 757
 Dauben, W. G. 497(405a), 592
 Daub, M. E. 610(80), 757
 Daughenbaugh, R. 283(471), 302, 1337(162), 1346
 Daukshas, V. K. 153(19), 167
 Dávalos, J. Z. 160(36), 161(39), 169
 Davey, M. 273(460), 302, 1336(154), 1346
 Davey, R. 273(460), 302, 1336(154), 1346
 Davidson, E. 1322(117), 1345
 Davidson, E. 1322(118), 1345
 David, A. 973(260), 996
 David, S. S. 974(263), 996
 Davies, A. G. 236(244), 245(245), 246(246), 286(558), 297, 305, 346(96a–c), 351(5), 354(113), 581, 584, 778(14), 827, 833(30), 894
 Davies, C. A. 15(15), 86
 Davies, C. J. 1256(252), 1275

- Davies, D. H. 381(174), 586
 Davies, D. R. 286(265), 297
 Davies, J. 223(207), 273(467), 275(487–489), 296, 302, 303, 1317(101), 1320(115), 1323(121), 1330(131, 132), 1332(92), 1337(165), 1344–1346
 Davies, M. J. 918(13, 14), 959(203), 968(240), 970(195a, b), 971(199b, c), 972(222b, 234, 252), 973(241, 247, 249a, b, 256, 257), 974(265), 975(261, 266), 986(321a, 324), 987(15, 325c, 327), 989, 993–996, 999
 Davison, V. L. 737(689), 772
 Davis, A. F. 672(484, 485), 768
 Davis, A. G. 783(18a–c), 824(117a), 827, 830
 Davis, F. 56(48b), 87
 Davis, K. M. 262(378), 300
 Davis, T. W. 674(503a), 768, 965(214), 994
 Davis, W. M. 825(121), 830
 Dawidzik, J. B. 933(58a), 990
 Day, V. W. 192(59), 293
 de Almeida Azzellini, M. A. 624(228), 761
 de Almeida Barbosa, L.-C. 608(56), 757
 de Arruda Campos, I. P. 1189(41b), 1208
 De Bernardinis, S. 1010(70), 1047
 de Boer, T. J. 1141(59), 1166
 de Bruin, B. 1062(42), 1119
 De Conciliis, M. A. 1074(134), 1121
 de Goeij, A. F. P. M. 969(245b), 995
 de la Guardia, M. 701(302), 763
 de la Moya Cerero, S. 520(449), 593
 de la Rosa, F. F. 646(343), 764
 De Lorenzo, F. 108(100), 141
 De Lucchi, O. 260(374–376), 300
 De Mol, P. 190(42), 292
 de Oro Osunar, S. 520(449), 593
 De Paoli, T. 675(504), 768
 de Serves, C. 604(6), 756
 de Suzzoni-Dezard, S. 1256(253), 1275
 de Tavernier, M. 659(419), 766
 de Visser, S. P. 84(163), 91, 472(143), 579(549), 585, 596, 1140(52a), 1166
 de Vivar, A. R. 134(198), 144
 De Voss, J. J. 1140(52c), 1166
 de Vos, D. E. 369(145), 446(328), 455(326, 329), 456(327), 457(330), 569(529), 585, 590, 595
 de Vries, B. 899(6), 912
 de Vries, M. E. 1069(44), 1119
 de Wildeman, S. 457(330), 590
 de Wolf, W. H. 199(85), 293
 De Zotti, M. 123(162), 143
 De Zwart, L. L. 670(124), 759
 Deakynne, C. A. 30(30), 87
 DeAngelis, W. 1250(223), 1275
 Dean, R. T. 614(142), 673(406), 691(143), 759, 766, 918(13), 956(200), 957(202), 959(203), 971(199b), 972(196a, 253a), 973(249b, 256, 257), 975(261, 266), 987(15, 325c, 327, 332), 989, 994–996, 999
 Debal, A. 621(178), 760
 Decarroz, C. 922(35a), 926(49), 938(48a, b, 63), 989, 990
 Dechy-Cabaret, O. 273(452), 284(541, 542, 548), 286(557), 302, 304, 305, 1320(43, 112, 113), 1343, 1345
 Decker, E. A. 658(415), 766
 Declercq, J.-P. 109(116), 141, 1069(65), 1120
 DeCorpo, J. J. 1261(321), 1277
 Decouzon, M. 874(170), 897
 Dedon, P. C. 981(306), 998
 Deegan, M. J. O. 12(7d), 85
 Deen, W. M. 611(85), 758
 Deforest, C. L. 642(7), 756
 Degan, P. 917(4), 988
 Degen, H.-G. 260(372), 300, 363(137), 373(152), 585, 869(145), 896, 1163(1m), 1165
 DeHart, J. 646(348), 764
 Deheza, M. F. 284(536, 538), 304
 Dehmlow, E. V. 1030(198), 1050
 Dejong, G. J. 1257(258, 259), 1276
 del Cerro, M. A. 689(390), 765
 del Fierro, J. 352(50), 582, 779(16a), 827
 del Río, L. A. 610(78), 757
 Del Todesco, M. 1109(393), 1127
 Delagoutte, T. 628(255), 762
 Delatour, T. 943(9b), 989, 1203(67b), 1209
 Delattre, J. 667(456), 767
 Delcastillo, M. D. 1242(190), 1274
 Della Bella, L. 656(402), 766
 Della Valle, G. 623(196), 761
 Della Védova, C. O. 702(591), 770
 Delmas, M. 622(186), 760
 Delogu, G. 260(375, 376), 300
 DeLong, J. M. 667(457), 676(458), 767
 Delpech, B. 1089(272), 1124
 Delpon, D. B. 1021(138), 1049
 DeLuca, D. 610(69), 757
 Demaison, J. 100(28b), 139
 DeMarco, R. A. 740(697), 772
 DeMasters, D. E. 155(25), 168
 Dembech, P. 778(12), 797(42, 45), 800(49, 50), 827, 828
 DeMello, N. C. 56(90a), 88, 1140(38), 1166
 Demerseman, P. 919(20), 989
 Deming, P. H. 532(474), 593
 Demirata-Öztiirk, B. 640(320), 764
 Demko, D. M. 1024(155), 1049
 Demole, E. 792(30b), 828
 Den Hertog, H. J. 899(6), 912
 Dengel, A. C. 1057(19), 1069(101, 112), 1118, 1120, 1121
 Deng, H. C. 190(27), 292
 Denicola, A. 741(699), 772, 951(167), 993
 Denise, B. 470(354), 590

- Denk, W. 861(5b), 893
- Denmark, S. E. 1021(134, 140), 1048, 1049, 1140(83, 86), 1163(11), 1164, 1167
- Denny, D. B. 1040(249), 1051
- Denny, R. W. 252(319), 299, 854(97), 888(190), 895, 897
- DePuy, C. H. 250(293), 298
- Derkosch, J. 163(46), 169
- Desai, P. V. 1314(97), 1344
- Desai, S. R. 192(59), 293
- Desai, U. V. 1027(174), 1029(193), 1049, 1050
- Deshayes, C. 918(10), 989
- Deshmukh, M. N. 480(377), 591, 1068(95), 1120
- DeSilva, R. 1198(33a), 1207, 1236(33), 1271
- Desjardins, A. E. 977(285), 997
- Desmaële, D. 1303(65), 1343
- DesMarteau, D. D. 102(54), 138(56a), 140, 1043(267), 1051
- Desousa, S. E. 1022(145), 1049
- Desrosiers, M. F. 963(226), 994
- Dessau, R. M. 900(12), 912
- Detomaso, A. 1153(109), 1168
- Detty, M. R. 572(545), 576(546, 547), 596
- Deubel, D. V. 48(114a), 56(88), 88, 89, 1075(152, 153), 1122, 1140(34), 1165
- Deufel, T. 263(383, 384), 300
- Devamanoharan, P. S. 655(397), 765
- Devaquet, A. 1227(86), 1272
- Devereux, M. M. 730(671), 772
- Devillers, M. 1069(65), 1120
- Dewaele, C. 1257(275, 279), 1276
- Dewar, M. J. S. 253(336), 299, 833(28), 894
- Dewick, P. M. 94(3c), 138
- Dey, D. 1116(423), 1128
- De, P. 709(600), 714(602), 770
- Dhanda, A. 380(161), 585
- Dhar, D. N. 1008(55), 1047
- Dhingra, V. 190(47), 292
- Di Furia, F. 185(41), 187, 477(372), 480(378), 591, 1020(124), 1031(207, 208), 1039(244), 1048, 1050, 1051, 1068(85–87, 89–92, 97, 98), 1069(103), 1070(108), 1072(24), 1074(134), 1076(133, 162), 1077(160), 1078(163, 165), 1095(4, 179, 306, 311–314), 1096(130, 324, 325), 1097(93, 329), 1098(129, 131), 1105(373, 374), 1107(164), 1110(392), 1115(315, 414), 1118, 1120–1122, 1125–1127, 1140(6), 1165
- di Mascio, P. 269(421, 423), 301, 941(80b), 943(85c, 86, 87, 91), 950(158, 159), 951(160, 161, 164), 954(193b), 967(238b, c), 977(274a, b), 984(292a, b, 294a–c), 991–993, 995–997
- di Renzo, F. 428(294), 589
- Di Valentin, C. 1075(148, 150, 151), 1121, 1122
- Diaz, A. 1161(103), 1167
- Diaz, J. 614(136), 759
- Díaz, M. 725(63), 757
- Díaz, S. 235(235), 297
- Díaz, U. 421(253), 588
- Dibrivnyi, V. N. 162(35), 169
- Dickey, F. H. 156(12), 167
- Dickman, M. H. 1063(18), 1118
- Dickson, J. 1257(294), 1277
- Dickson, M. 1257(294), 1277
- Dickson, S. 1252(245), 1275
- Didenko, Y. T. 606(42), 757
- Dieter, R. K. 1027(177), 1049
- Dietrich, P. 354(115), 584
- Dietz, R. 315(30), 582
- Dieu, C. 899(5), 912
- DiFuria, F. 432(302), 487(382), 589, 591
- Dignon, J. E. 605(36), 756
- Dihel, P. 172(6), 183(4), 186
- Dijksman, A. 1108(371), 1127
- Dikakov, S. I. 973(255a, b), 995
- Dikii, M. A. 154(11), 167
- Dikumar, E. A. 122(152), 142, 715(614), 771
- Dimitrov, A. 733(678b), 772
- Dimitrov, V. 177(14), 186
- Diñçkaya, E. 655(393, 394), 765
- Ding, H. 461(353), 466(355), 590, 591, 1083(219), 1123
- Ding, J.-Y. 317(27), 582, 1182(22), 1206
- Ding, J. 273(458), 302
- Dinoi, A. 40(98), 41(93), 47(103), 89, 1140(36), 1153(109), 1155(119b), 1160(143), 1161(145), 1163(1f, 1k, 152a), 1164, 1165, 1168, 1169
- Diodati, F. P. 102(55), 140, 713(613), 771
- Diogo, H. P. 149(9), 167
- DiPasquale, A. G. 118(123), 142
- DiPrete, R. 74(150), 90
- Dishington, A. P. 284(545), 304
- Diter, P. 480(375), 591, 1097(326), 1126
- Dittberner, U. 977(284), 997
- Diwu, Z. 643(67), 757
- Dixon, B. G. 1235(122, 123), 1273
- Dixon, B. 1232(116), 1272
- Dixon, D. A. 37(37b), 87, 101(52b), 140
- Dizdaroglu, M. 960(205), 976(272a), 994, 996
- Dmitrenko, O. 46(27a, b), 57(52, 131), 58(133, 134), 60(16b), 65(139), 73(19d), 75(147), 78(20b, c), 82(156), 86(21b), 86, 87, 90, 91, 94(11b), 139, 1140(22, 37), 1165
- Dobarganes, M. C. 673(498), 768
- Dobashi, S. 253(328), 299, 839(54), 895
- Dobbs, T. K. 728(665), 772
- Dobbyn, A. J. 12(7d), 85
- Dobosh, P. 6(6), 85
- Dobretsova, A. 1198(54), 1208

- Dobrolyubova, M. S. 736(686), 772
 Dobrzelewski, M. 732(677), 772
 Doddridge, A. Z. 943(97), 991
 Dodeigne, C. 697(183), 760, 1252(174), 1274
 Dodonov, V. A. 118(140), 142
 Doerge, D. R. 980(289b), 984(297a, 297g), 997, 998
 Dogan, B. 161(44), 165(62), 169
 Doggant, J. R. 1014(94), 1048
 Dogne, J. M. 190(42), 292
 Doi, T. 1020(119), 1048
 Dolan, P. 273(469, 470), 283(471), 302, 1337(162, 163), 1346
 Dolbneva, R. N. 161(34), 169
 Dolbneva, T. N. 148(6), 154(11), 167
 Dolco, K. 44(44a, b), 87
 Domagals, J. M. 56(48), 87
 Dombi, A. 678(252), 762
 Domine, M. E. 1084(235), 1124
 Domine, M. 421(253), 588
 Dominguez-Fernandez, B. 1140(85b), 1167
 Dominguez, J. N. 1322(117), 1345
 Donati, D. 107(87), 141
 Donchak, V. A. 162(35), 169
 Dong, H. Q. 237(248), 247(247), 297
 Dong, J. 663(435), 766
 Dong, S. 646(345), 653(385), 654(386), 764, 765
 Dong, Y. X. 190(44), 292, 1326(106), 1332(15, 105), 1342, 1344, 1345
 Dong, Y. 175(11), 186, 1066(74), 1120
 Donnoli, M. I. 487(387), 591, 1098(337), 1126
 Döpp, D. 536(483), 594
 Döpp, H. 536(483), 594
 Dorémieux-Morin, C. 1069(117), 1121
 Dornbos, D. L. 977(285), 997
 Dorn, A. 1332(15), 1342
 Dougherty, D. A. 873(166), 897
 Douki, T. 616(149), 759, 933(58b, 59), 935(64), 941(80a), 943(9a–c), 950(151), 975(268a, b, 269b), 976(270a, 270c), 977(275a–c), 984(294b), 988–992, 996, 997, 1203(67b), 1209
 Dourandin, A. 940(77), 991
 Doutheau, A. 918(10), 989
 Doweyko, W. M. 1282(25), 1342
 Dowidiet, P. 674(45), 757
 Downey, J. R. 15(15), 86
 Drago, R. S. 323(44), 582
 Drake, A. F. 382(181), 586
 Drake, M. D. 576(546), 596
 Draper, H. H. 977(277c), 996
 Drapper, C. S. 624(232), 761
 Drauz, K.-H. 378(166), 585
 Drauz, K. H. 379(163), 380(161), 585
 Dreeskamp, H. 1204(72a), 1209
 Drew, M. G. B. 727(639), 771
 Drozdov, A. 112(115), 141
 Druliner, J. D. 355(122), 584
 Drummond, J. 263(387), 300
 Druzhkov, O. N. 823(115), 830
 Dryuk, V. G. 48(115d), 89
 Duarte, V. 943(91, 93a), 991
 Dua, M. 1322(81), 1344
 Dubai, G. B. 217(182), 296
 Dubai, G. R. 217(181), 296
 Dubbelman, T. M. A. R. 969(245b), 995
 Dubey, I. 943(92), 991
 DuBois, J. L. 1069(54), 1119
 Ducherty, K. S. 690(11), 756
 Ducolomb, R. 921(32), 922(38), 928(37b), 933(54), 934(60a, b), 989, 990
 Dudas, A. 670(478), 768
 Duetsch, M. 480(375), 591, 1097(326), 1126
 Duez, P. 975(269b), 996
 Duggan, S. 986(321b), 999
 Duh, Y.-S. 617(158), 759
 Duim-Koolstra, E. T. 394(204), 586
 Dukhnovich, A. F. 1192(47b), 1208
 Dulog, L. 213(160), 295
 Dumais, J. J. 692(215), 761
 Dumbroff, E. B. 617(156), 759
 Dunach, E. 480(377), 591
 Duñach, E. 1068(95), 1120
 Dunbar, T. D. 685(544), 769
 Duncan, D. C. 1081(171), 1082(191, 192), 1122, 1123
 Dunlap, D. E. 706(597), 770
 Dunn, D. K. 1224(68), 1271
 Dunogues, J. 779(13a), 827
 Dunstan, H. 273(461), 302
 Dupont, A. C. 1252(247), 1275
 Dupres, D. 1114(11), 1118
 Dupuis, M. 12(7b), 85
 Dupuy, C. G. 269(428), 301
 Dupuy, N. 702(227), 761
 Duran, R. 1333(141), 1346
 Durazo, A. 1083(230), 1123
 Durbut, P. 426(274), 588
 Duretz, B. 976(270a), 996
 Durgaprasad, A. 512(411), 592
 Duschek, F. 1155(118a), 1168
 Dussalt, P. H. 869(83), 895
 Dussault, P. H. 217(180), 236(236), 241(241), 242(242), 243(243), 247(287), 260(373), 286(265), 288(288), 296–298, 300, 329(63b), 341(87), 346(97), 357(123), 583, 584, 888(194), 897
 Dussault, P. 329(63a), 352(62), 357(67, 83), 583
 Dust, J. M. 906(68), 913
 Dutta, D. K. 273(56), 293
 Dutton, H. J. 737(689, 692), 772
 Duvadie, R. K. 276(502), 303
 Duval, O. 238(257), 297, 892(65, 208), 895, 898

- Du, H. 418(252), 588
 Du, J. 975(267), 996
 Du, N. 973(258), 996
 Du, X. 47(108), 89
 Dwyer, C. L. 365(138), 585
 Dyer, A. 869(146), 896
 Dykstra, C. E. 1184(32), 1207, 1234(134), 1273
 Dyson, G. A. 1266(334), 1278
 Dziobak, M. P. 213(161), 295
 El-Essi, F. A. 631(294), 763
 Earle, F. R. 737(691), 772
 Eary, C. T. 243(243), 288(288), 297, 298
 Easton, C. J. 621(180), 760
 East, J. M. 273(453), 302, 1313(34), 1343
 Eberle, G. 981(307b), 998
 Ebersson, L. E. 1235(142), 1273
 Ebitani, K. 245(282), 298
 Eckert, C. R. 1242(193), 1274
 Eckert, F. 12(7d), 85
 Eckstein-Ludwig, U. 273(453), 302, 1313(34), 1343
 Economou, A. 647(354), 765
 Eddy, C. R. 105(63), 140, 160(37), 169
 Edwards, B. 1197(50), 1198(33c–f), 1199(48), 1200(53a, b), 1207, 1208, 1236(160, 163), 1256(249), 1273, 1275
 Edwards, G. 1326(106), 1345
 Edwards, J. O. 14(14), 73(149), 74(150), 86, 90, 796(43), 828, 1003(22), 1008(52), 1020(123, 124), 1021(130), 1046–1048, 1078(165), 1096(324), 1114(411), 1122, 1126, 1127, 1140(6), 1163(1a), 1164, 1165
 Edward, J. O. 785(29), 827
 Edward, J. T. 166(63), 169
 Eestévez, C. M. 94(11b), 139
 Effenberger, F. 1014(91), 1048
 Efferth, T. 273(459–461), 302, 1336(154–156), 1346
 Effkemann, S. 699(582a, b, 583), 770
 Egan, T. J. 1281(10, 11), 1283(29, 30), 1342, 1343
 Egar, A. L. 380(170), 586
 Eggelte, H. J. 273(325), 299, 730(673), 772, 783(26), 827
 Eggert, H. 861(5b), 893
 Egmore, K. 635(9), 756
 Ehrenshaft, M. 610(80), 757
 Ehrenson, S. 1244(177), 1274
 Ehrig, V. 324(51a), 582
 Eigen, M. 1264(330), 1277
 Einaga, H. 109(119), 142, 1064(69), 1069(118), 1120, 1121
 Einarsson, S. 960(204a), 994
 Eisenberg, G. M. 919(17), 989
 Eisenbraun, E. J. 728(665), 772
 Eisenstein, O. 310(3b), 581
 Eissenthal, K. B. 269(428), 301
 Eiserich, J. P. 951(174), 993
 Eissenbrand, G. 977(284), 997
 Ekersley, T. J. 1228(108), 1272
 Ekert, B. 919(20), 921(28b), 927(27), 989
 Ekmekcioglu, C. 611(82), 758
 Ekthawatchai, S. 273(472), 302
 El Ghissassi, F. 981(304), 998
 El Kordy, M. A. 112(72), 140
 El Kordy, M. 134(199), 144
 El-Feraly, F. S. 112(74), 134(197), 140, 144
 Elbert, S. T. 12(7b), 85
 Elbs, K. 1008(56), 1047
 Elder, R. H. 984(313), 998
 Eldsäter, C. 680(535, 536), 769
 Elemes, Y. 849(44, 67), 850(71), 853(85), 859(59), 894, 895
 Eley, C. D. 815(91b), 829
 Elferaly, F. S. 273(456, 465), 302, 1336(161), 1346
 ElIdreesy, T. T. 274(484), 303
 Eliel, E. L. 131(10), 139
 Elings, J. A. 1080(175), 1122
 Eling, T. E. 233(13), 292
 Elizarova, G. L. 1069(119), 1121
 Ellenberger, S. R. 1001(4), 1046
 Elliot, J. 672(485), 768
 Ellis, H. 605(27), 756
 Ellis, W. Y. 712(58), 757
 Ellwood, S. 422(256), 588
 Ell, A. H. 574(540), 595
 Elsegood, M. R. J. 367(140), 585
 ElSohly, H. N. 288(576), 289(578), 290(582), 583, 588–590, 305
 Elston, C. L. 392(199), 586, 1088(266), 1124
 Elzanowska, H. 650(363), 765
 Emanuel, C. J. 920(25), 989
 Emel'yanenko, V. N. 155(25), 168
 Emelin, V. D. 156(27), 168
 Emerit, J. 667(456), 767
 Emmons, W. D. 362(135), 585
 Emr, S. A. 688(555), 769
 Emsley, J. 94(3a), 138
 Emteborg, M. 1257(297), 1277
 Encinas, M. V. 909(92), 913
 Enders, D. 388(194), 392(173, 192), 520(454), 586, 593, 1088(262–264), 1124
 Endo, M. 413(233b), 587
 Endo, Y. 1335(147), 1346
 Engdahl, A. 98(34), 131(190), 139, 143
 Engelhardt, L. M. 112(79), 140
 Engel, P. C. 80(151), 91
 Engel, T. 1197(50), 1208, 1236(160), 1273
 Engström, S. 62(62), 88
 Enomoto, S. 429(289), 432(304), 433(295), 434(290), 589
 Ensley, H. E. 284(284), 298, 343(92), 584, 852(75), 895
 Epe, B. 1205(60a, b), 1209

- Epifano, F. 1027(178), 1028(180), 1029(188), 190, 194, 1049, 1050
- Eppinger, J. 1058(31), 1119
- Erdelmeier, I. 669(470, 471), 767
- Erden, I. 263(386, 387), 300
- Erickson, R. E. 734(681), 772
- Eriksen, J. 211(145), 295
- Eriksen, T. E. 1243(195, 196, 198), 1244(180), 1248(178, 216), 1274, 1275
- Erker, G. 196(73), 293
- Ernst, T. D. 794(39), 802(53), 828
- Ertaş, N. 655(394), 765
- Ervin, J. S. 665(446), 767
- Eržen, E. 182(22), 187
- Esaka, Y. 1011(83), 1047
- Escobar, R. 646(343), 764
- Eskın, N. A. M. 656(399), 766
- Esmayilpour, K. 1029(191), 1050
- Espenson, J. H. 466(360), 591, 1083(227), 1095(215), 1096(320), 1103(358), 1107(382, 383), 1123, 1125–1127
- Esposito, A. 1082(201), 1123
- Esser, G. 678(521), 769
- Esterbauer, H. 945(99, 105), 984(281b), 991, 997
- Estevez, C. M. 46(27a, b), 56(12b), 58(124), 60(16b), 66(138), 86, 87, 90
- Esteve, P. 418(247), 588
- Estornell, E. 1333(142), 1346
- Ettlinger, M. G. 323(45), 582
- Eun, M. Y. 616(153), 759
- Evansack, J. D. 1044(274), 1052
- Evans, D. A. 48(116), 89, 860(128), 896
- Evans, M. G. 907(77a, b), 913
- Evans, O. 686(547, 548), 769
- Evans, P. J. 655(258), 762
- Evans, R. N. 1257(273), 1276
- Evans, T. L. 1024(157), 1049
- Evans, W. H. 154(21), 168
- Everett, A. J. 104(23), 139
- Everitt, S. R. L. 904(75), 913
- Evmiridis, N. P. 742(334), 764
- Exner, O. 903(73), 913
- Eyring, H. 910(72a, b), 913
- Fabbri, D. 260(375, 376), 300
- Fabisiak, J. P. 660(110, 111), 758
- Fabre, M. 613(115), 758
- Fabris, F. 260(374–376), 300
- Fabrizi, G. 370(146), 560(511), 585, 594, 1111(400), 1127
- Facorro, G. 675(504), 768
- Fagan, J. M. 987(330), 999
- Fageron, I. S. 1008(55), 1047
- Fagian, M. M. 951(173), 993
- Fahey, R. C. 58(132), 90
- Fair, C. K. 1030(196), 1050
- Faisca Phillips, A. M. 562(498), 594, 1111(397), 1127
- Faist, J. 605(35), 756
- Falck, J. R. 352(10), 379(169), 582, 586
- Faler, G. R. 833(24), 894
- Fang, D.-C. 31(81), 88
- Fang, J.-M. 726(661), 772
- Fang, J. L. 984(297a, 297g), 998
- Fang, X. 964(228), 966(209), 994, 995
- Fantin, G. 1021(142), 1049
- Fan, A. 858(124), 896
- Fan, J. F. 273(29), 292
- Fan, K. N. 527(466), 593
- Fan, O. Y. 1317(103), 1344
- Fan, P. C. 1306(74), 1314(64), 1343, 1344
- Fan, P. 1286(41), 1343
- Fan, S. H. 645(340), 764
- Fan, X. 1336(157), 1346
- Fan, Y. L. 780(23), 827
- Farach, H. A. 675(504), 768
- Farag, I. S. A. 112(72), 140
- Fargere, T. 622(186), 760
- Farid, S. 208(127), 294, 870(156), 897
- Farina, A. 107(89), 141
- Farinotti, R. 1257(260), 1276
- Farkas, O. 12(7), 85
- Färnegardh, K. 574(538), 595
- Farona, M. F. 423(263, 265), 588
- Farooqi, M. 655(300), 763
- Farrall, M. J. 396(209), 587
- Farrant, G. 822(109), 829
- Farr, M. 945(102), 991
- Fauconneau, B. 614(135), 759
- Faulkner, D. J. 134(200), 144, 190(20–22), 292
- Faulkner, K. 1234(21), 1250(227), 1270, 1275
- Faulkner, L. R. 1226(69), 1272
- Fausto, R. 1184(26), 1207
- Favarger, F. 1293(36, 37, 51), 1343
- Favier, A. 943(87), 975(269b), 991, 996
- Fayos, J. 190(50), 293
- Fazal, N. 778(14), 827
- Fearn, T. 663(433), 766
- Federova, E. V. 156(27), 168
- Federsel, H. J. 1097(330), 1126
- Fedorova, V. A. 168(32), 168
- Fedtke, N. 981(298a, 307a), 998
- Feeder, N. 125(166), 126(165, 167), 127(168), 143
- Feldberg, L. 510(412), 592
- Feldman, K. S. 223(213–217), 296
- Felfer, U. 379(164), 585
- Felix, C. 963(221), 994
- Feller, D. 37(37b), 87
- Fell, R. T. 520(455b), 593, 1150(91), 1167
- Feng, M. 643(333b), 764
- Feng, X. 1150(95), 1167
- Feng, Y. 676(512), 768
- Ferguson, G. 134(134), 142, 511(413), 592
- Ferguson, J. F. 1225(64), 1271

- Feringa, B. L. 514(439), 516(444), 593,
1069(44, 48, 50), 1074(135), 1119, 1121
- Fernando, R. C. 981(299a), 998
- Fernie, C. E. 614(126), 759
- Ferrario, F. 1010(70), 1047
- Ferraro, J. R. 1030(196), 1050
- Ferraz, H. M. 1021(137), 1049
- Ferreira, A. M. 952(178), 993
- Ferreira, D. 379(168), 585
- Ferreira, P. 1086(252), 1124
- Ferrer-Sueta, G. 951(167), 952(178), 993
- Ferreri, C. 920(25), 989
- Ferrer, J. 1064(68), 1120
- Ferrer, M. 1154(19), 1155(118b), 1161(103),
1165, 1167, 1168
- Fessel, J. P. 612(91), 758
- Fey, O. 1163(154d, 154f), 1169
- Ficini, J. 259(361), 300
- Fickert, C. 1081(149), 1122
- Fiege, H. 1245(210), 1274
- Fiege, M. 253(344), 274(484), 299, 303
- Fielder, S. 217(188, 189), 296, 890(203), 898
- Fields, J. D. 1025(161), 1049
- Field, R. W. 1160(11b), 1165
- Fieser, L. F. 621(173), 760
- Fieser, M. 621(173), 760
- Figueras, F. 245(281), 298
- Filatov, M. J. 1075(145), 1121
- Filby, J. E. 317(27), 582, 1182(22), 1206
- Filik, H. 640(320), 764
- Filipiak, A. 972(253b), 995
- Filipkowski, M. 949(136), 992
- Filippova, N. Yu. 1192(47b), 1208
- Filson, G. W. 362(134b), 584
- Findeisen, M. 112(98), 141
- Fine, D. H. 163(49), 169
- Fink, S. P. 945(116), 984(311), 992, 998
- Finlay, M. R. V. 1145(68), 1167
- Finney, N. S. 1075(34), 1119
- Finn, M. G. 48(113a), 89, 567(528), 595,
1092(83), 1120
- Finn, M. 909(94), 913
- Finzel, R. 193(68), 195(69), 293
- Fiorani, T. 785(29), 827, 1094(305), 1125
- Fiorentino, M. 32(59), 88, 184(34), 187,
1140(13), 1145(7), 1146(70), 1155(115),
1160(11a, 13a, 139a, 142), 1163(25, 152a,
b), 1165, 1167–1169
- Fiorini, V. 1161(147), 1169
- Firentino, M. 1153(109), 1168
- Firestone, D. 663(436), 766
- Firouzabadi, H. 1019(117, 118), 1048
- Firth, C. A. 971(250), 995
- Fischer, C. M. 731(637), 771
- Fischer, J. 122(146), 131(131), 142, 426(276),
523(459), 539(495), 557(493), 588, 593,
594, 1115(161), 1116(56), 1117(432), 1119,
1122, 1128
- Fischer, N. H. 112(73), 140
- Fischer, R. W. 453(343a), 459(347, 348),
461(353), 466(342), 469(345), 529(471),
558(499), 569(534), 590, 593–595,
1062(39, 40), 1074(125), 1095(309),
1110(23, 396), 1116(424), 1118, 1119,
1121, 1125, 1127, 1128
- Fisher, G. J. 926(47), 990
- Fish, R. H. 444(316), 589, 1107(385), 1127
- Fitch, C. D. 1311(75), 1344
- Fitton, A. 1281(6), 1342
- Fitzgerald, G. 101(52b), 140
- Fleck, S. L. 284(540), 304, 1317(104),
1324(122), 1344, 1345
- Fleming, I. 503(420), 592, 808(65), 809(75),
828, 829
- Fleming, P. R. 18(18a), 86, 100(43), 140
- Fleming, S. A. 1236(167), 1274
- Flesch, G. C. 1004(33), 1046
- Fletcher, G. L. 960(206a), 994
- Fletouris, D. J. 669(466), 767
- Fletcher, R. J. 1322(118), 1345
- Flippen-Anderson, J. L. 107(86), 141,
273(440), 301
- Flippen, J. L. 938(69a), 967(213), 990, 994
- Flood, L. A. 563(402), 592
- Flood, R. W. 379(163), 381(176, 177),
382(178b), 585, 586
- Florio, S. 798(47), 828
- Flowerdew, B. E. 381(159), 585
- Flowers, A. E. 136(202), 144
- Floyd, R. A. 917(2c), 976(271), 988, 996,
1201(62c), 1209
- Flynn, C. R. 1244(202), 1274
- Flyunt, R. 616(152), 673(497), 674(503b),
740(244), 759, 762, 768
- Fochi, M. C. 107(89), 141
- Fogagnolo, M. 1021(142), 1049
- Foiles, P. G. 982(308), 998
- Fokin, V. V. 567(530b), 595
- Folli, U. 130(174), 143
- Fonaro, A. 650(361), 765
- Fong, L. G. 977(282a), 997
- Fonnum, F. 1250(228), 1275
- Fontana, A. 709(62), 757, 1333(142), 1346
- Fontana, F. 45(92, 106a–d), 89, 1160(35a–e),
1165
- Fontecave, M. 972(232), 995
- Foote, C. S. 211(145), 252(111), 255(349,
353, 354), 259(365), 263(385, 388),
269(52), 293–295, 299, 300, 325(56),
343(91b), 352(57), 583, 673(490, 491),
710(576), 768, 770, 832(6, 8, 13, 19, 20),
833(21, 22, 25, 35), 836(49, 50), 842(58),
844(61), 852(76), 853(85), 854(97, 99, 106),
856(112), 858(118, 121, 123, 124), 877(74),
878(53), 894–896, 941(82), 943(81, 83, 88,
89a, b), 948(131), 950(130, 152), 962(211),

- 969(243a, b), 991, 992, 994, 995, 1001(4),
1044(274), 1046, 1052, 1172(10b),
1173(17a), 1203(66), 1205, 1206, 1209
- Foote, S. 112(60), 140
- Ford, W. E. 962(211), 994
- Ford, W. T. 1021(129), 1048
- Foresman, J. B. 12(7), 44(100), 85, 89
- Forlani, R. 1021(142), 1049
- Formaggio, F. 123(162), 129(172), 143
- Fornes, V. 1111(403), 1127
- Fornés, V. 421(253), 564(506), 588, 594
- Forney, C. F. 667(457), 676(458), 767
- Forno, A. E. J. 315(30), 582
- Fortescue, W. F. 1265(332), 1277
- Fortin, J. J. 1199(48), 1208
- Fort, M. 531(322), 590
- Fossey, J. 213(158), 295
- Foster, B. 1337(164), 1346
- Foster, R. V. 354(113), 584
- Fowler, J. 185(35), 187
- Fowler, K. W. 1140(55b), 1166
- Fox, D. J. 12(7), 85
- Fox, W. B. 740(697), 772
- Fraile, J. M. 245(281), 298
- Francavilla, C. 576(546), 596
- France, C. J. 1097(328), 1126
- Francisco, J. S. 37(37b), 39(39), 87
- Francl, M. M. 28(28a), 87
- François, V. P. 1191(8b), 1205
- Franco, N. 1059(43), 1119
- Frankel, E. N. 323(42a, b), 582, 612(90),
669(468), 680(529), 758, 767, 769,
949(108), 991
- Franz, A. 605(36), 756
- Franz, R. 1178(19d), 1206
- Frappier, F. 238(257), 297
- Freccero, M. 37(91), 44(101), 46(110),
47(105, 111), 57(51b), 67(130a, b), 87, 89,
90, 1140(41), 1166
- Frechette, Y. 217(190), 296
- Frederich, M. 190(42), 292
- Freeburger, M. E. 811(82, 83), 829
- Freeman, B. A. 22(22a), 86, 741(699), 772,
951(174), 952(171), 953(172), 993
- Freeman, B. 951(170), 993
- Freeman, S. G. 276(502), 303
- Freitag, D. 638(188), 685(542), 707(308b),
760, 764, 769
- Freitas, A. C. C. 290(588), 305
- Frei, B. 250(296), 298, 680(537), 681(505),
768, 769, 956(201a), 977(279b), 994, 997
- Frei, H. 871(162), 897, 1082(206), 1123
- Frei, R. W. 1257(265, 267, 276, 278, 299),
1276, 1277
- Fréjaville, C. 973(254), 995
- Frelon, S. 933(58b), 975(268b), 976(270c,
273), 990, 996
- French, A. N. 1289(46), 1343
- Frenkel, K. 933(57), 990
- Frenking, G. 48(114a), 89, 1075(152, 153),
1122
- Frenzen, G. 267(418, 420), 301
- Freund, H. G. 933(58a), 990
- Frew, J. W. 659(260), 762
- Frey, J. 183(32), 187, 471(364), 591
- Friderich, W. 1002(13), 1046
- Fridgen, J. 1085(246), 1086(251), 1124
- Fridovich, I. 740(83), 758, 1243(197),
1250(226, 227), 1274, 1275
- Friedline, R. 909(94), 913
- Friedman, A. E. 572(545), 596
- Friedrich, H. B. 569(534), 595
- Friedrich, S. S. 901(30), 912
- Frimer, A. A. 252(320), 253(318, 327, 346),
273(325), 285(285), 298, 299, 310(6),
343(91c), 581, 584, 832(2), 835(41), 893,
894, 946(126c), 954(192b, c), 966(233d,
235), 992, 993, 995, 1174(18a), 1206,
1235(130), 1273
- Friquet, B. 984(317c), 998
- Frisch, M. J. 4(11a), 12(7), 44(100), 85, 86, 89
- Frisco, G. 183(30), 187
- Frisone, L. 1109(393), 1127
- Fristad, W. E. 889(199, 200), 898
- Fritchie, C. J. 99(40b), 139
- Fritsche, K. L. 660(423), 766
- Fritzsche, J. 253(324), 299
- Fritz, R. 622(192), 760
- Froba, M. 418(249), 588
- Froese, C. D. 617(156), 759
- Frohlich, L. 888(91, 92), 895
- Fröhlich, L. 112(71), 140
- Frohn, M. 1021(141), 1049, 1140(74, 75),
1146(71), 1150(93), 1163(1n), 1165, 1167
- Frommel, T. O. 987(331b), 999
- Fronczek, F. R. 112(73, 83), 114(91),
123(161), 140, 141, 143, 1062(62), 1119
- Fronza, G. 45(92, 106c, d), 89, 1160(35c–e),
1165
- Froudakis, G. E. 873(168), 880(181), 897
- Froudakis, G. 875(175), 897
- Fruvip, D. J. 15(15), 86
- Fuchs, K. 199(90), 294
- Fuchs, P. L. 1158(131), 1168
- Fueno, T. 833(29), 894
- Fugmann, B. 273(450), 302, 1317(68), 1343
- Fuhrer, J. 608(54), 757
- Fuhrmann, P. 112(94), 141
- Fujii, T. 352(48), 582
- Fujimori, K. 13(13c, d), 86
- Fujimoto, K. 680(538), 769
- Fujimoto, T. T. 844(62), 895
- Fujinaga, T. 918(8d), 988
- Fujino, I. 129(171), 143
- Fujisaka, T. 110(110), 111(111), 112(112),
113(113), 141

- Fujisawa, K. 118(135), 142
 Fujita, J. 1100(344), 1126
 Fujita, M. 208(132), 294
 Fujita, S. 923(42a), 990
 Fujiwara, M. 605(29), 756, 1115(412), 1127
 Fuji, K. 567(531g), 595
 Fukui, K. 833(27), 894
 Fukushima, T. 1257(284), 1276
 Fukushima, Y. 418(249b), 588, 664(441), 767
 Fukuzumi, S. 208(132), 294
 Fullerton, D. S. 497(405a), 592
 Fuller, D. L. 900(10), 912
 Fuller, M. P. 624(232), 761
 Fulton, N. 612(102), 758
 Fung, Y. 221(204), 296
 Funk, C. D. 214(167), 295
 Funk, J. O. 273(459, 460), 302, 1336(154), 1346
 Funk, M. O. 212(152, 153), 237(164), 295, 319(8), 581
 Furia, F. Di 1106(376), 1127
 Furin, G. G. 123(164), 143
 Furstemberger, G. 981(303), 998
 Furtado, M. M. 1314(97), 1344
 Furuichi, N. 857(117), 896
 Furukawa, H. 1094(302), 1125
 Furusawa, K. 1156(123b), 1168
 Furutachi, N. 325(53), 583, 854(88), 895
 Furutani, H. 743(704), 773
 Fusco, C. 41(93), 47(103), 89, 1140(13, 36), 1153(109), 1160(134, 139a, 142, 143), 1161(145), 1163(1k, 25, 152a, b), 1164, 1165, 1168, 1169
 Fusetani, N. 1334(144), 1346
 Fu, G. C. 48(116), 89, 860(128), 896
 Fu, H. N. 712(58), 757, 1326(106), 1345
 Fu, H. 476(71), 583, 1015(103), 1048
 Fu, M. X. 614(142), 759
 Fu, P. P. 980(289b), 997
 Fu, S.-L. 957(202), 994
 Fu, S. 614(142), 691(143), 759, 918(13), 956(200), 959(203), 972(253a), 973(256, 257), 987(15, 327, 332), 989, 994–996, 999
 Fu, X.-Y. 31(81), 88
 Gabe, E. J. 112(68), 140
 Gabriëls, M. 659(419), 766
 Gäb, E. 728(630, 666, 667), 771, 772
 Gab, S. 124(147), 142
 Gäb, S. 605(25), 638(314), 674(502), 678(522), 679(312, 313, 525–527), 708(546), 724(658), 756, 764, 768, 769, 772
 Gadelha, F. R. 951(173), 993
 Gadjev, I. 610(71), 757
 Gafney, H. 1189(44a), 1208
 Gaggero, N. 384(185), 476(368a, b, 369), 586, 591, 1157(12, 126, 128), 1165, 1168
 Gagnon, S. D. 1256(31), 1271
 Gajewski, J. J. 56(56b), 87
 Galal, A. M. 273(465), 302
 Galán, G. 643(331), 764
 Gallaher, K. L. 721(649), 771
 Galli, A. 667(456), 767
 Galli, R. 1010(71), 1047
 Galloo, J.-C. 605(10), 756
 Gallopo, A. R. 1003(22), 1046
 Galván, F. 646(343), 764
 Gal, A. W. 1062(42), 1119
 Gal, A. 981(300), 998
 Gal, J.-F. 874(170), 897
 Gambacoirta, A. 1162(151c), 1169
 Gambaro, M. 512(399), 592, 1094(305), 1106(377), 1125, 1127
 Gamiz-Gracia, L. 1240(173), 1257(288, 301), 1274, 1276, 1277
 Gandolfi, R. 37(91), 44(101), 46(110), 47(105, 111), 57(51b), 67(130a, b), 87, 89, 90, 1140(41), 1166
 Gandour, R. D. 112(83), 141
 Ganem, B. 385(189), 586
 Ganeshpуре, P. A. 539(20), 582, 1161(122), 1168
 Gansäuer, A. 459(349), 590
 Ganyushkin, A. V. 103(48), 140
 Gan, Y. 1148(79c), 1167
 Gao, F. G. 276(441), 302, 1314(95), 1344
 Gao, F. L. 276(494), 303
 Gao, F. 646(344), 764
 Gao, L. 217(179), 296
 Gao, R. 1059(43), 1119
 Gao, X. 265(402), 301
 Gao, Y. 400(208), 587, 1092(282), 1125
 Gara, M. 1081(184), 1091(186), 1107(185), 1122
 García Fraile, A. 520(449), 593
 García Martínez, A. 520(449), 593
 García-Campana, A. M. 1240(173), 1257(288, 301), 1274, 1276, 1277
 García-Domínguez, S. 646(343), 764
 García-Moreno, E. 688(558), 769
 Garcia, C. C. M. 984(292a), 997
 Garcia, H. 870(148c), 896
 García, H. 477(373b), 591
 Garcia, J. I. 245(281), 298
 Garcia, M.-A. 449(337), 590
 Garcia, N. A. 968(239c), 995
 García, P. 705(24), 756
 García, S. 641(309), 764
 Gardette, J.-L. 662(430), 692(569), 766, 770
 Gardiner, D. J. 101(53), 140
 Gardini, G. P. 1010(71), 1047
 Gardner, H. W. 946(126a), 977(283, 285), 992, 997
 Garland, D. 987(329c), 999
 Garneau, F. X. 196(77), 293
 Garner, R. C. 1140(55a, 55c, 56b, c), 1166
 Garnett, L. 1021(133), 1048

- Garrison, W. M. 955(194), 993
 Garson, M. J. 136(202), 144
 Gartner, P. 259(362–364), 300
 Garvie, M. 623(197), 761
 Garwood, R. F. 323(42a, b), 582
 Gasch, N. 382(179), 586
 Gasic, G. P. 190(14), 292
 Gasparoli, A. 656(402), 766
 Gasparrini, F. 47(103), 89, 1163(1k), 1164
 Gasparutto, D. 933(58b), 940(75a, 77),
 943(9b, c, 91), 989–991, 1203(67b), 1209
 Gassmann, E. 184(33), 187
 Gatilov, Y. V. 123(164), 143
 Gatter, K. C. 1335(149), 1346
 Gatti, R. M. 952(176), 993
 Gaudu, P. 972(232), 995
 Gaulier, J. M. 646(346), 764
 Gauss, J. 12(7c), 67(67), 72(72b, 72f), 85, 88
 Gauthier, R. 899(5), 912
 Gaut, J. P. 610(79), 757
 Gavagnini, R. 1109(122), 1112(123), 1121
 Gavagnin, M. 709(62), 757, 1333(142), 1346
 Gavagnin, R. 539(496), 559(515), 594
 Gavrilan, M. 201(91), 294
 Gavrilova, A. L. 1067(76), 1120
 Gay, C. A. 676(515), 768, 986(246), 995
 Gay, C. 986(322, 323), 999
 Gay, F. 280(529), 304, 1303(65), 1343
 Gazarian, I. G. 694(146), 759
 Geacintov, N. E. 940(77, 78), 991
 Gebhart, E. 273(459), 302
 Gebicki, J. M. 673(406), 674(250), 676(515),
 762, 766, 768, 972(196a–c, 222b, 253a, b),
 974(264), 975(267), 986(246, 321b, 322,
 323), 994–996, 999
 Gebicki, J. 945(99), 991
 Gebicki, S. 972(196a, b, 222b, 253a),
 974(264), 994–996
 Gee, C.-S. 607(48), 757
 Geiger, P. G. 687(550, 551), 769, 977(279c,
 d), 997
 Geiger, R. 1193(49a), 1208
 Geisberger, M. R. 466(344), 590, 1083(216),
 1123
 Geiser, F. 193(63), 293
 Gekhman, A. E. 528(467), 531(468), 593
 Gelalcha, F. G. 107(95), 112(97), 141
 Gelbard, G. 440(313a), 444(314), 589
 Geletii, Y. V. 40(40b), 87
 Geletneky, C. 177(15), 186
 Geller, T. P. 381(177), 586
 Geller, T. 380(161, 165), 585
 Gemmecker, G. 1076(157), 1122
 Gentile, A. 1010(69), 1047
 George, A. J. T. 616(147), 759
 George, P. 675(509), 768
 Georgiou, C. A. 656(401), 658(411), 766
 Georgiou, C. D. 628(68), 757
 Gérard-Monnier, D. 669(470, 471), 767
 Gerard, D. 284(540), 304, 1324(122), 1345
 Gerasimenko, A. V. 1058(37), 1119
 Gerber, M. J. 163(5), 167
 Gerena, C. H. Oh. L. 725(57), 757
 Gerena, L. 280(517, 518), 283(519), 303, 304,
 712(58), 757, 1298(18), 1326(106), 1342,
 1345
 Gere, E. P. 678(252), 762
 Gerlach, A. 569(535b), 595
 German, J. B. 680(529), 769, 984(317d), 999
 Gerothanassis, I. P. 185(37), 187
 Gerothanassis, I. 184(33), 187
 Gérot, O. 940(75a), 991
 Gerpe, L. D. 273(440), 301
 Gershanov, F. B. 533(475), 593
 Gerth, K. 1145(67c, d), 1166
 Gessup, W. 972(253a), 995
 Gevert, O. 888(140), 896
 Ghelli, S. 130(174), 143
 Ghigo, G. 253(338), 299
 Ghiladi, M. 1067(75), 1120
 Ghiotti, P. 1031(207), 1050
 Ghiron, A. F. 1068(84), 1120
 Ghodrati, K. 1004(28–30), 1046
 Ghorbani, M. 531(473), 593
 Ghormley, J. A. 131(188), 143, 674(503a),
 768, 965(214), 994
 Ghosh, A. 425(264), 588
 Ghosh, P. 128(169), 143
 Ghosh, S. K. 1074(128), 1121
 Ghosh, S. 617(156), 759
 Giannakakou, P. 1145(67e), 1166
 Giannattasio, S. 1076(158), 1122
 Gibian, M. J. 900(15), 912
 Gibson, D. H. 250(293), 298
 Gibson, D. T. 1200(58b), 1208
 Giernoth, R. 471(364), 591
 Gieseg, S. P. 971(250), 995
 Gieseg, S. 972(196a), 986(321b), 994, 999
 Giese, B. 213(162), 295
 Giguère, P. A. 99(40a), 133(189), 139, 143
 Gilbert, B. C. 449(334), 590, 973(248), 995
 Gilbert, D. L. 984(320), 999
 Gilbert, L. 418(247), 588
 Gilinski-Sharon, P. 285(285), 298
 Gillen, K. T. 685(543, 544), 769
 Gillette, G. R. 825(108b), 829
 Gillies, C. W. 721(595, 645, 649, 651),
 722(647), 770, 771
 Gillies, J. Z. 721(595), 770
 Gillmor, S. A. 1322(118), 1345
 Gill, C. D. 365(138), 585
 Gill, P. M. W. 12(7), 85
 Gilman, S. 564(501), 594
 Gilmore, D. W. 233(11), 237(237), 292, 297,
 317(16), 582
 Gilmore, D. 237(164), 295, 319(8), 581

- Gilner, D. 122(157), 143
 Gilson, D. F. 166(63), 169
 Gimeric, B. M. 2(2), 85
 Ginanneschi, M. 107(87), 141
 Giokas, D. L. 624(220), 761
 Giordano, C. 1008(51), 1010(77), 1047
 Giordano, F. 112(103), 118(118), 141, 142
 Girard, M. 567(531e), 595
 Girerd, J.-J. 1069(45), 1070(47), 1117(431), 1119, 1128
 Giri, B. P. 1198(33a, b), 1207, 1236(32, 33), 1271
 Girotti, A. W. 686(508), 687(550–552), 768, 769, 945(106, 124), 947(127), 948(132), 977(276, 277b, 277f, 279c, d), 991, 992, 996, 997
 Giroud, A. M. 921(32), 989
 Gisdakis, P. 48(114a), 89, 1075(148, 150, 151), 1121, 1122
 Gisin, M. 196(60), 198(79), 293
 Gitlin, S. N. 637(305), 648(307), 763
 Giuffre, L. 428(294), 589
 Giustarini, D. 986(326), 999
 Givens, R. S. 1188(40c, d), 1207, 1257(286), 1262(308, 311), 1263(316, 328), 1276, 1277
 Gladstone, M. T. 899(1), 911
 Glasstone, S. 910(72b), 913
 Glass, R. S. 1156(125), 1168
 Glas, H. 466(355), 591, 1069(115), 1076(156), 1083(219), 1121–1123
 Glaubitz, K. 382(179), 586
 Glazer, A. N. 680(537), 689(559), 769
 Glaze, W. H. 679(524), 769
 Gleeson, D. 1082(203), 1123
 Gleicher, G. J. 901(35), 912
 Gleicher, G. S. 901(31, 33), 912
 Gleim, R. D. 354(112), 584
 Gleiter, R. 861(94), 889(199), 895, 898
 Glende, E. A. 671(479), 768, 977(277d), 996
 Gleu, K. 1248(5), 1270
 Glidewell, C. 103(51), 140
 Glogar, H. D. 611(82), 758
 Glukhovtsev, M. N. 43(38), 47(107), 50(122), 56(12b, 48d), 58(124), 66(138), 73(19b, c), 86, 87, 89, 90, 1140(49, 50), 1160(53), 1166
 Goacolou, K. 1021(133), 1048
 Gobbato, K. I. 132(194), 144
 Gobert, F. 724(606), 770
 Gobey, J. S. 933(58a), 990
 Gocke, E. 273(273), 298, 608(59), 757, 1332(14), 1342
 Godbout, N. 185(39), 187
 Goddard, J. D. 1248(215), 1275
 Goddard, R. 1097(334), 1126
 Goddard, W. A. 28(61a), 88, 95(13a), 138(211), 139, 144, 832(16), 894
 Godde, F. 1069(45), 1119
 Goetz, M. 1145(67b), 1166
 Goggiamani, A. 560(511), 594, 1111(400), 1127
 Gogolinskii, V. I. 130(185), 143
 Gohda, R. 1257(284), 1276
 Goins, D. K. 276(498, 499), 303, 1286(41), 1314(64, 96), 1343, 1344
 Goins, K. 1306(74), 1344
 Goirine, R. A. 1039(245), 1051
 Gokhale, A. S. 516(435), 592
 Goldberg, K. I. 1064(70), 1120
 Goldberg, N. 68(143), 90, 97(31), 139
 Golden, D. M. 18(18b), 86, 100(44), 140
 Golding, B. T. 118(132), 142, 982(291d), 997
 Goldschmidt, B. M. 982(291a), 997
 Goldstein, B. 1040(249), 1051
 Goldstein, J. A. 963(225b), 994
 Goldstein, S. 611(84), 741(700), 758, 773, 952(179), 987(325a), 993, 999
 Gold, L. S. 917(1c), 988
 Golebiowski, A. 266(405, 406), 301
 Golic, L. 129(173), 143
 Gollnick, K. 135(201), 144, 205(119), 206(120), 208(125, 126, 128–130), 254(326, 348), 255(352), 260(369), 294, 299, 300, 324(49), 582, 832(14), 837(52), 854(98, 108), 861(130, 132), 894–896
 Golsch, D. 1096(323), 1126, 1143(60), 1154(110), 1155(118a, b), 1162(151a), 1166, 1168, 1169
 Gomes, O. F. 984(294a), 997
 Gómez Vara, M. E. 164(53), 165(54), 169
 Gomez, E. 612(102), 758
 Gomez, J. T. 1067(75), 1120
 Gómez, M. 610(78), 757
 Gomperts, R. 12(7), 85
 Goncalves, I. S. 471(296), 589, 1086(252), 1124
 Gong, B. Q. 1322(117, 118), 1345
 Gonon, L. 672(189), 760
 Gonzalez Cuervo, L. 1117(429), 1128
 Gonzalez-Núñez, M. E. 1155(117), 1160(138, 139a, b), 1161(105), 1167–1169
 González-Núñez, M. E. 1140(14), 1158(132), 1160(141), 1165, 1169
 Gonzalez, A. 974(262d), 996
 Gonzalez, C. 12(7), 50(122), 56(12b), 58(124), 68(141), 73(19b), 79(17b), 85, 86, 90, 97(32a), 139
 Gonzalez, L. 209(140, 141), 280(527), 295, 304, 1116(420), 1128, 1284(39), 1291(48), 1343
 Gonzalez, M. C. 1333(142), 1346
 Goodall, P. 635(298), 763
 Goodard, W. A. 28(61b), 88
 Goodman, J. L. 206(121, 122), 209(144), 294, 295
 Goodwin, S. 319(21), 582
 Goodyear, W. F. 1040(249), 1051

- Gooijer, C. 1257(265, 267, 276, 278, 297, 299), 1276, 1277
- Gopalan, P. 122(154), 142
- Gopinathan, G. 1116(419), 1128
- Gopinathan, S. 1116(419), 1128
- Gorb, L. 57(53), 87
- Gordon, G. 607(47), 757
- Gordon, M. S. 12(7b), 85
- Gorin, G. 629(261), 762
- Gorman, A. A. 253(342), 299, 832(15), 835(33, 40), 894
- Gorman, R. R. 233(10), 292
- Gormish, J. F. 1006(41), 1047
- Gornitzka, H. 284(548), 304
- Gorrichon, L. 201(91, 92), 294
- Gorst-Allman, C. P. 1140(56a), 1166
- Görth, F. 1155(118b), 1168
- Goschenhofer, D. 358(126), 584
- Goshe, M. B. 956(198), 994
- Gosser, D. K. 1312(78), 1344
- Goswami, P. 323(43), 582
- Goti, A. 536(484), 594, 1103(362), 1126
- Goto, M. 852(78, 79), 895
- Goto, S. 987(331a), 999
- Goto, T. 1214(30), 1244(203), 1271, 1274
- Göttlich, R. 793(38), 828
- Gottlieb, H. E. 285(285), 298
- Gottwald, T. 138(208), 144
- Gougoutas, J. Z. 105(14), 139
- Gould, E. S. 423(260, 261b), 588
- Gould, I. R. 835(40), 894
- Govorova, A. A. 129(176), 143
- Goyette, G. 660(424), 766
- Go, K. M. 911(71), 913
- Grabowski, S. 193(58), 196(64, 72), 293
- Graca, M. D. 1293(36), 1343
- Grace, J. M. 1317(107), 1345
- Grade, M. M. 1024(157), 1049
- Gräfenstein, J. 32(85b), 88
- Grandison, A. S. 634(89), 636(299), 758, 763
- Grandjean, D. 440(313a), 589
- Grand, A. 921(33), 922(39a, b), 989, 990
- Grant, K. E. 605(36), 756
- Grassian, V. H. 871(163), 897
- Grassi, J. 1256(253), 1275
- Grass, R. S. 1234(21), 1270
- Graupner, A. J. 718(634), 771
- Grau, A. 676(229), 761
- Grau, N. D. 889(201), 898
- Grayesi, M. L. 1257(257, 266, 291, 295, 300, 302), 1276, 1277
- Gray, P. 163(49), 169
- Graziano, M. L. 108(100), 141, 259(367), 300
- Grđina, M. B. 832(18), 871(3), 875(37), 893, 894
- Grđina, M. J. 343(91a), 583
- Greb, M. 138(207), 144, 1074(137), 1121
- Greci, L. 1155(119b), 1168
- Greenberg, A. 832(8), 894
- Greenberg, M. M. 920(24), 935(61, 62), 989, 990
- Greene, F. D. 1178(20a), 1206
- Greenhalgh, R. P. 1025(164), 1049
- Greenland, H. 323(47), 582
- Greenlee, L. 1250(226), 1275
- Greenspan, F. P. 1013(88), 1047
- Greenstock, C. L. 971(199a), 994
- Green, S. D. 1099(341), 1126
- Greer, A. 833(35), 894
- Grega, K. C. 1023(154), 1049
- Gregoire, F. 280(529), 304
- Greijdanus, B. 374(147b), 585
- Grellier, P. 238(257), 297
- Gremaud, E. 975(269b), 996
- Grever, M. R. 1145(67a), 1166
- Grey, C. P. 870(160), 882(182), 885(158), 897
- Griebenow, N. 1097(334), 1126
- Grieco, P. A. 564(501), 594
- Griesbaum, K. 175(11), 183(10), 186, 724(659), 772
- Griesbeck, A. G. 114(69), 140, 209(137), 252(322), 253(344), 263(383, 384), 274(484), 295, 299, 300, 303, 854(89), 895
- Griesbeck, A. 135(201), 144, 253(330, 333), 254(348), 255(352), 299, 300, 326(59), 408(86), 583, 852(72, 73), 854(98), 888(191, 192), 889(80), 895, 897, 1178(20b), 1206
- Griffin, G. W. 130(184), 143, 1035(227), 1051
- Griffiths, H. 681(144), 759
- Griffiths, M. J. 380(162), 585
- Griffith, W. P. 567(525), 595, 1057(19), 1058(30), 1069(101, 112), 1102(352), 1118–1121, 1126
- Grigoropoulou, G. 1080(175), 1122
- Grimme, S. 1204(72b), 1209
- Grimm, E. 1243(187), 1274
- Grobet, P. J. 457(330), 590
- Grof, P. 977(275a), 996
- Grohmann, K. 198(84), 293
- Grollman, A. P. 945(113), 992, 1201(62d), 1209
- Groot, M. 670(124), 759
- Grossmann, D. 638(314), 764
- Gross, E. 900(27), 912
- Groth, P. 726(662), 772
- Grubbs, R. H. 419(258), 425(244), 588
- Grundemann, E. 280(280), 298
- Grune, M. 943(85b), 991
- Grüne, M. 1204(71), 1209
- Grunheck, F. 1336(158), 1346
- Grunwald, E. 910(74), 913
- Guajardo, R. R. J. 1117(427), 1128
- Gualandi, G. 560(510), 594, 1111(399), 1127
- Gualtieri, A. F. 882(182), 897
- Guan, C. 1015(101), 1048

- Guan, J.-Q. 870(154, 155), 897
 Guardiola, F. 676(229), 761
 Gubitz, G. 1257(267), 1276
 Gude, M. 656(221), 761
 Gudipati, M. S. 253(344), 299
 Guengerich, F. P. 982(309), 984(310–313), 998, 1140(52d), 1166
 Guerchais, J. E. 425(267), 588
 Guerrini, A. 797(45), 800(49), 828
 Guichardant, M. 918(10), 989
 Guichard, Y. 984(297c, 297h), 998
 Guilbault, G. G. 638(311), 764, 1257(303), 1277
 Guilet, D. 892(65), 895
 Guillhem, J. 1069(45), 1119
 Guillén, M. D. 661(425–429), 666(408), 766
 Guillier, A. 976(270a), 996
 Guilment, J. 624(223, 226), 761
 Guiráim, A. 646(343), 764
 Guisnet, M. 1114(11), 1118
 Guitto, A. 112(103), 118(118), 141, 142, 273(438), 301
 Guixer, J. 380(155), 381(154), 585
 Gullotti, M. 476(368a, b), 591
 Gultekin, M. S. 264(400, 401), 301
 Gultekin, S. 264(394), 300
 Gunda, T. E. 1156(123a), 1168
 Gundermann, K. D. 1245(210–212), 1274, 1275
 Gundermann, K. 1250(224), 1252(246), 1275
 Gündoğan, M. 700(557), 769
 Gunn, C. 22(22b), 86
 Gunstone, F. D. 254(254), 297, 310(7a), 581
 Gunzner, J. L. 259(362–364), 300
 Gunz, W. G. 626(1), 756
 Guo, C. 1317(103), 1344
 Guo, Z.-X. 629(259), 762
 Guo, Z. 651(365), 765
 Gupta, N. 274(482, 483), 303, 1326(129), 1345
 Gurgan, S. 623(205), 761
 Gurtz, J. 608(54), 757
 Gusso, A. 558(513), 594, 1087(260), 1112(406), 1124, 1127
 Gustafsson, L. 987(325d), 999
 Gutbrod, R. 32(83), 78(78), 82(82a), 84(84), 88
 Guthlein, M. 260(371), 300
 Guthrie, J. P. 163(60), 169
 Gutsche, S.-H. 175(11), 186
 Gutteridge, J. M. C. 669(467), 767, 945(102), 977(286), 991, 997
 Gutz, I. G. R. 650(361), 765
 Gut, J. 1322(116), 1345
 Guzei, I. A. 1064(71), 1120
 Gu, D. 44(95), 89, 1140(45), 1156(120), 1166, 1168
 Gu, Y. 98(36), 139
 Gwaltney, S. R. 12(7c), 85
 Haanepen, M. J. 514(409b), 592
 Haase, W. 1067(77), 1120
 Haas, B. 102(49), 140
 Haas, W. 1074(126), 1121, 1140(51), 1166
 Hachey, D. L. 214(177), 295, 693(571), 703(593), 704(594), 770
 Haddadi, R. 1018(114), 1048
 Haddon, W. F. 978(287a), 980(289a), 997
 Hadd, A. G. 1261(319), 1262(318), 1277
 Hadjiara Poglou, L. 1021(131), 1048
 Hadjiarapoglou, L. P. 1163(1d), 1164
 Hadjiarapoglou, L. 1143(60), 1155(106d), 1158(32), 1163(1e), 1164–1166, 1168, 1178(20d), 1206
 Hadley, M. 977(277c), 996
 Haenel, F. 267(418, 419), 301
 Hafner, K. 1250(224), 1252(246), 1275
 Hagemann, H. 536(483), 594
 Hagen, R. 177(19), 187
 Hagen, T. 286(555), 305
 Hager, A. 675(504), 768
 Hage, R. 445(325), 590, 1069(44, 48, 50), 1074(135), 1119, 1121
 Hahn, B.-S. 927(50), 990
 Hahn, B. S. 938(69a), 990
 Hahn, W. 777(6), 827
 Haider, J. J. 461(353), 590, 1086(251), 1124
 Haines, L. G. 1267(71), 1272
 Haines, P. G. 1102(350), 1126
 Haissinsky, M. 921(26), 989
 Hajipour, A. R. 1018(114, 115), 1025(159, 160), 1027(173), 1028(182), 1031(209–213), 1032(214, 215), 1048–1050
 Halász, J. 1163(1g), 1164
 Halatsch, M. E. 273(459), 302
 Halcomb, R. L. 1154(113), 1168
 Halligudi, S. B. 1116(419), 1128
 Halliwell, B. 628(74), 655(258), 757, 762, 945(102), 991
 Hall, C. D. 824(117a), 830
 Hall, E. D. 675(507), 768
 Hall, L. M. 690(565), 770
 Halow, I. 154(21), 168
 Halpern, A. M. 1184(25a), 1207, 1228(94), 1272
 Halpern, J. 1189(44a), 1208
 Halper, J. B. 641(326), 764
 Halsted, C. H. 984(314), 998
 Halut, S. 1063(64), 1120
 Hamada, F. 1192(16b), 1206
 Hamakawa, S. 1095(307), 1125
 Hamann, H.-J. 112(117), 142, 329(65), 331(68, 69), 475(70), 493(66, 100, 101), 583, 584, 1099(343), 1126
 Hamano, T. 858(122), 896
 Hamberg, M. 190(6, 7, 9), 214(166), 292, 295, 737(92), 758, 949(134), 992

- Hamblett, I. 835(33, 40), 894
 Hambley, T. W. 212(148, 151), 295
 Hamel, E. 1145(67e), 1166
 Hamer, J. 254(326), 299
 Hamida, N. B. 823(116), 830
 Hamilton, G. A. 1035(228), 1051
 Hamilton, T. P. 31(31), 34(34), 35(35), 87
 Hammond, G. S. 907(79), 913
 Hampel, C. 12(7d), 85
 Hamstra, B. J. 1062(60), 1119
 Hamzaoui, M. 280(528, 529), 304
 Ham, A. J. L. 981(298c), 998
 Ham, A. J. 982(291f, g), 997
 Ham, J. 256(359), 273(464), 300, 302, 1338(166), 1346
 Hanada, Y. 680(530), 769
 Hanafusa, M. 432(299), 589, 1086(250), 1124
 Hanaoka, N. 1257(289), 1276
 Handelsgesellschaft, D. O. 1004(33), 1046
 Handler, P. 1250(226), 1275
 Handley, R. S. 1198(33a, b), 1207, 1236(32–34), 1271
 Handy, N. C. 12(7e), 85
 Haneda, Y. 1224(67), 1225(64), 1271
 Hanessian, S. 567(531e), 595
 Hang, C. 833(35), 894
 Hanks, T. W. 1020(120), 1048
 Hanna, P. M. 917(5e), 988
 Hanna, W. J. W. 1008(59), 1047
 Hanemann, K. 196(64, 71, 72), 293, 951(165), 993, 1224(58), 1271
 Hann, R. A. 1250(219), 1256(27), 1271, 1275
 Hanquet, G. 1021(133), 1048
 Hansen, L. F. 680(532), 769
 Hansen, N. 1085(244), 1124
 Hansen, R. T. 734(681), 772
 Hansen, S. H. 1322(120), 1345
 Hanser, C. F. W. 82(160), 91
 Hanson, J. C. 882(182), 897
 Hanson, P. 487(389), 591
 Hanson, R. M. 400(208), 479(385), 587, 591, 1092(282), 1125
 Hanspal, M. 1322(81), 1344
 Hanzlik, R. P. 55(120), 90
 Han, G. R. 503(425), 592
 Han, J. X. 273(458), 302
 Han, Q. 260(373), 300
 Hapangama, W. 283(471), 302, 1337(162), 1346
 Happ, J. W. 1250(223), 1251(238, 239), 1275
 Haq, A. 273(476), 303
 Harada, T. 250(294), 298
 Haraldson, C. A. 276(502), 303
 Harata, M. 1064(69), 1120
 Hara, R. 265(403), 301
 Hardcastle, K. I. 1082(193), 1123
 Harding, L. B. 28(61b), 88, 832(16), 894
 Harding, M. J. C. 1172(3), 1205
 Harding, M. M. 130(177–179, 186), 143
 Hardy, D. R. 617(157), 759
 Hardy, E. M. 56(56a), 87
 Hargrave, K. R. 675(509), 768
 Hari Prasad Rao, P. R. 531(469), 593
 Harigaya, Y. 374(151), 585
 Harijono, S. W. B. 605(29), 756
 Häring, D. 338(76, 77), 583
 Harkins, J. 734(681), 772
 Harmsen, D. 339(78), 583
 Harms, D. 637(239, 303, 304), 762, 763
 Harms, K. 118(122), 124(124), 142, 1067(57), 1119
 Harpp, D. N. 1156(120), 1168
 Harrison, B. 610(64), 757
 Harrison, J. G. 34(34), 35(35), 87
 Harrison, K. A. 739(694), 772
 Harris, K. D. M. 526(465), 593
 Harris, S. A. 1084(239), 1124
 Harris, T. M. 1140(57), 1166
 Harrup, M. K. 1082(198), 1123
 Hartmann, H. 832(14), 894
 Hartman, H. 161(43), 169
 Hartung, C. 112(93, 97), 141
 Hartung, J. 138(207, 208), 144, 1074(137), 1121
 Hartvigsen, K. 680(532), 769
 Hartz, N. 84(167), 91
 Hart, B. T. 645(340), 764
 Hart, E. J. 1189(44a), 1208
 Hart, H. 63(135), 90
 Hart, R. 1256(252), 1275
 Harvey, I. 1283(29), 1342
 Harvey, J. N. 84(165a), 91
 Harvey, L. M. 1251(231), 1275
 Harwood, L. M. 256(357, 358), 300
 Hasegawa, K. 1064(69), 1120
 Hasegawa, T. 196(76), 293
 Hasemann, L. 889(201), 898
 Hashida, I. 205(114), 208(103b), 294
 Hashidoko, Y. 218(192), 219(193, 194), 296
 Hashimoto, K. 650(360), 660(422), 765, 766
 Hashimoto, M. 1257(277), 1276
 Hashimoto, N. 1021(132), 1048
 Hashimoto, S. 318(9), 468(356), 582, 591, 743(704), 773, 817(95), 829
 Hashimoto, T. 444(311), 445(312), 589, 1081(177), 1089(178), 1122
 Hashizoe, M. 640(324), 641(100), 758, 764
 Hashizume, M. 481(381), 486(386), 591, 1097(331, 332), 1126
 Haskard, D. O. 616(147), 759
 Haslmayer, P. 611(82), 758
 Hasomi, A. 901(41), 912
 Hassall, C. H. 1003(18), 1046
 Hassaneen, H. M. 196(60), 293
 Hassan, D. 1021(127), 1048
 Hassner, A. 1181(11d), 1206

- Hastings, J. W. 1224(66, 67), 1226(65), 1235(132), 1271, 1273
 Hasty, N. M. 854(103), 896
 Hathaway, S. J. 263(382), 300
 Hatsui, T. 284(538), 304
 Hatta, Y. 682(474), 767
 Hattori, N. 612(108), 758
 Hatzelmann, A. 1242(191), 1274
 Hauenstein, E. 1004(32), 1046
 Haugland, R. P. 643(67), 757
 Hause, F. M. 1001(4), 1046
 Hauthal, H. G. 623(199), 761
 Havlin, R. H. 185(39), 187
 Havrilla, C. M. 214(177), 217(178, 179), 295, 296, 693(571), 714(96), 758, 770
 Hawco, F. J. 950(143), 992
 Hawkins, C. L. 968(240), 970(195a), 971(199c), 973(241, 249a), 986(321a), 993–995, 999
 Hawkins, E. G. E. 351(103b), 423(259), 584, 588
 Hawley, S. R. 1283(31), 1343
 Haw, J. F. 873(167), 897
 Hayaishi, O. 966(219), 994
 Hayakawa, K. 1257(290), 1276
 Hayakawa, T. 1095(307), 1125
 Hayakawa, Y. 805(60), 828
 Hayami, S. 1067(55), 1119
 Hayase, T. 1257(283), 1276
 Hayashi, M. 1105(370), 1127
 Hayashi, S. 255(350), 300, 497(405b), 592
 Hayashi, T. 809(71), 828, 1011(82), 1047
 Hayashi, Y. 514(432), 592, 1065(72), 1120
 Hayden, M. R. 341(87), 583
 Hayman, G. D. 138(209b), 144
 Haynes, R. K. 208(108), 211(106, 107, 109, 110, 146, 147), 212(148, 151), 213(156), 229(222), 273(39, 46, 449, 450), 288(565–567, 570, 572), 290(581, 591), 292, 294, 295, 297, 302, 305, 362(133), 584, 1301(59, 60), 1302(62), 1303(7), 1313(80), 1314(88), 1317(68, 87, 100), 1342–1344
 Hayon, E. 924(44), 990
 Hayter, B. R. 1140(85a, b), 1167
 Hazelhof, E. 190(8), 292
 Hazell, A. 1067(75), 1120
 Hazen, S. L. 963(225c), 994
 Hazlewood, C. 974(265), 996
 Ha, T.-K. 97(27b), 101(46), 139, 140
 Hdrich, J. 165(62), 169
 Head-Gordon, M. 9(9), 12(7), 85
 Headlam, H. A. 973(247), 986(324), 995, 999
 Heah, P. C. 174(9), 186
 Heaney, H. 795(40), 828
 Heaton, M. M. 310(3a), 581
 Héberger, K. 656(221), 761
 Hecher, M. 610(70), 757
 Hecht, E. 1081(171), 1122
 Heckel, F. 352(72), 583
 Hedman, B. 1069(54), 1119
 Heeg, M. J. 729(668), 772
 Hegarty, A. F. 902(65), 913
 Heggs, R. P. 385(189), 586
 Heiba, E. I. 900(12), 912
 Heicklen, J. 729(643), 731(640), 732(642), 771
 Heidary, M. A. 1016(106), 1048
 Heidenfelder, T. 192(62), 293
 Heiderich, E. W. 1040(247), 1051
 Heiffer, M. H. 1281(5), 1342
 Heikes, B. G. 604(4, 5), 698(310), 756, 764
 Heil, M. 1178(20c), 1181(11f), 1206, 1230(112), 1233(14), 1270, 1272
 Heinecke, J. W. 610(79), 757, 945(100), 963(225b, c), 991, 994
 Heinmüller, P. 678(522), 769
 Heisey, C. W. 138(210b), 144
 Helbock, H. J. 670(475), 767, 975(269a), 996
 Helder, R. 374(147), 585
 Held, S. 208(128, 129), 294
 Helesbeux, J. J. 238(257), 297
 Heller, C. A. 1261(322), 1277
 Helle, P. 1192(47e), 1208
 Hellpointner, E. 605(25), 679(312), 756, 764
 Hellring, S. D. 539(492), 594
 Hellström, K. E. 976(272b), 996
 Helly, P. J. 1257(266), 1276
 Helman, W. P. 262(345), 299, 966(233a), 971(199a), 994, 995
 Helsebeux, J. J. 892(65, 208), 895, 898
 Helsel, G. 667(459), 767
 Helz, G. R. 627(248), 642(249), 762
 Hemmingsen, A. 684(99), 758
 Hempelmann, E. 1281(11), 1342
 Henbest, H. B. 65(136a, b), 90
 Henderson, R. W. 900(8), 912
 Hendrickson, T. F. 276(494), 303
 Hendrickson, W. H. 909(95), 913
 Hengstler, J. G. 273(459), 302
 Hénin, F. 516(443), 593
 Henneke, H. F. 56(12a), 86
 Henne, A. 1228(107), 1272
 Hennig, L. 112(98), 141
 Henning, R. 809(75), 829
 Henriques, J. A. 670(478), 768
 Henry-Riyad, H. 122(148), 142
 Hensens, O. 1145(67b), 1166
 Hensley, K. 917(2c), 988
 Hentges, S. G. 567(526), 595
 Heravi, M. M. 1028(183), 1049
 Herberhold, M. 800(48), 828
 Herbert, K. 975(269b), 996
 Hercules, D. M. 1217(46), 1244(203), 1250(225), 1271, 1274, 1275
 Herderich, M. 338(77), 583
 Herkert, T. 198(82), 293
 Herkstroeter, W. G. 870(156), 897

- Hermanns, R. C. A. 670(124), 759
Hermann, A. 104(58), 140, 703(592), 770
Hermant, R. 1069(48), 1119
Hernández, F. 725(63), 757
Hernandez, R. 230(225–229), 297
Herrero, C. 641(309), 764
Herrmann, W. A. 48(114a), 89, 453(343a, b), 459(347, 348), 461(353), 466(342, 344, 355), 469(345), 529(346, 470, 471), 558(499), 569(534), 590, 591, 593–595, 1062(39, 40), 1074(125), 1083(216, 219), 1085(246), 1086(251), 1095(309), 1110(23, 213, 214, 396), 1116(424, 425), 1118, 1119, 1121, 1123–1125, 1127, 1128
Hertel, L. W. 861(94), 895
Hertzog, P. J. 1140(55c), 1166
Hescheler, J. 1336(158), 1346
Hesse, D. G. 165(17), 167
Hesse, M. 177(14), 186
Hesse, W. 735(685), 736(687), 772
Hetzler, G. 12(7d), 85
Hewgill, F. R. 112(79), 140
Hewitt, C. N. 678(26), 756
He, C. 1069(54), 1119
He, L. 1161(148a), 1169
He, M. 1140(74), 1167
He, Y. P. 1016(105), 1048
He, Y. 94(12b), 139, 1145(68), 1167
Hiatt, R. R. 423(261b), 533(477), 588, 594
Hiatt, R. 313(2), 581, 906(49), 912
Hibbs, D. E. 122(145), 142, 380(160), 585
Hickerson, R. P. 974(263), 996
Hickinbottom, W. J. 556(524), 595
Hicks, M. 674(250), 762
Hick, L. A. 691(143), 759, 956(200), 994
Higashidate, S. 1257(281, 282), 1276
Higa, T. 190(25), 292, 1333(138), 1345
Higgins, R. 673(491), 768
Higgs, D. E. 576(547), 596
Higson, A. P. 273(467), 302, 1337(165), 1346
Higuchi, T. 1188(40c), 1207, 1262(308), 1277
Hikichi, S. 118(126), 133(133), 142, 410(224), 444(315), 587, 589, 1064(51, 52), 1081(180), 1119, 1122
Hikino, H. 968(239a), 995
Hildebrand, J. P. 556(518a), 595, 1023(151), 1049
Hiley, C. 610(75), 757
Hilgetag, G. 1042(260, 261), 1051
Hillgärtner, N. 824(118), 830
Hillier, I. H. 1082(147), 1121
Hillier, M. C. 869(83), 895
Hillig, K. W. 722(653–655), 723(656), 771, 772
Hilliker, A. E. 211(147), 295
Hills, A. K. 672(483), 768
Hills, M. 175(11), 186
Hill, C. L. 40(40b), 87, 1081(171, 181), 1082(190–194, 197, 198), 1122, 1123
Hill, F. L. 678(519), 768, 946(128), 977(278c), 992, 997
Hiltunen, R. 1334(145), 1346
Hilvert, D. 338(81), 583
Hindahl, K. 1163(154b, 154e), 1169
Hindley, S. 275(489), 303, 1330(132), 1332(92, 93), 1344, 1345
Hino, T. 967(213, 215, 216, 237), 994, 995
Hinrichs, J. 123(163), 143
Hintzer, K. 1084(233), 1123
Hippler, H. 98(35a, b), 139
Hirama, M. 567(531a, b, 532a), 595
Hirano, M. 1023(152, 153), 1025(162, 163), 1049
Hirao, K. 40(40a), 87
Hirata, Y. 654(391), 765
Hiratsuka, A. 681(98), 758
Hirobe, M. 858(122), 896
Hiroi, S. 945(112), 991
Hiroshima, T. 1199(55), 1208, 1236(149), 1273
Hirota, K. 1011(82), 1047
Hirotzu, K. 118(129), 142
Hirt, R. C. 1225(70), 1272
Hisada, R. 1007(49), 1047
Hisatsune, I. C. 720(643), 731(640), 732(642), 771
Hiyama, T. 776(2b), 827
Hober, C. 12(7c), 85
Hobo, T. 674(253), 762
Hochanadel, C. J. 674(503a), 768, 965(214), 994
Hochstetler, A. R. 861(135), 896
Hoch, J. M. 1280(2), 1342
Hoch, U. 337(74, 75), 475(70), 583
Hock, F. 175(11), 186
Hock, H. 351(109), 584, 946(126b), 992
Hodges, D. M. 667(457), 676(458), 767
Hodges, G. R. 10(24b), 86
Hodgson, K. O. 1069(54), 1119
Hofer, T. 975(269b), 996
Hoffmann, G. 520(452), 593
Hoffmann, M. R. 29(66), 88
Hoffmann, R. V. 1045(250, 259), 1051
Hoffmann, R. W. 65(137b), 90, 128(128), 142, 864(138), 896
Hoffmann, R. 4(4), 85, 1092(283), 1125
Hoffman, B. M. 252(321), 299
Hoffman, M. R. 626(1), 756
Hoffman, R. V. 1006(43–45), 1007(46, 47), 1032(6), 1046, 1047
Hofheinz, W. 273(273), 277(503), 298, 303, 608(59), 757, 1332(14), 1342
Hofland, A. 1141(59), 1166
Höfle, G. 1145(67c, d), 1166
Hofmann, A. 800(48), 828

- Hofmann, B. 800(48), 828
 Hofmann, F. R. S. 1250(224), 1252(246), 1275
 Hofmann, J. 623(199), 761
 Hofstetter, D. 605(35), 756
 Höft, E. 329(65), 331(68, 69), 351(103a),
 475(70), 493(66, 100, 101), 583, 584,
 1099(343), 1126
 Hoganson, C. W. 963(224a), 994
 Hogg, J. S. 900(47), 912
 Hohman, J. R. 1263(316), 1277
 Höhne, G. 164(52), 169
 Hohorst, F. A. 138(56a), 140
 Holdcroft, S. 832(10), 894
 Holden, K. M. 233(12), 292
 Hölderich, W. F. 557(493), 594
 Hölderich, W. 539(495), 594
 Holland, P. L. 1117(434), 1128
 Hollist, G. O. 1024(156), 1049
 Holmes, E. W. 987(331b), 999
 Holme, A. D. 1326(106), 1345
 Holstege, A. 613(115, 116), 758
 Holthuis, J. J. M. 1257(262), 1276
 Holt, E. M. 728(665), 772
 Holt, S. 981(298b), 998
 Holzbecher, J. 1257(304), 1277
 Homma, H. 1257(284), 1276
 Homuth, G. 610(70), 757
 Honda, S. 984(281a), 997
 Honda, Y. 640(324), 641(100), 758, 764
 Honga, J. 685(542), 769
 Hong, J. I. 1093(291), 1125
 Hong, J. 638(188), 707(308b), 760, 764
 Hong, Y.-C. 605(37), 756
 Hon, Y.-S. 725(660), 772
 Hood, W. F. 106(80), 140
 Hool, K. 646(347), 764
 Hoos, R. 223(206, 210, 211), 296, 712(60),
 757, 1309(52), 1330(73), 1332(111),
 1343–1345
 Hoover-Litty, H. 1062(63), 1120
 Hopia, A. 680(529), 769
 Horiguchi, Y. 674(253), 762
 Horii, T. 271(271), 272(272), 298
 Horii, Z. I. 1010(74), 1047
 Hori, K. 524(460), 593, 918(8c), 988
 Hornero-Méndez, D. 658(418), 766
 Horner, L. 352(108), 584, 803(57), 828
 Horner, O. 1069(45, 49), 1119
 Hornish, R. E. 731(674), 772
 Horn, K. A. 1235(22, 137, 138), 1270, 1273
 Horowitz, N. 902(63), 913
 Horspool, W. M. 253(330), 299
 Horspool, W. 253(333), 299
 Hoshino, K. 340(85b), 583
 Hoshino, M. 1039(223), 1045(276), 1050,
 1052
 Hoshino, N. 1236(155), 1273
 Hoshino, Y. 542(213–215), 587,
 1093(288–290), 1125
 Hoshi, T. 651(371), 765
 Hoshi, Y. 209(144), 295
 Hosmane, R. S. 161(39), 169
 Hosomi, A. 901(14), 912
 Hosoya, N. 450(341), 590
 Hossel, P. 193(65), 293
 Hoss, W. P. 900(24), 912
 Houk, K. N. 37(37d, e), 40(96), 41(93),
 47(108), 55(55), 56(90a, b, 125, 129),
 87–90, 253(334, 335), 299, 833(29, 35),
 847(43), 861(137), 894, 896, 943(89a), 991,
 1044(274), 1052, 1140(36, 38, 39),
 1155(28), 1165, 1166
 Houmam, A. 206(121, 122), 294
 House, D. A. 1008(50), 1047
 House, H. O. 47(47a), 87
 Hou, H. 98(36), 139
 Hou, Q. X. 627(251), 762
 Hou, S.-Y. 1058(36), 1119
 Hou, X.-P. 701(589), 770
 Hou, Y. 122(155), 143
 Hoveyda, A. H. 48(116), 89, 860(128), 896
 Howard, J. A. 323(41), 360(131), 582, 584,
 901(16, 37, 40), 912, 949(142), 992
 Howarth, O. 1069(105, 116), 1121
 Howe, G. R. 533(477), 594
 Ho, C.-T. 665(444), 767
 Ho, D. G. 1059(43), 1119
 Ho, N. N. 1059(43), 1119
 Ho, R. Y. N. 1069(48, 50), 1119
 Ho, T.-L. 621(173), 760
 Ho, W. Y. 273(450), 302, 1317(68), 1343
 Ho, Y. S. 660(424), 766
 Hroch, A. 1076(157), 1122
 Hrovat, D. A. 269(428), 301
 Hrusak, J. 68(143), 90
 Hrůsák, J. 97(31), 139
 Hruska, F. E. 922(39a), 928(37b), 931(34b),
 989, 990
 Hrycko, S. 112(68), 140
 Hsi, L. C. 963(224a), 994
 Hsu, F. F. 963(225c), 994
 Hsu, H.-C. 612(106), 758
 Hsu, S.-Y. 503(425), 592
 Huang, D.-Z. 275(275), 298
 Huang, D. H. 259(363), 300
 Huang, D. Z. 277(505, 506), 303
 Huang, H. H. 68(142), 90
 Huang, H. 630(265), 639(315), 762, 764
 Huang, L. C. 1094(303), 1125
 Huang, L. 776(2b), 827
 Huang, M.-B. 77(77b), 88
 Huang, R. L. 901(23, 32, 36, 44), 912
 Huang, W.-J. 608(49), 757
 Huang, W.-w. 122(148), 142
 Huang, W. S. 392(193), 586, 1088(265), 1124

- Huang, X.-M. 630(268), 762
 Huang, X. R. 29(29), 87
 Huang, Y. 630(265), 762
 Hua, Y. 976(270b), 996
 Hubert, C. 623(196), 761
 Huber, F. 98(39a), 139
 Huber, R. 259(363), 300
 Huber, S. N. 291(596, 597), 305
 Hudlický, M. 492(396a), 591
 Hudson, C. E. 717(620), 771
 Hudson, R. F. 1045(250, 259), 1051
 Huff, G. F. 648(355a), 765, 1257(263), 1276
 Hughes, E. W. 99(40a), 139
 Hughes, M. N. 49(49), 87
 Huie, C. W. 742(703), 773
 Hui, S.-P. 693(570), 770
 Hull, L. A. 731(640), 771, 1140(15), 1165
 Hume, R. 610(75), 757
 Hummelen, J. C. 374(147), 585
 Hummer, W. 193(65), 293
 Hümmer, W. 1160(142), 1169
 Humpeler, S. 611(82), 758
 Humphrey, G. R. 503(426), 592
 Hundertmark, T. 408(86), 583
 Hunnius, W.-D. 733(678b), 772
 Hunter, E. P. L. 963(226), 994
 Hunter, N. R. 1031(203), 1050
 Huntington, J. 903(53), 912
 Hunt, J. V. 658(414), 766
 Hunt, J. W. 657(139), 759, 922(41b), 990
 Hunziker, D. 1332(15), 1342
 Hun, X. 701(590), 770
 Hurley, M. D. 692(19, 568), 756, 770
 Hursthouse, M. B. 125(149), 142, 380(160, 170), 585, 586
 Hursthouse, M. 122(145), 142
 Hurst, J. K. 952(177, 181, 182), 993
 Hurst, J. R. 834(38), 875(39), 894
 Hussein, A. 166(58), 169
 Huston, D. M. 351(105), 584
 Huta, O. M. 1253(241), 1275
 Hutchings, G. J. 422(256), 588
 Hutchison, J. E. 525(463), 593
 Huvenne, J. P. 702(227), 714(567), 761, 770
 Huyser, E. S. 901(28), 912
 Huy, D. N. 280(528), 304
 Hu, C. C. 935(65), 990
 Hu, C. 1011(78), 1047
 Hu, H. 278(511), 303
 Hu, J. K. 1317(107), 1345
 Hu, M.-L. 669(468), 767
 Hu, Q. S. 392(193), 586, 1088(265), 1124
 Hu, Z. Z. 112(85), 141
 Hviid, L. 1322(119), 1345
 Hwang, J. P. 1017(109), 1048
 Hwang, T.-M. 607(48), 757
 Hwang, Y.-S. 1116(422), 1128
 Hwu, J. R. 797(46), 828
 Hyeon, B. S. 856(110, 113), 896
 Hynes, R. C. 166(63), 169
 Hyodo, M. 1095(317), 1125
 Hyökyvirta, O. A. 623(198), 761
 Hølmer, G. 680(532), 769
 Iacazio, G. 339(82), 583
 Iamamoto, Y. 1140(52b), 1166
 Iannece, P. 408(99), 491(395), 584, 591, 1094(295), 1125
 Iannotta, A. V. 1266(305), 1277
 Iburg, J. E. 445(325), 590
 Ichihara, J. 478(297), 589, 1089(274), 1124
 Ichihara, O. 365(138), 585
 Ichikawa, H. 856(110), 896
 Ichikawa, T. 698(580), 770
 Ichikawa, Y. 476(71), 583
 Ichinohe, M. 1089(273), 1124
 Ichinose, N. 205(113, 115), 294
 Ilesce, M. R. 108(100), 112(103), 118(118), 141, 142, 259(367), 273(438), 300, 301
 Ignarro, L. 951(167), 993
 Iguchi, H. 659(420), 668(462, 463), 670(461), 766, 767
 Ihara, A. 698(193), 760, 1257(287), 1276
 Ihara, M. 288(577), 305
 Ihlo, J. 675(504), 768
 Ihmels, H. 1155(106b), 1168
 Ihrig, P. J. 1035(228), 1051
 Iida, S. 1236(36), 1271
 Iida, T. 793(38), 828
 Iishima, S. 664(441), 767
 Iitaka, Y. 113(76), 124(108), 136(203, 204), 140, 141, 144, 219(195), 296, 567(531h, 531j), 595
 Ijima, A. 792(30c), 828
 Ikeda, H. 206(121, 122), 209(135, 142, 144), 294, 295
 Ikeda, M. 396(211), 587, 904(75), 913
 Ikeda, T. 654(387), 765, 1040(253, 257), 1051
 Ikeda, Y. 122(144), 142
 Ikegami, A. 712(611), 727(664), 771, 772
 Ikegami, S. 419(257), 588, 1089(273), 1103(318), 1124, 1125
 Ikemoto, N. 320(34), 582
 Ikemura, T. 980(290a), 997
 Ikoma, K. 856(114–116), 896
 Illgen, K. 112(93, 94), 141
 Imada, Y. 567(532b), 595
 Imaizumi, N. 1257(290), 1276
 Imai, C. 1094(302), 1125
 Imai, H. 681(540), 769
 Imai, K. 1257(270, 272, 274, 275, 279–282, 284, 285), 1276
 Imai, M. 1268(336), 1278
 Imakura, Y. 278(511), 303
 Imamoto, T. 487(384), 591, 1098(335), 1126
 Imanishi, T. 1236(155), 1273
 Imato, T. 651(372, 373), 765

- Imazu, S. 326(58), 583
 Imbert-Bismuth, F. 613(116), 758
 Inagaki, H. 1094(302), 1125
 Inagaki, S. 418(249b), 588, 833(27), 894, 1011(83), 1047
 Inakazu, T. 1335(147), 1346
 Inamoto, N. 804(59), 828, 1157(127c), 1168
 Inanaga, J. 392(198), 586
 Indictor, N. 1055(9, 10), 1118
 Indira, V. 1116(419), 1128
 Ingallina, P. 1083(212), 1123
 Ingold, K. U. 10(24a, b), 86, 323(41), 582, 614(141), 759, 901(16, 37–40), 912, 949(142), 992, 1086(248, 249), 1124
 Inman, W. D. 276(494), 303
 Inomata, Y. 630(266), 762
 Inoue, A. 630(266), 762
 Inoue, H. 434(273), 588, 1089(271), 1124
 Inoue, K. 269(422), 273(437), 301, 698(193), 760, 962(210), 967(238a), 994, 995, 1244(203), 1257(287), 1274, 1276
 Inoue, M. 429(289), 432(304), 433(295, 298), 434(290), 589
 Inoue, S. 621(177), 760
 Inoue, Y. 904(75), 913
 Inzé, D. 610(71), 757
 Irgum, K. 648(356), 765, 1257(293, 297), 1259(314), 1277
 Irie, H. 1012(85), 1047
 Irie, M. 968(242), 995
 Irie, R. 450(341), 590
 Irschik, H. 1145(67c), 1166
 Irvine, D. S. 612(102), 758
 Irving, E. 273(467), 302, 1337(165), 1346
 Irwin, K. C. 423(261b), 588
 Isaac, R. 212(152), 237(164), 295, 319(8), 581
 Isacsson, I. 1242(185), 1274
 Isayama, S. 360(129), 584
 Isbell, T. A. 290(592), 305
 Ischiropoulos, H. 22(22b), 25(25), 86
 Iscimenler, B. D. 728(665), 772
 Iseki, Y. 621(177), 760
 Ishar, M. P. S. 199(88), 294
 Ishibashi, N. 651(372), 765
 Ishida, A. 208(131–133), 294, 295
 Ishida, N. 808(69, 70), 828
 Ishida, T. 413(233c), 587
 Ishigaki, H. 697(579), 707(598), 770
 Ishiguro, K. 1044(273), 1052
 Ishii, A. 1156(123b), 1157(124, 130a–c), 1168
 Ishii, Y. 434(273), 445(309), 525(308), 588, 589, 1080(173), 1081(174), 1087(256, 257), 1089(271), 1094(300, 301), 1102(353), 1106(172), 1108(388), 1122, 1124–1127
 Ishikawa, K. 1035(227), 1051
 Ishikawa, S. 1035(231), 1051
 Ishikawa, T. 945(112), 991
 Ishikawa, Y. 196(76), 293
 Ishiropoulos, H. 952(183), 993
 Ishitani, Y. 668(463), 767
 Ishizaki, S. 206(122), 294
 Isildar, M. 923(21), 989
 Iskra, J. 1327(130), 1345
 Islam, N. S. 1074(127, 128), 1109(21), 1118, 1121
 Islam, T. S. A. 148(10), 167
 Ismail, A. A. 662(431), 663(233, 235, 435), 761, 766
 Ismail, R. 1059(43), 1119
 Isobe, H. 1182(24c), 1207, 1228(96), 1272
 Isobe, K. 514(432), 592
 Isobe, R. 1236(149), 1273
 Isoe, S. 250(297), 252(298), 298, 856(110, 113, 114, 116), 896
 Isolani, P. C. 650(361), 765
 Itagaki, S. 271(271), 272(272), 298
 Itami, K. 776(2a), 810(77), 827, 829
 Iteya, K. 478(297), 589
 Itoh, K. 809(73), 829
 Itoh, Y. 804(59), 809(72), 828
 Itoi, Y. 429(289), 432(304), 433(298), 434(290), 589
 Itokawa, H. 136(203, 204), 144, 219(195), 296
 Ito, K. 379(157), 585, 1113(410), 1127
 Ito, S. 567(531b), 595
 Ito, T. 118(142, 143), 142, 223(218), 242(268), 269(269), 289(289), 296, 298, 472(365), 591, 712(610), 771
 Ito, Y. 819(106), 829
 Itsuno, S. 379(157), 585
 Itzstein, M. Von 1044(272), 1051
 Iuliano, L. 611(81), 758
 Ivashkevich, L. S. 129(176), 143
 Iversen, B. B. 1075(154), 1122
 Ives, J. L. 832(7), 894
 Iwado, A. 677(518), 768
 Iwaeda, T. 647(350, 351), 764, 1257(269), 1276
 Iwahara, T. 808(68), 828
 Iwahara, Y. 252(304), 298
 Iwai, T. 608(61), 757
 Iwama, T. 223(218), 296
 Iwamoto, H. 468(356), 591
 Iwasawa, Y. 1116(418), 1128
 Iwasa, J. 339(84), 583
 Iwata, Y. 118(135), 142
 Iyanar, K. 534(480), 594, 1103(359, 360), 1106(381), 1126, 1127
 Iyengar, R. 198(84), 293
 Iyer, R. S. 984(317b), 998
 Izumida, M. 1334(146), 1346
 Jablonski, C. R. 668(460), 767
 Jablonski, M. J. 34(34), 87
 Jablonsky, M. J. 951(174), 993
 Jackson, A. V. 604(3), 756
 Jackson, C. 945(121), 992

- Jackson, J. E. 122(154), 142
 Jackson, M. P. 381(159), 585
 Jackson, R. F. W. 366(139), 367(140),
 392(199), 585, 586, 1088(266, 267),
 1099(341), 1100(349), 1124, 1126
 Jackson, R. H. 101(52a), 140
 Jackson, W. P. 779(13b), 827
 Jacobsen, E. N. 48(114c), 89, 386(190b, c),
 487(389), 549(512b), 567(528), 586, 591,
 594, 595, 1092(286), 1125
 Jacobsen, J. N. 48(114d), 89
 Jacobsen, N. 1010(67), 1047
 Jacobson, R. R. 128(169), 143
 Jacobson, S. E. 492(397), 545(502), 566(494),
 592, 594, 1105(372), 1109(391), 1127
 Jacobs, P. A. 369(145), 446(328), 456(327),
 457(330), 569(529), 585, 590, 595
 Jacob, J. S. 963(225c), 994
 Jacob, P. 648(355b), 765
 Jacques, O. 1088(267), 1124
 Jacquier, Y. 1293(36, 37, 51), 1343
 Jaeschke, W. 648(307), 763
 Jaffe, L. 100(45a), 140
 Jagadeesh, M. N. 267(416), 301
 Jäger, V. 1160(142), 1169
 Jaggi, D. 113(75), 140, 284(537, 539, 540,
 546), 285(550), 304, 1324(122), 1345
 Jain, N. 1010(68), 1013(27), 1046, 1047
 Jakob, L. 184(33), 187
 Jalics, G. 777(8), 822(110), 824(111), 827, 829
 James-Krake, M. R. 660(423), 766
 Janasek, D. 647(349), 764
 Jang, S.-H. 122(154), 142
 Jang, Y. S. 612(107), 758
 Jankovic, I. 960(207c), 994
 Janoschek, R. 13(42), 87
 Janotaperret, K. 1228(60), 1271
 Janouch, M. 605(33), 756
 Jansen, E. G. 1251(238, 239), 1275
 Jansen, M. 735(683–685), 736(687), 737(688),
 772
 Janssen, C. L. 8(8c), 85
 Janzen, E. G. 1250(223), 1275
 Janzen, E. H. J. M. 1252(234), 1275
 Jan, B. I. 651(369), 765
 Jan, S.-T. 726(661), 772
 Jappar, N. 1108(387), 1127
 Jaquet, C. 273(273), 277(277), 298, 608(59),
 757, 1332(14), 1342
 Jardine, D. 667(454), 767
 Jaroszewski, J. W. 323(45), 582
 Jarosz, M. 636(243), 762
 Jaswal, J. S. 1069(102), 1120
 Jaworske, D. A. 627(248), 762
 Jayanthi, S. 709(601), 770
 Jayasinghe, L. R. 283(471), 302, 1337(162),
 1346
 Jayathirma Rao, V. 870(160), 897
 Jayatilaka, D. 12(7e), 85
 Jeandey, C. 1069(49), 719
 Jeanneret, F. 605(35), 756
 Jeannin, Y. 1069(117), 1121
 Jeffery, J. 125(149), 142
 Jefford, C. D. 861(133, 134), 896
 Jefford, C. W. 113(75), 122(159), 138(7), 138,
 140, 143, 255(351), 273(41, 443), 274(485,
 486), 278(509), 280(513, 514), 284(508,
 510, 535–540, 543–547, 549), 285(550),
 292, 300, 302–304, 326(52), 582, 727(578),
 770, 832(17), 854(104), 861(131), 894, 896,
 1293(36, 37, 51), 1296(53), 1324(122, 123),
 1325(20), 1332(13), 1342, 1343, 1345
 Jeffrey, G. A. 105(64), 111(121), 140, 142
 Jehle, H. 1163(154a), 1169
 Jelich, K. 196(73, 74), 293
 Jelinski, L. W. 692(215), 761
 Jemilev, U. M. 533(475), 593
 Jencks, D. A. 907(86), 913
 Jencks, W. P. 907(83, 86), 913, 1260(315),
 1277
 Jenker, A. 777(10), 827
 Jenkins, G. J. S. 616(148), 759
 Jenkins, I. D. 1044(272), 1051
 Jenningswhite, C. 275(492), 276(495–497),
 303, 1314(21, 22, 24, 94), 1342, 1344
 Jennings, W. B. 1155(106a), 1168
 Jenny, T. A. 269(428), 301
 Jensen, A. W. 1236(167), 1274
 Jensen, C. 666(447), 767
 Jensen, F. 849(44), 894
 Jensen, J. H. 12(7b), 85
 Jensen, K. B. 1069(46), 1119
 Jensen, R. 564(506), 594, 1111(403), 1127
 Jenson, C. 56(90b), 88, 1140(39), 1166
 Jeong, I. H. 273(462), 302
 Jeon, H. B. 280(523), 283(524), 304,
 1326(126), 1332(110), 1345
 Jerlich, A. 977(280a), 997
 Jessup, W. 673(406), 766
 Jewett, J. D. 835(41), 894
 Jeyadevan, J. P. 273(467), 302, 1337(165),
 1346
 Jeyaraman, R. 37(89), 58(58), 88, 1020(125),
 1021(139), 1048, 1049, 1140(8), 1151(98),
 1152(10), 1158(9), 1161(140), 1165, 1167,
 1169
 Jeziorek, D. 253(337), 299
 Jezkova, J. 651(367), 765
 Ježkova, J. 651(366), 765
 Jiang, H. 643(333b), 764
 Jiang, X.-K. 906(70a, b), 913
 Jiang, Y. 676(257), 762
 Jiang, Z.-Y. 658(412, 414), 676(256), 762, 766
 Jian, L. 741(702), 773
 Jiao, G. S. 1022(144), 1049
 Jierry, L. 1140(88), 1150(92), 1167

- Jie, O. Y. 252(305), 299
 Jie, T. 605(30), 756
 Jiménez, A. M. 643(331), 764, 1252(172), 1274
 Jiménez, P. 160(36), 161(39), 169
 Jiménez, R. 605(35), 756
 Jinap, S. 662(210), 761
 Jin, B. W. 1146(72), 1167
 Jin, F. 963(223), 964(227a, 228), 966(209), 968(239b), 994, 995
 Jin, H. W. 29(29), 87
 Jin, H. 966(209), 994
 Jin, S. J. 284(543, 544, 547), 304, 1324(123), 1345
 Jin, S. W. 1031(205), 1050
 Jin, X. 25(26a, b), 86
 Jitsukawa, K. 109(119), 142, 1064(69), 1120
 Ji, G.-Z. 906(70a), 913
 Ji, X. J. 511(416), 592
 Ji, X. 649(359), 765
 Jockusch, S. 1178(19d), 1206
 Joffe, A. 940(78), 991
 Joggi, D. 727(578), 770
 Johnson, B. F. G. 526(465), 593
 Johnson, B. G. 12(7), 85
 Johnson, C. R. 266(405, 406), 301
 Johnson, D. C. 651(370), 765
 Johnson, F. H. 1224(67), 1225(64), 1271
 Johnson, F. 945(113), 981(298c), 992, 998
 Johnson, K. A. 285(554), 286(555), 305
 Johnson, P. M. 976(272b), 996
 Johnson, P. 1024(158), 1049
 Johnson, R. A. 190(15), 233(10), 292, 315(33), 397(212c), 556(518b), 582, 587, 595
 Johnson, R. M. 660(424), 766
 Johnson, R. P. 1082(198), 1123
 Johnson, T. L. 276(500), 303
 Johnstone, R. A. W. 110(99), 141, 457(323), 590, 1094(303), 1125
 Johnston, A. E. 737(692), 772
 Johnston, L. J. 885(158), 897, 930(43c), 990
 Jolibois, F. 921(33), 922(39b), 989, 990
 Jolkkonen, S. 98(37), 139
 Jomaa, H. 190(43), 292
 Jonah, C. D. 1189(44b), 1208
 Jones, A. D. 984(317d), 999
 Jones, C. W. 1101(199), 1123
 Jones, D. W. 198(81), 293
 Jones, G. D. D. 943(97), 991
 Jones, G. R. 808(66), 828
 Jones, I. T. N. 951(163), 993
 Jones, M. R. 1034(224), 1050
 Jones, P. G. 122(146), 142
 Jones, P. W. 610(75), 757
 Jones, P. 659(260), 762
 Jones, R. H. 418(252), 588
 Jones, W. 99(41), 125(166), 126(165, 167), 127(168), 139, 143
 Jönsson, B. 62(62), 88
 Jonsson, M. 104(21), 139
 Jonsson, S. Y. 574(537–540), 595
 Jonsson, T. 1257(293), 1259(314), 1277
 Jordan, A. 815(91c), 829
 Jordan, J. E. 977(277f), 996
 Jordá, J. L. 421(253), 588
 Jörgensen, K. A. 1092(283), 1125
 Jorgensen, W. L. 56(90b), 88 1140(39), 1166
 Jorge, N. L. 164(53), 165(54), 169
 Jorg, W. G. 791(37), 828
 Jortner, J. 1217(45), 1271
 Josefsson, B. 960(204a), 994
 Joseph, J. 963(221), 994
 Joseph, R. 538(486), 594
 Joshi, P. C. 941(74b), 990, 1201(63a, b), 1209
 Joshi, P. 941(74a), 990
 Josimovic, L. J. 964(227b), 994
 Josimovic, L. 960(207c), 994
 Jost, C. 795(41), 828
 Jovanovic, S. V. 923(42b), 939(73), 960(207c), 962(212), 990, 994
 Joy, A. 870(147), 896
 Judd, D. A. 1082(197), 1123
 Juin, F. 614(135), 759
 Julia, S. 375(156), 379(153), 380(155), 381(154), 585
 Julich, W. D. 623(206), 761
 Julliard, M. 204(101), 294
 Jumonville, S. 900(10), 912
 Juneau, M. 638(311), 764
 Jung, B. C. 1035(226), 1038(241), 1051
 Jung, H. 290(579, 580), 305, 608(53), 757, 1314(90, 91), 1344
 Jung, J. C. 1014(92, 93, 96, 97), 1015(99), 1028(184), 1048, 1049
 Jung, M. K. 290(512, 584), 303, 305
 Jung, M. 256(359), 273(33, 48, 464), 289(578), 290(463, 579, 580, 582, 583, 585–590), 292, 300, 302, 305, 1314(90, 91), 1338(166), 1344, 1346
 Jung, Y. G. 1093(291), 1125
 Juo, R.-R. 1199(48), 1200(53b), 1208
 Jurczak, J. 348(18), 582
 Jurczak, M. 493(100), 584
 Jurgens, G. 945(99), 991
 Jurjev, V. P. 533(475), 593
 Just, G. 318(12), 582
 Juwiler, D. 1091(186, 280), 1122, 1125
 Jyothi, K. 569(535c), 595
 Jørgensen, K. A. 386(190), 586, 1075(144), 1089(25), 1118, 1121
 Kaanumalle, L. S. 870(147), 896
 Kabe, Y. 818(98), 825(121), 829, 830
 Káb, H. 1163(154e), 1169
 Kachurina, N. S. 156(26), 168
 Kacmarek, A. J. 172(5), 182(26), 186, 187
 Kadam, A. J. 1029(193), 1050

- Kadereit, D. 447(333), 458(332), 590
 Kagan, H. B. 432(300b), 472(191), 480(375, 377), 486(376), 487(379, 380), 586, 589, 591, 1068(95, 96), 1084(232, 233), 1089(269), 1097(94, 326, 327), 1120, 1123, 1124, 1126
 Kagan, V. E. 660(110, 111), 758
 Kahlos, K. 1334(145), 1346
 Kahn, M. 809(74), 829
 Kahr, B. 122(154), 142
 Kajikawa, S. 252(308), 299
 Kaji, K. 981(293), 997
 Kakeushi, T. 852(77), 895
 Kakinuma, K. 918(8d), 988
 Kako, M. 816(93), 817(97), 818(94, 98, 99), 819(100, 101, 103), 825(126), 829, 830
 Kakui, T. 808(67, 68), 828
 Kakuta, M. 657(407), 766
 Kalaitzakis, D. 883(183), 897
 Kalan, M. 1039(248), 1051
 Kalcher, K. 651(366, 367), 765
 Kalinowski, H.-O. 182(3, 27), 186, 187
 Kalita, B. 273(56), 293
 Kallio, H. 693(573, 574), 770
 Kallio, R. E. 1200(58b), 1208
 Kalnajs, J. 95(16), 139
 Kaltsoyannis, N. 1082(203), 1123
 Kalyanaraman, B. 953(172), 963(221), 993, 994
 Kamalakar, G. 538(487a, b), 594
 Kamalaprija, P. 284(540), 304, 1324(122), 1345
 Kamata, K. 410(224), 444(315), 587, 589, 1081(180), 1122
 Kamata, M. 207(118, 123), 209(138), 294, 295, 1291(49), 1343
 Kamat, V. P. 1013(89), 1048
 Kamaura, M. 392(198), 586
 Kambourakis, S. 858(119), 896
 Kamchonwongpaisan, S. 190(49), 273(34, 472), 292, 293, 302, 1283(32), 1343
 Kamigata, N. 1007(48), 1047
 Kaminaga, T. 1334(146), 1346
 Kaminsky, R. 1332(105), 1344
 Kaminsky, W. 118(123), 142
 Kamiyama, N. 205(112, 113), 294
 Kamiyama, T. 433(295), 589
 Kammel, T. 193(68), 293
 Kamminga, D. A. 1257(258, 259, 265), 1276
 Kammoun, M. 1021(135), 1048
 Kampf, J. W. 1062(60), 1119
 Kampinga, H. H. 273(456, 466), 302, 1336(161), 1346
 Kamura, A. 668(462), 767
 Kanai, M. 793(38), 828
 Kanamori, K. 1062(61), 1119
 Kanatani, R. 808(68), 828
 Kanazawa, A. 614(130), 759
 Kanda, A. 1021(132), 1048
 Kanda, S. 1257(285), 1276
 Kaneda, K. 245(282), 298, 1087(257), 1124
 Kaneda, M. 904(75), 913
 Kaneko, C. 264(390), 300
 Kaneko, T. 339(84), 583, 981(293), 984(281a), 997
 Kanemoto, S. 788(31), 789(32), 828
 Kaneti, J. 84(163), 91, 472(143), 585
 Kangas, L. 1334(145), 1346
 Kanger, T. 521(456, 457a, b), 553(516), 593, 594, 1113(407, 408), 1127
 Kang, C. H. 911(90), 913
 Kang, J.-G. 607(48), 757
 Kang, J.-W. 607(48), 757
 Kang, J. H. 275(490), 283(533), 303, 304, 1330(133), 1345
 Kang, P. 941(82), 943(83), 950(152), 969(243a, b), 991, 992, 995
 Kannan, R. 1283(33), 1343
 Kanner, R. C. 255(353), 300, 325(56), 583, 852(76), 895
 Kanno, H. 1334(146), 1346
 Kanofsky, J. R. 918(8a, b), 950(144), 988, 992
 Kano, K. 654(387), 765
 Kano, Y. 287(559), 305
 Kantam, M. L. 569(535c, d), 571(542, 543), 573(541), 595, 596
 Kanunnikova, E. N. 118(141), 142
 Kanwar, K. C. 669(103), 758
 Kao, H.-M. 870(160), 897
 Kapetanaki, S. 1303(66), 1343
 Kaplan, I. R. 604(2), 756
 Kaplan, J. K. 217(180), 296
 Kaplan, M. L. 264(389), 300, 732(493), 768
 Kapoor, S. 1058(33), 1119
 Kappert, W. 29(69), 72(72e), 88, 1154(112), 1168
 Kappes, D. 326(59), 583, 1178(20b), 1206
 Kapp, D. L. 211(149), 295
 Kapu, D. S. 275(489), 303, 1330(132), 1345
 Karakostas, K. X. 664(443), 767
 Karami, A. R. 649(357), 765
 Karasawa, S. 1067(55), 1119
 Karas, G. 1044(271), 1051
 Karayannis, M. I. 624(220), 630(271), 761, 762
 Kara, Y. 264(395, 397), 300, 301
 Karban, J. 726(663), 772
 Karbe, K. 1044(9), 1046
 Kardash-Strochkova, E. 663(438, 439), 766
 Kargar-Grisel, T. 1069(45), 1070(47), 1119
 Kariuki, B. M. 99(41), 139
 Karkalas, J. J. 630(267), 632(283), 762, 763
 Karlberg, A. T. 326(60), 583
 Karleskind, A. 672(400), 766
 Karle, I. L. 95(17c), 139, 938(69a), 990

- Karle, J. M. 276(502), 303, 1286(41), 1306(74), 1314(64), 1343, 1344
- Karlin, K. D. 128(169), 143
- Karlsson, A. 648(356), 765
- Karlsson, S. 680(535), 769
- Karlström, G. 30(75a), 62(62), 73(73), 88, 98(34), 139
- Karoui, H. 973(254), 995
- Karpukhin, O. 949(141), 992
- Karst, U. 637(303, 304), 699(582a, b, 583), 700(584), 708(605), 763, 770
- Karyakina, E. E. 655(392), 765
- Karyakin, A. A. 655(392), 765
- Kary, P. D. 380(171), 586
- Kasabayashi, S. 712(611), 727(664), 771, 772
- Kasai, H. 1201(62a, 63c), 1209
- Kasha, M. 950(157), 992
- Kashima, H. 265(403), 301
- Kashiwagi, H. 433(295), 589
- Kaspruk, B. I. 1043(263, 268), 1051
- Kasuga, N. C. 1192(16b), 1206
- Katagiri, R. 288(577), 305
- Katakai, R. 698(580), 770
- Kataoka, S. 967(215, 237), 994, 995
- Kataoka, T. 196(70), 223(218), 293, 296
- Katao, Y. 1236(152), 1273
- Katayama, T. 118(135), 142
- Katayama, Y. 1094(301), 1125
- Kateva, J. 184(33), 187
- Kato, K. 711(145), 759
- Kato, N. 657(407), 766
- Kato, S. 743(704), 773, 967(215, 237), 994, 995
- Kato, T. 805(60), 828
- Kato, Y. 647(350, 351), 764, 945(112), 984(318), 991, 999, 1251(236), 1257(269), 1275, 1276
- Katritzky, A. R. 1181(11g), 1206
- Katsuki, T. 48(114b), 89, 396(211), 397(212), 400(206), 419(257), 449(335), 450(341), 516(437a, b), 587, 588, 590, 593, 1092(286), 1097(12), 1099(338–340), 1100(348), 1105(285), 1113(410), 1118, 1125–1127
- Katsumura, S. 856(110, 113–116), 857(117), 896
- Katsuya, E. 968(239a), 995
- Katusin-Ražem, B. 676(511), 768
- Kauffmann, J.-M. 653(384), 765
- Kauppi, B. 972(232), 995
- Kawada, H. 1236(36), 1271
- Kawaguchi, D. 129(171), 143
- Kawaguchi, M. 374(148), 585
- Kawaguchi, S. 1257(268), 1276
- Kawahara, N. 630(266), 762
- Kawahara, S. 265(403), 301
- Kawai, K. T. 660(111), 758
- Kawai, K. 660(110), 758
- Kawai, S. 682(474), 767
- Kawai, T. 816(93), 829
- Kawai, Y. 1025(166), 1049
- Kawakami, M. 318(13), 582
- Kawakami, S. 605(29), 756
- Kawakami, T. 567(532b), 595, 833(31), 894, 1173(17b), 1206
- Kawakishi, S. 984(318), 999
- Kawamoto, H. 644(335), 645(337), 764
- Kawamura, S.-i. 711(608), 771
- Kawamura, S. 113(109), 141
- Kawanishi, M. 271(271), 272(272), 298
- Kawasaki, K. 516(437a, b), 593
- Kawasaki, T. 426(279), 589
- Kawashima, T. 630(264), 762, 1157(127c), 1168
- Kazakov, D. V. 1155(116), 1168
- Kazakov, V. P. 1155(116), 1168, 1181(11i), 1190(43, 45a–c), 1206, 1208
- Keaney, J. F. 681(505), 768
- Kearns, D. R. 253(341), 299, 854(103), 896
- Kearns, D. 1244(177), 1274
- Keating, K. P. 426(275), 588
- Keck, G. E. 1228(105, 106), 1272
- Keefer, R. M. 901(30), 912
- Keeney, M. 737(693), 772
- Kefala, E. T. 1058(38), 1119
- Keith, J. N. 172(5), 186
- Keith, T. A. 44(100), 89
- Keith, T. 12(7), 85
- Kelana, E. 605(29), 756
- Kelder, H. M. 605(31), 756
- Kelli, T. A. 640(323), 764
- Kellogg, C. 1227(89), 1272
- Kellogg, R. M. 854(100), 895
- Kellog, R. M. 1174(18b), 1206
- Kelly, D. R. 382(181), 586
- Kelly, J. 367(140), 585
- Kendrick, H. 290(580, 584), 305, 1314(91), 1344
- Kennard, C. H. L. 136(202), 144
- Kennard, O. 105(66), 140
- Kennedy, G. 982(291d), 997
- Kennedy, R. J. 1020(126), 1048
- Kensler, T. W. 273(469, 470), 283(471), 302, 1337(162, 163), 1346
- Kenyon, G. L. 1322(117, 118), 1345
- Kepler, J. A. 291(595), 305
- Keramidas, A. D. 1062(63), 1120
- Kerckow, A. 731(632), 771
- Kergomard, A. 1006(42), 1047
- Kermasha, S. 676(473), 767
- Kernan, M. R. 134(200), 144
- Kern, W. 977(282b), 997
- Kerr, A. F. 614(131), 759
- Kerr, B. 273(476), 303
- Kerr, J. A. 13(13e), 86, 94(4c), 138
- Kerschner, J. 445(325), 590

- Kerton, O. J. 422(256), 588
 Keshavarzian, A. 987(331b), 999
 Keszler, A. 656(221), 761
 Ketpirune, J. 1311(76), 1344
 Kettle, A. J. 966(231), 972(222a), 994, 995
 Kettrup, A. 638(188), 678(522), 679(313),
 685(542), 707(308b), 760, 764, 769
 Keul, H. 717(624, 627), 723(625), 771
 Khait, Y. G. 29(66), 88
 Khalilov, L. M. 729(669), 772
 Khambay, B. P. S. 323(42b), 582
 Khan, A. U. 252(320), 299, 812(85), 829,
 918(8b), 950(157), 988, 992
 Khan, I. A. 288(575), 305
 Khan, I. 276(498), 288(574), 303, 305,
 1314(96), 1344
 Khan, J. A. 217(185), 252(252), 296, 297
 Khan, S. I. 112(60), 140, 259(365), 263(385),
 300
 Khan, S. 943(83), 991
 Kharasch, M. S. 221(200), 296, 319(22),
 358(124), 582, 584, 899(1), 911
 Kharasch, M. 221(201), 296
 Kharazmi, A. 1322(119), 1345
 Khashab, A.-I. 731(637), 771
 Khenkin, A. M. 1082(188–190), 1091(186),
 1092(281), 1122, 1125
 Khoo, J. C. 612(104), 758
 Khot, S. N. 622(191), 760
 Khouri, F. F. 310(7c), 581
 Kho, E. 190(24), 292
 Khriachtchev, L. 98(37), 139
 Khrustalev, V. N. 110(70), 122(152), 140, 142
 Khuong, T.-A. V. 534(481), 594
 Khursan, S. L. 105(62a), 119(9), 139, 140,
 153(4), 167, 690(566), 770
 Khusainova, I. A. 1190(45b), 1208
 Khwaja, H. 425(264), 588
 Kibler, M. 638(314), 764
 Kiddle, J. J. 643(333a), 764
 Kieber, R. J. 642(7, 249), 643(333a), 756, 762,
 764
 Kiefer, W. 1081(149), 1122, 1155(116, 118a,
 b), 1168
 Kiguchi, T. 273(437), 301
 Kilford, J. 627(247), 762
 Kilic, H. 269(399), 301
 Kilpatrick, M. L. 362(134a), 584
 Kimoto, H. 1257(277), 1276
 Kimura, M. 112(85), 141, 273(453), 302,
 503(422a, b), 592, 1313(34), 1335(147),
 1343, 1346
 Kimura, R. 1025(166), 1049
 Kimura, T. 394(200, 200b), 586
 Kim, C. J. 911(88), 913
 Kim, C. S. 902(61), 911(91), 913
 Kim, C. 1031(205), 1050, 1117(430), 1128
 Kim, E. H. 1027(175, 176), 1049
 Kim, G. S. 1082(198), 1123
 Kim, H.-J. 650(230), 761
 Kim, H.-S. 113(102), 141
 Kim, H. B. 911(88), 913
 Kim, H. J. 275(491), 303, 1033(220), 1050
 Kim, H. O. 1006(43), 1047
 Kim, H. R. 911(88), 913
 Kim, H. S. 209(138), 225(220), 249(292),
 267(267), 288(577), 291(291), 295, 296,
 298, 305, 1282(27), 1291(49), 1332(108),
 1342, 1343, 1345
 Kim, H. 273(48, 464), 292, 302, 605(37), 756,
 1030(196), 1050, 1338(166), 1346
 Kim, J.-S. 65(136c), 90
 Kim, J. C. 1035(229), 1051
 Kim, J. Y. 612(107), 758, 1037(238), 1051
 Kim, J. 1117(430), 1128
 Kim, K. M. 616(153), 759
 Kim, K. S. 1001(7), 1028(184), 1032(219),
 1035(229), 1046, 1049–1051
 Kim, K. 1066(73), 1120
 Kim, L. 520(188), 586
 Kim, O. Y. 612(107), 758
 Kim, S.-J. 79(79), 88
 Kim, S.-Y. 605(37), 756
 Kim, S. K. 273(464), 302, 890(202), 898,
 1338(166), 1346
 Kim, S. S. 901(42, 43, 46), 902(61, 66, 67),
 906(54), 909(89), 911(71, 88, 90, 91), 912,
 913
 Kim, W.-J. 607(48), 757
 Kim, Y. H. 1001(5, 7, 8, 10, 11), 1014(92, 93,
 96–98), 1015(99, 100, 104),
 1017(108–111), 1018(112, 113), 1028(184),
 1032(218, 219), 1033(220, 221), 1034(222),
 1035(225, 226, 229), 1036(232), 1037(234,
 235, 237, 238), 1038(241–243), 1039(223),
 1042(251), 1045(252, 276), 1046(277),
 1046, 1048–1052
 Kim, Y. H. 1146(72), 1167
 Kim, Y. I. 1037(237, 238), 1051
 Kingzett, C. T. 627(246), 762
 King, G. R. 288(572), 305
 King, M. M. 950(145), 992
 King, T. P. 670(477), 767
 Kinkel, K. G. 706(596), 770
 Kinnison, D. E. 605(36), 756
 Kinnison, D. J. 94(4c), 138
 Kinoshita, H. 654(387), 765
 Kinoshita, T. 608(61), 757
 Kino, K. 940(75b), 991
 Kinsey, J. L. 1160(11b), 1165
 Kinstle, T. H. 1035(228), 1051
 Kiparisova, E. G. 163(47), 169
 Kiranas, E. R. 630(271), 762
 Kirby, A. J. 111(120), 142
 Kirby, G. C. 608(56), 757
 Kirby, S. P. 164(2), 167

- Kirfel, A. 112(72), 134(199), *140, 144*
 Kirksey, J. W. 190(50), 293
 Kirk, M. 951(174), 953(172), 993
 Kirrbach, S. 112(94), *141*
 Kirschfeld, A. 29(69), 60(60), 72(72e), 88,
 1154(16a, 112), *1165, 1168*
 Kirsch, J. F. 1260(315), *1277*
 Kirshenbaum, K. S. 432(301), 589, 1087(254),
 1124
 Kirtany, J. K. 1013(89), *1048*
 Kiryu, C. 918(8d), 988
 Kiseleva, E. V. 740(50), *757*
 Kiselewsky, M. 29(69), 88
 Kishida, E. 668(12, 462, 463), 670(461), 756,
 767, 1257(296), *1277*
 Kishikawa, N. 698(193), 760, 1257(287), *1276*
 Kishimoto, T. 812(86a), 829
 Kishi, E. 136(203, 204), *144*
 Kishi, M. 234(234), 297
 Kishi, Y. 1244(203), *1274*
 Kishore, K. 155(13, 24), *167, 168, 707(603),*
 709(601), 770
 Kissel, T. 1256(29), *1271*
 Kissner, R. 951(175), 993
 Kitagawa, T. 1064(69), *1120*
 Kitajima, N. 118(135), *142*
 Kitajima, T. 809(73), 829
 Kitamura, M. 270(430), *301*
 Kitaoka, T. 1335(147), *1346*
 Kitaura, K. 856(114, 116), 896
 Kita, K. 605(29), *756*
 Kita, Y. 426(279), 589
 Kiva, E. A. 113(59), *140*
 Kiyoto, I. 1082(196), 1117(195), *1123*
 Klamann, D. 536(483), *594*
 Klapdor, M. F. 132(194), *144*
 Klasinc, L. 32(32), 87
 Klayman, D. L. 273(30), 292, 1280(1, 2),
 1281(5), 1314(98), *1342, 1344*
 Kleiman, R. 737(691), *772*
 Kleinhenz, D. 1081(149), *1122*
 Klein, A. 1150(92), *1167*
 Klein, P. 213(160), 295
 Kliem, U. 291(593), 305
 Klimov, O. V. 1069(113), *1121*
 Klinedinst, D. 209(140, 141), 280(527),
 283(471), 295, 302, 304, 1284(39),
 1291(48), 1337(162), *1343, 1346*
 Klitzke, C. F. 967(238b), 995
 Klockow, D. 648(355b), 678(521), 765, 769
 Klotz, L. O. 950(153), 992
 Kluge, R. 47(103), 89, 520(452), 593,
 1003(24), *1046, 1163(1k), 1164*
 Klug, P. 888(140), 896
 Klug, R. 1140(26), *1165*
 Klunder, J. M. 400(208), 587, 1092(282), *1125*
 Klung, P. 889(195), 897
 Knapp, K. H. 352(108), 584
 Knifton, J. F. 426(275), 588
 Knipple, W. R. 1005(40), *1047*
 Knochel, P. 384(187), 560(39), 582, 586
 Knott, H. M. 973(249b), 995
 Knowles, P. J. 12(7d, e), 85
 Knowles, W. S. 1173(12a), *1206*
 Knutzen-Mies, K. 854(108), 896
 Kobayashi, A. 122(144), *142*
 Kobayashi, H. 1199(55), 1208, 1236(149, 152,
 153), *1273*
 Kobayashi, J. 1333(139, 140), *1346*
 Kobayashi, K. 792(30c), 828
 Kobayashi, M. 271(271), 272(272), 298,
 1006(38), 1007(49), *1046, 1047*
 Kobayashi, R. 12(7e), 85
 Kobayashi, S. 413(233, 233b–d), 587
 Kobayashi, T. 1069(118), 1115(412), *1121,*
 1127
 Kobayashi, Y. 392(196), 586, 651(371), 765
 Kobler, H. 1014(90), *1048*
 Kobori, N. 900(11), 912
 Kobylinski, T. P. 575(523), 595
 Kochi, J. K. 432(241), 457(320), 587, 590,
 1010(66), *1047, 1116(13), 1118*
 Koch, C. 382(179), 586
 Koch, E. 733(676, 678a), 740(672), 772
 Kočovský, P. 514(440), 593
 Koczkowski, R. L. 723(656), 772
 Koc, H. 982(291f), 997
 Kodato, S. 967(213, 237), 994, 995
 Koeberg-Telder, A. 199(87), 293
 Koehl, W. J. 900(12), 912
 Koek, J. H. 445(325), 590
 Koenig, M. 823(116), 830
 Koenig, T. 903(52, 53), 912
 Koerner, T. 57(51a), 87
 Kofod, P. 1067(75), *1120*
 Koga, K. 567(531c, 531h–j), 595
 Koga, S. 950(148), 992
 Kohlmeier, C. K. 720(641), 771
 Kohmoto, S. 113(75), 140, 278(509), 284(508),
 510, 537, 539, 540, 546, 547, 285(550),
 303, 304, 727(578), 770, 854(104), 896,
 1324(122, 123), *1345*
 Kohzuki, M. 610(73), 655(398), 757, 765
 Koike, R. 1268(336), *1278*
 Koizumi, C. 680(534), 769
 Kojima, H. 129(171), *143*
 Kojima, M. 208(131, 133), 294, 295,
 1100(344), *1126*
 Kojima, S. 382(178), 586
 Kojo, S. 659(420), 668(12, 462, 463),
 670(461), 756, 766, 767, 1257(296), *1277*
 Kokovinetz, O. S. 729(669), 772
 Kok, G. L. 637(305, 306), 648(307), 678(26),
 707(523), 756, 763, 769
 Kolberg, A. 107(96), *141*
 Kolb, H. C. 567(527), 595

- Kollar, J. 533(476), 593, 1085(240), *1124*
 Kolla, P. 708(605), *770*
 Koller, J. 131(192a), 132(193), *144*,
 182(20–22, 24, 25), *187*, 812(84), *829*
 Kollinger, M. 613(115), *758*
 Kollinge, M. 613(116), *758*
 Koll, P. 130(170), *143*
 Kolomiichuk, V. N. 1069(119), *1121*
 Kolopajlo, L. H. 732(642), *771*
 Kolsaker, P. 723(648), 725(644), *771*
 Kolthoff, I. M. 676(510), 768, 1010(72), *1047*
 Kol, M. 1140(29), *1165*
 Komala, N. 605(29), *756*
 Komaromi, I. 12(7), *85*
 Komatsuzaki, H. 118(126), *142*
 Komatsu, H. 650(364), *765*
 Komatsu, K. 209(138), 295, 1291(49), *1343*
 Komatsu, N. 481(381), 486(386), *591*,
 1097(331, 332), *1126*
 Komatsu, T. 612(88), *758*
 Komazaki, Y. 743(704), *773*
 Komhyr, W. D. 605(28), *756*
 Kommineni, C. 660(110), *758*
 Komoda, Y. 1236(37), *1271*
 Kondou, C. 56(121), *90*
 Kondo, A. 1100(348), *1126*
 Kondo, H. 476(71), *583*
 Kondo, K. 253(328), 299, 325(54), *583*,
 878(178), *897*
 Kondo, M. 664(441), 767, 1044(273), *1052*
 Kondo, T. 698(580), *770*
 Kondo, Y. 605(29), *756*
 Kongsaree, P. 190(49), 273(472), 293, *302*
 Kong, F. 77(77b), *88*
 Konieczny, M. 1043(269), *1051*
 Konings, A. W. T. 273(456, 465, 466), *302*,
 1336(161), *1346*
 Konishi, T. 1010(74), *1047*
 Konkoli, Z. 185(35), *187*
 Konno, A. 209(134, 135, 144), *295*
 Kono, Y. 50(50b), *87*
 Konstantinovskii, L. 223(206), 296, 712(60),
 757, 1330(73), *1344*
 Kooijman, H. 1069(44), *1119*
 Koola, J. J. 847(68), 854(95, 96), *895*
 Kooyman, E. C. 899(7), 900(29), *912*
 Koo, A. 273(28), *292*
 Koo, B. S. 1027(175, 176), *1049*
 Koo, H. M. 901(42), *912*
 Koo, J.-Y. 1184(29), *1207*, 1232(23, 81, 116,
 117), *1270*, *1272*
 Kopeckova, P. 973(259), *996*
 Kopecek, J. 973(259), *996*
 Kopeček, J. 973(244), *995*
 Kopecky, K. R. 317(27), 582, 1172(1, 9),
 1182(22), *1205*, *1206*, 1212(9), *1270*
 Kopf, J. 130(170), *143*
 Kopitzky, R. 104(58), 138(56b), *140*,
 703(592), 743(21), 744(22), *756*, *770*
 Koppenol, W. H. 22(22b), 25(25), 32(32), *86*,
 87, 612(86), 758, 917(5a, 5c), 951(166),
 952(183, 188), 966(208), 988, 993, *994*
 Koppenol, W. V. 951(175), *993*
 Koput, J. 100(28a), 101(26), *139*
 Korber, N. 737(688), *772*
 Korb, M. N. 408(220), 416(235b), 493(219),
 587, 1094(294), 1100(132), *1121*, *1125*
 Korkodilos, D. 240(261), *297*
 Korona, T. 12(7d), *85*
 Korotyuk, V. F. 156(7), *167*
 Korp, J. D. 112(92), *141*, 252(299, 300, 309),
 298, *299*
 Korp, J. 726(663), *772*
 Korshin, E. E. 223(205–212), 296, 712(60),
 757, 1309(52), 1323(121), 1330(73, 134),
 1332(111), *1343–1345*
 Korte, F. 124(147), *142*, 605(25), 724(658),
 728(630, 667), *756*, *771*, *772*
 Korytowski, W. 687(550–552), *769*,
 977(279c, d), *997*
 Koseki, S. 12(7b), *85*
 Kosinski, C. 974(262d), *996*
 Kosmas, G. 883(183), 885(185), *897*
 Kosnikov, A. Y. 103(47, 48), 122(158),
 123(104), 130(185), 131(180), *140*, *141*,
 143, 729(669), *772*
 Kosswig, K. 533(478), *594*
 Koster, H. 1255(38), *1271*
 Kostova, K. 177(14), *186*
 Kosugi, T. 690(563), *770*
 Kotamarthi, V. R. 138(210a), *144*
 Kottmann, H. 1014(91), *1048*
 Kot, S. C. 624(237), *761*
 Kouno, I. 1012(85), *1047*
 Koupal, L. 1145(67b), *1166*
 Koutek, B. 890(204), *898*
 Kouwatli, H. 1257(260), *1276*
 Kovacic, P. 1006(41), *1047*
 Kovac, F. 1160(144), *1169*
 Kovač, F. 182(25), *187*, 812(84), 813(87), *829*
 Kowalski, J. 803(56), 804(58), *828*
 Kowalski, R. J. 1145(67e), *1166*
 Koyama, J. 278(511), *303*
 Koyano, K. A. 418(249d), *588*
 Kozhevnikov, I. V. 1081(176, 182), *1122*
 Kozlova, A. 1116(418), *1128*
 Kozlov, A. 1116(418), *1128*
 Kozuch, S. 1140(52a), *1166*
 Ko, M. K. W. 138(210a, b), *144*
 Ko, S. Y. 400(208), 587, 1092(282), *1125*
 Kraebel, C. M. 223(217), *296*
 Kraka, E. 32(83, 85a, b), 40(94a), 70(70),
 72(72e), 78(78), 82(82a), 84(84), 88, 89,
 94(12b), *139*, 182(23), 185(35), *187*,
 1140(20), 1154(112), *1165*, *1168*

- Kramer, A. 623(206), 761
Kramps, L. 388(194), 392(173), 586,
1088(263, 264), 1124
Krasavin, M. 1337(163), 1346
Krasavin, M. 273(446, 470), 280(523),
283(520), 302, 304, 1332(110), 1345
Kratzer, R. M. 459(348), 461(353), 466(355),
569(534), 590, 591, 595, 1083(219), 1123
Kratz, T. 468(271), 588
Krauch, C. H. 326(38), 582
Krause, R. A. 1163(152a), 1169
Krauss, M. 10(33), 87
Krawczyk, T. 708(164), 760
Krebs, A. 1232(129), 1273
Krebs, B. 637(239, 303, 304), 762, 763,
1067(77), 1117(429), 1120, 1128
Krebs, H. 95(17b), 139
Krebs, O. 260(372), 300, 869(145), 875(174),
885(165), 896, 897
Kreevoy, M. M. 907(84), 913
Kreknin, D. A. 780(22), 827
Kresge, C. T. 418(248), 588
Kresinske, K. R. 624(222), 761
Kreutter, K. D. 202(95), 294
Kricka, L. J. 649(359), 765, 1184(25d),
1192(47c–e), 1199(48), 1200(53b), 1207,
1208, 1235(132), 1236(35), 1271, 1273
Krieger-Beck, P. 183(10), 186
Kriis, K. 1113(408), 1127
Krijnen, B. 445(325), 590
Krimmer, H.-P. 378(166), 585
Krishnan, S. 1035(228), 1051
Krishna, C. M. 926(49), 938(48a), 990
Krishna, N. R. 951(174), 993
Krishna, S. 273(453), 302, 1313(34), 1343
Kriska, T. 686(508), 768, 977(276), 996
Kristal, B. S. 978(287b), 997
Kristensen, D. 665(444, 445), 767
Kritsanapuntu, S. 1334(144), 1346
Kriz, D. 653(382), 765
Kriz, K. 653(382), 765
Kroger-Ohlsen, M. V. 665(444), 767
Krog, S. 623(197), 761
Krohn, K. 1104(364–367), 1108(389), 1126,
1127
Kropf, H. 234(239), 240(240), 297, 343(88),
351(109), 355(121), 357(117, 120),
358(126), 583, 584, 814(88), 829, 867(142),
896
Kropp, P. J. 1025(161), 1049
Kroutil, W. 380(158, 167), 381(175), 585, 586
Krow, G. C. 1108(390), 1127
Krow, G. R. 538(488a), 594
Krüger, T. 713(612), 771, 1067(81), 1120
Kruk, C. 183(31), 187
Ksebati, M. 980(290d), 997
Kubicki, M. 122(157), 143
Kubota, H. 698(580), 770
Kubota, I. 1003(20), 1046, 1244(203), 1274
Kubota, K. 122(144), 142
Kucharski, S. A. 12(7c), 85
Kuchkova, K. I. 122(101), 141
Kuck, D. 1163(152a, b), 1169
Kuczowski, R. L. 98(33), 139, 716(545, 616),
717(624), 721(649–651), 722(647,
653–655), 723(625, 657), 769, 771, 772
Kudin, K. N. 12(7), 85
Kudo, M. 621(177), 760
Kudsy, M. 605(29), 756
Kuge, N. 610(73), 655(398), 757, 765
Kuhan, Y. T. 984(316), 998
Kuhnen, L. 476(371), 591
Kuhn, D. G. 1035(228), 1051
Kuhn, F. E. 1083(216), 1086(252), 1110(214),
1123, 1124
Kühn, F. E. 453(343a, b), 461(353), 466(344),
529(470), 590, 593
Kuhn, T. 561(217), 587, 1093(292), 1125
Kühn, T. 542(216), 587
Kujime, M. 1064(52), 1119
Kuksis, A. 693(562a, 573, 574), 726(638),
739(695), 770–772
Kuliev, S. A. 652(380), 765
Kulig, M. J. 325(55a, b), 583, 946(128),
947(129), 992
Kulkarni, P. P. 1029(193), 1050
Kulkarni, S. J. 538(487a, b), 576(548), 594,
596
Kulmacz, R. J. 689(559), 769
Kuluncsics, Z. 977(275a), 996
Kumabe, R. 252(317), 299
Kumada, M. 806(63), 808(67–69), 815(62),
828
Kumagai, H. 630(266), 762
Kumakura, S. 1157(130a, b), 1168
Kumarathanan, R. 1031(203), 1050
Kumara, K. 901(41), 912
Kumar, A. S. 652(378), 765, 869(93),
889(197), 895, 897
Kumar, A. 1116(416), 1127
Kumar, D. 1140(52a), 1166
Kumar, G. S. 425(266), 588
Kumar, N. 1291(47), 1343
Kumar, P. 1094(304), 1111(401), 1125, 1127
Kumar, R. 414(228), 422(255), 527(246,
246b), 587, 588, 1094(304), 1111(401),
1125, 1127
Kumar, S. B. 1094(304), 1125
Kumazawa, S. 650(360), 765
Kunath, A. 329(65), 331(68), 475(70), 583
Kunikawa, S. 225(219, 220), 296
Kuntz, I. D. 1322(118), 1345
Kuo, J. S. 669(465), 767
Kupfer, B. 1335(150), 1346
Kupke, J. 1104(364–366), 1126
Kurbanyan, K. 974(262c, d), 996

- Kuriyama, Y. 208(103b), 294
 Kuroda, K. 253(328), 260(370), 299, 300, 418(249b), 588, 839(54, 55), 895
 Kuroda, N. 698(193), 760, 1257(268, 287), 1276
 Kurosawa, K. 112(92), 141, 252(299–309, 311–317), 298, 299
 Kurosawa, T. 693(570), 770
 Kurth, H.-H. 678(522), 679(313), 764, 769
 Kurusu, Y. 434(285), 501(417), 589, 592
 Kurzban, G. 1322(117, 118), 1345
 Kurz, A. 943(96), 991
 Kusabayashi, S. 108(107), 110(110), 111(111), 112(112), 113(113), 141, 734(679), 772, 1157(127a, b), 1168
 Kusama, H. 265(403), 301
 Kuselman, I. 624(242), 663(438, 439), 762, 766
 Kusmierek, J. T. 982(308), 998
 Kuwahara, Y. 1257(283), 1276
 Kuwajima, I. 265(403), 301
 Kuwana, T. 1263(328), 1277
 Kuwata, K. T. 55(55), 87, 833(35), 894
 Kuwata, S. 652(377), 765
 Kuwazawa, S. 651(371), 765
 Kuznik, N. 122(157), 143
 Kvick, Å. 100(42), 139
 Kwakman, P. J. M. 643(332), 764, 1257(258, 259), 1276
 Kwon, B.-M. 325(56), 583, 852(76), 854(106), 895, 896
 Kwon, Y. S. 616(153), 759
 Kyle, D. E. 1281(5), 1326(106), 1342, 1345
 Kyrikou, I. 1058(38), 1119
 L' Esperance, R. P. 174(9), 186
 La Crois, R. M. 1069(44, 50), 1119
 Laane, R. W. P. M. 374(147), 585
 Labaied, M. 238(257), 297
 LaBarge, M. S. 722(655), 723(625), 771, 772
 Labat, G. 1031(208), 1050
 Lachgar, M. 269(429), 270(431), 301
 Lachicotte, R. J. 1082(191), 1122
 Lacoste, J. 684(214), 761
 Laerdahl, J. K. 97(27a), 139
 Lagarde, M. 918(10), 989
 Lagerkvist, S. 960(204a), 994
 Lagrimini, L. M. 694(146), 759
 Laha, S. C. 422(255), 588
 Lahoz, F. J. 1064(68), 1120
 Laib, R. J. 981(307b), 998
 Laidig, K. E. 12(7e), 85
 Laidler, K. J. 910(72b), 913
 Laing, M. 95(18), 139
 Lai, D. K. W. 1075(146), 1121
 Lai, E. K. 950(145), 992
 Lai, H. 273(457), 302, 1336(151–153), 1346
 Lake, D. B. 1020(122), 1048
 Lakouraj, M. M. 368(144), 525(464), 585, 593, 1004(28–30), 1046
 Lakshminarasimhan, J. 1178(19c, d), 1206
 Lakshminarasimhan, P. H. 870(160), 897
 Lakshminarasimhan, P. 885(158), 897
 Lakshminarayana, V. 1028(186), 1050
 Lalbachan, B. 1140(15), 1165
 Lamata, M. P. 1064(68), 1120
 Lamberti, C. 1082(202), 1123
 Lambert, A. 558(491), 594, 1081(176), 1122
 Lambert, C. 835(33), 894
 Laming, G. 12(7e), 85
 Lamkat, R. 1163(154f), 1169
 Lam, K. S. 624(237), 761
 Lam, W. L. 1317(100), 1344
 Lam, Y. 124(153), 142
 Landau, R. 425(268), 588
 Landis, M. E. 317(29), 582, 1184(21), 1206, 1266(333), 1277
 Landi, L. 977(280a), 997
 Lands, W. E. M. 689(559), 769
 Land, E. J. 926(47), 945(125), 966(233b, c), 990, 992, 995
 Lane, B. S. 1082(168), 1122
 Langau, J. 269(428), 301
 Langer, V. 112(81), 113(82), 141, 514(440), 593
 Langley, W. D. 1008(60), 1047
 Langlois, R. 967(236), 995
 Langouët, S. 984(310, 311, 313), 998
 Langrand, G. 339(82), 583
 Lang, H. Q. 741(702), 773
 Lang, T. J. 58(128a), 90
 Lankat, R. 1163(154c, 154g), 1169
 Lapshin, N. M. 823(114, 115), 830
 Larcombe, B. E. 315(30), 582
 Lardet, G. 646(346), 764
 Larkin, I. 1067(78), 1120
 Larock, R. C. 492(396b), 592
 Larsen, F. K. 1075(154), 1122
 Larsen, S. C. 871(163), 897
 Larsen, S. 520(451), 593
 Larson, G. L. 776(1), 808(64), 827, 828
 LaScala, J. J. 622(191), 760
 Lasserre, L. 975(269b), 996
 Lasterra-Sánchez, M. E. 379(164), 380(158, 167), 585
 Latajka, Z. 84(164), 91
 Latarjet, R. 919(20), 921(28b), 989
 Latham, T. B. 1024(155), 1049
 Latour, J.-M. 1069(49), 1119
 Lattanzi, A. 408(99), 413(234), 482(14), 488(392), 491(395), 493(391, 393), 582, 584, 587, 591, 1094(295), 1097(333), 1125, 1126
 Lattimer, R. P. 721(651), 722(653), 771
 Lauderdale, W. J. 12(7c), 85
 Laurence, C. 111(22), 139

- Lauret, C. 382(180), 586
 Lauricella, R. 973(254), 995
 Lauterwein, J. 183(10), 186
 Lau, C. P. 425(244), 588
 Lau, M. L. 1257(302), 1277
 Laval, J. 984(313), 998
 Lawrence, J. R. 613(118), 758
 Laye, P. G. 163(48, 49), 169
 Lazarides, E. 1145(67b), 1166
 Lazarus, M. 337(75), 583
 Lazrus, A. L. 637(305, 306), 648(307), 763
 La, W. L. 1317(87), 1344
 Le Carpentier, J.-M. 1064(67), 1120
 Leach, A. G. 253(335), 299, 833(35), 894
 Leadbeater, N. E. 413(234), 587
 Leahy, D. F. 641(18), 756
 Leban, I. 129(173), 143
 Lebrun, C. 939(71), 990
 Lechtken, P. 1189(42), 1191(46a, 46c), 1208, 1222(53), 1224(56, 57), 1227(83), 1228(101), 1267(48), 1271, 1272
 Leckten, P. 164(52), 169
 Leclerc, G. 211(110), 294
 LeCloux, D. D. 1117(428), 1128
 Leddy, B. P. 238(238), 297
 Lederer, M. 354(114), 584
 Ledon, H. J. 421(243), 426(274), 587, 588
 Ledon, H. 1069(117), 1121
 Leenheer, J. A. 606(38), 756
 Leere Oiestad, A. M. 84(165b), 91
 Leeson, P. D. 1247(214), 1275
 Lee, A. G. 273(453), 302, 1313(34), 1343
 Lee, A. M. 12(7e), 85
 Lee, C.-H. 1116(417), 1128
 Lee, C.-M. 612(106), 758
 Lee, C. W. 1116(422), 1128
 Lee, C. 1256(28), 1271
 Lee, Chee-Seng 112(77), 140
 Lee, D. H. 1015(104), 1048
 Lee, F. L. 112(68), 140
 Lee, G.-H. 124(153), 142
 Lee, H. C. 185(38), 187
 Lee, H. J. 205(117), 294
 Lee, H. K. 1035(229), 1036(232), 1038(242, 243), 1051
 Lee, I. Q. 357(123), 584
 Lee, J.-T. 605(37), 756
 Lee, J. H. 612(107), 641(18, 325, 326), 756, 758, 764, 1262(326, 327), 1277
 Lee, J. J. 616(153), 759
 Lee, J. S. 1116(422), 1128
 Lee, J. 608(51), 757, 1224(62), 1225(64), 1243(63), 1244(203), 1271, 1274
 Lee, K.-H. 137(205), 144, 278(511), 303
 Lee, K. C. 1146(72), 1167
 Lee, K. H. 900(20, 21), 901(19, 23, 32, 34, 36, 44, 45), 902(66, 67), 912, 913
 Lee, K. J. 1027(176), 1049
 Lee, K. W. 902(63), 913
 Lee, K. 273(48, 464), 290(579, 580, 584), 292, 302, 305, 1314(90, 91), 1338(166), 1344, 1346
 Lee, M.-C.-i. 612(88), 758
 Lee, M. 604(4, 5), 698(310), 756, 764, 1314(98), 1344
 Lee, R. J. 241(241), 243(243), 297, 346(97), 584
 Lee, S.-G. 1146(72), 1167
 Lee, S. H. 981(295), 997
 Lee, S. J. 1027(175), 1049
 Lee, S. O. 526(465), 593
 Lee, S. Y. 1030(196), 1050
 Lee, S. 273(462, 464), 290(586, 587), 302, 305, 1003(23), 1046, 1317(102), 1338(166), 1344, 1346
 Lee, Y.-N. 650(13), 756
 Lee, Y.-T. 612(106), 758
 Lee, Y. W. 291(595), 305
 Leffler, J. E. 907(80), 910(74), 913
 Lefort, D. 213(158), 295
 Legendre, J. Y. 1257(260), 1276
 Legg, K. D. 1250(225), 1275
 Legrand, A. 667(456), 767
 Legrand, P. 702(227), 714(567), 761, 770
 Legros, J. 487(390), 591, 1021(138), 1049
 Lehman, L. S. 320(35a), 582
 Lehn, J. M. 1250(224), 1252(246), 1275
 Lehotay, D. C. 670(476), 767
 Leitich, J. 963(223), 964(227a), 968(239b), 994, 995
 Leitzke, A. 616(152), 673(497), 674(503b), 740(244), 759, 762, 768
 Leiva, L. C. A. 165(54), 169
 Leiva, L. C. 164(53), 169
 Lei, W. 86(86), 88
 Lei, X. 1178(19c, d), 1206
 Lejeune, R. 697(183), 760, 1252(174, 243), 1274, 1275
 Lemaire, J. 662(430), 692(569), 766, 770
 Lemercier, J. N. 14(46), 87
 Lemoigne, F. 973(254), 995
 Lemoine, L. M. 1062(63), 1120
 Lempers, E. L. M. 445(325), 590
 Lempers, H. E. B. 514(433, 434), 592, 1085(208), 1123
 Lenaerts, I. 1251(230), 1275
 Lenci, F. 253(333), 299
 Lendl, B. 662(432), 766
 Lenga, R. E. 621(170, 171), 760
 Lenhoff, H. M. 635(296), 763
 Lennartz, H.-W. 196(74), 293
 LeNoir, I. 286(555), 305
 Lenz, A. G. 987(329a, 329c), 999
 Léonardis, T. 605(10), 756
 Leonard, N. J. 938(69b), 990
 Leonce, S. 273(458), 302

- Leone, M. 1157(126), *1168*
 Leoni, L. 260(374), *300*
 Leonowicz, M. E. 418(248), *588*
 León, A. M. 610(78), *757*
 Leperchec, P. 842(57), *895*
 Leppard, D. G. 323(46), *582*
 Lercker, G. 690(564), 692(93), *758, 770*
 Lerdal, D. 842(58), *895*
 Lerman, C. L. 1184(21), *1206*
 Lerum, V. 1252(245), *1275*
 Leszczynski, J. 57(53), *87*
 Létard, S. 1117(431), *1128*
 Lett, P. 1089(270, 272), *1124*
 Leung, H.-K. 854(107), *896*
 Leung, H. K. 854(105), *896*
 Leung, Y. C. 1140(78), *1167*
 Levai, A. 373(152), *585*
 Lévai, A. 1143(60), 1163(1g), *1164, 1166*
 Leverich, E. P. 1059(43), *1119*
 Levett, G. 951(162), *993*
 Levina, A. 516(442, 443), *593*
 Levina, R. Ya. 153(19), *167*
 Levine, R. L. 986(328a, 328c), 987(325b, 329a, 329c), *999*
 Levi, E. M. 1006(41), *1047*
 Levy, D. 1026(170), *1049*
 Levy, H. A. 101(15), *139*
 Lewis, J. R. E. 960(204b), *994*
 Lewis, M. J. 634(89), 636(299), *758, 763*
 Lewis, S. E. M. 645(101), *758*
 Lewis, S. W. 1257(292, 298), *1276, 1277*
 Lex, J. 114(69), *140, 556(517), 595*
 Leyrer, U. 1084(233), *1123*
 Lezcano, I. 725(63), *757*
 Lhermitte, F. 384(187), *586*
 Liang, E. 124(153), *142*
 Liang, G. Y. 133(196b), *144*
 Liang, S. 649(358), *765*
 Liang, X. T. 190(27), *292*
 Liang, X. 273(28), *292*
 Liao, F. L. 892(210), *898*
 Liashenko, A. 12(7), *85*
 Lichtenberg, D. 671(113, 480), *758, 768*
 Licini, G. 487(382), *591, 1068(97, 98), 1096(130, 325), 1097(329), 1098(99, 100, 129, 131), 1115(315), 1120, 1121, 1125, 1126*
 Lick, C. 13(13b), *86*
 Liebler, D. C. 673(495), *768*
 Liebman, J. F. 147(16), 151(1), 155(22, 25), 160(3, 14, 36), 161(39, 42), 165(17), 167–169, 832(8), 894, 917(5a), *988*
 Liebman, Joel F. 153(19), *168*
 Liebscher, J. 112(117), *142, 493(66), 583*
 Liebsch, S. 1140(26), *1165*
 Liehr, J. G. 987(329b), *999*
 Liesch, J. 1145(67b), *1166*
 Lightsey, J. W. 953(186, 187), *993*
 Ligon, A. P. 638(314), *764*
 Ligtenbarg, A. G. J. 1074(135), *1121*
 Lijam, N. 1199(48), *1208*
 Liles, D. C. 103(51), *140*
 Lillien, I. 1013(87), *1047*
 Lillo, M. A. 1160(143), *1169*
 Lima, D. F. 1189(41a), *1208, 1230(111), 1260(309), 1272, 1277*
 Limbach, S. 707(308a), *763*
 Lim, H.-R. 650(230), *761*
 Lim, K. F. 1266(334), *1278*
 Lim, K. H. 882(182), *897*
 Lim, M. H. 1031(205), *1050*
 Lim, S. C. 1001(11), 1032(219), 1039(223), 1042(251), 1045(252, 276), 1046(277), *1046, 1050–1052*
 Lim, S. H. 909(89), *913*
 Lim, T. 1236(37), *1271*
 Linares, E. 953(185), *993*
 Lindahl, T. 917(1b), *988*
 Lindeman, S. V. 103(47, 48), 122(158), 123(104), 130(181, 182, 185), 131(180), *140, 141, 143, 729(669), 772*
 Linden, G. L. 423(263, 265), *588*
 Linde, S. A. 635(9), *756, 699(582), 770*
 Lindh, R. 12(7d), 30(75a), *85, 88*
 Lindsay Smith, J. R. 449(334), *590, 1140(55c, 56b), 1166*
 Lindsay, J. R. 1140(56c), *1166*
 Lindsey, R. L. 317(29), *582*
 Lind, J. A. 637(305), *763*
 Lind, J. S. 1242(194), *1274*
 Lind, J. 82(162), *91, 741(700), 773, 952(179, 180), 993, 1243(195, 196, 198), 1244(180), 1248(178, 216, 217), 1274, 1275*
 Lingeman, H. 1257(262), *1276*
 Ling, K. L. E. 612(95), *758*
 Ling, P. 744(705), *773*
 Linker, T. 112(71), *140, 265(404), 301, 888(91, 92), 895*
 Linnerborg, M. 326(60), *583*
 Linseisen, J. 614(127), *759*
 Linstrom, P. J. 160(3), *167*
 Linton, S. 987(325c), *999*
 Lin, A. J. 1280(2), 1314(98), *1342, 1344*
 Lin, B. 1257(275, 279), *1276*
 Lin, C.-C. 717(622), *771*
 Lin, F. 263(388), *300*
 Lin, J.-M. 742(703), *773*
 Lin, J. W.-P. 740(682), *772*
 Lin, J. 529(471), *593, 1116(424), 1128*
 Lin, M. C. 13(43), *87*
 Lin, M. S. 651(369), *765*
 Lin, M. 1008(53), *1047*
 Lin, N.-N. 669(465), *767*
 Lin, T.-S. 610(79), *757, 1116(417), 1128*
 Lin, W. 1082(206), *1123*
 Lin, X. Y. 1280(3), *1342*

- Lin, Z. M. 392(193), 586, 1088(265), 1124
 Lipka, R. 636(243), 762
 Lipke, M. 1003(24), 1046
 Lippard, S. J. 1066(73), 1067(79, 80),
 1069(54), 1117(428), 1119, 1120, 1128
 Lippert, J. L. 624(222), 761
 Lipscomb, W. N. 4(4), 85, 96(24), 139
 Lissi, E. A. 949(138), 992
 Lissi, E. 1242(190), 1274
 Litkovets, A. K. 780(19, 20), 827
 Littlechild, J. A. 381(175), 586
 Little, B. 1311(69), 1344
 Little, R. D. 193(67), 293
 Liu, A. 1015(102), 1048
 Liu, B. 902(66), 913
 Liu, C.-H. 634(195), 760
 Liu, C. Z. 1317(103), 1344
 Liu, D. 652(77), 757
 Liu, G. 12(7), 85
 Liu, H.-J. 288(571), 305
 Liu, H. H. 1299(57), 1303(67), 1343
 Liu, J. C. 779(16b, 17), 827, 1212(10), 1270
 Liu, J. D. 1015(103), 1048
 Liu, J. 41(93), 56(90a, b, 125), 88–90,
 652(77), 757, 984(317e), 999, 1140(36, 38,
 39), 1165, 1166
 Liu, L.-Z. 640(322), 764
 Liu, M.-Y. 273(29), 292
 Liu, M. 662(236), 761, 1015(102), 1048
 Liu, S.-X. 660(111), 758
 Liu, Y. 973(260), 996, 1156(125), 1168
 Liu, Z. 630(265), 639(315), 762, 764
 Livingstone, D. R. 917(4), 988
 Livshits, F. Z. 783(24), 827
 Liwo, A. 253(337), 299
 Li, B. 511(416), 592, 654(386), 765
 Li, C. B. 511(416), 592
 Li, C. 1094(299), 1125
 Li, D.-H. 639(316, 317), 640(319, 321), 764
 Li, H. R. 870(155), 897
 Li, H. X. 527(466), 593
 Li, H. 663(235), 761
 Li, J. R. 1336(153), 1346
 Li, J. 645(338), 646(342), 654(389), 674(328),
 678(329), 701(388), 764, 765
 Li, L. 629(259), 762
 Li, M. Y. 610(80), 757
 Li, M. 646(344), 764
 Li, Q. S. 29(29), 87
 Li, R. S. 1322(117, 118), 1345
 Li, W. Z. 265(402), 301
 Li, W. 503(426), 592, 963(225b), 994
 Li, X.-y. 652(374), 765
 Li, X. 289(578), 305, 854(107), 885(172), 896,
 897
 Li, Y.-Z. 639(318), 764
 Li, Y. 39(39), 87, 265(402), 273(32, 442, 458),
 292, 301, 302, 646(344), 764, 861(137),
 896, 1044(274), 1052, 1299(40), 1343
 Li, Z. 643(333b), 764, 1322(118), 1345
 Ljunggren, S. 1248(217), 1275
 Lloyd, A. W. 12(7d), 85
 Lloyd, R. V. 917(5e), 988
 Lobmaier, G. M. 1085(246), 1086(251), 1124
 Lobnik, A. 630(263), 762
 Locke, S. J. 614(141), 759
 Lockwood, P. A. 317(27), 582, 1182(22), 1206
 Locoge, N. 605(10), 756
 Loft, S. 917(2b), 988
 Lohmann, D. H. 900(47), 912
 Lohray, B. B. 1140(51), 1166
 Lohrenz, J. C. W. 118(122), 142
 Lohr, L. L. 45(45), 87
 Loh, L. S. 255(255), 297
 Loidl-Stahlhofen, A. 951(165), 993
 Lokensgard, D. 190(50), 293
 Longo, E. 1075(155), 1122
 Long, C. A. 253(341), 299
 Long, L. H. 628(74), 655(258), 757, 762
 Look, G. C. 476(71), 583
 Loomis, B. R. 1025(161), 1049
 Lopes, A. D. 1086(252), 1124
 Lopez Nieves, M. I. 324(51b), 582
 Lopez-Pedrosa, J.-M. 383(182), 586
 Lopez, L. 204(102), 294
 Lopp, M. 521(456, 457a, b), 553(516), 593,
 594, 1113(407, 408), 1127
 Lora Maroto, B. 520(449), 593
 Lorber, M. 497(405a), 592
 Lorenčák, P. 723(656), 772
 Lorentz, O. 718(631), 771
 Lork, E. 713(612), 771, 1067(81), 1120
 Losinskidang, L. 193(67), 293
 Loufty, R. O. 1234(136), 1273
 Loup, C. 284(548), 304
 Loureiro, A. P. M. 984(292a, b, 294a), 997
 Lovas, F. J. 57(57), 88, 721(595, 645), 770,
 771, 1140(5), 1165
 Loveitt, M. E. 238(251), 250(250), 297,
 317(26), 582
 Lovering, G. 253(342), 299
 Lovett, M. B. 1224(59), 1229(109), 1271,
 1272
 Love, S. G. 621(180), 760
 Lowry, T. H. 79(155b), 91
 Low, T. P. 901(34), 912
 Loy, M. 1266(305), 1277
 Lucas, T. 641(309), 764
 Lucchini, V. 888(192), 897
 Luck, R. L. 1062(62), 1119
 Lueras, A. M. K. 974(262d), 996
 Lukacs, Z. 339(78, 79), 583
 Lukey, C. A. 683(541), 769
 Lüke, H.-J. 700(584), 770

- Lumma, W. C. 740(682), 772
 Lumtscher, J. 1067(75), 1120
 Lundell, J. 98(37, 38), 139
 Lundin, A. 1192(47d), 1208
 Lundquist, K. 122(151), 142
 Lund, P. 680(532), 769
 Lunec, J. 681(144), 759
 Lunsford, J. H. 428(291), 429(292), 433(293), 589
 Luongo, J. P. 692(215), 761
 Luong, T. K. K. 549(512a), 594
 Luo, Q. 627(251), 762
 Luo, W. 943(93b, 94), 945(98), 991, 1204(69a–c), 1209
 Luo, X.-D. 273(439, 440), 301
 Luo, X. P. 670(476), 767
 Luo, X. 18(18a), 86, 100(43), 140
 Luo, Y. F. 1016(105), 1048
 Lupattelli, P. 1150(92), 1156(121a), 1160(136), 1161(147), 1162(151b, c), 1167–1169
 Lusinchi, X. 1021(133), 1048
 Lustri, J. P. 426(275), 588
 Luthe, C. 318(12), 582
 Lutsig, M. J. 928(37c), 989
 Lutzke, B. S. 675(507), 768
 Lutz, M. 1069(50), 1119
 Luxford, C. 975(261, 266), 996
 Lu, C.-S. 99(40a), 139
 Lu, C. 742(703), 773
 Lu, J. 622(191), 643(333b), 760, 764
 Lu, L. D. L. 1105(368, 369), 1126, 1127
 Lu, L. 725(660), 772
 Lu, Y. W. 1016(105), 1048
 Lvovich, V. 653(383), 765
 Lwamura, H. 1035(231), 1051
 Lyakhov, A. S. 129(176), 143
 Lyall, K. 614(126), 759
 Lymar, S. V. 952(177, 181, 182), 993
 Lyndon, J. 666(448), 767
 Lynn, K. R. 960(206b, 207b), 994
 Lyssenko, K. A. 110(70), 140
 Maayan, G. 444(316), 589, 1107(385), 1127
 Mabbs, F. 1304(63), 1343
 Macchi, P. 1075(154), 1122
 MacDonald, A. 647(352), 764
 MacDonald, S. J. F. 392(199), 586, 1088(266), 1099(341), 1100(349), 1124, 1126
 MacDonald, T. L. 1140(52d), 1166
 MacFaul, P. A. 1086(248, 249), 1124
 Machida, Y. 233(231), 297
 Machu, W. 1004(34), 1046
 Maciejewski, S. 348(18), 582
 Mackay, A. C. 196(77), 293
 Mack, H.-G. 94(11a), 104(58), 138(56b), 139, 140, 744(20, 22), 756
 Mack, H. G. 702(591), 770
 MacMillan, D. K. 693(562b), 770
 MacQuarrie, D. J. 558(491), 594
 Maddrell, S. J. 380(158, 167), 585
 Mader, M. M. 810(78), 829
 Madhavi, G. 538(487a, b), 594
 Madhi, S. 571(542), 573(541), 595, 596
 Maeda, H. 614(130), 759
 Maeda, K. 107(90), 141
 Maeda, M. 1069(107), 1121
 Maeda, Y. 1065(72), 1067(55), 1119, 1120
 Maeuchiara, N. 630(264), 762
 Maggini, M. 1155(106b), 1168
 Maggs, J. L. 274(274), 298, 1304(63, 71), 1314(83), 1324(124), 1332(93), 1343–1345
 Magnaval, J. F. 284(548), 286(557), 304, 305
 Magno, F. 1068(87), 1120
 Magnus, A. S. 1023(151), 1049
 Magnus, P. D. 211(109, 110), 294
 Magritte, H. 899(3), 912
 Maguhn, J. 638(188), 685(542), 707(308b), 760, 764, 769
 Mahadevan, A. 1158(131), 1168
 Mahammadpoor-Baltork, I. 1032(215), 1050
 Mahboubghah, N. 1028(182), 1049
 Mahindaratne, M. P. D. 221(197), 296
 Mahuteau, J. 249(249), 297
 Mahuzier, G. 1257(260), 1276
 Mah, D. A. 974(262d), 996
 Maidwell, N. L. 270(270), 298
 Maier, G. 819(105b), 829
 Maietti, S. 1021(142), 1049
 Maiorina, M. 614(128), 759
 Maiorino, M. 681(499, 539), 768, 769
 Mairata i Payeras, A. 449(334), 590
 Mair, R. D. 718(634), 771
 Maischak, A. 569(535b), 595
 Maistrenko, G. Y. 1155(116), 1168
 Majeste, R. J. 130(184), 143
 Majima, T. 208(132), 294
 Makide, Y. 743(704), 773
 Makino, Y. 945(112), 991
 Makiuchi, M. 918(8d), 988
 Maki, K. 1257(270), 1276
 Maki, Y. 1011(82), 1047
 Mąkosza, M. 1152(107, 108a, b), 1168
 Makrand, J. K. 1030(198), 1050
 Malanca, F. E. 705(24), 740(23), 756
 Malcolm, E. A. 613(118), 758
 Malick, D. K. 12(7), 85
 Malik, H. 274(481), 303, 1320(114), 1326(128), 1345
 Malik, K. M. A. 380(170), 586
 Malingre, T. M. 273(456), 302, 1336(161), 1346
 Maling, G. Q. 130(177–179, 186), 143
 Malins, D. C. 976(272b), 996
 Malisch, W. 477(373c), 591, 1094(17), 1118, 1163(154a–g), 1169
 Malkov, A. V. 514(440), 593

- Mallakpour, S. E. 1031(209–213), 1032(214, 215), 1050
- Mallard, W. G. 160(3), 167
- Mallégo, J. 662(430), 672(189), 692(569), 760, 766, 770
- Mallet, A. 612(105), 758
- Mallory, F. B. 172(6), 186
- Malone, M. E. 943(97), 991
- Malorey, L. S. 1055(8), 1118
- Malpezzi, L. 107(89), 141
- Maltz, H. 157(28), 168
- Mameniskis, W. A. 556(522), 595
- Manabe, T. 382(178), 586
- Manby, F. R. 12(7d), 85
- Mandard-Cazin, B. 253(343), 299, 833(34), 894
- Mandelli, D. 1116(426), 1128
- Mander, L. N. 131(10), 139
- Manescalchi, F. 575(533), 595
- Manes, L. V. 190(24), 292
- Mane, R. B. 1027(174), 1029(193), 1049, 1050
- Manfredi, A. 383(183, 184), 384(185, 186), 476(368a, b), 586, 591
- Mangold, D. 1009(64), 1047
- Manik, T. 605(29), 756
- Mani, J.-C. 856(111), 896
- Manner, J. A. 1005(39), 1046
- Mann, B. 1257(291), 1276
- Mann, J. 608(56), 727(639), 757, 771
- Mann, S. T. 288(566, 570), 305
- Manoj, P. 1011(84), 1047
- Manoj, V. M. 1011(84), 1047
- Manring, L. E. 255(353, 354), 300, 844(61), 854(99), 895
- Manrique, G. D. 622(192), 760
- Manson, D. 1039(246), 1051
- Mansuy, D. 443(319b), 455(318), 457(324), 531(322), 589, 590
- Mantegazza, M. A. 1082(202), 1123
- Mantell, G. J. 221(200), 296
- Mantis, A. J. 669(466), 767
- Mantoura, R. F. C. 606(39), 645(41), 757
- Mantovani, S. 1098(131), 1121
- Manzanares, I. 284(540), 304, 1324(122), 1345
- Mao, L.-Y. 630(268), 762
- Mao, L. 630(265), 634(295), 639(315), 762–764
- Maqsudur Rahman, A. F. M. 729(668), 772
- Marai, L. 693(562a), 726(638), 739(695), 770–772
- Maranzana, A. 253(338), 299
- Maran, F. 96(20), 123(162), 129(172), 139, 143
- Maraş, A. 891(205b), 898
- Marcantoni, E. 1103(357), 1126
- Marchetti, F. 112(115), 141
- Marcotullio, M. C. 1027(178), 1028(180), 1029(188, 190, 194), 1049, 1050
- Marcus, R. A. 907(85), 913, 1217(43–45), 1235(141), 1271, 1273
- Mareda, J. 284(540), 304, 1293(37, 51), 1324(122), 1343, 1345
- Mares, F. 211(105), 294, 492(397), 545(502), 566(494), 592, 594, 1105(372), 1109(391), 1127
- Marfat, A. 352(10), 582
- Margulès, L. 100(28b), 139
- Mariano, P. S. 1267(115), 1272
- Maria, P.-C. 874(170), 897
- Marini, S. 1156(121d), 1168
- Marioli, J. M. 968(239c), 995
- Marion, M. J. 984(297h), 998
- Markel, S. 624(225, 226), 761
- Markesbery, W. R. 945(101), 991
- Markler, M. T. 109(116), 141
- Marklund, S. 635(297), 763
- Marko, I. 567(528), 595
- Marko, J. 269(426), 301
- Marks, F. 981(303), 998
- Marks, N. E. 634(89), 758
- Marktl, W. 611(82), 758
- Mark, C. 432(300a, b), 589, 1084(232, 233), 1123
- Mark, G. 740(244), 762
- Marnett, L. J. 214(170), 295, 917(2a, 3b), 918(11a–c), 945(110, 116), 980(290c–f), 984(311), 988, 989, 991, 992, 997, 998
- Marques, S. A. 984(292a), 997
- Marquez, M. 56(12b), 58(124), 86, 90
- Marquis, E. T. 426(275), 588
- Marrero, J. J. 230(229), 297
- Marsch, M. 118(122), 124(124), 142, 1067(57), 1119
- Marsden, C. J. 102(54, 55), 140, 713(613), 771
- Marsella, A. 1117(433), 1128
- Marshall, H. 1002(16), 1046
- Marshall, J. A. 861(135), 896
- Marshall, P. A. 951(170), 993
- Marshall, P. M. 22(22a), 86
- Marsh, R. 1064(66), 1120
- Marsman, B. 374(147c), 585
- Martem'yanov, V. S. 153(4), 167
- Martens, R. J. 445(325), 590
- Martic, P. A. 870(156), 897
- Martinez, A. 1083(209), 1090(276), 1123, 1124
- Martínez, A. 418(247), 588
- Martinez, C. G. 184(33), 187
- Martinez, G. R. 269(423), 301, 941(80b), 943(85c, 86, 87, 91), 951(160, 161, 164), 967(238b, c), 977(274a, b), 991–993, 995, 996
- Martinho Simões, J. A. 160(14), 167
- Martins-Costa, M. T. C. 30(75b), 88
- Martins, A. P. B. 951(161), 993
- Martins, P. R. 1140(52b), 1166

- Martin, B. D. 943(95), 991
 Martin, C. N. 1140(55a, 56c), 1166
 Martin, C. S. 1198(54a), 1200(53a), 1208
 Martin, E. J. 156(20), 168
 Martin, E. 151(18), 167
 Martin, J. C. 34(34), 87, 901(25), 912
 Martin, J. E. 1189(44a), 1208
 Martin, K. F. 1020(120), 1048
 Martin, M. M. 901(33), 912
 Martin, R. L. 12(7), 85
 Martin, R. S. 284(284), 298, 343(92), 584, 852(75), 895
 Martin, S. W. 213(161), 295
 Martin, V. S. 396(211), 397(212), 587
 Maruyama, J. 1012(85), 1047
 Maruyama, T. 918(8c), 988
 Marz, D. W. 466(342), 590, 1110(23), 1118
 Masaki, Y. 118(142), 142
 Masamune, H. 400(208), 587, 1092(282), 1125
 Masamune, S. 825(121, 123), 830
 Masana, J. 375(156), 379(153), 380(155), 585
 Mascharak, P. K. 118(127), 130(130), 142, 1117(427), 1128
 Maschmeyer, T. 1085(247), 1086(248), 1124
 Masciadri, R. 273(273), 298, 608(59), 757, 1332(14), 1342
 Maseles, F. C. 1200(58b), 1208
 Mashiko, S. 858(122), 896
 Mashiko, T. 394(203), 586
 Maskiewicz, R. 1251(220, 221), 1275
 Maskos, Z. 966(208), 994
 Maslennikov, V. P. 1043(265, 266), 1051
 Maslen, P. E. 12(7e), 85
 Mason, D. Y. 1335(149), 1346
 Mason, H. S. 1055(7), 1118
 Mason, R. P. 917(5e), 973(255a, b), 988, 995
 Maspero, F. 1082(201), 1108(386), 1123, 1127
 Massa, A. 482(14), 483(15), 582
 Massa, W. 128(128), 142, 267(418, 420), 301
 Massey, V. 77(152b), 82(161), 91
 Masteropietro, G. 1161(146), 1169
 Masuda, H. 109(119), 142, 1064(69), 1065(72), 1069(118), 1120, 1121
 Masui, Y. 856(114), 896
 Masumoto, H. 50(50a), 87
 Masuyama, A. 108(106), 113(102), 141, 225(219, 220), 242(268), 249(292), 266(266), 267(267), 269(269), 288(560, 561), 289(289), 290(290), 291(291), 296–298, 305, 712(610), 771, 1282(27), 1332(108), 1335(147), 1342, 1345, 1346
 Masuyama, Y. 434(285), 512(398), 589, 592, 1105(375), 1127
 Mataka, S. 199(86), 293
 Mateos, R. M. 610(78), 757
 Matheson, M. S. 1189(44b), 1208
 Mathews, C. K. 1197(52), 1208
 Mathews, J. E. 380(170), 586
 Mathies, P. 250(296), 298
 Mathieu, B. 1069(65), 1120
 Mathurin, P. 613(116), 758
 Matile, H. 1332(15, 105), 1342, 1344
 Matoba, Y. 434(273), 588, 1089(271), 1124
 Matos, M. A. R. 161(42), 169
 Matschiner, H. 623(209), 761
 Matsubara, J. 1236(148), 1273
 Matsubara, S. 788(31), 789(32), 790(34, 35), 792(30a), 827, 828
 Matsubayash, G. E. 1020(119), 1048
 Matsuda, E. 1252(245), 1275
 Matsugo, S. 351(107), 584
 Matsuhashi, H. 1021(140), 1049, 1140(86), 1167
 Matsui, T. 1157(130a, b), 1168
 Matsumoto, H. 223(218), 296
 Matsumoto, K. 1140(82), 1167
 Matsumoto, M. 209(144), 253(327, 328), 259(366), 260(370), 295, 299, 300, 325(54), 583, 809(73), 829, 839(54, 55), 854(109), 878(178), 895–897, 1188(34b), 1192(16b), 1199(55, 57), 1206–1208, 1236(147–153, 156–158, 162), 1238(170), 1273, 1274
 Matsumoto, S. 113(76), 118(139), 124(108), 140–142
 Matsumura, M. 719(636), 771
 Matsunaga, N. 12(7b), 85
 Matsunaga, S. 1334(144), 1346
 Matsunaga, T. 1236(37), 1271
 Matsuoka, I. 255(350), 300
 Matsuo, M. 113(76), 124(108), 140, 141, 339(84), 583, 981(293), 984(281a), 997
 Matsushita, S. 949(109), 991
 Matsushita, Y. 497(405b), 592
 Matsutani, S. 674(253), 762
 Matsuura, T. 118(129), 142, 269(422), 301, 316(23), 318(13), 352(48), 582, 962(210), 967(216, 238a), 994, 995
 Mattay, J. 858(125), 896
 Mattes, S. L. 208(127), 294
 Matthew, J. A. 951(162), 993
 Matthijssens, F. 1251(230), 1275
 Mattingly, P. G. 1252(244), 1275
 Mattner, M. R. 466(344), 590, 1083(216), 1123
 Matusch, R. 262(379), 300, 885(187), 897
 Matusuno, K. 263(380), 300
 Matuszewski, B. 1188(40c, d), 1207, 1262(308, 311), 1277
 Matvienko, L. G. 1069(119), 1121
 Maulding, D. R. 1212(8), 1270
 Maumy, M. 254(347), 299
 Maurer, M. 272(436), 301
 Maurette, D. 270(431), 301
 Maurya, M. R. 1058(32), 1119
 Mavromoustakos, T. 1058(38), 1119
 Mavuso, W. W. 1283(30), 1343

- Mawatari, S. 675(464), 767
 Mawby, R. J. 125(149), 142
 Maxwell, J. P. 283(520), 304
 Maxwell, S. R. J. 1242(192), 1274
 Mayashi, M. 900(11), 912
 Mayer, A. 1199(56b), 1208, 1236(146), 1273
 Mayer, B. 13(42), 87
 Mayer, J. M. 118(123), 142
 Mayer, M. 945(120), 992
 Mayer, R. 134(199), 144
 Mayhew, S. G. 80(151), 91
 Mayon, P. 379(164), 380(158, 167), 585
 Mayoral, J. A. 245(281), 298
 Mayrargue, J. 217(191), 249(249), 280(525, 528, 529), 283(534), 296, 297, 304
 May, W. S. 1335(148), 1346
 Mazur, S. 1172(10b), 1205
 Mazur, U. 721(650), 771
 Mazzocchia, C. 428(294), 589
 Ma, H. 649(358), 765
 Ma, J. C. 873(166), 897
 Ma, K. 662(431), 663(233, 435), 761, 766
 Ma, Q. 649(358), 765
 Ma, W. 639(315), 764
 McAtee, J. L. 726(663), 772
 McBride, J. M. 130(183), 143
 McCague, R. 381(159), 585
 McCapra, F. 1172(4a, b, 6), 1191(8b), 1194(35a), 1205, 1207, 1227(82), 1235(131, 132), 1247(213, 214), 1250(219, 224), 1252(218, 232, 246), 1256(27, 233, 252), 1271–1273, 1275
 McCarrick, M. A. 253(334), 299
 McCarron, M. 1094(303), 1125
 McCarthy, B. J. 1192(47a), 1208
 McCarthy, T. J. 503(420), 592
 McCarty, M. F. 1336(160), 1346
 McCay, P. B. 950(145), 992
 McChesney, J. D. 289(578), 290(582, 583, 588–590), 305
 McClements, D. J. 614(133), 759
 McCloskey, C. J. 1140(43), 1166
 McCormick, M. L. 610(79), 757
 McCready, R. 351(102), 584
 McCullough, K. J. 107(61), 108(106, 107), 110(110), 111(111), 112(112), 113(102, 109, 113), 140, 141, 242(268), 249(292), 266(266), 267(267), 269(269), 273(53, 54, 476), 288(560), 290(290), 293, 297, 298, 303, 305, 711(608), 712(609–611), 727(664), 771, 772, 1282(27), 1342, 1327(125)1345
 McDonald, J. D. 834(38), 894
 McDonald, R. A. 15(15), 86
 McDonald, S. 906(69), 913
 McDouall, J. J. W. 56(48c), 67(140), 68(119, 141), 87, 89, 90, 97(32a, b), 139, 1140(44), 1166
 McDouall, J. W. 79(17a), 86
 McDougall, J. A. 1336(153), 1346
 McDowell, M. V. 1261(321), 1277
 McElhill, E. A. 901(22), 912
 McFarlane, I. M. 1097(328), 1126
 McGarvey, D. J. 1291(47), 1343
 McGoran, E. C. 122(159), 143, 284(549), 304
 McGrath, M. P. 28(28a, b), 87
 McGrouther, K. G. 628(255), 762
 McGuckin, M. R. 1155(106a), 1168
 McGuinness, A. 900(13), 912
 McGuire, S. O. 660(423), 766
 McIntosh, K. 1332(15), 1342
 Mckay, D. J. 133(191), 143
 McKee, M. L. 30(76), 54(54), 87, 88, 253(339), 299
 McKelvie, I. D. 645(340), 764
 McKenzie, C. J. 1067(75), 1069(46), 1119, 1120
 McKenzie, C. 1069(49), 1119
 McKerrow, J. H. 1322(117, 118), 1345
 McKillop, K. L. 825(108b), 829
 McKinney, K. A. 645(101), 758
 McLaren, S. E. 637(305, 306), 707(523), 763, 769
 McLaren, S. 648(307), 763
 McLean, W. G. 1326(106), 1345
 McLemore, J. L. 676(301), 763
 McMahan, T. B. 873(169), 897
 McMordie, R. A. S. 1200(58c), 1208
 McMorn, P. 422(256), 588
 McMullan, R. K. 99(40b), 139
 McNeil, B. 1251(231), 1275
 McNicholas, S. J. 12(7d), 85
 McPhail, A. T. 112(74), 134(197), 137(205, 206), 140, 144, 217(186, 187), 263(263), 278(511), 296, 297, 303
 McPhail, D. R. 134(197), 144, 278(511), 303
 McQueney, P. A. 1145(67b), 1166
 McRiner, A. J. 273(468), 302, 1337(164), 1346
 Meador, W. R. 161(40), 169
 Mebane, R. C. 233(11), 292
 Meche, F. S. 1320(112), 1345
 Medalia, A. I. 676(510), 768
 Medeiros, M. H. G. 269(423), 301, 941(80b), 943(85c, 86, 87, 91), 950(158, 159), 951(160, 161, 164), 967(238b, c), 977(274a, b), 984(292a, b, 294b, c), 991–993, 995–997
 Meerman, J. H. M. 670(124), 759
 Meerwein, H. 355(121), 584
 Meffre, P. 567(531e), 595
 Meguro, H. 660(422), 680(528), 766, 769
 Mehrabi, M. R. 611(82), 758
 Mehrotra, M. M. 812(85), 829
 Mehrotra, S. 276(441, 498–500), 302, 303, 1314(95, 96), 1344

- Mehrshikh-Mohammadi, M. E. 906(69), 913
 Mehta, G. 267(416, 417), 301
 Meijer, E. W. 819(105a), 829
 Meinershagen, J. L. 455(329), 590
 Meisel, D. 1189(44b), 1208
 Meisel, M. 733(678b), 772
 Meister, G. E. 1077(59), 1119
 Melchior, D. 674(502), 679(525), 768, 769
 Mele, A. 45(106d), 89, 1160(35d), 1165
 Melhler, A. H. 966(219), 994
 Mellon, F. A. 694(146), 759
 Mello, R. 32(59), 88, 184(34), 187, 806(61),
 828, 1140(13, 14), 1155(115, 117, 119a),
 1158(132), 1160(11a, 13a, 138, 139a, b,
 141, 142), 1161(105), 1163(1d, 25, 153),
 1164, 1165, 1167–1169, 1178(20d), 1206
 Melodieva, D. 966(229), 995
 Melrose, M. P. 3(3a), 85
 Melvin, T. 324(36a), 582
 Menasveta, P. 1334(144), 1346
 Mendenhall, G. D. 213(161), 295, 732(677),
 772, 854(102), 895, 950(149, 150), 992
 Menezes, S. L. 953(185), 993
 Mennucci, B. 12(7), 85
 Menzek, A. 267(409, 415), 301
 Menzel, D. B. 233(12), 292
 Menzies, I. D. 211(109, 110), 294
 Meou, A. 449(337), 590
 Mercer, A. E. 273(467), 302, 1337(165), 1346
 Merchan, M. 29(64), 88
 Merenyi, G. 82(162), 91, 1242(194),
 1243(195, 196, 198), 1244(180), 1248(216,
 217), 1274, 1275
 Merényi, G. 741(700), 773, 952(179, 180),
 993, 1248(178), 1274
 Merrill, Y. 137(206), 144
 Merk, C. 1097(334), 1126
 Merlic, C. 193(67), 293
 Merrigan, S. R. 56(125), 90
 Merritt, M. V. 315(33), 582
 Merritt, M. 315(31), 582
 Mertens, H.-J. 706(596), 770
 Meshnick, S. R. 273(34, 455), 280(518), 292,
 302, 304, 1281(8), 1283(32), 1291(47),
 1298(18), 1302(61), 1304(70), 1311(12, 69,
 77), 1312(78), 1342–1344
 Mesrobian, R. B. 149(8), 167
 Messeguer, A. 1154(19), 1155(118b),
 1161(103), 1165, 1167, 1168
 Metelitz, D. I. 426(277b), 588
 Meth-Cohn, O. 366(139), 585
 Metzinger, L. 777(6), 827
 Meunier, B. 273(449, 451, 452), 283(534),
 284(541, 542, 548), 286(557), 302, 304,
 305, 442(317), 538(488b), 589, 594,
 941(79), 943(92), 991, 1003(19), 1021(136),
 1031(202), 1046, 1048, 1050, 1069(45),
 1119, 1296(54, 55), 1298(56), 1303(7),
 1306(72), 1312(79), 1320(43, 112, 113),
 1342–1345
 Meyers, C. Y. 122(155), 143, 221(201), 296
 Meyer, J. 637(304), 763
 Meyer, L. 95(17a), 139
 Meyer, M. P. 833(35), 894
 Meyer, R. 101(46), 140, 166(59), 169
 Meyer, W. 12(7d), 85
 Mezzetti, A. 1084(237), 1124
 Mezzetti, M. 1161(146), 1169
 Mhasalkar, M. 718(633), 771
 Mialane, P. 1069(45), 1070(47), 1119
 Miaskiewicz, K. 44(99), 89, 1140(40),
 1159(135b), 1166, 1169
 Mican, A. N. 984(311), 998
 Michaelson, R. C. 410(225), 542(201),
 569(536), 586, 587, 595, 1092(287), 1125
 Michaels, H. B. 657(139), 759, 922(41b), 990
 Michael, P. R. 1226(69), 1272
 Michalczyk, M. 825(108a), 829
 Micejda, C. J. 900(24), 912
 Michelin, R. A. 1084(231, 236), 1123, 1124
 Michishita, S. 650(364), 765
 Michl, J. 825(108a), 829, 1244(201, 202),
 1274
 Micklitz, W. 1067(79), 1120
 Mick, M. S. 665(446), 767
 Midyanyj, S. V. 1253(241), 1275
 Mieglietz, K. 608(54), 757
 Mielke, K. 1155(106d), 1168, 1236(79, 159),
 1272, 1273
 Mifune, M. 677(518), 768
 Migita, T. 854(101), 895
 Miglietta, L. M. 982(308), 998
 Mignard, M. 423(262), 588, 1085(142),
 1116(56), 1119, 1121
 Migo, V. P. 719(636), 771
 Mihaljević, B. 676(511), 768
 Mihelich, E. D. 214(172, 173), 295
 Miki, K. 1117(431), 1128
 Mikolaiski, W. 128(128), 142
 Milas, N. A. 352(106, 111), 584, 1055(5–8),
 1084(239), 1118, 1124
 Milazzi, A. 986(326), 999
 Miles-Richardson, G. E. 918(8a), 988
 Mile, B. 717(628), 732(635), 771
 Milhous, W. K. 276(441), 280(514, 515, 517,
 518), 283(519), 284(546), 302–304,
 712(58), 725(57), 757, 812(86b), 829,
 1280(2), 1281(5), 1296(53), 1298(18),
 1314(95), 1325(20), 1326(106), 1342–1345
 Milhous, W. 273(440), 276(498), 301, 303,
 1314(96), 1344
 Millet, P. 1021(133), 1048
 Milius, W. 204(99), 294, 800(48), 828
 Millam, J. M. 12(7), 85
 Millasson-Schmidt, P. 1293(37, 51), 1343
 Miller, A. O. 123(164), 143

- Miller, A. 280(526), 304, 1332(93), 1344
 Miller, E. K. 1243(197), 1274
 Miller, H. 1082(187), 1091(186), 1122
 Miller, I. K. 1010(72), 1047
 Miller, J. A. 1140(56d), 1166
 Miller, J. F. 689(559), 769
 Miller, J. G. 160(31), 168
 Miller, K. 219(196), 296
 Miller, M. M. 433(287, 288), 589, 1062(63), 1120
 Miller, R. A. 503(426), 592
 Miller, R. E. 1322(117, 118), 1326(106), 1345
 Miller, R. W. 263(263), 297
 Miller, R. 276(498–500), 303, 1286(41), 1306(74), 1314(64, 96), 1343, 1344
 Miller, S. M. 1140(77b), 1167
 Miller, T. 1228(60), 1271
 Milligan, W. O. 726(663), 772
 Millot, C. 30(75b), 88
 Mills, K. A. 217(169, 181–183), 295, 296
 Milne, G. L. 977(280b), 997
 Milofsky, R. E. 1188(40f), 1207, 1262(324, 325), 1277
 Milofsky, R. 1257(294), 1277
 Mimoun, H. 48(115b), 89, 131(131), 142, 423(262), 426(276, 278), 432(280, 300b), 523(238, 458, 459), 587–589, 593, 1058(28, 29), 1061(58), 1072(14), 1075(141), 1078(159), 1084(232), 1085(142), 1089(269), 1115(161), 1116(56), 1117(432), 1118, 1119, 1121–1124, 1128
 Mimura, K. 199(86), 293
 Minas da Piedade, M. E. 149(9), 167
 Minato, H. 1006(38), 1007(49), 1046, 1047
 Minato, T. 56(121), 90
 Mincione, E. 370(146), 560(510), 585, 594, 1083(226), 1111(398, 399), 1123, 1127, 1156(121a–d), 1160(136), 1161(146, 147), 1162(151b, c), 1168, 1169
 Mínguez-Mosquera, M. I. 658(418), 766
 Ming, K. S. 870(155), 897
 Minidis, A. B. E. 516(435), 592
 Minisci, F. 45(92, 106a–d), 89, 1008(51), 1010(71, 77), 1047, 1160(35a–e), 1165
 Minkoff, G. J. 104(23), 139, 362(136a), 585
 Mink, J. 569(534), 595
 Minot, C. 310(3b), 581
 Mioskowski, C. 1256(253), 1275
 Mirajkar, S. P. 1094(304), 1125
 Miranda, M. S. 161(42), 169
 Mirbach, M. J. 1228(107), 1272
 Mirjalili, B. F. 1029(189), 1050
 Misawa, Y. 246(286), 298, 852(78, 79), 895
 Mischne, M. P. 291(596, 597), 305
 Mishnev, A. 493(101), 584, 1099(343), 1126
 Misiaszek, R. 940(78), 991
 Miska, W. 1193(49a), 1208
 Misono, M. 1082(196), 1094(302), 1117(195), 1123, 1125
 Misra, D. 274(479, 480), 284(545), 303, 304, 1326(127), 1345
 Misra, R. R. 984(297d), 998
 Mistry, N. 238(165), 295
 Mitchell, C. M. 410(223), 469(350), 477(373a), 478(374), 587, 590, 591, 1090(221, 276), 1091(278), 1096(319, 321), 1123–1125
 Mitchell, D. J. 310(3b), 581
 Mitchell, J. C. 358(128), 584, 672(483–485), 768
 Mitchell, J. M. 1075(34), 1119
 Mitchell, P. A. 847(43), 894
 Mitchell, R. H. 199(87), 293
 Mitschler, A. 426(276), 523(459), 588, 593, 1064(67), 1120
 Mitsudo, K. 810(77), 829
 Mitsui, H. 1104(356), 1126
 Miura, M. 112(112), 141, 374(150), 585, 712(611), 727(664), 734(679), 771, 772
 Miura, N. 650(364), 765
 Miyabe, H. 273(437), 301
 Miyachi, H. 273(461), 302
 Miyaji, T. 133(133), 142, 1064(52), 1119
 Miyake, M. 690(563), 770
 Miyake, T. 1242(188), 1274
 Miyamoto, A. 1082(205), 1123
 Miyamoto, F. 655(395), 765
 Miyamoto, H. 567(531g), 595
 Miyamoto, S. 680(533), 769, 951(160, 161, 164), 977(278d), 992, 993, 997
 Miyanari, S. 630(266), 762
 Miyano, S. 1105(368, 369), 1126, 1127
 Miyashita, K. 1236(155), 1273
 Miyashi, T. 206(121, 122, 124), 207(118, 123), 209(134–136, 139, 142–144), 294, 295
 Miyata, N. 1062(61), 1119
 Miyazaki, J. 918(8d), 988
 Miyazaki, M. 1257(290), 1276
 Miyazaki, S. 196(70), 293
 Miyazawa, T. 680(538), 769, 977(279a), 997
 Miyoshi, M. 680(533), 769, 977(278d), 997
 Miyoshi, Y. 1062(61), 1119
 Mizoguchi, Y. 1236(157), 1273
 Mizugaki, T. 245(282), 298
 Mizukoshi, E. 1251(236), 1275
 Mizuno, H. 711(145), 759, 792(30c), 828
 Mizuno, K. 205(112–115), 208(103a, b), 294, 429(292), 589
 Mizuno, N. 410(224), 444(315), 587, 589, 1081(180), 1082(196), 1117(195), 1122, 1123
 Mizuno, T. 1236(156), 1273
 Mizuno, Y. 612(108), 758
 Mizutani, F. 654(391), 765
 Mizutani, J. 218(192), 219(193, 194), 296

- Mlochowski, J. 540(505), 594
 Mobus, K. 118(122), 124(124), 142
 Möbus, K. 1067(57), 1119
 Mocchi, F. 186(44), 187
 Mochizuki, H. 1007(48), 1047
 Mochizuki, K. 670(461), 767
 Mock-Knoblauch, C. 475(73), 583
 Modena, G. 74(150), 90, 432(302), 477(372), 480(378), 487(382), 589, 591, 1039(244, 245), 1051, 1068(87, 89–92, 97, 98), 1072(24), 1076(162), 1077(160), 1078(163, 165), 1095(4, 179, 306, 313, 314), 1096(130, 324, 325), 1097(93, 329), 1098(99, 100, 129, 131), 1105(373, 374), 1107(164), 1115(414), 1118, 1120–1122, 1125–1127
 Modrego, J. 1064(68), 1120
 Moegling, J. K. 643(333a), 764
 Moerman, E. J. 987(325a), 999
 Moga-Gheorghe, S. 163(51), 169
 Moghaddari, M. 1227(91), 1272
 Mohajer, D. 1030(199), 1050
 Mohammadpoor-Baltork, I. 1032(214), 1050
 Mohammadpoor-Baltork, L. 1029(191), 1050
 Mohan, A. G. 1267(71), 1272
 Mohan, K. V. V. K. 576(548), 596
 Mohan, L. 37(89), 88, 1151(98), 1152(10), 1161(102, 140), 1165, 1167, 1169
 Mohnen, V. A. 648(307), 763
 Mohri, S. 687(553), 769
 Mohr, D. 956(201b), 994
 Moh, M. H. 662(210), 663(234), 761
 Moiseeva, N. I. 528(467), 593
 Moiseev, I. I. 528(467), 531(468), 593
 Moiseichuchk, K. L. 715(614), 771
 Moiseichuk, K. L. 122(152), 142
 Moleiro, J. 725(63), 757
 Molenkamp, C. R. 605(36), 756
 Molinari, H. 375(156), 380(155), 381(154), 585
 Molina, L. T. 138(209a), 144
 Molina, M. J. 138(209a), 144
 Möller, L. 975(268c), 996
 Möller, S. 1163(154a, 154d), 1169
 Molyneux, P. 96(8c), 139
 Momenteau, M. 185(36, 37), 187
 Monaghan, P. K. 134(134), 142
 Moncada, S. 214(166), 295
 Moncrieff, H. M. 1160(137), 1169
 Monfared, H. H. 531(473), 593
 Monier, R. 927(27), 989
 Monig, H. 945(125), 992
 Moniz, W. B. 740(697), 772
 Monroe, B. 966(233d), 995
 Montalban, A. G. 252(321), 299
 Montanari, F. 531(321), 590
 Montassier, C. 1114(11), 1118
 Montaudon, E. 710(575), 770
 Montecalvo, D. F. 198(78), 293
 Montes, O. 646(343), 764
 Montgomery, J. A. 12(7, 7b), 85
 Montgomery, R. E. 1158(4), 1165
 Monti, C. 1099(341), 1126
 Monti, D. 1313(80), 1344
 Moore, C. B. 31(80), 88
 Moore, J. A. 112(83), 141, 1252(244), 1275
 Moore, J. C. 1336(153), 1346
 Moorgat, G. K. 604(17), 678(16), 756
 Moorman, A. E. 1151(99a), 1167
 Moortgat, G. K. 638(314), 707(308a), 763, 764
 Mootz, D. 132(194), 144
 Morais, V. M. F. 161(42), 169
 Morales, G. A. 114(91), 141
 Morand, P. 112(68), 140
 Mordasini, T. Z. 82(160), 91
 More O'Ferrall, R. 907(82), 913
 Morello, M. J. 665(444), 767
 Moreno, J. J. 25(25), 86, 952(183), 993
 Moreno, Y. 201(92), 294
 Moretto, A. 123(162), 129(172), 143
 Morey, M. C. 291(595), 305
 Morgan, C. 616(148), 759
 Morgan, K. M. 157(28), 168
 Morgan, P. 380(158), 585
 Morihira, K. 265(403), 301
 Morikawa, T. 1040(256), 1051
 Morimitsu, Y. 945(112), 991
 Morimoto, T. 1023(152, 153), 1025(162, 163), 1049
 Morimoto, Y. 608(61), 757
 Morinello, E. J. 981(298c), 982(291g), 997, 998
 Morin, B. 941(74b), 959(203), 974(262a, b), 975(261), 990, 994, 996, 1201(63b), 1209
 Moritaka, Y. 129(171), 143
 Morita, H. 136(203, 204), 144, 219(195), 296, 899(2), 911
 Moriyama, H. 647(351), 764
 Moriya, M. 945(113), 992
 Mori, A. 621(177), 760
 Mori, H. 856(114–116), 857(117), 896
 Mori, K. 245(282), 298
 Mori, Y. 107(90), 141, 945(112), 991
 Morley, J. S. 960(204b), 994
 Morlière, P. 918(10), 945(115), 989, 992
 Moro-oka, Y. 118(126, 135), 133(133), 142, 1064(52), 1119
 Morokuma, K. 12(7), 85
 Morooka, Y. 426(277c), 588
 Moroz, C. 1335(150), 1346
 Moro, S. 1068(85–87), 1069(103), 1070(108–111), 1078(163, 165), 1095(311), 1096(130), 1098(99, 100), 1110(22), 1115(414), 1118, 1120–1122, 1125, 1127
 Morrison, H. 926(7), 988
 Morrison, J. D. 1092(83), 1120

- Morrison, V. 256(358), 300
 Morrisroe, K. 676(301), 763
 Morris, A. C. 672(483), 768
 Morris, G. W. 732(635), 771
 Morris, H. 163(48), 169
 Morrow, J. D. 217(178, 179), 296, 612(97),
 714(96), 758, 978(288), 997
 Morsa, S. 610(71), 757
 Mortensen, G. 656(404), 766
 Mortensen, J. 684(99), 758
 Mortensen, P. 635(9), 699(582a), 756, 770
 Morye, S. S. 622(191), 760
 Mosandl, T. 291(593), 305, 1181(11f),
 1205(60a), 1206, 1209, 1233(14), 1270
 Mosebach, M. 357(117), 584
 Mosher, H. P. 163(50), 169
 Mosher, H. S. 352(104), 584, 673(488),
 674(486), 697(487), 768
 Moskal, T. A. 273(456), 302, 1336(161), 1346
 Moskowitz, H. 280(525, 528, 529), 304
 Moss, G. P. 323(42b), 582
 Mosterz, J. 610(70), 757
 Mostowicz, D. 493(100, 101), 584, 1099(343),
 1126
 Motherwell, B. 324(36b), 582
 Motohashi, N. 677(518), 768
 Motoyoshiya, J. 255(350), 300, 1268(336),
 1278
 Motterle, R. 487(382), 591, 1098(129), 1121
 Mottola, H. A. 629(261), 762
 Mousseron-Canet, M. 856(111), 896
 Moussy, C. 286(555), 305
 Moustacchi, E. 977(275a), 996
 Mou, C.-Y. 1116(417), 1128
 Mou, S.-F. 701(589), 770
 Movassagh, B. 368(144), 525(464), 585, 593,
 1004(28–30), 1046
 Moysan, A. 945(115), 992
 Moze-Henry, N. 669(470), 767
 Mo, O. 874(170), 897
 Mpourmpakis, G. 880(181), 897
 Muccigrosso, D. A. 492(397), 592, 1105(372),
 1127
 Mueller, D. M. 963(225c), 994
 Mueller, S. 1243(187), 1274
 Muhle, S. A. 984(311), 998
 Mukaiyama, T. 360(129), 584
 Mukai, M. 1064(69), 1120
 Mukai, T. 206(124), 207(118, 123), 294,
 861(136), 896
 Mukherjee, S. 380(162), 585
 Mukhtar, A. 275(487), 303
 Mukundan, T. 155(24), 168
 Mulchandani, A. 687(549), 769
 Mulder, P. 10(24a), 86
 Mulholland, A. J. 82(159a, b), 91
 Müller, A. 1069(116), 1121
 Muller, B. L. 834(36), 894
 Müller, E. 355(121), 584, 1205(60a, b), 1209
 Müller, F. 77(152a), 91
 Muller, J. G. 920(23b), 943(93a, b, 94),
 945(98), 989, 991, 1204(69a–c), 1209
 Muller, K. A. 147(15), 167
 Müller, M. 520(453), 593, 982(309), 984(310,
 311), 998
 Mullica, D. F. 726(663), 772
 Mumford, C. 317(27), 582, 1172(9), 1182(22),
 1205, 1206, 1212(9), 1270
 Munakata, H. 1082(205), 1123
 Munch, E. 1069(50), 1119
 Muñoz-Fernandez, K. 449(336), 590
 Muñoz, K. 556(518a), 595
 Munjal, R. C. 1008(55), 1047
 Munro, D. J. 1008(59), 1014(94), 1047, 1048
 Munz, R. 1014(90), 1048
 Muraeva, N. P. 823(115), 830
 Murahashi, S.-I. 567(532b), 595
 Murahashi, S. I. 1104(356), 1126
 Murahashi, S. 360(130), 584
 Murai, T. 693(570), 770
 Murakami, H. 259(366), 300, 1236(36), 1271
 Murakami, K. 675(464), 767
 Murakami, N. 271(271), 272(272), 298
 Muralleedharan, K. M. 1314(97), 1344
 Muralidharan, D. 1010(65), 1047
 Murase, N. 542(213, 214), 587, 1093(288,
 289), 1125
 Murayama, J. 1236(157), 1273
 Murayama, T. 1333(139, 140), 1346
 Mura, M. E. 12(7d), 85
 Murcko, M. A. 156(20), 168
 Murphy, J. A. 920(23a), 989
 Murphy, O. J. 1236(35), 1271
 Murphy, O. 1198(33f), 1207
 Murphy, R. C. 690(565), 693(562b), 739(694),
 770, 772
 Murphy, S. 1182(24b), 1206, 1228(98),
 1229(110), 1272
 Murray, C. K. 283(471), 302, 1337(162), 1346
 Murray, C. W. 12(7e), 85
 Murray, P. J. 392(199), 586, 1088(266), 1124
 Murray, R. W. 37(89), 44(95), 58(58), 88, 89,
 177(19), 187, 264(389), 300, 534(480), 594,
 732(493), 740(682), 768, 772, 871(1), 893,
 1020(123, 125), 1021(139), 1039(248),
 1048, 1049, 1051, 1103(359, 360),
 1106(381), 1126, 1127, 1140(8, 45),
 1143(64), 1151(98), 1152(10), 1153(97b),
 1158(9), 1159(100a, b, 135a), 1160(137),
 1161(102, 140), 1163(1b, 1i), 1164–1167,
 1169
 Musaev, D. G. 40(40a, b), 87
 Mushrush, G. W. 617(157), 759
 Musumeci, M. 96(20), 139
 Mutanen, M. 981(302), 998

- Muthusamy, S. 29(69), 60(60), 72(72e), 88, 1154(16a, 112), 1165, 1168
- Mutoh, H. 1236(152), 1273
- Muto, T. 503(422a, b), 592
- Muursepp, A. M. 521(457a), 593
- Muzaffar, S. 963(225c), 994
- Muzart, J. 497(406), 503(421), 516(442, 443), 518(407, 424, 447), 592, 593
- Muzzi, R. M. 1021(137), 1049
- Mvula, E. 740(244), 762
- Mwesigye-Kibende, S. 118(132), 142
- Myall, C. J. 1004(35), 1046
- Myers, J. 606(40), 757
- Myher, J. J. 693(562a), 726(638), 739(695), 770–772
- Myhre, O. 1250(228), 1275
- Naberfeld, G. 1097(334), 1126
- Nadelmann, L. 1322(120), 1345
- Nadzan, A. M. 1140(55b), 1166
- Nagai, M. 1069(107), 1121
- Nagai, Y. 816(93), 829, 900(11), 912
- Nagano, T. 858(122), 896
- Nagano, Y. 149(9), 167
- Nagao, M. 981(299b), 998
- Nagao, T. 1257(281), 1276
- Nagasawa, H. 1157(124), 1168
- Nagase, S. 727(664), 734(679), 772, 816(93), 818(94, 99), 829
- Nagashima, H. 524(460), 593
- Nagata, R. 316(23), 318(13), 582
- Nagayama, S. 413(233, 233b), 587
- Nagayama, T. 1065(72), 1120
- Nagel, V. 1155(118b), 1168
- Nagiev, T. F. 652(380), 765
- Nagraba, K. 833(32), 894
- Nahm, K. 1044(274), 1052
- Naicker, K. P. 536(485), 594
- Nair, J. 981(296, 299a, b, 300–304), 984(297c, 297e, 297h), 998
- Nair, V. 667(453), 767, 980(290b), 982(291b), 997
- Naitoh, N. 478(297), 589
- Naito, T. 273(437), 301
- Najjar, F. 201(92), 294
- Nakadaira, Y. 325(53), 583, 854(88), 895
- Nakagawa, M. 967(215, 216, 237), 994, 995
- Nakagawa, N. 967(213), 994
- Nakagawa, Y. 681(540), 769, 809(72), 828
- Nakajima, K. 270(430), 301, 1100(344), 1126
- Nakajima, M. 468(356), 567(531c, 531h–j), 591, 595
- Nakajima, R. 1257(277), 1276
- Nakajima, S. 690(563), 770
- Nakajo, S. 1025(166), 1049
- Nakamura, A. 987(331a), 999
- Nakamura, E. 858(120), 896
- Nakamura, H. 1214(30), 1271, 1333(139), 1346
- Nakamura, J. 981(298c), 998
- Nakamura, M. M. 1257(261), 1276
- Nakamura, M. 612(87), 758, 1241(181), 1274
- Nakamura, N. 108(107), 110(110), 113(113), 141, 265(403), 301, 1236(37), 1271
- Nakamura, S. 1241(181), 1274
- Nakamura, T. 206(121, 122), 294, 1094(302), 1125
- Nakanishi, A. 472(365), 591
- Nakanishi, K. 325(53), 583, 854(88), 895
- Nakano, M. 857(117), 896, 918(8c), 950(146, 148), 988, 992
- Nakano, S. I. 984(281a), 997
- Nakano, S. 113(76), 140, 630(264), 762
- Nakase, Y. 949(136), 992
- Nakashima, K. 698(193), 760, 1257(268, 270, 280, 287), 1276
- Nakatani, S. 250(297), 252(298), 298
- Nakayama, H. 478(297), 589
- Nakayama, J. 1156(123b), 1157(124, 130a–c), 1168
- Nakayama, M. 497(405b), 592
- Nakayama, T. 650(360), 765
- Nakomoto, M. 1044(275), 1052
- Naldrett, M. J. 694(146), 759
- Nalwaya, N. 611(85), 758
- Nam, W. 1031(205), 1050
- Nanayakkara, A. 12(7), 85
- Nandrajog, S. 1116(416), 1127
- Nannelli, L. 1103(362), 1126
- Nano, G. M. 129(175), 143
- Naota, T. 360(130), 584
- Nappez, C. 984(281c), 997
- Naranjo, S. 1333(141), 1346
- Narasaka, K. 567(531f), 595
- Narasu, M. L. 190(47), 292
- Narayan, R. S. 1023(148), 1049
- Nardin, R. 931(34b), 989
- Narender, N. 576(548), 596
- Narita, S. 681(94), 758, 972(196a), 994
- Narsaiah, A. V. 1028(186), 1050
- Naruta, Y. 112(85), 141, 1067(55), 1119
- Nash, E. G. 1240(176), 1274
- Naso, F. 487(388), 591
- Nasu, S. 259(366), 300
- Natarajan, A. 870(147), 896
- Nath, J. 1116(423), 1128
- Nath, R. G. 945(117), 982(291e), 992, 997
- Nau, W. M. 192(62), 293, 943(85b), 991, 1203(65a), 1204(71), 1209
- Navarro, M. T. 422(250), 560(508), 588, 594, 1085(210), 1111(402, 404), 1123, 1127
- Navas Díaz, A. 644(336), 764
- Navas, M. J. 643(331), 764, 1252(172), 1274
- Navello, F. 1031(208), 1050
- Naviliat, M. 951(168), 993
- Navillat, M. 741(698), 772
- Nawa, H. 1257(272), 1276

- Naylor, R. D. 164(2), 167
 Nazarov, I. N. 278(278), 298
 Na, J. 861(137), 896
 Ncokazi, K. K. 1283(30), 1343
 Ndounga, M. 1320(112), 1345
 Neale, R. S. 900(27), 912
 Neckers, D. C. 425(266), 588
 Needleman, P. 214(166), 295
 Neelamkavil, S. 501(419), 592
 Neeleman, E. 512(408), 514(409a), 526(410), 592
 Neff, W. E. 949(108), 991
 Neimann, K. 368(141), 585
 Nelander, B. 98(34), 131(190), 139, 143, 732(629), 771
 Nelen, M. I. 576(547), 596
 Nelsen, S. F. 211(149, 150), 295
 Nelson, E. K. 190(1), 292
 Nelson, N. C. 1252(245), 1275
 Nelson, W. H. 812(86a), 829
 Nemes, C. 1143(60), 1156(123a), 1163(1g), 1164, 1166, 1168
 Nemeth, L. 560(508), 561(507), 564(506), 594, 1111(402, 403, 405), 1127
 Nencka, R. 885(165), 897
 Neri, C. 1082(201), 1123
 Neri, V. 1083(225, 226), 1123
 Nery, A. L. P. 1236(26, 74, 75, 77), 1271, 1272
 Neset, S. M. 1152(101), 1167
 Nestler, B. 343(89, 90), 345(93), 346(94), 583, 584, 853(82, 84), 865(139), 888(45, 46), 889(201), 894–896, 898, 1174(13a, b), 1206
 Neuenhofer, S. 1199(56b), 1208, 1236(146), 1273
 Neumann, M. B. 163(5), 167
 Neumann, R. C. 902(64), 903(55–58), 912, 913
 Neumann, R. 84(163), 91, 368(141), 408(222, 222b), 444(316), 472(143), 579(549), 585, 587, 589, 596, 1081(184), 1082(187–189), 1091(186, 279, 280), 1092(281), 1094(298), 1107(185, 384, 385), 1122, 1124, 1125, 1127
 Neuman, W. P. 824(118), 830
 Neumayer, M. 1163(154g), 1169
 Neunaber, H. 98(35b), 139
 Neuvonen, H. 1260(310), 1261(312), 1277
 Nevett, B. A. 1265(332), 1277
 Newcomb, M. 44(104), 89, 920(25), 989
 Newman, L. 641(18), 756
 Newman, P. D. 1086(234), 1124
 Newton, C. G. 1097(328), 1126
 Ngo, T. T. 635(296), 763
 Nguyen, C. 1117(427), 1128
 Nguyen, K. A. 12(7b), 85
 Nguyen, K. L. 974(262c, d), 996
 Nguyen, V. H. 252(306, 307, 313, 316, 317), 299
 Ng, S.-W. 1058(36), 1119
 Nice, L. E. 1027(177), 1049
 Nicklaß, A. 12(7d), 85
 Nicklin, H. G. 49(49), 87
 Nickon, A. 252(319), 299, 888(190), 897
 Niclas, D. 956(201a), 994
 Nicolaou, K. C. 1145(68), 1167
 Nicolaou, K. C. 190(14), 233(231), 259(362–364), 292, 297, 300, 315(32a), 582
 Nidy, E. G. 233(10), 292, 315(33), 582
 Nieh, E. 731(637), 771
 Nielsen, A. T. 1013(31), 1046
 Nielsen, J. H. 666(447, 448), 767
 Nielsen, L. P. 1069(46), 1119
 Nielsen, O. J. 692(568), 770
 Nielson, A. J. 567(525), 595
 Nieman, T. A. 646(347), 647(352), 764
 Niemela, O. 984(314), 998
 Niemeyer, J. 104(58), 140
 Nierlich, M. 1117(431), 1128
 Nieuwenhuyzen, M. 204(100), 294
 Nigon, F. 612(105), 758
 Nikishin, G. I. 130(181, 182), 143
 Nikje, M. M. A. 1028(183), 1049
 Nilanonta, C. 190(49), 293
 Niles, J. C. 943(85a), 991, 1204(68), 1209
 Nilsson, J. L. G. 326(60), 583
 Nilsson, S. E. G. 337(80), 583
 Nimz, H. 355(121), 584
 Ninkovic, S. 1145(68), 1167
 Nippert, U. 122(146), 142
 Nisbet, M. 672(485), 768
 Nishida, J.-i. 715(607), 770
 Nishida, K. 1062(61), 1119
 Nishida, Y. 1069(118), 1121
 Nishihara, H. 1108(388), 1127
 Nishihara, A. 1003(20), 1046
 Nishijima, W. 607(46), 757
 Nishikawa, A. 982(308), 998
 Nishikawa, E. 1094(302), 1125
 Nishimori, T. 265(403), 301
 Nishimura, K. 1088(268), 1124
 Nishimura, S. 1201(62a), 1209
 Nishinaga, A. 118(129), 142, 352(48), 582
 Nishino, H. 112(92), 141, 252(299–317), 298, 299
 Nishino, M. 833(31), 894, 1173(17b), 1206
 Nishino, S. 1069(118), 1121
 Nishitani, A. 1257(274, 285), 1276
 Nishiyama, H. 809(73), 829
 Nishiyama, M. 1236(157), 1273
 Nishiyama, Y. 445(309), 589, 1081(174), 1102(353), 1122, 1126
 Nishizawa, K. 118(129), 142
 Nishizawa, M. 394(200, 200b), 586
 Nishizono, I. 1236(36), 1271

- Nittala, S. S. 273(51), 293, 954(193a), 993
 Nitz, S. 728(630, 667), 771, 772
 Niu, Q. 950(149), 992
 Nivière, V. 972(232), 995
 Nivorojkine, A. 1069(45), 1119
 Nixon, J. R. 233(11), 241(258), 292, 297
 Nixon, J. 237(164), 295, 319(8), 581
 Nizova, G. V. 1117(429), 1128
 Ni, J.-M. 273(29), 292
 Ni, J. 984(297b), 998
 Ni, Z.-M. 701(589), 770
 Noar, J. B. 79(153c), 91
 Nofle, R. E. 1004(36), 1046
 Nojima, M. 108(106, 107), 110(110),
 111(111), 112(112), 113(102, 109, 113),
 141, 225(219, 220), 242(268), 249(292),
 266(266), 267(267), 269(269), 273(54),
 287(559), 288(560, 561), 289(289),
 290(290), 291(291), 293, 296–298, 305,
 711(608), 712(609–611), 727(664),
 734(679), 771, 772, 1157(127a, b), 1168,
 1282(27), 1327(125), 1332(108), 1335(147),
 1342, 1345, 1346
 Nolte, M. J. 95(18), 139
 Nomoto, T. 478(297), 589
 Nonami, Y. 1335(147), 1346
 Nooijen, M. 12(7c), 85
 Noone, B. C. 604(5), 698(310), 756, 764
 Norby, P. 882(182), 897
 Nord, L. 732(629), 771
 Norita, M. 129(171), 143
 Norrby, P.-O. 810(78), 829
 Northrop, J. 273(469, 470), 302, 1317(86),
 1337(163), 1344, 1346
 Notario, R. 155(25), 168
 Notari, B. 418(231, 245), 587, 588, 1082(200),
 1123
 Notou, M. 647(354), 765
 Nourooz-Zadeh, J. 612(95), 667(413),
 676(513, 514), 758, 766, 768
 Nouros, P. G. 658(411), 766
 Novello, F. 1031(207), 1050
 Novis, W. P. 1013(31), 1046
 Novotny, M. V. 984(319a), 999
 Nowitzki, M. 974(262c), 996
 Noyori, R. 397(212b), 444(310, 311),
 445(312), 496(400), 506(401), 525(462),
 587, 589, 592, 593, 784(27), 827,
 1081(177), 1089(178), 1095(317),
 1106(378–380), 1122, 1125, 1127,
 1173(12b), 1206
 Nozaki, C. 1082(196), 1117(195), 1123
 Nozaki, H. 137(205), 144, 788(31), 789(32),
 790(34, 35), 792(30a), 827, 828
 Nozaki, O. 644(335), 645(337), 647(350, 351),
 649(359), 764, 765, 1257(269), 1276
 Nudenberg, W. 221(200), 296
 Nugent, T. C. 380(160), 381(159), 585
 Nugent, W. A. 487(382), 591, 1096(130),
 1098(99, 100, 129, 131), 1120, 1121
 Nugteren, D. H. 190(5, 8), 292
 Nuhn, P. 652(376), 765
 Nukuna, B. N. 956(198), 994
 Nuntasri, D. 1083(211), 1123
 Nussbaum, S. 608(54), 757
 Nuttall, R. L. 154(21), 168
 Nuzum, E. O. 1322(117, 118), 1345
 Nyström, T. 987(325d), 999
 Nzila, A. 273(454), 302
 Oae, S. 13(13c), 86, 1001(7), 1032(218), 1046,
 1050
 Oakes, J. 449(334), 590
 Oakes, J. 449(334), 590
 Oberhammer, H. 94(11a), 102(49), 104(58),
 132(194), 138(56b), 139, 140, 144,
 702(591), 703(592), 744(20, 22), 756, 770
 O'Brien, P. J. 950(143), 963(225a), 992, 994
 O'Brien, P. 1022(145), 1049
 Ochiai, M. 118(142, 143), 142, 472(365), 591
 Ochterski, J. 12(7), 85
 O'Connor, D. E. 214(172, 173), 295
 O'Connor, P. F. 621(179), 760
 Oda, J. 374(148), 585, 677(518), 768
 Oddou, J. L. 1069(49), 1119
 Odegova, G. V. 1069(119), 1121
 Odinkov, V. N. 729(669), 772
 Odin, F. 976(273), 996
 O'Donnell, V. B. 951(174), 993
 O'Dowd, H. 202(96, 97), 273(470), 283(520),
 530, 294, 302, 304, 1337(163), 1346
 Odo, J. 630(266), 762
 Oe, T. 981(295), 997
 Offerman, R. J. 980(290b), 982(291b), 997
 Ogata, H. 1257(272), 1276
 Ogata, Y. 47(47b), 87, 1035(230),
 1040(253–257), 1051
 Ogawa, M. 434(273), 444(311), 445(312),
 525(308), 588, 589, 1080(173), 1081(177),
 1087(257), 1089(178, 271), 1094(300),
 1106(172), 1108(388), 1122, 1124, 1125,
 1127
 Ogawa, S. 1025(166), 1049
 Ogawa, T. 605(29), 756
 Oger, J. M. 892(208), 898
 Ogilby, P. R. 832(11), 894
 Ogle, C. A. 213(161), 295
 Ogliaro, F. 1140(52a), 1166
 Ogryzlo, E. A. 253(340), 299
 Oguchi, T. 1087(257), 1094(300), 1124, 1125
 Oguni, N. 1105(370), 1127
 Ogura, N. 267(267), 298, 1282(27), 1342
 Ogura, Y. 640(324), 641(100), 758, 764
 Ohaku, H. 206(122), 294
 Ohanessian, G. 873(169), 897
 O'Hara, S. M. 980(290c), 997
 Ohashi, Y. 122(144), 142

- Ohata, A. 680(528), 769
 Ohfune, Y. 564(501), 594, 1012(85), 1047
 Ohgaru, T. 654(387), 765
 Ohira, S. 497(405b), 592
 Ohishi, T. 1039(223), 1045(276), 1050, 1052
 Ohizumi, Y. 1333(139), 1346
 Ohkata, K. 382(178), 586
 Ohkita, M. 715(607), 770
 Ohloff, G. 861(130, 132), 896
 Ohme, R. 623(206), 761
 Ohmori, Y. 612(88), 758
 Ohno, T. 1040(254, 255), 1051
 Ohru, H. 660(422), 680(528, 530, 531), 766, 769
 Ohsaka, T. 699(581), 770, 1251(229), 1275
 Ohshima, H. 951(169), 993
 Ohshima, T. 680(529, 534), 769
 Ohta, B. K. 710(576), 770
 Ohta, C. 1100(348), 1126
 Ohta, H. 680(530), 769
 Ohta, M. 209(138), 295, 1291(49), 1343
 Ohta, Y. 825(121), 830
 Ohtsuka, Y. 1039(223), 1045(276), 1050, 1052
 Ohura, H. 651(372, 373), 765
 Oh, C. H. 275(490, 491), 280(515–518), 283(519, 533), 303, 304, 812(86b), 829, 1286(35), 1289(46), 1291(47), 1298(18), 1330(133), 1342, 1343, 1345
 Oh, H.-J. 607(48), 757
 Oh, J. T. 701(388), 765
 Oh, S. 273(462), 302, 1317(102), 1344
 Oiestad, E. L. 84(165a), 91
 Oishi, M. 542(213, 214), 587, 1093(288, 289), 1125
 Oishi, T. 567(531a, b, 532a), 595
 Oizumi, Y. 1333(140), 1346
 Ojima, I. 48(114b, 114d), 89, 397(212c), 472(191), 556(518a, b), 586, 587, 595
 Okabayashi, T. 434(273), 588, 1089(271), 1124
 Okada, H. 697(579), 707(598), 770
 Okada, K. 861(136), 896
 Okada, M. 607(46), 757, 1236(36), 1271
 Okada, S. 960(206a), 994
 Okajima, H. 967(213, 237), 994, 995
 Okajima, T. 68(144), 90, 97(30), 139, 1251(229), 1275
 Okamoto, K. 1062(61), 1119
 Okamura, F. 1105(370), 1127
 Okamura, H. 1065(72), 1120
 Okazaki, R. 804(59), 828, 1157(127c), 1168
 Okazoe, T. 790(34), 828
 Oka, M. 196(76), 293
 Okitsu, O. 209(135, 136), 295
 Oki, M. 129(171), 143
 Okovytyy, S. 57(53), 87
 Okuda, K. 858(122), 896
 Okuda, T. 980(290a), 997
 Okuda, Y. 255(350), 300
 Okun, N. 1082(193), 1123
 Okutani, T. 639(238), 761
 Okuyama, T. 682(474), 767
 Oku, A. 250(294), 298
 Oku, M. 374(150), 585
 Olah, G. A. 84(167), 91, 794(39), 802(53), 828
 Olbrich, A. 273(459), 302, 1336(155), 1346
 O'ldekop, Y. A. 783(24), 827
 Oldfield, E. 185(38, 39), 187
 Oldroyd, R. D. 1086(248, 249), 1124
 Oldziej, S. 253(337), 299
 Olesen, C. E. M. 1199(48), 1200(53a, b), 1208
 Oliphant, N. 12(7c), 85
 Oliva, A. 1111(398), 1127
 Oliveira, M. A. 1235(78), 1272
 Oliveiros, E. 184(33), 187
 Oliver, C. N. 987(325a, 329c), 999
 Oliver, J. P. 980(290c), 997
 Olivucci, M. 1182(24a, b), 1206, 1228(93, 98), 1272
 Oliw, E. H. 693(572), 770
 Olliaro, P. L. 273(449), 302, 1303(7), 1342
 Olliaro, P. 1313(80), 1344
 Olmstead, M. M. 118(127), 130(130), 138(138), 142
 Olmsted, J. 166(56), 169
 Olsen, C. E. 666(447, 448), 767
 Olson, L. P. 37(37d), 55(55), 87
 Olson, L. 1155(28), 1165, 1229(109), 1272
 Oltu, U. 623(205), 761
 Olzmann, M. 84(84), 88
 Omata, T. 1156(123b), 1168
 Omote, Y. 285(551), 304, 1242(188), 1274
 Onda, M. 374(151), 585
 O'Neal, H. E. 1227(84, 85), 1272
 O'Neill, M. A. A. 672(483), 768
 O'Neill, P. M. 223(207), 273(38, 445, 453, 454, 467), 274(274), 275(487–489), 280(526), 292, 296, 298, 302–304, 1283(31), 1298(45), 1304(63, 71), 1313(34), 1314(83), 1317(16, 101), 1320(115), 1323(44, 121), 1324(124), 1330(131, 132), 1332(92, 93), 1337(165), 1342–1346
 O'Neill, P. 902(65), 913
 O'Neill, Paul M. 1268(336), 1317(68), 1342, 1344
 O'Neil, S. V. 202(95, 98), 294
 Ong, S. H. 901(23), 912
 Onizawa, T. 362(134d), 585
 Ono, M. 643(211), 761
 Ooi, S. 118(129), 142
 Ookubo, T. 1065(72), 1120
 Oose, M. 1023(152, 153), 1049
 Opolon, P. 613(116), 758
 Orabona, I. 108(100), 141
 Oral, H. B. 616(147), 759
 Ordovas, J. M. 612(107), 758

- Orfanopoulos, M. 255(356), 300, 343(91a, b), 352(57), 583, 832(18–20), 833(21–23, 25), 836(49, 50), 849(44, 67), 850(71), 851(51), 853(87), 855(86), 858(119), 859(59), 860(127), 871(3), 874(171), 875(37), 877(74), 878(53), 880(56), 890(69), 893–897, 1173(17a), 1206
- Oribe, M. 668(12, 462, 463), 670(461), 756, 767
- Orita, H. 1095(307), 1125
- Orlova, G. 1248(215), 1275
- Orlovic, M. 1188(40d), 1207, 1262(311), 1277
- Orosz, G. 1188(40e), 1207, 1257(286), 1263(316), 1276, 1277
- Oro, L. A. 1064(68), 1120
- Ortega, M. J. 1333(141), 1346
- Ortiz-Maldonado, M. 77(152b), 82(161), 91
- Ortiz, J. V. 12(7), 85
- Ortmann, R. 190(43), 292
- Osawa, T. 945(112), 991
- Osborne, B. G. 663(433), 766
- O'Shea, K. E. 255(349), 299
- Oshima, K. 788(31), 789(32), 790(34), 828
- Ossowski, T. 253(337), 299
- Ostakhov, S. S. 1190(45a, b), 1208
- O'Sullivan, D. W. 604(4), 698(310), 756, 764
- O'Sullivan, D. 604(5), 756
- Oswald, A. A. 221(201), 296
- Oszwałdowski, S. 636(243), 762
- Otamiri, T. 945(104), 991
- Otsuji, I. 208(103b), 294
- Otsuji, Y. 205(112–115), 208(103a), 294
- Otsuka, K. 362(134d), 585
- Otsuka, M. 1257(277), 1276
- Otsuka, S. 432(299), 589, 1086(250), 1124
- Ottolina, G. 75(146), 90
- Ouahab, L. 440(313a), 589
- Ouellette, M. A. 259(364), 300
- Ouellette, M. 259(363), 300
- Ouerfelli, O. 259(361), 300
- Oumi, Y. 1082(205), 1123
- Ostdal, H. 972(252), 995Ø
- Ouyang, J. 252(311), 299
- Owensby, A. L. 29(63), 56(48c), 67(140), 68(119, 141), 79(17b), 86–90, 97(32a, b), 139, 1140(44), 1166
- Owens, G. S. 1083(229, 230), 1123
- Oyamaguchi, K. H. 1260(317), 1268(335), 1277, 1278
- Ozaki, A. 426(277c), 588
- Ozawa, N. 681(98), 758
- Ozawa, Y. 514(432), 592
- Özen, G. 640(320), 764
- Özyorük, H. 700(557), 769
- Pabon, R. 909(93), 913
- Pacey, G. E. 607(47), 757
- Pace, A. 870(159), 877(177), 897
- Packer, L. 671(479), 673(406), 676(513), 680(537, 538), 681(505, 539), 687(551), 689(559), 741(699), 766, 768, 769, 772
- Padeken, H.-G. 355(121), 584
- Padmaja, S. 14(46), 87
- Padmanilayam, M. 1332(15), 1342
- Padovani, C. 1077(160), 1122
- Padwa, A. 98(33), 139, 192(57), 293, 1163(1i), 1164
- Paetz, C. 1245(212), 1275
- Pagano, A. S. 362(135), 585
- Page, G. 614(135), 759
- Pagni, R. M. 196(60), 293
- Paik, I. H. 273(447, 468, 469), 280(523), 283(524), 302, 304, 1314(84), 1326(126), 1332(110), 1337(164), 1344–1346
- Paik, I. 273(37), 292
- Pais, G. C. G. 1094(304), 1125
- Pai, H. H. O. 1302(62), 1343
- Paju, A. 521(456, 457a, b), 553(516), 593, 594, 1113(407, 408), 1127
- Pakkanen, T. A. 80(158), 91
- Pakusina, A. P. 1058(37), 1119
- Pak, C. S. 890(202), 898
- Palamara, A. T. 1156(121d), 1168
- Palazzi, C. 545(503), 561(217), 587, 594, 1109(395), 1127
- Paleologos, E. K. 624(220), 761
- Palermo, R. E. 542(201), 574(521), 586, 595, 1092(287), 1125
- Palfey, B. A. 82(159c), 91
- Palke, W. E. 3(3b), 85
- Palma, J. M. 610(78), 757
- Palma, M. 610(69), 757
- Palmer, T. F. 1188(39, 40a, b), 1207, 1267(72, 323), 1272, 1277
- Palmieri, P. 12(7d), 85
- Palmisano, F. 688(556), 769
- Palm, W. U. 1204(72a), 1209
- Palombi, L. 414(232), 483(15), 493(394), 582, 587, 591
- Palomino, E. 729(668), 772
- Palucki, M. 487(389), 591
- Pamment, M. G. 516(436), 592
- Panasenko, A. A. 122(101), 141
- Panasenko, O. M. 673(494), 768
- Panchenko, Yu. V. 156(7), 167
- Panchuk-Voloshina, N. 643(67), 757
- Pandey, A. V. 1313(82), 1344
- Pande, C. S. 1010(68), 1013(27), 1046, 1047
- Paneghetti, C. 559(515), 594, 1112(123), 1121
- Pang, W. 418(252), 588
- Panin, A. I. 84(168), 91
- Panshin, S. Y. 165(17), 167
- Panyella, D. 445(312), 589, 1089(178), 1122
- Pan, H. Z. 1311(12), 1342
- Pan, J. 945(119), 992
- Pan, X. Q. 1302(61), 1343

- Pan, Y. 1252(244), 1275
 Papaefthymiou, G. C. 1067(80), 1120
 Papageorgiou, G. E. 669(466), 767
 Paquette, L. A. 199(90), 263(381, 382), 294, 300, 861(94), 889(199, 200), 892(206), 895, 898
 Paradisi, M. P. 1161(146), 1169
 Paradis, V. 613(115, 116), 758
 Paradkar, V. M. 1024(155), 1049
 Parapini, S. 1313(80), 1344
 Paredes, R. 47(103), 89, 1144(65), 1163(1k), 1164, 1166
 Parekh, N. J. 1188(40c), 1207, 1262(308), 1277
 Parekh, N. 1188(40d), 1207, 1262(311), 1277
 Parenteau, M. 623(200), 761
 Parhsarathy, S. 612(104), 758
 Pariente, R. 966(233b), 995
 Parker, D. C. 809(75), 829
 Parker, M. H. 273(470), 280(523), 302, 304, 1317(86), 1332(110), 1337(163), 1344–1346
 Parker, T. L. 211(145), 295
 Parker, V. B. 154(21), 168
 Parker, W. E. 105(63), 140, 160(37), 169
 Parkin, B. C. 1058(30), 1069(112), 1102(352), 1119, 1121, 1126
 Parkkila, S. 984(314), 998
 Parks, G. S. 163(50), 169
 Park, B. K. 273(467), 274(274), 275(488, 489), 298, 302, 303, 978(287b), 997, 1283(31), 1304(63, 71), 1314(83), 1317(101), 1324(124), 1330(131, 132), 1332(92, 93), 1337(165), 1343–1346
 Park, C. H. 902(66), 913
 Park, E. D. 1116(422), 1128
 Park, H. 608(51), 757
 Park, J. 825(121), 830
 Park, K. D. 185(38), 187
 Park, M. Y. 1017(110), 1018(112, 113), 1048
 Park, M. 273(48), 292
 Park, S. B. 280(521, 527), 304, 1262(327), 1277, 1282(17), 1284(39), 1342, 1343
 Park, T. K. 1093(291), 1125
 Parlar, H. 728(630, 667), 771, 772
 Parliment, M. W. 1008(55), 1047
 Parliment, T. H. 1008(55), 1047
 Parmon, V. N. 1069(119), 1121
 Parry, E. M. 616(148), 759
 Parry, J. M. 616(148), 759
 Parr, R. G. 3(3a), 85
 Parsons-Mair, H. N. 972(222b), 994
 Parsy, C. C. 110(99), 141
 Parvez, M. 134(134), 142, 223(213), 296
 Paryzek, Z. 114(114), 141, 696(577), 770
 Pasco, D. S. 987(331b), 999
 Pascual, C. 1242(190), 1274
 Paseshnichenko, K. A. 111(105), 141
 Pasini, E. 223(207), 296, 1323(121), 1345
 Pasta, P. 384(185), 476(368b, 369), 586, 591
 Pastore, P. 1068(87), 1120
 Pastorino, A. M. 681(499, 539), 768, 769
 Pastor, A. 869(144), 896, 1163(1m), 1165
 Patai, S. 13(13, 13b, c), 48(115), 67(1), 85, 86, 89, 105(14), 139, 151(1), 167, 171(1), 186, 253(318), 273(51), 293, 299, 360(131), 432(280), 584, 589, 954(192b, 193a), 993, 1032(6), 1046, 1090(1), 1118, 1142(61), 1163(155), 1166, 1169, 1181(11b), 1206, 1233(15), 1270
 Patel, A. 1256(252), 1275
 Paterson, J. R. 613(118), 758
 Pater, R. H. 1020(124), 1021(130), 1048, 1140(6), 1165
 Patonay, T. 373(152), 585, 1143(60), 1163(1g), 1164, 1166
 Patsalides, E. 614(131), 759
 Patsay, I. O. 1253(241), 1275
 Patterson, C. O. P. 606(40), 757
 Patyk, A. 72(72f), 88
 Paulmann, U. 205(119), 206(120), 294
 Pavlosky, T. A. 1116(421), 1128
 Pawlak, W. 845(63), 895
 Payne, G. B. 245(279), 273(473), 298, 302, 532(474), 593, 1001(1), 1046, 1087(255), 1124
 Payne, J. Q. 356(119), 584
 Pazdernik, L. 811(82, 83), 829
 Paziienza, A. 493(394), 591
 Pazzagli, M. 1184(25d), 1192(47d, e), 1207, 1208
 Peacock, R. D. 1086(234), 1124
 Pearson, A. J. 503(425), 592
 Pearson, J. 971(250), 995
 Pearson, R. E. 901(25), 912
 Pecoraro, V. L. 1062(60), 1069(104), 1119, 1121
 Pecorella, K. 1256(253), 1275
 Pedersen, B. F. 98(39b, c), 100(42), 139
 Pedersen, J. Z. 1069(46), 1119
 Pedley, J. B. 164(2), 167
 Pedrini, P. 1021(142), 1049
 Pedrotti, J. J. 650(362), 765
 Pegg, R. B. 668(460), 767
 Pehkonen, S. 98(38), 139
 Pehk, T. 521(456, 457a, b), 553(516), 593, 594, 1113(407, 408), 1127
 Pei, J. 652(374), 765
 Pelliccia, A. R. 1083(225, 226), 1123
 Pellmann, G. 358(125), 584
 Pelotier, B. 1100(349), 1126
 Peluffo, G. 741(698), 772, 951(168), 993
 Peña, R. M. 641(309), 764
 Pence, L. E. 1067(80), 1120
 Pendleton, R. B. 689(559), 769
 Peng, C. Y. 12(7), 85

- Peng, C. 4(11a), 86
 Peng, H.-S. 608(49), 757
 Peng, Z. Z. 1015(103), 1048
 Pentes, H. G. 112(73), 140
 Peover, M. E. 315(30), 582
 Perakylä, M. 80(158), 91
 Perales, A. 230(229), 297
 Perales, M. 1064(68), 1120
 Perchinunno, M. 1010(71), 1047
 Perdiz, D. 977(275a), 996
 Perego, G. 418(231), 587, 1082(200), 1123
 Pereira, M. M. 457(323), 590
 Perera, S. A. 12(7c), 85
 Pérez Pariente, J. 422(250), 588, 1083(209),
 1085(210), 1123
 Perez-Castorena, A. L. 134(198), 144
 Perez-Gálvez, A. 658(418), 766
 Perkel, A. L. 624(218), 674(501), 701(587),
 761, 768, 770
 Perlstein, D. L. 870(160), 897
 Pérot, G. 1114(11), 1118
 Perraud, X. 676(473), 767
 Perrier, S. 457(320), 590
 Perrin, J. L. 672(400), 766
 Perry, L. H. 352(111), 584
 Persy, G. 196(60), 293
 Perterson, M. E. 1043(270), 1051
 Perumal, P. T. 1010(65), 1047
 Pervaiz, S. 610(66), 757
 Petersen, A. C. 84(165b), 91
 Pettersson, G. A. 12(7), 85
 Peters, E.-M. 112(71), 123(163), 135(201),
 140, 143, 144, 193(68), 198(82, 83),
 260(371), 263(384), 272(434, 436),
 291(593), 293, 300, 301, 305, 869(93), 895
 889(201), 898, 1174(14b)1206
 Peters, J. M. 211(146), 295
 Peters, K. 112(71), 123(163), 135(201), 140,
 143, 144, 193(68), 198(82, 83), 260(371),
 263(384), 272(434, 436), 291(593), 293,
 300, 301, 305, 416(235, 236), 587, 869(93),
 144), 889(201), 895, 896, 898, 1143(63a),
 1166, 1174(14b), 1206
 Peters, L. D. 917(4), 988
 Peters, T. P. J. 1062(42), 1119
 Peters, W. 273(440, 450), 276(501), 277(277),
 284(540, 549), 298, 301–304, 1317(68,
 104), 1324(122), 1332(13), 1342–1345
 Petillot, Y. 972(232), 995
 Petricci, E. 1025(165), 1049
 Pétrignani, J.-F. 1059(41), 1119
 Petrini, G. 1082(202), 1123
 Petrini, M. 1103(357), 1126
 Petri, A. 569(535a), 595
 Petrovskaya, G. A. 156(26), 168
 Petrusevich, Y. I. 129(176), 143
 Petsch, W. 1248(5), 1270
 Pettersson, L. 1069(105, 106, 116), 1121
 Pettersson, M. 98(37, 38), 139
 Petter, W. 250(296), 298
 Pettinari, C. 112(115), 141
 Petty, S. A. 381(177), 586
 Pews, R. G. 1040(258), 1051
 Peyerimhoff, S. D. 37(37a), 87
 Peynet, J. 667(456), 767
 Peyronnet, D. 238(257), 297
 Pfaltz, A. 48(114c), 89, 386(190b, c),
 516(435), 549(512b), 586, 592, 594,
 1092(286), 1125
 Pfeiffer, A. 138(56b), 140, 744(22), 756
 Pfeiffer, S. 13(42), 87
 Pfenninger, A. 396(205), 587, 1092(284), 1125
 Pflederer, J. L. 1228(105), 1272
 Philip, A. 291(595), 305
 Phillipson, D. W. 190(26), 292
 Phillips, B. 185(38), 187
 Phillips, D. H. 981(299a), 998
 Phillips, D. 949(141), 992
 Phuwapraisrisan, P. 1334(144), 1346
 Pichorner, H. 966(229, 231), 995
 Pichota, A. 408(221), 587, 1094(296), 1125
 Pickett, J. B. 1250(223), 1275
 Pierce, T. E. 284(284), 298, 343(92), 584,
 852(75), 895
 Pierlot, C. 269(329, 421, 425, 426), 299, 301
 Pierrot, M. 1059(41), 1119
 Piers, E. 1142(62), 1166
 Pietikainen, P. 1030(200, 201), 1050
 Pietikäinen, P. 457(338), 458(340), 590
 Pietri, S. 973(254), 995
 Pike, R. A. 778(11), 783(25), 827
 Pilati, T. 122(156), 143
 Pilcher, G. 160(14), 167
 Pilgram, C. D. 1022(145), 1049
 Pilkington, L. G. 283(471), 302, 1337(162),
 1346
 Pillai, U. R. 559(509), 594
 Pillinger, M. 1086(252), 1124
 Pillinger, M. 471(296), 589
 Pilz, A. 267(418, 420), 301
 Pina, R. 198(84), 293
 Pinchuk, I. 671(113, 480), 758, 768
 Pincock, J. A. 1236(166), 1274
 Pincock, R. E. 700(586a), 770
 Pincock, R. 213(159), 295
 Piñeiro Avila, G. 701(302), 763
 Pingarrón, J. M. 688(558), 689(390), 765, 769
 Pinhey, J. T. 323(47), 582
 Pini, D. 569(535a), 595
 Pinkernell, U. 637(303), 699(582b, 583),
 700(584), 763, 770
 Pinnavaia, T. J. 418(249, 249c), 588
 Pinna, F. 539(496), 545(503), 549(514),
 558(513), 559(515), 594, 1084(236),
 1087(260), 1109(122, 393–395), 1112(123,
 406), 1117(433), 1121, 1124, 1127, 1128

- Piovella, F. 611(81), 758
 Piquemal, J.-Y. 1063(64), 1120
 Pischel, U. 943(85b), 991, 1204(71), 1209
 Piskorz, P. 12(7), 85
 Pitchen, P. 480(377), 591, 1068(95),
 1084(233), 1097(94, 328), 1120, 1123, 1126
 Piters, A. J. M. 605(31, 32), 756
 Piton, A. 613(116), 758
 Pitsevich, G. A. 130(185), 143
 Pitts, M. R. 383(182), 586
 Pitt, A. R. 977(280a), 997
 Pitzer, R. 12(7d), 85
 Pizzale, L. 690(564), 770
 Plaizier-Vercammen, J. 659(419), 766
 Platsch, H. 193(61, 65), 196(64), 293
 Plaut, H. E. 809(75), 829
 Pleacher, D. 1004(35), 1046
 Pleasic-Williams, S. 1062(63), 1120
 Pleier, A.-K. 1076(156), 1122
 Plesničar, B. 48(115), 49(118), 89, 131(192a),
 132(193), 144, 182(20–25), 187, 812(84),
 813(87), 829
 Plessi, L. 575(533), 595
 Ploypradith, P. 202(96), 223(209, 210),
 273(35, 470), 280(522), 283(471, 524, 530),
 292, 294, 296, 302, 304, 1282(19),
 1306(38), 1317(86), 1326(126), 1330(134),
 1332(109, 111), 1337(162, 163), 1342–1346
 Plucinski, P. 1081(176), 1122
 Pluim, H. 374(147d), 585
 Plumitallo, A. 183(32), 187
 Poelker, D. J. 1007(46), 1047
 Pokrovskaya, I. E. 118(141), 142
 Polanyi, M. 907(77a), 913
 Polborn, K. 209(137), 295
 Polimanti, O. 1103(357), 1126
 Polissiou, M. G. 658(411), 766
 Poll, W. 132(194), 144
 Polverelli, M. 938(66–68), 990
 Polyakova, N. P. 1155(116), 1168
 Polzer, J. 689(560), 769
 Pomelli, C. 12(7), 85
 Pomfret, A. 198(81), 293
 Pompella, A. 670(472), 767
 Pons i Prats, R. 449(334), 590
 Poole, C. P. 675(504), 768
 Poon, T. 1178(19c, d), 1206
 Pope, M. T. 1063(18), 1069(116), 1118, 1121
 Pople, J. A. 5(5), 6(6), 9(9), 12(7), 85
 Poppel, K. L. 1245(212), 1275
 Poprawski, J. 269(426), 301
 Porter, J. E. 1232(127), 1235(139), 1273
 Porter, M. J. 381(172), 586, 1087(261), 1124
 Porter, N. A. 94(1), 138, 212(152, 153),
 213(162), 214(168, 177), 217(169,
 178–187), 233(11–13, 155), 237(164, 237),
 241(258), 253(253), 263(263), 264(264),
 292, 295–297, 309(1), 310(7b, c), 317(16),
 319(8), 320(35a, b), 357(67), 581–583,
 612(97), 693(571), 703(593), 704(594),
 714(96), 758, 770, 977(280b, c), 997,
 1140(30), 1165
 Porzei, A. 1162(151a), 1169
 Poshni, F. I. 882(182), 897
 Posner, G. H. 202(96, 97), 209(140, 141),
 223(206, 208–210), 273(35–38, 445–447,
 467–470), 274(274), 280(515–518,
 521–523, 526, 527), 283(471, 519, 520,
 524, 530, 533), 292, 294–296, 298,
 302–304, 712(60), 725(57), 757, 812(86a,
 b), 829, 1281(8), 1282(17, 19), 1284(39),
 1286(35), 1289(46), 1291(47, 48), 1298(18,
 45), 1306(38), 1309(52), 1314(84),
 1317(86), 1323(44), 1324(124), 1326(126),
 1330(73, 134), 1332(93, 109–111),
 1337(162–165), 1342–1346
 Postel, M. 1115(161), 1122
 Potter, D. 984(297f), 998
 Pouchert, C. J. 621(168, 169), 760
 Pouget, J.-P. 941(80a), 943(9b), 975(268a, b),
 976(273), 977(275b), 989, 991, 996,
 1203(67b), 1209
 Pouget, J. P. 950(151), 976(270c), 992, 996
 Pouliot, R. 217(190), 296
 Poulou, M. 1257(260), 1276
 Poulsen, H. E. 917(2b), 975(268c), 988, 996
 Poulsen, J. R. 1257(267), 1276
 Poulsen, L. L. 79(154b), 91
 Povondra, P. 621(182), 760
 Powell, D. R. 825(108b), 829
 Power, M. B. 136(136), 142
 Powis, P. 616(150), 759
 Powland, F. S. 28(28b), 87
 Poynard, T. 613(115, 116), 758
 Poznyak, T. I. 740(50, 696), 757, 772
 Prados, P. 1257(281, 282), 1276
 Prakash, G. K. S. 84(167), 91, 802(53), 828
 Prandi, J. 1089(269), 1124
 Prange, R. K. 667(457), 676(458), 767
 Prange, T. 230(223–226), 297
 Prasad, M. R. 538(487a, b), 594
 Pras, N. 133(195), 144, 273(456, 465), 302,
 1336(161), 1346
 Prathapan, S. 250(295), 298
 Prather, M. J. 138(210a), 144
 Prato, M. 1155(106b), 1168
 Pratt, D. A. 217(184), 296, 1140(30), 1165
 Pratiel, G. 941(79), 943(92), 991, 1069(45),
 1119
 Prat, A. G. 949(139), 992
 Prat, D. 1089(270, 272), 1124
 Prat, F. 943(89a, b), 991
 Prechtl, F. 520(453), 593, 889(201), 898,
 1163(154b, 154e, 154g), 1169

- Prein, M. 94(2), 138, 271(331, 433), 272(432, 434–436), 299, 301, 889(4), 893, 1174(13c, 14a–c), 1206
- Prelog, V. 190(3), 292
- Prencipe, T. 1162(151b), 1169
- Prenzler, P. D. 667(454), 767
- Preut, H. 98(39a), 139
- Price, C. C. 734(680), 772, 899(2), 911
- Price, D. 606(39), 645(41), 757
- Price, M. E. 1224(59), 1271
- Priem, G. 1100(349), 1126
- Prilezajew, N. 48(112), 89
- Primon, S. 1107(166, 167), 1122
- Pritzkow, W. 147(15), 167, 623(199), 761
- Privezentzev, C. V. 984(313), 998
- Probert, M. K. 208(108), 294
- Proctor, D. D. 605(36), 756
- Prosen, E. J. 100(45a), 140
- Prosser-McCartha, C. M. 1081(181), 1122
- Provot, O. 280(525, 528, 529), 283(534), 304
- Pruz, W. A. 945(125), 992
- Pryor, R. W. 23(23), 86
- Pryor, W. A. 14(46), 25(25, 26a, b), 37(37e), 86, 87, 123(161), 143, 212(154), 295, 351(105), 584, 900(8, 10), 903(59, 60), 909(95), 912, 913, 952(183), 953(186, 187), 954(189), 993
- Psomiadou, E. 664(443), 767
- Puar, M. S. 137(206), 144
- Puchin, V. A. 148(6), 167
- Puchkov, S. V. 674(501), 768
- Puddephatt, R. J. 134(134), 142
- Pugach, S. P. 606(42), 757
- Pugh, M. D. 223(207), 275(489), 296, 303, 1323(121), 1330(132), 1345
- Pugh, M. 275(488), 303, 1317(101), 1330(131), 1344, 1345
- Puhl, H. 945(99), 991
- Pulido, R. 380(160), 585
- Punniyamurthy, T. 510(414, 415), 518(448), 592, 593, 1116(423), 1128
- Purdie, J. W. 960(206b), 994
- Puri, S. K. 274(481–483), 303, 1320(114), 1326(128, 129), 1345
- Purvis, G. D. 8(8b), 85
- Pu, L. 392(193), 586, 1088(265), 1124
- Pu, Y. M. 1314(85), 1344
- Pyne, S. G. 1027(173), 1049
- Pyun, H. Y. 73(149), 90
- Qian, C.-Y. 112(92), 141
- Qian, C. Y. 252(301–303, 309), 298, 299
- Qian, X. 616(154, 155), 759
- Qing, F. 1011(78), 1047
- Qin, C. J. 1067(76), 1120
- Quack, M. 97(27b), 139
- Quadri, L. E. N. 610(69), 757
- Qualls, S. 290(592), 305
- Quast, H. 198(82, 83), 293
- Quax, W. J. 133(195), 144
- Querci, C. 362(134c), 585
- Que, L. 1066(74), 1069(48, 50), 1117(430), 1119, 1120, 1128
- Quici, S. 122(156), 143, 531(321), 590
- Quilliam, M. 676(458), 767
- Quinlan, G. J. 977(286), 997
- Quinoa, E. 190(24), 292
- Quintarelli, C. 611(81), 758
- Raabe, G. 392(192), 586, 1088(262), 1124
- Rabalakos, C. 878(179), 880(181), 885(165), 897
- Rabek, J. F. 832(9), 894
- Rabinovich, I. B. 163(47), 169
- Rabin, P. 779(13a), 827
- Rabong, R. 678(522), 769
- Rabuck, A. D. 12(7), 85
- Racherla, U. S. 445(325), 590
- Rachlin, E. M. 943(93b, 94), 991, 1204(69a, 69c), 1209
- Radhakrishnan, T. P. 67(67), 88
- Radha, S. 1010(73), 1047
- Radi, M. 1025(165), 1049
- Radi, R. 22(22b), 86, 741(698, 699), 772, 951(167, 168, 173), 952(171, 176, 178), 953(172), 993
- Radschuweit, A. 652(375, 376), 744(207), 761, 765
- Radziszewski, B. 1212(3), 1270
- Rafaralahitsimba, G. 621(178), 760
- Rafecas, M. 676(229), 761
- Raffard, N. 1117(431), 1128
- Rafikov, S. R. 533(475), 593
- Raghavachari, K. 12(7), 85
- Raghavachari, K. 9(9), 85
- Raghavan, K. V. 538(487a, b), 569(535d), 571(543), 576(548), 594–596
- Rahhal, S. 917(5b), 988
- Rahman, A. F. M. M. 980(290c), 997
- Rahman, M. T. 252(310), 299
- Rahman, M. 30(76), 88
- Raison, F. 440(313a), 589
- Rajadhyaksha, S. N. 1161(102), 1167
- Raja, R. 526(465), 593
- Rajca, A. 192(59), 293
- Rajca, S. 192(59), 293
- Rajewsky, M. F. 981(307b), 998
- Rak, J. 1253(235, 241), 1275
- Raley, J. H. 156(12), 167
- Ramachandraiah, G. 580(550), 596
- Ramaker, G. 825(122), 830
- Ramalingam, T. 1028(187), 1029(192), 1050
- Ramamurthy, V. 870(147), 896
- Ramamurthy, V. 870(157, 160), 874(173), 885(158, 172), 897
- Ramaswamy, A. V. 531(469), 593
- Ramm, M. 122(160), 143
- Ramos, M. C. 644(336), 764

- Ranasinghe, A. 981(298c), 982(291f, g), 997, 998
 Ranby, B. 832(9), 894
 Randiais, Y. 808(66), 828
 Raney, J. K. 172(5), 182(26), 186, 187
 Raney, K. D. 1140(57), 1166
 Ranghino, G. 1082(202), 1123
 Rani, S. 1022(146), 1049
 Ranz, A. 1311(12), 1342
 Raoul, S. 941(74a, b), 943(90), 990, 991, 1201(63a, b), 1209
 Rao, C. B. 802(53), 828
 Rao, K. K. 518(446), 593
 Rao, K. V. 190(47), 292
 Rao, P. B. 363(137), 373(152), 561(217), 585, 587
 Rapaport, E. 1251(237, 240), 1275
 Raphael, P. 1322(81), 1344
 Rapi, G. 107(87), 141
 Rappoport, Z. 183(32), 187, 624(219), 761, 1142(61), 1166
 Raptis, C. 885(188), 897
 Raptopoulou, C. P. 1058(38), 1119
 Räsänen, M. 98(37, 38), 139
 Rastelli, A. 37(91), 44(101), 46(110), 47(105, 111), 57(51b), 67(130a, b), 87, 89, 90, 1140(41), 1166
 Rasul, G. 84(167), 91
 Rath, N. 1153(97b), 1167
 Ratnasamy, P. 527(246), 588
 Rauch, M. U. 459(347), 469(345), 590, 1062(39), 1119
 Rauch, P. 273(459), 302
 Rauhut, G. 12(7d), 85
 Rauhut, M. M. 1172(7), 1205, 1212(8), 1242(184), 1256(254, 255), 1258(307), 1266(305, 306), 1267(7, 71), 1270, 1272, 1274–1277
 Rauk, A. 37(37c), 47(109), 87, 89
 Rautenstrauch, V. 834(36), 854(64), 874(70), 894, 895
 Ravanat, J.-L. 269(423), 301, 616(149), 759, 922(40), 940(75a), 941(74a, 80a, b), 942(84), 943(9a–c, 85c, 86, 87, 91), 950(151), 951(164), 967(238c), 975(268a, b, 269b), 976(270a, 270c, 273), 977(274a, b), 988–993, 995, 996, 1201(63a), 1203(67b), 1209
 Ravikumar, K. S. 473(366), 591
 Ravindranathan, T. 538(486), 594
 Ravindranath, Y. 660(424), 766
 Ravindran, K. 155(13), 167
 Rawe, Sarah L. 1268(336), 1317(68), 1342, 1344
 Raynes, K. J. 274(274), 298, 1324(124), 1345
 Ray, T. 503(425), 592
 Ray, W. C. 177(17), 187
 Ražem, D. 676(511), 768
 Rebek, J. 48(115c), 89, 351(102), 584
 Rebeyrote, N. 921(28b), 989
 Rebien, F. 265(404), 301
 Recher, S. G. 833(24), 894
 Recknagel, R. O. 671(479), 768
 Recknager, R. O. 977(277d), 996
 Reddy, B. V. S. 1028(187), 1050
 Reddy, C. V. 571(543), 596
 Reddy, G. R. 945(116), 992
 Reddy, G. V. S. 518(446), 593
 Reddy, J. S. 527(246, 246b), 588
 Reddy, K. L. 468(351), 590, 1083(217), 1123
 Reddy, K. M. 379(169), 586
 Reddy, M. S. K. 1023(150), 1049
 Reddy, P. N. 1095(308), 1125
 Reddy, R. V. 576(548), 596
 Reddy, T. I. 411(230), 414(228), 587, 1089(275), 1090(276), 1124
 Reed, A. E. 4(11b), 86
 Reed, C. A. 185(36), 187
 Reed, J. W. 423(260), 588
 Reed, S. M. 525(463), 593
 Rees, C. W. 1181(11g), 1206, 1250(224), 1252(246), 1275
 Rees, W. W. 1178(20a), 1206
 Reetz, M. T. 1097(334), 1126
 Refsgaard, H. H. F. 945(111), 984(319b), 991, 999
 Reginato, G. 800(50), 828
 Régnard, K. 669(470), 767
 Reguero, M. 1182(24a, 24e), 1206, 1207, 1228(93, 100), 1272
 Rehder, D. 186(42), 187, 1069(106), 1070(120), 1121
 Reibenspies, J. 112(77), 140
 Reichard, P. 963(224b), 994
 Reichenbach, H. 1145(67c, d), 1166
 Reichwaldt, R. 343(88), 583, 867(142), 896
 Reiff, O. M. 362(134a), 584
 Reim, J. 1067(77), 1120
 Reina-Artiles, M. 531(322), 590
 Reinhardt, D. 1194(30), 1197(50), 1207, 1208, 1236(154, 160), 1256(144), 1273
 Reino, E. 1200(58b), 1208
 Reising, J. 1163(154c, 154e, f), 1169
 Reissenweber, G. 1009(64), 1047
 Reisz, E. 673(497), 740(244), 762, 768
 Reiter, R. 949(136), 992
 Reix, T. 1026(171), 1049, 1153(97a), 1167
 Rekers, J. W. 193(66), 293
 Rembaum, A. 100(45b), 140
 Remias, J. E. 1116(421), 1128
 Remin, M. 931(34b), 989
 Remund, J. 608(54), 757
 Renard, C. M. G. C. 623(196), 761
 Renard, P. Y. 1256(253), 1275
 Renard, P. 273(458), 302

- Renaud, J.-P. 443(319b), 455(318), 531(322), 589, 590
 Renaud, P. 213(156), 229(222), 295, 297
 Rennie, N. 977(280a), 997
 Renotte, R. 1252(243), 1275
 Renze, J. 866(141), 896
 Renzulli, M. 1025(165), 1049
 Renz, M. 411(230), 414(228), 416(235, 236), 538(488b), 560(508), 561(507), 564(506), 587, 594, 1089(275), 1090(276), 1111(402–405), 1124, 1127
 Ren, R. L. 1336(153), 1346
 Replogle, E. S. 12(7), 85
 Resch, U. 631(293), 667(459), 763, 767
 Ressick, R. F. 732(677), 772
 Retter, C. A. 1227(89), 1272
 Reuben, J. 172(8), 186
 Reviejo, A. J. 689(390), 765
 Revinskii, I. F. 283(283), 298
 Rexwinkel, R. 183(31), 187
 Reyes, S. 134(198), 144
 Reynaers, M. 456(327), 590
 Reynolds, G. T. 1224(67), 1271
 Reynolds, J. E. F. 623(174), 760
 Reynolds, M. S. 1095(88), 1120
 Rey, F. 421(253), 588, 1085(247), 1124
 Rezaeifard, A. 1030(199), 1050
 Rezzano, I. 701(381), 765
 Rheingold, A. L. 1067(76), 1120
 Riahii, A. 518(407), 592
 Ribeiro Gregorio, J. 470(354), 590
 Ricchiardi, G. 1082(202), 1123
 Ricci, A. 776(1), 778(12), 796(44), 797(42, 45), 800(49, 50), 827, 828
 Ricci, M. 362(134c), 444(305, 306), 529(472a, b), 585, 589, 593, 1079(169), 1122
 Rice, F. O. 362(134a), 584
 Rice, J. E. 12(7e), 85
 Richardson, A. 1256(252), 1275
 Richardson, D. G. 1172(4a, b), 1205, 1252(218), 1275
 Richardson, G. D. 274(485, 486), 303
 Richardson, G. 284(549), 304
 Richardson, K. S. 79(155b), 91
 Richardson, W. H. 356(118), 584, 1224(59), 1227(84, 85), 1228(60, 92, 102–104), 1229(109), 1271, 1272
 Richards, M. P. 676(512), 768
 Richards, S. J. 1088(267), 1124
 Richard, M.-J. 977(275b), 996
 Richert, S. 986(328c), 999
 Richeson, C. E. 10(24a), 86
 Riche, C. 280(529), 304, 1303(65), 1343
 Richomme, P. 238(257), 297, 892(65, 208), 895, 898
 Richter, H. P. 1261(322), 1277
 Richter, M. J. 853(81), 889(196, 198), 895, 897
 Rickard, R. C. 976(271), 996
 Ridder, L. 82(159a–c), 91
 Ridley, R. G. 190(45), 292
 Ridouane, F. 1059(41), 1119
 Rieche, A. 280(280), 298, 316(4, 25), 351(103a), 354(115, 116), 581, 582, 584, 776(3), 822(112), 824(113, 117c), 827, 829, 830, 977(278a), 997, 1042(260, 261), 1051
 Riedel, W. 669(469), 767
 Rieger, A. L. 901(26a, b), 912
 Rieger, H. 1104(365), 1126
 Riemersma, R. A. 614(125, 126), 759
 Riesz, P. 926(49), 938(48a), 990
 Rietjens, I. M. C. M. 80(157), 82(159a–c), 91
 Rigaudy, J. 167(64), 169, 254(347), 269(329, 427, 429), 270(431), 299, 301
 Riggins, J. N. 917(3b), 988
 Righi, G. 1161(149b), 1169
 Rigoulet, M. 987(325d), 999
 Rihm, B. 608(54), 757
 Riley, R. 323(44), 582
 Rimbault, C. G. 326(52), 582, 861(133, 134), 896
 Rinehart, K. L. 190(26), 292
 Rios, A. 273(474), 302
 Ripin, D. H. B. 1023(149), 1049
 Rispens, M. T. 516(444), 593
 Ritcher, H. W. 917(5b), 988
 Ritter, G. L. 624(232), 761
 Rivandi, A. 726(638), 771
 Rivas, E. V. 974(262d), 996
 Rivière, J. 933(59), 990
 Rizzo, T. R. 18(18a), 86, 100(43), 140
 Rnez, M. 1003(19), 1046
 Robards, K. 614(131), 645(339), 647(353), 667(454), 759, 764, 765, 767
 Robbins, J. 870(157), 897
 Robbins, M. J. 624(222), 761
 Robbins, R. J. 870(160), 874(173), 897
 Robb, M. A. 12(7), 85, 1182(24a, b), 1206, 1228(93, 98), 1272
 Robertson, J. 256(357, 358), 300
 Roberts, B. G. 1212(8), 1225(70), 1242(184), 1256(254), 1258(307), 1266(305, 306), 1270, 1272, 1274, 1275, 1277
 Roberts, B. P. 351(5), 581
 Roberts, C. 610(75), 757
 Roberts, D. H. 310(7b, c), 581
 Roberts, D. R. 1240(176), 1274
 Roberts, D. W. 984(297g), 998
 Roberts, J. S. 96(8b), 139
 Roberts, L. J. 612(91), 758, 978(288), 997
 Roberts, M. A. 418(252), 588
 Roberts, S. M. 378(166), 379(163, 164), 380(158, 160–162, 165, 167, 170, 171), 381(159, 174–177), 382(178b, 180, 181), 383(182), 585, 586, 1332(93), 1344

- Robert, A. 273(451, 452), 283(534), 284(541, 542, 548), 286(557), 302, 304, 305, 1296(54, 55), 1298(56), 1306(72), 1312(79), 1320(43, 112, 113), 1343–1345
- Robert, F. 1069(117), 1121
- Robine, A. 131(131), 142, 1117(432), 1128
- Robinson, A. L. 1261(319), 1277
- Robinson, B. L. 273(450), 276(501), 284(540, 549), 290(584), 302–305, 1317(68, 104), 1324(122), 1332(13), 1342–1345
- Robinson, C. E. 987(331b), 999
- Robinson, K. E. 250(295), 298
- Robinson, P. D. 122(155), 143
- Robinson, S. 681(144), 759
- Rocas, J. 380(155), 585
- Rocha, J. 471(296), 589, 1086(252), 1124
- Roch, I. S. D. 426(278), 588
- Rockenbauer, A. 973(248), 995
- Rock, J. C. 1262(326, 327), 1277
- Roda, A. 1184(25d), 1192(47d, e), 1207, 1208
- Rodenburg, P. H. M. 1257(262), 1276
- Roder, D. 1022(145), 1049
- Rodgers, M. A. J. 253(342), 299, 962(211), 994
- Roditi-Lachter, E. 440(313a), 589
- Rodrigues, C. R. 1282(26), 1342
- Rodriguez-Borges, J. E. 1086(252), 1124
- Rodriguez, A. 235(235), 297, 352(17), 582 730(673), 772, 785(28), 827, 1004(26), 1046
- Rodríguez, E. 1182(24e), 1207, 1228(100), 1272
- Rodríguez, J. M. 138(210a, b), 144
- Rodríguez, L. C. 1257(301), 1277
- Rodríguez, L. O. 1232(124), 1273
- Rodríguez, M. S. 230(227, 228), 297
- Roelfes, G. 1069(44, 48, 50), 1119
- Roe, A. N. 217(186, 187), 296
- Rogers, D. W. 155(23), 168
- Roger, N. A. 1228(108), 1272
- Rogoff, M. H. 1038(240), 1051
- Rogozhnikova, T. I. 736(686), 772
- Rohde, J.-U. 1069(50), 1119
- Rohou, Y. 623(196), 761
- Rokach, J. 318(11), 582
- Romano, L. J. 1199(56a), 1208
- Romano, U. 1082(201), 1108(386), 1123, 1127
- Romao, C. C. 1062(40), 1086(252), 1110(214), 1119, 1123, 1124
- Romão, C. C. 453(343b), 471(296), 529(470), 589, 590, 593
- Romao, C. 1111(397), 1127
- Romão, C. 562(498), 594
- Romero, A. 858(123), 896
- Romero, J. M. 164(53), 169
- Romoff, P. 1242(193), 1274
- Ronan, B. 1068(96), 1120
- Rondeau, D. 892(65), 895
- Rong, Y.-J. 283(532), 304
- Ronson, R. S. 612(87), 758
- Roof, A. A. M. 48(117c), 89
- Roof, A. A. 1140(42b), 1166
- Roos, B. O. 29(64), 73(73), 88
- Root, T. W. 1073(124), 1121
- Ropke, S. 1236(74), 1272
- Röpke, S. 1236(164), 1273
- Rosati, O. 1027(178), 1028(180), 1029(188, 190, 194), 1049, 1050
- Rosa, A. 1146(70), 1161(145), 1167, 1169
- Rosenthaler, G. V. 1013(89), 1048
- Roschmann, K. J. 477(373c), 493(219), 587, 591, 1094(17), 1100(132), 1118, 1121
- Rosch, N. 48(114a), 89
- Rösch, N. 1075(148, 150, 151), 1121, 1122
- Rosenberg, S. M. 617(157), 759
- Rosenthal, P. J. 1322(81, 116, 117), 1344, 1345
- Rosenthal, R. 520(450), 593
- Rosenthal, Z. 285(285), 298
- Rosewell, D. F. 1239(179), 1274
- Rose, A. L. 741(701), 773, 1241(182), 1274
- Rosini, C. 487(383, 387), 591, 1098(336, 337), 1126
- Rosito, V. 487(388), 591
- Rossan, R. N. 1281(5), 1342
- Rossier, J.-C. 274(485, 486), 284(540, 545, 547), 303, 304, 1296(53), 1324(122, 123), 1332(13), 1342, 1343, 1345
- Rossiter, B. E. 396(210), 414(227), 587
- Rossi, M. 1028(180), 1049, 1097(329), 1126
- Rossi, R. 986(326), 999
- Rossomando, A. J. 1062(63), 1120
- Ross, A. B. 262(345), 299, 966(233a), 971(199a), 994, 995
- Ross, B. O. 30(75a), 88
- Ross, D. D. 273(459), 302
- Ross, F. K. 1030(196), 1050
- Ross, H. B. 604(6), 756
- Ross, S. A. 1027(179), 1049
- Roswell, D. F. 1252(247), 1275
- Rothberg, R. 966(219), 994
- Rothenberg, G. 510(412), 592
- Röthlisberger, U. 44(44a, b), 87
- Roth, H. D. 870(148c), 896
- Roth, R. J. 288(562–564), 305
- Roth, W. J. 418(248), 588
- Roth, W. R. 196(73–75), 293
- Rotman, D. A. 605(36), 756
- Rottiers, P. 610(71), 757
- Roue, J. 425(267), 588
- Rouff, P. 721(646), 771
- Rougée, M. 253(343), 299, 833(34), 894, 966(233b), 995
- Rousseau, G. 842(57), 895
- Roussel, M. 523(458), 593
- Roux, M. V. 147(16), 155(25), 161(39), 167–169

- Rowan, D. D. 217(188, 189), 296, 890(203), 898
- Rowe, M. C. A. 815(91b), 829
- Rowland, J. M. 130(130), 142
- Rowlen, K. L. 1261(319), 1277
- Rowley, D. 945(102), 991
- Rozenberg, H. 223(212), 296
- Rozen, S. 1140(29), 1165
- Rozyczko, P. 12(7c), 85
- Ro, R. S. 47(47a), 87
- Rubbo, H. 951(167), 953(172), 993
- Rubino, M. F. 40(98), 89, 1163(1f), 1164
- Rubin, Y. 858(121, 126), 896
- Rubio, J. 951(169), 993
- Rubiralta, M. 1161(103), 1167
- Rubottom, G. M. 324(51b), 582
- Rüchardt, C. 161(44), 165(62), 169, 903(51), 912
- Rucker, G. 134(199), 144
- Rudaz, M. 284(540), 304, 1324(122), 1345
- Rudler, H. 470(354), 590
- Rudolph, D. C. 687(549), 769
- Rudolph, J. 468(351), 590, 1083(217), 1097(334), 1123, 1126
- Rudy, B. C. 1251(239), 1275
- Ruebner, B. 984(314), 998
- Ruiz-Lopez, M. F. 30(75b), 82(82b), 88
- Ruiz, M. A. 688(558), 769
- Rumbles, G. 252(321), 299
- Rummey, C. 1081(149), 1122
- Rush, J. D. 966(208), 994
- Russell, G. A. 360(132), 584, 900(9), 912, 951(46), 990, 1037(239), 1051
- Russell, J. L. 533(476), 593
- Russell, K. E. 900(47), 912
- Russell, R. A. 1257(273, 292, 298), 1266(334), 1276–1278
- Russell, S. W. 445(325), 590
- Russel, G. A. 901(18), 912
- Rust, F. F. 156(12), 167, 352(110), 584
- Rüttinger, H.-H. 652(375, 376), 744(207), 761, 765
- Ruíz, A. 662(432), 766
- Ryall, M. E. T. 1256(252), 1275
- Ryan, D. E. 1257(304), 1277
- Rychlewska, U. 114(114), 141, 696(577), 770
- Ryter, S. W. 950(154), 992
- Ryu, A. 858(122), 896
- Ryu, H. J. 612(107), 758
- Ryu, J. Y. 1031(205), 1050
- Sá e Melo, M. L. 516(427), 592
- Saad, M. M. A. 269(429), 301
- Saafeld, F. E. 1261(321), 1277
- Saak, W. 825(122), 830
- Sabater, M. J. 1084(235), 1124
- Saba, A. 1155(106c), 1168
- Sabelle, S. 1256(253), 1275
- Sabitha, G. 277(507), 303, 1023(150), 1029(195), 1049, 1050
- Sabnis, Y. A. 1282(26), 1342
- Sabourin, M. J. 623(197), 761
- Sadaoka, Y. 652(377), 765
- Sadasivamurthy, P. 714(602), 770
- Sadeghi, M. M. 1029(191), 1050
- Sadlek, O. 209(137), 295
- Sadoun, A. H. 892(206), 898
- Sadun, C. 1083(225), 1123
- Saeki, M. 655(395), 765
- Safari, H. 779(15c), 827
- Safont, V. S. 1075(155), 1122
- Sage, E. 977(275a, 275c), 996
- Saha-Möller, C. R. 65(139), 78(20), 86, 90, 271(332), 299, 337(74, 75), 338(76), 339(78, 79), 352(72), 363(137), 373(152), 408(221, 222, 222b), 410(223), 416(235b), 475(70, 73), 477(373a, 373c), 478(374), 493(219), 520(455b), 529(471), 561(217), 583, 585, 587, 591, 593, 884(184), 889(197), 892(207), 897, 898, 943(85b, 96), 949(140), 991, 992, 1083(223, 224), 1091(278, 279), 1094(17, 296, 298), 1096(319, 321), 1100(132), 1116(424, 425), 1118, 1121, 1123–1125, 1128, 1140(76), 1150(91), 1152(107), 1161(122), 1162(21, 150), 1163(1m, 1p, 154a), 1165, 1167–1169, 1174(15), 1181(11f, g), 1194(30), 1202(64b–d), 1203(65a, b), 1204(71), 1205(60a, b), 1206, 1207, 1209, 1233(14), 1256(144), 1270, 1273
- Sahal, D. 1283(33), 1343
- Sahle-Demessie, E. 559(509), 594
- Sahli, A. 329(63a), 352(62), 583
- Saiki, H. 651(371), 765
- Saint-Pierre, C. 943(86), 975(269b), 991, 996
- Sainton, J. 1069(45), 1119
- Sain, M. M. 623(200), 761
- Saito, B. 1099(339, 340), 1126
- Saito, I. 269(422), 273(51), 293, 301, 316(23), 318(13), 351(107), 582, 584, 833(31), 894, 940(75b), 954(193a), 962(210), 967(216, 238a), 991, 993–995, 1173(17b), 1182(24c), 1206, 1207, 1228(96), 1272
- Saito, M. 434(285), 589
- Saito, S. 434(285), 589
- Saito, T. 567(532b), 595
- Saito, Y. 677(518), 768, 966(219), 994
- Saiz, A. I. 622(192), 760
- Saji, T. 1234(135), 1273
- Sajus, L. 426(278), 588, 1058(28, 29), 1118
- Sakaguchi, K. 252(298), 298
- Sakaguchi, S. 445(309), 589, 1081(174), 1122
- Sakai, N. 1268(336), 1278
- Sakakura, M. 379(157), 585
- Sakamoto, M. 426(279), 589
- Sakamoto, N. 118(126), 142

- Sakanishi, K. 1251(236), 1275
 Sakan, T. 856(110, 113), 896
 Sakata, Y. 1087(256, 257), 1094(301),
 1102(353), 1124–1126
 Sakaue, S. 1102(353), 1126
 Sakemi, S. 190(25), 292, 1333(138), 1345
 Sakoh, T. 1334(146), 1346
 Sako, M. 1011(82, 83), 1047
 Sakugawa, H. 604(2), 756
 Sakuma, T. 1199(57), 1208, 1236(150, 157,
 158), 1273
 Sakurada, I. 793(38), 828
 Sakuragawa, A. 639(238), 761
 Sakurai, H. 815(91a), 829, 901(14, 41), 912,
 1062(61), 1119
 Sakurai, K. 1010(74), 1047
 Sakurai, M. 129(171), 143
 Sala-Pala, J. 425(267), 588
 Saladino, R. 560(510), 594, 1083(225, 226),
 1111(398, 399), 1123, 1127, 1156(121a–d),
 1161(146), 1168, 1169
 Salamci, E. 264(393, 398, 400), 300, 301,
 891(205a), 898
 Salast, L. J. 94(4b), 138
 Saleemuddin, M. 655(300), 763
 Salehi, P. 1019(117, 118), 1048
 Salerno, D. 1257(256), 1276
 Salgo, M. G. 123(161), 143
 Salifoglou, A. 1058(38), 1119
 Salimhanna, M. 1242(190), 1274
 Salles, L. 1069(117), 1121
 Salomon, I. J. 172(5), 186
 Salomon, M. F. 233(232, 233), 297, 354(112),
 584, 824(120), 830
 Salomon, R. G. 174(9), 186, 190(16), 233(232,
 233), 292, 297, 354(112), 584, 824(120),
 830, 984(317b), 998
 Salvadori, P. 569(535a), 595
 Salvador, A. 701(302), 763
 Salvador, J. A. R. 516(427), 517(445), 592,
 593
 Salva, J. 1333(141), 1346
 Sályi, S. 1156(123a), 1168
 Salzmann, R. 185(39), 187
 Salzner, U. 267(415), 301
 Šaman, D. 890(204), 898
 Samii, J. M. 681(505), 768
 Saminathan, S. 383(182), 586
 Sammartino, M. P. 664(440), 767
 Samokyszyn, V. M. 980(289b), 997
 Sampugna, J. 737(693), 772
 Sams, C. K. 1075(144), 1121
 Samuelsson, B. 190(4, 6, 7, 9), 214(166), 292,
 295, 949(134), 992
 Samuel, O. 486(376), 591, 1068(96), 1120
 San Filippo, J. 315(32b), 582
 Sanabia, J. 161(45), 169
 Sanceau, J.-Y. 567(531e), 595
 Sánchez-Baeza, F. 1154(19), 1155(118b),
 1161(103), 1165, 1167, 1168
 Sanchez, J. 1059(41), 1119
 Sandalio, L. M. 610(78), 757
 Sanderson, J. R. 426(275), 588
 Sanderson, P. E. J. 809(75), 829
 Sanderson, W. R. 110(99), 141
 Sanders, J. K. 624(216, 217), 761
 Sanders, L. K. 185(39), 187
 Sander, J. 378(166), 585
 Sander, W. 29(69), 60(60), 72(72a, 72e, f), 88,
 1154(16a, b, 112), 1165, 1168
 Sandison, M. D. 1236(34), 1271
 Sandmann, B. W. 1257(257, 295), 1276, 1277
 Sandu, V. 815(91c), 829
 Sanetti, A. 1160(136), 1169
 Sangaiiah, R. 982(291g), 997
 Sankar, G. 418(252), 526(465), 588, 593,
 1082(203), 1085(247), 1123, 1124
 Sano, Y. 918(8c), 988
 Santamaria, J. 204(101), 294
 Santarsiero, B. D. 125(125), 142, 1065(53),
 1119
 Santa, T. 1257(284), 1276
 Santos, A. M. 1086(252), 1124
 Santos, C. C. X. 953(185), 993
 Santos, C. X. C. 963(220), 994
 Santry, D. P. 5(5), 85
 Sanyal, D. K. 1058(35), 1119
 Saparbaev, M. 984(313), 998
 Sarabia, F. 1145(68), 1167
 Saracoglu, N. 267(410, 415), 301
 Saraiva, S. A. 1257(261), 1276
 Saraspriya, S. 605(29), 756
 Sardarian, A. R. 1019(117), 1048
 Sardella, D. J. 172(7), 186
 Sarikaya, H. Z. 608(52), 757
 Sarlet, G. 1252(243), 1275
 Sarmah, P. 273(56), 293
 Sarzi-Amade, A. 37(91), 44(101), 89
 Sarzi-Amade, M. 1140(41), 1166
 Sarzi-Amadé, M. 46(110), 47(105, 111),
 57(51b), 87, 89
 Sarzi-Amadé, M. 67(130a, b), 90
 Sasai, H. 390(197), 392(195, 196), 586
 Sasaki, S. T. 950(159), 992
 Sasaki, T. 1333(139), 1335(147), 1346
 Sasaki, Y. 468(356), 478(297), 589, 591
 Sasson, Y. 510(412), 592
 Sastry, M. S. 1058(33), 1119
 Sathyanarayana, D. N. 709(600), 714(602),
 770
 Satoh, M. 118(126), 142
 Satoh, W. 118(139), 142
 Sato, K. 444(310, 311), 445(312), 496(400),
 506(401), 525(462), 572(544), 589, 592,
 593, 596, 819(100, 101), 829, 1081(177),

- 1089(178), 1095(317), 1106(378–380),
1122, 1125, 1127
- Sato, N. 1003(21), 1046, 1157(130b), 1168
- Sato, R. 1025(166), 1049
- Sato, S. 825(125), 830
- Sato, T. 610(73), 655(398), 757, 765, 816(93),
829, 1065(72), 1120
- Sattler, W. 956(201b), 994
- Sauerbrey, A. 273(459, 461), 302
- Sauer, F. 604(17), 678(16), 707(308a), 756,
763
- Sauer, H. 1336(158), 1346
- Saul, R. L. 616(151), 759
- Sauriol, R. 166(63), 169
- Saussine, L. 131(131), 142, 423(262),
426(276), 588, 1078(159), 1085(142),
1115(161), 1116(56), 1117(432), 1119,
1121, 1122, 1128
- Saussman, S. 1055(5–7), 1118
- Sauter, M. 259(368), 300, 1143(63a–c), 1166,
1205(60b), 1209
- Sauvaigo, S. 943(9b, 87), 975(268a, b), 989,
991, 996, 1203(67b), 1209
- Savage, P. E. 97(29), 139
- Savina, J.-P. 623(196), 761
- Sawada, H. 183(28), 187
- Sawada, T. 199(86), 293
- Sawaki, Y. 1035(230, 231), 1040(254, 255),
1044(273), 1051, 1052
- Sawa, T. 614(130), 759
- Sawyer, B. C. 667(120–122), 758, 759
- Sawyer, D. T. 315(31), 582, 1032(216), 1050
- Saxena, G. 274(479, 480), 303, 1326(127),
1345
- Sayan, S. 267(415), 301
- Saygin, K. M. 114(69), 140
- Sayre, L. M. 973(260), 984(317b, 317e), 996,
998, 999
- Sbampato, G. 1068(98), 1120
- Sbardellati, S. 130(174), 143
- Sbrogio, F. 260(375, 376), 300
- Scaiano, J. C. 1140(31), 1165
- Scaiano, J. C. 909(92), 913, 1181(11e), 1206
- Scandola, F. 1234(114), 1272
- Scardellato, C. 1095(314), 1125
- Scarpati, R. 118(118), 142, 259(367),
273(438), 300, 301
- Scettri, A. 408(99), 414(232), 482(14),
483(15), 488(392), 491(395), 493(391, 393,
394), 582, 584, 587, 591, 1094(295),
1097(333), 1125, 1126
- Schaafsma, Y. 900(29), 912
- Schaap, A. P. 729(668), 772, 833(24),
854(102), 894, 895, 1172(10a), 1198(33a,
b), 1199(56a), 1205, 1207, 1208,
1236(32–34), 1255(248), 1256(29, 31, 250,
251), 1271, 1275
- Schachl, K. 651(366, 367), 765
- Schade, G. 837(52), 861(132), 895, 896
- Schaefer, H. F. 8(8c, d), 30(30), 68(142),
79(79), 85, 87, 88, 90, 185(35), 187
- Schafer-Ridder, M. 269(424), 301
- Schäfer, A. 825(122), 830
- Schäfer, C. 604(17), 678(16), 756
- Schäfer, M. 104(58), 140
- Schaffner, K. 1228(107), 1272
- Schalley, C. A. 68(143), 90, 97(31), 139
- Schambony, S. B. 271(332), 299, 1163(1m),
1165, 1174(15), 1206
- Schambony, S. 73(19d), 86, 1140(37), 1165
- Schaper, I. 744(20), 756
- Schara, M. 813(87), 829
- Scharf, C. 610(70), 757
- Schauberger, G. 605(33), 756
- Schaur, R. J. 977(280a), 984(281b), 997
- Scheeline, A. 653(383), 765
- Scheffler, A. 362(136b), 585, 1087(253), 1124
- Scheffler, D. 744(20), 756
- Scheinmann, F. 280(526), 304, 1314(83),
1332(93), 1344
- Scheller, M. E. 250(296), 298
- Scheller, N. 981(298b), 998
- Schenck, G. O. 254(326), 299, 322(37),
324(49), 326(38), 582, 691(489), 706(596,
597), 768, 770, 861(5a, b, 129, 130, 132),
893, 896
- Schenk, W. A. 477(373c), 591, 1094(17), 1118
- Schepartz, S. A. 1145(67a), 1166
- Scheper, T. 655(300), 763
- Scherer, W. 459(347), 469(345), 590,
1062(39), 1119
- Scheurer, C. 1332(15), 1342
- Schick, R. 740(244), 762
- Schiers, J. 673(500), 768
- Schiesser, C. H. 833(30), 894
- Schiffmann, D. 1205(60a, b), 1209
- Schiller, J. 673(494), 768, 1244(199), 1274
- Schilling, F. C. 695(496), 768
- Schinazi, R. F. 290(512), 303
- Schindler, G.-P. 539(495), 594
- Schindler, R. N. 32(83), 78(78), 82(82a), 88,
138(209a), 144
- Schindler, S. 1117(429), 1128
- Schinzler, D. 396(207), 587
- Schirmann, J. P. 183(29), 187
- Schlautman, M. A. 1262(326, 327), 1277
- Schlegel, H. B. 4(11a), 10(10a–c), 12(7),
29(63), 56(12b, 48c, d), 58(124), 60(16a),
67(140), 68(119, 141), 73(19a), 79(17b),
85–90, 96(8a), 97(32a, b), 138, 139,
310(3b), 581, 1140(44, 49), 1166
- Schlemper, E. O. 729(670), 772, 1030(196),
1050
- Schleyer, P. v. R. 1250(224), 1252(246), 1275
- Schlindwein, K. 175(11), 183(10), 186,
724(659), 772

- Schlingloff, G. 1100(346), 1126
 Schlitzer, M. 190(43), 292
 Schlomski, S. 638(314), 764
 Schlücker, S. 1155(116), 1168
 Schmalstieg, H. 1232(129), 1273
 Schmalwieser, A. W. 605(33), 756
 Schmickler, H. 556(517), 595
 Schmidt, E. 1181(11c), 1206, 1213(19), 1270
 Schmidt, G. 262(379), 300, 885(187), 897
 Schmidt, H. 186(42), 187, 623(199), 761, 1069(106), 1121
 Schmidt, M. W. 12(7b), 85
 Schmidt, M. 637(303), 763
 Schmidt, R. 269(329), 299
 Schmidt, S. P. 1184(29, 32), 1207, 1232(23, 116, 118), 1234(133, 134), 1235(80), 1248(41), 1270–1273
 Schmidt, T. 67(67), 72(72a), 88
 Schmid, G. 273(273), 277(503), 298, 303, 608(59), 757, 1332(14), 1342
 Schmid, K. S. 271(332), 299, 884(184), 892(207), 897, 898
 Schmid, K. 981(301), 998
 Schmitzer, S. 1163(154c, 154f, g), 1169
 Schmitz, E. 280(280), 298, 316(25), 582
 Schmitz, O. 679(525–527), 769
 Schnatterer, A. 208(125, 126, 130), 294
 Schneider, B. 112(93), 141
 Schneider, F. W. 1197(50), 1208, 1236(160), 1273
 Schneider, H. R. 183(4), 186
 Schneider, U. 869(93), 895
 Schneider, W. F. 692(19, 568), 756, 770
 Schnell, A. 623(197), 761
 Schnick, W. 735(683, 684), 772
 Schnitzer, E. 671(113), 758
 Schobert, R. 204(99, 100), 294
 Schofield, L. J. 422(256), 588
 Scholes, G. 659(260), 762, 919(16, 19), 920(22a, b), 921(28a), 923(18a–c, 18e), 989
 Scholten, M. 82(160), 91
 Scholz, B. P. 196(74, 75), 293
 Scholz, H. J. 623(199), 761
 Schomburg, D. 1145(67d), 1166
 Schönberger, A. 1202(64b–d), 1205(60b), 1209
 Schönfels, C. 1236(145), 1273
 Schore, N. E. 1191(46b, c), 1208, 1224(57), 1271
 Schorm, A. 1081(149), 1122
 Schowen, R. L. 1188(40c, d), 1207, 1257(286), 1262(308, 311), 1263(328), 1276, 1277
 Schrader, O. 946(126b), 992
 Schramm, G. 1042(260, 261), 1051
 Schram, E. 1192(47c), 1208
 Schreiber, S. L. 320(34), 327(61), 582, 583
 Schreier, P. 337(74, 75), 338(76, 77), 339(78, 79), 352(72), 475(70), 583
 Schrock, A. K. 1232(125), 1273
 Schroder, D. 68(143), 90
 Schröder, D. 97(31), 139
 Schröder, H. 357(120), 584
 Schröder, K. 72(72e), 88, 1154(112), 1168
 Schröder, M. 567(519, 525), 595
 Schroeter, S. 861(130, 132), 896
 Schuchardt, U. 1085(207), 1116(426), 1123, 1128
 Schuchmann, H.-P. 924(45), 964(228), 990, 995
 Schuchmann, M. N. 923(21), 989
 Schudde, E. P. 1069(50), 1119
 Schuhmann, W. 679(525), 769
 Schüller, E. 338(76, 77), 583
 Schulte-Elte, K.-H. 326(38), 582, 691(489), 768
 Schulte-Elte, K. H. 834(36), 854(64), 874(70), 894, 895
 Schulte-Frohlinde, D. 923(21), 930(56), 989, 990
 Schulte-Ladbeck, R. 708(605), 770
 Schulten, W. 824(118), 830
 Schultz, A. J. 1075(154), 1122
 Schultz, M. 977(278a), 997
 Schulz-Ekloff, G. 870(151), 896
 Schulze, B. 107(95, 96), 112(93, 94, 97, 98), 141
 Schulz, M. 47(103), 89, 440(313b), 520(452), 589, 593, 791(37), 795(41), 828, 1003(24), 1046, 1140(26), 1163(1k), 1164, 1165
 Schumacher, D. 260(372), 300
 Schumann, U. 12(7d), 85
 Schumaster, D. 869(145), 896
 Schumm, R. H. 154(21), 168
 Schurig, V. 432(300a, b), 589, 1084(232, 233), 1123
 Schuster, A. 1163(152b), 1169
 Schuster, B. G. 1281(5), 1342
 Schuster, G. B. 834(38), 875(39), 894, 1184(29, 31, 32), 1188(28), 1207, 1232(23, 81, 116–118, 125–127), 1234(114, 133, 134), 1235(22, 80, 122, 123, 137–139), 1248(41), 1267(20, 115), 1270–1273
 Schuster, G. 604(17), 678(16), 756, 1224(57), 1271
 Schütz, M. 12(7d), 85
 Schübler, M. 520(452), 593
 Schwarzenbach, G. 658(417), 766
 Schwarz, H. 68(143), 90, 97(31), 139
 Schweibert, M. C. 614(138), 759, 922(41a), 990
 Schwendt, P. 1058(20), 1118
 Schwenkreis, T. 456(339), 590
 Schwerdtfeger, P. 97(27a), 139
 Schwiens, E. 977(277g), 996
 Schwinn, J. 1244(199), 1274

- Sciacovelli, O. 32(59), 88, 183(30), 184(34),
187, 1076(158), 1122, 1155(115),
1160(11a), 1165, 1168
- Scialdone, M. A. 266(406), 301
- Scipionato, L. 123(162), 143
- Scorneaux, B. 1332(15), 1342
- Scorrano, G. 1155(106b), 1168
- Scott, G. 1257(264), 1276
- Scott, L. T. 267(408), 301
- Scovill, J. P. 1280(2), 1342
- Scrimgeour, C. M. 614(126), 759
- Scrimin, P. 1068(89, 90), 1095(314), 1120,
1125
- Scriven, E. F. V. 1181(11g), 1206
- Scurlock, R. D. 832(11), 894
- Scuseria, G. E. 8(8c, d), 12(7), 85
- Seal, J. R. 977(280c), 997
- Searle, N. L. 274(274), 298, 1304(63, 71),
1324(124), 1332(92), 1343–1345
- Sebastian, R. 922(39a), 990
- Sebbar, N. 103(57), 140
- Secen, H. 264(392–394, 398), 300, 301
- Secibu, G. C. 776(1), 827
- Seconi, G. 778(12), 797(42, 45), 800(49, 50),
827, 828
- Seddighi, M. 1019(117), 1048
- Sedman, J. 662(431), 663(233), 761, 766
- Seebach, D. 106(67), 140, 408(221, 222,
222b), 562(98), 584, 587, 1094(296, 298),
1113(297), 1125
- Seeber, A. 1262(318), 1277
- Seefeld, S. 94(4c), 138
- Seelbach, W. 1163(154d), 1169
- Segall, H. J. 978(287a), 980(289a), 997
- Segal, G. A. 5(5), 85
- Seguela, J. P. 284(548), 286(557), 304, 305
- Sehested, J. 692(568), 770
- Seip, H. M. 723(648), 771
- Seitz, G. 267(418–420), 301
- Seitz, W. R. 1244(200), 1257(263, 264), 1274,
1276
- Sekar, G. 516(438b), 593
- Sekino, H. 12(7c), 85
- Seliger, H. H. 812(86a), 829, 1191(8a), 1205,
1224(62), 1225(64), 1243(63), 1271
- Selke, M. 1059(43), 1087(258, 259), 1119,
1124
- Selley, M. L. 670(114), 758
- Sels, B. F. 456(327), 457(330), 590
- Seltzer, H. 724(658), 772
- Seltz, W. R. 648(355a), 765
- Selvam, T. 477(373a), 591, 1096(321), 1125
- Selva, A. 107(87), 141
- Selzer, P. M. 1322(118), 1345
- Selçuki, C. 29(74), 88
- Semsel, A. M. 1242(184), 1256(255),
1258(307), 1266(305, 306), 1274, 1276,
1277
- Senatore, A. 493(391), 591, 1097(333), 1126
- Seneviratne, V. 1151(99b), 1167
- Sengul, M. E. 267(414), 301
- Sensato, F. R. 1075(155), 1122
- Sen, A. 1008(53), 1047, 1116(421), 1128
- Sen, S. E. 870(148a), 896
- Seo, J. S. 901(46), 912
- Seraglia, R. 480(378), 591, 1095(179),
1097(93), 1120, 1122
- Seraphin, D. 238(257), 297, 892(65, 208), 895,
898
- Serbecic, N. 611(82), 758
- Seree de Roch, I. 1058(28, 29), 1118
- Sergeeva, V. P. 1043(265, 266), 1051
- Sergienko, V. I. 673(494), 768
- Serio, M. R. 1145(7), 1165
- Serradilla Razola, S. 653(384), 765
- Serrano, E. 614(136), 759
- Serravalle, M. 1010(69), 1047
- Serri, A. 45(106c), 89, 1160(35c), 1165
- Sessoli, R. 1067(80), 1120
- Setiowaty, G. 662(210), 761
- Seto, H. 980(290a), 997
- Seubold, F. H. 352(110), 584
- Sevanian, A. 614(128), 759
- Sevenard, D. V. 1013(89), 1048
- Severeyns, A. 569(529), 595
- Sever, R. R. 1073(124), 1121
- Sevimli, M. F. 608(52), 757
- Sevin, F. 253(339), 299
- Seya, K. 968(239a), 995
- Seçen, H. 891(205a, b), 898
- Shabalin, I. I. 113(59), 140
- Shacter, E. 986(328a), 999
- Shaffer, L. H. 778(11), 783(25), 827
- Shafirovich, V. 940(77, 78), 991
- Shahidi, F. 665(444), 668(460), 680(534), 767,
769
- Shahi, S. P. 803(55), 828
- Shah, A. 285(552), 286(556), 304, 305
- Shaik, S. 84(163), 91, 472(143), 579(549),
585, 596, 1140(52a), 1166
- Shailaja, J. 870(147, 157), 896, 897
- Shakespeare, D. 648(307), 763
- Shalhaf, H. 1016(106), 1048
- Shaltiel, S. 987(329a, 329c), 999
- Shalyaev, K. V. 185(40), 187, 1069(114),
1075(145), 1121
- Shamsipur, M. 649(357), 765, 1257(271), 1276
- Shank, K. 13(13b), 86
- Shantha, N. C. 658(415), 766
- Shan, F. 273(458), 302, 1299(40), 1343
- Shao, Q. Y. 511(416), 592
- Shapiro, T. A. 202(96), 209(140, 141),
223(209, 210), 273(447, 468–470),
280(521–523, 527), 283(471, 520, 524,
530), 294–296, 302, 304, 1282(17),
1284(39), 1289(46), 1291(48), 1314(84),

- 1326(126), 1330(134), 1332(109–111),
1337(162–164), *1342–1346*
- Sharipov, G. L. 1181(11i), 1190(43), *1206*,
1208
- Sharma, N. D. 1155(106a), *1168*, 1200(58c),
1208
- Sharma, P. K. 1140(52a), *1166*
- Sharma, R. P. 273(55), *293*
- Sharpless, K. B. 48(113a, b), 89, 94(5), *138*,
396(210, 211), 397(212c), 400(206, 208),
410(225), 414(227), 423(237), 426(277a),
432(301), 467(352, 359), 468(351, 357),
479(385), 503(428), 513(431), 534(481,
482), 542(201, 202), 556(518b),
567(526–528, 530b), 574(521), 575(520),
586–592, 594, 595, 789(33), 790(36),
802(54), 828, 1075(138–140), 1083(217,
220), 1087(254), 1090(218), 1092(82, 83,
243, 282, 287), 1097(12), 1105(368–370),
1118, *1120*, *1121*, *1123–1127*, 1161(149a),
1169, 1173(12c), *1206*
- Sharutina, O. K. 1058(37), *1119*
- Sharutin, V. V. 1058(37), *1119*
- Shas, L. 1015(102), *1048*
- Shavaleev, N. M. 1190(45c), *1208*
- Shaw, J. 457(323), *590*
- Shaw, R. G. 780(23), *827*
- Shchegoleva, T. M. 118(141), *142*
- Shearer, G. O. 55(120), *90*
- Sheats, J. R. 832(11), *894*
- Shea, K. J. 65(136c), *90*
- Sheehan, D. 1256(255), 1266(306), *1276*, *1277*
- Sheeto, J. 822(104), 829, 1172(5), *1205*
- Sheffield, S. A. 96(25), *139*
- Sheil, M. M. 691(143), 759, 956(200), *994*
- Sheldon, R. A. 368(142), 417(239), 426(240),
432(241), 462(361), 468(358), 497(403),
512(408), 514(404, 409a, b, 433, 434),
526(410), 560(500), 585, 587, 591, 592,
594, 1083(228), 1084(238), 1085(207, 208),
1108(371), 1116(13), *1118*, *1123*, *1124*,
1127
- Sheldrick, G. M. 103(51), *140*
- Shenai, B. R. 1322(116), *1345*
- Sheng, M. N. 426(269), 534(479), 556(522),
588, 594, 595, 1104(363), *1126*
- Sheng, M. 1084(241), *1124*
- Sheng, X. C. 950(150), *992*
- Shen, B. 270(430), *301*
- Shen, C.-C. 273(439), *301*
- Shen, D. M. 1228(60), *1271*
- Shen, H.-R. 973(244, 259), *995*, *996*
- Shen, H.-X. 629(259), 630(268), 640(322),
762, *764*
- Shen, H. X. 679(327), *764*
- Shen, L. 976(270b), *996*
- Shen, M. 30(30), *87*
- Shepherd, B. D. 820(107), *829*
- Sherburn, M. S. 217(188, 189), 296, 890(203),
898
- Sherman, D. G. 1228(102), *1272*
- Sherman, F. 624(242), *762*
- Sherman, P. A. 1257(304), *1277*
- Sherma, J. 977(278b), *997*
- Sherrington, D. C. 428(286), 433(287, 288),
589
- Sheu, C. 943(81, 83, 88), *991*, 1203(66), *1209*
- Shevlin, P. B. 30(76), *88*
- Sheyanov, N. G. 810(80), *829*
- She, X. 1022(143), *1049*, 1148(79a, b, 79d,
89, 90), *1167*
- Shibanov, V. V. 168(32), *168*
- Shibasaki, M. 233(231), 297, 315(32a),
390(197), 392(195, 196), 582, 586, 793(38),
828
- Shibata, F. 326(58), *583*
- Shibata, H. 50(50b), *87*
- Shibata, K. 804(59), *828*
- Shibata, Y. 1332(108), *1345*
- Shibutani, S. 1201(62d), *1209*
- Shideman, F. E. 1037(233), *1051*
- Shigenaga, M. K. 975(269a), *996*
- Shih, C. 238(174, 175), *295*
- Shih, N. Y. 238(174), *295*
- Shiliapintokh, V. 949(141), *992*
- Shiller, A. M. 645(341), *764*
- Shimada, M. 1012(85), *1047*
- Shimada, T. 1156(123b), *1168*
- Shimamoto, K. 1012(85), *1047*
- Shimazaki, Y. 1067(55), *1119*
- Shimizu, H. 196(70), 223(218), 293, 296,
1100(348), *1126*
- Shimizu, K. 1251(236), *1275*
- Shimizu, M. 1095(307), 1116(425), *1125*,
1128
- Shimizu, N. 326(58), *583*
- Shimizu, T. 352(48), *582*
- Shimizu, Y. 650(364), *765*
- Shimoji, K. 238(174, 175), *295*
- Shim, S. C. 205(116, 117), *294*
- Shindo, A. 208(132), *294*
- Shiner, C. S. 233(231), *297*
- Shing, T. K. M. 1140(78), *1167*
- Shinke, S. 497(405b), *592*
- Shinoda, K. 720(643), *771*
- Shin, W. S. 273(462), *302*
- Shioiri, T. 375(149), *585*
- Shiojima, N. 900(11), *912*
- Shiono, T. 1236(148), *1273*
- Shiori, T. 374(150), *585*
- Shiota, T. 1104(356), *1126*
- Shiraki, A. 382(178), *586*
- Shiratori, Y. 206(122), *294*
- Shirokii, V. L. 122(152), *142*
- Shiro, M. 118(142, 143), *142*
- Shishkin, D. I. 531(468), *593*

- Shi, G. Q. 259(362–364), 300
 Shi, S. H. 259(364), 300
 Shi, Y. 520(455a), 593, 1021(141), 1022(143), 1049, 1140(58, 74, 75, 77a, b), 1146(18, 71), 1148(79a–d, 89, 90), 1150(27, 93–95), 1163(1n, o), 1165–1167
 Shi, Z. P. 201(93), 202(94, 95), 294
 Shklover, V. E. 118(140), 130(181), 142, 143
 Shmuklarsky, M. J. 1281(5), 1342
 Shockravi, A. 649(357), 765
 Shoji, H. 612(88), 758
 Shono, T. 1032(219), 1050
 Shoulders, B. A. 717(626), 771
 Shroll, R. M. 45(45), 87
 Shtekher, S. M. 153(19), 167
 Shterman, N. 1335(150), 1346
 Shtivel, N. E. 156(27), 168
 Shubber, A. K. 824(119), 830
 Shul'pin, G. B. 1116(415, 420, 426), 1117(429), 1127, 1128
 Shumkina, T. F. 701(587), 770
 Shustov, G. V. 37(37c), 47(109), 87, 89
 Shu, C.-M. 617(158), 759
 Shu, L. 1148(79c, d, 89), 1150(27, 95), 1165, 1167
 Shvedova, A. A. 660(110), 758
 Shwaery, G. T. 681(505), 768
 Shweky, I. 1067(80), 1120
 Shyu, S.-C. 651(368), 765
 Siakotos, A. N. 977(282a), 997
 Sibi, M. 213(156), 229(222), 295, 297
 Sidebottom, H. W. 138(210b), 144
 Sidelmann, U. G. 1322(120), 1345
 Sideri, M. 628(68), 757
 Siders, P. 1217(44), 1271
 Siegfried, S. 204(100), 294
 Sieker, G. 1074(126), 1121
 Sieler, J. 107(96), 112(93, 97, 98), 141
 Sies, H. 50(50a), 87, 269(421), 301, 917(1a), 949(140), 950(147, 153, 156, 158, 159), 988, 992, 1155(118a), 1168, 1200(59a), 1201(62a), 1209
 Sigihara, Y. 1157(130a), 1168
 Sijwali, P. S. 1322(81, 116), 1344, 1345
 Silbert, L. S. 160(31), 168
 Silva, S. M. 1189(41d), 1208, 1260(317), 1267(18), 1268(140, 143, 335), 1270, 1273, 1277, 1278
 Simaan, A. J. 1070(47), 1119
 Simaan, A. 1069(45), 1119
 Simaan, J. 1117(431), 1128
 Simakov, P. A. 44(104), 89
 Simandiras, E. D. 12(7e), 85
 Simandi, L. I. 1068(98), 1120
 Simándi, P. 678(252), 762
 Simchen, G. 1014(90), 1048
 Simeonov, V. 605(35), 756
 Simic, M. G. 923(42b), 960(205), 962(212), 963(226), 990, 994
 Simic, M. 924(44), 990
 Simões, J. A. M. 149(9), 167
 Simonetta, M. 122(156), 143
 Simonov, Y. A. 122(101), 141
 Simons, D. M. 900(50), 912
 Simons, J. 744(705), 773
 Simon, A. 777(9), 827
 Simova, S. 177(14), 186
 Simpson, B. E. 629(261), 762
 Simpson, G. A. 1232(119), 1273
 Simpson, J. A. 972(196a), 994
 Simpson, J. S. A. 1256(252), 1275
 Simpson, R. E. 223(215, 216), 296
 Simpson, S. 433(287), 589
 Sims, P. 1009(62), 1047
 Singer, B. 980(290f), 982(308), 984(297f), 997, 998
 Singer, L. A. 902(63), 913, 1256(28), 1271
 Singh, A. 1322(116), 1345
 Singh, B. H. 94(4b), 138
 Singh, C. 274(478–483), 303, 1320(114), 1326(127–129), 1345
 Singh, M. 1143(64), 1153(97b), 1159(100a, b, 135a), 1160(137), 1163(1i), 1164, 1166, 1167, 1169
 Singh, N. P. 273(457), 302, 1336(151–153), 1346
 Singh, R. L. 1313(82), 1344
 Singh, R. 199(88), 294
 Singh, S. K. 680(535, 536), 769
 Singh, V. K. 516(438a, b), 593
 Singleton, D. A. 50(126), 56(125), 90, 833(35), 894
 Singleton, E. 95(18), 139
 Sinha, A. 443(319a), 590
 Sinigalia, R. 1084(236), 1124
 Siniscalchi, F. R. 482(14), 582
 Sink, C. W. 1265(332), 1277
 Sinnhuber, R. O. 667(451, 452), 767
 Sinzinger, H. 631(293), 667(459), 763, 767
 Siritanaratkul, N. 1311(76), 1344
 Sisemore, M. F. 1087(258, 259), 1124
 Sitzmann, E. V. 269(428), 301
 Sitzmann, M. E. 1013(31), 1046
 Sivaguru, J. 870(147, 157), 896, 897
 Sivakumar, M. 1024(156), 1049
 Sivák, M. 1058(20), 1077(160), 1118, 1122
 Sjødahl, R. 945(104), 991
 Sjövall, O. 693(562a, 573, 574), 739(695), 770, 772
 Skean, R. W. 291(594), 305
 Skibsted, L. H. 665(444, 445), 666(447, 448), 678(520), 767, 768
 Skidmore, J. 378(166), 379(163), 381(172, 177), 382(178b), 585, 586, 1087(261), 1124
 Sklorz, C. A. 509(331), 590

- Skogström, T. 693(572), 770
 Skrzynecka, B. 650(363), 765
 Skuratov, S. M. 153(19), 167
 Skurski, P. 1253(235), 1275
 Slaich, P. K. 982(291d), 997
 Slany, M. 1069(45), 1119
 Slater, T. F. 667(119–122), 758, 759,
 954(189), 977(277a), 993, 996
 Slayden, S. W. 151(1), 160(14), 167
 Slayden, Suzanne W. 153(19), 168
 Slebocka-Tilk, H. 57(51a), 87
 Slobodnick, C. 1069(104), 1121
 Sleczo, B. G. 987(330), 999
 Slemr, F. 604(15), 638(314), 756, 764
 Sloboda-Rozner, D. 1091(279), 1124
 Slooten, L. 610(71), 757
 Sloss, D. G. 260(373), 300
 Slovkhotov, Y. L. 128(50), 140
 Sluchevskaya, N. P. 824(117f), 830
 Sluchevskaya, V. P. 780(21), 827
 Smerz, A. K. 47(103), 89, 410(229), 587,
 1090(276), 1124, 1144(65), 1145(48),
 1160(47), 1163(1h, 1j, k), 1164, 1166
 Smerz, A. 1021(131), 1048
 Smiter, R. 1192(47a), 1208
 Smith, C. B. 382(178b), 586
 Smith, C. D. 22(22b), 86
 Smith, C. J. 973(244), 995
 Smith, C. W. 273(473), 302
 Smith, D. A. 44(99), 89, 1140(40),
 1159(135b), 1166, 1169
 Smith, H. W. 112(88), 141
 Smith, J. A. 381(176), 382(178b), 586
 Smith, J. P. 1232(116, 125), 1272, 1273
 Smith, K. C. 832(12), 894, 1200(59b), 1209
 Smith, K. J. 320(35a), 582
 Smith, K. 903(59, 60), 913
 Smith, L. L. 325(55a, b), 583, 678(519), 768,
 946(128), 947(129), 977(278c), 992, 997
 Smith, R. H. 627(247), 762
 Smith, R. J. 196(60), 293
 Smith, R. S. 356(118), 584
 Smith, S. M. 870(148a), 896
 Smith, W. A. 426(275), 588
 Smith, W. L. 214(170, 171), 295, 963(224a),
 994
 Smitrovich, J. H. 810(76), 829
 Smits, J. M. M. 1062(42), 1119
 Smit, R. 628(255), 762
 Smonou, I. 343(91b), 583, 833(22), 894
 Smyth, L. 614(126), 759
 Snelgrove, D. W. 1086(248, 249), 1124
 Snell, C. T. 676(254), 762
 Snell, F. D. 676(254), 762
 Snider, B. B. 201(93), 202(94, 95, 98), 294
 Snoonian, J. 44(100), 89
 Snyder, J. K. 567(531k), 595
 Sobczak, J. 433(284), 589
 Södergren, M. J. 514(441), 593
 Sodum, R. S. 981(305b), 982(291c), 997, 998
 Sofikiti, N. 885(186, 188), 897
 Sogah, D. 1251(220, 221), 1275
 Sohal, R. S. 954(189), 993
 Sohar, I. 987(330), 999
 Sohn, J. K. 616(153), 759
 Sohn, J. R. 433(293), 589
 Sohn, S. C. 901(43), 912
 Sojka, S. A. 740(697), 772
 Solaja, B. A. 109(116), 141
 Soleymani, M. 1016(107), 1048
 Solladié-Cavallo, A. 1140(88), 1150(92), 1167
 Solodar, S. L. 111(105), 141
 Solomon, I. J. 182(26), 187
 Soloway, A. H. 273(475), 303, 319(19), 582
 Soltermann, A. T. 968(239c), 995
 Sombret, B. 702(227), 714(567), 761, 770
 Sommer, R. D. 1067(76), 1120
 Sondheimer, F. 198(78), 293
 Sone, H. 981(299b), 998
 Song, C. E. 1027(175), 1049, 1146(72), 1167
 Song, J. S. 205(116), 294
 Song, J. 29(66), 88, 256(359), 300
 Song, P. 253(330), 299
 Song, S. H. 612(107), 758
 Soo, M. K. 1317(100), 1344
 Sorba, J. 213(158), 295
 Soriano, N. U. 719(636), 771
 Soriente, A. 493(391), 591, 1097(333), 1126
 Sosa, C. P. 70(70), 88
 Sosa, C. 32(85a), 72(72e), 88, 1154(112), 1168
 Sosnitsa, P. 655(300), 763
 Sosnovskikh, V. Y. 1013(89), 1048
 Sosnovsky, G. 319(22), 358(124), 582, 584,
 776(4), 827, 1008(54), 1042(261, 262),
 1043(264, 269), 1044(271), 1047, 1051
 Soszynski, M. 972(253b), 995
 Souma, Y. 1115(412), 1127
 Southan, M. 987(332), 999
 Spadoni, M. 383(184), 384(185, 186), 586
 Sparks, A. 1198(33c–f), 1207, 1236(163),
 1273
 Spector, E. 1037(233), 1051
 Špehar, K. 138(208), 144
 Spek, A. L. 1069(44, 50), 1119
 Spencer, B. 835(33), 894
 Spencer, G. F. 737(691), 772
 Spencer, M. D. 256(256), 259(259), 262(262),
 297
 Spialter, L. 810(81), 811(82, 83), 829
 Spickett, C. M. 977(280a), 997
 Spiegler, M. 1069(115), 1085(246), 1086(251),
 1121, 1124
 Spikes, J. D. 966(235), 973(244, 259), 995,
 996
 Spilling, C. D. 1091(222), 1123
 Spinney, R. 37(37c), 87

- Spiteller, G. 945(107, 122), 951(165), 977(282b), 991–993, 997
 Spiteller, P. 977(282b), 997
 Spiteri, M. A. 684(99), 758
 Spohn, U. 647(349), 764
 Spratley, R. D. 101(53), 140
 Springston, S. R. 604(14), 756
 Sprinz, H. 1244(199), 1274
 Spruell, C. 22(22b), 86
 Squadrito, G. L. 14(46), 23(23), 25(26a, b), 86, 87, 123(161), 143
 Sram, J. P. 871(164), 875(176), 877(177), 897
 Sribimawati, T. 605(29), 756
 Sridhar, S. 714(602), 770
 Srinivasan, C. 1010(73), 1047
 Srinivasan, K. 457(320), 590
 Srinivasu, P. 576(548), 596
 Srinivas, D. 1116(419), 1128
 Srinivas, P. 1028(181, 185), 1049
 Srinivas, R. 1028(187), 1029(192), 1050
 Staab, E. 255(355), 300, 888(191, 192), 897, 1145(69), 1167
 Stachulski, A. V. 1314(83), 1317(101), 1332(93), 1344
 Stadtman, E. R. 918(12), 945(111), 973(197a, b), 984(317a, 317c, 319b, 320), 986(328a–c), 987(325a, b, 329c), 989, 991, 994, 998, 999
 Staffelbach, T. A. 707(523), 769
 Staliński, K. 1152(108b), 1168
 Stalke, D. 260(372), 300, 869(145), 896
 Stalnaya, T. V. 111(105), 141
 Standen, M. C. 835(33), 894
 Standen, S. 1115(414), 1127
 Stanley, J. P. 212(154), 295
 Stanley, P. E. 1184(25d), 1192(47a, 47c–e), 1207, 1208, 1224(61), 1235(132), 1271, 1273
 Stante, F. 692(93), 758
 Stanton, J. F. 12(7c), 85
 Stapelfeldt, H. 656(404), 766
 Starikova, Z. A. 118(141), 142
 Starostin, E. K. 130(181, 182), 143
 Stavenulier, J. F. C. 1252(234, 242), 1275
 Stavroulakis, D. 883(183), 897
 Stearman, C. J. 1140(84), 1167
 Stec, W. J. 1026(168), 1049
 Steenhorst-Slikerveer, L. 672(481), 768
 Steenken, S. 614(137), 759, 909(92), 913, 923(42a), 939(73), 940(76), 990, 991, 1201(61a, b), 1209
 Steensma, D. H. 266(405, 406), 301
 Stefanovic, M. 109(116), 141
 Stefanov, B. B. 12(7), 85
 Steghens, J. P. 646(346), 764
 Stehle, R. 204(99), 294
 Steijger, O. M. 1257(262), 1276
 Steinbeck, M. J. 918(8b), 988
 Steinberg, D. 612(104), 758
 Steinberg, H. 1141(59), 1166
 Steinfatt, M. F. D. 1245(204, 205, 207, 208), 1266(206), 1274
 Steinfatt, M. 1245(210–212), 1274, 1275
 Steinmetzer, H.-C. 1191(46b), 1208
 Steinmetzer, H. C. 1191(46c), 1208, 1219(47), 1222(52), 1224(57), 1271
 Steinmetz, H. 1145(67d), 1166
 Steinwascher, J. 114(69), 140, 408(86), 583
 Stein, S. E. 160(3), 167
 Steliou, K. 256(360), 300
 Stelter, L. 930(56), 990
 Stemp, E. D. A. 974(262c, d), 996
 Stepanova, E. B. 652(380), 765
 Stephanon, S. E. 1020(122), 1048
 Stephenson, L. M. 343(91a, 91c), 583, 584, 832(2, 18), 833(23), 836(42), 871(3), 875(37), 893, 894
 Stephens, R. J. 977(282a), 997
 Sternhell, S. 323(47), 582
 Steryo, M. 974(262c, d), 996
 Stetter, J. 273(450), 302, 1317(68), 1343
 Stevani, C. V. 1189(41a–d), 1208, 1236(17), 1257(73), 1260(309, 317), 1263(320, 329), 1265(331), 1267(18), 1268(140, 335), 1270, 1272, 1273, 1277, 1278
 Stevens, E. D. 130(184), 143
 Stevens, S. E. 606(40), 757
 Stewart, D. 1008(59), 1047
 Stewart, J. M. 112(79), 140
 Steyn, P. S. 1140(56a), 1166
 Stigbrand, M. 648(356), 765
 Stiggallestberg, D. L. 1228(102, 104), 1272
 Stipa, P. 1155(119b), 1168
 Stirling, D. 1086(234), 1124
 Stocker, R. 956(201b), 973(256), 987(327), 994, 996, 999
 Stocks, P. A. 223(207), 275(487, 489), 296, 303, 1323(121), 1330(132), 1345
 Stock, A. M. 1020(126), 1048
 Stohler, H. R. 277(277), 298
 Stohler, H. 273(273), 298, 608(59), 757, 1332(14), 1342
 Stohrer, W. 1245(209), 1274
 Stok, J. E. 1140(52c), 1166
 Stoll, H. 12(7d), 85
 Stomberg, R. 122(151), 142, 1067(78), 1120
 Stone, A. J. 12(7d, e), 85
 Stone, K. 980(290d, e), 997
 Stone, M. 1140(57), 1166
 Stoop, R. M. 1084(237), 1124
 Stopper, H. 1205(60b), 1209
 Stork, G. 809(74), 829
 Storr, R. C. 274(274), 298, 1304(63, 71), 1324(124), 1332(92), 1343–1345
 Story, P. R. 177(17, 18), 187
 Stothers, J. B. 172(7), 186

- Stowasser, R. 1081(149), 1122
 Straight, R. C. 966(235), 995
 Strain, A. J. 981(299a), 998
 Strain, M. C. 12(7), 85
 Straka, M. R. 607(47), 757
 Strange, R. C. 610(75), 757
 Stratakis, M. 255(356), 300, 832(19), 833(25), 836(49, 50), 844(60), 849(44, 67), 850(71), 851(51), 853(87), 855(86), 859(59), 873(168), 874(171), 875(175), 878(53, 179), 880(181), 883(183), 885(165, 185, 186, 188), 890(69), 892(209), 894, 895, 897, 898, 1173(17a), 1206
 Stratmann, R. E. 12(7), 85
 Stratton, S. P. 673(495), 768
 Strauss-Blasche, G. 611(82), 758
 Strausz, O. P. 815(91c), 829
 Strong, R. 1198(33f), 1207
 Struchkov, Y. T. 103(47, 48), 118(140), 122(158), 123(104), 128(50), 130(181, 182, 185), 131(180), 140–143, 729(669), 772
 Strukul, G. 14(14), 86, 539(496), 545(503), 549(489, 514), 558(513), 559(515), 594, 1075(26), 1084(231, 236), 1087(260), 1095(312), 1109(122, 393–395), 1112(123, 406), 1114(411), 1117(121, 433), 1118, 1121, 1123–1125, 1127, 1128
 Studley, A. 1158(133), 1169
 Stunnenberg, F. 183(31), 187
 Stålfors, F. 567(530a), 595
 Suarez, E. 230(223–229), 297
 Subacheva, O. V. 1058(37), 1119
 Subba Rao, Y. V. 446(328), 456(327), 590
 SubbaReddy, B. V. 1029(192), 1050
 Subramaniam, P. 1010(73), 1047
 Subramanian, K. 707(603), 770
 Subramanyam, V. 273(475), 303, 319(19), 582
 Subra, R. 921(33), 989
 Such, S. 714(567), 770
 Suckling, I. D. 628(255), 762
 Sudalai, A. 538(486), 594, 1099(342), 1126
 Suenaga, K. 1334(143), 1346
 Suenram, R. D. 57(57), 88, 721(595, 645), 770, 771, 1140(5), 1165
 Sugamori, S. E. 1140(31), 1165
 Sukanuma, H. 854(109), 896, 1236(148, 152), 1273
 Sugden, K. D. 943(95), 991
 Sugihara, Y. 1157(124, 130b, c), 1168
 Sugimoto, A. 264(390), 300
 Sugimoto, H. 1065(72), 1120
 Sugimoto, T. 108(107), 141
 Sugino, K. 676(516), 768
 Sugioka, K. 950(146), 992
 Sugita, T. 481(381), 486(386), 591, 1097(331, 332), 1126
 Sugiyama, H. 940(75b), 991
 Sugiyama, N. 1242(188), 1274
 Suhardi, B. 605(29), 756
 Sukhikh, N. G. 1043(266), 1051
 Sulcek, Z. 621(182), 760
 Suleman, N. K. 909(94), 913
 Sulikowski, G. A. 112(77), 140
 Sulikowski, M. M. 112(77), 140
 Sullivan, G. A. 425(268), 588
 Sullivan, J. A. 253(253), 297
 Sullivan, K. A. 870(148a), 896
 Sumathi, R. 37(37a), 87
 Sumida, W. K. 182(26), 187
 Sumida, Y. 444(315), 589, 1081(180), 1122
 Sumimura, T. 904(75), 913
 Sum, F. W. 512(429), 592
 Sundberg, R. J. 79(155), 91, 963(218), 994
 Sundermeyer, J. 48(114a), 89, 440(313b), 589, 791(37), 795(41), 828, 1075(143, 152, 153), 1081(149), 1121, 1122
 Sunoj, R. B. 870(157), 897
 Sun, G. Y. 660(423), 766
 Sun, G. 973(260), 996
 Sun, H. 871(162), 897
 Sun, R. C. 623(201), 761
 Sun, Y. 679(327), 764
 Superchi, S. 487(383, 387), 591, 1098(336, 337), 1126
 Surgenor, D. M. 352(106), 584
 Suropto, A. 605(29), 756
 Surova, R. P. 823(115), 830
 Surowiec, M. 1152(108a), 1168
 Sur, S. 273(468), 302, 1337(164), 1346
 Süß-Fink, G. 1116(420), 1117(429), 1128
 Sutbeyaz, Y. 264(392–394, 398), 300, 301
 Sütbeyaz, Y. 891(205a, b), 898
 Sutherland, M. W. 945(123), 992
 Suurkuusk, M. 680(535, 536), 769
 Suyama, S. 697(579), 707(598), 770
 Sužnjević, D. 623(208), 652(379), 761, 765
 Suzuki, J. 854(101), 895
 Suzuki, K. 1095(307), 1125
 Suzuki, M. 784(27), 827, 1065(72), 1102(351), 1120, 1126
 Suzuki, N. 1236(36), 1244(203), 1271, 1274
 Suzuki, O. 657(407), 766
 Suzuki, T. M. 394(200, 200b), 586
 Suzuki, T. 209(144), 295, 680(538), 687(553, 554), 715(607), 769, 770
 Su, C. C. 423(260), 588
 Su, C. 693(572), 770
 Su, M.-D. 12(7e), 73(19a), 79(17c), 84(166), 85, 86, 91
 Su, M. 649(358), 765
 Su, S.-C. 634(195), 760
 Su, S. 12(7b), 85
 Švancara, I. 651(366, 367), 765
 Svendsen, H. M. 1069(46), 1119
 Svendsen, J. S. 567(528), 595
 Svensson, J. 190(9), 292

- Swain, H. A. 160(31), 168
 Swallow, A. J. 960(207a), 994
 Swallow, S. 256(357, 358), 300
 Swansiger, W. A. 811(82, 83), 829
 Swarthoff, T. 445(325), 590
 Sweet, D. V. 749(736), 774
 Sweet, L. J. 1062(63), 1120
 Swenberg, J. A. 981(298a–c, 307a), 982(291f, g), 984(297d), 997, 998
 Swern, D. 48(115e), 89, 105(63), 140, 160(37), 169, 313(2), 581, 796(43), 828, 1008(54), 1047, 1090(3), 1118
 Syamala, M. 1029(195), 1050
 Syed, A. 130(184), 143
 Sylwester, A. P. 902(64), 913
 Symonds, M. 901(16), 912
 Symonsbergen, D. J. 260(373), 300
 Syper, L. 540(505), 564(504), 594
 Syverud, A. N. 15(15), 86
 Sy, L.-K. 133(196a, b), 144, 288(567–569), 305
 Szalay, P. G. 12(7c), 40(94a), 85, 89, 1140(20), 1165
 Sze, N. D. 138(210a, b), 144
 Szpilman, A. M. 223(206, 210–212), 296, 712(60), 757, 1309(52), 1330(73), 1332(111), 1343–1345
 Sztaricskai, F. 1156(123a), 1168
 Szyrbicka, R. 30(76), 88
 Szwarc, M. 96(8b), 100(45a, b), 139, 140
 Szweda, L. I. 984(315, 317c), 998
 Szweda, P. A. 984(315), 998
 Szymanska-Buzar, T. 433(272), 588
 Szymanski, M. J. 833(35), 894
 Sæbø, S. 721(646), 771
 Sørensen, J. 656(404), 666(448), 766, 767
 Tabata, H. 1103(318), 1125
 Tabuchi, T. 1157(127a, b), 1168
 Tabushi, I. 47(47b), 87
 Tachi, Y. 112(85), 141, 1067(55), 1119
 Tadahiko, M. 858(122), 896
 Taddei, F. 105(62b), 129(172), 130(174), 140, 143
 Taddei, M. 778(12), 796(44), 797(42, 45), 800(49), 827, 828
 Tadokoro, K. 1192(16b), 1206
 Tae, J. 892(206), 898
 Tafeenko, V. A. 111(105), 141
 Tagliabue, S. 656(402), 766
 Taguchi, H. 640(324), 641(100), 758, 764
 Tahara, S. 218(192), 219(193, 194), 296, 339(84), 583
 Tainaka, R. 1236(155), 1273
 Tai, T.-a. 677(518), 768
 Tajaddini Sarmadi, J. 612(95), 758
 Tajaddini-Sarmadi, J. 667(413), 676(514), 766, 768
 Tajiri, K. 273(437), 301
 Takada, H. 784(27), 827
 Takada, N. 1334(143), 1346
 Takagi, J. 496(400), 506(401), 592, 1106(378–380), 1127
 Takagi, R. 382(178), 586
 Takaguchi, Y. 255(350), 300, 1268(336), 1278
 Takahashi, A. 650(360), 765
 Takahashi, H. 1089(273), 1103(318), 1124, 1125
 Takahashi, K. 234(234), 297
 Takahashi, T. 270(430), 301, 815(62), 828
 Takahashi, Y. 206(122, 124), 209(134–136, 139, 142–144), 294, 295
 Takai, K. 788(31), 789(32), 790(34, 35), 792(30a), 827, 828
 Takamatsu, Y. 1257(283), 1276
 Takama, K. 687(553, 554), 769
 Takami, S. 112(85), 141
 Takamuku, S. 208(131–133), 294, 295
 Takamura, T. 660(422), 766
 Takanashi, T. 640(324), 641(100), 758, 764
 Takano, Y. 1182(24c), 1207, 1228(96), 1272
 Takasaki, T. 209(144), 295
 Takasu, K. 288(577), 305
 Takata, T. 340(85a, b), 493(367), 583, 591, 1032(218), 1050
 Takeda, E. 1025(166), 1049
 Takeda, M. 259(366), 300
 Takehira, K. 1095(307), 1125
 Takenaka, S. 362(134d), 585
 Takeshita, M. 1201(62d), 1209
 Takesue, T. 980(290a), 997
 Takeuchi, E. 340(85b), 583
 Takeuchi, K. 246(286), 298
 Takeuchi, N. 1087(257), 1124
 Takeuchi, R. 108(106), 141
 Takeya, H. 630(266), 762
 Takeya, K. 136(203, 204), 144
 Takido, M. 1334(146), 1346
 Talbott, R. I. 1140(3), 1165
 Tallant, N. A. 256(256), 260(260), 285(553), 297, 305
 Tallman, K. A. 920(24), 989
 Talsi, E. P. 185(40), 186(43), 187, 1069(113, 114, 119), 1075(145), 1121
 Tamaddon, F. 611(82), 758
 Tamai, T. 205(114, 115), 208(103b), 294
 Tamao, K. 776(2a), 806(63), 808(64, 67–70), 809(72), 815(62), 827, 828
 Tamás, L. 1156(123a), 1168
 Tamchompoo, B. 190(49), 273(472), 293, 302
 Tamhankar, B. 1027(174), 1049
 Tamir, S. 981(300), 998
 Tamura, A. 1062(61), 1119
 Tamura, T. 1334(146), 1346
 Tamura, Y. 340(85a, b), 426(279), 583, 589
 Tanaka, C. 1182(24d), 1207, 1228(99), 1272
 Tanaka, J. 1182(24d), 1207, 1228(99), 1272

- Tanaka, K. 50(50b), 87, 567(531g), 595, 1065(72), 1120
 Tanaka, M. 572(544), 596, 612(108), 758, 1257(272), 1276
 Tanaka, S. 264(390), 300, 743(704), 773
 Tanaka, T. 808(69), 828
 Tanaka, Y. 129(171), 143, 288(577), 305, 1088(268), 1124
 Tanev, P. T. 418(249, 249c), 588
 Tang, B. 679(327), 764
 Tang, D. B. 1281(5), 1342
 Tang, I. N. 641(18, 325, 326), 756, 764
 Tang, M.-W. 1140(81a, b), 1146(17), 1165, 1167
 Tang, R. 211(105), 294, 545(502), 594, 1109(391), 1127
 Tang, Y.-C. 1155(28), 1161(148a, b), 1165, 1169
 Tang, Y. Q. 190(44), 292, 1332(15), 1342
 Tang, Y. 1140(74), 1167
 Taniai, T. 639(238), 761
 Tanimoto, H. 743(704), 773
 Tani, F. 1067(55), 1119
 Tani, K. 432(299), 589, 1086(250), 1124
 Tanko, J. M. 909(94), 913
 Tannahill, J. R. 605(36), 756
 Tannenbaum, S. R. 943(85a), 981(300), 991, 998, 1204(68), 1209
 Tanner, D. D. 901(26a), 912
 Tantanak, D. 1082(147), 1121
 Tanuma, T. 129(171), 143
 Tanyeli, C. 264(401), 301
 Tan, S. N. 654(389), 701(388), 765
 Tao, X. L. 209(140), 295, 1291(48), 1343
 Tao, Z.-F. 616(154, 155), 759
 Tappel, A. L. 669(468), 767
 Tarabarina, A. P. 780(22), 824(117b, 117d, e), 827, 830
 Taramaso, M. 418(231), 587
 Taramasso, M. 418(231), 587, 1082(200), 1123
 Taramelli, D. 1313(80), 1344
 Tarpey, M. M. 740(83), 758
 Tarroni, R. 12(7d), 85
 Tarunin, B. I. 810(79), 829
 Tarver, G. A. 678(329), 764
 Tasevski, M. 49(118), 89
 Tashiro, M. 199(86, 87), 293
 Taslakov, M. 605(35), 756
 Tassinari, R. 529(472a, b), 593
 Tategami, S. 252(299, 300), 298
 Tatsumi, T. 418(249d), 421(254), 588, 1083(211), 1108(387), 1123, 1127
 Tatsuzawa, H. 918(8c), 988
 Tatzber, F. 631(293), 667(459), 763, 767
 Taubert, K. 112(97, 98), 141
 Tauber, A. I. 918(8a), 988
 Tausch, M. W. 1245(209), 1274
 Taylor, A. R. 728(665), 772
 Taylor, R. J. K. 365(138), 585, 1024(158), 1049
 Taylor, R. T. 563(402), 592
 Taylor, R. 105(66), 140
 Taylor, T. E. 273(34), 292, 1283(32), 1343
 Tchertanova, L. 1069(45), 1119
 Tchir, P. 101(53), 140
 Teasley, M. F. 211(149), 295
 Teebor, G. W. 928(37c), 989
 Tehrani, K. 1227(89), 1272
 Teich, N. 1159(135b), 1169
 Teissèdre, G. 684(214), 761
 Tekavec, T. 132(193), 144, 182(20, 21), 187
 Tekwani, B. L. 1313(82), 1314(97), 1344
 Teles, J. H. 440(313b), 589, 791(37), 795(41), 828
 Telleri, R. 953(172), 993
 Tempesti, E. 428(294), 589
 Templado, J. 709(62), 757
 Temprado, M. 155(25), 161(39), 168, 169
 ten Brink, G.-J. 560(500), 594
 Teng, J. I. 946(128), 992
 Téoule, R. 921(31a, b), 922(38), 927(30a, b, 51, 52), 928(37a), 929(36a, 53), 930(29a, b, 43b), 931(34a), 933(54), 934(60a), 938(66, 67), 989, 990
 Terajima, A. 1102(351), 1126
 Terao, J. 680(533), 687(553, 554), 769, 949(109), 977(278d), 991, 997
 Terashima, S. 394(203), 586
 Tero-Kubota, S. 206(121, 122), 294
 Terzis, A. 1058(38), 1119
 Teshima, K. 108(107), 113(109), 141, 711(608), 712(609), 771
 Teso Vilar, E. 520(449), 593
 Testaferri, L. 1011(79–81), 1047
 Testard, I. 976(273), 996
 Testi, R. 1039(244), 1051
 Tew, K. D. 273(459), 302
 Textorius, O. 337(80), 583
 Thakur, V. V. 1099(342), 1126
 Thalhammer, T. 611(82), 758
 Thalji, R. K. 112(73), 140
 Than, R. 637(239, 303), 762, 763
 Thayer, A. L. 1256(29), 1271
 Theander, T. G. 1322(119), 1345
 Thebtaranonth, C. 190(49), 293
 Thebtaranonth, Y. 190(49), 273(472), 293, 302
 Thellend, A. 457(324), 590
 Themelis, D. G. 647(354), 765
 Thenard, L.-J. 138(212), 144
 Theoharides, A. D. 1280(2), 1342
 Theruvathu, J. A. 616(152), 759
 Thewalt, U. 1064(66), 1120
 Thewissen, S. 1062(42), 1119
 Thibault, J.-F. 623(196), 761
 Thielemans, W. 622(191), 760
 Thiele, W. 623(209), 761

- Thiel, W. R. 427(282), 434(283), 466(355), 589, 591, 1058(31), 1069(115), 1076(156, 157), 1083(219), 1085(244, 245), 1104(367), 1119, 1121–1124, 1126
- Thiel, W. 82(160), 91, 253(336), 299, 833(28), 894
- Thiemann, T. 199(86), 293
- Thiem, J. 355(121), 584
- Thierbach, D. 98(39a), 139
- Thomaidis, N. S. 656(401), 766
- Thomale, J. 981(307b), 998
- Thomas, A. A. 50(126), 90
- Thomas, A. F. 845(63), 895
- Thomas, A. H. 1191(8a), 1205
- Thomas, A. 1311(12), 1342
- Thomas, D. W. 977(282a), 997
- Thomas, J. M. 418(252), 526(465), 588, 593, 1082(203), 1085(247), 1086(248, 249), 1123, 1124
- Thomas, J. P. 977(277f), 996
- Thomas, P. J. 1040(258), 1051
- Thomas, S. C. 1281(9), 1342
- Thommen, W. 854(64), 895
- Thompson, D. M. 1097(328), 1126
- Thompson, J. A. 717(620, 626), 771
- Thompson, J. E. 617(156), 759
- Thompson, K. 637(306), 763
- Thompson, P. G. 1140(3), 1165
- Thompson, Q. E. 732(675), 772
- Thompson, R. C. 1030(196), 1050, 1068(84), 1120
- Thompson, W. 645(101), 758
- Thomsen, M. K. 665(445), 767
- Thomson, L. 951(173), 993
- Thomson, S. A. 1228(103), 1272
- Thorneley, R. N. F. 694(146), 759
- Thornton, E. R. 907(81), 913
- Thornton, S. R. 379(164), 380(158, 167), 585
- Thorpe, G. H. G. 1242(192), 1274
- Thorpe, S. R. 614(142), 759
- Thorsteinsson, T. 12(7d), 85
- Thorton, K. 676(301), 763
- Thouvenot, R. 440(313a), 589, 1069(117), 1121
- Thunus, L. 697(183), 760, 1252(174), 1274
- Tian, H. 1148(79a, b, 79d, 89), 1167
- Tidwell, T. T. 122(148), 142
- Tiecco, M. 1011(79–81), 1047
- Timari, G. 284(540, 545, 546), 304, 1324(122), 1345
- Timofeeva, T. V. 103(48), 128(50), 140
- Timoschtschuk, T. A. 426(277b), 588
- Timur, S. 655(394), 765
- Tinart, B. 109(116), 141, 1069(65), 1120
- Tingoli, M. 1011(79–81), 1047
- Tinucci, L. 1010(69), 1047
- Tirache, I. 945(115), 992
- Tishchenko, I. G. 283(283), 298
- Tits, M. 899(4, 5), 912
- Tjornelund, J. 1322(120), 1345
- Toba, T. 1105(370), 1127
- Tobias, H. J. 690(11), 756
- Tobolsky, A. V. 149(8), 167
- Tock, R. W. 622(190), 624(216, 217), 760, 761
- Todaro, L. 198(84), 293
- Todd, C. J. 379(164), 380(158, 167), 585
- Todorovic, N. M. 109(116), 141
- Tod, M. 1257(260), 1276
- Tofigh, S. 933(57), 990
- Tokitoh, N. 804(59), 828
- Tokles, M. 567(531k), 595
- Tokuvara, H. 290(290), 298
- Tokumaru, K. 208(103b), 294
- Tokumaru, S. 659(420), 668(462, 463), 766, 767, 1257(296), 1277
- Tokuyasu, T. 113(102), 141, 225(219, 220), 242(268), 249(292), 266(266), 267(267), 269(269), 289(289), 291(291), 296–298, 712(610), 771, 1282(27), 1342
- Tokyyama, H. 858(120), 896
- Tolman, W. B. 1117(434), 1128
- Tolson, M. R. 1140(56c), 1166
- Tolstikova, O. V. 190(19), 292
- Tolstikov, A. G. 190(19), 292
- Tolstikov, G. A. 190(19), 292, 533(475), 593, 729(669), 772, 1181(11i), 1190(43), 1206, 1208
- Tomadze, A. V. 783(18d), 824(117b), 827, 830
- Tomaru, J. 1025(162, 163), 1049
- Tomas-Vert, F. 29(64), 88
- Tomaselli, G. A. 185(41), 187, 432(302), 589, 1068(91), 1074(134), 1076(133), 1095(316), 1102(354, 355), 1120, 1121, 1125, 1126
- Tomasi, J. 12(7), 41(41), 44(102), 85, 87, 89
- Tomassetti, M. 664(440), 767
- Tomas, J. S. 1332(15), 1342
- Tome, M. E. 1336(156), 1346
- Tomikawa, Y. 605(29), 756
- Tomino, K. 1010(74), 1047
- Tomioka, K. 567(531c, 531h–j), 595, 1088(268), 1124, 1140(82), 1167
- Tomioka, N. 219(195), 296
- Tomita, H. 118(129), 142, 196(76), 293
- Tomita, M. 682(474), 767, 968(242), 995
- Tomizawa, K. 1040(253, 255–257), 1051
- Tomkinson, J. 623(201), 761
- Tonachini, G. 253(338), 299
- Tonellato, U. 900(10), 912
- Toniolo, C. 123(162), 129(172), 143
- Torao, Y. 288(561), 305
- Tordo, P. 973(248, 254), 995
- Torieda, M. 273(437), 301
- Torijas, M. C. 644(336), 764
- Torimura, M. 654(387), 765
- Torkler, A. 357(117), 584

- Tornabene, C. 976(270c), 996
 Torok, D. S. 1302(61), 1343
 Torre-Garcia, G. 858(125), 896
 Torrence, P. F. 273(446), 302
 Torrini, I. 1161(146), 1169
 Tor, I. 640(320), 764
 Toscano, R. M. 185(41), 187, 1074(134),
 1076(133), 1095(316), 1102(354, 355),
 1121, 1125, 1126
 Toscano, V. G. 1189(41a), 1208, 1260(309),
 1277
 Toschi, T. G. 692(93), 758
 Totherow, W. D. 901(31), 912
 Tóth, G. 265(404), 301, 1163(1g), 1164
 Totter, J. R. 1250(222), 1275
 Tourné, C. M. 1081(183), 1122
 Tourné, G. F. 1081(183), 1122
 Tovey, G. 1332(13), 1342
 Towers, T. D. 1022(145), 1049
 Townsend, J. M. 426(277a), 588, 1075(139),
 1121
 Townshend, A. 639(318), 764
 Toyota, M. 288(577), 305
 Toyota, S. 129(171), 143
 Tozer, D. J. 12(7e), 85
 Tozzola, G. 1082(202), 1123
 To, P. 974(262d), 996
 Trabanco, A. A. 252(321), 299
 Traber, B. 1093(291), 1125
 Tracey, A. S. 1069(102), 1120
 Tracey, A. 1058(20), 1118
 Tracey, J. 138(210b), 144
 Trahanovsky, W. S. 198(80), 293
 Trakatellis, A. G. 669(466), 767
 Traldi, P. 1098(99), 1120
 Tran Huu-Dau, M. E. 249(249), 297
 Travaglini, C. 1031(207), 1050
 Traven, Y. F. 816(92), 829
 Travis, B. R. 1023(147, 148), 1024(156),
 1030(197), 1049, 1050
 Trecarten, M. 396(209), 587
 Treiber, A. 1155(106d), 1168, 1202(64a), 1209
 Treibs, W. 358(125), 584
 Tremblay, S. 935(64), 990
 Tremmel, H. G. 604(15), 756
 Treseder, R. S. 156(12), 167
 Triantaphylidès, C. 339(82), 583
 Trimble, E. R. 613(117), 758
 Trinder, P. 630(270), 762
 Troe, J. 98(35a, b), 139
 Trofimov, A. V. 1184(25d, 25f), 1188(34a, b,
 36, 37a), 1194(35b), 1197(50), 1207, 1208,
 1236(79, 159, 160, 162), 1238(168–170),
 1272–1274
 Trofimov, A. 1155(116), 1168
 Trofimov, Alexei V. 1172(10b), 1188(40f),
 1206, 1208
 Troisi, L. 183(30), 187, 798(47), 806(61), 828,
 1021(130), 1048, 1076(158), 1122
 Troist, L. 785(29), 827
 Tromp, T. K. 138(210a), 144
 Tronche, C. 920(24), 989
 Trost, B. M. 503(420), 512(398), 592,
 1001(2), 1032(3), 1046, 1105(375), 1127,
 1250(224), 1252(246), 1275
 Trotman-Dickinson, A. F. 900(17), 912
 Trout, B. L. 71(148), 90
 Trowbridge, I. S. 1335(149), 1346
 Troyanov, S. 112(115), 141
 Trozzolo, A. M. 954(191), 993
 Trucks, G. W. 12(7), 85
 Trujillo, M. 953(172), 993
 Trunov, V. K. 118(141), 142
 Truscott, R. J. W. 918(14), 989
 Truscott, R. 987(332), 999
 Truscott, T. G. 966(233c), 995
 Trysberg, L. 1067(78), 1120
 Tsai, H.-H. 31(31), 35(35), 87
 Tsai, J.-H. M. 34(34), 36(36), 87
 Tsai, J.-H. 31(31), 87
 Tsai, J. H. M. 35(35), 87
 Tsai, L. 945(111), 984(315, 319b), 991, 998,
 999
 Tsai, M. 22(22b), 86
 Tsai, P.-J. 669(465), 767
 Tsai, W. 604(2), 756
 Tsangarakis, C. 883(183), 897
 Tsang, C. W. 624(237), 761
 Tsang, H. W. 1317(87, 100), 1344
 Tseng, M. C. 984(297b), 998
 Tseng, S. S. 1267(71), 1272
 Tsentsiper, A. B. 736(686), 772
 Tsimidou, M. Z. 664(443), 767
 Tso, T. L. 138(209a), 144
 Tso, W. W. 273(28), 292
 Tsuchiya, C. 1156(123b), 1168
 Tsuchiya, K. 1332(108), 1345
 Tsuda, S. 129(171), 143
 Tsuda, T. 1104(356), 1126
 Tsuge, H. 375(149), 585
 Tsuji, J. 524(460), 593
 Tsuji, S. 1044(273), 1052
 Tsuji, T. 715(607), 770
 Tsukagoshi, K. 1257(277), 1276
 Tsukamoto, I. 659(420), 766, 1257(296), 1277
 Tsukamoto, Y. 1257(270, 274), 1276
 Tsumuraya, T. 819(102), 825(124, 125), 829,
 830
 Tsumura, S. 516(437a), 593
 Tsunesada, T. 1182(24c), 1207, 1228(96), 1272
 Tsuno, Y. 326(58), 583
 Tsyba, I. 1059(43), 1119
 Tsyganash, N. E. 823(114), 830
 Tuccio, B. 973(254), 995

- Tuchkin, A. 902(61), 906(54), 911(71), 912, 913
- Tulub, A. V. 84(168), 91
- Tumolo, A. L. 734(680), 772
- Tung, C.-H. 870(152–155), 897
- Tung, J. C. 1025(161), 1049
- Tur'yan, Y. I. 663(439), 766
- Tur'yan, Ya. I. 663(438), 766
- Turkut, E. 264(401), 301
- Turner, G. A. 667(453), 767, 980(290b), 997
- Turner, J. J. 101(53), 140
- Turner, R. B. 161(40), 169
- Turner, W. B. 679(313), 764
- Turner, W. V. 124(147), 142, 605(25), 638(314), 678(522), 708(546), 756, 764, 769
- Turovskii, N. A. 103(47, 48), 123(104), 140, 141
- Turrens, J. F. 949(139), 992
- Turrión, C. 160(36), 169
- Turro, N. J. 112(84), 141, 167(64), 169, 269(427, 428), 301, 819(106), 829, 870(148b), 896, 1178(19a–e), 1189(42), 1191(46a–c), 1206, 1208, 1219(47), 1222(52), 1223(42), 1224(56, 57), 1227(83, 86), 1232(121), 1267(48), 1271–1273
- Tuter, M. 380(158, 167), 585
- Tuttle, T. 131(192a), 144, 182(23, 24), 187
- Tu, Y.-Y. 273(29), 292
- Tu, Y. 520(455a), 593, 1021(141), 1049, 1140(74, 75), 1146(18, 71), 1150(93), 1165, 1167
- Twigg, J. 612(102), 758
- Twist, J. P. 624(222), 761
- Tyblewski, M. 101(46), 140
- Tyeklar, Z. 128(169), 143
- Tyrrell, R. M. 945(114), 950(154), 992
- Tyurina, J. Y. 660(110, 111), 758
- Tyurin, V. A. 660(110), 758
- Tzanavaras, P. D. 647(354), 765
- Tzedakis, T. 201(91, 92), 294
- Tzouwara-Karayanni, S. M. 624(220), 630(271), 761, 762
- Uang, B. J. 542(218), 587, 892(210), 898, 1093(293), 1125
- Ucciani, E. 621(178), 760
- Uchida, K. 612(108), 758, 984(317a, 318), 998, 999
- Uchida, M. 643(211), 761
- Uchida, T. 1113(410), 1127
- Ueda, K. 1334(143), 1346
- Ueda, Y. 1236(155), 1273
- Uehara, A. 1065(72), 1120
- Uehara, K. 950(148), 992
- Uemura, D. 1334(143), 1346
- Uemura, S. 481(381), 486(386), 591, 1097(331, 332), 1126
- Ugarova, N. N. 1192(47b), 1194(51), 1208
- Uggerud, E. 84(165a, b), 91
- Ukita, T. 968(242), 995
- Ulber, R. 655(300), 763
- Ulic, S. E. 132(194), 144
- Ullrich, V. 94(6), 138, 1242(191), 1274
- Ulrich, J. 928(37a), 938(67), 989, 990
- Uma, R. 267(416, 417), 301
- Umbreit, M. A. 503(428), 592
- Umezawa, T. 1157(130c), 1168
- Umrigar, P. 130(184), 143
- Undheim, K. 1152(101), 1167
- Un, S. 1070(47), 1119
- Uozumi, Y. 809(71), 828
- Uppili, S. 870(147), 896
- Upton, P. B. 981(298c), 998
- Urabe, T. 612(108), 758
- Ura, T. 525(308), 589, 1080(173), 1094(300), 1106(172), 1122, 1125
- Urbanczyk-Lipkowska, Z. 493(101), 584, 1099(343), 1126
- Urban, M. W. 213(161), 295
- Urry, W. H. 822(104), 829, 1172(5), 1205
- Ursini, F. 614(128), 681(499, 539), 759, 768, 769
- Urwyler, H. 273(273), 298, 608(59), 757, 1332(14, 15), 1342
- Usachev, B. I. 1013(89), 1048
- Ushigoe, Y. 113(109), 141, 287(559), 288(560, 561), 305, 711(608), 771
- Ushio, H. 680(534), 769
- Usui, Y. 572(544), 596
- Utschick, G. 208(130), 294
- Uzieblo, A. 980(290e), 997
- Uzu, S. 1257(280), 1276
- Vaartstra, B. A. 1065(53), 1119
- Vaca, C. E. 981(302), 998
- Vaccaro, P. H. 1160(11b), 1165
- Vacque, V. 702(227), 714(567), 761, 770
- Valacchi, M. 447(333), 458(332), 590
- Valencia, S. 418(247), 561(507), 588, 594, 1111(405), 1127
- Valente, A. 471(296), 589
- Valentine, J. S. 315(32b), 582, 832(8), 894, 1032(216, 217), 1050, 1087(258, 259), 1124
- Valentini, M. 1084(237), 1124
- Valenzeno, D. P. 947(127), 992
- Valks, P. J. M. 605(31), 756
- Vallberg, H. 1145(68), 1167
- Valle, G. 260(375, 376), 300, 432(302), 589, 1068(97), 1105(374), 1120, 1127
- Valli, V. L. K. 512(411), 592
- Vallon, J. J. 646(346), 764
- Valsta, L. M. 981(302), 998
- van Asselt, A. 125(125), 142
- Van Baar, B. L. M. 670(124), 759
- van Berkel, W. J. H. 80(157), 91
- van Brazt, J. 899(6), 912
- van Breemen, R. B. 976(270b), 996
- Van Breusegem, F. 610(71), 757

- van de Voort, F. R. 662(431), 663(233–235, 435), 761, 766
- van den Berg, R. H. 1252(234), 1275
- van der A, R. J. 605(31, 32), 756
- van der Bergh, H. 605(35), 756
- Van Der Kelen, K. 610(71), 757
- van der Woerd, M. 34(34), 87
- van der Wolf, L. 445(325), 590
- van der Zee, J. 971(251), 995
- Van Dorp, D. A. 190(5), 292
- Van Duuren, B. L. 982(291a), 997
- van Es, D. S. 199(85), 293
- van Geffen, J. H. G. M. 605(31), 756
- van Goethem, I. D. A. 273(453), 302, 1313(34), 1343
- van Gunsteren, W. F. 82(160), 91
- Van Helden, R. 899(7), 912
- van Herwijnen, H. W. G. 870(161), 897
- van Holde, K. E. 1197(52), 1208
- van Hooff, J. H. C. 514(409b), 592
- van Kuijk, F. J. G. M. 977(282a), 997
- van Lier, J. E. 678(517), 695(140), 759, 768, 922(35a, b), 931(34c), 938(48a, b), 967(236), 989, 990, 995
- van Lier, J. 930(43c), 990
- Van Montagu, M. 610(71), 757
- van Oss, R. F. 605(31, 32), 756
- Van Santen, R. A. 1082(204), 1123
- van Steveninck, J. 969(245a, b), 995
- van Vliet, M. C. A. 368(142), 462(361), 468(358), 585, 591, 1083(228), 1123
- van Vliet, M. R. P. 445(325), 590
- Van-Chin-Syan, Yu. Ya. 148(6), 154(11), 156(7, 26), 167, 168
- Vanajatha, G. 1028(185), 1049
- Vandenabeele, S. 610(71), 757
- Vandenberg, M. 1062(63), 1120
- VanDerveer, D. 1082(198), 1123
- Vandoorn, J. A. 426(240), 587
- Vane, J. 214(166), 295
- Vanfleteren, J. R. 1251(230), 1275
- Vankar, V. D. 1022(146), 1049
- Vankar, Y. D. 803(55), 828
- VanNieuwenhze, M. S. 567(527), 595
- VanUden, W. 273(465), 302
- Vany, F. 779(17), 827
- Vanzoonen, P. 1257(265, 267, 276, 278, 299), 1276, 1277
- Varagnolo, A. 549(514), 594, 1109(394), 1127
- Varescon, F. 421(243), 426(274), 587, 588
- Vargas, F. 1205(60a), 1209
- Varghese, R. 1011(84), 1047
- Varma, R. S. 536(485), 594
- Varma, S. D. 655(396, 397), 765
- Varotsis, C. 1303(66), 1343
- Vartuli, J. C. 418(248), 588
- Vary, M. W. 130(183), 143
- Vasenkov, S. 871(162), 897
- Vasil'ev, R. F. 1181(11i), 1184(25b–f), 1188(37a), 1197(50), 1206–1208, 1228(95, 97), 1236(159, 160), 1238(168), 1272–1274
- Vasil'ev, V. P. 148(6), 167
- Vasilev, R. F. 1236(79), 1272
- Vasil'ev, R. F. 1184(25g), 1207
- Vaska, L. 95(19), 139, 1056(16), 1118
- Vásquez-Vivar, J. 952(176), 993
- Vasquez, P. C. 40(94b), 89, 221(198, 199), 296, 352(28), 582, 1140(46), 1160(144), 1166, 1169, 1227(90), 1272
- Vassell, K. A. 1096(320), 1125
- Vassilikogiannakis, G. 255(356), 300, 836(50), 892(209), 895, 898
- Vassilopoulos, V. N. 669(466), 767
- Vattanaviboon, P. 1311(76), 1344
- Vaughan, W. E. 156(12), 167, 352(110), 584
- Vaughn, S. F. 977(283), 997
- Vayssilov, G. N. 1082(204), 1123
- Vedde, J. 84(165b), 91
- Vedejs, E. 520(451), 593
- Veeger, C. 80(157), 91
- Vega, J. C. 379(153), 585
- Vehre, B. 1030(198), 1050
- Velarde, J. A. 280(514), 303, 1325(20), 1342
- Velarde, J. 280(513), 303
- Velasco, J. 673(498), 768
- Velazquez, S. M. 230(225, 226), 297
- Velic, I. 981(301, 302), 984(297e), 998
- Veloza, L. A. 47(103), 89, 1144(65), 1163(1k), 1164, 1166
- Velthorst, N. H. 1257(265, 267, 276, 278, 299), 1276, 1277
- Velusamy, S. 510(415), 518(448), 592, 593
- Velu, S. E. 1027(177), 1049
- Venegas, M. G. 193(67), 293
- Venezky, D. L. 1265(332), 1277
- Venhorst, J. 670(124), 759
- Venier, P. 917(4), 988
- Venkataram, U. V. 79(153c), 91
- Venkatesan, S. 276(498), 303, 1314(96), 1344
- Venkateswaran, R. V. 323(43), 582
- Vennerstrom, J. L. 190(44), 292, 712(58), 757, 1317(107), 1326(106), 1332(15, 105), 1342, 1344, 1345
- Venn, R. F. 960(204b), 994
- Venturello, C. 437(307), 444(305, 306), 512(399), 589, 592, 1079(169), 1080(170), 1094(305), 1106(377), 1122, 1125, 1127
- Venugopalan, B. 273(440), 301
- Vercesi, A. E. 951(173), 993
- Verevkin, S. P. 155(25), 165(62), 166(57), 168, 169
- Verevkin, S. 161(44), 169
- Verhoeven, T. R. 48(113b), 89, 94(5), 138, 414(227), 542(202), 586, 587, 789(33), 828, 1092(243), 1124
- Verissimo, E. 223(207), 296, 1323(121), 1345

- Verkade, P. E. 161(43), 169
 Verma, A. 669(103), 758
 Vermeulen, N. P. E. 670(124), 759
 Verney, V. 672(189), 760
 Vervoort, J. 80(157), 82(159a-c), 91
 Verwij, M. 969(245a), 995
 Vetter, A. H. 1100(347), 1126
 Viado, A. L. 858(126), 896
 Vialas, C. 941(79), 991
 Vial, H. 201(92), 284(548), 294, 304
 Vicente, H. 1293(36), 1343
 Vicente, M. G. H. 1293(37, 51), 1343
 Vicent, M. A. 1184(32), 1207
 Vichi, S. 690(564), 770
 Vicinanza, A. 408(99), 584, 1094(295), 1125
 Videla, L. A. 949(138), 992
 Vieira, T. deO. 1021(137), 1049
 Viertler, H. 1021(137), 1049
 Viet, M. T. P. 318(12), 582
 Viezee, W. 94(4b), 138
 Vignola, R. 529(472a, b), 593
 Vigny, P. 926(7), 988
 Vile, G. F. 945(114), 992
 Villanueva, J. 984(314), 998
 Villasenor, S. R. 833(24), 894
 Villiger, V. 1002(14), 1020(121), 1046, 1048, 1140(2), 1165
 Vilter, H. 186(42), 187
 Viña, J. 975(268c), 996
 Vincent, M. A. 1082(147), 1121, 1234(134), 1273
 Vincent, S. 1006(42), 1047
 Vincer, K. 877(177), 897
 Vinhado, F. S. 1140(52b), 1166
 Vinke, I. 1108(389), 1127
 Vinogradova, O. 984(315), 998
 Vinson, J. R. 323(42a), 582
 Vinson, M. A. 976(272b), 996
 Vinten-Johansen, J. 612(87), 758
 Violi, F. 611(81), 758
 Viré, J.-C. 653(384), 765
 Virgil, S. 567(531d), 595
 Vishwakarma, R. A. 1316(99), 1344
 Vismara, E. 1010(69), 1047
 Vis, J.-M. 560(500), 594
 Viterbo, D. 106(78), 125(150), 140, 142
 Viti, S. M. 1105(368, 369), 1126, 1127
 Vivas, L. 273(450), 302, 1317(68), 1343
 Vizcarra, L. S. 1267(71), 1272
 Vladimirov, Y. A. 673(494), 768
 Vladimir, A. 660(111), 758
 Vlad, P. F. 122(101), 141
 Vlessidis, A. G. 742(334), 764
 Voerste, A. 1302(62), 1317(87, 100), 1343, 1344
 Vogel, E. 269(424), 301
 Vogl, N. 408(221), 587, 1094(296), 1125
 Voigt, B. 1162(151a), 1169
 Voituriez, L. 922(39a, b), 931(34b), 989, 990
 Volk, M. 381(177), 586
 Volm, M. 273(459, 460), 302, 1336(154), 1346
 Voloshin, A. I. 1190(43, 45a-c), 1208
 Voltan, R. 917(4), 988
 von Gunten, U. 606(43, 44), 757
 von Schening, H. G. 869(93), 895
 von Schnering, H. G. 135(201), 144, 193(68), 198(82, 83), 263(384), 272(434, 436), 291(593), 293, 300, 301, 305, 889(201), 898
 von Sonntag, C. 616(152), 673(497), 674(45, 503b), 740(244), 757, 759, 762, 768, 923(21), 924(45), 930(56), 938(6), 963(223), 964(227a, 228), 966(209), 968(239b), 988-990, 994, 995
 von Woedtke, T. 623(206), 761
 Vonwallis, H. 234(239), 240(240), 297, 357(117), 584
 Vonwiller, S. C. 212(148, 151), 273(39), 288(565, 566, 570, 572), 290(581, 591), 292, 295, 305, 362(133), 584, 1301(59, 60), 1343
 Voronina, S. G. 624(218), 701(587), 761, 770
 Votoupal, K. L. 621(171), 760
 Vougioukalakis, G. C. 860(127), 880(56), 895, 896
 Vourloumis, D. 1145(68), 1167
 Voyiatzis, G. 1058(38), 1119
 Voyta, J. C. 1198(33c-f), 1199(48), 1200(53a, b), 1207, 1208, 1236(35, 163), 1256(249), 1271, 1273, 1275
 Vrajimasu, V. 1069(50), 1119
 Vrkoč, J. 890(204), 898
 Vroman, J. A. 273(40), 276(499-501), 288(574-576), 292, 303, 305, 1314(89), 1344
 Vučelić, D. 623(208), 652(379), 761, 765
 Vu, C. B. 1025(167), 1049
 Vyas, P. V. 580(550), 596
 Vyle, J. S. 1031(206), 1050
 Vytřas, K. 651(366, 367), 765
 Wada, A. 1064(69), 1120
 Wada, H. 1006(38), 1046
 Wada, M. 698(193), 760, 1257(268, 287), 1276
 Wada, T. 904(75), 913
 Waddell, W. H. 1191(46c), 1208
 Wadgaonkar, P. P. 1027(174), 1029(193), 1049, 1050
 Wadt, W. R. 28(61a), 88
 Wagman, D. D. 154(21), 168
 Wagner, J. R. 678(517), 695(140), 759, 768, 922(35a, b), 926(49), 930(43c), 931(34c), 935(64, 65), 938(48a, b, 63), 939(70a, b), 967(236), 989, 990, 995
 Wagner, J. 329(65), 583
 Wagner, K. 1268(140), 1273
 Wagner, P. J. 909(93), 913
 Wagner, P. 122(157), 143

- Wagner, R. D. 221(202, 203), 296
 Wagner, R. J. 929(36b), 989
 Wagner, R. 253(344), 299
 Wahlen, J. 369(145), 585
 Wahl, G. 440(313b), 589, 1081(149), 1122
 Wailes, J. S. 1021(133), 1048
 Wailes, J. S. 1140(85b), 1167
 Wainhaus, S. B. 976(270b), 996
 Waite, T. D. 741(701), 773, 1241(182), 1274
 Wai, J. S. M. 567(528), 595
 Wakabayashi, T. 190(9), 292
 Walker, N. P. C. 125(149), 142
 Walker, V. E. 981(298a), 998
 Walkinshaw, M. D. 712(611), 771
 Wallaart, T. E. 133(195), 144
 Wallace, P. A. 259(364), 300
 Wallace, T. J. 221(201), 296
 Wallasch, M. 723(625), 771
 Wallau, M. 1085(207), 1123
 Waller, R. L. 1045(250, 259), 1051
 Wallington, T. J. 692(19, 568), 756, 770
 Walling, C. 900(13, 15), 901(22, 26a, b), 907(62), 912, 913, 1008(58), 1047
 Walsh, C. 80(151b), 91
 Walsh, E. B. 727(639), 771
 Walsh, R. 815(91b), 829
 Walters, S. M. 1326(106), 1345
 Walter, P. B. 975(269a), 996
 Walton, D. J. 103(51), 140
 Walton, J. H. 362(134b), 584
 Walz, T. 193(68), 293
 Wang, B. 98(36), 139, 653(385), 654(386), 765, 832(11), 894
 Wang, C. H. 161(34), 162(35), 169
 Wang, C. M. 651(368), 765
 Wang, D. R. 1280(3), 1342
 Wang, D. S. 209(140), 280(518, 521, 527), 283(471), 295, 302, 304, 1282(17), 1284(39), 1289(46), 1291(48), 1298(18), 1337(162), 1342, 1343, 1346
 Wang, G. 1062(62), 1119
 Wang, H. J. 290(581), 305
 Wang, H. W. 870(155), 897
 Wang, H. 870(153), 897, 987(15), 989
 Wang, J. B. 284(536), 304
 Wang, J. L. 418(249, 249c), 588
 Wang, J. 689(390), 765
 Wang, K. M. 645(338), 764
 Wang, K. 679(524), 769
 Wang, L. 646(344), 764
 Wang, P. 621(180), 760, 1148(79c), 1167
 Wang, Q. 654(386), 765
 Wang, S. L. 892(210), 898
 Wang, S. Y. 927(50), 938(69a), 990
 Wang, T. J. 624(237), 761
 Wang, W. Q. 1336(159), 1346
 Wang, X.-C. 1140(81a, b), 1155(28), 1161(148a, b), 1165, 1167, 1169
 Wang, X. 854(89), 895
 Wang, Y. C. 1317(103), 1344
 Wang, Y. 284(535), 304, 679(327), 764
 Wang, Z.-X. 1140(58, 74, 75, 77a, b), 1146(18, 71), 1150(93, 94), 1165–1167
 Wang, Z. X. 1021(141), 1049
 Wang, Z. Z. 29(29), 87
 Wang, Z. 214(176), 295, 649(358), 654(386), 765
 Wannagat, U. 779(15a), 827
 Wan, H.-L. 1058(36), 1119
 Wan, J. 1015(101), 1048
 Wardman, P. 917(5d), 988
 Ward, F. E. 1021(128), 1048
 Ward, J. F. 923(18c), 989
 Ward, J. W. 731(637, 674), 771, 772
 Ward, M. B. 429(292), 589
 Ward, S. A. 223(207), 273(453, 454, 467), 274(274), 275(487–489), 296, 298, 302, 303, 1283(31), 1304(63, 71), 1313(34), 1317(101), 1320(115), 1323(121), 1324(124), 1330(131, 132), 1332(92, 93), 1337(165), 1343–1346
 Ward, S. R. 974(262c), 996
 Ware, J. 902(63), 913
 Warhurst, D. C. 280(514), 303, 1281(9), 1325(20), 1342
 Warhurst, E. 907(77b), 913
 Warnaar, J. B. 445(325), 590
 Warner, J. A. 288(566, 570), 305
 Warner, K. 656(399), 766
 Wartenberg, G. 1336(158), 1346
 Wartenberg, M. 1336(158), 1346
 Washington, I. 40(96), 56(129), 89, 90, 1178(19d), 1206
 Wasserman, D. J. 151(18), 156(20), 167, 168
 Wasserman, H. H. 832(7), 871(1), 893, 894, 1025(167), 1049, 1154(114), 1168
 Wasserman, J. 95(17a), 139
 Watanabe, A. 1113(410), 1127
 Watanabe, H. 967(213, 237), 994, 995
 Watanabe, K. 854(101), 895
 Watanabe, M. 1334(143), 1346
 Watanabe, N. 259(366), 300, 1192(16b), 1199(55, 57), 1206, 1208, 1236(148–150, 152, 153, 156–158), 1273
 Watanabe, S. 390(197), 392(195, 196), 586, 1104(356), 1126, 1157(127c), 1168
 Watanabe, T. 681(98), 758
 Watanabe, Y. 429(289), 433(298), 589, 697(579), 707(598), 770
 Wataya, Y. 113(102), 141, 209(138), 225(220), 249(292), 267(267), 288(577), 291(291), 295, 296, 298, 305, 1282(27), 1291(49), 1332(108), 1342, 1343, 1345
 Watson, B. D. 612(109), 758
 Watson, J. J. 976(271), 996
 Watson, S. P. 1266(334), 1278

- Watson, W. H. 264(395), 300, 317(29), 582
 Watson, W. P. 982(291d), 984(297f), 997, 998
 Wattimena, F. 417(242), 587
 Watts, J. D. 12(7c), 85
 Wayner, D. D. M. 206(121, 122), 294,
 614(141), 759, 1086(248), 1124
 Wayner, D. M. 96(20), 139
 Wayne, R. P. 94(4a), 138(210b), 138, 144
 Wearing, J. T. 534(480), 594, 1103(359, 360),
 1106(381), 1126, 1127
 Webb, K. S. 1151(99b), 1167
 Webb, K. S. 812(86a), 829, 1026(170), 1049
 Webb, R. J. 273(453), 302, 1313(34), 1343
 Weber, B. A. 320(35a), 582
 Weber, G. 1224(66), 1226(65), 1271
 Weber, H. O. 273(459), 302
 Wedge, P. J. 1236(166), 1274
 Weedon, B. C. L. 323(42a, b), 582
 Weeks, I. 1256(233), 1275
 Weenen, H. 320(35b), 582
 Wehling, R. L. 663(437), 671(231), 674(409),
 761, 766
 Wehr, N. B. 986(328c), 999
 Weichold, O. 477(373a, b), 591, 1083(223,
 224), 1096(321), 1123, 1125
 Weidenbruch, M. 825(122), 830
 Weiler, L. 512(429), 592
 Weinfeld, M. 941(74b), 990
 Weingartner, J. 204(100), 294
 Weinhold, F. 4(11b), 86, 95(13b), 139
 Weinkötz, S. 47(103), 89, 1163(1k), 1164
 Weinstein-Lloyd, J. B. 641(325, 326), 764
 Weinstein-Lloyd, J. 604(14), 641(8), 756
 Weissermel, K. 354(114), 525(461), 584, 593
 Weiss, D. 1236(75), 1268(140), 1272, 1273
 Weiss, J. 919(16, 19), 920(22a, b), 921(26,
 28a), 923(18a–d), 989
 Weiss, R. 131(131), 142, 523(459), 593,
 1064(67), 1115(161), 1116(56), 1117(432),
 1119, 1120, 1122, 1128
 Weistenstein, D. K. 138(210b), 144
 Weitz, E. 362(136b), 585, 1087(253), 1124
 Wei, D. 616(154), 759
 Wei, H. W. 1257(270), 1276
 Welcher, F. J. 627(245), 762
 Welch, A. M. 1140(55c), 1166
 Welch, F. 352(104), 584
 Welinder, E. 337(80), 583
 Weller, P. E. 980(290c), 997
 Welle, F. M. 166(57), 169
 Wells, J. R. 190(23), 292
 Wells, R. J. 1333(137), 1345
 Wen, J. 652(77), 757
 Werner, H.-J. 12(7d), 85
 Werner, R. 1067(77), 1120
 Wesche, D. L. 1317(107), 1326(106), 1345
 Weskamp, T. 1095(309), 1125
 Wesley, A. S. 1225(64), 1271
 Wessels, J. 962(211), 994
 Wessels, P. L. 1140(56a), 1166
 Wessel, J. 1031(204), 1050
 Westerheide, L. 637(304), 763, 1117(429),
 1128
 Westermeyer, T. A. 329(63b), 583
 Wester, R. T. 316(24), 582
 West, J. D. 917(3b), 988
 West, M. 917(2c), 988
 West, R. 815(90), 816(92), 820(107),
 825(108a, b), 829
 Wetmore, S. D. 1203(67a), 1209
 Wettermark, G. 1242(185), 1274
 Wexler, S. 673(490, 491), 768, 832(6), 894,
 1001(4), 1046
 Wheeler, C. M. 920(22b), 923(18a, b), 989
 Wheeler, D. R. 685(543), 769
 Wheeler, R. A. 1092(283), 1125
 Wheeler, R. R. 646(348), 764
 Whitacre, S. D. 665(446), 767
 Whitehead, T. P. 1242(192), 1274
 White, A. H. 112(79), 140
 White, A. J. P. 1058(30), 1119
 White, A. M. 354(113), 584
 White, D. A. 569(536), 595
 White, E. H. 1172(3), 1191(8a), 1205,
 1239(179), 1240(175, 176), 1251(237, 240),
 1252(247), 1274, 1275
 White, J. D. 291(594), 305
 White, S. 877(177), 897
 Whitman, R. H. 1256(254), 1266(305), 1275,
 1277
 Whittall, J. 383(182), 586
 Wiberg, K. B. 44(100), 89, 151(18), 156(20),
 157(28), 167, 168, 1010(76), 1047
 Wickman, H. B. 221(197), 296
 Wick, D. D. 1064(70), 1120
 Wieckol, A. 122(157), 143
 Wiedemann, E. 1212(2), 1270
 Wieland, P. 190(3), 292
 Wiemer, D. F. 938(69b), 990
 Wiener, H. 510(412), 592
 Wieprecht, W. 638(314), 764
 Wiering, J. S. 374(147), 585
 Wierzchowski, P. T. 708(561), 770
 Wiesenthal, G. 611(82), 758
 Wiesenthal, A. 166(63), 169
 Wiesler, D. 984(319a), 999
 Wiesner, J. 190(43), 292
 Wight, C. A. 744(705), 773
 Wight, P. A. 1198(54), 1208
 Wijsman, G. W. 199(85), 293
 Wikstrom, H. V. 273(465), 302
 Wilairat, P. 1311(76), 1344
 Wilbur, K. M. 666(450), 767
 Wild, D. 1205(60a, b), 1209
 Wild, O. 743(704), 773
 Wilen, S. H. 131(10), 139

- Wiles, D. H. 613(118), 758
Wiley, M. D. 130(186), 143
Wilkinson, F. 262(345, 377), 299, 300, 966(233a), 995
Willadsen, T. 723(648), 771
Willett, W. C. 917(1c), 988
Willey, J. D. 642(7), 756
Wille, U. 1012(86), 1047
Williamson, N. M. 380(162, 171), 585, 586
Williamson, R. C. 901(18), 912, 1037(239), 1051
Williams, B. L. 1160(137), 1169
Williams, D. C. 648(355a), 765, 1009(62), 1047, 1257(263), 1276
Williams, D. J. 1058(30), 1119
Williams, D. P. 273(467), 302, 1337(165), 1346
Williams, D. R. 426(277a), 588, 1075(139), 1121
Williams, G. I. 622(191), 760
Williams, H. R. 352(104), 584, 673(488), 674(486), 697(487), 768
Williams, I. D. 1317(87, 100), 1344
Williams, J. A. 986(328a), 999
Williams, P. A. 847(43), 894
Williams, P. H. 532(474), 593, 1087(255), 1124
Williams, R. B. 161(41), 169
Williams, S. D. 974(263), 996
Willis, C. L. 56(48), 87
Willi, A. 658(417), 766
Willner, H. 104(58), 132(194), 138(56b), 140, 144, 703(592), 705(24), 740(23), 743(21), 744(20, 22), 756, 770
Willson, A. L. 1006(43), 1047
Willson, R. J. 672(483), 768
Willstätter, R. 1004(32), 1046
Will, B. 888(192), 897
Will, G. 112(72), 134(199), 140, 144
Wilmot, I. D. 208(108), 211(146), 294, 295
Wilsey, S. 1182(24b), 1206, 1228(98), 1272
Wilson, A. A. 1252(247), 1275
Wilson, D. W. 978(287a), 997
Wilson, R. A. L. 65(136a), 90
Wilson, R. J. 672(484), 768
Wilson, R. M. 192(57), 193(58, 63, 65, 66), 196(64, 71, 72), 293
Wilson, R. 614(126), 759
Wilson, S. L. 875(39), 894
Wilson, T. 1181(11h), 1184(25a), 1206, 1207, 1227(40, 88), 1228(94), 1232(128), 1235(24, 25, 130), 1270–1273
Wilson, V. E. 1155(106a), 1168
Wiltng, J. B. M. 1062(42), 1119
Wimalasena, K. 221(197), 296
Wimmer, E. 101(52b), 140
Winchester, R. V. 960(207b), 994
Windaus, A. 253(2), 292
Winde, G. 981(301), 998
Winde, R. 47(103), 89, 1163(1k), 1164
Windig, W. 624(222–226), 761
Windus, T. L. 12(7b), 85
Winkler, R. E. 161(40), 169
Winship, D. H. 987(331b), 999
Winterbourn, C. C. 966(229, 231), 972(222a, b), 987(331c), 994, 995, 999
Winterfeldt, E. 122(146), 142
Winter, C. K. 980(289a), 997
Winter, H. 977(280a), 997
Winter, J. E. 60(16b), 65(97), 66(138), 79(17a), 86, 89, 90, 94(11b), 139
Winter, M. L. 987(329b), 999
Winter, M. W. J. 1140(42b), 1166
Winter, M. 792(30b), 828
Winter, W. J. 48(117c), 89
Winter, W. 432(300a), 589
Wirth, T. 65(137a), 90, 260(371), 271(332), 299, 300, 410(226), 587, 866(141), 869(143, 144), 896, 1089(277), 1124, 1145(66), 1166
Wirz, J. 193(61), 196(60, 64, 72), 198(79), 293
Wishnok, J. S. 943(85a), 991, 1204(68), 1209
Withopf, B. 338(77), 583
Witkop, B. 319(21), 582, 967(213, 237), 994, 995
Witnauer, L. P. 105(63), 140, 160(37), 169
Witte, G. 357(120), 584
Wittlin, S. 1332(15), 1342
Wittmann, G. 678(252), 762
Witt, P. 1245(212), 1275
Witzel, A. 198(82), 293
Witzum, J. L. 612(104), 758
Wocadlo, S. 267(418), 301
Woepel, K. A. 810(76), 829
Woerdenbag, H. J. 273(456, 465, 466), 302, 1281(4), 1336(161), 1342, 1346
Wogan, G. N. 981(300), 998
Wohl, C. J. 909(94), 913
Wohrle, D. 870(151), 896
Wöhrle, D. 1245(209), 1274
Wojdelski, M. 185(39), 187
Wolber, G. J. 58(128a, b), 90, 423(261a), 588
Wolfe, S. 310(3b), 581
Wolff, B. T. 1178(19e), 1206
Wolff, I. A. 737(691), 772
Wolff, J.-P. 672(400), 766
Wolff, S. P. 612(95), 658(412, 414), 667(413), 676(256, 257, 514), 758, 762, 766, 768, 986(230), 995
Wolfram, G. 614(127), 759
Wolf, A. 219(196), 296
Wolf, J. F. 211(105), 294
Wolf, R. 903(52), 912
Wolf, S. 1336(158), 1346
Woller, K. R. 247(287), 288(288), 298, 869(83), 888(194), 895, 897
Wolpers, J. 323(40), 582

- Wongpanich, V. 1317(107), 1345
 Wong, C. H. 476(71), 583
 Wong, G. T. F. 629(262), 679(330), 762, 764
 Wong, H.-F. 690(492), 768
 Wong, J. 418(249), 588
 Wong, M.-K. 1140(80, 81a, b), 1146(17),
 1154(111), 1161(148a, b), 1165, 1167–1169
 Wong, M. W. 12(7), 85
 Wong, P. K. 976(271), 996
 Won, H. S. 275(491), 303
 Woodall, A. A. 975(269a), 996
 Woodard, S. S. 396(211), 587
 Woodburn, H. M. 1013(88), 1047
 Woodhead, J. S. 1256(233, 252), 1275
 Woods, C. M. 1145(67b), 1166
 Woods, K. W. 52(127), 90
 Wood, J. K. 712(58), 757, 1326(106),
 1332(105), 1344, 1345
 Woolfrey, J. R. 1282(25, 26), 1342
 Woolf, E. J. 1257(266, 300), 1276, 1277
 Woollard, A. C. S. 658(412), 676(256, 257),
 762, 766
 Woolston, R. E. 1335(149), 1346
 Wool, R. P. 622(191), 760
 Woo, S. H. 273(470), 280(522), 302, 304,
 1317(86), 1332(109), 1337(163),
 1344–1346
 Woo, Y.-A. 650(230), 761
 Worgall, S. 610(69), 757
 Worsfold, P. J. 606(39), 645(41, 339),
 647(353), 757, 764, 765
 Wozniak, L. A. 1026(168), 1049
 Wozniak, L. 803(56), 804(58), 828
 Wright, A. 968(240), 973(241), 986(321a),
 995, 999
 Wright, J. J. K. 137(206), 144
 Wright, J. S. 133(191), 143
 Wright, J. 918(8a), 988
 Wróblewska, A. 1253(241), 1275
 Wulff, H. P. 417(242), 426(270), 587, 588
 Wu, B. 276(501), 303
 Wu, C.-Y. 575(523), 595
 Wu, G. D. 1336(159), 1346
 Wu, G. S. 273(458), 302
 Wu, H.-J. 717(622), 771
 Wu, H. L. 542(218), 587, 1093(293), 1125
 Wu, J. M. 273(458), 302
 Wu, K. C. 954(191), 993
 Wu, L.-Z. 870(152, 155), 897
 Wu, L. E. 380(160, 162, 171), 585, 586
 Wu, M. H. 48(114c), 89, 386(190c), 586
 Wu, P. 421(254), 588, 1083(211), 1123
 Wu, S. H. 275(491), 303
 Wu, W. L. 190(27), 292
 Wu, W. M. 1299(40), 1343
 Wu, X.-Y. 1022(143), 1049, 1148(90), 1167
 Wu, Y.-D. 1075(146), 1121
 Wu, Y.-L. 273(29), 283(531, 532), 292, 304,
 608(55), 757, 1299(50), 1343
 Wu, Y. D. 253(334), 299, 861(137), 896
 Wu, Y. K. 273(448), 302, 1299(40, 57),
 1302(58), 1303(67), 1343
 Wu, Y. L. 273(31, 32, 442), 292, 302,
 1299(40), 1343
 Wu, Y. 1299(50), 1343
 Wu, Z.-H. 273(29), 292
 Wu, Z.-Y. 1299(50), 1343
 Wu, Z. 1021(134, 140), 1048, 1049, 1140(83,
 86), 1163(11), 1164, 1167
 Wyandt, C. 276(498), 303, 1314(96), 1344
 Wynberg, H. 374(147, 147b–d), 585,
 819(105a), 829
 Xiangdong, Z. 605(30), 756
 Xiang, S. 1094(299), 1125
 Xiang, Y. 871(163), 897
 Xiao, D. 273(458), 302, 645(338), 764
 Xiao, H. 649(358), 765
 Xiao, J. 1065(53), 1119
 Xiao, X. L. 205(119), 294
 Xia, Q. 1108(387), 1127
 Xie, S. H. 527(466), 593
 Xie, S. J. 223(209), 273(468, 470), 280(522),
 283(520, 524, 530), 296, 302, 304,
 1326(126), 1330(134), 1332(109, 111),
 1337(163, 164), 1345, 1346
 Xie, S. 202(96), 223(210), 273(469), 294, 296,
 302
 Xie, Y. 30(30), 68(142), 87, 90
 Ximenes, V. F. 963(217), 994, 1193(49b),
 1208
 Xin, Q. 1094(299), 1125
 Xiong, Y. 976(270b), 996
 Xiujia, Z. 605(30), 756
 Xong, Z. 1150(96), 1167
 Xu, C. M. 1311(12), 1342
 Xu, F. 263(387), 300
 Xu, G. 646(345), 654(386), 764, 765, 833(26),
 894, 984(317e), 999
 Xu, J.-G. 639(316, 317), 640(319, 321), 764
 Xu, J. 1148(79b), 1167
 Xu, Q. 1115(412), 1127
 Xu, R. 418(252), 588
 Xu, T. 873(167), 897
 Xu, X. H. 870(155), 897
 Xu, X. X. 237(248), 247(247), 275(275),
 277(276, 505, 506), 297, 298, 303,
 1282(28), 1342
 Xu, X. 138(211), 144, 976(270b), 996
 Xu, Y. L. 511(416), 592
 Yabe, A. 818(94), 829
 Yabe, Y. 817(96), 829
 Yablokova, N. V. 780(21), 783(18d),
 824(117b, 117d–f), 827, 830
 Yablokov, V. A. 780(21, 22), 783(18d),
 824(117b, 117d–f), 827, 830

- Yabuki, S. 654(391), 765
 Yabushita, S. 833(29), 894
 Yacynych, A. M. 688(555), 769
 Yadan, J.-C. 669(470, 471), 767
 Yadav, J. S. 277(507), 303, 1023(150),
 1028(187), 1029(192, 195), 1049, 1050
 Yagi, K. 667(455), 767
 Yagyu, T. 1069(107), 1121
 Yakobson, G. G. 123(164), 143
 Yamabe, S. 56(121), 90
 Yamada, A. 1334(143), 1346
 Yamada, H. 525(308), 589, 1106(172), 1122,
 1257(283), 1276
 Yamada, K. 674(253), 762, 1334(143), 1346
 Yamada, M. 742(703), 773
 Yamada, S. I. 394(203), 586
 Yamada, S. 833(31), 894, 1173(17b), 1206
 Yamada, T. 252(299, 300, 302, 304), 298,
 567(531f), 595
 Yamada, Y. M. A. 1089(273), 1103(318),
 1124, 1125
 Yamada, Y. 396(211), 587
 Yamagishi, T. 278(511), 303
 Yamaguchi, H. 374(151), 585
 Yamaguchi, K. 245(282), 298, 410(224),
 444(315), 587, 589, 833(29, 31), 847(43),
 894, 1081(180), 1122, 1173(17b),
 1182(24c), 1206, 1207, 1228(96), 1272
 Yamaguchi, L. F. 943(91), 991
 Yamaguchi, M. 419(257), 588
 Yamaguchi, S. 478(297), 589
 Yamaguchi, Y. 1268(336), 1278
 Yamaizumi, Z. 1201(63c), 1209
 Yamamoto, H. 48(114c), 89, 285(551), 304,
 386(190b, c), 542(213–215), 549(512b),
 586, 587, 594, 1092(286), 1093(288–290),
 1125
 Yamamoto, K. 654(387), 765
 Yamamoto, M. 668(463), 767
 Yamamoto, T. 109(119), 142, 1157(127c),
 1168
 Yamamoto, Y. 118(139), 129(171), 142, 143,
 675(506), 680(537), 768, 769, 956(201a),
 977(279b), 994, 997
 Yamamoto, G. 129(171), 143
 Yamanaka, I. 362(134d), 585
 Yamanaka, M. D. 605(29), 756
 Yamanoi, Y. 487(384), 591, 1098(335), 1126
 Yamasaki, S. 651(372, 373), 681(98), 758,
 765, 793(38), 828
 Yamashita, O. 825(121), 830
 Yamato, T. 199(86), 293
 Yamauchi, R. 711(145), 759
 Yamawaki, K. 525(308), 589, 1080(173),
 1089(271), 1106(172), 1108(388), 1122,
 1124, 1127
 Yamazaki, I. 900(11), 912
 Yamazaki, S. 1010(75), 1014(95), 1047, 1048,
 1103(361), 1126
 Yamazaki, Y. 1010(75), 1014(95), 1047, 1048
 Yamazo, N. 650(364), 765
 Yanez, M. 874(170), 897
 Yang, C.-S. 669(465), 767
 Yang, D. 1022(144), 1049, 1140(81a, b, 87),
 1146(17), 1154(111), 1155(28), 1161(148a,
 b), 1165, 1167–1169
 Yang, G. C. 673(132), 759
 Yang, H.-H. 640(319, 321), 764
 Yang, J. 1015(101), 1048
 Yang, S. G. 1001(5), 1014(93, 96), 1015(104),
 1017(108–111), 1018(112, 113), 1046, 1048
 Yang, S. 185(38), 187
 Yang, W.-P. 701(590), 770
 Yang, X. H. 645(338), 764
 Yang, X. Y. 610(76), 757
 Yang, Y. Z. 1311(69), 1344
 Yang, Y. 976(270b), 996
 Yang, Z. 259(362–364), 300, 1145(68), 1167
 Yany, F. 1181(11d), 1206, 1232(119), 1273
 Yan, B. 645(339), 764
 Yan, M. G. 1016(105), 1048
 Yan, Q. J. 1015(103), 1048
 Yan, Q. 1015(102), 1048
 Yan, S. 1066(74), 1120
 Yan, Z. 1161(148a), 1169
 Yao, G. 256(360), 300
 Yao, Z. J. 1299(40), 1343
 Yardley, V. 290(580), 305, 1314(91), 1344
 Yarkony, D. R. 10(10c), 86
 Yarnell, A. 623(204), 761
 Yarysh, O. N. 674(501), 768
 Yasuda, K. 680(538), 769
 Yasuda, M. 681(94), 758
 Yasukawa, K. 1334(146), 1346
 Yasutake, M. 252(317), 299
 Yates, P. 196(77), 293
 Yatsenko, A. V. 111(105), 141
 Yazdanpanah, M. 670(476), 767
 Yazgan, M. S. 608(52), 757
 Yeh, H. J. C. 273(440), 301
 Yeh, P.-Y. 617(158), 759
 Yeh, W.-L. 288(571), 305
 Yekta, A. 1191(46a–c), 1208, 1219(47),
 1222(52), 1224(57), 1271
 Yen, T. Y. 981(298b), 998
 Yeo, H. C. 670(475), 767, 975(269a), 996
 Yermilov, V. 951(169), 993
 Yeung, H. W. 273(28), 292
 Yeung, K. W. 1140(78), 1167
 Ye, B. 283(531), 304
 Ye, J. 379(169), 586
 Yildiz, A. 700(557), 769
 Yildiz, G. 663(437), 671(231), 674(409), 761,
 766
 Ying, Y.-M. 870(153, 155), 897

- Yin, H. Y. 217(178, 179), 296
 Yin, H. 612(97), 703(593), 704(594), 714(96),
 758, 770, 1140(30), 1165
 Yip, W. P. 511(418), 592
 Yip, Y.-C. 1140(81a, b, 87), 1146(17),
 1154(111), 1165, 1167, 1168
 Yi, P. 980(289b), 997
 Yi, X. Y. 870(155), 897
 Yla-Herttuala, S. 984(314), 998
 Yokoi, T. 278(511), 303
 Yokoyama, T. 250(294), 298, 394(200, 200b),
 586
 Yokoyama, Y. 564(501), 594, 1006(38), 1046
 Yoneda, K. 339(84), 583
 Yonehara, K. 444(315), 589, 1081(180), 1122
 Yonemura, K. 360(130), 584
 Yon, D. J. 920(24), 989
 Yon, G. H. 1033(220), 1037(235), 1050, 1051
 Yoon, D. C. 1001(8), 1034(222), 1035(225),
 1046, 1050, 1051
 Yoon, J. 608(51), 757
 Yoon, M. H. 901(46), 912
 Yoo, C.-S. 96(25), 139
 Yoshida, J.-I. 776(2a), 810(77), 827, 829
 Yoshida, J. 250(297), 252(298), 298, 808(68),
 828
 Yoshida, M. 1007(48), 1047
 Yoshida, S. 199(89), 294
 Yoshida, T. 525(308), 589, 1080(173),
 1106(172), 1108(388), 1122, 1127,
 1335(147), 1346
 Yoshie, Y. 951(169), 993
 Yoshihiro, D. 1011(83), 1047
 Yoshimura, T. 693(570), 770
 Yoshino, F. 612(88), 758
 Yoshino, H. 612(108), 758
 Yoshioka, M. 196(76), 293
 Yoshioka, Y. 833(31), 894, 1173(17b),
 1182(24c), 1206, 1207, 1228(96), 1272
 Yoshizawa, T. 655(395), 765
 Young, I. S. 613(117), 758
 Young, V. G. 1066(74), 1120
 Youn, S. J. 911(88), 913
 Yuan, Q. 984(317e), 999
 Yuan, S. 645(341), 764
 Yuan, Z. Y. 870(155), 897
 Yuba, K. 316(23), 582
 Yudanov, I. V. 1075(148, 150, 151), 1121,
 1122
 Yudin, A. K. 467(359), 534(481, 482), 591,
 594, 790(36), 802(54), 828
 Yuen, P.-W. 567(531d), 595
 Yue, H. J. 211(105), 294
 Yue, Z. Y. 1299(57), 1343
 Yun, J. W. 1067(80), 1120
 Yurzhenko, T. I. 780(19, 20), 827, 1043(263,
 268), 1051
 Yuthavong, Y. 190(49), 273(449, 472), 293,
 302, 1303(7), 1311(76), 1342, 1344
 Yuvchenko, A. P. 122(152), 129(176), 142,
 143, 715(614), 771
 Yu, B. P. 945(121), 978(287b), 992, 997
 Yu, D. Q. 190(27), 292
 Yu, D. 290(589), 305
 Yu, H. B. 392(193), 586, 1088(265), 1124
 Yu, H. 520(455a), 593, 1140(74), 1148(79d,
 89), 1167
 Yu, Q. 605(30), 756
 Yu, T. C. 667(451, 452), 767
 Yu, W.-Y. 1140(80), 1167
 Yu, W. Y. 511(418), 592
 Zabarnick, S. 665(446), 767
 Zabeau, M. 610(71), 757
 Zabel, V. 317(29), 582
 Zabicky, J. 624(219), 718(633), 761, 771
 Zabrowski, D. L. 1151(99a), 1167
 Zafiriou, O. C. 1240(176), 1274
 Zagorski, M. G. 174(9), 186
 Zahradnfk, R. 1250(224), 1252(246), 1275
 Zaikin, I. D. 168(32, 33), 168
 Zajacek, J. G. 426(269), 534(479), 588, 594,
 1084(241), 1104(363), 1124, 1126
 Zaklika, K. A. 1256(27, 29), 1271
 Zakrzewski, V. G. 12(7), 85
 Zaman, F. 672(484, 485), 768
 Zamaraev, K. I. 185(40), 187, 1069(113, 114),
 1121
 Zambonin, L. 977(280a), 997
 Zambonin, P. G. 688(556), 769
 Zamboni, R. 318(11), 582
 Zambri, P. M. 566(494), 594
 Zamburlini, A. 614(128), 681(539), 759, 769
 Zanardi, G. 378(166), 585
 Zankl, H. 977(284), 997
 Zannella, S. 664(440), 767
 Zaret, E. H. 1042(262), 1043(264, 269), 1051
 Zarev, S. 612(105), 758
 Zarkadis, A. K. 824(118), 830
 Zatorsri, L. W. 708(561), 770
 Zauche, T. H. 1107(382, 383), 1127
 Zavoianu, D. 163(51), 169
 Zawadiak, J. 122(157), 143
 Zecchina, A. 1082(202), 1123
 Zehner, C. 605(31, 32), 756
 ZeiB, W. 468(271), 588
 Zenaro, L. 681(539), 769
 Zeng, H. 1082(198), 1123
 Zen, J.-M. 652(378), 765
 Zhai, L. 1322(119), 1345
 Zhang, C. J. 514(432), 592
 Zhang, D. M. 1015(103), 1048
 Zhang, D. 86(86), 88, 1015(102), 1048
 Zhang, F. 976(270b), 996, 1312(78), 1344
 Zhang, H. Z. 1280(3), 1342

- Zhang, H. 511(416), 592, 963(221), 994, 1015(101), 1048
 Zhang, J.-R. 675(507), 768, 1021(141), 1049, 1140(75), 1167
 Zhang, J. 511(416), 592, 653(385), 662(236), 761, 765, 873(167), 897
 Zhang, K. 425(266), 588, 634(295), 763
 Zhang, L.-P. 870(152), 897
 Zhang, L.-S. 629(262), 679(330), 762, 764
 Zhang, L. L. 984(297b), 998
 Zhang, L. P. 870(155), 897
 Zhang, L. 981(305a), 998
 Zhang, R. 86(86), 88, 408(221, 222, 222b), 587, 1091(279), 1094(296, 298), 1124, 1125
 Zhang, S. 684(99), 758
 Zhang, W.-H. 984(317e), 999
 Zhang, W.-H. 418(249), 588
 Zhang, W. Z. 418(249c), 588
 Zhang, W. 945(113), 992
 Zhang, X. J. 259(365), 300
 Zhang, X. Y. 192(62), 293
 Zhang, X. 263(385, 388), 300, 662(236), 761, 858(123, 124), 896, 1082(191, 192, 194), 1122, 1123
 Zhang, Y. 854(107), 896, 1094(299), 1125
 Zhang, Z.-J. 701(590), 770
 Zhang, Z. 610(76), 757
 Zhan, C. G. 37(37b), 87
 Zhan, D. 980(289b), 997
 Zhao, C.-G. 520(455b), 593, 1140(54, 76), 1146(73), 1150(23, 91), 1152(107, 108a, b), 1155(116), 1158(133), 1161(104), 1162(21, 150), 1163(1j, 1m, 1p), 1164–1169
 Zhao, L. 45(92, 106a, b), 89, 1160(35a, b, 35e), 1165
 Zhao, P. Y. 511(416), 592
 Zhao, S. H. 486(376), 591
 Zharinova, E. V. 1190(45b), 1208
 Zheng, H. 639(316, 317), 640(319, 321), 764
 Zheng, J.-H. 1140(81a), 1146(17), 1165, 1167
 Zheng, J. 604(14), 756
 Zheng, P. W. 511(416), 592
 Zheng, Q. Y. 283(471), 302, 1337(162), 1346
 Zheng, X. F. 392(193), 586, 1088(265), 1124
 Zheng, X. Q. 1095(317), 1125
 Zheng, X. 651(365), 765
 Zhou, C. M. 1299(40), 1343
 Zhou, F. 572(545), 596
 Zhou, G. 265(402), 301
 Zhou, H. J. 1336(157, 159), 1346
 Zhou, H. 662(236), 761
 Zhou, M. 643(67), 757
 Zhou, W.-S. 275(275), 277(276, 504–506), 298, 303
 Zhou, W. S. 1282(28), 1342
 Zhou, X. 270(430), 301, 650(13), 756
 Zhou, Z.-H. 1058(36), 1119
 Zhukovskaya, N. A. 715(614), 771
 Zhu, C.-Q. 639(316), 764
 Zhu, C. 646(344), 764, 854(105, 107), 896
 Zhu, J. Q. 388(194), 392(173, 192), 586
 Zhu, J. Y. 627(251), 762
 Zhu, J. 275(275), 277(505, 506), 298, 303, 1088(262–264), 1124, 1145(67b), 1166
 Zhu, M. 630(268), 762
 Zhu, N. Y. 511(418), 592
 Zhu, Q.-Z. 639(316, 317), 640(319, 321), 764
 Zhu, R. S. 13(43), 87
 Zhu, W. 1021(129), 1048
 Zhu, Y. P. 1281(4), 1342
 Zhu, Y. 520(455a), 593, 646(344), 764, 902(67), 913
 Zhu, Z. 1103(358), 1107(383), 1126, 1127
 Zhyan, Y. 1012(85), 1047
 Ziegenbein, W. 323(40), 582
 Ziegler, C. B. 310(7b, c), 581
 Ziegler, D. M. 79(154a–c), 91
 Ziegler, F. E. 316(24), 582
 Ziegler, K. 355(121), 584
 Ziemann, P. J. 690(11), 756
 Ziemer, B. 733(678b), 772
 Ziffer, H. 1302(61), 1314(85), 1343, 1344
 Zigler, J. S. J. 973(258), 996
 Ziller, J. W. 136(136), 142
 Zimmermann, K. 496(400), 592, 1106(379), 1127
 Zimmermann, T. 1184(25f), 1188(36), 1207, 1242(171), 1268(335), 1274, 1278
 Zimmerman, H. E. 1228(105, 106), 1236(165), 1272, 1274
 Zinczuk, J. 291(597), 305
 Zinke, H. 731(632), 771
 Zinner, K. 1192(16a), 1206, 1222(49), 1232(129), 1271, 1273
 Zinov'eva, T. I. 118(140), 142
 Ziolkowski, J. J. 433(272, 284), 588, 589
 Zolfigol, M. A. 1029(189), 1050
 Zoller, J. P. 1095(309), 1125
 Zollner, H. 984(281b), 997
 Zomer, G. 1252(234, 242), 1275
 Zondervan, C. 514(439), 516(444), 593, 1069(50), 1119
 Zonnevrijlle, F. 1081(183), 1122
 Zope, U. R. 236(236), 242(242), 243(243), 297, 329(63b), 583
 Zouhiri, F. 1303(65), 1343
 Zozom, J. 721(645), 771
 Zubia, E. 1333(141), 1346
 Zubieta, J. 128(169), 143
 Zulian, R. 1082(202), 1123
 Zuman, P. 623(208), 652(379), 761, 765
 Zuraw, P. J. 253(253), 264(264), 297
 Zvereva, T. D. 129(176), 143, 715(614), 771
 Zweier, J. L. 612(88), 758
 Zyat'kov, I. P. 103(47), 122(158), 123(104), 130(185), 131(180), 140, 141, 143

Subject Index

Entries are in letter-by-letter alphabetical order ignoring spaces and punctuation marks. Page numbers in *italic* refer to Figures and Tables not included in the relevant page ranges.

- Abasic sites, oxidative damage measurement, 670–1
- Abbreviations, 600–3, 1054–5
- Ab initio* calculations
- dioxetane chemiluminescent decomposition, 1181
 - peroxy vanadates, 1059
 - zeolite Na–Y cation– π interactions, 873
- Absorption spectrophotometry
- hydrogen peroxide determination, 627–37
 - hydroperoxide determination, 674–8
 - microplate spectrophotometry technique, 637
 - peroxide value, 658–9
- ABTS *see* 2,2'-Azinobis(3-ethylbenzothiazoline)-6-sulfonate
- Accelerated oxidation
- anisidine value, 666
 - peroxide value, 657, 661, 664
- Accelerated testing, surface coatings, 683
- Acetaminophen, hydrogen peroxide determination, 651
- Acetogenins, structural chemistry, 136–8
- Acetone, manufacture, 617
- Acetonitrile
- hydrolysis, 701–2
 - peroxydisulfate reactions, 1016–18
 - solvent for dioxirane oxidation, 1154
- Acetoxy alcohols, olefin oxidation synthesis, 792–3
- Acetylacetonate anion (acac), transition metal peroxides, 1086, 1089, 1090, 1092, 1095, 1100
- Acetyl peroxynitrate, structure, 103, 104
- Acetylsaturejol, triplet oxygen cycloaddition, 202, 204
- Acid-catalyzed synthesis, dialkyl peroxides, 351–8, 712
- Acidity value (ACV)
- colorimetric determination, 632
 - secondary oxidation products, 672
- Acid medium, W-catalyzed epoxidation, 437
- Acne formulations, benzoyl peroxide, 623
- Acridans, chemiluminescence, 1253, 1255–6
- Acridinium salts, chemiluminescence, 1251–6
- Acronyms, 600–3, 1054–5
- ACT *see* Activators
- Actinometry, chemiluminescence measurement, 1224, 1225
- Activated chemiluminescence, 1220–1, 1223
- Activated sludge process, bleaching waste, 623
- Activation parameters
- alkene epoxidation, 38, 40, 41, 43
 - tert*-butyl perbenzoate ETR reactions, 909–11
 - tert*-butyl phenylperacetate thermolysis, 903–4, 905, 906
 - chemiluminescence research, 1221–2
 - dioxirane decomposition, 1134
 - methyl substituted-benzyl carbonyl hypochlorite photolysis, 907–9
- Activators (ACT)
- chemiluminescence, 1220, 1221, 1222
 - peroxide decomposition, 1231, 1234
 - peroxyoxalates, 1189, 1190, 1256–7, 1266–7
- Active carbon, hydrogen peroxide determination, 638
- Active oxygen *see* Peroxide value
- ACV *see* Acidity value
- Acyclic allylic alcohols, dioxirane epoxidation, 1144–5
- Acyclic organic peroxides

- Acyclic organic peroxides (*continued*)
 formation, 94
 structural chemistry, 93–144
 hydrogen bonding, 103–5
 lone pair repulsion, 100
 orbital effects, 101–3
 steric effects, 101
- Acylation, trifluoroacetic anhydride, 1160
- Acyl peroxides
 detection and determination, 701
 enthalpies of formation, 159–60, 162–3
 enthalpies of reaction, 162–3
 homologous series, 162
 structural characterization, 702–4
 thermochemistry, 158, 162–3
- Adamantane, C–H bond dioxirane oxygen insertion, 1162
- Adamantyl trioxolanes, antimalarial drugs, 1320, 1321
- Addition reactions of hydroperoxides
 cyclization, 230, 233–52, 253
 thermochemistry, 157
- Aerosols, hydroperoxide determination, 678, 690
- Agarofuran, singlet oxygen cycloaddition, 265
- Aging
 polymers, 685
 thymidine oxidation, 616
- AIDS
 AZT synthesis, 315, 320
 4-hydroxynon-2-enal determination, 613, 670
- Air exposure, oxidative stability, 656, 664–5, 672
- Air pollutants
 benzoyl peroxide, 701
 hydrogen peroxide, 626, 638, 645–6
 ozone, 683
 peracetic acid, 698, 699
 plastic materials, 622
 see also Pollution
- Air transport, hazardous material labeling, 751–3
- Alcohols
 ether exchange reaction enthalpies, 157–8
 hydroperoxide oxidation, 692
 oxidation, 492, 496–503, 504–12, 787–90
 transition metal-catalyzed, 787–9, 1057, 1105–8
 ozone adducts, 734
 synthesis via silyl peroxides, 808–10
 see also Allylic alcohols
- Aldehydes
 abasic sites, 670–1
 catalyzed dioxirane epoxidation, 1150
 C–H bond unreactive to insertion, 1160
 core aldehydes, 719, 739
 detection and determination, 669–71
 IR spectrophotometry, 661, 662
 TBARS assay, 667
 hydroperoxide oxidation, 692
 lipid hydroperoxides, 977–8
 decomposition, 669
 DNA adducts, 978–84
 protein adducts, 984–5
 ozone adducts, 734
 ozonide reduction, 726
 ozonization characterization, 737, 739
 peroxydisulfate reactions, 1013, 1018
- Alkali metal ozonides, 735–7
- Alkaline peroxide process, pulp and paper bleaching, 623
- Alkaline phosphatase, chemiluminescent bioassays, 1193–200
- Alkanals, secondary oxidation products, 665
- n*-Alkanals, lipid peroxidation, 614
- Alkanes
 C–H bond dioxirane oxygen insertion, 1138
 dioxirane oxyfunctionalization, 1136, 1138
 oxidation, 531
- Alkanoyl peracids, crystal structure, 125–6
- 2-Alkenals, oxidative stress, 613
- Alkenes
 carbonyl oxide epoxidation, 35–40
 chiral
 diastereoselectivity, 883–6, 887
 dioxirane epoxidation, 1144–50
 dioxirane epoxidation, 35–40, 1136, 1139–50
 cis-alkenes, 1148
 chiral, 1144–50
 electron-poor alkenes, 1141–3
 electron-rich alkenes, 1139–40
 internal, 1145
 prochiral, 1145
 terminal, 1145, 1148
 trisubstituted, 1146
 unfunctionalized alkenes, 1140–1
 electron-poor
 dioxirane epoxidation, 1141–3
 intrazeolite photooxygenation, 877–8
 transition metal peroxide oxidation, 1087–9
 electron-rich, 1139–40
 intrazeolite photooxygenation, 874–8, 883–6, 887
 oxidation to ketones, 521–5
 peracid epoxidation
 allylic alcohols, 65–7
 early mechanistic studies, 48
 gas-phase, 58
 Hartree–Fock calculations, 48–50
 rate factors, 58–65
 synchronous/asynchronous transition states, 50–8
 prochiral, 341, 342, 1145

- regioselectivity
 cis and *trans* disubstituted alkenes, 842–4
 cyclic alkenes, 846–7
 electron-poor alkenes, 877–8
 functionalized alkenes, 852, 854
 geminal dimethyl alkenes, 844–5, 846
 intrazeolite photooxygenation, 874–8, 886, 887
 phenyl substituted alkenes, 839–42
 trisubstituted alkenes, 833–6, 844–5, 846, 874–7
- transition metal peroxide oxidation
 allylic and homoallylic alcohols, 1089–94
 cleavage, 1094–5
 electron-poor alkenes, 1087–9
 unfunctionalized alkenes, 1079–86
 triethylsilyl hydrotrioxide reactions, 812–13
 vicinal dihydroxylation, 556, 567–72, 573–5
- Alkenyl hydroperoxides, free radical
 cyclization, 212–18
- Alkoxide free radical, hydroperoxide
 determination, 675
- α -Alkoxyhydroperoxides, synthesis, 313
- Alkoxy groups, enthalpies of formation, 156, 157–8
- Alkoxy radical, lipid oxidation, 946
- Alkyd resin coatings
 differential scanning calorimetry, 672
 peroxide value, 658, 662
- Alkylbenzothiazoles, bis(trimethylsilyl)
 peroxide reactions, 798
- Alkyl(chloro)silyl peroxides, preparation,
 780–1
- Alkylgermanium peroxides, preparation,
 823–4
- Alkyl halides, hydroperoxide synthesis, 327–8
- Alkyl hydroperoxides
 anion ligands, 114–19
 covalent radii, 114, 118–19
 dihedral angles, 119
 geometric parameters, 115–8
 tetrahedral distortion, 119
 artemisinin formation, 133–4
 chlorotriorganosilane reactions, 779–83
 crystal structure, 105–14
 anomeric effect, 110–11
 geometric parameters, 106–9
 hydrogen bonding, 103–5, 111–14
 tetrahedral distortion, 110
 determination, 674
 enthalpy of formation, 144, 145–6, 147
 ether cocrystallization, 111, 113
 functionalization, 1055
 synthesis, 309, 310–29, 673
 synthetic use, 308–9
- s*-Alkyl hydroperoxides, molecular refraction,
 697
- Alkyl hydroperoxysilanes, preparation, 783
- Alkyl hydrotrioxides, structural chemistry, 132
- Alkyl iodides, dioxirane oxidation, 1158
- Alkyl methyl sulfonates, alkyl hydroperoxide
 synthesis, 673
- 2-(Alkyloxy)prop-2-yl hydroperoxide,
 hydroperoxide synthesis, 327–8
- Alkyl peroxides, enthalpies of reactions, 154
- s*-Alkylperoxy free radicals,
 chemiluminescence, 680
- 3-Alkylperoxyheptaorganotrisiloxanes,
 preparation, 781, 782
- Alkylperoxy hydridosilane, preparation, 783
- Alkyl phosphites, ozone adducts, 732
- Alkyl sodium alkyl peroxide,
 chlorohydridosilane reaction, 783
- Alkynes
 bis(trimethylsilyl) peroxide reactions, 800
 vicinal dihydroxylation, 556, 567–72, 573–5
- Allantoin, uric acid oxidation, 625
- Allene hydroperoxides, regioselectivity with
 twisted 1,3-dienes, 856–7, 858
- Allen's reagent
 hydroperoxide determination, 674
 ozonolysis, 606
- All-homolytic chain reactions, autoxidation,
 218–21
- Allylic alcohols
 acyclic, 1144–5
 asymmetric epoxidation
 chiral hydroperoxides, 401–6, 407–9
 chiral metal complex catalysis, 394–401
 chiral dioxetane synthesis, 1173–4
 chiral hydroperoxide synthesis, 331
 coupling with carbonyl compounds, 285–90
 epoxidation, 391–416, 789
 asymmetric, 394–406, 407–9
 dioxiranes, 1144–5
 ketone-catalyzed, 385–6
 peracids, 65–7
 Sharpless epoxidation, 789
 special synthetic utility, 406, 410–13, 414
- hydroperoxysilylation, 275, 1329, 1330
 isomerization, 789–90
 oxidation, 788–9
 transition metal peroxides, 1089–94
 photooxidation
 chiral allylic alcohols, 889
 diastereoselectivity, 864–6, 867
 site selectivity, 836, 837
 Sharpless epoxidation, 789
- Allylic amines, photooxidation site selectivity,
 836

- Allylic diradicals, bis(azoalkane) photolysis, 193, 194
- Allylic functionality, geminal regioselectivity, 845–9
- Allylic hydroperoxides
- coupling with carbonyl compounds, 285–90
 - singlet oxygen ene reaction, 673, 831–98
 - diastereoselective formation, 860–9
 - dye-sensitized intrazeolite
 - photooxygenation, 869–86, 887
 - allylic radical intermediate, 871
 - twin/twix* regioselectivity, 876–7
 - natural product synthesis, 888–93
 - regioselective formation, 833–60, 876–7
 - synthetic applications, 886, 888–93
- synthesis, 310–11, 324, 673
- Allylic oxidations, 503, 512–19
- 1,2-Allylic strain, dioxirane epoxidation, 1145
- 1,3-Allylic strain, dioxirane epoxidation, 1145
- Allylstannanes, chiral, 235–6
- Aluminum tetraaminophthalocyanine, hydrogen peroxide determination, 639–40
- Amberlyst IRA-400, ion exchange polymer, 569
- Amides
- C–H bond unreactive to insertion, 1160
 - nitrile hydrolysis, 701–2
 - selective dioxirane oxidation, 1152
- Amines
- allylic site selectivity, 836
 - dioxirane oxidation, 1151–2
 - primary amines, 1151
 - secondary amines, 1151–2
 - tertiary amines, 1152
- oxygen atom transfer from hydroperoxides, 67–70
- ozone adducts, 734
- peroxynitrous acid oxygen transfer, 14–17
- sulfonyl peroxide reactions, 1006–7
- transition metal peroxide oxidation, 1101–5
- Amino acid hydroperoxides, structure, 691
- Amino acid peroxides, protein secondary reactions, 972–5
- Amino acids
- free radical formation, 614, 615, 628
 - hydroperoxide determination, 674
 - radical reactions, 960–6
 - hydroxyl radical, 954–60
- side-chain peroxidation, 955–60
- singlet oxygen oxidation, 966–70
- TBARS assay, 669
- 4-Aminoantipyrine
- hydrogen peroxide determination, 630, 631, 632, 633
 - hydroperoxide determination, 676–7
- 3-(Aminomethyl)proxyl radical, spin label, 665
- N'*-Aminooxymethylcarbonylhydrazino-D-biotin, DNA oxidative damage, 736, 634
- 3-Aminophthalate, luminol oxidation, 643, 644, 1239–41, 1244–6
- 7-Amino-4-trifluoromethylcoumarin, hydrogen peroxide determination, 649
- Ammonium ion complex, mass spectrometry, 703, 704
- Ammonium molybdate
- hydrogen peroxide determination, 627, 651
 - hydroperoxide determination, 674
- Ammonium salts, selective dioxirane oxidation, 1152
- Amperometry
- diacyl peroxide determination, 701
 - dropping Hg electrode, 686, 687
 - hydrogen peroxide determination, 650, 651, 652, 653, 655
 - hydroperoxide determination, 686, 688
 - oxidative, 686
 - reductive, 686
- Amplex Red, hydrogen peroxide determination, 642–3
- Analytical methods, 624–774
- back trajectory analysis, 624
 - biological and biomedical systems, 608–17
 - central composite design, 624
 - chemometric approach, 624
 - cluster analysis, 624
 - environmental issues, 604–8
 - factorial design, 624
 - half-fractional, 624
- fitness for purpose, 624, 663
- hydrogen peroxide, 625–56
- industry, 617–24
- limits of detection, 625
- limits of quantitation, 625
- measurement uncertainty, 624
- method of standard addition, 624
- multiple linear regression, 624
- forward stepwise, 624
- multivariate analysis, 624, 702
- ozonolysis, 737–40
- partial least squares regression, 624
- principal component analysis, 624
- Analytical reagents, commercial codes, 621
- Animal tissue, TBATS assay, 669
- Anionites, molybdenum(VI) complexes, 427
- Anions
- acetylacetonate, 1086, 1089, 1090, 1092, 1095, 1100
 - alkyl hydroperoxide ligands, 114–19
 - hydrogen trioxide, 180–1
 - luminol radical anions, 1241–2, 1244, 1245
 - ozonide, 735–7
 - percarboxylate ligands, 127, 128
 - selective hydroperoxy anion transfer, 382
 - see also* Superoxide anion radical

- p*-Anisidine
absorption spectrophotometry, 636, 675
anisidine value, 666
diacyl peroxide determination, 701
Anisidine value (ANV), secondary oxidation products, 656, 663, 665–6
ANO₂, antitumour endoperoxide, 1335
Anomeric stabilization
alkyl hydroperoxides, 110–11
explosive triperoxides, 166
ozonides, 723
Antarctic air, hydrogen peroxide determination, 648
Anthocyanins, TBARS assay, 667
Anthracene, primary ozonides, 723–4
Anthropogenic emissions
atmosphere, 604, 605
hydrogen peroxide, 626
Antibodies, hydrogen peroxide determination, 1315
Antimalarial endoperoxides
biological targets, 1311–13
biomimetic Fe(II) chemistry, 1279–332, 1338, 1342
G3 factor, 199, 201, 202
mechanisms, 1309, 1310
NMR spectroscopy, 710
OZ 277 drug candidate, 1317, 1319, 1331
Plasmodium falciparum resistance, 608
synthetic, 1282, 1317–31
antimalarial activities, 1332
semi-synthetic artemisinin derivatives, 1313–17, 1332
triethylsilyl trioxide reactions, 813, 814
Antimicrobial activity, NMR spectroscopy, 725
Antimony(V) chloride, ozonide zwitterion complexes, 734
anti orientation, singlet oxygen ene reactions, 856
Antioxidants
capacity determination, 636
fluorescence quenching, 660
free radical trapping, 614
low-density lipoprotein, 610–11
luminol oxidation, 1242
TBARS assay, 668
see also Oxidants
Antiproliferative trioxane dimers, 283
Antitumour active trioxane dimers, 283
Antitumour endoperoxides, 1333–41
ANO₂, 1335
biomimetic Fe(II) chemistry, 1335–6
C10 carba dimers, 1337, 1340
mechanisms, 1335–6
natural products, 1333–5
synthetic, 1335
ANV (anisidine value), 656, 663, 666
Apoptosis
lipid oxidation, 660
reactive oxygen species, 610
Apple juice manufacture, 623
Apple pomace, hydrogen peroxide bleaching, 623
Arachidonic acid
H₂-isoprostane bicyclic endoperoxides, 612
lipid hydroperoxide determination, 681
Arene endoperoxides
spin-forbidden reactions, 166–7
thermochemistry, 166–7
Aromatic compounds
arene endoperoxide thermochemistry, 166
bis(trimethylsilyl) peroxide reactions
hydroxylation, 794–5
oxidation, 795
oxidation, 527–30
enzymatic, 77–82, 83
Aroyl peracids, crystal structure, 127
Arteflene antimalarial endoperoxide
Fe(II) degradation, 1304–9, 1310
synthesis, 243–4, 1282, 1324, 1326, 1332
Artemisia annua, artemisinin extraction, 1317
Artemisinic acid, artemisinin synthesis, 288, 289
Artemisinin (qinghaosu)
antimalarial activity, 1309, 1313
biological targets, 1311–13
ESR spin-trapping agents, 1291
Fe(II) degradation, 1283, 1293, 1295–6
heme adducts, 1298, 1311–12
heterolytic cleavage of peroxide bond, 1301–2, 1309
PfATP6 enzyme inhibition, 1313, 1320
antitumour activity, 1336–41
biosynthesis, 133–4
chemistry, 1314–17
extraction, 1280–1
natural occurrence, 190, 191, 608, 609
semi-synthetic derivatives, 1313–17, 1332
synthesis, 276–7, 278, 288–90
Artemisitene, artemisinin synthesis, 288, 289
Artificial photonucleases, naphthalimide hydroperoxides, 616–17
Aryl hydroperoxides, chlorotriorganosilane reactions, 779–83
Arylidene- β -ionones, triplet oxygen cycloaddition, 199, 201
Aryl phosphites, ozone adducts, 732
Aryl-substituted olefins, selenide-catalyzed epoxidation, 384–5
Ascaridole
natural occurrence, 608, 609
synthesis, 706
Ascorbic acid
free radical trapping, 614

- Ascorbic acid (*continued*)
 hydrogen peroxide determination, 245, 650, 651
 lipid peroxidation, 614
 low-density lipoprotein antioxidant, 611
 sperm motility, 669
- Aspergillus niger*, hydrogen peroxide biosensor, 655
- (+)-Asteriscanolide, synthesis, 891, 892
- Asymmetric dihydroxylation, ketones, 520–1
- Asymmetric epoxidation
 allylic alcohols
 chiral hydroperoxides, 401–6, 407–9
 chiral metal complex catalysis, 394–401
 electron-deficient olefins, 386–91
- Asymmetric metal-catalyzed sulfoxidations
 chiral catalysts, 478–85
 chiral hydroperoxides, 485–92, 493–5
- Asymmetric oxidation, metal-catalyzed sulfoxidations, 490
- Asymmetric synthesis, chiral auxiliaries, 868
- Asynchronous transition states, peracid alkene epoxidation, 50–8
- Atherogenesis, reactive oxygen species, 611, 612
- Atherosclerosis
 dietary lipid hydroperoxides, 614
o,o'-dityrosine residues, 610
- Athlete's foot formulations, benzoyl peroxide, 623
- Atmosphere
 dialkyl peroxides, 707
 hydrogen peroxide, 626, 637, 641–2, 645–6, 648
 hydroperoxides, 673, 678
 peracetic acid, 698, 699
 peroxide analysis, 604–5
- Autofluorescence, peroxide value, 660
- Autoxidation
 all-homolytic chain reactions, 218–21
 deterioration, 623
 dialkyl peroxide synthesis, 360, 362
 fatty acid hydroperoxides, 691
 free radical, 204
 hydrocarbons, 320
 hydrogen peroxide formation, 625
 hydroperoxide formation, 320–4, 656, 673
 jet fuel, 665
 lipids, 614, 623, 661
 polymers, 623
 ring enlargements, 219–21
 safety issues, 745
 stability on storage, 664–5
- Avidin–biotin–HRP reaction, DNA oxidative damage, 633
- Azadigermirane, photooxygenation, 825–6
- 2,2'-Azobis(3-ethylbenzothiazoline)-6-sulfonate (ABTS)
 dialkyl peroxide explosives, 708
 hydrogen peroxide determination, 636, 655
 hydroperoxide determination, 678
 peroxycarboxylic acid determination, 700
- Azoalkanes, benzophenone-sensitized laser photolysis, 193–5
- 2,2'-Azobis(2,4-dimethylvaleronitrile), TBARS assay, 668
- AZT, AIDS drug synthesis, 315, 320
- B3LYP, density functional theory, 4, 34–5, 38, 40, 41, 43
- Bacillus subtilis*, reactive oxygen species defense, 610
- Back electron-transfer (BET), peroxyoxalate chemiluminescence, 1268
- Back trajectory analysis, analytical methods, 624
- Bacteria, ozone disinfection, 616
- Bactericides, hydrogen peroxide, 623
- Baeyer–Villiger oxidation, 538–56, 557–66
 ketones, 784–7
 tin(IV) chloride, 786–7
 peroxyester determination, 700–1
- Base-catalyzed reactions
 dialkyl peroxide synthesis, 351–8
 epoxidation, 363–70
- Basicity, hydrogen bonding, 100
- Basidiomycetes, reactive oxygen species, 610
- BDE (bond dissociation energies), 5–7
- Beef, peroxide value, 658
- Beer
 autoxidation, 623
 hydrogen peroxide content, 643
- Bell–Evans–Polanyi principle, 907
- Benzaldehyde, primary ozonides, 720
- Benzeneearsonic acid, olefin epoxidation, 471–2
- 1,2-Benzisoselenazol-3(2H)-one (ebselen), peroxy-nitrous acid reaction, 117, 17
- Benzonitrile, hydrolysis, 701–2
- Benzophenone, laser photolysis, 193–5
- Benzoyl acetyl peroxide, structure, 703
- α -*N*-Benzoyl-L-arginine ethyl ester, malondialdehyde determination, 670
- Benzoyl peroxide
 biosensors, 664
 chemiluminescence, 646
 determination, 701
 flour bleaching, 622
 pharmaceutical preparations, 623, 672
 vibrational spectra, 702
- Benzyl carbonyl hypochlorites,
 methyl-substituted photolysis, 907–9
- Benzylic cations, homolytic cleavage, 911–12
- Benzyl ethers, sulfonyleperoxy radical reactions, 1037

- Benzylic oxidation, 503, 518–19
2-*O*-Benzylphosphatidylcholine,
 hydroperoxide determination, 690
- Bicyclic endoperoxides
 bridged, 193
 fused 1,2-dioxanes, 196, 197
 fused 1,2-dioxolanes, 193, 194
- Bicyclic monoterpenes, singlet oxygen ene
 reaction, 861, 863
- Bicyclic ozonides, acid-catalyzed
 condensation, 712
- 1,1'-Bicyclohexenyl, triplet oxygen
 cycloaddition, 211
- Bidentate ligands, molybdenum(VI)
 complexes, 427
- Bifurcated hydrogen bonds, alkyl
 hydroperoxides, 111, 112
- Bimetallic complexes, molybdenum(VI), 428
- Bioassays
 dioxetane chemiluminescence, 1173,
 1191–200, 1205
 alkaline phosphatase, 1193–200
 firefly bioluminescence, 1191–2
 β -galactosidase, 1193, 1198–9
 see also Immunoassays
- Biogenic emissions, atmosphere, 604, 605, 673
- Biological systems, 915–99
 analytical methods, 608–17, 740–2
 hydrogen peroxide determination, 626
 hydroperoxide determination, 679–80, 686
 ^{17}O NMR spectroscopy, 185–7
 oxidative processes, 918–19
 peroxide value, 659
 peroxynitrite determination, 740–2
- Bioluminescence (BL), 1212, 1255
 fireflies, 1182, 1191–2, 1213, 1232–3,
 1255, 1256
 imidazole, 1259
- Biomedical systems, 915–99
 analytical methods, 608–17
 detoxification, 611–12
 oxidative processes, 918–19
 see also Cellular indicators of
 hydroperoxides
- Biomimetic chemistry
 HRP catalysis, 639
 PGG₂ methyl ester synthesis, 214, 215
- Biomimetic Fe(II) chemistry
 antimalarial endoperoxides, 1279–332,
 1338, 1342
 antitumour endoperoxides, 1335–6
 Fe(II) sources, 1309
 haemoglobin degradation, 1281, 1283
 hydrogen peroxide determination, 652–5
 hydroperoxide determination, 687–9
 role of iron, 1283–310
 arteflene degradation, 1304–9, 1310
 carbon-centered radicals, 1283–99, 1309
 heterolytic cleavage of peroxide bond,
 1291, 1301–4, 1309
 homolytic cleavage of peroxide bond,
 1304
 non-heme iron, 1299–301
- Biosensors
 acyl peroxide determination, 701
 glucose determination, 650
 hydrogen peroxide determination, 652–5
 hydroperoxide determination, 664, 687–9,
 700
 oxygen electrodes, 655, 664
 peroxyester determination, 700
- Biotin markers, DNA basic sites, 633, 634
- 4-Biphenylboronic acid, chemiluminescence
 detection, 649
- Biradical intermediates
 chemiluminescence mechanism, 1181–2,
 1227–31
 ene reaction, 853
 see also Diradicals
- Bis(alkylperoxy)diorganosilanes, preparation,
 781, 782
- Bis(alkylperoxy)hydridosilanes, preparation,
 783
- Bis(azoalkane), allylic diradicals, 193, 194
- 2-Bis[bis(2-(1-methyl-4,5-diphenylimidazolyl)
 methyl)aminomethyl]-4-methylphenolate,
 1054, 1065–6
- Bis(*t*-butoxycarbonyl) peroxide, fragmentation,
 704
- Bis(butyltin)peroxide, peroxide transfer
 reactions, 824–5
- N,N'*-Bis(cyanomethyl)-*o*-phenylenediamine,
 hydrogen peroxide determination, 639
- Bis(2,4-dinitrophenyl) oxalate (DNPO),
 peroxyoxalate chemiluminescence, 1261,
 1262
- 1,2-Bis(diphenylphosphino)ethane (dppe),
 transition metal peroxides, 1064
- Bis(homoinositol), synthesis, 264
- Bishydroperoxides, enthalpies of formation,
 148
- Bis(hydroxymethyl) peroxide
 determination, 707
 hydrogen peroxide determination, 635, 650
- Bis(organosilyl) peroxides, preparation, 777–9
- Bis(pentachlorophenyl) oxalate (PCPO)
 light emission intensity calibration, 1225,
 1226
 peroxyoxalate chemiluminescence, 1262
- Bisperoxides, enthalpies of formation, 149
- Bisphenol A, ozonization elimination, 608
- 2-(Bis-pyridin-2-ylmethylamino)-*N*-[2-(5-2-
 (2-(*N*-methyl-*N*-pyridin-2-ylmethyl-
 amino)acetylamino]phenyl-[1,3,4]
 oxadiazol-2-yl)phenyl]acetamide, 1054,
 1067

- Bis(silyl) peroxide, preparation, 776–7
Bis(stannyl)peroxide, peroxide transfer reaction, 825
Bis(trialkyltin)peroxides, peroxide transfer reactions, 825
Bis(2,4,6-trichlorophenyl) oxalate (TCPO) chemiluminescence, 648, 1189, 1190, 1222, 1225, 1226, 1258, 1268–9
hydrogen peroxide determination, 637–8
hydroperoxide determination, 682
Bis(trifluoromethyl) peroxide, molecular structure, 713
Bis(trifluoromethyl) peroxydicarbonate, 705
Bis(trifluoromethyl) peroxydicarbonate, 705
Bis(trifluoromethyl) trioxide
IR spectrum, 740
¹⁷O NMR spectroscopy, 182
Bis(trifluoromethyl) trioxydicarbonate, 740
Bis(trimethylsilyl) monoperoxysulfate
Baeyer–Villiger oxidation, 785
catalytic epoxidation, 791–2
Bis(trimethylsilyl) peroxide (BTSP)
alcohol oxidation, 787–90
alkyne reactions, 800
aromatic compounds, 794–5
Baeyer–Villiger ketone oxidation, 784–7
demethylation, 798
heteroatom compound reactions, 802–8
iron(III) systems, 792, 800–1
nucleophile reactions, 795–800
olefin oxidation, 790–3
preparation, 778–9
saturated hydrocarbon oxidation, 800–2
tin(IV) chloride system, 786–7, 792–3
Bis(trimethylsilyl) peroxomonosulfate, preparation, 779
Bis(triphenylgermanium)oxide, germyl hydroperoxide formation, 822
BL *see* Bioluminescence
Bleaching
alkanoyl peracids, 125
commercial applications, 617, 622–3
hydrogen peroxide determination, 651, 652
ozone adducts, 734
percarboxylic acid, 699
Blood
lipid peroxides, 612
TBARS assay, 667
Bond angles
alkyl hydroperoxides, 105, 105–9, 110
anion ligands, 114, 115–7, 118–19
diacyl peroxides, 128, 130
dialkyl peroxides, 119–25
hydroperoxides, 690
¹⁷O NMR chemical shifts, 174, 177
peracids, 125–7
peresters, 127–8, 129
back side angles, 128, 129
Bond breaking, polar effects in decomposition, 900, 903, 905
Bond dissociation energies (BDE), 5–7
Bond lengths
C–O, π -type interactions, 102–3
O–O
acyclic organic peroxides, 105
alkyl hydroperoxides, 105–9
anion ligands, 114, 115–8
diacyl peroxides, 128, 130
dialkyl peroxides, 119, 122–3
MO calculations, 94–5
peracids, 125–7
peresters, 127–8, 129
Bonds
C–H
dioxirane oxygen insertion, 1138–9, 1158–63
oxyfunctionalization, 1159
ozonization, 178
secondary, 1161
tertiary, 1161
vinylid, 661
C–O–O–C, ¹⁷O NMR chemical shifts, 174, 177
double bonds
carbon–carbon, 230, 233, 238–45
ene adduct formation, 850–2
metal–O
alkyl hydroperoxide anion ligands, 114–19
geometric parameters, 135–8
O–O
bond dissociation energies, 5–7
heterolytic cleavage, 1291, 1301–4, 1309
homolytic cleavage, 1304
O insertion, 95–6
peroxynitrous acid homolysis, 7, 8
single-bonded oxygen functional group peroxides, 155–8
4-Boronobenzenepropanoic acid, chemiluminescence detection, 649
Bovine hematin, hydroperoxide determination, 678
Bovine serum albumin (BSA)
epoxidation catalysis, 383–4
 γ -radiation, 614, 691
prochiral sulfide dioxirane oxidation, 1157
Bowel inflammatory disease, 4-hydroxynon-2-enal determination, 670
Brain cortex, TBARS assay, 668–9
Brassinosteroid, C–H bond dioxirane oxygen insertion, 1162
Brevetoxin A, synthesis, 258, 259
Brewer spectrophotometer, atmospheric analysis, 605
Bridged bicyclic endoperoxides, synthesis, 193

- Bromine substitution, thymine/thymidine bromohydrins, 927–8
- β -Bromohydroperoxides, nucleophilic substitution cyclization, 233–4
- 2-(5-Bromo-2-pyridylazo)-5-diethylamino-phenol, hydrogen peroxide determination, 635–6
- Bromopyrogallol Red, hydrogen peroxide determination, 628–9
- Bronchial epithelial cells, IR spectrophotometry, 683
- Brønsted acids, olefin epoxidation, 471
- BSA *see* Bovine serum albumin
- BTSP *see* Bis(trimethylsilyl) peroxide
- 2-Butanone peroxide, hydroperoxide determination, 686, 688, 689
- E*-2-Butene, final ozonide, 721
- t*-Butoxy free radical, α -methylstyrene dimer reaction, 697
- Butter, peroxide value, 658, 660, 665
- t*-Butyl alcohol, tetroxide formation, 740
- t*-Butyl cumyl peroxide
air pollutant, 622
determination, 707
hydroperoxide determination, 685
- t*-Butyl hydroperoxide (TBHP)
catalyzed olefin epoxidation, 428, 432, 435
detection and determination, 675
diesel fuel additive, 624
Halcon Process, 428
HVP chemical, 622
hydrogen peroxide determination, 629, 637
hydroperoxide determination, 678, 685, 686, 688, 690
lipid oxidation, 693
perester formation, 127–8, 130
peroxide value, 660, 662
singlet oxygen generation, 673
tetrahedral distortion, 103, 110
toxic effects, 613
transition metal peroxides, 1070, 1082, 1096–9, 1108, 1113, 1114
epoxidation, 1088–90, 1092–3
oxidative cleavage, 1104–5
oxirane process, 1084–6
water-free, 395
- t*-Butyl peracetate, biosensor deactivation, 700
- t*-Butyl perbenzoates
air pollutants, 622
determination, 698, 700
dimethyl sulfide ETR reactions, 909–11
- t*-Butyl peresters, crystal structure, 127–8, 130
- 1-*t*-Butylperoxy-3-chlorotetramethyldisiloxane, preparation, 781
- t*-Butylperoxy ligand, covalent radii vs. M–O bond length, 114, 118–19
- t*-Butylperoxy(pentamethyl)disiloxane, preparation, 781
- t*-Butylperoxy-3-phenyltetramethyldisiloxane, preparation, 781
- t*-Butylperoxytrimethylsilane, peroxide transfer reaction, 824
- N*-*t*-Butylphenylnitron, spin trapping, 664
- t*-Butyl phenylperacetates
thermal decomposition, 900–7
thermolysis, 903–7
two-bond homolysis, 902
- t*-Butyl(trimethylsilyl) peroxide, 1,4-thioxane oxidation, 805–6
- C10 carba dimers, antitumour endoperoxides, 1337, 1340
- Cage structure
faujasite supercage structure, 869–70
radical polymerization, 697
- Calorimetry
differential scanning calorimetry, 672
enthalpy of formation determination, 155, 160, 163, 165
isothermal microcalorimetry, 672
oxidation stability evaluation, 672
- Capillary zone electrophoresis (CZE), 652, 687, 698–9, 744
- Carbenes, dioxirane preparation, 1132
- Carbocations, antimalarial endoperoxides, 1309
- Carbohydrate hydroperoxides, Mo-catalyzed olefin epoxidation, 432, 436
- Carbohydrates, TBARS assay, 669
- Carbonate esters, oxidative ozonolysis, 737, 738
- Carbon–carbon double bonds
epoxidation, 362–472
nucleophilic addition cyclization, 230, 233, 238–45
- Carbon-centered radicals
diradicals, 192
1,2,4-trioxane antimalarials, 1283–99, 1309
- Carbon–hydrogen bonds
dioxirane oxygen insertion, 1138–9, 1158–63
oxyfunctionalization, 1159
ozonization, 178
secondary, 1161
tertiary, 1161
vinylic, 661
- Carbon–hydrogen oxidation reactions, 503–31, 532
- Carbon number
conjugated dienes, 671
effective carbon number, 689, 690, 708
- Carbon–oxygen bonds
¹⁷O NMR chemical shifts, 174, 177
see also Dihedral angles
- Carbonyl compounds

- Carbonyl compounds (*continued*)
allylic hydroperoxide and alcohol coupling, 285–90
protein hydroperoxide decomposition, 986–7
secondary oxidation products, 656, 669–71
- Carbonyl functions, peroxyacetalization, 273–85
- Carbonyl group, nucleophilic addition
cyclization, 230, 233, 245–52, 253
- Carbonyl hydrate, hydroperoxide
hydrogenolysis, 156
- Carbonyl oxides
electronic structure, 29–32
nucleophilic addition cyclization, 243, 244
oxygen atom transfer, 32, 34–48
density functional theory, 34–5
epoxidation
alkenes, 35–40
relative rates in solution, 40–4
saturated hydrocarbon oxidation, 44–8
- Carboxylic acids
C–H bond unreactive to insertion, 1160
hydroperoxide oxidation, 692
- Cardamom peroxide, antimalarial, 190, 191
- Cardiac hypertrophy, reactive oxygen species, 611
- Cardiolipin, hydroperoxide determination, 675, 686
- Cardiovascular systems, reactive oxygen species, 611–12
- Caroate *see* Potassium peroxymonosulfate
- Carotenoids
flour bleaching, 622
peroxide value, 658
- (*R*)-Carvone, nucleophilic addition cyclization, 243, 244
- CASSCF *see* Complete active space calculation
- Catalase
hydrogen peroxide determination, 626, 642, 650, 655, 664, 674
hydroperoxide determination, 678
performic acid reaction, 698
peroxide explosive determination, 708
- Catalysis
chiral, 478–85
co-catalyzed hydroperoxysilylation, 1329, 1330
decomposition
chemiluminescence mechanism, 1231–8
dioxetanes, 1189–91
diphenoyl peroxide, 1213–14
dialkyl peroxide synthesis
acid- or base-catalyzed, 351–8
metal-catalyzed, 358–60
dioxiranes
epoxidation, 1146–50
preparation, 1130, 1132
epoxidation
chiral metal complexes, 394–401
metal-catalyzed, 386–472
in situ generated catalyst and acid, 437
olefins, 790–2
organo-catalyzed, 370–86
uncatalyzed and base-catalyzed, 363–70
sulfoxidation
enzyme-catalyzed, 474–6
metal-catalyzed, 476–92, 493–5
transition metal-catalyzed alcohol oxidation, 787–9, 1057, 1105–8
uric acid oxidation, 625
see also Cobalt catalysis
- Catalysis quenching, chemiluminescence, 647–8
- Catechol, hydrogen peroxide determination, 651
- Catecholamines, hydrogen peroxide determination, 625, 626, 647
- Cations
benzylic cleavage, 911–12
intrazeolite photooxygenation
cation- π interactions, 873–4
local minima structures, 873
regioselectivity, 874–7
radical cycloaddition, 204–12
- CCSD, density functional theory, 3, 34–5, 43
- β -CD-hemin, cyclodextrin condensation, 630
- CDV (conjugated dienes value), 663, 671–2
- Cell signaling, reactive nitrogen species, 611
- Cellular indicators of hydroperoxides
DNA oxidation products, 918, 975–7
lipid hydroperoxides, 918, 977–85
protein hydroperoxides, 918, 985–7
- Cellulose, grafted, 698
- Central composite design, analytical methods, 624
- Cerebral ischemia, lipid hydroperoxides, 612
- Cerium(III), hydrogen peroxide determination, 640
- Cerium(IV), hydrogen peroxide determination, 640
- Cesium ozonide, 735
- CFCs *see* Chlorofluorocarbons
- Chain flexibility, poly(styrene peroxide), 709
- Chain reactions
all-homolytic autoxidation, 218–21
free radicals, 225, 227, 229–30, 231–2
- Charge transfer complexes
chemiluminescence mechanism, 1232, 1233–4
 π -complexes with ozone, 731–2
- CHD (1,4-cyclohexadiene), 264, 1229–30
- Chemical industry
peroxide involvement, 617–24
safety issues, 744–9

- Chemically Initiated Electron Exchange Luminescence (CIEEL)
 acridinium salts, 1256
 alkaline phosphatase, 1193–8
 1,2-dioxetanes, 1182–200
 firefly bioluminescence, 1191–3
 intermolecular, 1213–15, 1231–6
 intramolecular, 1214–15, 1236–8
 luminol, 1247–8
 peroxyoxalates, 1188–9, 1266–70
- Chemical oxygen demand, pollution evaluation, 739
- Chemicals handling, regulatory agencies, 745–9
- Chemical shifts
 dioxiranes, 1132–3
 ¹⁷O NMR dihedral angles, 174, 177, 183
 ²⁹Si NMR spectroscopy, 182
 trioxides, 178–80
- Chemical titration, chemiluminescence quantum yields, 1223–4
- Chemiluminescence (CL), 1211–78
 activators, 1220, 1221, 1222
 peroxide decomposition, 1231, 1234
 peroxyoxalates, 1189, 1190, 1256–7, 1266–7
 basic principles, 1215–18
 bioassays, 1173, 1191–200, 1205
 catalysis quenching, 647–8
 chemiexcitation mechanism, 1213, 1214, 1215–18, 1232–3
 acridinium salts, 1253, 1255
 1,2-dioxetanes, 1186–8
 luminol oxidation, 1244–8
 meta-effect, 1186–8, 1236–7
 peroxyoxalates, 1257, 1258, 1266–70
 quantum yields, 1223, 1226, 1236, 1266–8
 reaction rates, 1221
- classification of reactions, 1218–21
 activated chemiluminescence, 1220–1, 1223
 direct chemiluminescence, 1218–19
 indirect chemiluminescence, 1219–20, 1221, 1223
- energy acceptors, 1223
- excited states, 1215–18
- Franck–Condon Principle, 1217
- heavy-atom effect, 1219
- high-energy intermediate, 1215, 1262, 1263
 activators, 1220, 1222
 peroxyoxalates, 1188–9, 1257, 1261–6, 1267, 1269
- history, 1212–15
- hydrogen peroxide determination, 643–9
- hydroperoxide determination, 680–3
- immunoassays, 1205, 1215, 1236
- lucigenin, 1212, 1239, 1248–56
- luminol oxidation, 643–6, 708, 741–2, 1238–48
- Marcus Theory, 1217–18, 1235
- mechanisms
 catalyzed peroxide decomposition
 dioxetanes, 1189–91
 diphenoyl peroxide, 1213–14
 intermolecular electron transfer, 1231–6, 1238
 intramolecular electron transfer, 1236–8
- CIEEL approach, 1213–15, 1231–8
- unimolecular peroxide decomposition, 1227–31
 asynchronous concerted mechanism, 1230
 biradical mechanism, 1227–31
 concerted mechanism, 1227, 1228–9, 1230
 merged mechanism, 1227, 1230
- peroxide intermediates, 1238–70
 luminol oxidation, 1238–48
 peroxyoxalates, 1188–9
- peroxyoxalates, 1188–90, 1220–1, 1225, 1226, 1235, 1239, 1248, 1256–70
- research methods, 1221–7
 actinometry, 1224, 1225
 activation parameters, 1221–2
 electronic excitation yields, 1221
 emission intensity calibration, 1224–7
 quantum yields, 1222–4
 chemical titration, 1223–4
 emission quantum yields, 1221, 1222–3
 energy transfer quantum yields, 1223
 excitation quantum yields, 1221, 1222–3, 1225
 reciprocal quantum yields, 1223
 rate constants, 1221–2
 singlet oxygen generation, 673
 see also 1,2-Dioxetanes; 1,2-Dioxetanones
- Chemometrics, analytical methods, 624
- Chemoselectivity, dioxirane epoxidation, 1150
- Chicken
 hydroperoxide determination, 676
 peroxide value, 658
- Chiral alkenes
 dioxirane epoxidation, 1144–50
 chirality centers, 1145
 prochiral alkenes, 1145
- intrazeolite photooxygenation
 diastereoselectivity, 883–6, 887
 regioselectivity, 886, 887
- Chiral allylic alcohols, photooxidation, 889
- Chiral allylstannanes, 1,2-dioxolane synthesis, 235–6
- Chiral auxiliaries, diastereoselective allylic hydroperoxide formation, 868–9

- Chiral catalysts, asymmetric metal-catalyzed sulfoxidations, 478–85
- Chiral 1,2-dihydronaphthalenes, photooxygenation, 265–6
- Chiral dioxetanes, stereoselective synthesis, 1173–8
- Chiral endoperoxides, synthesis, 260, 261
- Chiral hydroperoxides
- allylic alcohol asymmetric epoxidation, 401–6, 407–9
 - asymmetric metal-catalyzed sulfoxidations, 485–92, 493–5
 - (*E*)-configuration, 346
 - synthesis, 329–51
- Chiral metal complexes, allylic alcohol epoxidation catalysis, 394–401
- Chiral naphthalene derivatives, singlet oxygen cycloaddition, 271
- Chiral sulfides, dioxirane oxidation, 1156–7
- Chlamydomonas reinhardtii*, hydrogen peroxide determination, 646
- γ -Chlordene, isomers, 728
- Chlorella fusca*, hydrogen peroxide determination, 646
- Chlorinated ethylenes, ozone adducts, 720, 731–2
- Chlorobenzene, homolysis of *tert*-butyl phenylperacetates, 900–2
- Chlorofluorocarbons (CFCs)
- in atmosphere, 604
 - substitutes, 138
- Chloroform stability, lipid hydroperoxides, 676
- Chlorohydrosilane, alkyl sodium alkyl peroxide reaction, 783
- Chlorohydrins, olefin oxidation synthesis, 792–3
- Chloromethane, vibrational spectra, 692
- meta*-Chloroperbenzoic acid (*m*-CPBA)
- diastereoselectivity, 1144
 - transition metal peroxides, 1090, 1091
- p*-Chlorophenol, quinoneimine dyes, 630
- Chlorophyll, UV–visible spectrophotometry, 664
- Chlorotetramethyldisiloxane, preparation, 781
- Chlorotriorganosilanes, silyl peroxide preparation, 779–83
- CHLP protocol, enthalpies of vaporization, 147, 149, 150, 161, 165
- Cholestene hydroperoxides, electrochemical methods, 687
- Cholesterol
- lipid hydroperoxide determination, 681–2, 687
 - lipid oxidation, 946–7
- Cholesteryl acetate
- hydroperoxide determination, 682, 690
 - ozonolysis, 695–6
- Cholesteryl arachidonate, hydroperoxide formation, 693
- Cholesteryl esters
- hydroperoxide determination, 676, 680, 681, 682, 687, 692
 - photosensitized oxidation, 692
- Cholesteryl hydroperoxides, in skin, 612
- Cholesteryl linoleate, hydroperoxide formation, 693
- Choline phosphatide, ozonides, 719, 726
- Chondrollin
- antitumour activity, 1333
 - isolation, 190, 191
- CHP *see* Cumyl hydroperoxide
- CHRIS manual, hazards classification, 745
- Chromatography
- conjugated dienes value, 671–2
 - enantiomer/diastereomer separation, 329–30
 - gas liquid chromatography, 684–5, 719
 - liquid chromatography, 719
 - ozonide determination, 719
- Chromium catalysts
- alcohol oxidation, 787–8
 - olefin epoxidation, 425
- Cider manufacture, 623
- CIEEL *see* Chemically Initiated Electron Exchange Luminescence
- cis* effect
- regioselective allylic hydroperoxide formation, 834–5, 838, 839, 842
 - anti *cis* effect selectivity, 836–9, 840, 841
- (*R*)-(+)-Citronellal, artemisinin synthesis, 277
- CL *see* Chemiluminescence
- Clark-type electrode, hydrogen peroxide biosensor, 655
- Cleavage
- alkenes, 1094–5
 - Hock-cleavage, 946
 - see also* Bond breaking; Heterolytic cleavage; Homolytic cleavage
- Clinical samples
- catalysis quenching, 647
 - lipid hydroperoxide determination, 680
- Cloud water
- hydrogen peroxide determination, 638
 - hydroperoxide determination, 678
 - peroxide analysis, 604
- Cluster analysis, analytical methods, 624
- ¹³C NMR spectroscopy
- peroxyoxalate chemiluminescence, 1266
 - polyethylene thermal oxidation, 695
 - trioxide chemical shifts, 179
- Coatings
- autoxidation, 623
 - curing, 707
 - polymerization formulations, 622
 - see also* Surface coatings

- Cobalt catalysis
 hydroperoxysilylation, 1329, 1330
 luminol
 chemiluminescence, 698, 700, 701
 oxidation, 645
- Cobalt(II) complexes, peroxidation, 223, 225, 228–9
- Cobalt(II)–EDTA complex, hydrogen peroxide determination, 628, 639
- Cobalt(II)–hexacyanoferrate, hydrogen peroxide determination, 651
- Cobalt(III)–phthalocyaninetetrasulfonate, hydroperoxide determination, 677
- Cocrystallization, alkyl hydroperoxides–ether, 111, 113
- Coffee, instant, 610, 628
- Cold on-column injection, thermal analysis, 684–5
- Colorimetry
 dialkyl peroxide determination, 707–8
 hydrogen peroxide determination, 628–49
 hydroperoxide determination, 674–83
 peroxide value, 657, 658–61
 total polar phenols, 664
- Column chromatography,
 enantiomer/diastereomer separation, 330
- Combustion *see* Enthalpies of combustion
- Combustion aerosols, hydroperoxide determination, 678
- Combustion calorimetry, enthalpy of formation determination, 155, 160, 163
- Commercial products
 hydrogen peroxide determination, 630–1, 632–3, 634
 oxalate determination, 633, 635
 peroxides, 617, 618–21, 745
- Complete active space (CASSCF) calculation
 dioxymethane, 29
 peroxynitrous acid, 12
- Complexation model, intrazeolite
 photooxygenation, 878
- Computational chemistry
 dioxetane chemiluminescent decomposition, 1181–2, 1185–6
 dioxiranes, 1134–9, 1142–3
- Condensation reactions
 cyclodextrin, 630
 μ -peroxo transition metal complexes, 1060
- Conductivity, oxidation stability measurement, 664
- Configuration
 (*E*)-configuration, 346
 retention, 811
- Conformation
 acyclic organic peroxides, 100, 102, 104–5
 anomeric effect, 723
 chair conformations, 722, 723, 729
 envelope conformations, 721, 722–3, 724, 727–9
 final ozonides, 721–2
 peroxynitrous acid, 8–9
 primary ozonides, 721
 trioxides, 180
- Conjugated diene peroxides, conjugated dienes value, 671
- Conjugated dienes value (CDV), secondary oxidation products, 663, 671–2
- Coordination compounds
 ¹⁷O NMR spectroscopy, 185
 silyl peroxides, 808–10
- Coordination ionospray mass spectrometry, 693
- Co-oxygenation
 endoperoxide synthesis, 252
 thiol–olefin, 221–3, 224, 225, 226, 250, 251, 1330
- Copper(II) catalysis, chemiluminescence, 647
- Core aldehydes
 mass spectrometry, 689
 ozonides, 719, 739
- Corn oil, oxidation products, 693
- Corrosive substances
 hydrogen peroxide bleach, 623
 labeling codes, 621, 752
 UN classification, 746
- Cosmetics, keratinocytes, 613
- Coulomb repulsion, lone pairs, 100
- Coulometry
 hydroperoxide determination, 687
 peroxide value, 664
- Coumarin derivatives, hydrogen peroxide determination, 649
- p*-Coumaric acid, fluorescence enhancer, 644–5
- Covalent radii, alkyl hydroperoxide anion ligands, 114, 118–19
- CPMA (*meta*-chloroperbenzoic acid), 1090, 1091, 1144
- p*-Cresol, hydrogen peroxide determination, 639
- Criegee's mechanism, ozonolysis, 606, 685, 716–17, 721, 726, 729
- Criminals, dialkyl peroxide explosives, 708
- Cross-linking
 agents, 622, 697, 706
 IR spectrophotometry, 662
 protein hydroperoxides, 973–5
- Crown ethers, alkali metal ozonides, 736–7
- Cryptand[2.2.2], alkali metal ozonides, 736–7
- Crystallography *see* X-ray analysis; X-ray diffraction
- Crystal structure
 alkyl hydroperoxides, 105–14
 diacyl peroxides, 128, 130–1
 dialkyl peroxides, 119–25

- Crystal structure (*continued*)
 longilene peroxide, 136
 peracids, 125–7
 peresters, 127–8, 138, 139
 urea–hydrogen peroxide, 98, 99
see also Structure
- Cumyl allyl peroxide, determination, 708
 Cumyl free radical, 697
 Cumyl hydroperoxide (CHP)
 hydrogen bonding, 103–4
 hydrogen peroxide determination, 629, 637, 643, 680, 682–3
 hydroperoxide determination, 683, 686, 688, 689
 manufacture, 617, 622
 peroxide value, 659, 660
 sulfide oxidation, 1097
- Cumyl perbenzoate, synthesis control, 700
 Cumyl perbutyrate, synthesis control, 700
 Cumyl pervalerate, synthesis control, 700
 Cumyl 3-phenylpropyl peroxide, determination, 708
 Cumyl propyl peroxide, determination, 708
 Curing processes, 692, 707
 Curtin–Hammett principle, electron-poor alkene photooxygenation, 877
 Cyanine dye, TBARS assay, 667
 Cyanohydrins, bis(trimethylsilyl) peroxide reactions, 797
 Cyanopyridine, methyltrioxorhenium ligands, 460–1
 Cyclic alkenes, geminal regioselectivity, 846–7
 Cyclic disilanes, oxidation with molecular oxygen, 815–19
 Cyclic disilazanes, disila-2,3-dioxane preparation, 814–15
 Cyclic hydrocarbons, diastereoselective allylic hydroperoxide formation, 861–3, 864
 Cyclic olefins, final ozonides, 718
 Cyclic peroxides
 chemiluminescence, 1212–13, 1262, 1265, 1266, 1270
 disilirane singlet oxygenation, 818
 enthalpies of formation, 163–7
 oxidation, 1178
 ozonide oligomerization, 718
 synthesis, 189–305, 705
 halogen-mediated, 225, 227, 229–30, 231–2
see also Dioxetanes; Endoperoxides
 Cyclic peroxy hemiketals, triplet oxygen cycloaddition, 201, 203
 Cyclic silyl peroxides
 disilazane and urea–hydrogen peroxide reactions, 814–15
 oxidation with molecular oxygen
 disilanes, 815–19
 disilenes, 819–21
- Cyclic voltametry
 dialkyl peroxides, 715–16
 disposable electrodes, 652
 hydrogen peroxide determination, 652
- Cyclization
 alkenyl hydroperoxides, 212–18
 hydroperoxides, 230, 233–52, 253
- Cycloaddition
 [2 + 2] cycloaddition
 C3-aryl 1,2,4-trioxane synthesis, 1325–6, 1327, 1332
 1,2-dioxetanes, 255, 1172, 1173–8, 1224
 [3 + 2] cycloaddition, ozone to C=C bond, 247, 248
 [4 + 2] cycloaddition
 to dienes, 1324, 1325, 1332
 1,3-dienes, 211, 253–71
 fenozan synthesis, 1324, 1325, 1332
 [6 + 2] cycloaddition, 267
 singlet oxygen
 [2 + 2] cycloaddition
 chiral dioxetane synthesis, 1172, 1173–8, 1224
 1,2-dioxetanes, 255
 to vinyl ether, 1325–6, 1327
 dienes
 1,3-dienes, 252–73
 [4 + 2] cycloaddition, 253–71, 1324, 1325, 1332
- triplet oxygen
 [4 + 2] cycloaddition, 211
 cation radicals, 204–12
 diradicals, 192–204
- Cyclo(alkylperoxyorgano)siloxanes, reparation, 782–3
- Cyclobutane, ring-opening reaction, 164
 β -Cyclodextrin
 hemin condensation, 630, 639
 hydroperoxide determination, 687
 1,3-Cyclodigermoxanes, 825, 826
 1,3-Cyclodisiloxanes
 disiladioxetane rearrangement, 820–1
 disilirane oxidation, 816, 817
 3,5-Cycloheptadienol, TBS-protected, 266
 Cycloheptane, flame ionization detection, 689
 Cycloheptatriene, singlet oxygen
 cycloaddition, 267, 268
 1,3-Cyclohexadiene, singlet oxygen
 cycloaddition, 264
 1,4-Cyclohexadiene (CHD)
 chemiluminescence mechanism, 1229–30
 photooxygenation, 264
 Cyclohexane, C–H bond dioxirane oxygen insertion, 1158–9
 1,2-Cyclohexanediol acetal, C–H bond dioxirane oxygen insertion, 1161

- Cyclohexanone, C–H bond dioxirane oxygen insertion, 1158–9
- Cyclohexene, primary ozonide, 720
- Cyclohexyl hydroperoxide, flame ionization detection, 689
- Cyclopentadiene
peroxide synthesis, 706
photooxygenation, 263
- Cyclopentadisilane, oxidation with molecular oxygen, 815
- Cyclopentane bromohydroperoxides, stereoisomerism, 313, 314
- Cyclopentene, primary ozonide, 720
- Cycloperoxychlorination, 1,2-dioxolane synthesis, 238, 240
- Cyclopropanecarboxylic acid, peroxydisulfate reactions, 1010
- Cyclopropanes, 1,2,3-trisubstituted, 205, 206
- Cyclopropanols, nucleophilic addition cyclization, 249–50
- Cyclopropylcarbinyl–homoallyl rearrangement, radical-mediated reactions, 223, 226
- Cypridina*, bioluminescence, 1255
- Cytochrome C, lipid hydroperoxide determination, 681
- Cytosine hydroperoxides, 919
- Cytotoxic effects, lipid peroxides, 613
- CZE (capillary zone electrophoresis), 652, 687, 698–9, 744
- DABCO $2\text{H}_2\cdot\text{O}_2$ reagent, 778–9, 780
- Dairy products, oxidation stability, 664, 665, 666
- Dangerous materials, UN registration numbers, 621
- Data (thermochemical)
error bars, 147, 150
quality, 147, 150
sources, 146–7
- DBA (9,10-dibromoanthracene), 1219, 1223, 1226
- 1-Decahydronaphthylcyclohexylmethylsilane, ozonolysis, 811
- Decalin hydroperoxide, enthalpy of reaction, 153
- Decomposition
catalyzed, 1189–91, 1213–14, 1231–8
5,6-dihydrothymine, 930
hydroperoxides, 153
nucleobase hydroperoxides, 918, 975–7
polar effects, 899–913
protein hydroperoxides, 986–7
radiation-induced, 930
thymidine hydroperoxides, 930–3
unimolecular, 1227–31
see also Thermal decomposition
- Deep fat frying, oil autoxidation, 623, 662
- Deflagration, peroxides, 617
- Degradation
arteflene, 1304–9, 1310
enthalpies of degradation, 155
haemoglobin, 1281, 1283
- Dehydrative condensation, μ -peroxo transition metal complexes, 1060
- Demethylation, bis(trimethylsilyl) peroxide, 798
- Densitometry
hydroperoxide determination, 675, 678, 683
photodensitometry, 678
- Density functional theory (DFT)
B3LYP level, 4, 34–5, 38, 40, 41, 43
CCSD level, 3, 34–5, 43
dioxirane oxygen atom transfer, 34–5
QCISD level, 3, 34–5, 43
- 10-Deoxoartemisinin, synthesis, 289–90
- 10-Deoxoartemisinin, synthesis, 289–90
- Deoxyartemisinin, not antimalarial, 1280–1, 1283
- Deoxyepinephrine, chemiluminescence, 647
- Deoxygenation, hydroperoxides, 153
- DEPT (distortionless enhancement by polarization transfer), 725–6
- 6,9-Desdimethylartemisinin, synthesis, 288
- Desferrioxamine, PfATP6 enzyme inhibition, 1313
- DET *see* Diethyl tartrate
- Detergents, peracetic acid, 699
- Deterioration
indices, 625, 656–72
thermal autoxidation, 623
- Detonation, peroxides, 617
- Detoxification, reactive oxygen species, 611–12
- Deuteration, dimethyldioxirane epoxidation, 1143
- DFT *see* Density functional theory
- Diabetes, lipid peroxides, 613
- Diacetylene peroxides, thermal analysis, 715
- Diacyl peroxides
commercial availability, 620, 622
crystal structure, 128, 130–1
geometric parameters, 130
determination, 698, 700, 701
enthalpies of reaction, 162–3
formal hydrogenolysis, 162
peroxide value, 658
polymerization agents, 622
structure, 703
- Diagnosis, chemiluminescence, 643
- Dialkyl peroxides
analytical and safety aspects, 705–16
commercial availability, 619–20, 621
crystal structure, 119–25
detection and determination

- Dialkyl peroxides (*continued*)
 colorimetry, 707–8
 flame ionization detection, 708
 NMR spectroscopy, 708
 titration methods, 707
 UV–visible spectrophotometry, 707–8
 enthalpies of reactions, 153–4
 graft polymerization initiation, 706
 hydroperoxide determination, 685
 peroxide transfer synthesis, 824–5
 structural characterization, 708–16
 electrochemical analysis, 715–16
 electron diffraction, 713
 mass spectrometry, 714
 NMR spectroscopy, 709–11
 thermal analysis, 714–15
 vibrational spectra, 713–14
 X-ray crystallography, 711–13
 synthesis
 acid- or base-catalyzed, 351–8
 autoxidation, 360, 362
 metal-catalyzed, 358–60
 stannyl peroxides, 361, 362
 thermal decomposition, 706–7
 3,5-Dialkyl-1,2,4-trioxolane, IR
 spectrophotometry, 719
 Diallyl diradicals, triplet oxygen cycloaddition,
 196, 197
 Diamantane, bis(trimethylsilyl) peroxide
 reaction, 802
 Diamantanol, bis(trimethylsilyl) peroxide
 reaction, 802
 2,3-Diaminophenazine, hydrogen peroxide
 determination, 634
 Diaroyl peroxides, peroxide value, 658
 1,2-Diarylcyclopropane, photooxygenation,
 205, 206
 1,1-Diarylethylenes, photooxygenation, 207–8
 2,6-Diaryl-1,6-heptadienes, triplet oxygen
 cycloaddition, 209, 210
 2,2-Diaryl-1-methylenecyclopropanes,
 photooxygenation, 206–7
 3,6-Diaryl-2,6-octadienes, photooxygenation,
 209, 210
 1,2-Distearoyl-3-oleyl-*sn*-glycerol, synthesis,
 739
 Diastereomers, chromatographic separation,
 329–30
 Diastereoselectivity
 allylic hydroperoxide formation, 860–9
 cyclic hydrocarbons, 861–3, 864
 heteroatom substituents, 861, 863, 864
 photooxygenation
 allylic alcohols and amines, 836, 837
 chiral alkenes, 883–6, 887
 stereogenic center, chiral alkenes, 884–5,
 1144
 stereogenic center at α -position, 863–9
 attractive interactions, 864–6
 chiral auxiliaries, 868–9
erythro diastereoselectivity, 867
 repulsive interactions, 867–8
threo diastereoselectivity, 864–6, 867
 steric strain, 866
 synthetic applications, 886, 888–9, 891
 dioxirane epoxidation, 1144–5
 ene diol epoxidation, 413, 415–16
 π -facial diastereoselectivity, 272
 hydroxyl-group directivity, 1144–5
 Diazabicyclo[2.2.2]octane, superoxide
 reactions, 1034
 Diazaquinone, luminol oxidation, 1240–2,
 1244, 1245, 1246
 Diazene, furan ozonide decomposition, 730
 Diazo compounds, ozone adducts, 734
 Diazonium salts, TBARS assay, 667
 Dibenzoyl peroxide, determination, 698
 Z-Dibenzoylstilbene, tetracyclone bleaching,
 734–5
 9,10-Dibromoanthracene (DBA),
 chemiluminescence, 1219, 1223, 1226
 Dibromoarene, potassium peroxymonosulfate
 reactions, 1027
 3,6-Dibromocyclohexene, peroxydisulfate
 reactions, 1016
 3,5-Dibromo-4-nitrosobenzenesulfonic acid,
 spin trapping, 664
 E-Di-*t*-butylethylene, primary ozonide, 717
 Di-*t*-butyl peroxalate, synthesis, 700
 Di-*t*-butyl peroxide
 air pollutant, 622
 determination, 707, 708
 HVP chemical, 622
 hydrogen bond basicity, 100
 Di-*t*-butyl peroxydicarbonate, fragmentation,
 703–4
 [alpha,alpha]-Dicarbonyl-phosphoranes,
 dioxirane oxidation, 1154–5
 1,2-Dichloroaceneaphthylene, ozonides, 724
 E2,3-Dichloro-2-butene, ozonolysis, 685, 686,
 699, 724
 Dichlorodimethyltetroxanes, 685, 686
 1,2-Dichloroethene, π -complex with ozone,
 731–2
 1,2-Dichloroethylene, ozonolysis, 706
 1,1-Dichloroethyl hydroperoxide, 685, 686
 1,1-Dichloroethyl peracetate, determination,
 699
 Dichlorofluorescein, hydrogen peroxide
 determination, 626, 640
 3,5-Dichloro-2-hydroxyphenylsulfonate,
 hydrogen peroxide determination, 632,
 633
 3,5-Dichloro-2-hydroxyphenylsulfonic acid
 (Trinder's reagent), 630, 631

- 1,3-Dichloro(tetramethyl)siloxane, chlorotetramethyldisiloxane preparation, 781
- 3,6-Dichloro-1,2,4,5-tetraoxanes, formation, 706
- 7-(4,6-Dichloro-1,3,5-triazinylamino)-4-methylcoumarin, hydrogen peroxide determination, 649
- Dichlorotriphenylphosphorane, bis(trimethylsilyl) peroxide reactions, 804–5
- Diels–Alder reactions
cycloaddition of 1,3-dienes, 253
luminol oxidation, 1242, 1245, 1246
- Dienals, conjugated dienes value, 671
- Dienes
dioxirane asymmetric epoxidation, 1150
domino reactions, 221–3, 224, 225, 226–7
- 1,3-Dienes
cycloaddition, singlet oxygen, 252–73
[4 + 2] cycloaddition
singlet oxygen, 253–71, 1324, 1325, 1332
triplet oxygen, 211
twisted, 856–7, 858
- 1,5-Dienes, peroxidation, 223, 225, 228–9
- Diesel engine soot, hydroperoxide determination, 678
- Diesel fuel, *t*-butyl hydroperoxide additive, 624
- Dietary intake, lipid hydroperoxides, 614
- Diethyl tartrate (DET)
allylic alcohol epoxidation, 395
transition metal peroxides, 1088, 1092, 1113
- Differential scanning calorimetry (DSC)
alkyd resin coatings, 672
poly(methyl methacrylate peroxide), 714
- Difluorodioxirane, ¹⁷O NMR spectroscopy, 184–5
- Z-1,2-Difluoroethylene, ozonization, 722
- cis*-Difluoroethylene oxide, final ozonide, 722
- 1,2-Digermadioxetanes, 825, 826
- 1,2-Digermetrene, digermin formation, 819
- Digermin, 1,2-digermetrene reaction, 819
- Digermirane, photooxygenation, 825–6
- Digermolanes, 825–7
- Dihedral angles
¹⁷O NMR chemical shifts, 174, 177, 183
peroxy ligands, 119
steric effects, 101, 177
- Dihydroartemisinic acid, artemisinin synthesis, 288, 289
- Dihydroartemisinin, antimalarial, 1281
- Dihydrogen dioxide *see* Hydrogen peroxide
- Dihydrogen trioxide
formation mechanism, 181
¹⁷O NMR spectroscopy, 180–1
structural chemistry, 131–2
- Dihydrorhodamine, peroxydinitrite determination, 740, 741
- 5,6-Dihydrothymine, thymine hydroperoxides, 927, 928, 930
- Dihydroxybenzylamine, chemiluminescence, 647
- Dihydroxylation
alkene/alkyne vicinal dihydroxylation, 556, 567–72, 573–5
ketones, 520–1
- 3,4-Dihydroxyphenylalanine (DOPA), serum protein, 614, 615
- Diisopropyl tartrate (DIPT), allylic alcohol epoxidation, 395
- Dilauroyl peroxide, determination, 701
- Dimesityldioxirane, 26, 1133–4
- 3-(Dimethylamino)benzoic acid
hydrogen peroxide determination, 635
oxalate determination, 633
- Dimethylaniline, quinoneimine dyes, 630
- 2,3-Dimethyl-2-butene, primary ozonide, 720
- Dimethylcarbonyl oxide, ethylene epoxidation, 36–7
- Dimethyl-1,2-dioxetanone, chemiluminescence quantum yield, 1226–7
- Dimethyldioxirane
epoxidation
alkenes, 37–44
deuteriation, 1143
¹⁷O NMR spectroscopy, 184–5
preparation, 26, 1130–2
structure, 26
- 2,2-Dimethylloxazolidine derivatives of sorbic acid, singlet oxygen cycloaddition, 260, 261
- N,N*-Dimethyl-*p*-phenylenediamine dihydrochloride, hydroperoxide determination, 678
- Dimethylphenylsilyl hydrotrioxide
silane ozonolysis, 812
²⁹Si NMR spectroscopy, 182
- 3,5-Dimethylpyrazole (dmpz), transition metal peroxides, 1116
- β,β -Dimethyl styrene, photooxygenation, 839–41
- Dimethyl sulfide
tert-butyl perbenzoate ETR reactions, 909–11
hydroperoxide determination, 684, 696
oxidation, 74, 75
- 2,4-Dinitrophenylhydrazones (DNP)
aldehyde determination, 670
core aldehydes, 689
malondialdehyde determination, 669
ozonide reduction, 726
- gem*-Diols
hydroperoxide hydrogenolysis, 156
1,2,4,5-tetroxane formal reactions, 165

- 2,3-Dioxabicyclo[2.2.1]heptane, synthesis, 233
- 2,3-Dioxabicyclo[3.3.1]nonane, thiol-olefin
co-oxygenation, 222, 223
- 1,2-Dioxadigermins, oxidation with molecular
oxygen, 819
- 1,2-Dioxadisilins, oxidation with molecular
oxygen, 819
- 1,2-Dioxane synthesis, 192–273
fused bicyclic dioxanes, 196, 197
- 1,3-Dioxaphosphorinane, oxidation, 804
- Dioxasiletane, disilirane singlet oxygenation,
817, 818
- 1,2-Diox-4-ene ring system, dialkyl peroxide
formation, 706
- 1,2-Dioxetanedione, chemiluminescence,
1212–13, 1261, 1262, 1265
- Dioxetanes
C3-aryl 1,2,4-trioxane synthesis, 1325–6,
1327, 1332
chiral, 1173–8
contemporary trends, 1171–209
enthalpies of formation, 163–4
four-membered rings, 164, 1212–13
lipid hydroperoxides, 954
ring strain, 163
- 1,2-Dioxetanes
alkene conversion, 812–13
chemiluminescence, 1173, 1181–200, 1212,
1213, 1214–15, 1218–19, 1220
acridinium salts, 1256
bioassays, 1173, 1191–3, 1198–200
alkaline phosphatase, 1193–200
firefly bioluminescence, 1191–2
 β -galactosidase, 1193, 1198–9
catalytic decomposition, 1189–91, 1232,
1236–8
chemiexcitation, 1186–8
CIEEL approach, 1182–9
intermediates
 lucigenin chemiluminescence, 1249–50
 peroxyoxalate chemiluminescence,
 1188–9
 meta-effect, 1186–8, 1236–7
 methyl-substituted, 1228
 molecular biology, 1198–200
 quantum yields, 1222–4, 1225, 1226
 unimolecular decomposition, 1227–31
- 1,3-diene cycloaddition, 255
- photooxygenation
of DNA, 1200–5
synthesis, 1236
- syn* selective ene reaction, 839–40
- thermal decomposition, 1181–91, 1213,
1214, 1218–19, 1223, 1226
- 1,2-Dioxetanones, 1172
chemiluminescence
acridinium salts, 1252, 1253, 1255
mechanism, 1213, 1227, 1232, 1234,
1235
peroxyoxalates, 1265, 1266
quantum yields, 1223, 1226
synthesis, 1212
- Dioxiranes, 1129–69
acylation, 1160
Baeyer–Villiger ketone oxidation, 785
C–H bond oxygen insertion, 1138–9,
1158–63
configuration retention, 1163
overoxidation protection, 1160
chemoselectivity, 1150
diastereoselectivity, 1144–5
electronic structure, 29–32
enantioselectivity, 1145–50, 1162
epoxidation, 1135–8, 1139–50
 alkenes, 35–40, 1136, 1139–50
 asymmetric, 1146, 1149, 1150
 heteroarenes, 1143–4
 Weitz–Scheffer reaction, 1142
heteroatom oxidations, 1138, 1150–8
 halogens, 1157–8
 nitrogen, 1151–4
 oxygen, 1155
 phosphorus, 1154–5
 selenium, 1157
 sulfur, 1156–7
historical development, 1130, 1131
iodometric determination, 1158
mechanistic aspects, 1134–9
molecular orbital treatments, 27–9
¹⁷O NMR spectroscopy, 184–5
oxygen atom transfer, 32, 34–48
 agents, 1130
 catalysis, 1136
 density functional theory, 34–5
 epoxidation
 alkenes, 35–40
 relative rates in solution, 40–4
 mechanistic aspects, 1134–9
 saturated hydrocarbon oxidation, 44–8
 transition structures, 1135–9
ozonides, 716–17
preparation and isolation, 705–6, 1130–2
reactivity, 1134–5, 1139–63
regioselectivity, 1150, 1161
spectral characterization, 1132–4
stereoselectivity, 1139, 1144–50, 1163
strain energy, 1134–5
structure, 26, 27
theoretical chemistry, 26–48
 1,2,3-trioxolane decomposition, 721
1,2-Dioxolane synthesis, 192–273
 fused bicyclic dioxolanes, 193, 194
Dioxygenation, stereoselective, 339–48
Dioxymethane, molecular orbital treatment,
28–9

- Diphenoyl peroxide, chemiluminescence, 1213–14, 1226, 1227, 1232, 1235
- Diphenylanthracene (DPA), chemiluminescence, 1219, 1223, 1226
- 2,3-Diphenyl-2-bornene, ozonide, 728–9
- 1,2-Diphenylethane, dioxetane decomposition, 1230
- Diphenylmethane, chemiluminescence quantum yields, 1235, 1238, 1268
- Diphenyl-1-naphthylphosphine, peroxide value, 659
- Diphenyl-1-pyrenylphosphine hydroperoxide determination, 679–80 peroxide value, 659, 680
- Diphenyl sulfide, peroxyacid reduction, 700–1
- Dipolar intermediate, ene reaction, 853
- Dipole moments, dioxiranes, 1132
- DIPT (diisopropyl tartrate), 395
- Dipyridamole, low-density lipoprotein antioxidant, 611
- Diradicals
- 1,3-diradicals, 195–6
 - 1,4-diradicals, 196, 197
 - 1,5-diradicals, 192
 - allylic, 193, 194
 - carbon-centered, 192
 - diallyl, 196
 - Paterno–Büchi triplet 1,4-diradical, 290–1
 - singlet, 192–3
 - triplet oxygen cycloaddition, 192–204
 - see also* Biradical intermediates; Radicals
- Direct chemiluminescence, 1218–19
- Discoloration, deterioration evaluation, 664
- Disila-2,3-dioxane, preparation from cyclic disilazane, 814–15
- 1,2-Disiladioxetanes, disilene oxidation, 819–21
- Disilanes
- oxidation
 - bis(trimethylsilyl) peroxide reactions, 806–7
 - molecular oxygen, 815–19
 - tetracyanoethylene complexes, 816
- Disilaoxirane
- 1,2-disiladioxetane deoxygenation, 821
 - disilene oxidation, 820
- Disilazanes, urea–hydrogen peroxide reactions, 814–15
- Disilenes, oxidation with molecular oxygen, 819–21
- 1,2-Disilene, disilin formation, 819, 820
- Disilin, 1,2-disilene reaction, 819, 820
- 1,2-Disilirane
- oxidation with molecular oxygen, 816–19
 - disilirane–oxygen adduct, 817
 - UV absorption spectrum, 817
 - oxidation with singlet oxygen, 818
- Disilolanes, oxidation with molecular oxygen, 816–19
- Disinfection
- commercial applications, 617, 622–3
 - ozone
 - in drinking water, 606, 673, 740
 - mechanism, 616
 - percarboxylic acids, 699
- Disodium peroxide, bis(trimethylsilyl) peroxide preparation, 778
- Dispiro-1,2,4,5-tetraoxanes, synthesis, 608, 609, 706
- Dispirotrioxanes, synthesis, 1326, 1327, 1332
- Disposable electrodes, cyclic voltametry, 652
- Disproportionation, enthalpy of reaction, 154, 155
- Dissociation, peroxyxynitrous acid, 13–14
- Dissolved organic carbon (DOC), in water, 606, 607–8
- Distortionless enhancement by polarization transfer (DEPT), 725–6
- Disubstituted alkenes, regioselectivity, 842–4
- o*-Ditoluidine, glucose determination, 632, 634
- o,o'*-Dityrosine, low-density lipoprotein, 610
- DMD *see* Dimethyldioxirane
- DMDO *see* Dimethyldioxirane
- DNA
- biotin markers, 633, 634
 - lipid peroxidation aldehyde adducts, 978–84
 - mutations, 616
 - nucleic acid–protein cross-links, 974–5
 - nucleobase hydroperoxides, 918, 975–7
 - oxidation, 614, 633, 695, 975
 - cellular indicators of hydroperoxides, 918, 975–7
 - residues, 670–1
 - oxidative damage, 614, 633, 918
 - ozone effects, 616
 - peroxide value, 657, 660
 - photooxidation by 1,2-dioxetanes, 1200–5
 - TBARS assay, 669
- DNA hydroperoxides, 919–45
- cytosine components, 919, 935–9
 - guanine components, 939–43
 - 5-methyl-2'-deoxycytidine, 939
 - 8-oxo-7,8-dihydroguanine components, 943–5, 976–7
 - thymine components, 919, 921–33
 - uracil components, 919, 933–5
- DNP *see* 2,4-Dinitrophenylhydrazones
- DNPO (bis(2,4-dinitrophenyl)oxalate), 1261, 1262
- DOC (dissolved organic carbon), 606, 607–8
- Dodecyltrimethylammonium bromide, 744
- Domino reactions, thyl and selenyl radicals, 221–3, 224, 225, 226–7
- DOPA (3,4-dihydroxyphenylalanine), 614, 615

- Dopamine, hydrogen peroxide determination, 625, 626, 647, 651
- Double bond number, conjugated dienes, 671
- Double bonds
- carbon-carbon
 - epoxidation, 362-472, 695
 - nucleophilic addition, 230, 233, 238-45
 - ene adduct, 850-2
 - oxidative cleavage, 525-7
 - peroxide value, 661
 - unsaturation assessment, 740
- Downregulation of metabolism, 610
- 5-Doxylstearic acid methyl ester, spin label, 665
- DPA (diphenylanthracene), 1219, 1223, 1226
- Drinking water, ozone disinfection, 606, 673, 740
- Drugs
- dioxetane chemiluminescence, 1200
 - hybrids and pro-drugs, 1320-3, 1324, 1332, 1342
 - OZ 277 candidate antimalarial, 1317, 1319, 1331
 - see also* Pharmaceuticals
- Drying oils
- coating formulations, 622
 - curing process, 692
 - differential scanning calorimetry, 672
 - peroxide value, 658, 662
- DSC (differential scanning calorimetry), 672, 714
- Dyes, hydrogen peroxide determination, 628-35
- Dye-sensitized intrazeolite photooxygenation, allylic hydroperoxide formation, 869-86, 887
- Ebselen (1,2-Benzisoselenazol-3(2H)-one), 17, 18
- ECN (effective carbon number), 689, 690, 708
- Edible oils
- analysis, 636, 701
 - autoxidation, 614, 623, 661-2
 - peroxide value, 657, 658, 660-3
- EDTA
- Co(II) complex, 628, 639
 - masking, 629, 637
- Effective carbon number (ECN), flame ionization detection, 689, 690, 708
- EHS (extremely hazardous substances), 744
- Elastomers
- cross-linking agents, 622
 - hydroperoxide determination, 676, 684
- Electrocatalytic reduction, hydrogen peroxide, 654
- Electrochemical methods
- dialkyl peroxide structural characterization, 715-16
 - hydrogen peroxide determination, 650-5
 - hydroperoxide determination, 685-9
 - peroxide value, 663-4
- Electrochemiluminescence, 1213, 1214, 1234
- Electron addition, thymine hydroperoxides, 926-7
- Electron-deficient olefins, asymmetric epoxidation, 386-91
- Electron diffraction
- dialkyl peroxides, 713
 - ozonides, 721, 723
 - 1,2,4-trioxolanes, 740
 - see also* Gas electron diffraction
- Electron-donating substituents
- ene reactions, 841
 - sulfonyl peroxides, 1005-7
- Electronegative functional groups, hydrocarbon-substituted peroxides, 147
- Electronic excitation quantum yields, chemiluminescence, 1221, 1222-3
- Electronic structure
- dioxirane and carbonyl oxide, 29-32
 - hydroperoxide oxygen atom transfer, 72-6
- Electron paramagnetic resonance (EPR), arteflene Fe(II) degradation, 1304-5
- Electron-poor alkenes
- dioxirane epoxidation, 1141-3
 - intrazeolite photooxygenation, 877-8
 - transition metal peroxide oxidation, 1087-9
- Electron-rich alkenes
- alkyl hydroperoxide synthesis, 313
 - dioxirane epoxidation, 1139-40
- Electron spin resonance (ESR)
- deterioration evaluation, 656, 664
 - spin-trapping agents, 1291
- Electron transfer reactions (ETR)
- tert*-butyl perbenzoates, 909-11
 - negative charge, 909, 911
 - positive charge, 910, 911
 - tert*-butyl phenylperacetate thermolysis, 903, 905, 906
 - cation radical peroxidation, 204-12
 - chemiluminescence
 - back electron-transfer, 1268
 - CIEEL approach, 1182-8, 1213
 - intermolecular, 1213-15, 1231-6, 1238
 - intramolecular, 1214-15, 1236-8 - dioxetane-induced DNA photooxidation, 1201-2
 - see also* Single electron transfer
- Electron-withdrawing substituents
- ene reactions, 840-2
 - α -position, 852-3
 - β -position, 853-4
 - sulfonyl peroxides, 1006
- Electrophiles

- dioxiranes, 1135, 1142
- transition metal peroxides, 1072–4
- Electrophilic aromatic substitution, sulfonyl peroxides, 1005–6
- Electropolymerization, biosensor electrodes, 687–8
- Electrospray ionization mass spectrometry (ESI–MS)
 - negative ions, 693
 - transition metal peroxides, 1069–72
- Electrostatic interactions
 - alkyl hydroperoxides, 111
 - isobutenylarene intrazeolite photooxygenation, 882–3
- Elution factors, unsaturated triglycerides, 689–90, 739
- Emergency Response Guidebook, 747
- Emission quantum yields, chemiluminescence, 1221, 1222–3
- Enamel, percarbamide safety, 623
- Enantioconvergent processes, metal-catalyzed sulfoxidations, 490
- Enantiomers
 - chromatographic separation, 329–30
 - hydroperoxides, 691
- Enantiopure methyl 2,4-dideoxyhexapyranosides, 266
- Enantioselectivity
 - dioxiranes
 - C–H bond oxygen insertion, 1162
 - epoxidation, 1145–50
 - 3-(fluoroalkyl)-1,2,4-trioxane synthesis, 280, 281
 - sulfoxidation, 1069
- Endocrine disrupting chemicals, bisphenol A, 608
- Endogenous peroxides, TBARS assay, 667
- Endoperoxides
 - antimalarial activity, 1279–332, 1338, 1342
 - antitumour activity, 1333–41
 - arene endoperoxide thermochemistry, 166–7
 - bridged bicyclic, 193
 - chiral, 260, 261
 - diastereoselective intrazeolite photooxygenation, 885–6, 887
 - lipid hydroperoxides, 954
 - lone pair repulsion, 100
 - luminol chemiluminescence, 1244, 1248
 - peroxyacetalization, 277–85
 - rubrene bleaching, 734
 - steroidal, 1334–5
 - strained, 277–85
 - synthesis, 192–273, 705
 - synthetic, 1317–31
 - antimalarial activities, 1332
 - antitumour activities, 1335
 - chemistry, 1323–31
 - see also* Cyclic peroxides
- Endothelium
 - hydrogen peroxide damage, 616
 - peroxynitrite production, 611–12
- Ene diols, diastereoselective epoxidation, 413, 415–16
- Ene reactions
 - arteflene synthesis, 1324, 1326, 1332
 - biradical intermediates, 853
 - chiral dioxetane synthesis, 1173–7
 - 1,2-dioxolane synthesis, 236
 - dipolar intermediates, 853
 - double bond formation, 850–2
 - electron-donating substituents, 841
 - electron-withdrawing substituents, 840–2, 852–6
 - ene adduct, 838, 839, 850–2
 - ene products, 840
 - exciplex intermediate, 832–3, 835
 - hydroperoxide formation, 671, 735
 - mechanism, 832–3
 - perepoxide intermediate, 832–3, 835, 845, 846
 - endo*-perepoxide intermediate, 859
 - reactivity, 849
 - singlet oxygen, 673, 831–98, 1324, 1326, 1327, 1332
 - solvent effects, 854–6
 - spiro 1,2,4-trioxanes, 1326, 1327, 1332
- Energy acceptors, emission quantum yield, 1223
- Energy transfer quantum yields, chemiluminescence, 1223
- Enhanced chemiluminescence, 1219–20, 1221
- Enol esters, dioxirane asymmetric epoxidation, 1150
- Enol ethers, photooxidation site selectivity, 842
- Enones, Weitz–Scheffer epoxidation, 364–5, 370
- Enthalpies of combustion
 - ozonides, 165
 - peroxycarboxylic acids, 158, 160
 - 1,2,4,5-tetroxanes, 164
- Enthalpies of degradation, polymeric peroxides, 155
- Enthalpies of formation, 146
 - cyclic peroxides, 163–7
 - data quality, 147, 150
 - hydrocarbon-substituted peroxides, 147–55
 - linear least-squares analysis, 151, 158, 160, 162
 - linear regression analysis, 152, 158, 160, 162
 - multiply-linked peroxides, 163–7
 - oxygen functional group peroxides
 - double-bonded, 158–63
 - single-bonded, 155–8
 - ozonides, 165–6

- Enthalpies of formation, (*continued*)
 peroxy-carboxylic acids and derivatives,
 158–63
 methylene increment, 158
 regression constants, 151, 158
 1,2,4,5-tetroxanes, 164
 weighted least-squares regression, 158, 160,
 162
- Enthalpies of fusion, 146
 mixed hydroperoxides and peroxides, 155
 peroxy-carboxylic acids, 158–9
- Enthalpies of hydrogenation
 hydrocarbon-substituted peroxides, 155
 percarboxylate esters, 160, 161
- Enthalpies of isomerization,
 hydrocarbon-substituted peroxides,
 150–1
- Enthalpies of ozonation, 165
- Enthalpies of reactions
 acyl peroxides, 162–3
 arene endoperoxides, 166–7
tert-butyl perbenzoate ETR reactions,
 909–11
tert-butyl phenylperacetate thermolysis, 903,
 905
 dioxetanes, 163–4
 hydrocarbon-substituted peroxides, 151–5
 deoxygenation, 153
 disproportionation, 154, 155
 hydrogenation, 155
 steric strain, 154
 percarboxylate esters, 160–1
 single-bonded oxygen functional group
 peroxides, 155–8
 alcohol/ether exchange, 157–8
 1,2,4,5-tetroxanes, 165
 thermoneutrality, 154, 158, 164, 166
- Enthalpies of sublimation, 146
 percarboxylate esters, 161
 1,2,4,5-tetroxanes, 164–5
- Enthalpies of vaporization, 146
b constant, 149–50
 CHLP protocol, 147, 149, 150, 161, 165
 hydrocarbon-substituted peroxides, 147,
 149–50, 153–4
 aromatic substituents, 150
 peroxy-carboxylic acids and derivatives, 160,
 161
 single-bonded oxygen functional group
 peroxides, 156
 1,2,4,5-tetroxanes, 165
- Entropy
tert-butyl perbenzoate ETR reactions, 910,
 911
tert-butyl phenylperacetate thermolysis,
 903–4, 905, 906
- Environmental hazards
 chemicals, 747, 748
 labeling codes, 621, 751–3
 organic peroxides, 617
- Environmental issues
 analytical methods, 604–8
 hydrogen peroxide, 626, 643
 hydroperoxides, 678
- Environmental Protection Agency (USA)
 (EPA)
 occupational hazards, 749
 SIDS database, 622
 TSCATS database, 621, 745
- Enynes, dioxirane asymmetric epoxidation,
 1150
- Enzymes
 antimalarial endoperoxide targets, 1311–13,
 1320
 biosensors, 687–8
 catalyzed sulfoxidations, 474–6
 dioxetane chemiluminescence, 1191–200,
 1205
 fatty acid oxidation, 691
 heterocycle oxidation, 77–82, 83
 immobilized, 687–8
 milk pasteurization testing, 634
 PfATP6, 1313, 1320
 uric acid oxidation, 625
- EPA *see* Environmental Protection Agency
 (USA)
- Epinephrine, chemiluminescence, 647
- 6-Epiplakortolide E, synthesis, 256, 257
- Epithelial cells, ozone effects, 612
- Epothilone B, dioxirane epoxidation synthesis,
 1145
- Epoxidation
 alkenes
 carbonyl oxides, 35–40
 dioxiranes, 35–40, 1136, 1139–50
 hydrogen peroxide, 83–4
 peracids
 allylic alcohols, 65–7
 early mechanistic studies, 48
 gas-phase, 58
 Hartree–Fock calculations, 48–50
 rate factors, 58–65
 synchronous/asynchronous transition
 states, 50–8
 peroxy-nitrous acid, 17–20
 allylic alcohols, 65–7, 385–6, 391–416,
 789, 1144–5
 asymmetric, 391–406, 407–9
 special synthetic utility, 406, 410–13, 414
 carbon–carbon double bonds, 362–472, 405
 metal-catalyzed, 386–472
 organo-catalyzed, 370–86
 uncatalyzed and base-catalyzed, 363–70
 diastereoselective, 413, 415–16
 dioxiranes, 35–44, 1135–8, 1139–50
 asymmetric, 1146, 1149, 1150

- chirality centers, 1145
- epothilone B synthesis, 1145
- glabrescol synthesis, 1150
- relative rates in solution, 40–4
- ene diols, 413, 415–16
- isobutylene, 50, 52
- metal-catalyzed
 - carbon–carbon double bonds, 386–472
 - olefins, 790–2
 - unfunctionalized, 416–62, 463–70
- Sharpless epoxidation, 789
- Weitz–Scheffer reaction, 364–5, 370, 1142
- Epoxidation reagents, commercial codes, 621
- Epoxide-hydroperoxides, nucleophilic substitution cyclization, 236–7
- Epoxy compounds, π -complexes with ozone, 731
- EPR *see* Electron paramagnetic resonance
- Ergosterol 3 β -acetate, triplet oxygen cycloaddition, 211
- Ergosterol endoperoxide, isolation, 190, 191
- Erythrocytes
 - hydroperoxide determination, 690
 - phospholipid determination, 675
- ESI–MS (electrospray ionization mass spectrometry), 693, 1069–72
- ESR *see* Electron spin resonance
- Esters, C–H bond unreactive to insertion, 1160
- Etching, peroxodisulfate, 623
- Ethanolamine phosphatide, ozonides, 719, 726
- Ethers
 - alcohol/ether exchange reaction, 157–8
 - alkyl hydroperoxide cocrystallization, 111, 113
 - ozone adducts, 734
 - sulfonylperoxy radical reactions, 1037
- α -Ethoxy-*p*-nitrostyrene, ozonization, 717
- Ethylene
 - chlorinated, 720, 731–2
 - epoxidation
 - carbonyl oxides, 36–7
 - peroxynitrous acid, 17–20
 - fluorinated, 722
 - ozone explosion, 718
- Ethylene ozonides
 - dioxirane formation, 705–6
 - molecular models, 750
 - primary ozonides, 719–20, 721
- Ethyl hydroperoxide
 - Henry's law constants, 698
 - hydrogen peroxide determination, 629, 638
 - hydroperoxide determination, 678
- N*-Ethyl-*N*-(2-hydroxy-3-sulfopropyl)-3,5-dimethoxyaniline, 632, 634
- N*-Ethyl-*N'*-methyl imidazolium (emim), transition metal peroxides, 1083
- Ethyl plakortide Z, natural occurrence, 610
- N*-Ethyl-*N*-(3-sulfopropyl)-*m*-anisidine, triglyceride determination, 736, 634
- Ethynyl hydroperoxide, C–O distance, 102–3
- ETR *see* Electron transfer reactions
- Exchange reactions, alcohol/ether, 157–8
- Exciplex intermediate, ene reaction, 832–3, 835
- Excitation quantum yields,
 - chemiluminescence, 1221, 1222–3, 1225
- Excited states, chemiluminescence, 1215–18
- Explosion hazards
 - labeling codes, 621, 751
 - safety issues, 745, 746, 747
- Explosives
 - 2-butanone, 617
 - ethylene–ozone mixtures, 718
 - hexamethylene triperoxide diamine, 707–8
 - triacetone triperoxide, 707–8
 - trifluoroacetyl peroxide, 702–3
 - triperoxide thermochemistry, 166
- Exposure to chemicals, 747–8
- Extremely hazardous substances (EHS), 744
- π -Facial diastereoselectivity, singlet oxygen cycloaddition, 272
- Factorial design, analytical methods, 624
- Fast Blue B, lipid peroxidation visualization, 670
- Fats
 - oxidative stability, 656, 664–5
 - peroxide value, 657
- Fatty acids
 - conjugated dienes value, 671
 - hydroperoxide determination, 674, 676, 678, 680, 691
 - ozonolysis, 719
 - peroxide value, 661, 671
 - TBARS assay, 668
 - unsaturated, 661, 668, 671, 737, 945–6
- Faujasite supercage structure, 869–70
- Feedstuff, TBARS assay, 669
- Fenestrindane, C–H bond dioxirane oxygen insertion, 1162
- Fenestrindane monoalcohol, C–H bond dioxirane oxygen insertion, 1162
- Fenozan antimalarial endoperoxide
 - degradation, 1292–3
 - iron(IV) oxo species, 1292, 1293, 1294, 1309
 - synthesis, 1282, 1324, 1325, 1332
- Fenton's reagent, hydrogen peroxide determination, 641, 651–2
- Ferricyanide, performic acid determination, 699
- Ferrioxalates, actinometry, 1225
- Ferrocene biosensors
 - diacyl peroxides, 701

- Ferrocene biosensors (*continued*)
 hydrogen peroxide, 654
 hydroperoxides, 688
- Ferrocenecarboxylic acid, lipid hydroperoxide
 determination, 686–7
- Ferrocenol, bis(trimethylsilyl) peroxide
 reactions, 798–800
- Ferrocenol esters, preparation, 800
- Ferrocyanide, performic acid determination,
 699
- Final ozonides (FOZ), 716, 717, 718
 cis and *trans* isomers, 719, 720
 dialkyl peroxide formation, 706
 IR spectroscopy, 719
 mass spectrometry, 690
 microwave spectroscopy, 721–3
 molecular model, 750
 NMR spectroscopy, 724–5
 ozone water disinfection, 606
 X-ray crystallography, 726–30
- Fireflies
 bioluminescence, 1182, 1191–2, 1213,
 1232–3, 1255, 1256
 luciferin, 1172, 1191–2, 1213, 1232–3,
 1248, 1252, 1256
- Fish, peroxide value, 658
- Fish oil, oxidation stability, 665
- Fitness for purpose
 analytical methods, 624
 potentiometry, 663
- Flame ionization detection
 dialkyl peroxide determination, 708
 effective carbon number, 689, 690, 708
 hydroperoxide determination, 689
 relative mass response factor, 689
- Flame soot, hydroperoxide determination, 678
- Flammable substances
 risk and handling labels, 751
 safety issues, 745, 746, 747
- 4 α -Flavin hydroperoxide, enzymatic oxidation,
 77–82, 83
- Flavonoid ketones, lactone synthesis, 548–9,
 550
- Flour
 acyl peroxide determination, 701
 bleaching, 622
 dibenzoyl peroxide determination, 698
- Fluorescein isothiocyanate, DNA oxidative
 damage, 633, 634
- Fluorescence
 3-aminophthalate, 1239
 autofluorescence, 660
 hydrogen peroxide determination, 643
 peroxide value, 659–61
- Fluorescence quenching
 hydrogen peroxide determination, 626, 642
 peroxide value, 660
- Fluorinated peroxides, structure, 705
- 3-(Fluoroalkyl)-1,2,4-trioxanes, synthesis, 280,
 281
- Fluorocarbonyl peroxyhydrate
 gas electron diffraction, 744
 NMR spectroscopy, 743
 vibrational spectrum, 743
- Fluoroethylenes, final ozonide, 722
- Fluoroformyl peroxide, conformation, 702
- Fluorometry
 dialkyl peroxide determination, 707
 hydrogen peroxide determination, 637–43,
 707
 hydroperoxide determination, 678–80
 vitreous photofluorometry, 640
- 3-*p*-Fluorophenyl-1,2,4-trioxanes, synthesis,
 280, 281
- ¹⁹F NMR spectroscopy, peroxyoxalate
 chemiluminescence, 1263
- Food
 hydrogen peroxide
 bactericide, 623
 determination, 634, 643, 653, 655
 hydroperoxide determination, 678, 679–80
 oxidative stability, 656, 664–5
 long-term, 672
 peroxide value, 657, 659–60
 TBARS assay, 667–9
 unsaturated lipid deterioration, 614, 623
- Forbidden materials for transportation, 621
- Forensic analysis, dialkyl peroxide explosives,
 708
- Formaldehyde
 hydrogen peroxide determination, 635, 637
 1,2,3-trioxolane decomposition, 721
- Formal reactions
 acyl peroxides, 162
 hydrocarbon-substituted peroxides, 151–5
 percarboxylate esters, 160
 peroxycarboxylic acids, 158
 1,2,4,5-tetroxanes, 165
- N*-Formylkynurenine, 615
- Formyl-methionyl-leucyl-phenylalanine, 612
- Forward stepwise multiple linear regression,
 analytical methods, 624
- Fourier transform infrared spectroscopy
 (FTIR)
 anisidine value, 666
 hydroperoxides, 692
 imine peroxide, 744
 ozonides, 719
 peroxide value, 661, 662
 peroxynitrates, 743
 poly(methyl methacrylate peroxide), 714
 trifluoroacetyl peroxide, 702–3
 see also Infrared spectroscopy
- Fourier transform near-infrared
 spectrophotometry (FTNIR), 663

- Fourier transform NMR spectroscopy, polyethylene thermal oxidation, 695
- Fourier transform–Raman spectroscopy
hydroperoxides, 692
nitrile hydrolysis, 702
see also Raman spectroscopy
- Four-membered peroxides, 164, 1212–13
- FOX (Xylenol Orange–ferric complex) assay
hydrogen peroxide determination, 628, 632, 657, 658
hydroperoxide determination, 676
- FOZ *see* Final ozonides
- Franck–Condon Principle, chemiluminescence, 1181, 1217
- Free energy, chemiluminescence rate constants, 1234
- Free radicals
alkenyl hydroperoxide cyclization, 212–18
alkoxide, 675
s-alkylperoxy, 680
t-butoxy, 697
carbonate, 742
chain reactions, 225, 227, 229–30, 231–2
cumyl, 697
deterioration evaluation, 656, 664
dialkyl peroxide decomposition, 706–7
hydroxyl, 614, 681
lipids, 664
luminol, 742
performate, 742
serum protein scavenger, 614
spin labels, 665
tyrosyl, 610
see also Radicals
- Freezing point, peroxy-carboxylic acid enthalpy of fusion, 158–9
- FTIR *see* Fourier transform infrared spectroscopy
- FTNIR (Fourier transform near-infrared spectrophotometry), 663
- Fullerene adducts, regioselective self-sensitized oxygenation, 857–60
- Fungi cultures, hydrogen peroxide determination, 628
- Furan, ozonides, 730
- Furfuryl alcohol endoperoxide, ¹⁷O NMR spectroscopy, 184
- Furodysin hydroperoxide, isolation, 134–5
- Fused bicyclic 1,2-dioxanes, synthesis, 196, 197
- Fused bicyclic 1,2-dioxolanes, synthesis, 193, 194
- Fusion *see* Enthalpies of fusion
- γ -radiation
bovine serum albumin, 614, 691
free radical formation, 614, 615, 628
hydroperoxide determination, 674, 681, 685
polyethylene aging, 685
- G3 factor, antimalarial, 199, 201, 202
- β -Galactosidase, chemiluminescent bioassays, 1193, 1198–9
- Gamma-globulin (IgG), hydrogen peroxide biosensor, 655
- Gas electron diffraction (GED)
acyl peroxides, 702
peroxynitrates, 743–4
see also Electron diffraction
- Gas–liquid chromatography (GLC)
hydroperoxide determination, 684–5
ozonide determination, 719
- Gas-phase addition, hydroperoxides, 157
- Gas-phase epoxidation, alkenes, 58
- gauche* arrangement, acyclic organic peroxides, 102, 104–5
- GED (gas electron diffraction), 743–4
- Geminal regioselectivity
allylic hydroperoxide formation, 845–52
bulky allylic substituent, 845–9
bulky vinyl substituent, 849–50
cis alkyl substituents, 850–2
cyclic alkenes, 846–7
electron-withdrawing groups, 852–3
functionalized alkenes, 852
intraeolite photooxygenation, 875
non-bonded interactions, 850–2
- Geraniol
oxidation, 788–9, 790
1,2,4-trioxane synthesis, 274
- Germanium peroxides *see* Germyl peroxides
- Germyl hydroperoxides, 822–3
- Germyl hydrotrioxides, 823
- Germyl peroxides, 776, 819, 822–7
- GHS (globally harmonized system) of chemicals classification, 745–6
- Glabrescol, dioxirane epoxidation synthesis, 1150
- GLC *see* Gas–liquid chromatography
- Globally harmonized system (GHS), chemicals classification, 745–6
- Global Ozone Monitoring Experiment (GOME), 605
- δ -D-Gluconolactone, D-glucose determination, 625
- Glucose
colorimetry interference, 630
determination, 631, 632, 635, 637, 640
amperometry, 652
biosensors, 650, 654, 655
in human serum, 636, 644–5
in urine, 648
- D-Glucose, hydrogen peroxide determination, 625
- Glucose oxidase (GOX), glucose determination, 631, 636, 637, 647, 650, 654, 655
- Glutaraldehyde, fluorometry, 639

- Glutathione (GSH)
 Parkinson's disease, 613
 peroxide value, 659
- Glutathione peroxidase, 659, 687
- Glycaemia, lipid peroxides, 613
- Glycerol kinase, triglyceride determination, 633
- 1-Glycerol-3-phosphate oxidase (GPO), triglyceride determination, 633
- Glycerophosphocholine, unsaturated, 737
- Glycerophospholipid hydroperoxides, human plasma, 690
- Glyceryl esters, IR spectrophotometry, 661, 662
- 1-Glycerol phosphate
 human serum determination, 630
 hydrogen peroxide determination, 625, 626
 triglyceride determination, 633
- GOME (Global Ozone Monitoring Experiment), 605
- GOX (glucose oxidase), 631, 636, 637
- GPC (unsaturated glycerophosphocholine), 737
- GPO (1-glycerol-3-phosphate oxidase), 633
- Graft polymers
 cellulose, 698
 cross-linking initiators, 706
 ozonized polymers, 622
- Griesbaum co-ozonolysis, 1,2,4-trioxane antimalarials, 1331
- Ground state properties, peroxyxynitrous acid, 8–10
- GSH (glutathione), 613, 659
- Guanine
 oxidation residues, 670
 peroxide value, 661
 radical oxidation, 940–1
 singlet oxygen oxidation, 939, 941–3
- Gums, oxidation stability, 664
- G value, peroxide value, 657
- Haemoglobin
 hydrogen peroxide determination, 632, 634
 malaria parasite degradation, 1281, 1283
¹⁷O NMR spectroscopy, 185
- Hafnium(IV) complexes, olefin epoxidation, 417, 419, 422
- Halcon Process, *t*-butyl hydroperoxide, 428
- Half-fractional factorial design, analytical methods, 624
- Halogenation, hydrocarbons, 572, 575–81
- Halogen-containing compounds
 cyclic peroxide synthesis, 225, 227, 229–30, 231–2
 dioxirane oxidation, 1157–8
 olefin ozonization, 718
- Halosilanes, silyl peroxide preparation, 779–80
- Hammett reaction constants
tert-butyl perbenzoate ETR reactions, 909–10, 911
tert-butyl phenylperacetate thermolysis, 903, 904, 905, 906
 methyl substituted-benzyl carbonyl hypochlorite photolysis, 907, 908
 peroxyoxalate chemiluminescence, 1265, 1268
 polar effects, 899–903
- Hanalpinol, synthesis, 219, 220
- Handling
 IATA/ICAO labels, 751–3
 safety issues, 745
- Harmful substances, labeling codes, 621, 751–3
- Hartree–Fock calculations, peracid alkene epoxidation, 48–50
- Hazardous materials
 commercial codes, 621
 emergency response, 746–7
 environmental hazards, 747, 751–3
 labels, 751–3
 NIOSH Pocket Guide, 749
 occupational hazards, 747–9
 safety issues, 744–9
- HDL *see* High-density lipoprotein
- Heat of formation *see* Enthalpy of formation
- HEHP (1-hydroxyethyl hydroperoxide), 605, 638
- HEI *see* High-energy intermediate
- Hematin, peroxidase mimic, 640, 641, 642, 646
- Heme
 antimalarial endoperoxide targets, 1311–13
 artemisinin–heme adducts, 1298, 1311–12
 malaria parasite degradation, 1281, 1283
 mimetics, 628, 1309
 non-heme iron chelates, 1299–301
- Hemiketals, cyclic peroxy, 201, 203
- Hemin
 β -cyclodextrin condensation, 630
 horseradish peroxidase mimic, 628–9, 630
 hydrogen peroxide determination, 639
 hydroperoxide determination, 681, 708
- Hemoglobin *see* Haemoglobin
- Henry's law constants
 hydrogen peroxide determination, 638, 648
 hydroperoxide determination, 678
 peroxyacids, 698
- [4-(3-Heptyl)pyridine-2-carboxylic acid] (HPCA), transition metal peroxides, 1116
- Heteroarenes, dioxirane epoxidation, 1143–4
- Heteroatom oxidations
 bis(trimethylsilyl) peroxide reactions, 802–8
 disilanes, 806
 hydrosilanes, 807–8
 nitrogen, 829, 802–3

- phosphorus, 803–5
 - sulfur, 805–6
 - dioxiranes, 1138, 1150–8
 - halogens, 1157–8
 - nitrogen, 1151–4
 - oxygen, 1155
 - phosphorus, 1154–5
 - selenium, 1157
 - sulfur, 1156–7
 - transition metal peroxides, 1095–105
 - Heteroatom substituents, cyclic hydrocarbon diastereoselectivity, 861, 863, 864
 - Heterocycles, enzymatic oxidation, 77–82, 83
 - Heterogeneous osmium catalysts, 569
 - Heterolytic cleavage
 - biomimetic Fe(II) chemistry, 1291, 1301–4, 1309
 - tert*-butyl perbenzoate ETR reactions, 910, 911–12
 - Heteronuclear NMR, transition metal peroxides, 1069
 - Heteropoly acid, tungstate-based, 496, 497
 - Hexacoordinate silyl peroxides, 808–10
 - E,E*-Hexa-2,4-diene, photooxidation, 254–5
 - Hexamethyldisiloxane, oxidation, 806–7
 - Hexamethylene triperoxide diamine (HMTD)
 - enthalpy of formation, 166
 - explosive, 707–8
 - Hexanal, lipid oxidation assessment, 669
 - 1-Hexene, primary ozonide, 720
 - High-density lipoprotein (HDL)
 - oxidation, 612
 - TBARS assay, 667
 - High-energy intermediate (HEI)
 - chemiluminescence, 1215
 - activators, 1220, 1222
 - peroxyoxalates, 1188–9, 1257, 1261–6, 1267, 1269
 - structure, 1262, 1263
 - High volume production (HVP) chemicals, 622
 - Histidine, hydroperoxide formation, 614–15, 968–70
 - HIV-1
 - 4-hydroxynon-2-enal determination, 613, 670
 - lipid hydroperoxide determination, 676
 - serum analysis, 636
 - HMHP *see* Hydroxymethyl hydroperoxide
 - HMTD (hexamethylene triperoxide diamine), 166, 707–8
 - HNE *see* 4-Hydroxynon-2-enal
 - ¹H NMR spectroscopy
 - alkyl hydroperoxides, 104
 - trioxides, 179
 - Hock-cleavage, lipid oxidation, 946
 - HOI *see* Hypoiodous acid
 - Homoallylic alcohols, transition metal peroxide oxidation, 1089–94
 - Homoallylic peroxy-radicals, alkenyl hydroperoxide cyclization, 213–14
 - Homodesmic reactions, dioxetanes, 164
 - Homologous series
 - acyl peroxides, 162
 - hydrocarbon-substituted peroxides, 147
 - percarboxylate esters, 160
 - peroxycarboxylic acids, 158
 - single-bonded oxygen functional group peroxides, 157
 - Homolysis
 - tert*-butyl phenylperacetates, 900–2, 903
 - peroxynitrous acid, 7, 8
 - Homolytic cleavage
 - arteflene, 1304
 - benzylic cations, 911–12
 - tert*-butyl phenylperacetates, 903–6
 - methyl substituted-benzyl carbonyl hypochlorites, 907–9
 - Horseradish peroxidase (HRP)
 - diacyl peroxide determination, 701
 - dialkyl peroxide explosives, 708
 - hydrogen peroxide determination
 - absorption spectrophotometry, 628, 629, 631., 633, 636
 - biosensors, 652–5
 - chemiluminescence, 647, 648, 649
 - fluorimetry, 626, 637–41, 644–5
 - hydroperoxide determination, 675, 678–9, 688
 - luminol oxidation, 643, 1241
 - mimics, 628–9, 630, 639, 640, 646
 - quinoneimine dyes, 630
 - tyrosyl free radicals, 610
 - Horseradish peroxidase isoenzyme C (HRP-C), 616, 678
 - Household detergents, peracetic acid, 699
 - Household washing, perborate formulations, 623
 - HPCA ([4-(3-heptyl)pyridine-2-carboxylic acid]), transition metal peroxides, 1116
 - 15-HPETE (15*S*-hydroperoxy-5,8,11*z*, 13*E*-eicosatetraenoic acid), 214, 215, 681, 690
 - HRP *see* Horseradish peroxidase
 - HRP-C (horseradish peroxidase isoenzyme C), 616
 - Human serum
 - glucose determination, 636, 640, 644–5
 - 1-glycerol phosphate, 630
 - HIV analysis, 636
 - hydroperoxide determination, 676, 681
 - oxalate determination, 646
 - oxidative damage, 614
 - oxidized LDL antibodies, 633
 - protein damage, 614
 - TBARS assay, 667
- HVP (high volume production chemicals), 622

- Hyamine hydroxide, hydrogen peroxide determination, 655–6
- Hydrates, enthalpies of formation, 156, 157
- Hydrazones, aldehyde detection, 670
- Hydrocarbons
 autoxidation, 320
 cyclic diastereoselectivity, 861–3, 864
 heteroatom substituents, 861, 863, 864
 monocyclic, 861, 862
 polycyclic, 861, 863
 oxidation
 saturated hydrocarbons, 44–8, 800–2
 transition metal peroxides, 1114–17
 oxidative halogenation, 572, 575–81
 ozone adducts, 734
- Hydrocarbon-substituted peroxides
 electronegative functional groups, 147
 enthalpies of formation, 147–55
 enthalpies of isomerization, 150–1
 enthalpies of reactions, 151–5
 enthalpies of vaporization, 147, 149–50
 aromatic substituents, 150
 formal reactions, 151–5
 homologous series, 147
 polymeric peroxides, 155
- Hydrofluorocarbons, chlorofluorocarbon replacement, 604–5
- Hydrogen abstraction
tert-butyl perbenzoate ETR reactions, 909
 dioxetane-induced DNA photooxidation, 1201–2
 Hammett reaction constants, 899–902
 methane, 23, 25
- Hydrogen addition, thymine hydroperoxides, 926–7
- Hydrogenation
 hydroperoxides, 692
see also Enthalpies of hydrogenation
- 1,2-Hydrogen atom shift, hydrogen peroxide, 97
- Hydrogen bonding
 alkyl hydroperoxides, 103–5, 111–14
 basicity, 100
 bifurcated hydrogen bonds, 111
 cumene hydroperoxide, 103–4
 dioxirane epoxidation, 1136–8
 hydrogen peroxide–hydroxyl radical, 98
 hydroxyperoxides, 156
 intermolecular, 160
 intramolecular, 156, 180
 peracids, 125–7, 160
 trioxide NMR spectroscopy, 180
- Hydrogen-isoprostane bicyclic endoperoxides, 612
- Hydrogenolysis, diacyl peroxides, 162
- Hydrogen peroxide
 acridinium salt chemiluminescence, 1252
 in air, 626, 637, 638, 641–2, 645–6, 648
 allylic hydroperoxide formation, 673
 analytical and safety aspects, 625–56
 anhydrous, 778
 autoxidation determinations, 625–6
 chiral hydroperoxide synthesis, 348–51
 commercial availability, 618, 745
 complexes, 618, 621
 detection and determination, 625–56
 colorimetry, 628–49, 676
 commercial kits, 630–1, 632–3, 634
 electrochemical methods, 650–5
 NIR spectrophotometry, 649–50
 oxidation indices, 632–3
 oxidative coupling, 630, 635
 radiometric method, 655–6
 titration methods, 627, 674
 UV–visible spectrophotometry, 627–49, 707
 electrocatalytic reduction, 654
 endothelial cell damage, 616
 food application, 623
 1,2-hydrogen atom shift, 97
 hydrogen bonding with hydroxyl radical, 98
 hydroperoxide synthesis, 310–15, 316–9
 in juice, 653
 luminol oxidation, 1240–1, 1244, 1245, 1246
 manufacture, 617
 in milk, 653, 664
 milk pasteurization, 612, 631, 634, 636
 1,1'-oxalyldiimidazole reaction, 1189, 1190, 1260–1
 oxidation stability evaluation, 664–5
 oxidative stress, 613
 oxygen atom transfer, 67–76, 83–4
 peracetic acid determination, 699
 peroxide explosive determination, 708
 peroxyinitrite generation, 611
 in rainwater, 636, 637–8, 639, 641, 645, 648, 650, 651
 reactive oxygen species, 610
 in seawater, 606, 629, 639, 642, 645
 in snow, 648
 structure, 96–100
 synthesis, 362
 synthetic use, 308–9
 tautomerization, 97
 tetraoxane synthesis, 1326–8, 1332
 thiocyanate oxidation, 612
 thymine peroxide synthesis, 927–30
 in urine, 610, 628, 655
 in water, 606, 626, 629, 636, 639, 643
see also Urea–hydrogen peroxide
- Hydrogen peroxides, functionalization, 1055
- Hydrogen sesquioxide *see* Dihydrogen trioxide
- Hydrogen trioxide anion, 180–1
see also Dihydrogen trioxide
- Hydrolysis

- bis(trimethylsilyl) peroxide, 801
- peroxyesters, 329
- Hydroperoxide radical
 - oxygen atom transfer, 84
 - peroxynitrite generation, 611
- Hydroperoxides
 - alkenyl, 212–18
 - allylic, 831–98
 - analytical and safety aspects, 672–97
 - biological systems, 918
 - biosensors, 664, 687–9, 700
 - cellular indicators
 - DNA oxidation products, 918, 975–7
 - lipid hydroperoxides, 918, 977–85
 - protein hydroperoxides, 918, 985–7
 - commercial availability, 618
 - (*E*)-configuration, 346
 - cyclization
 - nucleophilic addition, 230, 233, 238–52, 253
 - nucleophilic substitution, 230, 233–8
 - decomposition to aldehydes, 669
 - deoxygenation, 153
 - derivatization, 691
 - detection and determination, 673–90, 977
 - absorption spectrophotometry, 627
 - biosensors, 664, 687–9, 700
 - colorimetry, 674–83
 - electrochemical methods, 685–9
 - flame ionization detection, 689
 - IR spectrophotometry, 683–4
 - mass spectrometry, 689–90
 - NMR spectroscopy, 685
 - ozonolysis, 626
 - thermal stability and GLC, 684–5
 - titration methods, 673–4
 - UV–visible spectrophotometry, 674–83
 - ene-reaction formation, 671, 735
 - enthalpies of formation, 151–3
 - double-bonded oxygen functional groups, 159–60
 - hydrocarbon-substituted, 148
 - single-bonded oxygen functional groups, 155–8
 - enthalpies of isomerization, 150–1
 - enthalpies of reactions, 151–3, 154–5, 157
 - formation by free radicals, 614–15
 - hydroxyl transfer, 72–6
 - mixed hydroperoxides and peroxides, 149, 154–5
 - oxygen atom transfer, 67–84
 - ozonide decomposition, 730
 - peroxide value, 657, 658, 659, 661, 662, 664
 - polymerization agents, 622
 - secondary oxidation products, 665
 - structural characterization, 690–7
 - mass spectrometry, 692–4
 - molecular refraction, 696–7
 - NMR spectroscopy, 694–5
 - vibrational spectra, 692
 - X-ray diffraction, 695–6
 - synthesis, 309–51
 - tertiary, 690–1
 - theoretical aspects, 67–84
 - thymine ozonolysis, 616
 - see also* Chiral hydroperoxides; DNA hydroperoxides; Lipid hydroperoxides; Protein hydroperoxides
- Hydroperoxyacetals
 - nucleophilic substitution cyclization, 234
 - 1,2,4-trioxane synthesis, 286, 287
- β -Hydroperoxyalcohols
 - ene diol diastereoselective epoxidation, 416
 - peroxyacetalization, 273–7, 278
- Hydroperoxy anion transfer, selective, 382
- 7 β -Hydroperoxycholesterol, lipid hydroperoxide determination, 681–2
- 15*S*-Hydroperoxy-5,8,11*Z*,13*E*-eicosatetraenoic acid (15-HPETE), 214, 215, 681, 690
- Hydroperoxyketal, nucleophilic addition cyclization, 241, 247, 248
- Hydroperoxyl group number, conjugated dienes, 671
- Hydroperoxysilylation
 - allyl alcohols, 275, 1329, 1330
 - spirotrioxane synthesis, 1329, 1330
- γ -Hydroperoxy- α,β -unsaturated ketones
 - photoisomerization, 246–7
 - 1,2,4-trioxane synthesis, 285
- Hydrophobic residue, chiral hydroperoxide synthesis, 338
- Hydrosilanes, oxidation, 807–8
- Hydrotrioxides
 - ozone adducts, 734
 - synthesis, 740
- Hydrotris(3,5-diisopropylpyrazolyl)borate, transition metal peroxides, 1060, 1064–6
- 4-Hydroxyalkenals
 - chromogenic activity, 669
 - secondary oxidation products, 665
- 4-Hydroxyalk-2-enals, oxidative stress, 613
- p*-Hydroxybenzene sulfonate, glucose determination, 632
- p*-Hydroxybenzoic acid, glucose determination, 632
- 1-Hydroxyethyl hydroperoxide (HEHP)
 - in atmosphere, 605
 - hydrogen peroxide determination, 638
 - hydroperoxide determination, 679
- Hydroxy-group directivity, allylic alcohol epoxidation, 65
- β -Hydroxyhydroperoxides, synthesis, 313–14
- Hydroxylamine, dioxirane oxidation, 1151
- Hydroxylation
 - aromatic compounds, 794–5
 - valine and leucine residues, 987

- α -Hydroxylation, ketones, 519–21, 522–3
- Hydroxyl groups
- allylic alcohol epoxidation, 65–7
 - dioxirane epoxidation directivity, 1144–5
 - enthalpies of formation, 155–8
 - transfer from hydroperoxides, 72–6
- Hydroxylhydroperoxides,
- 5-methyl-2'-deoxycytidine, 939
- Hydroxyl radical
- amino acid and peptide reactions, 954–60
 - biological system oxidation, 614
 - hydrogen peroxide hydrogen bonding, 98
 - lipid photooxidation, 948–9
 - luminol chemiluminescence, 681, 1243–4
 - thymine oxidation, 922–5, 976
- Hydroxymethyl hydroperoxide (HMHP)
- in atmosphere, 605, 641, 642, 674
 - Henry's law constants, 698
 - hydrogen peroxide determination, 626, 635, 638, 650
- 3-(Hydroxymethyl)oxindole, 616
- 2-Hydroxy-1-naphthaldehyde salicylhydrazone
- hydrogen peroxide determination, 641
 - hydroperoxide determination, 679
- 3-Hydroxy-2-naphthoic acid hydrazide,
- aldehyde determination, 670
- 4-Hydroxynon-2-enal (HNE)
- biomedical systems, 613–14, 670
 - colorimetric determination, 632, 669
- 3-Hydroxy-2-oxo-1-propyl phosphate,
- 1-glyceryl phosphate determination, 625, 626
- p*-Hydroxyphenylacetic acid, fluorometry, 637, 638, 639
- o*-Hydroxyphenylfluorone, hydrogen peroxide determination, 640
- 3-(4-Hydroxyphenyl)propionic acid, hydrogen peroxide determination, 639
- 6-Hydroxy-1,2,4-trioxanes, synthesis, 288
- Hypercholesterolemia, reactive oxygen species in blood, 612
- Hyperconjugation, lone pair orbital effects, 101
- Hyperthyroidism, endogenous peroxide determination, 667
- Hypoidous acid (HOI), generation in dioxirane oxidation, 1158
- Hypothiocyanite, from lactoperoxidase, 612
- ICAO (International Civil Aviation Organization), 751–3
- ICSC (International Chemical Safety Cards), 747, 749, 753–5
- IgB (gamma-globulin), 655
- Illumination, deterioration evaluation, 656
- Imidazole chemiluminescence, 647
- Imidazole peroxyoxalates, 1189, 1190, 1256–7, 1259–61, 1263, 1265
- Imine peroxide, analytical aspects, 744
- Imines, dioxirane oxidation, 1153
- Immobilized enzymes, biosensors, 687–8
- Immunoassays
- chemiluminescence, 1205, 1215, 1236
 - acridinium salts, 1252, 1256
 - see also* Bioassays
- Impact injury, hydrogen peroxide determination, 652
- Incidents, North American guidebook, 746
- Indamine dyes
- hydrogen peroxide determination, 635
 - oxalate determination, 633
- Indene ozonide, structure, 711–12
- Indigotrisulfonate, ozone measurement, 607
- Indirect chemiluminescence, 1219–20, 1221, 1223
- Indol-3-ylacetic acid, metabolic degradation, 616, 694
- Indoor ambients, hydrogen peroxide determination, 638
- Industry
- hydroperoxide determination, 680
 - peroxide involvement, 603, 617–24
- Inflammation, hydrogen peroxide damage, 616
- Inflammatory bowel disease,
- 4-hydroxynon-2-enal, 613
- Infrared spectrophotometry
- hydroperoxide determination, 683–4
 - ozonide determination, 718–19
 - peroxide value, 661–3
 - see also* Near-infrared spectrophotometry
- Infrared spectroscopy
- frozen Xe matrix, 720
 - FTIR spectra, 743, 744
 - hydroperoxides, 692
 - ozonides, 719–20
 - peroxynitrates, 742–3
 - see also* Fourier transform infrared spectroscopy
- Initiators, ozonides for polymerization, 622
- Inorganic peroxides, commercial availability, 620–1, 622
- in situ* generated catalyst, olefin epoxidation, 437
- Insoluble complexes, molybdenum(VI), 427
- Instant coffee
- hydrogen peroxide determination, 650
 - hydrogen peroxide in urine, 610, 628
- Intermolecular decomposition,
- chemiluminescence, 1213–15, 1231–6
- Intermolecular epoxidation, β -hydroperoxy alcohols, 416
- Intermolecular hydrogen bonding,
- peroxycarboxylic acids, 160
- Intermolecular isotope effect, intrazeolite photooxygenation, 872–3

- International Air Transport Association (IATA), hazard and handling labels, 751–3
- International Chemical Safety Cards (ICSC), 747, 749
peracetic acid, 753–5
- International Civil Aviation Organization (ICAO), hazard and handling labels, 751–3
- International Programme on Chemical Safety (IPCS), 747
- Intestinal carcinogenesis, dietary lipid hydroperoxides, 614
- Intramolecular decomposition, chemiluminescence, 1214–15, 1236–8
- Intramolecular hydrogen bonding hydroperoxides, 156
trioxides, 180
- Intramolecular nucleophilic reactions, hydroperoxide cyclization, 230, 233–52, 253
- Intramolecular peroxyketalization, artemisinin synthesis, 276–7
- Intrazeolite photooxygenation
allylic hydroperoxide formation, 869–86, 887
allylic radical intermediate, 871
chiral alkenes
diastereoselectivity, 883–6, 887
regioselectivity, 886, 887
dye-sensitized, 869–86, 887
electron-poor alkenes, 877–8
isobutenylarenes, 878–83
electrostatic interactions, 882–3
site selectivity, 880–3
zwitterionic intermediate, 880
kinetic isotope effect, 872–3
multicomplexation model, 878
(*R*)-(–)- α -phellandrene, 886
trisubstituted alkene regioselectivity, 874–7
type I and II processes, 871
zeolite Na–Y, 870–4
cation– π interactions, 873–4
diastereoselectivity, 885–6, 887
- Intrinsic reaction coordinate (IRC) analysis, saturated hydrocarbon oxidation, 45
- Iodide–molybdate method, hydroperoxide determination, 674
- Iodine, hydrogen peroxide titration, 627
- Iodine–iodide buffer, potentiometry, 699
- Iodine number, unsaturated polyolefins, 740
- Iodobenzene, dioxirane oxidation, 1158
- Iodohydrins, dioxirane oxidation, 1158
- Iodometry
dialkyl peroxide determination, 707
di-*t*-butyl peroxalate, 700
dioxirane determination, 1158
hydroperoxide determination, 673
ozonide determination, 718
peracid determination, 698
peroxide value, 657, 663
- Iodosobenzene, dioxirane oxidation, 1158
- Iodylbenzene, dioxirane oxidation, 1158
- Ion exchange polymers, heterogeneous catalysts, 569
- β -Ionones, 1,2,4-trioxane synthesis, 291
- IPCS (International Programme on Chemical Safety), 747
- IRC (intrinsic reaction coordinate analysis), 45
- Iridium oxide, amperometry, 650
- Iron(II) compounds
biomimetic Fe(II) chemistry
antimalarial endoperoxides, 1279–332, 1338, 1342
antitumour endoperoxides, 1335–6
arteflene degradation, 1304–9, 1310
carbon-centered radicals, 1283–99, 1309
heterolytic cleavage, 1291, 1301–4, 1309
homolytic cleavage, 1304
non-heme iron, 1299–301
role of iron, 1283–310
hydrogen peroxide biosensor, 652
hydroperoxide determination, 676
luminol chemiluminescence, 741–2
peroxide value, 658
potentiometry, 651
- Iron(II) hydroxyl radical, hydrogen peroxide determination, 641
- Iron(III) chloride, enol acetate oxidation, 792
- Iron(III) compounds
hydroperoxide determination, 676
potentiometry, 651
- Iron(III) *meso*-tetrakis(4-sulfonatophenyl) porphine, 646
- Iron(III) thiocyanate, hydrogen peroxide determination, 626, 628
- Iron(IV) oxo species, fenozan degradation, 1292, 1293, 1294
- Iron dioxygen complexes, ^{17}O NMR spectroscopy, 185
- Iron–protoporphyrin IX
diacyl peroxide determination, 701
hydrogen peroxide biosensor, 652
- Iron–tetrasulfonatophthalocyanine, hydrogen peroxide determination, 639, 640
- Irritant substances
labeling codes, 621, 753
RTECS data, 749
- IR spectroscopy
transition metal peroxides, 1069
see also NIR spectrophotometry
- Isoacetylsaturejol, triplet oxygen cycloaddition, 202, 204
- Isobutenylarenes, intrazeolite photooxygenation, 878–83

- Isobutylene, peroxyformic acid epoxidation, 50, 52
- Isofurans, H₂-isoprostane bicyclic endoperoxides, 612
- (+)-Isolimonene, artemisinin synthesis, 277
- Isoluminol, lipid hydroperoxide determination, 680, 681
- Isomerization
- allylic alcohols, 789–90
 - γ -chlordene, 728
 - enthalpies of isomerization, 150–1
 - exo:endo* ratio, 727
 - final ozonides, 719, 720, 727
 - peroxynitrous acid, 8–9, 25
 - photoisomerization, 246–7
 - positional isomers, 737
 - see also* Isotopomers; Stereoisomerism
- Isopropenyl hydroperoxide, bond dissociation energy, 6
- Isopropyl alcohol, hydrotrioxide formation, 740
- 5-Isopropyl-1,3-cyclohexadiene, singlet oxygen cycloaddition, 262–3
- Isopropyl ether, hydrotrioxide formation, 740
- 7-Isopropylidenenorbornenes, diastereoselective singlet oxygen ene reaction, 861, 864
- Isoprostane bicyclic endoperoxides
- H₂-isoprostane, 612
 - mass spectrometry, 714
 - synthesis, 612, 705
- Isoproterenol, chemiluminescence, 647
- (–)-Isopulegol, artemisinin synthesis, 277, 278
- Isothermal microcalorimetry, oxidation stability evaluation, 672
- Isotopomers
- alkali metal ozonides, 735
 - diacyl peroxides, 703
 - final ozonides, 721, 722–3
 - methyl nitrate, 744
 - primary ozonides, 720, 721
 - see also* Isomerization
- Jasmine lactone, preparation, 787
- Jet fuel, autoxidation, 665
- Jojoba oil, ozonized, 718
- Juice, hydrogen peroxide content, 653
- Keratinocytes, cosmetics, 613
- α -Ketoalkyl radicals, 252
- γ -Ketoalkyl radicals, 252
- α -Keto esters, benzylic oxidation, 518
- 2-Ketoglutarate, hydrogen peroxide determination, 655
- γ -Ketohydroperoxides, nucleophilic addition cyclization, 250, 251
- Ketone dienes, conjugated dienes value, 671
- Ketone peroxides
- commercial availability, 617, 619, 621
 - peroxide value, 658
- Ketones
- asymmetric dihydroxylation, 520–1
 - catalyzed epoxidation
 - allylic alcohols and olefins, 385–6
 - dioxiranes, 1146–50
 - C₂-symmetric, 1148
 - chiral, 1149
 - sugar derived, 1147
- C–H bond unreactive to insertion, 1160
- flavonoid, 548–9, 550
- hydroperoxide oxidation, 692
- α -hydroxylation, 519–21, 522–3
- IR spectrophotometry, 662
- oxidation
- of alkenes, 521–5
 - Baeyer–Villiger, 784–7
 - transition metal peroxides, 1108–14
 - α,β -unsaturated, 199–202, 246–7, 285, 666
- Ketoprofen, hydrogen peroxide determination, 625, 626, 652
- Kinetic isotope effect
- alkene photooxidation, 840
 - intrazeolite photooxygenation, 872–3
- Kinetic resolution
- chiral hydroperoxide synthesis, 330–9
 - metal-catalyzed sulfoxidations, 490
- Kingzett method, hydrogen peroxide determination, 627
- Lactate, determination, 625, 626, 632, 647
- γ -Lactones
- hydroperoxide oxidation, 692
 - IR spectrophotometry, 662
- Lactone synthesis, flavonoid ketones, 548–9, 550
- Lactoperoxidase
- milk pasteurization, 612, 631, 634, 636
 - tyrosyl free radicals, 610
- Lanthanide complexes, dioxetane decomposition, 1190–1
- Lard, IR spectrophotometry, 661
- Laser photolysis, azoalkanes, 193–5
- Laundry bleaches
- alkanoyl peracids, 125
 - hydrogen peroxide, 623, 652
 - percarboxylic acid, 699
- LC (liquid chromatography), 664, 719
- LDL *see* Low-density lipoprotein
- L-DOPA, chemiluminescence, 647
- LDPE (low-density polyethylene), 623, 692
- Lecitine (phosphatidylcholine)
- hydroperoxide determination, 675, 676, 678, 681, 683, 686, 687, 690

- peroxide value, 658–9
- quenching, 711
- Leffler–Hammond postulate (LHP), 907, 911
- Leucine
 - hydroperoxide formation, 956–8
 - protein hydroperoxide decomposition, 987
- Leucocites
 - contamination in semen, 612
 - superoxide generation inhibition, 612
- Leuco Crystal Violet
 - hydrogen peroxide determination, 629
 - hydroperoxide determination, 678
- Leuco Methylene Blue, hydrogen peroxide determination, 632, 633
- Leucotrienes
 - from arachidonic hydroperoxides, 612
 - lipid hydroperoxide determination, 681
- Leukemia cells, lipid hydroperoxide determination, 681, 687
- Lewis acids, dialkyl peroxide synthesis, 358
- LHP (Leffler–Hammond postulate), 907, 911
- Ligands
 - alkyl hydroperoxide anions, 114–19
 - percarboxylate anions, 127, 128
- Light emission
 - intensity calibration, 1224–7
 - singlet oxygen, 951
- Light-sticks, peroxyoxalate
 - chemiluminescence, 1256–7
- Lignin, hydrogen peroxide determination, 627, 628
- Limits of detection (LOD), 625
- Limits of quantitation (LOQ), 625
- Limonene
 - free radical domino reaction, 222, 223, 224
 - singlet oxygen ene reaction, 861, 862
- Linalool, oxidation, 790
- Linear least-squares analysis, enthalpy of formation, 151, 158, 160
- Linear low-density polyethylene (LLDPE), thermal oxidation in air, 623
- Linoleate hydroperoxide, hydroperoxide determination, 677
- Linoleic acid
 - conjugated dienes value, 671
 - hydroperoxide determination, 687, 692
 - oxidative ozonolysis, 737, 738
 - TBARS assay, 668
- Linolenic acid
 - hydroperoxide determination, 687, 692
 - TBARS assay, 668
- Linseed oil, vibrational spectra, 692
- Lipases
 - kinetic resolution of THPO, 332–3
 - triglyceride determination, 633
- Lipid hydroperoxides, 945–54
 - antimalarial targets, 1311
 - biomedical systems, 612–14
 - cellular indicators of hydroperoxides, 918, 977–85
 - aldehydes, 977–8
 - adducts to biomolecules, 978–85
 - degradation products, 977–85
 - hydroperoxide measurement, 977
 - conjugated dienes value, 671
 - detection and determination, 673–90
 - colorimetry, 632, 674–83
 - electrochemical methods, 686–7
 - fluorometry, 640
 - IR spectrophotometry, 683–4
 - titration methods, 673–4
 - UV–visible spectrophotometry, 674–83
 - dietary intake, 614
 - lipid oxidation, 945–7
 - autoxidation, 614, 661–2
 - nitrolipids, 952–4
 - photosynthesis interference, 617
 - TBARS assay, 667
- Lipid membranes, antimalarial endoperoxide targets, 1288, 1311–13
- Lipid peroxides
 - biological and biomedical systems, 612–14, 951–4
 - rat liver cells, 669
- Lipids
 - anisidine value, 666
 - autoxidation, 614, 623, 661
 - free radicals, 664
 - hydroperoxide determination, 673, 676, 687
 - oxidation, 667, 669, 693, 945–7
 - cholesterol, 946–7
 - unsaturated fatty acids, 945–6
 - peroxidation, 670, 918, 945, 974
 - peroxide value, 658, 661, 664
 - photooxidation, 947–51
 - hydroxyl radical, 948–9
 - one-electron, 948–9
 - singlet oxygen, 949–51
 - secondary oxidation products, 665
 - TBARS assay, 667
 - unsaturated, 683–4, 737
- Lipoproteins
 - high-density, 612
 - hydroperoxide determination, 681
 - low-density, 610–11, 612
 - TBARS assay, 667
- Liposomes
 - hydroperoxide determination, 674
 - peroxide value, 659
- Lipoxydase, phospholipid determination, 675
- Lipoxygenase
 - conjugated dienes value, 671
 - enzyme extraction, 670, 676
- Liquid chromatography (LC)
 - ozonide determination, 719
 - thermal blotter, 680

- Liquid chromatography (LC) (*continued*)
 Vitamin E, 664
- Lithium aluminum hydride, cholesteryl acetate
 ozonolysis, 696
- Lithium compounds, bis(trimethylsilyl)
 peroxide reactions, 796–8, 799
- Liver diseases, lipid hydroperoxides, 613
- Liver microsomes, 4-hydroxynon-2-enal,
 613–14
- DPE (linear low-density polyethylene),LLDPE
 (linear low-density polyethylene),623
- LOD (limits of detection), 625
- Lone pairs
 hyperconjugation, 101–2
 π -type interactions, 102–3
 repulsion, 100
- Longilene peroxide
 crystal structure, 136
 natural occurrence, 608, 609
- Long-term storage, calorimetric evaluation,
 672
- Lophine, chemiluminescence, 1212
- LOQ (limits of quantitation), 625
- Low-density lipoprotein (LDL)
 o,o' -dityrosine residues, 610
 hydroperoxide determination, 675
 oxidation, 610–11, 612, 613, 671
 oxidized antibody determination, 633
 TBARS assay, 667
- Low-density polyethylene (LDPE), thermal
 oxidation in air, 623, 692
- Luciferin, fireflies, 1172, 1191–2, 1213,
 1232–3, 1248, 1252, 1256
- Lucigenin
 chemiluminescence, 645, 1212, 1239,
 1248–56
 reactions, 1250, 1251
- Luminol
 free radical, 742
 light emission intensity calibration, 1224,
 1225
 oxidation chemiluminescence, 1238–48
 chemiexcitation, 1244–8
 CIEEL approach, 1247–8
 hydrogen peroxide determination, 643–6
 hydroperoxide determination, 680–1, 708
 hydroxyl radical, 1243–4
 mechanism, 1239–44, 1245
 peroxyacid determination, 698, 700, 701
 peroxydinitrite determination, 740, 741–2
 quantum yields, 1243
 radical anions, 1241–3, 1244, 1245
- Lysine, hydroperoxide formation, 614–15, 959
- Lysophosphatidylcholine, IR
 spectrophotometry, 683–4
- Lysophosphatidylethanolamine, IR
 spectrophotometry, 683–4
- Macrocyclic compounds, structure, 712
- Magnesium compounds, bis(trimethylsilyl)
 peroxide reactions, 795–6
- Malaria
 haemoglobin degradation, 1281, 1283
see also Antimalarial endoperoxides
- Malealdehydic acid, furan ozonide
 decomposition, 730
- Malondialdehyde (MDA)
 biomedical systems, 613, 614
 detection and determination, 669–70
 colorimetry, 632, 633
 TBARS assay, 667–8
 oxidation indices, 656, 665, 667
- Manganese complexes
 alkene/alkyne vicinal dihydroxylation, 556
 olefin epoxidation, 442–3, 445–53, 454–8
- Manganese–tetrasulfonatophthalocyanine
 hydrogen peroxide determination, 639, 646
 quinoneimine dyes, 630
- Marcus Theory, chemiluminescence, 1217–18,
 1235
- Margarine
 analysis, 636, 675, 701, 737
 peroxide value, 660
- Marine metabolites
 antitumour activity, 1333–4
 isolation, 190, 191
- Mass spectrometry
 coordination ionspray, 693
 dialkyl peroxides, 714
 hydroperoxides
 detection and determination, 689–90
 structural characterization, 692–4
 ozonides, 726
 peroxydinitrates, 743
 selected reaction monitoring, 693
 tandem techniques, 693, 703
see also Electrospray ionization mass
 spectrometry
- Mayonnaise
 hydroperoxide determination, 680
 oxidative stability, 660, 665
- Maytensifolin, isolation, 136, 137
- McLafferty rearrangements, acyl peroxides,
 704
- MCM-41, olefin epoxidation, 418, 421–2
- MCM-48, olefin epoxidation, 418
- MDA *see* Malondialdehyde
- Measurement uncertainties
 analytical methods, 624
 potentiometry, 663
- Meat
 hydroperoxide determination, 676, 678
 peroxide value, 658
 TBARS assay, 667
- Meldola Blue, hydrogen peroxide
 determination, 629–30

- (-)-Menthyl chloroformate, oxidative ozonolysis, 737, 738
- Metabolism, up/downregulation, 610
- Metal-catalyzed reactions
- dialkyl peroxide synthesis, 358–60
 - epoxidation, 386–472
 - asymmetric, 386–406, 407–9
 - unfunctionalized olefins, 416–62, 463–70
 - sulfoxidation, 476–92, 493–5
 - asymmetric, 478–92, 493–5
 - non-asymmetric, 477–8
 - transition metal-catalyzed alcohol oxidation, 787–9, 1057, 1105–8
- Metallo-organic systems, ¹⁷O NMR spectroscopy, 185–7
- Metal–oxygen bonds
- alkyl hydroperoxide anion ligands, 114–19
 - geometric parameters, 125–8
- Metal ozonides, 735–7
- Metal peroxides, commercial availability, 619
- Metal peroxy nitrates, theoretical studies, 9–10
- Metastable states, peroxy nitrous acid, 10–14, 22–5
- Methane
- hydrogen abstraction, 23, 25
 - peroxy nitrous acid oxidation, 22–5
- Method of standard addition (MOSA), 624, 636, 639
- 3-Methoxy-1,2,4-trioxolane
- rotational spectrum, 722–3
 - synthesis, 717
- N*-Methylacridan dioxetane, chemiluminescence, 1253, 1255
- 3-Methylbenzothiazolinone hydrazone
- hydrogen peroxide determination, 635
 - oxalate determination, 634, 633
- 2-Methylcyclohexanone peroxide, NMR spectroscopy, 709, 710
- 5-Methyl-2'-deoxycytidine
- hydroxylhydroperoxides, 939
 - methyl oxidation products, 939
- Methyl 2,4-dideoxyhexapyranosides, synthesis, 266
- 3-Methyl-3,4-dihydroquinoxalin-2(1*H*)-one, hydrogen peroxide determination, 639
- Methylenebisoxo dioxirane, molecular orbital treatment, 28–9
- Methylene Blue
- hydrogen peroxide determination, 632, 633, 654
 - lipid hydroperoxide determination, 676
- Methylenecyclohexene, final ozonide, 718
- Methylenecyclopentene, final ozonide, 718
- Methylene increment, peroxy carboxylic acids, 158
- 10-Methyl-9-(*p*-formylphenyloxycarbonyl)acridinium trifluoromethanesulfonate, 643
- Methyl hydroperoxide (MHP)
- Henry's law constants, 698
 - hydrogen peroxide determination, 629, 638, 641, 648
 - hydroperoxide determination, 678
- Methyl iodide, dioxirane oxidation, 1158
- Methyl linoleate, thermal oxidation, 691–2
- Methyl *p*-methoxycinnamate, ozonides, 720, 726
- 2-Methyl-1,4-naphthoquinone, thymidine photosensitization, 929
- Methyl nitrate, photolysis, 744
- Methyl oleate
- ozonization products, 725
 - triethylsilyl hydrotrioxide reaction, 813
- Methyl oxidation, 5-methyl-2'-deoxycytidine, 939
- 3-Methylphenol, quinoneimine dyes, 630
- N*-Methyl-2-phenylindole, malondialdehyde determination, 669
- Methylpropylphenyl phosphine oxide, reduction, 803
- N*-Methylpyrrole, hydroperoxide biosensor, 688
- 4-Methyl quinoline, peroxydisulfate reactions, 1010
- α -Methylstyrene dimer (MSD)
- dialkyl peroxide decomposition, 706–7
 - free radical capture, 697
- Methyl substitution
- benzyl carbonyl hypochlorite photolysis, 907–9
 - nucleophile peroxy nitrous acid oxidation, 15
- Methyl(trifluoromethyl)dioxirane (TFDO)
- alkene epoxidation, 39–40
 - ¹⁷O NMR spectroscopy, 184
 - preparation, 26, 1130–2
 - structure, 26, 27
- Methyltrioxorhenium (MTO)
- catalysis, 1057, 1083, 1096
 - olefin epoxidation, 453, 459–62, 463–70, 791, 1090–1
 - oxidation, 1074, 1106
 - nitrogen compounds, 534, 535, 803
 - pyridine/cyanopyridine ligands, 460–1
 - synthesis, 1058
- N*-Methyl-*N,N',N'*-tris(2-pyridylmethyl)ethane-1,2-diamine, transition metal peroxides, 1072
- MHP (methyl hydroperoxide), 629, 638, 641, 648
- Microalgae, hydrogen peroxide determination, 646
- Microbicides, pharmaceutical preparations, 623
- Microcalorimetric combustion, dioxetane enthalpy of formation, 163
- Microdialysis membrane, hydrogen peroxide determination, 651

- Microencapsulation, allylic alcohol epoxidation, 413
- Microperoxidase
hydrogen peroxide biosensor, 654
hydroperoxide determination, 679, 680, 681
- Microplate spectrophotometry, hydrogen peroxide determination, 637
- Microsomes, TBARS assay, 667
- Microspectrophotometry, lipid peroxidation visualization, 670
- Microwave spectroscopy
dioxiranes, 1132, 1133
hydrogen peroxide, 96
ozonide characterization, 721–3
1,2,4-trioxolanes, 720
- Milk
hydrogen peroxide content, 653, 664
pasteurization, 612, 631, 634, 636
- Mimetics *see* Biomimetic Fe(II) chemistry
- MO calculations, O–O bond, 94
- Molding, peroxide copolymer, 707
- Molecular biology, dioxetane substrates, 1198–200
- Molecular dynamics, poly(styrene peroxide), 709
- Molecular models, ethylene ozonides, 750
- Molecular orbitals, dioxiranes, 27–9
- Molecular oxygen
cyclic disilane oxidation, 815–19
disilene oxidation, 819–21
unpaired electrons, 166
see also Triplet oxygen
- Molecular refraction
hydroperoxides, 696–7
ozonides, 731
- Molecular sieves, chiral metal complex catalysis, 395
- Molozonides *see* Primary ozonides
- Molybdenum(VI) complexes
bimetallic complexes, 428
hydrogen peroxide determination, 635–6, 640
insoluble complexes, 427
Mo-peroxide, 427–8
olefin epoxidation, 425–542, 433–6
polymer immobilization, 427
- Molybdic acid, hydrogen peroxide spectrophotometry, 627
- Monodentate ligands, molybdenum(VI) complexes, 427
- Mononuclear complexes, manganese, 447
- Monoperoxyketals, dialkyl peroxide synthesis, 357–8
- Monoperoxyphosphonic acid, 1039–40
- Monoperoxyphosphoric acid, 1040
- Monopersulfuric acid, 1001–4
- Monoraphidium braunii*, hydrogen peroxide determination, 646
- Monoterpenic olefins, potassium peroxymonosulfate reactions, 1021
- Monounsaturated fatty acids, peroxide value, 661
- MOSA (method of standard addition), 624, 636, 639
- MSD (α -methylstyrene dimer), 697
- MTO *see* Methyltrioxorhenium
- Multicomplexation model, intrazeolite photooxygenation, 878
- Multiple linear regression, analytical methods, 624
- Multireference character, complete active space calculation, 12, 29
- Multivariate analysis
analytical methods, 624
SIMPLISMA program, 624, 702
- Mutations, DNA oxidative damage, 616
- Myeloperoxidase, tyrosyl free radicals, 610
- Myocardial ischemia, reactive oxygen species in blood, 612
- Myoglobin, ¹⁷O NMR spectroscopy, 185
- NADPH (nicotinamide adenine dinucleotide phosphate), 610, 643, 659
- Nafion membrane, hydrogen peroxide determination, 641–2, 645–6, 652, 653
- Naphthalene endoperoxide, synthesis, 269
- Naphthalimide hydroperoxides, artificial photonucleases, 616–17
- Naphthoquinone, peroxydisulfate reactions, 1010
- Natural products
antitumour activity, 1333–5
peroxide analysis, 608–10
photooxygenation synthesis, 886, 888–93
structural chemistry, 133–8
- Nature
atmospheric emissions, 605
peroxide involvement, 603–17
water composition, 607–8, 626
- Near-infrared spectrophotometry (NIR)
anisidine value, 666
Fourier transform, 663
hydrogen peroxide determination, 649–50
peroxide value, 663
PRESS technique, 624
- Negative ion electrospray mass spectrometry, 693
- Nerol, oxidation, 788–9, 790
- Neuroprostanes, H₂-isoprostane bicyclic endoperoxides, 612
- Neutron diffraction analysis, hydrogen peroxide, 96
- Nicotinamide adenine dinucleotide phosphate (NADPH), 610, 643, 659
- Niobium(V) complexes

- hydrogen peroxide determination, 635–6
olefin epoxidation, 422–5
- NIOSH
Pocket Guide to Chemical Hazards (NPG),
749
RTECS commercial data, 621, 749
- NIR spectrophotometry *see* Near-infrared
spectrophotometry
- Nitrate esters, hydroperoxide determination,
684
- Nitric oxide
effect on hydrogen peroxide analysis, 635
hydroperoxide determination, 684
peroxynitrite anion formation, 10
in vascular systems, 611–12
- Nitriles
C–H bond unreactive to insertion, 1160
hydrolysis, 701–2
- Nitrite, TBARS assay, 667
- Nitrite esters, hydroperoxide determination,
684
- 2-Nitrobenzene chloride, sulfonylperoxy
radical reactions, 1035, 1036
- 2-Nitrobenzenesulfonylperoxy intermediate,
superoxide reactions, 1034
- Nitrogen-containing compound oxidation
bis(trimethylsilyl) peroxide reactions,
802–3, 804
dioxiranes, 1151–5
primary aromatic amines, 1151
N-oxidation, 531–8, 539
- Nitrolipids, lipid hydroperoxides, 952–4
- Nitronate ions, dioxirane oxidation, 1152–3
- Nitrosation, malondialdehyde, 667
- Nitroso compounds, spin trapping, 664
- Nitrotyrosine, peroxynitrite determination,
740–1
- NMR spectroscopy
DEPT technique, 725–6
dialkyl peroxide determination, 708
Fourier transform, 695
hydroperoxides
detection and determination, 685
structural characterization, 694–5
nuclear spin relaxation, 709
ozonides
detection and determination, 719
structural characterization, 723–6
peroxynitrates, 743
spin–lattice relaxation, 695, 709
transition metal peroxides, 1069–70
see also Chemical shifts; ¹³C NMR
spectroscopy; ¹⁹F NMR spectroscopy;
¹H NMR spectroscopy; ¹⁷O NMR
spectroscopy; ²⁹Si NMR spectroscopy
- Non-asymmetric metal-catalyzed
sulfoxidations, 477–8
- Non-bonded interactions, regioselective allylic
hydroperoxide formation, 842–4, 850–2
- Nondrying oils
peroxide value, 662
plastics and resins, 622
- Nonisothermal DTA
furan ozonides, 730
phosphite–ozone adducts, 732–3
- Norcaradiene, peroxidation, 267, 268
- Norepinephrine, chemiluminescence, 647
- Norrish type II reaction, photochemical, 196,
197
- NPG (*NIOSH Pocket Guide to Chemical
Hazards*), 749
- Nuclear magnetic spectroscopy *see* NMR
spectroscopy
- Nuclear spin relaxation, poly(methacrylonitrile
peroxide), 709
- Nucleic acids, protein cross-links, 974–5
- Nucleobase hydroperoxides, decomposition,
918, 975–7
- Nucleophiles
bis(trimethylsilyl) peroxide reactions,
795–800
dioxirane oxidation, 1135
oxygen atom transfer from hydroperoxides,
70–2
peroxynitrous oxidation, 14–17, 18
transition metal peroxides, 1074–6
- Nucleophilic addition
dialkyl peroxide synthesis, 354–5
hydroperoxide cyclization
carbon–carbon double bonds, 230, 233,
238–45
carbonyl group, 230, 233, 245–52, 253
- Nucleophilic substitution, hydroperoxide
cyclization, 230, 233–8
- Nucleosides, oxidation, 975
- Occupational exposure limits (OEL), 749
- Occupational hazards, chemicals, 747–9
- Octalene, singlet oxygen ene reaction, 861,
863
- Δ Octalin, ozonation thermochemistry, 165
- 2-Octyl hydroperoxide, molecular refraction,
697
- Odour changes, deterioration evaluation, 656,
664
- OEL (occupational exposure limits), 749
- Oils
acyl peroxide determination, 701
conjugated dienes value, 671
hydroperoxide determination, 675, 680
oxidative stability, 656, 664–5, 666
ozonization products, 725
peroxide value, 657, 658, 659–63
TBARS assay, 667, 668

- ¹⁸O-labeled singlet oxygen, lipid photooxidation, 951
- Olefins
biogenic, 605
cyclic, 718
electron-deficient asymmetric epoxidation, 386–91
electron-withdrawing group regioselectivity, 852–3
halogen substituents, 718
ketone-catalyzed epoxidation, 385–6
metal-catalyzed epoxidation, 416–62, 463–70
oxidation, 790–3
 catalytic epoxidation, 790–2
 chlorohydrin and acetoxy alcohol synthesis, 792–3
 theoretical aspects, 83–4
 ozone π -complexes, 717–18
 ozonolysis, 673, 674
 pericyclic transformation, 94
 selenide-catalyzed epoxidation, 384–5
 terminal or aryl-substituted, 384–5
 thiol–olefin co-oxygenation, 221–3, 224, 225, 226, 250, 251, 1330
 unfunctionalized, 385–6, 416–62, 463–70
- Oleic acid
oxidation, 692–3
TBARS assay, 668
- Oligomers, ozonide decomposition, 706, 718, 730
- Oligopeptides, epoxidation catalysis, 381
- Olive oil
analysis, 636, 675, 701
anisidine value, 666
falsification, 661
oxidation stability, 664
peroxide value, 657, 661, 662, 664
- One-electron oxidation
lipid photooxidation, 948–9
methane with peroxyxynitrous acid, 22–5
8-oxo-7,8-dihydroguanine, 943–5
radical cation generation, 917–18
thymine, 925–6
- ¹⁷O NMR spectroscopy
advantages and drawbacks, 172
biological systems, 185–7
experimental/computation comparison, 184–5
hydroperoxide determination, 685
metallo-organic systems, 185–7
organic peroxides, 171–87
ozonolysis mechanism, 177–8
solid state, 185
substitution effects, 177
- Ophthalmopathological conditions, lipid hydroperoxides, 612
- Optical activity, diethyl and diisopropyl tartrate, 395
- Optodes
 luminol chemiluminescence, 646
 Meldola Blue, 629–30
- Oral hygiene, teeth whiteners, 623
- Orbital effects, acyclic organic peroxides, 101–3
- Organic ozonides, ozone adducts, 734–5
- Organic peracids, functionalization, 1055
- Organic peroxy compounds
 analytical methods, 624–774
 bond dissociation energies, 5–7
 chemiluminescence, 1211–78
 ¹⁷O NMR spectroscopy, 171–87
 safety aspects, 621, 625, 744–9, 751–5
 structural chemistry, 105–31
 theoretical aspects, 1–91
 UN classification, 746
 see also Peroxide group; Peroxides
- Organic solvents, peroxide value, 658
- Organic sulfur compounds
 with superoxide, 1032–9
 see also Sulfides
- Organo-catalyzed epoxidation
 bovine serum albumin, 383–4
 ketone-catalyzed, 385–6
 phase-transfer catalysis, 370–3
 polyamino acids, 373–83
 selenides, 384–5
- Organogermanium peroxides *see* Germyl peroxides
- Organonitrogen compounds *see* Nitrogen-containing compounds
- Organotris(alkylhydroperoxy)silanes, preparation, 782
- Organozinc compounds, alkyl hydroperoxide precursors, 322
- Osmium catalysts
 alkene/alkyne vicinal dihydroxylation, 556, 567–72, 673–5
 heterogeneous, 569
- Osmium(II) compounds
 diacyl peroxide biosensor, 701
 hydrogen peroxide biosensor, 652
- Oxadisiliranes, disilirane oxidation, 816, 817
- 4-Oxahomoadamantane, bis(trimethylsilyl) peroxide reaction, 802
- Oxalate, determination, 625, 626, 630, 633, 635, 646
- Oxalate oxidase, hydrogen peroxide generation, 646
- Oxalic acid derivatives, chemiluminescence, 648
- Oxalyl chloride, peroxyoxalate chemiluminescence, 1189, 1190, 1256–7, 1266
- 1,1'-Oxalyldiimidazole chemiluminescence

- hydrogen peroxide, 648
- peroxyoxalates, 1189, 1190, 1259, 1260–1
- Oxanthromycin, isolation, 136, 137, 138
- Oxaziridine, dioxirane imine oxidation, 1153
- Oxazolidinone, chiral dioxetane synthesis, 1175–8
- Oxazoline moiety, allylic oxidation, 514, 516, 517
- Oxidants
 - electrophilic, 1135, 1142
 - labeling codes, 621, 752
 - α -peroxylactones, 1178–80
 - UN classification, 746
 - see also* Antioxidants
- Oxidation
 - accelerated, 657, 661, 664, 666
 - alcohols, 492, 496–503, 504–12, 787–90
 - allylic alcohol isomerization, 789–90
 - transition metal-catalyzed, 787–9, 1057, 1105–8
 - alkanes, 531
 - alkenes to ketones, 521–5
 - allylic, 503, 512–19
 - amines, 67–70
 - aromatic compounds, 527–30
 - Baeyer–Villiger reaction, 538–56, 557–66, 784–7
 - benzylic, 503, 518–19
 - bis(trimethylsilyl) peroxide reactions, 784–93, 800–8
 - C–H reactions, 503–31, 532
 - dimethyl sulfide, 74, 75
 - dioxirane-mediated, 1135–63
 - disilanes, 806–7
 - disilenes, 819–21
 - DNA, 614, 633, 695, 975
 - cellular indicators of hydroperoxides, 918, 975–7
 - residues, 670–1
 - enzyme-catalyzed, 77–82, 83, 625, 634
 - hydrocarbons, 1114–17
 - saturated, 800–2
 - hydrosilanes, 807–8
 - ketones, 784–7, 1108–14
 - lipids, 667, 669, 693, 945–7
 - nucleophiles, 70–2
 - nucleosides, 975
 - olefins, 790–3
 - catalytic epoxidation, 790–2
 - chlorohydrin and acetoxy alcohol synthesis, 792–3
 - peroxynitrite anion, 21
 - protocols, 809–10
 - regioselective, 403
 - stability on storage, 664–5, 672
 - substrates in biological systems, 614–17
 - sulfides, 472–92, 493–5
 - thiol–olefin co-oxygenation, 221–3, 224, 225, 226, 250, 251, 1330
 - transition metal peroxides
 - alcohols, 1105–8
 - alkenes, 1079–95
 - electrophilic substrates, 1072–4
 - heteroatoms, 1095–105
 - hydrocarbons, 1114–17
 - ketones, 1108–14
 - mechanistic aspects, 1072–9
 - nucleophilic substrates, 1074–6
 - radical reactions, 1076–9
 - trimethylamine, 75, 76
 - types of reaction, 309
 - uric acid, 625
 - see also* One-electron oxidation; Oxygenation; Photosensitized oxidation; Thermal oxidation; Two-electron oxidation
- N-Oxidation, organonitrogen compounds, 531–8, 539
- Oxidation indices, 656–72
 - peroxide determination, 762–3
 - peroxide value, 656, 657–64
 - colorimetry, 658–61
 - definition, 657
 - direct titration, 657
 - electrochemical methods, 663–4
 - IR spectrophotometry, 661–3
 - NIR spectrophotometry, 663
 - UV–visible spectrophotometry, 658–61
 - secondary oxidation products, 656, 665–72
 - tests for stability on storage, 664–5, 672
 - thermal analysis, 672
- Oxidative amperometry, hydroperoxide determination, 686
- Oxidative cleavage
 - alkenes, 1094–5
 - double bonds, 525–7
- Oxidative coupling, hydrogen peroxide determination, 630, 635
- Oxidative damage
 - abasic site quantization, 671
 - DNA, 614, 633, 670–1, 918
 - proteins, 614, 918
 - secondary oxidation products, 665
 - thymidine, 616
 - tissue homogenizates, 669, 676
- Oxidative dimerization 4-hydroxyphenylacetic acid, 639
- Oxidative halogenation, hydrocarbons, 572, 575–81
- Oxidative ozonolysis, analytical methods, 737
- Oxidative stress
 - lipid hydroperoxides, 613, 614, 687
 - TBARS assay, 667
- Oxidative transformations, 309
- N-Oxides

- N*-Oxides (*continued*)
dioxirane oxidation, 1152, 1153–4
spin trapping, 664
- Oxidized LDL antibodies, immunoassay, 633
- Oxidized polyolefins, hydroperoxide detection, 673
- Oxidizing agents
peroxydisulfates, 1007–20
peroxymonosulfates, 1020–32
persulfonic acid, 1002–4
superoxides, 1032–9
- Oximes, aldehyde determination, 670
- 7-Oxocholesterol, oxidation indices, 666, 671
- 8-Oxo-7,8-dihydroguanine
one-electron oxidation, 943–5
singlet oxygen oxidation, 943, 944, 976–7
- Oxidiperoxo-chromium complex, alcohol oxidation, 787–8
- 8-Oxoguanine
DNA oxidative damage, 633
peroxide value, 661
- Oxone *see* Potassium peroxymonosulfate
- Oxorhenium species
catalyzed olefin epoxidation, 790
see also Methyltrioxorhenium
- Oxyfunctionalization, dioxiranes, 1135–63
- Oxygen
sensors, 652, 665
see also Molecular oxygen; Singlet oxygen; Triplet oxygen
- Oxygenation
fullerene adducts, 857–60
stereoselective dioxygenation, 339–48
thiol–olefin co-oxygenation, 221–3, 224, 225, 226, 250, 251, 1330
see also Oxidation
- Oxygen atom transfer
carbonyl oxides, 32, 34–48
dioxiranes, 32, 34–48
agents, 1130
catalysis, 1146
density functional theory, 34–5
epoxidation
alkenes, 35–40
relative rates in solution, 40–4
mechanistic aspects, 1134–9
saturated hydrocarbon oxidation, 44–8
transition structures, 1135–9
hydroperoxides, 67–84
amines, 67–70
electronic factors, 72–6
enzymes, 77–82, 83
nucleophiles, 70–2
peroxo bond, 82–4
peroxynitrous acid, 14–17, 18, 21–2
theoretical aspects, 67–84
- Oxygen-centered radicals, 1,2,4-trioxane
antimalarials, 1284–99, 1309
- Oxygen-containing compounds, dioxirane oxidation, 1155
- Oxygen electrodes, biosensors, 655, 664, 689
- Oxygen–oxygen bonds
bond dissociation energies, 5–7
heterolytic cleavage, 1291, 1301–4, 1309
homolytic cleavage, 1304
O insertion, 95–6
peroxynitrous acid homolysis, 7, 8
- Oxygen uptake
quartz microbalance, 665
TBARS assay, 668
- Ozone
in atmosphere, 605, 683
bronchial epithelial cell exposure, 683
chlorinated ethylene reactions, 731–2
[3 + 2] cycloaddition to C=C bond, 247, 248
demand, 739
disinfection, 606, 616, 740
DNA effects, 616
hydrotrioxide formation, 740
lipid hydroperoxides in epithelial cells, 612
in natural waters, 608
O₃-valley events, 605
ozonide synthesis, 718
 π -complexes, 717, 731–2
in soil, 608
in stratosphere, 605
- Ozone adducts
alkali metal ozonides, 735–7
organic ozonides, 734–5
ozonide zwitterionic complexes, 734
 π -complexes, 731–2
phosphite–ozone, 673, 706, 732–3
quaternary ammonium ozonides, 735–7
- Ozone resistance, rice, 616
- Ozonesonde studies, atmospheric analysis, 605
- Ozonide anion, alkali metal ozonides, 735–7
- Ozonide radical anion, alkali metal ozonides, 735–7
- Ozonides
analytical and safety aspects, 716–40
antimalarial activity, 1282, 1317, 1318
antimicrobial activity, 608
antitumour activity, 1335
atypical, 729
detection and determination
chromatography, 719
IR spectrophotometry, 718–19
NMR spectrometry, 719
titration methods, 718
organic, 734–5
ozone adducts, 731–7
peroxide formation, 705
polymerization initiators, 622
structural characterization
electron diffraction, 721, 722, 723

- IR spectroscopy, 719–20
- mass spectroscopy, 726
- microwave spectroscopy, 721–3
- molecular refraction, 731
- NMR spectroscopy, 723–6
 - ¹⁷O NMR spectroscopy, 173–8
 - thermal analysis, 730
 - X-ray crystallography, 711–12, 726–30
- thermochemistry, 165–6
- 1,2,4-trioxane synthesis, 290–1
- zwitterionic complexes, 734
- see also* Final ozonides; Primary ozonides
- Ozonization
 - analytical methods, 690, 737
 - bisphenol A elimination, 608
 - C–H bond, 178
 - enthalpies of ozonation, 165
 - multiple-stage, 607
 - wastewater decolorization, 608
- Ozonized polymers, graft polymers, 622
- Ozonolysis
 - Allen's reagent, 606
 - analytical methods, 737–40
 - biogenic olefins, 673
 - cholesteryl acetate, 695–6
 - Criegee's mechanism, 606, 685, 716–17, 721, 726, 729
 - E*,2,3-dichloro-2-butene, 685, 686, 699, 724
 - 1,2-dichloroethylene, 706
 - dioxirane preparation, 1132
 - FTIR spectroscopy, 718–19
 - Griesbaum co-ozonolysis, 1331
 - hydrogen peroxide determination, 626
 - hydroperoxide determination, 685, 686
 - hydroperoxide synthesis, 326–7
 - hydroperoxyketal formation, 241
 - mechanism, 177–8
 - mechanistic studies, 717
 - olefins, 673, 674
 - oxidative, 737
 - pollution evaluation, 739
 - reductive, 739
 - silanes, 810–14
 - silane trioxide intermediates, 811–14
 - synthesis applications, 716
 - tetroxide formation, 740
 - thymine, 616
 - trioxolane synthesis, 1331, 1332
 - vinylsilanes, 275–6
- π -type interactions, lone pairs, 102–3
- Packing class, commercial codes, 621
- Packing effect, dialkyl peroxides, 121
- Palm olein, oxidative deterioration, 662
- Panretinal laser photocoagulation, 640
- Paper, bleaching agents, 623
- Parasites
 - haemoglobin degradation, 1281, 1283
 - parasiticidal activity, 1309, 1313
- cis*-Parinaric acid, autofluorescence, 660
- Parkinson's disease, 4-hydroxynon-2-enal determination, 613–14, 670
- Partial least squares regression, analytical methods, 624
- Particle emissions, diesel fuel additive, 624
- Partition number, conjugated dienes, 671
- Pasteurization, lactoperoxidase, 612, 631, 634
- Paterno–Büchi triplet 1,4-diradical, 290–1
- PCPO *see* Bis(pentachlorophenyl) oxalate
- Pentacoordinate silyl peroxides, 808–10
- Pentacosane, thermal oxidation, 685
- O*-Pentafluorobenzylhydroxylamine, aldehyde determination, 670
- Pentafluorophenylhydrazine, aldehyde determination, 670
- Pentamethyldisilane, oxidation, 807–8
- 3-Pentyl hydroperoxide, molecular refraction, 697
- Peptides
 - radical reactions, 960–6
 - hydroxyl radical, 954–60
 - singlet oxygen oxidation, 966–70
- Peracetic acid
 - bleaching agent, 623
 - determination, 698, 699, 700
 - effect on hydrogen peroxide analysis, 635, 637, 638
 - hydroperoxide determination, 678
 - International Chemical Safety Card, 749, 753–5
 - oxidative ozonolysis, 737
- Peracids
 - alkene epoxidation, 48–67
 - allylic alcohols, 65–7
 - early mechanistic studies, 48
 - gas-phase, 58
 - Hartree–Fock calculations, 48–50
 - rate factors, 58–65
 - synchronous/asynchronous transition states, 50–8
 - commercial availability, 619, 621, 622
 - salts, 620–1, 622
 - crystal structure, 125–7
 - geometric parameters, 135
 - electrophilic oxidants, 1142
 - functionalization, 1055
 - hydrogen bonding, 104–5, 160
 - peroxyoxalate chemiluminescence, 1260–1, 1263–5, 1266, 1270
 - see also* Peroxycarboxylic acids
- Perborate
 - household washing formulations, 623
 - hydrogen peroxide determination, 630
- n*-Perbutanoic acid, determination, 699

- Percarbamide, pharmaceutical preparations, 623
- Percarboxylate anion ligands, crystal structure, 127, 128
- Percarboxylate esters
enthalpies of formation, 159, 160–2
formal enthalpy of hydrogenation, 160
homologous series, 160
thermochemistry, 158, 160–2
thermolysis, 161
see also Peresters
- Percarboxylic acids, determination, 699
- Perepoxide intermediate
ene reaction, 832–3, 835, 845, 846
endo-perepoxide intermediate, 859
nucleophilic substitution cyclization, 235–6
- Peresters
commercial availability, 619, 622
crystal structure, 127–8
geometric parameters, 130
hydroperoxide oxidation, 692
peroxide value, 658, 662
see also Percarboxylate esters
- Perfluoroacetyl peroxy nitrates, structure, 103, 104
- Performate free radical, 742
- Performic acid, determination, 698, 699
- Pericyclic transformation, olefins, 94
- Peroxalate, hydrogen peroxide determination, 643, 648, 649
- Peroxidase
hematin mimic, 640, 641, 642
hydrogen peroxide determination, 630, 631, 632, 633, 635, 638
peroxycarboxylic acid determination, 700
protein hydroperoxide formation, 972
- Peroxidation
cellular biomolecules, 917–88
Co(II) complex mediation, 223, 225, 228–9
lipids, 670, 918, 945, 974
protein backbone, 955
pyrimidine nucleosides, 929–30
thymine hydroperoxide synthesis, 927, 929–30
triplet molecular oxygen, 192–212
- Peroxide bonds
heterolytic cleavage, 1291, 1301–4, 1309
homolytic cleavage, 1304
O insertion, 95–6
- Peroxide group
analytical and safety aspects, 740–4
theoretical aspects, 1–91
- Peroxide precursors, hydroperoxide synthesis, 327, 328
- Peroxides
in atmosphere, 604–5
biological systems, 915–99
commercial availability, 617, 618–21
determination, 632–3
enthalpies of formation, 153–5
double-bonded oxygen functional groups, 159–10
hydrocarbon-substituted, 148–9
single-bonded oxygen functional groups, 318
enthalpies of reactions, 153–5
enthalpies of vaporization, 153–4
environmental hazards, 617
functionalization, 1055
handling, 617
hydrocarbon-substituted, 147–55
manufacture, 617, 622
multiply-linked, 163–7
in nature, 603–17
¹⁷O NMR spectroscopy, 183–5
plastic materials, 622
polymerization agents, 622
proteins, 970–2
single-bonded oxygen functional groups, 155–8
storage, 617
synthesis, 309–62
synthetic uses, 362–581
in technology, 603, 617–24
thermochemistry, 145–69
mixed hydroperoxides and peroxides, 149, 154–5
toxicity, 617
see also Cyclic peroxides; Organic peroxy compounds
- Peroxide transfer reactions, germyl peroxides, 824–5
- Peroxide value (POV), 656, 657–64
chromatography, 672
colorimetric determination, 632
rubber and elastomers, 676
- Peroxisomes, antioxidant in biological systems, 610, 611
- Peroxo complexes
¹⁷O NMR spectroscopy, 185–6
solid state structures, 1061–3
synthesis, 1057–9
- μ -Peroxo complexes
solid state structures, 1064–8
synthesis, 1059–61
- Peroxodisulfate
concentration monitoring, 744
etching formulations, 623
- Peroxomonosulfate, concentration monitoring, 744
- μ -Peroxo- μ -oxo-bis[bis(trimethylsilyl)methyl]tin, 729–30
- Peroxovanadates, ¹⁷O NMR spectroscopy, 186
- Peroxyacetalization of carbonyl functions
 β -hydroperoxyalcohols, 273–7, 278
strained endoperoxide systems, 277–85

- Peroxyacids
analytical and safety aspects, 697–705
detection and determination, 698–701
functional derivatives, 697–705
structural characterization, 701–5
thymine ozonolysis, 616
- Peroxycarbonates
hydrofluorocarbon decomposition, 604
photochemical synthesis, 740
polymerization agents, 622
polymerization initiation, 697
structural characterization, 705
- Peroxycarbonic esters, vibrational spectra, 705
- Peroxycarboximidic acids, structural characterization, 701–2
- Peroxycarboxylic acids
determination, 698–700, 701
enthalpies of formation, 159
enthalpies of vaporization, 160
formal reactions, 158
homologous series, 158
hydrogen bonding, 104–5, 160
polymerization, 698
thermochemistry, 158–63
see also Peracids
- Peroxycarboxylic esters
determination, 698, 701
radical polymerization initiation, 697
vibrational spectra, 705
- Peroxy compounds *see* Organic peroxy compounds
- Peroxydicarbonates, analytical methods, 740
- Peroxydisulfate, 1007–13
organic salts, 1001–2, 1014–20
- Peroxyesters
detection and determination, 700–1
hydrolysis, 329
polymerization agents, 622
polymerization initiation, 697
structural characterization, 705
synthesis, 705
thymine ozonolysis, 616
- Peroxyformic acid (PFA)
alkene epoxidation, 17–18, 38, 41, 43, 50–8
isobutylene, 50, 52
see also Peroxynitrous acid
- Peroxyhemiacetals, 1,2,4-trioxane synthesis, 286
- Peroxyiodination, nucleophilic addition
cyclization, 241–2
- Peroxyketalization, intramolecular, 276–7
- Peroxyketals, triplet oxygen cycloaddition, 201, 203
- Peroxylactol, triplet oxygen cycloaddition, 202, 204
- α -Peroxylactones, 1172
chemiluminescence, 1223, 1225, 1226, 1232
electron transfer decomposition, 1183, 1184
firefly bioluminescence, 1191–2, 1194
oxidants, 1178–80
see also 1,2-Dioxetanones
- β -Peroxylactone, synthesis, 230, 232
- Peroxymercuration, 1,2-dioxolane synthesis, 238, 239, 240–1
- Peroxymonosulfates
organic salts, 1030–2
potassium salt, 26, 1020–30, 1130
- Peroxynitrates
gas electron diffraction, 743–4
hydrofluorocarbon decomposition, 604
IR and Raman spectroscopies, 742–3
mass spectrometry, 743
NMR spectroscopy, 743
UV spectroscopy, 743
- Peroxynitric acid
1,2-rearrangement, 25
two-electron oxidation, 21–2
- Peroxynitrite anion
analytical aspects, 740–2
formation, 10
ground state, 8–10
oxidation, 21
- Peroxynitrites
dioxirane preparation, 1132
generation, 10, 611
lipid peroxides, 951–2
metal salts, 9–10
in vascular systems, 611–12
- Peroxynitrous acid
analytical aspects, 740–2
bond dissociation energy, 6, 7
conformers, 8–9
decomposition, 7–8
dissociative pathways, 13–14
epoxidation of ethylene and propylene, 17–20
generation, 611
ground state properties, 8–10
historical overview, 7–8
metastable states, 10–14, 22–5
one-electron oxidation, 22–5
O–O bond homolysis, 7, 8
reactivity, 14–25
1,2-rearrangement, 25
rotational isomers, 8–9
theoretical chemistry, 7–25
two-electron oxygen atom transfer, 14–17, 18, 21–2
- Peroxyoxalate chemiluminescence, 1239, 1256–70
activated, 1220–1, 1248
chemiexcitation, 1257, 1258, 1266–70
CIEEL approach, 1188–9, 1266–70

- Peroxyoxalate chemiluminescence, (*continued*)
 high-energy intermediate, 1188–9, 1257,
 1261–6, 1267, 1269
 mechanism, 1257–61
 quantum yields, 1225, 1226, 1235, 1266–8
- Peroxyoxalic acid, peroxyoxalate
 chemiluminescence, 1266, 1267
- Peroxyphosphorus radicals, 1044–6
- Peroxy polymers *see* Polymerization
- Peroxypropiolactone, synthesis, 230, 232,
 249–50
- Peroxy-radical cation, triplet oxygen reactions,
 204–5
- Peroxyulfates, analytical aspects, 744
- Peroxyulfenate, superoxide reactions, 1033
- Peroxyulfinate, superoxide reactions, 1033–5
- Perpendicular effect, methyl substituted-benzyl
 carbinyl hypochlorite photolysis, 907,
 911
- Per(poly)fluoroalkyl chlorides, peroxydisulfate
 reactions, 1011
- Persistent organic pollutants (POP), 747
- Persistent toxic substances (PTS), 747
- Personal care preparations, pharmaceuticals,
 621
- Persulfonic acid, 1002–4
- Perylene, chemiluminescence, 648
- PFA *see* Peroxyformic acid
- PfATP6 enzyme, 1313, 1320
- PGG₂, prostaglandin endoperoxide, 190, 191,
 214, 215
- PGH₂, prostaglandin endoperoxide, 190, 191
- Pharmaceuticals
 catalysis quenching, 647
 formulations, 623
 long-term stability, 672
 personal care preparations, 621
 see also Drugs
- Phase change enthalpies, 146
- Phase-transfer catalysis, organo-catalyzed
 epoxidation, 370–3
- pH dependence, CIEEL intensity, 1195–8
- (*R*)-(–)- α -Phellandrene, intrazeolite
 photooxygenation, 886
- 1,10-Phenanthroline, hydroperoxide
 determination, 675, 676
- Phenol
 manufacture, 617, 622
 quinoneimine dyes, 630, 632
- Phenolphthalin, hydrogen peroxide
 determination, 629
- Phenol Red, hydrogen peroxide determination,
 628–9
- Phenols
 nitronate ion dioxirane oxidation, 1152–3
 polar, 664
- Phenothiazine, hydrogen peroxide biosensor,
 653
- Phenylarsine oxide, hydrogen peroxide
 titration, 627
- 1-Phenylcyclopentene, ozonide, 712
- Phenyldimethylsilane, oxidation, 807–8
- o*-Phenylenediamine, hydrogen peroxide
 determination, 634, 646–7
- p*-Phenylenediamine, milk pasteurization
 testing, 634
- Phenyl hydroperoxide, C-O distance, 103
- ω -Phenylhydroperoxides, nucleophilic
 substitution cyclization, 234–5
- 1-Phenyl-3-methyl-3-butene, intrazeolite
 photooxygenation, 874–5
- Phenyl substituted alkenes, photooxidation site
 selectivity, 839–42
- Phenyltetramethylsiloxane, preparation, 781
- Phosgene, from tetrachloroethene, 731
- Phosphatidylcholines
 hydroperoxide determination, 675, 676, 678,
 681, 683, 686, 687, 690
 peroxide value, 658–9
 quenching, 711
- Phosphatidylethanolamine, hydroperoxide
 determination, 675, 683–4, 686, 690
- Phosphatidylglycerol, hydroperoxide
 determination, 690
- Phosphatidylinositol, hydroperoxide
 determination, 675, 683–4, 686
- Phosphatidylserine
 hydroperoxide determination, 675, 686
 oxidative stress, 613
- Phosphines
 nucleophile oxidation, 70–2
 peroxynitrous acid oxygen transfer, 14–17
- Phosphite–ozone adducts, 706, 732–3
- Phospholipase C, hydrolysis, 719
- Phospholipids
 hydroperoxide determination, 675, 678, 680,
 681, 683–4, 686, 687, 690
 TBARS assay, 668
- H-Phosphonates, oxidation, 805
- Phosphorus-containing compounds
 bis(trimethylsilyl) peroxide reactions, 803–5
 dioxirane oxidation, 1154–5
- Phosphorus oxides, phosphite–ozone adducts,
 733
- Phosphorus peroxides, 1039–46
 symmetrical, 1041–2
 unsymmetrical, 1042–4
- Photocalorimetry, ozonides, 165
- Photochemistry
 Norrish type II reaction, 196, 197
 syntheses, 740
 triplet oxygen cycloaddition, 196–204
- Photodensitometry, hydroperoxide
 determination, 678
- Photoisomerization α,β -unsaturated
 γ -hydroperoxyketone, 246–7

- Photolysis
 methyl substituted-benzyl carbonyl
 hypochlorites, 907–9
 perpendicular effect, 907, 911
- Photonucleases, artificial, 616–17
- Photooxidative stress, leukemia cells, 687
- Photooxidation
 dialkyl peroxide formation, 706
 DNA by 1,2-dioxetanes, 1200–5
 E,E-hexa-2,4-diene, 254–5
 lipids, 947–51
 singlet oxygen ene reaction regioselectivity,
 834–45, 846
 cis alkenes, 842–4
 allylic functionality, 845–9
 electron-donating groups, 841
 electron-withdrawing groups, 840–2,
 852–6
 fullerene adducts, 857–60
 geminal regioselectivity, 845–52
 kinetic isotope effect, 840
 Rose Bengal, 890
 synthetic applications, 886, 888, 889–92
 transition states, 859–60
 thymidine, 616
- Photooxygenation
 alkenes
 chiral diastereoselectivity, 883–6, 887
 electron-poor, 877–8
 trisubstituted regioselectivity, 874–7
 allene hydroperoxide, 857, 858
 allylic hydroperoxide formation, 869–86,
 887
 allylic radical intermediate, 871
 diastereoselectivity, 96, 836, 883–6, 887
 chiral 1,2-dihydronaphthalenes, 265–6
 1,4-cyclohexadiene, 264
 cyclopentadiene, 263
 digermolanes, 825–6
 1,2-dioxetane synthesis, 1236
 dye-sensitized intrazeolite, 869–86, 887
 kinetic isotope effect, 872–3
 multicomplexation model, 878
 type I and II processes, 871
 zeolite Na–Y, 870–4, 885–6, 887
- isobutenylarenes, 878–83
 electrostatic interactions, 882–3
 site selectivity, 880–3
 zwitterionic intermediate, 880
- synthetic applications, 886, 888–93
- TBS-protected-3,5-cycloheptadienol, 266
- 3-vinylindole derivatives, 259–60
- Photosensitized oxidation
 cholesteryl esters, 692
 dialkyl peroxide formation, 706
 ene reaction, 673
 lipid hydroperoxides, 676
 ozonide synthesis, 718, 728–9
- phosphite–ozone adducts, 732
- phytol, 690, 691
- γ -pyronene, 694, 709–10
- thymidine, 695
- Photosensitizers
 intrazeolite photooxygenation, 871
 2-methyl-1,4-naphthoquinone, 929
 oxadisilirane irradiation, 817
- Photosynthesis, lipid hydroperoxide
 interference, 617
- Phthalein dyes, hydrogen peroxide
 determination, 628–9
- Phthaloyl peroxide, luminol
 chemiluminescence, 1245
- Physiological matrices
 hydrogen peroxide determination, 644
 peroxynitrite determination, 741
- Phytol, photosensitized oxidation, 690, 691
- Phytoplankton, hydrogen peroxide in seawater,
 606
- Picket fence porphyrin, ^{17}O NMR
 spectroscopy, 185
- Pickling baths, capillary zone electrophoresis,
 744
- Picolinate-N-oxido anion (PICO), transition
 metal peroxides, 1058, 1095
- Picolinic acid (pic), transition metal peroxides,
 1054, 1058, 1067, 1076
- (–)- β -Pinene, artemisinin synthesis, 288, 289
- Plakorin, 191, 247, 1333
- Plakortin acid, 190, 191
- Plakortin, 190, 191
- Plant leaves, hydrogen peroxide formation, 636
- Plant tissue
 hydroperoxide determination, 676
 TBARS assay, 667
- Plasma
 hydroperoxide determination, 673, 676, 680,
 681, 687, 690
 4-hydroxynon-2-enal, 613
 malondialdehyde determination, 669
 oxidation level, 631
 peroxide value, 659
 protein free radical trapping, 614
 TBARS assay, 667
- Plasmodium falciparum*
 malaria parasite, 608, 1281, 1283
 PfATP6 enzyme, 1313, 1320
- Plutonium(IV) complexes, hydrogen peroxide
 determination, 635–6
- PNS (principle of nonperfect synchronization),
 907
- Polar effects
 tert-butyl perbenzoate ETR reactions,
 909–12
 negative charge, 909, 911
 positive charge, 910, 911

- Polar effects (*continued*)
 tert-butyl phenylperacetate thermolysis, 903–7
 decomposition, 899–913
 methyl substituted-benzyl carbonyl hypochlorite photolysis, 907–9
- Polarography, hydrogen peroxide determination, 652
- Polar phenols, colorimetry, 664
- Polar residue, chiral hydroperoxide synthesis, 338
- Pollution
 ozonolysis assessment, 739
 safety aspects, 747
 trifluoromethyl peroxyhydrate, 743
 see also Air pollutants
- Polyamines, hydrogen peroxide determination, 651
- Polyamino acids, epoxidation catalysis, 373–83
- Polyester–melamine coatings, hydroperoxide formation, 683
- Polyethylene
 γ -radiation, 685
 thermal oxidation, 623, 673, 695
- Polyethyleneglycol hydroperoxides, determination, 679
- Polymer immobilization, Mo-peroxide, 427
- Polymerization
 agents, 621, 622
 peroxide value, 661, 662
 peroxycarboxylic acids, 698
 radical polymerization, 697, 707
 styrene, 697, 720
 sulfonyl peroxides, 1005
 thermochemistry, 155
- Polymers
 aging, 685
 autoxidation, 623
 hydroperoxide determination, 685
- Poly(methacrylonitrile peroxide)
 NMR spectroscopy, 709
 radical polymerization, 707
- Poly(methyl methacrylate peroxide), structure, 714–15
- Poly(methylstyrene peroxide)
 radical polymerization, 707
 structure, 709
- Polyolefins
 oxidized, 673
 unsaturated, 740
- Polyoxides
 O insertion into O–O bond, 95–6
 structural chemistry, 133
- Polyoxo compounds, structural chemistry, 131–3
- Polyoxometallates (POM)
 catalyzed olefin epoxidation, 429–30
 transition metal substitution, 1057
- Poly-*o*-phenylenediamine, hydrogen peroxide determination, 647
- Poly(styrene peroxide)
 radical polymerization, 707
 structure, 709
- Polyunsaturated fatty acids
 conjugated dienes value, 671
 peroxide value, 661
- Poly(vinylferrocene), hydroperoxide biosensor, 688
- Poly(vinylferrocenium perchlorate), Hydroperoxide biosensor, 688
- POM (polyoxometallates), 429–30, 1057
- POP (persistent organic pollutants), 747
- Poppyseed oil, vibrational spectra, 692
- Porphyrin, ^{17}O NMR spectroscopy, 185
- Potassium carbonate, alcohol oxidation, 492
- Potassium hexacyanoferrate(II), hydrogen peroxide biosensor, 653
- Potassium hydrogen phthalate hemiperhydrate, 98–100
- Potassium ozonide, 735
- Potassium permanganate
 chemiluminescence, 643
 hydrogen peroxide titration, 627
 ozonide redox titration, 736
- Potassium peroxymonosulfate, dioxirane preparation, 26, 1020–30, 1130
- Potassium superoxide, commercial availability, 620
- Potentiometry
 biosensors, 664
 fitness for purpose, 663
 hydrogen peroxide determination, 650–1
 iodine–iodide buffer, 699
 measurement uncertainties, 663
 peroxide value, 663–4
 transition metal peroxides, 1069
- POV *see* Peroxide value
- POZ *see* Primary ozonides
- Precipitation waters, hydrogen peroxide determination, 637
- Predicted residual error sum of squares (PRESS), 624
- Preservatives, pharmaceutical preparations, 623
- PRESS technique, NIR spectrophotometry, 624
- Primary amines, dioxirane oxidation, 1151
- Primary ozonides (POZ), 716, 717
 dialkyl peroxide formation, 706
 IR spectroscopy, 718, 719–20
 microwave spectroscopy, 721
 molecular model, 750
 NMR spectroscopy, 709, 723–4
 octalin ozonation, 165
 ozone water disinfection, 606
 π -complexes with ozone, 732

- Principal component analysis, analytical methods, 624
- Principle of nonperfect synchronization (PNS), methyl substituted-benzyl carbonyl hypochlorite photolysis, 907
- Probulol
Fe(III) masking, 669
low-density lipoprotein antioxidant, 611
- Prochiral alkenes
allyl hydroperoxide synthesis, 341, 342
dioxirane epoxidation, 1145
- Prochiral sulfides, dioxirane oxidation, 1156–7
- Pro-drugs, antimalarials, 1320–3, 1324, 1332, 1342
- Propanal, TBARS assay, 667
- Propene, final ozonide, 721
- Propylene
peroxynitrous acid epoxidation, 17–20
primary ozonide, 720
- i*-Propylether–ozone adduct, 734–5
- Prostaglandin endoperoxides
isolation, 190, 191
lipid hydroperoxide biosensor, 690
peroxide transfer reaction, 825
- Prostaglandins, from arachidonic hydroperoxides, 612
- Protein hydroperoxides, 954–75
amino acid peroxide secondary reactions, 972–5
cellular indicators of hydroperoxides, 918, 985–7
carbonyl compounds, 986–7
global assessment, 986
hydroxylated valine and leucine residues, 987
decomposition, 986–7
histidine, 614–15, 968–70
leucine, 956–8, 987
lysine, 614–15, 959
tryptophan, 614, 615, 960–3, 966–8
tyrosine, 614, 615, 960, 963–6, 968, 969
valine, 614, 615, 956, 957, 987
- Proteins
cross-linking, 973–5
hydroperoxide determination, 673, 674
lipid peroxidation aldehyde adducts, 984–5
¹⁷O NMR spectroscopy, 185
oxidative damage, 614, 918
ozone disinfection, 616
peroxidation
amino acid side-chain, 955–60
protein backbone, 955
peroxide formation, 970–2
amino acid peroxide secondary reactions, 972–5
DNA and nucleoside oxidation, 975
lipid peroxidation, 974
nucleic acid–protein cross-links, 974–5
protein cross-links, 973–4
transfer within proteins, 973
peroxidase-mediated reactions, 972
radical reactions, 971–2
singlet oxygen oxidation, 972
see also Lipoprotein
- Protoporphyrin IX
diacyl peroxide biosensor, 701
hydrogen peroxide biosensor, 652
lipid hydroperoxide determination, 681
- Prussian Blue, hydrogen peroxide biosensor, 655
- Pseudomonas aureoginosa*, up/downregulation of metabolism, 610
- Pseudorotation, ozonides, 721, 722
- PTS (persistent toxic substances), 747
- Pulp
bleaching agents, 623
hydrogen peroxide determination, 627
- Pulse radiolysis, peroxynitrite generation, 611
- Purine bases, oxidative damage, 614
- 9*H*-Purine-6-thiols, dioxirane oxidation, 1156
- Purpurogallin, chemiluminescence, 649
- Pyrazole, transition metal peroxides, 1064, 1083
- Pyridine, methyltrioxorhenium ligands, 460–1
- Pyridine-2,6-dicarboxylate (dipic), transition metal peroxides, 1060, 1061
- Pyridinium dichromate, alcohol oxidation, 787–8
- Pyridoxine (Vitamin B₆), singlet oxygen detoxification, 610, 694–5, 710
- N*-(α -Pyridyl)-2-thioquinaldamide
hydrogen peroxide determination, 642, 643
hydroperoxide determination, 679
- Pyrimidine nucleosides, peroxidation, 929–30
- Pyrogallol, chemiluminescence, 649
- γ -Pyronene, photosensitized oxidation, 694, 709–10
- Pyronin B, fluorometry, 640
- Pyruvate, lactate determination, 625, 626
- Pyruvic acid, hydrogen peroxide determination, 655
- QCISD, density functional theory, 3, 34–5, 43
- Qinghaosu *see* Artemisinin (qinghaosu)
- Quality, deterioration evaluation, 656, 664
- Quantum chemical calculations,
1,2,4,5-tetroxane thermochemistry,
164–5
- Quantum yields
chemiluminescence research, 1222–7
emission quantum yields, 1221, 1222–3
energy transfer quantum yields, 1223
excitation quantum yields, 1221, 1222–3, 1225

- Quantum yields (*continued*)
 reciprocal quantum yields, 1223
 lucigenin oxidation, 1250
 luminol oxidation, 1243
 peroxyoxalate chemiluminescence, 1225,
 1226, 1235, 1266–8
 singlet, 858, 1211, 1222, 1223, 1224, 1226
 triplet, 1221, 1223, 1224
- Quartz microbalance, oxygen uptake, 665
- Quaternary ammonium ozonides, ozone
 adducts, 735–7
- proto*-Quercitol, synthesis, 264
- Quinine sulfate, light emission intensity
 calibration, 1225
- ortho*-Quinodimethanes, triplet oxygen
 cycloaddition, 198
- Quinoneimine dyes
 hydrogen peroxide determination, 630, 632
 hydroperoxide determination, 676–7
- o*-Quinones, dopamine determination, 625, 626
- Radiation-induced decomposition,
 5,6-dihydrothymine, 930
- Radiation stress, polymers, 685
- Radical polymerization
 dialkyl peroxides, 707
 peroxycarboxylic esters, 697
- Radicals
 allylic photooxygenation intermediate, 871
 amino acid and peptide reactions, 954–66
 biradical intermediates
 chemiluminescence mechanism, 1181–2,
 1227–31
 ene reactions, 853
 carbon-centered
 primary, 1283–4, 1292–9, 1309
 secondary, 1283–91, 1299, 1309
 1,2,4-trioxane antimalarials, 1283–99
 cation, 204–12
 dioxetane-induced DNA photooxidation,
 1202–5
 diradicals, 192–204
 DNA oxidation, 695
 electrochemiluminescence, 1213, 1214, 1234
 guanine oxidation, 940–1
 Hammett reaction constants, 899–903
 homoallylic peroxy, 213–14
 hydroperoxide radical, 84, 611
 hydroxyl
 biological system oxidation, 614
 hydrogen peroxide hydrogen bonding, 98
 iron(II), 641
 luminol chemiluminescence, 681, 1243–4
 α -ketoalkyl, 252
 γ -ketoalkyl, 252
 luminol radical anions, 1241–2, 1244, 1245
 oxygen-centered, 1284–99, 1309
 ozonide radical anion, 735–7
 peroxyphosphorus, 1044–6
 polymerization initiators, 697
 protein hydroperoxide formation, 971–2
 selenyl, 223, 227
 sulfate ion radical, 1014
 sulfonylperoxy, 1035–9
 thiyl, 221–3, 224, 225, 226
 transition metal peroxide oxidation, 1076–9
 trioxide formation mechanism, 180
 see also Biradical intermediates; Diradicals;
 Free radicals; Superoxide anion radical
- Radioactive materials
 risk and handling labels, 752
 UN classification, 746
- Radioactive standard, light emission intensity
 calibration, 1224
- Radiometric method, hydrogen peroxide
 determination, 655–6
- Rainwater
 hydrogen peroxide determination, 636,
 637–8, 639, 641, 645, 648, 650, 651
 hydroperoxide determination, 678
 peroxide analysis, 604
- Raman spectroscopy
 hydroperoxides, 692
 peroxynitrates, 742–3
 transition metal peroxides, 1069
 see also Fourier transform–Raman
 spectroscopy
- Rancidification, biosensors, 664
- RancimatTM, oxidation stability measurement,
 664, 672
- Rapeseed oil
 anisidine value, 666
 peroxide value, 657, 662, 665
- Rate constants
 chemiluminescence, 1221–2
 peroxyoxalates, 1258–9
 linear free-energy relationship, 1234
- Rat liver cells, lipid peroxide determination,
 669
- Reaction calorimetry, enthalpy of formation
 determination, 155, 160, 163
- Reaction rates
 tert-butyl perbenzoate ETR reactions,
 909–12
 tert-butyl phenylperacetate thermolysis, 903,
 904
 methyl substituted-benzyl carbonyl
 hypochlorite photolysis, 907–9
 peracid alkene epoxidation, 58–65
 perpendicular effect, 907, 911
 temperature studies, 903–12
- Reactions *see* Enthalpies of reactions; Formal
 reactions
- Reactive nitrogen species, biomedical systems,
 611–12

- Reactive oxygen species (ROS)
 biological and biomedical systems, 610–12,
 661, 669, 670
 hydroperoxide synthesis, 673
 water interactions, 605–8
- Reactivity
 dioxiranes, 1134–5, 1139–63
 peroxynitrous acid, 14–25
 transition metal peroxides
 alcohols, 1105–8
 alkenes, 1079–95
 electrophilic substrates, 1072–4
 heteroatoms, 1095–105
 hydrocarbons, 1114–17
 ketones, 1108–14
 mechanistic aspects, 1072–9
 nucleophilic substrates, 1074–6
 radical reactions, 1076–9
- Rearrangement reactions
 cyclopropylcarbinyl–homoallyl, 223, 226
 McLafferty rearrangement, 704
 peroxynitrous acid 1,2-rearrangement, 25
- Redox titration, alkali metal ozonides, 736
- Reduction, electrocatalytic, 654
- Reductive amperometry, hydroperoxide
 determination, 686
- Reductive ozonolysis, analytical methods, 739
- Regioselectivity
 allene hydroperoxide formation, 856–7, 858
 allylic hydroperoxide formation, 833–60
 allylic alcohols and amines, 836
 anti *cis* effect, 836–9, 840, 841
 chiral alkenes, 886, 887
 cis effect, 834–5, 838, 839, 842
 cis and *trans* disubstituted alkenes,
 842–4
 electron-donating substituents, 841
 electron-withdrawing substituents, 840–2,
 852–6
 ene products, 840
 fullerene adducts, 857–60
 geminal
 dimethyl trisubstituted alkenes, 844–5,
 846
 methyl groups, 875
 regioselectivity, 845–52
 intraeolite photooxygenation, 874–8,
 886, 887
 kinetic isotope effect, 840
 non-bonded interactions, 842–4, 850–2
 phenyl substituted alkenes, 839–42
 rotational barriers, 836, 847–9
 singlet oxygen ene reaction, 836
 site selectivity, 833–42
 solvent effects, 854–6
 syn selectivity, 834, 839–42
 synthetic applications, 886, 888, 889–92
 transition states, 859–60
 trisubstituted alkenes, 833–6, 844–5,
 846, 874–7
 twisted 1,3-dienes, 856–7, 858
 cholesteryl ester oxidation, 692–3
 dioxiranes
 C–H bond oxygen insertion, 1161
 epoxidation, 1150
- Regression analysis, enthalpies of formation,
 152, 158, 160, 162
- Regulatory agencies, safety issues, 745–9
- Relative mass response factor, flame ionization
 detection, 689
- Renilla*, bioluminescence, 1255
- Resorufin, hydrogen peroxide determination,
 642–3
- Retinal ischemia, lipid hydroperoxides, 612
- Rhenium catalysts
 nitrogen compound oxidation, 803
 olefin epoxidation, 790–2, 1090–1
 see also Methyltrioxorhenium
- Rhenium complexes, olefin epoxidation, 453,
 459–62, 463–70, 471
- Rhodamine, synthesis, 740, 741
- Rice, ozone resistance, 616
- Ring bending vibrations, ozonides, 721, 722
- Ring enlargement, autoxidation, 219–21
- Ring-opening reactions
 antimalarial endoperoxides, 1301–4
 cyclobutane, 164
- Ring twisting vibrations, primary ozonides,
 721
- Risk labels, IATA/ICAO, 751–3
- Risk phrases, 621, 748, 749
- River water, peroxide determination, 642
- RNA, ozone disinfection, 616
- ROS *see* Reactive oxygen species
- Rose Bengal sensitized photooxidation, 890
- Rotational barriers, regioselective allylic
 hydroperoxide formation, 836, 847–9
- Rotational isomers, peroxynitrous acid, 8–9
- Rotational spectra, ozonides, 721, 722–3
- RP-HPLC, hydrogen peroxide determination,
 627
- RTECS, commercial data, 621, 749
- Rubber, hydroperoxide determination, 676
- Rubidium ozonide, 735
- Rubrene
 bleaching, 734
 phosphite–ozone adduct detection, 732
- Rubrene peroxide, thermochemistry, 166
- Rugosal A, synthesis, 219
- Russell mechanism, lipid photooxidation,
 949–50
- Ruthenium complexes
 alcohol oxidation, 788–9
 alkene/alkyne vicinal dihydroxylation, 556
 dioxetane decomposition, 1189–90

- Ruthenium purple, hydrogen peroxide determination, 651
- σ -bonds, C–H dioxirane oxygen insertion, 1138–9, 1158–63
- trans*-Sabinene, synthesis, 891
- SADT (self-accelerated decomposition temperature), 746
- Safety aspects, 621, 625, 744–9, 751–5
- environmental hazards, 747, 751–3
 - occupational hazards, 747–9
 - regulatory agencies, 745
 - transportation, 745–6, 751–3
- Safety phrases, 621, 748, 749
- Safflower oil
- anisidine value, 666
 - peroxide value, 657, 661, 662
- Salen ligands, manganese complexes, 449–53
- Salicylideneaminato ligand (salen), transition metal peroxides, 1099, 1113–14
- Saturated hydrocarbon oxidation
- bis(trimethylsilyl) peroxide, 800–2
 - dioxiranes and carbonyl oxides, 44–8
- Schiff bases
- anisidine value, 666
 - hydroperoxide determination, 678
 - TBARS assay, 668
- Schiff's reagent, liquid chromatography, 719
- Sclerotium rolfsii*, reactive oxygen species, 610
- Scopoletin, hydrogen peroxide fluorometry, 627, 642
- Seafood, hydroperoxide determination, 680
- Seawater, hydrogen peroxide content, 606, 629, 639, 642, 645
- Secondary amines, dioxirane oxidation, 1151–2
- Secondary oxidation products
- oxidation indices, 656, 665–72
 - acid value, 672
 - anisidine value, 656, 666
 - carbonyl compounds, 656, 669–71
 - conjugated dienes value, 671–2
 - thiobarbituric acid reactive substances, 656, 666–9
- Secondary ozonides *see* Final ozonides
- Selected reaction monitoring (SRM), mass spectrometry, 693
- Selenides
- nucleophile oxidation, 70–2
 - organo-catalyzed epoxidation, 384–5
 - peroxynitrous acid oxygen transfer, 14–15, 17, 18
- Selenium-containing compounds, dioxirane oxidation, 1157
- Selenophenes, dioxirane oxidation, 1157
- Selenyl radicals, triplet oxygen domino reactions, 223, 227
- Self-accelerated decomposition temperature (SADT), 746
- Self-modeling multivariate analysis technique *see* SIMPLISMA
- Self-sensitized oxygenation, fullerene adducts, 857–60
- Semen, reactive oxygen species, 612
- Sensorial quality appreciation, oxidation stability, 664
- Serum protein
- oxidative damage, 614
 - see also* Human serum
- Sesquiterpenes, structural chemistry, 133–6
- SET *see* Single electron transfer
- Sharpless epoxidation, allylic alcohols, 789
- Shelf durability, peroxide value, 656
- Ship-in-the-bottle strategy, chiral dioxetane synthesis, 1176–7
- SIDS database, cumyl hydroperoxide, 622
- Silane hydrotrioxides, ozonolysis intermediates, 811
- Silanes
- ozone adducts, 734
 - ozonolysis, 810–14
- Silane trioxides, ozonolysis intermediates, 811–14
- Silanols, C–H bond dioxirane oxygen insertion, 1162
- Silanone, disilene oxidation, 821
- Silicon peroxides *see* Silyl peroxides
- Silicotungstate compound, olefin epoxidation, 440
- Silver fluoroboride, mass spectrometry, 693, 703
- Silyl alkyl peroxides
- from chlorotriorganosilanes, 779–83
 - from silyl enol ethers, 779
- Silyl aryl peroxides, from chlorotriorganosilanes, 779–80
- Silyl enol ethers
- dioxirane asymmetric epoxidation, 1150
 - silyl peroxide preparation, 779
- Silyl hydroperoxides
- preparation, 776–7
 - thermal stability, 777
- Silyl hydrotrioxides, silane ozonolysis, 812
- Silyl peroxides, 776–821
- alcohol synthesis via hexa- and pentacoordinates, 808–10
 - cyclic, 814–21
 - preparation, 776–83
- Silyl peroxosulfates, reactions, 840–64
- Silyl peroxyesters, preparation, 779
- SIMPLISMA
- multivariate analysis, 624
 - peroxycarboximide acids, 702
- Single-bonded oxygen functional groups thermochemistry, 155–8

- alkoxyl substituents, 156, 157–8
- gem*-dioxxygen substituents, 157
- homologous series, 157
- hydroxyl substituents, 155–8
- Single electron transfer (SET)
 - two-bond homolysis, 902
 - see also* Electron transfer reactions
- Singlet diradicals, triplet oxygen trapping, 192–3
- Singlet oxygen
 - amino acid and peptide oxidation, 966–70
 - cholesterol hydroperoxides in skin, 612
 - cycloaddition with dienes
 - 1,3-dienes, 252–73
 - [4 + 2] cycloaddition, 253–71, 1324, 1325, 1332
 - [2 + 2] cycloaddition
 - chiral dioxetane synthesis, 1172, 1173–8, 1224
 - to vinyl ether, 1325–6, 1327
 - dialkyl peroxide formation, 706
 - dioxirane
 - DNA photooxidation, 1201–2, 1203
 - oxidation, 1155
 - disilirane oxidation, 818
 - ene reaction allylic hydroperoxides, 673, 831–98
 - anti* orientation, 856
 - chiral auxiliaries, 868–9
 - cis* alkyl substituents, 850–2
 - cis* and *trans* disubstituted alkenes, 842–4
 - criss-cross flexibility, 835–6
 - cyclic hydrocarbons, 861–3, 864
 - diastereoselectivity, 860–9
 - dye-sensitized intrazeolite photooxygenation, 869–86, 887
 - heteroatom substituents, 861, 863, 864
 - quantum yield, 858
 - regioselectivity, 833–60
 - synthetic applications, 886, 888–93, 1324, 1326, 1332
 - germyl hydrotrioxide decomposition, 823
 - guanine oxidation, 939, 941–3
 - hydroperoxide synthesis, 324–6, 341, 342, 679, 681, 684, 696
 - lipid photooxidation, 948–9
 - ¹⁸O-labeled trapping, 951
 - light emission, 951
 - Russell mechanism, 949–50
 - 8-oxo-7,8-dihydroguanine oxidation, 943, 944, 976–7
 - ozonide synthesis, 718, 730, 734
 - pericyclic olefin transformation, 94
 - phosphite–ozone adducts, 732
 - prochiral alkene reaction, 341, 342
 - protein hydroperoxide formation, 972
 - silyl enol ether reaction, 779
 - trimethylsilyl hydrotrioxide, 812
 - Vitamin B₆ detoxification, 610, 694–5, 710
- ²⁹Si NMR spectroscopy, dimethylphenylsilyl hydrotrioxide, 182
- SIRE technique, hydrogen peroxide biosensor, 653
- Site selectivity
 - allylic hydroperoxide formation
 - allylic alcohols and amines, 836, 837
 - anti *cis* effect, 836–9, 840, 841
 - cis* effect, 834–5, 838, 839, 842
 - isobutenylarene intrazeolite photooxygenation, 880–3
 - kinetic isotope effect, 840
 - phenyl substituted alkenes, 839–42
 - syn* selectivity, 837, 839–42
 - trisubstituted alkenes, 833–6
- Skatolyl hydroperoxide, 616, 676, 678
- Skin, cholesterol hydroperoxides, 612
- Snow, hydrogen peroxide determination, 648
- SOD *see* Superoxide dismutase
- Sodium, zeolite Na–Y photooxygenation, 870–4, 885–6, 887
- Sodium borohydride, hydroperoxide determination, 687, 690, 691, 692
- Sodium hypochlorite, allylic hydroperoxides, 673
- Sodium metabisulfite, Meldola Blue optode, 630
- Sodium perborate, hydrogen peroxide determination, 652
- Soil, analysis of peroxides, 608
- Solar radiation, peroxides in river water, 642
- Solid phase extraction, hydrogen peroxide determination, 635
- Solid state ¹⁷O NMR spectroscopy, 185
- Solutions, transition metal peroxide characterization, 1068–72
- Solvated electron addition, thymine hydroperoxide formation, 926–7
- Solvents
 - dioxirane oxidation, 1154
 - ene reactions
 - diastereoselectivity, 860
 - regioselectivity, 854–6
 - organic solvents, 658
 - peroxide value, 658
 - polarity effects, 856, 860
 - safety issues, 745
- Soot, hydroperoxide determination, 678
- Sorbic acid, 2,2-dimethylloxazolidine derivatives, 260, 261
- Soybean lipoxxygenase, phospholipid oxidation, 668
- Soybean oil
 - anisidine value, 666

- Soybean oil (*continued*)
conjugated dienes value, 671
peroxide value, 661, 663
TBARS assay, 668
- Soybean peroxidase, hydrogen peroxide biosensor, 654
- Spectroscopic methods, peroxide value, 657
- Sperm motility
reactive oxygen species, 612
TBARS assay, 669
- Sphingomyelin, IR spectrophotometry, 683–4
- Spin delocalization, polar effects in decomposition, 903
- Spin labels, free radicals, 665
- Spin–lattice relaxation
oxidized functional groups, 695
poly(methylstyrene peroxide), 709
- Spin trapping
artemisinin ESR, 1291
free radicals, 665
- Spirobicyclic peroxides, synthesis, 238
- Spiro 1,2,4-trioxanes, synthesis, 1326, 1327, 1329, 1330, 1332
- Spontaneous decomposition, peroxidic compounds, 617
- SRM (selected reaction monitoring), 693
- Stability, oxidation indices, 656, 664–5
- Standard enthalpy of formation *see* Heat of formation
- Standards, light emission intensity calibration, 1224
- Stannyl peroxides, dialkyl peroxide synthesis, 361, 362
- Steam distillation, TBARS assay, 667
- 1-Stearoyl-2-arachidonoyl–GPC, 737, 738
- Stereogenic centers
chiral alkenes, 884–5, 1144
dihydrogen trioxide, 131
- Stereoisomerism
cyclopentane bromohydroperoxides, 313, 314
see also Isomerization
- Stereoselectivity
chiral dioxetane synthesis, 1173–8
chiral hydroperoxide synthesis, 339–48
dioxiranes, 1139
C–H bond oxygen insertion, 1163
configuration retention, 1163
epoxidation, 1144–50
hydroperoxy anion transfer, 382
- Steric effects
hydrogen dioxide, 96–7
peroxide dihedral angle, 101, 177
- Steric strain
diastereoselective allylic hydroperoxide formation, 866
enthalpies of reactions, 154, 163, 166
- Sterilization, hydrogen peroxide biosensors, 653
- Steroidal endoperoxides, antitumour activity, 1334–5
- Steroids, hydroperoxide determination, 678
- Stolonoxide A
natural occurrence, 608, 609
structure, 709
- Storage
long-term, 672
oxidation stability, 664–5, 672
peroxides, 617
- Strain, steric strain, 154, 163, 166, 866
- Strained endoperoxides, peroxyacetalization, 277–85
- Strain energy, dioxiranes, 1134–5
- Stratosphere, emissions model, 605
- Structure
acyclic organic peroxides, 93–144
dialkyl peroxides, 708–16
dimesityldioxirane, 26, 1133–4
dioxiranes, 26, 27
hydroperoxides, 690–7
natural products, 133–8
organic peroxy compounds, 105–31
peroxyacids and derivatives, 701–5
polyoxo compounds, 131–3
transition metal peroxides
peroxo complexes, 1061–3
 η^2 -peroxo complexes, 1061–3
 μ -peroxo complexes, 1064–8
zeolites, 869–70
Na–Y local minima structures, 873
see also Crystal structure
- Styrene
polymerization, 697
primary ozonide, 720
- Sublimation *see* Enthalpies of sublimation
- Substantia nigra*, Parkinson's disease, 613
- Substitution
aryl-substituted olefins, 384–5
tert-butyl phenylperacetate thermolysis, 903–4, 906
1,2-dioxetane chemiluminescence, 1228
meta-effect, 1186–8, 1236–7
disubstituted alkenes, 842–4
hydrocarbon-substituted peroxides, 147–55
aromatic substituents, 150
hydroperoxide cyclization, 230, 233–52, 253
meta-substitution, 899, 903, 1186–8, 1236–7
methyl substitution
benzyl carbonyl hypochlorite photolysis, 907–9
nucleophile oxidation, 15
 ^{17}O NMR spectroscopy, 177
para-substitution, 899, 903

- polar effects in decomposition, 899–913
- polyoxometallates, 1057
- single-bonded oxygen functional groups, 155–8
 - alkoxyl substituents, 157–8
 - hydroxyl substituents, 155–8
- sulfonyl peroxides, 1005–6
- thymine/thymidine bromohydrins, 927–8
- 1,2,3-trisubstituted cyclopropanes, 205, 206
- trisubstituted enol ethers, 842
- see also* Trisubstituted alkenes
- Substrates, oxidation in biological systems, 614–17
- Sugar-derived ketones, catalyzed dioxirane epoxidation, 1147
- Sulfanilamide, TBARS assay, 667
- Sulfate ion radical, peroxydisulfate organic salts, 1014
- Sulfides
 - dioxirane epoxidation, 1136, 1138
 - dioxirane oxidation, 1156
 - chiral, 1156
 - prochiral, 1156–7
 - nucleophile oxidation, 70–2
 - oxidation, 472–92, 493–5
 - peroxynitrous acid oxygen transfer, 14–17
 - transition metal peroxide oxidation, 1095–101
- Sulfinylperoxy intermediate, superoxide reactions, 1034
- Sulfonates, C–H bond unreactive to insertion, 1160
- Sulfones
 - C–H bond unreactive to insertion, 1160
 - dioxirane oxidation, 1156
- Sulfonic acids, C–H bond unreactive to insertion, 1160
- Sulfonyl endoperoxides
 - parasitocidal activity, 1309
 - synthesis, 1306–9, 1332
- Sulfonyl peroxides, 1001–2, 1004–7
- Sulfonylperoxy radical, superoxide reactions, 1035–9
- Sulfoxidation
 - enzyme-catalyzed, 474–6
 - metal-catalyzed, 476–92, 493–5
 - asymmetric, 478–92, 493–5
 - non-asymmetric, 477–8
 - transition metal peroxides, 1070
 - uncatalyzed, 472–4
- Sulfoxides, dioxirane oxidation, 1156
- Sulfur-containing compounds oxidation
 - bis(trimethylsilyl) peroxide reactions, 805–6
 - dioxiranes, 1156–7
 - with superoxide, 1032–9
- Sulfur dioxide, hydrogen peroxide determination, 637
- Sulfur peroxides, 1002–39
- Sunflower oil
 - anisidine value, 666
 - ozonization, 719, 725
 - peroxide value, 657, 662
- Supercritical fluid extraction
 - hydrogen peroxide determination, 638
 - hydroperoxide determination, 678
- Superoxide anion radical
 - amperometry, 653
 - Bacillus subtilis* defense mechanism, 610
 - bovine serum albumin γ -radiation, 614
 - generation inhibition, 612
 - hydroperoxide synthesis, 315, 320
 - lucigenin oxidation, 645, 1250–1
 - luminol oxidation, 643, 644, 1242–4
 - organic sulfur compounds, 1032–9
 - ozone water disinfection, 606
 - peroxynitrite generation, 10, 611–12
- Superoxide dismutase (SOD)
 - hydrogen peroxide biosensor, 653
 - lucigenin oxidation, 1250–1
 - luminol oxidation, 1242
- Superoxides, ozonides, 735–6
- Surface coatings
 - alkyd resin coatings, 658, 662, 672
 - durability testing, 683
 - peroxide value, 658, 662
 - polyester–melamine, 683
 - see also* Coatings
- Swern dimer, hydrogen bonding, 104, 105
- Synchronous transition states, peracid alkene epoxidation, 50–8
- syn* selectivity, regioselective allylic hydroperoxide formation, 834, 839–42
- Synthesis
 - artemisinin analogues, 1313–17
 - asymmetric synthesis, 868
 - chiral dioxetanes, 1173–8
 - cyclic peroxides, 189–305
 - dialkyl peroxides, 351–62
 - 1,2-dioxanes, 192–273
 - 1,2-dioxolanes, 192–273
 - endoperoxides, 192–273, 1317–31
 - chemistry, 1323–31
 - hydrogen peroxide, 362
 - hydroperoxides, 309–51
 - chiral hydroperoxides, 329–51
 - general methodology, 309–29
 - singlet oxygen ene reaction, 886, 888–93
 - synthetic methodologies, 309
 - thymine hydroperoxides, 927–30
 - transition metal peroxides
 - peroxo complexes, 1057–9
 - μ -peroxo complexes, 1059–61
 - 1,2,4-trioxanes, 273–91

- Tandem base modifications
 thymine hydroperoxides, 933
 uracil hydroperoxides, 935, 936
- Tantalum(V) complexes
 hydrogen peroxide determination, 635–6
 olefin epoxidation, 422–5
- Taste, deterioration evaluation, 664
- Tautomerization, hydrogen peroxide–water
 oxide, 97
- (–)-Taxol, synthesis, 265
- TBARS *see* Thiobarbituric acid reactive
 substances
- TBHP *see* *t*-Butyl hydroperoxide
- TBS-protected-3,5-cycloheptadienol,
 photooxygenation, 266
- TCPO (bis(2,4,6-trichlorophenyl) oxalate),
 1189, 1190, 1222, 1225, 1258, 1259,
 1268–9
- TDG (transport of dangerous goods), 745–6
- Technetium complexes, olefin epoxidation, 442
- Technological world, peroxide involvement,
 617–24
- Teeth whiteners, percarbamide, 623
- Temperature, reaction rates, 903–12
- Terminal olefins, selenide-catalyzed
 epoxidation, 384–5
- α -Terpinene, peroxide synthesis, 706
- α -Terpineol, preparation, 790
- Terrorists, dialkyl peroxide explosives, 708
- Tertiary amines, dioxirane oxidation, 1152
- Tertiary hydroperoxides, structural
 characterization, 690–1
- N,N,N',N'*-Tetraacetylenediamine, bleach
 production, 623
- Tetraalkylammonium hydroxide, 736
- Tetraalkylammonium ozonide, 736
- Tetraalkylammonium salts, transition metal
 peroxides, 1082
- Tetraalkylammonium superoxide, 736
- 1,1,2,2-Tetraarylcyclopropanes,
 photooxygenation, 205–6
- Tetrachloroethene, π -complex with ozone,
 731–2
- Tetracyanoethylene complexes, disilanes, 816
- Tetracyclone, bleaching, 734–5
- Tetraethylammonium ozonide, 736
- Tetragermabuta-1,3-diene, 825, 826
- Tetrahedral distortion
 acyclic organic peroxides, 103
 alkyl hydroperoxides, 110
 anion ligands, 119
- Tetrahydrobenzopyrans, 1,2,4-trioxane
 synthesis, 291
- 1,2,3,4-Tetrahydronaphthyl hydroperoxide
 (THPO), kinetic resolution synthesis,
 331–2
- Tetrahydropranyl ether, peroxydisulfate
 reactions, 1018
- N,N,N',N'*-Tetrakis(2-benzimidazolylmethyl)-
 1,3-diaminopropan-2-ol, hydrogen
 peroxide determination, 637
- N,N,N',N'*-Tetrakis[2'-(1'-ethylbenzimidazol-
 yl)-1,3-diamino-2-hydroxypropane],
 transition metal peroxides, 1066
- meso*-Tetrakis(4-sulfonatophenyl)porphine,
 luminol oxidation, 646
- 2,4,6,8-Tetrakis(thiomorpholino)pyrimido
 [5,5-*d*]pyrimidine, hydroperoxide
 determination, 681
- Tetralin hydroperoxide, enthalpy of reaction,
 153
- Tetramethylammonium ozonide, 736
- Tetramethyl-1,2-dioxetane (TMD)
 chemical titration, 1224
 chemiluminescence, 1221, 1234
 quantum yield standard, 1224, 1226
- N,N,N',N'*-Tetramethyl-*p*-phenylenediamine
 hydrogen peroxide determination, 735, 631,
 633
 hydroperoxide determination, 675, 678
- N,N,N',N'*-Tetramethyl-*p*-phenylenediamine
 dihydrochloride (Wurster's reagent), 678,
 684
- Tetraoxanes, synthesis, 1317, 1318, 1326–8,
 1332
- Tetraphenyl-distilbene, oxidation, 712–13
- 2,4,6,8-Tetrathiomorpholinopyrimidol[5,4-*d*]
 pyrimidine, 698
- 1,2,4,5-Tetroxanes
¹⁷O NMR spectroscopy, 174, 708
 thermochemistry, 164–5
- Tetroxides
 analytical aspects, 740
 structural chemistry, 133
 thymine oxidation, 924–5
- TFD *see* Methyl(trifluoromethyl)dioxirane
- TFDO *see* Methyl(trifluoromethyl)dioxirane
- Theoretical calculations
 dioxiranes, 26–48
 enzymatic heterocycle oxidation, 77–82, 83
 hydroperoxide oxygen atom transfer, 67–82
 metal-catalyzed peroxide oxidation, 1057
 peracid alkene epoxidation, 48–67
 peroxide group, 1–91
 historical perspective, 3–4
 peroxy-nitrous acid, 7–25
- Thermal analysis
 cold on-column injection, 684–5
 dialkyl peroxides, 714–15
 oxidation indices, 672
 ozonides, 730
 phosphite–ozone adducts, 732–3
- Thermal decomposition
 alkali metal ozonides, 735–6
tert-butyl phenylperacetates, 900–7
 dialkyl peroxides, 706–7

- 1,2-dioxetanes, 1181–91, 1213, 1214,
1218–19, 1223, 1226
 computational studies, 1181–2, 1185–6
 diphenoyl peroxide, 1213–14
 tricyclohexylgermyl hydroperoxide, 822–3
 see also Decomposition
- Thermal oxidation
 cholesteryl acetate, 690
 methyl linoleate, 691–2
 pentacosane, 685
 polyethylene, 623, 673, 695
 see also Oxidation
- Thermal stability, hydroperoxide
 determination, 684–5
- Thermal stress, polymers, 685
- Thermochemistry, 145–69
 cyclic peroxides, 163–7
 data sources, 146–7
 hydrocarbon-substituted peroxides, 147–55
 multiply-linked peroxides, 163–7
 peroxycarboxylic acids and derivatives,
 158–213
 single-bonded oxygen functional group
 peroxides, 155–8
- Thermogravimetric analysis, poly(methyl
 methacrylate peroxide), 714
- Thermolysis
 tert-butyl phenylperacetates, 903–7
 chemiluminescence, 680
 percarboxylate esters, 161
- Thermoneutrality, enthalpies of reactions, 154,
 158, 164, 166
- Thiacalixarene, quinoneimine dyes, 630
- Thiamine hydrochloride
 hydrogen peroxide determination, 641–2
 hydroperoxide determination, 678
- Thiobarbituric acid reactive substances
 (TBARS)
 oxidation stability, 664
 peroxide determination kit, 736
 secondary oxidation products, 656, 665,
 666–9
- Thiochrome, hydrogen peroxide determination,
 641–2
- Thiocyanate
 hydrogen peroxide determination, 626, 628
 hydroperoxide determination, 676
 lactoperoxidase oxidation, 612
 peroxide value measurement, 658
- Thioether, percarboxylic acid determination,
 699
- Thiol–olefin co-oxygenation (TOCO)
 cyclic peroxide synthesis, 221–3, 224, 225,
 226, 250, 251
 endoperoxide synthesis, 1330
- Thiols, dioxirane oxidation, 1156
- Thionin, zeolite Na–Y photooxygenation, 870,
 872, 880
- Thiophene, dioxirane oxidation, 1156
- Thiourea, dialkyl peroxide synthesis, 706
- 1,4-Thioxane, oxidation, 805–6
- Thiyl radicals, triplet oxygen domino
 reactions, 221–3, 224, 225, 226
- THPO (1,2,3,4-tetrahydronaphthyl
 hydroperoxide), 331–2
- Thromboxanes, from arachidonic
 hydroperoxides, 612
- Thylakoids, vesiculation mechanism, 617
- Thymidine
 hydroperoxide determination, 676, 695
 oxidation, 616, 922
 photosensitization, 929
- Thymidine bromohydrins, Br substitution,
 927–8
- Thymidine iodohydrins, halogen substitution,
 928–9
- Thymidine peroxides, decomposition, 930–3
- Thymine
 oxidation, 670, 922–6, 976
 ozonolysis, 616
 peroxide value, 657, 661
- Thymine bromohydrins, Br substitution, 927–8
- Thymine hydroperoxides
 characterization, 921–2
 base, 921
 nucleoside, 922
 decomposition, 930
 formation mechanism, 922–7
 hydroperoxides, 919, 921–33
 synthesis, 927–30
 tandem base modifications, 933
- Ti–HMS, olefin epoxidation, 418
- Tin(IV) chloride
 Baeyer–Villiger oxidation, 786–7
 fatty acid hydroperoxides, 690
 olefin oxidation, 792–3
- Tin complexes, Mo-oxide, 428
- Tiron, Fe(III) enhancement, 658, 659
- Tissue
 animal, 669
 plant, 667, 676
- Tissue homogenizates
 hydroperoxide determination, 676
 oxidative damage, 669
- Titanium, hydrogen peroxide corrosion, 623
- Titanium(IV) complexes
 hydrogen peroxide determination, 635–6
 olefin epoxidation, 417–22
- Titanium peroxyacid, hydrogen peroxide
 determination, 633, 635, 637
- Titanium silicalite (TS-1), transition metal
 peroxides, 1055, 1082–3, 1108
- Titanium tetraisopropoxide, allylic alcohol
 epoxidation, 395
- Titanyl sulfate, hydrogen peroxide
 determination, 632

- Titration
 coulometric, 664
 dialkyl peroxide determination, 707
 hydrogen peroxide determination, 627
 hydroperoxide determination, 673–4
 Kingzett method, 627
 ozonide determination, 718, 736
 peroxide value, 657, 663, 664
 see also Iodometry
- TMA (trimethylamine), 75, 76
- TMD *see* Tetramethyl-1,2-dioxetane
- TMSP (transition metal substituted polyoxometalates), 1081–2, 1091, 1107, 1116, 1117
- TOCO *see* Thiol–olefin co-oxygenation
- Tocopherols, TBARS assay, 668
- Torsion angles, hydroperoxides, 690
- Tosylhydrazones, superoxide reactions, 1036
- Total hydroperoxides *see* Peroxide value
- Total oxidative capacity, titration methods, 674
- Total polar phenols, colorimetry, 664
- Toxicity
 t-butyl hydroperoxide, 613
 organic peroxides, 617
 RTECS data, 749
 safety aspects, 745
- Toxic substances
 labeling codes, 621, 753
 UN classification, 746
- TPA (tris(2-pyridylmethyl)amine), 1117
- Transferrin, antitumour activity, 1335–6
- Transition metal catalysts, 1055–7
 alcohol oxidation, 787–9, 1105–8
 olefin epoxidation, 790–2
- Transition metal peroxides, 1053–128
 characterization in solution, 1068–72
 techniques, 1069
- enantioselective sulfoxidation, 1070
- reactivity
 alcohols, 1105–8
 alkenes, 1079–95
 electrophilic substrates, 1072–4
 heteroatoms, 1095–105
 hydrocarbons, 1114–17
 ketones, 1108–14
 mechanistic aspects, 1072–9
 nucleophilic substrates, 1074–6
 radical reactions, 1076–9
- solid state structures
 peroxo complexes, 1061–3
 η^2 -peroxo complexes, 1061–3
 μ -peroxo complexes, 1064–8
- synthesis
 peroxo complexes, 1057–9
 μ -peroxo complexes, 1059–61
- Transition metal substituted polyoxometalates (TMSP), 1081–2, 1091, 1107, 1116, 1117
- Transition states
 ethylene epoxidation, 36–7
 synchronous vs. asynchronous, 50–8
- Transportation
 forbidden materials, 621
 hazardous material labeling, 747–8, 751–3
 safety issues, 745–6
- Transport of dangerous goods (TDG), 745–6
- Trauma, plasma oxidation level, 631
- Triacetone triperoxide explosive, 707–8
- Triacylglycerides, mass spectrometry, 689
- Triarylgermyl hydroperoxide, formation, 822
- Triarylphosphine, hydroperoxide determination, 679
- Triaryl phosphite–ozone adducts, 706
- Tri(*n*-butyl)silyl peroxides, bis(trimethylsilyl) peroxide reactions, 796
- Trichloroacetyl chloride, from tetrachloroethene, 731
- Tricyclic isoalloxazine, enzymatic oxidation, 77
- Tricyclic trioxanes, synthesis, 282, 283
- Tricyclohexylgermyl hydroperoxide, thermal decomposition, 822–3
- Triethylsilane, oxidation, 807–8
- Triethylsilyl hydrotrioxide
 1,2-dioxetane synthesis, 812–14
 1,2,4-trioxane synthesis, 278–9, 813–14
- Trifluoroacetic acid, ozonide formation, 695–6
- Trifluoroacetic anhydride, dioxirane acylation, 1160
- Trifluoroacetyl anhydride, peroxycarbonate synthesis, 740
- Trifluoroacetyl peroxide, structure, 702–3
- Trifluoroacetyl peroxyxynitrate, IR spectrum, 743
- Trifluoromethyl fluoroformyl peroxycarbonate photochemical synthesis, 740
- vibrational spectra, 705
- Trifluoromethyl peroxyxynitrate, UV spectroscopy, 743
- Trifluorooperacetic acid, pyrimidine nucleoside peroxidation, 929–30
- Triglycerides
 determination, 633, 671–2
 hydroperoxide determination, 676, 678, 680, 681, 689–90
 oxidation, 693, 692
 ozonides, 719, 726
 peroxidized, 739
 unsaturated, 680, 689, 739
- Triiodide, peroxide value, 658
- Trimethylamine (TMA), oxidation, 75, 76
- Trimethyl(*t*-butylperoxy)silane, preparation, 783
- Trimethylsilyl hydroperoxide preparation
 bis(trimethylsilyl) peroxide hydrolysis, 801
 tetraethylsilane ozonolysis, 810
 trimethyl chlorosilane reaction, 776, 777

- Trimethylsilyl hydrotrioxide, singlet oxygen formation, 812
- α -Trimethylsilyl peroxyesters, preparation, 779
- Trimethylsilyl triflate, ketone oxidation, 89
- Trinder's reagent
(3,5-dichloro-2-hydroxyphenylsulfonic acid), 630, 631
- 2,3,5-Trioxabicyclo[2.1.1]hexane, final ozonide, 729
- 1,2,4-Trioxane antimalarials
C3-aryl, 1325–6, 1327, 1332
carbon-centered radicals, 1283–99, 1309
dimers, 283
endoperoxides, 1282–3
Griesbaum co-ozonolysis, 1331
spiro 1,2,4-trioxanes, 1326, 1327, 1329, 1330, 1332
synthesis, 273–91
allylic hydroperoxide and alcohol coupling, 285–90
peroxyacetalization of carbonyl functions
 β -hydroperoxyalcohols, 273–7, 278
strained endoperoxide systems, 277–85
triethylsilyl trioxide reactions, 813, 814
- Trioxaquinones, antimalarial drugs, 1320
- Trioxaquine-type antimalarial conjugates, 286
- 1,2,4-Trioxepanes, synthesis, 274
- Trioxides
analytical aspects, 740
 ^{13}C NMR chemical shifts, 179
 ^1H NMR chemical shifts, 179
 ^{17}O NMR spectroscopy, 178–82
structural chemistry, 131–2
- 1,2,3-Trioxolanes
nucleophilic addition cyclization, 247, 248
primary ozonides, 721
- 1,2,4-Trioxolanes
antimalarials, 1282, 1317–20, 1332
electron diffraction, 723
ozonides, 719, 721–2, 724, 725, 726–7, 728–9
zwitterion complexes, 734
see also Ozonides
- Trioxolaquinones, antimalarial drugs, 1320
- Trioxycarbonates, hydrofluorocarbon decomposition, 604
- Triperoxides, thermochemistry, 166
- Triphenylantimony, peroxyoxalate chemiluminescence, 1265–6
- Triphenylbromogermene, germyl hydroperoxide formation, 822
- Triphenylgermanol, germyl hydroperoxide formation, 822
- Triphenylgermyl hydroperoxide, formation, 822
- Triphenylgermyl peroxide,
triphenylsilyl(triphenylgermyl) peroxide formation, 824
- Triphenyl hydroperoxides, preparation, 776–7
- Triphenylmethyl hydroperoxide, tetrahedral distortion, 103, 110
- Triphenyl phosphate, ozone adducts, 732
- Triphenylphosphine
dioxirane oxidation, 1154
hydroperoxide determination, 676, 684, 687
ozonization, 718, 719, 726, 737
percarboxylic acid determination, 699
peroxide value, 662
- Triphenylphosphine oxide, dioxirane oxidation, 1154
- Triphenyl phosphite, ozone adducts, 673, 732
- Triphenylphosphite ozonide, 1,2,4-trioxane synthesis, 278–80
- Triphenylsilyl(triphenylgermyl) peroxide,
triphenylgermyl peroxide reaction, 824
- Triplet diradicals, triplet oxygen cycloaddition, 192, 193
- Triplet oxygen
dioxetane-induced DNA photooxidation, 1202–4
hydroperoxyxylation of allylic alcohols, 1329, 1330
peroxidation
[4 + 2] cycloaddition, 211
cycloaddition with cation radicals, 204–12
cycloaddition with diradicals, 192–204
thiyl and selenyl radicals, 221–3, 224, 225, 226–7
thiol–olefin co-oxidation, 221–3, 224, 225, 226, 1330
see also Molecular oxygen
- Tri(*n*-propyl)silyl peroxides, bis(trimethylsilyl) peroxide reactions, 796
- Tris(*p*-bromophenyl)aminium
hexachloroantimonate, oxadisilirane reaction, 817
- Tris(2-pyridylmethyl)amine (TPA), transition metal peroxides, 1117
- Tristimulus method, deterioration evaluation, 656
- 1,2,3-Trisubstituted cyclopropanes,
peroxidation, 205, 206
- Trisubstituted alkenes
photooxidation regioselectivity, 833–6
anti *cis* effect, 836–9
cis effect, 834–5, 838, 839
geminal dimethyl alkenes, 844–5, 846
intrazeolite photooxygenation, 874–7
- Trisubstituted enol ethers, photooxidation site selectivity, 842

- Triterpenes, structural chemistry, 136
- Tropopause, emissions model, 605
- Troposphere
ozone analysis, 605
trifluoromethyl peroxyxynitrate, 743
- Tryptophan
hydroperoxide formation
radical reactions, 614, 615, 960–3
singlet oxygen oxidation, 966–8
- TS-1 (titanium silicalite), 1055, 1082–3, 1108
- TSCATS database (EPA), hazardous
chemicals, 621, 745
- Tungstate-based heteropoly acid, alcohol
oxidation, 496, 497
- Tungsten oxide, amperometry, 653
- Tungsten(VI) complexes
hydrogen peroxide determination, 635–6
olefin epoxidation, 432, 436–42, 444–6
in situ generated catalyst in acid, 437
- Turkey, hydroperoxide determination, 678
- Two-bond homolysis, *tert*-butyl
phenylperacetates, 902, 903
- Two-electron oxidation
peroxyxynitric acid, 21–2
peroxyxynitrous acid, 14–17, 18, 21–2
- Tyrosine buffer, radiometry, 655
- Tyrosine
hydrogen peroxide determination, 651
hydroperoxide formation, 614, 615, 960,
963–6
radical reactions, 614, 615, 960, 963–6
singlet oxygen oxidation, 968, 969
- Tyrosyl free radicals, production, 610
- UHP *see* Urea–hydrogen peroxide
- Ultrasound treatment, hydrogen peroxide in
water, 606, 636
- Ultra-trace analysis, hydrogen peroxide
determination, 638
- Ultraviolet *see* UV
- Uncatalyzed sulfoxidations, 472–4
- Uncertainty, analytical methods, 624
- UN Environment Programme (UNEP)
chemicals safety, 745, 747
SIDS database, 622
- Unfunctionalized olefins
ketone-catalyzed epoxidation, 385–6
metal-catalyzed epoxidation, 416–62,
463–70
- Unimolecular peroxide decomposition
chemiluminescence, 1227–31
asynchronous concerted mechanism, 1230
biradical mechanism, 1181–2, 1227–31
concerted mechanism, 1227, 1228–9,
1230
merged mechanism, 1227, 1230
- United Nations (UN)
chemicals regulation, 745–6, 747
see also UN Environment Programme
- α,β -Unsaturated aldehydes, anisidine value,
666
- α,β -Unsaturated β -diketones, thiol–olefin
co-oxygenation, 250–2
- α,β -Unsaturated ketones
anisidine value, 666
synthesis methods, 199–202, 246–7, 285
- Unsaturated fatty acids
lipid oxidation, 946–7
TBARS assay, 668
- Unsaturated glycerophosphocholine (GPC),
ozonization, 737
- α,β -Unsaturated γ -hydroperoxyketone
photoisomerization, 246–7
1,2,4-trioxane synthesis, 285
- α,β -Unsaturated ketones, triplet oxygen
cycloaddition, 199–202
- Unsaturated lipids
cis unsaturation, 683–4
ozonization characterization, 737
- Unsaturated polyolefins, double bond content,
740
- Unsaturated triglycerides
hydroperoxide determination, 680, 689
reference derivatives, 739
- Upregulation of metabolism, 610
- Uracil
hydroperoxides, 919
hydroxyhydroperoxides, 933–4
tandem base modifications, 935, 936
- Uranium(VI) complexes, hydrogen peroxide
determination, 635–6
- Uranyl nitrate, effect on hydrogen peroxide
analysis, 635
- Urea–hydrogen peroxide (UHP)
crystal structure, 98, 99
disilazane reactions, 814–15
transition metal peroxides, 1083, 1089–90,
1099, 1103, 1113
- Uric acid
determination, 630, 632
enzyme-catalyzed oxidation, 625
free radical trapping, 614
hydrogen peroxide determination, 651
- Urine
glucose determination, 648
hydrogen peroxide concentration, 610, 628,
655
malondialdehyde, 614
- UV irradiation
cholesterol hydroperoxides in skin, 612
free radical formation, 615, 628
- UV spectroscopy, peroxyxynitrates, 743
- UV–visible spectrophotometry
chlorophyll, 664
dialkyl peroxide determination, 707–8

- hydrogen peroxide determination, 627–49
- hydroperoxide determination, 674–83
- peroxide value, 658–61
- Valine
 - hydroperoxide formation, 614, 615, 691, 956, 957
 - protein hydroperoxide decomposition, 987
- Valine hydroperoxides, structure, 691
- Vanadium catalysts
 - allylic alcohol asymmetric epoxidation, 402–6, 407–9
 - olefin epoxidation, 422–5
- Vanadium compounds, peroxovanadates, 186
- Vanadium(V) complexes, hydrogen peroxide determination, 635–6
- Vanadyl ion, hydrogen peroxide determination, 635
- Vanadyl peroxide, absorption spectrophotometry, 635
- van der Waals radii
 - alkanoyl peracids, 125–6
 - alkyl hydroperoxides, 111, 112
- Vaporization *see* Enthalpies of vaporization
- Varamine Blue, hydrogen peroxide determination, 631
- Varnish coatings, peroxide value, 658
- Vascular systems
 - hydrogen peroxide determination, 626
 - peroxynitrite analysis, 740
 - reactive oxygen species, 611–12
 - smooth muscle damage, 613
- Vasoconstriction, *t*-butyl hydroperoxide, 613
- Vegetable products
 - conjugated dienes value, 671
 - peroxide value, 658, 660
- Verruculogen, tremorgenic, 190, 191
- Vesiculation, lipid peroxide removal, 617
- Vibrational spectroscopy
 - dialkyl peroxides, 713–14
 - hydroperoxides, 692
 - imine peroxide, 744
 - peroxynitrates, 742–3
- Vicinal dihydroxylation, alkenes and alkynes, 556, 567–72, 573–5
- Vinyl chloride, π -complex with ozone, 720, 732
- Vinylcyclopropanes
 - domino reactions, 221–3, 224, 225, 226–7
 - peroxidation, 223, 225, 228–9
- Vinyl ether, [2 + 2] cycloaddition of singlet oxygen, 1325–6, 1327
- Vinyl fluoride, final ozonide, 722
- Vinyl hydroperoxide, C–O distance, 103
- Vinyl carbon–hydrogen bonds, peroxide value, 661
- Vinylc functionality, geminal regioselectivity, 849–50
- 3-Vinylindole derivatives, singlet oxygen photooxygenation, 259–60
- 2-Vinylnaphthalene, polyperoxide polymers, 155
- Vinylsilanes, ozonolysis, 275–6
- Viruses, ozone disinfection, 616
- Visible spectrophotometry *see* UV–visible spectrophotometry
- Vitamin B₆ (pyridoxine), singlet oxygen detoxification, 610, 694–5, 710
- Vitamin E
 - antioxidant capacity, 614, 615
 - fluorescence quenching, 660, 711
 - liquid chromatography, 664
 - low-density lipoprotein antioxidant, 611
 - TBARS assay, 668
- Vitreous photofluorometry, hydrogen peroxide determination, 640
- Volatile acids, oxidation stability measurement, 664
- Volatile organic compounds (VOC), in atmosphere, 604, 605
- Wagner–Meerwein rearrangement, sulfonyl peroxides, 1006
- Wastewaters
 - ozonization decolorization, 608
 - pollution level, 739
- Water
 - hydrogen peroxide content, 606, 626, 629, 636, 639, 643
 - ozone disinfection, 606, 673, 740
 - peroxide analysis, 605–8
 - pollution evaluation, 739–40
- Water oxide
 - formation, 97
 - structure, 96
 - tautomerization, 97
- Water tolerance, metal-catalyzed sulfoxidations, 481
- Weitz–Scheffer epoxidation
 - dioxiranes, 1142
 - enones, 364–5, 370
- Wheat flour, dibenzoyl peroxide determination, 698, 701
- Workplace air
 - benzoyl peroxide, 701
 - peracetic acid, 699
- Wurster's reagent, hydroperoxide determination, 678, 684
- X-ray analysis
 - dimesityldioxirane, 1133–4

- X-ray analysis (*continued*)
 hydrogen peroxide, 96
- X-ray diffraction
 acyclic organic peroxides, 105
 dialkyl peroxides, 711–13
 hydroperoxides, 695–6
 ozonides, 726–30, 736
- Xylenol Orange (FOX assay)
 hydrogen peroxide determination, 628, 632, 657, 658
 hydroperoxide determination, 676
- Yingzhaosu
 antimalarial activity, 1282
 natural occurrence, 190, 191, 608, 609
 total synthesis, 224, 226
 X-ray crystallography, 712
 yingzhaosu C synthesis, 217, 218
- Yttrium, zeolite Na–Y photooxygenation, 870–4, 885–6, 887
- Zeolites
 dye-sensitized intrazeolite photooxygenation, 869–86, 887
 cation– π interactions, 873–4
 diastereoselectivity, 884, 885–6, 887
 Na–Y, 870–4, 885–6, 887
 regioselectivity, 875
 thionin-supported, 870, 872, 880
 molybdenum(VI) complexes, 428
 ship-in-the-bottle strategy, 1176–7
 structural features, 869–70
- Zinc organometallics, alkyl hydroperoxide precursors, 322
- Zinc oxide, *t*-butyl hydroperoxide suspension, 624
- Zirconium(IV) complexes
 hydrogen peroxide determination, 635–6
 olefin epoxidation, 417, 419, 422
- Zwitterions
 isobutenylarene intrazeolite photooxygenation intermediate, 880
 ozonide complexes, 734

With kind thanks to Caroline Barlow for creation of this index.

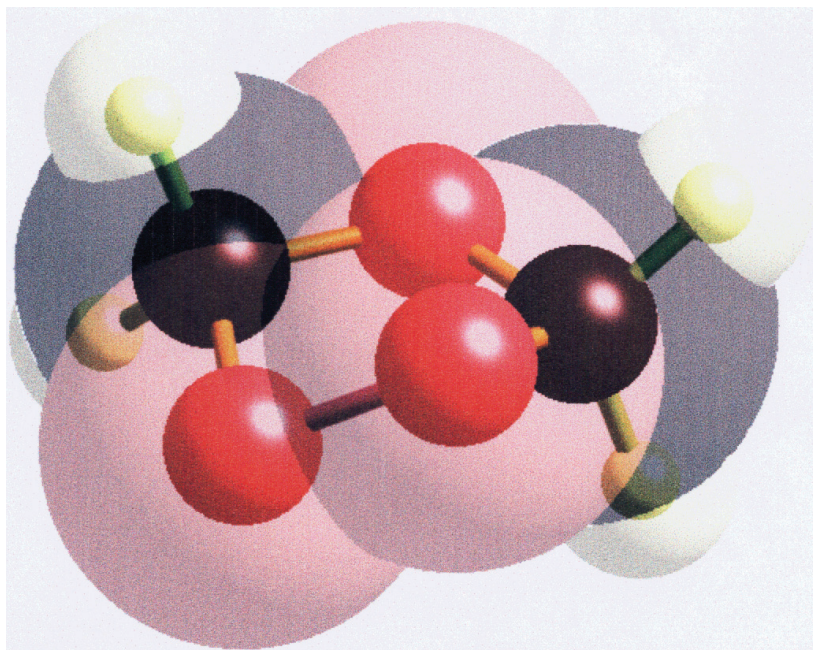
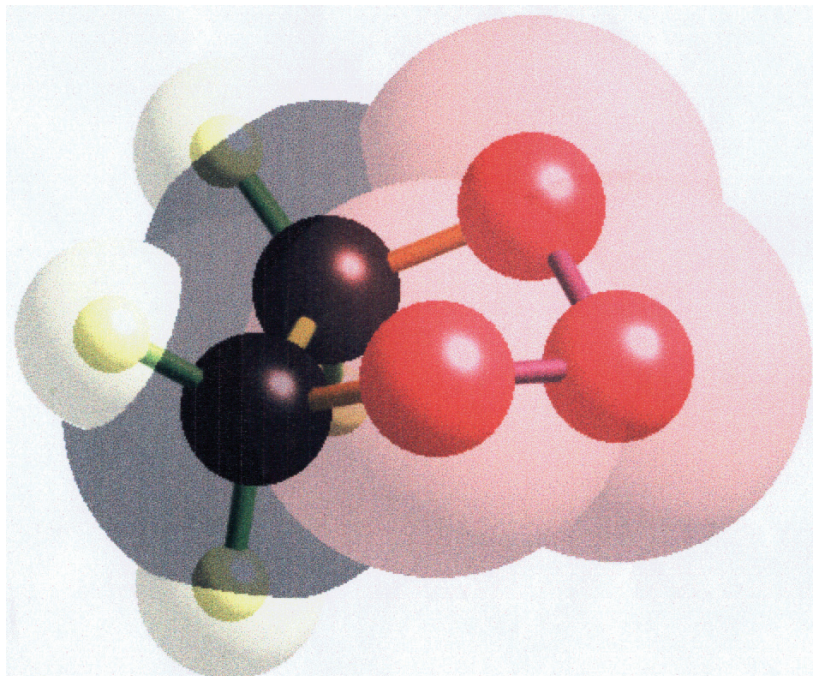


PLATE 1 (APPENDIX 1)

IATA/ICAO HAZARD AND HANDLING LABELS

Except for Radioactive and Handling Labels, text indicating the nature of risk on label is optional.

HAZARD LABELS



* Articles bearing the Explosive labels shown above and falling into Divisions 1.1, 1.2, 1.4F, 1.5 and 1.6 are normally forbidden.



PLATE 2 (APPENDIX 2) Reproduced by permission of the International Air Transport Association (IATA)

IATA/ICAO HAZARD AND HANDLING LABELS

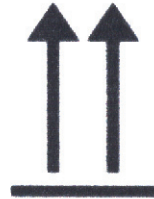
Except for Radioactive and Handling Labels, text indicating the nature of risk on label is optional.

HAZARD LABELS



PLATE 2 (APPENDIX 2) (continued)

HANDLING LABELS



MORE HAZARD LABELS



HARMFUL (Xn) or
IRRITANT (Xi)



ENVIRONMENTAL
HAZARD